Talanta, Vol. 30, No. 1, pp. 1–7, 1983
Printed in Great Britain.

0039-9140/83/010001-07 $03.00/0

TERNARY COMPLEXES OF THE Cu(II) AND Ni(II) CHELATES OF EDTA AND DCTA WITH CYANIDE AND ETHYLENEDIAMINE

J. KORSSE, L. A. PRONK, C. VAN EMBDEN, G. LEURS and P. W. F. LOUWRIER

National Institute for Nuclear Physics and High-Energy Physics Research [NIKHEF, Section K (formerly IKO)], P.O. Box 4396, 1009 AJ Amsterdam, The Netherlands

(*Received* 24 *February* 1982. *Revised* 2 *July* 1982. *Accepted* 25 *August* 1982)

Summary—The formation of the ternary complexes $CuEDTA(en)^{2-}$, $CuEDTA(CN)^{3-}$, $CuDCTA(CN)^{3-}$, $NiDCTA(CN)^{3-}$ and $NiEDTA(en)^{2-}$ has been established spectrophotometrically. The stability constants found were log $K = 2.87 \pm 0.03$, 3.76 ± 0.06, 2.64 ± 0.35, 2.41 ± 0.21 and 2.74 ± 0.35 respectively. For the system $CuDCTA^{2-}$ + en no ternary complex was observed, instead $Cu(en)_2^{2+}$ was formed. No reaction was found for the systems $CoEDTA^{2-} + N_3^-$, $CoDCTA^{2-} + N_3^-$, $NiDCTA^{2-}$ + en, $NiDCTA^{2-}$ + phen, $NiEDTA^{2-}$ + phen, $NiDCTA^{2-} + N_3^-$, $NiEDTA^{2-} + N_3^-$, $CrEDTA^-$ + NH_3, $CrEDTA^-$ + CN^-, $CuEDTA^{2-}$ + N_3 and $CuEDTA^{2-} + N_3^-$. The systems $CoEDTA^{2-}$ + en and $CoDCTA^{2-}$ + en involve more than one equilibrium. The absorption spectra of the ternary complexes between 500 and 850 nm are reported.

Ethylenediaminetetra-acetic acid (EDTA) and *trans*-1,2-diaminocyclohexane-*N*,*N*'-tetra-acetic acid (DCTA) form very stable 1:1 chelates with transition metal ions.[1–3] Since Schwarzenbach published his articles on these chelates much effort has been devoted to the elucidation of their structures.

In crystals containing the EDTA complexes of Cu^{2+},[4] Co^{3+},[5] Co^{2+},[6] Mn^{2+},[7] Fe^{3+},[8] and Zn^{2+},[9] the ligand is sexidentate. It is quinquedentate in crystals of the acidic complex $H_2NiEDTA$.[10]

In aqueous solutions sexidentate EDTA complexes are reported for Fe^{3+},[11] Co^{2+},[6] and Mn^{2+}.[12] In the case of Mn^{2+} it has been established by NMR that the co-ordination sphere includes a water molecule.[12] In acid solution the protonation of a carboxylic group leads to quinquedentate EDTA.[13] In the pH region 5–9 the complexes $AlEDTA^-$, $FeEDTA^-$, $CrEDTA^-$ and $MnEDTA^-$ take up an OH^- ion.[14] Complexes of EDTA and DCTA with Ni^{2+}, Co^{2+}, Cu^{2+}, Fe^{3+} and Hg^{2+} have been reported to form ternary complexes with CN^-, CNS^-, NH_3 and ethylenediamine.[14–17]

For our investigation of the reactivity of ternary complexes towards the hydrated electron[18] we needed the stability constants of the ternary complexes $CuEDTA(en)^{2-}$, $CuDCTA(en)^{2-}$, $CuEDTA(CN)^{3-}$, $CuDCTA(CN)^{3-}$, $NiEDTA(en)^{2-}$ and $NiDCTA(CN)^{3-}$. In this paper the results of our investigations on these complexes are reported.

The continuous-variation and molar-ratio spectrophotometric methods[19] were used to study the equilibria. The first was used only for assessment of the stoichiometry; the changes in the ΔA values were too small to be used for calculating reliable values for the stability constants.

EXPERIMENTAL

Reagents

All chemicals were of analytical grade (Merck, Fluka). They were used without further purification. Demineralized water was further purified by means of a Millipore "Milli Q2" apparatus, which removes most of the organic impurities. The conductivity was about 0.05 $M\Omega^{-1}.cm^{-1}$.

Molar-ratio method

For this method a stock solution A was prepared by dissolving an appropriate amount of the acid form of EDTA or DCTA with sodium hydroxide solution, in a small beaker, to give a neutral solution. The calculated amount of $CuSO_4.5H_2O$, $Ni(ClO_4)_2.6H_2O$ or $Co(ClO_4)_2.6H_2O$ was then added. Sodium perchlorate was added and the pH adjusted with sodium hydroxide solution to the value required for the experiments. The contents of the beaker were transferred quantitatively to a standard flask with a sodium hydroxide solution of the required pH, and this stock solution was then diluted to volume.

A second stock solution B was prepared by dissolving appropriate amounts of potassium cyanide or ethylenediamine hydrochloride and sodium perchlorate (in some cases EDTA or DCTA was also added). After adjustment of the pH this solution was transferred to a standard flask and diluted to volume with a sodium hydroxide solution of the required pH.

The concentrations of the complexing species in the stock solutions were ten times those in the final solutions to be measured, which were prepared by mixing stock solutions A and B in 100-ml standard flasks and diluting them to volume with 0.1*M* sodium perchlorate at the required pH. No special care was taken to prevent absorption of carbon dioxide from the air. The alkaline solutions were exposed to air as briefly as possible.

For the $CuEDTA^{2-}$ + en measurements

The samples contained:

(*i*) 2.002m*M* $CuEDTA^{2-}$; $c_{en} = [EDTA]_{excess} = 0$, 1.59,

3.18, 4.76, 6.35 and 7.94mM; 0.1M $NaClO_4$; pH = 11.0; T = 293 K.

(*ii*) 2.00mM $CuEDTA^{2-}$; $c_{en} = [EDTA]_{excess}$ = 0, 1.4, 2.0, 3.2, 4.8 and 6.4mM; 0.1M $NaClO_4$; pH = 10.85; T = 296.5 K.

For the CuDCTA + en measurements

2.00mM $CuDCTA^{2-}$; $[DCTA]_{excess}$ = 0.2mM; c_{en} = 0, 0.5, 0.75, 1.0, 1.5, 2.0, 4.0, 6.0, 8.0mM; 0.1M $NaClO_4$; pH = 11.0; T = 300 K.

For the $CuEDTA^{2-}$ + CN^- measurements

1.00mM $CuEDTA^{2-}$; $[EDTA]_{excess}$ = 5.0mM; c_{CN^-} = 0, 0,25, 0.38, 0.50, 0.75, 1.0, 1.5, 2.0, 2.5mM; 0.1M $NaClO_4$; pH = 10.8; ambient temperature.

For the $CuDCTA^{2-}$ + CN^- measurements

2.00m$M$$CuDCTA^{2-}$; $[DCTA]_{excess}$ = 1.99mM; c_{CN^-} = 0, 0.50, 0.75, 1.00, 1.50, 4.00, 6.00, 8.00mM; 0.1M $NaClO_4$; pH = 11.0; T = 300 K.

For the $NiEDTA^{2-}$ + en measurements

5.0mM $NiEDTA^{2-}$; $[EDTA]_{excess}$ = 1.0mM; c_{en} = 0, 2, 4, 7, 10, 15mM; pH = 11.1; no $NaClO_4$ added.

For the $NiDCTA^{2-}$ + CN^- measurements

5.01mM $NiDCTA^{2-}$; $[DCTA]_{excess}$ = 0.53mM; c_{CN^-} = 0, 0.4, 0.8, 2.0, 4.0, 6.0, 10.0, 15.0, 20.0mM 0.1M $NaClO_4$; pH = 11.0; ambient temperature.

Method of continuous variations

For this method two stock solutions were prepared, similarly to solutions A and B described above. From these stock solutions series of 11 solutions were prepared by mixing and diluting to volume with 0.1M sodium perchlorate. The following series were measured:

$c_{CuEDTA} + c_{en}$ = 1.0mM; $[EDTA]_{excess} = 2c_{en}$; 0.1$M$ $NaClO_4$; pH = 11.0.

$c_{CuEDTA} + c_{en}$ = 5.0mM; $[EDTA]_{excess} = 2c_{en}$; 0.1$M$ $NaClO_4$, pH = 11.0.

$c_{CuEDTA} + c_{CN^-}$ = 2mM; $[EDTA]_{excess} = c_{CuEDTA} + 1.67c_{CN^-}$; 0.1$M$ $NaClO_4$; pH = 11.0.

$c_{CuEDTA} + c_{CN^-}$ = 9.28mM; $[EDTA]_{excess} = c_{CuEDTA} + 1.5c_{CN^-}$; pH = 11.0; no $NaClO_4$.

$C_{CuDCTA} + c_{CN^-}$ = 4.92mM; $[DCTA]_{excess} = c_{CuDCTA} + c_{CN^-}$; pH = 11.25; no $NaClO_4$.

$C_{NiDCTA} + c_{CN^-}$ = 10.5mM; no excess of DCTA; no $NaClO_4$; pH = 12.

The formation of the ternary complexes was complete within the time necessary for preparing the samples. The solutions were not temperature-controlled, but the temperature variation within one series of measurements did not exceed 0.5°.

Spectra of the solutions were recorded with a Pye Unicam SP 1700 spectrophotometer directly after preparation of the samples. According to the manufacturer the reproducibility of the absorbance is 1% or 0.002, whichever is the larger.

The pH was measured with a Philips CA 11 combined glass electrode fitted to a Philips 9408 digital pH-meter. This system was calibrated with buffer solutions of pH = 7 and 11 or 12 (Merck Titrisol). No effects were observed that could be attributed to interference of perchlorate ions in the pH measurements.

RESULTS AND DISCUSSION

The concentration stability constant for the equilibrium:

$$ML + nX \rightleftharpoons MLX_n \qquad (1)$$

is given by:

$$K^{nX}_{MLX_n} = \frac{[MLX_n]}{[ML][X]^n} \qquad (2)$$

where M stands for the metal ion, L for EDTA or DCTA and X for the secondary ligand. Measurements for the determination of $K^{nX}_{MLX_n}$ must be made at constant ionic strength. Furthermore, interfering substitution reactions such as

$$ML + pX \rightleftharpoons MX_p + L \qquad (3)$$

have to be suppressed. This was done by the addition of an excess of L, ensuring that:

$$\frac{[MX_p]}{[ML]} = \frac{K^{pX}_{MX_p}[X]^p}{K^{L}_{ML}[L]} < 0.01. \qquad (4)$$

The occurrence of a chemical reaction such as (1) or (3) is usually accompanied by a change in the absorption spectrum with change in the ratio c_{ML}/c_X. In exploratory experiments at pH ~11 no changes whatsoever were observed for the following systems: $CoDCTA^{2-} + N_3^-$, $CoEDTA^{2-} + N_3^-$, $NiDCTA^{2-}$ + en, $NiDCTA^{2-}$ + phenanthroline, $NiEDTA^{2-}$ + phenanthroline, $NiDCTA^{2-} + N_3^-$, $NiEDTA^{2-} + N_3^-$, $CrEDTA^-$ + NH_3, $CrEDTA^-$ + CN^-, $CuEDTA^{2-} + N_3^-$ and $CuDCTA^{2-} + N_3^-$. There was evidence for a chemical reaction between ethylenediamine and $CoEDTA^{2-}$ or $CoDCTA^{2-}$. The results indicated that these systems contain more than two different absorbing species.

For the systems $CuEDTA^{2-}$ + en, $CuDCTA^{2-}$ + en, $CuEDTA^{2-}$ + CN^-, $CuDCTA^{2-}$ + CN^-, $NiEDTA^{2-}$ + en and $NiDCTA^{2-}$ + CN^- the results obtained with the molar-ratio method were analysed by the matrix diagonalization program TRIANG.[19] This showed that not more than two absorbing species were present in these systems. Thus only one equilibrium was taken into account. We established

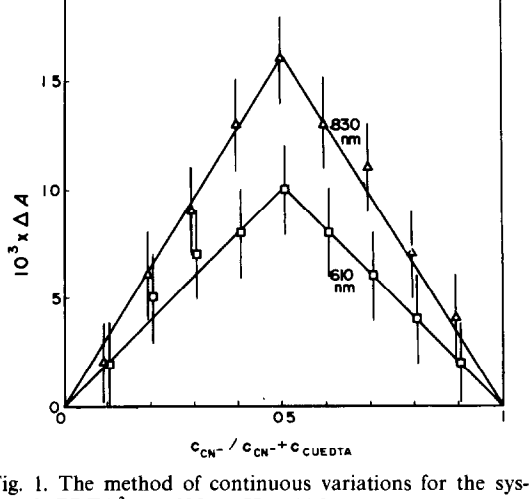

Fig. 1. The method of continuous variations for the system $CuEDTA^{2-}$ + CN^-: pH = 11.0; $c_{CuEDTA^{2-}} + c_{CN^-}$ = 9.28mM; light-path 10 mm.

Table 1. Stability constants of ternary complexes of some EDTA and DCTA chelates with cyanide and ethylenediamine

System	Conditions[a]	log K^{L}_{ML}[b]	log K^{X}_{MLX}	Ref.
$CuEDTA^{2-}$ + en	$\mu \sim 0.15$, pH = 11.0, 293 K	18.8	2.89 ± 0.04	c
	$\mu \sim 0.13$, pH = 10.85, 296.5 K	18.8	2.85 ± 0.05	c
$CuEDTA^{2-}$ + CN^-	$\mu = 0.15$, pH = 10.8	18.8	3.76 ± 0.06	c
$CuDCTA^{2-}$ + CN^-	$\mu = 0.12$, pH = 11.0, 300 K	22.0	2.64 ± 0.35	c
			3.59[d]	24
$NiEDTA^{2-}$ + CN^-	$\mu = 0.1$, pH = 11.0, 298 K	18.6	4.08	25
			3.76[e]	26
$NiDCTA^{2-}$ + CN^-	$\mu = 0.12$, pH = 11.0	20.3	2.41 ± 0.21[f]	c
$NiEDTA^{2-}$ + en	pH = 11.1	18.6	2.74 ± 0.35	c
$CoEDTA^{2-}$ + CN^-	$\mu = 0.2$, pH = 11.7, 298 K	16.3	3.30	27
$CoDCTA^{2-}$ + CN^-	$\mu = 0.1$, pH = 11.5, 298 K	19.6	1.59	25

[a]Measurements done at ambient temperature, unless specified otherwise.
[b]Literature values taken from ref. 3.
[c]This work.
[d]Value obtained by the mole-ratio method.
[e]Value from kinetic measurements.
[f]Unpublished results of Margerum and Hauer gave log K = 2.49 (ref. 22).

$n = 1$ in equation (1) for these systems, by using the method of continuous variations, except for the $CuDCTA^{2-}$ + en system, where no ternary complex is formed. Figure 1 shows the results of this method for $CuEDTA(CN)^{3-}$.

Taking $n = 1$ in equation (1), the following equation was used for the calculation of K^{X}_{MLX}:

$$\epsilon_{apparent} = \frac{(\epsilon_{ML} - \epsilon_{apparent})}{K^{X}_{MLX}[X]} + \epsilon_{MLX} \qquad (5)$$

where $\epsilon_{apparent} = A/lc_{ML}$, A is the absorbance, l the light-path and c_{ML} the analytical concentration of ML, which is kept constant while [X] is varied. Equation (5) is valid only if X and L do not absorb, which is the case for the wavelength intervals studied.

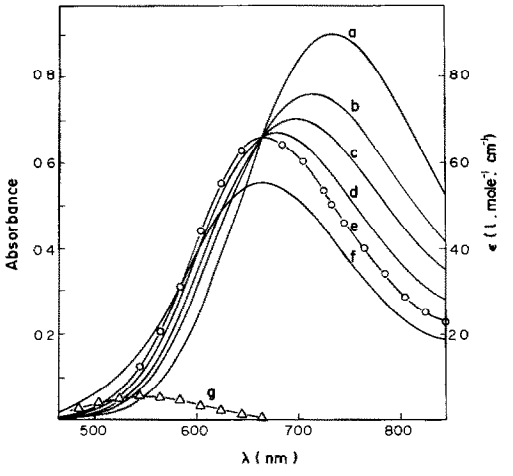

Fig. 2. The system $CuEDTA^{2-}$ + en: pH = 11.0; 0.1M $NaClO_4$; 20°C; $c_{CuEDTA} = 2.002mM$; $c_{en} = 0$, 1.59, 3.18 and 7.94mM for the curves a–d. Curve e: calculated spectrum of $CuEDTA(en)^{2-}$ [equation (5)]. Curve f: c_{en} = 41 mM; $c_{EDTA} = 0.55M$. Curve g: difference spectrum (f − 0.85e), *i.e.*, assuming 15% $Cu(en)_2^{2+}$. Light-path 50 mm. Molar absorptivities are given for curves a and e.

For about 8–10 wavelengths $1/(K^{X}_{MLX})$ was calculated by means of an iterative computer program. The iteration was stopped when two successive slopes of the plots of $\epsilon_{apparent}$ *vs.* $(\epsilon_{ML} - \epsilon_{apparent})/[X]$ differed by less than 1%. The unweighted average of the $1/(K^{X}_{MLX})$ values at the different wavelengths was calculated, giving K^{X}_{MLX}. This method of calculation was unsuccessful in the case of the $CuDCTA^{2-}$ + en system, where divergence occurred at every wavelength. For the other systems consistent sets of stability constants were obtained. The results are given in Table 1, together with some literature values. From the measured absorption curves and K^{X}_{MLX} the absorption spectra of the ternary complexes were determined (Figs. 2, 5–8).

Isomers

Assuming that the secondary ligand X co-ordinates to the metal ion by displacing one or two acetate groups, geometrical isomers have to be considered. For the unidentate CN^- ligand two isomers are possible, for the bidentate ethylenediamine there are three possible isomers (Schemes I and II). As each isomer

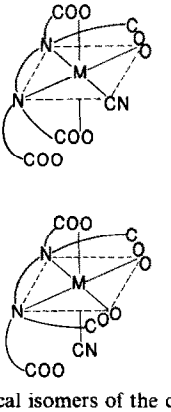

Scheme I. Geometrical isomers of the complex ML(CN).

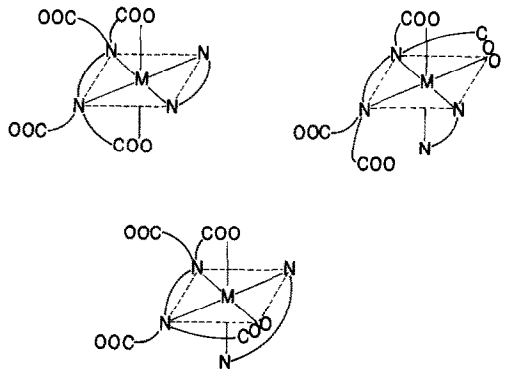

Scheme II. Geometrical isomers of the complex ML(en).

has its own stability constant, the K^{X}_{MLX} values and the absorption spectra have to be considered as average values for the possible isomers.

$CuEDTA^{2-}$ + en

Figure 2 shows some of the absorption spectra used for the evaluation of the stability constant. The $CuEDTA(en)^{2-}$ complex does not undergo any further reaction under the experimental conditions over a period of several months. The wavelength shift of the absorption maximum is about 80 nm (Fig. 2). This very large shift is in contrast with the zero shift for the pair $CuEDTA^{2-}$ and $CuEDTA(NH_3)^{2-}$.[15] This indicates that ethylenediamine is co-ordinated through both nitrogen atoms. Excluding co-ordination numbers higher than six for Cu(II), this means that two acetate groups are displaced by the ethylenediamine molecule (Scheme II).

When it was attempted to verify the calculated spectrum of $CuEDTA(en)^{2-}$, a third species interfered (Fig. 2, curve f). This was shown to be $Cu(en)_2^{2+}$, formed as a result of the high ionic strength of this particular solution ($\mu \simeq 5$). While K^{EDTA}_{CuEDTA} decreases

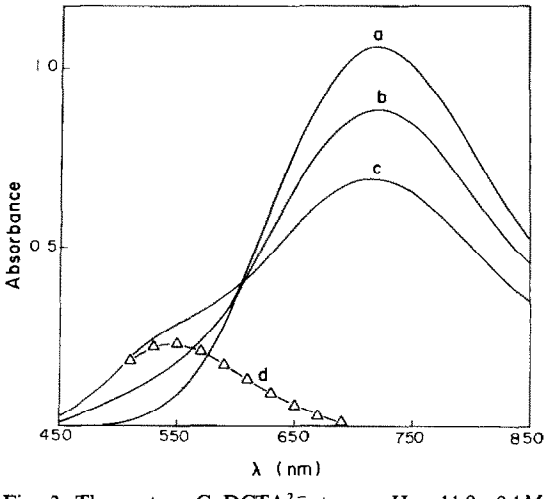

Fig. 3. The system $CuDCTA^{2-}$ + en: pH = 11.0; 0.1*M* $NaClO_4$; 27°C; c_{Cu} = 2.00m*M*; c_{DCTA} = 2.2m*M*; c_{en} = 0, 1.5, 16m*M* for the curves a–c. Curve d: difference spectrum (c − 0.65a), *i.e.*, assuming 35% $Cu(en)_2^{2+}$. Light-path 50 mm.

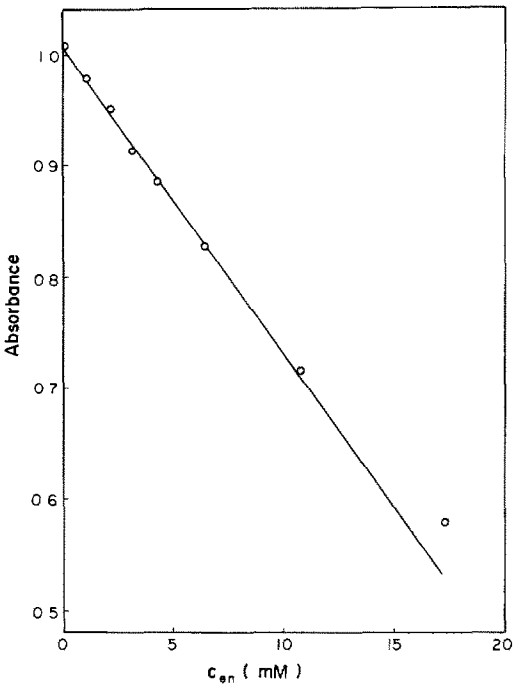

Fig. 4. The $CuDCTA^{2-}$ + en system: pH = 11.86; c_{Cu} = c_{DCTA} = 2.00m*M*. Light-path 50 mm; 720 nm.

with ionic strength, $K^{2en}_{Cu(en)_2}$ will remain practically constant, because the ethylenediamine ligand carries no charge.[20] From the spectra c and f in Fig. 2 we estimated $\Delta(\log K) = \log K^{2en}_{Cu(en)_2} - \log K^{EDTA}_{CuEDTA} =$ 1.7 at this ionic strength. This value seems reliable when compared with the value of $\Delta(\log K) = 0.8$ at zero ionic strength.

$CuDCTA^{2-}$ + en

Figure 3 shows some of the absorption spectra. From this and other experiments two general observations were made:

(*i*) the spectral changes caused by variation of [en] were smaller with larger excesses of DCTA;

(*ii*) at high [en] an absorption band at 550 nm appeared, which is due to $Cu(en)_2^{2+}$ (Fig. 3, d).

These observations indicate that the equilibrium:

$$CuDCTA^{2-} + 2\,en \overset{K_6}{\rightleftharpoons} Cu(en)_2^{2+} + DCTA^{4-} \quad (6)$$

occurs. As there are only two absorbing species present (*vide supra*) it can be assumed that this is the only equilibrium involved. For the evaluation of the equilibrium constant a series of measurements was performed without excess of DCTA. Taking $[CuDCTA^{2-}] = a - x$, $[en] = b - 2x$ and $[Cu(en)_2^{2+}] = ([DCTA^{4-}] + [HDCTA^{3-}]) = x$, we can deduce the approximate formula:

$$x \simeq (\sqrt{K_6 a})b \quad (7)$$

for $x \ll a$ and $x \ll b$.

This relation is confirmed experimentally (Fig. 4). Taking the molar absorptivities of $CuDCTA^{2-}$ and

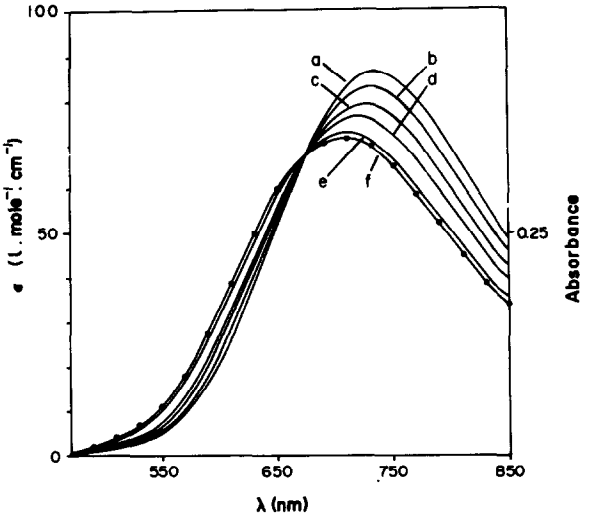

Fig. 5. The system $CuEDTA^{2-} + CN^-$: pH = 10.8; 0.1*M* $NaClO_4$; c_{CuEDTA} = 1.001m*M*; c_{CN^-} = 0, 0.25, 0.50, 0.75 and 2.50m*M* for the curves a–e. Curve f: calculated spectrum of $CuEDTA(CN)^{3-}$, assuming $K = 5.8 \times 10^3$. Light-path 50 mm.

$Cu(en)_2^{2+}$ at 720 nm as 107 and 10.9 l.mole^{-1}.cm^{-1} we calculated $K_6 \simeq 10^{-0.4}$ from the slope in Fig. 4. This value is not in agreement with the literature values of K^{DCTA}_{CuDCTA} and $K^{2en}_{Cu(en)_2}$,[3] from which we calculate $K_6 = 10^{-2.4}$. As we thought that this discrepancy might be due to an incorrect value for K^{DCTA}_{CuDCTA}, we tried to verify this value by studying the equilibrium

$$CuEDTA^{2-} + DCTA^{4-} \underset{}{\overset{K_8}{\rightleftharpoons}} CuDCTA^{2-} + EDTA^{4-}. \quad (8)$$

As K^{EDTA}_{CuEDTA} is well established,[2] a reliable estimate of K^{DCTA}_{CuDCTA} can be obtained from K_8. As (8) is a slow equilibrium, we let relaxation take place at ~330 K. We obtained $\Delta\log K \simeq 2$ at pH = 10.8, which is in agreement with the literature values, which give $\Delta\log K = 1.9$, after correction for protonation of EDTA and DCTA. The discrepancy mentioned above is therefore not understood.

$CuEDTA^{2-} + CN^-$ and $CuDCTA^{2-} + CN^-$

For both systems 1:1 complexes are formed. The spectra are shown in Figs. 5 and 6. With $CuEDTA^{2-}$ the introduction of CN^- leads to a shift of the absorption maximum by about 20 nm. There is no shift at all when CN^- is introduced into $CuDCTA^{2-}$; this indicates that cyanide is bonded differently in the ternary complexes $CuEDTA(CN)^{3-}$ and $Cu(DCTA)(CN)^{3-}$. In the presence of cyanide Cu(II) is reduced:[21]

$$2\ Cu(CN)_4^{2-} \rightarrow 2\ Cu(CN)_3^{2-} + (CN)_2 \quad (9)$$

Our results for the systems $CuEDTA^2 + CN^-$ and $CuDCTA^{2-} + CN^-$ indicate that this second order redox reaction had not interfered seriously at the time of measurement (within 1 hr after preparation). After one day, however, the blue colour of the solutions had faded significantly, possibly owing to reaction (9) or similar reactions.

$NiDCTA^{2-} + CN^-$ (Fig. 7)

The stability constant of $NiDCTA(CN)^{3-}$ is reported to be $10^{2.49}$ by Margerum *et al.*[22] This value is in good agreement with our value of log $K = 2.41 \pm 0.21$.

$NiEDTA^{2-} + en$ (Fig. 8)

The measurements on this system were not performed at constant ionic strength. However, the *K* value in Table 1 should be reasonably accurate, because the neutral ligand ethylenediamine is involved.[20]

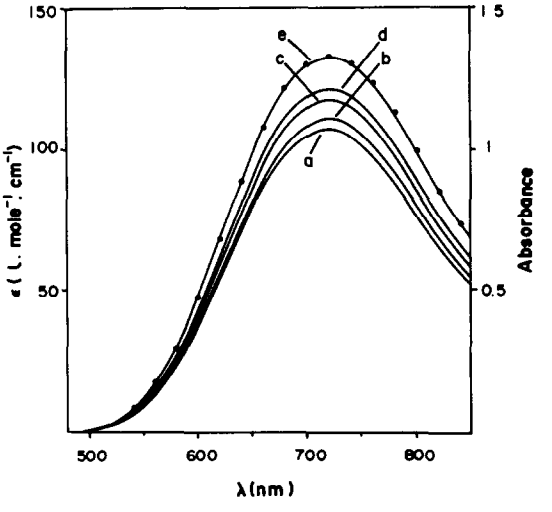

Fig. 6. The system $CuDCTA^{2-} + CN^-$: pH = 11.0; 0.1*M* $NaClO_4$; c_{Cu} = 2.00m*M*; c_{DCTA} = 3.99m*M*; c_{CN^-} = 0, 0.75, 2.0, 4.0m*M* for the curves a–d. Curve e: calculated spectrum of $CuDCTA(CN)^{3-}$, assuming *K* = 440. Light-path 50 mm.

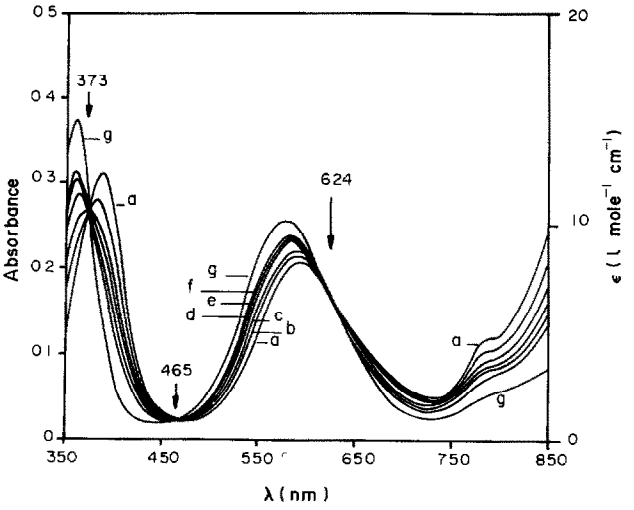

Fig. 8. The system $NiEDTA^{2-}$ + en, pH = 11.1, c_{NiEDTA} = 5.00m*M*, c_{en} = 0, 2.00, 4.01, 7.01, 10.02 and 15.03m*M* for curves a–f; curve g: calculated spectrum of $NiEDTA(en)^{2-}$, assuming K = 550. Light-path 50 mm.

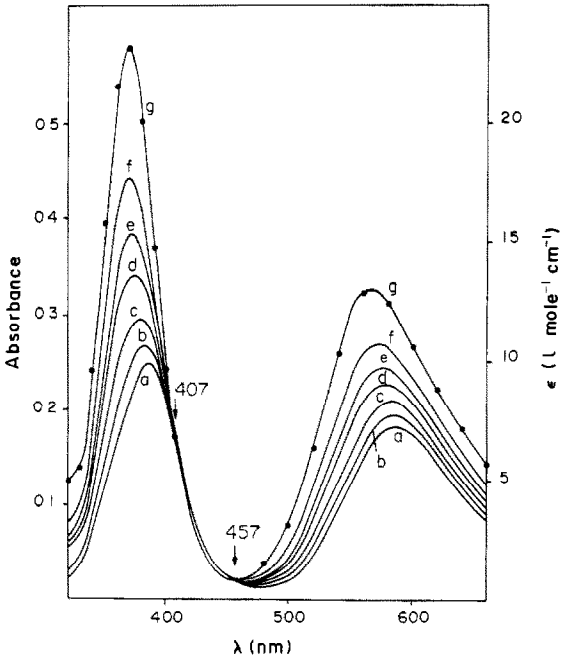

Fig. 7. The system $NiDCTA^{2-}$ + CN^-, pH = 11.0, 0.1*M* $NaClO_4$ c_{NiDCTA} = 5.01m*M*, c_{CN^-} = 0, 0.80, 2.01, 4.01, 6.02 and 10.03m*M* for curves a–f; curve g: calculated spectrum of $NiDCTA(CN)^{3-}$, assuming K = 267. Light-path 50 nm.

CONCLUSIONS

Formation of the ternary complexes $CuEDTA(en)^{2-}$, $CuEDTA(CN)^{3-}$, $CuDCTA(CN)^{3-}$, $NiDCTA(CN)^{3-}$ and $NiEDTA(en)^{2-}$ was established and concentration stability constants were evaluated. It appears that for all the systems reported in Table 1 the statement of Beck[23] applies, namely that the more stable the 1:1 chelate, the less stable the ternary complex:

$$K^{L_{(1)}}_{ML_{(1)}} > K^{L_{(2)}}_{ML_{(2)}};\quad K^{X}_{ML_{(1)}X} < K^{X}_{ML_{(2)}X} \qquad (10)$$

where $L_{(1)}$ and $L_{(2)}$ are different primary ligands. Inequality (10) also holds for the pairs $CuEDTA(en)^{2-}$/$CuDCTA(en)^{2-}$ and $NiEDTA(en)^{2-}$/$NiDCTA(en)^{2-}$, in view of the fact that $CuDCTA(en)^{2-}$ and $NiDCTA(en)^{2-}$ are not stable enough to be formed in detectable amounts under our experimental conditions.

Acknowledgements—The authors are indebted to Dr. J. Kragten, Natuurkundig Laboratorium of the Universiteit van Amsterdam for his valuable comments. This work is part of the research program of the National Institute for Nuclear Physics and High Energy Physics [NIKHEF, section K (former IKO)], made possible by financial support from the Foundation for Fundamental Research on Matter (FOM) and the Netherlands Organization for the Advancement of Pure Research (ZWO).

REFERENCES

1. G. Schwarzenbach and H. Flaschka, *Die komplexometrische Titration*, Enke Verlag, Stuttgart, 1965.
2. J. Bjerrum, G. Schwarzenbach and L. G. Sillén, *Stability Constants of Metal Complexes*, Part I, Chemical Society, London, 1957.
3. J. Kragten, *Atlas of Metal–Ligand Equilibria in Aqueous Solution*, Horwood, Chichester, 1978.
4. M. A. Porai-Koshits, N. V. Novozhilova, T. N. Polynova, T. V. Filippova and L. I. Martynenko, *Sov. Phys. Crystallog.*, 1973, **18**, 54.
5. H. A. Weakliem and J. L. Hoard, *J. Am. Chem. Soc.*, 1959, **81**, 549.
6. E. F. K. McCandlish, T. K. Michael, J. A. Neal, E. C. Lingafelter and N. J. Rose, *Inorg. Chem.*, 1978, **17**, 1383.
7. S. Richards, B. Pedersen, J. C. Silverton and J. L. Hoard, *ibid.*, 1964, **3**, 27.
8. Ya. M. Nesterova, T. N. Polynova and M. A. Porai-Koshits, *Koord. Khim.* 1975, **1**, 966.
9. A. I. Pozhidaev, T. N. Polynova, M. A. Porai-Koshits and N. N. Neronova, *Zh. Strukt. Khim.*, 1973, **14**, 570.
10. G. S. Smith and J. L. Hoard, *J. Am. Chem. Soc.*, 1959, **81**, 556.
11. G. Schwarzenbach and J. Heller, *Helv. Chim. Acta*, 1951, **34**, 576.
12. J. Oakes and E. G. Smith, *J. Chem. Soc. Faraday Trans.*, 1981, **2**, 77, 299.

13. A. A. McConnell, R. H. Nuttall and D. M. Stalker, *Talanta*, 1978, **25**, 425.
14. G. Schwarzenbach, *Helv. Chim. Acta*, 1949, **32**, 839.
15. T. R. Bhat and M. Krishnamurty, *J. Inorg. Nucl. Chem.*, 1963, **25**, 1147.
16. S. Koch and G. Ackermann, *Z. Chem.*, 1972, **12**, 149.
17. T. Nomura, T. Tawai and K. Izutsu, *Anal. Chim. Acta*, 1975, **77**, 263.
18. J. Korsse, G. A. Leurs and P. W. F. Louwrier, to be published.
19. F. R. Hartley, C. Burgess and R. M. Alcock, *Solution Equilibria*, Horwood, Chichester, 1979.
20. W. J. Moore, *Physical Chemistry*, 5th Ed., p. 454, Longmans, London, 1972.
21. R. Paterson and J. Bjerrum, *Acta Chem. Scand.*, 1965, **19**, 729.
22. Unpublished results mentioned in ref. 24.
23. M. T. Beck, *Chemistry of Complex Equilibrium*, p. 196. Van Nostrand, London, 1970.
24. D. W. Margerum, T. J. Bydalek and J. J. Bishop, *J. Am. Chem. Soc.*, 1961, **83**, 1791.
25. J. P. Jones and D. W. Margerum, *Inorg. Chem.*, 1969, **8**, 1486.
26. L. C. Coombs, D. W. Margerum and P. C. Nigam, *ibid.*, 1970, **9**, 2081.
27. S. Nakamura, *Ph.D. Thesis*, University of Chicago, 1964.

Talanta, Vol. 30, No. 1, pp. 9–14, 1983
Printed in Great Britain.

0039-9140/83/010009-06 $03.00/0

DETERMINATION OF TRACES OF SELENIUM IN HEAT-RESISTING ALLOYS BY GRAPHITE-FURNACE ATOMIC-ABSORPTION SPECTROMETRY AFTER CO-PRECIPITATION WITH ARSENIC

OSAMU KUJIRAI, TAKESHI KOBAYASHI, KUNIKAZU IDE and EMIKO SUDO*

Metallurgical Chemistry Division, National Research Institute for Metals, Nakameguro, Meguro-ku, Tokyo 153, Japan

(*Received* 11 *June* 1982. *Accepted* 23 *August* 1982)

Summary—Traces of selenium in complex nickel- and cobalt-based heat-resisting alloys have been determined by co-precipitation and graphite-furnace atomic-absorption spectrometry. The alloys are dissolved in a mixture of concentrated hydrochloric acid, concentrated hydrofluoric acid and 30% hydrogen peroxide. Selenium does not volatilize to any significant extent during the dissolution and concentration. Selenium is separated from the matrices as the element by co-precipitation with arsenic and is redissolved in nitric acid. Zinc is added to the solution to stabilize selenium during the ashing step and thus to enhance the absorbance in the atomization step. Standard solutions for the calibration are prepared in a similar manner to sample solutions after dissolution of the arsenic carrier. The detection limit for selenium is 0.3 ppm in the heat-resisting alloy.

Nickel- and cobalt-based heat-resisting alloys contain many refractory metals added to impart high strength and corrosion resistance. These heat-resisting alloys are used under severe circumstances where high strength at high temperatures is needed. However, it is known that traces of some impurities have harmful effects on the mechanical properties of nickel-based heat-resisting alloys.[1,2] Selenium is one of these harmful impurities: it reduces stress-rupture life and causes cracking during hot rolling.[3] The maximum allowable concentration in nickel alloy castings is given as 3 ppm, in the SAE Aerospace Material Specification 2280.[2]

The complex composition of the heat-resisting alloys limits the kinds and concentrations of the acids used for dissolution. Also, atomic spectroscopic methods are subject to severe chemical and spectral interferences. Traces of selenium in nickel-based heat-resisting alloys have so far been determined by X-ray fluorescence spectrometry[4] and graphite-furnace atomic-absorption spectrometry.[5–7] X-Ray fluorescence spectrometry[4] combined with a preliminary separation of the selenium has been found applicable to concentrations above 3 ppm. Graphite-furnace atomic-absorption spectrometry has been applied to the direct determination of traces of selenium in solutions of nickel alloys.[5] This method needed calibration with solutions of standard alloys or synthetic standard solutions matrix-matched to the samples. It is difficult to get a series of well-characterized standard heat-resisting alloys, and it is impractical to prepare sets of synthetic standard solutions for each alloy matrix encountered. Dulski and Bixler[6] used a direct method,[5] with a modified standard-additions procedure. Direct atomization of selenium from chips of nickel alloy[7] required standard alloys for the calibration and was less precise because the commercial graphite furnace was not designed for the analysis of solid samples.

At a wavelength as short as that used for the determination of selenium, an accurate direct determination is difficult because a deuterium background corrector often cannot compensate for the large background absorption[8] due to the salts of the major alloy constituents. Spectral interference from iron in the determination of selenium at 196.0 nm has been found[9–11] when a continuum source is used for background correction, so the direct method[5] cannot be applied to the determination of selenium in heat-resisting alloys which contain iron.

Traces of selenium should first be separated from the alloy matrix to avoid interferences when a continuum source is used for background correction. Various separation methods for traces of selenium have been reported.[12] Co-precipitation with arsenic as carrier is a simple preliminary separation method which gives a high recovery for traces of selenium from metallurgical,[13–15] geological and biological samples.[16,17] We have developed a simple analytical method for the determination of traces of tellurium in heat-resisting alloys, involving co-precipitation and graphite-furnace atomic-absorption spectrometry.[18] This method has now been applied to the determination of traces of selenium in heat-resisting alloys resulting in a simple method for which no special

*Present address: Fundamental Research Laboratories, Nippon Steel Corporation, Kawasaki 211, Japan.

laboratory apparatus is required and which is suitable for the routine determination of traces of selenium in heat-resisting alloys of varying composition, with a series of standard solutions for calibration.

EXPERIMENTAL

Apparatus

The atomic-absorption spectrophotometer, graphite furnace, auto-sampling system, recorder and temperature measurement were the same as used previously.[18] A deuterium lamp was used for background correction. The light-source for selenium determination was a Perkin–Elmer electrodeless discharge lamp (EDL) operated at 6 W with a Perkin–Elmer power supply. The analytical wavelength used was 196.0 nm. The spectral band-width was 0.7 nm. Solutions (20 μl) were injected into the graphite furnace. All absorbances were measured as peak heights. The furnace was purged with argon and the optics with nitrogen.

Reagents

Selenium stock standard solution (1 mg/ml). Prepared by dissolving 0.5 g of "Specpure" selenium metal (Johnson Matthey Chemicals) in the minimum volume of concentrated nitric acid, evaporating to a moist residue on a water-bath and dissolving in 500 ml of 0.2*M* hydrochloric acid. Working standard solutions were prepared from the stock standard solution immediately before use. Experiments were done at the 1.5-μg level of selenium except for absorbance enhancement experiments, where 5 μg of selenium were added. This amount of selenium (1.5 μg) was equivalent to a concentration of 0.030 μg/ml at the co-precipitation step and 0.060 μg/ml at the measurement step.

Arsenic solution (1 mg/ml). Prepared by dissolving 0.660 g of arsenic trioxide (Merck) in 10 ml of 5% potassium hydroxide solution with warming, and diluting to 500 ml with distilled water. Hypophosphorous acid (50%) was used as reducing agent.

Zinc solution (10 mg/ml). Prepared by dissolving high-purity zinc metal in concentrated nitric acid and diluting with distilled water to give a 0.6*M* nitric acid solution.

Other solutions. High-purity cobalt, nickel and copper metals and lithium carbonate of analytical reagent grade were dissolved in nitric acid and these solutions were used for absorbance enhancement experiments. Various metals used for the studies on matrix effects included Al, Ti, Cr, Mn, Fe, Co, Ni, Zr, Nb, Mo, Ta and W. The high-purity metals were dissolved in appropriate volumes of suitable solvents, such as hydrochloric acid, hydrochloric acid plus hydrogen peroxide, hydrochloric acid plus hydrofluoric acid, hydrofluoric acid, or hydrochloric acid plus hydrofluoric acid plus hydrogen peroxide. The other reagents were of analytical reagent grade.

Heat-resisting alloys

Table 1 summarizes the chemical compositions of the nickel and cobalt heat-resisting alloys used. The alloying elements present at 0.1% or above are shown.

Proposed procedure

Weigh 0.5 g of chips of heat-resisting alloy into a 100-ml Teflon beaker. Add 10 ml of concentrated hydrochloric acid and 5 ml of concentrated hydrofluoric acid. Cover the beaker and heat the solution on a hot-plate. Add 10–15 ml of 30% hydrogen peroxide little by little and decompose it by prolonged heating. After complete dissolution of the sample, concentrate the solution to about 15 ml. Add 2 ml of arsenic solution and about 25 ml of concentrated hydrochloric acid. Heat the solution to 80–100° and add 8 ml of 50% hypophosphorous acid (total volume 50 ml; matrix concentration 10 mg/ml). Continue heating for at least 20 min, then allow the solution to stand for at least 2 hr at room temperature to ensure complete coagulation of the precipitate. Filter off the precipitate of arsenic and selenium on a 9-cm Toyo Roshi No. 5B filter paper (4 μm average pore size, similar to Whatman No. 40 paper) and wash the precipitate on the filter paper and in the original beaker thoroughly with 1*M* hydrochloric acid and distilled water. Dissolve the precipitate in six 1-ml portions of hot 8*M* nitric acid, followed by 1 ml of hot concentrated nitric acid. Wash the filter paper and beaker with distilled water and collect the washings in a 25-ml standard flask. Add 1 ml of zinc solution and dilute to the mark with distilled water to give a final nitric acid concentration of about 2.5*M*.

Prepare standard solutions for the calibration in the following manner. Add appropriate volumes of the working standard selenium solutions to about 30 ml of concentrated hydrochloric acid and dilute to 40 ml. Add 2 ml of arsenic solution and heat. Add 8 ml of 50% hypophosphorous acid, then follow the same procedure as for the samples. Transfer the sample solutions and calibration solutions into the polystyrene cups on the turntable of the auto-sampling system. Push the start button, with the programme set as summarized in Table 2. Interrupt the flow of argon during the atomization. Measure the absorbance due to selenium, prepare a calibration curve and calculate the concentration of selenium in the samples.

Table 1. Chemical composition of nickel- and cobalt-based heat-resisting alloys used (% w/w)

Alloy	C	Al	Si	Ti	Cr	Mn	Fe	Co	Ni	Zr	Nb	Mo	Ta	W
NBS SRM 349*		1.2		3.1	19.5			14.0	57.2			4.0		
IN-792		3.4		3.9	12.6			9.1	61.0			1.8	4.1	4.0
IN-738 LC		3.4		3.4	15.8	0.1	0.2	8.3	61.6	0.1	0.8	1.8	1.7	2.6
MAR-M 246		5.5		1.5	10.1		0.3	9.9	57.7			2.6	1.5	10.9
Udimet CO263		0.5		2.2	20.1		0.3	19.9	50.9			5.8		0.2
JAERI-R9†		0.3	0.3		21.5	0.3	17.6	1 2	49.3			9.1		0.6
René 95	0.2	3.5		2.5	14.0			8.0	61.0		3.5	3.5		3.5
TM-51		5.0		2.7	13.0			4.1	66.4				2 3	6.5
NBS SRM 168§					20.3	1.5	3.4	41.2	20.3		3.0	4.0	1.0	4.0
Modified S-816					20.2	0.9	0.4	45.6	20.0		4.0	4.1		3.7
WI-52					21.2	0.3	2.0	62.5	0.8		1.8			10.4

*Waspaloy.
†Hastelloy X.
§Modified S-816.

Table 2. Operating parameters for GF/AAS determination of selenium

Drying temperature	100°
Drying time	30 sec
Ashing temperature	950°
Ashing time	30 sec
Atomization temperature	2550°
Atomization time	4 sec
Cleaning temperature	2500°
Cleaning time	3 sec

RESULTS AND DISCUSSION

Dissolution of sample

It has been reported that selenium is vaporized from solutions of hydrofluoric acid or when solutions of hydrochloric acid and hydrogen peroxide are taken to dryness.[12] It has also been found that the vaporization of selenium is considerably diminished in the presence of a large quantity of matrix.[12] Bajo reported that there was no loss of selenium from solutions of hydrofluoric acid and perchloric acid.[19] These results may imply that selenium does not vaporize in the presence of a large quantity of matrix and oxidizing agent even if hydrofluoric acid is present.

Therefore, the possibility of selenium vaporizing during the dissolution, concentration and co-precipitation steps was investigated with a nickel-based alloy, René 95. Chips of the alloy (0.5 g) were carried through the procedure already described,[18] except for the addition of zinc in place of the permanganate addition. In this dissolution method, the oxidizing agent (hydrogen peroxide) can easily be decomposed by prolonged heating and does not interfere with the reduction of the selenium. Selenium spikes (1.5 μg) were added (*a*) to the chips of the alloy before dissolution, (*b*) to the solution before concentration and (*c*) to the solution before co-precipitation. The recovery was calculated, after subtraction of the blank value, from the ratio of the absorbance of the sample solution to that of a standard calibration solution prepared from matrix-free and hydrofluoric acid-free solutions in the same manner as the sample solution. The recovery of selenium in (*a*) was about 90%, and in (*b*) and (*c*) about 91–93%. These results show that selenium is not appreciably vaporized during the dissolution of the alloy and the concentration of the solution, though about 10% of the selenium present may be lost during the co-precipitation step either by vaporization or by matrix effects.

Co-precipitation of selenium with arsenic

The best conditions for the co-precipitation of traces of selenium with arsenic were also established by experiments with René 95. The volume of the solution at the co-precipitation step was adjusted to 50 ml. The effect of the concentration of hydrochloric acid at the co-precipitation step was investigated from 3 to 8*M*, and the arsenic concentration was 80 μg/ml. The recovery increased with concentration of hydrochloric acid, becoming almost constant at concentrations above 6*M* (recovery: 96–98%); a concentration of approximately 7*M* was selected as optimal.

The recovery of selenium from the alloy solution was practically independent of the concentration of hydrofluoric acid from 0.5 to 2.7*M*: a working concentration of 2.7*M* was selected, giving 99% recovery. From a matrix-free solution, however, the recovery was lower, ranging from 64 to 90% over the hydrofluoric acid concentration range from 0.5 to 5.4*M*.

A second co-precipitation was done, to check for volatilization of selenium after adjustment of the hydrochloric acid concentration and addition of arsenic plus hypophosphorous acid: in this case the recovery of selenium was nearly zero, showing that some selenium did indeed volatilize from the matrix-free solution in the presence of hydrofluoric acid. Hence it is essential to work with standard selenium solutions which do not contain hydrofluoric acid.

The concentration of arsenic added as carrier was varied from 0.02 to 0.08 mg/ml, and the recovery of selenium remained constant within experimental error at 90–94% over this range. The recommended arsenic concentration is 0.04 mg/ml. The concentration of hypophosphorous acid had no effect on the recovery of selenium (94%) provided it was above 4% v/v: a level of 8% v/v (8 ml of 50% acid) was chosen as optimal.

Solutions were heated to 80–100° to assist reduction of the arsenic and collection of the selenium. Varying the duration of the heating step from 20 to 100 min had no significant effect on the recovery, but varying the standing time at room temperature did. It proved necessary to leave the solutions after precipitation for at least 2 hr, and preferably overnight, to obtain constant recovery (around 92%). This time is necessary to allow the precipitate to coagulate completely.

The bulk of the arsenic precipitate was dissolved in 6 ml of 8*M* nitric acid and the remainder in 1 ml of hot concentrated nitric acid. The solution was diluted to 25 ml after addition of 10 mg of zinc. The volumes of acid were chosen by considering the minimum amounts needed for dissolution and also the effect of the acid on the selenium absorbance. One graphite furnace tube could be used for more than 100 atomization cycles.

Enhancement of absorbance

It has been reported that nitric acid lowers the absorbance of selenium.[20,21] This negative interference is due to vaporization of selenium species during the pre-atomization heating step. To "fix" the selenium during this step, it has been recommended to add a metal which will react with selenium to form a selenide that will be stable during the pre-atomization heating step.[8,10,22–28] In the present work, several metals were tested for this purpose. The test metal

Table 3. Enhancement effect of metals on the relative absorbance of selenium

Metal added*	Relative absorbance
None†	1.0
Li	6.8
Co	7.7
Ni	8.3
Cu	7.6
Zn	9.1

*1 mg/ml.
†2.5*M* nitric acid solution containing 0.16 mg of arsenic and 0.20 μg of selenium per ml.

was added to the nitric acid solution of the arsenic and selenium precipitate. The relative absorbances summarized in Table 3 were obtained after an ashing step at 600°. The relative absorbance reading for selenium in the metal-free solution was set at 1.0. The enhancement effect was highest in the presence of zinc (9.1-fold).

Figure 1 shows the effect of ashing temperature on the selenium signal, in the presence of nickel and zinc. The ashing temperature can be raised to above 1000° without loss of selenium, if zinc is present. It has been reported that zinc selenide is formed when zinc selenate and carbon are heated in an electric furnace.[29] Zinc selenide, the melting point of which is above 1100°, may be formed in the carbon furnace under the conditions of this determination. The selenium absorption signal was found to increase with atomization temperature, becoming approximately constant at temperatures above 2550°, in the presence of zinc.

Figure 2 shows the effect of the matrix metal concentration on the enhancement of the selenium absorption signal. The enhancement became constant when the concentrations of cobalt, nickel and zinc exceeded 0.2, 0.2 and 0.4 mg/ml, respectively. In the

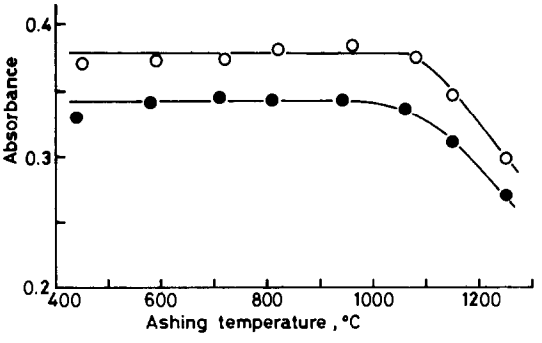

Fig. 1. Effect of ashing temperature on the selenium absorbance in the presence of nickel and zinc. ●: Ni (1 mg/ml); ○: Zn (1 mg/ml). 2.5*M* nitric acid solution containing 0.16 mg of arsenic and 0.20 μg of selenium per ml.

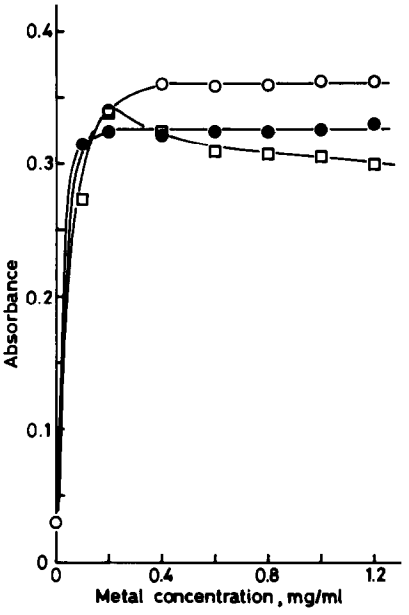

Fig. 2. Effect of metal concentration on the selenium atomic-absorption signal. ●: Ni, □: Cu, ○: Zn. 2.5*M* nitric acid solution containing 0.16 mg of arsenic and 0.20 μg of selenium per ml.

case of copper, however, the enhancement depended on the ratio of copper to selenium. The absorbance in the presence of zinc was almost constant when the concentration of arsenic was varied from 0.04 to 0.2 mg/ml in 2.5*M* nitric acid solution, but gradually increased as the concentration of nitric acid was raised 0.5 to 3*M*.

Matrix effects

Possible matrix effects in the co-precipitation step were studied separately. The chemical composition of the nickel and cobalt heat-resisting alloys was considered. The precipitate of arsenic plus selenium was washed with 3*M* hydrofluoric acid, if possible, before the washing with 1*M* hydrochloric acid and with distilled water. The following concentrations of the alloying elements did not interfere with the co-precipitation: Co and Ni 8.0 mg/ml; Cr 2.6 mg/ml; Ti, Mn, Zr and Nb 2.0 mg/ml; Al, Mo and Ta 1.5 mg/ml; W 1.0 mg/ml. However, selenium was not recovered quantitatively from a solution containing 2 mg of iron per ml, a higher concentration than that which would result from a 10-mg/ml solution of JAERI-R9. A considerable volume of the reducing agent was needed to reduce iron(III) to iron(II). The results of the second co-precipitation showed that some selenium had been lost by volatilization because it had not all been reduced before the co-precipitation.

Volatilization of selenium under these conditions can be prevented by using sufficient reducing agent and a large quantity of matrix. Selenium was re-

Table 4. Determination of selenium in nickel- and cobalt-based heat-resisting alloys (*ppm*)*

Alloy	Unspiked		Spiked (3.0 ppm)	
	Average value	Relative standard deviation, %	Average value	Relative standard deviation, %
NBS SRM 349	2.0	2.4	5.1	1.6
IN-792	0.5	10	3.4	1.9
IN-738 LC	1.7	2.5	4.8	2.2
MAR-M 246	0.3	13	3.3	2.2
Udimet CO263	0.6	10	3.5	1.8
JAERI-R9†	<0.3		3.2	1.0
René 95	<0.3		3.2	2.2
TM-51	<0.3		3.0	3.2
NBS SRM 168	<0.3		3.0	1.6
Modified S-816	0.4	13	3.4	0.9
WI-52§	<0.3		2.9	1.5

*Averages and standard deviations based on 10 replicate measurements on one solution of each alloy.
†Concentration of hypophosphoric acid: 12%.
§Concentration of hypophosphoric acid: 10%.

covered quantitatively from solutions containing 2 mg of iron per ml and 8 mg of nickel per ml if the concentration of hypophosphorous acid was increased to 12%.

Determination of Se in heat-resisting alloys

The proposed method was applied to the determination of traces of selenium in a wide variety of nickel- and cobalt-based heat-resisting alloys. The detection limit, defined as the concentration of selenium producing an absorbance twice the fluctuation of the baseline, was 0.3 ppm in the sample. Table 4 summarizes the results for unspiked and spiked (3.0 ppm of selenium) samples. The average value and relative standard deviation were obtained from 10 replicate measurements of the absorbance of selenium in the same solution. The concentration of hypophosphorous acid was increased in the cases of JAERI-R9 and WI-52 to ensure reduction of iron(III) in the solution of JAERI-R9 and to suppress oxidation by any residual hydrogen peroxide (fine bubbles were observed to be formed at the bottom of the beaker as the solution of WI-52 was being concentrated). The concentrations of selenium found agreed well with the amounts added as spikes, showing that interelement effects of the alloying elements were negligible. The reference value of 0.5 ppm for selenium in IN-792 was obtained by mass spectrometry. Analysis of different samples of JAERI-R9 (9 samples) and René 95 (10 samples), each taken through the complete procedure and spiked with 3.0 ppm of selenium added to the chips of the alloys, gave average values of 2.8 and 3.2 ppm, and relative standard deviations of 6.8 and 5.5%, respectively. Each value was calculated from the mean of three measurements. The method probably has a relative bias of −10% in view of the recoveries obtained in the dissolution and co-precipitation steps. It is possible to improve the detection limit if the final solution volume can be decreased by using a smaller filter paper and less nitric acid for dissolution of the precipitate.

REFERENCES

1. D. R. Wood and R. M. Cook, *Metallurgia*, 1963, **67**, 109.
2. R. T. Holt and W. Wallace, *Intern. Metals Rev.*, 1976, **21**, 1.
3. W. B. Kent, *J. Vac. Sci. Technol.*, 1974, **11**, 1038.
4. C. H. Albright, K. E. Burke and M. M. Yanak, *Talanta*, 1969, **16**, 309.
5. G. G. Welcher, O. H. Kriege and J. Y. Marks, *Anal. Chem.*, 1974, **46**, 1227.
6. T. R. Dulski and R. R. Bixler, *Anal. Chim. Acta*, 1977, **91**, 199.
7. J. Y. Marks, G. G. Welcher and R. J. Spellman, *Appl. Spectrosc.*, 1977, **31**, 9.
8. E. L. Henn, *Anal. Chem.*, 1975, **47**, 428.
9. D. C. Manning, *At. Absorp. Newsl.*, 1978, **17**, 107.
10. K. Saeed, Y. Thomassen and F. J. Langmyhr, *Anal. Chim. Acta*, 1979, **110**, 285.
11. F. J. Fernandez, S. A. Myers and W. Slavin, *Anal. Chem.*, 1980, **52**, 741.
12. R. Bock and D. Jacob, *Z. Anal. Chem.*, 1964, **200**, 81.
13. C. L. Luke, *Anal. Chem.*, 1959, **31**, 572.
14. G. L. Vassilaros, *Talanta*, 1971, **18**, 1057.
15. J. P. McKaveney, H. E. Baldwin and G. L. Vassilaros, *J. Metals*, 1968, **20**, No. 11, 54.
16. B. C. Severne and R. R. Brooks, *Talanta*, 1972, **19**, 1467.
17. W. H. Allaway and E. E. Cary, *Anal. Chem.*, 1964, **36**, 1359.
18. O. Kujirai, T. Kobayashi, K. Ide and E. Sudo, *Talanta*, 1982, **29**, 27.
19. S. Bajo, *Anal. Chem.*, 1978, **50**, 649.
20. G. C. Kunselman and E. A. Huff, *At. Absorp. Newsl.*, 1976, **15**, 29.
21. T. Kamada, T. Kumamaru and Y. Yamamoto, *Bunseki Kagaku*, 1975, **24**, 89.
22. R. M. Hamner, D. L. Lechak and P. Greenberg, *At. Absorp. Newsl.*, 1976, **15**, 122.
23. R. D. Ediger, *ibid.*, 1975, **14**, 127.

24. T. Kamada and Y. Yamamoto, *Talanta*, 1980, **27**, 473.
25. T. D. Martin, J. F. Kopp and R. D. Ediger, *At. Absorp. Newsl.*, 1975, **14**, 109.
26. R. F. Sanzolone and T. T. Chao, *Anal. Chim. Acta*, 1981, **128**, 225.
27. Y. Tada, T. Yonemoto, A. Iwasa and K. Nakagawa, *Bunseki Kagaku*, 1980, **29**, 248.
28. A. Meyer, Ch. Hofer and G. Tölg, *Z. Anal. Chem.*, 1978, **290**, 292.
29. Fonzes-Diacon, *Compt. Rend.*, 1900, **130**, 832.

Talanta, Vol. 30, No. 1, pp. 15–19, 1983
Printed in Great Britain

0039-9140/83/010015-05$03.00/0
Pergamon Press Ltd

SILICA GEL WITH ADSORBED ADOGEN 464 AS AN ANALYTICAL SAMPLING TOOL FOR ANIONS

P. BATTISTONI, S. BOMPADRE, G. FAVA and G. GOBBI
Istituto di Chimica della Facoltà di Ingegneria della Università degli Studi, 60100 Ancona, Italia

(*Received* 6 *November* 1981. *Revised* 26 *July* 1982. *Accepted* 23 *August* 1982)

Summary—A solid extractant made with the liquid anion-exchanger Adogen 464 supported on silica gel has been prepared and its potential as a resin-like exchange material has been evaluated. In acid media it furnishes a ready available, inexpensive tool for recovery of anionic metal complexes as well as simple anions and for elimination of complex matrices. Copper and cobalt have been recovered (with a concentration factor of 20) from sea-water, natural water, metal alloys and industrial electroplating baths and measured by atomic-absorption spectrophotometry. The detection limits for copper and cobalt are 0.2 and 0.4 ng/ml respectively and interferences are minimal. Chromium(VI) has been separated from chromium(III), and a concentration factor of 40 and a detection limit of 0.2 ng/ml have been achieved.

Liquid ion-exchangers have found wide use in the determination of metal ions.[1] In particular, anionic halide complexes have been used in extraction systems[2,3] and in multielement separative techniques for elimination of matrix effects.[4] Metal thiocyanate complexes have similarly been used.[5–7] However, a number of variables such as the organic solvents used, the ionic strength, and charge on the ions involved, can make this method time-consuming. A different approach is based on use of chelating resins (*e.g.*, Chelex 100) as a preconcentration tool for natural waters and sea-water.[8] Comparative studies[9] have shown almost quantitative recovery of zinc from sea-water but poor collection of cobalt and manganese, even with selectively silylated substrates.[10] Recently, anion-exchange resins loaded with ionic or non-ionic metal-chelating groups have been utilized as preconcentration substrates,[11,12] but show lack of stability in high ionic strength media. Water-insoluble chelating substrates supported on silica gel provide a rapid and selective method.[13,14]

In the present work we examine the use of liquid anion-exchangers supported on silica gel as a sorption system for anionic complexes, and establish its usefulness in the quantitative determination of copper, cobalt and chromium(VI) in systems such as natural waters or solutions of high ionic strength.

EXPERIMENTAL

Reagents

Stock copper and cobalt solutions (100 μg/ml) were used, and working solutions were made by diluting the stock solutions with $10^{-3}M$ potassium thiocyanate acidified with sulphuric acid. The stock dichromate solution was $10^{-3}M$, and was diluted with demineralized water to give working solutions. The standard chromium(III) solutions were obtained by dilution of Merck "Titrisol" chromium(III) solution. The silica gel (Merck Kieselgel 60) was sieved and the 60–80 mesh fraction was twice digested in nitric acid, washed with demineralized water and dried at 110° for a day. Adogen 464 was used as received from Aldrich Chemical Co. Analytical-grade chemicals were used throughout.

Apparatus

A Perkin–Elmer model 300 atomic-absorption spectrophotometer and HGA 2200 graphite-furnace atomizer were used for metal determination. The conditions are listed in Table 1. A Netzsch simultaneous thermal analysis model 429 and a Perkin–Elmer 298 infrared spectrophotometer were used to determine the amount of Adogen 464 on the silica gel.

In the chromium work, all glassware was soaked for at least an hour in 6*M* hydrochloric acid before use, and was never exposed to other chromium solutions.

Preparation of the loaded silica gel

Cleaned silica gel (100 g) was soaked in 250 ml of dichloromethane containing a weighed amount of Adogen 464. The mixture was stirred mechanically for 3 hr and then the solvent was evaporated under reduced pressure at room temperature and the air-dried product was stored in a bottle.

Elution of liquid anion-exchanger, as a function of pH

A 20-g sample of 10% Adogen 464/silica gel, loaded in a glass tube (bore 22 mm, bed height 90 mm), was eluted with demineralized water adjusted to the desired pH with hydrochloric acid, at a flow-rate of 4 ml/min. The silica gel was then extruded, dried at 120° for 3 hr and analysed for residual Adogen by differential thermal analysis and infrared spectroscopy.

Procedures for batch experiments

Extraction as a function of pH. A 0.5-g portion of 3% Adogen 464 silica gel was stirred mechanically with 50 ml of $10^{-3}M$ potassium thiocyanate at the desired pH and containing copper or cobalt (100 ng/ml), for 20 min. The solution was then filtered and analysed for metal by atomic-absorption spectrometry (AAS). For chromium, a 1-g portion of Adogen 464/silica gel was stirred mechanically for 20 min with 40 ml of 70-ng/ml chromium(VI) or chromium(III) solution acidified to the desired pH with sulphuric acid, and the solution was then analysed for chromium by electrothermal AAS.

Capacity study. The procedure just described was used to

Table 1. Conditions for AAS determinations

	Cu	Co	Cr
Resonance line, *nm*	324.7	240.7	357.9
Band-pass, *nm*	0.7	0.2	0.7
Ashing temperature, °C	700	700	900
Ashing time, *sec*	40	40	20
Atomization temperature, °C	2500	2500	2700
Atomization time, *sec*	5	5	5

determine the capacity of the 5% Adogen 464/silica system with respect to $10^{-2}M$ potassium thiocyanate containing 20 μg of copper and cobalt per ml, at the desired pH, or with respect to 500-μg/ml dichromate solution.

Rate of extraction. A 1-g portion of loaded silica gel was stirred with 40 ml of chromium solution buffered at pH 0.7 or 4.3, and portions of solution were abstracted at various intervals of time and analysed by electrothermal AAS.

General column procedure

For copper and cobalt a 6-mm bore glass column was loaded with 1.2–1.8 g of 3% Adogen 464/silica gel, which gave bed heights ranging from 6 to 8 cm. A known volume of $10^{-3}M$ potassium thiocyanate acidified to pH 1.7–1.8 with sulphuric acid and containing copper or cobalt was passed through the column at a rate of 2 ml/min under mild suction. After washing with 5 ml of demineralized water the column was stripped with 0.5 ml of concentrated nitric acid plus 0.5 ml of 30% hydrogen peroxide solution and the metal removed was determined by AAS.

For chromium the column had a bore of 0.8 cm and was loaded with 1.2 g of Adogen 464/silica gel (bed height 6 cm). Standard solutions [200 ml, containing 0.100–3.40 μg of Cr(VI) or Cr(III)] were prepared by dilution of 10-μg/ml stock solution and analysed within minutes of preparation. The solutions were adjusted to pH 2.0 with sulphuric acid and passed through the column at 2 ml/min. The column was washed with 10 ml of demineralized water and stripped with 2 ml of concentrated nitric acid. The strippings were diluted to the appropriate volume (5 or 10 ml) with water, and the chromium determined by electrothermal AAS.

Extraction of copper or cobalt from nickel electroplating baths. A sample of the bath solution was filtered through a 0.8-μm Millipore disc, and 100 ml were analysed as already described.

RESULTS AND DISCUSSION

The stability of the Adogen 464/silica gel was evaluated by leaching of the exchanger at different pH values from a column initially loaded at the 10% level (Fig. 1). Since the Blakeley and Zatka[15] method for determining the quaternary ammonium salt proved useless, differential thermal analysis and infrared spectroscopy (measurement of the 2930-cm^{-1} C–H stretching band) were used. The high retention of Adogen 464 at low pH makes the system similar to the modified anionic resins[11] or to the supported chelating substrates.[12]

The effect of pH on the extraction of the copper and cobalt thiocyanate complexes was examined by the batch method (Fig. 2). Copper is completely extracted over a wide range of pH, and the optimum pH range for cobalt is 1.4–2.5. The recovery, however, must be regarded as including the effect of the silica gel itself, since the hydroxyl groups of the gel are capable of complexing many metal ions. In particular, complete adsorption of copper, manganese, zinc and

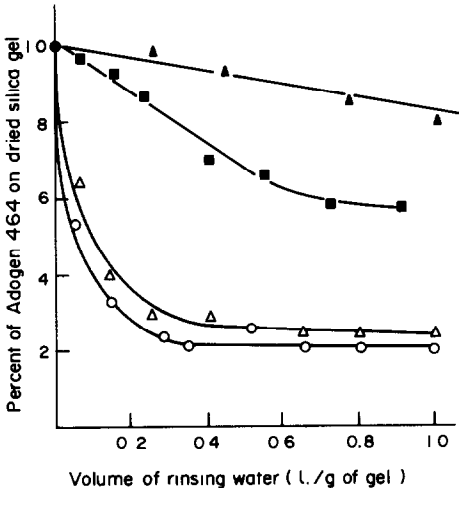

Fig. 1. Per cent of liquid anion-exchanger retained as a function of washing volumes: ▲ pH = 0, ■ pH = 2. △ pH = 4, ○ pH = 6.5.

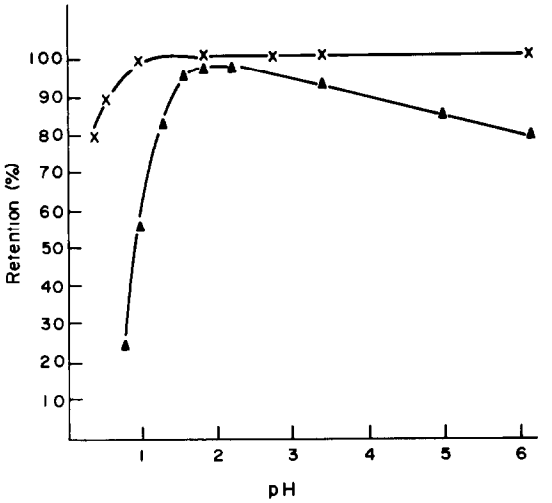

Fig. 2. Per cent retention as a function of pH: copper (×) and cobalt (▲).

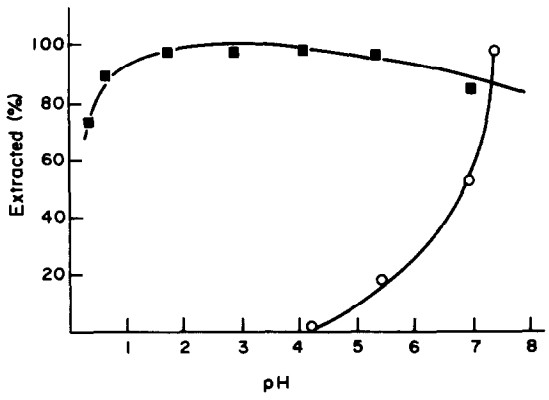

Fig. 3. Extraction of chromium on silica gel treated with Adogen 464, as a function of pH: ■ Cr (VI), ○ Cr (III).

silver at pH > 5 on untreated silica gel has been reported,[16] whereas cobalt ions are bonded only up to 5% from natural and sea-waters.

To maintain the selectivity and overall capacity, the thiocyanate metal complexes were adsorbed at pH 1.7–1.8. The capacity of the 5% Adogen 464/silica gel for the cobalt and copper thiocyanate complexes at pH 1.7 (20 min contact time) was found to be 0.028 and 0.025 mmole respectively, per gram of loaded silica. These values are consistent with sorption of hexathiocyanato metal complexes,[17] in contrast to the corresponding solvent extraction system. These capacities are in good agreement with those observed for silica-gel systems,[13,14] though less than a tenth of those for silylated immobilized reagents.[16]

Similar experiments were performed to obtain distribution curves for chromium(III) and chromium(VI), the results being shown in Fig. 3. The optimum pH is 2 for avoidance of sorption of chromium(III) and to keep the Adogen 464 loading as high as possible. The capacity for chromium(VI) at pH 2 (20 min contact time) is 0.020 mmole per gram of loaded silica. The rate of extraction of chromium(VI) is shown in Fig. 4.

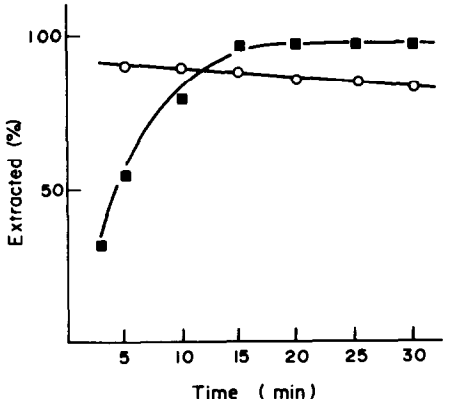

Fig. 4. Extraction of chromium (VI) on silica gel treated with Adogen 464, as a function of time: ○ pH = 0.7, ■ pH = 4.3

Table 2. Recovery of copper and cobalt ions from 100 ml of solution, on a column of silica gel treated with Adogen 464.

	Initial concentration, *ng/ml*	Adogen–SiO_2, *g*	Recovery, %
Co	100	1.5	100
	100	1.2	98.2
	10	1.8	99.2
	10	1.5	99.3
Cu	10	1.5	98.8
	10	1.8	97.9
	100	1.8	98.2
	100	1.5	98.9

The recovery of copper and cobalt in the concentration range from 10 to 100 ng/ml, from $10^{-3}M$ thiocyanate solution, is quantitative at flow-rates of 1–2 ml/min (Table 2). The most efficient stripping (*i.e.*, giving the lowest standard deviation) is obtained with concentrated nitric acid and hydrogen peroxide, whereas other systems such as ammonia solution or acetic acid fail to give satisfactory results. However, the method will give an enrichment factor of only about 10 or 20 (for final volumes of 10 or 5 ml respectively) since the recovery ratio is considerably lowered if water samples of more than 200–300 ml are used.

Other metals giving thiocyanate complexes, such as manganese and iron, have been examined for potential interference (Table 3). In the column system there is no interference in the recovery of traces of copper and cobalt. Since nickel does not inhibit the copper or cobalt recovery at any concentration, this method can safely be used for matrices such as nickel alloys, nickel electroplating baths, nickel ores, *etc.*, besides

Table 3. Recovery of copper and cobalt from 100 ml of solution, on a column of silica gel treated with Adogen 464, in the presence of added Zn, Fe, Mn and Ni

Initial concn., *ng/ml*			Ratio,	Recovery, %	
[Test ion], *ng/ml*		Foreign ion	[Test ion] [Foreign ion]	Co	Cu
Cu	10	Co	1:1	98.9	98.4
	10	Co	1:10	98.3	98.8
	100	Co	10:1		100.8
	100	Co	10:1	99.2	99.0
	10	Co	1:500		97.8
	10	Co	1:1000		101.2
	10	Zn	1:500		99.8
	10	Mn	1:500		97.8
	10	Fe	1:500		98.5
Co	10	Ni	1:10	99.1	
	10	Ni	1:50	98.7	
	10	Ni	1:500	99.4	
	10	Ni	1:1000	99.2	
Cu	10	Ni	1:50		99.3
	10	Ni	1:500		98.5

Table 4. Recovery of chromium (VI) in the presence of chromium (III)*

Cr(VI) taken, μg	Cr(III) taken, μg	Recovery, %
0.05	10	101
0.5	10	100
1	10	99
5	10	99
10	10	99
10	100	99
10	1000	105
17	100	102

*For 100 ml, pH 2.

solutions where the low metal content is not directly detectable because of matrix effects. These advantages are well illustrated by the examples below.

For chromium(VI) the recovery was quantitative for 100 ml of solution containing 0.05–17 μg of chromium (Table 4). Stripping was done most efficiently with a small volume of concentrated nitric acid. The method does not allow a concentration factor of more than 40, because the recovery is considerably lower if a large sample volume (>400 ml) is used. The detection limit for chromium(VI), defined as twice the standard deviation of the blank signal, is 0.2 ng/ml. The method is particularly useful for total chromium determination, since any chromium(III) can be oxidized with permanganate in acid medium, and the excess of oxidant need not be destroyed, since it is held at the top of the column, and the manganese(IV) produced does not interfere because it is not desorbed in the stripping process for chromium(VI). As use of sodium azide for reducing the excess of permanganate is thus avoided, there is no risk of loss of chromium(VI) by azide reduction (Table 5).

Copper determination in natural and sea-water

The direct AAS determination of metal traces in sea-water is well developed but satisfactory results have been achieved only for iron and zinc, whereas for lead, copper, nickel and cobalt, only higher concentrations are reliably determined.[18,19] The Adogen 464/silica gel system can conveniently be used to detect copper ions in either natural or sea-water at values as low as 0.2 ng/ml (Tables 6 and 7), but because of its low concentration (0.01–0.046 ng/ml in sea-water and 0.037–0.35 ng/ml in river water),[20] a 20-fold enrichment factor does not necessarily allow cobalt to reach its detection limit of 0.4 ng/ml and be safely detected.

Table 5. Recovery of total chromium

Taken*, ng		
Cr(VI)	Cr(III)	Recovery, %
10.0	1.0	99
10.0	5.0	99
10.0	10.0	97
0.5	—	98
1.0	—	102
10.0	10.0	89†
100	10.0	92†

*In 100 ml, pH 2.
†Sodium azide was used to destroy the excess of permanganate.

Table 6. Determination of copper in sea-water (Porto Novo harbour)

Cu added, ng/ml	Found, ng/ml	Std. devn., ng/ml
—	0.8	0.05
2	2.3	0.05
4	4.8	0.03

Table 7. Copper determination in natural water containing: Na^+ 3.4 μg/ml, K^+ 1.15 μg/ml, Ca^{2+} 65 μg/ml, Mg^{2+} 8.8 μg/ml, SO_4^{2-} 24.9 μg/ml

Cu added, ng/ml	Cu found, ng/ml	Std. devn., ng/ml
—	2.1	0.05
—	2.3	0.06
3	5.3	0.08
3	5.2	0.09
6	8.2	0.15
6	8.1	0.12

Copper and cobalt determination in other matrices

The reliability of the method has been verified by analysis of nickel electroplating baths, where contamination with cobalt and copper can cause loss of quality; satisfactory results can be achieved for Ni/Cu ratios of 5×10^5 and Ni/Co of 4×10^4 (Table 8). The amounts of organic substances such as surfactants and brightening agents usually present in the baths do not interfere. The analysis of standard alloys for copper (Table 9) provided standard deviations of 0.00095 and 0.0041% for copper contents of 0.045 and 0.170% respectively.

Table 8. Copper and cobalt determination in nickel electroplating bath

Cu added, ng/ml	Cu found*, ng/ml	Co added, μg/ml	Co found*, μg/ml
—	199 (6)	—	2.44 (0.03)
—	209 (8)	—	2.50 (0.02)
100	318 (6)	2.5	5.05 (0.05)
200	411 (12)	5.0	7.50 (0.08)

*Standard deviation (10 replicates) shown in brackets.

Table 9. Determination of copper in BCS standard 182/2 (Al alloy with 11% Si; Cu content 0.045%) and BCS standard 403 (low-alloy steel; Cu content 0.170%).

Sample	Cu found, %	Std. devn., % (10 replicates)
BCS 182/2	0.0454	0.0011
	0.0450	0.0008
	0.0448	0.0010
BCS 403	0.168	0.004
	0.171	0.004
	0.173	0.004

REFERENCES

1. H. Green, *Talanta*, 1973, **20**, 139.
2. F. G. Seeley and D. J. Crouse, *J. Chem. Eng.*, 1966, **11**, 424.
3. C. W. McDonald and F. L. Moore, *Anal. Chem.*, 1973, **45**, 983.
4. J. R. Clark and J. G. Vlets, *ibid.*, 1981, **53**, 61, 65.
5. R. Přibil and J. Adam, *Talanta*, 1973, **20**, 49.
6. H. M. N. H. Irving and A. D. Damodaran, *Anal. Chim. Acta*, 1970, **50**, 277.
7. A. R. Burkin, N. M. Rice and M. J. Rogers, *J. C. S. Dalton*, 1974, 213.
8. J. Lamathe, *Anal. Chim. Acta*, 1979, **104**, 307.
9. J. Smits, J. Nelissen and R. Van Grieken, *ibid.*, 1979, **111**, 215.
10. D. E. Leyden, G. H. Luttrell, A. E. Sloan and N. G. DeAngelis, *ibid.*, 1976, **84**, 97; D. E. Leyden, G. H. Luttrell, W. K. Nonidez and D. B. Werho, *Anal. Chem.*, 1976, **48**, 67.
11. M. Chikuma, M. Nakayama, T. Itoh, H. Tanaka and K. Itoh, *Talanta*, 1980, **27**, 807.
12. H. Akaiwa, H. Kawamoto and K. Ogura, *ibid.*, 1981, **28**, 337.
13. K. Terada and K. Nakamura, *ibid.*, 1981, **28**, 123.
14. K. Terada, K. Morimoto and T. Kiba, *Anal. Chim. Acta*, 1980, **116**, 127.
15. St. J. H. Blakeley and V. J. Zatka, *ibid.*, 1975, **74**, 139.
16. D. E. Leyden and G. H. Luttrell, *Anal. Chem.*, 1975, **47**, 1612.
17. P. W. West and C. G. de Vries, *ibid.*, 1951, **23**, 334.
18. R. J. T. Graham and A. Carr, *J. Chromatog.*, 1970, **46**, 293.
19. T. H. Donnelly and J. Ferguson, *Appl. Spectrosc.*, 1975, **29**, 158.
20. K. H. Wedepohl, C. W. Correns, D. M. Shaw, K. K. Turekian and J. Zemann, 1978. *Handbook of Geochemistry*, Vol. II/3, Springer-Verlag, New York.

Talanta, Vol. 30, No. 1, pp. 21–39, 1983
Printed in Great Britain

0039-9140/83/010021-19 $03.00/0

REFEREE ANALYSIS OF PRECIOUS METAL SWEEPS AND RELATED MATERIALS

SILVE KALLMANN and C. MAUL
Ledoux & Company, Teaneck, NJ 07666, U.S.A.

(*Received* 17 *March* 1982. *Accepted* 20 *August* 1982)

Summary—Sweeps samples are often complex mixtures containing from trace amounts to 20% of one or more precious metals distributed in matrices consisting of widely varying mixtures of base metals or their oxides. Three collection procedures are described that are suitable for the isolation of precious metals from base substances. One is based on direct fusion of the sample (high-grade sweeps) with sodium peroxide, and the others on collection of the precious metals by fire-assay techniques using either nickel sulphide or silver. The precious metals are then determined either gravimetrically or by atomic-absorption or plasma-emission spectrometry.

The precious metals silver, gold, platinum, iridium, palladium, rhodium, ruthenium, and to a lesser extent, osmium, are widely used in jewellery, coinage, photography and glass manufacture. They are also employed in a variety of chemical processes and are the effective ingredients of oil-reforming and pollution-control catalysts, particularly for purposes of automobile emission-control. Because of its great intrinsic value, precious metal scrap is invariably recycled. Osmium, however, is frequently not recovered.

High-grade scrap may consist of contaminated metals or alloys. It is usually purified by remelting or by chemical separation techniques. Low-grade scrap generally contains less than 5% of precious metals, which can be recovered by melting with copper, lead, nickel, aluminium or sulphur, or the scrap can simply be pulverized to yield "sweeps".

The term "sweeps" is derived from jewellers' "sweepings". Nowadays "sweeps" include a wide range of compositions which vary with the precious-metal source.

Sweeps may also result from neutralization and evaporation of precious-metal solutions or from burning and pulverization of electronic circuit boards and even resins and filters carrying precious metal. Some materials are sometimes called "sweeps" even though the precious metal content may exceed 20%; examples are "platinum metal residues" (or concentrates), "zincings" or "spent catalyst". These materials may contain from 5 to 50% of combined precious metals and a variety of base substances. The analytical methods described in this paper are equally applicable to these substances.

In a sweeps sample the precious metals are finely distributed in a matrix of base metals or their compounds. They are often a very complex mixture of any of the following elements or their oxides: lead, copper, bismuth, zinc, cadmium, tin, antimony, iron, nickel, silicon, aluminium, titanium, barium, zirconium, niobium, molybdenum, magnesium, calcium and chromium. Sweeps may also contain chlorides, bromides, iodides, sulphides, sulphates, carbonates and free carbon. This complexity arises mainly because material sent for recovery is often a mixture originating from many different sources. The analyst, in devising an analytical scheme, faces the problem of determining precious-metal concentrations ranging from μg/g to per cent levels, in the presence of high concentrations of widely varying matrix elements. The solution to the analytical problem may hence be simple or very complex, with the analyst constantly aware that small errors may correspond to very large differences in value.

Analytical requirements for sweeps depend entirely on the net weight of the lot being evaluated and the intrinsic value of the precious metals in it. With the price of gold, platinum, rhodium and iridium at about $350–$400 an ounce (1982), a sweeps sample containing as little as 100 ppm of any of these elements is worth at least $1000 a ton and, therefore, is of significant commercial value. With palladium at $75 and silver at about $7 an ounce, correspondingly larger tonnages are required to represent a viable commercial product. Comparatively large quantities of ruthenium (at about $45 an ounce), although adding to the complexity of the analysis, are often not determined and/or paid for, because of technical difficulties in the recovery of this element by the conventional smelting processes that are suitable for the other precious metals.

Differences in analytical results between buyer and seller can often be resolved only by engaging an umpire or referee laboratory. Although such differences may involve millions of dollars of value, they may be limited to one or a few of the precious metals in the sample. The referee laboratory is therefore required to devise an analytical scheme tailored to resolve specific differences between two parties, even

though the sample may also contain other precious metals. Thus, the referee analyst may be asked to determine only the iridium content of a sample of sweeps containing (unknown to him) 0–2 oz/ton (0–67 μg/g) of iridium in the presence of 0.1–2% or more of other (unspecified) precious metals in a matrix of 90% or more of the base metals. Obviously, a scheme covering only one, two or even three precious metals must be based on different criteria of selectivity and specificity than a scheme which includes the determination of all the precious metals.

Since, for various reasons, the parties involved in a dispute frequently fail to provide the referee laboratory with pertinent information regarding the composition of the sample, it is advisable to make preliminary tests to establish the matrix composition and the relative concentration of the various precious metals. This can be done most expeditiously by a complete X-ray fluorescence scan, and the results used for planning the analysis.

METHODS USED FOR DETERMINATION OF PRECIOUS METALS IN SWEEPS

All-instrumental methods

Because of the diverse and often complex compositions of sweeps and hence the lack of adequate standards, all-instrumental methods of analysis are limited to the few instances where the precious metals occur in quantities and in matrices which vary little from sample to sample. Thus X-ray fluorescence and neutron-activation have been used to a limited extent in the evaluation of spent alumina-base catalysts (sometimes included in the category of sweeps) when the standard and samples contain the precious metals within a narrow range of concentration in the same substrate.[1,2]

All-chemical methods

The main problem here is bringing the precious metals into solution, particularly when they are dispersed in a complex matrix, and decomposition with acids is required. Such methods may therefore be applicable only to special cases. Thus, it may be advantageous to determine the silver content of sweeps (Ag < 20%) by decomposing the sample by prolonged heating with sulphuric acid.[3] Decomposition by fusion with sodium peroxide is useful, provided a 2-g sample (the largest that can be handled conveniently) contains enough precious metal for a chemical procedure to be used. In practice, however, final measurements are usually made by instrumental procedures.[4,5] It is also possible to extract major amounts of precious or base metals with acids and subject the residue to a fire-assay procedure.[6] If rhodium is the only precious metal in the sample, and is present in sufficient quantities, it can be determined by atomic-absorption after fusion of the sample with sodium or potassium pyrosulphate or sodium peroxide.[7]

Fire-assay methods based on collection of precious metals in molten lead have been used for many centuries to determine gold and silver in a great variety of materials. There is a vast literature on the subject, the more recent[6,8–12] being the most useful. Other media have been suggested as collectors for precious metals.[13–15]

Fire-assay procedures are also widely used for the preliminary collection of platinum and palladium, in addition to gold and silver, from various metallurgical samples, including sweeps, by steps such as fusion and scorification and/or cupellation.[16,17] The resulting lead button or "silver prill" is analysed for its four components by gravimetric,[5] spectrophotometric,[13] atomic-absorption,[18] optical emission[19,20] and/or plasma emission methods.[21,22]

These methods are applicable only in the absence of rhodium, ruthenium or iridium, since these elements, after treatment with nitric acid and/or *aqua regia*, remain more or less as "acid insolubles", without any assurance that the other precious metals will be quantitatively found in the soluble fraction.

REFEREE METHODS FOR COLLECTING RHODIUM, RUTHENIUM AND/OR IRIDIUM IN ADDITION TO GOLD, PLATINUM, PALLADIUM AND SILVER

The methods to be described were developed in the laboratories of Ledoux & Company with the primary aim of obtaining master solutions containing all the precious metals in the sample (Methods A, A-1 and B). Where this is not required, *e.g.*, when one or two of the precious metals predominate, Method C is preferred; it provides two fractions, one containing the ruthenium, rhodium and iridium, the other the remaining precious metals, except silver and osmium. The methods are applicable to the various types of sweeps already mentioned. Methods A, A-1 and B are also attractive, in the absence of rhodium, ruthenium and/or iridium, for analysing samples relatively high in platinum (Pt > 100 mg), since there are difficulties in its determination after collection into a silver bead by fire-assay methods. Method A-1 is still being improved and is described here only tentatively. It requires the use of d.c. plasma equipment but is potentially applicable to most substances containing more than 0.5% of individual precious metals.

Sampling of sweeps

Since batches of sweeps are often heterogeneous mixtures, proper sampling procedures must be employed to ensure homogeneous and/or representative samples. The more important parameters of sampling were recently discussed at seminars of the International Precious Metals Institute.[23] For homogeneity reasons, the analytical referee methods suggested below require a minimum weight of 1 g of 300-mesh material for methods A and A-1 and up to 30 g of 200-mesh material for methods B and C.

*Collection procedures**

A. Sodium peroxide–sodium formate method. Transfer a sample of sweeps containing at least 10 mg and up to 500 mg of total precious metals into a 30–50 ml zirconium crucible. The maximum amount of sample which can be fused conveniently is 2 g. If the total amount of precious metals is less than 25 mg, add 25 mg of a precious metal that is not to be determined (usually ruthenium or osmium).

Add 4 g of sodium carbonate and 8 g of sodium peroxide, mix, and cover with an additional 4 g of sodium peroxide (or more if refractory oxides are present). Fuse over a burner, first at low temperature until the charge melts, then at dull red heat until a clear melt is obtained. Cool the crucible, put it in a 600-ml beaker and leach the melt with about 200 ml of cold water. Remove the crucible, and rinse it into the beaker with hot water. Add 15 ml of hydrochloric acid to the crucible, fill it up with hot water, then rinse the solution into a small beaker; evaporate this solution to dryness, dissolve the residue in a few drops of hydrochloric acid and a little water, and retain for later addition to the main solution.

Dilute the solution in the 600-ml beaker to about 350 ml and destroy the hydrogen peroxide by boiling gently for 10 min. Allow to cool for 5 min and add 15 ml of formic acid to reduce all the precious metals to insoluble lower-valency oxides or hydroxides. Heat on a steam-bath until the precipitate settles. (See Discussion section for modification to overcome the effect of chromium and large amounts of iron.) This usually takes 2–4 hr. Add 100 ml of methanol, mix and allow to cool.

Filter off on a 12-cm medium-texture paper and wash thoroughly with a 1:1 v/v mixture of water and methanol. If it is clear and colourless, discard the filtrate (it contains the fusion salts, and the silica and alumina contained in the sample). If the filtrate is slightly yellow, acidify it with hydrochloric acid and examine it for the presence of platinum (*e.g.*, by plasma emission). If the filtrate is more than slightly yellow the precipitation was faulty (see discussion).

Wash the precipitate into the precipitation beaker with hot water and place the beaker under the funnel. Pour 25 ml of hot dilute *aqua regia* ($HCl + HNO_3 + H_2O$, 3:1:4 v/v) through the paper, in two portions. Boil the mixture in the beaker until the precipitate has dissolved or reaction ceased. Dilute to about 150 ml, let cool to room temperature, filter through the same filter paper into a 250-ml beaker, and wash five times with nitric acid (2 + 98); this gives filtrate A. Put the paper in the 600-ml beaker and keep for further treatment.

If a silver determination is required, evaporate filtrate A to about 15 ml, dilute to 150 ml with hot water, cool, filter off the small amount of silver chloride and wash thoroughly with nitric acid (2 + 98). Put the filter (plus precipitate) into the 600-ml beaker, along with the one already there. If silver determination is *not* required, this step is omitted. In either case, put the filtrate (still designated A), onto a steam-bath to evaporate.

Add to the 600-ml beaker 30 ml of nitric acid, 10 ml of perchloric acid (72%), and 10 ml of sulphuric acid (but only the sulphuric acid if determination of ruthenium is required), cover the beaker, and evaporate to fumes of sulphuric acid. If necessary, add more nitric acid to give complete destruction of organic matter. The fuming should be vigorous enough to cause dissolution of silver chloride and/or any residual rhodium or iridium salts. Finally, raise the cover and evaporate to complete dryness. To the cold salts add 10 ml of nitric acid and 10 ml of water. Warm to dissolve the salts, and precipitate any silver by addition of 5 ml of hydrochloric acid. Boil for 2 min, then dilute to 150 ml with hot water and add the solution obtained from cleaning the zirconium crucible with acid.

Allow the silver chloride to settle, filter the cold solution through a 9-cm filter paper and wash with nitric acid (2 + 98). Add the filtrate to the main solution (filtrate A) evaporating on the steam-bath.

If the silver chloride looks discoloured, return the paper to the 600-ml beaker and repeat the fuming step.

Evaporate the combined filtrates, containing all the gold, platinum, palladium, rhodium, ruthenium and iridium, to dryness on a steam-bath, then add about 5 ml of hydrochloric acid, 1 ml of nitric acid and 5 ml of water, cover, and warm for a few minutes on the steam-bath to dissolve the salts. Transfer to a 100-ml or larger standard flask, dilute to volume, and mix. Analyse as described later.

The final precipitate obtained by this procedure contains all the silver in the sample. If a silver determination is required, use one of the following procedures.

(*a*) Put the paper containing the silver chloride in a scorifier (if Ag content is <25 mg) or an assay crucible (Ag content >25 mg). Obtain a silver bead by fusion or scorification and cupellation and weigh. Check the purity of the silver bead by dissolution in nitric acid and precipitation with hydrochloric acid.

(*b*) Transfer the paper and precipitate to a beaker, add nitric (20 ml), perchloric (5 ml) and sulphuric (15 ml) acids and heat to strong fumes, until the paper has been destroyed and the silver chloride converted into silver sulphate. Cool, dilute with water to 200 ml, heat to boiling, and allow to cool. Filter if necessary, then precipitate the silver with hydrochloric acid, filter off, and finally weigh as AgCl.

(c) Determine the silver by atomic-absorption spectrometry (AAS) after destroying the paper containing the silver chloride by fuming with nitric (20 ml) and perchloric (10 ml) acids, evaporating the solution to dryness and dissolving the residue in a measured amount of 2% potassium cyanide solution or 30% v/v hydrochloric acid.

A-1. The direct sodium peroxide/d.c. plasma method. Fuse up to 2 g of sample in a zirconium crucible with 12 g of sodium peroxide as described in method A. Leach the melt with water and remove the crucible. Acidify the solution carefully with hydrochloric acid.

Clean the crucible with hydrochloric acid and add to the main solution. Warm the solution, transfer it to a 500-ml standard flask containing 150 ml of concentrated hydrochloric acid, dilute to volume and mix. A clear solution should result unless the sample contains more than 150 mg of silver. If the sample contains species that yield hydrous oxides even in hydrochloric acid, such as Ta, Nb or W, filter the solution and wash the precipitate with 20% v/v hydrochloric acid. Determine the Au, Pt, Pd, Rh, Ru and Ir by d.c. plasma emission spectrometry (PES), as described later, and silver by AAS.

B. The nickel sulphide method. Fuse 1–20 g of sample, depending on the precious metal content, by the procedure suggested by Robèrt *et al.*,[15] modified when necessary.

If the total precious metal content of the sample taken is less than 25 mg, before the fusion add 25 mg of a precious metal which is not to be determined. (Ruthenium or osmium is best, since neither interferes in the proposed procedure; if desired, they can be volatilized later by fuming with perchloric acid.)

Pour the molten mass into an iron mould. In order to achieve a clean separation from the slag remove the nickel sulphide button while still warm (200–250°). Fuse the slag with more flux and recover the second nickel sulphide button.

Weigh the two buttons together, crush them, and pulverize to 60-mesh or finer powder. Weigh the powder and record the grinding loss for correction of the final results. Transfer the powder to a 600-ml beaker, warm the beaker

*All acids specified in these procedures are concentrated acids unless otherwise stated.

slightly, add 400 ml of hydrochloric acid and allow the vigorous reaction to proceed on a slightly warm hot-plate for about half an hour, then gradually increase the temperature until the volume of the solution has been reduced to 300 ml by vigorous boiling. Cool, dilute to 500 ml with water, add 0.5–1 ml of hydrofluoric acid to the cold solution, to dissolve any silica from small amounts of slag which may have adhered to the nickel sulphide buttons, stir and allow to stand for at least 2 hr.

Filter off the precious metal sulphides and wash the paper about 5 times with warm water to remove all but a small amount of the nickel salts. (The filtrate will contain a portion of the silver, which can be determined directly by AAS after transfer to a 1-litre standard flask, addition of 200 ml of concentrated hydrochloric acid, dilution to volume and mixing.) Wash the sulphide precipitate with hot water into the 600-ml beaker and place the beaker under the funnel. Pour two 20-ml portions of hot dilute *aqua regia* (HCl + HNO_3 + H_2O, 3:1:4 v/v) through the paper. Continue as described for procedure A, starting at the corresponding step in that method.

The final solution (filtrate A) contains all the platinum, palladium, rhodium, iridium, and ruthenium present in the sample or added as a collector, but the collection of gold is unfortunately not complete (see discussion). Analyse the solution as described later.

C. The silver bead method (*Fig. 1*). Fuse 5–15 g of sample, containing a minimum of 0.2 mg of any precious metal to be determined and not more than 0.25 g of total precious metals, in a clay assay crucible, with a lead flux containing the usual flux ingredients. The optimum flux composition can be varied to accommodate acid or basic ingredients of the sample and will usually contain the following ranges of the components.

Litharge	40–83%
Silica	0–20%
Soda ash	10–40%
Pearl ash	0–10%
Borax	0–15%

A high copper content in the sample will require comparatively large amounts of litharge in the flux, and a high alumina content comparatively large quantities of silica, borax and soda ash. The usual reducing agents are starch or flour, and potassium nitrate is used as an oxidizing agent. For details of fluxes and fire-assay techniques see the appropriate references.[6,8–12,16,17]

Before the fusion, add to the flux, unless already present in the sample, 5 g of silver for 50 mg of combined rhodium, ruthenium and/or iridium. If an iridium and/or rhodium determination is required, add for collection purposes 25 mg of ruthenium unless already present in the sample. If a ruthenium and rhodium determination is required, add 25 mg of iridium instead of ruthenium. If the sample portion itself should contain a total of 25 mg or more of these three elements (not counting the collector metal added), reduce the sample size so that the total (including collector) is <50 mg.

When the fusion is complete (final fusion temperature about 1150°), pour the melt into a metal mould, allow to cool, remove the lead button and fuse the slag with more flux. Combine the lead buttons and scorify to a convenient size.

Cupel the resulting lead button at about 920° in a cupel of convenient size. When the cupel has been taken out of the furnace, and the silver bead is just solidifying, loosen the bead by light tapping or pushing with a metal object, to prevent cementing of the bead to the cupel by the cooling lead oxide.

If the surface of the cupel appears discoloured, indicating the possible presence of a small quantity of precious metals, particularly the collecting element (Ru or Ir), "wash" the cupel by wrapping about 100 mg of silver into a 5-g sheet of lead foil and cupelling until the lead has disappeared. Combine the resulting silver bead with the bead containing the bulk of the precious metals.

If warranted by the low concentration of one or more of the precious metals, use more than one sample portion and combine the silver beads at this stage.

Dissolve the silver bead(s) in a 150-ml beaker by warming with 25 ml of nitric acid (1 + 3) per g of silver. Boil to remove brown fumes, then filter (9-cm medium-texture

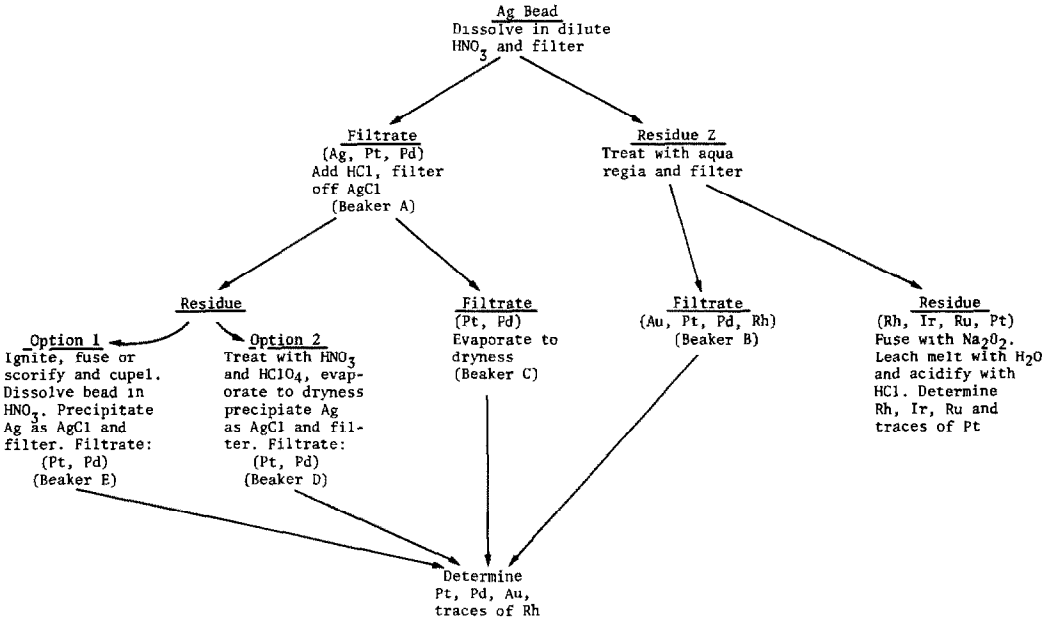

Fig. 1

paper) into a 250-ml beaker, washing the residue (Residue Z) thoroughly with nitric acid (2 + 98). If the determination of platinum and palladium is required, add to the filtrate hydrochloric acid (2.5 ml per g of silver) to precipitate the silver. Stir and heat on a steam-bath to coagulate the precipitate, then cool. The solution contains the bulk of the platinum and palladium (Fig. 1, Beaker A). If the determination of gold, platinum and palladium is required, return Residue Z to the 150-ml beaker with the aid of a fine stream of hot water, place the beaker under the funnel and pour through the filter paper 50 ml of a mixture of hot water and hydrochloric and nitric acids (3:3:1 v/v). Heat to boiling and filter through the same paper into a clean 150-ml beaker. Transfer the precipitate quantitatively to the filter with nitric acid (2 + 98), using a small piece of moistened filter paper to wipe the beaker. Wash the precipitate thoroughly with the dilute nitric acid. Evaporate the filtrate, which contains all the gold, residual platinum and palladium and possibly also traces of rhodium, to complete dryness on a steam-bath (Beaker B).

Ignite the precipitate (or Residue Z if Au, Pt, Pd are not to be determined), which contains all the iridium, rhodium and ruthenium in the sample or added as a collector (and possibly traces of platinum), in a 30-ml zirconium crucible at low temperature and fuse the residue with a mixture of 2 g of sodium carbonate and 4 g of sodium peroxide. Leach the cooled melt with 150 ml of water in a 400-ml beaker, remove the crucible and wash it with hot water. Fill the crucible with hydrochloric acid and use this acid to acidify the solution in the 400-ml beaker. Heat the solution until clear, evaporate it to less than 200 ml, and transfer to a 200-ml standard flask. Cool, dilute to volume, and mix. This solution is ready for the determination of rhodium, iridium and/or ruthenium (and possible traces of Pt) as described later.

Filter the solution in Beaker A through a 12-cm filter paper into a 250-ml beaker. Transfer the precipitate (AgCl) to the paper and wash it thoroughly with nitric acid (2 + 98). Evaporate the filtrate (containing the bulk of the platinum and palladium) to dryness on a steam-bath (Beaker C). The silver chloride may retain significant amounts of platinum and palladium and is treated by either of the following techniques.

(*a*) Return the precipitate to the original 250-ml beaker, add 25 ml of nitric acid and 30 ml of perchloric acid, evaporate slowly to perchloric acid fumes, then heat strongly, with the beaker covered, until the silver chloride appears to have been decomposed and a mere cloudiness remains. Raise the cover and evaporate slowly to complete dryness. Cool, and dissolve the salts in 20 ml of water and 10 ml of nitric acid. Stir to dissolve the salts, then add 2 ml of hydrochloric acid per g of silver and warm until brown fumes of nitrosyl chloride are freely evolved. Dilute to 150 ml with hot water, and allow the precipitate to settle. Cool, filter off on a 12-cm paper and wash the precipitate five times with nitric acid (2 + 98). Retain the silver chloride, if desired, for scrap recovery and evaporate the filtrate (which contains residual platinum and palladium), to complete dryness on a hot-plate (Beaker D).

(*b*) Place the filter paper in a 10-g assay crucible, ignite, and fuse with a suitable lead flux to provide a lead button which is then cupelled. Dissolve the resulting silver bead in nitric acid (1 + 3) (20 ml of the acid per g of silver). Precipitate the silver with 2.5 ml of hydrochloric acid per g of silver. Allow the precipitate to settle, then filter off and wash *etc.* as in (*a*) (Beaker E).

Add to the dry residues in beakers B, C, and D or E, about 3 ml of hydrochloric acid, 1 ml of nitric acid and 5 ml of water, cover, and warm for a few minutes on a steam-bath. Combine the solutions in a 100-ml or larger standard flask, dilute to volume, and mix. This solution is ready for the determination of gold, platinum, palladium and possible traces of rhodium as described later.

D. Supplementary lead-button method for the determination of silver and gold in sweeps rich in platinum metals. Sometimes the relative proportions of the precious metals make it advisable to determine gold and silver in separate portions of the sample, especially when their content in the sample is low compared with that of the other precious metals. The following method is recommended.

Fuse 1–20 g of the sweeps in a litharge-based flux to yield directly or after scorification a lead button weighing about 30–40 g. For flux compositions suitable for various matrices, see the appropriate references.[6,8,9,11,12]

Dissolve the lead button in about 10 ml of warm nitric acid (1 + 4) per g of lead, in a 600-ml beaker. Filter off the residue and wash it 20–30 times with cold nitric acid (2 + 98), receiving the filtrate in an 800-ml beaker. Precipitate the silver in the filtrate with 2 ml of concentrated hydrochloric acid, which is sufficient for 2 g of silver. Warm to coagulate the silver chloride.

Meanwhile, wipe the 600-ml beaker with a piece of moist filter paper and transfer this and the paper containing the residue to a 250-ml beaker. Add 30 ml of nitric acid and 25 ml of sulphuric acid and evaporate to fumes of sulphuric acid, adding more nitric acid, if required, to oxidize any organic matter completely. Finally fume strongly for at least 1 hr to break up the lead–precious metal compounds in the acid-insoluble residue. Allow to cool, dilute with about 150 ml of cold water, stir, heat to boiling, allow to cool, filter, and wash with cold water. Precipitate any silver in the filtrate by addition of several drops of hydrochloric acid. Warm and allow the silver chloride to settle.

Wash the sulphuric acid-insoluble residue back into the original 250-ml beaker, then pour through the paper 50 ml of a mixture of hydrochloric and nitric acids and hot water (3:1:4 v/v), receiving the filtrate in the same 250-ml beaker. Heat to boiling and filter into another 250-ml beaker, washing the paper with nitric acid (2 + 98). Discard the paper, which contains various platinum metals. Determine the gold in the filtrate or an aliquot, by AAS or PES.

Collect the two silver chloride precipitates separately. Wash the precipitate from nitrate medium 20–30 times with nitric acid (2 + 98). Wash the precipitate from sulphuric acid medium about 5 times with cold water.

Combine the precipitates and determine the silver as follows, depending on its amount.

(1) Ag < 10 mg. Decompose the paper with nitric and perchloric or sulphuric acids. Evaporate to dryness. Dissolve the residue in measured quantities of 2% potassium cyanide solution or 2*M* hydrochloric acid and determine the silver by AAS.

(2) Ag 10–500 mg. Ignite the paper in a 10-g assay crucible. Fuse with an appropriate lead flux to obtain a lead button. Cupel the button to obtain a silver bead and weigh on an assay balance.

(3) Ag > 500 mg. Decompose the combined papers by heating with 25 ml of nitric acid, 30 ml of sulphuric acid and 3 ml of perchloric acid. When sulphuric acid fumes appear, heat very strongly until the silver chloride is dissolved (2–3 hr). Cool, dilute with cold water, stir, heat to near boiling, cool, filter and wash with cold water. If a residue remains which does not appear to be lead sulphate, apply the same destruction treatment to the paper but with smaller amounts of the acids. From the filtrate(s) precipitate the silver as chloride with hydrochloric acid. Warm, allow to settle, cool, filter off on a tared Gooch crucible fitted with a fibreglass disc and wash thoroughly to remove all sulphuric acid. Dry for 5 hr at 125–136°, cool and weigh.

DETERMINATION PROCEDURES

The gravimetric and instrumental methods recommended are outlined below.

Gravimetric methods

Gravimetric determinations may be preferred when the precious metals are present in sufficient quantity and when a greater degree of accuracy is required than can normally be obtained by instrumental methods. A prerequisite is the absence of interfering elements.

Platinum. Platinum (>100 mg) is precipitated as ammonium chloroplatinate in the presence of 10 mg each of palladium, gold, rhodium and ruthenium, but not iridium.[5]

In the nickel sulphide procedure, the *aqua regia* solution from the dissolution of the precious metal sulphides is evaporated to dryness and, after repeated evaporations with hydrochloric acid to remove nitric acid, the platinum is precipitated in 0.1*M* hydrochloric acid medium (filtered if necessary) with ammonium chloride. The product is ignited to platinum metal. The filtrate is examined by AAS for traces of unprecipitated platinum, after destruction of ammonium salts with nitric acid. After the determination of this residual platinum, palladium can then be precipitated with dimethylglyoxime or can be determined together with rhodium, ruthenium and/or gold by AAS or plasma emission spectrometry (PES).

In the silver bead method, the combined *aqua regia* solutions can be used for the precipitation of the platinum as in the nickel sulphide procedure, and the resulting filtrate for the determination of the other precious metals.

In the sodium formate procedure, any iron, lead, zirconium (from the fusion in a zirconium crucible), and residual amounts of aluminium and silica must be removed. This can best be achieved by precipitation of the platinum with formic acid or sodium formate in sulphuric acid medium or with hydrogen sulphide.

Palladium. Palladium (>50 mg) can be precipitated with dimethylgloxime in the presence of not more than 10 mg of gold and up to 250 mg of platinum, rhodium, iridium, and ruthenium.[5,16]

In the nickel sulphide procedure, palladium can be precipitated directly after dissolution of the precious metal sulphides and dilution or evaporation (according to the amount of palladium) and filtration if necessary. The total amount of acid present should not exceed a sum of 5 ml of concentrated hydrochloric and nitric acids per 100 ml of solution. The precipitate is collected on a tared sintered-glass crucible, washed, dried and weighed. The filtrate is evaporated to remove the alcohol, then the residue is heated with nitric and perchloric acids until again dry. After dissolution of the residue in a small amount of hydrochloric acid or *aqua regia*, platinum, rhodium, iridium and/or ruthenium can be determined by AAS or PES. The combined *aqua regia* solutions from the silver bead collection can be used for the precipitation of the palladium as in the nickel sulphide procedure.

In the sodium formate procedure, the *aqua regia* solution must be silica-free. It may be advisable to evaporate it to dryness to remove any silica.

Gold. Gold (>100 mg), is preferably precipitated with oxalic acid, which gives quantitative separation from all platinum metals.[5,16] The precipitation is done in 0.1*M* hydrochloric acid medium, free from nitric acid, by boiling with 3 g of oxalic acid per 100 ml of solution.

In the silver bead method, if the sample contains more than 50 mg of gold, it is advisable not to combine the *aqua regia* solution containing the gold solution in Beaker B with the other gold-containing solutions. Instead, the gold is precipitated with oxalic acid from the solution in Beaker B. The filtrate is then evaporated to dryness after addition of nitric and perchloric acids. The residue is dissolved in a minimum of *aqua regia* and this solution combined with the other fractions containing the bulk of the platinum and palladium, prior to AAS or PES measurements.

Rhodium and iridium (nickel sulphide procedure). There are no specific precipitating agents for these two elements and separation procedures are unreliable.[16] If a gravimetric determination is preferred, both elements should first be isolated by treatment with bromide/bromate mixture,[24] followed by chlorination at 600° for purification.[6] The combined anhydrous chlorides of rhodium and iridium are converted into the metal by reduction in hydrogen and the element present in smaller amount is determined by an instrumental method such as XRF or by PES, after fusion with sodium peroxide and acidification with hydrochloric acid.

Ruthenium (nickel sulphide and sodium peroxide procedures). Ruthenium can be isolated by distillation from perchloric–sulphuric acid medium,[26] then precipitated either by hydrolysis at pH 6 or with hydrogen sulphide.[5,27]

Spectrophotometric methods

Since the collection procedures described involve the preparation of master solutions containing either all the precious metals or groups of them, they are not well suited for the spectrophotometric determination of precious metals, since few of the methods available are specific or even particularly selective.

Instrumental methods

We have found that XRF and optical emission measurements can be applied to a limited extent to the final products of the three collection procedures.

The work done so far indicates that various combinations of precious metals can be determined by XRF in the residue remaining after leaching the nickel sulphide with hydrochloric acid. The precious metal sulphides are collected on a Millipore or similar filter before XRF analysis. While the method is very sensitive, it requires the preparation of sets of appropriate standards. Since the precious metal sulphides may be accompanied by residual amounts of other elements, best results are obtained by incorporating a measured

amount of another precious metal to act both as a collector and an internal standard, *e.g.*, Ru for collection of Ir and Rh, or of Ir for collection of Rh and Ru. Another application of XRF is the determination of rhodium, iridium, and/or ruthenium in the *aqua regia*-insoluble residue in the silver bead procedure. Again the residue is collected on a Millipore or similar filter. Precision can be optimized by adding a known amount of one of the precious metals to serve as an internal standard. We also use XRF occasionally for semi-quantitative examination of the pulverized button in the nickel sulphide procedure.

For the determination of ultratrace amounts of rhodium, iridium and/or ruthenium in the *aqua-regia*-insoluble residue in the silver bead procedure, both optical emission spectroscopy (OES) and spark-source mass-spectrometry (SSMS) procedures have been used by us to a limited extent. The optimum concentration range for a 10-g sample is about 1–100 μg for the spark-source method and 0.01–200 μg for optical emission spectroscopy. With adequate standardization, results with a precision of 10% can be obtained by OES and 20% by SSMS.

Argon plasma techniques

With modern plasma-emission systems such as the argon plasma and inductively-coupled plasma (ICP), precious metals can now be routinely measured with a precision of 1–3% relative. These techniques are particularly suitable for use with the master solutions obtained by the collection procedures described.

While our experience is based on work with d.c. plasma units, many of our observations are undoubtedly equally applicable to ICP.

All work was performed with a Spectraspan III-A Echelle spectrometer. The 0.75-m spectrometer employs a 79 groove/mm echelle grating in conjunction with a 30° quartz prism which provides excellent dispersion and energy throughput, together with greater freedom from spectral interferences. The excitation source is the Spectrajet III, a three-electrode d.c. argon plasma jet. The plasma is an inverted "Y" configuration formed between two graphite anodes and a tungsten cathode. We prefer to use the instrument in the sequential mode since we have to measure small quantities of some precious metals in the presence of large quantities of others. We contend that it is difficult, if not impossible, to measure simultaneously all precious metals optimally in one dilution of the sample solution.

The sample is aspirated by pumping the solution through a ceramic nebulizer. After the aerosol has become stabilized in the plasma, the signal of the analyte of interest is integrated (in triplicate) for 10 sec. A dedicated microprocessor functions as data-collector and translates the information into concentration (on the assumption that the response/concentration relationship is linear) by use of two standards.

The fundamental principles of the d.c. plasma method, including ways to overcome random and systematic errors, have been discussed by Cooke.[21] His paper contains much valuable information on the linearity of response for the individual precious-metal emission spectra at various wavelengths, and techniques to overcome various sources of non-linearity.

The system is standardized with the standards prepared for the AAS measurements, which eliminates a source of error when comparing AAS and plasma emission results. These standards therefore contain 1.5% lanthanum chloride to act as a radiation buffer and releasing agent. The lanthanum salt is also added to all sample solutions to match the matrix of the standard solutions. Although lanthanum has a negligible effect on the signal intensity, it effectively stabilizes, but does not completely eliminate, the varying background contribution of the plasma and of the sample matrix.

The sample solutions subjected to PES measurements vary widely in composition. Some of the solutions contain only the isolated precious metals, whereas in the sodium peroxide method they contain salts of all the elements present in the sample. It is therefore necessary to provide a common matrix. It is well documented that the addition of salts of easily ionized elements, such as the alkali and alkaline-earth metals, will enhance the emission intensity of elements which otherwise may be difficult to excite.[28] The addition of 1% of sodium chloride to all standard and sample solutions caused a noticeable increase in sensitivity for all the precious metals. Sodium chloride was chosen because a relatively small amount will create a "matrix effect" and also because many of the samples are decomposed by sodium peroxide fusion and acidification with hydrochloric acid. Other alkali and alkaline-earth metal salts have not been investigated; they may well be as useful as sodium chloride. For gold, platinum and iridium, the signal is increased by about 5% if the sodium chloride concentration is 4%.

The sodium chloride virtually eliminates the effect of any base metals (remaining after the collection procedure) on the emission signals from the precious metals, and of major amounts of one or more precious metals on the emission of minor quantities of other precious metals. Interference effects can also be reduced or eliminated by matrix-matching of sample and standard solutions.[21,22]

Sodium chloride concentrations above 5% cause a significant decrease in signal intensity, possibly by a cooling effect on the plasma, and also cause rapid deterioration of the alumina ceramic sleeve at the cathode by vitrification and deformation. This will cause the plasma to be unstable and yield non-reproducible results. A maximum of 3% is chosen for safety.

Each instrumental technique has its own performance characteristics. The d.c. plasma technique has been reported to have a linear response range over at least two orders of magnitude in aqueous solutions. The composition of the precious metal samples analysed in our laboratory varies extremely widely. From

empirical observations, we have noted two distinct phenomena occurring in the d.c. plasma system which tend to reduce the linear range.

The first is spectrometer drift. This can be caused by changes in room temperature, air-currents, changes in the spectrometer-base casting, due to the warming effect of the plasma itself, and other external factors affecting the system. These effects can manifest themselves by relatively slow (10–15 min) cyclic increases and decreases in sensitivity, and may also cause a slight apparent shift of the wavelength peak. In such cases the wavelength must be reset to the peak, and restandardization may also be required. Spectrometer drift can be compensated by alternating sample and standard solutions. The ratio of the true and apparent concentrations of the standard is calculated and used as a correction for the sample value. The alternation between standards and samples allows instant corrections for drift. Although the correction factor can sometimes vary over a rather wide range without affecting the final results, we suggest that for precise work it should not vary by more than $\pm 20\%$.

The second phenomenon is a systematic positive absolute error of 2–3%. It is caused by background not compensated by the lanthanum salt and is correctable by deducting the signal of a reagent blank from the gross signal of the sample after the correction ratio has been applied. Corrected signal intensity is then plotted against concentration.

We have found a wide linear range can be obtained by deducting the background contribution (of the plasma system itself) from the total signal of each standard and sample. The correction factor for drift (external to the plasma system) is then applied to achieve true linearity. Table 1 lists the elements studied, with the wavelengths used and the optimum range for measurement. The wavelengths chosen are not necessarily the most sensitive available, but are the most free from interference by other precious and base metals. The first wavelength given is that of the primary analytical line, the others are secondary and can be used if matrix interference is encountered and also for confirmation of the precious metal concentration measured at the primary wavelength. Other investigators have recommended additional wavelengths for the analysis of specific materials.[21,22] We agree with their statements that no intensity measurement is perfectly linear over a wide dynamic range, which limits the accuracy of the plasma method if a wide-range calibration curve is used. Cooke[21] prefers to use bracketing of the sample by standards even outside the optimum range, rather than dilute the sample solution. For highest accuracy, we also recommend close bracketing, but within the linear portion of the calibration curve. The sample master solution should be diluted so that the signal is in the middle of the optimum range (Table 1). For improving the precision, aliquots taken by pipette should not be less than 5 ml and preferably 10 ml or greater. To ensure that measurements made by d.c. plasma meet the criteria of good quality-control techniques, more than one aliquot should be taken to place the analyte concentration at two different positions on the analytical curve.

Care should also be taken to ensure that the sodium chloride concentration is the same in all standards and samples. On the other hand, relative variations in acid concentrations (*e.g.*, 10–30%) do not effect either the sensitivity or the precision of the method. Unlike AAS analysis, there is no adverse effect caused by small amounts of sulphuric acid nor is there any interference caused by large concentrations of one or more precious metals in the determination of small amounts of others.

Atomic-absorption methods

The determination of individual precious metals in the absence of interfering base metals or other precious metals is comparatively simple. Suitable

Table 1. Parameters for plasma determination

Element	Wavelength, Å	Wavelengths of possible interferences, Å	Optimum range, μg/ml
Au	2675.95*	Rh 2676.11	0.3–100
	2082.09		5–100
Ir	2126.81		0.5–5
	2158.05	Rh 2158.194†	5–50
Pd	3242.70	OH band†	0.1–30
	2763.09	Fe 2763.03	1–50
		Cr 2763.06	
		Zr 2763.11	
Pt	2659.45		0.3–75
Rh	3434.89	Ru 3435.186†	0.1–50
Ru	3726.93		0.5–50

*This wavelength is usable for samples continuing Rh at concentrations less than 1000 μg/ml. It is separable from the Rh line by use of the narrowest slit-width.

†This interference is separable by use of the narrowest slit-width.

methods with detailed descriptions of instrumental parameters are given by Perkin–Elmer.[29]

The determination of the precious metals in their mixtures is more complex and subject to interference from various sources.[13,16,17,30] Valuable information has also been given in the publications of the South African National Institute of Metallurgy.[18,31,32]

The following observations indicate the degree of suitability of atomic-absorption methods for the determination of precious metals in the master solutions.

Silver bead method. The determination of gold, platinum and palladium in the presence of each other offers no problem. Lanthanum chloride should be used as releasing agent and the optimum ranges for the three elements are: Au (2428 Å) 3–50 μg/ml; Pd (3404 Å) 5–75 μg/ml; Pt (2660 Å) 10–100 μg/ml.

Rhodium and/or ruthenium can be determined in the hydrochloric acid solution of the sodium peroxide melt by use of either lanthanum chloride or uranium chloride as releasing agent. The optimum ranges are: Rh (3435 Å) 2–15 μg/ml; Ru (2696 Å) 5–25 μg/ml. The sensitivity for iridium is poorer [lower limit 10 μg/ml (2640 Å)] and this element is best determined by the plasma method.

Nickel sulphide procedure. The small amounts of sulphuric acid introduced by the dissolution of the sulphides can severely affect the determination of some of the platinum metals, particularly platinum, rhodium and iridium, unless the concentration of the test solution corresponds to dilution of the master solution to at least 500 ml (*e.g.*, a 20-ml aliquot drawn from a master solution prepared in a 100-ml standard flask must be diluted to at least 100 ml). In practical terms, this means that the solution to be measured should contain a minimum of 5 mg of platinum or 1 mg of rhodium. For smaller quantities of platinum or rhodium, the plasma technique is much to be preferred. The deleterious effect of sulphuric acid can be at least partially obviated by using lanthanum chloride as releasing agent (and not uranium chloride).[33] However, large amounts of platinum depress the rhodium signal and *vice versa*. In this case uranium appears to be a superior releasing agent. Iridium is more precisely measured by the plasma technique.

To detect interferences in the determination of the various precious metals in the master solutions, we use the technique of dilution. If a concentration X of precious metal gives an absorbance of Y, then dilution by a factor of 2 should give an absorbance of $Y/2$. If the value observed is greater than $Y/2$, interference is indicated and the solution should be further diluted (with adjustment of acid concentration and further addition of releasing agent) until the relationship between element concentration and absorbance becomes linear.

The determination of soluble silver in the nickel chloride solution by AAS is straightforward and without interference by the large concentration of nickel salts.

The sodium peroxide–sodium formate procedure. Most of what was stated for the nickel sulphide procedure is equally valid for the sodium peroxide–sodium formate procedure, but it must be remembered that the maximum amount of sample that can be handled is 2 g and that the range of application covers larger concentrations of precious metals. In this procedure, the depressive effect of sulphuric acid can be avoided by fuming any *aqua regia*-insoluble residue with nitric and perchloric acids (assuming, however, that no ruthenium determination is required).

We have found that zirconium (from the crucible used in the fusion) does not interfere with AAS measurements of precious metals and no interference has been noted from other elements that may be contained in the solution of the formate precipitate.

DISCUSSION

In the referee analysis of sweeps, Ledoux & Company employ, wherever feasible, two different collection procedures. Because of sample size considerations, the sodium peroxide method is best suited for the higher concentration range of the precious metals, and the silver bead method is optimal for the lower range. Because the nickel sulphide procedure can accommodate both small and large sample weights, it is always used as the second procedure in referee work.

The three collection procedures suggested here should prove superior to the lead collection technique widely used in the past.[5] They take less than half the time required for the lead collection procedures and avoid the tedious treatment and retreatment of various soluble and insoluble fractions.

The sodium peroxide–sodium formate procedure

The most attractive feature of this procedure is its ability to provide a medium which contains all the precious metals in one master solution. Because of its simplicity, it is our preferred method, as long as the relatively small sample weight gives an adequately representative sample containing a sufficient quantity of precious metal(s). The method is, therefore, particularly useful for the analysis of complex sweeps or precious metal residues containing more than 1% of the precious metal(s). It has the additional advantage of being applicable to collection of seven of the eight precious metals, only the determination of osmium requiring minor modifications. The addition of another precious metal, an innovative feature of all three methods, ensures the quantitative collection of trace amounts of precious metals. Ruthenium can always be used when its determination is not required, but the other precious metals work equally well.

With only a few precipitation and dissolution steps, a master solution is obtained containing all the precious metals in a form suitable for measurements by

gravimetric, atomic-absorption, and/or plasma-emission techniques.

Some difficulties may be encountered if the sample contains more than 10 mg of chromium (recognized by the distinct yellow chromate colour of the supernatant alkaline solution of the melt after the reaction with formic acid) or 250 mg of iron (recognized by the inability of the sodium formate to reduce the precious metals, particularly platinum, to the black hydroxides or oxides).

To avoid this problem, proceed as follows. After decomposition of the hydrogen peroxide, acidify the solution slightly with formic acid and heat on a steam-bath until reduction is complete, as recognized by the change in colour from yellow to black. Then alkalize the solution and add 25 ml of 10*M* sodium hydroxide. Continue heating until the precipitate settles. Add 100 ml of methanol and allow to stand for at least 2 hr. The supernatant solution should now be water-clear and ready for filtration. Some difficulties may also be encountered if the amount of rhodium plus iridium in the sample exceeds 200 mg. If, after two treatments with *aqua regia* and nitric and sulphuric or perchloric acid, an acid-insoluble residue remains, ignite it in a zirconium crucible and then fuse it with a minimum amount of sodium peroxide. Dissolve the cooled melt in water, in a 600-ml beaker, decompose the hydrogen peroxide by boiling, acidify the solution with hydrochloric acid and analyse it by the d.c. plasma technique either separately or after combination with the main solution.

As far as we are aware, the method of fusing the sample with sodium peroxide and reducing the precious metals in an alkaline medium with sodium formate to insoluble lower valence hydroxides has not been described before. Before choosing sodium formate we also experimented with formaldehyde and methanol as reducing agents.

Filtering off the precious metal oxides and hydroxides removes the alkali-metal salts introduced in the fusion and reduction steps, and also most of the silica and aluminium which are often major components of sweeps samples. Removal of the alkali-metal salts is important since they may not only complicate AAS measurements[4] but also make it difficult, if not impossible, to select optimum volumes for measuring the precious metals by instrumental techniques.

The alkali-metal salts can also be removed by use of the following hydrogen sulphide procedure.

Acidify the leached melt with hydrochloric acid, evaporate to dryness and dehydrate the silica. Dissolve the salts in dilute hydrochloric acid and filter off the silica (omit the dehydration step if the sample is low in silica). Wash the residue into a Teflon beaker and evaporate to dryness with hydrofluoric acid and a few drops of sulphuric acid. Dissolve the residue in a little hydrochloric acid and combine with the main solution. Saturate the hot solution with hydrogen sulphide. Reheat the solution and again saturate with hydrogen sulphide. Filter off the sulphides and after expelling the hydrogen sulphide test the filtrate by d.c. plasma emission for quantitative removal of iridium. Dissolve the metal sulphides in *aqua regia* and treat the solution as described in the nickel sulphide procedure. A further possibility for removing the fusion salts is to pass the silica-free solution through a column of Bio-Rad AG 50 W cation-exchanger.[4] This method, however, has the disadvantage that the amount of sodium peroxide which can be used is limited to 3 g, enough to fuse 0.5 g of a homogeneous residue sample, but not to fuse an adequate amount of most sweeps samples. Larger amounts of sodium peroxide cannot be used, since the sodium is not all retained by a cation-exchange column of reasonable size.

Validation of sodium peroxide procedure

Portions (10–30 mg) of gold, silver, platinum, palladium, rhodium, ruthenium and iridium were weighed into zirconium crucibles containing 2 g of sweeps-type residues containing only traces (<3 ppm) of any precious metals. The general compositions of the sweeps residues were as follows:

Sweeps Sample No. 1
SiO_2 40%; Al_2O_3 20%; FeO 12%; CaO 8%; MgO 7%; PbO 5%; CuO 3%; <1% each of Mn, Cu, Zr, Cr, Zn, Ni, Ti and Sn.

Sweeps Sample No. 2
SiO_2 22%; Al_2O_3 15%; CuO 15%; PbO 18%; Bi_2O_3 5%; ZrO_2 4%; CaO 5%; MgO 5%; FeO 2%; NiO 3%; Cr_2O_3 2%; TiO_2 3%; <1% of each of Sn, Zn, Ba.

These synthetic samples were fused and the precious metals collected into the master solution by (1) the sodium formate and (2) the hydrogen sulphide separation procedures. The filtrates from the sodium formate separations were examined for presence of precious metals by emission spectrography after application of the hydrogen sulphide technique in the presence of added copper(II) to act as collector.

The filtrates from the hydrogen sulphide separation procedure were examined by the plasma technique for the presence of precious metals, particularly iridium, an element which is not as easily precipitated with hydrogen sulphide as the other precious metals (<0.5 mg of iridium will typically be found in this filtrate).

The results presented in Table 2 indicate that the collection of the precious metals is substantially quantitative. The differences between the amounts added and found can largely be attributed to instrumental uncertainties. The slightly low silver results can be attributed to dissolution of some silver chloride during the repeated treatments with *aqua regia*. No attempt was made to determine the amount of silver remaining in solution, but this could easily be done by AAS.

Table 2. Sodium peroxide procedure

Element	Formate precipitation				H_2S precipitation	
	Sweeps sample No. 1		Sweeps sample No. 2		Sweeps sample No. 1	
	Added, *mg*	Found, *mg*	Added, *mg*	Found, *mg*	Added, *mg*	Found, *mg*
Au	10.2	10.9 (1)	33.5	32.7 (1)	30.3	30.8 (1)
	28.7	28.9 (1)	11.3	11.8 (1)		
	42.4	41.6 (2)	23.2	23.6 (2)		
Pt	30.2	29.8 (1)	30.3	30.0 (1)	31.2	31.6 (1)
	50.7	51.6 (2)	88.8	87.3 (2)		
	200.4	201.8 (3)	23.3	23.6 (2)		
Pd	28.6	29.0 (1)	34.7	34.1 (1,2)	28.6	28.4 (1)
	113.2	112.0 (3)	12.5	12.5 (2)		
	55.4	56.1 (2)	120.3	121.6 (3)		
Rh	33.5	32.0 (1)	16.4	16.9 (1)	26.5	26.0 (1)
	58.6	59.4 (2)	24.3	25.0 (2)		
	10.3	9.8 (2)	35.6	34.8 (2)		
Ru	25.9	26.4 (2)	33.4	34.2 (2)	30.5	31.2 (2)
	85.5	83.8 (2)	15.0	14.4 (2)		
	12.3	12.4 (2)	24.9	25.2 (2)		
Ir	25.2	25.9 (2)	33.1	32.1 (2)	27.7	26.9 (2,4)
	40.3	41.0 (2)	29.7	29.8 (2)		
	5.6	5.3 (2)	11.2	10.8 (2)		
Ag	110.5	109.3 (3)	35.6	34.8 (1)	30.3	30.0 (1)
	25.6	25.2 (1)	30.0	29.5 (1)		
	10.3	9.8 (1)	48.6	47.8 (1)		

(1) By AAS.
(2) By PES.
(3) Gravimetrically.
(4) 0.5 mg of iridium found in H_2S-filtrate by PES.

Direct sodium peroxide–d.c. plasma procedure

Strictly speaking, this is not a collection procedure, since it involves no separations, but it gives a master solution suitable for the direct determination of all the precious metals by the d.c. plasma technique, in which the presence of sodium chloride is beneficial. The limiting factor is the volume required to keep the sodium chloride concentration below 3%. A typical volume of sample solution is 500 ml, which would make the optimum range of application 5–500 mg of each precious metal. Since the maximum amount of sample that can be fused with sodium peroxide is 2 g, the method is less suitable for the analysis of lower-grade sweeps (any of the precious metals <100 oz/ton or $<0.35\%$), but it is extremely useful for the analysis of high-grade sweeps. We have noted some matrix effects in the d.c. plasma technique, for instance from high concentrations of aluminium, such as found in catalysts. It is therefore advisable to use standards matrix matched to the samples.

Since the method is extremely rapid, we use it largely semi-quantitatively to establish the analytical parameters for the more precise sodium formate, nickel sulphide and/or silver bead methods. If the hydrochloric acid concentration is kept at 3*M*, up to 200 mg of silver per litre will be kept in solution by the combined effect of the acid and sodium chloride present. The method is therefore well suited for the direct determination of silver in sweeps. Because of the close proximity of the zirconium and silver lines, AAS measurements are preferred to d.c. plasma measurements for silver. Some results are presented in Table 3. In these tests 5–100 mg portions of each of the precious metals and 2-g portions of sweeps sample No. 1 were fused with sodium peroxide in zirconium crucibles.

The nickel sulphide method

This method, based to a large extent on the excellent work of the investigators at the South African National Institute of Metallurgy[15,35] can accommodate both small and large sample weights, and small or large amounts of all the precious metals except gold. It is applicable to just about any sweeps matrix, including material that is difficult or impossible to fuse by conventional fire-assay techniques, such as samples simultaneously containing large amounts of nickel, copper, chromium, iron and aluminium. The authors of the nickel sulphide procedure suggested that the sample taken should contain a maximum of about 10 mg of precious metals. With only minor modifications, we have extended the scope of the method to as much as 1.5 g of precious metals, thus allowing the use of gravimetric methods when need

Table 3. Direct sodium peroxide–d.c. plasma procedure

Element	Added, *mg*	Found, *mg*	Element	Added, *mg*	Found, *mg*
Au	5.3	4.9	Ru	4.2	4.0
	10.5	11.3		23.6	22.5
Pt	12.0	12.9	Ir	5.5	5.2
	22.5	23.3		24.8	25.7
Pd	10.5	10.5	Ag*	6.9	6.5
	28.7	27.7		98.5	98.0
Rh	40.2	41.0			
	12.3	13.2			

*Determined by AAS.

for accuracy makes this desirable. (As much as 10 g of platinum, palladium and rhodium can be quantitatively collected without modification of the composition and quantity of flux.) On the other hand, the method can also be used for the determination of trace amounts of precious metals in sweeps when another precious metal, itself not to be determined, is added as a "collector".

We found that the procedure suggested by Robèrt *et al.*[15] for dissolving precious metal sulphides is inadequate for the larger quantities of precious metals found in most sweeps samples. Hot dilute *aqua regia* is significantly more effective than hydrochloric acid and hydrogen peroxide as a solvent for precious metal sulphides. If, after several treatments with *aqua regia*, some insoluble sulphides still remain (for instance, if the sample contains large amounts of rhodium and/or iridium), the residue can be decomposed by fuming with nitric acid and perchloric acid (or nitric acid and sulphuric acid, if ruthenium determination is required). After evaporation to dryness, the residue is treated with hot dilute nitric acid (to dissolve silver sulphate or perchlorate), then with hydrochloric acid to precipitate the silver. After filtration the filtrate is combined with the main solution. As in the case of the sodium peroxide–sodium formate procedure, an acid-insoluble residue can be transferred to a zirconium crucible and fused with sodium peroxide.

It has been reported[34] that tin causes losses of precious metals. It was conjectured that "the small amount of tin sulphide that enters the button promotes dissolution of the noble metals by the concentrated hydrochloric acid used for dissolving the button".

In a series of tests involving five sweeps samples of widely differing compositions, three 15-g samples were treated by the usual nickel sulphide collection technique, and to a fourth portion tin oxide (1.5 g) was added before the fusion. To a fifth portion tin metal (1.5 g) was added prior to the fusion. There was no statistical difference in the results obtained with and without addition of tin. In these tests, the filtrates containing nickel chloride were examined for the presence of precious metals as follows.

The hot filtrates were saturated with hydrogen sulphide in the presence of 100 mg of cupric chloride as collector. The sulphides were filtered off, ignited and examined for precious metals by emission spectrography. It was found that all portions contained, in addition to silver, only traces of precious metals (<0.1 mg of major components, <0.01 mg of minor ones), whether or not tin oxide or tin metal was originally added to the flux. These amounts of precious metals in the solutions would be insignificant in sweeps analysis. It is possible that the precious metal losses attributed by the earlier investigators[34] to the effect of tin may be due to differences in flux compositions.

The effect of prolonged heating of the sulphides with hydrochloric acid was also examined. Again no precious-metal losses were found, except for silver, even when the solutions were evaporated to incipient crystallization of nickel chloride.

We found it advantageous to modify the flux composition considerably in the nickel sulphide procedure, using the criteria for other fire-assay techniques, namely that for proper slag formation a basic sample matrix requires an acid component in the flux, and *vice versa*.

Thus, for the determination of precious metals in alumina-base catalysts and sweeps low in silica, we found it necessary to add at least 1 g of silica for each g of sample, to reduce the attack of the flux on the clay crucible. We have also replaced the borax and sodium carbonate, the basic components of the flux,[15] with potassium carbonate and boric acid, obtaining *in situ* formation of potassium tetraborate and/or metaborate. Three g of aluminium powder are also added to the flux to act as a deoxidant.

These changes in the flux composition make it easy to fuse refractory sweeps which otherwise could be fused only with some difficulty. The resulting nickel sulphide button has a silvery appearance and separates readily from the slag, which has a very low viscosity when poured and a very glossy obsidian-like appearance.

A typical flux–sample combination would be as follows.

Sample 2–20 g
Silica 5 g or equal to sample weight (whichever is the larger)
Potassium carbonate 100 g

Boric acid 60 g
Aluminium powder 3 g
Nickel carbonate 35 g
Sulphur 15 g

The resulting nickel sulphide button will weigh approximately 35 g.

The recovery nickel sulphide button is obtained by fusing the slag with 17 g of nickel carbonate and 8 g of sulphur.

In more recent tests we have replaced the nickel carbonate by nickel powder, mainly for economy since nickel powder is less than a fifth of the price of nickel carbonate per unit of available nickel. The reaction between the nickel powder and sulphur is as smooth as that between the carbonate and sulphur. We suggest using 17 g of the metal instead of 35 g of nickel carbonate.

Silver was not included in their investigations by the South African analysts. We found that silver is collected nearly completely by nickel sulphide. Only small amounts remain in the slag from the second fusion, and are recovered as described below. However, silver sulphide is partially decomposed by the concentrated hydrochloric acid treatment of nickel sulphide, and the silver liberated is held in solution by the high chloride concentration. Preliminary tests indicate that 20–100 mg of silver may remain in solution, even if the excess of hydrochloric acid is removed by evaporation and the solution diluted with water to 500 ml. This is due to the solubility of silver chloride in a concentrated nickel chloride solution. The conversion of silver sulphide into soluble silver chloride depends to a large extent on the amount of other precious metal sulphides.

The dissolved silver can easily be determined by AAS after transfer of the solution to a 1000-ml standard flask and dilution to volume with 30% v/v hydrochloric acid.

The incomplete collection of gold by the nickel sulphide procedure is a major disappointment. It can be assumed that most of the gold in samples of sweeps is present as the free metal, which does not readily form a sulphide, as shown by examination of the nickel sulphide slag. The slag contained a significant amount of gold, which was partially recovered by fusion of the slag with a lead flux containing silver as a collector. Though most of the gold was thus accounted for, the results were still significantly low. An examination of the assay crucible showed that part of the missing gold was embedded as free metal in the walls of the crucible.

A considerable effort was made to find a metal additive to the flux which might alloy with the gold during the fusion step. The best (but not completely satisfactory) results so far have been obtained by the addition of copper oxide to the flux in addition to aluminium powder. It appears that the molten aluminium produces, throughout the melt, copper metal which alloys with gold during the fusion step, before it and the gold are converted into their sulphides. A residual amount of gold passes into the slag, from which it can be recovered together with trace amounts of silver by a regular fire-assay technique, as follows.

The slag is crushed to 40-mesh powder, returned to the assay crucible and mixed with 4 g of starch and 250 g of a lead flux (PbO 85%, SiO_2 6%, Na_2CO_3 9%). The mixture is fused at about 1050°, and the resulting lead button is scorified to remove residual nickel. After cupellation, the resulting Ag/Au prill is weighed, then dissolved in nitric acid followed by hydrochloric acid (if the prill is mostly Ag) or directly in *aqua regia* (if mostly Au). The solution is evaporated to dryness, the residue dissolved in a measured amount of 2% potassium cyanide solution and the silver and/or gold determined by AAS.

Validation of nickel sulphide procedure

Portions of gold, silver, platinum, palladium, rhodium, ruthenium and iridium (5–250 mg) were weighed into 40-g assay crucibles containing 10 g of the sweeps-type residues used in validation of the sodium peroxide procedures. These synthetic sweeps samples were fused with the modified flux just described and the nickel sulphide buttons were treated and analysed by the procedures given.

The results are presented in Table 4. Except for gold the recovery of the precious metals is good, and the accuracy is limited only by the instrumentation used.

A considerable effort has been made to extend our investigation to other sulphide systems. The results will be reported in a future paper.

Silver bead method

The most attractive feature of this method is its ability to accommodate large sample weights. This approach is therefore best suited for the determination of small, even trace amounts, of the three "insoluble" precious metals (rhodium, iridium and ruthenium) in the presence of relatively large quantities of gold, silver, platinum and palladium.

To ensure the quantitative collection of trace amounts of these three "insoluble" precious metals, it is advisable to add to the fusion charge, unless enough is already present in the sample, up to 50 mg of one of the three elements for the collection of the other two. The addition of up to 5 g of silver serves to hold mechanically up to a total of 75 mg of the three insoluble metals. Beamish[16] has extensively described the appearance of silver beads containing precious metals. As a result of his investigations, he did not recommend silver as a collector for rhodium, iridium and ruthenium. It should be noted, however, that in the Beamish tests the silver to "insoluble" element ratio did not exceed 10:1, whereas in the method proposed here it exceeds 100:1. It should also be noted that all the precious metals are significantly soluble in an excess of molten silver. Separation starts only

Table 4. Nickel sulphide procedure

Element	Sweeps sample No. 1		Sweeps sample No. 2		Sweeps sample No. 2	
	Added, *mg*	Found, *mg*	Added, *mg*	Found, *mg*	Added, *mg*	Found, *mg*
Au	5.2	4.3 (1)	7.3	6.2 (1)	12.5	12.1 (2,4)
	75.3	68.2 (1)	120.0	116.5 (1)	23.2	23.0 (2,4)
	107.5	106.8 (2,4)	150.5	148.6 (1,4)	35.2	33.7 (2)
Pt	7.7	7.9 (2)	230.6	231.8 (3)	20.7	20.1 (2)
	74.6	73.0 (1)	12.8	12.1 (2)	50.8	49.5 (1,2)
	250.5	249.6 (3)	123.7	122.5 (2)	750.9	752.0 (3)
Pd	120.6	121.3 (3)	150.9	150.9 (3)	25.8	25.2 (2)
	22.5	22.0 (2)	15.3	15.9 (2)	70.6	70.8 (1,2)
	75.5	76.8 (3)	18.7	18.5 (1)	125.8	126.4 (3)
Rh	13.4	13.0 (2)	22.7	23.3 (1)	14.2	14.7 (2)
	130.7	129.6 (1)	27.3	27.9 (2)	30.9	31.6 (1)
	35.3	35.9 (2)	84.7	84.0 (2)	75.4	73.8 (1,2)
Ru	4.9	4.8 (2)	15.5	15.6 (2)	12.6	12.6 (2)
	30.2	29.5 (2)	45.3	44.5 (1,2)	55.9	57.0 (2)
	15.3	15.8 (2)	14.0	14.0 (2)	23.5	23.8 (2)
Ir	13.2	13.0 (2)	—	—	12.9	12.2 (2)
	40.7	40.0 (2)	55.5	54.3 (2)	30.3	30.4 (2)
	5.5	6.1 (2)	13.2	13.3 (2)	3.0	3.2 (2)
Ag	25.9	25.2 (3)	—	—	428.5	426.7 (3)
	120.5	120.0 (3)	65.3	65.0 (1)	75.3	73.8 (1)
	45.6	44.3 (3)	95.5	94.7 (3)	33.7	33.0 (1)

(1) By AAS.
(2) By PES
(3) Gravimetrically.
(4) Gold recovery improved by changes in flux composition and treatment of slag, see discussion.

when the silver solidifies on cooling. The amount of silver added is sufficient to prevent mechanical losses of the insoluble elements, since the element determined is always surrounded and protected by the added collector element. There are also the additional safeguards of "washing" the surface of the cupel with molten silver and of loosening the bead from the cupel at the solidification point.

The separation and collection of the various precious metals into two master solutions is achieved as shown in Fig. 1 (p. 24). The initial nitric acid solution contains all the silver and about 98% of the platinum and palladium. The filtrate in Beaker A contains about 96% of the platinum and palladium. After the reprecipitation of silver chloride, the filtrate in Beaker E or D contains more than 98% of the platinum and palladium retained by the first silver chloride precipitate.

The *aqua regia* solution in Beaker B contains all the gold and traces of platinum and palladium. It may also contain traces of rhodium, particularly if the gold content of the sample is significant. The combined *aqua regia* solution of the three fractions (Beakers B, C and D or E) therefore contains all the gold and palladium, all but traces of the platinum, and possibly traces of rhodium. The hydrochloric acid solution from the peroxide fusion of the acid-insoluble residue contains all the iridium and ruthenium and all but traces of the rhodium. It may also contain traces of platinum. The traces of precious metals mentioned are not disregarded, but are determined along with the major elements by PES.

Validation of silver bead collection procedure

Various amounts of precious metals ranging from 0.5 to 10 mg in the case of rhodium, iridium and ruthenium, and from 5 to 100 mg in the case of gold, platinum and palladium, were transferred to 30-g assay-crucibles holding 5 g of silver and 15 g of the sweeps-type samples used in the other validation work. Ruthenium or iridium were used as collectors. After fusion, scorification and cupellation, the silver beads were treated as described in the procedure. Two fractions resulted: one containing the gold, platinum and palladium and traces of rhodium, the other containing rhodium, iridium, ruthenium and traces of platinum. They were analysed as described in the experimental section. The results are presented in Table 5.

Supplementary lead-button method for determination of silver and gold in sweeps rich in platinum metals

The silver bead method obviously cannot be used for the determination of silver. The formate procedure and the direct sodium peroxide method are limited to sample weights of 2 g, which makes them most suitable for the determination of gold and silver in amounts greater than 0.25%. The modified nickel sul-

Table 5. Silver bead procedure

Element	Sweeps sample No. 1		Sweeps sample No. 2		Sweeps sample No. 2	
	Added, *mg*	Found, *mg*	Added, *mg*	Found, *mg*	Added, *mg*	Found, *mg*
Rh	0.50	0.48	4.3	4.1	0.85	0.81
	1.35	1.37	6.8	6.5	6.1	6.2
	8.4	8.5	1.52	1.52	3.2	3.0
Ir	2.33	2.39	5.2	5.3	0.55	0.50
	6.5	7.2	9.0	8.8	7.6	7.4
	25	ND*	25	ND	25	ND
Ru	25	ND*	25	ND	25	ND
	25	ND*	25	ND	25	ND
	4.7	4.6	8.3	8.4	1.62	1.70
Au	25.3	24.7	3.3	3.3	5	ND
	55.3	56.2	36.3	35.3	65	ND
	75.4	74.8	90.0	91.6	65	ND
Pt	7.3	7.3	90.5	89.0	26	ND
	23.5	22.9	30.3	30.8	40	ND
	85.3	87.2	55.1	55.7	60	ND
Pd	67.3	66.5	17.4	17.4	25	ND
	33.2	32.6	25.7	24.9	25	ND
	4.0	4.0	40.0	40.6	25	ND
Ag	5 g	ND*	5 g	ND*	5 g	ND*
	5 g	ND*	5 g	ND*	5 g	ND*
	5 g	ND*	5 g	ND*	5 g	ND*

ND Not determined.
ND* Not determined, added as collector.

phide method provides reasonably good results for gold and silver. For referee purposes, however, it is often desirable to use an alternative approach. The suggested supplementary procedure is suitable for the determination of both large and small quantities of gold and silver irrespective of the amounts of the platinum metals. No attempt is made, as in the classical lead button procedure,[5] to use the various fractions for the determination of any of the platinum metals, with the possible exception of ruthenium and iridium (but not rhodium), which remain in the residue after extraction of gold with *aqua regia*. The insoluble residue can be fused with sodium peroxide and used for the determination of ruthenium and/or iridium after acidification with hydrochloric acid.

Some of the gold and silver results obtained by application of this method to some typical sweeps samples received for analysis are given in Tables 6–12.

The d.c. plasma technique has one great advantage over the AAS method, namely superior sensitivity, allowing it to cover effectively a range difficult to achieve with AAS. This is particularly true in the case

Table 6. Analysis of sweeps sample 27303

Collection method	Analysis method	Content, %						
		Ru	Rh	Ir	Pt	Pd	Au	Ag
NiS	by PES	40.2	14.9	4.90	0.715	0.475	0.40	—
		40.5	15.2	4.95	0.707	0.479	0.39	—
	by AAS	39.8	15.2	4.6	0.703	0.477	0.38	1.50
		40.4	15.0	—	0.716	0.470	0.41	—
Direct Na_2O_2 fusion	by PES	39.8	14.9	4.63	0.70	0.46	0.42	1.45
	by AAS	40.3	14.8	—	—	—	—	1.47
Sodium formate	by PES	40.2	14.8	4.92	0.703	0.470	0.427	—
		39.9	15.0	4.94	0.707	0.478	0.420	—
	by AAS	40.3	15.0	—	0.712	0.473	0.415	1.43
Supplementary lead-button	by AAS	—	—	—	—	—	0.431	1.45

Table 7. Analysis of sweeps sample 92822-914

Collection method	Analysis method	Content, %						
		Ru	Rh	Ir	Pt	Pd	Au	Ag
NiS	by PES	0.028	0.408	0.155	0.511	0.094	0.012	—
		0.030	0.402	0.153	0.510	0.092	0.011	—
	by AAS	—	0.411	—	—	—	—	0.180
		—	0.408	—	—	—	—	—
Direct Na_2O_2 fusion	by PES	0.03	0.41	0.14	0.54	0.107	0.015	—
		—	—	—	—	—	0.014	—
	by AAS	—	—	—	0.55	0.095	—	0.220
Supplementary lead-button	by AAS	—	—	—	—	—	0.015	0.233
Sodium formate	by PES	0.031	0.406	0.147	0.511	0.094	0.013	—
		0.032	0.409	0.149	0.514	0.092	0.014	—
	by AAS	—	0.412	—	0.510	0.086	—	—
		—	0.412	—	—	—	—	—
Ag bead	by PES	—*	0.397	0.148	0.507	—	0.015	—
		—	—	0.152	0.509	—	—	—
	by AAS	—*	0.395	—	0.511	0.089	—	—
Outside laboratory No. 1, unknown method		0.028	0.402	0.154	0.525	0.099	0.023	0.238
Qutside laboratory No. 2, unknown method		0.003	0.390	0.127	0.510	0.091	0.015	0.15

*Ruthenium added as collector.

Table 8. Analysis of sweeps sample 92822-224

Collection method	Analysis method	Contents, %						
		Ru	Rh	Ir	Pt	Pd	Au	Ag
NiS	by PES	0.056	1.78	0.107	0.277	0.160	0.662	—
		0.054	1.76	0.104	0.271	0.163	0.656	—
	by AAS	—	1.77	—	0.277	0.167	0.650	6.85
Direct Na_2O_2 fusion	by PES	0.067	1.76	0.10	0.28	0.18	0.69	—
		0.065	1.76	0.10	0.27	0.19	0.69	6.87
	by AAS	—	1.74	—	—	—	—	—
Supplementary lead-button	by AAS	—	—	—	—	—	0.684	6.90§
Sodium formate	by PES	0.049	1.82	0.105	0.255	0.154	0.646	—
		0.052	1.80	0.103	0.257	0.158	0.663	—
	by AAS	—	1.76	—	0.255	0.157	0.660	6.91
Ag bead	by PES	*	1.79	0.106	0.271	0.162	0.694	—
		*	1.77	0.109	0.275	0.166	0.694	—
	by AAS	*	1.76	—	0.274	0.160	0.686	—
Outside laboratory No. 1		0.064†	1.78	0.110	0.294	0.171†	0.706	6.87†
Outside laboratory No. 2		0.052†	1.75	0.100	0.250	0.160†	0.630	7.16†

*Ru added to Ag beads.
†No referee analysis required.
§Silver determined gravimetrically as AgCl.

Table 9. Analysis of sweeps sample 92822-424

Collection method	Analysis method	Content, % Ru	Rh	Ir	Pt	Pd	Au	Ag
NiS	by PES	0.070	0.386	0.069	0.773	0.933	0.266	—
		0.072	0.388	0.066	0.770	0.946	—	—
	by AAS	—	0.400	—	0.769	0.928	0.260	1.13
		—	0.392	—	0.776	0.935	—	1.15
Direct Na_2O_2 fusion	by PES	0.05	0.41	0.076	0.76	0.94	0.28	—
	by AAS	—	0.40	—	0.75	0.94	0.28	1.09
		—	—	—	—	—	—	1.09
Supplementary lead-button	by AAS	—	—	—	—	—	0.276	1.14
Sodium formate	by PES	0.074	0.387	0.064	0.758	0.916	0.263	—
		0.074	0.394	0.068	0.764	0.925	0.269	—
	by AAS	—	0.389	—	0.768	0.920	0.260	—
Ag bead	by PES	*	0.380	0.068	0.766	0.938	0.284	—
			0.386	0.073	0.760	0.927	0.280	—
	by AAS	*	0.391	—	0.764	0.935	0.280	—
Outside laboratory No. 1		0.082†	0.388	0.081	0.835	0.966	0.294	1.17
Outside laboratory No. 2		—†	0.380	0.069	0.770	0.930	0.280	1.04

*Ru added as collector.
†No referee analysis required.

Table 10. Analysis of sweeps sample 33827-124

	Reported by shipper, %	Reported by receiver, %
Ru	0.017	0.014
Ir	0.0079	0.0050
Pt	0.010	0.010
Pd	0.034	0.036
Au	0.023	0.021
Ag	6.72	6.75
Rh	0.111	0.100

Umpire results for Rh by Ledoux & Co.

NiS	
by PES	0.117, 0.113
by AAS	0.112, 0.111
Ag bead	
by PES	0.107, 0.109
by AAS	0.109, 0.109
Direct Na_2O_2	
by PES	0.121
Sodium formate	
by PES	0.111

of iridium where the sensitivity of the plasma method is at least 50 times that of AAS. The fact that sodium chloride does not interfere with d.c. plasma measurements allows the use of fusion of precious-metals "insolubles" with sodium peroxide and acidification with hydrochloric acid. The direct sodium peroxide fusion method yields results ranging from semi-quantitative to quantitative, depending on the amount of potentially interfering elements present. For example, the presence of 1000 μg of alumina per ml, unless also present in the standards, will cause +5% relative error for rhodium and +10% relative error for platinum. The application of this method is also limited to sample solutions containing more than 1 mg of each precious metal.

In evaluating the data in Tables 6–12 it should be remembered that the precision of the d.c. plasma method, when based on a sufficient number of readings, is between 1 and 1.5% relative, whereas that of the AAS method varies between 1.5 and 3% relative. Any deterioration in the precision is attributable either to inadequacies in the collection procedures and/or the presence of interfering species.

Table 11. Analysis of sweeps sample 20292

Collection method	Analysis method	Content, % Ru	Rh	Ir	Pt	Pd	Au	Ag
NiS	by PES	0.051	1.40	0.0045	7.67	4.26	—	—
		0.052	1.42	0.0048	7.59	4.32	—	—
	by AAS	—	1.47	—	7.52	—	—	—
		—	1.52	—	7.67	—	—	—
Direct Na_2O_2 fusion	by PES	0.083	1.64	0.0046	7.87	4.49	0.568	—
		0.083	1.66	—	8.20	4.44	0.436	—
	by AAS	—	1.46	—	7.45	4.26	0.574	5.78
		—	1.45	—	7.46	4.26	0.55	5.76
Supplementary lead-button	by AAS	—	—	—	—	—	0.553	5.67†
Sodium formate	by PES	0.057	1.51	0.0056	7.81	4.39	0.551	—
	by AAS	—	1.52	—	7.60	—	—	5.56
*By CoS collection method**		0.050	1.52	0.011	7.42	4.28	0.542	5.50
Outside laboratory No. 1		—	1.45	—	7.78	4.33	0.55	5.47
Outside laboratory No. 2		—	(8.04!)	—	7.68	4.40	0.44	6.61

*Ledoux & Co. unpublished method.
†Silver determined gravimetrically as AgCl.

Table 12. Analysis of sweeps sample 20782

Method	Pt, %	Rh, %	Pd, %
NiS			
by PES	9.80	0.242	0.197
	9.87	0.242	0.195
by AAS	9.90	0.238	0.198
	9.92	0.240	0.196
Gravimetric	9.85	—	—
(15-g sample)	9.87	—	—
Direct Na_2O_2 fusion			
by PES	9.98	0.23	0.20
	9.96	0.23	0.20
Outside laboratory	9.90	0.23	0.20

Instrumental techniques applicable to other sulphide systems will be reported in a subsequent paper.

REFERENCES

1. V. P. Guinn and C. D. Wagner, *Anal. Chem.*, 1960, **32**, 317.
2. A. J. Lincoln and E. N. Davis, *ibid.*, 1959, **31**, 1317.
3. S. Kallmann, Unpublished results.
4. R. C. Mallet, E. J. Ring, H. R. Middleton and M. Dubois, *Natl. Inst. Met. Rep. S. Afr., Rept.*, No. 1555, 1975.
5. T. J. Walsh and E. A. Hausman, in *Treatise on Analytical Chemistry*, I. M. Kolthoff and P. J. Elving (eds.), Part II, Vol. 8, Interscience, New York, 1963.
6. Chemikerausschuss, *Edelmetall-Analyse*, Springer, Berlin, 1964.
7. S. Kallmann, *Anal. Chim. Acta*, 1970, **51**, 120.
8. F. W. Bowdish, *Fire Assaying for Gold and Silver*, paper at IPMI Meeting on Precious Metals, San Francisco, 1980.
9. E. E. Bugbee, *A Textbook on Fire Assaying*, 3rd Ed., Wiley, New York, 1940.
10. C. H. Fuston and W. J. Sharwood, *Manual of Fire Assaying*, McGraw-Hill, New York, 1929.
11. A. McGuire, *Classical Fire Assaying*, paper at IPMI Conference on Precious Metals, Morristown, N.J., 1978.
12. E. A. Smith, *The Sampling and Assay of the Precious Metals*, 2nd Ed., Griffin, London, 1947.
13. F. E. Beamish and J. C. Van Loon, *Recent Advances in the Analytical Chemistry of the Noble Metals*, Pergamon Press, Oxford, 1972.
14. G. H. Faye and P. E. Moloughney, *Talanta*, 1972, **19**, 269.
15. R. V. D. Robèrt, E. van Wyk and R. Palmer, *Natl. Inst. Met. Rep. S. Afr., Rept.*, No. 1371, 1971.
16. F. E. Beamish, *The Analytical Chemistry of the Noble Metals*, Pergamon Press, Oxford, 1960.
17. F. E. Beamish and J. C. Van Loon, *Analysis of Noble Metals*, Academic Press, New York, 1977.
18. R. C. Mallet, D. C. Pearton and E. J. Ring, *Natl. Inst. Met. Rep. S. Afr., Rept.*, No. 970, 1970.
19. C. L. Lewis, in reference 16.
20. *Idem*, in reference 17.
21. S. R. Cooke, *Analysis of Precious Metals, Using a D.C.*

Arc Plasma Spectrometer, paper at IPMI Conference on Precious Metals, Chicago, 1979.
22. H. Griffin, *Analysis of Fire Assay Collection Beads by D. C. Plasma Echelle-Grating Spectroscopy*, paper at IPMI Conference on Precious Metals, Morristown, N.J., 1978.
23. C. O. Ingamels, *General Sampling Theory*, paper at IPMI Conferences on Precious Metals in Morristown, N.J., 1978 and San Francisco, 1980.
24. R. Gilchrist and E. Wichers, *J. Am. Chem. Soc.*, 1935, **57**, 2565.
25. R. Gilchrist, *Chem. Rev.*, 1943, **32**, 277.
26. R. E. Thiers, W. Graydon and F. E. Beamish, *Anal. Chem.*, 1948, **20**, 831.
27. R. Gilchrist, *Bur. Stds. J. Research*, 1929, **3**, 993.
28. D. D. Nygaard and T. R. Gilbert, *Appl. Spectrosc.*, 1981, **35**, 52.
29. Perkin-Elmer, *Analytical Methods for Atomic Absorption Spectroscopy*, 1973.
30. J. C. Van Loon, *Analytical Chemistry of the Noble Metals*, paper at IPMI Conference on Precious Metals, San Francisco, 1980.
31. R. C. Mallet and R. J. Breckenridge, *Natl. Inst. Met., Rep. S. Afr., Rept.*, No. 1318, 1971.
32. R. C. Mallet, D. C. G. Pearton and E. J. Ring, *ibid., Rept.*, No. 1086, 1970.
33. R. C. Mallet and M. Dubois, *ibid.*, No. 1534, 1973.
34. R. V. D. Robèrt and E. Van Wyk, *ibid.*, No. 1705, 1975.
35. M. M. Kruger and R. V. D. Robèrt, *ibid.*, No. 1432, 1972.

Talanta, Vol. 30, No. 1, pp. 41–44, 1983
Printed in Great Britain.

0039-9140/83/010041-04$03.00/0

REACTIVITY OF POTASSIUM TETRACYANOMERCURATE WITH Ag(I), Ni(II) AND Co(II)*

ALESSANDRO DE ROBERTIS and ATHOS BELLOMO
Institute of Analytical Chemistry, University of Messina, Messina, Italy

(*Received* 14 *December* 1981. *Revised* 28 *May* 1982. *Accepted* 16 *August* 1982)

Summary—Potentiometric and conductometric studies on the reactions between $K_2Hg(CN)_4$ and Ag(I), Ni(II), Co(II) are reported. The possibility of determination of these metal ions has been evaluated and some titration data are reported.

The cyanide ion is a particularly strong ligand owing to its highly nucleophilic character. From formation-constants for the cyanide complexes of various cations[1,2] it can be seen that the reaction $M^{n+} + aCN^- = M(CN)_a^{(n-a)+}$ generally produces very stable species for $1 \leqslant a \leqslant n$, and less stable ones for $a > n$.

For the system Hg(II)–CN^- the values reported are $\log k_1 = 17.00$, $\log k_2 = 15.75$, $\log k_3 = 3.56$ and $\log k_4 = 2.66$ at 25°;[3] other authors[1,2] have obtained similar values. $Hg(CN)_2$ is so stable that it does not give the typical reactions of CN^- or Hg(II), except for HgS precipitation.[4] It can also be converted into the tetracyano-complex $Hg(CN)_4^{2-}$, which besides the two negative charges has lone pairs of electrons available on the four nitrogen atoms. We can therefore hypothesize some reactions of cations with $Hg(CN)_4^{2-}$ or with CN^- derived from it, on the basis of the stability constants of the resulting species and of possible hydrolytic reactions, since potassium tetracyanomercurate solutions have pH ~10. We decided it would be useful to study the reactions between $K_2Hg(CN)_4$ and Ag(I), Ni(II) and Co(II) to establish their stoichiometry and select those which are analytically useful; we also studied the interferences.

EXPERIMENTAL

Solutions and apparatus

The standard aqueous solution of $K_2Hg(CN)_4$ was prepared by dissolving the necessary quantity of the Merck reagent-grade salt, previously dried over phosphorus pentoxide, and analysed for purity (99.3%) by decomposing a known quantity with nitric acid and titrating the Hg(II) with thiocyanate by the Volhard method. All other solutions were made from analytically pure salts, and standardized by known methods.[5]

To determine the reacting ratio between $Hg(CN)_4^{2-}$ (henceforth abbreviated to HG) and M^{n+}, a known quantity of HG was titrated with standard solutions of the various metal ions in the absence of buffer. The equivalence points were found by potentiometry and low-frequency conductimetry.

Since each technique can reveal only what is allowed by its transducer,[6] a multiplicity of techniques was used in order to obtain complementary results, and thus determine and interpret the various reactions.

Potentiometric titrations of HG with hydrochloric acid (glass electrode) revealed only one equivalence point (EP), at a pH of about 5, with HG and HCl reacting in the ratio 1:2. When a mercury-selective electrode was used as indicator the same equivalence point was obtained, so the reaction is taken as being

$$Hg(CN)_4^{2-} + 2H^+ = Hg(CN)_2 + 2HCN \qquad (1)$$

Stoichiometry of reactions

$K_2Hg(CN)_4$ with $AgNO_3$. Figure 1 shows three typical titration curves of 1.0 mmole of HG with 0.0912*M* silver nitrate. There are three EP, corresponding to compounds in which the molar ratio (R) of Ag^+ to HG is 0.67, 1.00 and 2.00. We believe that the following successive reactions take place:

first EP, $R = 0.67$:

$$3Hg(CN)_4^{2-} + 2Ag^+ = Ag_2[Hg(CN)_4]_3^{4-} \qquad (2)$$

second EP, $R = 1.00$:

$$Ag_2[Hg(CN)_4]_3^{4-} + Ag^+ = 3AgHg(CN)_4^- \qquad (3)$$

third EP, $R = 2.00$:

$$3AgHg(CN)_4^- + 3Ag^+ = 3Hg(CN)_2 + 3Ag_2(CN)_2 \qquad (4)$$

The nitrate ions are omitted from these equations, since they affect only the conductivity. We should stress that both the ions involved in co-ordination with CN^-, *viz.* Hg(II) and Ag(I), are d^{10} cations and in aqueous solution are both typically soft acceptors.[7]

The initial decrease in conductivity is due to the gradual substitution [see reaction (2)] of the six charges of $3Hg(CN)_4^{2-}$ by the four charges of the anion $Ag_2[Hg(CN)_4]_3^{4-}$ and two charges of the NO_3^- ions. Further addition of Ag(I) leads to a compound having $R = 1.00$, according to reaction (3), and the conductivity increases slightly because of the higher mobility of the nitrate ion. In the compound $Ag_2[Hg(CN)_4]_3^{4-}$ the two silver ions (with co-ordination number 2) would act as bridges between the three $Hg(CN)_4^{2-}$ anions through the lone-pairs of electrons on the nitrogen atoms.

When the quantity of silver added reaches equimolarity with HG, the result is quantitative formation of $AgHg(CN)_4^-$. The increase in conductivity observed before

*Presented at the XIV Congress of the Società Chimica Italiana, Catania, 1981. Supported by C.N.R., Rome, Italy.

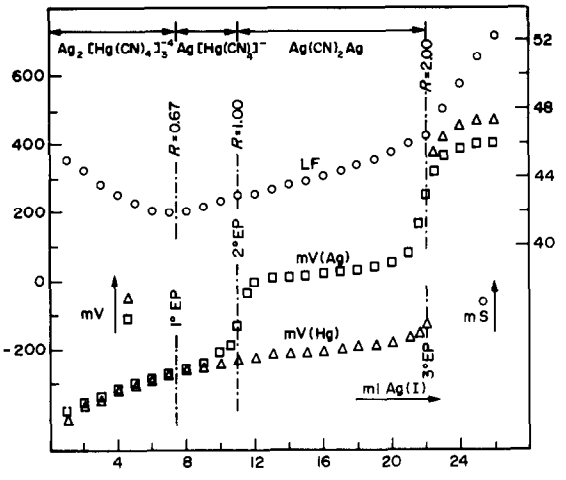

Fig. 1. Curves for titration of 1.0 mmole of $Hg(CN)_4^{2-}$/100 ml with 0.0912*M* Ag(I). LF = conductometric titration; mV(Ag) = potentiometric titration with an Ag-selective electrode as indicator; mV(Hg) = potentiometric titration with an Hg-selective electrode as indicator.

this second EP continues at the same rate even after it, because the substantial increase in $[NO_3^-]$ [see reaction (4)] is counterbalanced by the disappearance of the anion $AgHg(CN)_4^-$. The potentiometric titration with the Ag electrode gives a change in potential due to the quantitative transformation of $Ag_2[Hg(CN)_4]_3^{4-}$ into $AgHg(CN)_4^-$, whereas titration with an Hg electrode does not, since the $Hg(CN)_4^{2-}$ structure is preserved. The formation of $AgHg(CN)_4^-$ always take place through the lone-pairs of the nitrogen atoms; in such cases the co-ordination number 2 of Ag(I) would favour polymerization to yield compounds of the type $Ag_z[Hg(CN)_4]_z^{z-}$.

Once the second EP has been passed, addition of further Ag(I) causes reaction (4) until the third EP (for which R = 2.00) is reached. This is shown on the LF curve by the increase in conductivity due to the excess of silver nitrate. There is also an increase in potential with both electrodes, corresponding to the transformation of $AgHg(CN)_4^-$ (or its polymers) into the insoluble salt $Ag(CN)_2Ag$ (analysis of which confirms its composition), and release of the covalent compound $Hg(CN)_2$.

$K_2Hg(CN)_4$ with $NiSO_4$. Figure 2 shows the curves for titration of 1.0 mmole of HG with 0.0922*M* nickel sulphate. An overall view of the curves reveals three EP, with R equal to 0.25, 0.50 and 1.00 respectively. We hold that the reactions taking place are successively:

first EP, R = 0.25;

$$4Hg(CN)_4^{2-} + Ni^{2+} = Ni[Hg(CN)_4]_4^{6-} \quad (5)$$

second EP, R = 0.50:

$$Ni[Hg(CN)_4]_4^{6-} + Ni^{2+} = 2Ni(CN)_4^{2-} + 4Hg(CN)_2 \quad (6)$$

third EP, R = 1.00:

$$2Ni(CN)_4^{2-} + 2Ni^{2+} = 2Ni(CN)_4Ni \quad (7)$$

Sulphate ions are omitted from these equations since they affect only the conductivity measurements. The Ni(II) ion, d^8, possesses modest soft characteristics.[7]

In Fig. 2, the decrease of conductivity until the first EP is reached can be attributed to the gradual formation [reaction (5)] of a large ion carrying six negative charges, counterbalanced by the disappearance of four $Hg(CN)_4^{2-}$ ions and addition of one sulphate ion. We think that the $Ni[Hg(CN)_4]_4^{6-}$ is formed by interaction between Ni(II) and the lone-pairs of the cyanide nitrogen atoms, and that it is a square plane, similar to that of the tetracyanonickelate ion, nickel dimethylglyoximate,[8] *etc.*

Once the first EP is passed, addition of Ni(II) increases the conductivity owing to the destruction [reaction (6)] of the $Ni(HG)_4^{2-}$ and production of the smaller $Ni(CN)_4^{2-}$ ions and undissociated $Hg(CN)_2$. The quantitative formation of this last compound is demonstrated by the potentiometric EP (Hg electrode) at R = 0.50.

Further addition of Ni(II) precipitates solid $Ni(CN)_4Ni$,[9] in accordance with reaction (7). Thus we observe a decrease in conductivity (LF curve) until the third EP is reached, at which point the precipitation is quantitative. Beyond the third EP, the conductivity is increased by the excess of titrant.

$K_2Hg(CN)_4$ with $CoSo_4$. Figure 3, for titration of 1.0 mmole of HG with the d^7 cation Co(II). They clearly show two EP with R values of 0.40 and 1.00; the conductometric curve might also indicate equivalence in the region of R = 0.2 and 0.6, but we were able to hypothesize quantitative reactions concordant with these values, either on the basis of experiment or the literature on cobalt chemistry.[10-12]

The reactions which take place quantitatively are:

first EP, R = 0.40:

$$5\,Hg(CN)_4^{2-} + 2Co^{2+} = 2Co(CN)_5^{3-} + 5\,Hg(CN)_2 \quad (8)$$

second EP, R = 1.00:

$$2Co(CN)_5^{3-} + 3Co^{2+} = 5Co(CN)_2 \quad (9)$$

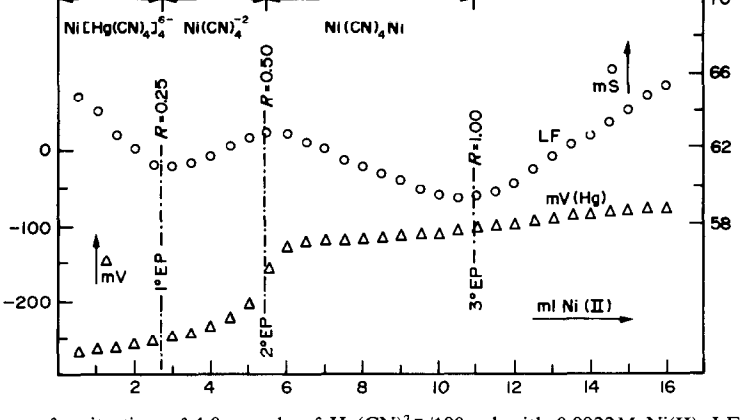

Fig. 2. Curves for titration of 1.0 mmole of $Hg(CN)_4^{2-}$/100 ml with 0.0922*M* Ni(II). LF = conductometric titration; mV(Hg) = potentiometric titration with an Hg-selective electrode as indicator.

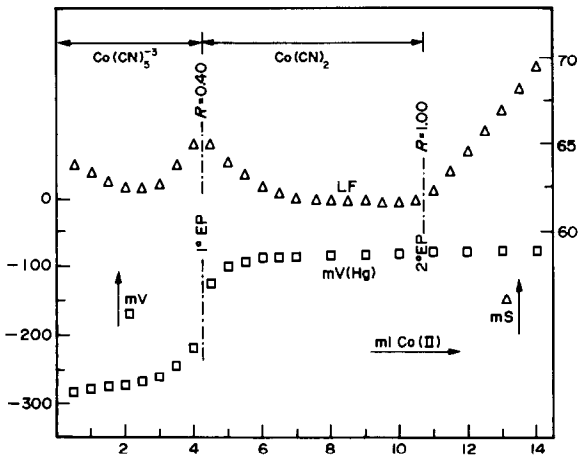

Fig. 3. Curves for titration of 1.0 mmole of $Hg(CN)_4^{2-}$/100 ml with 0.0935*M* Co(II). LF = conductometric titration; mV(Hg) = potentiometric titration with an Hg-selective electrode as indicator.

Reaction (8) was deduced from the inflection on the potentiometric curve, which indicates the liberation of $Hg(CN)_2$ and the formation of $Co(CN)_5^{3-}$, a reasonably stable complex already observed by others.[13,14] Reaction (9) was deduced from the LF curve and shows the quantitative formation of the brown $Co(CN)_2$ precipitate.

ANALYTICAL APPLICATIONS

The curves shown in Figs. 1–3 suggest possibilities for both conductometric and potentiometric direct and reverse titrations of HG, Ag(I), Ni(II) and Co(II).

We decided not to use the conductometric technique, since the titration curves give more than one EP, which could present interpretative problems.

Instead, we developed the potentiometric technique, which uses a cell of the type Hg/Hg(II)‖KNO_3‖SCE, where Hg denotes the Hg-selective electrode. The EP of the titrations corresponds to the quantitative formation of $Hg(CN)_2$ according to the overall reactions:

$$Hg(CN)_4^{2-} + 2Ag^+ = Hg(CN)_2 + Ag(CN)_2Ag \qquad R = 2.0$$

$$2Hg(CN)_4^{2-} + Ni^{2+} = 2Hg(CN)_2 + Ni(CN)_4^{2-} \qquad R = 0.5$$

$$5Hg(CN)_4^{2-} + 2Co^{2+} = 5Hg(CN)_2 + 2Co(CN)_5^{3-} \qquad R = 0.4$$

Standard stock solutions of Ag(I), Co(II), Ni(II) and HG were prepared and successively diluted to give the working solutions. The same method was used whichever solution was regarded as the determinand. A known volume of HG solution was diluted to about 100 ml and titrated with the appropriate cation solution. Since the titres of all the solutions were known, it was possible to compare the theoretical and experimental values. Table 1 shows some of the results obtained, which confirm the general validity of the method. The best results are obtained by titrations with (or of) Ni(II) and Co(II) to an EP which does not incur precipitation. The error is below ± 1% over a wide range of concentration. For Ag(I), however, the margin of error is wide for very low or very high concentrations. At low concentrations the error is

Table 1. Comparison between the theoretical and experimental values for HG, titrated potentiometrically with Ag(I), Ni(II), Co(II)

Ag(I)–HG system			Ni(II)–HG system			Co(II)–HG system		
HG_{theor}, μmoles	HG_{exper}, μmoles	Δ,%	HG_{theor}, μmoles	HG_{exper}, μmoles	Δ,%	HG_{theor}, μmoles	HG_{exper}, μmoles	Δ,%
19.80	20.20	+2.0	20.13	20.57	+2.2	19.35	20.05	+3.6
39.61	38.66	−2.4	40.26	40.98	+1.8	38.70	38.00	−1.8
69.31	70.56	+1.8	70.45	68.76	−2.4	67.73	69.22	+2.2
99.02	98.13	−0.9	100.6	101.9	+1.3	96.76	98.02	+1.3
148.5	147.6	−0.6	151.0	149.8	−0.8	145.1	146.0	+0.6
198.0	199.1	+0.6	201.3	202.0	+0.3	193.5	193.5	−0.2
247.6	248.2	+0.2	251.6	250.7	−0.4	241.9	240.9	−0.4
297.1	295.8	−0.4	301.9	300.2	−0.6	290.3	292.3	+0.7
346.6	347.7	+0.3	352.2	354.8	+0.7	338.7	337.3	−0.4
396.1	394.6	−0.4	402.6	401.3	−0.3	387.0	387.8	+0.2
445.6	446.0	+0.1	452.9	452.0	−0.2	435.4	438.0	+0.6
495.1	498.3	+0.6	503.2	508.1	+1.0	483.8	485.7	+0.4
742.7	740.3	−0.3	754.8	755.3	+0.1	725.7	727.2	+0.2
990	983	−0.7	1006	1010	+0.4	968	962	−0.6
1485	1475	−0.7	1510	1522	+0.8	1451	1464	+0.9
1980	1961	−1.1	2013	2004	−0.5	1935	1943	+0.4
2476	2440	−1.4	2516	2533	+0.7	2419	2434	+0.6
2971	2912	−2.0	3019	3049	+1.0	2903	2877	−0.9
3466	3394	−2.1	3522	3570	+1.3	3387	3333	−1.6
3961	3892	−1.7	4026	3970	−1.4	3870	3940	+1.8

Table 2. Interferences

Salt added	Ag(I)–HG system		Ni(II)–HG system		Co(II)–HG system	
	yes	no	yes	no	yes	no
$AgNO_3$	—	—	×		×	
$Ni(NO_3)_2$	×		—	—		×
$Co(NO_3)_2$	×			×	—	—
$Fe(NO_3)_3$		×		×	×	
$Cr(NO_3)_3$		×	×		×	
$Cd(NO_3)_2$		×		×		×
$Zn(NO_3)_2$		×		×	×	
$Pb(NO_3)_2$		×		×		×
$Cu(NO_3)_2$	×		×		×	
$MnSO_4$	—	—	×		×	
$FeSO_4$	—	—	×		×	
KCl	—	—	×		×	
KI	—	—	×		×	
$HgCl_2$	—	—	×		×	

— indicates not tested

always positive and attributable to precipitation difficulties; at high concentrations the error is always negative and suggests occlusion of HG in the precipitate already formed.

Interferences were studied, and are indicated in Table 2.

REFERENCES

1. L. G. Sillén and A. E. Martell, *Stability Constants of Metal-ion Complexes* 2nd Ed., pp. 107–113. The Chemical Society, London, 1964.
2. *Idem, ibid., Supplement No. 1*, pp. 53–57, 1974.
3. J. J. Christensen, R. M. Izatt and D. Eatough, *Inorg. Chem.*, 1965, **4**, 1278.
4. I. M. Kolthoff and P. J. Elving, *Treatise on Analytical Chemistry*, Part II, Vol. 3, p. 267. Interscience, New York, 1961.
5. A. I. Vogel, *Quantitative Inorganic Analysis*, 2nd Ed. Longmans, London, 1955.
6. A. DeRobertis, A. Bellomo and D. DeMarco, *Talanta*, 1976, **23**, 732.
7. C. F. Bell, *Principles and Application of Metal Chelation*, p. 32. Clarendon Press, Oxford, 1977.
8. B. Z. Shakhashiri, G. E. Dirreen and F. Juergens, *J. Chem. Educ.*, 1980, **57**, 900.
9. D. N. Hume and I. M. Kolthoff, *J. Am. Chem. Soc.*, 1950, **72**, 4423.
10. S. M. Nelson and T. M. Shepherd, *J. Chem. Soc.*, 1965, 3284.
11. F. A. Cotton, T. G. Dunne and J. S. Wood, *Inorg. Chem.*, 1964, **3**, 1495.
12. J. M. Pratt and R. J. P. Williams, *J. Chem. Soc. (A)*, 1967, 1291.
13. L. G. Sillén and A. E. Martell, *Stability Constants of Metal-ion Complexes*, 2nd Ed., p. 109, The Chemical Society, London, 1964.
14. *Idem, ibid., Supplement No. 1*, p. 54, 1974.

Talanta, Vol. 30, No. 1, pp. 45–48, 1983
Printed in Great Britain.

0039-9140/83/010045-04$03.00/0

SHORT COMMUNICATIONS

AN IMPROVED RADIOCHEMICAL PROCEDURE FOR LOW-LEVEL MEASUREMENTS OF AMERICIUM IN ENVIRONMENTAL MATRICES

S. BALLESTRA and R. FUKAI
International Laboratory of Marine Radioactivity, IAEA, c/o Oceanographic Museum, Principality of Monaco

(*Received* 9 *July* 1982. *Accepted* 25 *August* 1982)

Summary—The chemical yield and accuracy of measurements of ^{241}Am at low levels in marine environmental matrices have been substantially improved by applying the extraction procedure with DDCP (dibutyl-*N*,*N*-diethylcarbamylphosphonate). The improved procedure is described, and its advantages over the conventional procedure are discussed.

The results of several intercalibration exercises conducted in recent years on the measurements of transuranic radionuclides[1–4] demonstrate that the determination of americium at low levels, such as those encountered in environmental matrices, still poses serious analytical problems to a number of laboratories. Although the method for americium separation by extraction with HDEHP (di-2-ethylhexylphosphoric acid) together with anion-exchange in nitric acid–methanol medium, proposed previously by Holm *et al.*,[5] gives clean separation of americium and curium from interfering α-emitters and lanthanides, the radiochemical yield may sometimes be low owing to the effect of complex matrices, inadequate pH-control for the extraction step, *etc.* A more consistent recovery of americium can be achieved by extraction with DDCP (dibutyl-*N*,*N*-diethylcarbamylphosphonate) in strong acid medium instead of the HDEHP extraction, thus eliminating the delicate pH-control for the extraction step. The details of the improved procedure for americium separation are described below and the advantages of applying the new procedure are discussed.

EXPERIMENTAL

Reagents

Two-layer ion-exchange column. Bore 1 cm. Upper layer, 3 ml of Bio-Rad 50W-X8 cation-exchange resin (200–400 mesh); lower layer 3 ml of Bio-Rad AG1-X8 anion-exchange resin (100–200 mesh).

Anion-exchange column. Bio-Rad AG1-X4 (100–200 mesh), bore 1 cm, volume 6 ml.

Nitric acid (1M)–methanol (93% v/v) mixture. Mix 64 ml of concentrated nitric acid (15.7*M*) with 936 ml of pure methanol.

Hydrochloric acid (0.1)M–ammonium thiocyanate (0.5M)–methanol (80% v/v) mixture. Mix 100 ml of 1*M* hydrochloric acid and 100 ml of 5*M* ammonium thiocyanate with 800 ml of pure methanol.

Hydrochloric acid (1.5M)–methanol (86% v/v) mixture. Mix 122 ml of concentrated hydrochloric acid (12.4*M*) with 860 ml of pure methanol and dilute to 1000 ml with distilled water.

Americium yield monitor. Nitric acid (1*M*) solution of ^{243}Am or ^{244}Cm (1–2 dpm/ml).

Sample pretreatment

The procedures for pretreating large quantities of environmental matrices, such as sea-water (~200 l.), sediments (50–100 g), biological materials (20–100 g), for the measurements of transuranic nuclides have already been fully described.[5] After addition of the required yield monitors (^{243}Am or ^{244}Cm for the americium determination, 1–2 dpm per sample), sediment and biological samples are dry-ashed and then treated with hot *aqua regia*. Transuranic nuclides present in the resulting solutions are co-precipitated with iron hydroxide. Instead of two-step co-precipitation with first calcium–magnesium carbonate and then iron hydroxide,[6] transuranic nuclides in sea-water samples may be directly co-precipitated with large amounts of iron hydroxide (at least 10 mg of iron per litre of sea-water) after equilibration of the yield monitors added.

The precipitate of iron hydroxide obtained through the pretreatment procedures is dissolved with either concentrated hydrochloric acid or concentrated nitric acid. Plutonium is separated from americium and curium either by the anion-exchange procedure in the hydrochloric acid medium described by Talvitie[7] or by that of Wong,[8] in nitric acid medium.

Americium purification

The acid solution of the americium fraction (in either 9*M* hydrochloric acid or 8*M* nitric acid) is evaporated nearly to dryness and then the residue is dissolved in 600–800 ml of distilled water. Oxalic acid (~20 g) is added and, if necessary, 200–300 mg of Ca^{2+} (as calcium nitrate) and dissolved by stirring. The pH of the solution is

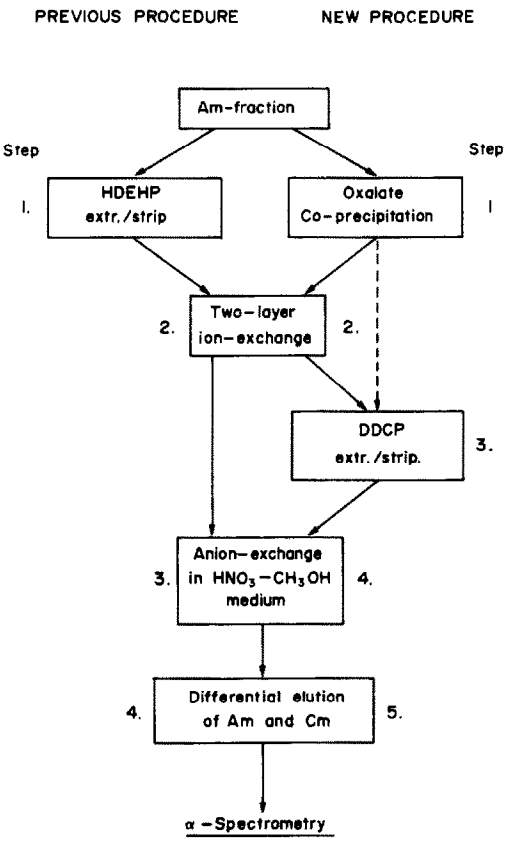

Fig. 1. Schematic flow-chart for the proposed procedure in comparison with that of the previous procedure (Holm *et al.*[5]).

adjusted to 2–3 by addition of ammonia until a precipitate of calcium oxalate appears. The solution is stirred for 1 hr and the precipitate is collected by decantation and centrifugation. The precipitate is then heated at 90° for 1 hr with ~50 ml of 0.1*M* sodium hydroxide. This leaves a hydroxide precipitate of the rare earths (R.E.), thorium, *etc.*, with americium. The precipitate is centrifuged and washed twice with ~20 ml of 2*M* ammonium nitrate. The hydroxide precipitate is dissolved in 9*M* hydrochloric acid (max. volume 20 ml) and the solution is passed through the two-layer ion-exchange column at a flow-rate of 0.5 ml/min. The column is washed with 5 column volumes of 9*M* hydrochloric acid.

The effluent from the column is evaporated to dryness and the residue is dissolved in 20 ml of 12*M* nitric acid. Americium and curium in the solution are extracted twice with 1 ml of DDCP by shaking in a separatory funnel for 30 sec. The organic phase is washed with two 5–10 ml portions of 12*M* nitric acid and then americium and curium are stripped with two 20-ml portions of 2*M* nitric acid, leaving accompanying thorium (and plutonium if present) in the organic phase.

The americium fraction in 2*M* nitric acid is evaporated nearly to dryness. The evaporation is repeated several times with the addition of concentrated nitric acid a few ml at a time. The residue is then dissolved in a minimal volume (5–20 ml) of 1*M* HNO_3–93% CH_3OH mixture and the solution is passed through the anion-exchange column at a flow-rate of 0.5 ml/min. The column is successively washed with 3–5 column volumes of the 1*M* HNO_3–93% CH_3OH mixture. Americium and curium are sorbed onto the column together with R.E. and any traces of lead, uranium, *etc.*, and traces of iron and bivalent metals pass through. The R.E. and any uranium are eluted in the washing. Finally, americium and curium are eluted with 5 column volumes of the 1.5*M* HCl–86% CH_3OH mixture. Remaining traces of lead, if any, stay on the column.

Electro-deposition and α-spectrometry

The cleaned-up americium–curium mixture is electrodeposited onto a stainless-steel disc from a sulphuric acid–ammonia medium at pH 3, as described by Talvitie.[9] The activity on the disc is counted with a silicon surface-barrier detector coupled with a multichannel analyser.

DISCUSSION

A schematic flow-chart for the new procedure is compared with that for the previous procedure[5] in Fig. 1. The new procedure has an additional major step, the HDEHP extraction step being replaced by two steps, the oxalate precipitation and the DDCP extraction, one before and the other after the two-layer ion-exchange. As has been pointed out,[5] the critical step for successful recovery of americium by the previous procedure is the HDEHP extraction, for which the pH of the solution should be controlled at 2–3. Even if the pH is properly controlled, the solutions originating from some samples, especially those from sediments, tend to start forming a precipitate in this pH-range, which may considerably lower the efficiency of the HDEHP extraction of americium. Although the extraction efficiency can be improved by mixing TBP (tri-n-butyl phosphate)[10] or HMEHP (monoester of HDEHP)[11] with the HDEHP, the efficiencies obtained are variable, depending on the success of the pH-control during the extraction step, as well as on the matrices of the samples analysed. In addition, since nitric acid itself is readily extractable with HDEHP, the presence of excess of nitric acid tends to reduce the extraction efficiency, owing to the competition between the nitric acid and the metal nitrate complexes. In contrast to uniodentate organophosphorus extractants such as TBP, DBBP (dibutylbutylphosphonate), HDEHP, *etc.*, bidentate organophosphorus reagents such as DDCP, DB-DECMP (dibutyl-*N*,*N*-diethylcarbamylmethylenephosphonate), *etc.* have much larger K_d-values for metal nitrate complexes than for nitric acid,[12] thus eliminating the effect of the presence of excess of nitric acid in the solution. Moreover, the K_d values of DDCP for metal complexes increase with increasing acidity, even above an acidity of 8*M*. This allows extraction from strong acid medium without disturbance by precipitate formation, especially for sediment samples.

Though all metals having oxidation states higher than 3+, such as Fe, R.E., Po, Th, U, Np, Pu, Am, Cm, *etc.* are, in principle, extracted with DDCP, univalent and bivalent cations, such as Ca, Pb, Ra, *etc.*, are not.[13] The stripping with 2*M* nitric acid brings Am and Cm together with R.E. into the aqueous phase, while traces, if any, of Th and Pu remain in the

Table 1. Efficiencies of the DDCP extraction and the 2*M* HNO_3 stripping, for various species

Species	Isotope used	Mode of counting	Extracted with DDCP, %	Stripped with 2*M* HNO_3, %
Bi^{3+}	^{207}Bi	γ	9	5.4
Po^{4+}	^{210}Po	α	47	40
Th^{4+}	^{229}Th	α	100	0
U^{6+}	^{233}U	α	97	61
Np^{5+}	^{235}Np	γ	99	71
Pu^{4+}	^{237}Pu	γ	97	3.2
Am^{3+}	^{241}Am	γ	99	92

organic phase. Table 1 presents the results for recovery of various elements by both the DDCP extraction and the 2*M* nitric acid stripping. The results show that these steps are very efficient for removing Th and Pu, while the loss of Am remains minimal. Since insufficient decontamination of Th has sometimes been experienced in analysis of Th-rich samples such as sediments by the previous procedure, the total elimination of Th through the DDCP extraction/stripping step substantially improves the accuracy of americium determinations on such samples. Thus, the combination of the oxalate precipitation, the two-layer ion-exchange and the DDCP extraction not only facilitates the analytical manipulation, but also ensures the elimination of interfering α-emitters, improving overall accuracy of the americium determinations. The oxalate precipitation as the preliminary clean-up step eliminates the remaining bulk of alkaline-earth metals and iron together with Al, Cr, Mn, Ni, *etc.*, while the two-layer ion-exchange removes traces of Fe, Po, Th, U, Pu, *etc.* The removal of these traces is further ensured by the DDCP extraction/stripping. Although it is prudent to adopt the three above-mentioned clean-up steps for completely eliminating traces of these elements, the two-layer ion-exchange step may not be absolutely necessary, in view of the high capability of the DDCP extraction/stripping for decontamination from Th and Pu. In fact, several sediment samples have been successfully analysed for americium without use of the two-layer ion-exchange step.

Since the abovementioned steps are incapable of eliminating R.E., the anion-exchange in nitric acid–methanol medium and successive differential elution of Am and Cm are still necessary to eliminate R.E. as well as any remaining ^{210}Pb.

In Table 2 the radiochemical yields achieved by the improved procedure are compared with those obtained with the previous procedure. These results clearly show that the new procedure substantially improves the overall recovery of ^{241}Am and gives higher accuracy.

Table 2. Comparisons between the chemical yields obtained for americium by the previous procedure and the new procedure

Previous procedure				New procedure			
Sample	Date of analysis	Chemical yield %	^{241}Am-content, *fCi/l.* or *fCi/g*	Sample	Date of analysis	Chemical yield, %	^{241}Am-content, *fCi/l.* or *fCi/g*
Sea-water				Sea-water			
AT-02-S	Nov. 78	59	0.07 ± 0.01	ET-R1-10 m	Oct. 81	73	1.2 ± 0.1
AT-02-100 m	Dec. 78	23	0.16 ± 0.03	ET-R1-100 m	Oct. 81	99	0.27 ± 0.03
AT-02-500 m	Apr. 79	16	0.35 ± 0.05	ET-R1-1000 m	Sep. 81	82	0.14 ± 0.02
AT-02-1000 m	Jan. 79	35	0.23 ± 0.02	ET-R2-10 m	Oct. 81	92	0.12 ± 0.02
AT-02-1500 m	Jan. 79	46	0.14 ± 0.02	ET-R2-250 m	Nov. 81	77	0.17 ± 0.03
AT-04-S	Nov. 78	38	0.05 ± 0.01	ET-R2-500 m	Nov. 81	61	0.03 ± 0.01
		Av. 36 ± 16		ET-R2-1000 m	Nov. 81	64	0.10 ± 0.02
						Av. 79 ± 15	
Sediment				Sediment			
SD-Nice-75	Feb. 76	20	0.10 ± 0.05	SD-N-1*	Dec. 80	68	14 ± 2
SD-Monaco-76	Jun. 76	22	7.2 ± 1.0	SD-N-1*	Dec. 80	83	13 ± 1
SD-M-1	Sep. 76	79	6.6 ± 0.6	SD-N-1*	Jan. 81	32	18 ± 2
SD-B-3*	May 78	16	120 ± 10	SD-N-1*	Jan. 81	68	14 ± 1
SD-B-3*	May 78	48	140 ± 20	SD-N-1*	Sep. 81	94	14 ± 1
		Av. 37 ± 27				Av. 69 ± 23	

*These sediment samples are the reference materials issued by the IAEA for environmental transuranic measurements.

REFERENCES

1. R. Fukai and C. N. Murray, *Reference Methods for Marine Radioactivity Studies II, Tech. Rept. Series*, No. 169, p. 107. IAEA, Vienna, 1975.
2. International Laboratory of Marine Radioactivity, *Intercalibration of Analytical Methods on Marine Environmental Samples, Prog. Rept.*, No. 14, IAEA, Monaco, June 1976.
3. *Idem, ibid.*, No. 17, IAEA, Monaco, July 1978.
4. R. Fukai, S. Ballestra and M. Thein, *Proc. Co-ordinated Research Meeting on Transuranic Cycling Behaviour in the Marine Environment* (May 1981).
5. E. Holm, S. Ballestra and R. Fukai, *Talanta*, 1979, **26**, 791.
6. S. Ballestra, E. Holm and R. Fukai, *Proc. Symp. Determination of Radionuclides in Environm. and Biol. Materials*, Paper No. 15. London, 1978. Central Electricity Generating Board.
7. N. A. Talvitie, *Anal. Chem.*, 1971, **43**, 1827.
8. K. M. Wong, *Anal. Chim. Acta*, 1971, **56**, 355.
9. N. A. Talvitie, *Anal. Chem.*, 1972, **44**, 280.
10. C. F. Baes, Jr., *Nucl. Sci. Eng.*, 1963, **16**, 405.
11. S. Tachimori, *J. Radioanal. Chem.*, 1979, **49**, 31.
12. T. H. Siddall III, *J. Inorg. Nucl. Chem.*, 1963, **25**, 883.
13. F. E. Butler and R. M. Hall, *Anal. Chem.*, 1970, **42**, 1073.

Talanta, Vol. 30, No. 1, pp. 49–50, 1983
Printed in Great Britain.

0039-9140/83/010049-02$03.00/0
Pergamon Press Ltd

DICHLOROHYDANTOIN AND DIBROMOHYDANTOIN AS NEW OXIDIMETRIC TITRANTS IN NON-AQUEOUS MEDIA

M. P. RADHAMMA and P. INDRASENAN*
Department of Chemistry, University of Kerala, Trivandrum-695034, India

(*Received* 15 *December* 1981. *Accepted* 4 *May* 1982)

Summary—Two new oxidimetric titrants, dichlorohydantoin and dibromohydantoin are introduced for use in acetic acid medium, and have been applied to direct potentiometric titration of AS(III), Sb(III), Sn(II), Fe(II), Tl(I), $Fe(CN)_6^{4-}$, I^-, SCN^-, hydrazine, phenylhydrazine, semicarbazide, hydroquinone, oxine and Reinecke's salt, in aqueous acetic acid medium.

As part of our programme for the development of new redox titrants[1–4] we now introduce two *N,N'*-dihalohydantoins, 1,3-dichloro-5,5-dimethylhydantoin (**I**) and 1,3-dibromo-5,5-dimethylhydantoin (**II**) for use as oxidimetric titrants. For convenience, they may be called dichlorohydantoin (DCH) and dibromohydantoin (DBH), respectively.

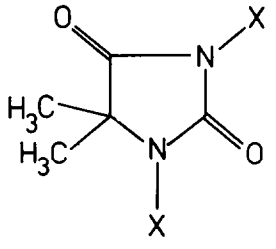

(I) X = Cl
(II) X = Br

They have been applied to direct potentiometric titration of a variety of common reductants in aqueous acetic acid medium.

EXPERIMENTAL

Apparatus

The apparatus and its use were the same as in earlier papers.[1–4]

Reagents

Dichlorohydantoin and dibromohydantoin. Prepared by halogenation of 5,5-dimethylhydantoin as reported by Okada *et al.*[5]

Stock solutions of DCH and DBH. DCH and DBH are insoluble in water and are fairly soluble in glacial acetic acid (DCH 118.5 g/kg, DBH 25.8 g/kg at 30°) and other common organic solvents. Approximately 0.25*M* (0.1*N*) solutions were prepared by dissolving 4.9 g of DCH (or 7.2 g of DBH) in a litre of glacial acetic acid and kept in amber coloured bottles. The solutions were fairly stable, the titre remaining constant for two or three days and then decreasing at the rate of about 0.1% per day. For accurate work daily standardization is recommended. The solutions were standardized iodometrically as for dibromamine-T.[1]

Reductants. These were of analytical-reagent grade, and standard solutions were prepared in appropriate solvents as described earlier,[1–4,6,7] and checked by standard methods.[8,9]

Procedure

A measured portion (5–10 ml) of reductant solution was taken in a titration cell, 10 ml of glacial acetic acid were added (and any other reagents, such as potassium bromide, hydrochloric acid, if required). The solution was diluted to 50 ml with water and titrated with DCH (or DBH). Near the end-point the titrant was added in 0.1-ml increments, and the solution was stirred magnetically for 1 min and the potential read after the stirring had been stopped. The titration was continued until there was no significant change in potential on further addition of the titrant, and the end-point was located in the usual way.

RESULTS AND DISCUSSION

The results are presented in Tables 1 and 2. The half-reactions of DCH and DBH are represented by the equation

$$RN_2X_2 + 2H^+ + 4e^- \rightleftharpoons RN_2H_2 + 2X^-$$

the reduction product being hydantoin, as shown by infrared spectroscopy. The conditional redox potentials in glacial acetic acid medium at 30° were found to be +1.19 and +1.13 V for DCH and DBH, respectively. In both cases a steady potential is attained quickly and at the equivalence point a potential jump of 100–350 mV is obtained on addition of 0.1 ml of either oxidant. The results show that all the titrations are accurate and precise. All the reductants tested undergo the oxidation schemes reported earlier.[1–4,8,9]

Both DCH and DBH have some advantages over the earlier *N*-halosulphonamides in non-aqueous media.[1,4,8] The stock solutions are a little more stable and the potentials become steady more quickly. More reductants can be titrated directly with DCH or DBH than with dichloramine-T,[8,9] dibromamine-T,[1] and

*Author for correspondence.

Table 1. Potentiometric titrations with dichlorohydantoin

Reductant	Reductant taken, *mmole*	Standard deviation,* *μmole*	Range studied, *mmole*	Maximum error, %
As(III)	0.2717	0.3	0.27–0.49	0.3
Sb(III)	0.2522	0.1	0.20–0.40	0.4
Sn(II)	0.1779	0.6	0.14–0.35	0.5
Fe(II)	0.2560	0.4	0.25–0.78	0.5
Tl(I)	0.1280	0.3	0.08–0.25	0.5
Ferrocyanide	0.5260	1.5	0.31–0.73	0.5
Iodide	0.4877	0.4	0.29–0.68	0.4
Hydrazine	0.1737	0.04	0.10–0.24	0.3
Phenylhydrazine	0.0724	0.07	0.03–0.18	0.5
Semicarbazide	0.0893	0.04	0.08–0.18	0.4
Hydroquinone	0.2598	0.1	0.25–0.51	0.3
Oxine	0.1320	0.1	0.10–0.21	0.4
Thiocyanate	0.0581	0.1	0.05–0.12	0.5
Reinecke's salt	0.0152	0.02	0.01–0.03	0.5

*Six replicates.

Table 2. Potentiometric titrations with dibromohydantoin

Reductant	Reductant taken, *mmole*	Standard deviation,* *μmole*	Range studied, *mmole*	Maximum error, %
As(III)	0.2503	0.1	0.20–0.45	0.4
Sb(III)	0.2517	0.2	0.20–0.40	0.4
Sn(II)	0.1726	0.3	0.13–0.34	0.4
Fe(II)	0.5030	0.1	0.20–0.60	0.3
Tl(I)	0.1663	0.2	0.08–0.24	0.5
Ferrocyanide	0.1769	0.2	0.17–0.53	0.4
Iodide	0.4877	0.4	0.29–0.68	0.4
Hydrazine	0.2113	0.1	0.16–0.25	0.4
Phenylhydrazine	0.0377	0.1	0.03–0.19	0.4
Semicarbazide	0.0654	0.02	0.06–0.13	0.4
Hydroquinone	0.2257	0.1	0.22–0.40	0.4
Oxine	0.1179	0.2	0.07–0.16	0.4
Thiocyanate	0.0607	0.06	0.06–0.12	0.4
Reinecke's salt	0.0148	0.01	0.01–0.03	0.3

*Six replicates.

chlorbromamine-T,[4] *e.g.*, thiocyanate and Reinecke's salt, which can only be determined by back-titration when these last three reagents are used.

Acknowledgements—We are thankful to Professor C. P. Joshua, Head of the Department of Chemistry, University of Kerala for all facilities kindly given to carry out this work, and also to the University Grants Commission, New Delhi, for the award of a fellowship to one of us (M.P.R.) under the Faculty Improvement Programme.

REFERENCES

1. C. G. R. Nair and P. Indrasenan, *Talanta*, 1976, **23**, 239.
2. C. G. R. Nair, R. Lalithakumari and P. I. Senan, *ibid.*, 1978, **25**, 525.
3. C. P. K. Pillai and P. Indrasenan, *ibid.*, 1980, **27**, 751.
4. K. D. Mahilamony and P. Indrasenan, *ibid.*, 1981, **28**, 627.
5. T. Okada, T. Kakutani and M. Ogawa, *Yuko Gosei Kagaku Kyokai Shi*, 1957, **15**, 295; *Chem. Abstr.*, 1957, **51**, 13852.
6. T. J. Jacob and C. G. R. Nair, *Talanta*, 1972, **19**, 347.
7. V. R. Nair and C. G. R. Nair, *ibid.*, 1973, **20**, 696.
8. I. M. Kolthoff and R. Belcher, *Volumetric Analysis*, Vol. III. Interscience, New York, 1957.
9. A. I. Vogel, *A Text Book of Quantitative Inorganic Analysis*, 3rd Ed. Longmans, London, 1964.

Talanta, Vol. 30, No. 1, pp. 51–53, 1983
Printed in Great Britain.

0039-9140/83/010051-03$03.00/0

NEW SPECTROPHOTOMETRIC METHOD FOR DETERMINATION OF CEPHAZOLIN

P. PAPAZOVA,† P. R. BONTCHEV* and M. KACAROVA†
Faculty of Chemistry, Sofia University, 1 A. Ivanov, Sofia 1126*
and Chemical Pharmaceutical Institute, Sofia, Bulgaria†

(*Received* 9 *February* 1982. *Accepted* 14 *July* 1982)

Summary—A simple, selective and accurate spectrophotometric method has been developed for the determination of the cephalosporin-type antibiotic cephazolin. The method is based on the fast preliminary acid hydrolysis of cephazolin and the spectrophotometric determination of one of its degradation products—2-mercapto-5-methylthiadiazole.

Cephazolin (I) is a semi-synthetic antibiotic of the cephalosporin group with a wide antimicrobial spectrum of activity, and containing a specific substituent, the 2-mercapto-5-methylthiadiazole group at position 3 in the β-lactam ring.

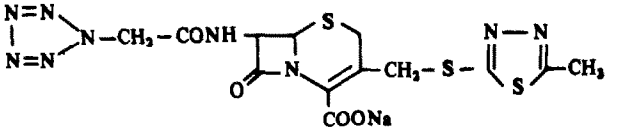

I

The analytical methods used for its determination are analogous to those applied for cephalosporins and penicillins and are usually based on determination of the degradation products formed in neutral or alkaline hydrolysis of the β-lactam ring. Examples are the iodimetric method,[1] which has been automated for the determination of some cephalosporins,[2] and the hydroxylamine[3] and bromosuccinimide[5] methods. Some direct methods have also been described such as alkalimetric titration[5] and potentiometric titration in non-aqueous medium.[6]

All these methods suffer from insufficient specificity. Thus when the iodimetric method is applied, all β-lactam antibiotics, as well as their degradation products or impurities, are oxidized by the iodine. When the hydroxylamine method (recommended[7] along with the microbiological method) is used, the presence of amides, esters, aldehydes, ketones, anhydrides *etc.*, which also react with hydroxylamine, leads to positive errors. The direct spectrophotometric method for cephalosporins[8] also does not find a practical application, because of the lack of specificity—all compounds containing the β-lactam ring absorb in the range 250–270 nm.

The aim of the present work was to develop a simple and accurate quantitative method for fast control analysis of cephazolin. For this purpose the antibiotic is firstly hydrolysed in acidic medium—a procedure which we have already proposed and used for determination of other cephalosporins.[9] The absorbance of the degradation product, 2-mercapto-5-methylthiadiazole (MMTD), is measured at 302 nm and used as a basis for determination of the parent antibiotic. A photometric procedure for MMTD was therefore developed first.

EXPERIMENTAL

Determination of MMTD

In aqueous solution MMTD shows an absorption band at 297 nm. The presence of sulphuric acid increases the intensity of the band and a bathochromic shift to 302 nm, due to the protonation of the compound, is also observed (Fig. 1).

Procedure

Dissolve 10.0 mg of MMTD in 2 ml of methanol, dilute to 100.0 ml with water, and then dilute 5.00 ml of this solution to 50.0 ml with water. Mix 5.00 ml of this working solution with 5.00 ml of 0.5% v/v sulphuric acid in a 25-ml test-tube and measure the absorbance at 302 nm in a 10-mm cell against 0.25% v/v sulphuric acid. Analyse sample solutions by similar treatment.

The sensitivity of the procedure is relatively high, the molar absorptivity being 1.3×10^4 l.mole^{-1}.cm^{-1}. Beer's law is valid over the range 1–10 μg/ml.

To estimate the precision and accuracy of the method 10 analyses were made of a commercial sample of the substance. The results are summarized in Table 1.

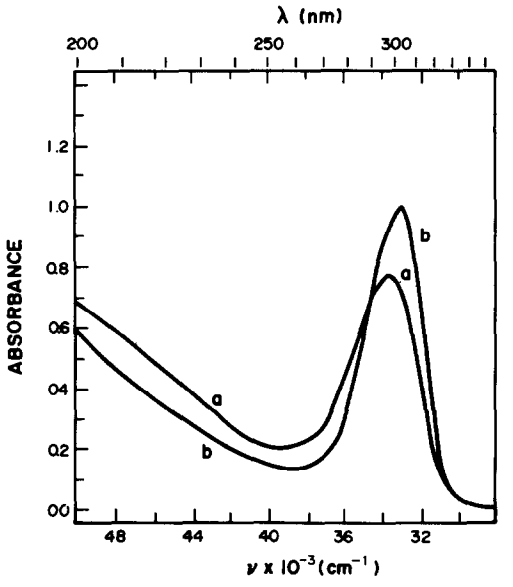

Fig. 1. Absorption spectra of MMTD: (a) 0.001% aqueous solution, (b) 0.001% solution in 0.25% v/v H_2SO_4.

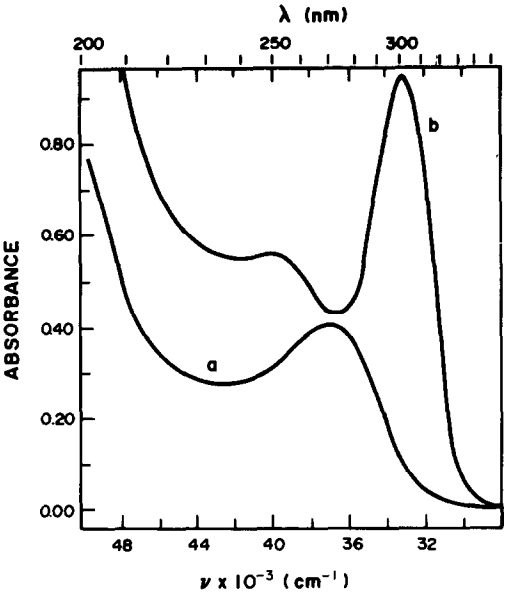

Fig. 2. Absorption spectra of cephazolin: (a) 0.0025% aqueous solution, (b) 0.005% solution after hydrolysis in 0.25% v/v H_2SO_4 for 20 min.

Table 1. Photometric determination of MMTD and cephazolin

	MMTD, %	Cephazolin, %
Number of determinations, n	10	10
Mean content, $\bar{x}$	95.5	90.2
Standard deviation, S	1.5	1.0
95% Confidence limit, $\Delta\bar{x} = S.t/\sqrt{n}$	1.1	0.7
Relative standard deviation, $100\ S/\bar{x}$	1.6	1.2
Relative error, $100\ \Delta\bar{x}/\bar{x}$	1.2	0.9

Determination of cephazolin

Cephazolin shows an absorption band at 270 nm, due to the β-lactam ring. This band cannot be used for a spectrophotometric determination, however, because of its low absorptivity and the lack of specificity. For example, 7-aminocephalosporanic acid (7-ACA), an impurity that can be present in the trade product, shows intense absorption at 262 nm. When cephazolin solution is heated in the presence of sulphuric acid the band at 270 nm disappears and a new band is observed at 302 nm (Fig. 2), due to the hydrolysis product MMTD, and there is also absorption at about 250 nm, by unidentified degradation products. The formation of such products was confirmed by TLC, with ethyl acetate–acetone–acetic acid–water (5:2:1:1) as developing agent. Irradiation with ultraviolet light (254 nm) shows that no cephazolin is present in the hydrolysed sample, but only MMTD and two other degradation products (that have not been identified).

The substituent at position 7 in 7-ACA (*viz.* tetrazolylacetic acid) does not interfere, since it shows no absorbance in the range 220–350 nm. The presence of 7-ACA as impurity or degradation product in the antibiotic also does not interfere. Its absorption band at 262 nm disappears after the substance has been heated with sulphuric acid, because the β-lactam ring opens. As no other hydrolysis product absorbs at ~300 nm, there is no need to extract the MMTD and the absorbance of the acidic solution can be measured directly.

The experimental conditions for quantitative hydrolysis of cephazolin to MMTD were investigated. The influence of acidity on the hydrolysis was studied by increasing the sulphuric acid concentration used, the mixtures being heated for 20 min on a steam-bath. The results obtained from three parallel determinations are presented in Table 2.

It can be seen that the antibiotic is partly hydrolysed by heating even in the absence of sulphuric acid, and TLC

Table 2. Influence of acidity on the absorbance after hydrolysis

H_2SO_4 in the solution, % v/v	Absorbance at 302 nm
0.00	0.160
0.10	0.370
0.15	0.375
0.25	0.375
0.50	0.370
2.50	0.365
5.00	0.360

Table 3. Results for determination of cephazolin content

Sample	Spectrophotometric method, %	Microbiological method, *E/mg*	Potentiometric titration, %
1	87.7	850	90.0
2	84.3	840	85.0
3	86.5	878	87.0
4	90.2	925	91.0
5	91.3	900	91.8
6	90.6	900	91.2

shows the presence of non-hydrolysed cephazolin. The extent of hydrolysis increases in the presence of sulphuric acid, and an acid concentration of 0.15% v/v is enough to give a quantitative yield of MMTD in 20 min.

Procedure

Dissolve 30.0 mg of pure cephazolin in water and make up to volume in a 100.0-ml standard flask and diluted 5.00 ml to 50.0 ml with water. Heat 5.00 ml of this solution with 5.00 ml of 0.5% v/v sulphuric acid on a steam-bath for 20 min. Treat a sample containing about 30 mg of cephazolin in the same way. After cooling, measure the absorbance of both solutions at 302 nm against 0.25% v/v sulphuric acid.

The cephazolin assay of the sample is determined by the absorbance of a cephazolin standard or of an MMTD standard [in which case a transformation coefficient of 3.61 (molecular-weight ratio cephazolin:MMTD)] is used. Beer's law is valid over the cephazolin range 5–50 μg/ml. The precision and accuracy of the determination (Table 1) were determined with a commercial product (Eli Lilly).

To compare the proposed method with the microbiological method and potentiometric titration[6] six samples were analysed according to the three methods. The results are given in Table 3, and are in good accordance, in view of the errors of the corresponding methods.

REFERENCES

1. J. F. Alicine, *Anal. Chem.*, 1961, **33**, 648.
2. E. B. Lindstrom and K. Nordstrom, *Antimicrob. Agents Chemother.*, 1972, **1**, 100.
3. W. W. Holl, M. O'Brien and J. Filan, *J. Pharm. Sci.*, 1975, **64**, 1232.
4. J. F. Alicino, *ibid.*, 1976, **65**, 300.
5. W. S. Wise and G. H. Twigg, *Analyst*, 1950, **75**, 106.
6. F. A. Zappala, W. W. Holl and A. Post, in *Analytical Profiles of Drug Substances*, K. Florey (ed.), Vol. 4, p. 1. Academic Press, New York, 1975.
7. *Food and Drugs*, Vol. 21, §442.11a, p. 398. U.S. Govt. Printing Office, Washington, 1980.
8. C. H. O'Callaghan, P. W. Muggleton and G. W. Ross, *Antimicrob. Ag. Chemother.*, 1968, 57.
9. P. Papazova, P. R. Bontchev and M. Kacarova, *Pharmazie*, 1977, **32**, 486.

Talanta, Vol. 30, No. 1, pp. 54–56, 1983
Printed in Great Britain.

0039-9140/83/010054-03$03.00/0

COULOMETRIC THERMOMETRIC TITRATION OF HALIDES IN MOLTEN CALCIUM NITRATE TETRAHYDRATE

ISTVÁN J. ZSIGRAI and DEZSÖ B. BARTUSZ
Institute of Chemistry, Faculty of Sciences, Novi Sad University, YU-21000 Novi Sad, Yugoslavia

(*Received* 19 *May* 1982. *Accepted* 13 *July* 1982)

Summary—A method for coulometric thermometric precipitation titrations of chloride, bromide and iodide in molten calcium nitrate tetrahydrate at 55° with coulometrically generated silver ions has been developed. The change in temperature during the titration is followed with the aid of a thermistor bridge coupled to a recorder. To minimize the temperature effect of the passage of current through the melt, two thermistors are connected in opposition in the bridge, with one in the anodic and the other in the cathodic cell compartment. Amounts of 62–80 μmole of halide have been determined with relative error below 0.4% and relative standard deviation less than 2.7%. The relative error in determination of 40 μmole of iodide was +2%.

In recent years there has been growing interest in developing analytical methods directly applicable for various determinations in molten salts. Electroanalytical methods have been most frequently used for this purpose.

The first thermometric titrations in molten salts were described by Jordan and co-workers,[1–5] who titrated halide and chromate ions in a eutectic $LiNO_3$–KNO_3 (34%w/w $LiNO_3$) salt melt, with silver nitrate in the same melt, at 158°, and also titrated Ag^+ and Pb^{2+} with potassium chromate. Besides this, they calculated the thermodynamic parameters for precipitation of silver halides and silver chromate. These determinations were done in anhydrous salt melts which required a relatively high temperature. The drawback of the method was the necessity to keep the titrant at high temperature, and the difficulty in manipulation.

In contrast, some hydrated salts melt at relatively low temperature, which allows use of the apparatus and technique normally used for titration in aqueous medium.

We have developed a method for thermometric titrations of halides in a $Ca(NO_3)_2 \cdot 4H_2O$ melt at 50–60° with a standard aqueous solution of silver nitrate, and *vice versa*.[6] Since the temperature used was only 25–30° above room temperature, it was possible to use the apparatus usually employed for aqueous media, and an aqueous titrant instead of a titrant in molten calcium nitrate.

We have now extended the method by using coulometric generation of the titrant.

Catalytic thermometric end-point detection in coulometric titrations of weak bases in non-aqueous solutions was introduced by Vajgand *et al.*[7,8] As far as we know, a purely thermometric (non-catalytic) method of monitoring coulometric titrations has not previously been described, and this work probably represents the first example of a thermometric titration with coulometric generation of titrant in a salt melt.

EXPERIMENTAL

Reagents

All chemicals were reagent grade. Calcium nitrate tetrahydrate (Kemika, Zagreb) was recrystallized from water and dried in air. Sodium chloride (Kemika, Zagreb) was recrystallized from water acidified with hydrochloric acid and dried by prolonged heating at 500°. Potassium bromide (Merck) and potassium iodide (Merck) were used without purification. The standard solutions of sodium chloride (1.365 and 0.8026*M*), potassium bromide (1.255 and 0.7395*M*) and potassium iodide (1.306 and 0.7907*M*) were prepared by dissolving the necessary amounts of the dried salts in redistilled water.

Apparatus

The coulometric cell for thermometric titration was made of Pyrex glass (Fig. 1) and consisted of the cathodic (60 ml) and anodic (55 ml) compartments, separated by a porosity-3 sintered-glass disc. Both compartments were closed by rubber bungs with suitable holes for thermistors and electrodes. The cell was placed in a cylindrical glass vessel, as shown in Fig. 1, which in turn was put into an electric oven (Instrumentaria, Zagreb), 36 litres in capacity. The oven temperature was kept constant within ± 0.2° in the range of 50–60°. The melt in the cell was stirred with a magnetic stirrer.

Silver ions were generated from a 2-mm diameter silver wire (purity 99.99%) with an effective surface area of about 2 cm^2, with a Metrohm-Herisau type E coulostat. The counter-electrode was a platinum wire. The temperature-monitoring system consisted of two thermistors (GM 104, ITT), Wheatstone bridge and a recorder (Goerz-Electro, type Servogor S RE 511). The circuit diagram of the thermistor and recorder coupling is also shown in Fig. 1.

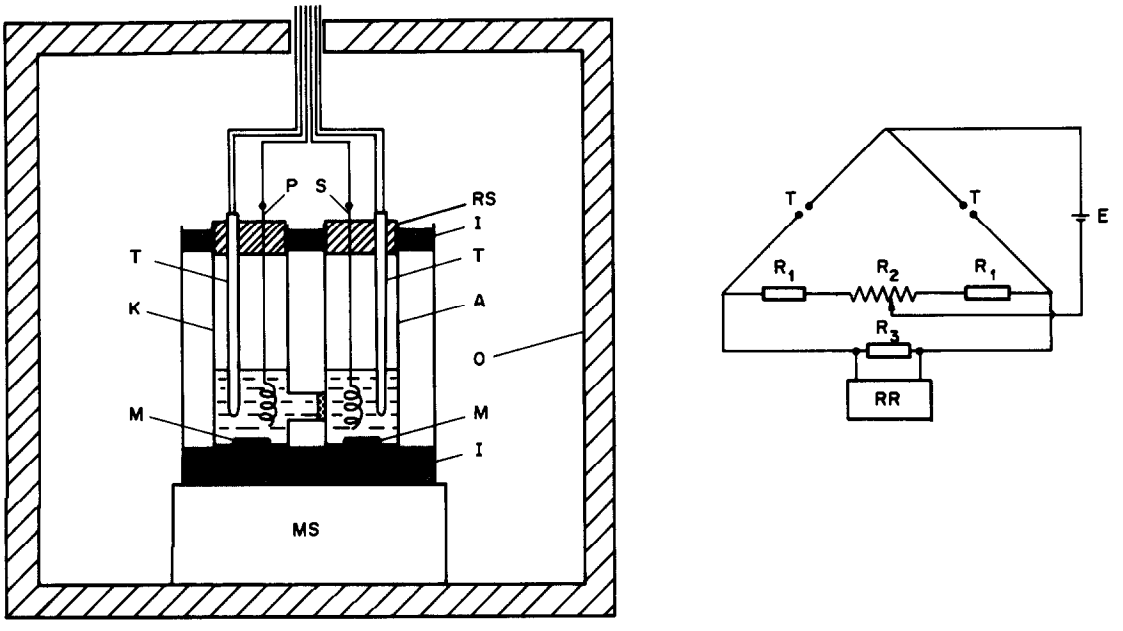

Fig. 1. Cross-section of the apparatus for coulometric thermometric titrations, and the circuit diagram of the thermistor and recorder coupling. A and B, anode and cathode compartment, respectively; S, silver anode; P, platinum cathode; T, thermistors (25 kΩ at 55°); I, polystyrene insulator; M, magnets; MS, magnetic stirrer; RS, rubber stopper; O, electric oven; R_1, 20-KΩ resistor; R_2, 10-kΩ potentiometer; R_3, 10-kΩ resistor; RR, recorder; E, 2.4-V battery.

The thermistors were sealed in glass and had the following specifications: resistance 100 kΩ at 25°, dissipation constant 0.7 mW/deg, effective resistance 25 kΩ at 55°. They were connected in opposition in a Wheatstone bridge, with one in the anodic and the other in the cathodic cell compartment. In this way the temperature effect of the passage of current through the melt was eliminated. The e.m.f. for the Wheatstone bridge was supplied from a 2.4-V battery. At the maximum sensitivity setting, the thermistor bridge yielded a temperature response of 0.16°/mV and the full-scale deflection on the recorder was 2 mV (20 cm).

Procedure

The salt melt was added to the same level in both cell compartments. The anodic compartment contained about 25 g of the melt, to which 50 or 100 μl of the standard halide solution were added by means of a calibrated micropipette (Oxford). Then the thermistors and electrodes were placed in both cell compartments and, after temperature equilibration, the recorder was switched on. The chart speed was 10 mm/min. After 1–2 min the titration was started by switching on the coulostat. The titration rate was 0.1 μmole/sec and the current density between 4.5 and 5.0 mA/cm^2. During the titration the melt in both cell compartments was stirred by magnetic stirrer.

RESULTS AND DISCUSSION

Examples of the coulometric thermometric titration curves, for determination of chloride and iodide, are shown in Fig. 2. The distance A–B′ was taken as a measure of the amount of silver ions corresponding to

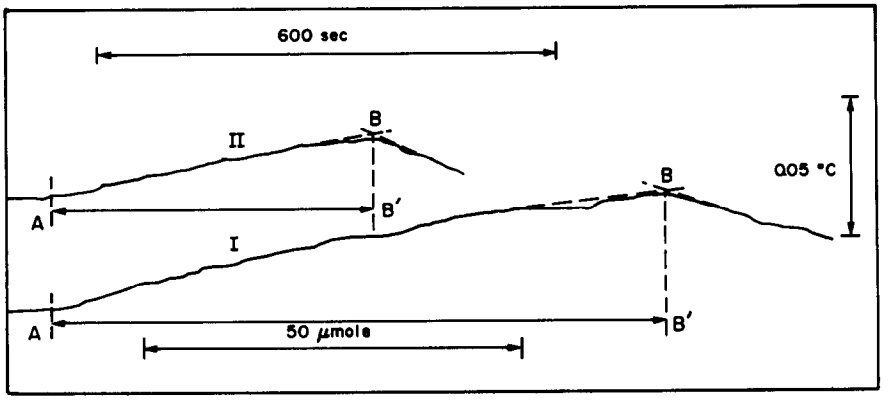

Fig. 2. Coulometric thermometric titration curves: I, 80.3 μmole of NaCl; II, 39.6 μmole of KI; A, start of titration; B, end-point; A–B′, stoichiometric measure of the amount of titrant required.

Table 1. Results of coulometric thermometric titration of halides in molten calcium nitrate tetrahydrate at 55°

Halide	No. of titns.	Taken, μmole	Found, μmole	Relative error, %	Relative std. devn., %
Cl^-	8	80.3	80.5	+0.3	0.5
	7	68.3	68.4	+0.1	1.1
Br^-	6	74.0	74.1	+0.1	1.4
	7	62.8	62.6	−0.3	2.7
I^-	6	79.1	78.8	−0.4	0.6
	6	65.3	65.2	−0.2	0.4
	6	39.6	40.4	+2.0	0.6

the end-point. The titration end-point (B) was taken as the intersection of the extrapolated best-fit straight lines before and after the equivalence point on the titration record. If the end-point break is sharp enough extrapolation may not be necessary. The sharpest break occurred for the iodide titration, and the most rounded for chloride, as might be expected from consideration of the solubility products. The height of the titration curve should correspond to the temperature change (or to the amount of heat liberated) due to chemical reaction in the anodic cell compartment, since the heat-effect of the current was minimized by connecting the thermistors in opposition. However, the temperature change is sometimes smaller and sometimes greater than that expected on the basis of the enthalpies of precipitation in a $Ca(NO_3)_2 \cdot 4H_2O$ melt,[9] and the heat capacity of the melt. This means that heating of the melt by the current passed cannot be completely eliminated in the way described. Several reasons can be given for this: difference in the thermistor characteristics, difference in the amount of melt in the two cell compartments, change in the heat capacity because of the precipitate formation, change in the electrode surface area, changes in frit resistance in repeated experiments, *etc.* However, none of these effects interferes significantly with the determination, since an adequate break on the titration curve is always attainable. At lower titration rates (0.05 μmole/sec lower) there is less heating of the melt by the passage of current but the titration time becomes too long and there is significant heat exchange with the surroundings. On the other hand, if only one thermistor is used, the temperature effect of the passage of current through the system is so large that it prevents the determination altogether.

The results are given in Table 1. As can be seen, in determination of 62–80 μmole of halides the relative error is below 0.4% and the relative standard deviation less than 2.7%. In determination of 40 μmole of iodide, the titration end-point is somewhat delayed and the relative error is +2%.

Acknowledgement—The authors acknowledge the financial support of the SCI for Research of the SAP Vojvodina.

REFERENCES

1. J. Jordan, J. Meier, E. J. Billingham, Jr. and J. Pendergrast, *Anal. Chem.*, 1959, **31**, 1439.
2. *Idem, ibid.*, 1960, **32**, 651.
3. *Idem*, *Nature*, 1960, **187**, 318.
4. J. Jordan and G. J. Ewing, *Bull. Chem. Thermochem.* (IUPAC), 1960, **3**, Sect. A-13 (a), 7.
5. J. Jordan, *Chimia*, 1963, **17**, 101.
6. I. J. Zsigrai and D. B. Bartusz, 3rd Yugoslav Symposium on Analytical Chemistry, Novi Sad, June 1982.
7. V. J. Vajgand, T. A. Kiss, F. F. Gaál and I. J. Zsigrai, *Talanta*, 1968, **15**, 699.
8. V. J. Vajgand, F. F. Gaál and S. S. Brusin, *ibid.*, 1969, **17**, 415.
9. B. Burrows and S. Noersjamsi, *J. Phys. Chem.*, 1972, **76**, 2759.

Talanta, Vol. 30, No. 1, pp. 57–59, 1983
Printed in Great Britain.

0039-9140/83/010057-03$03.00/0

PRECONCENTRATION OF SOME TRANSITION AND RARE-EARTH ELEMENTS BY DONNAN DIALYSIS

JAMES E. DINUNZIO,* ROBERT L. WILSON and F. PETER GATCHELL
Department of Chemistry, Wright State University, Dayton, OH 45435, U.S.A.

(*Received* 15 *December* 1981. *Revised* 4 *June* 1982. *Accepted* 13 *July* 1982)

Summary—A method using Donnan dialysis for the preconcentration of some transition and rare-earth elements is described. Enrichment factors of about 20 are obtained in 1 hr. Calibration curves that are linear over 2 orders of magnitude are obtained with a relative precision of about 3% when Co(II) is used as an internal standard. The effect of aluminium in the receiver electrolyte on the interference caused by phosphate in the sample solution is discussed.

Donnan dialysis[1] is a simple and reliable means of preconcentrating trace levels of ions. In this process an ion-exchange membrane separates two solutions of different ionic strength. Because of the potential developed across the membrane owing to the difference in ionic strength of the separated solutions, trace ions in the lower ionic strength solution (sample) will diffuse into the higher ionic strength solution (receiver electrolyte). Two properties of the Donnan dialysis system allow it to be used for preconcentration. First, the spontaneous diffusion of an ion across the membrane can occur against its concentration gradient. That is, an ion can diffuse from a region where it is in low concentration to one in which it is in higher concentration. Second, the concentration of an ion in the receiver electrolyte will be proportional to the initial concentration of that ion in the sample and to the time of preconcentration. By properly designing the dialysis system it is possible to obtain high enrichment factors in a reasonable time, thereby allowing Donnan dialysis to be used for preconcentration before analysis.

Donnan dialysis preconcentration of metals has been used in conjunction with a number of methods of analysis. These include atomic-absorption spectrophotometry,[2–4] voltammetry,[5,6] and high-pressure ion-exchange chromatography.[7] These procedures have focused almost exclusively on the development of systems for the Donnan dialysis preconcentration of transition metals, and although this technique should be applicable to any ion of a given charge sign, this has rarely been demonstrated. The purpose of this paper is to demonstrate its general applicability in this respect, and to report on a system suitable for preconcentration of both transition and rare-earth elements.

*Author for correspondence.

EXPERIMENTAL

Apparatus

The cation-exchange membranes used were Type R-1010 (RAI Research Corp., Hauppauge, Long Island, N.Y.). The membranes were pretreated as previously described,[8] and stored in the receiver electrolyte.

Metals were determined with a Varian Techtron Model AA-6 atomic-absorption spectrophotometer with a Model BC-9 simultaneous background corrector.

Reagents

Lanthanum nitrate hexahydrate (99.99%), europium oxide (99.99%), and lutetium oxide (99.99%) (Aldrich Chemical Co., Milwaukee, Wisconsin) were used to prepare solutions of the rare-earth elements. All other reagents were analytical reagent grade. All solutions were prepared with doubly-distilled demineralized water. All sample solutions were at pH 5.6.

Procedure

Metal enrichments were performed in a manner similar to that previously described.[2] In all cases, the diameter of the membrane in the dialysis cell was 3 cm, and 200-ml portions of sample and 4.0 ml of receiver electrolyte were used. The enrichment time was 1 hr unless otherwise stated. The receiver electrolyte consisted of 1.0*M* magnesium sulphate and $5.0 \times 10^{-3}M$ aluminium sulphate.

Enrichment was initiated by placing the membrane face of the dialysis cell (containing the receiver electrolyte) in contact with the magnetically-stirred sample solution. After the prescribed enrichment time the dialysis cell was removed from the sample and wiped, and the receiver electrolyte was transferred to a sample container. When necessary, the receiver electrolyte was filtered through 0.45-μm regenerated cellulose filters with a syringe filter. Metals in the receiver electrolyte were then determined by atomic-absorption spectrophotometry.

RESULTS AND DISCUSSION

The transfer of trace cations across an ion-exchange membrane in Donnan dialysis has been shown to be dependent on the difference in ionic strength between the sample solution and receiver electrolyte, as well as

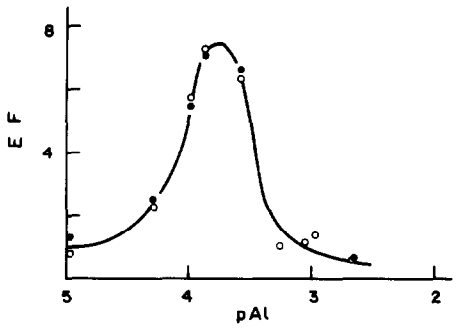

Fig. 1. Influence of aluminium on the transfer of trace metals. Receiver electrolyte 0.1*M* LiCl; enrichment time 0.5 hr, E.F. = enrichment factor, defined as the ratio of the ion concentration in the receiver electrolyte to that originally in the sample. Co(II): ○. Ni(II): ●.

the types of cation in the system.[2] Figure 1 shows that the presence of Al(III) in the sample increases the rate of transfer of Ni(II) and Co(II) across the membrane into 0.1*M* lithium chloride. This results in an increase in the enrichment factors.

The phenomenon demonstrated in Fig. 1 has been attributed to the relatively high selectivity of the membrane for Al(III).[6,9] The Al(III) in the system blocks the fixed negative exchange sites on the membrane, and allows the trace ions of lower selectivity to diffuse directly through the pore spaces in the membrane, resulting in higher enrichment factors over a given time. The decrease in transfer rate observed (Fig. 1) at higher Al(III) concentrations is due to the decrease in the difference between the ionic strengths of the sample solution and the receiver electrolyte.

On the basis of previous work,[2,3] a receiver electrolyte consisting of 1.0*M* magnesium sulphate and $5 \times 10^{-3}M$ aluminium sulphate was chosen, since it results in high enrichments and eliminates the dependence of ion transfer on the type and concentration of other ions in the sample.

The calibration graphs for the enrichment of Ni(II), Cd(II), La(III), Eu(III), and Lu(III) were all linear over a range of at least 2 orders of magnitude. The use of a fixed amount of Co(II) as internal standard (and plotting metal/cobalt ratio against initial metal concentration) results in improved precision in all cases.

Table 1 shows the precision obtained, with and without the internal-standard correction. The precision without the internal standard is about 8%, but is improved to about 3% by its use.

Table 1. Precision for Donnan dialysis preconcentration of heavy and rare-earth elements with and without an internal-standard correction

Metal	Average enrichment factor	Relative standard deviation, % Direct	Internal standard
Ni	22	8	2
Cd	22	8	2
La	18	8	6
Eu	18	7	3
Lu	16	10	3

The use of Co(II) as the internal standard also makes the method more generally applicable. Previously it was thought necessary to match the internal standard and analyte cations,[2] to minimize errors arising from the relative selectivity differences between them. However, the data in Table 1 show that this is not necessary. When receiver electrolytes of high ionic strength are used, any cation can be used as an internal standard. This readily expands the applicability of Donnan dialysis enrichment.

One of the advantages of Donnan dialysis enrichment is the relative lack of interferences.[5,6] This is because the analyte is removed from the sample and transferred to a standard matrix in the receiver electrolyte. Only those factors which influence the rate of transfer of the analyte across the membrane will interfere. We have previously reported[2] the interference of phosphate in Donnan dialysis enrichment of trace metals and given a method of eliminating it.

Table 2 shows data obtained for the enrichment of Ni(II) and Co(II) from solutions containing phosphate, at various pH values, into receiver electrolytes with and without Al(III). When Al(III) is present in the receiver electrolyte, the enrichment factor falls rapidly as the pH of the sample solution increases above pH 5.0. When Al(III) is not present in the receiver electrolyte the enrichment factors for cobalt and nickel do not change until the pH is above 8.5. The lower enrichment factors obtained in the absence of Al(III) in the receiver electrolyte are consistent with the data in Fig. 1.

The change in enrichment factor shown in Table 2 can be explained as due to some interaction between phosphate and Al(III). This could be either ion-pair formation between aluminium and phosphate, or the precipitation of $AlPO_4$ within the membrane. In the first case the formation of an ion-pair would reduce the affinity of aluminium for the membrane, resulting in an increased interaction between the fixed charges on the membrane and the nickel and cobalt ion migrating from the sample. This would result in a reduction in the transfer rates and lower enrichment factors in a fixed-time experiment. In the second case the

Table 2. Effect of aluminium on phosphate interference in Donnan dialysis

Receiver electrolytes: 1.0*M* $MgSO_4$/ $5 \times 10^{-3}M$ $Al_2(SO_4)_3$			Receiver electrolytes: 1.0*M* $MgSO_4$		
pH	Enrichment factor Ni	Co	pH	Enrichment factor Ni	Co
3.5	22.2	21.9	3.1	15.1	16.2
5.0	23.4	23.4	5.9	14.2	15.6
5.6	17.6	18.2	6.2	14.1	16.3
5.7	12.8	13.5	6.8	14.1	14.8
5.9	9.4	9.4	7.8	14.8	15 8
6.1	7.0	6.8	8.5	14.7	16.1
6.7	5.9	6.3	9.5	2.2	2.0

Total phosphate concentration = $10^{-3}M$; adjusted to constant ionic strength with NaCl.

precipitation of $AlPO_4$ could block the pores within the membrane and cause reduced transfer rates and lower enrichment. The fact that this phenomenon was not observed in the absence of Al(III) in the receiver electrolyte confirms that Al(III) plays an important role in the transfer of trace cations across the ion-exchange membrane.

REFERENCES

1. R. M. Wallace, *Ind. Eng. Chem. Process Des. Div.*, 1967, **6**, 423.
2. J. A. Cox and J. E. DiNunzio, *Anal. Chem.*, 1977, **49**, 1272.
3. R. L. Wilson and J. E. DiNunzio, *ibid.*, 1981, **53**, 692.
4. J. A. Cox and J. Carnahan, *Appl. Spectrosc.*, 1981, **35**, 447.
5. G. L. Lundquist, G. Washinger and J. A. Cox, *Anal. Chem.*, 1975, **47**, 319.
6. J. A. Cox and Z. Twardowski, *ibid.*, 1980, **52**, 1503.
7. M. H. Jubara and J. E. DiNunzio, unpublished work.
8. W. J. Blaedel and T. R. Kissel, *Anal. Chem.*, 1977, **44**, 2109.
9. J. E. DiNunzio, *Ph.D. Dissertation*, Southern Illinois University, 1977.

Talanta, Vol. 30, No. 1, pp 61–64, 1983
Printed in Great Britain.

0039-9140/83/010061-04$03.00/0

ANALYTICAL DATA

ALIZARIN-9-IMINE AS INDICATOR IN ACETONITRILE AND IN PYRIDINE MEDIA

M. BLANCO
Department of Analytical Chemistry, Faculty of Sciences, University Autonoma of Barcelona, Barcelona, Spain

and

J. BARBOSA
Department of Analytical Chemistry, Faculty of Sciences, University of Barcelona, Barcelona, Spain

(*Received* 8 *June* 1981. *Revised* 18 *March* 1982. *Accepted* 16 *August* 1982)

Summary—The behaviour of alizarin-9-imine as an indicator in acetonitrile and pyridine media has been studied. The protonation constant in acetonitrile, $K_I = a_{HI^+}/a_{H^+} . a_I = 10^{-3.4}$, has been determined. Organic acids, amino-acids, and aliphatic and aromatic amines have been titrated with errors below 2%.

Acetic acid is widely used as a medium for non-aqueous titration, but the end-point potential range is higher in many aprotic protophobic solvents,[1] such as acetonitrile,[2] which is being increasingly used in analysis. Commercial acetonitrile is variable in quality and contains impurities,[3] but for titrations the analytical-reagent grade can be used without previous purification.[4]

However, homoconjugation, which is important in acids but negligible in bases,[1] the decrease in hydrogen-ion activity in aged solutions,[5] and the instability of acetonitrile in the presence of strong bases lead to the solvent not being recommended for titration of acids but of interest for titration of bases[1,6] with perchloric acid in acetic acid as titrant.[7]

Many acid–base titrations in non-aqueous solvents, including acetonitrile, are described in the literature,[8] and potentiometric titrations with glass and calomel electrodes are frequently used.[9] However, routine titrations with visual indicators are faster and pa_{H+} can be spectrophotometrically determined if the indicator dissociation constant pK_I is known.[10]

Pyridine is a weak, stable base with a low dielectric constant ($\epsilon = 12.3$), and is a good solvent for many inorganic and organic substances. It is also an excellent medium for the titration of acids with quaternary ammonium hydroxides.[8,11] The dissociation constants of Brønsted acids are lower in pyridine than in water, as expected from the low dielectric constant.[11,12] The colour-change intervals of various indicators in pyridine have been found by Fritz and Gainer.[13]

The lack of indicators for acid–base titrations in acetonitrile and pyridine media has led us to study alizarin-9-imine for this purpose.

EXPERIMENTAL

Solutions

Acetonitrile was purified[14] for determination of the protonation constant. Perchloric acid solutions (0.1*M*) in acetonitrile[14] or acetic acid, and 0.1*M* tetrabutylammonium hydroxide solution in pyridine[15] or propan-2-ol/methanol were prepared.

Determination of the protonation constant in acetonitrile

This was done according to the method proposed by Kolthoff *et al.*[14] and is based on the equation

$$\log \{[ClO_4^-] - [HI^+]\} = \log[HI^+]/[I] - \log K_I$$

The graph of $\log \{[ClO_4^-] - [HI^+]\}$ *vs.* $\log[HI^+]/[I]$ is a straight line with $-\log K_I$ as intercept on the *y*-axis. The results are given in Table 1 and give a straight line with slope 0.98 and intercept 3.4.

Procedure

The basic (acid) substance was dissolved in acetonitrile (pyridine) and titrated with 0.1*M* perchloric acid in acetic acid (0.1*M* tetrabutylammonium hydroxide in propan-2-ol/methanol). The absorbance and potential were measured.

RESULTS AND DISCUSSION

Absorption spectra of alizarin-9-imine

In Fig. 1 the spectrum in acetonitrile is shown. Two isosbestic points can be seen, at 267 and 465 nm. The three forms show different colour. As the solvent is

Table 1. Determination of the protonation constant in acetonitrile

A	$[ClO_4^-]$,M	[I], μM	$[HI^+]$,μM	$\log\{[ClO_4^-] - [HI^+]\}$	$\log[HI^+]/[I]$
0.845	—	131.0	—	—	—
0.750	3.56×10^{-5}	115.5	15.5	−4.69	−0.87
0.540	1.78×10^{-4}	81.2	49.8	−3.89	−0.21
0.410	2.23×10^{-4}	60.0	71.0	−3.82	0.07
0.182	8.90×10^{-4}	22.7	108.3	−3.11	0.68
0.125	2.23×10^{-3}	13.4	117.6	−2.67	0.94
0.043	excess	—	131.0		

$c = 1.31 \times 10^{-4} M$; $\lambda = 535$ nm; $\epsilon_{HI} = 0.33 \times 10^3$ l.mole^{-1}.cm^{-1}; $\epsilon_I = 6.45 \times 10^3$ l.mole^{-1}.cm^{-1}.

recommended only for titration of bases, the most interesting colour change is from red to yellow, *i.e.*, from the molecular form **I** to a protonated species.

In the spectrum of alizarin-9-imine in pyridine (Fig. 2), there is one isosbestic point, at 430 nm. In pyridine solution the protonated form is not obtained even on addition of perchloric acid. The colour change when an acid is titrated in pyridine solution is from purple-blue to light rose and it corresponds to the passage of a mixture of the molecular form **I** and the singly dissociated form **II** into the doubly dissociated form **III**.

With the modified calomel reference electrode developed by Marple and Fritz,[16] excellent reproduction of potentials in pyridine medium is possible, certainly enough for measurement of indicator transition ranges in terms of the e.m.f. of a glass–calomel electrode system to be attempted.

For the pyridine system the photometric interval (measured at 500 nm) is between −220 and −400 mV, and the visual interval is between −255 and −360 mV.

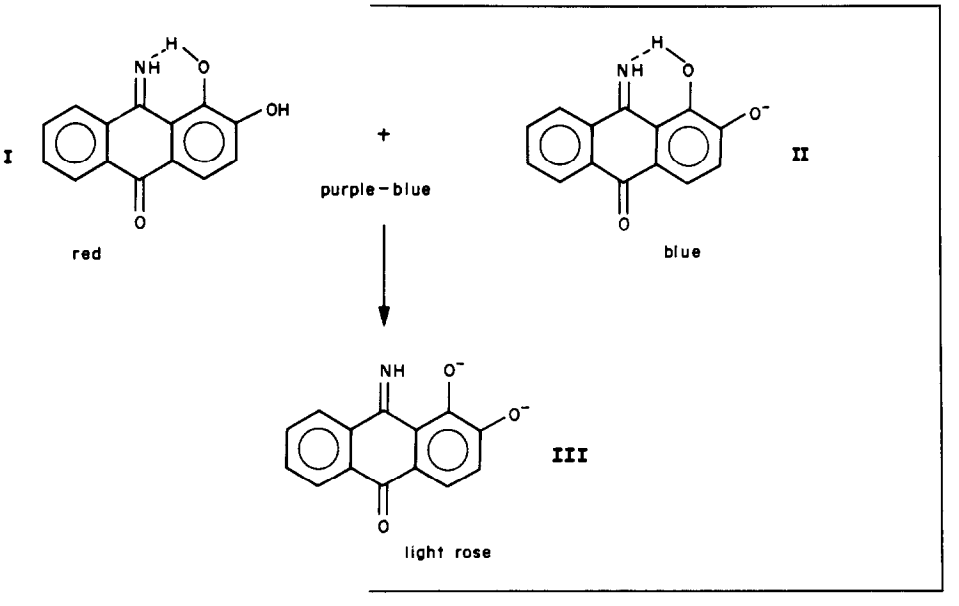

Study of alizarin-9-imine as an indicator

The colour-change intervals in acetonitrile medium have been determined, and are pH 2.5–4.3 for the photometric interval (at 535 nm) and pH 2.7–4.3 for visual observation.

The absorbance–potential graphs obtained in the titration of different bases (pyridine, butylamine, *etc.*) in acetonitrile with alizarin-9-imine as indicator show two marked breaks (Fig. 3): the first occurs at about 50% titration, and can be attributed to heteroconjugation of the indicator and the base titrated; the second indicates the titration end-point and determines the interval corresponding to the colour change from red to yellow.

These colour-change intervals correspond to a potentiometric range for which only one indicator has been studied, namely Thymol Blue,[16] which has a colour-change interval much greater than that of alizarin-9-imine.

The accordance between the potentiometric, spectrophotometric and visual end-points has been tested in a series of titrations, in acetonitrile as well as in pyridine medium, and the reversibility of the indicator has been confirmed in the same way.

In titration of acids in pyridine medium with TBAH solution in hydroxylic solvents (water, alcohols, *etc.*), with alizarin-9-imine as indicator at a final concentration higher than $5 \times 10^{-5} M$, a well-defined

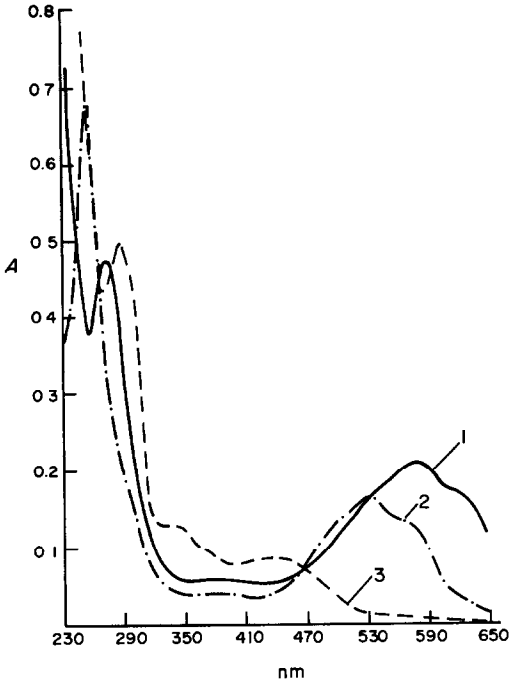

Fig. 1. Spectra of alizarin-9-imine in acetonitrile $c = 2.54 \times 10^{-5}M$. 1—Basic form (with TBAH, blue). 2—Molecular form (in acetonitrile, red). 3—Protonated form (with $HClO_4$, yellow).

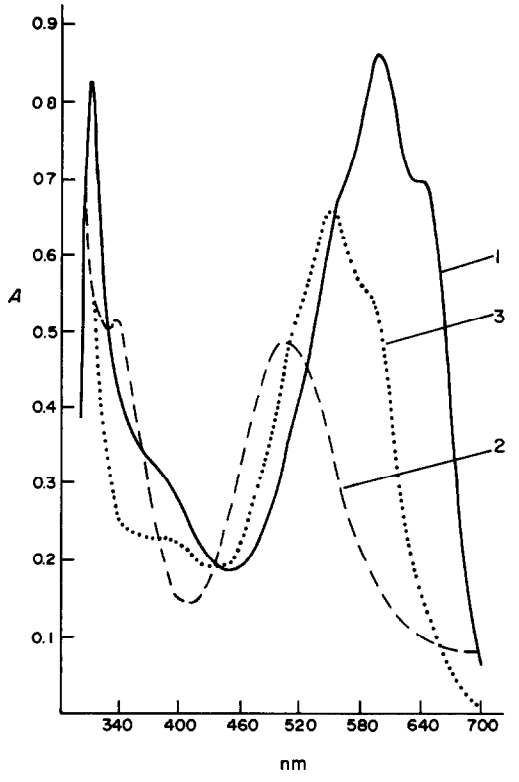

Fig. 2. Spectra of alizarin-9-imine in pyridine, $c = 8.2 \times 10^{-5}M$. 1—Monoionized form (TBAH in propan-2-ol/methanol). 2—Di-ionized form (TBAH in pyridine). 3—In pyridine.

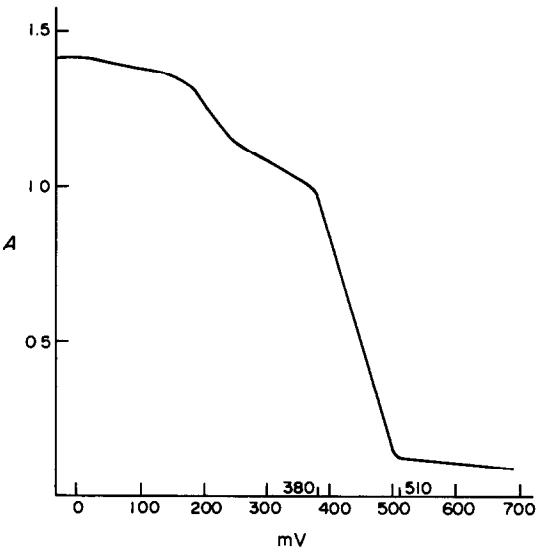

Fig. 3. Photometric interval of alizarin-9-imine in acetonitrile for titration of pyridine with $0.1M$ $HClO_4$ in acetic acid.

end-point is not obtained. This can be explained as due to stabilization of the singly ionized form of alizarin-9-imine by heteroconjugation with the solvent medium.[12]

However, a well-defined colour-change from purple-blue to light rose is seen when TBAH solution in pyridine is used or the final indicator concentration is lower than $5 \times 10^{-5}M$. Because of the strong colour of the indicator, this concentration is sufficient for visual detection of the colour-change.

Various bases and acids, in acetonitrile and pyr-

Table 2. Titration of bases in acetonitrile with $0.1M$ $HClO_4$

	Taken, *mg*	Found, *mg*
Pyridine	5.46	5.41
	5.52	5.57
	10.90	10.73
	22.7	22.3
	133.5	131.0
Butylamine	10.3	10.2
	20.3	10.0
	75.5	75.9
	186.9	185.0
	188.8	187.1
Aniline	4.67	4.70
	9.33	9.25
	23.3	22.9
α-Naphthylamine	8.26	8.24
	16.5	16.2
	16.7	16.5
Ethanolamine	6.57	6.68
	13.0	13.1
	13.14	13.23
Triethanolamine	9.04	9.01
	18.0	17.7
	44.7	43.8

Table 3. Titration of acids in pyridine with 0.1*M* TBAH

	Taken, *mg*	Found, *mg*
Benzoic acid	19.7	19.9
	22.7	22.6
	25.3	25.5
	25.7	25.9
	26.9	26.6
	47.8	47.7
	56.8	57.1
Nitrobenzoic acid	11.2	11.3
	22.3	22.6
	24.2	24.0
	34.5	35.0
	60.5	59.5
Nicotinic acid	8.20	8.24
	16.4	16.2
	41.0	40.6
Glutamine	51.7	50.7
	58.1	57.0
	60.5	59.4
Anthranilic acid	41.2	41.1
	47.9	47.4
	53.4	52.4
Methionine	48.5	48.7
	57.4	57.0
	58.2	59.0
α-Phenylglycine	62.4	62.6
	59.4	58.9
	61.8	61.5

idine respectively have been titrated with alizarin-9-imine used as indicator, with errors below 2%. Results are given in Tables 2 and 3.

REFERENCES

1. I. M. Kolthoff, *Anal. Chem.* 1974, **46,** 1992.
2. I. M. Kolthoff, M. K. Chantooni, Jr. and S. Bhowmik, *ibid.*, 1967, **39,** 1627.
3. H. Kiesele, *ibid.*, 1980, **52,** 2230.
4. L. E. I. Hummelstedt and D. N. Hume, *ibid.*, 1960, **32,** 576.
5. I. M. Kolthoff and M. K. Chantooni, Jr. *Chem. Analit. (Warsaw)*, 1972, **17,** 841.
6. G. A. Harlow and D. H. Morman, *Anal. Chem.*, 1968, **40,** 418 R.
7. J. F. Coetzee and R. J. Betozzi, *ibid.*, 1969, **41,** 860.
8. B. Kratochvil, *ibid.*, 1980, **52,** 151 R.
9. I. M. Kolthoff and M. K. Chantooni, Jr. *J. Am. Chem. Soc.*, 1965, **87,** 4428.
10. I. M. Kolthoff, M. K. Chantooni, Jr. and S. Bhowmik, *Anal. Chem.*, 1967, **39,** 315.
11. L. M. Mukherjee, *ibid.*, 1975, **47,** 325.
12. K. Tsuji and P. J. Elving, *ibid.*, 1969, **41,** 286.
13. J. S. Fritz and F. E. Gainer, *Talanta*, 1966, **13,** 939.
14. I. M. Kolthoff, S. Bruckenstein and M. K. Chantooni, Jr., *J. Am. Chem. Soc.*, 1961, **83,** 3927.
15. H. B. Heijde and E. A. F. Dahmen, *Anal. Chim. Acta*, 1957, **16,** 378.
16. L. W. Marple and J. S. Fritz, *Anal. Chem.*, 1962, **34,** 796.

Talanta, Vol. 30, No. 1, pp. 65–68, 1983
Printed in Great Britain.

0039-9140/83/010065-04$03.00/0

ANNOTATIONS

AN ALGORITHM FOR REDUCING STORAGE REQUIREMENTS IN COMPUTER CALCULATION OF CHEMICAL EQUILIBRIA

VIJAY S. TRIPATHI
Department of Applied Earth Sciences, Stanford University, Stanford, CA 94305, U.S.A.

(*Received* 25 *May* 1982. *Accepted* 15 *June* 1982)

Summary—An algorithm for storage of stoichiometric coefficients of the possible complexes and solids in a multi-component system of metals and ligands is described, along with FORTRAN code for its implementation. The proposed algorithm results in considerable saving in storage over the conventional use of a two-dimensional array. The saving in storage is especially useful for microcomputers, and for very large problems such as those encountered in geochemical calculations.

Almost all computer programs for calculation of equilibrium concentrations and evaluation of stability constants from titration data, such as MINIQUAD,[1] COMICS,[2] MINEQL[3] and COMPLEX[4] require the use of a two-dimensional array to store the stoichiometric coefficient of the ith component (reactant metal or ligand) in the jth complex or solid. Since the number of components in a complex seldom exceeds five, this two-dimensional array is sparse (*i.e.*, most entries are 0) whenever the total number of components is larger than five, as illustrated by a portion of the stoichiometric coefficient matrix for a system consisting of 10 components and 28 complexes shown in Table 1. Since in a system with NX components and NC complexes plus solids, (NX.NC—$\hat{n}$.NC) entries in the matrix will be zero, and the % sparsity of the matrix can be computed as follows:

$$\%\,\text{sparsity} = \left(1 - \frac{\hat{n}\,.\,\text{NC}}{\text{NX}\,.\,\text{NC}}\right).100$$

$$= \left(1 - \frac{\hat{n}}{\text{NX}}\right).100$$

Thus, although the total number of zeros in the coefficient matrix is a function of NX, NC and $\hat{n}$ (average number of components in complexes/solids), the % sparsity depends only on the number of components (NX) and $\hat{n}$. Figure 1 depicts the relationship between % sparsity of the stoichiometric matrix and the number of components, for $\hat{n} = 3$, 4 and 5 respectively.

SYMBOLS

A:	array containing stoichiometric coefficients.
AI:	a stoichiometric coefficient.
BETA:	array containing log (base 10) of stability constants.
C:	array containing molar concentrations of complexes/solids.
ID:	identification number of components.
IDC:	array containing ID of components present in complexes/solids. (corresponds to A).
IPINTR:	pointer.
ITEMP:	array for temporarily storing IDs of components present in complexes/solids. Its size is MAXCOM.
MAXCOM:	maximum number of components allowed in a complex/solid.
$\hat{n}$:	average number of components present in complexes/solids.
NC:	number of complexes/solids present in a problem.
NNC:	array containing the number of components present in each complex.
NX:	number of components in a problem.
PX:	array containing log (base 10) of the molar concentrations of free components.
SUMC:	total molar concentration of a component.
TEMP:	array for temporarily storing stoichiometric coefficients for a complex/solid. Its size is MAXCOM.
X:	array containing molar concentration of free components.

(All arrays are one-dimensional)

As the number of components and complexes (and solids) in a system increases, the size (NX.NC) of the array required to store the stoichiometric coefficients also grows, leading to growing overall storage requirements. This causes difficulty on smaller computers or with large problems, prompting the suggestion[5] that "for very large equilibrium systems or when the core space is limited ..." programs such as COMICS or COMPLEX may have to be preferred over faster programs such as MINIQUAD

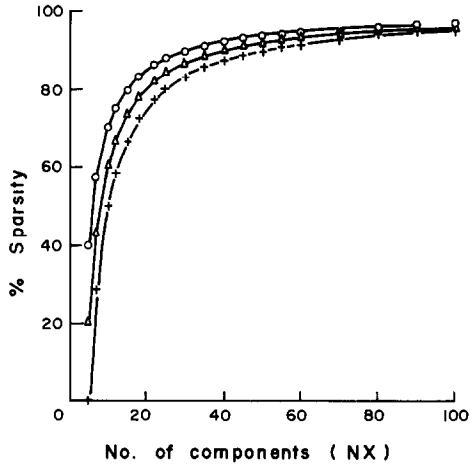

Fig. 1. Dependence of % sparsity on the number of components and $\hat{n}$: O—$\hat{n} = 3$, △—$\hat{n} = 4$, +—$\hat{n} = 5$.

(COMPLEX and COMICS are slower but require less memory). Additionally, referencing zeros (in the case of a sparse stoichiometric matrix A) during computation increases the number of times loops are executed, for example during calculation of concentrations of complexes, thus increasing the execution time of the program.

This problem becomes more severe for geochemical systems where the number of aqueous ions (components and complexes) as well as possible solids to be considered is very large. Problems of lack of storage space are particularly likely with the new generation of microcomputers, as well as "personal computers", which are reasonably fast but have limited main memory (usually 16–64 kbyte). Such a computer is the Hewlett Packard HP-85 personal computer, which is well suited for scientific problem-solving but has a maximum available memory of 32 kbyte. For a problem containing 50 components and 500 dissolved complexes plus possible solids, the array for storing stoichiometric coefficients alone would have 25,000 elements (and would require at least 100 kbyte of memory). For example, the computer program MINEQL has allocated a 400 × 30 array for this purpose.

It is thus evident that an algorithm which can permit storage and retrieval of only non-zero stoichiometric coefficients would considerably reduce storage requirements and allow solution of larger problems on smaller machines with limited memory. This paper presents such an algorithm, along with a suggested FORTRAN implementation and examples of its application for calculating concentration of complexes. The samples of FORTRAN code are intended to illustrate the algorithm and to ease the task, for potential users, of modifying existing computer programs so that they may be run on smaller machines. A program CHEMEQUIL,[6] at present being developed by the author, requires a total array storage of 9240 elements for problems involving 50 components and 500 complexes (solution phase only). COMPLEX and MINEQL require 27,000 and 30,000 elements respectively for the same size of problem.

ALGORITHM

STEP 0: POINTER = 0, I = 1, CLEAR arrays IDC, A, ITEMP, TEMP, NNC, *etc.*

STEP 1: READ information about the I-th complex or solid—Identification number (ID) and stoichiometric coefficient of each component present in the complex or solid along with its stability constant, and any other associated information.

Table 1. Part of the stoichiometric coefficient matrix in a system of 10 components and 28 complexes

	Components									
Complexes	UO_2	H	PO_4	CO_3	SO_4	F	Cl	H_2SiO_4	Hg	Cd
UO_2HPO_4	1	1	1	0	0	0	0	0	0	0
$UO_2H_2(PO_4)_2$	1	2	2	0	0	0	0	0	0	0
$UO_2H_2PO_4$	1	2	1	0	0	0	0	0	0	0
$UO_2H_4(PO_4)_2$	1	4	2	0	0	0	0	0	0	0
$UO_2H_6(PO_4)_3$	1	6	3	0	0	0	0	0	0	0
UO_2OH	1	−1	0	0	0	0	0	0	0	0
$UO_2(OH)_2$	1	−2	0	0	0	0	0	0	0	0
$(UO_2)_3(OH)_5$	3	−5	0	0	0	0	0	0	0	0
UO_2CO_3	1	0	0	1	0	0	0	0	0	0
$UO_2(CO_3)_2$	1	0	0	2	0	0	0	0	0	0
$UO_2(CO_3)_3$	1	0	0	3	0	0	0	0	0	0
UO_2F	1	0	0	0	0	1	0	0	0	0
UO_2F_2	1	0	0	0	0	2	0	0	0	0
UO_2F_3	1	0	0	0	0	3	0	0	0	0
UO_2F_4	1	0	0	0	0	4	0	0	0	0
UO_2SO_4	1	0	0	0	1	0	0	0	0	0
$UO_2(SO_4)_2$	1	0	0	0	2	0	0	0	0	0
$UO_2H(H_2SiO_4)$	1	1	0	0	0	0	0	1	0	0
HgOH	0	−1	0	0	0	0	0	0	1	0

Table 2. A representation of the method of storage of stoichiometric coefficients according to the proposed algorithm

	Array contents								
Array	UO_2HPO_4			$UO_2(HPO_4)_2$			$UO_2H_2PO_4$		
IDC	1	2	3	1	2	3	1	2	3
A	1	1	1	1	2	2	1	2	1
NNC		3			3			3	

In IDC, 1 = UO_2; 2 = H; 3 = PO_4.

Table 3. Array requirements of some programs as a function of the numbers of components and complexes

	No. of components × no. of complexes					
Program	6 × 20	10 × 50	20 × 50	20 × 100	30 × 400	50 × 500
CHEMEQUIL	400	880	1320	1920	6160	9240
COMPLEX	281	825	1435	2635	13945	27565
MINIQUAD	360	1010	1950	3200	15340	30720
COMICS	390	1320	2370	4620	26170	52770
MINEQL	744	1328	2178	3378	15128	30228

STEP 2: STORE the ID of components present in the complex or solid and their stoichiometric coefficients temporarily in arrays ITEMP and TEMP respectively.

STEP 3: COUNT (by using ITEMP) the number of components present in the complex and store it in NNC at I-th location, *i.e.*, NNC (I). (Note that in an actual implementation, counting can be done at step 1.)

STEP 4: TRANSFER contents of arrays ITEMP and TEMP to arrays IDC and A, at locations POINTER + 1 to POINTER + NNC(I) sequentially.

STEP 5: POINTER = POINTER + NNC(I), I = I + 1, CLEAR ITEMP and TEMP.

STEP 6: GO TO STEP 1 if there are more complexes or solids to READ.

STEP 7: NC = I − 1 (NC = number of complexes and solids).

For a simple problem containing 10 components and 28 complexes, a part of the stoichiometric matrix was shown in Table 1. Table 2 shows a representation of the stoichiometric information stored in a compact fashion without any zeros, according to the algorithm.

SAMPLE FORTRAN IMPLEMENTATION OF THE ALGORITHM

```
C     INSERT CODE FOR CLEARING (ZEROING) IDC, A, ITEMP
C     TEMP, NNC, ETC
C
      IPINTR = 0
      I = 1
C     READ INFORMATION ABOUT THE I-TH COMPLEX
  400 READ (5,5000) BETA (I), (ITEMP (K), TEMP (K), K = 1, MAXCOM)
      ICOUNT = 0
      DO 500 K = 1, MAXCOM
         IF (TEMP (K) EQ 0.0) GO TO 500
         ICOUNT = ICOUNT + 1
  500 CONTINUE
C
      NNC (I) = ICOUNT
      L = 1
      LSTART = IPINTR + 1
      LFINAL = IPINTR + NNC(I)
      DO 600 K = LSTART, LFINAL
         IDC (K) = ITEMP (L)
         A (K) = TEMP (L)
         L = L + 1
  600 CONTINUE
C
      IPINTR = IPINTR + NNC(I)
      I = I + 1
      DO 700 K = 1, MAXCOM
         ITEMP (K) = 0
         TEMP (K) = 0.0
  700 CONTINUE
C
C
C     INSERT CODE TO CHECK IF MORE COMPLEXES ARE TO
C     BE READ
C     IF SO, GO TO 400
C
      NC = I - 1
C     STOICHIOMETRIC INFORMATION IS NOW STORED FOR
C     ALL COMPLEXES
```

The proposed algorithm requires two one-dimensional arrays of size $\hat{n}$.NC, one one-dimensional array of size NC and two one-dimensional arrays of size MAXCOM (MAXCOM is rarely greater than 7 or 8). The total array requirement for the scheme is $(2\hat{n} + 1)$NC + 2MAXCOM. The conventional method of using a two-dimensional array would have required an array of size NC.NX. It is evident that in conventional method, the size of the NX.NC array the proposed scheme, the storage needed for stoichiometric coefficients depends only on the number of complexes plus solids and on $\hat{n}$. In other words, for fixed $\hat{n}$ and NC, the required storage is independent of the number of components in the problem. For the depends on both the number of complexes and the number of components. The total storage requirements of some programs (for solution phase computations alone), including CHEMEQUIL ($\hat{n} = 4$), are shown in Table 3.

EXAMPLES

These examples are intended to show how the required information can be retrieved during equilibrium calculation. The following FORTRAN loop can be used to find the identities of components and the corresponding stoichiometric coefficients for all complexes or solids in sequence (J from 1 to NC) where J is the index of the complex or solid and NC is the total number of complexes or solids in the problem.

```
C .   ID = ID OF COMPONENT
C     AI = STOICHIOMETRIC COEFFICIENT
C
      IPINTR = 0
C   . LOOP ON COMPLEXES (1 TO NC)
      DO 2000 J = 1, NC
          NNCJ = NNC(J)
C     GET ID AND AI OF ALL COMPONENTS PRESENT IN THIS
C     COMPLEX
          DO 1000 I = 1, NNCJ
              IIP = IPINTR + I
              ID = IDC(IIP)
              AI = A(IIP)
C
C     .ID AND AI NOW AVAILABLE FOR CALCULATIONS.
C     .E.G. JACOBIAN
C     .COMPUTATION
 1000     CONTINUE
C     .POSITION POINTER JUST BEFORE BEGINNING OF NEXT
C     .COMPLEX
          IPINTR = IPINTR + NNCJ
 2000 CONTINUE
```

To obtain random access to the identities and stoichiometric coefficients of all the components present in the J-th complex, proceed as follows:

```
C     COMPUTE STARTING LOCATION POINTER FOR J-TH
C     COMPLEX
      IPINTR = 0
      IF (J .EQ. 1) GO TO 6000
C     HERE FOR J > 1
      DO 5000 II = 1, J - 1
          IPINTR = IPINTR + NNC(II)
 5000 CONTINUE
 6000 CONTINUE
C
C
C     GET IDS AND COEEFICIENTS
      NNCJ = NNC(J)
      DO 7000 I = 1, NNCJ
          IIP = IPINTR + I
          ID = IDC(IIP)
          AI = A(IIP)
C
C   . HERE ID AND AI ARE SEQUENTIALLY AVAILABLE FOR
C     CALCULATIONS E.G. CONCENTRATION OF THE COMPLEX
C
 7000 CONTINUE
C
```

Finally, to compute the concentration of all complexes in which the I-th (ID = I) component is present, and the total number of moles of the I-th component bound in these complexes, the following code can be utilized:

```
C     COMPUTE CONCENTRATIONS OF ALL COMPLEXES IN
C     WHICH I-TH COMPONENT IS PRESENT AND ADD THEM
C     TO SUMC (INITIALIZED TO FREE CONC OF COMPONENT I)
C
      SUMC = X(I)
      IPINTR = 0
      DO 9000 J = 1, NC
C     .CHECK IF THE COMPONENT (ID = I) IS PRESENT IN
C     J-TH COMPLEX
          NNCJ = NNC(J)
          DO 8000 K = 1, NNCJ
              IIP = IPINTR + K
              ID = IDC(IIP)
              IF (ID .NE. I) GO TO 8000
              AI = A(IIP)
              GO TO 8200
 8000     CONTINUE
          GO TO 8600
C     NOW COMPUTE CONCENTRATION OF THE J-TH
C     COMPLEX
 8200     CJ = BETA(J)
          NNCJ = NNC(J)
          DO 8400 K = 1, NNCJ
              IIP = IPINTR + K
              ID = IDC(IIP)
              CJ = CJ + PX(ID)*A(IIP)
 8400     CONTINUE
          C(J) = 10.0**CJ
          SUMC = SUMC + C(J)*AI
 8600     IPINTR = IPINTR + NNCJ
 9000 CONTINUE
```

These simple examples perform tasks requiring manipulation of stoichiometric coefficients and represent some of the building blocks of computer programs for equilibrium calculation and stability-constant determination.

REFERENCES

1. A. Sabatini, A. Vacca and P. Gans, *Talanta*, 1974, **21**, 51.
2. D. D. Perrin and I. G. Sayce, *ibid.*, 1967, **14**, 833.
3. J. Westall, J. L. Zachary and F. M. M. Morel, *Tech. Note*, 1976, 18, Water Quality Lab. Dept. of Civil Eng., M.I.T.
4. G. Ginzburg, *Talanta*, 1976, **23**, 149.
5. D. J. Leggett, *ibid.*, 1977, **24**, 535.
6. V. S. Tripathi, in preparation.

Talanta, Vol. 30, No. 1, pp. 69–71, 1983
Printed in Great Britain.

0039-9140/83/010069-05$03.00/0

NOTE ON THE URANYL COMPLEXES OF EDTA

M. LURDES, S. S. GONÇALVES, A. M. ALMEIDA MOTA and
J. J. R. FRAÚSTO DA SILVA
Centro de Química Estrutural, Instituto Superior Técnico, Lisboa, Portugal

(*Received* 19 *February* 1982. *Accepted* 12 *July* 1982)

Summary—The nature of the EDTA complex of uranium(VI) is discussed, and it is concluded that there is no need to postulate stabilization of the complex by hydrogen-bonding between a protonated nitrogen atom and the uranyl ion.

In a previous paper[1] we reported that the stability constant of the MHL complex of the uranyl ion with EDTA is relatively high when compared with the value to be expected for a co-ordinating iminodiacetate moiety and suggested that this could be due to the formation of a hydrogen bond between the protonated nitrogen atom of the ligand and one of the oxygen atoms of the uranyl ion.

This view was criticised by Krishnamurthy and Morris,[2] who nevertheless also suggested the occurrence of a hydrogen bond, but involving bridging water molecules.

Later we extended our measurements to cover the series of diaminoalkanetetra-acetic acids with $n = 2$–6, n being the number of CH_2 groups in the alkane chain, and found that the values of log K_{UO_2HL} correlated linearly with the $pk_{H_2L^{2-}}$ values of the ligands but this correlation did not correspond to that of log K_{UO_2L} with pk_{HL^-} obtained for a series of iminodiacetic acids.[3] Since the deviations were smaller the larger the value of n, this fact seemed to support our hypothesis, but we have found that the same type of behaviour is given by the complexes of magnesium and calcium with the two families of ligands. In both cases two straight lines are obtained, one for the correlation of log K_{MHL} with $pk_{H_2L^{2-}}$ (for the diaminoalkanetetra-acetic acids) and the other for the correlation of log K_{ML} with pk_{HL} (for the iminodiacetic acids), these lines intersecting at about $n = 6$.

Since these two metal ions cannot form any hydrogen bonds of the types postulated for the uranyl complexes, the previous hypotheses are probably both wrong and the reason for the enhanced stabilities of the diaminoalkanetetracetate complexes found for all cations must be looked for elsewhere.

Thirty years ago, Schwarzenbach and Ackermann[4] noted that the values of $pk_{H_2L^{2-}}$ of the diaminoalkanetetra-acetic acids decreased with n but the drop was greater than was to be expected from inductive effects alone (due to the repulsion between protons bonded to the nitrogen atoms of the ligands) and calculated the $pk^{calc}_{H_2L}$ values that would correspond to this case. The differences between calculated and experimental values were ascribed to the formation of an intramolecular hydrogen bond in HL^{3-} species, between the carboxylate groups and the protonated nitrogen

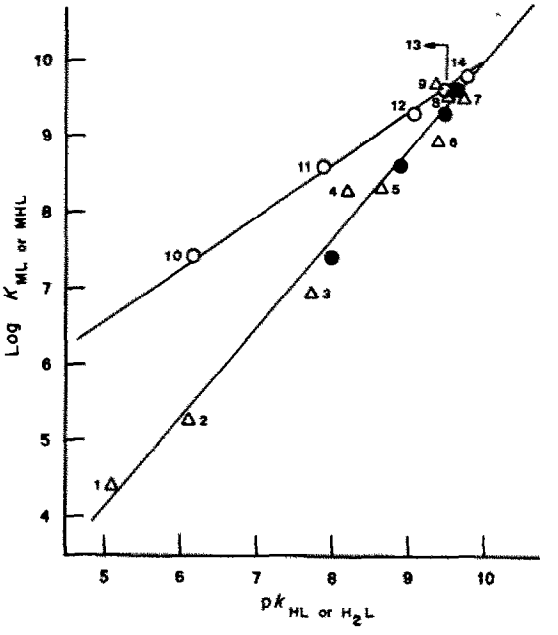

Fig. 1. Correlation of log K_{ML} for uranyl-iminodiacetate complexes or of log K_{MHL} for uranyl diaminoalkanetetra-acetate complexes with the dissociation constant of the ligands (pk_{HL} and pk_{H_2L}, respectively). The numbers from 1 to 9 correspond to iminodiacetate ligands, $RN(CH_2COOH)_2$, where R is: (1) C_6H_5; (2) C_6H_{10}; (3) $HOOCC_6H_4$; (4) C_5H_4N; (5) HOC_2H_4; (6) H; (7) CH_3; (8) $O_3N_2C_4H_3$ (barbiturate); (9) $HOOCCH_2$. The numbers from 10 to 14 correspond to diaminoalkanetetra-acetate ligands, $(HOOCCH_2)_2N(CH_2)_nN(CH_2COOH)_2$, where n is equal to: (10) 2; (11) 3; (12) 4; (13) 5; (14) 6. The points represented by ● correspond to the diaminoalkanetetra-acetate complexes correlated with calculated pk_{H_2L}, taking into account inductive effects alone.

Table 1. Experimental and calculated dissociation constants (pk_{H_2L}) of polyaminocarboxylate ligands, stability constants (log K_{MHL}) of their uranyl complexes, estimated net electrostatic interactions between the dissociating proton and the $>NH^+(CH_2COO^-)_2$ groups of the ligands [$\Delta G_{el}(H, N^+)$] and estimated free energy changes on the formation of the hydrogen bonds in HL^{3-} species (ΔG^*).

Ligand	n	$pk_{H_2L}^{exp}$ (experimental)	$pk_{H_2L}^{calc}$ (calculated in terms of inductive effects alone)	log $K_{MHL}^{\dagger}$	Estimated† $\Delta G_{el}(H, N^+)$§, *kcal/mole*	Estimated $-\Delta G^{*}$‡, *kcal/mole*
EDTA	2	6.2	8.0	7.40	2.4	2.4
PDTA	3	7.9	8.9	8.60	1.2	1.4
BDTA	4	9.1	9.5	9.32	0.4	0.5
PEDTA	5	9.5	9.6	9.59	0.3	0.1
HDTA	6	9.8	9.8	9.82	0.0	0.0

†Present work and reference 1.
‡$\Delta G^* = -2.3RT(pk_{H_2L}^{calc} - pk_{H_2L}^{exp})$.
§$\Delta G_{el}(H, N) = -2.3RT(pk_{H_2L}^{HDTA} - pk_{H_2L}^{calc}$; electrostatic interaction (H, N^+) assumed to be negligible for HDTA.

atoms, a view supported by infrared and NMR studies made by Chapman *et al.*[5] The data are given in Table 1.

Now, if $pk_{H_2L^{2-}}^{calc}$ values are used instead of the experimental $pk_{H_2L^{2-}}$ values in our correlations, it is found that all log K_{MHL} *vs.* $pk_{H_2L^{2-}}^{calc}$ values fall on the line obtained for the iminodiacetate complexes, *i.e.*, a single correlation is obtained for each metal ion (Fig. 1).

To explain this result it is convenient to consider two Born–Haber cycles, one for the formation of complexes with the iminodiacetates and the other for the formation of complexes with the diaminoalkanetetra-acetates.

For the iminodiacetates we have

$$M^{2+} + HL^- \xrightarrow{\pm\Delta\Delta G_h - \Delta G_{H,M}} ML + H^+$$
$$-\Delta G_1 \qquad\qquad +\Delta G_2$$
$$M^{2+} + L^{2-} + H^+$$

where

$\Delta\Delta G_h$ = net difference in the free energies of hydration of all species, *i.e.*,

$$-\Delta G_h(ML) - \Delta G_h(H^+) + \Delta G_h(M^{2+}) + \Delta G_h(HL^-)$$

$\Delta G_{H,M}$ = free-energy change on replacing a bonded proton for a bonded metal ion (in solution)

ΔG_1 = free-energy change on protonation of the L^{2-} ligand (in solution)

ΔG_2 = free-energy change on bonding M^{2+} to L^{2-} (in solution).

Since

$$|\Delta G_1| = 2.3RT \log K_{HL} = 2.3RT\, pk_{HL}$$
$$|\Delta G_2| = 2.3RT \log K_{ML}$$
$$\Delta G_2 = \Delta G_1 \pm \Delta\Delta G_h + \Delta G_{H,M}$$

it follows that

$$2.3RT \log K_{ML} = 2.3RT\, pk_{HL} + \Delta G_{H,M} \pm \Delta\Delta G_h$$

For the complexes of the diaminoalkanetetra-acetates some additional terms appear:

$$M^{2+} + H_2L^{2-} \xrightarrow{\pm\Delta\Delta G_h - \Delta G_{H,M} - \Delta G_{el}(H, \overset{+}{N}) \pm \Delta G_{el}(M, \overset{+}{N})} MHL^- + H^+$$
$$-\Delta G_1 + \Delta G^* + \Delta G_{el}(H, \overset{+}{N}) \qquad\qquad \Delta G_2 \pm \Delta G_{el}(M, \overset{+}{N}) - \Delta G^*$$
$$M^{2+} + HL^{3-} + H^+$$

where $\Delta G_{el}(H, \overset{+}{N})$ corresponds to the net electrostatic interaction between the ionizing proton and the $>N\overset{+}{H}(CH_2COO^-)_2$ group of the ligand; and $\Delta G_{el}(M, \overset{+}{N})$ is the net electrostatic interaction between the metal ion and the $>N\overset{+}{H}(CH_2COO^-)_2$ group.

If we represent by ΔG^* the free-energy change on the formation of the hydrogen bond in HL^{3-} species, we have for the formation of complexes of the diaminoalkanetetra-acetates

$$2.3RT \log K_{MHL} = 2.3RTpk_{H_2L}^{calc.} - \Delta G^* + \Delta G_{H,M} \pm \Delta G_{el}(M, N^+) + \Delta G_{el}(H, N^+) \pm \Delta\Delta G_h.$$

Following Schwarzenbach and Ackermann's calculations, the value of ΔG^* is estimated to be of the order of the electrostatic effect $\Delta G_{el}(H, N^+)$. Hence, for the correlation of log K_{MHL} *vs.* $pk_{H_2L}^{calc}$ to be superimposable with that of log K_{ML} *vs.* pk_{HL}, $\Delta G_{el}(M, N^+)$ must be close to zero, which means that the metal ion is effectively shielded by the co-ordinated iminodiacetate moiety and does not feel the effect of the other free $>NH^+(CH_2COO^-)_2$ group in the same molecule, in contrast to what happens with the proton.

The different behaviour of the two families of ligands is then due to the different contribution of the terms relative to the electrostatic interactions between the bonded proton or the co-ordinated metal ion and the second $>NH^{+}(CH_2COO^{-})_2$ group of the diamino alkanetetra-acetate and there is no need to postulate the formation of any stabilizing hydrogen bond whatsoever in the metal complexes. Naturally, the differences tend to cancel out when n increases and proton–proton repulsions become negligible.

REFERENCES

1. J. J. R. Fraústo da Silva and M. L. Simões Gonçalves, *Talanta*, 1968, **5**, 609.
2. M. Krishnamurthy and K. B. Morris, *Inorg. Chem.*, 1969, **8**, 2620.
3. J. J. R. Fraústo da Silva and M. L. Simões Gonçalves, *Rev. Port. Quim.*, 1970, **12**, 95.
4. G. Schwarzenbach and H. Ackermann, *Helv. Chim. Acta*, 1948, **31**, 1029.
5. D. Chapman, D. R. Lloyd and R. H. Prince, *J. Chem. Soc.*, 1963, 3645.

Talanta, Vol. 30, No. 1, pp. 72–74, 1983
Printed in Great Britain.

0039-9140/83/010072-03$03.00/0

ACTION DE L'ACIDE ASCORBIQUE SUR LES AMINES PRIMAIRES ET LES ACIDES α AMINES

D. BAYLOCQ, C. MAJCHERCZYK, A. RABARON et F. PELLERIN
Laboratoire de Chimie Analytique, Centre d'Etudes Pharmaceutiques de l'Université de Paris-Sud, Châtenay Malabry F92290, France

(*Reçu le* 5 *avril* 1982. *Accepté le* 29 *juin* 1982)

Résumé—Cette étude met en évidence la structure du dérivé obtenu par l'action de l'acide ascorbique sur les amines primaires et les acides α aminés; les méthodes utilisées sont la résonance magnétique nucléaire du ^{13}C, et la spectrophotométrie infra-rouge. La configuration chimique est comparable à celle du pourpre de Ruhemann obtenu par l'action de la ninhydrine sur les acides α aminés.

L'acide ascorbique en solution dans le diméthylformamide aqueux réagit sur les amines primaires telles que les acides α aminés et les alcoylamines (chlorhydrate de méthylamine, d'éthylamine, n-propylamine, n-butylamine et benzylamine) et conduit à une coloration rouge; cette réaction colorée est sélective pour les amines primaires, alors que les bases secondaires ou tertiaires réagissent trés peu.[1–3] Des essais réalisés sur la proline conduisent à un composé faiblement coloré, présentant des caractéristiques spectrales différentes.

Cette réaction a été appliquée au dosage colorimétrique des acides α aminés, des amines primaires et également de l'acide ascorbique; dans les deux cas, la réaction est quantitative et suit la loi de Beer-Lambert.

Mise à part la première étape de la réaction qui réside dans l'oxydation par l'air de l'acide ascorbique en acide déhydroascorbique, le mécanisme réactionnel et la structure du composé n'ont pas été décrits et font l'objet de la présente note (Fig. 1).

PARTIE EXPERIMENTALE

Réactifs

Réactif 1. Solution d'acide ascorbique à 0,1% dans le diméthylformamide aqueux (99:1 v/v).

Réactif 2. Solution aqueuse d'acide α aminé (0,005% à 0,05%).

Réactif 3. Plaque de silice 60 F 254; épaisseur 1 mm.

Réactif 4. Diméthylformamide.

Mode operatoire

Dans une fiole de 100 ml, introduire 5 ml de solution d'acide α aminé et 20 ml de réactif 1. Compléter à 100 ml avec du diméthylformamide. Agiter mécaniquement et porter le mélange à 100° au bain-marie bouillant pendant 10 min. Chromatographier le composé rouge ainsi formé, sur couche de silice (Réactif 3), en utilisant le diméthylformamide pur comme solvant de migration (Réactif 4).

Après élution, procéder à l'extraction des taches à l'aide du diméthylformamide. Centrifuger et évaporer le surnageant sous vide à 60°.

Resultats obtenus

Les mesures spectrophotométriques des absorbances maximales du composé coloré obtenu par l'action de l'acide ascorbique (Tableau 1) sur le glycocolle et une amine primaire (n-butylamine) présentent certaines analogies avec celles obtenues par la réaction classique de la ninhydrine sur les acides aminés (Fig. 2). Par ailleurs, une des propriétés de l'acide ascorbique est d'entrainer la libération d'ammoniaque par action sur les acides α aminés,[4] processus qui caractérise également la première phase de la réaction entre la ninhydrine et les acides aminés. Il nous est alors apparu intéressant de comparer les mécanismes de ces deux réactions colorées.

Malher et Cordes[5] ont étudié les réactions de la ninhydrine et des acides α aminés et ont proposé le mécanisme suivant (Fig. 1).

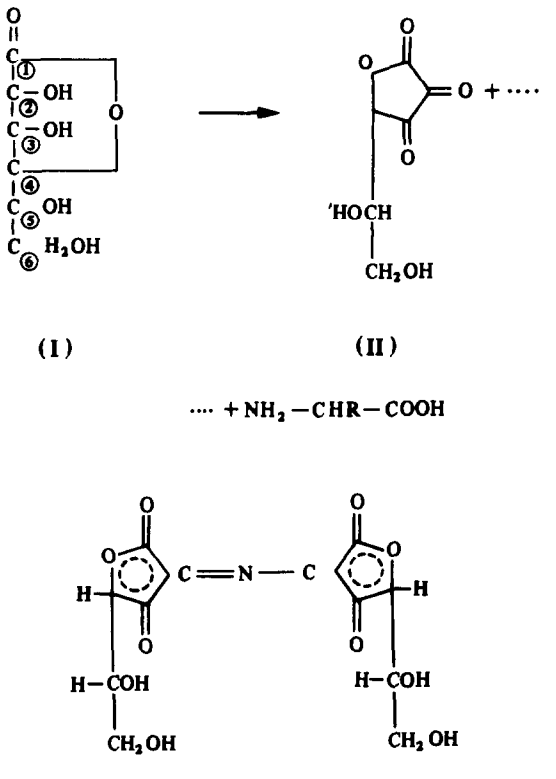

Fig. 1

Tableau 1. Caractéristiques spectrales du pourpre de Ruhemann et du composé rouge obtenu par l'action de l'acide ascorbique sur une amine primaire

Composé	Coloration	λ_{max}, nm	ϵ, $l.mole^{-1}.cm^{-1}$
Ninhydrine + acide α aminé ou amine primaire	Bleu violet	570	$0{,}9 \times 10^6$
Acide ascorbique + acide α aminé ou amine primaire	Pourpre	530	$0{,}75 \times 10^6$

Une molécule de ninhydrine (**IV**) est réduite par un acide α aminé pour donner l'hydrindantine (**V**); celle-ci réagit avec une nouvelle molécule de ninhydrine (**IV**), fixe l'ammoniaque libéré et conduit au pourpre de Ruhemann (**VI**).

Le composé obtenu avec l'acide ascorbique et le glycocolle font intervenir le pouvoir oxydant de l'acide déhydroascorbique (oxydation spontanée en présence d'air); la forme oxydée a été mise en évidence par titrage à l'iode 0,1*M* d'une solution d'acide ascorbique placée dans les conditions opératoires (10 min à 100°, dans le diméthylformamide aqueux). Il a été retrouvé 50% de l'acide ascorbique initial, sous forme d'acide déhydroascorbique.

L'acide déhydroascorbique agissant comme oxydant entraine la désamination oxydative de l'acide α aminé avec libération d'ammoniaque; le processus réactionnel est alors comparable à celui établi pour l'obtention du pourpre de Ruhemann (**VI**) dont la structure présente des analogies avec celle du composé rouge (**III**) (Figs 1 et 2). La configuration chimique est établie par l'analyse spectrale: résonance magnétique nucléaire du ^{13}C et spectrophotométrie infra-rouge.

Etude structurale par R.M.N. du ^{13}C du composé formé

Le spectre de R.M.N. du ^{13}C de l'acide ascorbique (**I**) présente six pics

—Trois d'entre eux sont attribuables à des carbones aliphatiques remplacés par un groupement oxygéné à 74,9–68,4 et 61,5 ppm et correspondent respectivement aux carbones (4, 5, 6) de l'acide ascorbique.

—Le signal 171,4 ppm correspond au carbonyle (1).

—Les signaux à 153 et 117,4 ppm sont attribués aux carbones insolubles (2, 3) portant chacunun groupe hydroxyle.

—Sur le spectre du produit préparé, on observe les signaux à 61,5 et 68,4 ppm de l'acide ascorbique, retrouvés à la même place, mais ils présentent un élargissement caractérisant une forte contrainte stérique qui diminue la libre rotation de la chaîne latérale $CHOH–CH_2OH$.

—Le signal à 74,9 ppm du carbone 4 est dédoublé à 72,9 et 75,6 ppm. Ce dédoublement proviendrait de la dimérisation de la molécule qui entraine, du fait des déplacements des doubles liaisons, un environnement magnétique différent pour les deux carbones des deux parties.

—L'apparition de quatre pics supplémentaires entre 83 et 108 ppm et leur déplacement chimique correspondent à une structure déhydroascorbique, ce qui suggère l'existence, dans le mélange analysé, d'une réduction partielle du dimère attendu. Ce mélange serait alors constitué de dimère ascorbique et d'autres dimères mixtes, ascorbique.

—Dans la région du carbonyle et des énamines 160–175 ppm, on relève la présence de cinq pics d'identités différentes, attribuables aux atomes de carbone doublement liés.

Ces observations permettent de considérer le produit analysé comme un mélange de plusieurs structures dimères d'acide ascorbique et–ou d'acide déhydroascorbique.

Des travaux en cours portant sur la séparation de ce mélange en ses différents constituants devraient permettre de préciser la structure et la répartition de ces dimères colorés.

Etude structurale par spectrophotométrie infra-rouge

L'étude structurale précédente a été complétée par l'analyse en spectrophotométrie infra-rouge de composé après isolement par évaporation sous vide.

On a préparé par compression une prise d'essai de 50 mg du composé précédent, mélangé à du bromure de potassium pur pour infra-rouge, et effectué le spectre infra-rouge et comparé ce spectra aux spectres obtenus, dans les mêmes conditions, d'acide ascorbique et d'acide déhydroascorbique.

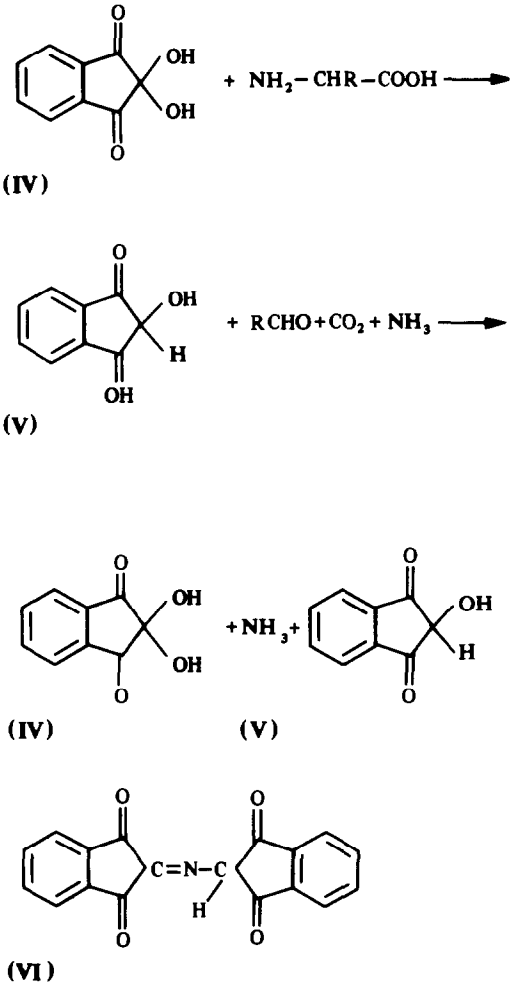

Fig. 2

Le spectre obtenu présente les caractéristiques suivantes.

—A 1740 cm^{-1}, une bande de vibration de valence du groupement CO caractéristique des γ lactones insaturés.

—Entre 1500 et 1700 cm^{-1}, une large bande correspondant à la zone d'absorption des vibrations des déformations des doubles liaisons C=O, C=N et C=C.

—Enfin, vers 1180–1200 cm^{-1}, une bande caractéristique des vibrations de déformation des groupements CO et CN.

—La présence de bandes entre 1600 et 1700 cm^{-1} met en évidence une zone d'absorption correspondant à une liaison C=N et confirme ainsi la configuration chimique de la fonction imine trop encombrée pour être détectable par résonance magnétique nucléaire du ^{13}C.

CONCLUSION

L'analyse spectrale du composé obtenu par l'action de l'acide ascorbique sur les acides α aminés et les amines primaires aliphatiques (R.M.N. du ^{13}C et spectrophotométrie I.R.) a permis d'en établir la structure et de préciser le mécanisme réactionnel; ce dernier est comparable à celui de la réaction de la ninhydrine sur les acides α aminés et les amines primaires (Fig. 1).

LITTERATURE

1. M. Pesez, *Pratique de l'analyse organique, colorimétrique.* Masson, Paris, 1966.
2. J. Bartos, *Ann. Pharm. Franc.*, 1964, **22**, 383.
3. M. Brunet, *ibid.*, 1968, **26**, 797.
4. M. Javiller et M. Polonovski, *Traité de Biochimie Générale.* Masson, Paris, 1962.
5. H. R. Malher et E. H. Cordes, *Biological Chemistry.* Harpers & Row, New York, 1966.

Summary—This study outlines the structure of the by-product obtained by the action of ascorbic acid on primary amines and α-amino-acids; the methods used are ^{13}C, NMR and infrared spectrophotometry. The chemical form is comparable to that of Ruhemann purple, obtained by the action of ninhydrin on α-amino-acids.

Talanta, Vol. 30, No. 2, pp. 75–80, 1983
Printed in Great Britain.

0039-9140/83/020075-06$03.00/0

SIMULTANEOUS FLUORESCENCE, PHOTOACOUSTIC AND TWO-PHOTON PHOTOIONIZATION DETECTION FOR LIQUIDS IN A CUVETTE

E. VOIGTMAN and J. D. WINEFORDNER*
Department of Chemistry, University of Florida, Gainesville, FL 32611, U.S.A.

(*Received* 7 *May* 1982. *Accepted* 15 *September* 1982)

Summary—A simple, sensitive liquid-phase photoionization detection scheme employing pulsed laser excitation has been developed. The system is an elaboration of an earlier simultaneous fluorescence and photoacoustic detection scheme employing a standard fluorescence cuvette. Factors affecting the analytical performance of the two-photon photoionization mode of operation are discussed, sensitive three-mode detection is demonstrated for a model compound (anthracene), and the effect of temperature on the photoionization mode provides an estimate of the ionic-charge carrier activation-energy in the conductance transport process.

Recently, we demonstrated a sensitive, liquid-phase, laser-excited photoacoustic detection system employing a standard (1 × 1 cm) quartz cuvette.[1] Various compounds, with fluorescence quantum efficiencies ranging from nearly zero (haemoglobin) to almost unity (Rhodamine 6G laser dye) were sensitively detected at the ng/ml level. Various laser systems were employed as excitation sources, and it was shown that the photoacoustic signal was indeed proportional to incident laser-pulse energy, as predicted by Tam and Patel,[2] and was independent of laser peak-power and power-density. The lowest detectable level of thermal energy (defined as a signal equal to three times the background noise) was found to be ~6 nJ, corresponding to a limiting detectable absorption coefficient of 4×10^{-6} cm^{-1}. Conventional absorbance measurements are actually transmittance measurements and therefore low absorbances require the determination of a small difference between two large quantities, *i.e.*, the transmitted-light intensity with and without the absorbing species present. Light-scatter of any kind is detrimental and usually limits the conventional technique to the measurement of absorbances greater than 10^{-4}. In contrast, the pulsed photoacoustic (PA) effect involves the measurement of a small acoustic signal, which is proportional to both the analyte absorbance and incident pulse energy, and is determined against only a small solvent background. For this reason, the PA effect is a so-called "zero-baseline" technique.

Despite the use of a "naked" piezoelectric transducer, it was found that the laser dye fluorescence emission did not generate spurious PA "signals". Consequently, the cuvette system was employed in a simultaneous fluorescence (FL) and PA detection scheme[3] with 30 strong fluorophors (polycyclic aromatic hydrocarbons, PAHs) as analytes of interest. The average PA detection limit for these PAHs, with excitation at 337.1 nm and 1.3 mJ/pulse, was $7 \times 10^{-9}M$ (2 ng/ml). This value is an order of magnitude lower than the best detection limit given by Harris[4] for laser calorimetric determination of small absorbances of solutions and is three orders of magnitude lower than the value for conventional transmittance techniques. Hence, the two-mode (FL and PA) cuvette system provides the advantages of both techniques, *i.e.*, the sensitivity and selectivity of fluorescence for analytes which fluoresce significantly, and the utility of a highly sensitive, zero-baseline technique for measuring small absorbances. This second mode is desirable because most substances have negligible fluorescence quantum efficiencies. It should also be noted that the PA signal is much less dependent on analyte fluorescence quantum efficiency than is the corresponding fluorescence signal.[3] Therefore, strong and weak fluorophors with similar molar absorptivities at the desired excitation wavelength do not produce greatly different PA signals (or PA limits of detection). Consequently, it was hoped that the PA mode could be used to complement the FL mode in the accurate determination of fluorescence quantum efficiencies in solution. Normally, such measurements are difficult since the necessary optical alignment and accurate calibration require great care. The process is further complicated if analytes of widely varying fluorescence quantum efficiency are to be studied. The synergistic use of one technique to compensate for difficulties in another is nicely shown in the PA determination of fluorescence quantum efficiencies by Adams *et al.*[5] (quinine sulphate) and by Sugitani and Kato[6] (uranium-mica compounds).

However, the customary assumption that the FL and PA effects are complementary is valid only if photochemical and other photophysical deactivation

*Author to whom correspondence should be addressed.

pathways, such as photoionization, can be neglected. This is certainly the case with most conventional (microphone detector and filtered xenon-arc excitation source) photoacoustic work, but is *not* the case for our system where typical pulse values of 1 mJ (energy), 10 nsec (duration), and 50 μm (beam focus) yield a power density of 3×10^9 W/cm^2. According to Hercules *et al.*,[7] power densities of 10^9–10^{10} W/cm^2 can produce ionization efficiencies ($\equiv$ ions produced/initial neutral species) of 10^{-2}–10^{-1}, while power densities below $\sim 10^8$ W/cm^2 yield much lower efficiencies of $\sim 10^{-5}$. This is in agreement with the value of 8×10^{-8} obtained by Locke *et al.*[8] for pyrene in hexane/2% 2-propanol with a microwave-excited xenon lamp continuum source. Note, however, that the potentially high ionization efficiencies obtained with moderately powered lasers can be used to advantage by adding an additional mode of operation to the FL and PA detection scheme.

In related work to develop a windowless flow-cell,[9–11] the two-photon photoionization (PI) mode was found to be at least as sensitive as the cuvette-system PA detection mode, despite the fact that the flow-cell was a first compromise between the differing optimization requirements of the three detection modes. It was found that the PI signal is *not* merely proportional to analyte absorbance, and can provide information not given by PA measurement. For example, *N,N,N',N'*-tetramethyl-*p*-phenylenediamine (TMPD) produced large PI and PA signals when excited at 337.1 nm, whereas TMPD·2HCl produced only a PA signal because the lone-pair electrons are no longer available. It was also found that a wide variety of substances (drugs) could be sensitively detected in the PI mode regardless of the dielectric constant, intrinsic conductivity, polarity and purity of the solvent.[10] The PI mode was employed, along with FL and PA detection, in a three-mode HPLC detector, and an average ionization efficiency of 3×10^{-2} was achieved for acridine, naphthalene, 7,8-benzoflavone, *N*-ethylcarbazole and anthracene in 70/30 v/v acetonitrile/water mixture.[11]

The desirability of adding an easily optimized PI detection mode to the already nearly optimized FL and PA detection modes arises from the observation that the cuvette system is substantially more sensitive (by a factor of about 100) in both the FL and PA detection modes than the flow-cell system[9,10] and that independent optimization of the detection modes is much easier with a cuvette system because of physical constraints in the flow-cell design. For example, it is very difficult to determine the effect on the PI signal of changing the electrode spacing in the flow-cell, since the analyte solution is held by surface tension between the flow-cell electrodes, and changes in spacing change the focusing of the excitation laser beam. In a cuvette, the electrode spacing may easily be varied without influencing the beam focus.

Accordingly, we have added the PI detection mode to the previous two-mode cuvette system, thereby providing the advantage of two distinct zero-baseline techniques, each more sensitive than conventional absorbance techniques and each applicable to the detection (and spectroscopic study) of a wide variety of substances. In addition, the sensitivity and selectivity of laser-excited fluorescence detection is retained. The use of a standard cuvette allows one or more of the detection modes to be added to existing instrumentation. Since the three detection modes are independent, it is possible, even with a single laser excitation pulse, to monitor simultaneously the three most important photophysical deactivation pathways available to molecules irradiated in solution.

In this paper, we describe the three-mode cuvette system and determine the effect on the PI detection process of factors such as incident laser pulse energy and analyte concentration. We also use the cuvette, and several modified versions of it, to determine the effect of factors which either could not be studied independently or could be studied only with great difficulty in the three-mode windowless flow-cell, namely laser beam focusing, electrode spacing, electrode geometry and composition, and solution temperature. The variation in PI signal with temperature is seen to be consistent with an ionic conductance transport process.

EXPERIMENTAL

The three-mode cuvette system is shown in Fig. 1. A bias voltage, typically -500 V, is supplied by a photomultiplier-tube supply (Pacific Precision Inst., Concord, CA, Model 226) to the high-voltage stainless-steel electrode (with respect to the grounded enclosure) through a current-limiting 10 MΩ resistor. Photocurrent signals are collected at the signal electrode and converted into signal voltages by an active current to voltage (I/V) converter composed of an operational amplifier (TL 071) with 20 MΩ feedback resistor in a classic I/V converter circuit For solvent sys-

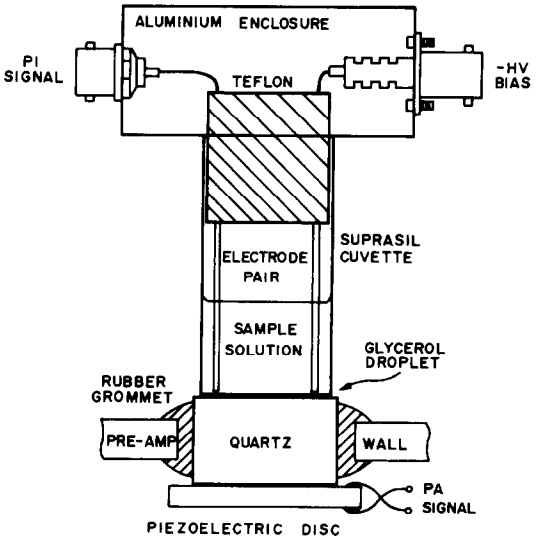

Fig. 1. The three-mode (fluorescence, photoacoustic, and two-photon photoionization) cuvette.

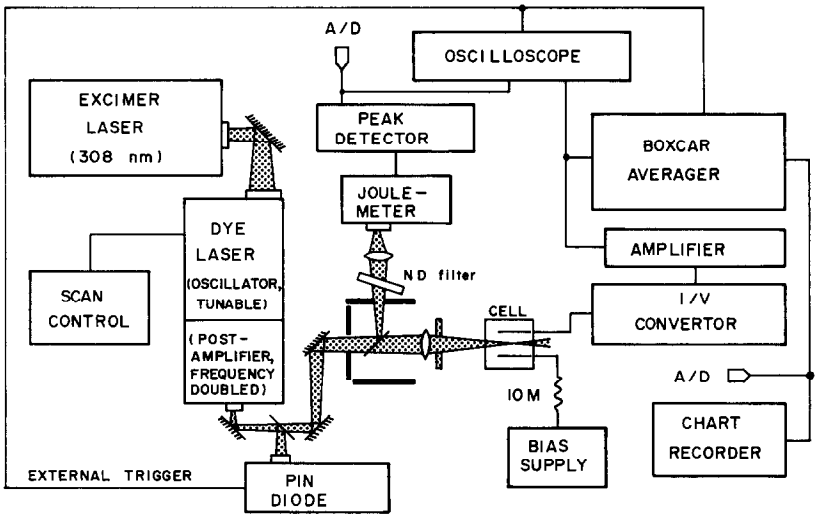

Fig. 2. Block diagram of the laser-excited photoionization detection scheme (N.D. filter = neutral density filter).

tems with substantial conductance, such as water and ethanol, an alternative I/V converter is used.[10] The amplified signals [EG&G Inc., Princeton Applied Research, PAR 211 amplifier, voltage gain (Av) = 1–1000, f_{-3db} = 1 Hz, 1 MHz] were acquired with a boxcar averager (PAR 160, 5-sec observed time constant) with either a chart-recorder or a home-made 10-sec integrator and digital voltmeter as the output device. The boxcar averager may be replaced with suitable peak-detection circuitry in all three modes, since the fluorescence signal may easily be stretched and the PA and PI signals are relatively low in frequency. Excitation illumination was provided by an excimer laser (Lumonics Research, Ontario, Canada, Model TE-861S) and laser pulse energies were measured with either a pyroelectric joulemeter (Molectron Corp., Sunnyvale, CA, Model J3-05DW, 0.89 V/mJ) or with a home-made, calibrated pyroelectric joulemeter and peak-detection circuit. Experimental details of the fluorescence and photoacoustic detection have been described previously.[1,3] A block diagram of the photoionization detection scheme is shown in Fig. 2. The tunable dye laser was not used in the present work.

To determine the effects of electrode separation and composition, a modified cuvette was built which did not have the FL and PA modes. A signal electrode (1.59 mm diameter stainless-steel rod) was attached to a cylindrical piece of Teflon which was in turn attached with heat-shrinkable tubing to a short, cylindrical alnico magnet. The assembly was made so that it would slide in a small rectangular Teflon block having a hole in it for the assembly and a milled channel for the signal electrode. A fixed, high-voltage electrode was also embedded in the Teflon block. A magnet provided non-rotational coupling to a micrometer anvil. The entire assembly was enclosed in a grounded aluminium minibox (Pomona Electronics, Pomona, CA, Model 4655) with appropriate milled electrode openings and BNC electrical connections.

The effects of solution temperature on the photoionization current were determined with another modified cuvette having a hollow stainless-steel signal-collection electrode which served as the housing for a calibrated thermistor (Omega Engineering, Inc., Stamford, CT, Model 44031). The solution temperature in the cuvette was varied by means of a Ranque-Hilsch vortex tube (Vortec Corp., Cincinnati, OH, Model 116 kit) with either the cold or the hot air-stream directed onto the front face of the sample cuvette. The principles of operation of the forced-vortex refrigeration device are described elsewhere[12] and in references therein. The vortex tube was operated with air at 140 psig pressure as the carrier gas and energy source. For the temperature and electrode-spacing experiments, solvents of lower volatility (n-nonane and n-dodecane) were used in preference to n-hexane and n-heptane. All solvents were HPLC grade except the n-dodecane, which was technical grade. Solvent purity was not a problem since impurities, *i.e.*, unwanted analytes, would merely produce a small additive offset in the PI signal. No such offsets were observed.

RESULTS AND DISCUSSION

Calibration curves for anthracene in n-hexane with excitation at 308 nm are shown in Fig. 3. The limits of detection, with 0.4-mJ laser pulse energy, are 0.2 ng/ml (FL), 60 ng/ml (PA), and 30 ng/ml (PI). The FL and PA detection limits are poorer by two orders of magnitude than the detection limits previously obtained with 337.1-nm excitation and 1.3-mJ incident pulse energy.[9] Even so, the PA result corresponds to a detection limit of 3×10^{-7} *M*, which is much better than conventional absorbance results, as discussed above. The PI result is five times as high as the flow-cell result because the increased signal due to a four-fold increase in bias voltage (V_b) is more than offset by the reduced laser pulse energy and increased electrode spacing (4.6 mm). It should also be noted that the results given above are conservative, since no effort was made to obtain the best possible detection limits. In fact, the electrodes in the cuvette partially blocked the fluorescence-emission optical path since they were not situated in opposite corners of the cuvette (this was necessary to allow study of beam-focusing effects).

The PI photocurrent increases linearly with bias voltage for voltages up to −2 kV (field strength = 4.35 kV/cm). The same behaviour is observed in the windowless flow-cell up to field strengths of

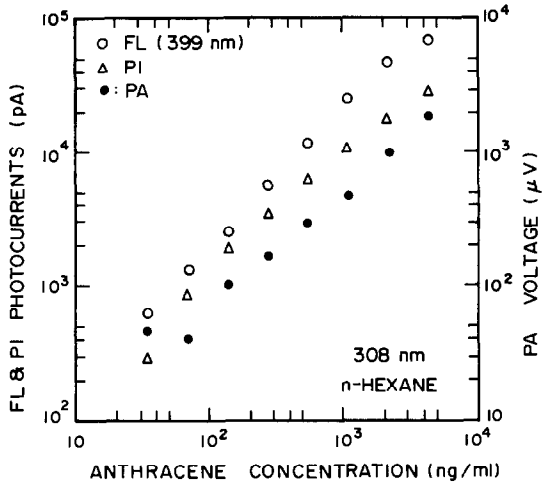

Fig. 3. Three-mode calibration graphs. Bias voltage was -2 kV and laser pulse energy (E_p) ~ 0.4 mJ.

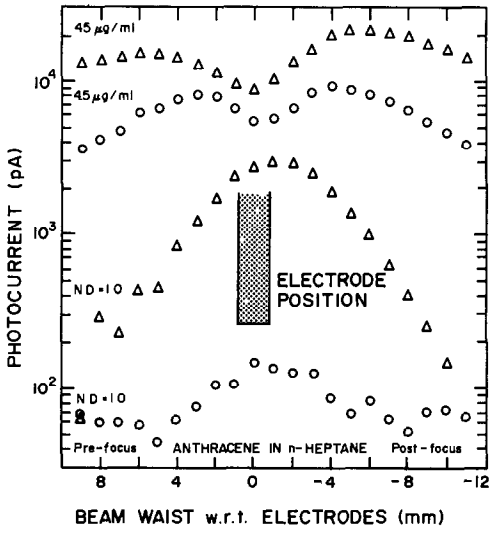

Fig. 5. Photoionization current as a function of position of laser-beam waist with respect to the position of the electrodes (*i.e.*, perpendicular to the plane of the electrodes; in the diagram, one electrode is behind the other). Triangles donote the more concentrated solution and a neutral density filter of absorbance 1.0 (N.D. = 1.0) The bias voltage was -1 kV and E_p = 1.3 mJ without the filter.

7.5 kV/cm. Considerable improvement should result from raising the bias voltage to yield field strengths of 25 kV/cm (the maximum tested field strength in the flow-cell) since the photocurrent is then[10] proportional to $V_b^{3/2}$.

The effect of laser pulse energy on the photoionization currents due to illumination of naphthalene, anthracene and pyrene is shown in Fig. 4 [in which an incident pulse energy (E_p) of ~0.5 mJ is normalized to unity]. Unlike the flow-cell, in which quadratic behaviour is exhibited for low pulse energies and analyte concentrations,[10] the slopes of the least-squares lines (not shown) fitting the data in Fig. 4 are approximately 1.4 ± 0.04, which is in reasonable agreement with the "Speiser-Jortner $\frac{3}{2}$-power law".[13] This behaviour is due to saturation in the interior portion of the focused beam and is a geometric effect rather than a so-called "sub-quadratic" photoionization phenomenon. This saturation effect may also be seen in Fig. 5 where PI photocurrent is plotted as a function of the position of the laser-beam waist (position of tightest focus). The asymmetry is due to the higher average photon flux in the post-focus positions. Note that the current is not maximized directly between the electrodes unless a neutral density filter of absorbance 1.0 is used to attenuate the incident laser beam tenfold. Reduction in the analyte concentration (unpublished data) also results in the photocurrent being maximal when the laser is focused directly between the electrodes.

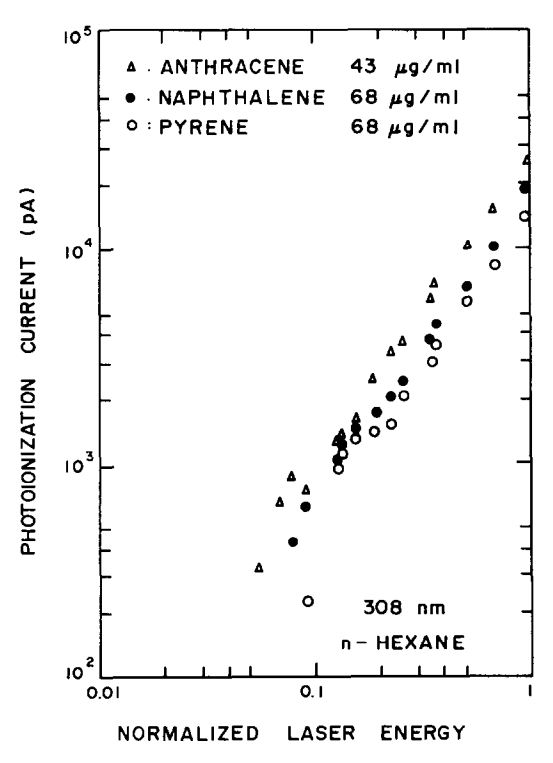

Fig. 4. Effect of laser pulse energy on the photoionization current (0.5 mJ ≡ 1).

For a well-studied photoconductor, such as cadmium sulphide, the photocurrent is inversely proportional to the square of the distance between the electrodes.[14] This is also the case for anthracene in n-nonane, as shown in Fig. 6 for three concentrations and two light intensities per concentration. It is obviously important to place the electrodes as close together as possible without direct illumination of the electrodes. It is also to be expected that parallel-plate electrodes would provide higher carrier-collection efficiency than thin rod electrodes and this is borne out by the results in Fig. 7. The largest photocurrent is obtained with the rectangular electrodes constructed

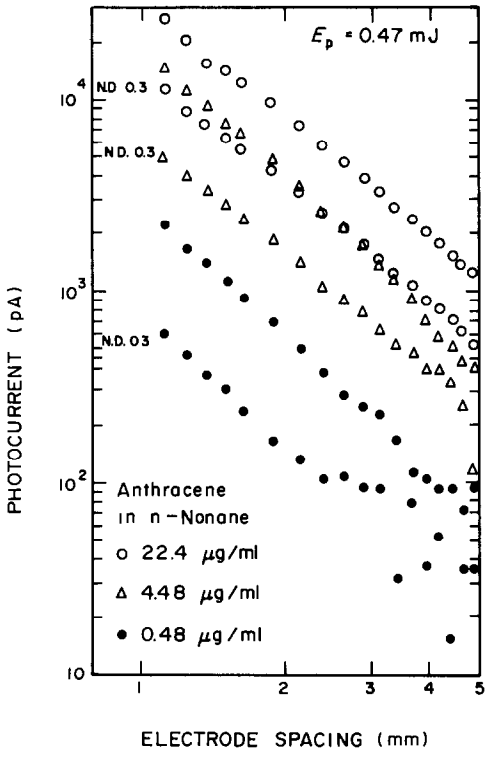

Fig. 6. Effect of electrode spacing on the photoionization current. Laser pulse energy = 0.5 mJ.

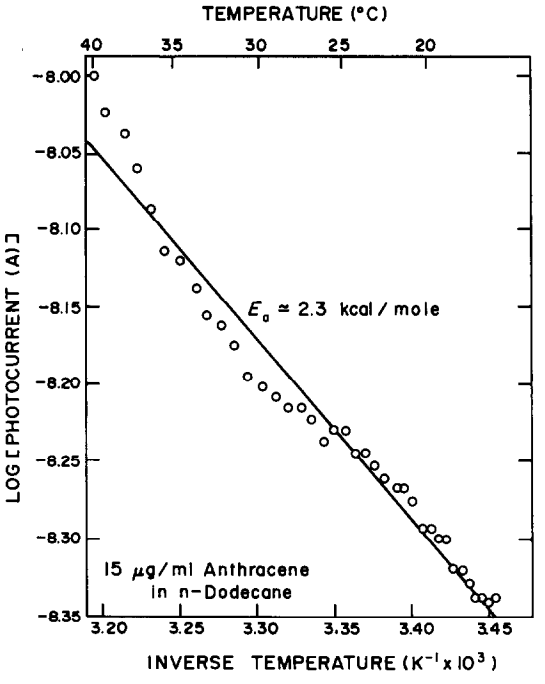

Fig. 8. Effect of temperature on the photoionization current, showing the expected Arrhenius relationship characteristic of the ionic conductance transport process. Laser pulse energy = 0.5 mJ.

of 30% w/w graphite-filled PTFE. The 6.35 mm diameter stainless-steel electrodes are only slightly less efficient and electrode composition seems to be relatively unimportant.

The one remaining factor of significance for the analytical use of two-photon photoionization is the determination of the effect of temperature on the PI current. As shown in Fig. 8, an increase in solution temperature causes an increase in photocurrent. Since the conduction of ionic charge-carriers is a transport process, it is expected that a corresponding activation energy will characterize the process. The activation energy may be obtained from an Arrhenius plot of the log of the photocurrent (which is proportional to the carrier mobility) *vs.* the reciprocal of the absolute temperature. For the results in Fig. 8, the slope of the least-squares line yields an activation energy of 2.3 kcal/mole. This agrees moderately well with the 3.2 kcal/mole obtained by Minday *et al.*[15] for ions in n-hexane.

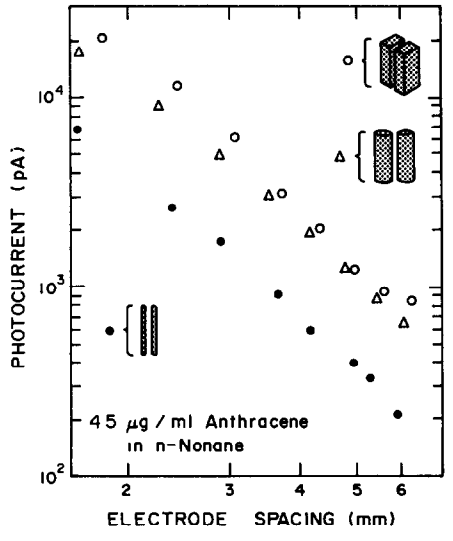

Fig. 7. Effect of electrode geometry and electrode composition on photoionization current. Laser pulse energy = 0.5 mJ.

CONCLUSIONS

The practicality and analytical utility of the three-mode cuvette system with pulsed laser excitation has been demonstrated and the effects on the two-photon photoionization current of bias voltage, analyte concentration, incident laser pulse energy, beam focus, electrode spacing, electrode geometry, and solution temperature have been evaluated. The cuvette system has been shown to possess two distinct zero-baseline operation modes for sensitively detecting non-luminescent as well as luminescent species. In addition, a sensitive and selective laser-excited fluorescence detection mode is simultaneously available. The cell may easily be optimized for PI detection and is already

near optimum for the FL and PA modes. Hence the amount of information available for analytical purposes is substantially increased and three-mode spectroscopy is easily possible. It is also possible, with appropriate signal acquisition systems, to obtain three-mode results with a single excitation laser pulse. The existence of a highly efficient two-photon photoionization pathway under the excitation and beam focusing conditions normally employed in pulsed photoacoustic detection also implies that PA "emission" is not complementary to fluorescence emission. Hence the PA effect cannot easily be used to aid in the determination of fluorescence quantum efficiencies because recombination of photogenerated ions and solvated electrons may disturb the excited singlet population by producing excited singlets.[16] This would alter the apparent fluorescence quantum efficiency.

Acknowledgement—This work was supported by U.S. Government Contracts NIH-GM-11373-19 and by DOE-DE-AS05-780R06022.

REFERENCES

1. E. Voigtman, A. Jurgensen and J. D. Winefordner, *Anal. Chem.*, 1981, **53**, 1442.
2. A. C. Tam and C. K. N. Patel. *Appl. Opt.*, 1979, **18**, 3348.
3. E. Voigtman, A. Jurgensen and J. D. Winefordner, *Analyst*, 1982, **107**, 408.
4. T. D. Harris, *Anal. Chem.*, 1982, **54**, 741A.
5. M. J. Adams, J. G. Highfield and G. F. Kirkbright, *ibid.*, 1977, **49**, 1850.
6. Y. Sugitani and K. Kato, *Bull. Chem. Soc. Japan*, 1979, **52**, 3499.
7. D. M. Hercules, R. J. Day, K. Balasanmugam, T. A. Dang and C. P. Li, *Anal. Chem.*, 1982, **54**, 208A.
8. D. C. Locke, B. S. Dhingra and A. D. Baker, *ibid.*, 1982, **54**, 447.
9. E. Voigtman, A. Jurgensen and J. D. Winefordner, *ibid.*, 1981, **53**, 1921.
10. E. Voigtman and J. D. Winefordner, *ibid.*, 1982, **54**, 1834.
11. *Idem, J. Liq. Chromatog.*, 1982, **5**(11), 2113.
12. C. D. Fulton, *Refrigerating Engineering*, 1950, **58**, 473.
13. S. Speiser and J. Jortner, *Chem. Phys. Lett.* 1976, **44**, 339.
14. S. M. Sze, *Physics of Semiconductor Devices*, p. 656. Wiley–Interscience, New York, 1969.
15. R. M. Minday, L. D. Schmidt and H. T. Davis, *J. Chem. Phys.*, 1971, **54**, 3112.
16. P. L. Piciulo and J. K. Thomas, *ibid.*, 1978, **68**, 3260.

Talanta, Vol. 30, No. 2, pp. 81–87, 1983
Printed in Great Britain.

0039-9140/83/020081-07$03.00/0

IONIC STRENGTH DEPENDENCE OF FORMATION CONSTANTS—I

PROTONATION CONSTANTS OF ORGANIC AND INORGANIC ACIDS

PIER G. DANIELE
Istituto di Analisi Chimica Strumentale dell'Università, via Bidone 36, 10125 Torino, Italy

CARMELO RIGANO
Seminario Matematico dell'Università, viale A. Doria 6, 95125 Catania, Italy

and

SILVIO SAMMARTANO
Istituto di Chimica Analitica dell'Università, via dei Verdi, 98100 Messina, Italy

(*Received* 1 *September* 1981. *Revised* 5 *May* 1982. *Accepted* 15 *September* 1982)

Summary—The protonation constants of formic, acetic, benzoic, oxalic, phthalic, maleic, malonic, succinic, DL-malic, DL-tartaric, aminoacetic, citric, nitrilotriacetic, ethylenediaminetetra-acetic, sulphuric and orthophosphoric acids have been determined from pH measurements, in tetraethylammonium iodide solution, at various ionic strengths in the range 0.01–1.0*M* (for phosphoric and sulphuric acids 0.01–0.5*M*). For each acid the dependence of the protonation constants on ionic strength was determined and an equation, valid for all the acids studied, to describe this was derived. The use of tetraethylammonium salts as background to avoid ion-pair formation is discussed.

The protonation constants of formic, acetic, benzoic, phthalic, maleic, oxalic, malonic, succinic, DL-malic, DL-tartaric, aminoacetic (glycine), citric, nitrilotriacetic (NTA), ethylenediaminetetra-acetic (EDTA), sulphuric and orthophosphoric acids have been widely studied at various temperatures and ionic strengths.[1–8] However, in only a few cases has the dependence of the protonation constants on ionic strength been systematically investigated. Furthermore, since carboxylic acids and some inorganic acids (such as sulphuric or phosphoric) can form complexes with alkali-metal ions, the literature values for the protonation constants obtained in potassium nitrate, potassium chloride, sodium nitrate, sodium chloride or sodium perchlorate media may be too low, because of reaction of the anions with Na^+ or K^+. Therefore we decided to re-investigate the protonation constants of these acids, at various ionic strengths and at 37°; tetraethylammonium iodide was used as background salt, since complex formation between the tetraethylammonium cation and the anions studied here may be considered negligible.

EXPERIMENTAL

Apparatus and procedure

Hydrogen-ion concentrations were measured potentiometrically with a Metrohm E 600 potentiometer, equipped with Metrohm glass and silver–silver chloride electrodes. The glass electrode was calibrated in the acid and in alkaline regions by titration of nitric acid (3–8m*M*) with standard 1*M* carbonate-free potassium hydroxide. The concentration of tetraethylammonium iodide was kept the same in all the test and calibration solutions. The E^0 and pK_w values were calculated as reported elsewhere.[9] The acid solutions (25–30 ml, 2–8m*M*) were titrated with the carbonate-free 1*M* potassium hydroxide delivered from a microsyringe (5000 divisions/ml). Other experimental details have been given before.[10,11] All the acids (Merck, *p.a.*) and the tetraethylammonium iodide (Fluka, *purissimum*) were used without further purification. The purity of the acids, checked by alkalimetric titrations, was always >99% and was taken into account in the calculations.

Calculations

The potentiometric data were analysed by computer. The program MINIQUAD 76A[12] refines the values of formation constants by minimizing the error-squares sum for the analytical concentrations. We modified this program in order to refine simultaneously the formation constants and the parameters which define the dependence on ionic strength (the linear parameters in a Debye–Hückel type equation). The program ACBA[13] refines the values of the protonation constants along with other parameters (namely analytical concentrations, E^0, *etc.*) of an alkalimetric titration, by minimizing the error-squares sum for the volume of titrant added. A modification to this program was made in order to obtain simultaneously the protonation constants and the parameters for the dependence on ionic strength.[14] The program REGRE[14] calculates the parameters of linear functions (see below).

The protonation constants are expressed as

$$K_j^H = [H_jL]/[H][H_{j-1}L]$$

and the stability constants of the potassium complexes are defined as

$$K_i = [KH_{i-1}L]/[K][H_{i-1}L]$$

(changes are omitted for simplicity).

Table 1. Protonation constants at 37°C*

Acid	C†	j	I 0.01	0.02	0.03	0.04	0.06	0.08	0.10	0.16	0.30	0.32	0.56	0.84	0.96	1.00
Formic	5–8	1	3.65(1)§		3.62(2)§				3.58(1)§		3.56(1)§					3.65(2)§
			3.66													
Acetic	5–8	1	4.68(1)		4.64(1)				4.61(1)		4.61(1)					4.76(1)
			4.69													
Benzoic	5–8	1	4.09(1)		4.05(1)				4.01(1)		4.01(1)					4.16(1)
			4.10													
Oxalic	4–5	1	4.141(6)	4.09(1)§	4.070(6)	4.06(1)§		4.025(7)§	3.99(1)		3.978(6)		4.08(1)§		4.18(1)§	
			4.195	4.13	4.095	4.08		4.04	4.00		3.985					
Phthalic	4–5	1	5.17(1)	5.15(2)		5.14(2)		5.12(2)		5.08(2)§		5.14(1)§	5.29(1)	5.46(2)§		
			5.22	5.18		5.16		5.13		5.09		5.15				
		2	2.86(1)	2.85(2)		2.84(2)		2.83(1)		2.80(1)		2.82(2)	2.94(1)	3.04(2)		
			2.87													
Maleic	3–5	1	6.13(1)	6.11(1)		6.06(1)		6.05(1)		6.01(1)		6.06(1)	6.22(1)		6.43(1)	
			6.17	6.13		6.07										
		2	1.92(3)	1.88(4)		1.855(15)		1.82(2)		1.79(2)		1.77(3)	1.87(2)		1.96(2)	
Malonic	3–5	1	5.54(1)	5.51(1)		5.47(2)		5.445(7)		5.39(1)		5.40(1)	5.50(1)		5.64(1)	
			5.59	5.54		5.49		5.46		5.40						
		2	2.82(2)	2.80(2)		2.77(2)		2.75(1)		2.68(1)		2.70(2)	2.77(2)		2.82(2)	
			2.83													
Succinic	4–5	1	5.45(1)	5.41(1)		5.39(1)		5.34(1)		5.27(1)		5.27(1)	5.30(1)		5.39(2)	
			5.50	5.44		5.40		5.35								
		2	4.11(1)	4.10(2)		4.08(1)		4.05(1)		4.01(1)		4.04(1)	4.14(1)		4.25(1)	
			4.12													
Malic	5–6	1	4.92(1)		4.85(2)				4.77(1)		4.75(1)					4.91(1)
			4.96		4.87				4.78							
		2	3.34(1)		3.31(1)				3.27(1)		3.29(1)					3.45(2)
			3.36		3.32											
Tartaric	3–4	1	4.13(1)		4.10(1)				3.99(1)		3.98(1)					4.12(2)
			4.18		4.11				4.00							
		2	2.895(7)		2.87(1)				2.84(1)		2.86(1)					3.03(2)
			2.91		2.88											

Glycine	5–7	1	9.33(1)		9.128(8)			9.28(1)	9.28(1)			9.32(1)
			9.35		9.135							
		2	2.30(2)		2.30(2)			2.31(2)	2.35(2)			2.47(2)
Citric	2 5–4	1	6.04(1)		5.98(1)			5.86(2)	5.82(2)			6.07(1)
			6.12		6.02			5.89	5.83			6.08
		2	4.569(10)		4.50(1)			4.40(2)	4.37(2)			4.505(8)
			4.595		4.51			4.41				
		3	2.99(2)		2.97(2)			2.92(2)	2.915(2)			3.065(15)
			3.00									
NTA	2–4	1			9.83(3)			9.72(3)	9.64(4)	9.58(3)		9.70(3)
					9.87			9.74	9.65			
		2			2.69(4)			2.60(5)	2.51(4)	2.57(4)		2.64(3)
					2.70							
		3			1.87(4)			1.71(5)	1.80(4)	1.85(5)		1.95(5)
EDTA	2–4	1			10.315(15)		10.22(3)	10.14(4)	10.07(3)	10.03(4)		10.10(4)
					10.41		10.28	10.20	10.09	10.04		10.11
		2			6.12(2)		6.08(2)	5.98(4)	5.94(4)	5.98(3)		6.04(2)
					6.16		6.11	6.00	5.95			
H_3PO_4	1.5–3	1		11.64(6)				11.49(5)	11.54(5)	11.74(4)		
				11.69				11.52	11.56	11.76		
		2		6.92(2)				6.855(15)	6.85(2)	6.94(2)		
				6.95				6.865	6.86			
		3		2.09(5)				2.06(4)	1.99(4)	1.95(4)		
				2.10								
H_2SO_4	4–8	1	1.90(2)			1.83(2)		1.78(1)	1.805(8)	1.93(1)		
			1.95			1.85		1.80	1.82	1.94		
OH^-	4–6	1	13.49(2)		13.46(2)			13.45(2)	13.47(2)	13.56(3)		13.70(2)
			13.50									

*First row: protonation constants not corrected for K^+ complex formation and I variation; second row: values corrected. Corrections <0.005 log units were not considered.

†Concentration (mM) of the acid in the titrations.

§The numbers in parentheses correspond to 3 times the standard deviation and have the same decimal places as the last significant figure(s).

RESULTS

The protonation constants, evaluated first without allowing for possible interactions between the anions of the acids and potassium ions from the titrant, and without taking into account the variation of ionic strength during the titrations were corrected as follows.

Potassium complex formation. In our previous work[7,8,15] and in the literature,[1,6,16] complex formation between alkali-metal ions and the ligands studied here was noted. If the formation constants K_i for the species $KH_{i-1}L$ are known, the protonation constants can be corrected by using the equation (see Appendix)

$$K_j^H = K_{j(app)}^H(1 + K_i[K]) \quad (i = j) \qquad (1)$$

where $K_{j(app)}^H$ is the constant calculated without allowing for potassium complexes.

Variation of ionic strength during the titrations. From the literature data[1,6] for zero ionic strength and from $K_{j(app)}^H$, approximate values of C_j can be estimated for the semi-empirical equation

$$\log K_j^H = \log {}^TK_j^H - G(I) + C_jI \qquad (2)$$

where

$$G(I) = z_j^* A\sqrt{I}/(1 + B_j\sqrt{I})$$

and $\log {}^TK_j^H$ is the protonation constant at infinite dilution; A is the parameter of the Debye–Hückel equation ($A = 0.523$ at 37°); $z_j^* = 2(1 - z - j)$ (z is the charge on the anion); C_j is an empirical parameter; B_j is set[7,8] equal to 1.5 (a small error in fixing B_j is absorbed in the linear term C_jI). If an approximate value of C_j is known†, the protonation constants can be corrected for the variation of ionic strength from I^* to I, by the equation

$$\log K_j^H(I) = \log K_j^H(I^*) - G(I,I^*) = C_j(I - I^*) \quad (3)$$

where

$$G(I, I^*) = z_j^* A\left[\frac{\sqrt{I}}{1 + 1.5\sqrt{I}} - \frac{\sqrt{I^*}}{1 + 1.5\sqrt{I^*}}\right]$$

where $I = [Et_4N]$ and I^* is the real ionic strength of the solution.

The values of $\log K_j^H(I)$ are reported in Table 1; when the corrections [equations (1) and (3)] are significant (>0.005 log units) the experimental values of $\log K_j^H$ are also reported.

The dependence of the protonation constants on ionic strength was then studied. A preliminary analysis of the data showed that if a fixed value is assigned to B_j, the fit with equation (2) is not always good over the whole range of ionic strength from 0.01 to 1*M*. This equation may be useful for small ranges of ionic strength but a better fit to the equation $\log K_j^H = f(I)$ is obtained by adding a further term of the form $D_jI^{3/2}$ (D_j is an adjustable parameter), as proposed by Datta and Grzybowski.[17]

Instead of taking $I = 0$ as reference [equation (2)], as has been common in the past, we chose a value, I', in the range experimentally studied.[7,8,18] The reasons for this are (*i*) the refinement of the experimental data, both with MINIQUAD 76A and ACBA, is sometimes divergent if $I' = 0$, but is always convergent when $I' = 0.1$–0.25; (*ii*) the error in $\log K_j^H$ values is always lower in the range experimentally studied, so it seems inappropriate to take an extrapolated value as reference; (*iii*) the value of $\log K_j^H$ is nearly always at its minimum at an ionic strength in the range 0.1–0.3*M* and is a "characteristic" of the curve $\log K_j^H = f(I)$. Therefore the data were fitted to the equation

$$\log K_j^H(I) = \log K_j^H(I') - G(I,I') + C_j(I - I') + D_j(I^{3/2} - I'^{3/2}) \quad (4)$$

where

$$G(I, I') = z_j^* A\left[\frac{\sqrt{I}}{1 + 1.5\sqrt{I}} - \frac{\sqrt{I'}}{1 + 1.5\sqrt{I'}}\right].$$

The values obtained for $\log K_j^H(I')$, C_j and D_j, collected in Table 2, were calculated by three different methods: the modified programs MINIQUAD 76 A and ACBA, that analyse primary potentiometric data, and REGRE, that calculates the linear parameters of the function

$$Y = \log K_j^H(I) + G(I,I') = \log K_j^H(I') + C_j(I - I') + D_j(I^{3/2} - I'^{3/2}) \quad (5)$$

where the $\log K_j^H(I)$ values are those shown in Table 1. It is noticeable that the introduction of the term $D_j(I^{3/2} - I'^{3/2})$ very often improves the fit of the data. For example, for the first protonation constant of EDTA, from equation (5) we obtain two sets of values depending on whether or not we take into account the term in D_j:

$C_1 = 1.63$, $D_1 = -0.8$, $r = 0.9993$, $\sigma(Y) = 0.025$ (with D_j)

$C_1 = 0.81$, $D_1 = 0$, $r = 0.9829$, $\sigma(Y) = 0.065$.

The correlation coefficients (r) and standard deviations [$\sigma(Y)$] show that there is a significant improvement in the fit when the D_j term is introduced. Equations similar to (2) and (4) can be used for $\log \beta_j^H$ as well, bearing in mind that

$$\log \beta_j^H = \sum_{i=1}^{j} \log K_i^H$$

(in this case $z_j^* = 1 - j - 2z$).

As can be seen from Table 2, the parameters which characterize the dependence of protonation constants on ionic strength show a regular trend and seem to be a function, as a first approximation, of only the z_j^*

†Under our conditions, a 10% error in C_j causes an error of 0.004 log units in the protonation constant.

Table 2. $\log\beta_j^H$, C_j and D_j values at 37°C; $I' = 0.1$; ACBA or REGRE calculations; $I' = 0.15$, MINIQUAD calculations

Acid	I'	$\log\beta_1^H$	C_1	$-D_1$	$\log\beta_2^H$	C_2	$-D_2$	$\log\beta_3^H$	C_3	$-D_3$
Formic	0.15	3.57(1)*	0.64	0.32						
	0.1	3.574(6)	0.76	0.44						
Acetic	0.15	4.60(1)	0.68	0.27						
	0.1	4.608(6)	0.77	0.34						
Benzoic	0.15	4.01(1)	0.64	0.22						
	0.1	4 015(9)	0.68	0.25						
Oxalic	0.15	3.99(1)	1.12	0.43						
	0.1	3.998(4)	1.07	0.38						
Phthalic	0.15	5.09(1)	1.35	0.37	7.89(3)*	2.01	0.47			
	0.1	5.101(9)	1.35	0 38	7.90(1)	1.93	0.38			
Maleic	0.15	6.02(2)	1.35	0.39	7.82(4)	1.75	0.40			
	0.1	6.022(7)	1.44	0.48	7 84(3)	1.84	0.48			
Malonic	0.15	5.39(1)	1.02	0.30	8.11(2)	1.49	0.45			
	0.1	5.429(12)	1.01	0.30	8.14(2)	1.33	0.30			
Succinic	0.15	5.29(2)	0.92	0.35	9.32(3)	1.56	0.50			
	0.1	5.317(10)	0.91	0.35	9.36(1)	1.39	0.35			
Malic	0.15	4.76(1)	1.06	0.44						
	0.1	4.788(7)	1.10	0.49	8.049(9)	1.53	0.49			
Tartaric	0.15	3.99(1)	1.05	0.46	6.83(3)	1.87	0.82			
	0.1	4.019(5)	1.11	0.52	6.859(6)	2.10	1.04			
Glycine	0.15	9.27(1)	0 70	0.40	11.59(5)	0.88	0.40			
	0.1	9.277(6)	0.89	0.60	11.56(3)	1.67	1.00			
Citric	0.15	5.83(2)	1.40	0.52	10.20(3)	2.35	0.90	13.08(5)*	2.95	1.10
	0.1	5.912(7)	1.63	0.74	10.324(9)	2.58	1.12	13.24(3)	3.18	1.32
NTA	0.15	9.69(4)	1.15	0.53	12.26(5)	1.94	0.83	14.11(9)	2.29	0.98
	0.1	9.73(5)	1.23	0.60						
EDTA	0.15	10.14(4)	1.52	0.70	16.13(5)	2.67	1.15			
	0.1	10.22(3)	1.62	0.80						
H_3PO_4	0.15	11.50(5)	1.85	0.45	18.34(5)	3.00	0.75	20.37(6)	3.05	0.75
	0.1	11.50(5)	1.20	0	18.34(5)	2.09	0	20.40(8)	2.30	0
H_2SO_4	0.15	1.79(1)	1.30	0.40						
	0.1	1.808(6)	1.21	0.31						
OH^-	0.15	13.42(2)	0.70	0.15						

*The numbers in parentheses correspond to 3 times the standard deviation and have the same decimal place(s) as the last significant figure(s).

value. We therefore studied the behaviour of C_j and D_j as a function of z_j^* in the equation

$$Y' = \log K_j^H(I) - \log K_j^H(I') + G(I,I')$$
$$= C_j(I - I') + D_j(I^{3/2} - I'^{3/2})$$
$$= f(I,z_j^*) \quad (6)$$

with all the protonation constants at the appropriate ionic strengths†. The following expressions were obtained for the linear parameters as a function of z_j^*:

$$C_j = 0.15p + 0.24z^* - 0.0033(z^*)^2$$
$$D_j = -0.11z^* \quad (7)$$

where $p = 1$ for $\log K_j^H$ and $p = j$ for $\log\beta_j^H$.

DISCUSSION

The mean deviation [$\epsilon(\log K_j^H)$] between the $\log K_j^H$ values in Table 1 and those calculated by equations (4) and (7) can be estimated by the equation

$$\epsilon(\log K_j^H) \leqslant 0.025z^* \mid I - 0.15 \mid \quad (8)$$

The error increases with increasing z^* value and with $\mid I - 0.15 \mid$. In any case, when $z^* \mid I - 0.15 \mid$ is $\leqslant 2$, the error is so low that equation (4), with the values of C_j and D_j calculated by equation (7), can be used to obtain $\log K_j^H$ values at different ionic strengths (in the range 0.01–1.0M), if a value determined experimentally in that range is available.

The species distribution can also be computed in order to estimate the error [$\epsilon(\%)$], in the calculated percentage of a species, resulting from an error in the $\log K_j^H$ value, by means of error propagation. These calculations were done by a modified version of the program DISDI.[14,24] As an example we considered a mixture of three hypothetical acids: monoprotic, with $\log K_1^H = 5.0$; diprotic, with $\log K_1^H = 5.5$ and $\log K_2^H = 2.5$; and triprotic, with $\log K_1^H = 6.0$, $\log K_2^H = 4.0$ and $\log K_3^H = 2.0$. From these calculations we found the empirical equation

$$\epsilon(\%) \leqslant 10^2\epsilon(\log K_j^H)(1 + \mid 50 - (\%) \mid /50) \quad (9)$$

where (%) is the percentage of the species of interest. From equations (8) and (9)

†In the calculations we also introduced some data for the protonation of adenosine-5′-triphosphate (ATP), $P_2O_7^{4-}$ and $P_3O_{10}^{5-}$, taken from the literature.[19–23]

$$\epsilon(\%) \leqslant 2.5z^* \mid I - I' \mid (1 - \mid 50 - (\%) \mid /50). \quad (10)$$

For example, for a diprotic acid, $\epsilon(\%)$ of HL^- is $\leqslant 2.6\%$, when $(\%) = 20$, $I = 0.7$ and $I' = 0.15$. Considering that $I \gg I'$, this error is, for many purposes, satisfactorily low.

As previously suggested,[18] the elimination of the influence of the formation of ion-pairs between the ligands and the cation(s) of the background makes it possible to formulate a general equation which correlates the protonation constant values with ionic strength, even if $I > 0.1M$, the limiting value indicated by Davies[25] for the validity of his equation for the evaluation of activity coefficients. The Davies equation, written with our symbols and referred to formation constants, becomes (with $B_j = 1$):

$$\log K_j^H(I) = \log K_j^H(I') - G(I,I') + 0.3z^*A(I - I'). \quad (11)$$

The mean error in $\log K_j^H$ for this case can be estimated, from our data (for I in the range 0.01–0.1M), by the equation

$$\log K_j^H \leqslant 0.2z^*(0.1 - I). \quad (12)$$

The mean error arising from the use of equations (4) and (7) is significantly lower than that from equations (8) and (12). Moreover, it is interesting that in the expression for C_j [equation (7)] there is a term which does not depend on z^*, and therefore the protonation constants of cationic acids, such as HL^+, for which $z^* = 0$, should be dependent on ionic strength, whereas according to equation (11) the protonation constants for $z^* = 0$ are not dependent on ionic strength. In this connection it may be remarked that the second protonation constant of amino-acids increases with increasing I.

The results reported here suggest that the ligands studied indeed do not interact significantly with the tetraethylammonium cation. The use of tetraethylammonium salts (tetramethylammonium ions can still form weak complexes,[23] and tetrabutylammonium salts are not sufficiently soluble) in order to avoid ion-pair formation seems advantageous. Also, it seems reasonable to explain the differences in the protonation constant values determined in various media (at the same ionic strength) in terms of alkali-metal complex formation (for $I < 1M$), since the results obtained by solubility measurements for the sodium–oxalate complex[26] and by ion-selective electrodes for alkali metal–citrate complexes are in good agreement with ours.[7,8,18]

Further studies in progress will check these results carefully. Extension of this investigation to the stability constants of binary and ternary metal complexes seems very important.

APPENDIX

The mass balance equations (for a monoprotic acid) can be written

$$[L]_T = [L] + K^H[L][H] + K[L][K] \quad (A1)$$

$$[H]_T = [H] + K^H[L][H] - K_w/[H] \quad (A2)$$

if potassium complexes are taken into account, or

$$[L]_T = [L]_{(app)} + K^H_{(app)}[L]_{(app)}[H] \quad (A3)$$

$$[H]_T = [H] + K^H_{(app)}[L]_{(app)}[H] - K_w/[H] \quad (A4)$$

if potassium complexes are neglected. By equating (A1) and (A3) and substituting for $[L]$ and $[L]_{(app)}$ from (A2) and (A4), we obtain

$$\frac{1}{K^H_{(app)}[H]} = \frac{1}{K^H[H]} + \frac{K[K]}{K^H[H]}$$

or

$$\log K^H = \log K^H_{(app)} + \log(1 + K[K]) \quad (A5)$$

If it is assumed that a polyprotic acid behaves as a mixture of monoprotic acids, equation (A5) becomes

$$\log K_j^H = \log K^H_{j(app)} + \log(1 + K_i[K]), (i = j). \quad (1)$$

This assumption, valid for calculation of K_j^H if $K_j^H/K_{j+1}^H > 10^3$, is also quite reasonable when the ratio of successive constants is greater than 10.

The potassium complexes are generally very weak and in equation (1) the free concentration $[K]$ can usually be set equal to the analytical concentration; otherwise the value of $[K]$ can be obtained iteratively.

REFERENCES

1. L. G. Sillén and A. E. Martell, *Stability Constants*, Chem. Soc. Spec. Publ., London, No. 17, 1964; No. 25, 1971.
2. D. D. Perrin, *Stability Constants, Organic Ligands*. Pergamon Press, Oxford, 1979.
3. E. Ogfeldt, *Stability Constants, Inorganic Ligands*. Pergamon Press, Oxford, 1982.
4. J. J. Christensen, L. D. Hansen and R. M. Izatt, *Handbook of Proton Ionization Heats and Related Thermodynamic Quantities*. Wiley, New York, 1976.
5. E. P. Serjeant and B. Dempsey, *Ionization Constants of Organic Acids in Aqueous Solution*. Pergamon Press, Oxford, 1979.
6. A. E. Martell and R. M. Smith, *Critical Stability Constants*, Vols. 1, 3, 4. Plenum Press, New York, 1974–1977.
7. P. G. Daniele, C. Rigano and S. Sammartano, *Ann. Chim. (Rome)*, 1980, **70**, 119.
8. *Idem, Thermochim. Acta*, 1981, **46**, 103.
9. P. Amico, P. G. Daniele, V. Cucinotta, E. Rizzarelli and S. Sammartano, *Inorg. Chim. Acta*, 1979, **36**, 1.
10. G. Ostacoli, P. G. Daniele and A. Vanni, *Ann. Chim. (Rome)*, 1973, **63**, 815.
11. G. Arena, R. Calì, M. Grasso, S. Musumeci, S. Sammartano and C. Rigano, *Thermochim. Acta*, 1980, **36**, 329.
12. A. Sabatini, A. Vacca and P. Gans, *Talanta*, 1974, **21**, 53; P. Gans, A. Sabatini and A. Vacca, *Inorg. Chim. Acta*, 1976, **18**, 237; A. Vacca, personal communication.
13. G. Arena, E. Rizzarelli, S. Sammartano and C. Rigano, *Talanta*, 1979, **26**, 1.
14. C. Rigano and S. Sammartano, work in progress.
15. P. G. Daniele, C. Rigano and S. Sammartano, work in progress.
16. D. Midgley, *Chem. Soc. Rev.*, 1975, **4**, 549, and references therein.
17. S. P. Datta and A. K. Grzybowski, *Trans. Faraday Soc.*, 1958, **54**, 1179.
18. V. Cucinotta, P. G. Daniele, C. Rigano and S. Sammartano, *Inorg. Chim. Acta*, 1981, **56**, L45.

19. R. C. Phillips, P. Eisenberg, P. George and R. J. Rutman, *J. Biol. Chem.*, 1965, **240,** 4393.
20. R. C. Phillips, P. George and R. J. Rutman, *J. Am. Chem. Soc.*, 1966, **88,** 2631.
21. R. P. Mitra, H. C. Malhotra and D. V. S. Jain, *Trans. Faraday Soc.*, 1966, **62,** 167.
22. R. R. Irani, *J. Phys. Chem.*, 1961, **65,** 1463.
23. R. M. Smith and R. A. Alberty, *ibid.*, 1956, **60,** 180.
24. R. Maggiore, S. Musumeci and S. Sammartano, *Talanta*, 1976, **23,** 43.
25. C. W. Davies, *Ion Association*, Chapter 3. Butterworths, London, 1962.
26. B. Finlayson, R. Roth and L. Dubois, *Intern. Symp. Renal Stone Res., Madrid*, 1972, pp. 1–7.
27. G. A. Rechnitz and S. B. Zamochnick, *Talanta*, 1964, **11,** 1061.

Talanta, Vol. 30, No 2, pp 89–93, 1983
Printed in Great Britain.

0039-9140/83/020089-05$03.00/0

DETERMINATION OF ARSENITE, ARSENATE AND MONOMETHYLARSONIC ACID IN AQUEOUS SAMPLES BY GAS CHROMATOGRAPHY OF THEIR 2,3-DIMERCAPTOPROPANOL (BAL) COMPLEXES

SYOZO FUKUI, TERUHISA HIRAYAMA, MOTOSHI NOHARA and YOSHIHIKO SAKAGAMI
Kyoto College of Pharmacy, Yamashinaku, Kyoto, 607 Japan

(*Received* 19 *June* 1981. *Revised* 22 *July* 1982. *Accepted* 9 *September* 1982)

Summary—Procedures are described for the determination of arsenite, arsenate and monomethylarsonic acid in aqueous samples. The arsenicals (after reduction of arsenic to the tervalent state) readily react with 2,3-dimercaptopropanol (BAL) to yield their BAL complexes. The products are extracted with benzene and introduced into a gas chromatograph equipped with a flame-photometric detector for sulphur. One aliquot of sample is treated with stannous chloride solution and potassium iodide solution to reduce arsenate and monomethylarsonic acid, then BAL is added and the complexes are extracted with benzene. The extract is analysed for total inorganic As plus monomethylarsonic acid. Magnesia mixture and phosphate solution are added to another aliquot to remove arsenate by co-precipitation with magnesium ammonium phosphate. The precipitate is filtered off and arsenite determined in the filtrate. The detection limits are 0.02 ng of As for arsenate and arsenite and 0.04 ng of As for monomethylarsonic acid.

Recently, in the environmental chemistry and biochemistry of arsenicals, greater emphasis has been placed on assessing arsenic in its various forms, especially as arsenate [As(V)], arsenite [As(III)], monomethylarsonic acid (MMAA) and dimethylarsinic acid (DMAA).[1–4] The methods currently most widely used for the purpose are based on the sequential volatilization technique described by Braman *et al.*,[5] where the arsenicals are volatilized as arsines. Several gas chromatographic methods based on the conversion of the arsenicals into volatile compounds have also been reported. Talmi and Norvell[6] have reported a method for inorganic As based on gas chromatographic separation of its triphenyl derivative. Butts and Rainey[7] chromatographed As(III) and As(V) as trimethylsilylates. Gudzinowicz and Martin[8] investigated the gas chromatographic behaviour of bromides of inorganic As and some organic arsenicals. Daughtrey *et al.*[9] reported a gas chromatographic method for total inorganic As, MMAA and DMAA after preparation of their diethyldithiocarbamates.

The present research sought a rapid, simple and quantitative method by which As(III), As(V) and MMAA in aqueous sample could be determined with specificity. The flame-photometric detector for sulphur would provide such a method if the arsenicals could be converted quantitatively into volatile stable sulphur-containing compounds. We found that 2,3-dimercaptopropanol (BAL) reacts readily with the arsenic(III) compounds to give products having such properties.

In a previous paper,[10] we reported a gas chromatographic method for the determination of DMAA. That method can be combined with the one presented here, to give selective determination of As(III), As(V), MMAA and DMAA.

EXPERIMENTAL

Apparatus

A Shimadzu Model GC-4CM gas chromatograph equipped with a Shimadzu Model FPD-1A flame-photometric detector for sulphur was used. The separation was performed on a 3-mm bore 2-m long glass column packed with 20% SE-30 on 80/100 mesh Chromosorb AWA DMCS. The transmission of the optical filter attached to the detector was maximal at 384 nm. The nitrogen carrier-gas flow-rate was 60 ml/min. The hydrogen and air pressures were 0.5 and 0.6 kg/cm^2, respectively. A Hitachi Model M-80 gas chromatograph mass spectrometer was used to confirm that the BAL–arsenical complexes were formed.

Reagents

As(III) and As(V) standards were prepared from As_2O_3 and NaH_2AsO_4 (Merck). MMAA was obtained from the Ventron Co. Stock solutions containing 100 μg of arsenic per ml were prepared for each of the acids, and diluted daily before use.

Reagent grade BAL (Wako Pure Chemical Ind., Ltd.) was distilled under reduced pressure, and a 0.2% aqueous solution prepared daily before use. Stannous chloride solution was prepared by dissolving 5 g of $SnCl_2.2H_2O$ in 100 ml of concentrated hydrochloric acid. Magnesia mixture was prepared by dissolving 55 g of $MgCl_2.6H_2O$ in 500 ml of water, adding 140 g of ammonium chloride and 130 ml of concentrated ammonia solution, and diluting with water to 1 litre. The phosphate solution was prepared by dissolving 0.158 g of K_2HPO_4 in 100 ml of water. Pesticide-grade benzene was used as the extraction solvent.

Procedure

Calibration graph. Take 0.5, 0.75, 1.0 and 1.5 ml of the 1-μg/ml As working standards for As(V) and MMAA, in eight graduated and glass-stoppered centrifuge tubes (one standard in each). Dilute each solution to 10 ml with water. The arsenic concentrations of these standard series are 0.05, 0.075, 0.10 and 0.15 μg/ml.

To each tube add 2 ml of the stannous chloride solution and 1 ml of 20% potassium iodide solution and let stand for 30 min. Add 1 ml of the BAL solution and dilute to 20 ml with water. Let stand for 60 min, add 5 ml of benzene, stopper and shake thoroughly. Centrifuge for 10 min at 3000 rpm. Withdraw 5 μl of the benzene layer and introduce it into the gas chromatograph by microsyringe.

Plot the peak height, H mm, against the arsenic concentration (μg/ml) on log–log paper, and calculate the slope n, of the log–log plots from $H = kC^n$.

Determination of total inorganic As and MMAA. Take 10 ml of sample in a graduated glass-stoppered centrifuge tube. Add the stannous chloride and potassium iodide solutions and proceed as described above. Measure the peak heights for inorganic As and MMAA. Calculate each $H^{1/n}$ and determine their arsenic concentrations in the sample with the aid of the calibration graphs.

Determination of As(III). Take 10 ml of the sample in a flask, add 1 ml of the magnesia mixture and 1 ml of the phosphate solution and let stand for 10 min. Filter the solution through a porosity-3 sintered-glass filter into a graduated glass-stoppered centrifuge tube. Wash the filter and residue with up to 4 ml of water, collecting the washings in the centrifuge tube. Proceed with the reduction *etc.* as before.

Determination of DMAA. Take 5 ml of sample in a glass-stoppered test-tube. Proceed as described in the previous report.[10]

RESULTS AND DISCUSSION

As(III), As(V) and MMAA react with BAL in the presence of hydrochloric acid and reducing agents to give benzene-extractable volatile complexes. The complexes chromatographed are detected by the flame-photometric detector for sulphur with high selectivity and sensitivity.

To determine the nature of the species eluted from the gas chromatograph, a gas chromatograph–mass spectrometer was employed. The fragmentation pattern of the BAL–monomethylarsonate complex was m/z = 212 ($C_4H_9OS_2As^+$), 197 ($C_3H_6OS_2As^+$), 166 ($C_2H_3S_2As^+$) and 107 (AsS^+), indicating the structure is 2-methyl-4-hydroxymethyl-1,3-dithia-2-arsacyclopentane as described by Stocken and Thompson.[11] The fragmentation pattern of the BAL–As(III) complex was m/z = 214, 212, 196, 166 and 107, from which it may be seen that the structure is 2-hydroxy-4-hydroxymethyl-1,3-dithia-2-arsacyclopentane.

The reaction sequence proposed is shown in Fig. 1. Dimethylarsinic acid is unable to form such a 5-membered ring by reaction with BAL, which may be why DMAA is not determined by the procedures.

Various parameters which might affect the complexation and reduction were examined. Maximum peak height was obtained by addition of at least 1 ml of concentrated hydrochloric acid and 1 ml of at least

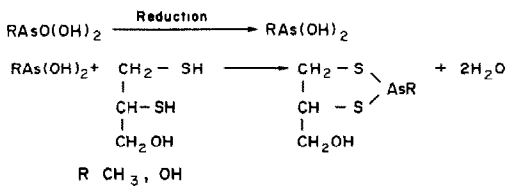

Fig. 1. BAL complexes of the arsenicals.

0.2% BAL solution to 10 ml of the As(III) standard, so 2 ml of concentrated hydrochloric acid and 1 ml of 0.2% BAL solution were chosen as sufficient quantities for the complexation. A standing time of at least 30 min after the addition of BAL was needed to complete the complexation; heating the reaction mixture did not shorten the standing time necessary.

When kept at ordinary temperature under room lighting, the solutions of the BAL–arsenical complexes gave constant peak heights on chromatography, over a period of at least 48 hr.

Arsenic(V) was completely reduced by addition of 2 ml of at least 1% stannous chloride solution to 10 ml of the standards, but MMAA required not only the addition of more concentrated stannous chloride solution but also the addition of potassium iodide for its complete reduction. The conditions described in the procedure give full reduction of both As(V) and MMAA. The addition of the stannous chloride solution also eliminates extraneous peaks resulting from excess of BAL, as shown in Fig. 2. This effect seems to depend on formation of a benzene-insoluble tin salt of BAL rather than on reduction, since a similar effect is given by addition of stannic chloride.

Typical gas chromatograms obtained by the present method are shown in Fig. 3. Peaks other than those due to the arsenicals scarcely appear in the chromatograms.

There is little difference in efficiency of separation of the BAL–arsenical complexes when non-polar silicone gums, *e.g.*, SE-30, OV-1, OV-17 and OV-101, are used as the stationary phase. We chose SE-30 because it gave the sharpest peak.

Butyl acetate, methyl isobutyl ketone, toluene, n-hexane and cyclohexane were also examined as the extraction solvents. Butyl acetate and methyl isobutyl ketone gave a large extraneous peak. Toluene, n-hexane and cyclohexane gave inferior extraction of the complexes. Benzene extracts the complexes efficiently but gives low extraction of the excess of BAL and/or its tin salts.

Typical calibration data are shown in Table 1. The response of the flame-photometric detector characteristically increases exponentially with increase in concentration of sulphur compounds. The H *vs.* C calibration graph therefore becomes linear on a log–log plot, and a normal plot of $H^{1/n}$ *vs.* C is also linear. The latter may be preferred for accurate analysis and estimation of the blank value.

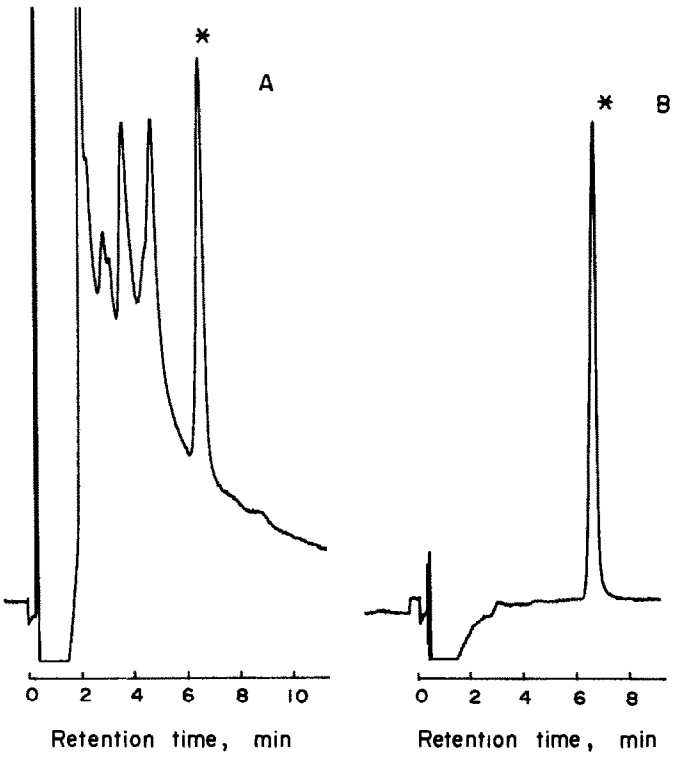

Fig. 2. Removal of extraneous peaks by the addition of stannous chloride solution. A: stannous chloride solution not added; B: added. * Peak for As(III).

As(III) was separated from As(V) by precipitation of ammonium magnesium arsenate in the presence of a large amount of ammonium magnesium phosphate as carrier, without loss of As(III), as shown in Table 2.

Table 3 shows the influence of foreign ions on the determination of inorganic arsenic. The determination can be done in the presence of considerable amounts of ferrous, zinc, calcium, magnesium, sulphate, sul-

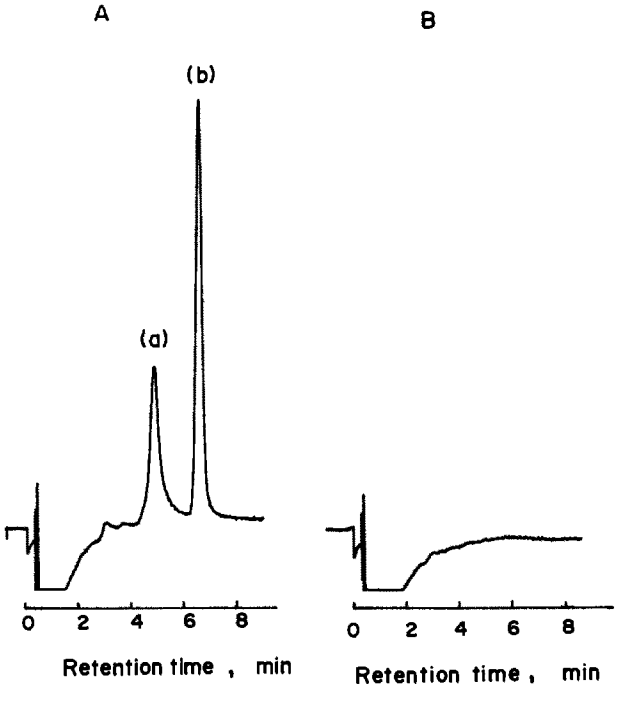

Fig. 3. Gas chromatograms of A: (a) monomethylarsonic acid, (b) inorganic As; B: blank.

Table 1. Calibration data*

Arsenical	Concentration, μg/ml (as As)	H,† mm	Range, mm	[H (mm)]$^{1/n}$	Range
Inorganic	0	0	—	0	—
As	0.050	20.0	18–21	6.7§	6.3–6.9
	0.075	35.3	34–37	9.7§	9.5–9.8
	0.100	64.6	63–67	14.2§	14.0–14.7
	0.150	119.7	118–121	21.1§	20.9–21.2
MMAA	0	0	—	0	—
	0.050	12.0	11–13	8.2‡	7.6–8.8
	0.075	17.5	17–18	11.3‡	11.0–11.6
	0.100	25.5	25–26	15.5‡	15.3–15.8
	0.150	40.0	39–41	22.7‡	22.3–23.2

*The detector conditions: sensitivity 10 MΩ; range 160 mV.
†Averages of 5 runs.
§n = 1.57.
‡n = 1.18.

Table 2. Removal of As(V) by the treatment with magnesia mixture

Species	Concentration, μg/ml	Peak height*, mm With treatment	Without treatment
As(V)	0.050	0	20.5 (19–21)
	0.075	0	36.0 (35.5–37)
	0.100	0	63.0 (62–65)
As(III)	0.050	19.5 (19–20)	20.0 (19.5–20.5)
	0.075	35.5 (34–37)	37.0 (36–38)
	0.100	62.0 (60–64)	63.0 (61–65)

*Average of 5 runs, range in parentheses.

phide and nitrate ions. Concentrations of ferric ion and cupric ion > 10 μg/ml cause a slight negative error.

The results for total inorganic arsenic obtained by the present method were compared with those obtained by the AOAC silver diethyldithiocarbamate method.[12] An aqueous extract of sea-weed (*Hijikia Fujiforme*) was used as the sample. The average and range obtained by the AOAC method were 0.144 ppm and 0.119–0.164 ppm, respectively, and those of the present method were 0.143 ppm and 0.130–0.160 ppm. Comparison of the results obtained for MMAA by the present method and by an independent method is difficult to make because of the lack of such a method.

The results of recovery tests for the four arsenicals added to urine are shown in Table 4. One of the major problems was the rapid oxidation of As(III) added to urine, but it was solved by heating the urine to about 60°, suggesting that the oxidation occurs enzymatically. The recovery tests were done on previously heated urine.

The present method, combined with the method previously reported,[10] was successfully applied to clarify the nature of the chemical forms of arsenicals excreted in the urine after eating *Hijiki*, which is a sea-weed containing arsenic naturally. A large portion of the arsenic in *Hijiki* is present as a form releasing inorganic As(V) in weak acid medium, but a large portion of the arsenic excreted in the urine was found to be in methylated forms such as MMAA and DMAA.[13,14]

Table 3. Permissible amount of foreign ions in the determination of 0.05 μg/ml inorganic As (to give < 10% error)

Ion	Added as	Concentration, μg/ml
Fe^{2+}	$FeSO_4(NH_4)_2SO_4.6H_2O$	500
Fe^{3+}	$Fe_2(SO_4)_3$	10
Cu^{2+}	$CuSO_4.5H_2O$	10
Zn^{2+}	$ZnSO_4.7H_2O$	500
Ca^{2+}	$CaCl_2$	500
Mg^{2+}	$MgSO_4.7H_2O$	500
SO^{2-}	Na_2SO_4	900
NO_3^-	KNO_3	100
S^{2-}	Na_2S	100

Table 4. Recovery tests of total inorganic As, As(III) and MMAA from urine

Arsenical	Added, μg/ml (as As)	Found,* μg/ml (as As)	Recovery, %
Total inorganic As	0	0.016 (0.015–0.017)	—
	0.050	0.068 (0.065–0.070)	103 (98–108)
	0.075	0.088 (0.085–0.092)	97 (92–101)
	0.100	0.109 (0.108–0.110)	93 (92–94)
	0.150	0.159 (0.158–0.161)	96 (95–97)
As(III)†	0	0.007 (0.006–0.0075)	—
	0.050	0.054 (0.050–0.056)	94 (88–98)
	0.075	0.081 (0.079–0.085)	99 (96–104)
	0.100	0.110 (0.097–0.115)	103 (97–108)
MMAA	0	0.038 (0.030–0.045)	—
	0.050	0.084 (0.082–0.087)	92 (88–98)
	0.100	0.135 (0.130–0.146)	97 (92–108)
	0.150	0.193 (0.190–0.196)	103 (101–105)

*Averages of 5 runs, ranges in parentheses.
†Analysed in the presence of 0.2 μg of As(V) per ml.

Acknowledgement—The work was supported by a grant for Environmental Preservation Research from the Environmental Agency.

REFERENCES

1. J. M. Wood, *Science*, 1974, **189**, 1049.
2. E. A. Woolson, *Environmental Health Perspectives*, 1977, **19**, 73.
3. R. S. Braman and C. C. Foreback, *Science*, 1973, **182**, 1274.
4. B. C. McBride and R. S. Wolfe, *Biochemistry*, 1971, **10**, 4312.
5. R. S. Braman, L. L. Justen and C. C. Foreback, *Anal. Chem.*, 1972, **44**, 2195.
6. Y. Talmi and V. Norvell, *ibid.*, 1975, **47**, 1510.
7. W. C. Butts and W. T. Rainey, Jr., *ibid.*, 1971, **43**, 538.
8. B. J. Gudzinowicz and H. F. Martin, *ibid.*, 1962, **34**, 648.
9. E. H. Daughtrey, Jr., A. W. Fitchett and P. Mushak, *Anal. Chim. Acta*, 1975, **79**, 199.
10. S. Fukui, T. Hirayama, M. Nohara and Y. Sakagami, *Talanta*, 1981, **28**, 402.
11. L. A. Stocken and R. H. S. Thompson, *J. Biochem.*, 1946, **40**, 548.
12. *Methods of Analysis of the AOAC*, 13th Ed., 1980, p. 387.
13. S. Fukui, T. Hirayama, M. Nohara and Y. Sakagami, *J. Food Hyg. Soc. Japan*, 1981, **22**, 513.
14. *Idem, Eisei Kagaku*, 1982, **28**, 35.

Talanta, Vol 30, No. 2, pp 95–100, 1983
Printed in Great Britain

0039-9140/83/020095-06$03.00/0
Pergamon Press Ltd

ION-EXCHANGER ULTRAVIOLET SPECTROPHOTOMETRY FOR URANIUM(VI)

HIROHIKO WAKI* and JOHANN KORKISCH
Institute of Analytical Chemistry, University of Vienna, Währingerstraße 38, A-1090 Vienna, Austria

(*Received* 21 *June* 1982. *Accepted* 5 *September* 1982)

Summary—A sensitive method based on solid-phase spectrophotometry has been developed for the microdetermination of uranium(VI) in water samples. Uranium is sorbed on the anion-exchanger QAE-Sephadex from thiocyanate solution and the absorbance of the exchanger is measured at 300 nm. This method is about 30 times more sensitive than solution spectrophotometry. Absorption spectra of various metals in the anion-exchanger phase are presented and their interferences discussed. A procedure for the cation-exchange separation of uranium from accompanying elements before spectral measurement of uranium is proposed.

Ion-exchanger colorimetry is a sensitive method based on measurement of light-absorption by an ion-exchanger that has sorbed coloured sample components.[1,2] A number of applications have been reported.[3–10] However, this method has so far not been applied to absorption of ultraviolet radiation, because of the extremely high background shown by most ion-exchange resins. The use of an ion-exchanger with a low background in the ultraviolet region may permit extension of solid-phase absorption photometry to the microdetermination of metals.

Although the spectrophotometric determination of uranium(VI) with thiocyanate is well known it is much less sensitive than the determination with reagents such as arsenazo III.[11,12] However, its sensitivity may be expected to be increased by use of solid-phase colorimetry. Uranium(VI) can be retained strongly on an anion-exchanger from thiocyanate solutions and effectively separated from many other metal ions. The combination of thiocyanate anion-exchange separation and colorimetry[12–14] or fluorimetry[14] has been employed for the determination of uranium at very low levels in water or rock samples.

In this work it was intended to determine uranium by direct measurement of the absorbance of the anion-exchanger with the uranium thiocyanate complexes retained on it. The commercially available anion-exchanger QAE-Sephadex A-25 was selected for this purpose, because of its low absorption background and very high sorption rate.

EXPERIMENTAL

Reagents

Ion-exchangers. The cross-linked dextran-type anion-exchanger, QAE-Sephadex A-25 (chloride form), was used in the original dry state, as obtained from the commercial source, for the collection of uranium from sample solutions. For the column separation of uranium the cation-exchange resin AG 50W-X8 (200–400 mesh, sodium form) was employed. The column dimensions were 8 mm × 18 cm (9.0 ml).

Metal ion solutions. These were prepared by dissolving $UO_2(NO_3)_2 \cdot 6H_2O$ (for U), $Mo_7O_{24} \cdot 4H_2O$ (for Mo) and K_2CrO_4 (for Cr) and the chlorides, nitrates or sulphates for other metals. Whenever necessary a small quantity of hydrochloric acid was added to each metal solution to prevent hydrolysis. Solutions of anions were prepared from the potassium salts. All chemicals employed were of analytical grade.

Apparatus

A Beckman DB-GT grating spectrophotometer was employed for all spectral measurements, with 1-cm quartz cells, except for the exchanger-phase spectrophotometry, for which a pair of 1-mm quartz cells was used.

Procedures

Ion-exchanger spectral measurements of uranium. To 200 ml of a solution, 1*M* in ammonium thiocyanate and 0.1*M* in hydrochloric acid, containing uranium(VI) (and other elements), 200 mg of QAE-Sephadex A-25 were added. In cases where the solution was coloured by contamination with iron, the minimum amount of ascorbic acid needed to remove the red colour was added. After stirring for 30 min the mixture was left to stand for about 5 min. The supernatant liquid was discarded and the remaining slurry poured into a 1-mm quartz cell. The absorbance of the slurry was measured at 300 nm (A_{300}) in the usual manner against a reference prepared by the same procedure, but without uranium or other sample components present. To compensate for the background due to the exchanger, the absorbance at 600 nm (A_{600}), where the absorbance of the uranium species is zero, was also measured and the difference $\Delta A_{600}^{300} = A_{300} - A_{600}$ calculated. The ΔA value thus obtained was directly proportional to the concentration of the sample species and was unaffected by a small difference in packing in the sample and reference cells.

Distribution ratio measurements. Portions of solutions (200 ml), 0.1*M* in hydrochloric acid, containing different concentrations of ammonium thiocyanate and 10 mg of uranium were each equilibrated for 30 min with 500 mg of QAE-Sephadex A-25. After equilibrium had been attained,

*Present address: Department of Chemistry, Faculty of Science, Kyushu University, Hakozaki, Higashiku, Fukuoka, 812 Japan.

the uranium concentration in the solution was measured spectrophotometrically from the absorbance at 300 nm. The distribution ratio D (ml/g) for uranium was calculated in the usual way from the initial and equilibrium concentrations in the solution.

Sorption rate measurements. Portions (200 ml) of a solution, 1M in ammonium thiocyanate and 0.1M in hydrochloric acid, were continuously stirred with 200 mg of QAE-Sephadex A-25. At fixed time intervals, small portions of the solution were analysed spectrophotometrically for uranium. The amount of uranium sorbed at each time was calculated from these values and the initial concentration.

Cation-exchange separation of uranium. When the sample solution contains interfering elements, uranium must first be separated by cation-exchange. For this purpose 200 ml of a 0.1M sodium chloride–0.01M hydrochloric acid solution containing uranium and the interfering elements were passed through a column of the cation-exchange resin. The resin bed was washed with 30 ml of 0.1M sodium chloride–0.01M hydrochloric acid solution to separate uranium from molybdate and other anionic species. Subsequently, 50 ml of 0.5M sodium thiocyanate–0.05M hydrochloric acid solution were passed through the column to elute cobalt, copper, vanadium(IV), nickel and iron(III). Finally uranium was eluted with 50 ml of 2M ammonium thiocyanate–0.2M hydrochloric acid solution and the eluate was adjusted to give 200 ml of 1M ammonium thiocyanate–0.1M hydrochloric acid solution by the addition of water, ammonium thiocyanate and hydrochloric acid, for the subsequent ion-exchanger spectrophotometry. All elutions were performed at a flow-rate of 0.6–0.7 ml/min and experiments were done at 20 ± 1°.

RESULTS AND DISCUSSION

Absorption background of the ion-exchanger

As mentioned previously, some ion-exchangers cannot be employed in this method because of the high absorption background due to the benzene rings in their structure. Cross-linked dextran-type ion-exchangers, such as QAE-Sephadex or SP-Sephadex, have a much lower background, which gradually increases with decreasing wavelength. These background spectra depend on the type and ionic form of the exchanger, the solution composition and the packing in the cell. Spectrum A (SCN^- form) in Fig. 1 shows a somewhat higher background than that in spectrum B (Cl^- form), owing to the greater shrinking of the exchanger in thiocyanate form. The sudden increase at wavelengths shorter than 270 nm is attributed to strong absorption by the thiocyanate counter-ions and this limits measurement to the region of wavelengths longer than 270 nm.

Anion-exchange distribution ratio of uranium(VI)

To find the optimum conditions for sorption of uranium by QAE-Sephadex, the distribution ratio of uranium was determined at various concentrations of ammonium thiocyanate: 0.1M hydrochloric acid was always added to stabilize the uranyl ions and for convenience in dealing with practical samples. As can be seen from Fig. 2, the distribution ratio ($D > 4 \times 10^3$) was attained for *ca.* 1–1.5M ammonium thiocyanate medium, and 1M ammonium thiocyanate was chosen as the optimal concentration. Small changes in hydrochloric acid concentration did not cause appreciable variation in the distribution ratio.

Sorption rate of uranium(VI)

A time of 30 min was sufficient for equilibrium to be reached under the experimental conditions (*i.e.*, 200 ml of solution and 200 mg of exchanger) and gave an equilibrium value of 80.3% uranium extraction. Complete collection is not necessary, provided the degree of extraction is reproducible. By this process it is possible to concentrate the uranium by a factor of several hundred. Since the sorption rate depends on the ratio of the amounts of the two phases, a different equilibration time is required when the conditions are changed. For instance, a time of only 10 min is necessary for 200 ml of solution and 500 mg of exchanger, but more than 80 min may be needed for 500 ml of solution and 200 mg of exchanger (for the same thiocyanate system).

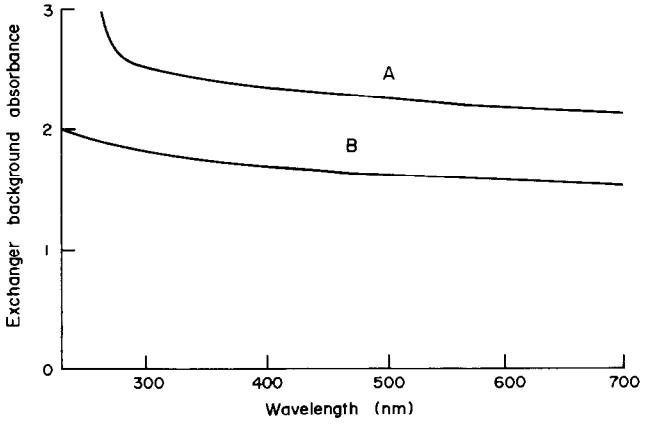

Fig. 1. Ion-exchanger background spectra. A, SCN^--form QAE-Sephadex A-25 equilibrated with 1M NH_4SCN–0.1M HCl; B, Cl^--form QAE-Sephadex A-25 equilibrated with H_2O. Cell length: 1 mm; reference H_2O.

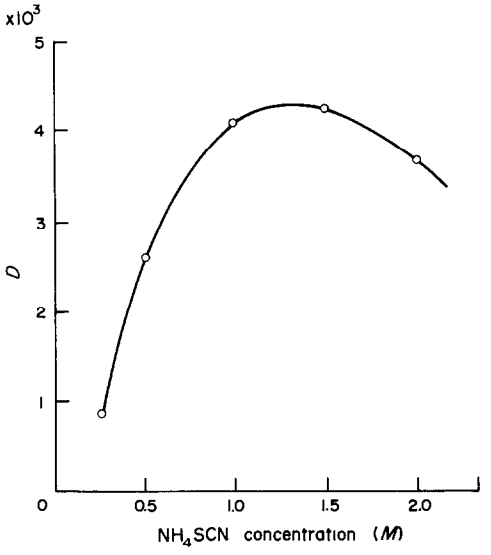

Fig. 2. Distribution ratio of uranium in the thiocyanate system. Anion-exchanger: QAE-Sephadex A-25, 500 mg. Solution: NH_4SCN–0.1*M* HCl containing 10 mg of U, 200 ml.

Calibration graph

The absorption spectrum of the uranium species sorbed from 1*M* ammonium thiocyanate–0.1*M* hydrochloric acid solution by QAE-Sephadex A-25 is similar to that of concentrated uranium thiocyanate solutions. The maximum absorptivity of the thiocyanate complexes is observed at *ca.* 300 nm and so this wavelength was selected for the uranium determination.

Solutions of different concentrations of uranium nitrate in 1*M* ammonium thiocyanate–0.1*M* hydrochloric acid were analysed according to the procedure given. The presence of small concentrations of nitrate ions did not affect the sorption behaviour of uranium, because of the predominance of the supporting thiocyanate salt. Figure 3 (Curve A) indicates that the ion-exchanger spectrophotometry has a much higher sensitivity than ordinary solution spectrophotometry under corresponding experimental conditions. The plot of ΔA_{600}^{300} against uranium concentration in solution is linear up to a uranium concentration of 0.5 μg/ml in the sample solution.

Absorption spectra and interference of other components

In the thiocyanate system, besides uranium a number of elements show absorbance in the ultraviolet region, and so do certain anions. In general, inert anions (*e.g.*, nitrate) are excluded from the anion-exchanger in the batch equilibration process by the presence of a large amount of strongly retained thiocyanates, and so do not interfere. On the other hand, most of the metals which interfere in the solution spectrophotometric determination of uranium with thiocyanate may also interfere in the present method, since they are strongly retained as thiocyanate complexes in the anion-exchanger phase. Figure 4 shows the absorption spectra for various species sorbed by 200 mg of QAE-Sephadex A-25 from 1*M* ammonium thiocyanate–0.1*M* hydrochloric acid solution, arranged in decreasing order of absorptivity at 300 nm. The extent of spectral interference by each species can easily be estimated by comparison of its absorptivity with that for uranium, taking their concentrations into consideration. Molybdenum interferes in the uranium determination to the largest extent, but can be removed with a cation-exchanger column, since it is not retained by the column from a solution of low acidity (Fig. 5). Vanadium(IV) also interferes considerably, but can also be separated from uranium with a cation-exchanger column, since it complexes strongly with thiocyanate and is eluted before the uranium. Iron(III) may interfere to the same extent as vanadium, but again is separable by cation-exchange, forming stable thiocyanate complexes. Contamination of the uranium fraction by a high concentration of iron(III) can be avoided by reduction of iron(III) to iron(II) with ascorbic acid. The absorbance of ascorbic acid itself is small at 300 nm, but even this can be eliminated by using a reference containing an equal amount of this reducing agent. Cobalt interferes appreciably if present in a concentration comparable to that of uranium, but can be separated completely from uranium on the cation-exchange column (Fig. 5). If necessary, copper and nickel can be separated in the same manner, though they interfere to a lesser extent than cobalt. Bismuth shows strong interference, having an absorptivity of the same order as that of uranium. However, it occurs in nature only at very low levels and hence will not present a problem in the analysis of water samples.

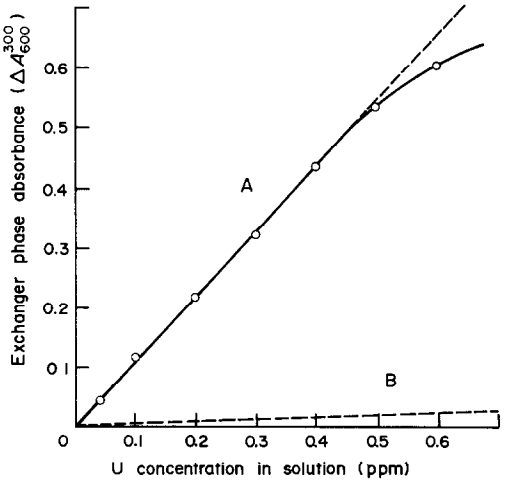

Fig. 3. Calibration graphs for the determination of uranium. A: ion-exchanger spectrophotometry. Solution: 1*M* NH_4SCN–0.1*M* HCl, 200 ml. Anion-exchanger: QAE-Sephadex A-25, 200 mg, path-length: 1 mm. B: solution spectrophotometry. 2*M* NH_4SCN–0.1*M* HCl, path-length: 1 cm.

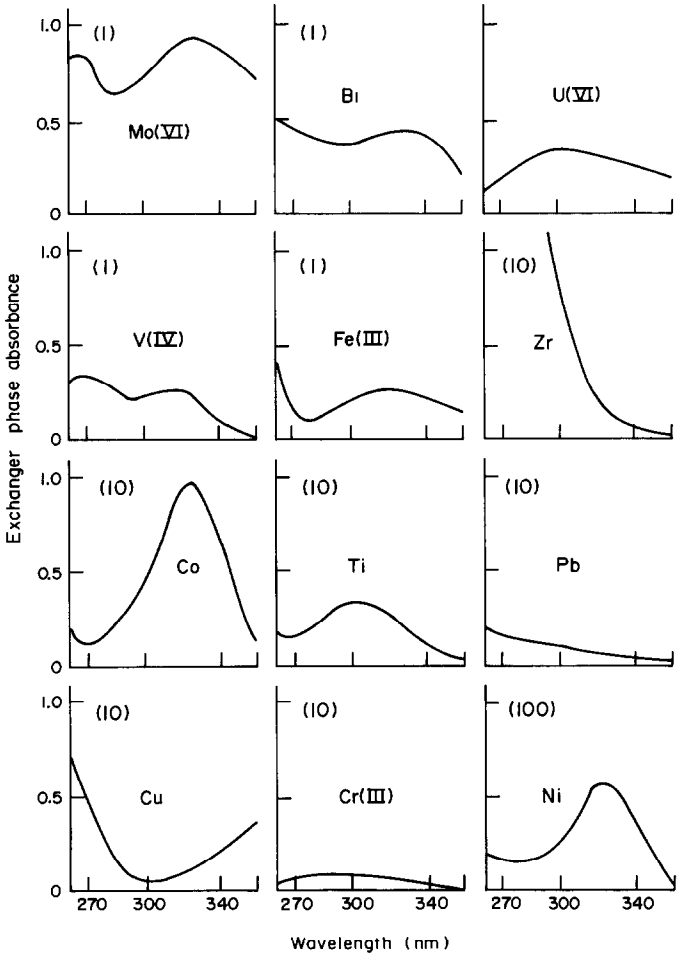

Fig. 4. Absorption spectra of QAE-Sephadex phase equilibrated with 1*M* NH_4SCN–0.1*M* HCl solution containing different metals. Solution: 200 ml, QAE-Sephadex A-25: 200 mg. Concentration of U 0.3 ppm. Number in parentheses is the weight ratio of each metal to the uranium contained in the solution.

Zirconium, titanium, lead and chromium cause appreciable spectral interferences when present in amounts comparable to that of uranium. Since they cannot be separated from uranium by use of the present cation-exchange procedure, this could sometimes present a problem in the determination of uranium in practical samples. The interference is reduced if a longer wavelength (*e.g.*, 340 nm) is used for the uranium determination, although the sensitivity then decreases.

Alkali metals, alkaline-earth metals, aluminium, thorium, manganese, zinc, cadmium, tin and iron(II) do not interfere, because they do not show any absorptivity at 300 nm.

The interference by sulphate is exceptional, as sulphate ions give a negative error through competition with the thiocyanate ligands for uranyl ions, when sulphate is present in large concentration.

Cation-exchange separation of uranium

To remove most of the interfering components, a cation-exchange column separation is done before the spectrophotometric determination of uranium. Figure 5 represents an elution curve showing the mutual separation of molybdenum, cobalt and uranium as a typical example. All the molybdenum is contained in the column effluent from passage of the original sample solution and the subsequent washing with 30 ml of 0.1*M* sodium chloride–0.01*M* hydrochloric acid solution. Other inert anions (not complexing with uranium) are also found in this effluent. At higher acidities (pH $\ll$ 2), molybdenum is increasingly retained by cation-exchangers. The 50 ml of effluent from the next elution with 0.5*M* sodium thiocyanate–0.05*M* hydrochloric acid contains all of the cobalt. The metals which form highly stable thiocyanate complexes, such as vanadium(IV), copper, nickel and iron(III), behave similarly to cobalt, although iron(III) tends to tail a little. The red colour of the iron(III) thiocyanate complex may therefore be used as a visual monitor to ascertain the approximate end of elution for the second group. The uranium is recovered quantitatively by the final elution with 50 ml

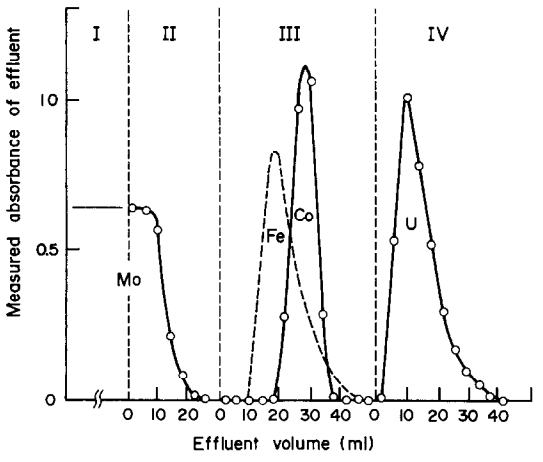

Fig. 5. Cation-exchange separation of uranium from other elements. Column: AG-50W-X8, Na^+ form (100–200 mesh), 9 ml (8 mm × 18 cm). Sample solution: 0.1*M* NaCl–0.01*M* HCl, 200 ml, containing 0.5 mg of U, 2 mg of Co and 2 mg of Mo. Elution sequence: I, passing of sample solution; II, washing with 0.1*M* NaCl–0.01*M* HCl; III, with 0.5*M* NaSCN–0.05*M* HCl; IV, with 2*M* NH_4SCN–0.2*M* HCl. Broken line is an elution curve for 3 mg of iron(III), in a separate run.

of 2*M* ammonium thiocyanate–0.2*M* hydrochloric acid, which is a more effective eluent than sodium thiocyanate. This last eluate also contains large amounts of sodium thiocyanate formed by exchange inside the resin phase, but it has been confirmed that the presence of considerable amounts of sodium ions does not affect the uranium determination. If present, bismuth, zirconium, titanium, lead and chromium will be found in the uranium eluate. Since the first three metals are subject to hydrolysis under the operating conditions employed, it is not easy to evaluate the extent of their interference. If the sample solution is acidified further, the situation is improved, but molybdenum may become less easily removed. The separation of chromium is also difficult, owing to its slow reaction rate with ligands.

Analysis of sample solutions

Solutions containing either uranium alone or in admixture with other elements were analysed by the present method (Table 1). The reproducibility was satisfactory for such a low level determination. The absorbance of the uranium thiocyanate complexes in the exchanger phase was stable for at least 3 hr if the sample and reference cells were kept in a dark place.

A measurement of uranium in the presence of a hundredfold amount of thorium was made in order to check whether there was an effect due to competition between uranium and other metal complexes for the ion-exchange sites on the exchanger. It was found that the sorption of metals such as thorium which show no light-absorption at around 300 nm does not affect either the distribution ratio or the exchanger-phase absorptivity of uranium.

The presence of 0.01*M* potassium nitrate in the sample solution caused no interference (as already explained) in spite of the high absorptivity of nitrate ions at 300 nm. On the other hand, the presence of 0.01*M* potassium sulphate produced an error of −10%. Therefore, sulphate ions should be removed. The proposed cation-exchange procedure can be used for this, but a higher concentration of sulphate may

Table 1. Analytical data for the determination of uranium by ion-exchanger ultraviolet spectrophotometry

Expt* No.	[U] taken, *ppm*	Other components	Absorbance measured, ΔA_{600}^{300}	Relative error, %†
1	0.400	None	0.432 ± 0.02§	
2	0.400	None	0.430‡	−0.5
3	0.300	None	0.318 ± 0.006 #	
4	0.300	Th/U = 100	0.312	−2
5	0.300	KNO_3 = 0.01*M*	0.315	−1
6	0.300	K_2SO_4 = 0.01*M*	0.285	−11
7	0.300	Mo/U = 10 Co/U = 10 Ni/U = 10 Cu/U = 10 V/U = 10 Fe/U = 10 Cl^-, NO_3^-, SO_4^{2-} KNO_3 = 0.01*M* NaCl = 0.1*M* HCl = 0.01*M*	0.320	+0.6

*1–6: batch equilibration + spectral measurement, 7: cation-exchange separation + batch equilibration + spectral measurement.
†Deviation from the average value when only U is present.
§Average from three different batches under identical conditions.
‡Absorbance measured after 3 hr in the dark.
#Average from two different batches under identical conditions.

disturb the elution behaviour of uranium from the cation-exchange column, by competitive strong complex formation, causing premature elution of uranium. The uranium sample solution must therefore not be prepared by use of sulphuric acid or other sulphate reagents.

When 200 ml of a sample solution (0.1*M* sodium chloride–0.01*M* hydrochloric acid) containing Mo, Co, Ni, Cu, V and Fe(III), each present in tenfold weight ratio to uranium (the corresponding counter-anions were chloride, nitrate or sulphate), and 0.01*M* potassium nitrate, were subjected to the cation-exchange separation and the subsequent spectrophotometric determination of uranium, there was no interference with the determination of uranium.

Sensitivity of the method

The sensitivity of the present method may be assessed by comparing the amounts of uranium in solution and in the exchanger phase which give the same absorbance. It is seen from Fig. 3 that the present method is approximately 30 times more sensitive than solution spectrophotometry. In ion-exchanger spectrophotometry, the ratio of the volume of the ion-exchanger to that of the sample solution may be adjusted to suit the requirements of the analysis. Thus, the volume of the sample solution may be increased to 1 litre for lower uranium concentrations, although more time is then necessary for equilibration. The shape and dimensions of the cuvettes can be modified so that a smaller amount of exchanger may be used, which again leads to an enhancement of sensitivity. Further, the volume of the sample solution before the cation-exchange separation can be adjusted as desired. For instance the volume of sample solution can be increased to 400 ml and passed through a column containing twice the amount of cation-exchange resin, without any alteration in equilibration and determination. If the electrolyte concentration of the water sample is very low, as in the case of river or lake water, a much larger volume may be passed through the cation-exchanger column, because the distribution ratio of bivalent ions, such as uranyl ions, decreases in inverse proportion to the square of the concentration of the bulk electrolyte cations. In this case, the sensitivity will be proportional to the volume of sample solution originally taken. If the preconcentration of uranium by ion-exchange is replaced by some other technique such as evaporation, more time is needed. Conversely, if the electrolyte concentration is too high, as in sea-water samples, the sample solution should be diluted to an overall concentration of about 0.1*M* before passage through the cation-exchanger column. In any case the scale of the preliminary cation-exchange separation should be in accordance with the practical situation (only one typical condition is presented in this paper).

Ion-exchanger spectrophotometry can be utilized for the sensitive determination of uranium in water samples, with appropriate conditions and procedures. We do not claim that the present method is the best and the most sensitive spectrophotometric method for uranium determination, but only emphasize that transfer to the ion-exchanger phase enhances sensitivity.

REFERENCES

1. K. Yoshimura, H. Waki and S. Ohashi, *Talanta*, 1976, **23**, 449.
2. *Idem*, *Kagaku No Ryoiki*, 1977, **31**, 885.
3. K. Yoshimura and S. Ohashi, *Talanta*, 1978, **25**, 103.
4. K. Yoshimura, H. Waki and S. Ohashi, *ibid.*, 1978, **25**, 579.
5. K. Yoshimura, Y. Toshimitsu and S. Ohashi, *ibid.*, 1980, **27**, 693.
6. K. Yoshimura and S. Ohashi, *Mem. Fac. Sci., Kyushu Univ., Ser. C*, 1978, **11**, 181.
7. S. Nigo, K. Yoshimura and T. Tarutani, *Talanta*, 1981, **28**, 669.
8. T. Tanaka, K. Hiiro and A. Kawahara, *Bunseki Kagaku*, 1979, **28**, 43; 1981, **30**, 131.
9. K. Ohzeki, T. Sakuma and T. Kambara, *Bull. Chem. Soc. Japan*, 1980, **53**, 2878.
10. Guo Wensheng and Meng Li, *Fenxi Huaxue*, 1978, **8**, 349.
11. H. Onishi and Y. Toita, *Bunseki Kagaku*, 1969, **18**, 592.
12. J. Korkisch and L. Gödl, *Talanta*, 1974, **21**, 1035.
13. *Idem*, *Anal. Chim. Acta*, 1974, **71**, 113.
14. J. Korkisch and I. Steffan, *ibid.*, 1975, **77**, 312.

Talanta, Vol 30, No. 2, pp. 101-105, 1983
Printed in Great Britain.

0039-9140/83/020101-05$03.00/0

MÖGLICHKEITEN ZUR VERBESSERUNG DER AUFLÖSUNG IN DER DÜNNSCHICHTCHROMATOGRAPHIE: EINE ÜBERSICHT

H.-P. FREY und G. ACKERMANN
Bergakademie Freiberg, Sektion Chemie, Lehrstuhl für Analytische Chemie, 9200 Freiberg, DDR

(*Eingegangen am* 14 *Dezember* 1981. *Revidiert am* 20 *Juli* 1982. *Angenommen am* 16 *August* 1982)

Zusammenfassung—Es wird eine Übersicht über Möglichkeiten zur Verbesserung der Auflösung in der Dünnschichtchromatographie gegeben. Der Beziehung $R = z_f'\Delta R/4\sigma$ entsprechend leiten sich diese im wesentlichen von einer Verlängerung der Trennstrecke, der Erhöhung der Trennphasenselektivität und der Verringerung der Fleckausdehnung ab.

Dünnschichtchromatographische Trennungen werden, wie andere Chromatographieverfahren auch, im Hinblick auf die Belastbarkeit des Trennbetts mit Analysensubstanz m, die erforderliche Trennzeit t und die gewünschte Auflösung R optimiert. Diese drei Variablen bilden das "magische Dreieck" der Chromatographie:

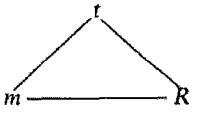

Zwischen diesen Größen sind immer nur Kompromisse möglich. Das bedeutet, daß unter keinen Umständen alle Größen gleichzeitig auf das höchste Niveau gebracht werden können. So wird man im präparativen Maßstab (großes m) noch schnell trennen können (kleines t), aber ganz sicher nicht die Auflösung erreichen, die bei wesentlich geringerer Belastung möglich wäre.

Für die Optimierung kommt der Auflösung eine besondere Bedeutung zu, da es eine nahezu unübersehbare Fülle von Möglichkeiten gibt, diese—mehr oder weniger gezielt—zu beeinflussen.

Die graphische Darstellung, auf die sich die den Textabschnitten vorangestellten Ziffern beziehen, faßt diese Möglichkeiten zusammen, ohne jedoch Anspruch auf eine vollständige Systematik zu erheben. Um die Übersichtlichkeit zu wahren, blieben manche "Querbeziehungen" zwischen den Verfahren und Methoden unberücksichtigt, so z.B. die Bedeutung von Volumengradienten für die Zirkularentwicklung.

THEORETISCHE VORBETRACHTUNG

Die Auflösung benachbarter Substanzzonen bzw. ihrer registrierten Konzentrationsprofile wird formal durch die folgende Gleichung beschrieben:

$$R = \frac{z_f'\Delta R_f}{4\sigma}$$

Es bedeuten R die Auflösung, z_f' die um die Distanz Fließmitteleintritt–Start verminderte Wanderungsstrecke der Fließmittelfront, ΔR_f die auf z_f' bezogene Differenz der Wanderungsstrecken der aufzulösenden Substanzen und σ die Standardabweichung beider mit Gaußform angenommenen Konzentrationsprofile (unter der vereinfachenden Annahme von $\sigma_1 \approx \sigma_2$).

Die Gleichung weist damit drei grundsätzliche Wege zur Verbesserung der Auflösung: 1. Verlängerung der Trennstrecke z_f', 2. Vergrößerung von ΔR_f (Selektivitätserhöhung), 3. Verringerung der Fleckausdehnung. Diese Wege werden schematisch in Abb. 1 zusammengestellt. Nicht alle Arbeitstechniken und methodischen Varianten lassen sich diesbezüglich so einfach klassifizieren; häufig sind die Wirkungen von z_f', ΔR_f und σ auf R gekoppelt. Abbildung 1 weist auf 20 Varianten.

DISKUSSION

(1,2) Die Verlängerung der Trennstrecke ist in experimenteller Hinsicht unproblematisch. Der damit erzielbare Gewinn an Auflösung erklärt sich aus der Zunahme der von den Substanzen überstrichenen Trennstufenzahl N. Wegen $N = R_f\, z_f'/h$ ist die Vergrößerung von z_f' nur solange sinnvoll, wie die Trennstufenhöhe h konstant bleibt: h aber steigt zu längeren Trennstrecken hin an, da sich auf Grund des Fließgesetzes der mobilen Phase, $z_f'^2 = \kappa t$ (κ ist die Fließkonstante), die Trennzeit t mit z_f' drastisch verlängert und zur Fleckverbreiterung durch Diffusion führt. Die Verlängerung der Trennstrecke geht also nicht nur zu Lasten der Analysenzeit; oberhalb einer bestimmten Grenze wird der Gewinn an Auflösung durch die Fleckverbreiterung wieder vernichtet. Auf "normalen" DC-Schichten liegt diese Grenze bei 8 bis 10 cm, auf Hochleistungsschichten wird sie bereits nach 3 bis 4 cm erreicht.

Aus der von Snyder[1] abgeleiteten Beziehung

$$R = \frac{1}{4}\left(\frac{k_1}{k_2} - 1\right)(1 - \overline{R_f})\sqrt{\overline{R_f}N}$$

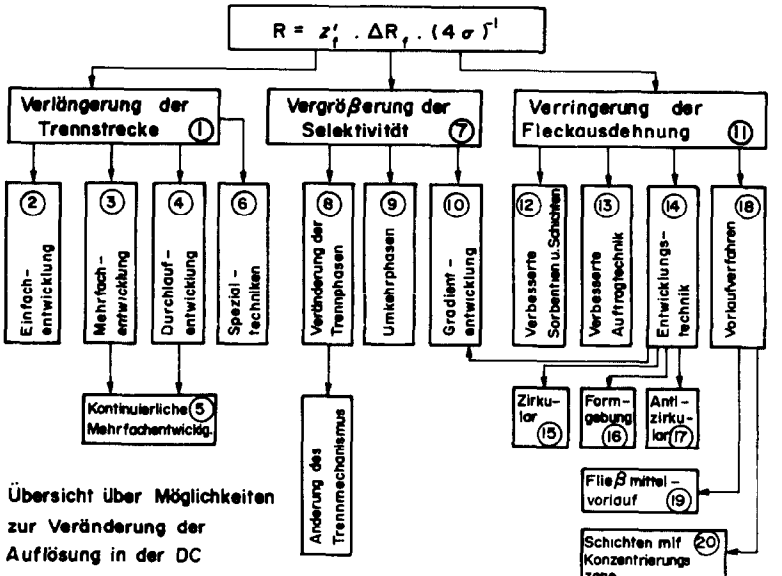

Fig. 1

mit $k = (1 - R_f)/R_f$ und $\overline{R_f} = (R_{f_1} + R_{f_2})/2$ folgt ein weiterer Grund für den nur beschränkten Auflösungsgewinn durch Verlängerung der Trennstrecke: die Auflösung wächst lediglich mit $\sqrt{N}$. So würde eine Verdoppelung der Trennstrecke—bei $h = \text{const.}$—höchstens zu einer 1,4-fachen Auflösung führen. Aus der Beziehung folgt weiterhin, daß die Auflösung ein Maximum aufweist, wenn der aus den R_f-Werten der zu trennenden Substanzen gemittelte R_f-Wert $\approx 0{,}3$ beträgt. Im R_f-Bereich von 0,20 bis 0,50 kann man mit mehr als 92% der unter den gewählten Bedingungen maximal möglichen Auflösung trennen.[2]

(3) Gegenüber einer einzigen Entwicklung über eine längere Distanz kann man an Auflösung und Zeit und damit an echter Trennleistung gewinnen, wenn man mehrfach über kurze Entfernungen (wenige Zentimeter) entwickelt. Dadurch bleibt man im Bereich der anfänglich hohen Fließmittelgeschwindigkeit und vermeidet so die diffusionsbedingte Fleckverbreiterung. Stark vereinfacht gesehen, addieren sich bei der wiederholten Entwicklung die Trennstufenzahlen, so daß diese Technik mit einer Verlängerung der Trennstrecke vergleichbar ist. Der Auflösungsgewinn bleibt allerdings in Grenzen, weil beim zweiten und jedem weiteren Lauf zunächst der untere (stärker retardierte) Fleck auf den darüberliegenden zubewegt wird, ehe dieser zu wandern beginnt. So verringert sich zunächst die Auflösung und dies umso mehr, je größer die anfänglichen R_f-Werte sind. Liegen diese oberhalb von *ca.* 0,45, so führt bereits die zweite Entwicklung grundsätzlich zu einer Verschlechterung der Trennung.[3] Je kleiner der R_f-Wert des kritischen Substanzpaares ($R_f \approx R_{f_1} \approx R_{f_2}$), desto mehr läßt sich seine Auflösung verbessern, desto größer wird aber auch die Zahl der dafür erforderlichen Entwicklungen. Diese Zahl kann mit $n \approx 1/R_f$ abgeschätzt werden. Sie stellt einen optimalen Wert dar, dessen Überschreitung ebenfalls nur eine Verminderung der Auflösung bringt. Die Notwendigkeit, kleine R_f-Werte zu erzeugen, liefert einen zusätzlichen Vorteil: man muß Fließmittel geringer Elutionskraft verwenden, welche eine höhere Selektivität bedingen, also zu einem zusätzlichen und echten Anstieg der ΔR_f-Werte führen [vgl. Abschnitt (6)].[4]

Es sei betont, daß die Vorteile der Mehrfachentwicklung vor allem auf HPTLC-Schichten bei entsprechender Auftragtechnik zum Tragen kommen. Hier bewährt sich diese Methode bei der Trennung komplexer Stoffgemische.[5–7]

Anmerkung. Es wird in diesem Zusammenhang zuweilen gesagt, die R_f-Werte würden erhöht bzw. der ΔR_f-Wert werde vergrößert. Streng genommen ist das falsch, denn der R_f-Wert ist—mit den erforderlichen Einschränkungen—eine thermodynamische Größe, die die Verteilung der Substanzen auf beide Trennphasen beschreibt und von der Anzahl der Entwicklungen, oder auch der Trennstreckenlänge, unabhängig ist. Was nach n Läufen gemessen wird, genügt zwar der Meßvorschrift, ist aber nur noch ein formaler R_f-Wert, der die relative Fleckposition angibt.

(4) Die Dünnschichtchromatographie mit Fließmitteldurchlauf (DDC) gilt als die leistungsfähigste DC-Technik, erfordert jedoch spezielle Trennkammern und ist daher nicht sehr verbreitet. Eine kritische Bewertung der DDC sowie einen Vergleich mit diversen Mehrfachentwicklungstechniken hat Geiss vorgenommen.[8] Der theoretisch erreichbaren Maximalauflösung nähert man sich in der DDC umso mehr, je weiter das Fleckpaar an die Abdampflinie heranrückt und je kleiner der R_f-Wert ist (günstige Werte: $\leqslant 0{,}2$). Besonders leistungsfähig wird die DDC, wenn man sie auf Dünnschichten mit Konzentrierungszone betreibt [vgl. Abschn. (20)].

(5) Die kontinuierliche Mehrfachentwicklung[9] ist eine weitere, nichtkonventionelle, DC-Entwicklungstechnik, deren Vorzüge ausschließlich auf Hochleistungsschichten sichtbar werden. Sie besteht in einer mehrfach wiederholten Durchlaufentwicklung.

(6) Bei der vom Saunders und Snyder[10] vorgeschlagenen Trommelentwicklung wird auf besondere Weise erreicht, daß sich Fließmitteleintauchlinie, Fließmittelfront und das Substanzpaar mit gleicher und konstanter Geschwindigkeit über die Trennschicht bewegen. Dadurch kann die zeitbezogene Auflösung um *ca.* eine Größenordnung erhöht werden. Eine drastische Herabsetzung der Trennzeit bei der Mehrfachentwicklung erreicht man nach Halpaap (zitiert in Geiss[3]) dadurch, daß man auf DC-Folien chromatographiert und diese nach jedem Lauf bis unterhalb des zu trennenden Fleckpaares abschneidet.

(7) Auch wenn die Größe ΔR_f selbst kein geeignetes Selektivitätsmaß ist, weist sie auf die generelle Bedeutung der Trennphasenselektivität für die Auflösung hin. Es läßt sich zeigen, daß die Erhöhung der Selektivität das wirksamste Mittel zur Verbesserung der Auflösung ist (vgl. dazu auch die obenstehende Auflösungsformel von Snyder[1]).

Der R_f-Wert ist gemäß $R_f = 1/(1 + k)$ mit dem Kapazitätsfaktor k und wegen $k = \rho K$ auch mit der thermodynamischen Separationskonstante K und mit dem Phasenquerschnittsverhältnis ρ verknüpft. Eine Vergrößerung von ΔR_f kann daher durch die qualitative (wirkt auf K) und/oder quantitative (wirkt auf ρ) Veränderung der Trennphasenkombination erreicht werden. Nach Thoma und Perisho[11] hängt aber ΔR_f linear von $\ln\rho$ ab, so daß mit praktisch relevanten ρ-Änderungen keine nennenswerten Auflösungsverbesserungen zu erzielen sind. Das wird durch die Praxis bestätigt.

(8) Im Extremfall zieht die Veränderung der stationären und/oder mobilen Phase eine Änderung des (dominierenden) Trennprinzips nach sich. Dann fallen ΔR_f-Änderungen oftmals drastisch aus; ebenso beobachtet man Änderungen der Retentionsfolge. Beispiele solcher Wechsel des Trennprinzips sind der Übergang Adsorption → Ausschluß bei der Verwendung genügend weitporiger Sorbentien oder der Übergang Verteilung → Austausch bei Veränderung des pH-Wertes der mobilen Phase. Derartige Eingriffe in das Trennmilieu werden umso effektiver sein, je mehr Informationen über die Natur der zu trennenden Substanzen vorliegen und je gezielter daher vorgegangen werden kann.

(9) In besonderem Maße gilt das für den Übergang zu Umkehrphasen. Da bei solchen Trennphasenkombinationen der Hydrophobizitätsgrad[12] der Substanzen ein entscheidendes Retentionskriterium ist, existiert ein dominierendes Selektivitätsprinzip, und die Struktur–R_f-Beziehungen werden überschaubarer.

(10) Selektivitätsänderungen kann man von Schicht zu Schicht, aber auch während einer Entwicklung vornehmen. Dementsprechend verläuft die Entwicklung isokratisch bzw. mit einem Gradienten. Dieser kann dem Fließmittel oder der Schicht aufgeprägt werden. Schichtgradienten, die bereits bei der Beschichtung erzeugt werden, also nicht durch nachträgliches Konditionieren einer an sich uniformen Schicht, haben Stahl und Mitarbeiter beschrieben und die hierfür erforderliche Technik vorgestellt.[13,14]

Fließmittelgradienten sind experimentell schwieriger zu realisieren[15,16] und überdies nicht so wirksam wie Schichtgradienten. Die Unterscheidung zwischen isokratischer und Gradiententwicklung hat oftmals nur formalen Charakter, denn es ist z.B. bei der allgemein üblichen DC-Technik, mit Verwendung einer Normalkammer, nicht möglich, die Ausbildung retentionswirksamer Vorbedampfungsgradienten gänzlich Zu unterdrücken. Nur mit Spezialtechniken und entsprechenden Ausrüstungen (z.B. Durchlauftechnik, VARIO KS-Kammer[17] oder andere Konditionierkammern,[18] oder U-Kammer[19]) kann man bezüglich der Trennkraft wirklich uniforme Schichten gewährleisten. Andererseits ist es auch erst mit speziellen Konditionierkammern möglich, nach Verlauf und Wirkung definierte Gradienten in der Schicht zu erzeugen. In Normalkammern bilden sich Gradienten mehr oder weniger spontan aus und sind nicht selten die eigentliche Ursache für gute Auflösungen—oft genug jedoch auch für schlechte Reproduzierbarkeit.

Aus theoretischer Sicht sollten Gradienten so angelegt sein, daß die Substanzen in Laufrichtung verzögert werden ("antiparalleler" Gradient[20]). Je stärker der Gradient "bremst" (mit anderen Worten: je steiler er ist), desto größer ist der R_f-Bereich, über den hinweg die Auflösung angehoben wird. Diese Auflösung ist jedoch kleiner, als die auf gradientfreier Schicht bei $R_f \approx 0{,}3$ erzielbare Maximalauflösung.[21] Gradienten helfen also nicht, die Trennung eines kritischen Fleckpaares zu verbessern. Sie machen unter Umständen das Chromatogramm eines heteropolaren Vielkomponentengemisches übersichtlicher.[22]

Interessante Trenneffekte mit guter Auflösung erhält man mit der "polyzonalen DC".[23] Bei dieser Gradienttechnik wird die Tatsache ausgenutzt, daß Substanzen in der Nähe steiler Polaritäts-(Elutions-)gradienten und quer zur Fließrichtung flache, elliptische Flecken bilden und sich daher besser auflösen lassen.

Abschließend sei auf den wohl allgegenwärtigsten Gradienten hingewiesen, den Fließmittelvolumengradienten (das "Fließmittelprofil"). Er ist besonders steil auf Schichten mit weitem Korngrößenspektrum bzw. mit sehr kleinem mittleren Korndurchmesser ($\bar{d} < 10\,\mu m$).[24] Diesem Gradienten ist es zuzuschreiben, daß startnahe Substanzen mit zu großem und frontnahe Substanzen mit zu kleinem R_f-Wert laufen. Außerdem wirkt dieser Gradient einer Fleckverbreiterung mit steigendem R_f-Wert entgegen. Dadurch wird im oberen R_f-Bereich die Trennung oft besser, als sie von der Schichtqualität her zu erwarten wäre.

(11,12) Dieser Komplex von Möglichkeiten steht teilweise in engem Zusammenhang mit der Wirkung von Gradienten. Die im Ergebnis der chromatogra-

phischen Entwicklung erhaltene Fleckbreite σ_{ges} wird wesentlich durch die Startbreite σ_0 bestimmt. Da sich nur die Varianzen additiv verhalten, gilt

$$\sigma^2_{ges} = \sigma^2_0 + \sigma^2_{chrom}$$

Es kommt also darauf an, sowohl die Startbreite wie auch die fleckverbreiternden Einflüsse während der Entwicklung (σ^2_{chrom}) auf ein Minimum zu reduzieren. Dies gelingt auf die vielfältigste Art und Weise. Auf schnellaufenden Schichten macht sich die zeitliche Verzögerung des Substanzübertritts zwischen den Trennphasen in Gestalt elliptisch längsverformter Flecken bemerkbar. Auf sehr langsamlaufenden Schichten, oder auch nach längeren Trennstrecken auf normallaufenden Schichten, beobachtet man dagegen konzentrische Fleckvergrößerung infolge Diffusion in der mobilen Phase (auch in der stationären, wenn diese flüssig ist). Folglich sollte man auf mäßig schnellaufenden Schichten bzw. nur über kürzere Distanzen trennen, dann sind beide genannten Einflüsse auf ein Minimum reduziert. Um außerdem konvektive Störungen im Substanztransport gering zu halten, muß ein Schichtmaterial mit genügend enger Kornmittlere Korngröße sollte dabei von 10 μm nicht wesentlich abweichen.[25,26] Den sehr komplexen Zusammenhang zwischen der Korngröße des Sorbens und Leistungsparametern der Dünnschichtchromatographie haben Guiochon und Mitarbeiter in einer sehr aufschlußreichen theoretischen Studie untersucht.[2]

(13) Geringe Startbreiten σ_0 lassen sich durch eine geeignete Auftragtechnik realisieren. In der Hochleistungs-DC sind Startbreiten <1 mm eine unabdingbare Forderung; dazu müssen Probenvolumina im Nanoliterbereich beherrscht werden.[27] Wenn unter einem, nötigenfalls vorgewärmten, Inertgasstrom aufgetragen wird, lassen sich kleine Startbreiten auch mit relativ großem Volumen erzielen.[28,29] Dies ist auch mit dem "contact spotting" möglich.[30]

Neben einer leistungsfähigen Auftragtechnik ist die richtige Wahl des Lösungsmittels für die Substanz wichtig. Wenn nicht andere Gründe dagegen sprechen, soll dieses leicht flüchtig und möglichst wenig polar sein; dann bleibt die Substanz am Auftragort auf kleiner Fläche konzentriert. Daß die strichförmige Auftragung der punktförmigen im Hinblick auf die erzielbare Auflösung überlegen ist, ist allgemein bekannt.

(14,15) Wenn keine geeignete Auftragtechnik vorhanden oder aus Gründen des Arbeitsablaufs nicht einsetzbar ist, so kann die Substanzauflösung vornehmlich im unteren R_f-Bereich durch Zirkularentwicklung verbessert werden. Hier breitet sich das Fließmittel kreisförmig aus. Die in Richtung des Kreisradius mitlaufenden Substanzen bilden ständig länger werdende Kreisbögen, wodurch sich zwangsläufig die radiale Fleckausdehnung (d.h. σ) verringert.

(16) In Form der von der Papierchromatographie übernommenen Keilstreifentechnik oder auch anderer Formgebungstechniken[31] läßt sich dieser Effekt mit der Linearentwicklung kombinieren.

(17) Soll die Auflösung von Substanzen vorwiegend höherer R_f-Werte verbessert werden, so gelingt dies auch mit der allerdings umständlichen "antizirkularen" Entwicklung, einer Variante der Hochleistungs-DC.[27] Neben einem Zeitgewinn, da die Lineargeschwindigkeit des Fließmittels nahezu konstant ist, erzielt man außerdem eine höhere Empfindlichkeit, denn mit der Entwicklung zum Kreismittelpunkt hin ist eine Substanzkonzentrierung verbunden. Auch bei der von Tyihák und Mitarbeiter[32] entwickelten "over pressure"-Technik (OPTLC) wird eine Verbesserung der Auflösung dadurch erreicht, daß, durch Druckförderung des Fließmittels in die hermetisch abgeschlossene Trennschicht (kein Gasraum) die quadratische Abhängigkeit der Fließmittelwanderung von der Zeit zu einer linearen gezwungen wird, also: $z'_f = \kappa t$. Damit wird Trennzeit gewonnen und die diffusionsbedingte Fleckverbreiterung vernachlässigbar klein gemacht.

(18) Neben diesen vorwiegend versuchstechnischen Möglichkeiten zur Erzielung geringer Startbreiten spielen die "Vorlaufverfahren" eine besondere Rolle. Diesen ist gemeinsam, daß man die Substanz vor der eigentlichen Trennung auf der Schicht praktisch retentionsfrei wandern läßt. Die Substanz läuft dann mit $R_f \approx 1$, d.h. in der Fließmittelfront als schmale Bande. Dieses Prinzip kann auf zwei grundsätzlich verschiedenen Wegen verwirklicht werden: (19) und (20).

(19) Man wählt ein hinreichend stark eluierendes Fließmittel, in dem die zu trennenden Substanzen mit $R_f \approx 1$ laufen, bricht diesen "Vorlauf" an geeigneter Stelle (nach 1 bis 2 cm) ab, entfernt das Fließmittel vollständig und startet dann die eigentliche Trennung mit dem "richtigen" Fließmittel.[33] Häufig ist die Desorption der Substanz am Auftragort verzögert, z.B. bei größeren Substanzmengen. Dann erzielt man erst nach mehrmaligem Vorlauf genügend schmale Banden. Man kommt bei dieser Vorlauftechnik mit einem Schichtmaterial aus, muß aber in Kauf nehmen, daß die Entwicklung durch den Fließmittelwechsel unterbrochen wird.

(20) Man läßt die Substanz auf einer der eigentlichen Trennschicht vorgelagerten Zone aus sorptionsinaktivem Material "vorlaufen". Ein Fließmittelwechsel ist hierbei nicht erforderlich. Bei richtiger Wahl des Schichtmaterials für die "Konzentrierungszone" (weitporiges Kieselgel,[34] bei 1200° geglühtes Kieselgel, Quarzmehl, α-Aluminiumoxid, Glaspulver,[35] Kieselgur[36]) und nicht zu hoher Konzentration der Substanzen werden diese vom Fließmittel spätestens am Schichtstoß zu schmalen Banden angereichert (Konzentrierungseffekt) und diese nach dem Übertritt in die eigentliche Trennzone mit vielfach hervorragender Auflösung getrennt.

Diese Vorlauftechnik macht die Substanzauftragung völlig problemlos; lediglich Überladung muß vermieden werden. Unabhängig vom Ort und von der

Form des Auftragtüpfels beginnt die Trennung präzise an der durch den Schichtstoß vorgegebenen Stelle. Das schafft die interessante Möglichkeit, diese Technik des "fliegenden Starts" mit der Durchlaufentwicklung in Schmalkammern zu kombinieren.

Diese Kammern bieten *a priori* bessere Voraussetzungen für die Übertragung von Retentionsdaten auf die Säule. Allerdings sind hierbei Fließmittelgemische ausgenommen, da diese in Schmalkammern adsorptiv entmischt werden. Entwickelt man aber mit Fließmitteldurchlauf und wartet den Durchgang der letzten Entmischungsfront ab, so schafft man mit einer anschließenden—sonst so problematischen, weil leistungsmindernden—Naß- in naß-Dosierung Verhältnisse, die bezüglich der Phasenzusammensetzung und der Dosierqualität (am eigentlichen Start) denen auf der HP-Säule weitgehend entsprechen.

LITERATUR

1. L. R. Snyder, *Principles of Adsorption Chromatography*. Dekker, New York, 1968.
2. G. Guiochon, F. Bresolle und A. Siouffi, *J. Chromatog. Sci.*, 1979, **17**, 368.
3. F. Geiss, *Die Parameter der Dünnschichtchromatographie*, S. 79. Vieweg, Braunschweig, 1972.
4. K. Y. Lee, C. F. Poole und A. Zlatkis, in W. Bertsch, S. Hara, R. E. Kaiser und A. Zlatkis (eds.), Instrumental HPTLC, S. 245. Hüthig, Heidelberg, 1980.
5. J. A. Perry, T. H. Jupille und L. J. Glunk, in E. S. Perry und C. J. Van Oss (eds.), *Separation and Purification Methods*, Vol. 4, S. 105. Dekker, New York, 1976.
6. J. A. Perry, *J. Chromatog.* 1975, **113**, 267.
7. T. H. Jupille, *J. Am. Oil Chemists Soc.*, 1977, **54**, 179.
8. F. Geiss, Zitat 3, S. 76.
9. J. A. Perry, *J. Chromatog.*, 1979, **165**, 117.
10. D. L. Saunders und L. R. Snyder, in A. Zlatkis (ed.) *Advances in Chromatography*, p. 307. Houston, 1970.
11. J. A. Thoma und C. R. Perisho, *Anal. Chem.* 1967, **39**, 745.
12. Cs. Horváth, W. Melander und J. Molnár, *J Chromatog.*, 1976, **125**, 129.
13. E. Stahl und J. Müller *ibid.*, 1980, **189**, 293.
14. *Idem, ibid.*, 1981, **209**, 484.
15. Th. Wieland und H. Determann, *Experientia*, 1962, **18**, 431.
16. A. Niederwieser und C. G. Honegger, *Helv. Chim. Acta*, 1965, **48**, 893.
17. F. Geiss und H. Schlitt, *Chromatographia*, 1968, **1**, 392.
18. H. P. Frey und G. Ackermann, *J. Chromatog.*, 1980, **198**, 357.
19. R. E. Kaiser, in *HPTLC-High Performance Thin-Layer Chromatography*, A. Zlatkis und R. E. Kaiser (eds.), S. 73–84. Elsevier, Amsterdam/New York, 1977.
20. A. Niederwieser, *Chromatographia*, 1969, **2**, 23.
21. L. R. Snyder und D. L. Saunders, *J. Chromatog.*, 1969, **44**, 1.
22. F. Geiss, Zitat 3, S. 244.
23. A. Niederwieser, *Chromatographia*, 1969, **2**, 519.
24. H. P. Frey, G. Ackermann und M. Loogk, unveröffentlicht.
25. A. Siouffi, H. Engelhardt, G. Guiochon und I. Halász, *J. Chromatog. Sci.*, 1978, **16**, 152.
26. H. P. Frey und G. Ackermann, Veröff. in Vorbereitung.
27. D. E. Jänchen, Zitat 4, S. 133.
28. M. E. Morgan, *J. Chromatog.*, 1962, **9**, 379.
29. U. Leonhardt, *Z. Med. Labortech.*, 1981, **22**, 103.
30. D. C. Fenimore und C. I. Meyer, *J. Chromatog.*, 1979, **186**, 555.
31. G. J. Kraus und G. Kraus, *Experimente zur Chromatographie*, S. 45. VEN Deutscher Verlag d. Wiss., Berlin, 1979.
32. E. Tyihák, E. Mincsovics und H. Kaláz, *J. Chromatog.*, 1979, **174**, 75.
33. J. Blome, in *Einführung in die Hochleistungs-Dünnschicht-Chromatographie*, S. 59. Bad Dürkheim, 1976.
34. H. Halpaap und K. F. Krebs, *J. Chromatog.*, 1977, **142**, 823.
35. H. P. Frey und G. Ackermann, unveröffentlicht.
36. A. Musgrave, *J. Chromatog.*, 1969, **41**, 470.

Summary—The possibilities for improving resolution in thin-layer chromatography are reviewed. According to the relationship $R = z'_f \Delta R_f / 4\sigma$ the important factors are seen to be the separation distance, the selectivity of the solvent system, and the reduction of spot width.

Talanta, Vol. 30, No 2, pp. 107–110, 1983
Printed in Great Britain.

0039-9140/83/020107-04$03.00/0

KINETIC FLUORIMETRIC DETERMINATION OF NANOGRAM AMOUNTS OF MANGANESE, BASED ON ITS CATALYSIS OF THE OXIDATION OF 2-HYDROXYBENZALDEHYDE THIOSEMICARBAZONE WITH HYDROGEN PEROXIDE

A. MORENO, M. SILVA, D. PEREZ-BENDITO and M. VALCÁRCEL
Department of Analytical Chemistry, Faculty of Science University of Córdoba, Spain

(*Received* 2 *June* 1981. *Revised* 29 *July* 1982. *Accepted* 18 *August* 1982)

Summary—A kinetic method is described for the determination of trace amounts of manganese(II), based on its catalytic effect on the oxidation of 2-hydroxybenzaldehyde thiosemicarbazone by hydrogen peroxide. The reaction is followed by measuring the rate of change of fluorescence (λ_{ex} 365 and λ_{em} 440 nm). The calibration is linear over the manganese range 2–9 ng/ml with a precision of ±1%. The proposed method suffers from few interferences.

Several kinetic fluorimetric determinations have recently been published, based on the catalytic effect of various metal ions on the aerial oxidation of azines and hydrazones.[1–6] The thiosemicarbazones have also been studied but the reactions have been followed by photometry.[7–10] In this paper 2-hydroxybenzaldehyde thiosemicarbazone (HBTS) has been employed for the first time in a kinetic system catalysed by trace metals. Its oxidation by hydrogen peroxide is used for the kinetic fluorimetric determination of manganese(II). The analytical properties and applications of this reagent have been described previously by several authors.

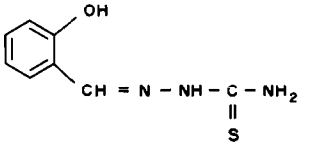

In recent years, many kinetic methods have been described for the determination of manganese(II), but only kinetic enzymatic methods have been followed by fluorimetry. This paper describes a fluorimetric determination based on a catalysed reaction not involving an enzyme. The method described is both very sensitive and selective, permitting the determination of manganese concentrations as low as 2 ng/ml, and with only a few foreign ions interfering.

EXPERIMENTAL

Reagents

All solvents and reagents were of analytical grade. The 2-hydroxybenzaldehyde thiosemicarbazone was synthesized according to the procedure of Sah and Daniels.[11] The standard manganese(II) solution was prepared from the nitrate (Merck) and standardized by titration with EDTA; it was diluted as required, just before use.

Apparatus

A Perkin–Elmer MPF-43A spectrofluorimeter equipped with recorder and thermostat for kinetic measurements, and a Perkin–Elmer model 402 recording spectrophotometer were used, both with 1-cm quartz cells. A Perkin–Elmer model 380 atomic-absorption spectrophotometer was used with an air–acetylene flame. All spectrofluorimetric measurements were made at a sensitivity setting of 0.1 and with 6-nm band-widths for the emission and excitation monochromators. Under these conditions a 1.28μM quinine sulphate solution gave a fluorescence signal that was 7.5% of full scale.

Procedure

To a solution containing up to 90 ng of Mn(II), in a 10-ml standard flask, add 0.25 ml of 0.1% reagent solution in ethanol, 1.5 ml of 0.3% v/v hydrogen peroxide solution and 4 ml of 1 *M* ammonia solution, then start the stop-clock. Make up to the mark with water, mix, and after 1 min transfer a portion to a 1-cm quartz fluorimeter cell maintained at 50 ± 0.1°. Wait 2 min before starting to record the fluorescence intensity (λ_{ex}365, λ_{em}440 nm) as a function of time. Follow the uncatalysed reaction under similar conditions, but without the addition of manganese. Calculate the reaction rate from the difference in the slopes of the fluorescence–time plots.

Preparation of samples

Water. To 250 ml of water add 2.5 ml of concentrated nitric acid. Warm gently for 30 min then concentrate by evaporating to 25 ml.

Milk. To 25 ml of milk in a 100-ml Erlenmeyer flask add 25 ml of concentrated sulphuric acid/nitric acid mixture (1:1 v/v) and warm gently for 15 min. To complete the destruction of the organic matter add several drops of concentrated hydrogen peroxide. Cool, transfer the solution to a 50-ml standard flask and dilute to the mark with distilled water.

Beer. Add 50 ml of beer to 4 g of sodium carbonate in a large porcelain crucible and evaporate to dryness. Heat at 500° for 1 hr, cool, add 10 ml of distilled water and 5 ml of

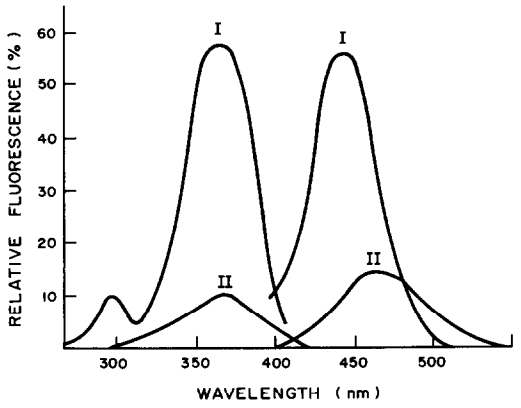

Fig. 1 Fluorescence spectra of HBTS before and after oxidation by hydrogen peroxide, catalysed by manganese(II). Conditions as described in the procedure. I—manganese 5 ng/ml; II—HBTS before oxidation.

concentrated hydrochloric acid and evaporate to dryness. Extract the residue with 25 ml of 1*M* hydrochloric acid, heat for 15 min, filter, and wash with distilled water, collecting the filtrate in a 50-ml standard flask.

Onion. Ash about 3 g of dried onion pieces in a porcelain crucible at 500° for 1 hr, then proceed as for beer.

RESULTS AND DISCUSSION

Catalytic effect of manganese(II)

Ammoniacal solutions of HBTS show a green fluorescence (λ_{ex} 380, λ_{em} 480 nm), but when they are treated with an oxidizing agent such as hydrogen peroxide, sodium periodate or potassium peroxodisulphate the fluorescence changes to blue and is then even more intense (λ_{ex} 365, λ_{em} 440 nm). This oxidation is catalysed only by manganese(II) when hydrogen peroxide is the oxidant. Figure 1 shows the fluorescence spectra of HBTS before and after catalytic oxidation.

Effect of reaction variables

The temperature was varied over the range 15–60° and the effect on both catalysed and uncatalysed reactions was examined. Both reactions proceed more quickly at higher temperatures, but at around 50–60° the rate appears to remain practically constant (Fig. 2). Accordingly, 50° was chosen for the final procedure.

Table 1. Choice of the method of adjusting temperature

Method	tan α*	% error
Proposed method	0.087	±1.0
Mix at room temperature and preheat to 50°		
record after 2 min	0.086	±1.2
record after 3 min	0.079	±1.7
Mix at 50° and record immediately	0.085	±2.1

*With 5 ng/ml manganese.

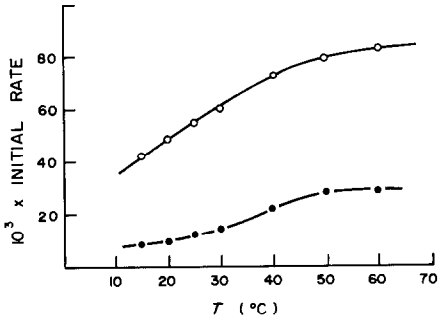

Fig. 2. Variation of the rate of the catalysed —○— and —●— uncatalysed reaction with temperature. Manganese concentration 5 ng/ml.

The activation energy calculated from the rates over the range 15–40° was 24.5 kJ/mole.

The approach to temperature control adopted in this paper is not the usual one for kinetic methods at elevated temperature, where all solutions are normally brought to the working temperature first and then mixed. However, the proposed method does give satisfactory performance, as shown by the comparative results in Table 1. Since the reaction is pseudo-first order, the initial rate is constant for any one manganese concentration, and following the change in fluorescence for a period starting 2 min after mixing does give a linear plot and hence a constant slope. (Fig. 3).

Changes in the order of addition of reagents, or in the ethanol concentration over the range 1–5% v/v, did not appreciably affect the performance of the method. Variations in ionic strength up to 0.1*M* did not affect the performance, but at higher ionic strengths (μ) the fluorescence was quenched somewhat, the effect levelling off at $\mu \sim 0.5M$ (Fig. 4). Samples containing appreciable concentrations of

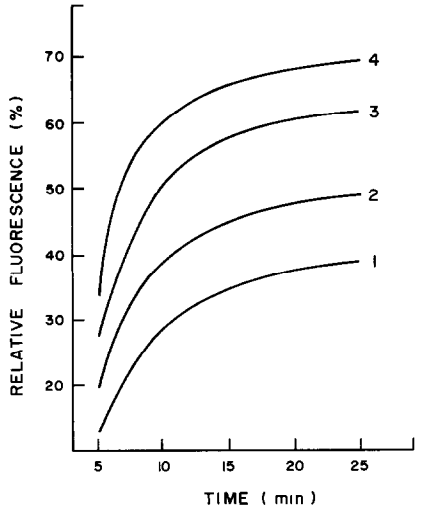

Fig. 3. Plots of fluorescence *vs.* time for different manganese concentrations. Conditions as for Fig. 1. Curve 1: 2 ng/ml; curve 2: 4 ng/ml; curve 3: 6 ng/ml curve 4: 9 ng/ml.

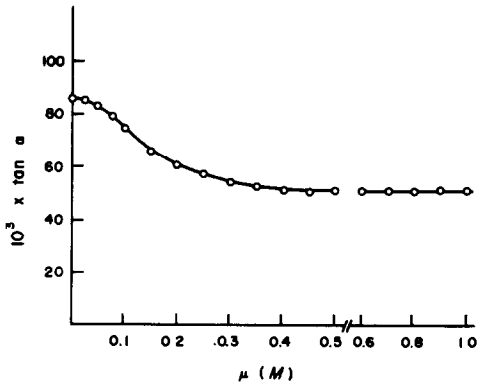

Fig. 4. Variation of initial rate (slope of plot) with ionic strength.

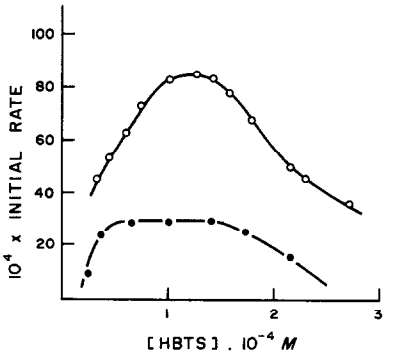

Fig. 5. Variation of initial rate with concentration of HBTS.

salts should be treated by addition of 2 ml of 2.5*M* sodium chloride to each 10-flask to give an ionic strength $\mu = 0.5M$. Calibration should be done under the same conditions.

The concentration of the HBTS reagent was varied over the range from 2.5×10^{-5} to $5 \times 10^{-4}M$ to investigate the effect on the rate of the reaction (Fig. 5). A log–log plot (Fig. 6) gave two linear sections, indicating that the reaction rate was proportional to the square root of the reagent concentration at low values. The initial rate of the uncatalysed reaction was independent of concentration over the range $0.8–1.3 \times 10^{-4}M$.

The rate of the catalysed reaction does not depend on the hydrogen peroxide concentration as long as it is above 0.01*M*. The concentration advocated in the procedure (1.5 ml of 0.3% peroxide solution in 10 ml) is 0.0145*M*. The rate of the catalysed reaction increases linearly with the ammonia concentration up to around 0.1*M*, then remains fairly constant till 0.4*M*, when the rate begins to decrease again. The recommended concentration in the procedure is 0.4*M*. The uncatalysed reaction showed a similar dependence on the ammonia concentration.

The catalysed reaction has also been studied in the presence of sodium hydroxide and nitrogenous bases such as butylamine and triethanolamine. In the alkali the catalytic effect of manganese(II) was minimal, but with the nitrogenous bases the behaviour observed was similar to that with ammonia.

Data manipulation

Three methods have been used for determination of low levels of manganese, and their performances compared (Table 2). The corresponding figures for media of ionic strength < 0.1*M* are as follows.

(*i*) The initial rate was plotted as a function of manganese concentration. Such calibration graphs

Table 2. Determination ranges and relative errors in the kinetic determination of manganese

Method	Range, *ng/ml*	Mean relative error, %
Initial rate	4–14	±1.2
Fixed-time	5–12	±1.3
Fixed-intensity	5–13	±1.8

*For ionic strength 0.5*M*.

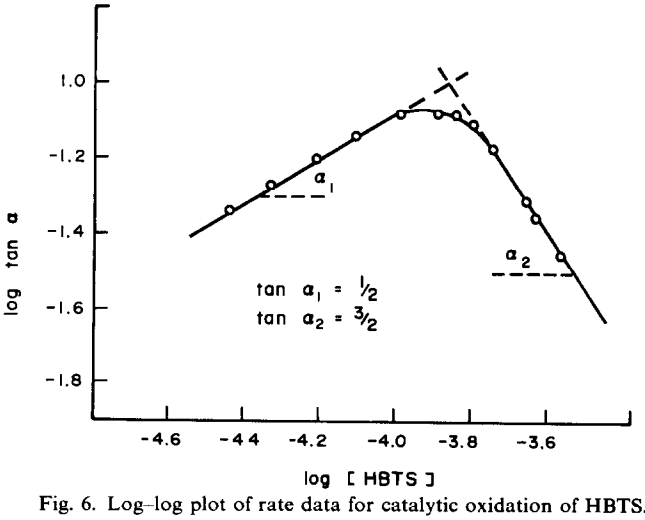

Fig. 6. Log–log plot of rate data for catalytic oxidation of HBTS.

Table 3. Interference levels of foreign ions in the kinetic determination of Mn at the 5.0 ng/ml level by the tangent method

Tolerance ratio (Ion)/(Mn^{2+})	Ion added
1000	Li^+, Na^+, K^+, Be^{2+}, Sr^{2+}, Ba^{2+}, Al^{3+}, V(V), In^{3+}, As(III and V), Se(IV), Ga^{3+}, UO_2^{2+}, Sb(III)*, Cl^-, Br^-, F^-, I^-, NO_2^-, NO_3^-, SCN^-, tartrate, citrate, oxalate, CO_3^{2-}, SO_4^{2-}, SO_3^{2-}, PO_4^{3-}, BrO_3^-, ClO_4^-, mercaptoacetic acid
400	Rb^+, Ca^{2+}, Cd^{2+}, Pd(II), Pt(IV), Bi^{3+}, Tl^+, Ce(IV), Mo(VI), Hg(II)†, S^{2-}, CN^-, IO_3^-, IO_4^-
200	Cu^{2+}, Sn^{2+}†, Rh(III), Th^{4+}, La^{3+}, Mg^{2+}, $S_2O_8^{2-}$
100	Zr^{4+}, W(VI), Hg(I), Ir(III)
50	Pb^{2+}†, Zn^{2+}†, Ag^+†, Cr^{3+}†
20	Co^{2+}
10	Fe^{3+}§

*Plus sodium thiosulphate (5 μg/ml).
†Plus mercaptoacetic acid (5 μg/ml).
§Plus sodium fluoride (5 μg/ml).

were linear over the range 2–9 ng/ml and the mean relative error was 1.2% ($P = 0.05$ and $n = 11$).

(*ii*) The fluorescence was measured at a fixed time after mixing: under these conditions the calibration graph was linear over the range 3–7 ng/ml.

(*iii*) The time to reach a preset fluorescence intensity was measured: here the linear range was 3–8 ng/ml of manganese, with a mean relative error of 1.7%.

Method (*i*) was selected on the basis of the smaller mean error and the wider linear range. In the non-linear portions of the calibration graphs the signal is lower than expected.

Interferences

The effect of many common ions on the rate of the catalytic reaction was examined to find any interferences. Tolerances for those ions investigated are given in Table 3. Of the cations, Fe(III), Pb(II), Zn(II), Ag(I), Sn(II) and Sb(III) all interfere and should be absent if accurate results are to be obtained. However, the tolerance for some interferences can be improved by addition of masking reagents such as mercaptoacetic acid, thiosulphate and fluoride. The strongest interference is given by EDTA (interfering at only twice the manganese concentration) since it forms a stable complex with manganese(II).

Applications

The proposed method has been used to determine manganese in a variety of foodstuffs, and the results have been compared with those obtained by atomic absorption. In all cases the standard addition method was applied (Table 4). Some results for the determination of manganese in a water sample by the standard-addition method are given in Table 5. The performance would seem to be quite satisfactory.

Table 4. Determination of manganese in water and foods

Sample	Subsample, *ml*	Manganese found,* Kinetic method	AAS method
Water†	2	3.8 ± 0.1 ng/ml	4.0 ± 0.1 ng/ml§
Milk†	0.2	310 ± 4 ng/ml	313 ± 2 ng/ml
Beer†	0.3	210 ± 2 ng/ml	214 ± 2 ng/ml
Onion	0.1	9.8 ± 0.1 μg/g	9.9 ± 0.1 μg/g

*Average of 8 separate determinations
†Fluoride added (5 μg/ml) to suppress interference from iron
§A litre of water acidified with HNO_3 was evaporated to 25 ml for this determination

Table 5. Determination of manganese in a water sample by the standard-addition procedure

Aliquot taken, *ml*	Manganese Added, *ng/ml*	Found, *ng/ml*	Recovery, %
1	—	0.72	
1	2.0	2.72	100.0
1	5.0	5.64	98.6
1	8.0	8.75	100.4
2	—	1.47	
2	2.0	3.45	99.6
2	3.0	4.42	98.9
2	5.0	6.49	100.3

REFERENCES

1. F. Grases, F. Garcia-Sanchez and M. Valcárcel, *Anal. Chim. Acta*, 1980, **119**, 359.
2. *Idem, An. Quim*, 1980, **76**, 124.
3. *Idem, Anal. Lett.*, 1979, **12**, 803.
4. F. Grases, J. Estela, F. Garcia-Sanchez and M. Valcárcel, *Analusis*, 1981, **9**, 66.
5. *Idem, Anal. Lett.*, 1980, **13**, 181.
6. M. D. Luque de Castro and M. Valcárcel, *Talanta*, 1980, **27**, 645.
7. M. D. Perez-Bendito, M. Valcárcel, M. Ternero and F. Pino, *Anal. Chim. Acta*, 1977, **90**, 405.
8. M. Ternero, F. Pino, M. D. Perez-Bendito and M. Valcárcel, *Microchem. J.*, 1980, **25**, 102.
9. J. Ferrer, *Doctoral Thesis*, University of Córdoba, 1980.
10. R. P. Igov, M. D. Jaredić and T. G. Pecev, *Talanta*, 1980, **27**, 361.
11. P. P. T. Sah and T. C. Daniels, *Rec. Trav. Chim.*, 1950, **69**, 1545.

Talanta. Vol. 30, No. 2, pp. 111–115, 1983
Printed in Great Britain

0039-9140/83/020111-05$03.00/0

DETERMINATION OF RARE EARTHS IN LANTHANUM OXIDE BY INDUCTIVELY-COUPLED PLASMA EMISSION DERIVATIVE SPECTROMETRY

HAJIME ISHII and KATSUHIKO SATOH
Chemical Research Institute of Non-Aqueous Solutions, Tohoku University, Katahira, Sendai-shi, 980 Japan

(*Received* 14 *January* 1982. *Accepted* 21 *April* 1982)

Summary—Rare-earth elements (REE) at ppm levels in lanthanum oxide can be determined without prior separation and preconcentration by use of high-resolution inductively-coupled plasma emission derivative spectrometry (ICPEDS). The calibration graphs are all linear and pass through the origin, even in the presence of large amounts of lanthanum, except those for dysprosium, holmium and ytterbium. The detection limit for each REE is 1–10 μg/g in lanthanum oxide. Investigation of various physical and/or spectral interferences shows that good selectivity is obtained by ICPEDS.

Inductively-coupled plasma emission spectrometry (ICPES) is in general a useful technique for trace analysis and has been applied to the determination of rare-earth elements (REE) in steel[1] and mineralogical samples[2] with high sensitivity, but its selectivity is not always satisfactory. However, we have recently found that much higher selectivity is obtained by inductively-coupled plasma emission derivative spectrometry (ICPEDS) with a high-resolution echelle spectrometer modified for wavelength modulation. We have reported its outline and characteristics together with its successful application to the determination of hafnium in zirconium oxide.[3] In the present work the same instrumentation is applied to the determination of REE at ppm levels in high-purity lanthanum oxide without any prior separation and preconcentration.

EXPERIMENTAL

Apparatus

The apparatus is the same as that described in our previous paper[3] and is outlined in Table 1. The wavelength is modulated sinusoidally by a refractor plate modulator included in the spectrometer and the second harmonic (*i.e.*,

Table 1. Instrumental facilities and operating conditions

Plasma	
R.F. generator	Model HFP-1500 D, Plasma-Therm Inc. (Kresson, N.J.)
Matching network	Model MN-1500 E, Plasma-Therm Inc.
Torch	Model PT-1500, Plasma Therm Inc.
Forward R.F. power	1.15 kW
Reflected power	<5 W
Argon flow-rates	
Coolant gas	10 l./min
Plasma gas	1 l./min
Aerosol carrier-gas	
Y, Ce, Gd, Yb, Lu	0.45 l./min
Other REE	0.48 l./min
Sample introduction system	Pneumatic nebulization with a concentric glass nebulizer
Sample solution uptake-rate	
Y, Ce, Gd, Yb, Lu	1.3 ml/min
Other REE	1.6 ml/min
Observation height	16 mm above work coil
Spectrometer	Wavelength-modulated echelle spectrometer with a modified Czerny-Turner mounting [commercially available as model UOE-1 from Yanaco Co., Ltd. (Japan)]. Reciprocal linear dispersion: 0.31, 0.62, 0.93, 1.2 Å/mm at 2000, 4000, 6000, 8000 Å, respectively, with 25-μm slit-width.
Entrance and exit slit-width	50 or 100 μm
slit-height	1000 μm
Integration time	15 sec
Modulation interval	See Table 2
Analysis line	See Table 2
Optical measurement unit	Model UM-1, Yanaco Co., Ltd. and model RC-125 chart recorder, Japan Spectroscopic Co., Ltd.

Table 2. Optimum analysis lines, modulation intervals, slit-widths and detection limits

Determinand	Analysis line, Å	Modulation interval, Å	Slit-width, μm	Detection limit, μg/g*
Y	3710.30	0.15	50	1
Ce	4040.76	0.22	100	10
Pr	4143.11	0.22	100	10
Nd	4303.53	0.20	100	10
Sm	3568.21	0.07	100	10
Eu	3819.17	0.30	50	2
Gd	3549.37	0.15	100	5
Tb	3509.17	0.20	100	4
Dy	3531.70	0.15	50	5
Ho	3456.00	0.20	100	2
Er	3372.71	0.20	100	2
Tm	3761.33	0.15	50	5
Yb	3289.37	0.07	50	1
Lu	2615.42	0.15	100	1

*As determinand (μg/g) in lanthanum oxide.

with twice the frequency of modulation) of the a.c. component of the signal is detected, so the second derivative emission spectrum or intensity is measured on a chart recorder, a distinction from the use of conventional apparatus.

Reagents

Stock solutions containing lanthanum (20.00 g/l.) or REE (3.000 g/l.) were prepared from 99.999% pure lanthanum oxide (Soegawa Chemicals Co., Ltd.) and 99.99% REE oxides (Shinetsu Chemicals Co., Ltd.), respectively, in the same way as the sample solutions (see below). The REE oxides used were ignited at about 700° before use, to decompose any carbonate present. Working solutions were prepared by dilution of the stock solutions with water. All other chemicals used were of analytical-reagent grade. All solutions were prepared with distilled demineralized water.

Preparation of sample solution

Place 1 g of sample in a 100-ml beaker, add 10 ml of 2*M* perchloric acid and heat gently until the solution is quite clear. After cooling, dilute the solution to 100 ml with water.

Operating conditions

On the basis of the experimental results described below, operating conditions for the determination of REE were decided as shown in Table 1.

RESULTS AND DISCUSSION

Selection of spectral lines, modulation intervals, slit-widths and slit-heights

There are many emission lines usable for the determination of individual REE, but most of them suffer spectral interference from other REE. Thus the level of mutual spectral interference among the REE as well as the spectral interference of lanthanum was examined at the sensitive lines for each REE, to find practically interference-free spectral lines suitable for the determination of each REE, as shown in Table 2. Only the lines of dysprosium, holmium and ytterbium were slightly subject to spectral interference by lanthanum. Any spectral interference could generally be suppressed by decreasing the slit-width or the modulation interval, but doing so also decreased the second derivative intensity and hence raised the detection limit. Consequently, an appropriate slit-width and modulation interval had to be selected for each REE. These are also shown in Table 2. The slit-height is also related to the spectral resolution, but the resolution is good with slit-heights up to 1000 μm.

Influence of perchloric acid concentration

As can be seen from Fig. 1, shown as an example, increasing the perchloric acid concentration in general decreases the second-derivative intensity of the REE, regardless of the plasma region observed, but the sample solution uptake-rate does not vary. The effect on the derivative intensity seems to be due to decrease in the nebulization efficiency on increase in

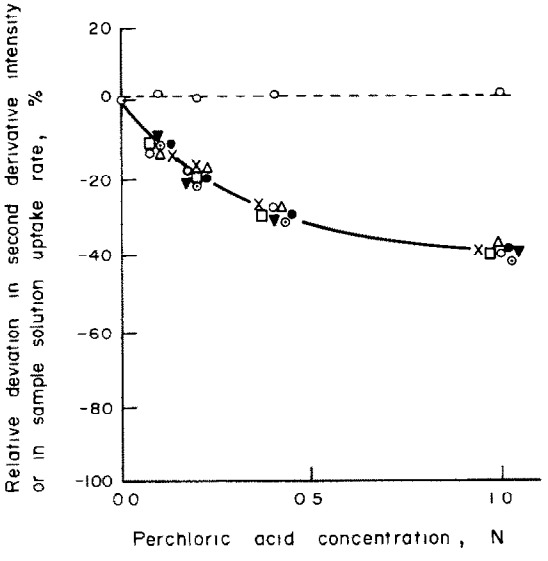

Fig. 1. Influences of perchloric acid concentration on the second derivative intensity (——) and sample solution uptake rate (– – – –). ○, Y; ⊙, Ce; ●, Sm; ×, Eu; △, Dy; ▼, Er; □, Lu.

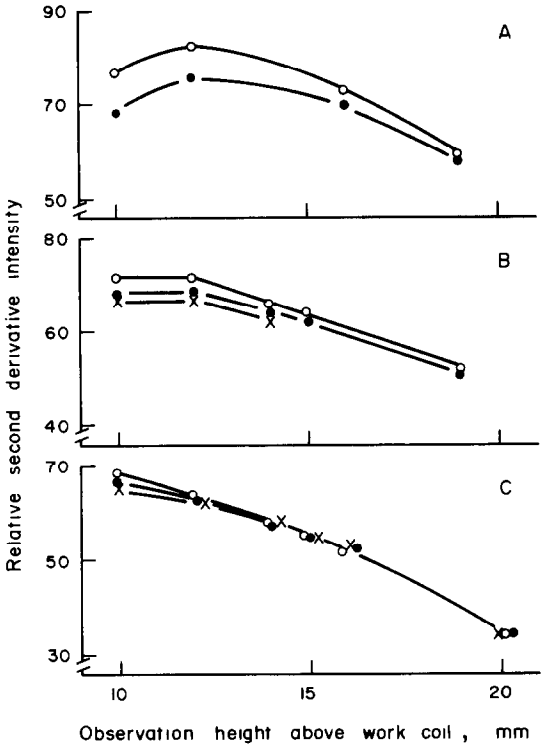

Fig. 2. Influences of observation height, nebulizer pressure and lanthanum concentration on the second derivative intensity of yttrium. Lanthanum concentration (ppm)—O, 0; ●, 5000; ×, 7500. Nebulizer pressure (psig)—A, 16.5; B, 14; C, 12.

the perchloric acid concentration. Hence the sample solutions and standard solutions should have as near as possible the same perchloric acid concentration.

Influence of lanthanum concentration

Freedom from chemical and physical interferences is one of the more important characteristics of ICPES. However, the matrix can cause the emission intensity of the determinand to increase, decrease, or show no change, depending on the plasma region observed.[4,5] In this study the second-derivative intensity of REE was also affected by the lanthanum concentration, to a degree which depended on the carrier-gas flow-rate and the R.F. power as well as on the plasma region observed. Figures 2 and 3 show the influence of the observation height in the plasma on the second-derivative intensity of yttrium and erbium, respectively, with varying lanthanum concentration and nebulizer pressure. Comparing Fig. 2 with Fig. 3 shows that the influence on yttrium differs from that on erbium. For yttrium, increasing the lanthanum concentration decreases the derivative intensity, and the effect decreases with decreasing nebulizer pressure, increasing R.F. power (not shown) or increasing observation height. For erbium, on the contrary, lanthanum increases the derivative intensity except as shown in Fig. 3A. Cerium, gadolinium, ytterbium and lutetium showed similar behaviour to yttrium, and the other REE behaved similarly to erbium. Since with our apparatus there is no significant spectral interference by lanthanum at the REE lines used, these phenomena are presumably due to changes in the population of excited determinand atoms and ions caused by introduction of large amounts of lanthanum into the plasma. Fortunately, however, there are conditions (as shown in Figs. 2C, 3A and 3B) under which all REE other than dysprosium, holmium and ytterbium (which are slightly subject to the spectral interference by lanthanum) can be determined directly in the presence of large amounts of lanthanum.

Spectral interference of REE and other ions

The mutual interferences among the REE and the interference by copper, iron, aluminium, sodium and potassium were studied. The results for the REE (expressed as apparent determinand concentration per 100 mg/l. of interferent) are summarized in Table 3, from which it is seen that lanthanum practically does not interfere with the determination of most REE, and that only cerium, dysprosium and erbium, and samarium and ytterbium give errors over 3% for the determination of praseodymium and terbium, respectively, when present in equal weight to the determinand. Even these errors, which are due to spectral interference as can clearly be seen from Figs. 4 and 5 (shown as examples) can easily be corrected for by utilizing Table 3.

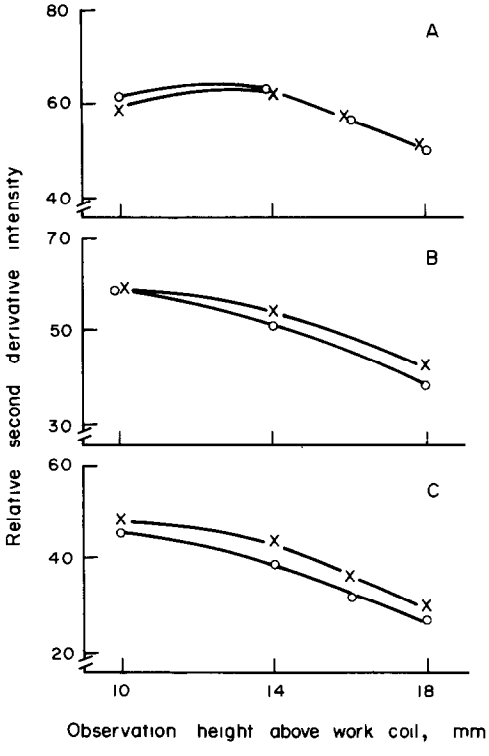

Fig. 3. Influences of observation height, nebulizer pressure and lanthanum concentration on the second derivative intensity of erbium. Lanthanum concentration (ppm)—O, 0; ×, 7500. Nebulizer pressure (psig)—A, 16; B, 14; C, 12.

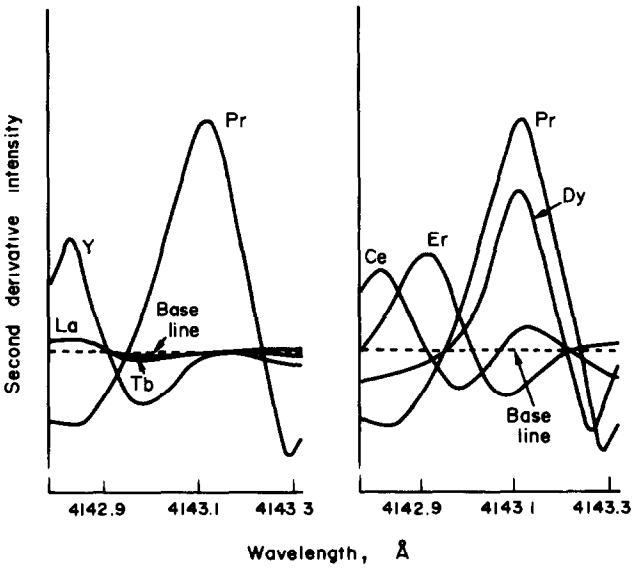

Fig. 4. Second derivative spectra of REE near the 4143.11 Å Pr line. Concentration (ppm)—Pr, 37; Y, 76; Ce, 70; Tb, 75; Dy, 77; Er, 80; La, 1% (as La_2O_3).

Interference by copper, iron, aluminium, sodium and potassium at concentrations up to 100 mg/l. is negligible. The results described here show the good resolution of our apparatus and, in addition, suggest the feasibility of direct determination of the REE as impurities not only in lanthanum but also in other REE, without prior separation.

Calibration graphs and detection limits

Plots of the second-derivative intensity against the determinand concentration were all linear, and the slopes were unaffected by the presence of lanthanum, as shown in Figs. 6 and 7. All the lines (except those for dysprosium, holmium and ytterbium in the presence of lanthanum) pass through the origin. These results show the outstanding characteristics, not obtained with the conventional apparatus, of our apparatus, and reveal that lanthanum, even in 10^5 w/w ratio to the determinand, does not interfere with the determination of other REE except for three mentioned.

The detection limit for each REE, defined as the determinand concentration (in a 1% solution of lanthanum oxide) that gives an average net derivative

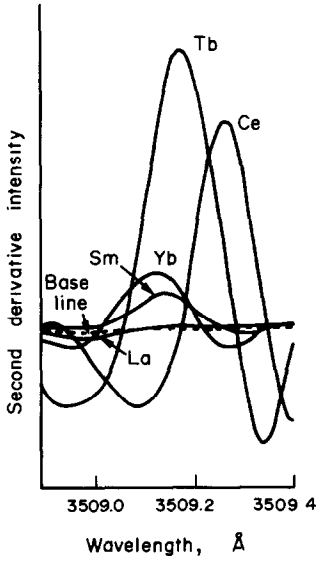

Fig. 5. Second derivative spectra of REE near the 3509.17 Å Tb line. Concentration (ppm)—Tb, 15; Ce, 70; Sm, 75; Yb, 76; La, 1% (as La_2O_3).

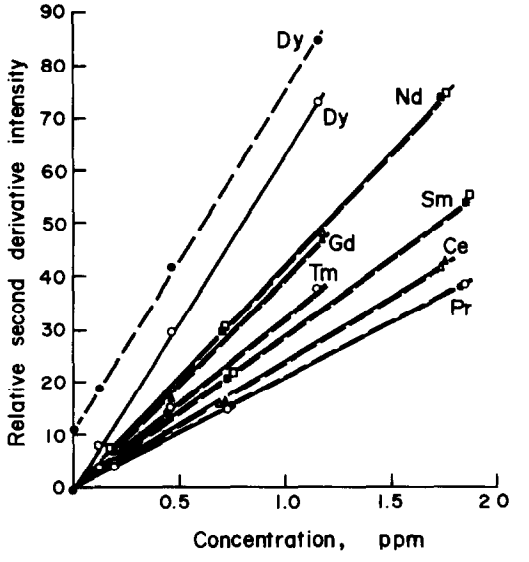

Fig. 6. Calibration curves in the presence or absence of lanthanum. Lanthanum oxide: ○, □, △—0%; ●, ■, ▲—1%.

Table 3. Interferences expressed in terms of determinand concentration (*μg/ml*) equivalent to signal from 100-μg/ml interferent concentration

Determinand	La*	Interferent Y	Ce	Pr	Nd	Sm	Eu	Gd	Tb	Dy	Ho	Er	Tm	Yb	Lu
Y	<DL							−0.62							
Ce	<DL			−2.37	2.61	−1.18			−0.65	−0.34	0.70	−3.91			
Pr	<DL	−0.41	5.30		−1.53			−1.18	−0.41	24.7		−6.30			
Nd	<DL		2.49	0.36			0.20	−0.72				−0.37			
Sm	<DL		−0.50		0.54							−0.41			
Eu	<DL														
Gd	<DL	−0.25		−0.27	0.39		−0.37		0.74	−2.27	−0.34	−0.50			
Tb	<DL		−1.51	−0.27	1.06	3.30				−0.30	0.63	−0.56		3.44	
Dy	0.17							0.96	−0.29						
Ho	−0.13		−0.18	0.34		−0.20		−1.23	0.54	−0.18					
Er	<DL								0.92	0.39	0.16				
Tm	<DL								0.50						
Yb	−0.04														
Lu	<DL														

*1%, added as lanthanum. DL = detection limit. Vacant spaces = <0.10 μg/ml.

Table 4. Determination of REE in lanthanum oxide and synthetic samples, *ppm*

Sample	Y	Ce	Pr	Nd	Sm	Eu	Gd	Tb	Dy*	Ho*	Er	Tm	Yb*	Lu
W_1	<1	<10	40	<10	<10	<2	<5	<4	<5	<2	<2	<5	<1	<1
N	<1	38	<10	22	<10	<2	5	<4	<5	<2	<2	<5	<1	<1
W_2	<1	<10	<10	<10	<10	<2	<5	<4	<5	<2	<2	<5	<1	<1
S_1	83	85	92 (80)†	84	76	80	80	49 (45)§	38	40	38	41	39	40
S_2	101	99	128 (104)†	103	90	102	97	113 (106)§	101	95	97	100	95	97

W_1, N, W_2: lanthanum oxide
W_1, sold as 99% La_2O_3; N, sold as 99.9% La_2O_3; W_2, sold as 99.99% La_2O_3.
S_1, S_2: synthetic samples
S_1, Y–Gd = 80 ppm; Tb–Lu = 40 ppm.
S_2, Y–Lu = 100 ppm.
*Corrected for interference from La.
†Corrected for interferences from Ce, Dy and Er.
§Corrected for interferences from Sm and Yb.

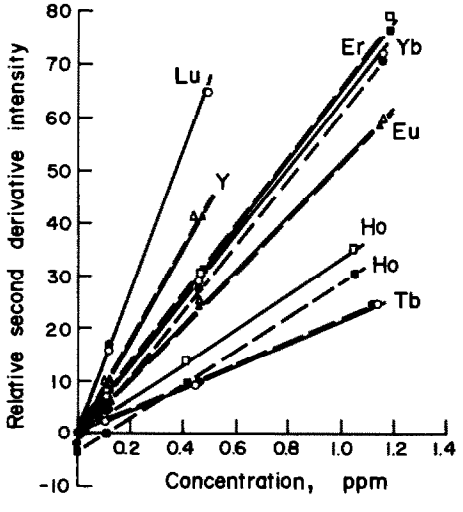

Fig. 7. Calibration curves in the presence or absence of lanthanum. Lanthanum oxide: ○, □, △—0%; ●, ■, ▲—1%.

signal equal to twice the standard deviation of the background noise, is listed in Table 2.

Determination of REE in lanthanum oxide and synthetic samples

REE in commercial high-purity lanthanum oxides and synthetic samples were determined with satisfactory results as shown in Table 4.

Acknowledgement—This study was partly supported by a scientific research grant from the Ministry of Education, Japan, to which our thanks are due.

REFERENCES

1. C. C. Butler, R. N. Kniseley and V. A. Fassel, *Anal. Chem.*, 1975, **47**, 825.
2. J. A. C. Broekaert, F. Leis and K. Laqua, *Spectrochim. Acta*, 1979, **34B**, 73.
3. H. Ishii and K. Satoh, *Talanta*, 1982, **29**, 243.
4. H. Kawaguchi, T. Ito, K. Ota and A. Mizuike, *Spectrochim. Acta*, 1980, **35B**, 193.
5. R. N. Savage and G. M. Hieftje, *Anal. Chem.*, 1980, **52**, 1267.

Talanta, Vol. 30, No. 2, pp. 117–120, 1983
Printed in Great Britain

0039-9140/83/020117-04$03.00/0
Pergamon Press Ltd

SHORT COMMUNICATIONS

DETERMINATION OF SILICON BY AN INDIRECT ATOMIC-ABSORPTION METHOD USING CARBON-ROD ELECTROTHERMAL ATOMIZATION

J. F. TYSON and W. S. WAN NGAH
Department of Chemistry, University of Technology, Loughborough, Leicestershire, England

(*Received* 5 *April* 1982. *Accepted* 16 *September* 1982)

Summary—An indirect procedure has been developed for the determination of trace amounts of silicon by atomic-absorption with carbon-rod electrothermal atomization. After dissolution, the silicon is extracted as silicomolybdic acid into a mixture of diethyl ether and pentan-1-ol (5 + 1). The co-extraction of excess of molybdate reagent is prevented by the addition of citrate, which also destroys phosphomolybdic and arsenomolybdic acids. The organic layer is washed with hydrochloric acid, μl quantities are transferred to the electrothermal atomizer and the molybdenum is measured. The method has been applied to analysis of several steels.

In attempting to extend the sphere of application of atomic-absorption spectrometry (AAS) in analytical chemistry both in terms of sensitivity (and consequently detection limit) and range of elements or species determined, the chemistry of the heteropolymolybdates offers several attractive possibilities, particularly when combined with electrothermal atomization devices.

The polymerization reaction which occurs when a solution of molybdate (MoO_4^{2-}) is acidified in the presence of a hereroelement has been used as the basis of analytical methods for about 10 of the possible 35 hetero-elements, namely P, Si, As, Ge, V, Th, Ta, Ti, Nb and Ce. Most of the previously reported methods use solution spectrophotometry or flame AAS as the final measuring stage in a procedure that almost always includes a solvent extraction stage to separate the heteropoly species, $H_nXMo_{12}O_{40}$ (where the value of n depends on the oxidation state of X) from the large excess of molybdate reagent, which polymerizes under the reaction conditions to give one or more of the isopolymolybdates.

The indirect determination of the hetero-element by determination of the molybdenum in the heteropoly species gives a considerable enhancement of sensitivity because of the 12:1 molar ratio of Mo to X.

Preliminary results for phosphorus and arsenic have already been reported[1] and the problems of the high blank values (due to co-extracted isopolymolybdate) and the difficulties in atomizing molybdenum from a carbon-rod electrothermal device outlined. In this paper the development of a method for silicon is described. The analysis of some standard steel samples, in which interference effects might be expected, is included to illustrate the application of the method.

Silicon has been determined by solution[2–7] and AAS amplification methods.[3,8–10] Ultraviolet spectrophotometric methods are based on the measurement of the absorbance of silicomolybdic acid [6,7] or its reduction product[4,5] ("molybdenum blue") or its decomposition product in a basic buffer.[2,3] The atomic-absorption methods[3,8,9] are based on the measurement of the molybdenum content of silicomolybdic acid. Concentration ranges of 0.1–0.4 and 0.1–1.2 ppm of silicon are covered by the indirect ultraviolet and atomic-absorption methods, respectively.[3] The direct determination of silicon by atomic-absorption has also been described (*e.g.*, Price and Roos[11]), but the sensitivity is poor.

Silicon in steel has been determined by atomic-absorption spectrophotometric,[4,11,12] colorimetric,[4,5,13] gravimetric,[13,14] titrimetric and electrochemical methods.[14] A differential pulse polarographic method has also been used for levels down to 0.002%.[15] The methods used by British Chemical Standards for the determination of silicon in steel are gravimetric and photometric.

Several workers have found that the addition of complexing agents such as citric, lactic, tartaric, oxalic and malonic acids, glycerol, mannitol and ethylene glycol to phosphomolybdic and arsenomolybdic acids destroys both acids, but not silicomolybdic acid.[16–18] Chalmers and Sinclair[16] found that certain complexing agents (notably citric, tartaric and oxalic acids, and mannitol) shift the absorption spectrum of isopolymolybdates by complexation, and have estab-

lished[17] that their differential effect on the heteropoly acids is kinetic in nature.

DEVELOPMENT OF THE METHOD

The extent of formation and extraction of the heteropolymolybdate and isopolymolybdate was studied as a function of acidity, molybdate concentration, reaction kinetics, nature of the extracting solvent, wash conditions and presence of a masking agent. The aim of these studies was to achieve an acceptable signal-to-blank ratio in a reasonable analysis time.

Acidity

In agreement with previous reports[19,20] it was found necessary to add the acid (hydrochloric) in two portions. The solution was first acidified to 0.12*M* to form the polymeric species and then to 1.0*M* to protonate the species for extraction. The formation reaction is reported to be slow and inhibited by a large excess of acid, owing to the formation of polysilicic acids.

Molybdate concentration

A large excess of molybdenum is necessary to achieve the required degree of formation. The best signal-to-blank ratio was obtained with a molar ratio of about 1400:1 molybdenum to silicon. In practice, a fixed amount of molybdenum was added as ammonium molybdate to not more than 6 μg of silicon.

Solvent system

Five different solvent systems were investigated as possible extractants: pentan-1-ol, butan-1-ol, 3-methylbutan-1-ol (isoamyl alcohol), 4-methylpentan-2-one (MIBK) and a mixture of diethyl ether and pentan-1-ol (5 + 1). The main criterion governing the choice of solvent was selectivity for extraction of silicomolybdic acid in presence of isopolymolybdic acid and other heteropoly acids. On this basis, the diethyl ether–pentan-1-ol mixture was used in the method eventually developed. It was found necessary to wash the organic layer with hydrochloric acid to reduce the blank level further.

Masking agents

The effect of six different masking agents on the extent of the isopolymolybdate extraction was investigated. These were oxalic, lactic, malonic and citric acids, glycerol and mannitol. Apart from lactic acid all of these complexing agents reduced the blank level. However, the greatest reduction was caused by citric acid and as citrate also masks possible interferences from other hetero-elements present in real samples, this was added at a concentration of about 0.4% after the final adjustment of the acidity.

Atomization procedure

A 1-μl portion of the organic phase was transferred to the carbon-rod atomizer. Some practice was needed to achieve reproducible transfer, since the solvent has a rather high vapour pressure. After evaporation, the residue was ashed at red heat and, after a 10-sec delay, atomized for 1.5 sec at a temperature just above the sublimation temperature of graphite. To avoid memory effects, a cleaning stage was applied before the rod was cooled (to below 30°) for transfer of the next sample. Oxygen-free nitrogen was used as sheathing gas. This procedure, although satisfactory with new rods, resulted in rod lifetimes of only a few firings and a rapid deterioration due to increased porosity. To overcome this problem, the rods were coated with pyrolytic graphite produced by the pyrolysis of acetylene bled (at 40–50 ml/min) into the nitrogen sheathing gas (flowing at 3.2 l./min). Two coatings were produced at the normal atomization temperature every thirty atomizations, prolonging the rod lifetimes to several hundred atomizations. The use of a hydrocarbon gas for the production of pyrolytic graphite coatings has been reported previously,[21] and methane appears to be preferred. However, the use of acetylene was found to be perfectly satisfactory and this gas is always readily available in a laboratory operating atomic-absorption instruments.

A comparison of the slope of the calibration graph for standard silicon solutions with that for standard molybdenum solutions showed that the combined degree of formation and extraction of the silicomolybdate was about 98%. However, the value varied from one analysis to another and as it seemed possible that the degree of atomization was affected by the chemical form of the molybdenum, calibration was done by applying the complete procedure to amounts of up to 4 μg of silicon. The absorbance due to the blank solution was subtracted before the calibration graph was plotted. As well as correcting for the small amount of isopolymolybdate co-extracted, this corrects for the small non-specific absorbance arising from the sublimation of a small amount of graphite from the rod surface during atomization.

EXPERIMENTAL

Apparatus

A Shandon Southern A3470 Flameless Atomizer and an A3400 Atomic Absorption Spectrophotometer were used. The output from the spectrophotometer was recorded by a Tarkan model 600 recorder. Graphite rods with a nominal capacity of 1 μl were used. Solutions were transferred with an Oxford microlitre pipette.

Reagents

Standard silicon solution, 100 ppm. Fuse 0.107 g of dry precipitated silica with 1.0 g of analytical grade anhydrous sodium carbonate in a platinum crucible. Cool the melt, dissolve it in demineralized water, dilute to 500 ml and store in a polythene bottle.

Hydrochloric acid, 5.1M and (1 + 9).

Ammonium molybdate solution, 1%. Dissolve 1 g of analytical grade ammonium molybdate in distilled water and dilute to 100 ml.

Table 1. Results of analysis of BCS steels

Steel sample	Silicon found, %	Certificate value, %
BCS 218/3 0.15% Carbon Steel	0.22 ± 0.03	0.22
BCS 365 Permanent Magnet Alloy	0.33 ± 0.04	0.34
BCS 434 Plain Carbon Steel	0.56 ± 0.07	0.51
BCS 254/1 Low Alloy Steel	0.22 ± 0.03	0.22
BCS 241/2 High Speed Steel	0.19 ± 0.02	0.21

Citrate solution, 10%. Dissolve 10 g of citric acid in about 80 ml of distilled water. Adjust to pH 3.2 with sodium hydroxide and dilute to 100 ml.

*Sulphuric acid, 1.5*M.

Ammonium persulphate solution, 12%.

Diethyl ether–pentan-1-ol mixture (5 + 1).

Preparation of steel sample solution[12]

Add 25 ml of 1.5*M* sulphuric acid to 0.3 g of steel in a Teflon beaker and heat until the sample is dissolved; add 10 ml of 12% ammonium persulphate solution, boil until clear, cool, and dilute to volume in a 50-ml standard flask with distilled water. Dilute a 2-ml aliquot of this solution to volume in a 100-ml standard flask with distilled water.

Extraction

Transfer 2 ml of the final solution into a 100-ml separating funnel and add 1 ml of 5.1*M* hydrochloric acid and 34 ml of distilled water. Add 4 ml of 1% ammonium molybdate solution, mix and allow to stand for 10 min. Add 8.8 ml of 5.1*M* hydrochloric acid and allow to stand for 10 min. Add 2 ml of citrate solution, mix and allow to stand for a further 10 min. The order of addition of reagents is important. Extract the silicomolybdic acid with 20 ml of solvent mixture by shaking for 1 min. Wash the organic extract three times with 25-ml portions of hydrochloric acid (1 + 9). For each wash, shake for 30 sec. Drain off the aqueous layer and transfer the organic layer into a 25-ml standard flask and dilute to the mark with the solvent.

Preparation of standards and calibration graph

Dilute the stock 100-ppm silicon solution to give a 1-ppm solution, just before use. Transfer 0, 1, 2, 3 and 4 ml to separating funnels and proceed as described for the sample solutions. Adjust the volume of water added so that the total volume is 37 ml before the addition of the ammonium molybdate.

Atomize 3 replicate 1-μl portions of the final organic phase, calculate the mean, subtract the mean blank value and plot absorbance against silicon concentration.

RESULTS AND DISCUSSION

Assuming 100% formation of silicomolybdate and 100% extraction in obtaining the calibration curve, the amount of silicon transferred to the rod for each atomization ranged from zero to 160 pg. This latter value represented the top of the linear range and corresponded to an absorbance value of 0.40. The blank absorbance value was typically around 0.03. A least-squares linear regression analysis of a five-point calibration graph had a slope corresponding to a characteristic amount of silicon (or sensitivity, *i.e.*, amount for 1% absorption) of 1.8 pg, a correlation coefficient of 0.998 and an intercept of 0.0060 on the absorbance axis. The standard deviation of the absorbance residuals was 0.0093, giving a limit of detection (on the basis of "intercept plus twice the absorbance residuals") of 5.2 pg. The relative standard deviation of 10 replicate atomizations of the solution corresponding to 40 pg of silicon transferred to the rod was 5.3% with a mean absorbance value of 0.12. The limit of detection calculated as twice this standard deviation corresponded to 4.4 pg.

The overall precision of the method, obtained from 5 replicate analyses of one of the standard steel samples (BCS 365) was 10% relative standard deviation. As the value for the atomization stage is 5.3%, the relative standard deviation of the formation and extraction stage is approximately 8.5%.

The effect of the addition of arsenic and phosphorus, both potential interferents in the analysis, was investigated for a solution corresponding to 80 pg of silicon taken for atomization. No interference was observed for up to 80 pg of arsenic and 120 pg of phosphorus.

In the absence of suitable certified reference materials containing low concentrations of silicon the accuracy of the method was evaluated by analysing five different British Chemical Standard steels. The results are shown in Table 1. The interval about the mean value is the 95% confidence interval calculated from the *t*-distribution.

Acknowledgements—One of us (WSWN) gratefully acknowledges financial support from the Public Services Department and the Universiti Sains Malaysia.

REFERENCES

1. J. F. Tyson and G. D. Stewart, *Anal. Proc.*, 1981, **18**, 184.

2. L. A. Trudell and D. F. Boltz, *Anal. Chem.*, 1963, **35,** 2122.
3. T. R. Hurford and D. F. Boltz, *ibid.*, 1968, **40,** 379.
4. Y. Kakita and H. Goto, *Talanta*, 1967, **14,** 543.
5. P. Pakalns and W. W. Flynn, *Anal. Chim. Acta*, 1967, **38,** 403.
6. H. W. Knudson, C. Juday and V. W. Meloche, *Ind. Eng. Chem., Anal. Ed.*, 1940, **12,** 270.
7. A. Ringbom, P. E. Ahlers and S. Siitonen, *Anal. Chim. Acta*, 1959, **20,** 78.
8. S. J. Simon and D. F. Boltz, *Anal. Chem.*, 1975, **47,** 1758.
9. T. V. Ramakrishna, J. W. Robinson and P. W. West, *Anal. Chim. Acta*, 1969, **45,** 43.
10. L. A. Trudell and D. F. Boltz, *Mikrochim. Acta*, 1970, 1220.
11. W. J. Price and J. T. H. Roos, *Analyst*, 1968, **93,** 709.
12. J. J. McAuliff, *At. Absorpt. Newsl.*, 1967, **6,** 69.
13. *Standard Methods of Analysis, of Iron, Steel and Associated Materials*, 5th Ed. The United Steel Companies Ltd., Sheffield, 1961.
14. BCIRA Methods of Analysis Sub-Committee, *Chemical Analysis for Ironfoundries, Selected Methods.* Allen & Unwin, London, 1967.
15. A. G. Fogg and A. A. Osakwe, *Talanta*, 1978, **25,** 226.
16. R. A. Chalmers and A. G. Sinclair, *J. Inorg. Nucl. Chem.*, 1967, **29,** 2065.
17. *Idem, Anal. Chim. Acta*, 1966, **34,** 412.
18. J. Paul, *Mikrochim. Acta*, 1965, **5,** 836.
19. C. H. Lueck and D. F. Boltz, *Anal. Chem.*, 1958, **30,** 183.
20. A. Halász, K. Polyák and E. Pungor, *Talanta*, 1971, **18,** 691.
21. K. C. Thompson, R. G. Godden and D. R. Thomerson, *Anal. Chim. Acta*, 1975, **74,** 289.

Talanta, Vol. 30, No. 2, pp. 121–123, 1983
Printed in Great Britain.

0039-9140/83/020121-03$03.00/0

CATHETER MICROELECTRODE ASSEMBLY FOR *IN-VIVO* AND *IN-VITRO* VOLTAMMETRIC ANALYSIS OF BODY FLUIDS

J. WANG* and L. D. HUTCHINS
Department of Chemistry, New Mexico State University, Las Cruces, NM 88003, U.S.A.

and

S. SELIM* and L. B. CUMMING
Primate Research Center, New Mexico State University, P.O. Box 1027, Holloman AFB, NM 88330, U.S.A.

(*Received* 6 *September* 1982. *Accepted* 24 *September* 1982)

Summary—An electrode assembly suitable for voltammetric analysis of very small sample volumes, *in vitro* or *in vivo*, has been constructed inside a catheter. Well-defined differential pulse current peaks have been obtained for acetaminophen, chlorpromazine and ascorbic acid at the submillimolar concentration level. Voltamperograms recorded for rhesus monkey blood *in vivo* and *in vitro* were similar.

The use of electrochemistry to measure analytes in very small volumes and *in vivo* has gained momentum in recent years,[1,2] Most of the *in-vivo* work achieved to date has focused on *in-situ* monitoring of neurotransmitter release in the brains of small animals[1] and of oxygen in blood.[2] The studies on brains utilized miniature carbon working electrodes, with chronoamperometry and normal pulse voltammetry as the measuring techniques. Amperometric oxygen monitoring has usually been done with a miniature Clark-type platinum working electrode.

Differential pulse voltammetry (DPV) has been shown to be an effective technique for the determination of drugs and other organic compounds at low concentrations. Studies have been reported on the measurement of drugs such as chlorpromazine[3] and diazepam[4] with various carbon electrodes. In the light of these developments and the increasing need to determine drugs in small sample volumes and *in vivo* (for therapeutic monitoring and bioavailability studies), it should prove useful and interesting to examine the applicability of DPV for this purpose.

This report describes the design of a microelectrode assembly (with carbon paste and silver wire as the working and reference electrodes) built into a catheter, and its applicability to *in-vitro* and *in-vivo* analysis for oxidizable compounds in monkey blood.

EXPERIMENTAL

Apparatus

A schematic drawing of the electrode assembly is shown in Fig. 1. The body consisted of a vein infusion catheter (16-gauge, 3.5-cm long, Travenol Lab. Inc) into which the Teflon and glass capillaries of the working and reference electrodes respectively were inserted. The working electrode material was a carbon paste (35/65 w/w mineral oil/graphite powder). The paste was packed into the end of a 5-cm long Teflon tube (0.3 mm i.d., 0.6 mm o.d.). The paste filled the tip to a height of about 2 mm, with electrical contact (to the inside end of the paste) made through a thin copper wire. A silver wire inserted into a 4.5-cm long glass

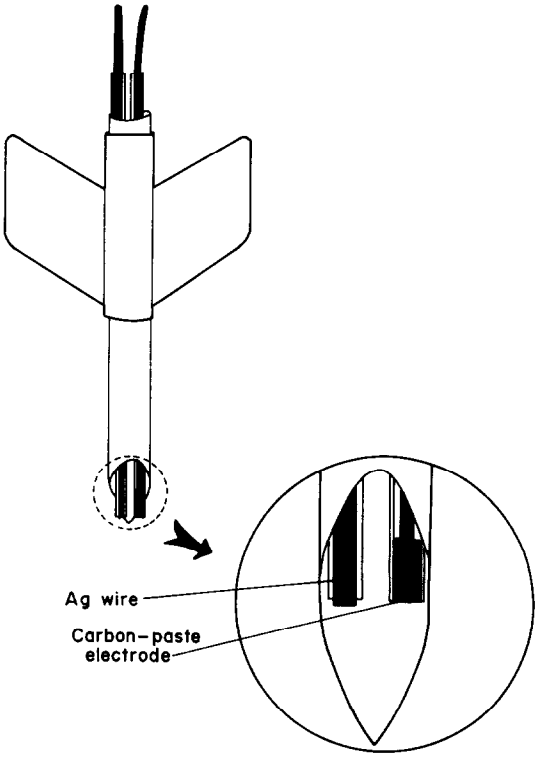

Fig. 1. Schematic drawing of the electrode assembly.

*Authors for correspondence.

capillary (0.2 mm i.d., 0.4 mm o.d.) served as the pseudo-reference electrode. A silicone-rubber sealant held the Teflon and glass capillaries in place, while allowing movement of the Teflon capillary as required for resurfacing the carbon paste.

A 2-ml (2.5-cm diameter, 1.5-cm high) Pyrex glass cell with a 2-hole Teflon cover was employed. Standard additions were made with a 50-μl Hamilton microsyringe. A tiny (1-mm thick, 6-mm long) magnetic stirring bar, placed at the bottom of the cell was used to mix the solution after each addition of analyte. All measurements were made with a Sargent-Welch Model 4001 Polarograph.

Reagents

Demineralized water was used to prepare all solutions. The 0.1M phosphate buffer (pH 7.4) was prepared from a 1:4 mixture of KH_2PO_4 and K_2HPO_4. Millimolar stock solutions of ascorbic acid and chlorpromazine (in water). and acetaminophen (in methanol) were prepared each day from Sigma Chemical Co. reagents. Monkey whole-blood samples, preserved with heparin, were stored at 4°.

Procedure

A 2-ml portion of supporting electrolyte solution or of the whole-blood sample was introduced into the cell. The working electrode was held at the potential for the start of the scan, and after the initial current had decayed an anodic differential pulse ramp was initiated.

In-vivo procedure. An 8.4-kg rhesus monkey was anaesthetized with ketamine hydrochloride. The area over the saphaneous vein (in the mid-calf region of the right leg) was shaved; an incision in the skin over the vein was made with a scalpel and the vein exposed. A small incision was made in the vein and the catheter electrode inserted into the lumen of the vein. Ligatures were used to prevent any possible blood leakage, and the electrode from slipping. The entire area was taped to provide additional support. The monkey was placed in a restraining chair and allowed to recover from sedation before the voltamperograms were recorded.

RESULTS AND DISCUSSION

Differential pulse voltammetry with the combined electrode assembly was evaluated first in phosphate buffer solutions. Typical voltamperograms obtained after successive standard additions of acetaminophen (A) and ascorbic acid (B) are shown in Fig. 2. Well-defined peaks, with height proportional to the analyte concentration, are obtained at the $10^{-4}M$ level. As expected for carbon paste electrodes, the background currents are low. On the basis of the signal-to-background characteristics of the response, the detection limits would be at the micromolar concentration level. Similar DPV response was observed for chlorpromazine, with a peak potential of +0.48 V (not shown).

Following the phosphate buffer experiments, DPV with the microelectrode assembly was tried for direct measurement of various drugs in rhesus monkey whole-blood samples. Figure 3 illustrates voltamperograms recorded after standard additions of acetaminophen (A) and chlorpromazine (B) to 2-ml blood samples. Surprisingly, relatively low background currents (a), similar to those observed in the buffer experiments (Fig. 2), are observed. Thus, most of the blood constituents do not give a DPV response in the range from −0.2 to +0.7 V. In some experiments, *e.g.*, Fig. 3 (A, a), a definite peak can be observed at +0.3 V for the blood background scan. The compound giving rise to this peak has not yet been identified. The peak currents for acetaminophen in blood are lower than those observed in phosphate buffer (compare Figs. 3A and 2A). This is attributed to interaction of the drug with some blood constituents. Even

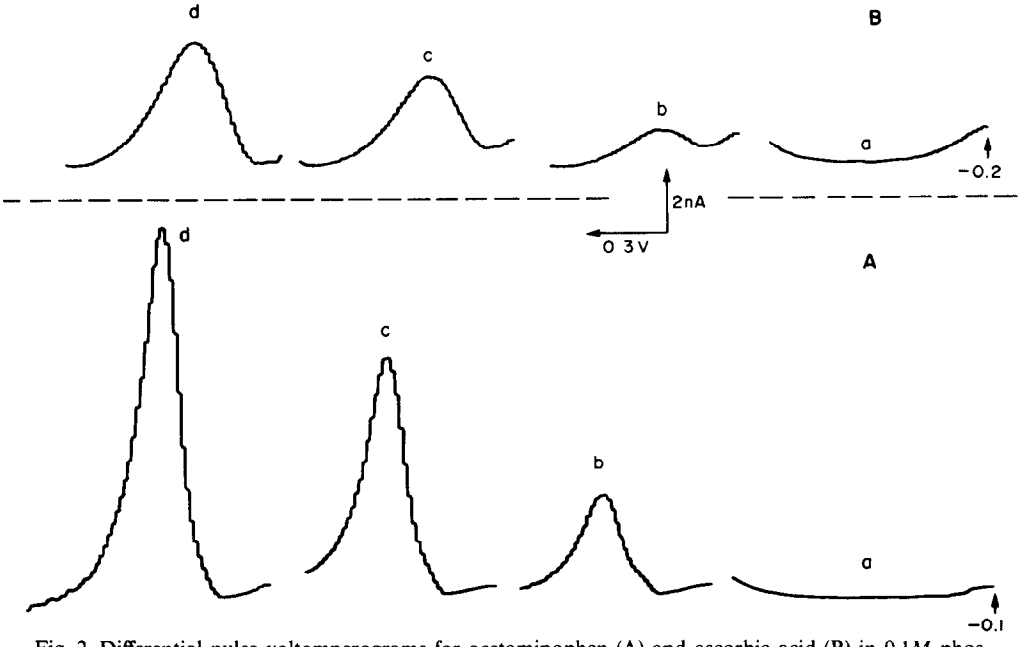

Fig. 2. Differential pulse voltamperograms for acetaminophen (A) and ascorbic acid (B) in 0.1M phosphate buffer: (a) background voltamperograms; (b)–(d), successive equal additions of $1.0 \times 10^{-4}M$ analyte. Scan-rate, 0.5 V/min. Amplitude, 50 mV.

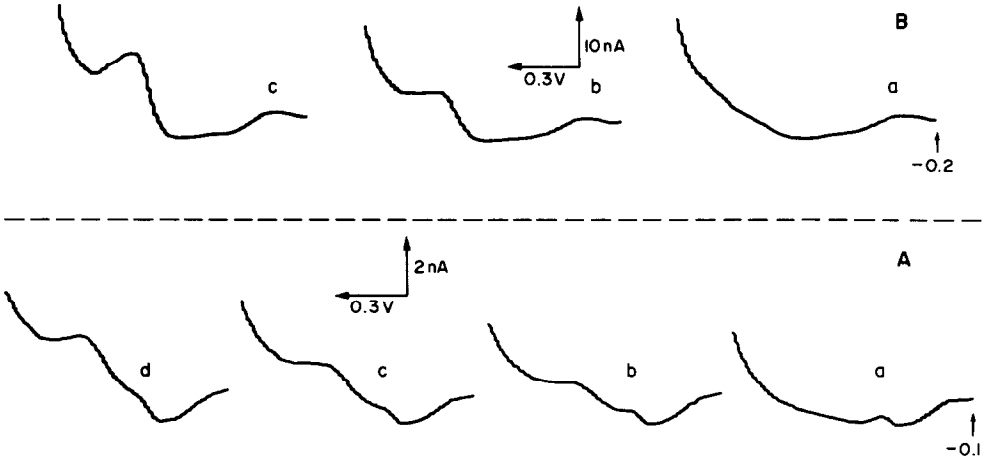

Fig. 3. Differential pulse voltamperograms for acetaminophen (A) and chlorpromazine (B) in monkey whole blood; (a) background voltamperograms; (b)–(d) successive equal additions of analyte—(A) 3.3×10^{-4} *M* acetaminophen, (B) 5×10^{-4} *M* chlorpromazine, with 3-min preconcentration. Scan-rate and amplitude as for Fig. 2.

lower sensitivity was observed for standard additions of 10^{-4}*M* ascorbic acid in blood (not shown). In contrast, relatively high peak currents are observed for chlorpromazine in blood (Fig. 3B). This is attributed to the tendency of chlorpromazine to adsorb on carbon electrodes and thus enhance its voltammetric response.[5] A 3-min preconcentration period (at 0 V with 500-rpm stirring) was employed in this experiment. In spite of the rising background current at around +0.7 V, chlorpromazine can be measured down to the submicromolar concentration level (especially when a subtractive method is used[6]).

Differential pulse voltamperograms were recorded also for 10^{-4}*M* dopamine (not shown); a well-defined peak was observed at around +0.2 V. The response was relatively stable, with about 15% decrease in the peak height over a 30-min period of continuous operation. This is attributed to gradual surface deterioration due to adsorption of surfactants present in the blood.

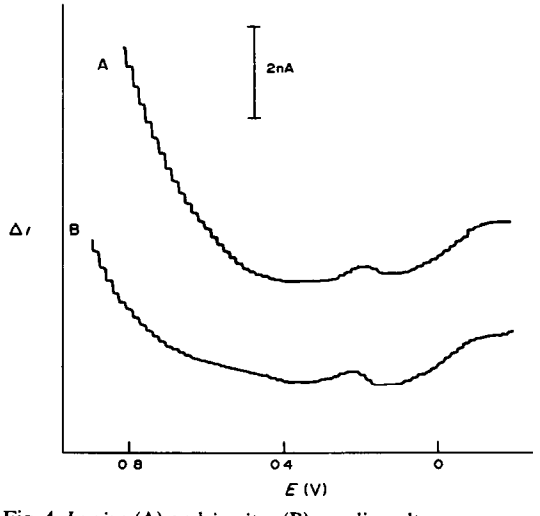

Fig. 4. *In-vivo* (A) and *in-vitro* (B) anodic voltamperograms of whole blood. Differential pulse conditions as for Fig. 2.

The suitability of the electrode for *in-vivo* application is demonstrated in Fig. 4. Voltamperograms A and B are the DPV responses recorded *in vivo* and *in vitro*, respectively. The *in-vivo* response was recorded with the electrode implanted into the saphaneous vein of the monkey's right leg. Similar responses (shape of background and characteristic peak at around +0.3 V) were observed for the *in-vivo* and *in-vitro* measurements. Curve A is part of a series of 4 voltamperograms, recorded *in vivo* at 5-min intervals, which yielded similar responses. The DPV scan takes 2 min; thus with the additional 30 sec needed for the current decay at the initial potential, *in-vivo* monitoring can be performed at a rate of about 20 measurements per hour.

In conclusion, the data presented in this communication demonstrate the utility of the catheter microelectrode assembly for DPV analysis in small sample volumes and *in vivo*. The electrode assembly is easily fabricated, and permits rapid renewal of the carbon paste surface. Further miniaturization of this design, which would allow implantation in smaller blood vessels or body tissues, may be achieved by using smaller (23–25 gauge) catheters. In the near future we will examine whether the implanted electrode can be used for direct sensing of changes in the levels of drugs in the blood stream after administration of therapeutic doses.

REFERENCES

1. R. N. Adams, *Anal. Chem.*, 1976, **48**, 1128A.
2. J. Koryta, M. Březina, J. Pradáč and J. Pradáčová, in *Electroanalytical Chemistry*, A. J. Bard (ed.), Vol. 11. p. 85. Dekker, New York, 1979.
3. T. B. Jarbawi and W. R. Heineman, *Anal. Chim. Acta*, 1981, **126**, 57.
4. T. P. DeAngelis, R. E. Bond, E. E. Brooks and W. R. Heineman, *Anal. Chem.*, 1977, **49**, 1792.
5. T. B. Jarbawi and W. R. Heineman, *Anal. Chim. Acta*, 1982, **135**, 359.
6. J. Wang and B. A. Freiha, work to be published.

Talanta, Vol. 30, No. 2, pp. 124–126, 1983
Printed in Great Britain.

0039-9140/83/020124-03$03.00/0

SIMULTANEOUS DETERMINATION OF STOICHIOMETRY, DEGREE OF CONDENSATION AND STABILITY CONSTANT

A GENERALIZATION OF THE MOLAR-RATIO METHOD

A. BELTRÁN-PORTER, D. BELTRÁN-PORTER, A. CERVILLA and J. A. RAMIREZ

Departamento de Química Inorgánica, Facultad de Ciencias Químicas, Universidad de Valencia, Burjasot (Valencia), Spain

(*Received* 5 *April* 1982. *Accepted* 21 *September* 1982

Summary—A generalization of the molar-ratio method is proposed, which allows study of relatively weak complexes. The method is based on treatment of the data from a molar-ratio saturation curve. From the mathematical expression derived, the stoichiometry, degree of condensation and stability constant are easily evaluated. Graphical representations of the results can be used advantageously.

The molar-ratio method[1] has been widely used for determination of the composition of AB_n complexes. Nevertheless, the basic method permits the evaluation of the stability constant and actual stoichiometry only in specially favourable cases.[2–4] Thus, Asmus[2] proposed his well-known "straight-line method" as an alternative procedure for determination of the stoichiometric ratio of relatively weak complexes.

In order to overcome the limitations of the method, Momoki *et al.*[5] developed a general theoretical equation that accurately predicts the shapes of experimental molar-ratio plots, but practical utility of their findings was criticized by Chriswell and Schilt,[6] who, through a detailed mathematical analysis of the molar-ratio method, have established several different techniques for identifying weak complexes in solution by use of computational procedures.

This paper shows a relatively simpler way for fixing the stoichiometry and particularly the degree of condensation of weak complexes from a molar-ratio experimental data-set. The only conditions are that a single complex is present in the solution and that the Lambert–Beer law is obeyed.

THEORY

The formation of a single complex can be described in terms of an equilibrium $mA + nB \rightleftharpoons A_mB_n$. For dilute solutions and constant ionic strength, the non-thermodynamic stability constant is

$$K = \frac{[A_mB_n]}{[A]^m[B]^n}. \quad (1)$$

If the concentration of A, C_A, is kept constant and the concentration of B, C_B, varied until it reaches a large excess, the limit of the equilibrium complex concentration will be proportional to the analytical concentration, C_A,

$$[A_mB_n]_{limit} = C_A/m. \quad (2)$$

For a given value of the added ligand concentration, $C_B(x)$, the equilibrium complex concentration is a fraction, x, of the limiting value:

$$[A_mB_n] = xC_A/m, \quad (0 \leqslant x < 1). \quad (3)$$

If we define

$$f_{m,n}(x) = \frac{C_B(x) - nC_Ax/m}{\left\{\frac{x}{m(1-x)^m}\right\}^{1/n}} \quad (4)$$

then equation (1) can be rewritten as

$$f_{m,n}(x) = K^* \quad (5)$$

where

$$K^* = \left(\frac{1}{KC_A^{m-1}}\right)^{1/n}.$$

Obviously only substitution of the correct m, n values into equation (4) will satisfy equation (5), because only in this case is K a constant. This fact is the keystone of a straightforward method for the determination of the stoichiometry and the equilibrium constant: the functions $f_{m,n}(x)$ can be evaluated for different m,n combinations over a wide range of x values and checked against equation (5). Once the correct m,n values have been determined, the evaluation of K is trivial.

Determination of $C_B(x)$

The application of this method involves the determination of the $C_B(x)$ values. $C_B(x)$ is defined as the

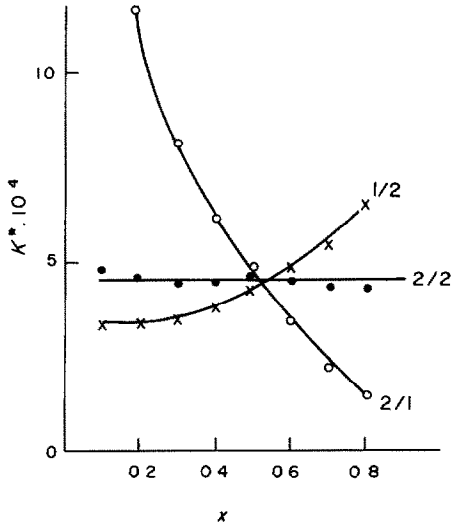

Fig. 1. $f_{m,n}$ *vs.* x for different stoichiometric ratios.

ligand concentration that implies an $[A_mB_n]$ value given by equation (3). Provided that the Lambert–Beer law is obeyed, we can write

$$\Delta Y = [A_mB_n]Y_{molar} = x[A_mB_n]_{limit}/Y_{molar} = x(\Delta Y)_{limit} \quad (6)$$

where ΔY is the contribution (due to the complex formation) to the measured physical property, Y. For very stable complexes a plot of ΔY *vs.* C_B allows direct estimation of $(\Delta Y)_{limit}$. However, a complex that undergoes appreciable dissociation in solution gives a continuous S-shaped curve from which the extrapolation to $(\Delta Y)_{limit}$ is uncertain.[1] In this case, a rather accurate value of $(\Delta Y)_{limit}$ can be obtained by measuring ΔY for a large enough C_B/C_A ratio.

$C_B(x)$ is the C_B value that corresponds, on a ΔY *vs.* C_B experimental plot, to $\Delta Y(x)$ calculated from equation (6).

EXPERIMENTAL

In order to show the usefulness of this kind of calculation we chose some experimental examples for which the classical application of the molar-ratio method was found unsuccessful.

Molybdenum (VI) and tartaric acid form a monomeric species, stable in weakly acidic medium, of stoichiometry Mo(VI)/tartaric acid = 1/2.[7,8] The monomeric character of this complex has been corroborated by saline cryoscopy in Glauber's salt. The Asmus straight-line method gave an apparent formation constant (at pH 6.75) of $K = 1.04 \times 10^3$. This small K value clearly indicates that the molar-ratio method will not be suitable for determining the stoichiometric ratio of the complex. In fact, when it is applied, an S-shaped curve is obtained, from which a direct determination of the stoichiometry is not possible.

†Gol'dshtein and Gur'yanova[11,12] proposed a general method based on the condition $(\partial K/\partial C_B)_{(C_A = \text{constant})} = 0$. However, its application implies polynomial sectional fitting of the experimental ΔY *vs* C_B curve in order to determine the derivative.

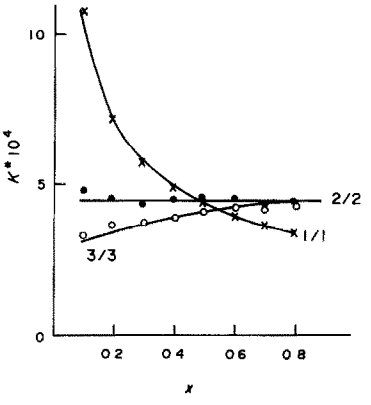

Fig. 2. $f_{m,n}(x)$ *vs.* x for a 1:1 stoichiometric ratio and different degrees of condensation.

When the procedure given here is applied, constancy in the $f_{m,n}(x)$ values (within experimental error) is attained only for $n = 2$, $m = 1$. Other m, n combinations leads to increasing $[f_{1,3}(x)$ or $f_{2,4}(x)]$ or decreasing $[f_{1,1}(x)]$ functions. A stoichiometry Mo(VI)/tartaric acid = 1/2 is thus derived by this approach. The equilibrium constant calculated is in excellent agreement ($K = 1.18 \pm 0.03 \times 10^3$) with our Asmus method result.

We have also studied[9] the formation of complexes between molybdenum (VI) and oxalic acid. At pH 2.75 the prevailing species in solution is dimeric (established by saline cryoscopy) and has the formula $[Mo_2O_5(OH)_2(C_2O_4)_2]^{-4}$. Klausen's extension of the Asmus method[10] gave an apparent formation constant $K = 9.52 \times 10^{10}$. As we shall now see, the application of the method proposed here greatly reduces the amount of work needed. From the absorbance increments obtained by varying the mole ratio of oxalic acid to Mo(VI) for a constant concentration of Mo(VI), we can calculate the data necessary to plot the graphs in Figs 1 and 2. A visual examination of these provides an unambiguous estimation of the stoichiometry as well as the degree of condensation. Only $n = m = 2$ gives a straight line of zero slope for $f_{m,n}(x)$ *vs.* x. The calculated K ($9.9 \pm 0.5 \times 10^{10}$) agrees very well with our previous result.

DISCUSSION

The uniqueness of the results obtained is implicit in the basis of the method. Thus, a correct calculation worked out from a fairly accurate experimental dataset must lead to the actual m,n values.

Furthermore, the results can be tested in a very simple way, by graphical expression in particular. Let us assume that we are dealing with an A_aB_b complex. Application of the method will lead to the solution $f_{a,b}(x) = K^*$.† It can be easily shown from equation (4) that the curves corresponding to the same stoichiometric ratio but different degrees of condensation $[f_{\alpha a,\alpha b}(x)]$ will intersect the $f_{a,b}(x)$ straight-line solution at $x = m\alpha^{1/(1-\alpha)}$. Further, a study of the first and second derivatives of these functions provides us with complete information about the theoretical curve shapes (see Table 1). Thus, in the case of a dimeric complex such as the one discussed above, $f_{1,1}(x)$ must be a concave decreasing curve whereas $f_{3,3}(x)$ will be a

Table 1. $f_{m,n}(x) = K^*$ functions and their first and second derivatives

	$\alpha > 1$	$\alpha < 1$
$f_{\alpha m,\alpha n} = \bar{K}x^{(\alpha-1)/\alpha n}$	$f(0) = 0$	$f(0) = +\infty$
$\bar{K} = K^{*\alpha n}\sqrt{\frac{\alpha}{m^{\alpha-1}}}$	$f(1) = \bar{K}$	$f(1) = \bar{K}$
$f'_{\alpha m,\alpha n}(x)$	>0 increasing	<0 decreasing
$(f''_{\alpha m,\alpha n}(x)$	<0 convex	>0 concave

convex increasing one. The intersections of these functions with $f_{2,2}(x)$ should be found at $x = 0.5$ and $x = 0.87$: the shape of the curves is as predicted.

A similar general study of the curves obtained for different stoichiometric ratios does not always give such a straightforward series of useful considerations. However, for each particular case it is possible to find some specific conditions that can help to verify the results. For example, the limit values of $f_{m,n}(x)$, that is to say $f_{m,n}(0)$ and $f_{m,n}(1)$, can always be readily evaluated. In this way we can also obtain an indication of the graphical shape of the functions. In the quoted example of a true 2:2 complex, these limit values of the functions obtained for 1:2 or 2:1 stoichiometries are $f_{1,2}(0) = K^*/\sqrt{2}$; $f_{1,2}(1) = +\infty$; $f_{2,1}(0) = +\infty$ and $f_{2,1}(1) = 0$. According to these $f_{1,2}(x)$ should be an increasing concave curve and $f_{2,1}(x)$ a decreasing concave one. As we can see from Fig. 1, all these predictions are correct in the case dealt with.

Our results are based on the fact that measurement of $(\Delta Y)_{\text{limit}}$ is experimentally accessible. However, a realistic determination of this parameter may occasionally not be achieved in practice, owing to experimental difficulties (*e.g.*, precipitation or formation of a new complex when B is in large excess). In general, the calculations based on an untrue estimation of $(\Delta Y)_{\text{limit}}$ lead to greatly dispersed K^* values. This difficulty can be obviated in the simplest cases ($m = n = 1$) through an alternative evaluation of the specific value of the measured physical property.[13] Nevertheless, an iterative application of the proposed method, involving successive $(\Delta Y)_{\text{limit}}$ and K^* estimations, has proved to be advantageous for any stoichiometry.

According to the theory of propagation of errors, the precision we can assign to the calculated K value is related to the dispersion of the estimate of K^* through

$$\frac{dK}{K} = n\frac{dK^*}{K^*} + (m-1)\frac{dC_A}{C_A}.$$

The statistically evaluated confidence limits of K^* (they have been calculated for the examples above at the 95% significance level[14]) include the errors in the physical property measurements as well as the imprecision of the estimated reagent concentrations. However, for polynuclear species, because of the dependence of K on C_A, the individual error in this last concentration must be included.

CONCLUSION

Usually, to establish the degree of condensation of a complex species with a given stoichiometric ratio is a more cumbersome problem than to determine the stoichiometric ratio itself. Besides the use of techniques for molecular weight determination there exist in the literature several papers dealing with photometric methods for differentiating mononuclear and polynuclear complexes.[10,15] In general, these methods require more than one independent set of measurements.

With the molar-ratio method proposed here it is possible to obtain both parameters from a single set of measurements. The method is valid for relatively weak complexes, for which the classic molar-ratio method does not work. Furthermore, it is also applicable to relatively stronger complexes, with satisfactory results as expected,[1-4] since we have not imposed any prior conditions on the magnitude of the K values.

The simplicity of the calculations and the ready graphical checking enable us to propose this generalization of the molar-ratio method as an alternative to the more sophisticated computational methods described in the literature.[4,6,13]

REFERENCES

1. J. H. Yoe and A. L. Jones, *Ind. Eng. Chem., Anal. Ed.*, 1944, **16**, 11.
2. E. Asmus, *Z. Anal. Chem.*, 1960, **178**, 104.
3. H. L. Schlafer, *Komplexbildung in Lösung*, p. 253, and references therein. Springer-Verlag, Berlin, 1961.
4. E. S. Shcherbakova, I. P. Gol'dshtein and E. N. Gur'yanova, *Russ. Chem. Rev.*, 1978, **47**, 1133.
5. K. Momoki, J. Sekino, H. Sato and H. Yamaguchi, *Anal. Chem.*, 1969, **41**, 1286.
6. C. D. Chriswell and A. A. Schilt, *ibid.*, 1975, **47**, 1623.
7. M. Cadiot and B. Viossat, *Rev. Chim. Min.*, 1969, **6**, 727.
8. A. Beltrán-Porter, *Doctoral Thesis*, Universidad de Valencia, 1979.
9. A. Beltrán, F. Caturla, A. Cervilla and J. Beltrán, *J. Inorg. Nucl. Chem.*, 1981, **43**, 3277.
10. K. S. Klausen and F. J. Langmyhr, *Anal. Chim. Acta*, 1963, **28**, 501.
11. I. P. Gol'dshtein and E. N. Gur'yanova, *Teor. Eksper. Khim.*, 1971, **7**, 410.
12. T. I. Perepelkova, E. S. Shcherbakova, I. P. Gol'dshtein and E. N. Gur'yanova, *Zh. Obshch. Khim.*, 1975, **45**, 656.
13. W. A. E. McBryde, *Talanta*, 1974, **21**, 979. This excellent review includes a careful discussion on this subject.
14. P. D. Lark, B. R. Craven and R. C. L. Bosworth, *The Handling of Chemical Data*, p. 97. Pergamon Press, London, 1968.
15. D. V. Gonzalez, A. Arrebola and M. Roman, *Talanta*, 1979, **26**, 215, and references therein.

Talanta, Vol. 30, No 2, pp. 127–130, 1983
Printed in Great Britain.

0039-9140/83/020127-04$03.00/0

ANALYTICAL DATA

EXTRACTION OF TETRA-ALKYLAMMONIUM BROMIDES INTO 1,2-DICHLOROETHANE + ALKANE MIXTURES

JAN CZAPKIEWICZ and ANNA WOLINSKA
Institute of Chemistry, Jagiellonian University, 30060 Kraków, Poland

(*Received* 18 *May* 1982. *Accepted* 9 *July* 1982)

Summary—The influence of an inert diluent on the extractability of tetradecyltrimethyl-, tetradecyltriethyl-, decyltriethyl- and tetra-amylammonium bromides into 1,2-dichloroethane + n-alkane mixtures at 25° has been determined. On the basis of the experimental data it is suggested that the bromide moiety of the ion-pair is solvated in the organic phase by 5–6 molecules of 1,2-dichloroethane.

The use of quaternary onium salts as liquid anion-exchangers in analytical and separation procedures is based on the displacement of anions according to the general scheme:

$$(Q^+X^-)_0 + Y^- \rightleftharpoons (Q^+Y^-)_0 + X^- \qquad (1)$$

where $(Q^+X^-)_0$ and $(Q^+Y^-)_0$ are ion-pairs in the low dielectric-constant organic phase and X^- and Y^- are singly charged anions in the aqueous phase. The equilibria of such processes are commonly expressed in terms of relative orders of extractability of anions, estimated through studies of the distribution ratios of quaternary ammonium salts of various types[1] or through spectrophotometric measurement of the extent of displacement in systems with coloured liquid anion-exchangers.[2,3]

The data available seem to suggest that the main factor governing the order of extractability of the anions is the difference in their free energy of transfer into the organic phase.[4–6] The calculation of the solvation free-energy of an ion suggested recently by Abraham and Liszi[7] affords a means of predicting absolute values of the free-energy of transfer, ΔG_t^0, of ions from water into an organic phase of low polarity. According to their one-layer model of solvation in less polar solvents, an ion is surrounded by an organized solvent layer the thickness of which is set equal to the solvent radius calculated from the bulk molar volume; beyond this organized layer there is only the bulk solvent. The calculations lead to values which are in good agreement with the free-energy for partition of the ions, ΔG_p^0, determined for the water–polychloroalkane systems among others.[8]

In solvents of low polarity the mode of solvation is presumably affected by extensive ion-pairing, the anion–cation interaction being an additional factor influencing the order of extractability of the anions. Although there is an ample literature on the partition of typical onium salts, little is known about the solvation of ion-pairs in polychloroalkanes. As far as we are aware, the only papers related to this problem are those of Higuchi and co-workers[9] and of Okazaki *et al.*[10] The former authors studied the effect of various anions on the extraction of dextromorphan as a function of chloroform concentration in cyclohexane and in carbon tetrachloride. They postulated stoichiometric complexes between the ion-pair and the solvating species in the organic phase and showed that the bromide, chloride and nitrate species are extracted as complexes associated with four or five molecules of chloroform. The iodide species appeared to require only four molecules of the solvating agent whereas the species obtained with less hydrophilic organic anions associated with 2–4 molecules of the solvating agent. Comparable results were reached by the latter authors[10] who suggested, on the basis of their infrared studies of several surfactants in chloroform, concentration-dependent solvation numbers varying in the range 2–5. According to Higuchi's simplified models of solvated ion-pairs,[9] the dextromorphan salts fall into the class of compounds with a large and lipophilic cation and a small anion carrying a relatively high negative charge per unit area. It thus seemed interesting to study the influence of the structure of the cationic co-ion on the solvation of the ion-pair. Tetra-alkylammonium bromides were chosen as model compounds for this purpose, and an attempt is made in this paper to estimate the solvation numbers for the salts in 1,2-dichloroethane through partition measurements in water–1,2-dichloroethane + n-alkane systems. In the presence of an apolar hydrocarbon diluent, the ammonium salt in the organic phase should exist predominantly in the form of ion-pairs and thus, following Higuchi's[9] assumption of stoichiometric solvation of the ion-pairs. the extraction of the ammonium salt into mixtures of 1,2-dichloroethane and diluent may be expressed by the overall reaction:

$$Q^+ + A^- + n\mathrm{DCE} = [\mathrm{QA(DCE)}_n]_{org} \qquad (2)$$

Table 1. Partition data for decyltriethylammonium bromide; $K_d = 1.0 \times 10^{-4}$

		Organic phase–0.1M aqueous NaBr $C_{init} = 1 \times 10^{-3}M$			Organic phase–0.05M aqueous NaBr $C_{init} = 0.5 \times 10^{-3}M$			Organic phase–water $C_{init} = 5 \times 10^{-3}M$		
C_{DCE}, M	ϵ	C^l, μM	n_{uncorr}	n	C^l, μM	n_{uncorr}	n	C^l, μM	n_{uncorr}	n
12.58*	10.3	650			294			600		
11.46	9.0	480	7.5	5.9	194	8.7	6.8	340	7.3	6.0
10.43	8.1	335	6.4	5.6	121	7.3	6.1	190	6.85	6.15
9.48	7.2	215	6.4	5.7	71	6.9	5.8	105	6.6	5.8
8.59	6.4	129	6.2	5.7	42	6.0	5.3	56	6.6	6.0
7.77	5.7	76	5.9	5.7	25	5.6	5.1	30	6.35	5.9
5.74	4.1	15	5.6	5.6						
4.85	3.6	6	5.5	5.5						

*Neat DCE.

where Q^+ and A^- are the hydrated quaternary ammonium cation and the anion in the aqueous phase and $[QA(DCE)_n]_{org}$ is the ion-pair solvated by n molecules of DCE in the organic phase. It follows that for high values of n the partition ratio of the salt should strongly depend on the concentration of DCE in the organic phase. Although the partition of ammonium salts in the water–DCE system has been studied in detail and it is well known that the solubility of such salts in alkanes is negligible, no quantitative prediction of the influence of hydrocarbon diluents on the extraction efficiency of the organic phase could be made. The results of Tribalat *et al.*,[11] who used kerosene to suppress the extraction of hexadecyltrimethylammonium bromide into chloroform, indicate that the effect is marked indeed.

EXPERIMENTAL

The preparation and purification of the quaternary ammonium bromides was described earlier.[12] n-Hexane, n-heptane, n-octane, n-decane and n-dodecane, were used as supplied. The DCE was washed several times with water, then dried over anhydrous calcium chloride and finally distilled. Analytical grade sodium bromide was oven-dried and then stored over phosphorus pentoxide. The partition technique has also been described.[13] The equilibrium concentration of the quaternary ammonium bromides was determined colorimetrically by adapting the Orange II method,[14,15] the phase chosen for analysis always being that which had the lower content of the quaternary ammonium salt. The concentration in the second phase was calculated from the mass balance. The total content of the salt in the two-phase system was checked occasionally when the partition ratio was close to unity. In the case of mixed organic solvents an aliquot was evaporated under reduced pressure, the residue was dissolved in water and the routine analytical procedure was then applied.

The partition experiments for the DCE/n-alkane–water systems could not be extended to concentrations of the diluent exceeding *ca.* 0.25 mole-fraction because the densities of both phases then tended to equalize, which rendered their separation difficult. On the alkane-rich side, where the phases were separable, the equilibrium concentrations of the partitioned salts in the organic phase were almost always at the limits of detection but this difficulty was overcome to some extent in the DCE/n-alkane–aqueous sodium bromide systems, for which a constant ionic strength was maintained. The concentration of sodium bromide was always at least two orders of magnitude higher than that of the partitioned quaternary ammonium bromide.

The two phases were not pre-equilibrated, it being assumed that their mutual solubility was low enough to have negligible effect on the initial composition of the sol-

Table 2. Partition data for tetra-amylammonium bromide, TAABr, $K_d = 2.14 \times 10^{-4}$ and tetradecyltrimethylammonium bromide, C_{14}TMABr, $K_d = 2.1 \times 10^{-5}$

		Organic phase–0.1M aqueous NaBr TAABr $C_{init} = 1 \times 10^{-3}M$			Organic phase–water TAABr $C_{init} = 1 \times 10^{-3}M$			Organic phase–water C_{14}TMABr $C_{init} = 1 \times 10^{-3}M$		
C_{DCE}, M	ϵ,	C^l, μM	n_{uncorr}	n	C^l, μM	n_{uncorr}	n	C^l, μM	n_{uncorr}	n
12.58*	10.3	991			490			315		
11.46	9.0	982	7.5	5.2	360	8.2	5.65	225	625	5.0
10.43	8.1				260	6.5	5.3	156	5.8	5.1
9.48	7.2	944	6.2	5.3	180	6.0	4.7	103	5.6	5.2
8.59	6.4	908	5.4	5.0	118	5.8	5.0	68	5.0	4.8
7.77	5.7				74	5.6	5.1	43	5.1	5.0
5.74	4.1	561	5.1	5.1	16	5.45	5.45			
4.42	3.5	241	5.3	5.3	4	5.0	5.0			
2.96	2.7	365	5.3	5.3						
2.22	2.5	9	5.0	5.0						

*Neat DCE.

Table 3. Partition data for tetradecyltriethylammonium bromide, $K_d = 1.0 \times 10^{-4}$

		Organic phase–water $C_{init} = 0.5 \times 10^{-3}M$			Organic phase–water $C_{init} = 1.04 \times 10^{-3}M$			Organic phase–0.05M aqueous NaBr $C_{init} = 0.5 \times 10^{-3}M$		
C_{DCE}, M	ϵ	C^I, μM	n_{uncorr}	n	C^I, μM	n_{uncorr}	n	C^I, μM	n_{uncorr}	n
12.58*	10.3	305			707		calculation	497		calculation
11.46	9.0	248	7.7	5.2	616	6.7	not			not
10.43	8.1	197	6.4	5.0	507	6.9	attempted			attempted
10.37	8.0							491	6.7	
9.48	7.2	148	6.1	5.2	391	6.8				
9.35	7.1							486	4.4	
8.66	6.4							482	3.5	
8.59	6.4	106	5.7	5.15	336	3.2				
7.77	5.7	73	5.4	5.1	285	3.0				

*Neat DCE.

vent mixtures. The dielectric constants (ϵ) of the mixtures were measured with a Hungarian precision dielectrometer.

RESULTS AND DISCUSSION

Preliminary tests with hexane, heptane, octane, decane and dodecane as the n-alkane diluents have shown that for a given salt, the partition ratio as a function of the molar DCE concentration is independent of the type of hydrocarbon. Further studies were therefore made only with n-heptane as diluent, and the results are given in Tables 1–3, where C^I is the molar equilibrium concentration of quaternary ammonium bromide in the organic phase and C_{init} is the initial DCE concentration in the aqueous phase; the final DCE concentration in the aqueous phase will be called C^{II}. According to equation (2) the relation

$$\log [QA(DCE)_n]/[Q^+][A^-] = \log K + n \log C_{DCE} \quad (3)$$

should hold, where K is the equilibrium constant of the extraction process, and C_{DCE} is the molar equilibrium concentration of DCE, the activity coefficients of the ions and ion-pairs being assumed to be unity. For systems where $[Q^+] = [A^-] = C^{II}$ and side-reactions such as dissociation of the ion-pairs or their polymerization in the organic phase or micellization in the aqueous phase may be neglected, the slope of the linear plot of $\log [C^I/(C^{II})^2]$ *vs.* $\log C_{DCE}$ should thus represent n, the solvation number of the ion-pair. When excess of bromide ions is used, *i.e.*, $[A^-]$ is constant, the value of n should be arrived at from $\log (C^I/C^{II})$ *vs.* $\log C_{DCE}$. Least-squares analysis of the partition data leads in almost all cases to values of n in the range of 5–6 with an apparently high correlation coefficient. A more careful analysis of the data indicates that in the DCE-rich concentration range the values of n are distinctly higher, and tend to fall to around 5 and exceptionally to lower values for systems with higher concentrations of the hydrocarbon diluent. The crude values of $n_{uncorr.}$, representing $\Delta \log [C^I/C^{II})^2]/\Delta \log C_{DCE}$ or $\Delta \log (C^I/C^{II})/\Delta \log C_{DCE}$, are given in the tables. An examination of the pattern of changes in n_{uncorr} indicates that account should be taken of ion-pair dissociation in the DCE-rich phases. The concentration dissociation constants of the salts in the DCE + alkane solvents were estimated on the basis of the known K_d values[16] by applying the simplified Denison and Ramsey[17] equation

$$pK_{d1}\epsilon_1 = pK_{d2}\epsilon_2 \quad (4)$$

where pK_{d1} and pK_{d2} are the negative logarithms of the dissociation constants of a salt in media of dielectric constants ϵ_1 and ϵ_2, respectively. Assuming that the mean ionic activity coefficient in the organic phase is equal to unity, the degree of dissociation, α, of the quaternary ammonium bromides in the organic phases was calculated and hence the concentration of the ion-pairs could be estimated. The values obtained served for the calculation of the solvation numbers, n, deemed to represent more closely the number of DCE molecules solvating the tetra-alkylammonium bromide ion-pair. The corrections were negligible at $\alpha < 0.01$. No corrections were attempted for the data in Table 3, where a sharp change in the values of n_{uncorr} is observed at comparatively high concentrations of tetradecyltriethylammonium bromide in the alkane-rich phases. This discrepancy is most probably due to aggregation of the long-chain electrolyte in the low dielectric-constant medium, leading to low effective values of n_{uncorr}.

The corrected solvation numbers, n, do not seem to depend on the structure of the tetra-alkylammonium cation and correspond fairly well to the number of DCE molecules forming a one-layer sheath around the bromide anion. Thus, as Abraham[18] has pointed out, his theory predicts that the bromide ion, with a radius of 1.95 Å, should be surrounded by a layer of DCE molecules with a volume of 350 Å^3, if the solvent molecule radius is 2.546 Å. The volume of the layer corresponds to 350/69 or 5.1 times the volume of a solvent molecule. Taking into account that the

bromide anion is presumably more strongly solvated than the tetra-alkylammonium cation (in a recent paper Krumgalz[19] even suggests that such hydrophobic cations are not solvated at all in organic solvents), it seems plausible to assume that upon ion-pairing the bromide ion retains its unimolecular solvation sheath. An octahedral arrangement of DCE molecules around the bromide anion might equally well be postulated. Upon ion-pairing one of the sites of the octahedron might be occupied by the polar end of the quaternary ammonium cation, leading to a tight ion-pair. An equilibrium between solvent-separated and tight ion-pairs would thus account for the observed n values.

Our preliminary studies on the effect of inert solvent on the partition of quaternary ammonium bromides in water-chloroform/diluent systems support the findings here reported. Assuming that the model of an ion-pair with the anion solvated by a one-layer sheath of the organic solvent is true for any solvent of low polarity, the influence of a diluent on the partition ratio of the quaternary ammonium salt may be predicted from the knowledge of the radius of the anion and the molar volume of the solvating agent.

Acknowledgement—We wish to thank Dr. Abraham for valuable comments and the Polish Academy of Sciences for financial support.

REFERENCES

1. N. A. Gibson and D C. Weatherburn, *Anal. Chim. Acta*, 1972, **58**, 159.
2. H. M. N. H. Irving and J. Hapgood, *ibid.*, 1980, **119**, 207 and references therein.
3. Y. Inoue and O. Tochiyama, *Bull. Chem. Soc. Japan*, 1980, **53**, 1618.
4. M. H. Abraham and A. F. Danil de Namor, *J. C. S. Faraday I*, 1976, **72**, 955.
5. M. H. Abraham, A. F. Danil de Namor and R. A. Schultz, *J. Soln. Chem.*, 1976, **5**, 529.
6. J. Czapkiewicz and B. Czapkiewicz-Tutaj, *J. C. S. Faraday I*, 1980, **76**, 1663.
7. M H. Abraham and J. Liszi, *ibid.*, 1978, **74**, 1604, 2858.
8. *Idem, J. Inorg. Nucl. Chem.*, 1981, **43**, 143.
9. T. Higuchi, A. Michaelis, T. Tan and H. Hurwitz, *Anal. Chem.*, 1967, **39**, 974; see also M. J. Harris, T. Higuchi and J H. Rytting, *J. Phys. Chem.*, 1973, **77**, 2694.
10. M. Okazaki, I. Hara and T. Fujiyama, *ibid.*, 1976, **80**, 64.
11. S. Tribalat, C. Piolet and M. F. Fontaine, *Bull. Soc. Chim. France*, 1978, 158.
12. B. Czapkiewicz-Tutaj and J. Czapkiewicz, *Roczniki Chem.*, 1975, **49**, 1353.
13. J. Czapkiewicz and B. Czapkiewicz-Tutaj, *J. Colloid Interface Sci*, 1977, **62**, 524.
14. A. Few and R. H. Ottewil, *ibid.*, 1956, **11**, 34.
15. G. V. Scott, *Anal. Chem.*, 1968, **40**, 768.
16. J. Czapkiewicz and B. Czapkiewicz-Tutaj, *Roczniki Chem.*, 1976, **50**, 1395
17. J. T. Denison and J. B. Ramsey, *J. Am. Chem. Soc.*, 1955, **77**, 2615.
18. M. H Abraham, private communication.
19. B. S. Krumgalz, *J. C. S. Faraday I*, 1980, **76**, 1887.

Talanta, Vol. 30, No. 2, pp. 131–133, 1983
Printed in Great Britain.

0039-9140/83/020131-03$03.00/0

HYDROXIDE COMPLEXES OF LANTHANIDES—V*

ERBIUM(III) IN PERCHLORATE MEDIUM

J. KRAGTEN
Natuurkundig Laboratorium der Universiteit van Amsterdam, Valckenierstraat 65, 1018 XE Amsterdam, The Netherlands

and

L. G. DECNOP-WEEVER
Laboratorium voor Analytische Chemie der Universiteit van Amsterdam, Nieuwe Achtergracht 166, 1018 WV Amsterdam, The Netherlands

(*Received* 15 *June* 1982. *Accepted* 26 *August* 1982)

Summary—From the precipitation borderline in the pM′–pC_H diagram, determined experimentally under CO_2-free conditions, stability constants for the mononuclear species of erbium hydroxide have been established. The values found were log $*\beta_1 = -6.3$, log $*\beta_2 = -14.5$, log $*\beta_3 = -23.1$, log $*\beta_4 = -36.8$ and log $*K_{s0} = 18.0$. The data refer to precipitates prepared at room temperature (21.5 ± 0.5°) in sodium perchlorate medium with an ionic strength of 1. The formation of polynuclear hydroxide complexes has been considered and rejected as unlikely to occur.

We have previously described the determination of the hydrolysis constants of cerium(III),[1] samarium(III),[2] gadolinium(III)[3] and ytterbium(III).[4] In this paper the hydrolysis of erbium(III) will be discussed.

The reported hydrolysis constants of erbium(III) (Table 1), like those of the other rare earths studied, show a fair diversity; moreover the set of constants is not completely known, so any description of its behaviour at pH > 7 is impossible.

Our experiments were done in sodium perchlorate medium ($I = 1.0$, temperature 21.5 ± 0.5°) and gave reproducible results when fresh precipitates were formed under nitrogen in a glove-box. All the manipulations in preparation of stock solutions and precipitate formation had to be standardized, as discussed before.[3,4] The pH-meter was calibrated in pC_H units.[3] The precipitate was formed by a procedure similar to that described for ytterbium.[4]

RESULTS AND CONCLUSIONS

The experimental results are shown in Fig. 1. No experiments were done at pEr′ < 1 as it would then be impossible to correct adequately for ionic strength > 1. The borderline of the precipitation region for Er consists of two nearly straight parts connected by a curve from pC_H 8.0 (pEr′ 4.4) to pC_H 9.0. Regression analysis of the steep part up to pEr = 4.4 shows that the slope can be estimated as 1.94 ± 0.15. This leads to the conclusion that polynuclear hydroxide complexes are not formed. $[Er_2(OH)_4^{2+}$ is unlikely for stereochemical and statistical reasons and so are $Er_3(OH)_7$ and higher species.[10]] We consider $Er(OH)^{2+}$ to be the major species "in equilibrium" with the precipitate below pC_H.[8]

According to the theory outlined before,[1–4] in which straight-line segments (see Table 2) determine the borderline of precipitation, we can assign the fol-

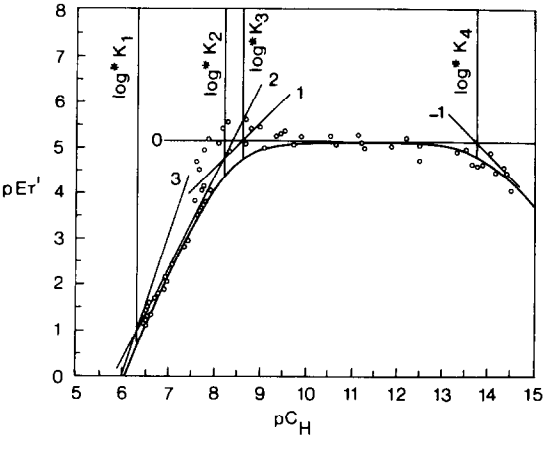

Fig. 1. The solid curve [the borderline of precipitation of Er $(OH)_3$] was constructed with the values given in Table 3. The numbers −1, 0, 1, 2 and 3 near the straight lines correspond to the slopes of the straight-line segments [equations (2a)–(2e) in Table 2] approximating the exact envelope curve. The circles denote the experimental results. The vertical lines separate the regions where Er^{3+}, $Er(OH)^{2+}$, $Er(OH)_3$ and $Er(OH)_4^-$, respectively, are the major species present.

*Part IV: *Talanta*, 1982, **29**, 219.

Table 1

Ref.	$\log {}^*\beta_1$	Polycomplex	$\log {}^*\beta_{q,p}$	$\log {}^*K_{s0}$	Medium	Method
5	−5.5				(H,Li)ClO_4, I = 0.1, 25°	solvent extraction and radiochemical indication
6		Er_2OH	−17.2		$LiClO_4$, 3M 25°	coulometry and pH determination
		$Er_2(OH)_2$	−13.72		2 days aging	
7	−9.0	$Er_2(OH)_2$	−13.72		$NaClO_4$, 3M 25°	potentiometric titration at various pH values
8	−7.85			15.0	I = 0	empirical relation
	−8.2				I = 0.05	empirical relation
	−9.4				I = 3	empirical relation
9	−8.26				$NaClO_4$, 0.3M	potentiometric titration

lowing equation to the steep part giving the best fit to the experimental points up to pEr′ = 4.4:

$$\mathrm{pEr}' = 2\mathrm{p}C_\mathrm{H} - (11.70 \pm 0.10) \quad (1)$$

Hence [according to equation (2b) in Table 2]

$$\log {}^*K_{s0} + \log {}^*\beta_1 = 11.70 \pm 0.10 \quad (3)$$

Equation (2d) can be assigned to the horizontal part of the borderline. The best fit corresponds to

$$\mathrm{pEr}' = 5.13 \pm 0.05 \quad (4)$$

from which follows

$$\log {}^*K_{s0} + \log {}^*\beta_3 = -5.13 \pm 0.05 \quad (5)$$

At high $\mathrm{p}C_\mathrm{H}$ the solubility increases again. Some values have been determined at $\mathrm{p}C_\mathrm{H} > 13.5$, although the ionic strength than exceeds 1.0 and the medium can no longer be regarded as only sodium perchlorate. So conclusions from this region ($\log {}^*\beta_4$) should be considered with some reserve. For the straight-line segment we deduce

$$\mathrm{pEr}' = -\mathrm{p}C_\mathrm{H} + 18.8 \quad (6)$$

so by comparison with equation (2c)

$$\log {}^*K_{s0} + \log {}^*\beta_4 = -18.8 \quad (7)$$

From equations (3), (5) and (7) the following equation can be deduced,[1–4] and this gives a good fit of the borderline of the precipitation region to the experimental points:

$$[\mathrm{Er}']_{max} = 10^{-2\mathrm{p}C_\mathrm{H} + 11.70} + 10^{-5.13} + 10^{\mathrm{p}C_\mathrm{H} - 18.8} \quad (8)$$

Addition of more terms does not improve the fit, which leads us to the following conclusions.

(*a*) The position of the straight-line segments corresponding to equation (2a) lies to the left of the experimental points. Thus $\mathrm{p}{}^*K_1 < 6.5$. On the other hand, in view of the radius of rare-earth ions (~0.84 Å) it is not likely[8] that hydrolysis becomes appreciable below $\mathrm{p}C_\mathrm{H}$ 6, and there is no reason to believe that erbium deviates in its behaviour from the other rare earths. Therefore we have chosen to make the region in which $Er(OH)^{2+}$ predominates as small as possible. The furthest right position of the straight-line segment leading to the negligible contribution to the envelope curve is then given by

$$\mathrm{pEr}' = 3\mathrm{p}C_\mathrm{H} - 18.0 \quad (9)$$

As equation (9) is equivalent to equation (2a),

$$\log {}^*K_{s0} = 18.0 \quad (10)$$

From equations (3) and (10), it follows that $\mathrm{p}{}^*K_1 = 6.3$.

(*b*) The straight-line segment corresponding to equation (2c) should not lie above the point of inter-

Table 2

Equation	p	q	Slope ($np - q$)	Equation for the borderline segment
2a	1	0	3	$\mathrm{pEr}' = 3\mathrm{p}C_\mathrm{H} - \log {}^*K_{s0}$
2b	1	1	2	$\mathrm{pEr}' = 2\mathrm{p}C_\mathrm{H} - (\log {}^*K_{s0} + \log {}^*\beta_1)$
2c	1	2	1	$\mathrm{pEr}' = \mathrm{p}C_\mathrm{H} - (\log {}^*K_{s0} + \log {}^*\beta_2)$
2d	1	3	0	$\mathrm{pEr}' = -(\log {}^*K_{s0} + \log {}^*\beta_3)$
2e	1	4	−1	$\mathrm{pEr}' = -\mathrm{p}C_\mathrm{H} - (\log {}^*K_{s0} + \log {}^*\beta_4)$

$$^*\beta_i = \frac{[\mathrm{Er(OH)}_i][\mathrm{H}^+]^i}{[\mathrm{Er}^{3+}]}.$$

Table 3

$\log {}^*\beta_1 = -6.3$	$\log {}^*\beta_4 = -36.8$
$\log {}^*\beta_2 = -14.5$	$\log {}^*K_{s0} = +18.0$
$\log {}^*\beta_3 = -23.1$	

section of lines (2b) and (2d), in order to prevent a reverse sequence in the magnitudes of $\log {}^*K_i$, as explained before.[1–4] If the line lies lower, the corresponding term can no longer be omitted from equation (8) and the line segment will give a contribution to the envelope curve.

Unfortunately the positions of the experimental points near this intersection point are not known as accurately as for the other rare earths. With the other lanthanides there was a slight tendency for the points to shift to lower pC_H with aging, but for these the shift could be kept within reasonable limits. In the case of erbium, there was much more uncertainty in the real position of the experimental points, making the position of line (2c) less conclusively determined. We chose to position the line slightly below the intersection-point, as that leads to a more regular sequence in the stepwise constants ($p^*K_1 < p^*K_2 < p^*K_3$, which is more likely than $p^*K_1 < p^*K_2 = p^*K_3$). Hence $p^*K_2 = 8.2$ and $p^*K_3 = 8.6$.

This completes the set of hydrolysis constants (Table 3), which can be regarded as useful for analytical practice.

It is difficult to discuss the accuracy of the individual constants. If the envelope curve is constructed, the position of the actual pEr'_{max} value is uncertain within 0.3 log unit, and this offers a measure for the spread around the line. This holds for both the steep parts and the horizontal part, assuming a "fresh precipitate" and CO_2-free conditions.

Acknowledgements—We are indebted to Mr. René Sepers and Mr. Alex Woldhuis for their valuable contributions to the experimental work.

REFERENCES

1. J. Kragten and L. G. Decnop-Weever, *Talanta*, 1978, **25**, 147.
2. *Idem, ibid.*, 1979, **26**, 1105.
3. *Idem, ibid.*, 1980, **27**, 1047.
4. *Idem, ibid.*, 1982, **29**, 219.
5. R. Guillaumont, B. Désiré and M. Galin, *Radiochem. Radioanal. Lett.*, 1971, **8**, 189.
6. T. Amaya, H. Kakihana and M. Maeda, *Bull. Chem. Soc. Japan*, 1973, 46, 1720.
7. K. A. Burkov, L. S. Lilich and Nguyen Din Ngo, *Izvest. Vyssh. Ucheb. Zaved. SSSR, Khim. i Khim. Tekhnol.*, 1975, **18**, 181.
8. C. F. Baes, Jr. and R. E. Mesmer, *The Hydrolysis of Cations*, pp. 129–138. Wiley–Interscience, New York. 1976.
9. U. K. Frolova, V. N. Kumok and V. V. Serebrennikov, *Izvest. Vyssh. Ucheb. Zaved. SSSR, Khim. i. Khim. Tekhnol.*, 1966, **9**, 176.
10. Ref. 8, p. 420.

Talanta, Vol. 30, No. 2, p. 134, 1983
Printed in Great Britain.

0039-9140/83/020134-01$03.00/0

HYDROXIDE COMPLEXES OF LANTHANIDES—VI*

J. KRAGTEN
Natuurkundig Laboratorium der Universiteit van Amsterdam, Valckenierstraat 65, 1018 XE Amsterdam, The Netherlands

and

L. G. DECNOP-WEEVER
Laboratorium voor Analytische Chemie der Universiteit van Amsterdam, Nieuwe Achtergracht 166, 1018 WV Amsterdam, The Netherlands

(*Received* 15 *June* 1982. *Accepted* 26 *August* 1982)

Summary—Experiments performed previously with cerium(III), samarium and gadolinium have been extended to conditions of high pC_H in order to discover any amphoteric character. Up to pC_H 14.6, the solubility of gadolinium hydroxide and of cerium(III) hydroxide does not increase, so the previously reported constants hold up to this pC_H. The solubility of samarium hydroxide increases at high pC_H, and the value $\log {}^*\beta_4 = -36.7$ can be deduced. This should be added to the previously reported set, now applicable up to pC_H 14.5.

In previous experiments on the hydrolysis constants of cerium(III), samarium and gadolinium[1-3] the pC_H was restricted to values up to 12. At that time we used a glass–calomel electrode system in a glove box and we were unable to determine higher pC_H values accurately enough.

These pC_H values are now determined acidimetrically with potentiometric end-point detection.[4] The pC_H is found from the titration result "C_{OH}" and the autoprotolysis constant (concentration product, pQ_W) of water for sodium perchlorate medium at $I = 1.0$ and temperature 21.5° ($pQ_W = 13.92 \pm 0.10$). The pC_H can be reproduced very well, but its accuracy only to ± 0.10. However, there is no need for greater accuracy, since above pC_H 13, pQ_W changes continuously as the medium changes into a hydroxide one, and above pC_H 14 the ionic strength will even increase.

The titrimetric pC_H determination has already been used to establish the amphoteric character of ytterbium[4] and erbium.[5] Recently experiments with cerium(III), gadolinium and samarium have been extended to high pC_H.

Up to pC_H 14.6, both for gadolinium hydroxide and for cerium(III) hydroxide the solubility remains constant within experimental error. Thus, the two sets of constants published before[1,3] can be regarded as giving a complete description of the borderline of the precipitation region.

The solubility of samarium hydroxide increases at pC_H above 13.8, however. The measurements have been continued to pC_H 14.5. Fitting of the envelope curve to the experimental points was found to be satisfactory with $p^*K_4 = 14.0$, so the value

$$\log {}^*\beta_4 = -36.7$$

can be added to the set of constants given before.[2]

Acknowledgements—We are indebted to Mr. René Sepers and Mr. Alex Woldhuis for their valuable contributions to the experimental work.

REFERENCES

1. J. Kragten and L. G. Decnop-Weever, *Talanta*, 1978, **25**, 147.
2. *Idem*, *ibid.*, 1979, **26**, 1105.
3. *Idem*, *ibid.*, 1980, **27**, 1047.
4. *Idem*, *ibid.*, 1982, **29**, 219.
5. *Idem*, *ibid.*, 1983, **30**, 131.

*Part V: *Talanta*, 1983, **30**, 131.

Talanta, Vol. 30, No. 2, pp. 135–137, 1983
Printed in Great Britain

0039-9140/83/020135-03$03.00/0
Pergamon Press Ltd

ANNOTATION

NICOLAE TECLU (1839–1916)

A PIONEER OF FLAME SPECTROSCOPY

G. E. BAIULESCU and S. MOLDOVEANU
Department of Analytical Chemistry, National Institute of Chemistry,
Splaiul Independenţei 202, 77207-Bacharest, Romania

and

T. S. WEST
The Macaulay Institute for Soil Research, Aberdeen, Scotland

(*Received* 4 *November* 1981. *Revised* 19 *May* 1982 *Accepted* 25 *August* 1982)

Summary—A brief account is given of Teclu's career and his contributions as a pioneer of the study of flames.

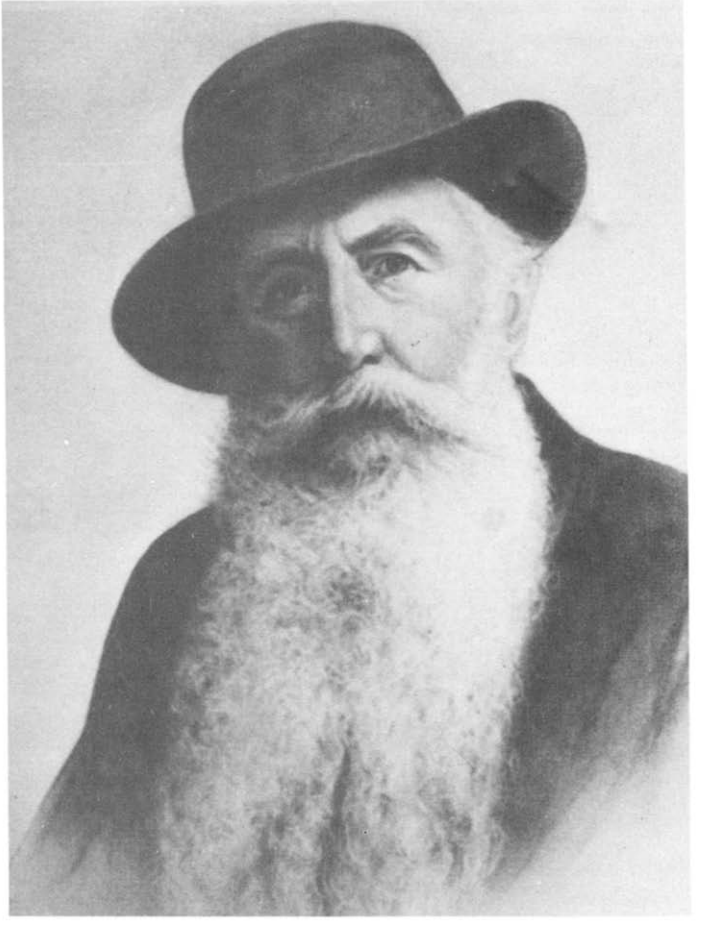

Nicolae Teclu

The Romanian chemist Nicolae Teclu was one of the pioneers of the systematic study of flames. Born in Braşov on 7 October 1839, he entered secondary school in his native city, but graduated from high school in Vienna. Subsequently he matriculated at the Polytechnic in Vienna and then, undecided as to his future career, went to Munich to study architecture at the Academy of Fine Arts. After graduation with a B.Sc. he returned to Romania and tried unsuccessfully to practice architecture before returning to Vienna and attending chemistry classes at the University.

As a young scientist he began his activity in chemistry in Vienna as assistant to Professor Ernest Ludwig. He distinguished himself as a skilled investigator and soon became Professor of Chemistry at the Technical Chemistry Department of the Vienna Trade Academy; at the same time he lectured on the chemistry of colours at the Academy of Fine Arts. It is worth noting that among other investigations he was always preoccupied with the construction of laboratory equipment, some of which is still in use.

Teclu ventured into a tremendous variety of investigations, *e.g.*, the burning process of combustible gases, the analysis of natural products, studies on the composition of paper, *etc.* However, this note will deal with only one of his most important contributions: the study of flames. He studied these with devices which he designed for the purpose and found that the combustion rate (for coal gas) depends on the oxygen content of the gaseous mixture. The position of a flame burning in a vertical tube (Fig. 1)[1] is the result of the descending movement of the flame in the tube, and of the ascending movement of the combustible mixture. Using this simple device, Teclu investigated flames with various compositions and found that any flame consists in fact of two parts—one burning on the outside and the other inside the tube; the former has a blue colour, points upward and is supplied with oxygen by the surrounding medium; the latter, very hot, has a green colour, points downward and burns on account of the oxygen contained in the gaseous mixture.

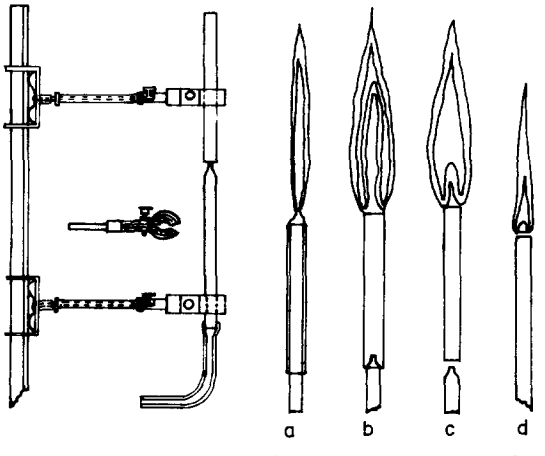

Fig. 1. Device used by Teclu[1] to study the splitting of a flame.

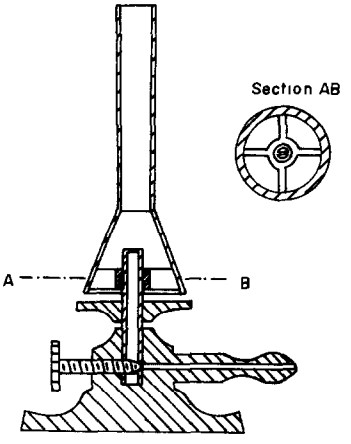

Fig. 2. The Teclu burner.[2]

By modification of the geometry of this simple device, the inner flame may be raised and placed on top of the tube, with its tip pointing upward. In this way a single flame is obtained, similar to the flame of a Bunsen burner.

As a result of these experiments, Teclu succeeded in improving the Bunsen burner and designed the almost perfect burner—now known as the Teclu burner—which is still used in laboratories the world over (Fig. 2).[2] This burner achieves virtually perfect control of gas mixing—previously the major problem with burner devices.

His first publication on the gas burner, "Ein neuer Laboratoriums Brenner,"[2,3] was issued in the *Journal für praktische Chemie* in 1892. The original burner was made of brass and patented by W. J. Rohrbeck's Nachfolger company in Vienna and the Franz Hugershoff company in Leipzig.

Teclu also demonstrated the presence of solid particles in flames,[4] using a photographic technique, and studied the spectra of various elements by using the spectral method discovered some twenty years earlier by Bunsen and Kirchhoff. He noticed and reported in his papers the stable position of the lines in a spectrum.[5]

In the same line of the study of flames, Teclu also investigated their shape and size[3] as a function of the flow of gases supplied and of burner geometry. From these experiments, Teclu obtained a series of results concerning the flame pressure.

Teclu's studies on flames, especially those on their transparency, represented outstanding achievements that have placed him, together with Kirchhoff and Bunsen, among the pioneers of modern analytical spectroscopic techniques such as flame-emission photometry and atomic-absorption spectrometry.

The major initial requirement for the determination of elements by flame techniques is to use an adequate burner and it is here that Teclu's pioneering work on burner design and flame transparency laid some of the foundations of the laboratory techniques of analytical atomic spectrometry.

Flame photometry was the first flame technique employed in analytical chemistry and its inception completely revolutionized the determination of the alkali and alkaline-earth metals. As an emission technique, it depends on excitation by energetic species in the flame. To make it suitable for determination of a larger number of elements, the flame temperature had to be high enough to provide more energetic species that could excite atoms other than those of the alkali metals, *etc.* Many studies have been dedicated throughout the years to improving excitation conditions, *e.g.*, by the use of various mixtures of fuel and support gases. In this field, too, Teclu did pioneering work; he estimated the heats of combustion of various mixtures of gases[6] and contributed significantly to the theoretical study of combustion rates. The studies continued in Romania by Radu Mavrodineanu, one of Teclu's eminent followers, are particularly worthy of mention. At that time theoretical knowledge was fairly advanced and, therefore, it became possible to envisage how a technically simple emission technique such as flame photometry could be applied to a considerably wider range of elements. Utilization of a hotter and more reducing flame, based on nitrous oxide as a support gas in place of air, extended the capability of the technique, but without solving many of its other problems.

In 1954/55 Walsh and, independently, Alkemade and Milatz worked out the principles and apparatus necessary for the evolution of a laboratory technique of flame atomic-absorption spectrometry. This has now extended the use of flames in analytical chemistry to the determination of traces of more than sixty elements. This technique, based on the idea of using the atoms in their ground state in an optically transparent flame, can be achieved (with a few exceptions) with conventional flames.

The evolution of atomic-absorption spectrometry represents an improvement of the analytical process itself, especially in terms of operational parameters. It is tempting to speculate whether Teclu could have imagined what an invaluable analytical tool would eventually be evolved from his studies of flames.

Whilst Teclu in his time succeeded in designing and building the equipment he needed for his own studies, nowadays advances result mainly from open competition between researchers and eventual collaboration between researchers and the manufacturers of scientific apparatus.

As a consequence of continuous progress in the perfection and design of laboratory equipment it is no surprise to note that flame atomic-emission spectrometry has already grown obsolete apart from its use (as originally) for the alkali metals. Some would even argue that atomic-absorption spectrometry may in due course be rendered obsolescent by the introduction of new and more sensitive emission techniques that do not use chemical flames. It is important to remember, however, that these new techniques arise as a logical result of studies with conventional flame equipment going back to the time of Teclu and others.

This brief historical outline underlines that progress in scientific research results from a process of continuous evolution arising initially from the discoveries and work of a few originators. It is our contention that the Transylvanian scientist Nicolae Teclu was one of the best of these in respect of modern analytical atomic spectroscopy.

REFERENCES

1. N. Teclu, *J. Prakt. Chem.* 1895, **52,** 145.
2. *Idem, ibid.*, 1982, **45,** 281.
3. C. Gh. Macarovici and G. Schmidt, *Nicolae Teclu.* Editura Ştiinţifică, Bucharest, 1971.
4. N. Teclu, *J. Prakt. Chem.* 1897, **56,** 178.
5. *Idem, România Jună*, Vienna, 1887–1888.
6. *Idem, J. Prakt. Chem.*, 1895, **52,** 277.

Talanta, Vol 30, No. 3, pp. 139–143, 1983
Printed in Great Britain.

0039-9140/83/030139-05$03.00/0

FLUORIMETRIC REACTION-RATE METHODS OF INORGANIC ANALYSIS: A REVIEW

M. VALCÁRCEL and F. GRASES

Departments of Analytical Chemistry, Faculty of Sciences, Universities of Córboda and Palma de Mallorca, Spain

(*Received* 24 *June* 1981. *Revised* 12 *July* 1982. *Accepted* 21 *September* 1982)

Summary—A review is given of the utilization in analytical chemistry of the rate of fluorescence reactions of inorganic species. These methods are of recent development and suggest the possibility of further analytical procedures. Two main types of methods, enzymatic and non-enzymatic, are distinguished, and their applications to inorganic analysis are discussed.

Fluorimetric methods of analysis can be divided into two large groups: equilibrium methods and kinetic methods. Within the latter group, four types of methods, with a wide variety of techniques and foundations, may be distinguished.

1. The first group, despite being inherently kinetic in nature (measurements are made before equilibrium is reached), is not normally distinguished from non-kinetic methods. The same methodology and instrumentation are employed, but measurements are made at various time intervals, the reaction being halted (for measurement purposes) by rapid cooling, pH-change, *etc.* Traces of Cu(II) and Hg(II) have been determined in this way by their catalysis of the self-oxidation of 2,2′-dipyridyl ketone hydrazone in neutral or slightly basic media, to give a product which shows maximum fluorescence in acid medium: acidification increases the fluorescence and halts the reaction.[1] When the reaction is slow, measurements can also be made after a time long enough for the reaction to be approaching completion and for the signal not to change rapidly with time. Au(III),[2] Co(II)[3] and Ti(IV),[4] cations that catalyse the aerobic oxidation of the reagents dipyridylglyoxal diphenylhydrazone, phenyl 2-pyridyl ketone hydrazone and picolinaldehyde nicotinoylhydrazone, respectively, producing intensely fluorescent products, have been determined in this way. Occasionally, from a purely formal viewpoint, this type of method may be considered to be non-kinetic.

2. The second group is of methods based on chemiluminescent reactions. In these, the analytical signal is the light emitted while the reaction is taking place. These methods generally record the intensity of emitted light as a function of time, and the maximum intensity is usually proportional to the concentration of the analyte. Occasionally the area under the intensity *vs.* time curve is integrated. This group of methods has been reviewed, and many inorganic species that act as catalysts for these reactions have been determined.[5–7] In these methods the kinetics of the reaction were not investigated and the time variable was not directly involved except in the following few cases. Thus, Musha *et al.*[8] determine cyanide, using the fact that this ion suppresses the chemiluminescence reaction of luminol with hydrogen peroxide; the incubation period is proportional to the cyanide concentration. Bovalini *et al.*[9] find that both the intensity and the duration of the light emitted by luminol with hydrogen peroxide and iron–haemin complexes are dependent on the concentration of both these substances. Pantel and Weisz[10] determine copper(II) by means of its catalysis of the chemiluminescent reaction between luminol and hydrogen peroxide. The intensity of the luminescence is used, through a photomultiplier and a current–voltage transducer, to regulate the addition of hydrogen peroxide from an automatic burette. The rate of addition needed to keep the luminescence constant is a measure of the copper(II) concentration.

3. The third group of methods is based on measuring the lifetime of the excited state of a chemical species. The decay curves are recorded, so the analytical measurement is made as the molecules pass from the excited state to the ground state, *i.e.*, under non-equilibrium conditions. This kind of technique has been applied to the analysis of mixtures of organic products with nearly identical excitation and emission spectra. Few applications to inorganic chemistry have been reported. Only the 8-quinolinolates of Ca^{2+}, Sc^{3+}, Zn^{2+}, Ga^{3+} and Ge^{4+},[11] the 5-sulpho-8-quinolinolates of Al^{3+}, Ga^{3+}, Mg^{2+} and Cd^{2+},[12] and the salicylidene-*o*-aminophenol complexes of In^{3+}, Ga^{3+} and Al^{3+},[13] seem to have been used.

4. The fourth group is based on measuring the rate of a chemical reaction in which one or more of the molecular species involved exhibits fluorescence. In these reaction-rate methods the "tangent", "fixed time" and "fixed fluorescence" methods are used.[14] If there is an induction period (*e.g.*, in the Landolt reaction), a fourth method, based on measurement of this period, can be applied.[15]

In this review we shall consider only the fluorimetric reaction-rate methods of inorganic analysis

and summarize the information published between 1960 and 1981. For kinetic methods in general, many reviews have been published. That of Mottola,[16] in which 39 reviews on this subject appeared before 1976 are listed, should be especially mentioned. After 1975 information referring to these publications is given in the biennial reviews of *Analytical Chemistry*.[17–19] It is important to reiterate here that the number of fluorimetric reaction-rate methods for determination of inorganic species is relatively limited, because few reactions are known in which inorganic compounds take part and fluorescent substances are formed or destroyed. It is for this reason that this area has become an important field of investigation in recent years.

FLUORIMETRIC REACTION-RATE METHODS

Fluorimetric reaction-rate measurements have primarily been applied to enzymatic reactions,[20,21] and in the field of organic and biochemical analysis the number of applications for these methods is quite large because of the inherent fluorescence of many of the compounds concerned. Several papers summarize the data in this field.[22–25] The general principles and practice of fluorimetric reaction-rate methods of analysis have been reviewed by Ingle and Ryan.[26] Most of the advantages of the reaction-rate methods lie in the selectivity and sensitivity of catalysis methods, the possibility of utilization of reactions which have unfavourable equilibrium constants and/or undergo side-reactions, the simultaneous *in situ* analysis of mixtures of closely related substances, saving of time, *etc.* However, there has been considerable resistance to use of the methods because of the obvious problem of adding time as an experimental variable.

Fluorimetric reaction-rate methods in inorganic analysis can be classified according to the nature of the substrates, into enzymatic and non-enzymatic reaction-rate methods.

Enzymatic methods

In these methods, the determination of the inorganic species is based on its action on the activity of an enzyme, the degree of inhibition or enhancement of the activity being proportional to the analyte concentration. More than 15 inorganic species have been determined in this way. Thus, a method for magnesium in plasma, based on the activation of isocitric dehydrogenase, was described by Baum and Czok.[27] With a constant amount of enzyme the rate is dependent on the magnesium concentration, down to $10^{-6}M$. A thorough study of this reaction was made by Adler *et al.*[28] and by Blaedel and Hicks,[29] who found that only Mg^{2+} and Mn^{2+} efficiently activate this enzyme. The useful analytical range extends to about 100 ng/ml for Mn^{2+} and $2 \times 10^{-4}M$ for Mg^{2+}; $10^{-5}M$ Hg^{2+} or Ag^{+} and $10^{-4}M$ Ca^{2+} completely inhibit the activation by Mn^{2+}.

The specific requirement for Mn^{2+} in the peroxidase-catalysed oxidation of 2,3-diketogulonate is utilized to produce hydrogen peroxide, and the signal observed in the fluorimetric "fixed time" procedure can be related to the Mn^{2+} concentration by using a modified standard-addition method.[30] The detection limit is $8\ \mu M$ Mn^{2+}, and the calibration range is up to $\sim 50\ \mu M$ Mn^{2+}. The analysis time is less than 30 min.

The enzyme glyceraldehyde-3-phosphate dehydrogenase is used for an oxidative arsenolysis of D-glyceraldehyde-3-phosphate.[31] The rate of reaction, measured by fluorescence, is first-order with respect to arsenic(V). The method gives a linear calibration plot for arsenic in the range 0.02–2.0 μg/ml. Samples of drinking water and river water can be analysed by this technique.

The inhibition of enzyme activity is the basis of a method for Cu^{2+} (0.2–0.6 μg/ml), Fe^{2+} (0.2–12 μg/ml) and CN^{-} (0.1–4 μg/ml), [32] which can be determined in the micromolar range with a relative precision of 2.3%. The method employs hyaluronidase-catalysed hydrolysis of indoxyl acetate to the highly fluorescent indigo white, and can also be used for the sensitive and precise determination of the enzyme itself.

Fluorescence methods have been described for the assay of the oxidative enzymes peroxidase, glucose oxidase and xanthine oxidase, based on the conversion of the non-fluorescent homovanillic acid into the highly fluroescent 2,2′-dihydroxy-3,3′-dimethoxybiphenyl-5,5′-diacetic acid.[33] Methods are given for various inorganic substances which inhibit these enzyme systems: CN^{-} (0.9–12 μg/ml), S^{2-} (0.3–3 μg/ml), $Cr_2O_7^{2-}$, SO_3^{2-}, Cu^{2+}, Fe^{2+}, Fe^{3+} (5–60 μg/ml), Mn^{2+} (0.6–12 μg/ml), Pb^{2+}, Co^{2+} (0.5–12 μg/ml), and Cd^{2+}. These ions can be determined with an average relative error of about 2%.

A fluorimetric method is described[34] for the determination of bismuth (1–70 μg/ml) and beryllium (0.01–0.30 μg/ml), with an average relative error of about 1.5% based on their inhibition of the activity of acid and alkalline phosphatase. The substrate umbelliferone phosphate is used, which is cleaved by phosphatase to the highly fluorescent umbelliferone.

Non-enzymatic methods

These methods include those in which the concentration of analyte is related to the rate of the reaction which takes place between a substrate and an inorganic species, or of one that is catalysed by this species. The reactions employed are generally redox reactions. The following species have been determined by this procedure: Co^{2+}, Cu^{2+}, V(V), Mn^{2+}, Ir^{4+}, Al^{3+}, Ag^{+}, Hg^{2+}, Pt^{4+}, Au^{3+}, Ti^{4+}, Ce^{4+}, Fe^{3+} and Tl^{3+}

Bozhevol'nov and Kreingol'd[35] have determined cobalt at the 0.1 ng/ml level. In this method 9-(2-hydroxyphenyl)-2,6-7-trihydroxyfluorone is oxidized by hydrogen peroxide, with cobalt as catalyst. Bozhevol'nov *et al.*[36] later examined three compounds in a comparative study of the kinetic determination of

traces of copper, and found benzamido(*p*-diethylaminobenzylidene)acetic acid the most sensitive. It is thought that the Cu^{2+} acts as catalyst in the formation of the fluorescent dimer of the reagent. Addition of sodium diethyldithiocarbamate further increases the sensitivity to 0.2–0.4 ng/ml.

The induction period of the bromate–bromide–ascorbic acid system is shortened by the catalytic action of vanadium. The bromine then liberated can be detected at pH 5 by its quenching action on the fluorescence of Rhodamine B, Cresyl Violet or trypaflavine. Vanadium in the concentration range 0.02–20 μg/ml can be determined in this way.[37]

Morgen *et al.*[38] developed a method for determining microamounts of manganese. The method is based on the ability to accelerate kinetically the aerial oxidation of the morin complex of beryllium. Cu^{2+}, Cr^{3+}, Fe^{2+}, Fe^{3+}, Co^{2+}, Ni^{2+} and Ag^{+} also catalyse this reaction. The sensitivity of the method under the conditions chosen is 0.5 ng/ml.

Shcherbov *et al.*[39] described a method for fluorimetric determination of 0.4–32 μg/ml Ir by its catalytic action on the reduction of cerium(IV) with arsenic(III) and antimony(III). Os and Ru interfere.

Silver can be determined by means of its enhancement of the reaction between 5-sulpho-8-quinolinol and persulphate.[40] The method gives a linear response to silver from 6 ng/ml to 3 μg/ml; extraction with dithizone is needed to eliminate interferences. The exact nature of the indicator reaction is not known, but the evidence suggests that the product is an oxidized form of the substrate (possibly a quinone) and that silver acts as a catalyst, probably through the usual Ag(I)/Ag(II) cycle. Aluminium interferes at very low levels, reacting slowly with the 5-sulpho-8-quinolinol to form a fluorescent product. This system was used in a kinetic procedure for trace aluminium in the range from 0.4 ng/ml to 10 μg/ml.[41] Again the nature of the reaction is not known.

A reaction-rate method for Hg^{2+}, with thiamine as reagent, has been developed;[42] the reaction is pseudo first-order in thiamine. It is assumed that Hg^{2+} is the oxidant in two reaction pathways.

In recent studies we have found that unsubstituted hydrazones and azines of 2,2′-dipyridyl ketone, phenyl 2-pyridyl ketone, and dipyridylglyoxal undergo aerial oxidation that is catalysed by Cu^{2+}, Co^{2+}, Hg^{2+}, Au^{3+} and Pt^{4+}, forming products that are intensely fluorescent at the appropriate pH. This fact allows the establishment of fluorimetric reaction-rate methods for determination of these cations.[3,43–45] The catalytic action of Cu^{2+} on the autoxidation (in neutral or slightly basic media) of the hydrazone of 2,2′-dipyridyl ketone had been exhaustively studied.[1] and the fluorescent product has been isolated and characterized. Picolinaldehyde nicotinoylhydrazone has been used for the kinetic fluorimetric determination of Ti^{4+},[4] based on its catalytic effect on aerial oxidation of the reagent. The catalytic action of Mn^{2+} on the oxidation of salicylaldehyde thiosemicarbazone by hydrogen peroxide has been utilized for its determination.[46] The reaction product has been isolated and characterized. The characteristics of these and the following methods are given in Table 1.

Anthraquinones with hydroxy and/or amino groups in appropriate positions react with oxidants such as V(V) and Ce^{4+} to produce intensely fluorescent products which can be used for kinetic fluorimetric determination of these oxidants.[47–50] In one case the product obtained has been isolated.[48]

1,4-Diamino-2,3-dihydroanthraquinone hydrolyses to give an intensely fluorescent product, which itself is oxidizable by Fe^{3+} and Tl^{3+} to another substance of identical fluorescence characteristics. This allows the determination of these species by fluorimetric reaction-rate methods.[51] The hydrolysis product has been isolated and characterized.

Instrumentation

The instrumentation suitable for this work can be classified into two groups according to whether it is used for fast reactions (15 sec or less) or slow ones which sometimes require several minutes for completion after the solutions have been mixed. In the first case, the use of most standard fluorimeters is unsatisfactory because of the time required for manual mixing of the solutions, and because of the generally slow response of the photodetector amplifiers. In general, the mixing cannot be completed in less than 5 sec, so reactions occurring in 15 sec or less cannot be accurately studied with such apparatus. For this reason it is necessary to employ special instrumentation, generally in association with stopped-flow systems.[52] In the second case, the normal instrumentation used in equilibrium-based measurements can be employed. However, the fluorimeter must have an independent signal-recorder to record the fluorescence intensity *vs.* time curves. To take full advantage of the specificity and sensitivity of fluorimetric kinetic measurements, the instrumentation must measure accurately and precisely very small changes in the fluorescence signal. The factors which affect the precision and signal-to-noise ratio (*S/N*) must also be well understood. The construction and operation of a fluorimetric reaction-rate instrument has been described by Wilson and Ingle.[53] This instrument was designed for maximum versatility and ease of operation in measuring initial reaction-rates of reactions involving the formation or disappearance of fluorescent species. The instrument consists basically of a molecular-fluorescence spectrometer, a ratemeter, and associated electronics to provide a digital read-out of the measured rate. The instrument's *S/N* characteristics for steady-state and reaction-rate measurements have been evaluated, and procedures presented for determining the precision of rate measurements under noise-limited conditions, and assessing the contribution of imprecision of sample-introduction to the total precision. In the ratemeter[54] the monitoring period is divided into two equal integration intervals. The difference between the

Table 1. Characteristics of various fluorimetric non-enzymatic reaction-rate methods

Cation determined	Reagent	pH or acidity	Range of applicability, *ppm*	λ_{ex}, λ_{em} *nm nm*	Ref.
Pt(IV)	2,2'-dipyridyl ketone hydrazone	2.6	0.2–0.6	359–435	43
Au(III)	2,2'-dipyridyl ketone azine	2.5	0.05–0.25	347–435	44
Cu(II)	2,2'-dipyridyl ketone azine	4.0	0.2–0.5	347–435	45
Cu(II)	2,2'-dipyridyl ketone hydrazone	6.3	0.1–1.0	359–430	45
Cu(II)	phenyl 2-pyridyl ketone hydrazone	9.0	0.1–0.6	308–435	45
Co(II)	phenyl 2-pyridyl ketone hydrazone	9.0	0.7–2.4	308–435	3
Co(II)	dipyridylglyoxal hydrazone	12.0	0.08–0.24	340–454	3
Ti(IV)	picolinaldehyde nicotinoylhydrazone	6.5	0.06–0.4	365–445	4
Mn(II)	salicylaldehyde thiosemicarbazone	NH_3	0.002–0.008	360–440	46
V(V)	1-amino-4-hydroxy anthraquinone	0.5*M* HCl	0.1–0.5	480–575	47
V(V)	sodium 4,8-diamino 1,5-dihydroxy anthraquinone-2,6-disulphonate	0.4*M* HCl	0.04–0.5	524–582	48
Ce(IV)	1-amino-4-hydroxy anthraquinone	0.6*M* HCl	0.1–0.9	480–575	49
Ce(IV)	sodium 4,8-diamino-1,5-dihydroxy anthraquinone-2,6-disulphonate	0.2*M* H_2SO_4	0.02–0.37	525–585	50
Fe(III)	1,4-diamino-2,3-dihydroanthraquinone	3.4	0.05–0.6	400–470	51
Tl(III)	1,4-diamino-2,3-dihydroanthraquinone	3.4	0.05–0.4	400–470	51

two integrals is directly proportional to the initial rate of the reaction.

Conclusion

Generally, the principal advantages of kinetic methods (to be exact, those based on the initial-rate method) over non-kinetic methods are the greater speed and selectivity of the former, because there is less time for the effects of the various interferences to become significant. Furthermore the kinetic methods have the advantage of easy adaptation to automation processes.

Many of the characteristics of fluorescence are ideal for kinetic methods. The principal reason for using fluorescence monitoring in place of absorbance monitoring is the greater sensitivity. Since only small concentration changes are measured in reaction-rate methods, the well-known sensitivity of fluorescence is especially important. A second advantage of fluorescence monitoring is greater specificity. This arises because only relatively few compounds exhibit significant fluorescence and because both the excitation and emission wavelengths can be chosen. In some cases interaction between the fluorescence and kinetic characteristics helps to annul an undesirable effect. For example, an increase in temperature generally increases the reaction rate, but decreases the fluorescence quantum efficiency, so there is partial compensation for temperature fluctuations. However, photolysis may place a constraint on reaction conditions or measurement times for equilibrium or kinetic fluorescence methods.

Examination of the historical development of fluorescence methods and reaction rate methods shows that it is only relatively recently that the two have been combined. Consequently fluorimetric reaction-rate methods have scarcely been applied up till now to inorganic analysis, the reason for this being the scarcity of reactions involving at least one inorganic component and showing appearance or disappearance of fluorescent products. In the field of organic and biochemical analysis, the number of applications for these methods is quite large, because of the inherent fluorescence of many of the compounds concerned.

Fluorescence instrumentation is more expensive and complex than absorbance instrumentation, because both excitation and emission optics must be incorporated. However, in some cases a simple filter fluorometer may be adequate if only low wavelength resolution is needed. As with any kinetic instrument, the added cost of the ratemeter circuitry and sample

and reagent delivery systems must be considered. Although rates may be obtained from chart recorder tracings, the use of electronic timing and rate-computation is more rapid, accurate, and precise.

REFERENCES

1. F. Grases, G. Garcia-Sanchez and M. Valcárcel, *Anal. Chim. Acta*, 1980, **119**, 359.
2. *Idem, Anal. Lett.*, 1979, **12**, 803.
3. Idem, An. Quim., 1980, **76(B)**, 402.
4. M. D. Luque de Castro and M. Valcárcel, *Talanta*, 1980, **27**, 645.
5. W. R. Seitz and M. P. Neary, *Contemp. Top. Anal. Clin. Chem.*, 1977, **1**, 49.
6. D. B. Paul, *Talanta*, 1978, **25**, 377.
7. W. R. Seitz, *Modern Fluorescence Spectroscopy*, E. L. Wehry (ed.), Vol. 1, pp. 193–209. Plenum Press, New York, 1976.
8. S. Musha, M. Ito, Y. Yamamoto and Y. Inamori, *Nippon Kagaku Zasshi*, 1959, **80**, 1285.
9. E. Bovalini and M. Piazzi, *Ann. Chim. Roma*, 1963, **53**, 1103.
10. S. Pantel and H. Weisz, *Anal. Chim. Acta*, 1975, **74**, 275.
11. F. E. Lytle, D. R. Storey and M. E. Juricich, *Spectrochim. Acta*, 1973, **29(A)**, 1357.
12. K. Hiraki, K. Morishige and Y. Nishikawa, *Anal. Chim. Acta*, 1978, **97**, 121.
13. T. L. Craven and F. E. Lytle, *ibid.*, 1979, **107**, 273.
14. H. B. Mark and G. A. Rechnitz, *Kinetics in Analytical Chemistry*. Interscience, New York, 1968.
15. K. B. Yatsimirskii, *Kinetic Methods of Analysis*. Pergamon Press, Oxford, 1966.
16. H. A. Mottola, *CRC Crit. Rev. Anal. Chem.*, 1975, **5**, 229.
17. R. A. Greinke and H. B. Mark, *Anal. Chem.*, 1976, **48**, 87R.
18. *Idem, ibid.*, 1978, **50**, 70R.
19. H. A. Mottola and H. B. Mark, *ibid.*, 1980, **52**, 31R.
20. G. G. Guilbault, *Practical Fluorescence Theory, Methods, and Techniques*. Dekker, New York, 1973.
21. *Idem, Enzymatic Methods of Analysis*. Pergamon Press, New York, 1970.
22. W. B. Dandliker, J. Dandliker, S. A. Levison, R. J. Kelly, A. N. Hicks and J. U. White, *Methods Enzymol.*, 1978, **48**, 380.
23. D. N. Kramer, *Pure Appl. Chem.*, 1976, **48**, 65.
24. D. Madge, *Q. Rev. Biophys.*, 1976, **9**, 35.
25. T. M. Jovin, *Biochem. Fluoresc.*, 1975, **1**, 305.
26. J. D. Ingle, Jr and M. A. Ryan, in *Modern Fluorescence Spectroscopy*, E. L. Wehry (ed.), Vol. 3, pp. 95–142. Plenum Press, New York, 1981.
27. P. Baum and R. Czok, *Biochem. Z.*, 1959, **332**, 121.
28. E. Adler, G. Gunther and M. Plass, *Biochem. J.*, 1939, **33**, 1028.
29. W. J. Blaedel and G. P. Hicks, *Advances in Analytical Chemistry and Instrumentation*, Vol. 3, p. 105. Interscience, New York, 1964.
30. V. L. Biddle and E. L. Wehry, *Anal. Chem.*, 1978, **50**, 867.
31. S. R. Goode and R. J. Matthews, *ibid.*, 1978, **50**, 1608.
32. G. G. Guilbault, D. N. Kramer and E. Hackley, *Anal. Biochem.*, 1967, **18**, 241.
33. G. G. Guilbault, P. Brignac Jr. and M. Zimmer, *Anal. Chem.*, 1968, **40**, 190.
34. G. G. Guilbault, M. H. Sadar and M. Zimmer, *Anal. Chim. Acta*, 1969, **44**, 361.
35. E. A. Bozhevol'nov and S. U. Kreingol'd, *Tr. Vses. Nauchn. Issled. Inst. Khim. Reactivov Osobo Chist. Khim. Vesshchestv*, 1966, **26**, 204.
36. E. A. Bozhevol'nov, S. U. Kreingol'd and L. I. Sosenkova, *ibid.*, 1967, **30**, 176.
37. J. Bognár and O. Jellinek, *Mikrochim. Acta*, 1968, 1013.
38. E. A. Morgen, N. A. Morgen, N. A. Vlasov and L. A. Kozhemyakina, *Zh. Analit. Khim.*, 1972, **27**, 2064.
39. D. P. Shcherbov, O. D. Inyutina and A. I. Ivankova, *ibid.*, 1973, **28**, 1372.
40. R. L. Wilson and J. D. Ingle, Jr., *Anal. Chem.*, 1977, **49**, 1066.
41. *Idem, Anal. Chim. Acta*, 1977, **92**, 417.
42. M. S. Ryan, *Ph.D. Thesis, Oregon State University, Corvallis*, 1980.
43. F. Grases, J. M. Estela, F. Garcia-Sanchez and M. Valcárcel, *Anal. Lett.*, 1980, **13**, 181.
44. *Idem, Analusis*, 1981, **9**, 66.
45. F. Grases, F. Garcia-Sanchez and M. Valcárcel, *Anal. Chim. Acta*, 1981, **125**, 21.
46. A. Moreno, M. Silva, M. D. Perez-Bendito and M. Valcárcel, *XVIII Reunion Bienal R.S.E.F.Q.*, Burgos, Spain, 1980.
47. F. Salinas, F. Garcia-Sanchez, F. Grases and C. Genestar, *Anal. Lett.*, 1980, **13**, 473.
48. F. Garcia-Sanchez, A. Navas, M. Santiago and F. Grases, *Talanta*, 1981, **28**, 833.
49. F. Salinas, C. Genestar and F. Grases, *Microchem. J.*, 1982, **27**, 32.
50. A. Navas, F. Sanchez-Rojas and F. Garcia-Sanchez, *Mikrochim. Acta*, 1982**I**, 175.
51. F. Salınas, C. Genestar and F. Grases, *Anal. Chim. Acta*, 1981, **130**, 337.
52. R. F. Chen, A. N. Dchechter and R. L. Berger, *Anal. Biochem.*, 1969, **29**, 68.
53. R. L. Wilson and J. D. Ingle, Jr., *Anal. Chem.*, 1977, **49**, 1060.
54. *Idem, Anal. Chim. Acta*, 1976, **83**, 203.

Talanta, Vol. 30, No. 3, pp. 145–149, 1983
Printed in Great Britain.

0039-9140/83/030145-05$03.00/0

KINETIC DETECTION OF THE END-POINT IN TITRATIONS INVOLVING SLOW REACTIONS

DIRECT TITRATION OF POLYHYDROXY-COMPOUNDS WITH PERIODATE

C. E. EFSTATHIOU and T. P. HADJIIOANNOU
Laboratory of Analytical Chemistry, University of Athens, 104 Solonos St., Athens 144, Greece

(*Received* 3 *April* 1982. *Revised* 24 *September* 1982. *Accepted* 4 *October* 1982)

Summary—A new titration technique is described in which the end-point is determined by measuring the relative reaction rate of the titration reaction. This technique is adequate for rather slow reactions where conventional direct titrations are not applicable. The titrations are done automatically under microcomputer control. The efficiency of this technique is demonstrated with direct titrations of certain polyhydroxy-compounds with standard periodate solution. Ethylene glycol and propylene glycol (0.05–0.3 mmole), glycerol (0.06–0.17 mmole) and mannitol (0.01–0.03 mmole) were determined with average relative errors of 0.1–0.3%.

A common requirement for direct titration is that the reaction should be fast, especially when automatic titrators are used. If the reaction is slow, it is customary to add excess of titrant, and back-titrate, but this increases the overall analysis time and decreases the accuracy.

The end-point is generally detected by observing a change in an indicator colour or some other parameter such as potential, polarization current or conductivity. During the last decade titration techniques have been developed in which kinetic parameters are used indirectly to locate end-points. In these techniques, known as catalytic titrations, the titrant and the titrand react stoichiometrically and the first excess of the former catalyses an indicating reaction that is used to locate the end-point of the titration.[1]

In this paper, we describe a titration technique which is applicable when rather slow but stoichiometric reactions take place between the titrant and titrand. This technique requires microcomputer control and the end-point is automatically detected when certain preselected requirements of a kinetic nature have been fulfilled. As a practical application of this technique, organic polyhydroxy-compounds have been directly titrated with a standard periodate solution.

PRINCIPLE OF THE METHOD

Compound C reacts rather slowly but stoichiometrically with compound T and is to be titrated with it according to the reaction

$$C + T \xrightarrow{k} \text{products} \qquad (1)$$

Suppose there is a transducer, with sufficiently fast response, capable of monitoring the concentration of T in the titrated solution. The following sequence of events (illustrated in Fig. 1) will take place:

(*i*) An initial volume, V_w, of solvent or buffer is transferred into the titration cell.

(*ii*) A predetermined volume, V_0, of titrant of concentration $[T]_0$ is delivered automatically to form a "base" titrant, with concentration $[T]_B$ which is given by

$$[T]_B = V_0[T]_0/(V_w + V_0) \qquad (2)$$

(*iii*) The corresponding "base" signal of the transducer, S_B, is measured and stored in the computer memory.

(*iv*) A sample volume, V_s, containing the whole amount of C to be titrated, is transferred into the reaction cell, to give an initial concentration $[C]_0$.

(*v*) The computer continuously receives the signal S from the transducer, and from it calculates and stores in memory the initial reaction rate, R_0 ($=|dS/dt|$), in arbitrary units, which is proportional to $-d[T]/dt$:

$$-d[T]/dt = k[C]_0[T]_B \qquad (3)$$

(*vi*) The burette is then actuated, and automatically delivers titrant until the signal from the transducer returns to the base signal S_B. Reaction (1) takes place during this addition, consuming T until the delivery rate surpasses the consumption rate and the concentration of T returns to $[T]_B$. The total volume of titrant delivered, V_1, is stored in memory. To avoid excessive overshoot of S_B, the delivery rate becomes progressively smaller as the signal S approaches S_B.

(*vii*) The computer, as in step (*v*), calculates the new reaction rate, R_1, which will be less than the

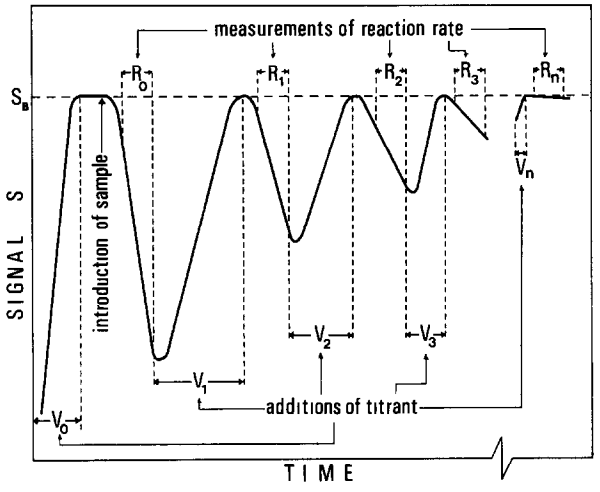

Fig. 1. Graphical presentation of the sequence of events taking place during a titration with kinetic detection of the end-point. The scale of the time axis is not uniform along its length. $V_0, V_1, \ldots V_n$ denote the time periods during which the titrant is delivered. $R_0, R_1, \ldots R_n$ denote the time periods during which measurements of reaction rate are taking place.

initial rate R_0, because part of the titrand C has been consumed.

Steps (*vi*) and (*vii*) are repeated with addition of volumes $V_2, V_3, \ldots, V_n$ and calculation of the corresponding reaction rates $R_2, R_3, \ldots, R_n$. The titration is terminated when the measured reaction rate R_n after the nth delivery of titrant is equal to or less than a predetermined fraction of R_0, typically $0.001R_0$, which denotes that 99.9% of the titrand originally present has reacted, *i.e.*, practically quantitative titration.

Calculation of the corrected (equivalent) volume of titrant

The total volume of titrant delivered for the titration of C, V_F, is equal to $V_1 + V_2 + \ldots + V_n$. V_0 is not included since it is delivered solely to form the base titrant concentration $[T]_B$ which is restored after the termination of the titration sequence. The equivalence volume, V_c, has to be calculated from V_F, allowance being made for the fact that dilution due to the sample volume and the additions of titrant will require addition of further titrant to restore its concentration in the final solution to $[T]_B$.

Hence at the end-point

$$[T]_B = \frac{\text{(total equivalents of T added)} - \text{(equivalents of T consumed by C)}}{\text{total volume in the titration cell}}$$

$$= \frac{(V_0 + V_F)[T]_0 - V_c[T]_0}{V_w + V_0 + V_s + V_F}. \quad (4)$$

Combining equations (2) and (4) gives

$$V_c = \frac{V_F V_w - V_0 V_s}{V_w + V_0}. \quad (5)$$

EXPERIMENTAL

Apparatus

A microcomputer-controlled potentiometric analysis system consisting of the following commercially available units was used: (*a*) an ALTAIR 8800B microcomputer equipped with a 32-kbyte RAM and the necessary peripherals (CRT, teletypewriter, cassette recorder), (*b*) an Orion 801 digital pH/mV-meter and (*c*) a Sargent-Welch S-11120-12 multispeed burette driven by a stepper motor.

The timing-control circuit of the digital pH/mV-meter was modified (by substitution of components of smaller values for a resistor and a capacitor), to make the range of display time 0.09–0.6 sec instead of the of original 0.6–5 sec. The internal square-wave clock of the burette, which controls the delivery rate, was disconnected and software-generated pulses from the computer, through an opto-isolator circuit, were directly fed to the driving circuit of the stepper motor, thus allowing direct control of the burette by the microcomputer; 4500 pulses (maximum frequency 120 Hz) corresponded to delivery of 1.000 ml of titrant. Homemade parallel interface circuits were used to transfer potentials to the microcomputer from the BCD output lines of the digital pH/mV-meter.

An Orion 92-81 perchlorate ion-selective electrode in conjunction with a double-junction silver/silver chloride reference electrode was used as a periodate-concentration transducer. The characteristics of this electrode have been described elsewhere.[2]

A double-walled 50-ml beaker kept at $33 \pm 0.1°$ was used as titration cell.

Software

Control programs were written in BASIC except for the potential-sampling routines, which were written in the 8080 microprocessor machine language.

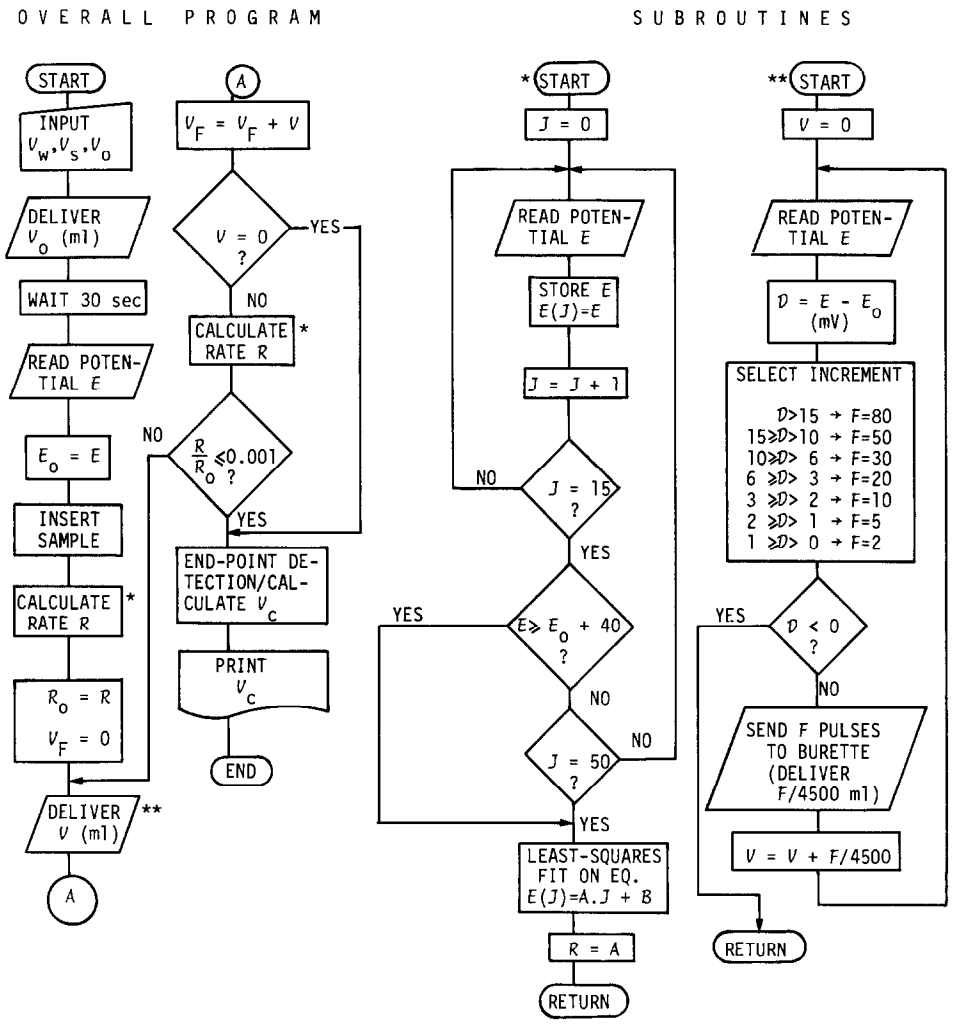

Fig. 2. Flow-charts of the overall control program and of two main subroutines "CALCULATE RATE R" (*) and "DELIVER V" (**).

A flowchart of the overall control program is shown in Fig. 2. In the same figure the flow-charts of two main subroutines (CALCULATE RATE R and DELIVER V) are also shown.

This program is suited for titrations monitored by potentiometric transducers. The operator tells the computer the sizes of V_w, V_s and V_0 and the initial amount V_0 ml of the titrant is delivered to form the "base" titrant (periodate) concentration. The "base" signal (potential E_0) is read after the delay period of 30 sec necessary to obtain a reasonably stable potential reading (within ± 0.1 mV). The sample is inserted manually and after a short mixing period (about 5 sec) the initial reaction rate (R_0) is measured by the CALCULATE RATE R subroutine and the incremental additions of titrant are started. The criterion for end-point detection is basically the kinetic condition $R/R_0 \leqslant 0.001$. Occasionally the quantization error of the potential measurement, combined with a low value of the initial rate (slowly reacting compounds—low sample concentrations) never allows this condition to be met. This case is dealt with (see Fig. 2) by examining the size of the last titrant increment and regarding the titration as completed if this is found to be zero.

Once the end-point has been detected the corrected volume of titrant (V_c) is calculated and printed.

In the CALCULATE RATE R subroutine at least 15 sequential potential readings are collected. This collection is terminated when 50 potential readings have been collected or the potential exceeds E_0 by 40 mV, whichever comes first. A least-squares fit is made and the reaction rate is calculated in terms of rate of increase of the perchlorate-electrode potential, in units of mV per display time period.

The DELIVER V subroutine undertakes the delivery of titrant in increments of sizes which always depend on the difference, D, between the actual potential, E, and the "base" potential E_0. The progressively diminishing size of each increment, as E approaches E_0, prevents an excessive overshoot of the "base" signal, E_0.

Reagents

Analytical-grade materials and demineralized distilled water were used throughout.

Sodium metaperiodate, 0.15M. Sodium periodate ($NaIO_4$, 32 g) is dissolved in water and the solution diluted to 1 litre. The solution is standardized iodometrically weekly.

Acetate buffer, pH 4.5. The pH of 0.10M acetic acid is adjusted to 4.5 ± 0.1 with 5M sodium hydroxide.

Polyhydroxy-compounds. Stock solutions of ethylene glycol, propylene glycol, glycerol and mannitol are dissolved in

Table 1. Effect of V_0 on the precision, accuracy and duration of the titration of 2.00 ml of 0.0779*M* propylene glycol with 0.1471*M* sodium metaperiodate

V_0, *ml*	$\bar{V}_c \pm s_{V_c}$,* *ml*	Approximate duration, *min*	Error, %
0.100	$1.061_5 \pm 0.007_2$	13	+0.2
0.200	$1.060_5 \pm 0.003_6$	7	+0.1
0.500	$1.065_8 \pm 0.002_3$	5	+0.6
1.000	$1.093_0 \pm 0.007_1$	3	+3.2

*Mean and standard deviation of three replicates.

water and standardized titrimetrically.[3] Working solutions are made by appropriate dilution of the stock solutions.

Procedure

The display time of the digital pH/mV-meter is adjusted to about 0.2 sec. Acetate buffer (30.00 ml) is transferred into the titration cell and the control program is initiated. The following parameters are given to the microcomputer: $V_w = 30.00$ ml, $V_s = 2.00$ ml, $V_0 = 0.200$ ml. The sample solution (2.00 ml) is pipetted into the titration cell and the titration is started and terminated automatically. The corrected titrant volume is computed and presented by the microcomputer.

RESULTS AND DISCUSSION

Selection of volume V_0

Volume V_0 determines the base concentration level of periodate, $[IO_4^-]_B$. The duration of the titration will depend on $[IO_4^-]_B$ and will be short if $[IO_4^-]_B$ is large enough. Unfortunately, in that case an overshoot of the base potential by even as little as 0.1–0.2 mV will cause a large positive analytical error. On the other hand, a smaller $[IO_4^-]_B$ will increase the duration of the titration and cause unstable potential readings, which may, in turn, cause large analytical errors in either direction. In Table 1 the effect of the selected V_0 on the precision, accuracy and duration of the titration of 2.00 ml of 0.0779*M* propylene glycol with 0.1471M sodium periodate is shown.

Analytical results

Table 2 gives typical analytical results for the titration of the polyhydroxy-compounds, with kinetic end-point detection.

The duration of these titrations was in the range 7–10 min for ethylene glycol, 5–9 min for propylene glycol, 5–7 min for glycerol and 7–9 min for mannitol. In most cases 5–10 titrant additions were needed.

Conclusions

The kinetic detection of the end-point in titrations involving rather slow reactions yields sufficiently accurate results, at least comparable with those obtained by back-titration. The necessity for computer control is no longer a problem since the advent of microcomputers.

A prerequisite for this type of titration is constant stoichiometry of the reaction. Titrations of tartrate and certain carbohydrates with periodate under the same conditions failed because of variable reaction stoichiometry. Such titrations took 30–40 min and gave non-reproducible results.

Another prerequisite of utmost importance is the reliability of the transducer used to monitor the concentration of the titrant.

The technique is in some degree complementary to the well-known technique of titration to a preset

Table 2. Results of the titration of polyhydroxy-compounds with kinetic detection of the end-point

Polyhydroxy-compound	Concentration, *m*M Taken	Found* $\pm s$	Error, %
Ethylene glycol	25.0_6	$25.1_0 \pm 0.1_0$	+0.2
	50.1_2	$49.9_4 \pm 0.1_6$	−0.4
	100.2	100.0 ± 0.2	−0.2
	150.4	150.3 ± 0.4	+0.1
			Av. 0.2_3
Propylene glycol	25.9_8	$26.1_3 \pm 0.0_8$	+0.6
	51.9_5	$51.9_3 \pm 0.2_0$	−0.0
	103.9	103.6 ± 0.1	−0.3
	155.8	155.5 ± 0.2	−0.2
			Av. 0.2_8
Glycerol	28.0_8	$28.1_6 \pm 0.1_3$	+0.3
	56.1_6	$55.9_9 \pm 0.1_2$	−0.3
	84.2_4	$84.1_3 \pm 0.3_4$	−0.1
			Av. 0.2_3
Mannitol	4.8_1	$4.8_1 \pm 0.01$	
	9.6_3	$9.6_6 \pm 0.02$	+0.3
	14.4_4	$14.4_4 \pm 0.02$	
			Av. 0.1_5

*Mean and standard deviation of three replicates.

end-point, for which slow reactions are rather unsuitable because of premature (false) end-point detection. Some preset end-point titrators overcome this problem by means of a delay circuit which slows down the response time of the electronic switch controlling the burette.[4] This delay is adjustable and some experimentation in needed to find the optimum setting. In essence this is a kinetic end-point detection. In the present work, such an adjustment is not necessary and the computer is left to decide when the preselected degree of reaction has been reached.

The applicability of this technique to certain Karl Fischer titrations which proceed rather slowly and to direct titrations of certain easily hydrolysed esters and alkyl halides with ethanolic potassium hydroxide solutions is under investigation.

REFERENCES

1. T. P. Hadjiioannou, *Rev. Anal. Chem.*, 1976, **3**, 82.
2. C. E. Efstathiou, T. P. Hadjiioannou and E. McNelis, *Anal. Chem.*, 1977, **49**, 410.
3. G. Dryhurst, *Periodate Oxidation of Diol and Other Functional Groups*, p. 121. Pergamon Press, Oxford, 1970.
4. G. Svehla, *Automatic Potentiometric Titrations*, p. 178. Pergamon Press, Oxford, 1978.

Talanta, Vol. 30, No. 3, pp. 151–154, 1983
Printed in Great Britain.

0039-9140/83/030151-04$03.00/0

STUDIES ON THE NATURE OF THE REACTIONS AND SPECIES INVOLVED IN POTENTIOMETRIC TITRIMETRIC DETERMINATION OF URANIUM

S. G. MARATHE, B. N. PATIL, VEENA BHANDIWAD and KESHAV CHANDER
Radiochemistry Division, Bhabha Atomic Research Centre, Trombay, Bombay-400 085, India

(*Received* 15 *October* 1981. *Revised* 22 *September* 1982. *Accepted* 4 *October* 1982)

Summary—The species and reactions involved in the determination of uranium by the Davies and Gray method have been investigated through the behaviour of the various species when present alone or in various combinations in the reaction medium. The studies indicate the formation of Fe(II) and V(III) in the titration system. These two species appear easily prone to oxidation by the titration medium. Probable reasons for the negative bias found when the titration is not completed in the stipulated time period, and for the sharpening of the end-point by the presence of vanadium(IV), are discussed.

For the determination of uranium in nuclear fuels, nuclear material accounting, laboratory-evaluation programmes *etc.*, the Davies and Gray method,[1] in the modified and improved form given by Eberle *et al.*,[2] is widely used. In the modified procedure U(VI) is reduced to U(IV) with Fe(II) in phosphoric acid medium, the excess of Fe(II) is oxidized by nitric acid in the presence of Mo(VI) as catalyst, and after dilution with 1*M* sulphuric acid the solution is titrated with potassium dichromate potentiometrically in the presence of V(IV), which helps to sharpen the end-point. The usefulness and applicability of this method have been reaffirmed.[3,4]

In spite of the importance of this method, little is known about the nature of the reactions involved and the species ultimately titrated with the dichromate. Eberle *et al.*,[2] on the basis of some qualitative spectrophotometric studies and spot-tests, concluded that U(IV)–Fe(III) and Fe(II)–V(IV) reactions occur and that V(III) is probably involved in the titration. To get a better understanding, we have attempted to probe the behaviour of the species involved and the nature of various redox reactions in the titration medium, and give a plausible explanation of the role of V(IV) in sharpening the potentiometric end-point.

EXPERIMENTAL

From consideration of the various redox couples involved in the procedure,[2] the oxidizable species are expected to be one or more of the species U(IV), Fe(II) and V(III). Since it is known[2] that negative errors arise if the titration takes more than 7 min, we resorted to studies of the effect of deliberate delay on the titration results obtained for uranium (in the analysis procedure) and for the individual species U(IV), Fe(II) and V(III) titrated in the titration medium, which consists of sulphamic acid, phosphoric acid, sulphuric acid, nitric acid and molybdenum(VI) as catalyst. A similar technique was used for studying possible reactions between various combinations of two species in the titration medium, namely U(IV)–V(IV), U(IV)–Fe(III), Fe(II)–V(IV) and Fe(III)–V(III).

For the potentiometric titrations, a known time was allowed to elapse between completion of addition of all the reagents and the start of titration. To study some reactions it was necessary to use a spectrophotometric technique, in which the concentration of a species was monitored by means of the change in absorbance as a function of time.

Reagents

Ferrous sulphate solutions (1*M* and 0.1*M*) were prepared by dissolving $FeSO_4.7H_2O$ (G.R. grade, Sarabhai Merck) in 1*M* sulphuric acid. Vanadyl sulphate solution (1 mg/ml) was made by dissolving $VOSO_4.5H_2O$ (Merck) in 1*M* sulphuric acid. Potassium dichromate solutions (~0.05 and 0.001 meq/g) were prepared by dissolving appropriate quantities of G.R. grade $K_2Cr_2O_7$ (Sarabhai Merck) in doubly distilled water. Sulphamic acid solution (Koch-Light) was made in distilled water. Analytical-reagent grade phosphoric, nitric and sulphuric acids were used.

U(IV) and V(III) solutions were prepared[5,6] by passing 1*M* sulphuric acid solutions of U(VI) and V(IV) respectively through a Jones reductor and allowing aerial oxidation of the U(III) and V(II) formed. The absorption spectrum of the V(III) solution was used to assess its purity.[7]

Apparatus

For the potentiometric titrations, an EMCO digital voltmeter was used, with a saturated calomel reference electrode and a platinum indicator electrode. For all spectrophotometric work, a Cary-14 spectrophotometer was used.

RESULTS AND DISCUSSION

Studies with the total uranium determination system

The decrease in the amount of uranium found with increase in elapsed time is shown by curve A in Fig. 1. The decrease is calculated as a fraction of the actual uranium content (as found by use of the usual procedure, with no waiting period after addition of

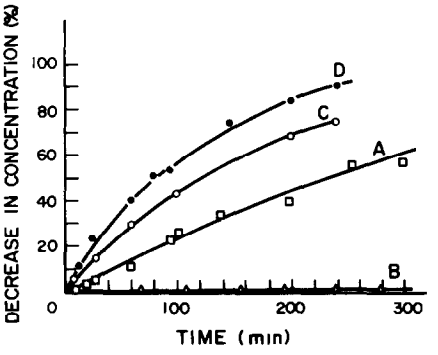

Fig. 1. (A) Decrease in uranium estimated, with time elapsed before titration; (B)–(D) oxidation of single species in the titration medium; (B) U(IV); (C) Fe(II); (D) V(III).

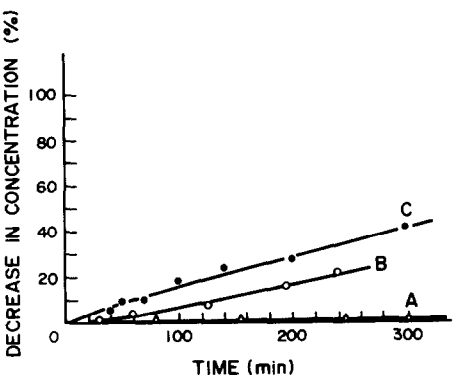

Fig. 2. Reactions between two species in the titration medium: (A) U(IV) + V(IV); (B) U(IV) + Fe(III); (C) U(IV) + Fe(III) in presence of V(IV).

the vanadyl sulphate). The effect of elapsed time is considerable.

Studies with single species in the titration medium

Curve B in Fig. 1 shows that there is practically no interaction of the titration medium with U(IV). Although the potentiometric end-point was sluggish in these titrations the reproducibility was within $\pm 1\%$. Curves C and D show the behaviour of Fe(II) and V(III) respectively in the titration medium [containing nearly the same quantities of Fe(III) and V(IV), respectively, as would be present in the determination of uranium]. These two curves show there is considerable interaction with the titration medium, probably due to molybdenum(VI)-catalysed oxidation by the nitric acid present in the medium. The contribution of aerial oxidation of Fe(II) and V(III) was studied and found to be less than 1% of the total oxidation.

Studies on the reactions between two species

U(IV) and V(IV). Several solutions containing these species in the titration medium [but no Fe(II) or Fe(III)] were prepared and titrated with dichromate after various elapsed times. The observed decrease in the concentration of titratable species with time is shown by curve A in Fig. 2; there is practically no decrease in U(IV) concentration with time.

If reaction had taken place between these two species, formation and subsequent partial reoxidation of V(III) in the medium would have been expected, with an accompanying decrease in apparent uranium concentration, the decrease becoming larger with increase in elapsed time. Hence this reaction does not occur. This was confirmed by monitoring the absorption spectra as a function of time and examining the U(IV) and V(IV) absorption maxima [at 660 and 800 nm respectively: V(IV) has its absorption maximum at 760 nm in sulphuric acid medium but at 800 nm in the titration medium]. No change in the absorbance at these maxima was observed even after 150 min standing time.

U(IV) and Fe(III). The reaction between these two species was studied by making solutions of U(IV) and Fe(III) in the titration medium and titrating with dichromate after known elapsed times. Curve B in Fig. 2 shows a decrease in concentration of titratable species with time, indicating the formation and partial reoxidation of Fe(II). The reaction was also studied in the presence of V(IV), and the rate of decrease observed was greater (Curve C).

Spectrophotometric experiments confirmed the occurrence of reaction between U(IV) and Fe(III), there being a decrease in the absorbance of U(IV) with time.

Fe(II) and V(IV). As already mentioned, both Fe(II) and V(III) are slowly oxidized in the titration medium. The oxidation of V(III) is only a bit faster than that of Fe(II). Hence if reaction between Fe(II) and V(IV) takes place in the reaction medium, the V(III) generated will be partially oxidized by the medium and the consumption of dichromate will be much the same (for a given elapsed time) whether reaction takes place or not, and potentiometric study of this reaction is not useful.

The reaction was therefore studied spectrophotometrically. A decrease in the original V(IV) concentration as well as formation of V(III) was observed at 410 and 650 nm (Fig. 3), showing that reaction between Fe(II) and V(IV) takes place.

It is worth noting that the reverse reaction between Fe(III) and V(III) could also be established by means of the appearance of the absorbance maximum of V(IV) and the decrease in absorbance of V(III).

Although the behaviour of the various species and their reactions was studied only when they were reacting in the titration medium, and not *in situ* during the titration with dichromate, we can form a qualitative idea of the species and reactions involved in the analysis procedure.

Curve A in Fig. 1 shows that the negative bias in the uranium determination increases with elapsed time, which explains the requirement[2] that the titration must be completed within 7 min from the addition of the vanadyl sulphate if the result is to be

correct within ±0.1%. From curve B it is seen that U(IV) itself is stable in the titration medium. It follows that in the complete titration system there cannot be only U(IV) titrated with the dichromate. Comparison of the curves A, C and D in Fig. 1 shows that the behaviour of the overall system is similar to that of the Fe(II) and V(III) systems. The species Fe(II) and V(III) are not present at the dilution step, but are probably slowly generated thereafter from Fe(III) and V(IV) through redox reactions. Oxidation of any Fe(II) and/or V(III) by the titration medium instead of dichromate will obviously lead to negative bias.

As pointed out above, no reaction between U(IV) and V(IV) seems to occur in the titration medium, whereas there is a definite reaction between U(IV) and Fe(III), especially in the presence of V(IV) (curve C in Fig. 2). This indirectly indicates the occurrence of an Fe(II)–V(IV) reaction, and corroborates the spectrophotometric observation (Fig. 3). The higher oxidation rate in the presence of V(IV) may be explained in two ways, based on the rates of the two reactions U(IV)–Fe(III) and Fe(II)–V(IV). We have not determined the rates of these reactions. If both reactions possess nearly the same rates, then because of the latter reaction and subsequent oxidation of V(III) along with Fe(II) by dichromate, one more channel is opened for the U(IV)–Fe(III) reaction to proceed in the forward direction. However, if the V(IV)–Fe(III) reaction is slow and the other is fast, then any Fe(II) produced will be quickly oxidized by V(IV) and the species oxidized by dichromate will be mainly V(III). The net effect will be to produce a catalytic cycle for the U(IV)–Fe(III) reaction, causing it to proceed faster.

These observations indicate that the following reactions take place in the medium:

$$U(IV) + 2Fe(III) \rightleftharpoons U(VI) + 2Fe(II)$$

$$Fe(II) + V(IV) \rightleftharpoons Fe(III) + V(III)$$

as suggested by Eberle *et al.*[2] The reverse reaction in the second equilibrium seems to be significant, according to the spectrophotometric observations.

It is known that the conditional potential of the Fe(III)/Fe(II) couple is lowered in phosphoric acid medium but the potentials for the U(VI)/U(IV) and V(IV)/V(III) couples are increased. Although the exact values of the potentials of these couples in the titration medium are not known, on the basis of available data[8] for phosphoric acid medium they seem to approach close to one another. The results of our studies also indicate that the conditional redox potentials (in the titration medium) of the various couples involved are close to each other so that either forward or backward reaction between the iron and vanadium couples is possible, depending on the relative concentrations of the species. The absence of reaction between U(IV) and V(IV) may be attributed to a high activation energy for formation and rupture of various metal–oxygen bonds.

Curves representing the behaviour of all the species and reactions studied are grouped together in Fig. 4 for ready comparison. Curves A and G represent similar species but the rates are different, because the starting species for curve A is U(VI) whereas that for curve G is U(IV), the consequence being that more Fe(II) remains unused in the latter case, necessitating consumption of nitric acid in its

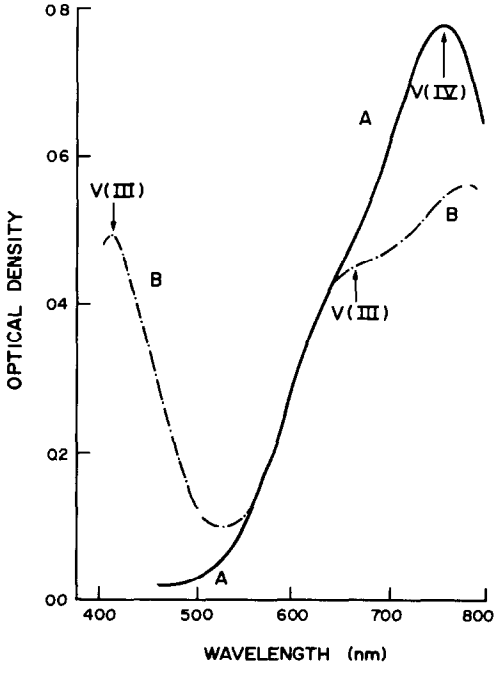

Fig. 3. Reaction between Fe(II) and V(IV) in the titration medium: (A–A) V(IV) in medium; (B–B) V(III)—generation due to reaction of V(IV) with Fe(II).

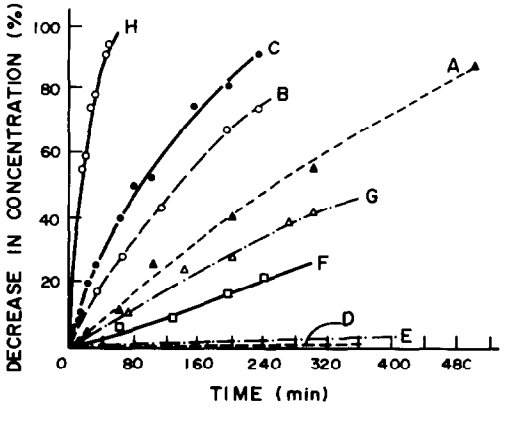

Fig. 4. Decrease in concentration of species with time in the titration medium. (A) Total system; (B) Fe(II); (C) V(III); (D) U(IV); (E) U(IV) + V(IV); (F) U(IV) + Fe(III); (G) U(IV) + Fe(III) in presence of V(IV); (H) Fe(II) and V(III) in absence of Fe(III) and V(IV) respectively.

oxidation. In effect the resulting lower nitric acid concentration leads to a lower rate of oxidation of the Fe(II) and/or V(III) produced *during* the titration, and hence to a smaller negative bias than for curve A.

The decrease in the concentration of Fe(II) and V(III) in the titration medium, as shown in curves B and C respectively, is that observed in the presence of relatively large amounts of Fe(III) or V(IV), which control the oxidation rates. Therefore, it was thought worth studying the effect of the medium in the absence of Fe(III) or V(IV). Curve H shows the rates of oxidation (decrease in concentrations) of Fe(II) or V(III) when the corresponding oxidized species is not initially present. In this experiment care was taken to see that the concentrations of Mo(VI) and nitric acid available for oxidation of Fe(II) or V(III) were of the same order as in the earlier experiments. The oxidation rates appear to be significantly high and nearly equal for both species, showing that both species are equally prone to oxidation by the medium. This can cause simultaneous consumption of both Fe(II) and V(III) during the titration with the dichromate. The oxidation of both species together would help in two ways: (*i*) acceleration of the main reaction U(IV)–Fe(III) in the forward direction and (*ii*) increase in the conditional potential in a *shorter time*. The latter effect will be mainly responsible for sharpening the end-point.

An alternative explanation can be given for the role of V(IV) in sharpening the end-point. It is well-known that platinum electrodes may give anomalous response owing to formation of oxide films, mixed potentials *etc.* It is possible that in the rather complex system used in the Davies and Gray method, the fastest electrode response is obtained through the mediation of the vanadium couple.

It is worth noting that Reeder and Delmastro[9] were able to obtain high precision and an error of less than 0.05% by lowering the temperature of the system to 18° before the titration. This may be attributed to the corresponding decrease in the rate of reaction of Fe(II) and V(III) with the reaction medium.

CONCLUSIONS

These studies on the reactions and species involved in the modified Davies and Gray procedure for uranium determination lead to the following conclusions.

(*i*) U(IV) appears to be stable in the titration medium.

(*ii*) Fe(II) and V(III) are produced and are slowly oxidized by the titration medium and thus can cause a negative bias in uranium determination if the titration is not completed within the specified 7 min.

(*iii*) The conditional potentials of the V(IV)/V(III) and Fe(III)/Fe(II) couples in the titration medium appear to be close.

(*iv*) The role of vanadyl ion in sharpening the end-point appears to be due either to the simultaneous consumption of both Fe(II) and V(III) species, thus accelerating the rate of main reaction and causing a quick rise in the conditional potential or to the dominance of the electrode response by the V(IV)/V(III) couple.

Acknowledgements—The authors thank Dr. P. R. Natarajan, Head of the Radiochemistry Division for his keen interest in the work and valuable suggestions. They also thank Dr. S. K. Patil for his encouragement during the course of this work. They wish to express their sincere thanks to Dr. R. A. Chalmers (University of Aberdeen) for his valuable comments and suggestions.

REFERENCES

1. W. Davies and W. Gray, *Talanta*, 1964, **11**, 1203.
2. A. R. Eberle, M. W. Lerner, C. G. Goldbeck and C. J. Rodden, *NBL Rept. No.* 252, 1970.
3. *1980 Annual Book of ASTM Standards*, Part 45, *Nuclear Standards*, p. 213.
4. F. B. Stephens, R. G. Gutmacher, K. Ernst and J. E. Harrar, *Rept.* NUREG-0256, 1977, p. 450; *Rept.* NUREG-75/010, 1975.
5. C. J. Rodden (ed.), *Analysis of Essential Nuclear Reactor Materials*, p. 76. USAEC, 1964.
6. G. Jones and J. H. Colvin, *J. Am. Chem. Soc.*, 1944, **66**, 1573.
7. S. C. Furman and C. S. Garner, *ibid.*, 1950, **72**, 1785.
8. J. A. Dean (ed.), *Lange's Handbook of Chemistry*. McGraw-Hill, New York, 1979.
9. S. D. Reeder and J. R. Delmastro, *ANS Topical Meeting*, Williamsburg, VA, 1978 (CONF-780522).

Talanta, Vol. 30, No. 3, pp. 155–159, 1983
Printed in Great Britain.

0039-9140/83/030155-05$03.00/0

EXTRACTION AND DETERMINATION OF ANIONIC SURFACTANTS WITH COPPER(II)–ETHYLENEDIAMINE DERIVATIVE COMPLEXES

KIYOSHI SAWADA,* SHIGEHIRO INOMATA, BUKICHI GOBARA and TOSHIO SUZUKI

Laboratory of Analytical Chemistry, Faculty of Science, Niigata University, Niigata 950-21, Japan

(*Received* 14 *December* 1981. *Revised* 27 *September* 1982. *Accepted* 3 *October* 1982)

Summary—Anionic surfactants, S^- [where S^- is dodecyl sulphate (DS) or dodecylbenzenesulphonate (DBS)] were extracted with a series of copper(II)–ethylenediamine derivative complexes, $Cu(R\text{-}en)_2^{2+}$, where R-en is ethylenediamine (en), *N,N'*-dimethylethylenediamine (NN'Me_2en), *N,N*-dimethylethylenediamine (NNMe_2en), *N,N*-diethylethylenediamine (NNE_2en) or 1,2-cyclohexanediamine (Cyen). The extraction constant of the ion-pair is $K_{ex} = [Cu(R\text{-}en)_2^{2+} \cdot 2S^-]_0/[Cu(R\text{-}en)_2^{2+}][S^-]^2$. The constants for extraction of the DS complexes with en, NN'Me_2en, NNMe_2en, NNEt_2en and Cyen into chloroform were found to be log $K_{ex} = 7.93$, 9.19, 8.88, 8.74 and 11.45 (± 0.05 at 25°C), respectively. The extractability of the ion-pair $Cu(en)_2^{2+} \cdot 2S^-$ gave a linear correlation with the acidity of the solvent. The $Cu(Cyen)_2^{2+}$ extraction system was applied to the determination of some anionic surfactants. With use of graphite-furnace atomic-absorption spectrophotometry, a limit of detection of 5 μg/l. was obtained with a 20-ml sample of river water or sea-water.

Ion-pair extraction methods for the determination of anionic surfactants have been extensively investigated.[1,2] The most commonly used and accepted method is the Methylene Blue method developed by Longwell and Maniece,[3] which has been improved and applied to the determination of anionic surfactants in many kinds of water.[1,2] Derivatives of Methylene Blue[4,5] and other cationic dyes such as Rhodamine B,[6] Crystal Violet,[7] and Remacryl Blue[8] have also been used as cationic extractants.

Cationic metal complexes such as tris(1,10-phenanthroline) iron(II),[9] tris(1,10-phenanthroline) copper(II),[10,11] and bis(ethylenediamine) copper(II)[12–14] have also been used for ion-pair extraction procedures. The analysis can be completed by determination of the extracted metal ion by radiometry or atomic-absorption spectrophotometry. With graphite-furnace atomic-absorption spectrophotometry it is possible to determine μg/l. levels of surfactant.

In spite of its frequent use, the extraction of anionic surfactants with cationic metal complexes has not been studied in detail. In the present paper the extraction of the ion-pair of an anionic surfactant with a copper(II)–ethylenediamine derivative complex has been investigated, and the effects of the solvent and particular substituted ethylenediamine have been examined. The copper(II)–cyclohexanediamine complex has been applied to the determination of surfactants in natural waters.

EXPERIMENTAL

Reagents

The sodium dodecyl sulphate (DS) and sodium dodecylbenzenesulphonate (DBS) used were of guaranteed reagent grade (>99.9% pure). Other reagents used were of analytical reagent grade.

Extraction procedure

Mix 20 ml of aqueous phase containing copper(II) sulphate, ethylenediamine derivative and surfactant with 20 ml of organic phase in a 50-ml stoppered centrifuge tube, at 25.0 ± 0.2°, and adjust the ionic strength to 0.1 with sodium sulphate. Shake the tube for 10 min (which is sufficient for complete equilibration). After separating the phases, determine the concentration of copper(II) in the aqueous phase by atomic-absorption spectrophotometry (AAS); alternatively, determine copper in the organic phase by AAS after stripping with 0.01*M* nitric acid.

Recommended analytical procedure

Add 1 ml of 0.02*M* copper(II) sulphate and 1 ml of freshly prepared 0.05*M* cyclohexanediamine solution to 20 ml of water sample in a 50-ml stoppered centrifuge tube. If necessary, neutralize the sample before adding the reagents. Add 20 ml of chloroform and shake the mixture for 10 min. Centrifuge the mixture, then draw off the aqueous phase with an aspirator. Transfer 10 ml of the chloroform phase to a 15-ml test-tube and shake with 1 ml of 0.01*M* nitric acid for 10 min. Let stand for 30 min, then determine the concentration of copper in the nitric acid phase by graphite-furnace AAS. If the surfactant concentration is very high, use a larger volume of nitric acid for the stripping, to optimize the copper concentration for the subsequent AAS measurements.

RESULTS AND DISCUSSION

Extraction equilibrium

Because of the large equilibrium constant for equa-

*To whom correspondence should be addressed.

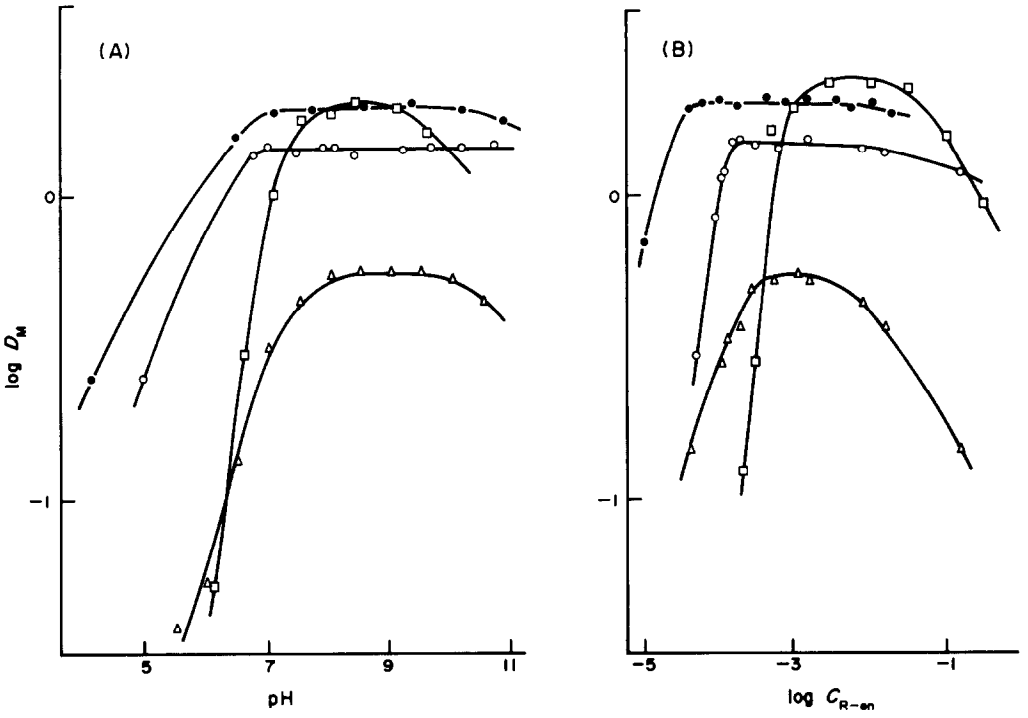

Fig. 1. The effects of pH (A) and ethylenediamine derivative concentration (B) on the extraction of DBS with metal–en and metal–Cyen complexes. Ethylenediamine complex: ○, Cu(II); □, Cd(II); △, Ni(II). (A) $C_{DBS} = 10^{-4}M$; $C_M = 5 \times 10^{-5}M$; $C_{en} = 10^{-2}M$. (B) pH = 9.0. Cyclohexanediamine complex: ●, Cu(II). (A) $C_{DBS} = 10^{-5}M$; $C_M = 6 \times 10^{-6}M$; $C_{Cyen} = 2 \times 10^{-4}M$. (B) pH = 9.0.

tion (1),[15] the presence of excess of R-en results in quantitative formation of the complex $Cu(R\text{-}en)_2^{2+}$ in the alkaline aqueous solution:

$$Cu^{2+} + 2\,R\text{-}en \rightleftharpoons Cu(R\text{-}en)_2^{2+} \quad (1)$$

where R-en is ethylenediamine (en), *N,N'*-dimethylethylenediamine (NN'Me$_2$en), *N,N*-dimethylethylenediamine (NNMe$_2$en), *N,N*-diethylethylenediamine (NNEt$_2$en) and cyclohexanediamine (Cyen). Thus, the equilibrium for extraction of the surfactant (S^-) with the $Cu(R\text{-}en)_2^{2+}$ complex can be written as

$$Cu(R\text{-}en)_2^{2+} + 2S^- \rightleftharpoons [Cu(R\text{-}en)_2^{2+} \cdot 2S^-]_o \quad (2)$$

where the subscript o denotes that the species is in the organic phase.

The extraction constant for the ion-pair, K_{ex}, is defined as:

$$K_{ex} = \frac{[Cu(R\text{-}en)_2^{2+} \cdot 2S^-]_o}{[Cu(R\text{-}en)_2^{2+}][S^-]^2} \quad (3)$$

and the distribution ratio of copper(II), D_M, as:

$$D_M = \frac{[Cu(R\text{-}en)_2^{2+} \cdot 2S^-]_o}{[Cu(R\text{-}en)_2^{2+}]} \quad (4)$$

Substitution of equation (3) into equation (4) leads to

$$\log D_M = \log K_{ex} + 2\log[S^-] \quad (5)$$

The distribution ratio of the surfactant is

$$D_S = \frac{2[Cu(R\text{-}en)_2^{2+} \cdot 2S^-]_o}{[S^-]} \quad (6)$$

or

$$\log D_S = \log 2K_{ex} + \log[Cu(R\text{-}en)_2^{2+}] + \log[S^-] \quad (7)$$

Effects of pH and ethylenediamine concentration

Dodecylbenzenesulphonate (DBS) was extracted with the Cu(II)–en and Cu(II)–Cyen complexes into chloroform at various pH values and ethylenediamine concentrations. The plot of log D_M as a function of pH is shown in Fig. 1 (A). Because of dissociation of the Cu–(R-en) complex caused by the protonation of R-en in the aqueous phase, the distribution ratio shows a steep decrease in the low pH region (pH < 6). When no acid or base is added, the pH of the solution after the addition of R-en is about 9. Thus the optimum extraction pH is obtained without any adjustment.

Table 1. Extraction constants of anionic surfactants with various copper(II)–ethylenediamine derivative complexes

R-en		en	NN'Me$_2$en	NNMe$_2$en	NNEt$_2$en	Cyen
log K_{ex}	DS	7.93	9.19	8.88	8.47	11.45 ± 0.05
	DBS	9.12				11.70 ± 0.05

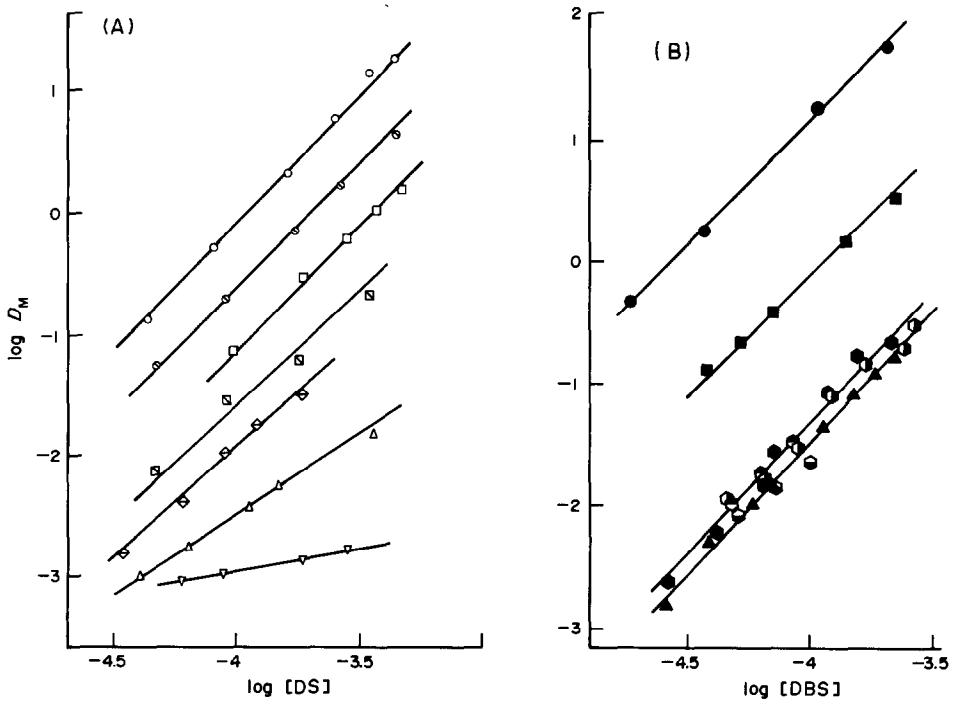

Fig. 2. The effect of organic solvents on the extraction of DS (A) and DBS (B) with copper(II)–ethylenediamine complex. ○ ●, chloroform; ⊘, chloroform–1,2-dichloroethane (1:1 v/v mixture); □ ■, 1,2-dichloroethane; ⧅, 1,2-dichloroethane–carbon tetrachloride (1:1 v/v mixture); ◇, methyl isobutyl ketone; △ ▲, carbon tetrachloride; ⬡ ⬢, benzene; ◑, toluene; ⬭, chlorobenzene; ⬙, *o*-dichlorobenzene. pH = 9.0; $C_{en} = 10^{-3}M$; $C_{Cu} = 10^{-4}M$.

In Fig. 1 (B), $\log D_M$ is plotted as a function of $\log C_{R\text{-}en}$, where $C_{R\text{-}en}$ is the initial concentration of ethylenediamine derivatives added in the aqueous phase. Although the distribution ratio decreases slightly at very high $C_{R\text{-}en}$, it is almost constant when the concentration of ethylenediamine derivative is sufficient to form the complex $Cu(R\text{-}en)_2^{2+}$, *i.e.*, $C_{R\text{-}en} > 2C_{Cu}$.

Extraction constant

Dodecyl sulphate and dodecylbenzenesulphonate were extracted into chloroform with various copper(II) R-en complexes. $\log D_M$ is a linear function of $\log [S^-]$, the value of $[S^-]$ being calculated from $[S^-] = C_S - 2[Cu(R\text{-}en)_2^{2+} \cdot 2S^-]_o$, where C_S is the total surfactant concentration. The plots all had a slope of 2, and thus the extraction equilibrium (2) was confirmed. The extraction constants K_{ex} obtained from the intercepts of the plots are listed in Table 1. Although increase in the molecular weight or molar volume of R-en tends to increase K_{ex}, there is not a good correlation; in particular, K_{ex} for the $NNEt_2$en complex is smaller than that for the $NN'Me_2$en and $NNMe_2$en complexes.

The extraction constant for DBS is larger than that for DS with both the $Cu(en)_2^{2+}$ and $Cu(Cyen)_2^{2+}$ systems. The difference between the $\log K_{ex}$ values for the Cu–Cyen complexes of DBS and DS is smaller than that for the Cu–en complexes. The volume of $Cu(Cyen)_2^{2+}$ is considerably larger than that of $Cu(en)_2^{2+}$. Thus, the extraction constant of the Cu–Cyen complex is less sensitive to change in the volume of surfactant.

Effect of the organic solvents

DS and DBS were extracted with the copper(II)–ethylenediamine complex into various solvents and their mixtures. $\log D_M$ is plotted as a function of log [DS] (A) and log [DBS] (B) in Fig. 2. The plots were all linear, with slopes (except for the

Table 2. Extraction constants of $Cu(en)_2^{2+}$ complexes, for various solvents and their mixtures

Solvent		$CHCl_3$	$CHCl_3$–DCE†*	DCE	DCE-CCl_4†	MIBK§	CCl_4	Bz#
$\log K_{ex}$	DS	7.93	7.39	6.89	6.43	6.06	5.54‡	—
	DBS	9.12		7.86			6.50	6.6

*1,2-Dichloroethane.
†1:1 v/v mixture.
§Methyl isobutyl ketone.
‡Tentative value estimated from data in the region of log [DS] from −4.4 to −3.8.
#Mean value for benzene and its derivatives.

DS–carbon tetrachloride and DS–benzene systems) of 2.0 ± 0.1. The extraction constants are listed in Table 2. The distribution ratio for n-hexane as solvent was too small for reliable data to be obtained. Thus, the efficiency of the extractants for the ion-pair $Cu(R\text{-}en)_2^{2+} \cdot 2S^-$ is in the order chloroform > 1,2-dichloroethane (DCE) > methyl isobutyl ketone (MIBK) > carbon tetrachloride $\simeq$ benzene and its derivatives (Bz) $\gg$ n-hexane for both surfactants. The D_M values for the benzene derivatives are of the same order of magnitude as that for benzene (Table 2) and show poor correlation with the polarity (*e.g.*, the E_T value[16] and Z value[17]) and dielectric constant of the solvents. The correlation of log K_{ex} with the solubility parameter[19] is also not very good, which is consistent with the poor correlation with the molar volume of the complex cation.

A plot of log K_{ex} as a function of the acceptor number, which is an indicator of the acidity of the solvent,[18] shows a good linear correlation, and the K_{ex} of n-hexane, which has an acceptor number of zero, is very small. Hence, the change in interaction of the acidic part of the ion-pair, *i.e.*, the complex cation $Cu(R\text{-}en)_2^{2+}$, with the solvent may not contribute very significantly to the change in the extractability of the ion-pair, whereas the interaction between the solvent and the basic part of the ion-pair, *i.e.*, the surfactant anion, may have the predominating effect on the change in extractability with change of solvent.

Extraction with cadmium and nickel complexes

DBS was also extracted into chloroform with the cadmium and nickel ethylenediamine complexes. Log D_M is plotted as a function of pH for the cadmium and nickel systems in Fig. 1 (A). The pH region for maximum extraction of these complexes is narrower than that for the Cu(II) complex.

The effect of the ethylenediamine concentration is shown in Fig. 1 (B). As the formation constants of the ethylenediamine complexes of Cd(II) and Ni(II) are smaller than that for Cu(II),[15] a higher ethylenediamine concentration is required to obtain the maximum distribution ratio. At high concentrations of ethylenediamine, there is a steep decrease in D_M for the cadmium and nickel systems, possibly because of formation of the larger tris-ethylenediamine complexes. The log K_{ex} values found for DBS were 9.12, 9.58 and 8.28 for the copper, cadmium and nickel ethylenediamine systems respectively.

ANALYTICAL APPLICATION

Recovery and calibration curve

The extraction constants for the anionic surfactants are much larger with the copper(II)–cyclohexanediamine complex than with copper(II)–ethylenediamine complex (Table 1). As can be seen from equation (7), the distribution ratio of the surfactant, D_S, decreases with decrease in the equilibrium concentration of surfactant in the aqueous phase, $[S^-]$, when the concentration of $Cu(R\text{-}en)_2^{2+}$ is kept constant. It follows that a fairly large value of K_{ex} is required for the determination of low concentrations of surfactant. For example, in the copper(II)–ethylenediamine method, the distribution ratio of a 10-μg/l. DS sample is 0.059 (*i.e.*, the degree of extraction of DS is about 5.6%) for equal volumes of the aqueous [$10^{-2}M$ $Cu(R\text{-}en)_2^{2+}$] and organic (chloroform) phases. On the other hand, in the copper(II)–cyclohexanediamine method, D_S is about 13 (*i.e.*, ~93% extraction of the surfactant) under the same conditions. Thus, the latter method is advantageous for the determination of low surfactant concentrations.

Over the DS concentration range of 100–10,000 μg/l. the recommended procedure gave an apparent $100 \pm 3\%$ extraction at high concentrations and over 90% at low, in agreement (within 5%) with that calculated by using the K_{ex} values shown in Table 1.

Limit of detection

It might be possible to lower the limit of detection by using a large volume of sample, but tests with surfactant-free water give blank values of several tenths of a μg of copper per litre, corresponding to a DS concentration of several μg/l. Thus, the limit of detection is taken as 5μg/l. (as DS).

Interferences

The effect of inorganic anions, which may be extracted as $Cu(Cyen)_2^{2+}$ ion-association complexes, on the detection limit, has been examined by use of extraction tests in the absence of surfactant. The concentrations of anions listed in Table 3 produce contributions below the detection limit for DS (<5 μg/l.). A large ion such as I^- or ClO_4^- is extracted at relatively low concentration levels, but the concentrations of these ions in natural waters are much less than those listed in Table 3.

The concentrations listed in Table 4 cause an error of less than $\pm 5\%$ in the determination of DS at the 100-μg/l. level. Sulphide ion up to the 5 mg/l. level does not interfere if iron(II) is added to give $[Fe^{2+}] = 50$ mg/l. When the concentration of sulphide ion is less than 0.5 mg/l., it is not necessary to add the iron(II). The cations and anions cause negative and positive interferences, respectively. The allowable concentrations of foreign ions listed in Tables 3 and

Table 3. Concentrations of anions giving a signal below the limit of detection for DS (5 μg/l.)

Anion	SO_4^{2-}	Cl^-	Br^-	I^-	NO_3^-	ClO_4^-
Concn., M	1	0.5	3×10^{-3}	10^{-3}	10^{-3}	10^{-4}

Table 4. Concentration of foreign ions causing $< \pm 5\%$ error for extraction of DS at the 100-μg/l. level

Concentration	Ion
0.75*M*	SO_4^{2-}, Cl^-, Na^+
1000 mg/l.	ClO_4^-, NO_3^-, Br^-, K^+, Ca^{2+}, Mg^{2+}, NH_4^+
500 mg/l.	Ni^{2+}, Zn^{2+}, Mn^{2+}, I^-
100 mg/l.	Co^{2+}, Al^{3+}
50 mg/l.	Fe^{2+}, Fe^{3+}
5 mg/l.	CN^-, S^{2-}*

*With 50 mg/l. Fe^{2+} added; 0.5 mg/l. in the absence of added Fe^{2+}.

4 are higher than those present in sea-water. As can be seen from Tables 1 and 2, the extraction constants for DBS larger than those for DS. Consequently, the interference of foreign ions is less significant in determination of DBS than of DS.

The concentrations of anionic surfactant found in some natural waters by the recommended procedure were as follows: sea-water (off-shore, Japan Sea, Niigata Prefecture), not detected; river water (Shin river, Niigata, Japan), 310 μg/l., expressed as DS; lake water (Toyano lake, Niigata, Japan), 590 μg/l., expressed as DS.

REFERENCES

1. R. A. Llenado and R. A. Jamieson, *Anal. Chem.*, 1981, **53**, 174R.
2. M. J. Fishman, D. E. Erdmann and T. R. Steinheimer, *ibid.*, 1981, **53**, 182R.
3. J. Longwell and W. D. Maniece, *Analyst*, 1955, **80**, 167.
4. L. K. Wang and P. J. Panzardi, *Anal. Chem.*, 1975, **47**, 1472.
5. K. Toei and H. Fujii, *Anal. Chim. Acta*, 1977, **90**, 319.
6. Z. Marczenko, *Microchim. Acta*, 1977 **II**, 651.
7. S. Motomizu, S. Fujiwara and K. Toei, *Anal. Chim. Acta*, 1981, **128**, 185; S. Motomizu, S. Fujiwara, A. Fujiwara and K. Toei, *Anal. Chem.*, 1982, **54**. 392.
8. S. Janeva and R. Borissova-Pangarova, *Talanta*, 1978, **25**, 279.
9. C. G. Taylor and J. Waters, *Analyst*, 1972, **97**, 533.
10. A. Le Bihan and J. Courtot-Coupez, *Anal. Lett.*, 1977, **10**, 759.
11. *Idem*, *Bull. Soc. Chim. France*, 1970, 406.
12. P. T. Crisp, J. M. Eckert and N. A. Gibson, *Anal. Chim. Acta*, 1975, **78**, 391.
13. P. T. Crisp, J. M. Eckert, N. A. Gibson, G. F. Kirkbright and T. S. West, *ibid.*, 1976, **87**, 97.
14. M. J. Gagnon, *Water Res.*, 1979, **13**, 53.
15. L. G. Sillén and A. E. Martell, *Stability Constants of Metal-Ion Complexes*. The Chemical Society, London, 1964.
16. K. Dimroth, C. Reichardt, T. Siepmann and F. Bohlmann, *Ann.*, 1963, **661**, 1; 1963, **669**, 95.
17. E. Kosower, *J. Am. Chem. Soc.*, 1958, **80**, 3253, 3261, 3267.
18. J. H. Hildebrand and R. L. Scott, *Regular Solutions*. Prentice-Hall, Englewood Cliffs, New York, 1962.
19. U. Mayer, V. Gutmann and W. Gerger, *Monatsh. Chem.*, 1975, **106**, 1235.

Talanta, Vol. 30, No. 3, pp. 161–167, 1983
Printed in Great Britain.

0039-9140/83/030161-07$03.00/0

GATEKEEPING* PATTERNS IN THE PUBLICATION OF ANALYTICAL CHEMISTRY RESEARCH

T. BRAUN
Institute of Inorganic and Analytical Chemistry, L. Eötvös University, P.O. Box 123, 1443 Budapest, Hungary

and

E. BUJDOSÓ
Department of Informatics and Science Analysis, Library of the Hungarian Academy of Sciences, P.O. Box 7, H-1361 Budapest, Hungary

(*Received* 14 *March* 1982. *Revised* 26 *July* 1982. *Accepted* 2 *October* 1982)

Summary—An analysis has been made of the nationalities of the members of advisory and editorial boards of analytical chemistry journals. Correlations were sought between their number and citation rates and between their number and the number of analytical papers published by scientists from the country in question. A comparison is given for the gatekeepers of organic and inorganic chemistry journals.

The invention of a mechanism for the systematic publication of scientific work may well have been the key event in the history of modern science.[1] The main channel through which this publication flows is provided by the scientific journals.

Thus Gordon[2] states: "Publication of papers in primary research journals is widely accepted as having a central role to play in the continuance of science as an intellectual and social activity. In particular it is recognised as being both a means by which researchers are able to establish and advance themselves professionally, and the medium through which contributions are made to a discipline's body of *ratified knowledge*. Consequently, journal editors, in controlling systems of manuscript evaluation and selection, occupy *powerful strategic* positions in the collective activity of their discipline. The practices and preferences which they adopt in their roles as editors are therefore of considerable significance."[2]

In an earlier paper[3] the same author had said "editors and referees who control the access to the coveted pages of scientific journals, particularly those who 'gatekeep' for the more prestigious publications, hold *vital strategic* positions in the orchestration of science."

There are three main groups of questions we consider of paramount importance in the whole complex problem of editorial gatekeeping in journals.

1. How does this gatekeeping system function and on what criteria do journal editorial board members base their decisions?

2. What is the structure of the powerful body of journal gatekeepers? In other words, who are chosen to perform gatekeeping tasks, and to which countries do they belong?

3. How can the evaluators be evaluated? In other words, what special characteristics give these individuals the right to sit in judgement?

In the present paper we concentrate on gatekeeping in analytical chemistry publications, to try to find answers to the last two questions.

We are not dealing with the first question, as we think that there is no answer to it that is specific to analytical chemistry. The gatekeepers of analytical chemistry journals use criteria similar to those used by science journal gatekeepers[4] in general, and these criteria have been quite thoroughly investigated.[2]

To find answers to the other two questions we have analysed the national composition of gatekeeping boards of analytical chemistry journals, and sought correlations between the number of gatekeepers, their citation rates and the number of analytical papers published by scientists from the country in question. A comparison has been made of the citation rates of the gatekeepers of organic chemistry, inorganic chemistry and analytical chemistry journals, and the citation data for the gatekeepers of analytical chemistry journals have been scrutinized.

EXPERIMENTAL

As a data-base, 14 analytical chemistry, 9 organic chemistry and 4 inorganic chemistry journals—considered among the most significant in their respective fields—were chosen.[5] The group of analytical

*The term "gatekeeping" is due to D. Crane, *American Sociologist*, 1967, **2**, 195.

chemistry journals was further divided into a subgroup of 7 broad-based analytical journals that deal with all branches of analytical chemistry[6] and 7 specialty journals. The inter-relationships between these two groups of journals were discussed in our previous paper dealing with the information flows in analytical chemistry.[7]

The broad-based journals were Analytical Chemistry, Analytical Letters A and B, Analusis, Analyst, Analytica Chimica Acta, Microchimica Acta and Talanta. The specialty journals were Chromatography, Journal of Chromatography, Journal of Radioanalytical Chemistry, Journal of Thermal Analysis, Radiochemical and Radioanalytical Letters, Spectrochimica Acta, Part A and Spectrochimica Acta, Part B.

These journals were examined with respect to the nationality of their gatekeepers. We considered as gatekeepers the editor(s)-in-chief, the editor(s), the managing editor, and the members of the editorial and advisory boards, but not the technical editor(s).[4] For the characterization of publication activities of the various countries in the field of analytical chemistry, papers published in the 14 analytical chemistry journals in 1978 were counted and grouped according to countries. In that year 1560 papers were published in the 7 broad-based journals and 3610 in the whole group of 14 analytical chemistry journals considered.

As a measure of "effectiveness", "eminence", "impact", "importance", "influence", "quality", "significance" or "utilization" of the scientific work of the gatekeepers,[8,9] the number of citations was considered. As a data-base the 1970–1974 cumulative volumes of the Science Citation Index[10] published by the Institute for Scientific Information (ISI), Philadelphia were chosen, and the citations under the gatekeepers' names were counted.

RESULTS AND DISCUSSION

National distribution of gatekeepers of analytical chemistry journals

Table 1 shows the national distribution and citation counts of the gatekeepers for the chosen analytical journals. The number of gatekeepers from various countries and their specific citation rates vary between wide limits. About half of the gatekeepers for analytical chemistry journals originate from only four countries (U.S.A., U.K., France and F.R.G.).

In co-opting scientists for journal gatekeeping functions, many points of view are probably taken into account. Here we would limit attention to only two factors affecting the "visibility" of an individual with regard to selection as a potential gatekeeper, namely publication productivity in some broad-based or specialized analytical field, and the impact of the research.

Accordingly correlations were sought, on the one hand between the number of gatekeepers from a given country and the number of papers published yearly in the two groups of journals (broad-based and specialty) from that country, and on the other between the number of gatekeepers and their citation rates. The results are shown in Fig. 1 as log–log plots; r and m represent the correlation coefficient and the slope, respectively. The overall correlation coefficient is $r = 0.8$. It appears that the two factors examined have an equal effect upon the selection of the gatekeepers.

The value of m in the relationship $y = ax^m$, *i.e.*, the exponent of publication productivity of quality, is usually below 1.0, its mean value being 0.71. This shows that the relationship is non-linear, in other words, to increase the number of gatekeepers from a given country, a progressively larger effort is necessary.

Along with the regression lines the standard deviation limits are also shown. Those cases that fall outside these limits are regarded as deviating significantly from the general group behaviour. For instance, taking the broad-based analytical journals as an example (Fig. 1b), the U.S.A., U.K., France, Belgium, Switzerland and Denmark give more gatekeepers than would be expected from their publication activity. In the citation rates of the gatekeepers of the same journals it is again the U.S.A., U.K., France and Belgium that figure foremost, along with Canada, the Netherlands and Italy. On the editorial boards of the broad-based analytical chemistry journals, India, South Africa and Israel are relatively under-represented.

Journals and gatekeepers in other subfields of chemistry

The impact factors*[11] of chemistry journals differ over about the same relative range as the citation rates of their gatekeepers. Do the scientific quality and distinction of the gatekeepers have a repercussion upon their gatekeeping activities?

We have tried to provide an answer to this question by comparing the impact factors of the journals with the citation rates of their gatekeepers. The data were taken from a previous paper.[12] Tables 2–4 contain data for organic, inorganic and analytical chemistry journals, respectively.

The citation frequencies of the gatekeepers are roughly in ratio 3:2:1 for the organic, inorganic and analytical chemistry journals, whereas the average impact factors are almost the same for the organic and inorganic journals, and that for the analytical journals is only about 25% lower (Table 5). These differences in impact factor are not significant. Figure 2 shows a plot of the data. Between the

*The impact factor is the number of citations in a given year to the papers published in the journal in question during the preceding two years divided by the number of those papers.

Table 1. National distribution and citation rates of gatekeepers of broad-based and specialty analytical chemistry journals: citation rates are given as the average number of citations per gatekeeper over a 5-yr period (1970–1974) and were rounded off by the program used

		Analytical chemistry journals		Broad-based analytical chemistry journals		Specialty analytical chemistry journals	
Rank*	Country	No. of gatekeepers	Citation rate	No. of gatekeepers	Citation rate	No. of gatekeepers	Citation rate
1	USA	154	220	81	260	73	180
2	UK	75	240	49	165	26	370
3	France	59	90	40	85	19	90
4	FRG	31	230	13	120	18	305
5	Hungary	30	120	5	415	25	65
6	Czechoslovakia	24	120	2	310	22	95
7	USSR	23	375	6	685	17	255
8	Japan	19	325	9	285	10	360
9	Canada	19	220	10	105	9	360
10	Belgium	18	75	12	80	6	60
11	Italy	17	95	4	30	13	115
12 eq	Switzerland	15	165	8	170	7	160
	Austria	15	120	6	115	9	130
14	The Netherlands	14	90	6	50	8	120
15	Sweden	12	300	8	320	4	260
16	Australia	9	290	7	345	2	120
17	Poland	8	150	4	235	4	65
18	Denmark	7	345	6	345	1	345
19 eq	GDR	6	85	2	120	4	70
	Israel	6	390	2	495	4	345
	South-Africa	6	330	2	845	4	70
	Yugoslavia	6	140	2	50	4	180
23 eq	Brazil	5	65	2	55	3	90
	India	5	260	1	140	4	290
	Roumania	5	300	3	200	2	440
26 eq	Mexico	3	1	2	1	1	1
	Norway	3	67	1	35	2	85
28 eq	Greece	2	36	2	35	—	—
	New Zealand	2	123	1	110	1	135
	Spain	2	15	—	—	2	15
31 eq	Egypt	1	—	1	—	—	—
	Argentina	1	7	—	—	1	7
	Other	6	15	5	20	1	2
	Total	608		302		306	
	Average		193		200		162

*According to the number connected with all 14 analytical chemical journals.

specific citation rates of the gatekeepers and the impact factors of their journals there is a significant correlation ($r = 0.6$). The slope of the regression line is 0.4, which means that the prestige of journals is only slightly raised by increasing the prestige of the gatekeepers.

The distribution of the gatekeepers of various countries and their citation rates is uneven, just as is the distribution of the scientific productivity,[13] area and national wealth of these countries. The Lorenz curve is a graphical presentation of the concentration, *i.e.*, the inequality of distribution, of various items over a population. A point on the Lorenz curve shows what percentage of the countries examined are endowed with a given percentage of the item plotted on the vertical axis. For example, in Fig. 3a we see that 25 (*i.e.*, 60%) of the 42 countries* dealt with can muster between them only 8% of the gatekeepers of broad-based analytical journals, the remaining countries having the other 92% of the gatekeepers. In this way Fig. 3 tells us that 72, 80 and 83% of the editors, and 74, 90 and 96% of the gatekeeper citations of analytical, inorganic and organic chemistry journals, respectively, stem from only 8 countries.

In the Lorenz-type graphs an even distribution is represented by the diagonal. The divergence of the Lorenz curve from the diagnonal is reflected in the Gini index, which is a measure of the normalized area between the diagonal and the Lorenz curve. It ranges from zero, *i.e.*, complete equality, to unity, *i.e.*, total inequality.

Upon comparing the Gini indices shown in Fig. 3 it becomes clear that the greatest inequality in the distribution of the citation rates of the gatekeepers appears for the inorganic and organic chemistry journals, $G = 0.81$ and 0.86, respectively. On the

*Forty-two countries are represented in the editorial boards of the international chemistry journals.[12] Our data are also referred to 42 countries in the case of analytical, inorganic and organic chemistry journals.

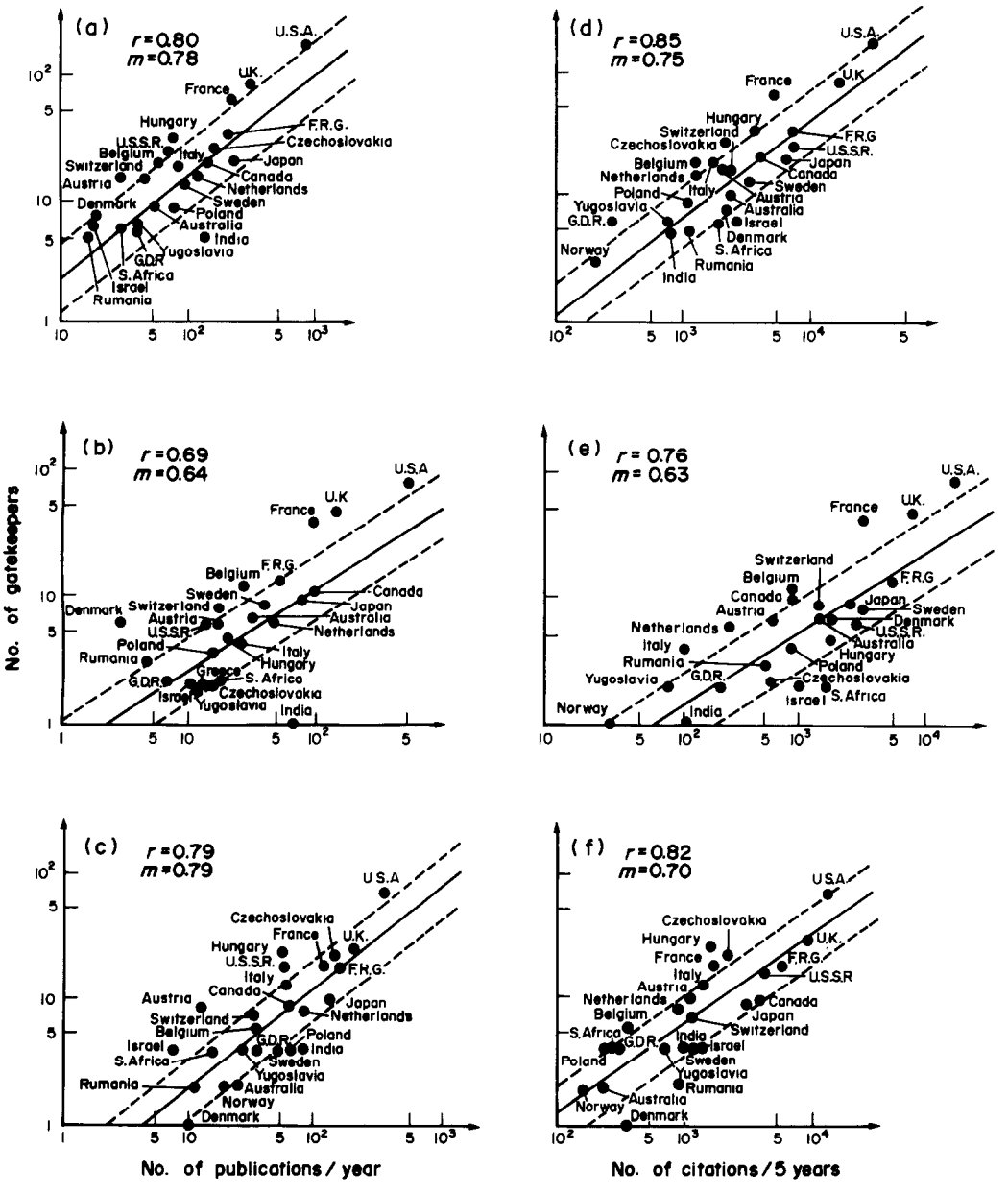

Fig. 1. Relationships between the number of gatekeepers and the number of pulications for a given country (a–c), and between the number of gatekeepers and their citation rates (d–f) for 14 analytical chemistry journals (a and d), 7 analytical chemistry journals of broad-based character (b and e) and 7 specialty analytical chemistry journals (c and f).

other hand, the national distribution of the gatekeepers of specialty analytical chemistry journals is the most even ($G = 0.62$). For comparison, the Gini-index of world scientific publication productivity is $G = 0.91$; the indices for the distribution of total national production and of population are $G = 0.85$ and 0.75, respectively.[13]

*"For unto every one that hath shall be given, and he shall have abundance: but from him that hath not shall be taken away even that which he hath" (Gospel according to St. Matthew).

The gatekeepers of analytical chemistry journals

Participation in gatekeeping for some scientific journal represents a form of reward for the person involved. Participation in many journals is naturally a cumulated reward, and in such cases no doubt the "Matthew-effect" is at work.[14]* It has been shown that scientists who are already known, *i.e.*, more "visible", are given more reward than others who may have similar scientific achievements but are less "visible" and/or less widely known.

Among the 608 gatekeepers of the 14 analytical

Table 2. Impact factors of organic chemistry journals and citation data for their gatekeepers

Journal	Impact factor	Gatekeepers No.	Gatekeepers Total citations	Gatekeepers Citations *per capita*
Carbohydrate Research	1.431	53	6638	125
Journal of Organometallic Chemistry	2.331	7	9888	1413
Monatshefte für Chemie	0.831	38	13584	357
Organic Magnetic Resonance	1.379	39	16553	424
Organic Mass Spectrometry	1.253	37	15178	410
Synthesis	1.758	24	27026	1126
Synthetic Communications	1.178	30	18360	612
Tetrahedron	1.745	71	60285	849
Tetrahedron Letters	2.114	65	60097	925

Table 3. Impact factors of inorganic chemistry journals and citation data for their gatekeepers

Journal	Impact factor	Gatekeepers No.	Gatekeepers Total citations	Gatekeepers Citations *per capita*
Inorganica Chimica Acta	2.859	79	42130	533
Inorganic and Nuclear Chemistry Letters	1.141	26	14441	555
Journal of Inorganic and Nuclear Chemistry	1.017	73	28635	392
Zeitschrift für anorganische und allgemeine Chemie	1.333	38	15220	400

chemistry journals considered, 61 are members of two editorial boards, and 19 participate in three or more.

The citation rate of gatekeepers of analytical chemistry journals can be well described by a logarithmic normal distribution curve (Fig. 4). The median corresponds to $M = 100$ citations per 5 yr; in other words, 50% of the gatekeepers receive over 20 citations per year, whereas 68% of them get between 3 and 100 yearly citations ($M \pm \sigma$).

CONCLUSIONS

The results of our study can be summarized as follows.

1. In the case of analytical chemistry journals, whether broad-based or specialized in character, a correlation has been shown to exist between the number of gatekeepers of a given nationality, and the number of analytical papers published in these groups of journals by scientists in the country concerned.

2. For the journals of analytical chemistry a correlation also exists between the number of gatekeepers and their citation rate. This correlation is of about the same strength for broad-based and specialized analytical chemistry.

3. The relationship between the number of gatekeepers (n) and their publication productivity, (*i.e.*, their citedness rate, N) is $n \sim aN^m$, where m shows values between 0.6 and 0.8. In other words, for the journals mentioned so far, the effort needed for a country to increase its number of gatekeepers by one, say from 50 to 51 or from 100 to 101, would be twice

Table 4. Impact factors of analytical chemistry journals and citation data for their gatekeepers

Journal	Impact factor	Gatekeepers No.	Gatekeepers Total citations	Gatekeepers Citations *per capita*
Analytical Chemistry	2.803	17	3193	188
Analytical Letters Parts A and B	0.884	62	15471	250
Analusis	0.774	50	6169	123
The Analyst	1.702	42	8664	206
Analytica Chimica Acta	1.488	40	7795	195
Chromatographia	1.394	33	8978	272
Journal of Chromatography	1.846	46	11543	251
Journal of Radioanalytical Chemistry	0.890	49	4535	93
Journal of Thermal Analysis	0.506	34	3625	107
Mikrochimica Acta	0.779	42	8830	210
Radiochemical and Radioanalytical Letters	0.515	74	6546	88
Spectrochimica Acta, Part A	1.023	34	5589	164
Spectrochimica Acta, Part B	1.621	33	15527	471
Talanta	0.907	51	10831	212

Table 5. Comparison of organic, inorganic and analytical chemistry journals (mean and standard deviation)

Characteristics	Organic chemistry	Inorganic chemistry	Analytical chemistry
Average impact factor	1.56 ± 0.47	1.59 ± 0.85	1.22 ± 0.62
Average number of gatekeepers per journal	40 ± 20	54 ± 26	43 ± 14
Average citations per gatekeeper	693 ± 415	470 ± 85	202 ± 97

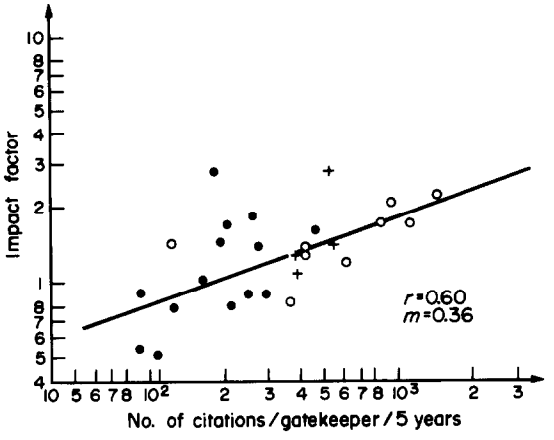

Fig. 2. Correlation between the citation rate of gatekeepers and journal impact factors: ● analytical chemistry, ○ organic chemistry, + inorganic chemistry.

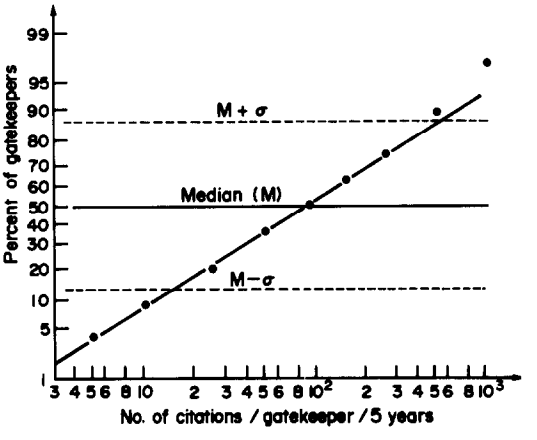

Fig. 4. Distribution of the number of citations for gatekeepers of journals in analytical chemistry, plotted on Gauss paper with logarithmic abscissa.

and thrice, respectively, as large as that necessary to effect an increase from 10 to 11.

4. There is yet another correlation between the impact factors (I.F.) of the journals and the citation rates of their gatekeepers. In the relationship $n \sim b\,(\text{I.F.})^m$, the exponent $m = 0.4$ is smaller than in the corresponding relationship involving the number of gatekeepers. The citation rate of the gatekeepers is therefore reflected in the impact factors of the journals.

5. The citation rates of the gatekeepers of organic and inorganic chemistry journals are 3 and 2.5 times (respectively) those for the gatekeepers of the analytical chemistry journals, and the impact factor of the latter journals is about 0.3 below that for the other two types of journal.

6. Of the 608 gatekeepers of analytical chemistry journals, 237 have an average citation rate of more than 20 per year, 113 have over 50 citations per year, and 58 are cited more than 100 times a year. The quality or impact of their research has an immediate effect on the prestige (impact factor) of the journals. Among the 608 editors, 61 are members of more than one, 19 of more than two, and 9 of more than three boards of analytical chemistry journals.

Our results show that 75% of the positions of power influencing the publication of new results in almost all areas of analytical chemistry are concentrated into the hands of scientists from no more than ten countries of the world.

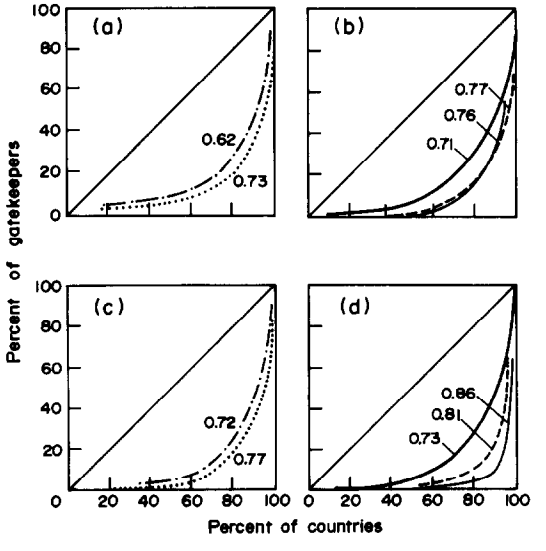

Fig. 3. Lorenz curves for the national distribution of gatekeepers of various groups of analytical chemistry journals (a and b), and of their citation rate (c and d): ··· broad-based; ·-·-· specialty; —— analytical chemistry (the sum of the first two groups); —— organic chemistry; --- inorganic chemistry. The corresponding Gini indices are also shown.

REFERENCES

1. J. M. Ziman, *Nature*, 1969, **224**, 318.
2. M. D. Gordon, *J. Res. Commun. Studies*, 1978, **1**, 139.

3. *Idem*, *New Scientist*, 1977, **73**, 342.
4. S. Zsindely, A. Schubert and T. Braun, *Scientometrics*, 1982, **4**, 57.
5. T. Braun, E. Bujdosó and W. S. Lyon, *Anal. Chem.*, 1980, **52**, 617A.
6. J. Petruzzi, in *Statistics*, R. F. Hirsh (ed.), Proc. 7th Eastern Analytical Symp., p. 277. Franklin Inst. Press, Philadelphia, Pa., 1978.
7. E. Bujdosó, T. Braun and W. S. Lyon, *Trends Anal. Chem.*, 1982, **13**, 223.
8. N. L. Geller, J. A. DeCani, R. E. Davies, *Lifetime citation rates as a basis for assessing the quality of scientific work*. Paper presented at the Belmont Conf. on the Use of Citation Data in the Study of Science, 1 April 1975, Elkridge, MD.
9. E. Garfield, *Scientometrics*, 1979, **1**, 359.
10. *Science Citation Index* 1970–1974; *Part Citation Index*. Institute for Scientific Information, Philadelphia, 1976.
11. E. Garfield, *Journal Citation Reports; A Bibliometric Analysis of Science Journals in the ISI Data Base*, Vol. 14. ISI Press, Philadelphia, 1979.
12. S. Zsindely, A. Schubert and T. Braun, *Scientometrics*, 1982, **4**, 69.
13. J. D. Frame, F. Narin and M. P. Carpenter, *Soc. Stud. Sci.*, 1977, **7**, 501.
14. R. K. Merton, *Science*, 1968, **159**, 56.

Talanta, Vol. 30, No 3, pp 169–172, 1983
Printed in Great Britain

0039-9140/83/030169-04$03.00/0

SIMULTANEOUS DETERMINATION OF SEVERAL TRACE METALS BY ASV AFTER PRECONCENTRATION BY ADSORPTION AS PADAP COMPLEXES ON C_{18}-BONDED GLASS BEADS

SHIGERU TAGUCHI, TAKAYUKI YAI, YASUKO SHIMADA, KATSUMI GOTO
Department of Chemistry, Faculty of Science, Toyama University, Toyama, Japan 930

and

MINORU HARA
Department of Chemistry, Faculty of Education, Toyama University, Toyama, Japan 930

(*Received* 30 *June* 1982. *Accepted* 24 *September* 1982)

Summary—Traces of zinc, lead, copper and cadmium are determined simultaneously by anodic-stripping voltammetry (ASV) combined with a preconcentration technique utilizing C_{18}-bonded glass beads. The metals are collected as their 2-(2-pyridylazo)-5-diethylaminophenol (PADAP) complexes on a column of the beads and the complexes are eluted with a small volume of ethanol–hydrochloric acid–chloroform mixture. The eluate is evaporated to dryness in the presence of hydrogen peroxide and the residue dissolved in a small volume of acetic acid–sodium acetate buffer. The concentrations of the metals are measured by ASV. Quantitative recoveries are obtained for 0.01-ng/ml levels of the metals. Many ions which interfere in the direct ASV procedure do not interfere in the present method.

Numerous preconcentration techniques for trace-element analysis of aqueous samples have been proposed and reviewed by many authors. The surface adsorption technique is one of the most versatile methods for the concentration and/or separation of trace elements from a variety of matrices.[1–14] In this technique, the trace element is adsorbed as a complex on an adsorbent such as a hydrophobic resin[2–5,8–14] or activated carbon.[6,7]

We have proposed C_{18}-bonded glass beads and polypropylene wool[11] as the adsorbent, on which traces of cobalt,[8] iron[12] and phosphorus[9–11] were collected as coloured complexes and eluted with a small volume of eluent, then determined spectrophotometrically. Since these adsorbents have no inner surfaces, adsorption and desorption of the complexes are very fast, and more than 100-fold concentration can easily be achieved.

Similar applications have been reported by Watanabe *et al.*[13] and Sturgeon *et al.*,[14] in which C_{18}-bonded silica gel was used for the preconcentration of several heavy metals in sea-water samples, and the concentrates were analysed by inductively-coupled plasma atomic-emission spectrometry (ICP–AES) or graphite-furnace atomic-absorption spectrophotometry.

In the present study, zinc, lead, copper and cadmium were collected as their 2-(2-pyridylazo)-5-diethylaminophenol (PADAP) complexes on a column of C_{18}-bonded glass beads and determined by anodic-stripping voltammetry (ASV). ASV is one of the most sensitive methods for trace analysis, and the instrumentation is generally inexpensive and often home-made, as in the present work. Simultaneous determinations can be done with a small volume of sample.

PADAP was chosen as the complexing reagent since it forms highly coloured water-soluble complexes with the metals concerned under conditions in which calcium and magnesium do not form complexes.[15]

EXPERIMENTAL

Reagents

C_{18}-bonded glass beads. Prepared by treating 100–120 mesh non-porous glass beads as reported previously.[12]

PADAP. Synthesized as reported previously,[16] and dissolved in 0.05*M* hydrochloric acid to give a 0.05% solution.

Buffer solution, pH 9.5. Prepared by mixing equal volumes of 0.05*M* sodium tetraborate and 0.05*M* sodium carbonate. The reagents were purified by recrystallization.

Eluent. A 7:2:1 v/v mixture of ethanol, 0.1*M* hydrochloric acid and chloroform.

Supporting electrolyte. Prepared by mixing equal volumes of 0.1*M* sodium acetate and 0.1*M* acetic acid. The sodium acetate was purified by recrystallization.

Hydroxylammonium chloride solution, 30%. Prepared with recrystallized hydroxylammonium chloride.

Standard metal solutions. Prepared by dissolving the nitrates or chlorides in hydrochloric acid, and standardized by complexometry.

Other chemicals used were reagent-grade. The water was doubly distilled.

Apparatus

ASV instrument. Constructed as described by Possley and Higgins.[17]

Electrochemical cell. This was essentially of the same type as that described by Barendrecht.[18] A hanging mercury drop electrode and a saturated calomel electrode were used as the working and reference electrodes, respectively. The volume of the cell was 1 ml.

Pump. A Taiyo Kagaku model 150-N tubing pump was used The flow-rate could be controlled over the range from 0.5 to 10 ml/min.

Column. The column was prepared in a glass tube, 10 mm in diameter and 300 mm in length, by adding a slurry of the beads in ethanol until the height of the bed was 250 mm. Before use, it was washed with water to remove the ethanol.

Procedure

To a sample solution containing less than 0.1 μg of zinc, lead, copper and cadmium, add 1.0 ml of the PADAP solution and adjust the pH to about 9.5 with the buffer solution. Set aside for more than 30 but less than 120 min, then pump the solution through the column at a flow-rate of about 10 ml/min. Pump the eluent slowly through the column (< 1 ml/min) and collect the coloured portion of the eluate in a beaker. Add 0.25 ml of 30% hydrogen peroxide, and heat slowly. When the solution has become colourless, add 3 ml of the hydroxylammonium chloride solution, and evaporate to dryness. Cool to room temperature and dissolve the residue with 2 ml of the supporting electrolyte. Transfer 1 ml of the solution into the electrochemical cell and measure the concentration by ASV under the following conditions: deposition period 5–20 min; deposition potential −1.2 V *vs.* SCE; sweep-rate 10 mV/sec

RESULTS AND DISCUSSION

Complexing reagent

PADAP is proposed as the complexing reagent, because it forms highly coloured complexes with many heavy metals under conditions in which calcium and magnesium do not form complexes, and because the reagent and its complexes are rather water-soluble.[15] 4-(2-Pyridylazo)-resorcinol, a well-known water-soluble complexing reagent, was also examined, but the adsorbed complexes were not easily eluted.

A large excess of PADAP does not affect the results. In this study, 1.0 ml of 0.05% PADAP solution (more than 600-fold excess for 0.1 μg of copper) is added.

Effect of pH

Figure 1 shows that pH values higher than 9.2 give quantitative recovery for the individual metals. A pH of 9.5 was therefore chosen for complex formation. For pH adjustment, a sodium tetraborate–sodium carbonate buffer was used, since these reagents can be easily purified by recrystallization.

Standing time before adsorption

Less than 30 min gives low recovery, since the complex formation is not complete. More than 2 hr also gives low recovery, owing to adsorption of the complexes on the beaker wall.

Effect of flow-rate

Recoveries of the metals did not vary with sample flow-rate in the range of 0.5–10 ml/min. A flow-rate of 10 ml/min (the maximum attainable with the pump used) was selected for use. The adsorbed complexes were eluted at flow-rates lower than 1 ml/min.

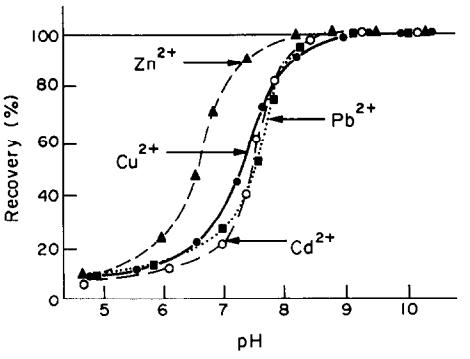

Fig. 1. Effect of pH on recovery (100-fold concentration factor). Concentration of each metal in the sample solution is 1.0 μg/l.

Adsorption capacity of the adsorbent

The adsorption capacity of the C_{18}-bonded glass beads used was found to be 0.2 μmole/g, by the column "breakthrough" technique,[19] with the Cd–PADAP complex as the indicator species. The small capacity is due to the small surface area of the non-porous glass beads used, but causes no problem, since the heavy metals with which PADAP reacts under the conditions used are present only at trace level in natural waters.

Eluent

Hydrochloric acid and several organic solvents were tested. The complexes are decomposed by 0.1*M* hydrochloric acid, but not completely eluted by it. Dimethylsulphoxide and dimethylformamide are effective eluents, but their low volatility makes it difficult to remove them by evaporation before the ASV measurement. Chloroform is one of the most effective solvents, but its high density causes mixing at the water–chloroform boundary during the elution. Various mixtures of ethanol, 0.1*M* hydrochloric acid and chloroform were studied. A 7:2:1 v/v mixture proved excellent, the adsorbed complexes being eluted with less than 10 ml of the eluent, and the eluate easily evaporated to dryness.

Treatment of the eluate before ASV measurement

Since ASV measurement could not be done directly in the eluate medium, the solvent was removed by evaporation before the ASV measurement, but recovery was poor if the PADAP was not decomposed, because of re-formation of the complexes in the supporting electrolyte medium. Addition of hydrogen peroxide to the eluate before the evaporation gave excellent recoveries.

Optimum conditions for ASV

Several media, such as acetic acid, sodium acetate, ammonium acetate, potassium nitrate, sodium potassium tartrate and sodium citrate were tested as supporting electrolytes. A mixture of equal volumes of

Table 1. Recoveries of the metals at various concentrations in various volumes

Metal concn., *μg/l.*	Volume, *ml*	Deposition period, *min*	Recovery, % Zn^{2+}	Cd^{2+}	Pb^{2+}	Cu^{2+}
1.0	100	5	99	99	99	105
			4*	3*	3*	5*
0.50	250	5	99	99	99	104
			4*	4*	4*	5*
0.10	250	10	97	98	97	103
			7*	6*	6*	8*
0.050	250	20	97	95	95	97
			6*	6*	6*	7*
0.010	500	20	94	94	92	95
			8*	7*	7*	9*

Recoveries are mean values of 10 determinations.
*Coefficient of variation, %.

0.1*M* sodium acetate and 0.1*M* acetic acid is proposed, because reproducible stripping potentials and peak currents were obtained with this medium.

The stripping potentials for zinc, cadmium, lead and copper are −0.96, −0.59, −0.42 and −0.05 V *vs.* SCE, respectively, in this supporting electrolyte. A potential of −1.20 V *vs.* SCE was chosen for deposition.

The peak current increased in proportion to the deposition period over the range 0–40 min. Sweep-rates ranging from 1.6 to 53.2 mV/sec were tested. Higher sweep-rates do not give reproducible results, and 10 mV/sec is recommended.

Recovery and precision

Table 1 shows the recoveries of the metals at various concentrations from various volumes of doubly distilled water. Spiking with standard solution was used. Better than 95% recovery was obtained at the 0.05-ng/ml level, with satisfactory precision. Better than 90% recovery was obtained with 500-ml sample volumes containing 5 ng of the metal.

Effect of diverse species

Table 2 shows the effect of various species on the determination of the metals by the present method, as compared with that on direct ASV. It is clear that many ions which interfere with the direct ASV method do not interfere in the proposed method. Large amounts of potassium, sodium and chloride do not affect the determination, nor do 1000 ppm of magnesium or 500 ppm of calcium (because they do not form complexes with PADAP under the conditions used).

Separation of the heavy metals from the matrices and from interfering ions in natural waters is a great advantage in this preconcentration technique. Cobalt(II), nickel, manganese(II) and iron(III) form

Table 2. Effect of diverse ions

Ion	Method	Concn., *mg/l.*	Recovery, % Zn^{2+}	Cd^{2+}	Pb^{2+}	Cu^{2+}
As^{3+}	direct ASV	1.0	29	97	95	71
	present method	10	98	98	98	101
Fe^{3+}	present method*	1.0	50	65	67	70
	present method	5.0	97	97	99	96
Sn^{2+}	direct ASV	1.0	110	98	†	†
	present method	10	96	98	98	98
Br^-	direct ASV	10	93	96	97	70
	present method	10	99	99	99	100
I^-	direct ASV	10	97	93	91	156
	present method	10	98	98	99	100
SCN^-	direct ASV	1.0	91	83	89	61
	present method	10	97	98	99	101
Gelatine	direct ASV	1.0	89	85	83	55
	present method	10	100	99	99	102

*In the absence of hydroxylammonium chloride.
†Cannot be measured.
100-fold concentration was performed in the present method.
Concentration of each metal was 0.1 mg/l. in the electrochemical cell.

reddish complexes with PADAP under the conditions used and are adsorbed on the glass beads. Of these, only iron(III) interferes with the determination of the four metals of interest, and this interference can be eliminated by addition of hydroxylammonium chloride, as shown in Table 2.

Chromium(III) slowly forms a PADAP complex, which is adsorbed on the glass beads, but large amounts of chromium(III) do not affect the ASV measurement.

In the presence of very high concentrations of these metals, large amounts of reagent and adsorbent should be used so that enough will be available for the complexation and adsorption of the metals to be determined.

CONCLUSIONS

Very high concentration factors are obtained by this simple preconcentration technique. A combination of the preconcentration technique with ASV is very promising for simultaneous determination of traces of heavy metals. PADAP is especially advantageous as the complexing reagent, forming water-soluble complexes with the four metals, but not with calcium and magnesium which are matrix species in natural waters.

Arsenic and tin, if present, seriously interfere with the determination of the four metals by direct ASV, but can be removed in the preconcentration step.

Since PADAP reacts with many heavy metals, this preconcentration technique will be applicable to the determination of many other metals in natural waters, if this separation method is combined with other instrumental methods such as ICP–AES, graphite-furnace atomic-absorption spectrophotometry and differential-pulse anodic-stripping voltammetry.

REFERENCES

1. D. E. Leyden and W. Wegscheider, *Anal. Chem.*, 1981, **53**, 1059A.
2. Y. Sugimura, *Bunseki*, 1981, 148.
3. A. Warshawsky, *Talanta*, 1974, **21**, 962.
4. R. B. Willis and D. Sangster, *Anal. Chem.*, 1976, **48**, 59.
5. Y. Sakai, *Talanta*, 1980, **27**, 1073.
6. M. Kimura and K. Kawanami, *ibid.*, 1979, **26**, 901.
7. M. Kimura, *Bunseki*, 1981, 297.
8. S Taguchi and K. Goto, *Talanta*, 1980, 27, 819.
9. S. Taguchi, K. Goto and H. Watanabe, *ibid.*, 1981, **28**, 613.
10. *Idem, Water Purification and Liquid Waste Treatment*, 1981, **22**, 13.
11. S. Taguchi, S. Amano and K. Goto, *Environmental Conservation Engineering Association*, 1981, **10**, 628.
12. S. Taguchi, C. Yoshikura and K. Goto, *Bunseki Kagaku*, 1982, **31**, 32.
13. H. Watanabe, K. Goto, S. Taguchi, J. W. McLaren, S. S. Berman and D. S. Russell, *Anal. Chem.*, 1981, **53**, 738.
14. R. E. Sturgeon, S. S. Berman and S. N. Willie, *Talanta*, 1982, **29**, 169.
15. S. Shibata, in *Chelates in Analytical Chemistry*, A. J. Barnard, Jr. and H. Flaschka (eds.), Vol 4, p. 194. Dekker, New York, 1972.
16. T. M. Florence, D. A. Johnson and Y. J. Farrar, *Anal. Chem.*, 1969, **41**, 1652.
17. N. L. Possley and G W Higgins, *J. Chem. Educ.*, 1974, **51**, 351
18. E. Barendrecht, in *Electroanalytical Chemistry*, A. J. Bard (ed.), Vol. 2, p 89. Dekker, New York, 1967.
19. J. R. Jezorek and H Freiser, *Anal. Chem.*, 1979, **51**, 366.

Talanta, Vol 30, No. 3, pp 173–178, 1983
Printed in Great Britain.

0039-9140/83/030173-06$03.00/0

STUDIES ON THE EXTRACTION OF PHOSPHOMOLYBDATE BY POLYETHER FOAM

ANJUM S. KHAN and A. CHOW
Department of Chemistry, University of Manitoba, Winnipeg, Manitoba, Canada

(*Received* 25 *June* 1982. *Accepted* 21 *September* 1982)

Summary—To establish the mechanism of heteropoly anion extraction, the sorption of phosphomolybdate by polyether-based polyurethane foam was investigated. The effect of several variables on the extraction was studied and the optimum conditions were ascertained. The results of this study indicate that the cation-chelation mechanism cannot account for the extraction of phosphomolybdate by polyether foam.

The extraction of phosphomolybdate by diethyl ether was described as early as 1864.[1] Later, Scroggie[2] reported that oxygen-containing organic solvents, such as ethers, esters, ketones and aldehydes, are good extractants for phosphomolybdate, and since then many reports have appeared on the extraction and separation of heteropoly anions with various oxygen-containing organic solvents. Phosphomolybdic acid has been extracted with ethyl acetate,[3] butyl acetate,[4] 2-methyl-1-propanol,[5] 3-methyl-1-butanol,[6] 1-octanol[7] and a mixture of butanol and chloroform.[8] Recently, high molecular-weight amines have also been introduced for the extraction of heteropoly anions.[9] The extraction and separation of heteropoly anions have been reviewed.[10,11]

Nevertheless, the mechanism of the extraction has not yet been established. Although several mechanisms have been proposed,[10] two in particular have been discussed most frequently. They are based on the assumption that a donor–acceptor interaction takes place between an oxygen atom of the organic solvent and the heteropoly complex. According to one of the mechanisms the oxygen atom of the solvent interacts with the molybdenum of the heteropolymolybdate and the changes in the absorption spectra of the extracts of heteropoly complexes are attributed to the increase in the co-ordination number of the molybdenum atom.[10,14] According to the other, which is commonly known as the hydrate–solvate mechanism, the extraction is due to interaction of the solvent with the cationic part of the heteropoly acid or salt.[13,14] It is obvious that the two mechanisms differ only in one respect, namely the part (cationic or anionic) of the extracted species that interacts with the oxygen atom of the solvent.

Since it has been observed that polyether foam extracts several metal anionic complexes through the cation chelation mechanism (CCM),[15] the extraction of phosphomolybdate by polyether foam was studied in the hope that the results would cast new light on the mechanism of heteropoly anion extraction and also extend the analytical value of polyether foam for the extraction of phosphorus, silicon, arsenic, germanium *etc.*, as heteropoly anions.

EXPERIMENTAL

Apparatus

A Varian 634S spectrophotometer, Fisher Accumet model 520 pH-meter and a Packard Tri-Carb model 3320 liquid scintillation spectrophotometer were used. A thermostatically-controlled multiple automatic squeezer was used for squeezing the foam in sample solutions.

Reagents

Phosphorus-32 ($t_{1/2}$ = 14.3 days) was obtained from New England Nuclear of Canada. Aqueous counting scintillant (ACS) was supplied by Amersham Ltd. All other chemicals used were of analytical grade. An acid-resistant polyether-type polyurethane foam was obtained from Union Carbide. Foam cubes, each weighing 70 ± 5 mg were washed according to the procedure described earlier.[16]

Stock solutions of sodium molybdate and sodium dihydrogen phosphate were prepared and stored in polyethylene bottles to avoid contamination from glass.

Procedure

Sample solutions were made by diluting the stock solutions to give the required concentrations. The solution containing the required amount of phosphate and other reagents was spiked with a sufficient amount of ^{32}P-labelled phosphate. The sample solution (100 ml) was then equilibrated with a foam cube in the extraction cell for 3–4 hr, which was found sufficient to establish equilibrium.

The degree of extraction (E) was determined by counting the radioactivity of a 2 ml aliquot of sample mixed with 10 ml of ACS "scintillation cocktail", before and after equilibrium with the foam:

$$E = \left(\frac{\text{Activity}_{\text{before}} - \text{Activity}_{\text{after}}}{\text{Activity}_{\text{before}}}\right) \times 100\%$$

The distribution coefficient (D) was calculated from the degree of extraction:

$$D = \frac{EV}{(100 - E)W}$$

where V is the sample volume (l.) and W the weight of foam (kg); D is thus expressed in l./kg.

RESULTS AND DISCUSSION

The results of preliminary studies showed that the heteropolymolybdates of phosphorus, silicon, arsenic and germanium, both in the reduced and non-reduced forms, are effectively extracted by the polyurethane foam. It was also noticed that the foam does not extract any detectable amount of the hetero-atom species in the absence of molybdate. The sorption of the yellow phosphomolybdate by polyurethane foam was studied in detail because the analytical literature contains a large number of papers describing the most appropriate conditions for the formation of yellow phosphomolybdate and its extraction into various organic solvents. In order to establish the optimum conditions for extraction of phosphomolybdate by polyurethane foam, the influence of various parameters was studied.

Effect of acid concentration

It has been reported[17] that the formation of phosphomolybdate is maximal between pH 1 and 2.0. However, the acidity range for the extraction of heteropoly anions has been found to depend on the nature of the organic solvent[10] and for most solvents is wider than the acidity range for formation of a given heteropoly anion.[17,18] The extraction curve for polyether foam is shown in Fig. 1. As can be seen, the distribution ratio of phosphomolybdate increases with increasing acidity of the aqueous phase. The distribution ratio reaches a maximum at about pH 2.5 and remains constant up to pH ~ 1.2. Further increase in the hydrogen-ion concentration results in a sharp decline in the distribution ratio. It is quite reasonable to assume that at higher acid concentration the sharp decrease in the extraction of phosphate results from the decomposition of the extractable species, *i.e.*, $H_3PMo_{12}O_{40}$, according to the equilibrium proposed by Souchay.[19] Similar extraction behaviour has been reported by other workers.[17,18] On the other hand, our study showed that the formation of heteropolymolybdate is maximal between pH 1.35 and 1.7. It is evident from these results that as with numerous solvent-extraction systems, the optimum acidity range for extraction of phosphomolybdate into polyether foam is wider than the acidity range for its formation.

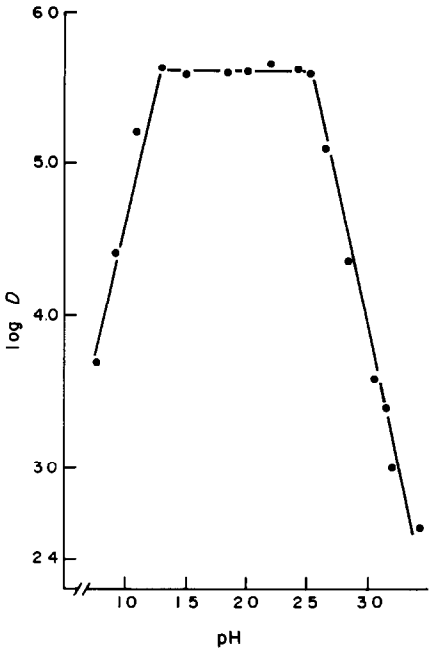

Fig. 1. Effect of pH on the extraction of phosphomolybdate. Conditions: 70 ± 5 mg of foam, 150 ml of solution $4 \times 10^{-5}M$ PO_4^{3-}, $1 \times 10^{-3}M$ MoO_4^{2-}, pH adjusted with HCl, LiCl added to maintain $0.5M$ ionic strength.

Effect of molybdate concentration

The extraction of phosphomolybdate was studied as a function of molybdate concentration. The results of one such study are shown in Fig. 2. Curve a dis-

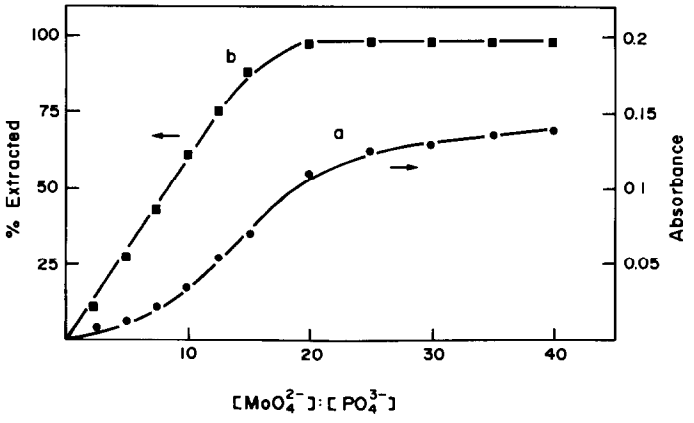

Fig. 2. Effect of molybdate on the formation and sorption of phosphomolybdate. Conditions: a, $[PO_4^{3-}] = 4 \times 10^{-5}M$, pH = 2.0 ± 0.1, λ = 420 nm; b, 70 ± 5 mg of foam, 150 ml of solution $4 \times 10^{-5}M$ in PO_4^{3-}, pH = 2.0 ± 0.1, $0.5M$ ionic strength maintained with LiCl.

plays the absorbance of the aqueous solution as a function of molybdate to phosphate ratio; the shape of the curve indicates that the formation of yellow 12-phosphomolybdate is not proportional to the amount of molybdate added. Similar results have been reported by Murata *et al.*,[17] who have suggested that a small amount of molybdate preferentially produces the colourless intermediate phosphomolybdate complexes which, on further addition of molybdate, are converted into yellow 12-phosphomolybdate. On the basis of these studies, they have proposed the following equilibria for the formation of 12-phosphomolybdate:

$$PO_4^{3-} + MoO_4^{2-} \underset{OH^-}{\overset{H^+}{\rightleftharpoons}} \text{(intermediate) complexes} \underset{OH^-}{\overset{H^+ + MoO_4^{2-}}{\rightleftharpoons}} PMo_{12}O_{40}^{3-}$$

It can be seen that the absorbance does not reach its maximum even at 40-fold excess of molybdate. This confirms the earlier reports that a large excess of molybdate is required to ensure the complete formation of 12-phosphomolybdate.

Curve b, in Fig. 2, represents the degree of extraction of phosphate as a function of molybdate concentration. As expected, the extraction increases with increasing molybdate concentration. The striking feature of this curve is that the extraction reaches a maximum at about 25-fold molar ratio of molybdate to phosphate. An excess of molybdate is used for the formation and subsequent extraction of phosphomolybdate into oxygen-containing organic solvents.[20,21] The results of other experiments with different amounts of phosphate and 25-fold molar ratio of molybdate confirm that this excess of molybdate is sufficient for extraction of more than 99% of phosphate as phosphomolybdate into foam.

In another study, phosphomolybdate was extracted from a series of solutions containing a fairly high concentration of molybdate. It is clear from Fig. 3, where log D is plotted against log of initial concentration of molybdate, that extraction of $4 \times 10^{-5}M$ phosphate remains practically constant up to $3 \times 10^{-2}M$ initial molybdate concentration (*i.e.*, up to 750-fold excess of molybdate), above which the distribution ratio steadily decreases with increasing molybdate concentration. The decrease in the extraction of phosphomolybdate is most likely due to increase in the simultaneous extraction of isopolymolybdate species into the polyether foam.

Effect of phosphate concentration

The extraction of phosphomolybdate was also studied as a function of phosphate concentration. Figure 4 shows the plot of log D *vs.* log initial concentration of phosphate. As can be seen, the D values are practically constant up to a certain concentration of phosphate, and then decrease at higher concentrations. All the distribution curves are similar except that the break in the curve is shifted towards lower phosphate concentration with increasing molybdate concentration. The drop in D values with increase in phosphate concentration might be attributed to either the polymerization or the dissociation of 12-phosphomolybdate. On the other hand, it is equally reasonable to assume that the drop in D values, caused by the increase in phosphate concentration, indicates the capacity of the foam. The capacity calculated from curve a (Fig. 2) is 0.75 meq/g. This capacity is slightly lower than that reported for other systems, *e.g.*, ~1 meq/g.[24] The lower foam capacity for phosphomolybdate is most likely due to the simultaneous extraction of isopolymolybdate species, which is further confirmed by the results in Fig. 4, which show a steady decrease in the foam capacity for phosphomolybate with increase in the initial concentration of molybdate.

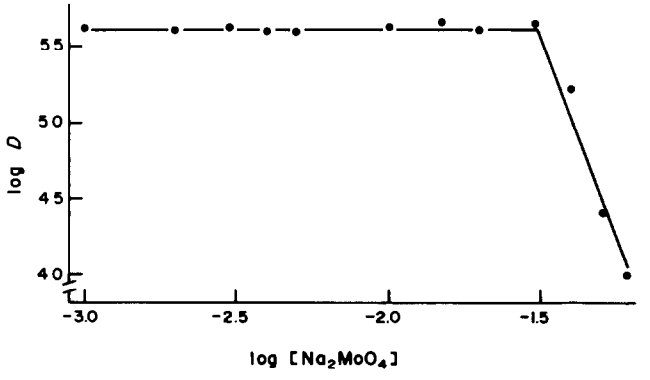

Fig. 3. Effect of varying the initial concentration of sodium molybdate on the extraction of phosphomolybdate. Conditions: 70 ± 5 mg of foam, 150 ml of solution $4 \times 10^{-5}M$ PO_4^{3-}, pH = 2.0 ± 0.1, 0.5M ionic strength maintained with LiCl.

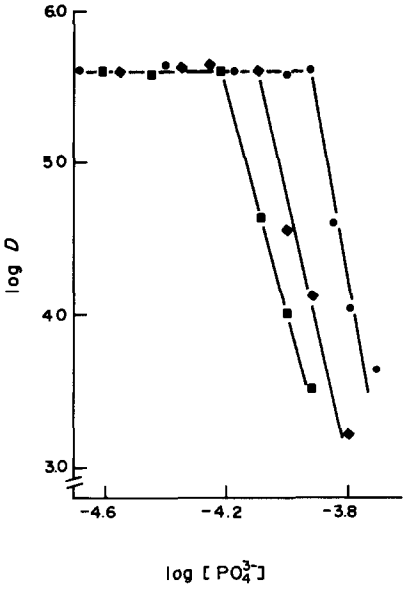

Fig. 4. Effect of varying initial concentration of phosphate on the extraction of phosphomolybdate. Conditions: 70 ± 5 mg of foam, 150 ml of solution, (■) $2 \times 10^{-2}M$, (◆) $1 \times 10^{-2}M$, (●) $6 \times 10^{-3}M$ MoO_4^{2-}, pH = 2.0 ± 0.1, 0.5*M* ionic strength maintained with LiCl.

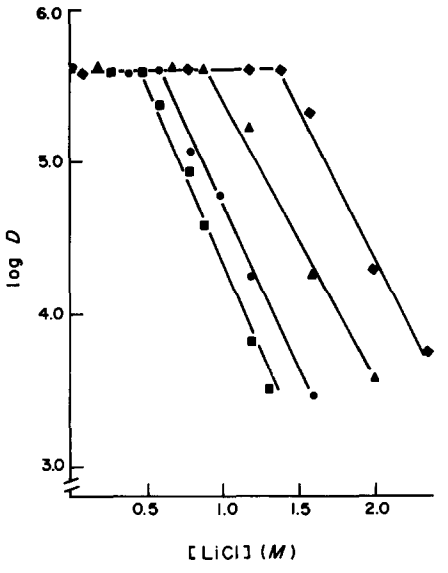

Fig. 5. Effect of varying the lithium chloride concentration on the sorption of phosphomolybdate. Conditions: 70 ± 5 ml of foam, 150 ml of solution, $4 \times 10^{-5}M$ PO_4^{3-}, pH = 2.0 ± 0.1, (●) $1 \times 10^{-3}M$, (▲) $5 \times 10^{-3}M$, (◆) $1 \times 10^{-2}M$, (■) $3 \times 10^{-2}M$ MoO_4^{2-}, LiCl added to maintain 0.5*M* ionic strength.

Effect of alkali metal chlorides

The effect of alkali-metal chlorides on the extraction of phosphomolybdate can be useful in evaluating possible mechanisms for the process.

It has been observed[15] that for the systems where the cation chelation mechanism (CCM) is at work, the nature and concentration of the cations present play an important role in the extraction of anions into polyether foam. The influence of neutral salts on the extraction of phosphomolybdate was studied in the hope that it might help in understanding the mechanism of extraction. The effect of lithium chloride on the extraction of phosphomolybdate was studied at different initial molybdate concentrations. The results of these studies are displayed in Fig. 5 and are also summarized in Table 1. It is clear that for a given initial concentration of molybdate, the distribution ratio remains constant up to a certain concentration of lith-

Table 1. Effect of lithium chloride on the extraction of phosphomolybdate

	Log distribution ratio (l./kg) at different concentrations of Na_2MoO_4			
Lithium chloride, M	1×10^{-3}M	5×10^{-3}M	1×10^{-2}M	3×10^{-2}M
0.0	5.62	5.6	—	—
0.1	5.60	—	5.60	—
0.2	5.62	5.64	5.61	—
0.3	—	—	—	5.61
0.4	5.60	—	5.63	—
0.5	—	—	—	5.61
0.6	5.61	—	5.62	5.37
0.7	—	5.62	—	—
0.8	5.08	5.61	5.61	4.95
0.9	—	5.61	—	4.52
1.0	4.78	5.4	—	—
1.2	4.25	5.22	5.61	3.81
1.3	—	—	—	3.50
1.4	—	—	5.61	—
1.6	3.46	4.25	5.32	—
2.0	—	3.58	4.29	—
2.3	—	—	3.76	—

Conditions: $[PO_4^{3-}] = 4 \times 10^{-5}M$, pH 2.0 ± 0.1, foam weight 70 ± 5 mg.

ium chloride, above which the extraction of phosphomolybdate deteriorates. On the other hand, for a given initial concentration of lithium chloride (*e.g.*, 0.8*M*), with increasing molybdate concentration the extraction increases to a maximum value and then declines. A similar effect in the extraction of 12-phosphomolybdate into butanol, with increasing sodium chloride concentration, has been observed by Anderson.[22] The decrease in the extraction of phosphomolybdate in the presence of sodium ions at concentrations $\geqslant 0.3M$ has also been reported by Russian workers and has been attributed to the low stability of 12-phosphomolybdate under these conditions.[25] Owing to the very complex chemistry of phosphomolybdate, it is very difficult to give any definite reason for the influence of lithium chloride on its extraction. However, the drop in D values with increasing concentration of lithium chloride tends to suggest that the CCM cannot account for the extraction of phosphomolybdate. This is further substantiated by the fact that phosphomolybdate is also extracted well by polyester-based polyurethane foam. The failure of polyether foam to extract the $PMo_{12}O_{40}^{3-}$ anion by the CCM may be attributed to the fact that according to that mechanism the extraction of a triply charged anion would require three cation-containing helices of polyether chains to be arranged around it. The possibility of such an arrangement is lower in the polymer. Al-Bazi[26] has observed that the extraction of the triply-charged $Rh(SCN)_6^{3-}$ complex anion cannot be explained on the basis of the CCM, although it has been proved that the extraction of several doubly charged metal thiocyanate complex anions $[M(SCN)_4^{2-}]$ takes place through this mechanism.

The oxonium type mechanism might be considered to account for the sorption of phosphomolybdate by polyether foam. According to this mechanism, the protonation of ethereal oxygen atoms of the polymer in acidic medium results in the formation of an oxonium type salt, which thus can extract the heteropoly anion ($PMo_{12}O_{40}^{3-}$) by an anion-exchange mechanism. Based on this, polyether foam may be regarded as a weak-base anion-exchanger. The high values of the distribution ratio (4×10^5) and of the foam capacity (0.75 meq/g) observed for the present system further support this idea. This possibility has also been mentioned by other workers.[24,27] In addition, sorption of the undissociated acid, $H_3PMo_{12}O_{40}$, may be very competitive, or perhaps the interaction of ethereal oxygen atoms with molybdate, as suggested for solvent extraction systems, may be responsible for the observed extraction.

Assuming that phosphomolybdate is extracted into polyether foam by any mechanism other than CCM, the decline in the D values with increase in concentration of lithium chloride may be attributed to the simultaneous extraction of Li^+, along with MoO_4^{2-} or any other suitable anion, into the polyether foam by the CCM. Since according to this mechanism, the extraction of Li^+ will be accomplished by the formation of a helical pattern of inwardly directed oxygen atoms of polyether chains around the cation, the adoption of such a geometry by polyether chains to encage the cation will certainly limit the availability of ethereal oxygen atoms for the extraction of phosphomolybdate, *i.e.*, would lower the degree of extraction. The decrease in the degree of extraction at high molybdate concentration can be explained by using the same argument. Since sodium molybdate was used as the source of molybdate, the addition of more of it not only increases the formation and thus the extraction of phosphomolybdate, it also enhances formation of the helical structure in the polymer owing to the extraction of sodium molybdate and thus decreases the number of "free" ethereal oxygen atoms to interact with phosphomolybdate.

In order to test this reasoning, the sorption of phosphomolybdate from sodium and potassium chloride solutions was studied. Since according to the CCM extractive power of polyether foam for alkali-metal cations increases in the order $Li \ll Na^+ < Cs^+ < Rb^+ < K^+$, greater interference would be expected from the more extractable cations if the explanation above is correct. The formation of precipitates did not permit the study of the effect of rubidium and caesium. The effect of potassium was studied but only over a small range of concentration (again because of precipitation). However, the extraction of phosphomolybdate was studied over a wide range of concentration of sodium chloride. The results are shown in Fig. 6, where they are compared with those of a similar study using lithium chloride. As expected, the extraction of phosphomolybdate in the presence of equal concentrations of alkali-metal cations decreases

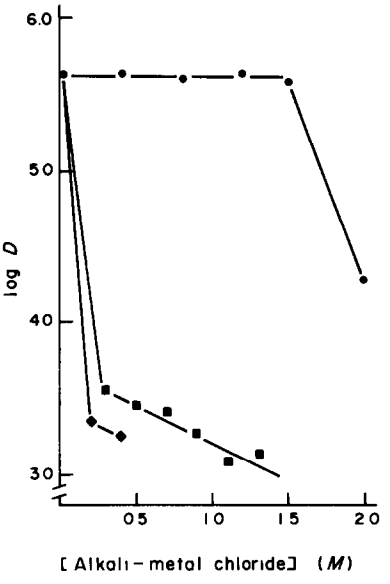

Fig. 6. Effect of varying initial concentration of alkali-metal chlorides on the extraction of phosphomolybdate. Conditions: 70 ± 5 mg of foam, 150 ml solution, $4 \times 10^{-5}M$ PO_4^{3-}, $6 \times 10^{-3}M$ MoO_4^{2-}, pH = 2.0 ± 0.1, (●) LiCl, (■) NaCl, (◆) KCl.

in the following order: $Li \gg Na^+ > K^+$. These results tend to suggest that the presence of a cation that can be chelated enhances formation of helical structure in the polymer and thus interferes with the sorption of species such as phosphomolybdate, which are not extracted through the CCM.

Acknowledgements—We gratefully acknowledge the financial support of the Natural Sciences and Engineering Research Council of Canada and of the University of Manitoba.

REFERENCES

1. C. Marignac, *Ann. Chim. Phys.*, 1864, **3**, 5.
2. A. G. Scroggie, *J. Am. Chem. Soc.*, 1929, **51**, 1057.
3. J. Hure and T. Ortis, *Bull. Soc. Chim. France*, 1949, 834.
4. R. J. L. Allen, *Biochem. J.*, 1940, **34**, 858.
5. I. Berenblum and E. Chain, *ibid.*, 1938, **32**, 286.
6. C. Rainbow, *Nature*, 1946, **157**, 268.
7. F. L. Schaffer, J. Fong and P. L. Kirk, *Anal. Chem.*, 1953, **25**, 343.
8. C. Wadelin and M. G. Mellon, *ibid.*, 1953, **25**, 1668.
9. V. I. Klitina, F. P. Sudakov and I. P. Alimarin, *Russ. J. Anal. Chem.*, 1966, **21**, 338.
10. I. P. Alimarin, F. P. Sudakov and V. I. Klitina, *Russ. Chem. Rev.*, 1965, **34**, 574.
11. E. N. Dorokhova and I. P. Alimarin, *ibid.*, 1979, **48**, 502.
12. L. I. Lebedeva and E. V. Vanchikhova, *Russ. J. Anal. Chem.*, 1974 **19**, 1978.
13. V. I. Lakshmanan and B. C. Haldar, *J. Indian. Chem. Soc.*, 1970, **47**, 231.
14. L. P. Tysganok, L. V. Sorokina and V. L. Spodina, *Russ. J. Inorg. Chem.*, 1977, **22**, 887.
15. R. F. Hamon, A. S. Khan and A. Chow, *Talanta*, 1982, **29**, 313.
16. A. S. Khan, W. G. Baldwin and A. Chow, *Can. J. Chem.*, 1981, **59**, 1490.
17. K. Murata and Y. Kiba, *J. Inorg. Nucl. Chem.*, 1970, **32**, 1667.
18. S. J. Simon and D. F. Boltz, *Anal. Chem.*, 1975, **47**, 1758.
19. P. Souchay, *Pure Appl. Chem.*, 1963, **6**, 61.
20. D. F. Boltz, T. DeVries and M. G. Mellon, *Anal. Chem.*, 1949, **21**, 563.
21. P. Pakalns, *Anal. Chim. Acta*, 1968, **40**, 1.
22. L. H. Anderson, *Acta Chem. Scand.*, 1959, **13**, 1743.
23. V. I. Klitina, F. P. Sudakov and I. P. Alimarin, *Russ. J. Anal. Chem.*, 1965, **20**, 1197.
24. H. J. M. Bowen, *J. Chem. Soc. (A)*, 1970, 1082.
25. L. I. Plekach, Yu. D. Averin and Z. V. Federova, *Russ. J. Anal. Chem.*, 1973, **28**, 2108.
26. S. J. Al-Bazi, *Ph.D. Thesis*, 1982, University of Manitoba, 1982.
27. J. J. Oren, K. M. Gough and H. D. Gesser, *Can. J. Chem.*, 1979, **57**, 2032.

Talanta, Vol. 30, No. 3, pp. 179–183, 1983
Printed in Great Britain.

0039-9140/83/030179-05$03.00/0

DETERMINATION OF MERCURY IN THE PRESENCE OF CHLORIDE BY MEANS OF THE TERNARY COMPLEX Hg(II)/XYLENOL ORANGE/AMBERLITE LA-2 IN NON-AQUEOUS MEDIA*

J. L. PERAL-FERNÁNDEZ, R. IZQUIERDO-HORNILLOS, A. CABRERA-MARTÍN and R. GALLEGO-ANDREU

Departamento de Química Analítica, Facultad de Ciencias Químicas de la Universidad Complutense de Madrid, Ciudad Universitaria, Madrid-3, Spain

(*Received* 4 *June* 1982. *Accepted* 19 *September* 1982)

Summary—The system Hg(II)/Xylenol Orange/Amberlite LA-2 dissolved in 1:1 v/v 3-methylbutan-1-ol/chloroform medium has been studied. A 3:2:2 complex is formed, which is suitable for analytical measurements at temperatures $<18°$. This complex allows the determination of mercury in the range 0.19–5.5 ppm with a molar absorptivity of 2.12×10^4 l.mole^{-1}.cm^{-1} at 600 nm and extraction pH of 7.4 (standard deviation 0.065 ppm). The proposed method has been applied to the determination of mercury in contaminated water with a high chloride content.

In a previous paper[1] a study of the reaction of Hg(II) and Xylenol Orange (XO) in aqueous solution was reported. To improve this spectrophotometric determination an attempt has been made to extract the ternary complex with Amberlite LA-2 as the second ligand, which is soluble in organic solvents.

The liquid anion-exchanger Amberlite LA-2 (*N*-lauryl-*N*-trialkylmethylamine) denoted here by LA-2 or HNR_1R_2, has been widely used in extraction processes,[2] because of its property of ion-pair formation. However, the nitrogen atom in LA-2 can provide an electron-pair to form a ternary co-ordination complex through the uncharged species HNR_1R_2, or can form ion-association complexes through the cationic species $H_2NR_1R_2^+$. In this paper a mechanism is suggested in which both species of LA-2 are involved in the extraction of the anionic Hg(II)/XO binary complex.

EXPERIMENTAL

Reagents

Xylenol Orange. Aqueous solution, $1.0 \times 10^{-3}M$.

Mercury(II) nitrate. Aqueous solution, $1.0 \times 10^{-3}M$, in $0.05M$ nitric acid.

Citric acid. Aqueous solution, $0.2M$.

Disodium hydrogen phosphate. Aqueous solution, $0.4M$.

Amberlite LA-2. Chloride form.

All chemicals were of analytical-reagent grade.

Procedure

The sample solution containing Hg(II) is mixed with 1.0 ml of $10^{-3}M$ XO and 5.0 ml of pH-7.4 citrate/phosphate buffer, diluted with water to 25.0 ml and shaken with 4.5 ml of LA-2 solution (0.6 ml of LA-2 and 3.9 ml of 1:1 v/v mixture of isoamyl alcohol and chloroform). Shaking for 30–60 sec is enough to reach equilibrium. The organic phase is centrifuged and separated, dried with anhydrous sodium sulphate and measured at 600 nm in 1-cm glass cells, against a spectrophotometric blank of XO, prepared in the same way.

RESULTS AND DISCUSSION

Selection of the solvent

The anion-exchanger LA-2 is soluble in water-immiscible alcohols having 4 or 5 carbon atoms: butan-1-ol, butan-2-ol, pentan-2-ol and 3-methylbutan-1-ol, were tested in the present work because these solvents have an oxygen donor-atom which can co-ordinate with mercury(II) during the extraction. Of these, 3-methylbutan-1-ol (isoamyl alcohol) proved the best, owing to its lower solubility in water. However, to keep the polarity of the solution as low as possible (dielectric constant ~ 10), with no substantial modification of the extractive power of the alcohol, the solvent should be mixed with chloroform, which increases the density of the mixture but takes no part in the extraction process.

A spectrophotometric study at 590 nm on solutions containing Hg(II) and XO has indicated that a 1:1 v/v mixture of alcohol and chloroform is optimal for the extraction. The optimal organic solvent:LA-2 ratio is 8:1 v/v.

Absorption spectra

The absorption spectra of the organic extracts of XO and its Hg(II) complex in the presence of LA-2 show two absorption maxima at 460 and 590 nm, the

*Paper presented at Euroanalysis IV, Helsinki, 1981.

complex being hyperchromic at the longer wavelength. These maxima are shifted bathochromically by 10 nm from those for aqueous solutions of XO and its Hg(II) complex, in the absence of an amine, such as hexamethylenetetramine, as the second ligand.[1,3,4] This behaviour may be attributed to the possible formation of a ternary complex in which LA-2 takes part as the second ligand, linked through its amine groups to the Hg(II) and the binary Hg(II)/XO complex. It may also be attributed to the alcohol present because of the change in the dielectric constant of the medium. If an amine, such as LA-2, with suitable pK_a value and solubility in organic media, is not present, there is no extraction. The difference spectrum indicates that 600 nm is the most suitable wavelength for analytical measurements.

Different absorption spectra are obtained if the pH of the XO solution is changed before the extraction. The absorption maximum at 460 nm can be assigned to the ionic species H_3XO^{3-} and its more acidic conjugated species, and the maximum at 590 nm to H_2XO^{4-} and its more basic conjugated species, if the ionic equilibria of XO, proposed by Rehák and Körbl,[5] apply to this non-aqueous medium. It may be assumed that this dissociation scheme will hold even when the pK_a values are changed by the medium, and can at least be qualitatively applied to this system.

Effect of pH

The influence of pH on the extraction of XO is shown in Fig. 1 (curve 2). As expected, the reagent is more extractable at lower pH values because the XO is then more protonated, and is nearly completely extracted at pH <7. The complex shows slightly different behaviour (Fig. 1, curve 1), the extraction maximum being reached near pH 7. The difference spectrum in this figure shows that the optimum range of pH for the extraction (pH_{ex}) is 7.2–7.5 (curve 3).

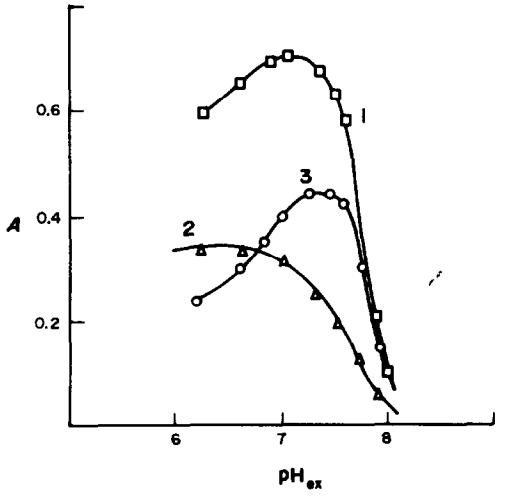

Fig. 1. Effect of pH. 1, Hg(II)/XO; 2, XO; 3, difference curve (1 *vs.* 2): λ, 600 nm; $C_{Hg(II)} = 2.0 \times 10^{-5} M$; $C_{XO} = 4.0 \times 10^{-5} M$.

Effect of the concentration of LA-2

The degree of extraction of XO increases with the LA-2 concentration, a constant absorbance value being reached when at least 0.5 ml of LA-2 per 4.0 ml of mixed organic solvent is used. It may be assumed that an outer-sphere (ion-association) complex is formed, which allows the extraction of XO. The counter-ion for the XO anion is thought to be $H_2NR_1R_2^+$, according to the equilibria:

$$\begin{array}{ccc} H_mXO^{n-}(w) + nH_2NR_1R_2^+(o) & \rightleftharpoons & [(H_mXO^{n-})(H_2NR_1R_2^+)_n]_{(o)} \\ \downarrow\uparrow & & \downarrow\uparrow \\ nH_2NR_1R_2^+(w) & \rightleftharpoons & [(H_mXO^{n-})(H_2NR_1R_2^+)_n]_{(w)} \end{array}$$

where, if $m = n = 3$, the species of XO is H_3XO^{3-} and λ_{max} 460 nm, but if $m = 2$ and $n = 4$, the species is H_2XO^{4-} and λ_{max} 590 nm.

The Hg(II)/XO system in the presence of LA-2 shows similar behaviour, but in the extraction process the mechanism may be different, since the water molecules co-ordinated to the mercury ion in the complex in aqueous medium may be removed in the extraction and substituted by uncharged molecules of solvent or amine (or both together) to complete the co-ordination number (synergistic effect).

To allow a safety margin for the LA-2 concentration, a mixture of 0.60 ml of LA-2 and 3.9 ml of organic solvent mixture was chosen.

Stability

The complex was found to be stable for at least 80 min at temperatures below 18°, and a temperature of 15° was used for all further investigations.

The thermal decomposition of the complex can be explained as due to the equilibrium:

$$\begin{aligned} &Hg(II)/XO/(HNR_1R_2)_p/(H_2NR_1R_2^+)_q \\ &\quad + 2[(Cl^-)/(H_2NR_1R_2^+)] \\ &\quad \overset{>18}{\rightleftharpoons} [(XO^{(q+2)-})(H_2NR_1R_2^+)_{q+2}] \\ &\quad + [Hg(HNR_1R_2)_p^{2+}(Cl^-)_2] \end{aligned}$$

since the spectra eventually obtained ($t \rightarrow \infty$) at >18° are those of XO under the same conditions. In any case, the complexes [Hg(II)LA-2] and $[Hg(LA\text{-}2)_p^{2+}(Cl^-)_2]$ do not absorb at 600 nm.

The presence of agar-agar, gelatin and gum arabic as stabilizing agents does not stop the decomposition of the complex at temperatures higher than 18°, nor does excess of XO give stabilization.

Composition and formation constant of the complex

The composition of the Hg(II)/XO complex was studied by the molar-ratio, continuous-variations and straight-line methods, in the presence of an excess of LA-2 (Fig. 2), since the ternary complex does not appear if a high concentration of LA-2 is not present. These methods gave evidence for a 3:2 Hg(II)/XO ratio in this complex. The combining ratio of LA-2 was found by Babko's equilibrium shift method.[6] The slope obtained indicated that the complex contains two LA-2 molecules. Therefore, it can be assumed that a 3:2:2 Hg(II)/XO/LA-2 complex is extracted.

The formation constant calculated from the continuous-variations data (with excess of LA-2 present) was 5.0×10^{20}.

Determination of the extraction constant and recovery

The method of Likussar and Boltz[7] was used to calculate the extraction constant from the expression

$$\log E_{M_3L_2L_2} = 0.7625 - 4 \log K + \log Y_{max} - 5 \log (1 - Y_{max})$$

where Y is the normalized absorbance[8] and $4.0 \times 10^{-5} M$ the value of K from the normalized continuous-variations plot. A value of 2.2×10^{21} was obtained for $E_{M_3L_2L_2}$.

The influence of pH on the recovery of XO and the complex is shown in Fig. 3. It can be observed that at $pH_{ex} \leqslant 6.85$, $99 \pm 1\%$ of the XO is extracted, whereas the complex is almost completely extracted in the range $pH_{ex} = 7.0$–7.3, but for determination of mercury it is best to use $pH_{ex} = 7.4$ because there is then maximal difference between the absorbance for XO and the complex.

Possible structure of the complex

Since the stoichiometry found for the Hg(II)/XO/LA-2 chelate is 3:2:2 at pH_{ex} 7.4, if Rehák and Körbl's equilibria[5] for XO are assumed, the formation equilibrium of this complex can be expressed by:

$$2H_3XO^{3-}_{(w)} + 3Hg(II)_{(w)} + 2HNR_1R_{2(o)} + 6H_2NR_1R_2^+ \cdot Cl^-_{(o)} \overset{<18°}{\rightleftharpoons} [(2XO/3Hg(II)/2HNR_1R_2)^{6-}//(H_2NR_1R_2^+)_6]_{(o)} + 6H^+_{(w)} + 6Cl^-_{(w)}$$

It is supposed, according to the theory of Bjerrum and Fuoss, that in this reaction, 6 monoprotonated LA-2 ions have reacted by ion-pair association with the anionic chelate to form an extractable neutral species. The release of 6 protons in the reaction has been verified from the slope of the plot of log $D_{Hg(II)} = f(pH_{ex})$. The solvation by the alcohol in the extraction medium is not shown in the equilibrium above, but is included in the structure suggested in Fig. 4 for this complex.

The proposed "superstoichiometry" could be explained on the basis of the low dieletric constant of the medium, which favours the formation of molecular aggregates. Kinetic studies showed that the complex is converted into the 1:1:1 complex when the temperature of the organic phase is higher than 18° (this being the complex obtained in other media or with another amine[1]). The rate of decomposition of the 3:2:2 complex increases with the mercury concentration, but in any case only the 1:1:1 complex is present after 17 min reaction time.

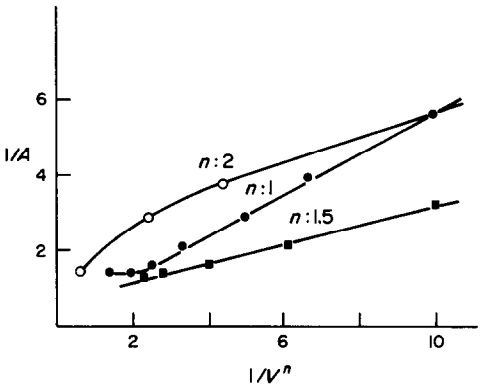

Fig. 2. Straight-line plot; λ 600 nm.

The analytical measurement must be made immediately after the extraction if the 3:2:2 complex is to be used; the higher molar absorptivity obtained indicates that it should.

Calibration graph

For pH_{ex} 7.4 and measurement at 600 nm Beer's law is obeyed over the range 0.19–5.5 ppm Hg(II), the molar absorptivity (referred to monomeric mercury) being 2.12×10^4 l.mole^{-1}.cm^{-1}. According to the method of Ringbom and Ayres, the range for minimal spectrophotometric error is 2.0–5.5 ppm Hg(II).

Statistics

The statistical parameters (for 4.0 ppm mercury, 14 replicates) of the proposed analytical method are: arithmetic mean (X) 4.0 ppm; standard deviation (s) 0.065 ppm; confidence limit ($X \pm st$) 4.0 ± 0.14 ppm (95% probability level).

Interferences

The interference due to the presence of other species was studied by mixing Hg(II) solution, potential interferent, reagent and buffer, in that order, diluting and extracting. The species tested were added in molar concentration 100 and 10 times that of the Hg(II).

The following ions showed no interference at either concentration: F^-, CO_3^{2-}, $S_2O_8^{2-}$, SO_4^{2-}, BO_2^-,

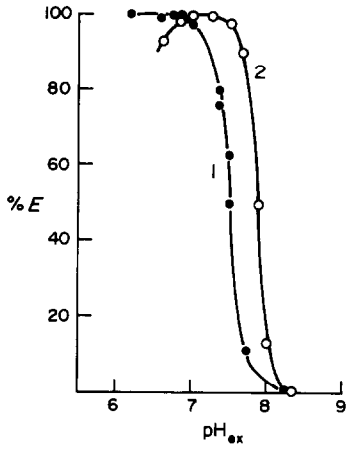

Fig. 3. Extraction curves. 1, XO; 2, Hg(II)/XO/LA-2 complex.

$C_2O_4^{2-}$, IO_3^-, CrO_4^{2-}, PO_4^{3-}, tartrate, citrate, Cl^-, SCN^-, BrO_3^-, CH_3COO^-, NO_3^-, ClO_4^-, Ag^+, Tl^+, As(V), Mo(VI), Al^{3+}, Mn^{2+}, Ce^{3+}, In^{3+}, Be^{2+}, Ba^{2+}, Mg^{2+}, Li^+, Na^+, K^+, Rb^+ and NH_4^+.

$Fe(CN)_6^{3-}$, $Fe(CN)_6^{4-}$, ClO_3^-, W(VI), As(III), Cr^{3+}, Zn^{2+}, Ce(IV), La^{3+}, Zr^{4+}, V(IV), U(VI) and Ca^{2+} did not interfere at the lower concentration level. The following ions interfered at 10-fold molar ratio to Hg(II): $S_3O_3^{2-}$, CN^-, I^-, Br^-, HS^-, EDTA, MnO_4^-, Pb^{2+}, Hg(I), Cd^{2+}, Cu^{2+}, Bi^{3+}, Sb(III), Sb(V), Fe^{3+}, Ni^{2+}, Co^{2+}, Th^{4+}, V(V) and Sr^{2+}.

$NaClO_4$, $NaNO_3$ and KNO_3 have no effect at concentrations below 0.002*M*, but higher concentrations cause incomplete extraction, especially $NaClO_4$.

Application

The method has been applied to determination of mercury in contaminated water containing 200 ppm of chloride. A recovery test was done by making standard additions. The results are shown in Table 1. The mercury was added in the form of its nitrate.

The method is less sensitive than the dithizone method, but also less laborious and less sensitive to light, and does not require removal of excess of reagent. The interferences are similar for both methods.

REFERENCES

1. A. Cabrera-Martín, J. L. Peral-Fernández and F. Burriel-Marti, *Talanta*, 1975, **22**, 489.
2. C. F. Coleman, C. A. Blake, Jr. and K. B. Brown, *ibid.*, 1962, **9**, 297.

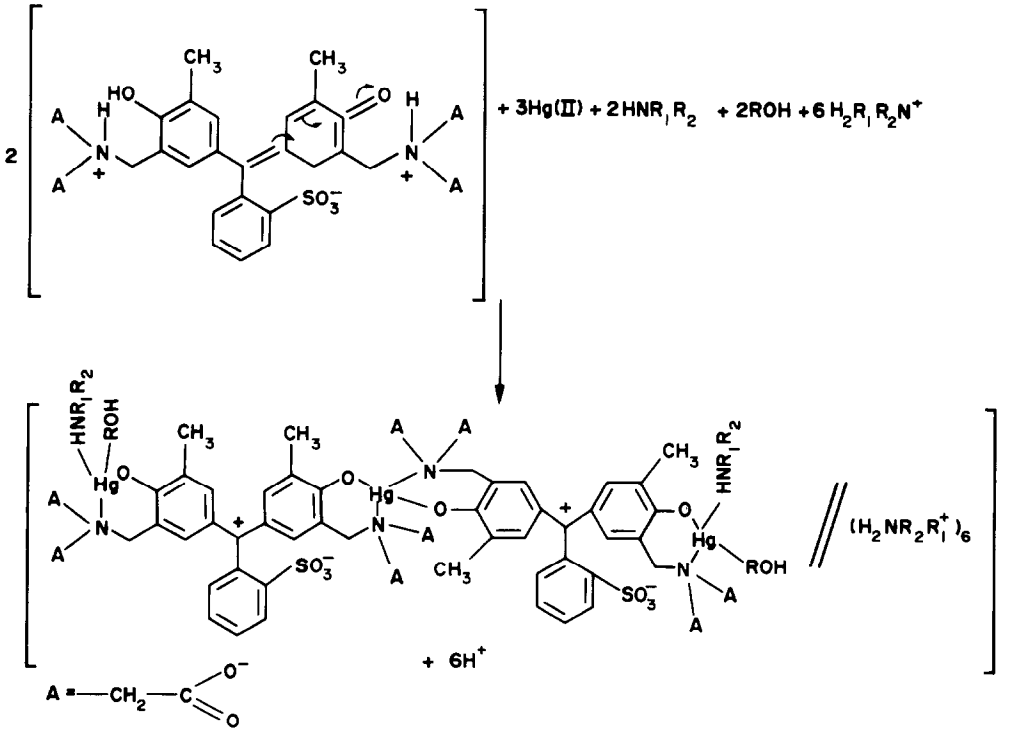

Fig. 4. Suggested reaction mechanism.

Table 1. Recovery studies for Hg(II) added to contaminated water

Added,* *ppm*	0	1.00	2.00	2.50	2.80	3.00	3.50
Found,* *ppm*	1.60	2.61	3.60	4.10	4.39	4.60	5.11

*Average of 5 determinations; s = 0.02 ppm.

3. A. Cabrera-Martín, J. L. Peral-Fernández, S. Vicente-Perez and F. Burriel-Martı, *ibid.*, 1969, **16,** 1023.
4. F. Burriel-Marti, A. Cabrera-Martín and J. L. Peral-Fernández, *Chem. Analit.* (*Warsaw*), 1972, **17,** 1125.
5. B. Rehák and J. Körbl, *Collection Czech. Chem. Commun.*, 1960, **25,** 797.
6. A. K. Babko, *Fizıko-khimicheskii analiz kompleskykh soedinenie vi rastvorakh*, Izdat. AN USSR, Kiev, 1955.
7. W. Likussar and D. F. Boltz, *Anal. Chem.*, 1971, **43,** 1971.
8. K. Momoki, J. Sekino, H. Sato and N. Yamaguchi, *ibid.*, 1969, **41,** 1286.

Talanta, Vol. 30, No. 3, pp. 185–186, 1983
Printed in Great Britain.

0039-9140/83/030185-02$03.00/0

SHORT COMMUNICATIONS

SPECTROPHOTOMETRIC DETERMINATION OF NO_2 IN THE WORKING ATMOSPHERE

B. G. ZHELYAZKOVA,*
Department of Chemistry, Sofia University, 1126 Sofia, Bulgaria

P. B. VARDEV
Institute of Hygiene and Professional Diseases, Medical Academy, 1431 Sofia, Bulgaria

and

N. D. YORDANOV
Institute of Organic Chemistry, Bulgarian Academy of Sciences, 1113 Sofia, Bulgaria

(*Received* 15 *April* 1982. *Revised* 20 *September* 1982. *Accepted* 4 *October* 1982)

Summary—A method is described for determining NO_2 in workplace atmospheres, based on its reaction with bis(diethyldithiocarbamato)copper(II) in toluene. NO_2 is absorbed from an air sample by a toluene solution of $Cu(dtc)_2$ and the decrease in the initial absorbance at 437 nm is measured. The method has been compared with the Saltzman method. The interference of NO, Cl_2, O_3, SO_2 and other gases has been studied. The NO_2 concentration range of the method is 1–500 mg/m^3.

In an earlier paper[1] we reported studies on the reaction of nitrogen dioxide with bis(diethyldithiocarbamato)copper(II), $Cu(dtc)_2$, in toluene. We found that $Cu(dtc)_2$ is destroyed as a result of stoichiometric reaction of NO_2 with the ligand. The main product yielded at an NO_2:$Cu(dtc)_2$ ratio of 2:1 was found to be the mixed-ligand complex $Cu(NO_3)(dtc)$, which has an absorption maximum at 400 nm. The final reaction products were, $Cu(NO_3)_2$ and thiuramdisulphide, obtained at an NO_2:$Cu(dtc)_2$ ratio of 4:1.[1]

EXPERIMENTAL

Reagents

Copper(II) diethyldithiocarbamate was prepared by mixing equimolar aqueous solutions of sodium diethyldithiocarbamate and cupric chloride in 2:1 ratio. The precipitate was washed with water and dried at 60°. The crude product was recrystallized twice from chloroform.[2]

Toluene was purified and dried before use. Toluene solutions of $Cu(dtc)_2$ were found to be stable for several months.

Nitrogen dioxide was obtained by thermal decomposition of dried reagent grade lead nitrate in a flow of oxygen.[3] A Teflon permeation tube was filled with liquefied NO_2. The permeation rate of the tube was determined gravimetrically and the tube was used to provide a working standard.

Saltzman absorption solution was prepared and stored according to the procedure described by NIOSH.[4,5] Solutions of sodium nitrite for the static calibration of the Saltzman method were prepared according to the same procedure.[4,5]

Apparatus

A dynamic mixing system[6] was used to obtain an air flow with a known NO_2 concentration. A stream of dry cylinder air, brought to 31.5 ± 0.1° and passed at a flow-rate of 82.5 ml/min over the NO_2 permeation tube was diluted with a stream of dried purified air, regulated with a needle valve and measured with a glass rotameter. Both streams were thoroughly mixed, and two glass T-pieces downstream of the mixer served as sampling ports. Various concentrations of NO_2 in air (in the mg/m^3 range) were obtained by varying the flow of dilution air. The system was kept running for about 20 hr before calibration, to achieve equilibration between adsorption and desorption of the contaminant on the walls of the system.

The humidity of the air was changed by mixing the dilution air with an air-stream saturated with water vapour. Relative humidities of 40% and 60% were produced by varying the flow-rates of both streams and were continuously monitored with a wet/dry psychrometer.

Procedure

Two all-glass fritted bubblers, each containing 10.0 ml of the Saltzman absorption solution, were attached in series to one of the ports. A second pair of all-glass fritted bubblers, each containing 5.0 ml of the toluene solution of $Cu(dtc)_2$, was attached to the other sampling port. The split gas stream was passed through both pairs of bubblers at a constant flow-rate of 150 ml/min, obtained by use of a critical orifice. Sampling times were arranged so that the absorbance of the Saltzman solutions was not more than 0.7 (in a 0.5-cm cell). The volume shrinkage caused by the volatility of toluene during the collection of the sample was corrected by addition of more toluene.

*Author to whom correspondence should be addressed.

The absorbance of the Saltzman solutions was measured at 550 nm, 15 min after collection of the sample. Calibration with nitrate solution was used.[4] The absorbance of the $Cu(dtc)_2$ toluene solution was measured at 437 nm before and after collection of the sample, and the difference ΔA was used in the calculations.

Calculations

The concentration of nitrogen dioxide in the sample is calculated as follows:

$$\text{Nitrogen dioxide, mg/m}^3 = 0.092 \times 10^6 \, v \, \Delta A / \varepsilon l V$$

where ΔA is the difference in absorbance at 437 nm of the $Cu(dtc)_2$ solution before and after sampling, v the volume of $Cu(dtc)_2$ solution in the bubbler (ml), ε the molar absorptivity of $Cu(dtc)_2$ at 437 nm (1.30×10^4 $l.mole^{-1}.cm^{-1}$), l the optical path-length (cm), V the volume of air sample, at 25° and 760 mmHg (litres).

RESULTS AND DISCUSSION

$Cu(dtc)_2$ concentration

It was found that the concentration of the $Cu(dtc)_2$ solution in toluene must be at least $1 \times 10^{-4}M$ to provide 2:1 stoichiometry of the reaction, but must not exceed $6 \times 10^{-4}M$ or the initial absorbance of the $Cu(dtc)_2$ solution measured in a 0.1-cm optical cell will be more than 0.7.

Collection efficiency

The collection efficiency experiments were performed to determine the amount of nitrogen dioxide absorbed in a single bubbler in a 15-min sampling period at a flow-rate of 150 ml/min. The experiment was performed over the NO_2 concentration range of 3–160 mg/m³ and with the $Cu(dtc)_2$ concentration in the range $1–6 \times 10^{-4}M$. The nitrogen dioxide not collected in the first bubbler was trapped in the second. Collection efficiencies of 93–99% were found, suggesting that no recovery correction is necessary.

Precision and accuracy

The reproducibility of the method (sampling and analysis) was determined by measuring the amount of NO_2 in 40 samples, over the range 1–500 mg/m³. The mean relative standard deviation was found to be 14%.

The overall accuracy of the sampling procedure and analysis was determined by comparison with the Saltzman method and with the permeation rate of the NO_2 tube used as a standard. The results are shown in Table 1. The absence of a systematic error was proved by a t-test.

Table 1. Determination of nitrogen dioxide

Actual concentration of NO_2, mg/m³	Nitrogen dioxide found		
	Present method		Saltzman method, mg/m³
	Value,* mg/m³	Coefficient of variation, %	
3.5	3.9	14.3	3.2
8.3	8.7	13.5	7.9
12.1	11.5	11.4	12.5
28.2	27.2	7.1	29.0
35.1	33.9	8.2	35.9
88.7	86.9	5.0	—
155.2	159.3	6.2	—

*Average of six determinations.

Sensitivity and analysis range

The method is suitable for the determination of nitrogen dioxide in the range 1–500 mg/m³. It is suitable for monitoring industrial atmospheres (the American and British TLV is 9 mg/m³).

Interferences

Strong oxidizing agents such as ozone and chlorine produce a similar effect. The interferences from NO, SO_2, CO_2, O_2 and air humidity (up to 60%) are negligible.

REFERENCES

1. N. D. Yordanov, B. G. Zhelyazkova and V. Terziev, *Inorg. Chim. Acta*, 1982, **58**, 213.
2. N. D. Yordanov and D. Shopov, *Compt. Rend. Acad. Sci. Bulg.*, 1970, **23**, 1239.
3. G. Brauer, *Handbook of Preparative Inorganic Chemistry*, 2nd Ed., Vol. 1, p. 488. Academic Press, New York, 1963.
4. *NIOSH Manual of Analytical Methods*, 2nd Ed., Method No. P&CAM 108. NIOSH, Ohio, 1977.
5. M. Katz, *Methods of Air Sampling and Analysis*, 2nd Ed. American Public Health Association, Washington, 1977.
6. F. P. Scaringelli, E. Rosenberg and K. A. Rehme, *Environ. Sci. Technol.*, 1970, **4**, 924.

Talanta, Vol. 30, No. 3, pp. 187–189, 1983
Printed in Great Britain.

0039-9140/83/030187-03$03.00/0

USE OF AN IMMOBILIZED GLUCOSE OXIDASE CATION-EXCHANGE RESIN COLUMN IN THE DETERMINATION OF GLUCOSE

NOBUTOSHI KIBA, YASUSHI ISHIDA, MASAKI TSUCHIYA and MOTOHISA FURUSAWA
Department of Chemistry, Faculty of Engineering, Yamanashi University, Takeda, Kofu-shi, 400, Japan

(*Received* 5 *July* 1982. *Accepted* 22 *October* 1982)

Summary—A thermal flow system for glucose determination is described, that utilizes a column of glucose oxidase immobilized on a cation-exchange resin (Amberlite CG50). The response is linear for glucose concentrations in the range 0.01–0.4m*M*. Stability and the factors influencing the response have been examined.

Many studies have been made of the immobilization of enzymes,[1,2] the simplest method of immobilization being adsorption on ion-exchange resins. The adsorption of glucose oxidase (EC 1.1.3.4) on cation-exchange resin (Amberlite CG50)[3] and macroreticular anion-exchange resins (Amberlite IRA938, 910, 93)[4] has been reported. Such immobilized enzymes have not been used in analytical chemistry because, in principle, the adsorption of an enzyme on a surface is a reversible process. Changes in pH and ionic strength could cause the bound enzyme to be desorbed and released into solution. In practice, good adsorption and activity can be maintained if the correct conditions of pH, ionic strength and temperature are chosen.

Enthalpimetric measurements based on immobilized enzymes have provided simple methods for the evaluation of the enzymes and for the determination of substrates and inhibitors.[2,5] There have been many reports on the application of immobilized enzymes and enthalpimetric sensors to glucose determination. Hexokinase,[6,7] glucose oxidase[7,8–13] and glucose oxidase–catalase coupled enzyme systems[14–16] have been used.

The present paper describes the application of glucose oxidase immobilized on cation-exchange resin (Amberlite CG50) in a flow enthalpimetric system for the determination of glucose.

EXPERIMENTAL

Reagents

Glucose oxidase (EC 1.1.3.4) (from *p. amagasakiense*, 102 U/mg) was purchased from Kanto Chemical Co., Japan. The enzyme activity was determined by the titration method.[17] Amberlite CG50 type I (H^+ form, 160–200 mesh) was purchased from Rohm and Haas Co., U.S.A. The buffer used was KH_2PO_4/Na_2HPO_4 (pH 5.8). Stock solution of glucose (0.1*M*) was made by dissolving analytical grade D-glucose (Merck) in the buffer. The solutions were allowed to come to anomeric equilibrium and were then refrigerated. Working solutions were made by appropriate dilution of the stock solution with the buffer before use.

Apparatus

The apparatus included a thermal detector, a pumping system, an injector and a strip-chart recorder. The thermal detector was manufactured by Japan Electron Optics Laboratory Co. Ltd. and has been described by others.[18,19] It consists of two thermistors sealed in glass tubes so that the beads extend into the columns. The reference column is filled with an inert material (glass beads, 20 mesh) and the detection column (bed dimensions: 0.8 cm diameter, 7 cm length) with Amberlite CG50. The thermistors form two arms of a Wheatstone bridge and respond to changes of temperature due to the heat of reaction, the bridge output being indicated on a chart recorder (at maximum sensitivity, full-scale deflection is equivalent to 0.001°). The piston pump (model KHU-52) and the loop injector (model KHP U1-130) were supplied by Kyowa Seimitsu Co.

Enzyme immobilization

A slurry of the resin (*ca.* 2.0 g), in the H^+ form, was poured into the detection column. The phosphate buffer (0.1*M*) was pumped through the column for 20 min at a flow-rate of 0.1 ml/min. A sample of glucose oxidase solution (2 mg/ml) in 0.1*M* buffer was circulated through the column at 25° for 8 hr at a flow-rate of 0.5 ml/min. The column was washed to remove any non-adsorbed enzyme by perfusion with the 0.1*M* buffer for 4 hr at 2.0 ml/min, followed by 0.05*M* buffer (pH 5.8) at 1.0 ml/min. When the enzyme on the column was to be replaced, the column was perfused with 0.1*M* hydrochloric acid for 20 min at a flow-rate of 1.0 ml/min, followed by water for 1 hr at 2 ml/min. Then 0.1*M* buffer was pumped through the column for 2 hr at a flow-rate of 1 ml/min, followed by enzyme solution circulated at 0.5 ml/min. An average activity of 140 ± 10 U/g of resin (10 runs) was obtained reproducibly.

Procedure

The buffer (0.05*M*) was passed through the system at 1.0 ml/min. The sample (2.0 ml) was introduced through the injector. The height of the peak obtained on the recorder was directly proportional to the glucose concentration in the sample.

RESULTS AND DISCUSSION

Choice of ion-exchange resin

It was found recently that the resistance of ion-exchange resins to oxidizing agents such as Cr(VI) is

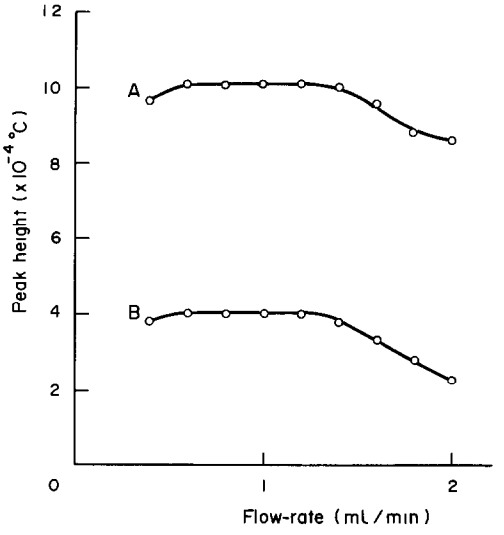

Fig. 1. Effect of flow-rate on temperature change. A $1.00 \times 10^{-4}M$ glucose; B $0.401 \times 10^{-4}M$ glucose. Sample volume 2.0 ml, pH 5.8 in $0.05M$ phosphate, column temperature 35°.

often poor.[20] The resistance to hydrogen peroxide, which is formed in the enzyme reaction, was therefore studied for five ion-exchange resins, *viz.* Amberlite CG50, CG120, CG00, IRA938 and IRA93. The last two were powdered in a mortar and all the resins were sieved to obtain the 160–200 mesh fractions. The resin (0.1 g) was added to 100 ml of $5 \times 10^{-4}M$ hydrogen peroxide solution in phosphate buffer ($0.05M$, pH 5.8) and the mixture was shaken at 30° for 4 hr. The ion-exchange capacities were then measured by the conventional method.[21] It was found that the capacities for CG50, CG120, CG400, IRA938 and IRA93 had decreased by 0.08, 0.08, 1.2, 1.2 and 1.0%, respectively.

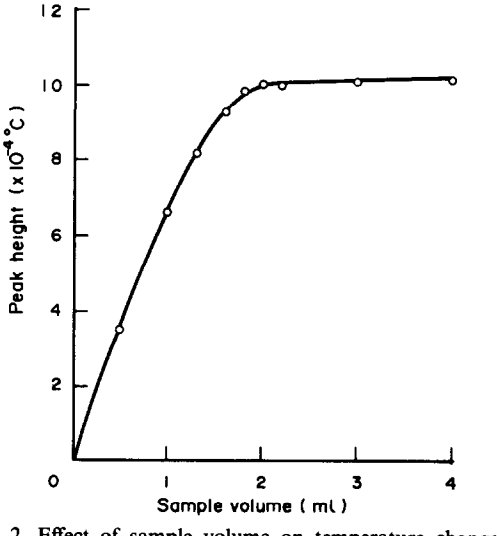

Fig. 2. Effect of sample volume on temperature change. $1.00 \times 10^{-4}M$ glucose, flow-rate 1.0 ml/min, pH 5.8 in $0.05M$ phosphate, column temperature 35°.

Table 1. Determination of glucose

Sample concn., 10^{-4}M	ΔT, 10^{-3} deg	C.V., %* ($n = 5$)
0.100	0.105	0.8
0.200	0.208	0.7
0.401	0.425	0.4
0.802	0.840	0.4
1.00	1.05	0.3
2.00	2.11	0.4
4.01	4.20	0.4

*C.V. = coefficient of variation.

Although an enzyme activity of about 300 units per g of resin was obtained by immobilization on the anion-exchange resins (CG400, IRA938 and IRA93), the activity was not maintained. The activities of the enzyme immobilized on CG50 (weak acid cation-exchanger) and CG120 (strong cation-exchanger) were about 140 and 60 units/g and stable enough for practical use. From these results, CG50 was chosen as the support for the glucose oxidase.

Properties of the immobilized glucose oxidase

The adsorption of the enzyme (2 mg/ml) on CG50 was complete after 3 hr at a flow-rate of 0.5 ml/min but circulation was continued for 8 hr. Immobilized enzyme with a steady activity was obtained by washing the resin with about 450 ml of $0.1M$ phosphate buffer (pH 5.8). The effect of pH on the activity of the immobilized enzyme was examined in phosphate buffer in the pH range 5.4–6.4. The optimum pH was 5.8 but similar activity was exhibited over the entire pH range. The effect of temperature was examined in the range 15–40° and it was found that the activity increased linearly with temperature. Leakage of the enzyme from the resin was not initiated by these changes of pH and temperature. In operation with 2-ml portions of $4 \times 10^{-4}M$ glucose at a flow-rate of 1.0 ml/min (phosphate buffer $0.05M$, pH 5.8), desorption of the enzyme occurred with a decrease in activity at the rate of 2% per 100 runs. When stored at 4° and 25° in buffer solution ($0.05M$) the immobilized en-

Table 2. Determination of glucose in mixtures of sugars

		Present, 10^{-4}M	Found, 10^{-4}M	C.V., % ($n = 5$)
Mixture 1	Glucose	1.00	1.01	0.6
	Fructose	1.14		
	Mannose	1.04		
Mixture 2	Glucose	0.802	0.804	0.6
	Xylose	1.12		
	Galactose	1.03		

Table 3. Analysis of white wines

Sample	Glucose, mM			Certificate value, mM
	n	$\bar{x}$	C.V.,%	
A	6	1.29	1.1	1.3
B	5	0.67	1.8	0.6

zyme was stable for at least 12 and 3 months, respectively.

Properties of the glucose oxidase reactor

The peak-height was independent of the pH of the buffer in the range 5.4–6.4. The dependence of peak-height on flow-rate was studied over the range 0.4–2.0 ml/min with a sample volume of 2.0 ml. The results are shown in Fig. 1. The peak-height was constant between flow-rates of 0.6 and 1.2 ml/min, but decreased rapidly at rates above 1.4 ml/min. Fall-off in peak-height was observed at flow-rates below 0.4 ml/min. Glucose is thus instantly converted into gluconic acid at flow-rates below 1.2 ml/min. Figure 2 shows that the peak-height is almost independent of sample volume in the range 2.0–4.0 ml. Even a 4-ml sample did not give a saturation signal, but the larger samples gave an increase in peak-width and a decrease in sample throughput. A flow-rate of 1.0 ml/min and a sample volume of 2.0 ml were therefore chosen.

The detection limit under these conditions was $1 \times 10^{-5}M$ glucose (for a 2-cm peak-height). A throughput of 15 samples per hr was possible without overlap of peaks. No decrease in peak-height was observed during the course of 500 runs with $4 \times 10^{-4}M$ glucose. Good linearity between peak-height and glucose concentration was obtained in the range 1×10^{-5}–$4 \times 10^{-4}M$. Table 1 summarizes the results obtained with solutions of known concentration, and those obtained in the presence of other sugars are given in Table 2. The method was also applied to the determination of glucose in white wine. The sample (5 ml) was boiled for 1 min in a tall beaker (30 ml), transferred to a 50-ml standard flask and made up to volume with $0.05M$ buffer. An aliquot (2 ml) was analysed by the procedure described. The results (Table 3) are in agreement with the certified values.

Acknowledgements—This work was partially supported by a Grant-in-Aid for Scientific Research from the Ministry of Education, Science and Culture, to which the authors' thanks are due.

REFERENCES

1. O. R. Zaborsky, *Immobilized Enzymes*, CRC Press, Ohio, 1974.
2. P. W. Carr and L. D. Bowers, *Immobilized Enzymes in Analytical and Clinical Chemistry*. Wiley, New York, 1980.
3. K. Miyamoto, T. Fujii and Miura, *J. Ferment. Technol.*, 1971, **49**, 565.
4. H. E. Klei, D. W. Sundstrom and R. Gargano, *Biotechnol. Bioeng.*, 1978, **20**, 611.
5. K. Mosbach and B. Danielsson, *Anal. Chem.*, 1981, **53**, 83A.
6. L. D. Bowers and P. W. Carr, *Clin. Chem.*, 1976, **22**, 1427.
7. J. C. Weaver, C. L. Cooney, S. P. Fulton, P. Schuler and S. R. Tannenbaum, *Biochim. Biophys. Acta*, 1976, **452**, 285.
8. A. Johansson, *Protides Biol. Fluids, Proc. Colloq.*, 1973, **20**, 567.
9. B. Mattiasson and C. Borrebaeck, *FEBS Lett.*, 1978, **85**, 119.
10. B. Mattiasson, *ibid.*, 1977, **77**, 107.
11. C. Tran-Mink and D. Vallin, *Anal. Chem.*, 1978, **50**, 1874.
12. B. Mattiasson, B. Danielsson and K. Mosbach, *Anal. Lett.*, 1976, **9**, 867.
13. K. Mosbach, B. Danielsson, A. Borgerud and M. Scott, *Biochim. Biophys. Acta*, 1975, **403**, 256.
14. B. Danielsson, K. Gadd, B. Mattiasson and K. Mosbach, *Clin. Chim. Acta*, 1977, **81**, 163.
15. B. Mattiasson, B. Danielsson and K. Mosbach, *Anal. Lett.*, 1976, **9**, 217.
16. H.-L. Schmidt, G. Krisan and G. Grenner, *Biochim. Biophys. Acta*, 1976, **429**, 283.
17. L. A. Underkofler, *Soc. Chem. Ind. Monograph*, No. 11, p. 72. Macmillan, New York, 1961.
18. K. Nagasawa, *J. Assoc. Off. Anal. Chem.*, 1968, **51**, 333.
19. N. Yoza, T. Ogata, Y. Ueno and S. Ohashi, *J. Chromatog.*, 1971, **61**, 295.
20. N. Ayuzawa, T. Suzuki and Y. Hayakawa, *Denki Kagaku*, 1981, **49**, 521.

Talanta, Vol 30, No. 3, pp. 190 to 192
Printed in Great Britain

0039-9140/83/030190-03$03.00/0
Pergamon Press Ltd

SPECTROPHOTOMETRIC DETERMINATION OF SILVER WITH CADION 2B AND TRITON X-100

WEI FU-SHENG and YIN FANG
Department of Chemistry, China University of Science & Technology, Hefei, China

(*Received* 3 *February* 1982. *Revised* 1 *June* 1982. *Accepted* 18 *October* 1982)

Summary—A highly sensitive and selective procedure for spectrophotometric determination of silver has been developed. At pH 9.2, in the presence of Triton X-100, silver forms a dark red-violet complex with cadion 2B which has an absorption maximum at 565 nm. The molar absorptivity is 1.0×10^5 $l.mole^{-1}.cm^{-1}$. Beer's law is obeyed for silver in the range 0.02–0.8 μg/ml. The colour reaction, if EDTA is used as a masking agent, is free from interference by the 20 cations and 19 anions investigated. Only Cl^-, Br^-, I^-, S^{2-} and CN^- interfere and must be absent. This method has been used to determine silver in waste-water.

Cadion 4′-(*p*-nitrophenyltriazeno)azobenzene and cadion 2B 4′-(4-nitronaphthyltriazeno)azobenzene have been used as spectrophotometric reagents for determination of cadmium, mercury and palladium.[1-3] The addition of the non-ionic surfactant Triton X-100 has been reported to increase the sensitivity for cadmium and mercury.[4-6] In our laboratory, extraction followed by spectrophotometry has been exploited for determination of silver, cadmium and nickel by means of the metal ion–1,10-phenanthroline–cadion ternary complexes.[7-9]

Cadion 2B has not been used as a spectrophotometric reagent for silver, but we have observed that it gives a sensitive colour reaction with silver in the presence of Triton X-100. This paper describes application of this reaction in a procedure for spectrophotometric determination of silver in waste-water.

EXPERIMENTAL

Reagents

Standard silver solution. Dissolve 0.1580 g of silver nitrate in distilled water, add one drop of concentrated nitric acid and dilute to volume in a 100-ml standard flask with distilled water. This solution contains 1.00 mg of silver per ml. Prepare a 10-μg/ml silver solution as a working standard.

Cadion 2B solution. Dissolve 0.040 g of the reagent in 100 ml of ethanol.

Triton X-100, 5% aqueous solution.

Sodium borate buffer, 5% solution (pH 9.2)

General procedure

Transfer a sample containing not more than 20 μg of silver into a 25-ml standard flask. Add, in the following order, 0.5 ml of 0.05*M* EDTA, 2 ml of sodium borate buffer, 1 ml of Triton X-100 solution and 1.5 ml of cadion 2B solution. Dilute to the mark with distilled water and mix well. Measure the absorbance at 565 nm in a 1-cm cell, using a reagent blank as reference.

Determination of silver in waste-water

To 50 ml of water sample, add 2 ml of concentrated nitric acid and 5 drops of sulphuric acid, and evaporate almost to dryness. Add 2 ml of concentrated nitric acid and evaporate again. Cool to room temperature, add distilled water to dissolve the residue, and make up to exactly 50 ml. Pipette an aliquot of this solution into a 25-ml standard flask and continue according to the procedure above.

RESULTS AND DISCUSSION

Absorption spectra

The absorption spectra of cadion 2B and its silver complex in the present of Triton X-100 at pH 9.2 are shown in Fig. 1. The absorbance maximum of the reagent is at 445 nm, and that of the dark red-violet complex at 565 nm.

Effect of Triton X-100 concentration

Cadion 2B is only slightly soluble in pH 9.2 aqueous medium and does not form an intensely coloured silver complex. However, if more than 0.5 ml of 5% Triton X-100 solution is added per 25 ml of solution,

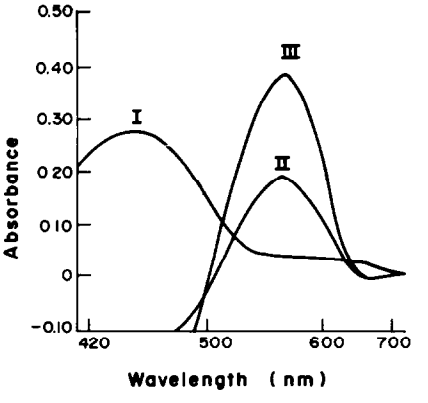

Fig. 1. Absorption spectra of cadion 2B and its silver complex (in presence of Triton X-100)
I—Cadion 2B, $8 \times 10^{-6}M$, against water (1-cm cell).
II—Silver 5 μg and 0.04% cadion 2B (1.0 ml), against reagent blank.
III—Silver 10 μg and 0.04% cadion 2B (1.0 ml), against reagent blank.

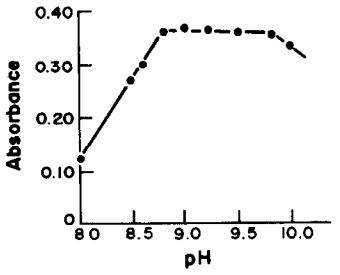

Fig. 2. Effect of pH. Absorbance of complex measured against corresponding reagent blank.

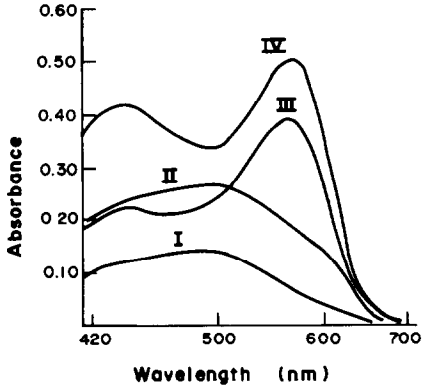

Fig. 3. Absorption spectra of the silver complex
I—$[Ag^+] = [L] = 8.0 \times 10^{-6} M$.
II—$[Ag^+] = 8.0 \times 10^{-6} M$, $[L] = 1.6 \times 10^{-5} M$.
III—$[Ag^+] = 4.0 \times 10^{-6} M$, $[L] = 1.6 \times 10^{-5} M$.
IV—$[Ag^+] = 4.0 \times 10^{-6} M$, $[L] = 2.4 \times 10^{-5} M$.
All measurements in 1-cm cells, against water.

a dark red-violet complex is formed within 1 min, and the coloured solution is stable at least for 24 hr. Addition of 1 ml of Triton X-100 solution is recommended.

Effect of cadion 2B concentration

The absorbance for 10 μg of silver at pH 9.2 in the presence of Triton X-100 and increasing amounts of cadion 2B is constant for use of 0.75–3.0 ml of the 0.04% reagent solution. Hence, 1.5 ml of the reagent is recommended.

Effect of pH

The absorbance, as shown in Fig. 2, is maximal and constant in the pH range 8.8–9.8 (borate buffers). A pH of 9.2 is therefore used in the procedure.

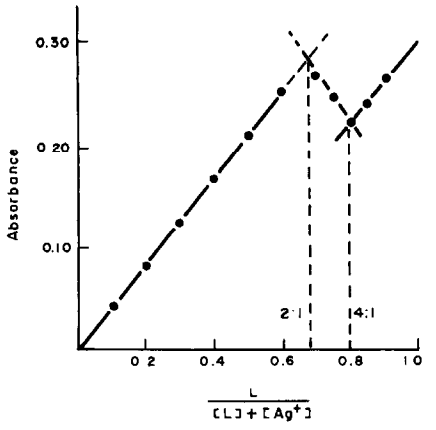

Fig. 4. Job's method
$[Ag^+] + [L] = 1.6 \times 10^{-5} M$. Measured at 500 nm in a 1-cm cell, against water.

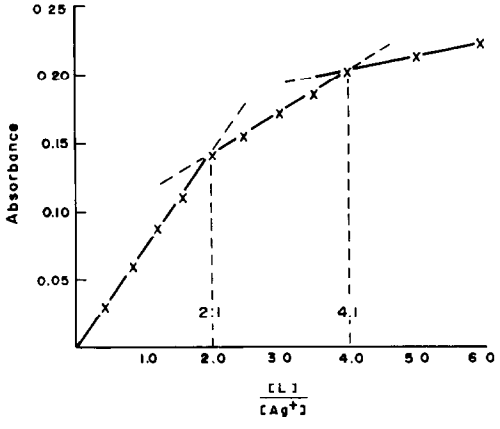

Fig. 5. Mole-ratio method; $[Ag^+] = 4.0 \times 10^{-6} M$. Measured at 500 nm in a 1-cm cell against water.

Beer's law

The absorbance is a linear function of silver concentration from 0.02 to 0.8 μg/ml. The molar absorptivity at 565 nm is 1.0×10^5 l.mole^{-1}.cm^{-1}.

Effect of foreign ions

In the determination of 10 μg of silver, the following ions (amounts given in milligrams) do not interfere: Li^+ (1.0), Na^+ (100), K^+ (10), NH_4^+ (10), Be^{2+} (0.1), Mg^{2+} (10), Ca^{2+} (1.0), Cr^{6+} (0.1), $B_4O_7^{2-}$ (100),

Table 1. Determination of silver in waste-water

Sample No.	Taken, *ml*	Ag found, μg	Ag added, μg	Recovery, %
1	1.0	8.6 8.9 8.6 8.3		
	1.0		5.0	93
2	5.0	6.7 6.5 6.7		
	5.0		10.0	99
3	10.0	4.6 4.7 4.4		
	10.0		5.0	102
	10.0		10.0	98
4	5.0	6.8 7.2 7.2 7.1 7.1 6.9		
	5.0		10.0	96

Table 2. Sensitivities of various methods for spectrophotometric determination of silver

Reagent	λ, nm	ε, $l.mole^{-1}.cm^{-1}$	Reference
Dithizone	462	3.05×10^4	10
p-Dimethylaminobenzylidenerhodanine	450	2.0×10^4	10
Bromopyrogallol Red/phenanthroline	635	5.1×10^4	11
Bromopyrogallol Red/phenanthroline/ nitrobenzene	590	3.2×10^4	12
2,4,5,7-Tetrabromofluoresceine/phenanthroline	550	3.5×10	13
1-(2-Pyridylazo)-2-naphthol/C_6H_6/isoBuOH	540	2.14×10^4	14
4-(2-Pyridylazo)/resorcinol	510	2.0×10^4	15
Thiodibenzoylmethane/benzene	420	1.07×10^4	16
4-Hydroxybenzalrhodanine	490	1.47×10^4	17
Ethyl Violet/Br^-/toluene	615	1.03×10^5	18
Cadion/phenanthroline/chloroform	525	5.7×10^4	7
Cadion 2B/Triton X-100	565	1.0×10^5	present method

EDTA (15), NO_3^- (10), SO_4^{2-} (10), PO_4^{3-} (10), PO_3^- (100), As^{3+} (1.0), WO_4^{2-} (1.0), MoO_4^{2-} (1.0), SeO_3^{2-} (0.1), TeO_3^{2-} (0.1), VO_3^- (0.1), BrO_3^- (1.0), IO_3^- (1.0), ClO_3^- (1.0), $S_2O_8^{2-}$ (1.0) and citrate (10).

To prevent hydrolysis or the colour reaction of the reagent with other heavy metal ions, EDTA is used as masking agent. If 0.5 ml of 0.05*M* EDTA is added before the cadion 2B, at least 1.0 mg each of Cd^{2+}, Cu^{2+}, Ni^{2+}, Pb^{2+}, Zn^{2+}, Mn^{2+}, La^{3+}, Fe^{2+}, Fe^{3+} and 0.1 mg each of Co^{2+}, Cr^{3+}, Al^{3+}, Y^{3+}, Hg^{2+}, Pd^{2+} will not interfere. However, 10 μg of Cl^-, Br^-, I^-, S^{2-} or CN^- will cause negative interference, but the effect can easily be overcome by adding nitric acid and boiling to evaporate almost to dryness.

Composition of the complex

In the complexation reaction system, when the molar ratio of the reagent to silver is less than 4, an orange complex is formed, but when the ratio is more than 4, a dark red-violet complex is formed. The absorption spectra for some different M:L (metal:ligand) ratios are shown in Fig. 3. A Job plot (at 500 nm) shows two break-points (Fig. 4) corresponding to an ML_2 and an ML_4 complex. A mole-ratio plot also indicates the existence of the two complexes (Fig. 5). Therefore, a sufficient excess of reagent must be used to favour the formation of the ML_4 complex.

Application to waste-water

The results for four waste-water samples are given in Table 1. The recovery of added silver is in the range 93.1–102.4%. The coefficient of variation for sample No. 4 is about 2% (six determinations).

Comparison with other reagents

Cadion 2B in the presence of Triton X-100 is one of the most sensitive reagents available for silver. The complex formed is very stable and has good selectivity. The present method is simple, rapid and accurate. The sensitivities of various reagents for silver are listed in Table 2 for comparison.

REFERENCES

1. P. Chavenne and Cl. Geronimi, *Anal. Chim. Acta*, 1958, **19**, 377.
2. G. R. Popa, A. F. Dănet and M. Popescu, *Talanta*, 1978, **25**, 546.
3. G. R. Popa and A. F. Danet, *Chim. Anal. (Bucharest)*, 1971, **1**, 86.
4. H. Watanabe and H. Ohmori, *Talanta*, 1979, **26**, 959.
5. Hsu Chung-gin, Hu Chao-sheng and Jing Ji-hong, *ibid.*, 1980, **27**, 676.
6. Hong Shui-jei and Wu Shui-shen, *J. Environ. Sci.*, 1981, **2**, No. 3, 20.
7. Shen Nai-kui, Qi Qi-ping and Wei Fu-sheng, to be published.
8. Shen Nai-kui, Wei Fu-sheng and Qi Qi-ping, *Anal. Lett.*, 1981, **14**, 20.
9. *Idem*, to be published.
10. Z. Marczenko, *Spectrophotometric Determination of Elements*, pp. 491–494. Horwood, Chichester, 1976.
11. R. M. Dagnall and T. S. West, *Talanta*, 1964, **11**, 1533.
12. *Idem, ibid.*, 1964, **11**, 1927.
13. M. T. El-Ghamry and W. F. Roland, *Anal. Chem.*, 1968, **40**, 1986.
14. M. C. Eshuar and B. Subrahmanyam, *Zh. Analit. Khim.*, 1976, **31**, 2319.
15. *Idem, Z. Anal. Chem.*, 1974, **272**, 44.
16. R. R. Mulye and S. M. Khopkar, *Anal. Chim. Acta*, 1975, **76**, 204.
17. T. Yoshimasa, Y. Saito, J. Odo and H. Omori, *Bunseki Kagaku*, 1980, **29**, 381.
18. N. L. Shestideyatnaya, L. I. Kotelyanskaya and I. A. Chuchulina, *Zh. Analit. Khim.*, 1975, **30**, 1303.

Talanta, Vol. 30, No 3, pp. 193–196, 1983
Printed in Great Britain.

0039-9140/83/030193-04$03.00/0

ANALYTICAL DATA

OXYDATION VANADIQUE DE LA *para*CHLOROBENZYL-4 DIMETHOXY-6,7 ISOQUINOLEINE EN MILIEU SULFURIQUE 5*M*

E. POSTAIRE, M. TSITINI-TSAMIS, M. HAMON
Laboratoire de Chimie Analytique II

et

C. VIEL

Laboratoire de Pharmacie Chimique II, ERA 317 du CNRS
Faculté des Sciences Pharmaceutiques et Biologiques de Paris-Sud, 3, rue J. B. Clément, 92290 Chatenay Malabry, France

(*Reçu le* 4 *mars* 1982. *Accepté le* 25 *Août* 1982)

Résumé—L'oxydation vanadique de diméthoxy-6,7 isoquinoléines substituées en 1 a montré le rôle essentiel que jouent les carbones situés en α d'un hétéroatome. La *para*chlorobenzyl-4 diméthoxy-6,7 isoquinoléine libre de tout substituant en ces positions, est ainsi sujette à une oxydation beaucoup plus poussée par le pentoxyde de vanadium en milieu sulfurique 5*M*. En effet, la consommation molaire en ions vanadyle est, dans ce cas, nettement supérieure à celle trouvée lors de l'oxydation des isoquinoléines substituées en 1. De plus, dans le milieu réactionnel ont été isolés des produits tels que l'acide succinique et le dioxyde de carbone, témoins d'une oxydation profonde de la molécule.

L'étude de l'action du pentoxyde de vanadium sur divers dérivés de l'isoquinoléine a montré le caractère particulier de cet oxydant. Ainsi ont été oxydées un certain nombre de dihydro-3,4 isoquinoléines pharmacologiquement actives, portant en position 1 des groupements phényle, benzyle et éventuellement des méthoxyles en 6 et 7,[1–3] ainsi que la papavéraldine.[4] Les résultats obtenus ont conduit à émettre l'hypothèse que seuls les atomes de carbone situés au voisinage immédiat d'un hétéroatome (oxygène carbonylé) pouvaient subir une oxydation. Pour confirmer cette hypothèse, nous avons oxydé la *para*chlorobenzyl-4 diméthoxy-6,7 isoquinoléine (**1**), une molécule à activité papavérinique,[5–9] caractérisée par la présence d'un groupe benzyle en position 4 et non plus en position 1 (Schéma 1).

PARTIE EXPERIMENTALE

Réactif

La solution sulfovanadique 0,1*M*,[10] a une concentration finale en acide sulfurique voisine de 0,72*M*, et est étalonnée par titrage avec une solution de sulfate de fer et d'ammonium.

Mode opératoire d'oxydation

Dans une fiole jaugée de 50 ml sont introduits 50 à 100 μmole de l'isoquinoléine **1**, 30 ml de la solution sulfovanadique, 16 ml d'acide sulfurique, 13*M*, et le volume est complété à 50 ml avec l'acide sulfurique 5*M*.

Le contenu de la fiole jaugée est transvasé dans un erlenmeyer surmonté d'un réfrigérant, puis placé dans un bain-marie à 100°. La cinétique de la réaction est suivie par dosage du pentoxyde de vanadium. Pour cela, une partie aliquote du mélange réactionnel est prélevée à temps déterminés jusqu'à oxydation complète de la molécule (Fig. 1), et l'excès de V_2O_5 est déterminé par titrage potentiométrique avec du fer(II) (électrodes platine–calomel).

Dosage du dioxyde de carbone

Les gaz libérés après réaction pendant 24 hr à 100° sont recueillis et analysés sur la cuve à mercure selon la technique de Chaigneau.[11] Le dioxyde de carbone est dosé à l'aide d'une solution concentrée d'hydroxyde de potassium; les autres gaz dégagés sont déterminés par spectrométrie de masse après élimination du dioxyde de carbone.

Isolement et dosage du formaldéhyde

Le formaldéhyde est isolé par entrainement à la vapeur d'eau dans un appareil de Parnas et Wagner, puis identifié et dosé par la réaction de Hantzsch (formation de dihydrolutidine), selon la méthode de Nash.[12] Cette réaction colorée est très spécifique du formaldéhyde. Nous l'avons utilisée du fait de la présence de *para*chlorobenzaldéhyde dans le milieu réactionnel, la méthode par formation d'une dinitrophénylhydrazone[13] dosant globalement ces deux aldéhydes.

Identification de l'acide et de l'aldéhyde para*chlorobenzoïques*

Après extraction éthérée du milieu réactionnel, ces deux composés ont été détectés et identifiés par chromatographie en phase gazeuse couplée à la spectrométrie de masse.

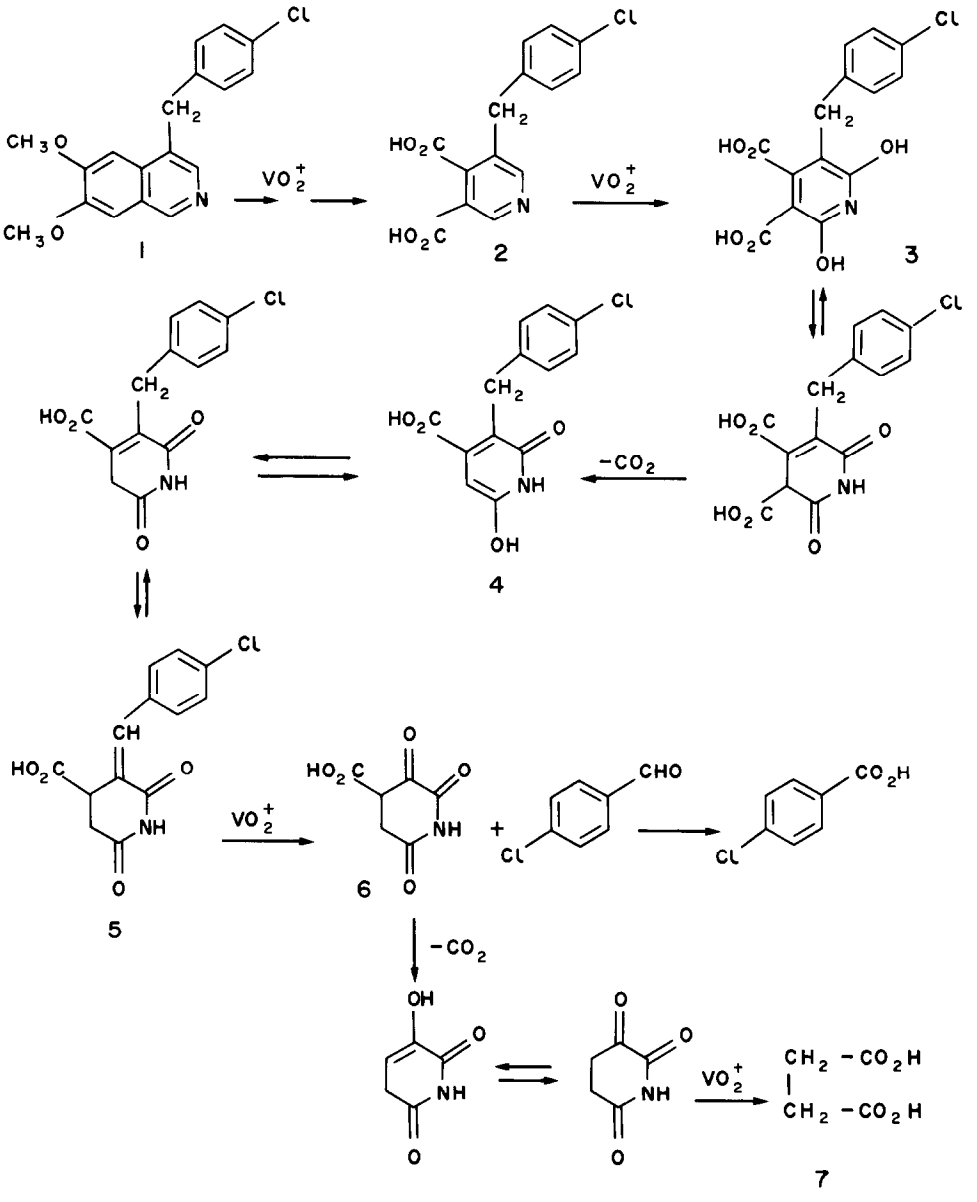

Schéma 1

Identification de l'acide succinique

Après 24 hr d'oxydation puis refroidissement, une partie aliquote de la solution réactionnelle est déposée sur plaque chromatographique de gel de silice GF 254 (solvant de migration: CH_3OH–NH_4OH–H_2O, 100:16:12 v/v). Après développement, la tache de R_f nul est récupérée et éluée avec du méthanol. Après évaporation du solvant sous azote le spectre infrarouge du résidu est enregistré en pastille de bromure de potassium.

Préparation du complexe acide succinique–pentoxyde de vanadium

A 100 ml d'eau bouillante, 10 mmoles d'acide succinique et 10 mmoles de pentoxyde de vanadium sont ajoutés. Le mélange est abandonné 1 hr au bain-marie bouillant puis 24 hr à l'obscurité et sous azote (afin d'éviter la formation du complexe carbovanadique). Le complexe formé a été isolé par chromatographie couche mince selon la méthode décrite au paragraphe précédent.

RESULTATS ET DISCUSSION

L'étude expérimentale a comporté un certain nombre de points qui nous ont permis de proposer un schéma reactionnel pour l'oxydation de la benzyl-4 isoquinoléine étudiée. Outre la détermination de la quantité de réactif oxydant consommé, les points essentiels sont l'identification et le dosage éventuel des substances formées, soit lors d'une phase intermédiaire, soit en fin de réaction.

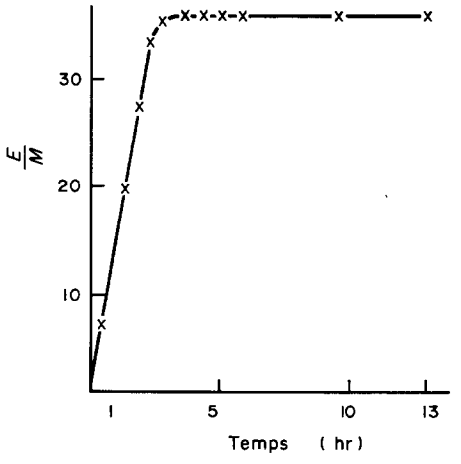

Fig. 1. Cinétique de l'oxydation de la *para*chlorobenzyl-4 diméthoxy-6,7 isoquinoléine (0,6 μM/ml), à 100°C en milieu acide sulfurique 5*M* (E/M = équivalents de V_2O_5 par mole de substance de départ).

Pour l'oxydation complète (3 hr), 35,5 moles d'oxydant par mole de produit de départ sont nécessaires.

La comparaison avec les résultats obtenus[3] lors de l'oxydation de la benzyl-1 dihydro-3,4 diméthoxy-6,7 isoquinoléine en milieu acide sulfurique 5*M* (consommation de 25,5 moles de réactif par mole de substance de départ) conduit à la conclusion que l'oxydation est ici beaucoup plus poussée.

La cinétique d'apparition du formaldéhyde montre que l'attaque initiale de l'oxydant s'effectue au niveau des groupements méthoxylés comme cela est toujours le cas lors de l'oxydation en milieu sulfurique 5*M*. L'apparition et la disparition du formaldéhyde sont plus rapides avec une isoquinoléine benzylée en 4 qu'avec une benzyl-1 isoquinoléine.[3]

Lors de l'oxydation, 7 molécules de dioxyde de carbone sont formées par molécule d'isoquinoléine. L'ouverture de l'homocycle isoquinoléique conduit à la formation de quatre molécules de CO_2,[2,3] les trois autres provenant d'une dégradation plus poussée de la molécule.

La mise en évidence de l'aldéhyde et de l'acide *para*-chlorobenzoïque implique une coupure oxydative au niveau du carbone benzylique de la benzyl-4 isoquinoléine étudiée, ce type de coupure ayant déjà été observé lors de l'oxydation de la benzyl-1 dihydro-3,4 diméthoxy-6,7 isoquinoléine dans les mêmes conditions.[3]

Des produits d'oxydation de la benzyl-4 isoquinoléine étudiée, nous avons isolé par chromatographie un composé organométallique dont le spectre infrarouge présente une large bande centrée sur 3400 cm^{-1} qui indique la présence d'un groupement hydroxyle. Quatre autres bandes sont également présentes, à 1590, 1400, 1340 et 1100 cm^{-1}. Par suite de la conservation du squelette benzylique de la molécule et du nombre de molécules de dioxyde de carbone formées au cours de la réaction, nous avons envisagé la formation d'acide succinique qui, selon Kharsan *et al.*[14] donne un complexe vanadique que nous avons obtenu. Le spectre du complexe et celui du produit isolé précédemment sont identiques. Nous avons noté la forte analogie entre le spectre du succinate de sodium et celui du complexe. Ce résultat conduit à penser que la formation du complexe met en jeu des liaisons ioniques faisant intervenir des fonctions carboxylates. La bande la plus caractéristique du spectre du complexe se situe à 1590 cm^{-1}. Ainsi, il est exclu que cette bande corresponde au CO d'un carboxyle ou d'un carboxylate libre. Ces bandes se situent respectivement à 1700 et 1660 cm^{-1} pour l'acide succinique et son sel de sodium.

Il existe néanmoins un déplacement de 60 cm^{-1} vers les faibles nombres d'onde entre le succinate et le complexe isolé. Cette différence peut s'expliquer par la diminution de la force de rappel du carboxylate lorsqu'il participe à une liaison avec le vanadium.[15]

La recherche d'ions chlorure s'est avérée négative. En outre, l'analyse des gaz n'a montré aucune trace de chlore gazeux.

Proposition d'un mécanisme réactionnel

Les résultats conduisent à envisager une attaque initiale par l'ion vanadyle de l'un des deux hétéroatomes: azote en 2 ou oxygène des méthoxyles en 6 et 7. Cependant, en milieu très acide le doublet électronique de l'azote est l'objet d'une compétition entre la protonation et la complexation avec l'ion vanadyle, avec oxydation ultérieure. Ceci favorise l'attaque de l'oxydant au niveau de l'un des atomes d'oxygène. L'attaque initiale porte probablement sur le méthoxyle en 7 car le doublet électronique de l'oxygène y est moins conjugué que dans le groupement méthoxyle en 6. La formation de radicaux méthyle est confirmée par l'analyse des gaz formés lors de la réaction, parmi lesquels ont été isolées des traces de méthane. Ces radicaux méthyle peuvent être oxydés en formaldéhyde puis en dioxyde de carbone.

La formation de deux moles de formaldéhyde montre que l'attaque de l'hétérocycle se poursuit au niveau du deuxième groupement méthoxyle pour donner probablement une *ortho*quinone qui, à son tour, s'oxyde et conduit à un diacide. Cependant, il n'a pas été possible de mettre en évidence l'acide pyridine dicarboxylique substitué (**2**).

Ainsi est-il plausible de supposer que la molécule initiale subit, simultanément ou non, une attaque au niveau de l'azote. Dans le cas où l'oxydation porterait simultanément sur les différents hétéroatomes, elle devrait avoir lieu sur les atomes de carbone 1 et 3 en α de l'azote.

La formation d'acide succinique conduit à émettre l'hypothèse de mécanisme suivant: l'absence d'hydrogène sur le carbone 4 empêche toute nouvelle oxydation à ce niveau. Il en résulte qu'un produit d'oxydation tel que l'acide dihydroxy-2,6 *para*chlorobenzyl-3 pyridine dicarboxylique-4,5 (**3**) peut se former intermédiairement par oxydation de l'acide pyridine dicarboxylique (**2**). A partir de l'acide **3**, la formation

d'acide succinique peut raisonnablement se concevoir en faisant intervenir une série de décarboxylations et d'oxydations (schéma 1). Dans le mécanisme réactionnel proposé, on peut donc envisager la formation intermédiaire d'un γ céto acide (**5**) porteur en β d'un groupement benzylidénique, cet acide résultant de la transposition de l'acide benzylique correspondant (**4**). A l'appui de cette proposition, on trouve mentionné dans la littérature que l'acide phényl-4 butène-2 oïque n'est pas stable et se transpose rapidement en acide phényl-4 butène-3 oïque.[16]

La coupure de la liaison éthylénique du groupement benzylidénique de l'acide **5** entraîne d'une part la formation d'aldéhyde puis d'acide *para*chlorobenzoïque et d'autre part, d'un groupement cétonique en β de la fonction carboxylique restant; il y a donc à nouveau décarboxylation de l'acide **6** ainsi formé puis rupture oxydative du cycle avec formation de l'acide succinique **7**, isolé non à l'état libre, mais sous forme de complexe vanadique. La consommation totale théorique en pentoxyde de vanadium est de 36 moles par mole d'isoquinoléine **1**. En fait, il s'agit de $36 + x$ ($0 \leqslant x \leqslant 2$) moles par mole de produit, où x correspond au pourcentage d'aldéhyde *para*chlorobenzoïque oxydé en acide *para*chlorobenzoïque, multiplié par 2. La valeur de x déterminée par un dosage protométrique de l'acide *para*chlorobenzoïque en milieu non aqueux est de 1,6. Comme nos résultats nous donnent une consommation en oxydant de 35,5 moles par mole de substance, nous pouvons signaler que l'oxydation n'a pas lieu à 100%, et donc qu'il reste des traces du produit de départ non oxydé.

CONCLUSION

La comparaison des résultats de l'oxydation de la *para*chlorobenzyl-4 diméthoxy-6,7 isoquinoléine (**1**) et de la benzyl-1 dihydro-3,4 diméthoxy-6,7 isoquinoléine[3] en milieu sulfurique 5*M* est particulièrement intéressante.

L'oxydation de **1** est beaucoup plus poussée que celle de la benzyl-1 dihydro-3,4 diméthoxy-6,7 isoquinoléine car on ne trouve pas d'acide pyridinedicarboxylique mais des composés témoignant d'une oxydation plus intense de la molécule, tel que l'acide succinique. Ceci est dû certainement à la position du groupe benzylique en 4 car le chlore ne semble jouer qu'un rôle mineur, favorisant peut être l'oxydation du CH_2 benzylique mais n'étant pas à l'origine de la formation d'acide succinique.

Nos résultats confirment donc le mécanisme déjà étudié de l'oxydation des isoquinoléines par le pentoxyde de vanadium et permet d'établir un nouveau mécanisme résultant de la destruction du noyau pyridinique.

Ils permettent d'espérer la mise au point de méthodes de dosage de ce type de produits à activité papavérinique.

LITTERATURE

1. M. Tsitini-Tsamis, M. J. Waechter, M. Chaigneau et M. Hamon, *Analusis*, 1979, **7**, 42.
2. M. Tsitini-Tsamis, M. Chaigneau, J. Likforman et M. Hamon, *ibid.*, 1980, **8**, 428.
3. M. Tsitini-Tsamis, M. J., Waechter, J. Likforman, J. P. Delcroix et M. Hamon, *ibid.*, 1981, **9**, 283.
4. M. Tsitini-Tsamis, Thèse de Doctorat, Université de Paris-Sud, 1980.
5. E. Prudhommeaux, Thèse de Doctorat, Université de Paris, 1973.
6. E. Prudhommeaux, C. Viel et B. Delbarre, *Chim. Thér.*, 1971, **6**, 358.
7. P. Bouvier, B. Marçot, C. Viel, B. Delbarre et G. Dumas, *ibid.*, 1971, **6**, 462.
8. P. Bouvier, D. Brancen, M. Prouteau, E. Prudhommeaux et C. Viel, *Eur. J. Med. Chem.*, 1976, **11**, 271.
9. P. Lejay, C. Viel et G. Uchida-Ernouf, *Il Farmaco, Ed. Sci.*, 1977, **32**, 3.
10. M. J. Waechter, J. Likforman et M. Hamon, *Analusis*, 1977, **5**, 34.
11. M. Chaigneau, *Bull. Soc. Chim. France*, 1970, 4133.
12. T. Nash, *Biochem. J.*, 1953, **55**, 416.
13. M. Pesez et J. Bartos, *Colorimetric and Fluorimetric Analysis of Organic Compounds and Drugs*. p. 258. Dekker, New York, 1974.
14. R. S. Kharsan, K. S. Patel, K. K. Deb et R. K. Mishra, *Microchim. Acta*, 1979 **2**, 53.
15. K. Nakamato et P. J. McCarthy, *Spectroscopy and Structure of Metal Chelate Compounds*, p. 269. Wiley, New York, 1968.
16. R. Truchet, *Traité de chimie organique*, V. Grignard, G. Dupont et R. Locquin (eds.), Vol. IX, p. 659. Masson, Paris, 1939.

Summary—The oxidation, by vanadium pentoxide, of 1-substituted 6,7-dimethoxyisoquinolines has shown the essential part played by the carbon atoms located α to a hetero-atom. Thus 4-(*p*-chlorobenzyl)-6,7-dimethoxyisoquinoline is more readily oxidized by vanadium pentoxide in presence of 5*M* sulphuric acid than 1-benzyl-6,7-dimethoxyisoquinoline. Carbon dioxide and succinic acid have been identified amongst the oxidation products, and indicate more extensive oxidation of the molecule.

Talanta, Vol. 30, No 3, pp 197–200, 1983
Printed in Great Britain

0039-9140/83/030197-04$03.00/0

DETERMINATION OF THE DISSOCIATION CONSTANTS OF OXALIC ACID AND THE ULTRAVIOLET SPECTRA OF THE OXALATE SPECIES IN 3*M* PERCHLORATE MEDIUM

J. J. CRUYWAGEN and J. B. B. HEYNS
Department of Chemistry, University of Stellenbosch, Stellenbosch 7600, Republic of South Africa

(*Received* 4 *June* 1982. *Accepted* 16 *August* 1982)

Summary—The dissociation constants for oxalic acid in 3.0*M* sodium perchlorate medium at 25.0° have been determined by potentiometric and spectrophotometric titrations. The values for the concentration constants are $K_{a1} = (5.32 \pm 0.15) \times 10^{-2}$ and $K_{a2} = (1.53 \pm 0.02) \times 10^{-4}$. The absorption spectra for the individual oxalate species are reported.

As part of a systematic study of the solution chemistry of molybdenum,[1] the formation of complexes between oxalate and molybdenum(VI) is currently being investigated by potentiometric and spectrophotometric methods. For the interpretation of our results accurate values for the dissociation constants of oxalic acid at 25° in 3.0*M* sodium perchlorate as well as information about the ultraviolet spectra of oxalic acid and its ions are necessary.

Although values for these dissociation constants are known for various ionic media and at different temperatures,[2,3] only one set of values pertaining to 3.0*M* sodium perchlorate at 25° has been reported in the literature.[4] Since these values were based on a very limited number of pH measurements it was felt that they could not be used without further verification. Further, the ultraviolet spectra of oxalic acid and its ions in the wavelength range 205–230 nm were not available from the literature. In this investigation the dissociation constants of oxalic acid were determined by a series of potentiometric titrations and confirmed by an independent spectrophotometric experiment. The data of the latter experiment also yielded the required absorption spectra of the different oxalate species.

EXPERIMENTAL

Reagents

All reagents were of analytical grade (Merck *p.a.*) and solutions were prepared with demineralized distilled water. The sodium perchlorate solution was prepared from the twice recrystallized solid and standardized by evaporating known volumes to dryness and heating at 130° to constant weight. Before recrystallization a saturated solution of the salt was allowed to stand for a week and then filtered. Perchloric acid was standardized by titration with sodium hydroxide that had been standardized by titration with potassium hydrogen phthalate. Sodium oxalate solutions were prepared from the solid, and used without further purification.

Potentiometric measurements

Titrations were done at 25.0 ± 0.1° (with the titration flask in a water-bath), starting with either 40.0 or 50.0 ml of 0.01811*M* sodium oxalate and adding perchloric acid from a 10-ml burette. All solutions were made 3.0*M* with respect to perchlorate by addition of sodium perchlorate. To prevent precipitation of sodium oxalate in this medium the concentration of oxalate had to be kept below ~0.019*M*. A stream of purified nitrogen was passed through 3.0*M* sodium perchlorate and then bubbled slowly through the titration solution, which both stirred the solution and excluded carbon dioxide from the system. The free hydrogen-ion concentration, *h*, was determined by measuring the potential to ± 0.2 mV with a Radiometer PHM64 Research pH-meter. The following cell was used:

Glass	Test solution,	0.1*M* NaCl	Hg_2Cl_2(s),
electrode	3.0*M* ClO_4^-	2.9*M* $NaClO_4$	Hg(s)

The electrodes used were a Radiometer glass electrode (G202C) and calomel reference electrode (K201), modified[5] as indicated in the cell. The advantage of this modification is that the internal solution of the electrode has the same ionic strength and nearly the same composition as the test solution. Before use and between experiments these electrodes were kept at 25°, the glass electrode in tap water and the calomel electrode in 0.1*M* sodium chloride/2.9*M* sodium perchlorate.

The relationship between the measured potential *E* (in mV) and the concentration of free hydrogen ions at 25° is given by

$$E = E^\circ - 59.15 \log h + E_j \qquad (1)$$

where E° includes the standard potentials of the electrodes, the asymmetry potential of the glass electrode, and the term 59.15 log γ_H (which is assumed to be a constant in the 3.0*M* sodium perchlorate medium used).

E_j is the liquid junction potential, which can be taken as proportional to the hydrogen-ion concentration.[6] Values for E° and E_j were determined from titrations of 3.0*M* sodium perchlorate with perchloric acid as described by Rossotti.[7] E_j was found to have the value 19*h* mV. *E* was corrected for E_j at $h > 0.008M$, *i.e.*, when E_j was significant. The equilibrium hydrogen-ion concentration was varied from 10^{-5} to $10^{-1.1}M$ by titrating with either 0.1 or 0.5*M* perchloric acid.

Spectrophotometric measurements

The spectrophotometric measurements were made with

a Beckman Acta MVI spectrophotometer. The titration procedure was similar to that for the potentiometric measurements, but a peristaltic pump was used to circulate the test solution from the reaction vessel to a flow-through cuvette (with adjustable path-length) set at 0.5 cm (actual path-length 0.497 cm).

A 50-ml portion of 0.001*M* sodium oxalate was titrated initially with 0.1*M* and eventually with 0.5*M* perchloric acid, h being thereby varied from $10^{-6.1}$ to $10^{-1.0}$. The perchlorate concentration of these solutions was 3.0*M*. The value of h was calculated from the measured potential, E, as described above. The absorbance of the solution at a particular E value was measured, against air as reference, at 2-nm intervals in the range 202–226 nm. In a similar blank titration (*i.e.*, without oxalate) the blank absorbances at the different wavelengths as well as a value for E° were determined.

RESULTS AND DISCUSSION

Constants from potentiometric data

The equilibria for the successive protonations of oxalate are represented by the equations

$$C_2O_4^{2-} + H^+ \rightleftharpoons HC_2O_4^- \quad (2)$$

$$HC_2O_4^- + H^+ \rightleftharpoons H_2C_2O_4 \quad (3)$$

The analytical concentrations of oxalate and acid, denoted by B and H, are given by

$$B = b + bh\beta_1 + bh^2\beta_2 \quad (4)$$

and

$$H = h + bh\beta_1 + 2bh^2\beta_2 \quad (5)$$

where b and h are the concentrations of free oxalate and hydrogen ions; and β_1 and β_2 are the overall protonation constants of oxalate, related to the dissociation constants by

$$K_{a1} = \beta_1/\beta_2; K_{a2} = 1/\beta_1 \quad (6)$$

The degree of protonation, Z, is defined by

$$Z = (H - h)/B \quad (7)$$

By substitution of equations (4) and (5) into (7), the following expression is obtained:

$$Z = \frac{h\beta_1 + 2h^2\beta_2}{1 + h\beta_1 + h^2\beta_2}. \quad (8)$$

Values for Z were calculated by means of equation (7) and are plotted in Fig. 1 as a function of $-\log h$. With use of these Z values and the corresponding h values, equation (8) was solved by a non-linear least-squares method, in which the error mean square $[\Sigma(Z_{expt} - Z_{calc.})^2]/(n-2)$ is minimized by stepwise Gauss–Newton iterations on the protonation constants β_1 and β_2, n being the number of data points. A package program, BMDX85,[8] has been adapted for this purpose. The values for the constants thus computed (error limits 2σ) were:

$$\beta_1 = (6.54 \pm 0.10) \times 10^3$$

$$\beta_2 = (1.23 \pm 0.03) \times 10^5$$

The standard deviation of Z was 0.006 (for Z from 0.100 to 1.650). The curve shown in Fig. 1 was calculated from these constants and fits the experimental points well.

Constants and ultraviolet spectra from spectrophotometric data

The molar absorptivity, ϵ, of a solution containing

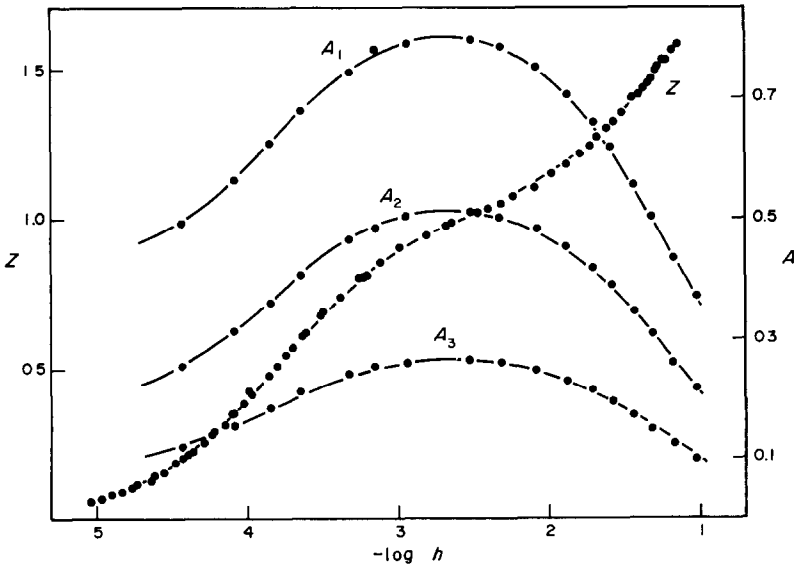

Fig. 1. The degree of protonation, Z, and the absorbance A, as a function of $-\log h$. A_1, A_2 and A_3 refer to wavelengths 208, 214 and 220 nm. The curves are calculated from the constants given in the text. Many of the dots on the Z-curve represent two closely spaced data points.

the various species is given by

$$\epsilon = \frac{A}{Bl} = \frac{\epsilon_0 + \epsilon_1\beta_1 h + \epsilon_2\beta_2 h^2}{1 + \beta_1 h + \beta_2 h^2} \qquad (9)$$

where A is the absorbance measured in a cuvette of path-length l cm, B is the total molar concentration, and ϵ_0, ϵ_1 and ϵ_2 are the molar absorptivities of $C_2O_4^{2-}$, $HC_2O_4^-$ and $H_2C_2O_4$ respectively at a particular wavelength. Because of overlap of the dissociation equilibria, ϵ_1 cannot be measured directly. To obtain a reliable value for ϵ_2 from direct absorbance measurements is also not feasible. For the practically complete protonation of $HC_2O_4^-$ to $H_2C_2O_4$, an acid concentration much higher than the ionic strength of the medium would be required, *e.g.*, 10.8M for 99.5% protonation. Moreover, at such a high hydrogen-ion concentration possible further protonation of oxalic acid itself would have to be considered. Although a value for ϵ_0 can be obtained directly by measuring the absorbance of an oxalate solution with $-\log h \gtrsim 6.5$, we preferred to regard ϵ_0 also as an unknown in the treatment of the data. To obtain the protonation constants from the spectrophotometric data, equation (9) must therefore be solved for five unknown parameters.

At first sight the spectrum of a solution containing oxalic acid and its ions does not seem to be suitable for stringent equilibrium analysis. The species absorb in the ultraviolet region at wavelengths shorter than ~235 nm and their absorption maxima occur at ≪200 nm. Consequently only the tail of the band, a rather steep sloping curve, is accessible for measurement. However, quite a significant change in absorbance takes place when $C_2O_4^{2-}$ is successively protonated to $HC_2O_4^-$ and $H_2C_2O_4$ (*cf.* Fig. 1). This observation and the fact that the overlap of the equilibria is rather small, have led us to attempt the spectrophotometric determination of the constants by employing the very useful computer program SQUAD.[9,10] By means of this program, absorbance data at a number of wavelengths can be handled simultaneously for the calculation of stability constants. In the present case the data consisted of 234 absorbance values measured at 13 wavelengths for 18 different hydrogen-ion concentrations. As typical results those for wavelengths 208, 214 and 220 nm are shown in Fig. 1. The following values for the overall protonation constants were computed from the spectrophotometric data (error limits 2σ):

$$\beta_1 = (6.93 \pm 0.20) \times 10^3$$

$$\beta_2 = (1.27 \pm 0.04) \times 10^5$$

The standard deviation of the absorbance was 0.0039 (for A from 0.016 to 1.027).

As was to be expected these constants could not be determined with the same accuracy as those evaluated from the potentiometric data. The agreement between the two sets of constants, however, is quite satisfactory. The spectral curves for the various species (Fig. 2) plotted from the molar absorptivities obtained in the calculation of the protonation constants can therefore be accepted as reliable. To the best of our knowledge complete ultraviolet spectra for the oxalate species in solution have not been published before, possibly because a spectrophotometric determination of the dissociation constants of oxalic acid has not previously been attempted. These spectra might be very useful for investigations of complex formation or kinetics of complex-formation involving oxalate as ligand.

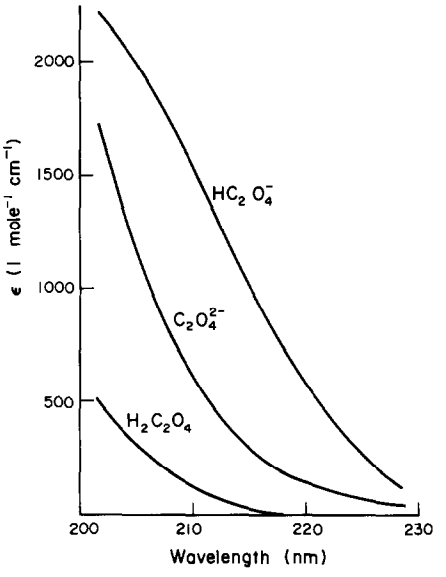

Fig. 2. Calculated absorption spectra of $H_2C_2O_4$, $HC_2O_4^-$ and $C_2O_4^{2-}$ in 3M Na(H)ClO$_4$ medium.

Alternative calculation of β_2

In the computation of the constants from the potentiometric as well as the spectrophotometric data, the hydrogen-ion concentrations used were obtained from potential measurements with a glass electrode. It is, of course, possible to calculate a value for β_2 from the absorbance data by using the analytical hydrogen-ion concentrations. Moreover, the equilibrium hydrogen-ion concentrations calculated (by iteration) from the analytical concentrations in the region above 0.01M will be more accurate than those obtained from potential measurements. The absorbance data were therefore treated again with the program SQUAD, but with the analytical acid concentrations in the region above 0.01M. The previously determined value for β_1 was used as a known constant to provide for the overlap of the equilibria. The new value for β_2 thus calculated was (error limits 2σ):

$$\beta_2 = (1.25 \pm 0.04) \times 10^5$$

The good agreement between the two values for β_2 indirectly confirms the reliability of the potentio-

metric measurements, especially at high acid concentrations where E had to be corrected for E_j.

As "best" values for the dissociation constants for oxalic acid we choose those determined by potentiometric titration. The values obtained are (error limits 2σ):

$$K_{a1} = (5.32 \pm 0.15) \times 10^{-2}$$

$$K_{a2} = (1.53 \pm 0.02) \times 10^{-4}$$

These values can be compared with those reported previously[4] for the same ionic medium and temperature (but each derived from only three pH-measurements) namely $(5.5 \pm 0.8) \times 10^{-2}$ for K_{a1} and $(1.58 \pm 0.02) \times 10^{-4}$ for K_{a2}.

Acknowledgements—Financial support by the South African Council for Scientific and Industrial Research is gratefully acknowledged. We thank Miss J. du Toit for assistance with some of the experimental work.

REFERENCES

1. J. J. Cruywagen, *Inorg. Chem.*, 1980, **19**, 552, and references therein.
2. A. E. Martell and R. M. Smith, *Critical Stability Constants*, Vol. 3, p. 93. Plenum Press, New York, 1977.
3. J. J. Christensen, L. D. Hansen and R. M. Izatt, *Handbook of Proton Ionization Heats*, p. 129. Wiley, New York, 1976.
4. E. G. Moorhead and N. Sutin, *Inorg. Chem.*, 1966, **5**, 1866.
5. M. Molina, C. Melios, J. O. Tognolli, L. C. Luchiari and M. Jafelicci, Jr., *J. Electroanal. Chem.*, 1979, **105**, 237.
6. G. Biedermann and L. G. Sillén, *Arkiv Kemi*, 1953, **5**, 425.
7. H. S. Rossotti, *Talanta*, 1974, **21**, 809.
8. *Biomedical Computer Programs*, X-Series Supplement, W. J. Dixon, (ed)., University Press, California 1972.
9. D. J. Leggett and W. A. E. McBryde, *Anal. Chem.*, 1975, **47**, 1065.
10. D. J. Leggett, *Complete listing of SQUAD II*, private communication, 1979.

Talanta, Vol 30, No 3, pp. 201–203, 1983
Printed in Great Britain.

0039-9140/83/030201-03$03.00/0

LONG-TERM STABILITY OF ION-SELECTIVE VALINOMYCIN MEMBRANES

J. J. GRIFFIN
D.M.T., Inc., 34 Tower St., Hudson, MA 01749, U.S.A.

and

G. D. CHRISTIAN
Department of Chemistry, University of Washington, Seattle, WA 98195, U.S.A.

(*Received* 14 *October* 1981. *Revised* 1 *July* 1982. *Accepted* 26 *August* 1982)

Summary—The response characteristics of freshly prepared membranes containing valinomycin are compared to those of membranes of identical composition prepared 2 and 10 years earlier. Independent melting point and infrared spectroscopy data on valinomycin of different ages are presented to substantiate its long-term stability. The separate-solution method was employed to establish selectivity coefficients for Rb^+, Cs^+, Li^+, H^+, Na^+ and NH_4^+ relative to K^+ for freshly prepared and aged membranes. The maximum values for Na^+ ranged from $10^{-4.69}$ for freshly prepared membranes to $10^{-4.27}$ for 10-year old membranes. The slope of the emf *vs.* potassium ion activity over the range 10^{-4}–$10^{-1}m$ was 58.5 mV/decade for freshly prepared membranes and 57.7 mV/decade for aged membranes. The time needed to reach 99% of the final emf was less than 1 min for freshly prepared and 2-year old membranes but 3–6 min for 10-year old membranes. Possible measures to increase the shelf life of these and similar membranes are suggested.

Numerous studies have been performed with valinomycin as an active agent in the selective transport of cations across membranes, since Moore and Pressman's discovery[1] of its ability to induce ion permeation in mictochondria. The ion-carrier capability of valinomycin led to its incorporation into organic matrices to give ion-selective membranes with electrochemical sensor applications (*e.g.*, ion-selective electrodes).

The stability of a 3-year-old membrane incorporating a potassium–valinomycin–tetraphenylborate salt in a block copolymer of poly(bisphenol-A carbonate) and poly(dimethylsiloxane) has been reported,[2] and Oesch and Simon[3] have indicated a methodology for assessing the lifetime, under continuous use conditions, of various ion-selective liquid membranes, including a system incorporating valinomycin as neutral carrier.

The purpose of this paper is to report the response characteristics of ion-selective valinomycin membranes prepared 2 and 10 years earlier and stored in conductance water. Melting point and infrared spectroscopy data confirming the long-term stability of valinomycin are also presented.

EXPERIMENTAL

Apparatus

A Health Digital Multimeter, Model IM-102, combined with a Heath Model EU 200-30 electrometer module, was used to measure cell emf values. All measurements were made with the membranes mounted on a snap-cap membrane electrode,[4] and facing silver–silver chloride electrodes (internal and external) prepared by the thermal decomposition method as described by Ives and Janz.[5] The right-hand side of all cells described was connected to the positive lead on the electrometer.

A Perkin–Elmer Model 710 infrared spectrophotometer was used to record the infrared spectra of the valinomycin samples. Melting points were determined with a Laboratory Devices 200-W "Mel-Temp".

Reagents

All reagents were of analytical grade except for "Ultrapure" grade NaCl, RbCl and CsCl supplied by Ventron Corporation, Alpha Industries. The impurities in the "Ultrapure" NaCl included potassium, rubidium and caesium at 5, 1 and 5 ppm, respectively. All solutions were prepared with distilled demineralized water. Solutions were maintained at $25 \pm 1°$ and magnetically stirred during measurements.

Valinomycin prepared in 1968 was supplied by Eli Lilly and Company, and Calbiochem supplied valinomycin prepared in 1974 and 1979. Mixtures of 2.5% w/w valinomycin with potassium bromide (infrared quality, Harshaw Chemical Company) were prepared and 70-mg quantities were compressed into pellets for infrared analysis.

Diphenyl ether, cyclohexanone, and dipentyl phthalate were purchased from Eastman Kodak Company, and the PVC resin was supplied by Stauffer Chemical Company.

Membrane preparation. Valinomycin, dissolved in diphenyl ether, was stirred into a 17% w/w solution of PVC in cyclohexanone, and then a 10% v/v quantity of dipentyl phthalate was added. After any air-bubbles had escaped, the mixture was cast onto a glass plate, masked to contain the fluid within a fixed area, and allowed to air-dry for up to 24 hr at room temperature. The valinomycin concentration in the "dried" membranes was approximately 4.5×10^{-4} and $5.1 \times 10^{-4}M$ for the membranes prepared in 1972 and 1980, respectively. Membranes (200 μm × 3.6 cm) were cut and either immersed in 0.10*m* potassium chloride (for immediate use) or stored together in 30–40 ml

of conductivity water within a sealed container (for future use). Before use, the latter membranes were cut, if necessary, to an appropriate size and conditioned for several hours in 0.10*m* potassium chloride. The 1972 membranes were prepared with valinomycin manufactured in 1968, and a 1979 sample of valinomycin was used in the preparation of the 1980 membranes. The 1972 membranes had also been used in a separate impedance study.

THEORETICAL

The cell used in the separate-solution method[6] of establishing selectivity coefficients can be described by

Ag–AgCl′/0.10*m* BCl//membrane//
0.10*m* KCl/Ag–AgCl″

where BCl represents the chloride activity of a univalent cation.

By use of silver–silver chloride electrodes exactly matched in potential, and equal chloride concentrations on each side of the membrane, or correcting the cell emf for any differences, the selectivity coefficient of the membrane for the univalent cation relative to the potassium ion can be readily determined from

$$k_{K,B}^{pot} = \frac{y_{K^+}}{y_{B^+}} \exp(FE_{membrane}/RT) \qquad (1)$$

where y is the activity coefficient of the ion indicated by subscript.

An attempt was made to establish the K^+/Na^+ selectivity coefficient by the recommended[6] fixed-interference method, but the high selectivity of the membrane for potassium (as well as rubidium and caesium) relative to sodium, coupled with the very small but significant concentrations of potassium in the ultrapure sodium chloride, precluded this determination.

The cell used to establish the response time and the slope of the calibration graph is described by

$$\text{Ag–AgCl}'\Big/\begin{Bmatrix} 10^{-1}m\,Cl^- \\ 10^{-1}\text{–}10^{-4}m\,K^+ \end{Bmatrix}\text{//membrane//0.10}m\text{ KCl/Ag–AgCl}''$$

The chloride activity was kept constant by addition of sodium chloride when necessary, when the potassium-ion concentration was changed from 10^{-4} to $10^{-1}m$.

RESULTS

The emf developed by 10-year old membranes was a linear function of potassium-ion activity over the range 10^{-4}–$10^{-1}m$ with a slope of 57.7 mV/decade.

For freshly prepared or 2-year old membranes the slope was 58.5 mV/decade over the same range. The relative standard deviation for the slope measurements was 1.7%.

For a thousandfold change in potassium-ion concentration (from 10^{-4} to $10^{-1}m$) the 10-year old membranes gave 90% of full response within 1 min and 99% (within 1 mV of the final emf) in 3–6 min. In comparison, 2-year old and freshly prepared membranes exhibited a 99% change in less than 1 min.

Table 1. Selectivity of coefficients of freshly prepared and aged membranes (of approximately identical composition) for different cations (chloride as the common anion)

	$-\log k_{K,B}^{pot}$		
B	10 Years*	2 Years*	0 Years*
Rb^+	−0.38	−0.40	−0.34
Cs^+	0.42	0.40	0.43
Li^+	3.78	3.82	3.85
H^+	3.55	4.40	4.43
Na^+	4.27	4.48	4.69
NH_4^+	1.74	1.82	1.83

*Age of membrane.

Measurements made in 1982 of the selectivity coefficients obtained for equimolal solutions of potassium and other univalent cations are shown in Table 1 for membranes prepared in 1972 and 1980, and are compared with those made in 1980 with freshly prepared membranes.

Samples of valinomycin prepared in 1968 and 1979 were analysed by infrared spectroscopy in 1980 and 1982, respectively. Little or no discernible difference in the spectra was observed, as shown in Fig. 1, although some differences were expected because of possible variations in purity and preparation by the two different laboratories.

The melting points, determined in 1980, for the valinomycin samples prepared in 1968, 1974 and 1979 were 187°, 187° and 186–187°, respectively.

DISCUSSION

Evidence from potentiometric measurements, infrared spectroscopy, and the melting points strongly suggests that valinomycin is stable when stored at room temperature in air or in an organic matrix immersed in conductivity water.

Ion-selective membranes containing valinomycin as the neutral carrier have been shown to have a shelf-life of at least 10 years, though there is some deterioration in response time and selectivity. When the membranes described here are stored in the open air, their lifetime is reduced from years to days because of loss of the more volatile constituents such as cyclohexanone. Repeated exposure to different test solutions can also result in the loss of one or more of the membrane components. Oesch and Simon[3] have demonstrated the importance of the concentration of the ion-carriers, including valinomycin, in a liquid ion-selective membrane system. Their data show that

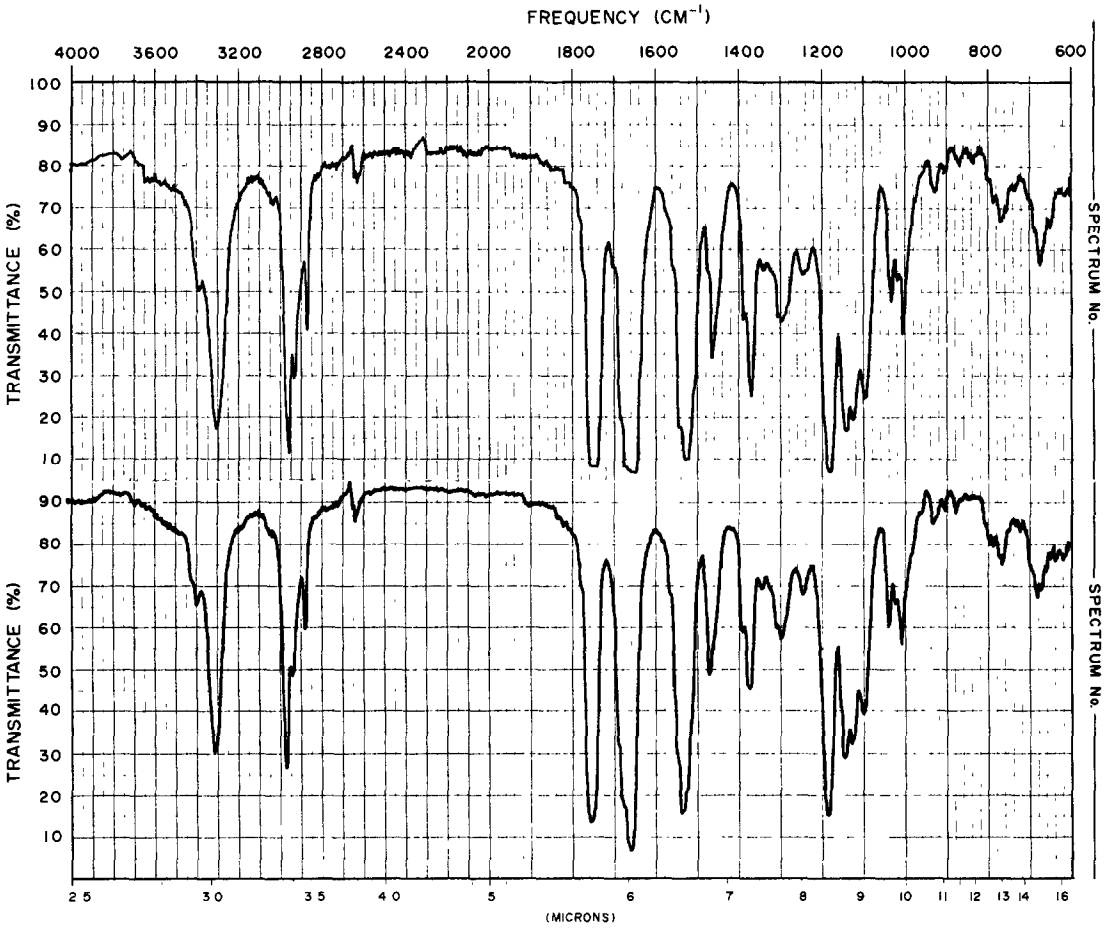

Fig. 1. Infrared spectra of valinomycin (2.5% w/w) in KBr. Upper spectrum—valinomycin prepared by Eli Lilly and Company in 1968. Lower spectrum—valinomycin prepared by Calbiochem in 1979.

changes in selectivity and departure from Nernstian behaviour can be expected if there is loss of the ion-carrier from the membrane.

Additional measures that can be taken to extend the shelf-life of this and similar membrane systems include addition of the water-soluble membrane components to the storage medium, to reduce the thermodynamic driving forces created by the concentration gradients between the membrane and the storage medium.

REFERENCES

1. C. Moore and B. C. Pressman, *Biochem. Biophys. Res. Commun.*, 1964, **15**, 562.
2. O. H. LeBlanc, Jr. and W. T. Grubb, *Anal. Chem.*, 1976, **48**, 1658.
3. U. Oesch and W. Simon, *ibid.*, 1980, **52**, 692.
4. J. J. Griffin and G. D. Christian, *Z. Anal. Chem.*, 1982, **311**, 126.
5. D. J. G. Ives and G. J. Janz, *Reference Electrodes, Theory and Practice*, pp. 208–209. Academic Press, New York, 1961.
6. G. G. Guilbault, R. A. Durst, M. S. Frant, H. Freiser, E. Hansen, T. S. Light, E. Pungor, G. Rechnitz, N. M. Rice, T. J. Rohm and J. D. R. Thomas, *Recommendations for Nomenclature of Ion Selective Electrodes.* I.U.P.A.C. Information Bulletin, No. 43, Jan. 1975.

Talanta, Vol. 30, No. 3, pp. 205–208, 1983
Printed in Great Britain.

0039-9140/83/030205-04$03.00/0

ANNOTATION

FAST pH CALCULATIONS IN AQUEOUS SOLUTION CHEMISTRY

MARIE-NOËLLE PONS, JEAN-LOUIS GREFFE and JACQUES BORDET
Laboratoire des Sciences du Génie Chimique, CNRS-ENSIC, 1, rue Grandville, F-54042, Nancy, France

(*Received* 17 *July* 1981. *Revised* 8 *October* 1982. *Accepted* 18 *October* 1982)

Summary—A technique for computation of the neutralization curves of acid–base solutions, based on an optimization search method, has been developed. The criterion function is the absolute value of the calculated difference between the numbers of positive and negative charges present in the solutions. This technique is generally applicable for solution chemistry, but because of its speed of resolution and its accuracy, it is particularly useful in the control of a real-time process by a computer.

In analytical chemistry, reactions in solution can be described by the equilibria and material balances involved. However, difficulties arise during numerical calculations for mixtures of acids and bases. For example, the calculation of the hydrogen-ion activity generally requires a powerful electronic calculator.[1–3] The usual approach is to write a polynomial equation in terms of hydrogen-ion concentration and then find a positive root.

We wished to control the pH in neutralization reactions taking place in a complex process requiring a sophisticated control system.[4] Computation of the neutralization curve was a necessary step in our control scheme, but was just one among many tasks to be done by the computer. The usual procedure for calculation of neutralization curves proved to be too time-consuming for real-time process control. We therefore developed a less sophisticated but powerful and fast procedure, suitable for a small process computer (MITRA 115-SEMS). Some attempts have been already made in this direction,[5] but we think that our simple technique could be a very valuable tool.

FORMULATION OF THE PROBLEM

A general equation for the dissociation of an n-protic acid with apparent dissociation constants $K'_{A1}, \ldots K'_{An}$ and thermodynamic dissociation constants $K_{A1} \ldots K_{An}$ is:

$$AH_{n-i+1}^{(i-1)-} + H_2O \rightleftharpoons H_3O^+ + AH_{n-i}^{i-}$$

$$K'_{A_i} = \frac{[AH_{n-i}^{i-}][H_3O^+]}{[AH_{n-i+1}^{(i-1)-}]} = K_{Ai}\frac{f_{AH_{n-i+1}}}{f_{AH_{n-i}}f_H}.$$

The concentrations of the species in solution are given by

$$[AH_{n-i}^{i-}] = \frac{C[H_3O^+]^{n-i}\prod_{k=1}^{i} K'_{Ak}}{[H_3O^+]^n + \sum_{k=1}^{n}[H_3O^+]^{n-k}\prod_{j=1}^{k} K'_{Aj}}$$

where C is the total (analytical) concentration of the acid. The mathematical expressions quickly become difficult to deal with when mixtures of many components are considered.

The activity coefficients are a function of the ionic strength, and may be predicted by various equations.[6]

pH computation

The calculation of pH for mixtures of acids and bases requires knowledge of the equilibria involved, and the material and charge balances have to be evaluted.

The resulting polynomial equation in $[H_3O^+]$ is often cumbersome to solve and requires great precision during the computation. The calculator we used first had a precision of only 1 in 10^5, *i.e.*, $1 + 10^{-6} = 1$. We then started looking for a method that was not based on iteration involving high-precision calculation. This led us to an iterative method using an optimization search technique, the "golden section" method.[7]

This method is a single-variable elimination method used when there is no information available (at least easily) about the derivatives used in such techniques as the Newton–Raphson method. It involves determining the optimum value of the independent variable by trial and error, with the search confined to progressively smaller intervals of size L_j ($j = 1, \ldots J$, and being finite) by elimination of unsuitable portions of the domain of search. The main characteristic of the method is that the intervals are successively decreased in geometric ratio τ, given by

$$\tau = L_{j-1}/L_j = (1 + \sqrt{5})/2$$

This method is similar to the Fibonacci search method used by McMillan *et al.*,[5] without requiring that the numbers of trials be known in advance.

Let F_1 be the number of negative charges per unit volume of solution and F_2 the corresponding number of positive charges. Charge balance gives $F_1 = F_2$. If this equality is obtained for only one value in the

possible domain of the variable pH′ ($= -\log [H_3O^+]$), $F_1 - F_2$ will take the value zero only once, so the absolute value $|F_1 - F_2|$, will have a unique minimum and therefore be a one-variable unimodal function. This is most important, and our discussion deals with this characteristic.

Consider titration of a single triprotic acid, AH_3, of total concentration C, with a strong monoprotic base, BOH. The species in solution are H_3O^+, B^+ and OH^-, AH_2^-, AH^{2-} and A^{3-}. Thus

$$F_1 = [OH^-] + [AH_2^-] + 2[AH^{2-}] + 3[A^{3-}]$$

$$F_2 = [H_3O^+] + [B^+].$$

Now, for a given titration data-point, consider how F_1 and F_2 will change as the value of $[H_3O^+]$ is changed, in order to find where $|F_1 - F_2|$ has its minimum. Since $F_2 = [H_3O^+] + [B^+]$, we have $dF_2/d[H_3O^+] = 1$. That is, F_2 increases when $[H_3O^+]$ increases.

F_1 can be written as

$$F_1 = \frac{K'_W}{[H_3O^+]} + C\frac{K'_{A1}[H_3O^+]^2 + 2K'_{A1}K'_{A2}[H_3O^+] + K'_{A1}K'_{A2}K'_{A3}[H_3O^+]^3}{[H_3O^+]^3 + K'_{A1}[H_3O^+]^2 + K'_{A1}K'_{A2}[H_3O^+] + K'_{A1}K'_{A2}K'_{A3}}$$

$$= G_1 + CK'_{A1}G_2.$$

Thus

$$\frac{dF_1}{d[H_3O^+]} = \frac{dG_1}{d[H_3O^+]} + CK'_{A1}\frac{dG_2}{d[H_3O^+]}$$

and

$$\frac{dG_1}{d[H_3O^+]} = -\frac{K'_W}{[H_3O^+]^2}$$

which is strictly negative.
Putting

$$Y = [H_3O^+]^3 + K'_{A1}[H_3O^+]^2 + K'_{A1}K'_{A2}[H_3O^+] + K'_{A1}K'_{A2}K'_{A3}$$

we have

$$\frac{dG_2}{d[H_3O^+]} = -\frac{[H_3O^+]^4 + 4K'_{A2}[H_3O^+]^3 + [K'_{A1}K'_{A2} + 9K'_{A2}K'_{A3}][H_3O^+]^2}{Y^2} - \frac{4K'_{A1}K'_{A2}K'_{A3}[H_3O^+] + K'_{A1}(K'_{A2})^2K'_{A3}}{Y^2}.$$

which is strictly negative.

Therefore $dF_1/d[H_3O^+]$ is strictly negative and F_1 decreases when $[H_3O^+]$ increases, *i.e.*, when pH′ decreases. Hence F_1 and F_2 change value in opposite directions when pH′ is changed, and the function $|F_1 - F_2|$ will be equal to zero when pH′ corresponds to the value for electrical balance. Therefore $|F_1 - F_2|$ is unimodal. The pH′ corresponding to the data point is calculated by applying the golden section method, starting with the boundary conditions pH′ = 0 and pH′ = 14. The calculation is repeated for each data point required.

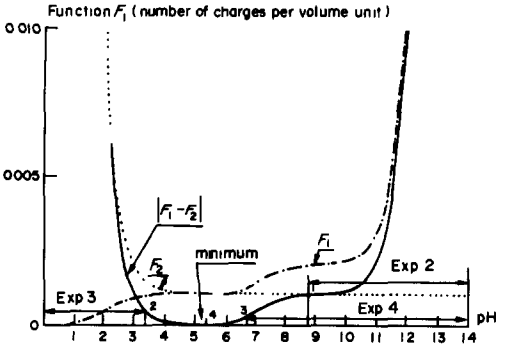

Fig. 1. Search for the minimum of $|F_1 - F_2|$. ——— F_1; ····· F_2; —— $|F_1 - F_2|$.

In this derivation, F_1 represents all the negative charges carried by the anions resulting from the dissociation of bases and/or acids existing in the mixture. For each dissociation sequence, we obtain a term G_2. F_2 represents all the positive charges carried by the cations resulting from the dissociation of bases and/or acids existing in the mixture. In the example taken the expression for F_2 is very simple, but in a more complicated dissociation of the type $H_nA^{n+}\ldots HA^+\ldots A$, there would be an additional term G_3 which increases as pH′ decreases (see Appendix), but a unimodal one-variable function $|F_1 - F_2|$ is still obtained, and its minimum can be computed by means of the golden section method.

The functions F_1 and F_2 are plotted in Fig. 1, which also illustrates the progressive size reduction of the search interval.

The true pH is calculated from pH′ by taking the activity coefficients into account, according to the procedure shown in Fig. 2.

IMPLEMENTATION

The computer used for the calculations presented in this paper was a MITRA 15 (SEMS) with 64 kbyte of memory with an 800-nsec machine cycle. The process computer MITRA 115 (SEMS) has the same memory capacity, but is faster.

The program was written in Fortran. The golden section technique subroutine, which can be found in most program libraries, requires 380 bytes of store. The user has to write his own subroutine to compute the function $|F_1 - F_2|$ for his particular problem.

The MITRA 15 computer took 0.1 sec to calculate one $-\log [H_3O^+]$ value (pH) with an accuracy of 0.01 pH unit. Convergence was obtained within two iterations, the convergence criterion (ε, the difference between two successive calculated pH values, see Fig. 2) being $\varepsilon = 0.01$.

Determination of neutralization curves

The method described was compared with the Newton–Raphson method for the determination of a

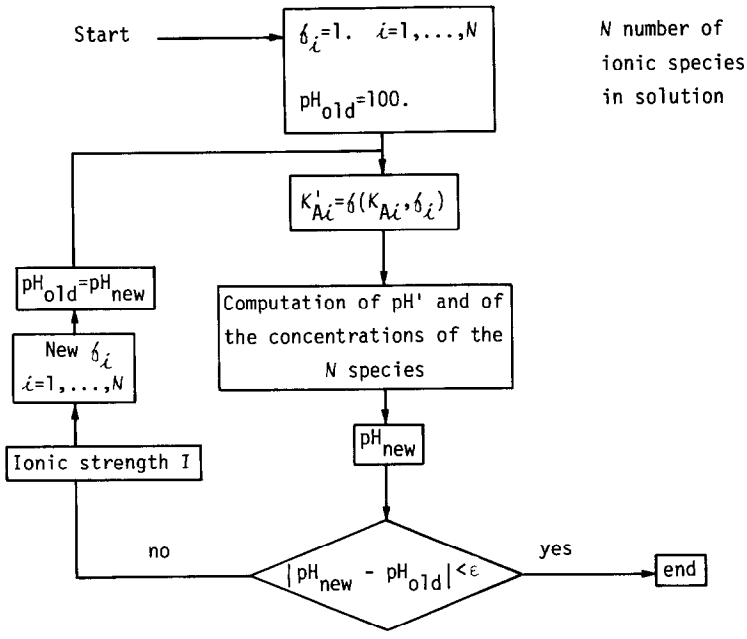

Fig. 2. Flow diagram for pH computation.

neutralization curve for 50 ml of 0.1*M* polyprotic acid ($pK_1 = 0.85$, $pK_2 = 1.49$, $pK_3 = 5.77$, $pK_4 = 8.22$) by 0.4*M* strong base. The calculation time was 5 sec. The golden section method used less core, and gave exactly the same results as the Newton–Raphson method.

Titration curves and distribution diagrams were calculated for citric acid ($pK_1 = 3.07$, $pK_2 = 4.75$, $pK_3 = 6.40$). The curves obtained were similar to those published elsewhere.[8]

The method was also used to determine the individual concentrations of hydrochloric, acetic and orthophosphoric acid in a mixture. The experimental curve for titration with 0.1*M* sodium hydroxide was evaluated by means of a multivariable search technique.[7]

CONCLUSION

A new method for determination of the pH of mixtures of acids and bases has been developed. It uses a "golden section" optimization technique, requires little computer memory and is relatively fast. It has been successfully implemented on a real-time process computer controlling a neutralization process. It could also be used on a microprocessor, because the golden section method is simple to program. The technique should be useful in other fields of the chemistry of solutions.

Acknowledgements—The authors are grateful to Professor J. Villermaux, Chairman of Laboratoire des Sciences du Génie Chimique, and wish to thank P. Bourret and G. Scacchi for their helpful discussions. The financial support of the Délégation Générale á la Recherche Scientifique Technique is gratefully acknowledged.

APPENDIX

For dissociation sequences of the type $H_nA^{n+} \ldots HA^+ \ldots A$, there is an additional term, G_3, in F_2:

$$G_3 = C\frac{[H_3O^+]\prod_{k=1}^{n-1} K'_{Ak} + 2[H_3O^+]^2\prod_{k=1}^{n-2} K'_{Ak} + \ldots + n[H_3O^+]^n}{[H_3O^+]^n + \sum_{k=1}^{n}[H_3O^+]^{n-k}\sum_{j=1}^{k} K'_{Aj}}$$

For example, when $n = 3$

$$\frac{dG_3}{d[H_3O^+]} = \frac{K'^2_{A1}K'^2_{A2}K'_{A3} + 4K'^2_{A1}K'_{A2}K'_{A3}[H_3O^+] + \{K'^2_{A1}K'^2_{A2} + 9K'_{A1}K'_{A2}K'_{A3}\}[H_3O^+]^2}{Y^2} + \frac{4K'_{A1}K'_{A2}[H_3O^+]^3 + K'_{A1}[H_3O^+]^4}{Y^2}$$

with $Y = [H_3O^+]^3 + K'_{A1}[H_3O^+]^2 + K'_{A1}K'_{A2}[H_3O^+] + K'_{A1}K'_{A2}K'_{A3}$; $dG_3/d[H_3O^+]$ is strictly positive; G_3 is increasing when $[H_3O^+]$ is increasing, *i.e.*, when pH′ is decreasing.

REFERENCES

1. D. D. Perrin and I. G. Sayce, *Talanta*, 1967, **14**, 833.
2. G. L. Breneman, *J. Chem. Educ.*, 1974, **51**, 812.
3. E. R. Rang, *Computers and Chemistry*, 1976, **1**, 91.
4. M. N. Pons, *Thèse Docteur Ingénieur*, Institut National Polytechnique de Lorraine, Nancy, June 1980.
5. G. D. McMillan, H. A. Grosby and R. C. Waggoner, *Instrum. Chem. Pet. Int.*, 1979, **15**, 27.
6. G. K. Pagenkopf, *Introduction to Natural Water Chemistry*. Dekker, New York, 1978.
7. W. H. Ray and J. Szekely, *Process Optimization*. Wiley, New York, 1973.
8. R. Rosset, D. Bauer and J. Desbarres, *Chimie analytique des solutions et microinformatique*. Masson, Paris, 1979.

Talanta, Vol. 30, No. 4, pp. 209–243, 1983
Printed in Great Britain.

0039-9140/83/040209-35$03.00/0

ANALYSIS OF DRUGS BY MICROCALORIMETRY

ISOTHERMAL POWER-CONDUCTION CALORIMETRY AND THERMOMETRIC TITRIMETRY

B. Z. CHOWDHRY,* A. E. BEEZER and E. J. GREENHOW
Department of Chemistry, Chelsea College, University of London, Manresa Road, London SW3 6LX, England

(*Received* 7 *April* 1981. *Revised* 25 *August* 1982. *Accepted* 5 *November* 1982)

Summary—Microcalorimetric analysis has been the subject of a few reviews in recent years, but these reviews have mainly dealt with the wide-ranging capabilities of calorimetric assay. This review, however, discusses the experimental basis and practical exploitation of the method in the particularly important area of pharmaceuticals. This field of analysis embraces both conventional chemical assays and bioassays which involve living microbial species. The review highlights the design of calorimetric instruments appropriate for study of microbial metabolism and interaction with drug substances. For comprehensiveness, both microcalorimetric and thermometric assay systems are discussed and critically assessed.

ISOTHERMAL POWER-CONDUCTION MICROCALORIMETRY

The analysis of drugs entails, essentially, the following:

(1) the quantitative, qualitative and relative bioactivity assay of pure and impure drugs in different matrices;
(2) elucidation of the mechanism of action of drugs at the molecular level;
(3) clinical evaluation, including assessment of site of action (*in vivo*) and side-effects, and methods of assaying development of resistance of cells to drug action.

Methods for quantitative and qualitative analysis of drugs are important in all three aspects. Quantitative drug measurements require to be of high reproducibility, precision and accuracy and are often required quickly. In clinical laboratories there is usually a very large number of samples derived from different sources to be dealt with.[1] Metabolic studies of drugs require detection at very low levels, often in the μg–ng range, in body fluids and tissues. Drug abuse also leads to a need for rapid qualitative and quantitative assay of drugs. The quantitative and qualitative analysis of drugs is also important in the pharmaceutical industry, but because dosage forms are of high purity and precisely known composition the limits of detection are not so demanding as in clinical medicine, and reasonably large quantities of sample are usually available.

*Present address: Sterling Chemistry Laboratory, Yale University, 225 Prospect Street, New Haven, CT 06520, U.S.A.

METHODS OF ANALYSIS OF ANTIMICROBIAL AGENTS

The methods currently available may be broadly divided into two categories:

(1) classical microbiological methods[2] and modifications thereof;[3]
(2) physicochemical techniques.[4–8]

Microbiological assays may be considered as variants of chemical assays in which a living organism or tissue is the reagent responding to the substance under investigation. The classical techniques are mainly based on inhibition of microbial growth and can be classified into (*a*) diffusion methods and (*b*) dilution techniques.

The diffusion methods are based on the uniform spread of an inhibitor into a solid medium from its point of application. As the inhibitor agent spreads, its concentration decreases. Organisms will grow only where the concentration of inhibitor is too low to stop growth. The diffusion methods are not well understood theoretically. The inhibition zone diameter is usually (but not always) proportional to the logarithm of the inhibitor concentration, and is affected by various experimental factors.

Synergistic or antagonistic effects of drug molecules on micro-organisms are also difficult, if not impossible, to assess by plate agar diffusion methods.

Respirometric methods depend on the ability of a drug to inhibit formation of carbon dioxide by either direct or indirect action. Radioactively labelled carbon dioxide, and Warburg or indicator methods can be used, but the indicators should not interfere by complexing with the drug.

Turbidimetric methods measure the inhibition of growth photometrically. The growth is assumed to be

inversely proportional to the drug concentration. Errors can be caused by variation in inocula, inoculum volume errors and light-absorption by the drug.

In dilution methods, several dilutions of the drug are incubated with an inoculum of test organisms, and the lowest concentration of drug producing complete inhibition of growth is taken as the inhibitory concentration.

Numerous variations of these techniques continue to be reported, and routinely practised in clinical and pharmaceutical laboratories. One of the primary reasons for this is that the structure of the drug need not be known. The methods are also usually cheap and simple and do not need elaborate apparatus, but are slow, have rather poor reproducibility and precision, are open to subjective error, and cannot be used qualitatively.

A wide variety of physicochemical methods have been employed, *e.g.*, spectroscopic, electrochemical and chromatographic, but their applicability to qualitative analysis of drugs is still problematic in certain cases. Antibiotics, for example, are usually non-homogeneous, and fermentation by-products present may affect the physicochemical qualitative assay. Nevertheless, these methods are the first choice for qualitative analysis of drugs.[4] The limits of detection, reproducibility, accuracy, *etc.* are usually better than those for the classical methods, but these methods do not fulfil the obligatory legal requirements of testing antimicrobial drugs against metabolically viable cells,[9] supply information on the susceptibility of organisms to drug molecules, or give ancillary information such as the kinetics of drug action. Moreover, a preliminary separation is often needed, making the methods slow.

Calorimetric techniques may be used for both qualitative and quantitative assay by measurement of the enthalpy change of reactions, and as micro-organisms may be regarded as assemblages of integrated chemical reactions their metabolic activity can be registered with a suitably sensitive calorimeter. Hence inhibitors of this activity can also be determined. This use of the calorimetric method has arisen only during the last ten years, and it is intended to give here a brief review of the developments in calorimetric instrumentation and experimental design[10–13] which have led to the use of isothermal power-conduction microcalorimetry for micro-organism–drug studies.

Instrumentation and experimental design

Calorimetric equipment has developed considerably since Black's pioneer work and Lavoisier's ice calorimeter[14] and modern instrumentation owes a large part of its success to the introduction of the thermistor,[15] which allows temperature changes as small as 10^{-5} deg to be detected with good accuracy. Thermistors have several other advantages: they are small, have a low heat capacity and respond rapidly to temperature changes. The thermistor gave great impetus to the development of the isoperibol[10] and adiabatic shield[16,17] "micro" calorimeters. Isoperibol calorimeters have a thermostatically controlled jacket. If the calorimeter vessel and the jacket differ in temperature, heat is transferred between them. This heat leakage can be calculated and allowed for, *e.g.*, by using Newton's law of cooling, and the enthalpy of the reaction calculated.

In adiabatic shield calorimeters, the temperature of the surroundings follows that of the vessel and theoretically no net heat exchange should take place with the environment. For exothermic processes this is achieved by inserting an adiabatic shield, consisting of a thin-walled metal envelope with a heater wound over its surface, between the calorimetric vessel and the thermostatic bath.

These calorimeters are not suited for studies of micro-organisms, however, because they depend on measurement of temperature rises for their operation, and also are of the batch type, with its attendant disadvantages.

Calorimeters operating on the basis of measurement of rate of heat transfer were developed in the 1940s and 1950s, and proved well suited for study of slow reactions, but still had rather large volumes and slow response time, and were still of the batch type.

The present ability to study micro-organism–drug interactions by calorimetry has arisen from the development of modern isothermal differential microcalorimeters designed to operate on small sample volumes (0.1–1.0 ml) and micromole quantities of reagents, and measure very low power output changes with high precision (0.1% at the 200-μW level).

The development of such calorimeters awaited the introduction of, amongst other components, semiconductor thermopiles and high-performance amplifiers.

Isothermal power-conduction microcalorimeters

Most of the microcalorimeters currently used for observations of cell–drug interactions have the same design principles (Fig. 1). They are built as twin instruments, with each calorimeter vessel sandwiched between semiconductor thermocouple plates surrounded by small aluminium blocks, the "primary heat sinks", the units being kept together by spring-loaded bolts and in good thermal contact with the main block through the primary heat sinks. The calorimetric block is enclosed in a steel container, positioned in a thermostatic air- or water-bath. The thermocouple plates surrounding each calorimetric vessel are arranged in series, and the two thermopiles thus formed are connected in opposition. The differential voltage signal is amplified and recorded (integrated). Calibration constants are normally determined electrically. The sensitivity of most designs is 10^{-7} W and the baseline stability 1 μW/day. For steady-state processes, the thermopile voltage (V) is

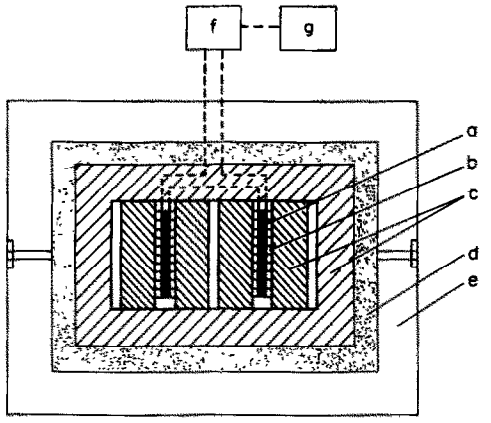

Fig. 1. Typical calorimetric arrangement: a—reaction vessel; b—thermocouple plate; c—heat-sink; d—insulation; e—thermostatic bath. From reference 12, with permission.

directly proportional to the rate of heat evolution [*i.e.*, the power, $(W = dQ/dt)$] in the calorimeter vessel. The calorimeter clearly acts as a wattmeter and the recorded voltage *vs.* time curve is directly related to the kinetics of the process studied ($V = \text{const.}dQ/dt$). Integration of this equation leads to $Q = \text{const.}Vt$. The quantity of heat evolved (Q) is thus proportional to the area under the voltage–time curve.

Batch calorimeters

Batch reaction calorimeter (*Fig. 2*). The reaction vessel consists of rectangular or square cans divided into two compartments by a partition connected by an air gap. The compartment volumes are usually 2 and 4 ml. The cans are made from steel, glass or gold. After the vessels have been charged and the block temperature adjusted, the calorimeter is allowed to equilibrate for about $1\frac{1}{2}$ hr. The reaction components are then mixed by rotation of the calorimetric block, one turn and back.

Ampoule drop calorimeter (*Fig. 3*). The sample is put in a steel ampoule, volume 1–10 ml, which is then brought (in a thermostat) to about the operating temperature of the calorimeter, and is transferred to the thermostatically controlled copper constriction (B) for a few minutes. It is then lowered to the aluminium block (D) for further temperature equilibration, and finally lowered into the thermopile zone (N). The calorimeter will reach equilibrium about 20 min after the ampoule is introduced into the heat-exchange system, depending on the size of the ampoule and its contents. The power–time (p–t) curve obtained with the reaction ampoule containing only the micro-organisms (no test sample) serves as the reference.

The great disadvantages of batch calorimeters are that the contents of the vessel are not easily accessible, and manipulations are difficult to perform (*e.g.*, drugs can be added only at the beginning of the experiment) and always cause thermal disturbance of the system. Batch techniques do not allow sampling or the use of physicochemical probes (for measuring pH, absorbance, *etc.*) during the experiment. Exact control of gaseous conditions, particularly aerobic atmospheres, is difficult to maintain. This means that obligate aerobes will not yield a usable p–t curve in a batch calorimeter unless a device permitting aeration of incubations is used. Beezer *et al.*[18] have

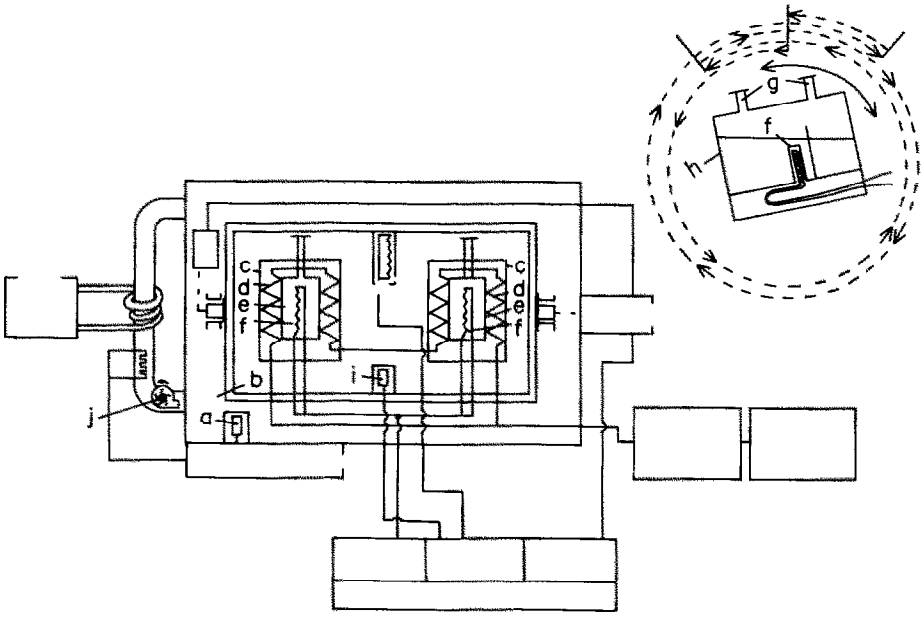

Fig. 2. Block diagram of a batch microcalorimeter: a—thermostatic-bath sensor; b—heat-sink in cylindrical, rotating casing; c—detectors; d—thermopiles; e—reaction vessels; f—calibration heaters; g—reaction-vessel filling ports; h—heat-sink heater; i—heat-sink sensor; j—circulation pump.

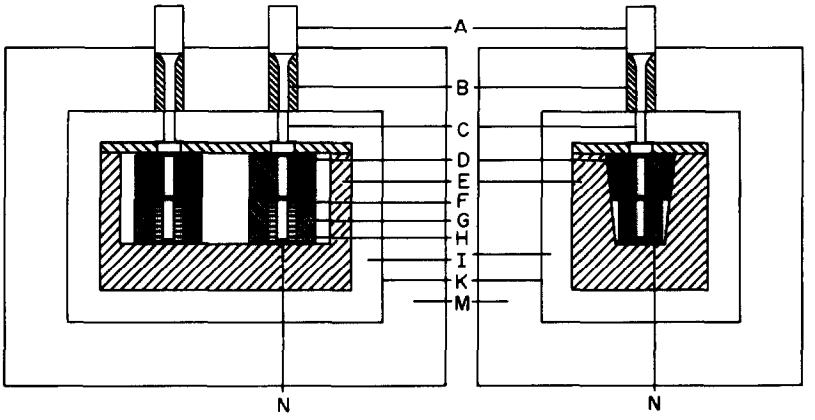

Fig. 3. Block diagram of an ampoule calorimeter: A—steel tube; B—copper constriction; C—steel tube; D—aluminium block; E—main heat-sink; F—air-space; G—aluminium block; H—thermocouple plate; I—air-space; K—steel container; M—water thermostat; N—aluminium plate with hole for ampoule. From reference 12, with permission.

shown by isothermal power-conduction flow microcalorimetry that the form of the p–t graphs for the growth and metabolism of micro-organisms varies with the nature of the atmosphere above the microbial incubation. Micro-organisms in unstirred suspensions in batch calorimeters settle out, and since their growth is normally followed over a period of 7–20 hr, cells originally in suspension may sediment, leading to differential gradients of cell density, nutrients and dissolved gas. The metabolic processes may result in pH stratification in the calorimetric vessel, and this may have at least two effects; metabolism may vary as a function of pH, and the heat of reaction will depend on the degrees of protonation of substrates and metabolites. Physical effects such as adsorption on the walls of the cells, mechanical effects, ionization and other side-reactions, as well as incomplete mixing, may also pose problems.

Experimental requirements for calorimetric studies of micro-organisms and their interactions with drugs

These studies require certain experimental conditions to be fulfilled. A reaction vessel which can be repeatedly sterilized is required, and a device for taking samples for culture is advantageous. A stirrer for the vessel contents is necessary. Control of the cell atmosphere, aerobic or anaerobic, is essential for standardization of experiments, because the metabolism of micro-organisms may alter according to the nature of the atmosphere. Provisions for analysing the cell suspension, *e.g.*, for monitoring the composition of the medium, are often required, and incubation media of defined chemical composition are therefore preferred. Measurement of temperature, pH, *etc.* of the cell suspension during the experiment is essential. Temperature control of the incubation vessel contents must be precise because variations in temperature will affect the kinetics of micro-organism–drug interactions.

The incubation vessel must therefore be designed with gas inlets and outlets, accommodation for sensors, and a means of easy and rapid addition of materials to the incubation vessel without altering the physical conditions of the system. Contamination of the incubation vessel with other micro-organisms must be avoided, especially in view of the long time-span of some experiments.

The test organism used must be susceptible to the drug under investigation, grow reasonably quickly in the assay medium, be non-virulent to man for reasons of safety, and be easy to maintain. Its susceptibility to the drug should not change with successive subcultivation. Whenever possible the same organism should be used. For example *E. coli* from one source may not give the same p–t curve as *E. coli* from another. The inoculum density and method of preparation require to be the same in each experiment.

The calorimetric instruments used should have high power sensitivity, allowing both large (10^7–10^8 cells/ml) and small cell concentrations (ideally 10^2–10^3 cells/ml) to be studied and subtle changes in properties (*i.e.*, cell metabolism) to be detected, and have long-term stability, high precision and good reproducibility. Since the different types of inocula studied may require different temperatures for optimal growth, the calorimeter should be able to operate isothermally at different temperatures. This is also important for monitoring temperature effects on the interactions. The microcalorimeter must also have low thermal inertia in order to detect kinetic phenomena. It is advantageous if the technique is non-invasive, *i.e.*, does not alter the properties of the system or introduce artefacts during the experiments. Removable microcalorimetric vessels of different internal design and dimensions are advantageous. Physical effects such as condensation, evaporation and surface adsorption phenomena must not occur in the calorimetric vesels. The microcalorimeter should be able to handle all types of cultures. The suspension employed should be homogeneous, but any stirring mechanism used should cause only negligible heat effects.

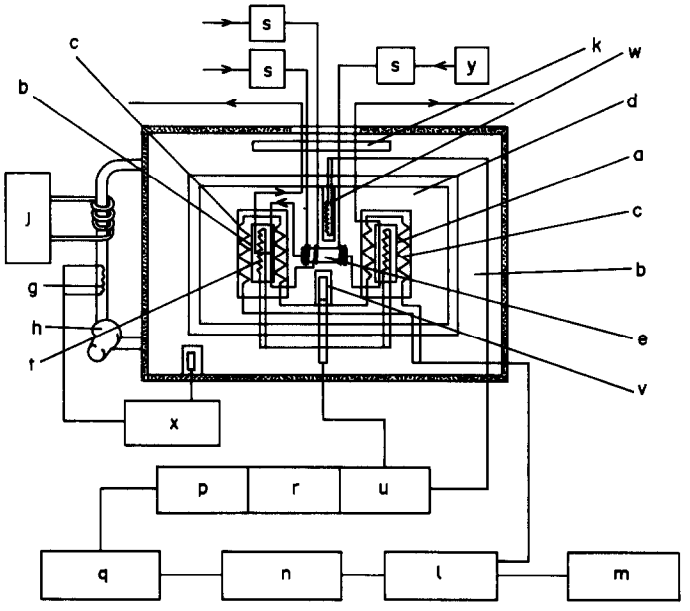

Fig. 4. Schematic diagram of flow microcalorimeter: a—flow-through vessel; b—mixing vessel; c—thermopile plates; d—heat-sink; e—heat-exchange unit; f—air-bath; g—air-bath heater; h—air-bath fan; j—external water-bath; k—primary heat-exchanger; l—amplifier; m—recorder; n—digital voltmeter; p—printer driver and timer; q—print-out; r—control-unit; s—peristaltic pumps; t—calibration heaters; u—temperature indicator; v—thermistor; w—heater; x—air-thermostat control; y—culture vessel.

An instrument with fast equilibration can considerably reduce the cycle time for repetitive assays. Simplicity of operation and calibration should be incorporated in the design. Multichannel instruments are preferable for industrial and clinical use, and computerized data-acquisition and treatment is desirable. Finally, it is advantageous if other analytical techniques can be used simultaneously with the calorimeter without disturbing its measurements. These criteria are met to a large extent by the flow microcalorimeter designed by Spink and Wadsö.[10]

The isothermal power-leak flow microcalorimeter shown in Fig. 4 is the one most commonly used for these studies. It contains a mixing vessel and a flow-through vessel. When the latter is used, the reaction mixture, *e.g.*, micro-organisms plus drug(s), is pumped through it from an incubation (reaction) vessel outside the calorimeter, by peristaltic pumps, and returned to the reaction vessel, to form a closed loop system. The instrument measures the power generation by the reaction process within the flow-through vessel, relative to power changes in the empty mixing vessel. The power output is amplified and recorded as a p–t curve.

Advantages and disadvantages of flow microcalorimeters for cell–drug studies

The advantages are as follows.

(1) Because of its sensitivity and the fact that the effect of drug(s) on the whole metabolism of the organism may be examined, microcalorimetry may reveal more and even new detail of micro-organism–drug interactions than extant methods can, especially those which use a specific reaction property for analysis.

(2) The calorimetric method requires only an observable difference between the power production in the treated and untreated (control) incubations, and unlike many other procedures does not require a transparent solution. Furthermore, measurements may be made directly without further addition of reagents. Coloured or turbid solutions or even suspensions can be put through the calorimeter. This is particularly important when examining certain pharmaceutical formulations.

(3) The system can be automated. This is of particular relevance for industrial and clinical applications.

(4) The kinetics of the action of antimicrobial drugs (or other cytotoxic agents) can be studied conveniently by means of the power–time curve.

(5) The mechanism of the drug action is immaterial; both antibacterial and antifungal drugs can be examined.

(6) Many of the problems with batch microcalorimeters are avoided. The flow microcalorimeter is connected to an external fermenter in which the culture grows. All manipulations are performed in the fermenter, so the thermal equilibrium of the calorimeter is not disturbed. Simultaneous measurements on the culture (for instance continuous determination of turbidity, pH, temperature, oxygen concentration, substrate consumption and viable cell counts) are readily made since the volume of the flow

Table 1. Methods for recording growth and metabolism in microbial cultures

Turbidity	Slow, low sensitivity, responds slowly to sudden changes in energy metabolism
Cell mass	Same as for turbidity
Production of acid	Directly related to growth and metabolism only in special cases, in aerobic cultures variable and depending on oxygen availability
Measurement of redox potential	Same as for production of acid
Dissolved oxygen tension (galvanic)	Rapid, but limited to aerobic cultures with oxygen in excess
Oxygen consumption (paramagnetic)	Fairly rapid, but limited to aerobic cultures
Carbon dioxide (formation, infrared)	Variable under different metabolic conditions
Heat production	Rapid (half-time responses ~2 min), directly dependent on catabolic reactions

(Reprinted from R. Eriksson and T. Holme, *LKB Application Note 267*, 1977 with permission).

lines is only a small fraction of the culture volume. Moreover, addition of special substances, such as additional drugs, is facilitated.

(7) The flow system is more akin to the *in vivo* state than are, for example, the systems used in diffusion assays.

(8) The flow systems represent the effect of drugs on the total metabolism of the micro-organisms. This again more closely approximates the *in vivo* state than do techniques which measure a single parameter of cell metabolism for analytical purposes.

(9) The appearance of cytoplasmic cell components, due to interaction of cells with drug(s), may also be monitored (providing suitable probes are available) to elucidate the mechanism of action of a drug or provide insight into the nature of the power–time curve.

(10) Table 1 shows that microcalorimetry does not possess the disadvantages shown by other methods for recording growth in microbial cultures.

The disadvantages of the microcalorimeters of this type currently available include the following.

(1) The calorimeters are not sufficiently sensitive to measure the power output from cell concentrations of 10^2–10^3/ml. The present detection limit is *ca.* 10^4–10^5 cells/ml. Moreover the metabolic process followed is catabolism; as yet anabolic processes cannot be examined microcalorimetrically.

(2) The lag time between the initiation and detection of a reaction. This means that very fast reactions (complete in 2–3 min) cannot be examined.

(3) Some difficulties, especially with respiring cultures with high cell density, arise because of the time taken for transfer from fermenter to calorimeter, during which a substrate of the medium, often oxygen, can change sufficiently in concentration for the metabolic conditions in the calorimeter to be different from those in the fermenter.

(4) Care has to be taken to avoid the presence of gas bubbles or the clumping of cells in the flow lines and microcalorimetric vessel, and the growth of micro-organisms on the microcalorimeter wall (otherwise, erroneous signals may be obtained).

(5) It is as yet very seldom that the signals from thermopile conduction calorimeters are corrected to give the true kinetic curves.[19] However, the biological processes are often so slow that the distortion is negligible.

Power–time curves

The simplest case of microbial metabolism to describe in terms of heat production is catabolism not coupled with anabolism, *i.e.*, metabolism without growth. Microbial cells, when washed, suspended in buffer and supplied with glucose, will establish a constant rate of glycolysis under anaerobic conditions. No work is done by the cells in increasing biomass or accumulating reserve material. A small amount of energy is expended in the translocation of glucose from the medium to the cell cytoplasm and in keeping the correct ionic balance between the cell and its environment. Therefore under conditions of respiratory metabolism a sigmoidal p–t curve is obtained by flow microcalorimetry. This curve is similar to those produced from an enzyme–substrate reaction or other chemical reactions exhibiting zero-order kinetics.[20,21]

When placed in a nutritionally adequate medium with glucose as the energy-supplying substrate, micro-organisms will grow, but still essentially convert all the glucose into metabolic products and build the cell mass from other compounds in the medium. In growing, the micro-organisms perform work in transporting and synthesizing materials and organizing the structure of the new biomass. The synthesis of biomass would be expected to reduce the amount of heat produced by catabolism, but this anabolic effect on the measured heat production is negligible. The rate of synthesis of new cell material, the degradation of carbon sources, and the power production are known to be described by the same type of exponential function. Therefore the kinetics of the effect of substances on the metabolism of growing cells can be examined.

The exact nature of the p–t curves for growing cells, obtained by isothermal power-conduction microcalorimeters, depends on the following factors.

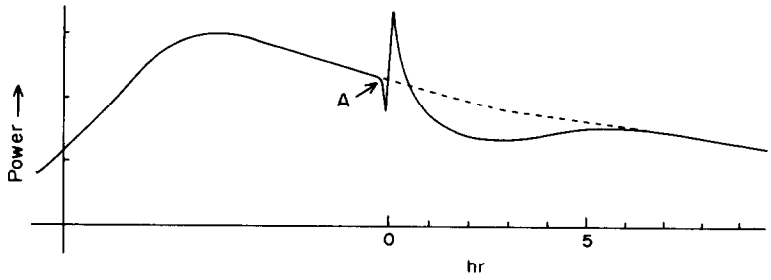

Fig. 5. Interaction of streptomycin with *E. coli* (Calvet batch instrument used). Reproduced with permission.[22]

(1) The microcalorimetric technique used (batch or flow). If a flow instrument is used then the microcalorimeter–incubation vessel assembly will also be a factor of importance.

(2) The constituents and pH of the medium, pO_2, temperature, homogeneity of the cell suspension, rate of stirring.

(3) Nature and prehistory of the micro-organisms and apparatus used for their preparation, and the inoculum density.

QUALITATIVE STUDIES

The earliest recorded calorimetric experiments on the effects of drugs on the metabolism of micro-organisms were conducted by Prat.[22] A batch Calvet instrument was used to demonstrate that the addition of 30.0 mg of streptomycin (in 1.0 ml) to 4.0 ml of a broth culture of *E. coli* (26-hr culture; mid-exponential growth phase) at 24.4° resulted in a marked fall in the power output, to one-tenth of the original value after 6.0 hr (Fig. 5). The cellular metabolism was found to be much more rapidly inhibited if the culture was stirred. Thus a limiting factor in the antimicrobial action of the antibiotic was its rate of diffusion through the medium in a static culture. The medium and atmospheric conditions were not specified.

The induction period for action of penicillin on *E. coli* (initial concentration 6×10^6 cells/ml) was found,[23] by modified isoperibolic calorimetry,[24] to depend on the phase of growth at which the antibiotic was added to the culture. At 25° the p–t curves for *E. coli*–penicillin interaction indicated that the induction period decreased with increase in the time spent by the cells in the logarithmic phase before the antibiotic was added (Fig. 6). The effects of streptomycin, chlortetracycline and oxytetracycline on *E. coli* were also studied. The p–t curves for streptomycin added to a culture in the logarithmic growth phase indicated an induction period of 15 min, that for oxytetracycline and chlortetracycline being only "a few minutes" (Fig. 7). In the same study it was also demonstrated that oxytetracycline added during the logarithmic phase of *S. typhi* (initial concentration 1.4×10^6 cells/ml) under the conditions used in the *E. coli* studies produced a similar change in the p–t curves of *S. typhi* as for *E. coli*, except that the induction period was longer (45 min). The concentration of antibiotics, the growth medium for prepa-

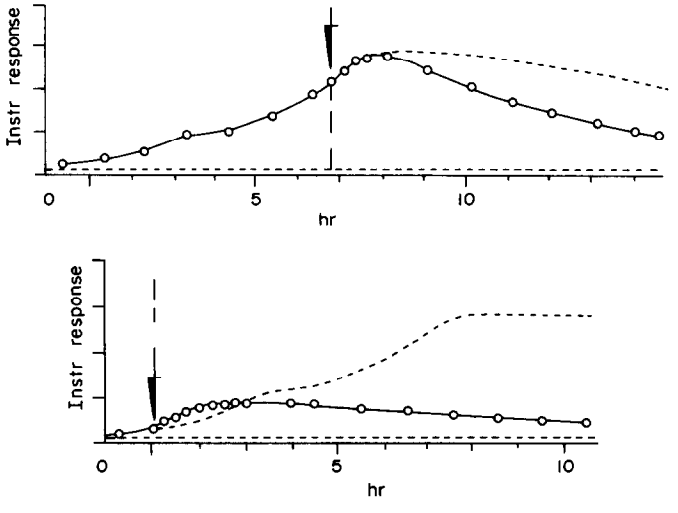

Fig. 6. Addition of penicillin to *E. coli* at different times during cell growth. Continuous curves denote experiment in which antibiotic was added, and the broken curves represent control experiments. Reproduced with permission.[23]

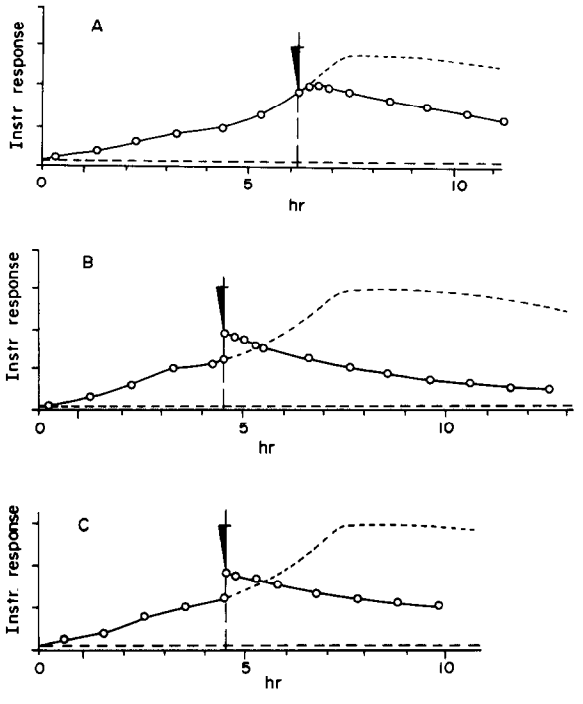

Fig. 7. Effects of streptomycin (A), oxytetracycline (B), and chlortetracycline (C) on a culture of *E. coli* in the logarithmic phase. Reproduced with permission.[23]

ration of the micro-organisms, and the atmospheric conditions of incubation were not specified.

Micro-organism–drug interactions monitored by an isothermal power-leak flow microcalorimeter were first reported by Wadsö.[25] Qualitative differences between the $p-t$ curves for *E. coli*–ampicillin cultures and *E. coli* alone were observed to occur 1 hr after addition of the antibiotic (Fig. 8); the tests were conducted in a complex medium at 28°.

Mardh *et al.*[26] have examined the biological activity of the tetracyclines minocycline, doxycycline, tetracycline and oxytetracycline on *E. coli* (source: infected urine, initial concentration 10^4 cells/ml). A temperature of 37° and trypticase soy broth (BBL), pH 7.2, as test medium were employed. The effect of the antibiotics on cells in the lag phase was examined with a batch microcalorimeter (with 1.0 ml of air as the initial gas phase). A flow microcalorimeter was used to study cell–drug interactions in the logarithmic phase of cell growth under aerated conditions (Figs. 9 and 10). The viable-cell count and minimum inhibitory concentration (MIC) for the cell cultures were also determined. The addition of half the MIC of minocycline and tetracycline (0.8 μg/ml) prolonged the lag phase of the cells by 8 hr. All four antibiotics decreased the power output immediately they were added to cells in the logarithmic growth phase but the extent and duration of the effect varied with the biological activity of the drugs. Although the antibiotics had the same MIC values, at levels above and below this they showed differences in ability to suppress the metabolism of the test organisms, the order being minocycline > doxycycline > oxytetracycline > tetracycline for both lag-phase and logarithmic-phase cells. It was suggested that the extent and duration of the inhibitory effect on the overall metabolism of *E. coli* could be combined with pharmokinetic information to establish dose intervals during antibiotic therapy. These experiments may be criticised because the experiments in the batch calorimeter started with aerobic conditions, but a shift to anaerobic metabolism of the bacteria may have occurred. It would have been advantageous to examine the effect of the tetracyclines on lag-phase cells by flow microcalorimetry to obtain a better comparison of the bioactivity of the drugs at different phases of the cell cycle.

Similar experiments on tetracycline hydrochloride, demethylchlortetracycline, doxycycline and minocycline have been reported by Semenitz and Tiefenbrunner[27] (Table 2). A flow microcalorimeter with a 1.0-ml steel ampoule measuring cell operated at 35° was used; the initial concentration was 10^6 cells/ml. Addition of tetracycline hydrochloride to a resistant strain of *S. aureus* caused an initial cessation in power production followed by an increase in the $p-t$ curve. The responses of sensitive and resistant strains to doxycycline and minocycline were identical, indicating no change in the mechanism of action. The immediate inhibition, by the tetracyclines, of power output from bacteria, observed by Mardh *et al.*, was verified in these experiments (Fig. 11).

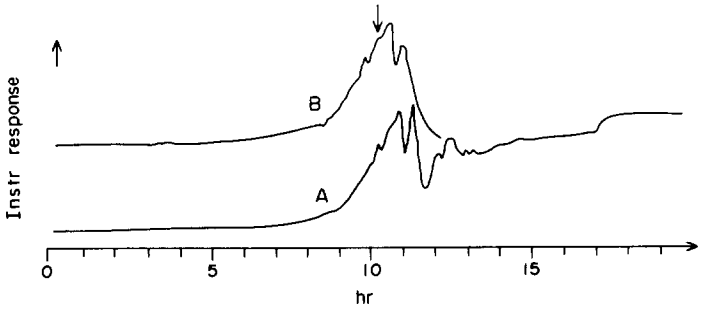

Fig. 8. Power–time curves of *E. coli* alone (A) and in the presence of ampicillin (B). The ampicillin was added at the point marked. Reproduced with permission.[25]

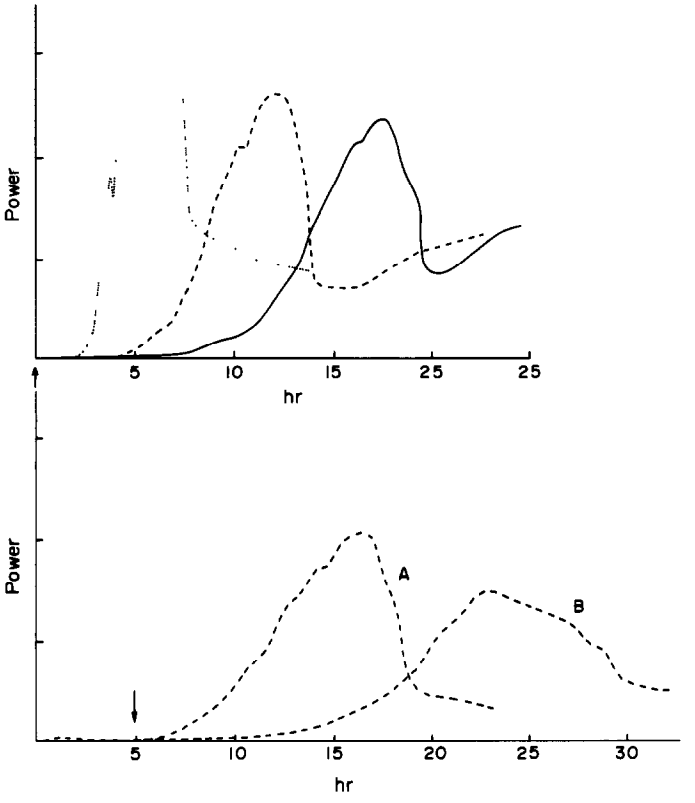

Fig. 9. Heat effects produced by *E. coli* cultured in the presence of tetracycline (----) and doxycycline (——). For comparison, the thermogram of a non-antibiotic-containing culture is shown (· · · ·). Reproduced with permission.[26]

Flow microcalorimetric experiments on *E. coli* (O 119, H 19) in the logarithmic growth phase indicated that cinoxacin (3.4 μg/ml) caused a decrease and delay in the power output of the microorganisms, followed by an increase in power output due to selection of cinoxacin-resistant mutant cells (Fig. 12).[28] The cells were examined at 37° in trypticase soy broth (pH 7.1) constantly aerated by sterile air bubbled through it. Exposure of the organism to the antibiotic also caused (1) a change of MIC from 1.7 μg/ml at the beginning of the experiment to 400 μg/ml after 17 hr; (2) appearance of elongated, filamentous bacterial forms within 1 hr; (3) lysis of a large percentage of the bacteria after 5 hr; (4) presence of normal bacterial cells again at the end of the experimental period.

The antibacterial activity of oleandomycin and erythromycin (both macrolide antibiotics) against *Staphylococci* and *Enterococci* has been compared by microdilution MIC tests and by flow microcalorimetry; the initial cell concentrations were 5.0×10^5 cells/ml.[29] The bacteria were grown in Columbia Broth (Difco). The p–t curves indicated that both antibiotics interfered with bacterial metabolism at concentrations significantly lower than their MICs (Fig. 13); the MIC of erythromycin for *S. aureus* strains was one-tenth and for *Enterococci* one-half that of oleandomycin. A 0.020–0.84 μg/ml concentration of the antibiotics altered the p–t curves of *S. aureus* in an identical manner. Although their *in vitro* activity measured by MIC tests differs, the two antibiotics apparently show similar clinical effectiveness and bioactivity; this may be a result of either different pharmacokinetics or of interference with bacterial metabolism at sub-MIC levels.

Beezer *et al.* have examined the effect of pH, metal ions (Ca^{2+}, Mg^{2+}) and sterols (ergosterol, cholesterol) on the interaction of polyene antibiotics with respiring yeast cells, by flow microcalorimetry.[30] The experiments were done at 30° with 0.1*M* glucose (in phthalate buffer) as substrate under anaerobic conditions. Standardized inocula recovered from liquid–nitrogen storage were employed. The bioactivity of nystatin was found to be pH-dependent; it was maximal at pH 3.0 and decreased with increasing pH. Both sterols and metal ions reduced the bioactivity of nystatin, amphotericin B and candicidin. The reduction in bioactivity was a function of the nature and concentration of sterol or metal ion added. No observable changes in the p–t curves of pimaricin were detected in the presence of either sterols or metal ions. The bioactivity of filipin was reduced in the presence of sterols but remained unaltered in the presence of metal ions. Possible explanations were given for these observations. Although similar conclusions have been reached by use

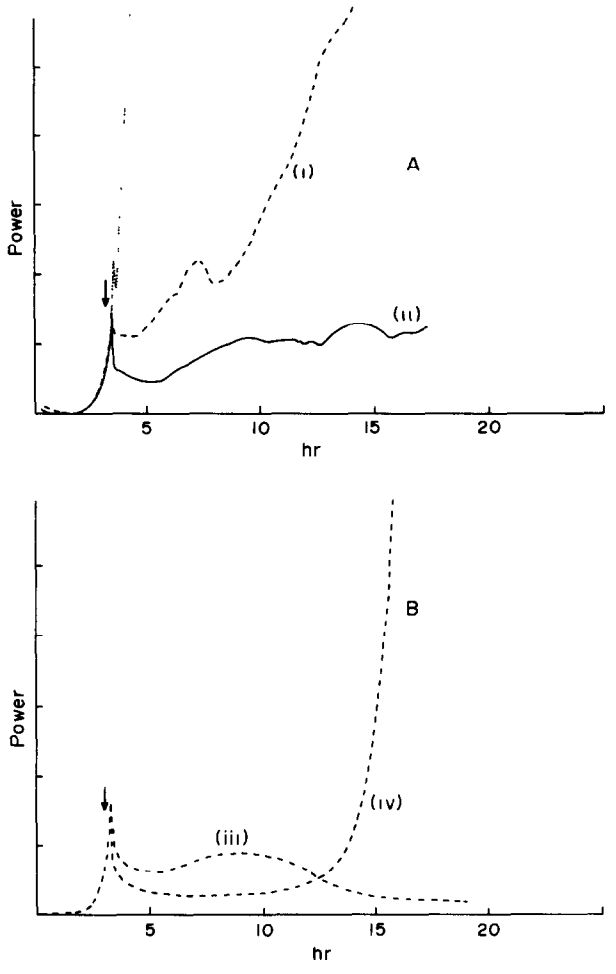

Fig. 10. Heat effects produced by *E. coli* in the presence of oxytetracycline (A) and minocycline (B). The concentration of the antibiotics was 0.4 μg/ml (0.5 × MIC). The arrows indicate point of addition. Reproduced with permission.[26]

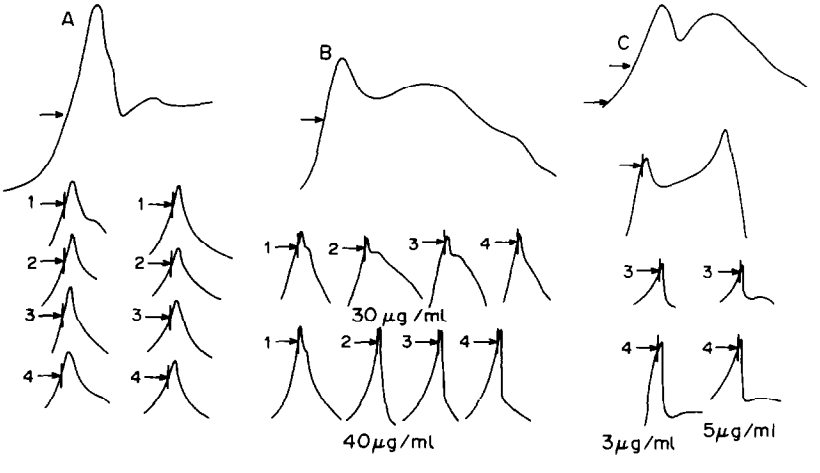

Fig. 11. Interaction of tetracyclines with (A) *E. coli* H3579 BBSUA, (B) *S. aureus* BBSUA and (C) *S. aureus* A2953 BBSUA: 1, tetracycline hydrochloride; 2, demethylchlortetracycline; 3, doxycycline; 4, minocycline. Reproduced with permission.[27]

Table 2

Organism	Source	Growth medium	MIC	Power–time curves
(1) *E. coli* H 3579 BBSUA	Urine, (cystitis patient)	Purple Broth + 1% dextrose	1.5 μg/ml culture medium	All antibiotics at concentrations of 3 and 40 μg/ml
(2) *Staph. aureus haem* A 3579 BBSU	Pus samples	Columbia Broth	0.7 μg/ml	All antibiotics at concentrations of 3 and 30 μg/ml
(3) *Staph. aureus haem* A 2953	Pus samples	Columbia Broth + physiological NaCl solution	250 μg/ml (a) 70 μg/ml (b) 15 μg/ml (c) 15 μg/ml (d)	Antibiotics (a) (c) and (d) at 30 μg/ml

(a) = tetracycline – HCl; (b) = demethyltetracycline; (c) = doxycycline; (d) = minocycline.
*From reference 27, by permission.

of other analytical techniques, previous experiments suffered from the drawback that a range of polyene antibiotics was not used in the same experiments, and only component reactions of cell–drug interactions were used for monitoring purposes instead of the effect on the whole metabolic activity of the micro-organisms.

The kinetics of action of benzylpenicillin, ampicillin and dicloxacillin on β-lactamase-producing (D349) and non-β-lactamase-producing (483) strains of *S. aureus* and on *E. coli* (O 119; H 19) have been investigated by flow microcalorimetry.[31] The bacteria were grown in trypticase soy broth at 37°; an initial concentration of 10^4 CFU/ml of these cells was added to the incubation vessel (CFU = colony-forming unit). The exposure of certain micro-organisms to benzylpenicillin and ampicillin gave a phenomenon termed the paradoxical zone (Table 3; Fig. 14), *i.e.*, the inhibitory effect of these agents on bacterial metabolism was smaller with intermediate concentrations than with low or high concentrations of the drugs. This phenomenon could have clinical importance. The study also indicates the importance of identification of micro-organisms so that optimal therapeutic doses of drugs can be prescribed if this phenomenon occurs *in vivo*.

Measurements of the action of nystatin on yeast cells by flow microcalorimetry, combined with measurements of oxygen consumption and percentage colony formation, have been used to assess the effect of glucose and ethanol on the bioactivity of this antimycotic agent.[32] Respiring (non-growing) cells suspended in phthalate buffer (pH 4.5) were used (Fig. 15). It was concluded that at concentrations of nystatin between 0 and 2 μg/ml the effect of the additive on the bioactivity of the drug was in the order 2% glucose < 0.1% glucose < 0.2% ethanol. However, the use of unstandardized inocula may have been enough to account for the difference between the bioactivity of nystatin in 0.1% and 2% glucose.

Semenitz[33] has hypothesized that flow microcalorimetry may be used to distinguish between drugs which are inhibitors of protein synthesis and those

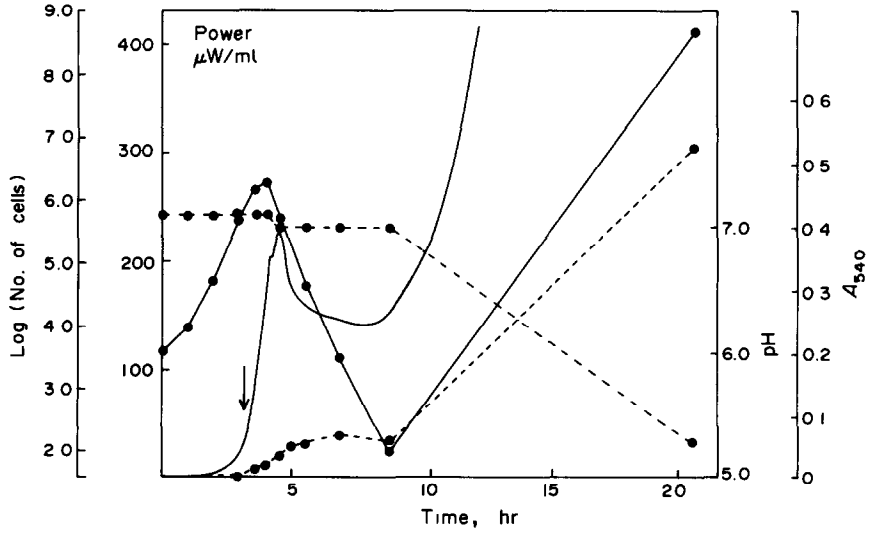

Fig. 12. Power–time curve produced in a flow microcalorimeter by *E. coli* exposed to 2 × MIC (3.4 μg/ml) of cinoxacin. Also shown are the number of colony-forming units, (CFU/ml, ●——●); absorbance (A_{540}), ●···●; pH (●–·–●). The arrow marks the addition of drug. Reproduced with permission.[28]

Table 3

Micro-organism	Drug	Order of bioactivity	Presence of paradoxical phenomenon
Non-β-lactamase *S. aureus*	Benzyl penicillin	10 μg/ml, 0.04 μg/ml 0.1–0.2 μg/ml	+
Non-β-lactamase *S. aureus*	Ampicillin	0.04–0.3 μg/ml 0.08 μg/ml	+
E. coli	Ampicillin	1.6 μg/ml, 4.0 μg/ml 8.0 μg/ml	+
β-lactamase *S. aureus*	Benzylpenicillin	–	–
β-lactamase *S. aureus*	Dicloxacillin	–	–

which interfere with the synthesis of the microbial cell envelope. Oleandomycin, erythromycin, and doxycycline gave *p–t* curves which were qualitatively the same but differed from those obtained with penicillins (epicillin, penicillin, ampicillin, oxacillin, carbenicillin and azvocillin (Fig. 16). *Staphylococcus aureus haem* 13665, and *E. coli haem* 3529 grown at 35° on Columbia Broth (Difco) plus 0.2% Tween 80, were employed as the test organisms. Continuous turbidimetric measurements supported the conclusion reached. However the flow microcalorimetric *p–t* curves contained more detail than the corresponding

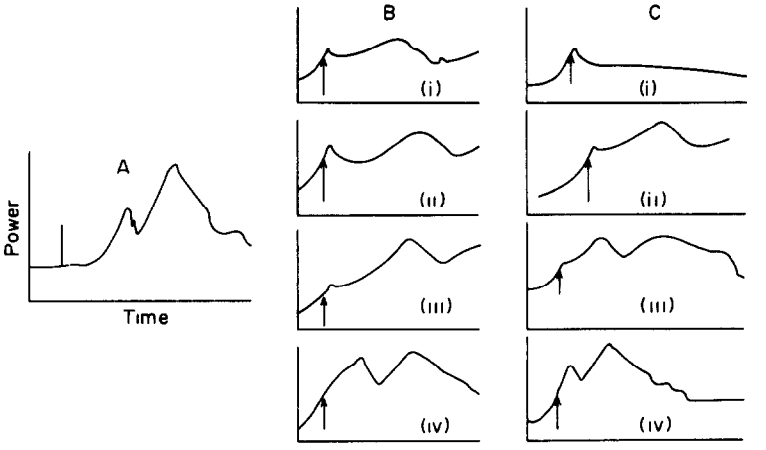

Fig. 13. Power–time curves for *S. aureus* A13665 alone (A) and in the presence of oleandomycin (B) and erythromycin (C). Concentration (μg/ml) of drug added at point marked: i, 0.4; ii, 0.2; iii, 0.08; iv, 0.02. Reproduced with permission.[29]

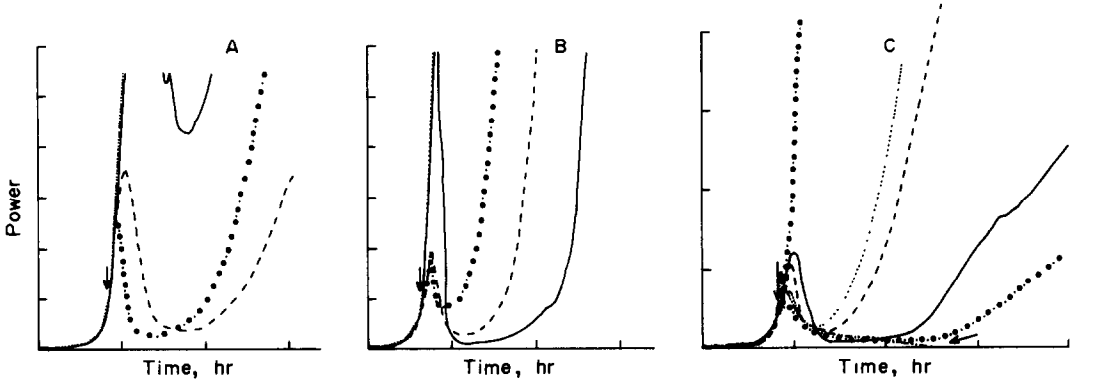

Fig. 14. Power–time curves for the interaction of *S. aureus* (Oxford Strain 483) with ampicillin (A), and benzylpenicillin (C), and for interaction of *E. coli* with ampicillin (B). Concentrations of drugs added at point marked: (A) (· · · ·) control; (——) 0.04 μg/ml ≡ 1 × MIC; (– – –) 0.08 μg/ml ≡ 2 × MIC; (·–·–·) 0.2 μg/ml ≡ 5 × MIC: (B), (· · · ·) control; (——) 1.6 μg/ml ≡ 2 × MIC; (– – –) 4.0 μg/ml ≡ 5 × MIC; (●–●) 8.0 μg/ml ≡ 10 × MIC: (C), (——) 0.04 μg/ml ≡ 2 × MIC; (· · · ·) 0.1 μg/ml ≡ 5 × MIC; (----) 0.2 μg/ml ≡ 10 × MIC; (●·●) 10 μg/ml ≡ 500 × MIC; (—·—·—·—) 200 μg/ml ≡ 1000 × MIC. From reference 31 with permission.

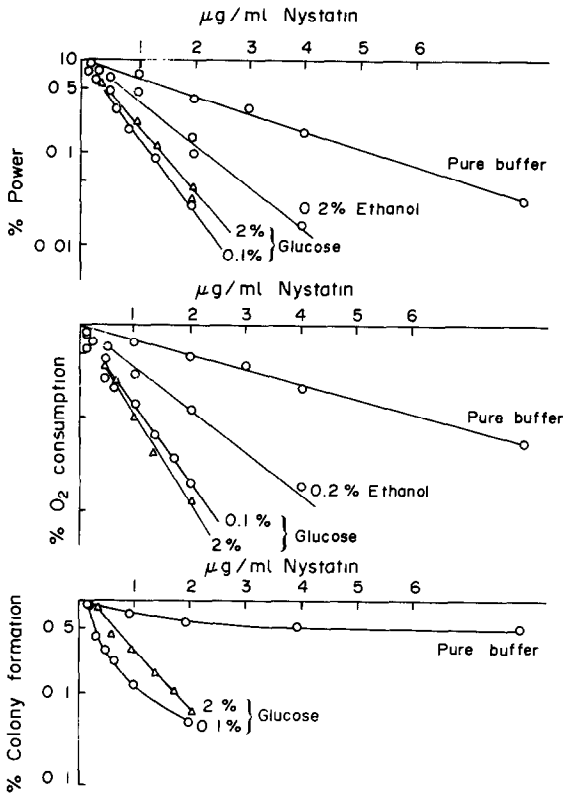

Fig. 15. Degree of production, O_2 consumption and colony-formation for respiration of *S. cerevisiae* in buffered glucose and its interaction with nystatin. From reference 32 with permission.

turbidimetric curves. The results could prove useful for distinguishing between the mechanism of action of newly discovered antimicrobial agents quickly, easily and conveniently.

QUANTITATIVE ANALYSIS OF DRUGS BY MICROCALORIMETRY

A method for the quantitative assay of tetracycline hydrochloride, based on the alteration in power output by the antibiotic during the exponential phase of *S. faecalis*, has been proposed (Fig. 17).[34] *S. faecalis* grown in rich medium at 37° was used. The Tronac isothermal calorimeter was also used for quantitative estimation of tetracycline hydrochloride in normal human serum (Fig. 18). No details of measurements of cell numbers or the composition of the atmosphere in the calorimeter were reported. Furthermore, no relationship between dose of antibiotic and calorimetric response was given and the method as described would be difficult to automate.

The *p–t* curves for doxycycline (at concentrations of 0–0.25 μg/ml) added to growing cultures of *Mycoplasma hominis* in a batch steel-ampoule power-leak calorimeter (Fig. 19) have been used for the determination of this antibiotic;[35] the experiments were conducted at 37° under essentially anaerobic conditions.

Though this batch technique may be valuable for studying the antibiotic susceptibility of organisms belonging to the order *Mycoplasmatales* the fact that the drugs may not be homogeneously mixed with the cell culture is of acute concern. The dose–response relationship between doxycycline concentration and instrument response was not reported.

Flow and ampoule microcalorimetric methods have been used to study the antibacterial action of cephalexin and cephaloridine against *E. coli* (O 119; H 19) and *S. aureus* 483;[36] the antibiotics were added to logarithmic-phase cells growing in undefined medium at 37°. Cephalexin added at concentrations of 5 MIC to *S. aureus* and 2 MIC to *E. coli* caused a decrease in power output (Fig. 20). Two–three hr after addition of the drug the power output became

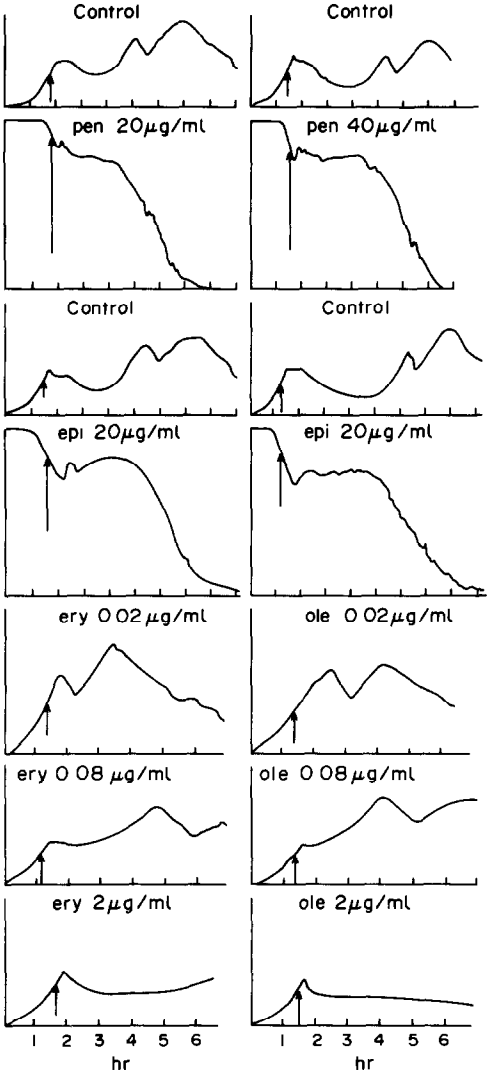

Fig. 16. Power–time curves and turbidimetric curves showing similarities between the interaction of penicillin and epicillin (both inhibitors of cell-wall synthesis); *p–t* curves for interaction of erythromycin and oleandomycin, both inhibitors of cell-wall synthesis. From reference 33 with permission.

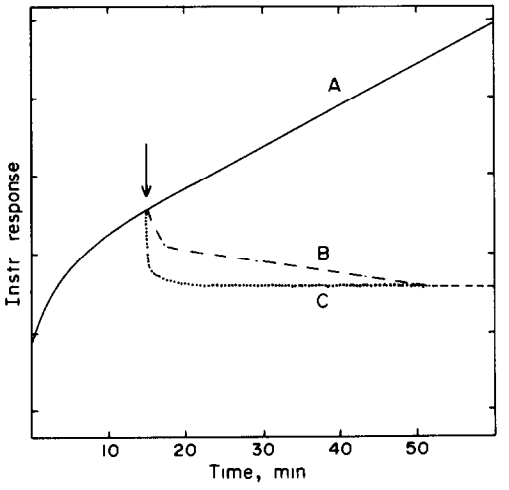

Fig. 17. Power–time curves for the interaction of tetracycline HCl with *S. faecalis*: (A) control; (B) 120 μg of tetracycline HCl/25 ml of broth; (C) 1180 μg of tetracycline HCl/25 ml. Reproduced from reference 34 with permission from the copyright holder, Elsevier Scientific Publishing Company, Amsterdam.

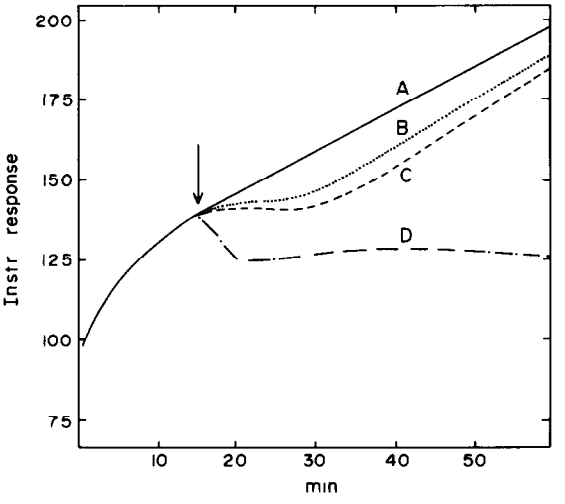

Fig. 18. Power–time curves for the interaction of tetracycline HCl with *S. faecalis* (A), control; (B), plus 200 μl inactivated human serum; (C), plus 200 μl of normal human serum; (D), plus 200 μg of 0.28 μg of tetracycline HCl per μl normal human serum. Reproduced from reference 34 with permission from the copyright holder, Elsevier Scientific Publishing Company, Amsterdam.

zero for the next 6–8 hr and then increased. A direct relationship between drug concentration and instrument response was found for 1–50 μg/ml added to cultures of *S. aureus*. The *p–t* curves obtained by ampoule microcalorimetry for the interaction of cephalexin and cephaloridine with *E. coli* indicated that the antibacterial activity of the two cephalosporins had similar kinetics. The power output in the cephaloridine-containing cultures occurred somewhat later than that with cephalexin, however.

The interaction of the polyene antibiotics nystatin, filipin, pimaricin, amphotericin B, candicidin and lucensomycin, and the synthetic antifungal imidazole drug clotrimazole with *Saccharomyces cerevisiae* NCYC 239 yeast cells has been examined in a number of studies by Beezer *et al.*[20,21,37,38] *S. cerevisiae* NCYC 239 was used as the responsive organism because it did not aggregate under the experimental conditions used, thus ensuring that maximal surface area of cells was exposed to the drugs. A flow microcalorimeter was used in all experiments, which were conducted under anaerobic conditions. The experiments were the first to employ cells recovered from liquid-nitrogen storage[39] for such studies. Furthermore they are the only example of studies of micro-organism–drug interactions using the same line of both non-growing but respiring mid-stationary phase cells and growing (mid-exponential phase) cells for studies of a series of structurally related compounds.

Cells recovered from liquid-nitrogen storage were used because the metabolic performance of inocula (which depends on inoculum size, inoculum history and phase of growth) is one of the major sources of variation in all microbiological assay methods. The use of inocula stored at liquid-nitrogen temperature instead of, for example, cultures grown overnight, minimizes these variations by allowing a standardized and highly reproducible inocululm to be used. Such inocula can be obtained by using a defined cell-

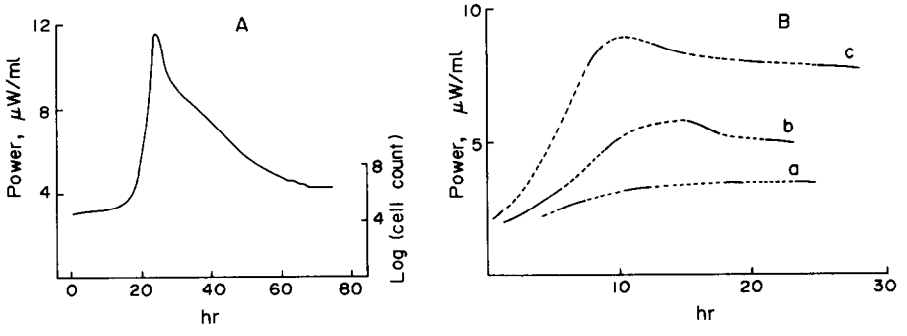

Fig. 19. (A) Typical *p–t* curve of *Mycoplasma hominis*; (B) *p–t* curves for *M. hominis* grown in the presence of (a) 0.25 μg/ml, (b) 0.10 μg/ml doxycycline or (C) in its absence. Readings were taken sequentially; the continuous lines indicate when each sample was being measured. From reference 35 with permission.

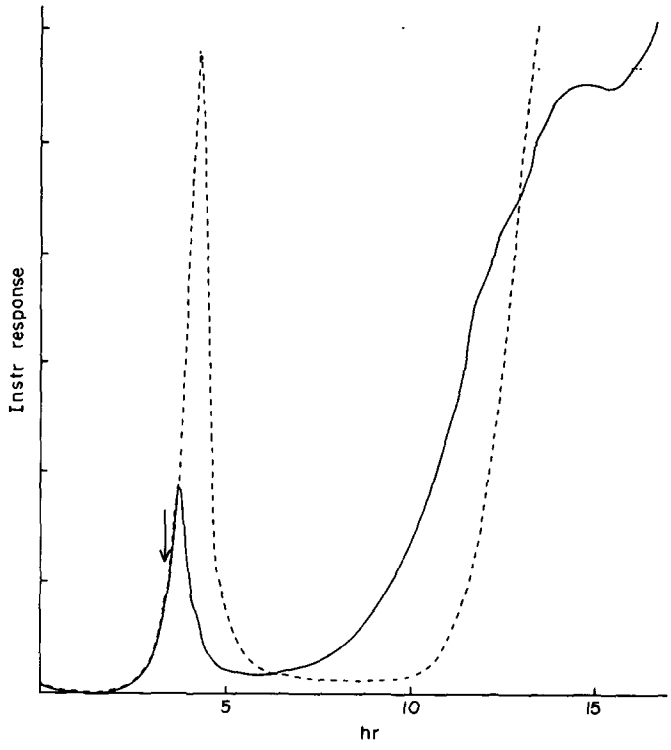

Fig. 20. Power–time curves produced by growth of *E. coli* in the absence of antibiotics (····) and when exposed to cephalexin (----; 9 μg/ml ≡ 2 × MIC) and cephaloridine (——; 6.0 μg/ml ≡ 2 × MIC). From reference 36 with permission from *Acta Path. Microbiol. Scand.*

growth regimen and rigorously standardizing the freezing and storage procedures. Liquid-nitrogen stored inocula can be regarded as bench reagents. Besides the advantage of allowing strict comparability between experiments, these inocula can be stored in bulk for long times (cells can be stored without significant changes in overall metabolism for periods in excess of 3 years). With frozen yeast-cell inocula the reproducibility of p–t curves for yeast-cell respiratory activity was found to be $\pm 2.5\%$ over a period of 3 years. The establishment of a dose-function *vs.* response curve for a given batch of inocula could suffice for large numbers of assays without recalibration. The freezing and thawing procedures for liquid-nitrogen frozen cells are simple and not time-consuming.

Eight-hour yeast-cell preparations (8.4×10^6 cells/ml) suspended at 25° in phthalate buffer (pH 4.5) containing glucose at 10m*M* concentration resulted in p–t curves which corresponded to simple zero-order kinetic processes (Fig. 21).[20] The addition of nystatin raw material to yeast cells gave a power output rate which first exceeded the maximum of that of the control but eventually fell below it when concentrations of nystatin of <5 units/ml were used. At higher concentrations of antibiotic (10–20 units/ml) this phenomenon was not observed (Fig. 21).

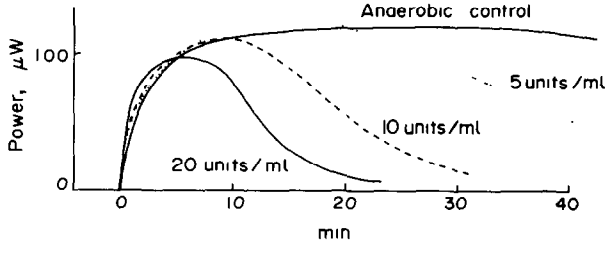

Fig. 21. Typical p–t curves obtained for respiration of *S. cerevisiae* in buffered glucose in the presence and absence of nystatin. Reprinted with permission from *Anal. Chem.*, 1977, **49**, 34. Copyright 1977, American Chemical Society.

Table 4. Sensitivity of yeast cells of different ages to nystatin

Age of cells, *hr*	Sensitivity range, *units/ml*
4.0	0.5–5.0
8.0	3.0–15.0
12.0	10.0–75.0

It was suggested that low concentrations of nystatin modified the yeast cell membrane in a way that permitted easier transport of glucose from the medium, thus giving rise to a temporary maximum power higher than that for yeast-cell controls.

A linear relationship was found between log of the nystatin dose and the time required for the signal to rise and fall from the first calorimetric response to some arbitrary level ($X\%$) above the baseline (*e.g.*, "B_{30}").

Microcalorimetric investigations of the action of nystatin on cell preparations of different incubation age before liquid-nitrogen freezing indicated that yeast cells were more susceptible to nystatin as the preparation age of the cells decreased (Table 4).

In the same study the potency of heat-treated nystatin samples was found to appear greater when determined by microcalorimetric techniques than by plate agar diffusion assay. This difference may possibly be attributed to the differing percentages of dimethylformamide used for solubilizing the nystatin in the two methods (0.3 and 10% respectively). Considerable differences in biological activity between heat-treated and non-heat-treated samples of nystatin were demonstrated.

In a follow up-study employing identical experimental conditions, except for a change in the temperature of the assay (30° instead of 25°) various dose–response relationships were obtained between the antibiotic concentration and instrument response,[21] the nature of the relationships depending on the identity and concentration of the antimicrobial agent (*e.g.*, Fig. 22). The microcalorimetric method showed distinct advantages over the agar diffusion test, in terms of lowest determinable concentration

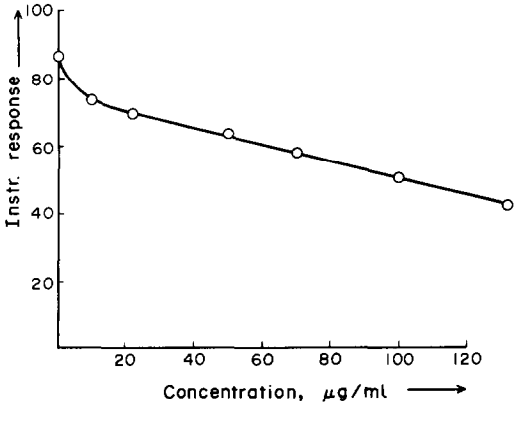

Fig. 22. Instrument response *vs.* dose curve for clotrimazole.

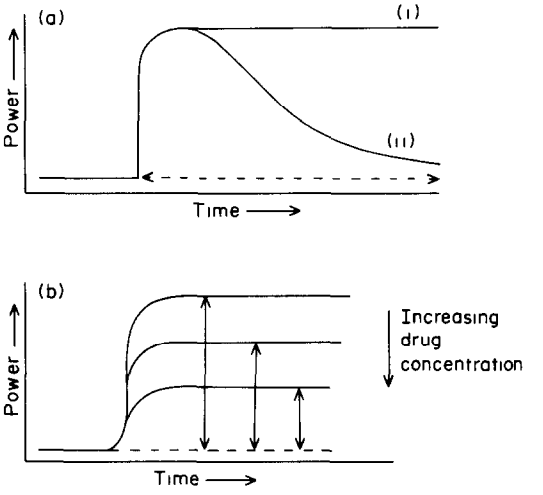

Fig. 23. Types of p–t curves obtained for the interaction of antifungal drugs with respiring cultures of *S. cerevisiae*: a(i) represents the response of yeast cells alone, a(ii) the response of yeast cells in the presence of nystatin, filipin, candicidin, amphotericin B and lucensomycin (the latter at concentrations of 5×10^{-6}–$1 \times 10^{-5} M/10^7$ yeast cells); b represents the types of p–t curves obtained with pimaracin, clotrimazole and lucensomycin (the latter at concentrations of 1–$5 \times 10^{-6} M$).

(0.120 unit/ml); usable concentration range (0.1–10 unit/ml) and speed (1 hr for microcalorimetry, 15 hr for diffusion assay).

The study indicated the importance of investigating dose–response relationships as a function of temperature, for establishing the optimum test temperature.

The order of bioactivity of the polyene antibiotics against respiring yeast cells was found to be nystatin > filipin > lucensomycin > pimaracin > candicin > amphotericin B.

It is interesting to note the concentration-dependence of the interaction of lucensomycin with respiring yeast cells between the two extremes of the observed microcalorimetric response (Fig. 23). Lucensomycin differs from pimaracin only in the alkyl side-chain R [$CH_3(CH_2)_3$– for the former and $-CH_3$ for the latter; Fig. 24] yet the two antibiotics show a completely different activity towards yeast cells in the

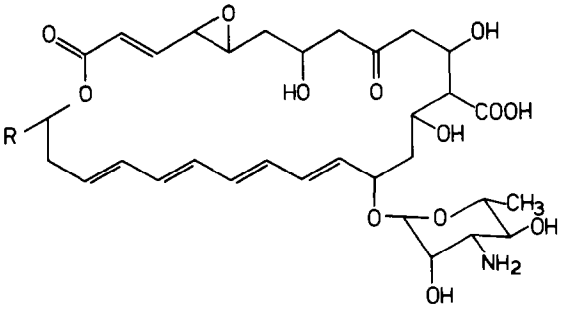

Fig. 24. Lucensomycin [$R = CH_3(CH_2)_3$] and pimaricin ($R = CH_3$).

concentration range 5×10^{-6}–$10^{-5}M$. The p–t curves indicate that the mode of action of lucensomycin may differ as a function of the concentration of the drug.

The experiments indicated that lucensomycin can act as both a fungistatic and fungicidal antibiotic, depending upon its concentration, whereas the other antifungals are either *only* fungicidal (nystatin, candicin, filipin, amphotericin B) or *only* fungistatic (pimaracin, clotrimazole). Thus the observed p–t curves reveal some of the differences in the mode of action of the antibiotics.

Comparisons of the p–t curves for interaction between respiring yeast cells and nystatin at 25° and 30° suggested that the kinetics and hence the mechanism of the interaction could not be dealt with by a simple mathematical treatment. However, the processes to which these p–t curves relate include at least adsorption, diffusion and enzyme inhibition, which are not, as yet, very clearly understood.

Comparisons of the bioactivity of nystatin and *N*-acetylnystatin towards respiring yeast cells (in $0.1M$ glucose in pH-4.5 phthalate buffer at 30° under anaerobic conditions) have been reported.[37] *N*-Acetylnystatin has a modified mycosamine moiety (–H replaced by $-COCH_3$). This small change in structure gives rise to a significant decrease in bio-

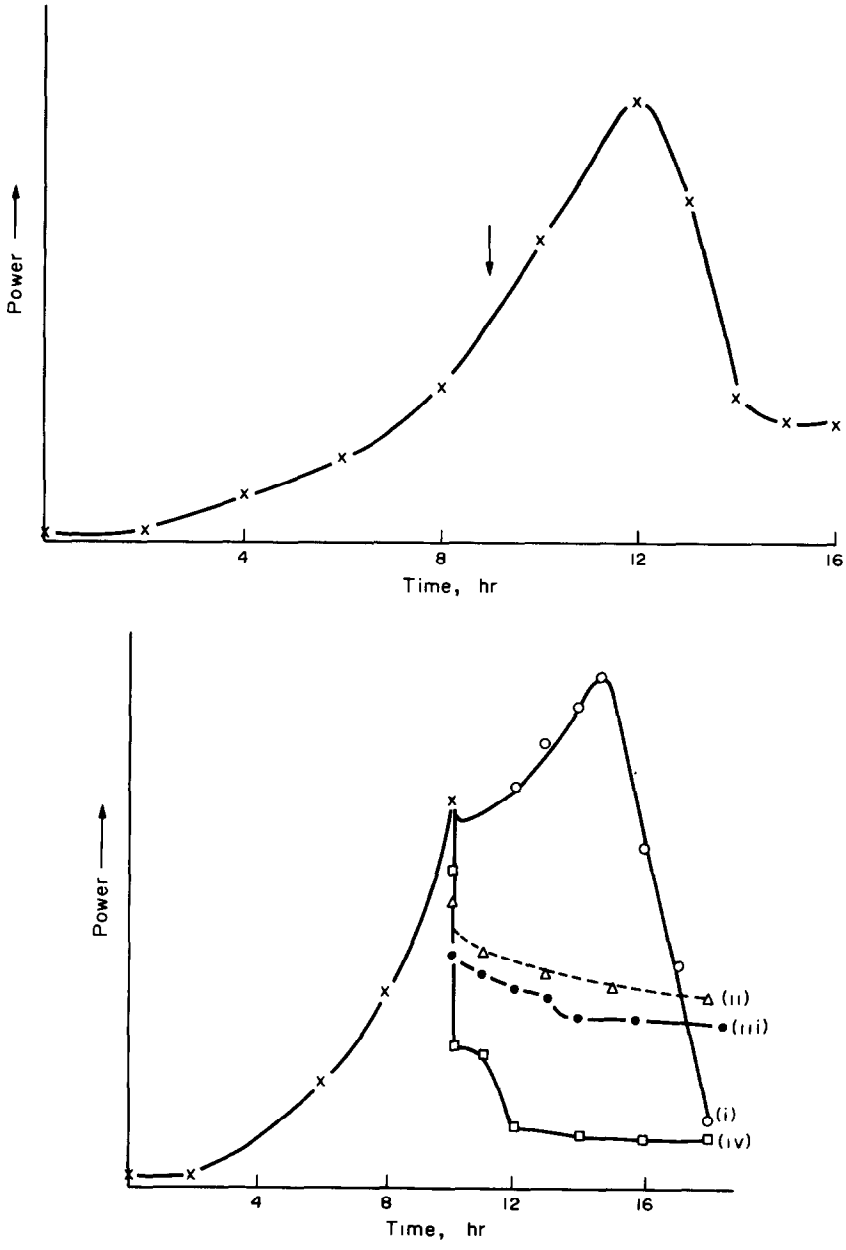

Fig. 25. Power–time for curves (a) *S. cerevisiae* in semi-defined medium at 30°C under anaerobic conditions, (b) *S. cerevisiae* in the presence of lucensomycin at concentrations of (i) $1 \times 10^{-6}M$; (ii) $6 \times 10^{-6}M$; (iii) $5 \times 10^{-6}M$); (iv) $1 \times 10^{-5}M$.

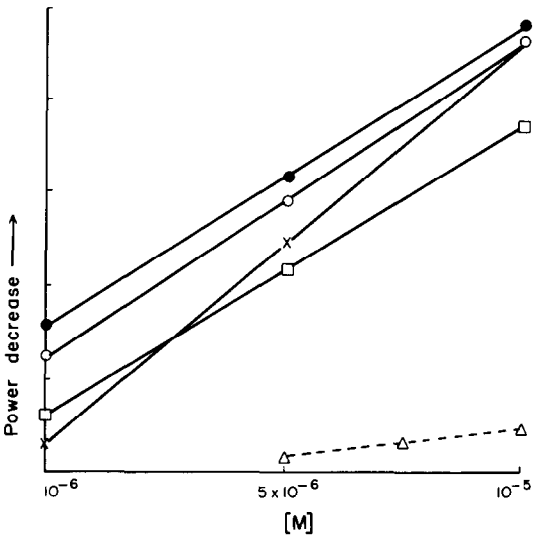

Fig. 26. Dose–response graphs for nystatin (●——●), amphotericin B (□——□), candicidin (○——○), lucensomycin (× —— ×) and pimaracin (△···△). The ordinate represents the immediate decrease of power upon addition of the antibiotics.

activity. A linear dose–response relationship for *N*-acetylnystatin was obtained over the range between 9×10^{-7} and $6 \times 10^{-6}M$ per 10^7 yeast cells.

The bioassay of other polyene antibiotic derivatives by flow microcalorimetry was recommended.

The interaction of different concentrations of polyene antibiotic with *S. cerevisae* NCYC 239 growing in semidefined medium at 30° under anaerobic conditions has also been recently studied,[38] the antibiotics being added during the mid-exponential growth phase of the yeast cells. The *p–t* curves indicated that at concentrations of 1×10^{-6}–$1 \times 10^{-5}M$ per 10^7 cells (initial cell numbers) the antibiotics have an almost immediate interaction with the cells.

The potency ranking of the antibiotics was assessed as lucensomycin > nystatin > candicidin > amphotericin B > pimaracin. The most potent antibiotic was taken to be that which inhibited microbial metabolism the most in the shortest time. The order given was confirmed by parallel experiments using flow nephelometry and is different from that obtained with mid-stationary phase cells undergoing respiration only. The reproducibility of the results was about ±3%.

Lucensomycin again showed a concentration-dependent behaviour towards mid-exponential phase cells, as it does with respiring yeast cells. In a growth medium a "biphasic activity" is shown by this antibiotic at high concentration, *e.g.*, $1 \times 10^{-5}M$ per 10^7 cells (initial number). This "biphasic" activity may be due to the fact that two processes or groups of processes occur during the interaction of yeast cells with lucensomycin (Fig. 25).

The inhibition of growth of yeast cells by polyene antibiotics was found to be useful for determination of the drugs (Fig. 26). This dose–response relationship could be significant in assessing drug bioavailability in body fluids after clinical administration of the drugs.

The addition of dicloxacillin at concentrations of 0.025–12.5 μg/ml was found to cause a concentration-dependent reduction in power output of an aerated exponential-phase culture of β-lactamase

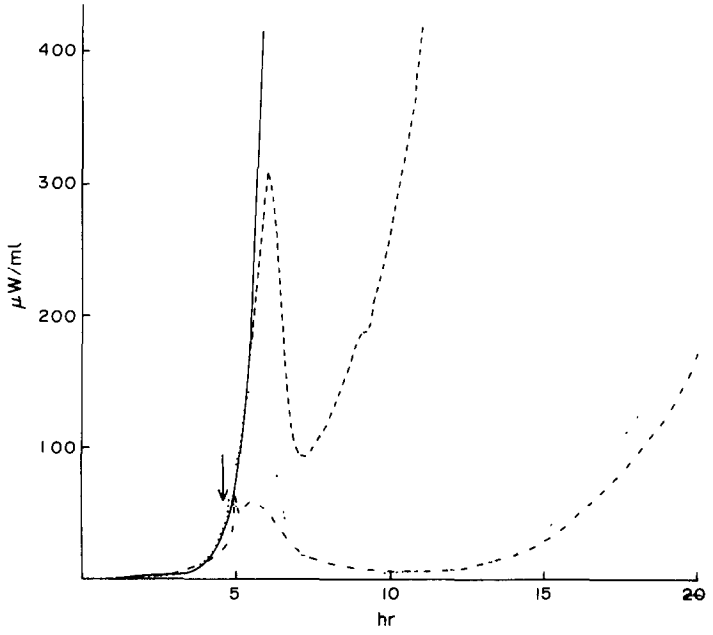

Fig. 27. Heat effects generated by a culture of a β-lactamase *S. aureus* exposed to increasing concentrations of dicloxicillin (—— 0.25, --- 0.63, ···· 1.25, .–.– 12.5 μg/ml). Reproduced with permission from reference 31.

S. aureus (Fig. 27);[31] the micro-organisms were grown in trypticase soy broth and monitored with a flow microcalorimeter at 37°. No dose–response relationship was given.

MICROCALORIMETRIC STUDIES OF MICRO-ORGANISM–DRUG COMBINATION INTERACTIONS

Microcalorimetry, especially flow microcalorimetry, is a powerful tool for the study of the effect of mixtures of drugs on microbial metabolism (Table 5, Figs. 28–30).[40–42] Classical microbiological assay techniques cannot deal with drug combinations adequately. Other methods of drug analysis also suffer from disadvantages for the study of such systems because more often than not they cannot measure the effect of drugs on microbial metabolism in a non-invasive manner or without also employing time-consuming ancillary techniques.

Measurement of drug susceptibility of micro-organisms by microcalorimetry

Binford *et al.* have reported results for susceptibility testing of *E. coli*, *γ-Streptococcus* and *Pseudomonas sp* to various antibacterial antibiotics, including (mg/ml) erythromycin (0.10), ampicillin (0.20), kanamaycin (0.4), colistin (0.20), gentamicin (0.066), cephalothin (0.60), carbenicillin (2.0), gantrisin (4.0).[43] Bacteria isolated from infected urines were grown in rich medium at 37° under both aerobic and anaerobic conditions. A stopped-flow version of the Beckman power-leak microcalorimeter, employing syringe pumps, was used. Different p–t curves were obtained for cultures grown at different oxygen concentrations. The experiments allowed distinction between bactericidal and bacteriostatic antibiotics (Fig. 31). Results were obtained 12–24 hr sooner than by the disc agar diffusion method for drug susceptibility of micro-organisms. The correlation with results obtained by the disc agar diffusion method was 27 and 87% under anaerobic and aerobic conditions respectively. The method described by Binford *et al.* still has the drawbacks of being time-consuming (1–1.5 hr), laborious, subject to problems in control of the pO_2 of the culture, and not easily automated.

The synthetic antifungal drug 5-fluorocytosine has no effect on the p–t curve of *S. cerevisae* NCYC 239

Table 5. Flow microcalorimetry studies on the effects of combinations of drugs on microbial metabolism

Drugs	Incubation conditions	Conclusions
(1) Amphotericin-B (2) Clotrimazole (3) 1 + 2	*Saccharomyces cerevisiae* SQ1600 semi-defined media, 30°C, exponential phase cells. Buffered glucose. Anaerobic conditions.	Drugs (1) and (2) show antagonism in both respiration and growth media[40] (Fig. 28).
(1) Doxycycline (2) Gentamicin (3) 1 + 2	*E. coli*, *S. aureus haem*, Purple Broth + 1% dextrose. Log phase cells, 35°C.	Drugs (1) and (2) show synergistic effect.[41] Cell metabolism altered by (3) in different way from individual inhibitory agents. (1) inhibits cell metabolism in doses lower by factors of 10–100 than those found with MIC tests (Fig. 29).
(1) Tetracycline (bacteriostatic) (2) Ampicillin (bactericidal) (3) 1 + 2	*E. coli* log phase Purple Broth (Difco) + 1% dextrose, 34°C.	(1) at 1–3 μg/ml gives immediate inhibition of power output. Bacterial density constant. (2) used at 3, 6 or 12 μg. Time of inhibition of microbial metabolism dependent on concentration of (2). Decrease in bacterial count. (3) 1μg of (1) + 3 μg of (2) gives immediate inhibition of microbial metabolism. Unchanged bacterial density[42] (Fig. 30).
(1) Nystatin (2) Pharmaceutical formulation excipients (3) 1 + 2	Mid-stationary phase respiring *Saccharomyces cerevisiae* NCYC239. Anaerobic, 30°C, glucose in phthalate buffer.	No synergistic effect for (1) + (2).[21]
(1) Nystatin (2) Tetracycline hydrochloride (3) 1 + 2	Conditions as above.[21]	(1) + (2) in ratio of 1:1→1:3 w/w same p–t curves as for nystatin alone.[21]

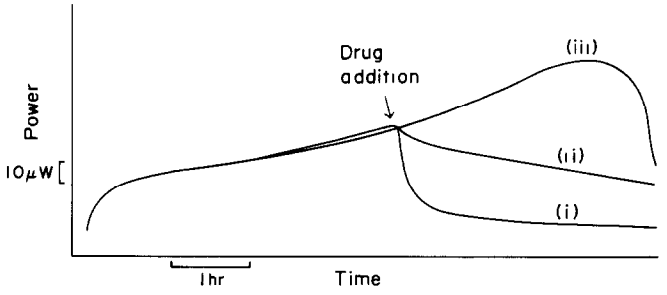

Fig. 28. Power–time curves for interaction of (i) 5 μg/ml amphotericin B, (ii) 5 μg/ml amphotericin B plus 5 μg/ml clotrimazole and (iii) 5 μg/ml clotrimazole, with *S. cerevisiae* in growth medium.[40] Reproduced with permission from the copyright holder, University of Chicago.

respiring in 0.1*M* glucose[18] in pH-4.5 phthalate buffer, but it does show bioactivity against yeast cells growing in a special medium under anaerobic conditions at 30° (Fig. 32). That 5-fluorocytosine does not interact with respiring yeast cells is expected, since this antimycotic interferes with deoxyribonucleic acid metabolism and would therefore only demonstrate its effects in growth medium.

This example illustrates the usefulness of microcalorimetry to distinguish easily and quickly between drugs which affect the respiratory activity of cells and those which interfere with other aspects of cellular metabolism.

The antibiotic sensitivity of two strains of *E. coli* (isolated from urine specimens) towards ampicillin, streptomycin, chloramphenicol, tetracycline and sulphadimidine has been determined rapidly by flow microcalorimetry.[44] The bacteria were grown in semidefined growth medium at 25°. The drug under test was added to the fermenter vessel 50 min after the addition of 2.0×10^7 cells per ml. The exponential power-output of the bacteria altered on addition of the antibiotics, the change depending on the type and concentration of antibiotic. Sensitive organisms showed a rapid response (4–8 min) to antibiotics added in the concentration range 1–2 MIC. Typical *p–t* curves from use of ampicillin are shown in Fig. 33.

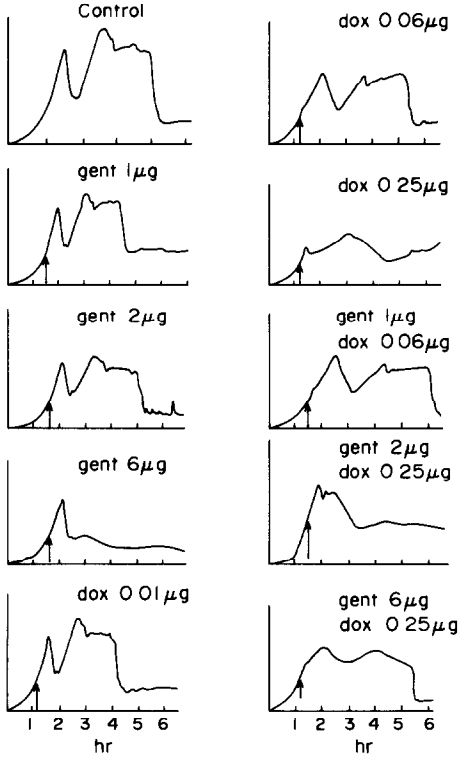

Fig. 29. Power–time curves for growth of *E. coli* 3579 in the presence of gentamycin and doxycycline and combinations of the two drugs. From reference 41 with permission.

Similar results were obtained for the other antibiotics. The antibiotics in half-MIC amounts had either no effect or only a marginal effect. MIC quantities prevented any further increase in power output or decreased it. Sulphadimidine was an exception, however, and produced no effect even at 29 × MIC levels. It was hypothesized that this could have been due to the high number of cells used in the microcalorimetric experiments (2×10^7 cells/ml) compared to the 2×10^5 cells/ml used in the classical MIC experiments, and also to the presence of sulphadimidine inhibitors, *e.g.*, *p*-aminobenzoic acid.

Microcalorimetric studies of model systems

The extreme complexity of biological phenomena often necessitates conducting experiments with model systems in order to help understand the system under investigation. Both batch and flow-leak isothermal microcalorimetry have been employed in this way.

For example, isothermal batch microcalorimetry has been used to study the binding of 5-methoxytryptamine (an acridine dye) to calf thymus deoxyribonucleic acid (DNA) and single-stranded poly(A) (a polymer of adenine).[45] The thermodynamic parameters for the binding of the dye to DNA and poly(A) were obtained by mixing DNA or poly(A) (in a 1 m*M* sodium cacodylate, 1 m*M* sodium chloride, 0.2 m*M* EDTA mixture at pH 7.0) with the dye (Fig. 34; Table 6). No difference in "calorific capacity" for the binding to DNA to dye was found between 25° and 40°. Thus it was inferred that the structure of the DNA–dye complex does not change between these

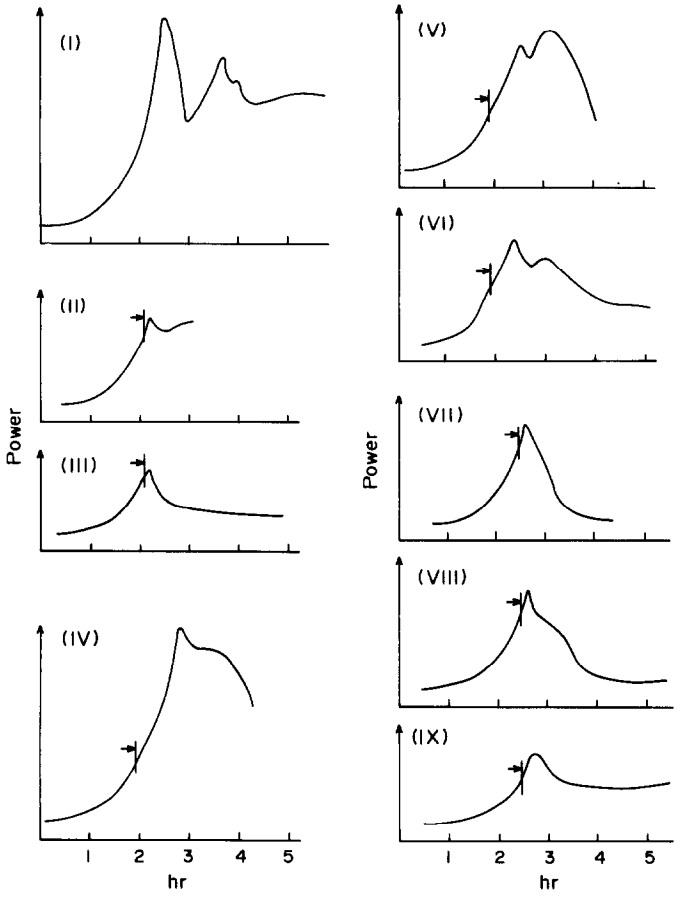

Fig. 30. Power–time curves for growth of *E. coli* H3579 BBSUA: (i) alone, and in the presence of (ii) 1 μg of tetracycline; (iii) 3 μg of tetracycline; (iv) 3 μg of ampicillin; (v) 6 μg of ampicillin; (vi) 12 μg of ampicillin; (vii) 1 μg of tetracycline + 1 μg of ampicillin; (viii) 1μg of tetracycline + 6 μg of ampicillin; (ix) 1 μg of tetracycline + 12 μg of ampicillin. From reference 42 with permission.

two temperatures. The formation of DNA–dye and poly(A)–dye complexes corresponds to quite similar reaction enthalpies. Various hypotheses were put forward to account for the similarity in ΔH for single- and double-stranded nucleic acids and for the entropy change being larger for interaction with poly(A) than with DNA.

Certain ion-selective neutral carrier antibiotics (ionophores) have been found to be able to translocate metal ions across cell membranes, including both plasma and mitochondrial membranes.[46] Some antibiotics, as well as certain synthetic carrier molecules, perform this function by forming complexes with metal ions on one side of a membrane. The

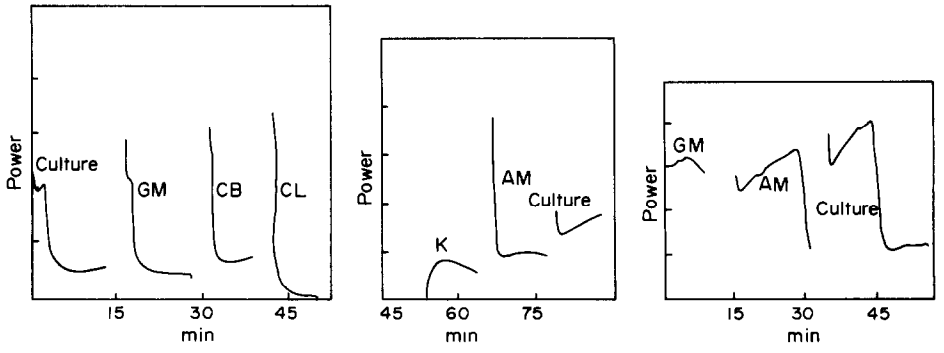

Fig. 31. Microcalorimetric antibiotic sensitivity tests. *E. coli* in the presence of gentamycin (GM), carbenicillin (CB), colistin (CL), kanamycin (K), ampicillin (AM). Reproduced with permission.[43]

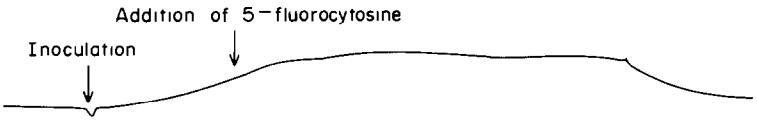

Fig. 32. Effect of 5-fluorocytosine on growth of *S. cerevisiae*. Reproduced with permission.[18]

complex then diffuses to the other side of the membrane where the metal ion is released and the carrier molecule can diffuse back across the membrane to pick up more metal ions.

A variety of techniques (including microcalorimetry) can be used for the determination of complex-formation constants for carrier antibiotic–metal complexes or synthetic carrier molecule–metal complexes. The advantages of microcalorimetry for such studies are that very small concentrations of the antibiotics can be used, and that the enthalpy (ΔH^0), free-energy (ΔG^0) and entropy (ΔS) changes of complex formation can be determined.[48] The influence of solvents and ligand structure on the thermodynamics of complexation reactions between metal ions (*e.g.*, K^+ and Na^+) and ionophores (*e.g.*, nigericin and monensin) has been determined by Fruh and Simon[47] by batch isothermal power-leak microcalorimetry of mixtures of the ionophores with metal thiocyanates. The thermodynamic values obtained were in excellent agreement with those found by less direct and convenient methods such as emf measurement and relaxation techniques (Table 7). Furthermore the cation selectivity for nigericin ($K^+ > Na^+$) and monensin ($Na^+ > K^+$) agreed with that observed in biological systems.

Table 6. Thermodynamic parameters for the binding of 5-methoxtryptamine on calf thymus DNA and poly(A) (from reference 45, by permission)

	T,°C	K	ΔH; kJ/mole	ΔS, $J \cdot mole^{-1} \cdot deg^{-1}$
DNA	25	2×10^4	−0.59	2.63
	40	1.6×10^4	−0.59	2.63
Poly(A)	25	0.5×10^4	−0.47	5.26

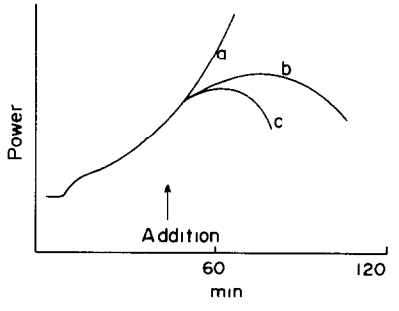

Fig. 33. Addition of ampicillin to a sensitive strain of *E. coli* (a, 1 μg/ml ≡ to control; b, 2 μg/ml; c, 5 μg/ml). A resistant strain of *E. coli* when similarly examined showed no reaction toward 5000 μg/ml of ampicillin. Reproduced with permission.[44]

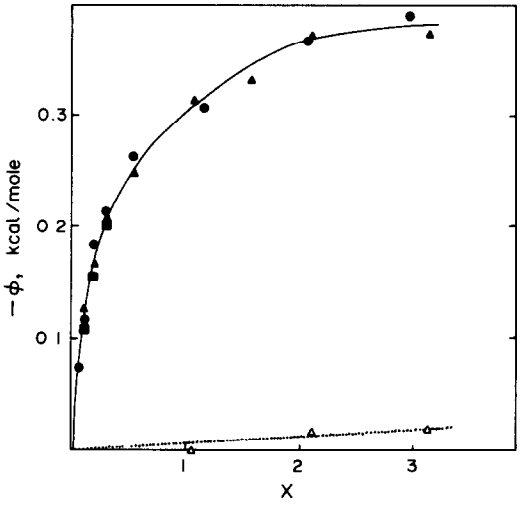

Fig. 34. Heat of binding ($-\phi$) of 5-methoxytryptamine to calf thymus DNA (kcal per mole of phosphate) (——); × is the final molar concentration ratio of amine to DNA. The concentration of DNA was constant and equal to $10^{-3}M$). Symbols (● ■ ▲) correspond to different series of experiments. Heat of dilution of 5-methoxytryptamine (△——△). Buffer; 1m*M* NaCl, 1m*M* sodium cacodylate, $2 \times 10^{-4}M$ EDTA, pH 7.0; 298 K. Reproduced with permission.[45]

The enthalpy changes associated with lipid–protein interactions have also been examined by batch isothermal power-leak microcalorimetry.[48] The enthalpy of binding may again be measured with very much smaller samples than by other physical methods; most microcalorimetric experiments require only 2 ml of protein solution at a concentration of about $5 \times 10^{-5}M$ and a ligand concentration of the same order of magnitude or greater, depending upon the complex stoichiometry. Microcalorimetry can also provide important information on the stability of lipid–protein complexes, which might be useful in the formulation of a mechanism for the formation of these complexes *in vivo*. Although the experiments reported did not investigate the interaction of membrane proteins with membrane lipids (plasma apolipoproteins and phospholipids were examined instead) it does, nevertheless, indicate the potential for doing so. Investigations of the thermodynamics of such interactions may give further understanding of cell membrane behaviour, which in turn may help in the elucidation or clarification of membrane–drug phenomena.

The inhibition of power (heat) production associated with protein biosynthesis in cell-free systems of yeast (*Saccharomyces*) by antibiotics has been exam-

Table 7. Thermodynamic parameters for the interaction of nigericin and monensin with Na^+ and K^+ ions

Antibiotic	Metal ion	$\Delta H°$, *kJ/mole*	$\Delta G°$, *kJ/mole*	$\Delta S°$ $J \cdot mole^{-1} \cdot deg^{-1}$	log *K*	*K*
Nigericin	Na^+	$+6.9 \pm 11\%$	-22.2	$+98$	3.9	8×10^3
	K^+	$-9.7 \pm 7\%$	-32.0	$+93$	5.6	4×10^5
Monensin	Na^+	$-16.2 \pm 2\%$	-39.3	$+61$	6.0	1×10^6
	K^+	$-15.6 \pm 2\%$	-26.0	$+35$	4.6	4×10^4

ined with a Calvet batch microcalorimeter;[49] the object was to try to distinguish between the heat produced by protein biosynthesis and that produced by interfering reactions (Table 8), but owing to the complexity of the system no definite conclusions could be drawn.

Perrin and co-workers[50,51] have estimated the binding constants and thermodynamic parameters, and obtained structure–activity relationships for a variety of pharmaceutical complexes by isothermal flow power-leak microcalorimetry. The complexation of barbituric acids, prostaglandin E_2 and the antibiotic chloropromazine with B cyclodextrin[50] and the drugs salicylate, sulphaethidole, fenoprofen, indomethacin and flufenamic acid with human serum albumin were investigated.[51] The air-bath of the microcalorimeter was replaced by a water-bath giving a short-term temperature stability of $\pm 2 \times 10^{-4}$ deg.

A titration procedure was used to obtain values of K_B and thermodynamic parameters, *i.e.*, the drug or the biopolymer concentration was kept constant and the concentration of the other was varied exponentially.

ΔH was obtained from the relationship

$$\Delta H = V_{max} \times \frac{1}{\text{calibration constant}} \times \frac{1}{\text{total flow rate}} \text{ J/mole}$$

where V_{max} is the voltage obtained after completion of the reactions.

K_B was determined as the slope of a plot of $1/V$ *vs.* $a/(b-c)$ (where a and b are the initial concentrations of the reactants and c is the concentration of complex formed).

Data for the binding mechanism were obtained by measuring the enthalpy changes of complexation as a function of temperature. The method was found to be satisfactory for the study of complexation of molecules for which the residence time in the reaction vessel (1 min) is many orders of magnitude larger than the equilibration time for small molecules, and formation of complexes is diffusion-controlled.

Microcalorimetric values for small binding constants were found to be more reliable than those obtained by ultraviolet and circular dichroism measurements (Table 9).

Table 8. Incorporation of ^{14}C-phenylalanine into the complete system of yeast, and resultant heat production (from reference 49, by permission)

	Inhibitor conc. and polypeptide formation as % of the complete system				Heat production, *mJ*	
	Data by the author[49]		Data by other authors			
Conditions					Q^+*	Q^-†
Complete system		100		100	404 ± 84	361 ± 84
Cycloheximide	1 m*M*	22 ± 8	1.0 m*M*	15–30	322 ± 84	27 ± 29
			0.01 m*M*	14		
Puromycin	1 m*M*	29 ± 10	0.1 m*M*	0	94 ± 42	21 ± 20
			0.1 m*M*	38		
Fusidic acid	1 m*M*	17 ± 10	1.0 m*M*	7	No significant difference from complete system	

*Endothermal part of the *p–t* curve.
†Exothermal part of the *p–t* curve.

Table 9. Binding constants and derived thermodynamic parameters for 1:1 complexes between the drug and HSA (from Otagari *et al.*,[51] by permission)

Drug	*K*	$\Delta H°$, *kJ/mole*	$\Delta G°$, *kJ/mole*	ΔS, $J.mole^{-1}.deg^{-1}$	K_{lit}
Salicyclic acid	2.1×10^5	1.735	1.355	+1.27	1.2×10^5
Sulfaethidole	1.1×10^5	1.644	1.323	+1.08	1.2×10^5
Fenoprofen	3.4×10^5	1.803	1.501	+1.00 (4)	1.9×10^5
Indomethacin	7.5×10^5	1.915	1.269	+2.17 (5)	3.0×10^5

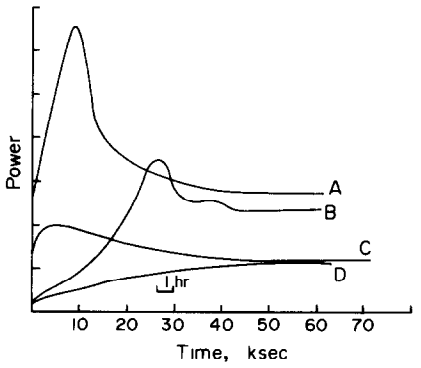

Fig. 35. Power–time curves showing the effects of variation in both glucose concentration and inoculum density (all inocula derived from 5-litre growth). A, 10m*M* glucose, 5×10^8 cfu/150 ml; B, 10m*M* glucose, 5×10^7 cfu/150 ml; C, 1m*M* glucose, 5×10^8 cfu/150 ml; D, 1m*M* glucose, 5×10^7 cfu/150 ml. With permission.[52]

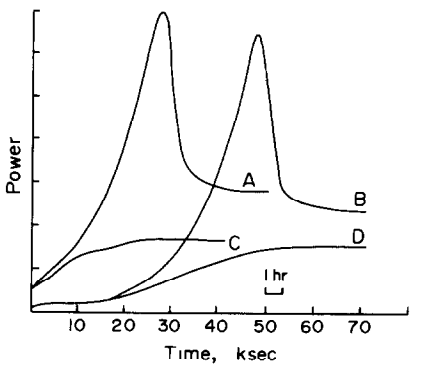

Fig. 36. As for Fig. 35. A, 20m*M* glucose, 1×10^8 cfu/150 ml; B, 20,*M* glucose, 1×10^7 cfu/150 ml; C, 2m*M* glucose, 1×10^8 cfu/150 ml; D, 2m*M* glucose, 1×10^7 cfu/150 ml. With permission.[52]

It was concluded that cyclodextrins bind a wide range of both acidic and basic drugs equally well, but there appear to be differences in the mechanism of binding of cyclic barbiturates and linear barbiturates.

The enthalpy and entropy changes for the reactions of drugs with human serum albumin (Table 9) were interpreted as primarily due to the changes in the behaviour of the solvent, water, on complex-formation.

DISCUSSION

Isothermal power-leak microcalorimetric techniques can be used, as these examples show, for a variety of purposes in the analysis of drugs, but not for identification of drugs or biotransformation and metabolic studies or determination of ratios of bound drug concentrations to free, in body fluids.

Both batch and flow microcalorimetric methods are used with viable organisms, but the flow assays have distinct advantages.

It is to be hoped that such studies will be extended to the many antimicrobial agents which have not hitherto been examined in this way, and that the information gained will be extensively compared with that from more conventional methods.

These advantages may not always be apparent, however, and are in some ways dependent on the ingenuity of the experimentalist in design of the experiments; dosage–response relationships for bioassays are a case in point.

The quantitative analysis of drugs by microcalorimetric techniques is sensitive down to microgram levels, but many of the methods have not yet been optimized and improvements in the sensitivity of microcalorimeters combined with good experimental design should allow detection limits for drugs down to 10^{-9}–10^{-10}*M*. Though certain physicochemical methods already have such detection limits for drugs, they do not give determination of biologically active drugs or the total bioactivity of pharmaceutical formulations.

Improvements in methodology, such as use of standardized inocula stored at liquid-nitrogen temperature, will also help in optimizing micro-organism–drug studies. It may be noted that drugs can also be stored in this way, without change in bioactivity, allowing strict comparisons of micro-organism–drug behaviour.

At present there is a great diversity in the nature of the micro-organisms, environmental conditions, pH, temperature, pO_2, media *etc.*, used for drug analysis, and such parameters need to be standardized so that comparisons can be made at the intra- and interlaboratory level. For example, defined growth media should be used.

Using inocula stored at liquid-nitrogen temperature, Perry *et al.*[52] have shown that pronounced differences occur in the p–t curves when either the inoculum density or the substrate concentration is changed; inoculum variations, *e.g.*, in size, history, phase of growth, cause alterations (of lag time, peaks, troughs, *etc.*) in the p–t curve. Variations in the p–t curve profiles were also found for liquid-nitrogen stored inocula prepared from growths in different batches of the same complex medium (Figs. 35–38). When a defined medium and liquid-nitrogen stored inocula are used, differences in design of the fermenters employed in the inoculum preparation may cause differences in the p–t curves. Rigorous standardization of all experimental parameters is therefore essential for obtaining reproducible and analytically useful p–t curves.

Flow power-leak microcalorimetry has been shown to be a simple and rapid method for the enumeration of micro-organisms in urine.[53,54] The methods described can distinguish between 10^4, 10^5 and 10^6 organisms/ml. By using multichannel flow instruments which could detect 10^2–10^5 organisms/ml it should be possible to conduct micro-organism enumeration and drug-susceptibility testing simultaneously. This is because there seems to be no reason why body fluids (such as serum) containing micro-organisms should not be examined by microcalorimetry for assessment of microbial susceptibility to

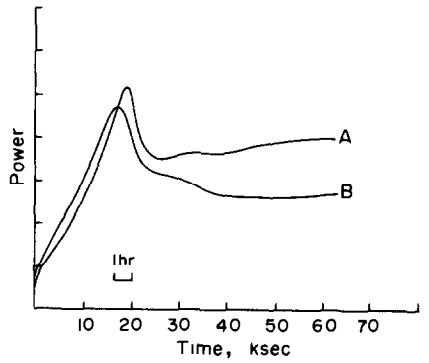

Fig. 37. Power–time curves showing the variations produced by inocula prepared from growth in two batches (A and B) of the same complex medium (modified Antibiotic Medium No. 3, Oxoid); calorimetric incubation medium in both cases modified Cutts and Rainbow medium: 10m*M* glucose, 1×10^8 cfu/150 ml. Reproduced with permission.[52]

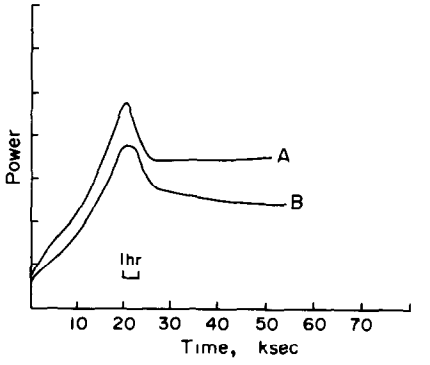

Fig. 38. Power–time curves showing the effects of fermenter conditions (*e.g.*, aeration efficiency, stirring rate, surface-to-volume ratio, *etc.*) on the derived inocula. Calorimetric incubations in modified Cutts and Rainbow medium: 10m*M* glucose, 1×10^8 cfu/150 ml. A, inocula derived from 5-litre growth; B, inocula derived from 1-litre growth. Reproduced with permission.[52]

drugs and for measurements of the number of microbes before and after drug treatment. This may be particularly useful when the susceptibility of the micro-organism to a certain drug is in doubt. This application would, of course, again require modification of present instrumentation. The sensitivity would have to be 10–20 times that of currently available calorimeters, without loss of stability or the ability to monitor the culture with other probes, *e.g.*, miniature pO_2 electrodes. Ideally, in such a calorimeter the calorimetric vessel would also be the culture vessel, and designed to allow good atmospheric control for both anaerobic and aerobic cultures. Homogeneity of cell contents would also be essential.

There have been many reports of the disagreement in the drug-susceptibility of micro-organisms as measured by MIC methods and microcalorimetric methods. The MIC specifies the minimum concentration of a drug which keeps the cell inoculum below an arbitrary absorbance threshold at the time of inspection in the particular test environment. Semenitz *et al.*,[27] in tests with tetracycline antibiotics, have also high-lighted this problem. There is, then, a need to re-examine interpretations of the value and meaning of MIC tests. Furthermore, in our view a comparison of MIC values and microcalorimetric tests should be made with the same conditions of inoculum density, temperature, *etc.*, in order to try to establish the significance, if any, of MIC tests.

Future studies of interest in drug analysis by microcalorimetry could include the following:

(1) the interaction of biopolymers and other biologically relevant molecules with drugs, for studies of mode of action and/or bioavailability of drugs in body fluids;

(2) the investigation of the effect of raw drug materials, combinations of drugs or pharmaceutical formulations, on mixed microbial populations of clinical relevance;

(3) studies of the interaction of erythrocytes with drugs, which could be especially valuable in instances where it is known that a series of structurally related drugs may cause side-effects such as interference with red blood-cell metabolism (although such studies have not been reported to date, many investigations of erythrocytes by microcalorimetry have been conducted);[18]

(4) investigation of the efficiency of protective agents in pharmaceutical formulations *etc.* [no such investigations have yet been made by microcalorimetry; at present, a protective effect (*i.e.*, no increase in microbial population) has to be demonstrated on an initial inoculum of 10^5–10^6 organisms/ml over a 28-day period;[55] this is well within the detection limits of presently available calorimeters[54]].

Although this section has dealt with studies of micro-organism–drug interactions, it is, perhaps, important to note that studies of the interaction of other substances with microbial populations by isothermal power-leak microcalorimetry may also be rewarding, disinfectants and detergents being two examples.

THERMOMETRIC TITRIMETRY

Three distinct, and fundamentally different, analytical procedures may be considered under the general heading of "thermometric titrimetry".

(1) Conventional thermometric titrimetry, also known as thermometric enthalpy titration (TET).[56]

(2) Catalymetric or catalytic-thermometric titrimetry (CTT).[57,58]

(3) Direct injection enthalpimetry (DIE).[59]

In (1), the temperature of the titrand is monitored as titrant is added, and variations in the rate of temperature change, shown as inflections in the recorded temperature–titrant volume graph, serve to

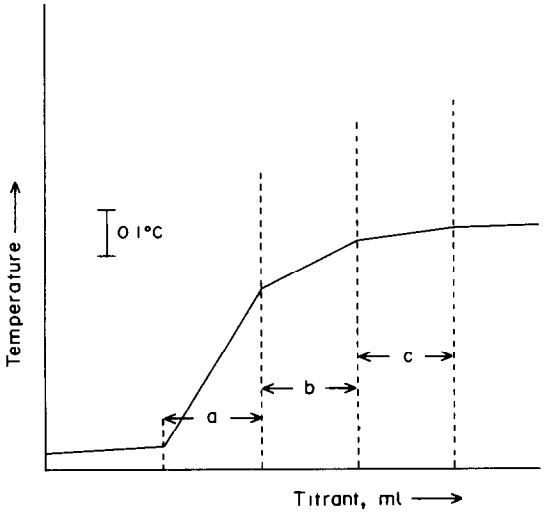

Fig. 39. Thermometric enthalpy titration (TET) of a mixture of three constituents (a, b and c).

indicate the virtual completion of reactions between the titrant and titrand (Fig. 39).

In (2), a thermometric-indicator reagent is included in the titrand solution, and when the first excess of titrant initiates an exothermic indicator reaction, the accompanying rise in temperature locates the end-point (Fig. 40).

In (3), an excess of titrant is added rapidly to the titrand and the rise in temperature is measured (Fig. 41). No attempt is made to measure the amount of titrant required for a stoichiometric reaction with the sample substance. The temperature rise can be related to the reaction enthalpy, and therefore to the concentration of the determinand. The apparatus is very similar to that employed in (1) and (2) and it is convenient to consider the three procedures together, although DIE more closely resembles conventional calorimetry in principle.

In addition to these three "batch" titrimetric methods, continuous-flow techniques are increasingly used, and are particularly suitable for routine analysis.[60,61] Three procedures are employed: (*a*), the continuous mixing of the sample and titrant (Figs. 42 and 43), (*b*), the intermittent addition of titrant to the sample, and (*c*), the injection of the sample in pulses to a continuous flow of titrant (Fig. 44). Both (*a*) and (*b*) are referred to as "continuous-flow enthalpimetry", while (*c*) is distinguished by the name of "peak enthalpimetry". In all three the temperature rise is related to the sample concentration, so the methods can be considered an extension of DIE.

TET and DIE can, in theory, be applied to any chemical reaction resulting from the mixing of two reagents, while CTT is applicable if an appropriate indicator reagent is available.

An advantage of CTT is that large amounts of the indicator reagent can be used—often the indicator is itself a solvent—and the temperature change at the end-point is usually much greater than that possible in TET and DIE, particularly when the analyte concentration is low. Thus the effect of the environment and heat of dilution of titrant with titrand is less important and the titration apparatus can be of simple design, as shown in Fig. 45, for example.

Measurement of temperature change is in principle non-selective, and in thermometric titrimetry selectivity has to be achieved by the use of selective reagents and masking reactions, the adjustment of reaction conditions (*e.g.*, pH) and taking advantage of differences in solubility, stability constants and the rates of reaction of the analyte and interferents with the titrant.[62]

TET, like potentiometric titrimetry, can be used for serial titration, *i.e.*, for the selective consecutive determination of several components in a mixture. In contrast, methods (2) and (3) would normally give the

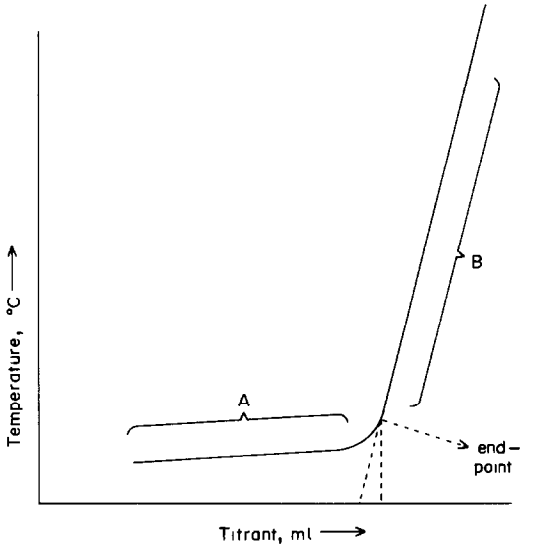

Fig. 40. Catalytic thermometric titration (CTT): A, determinative reaction; B, indicator reaction.

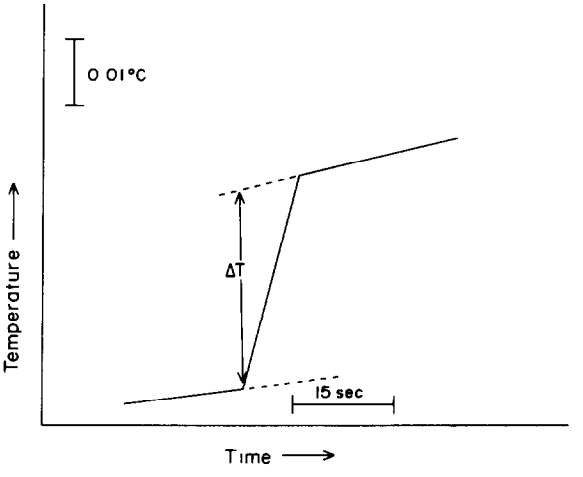

Fig. 41. Direct injection enthalpimetry (DIE). The excess of titrant is added over the first few seconds.

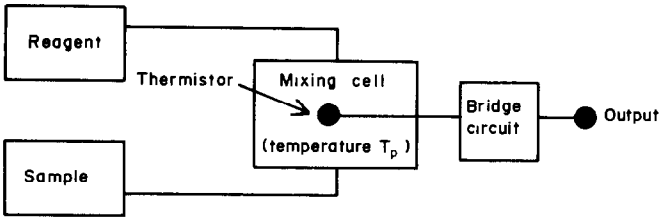

Fig. 42. Schematic diagram for flow enthalpimetry. Reprinted with permission from *Anal. Chem.*, 1976, **48**, 427A. Copyright 1976 American Chemical Society.

total functional-group content, although by manipulation of the chemistry it is sometimes possible to determine separately weak and very weak acidic functions in samples by CTT.[63]

Instrumentation

Apparatus for discrete, as distinct from continuous-flow, thermometric titrimetry, comprises a burette, preferably motor-driven, a titration vessel and a temperature-measuring device. It is usually designed to maximize the observable temperature changes resulting from the heat of the determination reaction or, in the case of CTT, the indicator reaction, and to minimize the effects of variations in the temperature of the immediate environment. The first requirement can be realized by the use of an insulated reaction vessel, *e.g.*, a glass Dewar flask (Fig. 46) or a vessel insulated with polystyrene foam. Environmental effects on the temperature of the burette have been minimized in DIE by immersing the burette in a rather large titration beaker[64] (Fig. 47), but in TET the more general practice has been to carry out titrations with a well-insulated apparatus (Fig. 46) or in a temperature-controlled room. An alternative is to use an isoperibolic titration calorimeter in which the burette and insulated reaction vessel are immersed in a water-bath controlled to about $\pm 2 \times 10^{-4}$ deg;[65] a suitable vessel is shown in Fig. 48.

Isothermal titration calorimeters are also used (Fig. 49). The reaction vessel is made of an inert metal with good heat conduction (Fig. 50). The vessel has an air-jacket and is immersed in a constant-temperature water-bath. The contents of the reaction vessel are kept at constant temperature by use of a Peltier thermoelectric cooler and a wafer control-heater.[66] The heat input under constant cooling conditions can be related to the heat of reaction and therefore to the content of the reactive species.

The design of apparatus for continuous-flow titration has been discussed by Jordan *et al.*[61] Details of apparatus used for thermometric titrimetry are given in the monographs by Vaughan[67] and Barthel,[68]

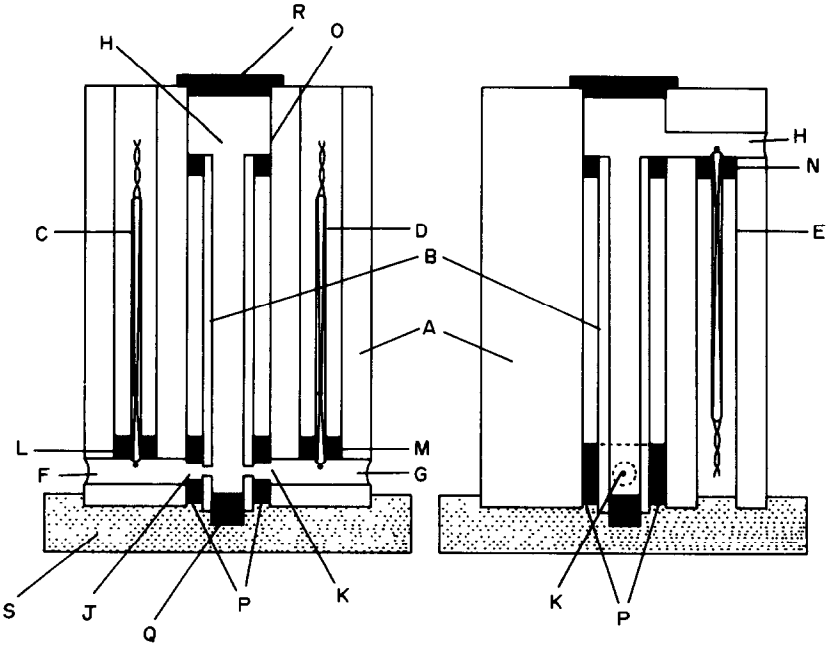

Fig. 43. Reaction vessel for continuous-flow enthalpimetry: (a) cross-section of front elevation; (b) cross-section of side elevation: A, perspex cylinder; B, perspex mixing tube; C, D and E, thermistors; F and G, inlet ports; H, outlet port; J and K, mixing jets; L, M, N, O and P, rubber seals; Q and R, rubber plugs; S, polythene base. Reproduced with permission.[60]

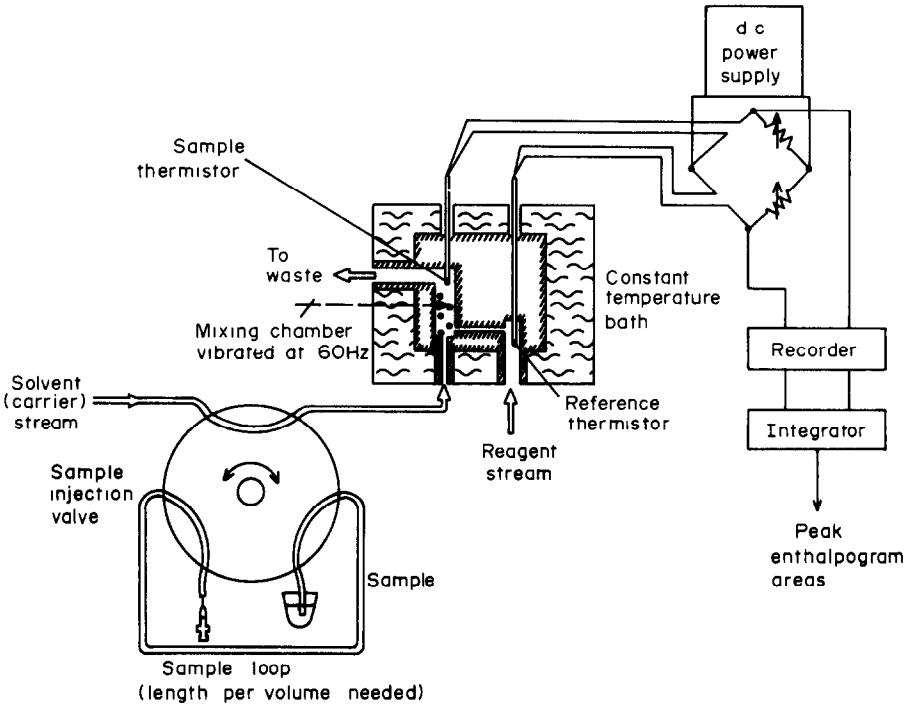

Fig. 44. Schematic diagram of peak enthalpimetry apparatus. Reprinted with permission from *Anal. Chem.*, 1976, **48**, 427A. Copyright 1976 American Chemical Society.

and more recent developments have been reviewed by Eatough,[69] Brandstetr[70] and Martin and Marini.[71]

Applications

Titrimetric methods are widely used in assays of pharmaceutical substances and formulations, including tablets and capsules. In Pharmacopoeias, many of the recommended procedures involve the titration of weakly acidic or basic functional groups, usually in non-aqueous media, with potentiometric or visual indication of the end-point. Aniline derivatives, particularly sulpha drugs, are determined by the "dead-stop" method with aqueous sodium nitrite as the titrant. A few oxidation–reduction titrations are listed, *e.g.*, the determination of isoniazid, antimony sodium tartrate and ascorbic acid with bromine, iodine and cerium(IV) respectively.[72]

Thermometric titrimetry has been evaluated for the determination of pharmaceutical products and in clinical analysis generally, but its advantages remain to be appreciated, especially for routine work.

In clinical investigations, the analyst is concerned not only with drugs and their metabolites but also with substances occurring "naturally" in the body. Determinations of the latter are included in this review for completeness.

Applications can conveniently be considered under two headings:

(*a*) determination of pharmaceutical substances and formulations; (b) clinical and biochemical determinations.

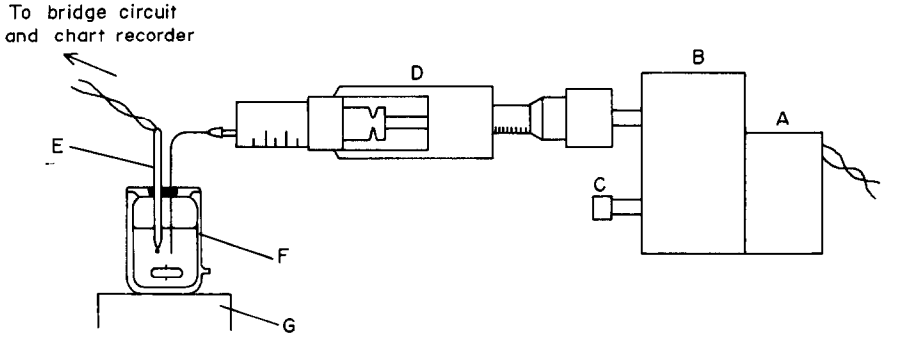

Fig. 45. Apparatus for catalytic thermometric titrimetry: A, synchronous motor; B, gear box; C, gear change; D, micrometer syringe; E, thermistor; F, Dewar beaker; G, magnetic stirrer.

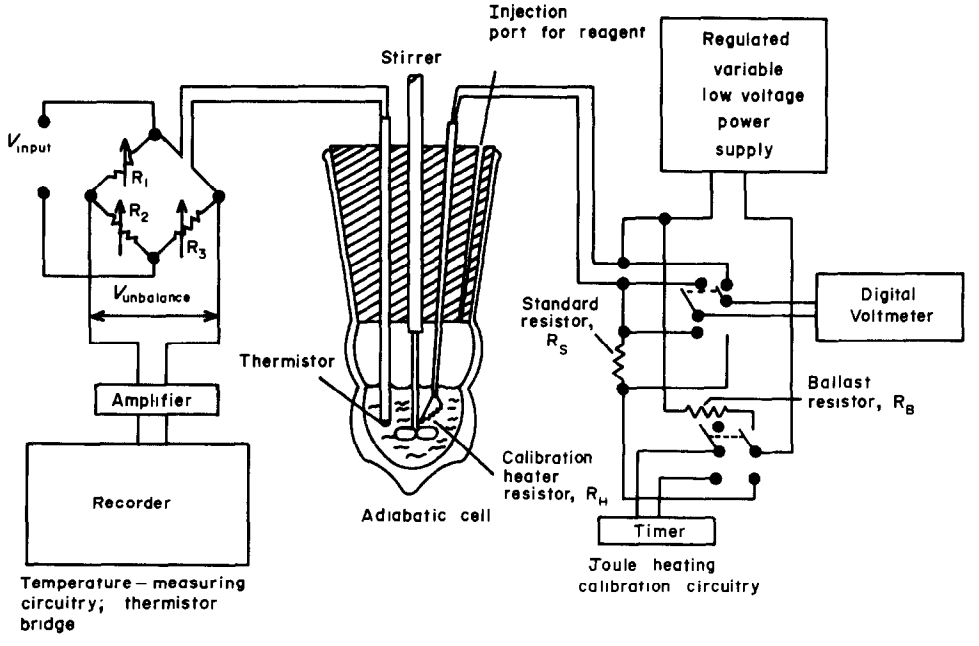

Fig. 46. Diagram of circuitry and apparatus used in enthalpimetric analysis. Reprinted with permission from *Anal. Chem.*, 1976, **48**, 427A. Copyright 1976 American Chemical Society.

Pharmaceutical substances and formulations

Thermometric enthalpy titrations. TET is generally more versatile than CTT, and has been used not only for acid–base titrations, but also for titrations involving reagents such as silver nitrate,[73] sodium hypochlorite,[74] *N*-bromosuccinimide[75] and iodine chloride.[76]

DeLeo and Stern[77] have discussed the titration of bases of pharmaceutical interest. They have shown that satisfactory results can be obtained in aqueous media for determination of nicotinamide, niacinamide and chlorpheniramine maleate by titration with hydrochloric acid, of aminophylline, hydrochlorothiazide and chlorpromazine hydrochloride by titration with sodium hydroxide, and of aminophylline by titration with silver nitrate. Only in the analysis of chlorpheniramine maleate tablets was interference from excipients in solid dosage forms

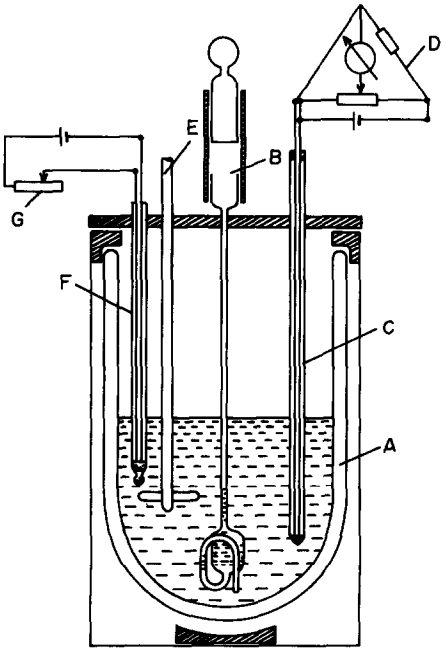

Fig. 47. Apparatus for direct injection enthalpimetry: A, Dewar flask; B, immersion pipette; C, thermistor; D, Wheatstone bridge; E, stirrer; F, calibration heater; G, heater control. Reproduced with permission.[64]

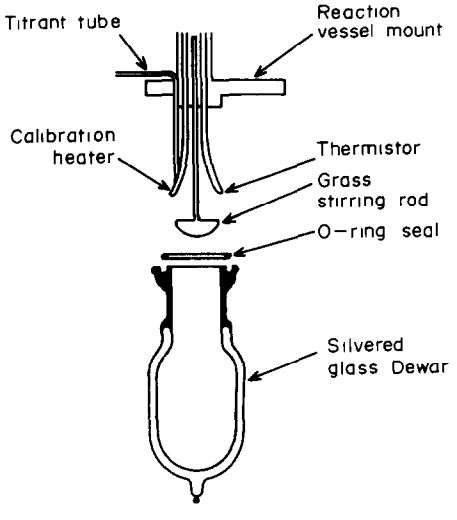

Fig. 48. Isoperibolic rapid-response glass Dewar reaction vessel. Reproduced with permission of Tronac Inc.

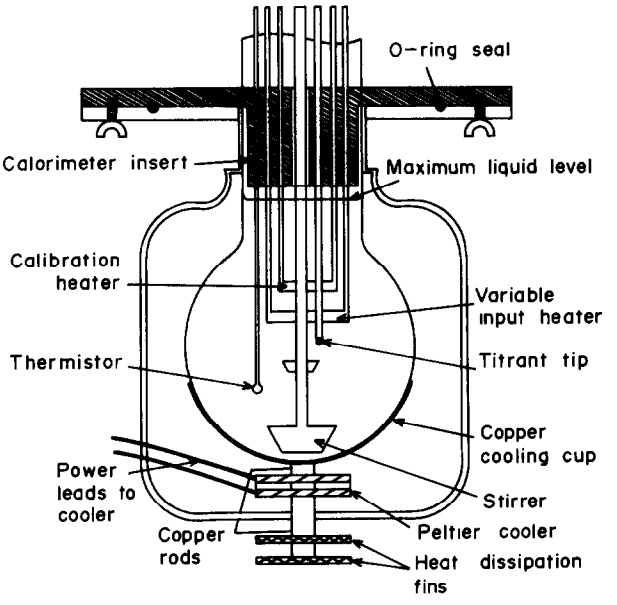

Fig. 49. Isothermal titration calorimeter. Reproduced with permission.[66]

observed, but the results were generally less reliable for titrations of syrups and elixirs.[78] These authors claim that TET has advantages over the non-aqueous titrimetric procedures of the British and United States Pharmacopoeias. The relative standard deviations and recoveries, 0.25–0.8% and 98.6–100.2%, respectively, are claimed to be acceptable.

More recently, promethazine hydrochloride, thioproperazine bis(methyl sulphate), aminopromazine fumarate and alimemazine tartrate have been determined by titration of their acidic functions with sodium hydroxide,[79] and benzodiazapines[80] (oxazepam, diazepam, nitrazepam and chloridiazepoxide) have been titrated as bases, with hydrochloric acid.

Ascorbic acid, pure and in tablets, has been determined by titration with iodine chloride.[76,81] Apparently, excipients in the tablets do not interfere significantly, but it is necessary to add Hg(II) to complex iodide or it will be oxidized to iodine and

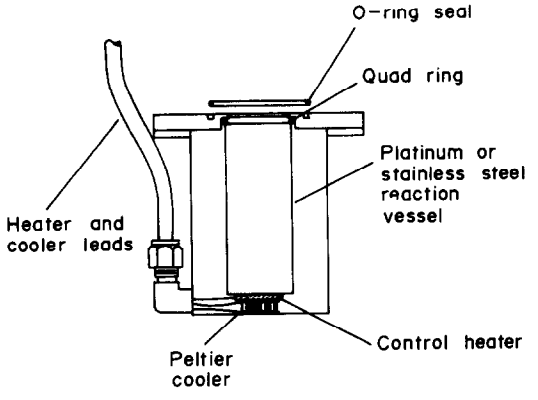

Fig. 50. Metal isothermal reaction vessel. Reproduced with permission of Tronac Inc.

influence the titration value. An aqueous solution of *N*-bromosuccinimide is also suitable as a reagent for the determination of ascorbic acid.[75] Physiologically active alkaloids, and vitamin B_1 in tablets and injection dosage forms, can be determined without the usual separation procedures, by precipitation titration with aqueous silicotungstic acid solution.[82] The common excipients—magnesium stearate, lactose, sucrose, starch and chalk—do not interfere, and titration errors are approximately $\pm 1\%$.

Sulphonamides have been determined by TET with silver nitrate,[73] sodium nitrite[83] and sodium hypochlorite[74] as reagents. Excipients do not interfere in the titration with silver nitrate, and it is claimed that this reagent is superior to hypochlorite, which might be expected to oxidize excipients as well.

Catalytic thermometric titrimetry. The assays of pharmaceutical substances by CTT so far investigated have been done in non-aqueous solution, because the response of thermometric indicators currently used is adversely affected by water. Thus the solvent systems differ significantly from those favoured in the TET determinations.

For titration of acidic functions, acetone,[84] acrylonitrile[85] and some acrylic esters have been evaluated. Acetone is suitable as both an indicator and a solvent, but when acrylonitrile is the indicator a co-solvent, usually dimethylformamide, is required. Acetone is suitable for the determination of very weak acids, such as phenols.[84] The acrylonitrile indicator was found suitable for the determination of the catecholamines, adrenaline, noradrenaline, dopamine, dopa, methyldopa, and Corbasil,[86] and twelve pharmaceutically-important sulphonamides (Fig. 51).[87] Both acetone and acrylonitrile have been evaluated as indicators for the determination of barbiturates.[88] The titration of tablet dosage forms of

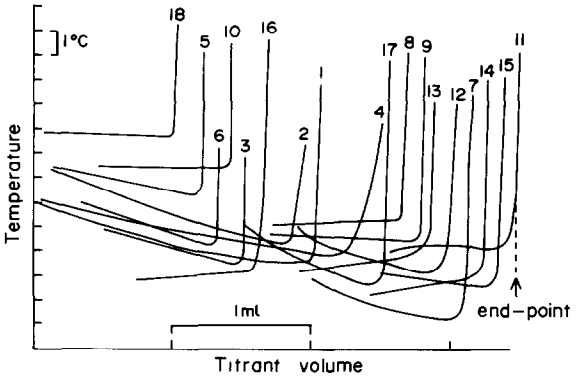

Fig. 51. Catalytic thermometric titration curves for sulphonamides in different solvent systems; 1, phthalylsulphathiazole; 2, succinylsulphathiazole; 3 and 4, sulphadiazine; 5, sulphamerazine; 6, sulphamethizole; 7, 8 and 9, sulphapyridine; 10, sulphaquinoxaline; 11–17, sulphathiazole; 18, sulphaurea. Reprinted with permission from *Anal. Chem.*, 1975, **47**, 1384. Copyright 1975 American Chemical Society.

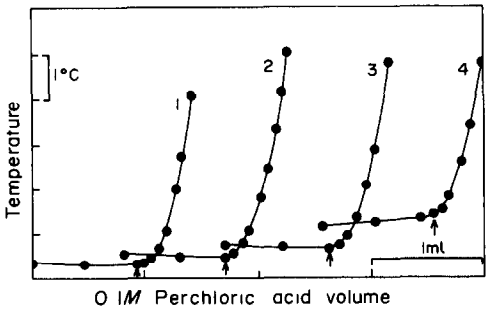

Fig. 53. Catalytic thermometric titration of the basic functions of catecholamines by a manual method: 1, L-dopa; 2, (−)-adrenaline; 3, L-noradrenaline; 4, dopamine hydrochloride. Arrows indicate theoretical end-points. Reproduced with permission.[86]

catecholamines, sulphonamides and barbiturates (tablets) indicated that the excipients did not interfere in titrations for acidic functions, but acidic excipient material in capsule doses of L-dopa gave rise to a high value for the content of active constituent.[86]

The thermometric-indicator reagents available at present for the titrimetric determination of bases are mixtures of acetic anhydride and water,[89] mixtures of acetic anhydride and alkanols,[90] α-methylstyrene[91] and vinyl alkyl ethers.[91] Perchloric acid in acetic acid is the preferred titrant with the first three indicators, but it is too active for use with the vinyl ethers, and a "milder" acid, boron trifluoride etherate in dioxan, is more suitable.

Vajgand and co-workers used the acetic anhydride–water indicator in the determination of tertiary amines and metal carboxylates, including brucine, antipyrine, cinchonine, pyridoxine hydrochloride, Flagyle, Intra-iodine, Inversal and sodium salicylate,[89,92] and developed a non-aqueous coulometric method for generation of the titrant.[92,93]

Greenhow has used mixtures of acetic anhydride and different alkanols to indicate the end-point in the determination of weak bases, including antipyrine, caffeine, theophylline and sodium salicylate (Fig. 52).[90] The mixture with alcohols is more effective than that with water for the determination of very weak bases, such as caffeine.

The α-methylstyrene indicator has been used in the titration of ephedrine hydrochloride and sulphate, codeine phosphate, and the alkaloids atropine, caffeine, nicotine, papaverine, quinine and its hydrochloride, strychnine and theophylline,[94] and the catecholamines listed above (Fig. 53).[86] Nicotine can be determined at the 8.5-μg level with 0.001*M* perchloric acid as titrant.

It is not necessary to add mercury(II) acetate in the titration of the amine hydrochlorides, although this addition is necessary in non-aqueous potentiometric titrimetry. In the titration of dosage forms, the presence of the excipient magnesium stearate can give rise to high titration values because, like other metal carboxylates, it is titrated as a base when it is soluble in the sample solvent.[86]

The end-point in iodimetric titration of non-aqueous solutions can be detected thermometrically

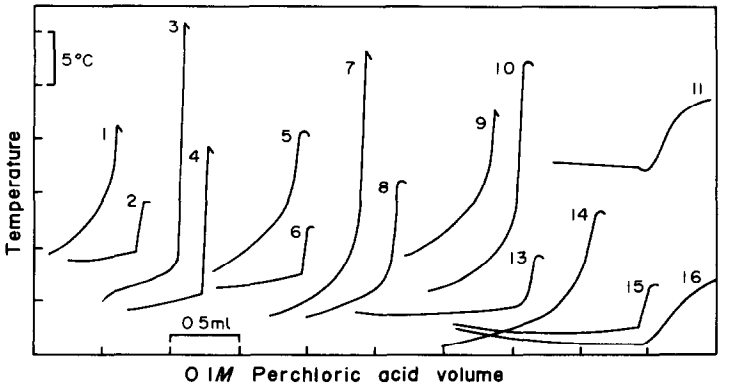

lytic thermometric titration, in different indicator systems, of antipyrine, caffeine, theo- with 0.1*M* perchloric acid in acetic acid: 1–4, antipyrine (9.4 mg); 5–12, caffeine , 14, theophylline (25.0 mg); 15, 16, urea (9.0 mg). Reproduced with permission.[90]

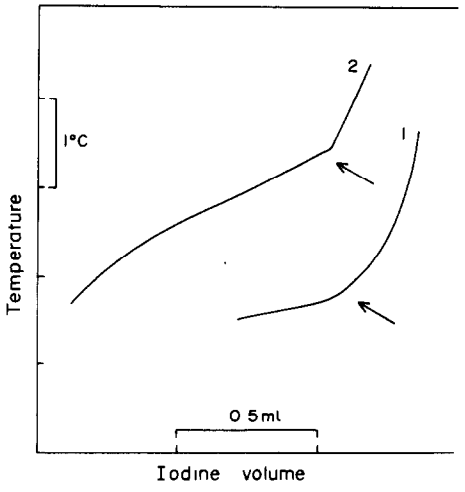

Fig. 54. Catalytic thermometric titration of isoniazid with iodine in dimethylformamide; 1, 0.85 mg, 0.05*M* titrant; 2, 0.54 mg, 0.01*M* titrant. Arrows indicate end-points.

with ethyl vinyl ether as the indicator reagent, because the first excess of iodine catalyses the cationic polymerization of the indicator. This iodimetric method has been applied successfully to the determination of primary, secondary and tertiary amines, which form iodine complexes, and isoniazid, which undergoes oxidation.[95] Typical titration curves for isoniazid are shown in Fig. 54.

Direct injection enthalpimetry. DIE is faster than TET or CTT because the excess of titrant is injected into the sample solution as quickly as possible. It lends itself well to "inverse" reactions, in which the sample is injected into an excess of reagent; this procedure should be useful for routine work because several samples can be injected into the same lot of reagent.[96]

A reduction reaction has been applied to the DIE determination of hydrogen peroxide in Hyperol tablets (a mixture of hydrogen peroxide and urea) with acidified potassium iodide in the presence of a molybdate catalyst.[96] Amino-acids, urea, thioglycollic acid, salicylic acid, acetylsalicylic acid and ascorbic acid have been determined by oxidation reactions—ascorbic acid by reaction with hexacyanoferrate[97] and the other analytes by reaction with sodium hypobromite.[98] In the ascorbic acid determination, starch, calcium lactate and talc excipients are unaffected by the reagent.[97]

Bark and Grime have determined organic nitrogen bases by titration with sodium tetraphenylborate.[99] An excess of reagent is added and back-titrated with aqueous potassium chloride solution. The method has been applied to the determination of several primary, secondary and tertiary amines, quaternary ammonium salts and hexamethylenetetramine.

Grime and Tan[100] have determined some penicillins in "pure" form, and in tablets, capsules and vials without further purification, by an enzymatic procedure. The sample, in aqueous solution, is injected into a buffered solution of penicillinase and the temperature rise is measured. The enzymatic reaction takes only 80 sec, and ten samples can be injected consecutively into one batch of enzyme. The relative standard deviations range from 0.6 to 4.0%. The limit of detection is $10^{-3}M$.

Clinical and biochemical determinations

Clinical samples are complex mixtures, and to determine specific constituents by the thermometric method it is usually necessary to use specific or highly selective reagents. Enzymes come under the former heading, and enzyme–substrate reactions, in the absence and presence of inhibitors, have been investigated for the purpose of determining the concentration of substrate, the enzyme activity or the concentration of inhibitor. Another "specific" reaction that has not, as yet, received the same wide attention as enzymic processes, is that between antibody and antigen.

Thermometric enthalpy titrations

The protein content of 1 ml of human serum has been determined with a precision of 0.5% by titration with 12-phosphotungstic acid, which reacts stoichiometrically with the protonated basic amino-acid residues of the protein.[101] Aqueous solutions containing 1 g of bovine serum albumin per litre have been examined.

Baldridge and Jesperson have used an enzymatic reaction to determine silver, which is a non-competitive inhibitor of the urease-catalysed hydrolysis of urea.[102] The inhibitor is pumped into the enzyme–substrate mixture, and its concentration is calculated from the kinetic data.

The TET method has been used to study the binding of ADP (adenosine diphosphate) to bovine liver glutamate dehydrogenase by injection of a solution of the former into a buffered solution of the latter. From the temperature changes, the values of the standard enthalpy and free-energy changes are calculated.[103]

Direct injection enthalpimetry

McGlothlin and Jordan have used DIE for determining glucose enzymatically in serum, plasma and whole blood by measuring the heat changes when glucose is phosphorylated by magnesium adenosine triphosphate [$Mg(ATP)^{2-}$] reagent in the presence of hexokinase.[104,105] The samples are injected sequentially into an excess of the reagent, containing hexokinase and tris buffer. A precision and accuracy of 2% are claimed. The authors have used a similar procedure for determining the enzyme activity of hexokinase; here the limit of detection was 0.5 E.A. units.[106]

Grime *et al.* have used the DIE method to measure the Michaelis constant for the hydrolysis of *N*-acetyl-L-tyrosine ethyl ester (ATEE), catalysed by bovin pancreas α-chymotrypsin.[107] The enzyme is rapid

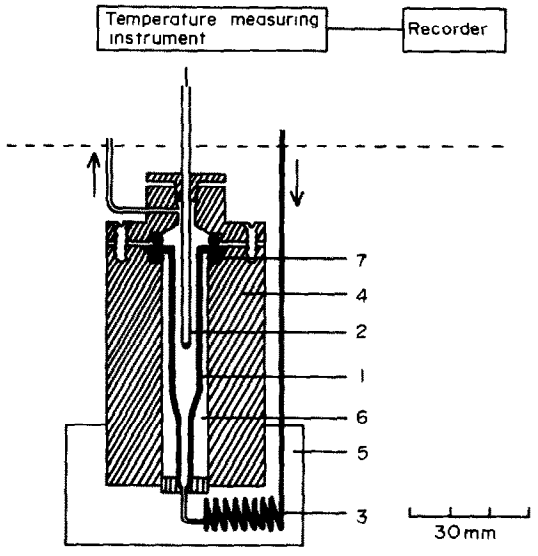

Fig. 55. Apparatus for continuous-flow enthalpimetry with an immobilized enzyme in the reaction compartment (the "enzyme thermistor"): 1, reaction microcolumn; 2, thermistor; 3, heat-exchanger; 4, Perspex cylinder; 5, water-jacket; 6, air-gap; 7, O-rings to seal the lid. The entire unit is immersed in a water-bath (level shown by dotted line). Reproduced from reference 112 with permission from the copyright holder, Elsevier/North-Holland Biomedical Press, Amsterdam.

injected into the titration cell containing ATEE, ethanol and buffer, the data are evaluated kinetically, and the effect of inhibition by ethanol is assessed.

Continuous-flow methods

A number of workers have used flow microcalorimetry to study protonation of proteins. Heats of protonation are measured and the ΔH values for different groups titrated are calculated from the ΔH *vs.* pH titration curves. Proteins examined include those of the chymotrypsinogen family,[108] lysozyme,[109] ribonuclease A and its complex with 3′-cytosine monophosphate,[110] and a group of globular proteins, including lysozyme, chymotrypsinogen A and oxidized Cytochrome C.[111]

In recent years there has been considerable interest in the use of immobilized enzymes in flow enthalpimetric analysis. The enzymes are usually bonded to controlled-porosity glass beads by reaction with a bifunctional silane reagent and glutaraldehyde.

Mosbach *et al.*[112] have used immobilized glucose oxidase, penicillinase, trypsin and urease as catalysts for the determination of glucose, penicillin G, benzoyl-L-arginine ethyl ester and urea, respectively, with appropriate reagents. The substrate and reagent solutions are allowed to flow through a column packed with immobilized enzyme and containing a thermistor (the "enzyme thermistor") (Fig. 55). Figure 56 shows titration curves for discrete and continuous sample addition.

Bowers and co-workers have used a similar system for the determination of urea in serum.[113,114] Bilirubin haemoglobin did not interfere[114] and the results compared well with those obtained by the biacetyl monoxime and urease/indophenol methods.

Bowers and Carr also determined glucose in serum by phosphorylation, using immobilized hexokinase as catalyst.[115] These authors have reviewed the analytical applications of immobilized enzymes in general, and have quoted these two determinations as examples of the use of thermometric procedures.[113] They suggested that determinations at the rate of 60/hr are possible.

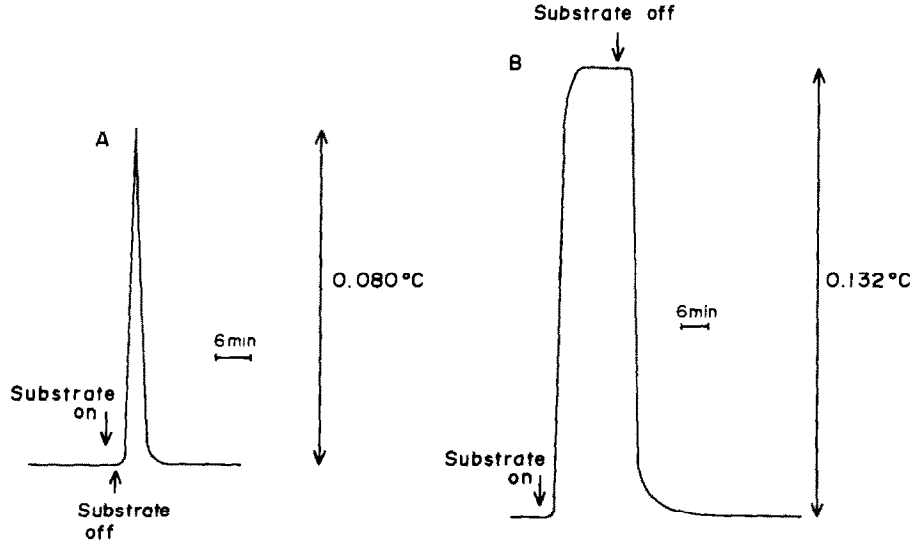

Fig. 56. Experimental curves obtained after injecting 10m*M* penicillin through the enzyme thermistor: A, pulse of 1.5 ml; B, continuous flow. Reproduced from reference 112 with permission from the copyright holder, Elsevier/North-Holland Biomedical Press.

Conclusions

All three titrimetric procedures, TET, CTT and DIE (including continuous-flow methods) are suitable for the analysis of pure compounds, formulations and complex mixtures, such as clinical samples, provided that a suitable selective reaction is available (and with CTT an appropriate indicator reagent). Selectivity cannot be achieved instrumentally when the response is measured thermometrically, unless the kinetics are very favorable, *i.e.*, the reaction rates for the determinand(s) and interferent(s) are very different.

In theory, the time needed for a thermometric titration will depend only on the speed of the determination reaction. In practice, DIE is the fastest method because it requires only measurement of the temperature rise, whereas in TET and CTT an accurate measurement of the titrant volume is necessary. Another advantage of DIE is that the large excess of reagent injected ensures the rapid completion of the reaction. A disadvantage of DIE is the need to construct a calibration graph relating ΔT to sample concentration.

According to Jordan and Carr,[116] TET is more precise than DIE, the relative standard deviations lying in the ranges 0.2–0.5% and 3–5%, respectively. The precision of CTT is generally of the same order as that of DIE when titrants of the same molarity are used.

However, CTT has the advantage of being applicable to the determination of much smaller sample concentrations, *e.g.*, at the 10-μg/ml level, because the response of the indicator reagent is not influenced by sample size. Major disadvantages of CTT are (1) the lack of suitable indicators for the determination of organic compounds by oxidation–reduction and precipitation reactions, and (2) the need to use non-aqueous solvents for the organic analyses. The latter disadvantage has been overcome to some extent in the determination of weak acids, by the introduction of acetaldehyde as a thermometric indicator.[117] With it, carboxylic acids, including amino-acids, can be determined in aqueous solution by titration with aqueous alkali.

The rate of the determination reaction in thermometric titrimetry has some influence on the choice of instrument. Thus for reactions that are reasonably fast and can be initiated and stopped at will, pseudo-adiabatic, including isoperibolic, titration calorimeters are satisfactory, but for slow reactions that may continue for hours, isothermal calorimeters are much to be preferred.

To summarize: on the ground of sensitivity, simplicity, convenience, and low cost and ease of transportation of the apparatus, CTT would probably be the thermometric method of choice, but its scope is limited by the availability of suitable thermometric indicators. Both DIE and TET have a wide range of applications, since any analyte for which there is a selective chemical reaction can be determined. Of these two methods, DIE would be chosen for rapid analyses, and also for multiple analyses by successive injection of several discrete samples into one lot of reagent or by use of one of the continuous-flow modifications. On the other hand, of the three techniques only TET is, at present, generally suitable for the determination of several constituents or reactive functions in the same sample.

Acknowledgement—The authors wish to thank the copyright owners for permission to reproduce figures and tables cited in the text.

REFERENCES

1. G. Swidler, *Handbook of Drug Interactions*. Wiley Interscience, New York, 1971.
2. F. Kavanagh (ed.), *Analytical Microbiology*, Vol. 1. Academic Press, New York, 1963.
3. C. H. Collins and P. M. Lyne, *Microbiological Methods*. Butterworths, London, 1976.
4. K. Florey (ed.), *Analytical Profiles of Drugs*, Vols. 1–8. Academic Press, New York, 1972–1978.
5. I. Nadzinge, C. D. Peters and A. H. Thomas, *Analyst*, 1977, **102**, 328.
6. R. F. Cosgrove and J. E. Fairbrother, *Antimicrob. Ag. Chemother.*, 1977, **11**, 31.
7. A. E. Beezer and P. Sharma, *Talanta*, 1979, **26**, 411.
8. B. Z. Chowdhry, *M.Sc. Thesis*, London University, 1975.
9. D. W. Hughes and W. L. Wilson, *Can. J. Pharm. Sci.*, 1973, **8**, 67.
10. C. Spink and I. Wadsö, *Meth. Biochem. Anal.*, 1975, **23**, 2.
11. I. Wadsö, *Quart. Rev. Biophys*, 1970, **3**, 383.
12. *Idem, Biochem. Soc. Trans.*, 1976, **4**, 565.
13. D. S. Reid, *J. Phys. E., Sci. Instr.*, 1976, **9**, 601.
14. H. A. Skinner, in *Biochemical Microcalorimetry*, H. D. Brown (ed.). Academic Press, New York, 1969.
15. H. J. V. Tyrrell and A. E. Beezer, *Thermometric Titrimetry*, p. 38. Chapman & Hall, London, 1968.
16. J. M. Sturtevant, *Meth. Membrane Biol.*, 1978, **9**, 237.
17. P. Privalov, *Pure Appl. Chem.*, 1980, **52**, 479.
18. A. E. Beezer, in *Applications of Calorimetry in Life Sciences*, I. Lamprecht and B. Schaarschmidt (eds.), pp. 109–118. de Gruyter, Berlin, 1977.
19. S. L. Randzio and J. Suurkuusk, in *Biological Microcalorimetry*, p. 311. A. E. Beezer (ed.). Academic Press, New York, 1980.
20. A. E. Beezer, R. D. Newell and H. J. V. Tyrrell, *Anal. Chem.*, 1977, **49**, 34.
21. A. E. Beezer, B. Z. Chowdhry, R. D. Newell and H. J. V. Tyrrell, *ibid.*, 1977, **49**, 1781.
22. H. Prat, *Rev. Can. Biol.*, 1953, **12**, 19.
23. B. Zablocki and E. Czerniaski, *Bull. Acad. Pol. Sci. Ser. Cl. II*, 1962, **10**, 209.
24. B. Zablocki, J. Goscicki and E. Czerniaski, *Bull. Acad. Pol. Ser. Sci. Biol.*, 1959, **7**, 409.
25. I. Wadsö, *Svensk. Kemisk Tidskrift*, 1969, **81**, 28.
26. P. A. Mardh, T. Ripa, K. E. Anderson and I. Wadsö, *Antimicrob. Ag. Chemother.*, 1976, **10**, 604.
27. E. Semenitz and F. Tiefenbrunner, in *Applications of Calorimetry in Life Sciences*, I. Lamprecht and B. Schaarschmidt (eds.), pp. 251–260. de Gruyter, Berlin, 1977.
28. P. A. Mardh, M. Arhammer, S. Colleen and K. E. Andersson, *J. Antimicrob. Chemother.*, 1978, **4**, 73.
29. E. Semenitz, *ibid.*, 1978, **4**, 455.
30. A. E. Beezer and B. Z. Chowdhry, *Microbios*, 1980, **28**, 107.
31. P. A. Mardh, M. Arhammer and K. E. Andersson, *Chemotherapy*, 1979, **25**, 106.

32. B. Schaarschmidt, I. Lamprecht and M. Simonis, in *Angewandte Chemische Thermodynamik und Thermoanalytik*, E. Marti, H. R. Osland and H. G. Weidemann (eds.). Birkhauser, Basel, 1979.
33. E. Semenitz, *Immunitat. Infektion*, 1978, **6**, 260.
34. T. E. Jensen, L. D. Hansen, D. J. Eatough, R. J. Sagers and R. M. Izatt, *Thermochim. Acta*, 1976, **17**, 65.
35. K. Ljungholm, I. Wadsö and P. A. Mardh, *J. Gen. Microb.*, 1976, **96**, 283.
36. M. Arhammer, P. A. Mardh, T. Ripa and K. E. Andersson, *Acta Path. Microbiol. Scand., Sect. B*, 1978, **86**, 59.
37. A. E. Beezer and B. Z. Chowdhry, *Talanta*, 1980, **27**, 1.
38. *Idem*, *Experientia*, 1981, **37**, 828.
39. A. E. Beezer, R. D. Newell and H. J. V. Tyrrell, *J. Appl. Bact.*, 1976, **41**, 197.
40. R. F. Cosgrove, A. E. Beezer and R. J. Miles, *J. Infect. Dis.*, 1978, **138**, 681.
41. E. Semenitz, *Zentralbl. Bakteriol. Parasitenk. Infektionskr. Hyg. Abt. 1, Orig. Reihe A*, 1979, **243**, 372.
42. E. Semenitz and F. Tiefenbrunner, *Arzneim. Forsch.*, 1977, **27**, 2247.
43. J. S. Binford, L. F. Binford and P. Adler, *Am. J. Clin. Path.*, 1973, **59**, 86.
44. A. E. Beezer, R. J. Miles, E. J. Shaw and P. Willis, *Experientia*, 1979, **35**, 795.
45. M. Durand, T. C. Maurizot and C. Helene, *FEBS Lett.*, 1976, **71**, 9.
46. D. W. Urry, *Intern. J. Quantum Chem. Quantum Biol. Symp.*, 1975, **2**, 221.
47. P. U. Fruh and W. Simon, in *Protides of the Biological Fluids*, H. Peeters (ed.), **20**. Pergamon Press, Oxford.
48. M. Rossenau and W. Dekeersigierter, *J. Cal. Anal. Therm.*, 1978, **9B, C11**, 63.
49. L. Berti-Corti, in *Application of Calorimetry in Life Sciences*, I. Lamprecht and B. Schaarschmidt (eds.), pp. 85–95. de Gruyter, Berlin, 1977.
50. G. E. Hardee, M. Otagiri and J. H. Perrin, *Acta Pharm. Suecie*, 1978, **15**, 188.
51. M. Otagiri, G. E. Hardee and J. H. Perrin, *Biochem. Pharmac.*, 1978, **27**, 1401.
52. B. F. Perry, A. E. Beezer and R. J. Miles, *J. Appl. Bact.*, 1979, **47**, 527.
53. A. E. Beezer, K. A. Bettelheim, R. D. Newell and J. Stevens, *Science Tools*, 1974, **21**, 13.
54. A. E. Beezer, K. A. Bettelheim, A. S. Sabria and E. J. Shaw, *ibid.*, 1977, **25**, 6.
55. *U.S. Pharmacopeia*, 1975.
56. J. Jordan and P. W. Carr, in *Analytical Calorimetry*, Vol. 2, R. S. Porter and J. F. Johnson, (eds.), p. 203. Plenum Press, New York, 1970.
57. V. J. Vajgand and F. F. Gaál, *Talanta*, 1967, **14**, 345.
58. H. A. Mottola, *ibid.*, 1969, **16**, 1267.
59. J. S. Wasilewski, P. T-S. Pei and J. Jordan, *Anal. Chem.*, 1964, **36**, 2131.
60. P. T. Priestley, W. S. Sebborn and R. F. W. Selman, *Analyst*, 1965, **90**, 589.
61. J. Jordan, J. K. Grime, D. H. Waugh, C. D. Miller, H. M. Cullis and D. Lohr, *Anal. Chem.*, 1976, **48**, 427A.
62. I. Sajó, *J. Thermal Anal.*, 1969, **1**, 349.
63. E. J. Greenhow and A. A. Shafi, *Analyst*, 1976, **101**, 421.
64. I. Sajó and B. Sipos, *Mikrochim. Acta*, 1967, 248.
65. J. J. Christensen, H. D. Johnston and R. M. Izatt, *Rev. Sci. Instrum.*, 1968, **39**, 1356.
66. J. J. Christensen, J. W. Gardner, D. J. Eatough, R. M. Izatt, P. J. Watts and R. M. Hart, *Anal. Chem.*, 1973, **44**, 481.
67. G. A. Vaughan, *Thermometric and Enthalpimetric Titrimetry*. Van Nostrand Reinhold, London, 1973.
68. J. Barthel, *Thermometric Titration*. Wiley, New York, 1975.
69. D. J. Eatough, *J. Thermal Anal.*, 1978, **14**, 45.
70. J. Brandstetr, *ibid.*, 1973, **14**, 157.
71. C. J. Martin and M. A. Marini, *CRC Crit. Rev. Anal. Chem.*, 1979, **8**, 221.
72. *The British Pharmaceopeia.*, H. M. Stationery Office, London, 1973.
73. L. S. Bark and J. K. Grime, *Analyst*, 1973, **98**, 452.
74. H. Schafer and E. Wilde, *Z. Anal. Chem.*, 1949, **130**, 396.
75. L. S. Bark and P. Prachuapaibul, *Anal. Chim. Acta*, 1976, **87**, 505.
76. L. S. Bark and J. K. Grime, *Analyst*, 1974, **99**, 38.
77. A. B. DeLeo and M. J. Stern, *J. Pharm. Sci.*, 1964, **53**, 993.
78. *Idem. ibid.*, 1966, **55**, 173.
79. J. L. Burgot, *Talanta*, 1978, **25**, 339.
80. P. Marcu and I. Grecu, *Pharmazie*, 1976, **31**, 167.
81. L. S. Bark and J. K. Grime, *Talanta*, 1975, **22**, 443.
82. *Idem*, *Anal. Chim. Acta*, 1973, **64**, 276.
83. J. Jordan, R. A. Henry and J. C. Wasilewski, *Microchem. J.*, 1966, **10**, 260.
84. G. A. Vaughan and J. J. Swithenbank, *Analyst*, 1965, **90**, 594.
85. E. J. Greenhow and L. E. Spencer, *ibid.*, 1973, **98**, 90.
86. *Idem*, *ibid.*, 1973, **98**, 485.
87. *Idem*, *Anal. Chem.*, 1975, **47**, 1384.
88. L. S. Bark and O. Ladipo, *Analyst*, 1976, **101**, 203.
89. V. J. Vajgand and F. F. Gaál, *Talanta*, 1967, **14**, 345.
90. E. J. Greenhow, *Analyst*, 1977, **102**, 584.
91. E. J. Greenhow and L. E. Spencer, *ibid.*, 1973, **98**, 81.
92. V. J. Vajgand, T. A. Kiss, F. F. Gaál and I. J. Zsigrai, *Talanta*, 1968, **15**, 699.
93. V. J. Vajgand, F. F. Gaál and S. S. Brusin, *ibid.*, 1970, **17**, 415.
94. E. J. Greenhow and L. E. Spencer, *Analyst*, 1973, **98**, 98.
95. *Idem*, *ibid.*, 1974, **99**, 82.
96. P. Marik-Korda, *J. Thermal Anal.*, 1978, **13**, 357.
97. L. S. Bark and L. Kershaw, *Analyst*, 1975, **100**, 873.
98. N. Malingerová and M. Malinger, *J. Thermal Anal.*, 1978, **13**, 149.
99. L. S. Bark and J. K. Grime, *Analyst*, 1972, **97**, 911.
100. J. K. Grime and B. Tan, *Anal. Chim. Acta*, 1979, **107**, 319.
101. E. B. Smith and P. W. Carr, *Anal. Chem.*, 1973, **45**, 1688.
102. J. N. Baldridge and N. D. Jesperson, *Anal. Lett.*, 1975, **8**, 683.
103. N. V. Beaudette and N. Langerman, *Anal. Biochem.*, 1978, **90**, 693.
104. C. D. McGlothlin and J. Jordan, *Clin. Chem.*, 1975, **21**, 741.
105. *Idem*, *Anal. Chem.*, 1975, **47**, 786.
106. *Idem*, *ibid.*, 1975, **47**, 1479.
107. J. K. Grime, K. Lockhart and B. Tan, *Anal. Chim. Acta*, 1977, **91**, 243.
108. R. Biltonen, A. T. Schwartz and I. Wadsö, *Biochem.*, 1971, **10**, 3417.
109. C. Bjurulf, *Eur. J. Biochem.*, 1972, **30**, 33.
110. M. Flogel and R. L. Biltonen, *Biochem.*, 1975, **14**, 2603.
111. D. D. F. Shiao and J. M. Sturtevant, *Biopolymers*, 1976, **15**, 1201.
112. K. Mosbach, B. Danielsson, A. Borgerud and M. Scott, *Biochim. Biophys. Acta*, 1975, **403**, 256.
113. L. D. Bowers and P. W. Carr, *Anal. Chem.*, 1976, **48**, 545A.
114. L. D. Bowers, L. M. Canning Jr., C. N. Sayers and P. W. Carr, *Clin. Chem.*, 1976, **22**, 1314.
115. L. D. Bowers and P. W. Carr, *ibid.*, 1976, **22**, 1427.
116. J. Jordan and P. W. Carr, *U.S. At. Energy Comm. Rept.*, NYO-2133-48, 1967.
117. E. J. Greenhow and L. E. Spencer, *Talanta*, 1977, **24**, 201.

Talanta, Vol. 30, No. 4, pp. 245–250, 1983
Printed in Great Britain.

0039-9140/83/040245-06$03.00/0

METAL CHELATES OF AZO-PYRIDAZINE DYES

CHELATING TENDENCIES OF BENZOYLACETONE-MONOHYDRAZONE-3-HYDRAZINO-4-BENZYL-6-PHENYLPYRIDAZINE (BAHP)

ATEF A. T. RAMADAN and MAGDY H. SEADA
Faculty of Education, Ain Shams University, Roxy, Cairo, Egypt
and
EMIL N. RIZKALLA*
Faculty of Science, Ain Shams University, Abbassia, Cairo, Egypt

(*Received* 15 *March* 1982. *Revised* 25 *June* 1982. *Accepted* 5 *November* 1982)

Summary—The synthesis, acid–base equilibria and metal-ion chelating tendencies of BAHP are reported. From potentiometric equilibrium measurements of hydrogen-ion concentration at 30° and ionic strength 0.10*M* (KNO_3), in 75% dioxan–water medium, the values of the stability constants of some BAHP complexes with transition, non-transition and lanthanide ions have been evaluated. Probable structures of the metal chelates are inferred from the electronic absorption spectra and infrared examination of the solid copper complex. The use of BAHP as an analytical reagent for the spectrophotometric determination of copper, nickel and cobalt ions is discussed.

Azo-dyes form the largest group of synthetic dyestuffs and feature prominently in almost every type of application. β-Diketones are a well-known class of ligand, capable of forming stable complexes with various metal ions.[1,2] Species containing both these types of functional group might be expected to combine the features of both classes of ligand.

A condensation reaction between a hydrazino group and a β-diketone species can take place through one of the carbonyl groups or the active methylene group to give ligands with the chromophoric groups **I** and **II** respectively.

*To whom correspondence should be addressed.

Both arrangements can be useful in explaining the different co-ordinating properties. Most of the studies reported on these systems are limited to isolation of the solid complexes[3] or characterization of the absorption spectra.[4]

The metal-binding characteristics of a series of ligands with donor groups **I** or **II** have been studied. In some cases, auxiliary strong co-ordinating groups such as carboxylate or amino groups have been incorporated. In the present communication, the metal-binding characteristics of one of the representative ketonic hydrazones, *viz.* benzoylacetone-monohydrazone-3-hydrazino-4-benzyl-6-phenylpyridazine (BAHP) (**III**), is described.

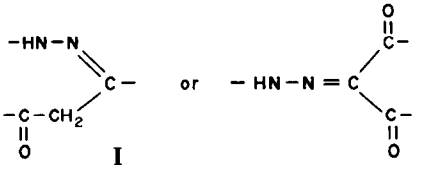

I **II**

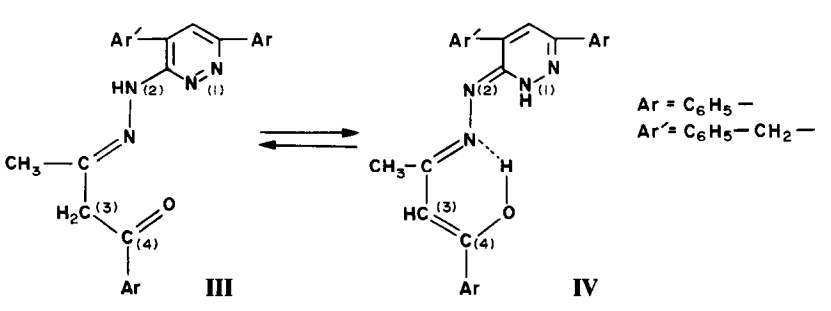

III **IV**

EXPERIMENTAL

Preparation of the solid ligand and its copper chelate

BAHP was prepared as described in an earlier publication.[5] The copper chelate was prepared by adding a dioxan solution of the ligand (0.025 mole) to an aqueous solution of copper nitrate (0.025 mole). The pH of the solution was then increased to *ca.* 4 and the mixture was refluxed for 1 hr. The reddish brown precipitate obtained was filtered off, washed, recrystallized from ethanol and dried under vacuum. Found: C 64.8%; H 5.0%; N 11.2%; $C_{27}H_{22}N_4OCu \cdot H_2O$ requires C 64.93%; H 4.81%; N 11.22%.

Determination of stability constants

Reagent-grade metal nitrates were used for making stock solutions, which were standardized with EDTA.[6] Carbon dioxide-free potassium hydroxide solution was prepared and standardized as recommended.[7] Dioxan was purified by refluxing it with $Na/LiAlH_4$ for 8–10 hr, followed by distillation. The procedure was repeated twice to insure the disappearance of acetals.

Appropriate aliquots of standard solutions of metal nitrates and BAHP in 75% dioxan–water medium were titrated potentiometrically with 0.04*M* potassium hydroxide (Beckman SSR 2 pH-meter fitted with a combined glass–calomel electrode). The correction for pH values in 75% dioxan–water was taken as 0.28.[8] The temperature was maintained at 30° by use of jacketed cells with water circulated from a constant-temperature bath. Purified nitrogen was passed through the solution during the measurements. The ionic strength of the medium was kept virtually constant at 0.10*M* with potassium nitrate as background electrolyte.

All the titrations were repeated at least twice and the titration curves agreed within ±0.02 pH unit.

Spectroscopy

Infrared spectra (potassium bromide discs) were recorded on a Perkin–Elmer 437 spectrometer (4000–300 cm^{-1}). The electronic spectra were measured at 25° with a Prolabo UV–visible spectrometer, with 1-cm matched quartz cells.

Determination of Cu(II), Ni(II) and Co(II)

Copper, nickel and cobalt were determined spectrophotometrically at 360, 346 and 370 nm respectively, over the concentration range 0.9–8.0 μg/ml, in 75% dioxan–water medium.

RESULTS AND DISCUSSION

Potentiometric measurements

The pH-titration curves for free and complexed BAHP are shown in Fig. 1. Between $a = 0$ and $a = 1$, and in the presence of different metal ions, only one proton dissociates (a = moles of base added per mole of ligand present). This suggests that under these conditions the ligand behaves as a monoprotic species, with the dissociation of either the hydrazo or the enolic OH-group proton. The acid dissociation constant, K^H, was calculated by using the relationship;

$$\log K^H = \log \frac{aC_L - [H^+] + [OH^-]}{(1-a)C_L + [H^+] - [OH^-]} + \text{pH}. \quad (1)$$

Since the ionic product, pK_w, of water in 75% dioxan–water medium is approximately 18.7,[9] both the hydrogen-ion and hydroxyl-ion concentration terms in equation (1) are negligible in the region of proton dissociation.

The titration curves obtained in the presence of

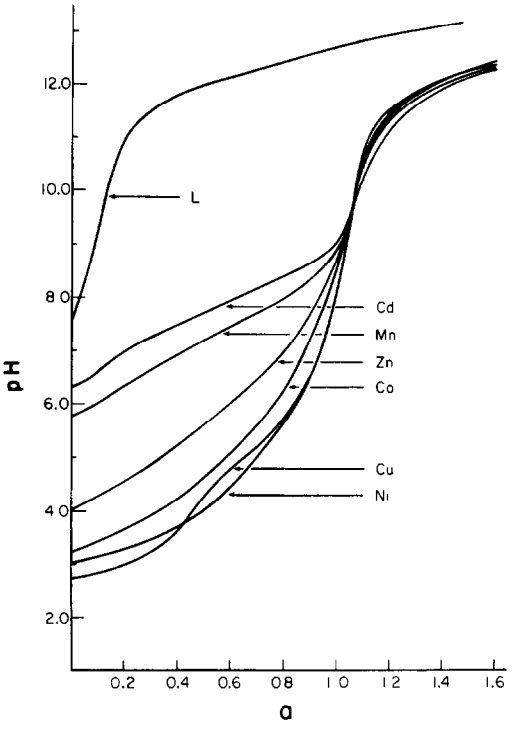

Fig. 1. Potentiometric titration curves of BAHP and its complexes with Mn(II), Co(II), Ni(II), Cu(II), Zn(II) and Cd(II) ions, at 30°C; 0.10*M* KNO_3. L = Free ligand; a = moles of base added per mole of BAHP. [M] = 0.001*M*; [L] = 0.002*M*.

bivalent cations showed an inflection at $m = 2$ (where m = moles of base added per mole of metal), corresponding to formation of the bis-chelates, represented by the equilibrium

$$M^{2+} + 2HL \rightleftharpoons ML_2 + 2H^+$$

but in the case of copper an additional inflection was observed at $m = 1$, corresponding to the formation of an ML species.

Values of the stability constants β_{ML} and β_{ML_2} were obtained from the intercept and slope of the linear relationship

$$\frac{\bar{n}}{(1-\bar{n})[L]} = \frac{2-\bar{n}}{1-\bar{n}}[L]\beta_{ML_2} + \beta_{ML}. \quad (2)$$

The best straight line was obtained by the method of least squares.

The hydrolytic tendencies of the lanthanide chelates in moderately alkaline media and beyond $a = 1$ did not allow useful estimates of $\bar{n}$ values in the region of formation of the bis-chelates. Accordingly, only the values of β_{ML} were considered. A summary of the constants obtained is given in Table 1.

Spectroscopy

The electronic absorption spectrum of the free ligand (in 75% dioxan–water mixture) displays two absorption bands, with λ_{max} 220 and 291 nm, and molar absorptivities of 4.5×10^4 and 1.8×10^4

Table 1. Stability constants of BAHP–metal complexes (30°C, 75% dioxan–water, 0.10*M* KNO_3)

Cation	log β_{ML}	log β_{ML_2}	K_{ML}/K_{ML_2}
H^+	11.98		
Mn^{2+}	7.95	15.31	4
Co^{2+}	11.03	20.38	48
Ni^{2+}	11.76	22.00	33
Cu^{2+}	12.18	21.84	333
Zn^{2+}	9.87	18.37	23
Cd^{2+}	7.35	14.13	4

Cation	log β_{ML}	Cation	log β_{ML}
La^{3+}	7.64	Tb^{3+}	8.43
Ce^{3+}	7.52	Dy^{3+}	8.50
Pr^{3+}	7.68	Ho^{3+}	8.64
Nd^{3+}	7.82	Er^{3+}	8.75
Sm^{3+}	8.10	Tm^{3+}	8.82
Eu^{3+}	8.36	Yb^{3+}	8.74
Gd^{3+}	8.40	Lu^{3+}	8.84

$l.mole^{-1}.cm^{-1}$ respectively. Like those reported for the pyridazine ring at 245 and 295 nm,[10] these two bands are attributed to an enhanced $\pi \rightarrow \pi^*$ transition (*K*-band) over the whole conjugated system and an enhanced $n \rightarrow \pi^*$ transition (*R*-band) respectively. In the presence of copper, nickel or cobalt, the latter band shows a bathochromic shift, with the appearance of additional bands (*cf.* Figs. 2 and 3). The intensities of the peaks observed are a function of both the pH of the medium and the molar ratio of metal to ligand. In the case of the copper complex, a maximum is reached at an M:L molar ratio of 1:2 (see Fig. 2B), whereas, in the case of cobalt and nickel the maximum is observed at a molar ratio of 1:3.

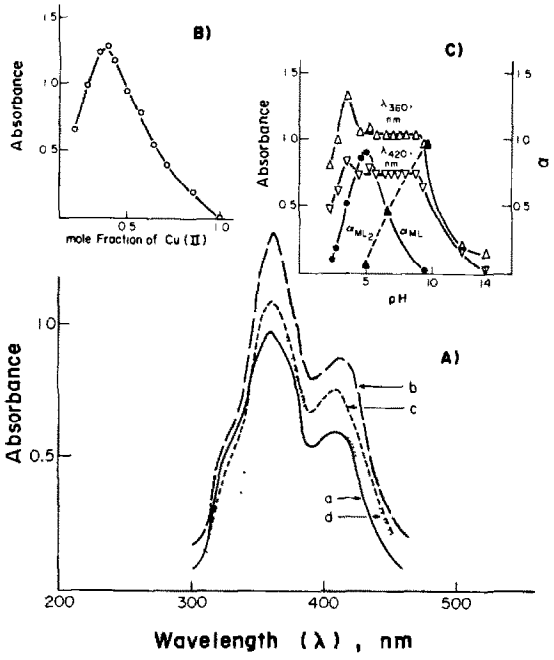

Fig. 2. Electronic absorption spectra of Cu-BAHP (A) Spectra of the bis-chelates at pH (a) 2.70; (b) 3.50; (c) 6.55; (d) 9.40. (B) Job's plot for 0.45m*M* Cu(II) in 75% dioxan–water, measured at 420 nm. (C) Absorption–pH and mole-fraction–pH relationships for the copper chelates.

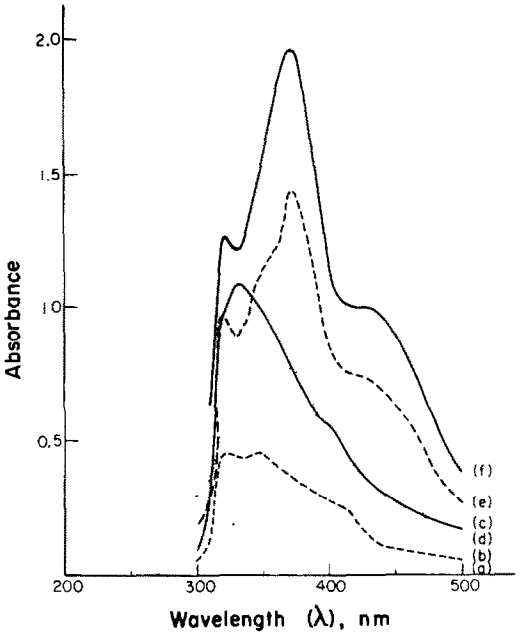

Fig. 3. Electronic absorption spectra in 75% dioxan–water for Ni (a, b and c) and Co (d, e and f) chelates at molar ratios 1:1 (a and d), 1:2 (b and e) and 1:3 (c and f), at 25°C.

The infrared spectra of the ligand and of the solid copper complex are presented in Table 2. The assignments reported were made by comparison with known systems.[10-12]

Conclusions

BAHP is a monobasic ligand with a structure which can be considered as consisting of a pyridazine-hydrazo group condensed with benzoylacetone. The structure can be represented in different tautomeric forms, among which are structures **III** and **IV**. An important feature of species **IV** is the existence (and strength) of the intramolecular hydrogen-bond between the enolic OH group and the aliphatic azomethine (>C=N–) group. The enolic form is further stabilized by the extension of the conjugated system. Evidence for this assignment is gained from both the infrared and ultraviolet spectroscopy.

In both the dissolved and solid states, the enol form is predominant. The absence of a strong carbonyl stretching band in the region of *ca.* 1700 cm^{-1} and the presence of a broad band at 3470 cm^{-1} (tentatively assigned to an intramolecular hydrogen-bonded OH stretching band) in the spectrum of the free ligand agrees with the proposed structure **IV**, but it was difficult to decide from the infrared spectrum alone whether the hydrazo hydrogen atom is mainly located on the hydrazo group or on the pyridazine nitrogen atom. The ultraviolet spectrum shows the presence of two intense bands assigned to a $\pi \rightarrow \pi^*$

Table 2. Some important infrared spectral bands of BAHP and its copper complex

Assignment	BAHP, cm^{-1}	Cu–BAHP, cm^{-1}
ν_{O-H}, intramolecular H-bond	3470, mb	
ν_{HOH}		3350, sb
ν_{N-H}	3250, m	
ν_{C-H}	3050, m 2910, w	3000, m 2865, m
$\nu_{C=C}$	1630, m	1612, m
ν_{C-N}	1590, m	1578, m
δ_{O-H}	1385, m	
$\nu_{C-N(1)}$, (structure **IV**)*	1310, s	
$\nu_{C-N(2)}$, (structure **III**)*	1250, m	1272, s
ν_{C-O}	1105, w	1070, m
$\delta_{>C(3)=C(4)<}$ (structure **IV**)*	975, s	990, m
ν_{N-N}	870, m	910–840, b
ν_{M-O}		500, w
ν_{M-N}		390, m
$\nu_{M-N'}$		340, m

*The atoms are numbered in the structures.
s = strong; m = medium; w = weak; b = broad.

and an $n\rightarrow\pi^*$ transition. The molar absorptivity for the first transition is more than twice that reported[10] for two aromatic rings conjugated as in structure **III**. This enhanced transition can be explained only in terms of further conjugation in the aliphatic chain linking the aromatic groups. The origin of the enhanced $n\rightarrow\pi^*$ transition is not known. Any of the nitrogen or oxygen lone pairs could contribute to such a transition.

Titration of the ligand with alkali shows the presence of only one ionizable proton. The value of log K^H obtained (11.98 in 75% dioxan–water) is close to that reported for benzoylacetone under similar experimental conditions (*ca.* 12.85, corrected for the differences in ionic strength[13]). In contrast, ligands containing the grouping Ar–NH–N=C<R are normally ionized in moderately alkaline media, and have pK^H values ranging[14,15] between 6 and 9. This suggests that in BAHP it is the BAHP enolic OH group that loses a proton. The ionization of the hydrazo proton has been observed only under drastic conditions of reflux and in the presence of metal ions (see below). This extra basicity is supporting evidence that the hydrazo group is not present as such, but that its proton is more likely attached to the pyridazine ring nitrogen atom, where it is less ionizable.

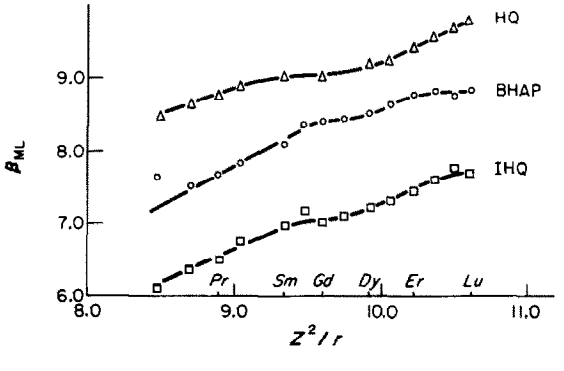

Fig. 4. Log β_{ML} as a function of ionic potential, Z^2/r, for various rare-earth complexes. Radii from reference 16. HQ = 8-hydroxyquinoline; IHQ = 8-hydroxy-5,7-di-iodoquinoline.

The metal–ligand interactions can be divided into three groups: those of copper, nickel and cobalt which have high affinities for nitrogen donor atoms; those of the rare-earth ions, which are normally considered to give purely electrostatic interactions, with high affinities for oxygen donor atoms; and those of manganese, zinc and cadmium, with intermediate affinities for both nitrogen and oxygen atoms.

In Fig. 4, the values of log β_{ML} for the rare-earth complexes are plotted against the ionic potential, Z^2/r. Instead of the expected linearity, a curve is obtained with a gradual increase in stability between lanthanum and europium followed by a plateau in the region of gadolinium–terbium, and a slight increase for the earlier heavy lanthanides, levelling off in the thulium–lutetium region. This kind of behaviour has been observed before for a variety of ligands, among which are quoted here those of 8-hydroxyquinoline (HQ)[17] and 8-hydroxy-5,7-di-iodoquinoline (IHQ)[18] (see Fig. 4). This deviation from linearity beyond gadolinium has been attributed by various authors to changes in hydration along the cationic series.[19–21]

BAHP is analogous to HQ and IHQ in that it is expected to form chelates with lanthanide ions by using the enolic OH group and the nitrogen atoms of the azomethine groups. A comparison of log β_{ML} for the complexes of a specific element with the three reagents shows that its value is in rough proportionality to Σ log K^H. The extra stability of the HQ chelates relative to the BAHP chelates can be attrib-

uted to the rigidity of the first group of chelates and the differences in the chelate ring sizes.

In addition to their ability to form 1:1 chelates with BAHP, manganese, cadmium and zinc are capable of forming 1:2 chelates. The most probable chelation sites in BAHP are shown in **V**:

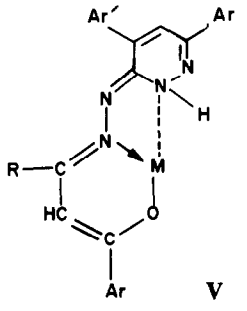

V

Addition of a second ligand might lead to breakdown of the pyridazine–metal bond to relieve steric hindrance. A comparison of the stepwise formation constants might even raise doubts about the extent of participation of this particular donor site in the bonding. The K_{ML}/K_{ML_2} ratio (Table 1) is probably too small to be accounted for by appreciable steric hindrance effects,[22] except in the case of the copper chelates. In addition, the spectral studies show that tris-chelates are formed with nickel and cobalt (see Fig. 3), which suggests that BAHP acts only as a bidentate ligand.

The titration curve for copper shows the presence of two distinct buffer regions separated by a sharp inflection at $m = 1$. From the ratio K_{ML}/K_{ML_2}, it is possible to suggest that in this particular case BAHP behaves as a terdentate ligand. In an attempt to study the 1:1 chelate, the solid complex was prepared. Under the drastic conditions used, the ligand molecule loses two protons, and the species Cu(OH)L (or $CuH_{-1}L \cdot H_2O$) separates. The infrared spectrum of the solid shows a systematic shift of the $\nu_{C=C}$, $\nu_{C=N}$ and ν_{C-O} bands to a lower frequency with the simultaneous disappearance of the ν_{N-H} and ν_{O-H} bands. The new bands observed at 500, 390 and 340 cm^{-1} are assigned to ν_{M-O}, ν_{M-N} and $\nu_{M-N'}$ respectively, with N and N′ being the nitrogen atoms of the azomethine and pyridazone groups, or *vice versa*.

The ultraviolet spectrum of the copper complex shows the presence of two bands, with λ_{max} at 360 and 410 nm. Also the spectrum shows the presence of a shoulder at 320–340 nm. The molar absorptivities of the bands are around $0.3–2.5 \times 10^4$ $l.mole^{-1}.cm^{-1}$, implying allowed electron transitions. The intensities of these bands are also a function of the pH of the medium. As is clear from Fig. 2c, the absorbance has a maximum in the pH region 3.5–4.0 followed by a plateau in the pH region 5–9. In addition to the pH-absorbance plots, the distribution curves for CuL and CuL_2 are shown as a function of the pH of the solution. A comparison of the plots shows that at $pH > 5$ and in the region of formation of the ML_2 species, the absorbance is constant, indicating perhaps that both ML and ML_2 are absorbing to the same extent ($\varepsilon_{ML} = \varepsilon_{ML_2}$). In strongly acidic media and in the region of very small fractions of the ML species, the copper–BAHP mixture still displays strong ultraviolet bands. These bands might be attributed to the presence of a significant proportion of the protonated complex, MHL. Similar spectra are also observed for the nickel and cobalt chelates, but slightly modified as a result of the differences in the mode of bonding between the ligand and the metal ions.

The band located at *ca.* 310 nm may be due to the spin-allowed $n \rightarrow \pi^*$ transitions. The other bands are relatively broad, indicating high oscillator strength, and are therefore perhaps charge-transfer in origin,[23] with the band at the lower frequency due to M→L transitions and that at the higher frequency due to L→M transitions. Copper(II) being the most difficult of the three ions to oxidize further, is expected to absorb at the highest frequency, whereas the most readily oxidizable cobalt(II) is expected to absorb at the lowest energy, with a high value of ε. This is in good agreement with the order observed for the assigned $d \rightarrow \pi$ transitions. The same argument could also be used to account for the order observed in the

Table 3. Ultraviolet absorption spectra of the ligand and metal chelates in 75% dioxan–water

Species	λ_{max}, *nm*	log ε	Assignment
H(BAHP)	220	4.65	$\pi \rightarrow \pi^*$ (*K*-band)
	291	4.26	$n \rightarrow \pi^*$ (*R*-band)
Cu-chelate	320–336	3.53–3.83	$n \rightarrow \pi^*$
	360	4.04	$\pi \rightarrow d$
	410	3.88	$d \rightarrow \pi$
Ni-chelate	323	3.80	$n \rightarrow \pi^*$
	345	3.80	$\pi \rightarrow d$
	412	3.66	$d \rightarrow \pi$
Co-chelate	320	5.03	$n \rightarrow \pi^*$
	340–357	5.08–5.13	$\pi \rightarrow d$
	370	5.20	
	410–430	4.92	$d \rightarrow \pi$

$\pi \rightarrow d$ transitions. Table 3 summarizes all the results obtained.

In the case of nickel, the enhanced $\pi \rightarrow d$ transition at higher L:M ratio results in the apparent disappearance of the $n \rightarrow \pi^*$ transition. However, the presence of the small shoulder in the region of 325–350 nm is still indicative of this transition. Similar considerations may be applied to the two $\pi \rightarrow d$ transitions for the cobalt species. A summary of the results obtained is given in Table 3.

Analytical applications

Copper, nickel and cobalt can be determined spectrophotometrically with BAHP. The colour is stable for more than 24 hr and reaches maximum intensity within 5 min of mixing. The optimum pH is 3.5 for copper and cobalt and 4.0 for nickel. The systems obey Beer's law in the metal concentration range 0.9–10.0 μg/ml. Under optimum conditions, the relative standard deviation of the absorbance was 0.6% for Cu, 1.6% for Ni and 1.8% for Co (all at approximately the 3.5 ppm level).

REFERENCES

1. A. E. Martell and R. M. Smith, *Critical Stability Constants*, Vol. 3. Plenum Press, New York, 1977.
2. D. D. Perrin, *Stability Constants of Metal-Ion Complexes, Part B, Organic Ligands*, IUPAC Chemical Data Series No. 22. Pergamon Press, Oxford, 1979.
3. A. K. Jain, R. N. Gayal and D. D. Agarwal, *J. Inorg. Nucl. Chem.*, 1981, **43**, 2005.
4. Y. Yagi, *Bull. Chem. Soc. Japan*, 1963, **36**, 487, 492, 500, 506, 512.
5. H. Jahine, H. A. Zaher, A. Sayed and M. Seada, *Indian J. Chem.*, 1977, **15B**, 352.
6. T. S. West, *Complexometry with EDTA and Related Reagents*. Broglia Press, London, 1969.
7. A. I. Vogel, *Quantitative Inorganic Analysis*, 4th Ed. Longmans, London, 1966.
8. H. M. N. H. Irving and U. S. Mahnat, *J. Inorg. Nucl. Chem.*, 1968, **30**, 1215.
9. D. E. Goldberg, *J. Chem. Educ.*, 1963, **40**, 341.
10. R. M. Silverstein, G. C. Bassler and T. C. Morrill, *Spectrophotometric Identification of Organic Compounds*, 4th Ed. Wiley, New York, 1981.
11. D. M. Adams, *Metal-Ligand and Related Vibrations*. Spottiswoode & Ballantyne, London, 1967.
12. K. Nakanishi, *Infrared Absorption Spectroscopy*. Holden-Day, San Francisco, and Nakodo, Tokyo, 1964.
13. V. V. Sukhan, E. Uhlemann and L. Wolf, *Zh. Neorgan. Khim.*, 1967, **12**, 455.
14. F. A. Snavely and C. H. Yoder, *J. Inorg. Nucl. Chem.*, 1971, **33**, 2699.
15. R. W. Green and W. G. Goodwin, *Austral. J. Chem.*, 1969, **22**, 2333.
16. S. G. Ashcroft and C. T. Mortimer, *Thermochemistry of Transition Metal Complexes*, p. 383. Academic Press, London, 1970.
17. R. D. Gupta, G. S. Manku, A. N. Bhat and B. D. Jain, *Austral. J. Chem.*, 1970, **23**, 1387.
18. G. C. S. Manku, *J. Inorg. Nucl. Chem.*, 1971, **33**, 285.
19. G. Degischer and G. R. Choppin, *ibid.*, 1972, **34**, 2823.
20. I. Grenthe, *Acta Chem. Scand.*, 1964, **18**, 293.
21. L. A. K. Staveley, D. R. Markham and M. R. Jones, *J. Inorg. Nucl. Chem.*, 1968, **30**, 231.
22. F. J. C. Rossotti, in *Modern Coordination Chemistry*, J. Lewis and R. G. Wilkins (eds.), p. 37. Interscience, New York, 1960.
23. A. B. P. Lever, J. Lewis and R. S. Nyholm, *J. Chem. Soc.*, 1962, 5262.

Talanta, Vol. 30, No. 4, pp. 251–260, 1983
Printed in Great Britain

0039-9140/83/040251-10$03.00/0
Pergamon Press Ltd

TRACE DETERMINATION OF THE ANTIHISTAMINES TRIPELENNAMINE HYDROCHLORIDE, THENYLDIAMINE HYDROCHLORIDE, AND CHLOROTHEN CITRATE IN ADMIXTURE IN ANIMAL FEED, HUMAN URINE, AND WASTEWATER BY HIGH-PRESSURE LIQUID CHROMATOGRAPHY AND USE OF A FLUORESCENCE DETECTOR

HAROLD C. THOMPSON, JR., CLAUDE L. HOLDER and JAMES R. ALTHAUS
Department of Health and Human Services, Food and Drug Administration, National Toxicology Program, National Center for Toxicological Research, Jefferson, AR 72079, U.S.A.

(*Received* 25 *August* 1982. *Accepted* 28 *October* 1982)

Summary—Tripelennamine hydrochloride, thenyldiamine hydrochloride, and chlorothen citrate have been used as antihistamines and for the treatment of asthma and bronchitis. Toxicological evaluation of these drugs was scheduled as part of a structure–activity relationship study of antihistamines in rats and mice, because of the paucity of such information. Prerequisite for the evaluation was the development of analytical chemical procedures to certify the concentration, homogeneity, and stability of the drugs in dosed feed, to monitor the urine of laboratory personnel to signal their possible exposure to the drugs, and to monitor the wastewater to ensure that the test agents were not discharged into the environment. A high-pressure liquid chromatographic procedure with fluorescence detection was developed for determination of the three antihistamines in admixture in animal feed, human urine, and wastewater at levels of 500, 10 and 10 ng/g, respectively. Data on the partition values and use of a silica gel column to aid in the clean-up of sample extracts from the three substrates are reported for the three test agents. Extraction efficiencies and data concerning the stability of tripelennamine hydrochloride and thenyldiamine hydrochloride in animal feed are presented. Description of a new route for synthesis of chlorothen citrate and ancillary data concerning the gas chromatographic analysis for the three drugs in admixture in animal feed at levels as low as 10 μg/g are also reported.

The antihistamines tripelennamine hydrochloride (2-[benzyl(2-dimethylaminoethyl)amino]pyridine hydrochloride), thenyldiamine hydrochloride (2-[(2-dimethylaminoethyl)-3-thenylamino]pyridine hydrochloride), and chlorothen citrate (2-[(5-chloro-2-thenyl)(2-dimethylaminoethyl)amino]pyridine citrate), (formulae shown in Fig. 1), are antihistaminic drugs that have been used for treatment of asthma, bronchitis and bronchoconstriction.[1–5]

As early as 1950, Haley and Andem[6] reported toxicological studies of tripelennamine hydrochloride and thenyldiamine hydrochloride, which demonstrated the ability of these drugs to modify capillary blood flow and affect the mammalian capillary bed. More recently, Chaudhuri *et al.*[7] demonstrated that tripelennamine is metabolized in man, identifying four metabolites in the urine; desmethyltripelennamine was not detected, however. Probst and Neal[8] reported that tripelennamine hydrochloride could cause unscheduled DNA synthesis in primary cultures of adult rat hepatocytes, and suggested further mutagenic or carcinogenic potential test systems. Rao *et al.*[9,10] reported the *in vitro* and *in vivo* (rats) conditions necessary for formation of the chemically reactive metabolite, *N*-nitrosodesmethyltripelennamine, which has high carcinogenic potential. However, no incidence or evidence of mutagenic or carcinogenic potential of antihistaminic drugs in humans has been reported. In view of this information and the similarity of the structure of these drugs to that of other antihistamines currently used in the United States, toxicological evaluation of these antihistamines was scheduled at the National Center for Toxicological Research (NCTR) as part of the National Toxicology Program (NTP).

However, before such toxicological tests could begin, analytical procedures were required for ensuring proper concentration, homogeneity and stability of the test chemicals in dosed animal feed used in animal feeding studies. Also, trace level procedures were required for determination of the test chemicals in the urine of laboratory personnel (to monitor their possible exposure to the drugs) and in the wastewater to ensure that the drugs had been adequately removed from the water before its discharge into the environment.

Various thin-layer chromatographic (TLC) and ultraviolet spectrophotometric techniques for assaying basic antihistaminic drugs have been reported.[11–13] Wilson *et al.*[14] based their method on the fluorescence and phosphorescence of antihistamines containing the 2-aminopyridine group. Moffat,[15] and

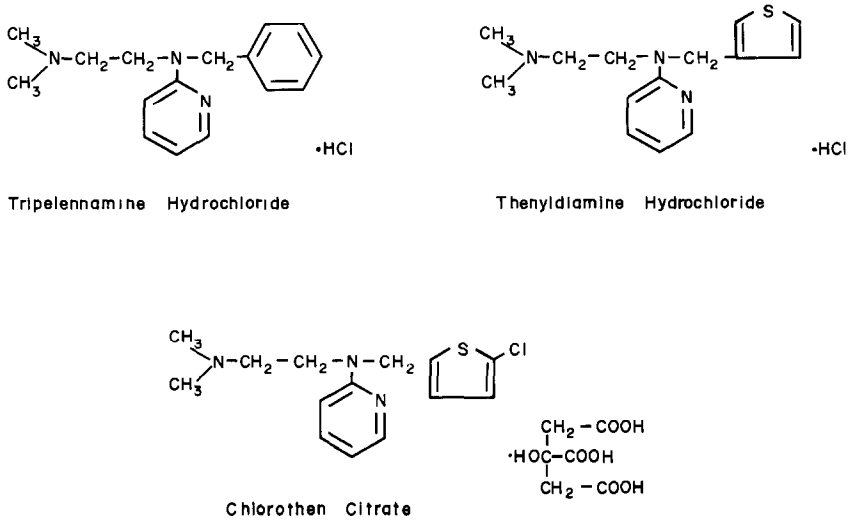

Fig. 1. Formulae of tripelennamine hydrochloride, thenyldiamine hydrochloride, and chlorothen citrate.

McLinden and Stenhouse,[16] reported gas chromatographic methods for determination of the antihistamine drugs in the absence of biological matrices. Pierce *et al.*[17] reported a gas chromatographic procedure for determining basic drugs (including antihistamines) in blood. Massart and Detaevernier[18] reported a high-pressure liquid chromatographic (HPLC) system for basic antihistamines. However, none of these methods was suitable for use in our proposed work.

This paper describes an HPLC procedure (with fluorescence detection) for determination of the three antihistamines in admixture in animal feed, human urine, and wastewater after liquid–liquid partitioning and silica gel column clean-up at levels as low as 500, 10 and 10 ng/g, respectively. Data concerning the stability of two of the test compounds in animal feed, extraction efficiencies from animal feed into various solvents, the constants for partition of all three drugs between dichloromethane and aqueous solutions at various pH values, and ancillary data concerning determination of the three drugs in animal feed by gas chromatography using a nitrogen–phosphorus detector (N/P-GC) at levels as low as 10 μg/g are also reported.

EXPERIMENTAL

Reagents

Tripelennamine hydrochloride (Ciba Pharmaceutical Co., Summit, N.J., U.S.A.) and thenyldiamine hydrochloride (Sterling Organics, Dudley, Cramlington, Northumberland, England) were used as received. Determination by HPLC and flame ionization–gas chromatography (FID/GC) indicated that both were essentially 100% pure. The structures of tripelennamine and thenyldiamine were confirmed by mass spectrometry (MS). The antihistamine chlorothen citrate was unavailable commercially and was synthesized at this laboratory by a new route to *N*-substituted 2-aminopyridines, as described below. Analysis by HPLC and FID/GC indicated it was 99% pure, and contained 1% of an impurity which was identified as methapyrilene. The structure of the major component was confirmed by nuclear magnetic resonance (NMR) (Bruker WH-500 Spectrometer ^1H probe operated at 500 MHz) and mass spectrometry (Finnigan 4023 GC–MS Data System operated in the electron-impact mode).

The silica gel (J. T. Baker Chemical Co., Phillipsburg, NJ) was heated overnight in an oven at 130° and cooled in a desiccator before use. All solvents were of "ultraviolet" grade and all other reagents were CP grade.

Synthesis of chlorothen citrate

Chlorothen (2-[(5-chloro-2-thenyl)(2-dimethylaminoethyl)amino]pyridine) (Fig. 2, **I**) has been prepared before,[19] but the method described here reports a new route to the *N*-substituted 2-aminopyridines. A small crystal of *p*-toluenesulphonic acid was added to 2-aminopyridine (8 g, 0.025 mole) dissolved in 11 g (0.075 mole) of 5-chloro-2-thiophenecarboxaldehyde, and the solution was stirred at ambient temperature until it solidified to a slightly yellow crystalline mass (about 2 hr being needed). Mass spectral analysis indicated the product to be the Schiff's base (**II**, [*N*-(2-pyridyl)(5-chloro-2-thenyl)imine]) desired for immediate use in the next step without purification. The Schiff's base was dissolved in 100 ml of methanol containing 4.5 g (0.075 mole) of acetic acid, and sodium cyanotrihydridoborate (6 g, 0.1 mole) was added during a period of 1 hr. The solution was then stirred overnight, under a blanket of argon. Analysis of the mixture by high-pressure liquid chromatography (HPLC) indicated complete conversion into a new product, which was isolated as follows. Sufficient hydrochloric acid was added to destroy any remaining reducing agent and produce the hydrochloride of the product, followed by the evaporation of the bulk of the methanol, addition of water (150 ml), and extraction with chloroform to remove any neutral species (the starting aldehyde or benzyl alcohol) formed during reduction of the Schiff's base. The aqueous phase was adjusted to pH 9 with potassium hydroxide solution and extracted with two 150-ml portions of chloroform. The combined chloroform extracts were dried with solid potassium carbonate, filtered, and evaporated. *N*-(2-Pyridyl)-*N*-(5-chloro-2-thenyl)amine (**III**) crystallized during the evaporation to a mass of off-white crystals, having a yield of 16.9 g (95.4% based on the starting aldehyde), m.p. 86–88.6° (uncorrected), and yielding a molecular ion (^{35}Cl) at m/z 224 (44%).

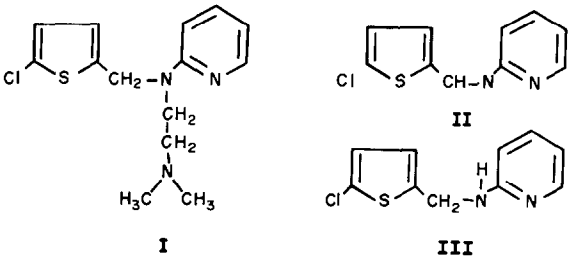

I II III

Fig. 2. Formulae of the synthesized test chemical, chlorothen (I), the Schiff's base (II), and a residual product (III), [*N*-(2-pyridyl)-*N*-(5-chloro-2-thenyl)amine].

The final product was obtained by the alkylation procedure of Hunttrer *et al.*[20] III (12.4 g, 0.55 mole), was heated under reflux in dry toluene (dried with sodium) with 5 g of sodamide under a blanket of argon for 2 hr, then *N*,*N*-dimethylaminoethyl chloride hydrochloride (10 g, 0.069 mole) was added, and the heating and stirring under argon was continued for an additional 22 hr. HPLC of the mixture indicated about 60% conversion into a new substance having chromatographic properties similar to those of methapyrilene. The reaction mixture was filtered and evaporated, then 100 ml of 2*M* hydrochloric acid were added, and the solution was extracted with three 100-ml portions of dichloromethane, the organic phase being discarded. The acid solution was adjusted to pH 9 with potassium hydroxide solution and extracted with three 100-ml portions of dichloromethane. The extracts were combined, dried with solid potassium carbonate, filtered and evaporated, yielding 13.0 g of a dark oil, about 60% of which was the desired product. The oil was distilled under reduced pressure and the fraction distilling at 150–155° (0.1 mmHg) was redistilled, the same fraction being collected. This procedure yielded 6.5 g (~40%) of the chlorothen. To this product a solution of 4.3 g of anhydrous citric acid in 20 ml of methanol was added. The methanol was evaporated. Repeated evaporation, and addition of ethanol, followed by immersion of the flask in liquid nitrogen initiated crystallization, yielding 7.5 g of pure white citrate crystals with a purity of at least 99% as determined by HPLC; the impurity had the same chromatographic behavior as the authentic methapyrilene, and may have arisen from unchlorinated aldehyde used in the production of the Schiff's base. The free base liberated from the purified salt was examined spectroscopically. The ^{1}H NMR ($CDCl_3$) spectrum at 500 MHz could be interpreted as a first-order spectrum indicating the presence of 5-chlorothenylamino, 2-aminopyridyl and *N*,*N*-dimethylethylamino functional groups. The mass spectrum yielded a molecular ion (^{35}Cl) at *m*/*z* 295 (15%) and diagnostic fragment ions corresponding to the functional groups on the tertiary nitrogen atom.

Preparation and operation of silica-gel clean-up column

The silica-gel columns (12 mm bore) used for the clean-up of extracts from animal feed, human urine, and wastewater were prepared just before use by adding successively a plug of glass wool, 2 g of anhydrous sodium sulphate, 2 g of silica gel (activated at 130° overnight and cooled in a desiccator), and 2 g of anhydrous sodium sulphate. The columns were washed with four 5-ml portions of 0.01*M* triethylamine (TEA) in dichloromethane, which was discarded. [Note—the activated silica gel was evaluated before use to ensure that the three antihistamines (chlorothen, tripelennamine and thenyldiamine) would be eluted as indicated in the analytical method.] The residue (see next section) from the animal feed, human urine, or wastewater extract was dissolved in 5 ml of 0.01*M* TEA in dichloromethane and transferred to the silica-gel column with three additional 5-ml portions of the 0.01*M* TEA in dichloromethane, the resulting effluent from the column being discarded. The column was then eluted with 5 ml of 0.01*M* TEA in dichloromethane containing 5% v/v methanol, this eluate also being discarded. Finally, the mixture of the three antihistamine free bases was eluted with 20 ml of the same methanolic eluent and collected in a 100-ml round-bottomed flask. The contents of the flask were evaporated to dryness with a rotary evaporator at ambient temperature and reduced pressure (water pump). The residue (from 1 g of animal feed or 50 g of human urine or wastewater) was dissolved in a known volume (1 ml or more) of the appropriate solvent for analysis by HPLC with fluorescence detection or by gas chromatography with a nitrogen–phosphorus detector.

Extraction and clean-up of animal feed

A 20-g sample of animal feed was weighed into a 250-ml Erlenmeyer flask fitted with a Teflon-lined screw cap and extracted for 1 hr with 100 ml of methanol/1*M* hydrochloric acid (4:1 v/v) on a reciprocating shaker (Eberbach Corp., Ann Arbor, MI) operating at 200 excursions/min. The feed particles were then allowed to settle (*ca.* 10 min) and part of the extract was decanted into a 50-ml culture tube. The tube was sealed with a Teflon-lined screw cap and centrifuged for 5 min at 1000 rpm to remove any suspended particles. (Note—all culture tubes were made of borosilicate glass and fitted with Teflon-lined screw caps.) A 5-ml aliquot of the feed extract (equivalent to 1 g of sample) was pipetted into a 30-ml culture tube containing 10 ml of 1*M* hydrochloric acid and 10 ml of dichloromethane, and the mixture was shaken vigorously, then centrifuged for 2 min at 1000 rpm. The dichloromethane was removed with a syringe and cannula and discarded. The aqueous layer was extracted with two additional 10-ml portions of dichloromethane, which were also discarded. The mixture of antihistamines (tripelennamine, thenyldiamine and chlorothen as free bases) was removed from the aqueous phase after the addition of 1.2 ml of 10*M* sodium hydroxide, 2 ml of 1*M* dipotassium hydrogen phosphate solution (pH 9.4), and 10 ml of dichloromethane. The dichloromethane phase was removed with a syringe and cannula and percolated through a plug of anhydrous sodium sulphate (*ca.* 18 mm diameter × 30 mm thick) into a 100-ml round-bottomed flask. The extraction was repeated with two further 10-ml portions of dichloromethane. The combined extract was evaporated to dryness with a rotary evaporator at ambient temperature and reduced pressure (water pump). The residue was reserved for clean-up on a column of silica gel as described above.

High-pressure liquid chromatography

The HPLC system consisted of a Waters Associates, Inc., Model 6000A solvent delivery system, a Rheodyne, Inc., Model 7120 septumless injector, a guard column 40 mm long, 3.2 mm bore, packed with 37–50 μm Corasil Si (Waters Associates, Inc.), an Altex 5-μm Si Ultrasphere

column, 25 cm long, 4.6 mm bore, and a Farrand HPLC fluorescence monitor. The mobile phase was 0.005*M* TEA in dichloromethane/2-propanol mixture (99:1 v/v), flowing at 2.0 ml/min. The fluorescence detector was set with $\lambda_{Ex} = 310$ nm and $\lambda_{Em} = 360$ nm (0-52 emission filter) and a 10-nm slit programme, for all three antihistamines. Under these conditions, the retention times (t_R) for chlorothen citrate, tripelennamine hydrochloride and thenyldiamine hydrochloride were 6.5, 7.4 and 8.4 min, respectively. All sample injections were 50 μl in size. Residues containing all three antihistamines (each at levels of 0.5, 1.0, 10, 100 and 1000 ppm), and derived from the equivalent of 1 g of animal feed, were analysed by HPLC after the silica-gel column clean-up. Residues from the silica-gel column clean-up were dissolved in 1 ml (for the 0.5 ppm level) or more of dichloromethane (accurately measured) for higher levels, as appropriate. The standard solutions were made by evaporating to dryness known volumes of a stock solution of the three antihistamine salts in methanol (each at a concentration equivalent to 1 mg of free base per ml), and taking up the residues in known volumes of dichloromethane.

Gas chromatography

A Tracor Model 560 instrument equipped with a Tracor Model 702 sensitized rubidium-bead nitrogen/phosphorus detector and a 6-ft glass column (2 mm bore) containing 5% w/w Dexsil 300 on Chromasorb W HP (80–100 mesh), conditioned at 260° overnight before use, was operated at 220° with a helium carrier-gas flow of 25 ml/min and hydrogen and air flows to the detector of 2 and 120 ml/min, respectively. The injection port and detector were operated at 230 and 280°, respectively. The retention times for tripelennamine, thenyldiamine and chlorothen were 4.2, 4.8 and 8.0 min, respectively. Reference standards of atrazine dissolved in acetone, over the concentration range 0.1–10 μg/ml, were used to test the linearity of response of the detector bead. Peak-heights were used for quantification. Appropriate dilutions of an acetone stock solution containing the three antihistamine salts at concentrations equivalent to 1 mg/ml of each as the free amine, were used as the standards for calibration. A 2-μl volume of sample or standard was injected.

Preparation of dosed feed for stability experiments

Batches of animal feed (2 kg) (Laboratory Chow, Type 5010 M, Ralston Purina Co., St. Louis, MO) spiked with 0, 114 or 2280 ppm of tripelennamine hydrochloride or thenyldiamine hydrochloride to yield the equivalent of 0, 100 or 2000 ppm of the free base, were prepared by adding the appropriate amount of test chemical dissolved in 50 ml of 95% ethanol to the feed through the intensifier bar of the blender, followed by 50 ml of 95% ethanol added through the bar as a rinse. The feed was mixed for 40 min in a Model LV Twin-Shell Lab Blender (Patterson-Kelly Co., East Stroudburg, PA) with the shell of the blender operated at 20 rpm. The intensifier bar was operated at 3300 rpm during the first 35 min of mixing, then turned off. After blending, each batch was transferred to a stainless-steel pan and dried for 1 hr in an autoclave at reduced pressure (305 mmHg) and ambient temperature. Each batch was then divided into a 500-g and a 1500-g portion and reserved for the following stability experiments.

Stability experiments

The 500-g portion of the batch of dosed feed was placed in a crystallizing dish (*ca.* 19 cm in diameter × 10 cm deep) and allowed to stand in the open vessel in a fume hood under tungsten-lamp lighting at ambient temperature. These portions were used for short-term stability tests to simulate animal test conditions. Duplicate 20-g samples were taken from each dish immediately, and 1, 2, 4, 8 and 16 days later, for determination of tripelennamine or thenyldiamine by HPLC. The feed was thoroughly mixed just before the removal of each sample. The 1500-g portion of the batch was sealed in an amber bottle and stored in a light-free cabinet at ambient temperature, and used for long-term stability tests under simulated storage conditions. Duplicate 20-g samples were taken from each bottle immediately, and 1, 2, 4, 8 and 16 weeks later, and analysed by the HPLC method. Stability experiments for chlorothen citrate in feed were not performed, owing to the small amount of this chemical that was available.

Extraction of human urine and wastewater

Fifty ml of human urine or wastewater (the pH of both was 6.8) were pipetted into a 70-ml culture tube, 20 ml of dichloromethane were added, and the tube was gently shaken by hand for 1 min. (Note—if the pH of the sample is not near pH 7 or above, it must be adjusted by addition of sodium hydroxide solution.) The tube was then centrifuged at 500 rpm for 2 min, and the dichloromethane layer was removed with a syringe and cannula, percolated through a plug of anhydrous sodium sulphate, and collected in a 100-ml round-bottomed flask. The extraction was repeated in the same manner with two additional 20-ml portions of dichloromethane and the combined extract (60 ml) evaporated to dryness, as described above for extraction and clean-up of animal feed. The residue (equivalent to 50 g of human urine or wastewater) was subjected to clean-up on the silica-gel column.

Recovery experiments

Triplicate 20-g samples of animal feed were spiked with 1 ml of methanol containing enough chlorothen citrate, tripelennamine hydrochloride and thenyldiamine hydrochloride to give sample levels equivalent to 0, 0.5, 1.0, 10, 100 and 1000 ppm of each free amine. The samples were allowed to stand for 16 hr at ambient temperature before extraction, partitioning, silica-gel column clean-up, and analysis by HPLC with fluorescence detection or by gas chromatography with nitrogen/phosphorus detection as already described.

Triplicate 50-ml samples of human urine or wastewater in 70-ml culture tubes were similarly spiked at the 0, 10, 100, 500 and 1000 ng/ml levels of each of the free bases. The tubes were sealed and the contents thoroughly mixed and allowed to stand for 16 hr in the refrigerator at 5° before extraction, clean-up on a column of silica gel, and analysis by HPLC as already described.

RESULTS AND DISCUSSION

Both gas chromatography with a rubidium-sensitized N/P detector and HPLC employing fluorescence detection were investigated as means of determining the three antihistamines. After the appropriate instrumental parameters for determination of the drugs by both techniques had been established, an efficient procedure for extracting the chemicals from animal feed was sought. When feed spiked at the 100-ppm level with tripelennamine or thenyldiamine was extracted with methanol the recovery varied inversely with the length of time that the drug was in contact with the feed. Extraction with chloroform resulted in low recoveries, *e.g.*, approximately 50% after contact for 16 hr. However, when the feed was treated with 1*M* hydrochloric acid (to release test agent from potential binding sites on the feed) before extraction with methanol, good recoveries (96%) were obtained even after the drug(s) had been in contact with the feed for 96 hr. Data for recovery of tripelennamine and thenyldiamine with three different

Table 1. Tripelennamine hydrochloride and thenyldiamine hydrochloride recovered (as their free bases) from animal feed after various contact times*

Solvent	Contact time, *hr*†	Recovery, %§ Tripelennamine	Thenyldiamine
Chloroform	16	50	52
Methanol	0.25	84	87
Methanol	90	70	72
Methanol (80 ml)/1*M* HCl (20 ml)‡	16	97	97
Methanol (80 ml)/1*M* HCl‡ (20 ml)‡	96	96	96

*Twenty g of animal feed and 100 ml of solvent were used in all tests.
†Time elapsed between spiking and addition of extraction solvent.
§Assay performed by HPLC.
‡Twenty ml of acid were added to the animal feed sample, followed by the 80 ml of methanol.

solvent systems from feed spiked at the 100-ppm level are reported in Table 1. Since the acid treatment coupled with extraction into methanol gave good recoveries, this method was chosen for incorporation into the analytical procedure.

The partition constants for distribution of tripelennamine and thenyldiamine between dichloromethane and aqueous solutions at various pH values were investigated for possible use in liquid–liquid extraction clean-up of feed extracts (Table 2). This was necessary because these extracts contained appreciable amounts of components that interfered with both the GC and HPLC analyses, reducing the accuracy. For both tripelennamine and thenyldiamine the partition constant for pH 1 or less was zero, and this property was useful in separating the drugs from feed and some of the co-extractives which otherwise interfered with the determination of the two drugs.

GC analyses for the three antihistamines in animal feed extracts that had been subjected to liquid–liquid extraction indicated that further clean-up was necessary for assays below the 10-ppm level. Therefore, additional experiments were done with gravity-flow columns of silica-gel (activated at 130° overnight before use) and elution with 0.01*M* TEA in dichloromethane containing 5% v/v methanol. From these columns there was essentially complete elution of all of the drugs applied at each level that was investigated in feed, and the co-extractives were retained sufficiently to allow GC analysis for the drugs with a minimum detectable level (defined as twice the background noise) of about 2 ppm for each. However, measurement below the 10-ppm level was not attempted because of loss of detector response, caused by the interaction of the antihistamines and co-extractives on the GC column, as already reported.[21] Although this phenomenon also occurs for these antihistamines at levels above 10 ppm, acceptable correction factors can be determined as follows and applied to the recovery data.

Table 2. Partition of the three antihistamines between dichloromethane and aqueous solution at various pH values (1.00 = 100% extraction into organic phase)

pH	Tripelennamine hydrochloride	Thenyldiamine hydrochloride	Chlorothen citrate
0	0.00	0.00	0.00
1	0.00	0.00	0.00
3	0.04	0.02	0.02
5	0.64	0.74	0.75
7	1.00	1.00	1.00
9	1.00	1.00	1.00
11	1.00	1.00	1.00

Three portions of cleaned-up dry residues of control feed-extracts corresponding to 0.1, 0.1 and 0.01 g of feed were spiked with 1 ml of acetone solution containing the equivalent of 1 μg of each of the three antihistamine free bases (for the first portion) and the equivalent of 10 μg of each free base for the other two portions. These samples correspond to feed spiked with 10, 100 and 1000 ppm of each base, respectively. The ratio of the responses of 1, 10 and 10 μg/ml free base standards in acetone, to the responses obtained from each of the spiked extracts, served as the correction factors for obtaining recoveries from the amounts of the antihistamines detected (Table 3). An atrazine standard was used to monitor the performance of the rubidium-sensitized detector during the course of all experiments using this detector. Correction factors determined for antihistamine levels below 10 ppm were greater than 2.0 and considered unacceptable.

Because the GC procedure for feed analysis was not adequate for levels below 10 ppm, the procedure employing HPLC with fluorescence detection was developed. Several solvent systems were examined for their efficiency in separation of the three antihistamines, coupled with adequate fluorescence response (Table 4). Although dichloromethane gave the highest relative fluorescence intensity for each antihistamine it did not provide adequate separation. The system consisting of 0.005*M* triethylamine in dichloromethane/2-propanol mixture (99:1 v/v) gave the best separation and adequate sensitivity. After the

Table 3. Results of N-P/GC anaylsis of animal feed spiked with chlorothen citrate, tripelennamine hydrochloride and thenyldiamine hydrochloride*

Amount of free base added, *ppm**	Equivalent sample weight injected, *mg*†	Antihistamine detected, *ppm* ($\bar{x} \pm$ SD)	Correction factors for amines lost on GC column	Antihistamine recovered, ($\bar{x} \pm$ SD)§	
				ppm	%
Chlorothen					
(control)	2.0	—		0.050 ± 0.01	—
10	0.2	7.87 ± 0.14	1.21	9.52 ± 0.17	95.2 ± 1.7
100	0.2	91.5 ± 1.6	1.07	97.9 ± 1.7	97.9 ± 1.7
1000	0.02	965 ± 11	1.01	975 ± 11	97.5 ± 1.1
Tripelennamine					
0 (control)	2.0	—		0.100 ± 0.02	—
10	0.2	7.62 ± 0.24	1.27	9.68 ± 0.3	96.8 ± 3.0
100	0.2	92.3 ± 2.1	1.09	100.6 ± 2.3	100.6 ± 2.3
1000	0.02	972 ± 21	1.01	982 ± 21	98.2 ± 2.1
Thenyldiamine					
0 (control)	2.0	—		0.560 ± 0.10	—
10	0.2	7.33 ± 0.25	1.29	9.46 ± 0.32	94.6 ± 3.2
100	0.2	92.6 ± 2.3	1.09	100.9 ± 2.6	100.9 ± 2.6
1000	0.02	977 ± 29	1.01	987 ± 29	98.7 ± 2.9

*To 20 g of animal feed.
†Samples assayed by N/P-GC were injected in 2 μl of acetone.
§Mean and standard deviation for triplicate assays; spiked samples are corrected for background of (control) samples and loss of amine on GC column.

HPLC parameters for determination of the three antihistamines in animal feed had been determined, recovery experiments were performed to determine the accuracy and precision of the method (Table 5). The recoveries increased with concentration. The unspiked animal feed appeared to contain 0.25 ppm chlorothen and 0.10 ppm each of tripelennamine and thenyldiamine. Typical HPLC recordings of a mixture of the three antihistamine standards, for unspiked animal feed extracts carried through the analytical procedure, and for cleaned-up feed extract spiked at the 0.5 and 1.0 ppm levels with the three antihistamines are shown in Fig. 3.

Recovery experiments were also performed on the analysis of wastewater and human urine by the HPLC procedure (Table 6). The recoveries again increased with concentration, but failed to reach 100%. For the unspiked urine the apparent concentrations of chlorothen, tripelennamine, and thenyldiamine were 0.40, 0.60 and 0.60 ng/ml, respectively, and for the unspiked wastewater 0.40, 0.30 and 0.40 ng/ml, respectively. Typical chromatograms are shown in Fig. 4.

After development and validation of the analytical procedure, experiments were conducted to determine the stability of tripelennamine and thenyldiamine in animal feed. The stability of chlorothen citrate in feed was not determined because not enough of the drug was available. It was decided that synthesis of enough of this drug for the scheduled bioassay tests was too expensive, so the tests were cancelled. Results of the short- and long-term stability tests for the two antihistamines in animal feed are presented in Table 7. The 100 and 2000 ppm tripelennamine preparations showed 12 and 11% reduction in the amount of recoverable drug after 16 days in the short-term study, whereas for thenyldiamine the reduction was only 5 and 9% for the same levels. In the long-term study, there was only a slight decrease in recoverable residues of both drugs at both levels after 16 weeks.

Table 4. Spectrofluorometric investigation of the antihistamines, for determining optimum HPLC solvent system (λ_{Ex} 310 nm, λ_{Em} 360 nm)

Solvent	Relative intensity of antihistamine solution (10 μg/ml)		
	Chlorothen	Tripelennamine	Thenyldiamine
Dichloromethane	21	50	45
2-Propanol	8.6	14	12
Methanol	2.1	3.3	2.1
Methanol–buffer (9/1; 0.01 M KH_2PO_4, pH 7)	2.6	4.2	2.7
Dichloromethane/2-propanol (99:1 v/v; 0.005*M* triethylamine)*	18	42	31
Acetonitrile	7.5	18	25
1*N* Sulphuric acid	0.3	1.0	0.6

*This HPLC solvent system was selected for use as the mobile phase and afforded the best separation of the three antihistamines on an Altex Ultrasphere Si (5 μm) column, without excessive loss of fluorescence response.

Table 5. Results of HPLC fluorescence analysis of animal feed spiked with chlorothen citrate, tripelennamine hydrochloride, and thenyldiamine hydrochloride

Free amines added, *ng/g**	Equivalent amount of sample injected,† *mg*	Antihistamine recovered ($\bar{x} \pm$ SD)§					
		Chlorothen		Tripelennamine		Thenyldiamine	
		ng/g	%	*ng/g*	%	*ng/g*	%
0 (control)	50	0.250 ± 0.10	—	0.100 ± 0.020	—	0.100 ± 0.040	—
0.5	50	0.305 ± 0.015	61.0 ± 3.0	0.407 ± 0.013	81.4 ± 2.6	0.393 ± 0.007	78.6 ± 1.4
1.0	50	0.839 ± 0.01	83.9 ± 1.0	0.853 ± 0.01	85.3 ± 1.0	0.866 ± 0.0	86.6 ± 0.0
10	5	9.12 ± 0.25	91.2 ± 2.5	9.32 ± 0.21	93.2 ± 2.1	9.42 ± 0.4	94.2 ± 4.0
100	5	94.7 ± 1.4	94.7 ± 1.4	96.2 ± 0.6	96.2 ± 0.6	96.8 ± 0.35	96.8 ± 0.4
1000	0.5	996 ± 4	99.6 ± 0.4	999 ± 7	99.9 ± 0.7	1000 ± 7	100.0 ± 0.7

*To 20 g of animal feed.
†Injected in 50 μl of dichloromethane.
§Mean and standard deviation of triplicate samples; results for spiked samples are corrected for background of control samples.

It was concluded that the two antihistamines were sufficiently stable in feed for bioassay tests involving administration of the drugs in feed to be satisfactory.

The analytical methodology for determination of the three antihistamines was developed with mixtures rather than the individual drugs, to reduce the time required for methods development. The procedures and ancillary data reported here have allowed the toxicological evaluation of tripelennamine hydrochloride and thenyldiamine hydrochloride in laboratory animals, which would otherwise not have been possible.

Acknowledgements—The authors thank R. K. Mitchum and J. P. Freeman from NCTR for performing the MS analyses and F. E. Evans and D. W. Miller also from NCTR for the NMR analyses. We also thank Bobbye James and Lyle Davis for typing the manuscript.

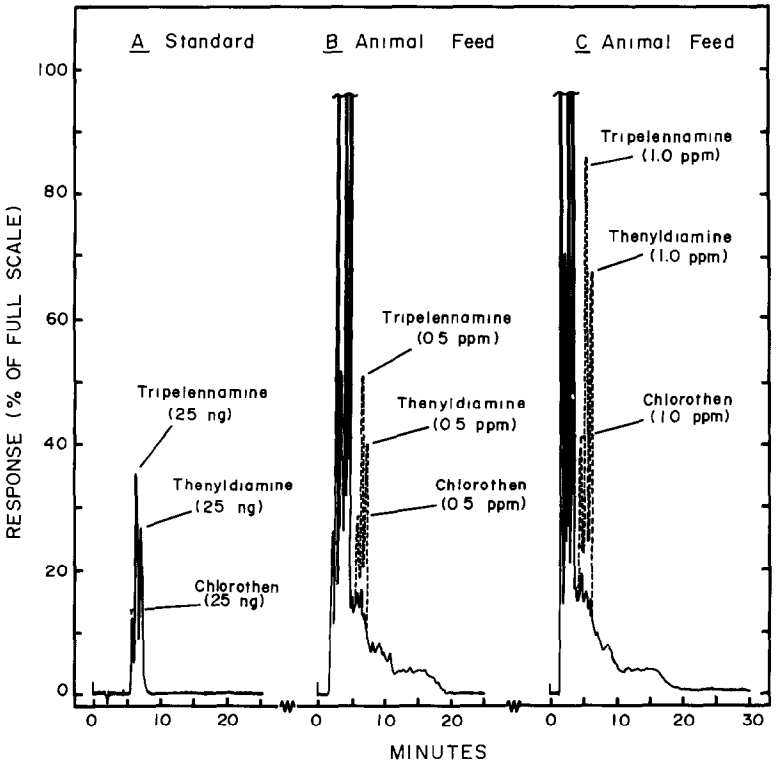

Fig. 3. High-pressure liquid chromatograms. A is a standard containing 0.5 μg/ml each of tripelennamine hydrochloride, thenyldiamine hydrochloride and chlorothen citrate. In B and C solid lines represent unspiked cleaned-up extracts of animal feed (each injection is equivalent to 50 mg of sample); broken lines (superimposed) illustrate responses for the three antihistamines in quantities equivalent to 0.5 and 1.0 μg/g (ppm) levels of their free bases (in the sample). Extracts were spiked with a mixture of the three antihistamines after the partitioning and silica-gel column clean-up steps. All injections were 50 μl of dichloromethane solution. In all chromatograms the fluorescence detector was set at 0.1 × full scale.

Table 6. Results of HPLC fluorescence analysis of human urine and wastewater spiked with the three antihistamines

Free base added,* ng/ml	Equivalent amount of sample injected, mg	Antihistamines recovered ($\bar{x}$ + SD)†					
		Chlorothen citrate§		Tripelennamine hydrochloride§		Thenyldiamine hydrochloride§	
		ng/ml	%	ng/ml	%	ng/ml	%
		Human urine					
0	2.5	0.40 ± 0.1	—	0.60 ± 0.2	—	0.60 ± 0.2	—
10	2.5	7.68 ± 0.3	76.8 3.0	6.34 ± 0.2	63.4 ± 2.4	7.86 ± 0.5	78.6 ± 5.0
100	2.5	87.5 ± 0.5	87.5 ± 0.5	85.0 ± 0.4	85.0 ± 0.4	89.9 ± 2.0	89.9 ± 2.0
500	1.0	444 ± 4	88.8 ± 0.8	450 ± 4	90.0 ± 0.8	445 ± 6	89.0 ± 1.2
1000	0.5	914 ± 10	91.4 ± 1.0	921 ± 14	92.1 ± 1.4	901 ± 20	90.1 ± 2.0
		Wastewater					
0	2.5	0.40 ± 0.1	—	0.30 ± 0.1	—	0.40 ± 0.1	—
10	2.5	8.18 ± 0.2	81.8 ± 2.0	6.96 ± 0.15	69.6 ± 1.5	8.48 ± 0.3	84.8 ± 3.0
100	2.5	89.9 ± 2.3	89.9 ± 2.3	83.4 ± 3.2	83.4 ± 3.2	87.8 ± 4.0	87.8 ± 4.0
500	1.0	465 ± 4.0	93.0 ± 0.8	488 ± 9	97.6 ± 1.8	478 ± 9	95.6 ± 1.8
1000	0.5	924 ± 15	92.4 ± 1.5	967 ± 16	96.7 ± 1.6	933 ± 13	93.3 ± 1.3

*To 50 ml of sample.
†Mean and standard deviation from triplicate assays; spiked samples are corrected for background of control samples.
§Based on the free amine content.

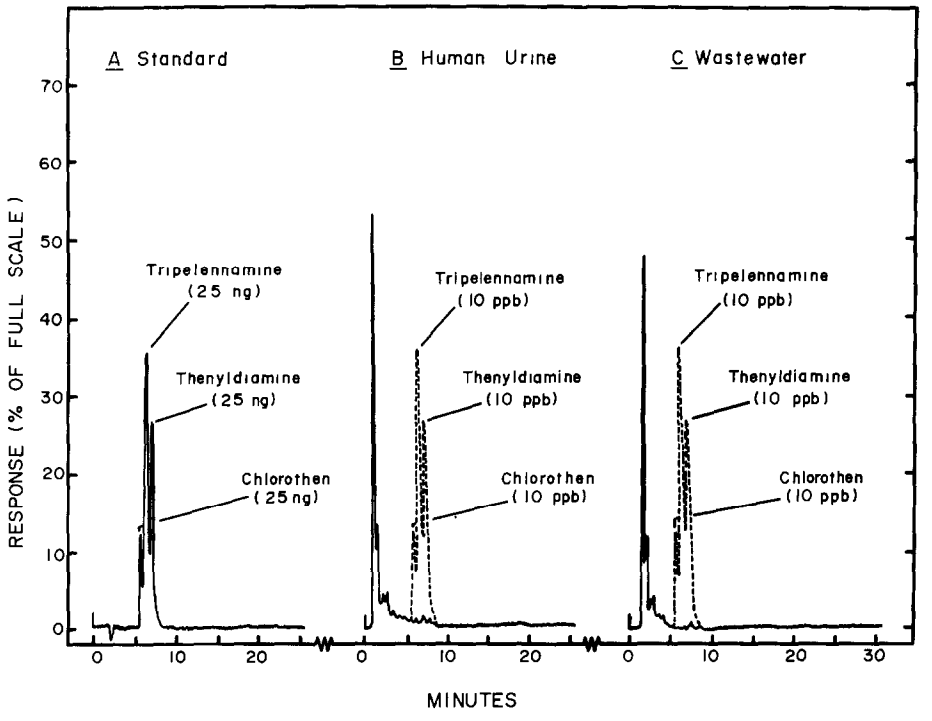

Fig. 4. High-pressure liquid chromatograms. A is a standard containing 0.5 μg/ml each of tripelennamine hydrochloride, thenyldiamine hydrochloride and chlorothen citrate. In B and C solid lines represent unspiked cleaned-up extracts of human urine and wastewater (each injection is equivalent to 2.5 mg of sample); broken lines (superimposed) illustrate responses for amounts of the three antihistamines equivalent to 10 ng/ml (ppb) levels of the free bases (in the sample). Extracts were spiked after the partitioning and silica gel column clean-up steps. All injections were 50 μl of dichloromethane solution. In all chromatograms the fluorescence detector was set at 0.1 × full scale.

Table 7. Results from stability studies with tripelennamine hydrochloride and thenyldiamine hydrochloride in animal feed spiked at two levels*

	Antihistamine recovered, $\mu g/g$†					
	Tripelennamine hydrochloride§			Thenyldiamine hydrochloride§		
Sampling intervals	Control (0)	100	2000	Control (0)	100	2000
	Short-term study‡					
Days						
0	0.400 ± 0.10	101 ± 2	2020 ± 20	0.770 ± 0.10	102 ± 1	2030 ± 10
1	0.400 ± 0.20	102 ± 2	2040 ± 25	0.770 ± 0.10	98 ± 2	1960 ± 10
2	0.440 ± 0.10	99 ± 4	1980 ± 20	0.920 ± 0.10	101 ± 1	1980 ± 40
4	0.730 ± 0.20	100 ± 2	2000 ± 0	0.980 ± 0.20	96 ± 1	1900 ± 30
8	0.400 ± 0.10	96 ± 1	1930 ± 15	0.800 ± 0.10	98 ± 1	1920 ± 10
16	0.420 ± 0.10	89 ± 1	1800 ± 0	0.600 ± 0.20	97 ± 1	1840 ± 30
	Long-term study #					
Weeks						
0	0.400 ± 0.10	101 ± 2	2020 ± 20	0.770 ± 0.10	102 ± 1	2030 ± 10
1	0.610 ± 0.10	100 ± 1	1990 ± 20	0.700 ± 0.10	99 ± 0	1950 ± 20
2	0.420 ± 0.10	99 ± 0	1980 ± 0	0.600 ± 0.20	97 ± 2	1890 ± 0
4	0.470 ± 0.10	96 ± 3	1970 ± 70	1.00 ± 0.20	101 ± 2	2020 ± 40
8	0.730 ± 0.20	101 ± 2	1980 ± 20	1.00 ± 0.20	99 ± 1	1980 ± 60
16	0.620 ± 0.20	95 ± 2	1970 ± 10	0.600 ± 0.10	100 ± 1	1970 ± 0

*Assays performed by reverse phase HPLC with UV detector set at 254 nm, and mobile phase of 90% methanol-10% buffer (0.01M KH_2PO_4, pH 7) flowing at 1 ml/min.
†Mean and standard deviation from duplicate assays; corrected for background of control samples and recovery.
§Based on the free amine content.
‡Open container, incandescent lighting, and ambient temperature.
Sealed container, light-free cabinet, and ambient temperature.

REFERENCES

1. M. Mattila and A. Muittari, *Acta Med. Scand.*, 1966, **180,** 421.
2. J. S. Finch, T. R. Adiska and T. J. DeKornfeld, *Clin. Med.*, 1969, **76,** 34.
3. C. Warlow, D. Ogston and A. S. Douglas, *7th Europ. Conf. Microcirculation*, 1973, Part II, 249.
4. B. Spilker and H. Minatoya, *Arch. Intern. Pharmacodyn.*, 1975, **217,** 201.
5. Z. E. Mielens, *Pharmacology*, 1979, **18,** 311.
6. T. J. Haley and M. R. Andem, *J. Pharm. Exp. Ther.*, 1950, **100,** 393.
7. N. K. Chaudhuri, O. A. Servando, M. J. Manniello, R. C. Luders, D. K. Chao and M. F. Bartlett, *Drug Metab. Dispos.*, 1976, **4,** 372.
8. G. S. Probst and S. B. Neal, *Cancer Lett.*, 1980, **10,** 67.
9. G. S. Rao, G. Krishna and J. R. Gillette, *Biochem. Pharmacol.*, 1975, **24.** 1707.
10. G. S. Rao and G. Krishna, *J. Pharm. Sci.*, 1975, **64,** 1579.
11. K. K. Kaistha and R. Tadrus, *J. Chromatog.* 1978, **155,** 214.
12. W. W. Fike, *Anal. Chem.*, 1966, **38,** 1697.
13. F. Boonen, *J. Pharm. Belg.*, 1973, **28,** 410.
14. D. L. Wilson, D. R. Wirz and G. H. Schenk, *Anal. Chem.*, 1973, **45,** 1447.
15. A. C. Moffat, *J. Chromatog.* 1975, **113,** 69.
16. V. J. McLinden and A. M. Stenhouse, *Forensic Sci. Intern.*, 1979, **13,** 71.
17. W. O. Pierce, T. C. Lamoreaux, F. M. Urry, L. Kopjak and B. S. Finkle, *J. Anal. Tox.*, 1978, **2,** 26.
18. D. L. Massart and M. R. Detaevernier, *J. Chromatog. Sci.*, 1980, **18,** 139.
19. R. C. Clapp, J. H. Clark, J. R. Vaughan, J. P. English and G. W. Anderson, *J. Am. Chem. Soc.*, 1947, **69,** 1549.
20. C. P. Hunttrer, C. Djerassi, W. L. Beears, R. L. Mayer and C. R. Scholz, *ibid.*, 1946, **68,** 1999.
21. H. C. Thompson, Jr., C. L. Holder and M. C. Bowman, *J. Chromatog. Sci.*, 1982, **20,** 373.

Talanta, Vol. 30, No. 4, pp. 261–264, 1983
Printed in Great Britain.

0039-9140/83/040261-04$03.00/0

ANION-EXCHANGE SEPARATION AND SPECTROPHOTOMETRIC DETERMINATION OF VANADIUM IN SILICATE ROCKS

T. KIRIYAMA
Laboratory for Chemistry, Faculty of Education, Kagoshima University, Kagoshima, Japan

and

R. KURODA
Laboratory for Analytical Chemistry, Faculty of Engineering, University of Chiba, Yayoi-cho, Chiba, Japan

(*Received* 9 *September* 1982. *Accepted* 20 *October* 1982)

Summary—A combined anion-exchange–spectrophotometric method has been developed for the determination of vanadium in silicate rocks. A rock sample weighing about 0.1 g is decomposed with a mixture of sulphuric and hydrofluoric acids and after removal of HF the residue is taken up with dilute sulphuric acid. This solution is adjusted to be 0.05*M* in sulphuric acid and contain 0.3% hydrogen peroxide, and is passed through a column of Amberlite CG 400 (sulphate form). The sorbed vanadium is eluted with 30 ml of 1*M* hydrochloric acid. The effluent is evaporated to dryness, made 0.1*M* in hydrochloric acid and 3% in hydrogen peroxide content, and passed through a column of Amberlite CG 400 (chloride form) to get rid of accompanying thorium and zirconium. Vanadium is stripped by elution with 20 ml of 1*M* hydrochloric acid and subsequently determined spectrophotometrically with 4-(2-pyridylazo)resorcinol. The detection limit is 0.4 ppm.

A number of reagents have been reported for the spectrophotometric determination of vanadium.[1] Among them, phosphotungstate,[2] *N*-benzoyl-*o*-tolylhydroxylamine,[2] diaminobenzidine,[2] 4-(2-pyridylazo)resorcinol,[3–6] *N*-phenylbenzohydroxamic acid,[7] 2-(3,5-dibromo-4-methyl-2-pyridylazo)-5-diethylaminophenol[8] and 2-nitroso-5-dimethylaminophenol[9] have been applied effectively to determine trace vanadium in a variety of silicate rocks, owing to their sensitivity and/or selectivity. However, direct spectrophotometric determination of vanadium in silicates is seldom possible, because of inadequate specificity. Separation or extensive use of masking agents (*e.g.*, fluoride when *N*-benzoyl-*o*-tolylhydroxylamine,[2] *N*-phenylbenzohydroxamic acid[7] or pyridylazophenol[8] is used) is necessary before the final determination of vanadium.

Ion-exchange chromatography has already been used in systematic rock analysis for major and minor elements, including vanadium.[4,5,10,11] If determination of vanadium is the primary objective, however, these methods are often too tedious for routine use. Cation-exchange procedures for the isolation of vanadium in silicate rocks have been reported by Chan and Riley[12] and Strelow and Victor.[6] Because of the sorption of major rock elements on the cation-exchange resin in these methods, very large columns have to be used. Korkisch *et al.*[13] developed analytical schemes for determining vanadium as well as several other metals in silicate rocks. For vanadium an aliquot of the sample solution, adjusted to 90% methanol–10% 6*M* hydrochloric acid, was passed through a column of the strongly basic resin Dowex 1 × 8. Vanadium was then eluted together with other metals, including alkaline-earth metals, aluminium, nickel, chromium, manganese, *etc.*[14] Accordingly, a specific or at least highly selective method was needed for the final determination of vanadium in the eluate.

In this work we have developed a method for anion-exchange chromatographic separation and spectrophotometric determination of vanadium in silicate rocks. Anion-exchange sorption of vanadium first from sulphuric acid–hydrogen peroxide medium and then from hydrochloric acid–hydrogen peroxide medium provides a basis for the selective separation of vanadium before its spectrophotometric determination with the highly sensitive, but unselective reagent 4-(2-pyridylazo)resorcinol (PAR). In the first anion-exchange system only a few of the trace metals found in silicate rocks are sorbed on the resin, and more of the major elements.[15] The second anion-exchange system removes thorium and zirconium, giving a wide choice for the final determination of the vanadium.

EXPERIMENTAL

Reagents and apparatus

Vanadium (IV) and vanadium (V) solutions. Dissolve vanadium(IV) sulphate and ammonium metavanadate in distilled water to give 2-mg/ml solutions of vanadium(IV) and vanadium(V), respectively. Standardize these solutions by titration with 0.01*M* EDTA, using copper–PAN as the indicator [*i.e.*, a mixture of copper–EDTA and 1-(2-pyridylazo)-2-naphthol].

PAR-solution. Dissolve 0.25 g of 4-(2-pyridylazo)-resorcinol in 8.5 ml of 1% sodium hydroxide solution and dilute to 250 ml with distilled water.

Bromine–sodium hydroxide solution. Mix 6 ml of saturated bromine water and 100 ml of 1*M* sodium hydroxide.

Phosphate buffer solution (pH 6.5). Prepare by mixing 25 parts of 0.5*M* disodium hydrogen phosphate and 24 parts of 0.5*M* sodium dihydrogen phosphate (v/v).

Ion-exchange column A. A glass tube approximately 3.8 cm in length and 1.5 cm in bore, containing a slurry of 3.0 g of Amberlite CG 400 (100–200 mesh) in the sulphate form.

Ion-exchange column B. A glass tube approximately 6 cm in length and 1.0 cm in bore containing a slurry of 2.0 g of Amberlite CG 400 (100–200 mesh) in the chloride form.

Determination of distribution coefficients

The distribution coefficients, K_d, for vanadium(IV, V) on Amberlite CG 400 in the sulphate form were measured by a batch equilibrium method. Weighed portions of dried resin (1.0 g each) were placed in glass-stoppered Erlenmeyer flasks, to which 41-ml portions of 0.3% hydrogen peroxide solutions of varied sulphuric acid concentration were added. The mixed solutions contained either 0.0412 mmole of V(IV) or 0.0430 mmole of V(V). After mechanical shaking for 6 hr at room temperature, the two phases were separated by filtration. Vanadium in the filtrate was determined spectrophotometrically with PAR as described below. K_d was calculated from:

$$K_d = \frac{\text{amount of vanadium in resin phase/g of resin}}{\text{amount of vanadium in solution phase/ml of solution}}.$$

Similarly, the K_d values for vanadium(IV, V) with Amberlite CG 400 in the chloride form in 3% hydrogen peroxide–hydrochloric acid media were measured as a function of hydrochloric acid concentration.

Spectrophotometric determination of vanadium

Evaporate the sample solution to dryness. Take up the residue with 5 ml of distilled water and 2 ml of the bromine–sodium hydroxide solution and let it stand for 30 min. To this solution add 0.5 ml of 1.2% aqueous phenol solution and 2.5 ml of the phosphate buffer solution (pH 6.5). Adjust the pH to 6.5 with 1*M* hydrochloric acid, if necessary. Add 2 ml of 0.01*M* *trans*-1,2-diaminocyclohexane tetra-acetic acid (DCTA) and mix. Add 1.0 ml of 0.1% PAR solution, dilute to 25 ml with distilled water and let stand for 5 min. Measure the absorbance at 545 nm against a reagent blank.

Procedure

Weigh ~0.1 g of rock sample into a platinum dish. Heat with 2 ml of sulphuric acid (1 + 1) and 2 ml of concentrated hydrofluoric acid. Repeat the decomposition with an additional 1 ml of hydrofluoric acid and evaporate to dryness. Dissolve the residue with 1.0 ml of 2.5*M* sulphuric acid and 20 ml of distilled water. Dilute to 50 ml with distilled water and add 0.5 ml of 30% hydrogen peroxide. Pass this solution through column A previously conditioned with 20 ml of 0.05*M* sulphuric acid–0.3% hydrogen peroxide solution. Wash the column with 50 ml of the same solution. Elute vanadium with 30 ml of 1*M* hydrochloric acid. Evaporate the eluate to dryness. Moisten the residue with 0.5 ml of 6*M* hydrochloric acid and add 10 ml of water to dissolve the residue. Add 17 ml of water and 3 ml of 30% hydrogen peroxide and pass the solution through column B, previously conditioned with 10 ml of 0.1*M* hydrochloric acid–3% hydrogen peroxide solution. Wash the column with 25 ml of 0.1*M* hydrochloric acid–3% hydrogen peroxide solution. Elute the vanadium with 20 ml of 1*M* hydrochloric acid. Determine the vanadium spectrophotometrically as described above.

Table 1. Distribution coefficients of vanadium on Amberlite CG 400 in both H_2SO_4* and HCl† media

	CG 400 (SO_4^{2-})			CG 400 (Cl^-)		
	H_2SO_4, *M*			HCl, *M*		
	0.0050	0.050	0.50	0.010	0.10	1.0
V(V)	433	89	3	760	73	5
V(IV)	305	85	3	540	67	4

*0.3% H_2O_2 present.
†3% H_2O_2 present.

RESULTS AND DISCUSSION

The data for distribution of V(IV) and V(V) between Amberlite CG 400 in the sulphate form and sulphuric acid–0.3% hydrogen peroxide media as a function of the acid concentration, are listed in Table 1. The magnitude of sorption of V(V) is in agreement with the data of Strelow and Bothma,[16] and about the same as that of V(IV), increasing rapidly with decreasing acid concentration. The presence of peroxide apparently increases the sorption of V(IV), which is reported[16] to be low in the absence of peroxide. From a practical point of view, use of 0.050*M* acid medium may be best for concentration of vanadium from a silicate sample solution. The vanadium can be eluted quantitatively with 1.0*M* hydrochloric acid (Fig. 1).

PAR is a highly sensitive colorimetric reagent for vanadium, but not selective. Results of an interference study with this reagent are summarized in Table 2; only elements which both react with PAR and are likely to be present in common rocks were tested. As only a 0.1-g sample is used, only zirconium and thorium seem likely to interfere with the determination of vanadium in silicate rocks. Except for zirconium and thorium, none of the metals listed is

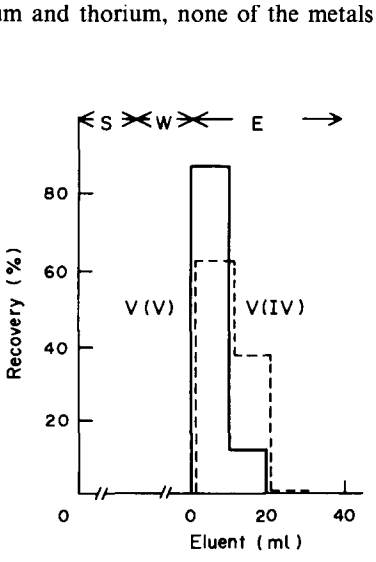

Fig. 1. Sorption and elution of vanadium. S: sample solution (50 ml), 0.05*M* H_2SO_4–0.3% H_2O_2. W: wash solution (50 ml), 0.05*M* H_2SO_4–0.3% H_2O_2. E: eluent, 1*M* HCl. Approximately 90 μg each of V(IV) or V(V) loaded and chromatographed. --- V(IV); —— V(V).

Table 2. Effect of diverse ions

Foreign ion	Added, μg	V(V), μg Added	Found	Relative error, %
Ce(IV)	338	7.00	6.97	−0.4
Cu(II)	133		7.53	7.6
	53.4		7.11	1.6
Ga(III)	75.9		8.17	16.7
	30.4		7.11	1.6
La(III)	266		7.00	0.0
Mn(II)	848		7.60	8.6
	424		7.22	3.1
Pb(II)	208		7.21	3.0
Th(IV)	15.6		6.48	−7.4
	7.8		6.70	−4.3
Y(III)	160		7.26	3.7
Zn(II)	616		7.53	7.6
	308		7.08	1.1
Zr(IV)	10.2		7.82	11.7
	2.0		7.26	3.7

Table 3. Anion-exchange separation of vanadium in simulated solutions of rock sample

No.	Added, μg V(IV)	V(V)	Found, μg		
1	6.72		6.65	6.90	7.10
			6.94	av.	6.90
2		7.00	7.04	6.89	7.11
			7.40	av.	7.11
3			0.30	0.41	0.19
			0.22	av.	0.28
4	6.72		6.83	6.87	
5		7.00	7.19	7.04	
6			0.22	0.42	

*The solution consisted of 7.5 mg Al, 12 mg Fe(III), 2.6 mg Mg, 5.1 mg Ca, 2.8 mg Na, 1.8 mg K, 1.3 mg Ti(IV), 5.3 mg Mn(II), 1.0 mg Th and 2.5 mg Zr in a total volume of 50 ml, 0.05*M* in H_2SO_4 and 0.3% in H_2O_2. For Nos. 4–6, 663 mg of Na_2SO_4 were also added.

retained to any great extent by the resin in sulphuric acid–hydrogen peroxide medium. The zirconium and thorium are also stripped by 1*M* hydrochloric acid, so they should be separated before the spectrophotometric determination of vanadium with PAR. For this purpose we incorporated the additional anion-exchange system, with the hydrochloric acid–hydrogen peroxide medium. The distribution coefficients of V(IV) and V(V) on Amberlite CG 400 (Cl^-) in this system are shown in Table 1. There is moderate sorption of V(IV) and V(V) but none of thorium and zirconium. The vanadium can be eluted with 20 ml of 1*M* hydrochloric acid. Molybdenum is sorbed like vanadium in the sulphuric acid–hydrogen peroxide system but is not appreciably stripped during elution of the vanadium. The few ppm of molybdenum in common silicate rocks will not affect the determination of vanadium. The proposed procedure gives selective determination of vanadium in silicate rocks. Table 3 lists the results obtained for determination of known amounts of vanadium added to a solution made up to simulate a 0.10-g sample of basalt rock BCR-1. To test the effect of thorium and zirconium 2.5 mg of zirconium and 1 mg of thorium were also added. The separation of vanadium is satisfactory. This is also the case even when much sodium sulphate is present, as would happen if

Table 4. Determination of vanadium in typical igneous rocks

Rock (location)	Sample, *mg*	Added, *μg*	Found, *μg*	Content in original rock, *ppm*
Basalt	95.10	0	16.5	174
(Tanegashima)	92.30	0	16.8	182
	97.98	0	16.3	166
	91.73	14.0	29.3	167
	98.76	28.0	44.5	167
				av. 171 ± 7
Andesite	108.24	0	10.8	99.8
(Sakurajima)	102.28	0	10.7	105
	100.78	0	10.0	99.2
	102.21	7.0	17.0	97.8
	102.57	14.0	23.5	92.6
				av. 98.9 ± 4.4
Granite	296.55	0	9.71	32.7
(Yakushima)	290.83	0	9.34	32.1
	299.84	0	9.94	33.2
	292.00	7.0	17.3	35.3
	303.45	14.0	24.2	33.6
				av. 33.4 ± 1.2
Granite	299.65	0	4.93	16.5
(Takakuma)	311.49	0	5.04	16.2
	301.98	0	4.59	15.2
	326.39	3.5	8.85	16.4
	300.16	7.0	11.6	15.3
				av. 15.9 ± 0.6

Table 5. Determination of vanadium in standard rocks

Sample	Vanadium, *ppm*			
	Average This work	Average (Flanagan)[17]	(Ando)[18]	Reported values
W-1 (diabase)	261, 270	264		272, 274[a]; 281[b]; 273[d]; 272 ± 1.6[e]; 284[g]; 265[h]
G-2 (granite)	37.1, 37.2	35.4		35.5, 35.5[a]; 34[b]; 36.3[f]; 35.7[h]
AGV-1 (andesite)	125, 122	125		121, 122[a]; 121[b]; 121[d]; 121 ± 0.7[e]; 123[f]; 123 ± 4[h]; 124[j]
JG-1 (granite)	25.2, 23.2		24	21[b]; 23.3 ± 1.1[c]; 24.8[f]; 23.6 ± 0.1[h]; 21[i]; 24.9[j]
JB-1 (basalt)	201, 211		211	215[b]; 178 ± 7.4[c]; 198[f]; 249[g]; 224[h]; 225[i]; 215[j]

a. Donaldson;[7] b. Terashima;[19] c. Akaiwa *et al.*;[3] d. Strelow *et al.*;[5] e. Strelow and Victor;[6] f. Kiss;[8] g. Uchida *et al.*;[9] h. Kojima *et al.*;[20] i. Ohta and Suzuki;[21] j. Uchida *et al.*[22]

sodium carbonate fusion were used for opening-out a rock sample. The results for three representative types of igneous rocks are shown in Table 4, along with results for samples spiked with known amounts of vanadium. The recoveries are again satisfactory. The method was also applied to the analysis of standard rocks of the U.S. Geological Survey and the Geological Survey of Japan, the results being listed in Table 5. The agreement with the reference values is generally excellent. The anion-exchange separations developed in this work may be combined with other determination methods, because of the effective and extensive removal of major elements as well as most minor or trace metals present in silicate rocks.

REFERENCES

1. F. D. Snell, *Photometric and Fluorometric Methods of Analysis, Metals*, Part 2, p. 1191. Wiley, New York, 1978.
2. P. G. Jeffery, *Chemical Methods of Rock Analysis*, 2nd Ed., p. 484. Pergamon Press, Oxford, 1975.
3. H. Akaiwa, H. Kawamoto and K. Kondo, *Bunseki Kagaku*, 1974, **23**, 402.
4. F. W. E. Strelow, C. J. Liebenberg and F. Von S. Toerien, *Anal. Chim. Acta*, 1969, **47**, 251.
5. F. W. E. Strelow, C. J. Liebenberg and A. H. Victor, *Anal. Chem.*, 1974, **46**, 1409.
6. F. W. E. Strelow and A. H. Victor, *J. S. Afr. Chem. Inst.*, 1975, **28**, 272.
7. E. M. Donaldson, *Talanta*, 1970, **17**, 583.
8. E. Kiss, *Anal. Chim. Acta*, 1975, **77**, 205.
9. F. Uchida, S. Yamada and M. Tanaka, *ibid.*, 1976, **83**, 427.
10. K. Govindaraju, *Analusis*, 1973, **2**, 367.
11. R. Frache, A. Muzzucotelli, A. Dadone, F. Baffi and P. Cescon, *ibid.*, 1978, **6**, 294.
12. K. M. Chan and J. P. Riley, *Anal. Chim. Acta*, 1966, **34**, 337.
13. J. Korkisch, I. Steffan and H. Groß, *Mikrochim. Acta*, 1976, **I**, 503.
14. J. Korkisch and I. Hazan, *Talanta*, 1964, **11**, 1157.
15. K. Kawabuchi and R. Kuroda, *ibid.*, 1970, **17**, 67.
16. F. W. E. Strelow and C. J. C. Bothma, *Anal. Chem.*, 1967, **39**, 595.
17. F. J. Flanagan, *Geochim. Cosmochim. Acta*, 1973, **37**, 1189.
18. A. Ando, *Bunseki*, 1978, 526.
19. S. Terashima, *Bunseki Kagaku*, 1973, **22**, 1317.
20. I. Kojima, T. Uchida, M. Nanbu and C. Iida, *Anal. Chim. Acta*, 1977, **93**, 69.
21. K. Ohta and M. Suzuki, *ibid.*, 1979, **108**, 69.
22. H. Uchida, T. Uchida and C. Iida, *ibid.*, 1980, **116**, 433.

Talanta, Vol. 30, No. 4, pp. 265–270, 1983
Printed in Great Britain.

0039-9140/83/040265-06$03.00/0

DETERMINATION OF TRACE ARSENIC, ANTIMONY, SELENIUM AND TELLURIUM IN VARIOUS OXIDATION STATES IN WATER BY HYDRIDE GENERATION AND ATOMIC-ABSORPTION SPECTROPHOTOMETRY AFTER ENRICHMENT AND SEPARATION WITH THIOL COTTON

MU-QING YU and GUI-QIN LIU
Changchun Institute of Geography, Chinese Academy of Science

and

QINHAN JIN*
Department of Chemistry, Jilin University, Changchun, People's Republic of China

(*Received* 4 *March* 1982. *Revised* 9 *October* 1982. *Accepted* 20 *October* 1982)

Summary—A novel procedure for determination of trace As(III) and As(V), Sb(III) and Sb(V), Se(IV) and Se(VI), Te(IV) and Te(VI) in water by atomic-absorption spectrophotometry after separation and enrichment with "thiol cotton" and hydride generation has been established. The sorption behaviour of various oxidation states of arsenic, antimony, selenium and tellurium, and the conditions of quantitative sorption and desorption of these species were studied. The procedures for reducing species from higher oxidation states were optimized. Interferences from other species and their elimination were investigated. The selectivity of the procedure for the determination of species in higher and lower oxidation states was examined. The procedure has been successfully used to determine arsenic, antimony, selenium and tellurium in water, in the range from pg/ml to ng/ml. The recoveries for added spikes were in the range 90–110%, with coefficients of variation in the range 3–8%.

It has been shown by more and more facts that the transport and conversion processes as well as the biological toxic effects of a variety of trace elements, such as mercury, chromium, arsenic, antimony, selenium and tellurium, in the environment are closely related to the oxidation states and compounds present. It is obvious that ignoring this fact can lead to inadequate or even totally wrong evaluation of environmental quality. For this reason the investigation of methods for specification of trace elements has been of interest for several years.

Various methods for determining chromium,[1–5] arsenic,[6–11] antimony,[12–14] selenium[15–21] and tellurium[22–24] in various oxidation states, after separation by co-precipitation, solvent extraction, ion-exchange, hydride generation and stepwise reduction, have been established, but most of them are limited in their application.

It has been shown that the thiol group has very strong affinity for heavy-metal ions and that cotton impregnated with thioglycollic acid ("thiol cotton") quantitatively adsorbs a variety of trace elements from water,[25–27] but its adsorptive power depends significantly on the oxidation state of the element concerned. In general, the lower oxidation states are readily adsorbed whereas the higher states are not. It should therefore be possible to adsorb the lower states selectively, and then to reduce the higher states and adsorb the products.

On the basis of investigations on the enrichment in this way of more than twenty trace species, including Pt(II), Pd(II), Au(III), Se(IV), Te(IV), As(III), Hg(II), Sb(III), Bi(III), Sn(II), Ag(I), Cu(II), In(III), Pb(II), Cd(II), Zn(II), Co(II) and Ni(II),[25–28] we have established this procedure for determining trace As(III), As(V), Sb(III), Sb(V), Se(IV), Se(VI), Te(IV) and Te(VI) in water by hydride generation and atomic-absorption spectrophotometry after separation and enrichment with thiol cotton.

EXPERIMENTAL

Apparatus

A Pye-Unicam SP 1900 atomic-absorption spectrophotometer and a home-made hydride-generator (Fig. 1) were used, under the conditions listed in Table 1.

A 250-ml (or 500-ml) Pyrex separatory funnel fitted with a thiol-cotton tube was used for separation and enrichment of various trace species. The thiol-cotton tube was a glass tube with about 0.1 g of thiol cotton in it. It was 8 mm in bore and 100 mm long, and one of the ends was narrowed.

Reagents

Suprapur-grade hydrochloric acid and nitric acid were used. All the other reagents were analytical-reagent grade. All water used was redistilled.

Standard antimony(III) solution (1000 ppm). Prepared from antimony potassium tartrate.

*To whom correspondence should be addressed.

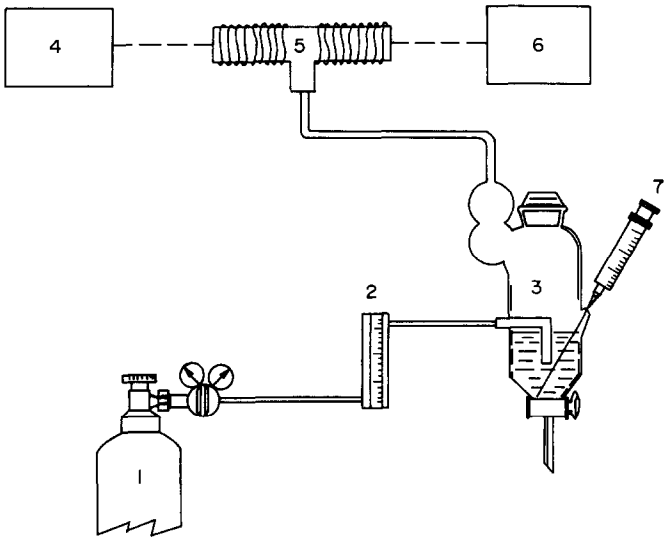

Fig. 1. Equipment for hydride-generation determination. 1, N_2 cylinder; 2, flowmeter; 3, hydride generator (25 mm bore, 80 mm long); 4, light source; 5, quartz-tube atomizer (8 mm bore, 150 mm long); 6, detector; 7, syringe.

Standard antimony(V) solution (10 ppm). Prepared by oxidizing the standard antimony(III) solution with permanganate.

Standard arsenic(III) solution (1000 ppm). Prepared from arsenious oxide.

Standard arsenic(V) solution (1000 ppm). Prepared from sodium arsenate.

Standard selenium(IV) solution (1000 ppm). Prepared from selenium dioxide.

Standard tellurium(IV) solution (1000 ppm). Prepared from tellurium powder.

Standard tellurium(VI) solution (1000 ppm). Prepared from telluric acid.

Potassium iodide (20%)–thiourea (2%) solution.

Potassium iodide (20%)–ascorbic acid (4%) solution.

Potassium borohydride solution (2%). Prepared in 0.5% sodium hydroxide solution.

Titanium(III) chloride, 15–20% solution.

Hydrogen peroxide, 30% solution.

Thiol cotton. Thioglycollic acid (50 ml), acetic anhydride (35 ml), glacial acetic acid (16 ml), concentrated sulphuric acid (0.15 ml) and water (5 ml) were put in that order into a bottle and mixed well, and then 15 g of absorbent cotton were added. The bottle was closed, then left in an oven at 40–50° for 4–5 days. The cotton was collected on a sintered-glass funnel and washed with water till the washings were neutral, then dried at 40–50° and kept in a brown bottle.

Procedures

Separation and enrichment. Put a selected volume of water sample into the separation assembly, adjust its acidity to the value indicated in Table 2 and then pass it through the thiol-cotton tube at a suitable flow-rate to extract the Sb(III), As(III), Se(IV) or Te(IV). Treat the effluent solution with the appropriate reagents (as indicated in Table 3) to reduce Sb(V), As(V), Se(VI) or Te(VI) to the next lower oxidation state, and collect the reduced species in another thiol-cotton tube.

Desorb the As(III), Sb(III), Se(IV) or Te(IV) as follows.

Arsenic. Elute slowly with 3 ml of hot concentrated hydrochloric acid. Collect the eluate in a 10-ml graduated tube. Add 0.2 ml of potassium iodide solution to the eluate and dilute to 10 ml with water.

Antimony. Elute slowly with 3 ml of 5*M* hydrochloric acid into a 10-ml graduated tube. Add 0.2 ml of potassium iodide solution to the eluate and dilute to 10 ml with water.

Selenium. Put the cotton into a 10-ml graduated tube. Add 2.5 ml of concentrated hydrochloric acid and 1 drop of concentrated nitric acid. Heat in a boiling water-bath for 3 min. Cool to room temperature and dilute to 10 ml with water.

Tellurium. Place the cotton in a 10-ml graduated tube. Add 2.5 ml of concentrated hydrochloric acid. Heat in a boiling water-bath for 3 min. Cool to room temperature and dilute to 10 ml with water.

Use a separate sample for each element, but if desired, antimony(III) can be selectively eluted first.

Determination. Set the AAS instrument according to Table 1. Place a known amount of sample solution in the

Table 1. Conditions for hydride generation and AAS determination

Parameter	Sb	As	Se	Te
Light-source	Pye hollow-cathode lamps			
Wavelength, *nm*	217.6	193.7	196.0	214.2
Lamp current, *mA*	12	10	6	10
Slit-width setting	0.2	0.2	0.2	0.2
Temperature of quartz tube, *°C*	900	900	900	900
Flow-rate of carrier-gas (N_2), *l./min*	0.6	0.6	0.6	0.6
Acidity of solution analysed, *N*	1.5	3	3	3

Table 2. Acidity for enriching As(III), Sb(III), Se(IV) and Te(IV)

Species	Acidity of water sample
Sb(III)	pH 6–8
As(III)	1*M* HCl
Se(IV)	0.3*M* HCl
Te(IV)	0.3*M* HCl

hydride generator and make up to 5 ml with hydrochloric acid of the same concentration as the sample. Close the generator and with a syringe rapidly add 1.5 ml of potassium borohydride solution to the lower part of the solution. From the recorded absorbance calculate the content of the species in the sample.

RESULTS AND DISCUSSION

Adsorption behaviour of thiol cotton towards arsenic, antimony, selenium and tellurium

It is clear from Figs. 2 and 3 that the adsorption behaviour of those elements depends greatly on the acidity of the solution and the oxidation state of the element. Thiol cotton efficiently adsorbs only As(III), Sb(III), Se(IV) and Te(IV), the ranges of acidity for quantitative adsorption being Sb(III), pH 8–2*M* HCl; As(III), 0.5–7*M* HCl; Te(IV) pH 8–9*M* HCl; Se(IV), pH 2–10*M* HCl. It was also noticed that within certain ranges of hydrochloric acid concentration, some species in higher oxidation states could be reduced by the thiol group and then adsorbed by the thiol cotton. The degree of reduction depends on the species concerned and the acidity but is never quantitative. For example, Sb(V) is partly reduced to Sb(III) in dilute hydrochloric acid. Therefore, this species can be adsorbed significantly (~50% maximum) at pH ≤ 5, but Se(VI), Te(VI) and As(V) can only be slightly reduced and adsorbed at acidities below 5*M* hydrochloric acid.

The range of acidity for quantitative adsorption shown in Figs. 2 and 3 will change slightly with the composition of the solution, the concentration of the trace element and the quality of the thiol cotton. The conditions shown in Table 2 are recommended as optimal.

Choice of desorption procedures

The adsorptive power of thiol cotton for Sb(III) is rather poor, and this species can be desorbed quantitatively with 5*M* hydrochloric acid.

To desorb As(III), the thiol cotton should be dipped into concentrated hydrochloric acid for several minutes.

Se(IV) and Te(IV) are adsorbed very firmly by thiol cotton, so it is necessary to heat the cotton with concentrated hydrochloric acid in a boiling water-bath to desorb these species quantitatively; this process also attacks the cotton itself.

Table 3. Conditions for reducing As(V), Sb(V), Se(VI) and Te(VI)

Species	Acidity	Amount of reductant used, and reduction procedure
Sb(V)	0.3*M* HCl	Add KI to 0.1% and ascorbic acid to 0.02%; let stand for 10 min at room temperature
As(V)	1*M* HCl	Add KI to 0.2% and thiourea to 0.02%; heat for 3–5 min in a boiling water-bath (the temperature of the solution reaches 80°)
Se(VI)	0.3*M* HCl	Add $TiCl_3$ to 0.1%; after 30 min add H_2O_2 to 0.1% and heat for 5 min in a boiling water-bath
Te(VI)	0.3*M* HCl	Add $TiCl_3$ to 0.1%; after 10 min add H_2O_2 to 0.1% and let stand for 5 min at room temperature

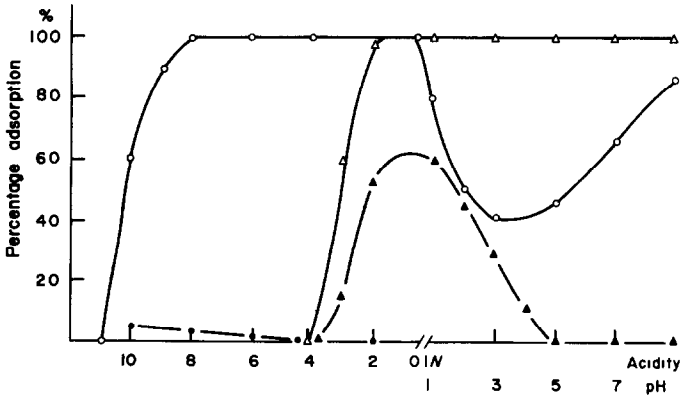

Fig 2. The effects of acidity on the adsorption of As(III), As(V), Sb(III) and Sb(V) (all 10 ng/ml concentration) on thiol cotton. (○) As(III); (●) As(V); (△) Sb(III); (▲) Sb(V).

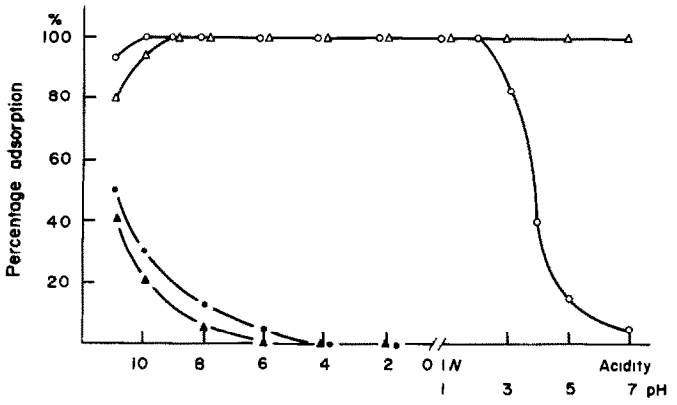

Fig. 3. The effects of acidity on the adsorption of Se(IV), Se(VI), Te(IV) and Te(VI) (all 10 ng/ml concentration) on thiol cotton. (○) Se(IV); (●) Se(VI); (△) Te(IV); (▲) Te(VI).

The procedure for determination of arsenic, antimony, selenium and tellurium by hydride-generation atomic-absorption spectrophotometry is also related to the oxidation state. Therefore, the oxidation state of the species to be determined in the desorbed solution should be consistent with the requirements of this technique. For this reason, a small amount of nitric acid is added when selenium is to be desorbed, to ensure the selenium is in the quadrivalent state.

Choice of reduction procedures

Since As(V), Sb(V), Se(VI) and Te(VI) must be reduced to As(III), Sb(III), Se(IV) and Te(IV) before they can be quantitatively adsorbed by thiol cotton, the reduction procedure should be compatible with the enrichment technique. Those selected are as follows.

Sb(V) can be rapidly reduced by adding potassium iodide to the dilute hydrochloric acid sample solution.

As(V) is more difficult to reduce than Sb(V). It is necessary to add potassium iodide and thiourea to a sample solution that is 1*M* in hydrochloric acid and heat in a boiling water-bath for several minutes.

Se(VI) and Te(VI) are difficult to reduce selectively to Se(IV) and Te(IV) because they are very easily reduced to the elements in hydrochloric acid medium. We have found that if enough titanium trichloride to reduce Te(VI) to Te(IV) and Se(VI) to Se is added to a dilute hydrochloric acid solution followed by enough hydrogen peroxide to oxidize the excess of titanium trichloride and to form a complex with it, a stable Te(IV) solution is formed and the elemental selenium is oxidized to Se(IV). The concentration of hydrochloric acid, the amounts of titanium trichloride and hydrogen peroxide used and the temperature and time of reduction all affect the efficiency of reduction. Table 3 shows the recommended reduction conditions. This reduction procedure is simple, rapid and easy to operate, and Se(VI) and Te(VI) can be converted into Se(IV) and Te(IV) simultaneously and quantitatively.

Amount of thiol cotton to use and flow-rate of sample solution

The adsorption capacity of thiol cotton for the species concerned and the flow-rates for quantitative adsorption are shown in Table 4. The operational adsorption capacities are between a third and a half of the corresponding saturation capacities.

On the basis of the concentration ranges of these species that can be adsorbed by thiol cotton and those existing in practical environmental water samples, about 0.1 g of thiol cotton is adequate for enrichment.

Selectivity for higher or lower oxidation states

The selectivity for enriching and determining species in their higher or lower oxidation states is quite good. The maximum ratios allowed between higher and lower oxidation-state species, for an error of 10%, are shown in Table 5.

To obtain selective determination the following measures should be taken.

1. The thiol-cotton tube should first be rinsed with water or with hydrochloric acid of appropriate concentration to bring it to the optimum state for the adsorption.
2. If the concentration ratio of lower to higher oxidation state species in the water sample is very high, to adsorb the lower-valence species the amount of thiol cotton used should be increased accordingly and the flow-rate should be reduced.
3. If the higher to lower oxidation state concentration ratio is high, the lower-valence species ad-

Table 4. Saturation adsorption capacity of thiol cotton and flow-rate of water sample

	As(III)	Sb(III)	Se(IV)	Te(IV)
Saturation capacity, *mg/g* of thiol cotton	4–5	5–7	7–9	8–11
Flow-rate, *ml/min**	≤2	≤10	≤5	≤10

*For 0.1 g of thiol cotton.

Table 5. Selectivity for determining As, Sb, Se and Te at higher or lower valence respectively,* with ±10% error

	As	Sb	Se	Te
Maximum ratio of higher valence/lower valence species for determination of lower valence species	30	20	40	50
Maximum ratio of lower valence/higher valence species for determination of higher valence species	20	20	20	30

*The volume of water sample enriched was 100–200 ml and the concentration of As, Sb, Se or Te was 2–4 ng/ml.

sorbed on the thiol cotton should be washed with water or the appropriate concentration of hydrochloric acid to remove any residual higher oxidation state species on it.

Interference studies

It has been shown that except for some slight interference in adsorption of Sb(III) from higher concentrations of humic acid, the species usually found in environmental water, such as Cl^-, Br^-, SO_4^{2-}, SO_3^{2-}, CO_3^{2-}, HCO_3^-, NO_2^-, NO_3^-, HPO_3^{2-}, K^+, Na^+, Ca^{2+}, Mg^{2+}, Fe^{3+}, Al^{3+} and various heavy metal ions, as well as fulvic acid, glycine, cysteine, citric acid and the like, do not interfere in the quantitative adsorption of As(III), Sb(III), Se(IV) and Te(IV) by thiol cotton.

It has also been shown that the direct determination of As, Sb, Se and Te by hydride-generation atomic-absorption spectrophotometry would suffer interferences from Co^{2+}, Ni^{2+}, Fe^{3+}, Cu^{2+}, Pb^{2+}, Sn^{4+}, Bi^{3+} and Ag^+ ions, and between the four elements themselves, but after enrichment with thiol cotton and stepwise desorption these interferences are effectively eliminated.

Co^{2+}, Ni^{2+}, Cu^{2+}, Sn^{4+}, Bi^{3+}, Pb^{2+} and Ag^+ adsorbed by thiol cotton can be removed quantitatively by eluting with 1–2*M* hydrochloric acid.

Table 6. Analysis of real water samples and recovery of the procedure

		Standard added, *ng/ml*		Found			
				Lower valency		Higher valency	
Element		Lower valency	Higher valency	Total, *ng/ml*	Recovery of added standard,* %	Total, *ng/ml*	Recovery of added standard,* %
Arsenic	Spring water	0	0	3.05		5.44	
		4.00	4.00	6.95	98	9.90	117
	Natural river water	0	0	0.40		0.76	
		2.00	2.00	2.54	107	2.60	92
	Polluted river water	0	0	6.58		135	
		2.00	10.00	8.80	115	22.0	85
		6.00	6.00	12.3	97	19.4	98
		10.00	2.00	15.7	92	15.4	95
Antimony	Natural river water	0	0	<0.01		0.26	
		1.00	2.00	0.95	95	2.30	102
		2.00	1.00	1.75	88	1.30	104
	Polluted lake water	0	0	0.10		1.10	
		1.00	3.00	1.00	90	4.25	98
		3.00	1.00	2.90	93	2.00	90
	Polluted river water	0	0	1.05		0.65	
		1.00	2.00	1.92	87	2.90	112
		1.00	1.00	2.00	95	1.68	103
		2.00	1.00	2.80	88	1.73	108
Selenium	Well water	0	0	0.04		0.64	
		0.50	0.50	0.58	108	1.15	102
	Natural river water	0	0	0.10		<0.01	
		1.00	1.00	1.18	108	0.95	95
	Polluted river water	0	0	0.28		0.37	
		1.50	0.50	1.66	92	0.92	110
		1.00	1.00	1.27	99	1.30	93
		0.50	1.50	0.77	98	1.66	86
Tellurium	Natural river water	0	0	<0.01		<0.01	
		2.00	1.00	1.95	98	0.98	98
		1.00	2.00	1.05	102	2.09	105
	Sea-water	0	0	<0.01		0.06	
		2.00	1.00	1.91	96	1.06	100
		1.00	2.00	1.12	112	2.16	105
	Polluted river water	0	0	0.27		0.23	
		0.50	2.00	0.83	110	2.15	96
		1.00	1.00	1.28	101	1.10	87
		2.00	0.50	2.25	99	0.75	104

*Average of three replicates.

Table 7. Sensitivity and precision of the procedure

		As	Sb	Se	Te
Sensitivity (1% absorbance),* *ng/ml*		0.11	0.09	0.20	0.16
Detection limit,† *ng/ml*		0.006	0.005	0.010	0.008
Coefficient of variation,§ %	Lower valency	3.5	7.9	2.8	2.7
	Higher valency	5.4	5.0	3.2	3.4

*The volume analysed was 5 ml.
†The volume of water sample enriched was 200 ml.
§Based on 11 samples.

To isolate antimony, the thiol cotton is eluted with 5*M* hydrochloric acid. As, Se and Te are retained and the Sb desorbed.

When selenium is being determined, any co-existing arsenic is oxidized to As(V) and so does not interfere.

When arsenic is being determined, the only interference is from selenium, but this can be eliminated by adding a small amount of potassium iodide.

The interference from selenium and arsenic in determination of tellurium can be largely eliminated by enrichment with thiol cotton and desorption.

Sensitivity and precision

As, Sb, Se and Te in various oxidation states in various environmental water samples were determined by this procedure. The recoveries were in the range 90–110%, as shown in Table 6.

The sensitivity and the coefficient of variation (11 replicates) for these elements in the range 2–4 ng/ml are shown in Table 7.

Conclusions

The procedure has the following characteristics.

1. The enrichment efficiency is high, the enrichment factor ranging up to several hundred. The detection limit can be as low as a few ng/l.

2. The separation procedure is simple and the higher and lower oxidation-state species can be separated and enriched separately. Therefore the error introduced by the subtraction technique adopted in some other methods is avoided.

3. The selectivity is good. There is no mutual interference between higher and lower valence species when their concentration ratio is not more than 20–50, depending on the particular system.

4. The accuracy is good. Interference from various concomitant species is eliminated and the method can be used to analyse various environmental water samples.

REFERENCES

1. T. Goto and S. Ginba, *Bunseki Kaguku*, 1974, **23,** 517.
2. T. Matsuo, J. Shida, M. Abiko and K. Konno, *ibid.*, 1975, **24,** 723.
3. K. Hiiro, T. Owa, M. Takaoka, T. Tanaka and A. Kauahara, *ibid.*, 1976, **25,** 122.
4. M. Q. Yu and Y. J. Zhao, *J. Environ. Sci.* (*Chinese*), 1979, No. 1, 20.
5. S. R. Wang, F. Z. Xu, H. F. Zhou and X. L. Jin, *ibid.*, 1980, No. 3, 11.
6. T. Kamada, *Talanta*, 1976, **23,** 835.
7. J. Aggett and A. C. Aspell, *Analyst*, 1976, **101,** 341.
8. D. J. Myers and J. Osteryoung, *Anal. Chem.*, 1973, **45,** 267.
9. F. T. Henry, T. O. Kirch and T. M. Thorpe, *ibid.*, 1979, **51,** 215.
10. Y. Talmi and D. T. Bostic, *ibid.*, 1975, **47,** 2145.
11. M. O. Andreae, *ibid.*, 1977, **49,** 820.
12. T. Kamada and Y. Yamamoto, *Talanta*, 1977, **24,** 330.
13. I. Valente and H. J. M. Bowen, *Analyst*, 1977, **102,** 842.
14. K. S. Subramanian and J. C. Meranger, *Anal. Chim. Acta*, 1981, **124,** 131.
15. O. Yoshil, K. Hiraki, Y. Nishikawa and T. Shigematsu, *Bunseki Kagagu*, 1971, **26,** 91.
16. Y. Shimoshi and K. Toei, *Anal. Chim. Acta*, 1978, **100,** 15.
17. T. Kamada, T. Shiraishi and Y. Yamamoto, *Talanta*, 1978, **25,** 15.
18. G. A. Cutter, *Anal. Chim. Acta*, 1978, **98,** 59.
19. Y. Sugimura and Y. Suzuki. *J. Oceanogr. Soc. Japan*, 1977, **33,** 23.
20. C. I. Measures and J. D. Burton, *Anal. Chim. Acta*, 1980, **120,** 177.
21. H. J. Robberecht and R. E. Van Grieken, *Anal. Chem.*, 1980, **52,** 449.
22. T. Kamada, N. Sugita and N. Yamamoto, *Talanta*, 1979, **26,** 337.
23. K. Jin, M. Taga, H. Yoshida and S. Hikime, *Bull. Chem. Soc. Japan*, 1979, **52,** 2276.
24. X. Q. Shan and Z. M. Ni, *Acta Scientiae Circumstantiae* (*Chinese*), 1981, **1,** 80.
25. S. Nishi, Y. Horimoto and R. Kobayashi, *Intern. Symp. Identification and Measurement of Environmental Pollutants*, p. 201. NRCC, Ottawa, 1971.
26. M. Q. Yu, G. Q. Liu and S. H. Wang, *J. Environ. Sci.* (*Chinese*), 1979, No. 5, 46.
27. M. Q. Yu and G. Q. Liu, *Acta Scientiae Circumstantiae* (*Chinese*), 1981, **1,** 180.
28. *Idem, J. Environ. Chem.* (*Chinese*), 1982, No. 1, 12.

Talanta, Vol 30, No. 4, pp. 271–274, 1983
Printed in Great Britain

0039-9140/83/040271-04$03 00/0

DETERMINATION OF ALPHA-EMITTING URANIUM ISOTOPES IN SOFT TISSUES BY SOLVENT EXTRACTION AND ALPHA-SPECTROMETRY

NARAYANI P. SINGH and MCDONALD E. WRENN
Radiobiology Division, Department of Pharmacology, University of Utah, College of Medicine, Salt Lake City, UT 84112, U.S.A.

(*Received* 19 *May* 1982. *Accepted* 16 *October* 1982)

Summary—A radiochemical procedure has been developed for the determination of alpha-emitting isotopes of uranium (^{238}U, ^{235}U and ^{234}U) in soft tissues. Known amounts of sample are spiked with ^{232}U internal tracer and wet-ashed. Uranium is co-precipitated with iron hydroxide as carrier, and extracted into 20% trilaurylamine solution in xylene after dissolution of the precipitate in 10*M* hydrochloric acid. The uranium, after stripping into an aqueous phase, is electro-deposited onto a platinum disc and counted by alpha-spectrometry. The radiochemical recovery ranges from 60 to 85% for bovine liver samples. The average radiochemical recoveries for human tissues vary from 53 to 78%.

Uranium is found in many varieties of rocks and soils. In addition, it may be distributed locally in the vicinity of uranium mining, milling, refining and fuel fabrication plant and occurs (from natural sources) at low levels in human tissues. Good analytical techniques are required to determine the normal low levels of uranium in human tissues. Earlier, fluorometry and neutron activation were used,[1,2] both of which are capable of detecting nanogram quantities of uranium but incapable of determining concentrations of individual uranium isotopes. A knowledge of relative isotopic content may be useful in establishing the origin of the uranium found in tissues (*i.e.*, natural uranium or uranium enriched in ^{235}U). Methods have been reported for the determination of isotopic composition in sediments, soil and bio-assay samples,[3–6] but none has been described for determination of isotopes of uranium in soft tissues.

A simple analytical procedure has now been developed, based on solvent extraction and solid-state alpha-spectrometry. Trilaurylamine was chosen as the extracting agent because of its successful application in determination of thorium and plutonium in soft tissues and bone.[7–9]

EXPERIMENTAL

Reagents

All the reagents used were of analytical grade. A 20% v/v trilaurylamine (TLA) solution was prepared in xylene and shaken with one third of its volume of 10*M* hydrochloric acid for 10 min. The mixture was centrifuged and the organic phase separated before use. Dilute acids were prepared with demineralized distilled water. Other reagents included ^{232}U tracer, Thymol Blue indicator, 5% sodium bisulphate solution in 9*M* sulphuric acid, 1*M* ammonium sulphate adjusted to pH 3.5, ethyl alcohol, concentrated ammonia solution, and ferric chloride solution (10 mg/ml).

Sample preparation

Weigh the soft tissue (0.3–1100 g depending on type), transfer it to a beaker of appropriate size and spike it with 1–2 dpm of ^{232}U tracer. Wet-ash with nitric acid followed by a mixture of nitric and sulphuric acids with occasional additions of nitric acid and hydrogen peroxide until all the organic material is destroyed, giving a clear colourless solution. Evaporate most of the sulphuric acid by continuous heating, but do not heat to dryness. In the case of lung and lymph nodes, heat the tissues with hydrofluoric and nitric acid mixtures and remove surplus hydrofluoric acid by continuous heating.

Add 100 ml of hydrochloric acid (1 + 3) to the clear solution of the tissues and 1 ml of iron carrier solution. Boil for several minutes and cool. Add concentrated ammonia solution very slowly until the pH is 10–11. Boil for 10–15 min and let the precipitate settle. Transfer the whole to a 250-ml centrifuge tube and centrifuge for 10 min. Discard the supernatant liquid, dissolve the precipitate in 125–130 ml of 1*M* nitric acid and reprecipitate with ammonia, adjusting the pH to 9–10. Repeat twice more to ensure complete removal of sulphate. Finally, dissolve the precipitate in a known minimal volume (usually 10–15 ml, depending on the sample) of concentrated hydrochloric acid and adjust the acidity to 10*M* (titrate 0.1 ml of the solution with 0.1*M* sodium hydroxide and calculate how much concentrated acid to add).

Solvent extraction

Extract the uranium into an equal volume of 20% TLA solution in xylene (pre-equilibrated with 10*M* hydrochloric acid) from the solution obtained in the sample preparation, shaking for 10 min. Centrifuge to separate the phases, then transfer the mixture to a 250-ml separatory funnel, run the aqueous phase back into the centrifuge tube, add an equal volume of 20% TLA solution and repeat the extraction by shaking for 10 min. Centrifuge, then transfer the solution into the separatory funnel containing the organic phase from the first extraction. Remove the aqueous phase and discard it. Wash the organic phase twice by shaking it (10 min each time) with an equal volume of 10*M* hydrochloric acid, discarding the aqueous phases. Strip uranium from the organic phase by shaking it with an equal volume of 0.1*M* hydrochloric acid for 10 min. Separate the aqueous

phase and transfer it to a beaker. Repeat the stripping and combine the aqueous phases. Remove any iron quantitatively from the aqueous phase before electro-deposition, as follows. Evaporate the aqueous solution almost to dryness and add 4–5 ml of concentrated sulphuric acid. Heat strongly, with occasional addition of concentrated nitric acid to remove any traces of organic contaminants. Finally, remove the sulphuric acid by heating strongly. Cool, and dissolve the residue in 8–10 ml of concentrated hydrochloric acid. Transfer the solution into a 50-ml polypropylene tube, add an equal volume of isopropyl ether, shake the tube for 2 min and heat the tube for 2–3 min in a hot water-bath (95°). Transfer to a separating funnel,separate the aqueous phase and return it to the same polypropylene tube. Repeat the extraction with an equal volume of isopropyl ether, heating as before (the extraction of iron is then quantitative). The organic phases contain all the iron, leaving uranium in the aqueous phase. Evaporate the aqueous phase almost to dryness and add 5 ml of 5% sodium bisulphate solution in 9*M* sulphuric acid. Heat strongly with occasional additions of nitric acid to remove any traces of organic matter. Evaporate the solution to dryness without baking. Finally, dissolve the residue in 5 ml of 1*M* ammonium sulphate solution, warming if necessary.

Electro-deposition

Details of the apparatus used are given elsewhere.[7-10]

Transfer the ammonium sulphate solution of the residue into the plating cell, rinsing it with two 1-ml portions of 1*M* ammonium sulphate. Add one drop of Thymol Blue indicator and then concentrated ammonia solution dropwise until the solution just turns yellow (it is important not to add excess). Bring back to a salmon pink colour by adding 2*M* sulphuric acid drop by drop. Deposit the uranium at a current of 1.2 A for 1 hr. Quench the electrolyte with an excess of 10% ammonia solution, letting the stirrer run for 1 min more. Dismantle the cell and rinse the platinum disc with water and then alcohol. Heat the disc to red heat with a burner. Determine the recovery and the isotopic composition of uranium by counting the disc in an α-spectrometer, using a surface-barrier silicon diode and a multichannel analyzer.

RESULTS AND DISCUSSION

Uranium was extracted from 1–10*M* hydrochloric acid medium into equal volumes of 20% TLA solution in xylene, pre-equilibrated with hydrochloric acid of the corresponding molarity. The extraction was almost quantitative from 6–10*M* hydrochloric acid, but in further experiments the 10*M* hydrochloric acid medium was used, because it is optimal for decontamination from thorium.

Uranium-232 tracer was added to beef liver, which was then decomposed and processed as described, except that the extraction of iron with isopropyl ether was omitted. The recoveries were very poor, ranging from 5 to 20%, owing to large amounts of iron being electrolytically co-deposited with uranium on the platinum discs and causing self-absorption of the emitted alpha-particles. However, when the iron was removed by extraction with isopropyl ether, the recoveries improved.

Attempts to extract the iron with 0.2*M* thenoyltrifluoroacetone (TTA) in xylene gave only partial removal. Attempts to strip iron selectively from the TLA phase by shaking with an equal volume of a 3:1 v/v mixture of 6*M* hydrochloric and concentrated hydriodic acids failed because results indicated that although removal of iron was complete, a large percentage of the uranium was also removed. The isopropyl ether extraction was the most suitable method.

Replicate experiments on different sample sizes of beef liver (50–400 g) spiked with ^{232}U tracer showed (Table 1) no effect of sample size (up to 400 g) on the percentage recovery of uranium. The overall recovery was found to be $73 \pm 4\%$ which is quite high and satisfactory for such large samples of biological tissues.

Once the method had been established with beef liver it was applied to samples of human tissues, including lung, liver, lymph nodes, spleen, kidney, thyroid and gonads. The results of radiochemical recoveries are given in Table 2. The recoveries for all organs except liver were comparable to those ob-

Table 1. Recovery of uranium from beef liver

Sample, *g*	No. of detns.	Recovery, % Range	Recovery, % Mean
50	3	69–85	77
100	6	65–75	71
150	3	65–78	73
200	4	66–82	76
250	3	65–71	68
400	3	60–80	70

Table 2. Recovery of ^{232}U added to human tissues and ^{238}U and ^{234}U concentrations found

Tissue type	Amount, *g*	No. of detns.	Recovery, % Range	Recovery, % Mean	Concentrations of U isotopes human tissues, *pCi/kg* (wet wt.) ^{238}U Range	^{238}U Mean	^{234}U Range	^{234}U Mean
Lung	219–538	6	66–79	68	0.19–0.82	0.59	0.27–2.14	0.58
Liver	360–1102	6	47–61	53	0.01–0.31	0.10	0.07–0.50	0.20
Lymph nodes	0.3–6.4	6	59–78	72	2.07–14.75	7.30	0.84–31.2	12.5
Spleen	54–287	6	59–90	73	0.04–0.33	0.14	0.02–1.40	0.36
Kidney	69–174	6	61–91	78	0.04–0.57	0.21	0.06–0.92	0.33
Thyroid	8–18	5	66–81	74	−(1.80–0.95)	−0.10	0.04–5.35	1.10
Gonads	8–39	5	61–89	75	0.07–1.87	0.20	0.41–1.84	0.56

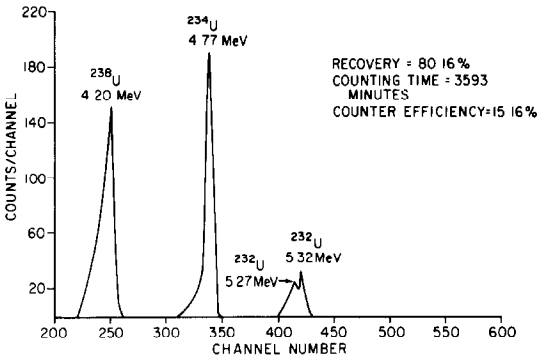

Fig. 1. Alpha-spectrum of human lung with added ^{232}U tracer.

tained for beef liver. The recoveries for human liver were lower, probably because of the larger sample size processed (>800 g). The overall recovery (excluding liver) was 73 ± 3%. The major loss of uranium occurs in the electro-deposition stage (10–15%), but some losses are observed in the precipitation, solvent extraction and back-extraction steps.

The implications (for metabolism and radiological health hazards) of the concentrations of uranium found in different human organs are beyond the scope of this paper. However, mean values found for ^{238}U and ^{234}U in some soft tissues from six persons not occupationally exposed to uranium are given in Table 2. The alpha-spectra of uranium in a human lung and kidney are given in Figs. 1 and 2 and demonstrate the applicability of this technique in determining the environmental level of uranium isotopes in human tissues.

There are certain other radionuclides present in the environment which are accumulated in human organs either by inhalation or ingestion, and their alpha-energies are very close to the alpha-energies of the uranium isotopes of interest. For example, that of ^{226}Ra (4.78 MeV) is very close to those of ^{234}U (4.77 and 4.72 MeV), and the alpha-energies of ^{210}Po (5.305 MeV) and ^{228}Th (5.43 and 5.34 Mev) are very close to the alpha-energies of ^{232}U (5.32 and 5.27 MeV), used as the internal tracer. It is therefore essential to separate uranium from radium, thorium, and polonium before the electro-deposition and counting by alpha-spectrometry, to avoid any interferences due to ^{210}Po, ^{228}Th and ^{226}Ra. Under the present experimental conditions, radium is partially eliminated in the precipitation stage, with further elimination in the solvent extraction and electro-deposition stages. The extraction of polonium is poor with high molecular-weight amines and only about 1.5% of the polonium present is electro-deposited in ammonium sulphate–sulphuric acid medium. Further, polonium, being highly volatile, is removed from the platinum disc when it is heated. In the method described the discrimination against polonium exceeds 5×10^3. The decontamination from thorium is achieved in the solvent extraction step. In our method, when uranium is extracted from 10*M* hydrochloric acid, thorium is quantitatively left in the aqueous phase. The discrimination against thorium exceeds 3×10^4.

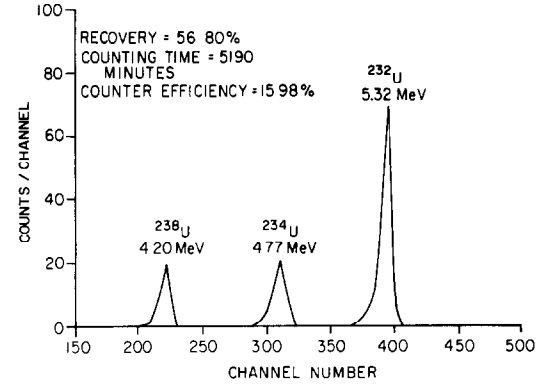

Fig. 2. Alpha-spectrum of human kidney with added ^{232}U tracer.

Plutonium isotopes (239, 240 and 238) are distributed in the environment, owing to fall-out from nuclear testing and burn-up of nuclear-powered satellites. They are accumulated in humans (mostly in the liver and skeleton) primarily through inhalation. The alpha-energies of ^{238}Pu (5.50 and 5.46 MeV) and ^{239,240}Pu (5.11, 5.12, 5.16 and 5.17 MeV) are far from those of the naturally occurring isotopes of uranium (^{234}U, ^{235}U and ^{238}U, alpha-energies 4.72 and 4.77 MeV, 4.58, 4.40 and 4.37 MeV and 4.15 and 4.20 MeV, respectively) and therefore do not interfere in the alpha-spectrometry. The alpha-energies of ^{232}U (5.27 and 5.32 MeV), used as internal tracer for radiochemical recoveries, are between those of ^{239,240}Pu and ^{238}Pu, but sufficiently different from them (>100 keV) for there not to be any interference unless a particularly large mass of metal is deposited, in which case the resolution becomes poor and the alpha-spectra may overlap. Any interference by plutonium can be made negligible by increasing the concentration of ^{232}U tracer, but if this is not satisfactory in certain circumstances, the plutonium can be separated from uranium before the latter is stripped from the TLA phase. An equal volume of 8*M* hydrochloric acid containing 0.05*M* ammonium iodide is added to the organic phase and shaken with it for 10 min. Plutonium is reduced to the tervalent state and is brought into the aqueous phase, leaving the uranium quantitatively in the TLA phase. Uranium is then back-extracted into the aqueous phase by shaking with an equal volume of 0.1*M* hydrochloric acid as described earlier.

Acknowledgement—The authors' sincere thanks are due to Carol Zimmerman and Laura L. Lewis for their technical assistance and to the Department of Energy for supporting this work.

REFERENCES

1. G. A. Welford and R. Baird, *Health Phys.*, 1967, **13,** 1321.
2. E. I. Hamilton, *ibid.*, 1972, **22,** 149.
3. C. W. Sill, K. W. Puphal and F. D. Hindman, *Anal. Chem.*, 1974, **46,** 1725.
4. T. M. Beasley, *Health Phys.*, 1965, **14,** 1059.
5. J. C. Veselsky, P. C. Kirl and N. J. Sezginer, *J. Radioanal. Chem.*, 1974, **21,** 97.
6. F. E. Butler, *Health Phys.*, **15,** 19.
7. N. P. Singh, S. A. Ibrahim, N. Cohen and M. E. Wrenn, *Anal. Chem.*, 1979, **51,** 207.
8. *Idem, ibid.*, 1978, **50,** 357.
9. *Idem, ibid.*, 1979, **51,** 1978.
10. *Health and Safety Manual.* Environmental Measurement Laboratory, U.S. Department of Energy, 1976.

Talanta, Vol. 30, No. 4, pp. 275–276, 1983
Printed in Great Britain.

0039-9140/83/040275-02$03.00/0

SHORT COMMUNICATIONS

A HIGHLY SENSITIVE SPECTROPHOTOMETRIC METHOD FOR DETERMINATION OF MICRO AMOUNTS OF ARSENIC

WU QIAN-FENG and LIU PENG-FEI
Shaanxi Monitoring Station of Environmental Protection, 25 Chang An Road (N.), Xian, People's Republic of China

(*Received* 9 *July* 1982. *Accepted* 21 *October* 1982)

Summary—A highly sensitive spectrophotometric method for determination of arsenic, based on the formation of an ion-association complex between arsenoantimonomolybdenum blue and Malachite Green, has been developed. The ion-association complex is soluble in the presence of Triton X-305, so arsenic can be determined directly in aqueous solution. The apparent molar absorptivity for arsenic is 1.13×10^5 l.mole^{-1}.cm^{-1} at 640 nm. Beer's law is obeyed for 0–5 μg of arsenic. The lower limit of determination (absorbance = 0.01) is 4 ng/ml in the final solution.

Arsenomolybdenum blue has long been used for spectrophotometric determination of arsenic.[1-3] A later modification uses the reduced ternary heteropoly acid arsenoantimonomolybdenum blue,[4,5] and is more sensitive than the methods based on the binary heteropoly acid. In recent years, the reaction of the arsenomolybdenum blue and triphenylmethane dyes has been exploited.[6]

We now recommend a simple and highly sensitive colour reaction for the spectrophotometric determination of arsenic by means of the arsenoantimonomolybdenum blue– Malachite Green complex in presence of Triton X-350 as solubilizing agent. The arsenic can be determined directly in aqueous solution, with no need for extraction into an organic solvent.

The method is one of the most sensitive available and compares favourably with others for the spectrophotometric determination of arsenic.

EXPERIMENTAL

Reagents

Stock solution of arsenic (100 μg/ml). Dissolve 0.0660 g of As_2O_3 in 5 ml of 3% sodium hydroxide solution, adjust to pH 1.5 with 1*M* sulphuric acid and dilute to 500 ml with 0.2% v/v sulphuric acid.

Working solution of arsenic (1.0 μg/ml). Heat and oxidize 5 ml of stock solution with 1 or 2 drops of 3% potassium permanganate solution, then add 1% sodium nitrite solution until the excess of oxidant has been destroyed. Cool, transfer the solution into a 500-ml standard flask and make up to the mark with water.

Antimony solution (100 μg/ml). Dissolve 0.05 g of pure antimony powder in 10 ml of concentrated sulphuric acid, heating until it is completely dissolved. Cool, then add 326 ml of water and 164 ml of concentrated sulphuric acid (with cooling) to give a final acid concentration of 12.5*N*.

Triton X-305/Malachite Green solution. Dissolve 0.1 g of Triton X-305 in lukewarm water, add 0.1 g of Malachite Green (MG) and dilute to 100 ml with water.

All chemicals used were of analytical grade whenever possible.

General procedure

To the test solution, containing not more than 5 μg of arsenic, in a 25-ml standard flask, add 4 ml of 2% ammonium heptamolybdate solution, 2 ml of antimony solution, 4 ml of 2% ascorbic acid solution and 3 ml of Triton X-305/MG solution. Dilute to volume with water and mix well. Measure the absorbance at 640 nm in a 2-cm cell against a reagent blank after 20 min.

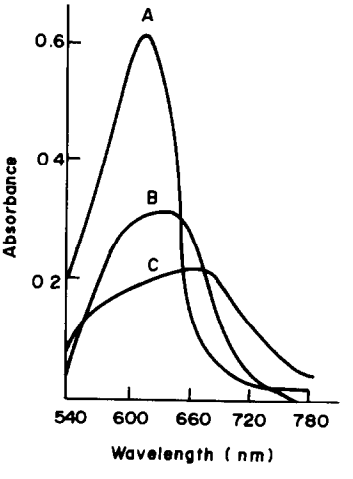

Fig. 1. Absorption spectra. (A) Reagent blank with Triton X-305, measured against water; (B) ion-association complex with Triton X-305, measured against reagent blank; (C) ion-association complex measured against reagent blank in absence of Triton X-305; As taken, 5 μg; 1-cm cells.

Table 1. Sensitivities of methods for the spectrophotometric determination of arsenic

Method	λ, nm	$l.mole^{-1}.cm^{-1}$	Ref.
Silver diethyldithiocarbamate (AgDDC)	535	1.4×10^4	8
Arsenomolybdenum blue	650	2.6×10^4	1,2
Arsenoantimonomolybdenum blue	860	2.1×10^4	4,5
4-Nitrosocatechol/Brilliant Green	637	1.09×10^5	7
Present method	640	1.13×10^5	This paper

Table 2

	Present method				
Sample	Found, *ng/ml*	Added, *ng/ml*	Total, *ng/ml*	Recovery, %	AgDDC method,[8] *ng/ml*
1	14.0	120	128	95	10
	14.4	120	132	98	
	16.0	120	134	98	
2	41.8	40.0	83.4	104	38
	38.6	40.0	82.2	109	
	39.6	40.0	82.8	108	
			Average	102	
			Std. devn.	6	

RESULTS AND DISCUSSION

Absorption spectra

The absorption spectra of the ion-association complex and the reagent blank in presence of Triton X-305 have been measured over the range 540–780 nm. The absorption maximum of the complex is at 640 nm and that of the reagent blank at 610 nm (Fig. 1). The molar absorptivity of the complex is increased 35% by the presence of Triton X-305. Consequently, in further experiments, the absorbance was measured at 640 nm against a reagent blank in presence of Triton X-305.

Effect of acidity

The optimum acidity for formation of the complex was found to be 0.8–1.2*N* sulphuric acid. If the sulphuric acid concentration is less than 0.8*N* or more than 1.2*N*, the complex is less easily formed; the antimony(III) will be hydrolysed at lower acidity. Hence 1.0*N* sulphuric acid was chosen for the colour development.

Effect of amounts of reagents

In 25 ml of final solution, 2–5 ml of 0.1% Triton X-305/MG solution gives maximum and constant absorbance with 5 μg of arsenic, so use of 3 ml of the mixed reagent solution is recommended for the determination. The amounts of other reagents given in the procedure are optimal.

Characteristics of the complex

At room temperature, the complex is completely formed in 20 min, and the absorbance remains stable for about 90 min.

Beer's law is obeyed over the range 0–5 μg of arsenic in 25 ml of solution, at 640 nm. The apparent molar absorptivity (with respect to arsenic) is 1.13×10^5 l.mole^{-1}.cm^{-1} at 640 nm. For 10 parallel determinations of 5 μg of arsenic, the standard deviation found was 0.04 μg.

Comparison with other methods

The method described is one of the most sensitive available and compares favourably with others for the spectrophotometric determination of arsenic. The sensitivities of various methods are listed in Table 1. The method can be used for determining arsenic in waters, rocks and steels, if combined with separation of the arsenic by evolution as arsine, which is absorbed in a solution of iodine in sodium bicarbonate solution; the arsenate thus produced is then determined by the procedure described. Only the inorganic arsenic compounds in water samples are thus determined.[8] The components of the absorption solution do not interfere. Some results for water analysis are given in Table 2.

Acknowledgement—We wish to thank Professor Deng-Ze Xue of Northwest Agricultural College, China, for valuable discussions during the course of this work.

REFERENCES

1. D. Rogers and A. E. Heron, *Analyst*, 1946, **71**, 414.
2. M. Daniels, *ibid.*, 1957, **82**, 133.
3. R. Milton and W. D. Duffield, *ibid.*, 1942, **67**, 279.
4. Huang Zu-Xian, *Fenxi Huaxue*, 1981, **3**, 329.
5. E. Kitazume and K. Yagi, *Bunseki Kagaku*, 1981, **30**, 608.
6. Z. A. Karapelyan, F. V. Mirzoyan, V. M. Taravan and L. G. Mushegyan, *Arm. Khim. Zh.*, 1980, **33**, 206.
7. K. Kuwada, S. Motomizu and K. Toei, *Bunseki Kagaku*, 1977, **26**, 609.
8. *Standard Methods for the Analysis of Water and Waste Water*, 14th Ed., P. 283. American Public Health Association, Washington, D.C., 1976.

Talanta, Vol. 30, No. 4, pp 277–278, 1983
Printed in Great Britain

0039-9140/83/040277-02$03.00/0
Pergamon Press Ltd

SIMULTANEOUS DETERMINATION OF DECACHLOROBIPHENYL, OCTACHLORONAPHTHALENE AND DECACHLORO-1,4-DIHYDRONAPHTHALENE IN MIXTURES, BY HPLC

ZLATA IVANOV, R. J. MAGEE and L. MARKOVEC
Department of Inorganic and Analytical Chemistry, La Trobe University, Bundoora, Victoria 3083, Australia

(*Received* 22 *July* 1982. *Accepted* 21 *October* 1982)

Summary—Gas–liquid chromatography cannot distinguish between octachloronaphthalene and decachloro-1,4-dihydronaphthalene, because of the dechlorination of the latter during the chromatographic separation. High-pressure liquid chromatography on S50DS in the reverse-phase mode, with methanol as the solvent, has been successfully used in analytical (both qualitative and quantitative) and semi-preparative applications, involving the major products of the perchlorination of PCBs and PCNs: decachlorobiphenyl, octachloronaphthalene and decachloro-1,4-dihydronaphthalene.

The discovery of polychlorinated biphenyls (PCBs) in environmental samples brought about investigations into their separation. Most industrial and environmental samples also contain various amounts of polychlorinated naphthalenes (PCNs), which themselves have been recognized as serious environmental pollutants. The quantitative analysis of environmental samples is routinely based on a comparison of the gas–liquid chromatographic pattern of the sample with the GLC profiles of commercial products (e.g., Aroclors®) usually for one (or a few) prominent peak(s) in the chromatogram. The actual presence of PCNs is frequently either unnoticed or neglected, regardless of the fact that the relationship between the toxicity and degree of chlorination of PCNs does not follow the pattern for PCBs.[1]

To simplify the analysis of PCBs, PCNs and their mixtures, it has been suggested that all the members of a given series be converted into a single compound. This might be achieved either by complete dechlorination[2] to naphthalene and biphenyl, or by perchlorination[3–6] to octachloronaphthalene (OCN) and decachlorobiphenyl (DCB), respectively. In the latter case, DCB is the final product of chlorination of PCBs, but PCNs could easily be overchlorinated to decachloro-1,4-dihydronaphthalene (DCDHN).[4,7] In this paper, some problems connected with both the qualitative and quantitative determination of DCB, OCN and DCDHN in their mixtures have been examined in detail.

It was found that DCDHN easily loses chlorine during any analytical treatment involving higher temperatures. It is fully converted into OCN during GLC, which renders the GLC methods useless, as OCN and DCDHN then both give identical GLC traces. Similarly, DCDHN loses chlorine during mass-spectroscopic examination. However, in contrast to Hutzinger *et al.*,[4] we have been able to recognize the presence of DCDHN in the mass spectrum. Although the parent (molecular) ion of DCDHN is undetectable under normal conditions, the $C_{10}Cl_9^+$ ion (*i.e.*, the $[M - Cl]^+$ ion) always gives a strong and detectable signal even at low concentrations of DCDHN in the sample. However, it is difficult to confirm or exclude the presence of OCN in such a sample, as under electron impact DCDHN loses even more chlorine and the most predominant ion $[M - 2Cl]^+$ has the same m/z as the molecular ion of OCN.

Because of the shortcomings found in the use of GLC, attention was turned to high-pressure liquid chromatography (HPLC), which does not require the use of high temperatures. By this means previous methods for the separation of OCN and DCB[6–8] have been improved and simultaneous separation of these two compounds from DCDHN and other minor components present in mixtures from the perchlorination of naphthalene or PCNs has been achieved.

As an extension to the work, standard DCDHN was prepared by means of the BMC chlorination of naphthalene[7,9] with subsequent semi-preparative HPLC separation of the DCDHN from the reaction products, which also contained substantial quantities of a $C_{10}Cl_{10}H_2$ compound (which was not examined further) and smaller amounts of OCN and other compounds.

A routine HPLC separation of all three compounds (DCB, DCDHN and OCN), together with $C_{10}Cl_{10}H_2$ and other impurities, is shown in Fig. 1. Any of these components may be determined by use of standard compounds. Changing the detection wavelength (see Fig. 1) may improve the accuracy and sensitivity.

EXPERIMENTAL

The reagents used and the standard DCB and OCN were commercially available. DCDHN was prepared by perchlorination of naphthalene by means of a modified

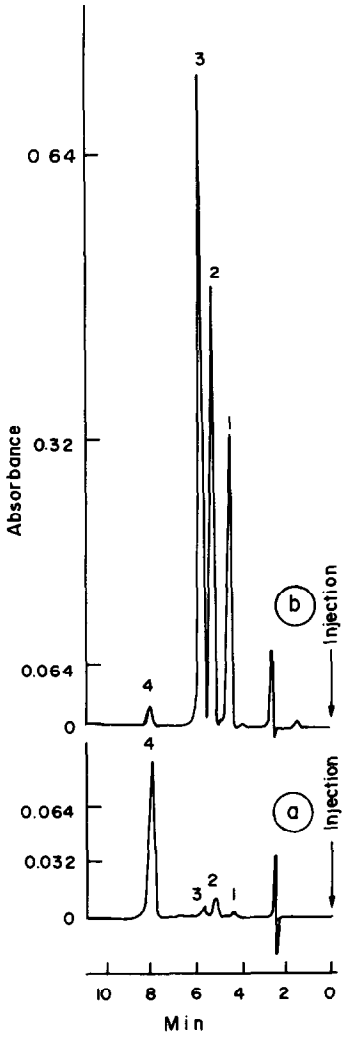

Fig. 1. HPLC separation of a mixture of standard DCB, standard OCN and crude DCDHN: (1) $C_{10}Cl_{10}H_2$; (2) DCDHN ($C_{10}Cl_{10}$); (3) DCB ($C_{12}Cl_{10}$); (4) OCN ($C_{10}Cl_8$); (a) 270 nm, attenuation 64; (b) 230 nm, attenuation 128. Column 150 × 4.6 nm S50DS. Precolumn 50 × 4.6 mm S50DS. Solvent flow 1 ml/min MeOH. Injection 20 μl. Sample: 50 ppm DCB, 30 ppm OCN and 90 ppm of the recrystallized product of naphthalene perchlorination, all dissolved in a mixture of equal volumes of MeOH and CH_2Cl_2.

BMC chlorination method.[9] The reaction always yielded 60–70% DCDHN together with other chlorination products, *e.g.*, the $C_{10}Cl_{10}H_2$ compound (product of simultaneous chlorination and hydrochlorination of naphthalene), OCN and minor impurities. The crude reaction product was recrystallized from diethyl ether and separated by preparative HPLC. The resulting DCDHN was more than 99.8% pure. The melting point of 208° (DTA), ultraviolet spectrum (absorption maximum at 233 nm) and facile transition into OCN with loss of chlorine were in agreement with published data.[4,7,9]

The analytical HPLC system consisted of an Altex 100A pump, an Altex 210 injection valve with a 20-μl injection loop, a Perkin–Elmer LC75 variable wavelength ultraviolet detector and a Perkin–Elmer Model 561 recorder. A 150 × 4.6 mm column with a 50 × 4.6 mm precolumn, packed with Spherisorb[R] S50DS, was found most suitable. The column and precolumn were purchased from Chromatographic Systems, Melbourne. Satisfactory separations were achieved with pure methanol at a flow-rate of 1 ml/min (see Fig. 1). Even better separations could be achieved with aqueous methanol, or longer columns, but the system described was preferred because of the conveniently short elution times.

The semi-preparative HPLC system was similar to the analytical one, but the injection loop was increased to 50 μl and the column to 245 × 10 mm with a 50 × 10 mm precolumn, again with S50DS packing. The flow-rate of methanol was 4 ml/min. The sample was injected as a 1.3% solution (in dichloromethane) of the recrystallized product from the chlorination of naphthalene.[9] Fractions were collected manually. The solvent was evaporated on a rotary evaporator under reduced pressure. Because of the sensitivity of DCDHN to changes during solvent evaporation, the use of aqueous methanol in preparative runs was avoided.

REFERENCES

1. M. A. Campbell, S. Bandiera, L. Robertson, A. Parkinson and S. Safe, *Toxicology*, 1981, **22**, 123.
2. A. De Kok, R. B. Geerdink, R. W. Frei and U. A. Th. Brinkman, *Intern. J. Environ. Anal. Chem.*, 1981, **9**, 301.
3. J. A. Armour, *J. Assoc. Off. Anal. Chem.*, 1973, **56**, 987.
4. O. Hutzinger, S. Safe and V. Zitko, *Intern. J. Environ. Anal. Chem.*, 1972, **2**, 95.
5. O. Hutzinger, W. D. J. Jamieson, S. S. Safe and V. Z. Zitko, *J. Assoc. Off. Anal. Chem.*, 1973, **56**, 982.
6. U. A. Th. Brinkman, G. DeVries, A. De Kok and A. L. De Jonge, *J. Chromatog.*, 1978, **152**, 97.
7. M. Ballester, J. Castaner, J. Riera and J. Pares, *An. Quim., Ser. C*, 1980, **76**, 157.
8. U. A. Th. Brinkman and H. G. M. Reymer, *J. Chromatog.*, 1976, **127**, 203.
9. A. F. Andrews, C. Glidewell and J. C. Walton, *J. Chem. Res. (M)*, 1978, 3683.

Talanta, Vol. 30, No. 4, pp. 279–281, 1983
Printed in Great Britain

0039-9140/83/040279-03$03.00/0
Pergamon Press Ltd

DETERMINATION OF NITRITE AND MIXTURES OF BROMIDE AND IODIDE WITH *o*-IODOSOBENZOATE

KRISHNA K. VERMA and ANIL K. GULATI
Department of Chemistry, University of Jabalpur, Jabalpur 482001, India

(*Received* 5 *July* 1982. *Accepted* 1 *November* 1982)

Summary—Nitrite diazotizes sulphanilamide, which then does not undergo 3,5-dibromination. Nitrite can therefore be determined by reaction with excess of sulphanilamide, the surplus of which is then titrated with *o*-iodosobenzoate or chloramine-T in the presence of potassium bromide, with Methyl Red as indicator. Mixtures of iodide and bromide can be analysed by oxidation of the iodide with excess of *o*-iodosobenzoate at pH 4–6, followed by extraction of the iodine (which is then titrated with thiosulphate) and then oxidation of the bromide in dilute sulphuric acid medium in the presence of sulphanilamide as bromine scavenger, the residual oxidant being evaluated iodometrically.

A number of analytical methods using *o*-iodosobenzoate have been reported[1] and this communication describes some further applications.

EXPERIMENTAL

Reagents

o-Iodosobenzoate solutions, 0.05 and 0.02M. Prepared as described previously.

Chloramine-T solution, 0.02M. Standardized iodometrically.[2]

Sulphanilamide solution, 0.01M. Treat 0.43 g of sulphanilamide with 2 ml of glacial acetic acid and dilute to 250 ml with water.

Sulphanilamide solution, 1%, in 2% sulphuric acid.

Methyl Red. A 0.04% solution in ethanol.

Sodium thiosulphate solution, 0.04M.

Samples

High-purity test materials were dissolved in water and the solutions standardized, the nitrite solutions by oxidation with chloramine-T,[3] and the halide solutions by argentometry.[4]

Determination of nitrite

Dissolve an accurately weighed amount of sample in 20 ml of water, or take an aliquot of a solution of it, add a measured (and excessive) volume of 0.01*M* sulphanilamide and 2 ml of 5% sulphuric acid. Swirl for 30 sec, add 0.5 g of potassium bromide, 5 ml of 5% sulphuric acid, 20 ml of methanol and 2 or 3 drops of Methyl Red indicator, and titrate the residual sulphanilamide with 0.02*M* *o*-iodosobenzoate or chloramine-T till the indicator is bleached. Run a blank determination on the same volume of sulphanilamide.

$$NO_2^-\,(\text{mg}) = 11.5\ m\Delta V$$

where ΔV is the difference between the two titration volumes (ml) of *o*-iodosobenzoate or chloramine-T (molarity m).

Determination of bromide

To an aliquot of sample solution, add 5 ml of 1% sulphanilamide solution (in sulphuric acid), 5 ml of 5% sulphuric acid, and a measured (excessive) volume of 0.05*M* *o*-iodosobenzoate. Swirl for 30 sec, add 1 g of potassium iodide and titrate the liberated iodine with 0.04*M* thiosulphate. Do a blank determination on the same volume of *o*-iodosobenzoate.

$$Br^-\,(\text{mg}) = 40\ m'\Delta V'$$

where $\Delta V'$ is the difference in titration volume (ml) and m' the molarity of the thiosulphate solution.

Analysis of mixtures of iodide and bromide

Take an aliquot of sample solution in a 150-ml separatory funnel, add 5 ml of acetate buffer (pH 4), 30 ml of water, 10 ml of chloroform and a measured (excessive) volume of 0.05*M* *o*-iodosobenzoate. If a precipitate of *o*-iodosobenzoic acid appears at this stage, discard the solution and repeat the determination, adding more water before introducing the reagent. Shake the contents for 1 min and extract the liberated iodine with three 10-ml portions of chloroform (*o*-iodosobenzoic acid is not soluble in chloroform or carbon tetrachloride.) To the combined chloroform extracts add 50 ml of water and 1 g of potassium iodide and titrate with 0.04*M* thiosulphate.

$$I^-\,(\text{mg}) = 127\ V''m''$$

where V'' is the volume of thiosulphate (molarity m'') used.

Transfer the aqueous phase from the extraction to a 250-ml Erlenmeyer flask, add 5 ml of 1% sulphanilamide solution (in sulphuric acid) and 5 ml of 5% sulphuric acid. Shake for 30 sec, add 1 g of potassium iodide and titrate with 0.04*M* thiosulphate. Run a blank determination on the same volume of *o*-iodosobenzoate.

$$Br^-\,(\text{mg}) = 40(\Delta V' - V'')m''$$

where $\Delta V'$ is the difference between the two titration volumes of thiosulphate (molarity m'') for the blank and residual *o*-iodosobenzoate.

If desired, use 0.04*M* thiosulphate (molarity m'') for the iodide determination and 0.05*M* (molarity m''') for the bromide. In that case

$$Br^-\,(\text{mg}) = 40(\Delta V'm''' - V''m'')$$

RESULTS AND DISCUSSION

Over the pH range 4–6, only iodide is oxidized to iodine by *o*-iodosobenzoate:

$$2HI + OI\cdot C_6H_4\cdot CO_2H \rightarrow I_2 + H_2O + I\cdot C_6H_4\cdot CO_2H$$

The extracted iodine can be titrated with thiosulphate or with *o*-iodosobenzoate to an Andrews

end-point. Alternatively, a 6-fold amplification method[5,6] may be used, involving stripping the iodine by shaking with 2 ml of 1% ascorbic acid solution, oxidizing the resulting iodide to iodate with bromine, and titrating it iodometrically after destroying the surplus bromine by reaction with formic acid. With this amplification method the equations are

$$I^-(mg) = 21.17\ V''m''$$

$$Br^-(mg) = 40\ (\Delta V'm''' - V''m''/6)$$

where the symbols have the same meaning as before.

Bromide is oxidized to bromine by *o*-iodosobenzoate in sulphuric acid medium, the liberated bromine being immediately consumed in a substitution reaction with sulphanilamide:

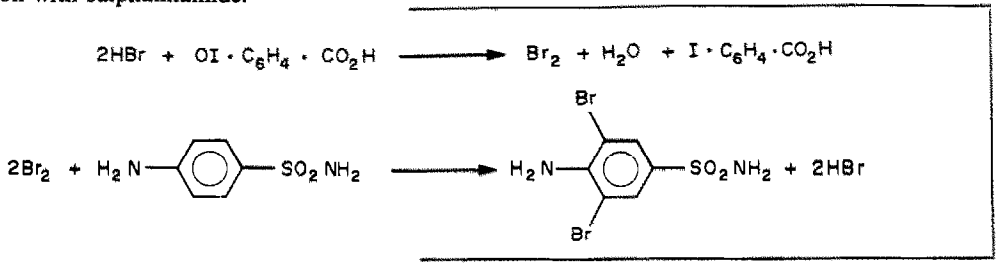

The bromide thus formed is again oxidized by *o*-iodosobenzoate and this reaction sequence continues till all the bromide has been used up in substitution. Thus

$$Br^- \equiv OI \cdot C_6H_4 \cdot CO_2H \equiv 2S_2O_3^{2-}$$

Neither *o*-iodosobenzoate nor the iodine released in the iodometric evaluation of the surplus oxidant reacts with sulphanilamide.

Nitrite diazotizes the amino-group of sulphanilamide in acid medium, blocking the 3,5-dibromination reaction.[3] Hence

$$NO_2^- \equiv H_2N \cdot C_6H_4 \cdot SO_2NH_2$$

$$\equiv 2Br_2 \equiv 2OI \cdot C_6H_4 \cdot CO_2H$$

The diazotized sulphanilamide does not interfere in the bromometric titration of the residual sulphanilamide.

The most widely used method for the titrimetric determination of nitrite involves oxidation with permanganate,[7] but the reaction is slow and suffers from decomposition and aerial oxidation of the nitrite. Oxidation with chloramine-T is rapid and yields precise results.[3] Reduction of nitrite with ascorbic acid has also been used[8] but seems to have little value; it is a reverse filtration (with the sample solution in the burette), and nitrate interferes quantitatively.

Table 1. Determination of nitrite, bromide and iodide

Substance taken, *mg*		Substance found*			
I	II	I, *mg*	CV, %	II, *mg*	CV, %
$NaNO_2$					
0.34		0.34	0.3		
0.42		0.43	0.3		
0.51		0.51	0.2		
0.59		0.59	0.1		
1.79		1.77	0.1		
3.59		3.56	0.2		
4.47		4.45	0.2		
5.38		5.34	0.3		
6.28		6.25	0.3		
KBr					
0.69		0.70	0.2		
1.21		1.18	0.2		
3.68		3.66	0.3		
6.24		6.26	0.1		
10.36		10.32	0.1		
15.66		15.68	0.2		
20.58		20.52	0.3		
25.29		25.34	0.4		
KBr	KI				
0.66	30.18	0.67	0.4	30.06	0.2
1.24	25.76	1.25	0.3	25.62	0.3
3.86	20.60	3.85	0.2	20.52	0.3
6.52	15.21	6.55	0.2	15.16	0.1
12.39	8.37	12.26	0.1	8.30	0.1
16.25	3.14	16.12	0.2	3.16	0.2
20.66	1.82	20.59	0.3	1.83	0.3
25.78	0.60	25.59	0.4	0.59	0.3
30.63	0.52	30.86	0.4	0.52	0.3

*Average of 6 replicates; CV = coefficient of variation.

The amplification method for iodide involving oxidation with bromine[5,6] naturally tolerates large quantities of bromide but that using periodate gives higher blank values if bromide is also present.[9,10] Determination of bromide in the presence of iodide is troublesome, the best procedure perhaps being argentometric titration, with use of adsorption indicators.[4]

The methods described here do not require any critical control of reaction conditions and the results are accurate and precise (Table 1).

Interferences

Any reducing species in the sample will cause a positive error. Sulphite, thiosulphate, sulphide, thiocyanate, arsenic(III), antimony(III) interfere severely.

Acknowledgement—Thanks are due to the Council of Scientific and Industrial Research (New Delhi) for a Senior Research Fellowship to AKG.

REFERENCES

1. K. K. Verma and A. K. Gupta, *Talanta*, 1982, **29**, 779, and references therein.
2. A. Berka, J. Vulterin and J. Zýka, *Newer Redox Titrants*, p. 37. Pergamon Press, Oxford, 1965.
3. J. Agterdenbos, *Talanta*, 1970, **17**, 238.
4. A. I. Vogel, *Text-Book of Quantitative Inorganic Analysis*, 4th Ed., p. 339. Longmans, London, 1978.
5. R. Belcher, S. S. T. Liao and A. Townshend, *Talanta*, 1976, **23**, 541.
6. D. Amin and M. S. Al-Ajely, *ibid.*, 1981, **28**, 955.
7. I. M. Kolthoff, R. Belcher, V. A. Stenger and G. Matsuyama, *Volumetric Analysis*, Vol. III, p. 69. Interscience, New York, 1957.
8. N. Rukmini, V. S. N. P. Kavitha and K. R. Rao, *Talanta*, 1980, **27**, 593.
9. R. Belcher, J. W. Hamya and A. Townshend, *Anal. Chim. Acta*, 1970, **49**, 570.
10. S. A. Rahim, S. W. Bishara and D. Amin, *Talanta*, 1977, **24**, 681.

Talanta, Vol. 30, pp 282–284, 1983
Printed in Great Britain.

0039-9140/83/040282-03$03.00/0

PHOTOCHEMICAL THALLIMETRIC OXIDATIONS—ESTIMATION OF FORMIC ACID*

S. R. SAGI, K. APPA RAO and M. S. PRASADA RAO
Inorganic Chemistry Laboratories, Andhra University, Waltair 530003, India

(*Received* 27 *August* 1982. *Accepted* 1 *November* 1982)

Summary—A simple, rapid and convenient redox method has been developed for the estimation of formic acid. Formic acid is photochemically oxidized with thallium(III) in the presence of bromide as catalyst, and the thallium(I) formed is determined by titration with potassium bromate. The procedure can also be used for the estimation of thallium(III) with formic acid as reductant.

Den Boef and Polak[1] have surveyed the oxidation of organic compounds by strong oxidants, and concluded that the main difficulty in use of moderately strong oxidants is that the reactions generally do not proceed to give the ultimate oxidation products, *viz.* carbon dioxide and water, and are not stoichiometric. This lack of stoichiometry does not arise with strong oxidizing agents, which usually give complete oxidation to carbon dioxide and water, and is achieved by selecting the reaction medium, changing the pH of the medium at a particular stage of the reaction, or using a suitable catalyst.

Many organic compounds are easily oxidized to formic acid, but further oxidation to carbon dioxide and water is very difficult, especially in acid medium. Hence, any method by which formic acid can be quantitatively oxidized to a definite oxidation stage should yield good results, with a definite stoichiometry.

The redox methods available for the estimation of formic acid involve oxidation with mercuric chloride,[2–8] lead tetra-acetate,[9] telluratoargentate(III),[10–12] telluratocuprate(III),[10,12,13] periodatocuprate(III),[10,11] iodine,[14] bromine,[15,16] *N*-bromosuccinimide,[17] *N*-bromoacetamide,[18] iodine chloride,[19] potassium manganate,[20] potassium permanganate[21] and cerium(IV).[22–24] Most of the methods are indirect determinations with tedious procedures and have various limitations. Hence there is a need for a simple, convenient, and direct method for the estimation of formic acid at room temperature.

Following our successful use of thallium(III) for photochemical oxidation of oxalic acid[25] we have applied the same technique to estimation of formic acid.

EXPERIMENTAL

Reagents

Thallium(III) hydroxide was prepared as reported earlier[26] and dissolved in suitable amounts of perchloric or sulphuric acid. The thallium content was estimated iodometrically[27] and verified by other methods.[26,28] Formic acid solutions were prepared by appropriate dilution of the concentrated acid. They were standardized by the potassium permanganate method.[21] All other reagents were of analytical reagent grade.

Apparatus

Though the photochemical reaction used takes place much faster under direct sunlight, the light-intensity is variable, so all the investigative work was done with a Phillips high-pressure mercury vapour lamp (200/250 V; 125 W) as the light-source. The solutions were irradiated in colourless glass containers.

Recommended procedure

To an aliquot containing 0.1–1.0 mmole of formic acid, in a 200-ml beaker, add 20 ml of 1*M* perchloric acid, 0.75 mmole of bromide, 3 mmole of thallium(III) and dilute to 100 ml. Stir and expose to light from a high-pressure mercury vapour lamp for 30 min (or keep in bright sunlight for 5 min). Add 25 ml of concentrated hydrochloric acid and 0.1 ml of 0.1% Methyl Orange solution, heat to 60° and titrate with 0.05*N* potassium bromate (1.392 g/l.) until the indicator is destroyed. The blank correction is negligible. This method is also applicable in dilute sulphuric acid medium.

Procedure for estimation of thallium(III)

To an aliquot containing 0.1–0.5 mmole of thallium(III) in a 200-ml beaker add 20 ml of 1*M* perchloric acid 0.025 mmole of bromide, 1.5 mmole of formic acid and dilute to 100 ml with water. Expose the reaction mixture to the light from the mercury vapour lamp for 90 min (or keep under bright sunlight for 15 min). Determine the thallium(I) formed, as already described. The results obtained are quite satisfactory. This method is also applicable in sulphuric acid medium.

RESULTS AND DISCUSSION

Effect of light on the redox reaction

Nitric acid oxidizes organic material in the presence of light,[29,30] so only perchloric acid and sulphuric acid were used. Since the medium effects are minimal in perchloric acid, this acid was used first. It was found that in this medium formic acid is quantitatively oxidized with thallium(III) in about 5 hr at room temperature, under the direct light from the mercury vapour lamp. In the dark the oxidation is not complete at room temperature even after 24 hr.

*This article is dedicated to the late Professor G. Gopala Rao, former Regional Editor, *Talanta*, and pioneer in the utilization of photochemical reactions in analytical chemistry.

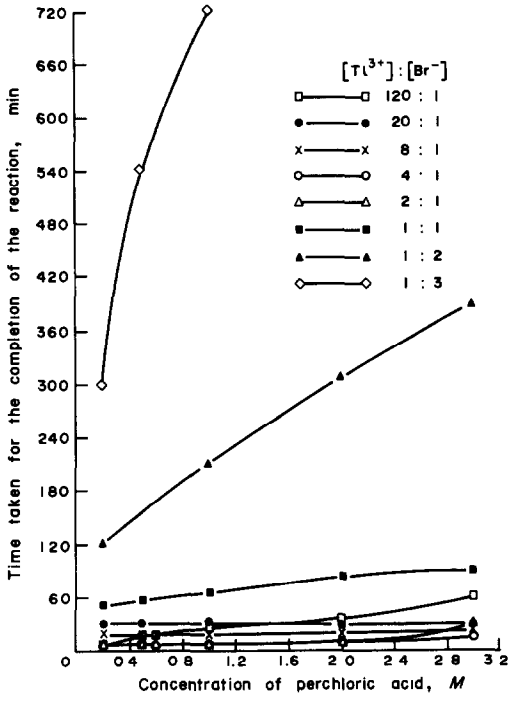

Fig. 1. Effect of $[H^+]$ and $[Br^-]$ on the rate of photochemical oxidation of formic acid by thallium(III). Volume of reaction mixture, 100 ml; amount of thallium(III), 0.75 mmole; amount of formic acid, 0.125 mmole.

Effect of halide

Low concentrations of chloride and bromide catalyse the photochemical reaction of thallium(III) with oxalic acid,[25] but only bromide catalyses the formic acid reactions. Chloride retards the reaction at all concentrations, bromide at low concentrations catalyses the reaction and fluoride has no effect.

Formic acid does not interfere[31] in the titration of thallium(I) with bromate,[32-34] so this titration was used for monitoring the progress of the photochemical reaction. In $\geqslant 2M$ perchloric acid medium the decolorization of Methyl Orange (as indicator) is slow, therefore Brilliant Ponceaux 5R was used instead. In the other media either indicator could be used.

Thallium(III) and formic acid were found to react in 1:1 molar ratio and the rate of the reaction was found to increase with increase in thallium(III) concentration but become maximal and constant when the concentration ratio of thallium(III) to formic acid is $\geqslant 6$. Hence this was taken as the initial ratio and the effect of acid and bromide concentration on the photochemical reaction was studied in perchloric acid medium. The results are presented in Fig. 1, from which it is clear that bromide at relatively low concentrations catalyses the reaction, the optimal concentration being a quarter of that of the thallium(III). The effect of the acid concentration under these conditions was then examined, and gave the results summarized in Table 1.

The results in Table 1 indicate that when the concentration of perchloric acid is about $1.0M$ and the thallium(III)/formic acid ratio is at least 3, quantitative photochemical oxidation takes place in about 15 min.

Typical results obtained by the recommended procedure are given in Table 2.

Table 2. Estimation of formic acid

Taken, *mmole*	Found, *mmole*
0.1071	0.1075
0.1284	0.1285
0.2550	0.2540
0.3400	0.3405
0.4250	0.4230
0.5024	0.5020
0.5874	0.5870
0.8746	0.8760

Interferences

Chloride and nitrate interfere. Zn^{2+}, Cu^{2+}, Cd^{2+}, Mg^{2+} and Na^+ do not interfere. Fe^{3+}, Mn^{2+} and Cr^{3+} drastically inhibit the reaction even when present in only small amounts.

REFERENCES

1. G. den Boef and H. L. Polak, *Talanta*, 1962, **9**, 271.
2. F. Auerbach and W. Plüddemann, *Arb. Kais. Gesundheitsamt*, 1909, **30**, 178; *Chem. Abstr.*, 1910, **4**, 2080.
3. H. Franzen and G. Greve, *J. Prakt. Chem.*, 1929, **78**, 125.
4. S. Bose, *J. Indian Chem. Soc.*, 1958, **35**, 320.
5. R. M. Verma and S. Bose, *ibid.*, 1960, **37**, 47; *Proc. Natl. Acad. Sci. India*, 1961, **30**, 171.
6. L. Maros, M. Pintér-Szakács and E. Schulek, *Anal. Chim. Acta*, 1961, **25**, 546.
7. P. Fuchs, Z. *Anal. Chem.*, 1929, **78**, 125.
8. R. G. C. Oldeman, *Pharm. Weekblad*, 1931, **68**, 379.
9. A. S. Perlin, *Anal. Chem.*, 1954, **26**, 1053.

Table 1. Effect of thallium(III) and perchloric acid concentration on the rate of photochemical oxidation of formic acid (0.125 mmole) with thallium(III), (total volume 100 ml, bromide one quarter of the molar amount of thallium)

	Time for the completion of the reaction, *min*						
$[HClO_4]$, M	0.125*	0.25*	0.375*	0.50*	0.75*	1.00*	1.25*
0.1	Thallium(III) hydrolysed						
0.2	360	25	15	15	10	10	10
0.5	420	25	15	15	10	10	10
1.0	>420	30	15	15	10	10	10
2.0	>420	40	25	25	15	15	10
3.0	>420	40	30	25	15	15	15

*Amount of Tl(III) taken, *mmole*.

10. P. K. Jaiswal and K. L. Yadava, *J. Indian Chem. Soc.*, 1979, **56,** 425.
11. P. K. Jaiswal, *Mikrochem. J.*, 1972, **17,** 200; *Chim. Anal. (Paris)*, 1971, **53,** 631.
12. P. K. Jaiswal and S. Chandra, *Chim. Anal. (Paris)*, 1969, **51,** 493.
13. S. Bose and N. Nair, *J. Indian Chem. Soc.*, 1974, **51,** 505.
14. R. M. Verma and S. Bose, *ibid.*, 1961, **38,** 109.
15. *Idem, ibid.*, 1962, **39,** 329.
16. J. V. L. Longstaff and K. Singer, *Analyst*, 1953, **78,** 491.
17. M. H. Hashmi, M. Sarwar and A. Rashid, *Pakistan J. Sci. Res.*, 1964, **16,** 158.
18. Gh. Balica, V. Piscati and S. Simion, *Rev. Chim. (Bucharest)*, 1968, **19,** 419.
19. P. P. Suprun, *Farm. Zh. (Kiev)*, 1967, **22,** 70; *Chem. Abstr.*, 1968, **68,** 48988j.
20. H. L. Polak, *Z. Anal. Chem.*, 1960, **176,** 34.
21. A. I. Vogel, *Quantitative Inorganic Analysis*, 3rd Ed., p. 301. Longmans, London, 1968.
22. N. N. Sarma and R. C. Mehrotra, *Anal. Chim. Acta*, 1955, **13,** 419.
23. N. K. Mathur, S. P. Rao and D. R. Chowdhury, *ibid.*, 1961, **24,** 533.
24. I. Khan and S. Bose, *Indian J. Appl. Chem.*, 1969, **32,** 165.
25. S. R. Sagi, G. S. P. Raju, K. A. Rao and M. S. P. Rao, *Talanta*, 1982, **29,** 413.
26. S. R. Sagi and K. V. Ramana, *ibid.*, 1969, **16,** 1217.
27. J. Proszt, *Z. Anal. Chem.*, 1928, **73,** 401; I. M. Kolthoff and R. Belcher, *Volumetric Analysis*, Vol. III, p. 370. Interscience, New York, 1957.
28. S. R. Sagi and M. S. P. Rao, *Talanta*, 1979, **26,** 52.
29. A. E. Tylor, G. E. Heckler and D. R. Percival, *ibid.*, 1961, **7,** 232.
30. R. Cultrera and G. Ferrari, *Anal. Chim. (Rome)*, 1958, **48,** 1410, 1419.
31. H. N. Halvorson and J. Halpern, *J. Am. Chem. Soc.*, 1956, **78,** 5562.
32. I. M. Kolthoff, *Rec. Trav. Chim.*, 1922, **41,** 172.
33. E. Zintl and G. Rienäcker, *Z. Anorg. Allgem. Chem.*, 1926, **153,** 276.
34. G. Rienäcker and G. Knauel, *Z. Anal. Chem.*, 1947, **128,** 459.

Talanta, Vol. 30, No. 4, pp 285–287, 1983
Printed in Great Britain

0039-9140/83/040285-03$03.00/0
Pergamon Press Ltd

A POLYSTYRENE-BASED MEMBRANE ELECTRODE SENSITIVE TO MOLYBDATE IONS

S. K. SRIVASTAVA, A. K. SHARMA and C. K. JAIN
Chemistry Department, Roorkee University, Roorkee (U.P.), India

(*Received* 17 *December* 1981. *Revised* 24 *August* 1982. *Accepted* 27 *October* 1982)

Summary—A polystyrene-based zirconium oxide membrane has been used to determine the concentration of molybdate ions in the range 0.5–$10^{-3}M$ and pH range 7–11. The response time is about 20 sec and the electrode remains usable for at least 6 months. It can also be used as an indicator electrode for titrations involving molybdate ions. Univalent anions interfere more strongly than bivalent and multivalent anions.

Inorganic gels, besides being used for separatory purposes, have been tried as membrane electrodes.[1,2] Hydrous zirconium oxide exhibits anion-exchange properties.[3,4] Investigations of the salt-rejection properties of dynamically formed hydrous zirconium oxide membranes[5,6] and of those formed on a microporous support[7] have been reported. We have examined the utility of this compound as a sensor material for a membrane electrode and found that a polystyrene-based membrane containing this compound shows promising selectivity for molybdate ions. The characteristics of this are reported in this paper.

EXPERIMENTAL

Reagents

All reagents used were analytical-grade. The hydrous zirconium oxide (HZO) gel was prepared and characterized by the method reported by Shor *et al.*[6]

Preparation of the membrane

Unsupported membranes of HZO could not be prepared. Membranes supported with a binder (polystyrene) were found to be quite stable and were therefore employed in these investigations. The following method[8] was used.

Polystyrene granules were heated in a glass tube in an oil-bath. The molten mass was allowed to cool and then ground to yield a product of 50-mesh particle size. The minimum amount of polystyrene needed for a fairly stable membrane was determined by trial and error. Membranes were obtained by mixing polystyrene and HZO in 1:9 w/w ratio and heating the homogeneous mass in a die of diameter 2.5 cm in a metallurgical-specimen mounting press at 120° under a pressure of 6500–7000 psi. By this method, membranes that were both mechanically and chemically fairly stable were obtained and were checked under a high-resolution microscope for any deformities or cracks.

Equilibration of membranes and potential measurements

Membranes thus obtained were equilibrated in 0.01M sodium molybdate for 2–3 days. The solution was changed four or five times at intervals during this period. Excess of the sodium molybdate solution was washed from the surface of the membrane. The equilibration time was determined in a preliminary investigation and it was observed that membranes equilibrated for shorter times did not give stable potentials.

The electrode assembly used for potential measurements was the same as that reported earlier,[2] and the reference solution was 0.01M sodium molybdate. All emf measurements were made at 25 ± 0.1° with a Radiometer (model PHM64) millivoltmeter coupled to a Servoscribe recorder. Ceramic-junction calomel reference electrodes were used.

RESULTS AND DISCUSSION

The potentials recorded with this membrane in contact with molybdate ions (concentration range 0.5–$10^{-5}M$) are shown in Fig. 1(a). The response is linear and practically Nernstian (slope −30 mV/pMo) over the concentration range 0.5—$10^{-3}M$.

The electrode response is fast, stable potentials being obtained within a few seconds, and no deviations are observed within an hour, after which a slow drift in potential occurs. The response time (static) was found to be 20 sec in dilute solutions ($10^{-3}M$) and a little more (30 sec) in more concentrated solution (0.1M). Repetition of the potential measurements gave a standard deviation of 0.5 mV in the higher concentration range and 0.6 mV in the low concentration range. It can be used for 6 months in a working range of two orders of magnitude of molybdate ion activity without showing any drift. If some

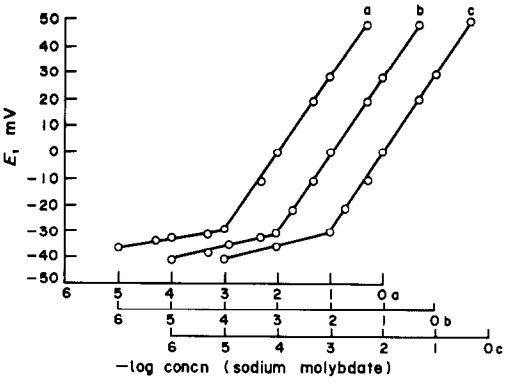

Fig. 1. Potential *vs.* log concentration of medium: (a) MoO_4^{2-}; (b) $Cl^- + MoO_4^{2-}$; and (c) $NO_3^- + MoO_4^{2-}$.

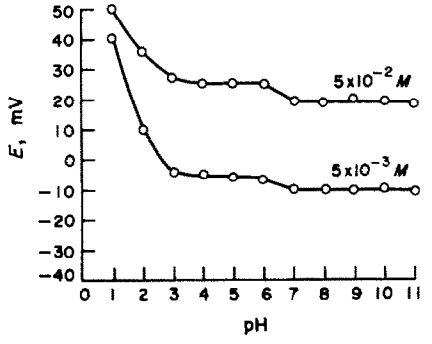

Fig. 2. Variation of membrane potential with pH, for two concentrations of molybdate.

contamination occurs, it can be removed by equilibrating the membrane with 0.01M sodium molybdate for 2–3 days. If this treatment fails, it is advisable to discard the electrode and prepare a new one.

The pH range in which this electrode can be used has also been determined (Fig. 2) at two molybdate concentrations and found to be 7–11. The sharp decrease in response slope on acidification, may be attributed to the formation of para-, tri- and tetramolybdate ions.[9] The electrode also appears to respond to protons at low pH.

The electrode assembly can also be used to measure molybdate ion concentration in partially non-aqueous media, up to a maximum of 25% v/v non-aqueous content. The response in 25% v/v methanol, ethanol and acetone is linear but not quite Nernstian (slopes of −32, −31 and −33 mV/pMo respectively). This, however, does not effect the functioning of the electrode system. The response time remains almost the same. If the non-aqueous content exceeds 30% there is an increase in response time and a drift in potential.

The performance of the electrode has been assessed in the presence of other ions and reported in terms of the selec-tivity coefficients ($k^{pot}_{A,B}$), determined by the fixed interference method.[10] The values obtained at two concentrations of the interfering ions are given in Table 1.

Table 1. Selectivity coefficient ($k^{pot}_{A,B}$) values for the hydrous zirconium oxide membrane electrode at 10^{-4} and $10^{-2}M$ concentrations of interfering ions, as determined by the fixed interference method

	$k^{pot}_{A,B}$	
Ion	$10^{-4}M$	$10^{-2}M$
Cl^-	12	15
SCN^-	14	18
ClO_4^-	14	18
NO_3^-	12	13
$C_2O_4^{2-}$	0.11	0.14
WO_4^{2-}	0.21	0.23
SO_4^{2-}	0.12	0.14
AsO_4^{3-}	0.029	0.034
PO_4^{3-}	0.016	0.020
$Fe(CN)_6^{4-}$	0.021	0.023

It is observed that the bivalent and multivalent anions have very low $k^{pot}_{A,B}$ values and would not interfere even if present at the same concentration as the molybdate. The selectivity coefficients for univalent anions are about 12–14. Normally a zero value of $k^{pot}_{A,B}$ is ideal but the values obtained for univalent anions are negligibly small in comparison with the values corresponding to equal electrode response to primary and interfering ion, calculated from the expression:[11] $a_A = k^{pot}_{A,B}(a_B)^{z/y}$, where z is the charge on the primary ion A (activity a_A) and y is the charge on the interfering ion B (activity a_B). Thus the molybdate electrode would exhibit equal response to molybdate and a univalent interfering ion at 10^{-2} for $k^{pot}_{A,B} = 10^2$, and $10^{-4}M$ for $k^{pot}_{A,B} = 10^4$.

When mixed-solution runs were made with chloride–molybdate and nitrate–molybdate mixtures at a fixed interfering ion concentration of $10^{-3}M$ and primary (molybdate) ion concentration varied from 10^{-5} to 0.5M, the potentials [Fig. 1(b), (c)] were the same as those in the calibration plot for molybdate [Fig. 1(a)] except at concentrations $< 10^{-3}M$ (where this electrode system is not usable anyway). At molybdate concentrations $< 10^{-3}M$, the ratio of interfering ion to molybdate was > 1, and there was a slight increase in slope (relative to that for molybdate alone).

The electrode has also been used as an end-point indicator in titrations involving molybdate ions. The titration of sodium molybdate with thorium nitrate is shown in Fig. 3. The break in the curve is quite sharp and reproducible, and corresponds to precipitation of $Th(MoO_4)_2$. The standard deviation (ten replicates) of these particular titrations was 0.07 ml.

The determination of molybdate ions with this membrane electrode is faster than the usual spectrophotometric procedures,[12] and more convenient.

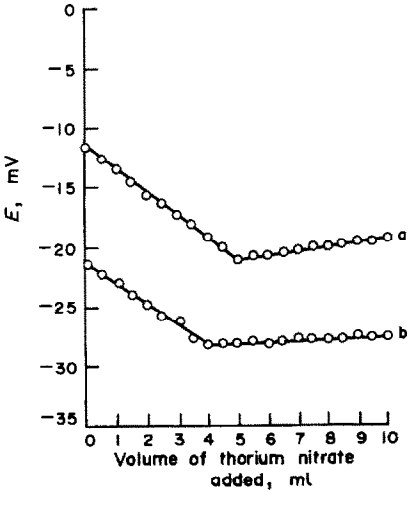

Fig. 3. Curves for titration of (a) 20 ml of 0.005M sodium molybdate with 0.01M thorium nitrate at pH 8; (b) 20 ml of 0.002M sodium molybdate with 0.005M thorium nitrate at pH 7.

REFERENCES

1. W. U. Malik, S. K. Srivastava and S. Kumar, *J. Electroanal. Chem.*, 1976, **72,** 111.
2. S. K. Srivastava, R. P. Singh and S. Agarwal, *J. Chem. Tech. Biotech.*, 1977, **27,** 680.
3. K. A. Kraus and H. O. Phillips, *J. Am. Chem. Soc.*, 1956, **78,** 249.
4. N. J. Singh and S. N. Tandon, *Talanta*, 1977, **24,** 459.
5. A. E. Marcinkowsky, K. A. Kraus, H. O. Phillips, J. S. Johnson, Jr., and A. I. Shor, *J. Am. Chem. Soc.*, 1966, **88,** 5744.
6. A. J. Shor, K. A. Kraus, W. T. Smith and J. S. Johnson, Jr., *J. Phys. Chem.*, 1968, **72,** 2200.
7. D. Freilich and G. B. Tonny, *J. Colloid Interface Sci.*, 1978, **64,** 362.
8. M. R. J. Wyllie and H. W. Patnode, *J. Phys. Chem.*, 1950, **54,** 204.
9. F. G. R. Gimblett, *Inorganic Polymer Chemistry*, p. 195. Butterworths, London, 1963.
10. G. G. Guilbault, *Ion-Selective Electrode Review*, 1979, **1,** 139.
11. G. E. Baiulescu and V. V. Coşofreţ, *Applications of Ion-Selective Membrane Electrodes in Organic Analysis*, p. 17. Horwood, Chichester, 1977.
12. Z. Marczenko, *Spectrophotometric Determination of Elements*. Horwood, Chichester, 1976.

Talanta, Vol. 30, No. 4, pp. 288–290, 1983
Printed in Great Britain.

0039-9140/83/040288-03$03.00/0

DETERMINATION OF PLATINUM IN URINE BY DIFFERENTIAL PULSE POLAROGRAPHY

O. VRÁNA, V. KLEINWÄCHTER and V. BRABEC*
Institute of Biophysics, Czechoslovak Academy of Sciences, 612 65 Brno, Czechoslovakia

(*Received* 18 *June* 1982. *Revised* 24 *August* 1982. *Accepted* 26 *October* 1982)

Summary—A method has been developed for determination of platinum in urine, after administration of *cis*-dichlorodiammineplatinum(II). The diethyldithiocarbamate complex of the platinum(II) is formed and extracted into chloroform, then mineralized with *aqua regia*. After removal of nitric acid the platinum is complexed with ethylenediamine. This chelate yields a catalytic current at a dropping mercury electrode, which is measurable by differential pulse polarography. The detection limit is ~10 ng/ml. The calibration graph is linear over the range 20–800 ng/ml.

The discovery of the potent anti-tumour activity of *cis*-dichlorodiammineplatinum(II) (*cis*-DDP) led to extensive development of methods for the detection and determination of platinum in biological materials. Several methods for routine determination of platinum in biological fluids have been published,[1–8] but the accuracy of most of them depends on the sample matrix. To eliminate matrix effects procedures have been based on wet or dry ashing of the sample[4,9,10] or on formation of an extractable platinum complex and its determination by ultraviolet spectroscopy,[5] liquid chromatography[5,6] or atomic-absorption spectroscopy (AAS).[7] Another AAS method overcomes the sample matrix effect by careful optimization of the instrument parameters.[8] Here we describe a procedure based on isolation of the platinum as its complex with sodium diethyldithiocarbamate (DDTC), and subsequent determination by differential pulse polarography (DDP). DPP is comparable to AAS in sensitivity and precision, but uses simpler instrumentation.

EXPERIMENTAL

Apparatus

DPP was performed with a PA 2 polarographic analyser (Laboratory Instruments, Prague) with a three-electrode system comprising a dropping mercury electrode (DME), spectroscopic-grade graphite counter-electrode and a saturated calomel reference electrode. The DME had a mercury flow-rate of 0.927 mg/sec. Polarograms were obtained with a pulse amplitude of −50 mV and a sweep-rate of 2 mV/sec. The drop-time control of the PA 2 analyser was set at 2.0 sec. The initial potential was −1.3 V.

Materials

The *cis*-DDP (Lachema, Czechoslovakia) was used without further purification. Standard platinum solution, 70 μg/ml, was prepared fresh each working day by dissolving *cis*-DDP in doubly distilled water. DDTC (Lachema) was dissolved in 0.1*M* sodium hydroxide, to make a 10% solution, prepared fresh each working day. Ethylenediamine and spectral grade chloroform were purchased from Fluka (Switzerland) and Lachema respectively. Human urine was obtained from volunteers not undergoing *cis*-DDP therapy, unless stated otherwise. All other chemicals were of analytical grade.

Preparation of calibration graph

Six 9-ml portions of platinum-free urine from the subject, withdrawn before administration of the *cis*-DDP, are mixed with 0, 5, 10, 20, 50 and 100 μl of standard platinum solution in glass test-tubes, and allowed to stand for 30 min. Then 1 ml of DDTC solution is added to each and the test-tubes are sealed and heated in a steam-bath for 15 min. The tubes are allowed to cool to room temperature, then opened, and exactly 4 ml of water-saturated chloroform are added to each. The mixture is vigorously mixed with a vortex-mixer for approximately 5 min, then 1 ml of 0.1*M* sodium hydrogen sulphide is added. After vigorous mixing for an additional 2–3 min, the mixture is centrifuged for 10 min at 1200 g, and after a brief "vortex" mixing, is centrifuged for 5 min. Exactly 2 ml of the chloroform extract are placed in a 50-ml glass beaker and evaporated to dryness on a steam-bath. The residue is converted into the platinum–ethylenediamine complex by dissolution in 4 ml of freshly prepared *aqua regia*, evaporation to dryness, dissolution in 2 ml of 12*M* hydrochloric acid, evaporation, dissolution in 2 ml of 0.025*M* ethylenediamine, evaporation, and dissolution in 2 ml of 0.01*M* ethylenediamine and a final evaporation. The residue is dissolved in 2 ml of supporting electrolyte (0.4*M* ethylenediamine–0.1*M* potassium chloride). After 2–10 min the sample is deoxygenated for 5 min with nitrogen and analysed by DPP. The height of the DPP peak (*I*) is measured at −1.65 V (Fig. 1) and a working graph of *I* *vs.* platinum concentration is plotted.

Sample preparation

A 9-ml sample of urine is placed in a glass test-tube, 1 ml of DDTC solution is added, and the mixture is then heated, *etc.*, as described above. The concentration of platinum is obtained from the working graph. If the DPP peak is markedly higher than the DPP peak of the highest standard, the solution for polarography is diluted in known ratio with a solution obtained by taking platinum-free urine through the analysis scheme, and the polarography is repeated.

*To whom correspondence and reprint requests should be directed.

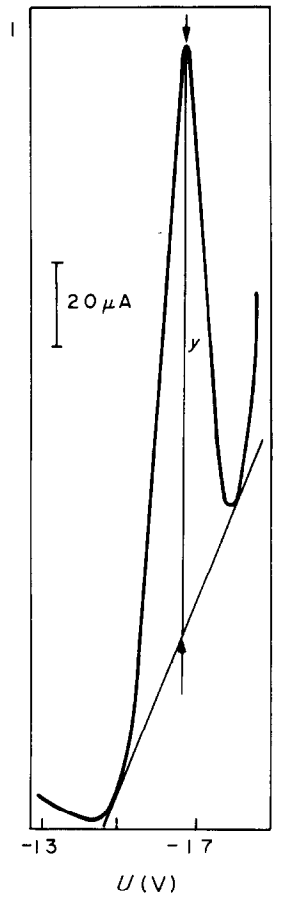

Fig. 1. Differential pulse polarogram of platinum–ethylenediamine complex in 0.1*M* potassium chloride–0.4*M* ethylenediamine medium. The complex was formed from *cis*-dichlorodiammineplatinum(II) in urine by the method outlined. The platinum concentration in the urine was 321 ng/ml. The height of the peak was taken as *y*.

RESULTS AND DISCUSSION

In the initial work on this determination, we used urine that had either received no pretreatment or had been digested with various mixtures of nitric, perchloric, hydrochloric and sulphuric acids and hydrogen peroxide, at various temperatures. However, no DPP response was obtained which could be exploited for determination of platinum in urine.

Recently a procedure for the determination of platinum in ores was proposed,[11] based on releasing platinum from the sample by successive treatment with *aqua regia* and hydrochloric acid, and subsequent formation of its ethylenediamine complex. This chelate was found to produce a well-defined DPP peak when polarographed in potassium chloride–ethylenediamine supporting electrolyte.[11,12] This peak has been supposed to correspond to a catalytic electrode reaction during which the platinum in the complex is reduced to a lower oxidation state which is highly reactive and reduces protons to hydrogen.[11,12] We tried, therefore, to exploit this procedure for determination of platinum in urine. The platinum–ethylenediamine chelate was first formed directly in the digest obtained by heating urine with *aqua regia*, evaporating to dryness and heating again with hydrochloric acid. However, the DPP peak corresponding to this chelate was poorly reproducible. The results so far described thus indicate that analysis of urine for platinum by DPP is unfavourably influenced by the matrix even after the digestion with acids.

Table 1. DPP peak-heights for platinum standards in urine obtained from different volunteers

Platinum, *ng/ml*	DPP peak-height,* *μA*		
	Sample 1†	Sample 2§	Sample 3‡
39	1.81	1.97	1.69
78	3.61	4.06	3.39
155	7.2_2	7.7_0	6.7_2
387	18.5_2	18.0_2	16.9_2
769	36.5	39.1	33.7

*Average of three determinations.
†From a man 26 years old.
§From a man 43 years old.
‡From a man 61 years old.

Chemical treatment of platinum in urine, aimed at yielding an extractable product, has proved useful as an approach to eliminate the matrix effects. We therefore decided to develop a method based on the initial formation of the platinum complex with DDTC,[5,6] but this complex proved to be DPP-inactive or to yield only a small, poorly reproducible peak at around −0.8 V in various supporting electrolytes. If, however, the complex was further decomposed with *aqua regia* and hydrochloric acid, and the platinum subsequently converted into its ethylenediamine complex, a reproducible and well-defined DPP peak at −1.65 V (Fig. 1) was obtained which was suitable for quantitative work.

Table 1 contains the DPP peak-heights thus obtained from a typical calibration graph for platinum in urine: such graphs were linear over the platinum concentration range 20–800 ng/ml, with a correlation coefficients of 0.99. The detection limit of the procedure is 10 ng/ml. To the best of our knowledge, a substantially better limit has not been reached by any method so far used for the determination of platinum in biological liquids. However, this concentration limit is valid only if the whole procedure is used without any modification. The method outlined here uses 9 ml of urine for each determination. During the procedure the platinum present is concentrated by a factor of 2.25. In some cases, however, insufficient urine may be available (for instance, in the case of some experimental animals). It is then necessary to take into consideration the changed concentration conditions resulting from the smaller initial volume of urine.

DPP peaks for urine containing known amounts of platinum (30–500 ng/ml) and treated as described in the procedure, were compared with those obtained for

Table 2. DPP peak-heights for urine samples (Pt added, 111 ng/ml) obtained from one volunteer during 48 hr

Time of withdrawal, *hr*	DPP peak-height,† *μA*	Recovery,§ %
0	5.16	—
0*	5.31	103
8	5.16	100
16	5.42	105
24	5.06	98
32	5.00	97
48	5.26	102

*Urine diluted tenfold with distilled water.
†Average of three determinations.
§Platinum standards made with the sample withdrawn at the beginning of the experiment.

similarly treated pure solutions of platinum in distilled water or in 0.15*M* sodium chloride. The recoveries ranged from 63 to 85%. Moreover, the DPP peak-heights obtained for urine samples from different volunteers, to which the same amount of *cis*-DDP was added and which were taken through the analysis scheme, differed by 10–20%. These results demonstrate that the calibration graph cannot be prepared by use of standards made up with distilled water or a simple inorganic electrolyte or urine from different source. Table 2 gives the DPP peak-heights for a fixed amount of platinum added to urine samples obtained over a 48-hr period from a man 26 years old. The recoveries were in the range $101 \pm 4\%$. Thus in a pharmacokinetic investigation of a patient receiving *cis*-DDP the best results can be obtained if the calibration graph is prepared by use of platinum-free urine from the patient, taken just before the *cis*-DDP administration. The use of a calibration graph is suitable only when a sufficient amount of sample is available. When not much sample is available (for instance when urine is taken from small experimental animals) it is better to use the standard addition method. The highest precision is then obtained if the stock solution for the standard additions is prepared with platinum-free urine from the patient.

The precision of the estimation was found to be 5% at the 111 ng/ml level (ten replicates). The effect of metal ions on the platinum catalytic peak was also studied. Treatment of the chloroform extract with NaSH decomposed the DDTC complexes of Fe^{2+}, Mn^{2+} and Zn^{2+}. Moreover, Ca^{2+} and most transition-metal ions interfered with the DPP peak of the platinum–ethylenediamine chelate only when present in at least 400:1 ratio to platinum. Other interference studies yielded essentially the same results as those obtained for DPP determination of platinum in ores.[11]

It is obvious that during metabolism *cis*-DDP is converted into various platinum species, which could differ in their reactivity with DDTC. In that case the determination of total platinum in urine by any method based on formation of the platinum–DDTC complex would not be reliable. This problem has already been examined by Bannister *et al.*,[6] who concluded that *cis*-DDP is converted into species which react in urine with DDTC in a manner similar to that of *cis*-DDP.

The utility of the method was tested by administering *cis*-DDP (Platidiam, Lachema, Czechoslovakia), by intravenous infusion into a 45-year old female patient with a liposarcoma, at a dose of 160 mg per m^2 of body surface, over a period of 4 hr. The platinum level found in the urine of this patient immediately after completion of the infusion was 16.0 ± 0.4 μg/ml (average ± standard deviation; four samples). The level in urine taken after a further 12 hr was 6.1 ± 0.2 μg/ml. Identical results were obtained if $PtCl_2$ was used instead of *cis*-DDP for preparing the standard curve.

CONCLUSIONS

This report describes a clinically useful method for determination of platinum in urine. The procedure has a high degree of specificity, circumventing any matrix effects, and also has the high sensitivity provided by differential pulse polarography. As simple differential pulse polarographs are now available at reasonable prices the determination is inexpensive; it is also suitable for automation to accommodate large numbers of samples, but in that case the sample preparation may limit the sample throughput.

Acknowledgement—The authors are indebted to Dr. J. Drobnik for initiation of this work and for critical reading of the manuscript.

REFERENCES

1. A. H. Jones, *Anal. Chem.*, 1976, **48,** 1472.
2. C. L. Litterst, T. E. Gram, R. L. Dedrick, A. F. LeRoy and A. M. Guarine, *Cancer Res.*, 1976, **36,** 2340.
3. S. J. Bannister, Y. Chang, L. A. Sternson and A. J. Repta, *Clin. Chem.*, 1978, **24,** 877.
4. M. F. Pera and M. C. Harder, *ibid.*, 1977, **23,** 1245.
5. R. F. Borch, J. H. Markovitz and M. E. Pleasants, *Anal. Lett.*, 1978, **12,** 917.
6. S. J. Bannister, L. A. Sternson and A. J. Repta, *J. Chromatog.*, 1979, **173,** 333.
7. D. A. Hull, N. Muhammad, J. G. Lanese, S. D. Reich, T. F. Finkelstein and S. Fandrich, *J. Pharmaceut. Sci.*, 1981, **70,** 500.
8. D. Priesner, L. A. Sternson and A. J. Repta, *Anal. Lett.*, 1981, **14,** 1255.
9. R. G. Miller and J. H. Doerger, *At. Abs. Newslett.*, 1975, **14,** 66.
10. M. L. Denniston, L. A. Sternson and A. J. Repta, *Anal. Lett.*, 1981, **14,** 451.
11. P. W. Alexander, R. Hoh and L. E. Smythe, *Talanta*, 1977, **24,** 549.
12. *Idem, ibid.*, 1977, **24,** 543.

Talanta, Vol. 30, No 4, pp. 291–293, 1983
Printed in Great Britain.

0039-9140/83/040291-03$03.00/0

SPECTROPHOTOMETRIC DETERMINATION OF ALUMINIUM WITH CHLOROPHOSPHONAZO I

ZHU YING-QUAN, ZHANG LIN and LI JUN-YI

Department of Chemistry, Huazhong Normal College, Wuchang Gui-zi Shan, Wuhan, China

(*Received* 14 *May* 1981. *Revised* 21 *February* 1982. *Accepted* 2 *May* 1982)

Summary—Aluminium reacts with Chlorophosphonazo I at pH 4–6 to form a water-soluble 1:1 red-violet complex. The absorption maximum is at 610 nm and the apparent molar absorptivity is 1.96×10^4 l. mole^{-1}. cm^{-1}. The apparent instability constant has been calculated to be 1.8×10^{-4}. The colour of the complex is stable for 24 hr. Beer's law is obeyed over the concentration range up to 0.8 μg/ml. Titanium and zirconium interfere seriously.

Chlorophosphonazo I (CPA I) has been used for the spectrophotometric determination of several elements, including uranium, copper and yttrium, but not aluminium. We have therefore explored the analytical value of this colour reaction.

EXPERIMENTAL

Reagents

CPA I solution (0.1%).

Standard aluminium solution (100 μg/ml). Dissolve 1.759 g of $KAl(SO_4)_2 . 12 H_2O$ in water containing 3 ml of concentrated sulphuric acid, and dilute to volume with water in a 1-litre standard flask. Prepare a 10-μg/ml solution by dilution.

Acetate buffer solution (pH 5.1). Dissolve 4 g of sodium acetate in 250 ml of water, add 0.8 ml of glacial acetic acid, and dilute with water to 500 ml.

Procedure

To the test solution containing not more than 40 μg of aluminium, in a 50-ml standard flask, add the following reagents in the order given, mixing between additions: *ca.* 13 ml of water, 10 ml of acetate buffer solution and 7 ml of CPA I solution. Dilute to the mark with water and measure the absorbance at 610 nm in a 1.0-cm cell against a reagent blank prepared under identical conditions.

RESULTS AND DISCUSSION

All experiments were done at room temperature (25 ± 1°).

Absorption spectra

The absorption spectra of the aluminium–CPA I complex and the reagent blank were measured against water in the range 520–660 nm in 1.0-cm cells and are shown in Fig. 1.

In the subsequent experiments, the absorbances were measured at 610 nm against a reagent blank.

Maximum and constant absorbance was obtained in the pH range 4–6 by the procedure described (Fig. 2). For further work a pH of 5.1 was selected.

For 50 ml of final solution, 6.0–10.0 ml of 0.1% CPA I solution gave maximum and constant absorbance with 20 μg of aluminium, so 7.0 ml were added for determinations. Addition of up to 10 ml of the acetate buffer (pH 5.1) did not affect the absorbance of a fixed amount of aluminium.

At 25°, the complex was formed instantaneously and the absorbance remained stable for 24 hr.

Composition of the complex

The molar composition of the complex was studied by Job's method and the mole-ratio method and both indicated a 1:1 ratio of aluminium and CPA I in the complex, which thus probably has the structure

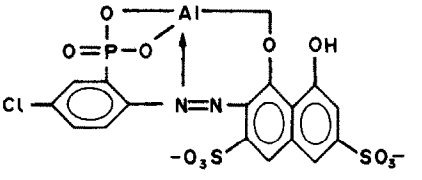

The apparent instability constant was determined by the Bent and French method, and found to be 1.8×10^{-4}.

Beer's law was found to be obeyed for aluminium concentrations up to 0.8 μg/ml in the final solution, and the apparent molar absorptivity was found to be 1.96×10^4 l. mole^{-1}. cm^{-1}.

Effect of other ions

Synthetic solutions containing known amounts of aluminium and varying amounts of other ions were prepared and the aluminium was determined. The levels (in μg) at which various ions do not interfere in the determination of 20.0 μg of aluminium are given below (in parentheses). Co(II) and V(V) (150), Ba(II) and Sr(II) (1500), Mg(II) (450), Ca(II) (1200), Ni(II) (70), Fe(III) (masked with 0.1*M* EDTA–Zn) (5000), Cu(II) and Bi(III) (350), Mn(II) (100), Cr(VI) (500), W(VI) (400), Sn(II) and Sb(III) (200), Mo(VI) (90)

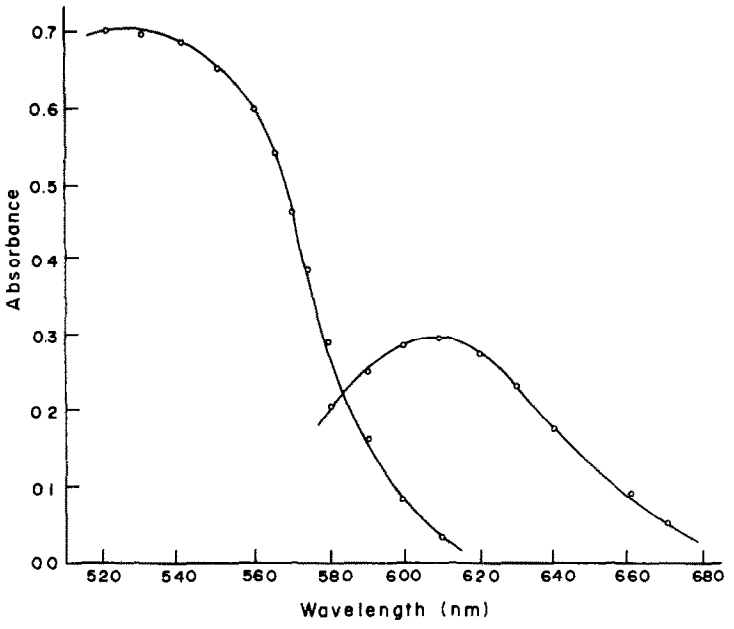

Fig. 1. Absorption spectra of: I, reagent blank against water, and II, aluminium–CPA I complex (Al taken, 20 μg; 1.0-cm cell).

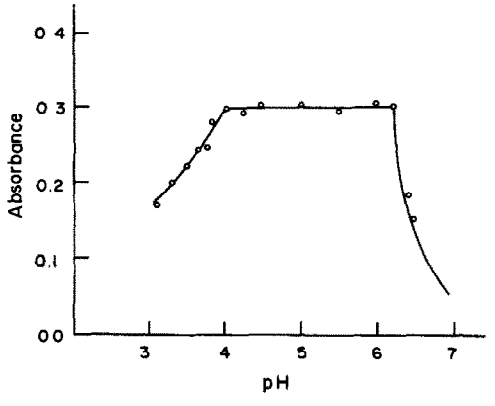

Fig. 2. Effect of pH on Al–CPA I complex.

and Ce(III) (10). As expected, aluminium-complexing anions such as fluoride, tartrate, citrate and oxalate have a marked influence on the absorbance.

Application

The method was applied to determination of aluminium in cobalt oxide. It was necessary to separate the bulk of the cobalt first. This was done by gently heating the sample (containing not more than 40 μg of aluminium) with 10 ml of concentrated hydrochloric acid until dissolved, evaporating to dryness, taking up with 10 ml of 2*M* hydrochloric acid, adding 20 ml of 50% ammonium thiocyanate solution and extracting the cobalt thiocyanate by shaking with 35 ml of methyl isobutyl ketone (MIBK) for 1 min, discarding the organic phase and again extracting with 15 ml of MIBK. The aqueous phase was then treated as described in the general procedure.

The results, together with those obtained by the Chrome Azurol S method, are given in Table 1, and indicate that the procedure is satisfactory.

Comparison with other spectrophotometric methods for aluminium

Table 2 shows a comparison between various methods. The present method is simple and rapid, works over a wider range of pH and gives a complex that is stable for a long time.

Table 1. Determination of aluminium in cobalt oxide

Sample	Al found,* %		Relative standard deviation, %
	CPA I method	CAS method	
1	0.045	0.043	7
2	0.086	0.085	2
3	0.10	0.11	7
4	0.24	0.25	3

*Mean of 5 determinations.

Table 2. Comparison of methods

Method	λ_{max}, *nm*	Optimum pH	ε, $l.mole^{-1}.cm^{-1}$	Reference
Chrome Azurol S	610	6.0 ± 0.2	4.9×10^4	1
Eriochrome Cyanine R	535	6.1 – 6.2	$\sim 6.5 \times 10^4$	2
Stilbazo	496	5.6	1.8×10^4	3
Xylenol Orange	555	3.4	2.1×10^4	4
Methylthymol Blue	590	3 – 4	1.9×10^4	5
CPA I	610	4 – 6	1.96×10^4	Present method
Aluminon	525	4 – 4.9	1.4×10^4	6
Oxine	390	9.0	7.3×10^3	7

REFERENCES

1. L. Buck, *Chim. Anal. (Paris)*, 1965, **47**, 10.
2. Z. Marczenko, K. Kasiura and M. Mojski, *Chem. Anal. (Warsaw)*, 1971, **16**, 203.
3. C. U. Wetlesen and S. H. Omang, *Anal. Chim. Acta*, 1961, **24**, 294.
4. D. T. Pritchard, *Analyst*, 1967, **92**, 103.
5. V. N. Tikhonov, *Zh. Analit. Khim.* 1966, **21**, 275.
6. E. B. Sandell, *Colorimetric Determination of Traces of Metals*, 3rd Ed., p. 175. Interscience, New York, 1959.
7. Z. Marczenko, *Spectrophotometric Determination of Elements*, p. 112. Horwood, Chichester, 1976.

Talanta, Vol. 30, No. 4, pp. 295–298, 1983
Printed in Great Britain.

0039-9140/83/040295-04$03.00/0

ANALYTICAL DATA

FORMATION CONSTANTS FOR THE COMPLEXES OF LEVULINATE AND ACETATE WITH MANGANESE(II), COBALT(II), NICKEL(II), COPPER(II), ZINC(II) AND HYDROGEN IONS

PETER W. LINDER, RALPH G. TORRINGTON and UTE A. SEEMANN
School of Chemical Sciences, University of Cape Town, Rondebosch 7700, South Africa

(*Received* 14 *September* 1982. *Accepted* 18 *November* 1982)

Summary—Formation constants are reported for the levulinate complexes of manganese(II), cobalt(II), nickel(II), copper(II) and zinc(II) at 25° in 0.1*M* chloride medium. In addition, results are presented for the corresponding acetate complexes for comparison. Protonation constants for the two ligands are also reported.

In a current project on equilibria of metal ions in soil solutions, we require the formation constants for complexes formed between various metal ions and certain ligands that we postulate as models for the cation-binding sites on fulvic acid molecules. Though for many of the systems concerned the constants are available from the literature and, where necessary, ionic strength corrections can be applied,[1] for the remaining systems we need to determine the constants. Metal complexes formed with the levulinate (4-oxopentanoate) anion fall into the latter category and in this paper we report our findings for these systems together with a study of the corresponding acetate complexes, made for comparative purposes.

EXPERIMENTAL

Sodium hydroxide solutions (0.1*M*) were prepared freshly and frequently under nitrogen from BDH CVS ampoules and standardized with potassium hydrogen phthalate (BDH "AnalaR"). Stock solutions (*ca.* 0.1*M*) of levulinic acid (Sigma) or acetic acid (BDH "AnalaR") were standardized with the sodium hydroxide solutions by Gran's method.[2] To control the ionic strength, the sodium hydroxide, levulinic acid and acetic acid solutions were prepared with a chloride concentration of 0.1*M* by the addition of dried sodium chloride (BDH "Aristar"). Metal(II) chloride solutions (0.05*M*) were prepared from Merck GR reagents and standardized with EDTA (BDH AVS) which in turn had been standardized against zinc pellets (Merck GR). Since each of the metal(II) chloride solutions was prepared with a concentration as close as possible to 0.05*M*, their chloride concentrations were also 0.1*M*.

Protonation constants for the ligands and the formation constants for the metal complexes were determined by potentiometric titrations, in a Metrohm EA876-20 titration vessel maintained at 25°. The electrodes were a Metrohm EA109 glass electrode and a Metrohm EA404 calomel electrode containing 5*M* sodium chloride as electrolyte. During the titrations a purified nitrogen atmosphere was maintained in the titration vessel.

In the determination of the protonation constants, solutions containing the acid and sodium chloride were titrated with the sodium chloride/hydroxide solution, added from a Metrohm Dosimat (E635) piston-burette controlled by a Metrohm Titroprocessor (E636) which also measured and recorded the emf of the cell. The pH-range covered was approximately 2.5–11. The data obtained were used to calibrate the electrodes and determine the protonation constants simultaneously.

For the complexation titrations, the acid plus sodium chloride was first titrated with sodium hydroxide as just described, but only until a preselected pH was approximately reached. Immediately after this, metal chloride solution was added to the solution from a 50-ml manual piston-burette (Metrohm EA274). In this second stage, emf readings were taken on a Radiometer PHM64 pH-meter. This two-stage procedure has two advantages. First, the initial titration of ligand with alkali provided data which were used for calibrating the electrodes specifically for each individual titration. Secondly, by use of the metal chloride as titrant, a considerably greater range of extent of complexation was attainable, without interference by precipitate formation, than by the more usual procedure of adding alkali to a solution containing ligand and metal. An adequate range of pH in the complexation measurements was obtained by doing a large number of titrations, covering a suitable range of starting pH-values.

The electrode calibration parameters were determined by running the titration data (from titration of the acid with sodium hydroxide) on the MAGEC[3] and MINIQUAD[4] programs alternately, according to the procedure described by May *et al.*[3] The complexation data were processed initially by ZPLOT[5] in order to obtain formation curves and subsequently by MINIQUAD[4] in order to obtain best-fitting chemical models and refined formation constants. The formation constants were supplied to PSEUDOPLOT,[6] which generated theoretical formation curves for comparison with the experimental formation curves, thereby facilitating hypothesis-testing. The computational procedure is described in greater detail in references 7 and 8.

NMR spectra of D_2O solutions of levulinic acid and levulinic acid plus copper(II) chloride were obtained with a Varian XL100 spectrometer.

Table 1. Logarithms of formation constants (β_{pqr}*) for proton and metal(II) complexes of levulinate and acetate at 25°C and $I = 0.1M$ [Cl^-]

Ligand	Acceptor	p	q	r	log β_{pqr}	d	n	Literature data: log β (temp., °C, I, M, [medium], ref.).
Levulinate	H^+	1	0	1	4.498	0.0005	195	
	Mn^{2+}	1	1	0	0.75	0.01	66	
		2	1	0	1.59	0.04	66	
	Co^{2+}	1	1	0	0.80	0.01	49	
		2	1	0	1.89	0.03	49	
	Ni^{2+}	1	1	0	0.79	0.01	41	
	Cu^{2+}	1	1	0	1.70	0.002	226	
		2	1	0	2.55	0.009	220	
	Zn^{2+}	1	1	0	1.13	0.004	59	
Acetate	H^+	1	0	1	4.499	0.0004	197	4.53 (25°, 0.1);[15] 4.64 (25°, 0.2 [KNO_3]);[16] 4.42 (25°, 0.3 [$NaClo_4$];[17] 4.55 (20°, 0.1 [$NaClO_4$]).[18]
	Mn^{2+}	1	1	0	0.80	0.004	38	1.40 (25°, 0);[19] 1.20 (25°, 0);[20] 0.61 (25°, 0.16).[21]
	Co^{2+}	1	1	0	0.82	0.01	54	1.46 (25°, 0);[19] 1.29 (25°, 0);[22] −0.22 (25°, 0.2).[23]
	Ni^{2+}	1	1	0	0.87	0.01	49	1.43 (25°, 0);[19] 1.80 (25°, 0);[20] 1.0 (25°, 0.1);[15] 0.81 (25°, 0.2);[24] 2.12 (20°, 0.1 [$NaClO_4$]).[25]
	Cu^{2+}	1	1	0	1.75	0.003	196	2.23 (25°,0);[19] 2.24 (25°, 0);[26] 1.18 (25°, 0.1);[15] 0.25 (25°, 0.2);[23] 1.89 (20°, 0.1) [$NaClO_4$]);[18] 2.38 (20°, 0.1 [$NaClO_4$]).[25]
		2	1	0	2.43	0.02	196	3.63 (25°, 0);[19] 3.09 (20°, 0.1 [$NaClO_4$]).[18]
	Zn^{2+}	1	1	0	1.14	0.01	44	1.57 (25°, 0);[19] 1.0 (25°, 0.1);[15] 0.66 (25°, 0.2);[23] 1.28 (20°, 0.1 [$NaClO_4$]);[18]
		2	1	0	—	—	—	2.09 (20°, 0.1 [$NaClO_4$]).[18]

*β_{pqr} refers to the general complex $A_pB_qH_r$ where A = ligand, B = metal ion and H = proton.
d = standard deviation of log β; n = number of observations.

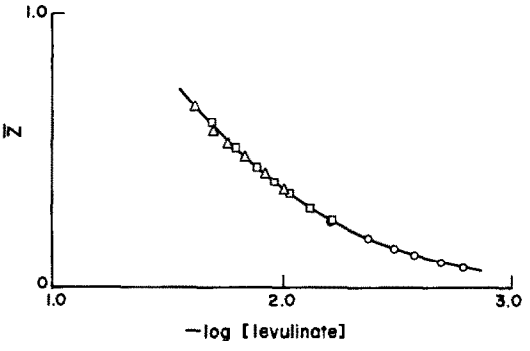

Fig. 1. PSEUDOPLOT curve calculated from the levulinate–proton and –copper(II) β values in Table 1, plotted on a selection of the experimental ZPLOT points from three of the titrations. Initial concentrations of levulinate and −log(unbound proton concentration) values were □ 68.74 m*M*, 4.439; ○ 93.7 m*M*, 3.460; △ 57.39 m*M*, 5.015. The titrant was 49.75 m*M* $CuCl_2$.

RESULTS AND DISCUSSION

Four protonation titrations were done for each ligand. Processing of the data obtained by the MAGEC/MINIQUAD cycling procedure[3] gave converging values for the electrode parameters and the protonation constants. Satisfactory statistical fits between the parameters and the data were indicated by reasonable values obtained for the MAGEC objective function and the MINIQUAD *R*-factor. Only the formation of the monomeric acid could be detected, for either ligand; no evidence for dimeric species[9] could be found. The values obtained for the protonation constants are given in Table 1. The acetic acid constant agrees acceptably with the literature values, taking into account the variation in background medium.

The individual metal-complexation titrations yielded overlapping formation curves, as computed by ZPLOT, for each system, indicating that under the conditions studied, only mononuclear binary complexes were formed.[6] For each system, initial stepwise formation constants were inferred from the formation curves by Bjerrum's method.[10] The corresponding overall constants were subsequently refined by MINIQUAD. Series of chemical models incorporating metal hydrolysis reactions of the sort described by Baes and Mesmer[11] were tried but in no case could significant concentrations of hydrolysed metal species be detected; this is consistent with the overlapping character of the formation curves. The "best" constants found, as judged by the MINIQUAD *R*-factor, were tested for validity by using them in PSEUDOPLOT to generate theoretical formation curves. In each case, the visual match obtained between the experimental and theoretical formation curve was excellent. As an example, the experimental ZPLOT points and corresponding PSEUDOPLOT curves for the levulinate–copper(II) system are shown in Fig. 1. Table 1 lists the complete set of "best" constants for all the systems studied, together with literature values for acetate–metal systems. The agreement of our values with the literature is satisfactory, considering the variation in background conditions.

No marked differences are apparent, amongst our results, between the levulinate and the corresponding acetate complex-formation constants. In order to make suitable, though rough, comparisons, it is useful to consider ranges of values spanning three standard deviations on either side of each log β_{pqr} value. (For the significance of β_{pqr}, please refer to the footnote of Table 1.) On the basis of this criterion, significant differences are observed between levulinate and acetate complexes of manganese(II) and nickel(II) (log β_{110}) and of copper(II) (log β_{110} and log β_{210}) but the differences are very small. None of the other log β_{pqr} values show significant differences between the levulinate and acetate complexes. Thus these results indicate that, as might be expected, the binding of metal to levulinate is of the same type as to acetate, namely through the carboxylate group. The carbonyl group is evidently not involved. This conclusion was confirmed by running NMR spectra; broadening as a result of addition of copper(II) chloride was observed for only the 2-methylene protons of levulinic acid.

Our results suggest, further, that levulinate shows a greater propensity than acetate for *bis*-complex formation. Moreover, log β_{210} is significantly greater for $(levulinate)_2Cu$ than for $(acetate)_2Cu$ in spite of the fact that (levulinate)Cu has a significantly smaller formation constant than (acetate)Cu. This apparent ability of the first ligand co-ordinated to enhance the binding of a second is demonstrated more clearly in Table 2, in which the second stepwise constants for the levulinate– and acetate–copper systems are compared. The errors were estimated from the correlation coefficients determined by MINIQUAD, in the manner described by Micheloni *et al.*[12] The possible co-operative binding effect of levulinate is further indicated by the values of log β_{210} for the manganese and cobalt complexes. These appear to be anomalously high (more than double the log β_{110} values) in comparison with the statistically expected relationship between successive stepwise constants[13] and the observed ratios for the majority of normally behaved systems.[14] The co-operative effect observed is small, but we believe it to be significant. We have considered published data for other similar systems but are unable to find a satisfactory explanation.

Table 2. Logarithms of stepwise formation constants (K_2) and the standard deviations (d_2) of log K_2, for the reaction $A + ACu \rightleftharpoons A_2Cu$

	$(acetate)_2Cu$	$(levulinate)_2Cu$
log K_2	0.68	0.85
ρ	−0.81	−0.79
d_2	0.02	0.01

A = levulinate or acetate; ρ = correlation coefficient between the standard deviations (d) of log β_{210} and log β_{110}.

Finally, it may be noted that the sequence of log β_{110} values for each of the acetate and levulinate complexes is consistent with the Irving–Williams order.

Acknowledgements—Grateful acknowledgement is expressed to the University of Cape Town and the South African Council for Scientific and Industrial Research for generous grants. We also thank the University of Cape Town Computer Service for the smooth running of our programs on the Univac 1100/81.

REFERENCES

1. P. W. Linder and K. Murray, *Talanta*, 1982, **29**, 377.
2. G. Gran, *Analyst*, 1952, **77**, 661.
3. P. M. May, D. R. Williams, P. W. Linder and R. G. Torrington, *Talanta*, 1982, **29**, 249.
4. A. Sabatini, A. Vacca and P. Gans, *ibid.*, 1974, **21**, 53.
5. D. R. Williams, *J. Chem. Soc. Dalton Trans.*, 1973, 1064.
6. A. M. Corrie, G. K. R. Makar, M. L. D. Touche and D. R. Williams, *ibid.*, 1975, 105.
7. G. V. Fazakerley, P. W. Linder, R. G. Torrington and M. R. W. Wright, *ibid.*, 1979, 1872.
8. P. W. Linder and R. G. Torrington, *S. Afr. J. Chem.*, 1980, **33**, 55.
9. D. L. Martin and F. J. C. Rossotti, *Proc. Chem. Soc.*, 1959, 60.
10. F. J. C. Rossotti and H. Rossotti, *The Determination of Stability Constants*, p. 107. McGraw-Hill, New York, 1961.
11. C. F. Baes, Jr. and R. E. Mesmer, *The Hydrolysis of Cations*. Wiley Interscience, New York, 1976.
12. M. Micheloni, A. Sabatini and A. Vacca, *Inorg. Chim. Acta*, 1977, **25**, 41.
13. M. T. Beck, *Chemistry of Complex Equilibria*, p. 34. Van Nostrand Reinhold, London, 1970.
14. L. G. Sillén and A. E. Martell, *Stability Constants of Metal–Ion Complexes*, Spec. Publ. Nos. 17 and 25, Chemical Society, London, 1964 and 1971.
15. M. Yasuda, K. Yamsaki and H. Ohtaki, *Bull. Chem. Soc. Japan*, 1960, **23**, 1067.
16. I. Feldman and L. Koval, *Inorg. Chem.*, 1963, **2**, 145.
17. P. H. Tedesco and J. A. G. Quintana, *J. Inorg. Nucl. Chem.*, 1970, **32**, 2689.
18. R. S. Kolat and J. E. Powell, *Inorg. Chem.*, 1962, **1**, 293.
19. D. W. Archer and C. B. Monk, *J. Chem. Soc.*, 1964, 3117.
20. K. B. Yatsimirskii and T. I. Fedorova, *Zh. Neorgan. Khim.*, 1956, **1**, 2310.
21. N. C. Li, W. M. Westfall, A. Lindenbaum, J. M. White and J. Schubert, *J. Am. Chem. Soc.*, 1957, **79**, 5864.
22. R. G. Seys and C. B. Monk, *J. Chem. Soc.*, 1965, 2452.
23. N. Tanaka and K. Kato, *Bull. Chem. Soc. Japan*, 1960, **33**, 417, 1412.
24. E. Ohyoshi, *ibid.*, 1973, **46**, 2758.
25. G. S. Manku, A. N. Bhat and B. D. Jain, *J. Inorg. Nucl. Chem.*, 1969, **31**, 2533.
26. M. Lloyd, V. Wyckerley and C. B. Monk, *J. Chem. Soc.*, 1951, 1786.

Talanta, Vol 30, No 5, pp 299–315, 1983
Printed in Great Britain

0039-9140/83/050299-17$08 50/0

TALANTA REVIEW*

CHEMICAL AND INSTRUMENTAL ANALYSIS OF FERRITES

C. McCRORY-JOY and DAVID C JOY
Bell Telephone Laboratories, Materials Science and Engineering Division, Murray Hill, NJ 07974, U S A

(*Received* 4 *December* 1981 *Accepted* 14 *October* 1982)

Summary—More than thirty years since the manufacture of the first commercial ferrites, research and development efforts continue to produce ferrites with enhanced performance and new applications Analytical chemistry has maintained a substantial role in the ferrite industry in the characterization of both raw materials and products, and the analytical literature of ferrites has grown accordingly The continuing importance of ferrites to the electronic device industry requires further development of analytical methods suitable for characterization of ferrites so that their chemical composition may be related to performance and to the manufacturing processes used As modern analytical techniques have been developed, their application to the characterization of ferrites and the detection of heterogeneity in these materials is increasing

Ferrites are magnetic oxides containing iron oxide as a major constituent The ferrites of greatest industrial importance are members of three crystallographic classifications, the spinel ferrites, the orthoferrites or garnets, and the hexagonal ferrites or magnetoplumbites.[1-3] Spinel ferrites have the general chemical composition MFe_2O_4 where M is a bivalent metal such as iron, manganese, cobalt, nickel, copper, zinc, magnesium or cadmium. Orthoferrites are represented by the general formula $RFeO_3$ where R is a tervalent metal such as aluminium or one of the lanthanides, and the garnets are specifically designated by the formula $R_3Fe_5O_{12}$ Hexagonal ferrites are structurally derived from the naturally-occurring magnetoplumbite, $PbFe_{12}O_{19}$, with bivalent metals such as barium, iron, cobalt or nickel substituting for lead

The behaviour of magnetite, Fe_3O_4, was recognized long before the special properties of natural ferrites were investigated methodically late in the nineteenth century. The first synthetic ferrites were prepared in 1909, followed by theoretical studies spanning several decades. These provided the basis of the science and technology of ferrites and the preparation of the first usable modern ferrites in 1946.[4]

The characteristics of ferrites depend upon the crystal structure, chemical composition and conditions of manufacture, in particular any processes involving heat treatment Significant properties such as resistivity, permeability, saturation, Curie temperature, magnetostriction and ferrimagnetic behaviour in general are routinely measured in the characterization of ferrites Variations in chemical composition and structure lead to a wide variety of magnetic and electrical properties and allow the formulation of ferrite materials for specific applications.

Magnetic performance properties lead to the classification of ferrites into five groups:[5] soft, square-loop, hard, microwave and single-crystal, referring to the behaviour of the material on magnetization and subsequent demagnetization, the mode of application, or the form of the device Table 1 summarizes these categories by type, structural classification, examples and typical applications.

The manufacture of ferrite materials and devices is necessarily a precisely controlled procedure, since reproducible electrical, magnetic and mechanical properties must be ensured.[1,2,6] First, high-purity raw materials must be weighed accurately to obtain the desired composition In a typical process, the metal oxides chosen are thoroughly mixed, then presintered at high temperatures, typically 1000°, and broken into granules of uniform size. The granules are mixed with a binder or lubricant and formed into devices by pressing or extrusion Finally, the devices are sintered in a controlled atmosphere for several hours, followed by cooling at a controlled rate. Since ferrite devices come in a large variety of shapes, such as the toroids used in the memories of large computers, the small cylindrical devices used as magnetic cores in speakers or as posts in microwave guides, or as single-crystal thin garnet plates used in microwave circuits or magnetic bubble devices, a variety of ceramic machining techniques such as grinding, ultrasonic drilling and diamond-saw cutting are used to shape the final product

The composition of ferrites prepared by the classic ceramic procedure described, at temperatures at which the raw material oxides are not volatilized, should not deviate significantly from the expected

*For reprints of this review, see Publisher's announcement near the end of the issue

Table 1 Examples of ferrite compositions and applications

Type	Crystal structure	Typical composition	Application
Soft	Spinel	MO Fe_2O_3 M = MnZn, NiZn, LiZn or MgZn	Inductors for telecommunications inductors and transformers for television, transducers, radio antennas
Hard	Hexagonal	Ba–Fe Sr–Fe	Generators, relays, small motors, permanent magnets, loudspeakers
Square-loop	Spinel	Mg–Mn–Zn–Fe Li–Ni–Fe	Computer memories, logic devices
Microwave	Garnet	$Y_3Fe_5O_{12}$ (YIG) with rare earth or Al substitution	Phase shifters, switches, tunable devices, isolators
	Spinel	MFe_2O_4 Sr, Ni, Co, Al substitution	
Single crystal	Spinel, garnet	$Y_3Fe_5O_{12}$ with rare earth substitution	Magnetic bubble devices, recording heads, microwave filters, magneto-optical devices

composition based on the quantities of oxides used in formulation Ferrites prepared from complex compounds such as oxalates or acetates, or by crystallization from a melt, may exhibit greater deviation from the theoretical composition.

The particular shape of the device may be of interest in the application of instrumental analytical techniques The metal oxide raw materials and the polycrystalline ferrite products are usually soluble in mineral acids such as hydrochloric acid, but because of the crystalline nature of these materials, a considerable amount of time may be required to effect complete dissolution Much attention has therefore been given to sample treatment Compounds that are particularly hard to dissolve, such as certain garnets or samples containing chromium, may require a preliminary fusion at high temperature Another approach is dissolution in sealed ampoules at elevated temperatures This method minimizes the amount of acid required and results in an initial solution of known acidity, an inert atmosphere may be used, and the procedure allows decomposition of a number of samples which may then be stored without contamination for analysis later

The relationship of the properties of ferrites to their chemistry was documented early in their commercial development [7] Several reviews concerning the chemical analysis of ferrites and metal oxide raw materials have been published,[8-12] the most recent in 1971 Their scope was limited almost entirely to complexometric titrimetry, since few other procedures had been used at the time of their publication

When considering the analysis of ferrites, five levels of detail can be distinguished

(1) Stoichiometry

(2) Verification of the oxidation states of cations

(3) Identification and measurement of trace elements

(4) Measurement of differences in composition between grains

(5) Tests for the segregation of impurities, or trace elements, to grain boundaries, *etc*

Chemical techniques generally require homogenization of the sample by dissolution in an appropriate medium, but they may offer high sensitivity and accuracy, good precision and the ability to determine oxidation states, and thus can be used for the first three types of analysis Instrumental techniques, on the other hand, usually have some degree of spatial resolution, but in some cases less sensitivity and lower precision Chemical techniques are by their nature destructive, whereas the instrumental techniques described are generally non-destructive, and are often more suited to the last two types of analysis While this division is not absolute, it does indicate that the property of interest and its relationship to the microstructure of the ferrite will usually decide which is the best technique to use The development of analytical methods for ferrites during the period 1967–1981 is represented by a literature consisting largely of classical wet analytical procedures in the early years, with a trend toward sophisticated instrumental techniques which offer speed of analysis or allow the detection of heterogeneity

The sensitivity of ferrite properties to chemical composition requires the continuing development of better characterization procedures as their applications and requirements continue to be more specifically defined Descriptions of recent advances and the current status of the science and technology of

ferrites[13–18] have suggested a number of areas for future investigation which impose increased demands on analytical capabilities These areas include a detailed study of the influence of additives or dopants such as CaO or SiO_2 in soft ferrites on the technology, structure and properties of the product The concentration of additives is often critical, resulting in severe requirements for reproducibility of chemical composition Secondary structural parameters such as cation distribution must be examined to understand more thoroughly their effects on the magnetic properties of ferrites

SUMMARY OF CHEMICAL ANALYSIS PROCEDURES

Gravimetry and titrimetry

This category includes the classical methods of gravimetry and titrimetry, and any separation techniques required to perform them, such as chromatography and ion-exchange However, gravimetric procedures for the analysis of ferrites are scarcely mentioned in the literature The sensitivity of the properties of ferrites to impurities and microstructure indicates that these factors must be considered as significant as the elemental stoichiometry of a material Consequently the growing importance of the characterization of microstructure and cation distribution does not justify lengthy analytical procedures, no matter how accurate they might be

Titrimetry has been used extensively, particularly complexometric titration with ethylenediaminetetraacetic acid (EDTA), with a variety of end-point detection methods, including electrometric and colorimetric techniques. The extensive documentation of titrations involving EDTA for ferrites or metal ions in general[9,19–22] provides a good source for planning the titrimetric analysis of new materials The conveniences of using EDTA, which forms stable 1 1 complexes with a large number of metal ions, as shown in Table 2,[22] include speed combined with accuracy and considerable selectivity attainable by use of separation and masking reactions

Reports of titrimetric procedures generally deal with a single type of ferrite The diversity of ferrite and garnet compositions makes concise summary of these procedures difficult The discussion here is organized on the basis of decreasing complexity of the ferrite and the extent of sample characterization For purposes of this review complex ferrites are those containing four or more difficult cations, and simple ferrites are those containing three or fewer In some cases every cation present is determined, while in others, characterization of the sample is less exhaustive, often involving determination of only one constituent

Several procedures[23–30] for the characterization of a number of ferrites are summarized in Table 3 The errors reported are more likely to arise from the separation techniques than the titrations Other procedures are summarized in terms of the determination of individual components Some lengthier procedures which cannot be conveniently summarized in Table 3 are worth describing in more detail for certain materials Funke[9] has published a collection of complete analytical procedures for the semimicro titrimetric determination of cation in 2-, 3- and 4-component ferrites

Table 2 Stability constants of selected metal–EDTA complexes

Metal	log *K*
Fe^{3+}	25 1
Cr^{3+}	23 0
Cu^{2+}	18 8
Ni^{2+}	18 6
Y^{3+}	18 1
Pb^{2+}	18 0
Zn^{2+}	16 5
Co^{2+}	16 3
Al^{3+}	16 1
Fe^{2+}	14 3
Mn^{2+}	14 0
Mg^{2+}	8 7
Ba^{2+}	8 7

Iron Determination of iron by EDTA titration is relatively simple, owing to the high stability of the iron(III) EDTA complex Dissolution in acid, usually hydrochloric acid, is generally followed by oxidation (*e g*, with hydrogen peroxide) to iron(III) Since iron(III) may be titrated at pH 1–2 with little or no interference from cations forming weaker complexes, no further treatment other than dilution is generally required The error can be as low as 0 2 or 0 3% in the analysis of Fe–Ni–Co–Zn[23] and Fe–Mn–Zn–Mg[31] compounds respectively Iron interferes in the determination of other cations, and must therefore be masked or separated by extraction, precipitation, or ion-exchange before their titration For example, Přibil and Veselý[24,28] extract iron(III) with cupferron into 1 1 isoamyl alcohol–benzene mixture or from hydrochloric acid into ether, before use of a series of indirect determinations based on back-titration (see Table 3) The use of benzene is now considered by some to be hazardous, and other solvents may be substituted for it The further chemical treatment of the sample depends on the number and nature of the metal oxides used to prepare the ferrite, but even a glance at Table 2 indicates that separation or masking will be necessary even for the simpler materials

In the procedures outlined by Funke,[9] iron is determined as iron(II) by titration with cerium(IV) sulphate, with a relative error of <0 5% Other metals, including magnesium, manganese, aluminium, zinc and cobalt, are determined by EDTA titrations, usually after ion-exchange separations, with <1 0% relative error for 2-component systems and $<2\%$ for complex ferrites Iron may be separated by cupferron extraction or by ether extraction of the chloro-complex

Table 3 Titrimetric procedures for analysis of selected ferrites

Type of ferrite or garnet	Procedure	End-point detection	Cation determined	Relative error, %
Fe–Co–Ni–Zn[23]	Dissolve in 9*M* HCl + H_2O_2 Separate by anion-exchange Adjust each fraction to pH 4 8 (acetate buffer), add excess of EDTA, back-titrate with Cu^{2+}	PAN	Fe^{3+} Co^{2+} Ni^{2+} Zn^{2+}	0 2 3 0 1 6 2 9
Fe–Co–Mn–Mg[24]	Dissolve in *aqua regia* Extract Fe(III) with HCl and ether Aliquot (1) add excess of EDTA, adjust to pH 5 0–5 5 (hexamine), heat to 90–95°, back-titrate with Pb^{2+}, gives Mn + Co	Xylenol Orange	Co^{2+} Mn^{2+} Mg^{2+}	3 1 3 0 5 8
	Aliquot (2) add excess of EDTA, add ascorbic acid, back-titrate with Mg^{2+}, gives Co + Mn + Mg Add KCN, heat to 40°, titrate with Mg^{2+}, gives Co Mg by difference	Thymolphthalexone		
Fe–Mn–Zn–Mg[25]	Dissolve in conc HCl Extract Fe(III) with cupferron into 1 1 v/v isoamyl alcohol/benzene Titrate Mn + Zn + Mg at pH 10 (NH_3 buffer) with EDTA Add NH_4F and titrate with Mn^{2+}, gives Mg Add KCN, titrate with Mn^{2+}, gives Zn Mn by difference	Eriochrome Black T	Mn^{2+} Zn^{2+} Mg^{2+}	
Fe–Mn–Zn–Mg[26]	Dissolve in 6*M* HCl, oxidize with HNO_3, extract Fe(III) into MIBK Adjust to pH 6 5–8 5, extract with diethyldithiocarbamate and trichloroethylene Titrate Mg in aqueous phase at pH 9–10 (NH_3) with EDTA Strip Mn and Zn from organic phase with methanol and NaOH Add KCN and ascorbic acid, titrate Mn with EDTA (pH 9–10) Demask Zn with formaldehyde, titrate with EDTA (pH 9–10)	Eriochrome Black T	Mn^{2+} Zn^{2+} Mg^{2+}	
Fe–Zn–Ba[29]	Dissolve in hot conc HCl + H_2O_2 Extract Fe(III) with isopropyl ether Strip with H_2SO_4, add excess of EDTA, back-titrate with Fe^{3+} at pH 5 (acetate buffer)	Potentiometric	Fe^{3+}	0 1
	Precipitate $BaSO_4$ from extraction aqueous phase, filter off, dissolve in excess of ammoniacal EDTA, add Hg-EDTA and back-titrate with Zn^{2+}		Ba^{2+}	0 2
	Adjust filtrate to pH 5 (acetate buffer), add excess of EDTA and back-titrate with Fe^{3+}		Zn^{2+}	0 3
Fe–Ba–Bi[30]	Dissolve in conc HCl, reduce Fe^{3+} ($SnCl_2$ procedure), titrate with $K_2Cr_2O_7$	Diphenylamine	Fe^{3+}	

Table 3 (*cont.*)

Type of ferrite or garnet	Procedure	End-point detection	Cation determined	Relative error, %
	Dissolve in *aqua regia*, add ascorbic acid, titrate with EDTA at pH about 1	Xylenol Orange	Bi^{3+}	
	Dissolve in *aqua regia*, neutralize with pH-10 buffer, add NH_2OH HCl to dissolve and reduce Fe(III), add KCN, and ascorbic acid pH-10 buffer, and titrate	Eriochrome Black T	Ba^{2+}	
Fe–Mn–Mg[27]	Dissolve in hot conc HCl, extract Fe(III) with cupferron into 1 1 v/v isoamyl alcohol/benzene Add NH_2OH HCl to aqueous phase, titrate at 40° and pH 10 (NH_3 buffer), gives Mn + Mg Add NaF to decompose Mg complex, add excess of Mn^{2+} and back-titrate with EDTA, gives Mg	Eriochrome Black T	Mn^{2+} Mg^{2+}	0 1 0 1
Fe–Mn–Mg–Zn[27]	Decompose, extract Fe and titrate as for Fe–Mn–Mg, gives Mn + Zn + Mg Add KCN, then excess of Mn^{2+} and back-titrate with EDTA, gives Zn Add NaF and determine Mg as for Fe–Mn–Mg	Eriochrome Black T	Mn^{2+} Zn^{2+} Mg^{2+}	0 1 0 1 0 1
Fe–Mg–Ni–Pb[28]	Dissolve in *aqua regia* Evaporate to dryness, add HCl, extract Fe(III) with ether Reduce to Fe(II) and titrate with $KMnO_4$		Fe^{3+}	
	Aqueous phase			
	Procedure A To an aliquot add excess of EDTA (*a*), alkalize with NaOH, acidify with HNO_3, adjust to pH 5–6 with hexamine, back-titrate with Pb^{2+} (*b*) Add excess of EDTA (*c*) and pH-10 buffer and back-titrate with Ca^{2+} (*d*) Add KCN and titrate at 40° with Ca^{2+} (*e*) (*a*) − (*b*) = Ni + Pb, (*c*) − (*d*) = Pb + Mg, (*e*) = Ni	Methylthymol Blue	Ni^{2+} Pb^{2+} Mg^{2+}	
	Procedure B To an aliquot add excess of EDTA (*a*) and pH-10 buffer Back-titrate with Ca^{2+} (*b*) Add sodium thioglycollate and titrate with Ca^{2+} (*c*) Add KCN and titrate at 40° with Ca^{2+} (*d*) (*a*) − (*b*) = Ni + Pb + Mg, (*c*) = Pb, (*d*) = Ni, Mg by difference	Thymolphthalexone	Ni^{2+} Pb^{2+} Mg^{2+}	

Zinc The titrimetric procedures for zinc refer almost exclusively to manganese–zinc ferrites Zinc is usually titrated in ammonia buffer, pH 9 0–10 0, with Eriochrome Black T (EBT) as indicator In one case[32] the zinc–diantipyrinylmethane complex is extracted with dichloroethane, followed by titration in the organic phase, with a relative error of $<2\%$ for $\sim 10\%$ zinc Nickel, cobalt, manganese, iron(II), aluminium, chromium, calcium, magnesium, barium and silicon do not interfere

Anion-exchange is useful for the separations required for Mn–Zn ferrites Iron and manganese are typically eluted with 2*M* hydrochloric acid and zinc with 0 1*M* nitric acid [33] Iron is reduced to iron(II)

with ascorbic acid before complexation of zinc with dioctylmethylamine in either dichloro- or trichloroethylene and extraction of the zinc [34] Caution should be exercised in the use of chlorinated solvents Another procedure[35] involves the extraction of zinc with Azo-azoxy BN in 4 1 v/v carbon tetrachloride–tributyl phosphate mixture and stripping with 0 1*M* hydrochloric acid The pH is then adjusted to 9–10 for the EDTA titration (sulpharsene indicator) A relative error of <2 5% was reported

Nickel Iron and zinc can both be extracted with diantipyrinylmethane in dichloroethylene from 3*M* hydrochloric acid Titration of nickel after addition of ammonia buffer allows determination of ~12% NiO with a relative error of <2%[36] Nickel–zinc ferrites are not always completely dissolved by hydrochloric acid, so decomposition under pressure[9] or by fusion with pyrosulphate[30,37] is sometimes recommended Nickel may be separated by precipitation from ammoniacal solution with dimethylglyoxime [37] The precipitate is then dissolved in warm 1 1 nitric acid, the solution neutralized with 1 1 ammonia solution and adjusted to pH 4 with acetate buffer Copper is masked with sodium thiosulphate, then excess of EDTA is added and the surplus back-titrated with a standard indium solution (PAN as indicator)

Other metal ions Manganese in Mn–Zn ferrites can be titrated with EDTA after extraction of zinc and iron with diantipyrinylmethane in dichloroethane from 3*M* hydrochloric acid [38] Magnesium–manganese ferrites can be analysed after extraction of iron by this procedure, followed by the titration of manganese and magnesium [39] Magnesium oxide in ferrites has been determined selectively[40,41] with a relative error of <0 2% by precipitation of other metals with sodium diethyldithiocarbamate, Chromogene Black ETOO was used as the indicator Magnesium in Fe–Mg–Cr ferrites has been titrated after extraction of dichromate with benzylamine in dichloroethane, then of the iron–thiocyanate–diantipyrylmethane complex [42]

Aluminium in multicomponent ferrites has been determined by back-titration of excess of EDTA with zinc sulphate (Xylenol Orange as indicator) after precipitation of iron and titanium with concentrated sodium hydroxide solution [43] Barium and lead in Fe–Ba–Pb ferrite can be titrated after the reduction of Fe(III) to Fe(II), in addition of cyanide and adjustment to pH 10 with ammonia [30] Both metals are titrated together, then diethyldithiocarbamate is added and the EDTA released from the Pb–EDTA complex is titrated with magnesium solution, with EBT as indicator Barium in hard barium ferrites may be precipitated as barium sulphate, which is then dissolved in alkaline EDTA solution, and the excess of EDTA is titrated in pH-10 ammonia buffer with magnesium solution (EBT indicator) [44] More complex ferrites such as Fe–Ba–Zn and Fe–Ba–Co compounds may be similarly analysed after extraction of iron as its acetylacetonate and of zinc and cobalt as the dithizonates [45] Synthetic mixtures containing various quantities of iron, zinc and barium were analysed and average errors for these metals ranged from 0 2 to 1 7%, 0 to 1 0%, and 0 1 to 1 1% respectively

The garnets contain tervalent metals, usually lanthanides, aluminium or gallium If more than one lanthanide is present, ion-exchange separation will be necessary Since garnets are generally more difficult to dissolve, fusion of the sample may be required

Yttrium and aluminium in YAG crystals[46] are titrated with EDTA after fusion with borax, dissolution of the cooled melt in sulphuric acid and adjustment to pH 5.0–5.8 The yttrium content is first determined by titrating with EDTA after the addition of sulphosalicylic acid to mask aluminium, and Xylenol Orange as indicator The sum of aluminium and yttrium is found by addition of excess of EDTA and back-titration with zinc sulphate The absolute standard deviations reported for yttrium and aluminium were 0 16 and 0 02% respectively but the results were low by 0 9 and 0 4% absolute respectively Yttrium iron garnets containing gallium and gadolinium have been analysed[47] after separation of the components with a cation-exchange resin and stepwise elution of iron with 3*M* hydrochloric acid and of gallium with 4*M* hydrochloric acid Yttrium and gadolinium remain on the column under these conditions, but yttrium can be eluted with 0 1*M* ammonium hydroxyisobutyrate at pH 4 6 and gadolinium with a 0 5*M* concentration of this reagent at pH 6 A relative error of 4% was reported for titration of all four cations

Gallium and gadolinium in Ga–Gd garnet crystals have been determined together by addition of excess EDTA and back-titration with zinc sulphate (EBT indicator), followed by addition of fluoride to liberate EDTA from the gadolinium complex, and further titration with zinc sulphate The reproducibility reported was 0 18% for gallium and 0 12% for gadolinium,[48] but the results were about 1% absolute low for Ga and 1 0% high for Gd

General remarks Some of the errors reported seem very large by the standards of classical titrimetry, and further research to establish the causes of such errors seems called for

Electroanalytical techniques

Electroanalytical procedures for ferrite analysis include polarography, voltammetry at solid electrodes, and coulometry, particularly constant-current coulometric titration Several considerations determine the applicability of electrochemical methods Many metal ions exhibit well-defined polarographic reduction waves in a variety of media, but others are either not polarographically active or give a response only in a limited number of electrolytes This may impose limitations on the chemical preparation of samples or preclude the complete analysis of a ferrite by a single procedure For ferrites containing two or

more electroactive cations, the conditions may require adjustment to ensure selective determination. Such adjustments include complexation to increase the separation of half-wave potentials, precipitation of one or more cations, or the use of more than one medium

Nearly all research on polarographic analysis of ferrites was reported before 1971. Techniques such as normal pulse and differential pulse polarography have much greater sensitivity and resolution than classical d c polarography[49,50] with the conventional dropping mercury electrode Pulse polarography offers sensitivity two orders of magnitude better than d.c polarography In situations where the d c technique might provide no analytically useful information, *e g*, analysis of a solution containing several electroactive cations, several distinct peaks may be obtained with the differential pulse technique These techniques may therefore offer a reasonably fast, and possibly simultaneous, cation analysis of ferrite products.

The other electroanalytical technique most commonly employed for ferrite analysis is constant-current coulometric titrimetry, which can be very useful for accurate determination of stoichiometry

Coulometric titrations require a suitable titrant which can be generated electrolytically at 100% current efficiency and react rapidly, selectively and stoichiometrically with the cation of interest, and also a suitable end-point detection method Separations or choice of solution conditions may be required to ensure selective titration Frequently used detection methods include amperometry, potentiometry and colorimetry, the first usually offering the greatest sensitivity and precision As little as a few micrograms may be determined and the precision obtainable for a few milligrams of sample is often in the parts per thousand range Determination of both trace and major constituents is therefore possible

Iron and nickel in nickel ferrites have been simultaneously determined polarographically with a precision of $\pm 2\%$, in supporting electrolytes containing an excess of sulphosalicylic acid and either 1*M* ammonia/ammonium chloride or 0 5*M* pyridine/1*M* ammonium chloride buffer [51]

Nickel and zinc have been determined polarographically in Mn–Zn and Ni–Zn ferrites,[52] the supporting electrolyte being 0 1*M* potassium thiocyanate/0.04*M* tartrate The tartrate complexes the iron and the thiocyanate allows sufficient separation of the half-wave potentials of nickel and zinc The method was compared with an EDTA procedure involving separation of zinc by anion-exchange and precipitation of nickel with dimethylglyoxime The titrimetric approach was more accurate with a reported relative error of 1 5% but the polarographic procedure was faster, with a 2 5% relative error The same workers examined the use of triethanolamine–potassium hydroxide–sodium sulphate electrolytes

Another procedure[53] for nickel and zinc employed an electrolyte consisting of ammonium cyanide, 0 15*M* phosphoric acid and 0 02*M* sodium acetate Nickel and zinc were determined with a relative error of ± 1 5%. Iron and zinc in zinc ferrites may be determined simultaneously in a 1*M* ammonium tartrate/ammonia medium at pH ~9 7.[54]

A more comprehensive investigation has considered the determination of iron, nickel, manganese, zinc, copper and other cations in magnetic materials [55] Samples were dissolved by heating with concentrated hydrochloric acid in a sealed hard-glass tube at 120–160° Various electrolytes were studied, though none gave perfect resolution and definition of the polarographic waves, all had advantages, depending on the type of ferrite to be analysed. A re-examination of these by modern polarographic techniques might be beneficial The pyridine–pyridinium chloride electrolyte tried is interesting in that the polarographic waves of cadmium, nickel, zinc and iron(II) can be resolved and might be used routinely for analysing Fe–Ni–Zn ferrites Iron(III) must first be reduced (with ascorbic acid) to prevent its precipitation in this medium Cobalt may also be determined except when zinc is present (they are reduced at similar potentials) The procedures developed in this investigation permit the analysis of as little as 20 mg of sample, with an overall error estimated at ± 0 3%, which includes weighing, dilution, sampling and instrumental error However, the errors found experimentally were rather larger (coefficient of variation 1–2% for iron, for example)

Coulometric titrations of total iron, manganese and chromium have been reported Iron(III) in iron oxide and finished ferrite products was determined by titration with electrolytically generated copper(I) in an electrolyte consisting of 0 1*M* hydrochloric acid, 0 36*M* sulphuric acid and 0 01*M* copper sulphate, without interference from Mg, Co(II), Mn(II), Y, Zn or Ti(IV) [56] Samples weighing 0.3–0.5 g were dissolved in hydrochloric or sulphuric acid, and iron(II) was oxidized with hydrogen peroxide A variety of ferrites were analysed, including Fe–V–Al, Fe–Mg–Cr–Cu, Fe–Mn–Mg–Co, Fe–Mn–Zn–Cr–Ca, Fe–Mn–Zn–Co–Ti, Fe–Ni–Zn–Co–Ti–Si and Fe–Li–Na–Ti, with reproducibility ranging from 0 08 to 0 14%

Manganese in ferrites can be oxidized to Mn(VII) with ammonium persulphate in the presence of silver ions, before coulometric titration with electrogenerated iron(II)[57] with a reproducibility of ± 0 26%

Spectrophotometry and colorimetry

Spectrophotometry and colorimetry were formerly more important in the analysis of ferrites than they are now Their speed, sensitivity and relatively simplicity contribute to their importance in routine analysis The measurement time is relatively short, but sample preparation may be quite long Procedures for a wide variety of species are available.[58] These may be

used as guides for the development of an appropriate analytical procedure for a given ferrite

The sensitivity of spectrophotometric measurements generally permits determination of species at concentrations of 10^{-4}–$10^{-5}M$, and sometimes even as low as $10^{-7}M$ Proper choice of conditions may allow highly selective determinations The relative error is typically 1–3%, but may be reduced by use of differential methods

Spectrophotometric methods for ferrites most often involve determination of iron or manganese Several procedures are concerned with the determination of one oxidation state in the presence of another, and are included in the section on variable-valence analysis

Iron and copper have been determined simultaneously in the analysis of copper ferrites [59] After dissolution of a 10-mg sample in concentrated sulphuric acid, the solution is diluted and ascorbic acid is added to reduce iron(III) to iron(II) *Syn*-phenol α-pyridyl ketoxime (HPPK) solution is added and the pH adjusted to 10 with sodium carbonate solution The iron(II) and copper(II) complexes of HPPK are extracted into chloroform and the absorbances measured at 475 and 550 nm respectively The two elements are determined by solving the appropriate simultaneous equations. Iron is determined with a relative error of 1 8% or less and a relative standard deviation of 0 7%, the corresponding values for copper being 1 5% and 1 1%

Total manganese in Mn–Mg ferrites can be determined by dissolving the sample in phosphoric acid, adding potassium pyrophosphate and potassium bromate, diluting and measuring the absorbance of the Mn(III) at 520 nm against a reagent blank [60] Manganese levels of 1–2 5% can be determined within 20 min with a relative error $<3\%$ Manganese in garnets has been determined[61] with gluconic acid as a colorimetric reagent The samples were fused with sodium carbonate, followed by dissolution of the melt in hot hydrochloric acid Gluconic acid was added to the manganese(II) solution at pH > 11 5 to produce a complex having maximum absorption at 440 nm The calibration plot for manganese(II) was linear over the range 9–47 μg/ml The maximum relative error for three series of measurements was 2 4% Manganese may also be determined after oxidation to manganese(VII) with potassium periodate [62]

Copper may be determined photometrically at the 0 1% level in Ni–Zn and Mn–Zn ferrites with diethyldithiocarbamate at 440 nm with a relative error of $<4\%$ The metal may be also be determined with 2,2-bicinchoninic acid [63] Titanium in manganese–zinc ferrites may be measured quantitatively as the coloured diantipyrinylmethane complex in $3M$ hydrochloric acid solution [64] Zinc, manganese, cobalt and iron(II) do not interfere Iron(III) is reduced beforehand with ascorbic acid The reported sensitivity of the method was 0 5 μg/ml and the relative error 8% for a titanium content of 0 2% Lithium at the 1–5% level in bismuth ferrites can be determined (after removal of iron and bismuth as the hydroxides) with a solution of 4-(5-nitrophenyl)-1-phenyl-3-methyl-5-pyrazolone in dimethylformamide [65]

Procedures for the colorimetric determination of cobalt, nickel, copper, manganese and chromium as impurities in a variety of ferrites and starting materials have been described [11] Impurity concentrations of 0 01–0 001% were measured as follows cobalt with β-nitroso-α-naphthol at 530 nm, nickel with dimethylglyoxime at 460 nm, copper as copper(I) with cuproin at 530 nm, manganese as permanganate at 530 nm, and chromium with diphenylcarbazide at 546 nm The relative error was $\leqslant 10\%$

Atomic-absorption and flame photometry

Atomic-absorption and flame photometry provide a means of highly sensitive determination for most metals and both have become increasingly important in the determination of metals present as major and trace constituents of ferrites Detection limits for metals lie in the range of 0 01–10 0 μg/l, and the relative error is typically 1–2%, which may be reduced to a few tenths of a per cent with optimization of the procedure Interferences may be encountered whatever type of excitation is used Cation interferences are relatively rare, which is of course beneficial in ferrite analysis, but anion interferences are observed more frequently To avoid such interferences, consideration must be given to the chemical treatment and sample solution conditions.

The methods have several advantages over titrimetric and electroanalytical techniques, including selectivity, sensitivity and speed, and can offer reasonably good precision and accuracy with proper preparation of standards and sample solutions These techniques can be used for the determination of several elements and are therefore valuable as control methods for both simple and complex ferrites once suitable procedures have been developed Atomic absorption has been used mainly for the determination of a number of transition metal and rare-earth cations in a variety of ferrites and garnets, and flame photometry has been employed for alkali metals and alkaline-earth metals (such as calcium) Both major constituents and trace impurities may be determined by these techniques

Several Mn–Zn, Mn–Cu, Li–Ni and Cu ferrites have been analysed for iron, lithium, nickel, manganese, copper and zinc with an average relative error of $\pm 3\%$ or less and a precision of $\pm 1\%$ [66] The pH of the analyte solution, a hydrochloric acid medium, was in the range 2 3–2 5 An upper pH limit of ~ 4 was established, above which colloidal $Fe(OH)_3$ was formed Traces of aluminium, chromium, copper, magnesium, manganese, sodium, nickel, lead, tin and zinc were detected by emission spectrography and determined without difficulty in the presence of major constituents An air–acetylene flame was used for all elements except aluminium, for which an N_2O–

acetylene flame was used A multielement Cr–Cu–Mn–Co–Ni lamp and Ca–Mg and Zn–Ca lamps were employed for these elements and single-element hollow-cathode lamps were used for all others

The copper and cobalt contents of Ni–Cu–Fe–Co ferrites, in the ranges 0 1–2 5% and 0 1–4% respectively, were determined by using an air–acetylene flame, after dissolution of the sample in hydrochloric acid [67] The Co 204 7-nm and Cu 324.7-nm lines were used Iron and nickel present at considerably higher concentrations did not interfere and no interference from the matrix acid was observed

Rare-earth elements in garnet crystals have been determined by various procedures A detailed study of the AA analysis of garnet single crystals containing ytterbium, europium, gadolinium, dysprosium, holmium and erbium has been made, to establish the optimum conditions for determination [68] High-temperature flames such as nitrous oxide–acetylene are required to produce complete atomization In air–acetylene flames, rare-earth elements are not completely atomized, and the sensitivity is poor A further problem encountered with rare-earth elements is that they are often easily ionized and also affected by other elements present Easily ionized elements such as alkali metals and lanthanum are usually added to suppress the ionization The garnets studied[68] were dissolved in hydrochloric acid, which does not interfere, whereas nitrate and nitric acid do Analytical lines used were Y 410 2 nm, Eu 459 4 nm, Gd 368 4 nm; Dy 421 2 nm, Ho 410 4 nm, Er 400 8 nm Sample weights of 10–20 mg were used and relative errors ranged from 0 4 to 3 9%

Neodymium in YAG crystals has been determined with a nitrous oxide–acetylene flame [69] Samples weighing 250 mg were dissolved by fusion with lithium carbonate in a platinum crucible at 1000°, followed by dissolution in 1*N* sulphuric acid and dilution The 489 7-nm line from an Nd hollow-cathode lamp was used for analysis A relative error of $\leqslant 1$ 75% was reported

The major constituents iron, gallium, yttrium, copper, gadolinium and erbium, and any lead present as an impurity, in flux-grown magnetic garnets have been determined by atomic-absorption [70] Samples weighing 10–20 mg were dissolved in concentrated hydrochloric acid and the solutions appropriately diluted Lanthanum chloride was added to eliminate interference effects A nitrous oxide–acetylene flame and individual commercial hollow-cathode lamps were used for all elements determined Relative errors of 1–2% were reported for rare earths, iron, gallium and lead. The error for attempts to determine europium in the absence of $LaCl_3$ was 5 2%

A flame-photometric method has been reported for the determination of lithium in Li–Fe, Li–Cr–Fe, Li–Ti–Fe and Li–Zn–Ni–Fe ferrites used in various microwave devices [71] An air–acetylene flame was used, and the samples were dissolved in a mixture of sulphuric acid and orthophosphoric acid, and diluted A maximum relative error of 4 2% was reported

Sodium, magnesium and calcium at the 10^{-3}–0 2% level in various ferrites have been determined by atomic-absorption with use of the standard-additions method [72] Samples weighing 0 5 g were dissolved in hydrochloric acid and appropriate dilutions were made The resonance lines at 589.0, 285 2 and 422 7 nm were employed The reported relative error was 1 3% for sodium, 1 1% for magnesium and 2 0% for calcium Addition of acetone increased the sensitivity for sodium, but reduced it for magnesium and calcium Atomic-absorption analysis has also been used for the determination of potassium, sodium, calcium, magnesium, titanium, silicon and aluminium in manganese–iron garnets [73]

Emission spectrography

Emission spectrography is not as well represented as other instrumental techniques in the literature of ferrite analysis, but has several features that make it useful for certain aspects of ferrite analysis. It is applicable to some 70 metal and metalloid elements, and is virtually unrivalled in its capability for qualitative analysis Speed, specificity and high sensitivity, allowing detection limits in the range from ng/g to μg/g, with little or no preliminary sample treatment, are further advantages However, quantitative applications suffer from lack of precision. Relative errors of 10–20% are not unusual although with great effort they may be reduced to 1–2% The emission techniques are relatively useless for determination of major and minor components of ferrites, because of the demand for reproducible composition of products, but for some applications such as screening tests for impurities (especially at low level in raw materials) may be useful on account of speed and convenience

Emission spectrography has been used in determining major and trace impurities of rare earth and aluminium garnets.[74] One procedure for the Fe–Y–Gd–Al system used powdered samples homogenized with sodium chloride and ethanol Five mg of the mixture and 10 mg of carbon powder were mixed and placed in the crater of a carbon electrode, and several elements, including yttrium, ytterbium, gadolinium, gallium, cobalt, iron, indium and aluminium were determined with coefficients of variation of 3–7%, except for aluminium for which the value was stated to be much greater

Silicon, aluminium, iron, magnesium, calcium, manganese, titanium and chromium have been determined in small particles of garnets weighing 0 03–0 3 mg,[75] by a c arc evaporation from the channel of a carbon electrode, with an exposure time of 150 sec Garnet particles of known composition were used as internal standards for preparing calibration curves, and a reproducibility of 10% was obtained in most cases

Nd present in Y–Al(YAG) and Y–Fe(YIG) gar-

nets at the 0 2–7% and 10^{-3}–0 3% levels respectively was determined after dilution of the sample with a large amount of carbon powder, by evaporation of the mixture in an a c or d c arc [76] Aluminium and iron were used as internal standards for the two garnets

Another determination of neodymium and various impurities such as barium, iron, silicon, magnesium, manganese, copper, tin, antimony, lead and titanium in YAG has been reported [77] Standards were prepared by mixing the oxides of the impurity metals and aqueous copper and lead nitrate solution with YAG powder, followed by calcination for one hour at 800° Impurities were detected at various levels over the range 2×10^{-3}–0 1% The relative standard deviation for neodymium was 5% and for impurities 8–18%.

Silicon in YIG samples and in iron oxide and yttrium oxide raw materials was detected at levels of 0 085–5, 8×10^{-4}–10^{-3} and 10^{-3}–10^{-2}% respectively, with a relative standard deviation of 10–20% [78] Samples were ground, mixed with carbon powder and excited in an a c arc

Yttrium aluminium garnets and the alumina raw materials as well as YAG alloyed with Nd_2O_3 have been analysed for a number of impurity elements, including lead, manganese, tin, cobalt, bismuth and magnesium [79] Detection limits ranged from 10^{-5} to 10^{-4}%, with a relative standard deviation of 16–20% Samples were first mixed with silver chloride and carbon powder, and an a c arc was used

A general method has been developed for the spectroscopic analysis of various inorganic compounds containing lanthanides, including rare earth oxides and garnets [80] Samples, *e g*, YAG, are first dissolved in dilute mineral acid. The solution is delivered to a spark discharge through a porous electrode or by aerosol nebulization Rare earths present as additives at the 10^{-1}–10^{-3} % level, and as main components, have been determined by this procedure, which was reported to give increased precision and efficiency as well as greater ease of standardization with solutions

Barium, strontium, calcium and aluminium in hard ferrites have been determined by emission spectrography with an a.c arc, with a 3–4% error for each component [81] Ferrite samples weighing 0 1 g were prepared by grinding with sodium chloride Copper, cobalt, titanium and silicon additives in Ni–Zn and magnetostrictive Ni–Cu–Co ferrites were determined by a similar procedure, the samples being mixed with sodium chloride and carbon powder For Ni–Zn ferrites the relative standard deviations for titanium, cobalt and silicon were 6, 6 and 9% respectively Copper and cobalt in magnetostrictive ferrites have been determined with relative standard deviations of 15 and 7% respectively

Detection and determination of variable-valence cations

The oxygen content of a particular ferrite, for example one with the spinel stoichiometry $Me_xFe_{3-x}O_4$, is a major factor influencing ferrite performance Measurements of oxygen partial pressure may be used to monitor ferrite composition during the heat-treatment steps of manufacture An oxygen deficiency manifests itself through the presence of a lower oxidation state of one of the metallic components, *e g*., iron(II) Conversely an oxygen excess is indicated by the presence of ions in higher oxidation states, *e g* , manganese(III)

A number of chemical procedures have been described for the measurement of negative deviations from oxygen stoichiometry by determination of iron(II) and of positive deviations by determination of manganese(III) In addition, procedures for the simultaneous determination of both these species have been developed in attempts to obtain structural information related to the oxidation state of the ions as they exist in the ferrite matrix Techniques applied to variable-valence analysis include voltammetric and coulometric titrations, with amperometric, potentiometric, and visual end-point detection with various indicators Spectrophotometric methods and electron paramagnetic resonance (EPR) spectroscopy have also been employed A significant problem encountered in the chemical procedures is the development of dissolution techniques which will ensure that oxidation states of the metals in solution will be the same as in the original sample Certain preparation procedures such as grinding may affect the result In the case of finished ferrite devices the sample to be analysed must be representative of the whole material Chemical preparation steps must avoid the reaction of one species with another, *e g*, $Fe(II) + Mn(III) \rightarrow Fe(III) + Mn(II)$

The use of EPR and Mossbauer spectroscopy, where applicable, might avoid the sample treatment problems but would not provide quantitative analytical results as accurate and precise as those from a technique such as coulometric titration Furthermore, Mossbauer and EPR spectroscopy are relatively limited in application The first depends on the existence of a nuclear configuration possessing a quadrupole moment, and the second requires electrons with unpaired spins, and is therefore not likely to be applicable to both oxidation states, whereas certain titrimetric and electrometric techniques might be

Magnetic-moment measurements for manganese ferrites, and theoretical considerations, suggest that the ion-pair [Fe(II)–Mn(III)] is actually more stable than [Fe(III)–Mn(II)] in the octahedrally coordinated sites of spinel ferrites,[82] which is the opposite of the situation in aqueous solution. The amounts and distribution of Fe(II), Fe(III), Mn(II) and Mn(III) depend on the sintering conditions It has been found that in sintered ferrite toroids, the Fe(II) and Mn(III) content may vary radially around the sample,[83] the variation in oxidation state depended on the gas flow and positioning in the sintering furnace

Several methods have been proposed for the determination of iron(II) and manganese(III) in manganese–zinc ferrites Nagato devised two procedures, one a spectrophotometric method[84–86] and the other based on potentiometric titration.[87] In the first procedure a ferrite sample weighing about 0 2 g was dissolved rapidly in 30·1 phosphoric acid–perchloric acid mixture at 265° and the absorption of Mn(III) was measured at 520 nm after dilution to 100 ml For the determination of iron, another 0 2 g of sample was dissolved at the same temperature in 30 ml of phosphoric acid containing a known amount of Mn(III) and the change in the absorption at 520 nm was measured The amount of Fe(II) was then calculated from the two results A set of samples containing 0.6–1 3% Fe(II) and 2.6–2 0% Mn(III) was analysed by this procedure and the results were related to the quenching temperatures employed The method satisfies two requirements, the first that the oxidation potential of the solvent be higher than that of the oxidizing cation Mn(III), and the second that the time required for dissolution be very short At the high temperatures employed, phosphoric acid is converted into polyphosphoric acid and the ease of dissolution is so enhanced that ferrites which are hard to dissolve under ordinary conditions are completely dissolved in 10 sec This procedure was used to determine the composition of sintered iron oxides, manganese oxides and Mn–Zn ferrites prepared under different sintering conditions Statistical analysis of the relationship between ferrite composition and sintering conditions gave a reproducibility of 0 2% for Fe(II) and 0 8% for Mn(III) at the 95% confidence level

For the potentiometric titration method[87] a sample was dissolved in condensed phosphoric acid (in a nitrogen atmosphere, and at 240°) containing 2 g of oxalic acid Manganese was reduced to Mn(II) and the surplus oxalic acid destroyed in this process The Fe(II) present was titrated with potassium permanganate, and the difference in the amounts of Fe(II) and Mn(III) was determined by titration of a sample dissolved in phosphoric acid alone The author reported reproducibility to better than 0.2% for samples weighing 0 2–0 3 mg and analysed under carefully controlled conditions Samples produced under various temperature and atmospheric conditions contained 2 6–5 1% Fe(II) and 0 2–0 5% Mn(III)

Other investigators[88] have attempted to avoid the reaction of Fe(II) and Mn(III) by dissolving samples in the presence of dichromate, which reacts with Fe(II) more readily than does Mn(III) during dissolution After dissolution the Mn(III) is reduced with sodium azide, the excess of which is decomposed by boiling, and the surplus dichromate is titrated with ferrous ammonium sulphate Blanks, run to allow correction for the reaction of azide with dichromate, were found to increase with increasing Mn(II) content Iron(II) and manganese(III) were determined with reproducibilities of 3 1 and 3 4% respectively (at the 99% confidence level) Other analysts[83,89] found that potassium dichromate was less stable in boiling solution than at room temperature, and also that the method was suitable only for ferrites containing low concentrations of Fe(II) and Mn(III) As the content of these cations increases, Cr(III) formed by the oxidation of Fe(II) with dichromate reacts with the Mn(III) in solution It has been established that ferrites containing more than 2 0% Mn(III) cannot be analysed accurately by this method Problems due to the instability of dichromate are reportedly eliminated by dissolving the sample at 80° [83]

A comparison of the effectiveness of sodium sulphate and oxalic acid as reducing agents for Mn(III) showed that oxalic acid has certain advantages,[90] so a mixture of phosphoric and oxalic acids has been used to dissolve ferrite samples For samples containing >1 5% Mn(III) the Mn(III) was determined by spectrophotometry with a filter having maximum transmission at 490 nm For Mn(III) content <1 5% amperometric titration with ferrous ammonium sulphate was employed. The limiting amount of Fe(II) which could be tolerated in the determination of Mn(III) was 1 3%

A spectrophotometric method for Mn(III) in ferrospinels has been reported,[91] which should be applicable to ferrite analysis Powdered samples are dissolved in phosphoric acid containing iodic acid Iron(II) reduces iodate to iodine, which may be removed by extraction with carbon tetrachloride After removal of the iodine the Mn(III) is determined by measuring the absorbance at 500–510 nm At least a 200-mg sample is required and the detection limit is 1 5% Mn(III)

Another variable-valence combination is found in cobalt-containing ferrites, which have been analysed for Fe(II) and Co(III) [92] The samples were dissolved in phosphoric acid containing oxalic acid The maximum content of Co(III) which does not interfere by reaction with Fe(II) (in a 0 1-g sample) is 1 4% For higher Co(III) levels the amount of sample is reduced Ferrite samples weighing typically 0 1 g were dissolved in the phosphoric acid–oxalic acid mixture under a carbon dioxide atmosphere in a flask fitted with a reflux condenser The solution was diluted and sulphuric acid was added, followed by titration of iron(II) with ceric sulphate, with ferroin as indicator Cobalt(III) was determined indirectly by dissolving a sample of ferrite together with a known quantity of iron oxide [containing a known amount of Fe(II)] in 6*M* hydrochloric acid under carbon dioxide After addition of a mixture of sulphuric acid and phosphoric acids and dilution the mixture was titrated with ceric sulphate The excess of iron remaining after reaction of Fe(II) with Co(III) was titrated in this step and the Co(III) content was calculated

A procedure has been developed[93] for the determination of several oxidizing and reducing cations by dissolving the sample in dilute sulphuric acid contain-

ing vanadium(V) and vanadium(IV) sulphate Strongly oxidizing cations such as Co(III), Mn(III) and Mn(IV) oxidize V(IV), and reducing cations such as Fe(II), V(III) and Ti(III) reduce V(V) in such solutions The V(IV) produced may be titrated with potassium permanganate The method was applied in stoichiometry studies of materials such as $Y_3Fe_5O_{12}$, solid solutions such as Fe_2GeO_4–$ZnFe_2O_4$, Fe_2VO_4–FeV_2O and $MgFe_2O_4$–Mn_3O_4 V_2O_3, Mn_2O_3 and Co_3O_4, were reportedly determined with a relative error $\leqslant 0\,6\%$ and reproducibility $\leqslant 2\,5\%$ The stability of the vanadium solutions is an advantage, since for some samples, *e g*., $Y_3Fe_5O_{12}$, several days are required for dissolution

Several procedures involve dissolution of the ferrite sample in a standard ferrous ammonium sulphate solution in an inert atmosphere, followed by titration with cerium(IV) [94,95] This approach allows the indirect determination of Mn(III) and Mn(II).

Certain procedures describing the determination of oxidation states of cations in ferrites also use the terms "active" or "bound" oxygen determination, since they are used for measuring the oxygen deficit or excess arising from variations in oxidation states Chemical analysis by cerimetric titration and spectrophotometric determination of Fe(II) as the 1,10-phenanthroline–iron(II) complex has been used in conjunction with thermogravimetric studies and studies of variation in the atmosphere used in ferrite production [96] Bound oxygen in ferrites has also been determined indirectly[97] after dissolution of the sample in a mixture (dehydrated with acetic anhydride) of phosphoric acid, dichloroacetic acid and acetic acid During dissolution, water is liberated in a quantity equivalent to the bound oxygen in the ferrite, and is determined by titration with Karl Fischer reagent, with a relative error of $\pm 1\%$

The use of a hot phosphatocerate solution as solvent allows the determination of ferrous oxide in nickel ferrite and zinc germanium ferrite with a relative error $\leqslant 2\%$.[98] Excess of the phosphatocerate is titrated with ferrous ammonium sulphate, with ferroin as indicator

Finely powdered samples of 30–100 mg require 15–30 min for dissolution Citing pulverization of the sample as a source of error, other workers[99] have dissolved ferrite samples (as obtained) by heating them in sealed tubes containing 6*M* hydrochloric acid, a known quantity of iron(II), and nitrogen to give an inert atmosphere Iron(II) was titrated with ceric sulphate with ferroin as indicator "Active" oxygen, due to the presence of iron, manganese, chromium, nickel or lead in the tervalent or quadrivalent state, oxidizes part of the iron(II) in solution As little as 2 μg of active oxygen of 10 μg of iron(II) may be determined A blank is essential, since hydrochloric acid is known to contain small amounts of Cl_2, which reacts with iron(II)

Yttrium–iron garnets have been analysed[100] for iron(II) content by its biamperometric titration with ammonium vanadate after dissolution of the sample with hydrochloric acid Triplicate determinations of 0 1–2% of iron(II) had a relative error of 5–15%

A coulometric titration with potentiometric end-point detection used for analysis of Mn–Zn or Ni–Zn–Co ferrites may also be used for either iron(II) or active-oxygen determination [101] Samples are dissolved in sealed tubes containing hydrochloric acid, followed by titration of iron(II) with Cl_2 generated from the solvent, at a platinum electrode Blanks are run and if the presence of active oxygen is suspected, a known quantity of ferrous ammonium sulphate is added to the ferrite sample before dissolution Iron(II) contents ranging from 0 07 to 3.84% have been determined in Ni–Zn–Co ferrites Since hydrochloric acid is the solvent, Cl_2 is the most convenient electrogenerated titrant. Samples prepared by dissolution of 17 9 μeq of iron wire or 17 9 μeq of ferrous ammonium sulphate were titrated with average errors of 0 6 and 1 9% respectively Certain other coulometric procedures described in the section on electrochemical analysis can be modified for oxidation-state analysis, *e g* , procedures involving titration of iron with copper(I)

Iron(II) in magnesium–aluminium ferrites has been determined spectrophotometrically[102] by means of its 2,2′-bipyridyl complex As little as 2 5 mg of Fe(II) was determined Iron(III) was extracted with acetylacetone in carbon tetrachloride

A sensitive and accurate method has been developed for the determination of microgram quantities of Fe(II) in single crystal samples weighing only a few milligrams [103] The iron(II) was complexed with 4,7-diphenyl-1,10-phenanthroline, followed by extraction into a chloroform–ethanol medium The absorbance was measured at 540 nm against a solvent blank Iron(III) was masked with ammonium dihydrogen phosphate, and cobalt, copper and nickel did not interfere The lowest level determined in ferrite samples was 0 02% Fe(II) A precision better than 10% was obtained for Fe(II) standards Synthetic samples containing iron(II) in combination with cobalt, nickel, zinc, manganese or copper were analysed with average errors of 4% and 2% for samples containing 10 and 50 μg of iron(II) respectively

The EPR signal due to Pb(III) has been used to detect this ion as an impurity in yttrium–gallium garnet [104] It was found that Pb(III) ions occupy the dodecahedral sites in the garnet lattice

SUMMARY OF INSTRUMENTAL ANALYSIS PROCEDURES

Analysis by X-ray or electron excitation

Irradiation can excite an atom to a higher energy state by promoting an electron to an orbital of higher energy or removing it completely This excited state is unstable, so the atom returns to its ground state by one of two de-excitation processes In the first an outer-orbital electron fills the vacancy and loses

energy which is emitted as a photon Alternatively an electron from an inner orbital fills the vacancy and another electron from the same orbital is ejected as an Auger electron carrying the energy released. These two processes are competitive, so the probability of an excited atom emitting an X-ray (the fluorescence yield ω) and the probability of Auger emission sum to unity In general, atoms of low atomic number are de-excited by Auger emission, whereas those of higher atomic number are de-excited by X-ray production Since in either case the energy of the X-ray or the Auger electron represents the difference between the binding energies of one inner-shell and another shell or the vacuum level, the energy is uniquely characteristic of a particular atom A measurement of this energy is therefore sufficient for identification of the element. When individual atoms are combined into a solid the binding energies can be changed by an amount depending on both the inner-shell involved and the nature of the valence bonds formed, so measurements of the energy shift can provide information on the chemical state of the atoms examined The incident radiation can be either photons or electrons, the only requirement being that the beam has sufficient energy to eject an electron in one or more of the shells in all the atoms of interest Three combinations have been applied to ferrite studies and will be considered here

(*a*) Fluorescent X-rays stimulated by X-rays (XRF)

(*b*) Fluorescent X-rays stimulated by electrons, combined with electron probe microanalysis (EPMA)

(*c*) Auger electrons stimulated by electrons (AES)

X-Ray fluorescence (XRF)

XRF has been applied widely to the study of ferrites, because it can offer a useful combination of advantages The conventional arrangement involves a suitable source of X-rays, such as a rotating-anode X-ray generator, the output of which is collimated to produce an illuminating beam a few hundred μm or more in diameter The beam irradiates the sample, which can be in any convenient form, and the fluorescence X-rays produced are collected and analysed with either a crystal spectrometer or an energy-dispersive spectrometer. The crystal spectrometer functions by an application of Bragg's law, and offers high energy-resolution It can thus differentiate between X-ray lines of similar energy, a factor which is important in multi-element systems, or accurately measure chemical shifts By appropriate choice of crystals all elements with atomic number $\geqslant 5$ can be detected However, only one element at a time can be measured with a single-crystal analyser and complex systems therefore require several crystals and several separate measurements per crystal to cover all the elements present While such a procedure can be employed to verify the presence of a given set of elements, the probability of an unsuspected element such as a contaminant being detected is very small unless a time-consuming angular sweep of each crystal is performed.

The energy-dispersive X-ray spectrometers use a lithium-doped silicon detector interfaced with a multi-channel analyser In this approach all the elements present are analysed for simultaneously, so it is ensured that even unsuspected elements are found However, in general only elements with atomic number greater than that of sodium can be determined directly Because relatively large numbers of counts can be accumulated quickly, this approach is particularly suited to quality-control operations The sample spectrum can be compared with a previously stored control spectrum by a computer and any discrepancy outside some preset limits used to start an alarm or terminate the process. Since the technique is non-destructive, rapid and fully automated, it has obvious benefits

For many detailed analyses, however, this qualitative comparison must be replaced by a quantitative technique Ideally, the composition of a ferrite could be directly determined by comparing the intensities of the X-ray line for a particular element in the unknown and in a suitable standard The ratio gives the atomic fraction of the element This simple scheme is upset by several factors First the radiation from an element can be absorbed by another element, so the intensity observed is reduced Secondly the radiation from one element can excite fluorescence from another, and thus increase the intensity of the X-ray line of the latter element Lastly, since the incident X-ray beam penetrates a substantial depth of material it is necessary to ensure that the beam is fully absorbed in both the unknown and the standard, which may be difficult if one or the other is thin or of variable thickness An accurate quantitative analysis therefore requires either that matrix corrections be made for these effects, or that an experimental technique be used which eliminates the necessity for them The following examples, drawn from the extensive literature, are illustrative of the commonly applied techniques

A typical approach of the first type is that reported by Raevskaya *et al* [105] for the determination of Fe_2O_3, MnO and MgO The manganese and magnesium contents were obtained directly from measurements of pure mixed binary standards of the two oxides, and shown to be linear functions of the observed intensities, but the intensity of the iron K_α and K_β lines for varying Fe_2O_3 content was found to depend on the relative concentrations of manganese and magnesium By using mixed pure oxide standards a series of coupled linear equations, representing the matrix-correction calibrations, was obtained and then used for the analysis An error of 0 1% was claimed, although no actual count statistics were supplied to justify this claim A similar technique was

employed by Magathan *et al*,[106] who generated a table of interelement correction coefficients based on data from mixed binary standards, to give a claimed error of $<1\%$ A variant of this approach is to use intensity ratios instead of absolute intensities for calibration Thus Murata[107] studied Mn–Zn ferrites by using a direct calibration for ZnO against a standard, but measuring the intensity ratio of the iron K_α and manganese K_α lines to obtain the content of MnO and Fe_3O_3 by comparison with the intensity ratios for mixed standards This approach reduces the number of variables in the equation and consequently simplifies the numerical analysis This procedure was claimed to produce an error of 0 2% A different normalization was employed by Florestan[108] in a determination of Nb, Dy, Mn and Al in garnets Here the scattered Compton radiation from standards was recorded in addition to the chosen X-ray lines, and it was shown that when normalized by means of the Compton component a set of linear calibration plots was obtained Finally, when only the variation of one element is of concern the process can be simplified still further, as was done by Bhawalkar *et al*[109] in their study of calcium in Mn–Zn ferrites Ferrites of the correct composition but containing different amounts of calcium were used as standards A plot of the calcium K_α intensity normalized by means of the iron K_β intensity gave a direct measure of the calcium content

The alternative method involves putting the sample into a form for which the matrix corrections are negligible The most convenient form is fine powder, since for sufficiently small particle diameters neither absorption nor self-fluorescence will be significant However, since the sample thickness is then small, only a fraction of the beam intensity, dependent on the thickness, is absorbed. Instead of measuring absolute intensities it is therefore necessary to record the intensity ratio of chosen lines instead Barlow and Van Valkenburg[110] used ion-exchange (for Gd–Fe systems) to produce powders supported on filter paper suitable for analysis, using the Fe/Gd intensity ratios for the measurement A benefit of this approach is that, in addition to avoidance of the matrix correction, standards can be prepared by simple solution chemistry techniques An error of ± 0 5% was claimed An alternative approach has been described by Luke,[111] who uses co-precipitation to obtain powders of Mn, Ni and Zn ferrites, with Cu or Fe as the co-precipitating ion Intensity ratios, compared with those for standards similarly prepared, give a direct determination of each element present, with a claimed error of 0 6% Though these techniques have been successfully applied, the sample preparation required is sufficiently lengthy to remove much of the advantage of speed and convenience that is characteristic of the XRF method Most studies have therefore relied on either qualitative comparisons with standards, or on computer-calculated matrix corrections

Electron probe microanalysis (EPMA)

The electron probe microanalyser uses an energetic beam of electrons to generate the fluorescent X-rays from the sample, rather than the X-ray flux used in XRF The most important single advantage of this is that the electron beam can be focused to a fine probe to allow spatially resolved microanalysis The degree of resolution obtained will depend on the energy of the beam and on the sample, because the beam scatters as it travels through the specimen, but typically a volume 5–10 μm in diameter can be selected and analysed In addition, since the penetration of the beam is much less than that of an X-ray beam, thin samples can be analysed without having to be removed from their substrate. However the advantages are obtained at the cost of a rather poorer peak-to-background ratio in the spectra than for XRF, and by the additional complication of the good vacuum system needed for the electron beam The techniques for collecting, detecting and analysing the X-rays are identical to those for the XRF technique, and in general an electron probe will use both energy-dispersive and crystal spectrometers, the first for rapid analysis of major constituents, the second for trace elements or for cases where peak overlaps are a problem In addition provision is made to produce a two-dimensional map indicating the relative concentration of one or more chosen elements The accuracy of the analytical result will depend on the counting statistics, and on the quality of the matrix corrections Since the electron beam penetrates only a relatively small distance the corrections are more straightforward than for XRF Most published studies rely on the use of calibration curves derived from suitable standards For example Van Hook and Guentert[112] studied Y–Gd–Ga–Fe–O by using calibration curves derived from gadolinium and gallium YIG standards Relying on the limited electron beam penetration, they left the samples on their GGG (gallium gadolinium garnet) substrates The results demonstrated minor variations in the Gd/Gd ratio, which it was possible to correlate with changes in the saturation magnetization A similar technique was used by Szaplonczay[113] in a study of epitaxially grown garnets Here bulk standards were employed, and films of different thickness were examined to show that the gadolinium concentration fell with increasing thickness No specific accuracy limits were claimed for these observations, but comparable studies[114] have indicated probable error limits of about 1–2% The alternative procedure using pure element standards and "ZAF" routines, which compute the matrix corrections for atomic number (Z), absorption (A) and fluorescence (F) effects, has been widely applied A study by Kurosawa[115] of epitaxial garnet films on GGG, similar to that discussed above, yielded data which showed deviations of up to 5% from figures obtained by plasma emission spectroscopy Because the computer corrections rely on

many fitted parameters and operate iteratively until convergence is obtained, such an error can easily occur under conditions where the corrections required are significant In that event recalculation of some of the correction parameters is required Weisweiler,[116] in a study comparing EPMA and wet analysis results for several ferrites, found it necessary to derive new ionization cross-sections and mass-absorption correction factors by back-calculation in order to harmonize the data Once this has been done, however, good accuracy can be obtained from the EPMA technique alone for other similar specimens

In addition to the elemental composition, the valence state can be determined, by a measurement of the change in energy of the X-ray peak The magnitude of the shift is rather small (0 5–5 eV) because the transitions used in the X-ray analysis arise from inner-shell levels which are screened from the valence electrons However, using such a method Kirichok and Karalnik[117] studied the relative concentration of Fe(II) and Fe(III) in ferrites and spinels It was found that Fe(II) could be detected both in non-ferromagnetic spinels and at a low concentration in ferrites The potential of this technique is considerable, but it requires very accurate wavelength calibration and carefully optimized crystal spectrometers and this may limit its practical application

The fact that the electron beam can be focused to probe volumes of small diameter allows direct measurements of spatial inhomogeneities in a material Thus, for example, Andrushchenko *et al*[118] studied the distribution of gallium across as-grown crystals of Y–Ga garnets in order to correlate changes in physical properties with compositional gradients This measurement was made by observing the point to point variation in the ratio of a chosen gallium line with that from a standard, but a direct plot of such a distribution can be obtained by displaying a signal (on the cathode-ray tube) proportional to the instantaneous count-rate of the line as the area of interest is scanned by the probe The limit of spatial resolution will be determined by the spreading of the electron beam within the sample, and this is typically a few μm This limit can be removed by using material thin enough to be transparent to electrons, allowing microanalysis at the level of a few hundred Å penetration but at the expense of much worse counting statistics However, this ability to perform spatially resolved analysis rarely seems to be the reason for choosing the EPMA in preference to some other technique Rather it seems that it is the convenience and high degree of automation of the electron probe that makes it attractive

The third technique is to measure the Auger electron spectrum (AES) This is a surface-sensitive technique because the escape depth for Auger electrons is only 1–5 nm, and this fact is often used to obtain depth profiles of composition by performing Auger analysis in conjunction with ion sputtering[119] In addition, newer Auger systems can analyse, and image, sub-μm diameter regions, suggesting the application of AES to study of grain boundaries in ferrites as a potentially worthwhile field Although the sensitivity of AES is high, the quantitation of the data is difficult and the technique would appear to be best suited as a research tool at the moment

CONCLUSION

The most suitable method of analysis for characterizing raw materials and finished ferrite products is chosen after considering the ultimate use of the analytical information to be obtained Two distinct situations are encountered, the first involving analysis of materials subject to fundamental investigations such as those seeking to relate precisely the nature of the product obtained to varying conditions of manufacture in order to optimize the process, or studies in which physical and performance properties are correlated with ferrite compositions The other application of analysis is, of course, the routine screening of raw materials and ferrite products on an industrial production level The nature of the first application requires more precise procedures and tolerates more time-consuming methods Methods can be selected on the basis of a knowledge of the qualitative composition of the ferrite to be analysed, including information about the major and trace constituents, which could be obtained from more routine methods suitable for the second type of analytical application

The wide variety of analytical methods discussed here makes it possible to find a suitable technique optimized for any particular requirements. Among the considerations leading to the selection of a method are homogeneity of the sample, the importance of major constituent stoichiometry, the presence of trace impurities, whether a qualitative, semi-quantitative or quantitative analysis is required, and the speed needed The chemical techniques described here offer a high degree of accuracy, precision and suitable specificity, but for many purposes their application would be too time-consuming or costly In such situations it may be advantageous to use a suitable chemical technique for standardization and then rely on a secondary instrumental method for rapid, or routine, testing Techniques such as XRF or EPMA readily lend themselves to this type of application since they are inherently highly automated, rapid, require little sample preparation and are highly accurate when properly standardized Emission spectrography is certainly useful for screening raw materials and ferrites to determine, at least qualitatively, the major and trace constituents For more detailed investigations and for fundamental research, the conventional techniques of wet analysis, atomic-absorption and electrochemistry remain important tools, especially with the improvements in sensitivity and accuracy made possible by advances in instrumentation

Clearly no single technique is able to fully characterize a sample in all the aspects that might be required, and a combination of methods chosen to minimize problems from the conflicting requirements of specimen preparation will be required Although the basic differences between techniques which assume homogeneity in the sample and those which have some spatial discrimination are clear, it must also be realized that the volume sampled by different techniques can vary even more widely than the lateral resolution Thus the volume sampled by a typical Auger analyser, 10 μm × 10 μm × 1 nm is about 10^{-9} of the volume sampled by a spark technique or a typical wet chemical analysis

Microstructural characterization, using such techniques as electron microscopy and electron diffraction, possibly combined with X-ray or electron spectroscopy, has not been explicitly considered here However, as the grain-size of ferrites is made smaller the importance of microstructure and particularly of the grain boundary region becomes even greater As a consequence, this type of investigation is likely to be of value in fundamental studies of ferrite behaviour, although its value for routine analysis is very limited because of the time required for sample preparation and examination

The literature cited in this review is not necessarily exhaustive in its representation of the application of various techniques to ferrite analysis, but sufficient examples are included to provide a guide for those interested in developing analytical procedures for various applications Information concerning the most frequently encountered ferrite compositions is certainly adequate for this purpose

REFERENCES

1 R F Soohoo, *Theory and Application of Ferrites*, Chap 1 Prentice-Hall, Englewood Cliffs, 1960
2 J Smit, *Magnetic Properties of Materials*, Chap 2 McGraw-Hill, New York, 1971
3 G Y Chin, *Ferrite*, in *McGraw-Hill Encyclopedia of Science and Technology*, 5th Ed , to be published 1982
4 J L Snoek, *Philips Tech Rev* , 1946, **8,** 353
5 W H von Aulock, *Ferrites*, in *Encyclopedia Brittanica*, Oxford University Press, 1974, **1,** 248
6 H B Ries, *Interceram*, 1966, No 1, 84
7 E W Gorter, *Proc IRE*, 1955, **43,** 1945
8 E Varzaru and A Cormos, *Rev Chim Bucharest*, 1967, **18,** 623, *Chem Abstr* , 1968, **68,** 101604
9 A Funke, *Z Anal Chem* , 1969, **244,** 105
10 J Novák and R Gerber, *Chem Listy*, 1969, **63,** 395, *Chem Abstr* , 1969, **71,** 45295
11 A Funke and H J Laukner, *Z Anal Chem* , 1970, **249,** 26
12 R C Hughes, R C Sweet and R Mavrodineanu, *Ferrites* in *Encyclopedia of Industrial Chemical Analysis*, Vol 12, p 514 Interscience, New York, 1971
13 T Inui and N Ogasawara, *IEEE Trans Mag* , 1977, **13,** 1729
14 B B Ghate, *Mater Sci Res* , 1978, **11,** 369
15 L R Whicker, *IEEE MTT-S Intern Microwave Symp Dig* , 1979, 367
16 B G Street, *Powder Metall* , 1979, **22,** 62
17 T G Reynolds in *Kirk-Othmer Encyclopedia of Chemical Technology*, Vol 9, p 881 Wiley, New York, 1980
18 S Krupicka, *J Magn Mater* , 1980, **19,** 88
19 G Schwarzenbach, *Complexometric Titrations*, 2nd Ed Methuen, London, 1957
20 F J Welcher, *The Analytical Uses of Ethylenediaminetetraacetic Acid* Van Nostrand, Princeton, 1958
21 H A Flaschka and A J Barnard, Jr , in *Comprehensive Analytical Chemistry*, Vol Ib, C L Wilson and D W Wilson (eds), Chap VII Elsevier, Amsterdam, 1960
22 R Přibil, *Applied Complexometry* Pergamon Press, Oxford, 1982
23 D H Wilkins, *Anal Chim Acta*, 1959, **20,** 271
24 R Přibil and V Veselý, *Chemist-Analyst*, 1961, **50,** 108, *Chem Abstr* , 1962, **56,** 12303*i*, 12309*a*
25 C Rózycki, *Chem Analit Warsaw*, 1967, **12,** 573, *Chem Abstr* , 1968, **68,** 65438
26 E Chiaki, Y Tomita and M Ezawa, *Bunseki Kagaku*, 1966, **15,** 1047, *Chem Abstr* , 1967, **66,** 121771
27 W G Scribner, *Anal Chem* , 1959, **31,** 273
28 R Přibil and V Veselý, *Chemist-Analyst*, 1961, **50,** 73
29 V Fano and F Licci, *Analyst*, 1975, **100,** 507
30 T Mutsunobu, *Bunseki Kagaku*, 1966, **15,** 1384, *Chem Abstr* , 1967, **67,** 7706
31 V Bărcănescu, E Potamian and S Călugareanu, *Rev Chim Bucharest*, 1964, **15,** 561, *Chem Abstr* , 1966, **64,** 1353*a*
32 I A Shevchuk and T N Simonova, *Metody Analit Khim Reaktovov Prep* , 1967, **14,** 65, *Chem Abstr* , 1968, **69,** 64410
33 O Miyamoto, Y Tanaka and M Kurukawa, *Nagoya Kogyo Giyutsu Shikensho Hokoku*, 1962, **11,** 224, *Chem Abstr* , 1962, **57,** 1543*e*
34 T R Andrew and P N R Nichols, *Analyst*, 1961, **86,** 676
35 F P Gorbenko and L I Degryarenko, *Tr Vses Nauch -Issled Inst Khim Reaktivov Osobo Chist Khim Veshchestn* , 1966, **29,** 69, *Chem Abstr* , 1968, **68,** 26684
36 I A Shevchuk, N N Nikol'skaya and T N Simonova, *Metody Analit Khim Reaktivov Prep* , 1967, **14,** 63, *Chem Abstr* , 1968, **69,** 64364
37 H Kitagawa and N Shibata, *Bunseki Kagaku*, 1962, **11,** 358, *Anal Abstr* , 1964, **11,** 169
38 I A Shevchuk, N N Nikol'skaya and T N Simonova, *Metody Analit Khim Reaktivov Prep* , 1967, **14,** 74, *Chem Abstr* , 1968, **69,** 64359
39 I A Shevchuk, N N Nikol'skaya and T N Simonova, *ibid* , 1967, **14,** 71, *Chem Abstr* , 1968, **69,** 64354
40 G P Pedan, Y Karavanskays and G V Kukhtenkova, *Zavodsk Lab* , 1964, **30,** 1448, *Chem Abstr* , 1965, **62,** 5892*f*
41 *Idem, Ukr Khim Zh* , 1965, **31,** 722, *Chem Abstr* , 1965, **63,** 14043*b*
42 I A Shevchuk and T N Simonova, *ibid* , 1964, **30,** 983, *Chem Abstr* , 1965, **62,** 3384
43 F P Gorbenko, E D Kuchkina and E U Volodko, *Tr Vses Nauch -Issled Inst Khim Reaktivov Osobo Chist Khim Veschchestn* , 1966, **29,** 121, *Chem Abstr* , 1968, **68,** 18369
44 W Kemula and C Brajter, *Chem Analit Warsaw*, 1961, **6,** 343
45 V Fano and F Licci, *Mikrochim Acta*, 1975 **II,** 561
46 W Grosskreutz, D Schultze and K T Wilke, *Z Anal Chem* , 1967, **232,** 278
47 F Tanos, *Tavkoslesi Kut Intez Kozl* , 1973, **18,** 47, *Chem Abstr* , 1973, **78,** 52165
48 J Novák, *Z Anal Chem* , 1977, **285,** 126
49 A J Bard and L R Faulkner, *Electrochemical Methods*, Chap 5 Wiley, New York, 1980
50 A M Bond, *Modern Polarographic Methods in Analytical Chemistry*, Chap 6 Dekker, New York, 1980
51 S L Phillips and E Morgan, *Anal Chem* , 1959, **31,** 1467

52 W Kemula, K Brajter and S Rubel, *Chem Analit Warsaw*, 1961, **6,** 331, *Chem Abstr*, 1962, **56,** 2882i
53 L A Mikhailova, *Tezisy Dokl Mezhotrasl Soveshch Metod Poluch Anal Ferritovykh, Segneto-, P'ezoelektricheskikh Kondens Mater Syr'ya Nikh, 4th*, 1971, 1972, 134, *Chem Abstr*, 1974, **81,** 130497
54 W Gorzelany and M Mielczarek, *Chem Analit Warsaw*, 1966, **11,** 77, *Chem Abstr*, 1966, **64,** 18404b
55 E L Bush and E J Workman, *Analyst*, 1965, **90,** 346
56 L N Nikolaeva, O N Fedorov and T E Komissarova, *Zavodsk Lab*, 1971, **37,** 913, *Anal Abstr*, 1972, **22,** 4006
57 L N Nikolaeva and T E Komissarova, *Zh Analit Khim*, 1974, **29,** 1658, *Chem Abstr*, 1975, **82,** 50956
58 Z Marczenko, *Spectrophotometric Determination of Elements* Horwood, Chichester, 1976
59 C K Bhaskare and S G Kawatkar, *Talanta*, 1975, **22,** 189
60 E Chiaki, Y Tomita and M Ezawa, *Bunseki Kagaku*, 1968, **17,** 13, *Anal Abstr*, 1969, **17,** 2103
61 F Bermejo and G Branas, *Mikrochim Acta*, 1971, 489
62 S Grinshpun, M B Fisherman and Yu M Belava, *Prom Khim Reaktivov Osoba, Chistykh Veshchestn Gos Kom Khim Neft Prom pri Gosplone SSSR, Inform Byul*, 1963, **1,** 24, *Chem Abstr*, 1964, **61,** 2470c
63 V T Vasilenko, *Zavodsk Lab*, 1965, **31,** 1070, *Chem Abstr*, 1965, **63,** 17131b
64 I A Shevchuk, F P Gorbenko and T N Simonova, *Metody Analit Khim Reaktivov Prep*, 1967, **14,** 68
65 N F Budyak, *Zh Prikl Khim*, 1971, **44,** 669, *Chem Abstr*, 1971, **74,** 150757
66 S L Levine, *Anal Chem*, 1968, **40,** 1376
67 G V Plyushch, *Zavodsk Lab*, 1968, **34,** 1471, *Chem Abstr*, 1969, **70,** 63860
68 K Ametani, *Bull Chem Soc Japan*, 1974, **49,** 2238
69 K-H Konig and P Neumann, *Anal Chim Acta*, 1973, **65,** 210
70 K Ametani, *Talanta*, 1978, **25,** 317
71 V P Borzov, G V Plyushch and N G Yanklovich, *Zavodsk Lab*, 1966, **32,** 1471, *Chem Abstr*, 1977, **66,** 82106
72 Y Yamamoto, T Kumamaru and Y Otani, *Kogyo Kagaku Zasshi*, 1971, **74,** 779, *Chem Abstr*, 1971, **75,** 45555
73 V M Novikov and V A Shiryaeva, *Ezheg Rab*, 1971, **1970G,** 417, *Chem Abstr*, 1972, **77,** 147214
74 V P Borzoz, M G Mal'tsev, G V Plyushch and T F Luk'yanova, *Specktrosk Tr Sib Soveshch, 4th, 1965*, 1969, 354, *Chem Abstr*, 1971, **74,** 9353
75 V A Gubanov, *Analit Metody Geokhim Issled, Mater Geokhim Konf, 4th, 1970*, 1972, 76, *Chem Abstr*, 1974, **80,** 115702
76 M Z Nesanelis, E S Zolotovitskaya and V K Shevchenko, *Monkrist Tech*, 1971, **5,** 141, *Chem Abstr*, 1973, **78,** 105617
77 S K Bondarenko, Zh A Mamot and S V Prokop'eva, *Zavodsk Lab*, 1970, **36,** 945, *Chem Abstr*, 1971, **74,** 9257
78 K Dittrich and R Wennrich, *Chem Analit Warsaw*, 1974, **19,** 475, *Chem Abstr*, 1974, **81,** 145148
79 A Y Vidisheva and T M Zinchenko, *Zh Analit Khim*, 1976, **31,** 1688, *Chem Abstr*, 1977, **86,** 132902
80 L I Karpenko, L A Fadeeva and L D Shevchenko, *Zh Analit Khim*, 1979, **34,** 275, *Chem Abstr*, 1979, **90,** 214632
81 E Cruceanu, P Miron and J Neuberger, *Lucr Conf Nat Chim Anal 3rd*, 1971, **2,** 27, *Chem Abstr*, 1972, **77,** 83213
82 A Miller, *J Appl Phys*, 1960, **31,** 261S
83 A M Szaplonczay, *J Can Ceram Soc*, 1969, **38,** 111
84 H Nagato, *Bunseki Kagaku*, 1961, **10,** 985, *Anal Abstr*, 1963, **10,** 4159
85 *Idem, Rev Elec Comm Lab*, 1961, **9,** 300
86 *Idem, Bunseki Kagaku*, 1962, **11,** 1291, *Anal Abstr*, 1964, **11,** 1736
87 *Idem, ibid*, 1966, **15,** 129, *Anal Abstr*, 1967, **14,** 6132
88 W Bonsels and I Linnemann, *Z Anal Chem*, 1965, **214,** 422
89 G Schnitt and A Funke, *ibid*, 1967, **230,** 338
90 T E Komissarova and E A Pozdnyakova, *Zh Analit Khim*, 1974, **29,** 306
91 J Marinenko, *Anal Lett*, 1976, **9,** 775
92 E A Pozdnyakova, T E Komissarova and A M Barssukova, *Zh Analit Khim*, 1971, **26,** 1128
93 D G Wickham, *Talanta*, 1963, **10,** 314
94 P Kleinert, *Acta Chim Acad Sci Hung*, 1962, **31,** 339, *Chem Abstr*, 1963, **58,** 1904g
95 E A Pozdnyakova and T E Komissarova, *Zh Analit Khim*, 1971, **26,** 2046
96 R Marineau and M Paulus, *Phys Stat Sol*, 1973, **20,** 373
97 K Hochmann-Fischer, *Z Anal Chem*, 1966, **220,** 346
98 K L Cheng, *Anal Chem*, 1964, **36,** 1666
99 G W van Oosterhout and J Visser, *Anal Chim Acta*, 1965, **33,** 330
100 A M Bulgakova, G A Antipova and A P Mirnaya, *Zavodsk Lab*, 1971, **37,** 914, *Anal Abstr*, 1972, **22,** 3148
101 P K Gallagher, *Am Ceram Soc Bull*, 1978, **57,** 576
102 K H Lieser and H Schroeder, *Z Anal Chem*, 1960, **174,** 569
103 F Licci, *Mikrochim Acta*, 1977 **I,** 37
104 B Andlauer, J Schneider and W Tolksdorf, *Phys Rev B*, 1973, **8,** 1
105 T N Raevskaya, N I Korepanova and V T Vasilenko, *Zavodsk Lab*, 1973, **39,** 1474, *Chem Abstr*, 1974, **80,** 103462
106 E M Magathan, D W Short and R L Yocom, *Adv X-Ray Analysis*, 1975, **18,** 327
107 M Murata, *X-Ray Spectrom*, 1973, **2,** 111
108 J Florestan, *CEN Commis Energ Ab France, Rept*, CEA-CONF-2590, 1972, *Chem Abstr*, 1975, **82,** 105924
109 R H Bhawalkar, K C Nagpal and S Z Ali, *Indian J Tech*, 1972, **10,** 388
110 I C Barlow and R K Van Valkenburg, *Mikrochim Acta*, 1968, 827
111 C L Luke, *Anal Chim Acta*, 1968, **41,** 237
112 H J Van Hook and O J Guentert, *Am Inst Phys Conf on Magnetism and Magnetic Materials*, 1973, **10,** 419, *Chem Abstr*, 1973, **79,** 13192
113 A M Szaplonczay and H Quon, *Can J Spectrosc*, 1975, **20,** 6
114 D Keji and M Saburo, *Natl Tech Rept*, 1964, **10,** 449
115 S Kurosawa, *Bunseki Kagaku*, 1977, **26,** 833, *Chem Abstr*, 1978, **89,** 16159
116 W Weisweiler, *Arch Eisen*, 1978, **49,** 555, *Chem Abstr*, 1979, **90,** 66188
117 P P Kirichok and S M Karalnik, *Izv Akad Nauk SSR*, 1967, **31,** 1027, *Chem Abstr*, 1967, **67,** 95315
118 N S Andrushchenko, R A Petrov, Y G Suksonov and A G Titova, *Bull Acad Sci USSR*, 1971, **35,** 1158, *Chem Abstr*, 1977, **87,** 47697
119 R G Hart and G W Simmons, *J Vac Sci Tech*, 1978, **15,** 716

Talanta, Vol 30, No 5, pp 317–322, 1983
Printed in Great Britain

0039-9140/83/050317-06$03 00/0

EVALUATION OF DIFFERENTIAL PULSE VOLTAMMETRY AT CARBON ELECTRODES

JOSEPH WANG* and BASSAM A. FREIHA
Department of Chemistry, New Mexico State University, Las Cruces, NM 88003, U S A

(*Received* 22 *August* 1982 *Accepted* 8 *December* 1982)

Summary—The background and analytical responses of differential pulse voltammetry at carbon electrodes have been evaluated Transient currents associated with small potential steps have been examined and are attributed mainly to redox reactions of various groups on the electrode surface Instrumental parameters have been thoroughly investigated and optimized for improving the signal-to-background response Glassy-carbon and carbon-paste disk electrodes have been compared, and the latter found to yield better response owing to the lower background current Dopamine, epinephrine, chlorpromazine, ascorbic acid, homovanillic acid and ferrocyanide were used as test systems

Differential pulse voltammetry (DPV) is the most sensitive and widely used voltammetric technique other than anodic stripping voltammetry The technique was designed for achieving a large differential between the analytical current and charging current at the end of the life of the mercury drop With the increasing need for trace analysis for important oxidizable compounds (*e.g.*, drugs, vitamins, carcinogens) the technique has been used with various solid electrodes, such as carbon or platinum, which have a wider anodic potential range than mercury electrodes [1–9] Although for certain compounds detection limits around the $10^{-8}M$ concentration level have been reported,[1,3,7] in most cases the detection limits are around the $10^{-6}M$ level.[6,8,10]

The reason for the inferior sensitivity of DPV at solid electrodes (compared to that at mercury electrodes) is the additional background current component due to redox reactions of the electrode surface Consider the surface of solid carbon electrodes, for instance Studies of various carbon surfaces have indicated the existence of various functional groups such as carbonyl, carboxyl, phenolic and quinonoid [11,15] As the potential is stepped (as in DPV), the oxidation states of these functional groups are changed, and a current flows The resulting faradaic background current decays very slowly (over some minutes) in comparison with the rapid (a few msec) decay of the accompanying double-layer charging current [10] Most commercial polarographic analysers, *e g* , the Princeton Applied Research Model 174, are designed for use with a dropping mercury electrode and ~50 msec pulse duration, which is sufficiently long for complete decay of the charging current. Thus, utilizing carbon surfaces, the current sampled toward the end of the pulse contains a significant contribution from the surface transient background current

This work was initiated in order to characterize more fully the nature of the background current in DPV at carbon electrodes (to which little attention has been given). For this purpose, small potential steps (ΔE = 10–100 mV) are applied to the working electrode, immersed in the supporting electrolyte solution, from the magnitude and shape of the resulting transient currents important information is obtained about the DPV background current Larger potential steps (ΔE = 400 mV) were applied[16] to investigate the behaviour of carbon electrodes in normal pulse voltammetry In addition to the characterization of the background current, data have been obtained on the effects of pulse amplitude, repetition time, scan-rate, and rotation speed on the analytical response These data are used for optimizing the experimental parameters for DPV at carbon electrodes

EXPERIMENTAL

Apparatus

A 100-ml (6 5-cm diameter, 5 0 cm high) Pyrex glass cell with a 5-hole "Plexiglas" cover was employed A 0 75-cm diameter glassy-carbon disk (Model DDI, Pine Instruments Co , Grove City, PA) and 0 75-cm diameter "homemade" carbon-paste disk served as the working electrodes The working electrode was mounted on a rotating disk assembly (Model PIR, Pine Instruments Co) The working electrode, the Ag/AgCl(3*M* NaCl) reference electrode, the spectroscopic-graphite auxiliary electrode, and the nitrogen delivery tube entered the cell through the holes in its cover The glassy-carbon face was polished with a 5-μm alumina suspension The carbon paste was prepared by thoroughly mixing 2 5 g of graphite powder (Acheson Graphite, Grade 38, Fisher) and 1 5 g of Nujol oil The paste surface was smoothed with a computer card A fresh electrode surface was used for each experiment All experiments were performed with a Princeton Applied Research Model 174 Polarographic Analyzer, in conjunction with a Houston Omniscribe strip-chart recorder

Reagents

All solutions were prepared with demineralized water The chemicals and reagents used were those described previously,[17] unless otherwise stated Millimolar and submillimolar stock solutions of homovanillic acid and chlorpromazine (Sigma Chemical Co), respectively, were pre-

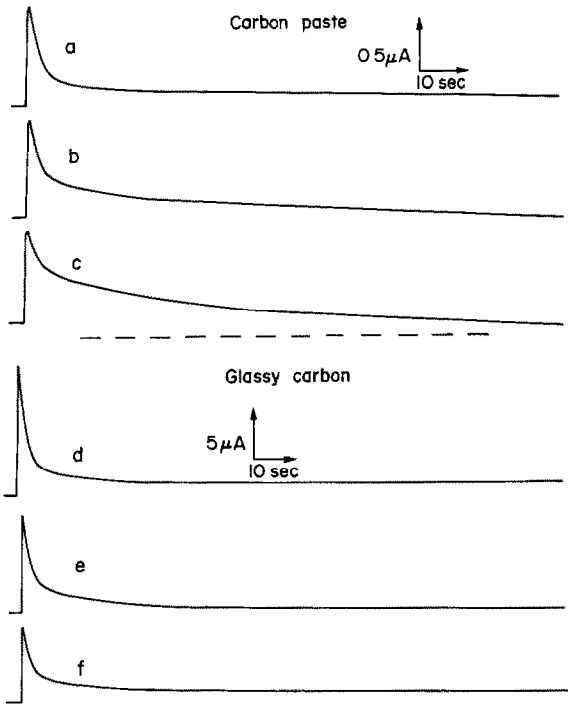

Fig 1 Current–time relationships after the application of potential steps from 0 to 0 1 V (a, d), 0 3 to 0 4 V (b, e), and 0 6 to 0 7 V (c, f) Carbon-paste (a–c) and glassy-carbon (d–f) stationary disk electrodes, 0 1*M* phosphate buffer (pH 7 4)

pared fresh every day The supporting electrolytes were 0 1*M* potassium chloride, 0 1*M* phosphate buffer (pH 7 4) and 0 5*M* sulphuric acid

Procedure

A 100-ml portion of supporting electrolyte solution was deaerated with nitrogen for 10 min, then the nitrogen delivery tube was raised above the solution The working electrode was pretreated by cycling the applied potential between −1 1 and +1 1 V for 12 min, allowing 2 min at each potential and ending at the positive potential Then the electrode was held at the starting potential for the scan, and after decay of the transient currents a differential pulse ramp was initiated DPV measurements were performed under various experimental conditions, as described later in the paper Potential steps were applied at the working electrode (with the supporting electrolyte solution in the cell) by switching between the HOLD and INITIAL settings of the polarographic analyser

RESULTS AND DISCUSSION

Background current characterization

In order to investigate the nature of the background current in DPV at carbon electrodes, small potential steps were applied to the working electrode in the supporting electrolyte solution Figure 1 shows the current–time relationships obtained for the glassy-carbon and carbon-paste electrodes after the application of 100-mV potential steps in different potential regions For both electrodes and at the various potential regions the potential steps yield large transient currents which settle down very slowly From the long time required to reach a steady state it is clear that the current (after ~20 msec) is due to the slow faradaic reorganization of functional groups at the electrode surface and not to double-layer charging The absence of oxidizable impurities in the supporting electrolyte solution was examined and verified by using sensitive stopped-rotation measurements[18] over the 0–1 0 V region Two interesting points are noticed from Fig 1 First, the current–time profile depends on the potential region employed, possibly because of potential-dependent reactions of different surface groups (surface reactions of the quinone–hydroquinone couple (~ +0 4 V) and formation of carboxyl groups (~ +1 0 V) were identified by cyclic voltammetry[15]) Secondly, although the two electrodes have the same surface area, much larger currents are observed at the glassy-carbon electrode (as indicated by the different current scales) Detailed examination of the transient currents in Fig 1 is given in Table 1 In all cases, it takes more than a minute to reach a steady-state current (the currents after 60 sec range between 3 and 18% of the initial currents) The currents measured 5 sec after the potential step correspond to 40–65% of the initial currents Though larger currents are observed at the glassy-carbon electrode, they decay faster than those at the carbon-paste electrode Finally, in most cases the currents decay faster as the potential region becomes less anodic

A log–log plot of current against time can provide important information regarding the rate of surface current decay following steps in the potential Such plots were made for the 0 3–0 4 V steps shown in Fig 1, over the 5–30 sec period following the step The resulting plots (not shown) were linear with slopes of −0 47 and −0 69 for the carbon paste and glassy carbon electrodes, respectively. Thus, though the rate of decay is not uniform, the slopes (around −0 5) are similar to that of the analytical diffusion-controlled faradaic current following a potential step In view of the similar decay rates of the

Table 1 Current–time profiles after 100-mV potential steps at carbon electrodes (conditions as for Fig 1)

Current ratio*	Potential step	Carbon paste			Glassy carbon		
		0→0 1 V	0 3→0 4 V	0 6→0 7 V	0→0 1 V	0 3→0 4 V	0 6→0 7 V
i_5/i_0		0 40	0 49	0 65	0 26	0 32	0 37
i_{10}/i_0		0 23	0 35	0 52	0 17	0 20	0 25
i_{30}/i_0		0 14	0 20	0 31	0 10	0 09	0 15
i_{60}/i_0		0 10	0 13	0 18	0 07	0 03	0 10

*The subscripts designate the time elapsed (sec) after the potential step, when the current is measured

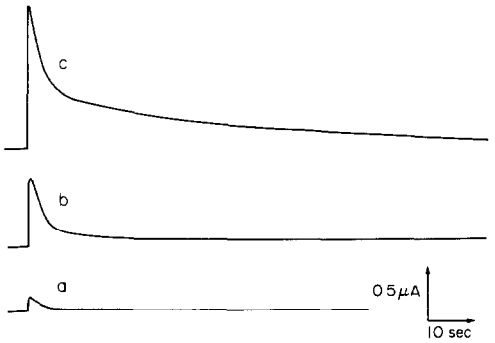

Fig 2 Current–time relationships after the application of 10-mV (a), 50-mV (b), and 100-mV (c) potential steps to 0 4 V Carbon-paste stationary disk electrode, 0 1*M* phosphate buffer

analytical and background currents, little advantage is expected from using longer DPV pulses and/or for measuring the difference between two currents sampled during the pulse [19] The latter approach was found profitable with platinum electrodes,[8] where the nature of the surface redox reactions is different from that for carbon electrodes.

The current–time relationship depends on the magnitude of the potential step (Fig. 2) The greater the step the larger the current associated with it the transient surface currents measured 2 sec after application of steps of 10, 50 and 100 mV, are 0.1, 0 5 and 1 1 μA, respectively

We examined the effect of the electrode treatment on the current–time response associated with 100-mV potential steps at the stationary glassy-carbon disk electrode This experiment yielded some surprising data (not shown graphically) After recording of the current–time relationships in the same manner as for Fig 1, an additional 10-min cathodic reduction of the surface (at -1 1 V) was applied This resulted in increases of the initial currents associated with the 100-mV potential steps 95% increases for steps from 0 to 0 1 V and from 0 3 to 0 4 V, and 50% increase for the step from 0.6 to 0 7 V Following this, an anodic treatment (10 min at $+1$ 1 V) was applied, the resulting initial currents for the potential steps were reduced by 25% for the 0–0 1 V step and by 30% for the 0 3–0 4 V and 0 6–0 7 V steps With an additional 10-min cathodic reduction of the surface at 1.1 V, the potential-step initial currents increased again to the level they had before the anodic oxidation. The surprising aspect of these data is the reduction of the potential-step currents following the anodic treatment of the surface It is known that additional surface functional groups become attached to the electrode surface during electrode treatment, mainly in anodic treatment [9 12] Thus, we expected an increase of the potential-step transient currents following surface oxidation However, our data indicate that functional groups formed by cathodic treatment, or the reduced form of groups formed in anodic treatment, are mainly responsible for the potential-step transient currents.

Another characteristic of DPV at carbon electrodes is the reproducibility of the background current It has been claimed that the slow faradaic surface reactions make it difficult to obtain a reproducible surface state [10] Figure 3 examines the stability of the background current in DPV at stationary glass-carbon and carbon-paste disk electrodes Eight repetitive runs were performed on each electrode, within 80 min For both electrodes only negligible changes of the background current are observed over these prolonged series. Changes in the background current during DPV measurements at carbon electrodes may therefore be attributed to adsorption of the analyte (a common occurrence with organic compounds) and not to the redox reactions of surface groups Also shown in Fig. 3, and as already indicated in the potential-step experiments, the DPV background current of the carbon-paste electrode is much lower than that of the glassy-carbon electrode (notice the different current scales employed). Since the surface functional groups depend on the structure of the carbon material employed, glassy carbon from different sources or carbon paste prepared by a different procedure, may yield different DPV background currents. For the same reason, the currents may be affected by the procedures used for polishing the glassy-carbon and surfacing the carbon-paste electrodes

Analytical response

The overall DPV response depends on the signal-to-background characteristics Figures 4 and 5 show

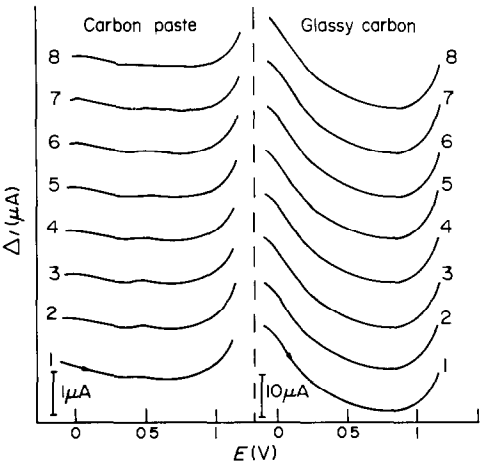

Fig 3 Successive differential pulse voltamperograms for the 0 1*M* phosphate buffer blank solution, at the stationary glassy-carbon and carbon-paste electrodes Voltamperograms recorded at 10-min intervals, with the number on each representing the run number Conditions scan-rate, 5 mV/sec, amplitude, 50 mV, repetition time, 0 5 sec The zero current of the individual curves is displaced for clarity

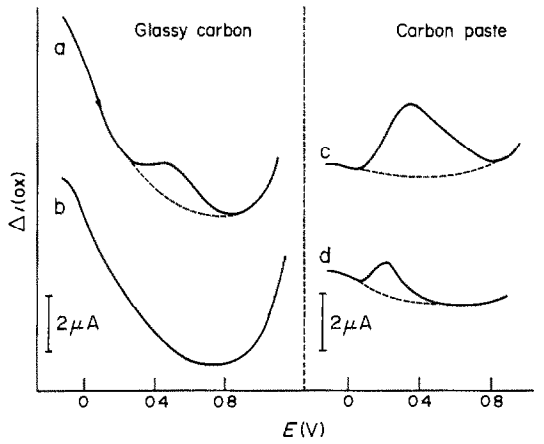

Fig 4 Differential pulse voltamperograms for $5 \times 10^{-5}M$ ferrocyanide at glassy-carbon (a, b) and carbon-paste (c, d) disk electrodes Conditions rotation speeds 2500 (a, c) and 0 (b, d) rpm, amplitude, 50 mV, scan-rate, 5 mV/sec, repetition time, 1 sec, supporting electrolyte, 0 1M KCl

differential pulse voltamperograms for $5 \times 10^{-5}M$ ferrocyanide and $5 \times 10^{-6}M$ epinephrine, respectively, recorded at the glassy-carbon and carbon-paste disk electrodes. Although electrode reactions on carbon paste are generally slower than at glassy-carbon electrodes,[20,21] the significantly lower background current of the paste (dotted lines) makes it superior to glassy carbon with respect to the overall signal-to-background characteristics This, combined with its low price and easy preparation, makes carbon paste the electrode material of choice in many applications However, in certain cases, such as use of organic solvents or cathodic reductions, glassy carbon has the advantages of better solvent-resistance and wider negative-potential limit (the carbon-paste electrode is affected by the oxygen incorporated in it[22])

Also shown in Figs 4 and 5 is the effect of electrode rotation on the DPV response Most DPV measurements at solid electrodes have been performed without forced convection (*i e.*, with a stationary electrode and quiescent solution).[1-9] In a few cases pulse voltammetry has been employed in studies using the rotating-disk electrode[23] or flow-through electrode [24] From the data of Figs 4 and 5 it is clear that DPV with a rotating electrode (voltamperograms a and c) has an advantage over similar measurements at a stationary electrode (voltamperograms b and d), giving about twice as large a peak current The ferrocyanide peak, which is detectable with the rotating glassy-carbon electrode (Fig 4a), is totally masked by the background current at the stationary electrode (Fig. 4b) From the signal-to-background characteristics of the voltamperograms at the rotating carbon-paste electrode, the detection limits for epinephrine and ferrocyanide would be around $2\,5 \times 10^{-7}M$ and $4 \times 10^{-6}M$, respectively Similar voltamperograms recorded for $5 \times 10^{-5}M$ ascorbic acid in 0.5M sulphuric acid yielded a detection limit of about $2 \times 10^{-6}M$ (not shown, conditions as in Fig 4c) The lower detection limits ($\sim 10^{-8}$–$10^{-9}M$) reported for some DPV/solid-electrode studies[1,3,7] are attributed to adsorption or extraction of the analyte, and do not reflect the detectability of solution-phase DPV Species in solution can be measured down to the $10^{-8}M$ level by use of various hydrodynamic modulation voltammetric procedures,[25] which are not commercially available

To check the dependence of the DPV peak current on rotation speed, three oxidizable compounds, ferrocyanide, dopamine, and chlorpromazine, were employed (Fig 6) Though for all compounds an increase in peak current with rotation speed is obtained, there are different relationships between the three On a log–log plot, the data of Fig 6 yield straight lines over the 900–3600 rpm range (not

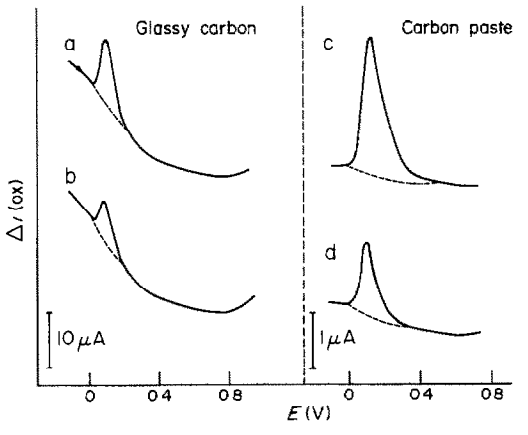

Fig 5 Differential pulse voltamperograms for $5 \times 10^{-6}M$ epinephrine at glassy-carbon (a, b) and carbon-paste (c, d) disk electrodes Conditions as for Fig 4, except that the supporting electrolyte was 0 1M phosphate buffer (pH 7 4)

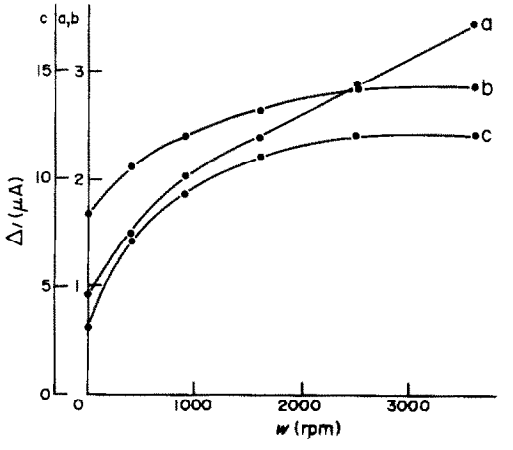

Fig 6 Dependence of peak current on rotation speed for $5 \times 10^{-5}M$ ferrocyanide (a), $5 \times 10^{-6}M$ dopamine (b) and $5 \times 10^{-6}M$ chloropromazine (c) Carbon-paste electrode Differential pulse ramp, as in Fig 4 Supporting electrolyte, 0 1M phosphate buffer (pH 7 4)

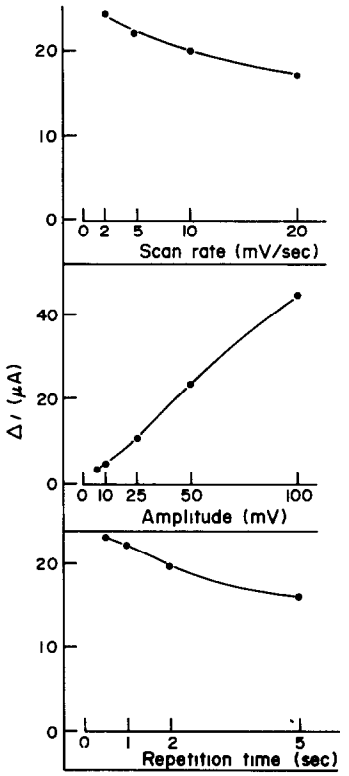

Fig 7 Effect of individual parameters on DPV response Peak currents are for $5 \times 10^{-4}M$ ferrocyanide in 0 1M KCl Rotating (2500 rpm) carbon-paste electrode Scan-rate study 1-sec repetition time and 50-mV amplitude Amplitude study 5 mV/sec scan-rate and 1-sec repetition time Repetition time study, 50-mV amplitude and 5-mV/sec scan-rate

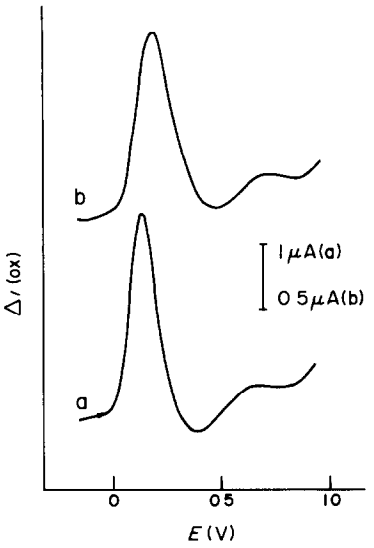

Fig 8 Differential pulse voltamperogram for $5 \times 10^{-6}M$ dopamine and $7\,5 \times 10^{-6}M$ homovanillic acid at rotating (2500 rpm) carbon-paste electrode Scan-rates, 5 (a) and 20 (b) mV/sec Amplitude, repetition time and supporting electrolyte as for Fig 3

shown), with slopes of 0.22, 0 36 and 0 40 for dopamine, chlorpromazine and ferrocyanide, respectively For reversible reactions, when longer pulse widths and high rotation speeds are used, "Levich" behaviour (slope 0 5) is expected [23] For compounds known to interact with the electrode surface, such as chlorpromazine,[26] deviation from the theoretical behaviour is obvious Notice also the larger currents observed in the case of chlorpromazine, due to its accumulation at the surface.

The effects of the DPV ramp parameters (scan-rate, amplitude, and repetition time) on the response were also evaluated. Ferrocyanide oxidation at the rotating carbon-paste electrode was used as a model system The results summarized in Fig. 7 demonstrate the effect of each individual parameter on the peak current. It can be seen that reductions of 31% and 27% respectively in the peak current are obtained by increasing the scan-rate from 2 to 20 mV/sec or the repetition time from 0 5 to 5 sec At the same time, ~40% increase of the peak half-width is obtained for the same changes of scan-rate or repetition time (not shown). In addition, the peak current increases approximately directly, with the pulse amplitude However, it should be noted that the background surface current increases in a similar way with the amplitude, as was shown in Fig. 2 According to the treatment for reversible systems at rotated electrodes,[23] the DPV peak current should be independent of repetition time and scan-rate Ferrocyanide is known to behave quasi-reversibly at a carbon-paste electrode [6] Similar dependences were obtained when the oxidation of ascorbic acid was used as a representative irreversible reaction[27] (not shown) In this study (employing $5 \times 10^{-4}M$ ascorbic acid in 0.5M sulphuric acid, and a carbon-paste disk rotated at 2500 rpm), the peak currents were decreased by 22% and 27% when the scan-rate was increased from 2 to 20 mV/sec and the repetition time from 0.5 to 5 sec, respectively Also, a direct proportionality was obtained between the peak current and the pulse amplitude Increasing the scan-rate from 2 to 20 mV/sec resulted in 120 and 250-mV anodic shifts of the ascorbic acid and ferrocyanide peak potentials, respectively. For analytes that accumulate on the carbon surface, a different dependence on DPV parameters has been reported.[3]

Most DPV measurements at solid electrodes have been made at a scan-rate of 5 mV/sec, *i.e.*, about 4 min are required for recording the voltamperogram. The data of Fig 7 indicate that a compromise between speed and sensitivity may result in a significant gain in time and only a slight loss in sensitivity Such a compromise is shown in Fig 8 A mixture of 5μM dopamine and 7 5μM homovanillic acid was analysed at scan-rates of 5 (a) and 20 (b) mV/sec The slight losses in sensitivity and selectivity are compensated by the significant (factor of 4) reduction in time Thus, mixtures of oxidizable compounds at the micromolar concentration level can be analysed within less than a minute

REFERENCES

1 W M Chey, R N Adams and M S Yllo, *J Electroanal Chem*, 1977, **75,** 731
2 J M Séquaris, P Valenta and H W Nurnberg, *ibid*, 1981, **122,** 263
3 T B Jarbawi, W R Heineman and G J Patriache, *Anal Chim Acta*, 1981, **126,** 57
4 S C Rifkin and D H Evans, *Anal Chem*, 1976, **48,** 2174
5 J Wang, *ibid*, 1981, **53,** 2280
6 P Soderhjelm, *J Electroanal Chem*, 1976, **71,** 109
7 R P Baldwin, D Packett and T M Woodcock, *Anal Chem*, 1981, **53,** 540
8 W F Sokol and D H Evans, *ibid*, 1981, **53,** 578
9 F G Gonon, C M Fombarlet, M J Buda and J F Pujol, *ibid*, 1981, **53,** 1386
10 P T Kissinger, *ibid*, 1976, **48,** 17R
11 B D Epstein, E Dalle-Molle and J S Mattson, *Carbon*, 1971, **9,** 609
12 E Theodoridou, J O Besenhard and H P Fritz, *J Electroanal Chem*, 1981, **122,** 67.
13. W E van der Linden and J W Dieker, *Anal Chim Acta*, 1980, **119,** 1
14 R E Panzer and P J Elving, *Electrochim Acta*, 1975, **20,** 635
15 D Laser and M Ariel, *J Electroanal Chem*, 1974, **52,** 291
16 J W Dieker, W E van der Linden and H Poppe, *Talanta*, 1978, **25,** 151
17 J Wang, *Anal Chim Acta*, 1981, **129,** 253
18 *Idem, Anal Chem*, 1981, **52,** 1528
19 N Klein and C Yarnitzky, *J Electroanal Chem*, 1975, **61,** 1
20 M Štulíková and K Štulík, *Chem Listy*, 1974, **68,** 800
21 R J Taylor and A A Humffray, *J Electroanal Chem*, 1973, **42,** 347
22 R M Wightman, E C Paik, S Borman and M A Dayton, *Anal Chem*, 1978, **50,** 1410
23 D J Myers, R A Osteryoung and J Osteryoung, *ibid*, 1974, **46,** 2089
24 A MacDonald and P D Duke, *J Chromatog*, 1973, **83,** 331
25 J Wang, *Talanta*, 1981, **28,** 369
26 T B Jarbawi and W R Heineman, *Anal Chim Acta*, 1982, **135,** 359
27 J Lindquist, *Analyst*, 1975, **100,** 339

Talanta, Vol 30, No 5, pp 323–327, 1983
Printed in Great Britain

0039-9140/83/050323-05$03 00/0
Pergamon Press Ltd

PYRIMIDINETHIOL AS A REAGENT FOR EXTRACTION SEPARATION OF PLATINUM METALS AND GOLD

DETERMINATION OF Pd(II), Os(VIII) AND Ru(III)

M A. ANUSE, N A MOTE and M B CHAVAN
Department of Chemistry, Shivaji University, Kolhapur 416008, India

(*Received* 4 *September* 1981 *Revised* 30 *November* 1982 *Accepted* 8 *December* 1982)

Summary—The solvent extraction separation of Pt(IV), Pd(II), Os(VIII), Ru(III) and Au(III) from one another and also from Rh(III) and Ir(III) with 1-(2′-nitro-4′-tolyl)-4,4,6-trimethyl-(1H, 4H)-2-pyrimidinethiol has been investigated Photometric procedures have been developed for the determination of Pd(II), Os(VIII) and Ru(III) with the same reagent The reagent allows the enrichment of Pd(II) and Au(III) at the trace level from a large volume of aqueous medium even in the presence of base metals The method can be used for the determination of platinum metals and gold in alloys

This communication describes systematic studies on the use of 1-(2′-nitro-4′-tolyl)-4,4,6-trimethyl-(1H, 4H)-2-pyrimidinethiol in the solvent-extraction separation of platinum metals and gold, and the photometric determination of Pd(II), Os(VIII) and Ru(III) Several 1-substituted pyrimidinethiols have been reported by Singh *et al.* as selective spectrophotometric reagents for the determination of palladium,[1,2] osmium,[2–4] ruthenium[4] and iridium [5] However, the use of such compounds as extractants for the platinum metals and gold has not been investigated The present studies were made in order to extend the application of pyrimidinethiols to the solvent extraction of all the platinum-group metals and gold.

EXPERIMENTAL

Reagents

Standard solutions Standard solutions of Pd(II), Pt(IV), Rh(III), Ir(III), Ru(III) and Au(III) were prepared separately by dissolving the corresponding metal chlorides (Johnson Matthey) in dilute hydrochloric acid, and were standardized by standard methods The Os(VIII) solution was made by dissolving osmium tetroxide (Johnson Matthey) in 0 2*M* sodium hydroxide and standardized [6]

Pyrimidinethiol solution 1-(2′-Nitro-4′-tolyl)-4,4,6-trimethyl-(1H, 4H)-2-pyrimidinethiol was prepared by the method of Mathes [7] A 0 01*M* stock solution was prepared by dissolving the requisite amount of the pyrimidinethiol in chloroform Solutions of the pyrimidinethiol in dimethylformamide (DMF) (0 04*M*) and in dioxan (0 08*M*) were also prepared All solutions were made up freshly and stored in amber-coloured bottles

Procedures

Dissolution of osmiridium alloy The alloy is dissolved according to the procedures given by Schoeller and Powell[8] or Beamish and Van Loon [9] This brings the elements present into the proper oxidation states for reacting with the pyrimidinethiol A sample of the alloy (if available as coarse grains) is fused with five times its weight of pure zinc in order to obtain it as a spongy mass It is then powdered, fused with sodium peroxide, leached with water and acidified, the acid concentration being adjusted to 2*M* in hydrochloric acid This gives the oxidation states Os(VIII), Ru(III), Au(III) and Pt(IV) and the sample is ready for analysis

Dissolution of jewellery and solder [8] An accurately weighed amount of sample (about 50 mg) is transferred into a covered 100-ml beaker and heated with 5 ml of *aqua regia* The solution is evaporated almost to dryness and treated with three successive 2-ml portions of hydrochloric acid (1 + 1), the solution being evaporated almost to dryness between additions, in order to remove nitrogen oxides The residue is dissolved in dilute hydrochloric acid, 0 1 g of sodium chloride is added and the solution evaporated on a steam-bath to a moist residue Ten ml of concentrated hydrochloric acid are added and the solution is made up to volume in a 500-ml standard flask with distilled water Appropriate aliquots are used for the determination of each of the noble metals separately

Photometric determination of Pd(II) Adjust the acidity of a Pd(II) solution to 2*M* in hydrochloric acid Shake for 10 min with 5 ml of 0 01*M* pyrimidinethiol in chloroform (Table 1) Collect the organic phase and make up to a known volume Measure the absorbance at 430 nm against a reagent blank Compute the metal content from a calibration graph

Table 1 Extraction of 200 μg of Pd(II) from 2*M* HCl with 0 01*M* pyrimidinethiol in chloroform, as a function of time

Shaking time, *min*	Extraction, %		
	27°	11°	0°
0 1	0 0	0 0	0 0
0 2	1 1	0 0	0 0
0 3	7 0	0 0	0 0
0 5	25 1	0 0	0 0
1 0	41 3	0 0	0 0
2 0	62 5	0 0	0 0
3 0	67 3	18 8	0 0
5 0	71 9	27 1	0 0
7 0	93 8	37 5	0 0
10 0	100 0	62 5	0 0
20 0	100 0	100 0	18 3
40 0	100 0	100 0	75 0
60 0	100 0	100 0	95 3
120 0	100 0	100 0	100 0

Table 2 Characteristics of metal complexes of pyrimidinethiol

Characteristic	Pd(II)	Os(VIII)	Ru(III)
λ_{max}, *nm*	430	500	620
ε_{max}, *l mole*$^{-1}$ *cm*$^{-1}$	4.2×10^3	4.6×10^3	4.6×10^3
Acidic medium for maximum colour development	0.1–5*M* HCl 0.1–10*N* H_2SO_4 0.1–5*M* $HClO_4$ 0.1–3*M* HNO_3	0.3–0.7*M* HCl	5.7–6.2*M* HCl
Stability in chloroform, *hr*	24	24	>48
Beer's law range, *ppm*	2–12	8–64	3–40
Molar composition (metal ligand)	1 2	2 3	—
Standard deviation* (5 samples)	0.006	0.006	0.009
Molar ratio of thiol to metal needed for complete complexation	16	10	200

*For absorbance of 8, 20 and 20 ppm of Pd(II), Os(VIII) and Ru(III), respectively

Photometric determination of Os(VIII) and Ru(III) Adjust the acidity of an Os(VIII) or Ru(III) solution (Table 2) in a total volume of 25 ml Add 5 ml of 0.04*M* pyrimidinethiol in DMF for Os(VIII), or 10 ml of 0.08*M* pyrimidinethiol in dioxan for Ru(III) Digest the mixture on a boiling water-bath for 5 min and cool Extract the reddish-brown complex of osmium or the green complex of ruthenium with two 5-ml portions of chloroform Measure the absorbance of the Os(VIII) and Ru(III) complexes at 500 and 620 nm, respectively, against a reagent blank

Extraction procedure for Os(VIII) and Au(III) Adjust the acidity of an Os(VIII) solution to 1–5*M* or of an Au(III) solution to 0.5–8*M* in hydrochloric acid Extract for 2 min with 10 ml of 0.01*M* pyrimidinethiol in chloroform Collect the organic phase Strip Os(VIII) by equilibrating with 1*M* potassium hydroxide (6 ml) and determine as described above For the determination of Au(III), evaporate the organic phase to dryness and destroy the complex by treatment with 1–2 ml of concentrated perchloric and hydrochloric acids Dissolve the residue in hydrochloric acid and a few drops of nitric acid Evaporate the solution with hydrochloric acid to remove oxides of nitrogen, taking care not to evaporate to dryness, and so avoid loss of gold [10]

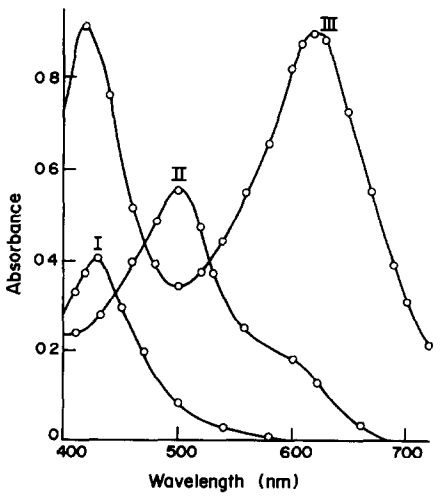

Fig 1 Absorption spectra of thiol complexes of I, Pd(II), 10 ppm, II, Os(VIII), 24 ppm, III, Ru(III), 20 ppm

Dissolve the residue in dilute hydrochloric acid and determine gold photometrically by the stannous chloride method [11]

Extraction procedure for Pt(IV) Add 5 ml of 0.08*M* pyrimidinethiol solution in dioxan to the sample solution Adjust the hydrochloric acid concentration of the solution to be 3.5–4.5*M* after dilution to 25 ml with distilled water Allow to stand at room temperature for 25 min and extract with 10 ml of chloroform Destroy the organic matter in the extract as described for Au(III) in the preceding paragraph, then determine by the stannous chloride method [11]

RESULTS AND DISCUSSION

The absorption spectra of solutions of the complexes formed by Pd(II), Os(VIII) and Ru(III) with the pyrimidinethiol are shown in Fig 1 A chloroform solution of the pyrimidinethiol is slightly yellow and absorbs in the visible region, so a reagent blank is required A chloroform solution of the pyrimidinethiol extracts Pd(II) quantitatively from hydrochloric acid medium with 10 min of shaking, whereas the colourless complexes of Os(VIII) and Au(III) are quantitatively extracted in a single extraction in 5–10 sec Os(VIII) and Ru(III) in hot solution form reddish-brown and green complexes in the presence of 18–24% DMF or more than 18% dioxan, respectively Pt(IV) reacts with the pyrimidinethiol on standing for 25 min at room temperature in the acidity range 3.5–4.5*M* hydrochloric acid in the presence of dioxan (18% or more in the aqueous medium) All these complexes are soluble in chloroform

The extraction of Pd(II), Os(VIII) and Au(III) from 2*M* hydrochloric acid with 0.01*M* pyrimidinethiol in chloroform at 27°, 11° and 0° was studied as a function of time. The extraction of Os(VIII) and Au(III) was quantitative and unaffected by both temperature and the period of shaking over the range from 5 sec to 30 min. Studies on the kinetics of extraction of Pd(II) (Table 1) indicate that the successive separation and determination of Pd(II) and

Table 3 Extraction scheme for separation and determination* of Pt(IV), Pd(II), Os(VIII), Ru(III) and Rh(III) or Ir(III)

Rhodium/Iridium		Platinum		Palladium		Osmium		Ruthenium		Gold	
Taken, μg	Recovery, %	Taken, μg	Recovery, %	Taken, μg	Recovery, %	Taken, μg	Recovery, %	Taken, μg	Recovery, %	Taken, μg	Recovery, %
—	—	190	100 0	200	99 5	200	100 0	225	99 5	200	98 4
Rh 200	99 7	400	99 8	225	99 5	300	99.8	200	99 4	300	98 5
Ir 210	99 2	300	100 2	200	98 9	250	100 0	150	98 9	250	98 3
—	—	—	—	250	99 7	275	100 0	100	99 7	220	98 8
—	—	—	—	100	99.0	350	99 7	300	99 4	—	—
—	—	—	—	—	—	400	101 0	200	99 1	200	99 0
—	—	—	—	180	100 0	—	—	225	99 3	200	99 2
—	—	—	—	230	100 0	500	100 0	—	—	—	—
—	—	—	—	150	100 0	—	—	250	100 0	—	—
—	—	—	—	175	100 0	—	—	—	—	250	99 1
—	—	—	—	—	—	450	101.0	175	100 0	—	—
—	—	—	—	—	—	300	100 0	—	—	275	99 0
—	—	—	—	—	—	—	—	200	100 0	300	99 2

*Analyses in triplicate

Au(III) and also of Pd(II) and Os(VIII) is possible, with quantitative recoveries.

The characteristics of the metal complexes of the pyrimidinethiol are summarized in Table 2.

Extraction scheme for the separation and determination of Pt(IV), Pd(II), Os(VIII), Ru(III), Au(III) and Rh(III) or Ir(III)

The extraction study shows that it is possible to separate Pt(IV), Pd(II), Os(VIII), Ru(III) and Au(III) from one another and also from Rh(III) or Ir(III). The scheme is presented as a flow-chart on the next page, and the results are reported in Table 3

Synthetic mixtures containing platinum metals and gold(III) in amounts corresponding to jewellery alloy (95 5% palladium and 4.5% ruthenium), solder (60% gold, 30% palladium, 10% platinum) and osmiridium alloy were analysed for metal content by this separation scheme. Triplicate analyses gave average relative errors (without regard to sign) of Pd 0.3%, Ru 1 3% for jewellery alloy, Au 1 1%, Pd 0.4%, Pt 0.6% for solder, Os 0 4%, Pt 0.4%, Ru 1.1%, Au 1.8% for osmiridium alloy.

Effect of foreign ions

The effect of foreign ions commonly associated with the test metals was studied by the recommended

Table 4 Effect of foreign ions on the determination of Pd(II), Pt(IV), Os(VIII), Ru(III) and Au(III) with pyrimidinethiol

Foreign ion added	Amount tolerated (*mg*) in the determination† of				
	Pd(II)	Pt(IV)	Os(VIII)	Ru(III)	Au(III)
V(V)	3	5	5	5	2
Cr(VI)	1	2 5	1	5	1
Mn(II)	10	5	5	3	10
Fe(III)	20	10	1	1	15
Co(II)	20	5	5	10	15
Ni(II)	20	3	5	1	15
Cu(II)	20	5	5	10	20
Zn(II)	15	10	0 4	10	10
Ga(III)	2	2	5	0 2	1 5
Mo(VI)	5	2	4	2	3
Ru(III)	1	2	2	—	1
Rh(III)	5	5	2	5	5
Pd(II)	—	co-extracted	interferers	1	co-extracted
Cd(II)	10	2	5	2	10
W(VI)	15	1	2	1	15
Os(VIII)	0 1	co-extracted	—	0 2	co-extracted
Ir(III) or (IV)	5	5	5	5	5
Pt(IV)	20	—	2	1	20
Au(III)	1	co-extracted	0 2	1	—
Hg(II)	20	10	2	10	15
Pb(II)	5	3	1	3	5
U(VI)	20	10	5	10	20
Ag(I)*	0 2	0 5	0 2	5	0 2
Zr(IV)	2	2.5	1	1	2 5

*Centrifuge AgCl

†Amount (μg) of platinum metal taken. Pd(II) 200, Pt(IV) 300, Os(VIII) 200, Ru(III) 200, Au(III) 300

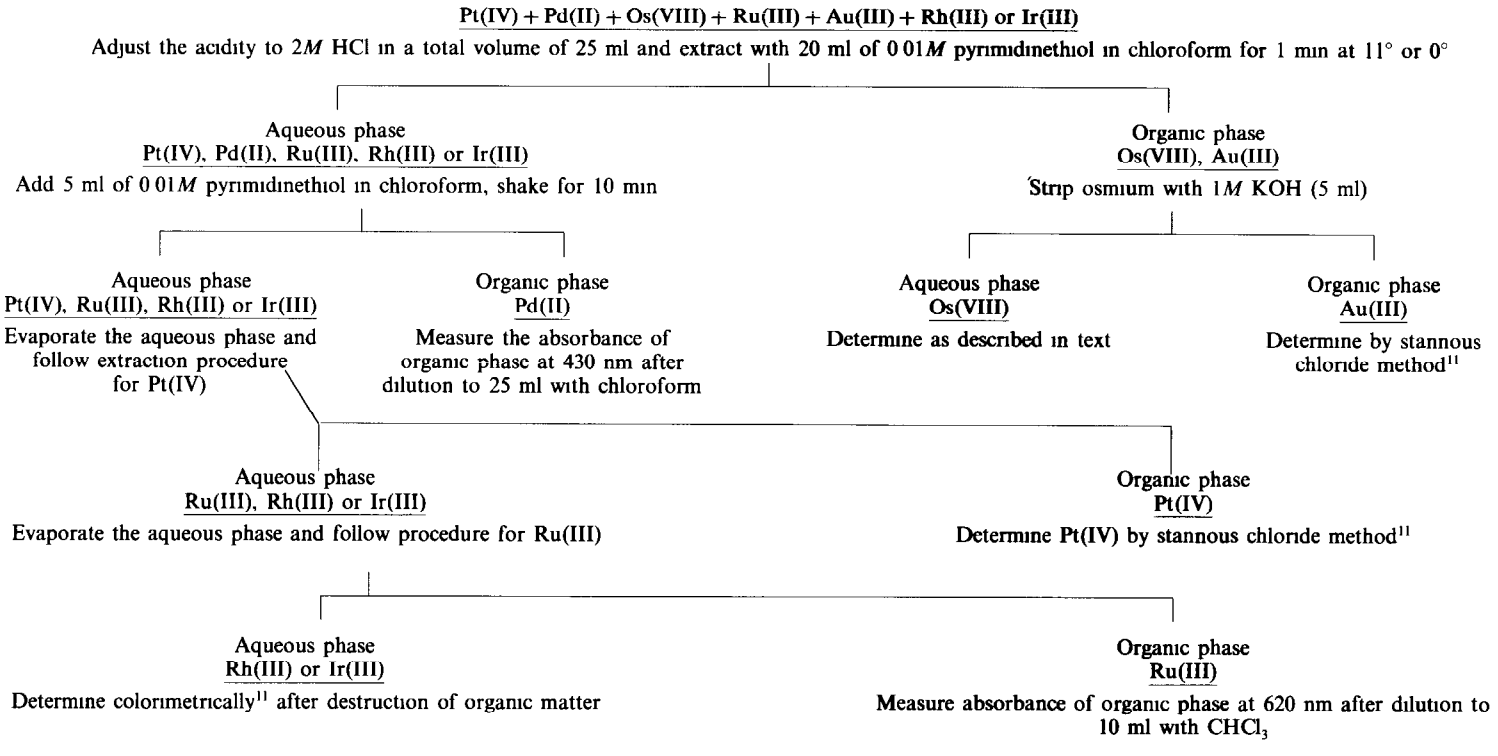

Separation Scheme

Table 5 Determination of Pd(II) or Au(III) at the ng/ml level*

Pd(II) taken, *ng/ml*	Pd(II) found, *ng/ml*	Au(III) taken, *ng/ml*	Au(III) found, *ng/ml*
40	40 0	36	35 6
60	59 4	70	69 1
80	79 8	90	88 9

*Sample was 2500 ml of water adjusted to 2*M* in hydrochloric acid and extracted with pyrimidinethiol solution

procedure The criterion for interference was an error greater than 2% in the transmittance The tolerance limits for the ions tested are given in Table 4 Thiourea and thiosulphate interfere seriously in the determination of each element Fe(II) interferes in the extraction of Au(III) by reducing it to the metal

Enrichment studies on Pd(II) and Au(III)

Extraction of different amounts of Pd(II) or Au(III) at trace levels from 25, 50, 100, 500, 1000 and 2500 ml of 2*M* hydrochloric acid containing 20-mg amounts each of Fe(III), Cu(II), Ni(II) and Co(II), and subsequent determination, showed that the recovery of Pd(II) or Au(III) was quantitative and that the results were reproducible. The recoveries of Pd(II) and Au(III) from 2500 ml of 2*M* hydrochloric acid with 10 ml of 0 01*M* pyrimidinethiol in chloroform, with 60 and 30 min shaking respectively, are shown in Table 5

Acknowledgements—One of the authors (M A A) gratefully acknowledges financial assistance provided by C S I R in the form of a Junior Research Fellowship The authors also express their gratitude to Professor M H Jagdale, Head of the Chemistry Department, for providing laboratory facilities and kind encouragement

REFERENCES

1 A K Singh, M Katyal, A M Bhatti and N K Ralhan, *Talanta*, 1976, **23**, 337
2 A K Singh, M Katyal and R P Singh, *ibid*, 1976, **23**, 851
3 A K Singh and R P Singh, *J Indian Chem Soc*, 1979, **56**, 423
4 V Kushwaha, P Jain, M Katyal and R P Singh, *J Chin Chem Soc, Taipei*, 1976, **23**, 43
5 A K Singh, M Katyal and R P Singh, *Rev Roum Chim*, 1978, **23**, 1153
6 G M Ayres and W N Wells, *Anal Chem*, 1950, **22**, 317
7 R A Mathes, *J Am Chem Soc*, 1953, **75**, 1747
8 W R Schoeller and A R Powell, *Analysis of Minerals and Ores of the Rare Elements*, pp 387, 336 Griffin, London, 1955
9 F E Beamish and J C Van Loon, *Analysis of Noble Metals, Overview and Selected Methods*, p 272 Academic Press, New York, 1977
10 K Beyermann, *Z Anal Chem*, 1964, **200**, 183
11 E B Sandell, *Colorimetric Determination of Traces of Metals*, 3rd Ed Interscience, New York, 1965

Talanta, Vol 30, No 5, pp 329–332, 1983
Printed in Great Britain

0039-9140/83/050329-04$03 00/0

DETERMINATION OF TRACES OF LEAD AND CADMIUM IN HIGH-PURITY TIN BY POLARIZED ZEEMAN ATOMIC-ABSORPTION SPECTROMETRY WITH DIRECT ATOMIZATION OF SOLID SAMPLE IN A GRAPHITE-CUP CUVETTE

KUNIO TAKADA and KICHINOSUKE HIROKAWA
The Research Institute for Iron, Steel and Other Metals, Tohoku University, Sendai, 980, Japan

(*Received* 7 *September* 1982 *Accepted* 8 *December* 1982)

Summary—Lead at the μg/g level and cadmium at ng/g–μg/g levels in high-purity tin have been determined by polarized Zeeman atomic-absorption spectrometry with direct atomization of the solid sample Pieces of high-purity tin weighing up to 5 mg for lead and 20 mg for cadmium were analysed Calibration graphs were constructed by use of standard solutions of lead and cadmium in the presence of pure tin having lead and cadmium contents below the detection limit The tin matrix remained in the graphite-cup cuvette after atomization and did not adhere to the wall of the cuvette, so it could be easily removed and the same cuvette repeatedly used

Atomic-absorption spectrometry with direct atomization of a solid sample has the following advantages high sensitivity, short analysis time and no contamination with (or loss of) determinand, since there is no chemical treatment, microamounts of sample can be analysed This technique has therefore been applied to a variety of samples.[1] On the other hand, non-specific absorption (background absorption) has to be considered, and repeated use of a cuvette is limited[2–4] by change in its characteristics through reactions with samples

High-purity tin is used as the starting material for making certain semiconductors (PbSnTe, PbSnSe *etc*) or superconductors (Nb_3Sn *etc.*), and the advantages of atomic-absorption spectrometry with direct atomization of solid sample suggest it as a method of choice for its analysis Frech *et al* [5] have reported that complete volatilization of traces of lead from tin is difficult because of the solubility of lead in tin However, the lead content can be reduced to below the detection limit by selection of an appropriate atomization temperature and time, amount of sample, and concentration of lead in it. Cadmium is also soluble in tin, and traces of cadmium in tin can be determined by a procedure similar to that for lead Any non-specific absorption signals should be corrected for by use of the Zeeman effect, [6–8] a deuterium lamp or two hollow-cathode lamps In this study, correction by means of the Zeeman effect was employed Standard reference materials made from the matrix element are not always available, and standard solutions of the analyte elements,[4,5 9–12] standard solid samples made from other matrix components,[2] or series of "home-made" solid samples of similar composition to the analytical samples, are used for standardization The analytical results obtained by use of these standards should be checked by comparison with those values obtained by other methods In this study, satisfactory results were obtained by standardization with standard solutions of lead or cadmium together with pure tin

EXPERIMENTAL

Apparatus

A Hitachi 180-80 polarized Zeeman atomic-absorption spectrometer, Hitashi 056 chart-recorder and Tokyo Kagaku RD-202 digital integrator were used, with a graphite-cup cuvette as electrothermal atomizer Solid samples were weighed on a Shimadzu LM-20 balance (standard deviation 5 μg) An Eppendorff micropipette was used for placing standard solutions (10 μl) in the graphite-cup cuvette

Standard solutions

Known amounts of lead and cadmium were dissolved in a small amount of nitric acid, and the solutions diluted with redistilled water in polypropylene standard flasks Further dilution gave working solutions covering the range 0–500 ng/ml for lead and 0–10 ng/ml for cadmium These were used within 5 hr for constructing calibration graphs The concentration of nitric acid in these solutions was so low (below $3.5 \times 10^{-5} M$) that a study of its effect on the atomic-absorption signals was considered unnecessary

Procedure

A small sample (0 1–20 mg), of irregular form, was carefully cut off a tin ingot with a pair of nippers A single particle of sample was weighed, put into a graphite-cup cuvette and atomized by electrothermal heating under the analytical conditions in Table 1 The profile and area of the atomic-absorption signal of lead or cadmium were recorded Further sample particles were successively analysed in the same cuvette Ten μl of standard lead or cadmium solution were similarly atomized in the presence of the "pure" tin which remained in the graphite-cup cuvette after analysis of the samples The atomic-absorption signals were automatically corrected for non-specific absorption, by the polarized Zeeman atomic-absorption spectrometer

Table 1 Instrumental parameters

Parameter	Pb	Cd
Drying temperature, °C	400	300
current, *A*	118	102
time, *sec*	15	15
Ashing temperature, °C	400	300
current, *A*	118	102
time, *sec*	15	15
Atomizing temperature, °C	2000	1500
current, *A*	261	216
time, *sec*	40	30
Cleaning temperature, °C	2400	1800
current, *A*	308	241
time, *sec*	3	3
Wavelength, *nm*	283 3	228 8
Spectral bandwidth, *nm*	1 3	1 3
Lamp current, *mA*	7 5	7 5
Argon flow, *l/min*		
sheath gas	3	3
carrier gas	None	None

RESULTS AND DISCUSSION

Absorption signal

The signals for lead from a standard solution, a tin sample, and a standard solution added to "pure" tin left in the cuvette, are shown in Fig 1 The tin metal remaining in the cuvette after the atomization of lead is in spherical form, and gives no lead signal, it will henceforth be referred to as "pure" tin The absorption signal for lead from a standard solution is a sharp single peak (Fig 1A) whether the lead is atomized in a fresh cuvette or in a used cuvette from which residual tin matrix has been removed, but the peak area is 10–15% larger when a fresh cuvette is used The area obtained with the used cuvette is equal to that for the same volume of standard solution added to "pure" tin in the cuvette, but the latter system results in a double peak, as shown in Fig 1C The greater the amount of "pure" tin in the cuvette, the smaller the area of the first peak and the larger is the area of the second peak The two peaks arise because the lead in the standard solution is reduced to the metallic state by the graphite of the cuvette, and part is atomized (first peak) while the rest is dissolved in the tin in the cuvette, and only gradually atomized (giving the wide second peak) This mechanism was confirmed by experiments similar to those described earlier [13] The slow volatilization from the solution of lead in molten tin also accounts for the broad peak obtained for the tin samples (Fig 1B)

When the samples are analysed successively in the same cuvette without removal of the tin, the amount of "pure" tin in the cuvette increases so the signal peak should get broader For a fixed amount of lead, if the degree of atomization is constant the peak-area should remain constant but the peak-height should decrease as the number of samples increases

This hypothesis was tested by analysing for lead after successive additions of small samples (0 25–0 45 mg, accurately weighed) of BCS 192f (Pb 3 5 μg/g) The results (expressed as signal per 0 1 mg of tin

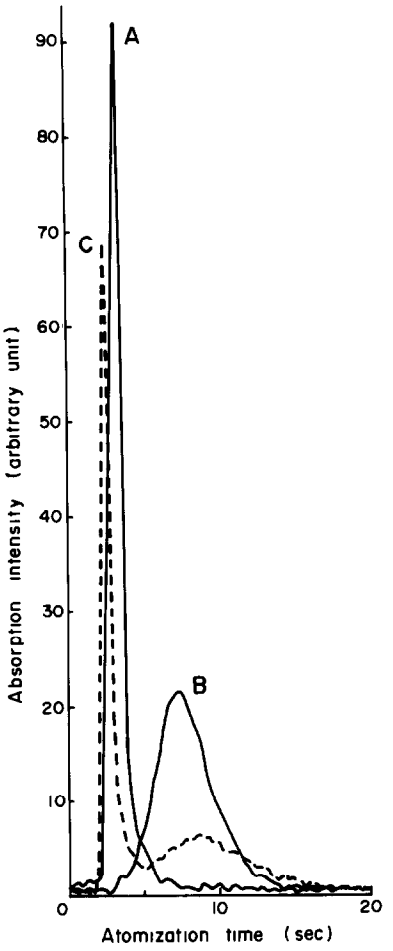

Fig 1 Profiles of atomic-absorption signal for lead A, lead standard solution (Pb 1 01 ng), B, tin metal (BCS 192f, Pb 3 5 ppm) 0 245 mg, C, lead standard solution (Pb 1 01 ng) with 2 818 mg of "pure" tin Atomization temperature 2000°C

added, *i e*, as a specific signal) are shown in Fig 2 The specific peak-area was constant in spite of increase in the amount of residual tin in the cuvette (the coefficient of variation of peak-area in 10 determinations was 7 6%), but the peak-height decreased

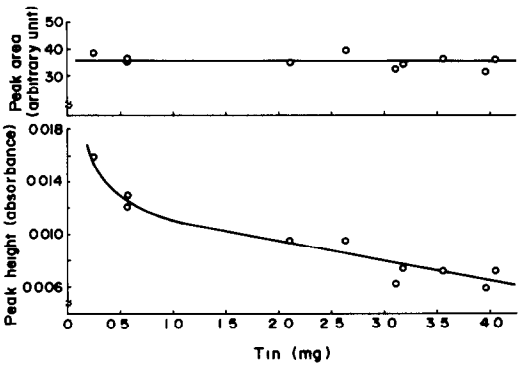

Fig 2 Effect of the amount of "pure" tin in the graphite-cup cuvette on peak-area and peak-height of absorption signal of lead in tin Atomization temperature 2000°C Each plotted value corresponds to the specific absorption signal of lead in 0 1 mg of tin (BCS 192f, Pb 3 5 ppm)

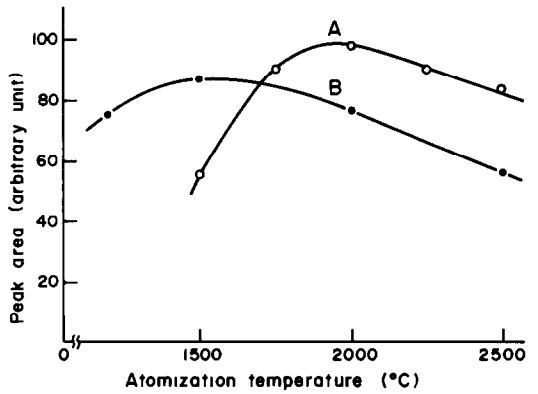

Fig 3 Effect of atomization temperature on the peak-area of lead and cadmium A, lead standard solution (Pb 1 01 ng) with 4 50 mg of "pure" tin metal, B, cadmium standard solution (Cd 0 050 ng) with 10 0 mg of "pure" tin metal

and the peak-width increased Therefore, the absorbance of the lead was always evaluated from the peak-area and the amount of the tin remaining in the cuvette was kept below 5 mg The peak-area for cadmium was not affected by the amount of residual tin until this exceeded about 20 mg When the amount of tin in the cuvette exceeded these tolerable amounts (5 mg for lead, 20 mg for cadmium), it was carefully removed, and the same cuvette could then again be employed for atomization of tin samples Therefore, one cuvette could be used about 250–300 times

Drying, ashing and atomization conditions

The effect of atomization temperature on the peak-area for the absorption signal from lead in tin is shown in Fig 3A

To find the optimum conditions for lead, atomization at 1500, 1750, 2000, 2250 and 2500° for periods of 60, 50, 50, 40 and 20 sec, respectively, was examined At temperatures below 1750°, the time for removing lead from tin was longer and the peak-area for lead was smaller than at 2000° At temperatures above 2250°, the instrument was contaminated by volatilized tin, and the peak-area for lead became smaller than that at 2000° Therefore an atomization temperature of 2000° was chosen because the peak-area was largest, the rate of volatilization of lead from tin was comparatively high, and practically no tin was volatilized When lead at the $\mu g/g$ level in tin was determined and there was <5 mg of residual tin in the cuvette, an atomization time of 40 sec was sufficient at a temperature of 2000° When cadmium in tin was atomized at 2000° it was rapidly volatilized, but the absorption signal was smaller than that at 1500°, as shown in Fig 3B Further, if there was more than 10 mg of residual tin, it jumped out of the cuvette during the heating at 2000° Therefore, cadmium in tin was atomized at 1500° For cadmium at the $\mu g/g$ level in tin, with <20 mg of "pure" tin in the cuvette, an atomization time of 30 sec was sufficient at 1500°

The absorption signal for lead was not affected by varying the drying temperature from 100° to 400° (15-sec drying), or (with drying for 15 sec at 400°) by ashing either for 5–60 sec at 400° or for 15 sec at 500–1000° Similar investigations were made for cadmium The drying and ashing procedures finally selected are shown in Table 1. The cleaning step was introduced to avoid contamination of the cuvette by condensation of sample vapours on the cooler parts (the connections to the instrument)

Calibration graphs for 0–5 ng of lead and 0–0 1 ng of cadmium were constructed with standard solutions of lead and cadmium in the presence of "pure" tin as described in the procedure

Determination of lead and cadmium

Lead and cadmium in high-purity tins were determined by the proposed method and the results obtained are shown in Tables 2 and 3. They agree with the certified values or those obtained by flameless atomic-absorption spectrometry This suggests that standardization with standard solutions of lead and cadmium is suitable for use in analysis of tin In this method a sample of only 0 1–20 mg is needed, but in the check method (solution/flameless AAS), samples of 0 3–10 g were used, with a final solution volume of 50 ml

Table 2 Determination of lead in high-purity tin

Sample	Proposed method: Number of determinations	Proposed method: Pb found, $\mu g/g$	Proposed method: Coefficient of variation, %	Pb found by other method*, $\mu g/g$	Pb, certified value, $\mu g/g$
Tin A (99 9999%)	34	$0\,5_9$	3 6	$0\,5_0$ $0\,5_1$	—
Tin B (99 999%)	28	$2\,3_5$	9	$2\,5_5$ $2\,6_2$	—
Tin C (BCS 192f)	59	$3\,6_7$	6	$3\,9_8$ $3\,9_6$	3 5
Tin D (special grade reagent)	7	16 2	16	14 5 14 7	—

*Tin was removed as $SnBr_4$ after dissolution in nitric acid, and determined by flameless (graphite cuvette) atomic-absorption spectrometry

Table 3 Determination of cadmium in high-purity tin

Sample	Proposed method: Number of determinations	Proposed method: Cd found, $\mu g/g$	Proposed method: Coefficient of variation, %	Cd found by other method,* $\mu g/g$	Cd, certified value, $\mu g/g$
Tin A (99 9999%)	9	$0\,0004_3$	30	Not detected	—
Tin B (99 999%)	15	$0\,022_2$	9 5	$0\,023_5$ $0\,023_2$	—
Tin C (BCS 192f)	9	0 0011	12	Not detected	<0 5
Tin D (special grade reagent)	8	2 83†	21	$2\,6_6$ $2\,6_5$	—
Tin E (foil)	10	$0\,12_4$	5	$0\,12_6$ $0\,12_6$	—

*See Table 2
†With carrier gas flowing through cuvette

The relative standard deviations of the peak areas for lead and cadmium standards with "pure" tin in a cuvette were 1 8% for lead (Pb 1 03 ng, 7 determinations) and 4 3% for cadmium (Cd 50.5 pg, 8 determinations). The corresponding values for analysis of high-purity tins were 3 6–9% for lead and 5–12% for cadmium (Tables 2 and 3) These values were good enough for lead to be determinable at the $\mu g/g$ level and cadmium at the ng/g–$\mu g/g$ level The large relative standard deviations for tin sample D might be due to segregation of the lead and cadmium The very large relative standard deviation for cadmium in tin sample A might be due to the very low absorption signal from the very small amount of cadmium in the sample

The detection limits were 37 pg for lead and 1.5 pg for cadmium. These values correspond to $7\,4 \times 10^{-3}$ ppm of lead in 5 mg of tin and $7\,5 \times 10^{-5}$ ppm of cadmium in 20 mg of tin. Here, the detection limit is defined as the weight of element giving a signal equal to twice the standard deviation of the instrumental noise signal

By use of the polarized Zeeman atomic-absorption spectrometer, the atomic-absorption signal at 283 3 nm for lead and at 228 8 nm for cadmium was automatically corrected for non-specific absorption by any matrix tin volatilized (absorbance <0 05 in this work)

The calibration graphs constructed from the results for the lead and cadmium standards made with the "pure tin" metal can, then, be applied for the determination of low levels of these elements in tin by direct atomization with very small samples (0 1–2 mg for lead and 0 2–20 mg for cadmium) Traces of zinc, bismuth, copper and silver in tin can similarly be determined Passage of carrier gas (Ar, 200 ml/min) into the cuvette makes the absorption lower by a factor of 15–20 than that with no flow of carrier gas Therefore the comparatively large amount of cadmium in tin D (Table 3) was determined with carrier gas flowing through the cuvette

REFERENCES

1 F J Langmyhr, *Analyst*, 1979, **104**, 993
2 K Hirokawa and K Takada, *Bunseki Kagaku*, 1980, **29**, 675
3 K Takada and K Hirokawa, *Z Anal Chem*, 1982, **312**, 109
4 T Kobayashi, K Ido and E Sudo, *J Jap Inst Metals*, 1982, **46**, 603
5 W French, E Lundberg and M M Barbooti, *Anal Chim Acta*, 1981, **131**, 45
6 H Koizumi, *Hitachi S I News*, 1982, **25**, 25
7 H Koizumi and K Yasuda, *Spectrochim Acta*, 1976, **31B**, 523
8 H Koizumi, K Yasuda and M Katayama, *Anal Chem*, 1977, **49**, 1106
9 A Goda, K Moriyama and S Harimaya, *Trans Iron Steel Inst Japan*, 1980, **20**, B405
10 W Ishibashi, M Sato and M Hashimoto, *Bunseki Kagaku*, 1974, **23**, 597
11 W Ishibashi, R Kikuchi and K Yamamoto, *ibid*, 1979, **28**, 394
12 T Hadeishi and H Kimura, *J Electrochem Soc*, 1979, **126**, 1988
13 K Takada and K Hirokawa, *Talanta*, 1982, **29**, 849

Talanta, Vol 30, No 5, pp 333–338, 1983
Printed in Great Britain

0039-9140/83/050333-06$03 00/0

DETERMINATION OF TRACE AMOUNTS OF PHOSPHATE IN RIVER WATER BY FLOW-INJECTION ANALYSIS

SHOJI MOTOMIZU, TOSHIAKI WAKIMOTO and KYOJI TÔEI
Department of Chemistry, Faculty of Science, Okayama University, Tsushima-naka, Okayama-shi, Japan

(*Received* 29 *March* 1982 *Revised* 15 *November* 1982 *Accepted* 22 *November* 1982)

Summary—A flow-injection analysis system for the determination of trace amounts of phosphate in river water has been developed The phosphate is reacted with molybdate and Malachite Green in acidic medium to form a green species, the absorbance of which is measured at 650 nm Phosphorus (as inorganic phosphate) can be determined at the level of several ng/ml in water Analyses can be done at a rate of up to 40 per hour

Flow-injection analysis (FIA), a simple technique that allows the rapid and automated determination of a wide range of species, is based on continuous-flow measurements and has already proved very useful in many practical applications, in such fields as environmental, clinical and agricultural analysis.[1] The FIA determination of phosphorus has been studied by several workers,[2–11] all these methods were based on formation of yellow molybdophosphate or molybdenum blue Itaya *et al*[12] have reported that the molybdophosphate formed in acidic medium will react with Malachite Green to form a coloured complex, which can be used for spectrophotometric determination of phosphorus The method was subsequently modified and applied to the determination of phosphate in serum, plasma and urine.[13–20] Altmann *et al*[21] concluded that the ion-association complex (Malachite green)$_3$($PMo_{12}O_{40}$) was formed in acid medium. The spectrophotometric method with Malachite Green is very sensitive (the molar absorptivity at 650 nm is about 1×10^5 l mole^{-1} cm^{-1}, but the colour intensity is affected by temperature and reaction time The addition of non-ionic surfactant has an enhancement effect on the colour reaction Belle[22] adapted the method to automatic determination of inorganic phosphate (with the Auto-Analyzer) but using Methyl Green as counter-ion and Brij-35 as non-ionic surfactant, and applied the method at the μg/ml level to serum analysis. In environmental analysis, however, a method suitable for ng/ml levels is required

This paper describes a very sensitive FIA procedure, operable at high sampling rate, for the determination of trace amounts of phosphorus in river water with molybdate and Malachite Green, without use of non-ionic surfactant.

EXPERIMENTAL

Reagents

All chemicals used were of analytical-reagent grade
Standard phosphate solution Dissolve potassium dihydrogen phosphate in distilled water to give a $2 \times 10^{-3}M$ stock solution, dilute it accurately before use

Reagent solution A Dissolve 19 4 g of ammonium heptamolybdate tetrahydrate, 0 092 g of Malachite Green (oxalate) in about 500 ml of distilled water, add 250 ml of ethanol and 70 ml of concentrated sulphuric acid, and dilute to 1000 ml with distilled water This solution is 0 11M in molybdenum and $2\,2 \times 10^{-4}M$ in Malachite Green Filter through a 0 45-μm membrane filter before use This solution is stable for at least one month if stored in the dark

Reagent solution B Prepare in the same way as solution A, but without the ethanol

Carrier solution Sulphuric acid (0 35M)

Apparatus

The absorbance was measured with a Shimadzu UV-140-02 double-beam spectrophotometer with a 10-mm micro flow-cell (18 μl) and recorded with a Toa Dempa FBR-251A recorder A double-plunger micropump (Kyowa Seimitsu KHU-W-104) was used for the reagent solution and the carrier solution The sample was injected by a 6-way injection valve (Kyowa Seimitsu KMH-6V) into the carrier stream (sample volume 240 μl for use of reagent A and 40 μl with reagent B) The flow lines were made from Teflon tubing The reaction coils were 7 5 m long (1 mm bore) for use of reagent A and 5 m long (0 5 mm bore) for reagent B, and were wound on glass rods To cancel the pulse from the reciprocal pump, 10-m damping coils (0 5 mm bore) and an air damper (volume 24 ml) were used The back-pressure tubing (0 25 mm bore) was 3 m long, to prevent formation of air bubbles A diagram of the flow system (with dimensions) is shown in Fig 1

RESULTS AND DISCUSSION

Experimental variables in use of reagent B

Flow-rate As shown in Fig 2, the signal (peak height) increased with flow-rate but was practically constant over the flow-rate range 1 25–1 7 ml/min, a flow-rate of 1 3 ml/min was selected

Malachite Green concentration It was found that the larger the concentration of Malachite Green, the poorer the stability of the base-line As shown in Fig 3, the calibration graphs were all linear up to the 200-ng/ml phosphorus level at a Malachite Green concentration of 1.1×10^{-4}–$4\,4 \times 10^{-4}M$ A $2.2 \times 10^{-4}M$ Malachite Green solution was found to

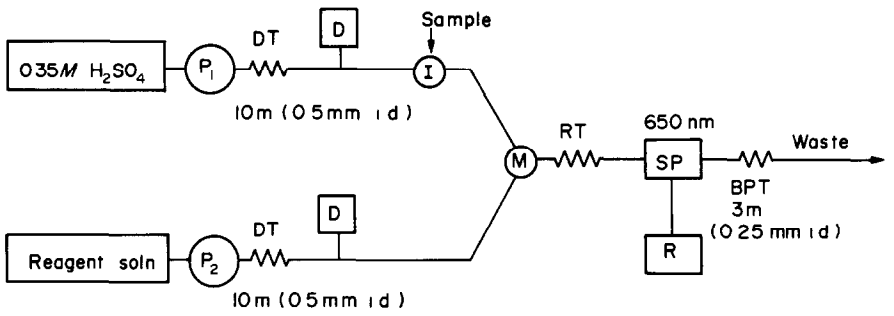

Fig 1 Schematic flow diagram P_1 and P_2, pumps, DT, damping coil (0.5 mm × 10 m), D, air damper, I, sample injector, M, mixing joint, RT, reaction coil (1 mm × 7.5 m or 0.5 mm × 5 m), SP, spectrophotometer with flow-cell, R, recorder, BPT, back-pressure coil (0.25 mm × 3 m)

give a good compromise between sensitivity and base-line stability

Molybdate concentration As shown in Fig 4, the peak height increased with increase of molybdate concentration, but again at the cost of increasing instability of the base-line and decreasing linearity of the calibration graphs A concentration of 0.11*M* molybdate was chosen as a compromise

Sulphuric acid concentration From the results shown in Fig 5, a concentration of 1.3*M* sulphuric acid was chosen

Length of reaction coil As the reaction coil was increased in length from 2.5 to 7.5 m, the peak height decreased, but the base-line became more stable A 5-m coil (0.5 mm bore) was chosen from a consideration of peak height, base-line stability and retention time

Sample injection volume (Fig 6) Though the peak height increased with sample size, the tailing of the peak became larger A 20-cm sample loop (0.5 mm bore) was selected for use

Calibration graph With use of the flow system in Fig 1 (reaction coil 5 m long, 0.5 mm bore), the calibration graph was linear up to 200 ng of phosphorus per ml

Development of the method for > 200 ng of phosphorus per ml (reagent A)

When reagent B is used for phosphorus concentrations above 200 ng/ml, the complex becomes coagulative and easily adsorbed on the surface of the Teflon tubing This effect can be prevented by addition of ethanol to the reagent (giving reagent A) The effect of varying the ethanol concentration is shown in Fig 7 The optimal ethanol content in the reagent solution is 25%, which gives a graph calibration that is linear up to 0.8 ppm of phosphorus In this case, the reaction coil (7.5 m long, 1 mm bore) is wound in a figure-of-eight on two parallel rods (diameter about 5 mm), as this is found to result in less tailing of the peaks The decrease in tailing allows a higher sampling rate and use of a larger volume of sample solution With reagent A, 240 μl of sample solution can be used

Examination of the experimental variables gave the results summarized in Figs 8–11, from which the

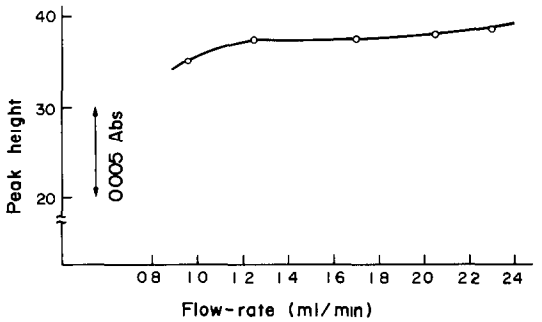

Fig 2 Effect of flow-rate (reagent B) Phosphorus 100 ng/ml

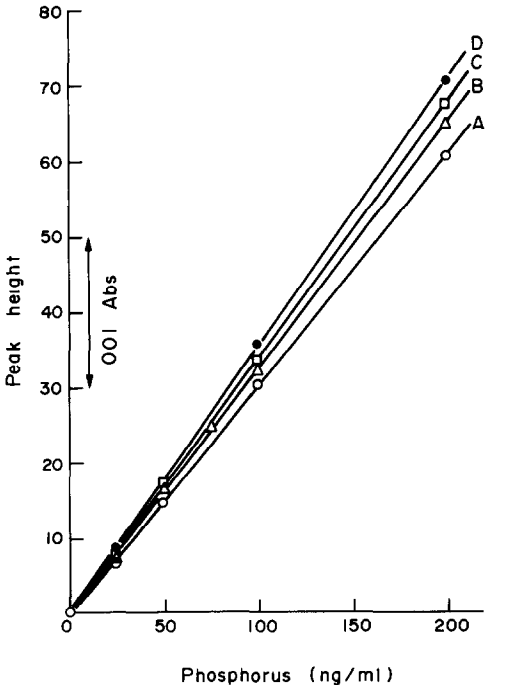

Fig 3 Effect of Malachite Green (reagent B) A, $1.1 \times 10^{-4}M$, B, $2.2 \times 10^{-4}M$, C, $3.3 \times 10^{-4}M$, D, $4.4 \times 10^{-4}M$

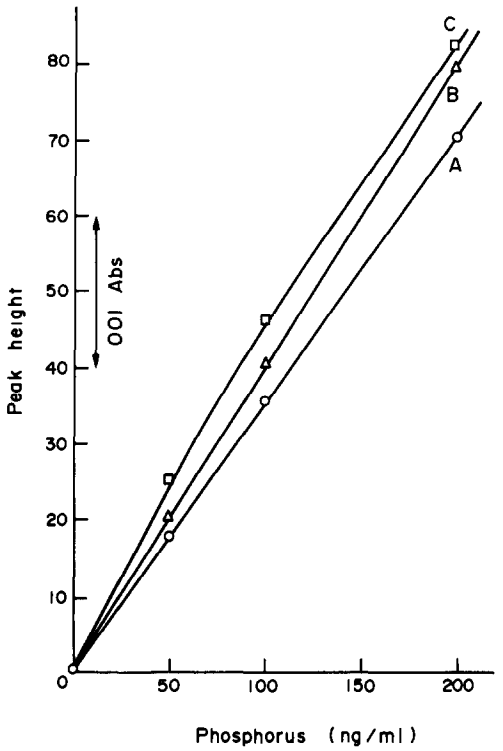

Fig 4 Effect of molybdate (reagent B) A, 0 11*M*, B, 0 18*M*, C, 0 24*M*

conditions regarded as optimal were deduced, namely a flow-rate of 2.1 ml/min and a reagent (A) containing 250 ml of ethanol, 70 ml of concentrated sulphuric acid and 0 11 mole of molybdenum per litre.

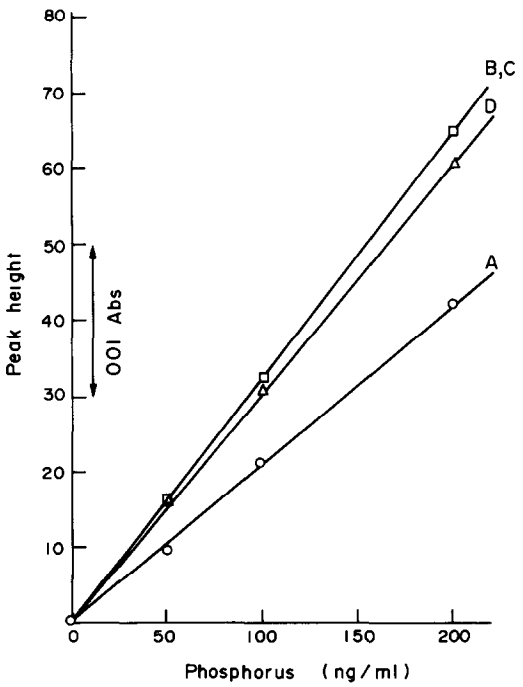

Fig 5 Effect of sulphuric acid (reagent B) A, 0 8*M*, B, 1 3*M*, C, 1 7*M*, D, 2 1*M*

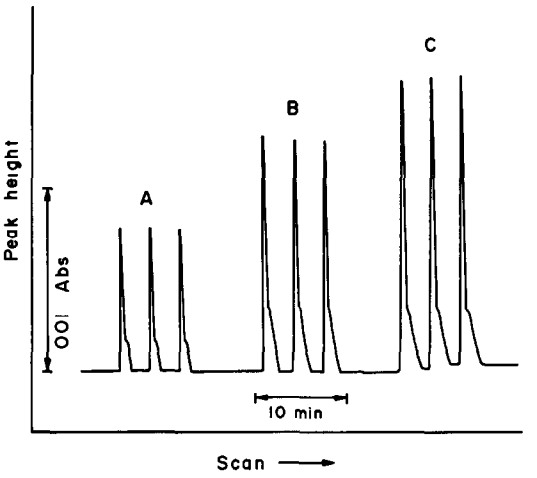

Fig 6 Effect of sample volume (reagent B). Length of sampling loop (0.5 mm bore tubing) A, 10 cm (20 μl), B, 20 cm (40 μl), C, 30 cm (60 μl) (phosphorus 75 ng/ml)

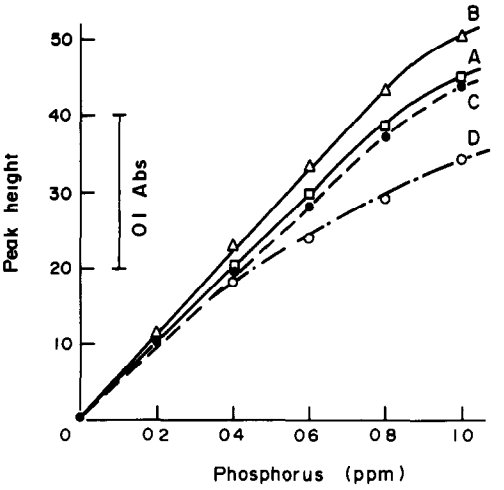

Fig 7 Effect of ethanol A, 20%, B, 25%, C, 30%, D, 40% (flow-rate 2 1 ml/min)

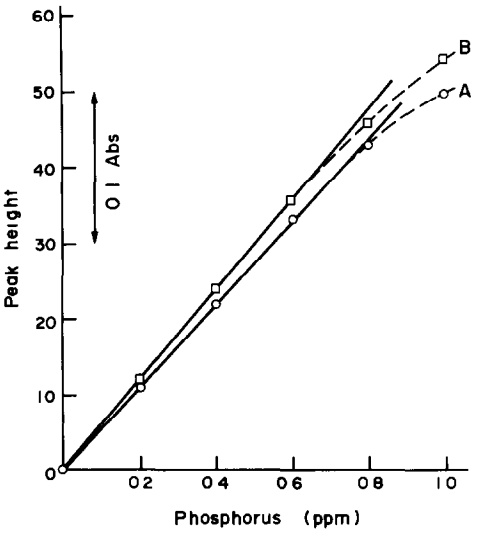

Fig 8 Effect of flow-rate (reagent A) Flow-rate A, 2 0 and 2 1 ml/min, B, 2 2 ml/min

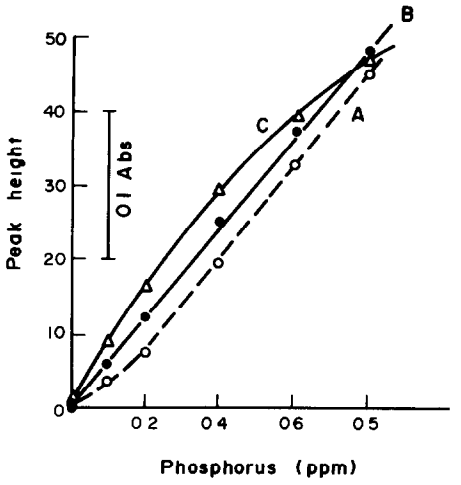

Fig 9 Effect of molybdate (reagent A) A, 0·06*M*, B, 0·11*M*, C, 0·17*M*

The Malachite Green concentration was again important The graphs (Fig. 10) were all linear up to the 800-ng/ml phosphorus level, but the higher the Malachite Green concentration the less stable the baseline. The sensitivity first increased and then decreased with increasing dyestuff concentration

Calibration graph (reagent A) The flow system in Fig 1 (reaction coil 7·5 m long and 1 mm bore) was used for preparing the calibration graph. The sample solution was injected from a sample loop of 30 cm of 1-mm bore Teflon tubing (sample volume about 240 μl) Typical signals are shown in Fig 12. The calibration graphs are linear up to 120 and 800 ng/ml (at different recorder sensitivities)

Determination of phosphorus in river water

Phosphorus at concentrations below 200 ng/ml can be determined with either reagent, but for higher

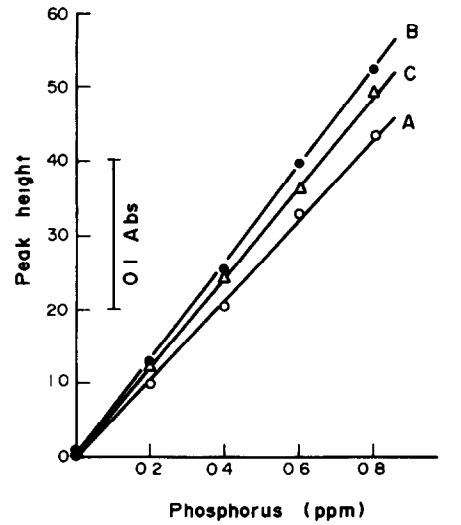

Fig 10 Effect of Malachite Green (reagent A) A, $1·1 \times 10^{-4}M$, B, $2·2 \times 10^{-4}$, C, $3·3 \times 10^{-4}$

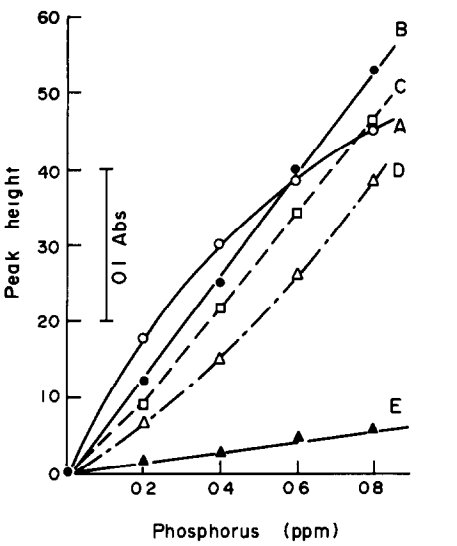

Fig 11 Effect of sulphuric acid concentration in reagent A Concentrated sulphuric acid added (ml per litre of reagent solution) A, 45 ml, b, 70 ml, C, 75 ml, D, 93 ml, E, 115 ml

Table 1 Tolerable concentrations of co-existing ions

Ion	Maximum tolerable concentration, *M*
Na^+, Cl^-	0·1
Mg^{2+}, Ca^{2+}	0·01
Al^{3+}, K^+, Fe^{3+}, NO_3^-, HCO_3^-	10^{-3}*
SiO_3^{2-}	10^{-4}
WO_4^{2-}, VO_3^-	10^{-5}
AsO_4^{3-}	2×10^{-6}

Phosphorus taken 120 ng/ml
*Maximum tested

Table 2 Determination of phosphorus in river water

Sample	Phosphorus, *ng/ml*	Reference value,* *ng/ml*
Zasu River		
A	69	71
B	80	79
Takahashi River		
A	30	
B	16	
C	20	22
D	14	
Yoshii River		
A	25	
B	23	
C	38	38
D	32	
Asahi River		
A	39	38
B	17	
C	11	

The Takahashi, Yoshii and Asahi Rivers are the three largest rivers in Okayama Prefecture The waters were sampled on 10 September 1981 The Zasu River is one of the branches of the Asahi River Domestic wastewater flows into the Zasu River Symbols A–D denote order of sampling down stream

*Obtained by the solvent extraction–spectrophotometric method [23]

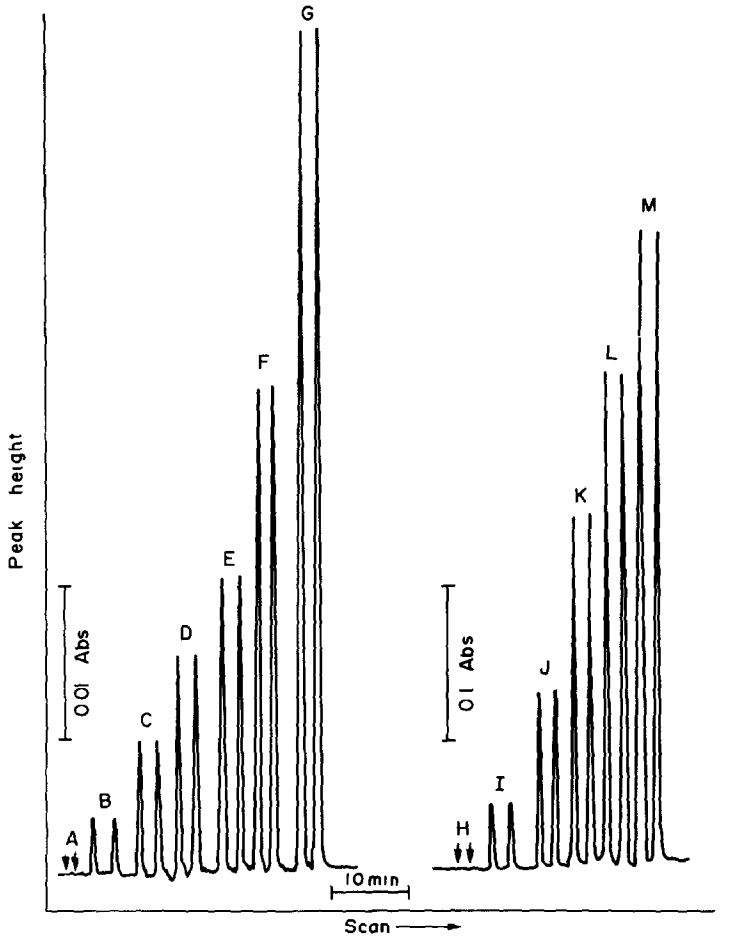

Fig 12 Flow-injection signals for determination of phosphorus Phosphorus (μg/ml) A, 0, B, 0·01, C, 0·02, D, 0·03, E, 0·04, F, 0·06, G, 0·12, H, 0, I, 0·1, J, 0·2, K, 0·4, L, 0·6, M, 0·8

levels the reagent A is recommended because of the wider linear span of the calibration graph (larger sample volumes are then needed though).

Interferences were examined with the reagent A system, and the results are shown in Table 1 The amounts of these ions generally found in river water are smaller than those listed in Table 1

Phosphorus occurs in natural waters as orthophosphate, condensed phosphates (pyro-, meta- and poly-phosphate) and organically bound phosphorus. By our method only orthophosphate can be determined However, the condensed phosphates can be easily hydrolysed to orthophosphate by heating the acidified solution for 30 min in a water-bath at about 90° [23] In this work, the water samples were made 0·35*M* in sulphuric acid in stoppered test-tubes, heated for about 45 min in a water-bath at about 95°, cooled to room temperature, and injected into the carrier stream The results are shown in Table 2. Phosphorus below the 100 ng/ml level in river water was determined The results obtained by using the solvent extraction–spectrophotometric method[23] are almost the same as those obtained by FIA

Acknowledgement—The authors express their thanks to Nissan Science Foundation for financial support

REFERENCES

1 J Růžička and E H Hansen, *Flow Injection Analysis* Wiley, New York, 1981
2 *Idem, Anal Chim Acta*, 1975, **78**, 145
3 J Růžička and J W B Stewart, *ibid*, 1975, **79**, 79
4 J W B Stewart, and J Růžička, *ibid*, 1976, **82**, 137
5 E H Hansen and J Růžička, *ibid*, 1976, **87**, 353
6 H Bergamin F, E A G Zagatto, F J Krug and B F Reis, *ibid*, 1978, **101**, 17
7 Y Hirai, N Yoza and S Ohashi, *ibid*, 1980, **115**, 269
8 J Růžička, E H Hansen, H Mosbaek and F J Krug, *Anal Chem*, 1977, **49**, 1858
9 E H Hansen, F J Krug, A K Ghose and J Růžička, *Analyst*, 1977, **102**, 714
10 A G Fogg and N K Bsebsu, *ibid*, 1981, **106**, 1288
11 Y Hirai, N Yoza and S Ohashi, *Bunseki Kagaku*, 1981, **30**, 465
12 K Itaya and M Ui, *Clin Chim Acta*, 1966, **14**, 361
13 I Štěpánová, *ibid*, 1967, **16**, 330
14 A J Bastiaanse and C A M Meijers, *Z Klin Chem Klin Biochem*, 1968, **6**, 48

15 *Idem*, *ibid*, 1968, **6**, 109
16 W Hohenwallner and E Wimmer, *Clin Chim Acta*, 1973, **45**, 169
17 A Kallner, *ibid*, 1975, **59**, 35
18 C L Penney, *Anal Biochem*, 1976, **75**, 201
19 B Anner and M Moosmayer, *ibid*, 1975, **65**, 305
20 D J Stewart, *ibid*, 1974, **62**, 349
21 H J Altmann, E Furstenau, A Gielewski and L Scholz, *Z Anal Chem*, 1971, **256**, 274
22 H V Belle, *Anal Biochem*, 1970, **33**, 132
23 S Motomizu, T Wakimoto and K Tôei, *Anal Chim Acta*, 1982, **138**, 329

Talanta, Vol 30, No 5, pp 339–345, 1983
Printed in Great Britain

0039-9140/83/050339-07$03 00/0
Pergamon Press Ltd

EVALUATION OF AN INDUCTIVELY-COUPLED PLASMA WITH AN EXTENDED-SLEEVE TORCH AS AN ATOMIZATION CELL FOR LASER-EXCITED FLUORESCENCE SPECTROMETRY

M A KOSINSKI, H UCHIDA* and J D WINEFORDNER†
Department of Chemistry, University of Florida, Gainesville, FL 32611, U S A

(*Received* 27 *August* 1982 *Accepted* 12 *November* 1982)

Summary—An inductively-coupled plasma (ICP) with an extended-sleeve torch has been evaluated as an atomization cell for laser-excited fluorescence spectrometry Limits of detection for 20 lines are given The detection power is almost equivalent to that obtained by excitation with a hollow-cathode lamp Interelement effects and spectral interferences are discussed

The inductively-coupled plasma (ICP) is the best source for simultaneous multielement excitation in emission spectrometry (ES) for the determination of major, minor and trace elements in various materials, because of the resulting high sensitivities (especially for refractory elements), wide dynamic ranges and freedom from chemical and ionization interferences In spite of these advantages, there are a number of difficulties associated with the use of ICP–ES systems, notably the occurrence of spectral interferences, the need for careful optimization to minimize multiplicative interferences, and the variation in nebulization efficiency caused by variation in solution viscosities [1,2] Because of the high temperature in the ICP, the spectra are rich in lines and even the use of a high-resolution monochromator does not enable all the analytically useful lines to be used in certain analyses

In principle, fluorescence techniques, although requiring an intense primary excitation source, should be effective in avoiding spectral interferences Atomic-fluorescence techniques based on use of a xenon arc lamp,[3] electrodeless discharge lamps (EDL),[4] hollow-cathode lamps (HCL),[5] ICP emission[6] or a pulsed tunable dye-laser[7] as primary excitation sources have been employed with flame atomization systems Laser excitation has been found to result in an improvement of detection limits,[8] some of which were equivalent to or better than those obtained by flame atomic-absorption spectrometry (AAS) and ICP–ES However, chemical and ionization interferences often occur in flames, and for refractory elements poor detection cannot be avoided The detection power should be improved by using the ICP as an atomization cell, because of its high temperature and the relatively long residence time of the analyte The high volatilization efficiency achieved in the ICP should also minimize the scattering of excitation radiation. Furthermore, quenching effects caused by molecular species should be less than those in combustion flames

The first study using the ICP as an atomization cell for fluorescence was reported by Montaser and Fassel,[9] EDLs were used as excitation sources and special torches with extended sleeves were investigated Montaser and Fassel studied only cadmium, zinc and mercury, for which intense EDLs were available Demers and Allemand[10,11] investigated pulsed HCLs for excitation of atomic fluorescence in the ICP and reported detection limits for 32 elements (with linear dynamic ranges of 4–5 orders of magnitude) that were comparable to those obtainable by flame AAS

For laser-excitation of atoms in the ICP, dye-lasers pumped by a continuous-wave argon-ion laser,[12] a pulsed flash-lamp pumped laser[13] and a pulsed nitrogen laser[13,14] have been investigated In addition, the laser-excitation technique has also been applied to the measurement of relative analyte atom distributions in the ICP, without the need for Abel inversion [14,15] The present paper describes the use of the combination of a tunable dye-laser pumped with a pulsed nitrogen-laser (as the primary excitation source) and an ICP with an extended-sleeve torch (as an atomization and/or ionization cell) for fluorescence spectrometry

EXPERIMENTAL

Figure 1 gives a schematic diagram of the system The organic dyes PBD, BBQ, DPS, Bis-MSB, C120, 7D4MC, C500 and C495 (Molectron Corp) were used in the dye-laser (Molectron Corp , DL-300), which was pumped by a nitrogen-laser (Molectron Corp , UV-14) The operating conditions of this laser system were similar to those described by Weeks *et al* ,[8] except for the optical trigger The photoelectric pulse from the photodiode circuit was used as a trigger signal for the boxcar averager

The ICP (Plasma Therm, HFP-1500D) was operated under the following conditions RF power 0 7, 1 0 or 1 2 kW, plasma support-argon flow-rate 15 l /min, no auxiliary

*On leave from Industrial Research Institute of Kanagawa Prefecture, Yokohama 236, Japan
†Author to whom correspondence should be addressed

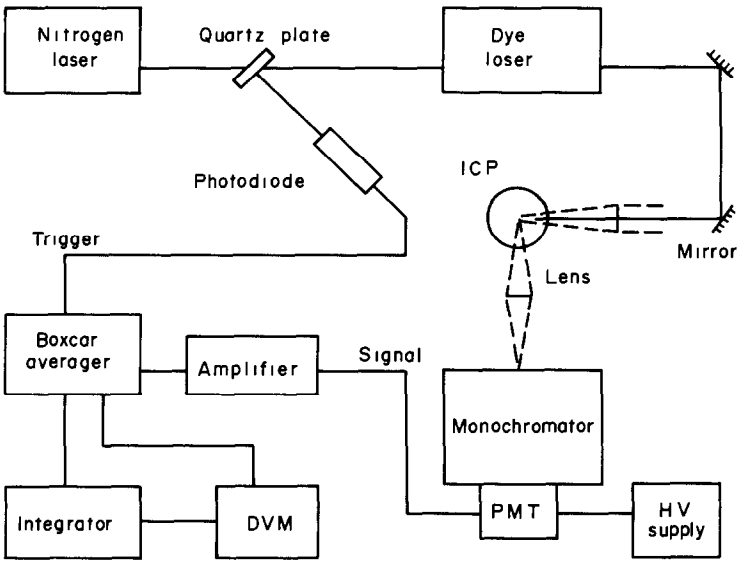

Fig 1 Schematic diagram of laser-excited ICP–FS system

argon, nebulizing-gas pressure 40 psig, for a cross-flow type nebulizer (Nippon Jarrell-Ash) A long-sleeve torch (Baird Corp) was used, with a coolant tube extending 63 mm beyond the nozzle of the aerosol tube

The diameter of the dye-laser beam in the plasma was about 3 mm for the exploratory studies and 10 mm for the investigation of calibration graphs and detection limits The fluorescence was imaged on the entrance slit of the monochromator (Heath Co , EU-700, 350-mm focal length, grating with 1180 grooves/mm) The entrance and exit slit-widths were set to 1 mm, and the slit-height was 3 mm for the initial studies and 10 mm for determination of the detection limits The output signal from the photomultiplier (Hamamatsu TV, R928) was connected to the boxcar averager (Princeton Applied Research, 162/164) through an amplifier with a gain of 10 (Comlinear Corp , CLC100) The photomultiplier base was modified for pulsed high-current operation [16] The output from the boxcar was integrated for 10 sec with a laboratory-constructed integrator and the output displayed on a digital voltmeter (Fluke 8000A)

Stock solutions (1000 μg/ml) of aluminium, barium, calcium, gallium, molybdenum, scandium, strontium, thallium, vanadium, lead, yttrium and zirconium were prepared and successively diluted with distilled/demineralized water For the interference studies, 20-mg/ml sodium, aluminium and iron solutions were prepared, and commercially available phosphoric acid (special grade) was used

RESULTS AND DISCUSSION

Fluorescence intensities in the ICP depend primarily on the following three factors (*i*) population density of the lower level in the laser-excitation process, (*ii*) output power of the laser, (*iii*) spontaneous transition probability of the fluorescence line Laser-excitation from the ground state and saturation of the spectral transition are both advantageous However, excited-state fluorescence and thermally-assisted fluorescence[17] are more useful than in flames, because of the higher temperature of the ICP [14] One of the most significant differences between flames and the ICP is that the resonance fluorescence of ionic lines is strong in the latter [14] Hollow-cathode lamps are not suitable for the excitation of ionic lines, except for those of barium [10,11] In this work, we did not consider the use of sensitive lines at wavelengths shorter than 350 nm, because of poor laser energy in the frequency-doubled mode and difficulty in keeping the doubled line tuned

Extended-sleeve torch and carrier-argon flow-rate

Basically, the temperature in the analytical region of the ICP (10–25 mm above the induction coil) is too high for analytical fluorescence measurements[12,14] because it decreases the ground-state population and causes strong background emission Most of the sensitive fluorescence lines involve resonance transitions with excitation from the ground state Three methods are available for decreasing the ICP temperature reducing the power, increasing the carrier-argon flow-rate,[18] and using a higher observation point When 40 psig nebulizing-gas pressure was used [at which the argon flow and solution uptake rates were 1 7 l /min and 2 2 ml/min (water), respectively], the fluorescence intensity at the Ca II 393 4-nm line was about four times that obtained at 30-psig nebulizing pressure A similar result was obtained for other lines, both atomic and ionic At observation points above the induction coil, the analyte population is less dense than in lower positions, owing to diffusion into the surrounding air, as shown in emission,[19] absorption[20] and fluorescence measurements [15] An extended-sleeve torch[10,11] was therefore used to minimize the diffusion Furthermore, this torch should be more effective than a short one for transfer of collisional energy from the plasma to the analyte atoms [20] In addition, scattering caused by water droplets[15] should be decreased

Horizontal distribution of the fluorescence intensity

Figure 2 shows the horizontal distribution of the

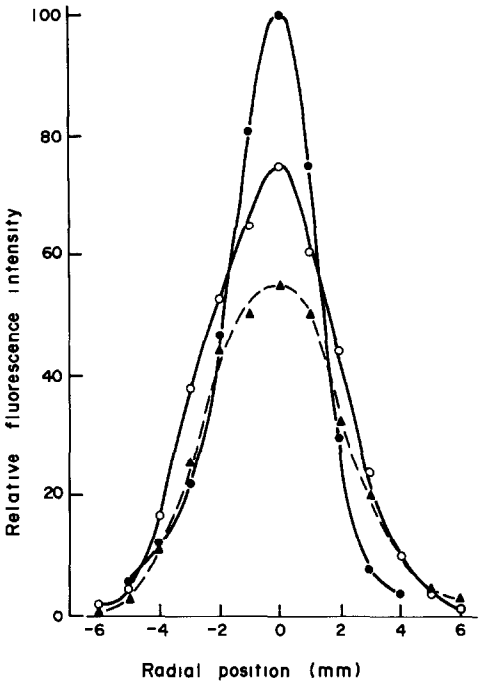

Fig 2 Horizontal distribution of resonance ionic fluorescence intensity for calcium ions at 393 4 nm RF power 1 0 kW, observation height ● 5 mm, ○ 15 mm, ▲ 25 mm from top of torch (45 mm, 55 mm, 65 mm above induction coil)

ionic resonance-fluorescence intensity for the Ca II 393 4-nm lines at three heights The heights of 5, 15 and 25 mm above the top of the extended-sleeve torch correspond to 45, 55 and 65 mm above the induction coil In this experiment, the dye-laser diameter at the ICP position was about 3 mm, and the width and height of the monochromator slit were 0 5 and 3 mm respectively These distributions indicate the spatially resolved relative population densities for calcium ions above the long torch All the distributions are symmetrical, with the maximum on the central axis of the plasma The fluorescence intensity decreases and the distribution profile becomes slightly wider with increase in observation height Comparison of these distributions with those obtained with a conventional

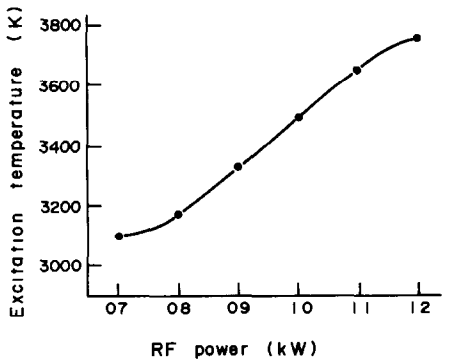

Fig 3 Effect of RF power on excitation temperature Observation height 5 mm above top of the torch (45 mm above the coil)

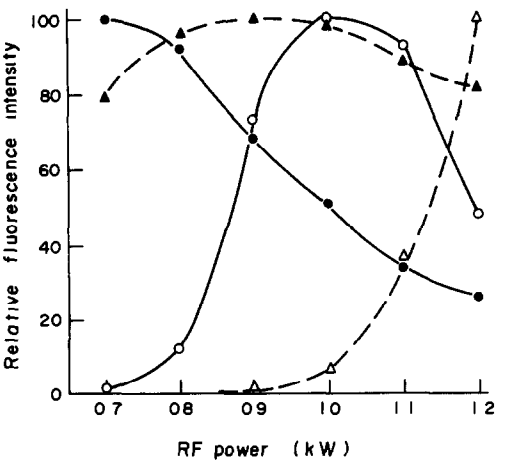

Fig 4 Effect of RF power on fluorescence intensity Observation height 5 mm above top of the torch (45 mm above the coil) Fluorescence line ● Ga I 403 3 nm, ○ Mo I 386 4 nm, ▲ Ca II 393 4 nm, △ Y II 508 7/371 0 nm

short torch[14] shows that the extended-sleeve torch is fairly effective in preventing diffusion of analyte atoms into the surrounding air For all further fluorescence measurements the central axis of the plasma was observed

Effect of RF power on excitation temperatures and fluorescence intensities

The RF power of the ICP is one of the significant parameters affecting plasma temperature and fluorescence intensity The excitation temperature is easily obtained from relative emission intensities and often used to describe plasmas [18-21] Figure 3 shows the effect of the RF power on the excitation temperature for iron at 5 mm above the top of the extended-sleeve torch (45 mm above the induction coil) The temperatures were obtained from the slope calculated from the iron atomic lines at 382 0, 382 4 and 382 6 nm Spectral data for these lines were summarized previously [18] As shown in the figure, the temperature increases with increase in RF power and is close to that of some flames The excitation temperature measured in the same way 20 mm above the induction coil of a conventional torch (1 0 kW RF power and 22 psig nebulizing-gas pressure) was found to be 4500 K

Figure 4 indicates the effect of power on the resonance-fluorescence intensities for the Ga I 403 3 nm, Mo I 386 4 nm and Ca II 393 4 nm lines and the fluorescence intensity for the Y II 508 7/371 0 ($\lambda_{ex}/\lambda_{fl}$) transition, measured at 5 mm above the top of the extended-sleeve torch (45 mm above the coil) The intensity of the atomic line for gallium (a non-refractory element) decreases with increase in RF power As can be seen from Fig 4, an even lower temperature might be optimal for gallium, but RF powers below 0 7 kW were not investigated The atomic line for molybdenum (a refractory element) gives a maximum fluorescence peak at 1 0 kW (3500

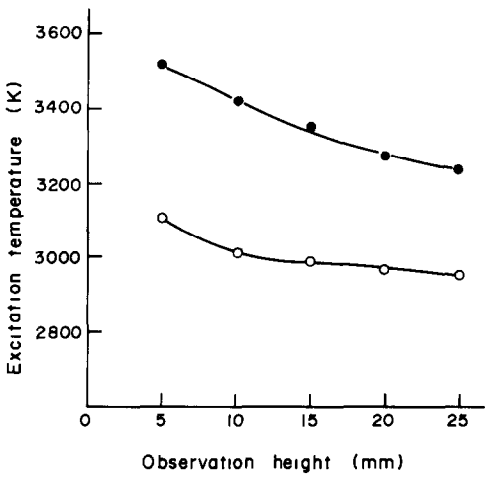

Fig. 5 Vertical distribution of excitation temperature. RF power, ○ 0 7 kW; ● 1 0 kW

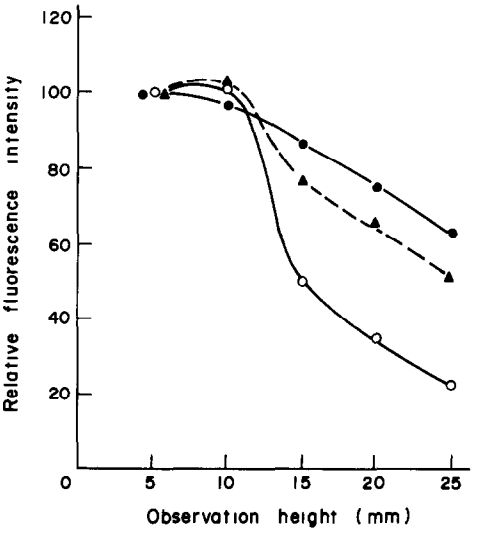

Fig 6 Vertical distribution of the fluorescence intensity Fluorescence line· ● Ga I 403 3 nm (0 7 kW), ○ Mo I 386 4 nm (1 0 kW), ▲ Ca II 393 4 nm (1 0 kW)

K), and for calcium the ionic fluorescence is maximal at about 0 9 kW (3300 K). Similar results were obtained for resonance ionic fluorescence for barium at 455.4 nm and for strontium at 407.8 and 421.6 nm.

In contrast, the yttrium ionic fluorescence at 508 7/371.0 nm (anti-Stokes fluorescence[17]) should be measured at high power, as also shown in Fig 4. One of the reasons for this might be that the lower level of the laser excitation at 508.7 nm is fairly high above the ground state (8743 cm^{-1}). However, similar results were also obtained for other yttrium ionic lines, involving the line excited from the ground state (Y II 363 3 nm), and also for Zr II 431 7/349 6 nm

The background intensity level and its reproducibility were about the same at each RF power

Vertical distributions of excitation temperature and fluorescence intensity

Vertical distributions of the iron excitation temperatures at 0 7 and 1 0 kW power, along the central axis of the ICP, are shown in Fig 5. For both powers, the temperature decreases with increasing observation height. At 0.7 kW, the temperature is roughly that of a nitrous oxide–acetylene combustion flame, especially at the higher positions

The vertical distributions of resonance-fluorescence intensities along the central axis of the plasma for Ga I 403.3 nm (at 0 7 kW RF power), Mo I 386.4

Table 1 Limits of detection (LOD) by laser–ICP–FS and two other ICP methods

	Laser–ICP–FS (this work)		Laser–ICP–FS[14] (conventional short torch)		HCL–ICP–FS[10]		ICP–ES[22]	
Line	$\lambda_{ex/fl}$,* *nm*	LOD, *ng/ml*	$\lambda_{ex/fl}$,* *nm*	LOD *ng/ml*	$\lambda_{ex/fl}$, *nm*	LOD, *ng/ml*	$\lambda_{Emission}$ *nm*	LOD, *ng/ml*
Al(I)	394 4/396 2	5			309 2	20	396 2	1
Ba(I)	553 5	2000						
Ba(II)	455 4	1	455 4	40	455 4	50	455 4	0 05
Ca(I)	422 7	100			422 7	0 08	422 7	3
Ca(II)	393 4	1	393 4	8			393 4	0 04
Ga(I)	403 3	10					403 3	5
	403 3/417 2	4					417 2	3
Mo(I)	386 4	100	386 4	3000	313 3	30	386 4	2
Pb(I)	405 8	70	405 8	6000	283 3	25	405 8	20
	405 8/283 3	100					283 3	40
Sc(II)	364 3	30					364 3	0 13
Sr(I)	460 7	7			460 7	0 7	460 7	2
Sr(II)	407 8	0 5					421 6	0 03
Tl(I)	377 6	8	377 6	8000	377 6	7	377 6	11
	377 6/535 0	10					535 0	9
V(I)	411 2	400					411 2	9
V(II)	390 3/290 9	10,000	390 3/290 0	700			290 9	0 7
Y(I)						500†		
Y(II)	371 0	10					371 0	0 08
	508 7/371 0	70	508 7/371 0	30				
Zr(II)	431 7/349 6	6000					349 6	0 9

*Excitation and fluorescence wavelengths, only the one is given if they are identical
†Reported by Demers *et al*.,[11] wavelength not stated

nm (1.0 kW), and Ca II 393.4 nm (1 0 kW) are shown in Fig. 6 All three elements are affected by lateral diffusion to the same extent, but in the case of calcium, the decreasing temperature (see Fig. 5) would result in a depopulation of the first ionic state. Furthermore, the molybdenum intensity decreases even more because of the formation of monoxides.

The background intensity level was slightly larger at 5 mm above the top of the extended-sleeve torch than at higher positions, but the noise level was almost the same at all heights examined.

Limits of detection and calibration curves

The use of an expanded dye-laser beam (about 10 mm diameter at the ICP position) and 10-mm monochromator slit-height to improve the sensitivity was investigated Fluorescence intensities were 3–5 times as large as those obtained with the 3-mm beam and 3 mm slit-height The background intensity caused by scattering also increased, but the increase in noise was small As a result, the fluorescence signal-to-noise ratio (SNR) was improved appreciably, depending on the type of fluorescence line observed. The SNR was much better for non-resonance lines The centre of the expanded-dye laser-beam was located 10 mm from the top of the torch in order to avoid hitting the torch and increasing the scatter signal

Table 1 shows the limits of detection together with those obtained from laser–ICP–FS with a conventional short torch,[14] HCL–ICP–FS[10,11] and ICP–ES [22] For measuring the limits of detection (LOD), the boxcar output was integrated for 10 sec. The LOD was taken to be the concentration corresponding to a signal twice as large as the standard deviation of 16 consecutive, integrated blank readings The RF powers used were 0 7 kW for the atomic lines of calcium, gallium, strontium, thallium and lead, and 1.0 kW for the atomic lines of aluminium, molybdenum and vanadium and for all ionic lines, except for those of yttrium and zirconium, for which 1 2 kW was used.

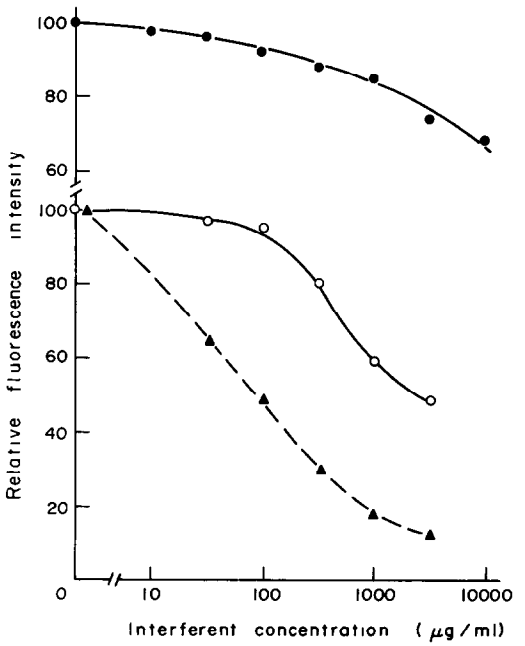

Fig 7 Effect of phosphorus and aluminium on fluorescence intensity of Ca II 393 4 nm Interferent ● phosphoric acid (1 0 kW), ▲ aluminium (0 7 kW), ○ aluminium (1 0 kW)

With the present method, ionic fluorescence is generally more sensitive than atomic fluorescence for a given element, as shown for barium, calcium and strontium In the case of vanadium however, the ionic line is less sensitive, probably because the laser-excitation occurs from an excited state which is not well populated This might also be true of zirconium, although we have no data on the atomic fluorescence for this element

Comparison of the LOD values for the present method with those obtained with a conventional short torch under the conditions of 1 0 kW RF power, 22 psig carrier-argon pressure and 20 mm observation height[14] shows that the short torch provided superior LOD values for ionic excited-state fluorescence and for the refractory elements, as is shown for vanadium and yttrium For the other lines, the long torch gives limits of detection better by 1–3 orders of magnitude than those obtained with the short torch. There is little to choose between laser and HCL excitation of fluorescence, for practical use The HCL system gives good limits of detection for atomic fluorescence[10,11] but the laser excitation of ionic lines is useful

Calibration graphs were plotted for each line and indicated linearity over a range of 4 orders of magnitude from the LOD levels At higher concentrations the calibration graphs levelled off because of saturation of the photomultiplier (anodic current) and self-absorption of the fluorescence The linear range could be extended upwards by 1–2 orders of magnitude by using neutral density filters to decrease the light intensity introduced into the monochromator

Interelement effects

In low-temperature combustion flames, the presence of phosphorus sometimes reduces the absorption or fluorescence signal intensity because of the formation of refractory compounds Figure 7 indicates the effect of phosphorus on the ionic fluorescence of calcium The intensity was slightly lowered by the presence of phosphorus, but this is partly due to the increase in sample viscosity,[1,2] so chemical interference is probably negligible A similar result was obtained at 0.7 kW power

The effect of the presence of aluminium on calcium intensity at 0 7 and 1 0 kW RF power is also shown in Fig 7 At 0 7 kW power, the fluorescence intensity decreased with increase in the aluminium concentration, because of refractory compound formation between calcium and aluminium affecting the solute vaporization process This reaction should occur to a

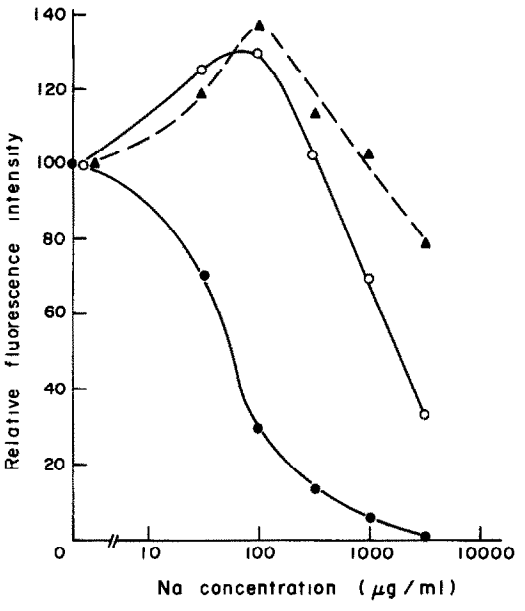

Fig 8 Effect of sodium on fluorescence intensity of Ca II 393 4 nm RF power ● 0 7 kW, ○ 1 0 kW, ▲ 1 2 kW

lesser extent at higher temperatures, as is shown at 1 0 kW power

The effect of the presence of sodium on the calcium ionic line is shown in Fig 8 The results are quite complicated At 0 7 kW, the calcium fluorescence intensity decreases rapidly with increase in sodium concentration, which seems to be due to an ionization interference In contrast, at 1 0 and 1 2 kW RF power the intensity increases to a maximum at about the 100-μg/ml sodium level and then falls again This enhancement is not due to an ionization interference Similar enhancements were observed at higher carrier-gas flow-rates (> 1 0 l /min) and 15 mm above the coil, for use of a conventional torch with an ICP,[18] and also with a capacitively-coupled microwave plasma [23] In the latter case, Murayama[24] reported that the enhancement was caused by a change in the atom and ion distributions in the plasma The suppression at high concentration of sodium is at least partly due to the change in sample solution viscosity

These interelement effects can probably be reduced by further optimization of the power and carrier-gas flow-rate

Spectral interference

One of the major disadvantages in the ICP–ES method is spectral interference, in the form of the change in background emission caused by stray light and overlap of emission spectra. The fluorescence technique should be considerably less susceptible to spectral interference since multiple excitation is minimized (the laser excitation line is only 0 03 nm wide[7]), and fluorescence spectra contain fewer lines than do spectra produced by collisional excitation

The fluorescence excitation and emission spectra (~370–372 nm) for a 100-μg/ml yttrium solution containing 5000 μg of iron per ml as matrix, are shown in Fig 9 Emission measurements were made under conditions of 1 0 kW RF power, 20 psig nebulizing-gas pressure and 15 mm observation height above the coil, with a conventional short torch, the monochromator entrance and exit slit-widths being 20 μm (bandpass 0 04 nm) The fluorescence spectrum was obtained with a fixed monochromator wavelength and 1-mm slit-width (bandpass 2 nm). Even with the 50-fold bandpass, the spectral profile for fluorescence shows no overlap between the Y II 371 030 nm line and the Fe 370 925 nm line, in contrast to the emission spectrum, as shown in the figure The yttrium emission at 371 030 nm slightly overlaps the iron at 370 925 nm In ICP–ES such overlap becomes a significant interference when the analyte concentration is low and especially when less sensitive lines are being used

Conclusion

The limits of detection obtained with this system for 20 lines (12 elements) are practically equivalent to

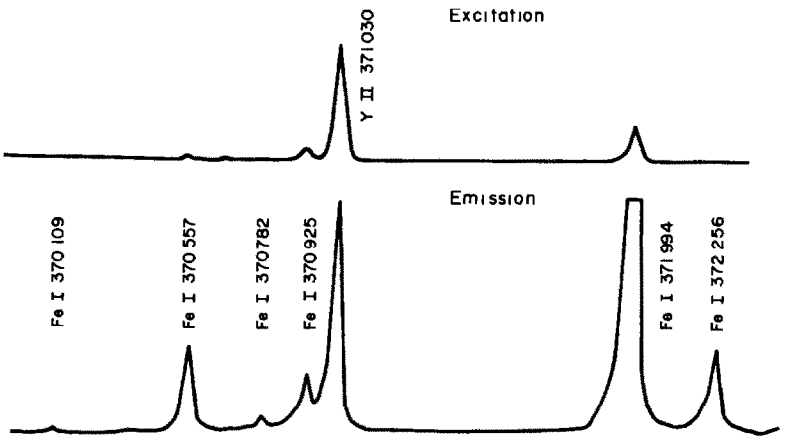

Fig 9 Emission and fluorescence excitation spectra for 100-μg/ml yttrium solution containing 5000 μg of iron per ml as matrix Slit-width of monochromator 1 mm (fluorescence), 0 02 mm (emission)

those obtained with the HCL–ICP–FS system Operating parameters, such as RF power and carrier-gas flow-rate, should be optimized to minimize interelement effects At present, the detection limits are inferior to those in ICP–ES, except for the atomic lines of non-refractory elements, but the relative freedom from spectral interference is useful for trace analysis.

Acknowledgements—The authors wish to thank Edward Voigtman for his advice and construction of the integrator and photodiode trigger circuit This research was supported by a grant from AFOSR-F49620-80-C-0005 MOD P00004

REFERENCES

1 S Greenfield, H M McGeachin and P B Smith, *Anal Chim Acta*, 1967, **84,** 76
2 H Uchida and H Matsui, *Bunko Kenkyu*, 1978, **27,** 110
3 D R Demers, *Appl Spectrosc*, 1968, **22,** 797
4 J M Mansfield, Jr, M P Bratzel, Jr, H O Norgordon, D O Knapp, K E Zacha and J D Winefordner, *Spectrochim Acta*, 1968, **23B,** 389
5 R M Lowe, *ibid*, 1971, **26B,** 201
6 M S Epstein, S Nikdel, N Omenetto, R Reeves, J Bradshaw and J D Winefordner, *Anal Chem*, 1979, **51,** 2071
7 L M Fraser and J D Winefordner, *ibid*, 1971, **43,** 1693
8 S Weeks, H Haraguchi and J D Winefordner, *ibid*, 1978, **50,** 360
9 A Montaser and V A Fassel, *ibid*, 1976, **48,** 1490
10 D R Demers and C D Allemand, *ibid*, 1981, **53,** 1915
11 D R Demers, D A Busch and C D Allemand, *Am Lab*, 1982, March, 167
12 B P Pollard, M B Blackburn, S Nikdel, A Massoumi and J D Winefordner, *Appl Spectrosc*, 1979, **33,** 5
13 M S Epstein, S Nikdel, J D Bradshaw, M A Kosinski, J N Bower and J D Winefordner, *Anal Chim Acta*, 1980, **113,** 221
14 H Uchida, M A Kosinski and J D Winefordner, *Spectrochim Acta*, in the press,
15 N Omenetto, S Nikdel, R D Reeves, J D Bradshaw, J N Bower and J D Winefordner, 1980, **35B,** 507
16 L M Fraser and J D Winefordner, *Anal Chem*, 1972, **44,** 1444
17 N Omenetto and J D Winefordner, *Appl Spectrosc*, 1972, **26,** 555
18 H Uchida, *Spectrosc Lett*, 1981, **14,** 655
19 D J Kalnicky, R N Kniseley and V A Fassel, *Appl Spectrosc*, 1977, **31,** 137
20 Y Nojiri, K Tanabe, H Uchida, H Haraguchi, K Fuwa and J D Winefordner, *Spectrochim Acta*, in the press
21 H Uchida, K Tanabe, Y Nojiri, H Haraguchi and K Fuwa, *ibid*, 1981, **36B,** 711
22 P W J M Boumans and M Bosveld, *ibid*, 1979, **34B,** 59
23 P W J M Boumans and F J de Boer, *ibid*, 1977, **32B,** 365
24 S Murayama, *ibid*, 1970, **25B,** 191

Talanta, Vol 30, No 5, pp 347–354, 1983
Printed in Great Britain

0039-9140/83/050347-08$03 00/0

INFLUENCE OF COLLOIDAL CHARGE ON RESPONSE OF pH AND REFERENCE ELECTRODES: THE SUSPENSION EFFECT

DONALD P BREZINSKI*
Corning Glass Works, Sullivan Research Park, Corning, NY 14831, U S A

(*Received* 3 *February* 1982 *Revised* 5 *July* 1982 *Accepted* 21 *October* 1982)

Summary—The pH measured in a charged sediment is often very different from that of the supernatant solution This effect has been studied to determine whether it is caused by an anomalous junction potential at the reference electrode, as commonly thought, or by Donnan partitioning of hydrogen ions Electrical conductivities in sediments of a strong cation-exchange resin were much higher than predicted by the junction artifact theory, electrode measurements of pH in sediments corresponded to titratable H^+-content, and pH-changes induced by titration and salt addition were in accord with partitioning theory These findings suggest that most pH differences observed between colloidal sediments and supernatants are real, not junction artifacts Guidelines for interpretation of pH measurements on colloids are suggested

The use of ion-selective electrodes to measure ionic concentration or activity within colloids is inhibited by uncertainty regarding the effect of colloidal charge and inhomogeneity on the reading. Pallman and Wiegner observed that a colloidal suspension and its ultrafiltrate may differ in measured pH, termed this the "suspension effect," and attributed it to hydrogen ions sorbed by the dispersed phase [1-3] However, a difference in pH is by itself inadequate to explain the effect because the pH reading depends on the position of the reference electrode, not of the pH electrode (Fig 1) [4-6] Two major conflicting explanations have been provided the Donnan explanation holds that there is unequal partitioning of hydrogen ions between the supernatant and the charged sediment, in response to a phase boundary potential,[7] the reference artifact explanation, proposed by Jenny *et al*, holds that the effect is a liquid-junction anomaly caused by unequal diffusional mobility of K^+ and Cl^- within the charged sediment.[6] According to the former view the pH difference is real, according to the latter view, it is wholly artifact Considering that the pH shift may exceed 5 units in certain systems,[6] the difference in interpretation is of considerable consequence

Subsequent debate has not resolved the issue Donnan advocates have pointed out that ion partitioning is central to colloidal theory and that voltaic expressions derived from Meyer–Sievers–Teorell (charged-membrane) or Guoy (double-layer) theory could provide a somewhat better fit to the data of Jenny *et al* [8-10] Overbeek equated the Donnan emf and the suspension effect,[11] but his calculation method *seemingly* attributes the potential to the reference junction interface, consequently, a bridge electrolyte of low potassium chloride concentration (matching the colloid) was recommended for accurate measurement [12] Marshall attributed the potential to the sediment/supernatant interface, and recommended that the bridge electrolyte be much more concentrated than the colloidal electrolyte [13] While Donnan-type views seem favoured by colloidal chemists, the Jenny view seems to have gained considerable informal acceptance among analytical chemists, who typically cite the suspension effect as a drastic example of junction error Reference texts mention both views, leaving them unresolved.[14-16] Finally, the uncertainty regarding interpretation of pH readings for colloids has led to the opinion that the pH value of neither the sediment nor the supernatant is very meaningful or useful for characterizing colloids [15,17]

Presuming that sense can be made of pH readings for colloids, the current lack of consensus regarding the origin and significance of the suspension effect is highly unfortunate, as it may occasion improper methodology, incorrect interpretation, or unwarranted general avoidance of potentiometric methods in work on colloids Thus the purpose of this study is to provide a clearer theoretical perspective and to support it by electrode measurement on a model colloid The view proposed is that the sediment effect arises from a true difference in pH induced by a Donnan potential at the sediment/supernatant interface, but that significant uncertainty may be introduced by conventional junction errors and by inhomogeneity of colloidal charge

*Address correspondence to 54798 CR653, Paw Paw, MI 49079, U S A

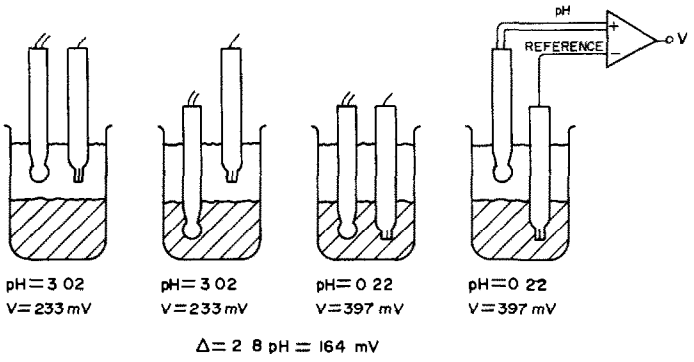

Fig 1 Suspension effect in pH measurement of H_2O-washed H^+-form cation-exchange resin (Bio-Rad AG 50W-X8, 50–100 mesh, hydrogen form, 1 7 meq/ml nominal resin-bed capacity) Electrodes were calibrated in standard pH 2 00 and 4 00 buffers

THEORY

According to Donnan theory, a phase boundary potential arises from the tendency of mobile counter-ion charge to diffuse from the charged sediment into the supernatant Assuming a 1–1 electrolyte, let $C_1^+ = C_1^- = C_1$ be the cation and anion concentrations in the supernatant phase, C_0^+ and C_0^- be their respective concentrations in the sediment aqueous phase, and σ be the concentration of fixed charge (of known sign and presumed to be uniform) in the sediment phase At the sediment boundary, where local equilibrium can be assumed, the diffusional and electrophoretic fluxes for each ionic species are very large and must essentially cancel Equating these fluxes, solving for the electric field, and integrating through the interface, yields the potential difference between the phases

$$\Delta U = U_0 - U_1 = -(RT/F)\ln(C_0^+/C_1)$$
$$= -(RT/F)\ln(C_1/C_0^-)$$

where RT/F is the electrochemical slope factor Solving the simultaneous equations $C_0^+/C_1 = C_1/C_0^-$ and $C_0^+ + \sigma = C_0^-$ (electroneutrality) gives $C_0^+ = \sqrt{C_1^2 + (\sigma/2)^2} - \sigma/2$ and $C_0^- = \sqrt{C_1^2 + (\sigma/2)^2} + \sigma/2$. Thus the change in potential upon entering the sediment from the supernatant is

$$\Delta U = U_0 - U_1$$
$$= (RT/F)\ln(\sqrt{1 + (\sigma/2C_1)^2} + \sigma/2C_1)$$

which yields $\Delta U \approx \pm(RT/F)\ln(\pm\sigma/C_1)$ for $C_1 \ll |\sigma|$, and $\approx (RT/F)\sigma/2C_1$ for $C_1 \gg |\sigma|$ (A Nernst-like potential occurs across a sediment interface with a dilute solution, but this potential disappears for a concentrated solution) The expression derived for ΔU is a single-boundary equivalent of the Meyer–Sievers–Teorell membrane potential [18,19] If activity coefficients are not ignored, the corresponding activities give $a_0^+/a_1 = a_1/a_0^-$ and $C_0^+ + \sigma = C_0^-$, which yield

$$\Delta U = (RT/F)\ln(\sqrt{1 + (\gamma_0\sigma/2a_1)^2} + \gamma_0\sigma/2a_1)$$

where $\gamma_0 \equiv \sqrt{\gamma_0^+\gamma_0^-}$ is the mean activity coefficient for the mobile species within the colloid

At equilibrium, H^+ should partition across the sediment/supernatant interface analagously to the major cation species, so $(RT/F)\ln(H_0^+/H_1^+) = U_1 - U_0$ Response of the pH electrode is deduced by noting that the potential of the reference buffer within the pH sensor is equal to the potential of the external phase plus the potential across the sensor membrane In moving from the supernatant into a negatively charged sediment, the pH electrode experiences a decrease in phase potential, $U_0 - U_1 (< 0)$, but the sensor membrane potential increases by the Nernstian response, $(RT/F)\ln(H_0^+/H_1^+) = U_1 - U_0$, for zero net change Thus, in an equilibrated system, the response of the pH electrode [which senses electrochemical potential, $U + (RT/F)\ln H^+$], is invariant even though pH may change from phase to phase. In contrast, if the boundary potential between the reference electrolyte and sediment is small ($\sigma \ll 4M$), then the reference electrode experiences only the shift in electric potential $(U_0 - U_1)$ upon entering the sediment, thereby yielding the proper reference potential for pH measurement in that phase. The position of the reference electrode, not that of the ion-sensor, would determine the phase measured

The junction artifact theory of Jenny *et al* is based on the following findings and conclusions.[6] Fluid removed by rapid filtration of cation-exchange resin sediment was identical to the supernatant, hence, ion partitioning does not occur The magnitude of the suspension effect varied greatly with the concentration of junction electrolyte (Table 1), thus, the suspension effect must arise at the junction, rather than at the remote sediment/supernatant interface The relative transference of K^+ and Cl^- in the sediment varied greatly with the activity $(a_\pm)$ of potassium chloride in the interstitial fluid. By assuming $a_K = a_{Cl} = a_\pm$ in the sediment and substituting an observed transference dependence of the form $t_- \approx 0\,4\ ka_\pm/(1 + ka_\pm)$ into the diffusion potential expression

$$\Delta U = (RT/F)\int \sum_i t_i\, d\ln a_i,$$

Table 1 Junction potentials in colloidal sediment

KCl mean activity, M			$U_1 - U_2$, mV	
a_1	a_2	Measured*	Calculated from artifact theory[6]	Calculated from Donnan theory†
0 00463	0 00902	18 0	17 7	16 8
0 00463	0 0441	53 7	53 7	56 4
0 00463	0 296	91 7	85 2	93 1
0 00463	0 432	96 5	89 3	96 7
0 00463	2 323	113 0	102 0	103 0

*Data from Jenny *et al*[6] for Dow Ion-X cation-exchanger (3 7 meq/g) in the following cell

Reference junction: X_2; Sediment interface: X_1

$$\mathrm{Hg}|\mathrm{Hg_2Cl_2}|\mathrm{KCl\ (satd)}|\mathrm{KCl}\ (a=a_2)|\text{cation-exchanger}+\mathrm{KCl}\ (a_1)|\mathrm{KCl}\ (a=a_1)|\mathrm{KCl\ (satd)}|\mathrm{Hg_2Cl_2}|\mathrm{Hg}$$
$$(U_2) \qquad\qquad (U_1)$$

†Values derived from
$U_1 - U_2 = (59\ \mathrm{mV})\ \log\ [(\sqrt{1+(\sigma'/2a_1)^2}+\sigma'/2a_1)/(\sqrt{1+(\sigma'/2a_2)^2}+\sigma'/2a_2)]$, where $\sigma' = \gamma_0\sigma = -0\ 3$ meq/ml

the suspension effect could be roughly calculated The sediment effect was therefore attributed to an anomalous junction potential caused by alteration of the relative diffusional mobility of K^+ and Cl^- within the sediment, and the ionic activities in the sediment and supernatant were claimed to be identical

The two theories cannot be directly distinguished potentiometrically even though the interfacial potentials predicted are radically different The potential across a single colloidal interface cannot be measured directly, because of additional phase boundaries with the measuring electrodes Reference electrodes impose an electrolyte boundary, ion-sensor electrodes impose an interstitial solution boundary where the activity of the sensed ion is *per se* at issue. Therefore, potentiometric evidence for a colloidal theory has to be judged by the plausibility and consistency of the postulated interfacial contributions to the total cell potential

EXPERIMENTAL

Electrical impedances of colloidal phases were measured at 1 kHz frequency with an ESI Impedance Bridge, Model 250DA (Portland, OR) and a cell consisting of two stainless-steel rods (25 mm long, 3 mm diameter) protruding axially into the ends of a 25-cm long 14-mm diameter glass tube The cell was filled with sediment by gravitational settling of a slurry Interstitial fluid in the sediment was changed by perfusion Contact impedance was compensated by subtracting the results obtained in a minimal-path cell having the rods parallel and 5 mm apart

pH was measured with a Corning 130 meter, a Corning 476022 pH electrode, and a Vycor-barrier reference electrode[20] having a ceramic outer junction with 10-μl/hr outward flow of pure 4M potassium chloride Corning standard pH buffers were used for calibration Other experimental details are given in the figure legends

Ion-exchange resins were obtained from Bio-Rad Laboratories, Richmond, CA 94804, and Fisher Scientific Company, Pittsburgh, PA 15219

RESULTS AND DISCUSSION

The anomalous junction-potential expression derived by Jenny *et al* is based on their interpretation that the observed transference imbalance is not attributable to the known difference in K^+ and Cl^- concentrations within the sediment, but to a charge-induced difference in their relative mobility This requires the seemingly paradoxical hypothesis that K^+ counter-ions are rendered immobile and inactive by the fixed charge, but Cl^- is also rendered less mobile than the non-counter-ionic K^+ This interpretation seems strained, particularly since their empirical expression for t_- would have similar form if surplus cations and anions were equally mobile, and counter-ions to the fixed charge made a constant contribution to the conductivity These alternatives could have been distinguished by use of sediment and supernatant conductivity data, which were not provided Table 2 gives the electrical conductivity observed in a sediment of K^+-form cation-exchange resin at different values of interstitial potassium chloride concentration The conductivity of the sediment was substantial even when interstitial conductivity was negligible, showing that counter-ionic K^+ in the resin was mobile The interstitial-fluid conductivity had a strong indirect influence on the sediment conductivity, probably by governing the conduction between adjacent particles and the tortuosity of the electrical path Sediment conductivity remained higher than supernatant conductivity up to a supernatant concentration of 0 4M potassium chloride

Table 2 Relative conductivity of supernatant and K^+-form cation-exchanger sediment

Supernatant composition, [KCl], M	Supernatant conductivity, $\mu mho/cm$	Sediment conductivity, $\mu mho/cm$
H_2O wash	0 015	3 1
10^{-3}	0 15	4 4
10^{-2}	1 4	10 6
10^{-1}	13	28
1	104	64

Bio-Rad AG 50W-X8 H^+-form resin, 50–100 mesh, ~1 7 meq/ml exchange capacity, titrated with KOH and washed exhaustively with distilled water

(interpolated value) This is inconsistent with the artifact theory, which predicts that the sediment conductivity should always be lower, because the K^+ and Cl^- activities are equal in the supernatant and sediment, but the Cl^- mobility is reduced in the latter The mechanism of the Donnan equilibrium potential is not mobility-dependent, but it is noteworthy that the equal conductance of the two phases at 0 4*M* potassium chloride concentration implies that the average specific ionic conductance of K^+ and Cl^- in the resin was at least 30% of the free-solution value Thus, the unfixed ionic charge in this resin was *very* mobile

According to the artifact theory, the junction potential must increase anomalously with potassium chloride activity in order to explain the data in Table 1 However, the observed cell potential, $U_1 - U_2$, could also increase with junction electrolyte activity (a_2) because reduction of a Donnan potential at the reference interface (X_2) progressively reveals a Donnan potential at the supernatant interface (X_1) As shown in Table 1, a reasonable fit to the data of Jenny *et al* is provided by an approximate Donnan expression which assumes a fixed value of $\gamma_0\sigma = 0\,3$ A much closer fit (not shown) is possible if $\gamma_0\sigma$ is presumed to increase from 0 4*M* to 0 7*M* as a_2 increases to 0 4*M* This apparent increase in γ_0 may be the consequence of a heterogeneous distribution of fixed charge within the resin bed, which would yield a composite curve Eriksson[9] showed that a very good fit to the data is obtained by assuming that the boundary potential varies as $1/\sqrt{a_2}$, as derived in double-layer theory Both of these theories provide a better fit to the interfacial potential data than does the junction artifact theory

pH measurements were performed on cation-exchange resin sediments and supernatants to determine which theoretical interpretation of the data was the more plausible pH measurements on H^+-form resin exhibited overshoot When the reference electrode was transferred to H^+-form sediment from a low ionic-strength supernatant, the indicated pH dropped quickly to a broad minimum, then drifted slowly upward ($\sim$0 04 pH/min) Agitating the electrode in the sediment caused repetition of the time-dependent behaviour This effect is probably caused by a small adjustment of the junction potential as potassium chloride penetrates beyond the nearest layer of resin particles When such drift occurred, pH readings were recorded as the preceding minimum value

The following experiment showed that pH measurement of the resin bed, adjusted for a conventional residual junction potential, corresponded closely to the hydrogen-ion concentration In turn, a close correspondence between hydrogen-ion concentration and activity within the resin can be expected because the sulphonic acid exchange groups are very concentrated and strongly acidic With the reference electrode inserted in the H^+-form sediment (Fig 2), the measured pH was 0 16, which was within half a unit of the pH corresponding to the actual H^+ content of the sediment, as indicated by the titration with base (1 90*M* $\equiv$ pH $-0\,28$) and only 0 17 higher than the pH value of $-0\,01$ measured for 1 9*M* sulphuric acid Compensation for a calculated residual junction potential of roughly -34 mV (consisting of a Donnan potential of -9 mV between 4*M* potassium chloride and the K^+-exchanged surface of the resin particles, plus an additional Henderson diffusion potential[21] of -25 mV between the particle surface and its H^+-exchanged interior) yielded a corrected reading of pH $-0\,43 \equiv 2\,67M$ activity, which agreed closely with the hydrogen-ion concentration calculated for the interior of the close-packed spherical resin particles, $1\,9M/0\,7 = 2\,7M$ A 34-mV junction potential is large, but not drastically greater than the potential calculated for comparably concentrated solutions of strong acid (*e g*, 20 mV for 2 7*M* sulphuric acid) and should diminish nearly to the Donnan equilibrium value if H^+ in the resin is replaced by less mobile ions, such as Na^+ or K^+ Thus, rather than being anomalous, the response of the electrodes in the sediment was analogous to that obtained for conventional strong acids with mobile anions Why the pH reading may correspond to the intraparticle H^+ content rather than the mean H^+ content of the bed is discussed later

Addition of alkali or salt to the system gave pH readings that reflected the changes in H^+ distribution expected from Donnan theory For example, the H^+ content of the supernatant was largely determined by the concentration of free anion as shown in Fig 2, partial titration of the sediment with sodium hydroxide had negligible effect on the difference between the pH of the sediment and supernatant, since H^+ is replaced by Na^+ without introduction of additional ions After the equivalence point, however, the

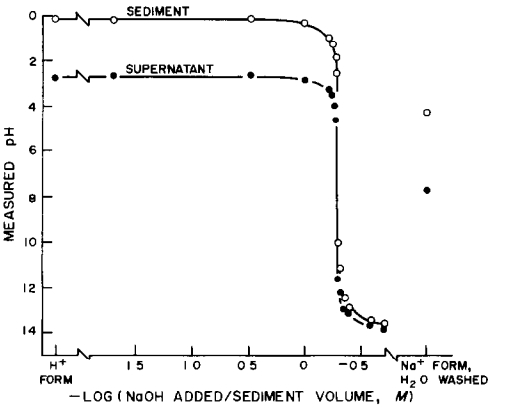

Fig 2 Effect of alkali addition on measured pH of supernatant and sediment of H^+-form Bio-Rad cation-exchange resin The pH was measured by placing the reference electrode in the supernatant or sediment, respectively, with the pH electrode placed in either phase Initially equal volumes of sediment and supernatant, followed by addition of 10*M* NaOH Sediment values are peak readings which preceded a slow drift

accumulation of sodium hydroxide in the supernatant caused progressive reduction of the partitioning of hydrogen ions Partitioning was restored by washing the Na^+-form resin with water, which removed the sodium hydroxide Just before the equivalence point, H^+ in the resin had been almost entirely replaced by Na^+, which is only one-seventh as mobile, yet the magnitude of the suspension effect remained essentially the same This lack of dependence on cation mobility is evidence that the suspension effect is due to a charge-dependent equilibrium process, such as Donnan partitioning, rather than to a mobility-dependent kinetic process, such as the diffusion potential. The effect of adding solid potassium chloride to H^+-form resin is shown in Fig. 3. Adding small amounts of the salt caused a roughly equivalent amount of H^+ to be liberated into the supernatant, as expected from reduction of the Donnan potential, and ion-exchange. When equal volumes of supernatant and sediment were present, the sediment pH remained essentially constant as salt was added, while the supernatant pH decreased until the two values were equal The pH of the sediment might be expected to increase by about 0.3 as H^+ is liberated into the supernatant, but this change is probably compensated by the effect of potassium chloride in decreasing the residual junction potential When potassium chloride was added to a supernatant-free sediment, the measured pH decreased by about 0 5, yielding agreement with the H^+ content determined by the titration

Moving the reference electrode into a sediment of strong *anion*-exchange resin (Fisher Rexyn 201 polystyrene alkyl quaternary amine, hydroxyl form) caused a substantial *increase* in measured pH, as expected for fixed positive charge

Interpretation of the sediment data in terms of the junction artifact theory seems strained The artifact theory proposes that the hydrogen-ion activity in water-washed H^+-form strong cation-exchanger is

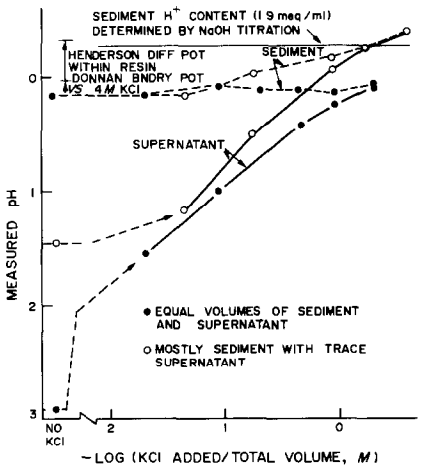

Fig 3 Effect of adding solid KCl on measured pH of sediment and supernatant of H^+-form Bio-Rad resin

the same as in the supernatant (very low), but hydrogen-ion activity is high for strong-acid solutions in which the anion is mobile, and the fixation of negative charge within the resin seems unlikely to curtail the activity drastically. For Fig 3, the artifact theory would imply that the hydrogen-ion activity in the colloidal matrix is determined primarily by the free anion (Cl^-) concentration rather than the hydrogen-ion concentration, and that the maintenance of a constant, fairly correct indication of sediment H^+content during salt addition is the fortuitous result of compensatory changes in the pH-electrode potential and the anomalous junction potential

The pH behaviour of supernatants, as shown in Figs. 2 and 3, is not in obvious conflict with the junction artifact theory, because the general features of the supernatant-pH dependence can be explained in terms of ion-exchange and mass action alone, without invoking a distinct phase boundary potential. Similarly, the sediment filtration experiment of Jenny *et al* was inherently incapable of detecting Donnan partitioning; a positive result would require gross separation of the fixed resin charge from its mobile counter-ionic charge. (Moreover, the interstitial fluid between macroscopic porous exchanger particles should be nearly identical to the supernatant.) The key question is the actual meaning of hydrogen-ion activity in the resin. In both theories, binding of H^+ to the resin is presumed to be electrostatic The artifact theory must therefore postulate that counter-ionic H^+ is confined to local potential wells around the SO_3^- sites, and that these wells constitute a negligible fraction of the intraresin aqueous phase Then species such as neutral molecules entering the resin would not "experience" the H^+ counter-ions, but only the H^+ ions associated with Cl^- co-ions, both of which have equal activity in the resin aqueous phase and supernatant In the Donnan theory, however, these wells must effectively merge so that the resin aqueous fraction is generally characterized by low potential and high H^+ activity, and anions such as Cl^- would be excluded Thus hydrochloric acid liberated by adding small amounts of potassium chloride to H^+-form resin should be distributed uniformly throughout the sample volume according to the Jenny theory, but be excluded from the resin particles according to Donnan theory Supernatant H^+ concentrations did show some enhancement in the experiment illustrated in Fig 3, but this is inconclusive because of uncertainty about the relative volume of the resin aqueous phase However, exclusion of hydrochloric acid at low ionic strength has already been demonstrated for this resin, by ion-exclusion chromatography, which is based on the inability of dilute electrolytes to penetrate ion-exchange resins [22] Relative homogeneity of the potential, contrary to the artifact hypothesis, is also suggested by the comparably small pore-size and charge spacing in this resin (~ 10 Å, calculated)

Even if electrolyte does slowly penetrate a heterogeneous colloidal matrix, the associated potential is not, strictly speaking, a "diffusion" potential if the imbalance in ionic mobility is due to purely electrostatic rather than physical (*e g*, steric) causes. on the microscopic level, it is not the low mobility of, say, Cl^- that generates the potential, but rather that the blocking of conductance channels by Donnan-like potentials reduces the apparent Cl^- mobility This distinction is manifested by the response of a thin ion-exchange layer on a blocked interface, *viz* a coated-wire electrode [23] such electrodes would not function stably if the membrane potential were a diffusional phenomenon ceasing at equilibrium

CONCLUSIONS

The purpose of the foregoing has been to eliminate the junction artifact theory as a possible comprehensive explanation of the suspension effect The observations of substantial counter-ion mobility, co-ion exclusion, and close correspondence between pH measurements and expected H^+ activities in a strong cation-exchanger, are all incompatible with the artifact theory and in accord with equilibrium partitioning theories More basically, the existence of a phase boundary potential between a charged sediment and dilute supernatant cannot be denied without abandoning the very foundation of the present theory of electrolytes

However, even with acceptance of the basic Donnan view that the suspension effect largely corresponds to a real difference in pH, the interpretation of the readings still remains problematic Ionic and potential profiles for a particular colloidal interface at equilibrium can be modelled in relative detail by double-layer theory [24] Uncertainty still arises, however, at the non-equilibrium interface where junction electrolyte diffuses into the colloidal interior The key issue is the relationship between the reference electrolyte potential and the often non-uniform potential profile deep within the colloid Several cases can be distinguished on the basis of colloidal charge homogeneity The following interpretations are offered tentatively, but seem indicated by the evidence presented above and by earlier investigators

Homogeneous gel

If the fixed charge is uniformly spaced by less than the double-layer thickness (the Debye length),[25] the electrical potential and ionic activities within the gel can be presumed to be spatially uniform. Measurement of ions *within* the gel should be obtainable by placing the ion-sensor and reference junction on the gel surface, as is common practice The reference potential will be that of the gel interior, shifted by a residual junction potential consisting of a Donnan boundary potential plus a conventional diffusion potential between the surface and the interior of the gel This residual junction potential can be a significant source of error (*e g*., see Fig 3), and may reflect modifications of ionic mobility, however, such errors are not equivalent to the suspension effect and generally are minimized by a concentrated, equitransferent junction electrolyte The result will be in error if the surface concentration of the measured ion is not at electrochemical equilibrium with the gel interior (*e g*, steric exclusion from the gel).

Sediments of homogeneous, porous charged particles

Here the aqueous component is inhomogeneous, consisting of both fluid within the particles and interstitial fluid between the particles. Simultaneous contact of junction electrolyte with phases of different potential makes the reference potential seem uncertain. From considering the extreme cases, however, it is apparent that the resultant potential is determined by the relative conductance of the two phases Figure 4 shows the predictions made from a crude model in which the junction/sediment interface consists of a single porous particle generating a membrane potential, shunted by a parallel volume of interstitial fluid When the relative conductance of the interstitial fluid is low ($2C_1/\sigma < 0.1$), the reference level corresponds to the porous interior of the particles, but when the interstitial conductance is high ($2C_1/\sigma > 1$), the reference potential corresponds to the average pH of the

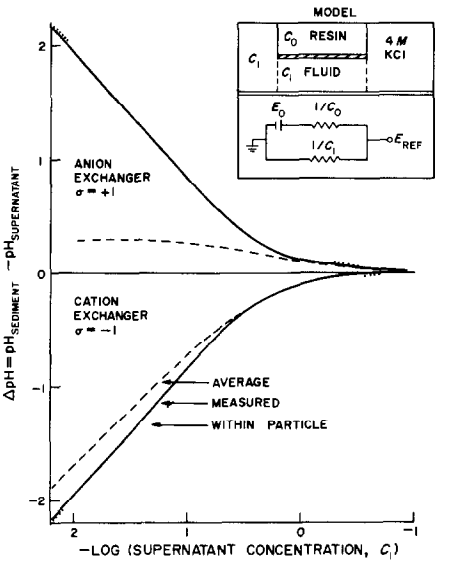

Fig 4 Model and predicted results for colloidal pH measurement with 4*M* KCl reference electrode in simultaneous contact with a porous particle and surrounding interstitial fluid Interstitial fluid concentration C_1, resin charge density $\sigma = \pm 1$, intraparticle mean concentration $C_0 \equiv C_0^+ + C_0^-$ and supernatant boundary potential $E_0 = U_0 - U_1$, are related as described in text Resultant reference potential $E_{ref} = E_0 C_0/(C_0 + C_1)$ where the relative conductances are the particle and fluid phases is presumed proportional to their free ionic content C_0, C_1 If pH_1 is the supernatant (and interstitial) pH, then the within-particle pH is $pH_0 = pH_1 + E_0F/RT$, the average pH of sediment is $pH_{sed} = -\log\ [(H_0 + H_1)/2]$, and the measured pH is $pH_{meas} = pH_1 + E_{ref}F/RT$

sediment bed, which is nearly the same as the pH within the particles because of the lack of significant partitioning. Maximum bias away from the value for the particles, about 0 2 pH unit, occurs when the observed sediment effect is moderate (0.1–1 pH unit). The corresponding steepening of the "measured" curve with concentration (Fig 4) would help to explain the apparent increase in $\gamma_0\sigma$ required to fit the data in Table 1 Other evidence for this model is the correspondence between corrected sediment pH value and intraresin H^+ concentration discussed for Fig 2, and the constancy of the sediment pH value on addition of solid potassium chloride though the supernatant effect was greater than 1 pH unit (Fig 3) Thus, when the supernatant effect is large, readings taken with the reference electrode immersed in a sediment of macroscopic porous particles should indicate the ionic environment inside the particles, whereas readings taken with the reference electrode in the supernatant should indicate the interstitial fluid environment between particles. Extension of this model to a generally inhomogeneous conductive matrix suggests that the reference potential corresponds to a number-weighted mean pH $[(-\sum_i n_i \log H_i)/\Sigma_i n_i]$, where n_i is the relative number of H^+ ions at concentration H_i However, the pH reading may be ill-defined if the colloidal charge is heterogeneous, with the measured ion differing in sign or size of charge from some major counter-ionic species (*e g*, in a mixed-resin bed)

It is significant for ion-exchange chromatography that the pH within the resin may differ from that of the running eluent and depend on both its pH and ionic strength For example, cation-exchanger that had been titrated with sodium hydroxide was made markedly acidic by washing with distilled water (Fig 2) Such interactions may affect the charge and stability of sorbed materials and the dissociation of weakly exchanging resins

Charged solid particles

Improper boundary potentials seem likely if the charged particles aggregate in the presence of junction potassium chloride Stable (viscous) dispersions and particulate sediments may yield valid readings. If the Debye length is comparable with the mean distance between charged surfaces, the situation seems analogous to a gel However, if the Debye length is much smaller than that distance, the interstitial fluid will typically be quite inhomogeneous in composition and potential This case is illustrated by a surface-charged capillary connecting reservoirs of dilute electrolyte and 4*M* potassium chloride, containing, respectively, an electrode selective for the counter-ion and a reference electrode The reference potential relative to the external dilute electrolyte will be established somewhere between the axial and wall potentials at the dilute end of the capillary, depending on the relative conductances for these positions For this reason, Peech *et al*[26] and Marshall[27] concluded that electrode measurements cannot lead to characterization of any intrinsic property of particulate suspensions. According to Overbeek, however, the reference potential for the capillary should be determined primarily by the ratio of its specific surface conductance (due to counter-ions) divided by the conductance of the external dilute solution [11] It can be shown that if the ionic mobilities are unchanged within the capillary, then the capillary reference potential, if large, should correspond to the average concentration of counter-ions per capillary volume, even though those ions are primarily confined to the double layer Thus, a valid space-averaged concentration is obtained, and such space-averages rather than thermodynamic quantities are likely to be of primary interest to analytical chemists. Similar potentiometry of a parallel (shunt) assembly of capillaries of equal lengths and various constant radii would yield a number-weighted mean pI indication for the counter-ion within the several capillaries Internal bulges or length variation in the section of the capillaries that contains dilute solution would make this correspondence obviously invalid. Thus, the obtaining of quantitatively valid space-averages requires a certain uniformity rather than strict homogeneity of physical structure and ionic mobility The requirement for physical uniformity seems likely to be satisfied by having the junction electrolyte make contact with a representative cross-section of heterogeneous colloid The constraints on ionic mobility seem much more problematic. to yield a valid result, the measured ion should partition comparably to the major counter-ion species, which in turn may be required to have a mobility similar to those in the connecting phases. According to Overbeek,[11] however, double-layer mobilities may be considerably altered or even reversed because of field-induced compositional differences and electrical and hydrodynamic interactions. As these models are not free from assumptions and have not been thoroughly verified, the quantitative significance of the predicted errors remains uncertain. However, Marshall cites a number of studies showing good correlation between potentiometric and comparison methods of ion determination in dilute particulate colloids [13]

On the basis of reduction of the Donnan cell emf for Vorclay and alumina suspensions, Peinemann and Helmy recommended that a potassium chloride bridge solution matching the concentration of the supernatant should be used during ion-potentiometry in such colloids [12] This recommendation, unsubstantiated by actual ionic measurements, is the result of their attributing the Donnan potential seen at high bridge-concentrations to the bridge interface This interpretation is suggested by use of Overbeek's reference-ion expression for the cell emf, which involves only transference integrals at the supernatant and sediment reference junctions However, it cannot be concluded that those interfaces are solely re-

sponsible for the potential, otherwise, the reference electrode in the supernatant would have to act as an ion-sensor to yield a Donnan dependence

The measured pH of blood changes by about −0 01 unit if red blood cells (erythrocytes) are admitted to the vicinity of the reference junction [28,29] This has been interpreted as a junction potential artifact, but in theory it could also correspond to a colloidal pH difference between blood and plasma (its filtrate) The electrophoretic mobility of human erythrocytes indicates a cellular surface charge[30] of approximately $-1\ 1 \times 10^{-6}$ C/cm^2, which yields a fixed-charge concentration (σ) of roughly −0 16mM with respect to the interstitial fluid of 50% haematocrit blood At physiological salt concentrations (145mM) this should cause a pH shift of $\sigma/2C \approx -5 \times 10^{-4}$, which is only about one twentieth of the observed effect Thus, the pH shift does indeed seem to be an artifact, perhaps caused by electrical coupling of junction electrolyte to the cell interiors, which are biased about −8 mV with respect to the external solution,[31] or by asymmetric reduction of the −1 V surface potentials of erythrocytes embedded in the potassium chloride gradient.

Design deficiencies of the reference electrode can contribute to erroneous readings in colloids When the flow of a reference electrode in ion-exchanger sediment was reversed so that interstitial fluid was drawn into the junction, the pH reading shifted to that of the supernatant and the suspension effect disappeared This behaviour is attributable to displacement of 4M potassium chloride from the sediment boundary Thus, in order to obtain accurate reference potentials in colloids, an adequate outward flux of potassium chloride to the junction surface must be provided by either diffusion or flow Use of non-flowing, gel-type reference electrodes with thick junctions for measurements on sediments will tend to give readings that are erroneously similar to the values for the supernatant

These findings pertain to all colloidal measurements with ion-selective electrodes, not just measurements of pH If the junction artifact theory of the suspension effect is valid, then the whole issue of potentiometry in colloids is rendered meaningless This study comes to the contrary conclusion that the effect is best explained by a Donnan-like potential at the sediment/supernatant boundary Readings in homogeneous, gel-type colloids are likely to be useful, and the accuracy of H^+ indication as a function of fixed-charge density should be investigated Though the case of solid particulate suspensions at present remains uncertain, more realistic models of the reference junction potential should be amenable to double-layer theory, and the actual utility of such readings can be determined empirically In any case, colloidal potentiometry warrants further study rather than avoidance

Acknowledgements—I thank Dr W A Baase (University of Oregon, Eugene) for helpful discussions and Dr I Tinoco, Jr and B Dengler (University of California, Berkeley) for providing facilities for the conductance measurements

REFERENCES

1 H Pallman, *Kolloidchem Beihefte*, 1930, **30,** 334
2 G Wiegner, *Kolloid-Z*, 1930, **51,** 49
3 G Wiegner, H Pallmann, A Musierowicz and J M Albareda, *Polish Agr Forestal Ann* 1932, **28,** 323
4 C Du Reitz, *Thesis*, Tekn Hogskolan, Stockholm, 1938
5 L E Davis, *Thesis*, University of California, 1941
6 H Jenny, R R Nielsen, N T Coleman and D E Williams, *Science*, 1950, **112,** 164
7 J Loeb, *Proteins and the Theory of Colloidal Behavior*, McGraw-Hill, New York, 1922
8 C E Marshall, *Science*, 1951, **113,** 43
9 E Eriksson, *ibid*, 1951, **113,** 419
10 L G Longsworth, *J Am Chem Soc*, 1964, **86,** 3912
11 J Th G Overbeek, *J Colloid Sci*, 1953, **8,** 593
12 N Peinemann and A K Helmy, *Soil Sci*, 1973, **115,** 331
13 C E Marshall, *The Physical Chemistry and Mineralogy of Soils*, Vol 1, pp 35–39, Wiley, New York, 1964
14 G Mattock, *The Glass Electrode*, pp 62, 110 Wiley–Interscience, New York, 1965
15 R G Bates, *Determination of pH*, pp 322–23 Wiley, New York, 1973
16 R A Durst, in *Ion-selective Electrodes in Analytical Chemistry*, H Freiser (ed), Vol 1, p 326 Plenum Press, New York, 1978
17 G Mattock, *pH Measurement and Titration*, p 173 Heywood, London, 1961
18 T Teorell, *Proc Soc Exptl Biol Med*, 1935, **33,** 282
19 K H Meyer and G F Sievers, *Helv Chim Acta*, 1936, **19,** 649
20 D P Brezinski, *Anal Chim Acta*, 1982, **134,** 247
21 D A MacInnes, *Principles of Electrochemistry*, p 231 Dover Publications, New York, 1947
22 R M Wheaton and W C Bauman, *Ind Eng Chem*, 1953, **45,** 228
23 H Freiser, in *Ion Selective Electrodes in Analytical Chemistry*, H Freiser (ed), Vol 2, p 85 Plenum Press, New York, 1980
24 G H Bolt and M Peech, *Soil Sci Soc Am Proc*, 1953, **17,** 210
25 J O'M Bockris and A K N Reddy, *Modern Electrochemistry*, Vol 1, p 199 Plenum Press, New York, 1970
26 M Peech, R A Olsen and G H Bolt, *Soil Sci Soc Am Proc*, 1953, **17,** 214
27 C E Marshall, *ibid*, 1953, **17,** 218
28 J W Severinghaus, M Stupfel and A F Bradley, *J Appl Physiol*, 1956, **9,** 189
29 A H J Maas, *NBS Spec Publ* 1977, **450,** 195
30 M Bier, *Electrophoresis*, p 481 Academic Press, New York, 1959
31 A W L Jay and A C Burton, *Biophys J*, 1969, **9,** 115

Talanta, Vol 30, No 5, pp 355–358, 1983
Printed in Great Britain

0039-9140/83/050355-04$03 00/0
Pergamon Press Ltd

SHORT COMMUNICATIONS

APPLICATION OF XYLENOL ORANGE TO THE SEPARATION OF METAL IONS ON AMBERLYST A-26 MACRORETICULAR ANION-EXCHANGE RESIN

KRYSTYNA BRAJTER and EWA OLBRYCH-ŚLESZYŃSKA
Department of Chemistry, University of Warsaw, Warsaw, Poland

(*Received* 23 *July* 1981 *Revised* 20 *August* 1982 *Accepted* 8 *December* 1982)

Summary—The possibility of using a sulphonated aromatic organic complexing agent—Xylenol Orange—for separation of metal ions on the macroreticular anion-exchanger Amberlyst A-26 has been investigated The dependence of retention on pH was determined by the batch method for Al^{3+}, Cr^{3+}, Mn^{2+}, Fe^{3+}, Co^{2+}, Ni^{2+}, Cu^{2+}, Zn^{2+}, Ga^{3+}, Rh^{3+}, Cd^{2+}, In^{3+}, Ir^{3+}, and Pb^{2+} The selectivity differences make possible the separation of some of these metal ions The following mixtures, of practical importance, have been separated Al^{3+}–In^{3+}, Ga^{3+}–In^{3+}, Zn^{2+}–In^{3+}, Cu^{2+}–Mn^{2+}, in various ratios The method has been applied to analysis of Ga–In alloy

Aromatic complexing agents containing sulphonic acid groups are particularly useful in separation of metal ions on anion-exchange resins, as shown earlier by us[1–7] and confirmed by others.[8–10] The aim of this paper was to investigate the usefulness of Xylenol Orange (XO) (tetrasodium salt) for modification of the macroreticular exchange resin Amberlyst A-26.

XO forms complexes of different stability with a large number of metal ions,[11] which makes it especially useful for separation of these ions The very large size of the XO molecule increases its strength of interaction with a sorption matrix, and results in an increase of affinity of an anion-exchanger for XO and its complexes with metal ions It is thought that a macroreticular anion-exchanger should be more convenient for use with large aromatic complexing agents Partial exclusion of large molecules by sieve action and the swelling-pressure effect might occur if common anion-exchangers were used

EXPERIMENTAL

Ion-exchanger

For static and dynamic investigations the macroporous strong-base anion-exchange resin Amberlyst A-26 (Rohm and Haas) was used in its chloride form The exchange capacity determined by titration was 3 46 meq/g Sample weights were calculated with allowance made for the moisture content of the exchanger (average, 20%)

Metal-ion solutions

These were generally prepared by dissolving appropriate weights of the sulphates or nitrates of the metals in doubly distilled water, and standardized by EDTA titration The Rh(III) solution was prepared from $RhCl_3$ $3H_2O$ dissolved in hydrochloric acid (and standardized gravimetrically with thionalide) The Ir(IV) solution was prepared from a 3 42% w/w solution of chloroiridic acid The stock solutions were diluted as required

Solutions of XO of the required concentrations were made directly before the experiment by dissolving appropriate weights in doubly distilled water They were found to be stable for 3–4 days when stored in the dark The XO was recrystallized before use

Apparatus

A Perkin–Elmer model 300A atomic-absorption spectrophotometer with HGA-72 graphite furnace and a Hitachi/Perkin–Elmer model 159 recorder and Beckman model 1248 and Analog model 1272 spectrophotometers were used

Determination of metal-ion retention, by batch method

The test solutions all had a 1 10 molar ratio of metal ion to XO For measurements a constant amount (equivalent to 0 200 g dry weight) of ion-exchanger (chloride form) was mixed with 20 ml of solution containing 0 10 mg of metal ion and the appropriate amount of XO to give the desired molar ratio (and adjusted to the desired pH with sodium hydroxide or sulphuric acid) and the mixture was shaken for 10 hr The equilibrium hydrogen-ion and metal-ion concentrations were determined 12 hr later The metal ions were determined by AAS under the conditions given in Table 1

The retention of metal ion was calculated as a fraction of the initial quantity of metal ion in the solution

Separation procedure

Portions (equivalent to 2 00 g dry weight) of Amberlyst A-26 (chloride form) were shaken with XO (20 ml of aqueous solution, pH 6 5) and then placed in glass tubes 10 cm long and 0 8 cm in bore A 10-ml volume of solution containing a mixture of metal ions was then passed through the column of exchanger and the metal ions were eluted at a flow-rate of 1 ml/min with the eluents given in Table 2

Analysis of Ga–In alloy

The sample of alloy (0 16 g) was dissolved in 10 ml of sulphuric acid (1 + 1), then the solution was evaporated to low bulk, cooled and diluted with doubly distilled water to 10 ml in a standard flask. A 1-ml aliquot was diluted to 10 ml and adjusted to pH 2 0 and passed through the column

Table 1 AAS conditions used for the metal determinations

Method	Metal	Wavelength, *nm*	Band-pass, *Å*	Sample volume, *µl*	
Flameless AAS	Al	237 9	2	10, 20	
		309 3		10	
	Cr	358 0	7	10	
	Mn	403 4	2	10	
	Fe	306 0	2	10	
		248 0		10	
	Co	304 4	2	20	
	Ni	346 4	2	20	
	Cu	223 0	2	10	
		217 0		10	
	Zn	308,0	7	10, 20	
	Ga	287 4	7	10	
	Rh	350 4	2	10	
	Cd	326 2	7	5	
	In	303 9	7	10	
	Ir	263 9	2	20	
	Pb	283 3	7	5, 10	
				Gas pressure, *bar*	
				C_2H_2	air
Flame AAS	Zn	213 9	4	0 40	2 10
	Ga	287 4	5	0 40	1 90
	In	303 9	5	0 40	1 90

The gallium was eluted with 0 03*M* sodium hydroxide, and the indium with 0 2*M* sulphuric acid, for determination by AAS

RESULTS AND DISCUSSION

The retention of metal ions (as a function of pH) on the Amberlyst A-26 in the presence of XO is presented in Fig 1, and the results suggest that this system can be used for separation of some of these metal ions The amphoteric cations such as Al^{3+} can be eluted with alkali, giving greater scope for separation

The possibility of separation of metal ions of similar properties was studied with three pairs of ions, chosen for their practical importance Al^{3+}–In^{3+}, Ga^{3+}–In^{3+}, Zn^{2+}–In^{3+} and also with Cu^{2+}–Mn^{2+} (Figs 2 and 3) Metal ions not retained by the exchanger in the static system can be eluted with water, but it is better to use a slightly acid solution for aluminium to avoid hydrolysis problems In^{3+} is strongly held by the anion-exchanger in the presence of XO over a wide range of pH, which makes it possible to separate it from a large excess of Ga^{3+} The double peak for gallium is attributed to formation of two complexes having different sorption characteristics Mixtures of indium and gallium in molar ratios of 1 100, 1 500 and 1 1000 were successfully separated (Table 2) Aluminium, gallium and zinc can all be separated from indium (Table 2) The method for separation of gallium and indium was

Table 2 Separation of metal ions on Amberlyst A-26 (average for 6 determinations, each with 12 measurements)

No	Metal	Elution agent	Amount of metal, *mg*		Standard deviation, *µg*
			Added	Found	
	Al	0 001*M* HCl, 200 ml	1 00	1 00	19
1	In	0 100*M* H_2SO_4, 210 ml	1 00	1 00	0
	Zn	H_2SO_4, pH = 4 0, 100 ml	1 00	1 00	18
2	In	0 030*M* H_2SO_4, 240 ml	1 00	1 00	0
	Ga	0 030*M* NaOH, 140 ml	1 00	0 99	4 5
3	In	0 030*M* H_2SO_4, 240 ml	1 00	1 00	
	Ga	0 030*M* NaOH, 200 ml	5 56	5 51	28
4	In	0 100*M* H_2SO_4, 100 ml	0 09	0 09	
	Ga	0 030*M* NaOH, 200 ml	13 9_0	13 7_6	14
5	In	0 200*M* H_2SO_4, 100 ml	0 046	0 046	
	Ga	0 030*M* NaOH, 400 ml	27 8_0	27 5_5	39
6	In	0 200*M* H_2SO_4, 100 ml	0 046	0 046	0
	Mn	H_2SO_4, pH = 4 0, 100 ml	1 00	1 00	23
7	Cu	1 00*M* HCl, 100 ml	1 00	1 00	6 3

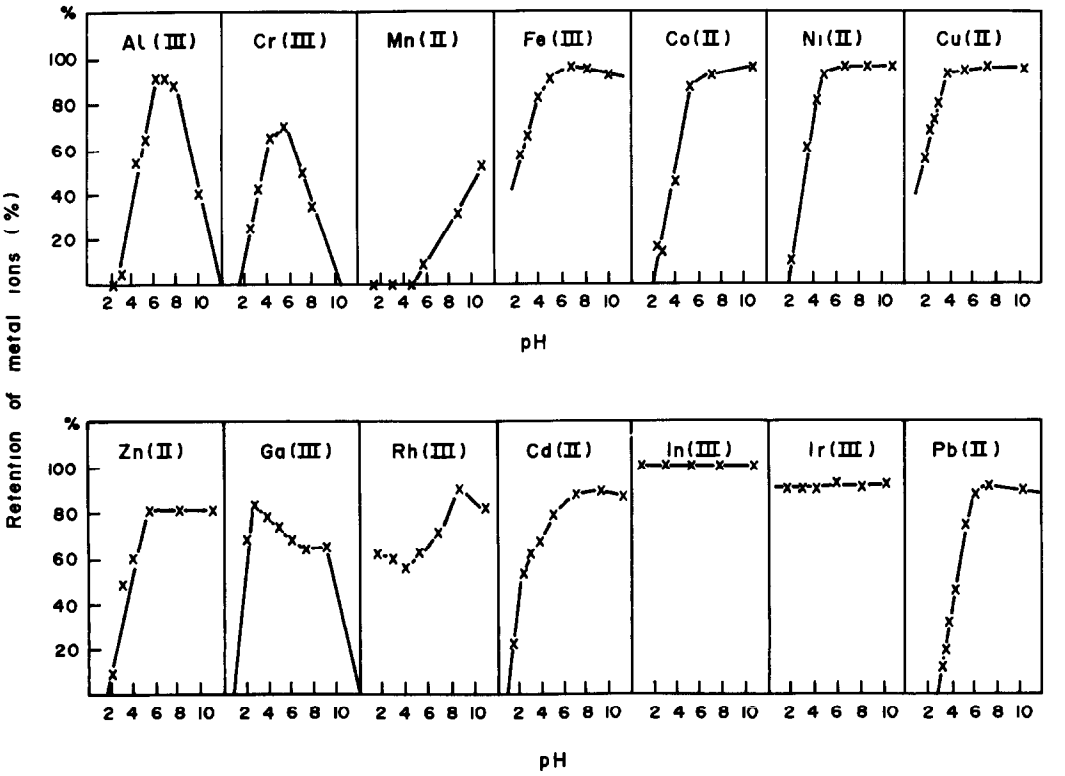

Fig 1 Retention of metal ions as a function of pH in the system Amberlyst A-26/metal-ion/XO

applied to the analysis of a Ga–In alloy for indium (found 0 614% In, standard deviation 0 002%, composition 99 38% Ga, 0.615% In)

The behaviour of copper(II) was particularly interesting In the batch experiments the copper(II) and Xylenol Orange solutions were mixed before being equilibrated with the exchanger and there was 78–92% uptake of the copper (0 100 mg taken) by 0 200 g dry weight of resin In the column experiments, however, there was complete uptake of 1 00 mg of copper by 2 00 g dry weight of resin, but here the Xylenol Orange was loaded onto the column

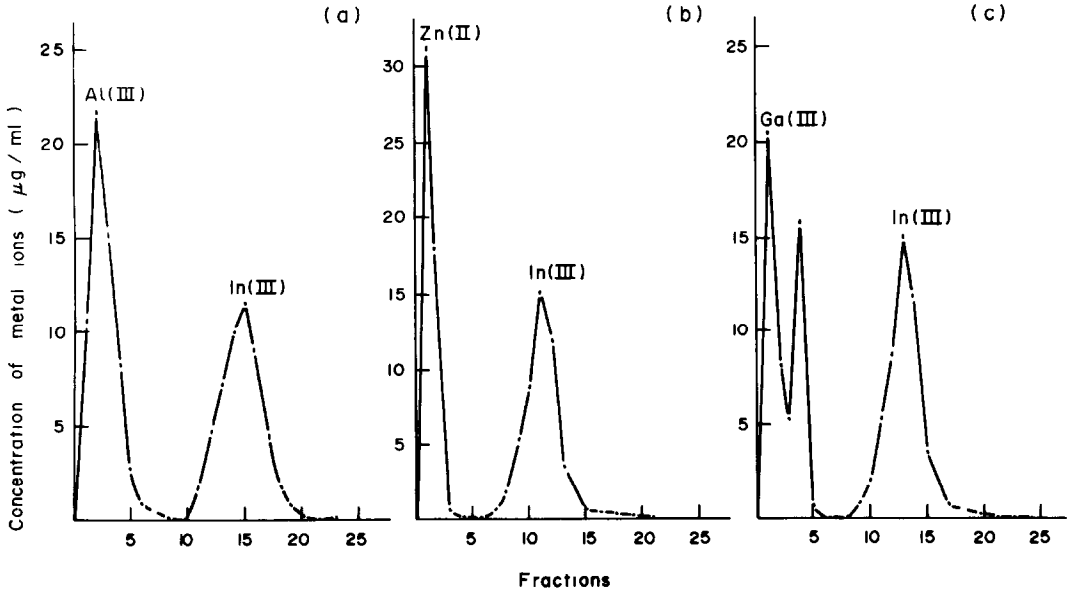

Fig 2 Elution curves showing the separation of metal ions on Amberlyst A-26 with the reagents indicated in Table 2

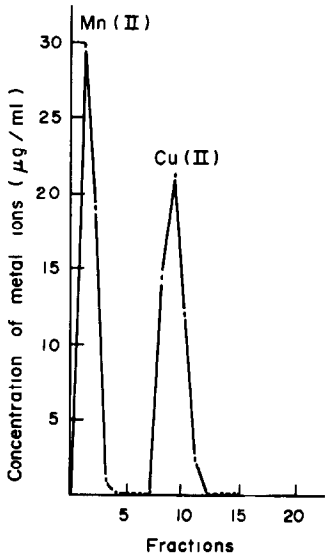

Fig 3 Elution curve showing the separation of Cu^{2+} from Mn^{2+} on Amberlyst A-26

before the copper was added We attribute this difference in behaviour to the inert nature of the Cu–XO complex (which is known[12] to be responsible for "blocking" of the indicator) and consider that in the batch experiments, where the XO is added in 10-fold molar ratio to the copper(II), there will be competitive uptake of the free XO and of the Cu–XO complex by the resin, followed by slow exchange of copper between unsorbed Cu–XO and sorbed but uncomplexed XO In the column work, there is simply direct complexation by the XO on the resin This view is supported by the fact that it was necessary to use 1*M* hydrochloric acid to elute the copper from the column

These investigations confirm the usefulness of this macroporous anion-exchanger for separation of metal ions in the presence of XO XO and its complexes with metal ions all have strong affinity for Amberlyst A-26, especially XO itself, since on elution of the metal ions from the column only traces of XO were found in the effluent

No sieve action was observed for XO On the contrary, the total exchange capacity of Amberlyst A-26 for XO appeared to 116% of the theoretical capacity, probably because of adsorption as well as ion-exchange It is interesting that for large aromatic molecules such as Bromopyrogallol Red only 30% of the total exchange capacity is available [13] Such molecules are too large to enter most of the anion-exchanger pores

REFERENCES

1 W Kemula and K Brajter, *Chem Anal (Warsaw)*, 1968, **13,** 305
2 *Idem, ibid*, 1968, **13,** 503
3 *Idem, ibid*, 1970, **15,** 351
4 K Brajter, *ibid*, 1973, **18,** 125
5 *Idem, J Chromatog*, 1974, **102,** 385
6 *Idem, Proc 3rd Symposium Ion-Exchange*, Balatonfured, Hungary, 28–31 May 1974
7 K Brajter and E Dąbek-Złotorzyńska, *Talanta*, 1980, **27,** 19
8 J E Going, G Wesenberg and G Andrejat, *Anal Chim Acta*, 1976, **81,** 349
9 H Tanaka and M Chikuma, *Talanta*, 1976, **23,** 489
10 K S Lee, W Lee and D W Lee, *Anal Chem*, 1978, **50,** 255
11 S Rani, Ch D Dwivedi and S K Banerjee, *Chem Era*, 1978, **13,** 372
12 R Přibil, *Talanta*, 1959, **3,** 91
13 K Brajter, *Chem Anal (Warsaw)*, 1976, **21,** 1195

Talanta, Vol 30, No 5, pp 359–362, 1983
Printed in Great Britain

0039-9140/83/050359-04$03 00/0

DETERMINATION OF THIOCYANATE WITH AROMATIC HALOSULPHONAMIDES IN ACID AND ALKALINE MEDIA

B THIMME GOWDA*
Department of Chemistry, Hydrocarbon Research Institute, University of Southern California, Los Angeles, CA 90089, U S A

and

D S MAHADEVAPPA
Department of Chemistry, Manasa Gangotri, University of Mysore, Mysore 570006, Karnataka, India

(*Received* 2 *March* 1982 *Revised* 22 *November* 1982 *Accepted* 8 *December* 1982)

Summary—Ten organic aromatic halosulphonamides, both mono and dihalo compounds, ranging from chlorosulphonamides to iodosulphonamides, have been prepared and characterized by their infrared and NMR spectra and successfully used for determining thiocyanate in its metal salts and complexes The proposed procedures are simple, rapid and reproducible, with an error of about ±0 8% These procedures are also useful for computing the number of thiocyanate ligands present in the complexes Comparison of the present results with those from the argentometric method shows excellent agreement The oxidation involves an 8-electron change per thiocyanate ion with the chloro and bromosulphonamides and a 6-electron change with iodosulphonamides

Thiocyanates find a number of industrial applications, in photography, printing, textile dyeing, medicines, freezing mixtures, manufacture of synthetic dyestuffs, sulphocyanides, thioureas and mustard oil, and as reagents in analytical chemistry. In view of the importance of this class of compounds, rapid and accurate analytical techniques are essential for their estimation in solution. Although there are a number of reports on the oxidation of thiocyanates, very few analytical procedures for their determination in solutions are available Conventional methods involving the estimation of the –NCS group in thiocyanates have been developed, but these are laborious and have a number of experimental restrictions [1] The methods reported so far include the use of hypohalite,[2] bromine,[3] iodine,[4] iodate,[5] hydrogen peroxide,[6] some aromatic halosulphonamides[7–12] and lead tetra-acetate [13] Although we have used some of the aromatic halosulphonamides individually for determining thiocyanates,[11,12] general procedures for their determination with halosulphonamides are lacking In the present investigation the general behaviour of halosulphonamides as oxidimetric reagents towards the NCS^- ion in its metal salts and complexes has been critically examined and general procedures for its determination have been developed

The chemistry of *N*-halo-*N*-sodio (or potassio) and *N,N*-dihaloaromatic sulphonamides

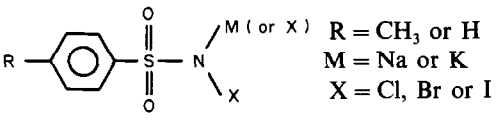

has awakened considerable interest as these compounds are sources of halonium cations, hypohalite species and *N*-anions which act both as bases and nucleophiles [14–18] They interact with a wide range of functional groups in aqueous, partially aqueous and non-aqueous media in presence of acids or alkalis, effecting an array of molecular transformations Generally monohaloamines undergo a two-electron change while dihaloamines are four-electron oxidants The reduction products are the respective sulphonamide and NaX or HX Although the haloamines derived from toluene are well known, there is little information about the derivatives of benzene

EXPERIMENTAL

Potassium thiocyanate (Merck, analytical grade) was dried at 150° and its purity was checked by the argentometric method [19] The metal thiocyanates LiNCS, NaNCS, $Cd(NCS)_2$, $Zn(NCS)_2$, $Ni(NCS)_2 0\ 5H_2O$, $Pb(NCS)_2$ and $UO_2(NCS)_2\ 3H_2O$ and complexes $K_2Cd(NCS)_4\ 2H_2O$, $K_2Zn(NCS)_4\ 4H_2O$, $K_4Ni(NCS)_6\ 4H_2O$, $KUO_2(NCS)_3\ 2H_2O$, and $K_4Pb(NCS)_6$ were prepared by standard methods reported elsewhere and their composition was checked by elemental analysis

Preparation of oxidants

Chloramine-T (Merck) was purified by the method of Morris *et al* [16] Dichloramine-T (DCT) was prepared by the

*To whom correspondence should be addressed Present address Department of Chemistry, Mangalore University, Mangalagangothri 574152, Mangalore, Karnataka, India

chlorination of CAT solutions,[20] and bromination of CAT yielded dibromamine-T (DBT) [21] Partial debromination of DBT by dissolving it in 4*M* sodium hydroxide gave bromamine-T (BAT) [22] Chloramine-B (CAB) was prepared by the partial chlorination of benzenesulphonamide[23] in 4*M* sodium hydroxide for 1 hr at 70° Further chlorination produced dichloramine-B (DCB) [24] Dibromamine-B (DBB) was prepared by adding liquid bromine to aqueous CAB solutions[25] and bromamine-B was obtained by the partial debromination of DBB [26] Iodamine-T (IAT)[27] and iodamine-B (IAB)[28] were prepared by the iodination of *p*-toluenesulphonamide and benzenesulphonamide respectively

The purity of all the oxidants was checked by estimating, iodometrically, the amounts of active halogen present in them They were further characterized by their infrared spectra (recorded on a Perkin–Elmer 298 grating infrared spectrophotometer) and Fourier transform ^{1}H and ^{13}C NMR spectra (obtained on a Bruker WH 270-MHz nuclear magnetic resonance spectrometer, with TMS as the internal standard)

Approximately decinormal solutions of the monohalosulphonamides (except IAT and IAB) were prepared by dissolving the requisite quantities of the solids in triply distilled water IAT and IAB were dissolved in 0 1*M* potassium hydroxide solution Solutions of dihalosulphonamides were prepared in water-free acetic acid (glacial acetic acid containing 10% v/v acetic anhydride) All the solutions were standardized iodometrically and stored in amber-coloured bottles

Solutions (~2 mg/ml) of thiocyanates [except $Pb(NCS)_2$] in triply distilled water, or acids of various concentrations, or buffer solutions (pH 1–10), or alkalis of different concentrations were prepared $Pb(NCS)_2$ was dissolved in dilute acetic acid

Standard buffer systems were employed [29] All other reagents used were of analytical-reagent grade

Preliminary studies

Known quantities of the reductant solutions were added to known excessive volumes of the oxidants in separate iodine flasks (only aqueous solutions of the reductants were used with the dihalosulphonamides) The reaction mixtures were set aside for various intervals of time at room temperature (~300 K) with occasional shaking The excess of oxidant left unconsumed in each flask was iodometrically determined by back-titration with sodium thiosulphate

It was observed that with monochlorosulphonamides (CAT and CAB) the oxidation of thiocyanates is fast in the pH range 1–6 (fastest at pH 4) and in acid solutions, but slow in alkaline solutions The eight-electron stoichiometric oxidation (of the NCS^- ion) takes place in less than 15 min with all the thiocyanates in acid solutions and buffer solutions of pH 1–6 The oxidation of thiocyanates by monobromosulphonamides (BAT and BAB) is sluggish in acid solutions and in buffer solutions of pH 1–10 but rapid in alkaline solutions The eight-electron stoichiometric oxidation of NCS^- takes 5–10 min in 0 05–0 2*M* sodium hydroxide for all the thiocyanates with both the oxidants The same eight-electron stoichiometry was observed with the dihalosulphonamides in partially aqueous medium (oxidant solutions in water-free acetic acid and thiocyanate solutions in water), the reaction taking 15–20 min for all the thiocyanates These oxidation times refer to reaction with about 50% excess of oxidant If a smaller excess is used the stoichiometric oxidation takes longer

Recommended procedures

With monochlorosulphonamides (CAT and CAB) Adjust the pH of the thiocyanate solution to any value between 1 and 6 Add aliquots of this solution to known excessive volumes (~50% excess) of 0 1*N* oxidant (CAT or CAB) in iodine flasks and set aside the reaction mixtures for about 15 min with occasional shaking Rinse down with about 20 ml of water, add 20 ml of 1*M* sulphuric acid and 10 ml of 20% potassium iodide solution and titrate the liberated iodine with 0 05*M* sodium thiosulphate to a starch end-point (V_1 ml) Run blanks with the same volumes of the oxidant alone (CAT or CAB) (V_2)

With monobromosulphonamides (BAT and BAB) Add aliquots of the reductant solution to known excessive volumes (~50% excess) of decinormal oxidant (BAT or BAB) in iodine flasks containing enough sodium hydroxide to maintain an overall concentration of 0 05–0 20*M* alkali Set the reaction mixtures aside for about 10 min, shaking occasionally Complete the titration as above after adding sufficient acid (20 ml of 2*M* sulphuric acid)

With dihalosulphonamides (DCT, DBT, DCB and DBB) Add aliquots of thiocyanate solution to known volumes (~50% excess) of 0 1*N* oxidant solution (DCT, DBT, DCB or DBB) in iodine flasks and set aside the reaction mixtures for 20 min Rinse down with about 50 ml of water, add 10 ml of 20% potassium iodide solution and complete the titration as before

The amount of thiocyanate (X μmole) in the sample solution is given by $X = 10^3M(V_2 - V_1)/E$, where M is the molarity of the thiosulphate solution and E is the number of electrons exchanged per molecule of thiocyanate $E = 8$ for Li, Na and K thiocyanates, 16 for Zn, Cd, Ni, Ba, Pb and UO_2 thiocyanates, and 24, 32, 32, 48 and 48 for UO_2, Zn, Cd, Ni and Pb complex thiocyanates, respectively

Direct titrations Andrews type titration of thiocyanates with most of the oxidants was found practicable in the presence of sodium acetate and potassium bromide (and acetic acid in titrations with monochlorosulphonamides except BAT and BAB) Sodium acetate was found to catalyse the oxidations Add sodium acetate (20% solution, 3–5 ml), potassium bromide solution, (1*M*, 5 ml) and carbon tetrachloride (1 ml) (and 5 ml of glacial acetic acid with monochlorosulphonamides) to aliquots of thiocyanate solution and titrate with the oxidant with stirring till the appearance of a faint yellow colour in the organic layer

The blank correction is found to be about 0 05 ml of 0 1*N* oxidant Alternatively a potentiometric method can be used for the detection of the end-point, a potential jump of ~200–400 mV being obtained for addition of 0 1 ml of 0 1*N* oxidant in the equivalence-point region

The blank correction, addition of sodium acetate and pipetting of poisonous thiocyanate solutions can be avoided by reversing the procedure above The reductant is added to a suitable volume of the oxidant, containing potassium bromide and with 1 ml of carbon tetrachloride added The volatility of bromine is the only source of error in this procedure, but can be minimized by a proper choice of the titration assembly

Back-titration gives more reproducible results than direct titrations do

Titrations with iodamine-T and iodamine-B The Pillai and Indrasenan method[27] is used Take equal volumes of thiocyanate solution and saturated mercuric chloride solution in a titration flask Add 10 ml of concentrated hydrochloric acid and 5 ml of carbon tetrachloride Dilute the reaction mixture to 100 ml and titrate with IAT or IAB solution with vigorous shaking after each addition till a permanent faint pink colour appears in the organic layer Run blanks under identical conditions

RESULTS AND DISCUSSION

All the thiocyanates undergo stoichiometric oxidations, with an eight-electron change per NCS^- ion, with all the oxidants except IAT and IAB, with which a six-electron stoichiometry was observed

The results of typical analyses are shown in Table 1 It may be seen that the maximum error is

Table 1 Determination of thiocyanate ion in metal salts and complexes with aryl halosulphonamides

Thiocyanate	Ranges studied, μmole	Maximum error in recovery, %										
		CAT	DCT	BAT	DBT	IAT	CAB	DCB	BAB	DBB	IAB	$AgNO_3$
LiNCS	30 8–769	0 6	0 5	0 5	0 6	0 7	0 5	0 4	0 3	0 3	0 7	0 6
NaNCS	24 7–617	0 5	0 5	0 5	0 5	0 7	0 5	0 8	0 4	0 4	0 6	0 3
KNCS	20 6–515	0 2	0 5	0 5	0 4	0 6	0 2	0 8	0 5	0 5	0 4	0 6
$Zn(NCS)_2$	11 0–275 4	0 3	0 5	0 6	0 3	0 5	0 4	0 4	0 2	0 2	0 5	0 6
$Cd(NCS)_2$	8 8–219 8	0 6	0 6	0 7	0 5	0 4	0 5	0 8	0 5	0 5	0 6	0 6
$Ni(NCS)_2$ 0 $5H_2O$	10 9–271 9	0 5	0 5	0 3	0 2	0 3	0 6	0 8	0 5	0 5	0 5	0 4
$Ba(NCS)_2$ $2H_2O$	6 9–172 7	0 6	0 6	0 5	0 4	0 6	0 4	0 6	0 4	0 4	0 6	0 6
$Pb(NCS)_2$	6 2–154 6	0 5	0 5	0 6	0 6	0 7	0 3	0 7	0 5	0 5	0 7	0 5
$UO_2(NCS)_2$ $3H_2O$	4 5–113 6	0 5	0 5	0 5	0 5	0 6	0 5	0 8	0 4	0 4	0 5	0 8
$KUO_2(NCS)_3$ $2H_2O$	3 9–96 3	0 4	0 5	0 4	0 6	0 5	0 5	0 8	0 4	0 5	0 4	0 8
$K_2Zn(NCS)_4$ $4H_2O$	4 5–111 6	0 4	0 4	0 1	0 1	0 2	0 6	0 5	0 5	0 5	0 2	0 8
$K_2Cd(NCS)_4$ $2H_2O$	4 4–108 9	0 5	0 4	0 4	0 4	0 3	0 7	0 9	0 5	0 5	0 3	0 7
$K_4Ni(NCS)_6$ $4H_2O$	3 2 78 7	0 5	0 5	0 5	0 0	0 1	0 5	0 6	0 5	0 5	0 1	0 8
$K_4Pb(NCS)_6$	2 8–70 2	0 5	0 5	0 5	0 7	0 4	0 6	0 7	0 5	0 4	0 6	0 7

about ±0 8% For comparison, the results of the argentometric method are also included in Table 1

Metal salts of monohaloamines (RNXM, where R = $C_6H_5SO_2$ or p-$CH_3C_6H_4SO_2$, X = Cl, Br or I and M = Na or K) behave like electrolytes [15] The possible oxidizing species in acidified haloamine solutions are RNHX, RNX_2, HOX and possibly H_2OX^+ (and X_2 in presence of X^-) In alkaline solutions the probable species are $(RNX)^-$ and OX^-

Hence the observed eight-electron stoichiometry can be shown by the following equations

$$NCS^- + 4RNHX \text{ (or } 2RNX_2) + 5H_2O \rightarrow SO_4^{2-} + CNO^- + 4RNH_2 \text{ (or } 2RNH_2) + 4X^- + 6H^+$$

$$NCS^- + 4RNX^- + 3H_2O + 2OH^- \rightarrow SO_4^{2-} + CNO^- + 4RNH_2 + 4X^-$$

When the six-electron stoichiometry occurs, cyanide will be produced instead of cyanate

In the direct titrations, bromine formed from the oxidants interacts with the thiocyanate

$$RNHX + 2Br^- + H^+ \rightarrow RNH_2 + Br_2 + X^-$$

$$RNX_2 + 4Br^- + 2H^+ \rightarrow RNH_2 + 2Br_2 + 2X^-$$

$$NCS^- + 4Br_2 + 4H_2O \rightarrow SO_4^{2-} + CNBr + 8H^+ + 7Br^-$$

The bromine cyanide formed can be quantitatively estimated by the iodometric method [30]

The presence of sulphate, cyanide and cyanate in the reaction products was detected by standard tests [31–33] Benzenesulphonamide formed in the reactions with the benzene derivatives was detected by TLC [34]

Common anions such as SO_4^{2-}, PO_4^{3-}, ClO_4^-, NO_3^-, F^- and Cl^- do not interfere, but Br^-, I^-, CN^-, hydrazine, urea and thiourea all interfere

It can be concluded that the proposed analytical procedures are simple, rapid and reproducible and are useful for determining thiocyanates in solution and for computing the number of ligands present in the complexes

Acknowledgements—One of us (B T G) is grateful to the Government of India, New Delhi, for the award of a National Scholarship for post-doctoral research abroad We thank the Bangalore NMR Facility, Indian Institute of Science, Bangalore, India, for the NMR spectra

REFERENCES

1 I M Kolthoff and R Belcher, *Volumetric Analysis*, Vol III Interscience, New York, 1957
2 O Tomiček and M Jesek, *Collection Czech Chem Commun*, 1938, **10**, 353
3 F P Treadwell and C Mayr, *Z Anorg Chem*, 1915, **92**, 127
4 E Rupp and A Schied, *Ber*, 1902, **35**, 2191, *Arch Pharm*, 1907, **243**, 460
5 E W Hammock, D Beavon and E H Swift, *Anal Chem*, 1949, **21**, 970
6 I R Wilson and G M Harris, *J Am Chem Soc*, 1960, **82**, 4515
7 A S Komarovsky, W F Filanova and I M Korenman, *Z Anal Chem*, 1934, **96**, 321
8 B Singh and K C Sood, *Anal Chim Acta*, 1955, **13**, 301
9 V R S Rao and A R V Murthy, *Curr Sci India*, 1961, **30**, 176
10 E Bishop and V J Jennings, *Talanta*, 1962, **9**, 581
11 B T Gowda, *Ph D Thesis*, University of Mysore, Mysore, India, 1978, and references therein
12 K S Rangappa, *Ph D Thesis*, University of Mysore, Mysore, India, 1982, and references therein
13 B T Gowda and D S Mahadevappa, *J Indian Chem Soc*, 1977, **54**, 980
14 M M Campbell and G Johnson, *Chem Rev*, 1978, **78**, 65

15 E Bishop and V J Jennings, *Talanta*, 1958, **1**, 197
16 J C Morris, J A Salazar and M A Wineman, *J Am Chem Soc*, 1948, **70**, 2036
17 T Higuchi, K Ikeda and A Hussain, *J Chem Soc (B)*, 1967, 546, 1968, 1031
18 B T Gowda and D S Mahadevappa, *J Chem Soc Perkin II*, in the press
19 A I Vogel, *A Text Book of Quantitative Inorganic Analysis*, 3rd Ed, p 264 Longmans, London, 1961
20 T J Jacob and C G R Nair, *Talanta*, 1972, **19**, 347
21 C G R Nair and P Indrasenan, *ibid*, 1976, **23**, 239
22 C G R Nair, R L Kumari and P Indrasenan, *ibid*, 1978, **25**, 525
23 A Chrząszczewska, *Bull Soc Sci Lettres Lódź, Class III*, 1952, **3**, No 16, *Chem Abstr*, 1955, **49**, 212
24 H S Yathirajan, D S Mahadevappa and Rangaswamy, *Talanta*, 1980, **27**, 52
25 D S Mahadevappa and M S Ahmed, *ibid*, 1979, **26**, 590
26 M S Ahmed and D S Mahadevappa, *ibid*, 1980, **27**, 669
27 C P K Pillai and P Indrasenan, *ibid*, 1980, **27**, 751
28 E Roberts, *J Chem Soc*, 1923, 849
29 A Findlay, *Practical Physical Chemistry*, 8th Ed, p 268 Longmans, London, 1954
30 E Schulek, *Z Anal Chem*, 1923, **62**, 337
31 F Feigl, *Spot Tests in Inorganic Analysis*, 5th Ed Elsevier, Amsterdam, 1958
32 E A Werner, *J Chem Soc*, 1923, **123**, 2577
33 D Van Nostrand, *International Encyclopedia of Chemical Science*, New York, 1964
34 E Stahl, *Thin-layer Chromatography A Laboratory Handbook*, p 305 Springer, New York, 1969

Talanta, Vol 30, No 5, pp 363–364, 1983
Printed in Great Britain

0039-9140/83/050363-02$03 00/0

SPECTROFLUORIMETRIC DETERMINATION OF TRACES OF PERCHLORATE BY EXTRACTION WITH RHODAMINE 6G

S JAYA,* T PRASADA RAO† and T V RAMAKRISHNA
Department of Chemistry, Indian Institute of Technology, Madras 600 036, India

(*Received* 18 *June* 1982 *Revised* 21 *October* 1982 *Accepted* 18 *November* 1982)

Summary—A method for the spectrofluorimetric determination of perchlorate is described, it is based on extraction of the perchlorate–Rhodamine 6G ion-pair into benzene The procedure is sensitive, highly reproducible and useful for the determination of 0 04–1 0 ppm of perchlorate The determination of traces of perchlorate in chlorate is described

Burns and Hanprasopwattana[1] have listed the few spectrophotometric methods so far suggested for determination of perchlorate. These procedures generally make use of ion-pair extraction or redox or precipitation reactions Triphenylmethane dyes have mainly been exploited for ion-pair extraction, xanthene dyes do not seem to have been tried The only spectrofluorimetric procedure reported is based on extraction of the perchlorate–amiloride ion-pair at pH 4 into isobutyl methyl ketone,[1] but is not entirely satisfactory as it depends critically on pH (the fluorescence intensity increases by 20% per pH unit in the range 3–7) It therefore seemed worth while investigating the use of xanthene dyes for a similar spectrofluorimetric determination Rhodamine 6G is found to be superior to Rhodamine B and Pyronine G, and can be used for determination of traces of perchlorate in chlorate

EXPERIMENTAL

Reagents

Perchlorate solution Dissolve 0 3482 g of pure potassium perchlorate in water and dilute to 250 ml Dilute this 1000 ppm solution to obtain a 5 ppm solution

Rhodamine 6G solution, 0 1%

Citrate buffer, pH 4, 0 1M

Apparatus

A Carl Zeiss PMQ-II spectrophotometer with ZFM-4 fluorescence attachment, 10-mm quartz cells and mercury lamp

Procedure

Transfer 2 5–25 μg of perchlorate into a 60-ml separatory funnel Add 1 ml of citrate buffer followed by 3 ml of Rhodamine 6G solution and dilute to 10 ml with water Equilibrate with two 10-ml portions of benzene, shaking for 1 min Combine and centrifuge the organic extracts and transfer into a 25-ml standard flask Make up to volume with benzene and measure the fluorescence in a 10-mm cell at 560 nm, excite the fluorescence by irradiation at 365 nm Read the perchlorate concentration from a calibration graph similarly prepared

RESULTS AND DISCUSSION

Effect of pH

The optimum pH range for the extraction of perchlorate with Rhodamine 6G into benzene was studied in the range from 0 to 9. The fluorescence intensity was found to be maximal in the pH range 1–6 (Fig 1) Though the extraction characteristics of the dye or ion-pair are not affected by citrate, acetate or phosphate buffers, pH-4 citrate buffer was preferred as it improves the selectivity

Effect of Rhodamine 6G concentration

Figure 2 shows that for maximum fluorescence intensity, the extraction should be done with 5–8 ml of 0 05% Rhodamine 6G solution

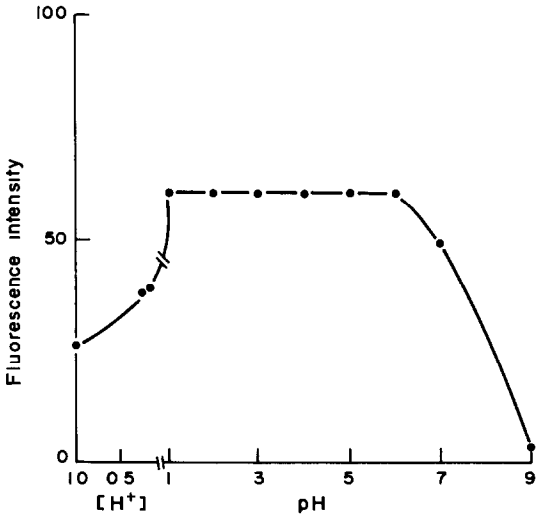

Fig 1 Effect of pH on the extraction of perchlorate–Rhodamine 6G ion-pair into 10 ml of benzene, 20 μg of perchlorate and 3 ml of 0 1% Rhodamine 6G solution in 10 ml of aqueous phase

*Indian Institute of Science, Bangalore 560 012, India
†Manager, R & D, Purex Laboratories (India) Private Limited, Bangalore 560 038, India, to whom correspondence should be addressed

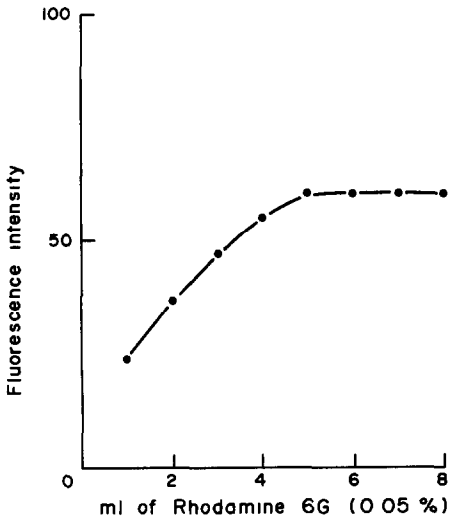

Fig 2 Effect of Rhodamine 6G concentration on the extraction of the perchlorate ion-pair into 10 ml of benzene, 20 μg of perchlorate, 10 ml of aqueous phase

Choice of solvent

The solvents tested included representatives from most classes of organic solvent, such as alcohols, ketones, esters, ethers, and aliphatic, chlorinated and aromatic hydrocarbons Chloroform and nitrobenzene extracted the free dye and ion-pair equally well The extraction behaviour of the other solvents is shown in Table 1, from which it is clear that only benzene is suitable

Equilibration time

It was found that shaking 10 ml of the aqueous phase with 10 ml of benzene for periods ranging from 30 sec to 5 min gave the same fluorescence intensity of the benzene extract, and extracted 90% of the perchlorate Extraction with two 10-ml portions of benzene, with shaking for 1 min, gave at least 99% extraction, and reproducible results A third extraction is unnecessary

Calibration graph

The recommended procedure gives a calibration graph that is linear up to 25 μg of perchlorate in 25 ml of benzene and passes through the origin. The extract can also be used for the spectrophotometric determination of 0 2–2 0 ppm of perchlorate, the molar absorptivity being $3\,4 \times 10^4$ l mole^{-1} cm^{-1} at 530 nm

The coefficient of variation (10 determinations of 10 μg of perchlorate) was found to be 1 2%

Table 1 Choice of solvent

Solvent	Fluorescence intensity
Benzene	60
Toluene	14
Cyclohexane	Nil
Xylene	2 5
Carbon tetrachloride	Nil

Table 2 Determination of perchlorate in chlorate samples

Sample	$KClO_4$ added, $\mu g/g$	Total $KClO_4$ found, $\mu g/g$	$KClO_4$ in $KClO_3$, %
Technical grade	0	61 2	0 00614
		61 2	
		61 8	
	25	86 0	
		86 6	0 00612
		87 2	
	50	110 6	
		111 2	0 00612
		111 8	
	100	161 2	
		161 2	0 00613
		161 5	
Riedel-de Haen	0	0 0	—
	5	5 0	—
	10	10 0	—
	20	20 6	—

Interference studies

Only anions commonly found in association with perchlorate were examined as potential interferents, along with a few inorganic cations There was no interference from 200 mg of chloride or 10 mg each of sulphate, bromide, nitrate, citrate, acetate, iodate, Mn^{2+}, Ni^{2+}, Co^{2+}, Zn^{2+}, Cu^{2+} or Fe^{3+} Up to 10 mg of Hg^{2+} can be masked with EDTA and the procedure can tolerate a 50-fold w/w ratio of chlorate, 10-fold ratio of iodide or 1 1 ratio of thiocyanate to perchlorate

Analysis of potassium chlorate

Perchlorate is often found associated with chlorate The presence of traces of perchlorate in chlorate is known to increase the combustion temperature and its presence in batches of potassium chlorate used for pyrotechnic purposes must be closely monitored [2] As more than 1 mg of chlorate interferes in the present determination, it is necessary to remove or destroy it by evaporation with concentrated hydrochloric acid[3] before the extraction of perchlorate

For the analysis, weigh a 5-g sample into an evaporating dish and heat with 100 ml of concentrated hydrochloric acid as described elsewhere [3] Dissolve the residue in distilled water and make up to volume in a 100-ml standard flask Apply the procedure already described, to a 5-ml aliquot of this solution The results presented in Table 2 show that the method is satisfactory for determination of perchlorate in chlorate samples

The procedure is almost three times as sensitive as the one developed by Burns and Hanprasopwattana,[1] and has the advantage of giving a constant signal over a wide range of pH

REFERENCES

1 D T Burns and P H Hanprasopwattana, *Anal Chim Acta*, 1980, **118**, 185
2 A G Briggs, W P Hayes, P A Howling and D T Burns, *Microchim Acta*, 1970, 888
3 A G Fogg, D T Burns and E H Yesowart, *ibid*, 1970, 974

Talanta, Vol 30, No 5, pp 365–367, 1983
Printed in Great Britain

0039-9140/83/050365-03$03 00/0
Pergamon Press Ltd

IODOMETRIC MICRODETERMINATION OF BORIC ACID AND BORAX SEPARATELY OR IN A MIXTURE

R SAXENA and R M VERMA
Department of Chemistry, University of Jabalpur, Jabalpur (M P) 482001, India

(*Received* 26 *August* 1982 *Accepted* 8 *December* 1982)

Summary—Boric acid is determined by first treating it with mannitol and then with solid potassium iodate and potassium iodide The iodine liberated is titrated with thiosulphate Borax is determined by reacting it with a known and excessive volume of hydrochloric acid and determining the surplus acid by iodometry From the amount of acid consumed, the quantity of borax is calculated Mixtures of borax and boric acid are analysed by combination of the two methods Borax is determined first, then the mannitol procedure is applied to a second sample and the total boric acid (original plus that produced in the borax–HCl reaction) is determined iodometrically The boric acid content of the sample is obtained by difference The procedures can be used for determining 0 01–0 1 mmole of these substances with an average deviation of 0 1–0 4% The end-points obtained are sharper than those for potentiometric acid–base titrations Furthermore, the procedures are applicable at much lower concentrations

Boric acid acts as a weak monobasic acid and can be titrated directly with alkali only at high concentration ($\sim 1M$), with Tropeolin O or nitramine as indicator [1] Titration with phenolphthalein as indicator is very incomplete However, its complexation reaction with certain polyhydroxy compounds, such as glycerol, mannitol or dextrose, releases protons and it then behaves as a relatively strong monobasic acid, and can be titrated with strong alkali to a phenolphthalein end-point,[2] but with dilute sample and titrant solutions there is rapid fading of the phenolphthalein colour at the end-point,[3] making judgment of the end-point difficult Potentiometric titration is better, but at low concentrations the potential jump near the end-point is too small to be of use Spectrophotometric titration is then superior

The present communication describes an application of the iodometric microprocedure already used for weak organic acids, based on the determination of acids by means of the iodate–iodide reaction [4] Boric acid is determined by adding mannitol and an excess of solid potassium iodide and potassium iodate, and titrating the iodine liberated Borax is determined by adding a measured excessive volume of hydrochloric acid, and titrating the surplus by the iodate–iodide procedure

A mixture of borax and boric acid can be analysed by first determining borax as described above, calculating how much boric acid it would produce by stoichiometric reaction with hydrochloric acid, and substracting this from the total boric acid found after treatment of a sample with the stoichiometric amount of hydrochloric acid

EXPERIMENTAL

Reagents

Analytical grade chemicals and conductivity water were used

*Oxalic acid, 0 1*N *solution* Prepared by dissolving the calculated amount of the acid in water Further diluted as required, to obtain solutions of lower concentration

*Sodium hydroxide, 0 1*M *solution.* Standardized with the 0 1*N* oxalic acid, diluted to lower concentrations as required

*Sodium thiosulphate, 0 1*M *solution* Standardized with potassium iodate,[2] and diluted as required

Potassium iodate solution, 5%

*Boric acid, 0 1*M *solution* Standardized by titration with alkali after addition of mannitol [2] Suitably diluted to obtain test solutions

*Borax, 0 1*M *solution* Standardized by titration with hydrochloric acid [2] Test solutions were obtained by suitable dilution

Determination of boric acid

Visual method Take 5 or 10 ml of sample solution (containing 0 2–1 meq of boric acid) in a 100-ml iodine flask, add 1 5 g of mannitol and swirl the flask for 2 min Add 1 g each of potassium iodate and potassium iodide and again swirl for 5 min Titrate the liberated iodine with 0 02–0 1*M* thiosulphate, with starch as indicator

1 ml of 0 1*M* thiosulphate ≡ 6 18 mg of boric acid

Potentiometric titration Take 5 or 10 ml of test solution (containing 0 01–0 2 meq of boric acid) in a 100-ml beaker, add 1 5 g of mannitol and stir for 2 min (magnetic stirrer) Add 1 g each of potassium iodate and potassium iodide, stir for 2 min, cover the beaker, and allow 5 min for the reaction Insert platinum and calomel electrodes and titrate the liberated iodine potentiometrically with 0 001–0 01*M* thiosulphate Locate the end-point on a plot of $\Delta E/\Delta V$ against volume (V) Standardize the thiosulphate solution potentiometrically with oxalic acid solution by the same

procedure except for the addition of mannitol. (The oxalic acid concentration should be comparable to that of the boric acid in the sample solution.)

1 ml of 0.001*M* thiosulphate ≡ 61.8 μg of boric acid

Determination of borax

Visual method Take 5 or 10 ml of sample solution (containing 0.025–0.1 mmole of borax) in a 100-ml iodine flask. Add a known and excessive volume of hydrochloric acid, followed by 0.5 g of potassium iodide and 5 ml of 5% potassium iodate solution. Swirl the flask and titrate the liberated iodine with thiosulphate solution, using starch as indicator. In the same way run a blank with the same volume of hydrochloric acid. The difference between the blank and the test titrations gives the amount of the acid equivalent to the borax in the test solution.

1 ml of 0.1*N* thiosulphate ≡ 10.07 mg of $Na_2B_4O_7$

Potentiometric titration Take 5 or 10 ml of test solution (containing 0.01–0.1 mmole of borax) in a 100-ml beaker. Treat with hydrochloric acid, iodate and iodide as for the visual titration (but use magnetic stirring). Insert platinum and calomel electrodes and titrate the liberated iodine potentiometrically with 0.001–0.01*M* thiosulphate. Plot $\Delta E/\Delta V$ against volume of titrant to locate the end-point. Run a blank with the same volume of acid. Standardize the thiosulphate solution potentiometrically with standard oxalic acid.

1 ml of 0.001*M* thiosulphate = 100.7 μg of $Na_2B_4O_7$

Analysis of a mixture of borax and boric acid

Determine borax in a portion of sample, as already described. Calculate the volume (*X* ml) of hydrochloric acid consumed, the quantity of borax, and the amount (*A*) of boric acid produced during the reaction between borax and hydrochloric acid.

To an equal volume of sample add the volume (*X* ml) of hydrochloric acid calculated as used in the first experiment. Then determine the total boric acid (original plus that produced from the borax). From this total amount (*B*) subtract the amount (*A*) liberated from the borax reaction, to obtain the quantity of boric acid present in the sample solution.

RESULTS AND DISCUSSION

Boric acid cannot be titrated accurately with standard alkali.[2] Although satisfactory results are obtained when mannitol is added, the phenolphthalein end-point is not sharp for dilute solutions, and carbon dioxide interferes. For these reasons there is a progressively increasing positive error with increasing dilution of the titrand and the titrant. Preliminary experiments showed that addition of 1.5 g of mannitol and 1 g each of potassium iodate and potassium iodide in solid form to a boric acid sample solution would liberate iodine quantitatively within 5 min. These observations were used in developing the methods described. The results in Table 1 show that these procedures can be applied to determine 0.01–1 meq of boric acid with an average deviation of 0.1–0.4%.

Table 1 Determination of boric acid

Method	Boric acid, *mg*		Relative standard deviation, %
	Taken	Found*	
Visual	61.84	61.9	0.2
	30.9	30.9	0.2
	15.46	15.48	0.2
	12.37	12.39	0.2
Potentiometric	6.184	6.193	0.2
	3.092	3.100	0.3
	1.236	1.239	0.4
	0.773	0.776	0.4
	0.618	0.620	0.5

*Average of six determinations

Table 2 Determination of borax

Method	Borax, *mg*		Standard deviation, %
	Taken	Found*	
Visual	100.7	100.7	0.2
	20.13	20.14	0.2
	10.06	10.07	0.2
	5.03	5.04	0.2
	2.51	2.52	0.3
Potentiometric	10.07	10.07	0.2
	5.03	5.04	0.2
	1.677	1.680	0.2
	1.258	1.261	0.3
	1.006	1.009	0.4

*Average of six determinations

Methyl Orange has been recommended as the indicator for titration of borax with 0.1*M* hydrochloric acid[2] but this method is not satisfactory on the micro scale. Addition of excess of hydrochloric acid and back-titration with alkali fails because of interference by the boric acid liberated during the reaction between borax and hydrochloric acid. However, it was observed that if the surplus acid is determined iodometrically there is no interference due to boric acid. This fact was used in working out the method given here. The method using starch as indicator can be applied to determine 0.025–0.1 mmole. These procedures have an average deviation in the range 0.1–0.4% (Table 2).

The methods can be coupled for determining borax and boric acid, as already explained. Consecutive titration of both components in the same solution (borax first, followed by total boric acid), though

Table 3 Potentiometric analysis of mixtures of borax and boric acid

Taken, *mg*		Found,*			
Borax	Boric acid	Borax, *mg*	r.s.d.,† %	Boric acid, *mg*	r.s.d.,† %
20.13	3.092	20.15	0.2	3.10	0.3
10.07	6.184	10.08	0.2	6.20	0.3
10.07	12.37	10.08	0.2	12.39	0.2
6.04	0.618	6.05	0.3	0.620	0.3
2.013	1.854	2.017	0.3	1.857	0.3
1.006	0.618	1.009	0.4	0.620	0.4
1.006	0.927	1.009	0.4	0.930	0.3

*Average of six determinations
†Relative standard deviation

attractive in principle, is not fully satisfactory in practice If starch is used as indicator, it is present from the start of the titration, which is contrary to recommended practice If potentiometric titration is used, the first end-point must be overshot so that the equivalence point can be located, and the excess could perhaps influence the second titration.

The combined procedure can be applied to mixtures containing 0 01–0 1 mmole of the two substances The results in Table 3 show that the average deviation is in the range 0 1–0 5%

Acknowledgement—The authors' sincere thanks are due to the Council of Scientific and Industrial Research, New Delhi, for the award of a Fellowship to R S

REFERENCES

1 I M Kolthoff and V A Stenger, *Volumetric Analysis*, Vol II, p 114 Interscience, New York, 1961
2 A I Vogel, *A Text Book of Quantitative Inorganic Analysis*, 3rd Ed , pp 245, 246, 334 Longmans, London, 1960
3 N D Cheronis and T S Ma, *Organic Functional Group Analysis*, p 485 Wiley, New York, 1964
4 S N Nema and R M Verma, *Talanta*, 1978, **25**, 400

Talanta, Vol 30, No 5, pp 368–370, 1983
Printed in Great Britain

0039-9140/83/050368-03$03 00/0

HIGH-PRESSURE LIQUID CHROMATOGRAPHY COMBINED WITH FLUORESCENCE DETECTION AND SOLVENT EXTRACTION FOR SIMULTANEOUS DETERMINATION OF COPROPORPHYRINS I AND III IN HUMAN URINE

YASUHISA HAYASHI and MISAKO UDAGAWA
Department of Chemistry, Joetsu University of Education, Joetsu 943, Japan

(*Received* 23 *September* 1982 *Accepted* 22 *November* 1982)

Summary—A precise and reproducible high-pressure liquid chromatography (HPLC) method for the determination of coproporphyrin I and III isomers (cp isomers) in urine was investigated The cp isomers were extracted into diethyl ether, the solution was evaporated and the residue dissolved prior to HPLC The recoveries of both cp isomers were 87 8 ± 3 2 and 90 0 ± 2 1% and detection limits ($S/N = 3$) were 0 07 ng, respectively

The separation and determination of coproporphyrin I and III isomers (cp isomers) are important both in clinical diagnosis and research on porphyrins A number of methods have been investigated for the determination of cp isomers in biological fluids The thin-layer[1,2] and paper[3,4] chromatography methods are time-consuming, tedious and difficult to make quantitative In recent years, HPLC has been developed as a most convenient method for the routine identification and determination of porphyrins in biological fluids [5–7] Recently, Englert *et al* [8] have reported a direct method for the determination of cp isomers by use of HPLC and fluorometric detection Unfortunately, their method is not fully satisfactory for the determination of cp isomers in urine, because of the complexity of the chromatographic procedure and the poor precision The present paper describes a precise and reproducible HPLC procedure for the determination of both cp isomers in urine

EXPERIMENTAL

Reagents

Cp I standard solution (1 0 μg/ml) Free cp I (5 μg/vial, Sigma Chemical Co) was dissolved and diluted to 5 ml with 0 1*M* hydrochloric acid

Cp III stock solution (15 0 μg/ml) Cp III tetramethyl ester (15 mg, Sigma Chemical Co) was hydrolysed overnight in 15 ml of 7*M* hydrochloric acid at room temperature in the dark, and the reaction mixture was then diluted to 1000 ml with water The standard solution was prepared by diluting the stock solution with 0 1*M* hydrochloric acid just before use The concentration of free cp III was calculated from the absorbance and molar absorptivity [9]

All other reagents used were of reagent grade or better

Apparatus

A Hitachi Model 635T HPLC apparatus was equipped with a Hitachi Model 204S fluorescence detector, operated at 392 nm for excitation and 610 nm for emission, for fluorometric detection, and with a Hitachi 056 dual-pen recorder The reversed-phase chromatographic column was a Hitachi 3053, consisting of octadecylsilane bonded to 5-μm silica in a stainless-steel tube, bore 4 mm and length 150 mm

Sample collection and preparation

A 24-hr urine sample is collected and 3 g of EDTA (disodium salt) are added as a preservative, the sample is kept at 4° until analysed (which is done as soon as possible)

The extraction method used is a modification of that developed by Aziz *et al* ,[10] in which the organic solvent used was ethyl acetate In this modified procedure the urine sample (10 ml) is acidified with acetic acid to pH 4–5, and then shaken with 20 ml of diethyl ether The phases are separated and the ether extraction repeated until the aqueous phase no longer shows any red fluorescence under ultraviolet light The pooled extract is evaporated to dryness in a rotary evaporator at about 30° The residue is dissolved with 0 5 ml of 0 1*M* hydrochloric acid and the solution filtered through a 0 45-μm membrane filter, before the HPLC

Chromatographic procedure

A 10-μl aliquot of sample containing up to 10 ng of cp I and 15 ng of cp III is injected into the column, and separated with a mobile phase composed of acetonitrile–2% v/v acetic acid–0 1% potassium dihydrogen phosphate solution (2 1 1 v/v at a flow-rate of 1 3 ml/min

RESULTS AND DISCUSSION

It was found experimentally that, as expected, the ratio of acetonitrile to buffer solution in the mobile phase had an important influence on the retention volume and resolution The resolution of the cp isomers was found to increase with the acetonitrile content of the mobile phase The effect of acetic acid and potassium dihydrogen phosphate concentration in the mobile phase was also studied, and good separation was obtained with a concentration range of 0 25–1% v/v acetic acid and 0 01–0 04% w/v

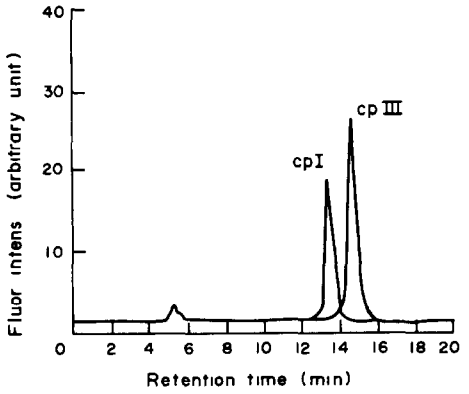

Fig 1 Chromatogram of cp isomers in human urine, obtained by the standard procedure

potassium dihydrogen phosphate in 1 1 v/v acetonitrile–water medium A mobile phase consisting of acetonitrile–2% v/v acetic acid–0 1% potassium dihydrogen phosphate solution (2 1.1 v/v) is therefore recommended A typical chromatogram of the cp isomers in a urine sample is shown in Fig 1 The peaks were identified by adding authentic cp isomers to the sample

Table 1 Recoveries of cp isomers (cp I 25 0 ng/ml, cp III 37 5 ng/ml) added to a urine sample

Found, *ng/ml*		Recovery, %	
cp I	cp III	cp I	cp III
22 1	32 8	88 4	87 5
21 5	34 7	86 0	92 5
23 2	33 4	92 8	89 1
21 9	34 1	87 6	90 9
21 1	33 2	84 4	88 5
22 4	35 4	89 6	92 0
21 4	33 6	85 6	89 6

Calibration graphs and precision

The relationship between the cp I and III concentration and fluorescence intensity was linear over the concentration range studied, 0–1 0 ng/μl for cp I and 0–1 5 ng/μl for cp III The detection limit (defined as the concentration giving a signal equal to 3 times the standard deviation of the blank signal) was found to be 0.007 ng/μl for each isomer To determine the extraction efficiency of the diethyl ether–acetic acid method, a urine sample was spiked with known amounts of the pure isomers and then analysed by the

Table 2 Values found for excretion of coproporphyrins in urine from 12 volunteers

Sample No	cp I, $\mu g/day$*	cp III, $\mu g/day$*	cp III/total cp, %
1	27 1	66 5	71 0
2	17 6	41 1	70 0
3	49 7	72 0	59 2
4	30 0	50 6	62 8
5	36 5	68 3	65 2
6	25 2	120 1	82 7
7	23 1	28 9	55 6
8	25 8	77 4	75 0
9	15 6	30 1	65 9
10	6 9	45 7	86 9
11	11 0	19 2	63 6
12	30 2	27 8	47 9
Mean ± SD	24 9 ± 11 6	54 0 ± 28 5	67 1 ± 11 0

*Mean of three determinations on each sample

Table 3 Values reported for cp isomers in normal urine

Authors	Number of subjects	Total cp* (Mean ± SD), $\mu g/day$	Cp III/Total* %	Analytical technique
Aziz *et al* [10]	20 (Men, age 18–36)	146 6 ± 38 (100–230)	65 4 ± 5 6 (50–75)	
	11 (Women, age 18–62)	103 ± 15 9 (72–122)	65 4 ± 5 6 (53–83)	PC
	9 (Children, age 4–10)	78 ± 19 (60–120)	81 ± 3 (77–87)	
Fernandez[11]	34 (Adult)	(0–161)		Spectrometry
Sobel *et al* [6]	48	117 (32–235)		LC
Schermuly *et al* [1]	15		77 5 ± 6 4	TLC
Englert *et al* [8]	14	61 (1–162)	79 (63–100)	HPLC
Ford *et al* [7]	57 (Men and women)	39 ± 23 (3–109)		HPLC
Present study	12 (Age 10–25)	79 ± 35 (30–145)	67 ± 11 (48–87)	HPLC

*Range given in parentheses

procedure given The concentrations were calculated from calibration graphs prepared at the same time, and corrected for the amounts of each isomer already found present in the sample The results, summarized in Table 1, indicate that each isomer was recovered with an efficiency of 88% for cp I (s d 2 8%) and 90% for cp III (s d 1 8%)

Table 2 presents the results obtained for urinary excretion of the two cp isomers The cp III content seems generally significantly higher than that of cp I

The cp III values were generally higher than those for cp I, forming 47 9–86 9% of the total cp (average 67%) and this preponderance of cp III appears to be independent of the excretion level of total cp in healthy human urine As shown in Table 3, widely divergent values of the total cp have been reported, varying from 39 to 146 μg/day, but it is generally agreed that the cp III is preponderant and forms an almost constant fraction of the total cp in normal urines

The HPLC–solvent extraction method proposed here has sufficient precision and reproducibility for the determination of urinary cp isomers, and is useful for routine analysis in clinical diagnosis

REFERENCES

1 E Schermuly and M Doss, *Z Klin Chem Klin Biochem*, 1975, **13,** 299
2 J Jensen, *J Chromatog*, 1963, **10,** 236
3 T C Chu, A A Green and E J Chu, *J Biol Chem*, 1951, **190,** 643
4 L Eriksen, *Scand J Clin Lab Invest*, 1958, **10,** 319
5 R Horchner and T Rietveld, *J Chromatog*, 1976, **123,** 414
6 C Sobel, C Cano and R E Thiers, *Clin Chem*, 1974, **20,** 1397
7 R E Ford, C N Ou and R D Ellefson, *ibid*, 1981, **27,** 397
8 E Englert, Jr, A W Wayne, E E Wales, Jr, and R C Straight, HRC & CC, 1979, **2,** 570
9 C Rimington, *Biochem J*, 1960, **75,** 620
10 M A Aziz, S Schwartz and C J Watson, *J Lab Clin Med*, 1964, **63,** 585
11 A A Fernandez, R J Henry and H Goldenberg, *Clin Chem*, 1966, **12,** 463

Talanta, Vol 30, No 5, pp 371–373, 1983
Printed in Great Britain

0039-9140/83/050371-03$03 00/0

SEPARATION OF ARSENIC(III) AND ARSENIC(V) IN GROUND WATERS BY ION-EXCHANGE

WALTER H FICKLIN
U S Geological Survey, Box 25046, Denver, CO 80225, U S A

(*Received* 17 *August* 1982 *Accepted* 5 *November* 1982)

Summary—The predominant species of arsenic in ground water are probably arsenite and arsenate These can be separated with a strong anion-exchange resin (Dowex 1 × 8, 100–200 mesh, acetate form) in a 10 cm × 7 mm column Samples are filtered and acidified with concentrated hydrochloric acid (1 ml per 100 ml of sample) at the sample site Five ml of the acidified sample are used for the separation At this acidity, As(III) passes through the acetate-form resin, and As(V) is retained As(V) is eluted by passage of 0 12*M* hydrochloric acid through the column (resulting in conversion of the resin back into the chloride form) Samples are collected in 5-ml portions up to a total of 20 ml The arsenic concentration in each portion is determined by graphite-furnace atomic-absorption spectrophotometry The first two fractions give the As(III) concentration and the last two the As(V) concentration The detection limit for the concentration of each species is 1 μg/l

Arsenic in ground waters occurs in the oxidation states As(III) and As(V) Recently Cherry *et al*[1] proposed that the concentrations of As(III) and As(V) could be used to calculate the oxidation–reduction potential of a ground water sample. The redox potential is an important factor in the study of ground waters as a sample medium for geochemical exploration

A popular method[2,3] for determining low levels of As(III) and As(V) involves generation of arsine, coupled with atomic-absorption detection Careful control of sample pH is required in order to generate arsine selectively from As(III)[2,3] The sample must also be analysed very soon after collection or stabilized in some way to prevent oxidation of As(III) Acidification with hydrochloric acid prevents the oxidation[4] but the pH must then be carefully adjusted before the analysis Nakashima[5] added Zr(IV) and potassium iodide to the acidified sample to generate arsine selectively from As(III) All the methods require complex equipment and procedures

A simple separation of As(III) and As(V) based on ion-exchange is presented here The sample can be stored in acidified solution or the separation can be performed at the sample site before any chemical change can take place The use of an anion-exchange resin for separation of arsenic species in water has been investigated by Henry and Thorpe,[6] but they used separate portions of sample water for determinaton of As(III) and As(V) Pacey and Ford used a similar ion-exchange method to determine organic and inorganic arsenic species,[7] with detection by graphite-furnace atomic-absorption spectrophotometry (GFAAS)

GFAAS determination of arsenic, with addition of nickel, is well established[8] Small volumes of sample are required and a detection limit of 1 μg/l. is readily achieved GFAAS was therefore chosen for the determinations in the present work.

EXPERIMENTAL

Apparatus

A Perkin–Elmer model 703 atomic-absorption spectrophotometer* equipped with a deuterium arc background corrector and an HGA-2200 graphite furnace was used for arsenic determination Glass "econo-columns" were obtained from Bio-Rad Laboratories (Richmond, California) The samples were injected manually by Eppendorff pipette or with a Perkin–Elmer As-1 auto sampler

Reagents

Hydrochloric acid, nitric acid, acetic acid, sodium arsenite, disodium hydrogen arsenate heptahydrate, sodium hydroxide and nickel nitrate 6-hydrate were "Baker Analyzed", supplied by J T Baker Chemical Co Dowex 1 × 8 anion-exchange resin (100–200 mesh) was supplied by Bio-Rad Laboratories Demineralized water was obtained from a Millipore Milli-Q water system

Column preparation

Glass "econo-columns" (10 cm × 7 mm) were used for all separations Enough resin (2 3 g) was slurry-packed into the column to fill it to within 1 or 2 mm of the top The resin was supplied in the chloride form and required conversion into the acetate form through the hydroxide form as intermediate This was achieved by allowing 3 ml of 1*M* sodium hydroxide to drain through the resin, followed by 15 ml of water and then 5 ml of 1*M* acetic acid The resin was rinsed once more with water, leaving the resin in the acetate form A small amount of water was added to the columns to keep the resin moist The columns were capped to prevent contamination from dust

Procedure

At the sample site, 50 ml of water were filtered through a 0 45-μm membrane filter (to remove particulate matter that might contain soluble or acid-leachable arsenic), and

*Any use of trade names is for descriptive purposes only and does not imply endorsement by the U S Geological Survey

Table 1 Instrumental parameters for graphite-furnace atomic-absorption spectrometer

Drying	60 sec	100°C	
Charring	20 sec	950°C	
Atomizing	6 sec	2700°C	Interrupt mode
Purge gas	Argon		
Source	Electrodeless discharge lamp		

then acidified with 0 5 ml of concentrated hydrochloric acid Five ml of the acidified sample were allowed to pass through the resin in the column, followed by 15 ml of 0 12*M* hydrochloric acid as eluent, added in three separate 5-ml portions The successive 5-ml fractions of effluent (one from the sample, three from the eluent) were collected in 6-ml vials, which were then capped The As(III) from the sample was in the first two fractions and the As(V) in the last two

Table 2 Results for arsenic speciation in ground waters and acid mine waters

Sample	As(III), μg/l	As(V), μg/l	Total As, μg/l
M002*	23	7	30
M021*	<1	3	3
M022*	2	5	7
M027*	1	18	18
M030*	2	6	8
M043	1	6	8
M045*	54	16	69
BV-012*	8	6	14
BV-020*	2	4	5
BV-039*	<1	5	5
BV-041*	<1	5	5
BV-046*	1	10	11
MS-02†	13	1	15
MS-03†	5	2	7
MS-04†	5	2	7
MS-06†	5	1	6
MS-08†	4	1	6
Salt Spring, Utah	1400	1180	2450

*Irrigation well water, Beaver Area, Utah
†Acid mine water, Colorado

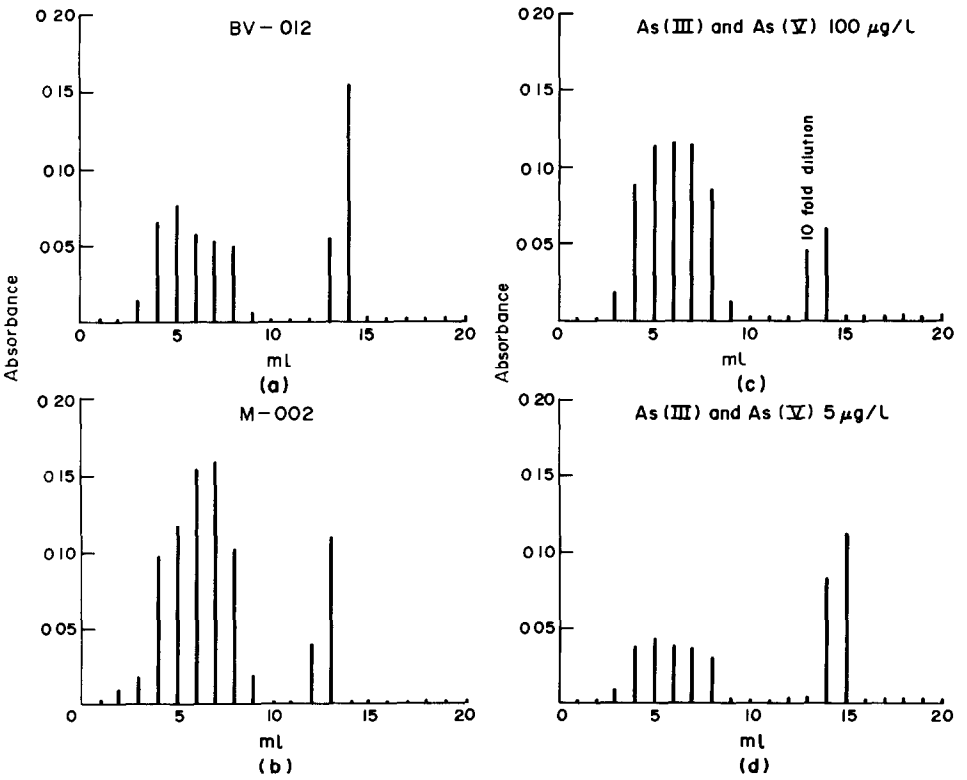

Fig 1 Separation of As(III) and As(V) a, b, d, 25-μl samples, interrupted mode, c, 10-μl sample, normal mode

Table 3 Recovery of added arsenic

Sample	As(III), μg/l	As(V), μg/l	As(III),* μg/l	As(V),* μg/l
M-027	1	18	6	24
BV-012	6	5	12	10
BV-041	<1	5	5	11
BV-046	1	10	7	16
Virginia Canyon Mine	2	1	6	6
Lucania Mine	1	<1	6	6

*Spiked with 5 μg of arsenic per litre

Table 4 Sample-site separation compared to laboratory separation

	Sample site		Laboratory		
	As(III), μg/l	As(V), μg/l	As(III), μg/l	As(V), μg/l	Total, μg/l
Rockford Tunnel	3	<1	3	<1	3
Virginia Canyon Mine	2	1	2	1	3
Idaho Spring Mine	14	<1	15	<1	13
Lucania Mine	1	<1	<1	<1	1

The unused sample was brought back to the laboratory for further study by the same procedure

Arsenic was determined in each portion of sample by graphite-furnace atomic-absorption spectrophotometry An equal volume of 200-mg/l nickel solution was added to the volume of sample in the graphite furnace (generally, 25 μl) The instrumental parameters are shown in Table 1 A calibration graph was constructed by analysing standards in the same way Total arsenic for each sample was determined directly in the same manner, with an appropriate aliquot of the original sample

RESULTS

Two ground-water samples and two laboratory standards with measurable concentrations of both As(III) and As(V) were introduced into the columns described The effluent was collected in twenty successive 1-ml portions, each of which was analysed for arsenic Plots of absorption signals (peak-heights) *vs* eluate volume showed a definite chromatographic separation of two arsenic species (Fig 1) All of the As(III) is eluted in the first 10 ml of effluent, there being little or no retention of As(III) by the acetate form of the resin As the eluent (hydrochloric acid) passes through the column, the resin is converted from the acetate form into the chloride form, which has little or no affinity for As(V) in the acidic medium, and the arsenic(V) is eluted in the 13th and 14th 1-ml fractions The change from acetate form to chloride form is evidenced by an accompanying slight colour change proceeding down the column As(III) and As(V) in 13 ground-water samples from Utah and 5 acid mine waters from Colorado, that had been filtered and acidified at the sample site, were separated in the laboratory The results are shown in Table 2

Recovery studies involved adding As(III) and As(V) (each at the 5-μg/l level) to each of six samples The results in Table 3 for the spiked and original samples show that the recoveries of As(III) and As(V) ranged from 80 to 120% respectively, which is satisfactory at this level That all of the arsenic is recovered can also be seen from the data in Table 2

Table 5 Mean and standard deviation (*S*) for six separations of two samples

M002		BV012	
As(III), μg/l	As(V), μg/l	As(III), μg/l	As(V), μg/l
24	7	10	6
24	6	8	7
22	8	8	7
23	8	9	7
25	6	9	6
21	7	8	6
Mean = 23 3	7 0	8 7	6 5
S = 1 4	0 9	0 8	0 6

Separations of the arsenic species in some acid mine waters collected in the front range area of Colorado were done at the sample site and later in the laboratory The values shown in Table 4 show satisfactory agreement between the two sets of results

Two samples (M-002 and BV-012) were analysed six times each The values, means and standard deviations are listed in Table 5

A separation in the field takes about 15 min In the laboratory, several columns can be used simultaneously for analysis of a number of samples The columns are inexpensive and can be used several times before the resin must be replaced

REFERENCES

1 J A Cherry, A U Shaikh, D E Tallman and R V Nicholson, *J Hydrol*, 1979, **43**, 373
2 J Aggett and A C Aspell, *Analyst*, 1976, **101**, 341
3 A U Shaikh and D E Tallman, *Anal Chim Acta*, 1978, **98**, 251
4 C Venghout and H Agemian, *Analyst*, 1980, **105**, 737
5 S Nakashima, *ibid*, 1979, **104**, 172
6 F T Henry and T M Thorpe, *Anal Chem*, 1980, **52**, 80
7 G E Pacey and J A Ford, *Talanta*, 1981, **28**, 935
8 K C Tam, *Env Sci Techn*, 1974, **8**, 734

Talanta, Vol 30, No 5, pp 374–376, 1983
Printed in Great Britain

0039-9140/83/050374-03$03 00/0

SPECTROPHOTOMETRIC DETERMINATION OF MICRO AMOUNTS OF NITRITE IN WATER AND SOIL

QIAN-FENG WU and PENG-FEI LIU
Shaanxi Monitoring Station of Environmental Protection, 25 Chang An Road (N), Xian, People's Republic of China

(*Received* 20 *April* 1982 *Revised* 10 *October* 1982 *Accepted* 29 *October* 1982)

Summary—A spectrophotometric method for determination of micro amounts of nitrite in water and soil with *p*-aminoacetophenone and resorcinol is described The interference of foreign ions can be eliminated by masking with complexing agents Beer's law is obeyed up to 20 μg of NO_2^- in 60 ml of solution and the molar absorptivity at 435 nm is $5\,27 \times 10^4$ 1 $mole^{-1}$ cm^{-1} The colour is stable for 10 hr Results obtained by using the proposed method for water and soil samples agree well with those obtained by the Saltzman standard method

As nitrite can react with secondary amines present in the body it may form carcinogenic nitrosamines, so determination of nitrite is important [1,2] Numerous methods are available. The generally acknowledged methods are the Griess[3] and Saltzman[4] methods. The two most sensitive methods have been reported by Sawicki *et al*,[5,6] in an extensive survey in which they mentioned various sensitive reactions based on diazotization of *p*-aminoacetophenone and coupling with 1-naphthylamine, 1-anilinonaphthalene *etc* Celardin[7] used phenyl-1-naphthylamine or phenyl-β-naphthylamine as coupling agent, but these are carcinogenic [8] Other coupling agents have been reported [9–11] However, these methods are all limited by fairly rapid fading of the colour, and by interference by Cu(II), Fe(III), S^{2-}, I^- *etc*

We present here a sensitive colour reaction for nitrite, based on diazotization of *p*-aminoacetophenone (AAP) followed by coupling with resorcinol (RSC) in sodium carbonate/sodium acetate medium, to form a bright gold water-soluble azo-dye Foreign ions are masked with a composite EDTA–sodium hexametaphosphate reagent The interference of sulphide can be eliminated by addition of mercuric chloride The method is simple, rapid and more sensitive than the Saltzman procedure

EXPERIMENTAL

Reagents

Colour developing solution Dissolve 2 g of AAP and 1 g of RSC in 100 ml of hydrochloric acid (1 + 4) Keep the solution in a brown bottle, in the refrigerator

Complexing agent solution Dissolve 10 g of sodium hexametaphosphate and 10 g of EDTA in 90 ml of water, heating until completely dissolved, cool and dilute to 100 ml with water

Mixed alkali solution Dissolve 10 g of anhydrous sodium carbonate and 8 6 g of anhydrous sodium acetate in 50 ml of water, add 17 ml of dimethylformamide and dilute to 100 ml with water

Standard nitrite solution Dissolve 0 1500 g of sodium nitrite in water and dilute to 1000 ml Add 1 ml of chloroform to inhibit bacterial growth Dilute 100-fold to give a 1.0-μg/ml working standard solution

All reagents used were of analytical grade, and demineralized water was used throughout

Procedure

To a 100-ml Nessler tube (graduated at 50 ml) add an appropriate volume of test solution, containing <20 μg of nitrite, make up to the 50-ml mark with water, add 2 0 ml of complexing agent solution and 2 0 ml of colour developing solution, and mix After 5 min add 6 0 ml of mixed alkali solution Measure the absorbance at 435 nm in a 2-cm cell against a reagent blank prepared in the same manner but containing no nitrite

Sample preparation

Waters Place 100 ml of water sample in a beaker, and add 2 ml of 5% mercuric chloride solution Let stand for 5 min, then filter to remove mercuric sulphides and iodide Analyse a known volume of the filtrate by the procedure above

Soils Weigh 1 0 g of fresh soil sample into a 100-ml beaker Add 20 ml of water, let stand for 5 min, add 0 5 ml of 5% mercuric chloride solution and 1 ml of sodium sulphide solution, filter into a Nessler tube, dilute to the 50-ml mark with water, and analyse for nitrite as already described Determine the water content of the soil with a separate 20-g sample and calculate the nitrite content on a moisture-free basis

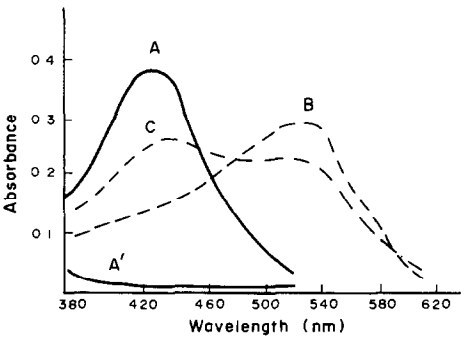

Fig 1 Absorption spectra of the azo dye in various alkaline media A, in Na_2CO_3–NaAc medium at pH 9, B, in 0 33–1 2*M* KOH, C, in 0 17*M* KOH, A', reagent blank in Na_2CO_3–NaAc medium at pH 9 (NO_2^- 10 μg, 2-cm cell)

RESULTS AND DISCUSSION

Absorption spectra and reaction mechanism

When coupled with RSC at various degrees of alkalinity, the diazonium salt gave different colours The absorption spectra of the products are shown in Fig 1 Curve A shows maximum absorption at 435 nm for the product obtained in sodium carbonate–sodium acetate medium (pH 9) The dye is bright golden, with apparent molar absorptivity $\varepsilon_{435} = 5\,27 \times 10^4$ l mole^{-1} cm^{-1} Curve B shows that absorption is maximal at 525 nm for the dye obtained in 0 33–1 2*M* potassium hydroxide medium. This azo dye is red, with $\varepsilon_{525} = 4\,07 \times 10^4$ l mole^{-1} cm^{-1} Curve C, for the product obtained in 0 17*M* potassium hydroxide medium, shows two absorption maxima, at 450 and 520 nm This product is orange-red, with an apparent $\varepsilon_{450} = 3\,56 \times 10^4$ l mole^{-1} cm^{-1} The preferred coupling medium is the pH 9 sodium carbonate–sodium acetate mixture The suggested reaction sequence is

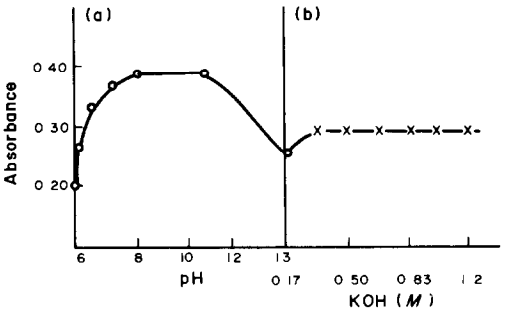

Fig 2 Effect of alkalinity on the coupling reaction for 10 μg of NO_2^- (a) $\lambda = 435$ nm, (b) 525 nm, 2-cm cell

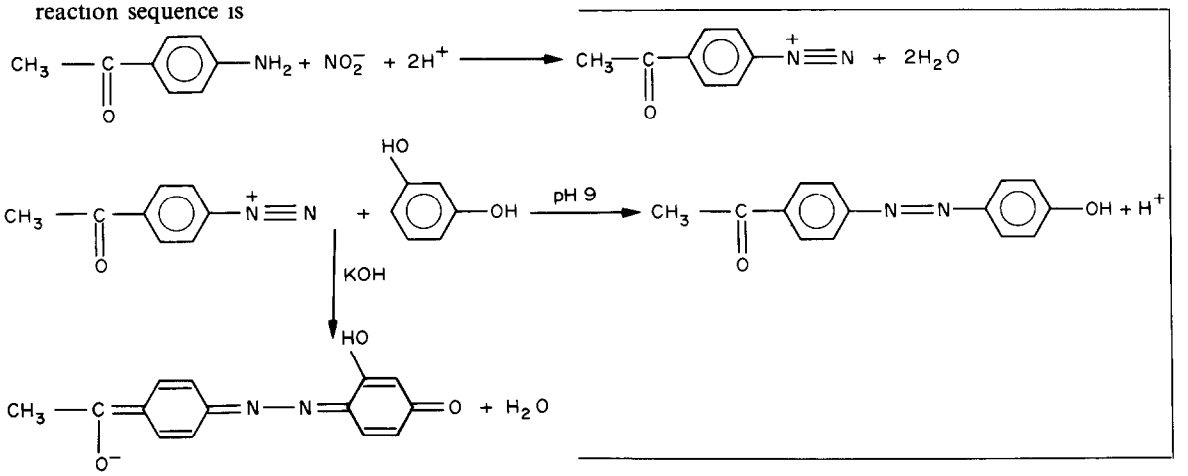

Effect of colour reagent concentration

With resorcinol as coupling agent, sulphanilic acid and *p*-aminoacetophenone (AAP) were tested as the substrates for diazotization, but only AAP gave a water-soluble dyestuff The effect of AAP and RSC concentration on the colour intensity was studied by using a fixed nitrite concentration and varying the AAP and RSC concentration The results showed that use of 2 ml of mixed reagent solution containing 1–4% AAP and 0 5–3% RSC gave constant and maximal absorbance Therefore use of 2 ml of 2% AAP–1% RSC solution is recommended

Effect of pH

The absorbance for a fixed amount of nitrite was determined at various pH values in the range 6–10 and also in strongly alkaline solution (Fig 2) The highest absorbance was obtained at pH 8–10, so pH 9 is recommended, and is attained by use of 6 ml of the mixed alkali solution. An alternative would be to use 0 5–1 0*M* potassium hydroxide medium, with rather lower sensitivity We attribute this pH effect to a combination of (*a*) competition between the coupling reaction and decomposition of the diazonium salt in very alkaline medium and (*b*) the deprotonation and structural change of the product at high pH The absence of the isosbestic point in the spectra (Fig 1) expected from (*b*) is due to the effect of (*a*)

Table 1 Effect of various ions on determination of 10 μg of nitrite

Foreign ion	Taken, *mg*	Ion/NO_2^-, *w/w*	NO_2^- found, μg
Zn(II)	2 0	200	9 8
Ni(II)	2 0	200	10 0
Mn(II)	2 0	200	10 0
Mo(VI)	2 0	200	10 0
Hg(II)	74 0	7400	10 0
Fe(III)	0 5	50	9 8
Bi(III)	0 5	50	10 0
Zr(IV)	0 5	50	10 0
Pb(II)	0 25	25	10 0
Cu(II)	0 10	10	10 2
Ag(I)	0 10	10	10 0
Se(IV)	0 10	10	10 0
Ce(IV)	0 05	5	10 0
V(V)	0 025	2 5	10 0
S^{2-}	7 0	700	10 1*
$S_2O_3^{2-}$	3 3	330	9 8*
$S_2O_4^{2-}$	2 5	250	9 8*
SO_3^{2-}	1 0	100	10 0*
I^-	5 0	500	10 2*
F^-	2 0	200	9 9

*After addition of 2 ml of 5% mercuric chloride solution, letting stand for 5 min, filtering off and washing with water

Table 2 Recovery of nitrite spikes from water and soil samples

Sample	Amount taken, *ml* or *g*	Nitrite, *μg*				
		Native	Added	Total	Recovered*	Error
Well water	40 0	0 87	5 0	6 0	5 13	+0 13
			10 0	10 9	10 02	+0 02
River water 1	40 0	3 04	2 0	5 4	2 36	+0 36
			5 0	8 1	5 06	+0 06
Lake water	40 0	6 40	2 0	8 1	1 70	−0 30
			5 0	11 2	4 80	−0 20
Sewage	1 0	6 60	2 0	8 8	2 20	+0 20
			5 0	11 7	5 10	+0 10
Red soil	1 0	0 92	5 0	5 7	4 78	−0 22
Alluvial soil 2	1 0	2 30	5 0	7 4	5 10	+0 10

*Recovered = total − native

Table 3 Comparison of nitrite determination in sample by proposed method and Saltzman method

Sample	Proposed method,* *ppm*	Saltzman method, *ppm*
Well water	0 022	0 024
River water 1	0 076	0 074
River water 2	0 022	0 030
Lake water	0 160	0 155
Sewage	6 60	6 70
Red soil	0 92	—
Black soil	0 83	0 81
Loess	1 60	1 60
Alluvial soil 1	1 96	1 92

*Mean of 3–6 determinations

Colour stability

Under the optimized conditions, the bright gold azo dye develops instantaneously and remains stable for 10 hr A temperature range of 15–30° gives the most useful results The limit of detection of nitrite by this method is 0 005 μg/ml. A statistical study of 6 water samples, each containing 75 7 ng of nitrite per ml, gave a relative standard deviation of 2 3%

Effect of foreign ions

The effect of various amounts of 20 foreign ions on the determination of nitrite was examined The results are listed in Table 1. Most of the cations and common anions do not interfere, S^{2-}, $S_2O_3^{2-}$, SO_3^{2-}, $S_2O_4^{2-}$ and I^- interfere but their effect can be mitigated by adding 2 ml of 5% mercuric chloride solution before the determination (Table 1)

Determination of nitrite in samples

The nitrite contents of water and soil samples were determined by the proposed method The results shown in Tables 2 and 3 are in reasonable agreement with those obtained by the standard Saltzman method No volume correction was applied for the mercuric chloride solution added, but is easily made if desired

REFERENCES

1 L J Dombrowski and E J Pratt, *Anal Chem*, 1972, **44**, 2268
2 D Jenkins, *Prog Water Technol*, 1977, **8**, 31
3 J P Griess, *Ber Dtsch Chem Ges*, 1949, **12**, 427
4 B E Saltzman, *Anal Chem*, 1960, **32**, 135
5 E Sawicki, T W Stanley, J Pfaff and A D'Amico, *Talanta*, 1963, **10**, 641
6 E Sawicki, *Anal Chem*, 1963, **35**, 2183
7 F Celardin, M Marcantonatos and D Monnier, *Anal Chim Acta*, 1974, **68**, 61
8 S E Allen, *Chemical Analysis of Ecological Materials*, p 203 Blackwells, Oxford, 1974
9 J A Dougherty and G A Laban, *Anal Chem*, 1975, **47**, 1130
10 B S Gard, Y L Mehta and M Katyal, *Talanta*, 1976, **23**, 71
11 J Gabbay, *Analyst*, 1977, **102**, 371

Talanta, Vol 30, No 5, pp 377–380, 1983
Printed in Great Britain

0039-9140/83/050377-04$03 00/0

ANALYTICAL DATA

A STUDY OF SOME NUCLEAR REACTION INTERFERENCES IN DETERMINATION OF NITROGEN CONTENT OF PLANT MATERIALS BY 14-MeV NEUTRON-ACTIVATION ANALYSIS

CH L NDIOKWERE* and P JERABEK
Chemistry Department, University of California, Irvine, CA 92717, U S A

(*Received* 1 *March* 1982 *Revised* 13 *July* 1982 *Accepted* 30 *November* 1982)

Summary—The nitrogen content of 10 medicinal plant species has been determined by fast-neutron activation analysis (FNAA) Correction factors for the effects of the $^{16}O(p, \alpha)^{13}N$ knock-on proton-induced reaction and the (n, 2n) reactions, which produce interfering positron-emitting radionuclides, have also been determined The total relative interference from the $^{16}O(p, \alpha)^{13}N$ and (n, 2n) reactions of K, Cl, Fe and Br was found to be 5 1–32 1% for the plant samples

In recent years much attention has been paid to the chemical composition and pharmacology of some Nigerian medicinal plant materials,[1–3] but their elemental composition has not yet been reported This study was aimed at determining the nitrogen content of these species by fast-neutron activation analysis (FNAA) based on the $^{14}N(n, 2n)^{13}N$ reaction Several authors have used nuclear methods for this purpose,[4–10] since FNAA is claimed to be better than the traditional Kjeldahl method in terms of rapidity, precision and accuracy A further disadvantage of the Kjeldahl method is that it cannot be used to determine nitrogen in nitrogen–oxygen groups satisfactorily The main problem encountered with FNAA for nitrogen is that in some complex samples a number of induced activities, which are also positron emitters, contribute to the 511-keV activity measured in the analysis Corrections for these contributions are therefore very important Although a number of authors[8,10–13] have discussed some of these interferences, little or no comprehensive quantitative study of the interfering reactions has been made In this work correction factors have been determined to account for the contribution of the reaction $^{16}O(p, \alpha)^{13}N$ and the (n, 2n) reactions of K, Cl, P, Fe, Cu and Br, to the nitrogen found. The same FNAA method can be used to determine the oxygen content, without any significant interference and with good precision This information is necessary to evaluate the contribution due to the $^{16}O(p, \alpha)^{13}N$ reaction

EXPERIMENTAL

Samples and standards

The parts of the plants analysed were mainly the roots, bark and leaves, which were collected fresh from the plants, sponged briefly in water and well rinsed with demineralized water to remove any surface contamination All the samples were air-dried, crushed and pulverized to pass a 200-mesh sieve

Benzoic acid (26 2% oxygen) and diphenylamine (8 3% nitrogen) were used as standards for the determination of oxygen and nitrogen respectively The samples and standards (in the range 0 5–1 0 g) were accurately weighed by difference, firmly packed in special polyethylene vials (volume about 2 5 ml) to ensure a minimum of trapped air, and heat-sealed for irradiation

Determination of oxygen

Oxygen was determined on the basis of the $^{16}O(n, p)^{16}N$ reaction by counting the 6 13 and 7 12 MeV spectral region for gamma-rays emitted by 7 1-sec half-life ^{16}N This high-energy gamma-radiation from the decay of ^{16}N is almost free from other spectral interferences The automated dual-activation facility (using the Kaman A-711 sealed-tube 14-MeV neutron generator, connected with a single-tube pneumatic-transfer and counting system of the University of California, Irvine) used for the determination of oxygen, which has been described in detail elsewhere,[14] is shown in Fig 1 The multiscaler counting of the spectral region was done with a 4 × 4 in NaI(Tl) detector and a Nuclear Data (ND 100) multichannel analyser The sample and standard pair was irradiated for 20 sec, allowed to decay for 20 sec, and counted for 20 sec

The pair was then reversed, irradiated and counted under the same conditions This process was repeated four times for each plant sample Average background counts were also determined for the sample and standard and appropriate corrections applied The calculated oxygen content of each sample was taken as the average of the four determinations

Determination of nitrogen

The apparent nitrogen content was determined by using the $^{14}N(n, 2n)^{13}N$ reaction induced by exposing the sample and standard to 14-MeV neutrons produced by the Kaman A-711 sealed-tube neutron generator at a flux of about $2\,0 \times 10^{11}$ n/sec The flux was monitored with a BF_3 counter shielded with a paraffin moderator The 511-keV positron-annihilation gamma-rays associated with the decay of ^{13}N were counted with a 3 × 3 in NaI(Tl) scintillation counter,

*Department of Chemistry, University of Benin, Benin City, Nigeria

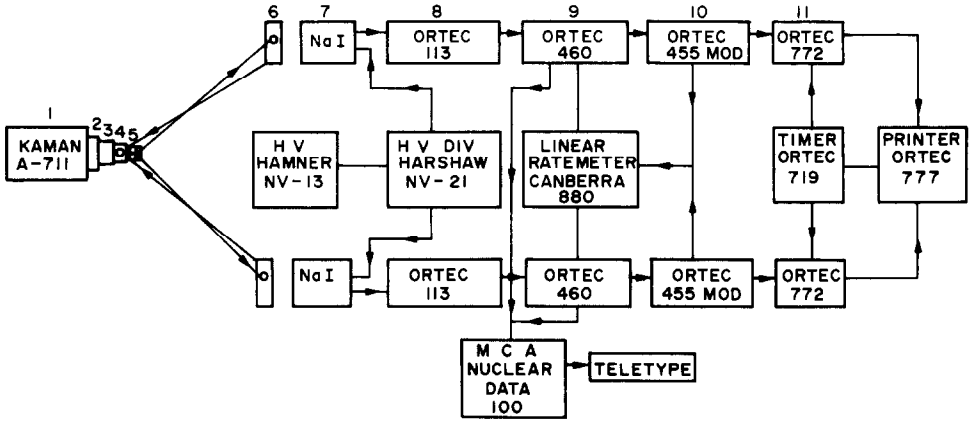

Fig 1 Dual-activation system for determination of oxygen (Reactor Facility, Chemistry Department, University of California) 1 Sealed-tube neutron generator 2 Target 3 Single-tube irradiation port 4 Dual-tube small sample irradiation port and rotation 5 Path of "vial" 6 Sample-counting ports 7 4-in NaI(Li) crystals and photomultiplier tubes 8 Preamplifiers 9 Amplifiers 10 Single-channel timing analysers 11 Printing scalers

Table 1 Possible interferences in nitrogen determination by the $^{14}N(n, 2n)^{13}N$ reaction

Reaction	Target nuclide abundance	14-MeV neutron cross-section, *mbarn*	Product half-life, *min*	Gamma-ray energy
$^{14}N(n, 2n)^{13}N$	99 63	5 7	9 96	β^+(511 keV)
$^{16}O(p, \alpha)^{13}N$	99 76	?	9 96	β^+
$^{13}C(p, n)^{13}N$	1 11	?	9 96	β^+
$^{12}C(p, \gamma)^{13}N$	98 89	?	9 96	β^+
$^{39}K(n, 2n)^{38}K$	93 09	4	7 71	β^+, pair production
$^{31}P(n, 2n)^{30}P$	100	11	2 5	β^+
$^{63}Cu(n, 2n)^{62}Cu$	69 1	550	9 76	β^+
$^{79}Br(n, 2n)^{78}Br$	50 52	1141	6 46	β^+
$^{81}Br(n, 2n)^{80}Br$	49 48	700	17 6	β^+
$^{54}Fe(n, 2n)^{53}Fe$	5 84	15	8 5	β^+
$^{35}Cl(n, 2n)^{34m}Cl$	75 77	?	32 2	β^+
$^{27}Al(n, p)^{27}Mg$	100	80	9 5	pair production
$^{28}Si(n, p)^{28}Al$	92 27	235	2 31	pair production
$^{30}Si(n, \alpha)^{27}Mg$	3 12	46	9 5	pair production
$^{56}Fe(n, p)^{56}Mn$	91 68	103	154 6	pair production

Table 2 Some correction factors for nitrogen determination

Compound	Element	Reaction	Counts/mg of element	Correction factor*
H_2O	O	$^{16}O(p, \alpha)^{13}N$	$3\,2 \pm 0\,03$	$(6\,8 \pm 0\,1) \times 10^{-3}$
Fe_2O_3	Fe	$^{54}Fe(n, 2n)^{53}Fe$	$14\,6 \pm 0\,4$	$(3\,1 \pm 0\,04) \times 10^{-2}$
$Ca_3(PO_4)_2$	P	$^{31}P(n, 2n)^{30}P$	$42\,0 \pm 0\,3$	$(9\,0 \pm 0\,1) \times 10^{-2}$
NaCl	Cl	$^{35}Cl(n, 2n)^{34m}Cl$	$92\,0 \pm 0\,2$	$0\,2 \pm 0\,02$
K_2SO_4	K	$^{39}K(n, 2n)^{38}K$	$74\,5 \pm 0\,4$	$0\,16 \pm 0\,002$
NaBr	Br	$^{79}Br(n, 2n)^{78}Br$	3419 ± 22	$7\,3 \pm 0\,1$
$CuSO_4$	Cu	$^{63}Cu(n, 2n)^{62}Cu$	4481 ± 12	$9\,5 \pm 0\,1$

*Apparent mg of nitrogen per mg of element, average counts/mg of $N = 471 \pm 5$

Table 3 Br, Cl, Fe and K concentrations in some Nigerian medicinal plants by thermal-neutron activation analysis

Sample	Br, *μg/g**	Cl, *mg/g**	Fe, *μg/g**	K, *mg/g**
P1	$3\,4 \pm 0\,1$	$0\,07 \pm 0\,02$	$17 \pm 0\,8$	$1\,53 \pm 0\,05$
P2	$19\,7 \pm 0\,3$	$0\,21 \pm 0\,03$	$26 \pm 0\,6$	$2\,72 \pm 0\,06$
P3	$6\,5 \pm 0\,2$	$0\,64 \pm 0\,05$	$61 \pm 1\,0$	$9\,9 \pm 0\,2$
P4	$16\,2 \pm 0\,2$	$0\,46 \pm 0\,05$	$113 \pm 1\,5$	$8\,5 \pm 0\,1$
P5	$13 \pm 0\,2$	$1\,89 \pm 0\,07$	$114 \pm 3\,4$	$6\,4 \pm 0\,1$
P6	$8\,5 \pm 0\,2$	$10\,6 \pm 0\,3$	$52 \pm 0\,4$	$29\,9 \pm 0\,6$
P7	$29\,5 \pm 1\,5$	$6\,8 \pm 0\,2$	$69 \pm 4\,2$	$37\,9 \pm 0\,7$
P8	$18\,2 \pm 1$	$2\,85 \pm 0\,12$	$81 \pm 2\,4$	$22\,6 \pm 0\,2$
P9	$20\,7 \pm 1\,4$	$5\,00 \pm 0\,2$	$99 \pm 2\,6$	$17\,5 \pm 0\,4$
P10	$15\,8 \pm 0\,9$	$1\,06 \pm 0\,05$	$88 \pm 1\,1$	$11\,8 \pm 0\,2$

*Dry weight

Table 4 Interference (%) of O, K, Cl, Fe and Br in nitrogen determination under the specified conditions

Sample	$^{16}O(p, \alpha)^{13}N$	$^{39}K(n, 2n)^{38}K$	$^{35}Cl(n, 2n)^{34m}Cl$	$^{54}Fe(n, 2n)^{53}Fe$	$^{79}Br(n, 2n)^{78}Br$	Total
P1	22 6	1 6	0 09	0 004	0 16	24 5
P2	12 1	1 5	0 14	0 003	0 50	14 3
P3	3 2	1 7	0 14	0 002	0 05	5 1
P4	10 2	4 2	0 28	0 010	0 37	15 1
P5	22 6	6 5	2 4	0 023	0 61	32 1
P6	4 5	7 5	3 3	0 003	0 10	15 3
P7	5 4	10 2	2 3	0 004	0 36	18 3
P8	4 9	6 0	0 94	0 004	0 22	12 1
P9	5 4	5 2	1 9	0 006	0 28	12 7
P10	7 1	4 6	0 50	0 006	0 29	12 5

connected through a linear amplifier to a single-channel analyser After irradiation for 5 min, the sample and standard were allowed to cool for 11 min before being counted for 10 min The contribution of the ^{30}P (half-life = 2 5 min) activity from the $^{31}P(n, 2n)^{30}P$ reaction, to the 511-keV spectral region, was significantly reduced by allowing this decay time The sample and standard were reversed and again irradiated and counted The net photopeak counts for each sample and standard pair were normalized and summed to give the total counts for sample and standard respectively The calculated apparent nitrogen content of each plant sample was the average of two determinations

The possible interfering positron-emitting activities induced mainly by the (n, 2n), (p, α) and (n, p) reactions are summarized in Table 1 [15] The determination of the correction factors for some of the reactions is described in the following section

Determination of correction factors for nitrogen

To assess the interferences in the nitrogen determination, standard compounds containing the elements of interest were run under the same conditions of irradiation, decay and counting as the plant materials For each element of interest two standard compounds were prepared Each pair was irradiated and counted, the pair was then reversed and the process repeated The net photopeak count for each run was irradiated and counted, the pair was then reversed and the process repeated The net photopeak count for each run element in the sample to give counts/mg of element Each pair was measured five times Similarly two samples each of various organic nitrogen compounds such as urea, piperidine, melamine, adenine, phenylenediamine and diphenylamine, were prepared and run as described above to determine counts/mg of nitrogen under the same irradiation, decay and counting conditions, each pair again being measured five times Where appropriate, corrections were applied to allow for the contribution of ^{13}N activity from oxygen The average for the six nitrogen compounds was taken as 471 ± 5 counts/mg of nitrogen, and was used to evaluate the correction factor for a given element This was arrived at by dividing the counts/mg of interfering element by counts/mg of nitrogen, to give apparent mg of N/mg of interfering element, as summarized in Table 2 Demineralized water was used to determine the correction factor from the $^{16}O(p, \alpha)^{13}N$ knock-on proton-induced reaction Duplicate samples run under the same conditions gave an average of 3 2 counts/mg of oxygen This interference and those from the (n, 2n) reactions were evaluated, and where necessary corrections were applied to the apparent nitrogen values found

The K, Cl, Br and Fe concentration levels in the plant materials, previously determined by instrumental thermal-neutron activation analysis, are presented in Table 3 These concentrations were used for the evaluation of percentage interference and corrected nitrogen concentrations

RESULTS AND DISCUSSION

The oxygen and corrected nitrogen concentrations obtained for the 10 plant species are presented in Table 5 The nitrogen concentration range of 0 8–2 2% for the woody roots and bark is within the reported range for woody angiosperms (1 2–3.8%), and that for the leaves (3 5–5 1%) compares satisfactorily with the range 3–7 5% reported for herbaceous vegetables and 4 3% for Bowen's kale [16] The oxygen concentration was in the range 41 6–51 5%, that reported for woody angiosperms and herbaceous vegetables is 41% and for Bowen's kale 39 7% [16]

The correction factors due to interference of the $^{16}O(p, \alpha)^{13}N$ and some (n, 2n) reactions are also given in Table 4 The predominant interferences in this study are the $^{16}O(p, \alpha)^{13}N$ $^{39}K(n, 2n)^{38}K$ and $^{35}Cl(n, 2n)^{34m}Cl$ reactions (Table 4) The correction factor for oxygen $6\,8 \times 10^{-3}$, is relatively high when

Table 5 Nitrogen and oxygen content (% dry weight) of some Nigerian plant species

	Plant sample	Part used	Oxygen	Nitrogen
P1	Khaya Ivorensis	bark	49 6 ± 0 4	1 0 ± 0 02
P2	Syncalasia Scabraida	root	50 7 ± 0 5	2 2 ± 0 04
P3	Nauclea Sp	root	41 8 ± 1 0	2 1 ± 0 07
P4	Clausenia Anisata	root	48 2 ± 0 5	2 1 ± 0 05
P5	Dennetia Tripetela	root	51 5 ± 0 5	0 8 ± 0 02
P6	Ageratum Conzoides	leaves	41 6 ± 0 4	4 6 ± 0 06
P7	Boerhavia Diffusa	leaves and small tubers	46 2 ± 0 4	4 0 ± 0 05
P8	Cassia Favanica	leaves	42 4 ± 0 4	5 1 ± 0 05
P9	Ocimum Bacilicum	leaves	41 6 ± 0 4	4 1 ± 0 05
P10	Azadirachita Indica	leaves	42 0 ± 0 4	3 5 ± 0 04

compared with the values of 1.6×10^{-3} and 2.6×10^{-3} reported by Nargolwalla and Przybylowicz[15] and by Bibby and Champion,[8] and it is difficult to account for this discrepancy. Since the samples were activated and counted in polyethylene vials, a blank correction for the small oxygen content of the polyethylene could be applied to the 3.2 counts/mg reported in Table 2, but it is most unlikely that it would be significant. The ranges of interference found in this study (oxygen 3.2–22.6% K 1.5–10.2% and Cl 0.09–3.3%) compare quite favourably with the corresponding values 19, 1.15 and 0.8% obtained by Leach *et al*.[12] under similar irradiation, decay and counting conditions. The contributions from carbon through $^{13}C(p, n)^{13}N$ and $^{12}C(p, \gamma)^{13}N$ reactions were not determined. They are presumably negligible compared to the errors of the analysis. Atmospheric nitrogen trapped in the irradiation vial could be a potential source of error, but since air was quantitatively displaced by the sample or standard, the error was likely to be negligible.

Acknowledgements—The authors wish to express their appreciation to the Chemistry Department, University of California, Irvine, for the provision of irradiation and other facilities. Financial support to the first author for this work from the IAEA, Vienna, is also gratefully acknowledged.

REFERENCES

1 O. O. Ogunkoya, O. O. Olubajo and D. S. Sondha, *Phytochemistry*, 1972, **11**, 2361
2 S. O. Fadulu, *J. Med. Plant Res.*, 1975, **27**, 122
3 A. A. Olaniyi, E. A. Sofowara and B. O. Oguntimehin, *ibid.*, 1975, **28**, 186
4 A. A. Prapuolenis and J. M. Bakes, *Radiochem. Radioanal. Lett.*, 1969, **1**, 19
5 W. H. Doty, D. E. Wood and E. L. Schneider, *J. Assoc. Offic. Anal. Chemists*, 1969, **32**, 953
6 D. E. Wood, W. H. Doty and E. L. Schneider, *Trans. Am. Nucl. Soc.*, 1971, **14**, 98
7 D. Brune and A. Arrayo, *Anal. Chim. Acta*, 1971, **56**, 473
8 P. M. Bibby and H. M. Champion, *Radiochem. Radioanal. Lett.*, 1974, **18**, 177
9 C. Segebade, *Z. Anal. Chem.*, 1977, **284**, 23
10 L. S. Chuang, D. A. Miller, W. P. Lay and W. Y. Chiu, *J. Radioanal. Chem.*, 1977, **38**, 279
11 W. D. James, W. D. Ehmann, C. E. Hamrin and L. L. Chyi, *ibid.*, 1976, **32**, 195
12 M. O. Leach, B. J. Thomas and D. Vartsky, *Intern. J. Appl. Radn. Isotopes*, 1977, **28**, 263
13 C. E. Hamrin, W. D. Ehmann and L. L. Chyi, *Fuel*, 1979, **58**, 48
14 A. Volborth, G. E. Miller and C. K. Garner, *Proc. Third Conf. Use of Small Accelerators*, Denton, Texas, 1974
15 S. S. Nargolwalla and E. P. Przybylowicz, *Activation Analysis with Neutron Generators*. Wiley, New York, 1973
16 H. J. M. Bowen, *Environmental Chemistry of the Elements*, pp. 92–93. Academic Press, New York, 1979

Talanta, Vol 30, No 5, pp 381–383, 1983
Printed in Great Britain

0039-9140/83/050381-03$03 00/0

CELLULOSE: A BIOPOLYMERIC SORBENT FOR HEAVY-METAL TRACES IN WATERS

P BURBA and P. G WILLMER
Institut fur Spektrochemie und angewandte Spektroskopie, Postfach 778, D-4600 Dortmund 1, Federal Republic of Germany

(*Received* 17 *November* 1982 *Accepted* 14 *December* 1982)

Summary—The sorption of dissolved heavy-metal traces on natural cellulose is characterized for the lower μg/l range It proceeds relatively rapidly, with half-times of about 1.5 min At neutral pH-values the distribution coefficients (K_d) of many cations, of various types, *e g*, Al^{3+}, Be^{2+}, Cd^{2+}, Cr^{3+}, Fe^{3+}, Pb^{2+}, Zn^{2+}, between cellulose and electrolyte solutions (*e.g*, NaCl) are of the order 10^1–10^4 In alkaline salt solutions K_d as high as 10^5 can be attained The role of cellulose as a sorbent for metal traces in natural waters is discussed

Cellulose has a highly porous and hydrophilic structure Like other hydroxyl-containing materials (*e g*, Al_2O_3 aq, SiO_2 aq), it tends to have manifold sorption interactions This characteristic is mainly exploited for the chromatographic separation of organic macromolecules (*e g*, enzymes, hormones, proteins),[1] but to some extent also for the separation of ions. However, there is little information on the sorption behaviour of cellulose towards dissolved trace elements in the ng/l–μg/l. range,[2-4] which is predominant for many heavy metals in natural waters Multifarious interactions (*e g.*, ion-exchange, sorption) between the aqueous and the solid phase (*e.g*, sediments, suspended matter) govern the solution concentrations and the transport of toxic metals in the aquatic environment. A considerable fraction of the solid matter in the hydrosphere, particularly in surface waters, consists of many organic materials,[5,6] for example cellulose and its derivatives In this respect, detailed information about possible sorption and enrichment of heavy metal traces on cellulose is important The aim of the present investigation was to characterize the sorption of metal traces on cellulose in the μg/l range

EXPERIMENTAL

Cellulose

Standardized short-fibred celluloses (*e g*, Schleicher & Schull 123/3, 124a and 180a, Merck Avicel® and No 2351), already available for liquid chromatography, were used For purification, each cellulose (10 g) was stirred in 2*M* hydrochloric acid (p a, 500 ml) for 5 hr at room temperature and then in acetone (p a, 500 ml) for 2 hr. After filtration it was air-dried

Reagents

Stock solutions of the elements Solutions containing 10 elements (100 μg/l concentration of each) were prepared from Merck Titrisols®

Sodium chloride solutions Prepared by dissolving the Merck "*Suprapur*" salt in triply distilled water Possibly interfering heavy-metal traces could be removed by means of a selective ion-exchanger (Cellulose-Hyphan®, Riedel de Haen)

Hydrochloric acid, 2M Prepared by dilution of the Merck "*Suprapur*" acid with triply distilled water

All other reagents were of analytical grade

Procedure

The distribution coefficients K_d (w/v) of metal traces between cellulose and saline solutions were determined from the metal loading of the cellulose, by the batch method For this purpose, the trace elements, each at the 20-μg/l level, were shaken separately or together with 0 1 g of cellulose in 500 ml of 0 5*M* sodium chloride for 1 hr The kinetics of the metal sorption could be determined in a similar manner, the cellulose being separated by a fast filtration step at appropriate intervals of time The trace metals adsorbed on the cellulose were eluted with 2 ml of 2*M* hydrochloric acid and subsequently determined in the eluate by a flame-AAS micromethod (the injection method) [7] A Pye–Unicam SP 9 instrument was used under standard conditions for flame-AAS

RESULTS AND DISCUSSION

Figure 1 shows the kinetics of sorption of Fe^{3+} and

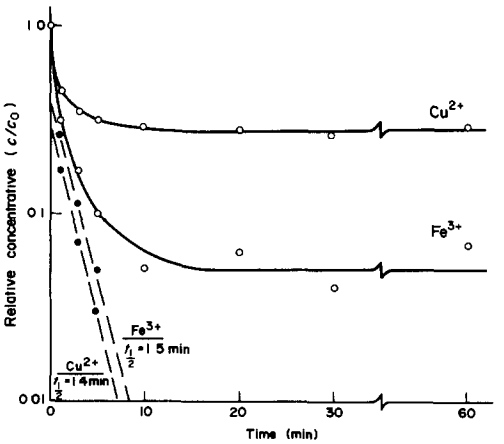

Fig 1 Sorption of iron(III) and copper(II) traces (20 μg/l) on 0 1 g of cellulose as a function of time, from 1-g/l NaCl, 200-mg/l Ca^{2+} solution (100 ml, pH 9), —●—●— $\triangleq (c - c_{equilibrium})/c_0$

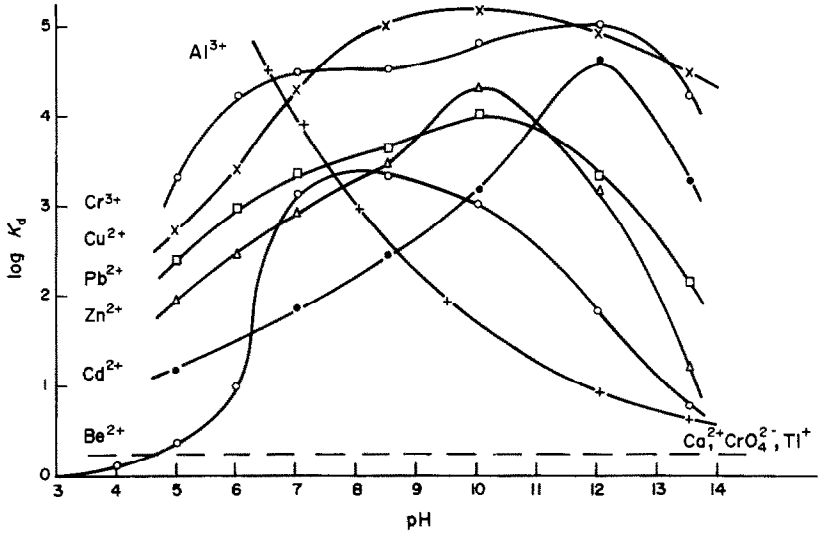

Fig 2 Distribution coefficients (K_d) of metal ion traces (each 20 μg/l) between cellulose and 0 5*M* NaCl, as a function of pH

Cu^{2+} (each 20 μg/l) on cellulose (0 1 g) in 100 ml of saline solution (containing 0 1 g of sodium chloride and 10 mg of Ca^{2+}, pH 9 0) When the concentration ratio c/c_0 (c_0 = initial concentration) is logarithmically plotted as a function of time, half-times of about 1 5 min can be established for the sorption of Cu^{2+} and Fe^{3+} on short-fibred cellulose Other heavy-metal traces are adsorbed on cellulose at similar rates Thus, equilibrium between cellulose and a saline solution can be attained within a few minutes, even if only a small amount of the solid matter is distributed in a large volume of solution The trace sorption on cellulose proceeds considerably faster than on many inorganic sorbents (*e g*, Al_2O_3 aq, SiO aq, TiO_2 aq),[8,9] which are substantial mineral components of natural sediments and suspended matter

Some distribution coefficients (K_d) of metal traces between short-fibred cellulose and 0 5*M* sodium chloride are shown as functions of pH in Fig 2 These K_d-values are more or less dependent on the pH, with the exception of those for Ca^{2+}, CrO_4^{2-} and Tl^+, which exist as free ions over a wide pH range Even in neutral solutions (pH 5–8) many metals are enriched on cellulose by a factor of 10^2–10^4, among them are the toxic species Be^{2+}, Cd^{2+} and Pb^{2+} Therefore cellulose, as a component of the solid phase in aquatic systems, can play an important role with regard to the binding and the remobilization of metal traces in waters On the other hand, the distribution coefficients of about 10^5 that can be reached on cellulose in alkaline solutions (pH 10–12) are very interesting for analytical trace enrichment [4]

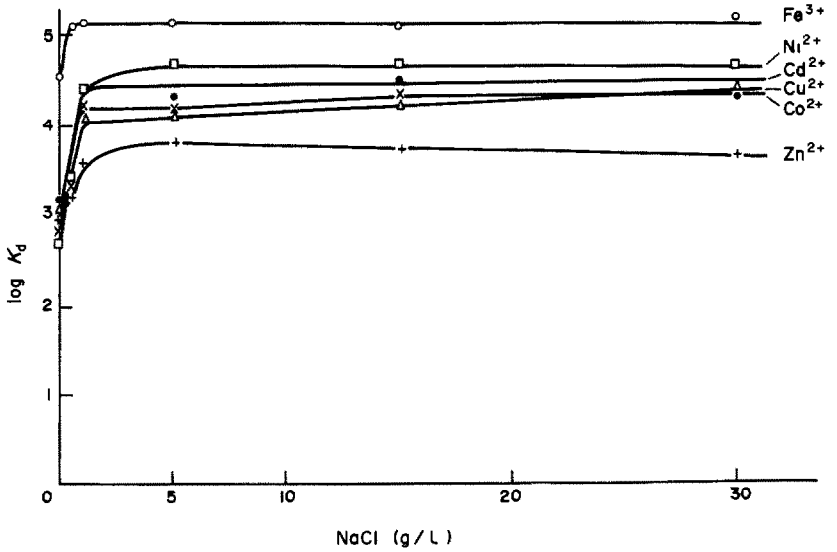

Fig 3 Influence of electrolyte solution concentration (0–30 g/l NaCl) on heavy-metal sorption (Cd^{2+}, Co^{2+}, Cu^{2+}, Fe^{3+}, Ni^{2+}, Zn^{2+}, each 20 μg/l) on cellulose

Table 1 Distribution coefficients (w/v) on different celluloses for metal ions at the 20-μg/l level (pH 11 0)

	log K_d					
Element	Cellulose S & S* 123/3	Cellulose S & S* 123ag	Linters S & S* 124a	Powder S & S* 180a	Powder Avicel® Merck 2330	Native cellulose Merck 2351
Cd^{2+}	3 73	3 58	3 51	3 80	3 85	3 74
Co^{2+}	4 99	4 30	3 85	4 60	4 57	4 98
Cu^{2+}	4 25	4 12	4 10	4 50	3 75	4 75
Fe^{3+}	$\geq$ 5 0	$\geq$ 5 0	$\geq$ 5 0	$\geq$ 5 0	$\geq$ 5 0	$\geq$ 5 0
Mn^{2+}	4 0	3 95	3 72	4 05	3 94	4 40
Pb^{2+}	3 67	3 90	3 70	3 80	3 85	3 85

*Schleicher & Schull

Another remarkable result is the very different sorption of Cr(III) and Cr(VI) species on cellulose For example, it makes possible their analytical separation and speciation in natural waters

The K_d-values found for individual species, *e g*, Cu^{2+}, Zn^{2+}, at neutral pH (*e g*, pH 8) in 0 5*M* sodium chloride prove to be nearly constant (*e g*, 10^3 for the two just mentioned) over large concentration ranges (*e g*, from 200 ng to 1 mg per litre) However, in the presence of other trace metals [*e g*, iron(III) at concentrations of some 100 μg/l], a considerable synergistic enhancement of the distribution coefficients occurs

Figure 3 shows the influence of electrolyte concentration (sodium chloride, 0–30 g/l) on the heavy-metal sorption (Cd^{2+}, Co^{2+}, Cu^{2+}, Fe^{3+}, Ni^{2+}, Zn^{2+}, each at the 20-μl level), on cellulose at pH 11 In the absence of sodium chloride, the distribution coefficients reach values of 500–2000, with the exception of Fe^{3+} However, even a 1 5–2 g/l concentration of sodium chloride will enhance the K_d-values by a factor of about 30 At higher salt levels, the distribution equilibria seem to be nearly constant Similar salt effects can be observed in neutral suspensions of cellulose In contrast to these results, other materials investigated as sorbents in natural waters[10–12] tend to give remobilization of fixed heavy-metal traces at higher salt concentrations

Different kinds of cellulose (*e g*, wood and linters cellulose, amorphous and microcrystalline cellulose) are compared in Table 1 in terms of the distribution coefficients of heavy metals at pH 11 As the comparison establishes, the distribution coefficients for a given element are practically independent of the species of cellulose used

In this paper we indicate the important role which can be attributed to cellulose (besides humic substances) in the various processes for distribution of essential and toxic metal traces between the solid and solution phase in the hydrosphere Presumably, the results of the investigation can be transferred to native cellulose-species in waters Ion-exchange and/or chemisorption are possible binding mechanisms for the metal traces The knowledge of such processes and the resulting binding of heavy-metal traces in the aquatic environment is of increasing importance

REFERENCES

1 E A Peterson, *Cellulose Ion-Exchangers* North-Holland Publishers, Amsterdam, 1970
2 H Farrah and W F Pickering, *Austr J Chem*, 1978, **31**, 1501
3 P Burba and W Schafer, *Erzmetall*, 1981, **34**, 582
4 P Burba and P G Willmer, *Vom Wasser*, 1982, **59**, 139
5 U Forstner and G Muller, *Schwermetalle in Flussen und Seen*, p 78 Springer Verlag, Berlin, 1974
6 U Forstner and G T W Wittmann, *Metal Pollution in the Aquatic Environment*, p 220 Springer Verlag, Berlin, 1979
7 H Berndt and E Jackwerth, *At Abs Newsl*, 1976, **15**, 109
8 F Ambe, P Burba and K H Lieser, *Z Anal Chem*, 1979, **295**, 13
9 K Lieser, S Quandt and B Gleitsmann, *ibid*, 1979, **298**, 378
10 W Calmano and K H Lieser, *ibid*, 1981, **307**, 356
11 U Forstner and W Calmano, *Vom Wasser*, 1982, **59**, 83
12 J Slavek, J Wold and W F Pickering, *Talanta*, 1982, **29**, 743

Talanta, Vol. 30, No. 6, pp. 385–400, 1983
Printed in Great Britain.

0039-9140/83/060385-16$08.00/0

TALANTA REVIEW*

TRACE ELEMENT ANALYSIS BY PARTICLE AND PHOTON-INDUCED X-RAY EMISSION SPECTROSCOPY

B. GONSIOR and M. ROTH
Institut für Experimentalphysik, Ruhr-Universität Bochum, Postfach 102148, D-4630 Bochum, F.R.G.

(*Received* 7 *January* 1982. *Revised* 29 *June* 1982. *Accepted* 27 *December* 1982)

Summary—The analytical use of particle- and photon-induced X-ray emission spectroscopy has become an important tool in trace element analysis, especially when only small amounts of sample material are available. The physical basis, experimental procedure and typical examples are reviewed.

Moseley's law was the starting point for the application of characteristic X-ray emission to elemental analysis. Since then there have been many developments, culminating in the wide range of modern techniques.

Matter can be analysed in two main ways, either by determination of the mean elemental composition or by examination of the local microstructure. Over the past ten years there has been a broad development of techniques based on characteristic X-ray emission for both types of analysis. This was assisted by the availability of particle accelerators and of semiconductor detectors with high energy-resolution. Ion beams from accelerators have been used as well as photons to induce characteristic X-rays.

The physical principles of induced X-ray emission and examples of applications have been reviewed.[1–4] Conferences have been devoted to this topic[5,6] and particle-beam analytical work and trace element analysis have also been discussed.

The aim of this paper is to review the use of induced X-ray emission for quantitative analytical purposes over a wide range of concentrations down to the ppm level. The main interest will be restricted to the determination of trace elements.

INDUCED X-RAY EMISSION

Characteristic X-ray emission

Moseley's law gives a relationship between the wavelength of the emitted radiation and the atomic number Z of the element. Characteristic X-rays are emitted whenever vacancies in inner atomic shells are filled by outer electrons. The wavelength is related to the difference in binding energy of the electronic shells participating in the transition and is therefore characteristic of the emitting atom. There are also radiationless processes in which the transition energy is used for the ejection of outer shell electrons (Auger effect) or to promote transitions between subshells (Coster–Kronig transitions). These processes reduce the probability of X-ray emission from lower shells. The ratio of vacancies filled by emission of X-ray quanta to the total number of vacancies in a shell is called the fluorescence yield ω. The K- and L-shell fluorescence yields of the elements have been tabulated but yields from the M-shells are only poorly known.[7] The dependence of K-shell fluorescence yield on atomic number is represented in Fig. 1. The L-shell fluorescence yield depends on the subshell under consideration, *e.g.*, for lead,[7] $\omega_{L_1} = 0.1$, $\omega_{L_2} = 0.4$, $\omega_{L_3} = 0.35$. There are various types of electromagnetic transition but for elemental analysis only the electric dipole type is relevant. In Fig. 2 an energy-level scheme is given, showing the main X-ray transitions. Unfortunately, for historical reasons there is some confusion in labelling the different transitions and here we use that given by Bearden.[8] The K-radiation consists of two groups, K_α and K_β, which can be resolved by use of silicon solid-state

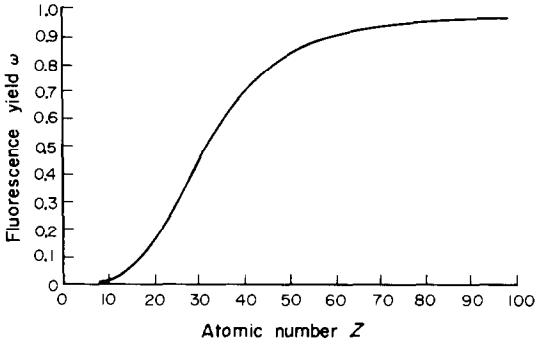

Fig. 1. Variation of K-shell fluorescence yield ω with atomic number, Z.

*For reprints of this review see Publisher's announcement near the end of the issue.

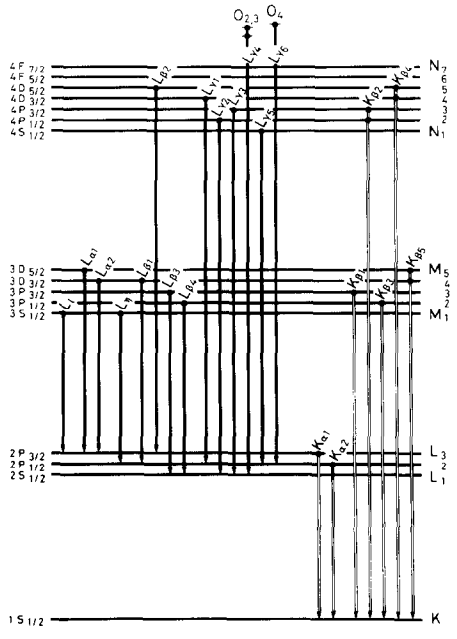

Fig. 2. Energy level scheme for the most intense X-ray transitions.

detectors. The L-radiation also consists of several groups which may be separated if the resolving power of the detector is high enough.

Inner shell ionization

The production of a vacancy in an inner atomic shell, by means of photons, electrons or ions, arises from the electromagnetic interaction between the bound electron and the incident particle. The necessary condition is that the energy of the projectile should exceed the binding energy E_B of the electron under consideration.

Whenever a vacancy is generated by ejection of an electron, characteristic X-ray quanta are emitted. The probability of emission is described by the cross-section for production of X-rays, σ_x, defined as

$$\sigma_x = \frac{(\text{number of X-ray emitting reactions}) \times (\text{target particle})^{-1}.\text{sec}^{-1}}{(\text{number of incident particles}).\text{sec}^{-1}.\text{cm}^{-2}}$$

The unit for the cross-section is 1 barn $= 10^{-24}$ cm^2. We can describe σ_x as the product of the fluorescence yield ω and the cross-section for producing vacancies in a certain inner shell σ_I:

$$\sigma_x = \omega\sigma_I$$

The analytical aim is to find the number of emitting atoms and this may be expressed as the mass of these atoms per unit area of the sample surface penetrated by the beam, the so-called mass layer of the target (units g/cm^2). From the known area under irradiation we can derive the mass of the substance (in g). In this way a measure of the amount of substance under investigation with respect to the total target specimen, *i.e.*, the concentration, is obtained.

The excitation or ionization of inner shells has been investigated for many years[9,10] and cross-sections can now be fairly confidently predicted.[11,12]

Excitation by incident ions. Ionization with high-velocity ions can be described in terms of the Coulombic interaction of the projectile (assumed to be a point charge) with an electron in the target atom. This is valid when the atomic number Z_p of the projectile is much smaller than that of the target atom, Z, *e.g.*, for protons and $Z > 12$.

For quantitative work based on the intensity of the experimentally detected X-rays, the ionization cross-sections must be known. These can be measured beforehand or theoretical predictions can be used. Both methods give results in good agreement when protons are used as the projectiles. Alternatively, standard samples can be used, a common procedure in analytical work. In any case it is useful to inspect the ionization cross-section for the electron shell considered, as a function of the projectile energy, mass and charge and of the atomic number of the atom to be ionized, since the sensitivity and the optimum experimental conditions can then be estimated. The cross-section rises with increasing projectile energy (E_p),[13] reaching a maximum when the projectile velocity equals the orbital velocity of the electron. At higher projectile velocities the cross-section decreases at a rate roughly proportional to $1/E_p$. This relationship between cross-section and the energy of the projectile is represented in Fig. 3, where the energy is given in units of $(m_p/m_e)E_B$. For example, with proton-excitation the cross-section for K-shell ionization of iron ($Z = 26$, $E_B = 7.1$ keV) rises as the energy of the protons is increased to 14 MeV. The ionization cross-section decreases drastically with increase in Z because of the increase in binding energy of the electrons. This is represented in Fig. 4, for K- and L-shell ionizations.

There is also a relationship between the ionization cross-section and the atomic number of the projectile, which can be described by the scaling law

$$\sigma_I(\text{projectile } p, E_p) = Z_p^2\,\sigma_I(\text{proton}, E_p/A_p)$$

which relates σ_I for any projectile with mass number A_p, atomic number Z_p and energy E_p to σ_I for a proton with energy E_p/A_p.

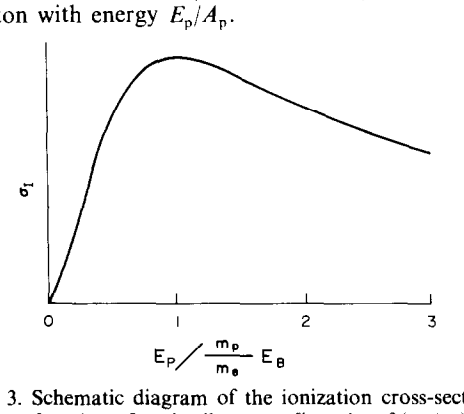

Fig. 3. Schematic diagram of the ionization cross-section, σ_I, as a function of projectile energy [in units of $(m_p/m_e)E_B$].

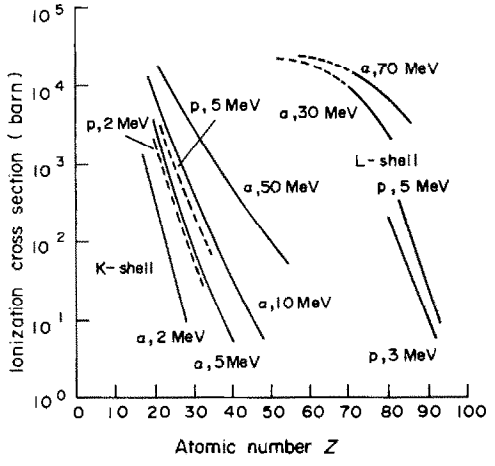

Fig. 4. Variation of K- and L-shell ionization cross-sections with atomic number Z for protons and α-particles of different energies.

Excitation by photons. If the energy of a photon exceeds the binding energy of an electron in a given atomic shell, then in the energy of 1–200 keV, absorption takes place with the photoionization of inner-shell electrons. Figure 5 shows the dependence of some experimentally determined photoionization cross-sections of the K-shell on the exciting photon energy. Photoelectric absorption cross-sections have been tabulated by Veigele[14] for photon energies ranging from 0.1 keV to 1 MeV. The error is said to be 2–5% for energies higher than that corresponding to the K-absorption edge.

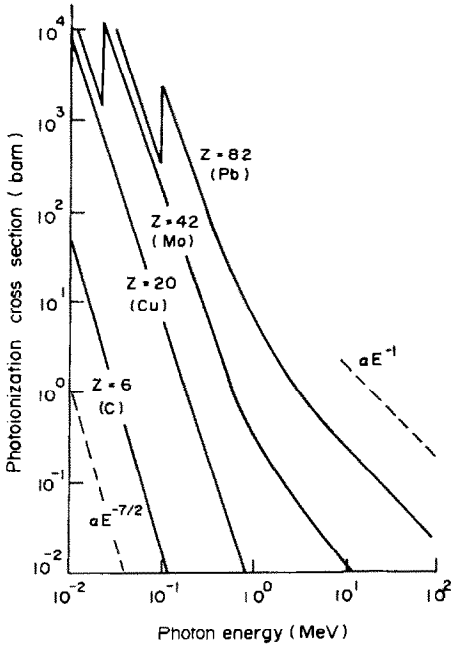

Fig. 5. K-shell photoionization cross-section of different elements as a function of photon energy.

From these numbers cross-sections $\sigma_{K_\alpha,L_\alpha}(E_0, Z)$ for the production of K_α or L_α X-rays, can be obtained by using the formula

$$\sigma_{K_\alpha,L_\alpha}(E_0, Z) = \sigma_{\text{photo}}(E_0, Z) \times j_{K,L_3}(Z) \times t_{K_\alpha,L_\alpha}(Z) \times \omega_{K,L_3}(Z)$$

where $\sigma_{\text{photo}}(E_0, Z)$ is the total photoelectric absorption cross-section, E_0 is the photon energy, $j_{K,L_3}(Z)$ is the relative contribution of the K or L_3 shell to the total photoelectric absorption cross-section when the K_α or L_α radiation is analysed, $t_{K_\alpha,L_\alpha}(Z)$ is the relative rate of emission of the K_α or L_α radiation compared to the K or L radiation, respectively, and ω_{K,L_3} is the fluorescence yield for the K or L_3 shell. The values for j_K,[15] t,[16] and ω have also been tabulated.

The cross-sections for the production of K_α X-rays (which depend upon the atomic number of the trace element), calculated in this way, are shown in Fig. 6 for the different excitation sources used in X-ray fluorescence. From Fig. 6 it is possible to identify the appropriate photon energy for the determination of an element, since this will be just above the K-absorption edge for the element.

PRINCIPLES OF THE USE OF INDUCED X-RAY EMISSION FOR TRACE ELEMENT ANALYSIS

Wavelength-dispersive methods are limited in application and will not be discussed. In energy-dispersive X-ray spectrometry the gas proportional counter is a widely used and simple detector.[17,18] It is relatively inexpensive but its usefulness is limited owing to its poor energy resolution, typically about 15% FWHM [full (peak) width at half maximum] for 5.9-keV (Mn) X-rays. This instrument is particularly handy when interest is centred on a small number of elements.

The semiconductor (Si and Ge) detectors are more widely applicable and their rapid development has brought X-ray spectrometers widely into use for trace

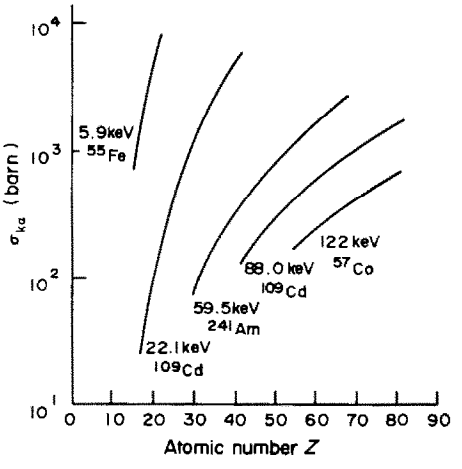

Fig. 6. K_α-production cross-section *vs.* atomic number for different X-ray sources.

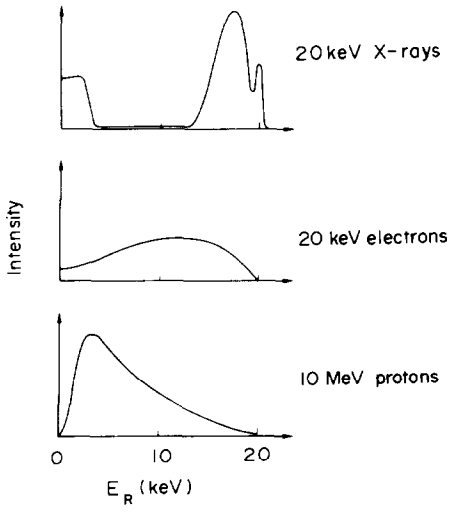

Fig. 7. Background spectra obtained with the three different excitation mechanisms used in X-ray analysis.

element analysis. This is true for ion-, photon- and electron-induced X-ray fluorescence. The last two methods have long been in use but the first application of particle-induced X-ray emission (PIXE) was not published until 1970.[19] The energy resolution of semiconductor detectors is sufficient to resolve the K_α or L_α lines of neighbouring elements, rendering possible the simultaneous determination of these elements. As can be seen from Fig. 4, either K or L radiation can be used for analysis, according to whether K- or L-shell ionization results in a higher yield in the detector. Although the energy resolution is generally adequate, problems may arise in certain cases, *e.g.*, in determination of a trace element in the presence of large amounts of neighbouring elements. There are also interference problems when the K-line of one element falls close to the L-line of another, *e.g.*, As K_α and Pb L_α. To arrive at a quantitative analysis, a relation between the intensity of the characteristic X-ray line and the amount of the trace element under investigation has to be established.

The applicability and sensitivity of the method depend on the ratio of the characteristic X-ray yield to the amount of background radiation in the energy region of the X-ray line. Therefore an estimation of the sensitivities achievable requires not only a knowledge of the ionization cross-section and fluorescence yield, but also a consideration of the background contributions. The background spectra for the three different excitation methods are shown schematically in Fig. 7. The background in PIXE is dominated by bremsstrahlung created by the stepwise slowing down of energetic secondary electrons arising as a result of scattering of the ion-beam in the target, resulting in continuous spectrum. In excitation by electrons, the background is dominated by the slowing down of the primary electrons in the target. In a broad energy region this background is much higher than that obtained by excitation with ions or photons, and the sensitivity is lower by about two orders of magnitude. Finally, the background spectrum obtained by using photon excitation contains mainly the primary line of the exciting photons, arising from Rayleigh scattering in the target, and a continuous region at lower photon energies, due to Compton scattering in the target. The background contribution depends on the experimental conditions and an estimation of the sensitivity refers only to a given experiment since the sample matrix is the main source of the background.

It has been shown in some fundamental investigations[1,2,20] that in PIXE analysis, sensitivities in the ppm region can be achieved for all elements. Less than 1 mg of sample may be sufficient. The detection limits obtained depend on the sample area irradiated. With a beam of 5 mm^2 cross-section, a sample density of 10 μg/cm^2 and a sensitivity of 1 in 10^5, quantities as low as 5 pg can be detected. Collimating the beam to a smaller diameter results in an even lower detection limit. With a beam diameter of 10 μm and a beam current of 1 nA, quantities of 10^{-16} g become detectable. It has been demonstrated that well-collimated ion beams and PIXE can be used to investigate lateral trace element distributions with high spatial resolution and sensitivity.[21–23] The sensitivity obtainable with photon excitation is only slightly smaller than that with proton excitation.[1,24]

Particle-induced X-ray emission (PIXE)

The observed ion-induced X-ray spectra contain the characteristic spectral lines of the trace elements and a continuous background in the same energy range. Two processes mainly contribute to the background: Compton scattering[25] and production of bremsstrahlung by secondary electrons. Figure 8 shows the bremsstrahlung background in the X-ray

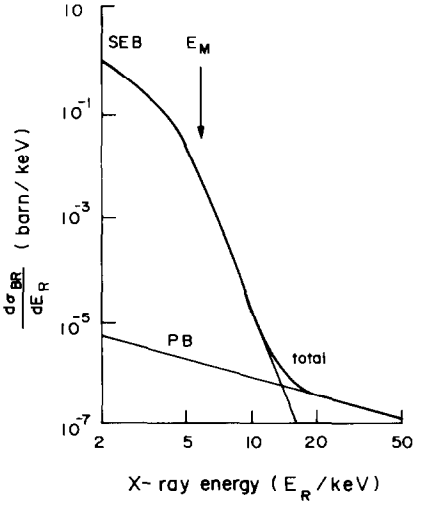

Fig. 8. Differential bremsstrahlung cross-section for 3-MeV proton irradiation of a carbon matrix. The background consists of secondary electron bremsstrahlung (SEB) for lower energies and of proton bremsstrahlung (PB) for higher energies.

energy region used for analysis, in the case of 3-MeV protons impinging on a carbon foil. The secondary electron bremsstrahlung (SEB) dominates at energies below and around E_M, the highest amount of energy transferable to a free electron (mass m_e) at rest by a projectile of mass m_p and energy E_p ($E_M \sim 4E_p m_e/m_p$). The cross-section for bremsstrahlung production decreases with increasing X-ray energy, slowly at energies $< E_M$ but rapidly at $> E_M$. At higher energies production of projectile bremsstrahlung (PB) dominates and is almost independent of the X-ray energy.

The Compton scattering increases with projectile mass and energy.[25] To suppress this background contribution, nuclei with low-energy nuclear levels, such as ^{19}F and ^{23}Na, should be absent from the target and environment.

Yield of characteristic X-rays. The measured X-ray yield is determined by physical quantities such as X-ray emission cross-section (which is dependent on projectile energy and atomic number, the fluorescence yield, the efficiency of the X-ray detector, the absorption in any material between sample and X-ray detector, and the solid angle of the X-ray detector. The relationship between the measured X-ray yield for a certain K or L spectral line and the mass of a specific element is thus given by the formula:

$$Y_x = \frac{\sigma_I \omega T_M N_A \Omega \epsilon n}{4\pi A \sin\theta}$$

where Y_x is the measured X-ray yield, σ_I the ionization cross-section, ω the fluorescence yield, T_M the mass layer (g/cm^2), N_A Avogadro's number, A the relative molar mass, Ω the solid angle of the Si(Li) detector, ϵ the efficiency (including all absorbing components of the set-up), n the total number of projectiles and θ the target angle with respect to the beam axis. Depending on the atomic number Z of the element under consideration, the physical and instrumental factors can be combined to give the so-called "yield factor" for characteristic X-rays, ρ_x, defined as

$$\rho_x = \frac{\sigma_I \omega \Omega \epsilon N_A}{4\pi \sin\theta}$$

and the experimentally determined mass layer is given by

$$T_M = \frac{Y_x A}{\rho_x n}$$

From these equations and the measured X-ray yield, the mass layer of the trace element under investigation, *i.e.*, the mass per unit area, can be determined by one of the following methods. By use of the theoretical ionization cross-sections,[11,12] the tabulated values of fluorescence yield[7] and the measured X-ray yield, the mass layer can be determined provided that the detector efficiency, detector solid angle, corrections for absorption and total number of projectiles are known. This is difficult and subject to error.

The method of X-ray yield curves is recommended in those cases where a large number of analyses is to be performed with the same apparatus. The yield factors ρ_x can then be determined for a set of elements by using pure targets of known thickness. Since the yield factors include the properties of the detector system they are only valid for the same system. The smooth dependence on Z allows fitting of the experimental yield factors of different elements and the interpolation of the yield factors for all elements, resulting in the so-called "yield curves". The determination of the yield factors and the resulting yield curves has been described elsewhere.[26] A similar method may be used for the routine determination of a few trace elements when standard samples are available. Quantitative analysis of the sample is then possible by direct comparison with the standard. The sample and standard must be similar in chemical composition, thickness and analyte concentration.

Detection limits. These depend on the ratio of X-ray yield to background and hence on the nature and energy of the projectile. The detection limit can be defined as the ratio of X-ray peak to background radiation, both measured in the energy region given by the peak energy $\pm$FWHM. This ratio should be at least unity. This criterion for the detection limit is independent of experimental conditions such as measurement time or intensity of the exciting beam. A disadvantage of this definition arises from the relationship of certainty of identification to statistical accuracy of the measurement. It is more useful to define the detection limit as the mass layer for which the number of pulses in the peak, N_{min}, is given by $N_{min} = 3\sqrt{N_b}$, where N_b is the number of background pulses measured over the same energy range as the peak (peak maximum $\pm$ FWHM). The detection limit derived in this manner depends on experimental parameters such as detector solid angle, detector resolution, number of projectiles and target thickness.

To minimize the limit of detection, the support material for the sample has to be chosen so as to keep the background small. It should therefore have low atomic number, and also high thermal and electrical conductivity to give rapid dissipation of heat and charge arising from the impact of the particle beam on the target. Samples are therefore usually deposited on carbon or organic materials, *e.g.*, "formvar", "hostaphane", "nuclepore", and basic investigations can be performed with thin carbon foils. In Fig. 9 minimum detectable concentrations are given as a function of the atomic number of the trace element under investigation, for protons of several energies and for ^{16}O-ions. Similar curves have been published by many authors.[1,2,20,27] These permit the following conclusions to be drawn.

Concentrations of less than 1 μg/g can be detected in thin samples.

Protons are preferable to heavy ions because of the lower background due to Compton scattering.

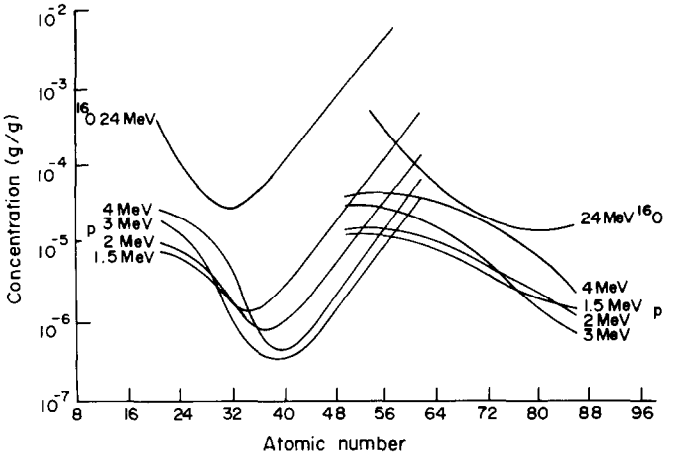

Fig. 9. Minimum detection limits *vs.* atomic number for protons of four different energies between 1.5 and 4 MeV and for ^{16}O ions of 24 MeV, *i.e.*, 1.5 MeV/amu.

For elements with $Z < 50$, measurement of K X-rays gives the highest sensitivity. For elements with $Z > 50$ higher sensitivity is obtained by using the L X-rays (neglecting peak interference).

The position of the minimum in the detection-limit curve depends upon the nature and energy of the projectile.

The highest sensitivity is obtained for elements with Z between 20 and 30.

Photon-excited X-ray fluorescence (XRF)

Background radiation. Photon excitation also generates background radiation from the matrix material, which limits the sensitivity of the method. The main contribution to this background is from scattering of the primary photons. The primary photons can be scattered by the bound electrons (Rayleigh scattering) without energy loss by ionization or excitation. This results in the so-called "coherent peak" in the X-ray spectrum, at the incident photon energy. There is also Compton scattering of the primary photons by free electrons. The scattered photon has an energy lower than the incident energy E_0. This results in the Compton peak in the X-ray spectrum at the energy

$$E_c = E_0 \Big/ \left[1 + \frac{E_0}{m_e c^2}(1 - \cos\alpha) \right]$$

where m_e is the electron mass, c the velocity of light and α the angle between the incident and scattered photons. The photoelectric interaction of the primary photons with the atoms of the matrix results in the emission of photoelectrons. In many cases the matrix consists of material with low Z, and hence electrons with low binding energy. As a result the total energy of the incident photon can be transferred to the electron. The bremsstrahlung of these electrons forms a continuous background, up to the energy E_0.

The detection process can make further contributions to the background radiation. After the interaction of photons with the detector material, photoelectrons may escape from the surface layer and their energy be lost in the detection process. In a similar way bremsstrahlung and characteristic X-ray quanta may escape from the detector. All these processes give rise to escape lines and to a continuous background in the X-ray spectrum.

Yield of characteristic X-rays. Information on the dependence of X-ray yield on the energy of the primary photons and the atomic number of the analyte elements is also of importance for XRF analysis, but not strictly necessary, since in practice the use of standards is more convenient. Nevertheless, to define experimental conditions for highest sensitivity, information about the X-ray production cross-section and its energy-dependence is essential.

The cross-section for production of K and L X-rays is derived from the photoelectric cross-section and the fluorescence yield and relates the mass layer of an element to the measured characteristic X-ray yield. Also included are experimental parameters such as efficiency and the solid angle of the detector, numbers of impinging photons and the geometry of the experiment. Assuming a fixed geometry and a given photon energy the mass layer (T_M) may be expressed as:

$$T_M = \frac{Y_x A}{\rho_x I}$$

where I is the number of impinging photons and the yield factor ρ_x combines various factors as before. For analytical work the yield factors can be determined for a set of elements by using standard targets for calibration to determine the absolute amount of trace element(s) present.

Detection limits. As in the case of ion-excitation, the detection of trace elements by their characteristic X-ray yield is limited by the interference of the background in the same spectral region. The detection limits depend on the photon source used. For

example Rhodes *et al.*[28] quote detection limits for the analysis of air samples (deposits on cellulose filters); with photon excitation and optimum experimental conditions[1,24] a sensitivity close to that attainable with PIXE could be achieved. The lowest detectable concentrations were 10^{-5}–10^{-6} μg/g, compared with 10^{-7} by PIXE.

Figure 10 shows a plot of detection limit *vs.* Z for a general-purpose experimental set-up using 20 mCi of ^{109}Cd as photon source.[29] The detection limits quoted are based on a 1-day measurement of a 5-μm thick "nuclepore" filter. It is obvious that the detection limit falls off with increasing atomic number (corresponding to the curves in Fig. 2).

Comparison between PIXE and XRF

An exact comparison between PIXE and XRF is difficult (and not especially useful) because the experimental conditions are not necessarily the same for optimum sensitivity. In ion irradiation the sample must be resistant to heat so thin targets are advisable. On the other hand the energy loss of the ions in penetrating the sample allows the possibility of selecting the depth of the layer being analysed by adjustment of the incident energy. Photon irradiation is to be preferred for thick targets, which deteriorate in an ion-beam. A further advantage of photon excitation is that trace element detection is possible at a greater depth of the sample material. Generally the selection of the method is determined by practical considerations such as the availability of an accelerator and the methods are complementary rather than competitive.

EXPERIMENTAL ARRANGEMENTS

A system for trace element analysis by emission of characteristic X-rays consists of an irradiation source, a holder for the sample target and an X-ray detector.

Irradiation sources

Irradiation with ions. The technical details of PIXE have been reviewed from the point of view of physics.[1,2,4,30–32] Low-energy particle accelerators suitable as sources for trace analysis are available in laboratories devoted to nuclear, atomic and solid-state physics and materials science. The most useful sources are single-stage or tandem accelerators, producing proton or α-particle beams of a few MeV energy. Beam currents range from 1 to 100 nA. The chamber containing the sample target is connected to the beam line from the accelerator and is normally under vacuum. This restricts the kind of samples to be investigated since the sample has to be stable under vacuum conditions and must not be destroyed by overheating during particle irradiation. Integral with this chamber is a target holder, which for the purpose of routine analysis should hold as many targets as possible, to allow rapid target change. The so-called "target ladders" or "target wheels" are most useful in this respect. The X-ray detector is mounted close to the irradiation chamber and separated from it by a thin beryllium window. To achieve high sensitivity, the solid angle of the target seen by the detector should be large; this means that the detector should be as close as possible to the target spot irradiated by the ion beam. The detector may be mounted at 90° to the beam axis, and the target surface inclined at 45° to the beam and detector axes. Care must be taken to avoid background contributions from ions scattered in the neighbourhood of the target and in the irradiation chamber as a whole. It is advisable to use high-purity materials with low atomic number, *e.g.*, aluminium, in the construction of the chamber. Some workers line the inner walls with carbon or plastics and also use these materials to construct the inner parts. The energy of the characteristic X-rays emitted from materials containing elements of low atomic number is low enough to permit their absorption in the beryllium window in front of the detector.

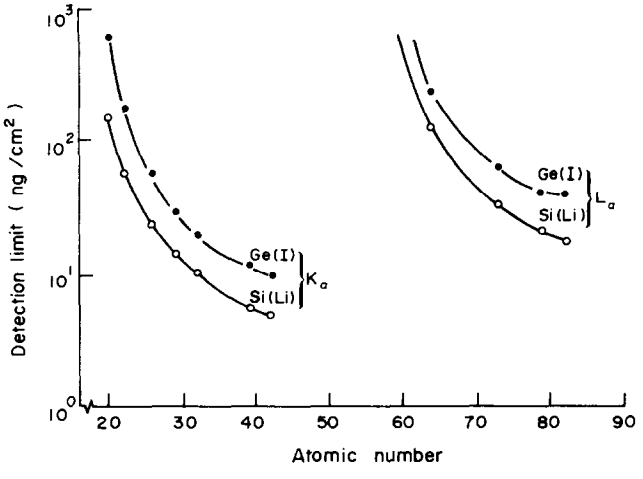

Fig. 10. Minimum detection limits *vs.* atomic number for measurements with Ge(I) and Si(Li) detectors.

To confine the beam to a certain diameter collimators made from carbon are positioned at the target-chamber entrance. The beam spot at the target position is generally a few mm^2 in area, but highly focused microbeams a few μm in diameter are used for special purposes.

When the elements in the sample target are not homogeneously distributed, care must be taken that a homogeneous intensity distribution of the beam is maintained across the irradiated surface. This can be achieved by deflecting the beam across the entrance collimator or inserting a thin diffuser foil into the beam. For measurement of absolute concentrations the beam current must be measured; for thin targets this can be done by counting the ions (*e.g.*, protons) crossing the target, by measuring the charge accumulated in a Faraday cup mounted behind the target. With thick targets special measures are necessary to determine the beam current since the beam is stopped in the target.[33–35] It must also be ensured that the charge accumulated in the target during irradiation is carried off through the target mount. In the case of non-conducting thick targets, such as biological samples, special care must be taken and the external-beam technique may be preferred (see below). There must also be no modification of the sample, caused by evaporation or overheating, and this limits the applicability of the method in the case of organic samples, with their poor thermal conductivity (*e.g.*, samples of biological or medical origin). To overcome this difficulty PIXE analysis has been used in combination with the external-beam technique.[36–38] The particle beam leaves the vacuum system through a thin foil and impinges on the sample, located about 10 mm away. Heating of the sample is reduced by air cooling. There is a small reduction in sensitivity, owing to a slight increase in background caused by interaction of the ions with the exit foil and any gases (*e.g.*, air in the system).

A powerful analytical tool for the investigation of microstructures is the nuclear microprobe. In some cases it is desirable to determine trace element distributions over small areas. For this, beams of accelerated protons with spot sizes as small as 1 μm in diameter have been produced, a series of quadrupole magnets being used to focus the particle beam. A series of collimators can also be used. Comprehensive reviews of this topic have been published.[21–23,39–41] The electron microprobe is already a standard tool in many laboratories, but the limit of detection is greater by a factor of 10^2 than that of the proton microprobe. This is due to the high bremsstrahlung background from the primary electrons. On the other hand, spot sizes of 0.1 μm can be achieved with an electron microprobe, but not with proton microprobes.

Irradiation by photons from radioactive sources. In XRF the scattering of the primary photons in the sample material is the main source of background and therefore a crucial factor for the sensitivity. For this reason the excitation sources used should preferably have strong photon activity in the range of energies just greater than that of the *K*-absorption edge of the element under investigation and a negligible activity in the energy region where the characteristic X-rays are to be expected. There is thus a need for monochromatic photon sources, to permit simultaneous analysis for several elements, which might otherwise be hindered partly by interference due to the primary photons. This can be achieved by the use of a set of radioactive sources with suitable excitation energies. X-Ray tubes with secondary targets may also be considered as monoenergetic sources. The use of radionuclide sources is advantageous in so far as they can be fabricated as point sources to provide experimental arrangements with narrow geometry. The decay time of the source should not be too short (typically about 1 yr). The minimum intensity to achieve an X-ray yield sufficient for an analysis in a suitable measuring time is 10^8 photons/sec. Source activities of around 10 Ci (3.7×10^{11} photons/sec) are required to detect trace element concentrations in the ppm region in a measuring time of a few minutes.[3] LaBrecque[42] describes the application of a 100-mCi Am source, with typical measuring times of 100 sec. However, this is a case where higher concentrations were under investigation and therefore the sensitivity requirements were only moderate. XRF with radioactive sources is widely applicable.[43–47] Table 1 lists various radionuclides useful for this purpose, together with their main properties.[48]

To obtain the highest sensitivities for certain elements, secondary scatter systems are used. The photons emitted from a primary source cause X-ray emission (of more suitable energy for the analysis) from a secondary target.[3] The geometry of a ring source is usually chosen. The best sensitivities can be obtained with X-ray tubes and a secondary target. Using a pulsed X-ray tube can improve the yield still further. The tube is shut down whenever a detection pulse is registered.[49] In this way sensitivities close to those achieved with the PIXE technique can be obtained.[1,24]

Semiconductor-detector spectrometer

The two main spectroscopic procedures based on characteristic X-rays, use either energy-dispersive or wavelength-dispersive detectors. With the older wavelength-dispersive procedure Bragg crystal spectrometers are used to detect the spectral X-ray lines. These spectrometers offer excellent energy resolution, so that even chemical effects on the spectral lines, *i.e.*, the chemical states of the elements, can be determined.[50] However, unlike the energy-dispersive semiconductor detectors, these crystal spectrometers have a low detection efficiency and the solid angle of acceptance is small. Also, since scanning through small wavelength intervals is necessary, the measurements are time-consuming. Therefore in trace-element analysis this method is almost exclusively

Table 1. Radioactive sources for photon-induced X-ray fluorescence analysis

Nuclide	Half-life	Main emission energies, *keV*	Photons emitted per 100 decays
^{241}Am	458 yr	Np-*L*-series	
		11.9–22.2	37
		Gamma-emission	
		59.5	36
^{109}Cd	453 d	Ag-*K*-series	
		22.1, 25.0	101
		Ag-*L*-series	
		2.63–3.75	10.8
		Gamma-emission	
		88.0	4.0
^{57}Co	270 d	Fe-*K*-series	
		6.4, 7.1	48
		Gamma-emission	
		14.4,	8
		121.9,	85
		136.3	11
^{153}Gd	242 d	Eu-*K*-series	
		41.3, 47.3	110
		Gamma-emission	
		69.7,	2.6
		97.4,	30
		103.2	20
^{55}Fe	2.7 yr	Mn-*K*-series	
		5.9, 6.5	25
^{125}I	60 d	Te-*K*-series	
		27.4, 31.1	141
		Gamma-emission	
		35.4	7
^{210}Pb	22 yr	Bi-*L*-series	
		9.4–16.4	24
		Gamma-emission	
		46-5	4
^{238}Pu	86 yr	U-*L*-series	
		11.6–21.7	13
^{170}Tm	127 d	Yb-*K*-series	
		52.0, 59.7	4.5
		Gamma-emission	
		84.3	3.3
^{244}Cm	17.6 yr	Pu-*L*-series	
		14.1, 21.4	13

used in combination with high-power X-ray tubes. The increasing availability of energy-dispersive semiconductor detectors in the 1960s stimulated the development of induced X-ray emission as an analytical method. Nowadays lithium-drifted silicon detectors [Si(Li)] are mainly in use, but germanium detectors [Ge(Li)] or the so-called "intrinsic germanium detectors" [Ge(I)] are also applied. A semiconductor-detector spectrometer consists of the detector system, the recording electronics and a data-handling system. Commercially-available detectors have an active detecting surface 10–80 mm^2 in area. Silicon detectors are mostly used at X-ray energies of <20 keV whereas germanium detectors are most useful at higher X-ray energies. This is due to the atomic number of germanium being sufficiently high to give appreciable cross-sections for X-ray absorption in this energy region. The efficiency of a silicon detector decreases at energies >20 keV and is also limited at low energies owing to absorption of the X-rays by the beryllium window separating the detector system from the measuring chamber. The energy resolution of semiconductor detectors is limited by the statistical spread of energy losses during the detection process and is proportional to $\sqrt{E_x}$; it is typically given by $\Delta E \sim 160$ eV (FWHM) at $E_x = 5.9$ keV.

The strong absorption of low-energy X-rays can be utilized to suppress interfering radiation in this energy region. This can be achieved by insertion of other absorbers. In this way problems associated with high counting rates can be obviated. The so-called "dead-time losses" due to overloading of the electronics are thus avoided. As an example, an intense line at a low X-ray energy may be partly suppressed by use of an absorption foil with a small hole in it and low absorption for higher energy X-ray lines.

The charge-carriers produced in the detector by the X-rays are collected and cause charge pulses which are converted into voltage pulses by a charge-sensitive preamplifier, followed by a main amplifier. Sophisticated electronics for X-ray spectrometry, including special units for pile-up rejection and dead-time correction, are commercially available. A discussion of this development is given by Woldseth.[51] With modern equipment count-rates of up to 5000 counts/sec can be handled.

The X-ray spectrum is identified by pulse-height analysis which determines the energies and measures the intensities of the X-ray peaks, with the aid of a multichannel analyser. Computer-based codes are used in the spectrum evaluation. This procedure combines energy calibration, separation of interfering peaks, peak identification for the element(s) of interest, peak integration and efficiency calibration. The final result is the amount of the element(s) sought.

Many details of semiconductor spectrometers for X-ray analysis and data acquisition have been given explicitly in a number of review articles.[1-3]

Target preparation

The preparation of sample targets is one of the main problems in induced X-ray emission analysis. Whereas in the case of XRF any kind of target is suitable, the requirements and limitations are more severe in PIXE. This is especially the case for those targets which are not stable under vacuum conditions or which cannot be irradiated with particles without being destroyed by overheating. Thin targets are the simplest to investigate, *i.e.*, those targets in which the energy loss of the incident particles in passing through the target is small compared with the initial energy. Aerosol or solution samples may be deposited on filters, *e.g.*, "nuclepore" filters, and these substrates may be considered as thin films. Alternatively thin carbon foils may be used, but although strong they often contain unacceptably high amounts of impurities.

Biological and medical specimens can be irradiated directly if prepared as microscopic sections. The same

procedure can be adopted for materials science or geological specimens.

For some samples it is possible to improve the detection limit by some orders of magnitude by use of preconcentration procedures.[38,52–54] In that case large samples are required, but it must be emphasized that induced X-ray emission gives highly sensitive non-destructive analysis even with extremely small samples.

APPLICATIONS

Trace elements in water samples

Water contains essential trace elements as well as toxic elements from industrial activities. More than 60 trace elements are now regarded as essential, but many of them appear to be toxic if present in too large an amount. Generally there is a difference of some orders of magnitude between the essential and toxic levels of these elements, but for a few, such as selenium, the "gap" is rather narrow, and accurate methods of analysis are of considerable importance.

Target preparation from water solutions is simple if only a knowledge of relative amounts of elements, or "fingerprinting", is required. Carbon films, prepared by vacuum evaporation onto glass, can be floated in the water under investigation and used as supports. Addition of an internal standard to the solution permits the determination of approximate absolute concentrations. The carbon film can be picked up on a target frame. Since in most cases the water under investigation is available in large amounts this method is very often used. When this is not the case, drops of water can be dried on the carbon film. Alternatives to carbon film are "nuclepore", "formvar", polystyrene or "hostaphane" membranes, *etc.* Campbell[55] has reviewed target-backing and specimen-preparation techniques in detail. Crystallization of a substance from solution often results in a non-uniform distribution,[56] which is difficult to avoid even if insulin is added as recommended in the literature.[1]

Analysing for trace metals in water sometimes requires preconcentration techniques.[38,52–54,57,58] One of the simplest methods is chelation of the trace metals and adsorption of the complexes on activated carbon. However, activated carbon is a natural product and contains large amounts of trace elements.[38] A different technique with lower blank values, described by Raith *et al.*,[38] gives detection limits of 0.4 ng/g for Fe, 0.5 ng/g for Zn, 2 ng/g for Pb and 8 ng/g for Cd.

Deconninck[59] has described a method in which drops of a liquid are examined by use of an external beam. Good sensitivity is achieved without chemical preparation.

Trace elements in body fluids

Body fluids, such as blood or urine, have been extensively investigated.[60–62] In the case of whole blood, analysis for low concentrations of trace elements, *e.g.*, Pb, is difficult because of the high count-rate due to the iron peak. Serum does not present this problem, as the iron concentration is much lower, but there is the disadvantage that serum is not representative of whole blood. Since this kind of investigation is used more and more in clinical work, automatic systems have been developed for determination of trace element concentrations.[63] Kleimola *et al.*[64] have investigated trace elements in serum, with emphasis on the routine analysis of samples from healthy persons. No preconcentration steps were used. Fe, Zn and Cu were measured at the ppm level and comparisons were made with the results obtained by other methods. Urine samples can be similarly investigated, with use of simple preconcentration techniques if required.[65]

Trace elements in biological materials

Owing to the role of trace elements in living organisms, especially in metabolic processes, there has been a great increase in the investigation of biological materials over the past few years. Normal biological behaviour depends on the presence of relatively narrow absolute concentration ranges of certain trace elements as well as on their relative amounts. It is therefore possible to determine the normal concentrations in biological material and detect any deviations from the normal.

There has been much work on the normal trace element concentrations in different parts of the human organism (Table 2). Nutritional requirements can also be identified by such analysis.[66] Reviews of these aspects of the subject have recently been published.[60,67]

There are many industrial diseases caused by abnormal environmental exposure, in some cases resulting in an attack on the lungs. Weber *et al.*[68] have investigated lung tissue obtained by biopsy and reported the trace element concentrations and diagnoses for a number of patients. Dermatological studies of microscopic sections of the human epidermis have been performed with a proton microprobe.[22] Lateral variations of S, Cu, Zn, Pb concentrations have been measured by scanning the sample with a 6-μm diameter beam.

Another field of investigation is the analysis of cancer tissue and the results have been compared with those obtained for normal tissue.[69] This work also made a careful study of the reproducibility of PIXE analysis and a comparison with neutron-activation analysis. A major criticism of many other analytical papers is the lack of information concerning the accuracy of the results and the precision of the methods used. Analytical results should always be related to standard reference materials.

An extensive comparison of Cu/Zn ratios and of the concentrations of Cd, Se and Pb in normal and diseased tissue (taken from the same patient) was made by Guffey *et al.*[70] by PIXE analysis. They investigated dried tissue samples (100 μg) from kid-

Table 2. Analytical applications of PIXE

Sample	Elements investigated	Reference	Comments
Biological			
Human hair	Zn, Cu, Ca	80	Correction factors for energy loss and self-absorption
Proteins, liposomes, serum, broncho-alveolar lavages	Fe, Cu, Zn, Ni, Co, Br, Pb	68	Biophysics, cancer therapy, lung pathology related
Kidney, serum, NBS bovine liver	Many between K and Pb	69	Reproducibility determination, comparison with neutron-activation analysis, investigation of cancerous and normal tissue
Cells and tissue of different biological and medical specimens	Between Na and Pb	23	Scanning proton microprobe
Serum		81	Rheumatoid polyarthritis treated chrysotherapeutically
Serum		82	Low-temperature ashing as preconcentration method
Serum	Ca, Fe, Cu, Zn, Br	83	Trace elements in pregnancy, yttrium as internal standard; serum dried on Nuclepore polycarbonate filter membrane
Serum, cerebrospinal fluid, hair, retina of eye	$Z \geq 19$	84	Clinical applications
Animal eye lenses	P, S, Cl, K, Ca	85	Cataracts, α-particle microbeam (200 μm)
Serum	K, Ca, Fe, Cu, Zn, Br, Au	63	Automatic data aquisition and on-line analysis
Whole blood, liver, kidney	Fe, Cu, Zn, Pb, Cd	86	Freeze-dried, homogenized blood pressed into pellets, tissue section, comparison with other methods
Bone, tissue	Sb, As, Cd, Cu, Pb, Hg, Se Ag, Sn, Zn	87	Industrially exposed workers combined use of AAS, NAA, PIXE in a microprobe
Human blood, liver tissue	Fe, Cu, Zn	88	PIXE
Human blood, serum	Si, Ti, Cr, Mn, Ni, Cu, Zn, Ga, Se, Br, Pb, macroelements	89	PIXE, external beam, correlation between geographical area and trace element composition, sample freeze-dried
Human whole blood	Fe, Cu, Zn, Br, Rb, Pb, macroelements	90	PIXE, external beam, freeze-dried pellets, NBS standard used
Liver	Mn, Fe, Cu, Zn, Se, Rb, Mo, Cd, Pb	91	PIXE
Dental enamel	F	92	PIXE and resonance reaction ^{19}F (p,$\alpha\gamma$) ^{16}O, microprobe, depth determination
Human hair	Ca, Cr, Fe, Co, Cu, Br, I, Pb, relative to Zn	93	PIXE, target preparation described in detail
Human bone	Cr, Mn, Fe, Ni, Cu, Zn, Br, Sr, Pb	94	PIXE, external beam, target preparation described in detail
Blood, serum	Br	95	Comparison with NAA
Organic and biological matrices	Se	96	
Environmental			
Aerosols	Be, Cu, Se	97	PIXE combined with proton elastic scattering analysis
Epiphytic lichens	Pb, Br, F	140	PIXE and nuclear reaction analysis
River water	from Na to Fe	98	Asbestos concentration in correlation with elemental concentrations
Ambient aerosols	S, other elements	99	Sampling by cascade impactor, chemical state of particulate S determined
Sediments	from Ti to Zr	100	XRF
Leaves	Pb	101	X-ray tube
Water, aerosols, oil	S and from V to Pb	102	XRF

(*continued*)

Table 2—*continued*

Sample	Elements investigated	Reference	Comments
Aerosols	Zn, Pb	103	XRF
Soil, milk	from Ca to Pb	104	PIXE
Aerosols	S	105	XRF
Aerosols	mainly Pb and Br	106	XRF, detection of air pollution sources
Water	Se	107	
Sea-water, urban particulates, also urine	Ni, Mn, Zn, Cu, Pb	108	Preconcentration by cation-exchange resin filters
Materials science			
Cadmium telluride	Si, Cl, Ge, As	109	PIXE using heavy ions combined with secondary mass spectroscopy
Catalysts	Pb, Br, others	74	Catalyst poisoning
Aluminium	Zn, Mg	110	Depth profile to 30 μm after annealing
Cr–Ni–Ti-alloys	N, Ti	111	Combining nuclear reactions with PIXE, microprobe, N–Ti correlation
Copper	Pd	112	PIXE
Catalysts	Co, Ni, Mo	113	XRF, computerized system
Cu blisters	Ag, Pb	114	XRF, annular sources
Geological			
Rock and ore	Th, U	76	Comparison with NAA
Apatite	Y, La, Ce, Nd	115	18 MeV α-particles, dissolution of apatite in concentrated perchloric acid, extraction with di(2-ethylhexyl)phosphoric acid, comparison with other methods
Rock	Rb, Sr	116	XRF
Kaolin	Ti, Fe	117	XRF
Laterite	Ti	118	XRF
Crude oil	S, Cl	119	XRF
Laterite	Ni	120	XRF, portable unit
Laterite	Ba, La, Cl	121	XRF
Rock	U	122	XRF
Laterite	Sr, Y	123	XRF, region of 100–1000 ppm, comparison with wavelength dispersive method
Geochemical	40 elements	124	XRF
Oil	V, Fe, Ni, Mo, Zn, As, Se	125	
Deep-sea ferromanganese nodules	$11 < Z < 82$	126	Thin sample targets on Nuclepore filter
Apatite minerals	La, Ce, Pr, Nd	127	Preconcentration by anion-exchange extraction
Arts and artefacts			
Obsidian, pottery, metal	$Z \geq 11$	128	PIXE and proton-induced gamma rays
Archeological	main components	129	XRF
Obsidian	K, Ca, Ti, V, Mn, Fe, Rb, Y, Sr, Zr, Nb, Ta, Pb	130	Thick targets
Miscellaneous			
Al layer	Ar	131	Density of implanted Ar, heavy-ion beam
Pharmaceutical	Br, Ag, I	132	XRF
Gun residues	S, Ba, Fe, Pb	133	Forensic science, PIXE
Aqueous solutions	noble metals	134	XRF
Glasses	from Ca to Pb	135	Forensic science, PIXE and inelastic proton scattering
Standard targets		136	Preparation of standard targets
Variable composition and thickness	$17 < Z < 82$	137	Absorption correction from scattered radiation
		138	Use of carbon foils for elimination of charging effects in PIXE
Human hair	Fe, Cu, Zn	139	Trace element profiles

ney, breast, liver, lung, colon and aorta. The intake of trace elements may also be of considerable importance in pharmaceutical medication. During investigations by the external-beam technique with thick targets,[71] trace element concentrations of up to 70 ppm of Ti, Mn, Cu, Zn, Br and Sr were measured.

Trace elements in materials science

Table 2 gives a number of examples of the use of trace element analysis by induced X-ray emission in materials science. In the fabrication of high-frequency and optoelectronic devices, impurities of low atomic number have been used extensively. Takai *et al.*[72] have investigated the lattice locations of such impurities in gallium arsenide. An undoped GaAs single crystal has been implanted with S and Mn ions and subsequently examined by ion-induced X-ray analysis. Protons, as well as $^4He^+$ ions, were used for the irradiation. To assign the lattice location, the X-ray yield as well as back-scattering of the ions was measured in angular scans. A detailed analysis of the background radiation was made, by use of the channelling effect. The atomic composition of bielemental thick targets has been investigated by Baeri *et al.*,[73] by ion-induced X-ray analysis. These authors determined the angular dependence of the X-ray yield, using proton and helium-ion beams. The thick-target yields were analysed by computer, the depth dependence, *i.e.*, energy dependence of the ionization cross-sections, X-ray absorption coefficients and secondary fluorescence being included. A comparison of these results with those of theoretical calculations was also included. The method gave the atomic compositions of homogeneous bulk targets of GaAs, ZnTe and PbTe.

The preparation and investigation of heterogeneous catalysts is another interesting application of PIXE analysis, and Cairns *et al.*[74] have described its use in the development of new catalysts. A proton microprobe focused down to a 10-μm diameter spot was used, so that scans over narrowly restricted areas of the catalyst were possible. In this way the physical properties could also be monitored and changes during use studied, thus giving information about the process of catalyst poisoning. Catalysts designed for vehicle exhaust-emission control have been examined. Hanson *et al.*,[75] using a proton microprobe, investigated the migration of molybdenum in reactor-grade graphite at temperatures between 1800 and 3100° in a study of the safety of high-temperature gas-cooled reactors. They observed the formation of molybdenum carbide as a result of nuclear fission. The presence of a microstructure in the Mo distribution, after the graphite had been heated together with molybdenum, was established. The authors discussed the probable migration processes and determined a diffusion coefficient. Chemical techniques cannot be used in this case since the Mo distribution changes too rapidly after the heat treatment. The use of an electron microprobe is also excluded, since the concentrations examined are too low.

Miscellaneous applications

Cohen *et al.*[76] have investigated thorium and uranium concentrations in ore samples. A variety of naturally occurring ores were studied, covering a broad range of concentrations between 10 and 10^4 μg/g, *L* X-ray emissions being measured for elements with high *Z*. This work is a good example of careful analysis of background contributions. The spectra were related to those of standard samples and the problem of adjacent peak interferences was painstakingly handled. Since thick targets were used the associated problems were examined in detail. A comparison of the results from the PIXE measurements with those from delayed fission-neutron analysis and from neutron-activation analysis showed the intrinsic reliability of the methods used.

Rowson and Hontzeas[77] have investigated uranium ores with a 10-mCi ^{57}Co point source for photon excitation. The aim of this type of X-ray analysis was the on-stream determination of elemental composition in an industrial environment. The advantage of using photons for the excitation lay in their penetration ability, which made possible direct excitation through the walls of vessels or pipelines. Since thick samples were analysed, the influence of the thickness and matrix was evaluated by simultaneously measuring the Compton scattering and peak intensities transmitted. The authors described the procedure in detail and discussed the results with respect to both precision and possible applications.

Investigations in the fields of fine arts and archeology may be conveniently made by the X-ray technique because it is both sensitive and non-destructive. The PIXE technique using the external-beam method has been applied by Chen *et al.*[78] to the study of the elemental composition of famous ancient swords. This method is especially useful for analysing large objects non-destructively. The authors were able to extract from their results information on the surface treatment technology used in ancient times. They also reported on measurements of human hair specimens and compared their results with those obtained by atomic-absorption spectrometry. The agreement was good but it must be emphasized that in applying PIXE analysis to hair samples the external-beam technique should be applied, since the cooling by convected air avoids destruction of the sample. In another study Tove *et al.*[79] combined X-ray investigations with ion back-scattering to determine the elemental composition of the surface layers of violin varnish and wood. In this way the presence of trace elements can be established, which may aid in the identification of the methods and materials used by famous instrument makers. The method is also useful in authentication of instruments.

Conclusions

PIXE and XRF are reliable trace-analysis methods for simultaneous determination of elements with $Z > 12$. A disadvantage is that interferences between the K and L X-rays from light and heavy elements may limit the number of elements detectable, at least near the detection limit of 0.1–1 μg/g. Very small amounts of a sample can be analysed non-destructively in a time of only 10 min. By use of a proton microprobe with the present lower limit of resolution, structures as small as 1 μm in diameter can be investigated. This corresponds to a minimum detectable amount of a trace of about 10^{-16} g.

Acknowledgements—The authors have benefited from discussion with numerous colleagues over the years, all of whom are gratefully thanked. In particular, thanks are due to B. Raith and H.-R. Wilde, both of whom took leading parts in many experiments, the results of which have been incorporated in this article. They also wish to thank Mrs. Elsbeth Grieger for her patience during the preparation of the manuscript. The work was supported in part by the Minister für Wissenschaft und Forschung des Landes Nordrhein-Westfalen, and by the Bundesminister für Forschung und Technologie.

REFERENCES

1. S. A. E. Johansson and T. B. Johansson, *Nucl. Instrum. Methods*, 1976, **137,** 473.
2. F. Folkmann, *J. Phys.*, 1975, **E8,** 429.
3. F. S. Goulding and J. M. Jaklevic, *Ann. Rev. Nucl. Sci.*, 1973, **23,** 45.
4. G. L. Macdonald, *Anal. Chem.*, 1978, **50,** 135R.
5. *Proc. Intern. Conf. Particle-Induced X-ray Emission and its Analytical Applications, Nucl. Instrum. Methods*, 1977, **142.**
6. *Proc. Intern. Conf. Particle-Induced X-ray Emission and its Analytical Applications, ibid.*, 1981, **181.**
7. W. Bambynek, B. Crasemann, R. W. Fink, H. U. Freund, H. Mark, C. D. Swift, R. E. Price and P. V. Rao, *Rev. Mod. Phys.*, 1972, **44,** 716.
8. J. A. Bearden, *ibid.*, 1967, **39,** 78.
9. J. D. Garcia, R. J. Fortner and T. M. Kavanagh, *ibid.*, 1973, **45,** 111.
10. D. H. Madison and E. Merzbacher, in *Atomic Inner-Shell Processes*, Vol. 1, B. Crasemann (ed.), p. 1. Academic Press, New York, 1975.
11. G. S. Khandelwal, B. H. Choi and E. Merzbacher, *At. Data*, 1969, **1,** 103.
12. B. H. Choi, E. Merzbacher and G. S. Khandelwal, *ibid.*, 1973, **5,** 291.
13. E. Merzbacher and H. W. Lewis, in *Encyclopedia of Physics*, Vol. 34, S. Flügge (ed.), p. 166. Springer-Verlag, Berlin, 1958.
14. W. M. J. Veigele, *At. Data*, 1973, **5,** 51.
15. E. Storm and H. I. Israel, *Nucl. Data Tables*, 1970, **A7,** 565.
16. S. I. Salem, S. L. Panossian and R. A. Krause, *At. Data Nucl. Data Tables*, **14,** 91.
17. R. Cesareo, F. V. Frazzoli and S. Sciuti, *J. Radioanal. Chem.*, 1976, **34,** 157.
18. R. Cesareo and G. E. Gigante, *Intern. J. Appl. Radiat. Isot.*, 1977, **28,** 301.
19. T. B. Johansson, R. Akselsson and S. A. E. Johansson, *Nucl. Instrum. Methods*, 1970, **84,** 141.
20. B. Raith, M. Roth, K. Göllner, B. Gonsior, H. Ostermann and C. D. Uhlhorn, *ibid.*, 1977, **142,** 39.
21. J. A. Cookson, *ibid.*, 1979, **165,** 477.
22. H. R. Wilde, W. Bischof, B. Raith, C. D. Uhlhorn and B. Gonsior, *ibid.*, 1981, **181,** 165.
23. G. J. F. Legge and A. P. Mazzolini, *ibid.*, 1980, **168,** 563.
24. F. S. Goulding and J. M. Jaklevic, *ibid.*, 1977, **142,** 323.
25. T. A. Cahill, R. G. Flocchini, P. J. Feeney and D. J. Shadoan, *ibid.*, 1974, **120,** 193.
26. R. L. Walter, R. D. Willis, W. F. Gutnecht and J. M. Joyce, *Anal. Chem.*, 1974, **46,** 843.
27. R. C. Bearse, D. A. Close, J. J. Malanify and C. J. Umbarger, *ibid.*, 1974, **46,** 499.
28. J. R. Rhodes, A. H. Predzynski, C. B. Hunter, J. S. Payne and J. L. Lindgren, *Environ. Sci. Technol.*, 1972, **6,** 922.
29. H. H. Horn, A. Trapp, M. Roth and B. Gonsior, *Progress Report* 3038, Westdeutscher Verlag GmbH, Opladen, 1981.
30. G. L. Macdonald, *Anal. Chem.*, 1980, **52,** 100R.
31. T. B. Johansson, M. Ahlberg, R. Akselsson, G. Johansson and K. Malmqvist, *J. Radioanal. Chem.*, 1976, **32,** 207.
32. R. D. Vis and H. Verheul, *ibid.*, 1975, **27,** 447.
33. F. Folkmann, in *Ion Beam Surface Layer Analysis*, Vol. 2, O. Meyer, G. Linker and F. Käppeler (eds.), p. 747. Plenum Press, New York, 1976.
34. M. S. Ahlberg, *Nucl. Instrum. Methods*, 1977, **142,** 61.
35. P. M. A. Van der Kam, R. D. Vis and H. Verheul, *ibid.*, 1977, **142,** 55.
36. G. G. Seaman and K. C. Shane, *ibid.*, 1975, **126,** 473.
37. A. Katsanos, A. Xenoulis, A. Hadjiantoniou and R. W. Fink, *ibid.*, 1976, **137,** 119.
38. B. Raith, A. Stratmann, H. R. Wilde, B. Gonsior, S. Brüggerhoff and E. Jackwerth, *ibid.*, 1981, **181,** 199.
39. J. A. Cookson, A. T. G. Ferguson and F. D. Pilling, *J. Radioanal. Chem.*, 1972, **12,** 39.
40. J. A. Cookson, J. W. McMillan and T. B. Pierce, *ibid.*, 1979, **48,** 337.
41. F. Bosch, A. El Goresy, W. Herth, B. Martin, R. Nobiling, B. Povh, H.-D. Reiss and K. Traxel, *Nucl. Sci. Appl.*, 1980, **1,** 33.
42. J. J. LaBrecque, *J. Radioanal. Chem.*, 1979, **53,** 213.
43. C. Shenberg, A. Aladjem and S. Amiel, *ibid.*, 1974, **20,** 77.
44. R. Cesareo and C. Mancini, *ibid.*, 1976, **34,** 151.
45. H.-P. Weise and Chr. Segebade, *ibid.*, 1977, **37,** 195.
46. J. Leonowich, S. Pandian and I. L. Preiss, *ibid.*, 1977, **40,** 175.
47. R. D. Giauque, R. B. Garrett and L. Y. Goda, *Anal. Chem.*, 1979, **51,** 511.
48. H.-W. Thümmel, *Isotopenpraxis*, 1975, **11,** 87.
49. J. M. Jaklevic, F. S. Goulding and D. A. Landis, *IEEE Trans., Nucl. Sci.*, 1972, **NS19,** 392.
50. R. L. Watson, A. K. Leeper, B. I. Sonobe, T. Chiao and F. E. Jenson, *Phys. Rev. A*, 1977, **15,** 914.
51. R. Woldseth, *X-Ray Energy Spectrometry*. Kevex Corporation, Burlingame, California, USA, 1973.
52. R. Cesareo and G. E. Gigante, *Water, Air, Soil Pollut.*, 1978, **9,** 99.
53. D. E. Leyden and G. H. Luttrell, *Anal. Chem.*, 1975, **47,** 1612.
54. K. Wundt, H. Duschner and K. Starke, *ibid.*, 1979, **51,** 1487.
55. J. L. Campbell, *Nucl. Instrum. Methods*, 1977, **142,** 263.
56. H. R. Wilde, M. Roth, C. D. Uhlhorn and B. Gonsior, *ibid.*, 1978, **149,** 675.
57. C. H. Lochmüller, J. W. Galbraith and R. L. Walter, *Anal. Chem.*, 1974, **46,** 440.
58. W. Blommaert, R. Vandelannoote, L. van't Dack, R. Gijbels and R. van Grieken, *J. Radioanal. Chem.*, **57,** 383.
59. G. Deconninck, *Nucl. Instrum. Methods*, 1977, **142,** 275.

60. V. Valkowic, *Analysis of Biological Material for Trace Elements Using X-ray Spectroscopy*. CRC Press, Boca Raton, Florida, 1980.
61. L. Kaufman, D. C. Price, M. A. Holliday, B. Payne, D. C. Camp, J. A. Nelson and F. Deconninck, *J. Radioanal. Chem.*, 1978, **43,** 321.
62. M. Berti, G. Buso, P. Colautti, G. Moschini, B. M. Stievano and C. Tregnaghi, *Anal. Chem.*, 1977, **49,** 1313.
63. R. Lecomte, P. Paradis, S. Monaro, M. Barrette, G. Lamoureux and H. A. Menard, *Nucl. Instrum. Methods*, 1978, **150,** 289.
64. V. Kleimola, J. Dahlbacka, P. Pakarinen, T. T. Salmi and V. Näntö, in *Trace Element Analytical Chemistry in Medicine and Biology*, P. Brätter and P. Schramel (eds.), p. 331. de Gruyter, Berlin, 1980.
65. M. Agarwal, R. B. Bennett, I. G. Stump and J. M. D'Auria, *Anal. Chem.*, 1975, **47,** 924.
66. E. J. Underwood, *Trace Elements in Human and Animal Nutrition*, 4th Ed. Academic Press, New York, 1977.
67. *Trace Element Analytical Chemistry in Medicine and Biology*, P. Brätter and P. Schramel (eds.). de Gruyter, Berlin, 1980.
68. G. Weber, G. Robaye, J. M. Delbrouck, I. Roelandts, O. Didebers, P. Bartsch and M. C. de Pauw, *Nucl. Instrum. Methods*, 1980, **168,** 551.
69. W. Maenhaut, L. de Reu, H. A. van Rinsvelt, J. Cafmeyer and P. van Espen, *ibid.*, 1980, **168,** 557.
70. J. A. Guffey, H. A. van Rinsvelt, R. M. Sarper, Z. Karcioglu, W. R. Adams and R. W. Fink, *ibid.*, 1978, **149,** 489.
71. B. Gonsior and E. Szirmai, *Agressologie*, 1981, **22,** 143.
72. M. Takai, K. Gamo, H. Yagita, K. Masuda, S. Namba and A. Mizobuchi, *Nucl. Instrum. Methods*, 1978, **149,** 457.
73. P. Baeri, S. U. Campisano, G. Immé, E. Rimini and G. Della Mea, *ibid.*, 1978, **149,** 435.
74. J. A. Cairns and J. A. Cookson, *ibid.*, 1980, **168,** 511.
75. A. L. Hanson, R. E. Shroy, H. W. Kraner, K. W. Jones and E. Uneberg, *Proc. Conf. Application of Accelerators in Research and Industry, Denton, Texas*, 3–5 November 1980; *IEEE Trans. Nucl. Sci.*, 1981, **NS28,** 1421.
76. D. D. Cohen, P. Duerden, E. Clayton and T. Wall, *Nucl. Instrum. Methods*, 1980, **168,** 523.
77. J. W. Rowson and S. A. Hontzeas, *ibid.*, 1979, **163,** 555.
78. Jian-Xin Chen, Hong-Kou Li, Chi-Gang Ren, Guo-Hun Tang, Xi-De Wang, Fu-Chia Yang and Hui-Ying Yao, *ibid.*, 1980, **168,** 437.
79. P. A. Tove, D. Sigurd and S. Petersson, *ibid.*, 1980, **168,** 441.
80. E. C. Montenegro, G. B. Baptista, L. V. De Castro Faria and A. S. Paschoa, *ibid.*, 1980, **168,** 479.
81. S. Monaro, R. Lecomta, P. Paradis, M. Barrette, G. Lamoreux, H. Ménard and C. H. U. Sherbrooke, *Rapp. Act.* No. 15, Université De Montréal, Département De Physique, 1980, 108.
82. S. Monaro, R. Lecomte, P. Paradis, S. Landsberger and G. Desaulniers, *ibid.*, 1980, 110.
83. P. Kiilholma, M. Grönroos, V. Kleimola, P. Pakarinen, J. Dahlbacka and V. Näntö, *Mineral Elements '80, Proc. Nordic Symp. Helsinki*, 1980, **1,** 259.
84. V. Näntö, J. Dahlbacka, P. Pakarinen, T. Markkanen, V. Kleimola, L. Salminen and H. Frey, *ibid.*, 1980, **2,** 439.
85. H. Koyama-Ito, A. Jahnke, E. Wada, T. Tsumita and T. Yamazaki, *Nucl. Instrum. Methods*, 1979, **166,** 269.
86. A. E. Simpson and N. A. Dyson, *ibid.*, 1977, **146,** 473.
87. U. Lindh, D. Brune, G. Nordberg and P. O. Wester, *Sci. Total Environ.*, 1980, **16,** 109.
88. N. A. Dyson, A. E. Simpson and J. T. Dabek, *J. Radioanal. Chem.*, 1978, **46,** 309.
89. G. J. Boulle, M. Peisach, W. S. Dempster and H. de V. Heese, *ibid.*, 1979, **52,** 153.
90. A. H. Khan, M. Khaliquzzaman, M. B. Zaman, M. Husain, M. Abdullah and S. Akhter, *ibid.*, 1980, **57,** 157.
91. W. Koenig, F. W. Richter, J. Ch. Bode and B. Meinel, *ibid.*, 1980, **58,** 327.
92. U. Lindh and A. B. Tveit, *ibid.*, 1980, **59,** 167.
93. A. E. Pillay and M. Peisach, *ibid.*, 1981, **63,** 85.
94. M. Hyvönen-Dabek, J. Räisänen and J. T. Dabek, *ibid.*, 1981, **63,** 163.
95. M. S. Rapaport, M. Mantel and R. Nothmann, *Anal. Chem.*, 1979, **51,** 1356.
96. S. E. Raptis, W. Wegscheider, G. Knapp and G. Tölg, *ibid.*, 1980, **52,** 1292.
97. G. M. Hudson, H. C. Kaufmann, J. W. Nelson and M. A. Bonacci, *Nucl. Instrum. Methods*, 1980, **168,** 259.
98. S. Monaro, R. Lecomte, P. Paradis, S. Landsberger and G. Desaulniers, *Rapp. Act.* No. 15, Université De Montréal, Département De Physique, 1980, 115.
99. M. S. Ahlberg, A. C. D. Leslie and J. W. Winchester, *Nucl. Instrum. Methods*, 1978, **149,** 451.
100. P. V. Kulkarni and I. L. Preiss, *J. Radioanal. Chem.*, 1975, **24,** 423.
101. J. S. C. McKee, M. L. H. Wise, J. R. Holt and A. Meredith, *ibid.*, 1976, **31,** 461.
102. H. Meier and E. Unger, *ibid.*, 1976, **32,** 413.
103. M. Gallorini, N. Genova, E. Orvini and R. Stella, *ibid.*, 1976, **34,** 135.
104. T. C. Chu, V. R. Navarrete, H. Kaji, G. Izawa, T. Shiokawa, K. Ishii, S. Morita and H. Tawara, *ibid.*, 1977, **36,** 195.
105. Y. Matsuda and T. Mamuro, *ibid.*, 1977, **36,** 209.
106. M. Boazi, J. Gabey, S. Devir and C. Shenberg, *ibid.*, 1978, **45,** 395.
107. H. J. Robberecht and R. E. Van Grieken, *Anal. Chem.*, 1980, **52,** 449.
108. H. Kingston and P. A. Pella, *ibid.*, 1981, **53,** 223.
109. C. Scharager, R. Stuck, P. Siffert, J. Cailleret, Ch. Heitz, G. Lagarde and D. Tenorio, *Nucl. Instrum. Methods*, 1980, **168,** 367.
110. J. Végh, D. Berényi, E. Koltay, I. Kiss, S. Seif El-Nasr and L. Sarkadi, *ibid.*, 1978, **153,** 553.
111. J. W. McMillan, P. M. Hirst, F. C. W. Pummery, J. Huddleston and T. B. Pierce, *ibid.*, 1978, **149,** 83.
112. G. Demortier, *J. Radioanal. Chem.*, 1975, **24,** 47.
113. J. J. LaBrecque, C. A. Pena, E. Marcano and W. C. Parker, *ibid.*, 1980, **60,** 247.
114. J. L. Parus, G. Kuc and J. Kierzek, *ibid.*, 1978, **44,** 189.
115. I. Roelandts, G. Y. Weber and L. Quaglia, *Nucl. Instrum. Methods*, 1978, **157,** 141.
116. J. Bacso and K. Balogh, *J. Radioanal. Chem.*, 1974, **22,** 157.
117. N. Bialy, J. Kierzek and J. Parus, *ibid.*, 1976, **34,** 365.
118. J. J. LaBrecque, *ibid.*, 1978, **43,** 253.
119. J. Csikai and S. M. Al-Jobori, *ibid.*, 1979, **53,** 225.
120. Z. Augustyński, B. Dziunikowski and J. Meitin, *ibid.*, 1981, **63,** 325.
121. J. J. LaBrecque, W. C. Parker and D. Adames, *ibid.*, 1980, **59,** 193.
122. H. Kumpulainen, *ibid.*, 1980, **59,** 635.
123. J. J. LaBrecque, E. Marcano, C. A. Peña and W. C. Parker, *ibid.*, 1981, **63,** 73.
124. R. D. Giauque, R. B. Garrett and L. Y. Goda, *Anal. Chem.*, 1977, **49,** 1012.
125. H. Kubo, R. Bernthal and T. R. Wildeman, *ibid.*, 1978, **50,** 899.
126. S. J. Kirchner, H. Oona, S. J. Perron, Q. Fernando, J. Jong-Hae Lee and H. Zeitlin, *ibid.*, 1980, **52,** 2195.
127. I. Roelandts, *ibid.*, 1981, **53,** 676.

128. P. Duerden, J. R. Bird, M. D. Scott, E. Clayton, L. H. Russell and D. D. Cohen, *Nucl. Instrum. Methods*, 1980, **168,** 447.
129. C. Shenberg and M. Boazi, *J. Radioanal. Chem.*, 1975, **27,** 457.
130. P. Duerden, D. D. Cohen, E. Clayton, J. R. Bird, W. R. Ambrose and B. F. Leach, *Anal. Chem.*, 1979, **51,** 2350.
131. I. V. Mitchell, W. N. Lennard and J. B. Sanders, *Nucl. Instrum. Methods*, 1980, **168,** 121.
132. J. Švitel and P. Schiller, *J. Radioanal. Chem.*, 1970, **5,** 343.
133. B. K. Barnes, L. E. Beghian, G. H. R. Kegel, S. C. Mathur and P. Quinn, *ibid.*, 1973, **15,** 13.
134. B. Holynska, S. Kalita, M. Lankosz, A. Markowicz and M. Wasilewska, *ibid.*, 1977, **35,** 361.
135. R. D. Vis, K. J. Wiederspahn and H. Verheul, *ibid.*, 1978, **45,** 407.
136. R. Baum, W. F. Gutknecht, R. D. Willis and R. L. Walter, *Anal. Chem.*, 1975, **47,** 1727.
137. P. M. Van Dyck and R. E. Van Grieken, *ibid.*, 1980, **52,** 1859.
138. H. Oona, S. J. Kirchner, P. L. Kresan, Q. Fernando and H. Zeitlin, *ibid.*, 1979, **51,** 302.
139. J. L. Campbell, S. Faiq, R. S. Gibson, S. B. Russel and W. Schulte, *ibid.*, 1981, **53,** 1249.
140. A. Z. Hrynkiewicz, S. Szymczyk, J. Kajfosz and M. Olech, *Nucl. Instrum. Methods*, 1980, **168,** 517.

Talanta, Vol. 30, No. 6, pp. 401–404, 1983
Printed in Great Britain.

0039-9140/83/060401-04$03.00/0

KINETIC DETERMINATION OF MICROAMOUNTS OF SOME SULPHUR-CONTAINING LIGANDS

MADHU PHULL and P. C. NIGAM*
Department of Chemistry, Indian Institute of Technology, Kanpur 208016, India

(*Received* 30 *November* 1981. *Revised* 3 *December* 1982. *Accepted* 6 *January* 1983)

Summary—Some sulphur-containing ligands have been shown to inhibit the Hg(II)-catalysed substitution of *p*-nitrosodiphenylamine (*p*-NDA) for cyanide in hexacyanoferrate(II), by binding the mercury(II). This effect is used for determination of microamounts of cysteine, thioglycollic acid and thiosulphate. The reactions are followed spectrophotometrically at 640 nm (λ_{max} of $[Fe(CN)_5 \cdot p\text{-NDA}]^{3-}$). The determination range depends on the amount of mercury(II) added and the stability of the Hg(II)–ligand complex. Under specified conditions, the detection limits are: thioglycollic acid $1 \times 10^{-7}M$, cysteine $1 \times 10^{-6}M$ and thiosulphate $4 \times 10^{-7}M$.

Trace amounts of many species have been determined by their catalytic effect on suitable indicator reactions.[1] Addition of a complexing agent to such a system may either promote or inhibit the catalytic effect.[2] A linear relationship between reaction rate and concentration of added ligand can often be obtained by simple empirical treatment of the rate data. This forms the basis of the so-called "kinetic method".

We reported earlier[3] that Hg(II) catalyses displacement of cyanide from hexacyanoferrate(II) by *p*-nitrosodiphenylamine and can thus be determined in concentrations as low as $2 \times 10^{-8}M$.

We now report use of the same indicator reaction for determination of ligands containing a nitrogen, oxygen or sulphur donor atom. The Hg(II) complexes with sulphur-containing ligands are usually more stable than those containing nitrogen or oxygen donor atoms, even at low pH, and are thus better suited for the proposed method. We have, therefore, examined three such ligands, thioglycollic acid (TGA), cysteine and thiosulphate, all of which inhibit the indicator reaction.

The concentrations of the other reactants are high compared with that of the catalyst. Because of the high molar absorptivity of the product it is easy to monitor the reaction-rate even in presence of an inhibitor. The reaction-rate method is satisfactory if a measurable change in rate is caused by a 10–20% change in the catalyst concentration. For a typical concentration (C_C) of $4 \times 10^{-7}M$ for a catalyst forming a 1:1 complex with an inhibitor, the concentration of the inhibitor (C_I) would need to be at least $4 \times 10^{-8}M$ for detection. If the inhibitor is regarded as 99% complexed under these conditions, the conditional formation constant of the complex, K'_{CI}, would be approximately $3 \times 10^{-8}M$. It can likewise be calculated that for equal concentrations of catalyst and inhibitor (forming a 1:1 complex) the catalytic reaction would effectively cease[4] (99% complexation) under conditions where K'_{CI} is $> 10^4/C_C$.

If K'_{CI} is too low, only partial complexation and hence partial inhibition will occur, so the pH will be a critical factor, since practically all inhibitors will be strong bases. It follows that the sensitivity towards inhibitors will be maximal if the optimum pH for the indicator reaction is higher than the pH at which the side-reaction coefficient for protonation of the inhibitor species becomes significantly greater than unity.

EXPERIMENTAL

Reagents

Stock solutions of potassium hexacyanoferrate(II), mercuric chloride and *p*-nitrosodiphenylamine were prepared as reported earlier.[3] Cysteine hydrochloride is readily oxidized by atmospheric oxygen at room temperature[5] so a stock solution was stored at low temperature and standardized with hexacyanoferrate(III)[6] every time before use. The thioglycollic acid was standardized with periodate, with iodide and starch as indicator.[7] Thiosulphate was standardized iodometrically against standard dichromate solution.[8] The pH of the reaction mixture was kept constant as desired, with phthalate–sodium hydroxide buffer. All solutions were thermally equilibrated for half an hour in a thermostat at $25 \pm 0.1°$ before the kinetic runs.

Procedure

To 1 ml of Hg(II) solution of fixed concentration, add 1 ml of inhibitor (or complexing agent) and let stand for 10 min to ensure formation of the mercury complex. Then add 6 ml of buffer and 1 ml of *p*-nitrosodiphenylamine solution of fixed concentration. Initiate the reaction by adding 1 ml of hexacyanoferrate(II) solution. Shake the reaction mixture well and transfer it to a 1-cm cuvette in a constant-temperature cell compartment ($25 \pm 0.1°$). Use the fixed-time procedure to find the initial rate of reaction.

Use the reagent concentration given below, pH 5 ± 0.2, and an ionic strength of $0.15M$ (obtained by adding an appropriate amount of potassium nitrate along with the buffer.

*Author for correspondence.

Determinand (I)	$[Fe(CN)_6^{4-}]$, M	[p-NDA], M	$[Hg^{2+}]$, M	$[I]/[Hg^{2+}]$
Thioglycollic acid	9×10^{-3}	2.5×10^{-4}	4×10^{-7}	0.1–1.1
Cysteine	1×10^{-2}	2.5×10^{-4}	5×10^{-7}	0.1–6
Thiosulphate	9×10^{-3}	2.5×10^{-4}	4×10^{-7}	0.1–5

Caution

Sometimes a higher initial absorbance is observed for a kinetic run when the observation cell has been used for many runs. This is due to deposition of the highly absorbing green complex $[Fe(CN)_5 \cdot p\text{-NDA}]^{3-}$ on the optical walls of the cuvette. The cell should, therefore, be cleaned with acetone after each run.

RESULTS AND DISCUSSION

The basic considerations concerning preparation of solutions, reagent concentrations and pH control are similar to those reported previously.[3] Maintenance of the reaction mixture at pH 5 ± 0.2 is critical, since TGA and cysteine will be present in various forms, the relative amounts of which are a function of pH. Because this pH is quite critical[3] for the indicator reaction, it has to be used for determination of the inhibitor, though it results in a higher detection limit and poorer sensitivity. As reported earlier,[11] temperature does not appreciably affect the sensitivity of the reaction and 25° was chosen for convenience.

The absorbance change over a short reaction time, denoted by A_t, can be taken as a measure of the initial rate. For the inhibitors tested, plots of A_t *vs.* mole ratio are shown in Fig. 1, and are non-linear. Plotting A_t *vs.* e^{-x} (where $x = C_I/C_C$), as was done by Klockow *et al.*,[9] gives good linear relationships over a moderate range of concentrations, as shown in Fig. 2. It can be seen (Fig. 1) that TGA has maximum inhibitory effect at $x \sim 1.1$ and that further addition

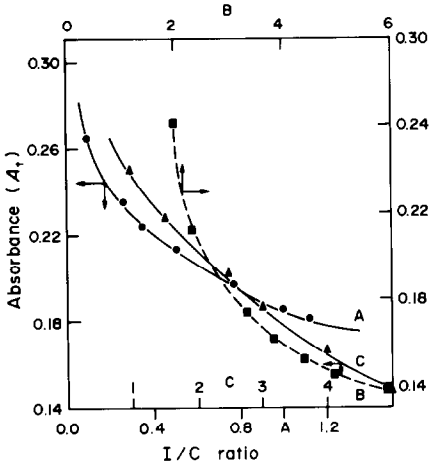

Fig. 1. Plot of absorbance after fixed time *vs.* (inhibitor)/(catalyst) mole ratio. (A) TGA: $[Fe(CN)_6^{4-}] = 9 \times 10^{-3}M$, [$p$-NDA] $= 2.5 \times 10^{-4}M$, $[Hg^{2+}] = 4 \times 10^{-7}M$, pH $= 5 \pm 0.2$, time $= 15$ min. (B) Cysteine: $[Fe(CN)_6^{4-}] = 1 \times 10^{-2}M$, [$p$-NDA] $= 2.5 \times 10^{-4}M$, $[Hg^{2+}] = 5 \times 10^{-7}M$, pH $= 5 \pm 0.2$, time $= 20$ min. (C) Thiosulphate: $[Fe(CN)_6^{4-}] = 9 \times 10^{-3}M$, [$p$-NDA] $= 2.5 \times 10^{-4}M$, $[Hg^{2+}] = 4 \times 10^{-7}M$, pH $= 5 \pm 0.2$, time $= 20$ min.

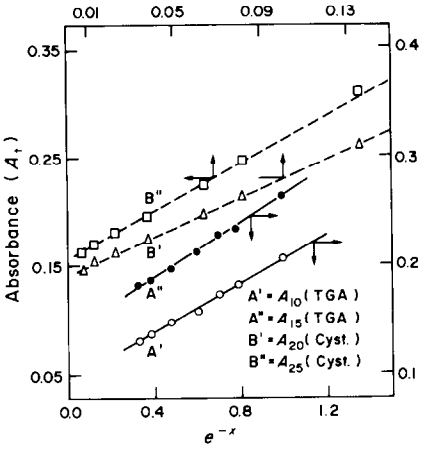

Fig. 2. Calibration curve for determination of TGA and cysteine—plot of absorbance after fixed time *vs.* e^{-x}. Conditions as for Fig. 1, (A) and (B).

of TGA has little or no more inhibitory effect. Cysteine has no appreciable inhibitory effect until x approaches 2. A linear plot is obtained between A_t and e^{-x} for x ranging from 2.0 to 6.0. Similarly

Table 1. Determination of TGA

Taken, 10^{-7}M	Found,* 10^{-7}M	
	A_{10}	A_{15}
4.60	4.4_0	4.4_6
3.97	3.8_7	3.8_2
3.02	3.0_2	3.0_2
2.04	1.9_1	2.0_4
1.42	1.4_0	1.4_0
1.05	1.0	1.0_5

$[Hg^{2+}] = 4 \times 10^{-7}M$; $[Fe(CN)_6^{4-}] = 9 \times 10^{-3}M$; [$p$-NDA] $= 2.5 \times 10^{-4}M$; pH $= 5.0 \pm 0.2$; $\mu = 0.15M$; temperature $= 25 \pm 0.1$°C; A_{10} and A_{15} refer to measurement after 10 and 15 min respectively.
*Mean of three results; standard deviation $0.1 \times 10^{-7}M$ throughout.

Table 2. Determination of cysteine

Taken, 10^{-6}M	Found,* 10^{-6}M	
	A_{20}	A_{25}
2.49	2.48 ± 0.20	2.42 ± 0.20
2.21	2.09 ± 0.05	2.20 ± 0.03
1.88	1.83 ± 0.03	1.87 ± 0.01
1.63	1.66 ± 0.01	1.66 ± 0.01
1.38	1.39 ± 0.03	1.38 ± 0.01
1.25	1.25 ± 0.05	1.25 ± 0.03
1.00	0.96 ± 0.03	0.98 ± 0.01

$[Hg^{2+}] = 5 \times 10^{-7}M$; $[Fe(CN)_6^{4-}] = 1 \times 10^{-2}M$; [$p$-NDA] $= 2.5 \times 10^{-4}M$; pH $= 5.0 \pm 0.2$; $\mu = 0.15M$; temperature $= 25 \pm 0.1$°C; A_{20} and A_{25} refer to measurement after 20 and 25 min respectively.
*Mean of three determinations ($\pm$ = standard deviation).

Table 3. Determination of thiosulphate

Taken, 10^{-7}M	Found,* 10^{-7}M	
	A_{15}	A_{20}
4.0	$4.0 \pm 0.1_3$	$3.7 \pm 0.1_3$
6.0	$6.4 \pm 0.1_3$	$6.4 \pm 0.1_3$
8.1	$8.0 \pm 0.2_4$	$7.9 \pm 0.2_4$
10.0	$11.0 \pm 0.0_3$	$9.9 \pm 0.1_3$
12.5	$12.9 \pm 0.0_3$	$12.6 \pm 0.0_3$
16.2	$15.5 \pm 0.1_3$	$15.8 \pm 0.1_3$

$[Hg^{2+}] = 4 \times 10^{-7}M$; $[Fe(CN)_6^{4-}] = 9 \times 10^{-3}M$; [*p*-NDA] $= 2.5 \times 10^{-4}M$; pH $= 5.0 \pm 0.2$; $\mu = 0.15M$; temperature $= 25 \pm 0.1$°C; A_{15} and A_{20} refer to measurement after 15 and 20 min respectively.
*Mean of three determinations ($\pm$ = standard deviation).

thiosulphate has no perceptible effect for $x < 1$, and the linear relationship holds from $x = 1$ to $x = 5$ when A_t is plotted against $[S_2O_3^{2-}]^{1/2}$. Higher concentration ratios do not affect the rate further and it thus approaches a limiting value.

Mercury(II) concentrations below $4 \times 10^{-7}M$ were also tested but the catalytic effect was insufficient to give a measurable change in the reaction rate under the chosen experimental conditions. Increasing the catalyst concentration increases the sensitivity and extends the concentration range over which the inhibitors can be determined. It also decreases the detection limit except for TGA.

The relative standard deviations for triplicate determinations are given in Tables 1–3. The relevant equations for calibration curves can be obtained by a least-squares fit and they give a positive intercept on the ordinate.

The kinetic role of sulphur-containing ligands as inhibitors for the reaction of $Fe(CN)_6^{4-}$ and *p*-NDA in the presence of Hg(II) as catalyst can be understood if we assume that the inhibitor competitively forms a non-reactive complex with the catalyst. The inhibitor lowers the free catalyst concentration and hence the reaction rate. The reaction scheme proposed earlier,[3] modified to include the role of the inhibitor (I), can be given in general form as:

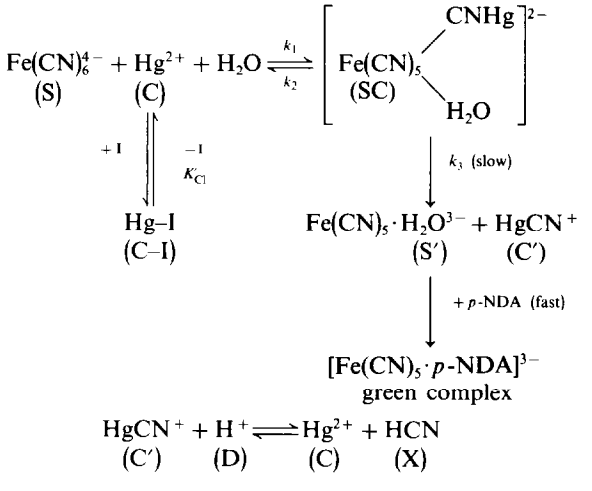

$Fe(CN)_6^{4-}$ (present in large excess) is denoted by S (substrate) and its initial concentration by $[S_0]$. C represents the catalyst, I the inhibitor, SC and CI the complexes of the catalyst with the substrate and inhibitor respectively, S′ the intermediate that gives the final product and C′ and D the species which regenerate the catalyst (D is usually H^+, OH^- or H_2O). It is then a simple matter to derive the rate expression for the conditions that $[S_0]$ is large and $[I_0] > [Hg\text{–}I]$:

$$v_I = \frac{v_{max}}{\frac{K_m}{[S_0]}\left(1 + \frac{[I_0]}{K'_{CI}}\right) + 1} \qquad (1)$$

where $K_m = (k_2 + k_3)/k_1$.

Here v_{max} denotes the maximum attainable velocity when the rate becomes independent of substrate concentration but is dependent on the catalyst concentration (in absence of the inhibitor); v_I denotes the reaction velocity in the presence of inhibitor. K_m (the equivalent of the Michaelis–Menton constant) is approximately equal to the dissociation constant of the catalyst–substrate complex and K'_{CI} the conditional dissociation constant of the catalyst–inhibitor complex. Expression (1) is derived in a manner similar to that for an enzyme-catalysed reaction of a single substrate in presence of an inhibitor. It is also formally similar to the rate equation for heterogeneously catalysed unimolecular gas-phase reactions proceeding by the Langmuir mechanism. A passing reference to this similarity was made by Klockow *et al.*[9] in deriving an expression for determination of F^- by its inhibiting effect on the Zr-catalysed oxidation of I^- by perborate, but was not dealt with by them in any detail. Equation (1) can be rearranged by the Lineweaver–Burk transformation[10] to yield

$$\frac{1}{v_I} - \frac{1}{v_{max}} = \frac{K_m}{v_{max}[S_0]} + \frac{K_m[I_0]}{v_{max}[S_0]K'_{CI}} \qquad (2)$$

The value of v_{max} is obtained from the intercept of the plot of $1/v$ *vs.* $1/[S_0]$ for the system in the absence of the inhibitor.

If equation (2) holds, a plot of the left-hand side *vs.* $[I_0]$ should give a straight line with intercept $K_m/v_{max}[S_0]$ and slope $K_m/v_{max}[S_0]K'_{CI}$. Thus K_m and K'_{CI} can be obtained. The K_m values obtained from such plots (not shown) are given in Table 4. The reciprocal of K_m so obtained is approximately equal to the stability constant K_s ($= k_1/k_2$; log $K_s = 2.42 \pm 0.02$) of the catalyst–substrate complex reported by us earlier.[3] The average values of K_m (this work), K_s and k_3 (16.7 ± 0.8)[3] thus obtained enable us to estimate $k_1 = 6 \times 10^5$ l.mole^{-1}.sec^{-1} and $k_2 = 2.3 \times 10^3$ sec^{-1}. Since the value of k_3 is quite small compared to k_2, the near equality of K_m^{-1} and K_s is understandable. The stability constants (K_{CI}) of the three catalyst–inhibitor complexes (reciprocals of K'_{CI}), which are actually conditional equilibrium constants, are also given in Table 4.

Table 4. Conditional constants (under conditions given in experimental section)

Inhibitor	log K_{CI}	log K_M
Thioglycollic acid	6.51 ± 0.02	-2.49 ± 0.02
Cysteine	5.92 ± 0.1	-2.40 ± 0.01
Thiosulphate	6.19 ± 0.01	-2.36 ± 0.01

Alternatively, the catalyst–inhibitor complex formed may dissociate appreciably, especially in the presence of a high concentration of the reactants or products of the indicator reaction (for example CN^- in this case). In such cases the degree of inhibition will fall below the limit for giving 10–20% change in catalyst concentration and it will be difficult to differentiate the inhibited part of the catalyst from the reactive part and with increase of time the reaction will follow the rate of the catalysed reaction only. This may be the reason why no perceptible change in rate is seen in the case of cysteine till a metal:inhibitor ratio of 1:2 is reached. The competitive, non-competitive and uncompetitive behaviour of inhibiting ligands can also be differentiated but this has not been attempted here. Some observation is called for about the dependence of the indicator reaction rate on the concentration of thiosulphate. Unlike the case of TGA and cysteine there is a linear relationship between the square root of the thiosulphate concentration and A_{15} or A_{20}. This behaviour is not well understood at present. An attempt will be made to provide an explanation for this anomaly in future work.

Interferences

The interferences for the indicator reaction have already been enumerated[11] and will be the same here. In addition, any complexing agents giving mercury complexes more stable than the one of analytical interest will also interfere. It is also reasonable to assume that the few metal ions which can complex more strongly than Hg(II) under the given conditions with the three ligands investigated, should be absent. Among the metals giving less stable complexes than the Hg(II) complexes, Zn^{2+}, Cd^{2+} and Bi^{3+} were tested for interference. None of them interferes until a metal:catalyst molar ratio of 2 is reached, and this is assumed to be the tolerance limit for such metals.

The inhibitory effect of TGA starts at an [I]/[C] ratio of 0.1, while for cysteine and thiosulphate the effect starts at ratios of 1 and 2 respectively (Fig. 1). We have verified experimentally that there is no interference in the determination of TGA in presence of cysteine and thiosulphate up to [interferent]/[C] ratios of 1 and 2 respectively. Similarly cysteine can be determined in the presence of thiosulphate when the $[S_2O_3^{2-}]$/[C] ratio does not exceed 2. Neither cysteine nor thiosulphate can be determined in the presence of TGA, however.

We have made the interesting observation[12] that some non-sulphur-containing amino-acids, *viz.* histidine, isoleucine and iminodiacetic acid, accelerate the indicator reaction used. Such an acceleration has also been observed by previous workers.[13–15] The kinetic method discussed here can, therefore, also be used for a qualitative distinction between sulphur-containing and non-sulphur-containing amino-acids. The latter will obviously interfere in determination of the former. The activators can also be used to increase the sensitivity of an indicator reaction for a given analyte.

Acknowledgements—One of us (M.P.) is thankful to the University Grants Commission, Government of India, for the award of a fellowship under their Faculty Improvement Programme. The other (P.C.N.) is thankful to the Department of Science and Technology, Government of India, for partial support of this work.

REFERENCES

1. H. B. Mark, Jr. and H. A. Mottola, *Anal. Chem.*, 1980, **52**, 31R.
2. A. E. Martell, *Pure Appl. Chem.*, 1968, **17**, 129.
3. M. Phull and P. C. Nigam, *Talanta*, 1981, **28**, 591.
4. H. Muller, *ibid.*, 1979, **26**, 785.
5. P. J. Morando, E. B. Borghi, L. M. de Scheingart and M. A. Blesa, *J. Chem. Soc. Dalton Trans.*, 1981, 435.
6. H. L. Mason, *J. Biol. Chem.* 1930, **86**, 623.
7. S. Bose, *Curr. Sci. India*, 1977, **46**, 562.
8. A. I. Vogel, *A Textbook of Quantitative Inorganic Analysis*, 3rd Ed., p. 350. Longmans, London, 1962.
9. D. Klockow, J. Auffarth and C. Kopp, *Anal. Chim. Acta*, 1977, **89**, 37.
10. H. Lineweaver and D. Burk, *J. Am. Chem. Soc.*, 1934, **56**, 658.
11. M. Phull, H. C. Bajaj and P. C. Nigam, *Talanta*, 1981, **28**, 610.
12. P. C. Nigam, M. Phull and S. R. Naidu, communicated.
13. D. P. Nikolelis and T. P. Hadjiioannou, *Analyst*, 1977, **102**, 591.
14. H. A. Mottola and C. R. Harrison, *Talanta*, 1971, **18**, 683.
15. H. A. Mottola and G. L. Heath, *Anal. Chem.*, 1972, **44**, 2322.

Talanta, Vol. 30, No. 6, pp. 405–408, 1983
Printed in Great Britain

0039-9140/83/060405-04$03.00/0
Pergamon Press Ltd

EXTRACTION OF ZINC, CADMIUM AND MERCURY SALICYLATES

VASUDHA V. MUDSHINGIKAR and V. M. SHINDE
Analytical Laboratory, Department of Chemistry, Shivaji University, Kolhapur 416004, India

(*Received* 23 *November* 1981. *Revised* 10 *December* 1982. *Accepted* 23 *December* 1982)

Summary—A systematic study of the solvent extraction of Zn, Cd and Hg salicylates is reported. Optimum conditions for extraction and separation of Zn, Cd and Hg are evaluated from a critical study of pH, sodium salicylate concentration, mesityl oxide concentration, period of equilibration, and effect of diverse ions. A separation scheme is described and results are reported for analysis of synthetic mixtures and commercial samples.

Mesityl oxide has been used by Khopkar and Shinde for the extraction of transition elements from halide solutions.[1] In this communication we propose a method for extraction of zinc, cadmium and mercury as their salicylates, with mesityl oxide as extractant. The extracted metal ions are stripped with either distilled water or 5*M* sodium hydroxide solution, and determined complexometrically.[2,3]

Various methods for the solvent extraction of zinc, cadmium and mercury have been summarized and critically reviewed[4,5] but a method for their extractive separation is lacking. The proposed method permits separation of mercury(II) from zinc, cadmium, copper(II), lead and thallium(III) and that of zinc and cadmium from iron(III), molybdenum(VI), chromium(VI) and bismuth(III).

EXPERIMENTAL

Reagents

Analytical grade chemicals were used whenever possible. The stock solutions of mercury, zinc and cadmium were prepared by dissolving 1.67 g of mercuric chloride, 5.49 g of $ZnSO_4.7H_2O$ and 2.85 g of $3CdSO_4.8H_2O$ in 250 ml of distilled water containing the minimum amount of the appropriate acid to prevent hydrolysis. The solutions were standardized by known methods[3] and test solutions of lower concentration were prepared by suitable dilution.

The mesityl oxide used was doubly distilled (b.p. 128°). Buffer solution of pH 10 was prepared by adding 142 ml of concentrated ammonia solution to 17.5 g of ammonium chloride and diluting to 250 ml with distilled water. The buffer solution (also pH 10) used for spectrophotometric determination of mercury was prepared from 0.01*M* sodium carbonate and 0.01*M* sodium bicarbonate. A 0.1% methanolic solution of 1-(2-pyridylazo)-2-naphthol (PAN) was used for the mercury determination.

Procedure for mercury

Take a portion of test solution containing 1 mg of mercury, dilute it to 25 ml, add 2 g of sodium salicylate, and adjust the pH to 7 with dilute hydrochloric acid and sodium hydroxide. Transfer the solution into a 100-ml separatory funnel and shake it for 3 min with 10 ml of mesityl oxide. Separate the phases and strip mercury from the mesityl oxide layer by shaking this with two 10-ml portions of 5*M* sodium hydroxide. Determine mercury in the aqueous phase complexometrically.[2] For micro amounts (10–50 μg), determine the mercury spectrophotometrically in the mesityl oxide phase as follows: add 5 ml of bicarbonate buffer solution (pH 10) and 1 ml of 0.1% PAN solution and shake for 1 min. Measure the absorbance at 555 nm against a reagent blank similarly prepared.

Procedure for zinc and cadmium

Take a portion of test solution containing 1 mg of zinc or cadmium, dilute it to 25 ml, add 1.6 g of sodium salicylate for Zn or 1.4 g for Cd, and adjust the pH to 5.2–5.8 for Zn or 6.5–7.5 for Cd, and shake it for 2 min with 10 ml of mesityl oxide in a 100-ml separatory funnel. Separate the phases, strip the metal from the mesityl oxide phase with two 10-ml portions of distilled water, and determine it in the combined aqueous phase complexometrically.[3]

RESULTS AND DISCUSSION

Extraction conditions

By varying the pH (4.5–10), salicylate concentration (0.05–0.6*M*) and mesityl oxide concentration (10–100%, with benzene as diluent), it was shown that a single extraction (2–3 min shaking) with 10 ml of undiluted mesityl oxide is adequate for quantitative extraction of zinc, cadmium and mercury. The optimum extraction conditions are given in Table 1 and in Figs. 1 and 2.

Spectral characteristics

The extracted mercury may be determined spectrophotometrically in the mesityl oxide phase with PAN. The orange Hg–PAN complex in the organic phase has maximal absorption at 555 nm and obeys Beer's law over the concentration range 1–5 μg/ml in the organic phase. The colour is stable for 24 hr. The molar absorptivity is 1.21×10^4 l.mole^{-1}.cm^{-1}. The coefficient of variation is 2% at the 5 μg/ml level.

Nature of the extracted species

The log–log plots of distribution ratio *vs.* salicylate concentration (at fixed pH and mesityl oxide concentration) and *vs.* mesityl oxide concentration (at fixed pH and salicylate concentration) indicate a molar ratio of 1:2 with respect to both extractant and salicylate. Hence the extracted species is probably

Table 1. Optimum conditions for extraction of zinc, cadmium or mercury with undiluted mesityl oxide

Metal ion		Salicylate concentrations, M	pH
Zinc(II)	1–5 mg	0.4	5.2–5.8
Cadmium(II)	1–5 mg	0.35	6.5–7.5
Mercury(II)	10–50 μg 1–5 mg	0.5	6.8–7.2

$MSal_2.2MeO$, where M stands for either Zn(II), Cd(II) or Hg(II), Sal the salicylate ion and MeO mesityl oxide. The extraction is due to solvation of the metal salicylate and the solvation number for all three metal ions is 2.

Effect of diverse ions

An interference study showed that for the extraction and complexometric determination of Zn, Cd and Hg by the proposed procedure, a large number of cations and anions did not interfere (as shown by less than 1% deviation in analyte recovery). The few cations and anions that do interfere are listed in Table 2.

Separation of Hg(II) from Cu(II), Pb(II), Tl(III), Zn(II) or Cd(II)

Copper(II) remains quantitatively in the aqueous phase when mercury(II) is extracted into mesityl oxide from 0.5*M* sodium salicylate solution at pH 7. The unextracted copper can be estimated in the aqueous phase complexometrically,[2] and the mercury is stripped and determined as described above; zinc, cadmium, lead and thallium(III) are partially extracted with the mercury, but can be removed by washing the mesityl oxide phase with water (2 × 10 ml), and this extract is combined with the aqueous phase from the extraction, containing the rest of these metal ions.

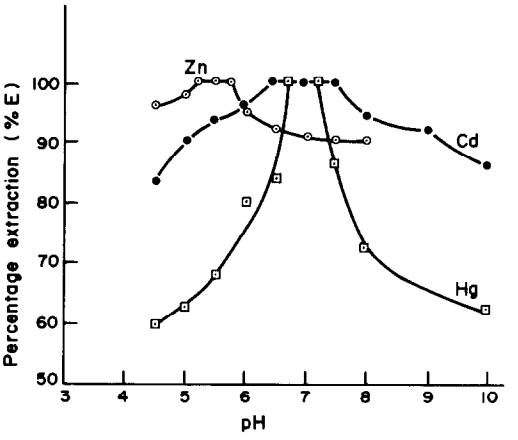

Fig. 1. Extraction of Zn, Cd, Hg as a function of pH.

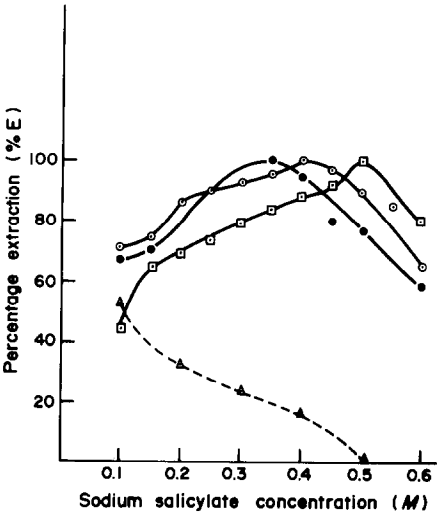

Fig. 2. Extraction of Zn, Cd, Hg, Cu as a function of salicylate concentration. ⊡——⊡, Hg; ●—●, Cd; ⊙——⊙, Zn; △---△, Cu.

Table 2. Effect of diverse ions on extraction of 1 mg of Zn(II), Cd(II) or Hg(II)

Tolerance limit, *mg*	Zinc	Cadmium	Mercury
20	Cr(VI)	Ag(I), Au(III), Cr(VI)	—
15	W(VI), Mo(VI)	W(VI)	Cr(VI)
10	Ag(I), Hg(II), Au(III), Fe(III), Bi(III), PO_4^{3-} F^-, Cl^-, ascorbate, SCN^-	Ca(II), Sr(II), Ba(II), Hg(II), Fe(III), Mo(VI), Bi(III), PO_4^{3-}, F^-, Cl^-, ascorbate$^-$, SCN^-	Ag(I), Au(III), Fe(III), V(V), W(VI), Mo(VI), Cl^-, tartrate,
7.5	V(V)	V(V)	—
5	Ca(II), Sr(II), Ba(II), Ti(IV), citrate, oxalate, tartrate, NO_3^-, SO_4^{2-}, thiourea	Ti(IV), citrate oxalate, tartrate, NO_3^-, SO_4^{2-}, thiourea	Ca(II), Sr(II), Ba(II), Ti(IV), citrate, oxalate, NO_3^-, PO_4^{3-}, SO_4^{2-} SCN^-, ascorbate
2.5	—	—	Bi(III), thiourea
Ions not tolerated	Cd(II), Cu(II), Mn(II)	Zn(II), Cu(II), Mn(II)	Zn(II), Cd(II), Mn(II), Pd(II), Pt(IV), Sn(II)

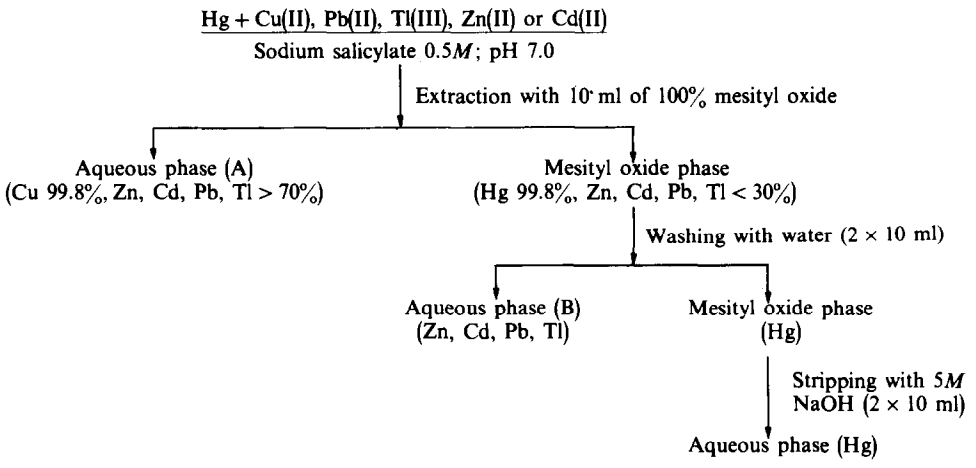

Fig. 3. Flow-sheet for separation scheme.

In the combined aqueous phase Zn, Cd, Pb and Tl(III) are estimated complexometrically.[2,3] The extracted mercury is stripped from the mesityl oxide with 5*M* sodium hydroxide and estimated complexometrically as already described. The separation scheme is shown in Fig. 3. The separation of mercury is quantitative and results of analysis of some synthetic mixtures are reported in Table 3.

Separation of Zn(II) or Cd(II) from Fe(III), Mo(VI) and Cr(VI)

The quantitative extraction of zinc and cadmium into mesityl oxide from sodium salicylate solution (0.4*M* at pH 5.5 ± 0.3 for Zn and 0.35*M* at pH 7.0 ± 0.5 for Cd) facilitates their separation from iron(III), molybdenum(VI) and chromium(VI), which remain quantitatively in the aqueous phase, where they can be estimated spectrophotometrically.[6] Zinc and cadmium are stripped from the mesityl oxide phase and determined as already described. Iron and molybdenum are estimated colorimetrically with thiocyanate, and chromium with diphenylcarbazide.[6] The results for some separations are reported in Table 4.

Table 3. Analysis of synthetic mixtures containing mercury

No.	Composition, *mg*	Recovery of mercury,* %	Recovery of added ion,* %
1	Hg(II), 1; Zn(II), 1	99.8	99.7
2	Hg(II), 1; Zn(II), 2	99.6	99.7
3	Hg(II), 2; Zn(II), 1	99.4	99.8
4	Hg(II), 1; Cd(II), 1	99.8	99.9
5	Hg(II), 1; Cd(II), 2	99.8	99.9
6	Hg(II), 2; Cd(II), 1	99.6	99.7
7	Hg(II), 1; Pb(II), 1	99.8	99.6
8	Hg(II), 1; Cu(II), 1	99.8	99.8
9	Hg(II), 1; Tl(III), 1	99.8	99.5
10	Hg(II), 1; Fe, 2; Cr, 2; Mo, 1; W, 1	99.8	—
11†	Hg(II), 1; Zn, 2; Cd, 2; Pb, 1; Mn, 1	99.6	—
12	Hg(II), 1; Au, 2; Ag, 2; Cu, 1	99.7	—

*Mean of three results.
†Zn, Cd, Pb and Mn removed by scrubbing with distilled water after extraction.

Table 4. Separation of zinc and cadmium from synthetic mixtures

No.	Composition, *mg*	Recovery of Zn or Cd,* %	Recovery of added ion,* %
1	Zn(II), 1; Fe(II), 1	99.7	99.3
2	Zn(II), 1; Fe(III), 2	99.7	99.0
3	Cd(II), 1; Fe(III), 2	100.0	100.0
4	Zn(II), 1; Cr(VI), 1	99.8	99.7
5	Zn(II), 1; Cr(VI), 2	99.7	99.7
6	Cd(II), 1; Cr(VI), 2	99.7	99.8
7	Zn(II), 1; Mo(VI), 1	99.6	99.7
8	Cd(II), 1; Mo(VI), 1	99.5	99.5
9	Zn(II), 1; Bi(III), 1	99.5	99.8
10	Cd(II), 1; Bi(III), 1	99.5	99.8
11	Zn(II), 1; Fe, 1; Cr, 1; Mo, 1; W, 1	99.4	—
12	Zn(II), 1; Au, 1; Ag, 1	99,7	—
13	Zn(II), 1; Hg, 2; Bi, 1	99.3	—
14	Cd(II), 1; Fe, 1; Cr, 1; Mo, 1; W, 1	99.4	—
15	Cd(II), 1; Au, 1; Ag, 1	99.5	—
16	Cd(II), 1; Hg, 2; Bi, 1	99.6	—

*Mean of three results.

Table 5. Precision data (6 replicates)

	Taken, *mg*	Found, *mg*	Std. devn., *μg*	Relative Std. devn., %
Hg	1	0.991–1.003 (mean 0.997)	4	0.4
	2	1.985–1.995 (mean 1.990)	3	0.2
Zn	1	0.990–1.002 (mean 0.996)	5	0.5
Cd	1	0.990–1.002 (mean 0.996)	5	0.5

Table 6. Analysis of commercial items (6 replicates)

Item	Manufactured by	Composition	Nominal amount of metal, %	Present method		Spectrophotometrically[7,8]	
				Found, %	Std. devn., %	Found, %	Std. devn., %
"Nycil" (Prickly heat powder)	Glaxo Laboratories (India) Ltd.	Chlorphenesin BP1%, boric acid IP 5% zinc oxide IP 16%, starch IP 51%, talc purified IP to 100%	12.8	11.1–12.6 (mean 11.9)	0.5	11.9–13.0 (mean 12.4)	0.4
"Siloderm" (Skin protective barrier ointment)	Neo-Pharma Pvt. Ltd. (India)	Dimethicene 20 BPC 20%, zinc oxide IP 7.5%, calamine IP 1.5%, centrimide IP 1.125%	6.0	6.2–6.8 (mean 6.5)	0.2	6.0–6.2 (mean 6.1)	0.1
"Neko" (Medicated soap)	Parke-Davis (India) Ltd.	Mercuric iodide 1% w/w	0.54	0.41–0.49 (mean 0.45)	0.03	0.47–0.55 (mean 0.51)	0.03

Separation of Zn(II) or Cd(II) from Bi(III)

Bismuth is co-extracted with zinc and cadmium but can be separated from them by selectively stripping them with water. The bismuth can be stripped from the mesityl oxide phase with two 10-ml portions of 1*M* sodium hydroxide, and determined complexometrically with EDTA.[2] Some results are reported in Table 4.

Precision

The results in Table 5 show that the relative standard deviation for determination of 1 mg of mercury, zinc or cadmium is 0.4–0.5%.

Analysis of commercial samples

"Nycil" talc powder and "Siloderm" skin protective ointment. The samples (20–50 mg) were treated with the minimum amount of concentrated sulphuric acid needed to dissolve the zinc oxide present. The solutions were diluted to 25 ml with distilled water and extracted with 10 ml of mesityl oxide after adjustment to the optimum extraction conditions for zinc. Zinc was stripped from the mesityl oxide phase with water and estimated complexometrically with EDTA.[2]

"Neko" medicated soap. A 200-mg sample was dissolved in 25 ml of water containing 2 or 3 drops of concentrated hydrochloric acid. The solution was heated for 5 min and extracted with mesityl oxide after adjustment to the optimum extraction conditions for mercury. Mercury was stripped from the organic phase with 5*M* sodium hydroxide and estimated complexometrically with EDTA.[2]

The results were satisfactory and are reported in Table 6.

Acknowledgements—The authors are thankful to Dr. R. A. Chalmers for helpful suggestions, and gratefully express their thanks to the Council of Scientific and Industrial Research, New Delhi, India, for awarding a fellowship to one of them (VVM).

REFERENCES

1. V. M. Shinde and S. M. Khopkar, *Anal. Chim. Acta*, 1968, **43**, 146; *Talanta*, 1969, **16**, 525; *Indian J. Chem.*, 1969, **7**, 504; *Sepn. Sci.*, 1969, **4**, 161; *Chem. Analit. Warsaw*, 1969, **14**, 749; *Z. Anal. Chem.*, 1970, **249**, 239; *Anal. Chem.*, 1971, **43**, 473; *Sepn. Sci.*, 1972, **7**, 97.
2. F. J. Welcher, *The Analytical Uses of Ethylenediamine Tetraacetic Acid*, pp. 164, 234, 382. Van Nostrand, New York, 1961.
3. A. I. Vogel, *A Textbook of Quantitative Inorganic Analysis*, 3rd Ed., pp. 433, 444, 442. Longmans, London, 1961.
4. J. Starý, *The Solvent Extraction of Metal Chelates*. Pergamon Press, London, 1964.
5. A. K. De, S. M. Khopkar and R. A. Chalmers, *Solvent Extraction of Metals*. Van Nostrand, London, 1970.
6. E. B. Sandell, *Colorimetric Determination of Traces of Metals*, 3rd Ed., pp. 397, 524, 644. Interscience, New York, 1965.
7. S. Ahrland and R. G. Herman, *Anal., Chem.*, 1975, **47**, 2422.
8. Li-Shu Ho, Ching-Nan Kuo, Chihsheng Shih and Wu-Chiang, *Chem. Bull. Peking*, 1965, **4**, 250.

Talanta, Vol. 30, No. 6, pp. 409–412, 1983
Printed in Great Britain.

0039-9140/83/060409-04$03.00/0

SPECTROPHOTOMETRIC DETERMINATION OF TRACE AMOUNTS OF SELENIUM WITH 4,5,6-TRIAMINOPYRIMIDINE

MARIO E. BODINI* and OMAR ALZAMORA E.
Pontificia Universidad Católica de Chile, Facultad de Química, Casilla 114-D, Santiago, Chile

(*Received* 1 *April* 1981. *Revised* 3 *November* 1982. *Accepted* 23 *December* 1982)

Summary—4,5,6-Triaminopyrimidine reacts in acidic aqueous media with selenium(IV) to give a piazselenol which has an absorption maximum at 362 nm with a molar absorptivity of 1.72×10^4 $l.mole^{-1}.cm^{-1}$. The compound is stable but not extractable into non-polar solvents. The calibration graph is linear up to 10 ppm of selenium, with a detection limit of 0.1 ppm in the sample solutions. Of the many different ions tested only iron(III) (in the presence of chloride) and tin(II) interfere. The method has good reproducibility, with a relative standard deviation of 1.5% for pure solutions. The application of this method to analysis of water and electrolytic copper is described.

The most frequently utilized spectrophotometric methods for the determination of selenium at trace levels are those in which this element reacts with an aromatic *o*-diamine to yield the corresponding piazselenol.[1] Hoste and Gillis[2,3] introduced 3,3′-diaminobenzidine as a selective colorimetric reagent for selenium(IV), which forms an intensely yellow product in acidic medium:

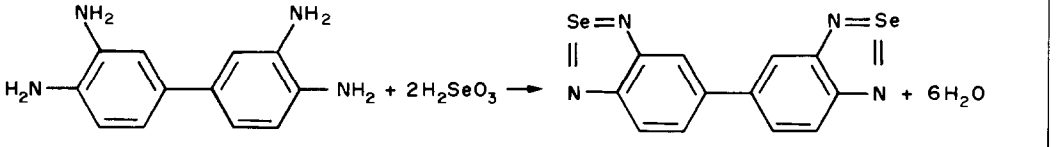

The piazselenol can be extracted[4] and the quantity of selenium determined from the absorbance at 420 nm. Several reagents with similar structural characteristics have since been studied,[5–7] but most of these reagents give a poor reproducibility when applied to samples of electrolytic copper;[8] in addition, 3,3′-diaminobenzidine is being banned as an analytical reagent in view of its reported toxicity.

Since the reaction takes place with the *o*-diamino grouping, we considered it of interest to study the reaction of 4,5,6-triaminopyrimidine with selenium(IV).

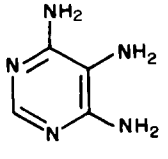

4,5,6-Triaminopyrimidine

This molecule has three vicinal amino groups so the reaction with selenium should be favoured.

The present work describes the study of this reaction and its application, to determination of selenium in electrolytic copper and in water.

EXPERIMENTAL

Reagents

4,5,6-Triaminopyrimidine (TAP) was obtained as the hydrated sulphate from Aldrich Chemical Co., Inc. Stock solutions (0.01*M*) in 1*M* hydrochloric acid and in 3.5*M* phosphoric acid were purified by stirring with activated charcoal for 15 min. The purified stock solutions were stored in the refrigerator, after saturation with nitrogen, and did not decompose appreciably for three weeks.

The standard selenium(IV) solution was prepared by diluting the contents of a Merck "Titrisol" (containing 1000 g of Se) to 500 ml with doubly distilled water. The 250-ppm stock solutions of selenium(IV) were prepared by dilution of this solution. Class A volumetric glassware was used for this purpose.

The copper sulphate used in exploratory work was analysed by neutron-activation analysis at the Chilean Nuclear Energy Commission and found to contain <0.05 ppm selenium.

All other chemicals used were reagent grade.

Procedure for analysis of electrolytic copper

Clean the sample with dilute nitric acid (1 + 9), wash it with distilled water and then acetone, and dry it. Dissolve 10 g of the cleaned sample in 90 ml of nitric acid (1 + 1), with mild heating. Add 10 ml of concentrated sulphuric acid and heat until the solution is evaporated almost to dryness. Take up the cooled residue in water, adjust to pH 3 with ammonia and dilute to about 200 ml. Add 2 ml of ferric nitrate solution (Fe 5 mg/ml). Adjust the pH to 4.0 with dilute ammonia solution. Stir for 1 hr, then filter off the iron precipitate with a porosity-4 sintered-glass crucible and

*Author for correspondence.

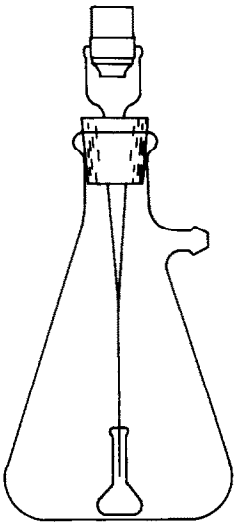

Fig. 1. Apparatus used to dissolve the ferric hydroxide precipitate with phosphoric acid and to collect the resulting solution in a 10-ml standard flask.

wash it with 10 ml of 0.5% ammonium nitrate solution. Add 4 ml of 3.5*M* phosphoric acid to the crucible containing the precipitate and collect the resulting solution in a 10-ml standard flask placed inside a 2-litre filter flask, as shown in Fig. 1. Then add 5 ml of 0.01*M* TAP solution in 3.5*M* phosphoric acid and finally make up to volume with distilled water. Measure the absorbance at 360 nm after 13 hr at room temperature, or 2 hr at 40°. Run a blank with a selenium-free copper solution by the same procedure.

Procedure for water analysis

To an appropriate volume of sample (*e.g.*, 100 ml) add 2 ml of ferric nitrate solution (Fe 5 mg/ml) and adjust to pH 9 with dilute sodium hydroxide solution. Stir for 15 min, then filter off the precipitate, wash it, dissolve it and continue as described for analysis of copper samples.

RESULTS AND DISCUSSION

The reagent 4,5,6-triaminepyrimidine (TAP) reacts with selenium(IV), in aqueous acidic media, yielding a compound that shows an absorption maximum at 362 nm. Figure 2 shows the spectrum obtained from 0.3*M* hydrochloric acid containing 3 ppm of Se(IV) and 484 ppm of TAP, after a reaction time of 13 hr at room temperature.

The concentration of acid is an important variable of the reaction, and it has been found that the minimum concentration of hydrochloric acid required to obtain a good result is between 0.2 and 0.3*M*.

In this case the reaction product is not extractable into the non-polar solvents normally used, such as toluene, chloroform, ether and carbon tetrachloride. Apparently this is due to the presence of the third amino group in TAP being protonated under the working conditions, and giving polar character to the piazselenol formed.

If phosphoric acid is used instead of hydrochloric, the results illustrated in Fig. 3 are obtained, which indicate that the optimum concentration of phosphoric acid is 3.5*M*. The reason for using phosphoric acid instead of hydrochloric is that ferric hydroxide is known to be a very good collecting agent for selenium(IV)[9] and we therefore chose this procedure to concentrate the selenium from the solutions. Dissolution of this precipitate with hydrochloric acid produces iron(III)–chloride complexes that interfere in the determination of selenium at 362 nm. The complex formed in phosphoric acid does not show this effect.

Since the protonated species of the corresponding diamine is known to be the one reacting with selenium(IV),[4] it is reasonable that a higher concentration of acid is needed when phosphoric acid is used, since it is weaker than hydrochloric acid.

Another important variable is the TAP:Se(IV) concentration ratio in the solutions. Figure 4 illustrates the dependence of the absorption maximum on this ratio, with 3.5*M* phosphoric acid and 2.5 ppm of selenium(IV) in the solutions, and 12 hr reaction time. The absorbance becomes constant for a TAP:Se(IV) molar ratio of 50 or more.

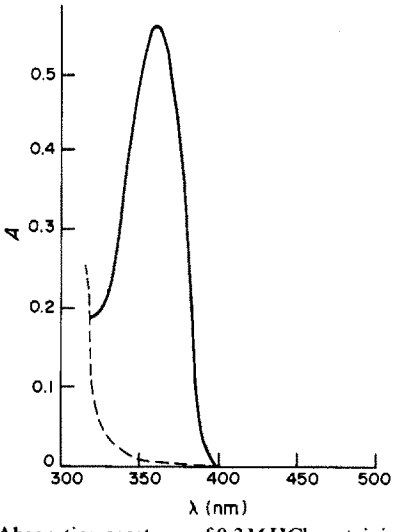

Fig. 2. Absorption spectrum of 0.3*M* HCl containing 3 ppm of selenium(IV) and 484 ppm of TAP, after a reaction time of 13 hr at room temperature. ——, Sample; – – –, blank.

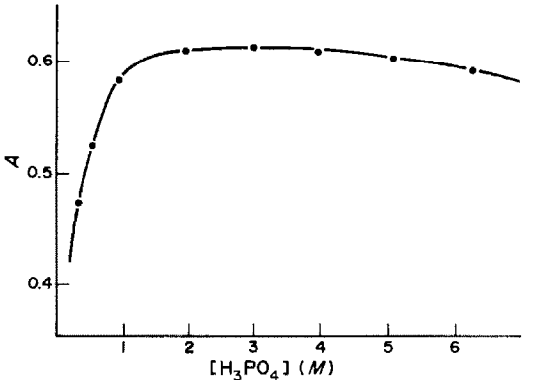

Fig. 3. Dependence of the absorbance of solution containing 3.5 ppm of selenium(IV) and 500 ppm of TAP, on the concentration of phosphoric acid.

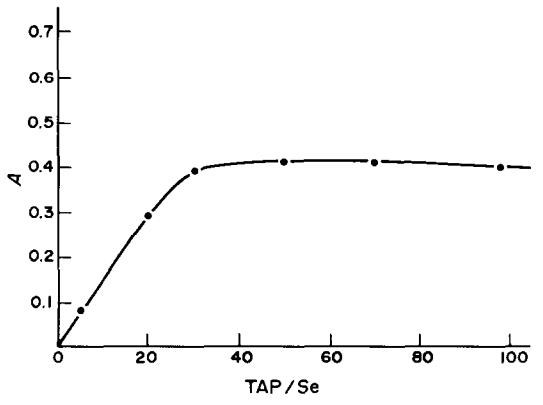

Fig. 4. Effect of the TAP:Se molar concentration ratio on the absorbance of solutions containing 2.5 ppm of Se(IV) in 3.5*M* H_3PO_4, after a reaction time of 12 hr.

The last variable studied was the reaction time. It was found that in 1*M* hydrochloric acid the reaction goes to completion in 11 hr whereas in 3.5*M* phosphoric acid the time needed is only 5.5 hr. These results confirm that the kinetics of the reaction involved strongly depend on the acid concentration.

If the temperature of the system is increased the reaction time becomes shorter. Thus, at 40° the absorbance readings become constant after 90 min, which is more convenient for practical purposes. At higher temperature the reaction time becomes even shorter but, in turn, the reaction product decomposes very rapidly, making the analysis less reliable.

The calibration graph obtained with 3.5*M* phosphoric acid, 600 ppm of TAP and measurement of the absorbance at 360 nm after a reaction time of 2 hr at 40° is linear up to 10 ppm of selenium and the molar absorptivity is 1.72×10^4 $l.mole^{-1}.cm^{-1}$. The detection limit is 0.1 ppm of Se. A reproducibility study gave a relative standard deviation of 1.5% in a series of 10 determinations on pure solutions containing 3 ppm of selenium.

The reaction stoichiometry was found to be 1:1 by the Job method,[10] so the reaction involved is one in

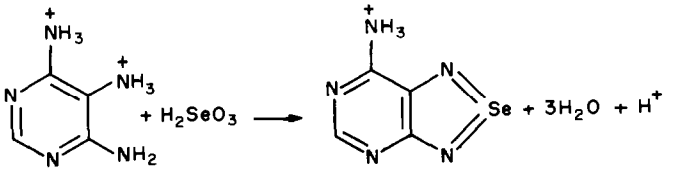

which the TAP must be protonated to favour formation of the piazselenol.

Of the ions normally present in the samples of interest it has been found that Cu^{2+} (100 ppm), Mn^{2+} (100 ppm), Sb^{3+} (50 ppm), Ag^{+} (100 ppm), Pb^{2+} (500 ppm), As^{3+} (50 ppm), and Te^{4+} (100 ppm) do not interfere when present at the levels shown in brackets. However, Sn^{2+} interferes by reducing Se(IV) to Se, and Fe^{3+} causes interference if hydrochloric acid is used instead of phosphoric (its chloride complex absorbs strongly at 360 nm). Nitrate, sulphate and chloride do not interfere even at high concentration, but a very high concentration of chloride should be avoided when selenium(IV) is co-precipitated with ferric hydroxide.

Table 1. Analysis of spiked water samples

Sample volume, *ml*	Selenium(IV), *μg*	
	Added	Found
100	3.0	2.9
100	7.5	7.5
1000	3.0	2.9

An attempt was made to apply the flotation technique, described by Nakashima[11] and by Tzeng and Zeitlin,[12] for separation of selenium from sample solutions, but we found it impossible to reproduce their results because it was very difficult to stabilize the colloidal ferric hydroxide and consequently it did not float quantitatively. That was why we decided to co-precipitate the selenium(IV) with ferric hydroxide, collect the precipitate, and dissolve it in phosphoric acid. This step was necessary in order to separate selenium from the extremely high concentration of copper in the sample solutions and, at the same time, concentrate the selenium content of the samples to a level at which the spectrophotometric method is applicable.

Ten simulated samples of electrolytic copper, made by dissolving high-purity copper sulphate and adding a known amount of selenium (0.30 ppm), were analysed. The amounts of selenium found ranged from 0.24 to 0.36 ppm, mean 0.295 ppm, standard deviation 0.036 ppm. In view of the low selenium concentration the reproducibility seems good and the method very suitable for the analysis of this kind of sample. Three commercial samples of electrolytic copper were also analysed by the TAP method, the results being 0.34 (0.36), 0.27 (0.30) and 0.30 (0.31) ppm, the values in brackets being obtained by neutron-activation analysis. In addition three spiked samples of water were analysed, the selenium(IV) being co-precipitated with ferric hydroxide at pH 8–9, and the solutions allowed to stand for 15 min before filtration. The results shown in Table 1 indicate very good recovery.

We conclude that this method has proved to be accurate and precise for analysis of electrolytic copper and water.

Acknowledgements—This work was supported by the Dirección de Investigación (DIUC) of the Pontificia Universidad Católica de Chile under Grant No. 106/79. We thank Mr. Eduardo Cortés, from the Chilean Nuclear Energy Commission, for the selenium analysis of the copper sulphate utilized in this work.

REFERENCES

1. V. I. Murashova and S. G. Sushkova, *J. Anal. Chem. USSR*, 1969, **24,** 729.
2. J. Hoste, *Anal. Chim. Acta*, 1948, **2,** 402.
3. J. Hoste and J. Gillis, *ibid.*, 1955, **12,** 158.
4. H. Ariyoshi, M. Kiniwa and M. Toei, *Talanta*, 1960, **5,** 112.
5. L. M. Cummins, J. L. Martin and D. D. Magg, *Anal. Chem.*, 1965, **37,** 430.
6. P. F. Lott, P. Cukor, G. Moriber and J. Solga, *ibid.*, 1963, **35,** 1159.
7. Y. Shimoishi, *J. Chromatog.*, 1977, **136,** 85.
8. J. Hernández, División Chuquicamata, CODELCO-Chile, personal communication.
9. Y. K. Chau and P. J. Riley, *Anal. Chim. Acta*, 1965, **33,** 36.
10. I. Ostromisslensky, *Ber.*, 1911, **44,** 268.
11. S. Nakashima, *Anal. Chem.*, 1979, **51,** 654.
12. J. Tzeng and H. Zeitlin, *Anal. Chim. Acta*, 1978, **101,** 71.

Talanta, Vol. 30, No. 6, pp. 413–418, 1983
Printed in Great Britain.

0039-9140/83/060413-06$03.00/0

CATION-EXCHANGE IN THIOUREA–HYDROCHLORIC ACID SOLUTIONS*

C. H.-SIEGFRIED W. WEINERT and FRANZ W. E. STRELOW
National Chemical Research Laboratory, P.O. Box 395, Pretoria 0001, Republic of South Africa

and

REINHARD G. BÖHMER
Department of Chemistry, University of Pretoria Hillcrest, Pretoria 0083, Republic of South Africa

(*Received* 1 *November* 1982. *Accepted* 22 *December* 1982)

Summary—Ion-exchange distribution coefficients are reported for several transition and post-transition elements in solutions of hydrochloric acid (0.1–3.0*M*) and thiourea on AG50W resins. Some typical elution curves illustrate use of the systems with special reference to the separation of small amounts of gold, palladium, platinum, rhodium and iridium from large amounts of numerous base metals by using 1.5*M* hydrochloric acid–0.1*M* thiourea as eluent. Also illustrated is the use of a bromine-containing solution to strip thiourea complexes from a cation-exchange column.

The first application of thiourea as a complexing agent for the separation of elements by cation-exchange chromatography was reported by Berg and Senn[1] who separated rhodium as a cationic thiourea complex from iridium. Since then similar procedures have been employed by Bykov[2] to separate copper from zinc, nickel, cobalt, iron and cadmium, by Skorokhod and Varavva[3] to separate cadmium from zinc, and by Abrao[4] to separate tellurium from iodide. Toerin and Levin[5] included solutions containing thiourea in a cation-exchange chromatographic separation scheme for rhodium (plus iridium), gold, silver, and palladium (plus platinum). Skorokhod and Varavva[3,6] have shown that Na^+, K^+, Mg^{2+}, Mn^{2+}, Co^{2+}, Ni^{2+} and Cr^{3+} do not form thiourea complexes on a strongly acidic cation-exchange resin (KU-2), but H^+, Zn^{2+}, Pb^{2+} and Cd^{2+} apparently do. Their measurements indicated that the complexes of Pb^{2+} and Cd^{2+} were significantly more stable in the resin phase than in the aqueous phase. Significant extra stabilization in the resin phase was also reported for the silver complex, $AgTu^+$ (Tu = thiourea).[7] Several elements which are normally present as anions in aqueous solution are known to form cationic complexes with thiourea which are strongly sorbed by cation-exchange resins. These include Te(IV),[4] Ru(III),[8] Tc(VII)[9] and Re(VII).[10]

Thus, cation-exchange chromatography with thiourea-containing eluents offers several interesting separation possibilities. However, at present no systematic data seem to be available, and the present paper is an attempt to remedy the situation.

EXPERIMENTAL

Reagents

The AG50W-X8 and AG50W-X4 sulphonated polystyrene cation-exchangers marketed by Bio-Rad Laboratories (Richmond, Ca.) were used. Resins of 100–200 mesh particle size were employed for the determination of distribution coefficients. AG50W-X4 resin of 200–400 mesh particle size was used for column work.

The water used was distilled, and for further purification, passed through an Elgastat demineralizer.

Only analytical-grade reagents were used. Stock solutions, each 0.05*M* in a given metal, were prepared from suitable analytical grade salts [of Ag^+, Tl^+, Cu^{2+}, Cd^{2+}, Zn^{2+}, Co^{2+}, Hg^{2+}, Pb^{2+}, Mo(VI), Sb(III), Sn^{4+}], or from the pure (>99.9%) metals (Bi, Te, Au, Pd, Pt, Rh, Ir, Ru, Os). The metals were dissolved with a suitable combination of hydrochloric and nitric acids on a hot-plate (Bi, Te, Pd, Pt, Au), or in a Teflon (PTFE)-lined pressure bomb at about 280° (Rh, Ir, Os, Ru). The salts were assumed to be stoichiometric within the limits of purity specified by the manufacturers.

All stock solutions contained 1*M* hydrochloric acid, in some cases with subordinate amounts of nitric acid (<0.15*M*), except those of Ag^+, Tl^+ and Pb^{2+} which contained 0.1*M* nitric acid only.

Apparatus

Borosilicate glass tubes, 20 mm in internal diameter and about 400 mm in length, were used as columns. These were fitted with porosity-2 sintered-glass plates and burette taps at the bottoms and B19 ground-glass joints at the tops to receive 500-ml separating funnels to serve as reservoirs for the elements. The columns were filled with a slurry of AG50W-X4 resin (200–400 mesh, H^+-form) until the settled resin bed volume was 43 ml, corresponding to 10 g of dry resin. Atomic-absorption (AA) measurements were made with a Varian–Techtron AA-5 instrument. A Zeiss PMQII instrument was used for spectrophotometric measurements. Matrix-matched standards were used. Copper nitrate was

*This paper represents part of a D.Sc. Thesis by C. H.-S. W. Weinert to be submitted to the University of Pretoria, Republic of South Africa.

Table 1. Cation-exchange distribution coefficients in aqueous hydrochloric acid solutions in the presence and absence of thiourea

Species[a]	Amount, *mmole*	[Tu], M	[HCl], M 0.1	0.2	0.5	1.0	2.0	3.0
Pt(IV)[b]	2.5	Nil	1.4	1.1	1.2	1.4	1.3	1.2
Pt(IV)	2.5	0.2	1.5×10^4	8.8×10^3	3.5×10^3	1.5×10^3	340	210
Pd(II)[b]	2.5	Nil	1.6	1.3	0.9	0.8	0.6	0.6
Pd(II)	2.5	0.2	2.5×10^3	3.5×10^3	3.2×10^3	1.1×10^3	440	345
Au(III)[b]	1.67	Nil	<0.5	<0.5	<0.5	<0.5	<0.5	<0.5
Au(III)	1.67	0.2	1.7×10^4	5.5×10^3	1.6×10^3	670	265	135
Ag(I)[d]	0.50	0.1				203	160†	23.3
Cu(II)[b]	2.5	Nil	990	320	64	16.1	3.5	1.6
Cu(II)	2.5	0.2	3.8×10^3	1.9×10^3	900	370	160	91
Cu(II)[d]	0.50	0.1	2.7×10^3	1.3×10^3	440	192		
Cd(II)[b]	2.5	Nil	370	84	6.5	1.6	0.6	<0.5
Cd(II)	2.5	0.2	6.1×10^3	1.2×10^3	142	29.3	7.9	7.5
Zn(II)[b]	2.5	Nil	1.0×10^3	336	64	16.6	3.7	1.7
Zn(II)	2.5	0.2	900	290	62	15.3	3.2	1.7
Co(II)[b]	2.5	Nil	1.1×10^3	340	72	21.3	6.2	2.7
Co(II)	2.5	0.2	800	270	60	17.0	5.5	2.8
Hg(II)[b]	2.5	Nil	1.6	0.9	0.5	0.3	0.3	0.2
Hg(II)	2.5	0.2	$>10^5$	2×10^4	6.2×10^3	1.2×10^3	285	†
Hg(II)[d]	0.50	0.1	$>2 \times 10^4$	1.6×10^4	2.4×10^3	470		
Bi(III)[b]	1.67	Nil	†	†	0.9	<0.5	<0.5	<0.5
Bi(III)[d]	0.50	0.1	3.3×10^4	9.4×10^3	370	18.1		
Pb(II)[b]	0.10	Nil	†	†	62	5.8	1.3	0.5
Pb(II)[d]	0.50	0.1	3.6×10^3	720	42	4.6		
Tl(I)[b]	0.10	Nil	386	129	37.7	11.6		
Tl(I)[d]	0.50	0.1	210	81	26.1	15.0†		
Te(IV)[b]	2.5	Nil	39.3	17.0	4.7	1.4	0.7	<0.5
Te(IV)[d]	0.50	0.1	4.5×10^4	3.3×10^3	1.5×10^3	900		
Mo(VI)[b]	2.5	Nil	0.9	0.8	0.6	<0.5	<0.5	<0.5
Mo(VI)[d]	0.50	0.1		117	31	6.7	2.3	
Sn(IV)[b]	2.5	Nil	†	99	6.3	1.7	0.5	<0.5
Sn(IV)[d]	0.50	0.1	†	†	1.4	0.45	0.3	0.15
Sb(III)[b]	1.67	Nil	†	†	†	†	2.8	1.3
Sb(III)[d]	0.50	0.1	620†	540	124	32.4	5.4	2.5
Rh(III)[b]	1.67	Nil	4.2	2.0	1.4	0.9	0.7	0.8
Rh(III)[d]	0.50	0.1	67		54	51		
Rh(III)[d,f]	0.50	0.1	225		200	180	150	
Rh(III)[d,g]	0.50	0.1	390		220	180		
Rh(III)[d,h]	0.50	0.1	2.7×10^3		1.0×10^3	615	170	
Rh(III)[d,i]	0.50	0.1	11.8		2.8	1.1		
Rh(III)[d,g,i]	0.50	0.1			3.7	8.4		
Ir(IV)[d]	0.50	0.1	3.5	3.2	2.7	3.6	5.2	
Os(IV)[d]	0.50	0.1	6		5	4.5		
Ru(III)[d]	0.50	0.1			150	180	200	

[a]Oxidation state in stock solution.
[b]Reference 12.
[c]Hydrogen peroxide present.
[d]AG50W-X4 resin.
[e]60-hr equilibration.
[f]7 days equilibration.
[g]Rh(III) brought to dryness three times with conc. hydrochloric acid immediately before transfer to equilibration mixture.
[h]70 (±1)°.
[i]5 (±1)°.
†Precipitation.

used as releasing agent in the AA determination (nitrous oxide–acetylene flame) of some of the noble metals (Rh, Ir, Ru, Os).

Distribution coefficients

The resin was dried at 80° in a ventilated drying oven, and stored in a desiccator over anhydrous silica gel. Residual water was determined by drying at 120°, and the weights of resin were corrected accordingly.

Distribution coefficients were determined by shaking 2.500 g of dry resin (AG50W-X8 unless indicated otherwise in Table 1), in the H^+-form, with 250 ml of solution for 24 hr (unless indicated otherwise in Table 1) in a mechanical shaker, normally in a room maintained at 20°. Some equilibrations were done at 5° and 70° in a cold-room and a temperature-controlled water-bath respectively.

When the resin could be ignited without loss of the element concerned, it was filtered off on paper and ashed at low temperature, and the ash was dissolved or weighed directly. Otherwise the resin was transferred to a short large-diameter column, and sorbed metal was eluted with some suitable eluent such as 3*M* HCl or 1.5*M* HCl–2% w/w

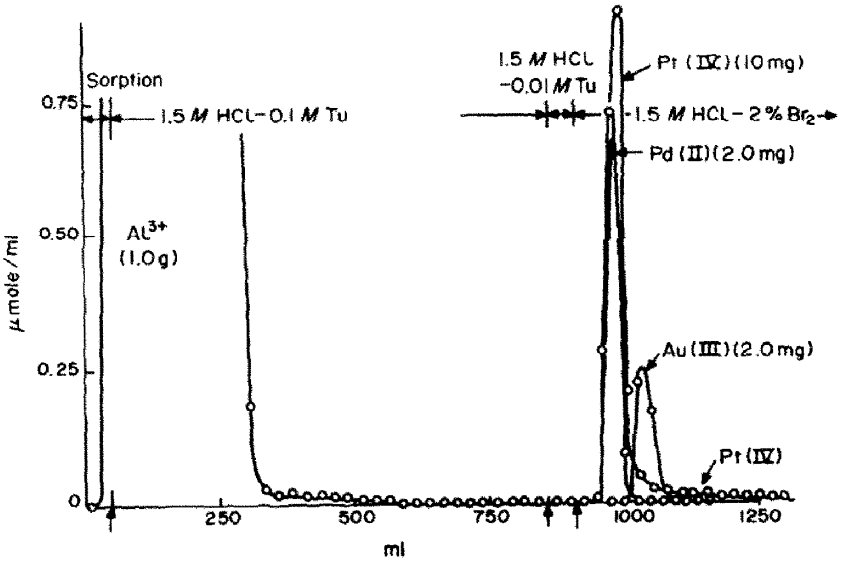

Fig. 1. Elution curves for the pairs Al^{3+} (1.0 g)–Au(III) (2.0 mg), Al^{3+} (1.0 g)–Pd(II) (2.0 mg), Al^{3+} (1.0 g)–Pt(IV) (10 mg). Column: 10 g (43 ml) of AG50W-X4, 200–400 mesh, H^+-form; internal diameter 2.0 cm. Flow-rate 3.0 ± 0.3 ml/min.

Br_2. The amounts of the elements in the aqueous and resin phases were then determined by appropriate analytical methods. The distribution coefficients, D, were calculated from[11]

$$D = \frac{\text{(amount of element in resin) (ml of solution)}}{\text{(amount of element in solution) (g of dry resin)}}$$

and are presented in Table 1.

Elution curves

The columns were first equilibrated by passing through them 100 ml of 1.5*M* HCl–0.1*M* Tu. This was followed by:

(*a*) 50 ml of 1.5*M* HCl–0.5*M* Tu containing the metal or metals of interest,
(*b*) four rinses, with a total of 50 ml of 1.5*M* HCl–0.1*M* Tu,
(*c*) 750 ml of 1.5*M* HCl–0.1*M* Tu,
(*d*) 50 ml of 1.5*M* HCl–0.01*M* Tu to displace most of the excess of thiourea from the column,
(*e*) 500 ml of 1.5*M* HCl–2% w/w Br_2, and
(*f*) 250 ml of 1.5*M* HCl to remove bromine from the column.

Step (*f*) followed (*e*) without delay. Under these conditions the bromine did not seem to have any detrimental effect and the exchange capacity of the resin was not significantly altered even after at least 20 runs with the same elution sequence on a single column.

The flow-rate was maintained at 3.0 ± 0.3 ml/min throughout. The column was allowed to drain completely after each addition of solution. Care was taken to minimize disturbance of the resin bed surface.

Fractions (25 ml in volume) were taken with an automatic fraction-collector from the beginning of the sorption step, and the amounts of the elements in each fraction were determined by an appropriate method. Some of the experimental curves are shown in Figs. 1–3.

DISCUSSION

The data presented in Table 1 show that the presence of an excess of thiourea increases the distribution coefficients of a number of elements in hydrochloric acid media by several orders of magnitude. For some other elements there is little or no effect. (The slight decrease in D-values in the presence of thiourea, under conditions which are otherwise similar to those in its absence, can be attributed to batch-to-batch changes in the exact composition of the resin, or to the competitive sorption of thiourea, the possibility of which follows from observations recorded by Skorokhod and Varavva.[6]) Some practical implications of the changes in distribution coefficients caused by the presence of thiourea, and their effects on separations are discussed by reference to Fig. 1.

The Al^{3+} ion may be taken to represent a large group of elements which have little or no tendency[13] to form complexes with thiourea. The chromatographic behaviour in the presence of thiourea is similar to that in its absence, and can be predicted from the comprehensive lists of D-values in hydrochloric acid media already available.[11,12] Included in this group are Li^+, Na^+, K^+, Rb^+, Cs^+, Tl^{+}*, Be^{2+}, Mg^{2+}, Ca^{2+}, **Sr^{2+}** (0.1 g), Mn^{2+}, **Fe^{2+}** (1.0 g), **Co^{2+}** (1.0 g)*, Ni^{2+}, **Zn^{2+}** (1.0 g)*, **Pb^{2+}** (10 mg)*, **V(IV)** (0.5 g), **U(VI)** (0.1 g) and Sn(IV)*, all of which are expected to be eluted approximately together with, or ahead of Al^{3+} (1.0 g). This was experimentally verified for the species printed in bold type, in the amounts shown in brackets. The elements marked with an asterisk are included in Table 1. Ba^{2+}, Sc^{3+}, Y^{3+}, La^{3+}... Lu^{3+}, Th^{4+}, Hf^{4+} and Zr^{4+} are very strongly sorbed in the aquo-form, and can be eluted only partially or not at all with 750 ml of 1.5*M* HCl (with or without 0.1*M* Tu).

Aluminium at low concentrations shows extended tailing. Zinc behaves similarly, but is eluted ahead of

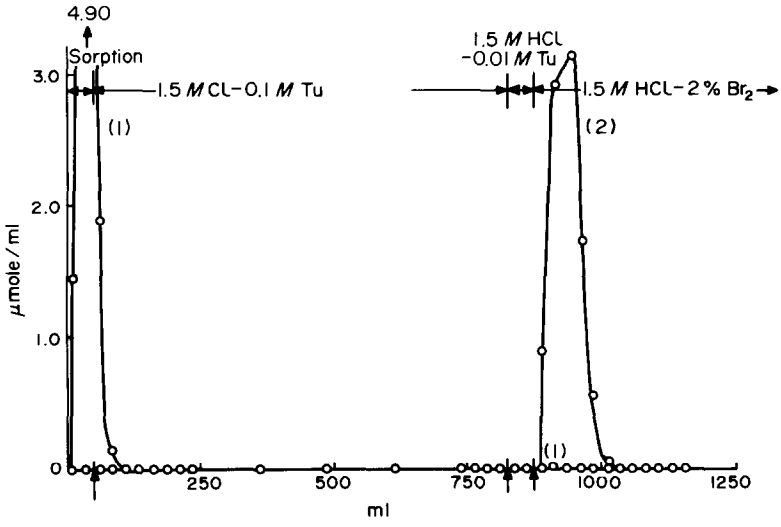

Fig. 2. Elution curves for Ir(IV, III) (50 mg). Column and flow-rate as for Fig. 1. Curve (1): solution transferred directly onto column; (2) solution heated for 24 hr before transfer to column.

Al^{3+}. None of the other elements examined showed this effect. Tl^{+} and Pb^{2+} are poorly soluble in hydrochloric acid (with or without Tu present), and any excess precipitated is eluted only gradually. Provided no solution channels are formed in the precipitates, elution seems to proceed roughly at a concentration level corresponding to the solubility of the precipitates in the eluent (*ca.* 200 µg/ml for Pb^{2+} in 1.5*M* HCl–0.1*M* Tu at *ca.* 25°).

Vanadium and iron were originally added in oxidation states (V) and (III) respectively, but both are rapidly reduced by excess of thiourea (in the case of Fe^{3+} this occurs through transient red species which may be[14] $FeTu^{3+}$ and/or $FeTu_2^{3+}$), and are eluted well ahead of Al^{3+}, as the blue vanadium(IV) and pale greenish iron(II) aquo complexes respectively.

Ti^{4+} (10 mg) hydrolyses slowly in 1.5*M* HCl–0.1*M* Tu, and cannot be eluted quantitatively. An attempt to keep it in solution with hydrogen peroxide failed because thiourea destroyed the peroxo-complex.

According to Lederer,[15] thiourea forms moderately to very stable complexes with Tc(IV), Re(IV), **Ru(III), Os(III), Rh(III), Pd(II), Pt(II), Au(I), Cu(I), Hg(II), Sb(III), Bi(III), Te(II)** and Po(II). To this group may be added **Cd^{2+}**,[6] **Ag^{+}**,[7] and, according to present evidence, **Mo(V?)** and **Ir(III)**. (Elements given in bold type are included in the present study.) Many of these elements are normally present in solution in a higher oxidation state, and then often as anionic complexes, *e.g.*, ReO_4^-, $OsCl_6^{2-}$, $IrCl_6^{2-}$, $PtCl_6^{2-}$, $AuCl_4^-$, TeO_3^{2-} and MoO_4^{2-} (polymeric). These, as well as Cu^{2+}, are reduced by thiourea to the oxidation state indicated above, at rates which may vary greatly from species to species,[13,16] and unlike the case of iron(III) and vanadium(V), the reduced forms are strongly complexed by excess of thiourea.[13] The formation of the thiourea complexes (after reduction, if this applies), and any subsequent exchange of ligands, may also take place at rates which can vary greatly from species to species. Thus, while the formation of cationic thiourea complexes is tolerably rapid for most of the species investigated, it is slow to extremely slow in the case of Rh(III) and Ir(IV). In the latter case, reduction is extremely rapid,[19] as evidenced by a change in colour from deep red to light yellow or colourless, depending on the concentration of Ir(IV), but the initial product passes through the column practically unsorbed (Fig. 2). However, on heating with an excess of thiourea for 24 hr on a steam-bath, this product is changed, apparently quantitatively, into a complex which is strongly retained by the column. Rh(III) behaved on the column much like Ir(IV, III) except that the conversion into the strongly sorbed complex by heating for 24 hr on the steam bath was less quantitative (Fig. 3). Distribution coefficients have been included in Table 1 to illustrate the effect of time, temperature, and pretreatment on the formation of the sorbable Rh(III)–Tu complex (or complexes). Evaporating an Rh(III) solution three times with hydrochloric acid to displace water at least partially from the inner coordination sphere of Rh(III) resulted in an increase in the distribution coefficients to a value commensurate with that obtained after 7 days of equilibration without such pretreatment.

It must be stressed that most of the *D*-values obtained for Rh(III) in the presence of thiourea are not equilibrium values. They reflect essentially the formation of the most strongly sorbed complex which, as can be seen from Fig. 3, is very strongly sorbed indeed. The same applies to Ir(IV, III) (see Fig. 2), Os(IV, III) and Ru(III).

Osmium in its various oxidation states ($\geqslant$III) and Ru(IV, III) form well-known coloured complexes with thiourea (red in the case of Os, and blue in the case of Ru).[17] Column experiments (conditions as in

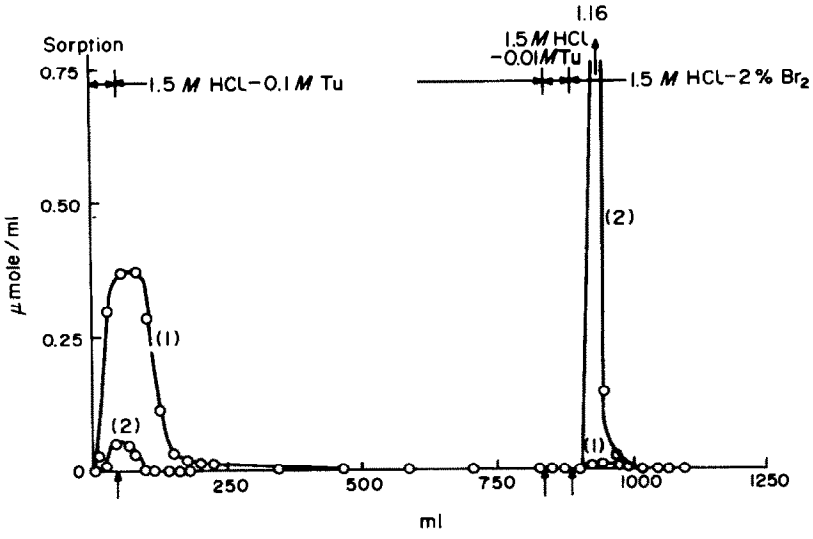

Fig. 3. Elution curves for Rh(III) (5 mg). Column and flow-rate as for Fig. 1. Curves (1) and (2): as for Fig. 2.

Figs. 1–3) showed that both these complexes are retained strongly and quantitatively, and are eluted together with Pd(II) *etc.* The fraction of the sorbable species in the case of Os(IV) (0.1 μM) was found to increase at room temperature from about 5% after 24 hr to about 30% after 30 days in 0.5*M* HCl–0.05*M* Tu. Both Os(IV) and Ru(III) were found to be only partially converted into the strongly sorbed complex on heating in 1.5*M* HCl–0.5*M* Tu for 24 hr on the steam-bath. However, these are probably not the optimum conditions for forming the complexes.[17] Molybdenum(VI) is slowly reduced by thiourea to molybdenum blue, but it is not the latter which is sorbed. The sorbed species appears to be essentially colourless. Inspection of the solutions during equilibration showed that the blue product is transient in nature, and disappears completely during $2\frac{1}{2}$ days of equilibration.

Of the other elements investigated, Cd^{2+} is rapidly eluted with 1.5*M* HCl–0.1*M* Tu, but the amount that can be tolerated is limited by its reduced solubility at relatively high concentrations of hydrochloric acid and thiourea (1.3 mg/ml and 45 mg/ml in 1.5*M* HCl–0.5*M* Tu and 1.5*M* HCl–0.1*M* Tu respectively at 27°). Analysis showed the precipitate to correspond to $CdTu_2Cl_2$.

More or less extensive precipitation was also observed with Ag^+ (as $AgTu_2Cl$), Pd(II) (as $PdTu_4Cl_2$) and Pt(IV, II) (as $PtTu_4Cl_2$) in 1.5*M* HCl–0.5*M* Tu. A solubility determination for Pt(IV, II) in 0.5*M* HCl–0.1*M* Tu gave 0.56 mg/ml at 23°. This was decreased by a factor of at least five for 2*M* HCl–0.1*M* Tu medium. In these cases, however, precipitation had no serious consequences during the chromatographic procedure, because the metal complexes moved into the top of the column as elution proceeded, and in no case was an unexpectedly early breakthrough observed. The first traces of Ag^+ (0.1 g) appeared just after the main portion of Al^{3+} had passed through the column, and Cu^+ (0.1 g) followed about 150 ml later. No trace of platinum, palladium or gold could be detected in the eluate until after the change of eluent to 1.5*M* HCl–2% w/w Br_2. The latter elutes palladium (2 mg), gold (2 mg) and any strongly sorbed complexes of iridium, rhodium, ruthenium and osmium virtually quantitatively, but not platinum (10–100 mg), copper (100 mg) and silver (100 mg). In the case of Pt(IV, II), incomplete recovery was associated with the formation of a thin dark red band close to the top of the column. The recovery was considerably improved by passing 50-ml quantities of 1.5*M* HCl, containing alternately 0.1*M* Tu and 2% w/w Br_2, through the column. Copper and silver were not investigated further.

Analytical implications

The results presented here show that excellent chromatographic separations of a number of the noble metals from large amounts of many matrix elements are possible on AG50W-X4 resin, with 1.5*M* HCl–0.1*M* Tu as eluent. Some care is needed in order not to exceed the solubility products of some of the rarer matrix elements such as Cd^{2+} and Pb^{2+}. Several elements will accompany the noble metals at least partially. They include Ba^{2+} *etc.*, as mentioned earlier, silver, copper and, according to their *D*-values, tellurium and mercury. Rhodium(III) and Ir(IV, III) normally pass through the column almost quantitatively, but treatment with Tu at higher temperatures can result in almost quantitative retention. Osmium and ruthenium will occur in both fractions, but these two elements can easily be separated by distillation.[17]

Several additional separations can be predicted from the D-values presented in Table 1, and D-values available for pure hydrochloric acid media.[11,12] For example it should be possible to separate Ag^+ from large amounts of elements such as Sr^{2+} and Co^{2+} which do not show extensive tailing.

Hydrochloric acid (1.5M) containing bromine (2% w/w) was found to be an effective eluent for most of the noble metals retained. Platinum(IV, II) cannot be eluted satisfactorily with purely aqueous eluents. Quantitative elution can be obtained by using 0.87M HBr-0.01M Tu in 90% acetone.

Thiourea solutions almost always contain small amounts of finely dispersed sulphur. This, and any additional sulphur formed in the presence of various oxidizing agents, did not present serious problems in the separations. When an impervious sulphur layer formed at the top of a column and impeded the flow of the eluent, it could simply be broken up with the tip of a glass rod.

Free sulphur and thiourea can be oxidized fairly effectively by bromine. The oxidation products (sulphuric acid *etc.*) as well as thiourea itself may have to be taken into account in the subsequent analysis.

Acknowledgements—The authors are grateful for microanalyses performed by Mr. H. Lachmann and Mrs. J. Smit of the NCRL, and assistance in the determination of some of the distribution coefficients by Mr. R. J. Rogers during university vacations.

REFERENCES

1. E. W. Berg and W. L. Senn, Jr., *Anal. Chem.*, 1955, **27,** 1255.
2. I. E. Bykov, *Izv. Sib. Otd. Akad, Nauk SSSR*, 1961, No. 12, 72.
3. O. R. Skorokhod and A. G. Varavva, *Russ. J. Phys. Chem.*, 1974, **48,** 247.
4. A. Abrao, *Publ. I.E.A.*, 1975, No. 371.
5. F. von S. Toeries and M. Levin. *J.S. Afr. Chem. Inst.*, 1974, **27,** 91.
6. O. R. Skorokhod and A. G. Varavva, *Russ. J. Phys. Chem.*, 1972, **46,** 980.
7. A. Maes and A. Cremers, *J. Chem. Soc., Faraday Trans. I*, 1978, **74,** 2740.
8. A. T. Pilipenko, I. P. Sereda, Z. A. Semchinskaya and V. I. Golub, *Russ. J. Inorg. Chem.*, 1971, **16,** 1635.
9. R. Kopunec, F. Macašek, P. Rajek and D. Hudecová, *J. Radioanal. Chem.*, 1979, **51,** 401.
10. R. Morpurgho, *Inorg. Chim. Acta*, 1968, **2,** 169.
11. F. W. E. Strelow, *Anal. Chem.*, 1960, **32,** 1185.
12. *Idem, Cation Exchange Distribution Coefficients in HCl: New Revised List*, unpublished.
13. C. H.-S. W. Weinert, *The Reactions and Reactivity of Thiourea; Review*, unpublished.
14. N. Pustelnik and R. Soloniewicz, *Monatsh. Chem.*, 1978, **109,** 33.
15. M. Lederer, *J. Chromatog.*, 1960, **4,** 414.
16. W. Robb, Table 17 in A. Warshawsky, M. M. B. Fieberg, P. Mihalik, T. G. Murphy and Y. B. Ras, *Sep. Purif. Methods*, 1980, **9,** 209.
17. E. B. Sandell, *Colorimetric Determination of Traces of Metals*, 3rd Ed. Interscience, New York, 1959.

Talanta, Vol. 30, No. 6, pp. 419–422, 1983
Printed in Great Britain

0039-9140/83/060419-04$03.00/0
Pergamon Press Ltd

ANALYSIS OF MIXTURES OF SULPHIDE, THIOSULPHATE, DITHIONITE AND SULPHITE

WILLIAM P. KILROY
Naval Surface Weapons Center, White Oak Laboratory, Silver Spring, MD 20910, U.S.A.

(*Received* 27 *August* 1982. *Accepted* 16 *December* 1982)

Summary—This paper reports a procedure for the accurate determination of sulphide, dithionite and thiosulphate and an estimation of sulphite in heterogeneous and/or inaccessible mixtures.

A procedure for the analysis of certain mixtures of sulphur compounds, such as a mixture containing both sulphide and dithionite, has not hitherto been reported. There appear to be several reasons for this. (1) Sulphide and dithionite are both generally determined by employing their strong reducing power to reduce salts of mercury, lead or silver. (2) Conditions under which both co-exist may be rare, or if they do co-exist, this may occur under conditions which make them inaccessible to convenient methods of analysis; separation by dissolution complicates matters since both sulphide and dithionite are unstable in aqueous solution, readily hydrolysing or undergoing aerial oxidation. (3) In mixtures, dithionite has been determined in the presence of sulphite,[1] thiosulphate[2] and mixtures of both.[3–6] Sulphide has also been determined in a mixture containing sulphite and thiosulphate by an iodometric method similar to that used for analysis of the corresponding dithionite mixture.[7] However, in all the procedures reported, sulphide interferes with the dithionite determination and *vice versa*.

This paper reports a method of analysing mixtures of soluble sulphides, thiosulphate, dithionite and sulphite. The selected method permits analysis of heterogeneous samples or samples not conveniently separated. The scheme combines several methods, including the iodometric procedure for analysis of inaccessible mixtures containing dithionite,[8] modification of the dithionite determination with Methylene Blue,[9] and the analysis of soluble sulphides by the iodate method of Bethge.[10]

EXPERIMENTAL

Reagents

A "purified" sample of J. T. Baker sodium dithionite, iodometrically analysed and found to be 89.9% dithionite, 6.9% sulphite and 2.5% thiosulphate, was used throughout. Anhydrous reagent-grade sodium thiosulphate and ultrapure lithium sulphide were analysed for purity under helium by the iodimetric and iodate methods[10] respectively. A standard aqueous 0.025*M* solution of Methylene Blue (99.9% purity, Matheson, Coleman and Bell) was prepared. The concentration was verified by titration of an oxygen-free aliquot of a solution of dithionite previously analysed by iodometric methods. Fresh zinc carbonate was prepared by mixing equal volumes of 1.0*M* solutions of zinc sulphate and sodium carbonate just before use. The sodium acetate–acetic acid buffer was 3.5*M* in each constituent.

The concentrations of the standard iodine solutions are expressed in moles of I_2 per litre.

Solution preparation

Argon (99.999% pure), after passing through acidic chromous chloride solution, was used to deaerate 500 ml of 0.1*M* sodium hydroxide in a 1-litre three-necked flask and maintain it oxygen-free. The flask was kept in an ice bath. Sulphide was introduced into the alkali and dissolved, and an aliquot was withdrawn for analysis to verify the sulphide concentration. Known amounts of thiosulphate, dithionite and sulphite were then introduced into the remaining solution. The apparatus is shown in Fig. 1.

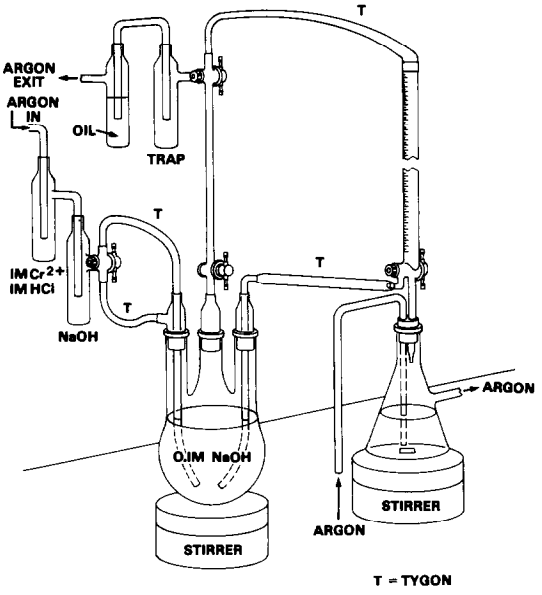

Fig. 1

Analysis

The solution was forced under argon into an argon-filled burette. Measured 5–20-ml portions of this solution, accurately measured, were added to rapidly swirled solutions of iodine, *etc.* as described below.

Titration A. To a 250-ml filter flask containing a magnetic stirring bar, add a mixture of approximately 100 ml of 0.1*M* sodium hydroxide and 100 ml of methanol. Deaerate the solution by bubbling oxygen-free argon through it for 20 min. When the deaeration is complete, add the sample solution from the burette where it is kept under argon. Use

5 ml of sample solution for solutions ~0.03*M* in dithionite, and 10 ml for solutions ~0.01*M* in dithionite. Maintain the argon atmosphere in the filter flask, and replace the sample-solution burette with another containing standard Methylene Blue solution under argon. Titrate rapidly with the Methylene Blue, at room temperature. The end-point is characterized by a colour change from clear gold to a persistent purple. As the dithionite concentration decreases, the intensity of the gold colour decreases until the solution is nearly colourless, before the end-point change to a blue-violet. Let the number of mmoles of dithionite in 20 ml of the sample solution be *A*.

Titration B. Add a 10 or 20 ml portion of the sample solution (accurately measured) rapidly to a swirled flask containing approximately 12 ml of zinc carbonate suspension, 5 ml of water and four drops of 10*M* sodium hydroxide. Use a 10-ml sample for higher sulphide concentrations (~0.03*M*) and the 20-ml sample for lower (~0.01*M*) concentrations. Immediately filter off the precipitate on a medium porosity sintered-glass filter, into a flask containing a mixture of approximately 6–10 ml of 0.5*M* iodine, 5 ml of water and 4 ml of acetic acid–acetate buffer. Wash with 0.1*M* sodium hydroxide, then with several small portions of water. (The precipitate should be stirred in the washings and many washings applied; the precipitate must be thoroughly washed, otherwise the sulphide result will be high.) Transfer the filtrate quantitatively to a standard flask; the pH should be between 4 and 5, and sufficient excess of iodine should be left for the solution to be dark brown. Remove the excess of iodine with 10% sodium sulphite solution and add an additional 7 or 8 ml of sulphite solution. Neutralize the solution to phenolphthalein by dropwise addition of 10*M* sodium hydroxide. Let stand for 5 min, add 4 ml of 37% formaldehyde solution and dilute to the mark with 20% v/v acetic acid. Remove an aliquot, adjust the pH to 4–4.5 with 20% acetic acid, and titrate with 0.005*M* iodine to a starch end-point. Let the number of mmoles of iodine consumed for 20 ml of the original sample solution be *B*.

Titration C. Transfer the zinc sulphide precipitate (from the titration B procedure) to a flask containing ~15 ml of 10*M* sodium hydroxide and a known excessive volume of standard 0.05*M* potassium iodate. Boil gently for 10 min after the solution is clear, then cool in an ice-bath. Add excess of potassium iodide solution and slowly acidify with 4*M* sulphuric acid, adding about 3 ml more once iodine has appeared permanently. Titrate the iodine with 0.1*M* thiosulphate. The number of mmoles of sulphide is equal to three-fourths of the number of mmoles of iodate consumed. Let the number of mmoles of sulphide from 20 ml of original sample solution be *C*.

Titration D. Add 20 ml of the sample solution to a partially evacuated flask fitted with a one-hole stopper and containing a well stirred solution of 10–25 ml of water, 3 ml of acetic acid–acetate buffer and a known volume of standard iodine solution (in large excess). Let stand for 20 min in the stoppered flask. Titrate the remaining iodine with standard thiosulphate solution. Let the number of mmoles of iodine consumed by 20 ml of the sample solution be *D*.

THEORY

Titration A.

When Methylene Blue is added to an oxygen-free alkaline methanol solution containing dithionite, sulphide, thiosulphate, and sulphite, it reacts with only the dithionite (rapidly and quantitatively) at room temperature. The Methylene Blue is reduced from the intensely blue form to a solid leuco form that is soluble in the methanol. The colour intensity of the leuco form in the solution increases as more and more dithionite is consumed. Consequently, the colour change at the end-point is dependent on the dithionite concentration in solution. The end-point is characterized by the persistence of the intense Methylene Blue colour. The number of mmoles of dithionite consumed in titration A is equal to the number of mmoles of Methylene Blue used.

Titration B

A sample containing sulphide, dithionite, thiosulphate and sulphite reacts with excess of iodine in acetic acid–acetate buffer as follows:

$$S^{2-} + I_2 \rightarrow S + 2I^- \quad (1)$$

$$S_2O_4^{2-} + 3I_2 + 4H_2O \rightarrow 2HSO_4^- + 6HI \quad (2)$$

$$2S_2O_3^{2-} + I_2 \rightarrow S_4O_6^{2-} + 2I^- \quad (3)$$

$$HSO_3^- + I_2 + H_2O \rightarrow HSO_4^- + 2HI \quad (4)$$

If the sample is first added to a suspension of freshly precipitated zinc carbonate, the sulphide is quantitatively precipitated, and the filtrate reacts with an acidic iodine solution according to reactions (2), (3) and (4). Excess of sulphite is then added (*a*) to remove unreacted iodine and (*b*) after alkalization of the solution, to convert the tetrathionate, $S_4O_6^{2-}$, formed from reaction (3), quantitatively into half the original amount of thiosulphate:

$$S_4O_6^{2-} + SO_3^{2-} \rightarrow S_2O_3^{2-} + S_3O_6^{2-}. \quad (5)$$

The unreacted sulphite is complexed by formaldehyde in acetic acid, and the thiosulphate produced by reaction (5) is titrated with standard iodine (*B* mmoles of I_2). Then $4B$ = the number of mmoles of $S_2O_3^{2-}$ originally present.

Titration C

Hot alkaline iodate (in excess) oxidizes sulphide quantitatively according to the reaction

$$3S^{2-} + 4IO_3^- \rightarrow 3SO_4^{2-} + 4I^-. \quad (6)$$

Addition of iodide followed by acidification converts the unreacted iodate into iodine, which is titrated with standard thiosulphate solution. The number of mmoles of sulphide is given by

$$c = \tfrac{3}{4}\,[(\text{mmoles of iodate taken}) - \tfrac{1}{6}\,(\text{mmoles of thiosulphate used})].$$

Titration D

The number of mmoles of I_2 consumed by the sample in titration *D* is the result of reactions (1)–(4). Consequently, the number of mmoles of SO_3^{2-} present is given by $(D - 3A - 2B - C)$.

DISCUSSION

The effects of temperature, concentrations of reagents, alkalinity, stability in solution, dilution, *etc.* were investigated to assess the procedure for the determination of each anion in the presence of the others. The procedure found most suitable is that

detailed in the experimental section. However, some of the variables cited above can influence the analysis and therefore some comments are appropriate.

The anion stability and the possibility of anion interaction in the alkaline solution were investigated. A solution of each anion was prepared and analysed. In turn, each of the other anions was added and the solution re-analysed approximately 1 hr after each addition. Finally, a standard solution of all four anions (S^{2-}, $S_2O_4^{2-}$, $S_2O_3^{2-}$, SO_3^{2-}) was prepared, and analysed immediately and again 6 hr later. No changes in concentration were observed. This was reconfirmed on several occasions during the course of the experiments. Interestingly, the yellow colour imparted to the solution by the sulphide slowly disappeared on addition of the dithionite. Analysis revealed that no change in either the sulphide or dithionite concentration had occurred. To ensure stability of the solution, it should be kept oxygen-free and preferably at below 25°. The stability of dithionite in solution is a function of its concentration, temperature, and pH.[11] Analysis of higher concentrations of dithionite may warrant a different concentration of alkali solution.

Sulphide and thiosulphate. For the determination of these anions, the complete recovery, effective separation and decomposition or oxidation of dithionite were the primary problems studied. Sulphide solutions, 0.01 and 0.03*M*, were prepared. Aliquots were analysed by iodate titration and then re-analysed by precipitation with freshly prepared zinc carbonate suspension. Recovery was 100% efficient. However, smaller sample volumes, 10 ml instead of 20, appeared to give slightly better reproducibility for the 0.03*M* solution when other anions were present. Other anions were added to the standard sulphide solution to determine their effect on the analysis. Thiosulphate had no effect on recovery of sulphide. Dithionite and sulphite increased the apparent sulphide value by approximately 4% and 2% relative respectively. The problem with dithionite was eliminated by adding several drops of 10*M* sodium hydroxide to the zinc carbonate suspension before adding the sulphide–dithionite solution. Increasing the pH evidently stabilizes the dithionite sufficiently for it to be unaffected by the exposure to air for the 1–2 min required for the filtration. The apparent increase in sulphide in the presence of sulphite seems to be due to formation of some zinc sulphite. Thorough washing, first with 0.01*M* sodium hydroxide and then with many small volumes of water, minimizes the sulphite interference.

No apparent interference by any of the other anions was observed in the thiosulphate determination. In mixtures, the results were generally ~1.5% high, especially for the more dilute (0.01*M*) thiosulphate solutions.

Dithionite. The best method for determination of dithionite in the presence of thiosulphate and/or sulphite and absence of sulphide has already been reported.[8] Results from attempts to expand this method by adding an aliquot of sample solution to alkaline formaldehyde containing zinc carbonate or by adding the zinc carbonate later after permitting the formaldehyde mixture to stand for ~15 min, followed by filtration of the sulphide, were generally ~3% low and less reproducible. The use of Methylene Blue gives better results provided the analyst is familiar with the method. If the solution containing dithionite is used to titrate a standard solution of Methylene Blue in alkaline methanol, very erroneous and irreproducible results are obtained, especially with more concentrated dilthionite solutions. Instead, the sample solution must be added to a totally oxygen-free mixture of methanol and sodium hydroxide solution and this mixture titrated with Methylene Blue.

The titration should be performed rapidly, under an inert gas and at room temperature. The same results are obtained if an additional 5 ml of 0.1*M* sodium hydroxide are added to the methanol–hydroxide mixture or if the methanol is replaced by acetone. Large volumes of the methanol–hydroxide solution are recommended for two reasons. First, to solubilize the relatively insoluble leuco form produced when Methylene Blue is reduced, because the insoluble leuco form appears to adsorb Methylene Blue and make the end-point more drawn-out and difficult to locate. Secondly, the larger volume decreases the overall concentration of dithionite present and thereby enhances detection of the end-point. Best results are obtained by using a small sample volume, preferably 5 ml, large amounts of methanol–hydroxide mixture, and a preliminary titration to become familiar with the end-point. The end-point is remarkably sharp for dilute solutions of dithionite (~0.005*M*) but at concentrations of ~0.03*M*, the methanol–hydroxide–dithionite solution progressively becomes more deeply golden in colour as the Methylene Blue is added. Even under these latter conditions, however, the end-point, characterized by the persistence of a purple colour in the solution, due to unreacted Methylene Blue, is remarkably reproducible.

Sulphite. Sulphite can be determined by difference provided all four anions can be quantitatively oxidized. Two methods were examined; oxidation by hot alkaline iodate and oxidation by acidic iodine. Alkaline iodate was found unsuitable owing to slow oxidation of the dithionite (accompanied by some decomposition). If the solution containing the sulphur anions is added to a rapidly stirred solution containing excess of iodine and a few ml of the acetic acid–acetate buffer, good agreement is consistently found between the amount of iodine consumed and the theoretical amount needed. However, if a large excess of iodine is not used or if too much water (~100 ml) is added along with the iodine, the analysis is generally low by ~2%. Analysis for the individual anions shows that the dithionite is re-

Table 1. Determination of thiosulphate, sulphide, dithionite, and sulphite*

	$S_2O_3^{2-}$, *mmole*		S^{2-}, *mmole*		$S_2O_4^{2-}$, *mmole*		SO_3^{2-}, *mmole*	
Run†	Present	Found	Present	Found	Present	Found	Present	Found§
1	0.111	0.113	0.205	0.206	0.591	0.586	—	—
2	0.205	0.207	0.214	0.215	0.200	0.198	—	—
3	0.202	0.205	0.628	0.630	0.202	0.201	—	—
4	0.210	0.212	0.198	0.196	0.627	0.637	—	—
5	0.596	0.602	0.625	0.631	0.604	0.599	—	—
6	0.210	0.215	0.211	0.211	0.205	0.202	0.206	0.204 (0.197)
7	0.224	0.228	0.614	0.605	0.624	0.628	0.251	0.233 (0.237)
8	0.208	0.212	0.195	0.199	0.204	0.203	0.598	0.575 (0.578)
9	0.612	0.615	0.209	0.206	0.614	0.624	0.251	0.239 (0.259)
10	0.605	0.600	0.202	0.202	0.207	0.207	0.203	0.200 (0.198)

*Expressed as mmoles per 20 ml from the original 500 ml of solution.

†Run 5—the solution contained ~0.5 g of carbon black; run 10—the solution contained LiBr (0.02*M*).

§The value in parentheses is the number of mmoles of sulphite found by using the original initial concentrations of S^{2-}, $S_2O_3^{2-}$, $S_2O_4^{2-}$ (as opposed to those experimentally found).

sponsible for this error, apparently undergoing some acidic decomposition.

The procedure described for titration D consistently gives a consumption of iodine that agrees with the theoretical consumption within ±1%. Consequently, in theory, the determination of sulphite should be correct, but in practical analyses, of course, the sulphite result is affected by the errors in all four titrations, especially A and B [because of the stoichiometry of reactions (1)–(4)]. Careful analysis permits sulphite to be determined with a relative error below 5%.

High surface-area (60 m^2/g) carbon black and the presence of 0.02*M* lithium bromide has no effect on either catalysing the solution interactions or influencing the analysis scheme.

RESULTS

Table 1 summarizes the analyses of solutions containing a variety of anion concentrations, corrected for the thiosulphate and sulphite present in the dithionite sample. The findings are reported as mmoles per 20 ml of the original 500 ml of test solution, corresponding to the sample volumes most frequently taken for analysis. Two analyses were performed for each constituent of each sample solution. Excellent agreement was found and the average values are reported. The experimental conditions under which titration D gives successful analyses for sulphite were discovered during the later part of the analytical investigation. Consequently, the first part of Table 1 does not include sulphite in the test mixtures. Additional investigation of titration D was done with mixtures similar to those of runs 6 and 8. The experimental iodine titration volume used was found to be within 1% of the theoretical value predicted from the composition of a standard solution of the four anions. Table 1 reports the sulphite values found by use of both the original concentrations of the anions and those experimentally measured.

REFERENCES

1. R. L. Kaushik and R. Prosad, *J. Indian Chem. Soc.*, 1969, **46**, 405.
2. F. Solymosi and A. Varga, *Magy. Chem. Folyoirat*, 1959, **65**, 52.
3. R. Wollak, *Z. Anal. Chem.*, 1930, **80**, 1.
4. V. R. Nair and C. R. Nair, *Res. Ind.*, 1971, **16**, 47.
5. W. P. Kilroy, *Talanta*, 1978, **25**, 359.
6. *Idem*, *ibid.*, 1979, **26**, 111.
7. A. Kurtenacker and R. Wollak, *Z. Anorg. Allgem. Chem.*, 1927, **161**, 201.
8. W. P. Kilroy, *Talanta*, 1980, **27**, 343.
9. E. Knecht and E. Hibbert, *Ber.*, 1907, **40**, 3819.
10. P. Bethge, *Anal. Chim. Acta*, 1954, **10**, 310.
11. W. P. Kilroy, *J. Inorg. Nucl. Chem.*, 1980, **42**, 1071.

Talanta, Vol. 30, No. 6, pp. 423–426, 1983
Printed in Great Britain.

0039-9140/83/060423-04$03.00/0

PRECIPITATION OF MOLYBDENUM α-BENZOIN OXIMATE FROM HOMOGENEOUS SOLUTION

T. P. S. ASARI and C. S. P. IYER
Analytical Chemistry Division, Bhabha Atomic Research Centre, Trombay, Bombay-85, India

(*Received* 21 *May* 1980. *Revised* 20 *May* 1982. *Accepted* 15 *December* 1982)

Summary—Molybdenum α-benzoin oximate is precipitated from homogeneous solution by hydrolysis of ethyl monochloroacetate to decrease the pH of an originally alkaline solution containing molybdenum and the oxime. The method can be used for assay of molybdenum compounds and ferromolybdenum.

Precipitation from homogeneous solution (PFHS) is a well-known technique for obtaining precipitates that are dense, crystalline and, under certain conditions, practically free from contamination by co-precipitation.[1–3] Among the various methods of PFHS, the most widely used is that involving change in pH, generally by increasing it. Monoethyl glycollate[4] is perhaps the only reagent that has been used *in situ* for decreasing the pH, although acid vapour has been used for the same purpose.[5] This is rather surprising as the pH can easily be decreased by the hydrolysis of various esters. The major problem in the use of esters is probably their insolubility in water, but this can be overcome by using alcohol–water mixtures.

Here we describe the PFHS of molybdenum α-benzoin oximate from aqueous alcohol medium by the decrease in pH resulting from hydrolysis of ethyl monochloroacetate. We also give some applications.

EXPERIMENTAL

Reagents

Molybdenum solution (1 ml = 10.11 mg of Mo) was prepared by dissolving 25.50 g of GR grade sodium molybdate dihydrate in 400 ml of water and diluting to 1 litre, and was standardized.

^{99}Mo tracer was prepared by irradiating 5 mg of MoO_3 (Johnson and Matthey "Spec. Pure") in the Apsara reactor, BARC, at a flux of about 10^{11} n.cm^{-2}.sec^{-1} for 20 hr. The product was dissolved in 2% sodium hydroxide solution and the solution was made 6*M* in hydrochloric acid. The molybdenum was extracted into petroleum ether (b.p. 60°–80°), pre-equilibrated with 6*M* hydrochloric acid, then stripped into water and diluted to volume in a 50-ml standard flask.

All other reagents used were of analytical grade.

Procedure

In a tall, clean scratchless 250 ml beaker, place 0.6 g of α-benzoin oxime and 10 ml of 10% sodium hydroxide solution. After dissolution of the oxime, add the molybdenum solution, containing up to 50 mg of Mo, 25 ml of water and 50 ml of ethanol. Put the beaker in a thermostat at 50°. After 30 min, add 10 ml of ethyl monochloroacetate to the beaker and leave in the thermostat for at least $4\frac{1}{2}$ hr. Remove the beaker and cool it to room temperature. Filter off the precipitate with a tared sintered-glass crucible, porosity 4, wash thrice with ethanol, then twice with water and finally thrice with ethanol, dry at 110° for 1 hr and weigh. Make up the filtrate to volume in a 200-ml standard flask, with ethanol, and determine the residual Mo by the thiocyanate method,[6] using a 20-ml aliquot. Compute the total molybdenum.

Determination of Mo in ferromolybdenum

Weigh 0.2–0.5 g of ferromolybdenum into a clean 250-ml beaker and add 5 ml of concentrated nitric acid and 15 ml of concentrated hydrochloric acid. After dissolution is complete, boil gently for 5 min, cool, and add 20 ml of water. Add 10% sodium hydroxide solution dropwise till a turbidity appears, and clear it by adding a few drops of concentrated hydrochloric acid. Add the solution dropwise to 40–45 ml of nearly boiling 10% sodium hydroxide solution, with stirring. Cool, then make up to volume in a 200-ml standard flask and filter (dry paper) into a clean dry beaker, discarding the first few ml of filtrate. Transfer 50 ml of the filtrate into a tall scratchless beaker containing 0.6 g α-benzoin oxime in 65 ml of ethanol. Heat the beaker in the thermostat at 50° and follow the hydrolysis procedure given above.

Assay of molybdic acid and sodium molybdate

Transfer a suitable weight of sample (as the solid or in solution) into a tall scratchless 250-ml beaker, containing 0.6 g of α-benzoin oxime in 10 ml of 10% sodium hydroxide solution. Add 20 ml of water and 50 ml of ethanol. Heat in the thermostat and follow the procedure already given.

RESULTS AND DISCUSSION

The choice of ester for decreasing the pH depends on the dissociation constant of the corresponding acid and the rate of hydrolysis of the ester. Three esters were chosen for test; ethyl acetate (acetic acid, $pK = 4.76$), monoethyl glycollate (glycollic acid $pK = 3.88$) and ethyl monochloroacetate (monochloroacetic acid, $pK = 2.86$). Preliminary experiments showed that alcohol is necessary to keep these esters in solution, except for monoethyl glycollate. At high alcohol concentrations (above 60% v/v) the rate of hydrolysis was found to be very slow. The rate was found to be optimum when the water to alcohol ratio was maintained at 4:5. However, although the pH dropped very rapidly in the first 3–4 min, further reaction was comparatively slow, and only ethyl monochloroacetate gave a sufficient decrease in pH for the molybdenum to be precipitated (Fig. 1).

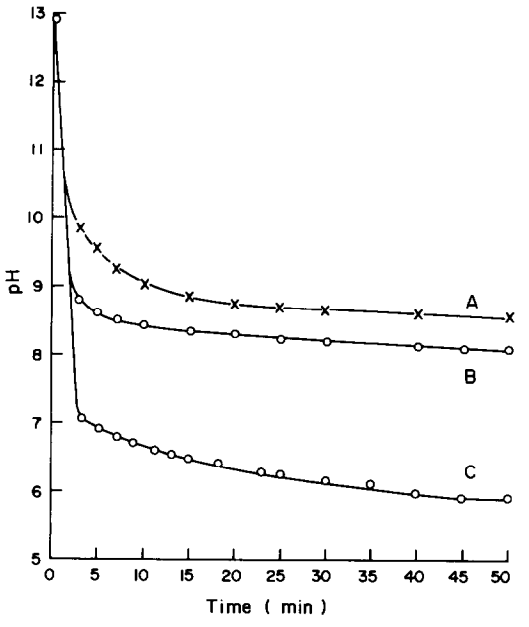

Fig. 1. Rate of hydrolysis of esters in presence of Mo(VI) and α-benzoin oxime. Mo 50.6 mg, α-benzoin oxime 0.6 g, 2.5*M* NaOH 10 ml, ester 10 ml, temperature 50°C. A—ethyl acetate, B—β-hydroxyethyl acetate, C—ethyl monochloroacetate.

The concentrations of sodium hydroxide, molybdenum, alcohol and oxime were then kept constant and the concentration of ethyl monochloroacetate was varied. The pH and time at which the precipitate just appeared were noted (Table 1). Similarly, the amount of oxime was varied from 300 to 1000 mg, with the other parameters kept constant, and the amount of molybdenum left in solution was determined spectrophotometrically as the thiocyanate.[6] The results given in Fig. 2 show that a minimum of 600 mg of the oxime is required for 50 mg of molybdenum.

The effects of reaction temperature and solvent system were next examined. In aqueous ethanol medium the precipitation is rather slow at 50° (40 min for initiation) slightly faster at 70° (20 min) and very fast at 90° (10 min), but at 90° the solution turns blue owing to reduction of the molybdenum. At 50°, in aqueous methanol medium, a precipitate appeared after 20 min whereas in aqueous propan-2-ol medium the start of precipitation took 60 min.

Table 1. Rate of change in pH with different concentrations of ethyl monochloroacetate [600 mg of oxime, 10 ml of 2.5*M* sodium hydroxide, 5 ml of molybdenum solution (Mo 50.6 mg), 25 ml of water, 60 ml of ethanol + ester, total volume 100 ml]

Ester, *ml*	Concn. of ester, M	Time, *min*	pH	Observations
3	0.28	180	7.0	No precipitation
5	0.47	120	6.5	
7	0.66	60	5.9	Precipitation first appears
10	0.94	40	5.9	

The degree of precipitation was determined by using ^{99}Mo tracer, keeping the experimental parameters the same as in the recommended procedure, filtering aliquots of reaction mixture taken out at various intervals of time, and counting the activity of the filtrate. A funnel kept at 50° was used for the filtration. A reference activity was obtained by simultaneous counting of the activity of the tracer in an identical test solution not subjected to hydrolysis. Hydrolysis for at least $4\frac{1}{2}$ hr was necessary to complete the precipitation.

A known weight of the oximate was carefully ignited to MoO_3, with slow heating to 520°, and keeping for 1 hr at that temperature, then collected and weighed. The molybdenum content of the oximate was found to be 16.56% which corresponds to the formula $MoO_2(C_{14}H_{12}O_2N)_2$.

pH of precipitation

It was found in our method that molybdenum starts to be precipitated at pH 5.9, whereas in the literature it is stated that molybdenum α-benzoin oximate does not precipitate at pH above 1, but that value referred to precipitation from aqueous acetone medium (acetone 20% v/v) by the conventional method.[7]

Nature of the product

The precipitates obtained by PFHS and by the Hoenes and Stone method[7] were examined by scanning electron microscopy. The PFHS products were all crystalline whereas that obtained by heterogeneous precipitation was amorphous.

In our work, the Hoenes and Stone method gave a precipitate that was difficult to collect and some tended to pass through the filter, whereas PFHS gave a precipitate that was easy to collect and wash. The conventional method[8] gives a product contaminated with reagent, so it must be ignited to the oxide. In the Hoenes and Stone method the acetone keeps the oxime in solution. The alcohol serves the same purpose in the PFHS method.

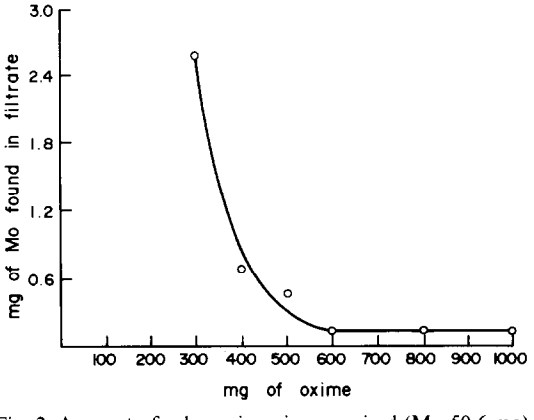

Fig. 2. Amount of α-benzoin oxime required (Mo 50.6 mg).

Table 2. Determination of molybdenum in ferromolybdenum (certified Mo content 74.00%)

Sample*	Mo-oximate obtained, *mg*	Mo, *mg*	Mo left in solution, *mg*	Total Mo found, *mg*	Mo by PFHS method, %
A	226.8	37.5	0.13	37.6	74.0
A	226.7	37.5	0.14	37.6	74.0
B	446.5	73.9	0.14	74.0	73.9
B	446.7	73.9	0.14	74.0	73.9

*A: 0.2035 g in 200 ml; 50-ml aliquot taken. B: 0.5006 g in 250 ml; 50-ml aliquot taken.

Rate of hydrolysis

The three esters hydrolyse at different rates, as shown in Fig. 1, and only the ethyl monochloroacetate gives a pH low enough for precipitation of the molybdenum (pH 5.9, reached in about 45 min). Under the starting conditions used, 7 ml of the monochloroacetate ester are needed for pH 5.9 to be reached, and for convenience it is recommended to use 10 ml (Table 1). The precipitation then starts after 40 min and is complete in about $4\frac{1}{2}$ hr, as is evident from experiments with ^{99}Mo as tracer.

Temperature affects the rate of hydrolysis and hence the rate of precipitation of the molybdenum. At 50° it takes 40 min for the first visible turbidity to appear, 20 min at 70° and 10 min at 90°, but at this temperature the system rapidly turns blue owing to reduction. Hence the precipitation can be safely done at temperatures up to 70°, contrary to the accepted belief that the precipitation should be done only in the cold.[8]

The ratio of water to alcohol is also an important factor as it affects the dielectric strength of the medium and hence the rate of hydrolysis. At high ratios of alcohol to water, precipitation takes much longer whereas at low ratios the ester separates out. Conditions are ideal when the ratio of water to alcohol is kept at 4:5, though precipitation can be done at 1:2 ratio over a longer period.

The lower the dielectric constant of the alcohol, the slower the precipitation, which is fast in methanol medium, moderately slow in ethanol and slowest in propan-2-ol medium, though quantitative in all three.

Accuracy

The precision is good, and the accuracy is further improved by correcting for the amount of molybdenum left in solution. For 50 mg of molybdenum the amount left in solution was 0.12–0.16 mg (6 replicates) and the standard deviation for the amount precipitated was 0.02 mg and for the total recovered 0.01 mg.

The values found for BCS Ferromolybdenum 231 by the PFHS method show good agreement with the certified value, as shown in Table 2. The recommended method for certification uses precipitation as 8-hydroxyquinolinate[9] after separation of iron with sodium hydroxide. The advantage of the present method is the lower conversion factor, 0.1655 compared to 0.2307 for the oxinate method. Also, strict pH control is not needed.

The values obtained by PFHS and by the standard redox method for molybdic acid and sodium molybdate, given in Table 3, also show good agreement. The PFHS method is simpler and easier to handle than the Jones reductor method, though much slower.

Interferences

Vanadium(V) is completely precipitated along with molybdenum and could be corrected for. Tungsten is partially precipitated and must be removed beforehand. Chromium(VI) can be tolerated up to 1 mg and silicon and aluminium up to 5 mg. Iron(III), Cu(II), Cr(III) and Mn(II) are precipitated by the alkali added in adjusting the initial conditions, and filtered off, so cannot interfere. Niobium and tantalum should be absent. Sulphate interferes by precipitation as sodium sulphate in the alcohol medium, but this can be washed out of the precipitate with water, after removal of the excess of oxime with alcohol. Fluoride and phosphate interfere by complex-formation with molybdenum, and must be absent.

Table 3. Assay of molybdic acid and sodium molybdate

	Jones reductor method[9]		PFHS method				
Sample*	Sodium molybdate found, *mg*	MoO_3 found, *mg*	Mo-oximate found, *mg*	Mo left in solution, *mg*	Total Mo found, *mg*	Sodium molybdate, found, *mg*	MoO_3 found, *mg*
1	160.7	—	383.2	0.15	63.6	160.3	
2	160.3	—	383.3	0.14	63.6	160.3	
3	—	90.3	360.4	0.16	59.8	—	89.7
4	—	90.1	360.3	0.17	59.8	—	89.7

*1,2: sodium molybdate dihydrate 160.3 mg. 3,4: molybdic acid 100.0 mg (≡90.0 mg of MoO_3).

Acknowledgements—The authors express their sincere thanks to Dr. M. Sankar Das, Head, Analytical Chemistry Division, for his guidance and encouragement and Dr. R. N. Bhatnagar, Analytical Chemistry Division, for help in the experimental work involving the hydrolysis of esters.

REFERENCES

1. H. H. Willard and N. K. Tang, *J. Am. Chem. Soc.*, 1937, **59,** 1190.
2. P. F. S. Cartwright, E. J. Newman and D. W. Wilson, *Analyst*, 1967, **92,** 663.
3. L. Gordon, M. L. Salutsky and H. H. Willard, *Precipitation from Homogeneous Solution*. Wiley, New York, 1959.
4. L. Gordon, J. J. Peterson and B. P. Burtt, *Anal. Chem.*, 1955, **27,** 1770.
5. F. H. Firsching and P. H. Warner, *Talanta*, 1972, **19,** 790.
6. E. B. Sandell, *Colorimetric Determination of Traces of Metals*, 3rd Ed., p. 644. Interscience, New York, 1959.
7. H. J. Hoenes and K. G. Stone, *Talanta*, 1960, **4,** 250.
8. H. B. Knowles, *Bur. Stds. J. Res.*, 1932, **9,** 1.
9. R. Přibil and M. Malát, *Collection Czech. Chem. Commun.*, 1950, **15,** 120.

Talanta, Vol. 30, No. 6, pp. 427–432, 1983
Printed in Great Britain.

0039-9140/83/060427-06$03.00/0

LIQUID-MEMBRANE DICYANOARGENTATE-SENSITIVE ELECTRODES BASED ON QUATERNARY AMMONIUM SALTS

RU-QIN YU and SHA-SHENG HUANG
Department of Chemistry and Chemical Engineering, Hunan University, Changsha, People's Republic of China

(*Received* 14 *July* 1982. *Accepted* 3 *December* 1982)

Summary—Several quaternary ammonium salts have been synthesized and comparisons made of their efficiency as exchange substrates in dicyanoargentate-sensitive electrodes. The electrode prepared from hexadecyltrioctylammonium dicyanoargentate shows the best performance characteristics and has been studied in more detail. Its Nernstian response range is 10^{-1}–$10^{-4}M$, the optimum pH range is 10.6–12.6, and the detection limit is $3 \times 10^{-5}M$. It is suggested that the detection limit of the electrode is controlled by interference from cyanide ions, and the difference between detection limits obtained with the various electrodes is discussed in the light of this. Selectivity coefficients for various interfering ions have been determined and related to the extractability of the ions. The electrode has been applied to determination of silver in cyanide-containing plating solutions.

The determination of silver in cyanide media such as silver-plating solutions is time-consuming because of the need to destroy the cyanide ions before the determination. An electrode which could be used for direct determination of silver in such solutions is thus of considerable interest. The dicyanoargentate ion is relatively large and polarizable. The large and easily polarized positively-charged complexes of transition-metal ions and 1,10-phenanthroline derivatives have proved suitable for preparation of electrodes sensitive to polarizable ions such as nitrate,[1] but unfortunately cannot be used for a dicyanoargentate-sensitive electrode, because cyanide ions preferentially complex the central metal ions in these complexes. Shavnya *et al.*[2,3] tried tetraphenylarsonium salts for construction of a dicyanoargentate-sensitive electrode. Various long-chain quaternary ammonium salts have been used in preparation of anionic ion-selective membrane electrodes. Recently it was shown[4,5] that better electrode characteristics for BF_4^- and TaF_6^- ions could be obtained when an unsymmetrical long-chain quaternary ammonium species such as the dodecyltriheptylammonium ion was used as counter-ion. We have synthesized and tested several such salts, including hexadecyltrioctylammonium iodide (HTOA-I), butyltrioctylammonium iodide (BTOA-I), hexadecyltributylammonium iodide (HTBA-I) and decyltrioctylammonium iodide (DTOA-I).

As the quaternary ammonium salts are more stable than tetraphenylarsonium salts, we have examined the use of these quaternary ammonium salts for preparing dicyanoargentate ion-selective electrodes for direct potentiometric determination of silver in cyanide-containing solutions.

EXPERIMENTAL

Apparatus

Potential differences were measured with a PHS-2 pH-meter (Analytical Instruments, Shanghai) in conjunction with a UJ-25 d.c. potentiometer (Electric Meters, Shanghai). For automatic determinations of silver concentration by the known-addition method, an Orion 901 microprocessor "Ionalyzer" was used. A PZ8 digital voltmeter and an LY4 digital typewriter (Electric Meters, Shanghai) were used for response-time measurements.

Reagents

All reagents were of analytical grade except when stated otherwise. Demineralized water was used throughout.

A standard solution of potassium dicyanoargentate was made by dissolving silver nitrate (G.R., dried at 110°) in $0.3M$ potassium cyanide and diluting to a silver concentration of $0.1M$, and was further diluted with $0.1M$ potassium cyanide as required.

Synthesis of quaternary ammonium salts

HTOA-I was prepared by refluxing 0.28 mole of hexadecyl iodide and 0.25 mole of trioctylamine in 200 ml of ethanol at 90° for 65 hr. The product was dissolved in ethanol, reprecipitated by addition of ammonia, filtered off and dried (yield *ca.* 60 g). The crude product was redissolved in hot ethyl acetate (150 ml) then the beaker was immersed in a hot water bath and allowed to cool slowly. This recrystallization was done five times. After drying, a white product, m.p. 96.5–98.5°, was obtained. Analysis: $C_{40}H_{84}IN$ requires 1.98% N, 18.0% I; found, 1.94 ± 0.03% N, 17.6 ± 0.6% I. The principal infrared bands were at 2925, 2865, 1465, 1380, 745 and 715 cm^{-1}.

BTOA-I was similarly prepared from trioctylamine and butyl iodide in ethanol. Substances with low b.p. were separated off under partial vacuum. The crude product was obtained by pouring the reaction mixture into water (yield *ca.* 80 g) and recrystallized five times from ethyl acetate. A white product (m.p. 103–105°) was obtained. Analysis: $C_{28}H_{60}IN$ requires 2.60% N, 23.6% I; found, 2.62 ± 0.16% N, 23.2 ± 0.6% I. The principal infrared bands were

at 2940, 2865, 1468, 1439, 1415, 1378, 730 and 718 cm^{-1}.

HTBA-1 was synthesized from 71 g of hexadecyl iodide and 33.3 g of tributylamine in a similar way (yield *ca.* 74 g). The white product, recrystallized six times from ethyl acetate, had m.p. 94–96°. Analysis: $C_{28}H_{60}IN$ requires 2.60% N, 23.6% I; found 2.63 ± 0.17% N, 23.8 ± 0.6% I. The principal infrared bands were at 2930, 2865, 1468, 1438, 1412, 1376, 730 and 718 cm^{-1}.

The infrared spectra of the compounds synthesized were quite similar to those of authentic dodecyltriheptylammonium iodide (DTHA-I, principal bands at 2930, 2865, 1465, 1455, 1400, 1378, 760 and 715 cm^{-1}) and trioctylpropylammonium iodide.[6]

Decyltrioctylammonium iodide was also synthesized, but the product was a viscid liquid difficult to refine. Of all the purified quaternary ammonium salts, BTOA-I was the simplest to synthesize and purify.

Preparation of electroactive material

The quaternary ammonium iodide, dissolved in *o*-nitrotoluene (*o*-NT), was converted into the dicyanoargentate form by successive extractions with solutions of potassium dicyanoargentate, until the aqueous phase gave a negative test for iodide. The organic phase was dried with anhydrous sodium sulphate.

o-Nitrotoluene is preferred to dialkyl phthalates as the solvent because the electroactive materials are more soluble in it.

RESULTS

Comparison of liquid and poly(vinyl chloride) (PVC) membrane electrodes

Figure 1 shows the configuration of the liquid-membrane electrode with a thin porous poly(vinylidene fluoride) (PVF) membrane attached to the end of a PVF tube. The membrane holds a solution of the electroactive material, prepared by the method described above, to form the liquid membrane. The inner reference system consists of a silver/silver chloride electrode inserted into a glass tube filled with a saturated solution of potassium and silver chlorides in 4% agar.

The PVC membrane electrodes were prepared by the standard procedure,[7] by dissolving 0.20 g of PVC powder and 0.58 g of *o*-nitrotoluene solution of electroactive material in 3 ml of tetrahydrofuran, for casting an approximately 9-cm^2 membrane on a glass plate.

The dicyanoargentate complex seemed readily reducible to silver metal in the PVC membrane phase. The rate of reduction decreased with decreasing concentration of the electroactive material. A PVC membrane electrode made with a $10^{-3}M$ solution of

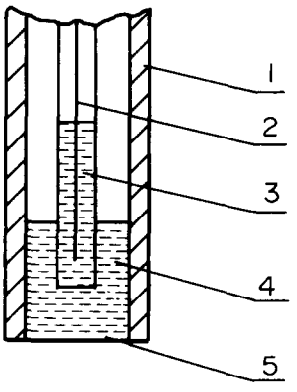

Fig. 1. Schematic diagram of the liquid-membrane electrode assembly. 1, PVF tube; 2, Ag/AgCl electrode; 3, saturated KCl–AgCl solution in 4% agar; 4, electroactive material dissolved in *o*-nitrotoluene; 5, porous PVF membrane.

quaternary ammonium salt in *o*-nitrotoluene has a life-time of several days. The characteristics of such electrodes are listed in Table 1. Repeated experimental efforts were, unfortunately, unsuccessful in lengthening the life of the PVC dicyanoargentate electrodes. The liquid-membrane electrodes have a much longer life and greater reproducibility of potential, probably because the fresh liquid electroactive material can always diffuse from the reservoir to the surface of the membrane to replace that which has deteriorated. As the internal reservoir of active material is large enough for virtually indefinite replenishment of the liquid material, the lifetime depends on the serviceable life of the microporous membrane. The liquid-membrane electrode was used for the rest of this work.

Comparison of various quaternary ammonium counter-ions

Five different quaternary ammonium salts in dicyanoargentate form (denoted by the suffix CA: HTOA-CA, HTBA-CA, BTOA-CA, DTHA-CA and 7402-CA*) were incorporated into liquid-membrane electrodes. Potential measurements were made relative to a saturated calomel electrode.

The electrode parameters are summarized in Table 2 and the calibration curves are shown in Fig. 2. The detection limits were calculated according to the IUPAC recommendation[8] and the d.c. resistances of the membranes were determined by the method of Eckfeldt *et al.*[9] It can be seen that the limit

*A crude product with main component $(C_nH_{2n+1})_3CH_3NCl$, where $n = 8$–9.

Table 1. Response characteristics of PVC dicyanoargentate electrodes (8–10°C)

Electrode	Slope, *mV/decade*			
	1×10^{-1}–$1 \times 10^{-2}M$	1×10^{-2}–$1 \times 10^{-3}M$	1×10^{-3}–$1 \times 10^{-4}M$	1×10^{-4}–$1 \times 10^{-5}M$
1	56	54	52	53
2	57	52	52	52
3	55	54	47	49

Table 2. Comparison of various quaternary ammonium sites

Electroactive material	HTOA-CA	DTHA-CA	BTOA-CA	HTBA-CA	7402-CA
Detection limit, M	3×10^{-5}	9×10^{-5}	1×10^{-4}	1.2×10^{-4}	1.6×10^{-4}
Electrode slope, *mV/decade*	55	51	52	44	46
Membrane d.c. resistance, *kΩ*	83.6	88.5	66.6	100	375
$K^{ext.}_{Ag(CN)_2^-,I^-}$	6.39	4.29	4.29	3.13	0.945
$K^{ext.}_{CN^-,I^-}$	0.0158	0.019	0.0182	0.0182	0.0169

of detection and the slope for the HTOA-CA electrode are slightly better than those obtained with other membranes. The lack of purity of the 7402-CA salt seems to have a pronounced effect on the resistivity of the membrane.

Effect of concentration of HTOA-CA in the liquid membrane

The results of a study of effect of the concentration of HTOA-CA in the liquid-membrane phase on the electrode properties are shown in Fig. 3. Better electrode characteristics are obtained with relatively higher (*ca.* $10^{-2}M$) HTOA-CA concentration. Above $10^{-2}M$, the quantitative conversion of the HTOA-I into the HTOA-CA form requires unreasonably lengthy and repeated extraction with highly concentrated aqueous solutions of dicyanoargentate.

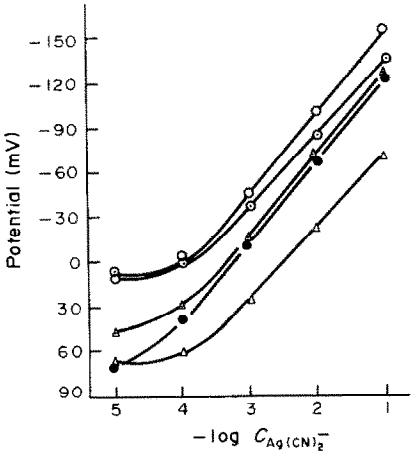

Fig. 2. Comparison of various quaternary ammonium counter-ions △, HTBA-CA; ●, HTOA-CA; △, BTOA-CA; ⊙, 7402-CA; ○, DTHA-CA.

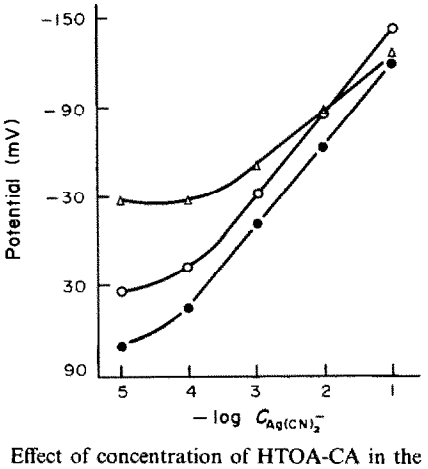

Fig. 3. Effect of concentration of HTOA-CA in the liquid membrane. ●, $10^{-2}M$ HTOA-CA; △, $10^{-3}M$ HTOA-CA; ○, $10^{-1}M$ HTOA-CA.

Effect of concentration of free cyanide ions in the sample solution

Figure 4 shows the effect of free cyanide-ion concentration on the electrode properties. The detection limit of the electrode improves with decreasing free cyanide concentration. However, solutions having a relatively high concentration of dicyanoargentate are unstable if the concentration of free cyanide is too low. As the presence of free cyanide ions affects the electrode potential, it is essential to keep the free cyanide concentration in the standard and sample solutions at the same level. A cyanide concentration of $0.1M$ is recommended as suitable for most practical situations.

Potential–pH curves

The pH of a standard dicyanoargentate solution was adjusted to various values by addition of dilute sodium hydroxide or hydrochloric acid. Figure 5 shows the potential as a function of pH for two

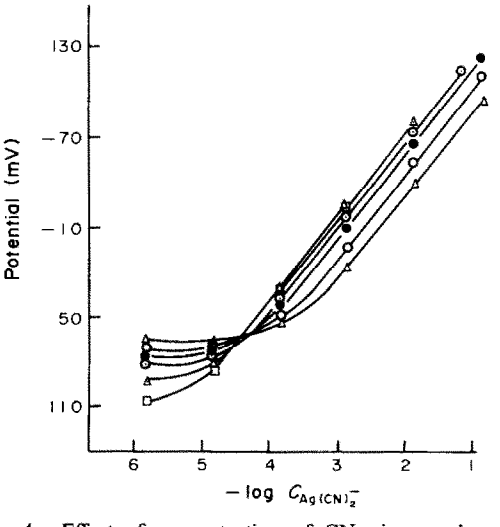

Fig. 4. Effect of concentration of CN^- in sample solution. △, $0.4M$; ○, $0.2M$; ●, $0.1M$; ⊙, $0.05M$; △, $0.01M$; □, $0.001M$.

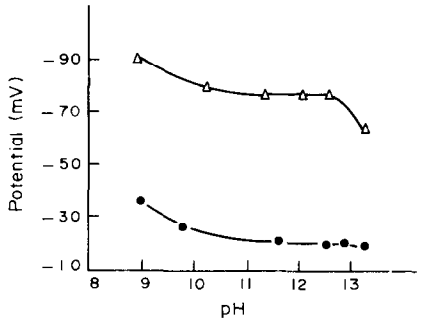

Fig. 5. Electrode response as a function of pH. △, $10^{-2}M$ $Ag(CN)_2^-$; ●, $10^{-3}M$ $Ag(CN)_2^-$.

dicyanoargentate concentrations, 10^{-3} and $10^{-2}M$. Because cyanide is liberated as HCN at low pH, the electrode can be used only in basic solutions. The useful working pH-range is 10.6–12.6. In strongly alkaline medium a slight deterioration in electrode performance was noted.

Temperature effect and response-time

The effect of temperature was tested by recording calibration graphs at 8, 25 and 45° (Fig. 6). The response-time of the electrode under static conditions was determined by use of a PZ8 digital voltameter in conjunction with an LY4 digital typewriter. In 10^{-5}–$10^{-1}M$ solutions of dicyanoargentate, stable readings were obtained within 1–3 min. The response-time does not depend appreciably on the concentration of dicyanoargentate ion. A newly constructed electrode seems to respond slightly more slowly. For several weeks after construction of the electrode a steady reading should be obtained in less than 2 min after the dicyanoargentate concentration has been changed.

Interferences

The selectivity coefficients listed in Table 3 were determined by the mixed-solution method with a fixed level of interferent ion. Most common anions do not affect the electrode response. However, $Au(CN)_2^-$ causes a large response and it seems possible that an excellent $Au(CN)_2^-$ ion-selective electrode could be made.

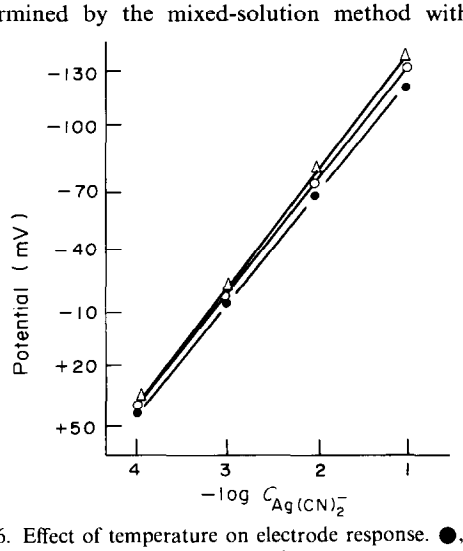

Fig. 6. Effect of temperature on electrode response. ●, 8°; ○, 25°; △, 45°.

Stability and lifetime

The electrode potentials were reproducible to ±1 mV over a day and +5 mV over 8 days (Table 4). Some electrodes lasted for 6 months before needing renewal.

DISCUSSION

There are currently two general models which account for the low-level responses of ion-selective electrodes. The first model assumes that the detection limit is controlled by dissolution of the membrane material. The other, an interference model, asserts that the electrode response in a dilute analyte solution is controlled by interference from ions in the sample solution. For the first model an equation describing the potential of a liquid-membrane electrode was derived by Kamo *et al.*[10]

$$E = E^\circ - \frac{RT}{F} \ln[(C + \sqrt{C + A_x})/2] \qquad (1)$$

where C is the concentration of the primary ion that the electrode is designed to measure, and the detection limit of the electrode is dependent on A_x. When the ion-exchanger dissociates completely in the membrane phase, A_x is given by $4\sigma^2/b_x$, where σ represents the concentration of ion-exchanger in the liquid membrane, and b_x is a quantity related to the ion-selectivity. This model was verified by Kamo *et al.* with a Crystal Violet–iodide system and by Mathis *et al.*[11] with quaternary ammonium nitrate membranes. Our experimental results suggest that the detection limit with the dicyanoargentate electrode is probably controlled by cyanide ion interference. If the detection limit of the electrode were controlled by dissolution of the electroactive material in aqueous solution, it should improve with decreasing concentration of electroactive material in the membrane phase, but our results (Fig. 3) show the reverse. In addition, the amount of silver lost from the membrane into aqueous solution was determined spectrophotometrically and found to be $< 10^{-6}M$, which was much lower than the experimentally determined detection limit of the electrode. Figure 4 also shows that a decrease of free cyanide concentration leads to improvement in the detection limit of the electrode, as expected for the interference mechanism. Also, for dissolution-controlled membrane electrodes, response times are generally longer at lower concentrations, particularly in the region between the limit of linear response and the limit of detection. Again, this is not true for the dicyanoargentate electrode. Even at a concentration below the detection limit, the time needed to reach an emf within 1 mV of the final

Table 3. Selectivity coefficients

Interferent, N^{n-}	$K^{pot}_{Ag(CN)_2^-,N^{n-}}$	Interferent, N^{n-}	$K^{pot}_{Ag(CN)_2^-,N^{n-}}$
$Au(CN)_2^-$	$58(1 \times 10^{-5}M)$*	$Fe(CN)_6^{3-}$	$1.26 \times 10^{-4}(0.50M)$
Br^-	$3.64 \times 10^{-3}(0.5M)$	$Fe(CN)_6^{4-}$	$10^{-5}(0.5M)$
CN^-	$3.70 \times 10^{-4}(0.1M)$	I^-	$0.24(1 \times 10^{-2}M)$
Cl^-	$5.00 \times 10^{-4}(0.5M)$	NO_3^-	$1.04 \times 10^{-2}(1 \times 10^{-2}M)$
ClO_4^-	$10.9(1 \times 10^{-3}M)$	PO_4^{3-}	$1.66 \times 10^{-4}(0.5M)$
CO_3^{2-}	$10^{-5}(0.5M)$	SO_4^{2-}	$10^{-5}(0.5M)$

*Values in parentheses are interferent concentrations.

equilibrium value is 1–2 min. It seems that in this case the contribution of the activity of the ion, $a_{Ag(CN)_2^-}$, to the electrode potential in the modified Nernst equation

$$E = \text{Const.} + \frac{2.303RT}{F} \log(a_{Ag(CN)_2^-} + K^{pot}_{Ag(CN)_2^-,CN^-} a_{CN^-} + \ldots) \quad (2)$$

becomes negligible and the contribution of the cyanide interference term $K^{pot}_{Ag(CN)_2^-,CN^-} a_{CN^-}$ becomes dominant, the activity of the cyanide ion a_{CN^-} (*ca.* $0.1M$) being in the typical range for fast response of ordinary electrodes.

The differences between the detection limits for electrodes prepared from various quaternary ammonium counter-ions will depend on the differences in the relative affinities for the dicyanoargentate and cyanide ions. Dicyanoargentate is polarizable and larger than the cyanide ion. It seems that larger counter-ions with lower charge density prefer larger and polarizable ions.[12] The HTOA cation was the largest of the quaternary ammonium ions tested, so it would be expected to have the greatest affinity for the dicyanoargentate. Consider the competitive distribution between dicyanoargentate and cyanide ions in the aqueous phase and the iodide ion in the organic membrane phase:

$$(Q^+, I^-)_o + Ag(CN)_{2,w}^- \rightleftharpoons [Q^+, Ag(CN)_2^-]_o + I_w^- \quad (3)$$

and

$$(Q^+, I^-)_o + CN_w^- \rightleftharpoons (Q^+, CN^-)_o + I_w^- \quad (4)$$

where Q^+ is the quaternary ammonium ion. The equilibrium constants for these processes are (activity coefficient effects being neglected):

$$K^{ext.}_{Ag(CN)_2^-,I^-} = \frac{[(Q^+, Ag(CN)_2^-)]_o[I^-]_w}{[(Q^+, I^-)]_o[Ag(CN)_2^-]_w} \quad (5)$$

and

$$K^{ext.}_{CN^-,I^-} = \frac{[(Q^+, CN^-)]_o[I^-]_w}{[(Q^+, I^-)]_o[CN^-]_w} \quad (6)$$

For the experimental determination of $K^{ext.}_{Ag(CN)_2^-,I^-}$ and $K^{ext.}_{CN^-,I^-}$ the concentrations of the various species in the aqueous and organic phases were measured spectrophotometrically. The competitive extraction constants calculated from equations (5) and (6) are listed in Table 2. The extractability of $Ag(CN)_2^-$ by the quaternary ammonium counter-ions, as measured by

Table 4. Reproducibility of electrode potential (*mV*)

	Day						
$[Ag(CN)_2^-]$	1	2	3	4	5	6	8
$10^{-3}M$	−13	−14	−12	−11	−10	−10	−10
$10^{-2}M$	−70	−70	−69	−69	−66	−67	−65

Table 5. Determination of silver concentration in silver cyanide plating solutions

Sample	Silver added, *mmole*	Silver found, *mmole*	
		Electrode method	Argentometry
Synthesized Plating bath	5.00	5.10; 4.89; 4.82	
	1.00	1.04; 1.03; 1.01	
N1	0	30.3; 30.1; 30.0	30.5
N2	0	31.0; 31.2; 31.9	32.6
N3	0	3.01	Recovery, %
N3	0.50	3.50	98
N3	1.00	3.98	97

$K^{ext.}_{Ag(CN)_2^-,I^-}$, generally increases with the number of carbon atoms in the cation, but the size of the cation has a smaller effect on the values of $K^{ext.}_{CN^-,I^-}$. Thus the largest counter-ion (HTOA) has greater selectivity for $Ag(CN)_2^-$ with respect to CN^-. According to the interference model, the electrode prepared from HTOA-CA should have a lower detection limit for $Ag(CN)_2^-$ in the presence of free cyanide (Table 2).

James *et al.*[13] related the selectivity coefficients of electrodes to ion-pair extractability. For the dicyanoargentate electrode the following distribution should be considered:

$$n(Q^+, Ag(CN)_2^-)_o + N_w^{n-} \rightleftharpoons (nQ^+, N^{n-})_o + nAg(CN)_{2,w}^- \quad (7)$$

The equilibrium constant is:

$$K^{ext.}_{Ag(CN)_2^-,N^{n-}} = \frac{[Ag(CN)_2^-]_w^n[(nQ^+, N^{n-})]_o}{\{[Q^+, Ag(CN)_2^-]\}_o^n[N^{n-}]_w} \quad (8)$$

The equilibrium constants given by equation (8) were determined for a number of anions N^{n-} by spectrophotometry. A plot of log $K^{pot}_{Ag(CN)_2^-,N^{n-}}$ (X) *vs.* log $K^{ext.}_{Ag(CN)_2^-,N^{n-}}$ (Y) is approximately linear with correlation coefficient 0.91, the regression line being

$$Y = -1.08 + 0.92X \quad (9)$$

PRELIMINARY APPLICATIONS

The silver concentration of cyanide-containing plating solutions has for many years been determined by argentometric titrations, but time-consuming and potentially hazardous operations are required to destroy cyanide ions before the analysis. The dicyanoargentate electrode provides a faster and simpler alternative method for this determination. The only sample pretreatment required is a tenfold dilution of the sample with water. The method was validated by analysing synthesized and industrial samples of silver cyanide plating solutions by the standard-addition method. Table 5 shows that the results obtained by the electrode method are in reasonable agreement with those from the argentometric procedures.

REFERENCES

1. J. W. Ross, in *Ion-Selective Electrodes*, R. A. Durst, (ed.), N.B.S. Spec. Publ. No. 314, p. 70. Washington, D.C., 1969.
2. Yu. V. Shavnya, A. S. Bychkov, O. M. Petrukhin, V. A. Zarinskii, L. V. Bakhtinova and Yu. A. Zolotov, *Zh. Analit. Khim.*, 1978, **33,** 531.
3. A. S. Bychkov, O. M. Petrukhin, Yu. V. Shavnya, V. A. Zarinskii and Yu. A. Zolotov, *VINITI Deposited Doc.* 1977, 3564-77; *Chem. Abstr.*, 1979, **90,** 194625j.
4. Q. Yuan and J. C. Luo, *Fenxi Huaxue* (Analytical Chemistry), 1981, **9,** 319.
5. K. X. Chang, H. C. Fu, W. X. Chen, H. C. Wang and Q. Yuan, *Acta Chimica Sinica*, 1980, **38,** 223.
6. Sadtler Research Laboratories, Inc., *Standard Infrared Prism Spectra*, 46687, Propyltrioctylammonium iodide, Researchers, Ed. & Publ., Philadelphia, 1974.
7. G. J. Moody and J. D. R. Thomas, *Ion-Selective Electrode Rev.*, 1979, **1,** 3.
8. IUPAC, *Pure Appl. Chem.*, 1976, **48,** 127.
9. E. L. Eckfeldt and C. A. Perley, *J. Electrochem. Soc.*, 1951, **98,** 37.
10. N. Kamo, N. Hazamoto and Y. Kobatake, *Talanta*, 1977, **14,** 111.
11. D. E. Mathis, R. M. Freeman, S. T. Clark and R. P. Buck, *J. Membrane Sci.*, 1979, **5,** 103.
12. J. W. Ross, Lecture read at ISE Seminar held at Hunan University, Changsha, 15–19 Nov. 1981.
13. H. J. James, G. P. Carmack and H. Freiser, *Anal. Chem.*, 1972, **44,** 853.

Talanta, Vol. 30, No. 6, pp. 433–436, 1983
Printed in Great Britain.

0039-9140/83/060433-04$03.00/0

SOME INVESTIGATIONS ON NEW POLYPHOSPHATES BY THE ANION-EXCHANGE METHOD

TOSHIO NAKASHIMA* and HIROHIKO WAKI
Department of Chemistry, Faculty of Science, Kyushu University, Hakozaki, Higashi-ku, Fukuoka 812, Japan

(*Received* 27 *August* 1982. *Accepted* 5 *November* 1982)

Summary—The structure of the pentamer (a new P–P bonded phosphate) produced by the hydrolysis of dodecaoxohexaphosphoric(III) acid (ring hexamer) has been examined by an anion-exchange distribution method after complex formation with copper(II) and found to be HPO(OH)PO(OH)PO(OH)PO(OH)PO(OH)H. The hexamer and pentamer salts of these P–P bonded linear phosphorus anions have been prepared. The yield of each species was about 1 mole% of the parent material.

New linear phosphorus oxo-acids (hexamer and pentamers) with P–P bonds can be prepared by the hydrolytic cleavage of their parent ring hexamer.[1] Theoretical considerations of the hydrolysis predict that only one hexameric species exists but there may be three pentamers in which the oxidation numbers of the terminal phosphorus atoms are different. In order to make clear which component is predominant among these pentamers, the structures have been investigated by anion-exchange methods. Anion-exchange charge analysis is considered to be an effective method for the determination of the structure of dissolved sample components.[2–5] In the present case, however, direct application to the oxo-anion itself may lead to ambiguous results because of uncertainties about the protonation of the terminal phosphorus units. Complexation of these oxo-anions with suitable metal ions expels bound protons, and more information may thus be obtained on the charge state of the original sample anion. Charge determination after complexation of the pentamer with a suitable metal ion is possible because labile protons bound to the anion should be released when the anion is strongly co-ordinated to a multivalent metal ion. Copper(II) was selected as a suitable metal ion because of its strong affinity for the terminal phosphate unit of the linear polymer.

Although the hexamer and pentamers are fairly stable in aqueous solution, they are hydrolysed on standing for a long time. The best way of preserving these oxo-acids is by solidification as their salts. Desalting by a gel chromatographic separation, followed by concentration in vacuum, is not suitable for the hexamer because decomposition occurs on contact with a Sephadex gel. When a very small amount of the sample component is to be prepared from a large amount of electrolyte solution, anion-exchange concentration may be useful, since the decomposition of the polyphosphate anion is suppressed in the anion-exchange resin phase.[6] However it is necessary to establish strictly the equilibration conditions such as solution volume, electrolyte concentration and amount of exchanger.

*Present address: Institut für Chemische Technologie, Kernforschungsanlage Jülich GmbH, 5170 Jülich, F.R.G.

EXPERIMENTAL

Reagents

Analytical grade copper(II) chloride dihydrate was used without purification. The potassium sodium salt of dodecaoxohexaphosphoric(III) acid was prepared by the Blaser and Worms procedure.[7] Commercial tetramethylammonium chloride and 10% tetramethylammonium hydroxide solution were used without purification. For preparation of $[N(CH_3)_4]_6(PO_2)_6$ solution, a solution of the potassium sodium salt of dodecaoxohexaphosphoric(III) acid was passed through a column containing Dowex 50W-X4 resin (50–100 mesh) in the tetramethylammonium form. The conditions for hydrolysis of the parent hexamer and a method of separation of the decomposition products have already been described.[1]

Distribution measurements for the copper complex

Ring hexamer. Distribution ratios of copper ions between the resin and the solution phase were measured by the normal batch equilibrium method. A series of $10^{-4}M$ copper(II) chloride/$5.2 \times 10^{-4}M$ ring hexamer solutions (pH 7) containing different concentrations of tetramethylammonium chloride were equilibrated with 1 g of Dowex 1-X4 resin (100–200 mesh) in the chloride form at $20 \pm 1°$ for 1 hr. After settling, the mixture was filtered and the copper concentration in the filtrate determined with a Perkin–Elmer model 403 atomic-absorption spectrophotometer and a Hitachi 056 type recorder. The copper AAS signal was enhanced by about 10% by the presence of phosphorus atoms and the distribution ratio of copper(II), D_{Cu}, was corrected accordingly:

$$D_{Cu} = \frac{[\text{concentration of copper(II) in the resin (air-dry weight)}]}{[\text{concentration of copper(II) in solution}]} \quad (1)$$

The phosphorus concentration was determined as described by Hosokawa and Oshima.[8]

Pentamers. The solutions containing the pentamers separated by anion-exchange chromatography were diluted to 250 ml with water and the absorbances at the characteristic peak (255 nm) were measured to estimate the amount of the species. The pentamer was then sorbed on 1 g of Dowex 1-X4 resin (100–200 mesh) in the chloride form and eluted with 15 ml of 1.0*M* tetramethylammonium chloride (to transform it into its tetramethylammonium salt) and the eluate was diluted to 50 ml with water. The chloride concentration in this stock solution was measured by Volhard titration. A fixed volume of tetramethylammonium chloride solution was put into a beaker containing 10 ml of the stock solution and 5 ml of $1 \times 10^{-3}M$ copper(II) chloride and made up to 50 ml. The pH of the solution was adjusted to 8.5. No precipitation of copper hydroxide occurred at this pH in the presence of excess of phosphorus oxo-anion ligand. A series of such mixtures was shaken at $20 \pm 1°$ for 1 hr with 1 g of Dowex 1-X4 resin (100–200 mesh) in the chloride form and the copper remaining in solution was determined as described above.

Concentration and solidification

The effluent fractions (containing 0.14 meq of the linear P–P hexamer and 15 meq of chloride from the eluent) separated by anion-exchange chromatography were collected, and the total concentration of the hexamer was measured spectrophotometrically. The solution was diluted to 500 ml with water and the hexamer sorbed on 0.1 g (0.2 meq) of Dowex 1-X4 resin (100–200 mesh) in the chloride form: here 0.14 meq (total phosphate)/0.20 meq (resin used) = 0.7, so 70% of the sites available on the resin were occupied by phosphate anions at this stage. The resin sample containing the hexamer was filtered off and packed into a small column (bore 0.4 cm, length 1.0 cm). The hexamer was eluted with 1 ml of 1.0*M* potassium chloride (degree of desalting at least 93%), and 1.0 ml of 1.0*M* magnesium chloride was added to the eluate. A few ml of 99.9% methanol were added to this solution, and the magnesium salt was precipitated, filtered off, washed with a small amount of methanol and dried in air. The yield was 4 mg (1% of the parent compound in molar ratio). The pentamers were obtained as solids by the same method, the yield being 1.1% of the parent compound.

Elemental analysis

A portion of the magnesium salt of the pentamer was dissolved in 20 ml of water, then the solution was passed through a column of anion-exchange resin (Bio-Rad AG1-X8, nitrate form, 100–200 mesh, bore 1.2 cm, length 3.0 cm) to elute the magnesium as nitrate. The magnesium was determined by EDTA titration. Potassium coprecipitated with the magnesium salt was determined potentiometrically. Then 20 ml of 1*M* sodium perchlorate were passed through the column to elute the anions. The chloride concentration in the effluent was determined potentiometrically.[8]

RESULTS AND DISCUSSION

The distribution ratio, D_M, of the metal ion, M^{m+}, in the presence of polyanion L^{l-} between the anion-exchanger phase and aqueous phase may be written as

$$D_M = \frac{\Sigma[M^{m+}]_R}{\Sigma[M^{m+}]} = \frac{[ML^{(l-m)-}]_R + [ML_2^{(2l-m)-}]_R + \cdots}{[M^{m+}] + [ML^{(l-m)-}] + [ML_2^{(2l-m)-}] + \cdots} \quad (2)$$

Assuming the presence of only an ML complex for a ligand of high anionic charge, because the stability of

Table 1. Anion-exchange distribution data for copper(II) complex with ring hexamer

No.	$[Cu]_R$, *mmole/g of resin*	D_{Cu}, (volume basis)	$^*C_R$, *mmole/g of resin*	$\Sigma[P]_R$, *mmole/g of resin*	$[Cl^-]_R$, *mmole/g of resin*	$[Cl^-]_R$,† relative (volume basis)	$[Cl^-]$, M	$[Cl^-]/[Cl^-]_R$, M
1	0.0049	1552	2.108	0.0259	1.962	1.000	0.150	0.150
2	0.0045	478	2.111	0.0255	1.967	1.009	0.200	0.198
3	0.0041	208	2.114	0.0249	1.973	1.017	0.250	0.246
4	0.0034	109.9	2.118	0.0229	1.999	1.030	0.300	0.291

*C_R means effective resin capacity after corrections for invasion of cations into the exchanger.
†Relative $[Cl^-]_R$ is used here, referred to solution number 1, after corrections from weight basis to volume basis.

an ML_2 complex will be low on account of electrostatic repulsion between the ligand anions, then,

$$D_M = \frac{[ML^{(l-m)-}]_R}{[M^{m+}] + [ML^{(l-m)-}]} = \frac{[ML^{(l-m)-}]_R}{[ML^{(l-m)-}]} \times \frac{K_c[L^{l-}]}{1 + K_c[L^{l-}]} \quad (3)$$

where

$$K_c = \frac{[ML^{(l-m)-}]}{[M^{m+}][L^{l-}]} \quad (4)$$

If the total concentration of ligand anion is much higher than that of the metal ion, $K_c[L^{l-}] \gg 1$ if K_c is sufficiently high, and then equation (3) simplifies to

$$D_M = \frac{[ML^{(l-m)-}]_R}{[ML^{(l-m)-}]} \quad (5)$$

is identical with the slope of the log–log plot of the distribution ratio *vs.* the supporting anion concentration. The validity of this interpretation is supported by the results obtained with the copper(II) complex of the ring hexamer having an anionic charge of 4−. The slope of the log–log plot of D_{Cu} *vs.* $[Cl^-]/[Cl^-]_R$ was −4.0 in agreement with the theoretical charge. Table 1 shows the anion-exchange distribution data after corrections (for invasion of cations into the resin, loading of sample species and resin volume change[9]) by computer iterative calculation.[1,10] The constancy of the selectivity coefficient, K_{Cl}^{CuP}, was confirmed from the agreement between the theoretical and experimental values. The method was next applied to the copper(II)–linear pentamer sample. The slope of the log D_{Cu} *vs.* log $[Cl^-]/[Cl^-]_R$ plot was −3.18, indicating that the following process (A) is predominant in the formation of the linear pentamer, with a much smaller contribution from process (B). The low yields of hexamer and pentamer

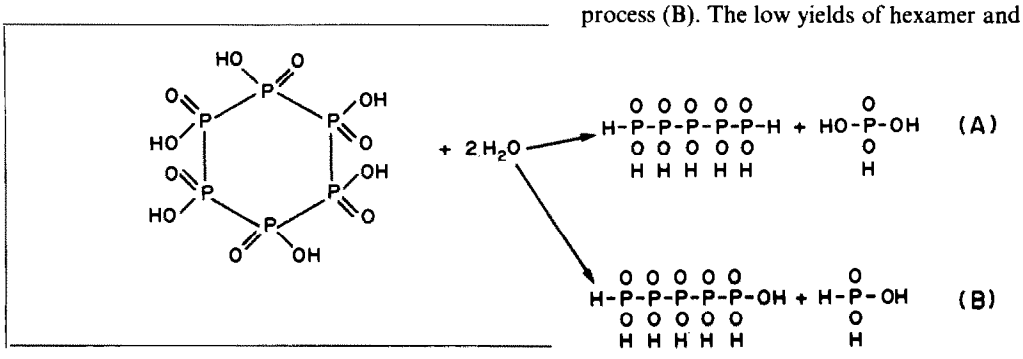

from the ring hexamer and the high solubilities of their salts in water necessitate extreme concentration of the sample component. In order to obtain as much of the polyphosphates as possible, information about the free anionic charge of the polyphosphates in aqueous solution, the ion-exchange selectivity coefficient K_{Cl}^{P} and the absolute values of the distribution ratios, D_{P6} and D_{P5}, is needed. These quantities may be obtained from previous work,[1] to give the following equations.

$$K_{Cl}^{P6} \equiv D_{P6}\left(\frac{[Cl^-]}{[Cl^-]_R}\right)^6 = 0.004 \quad (11)$$

$$K_{Cl}^{P5} \equiv D_{P5}\left(\frac{[Cl^-]}{[Cl^-]_R}\right)^{4.8} = 0.022 \quad (12)$$

The relationship between the resin weight to be used and the dilution volume for a given recovery of the desired polyanion from the aqueous phase can be established by use of these equations. A general recovery curve for differently charged polyanions can be constructed when the charge and the selectivity coefficient at neutral pH are known. Figures 1 and 2 show the theoretical recovery curves for hexamer and pentamer, obtained by using equations (11) and (12). The ordinate is the logarithm of dilution volume (ml). The abscissa is the ratio of the resin capacity (meq) to the amount of sample (meq). The upper region of

With use of the Donnan equations:

$$[B^+]^{(l-m)}[ML^{(l-m)-}](\gamma_B)^{(l-m)}\gamma_{ML} = [B^+]_R^{(l-m)}[ML^{(l-m)-}]_R(\bar{\gamma}_B)^{(l-m)}\bar{\gamma}_{ML} \quad (6)$$

$$[B^+][A^-]\gamma_B\gamma_A = [B^+]_R[A^-]_R\bar{\gamma}_B\bar{\gamma}_A \quad (7)$$

where γ and $\bar{\gamma}$ represent the activity coefficients for the solution and resin phase respectively, and B^+ and A^- the singly-charged cation and anion, equation (5) can be rewritten in the form

$$D_M = K_A^{ML}\left(\frac{[A^-]_R}{[A^-]}\right)^{(l-m)} \quad (8)$$

where K_A^{ML} represents the activity coefficient quotient:

$$K_A^{ML} = \left(\frac{\bar{\gamma}_A}{\gamma_A}\right)^{(l-m)}\frac{\gamma_{ML}}{\bar{\gamma}_{ML}} \quad (9)$$

which is assumed to be constant when the variation of the ionic strength of the solution is not large. Differentiation of the logarithmic form of equation (8) gives

$$\frac{d\log(D_M)}{d\log([A^-]/[A^-]_R)} = \frac{d\log(K_A^{ML})}{d\log([A^-]/[A^-]_R)} - (l-m) = -(l-m) \quad (10)$$

This equation means that the charge on the complex

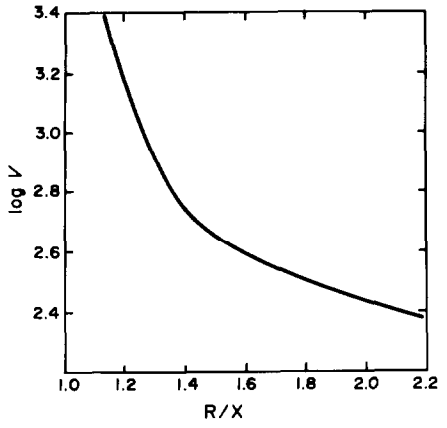

Fig. 1. Theoretical recovery curve (99.5%) with Dowex 1-X4 resin for the hexamer. R: Resin capacity used (meq); X: amount of hexamer (meq).

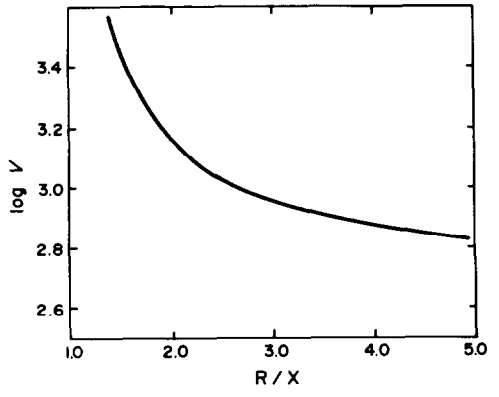

Fig. 2. Theoretical recovery curve (99.0%) with Dowex 1-X4 resin for the pentamer. R: Resin capacity used (meq); X: amount of pentamer (meq).

the line corresponds to more than 99% sorption of the hexamer and pentamer under the given conditions. In our experiments R/X is 1.43 and 2.43, and log V 2.7 and 3.0 for the hexamer and pentamer, respectively. The solid hexamer was dissolved in water and converted into the potassium salt by ion-exchange. The ultraviolet absorption spectra of these solutions were identical with those of the original solutions, indicating that no decomposition had taken place during solidification. This technique may be useful for obtaining in solid form unstable polyanion salts only available in small amounts.

Stoichiometric analysis of the magnesium linear-pentamer salt produced was attempted. The ratio of magnesium to phosphate is 2.56 ± 0.13, suggesting that route (A) is the major one in the formation of linear pentamer from the parent ring hexamer, because theoretically 2.5 ions of magnesium should be bound to one anion of linear pentamer for charge balance.

REFERENCES

1. T. Nakashima, H. Waki and S. Ohashi, *J. Inorg. Nucl. Chem.*, 1977, **39**, 1751.
2. F. Nelson, R. A. Day, Jr. and K. A. Kraus, *ibid.*, 1960, **15**, 140.
3. K. A. Kraus and F. Nelson, *Proc. Int. Conf. United Nations, Geneva*, 1955, **7**, 113.
4. *Idem, Anion Exchange Studies of Metal Complexes* in *The Structure of Electrolytic Solutions*, W. J. Hamer, (ed.). Wiley, New York, 1959.
5. H. Waki, Y. Hisazumi and S. Ohashi, *J. Inorg. Nucl. Chem.*, 1977, **39**, 349.
6. H. Waki, *unpublished data.*
7. B. Blaser and K. H. Worms, *Z. Anorg. Allg. Chem.*, 1959, **300**, 237.
8. I. Hosokawa and F. Ohshima, *Water Res.*, 1973, **7**, 283.
9. M. Yoshio, H. Waki and N. Ishibashi, *J. Inorg. Nucl. Chem.*, 1970, **32**, 1365.
10. T. Nakashima, *Ph.D. Thesis*, Kyushu University, Fukuoka, Japan.

Talanta, Vol. 30, No. 6, pp. 437–439, 1983
Printed in Great Britain.

0039-9140/83/060437-03$03.00/0

SHORT COMMUNICATIONS

DECOMPOSITION OF ORGANIC MATTER WITH MOLTEN ALKALI: DETERMINATION OF ARSENIC AND ANTIMONY IN ORGANIC COMPOUNDS

F. Bosch Reig and J. V. Gimeno Adelantado*
Department of Analytical Chemistry, Faculty of Chemistry, University of Valencia, Valencia, Spain

(*Received* 25 *August* 1982. *Revised* 11 *November* 1982. *Accepted* 6 *January* 1983)

Summary—Decomposition of organic matter with molten alkali has been examined as a method of opening out organic matrices for elemental detection and/or determination. The fusion product is readily soluble. Arsenic and antimony in organic compounds can be determined iodimetrically after mineralization by this fusion method.

The methods commonly used for opening out organic samples usually involve total destruction of the organic matter.[1] Both wet oxidation and dry-ashing procedures are used.[2]

The wet-way techniques use digestion with acids such as sulphuric, nitric and perchloric. The sulphuric acid methods are essentially modifications of the Kjeldahl method, which dates from 1883 and generally needs an auxiliary oxidant; Kjeldahl originally used potassium permanganate, but there have been many modifications, including the use of catalysts.[3] Hydrogen peroxide is particularly popular, and in association with sulphuric acid produces rapid oxidation of many substances.[4]

Hot concentrated nitric acid is a very good oxidant, but because it tends to volatilize before destruction of the sample is complete it is generally used together with sulphuric acid, small amounts of which aid the destruction and minimize the explosion hazards;[5] other mixtures of nitric and sulphuric acids are also effective.[6] Nitric acid or its mixture with hydrofluoric acid can be used under pressure in a Teflon tube to decompose biological materials for determination of volatile elements;[7] a mixture of nitric, hydrofluoric and boric acids, used in a Teflon bomb, has been found an excellent medium for oxidation and dissolution of coal.[8] Refluxing with nitric acid alone in a Soxhlet extractor is also satisfactory, although ammonium bromide must be added to inhibit formation of alkali metal nitrates (explosion hazard) or metal chlorides (more volatile).[9]

Perchloric acid, when hot and concentrated, can cause explosive decomposition of organic matter, and is therefore generally used mixed with nitric acid;[10–13] automated systems have been designed for the purpose.[14] The oxidation potential of perchloric acid is a function of temperature and concentration, and can be controlled by suitable additions of nitric and/or sulphuric acid, the explosion hazards being decreased.[15] A decided advantage of wet oxidation with the sulphuric, nitric and perchloric acid mixture is that no explosion or ignition occurs; furthermore, the use of catalysts considerably diminishes both charring and foaming,[16] though interferences can occur.

Dry-ashing consists of oxidizing the organic matter with oxygen in either an open or a closed system, at a much higher temperature than that of wet-ashing. The dry-ashing procedures in open systems generally use ashing aids such as alkali-metal nitrates, to allow the recovery of elements such as arsenic.[17–19] To avoid volatilization losses the dry-ashing can be done in a closed system, such as the Schöniger flask.[20,21]

Fusion techniques have also been used for destroying organic matter, typical examples being oxidizing fusion with sodium peroxide in a Parr bomb,[22] and reductive fusion with alkali metals[23] and other metals.[24] Bowen[25] proposed fusion with an equimolar mixture of sodium and potassium nitrates at 390°, which oxidizes many organic materials in a few minutes; enough of the mixture must be added to avoid pyrophoric or explosive effects;[25] the explosion danger has been reported.[26]

Fusion with sodium hydroxide has been but little used to destroy organic matrices. Klimova and Vitalina[27] determined germanium after decomposing "difficult" organogermanium compounds by fusion with potassium or sodium hydroxide in a nickel bomb at 700–750° for 40–45 min; the method even allowed the destruction of polymers. For determination of fluorine in vegetation Baker[28] mixed the

*Author for correspondence.

sample with 10 ml of 67% sodium hydroxide solution in a nickel crucible and dried the mixture at 150° for 2 hr, then heated the crucible in a muffle furnace at 550° for 2 hr to fuse the alkali and destroy the sample.

In our opinion fusion with alkalis has been far from fully exploited, and it should be particularly useful for retention of elements such as arsenic and antimony which can form stable oxy-anions but may otherwise be lost by volatilization.

In the present work we propose a general method for destruction of organic matter through the action of molten alkali-metal hydroxides, together with auxiliary oxidizing agents if necessary. The method simplifies the procedures described in the literature, and is simple, rapid and free from explosion hazards. Two methods for the destruction of organic arsenic or antimony compounds have been established; they are compared with a reference method based on digestion with a mixture of nitric and perchloric acids.[12,13] An iodimetric method for arsenic determination[29] has been slightly modified for determination of the arsenic and antimony.

EXPERIMENTAL

Procedure

Alkaline fusion. In a 50-ml nickel or silver crucible, fuse 2–3 g of sodium or potassium hydroxide or a eutectic mixture of the two (41:59 w/w). When the alkali appears to have solidified on the bottom and lower side walls of the crucible, cool it to room temperature. Transfer a known weight of sample containing about 40 mg of arsenic or 60 mg of antimony into the crucible. Heat gently with a Bunsen burner until the alkali begins to fuse, mixing in the sample by gentle swirling of the melt. If a more oxidizing medium is wanted in this first step, cautiously add small amounts of sodium peroxide. Then heat more strongly while continuing the swirling, until a clear melt is obtained. If necessary, add sodium or potassium nitrate, in small amounts at a time, as auxiliary oxidant. Cool the melt to room temperature, then dissolve it immediately with hot water, and transfer it quantitatively into a 250-ml beaker. Acidify the cold solution to about 1*M* acid concentration, with 50% v/v hydrochloric or sulphuric acid. Transfer to a 100-ml standard flask and dilute to the mark. Add 5 ml of 66% potassium iodide solution to a 20-ml aliquot, and keep at 100° for 30 min. Cool, add a little starch solution and then 0.01*M* sodium thiosulphate solution until the starch–iodine colour is discharged. Then add 0.02*N* iodine until the indicator colour just reappears. Slowly neutralize with 2*M* sodium hydroxide, add excess of sodium bicarbonate and titrate with 0.02*N* iodine till the starch–iodine colour persists. For the antimony determination add 3 g of tartaric acid before the titration of antimony(III) with iodine.

Acid digestion. For samples containing arsenic, weigh an appropriate amount of sample containing about 40 mg of arsenic and transfer it quantitatively into the bottom of a 100-ml Kjeldahl flask. Add cautiously 5–6 ml of 1:1 v/v mixture of nitric acid and perchloric acid, homogenize with the sample and heat carefully until expulsion of nitrogen dioxide is complete and white fumes appear (this takes several hours), and a clear colourless solution is obtained. Increase the amount of acid mixture and the time or temperature, if necessary. Dilute the resulting acid solution, once it is cold, and neutralize it with 2*M* sodium hydroxide. Acidify an aliquot and titrate as above.

RESULTS AND DISCUSSION

Destruction of organic matter

The proposed method has been applied to destroy diverse organic samples. During the process three stages can be distinguished: (1) evaporation of moisture and homogenization of the alkali–organic material mixture; (2) dissolution or volatilization of pyrolysis or oxidation products; (3) progressive oxidation until destruction of organic material or charred residue is complete. This sequence occurs whether an auxiliary oxidant (nitrate or peroxide) is used (method A_{ox}) or not (method A).

Although the heating is normally done with a Bunsen burner, a muffle furnace can also be used (at a preset temperature from 350 to 650° according to sample type), but the decomposition then takes longer and the crucible has to be repeatedly taken out and put back, to allow observation and swirling of the melt and addition of oxidant.

The minimum amount of alkali needed depends on the nature of the sample; for pure compounds 10–15 times the sample weight is enough, and 15–20 times for vegetable or animal material.

The melt quantitatively retains many important elements capable of forming volatile species, such as arsenic and antimony, and when cooled is easily soluble.

The method is inapplicable if volatilization can take place at a lower temperature than that required for fusion of the alkali, but such samples will also cause difficulty if dry-ashing is used, and sometimes with wet oxidation.

Table 1

		Phenylarsonic acid			Arsenazo I			Arsenazo III		
	Decomposition	As found, %			As found, %			As found, %		
Series	method	*n*	$\bar{x}$	*s*	*n*	$\bar{x}$	*s*	*n*	$\bar{x}$	*s*
I	Method A*	10	36.81	0.06	10	9.92	0.20	10	16.79	0.19
II	Method A†	10	36.80	0.06	10	9.91	0.16	10	16.82	0.20
III	Method A_{ox}*	5	36.81	0.08	5	9.87	0.17	5	16.74	0.16
IV	Acid digestion*	10	36.77	0.06	10	9.91	0.19	10	16.71	0.21

Method A: alkaline fusion without auxiliary oxidant. Method A_{ox}: alkaline fusion with oxidant.
*Iodimetric titration in HCl medium.
†Iodimetric titration in H_2SO_4 medium.

The complete destruction of organic material in different matrices has been confirmed. Organic compounds tested which are destroyed by both methods include phenylarsonic acid, arsenazo I, arsenazo III, triphenylantimony and tartar emetic, but glucose and mixtures of glucose with antimony(III) oxide or tartar emetic require use of method A_{ox}, because of production of an abundant charred residue which necessitates use of a more oxidizing medium. Natural samples destroyed include leaves, fruits, seeds, hair, skin and nails. Technical samples that have also been completely decomposed include fertilizers, detergents and plastics.

Determination of arsenic and antimony

The method was tested with arsenic(III) oxide and tartar emetic as standards. The recoveries had a relative standard deviation of 0.03% for arsenic and 0.15% for antimony with systematic errors of 0.05 and 0.3% respectively; the iodimetric method modified for application after the alkaline fusion is thereby shown to give correct results.

The determination of arsenic in phenylarsonic acid, arsenazo I and arsenazo III was extensively examined, and the results obtained are shown in Table 1. There is excellent agreement between all the results, as shown by *t*-test and *F*-test.

The experimental conditions were found not to be critical. The possible effect of chloride was examined by adding sodium chloride to the test samples, but no interference (*e.g.*, by volatilization of antimony or arsenic chloride) was found. The average value obtained for ten arsenazo I samples was 9.89% of arsenic (standard deviation 0.13%). The serious loss of arsenic which could be caused by the presence of chloride in other procedures for mineralization of arsenic[30,31] is evidently avoided.

Antimony was determined in artificial samples formed by mixing tartar emetic and glucose; these also required method A_{ox}. The antimony recovery in two series of five analyses was satisfactory. In hydrochloric acid medium an average antimony recovery of 99.8% (standard deviation 0.1%) was obtained and in sulphuric acid medium an average recovery of 99.7% (standard deviation 0.1%). The addition of excess of ammonium chloride to the sample had no effect, in contrast to dry oxidation.[32]

Conclusions

Fusion with alkali-metal hydroxides is an accurate, effective and rapid method for the destruction of organic matter in different matrices: pure compounds, natural samples (vegetable and animal), technical materials, and so on. The easy mineralization and the retention of a large number of elements in the melt make it useful for elemental identification or determination.

REFERENCES

1. E. C. Dunlop and C. R. Ginnard, in *Treatise on Analytical Chemistry*, I. M. Kolthoff and P. J. Elving (eds.), 2nd Ed., Part I, Vol. 5, p. 23. Interscience, New York, 1982.
2. T. T. Gorsuch, *The Destruction of Organic Matter*. Pergamon Press, Oxford, 1970.
3. R. B. Bradstreet, *The Kjeldahl Method for Organic Nitrogen*. Academic Press, New York, 1965.
4. Analytical Methods Committee, *Analyst*, 1967, **92**, 403.
5. G. Middleton and R. E. Stuckey, *ibid.*, 1954, **79**, 138.
6. R. A. Chalmers and D. A. Thomson, *Anal. Chim. Acta*, 1958, **18**, 575.
7. L. Kotz, G. Kaiser, P. Tschöpel and G. Tölg, *Z. Anal. Chem.*, 1972, **260**, 207.
8. A. M. Hartstein, R. W. Freedman and D. W. Platter, *Anal. Chem.*, 1973, **45**, 611.
9. M. M. Schachter and K. W. Boyer, *ibid.*, 1980, **52**, 360.
10. G. F. Smith, *Anal. Chim. Acta*, 1953, **8**, 397.
11. K. May and M. Stoeppler, *Z. Anal. Chem.*, 1978, **293**, 127.
12. H. R. Griffin, M. B. Hocking and D. G. Lowery, *Anal. Chem.*, 1975, **47**, 229.
13. F. Peter, G. Growcock and G. Strunc, *Anal. Chim. Acta*, 1979, **104**, 177.
14. M. K. John, *Anal. Chem.*, 1972, **44**, 429.
15. G. F. Smith, *Talanta*, 1959, **2**, 209.
16. G. D. Martinie and A. A. Schilt, *Anal. Chem.*, 1976, **48**, 70.
17. C. C. Cassil, *J. Assoc. Off. Agric. Chem.*, 1937, **20**, 171.
18. D. J. Lisk, *J. Agric. Food Chem.*, 1960, **8**, 121.
19. H. Woidich and W. Pfannhauser, *Z. Anal. Chem.*, 1975, **276**, 61.
20. W. Schöniger, *Mikrochim. Acta*, 1955, 123.
21. A. D. Campbell, *ibid.*, 1980 **I**, 139.
22. A. Elek and D. W. Hill, *J. Am. Chem. Soc.*, 1933, **55**, 2550, 3479.
23. P. J. Elving and W. B. Ligett, *Ind. Eng. Chem., Anal. Ed.*, 1942, **14**, 449.
24. M. Jureček and J. Jeník, *Chem. Listy*, 1956, **50**, 84.
25. H. J. M. Bowen, *Anal. Chem.*, 1968, **40**, 969.
26. T. Greweling, *ibid.*, 1969, **41**, 540.
27. V. A. Klimova and M. D. Vitalina, *Zh. Analit. Khim.*, 1964, **19**, 1254.
28. R. L. Baker, *Anal. Chem.*, 1972, **44**, 1326.
29. J. A. Pérez Bustamante and F. Burriel Martí, *Inform. Quim. Anal.*, 1968, **22**, 25.
30. J. L. Down and T. T. Gorsuch, *Analyst*, 1967, **92**, 398.
31. S. Imai, *Bunseki Kagaku*, 1978, **27**, 611.
32. T. T. Gorsuch, *Analyst*, 1962, **87**, 112.

Talanta, Vol. 30, No. 6, pp. 440–442, 1983
Printed in Great Britain

0039-9140/83/060440-03$03.00/0
Pergamon Press Ltd

TITRIMETRIC MICRODETERMINATION OF CERTAIN SULPHUR-CONTAINING ORGANIC COMPOUNDS BY OXIDATION WITH ALKALINE POTASSIUM PERMANGANATE

K. K. TIWARI and R. M. VERMA*
Department of Chemistry, University of Jabalpur, Jabalpur 482001, India

(*Received* 25 *February* 1982. *Revised* 29 *November* 1982. *Accepted* 23 *December* 1982)

Summary—A titrimetric procedure is described for the microdetermination of some mercaptans and sulphur-containing amino-acids by oxidation with alkaline potassium permanganate at room temperature in presence of barium ions. The procedure can be applied to 0.002–0.025*M* solutions with an average deviation of 0.1–0.5%. The effect of variation in the amount of alkali and barium chloride and in the reaction period, on the stoichiometry of the oxidation reactions, has also been studied.

Mercaptans and sulphur-containing amino-acids are important because of their high reactivity, and presence in a large number of biological materials. Several oxidants have been utilized for quantitatively oxidizing mercaptans, usually to the corresponding disulphides, but there is sometimes irreproducible partial overoxidation of the disulphide.[1,2]

This difficulty might be overcome by using stronger oxidants which would oxidize the mercaptans to a higher stable oxidation state, but this has rarely been exploited.

According to Ashworth,[3] potassium permanganate has not been much used for titration of sulphur-containing organic compounds, perhaps because of uncertainty in the stoichiometry of the reactions. Kalinowski *et al.*[4] suggested an indirect determination of methyl thiouracil with acidic permanganate, and Willgerodt[5] titrated *p*-nitrothiophenol in sulphuric acid medium with potassium permanganate.

The mechanism of oxidation with permanganate is complicated. Generally the titrations are done in acidic medium but with some nitrogen- or sulphur-containing compounds such as hydrazine, sulphide, sulphite, thiosulphate, the oxidation is more smooth and rapid in alkaline medium.[6] In the present work this fact is utilized in the titration of some mercaptans, cystine and methionine.

The reduction of permanganate in alkaline medium can take place in two steps:[6]

$$MnO_4^- + e^- \rightarrow MnO_4^{2-} \qquad (I)$$

$$MnO_4^{2-} + 2H_2O + 2e^- \rightarrow MnO_2 + 4OH^- \qquad (II)$$

Reaction (II) makes the system unsuitable for quantitative analysis, but the reduction can be stopped at the end of step (I) by addition of barium chloride to give insoluble barium manganate and consequent suppression of step (II). The precipitate settles well and its colour does not interfere with detection of the end-point.[7] This technique has been used for determining some sulphur-containing organic compounds. The various factors governing the stoichiometry of the reactions are the alkalinity of the reaction mixture, amount of barium chloride added and the duration of the reaction. These have been examined and suitable conditions found for titration of 2- and 3-mercaptopropionic acids, thioglycollic acid, thiomalic acid, cysteine, glutathione, cystine and methionine.

EXPERIMENTAL

Reagents

*Potassium permanganate solution, 0.1*M. About 16.5–17 g of potassium permanganate was boiled with 1 litre of water for 15–30 min. The solution was cooled and filtered through a plug of glass wool. This solution was standardized with sodium oxalate.[8]

Barium chloride. Saturated solution in water.

*Sodium hydroxide, 1*M.

Sample solutions. Standardized by different procedures as shown in Table 1.

Procedure

Take 25 ml of 0.1*M* potassium permanganate and 10 ml each of 1*M* sodium hydroxide and saturated barium chloride solution in a 250-ml Erlenmeyer flask (for 5 or 10 ml of 0.1*M* permanganate use 5 ml each of the other two solutions). Heat the mixture to 70–80° and slowly titrate with the analyte solution, with constant shaking. This gives an approximate result which is slightly low because of the increased reduction of permanganate by water in alkaline medium at 80°.

Prepare a second permanganate solution in the same way, but do not heat it. Add (as rapidly as possible) the volume of titrant found as above. Let the mixture stand for 10 min, but swirl it frequently. Complete the titration dropwise, at room temperature, letting the green precipitate settle after each addition and inspecting the colour of the supernatant liquid. Disappearance of the pink colour marks the end-

*226, Napier Town, Jabalpur, M.P., India 482001.

Table 1. Microdetermination (six replicates) of some sulphur-containing organic compounds with alkaline permanganate

Compound	0.1*M* $KMnO_4$ taken, *ml*	Molarity of sample solution, M	Moles of electrons per mole of reductant	Equivalent weight	Titre, *ml*		Average error, %	Relative standard deviation, %	Standardization method
					Expected	Mean observed			
2-Mercaptopropionic acid	25.0	0.025	10	10.61	10.00	10.02	0.2	0.3	Mercuric chloride[23]
	25.0	0.0125			20.00	20.03	0.2	0.2	
	10.0	0.005			20.00	20.04	0.2	0.1	
	5.0	0.0025			20.00	20.10	0.5	0.1	
3-Mercaptopropionic acid	25.0	0.025	6	17.69	16.67	16.72	0.3	0.2	Iodate[24]
	10.00	0.01			16.67	16.70	0.2	0.2	
	10.00	0.005			33.34	33.40	0.2	0.1	
	5.00	0.0025			33.34	33.50	0.5	0.2	
Thioglycollic acid	25.00	0.025	12	7.67	8.34	8.35	0.1	0.1	Iodine[9]
	10.00	0.01			8.34	8.37	0.4	0.3	
	10.00	0.005			16.67	16.71	0.3	0.2	
	10.00	0.0025			33.34	33.45	0.4	0.1	
Thiomalic acid	25	0.02	16	9.38	7.81	7.83	0.3	0.3	Mercuric chloride[23]
	25	0.01			15.62	15.65	0.2	0.1	
	10	0.005			12.50	12.53	0.3	0.3	
	10	0.0025			25.00	25.04	0.2	0.2	
Cysteine	25	0.02	17	7.13	7.35	7.37	0.3	0.4	Iodate[24]
	25	0.01			14.70	14.75	0.3	0.3	
	25	0.005			29.4	29.51	0.3	0.2	
	10	0.0025			23.53	23.60	0.3	0.1	
Glutathione	25	0.02	25	12.29	5.00	5.02	0.4	0.5	Bromine chloride[25]
	25	0.01			10.00	10.02	0.2	0.3	
	25	0.005			20.00	20.02	0.1	0.1	
	10	0.002			20.00	20.03	0.2	0.2	
Methionine	25	0.02	15	9.95	8.33	8.37	0.5	0.3	Bromine chloride[25]
	25	0.01			16.67	16.70	0.2	0.1	
	10	0.005			13.34	13.36	0.2	0.2	
	10	0.0025			26.67	26.72	0.3	0.1	
Cystine	25	0.01	26	9.24	9.62	9.63	0.1	0.3	Bromine chloride[25]
	25	0.005			19.23	19.26	0.2	0.1	
	10	0.002			19.23	19.27	0.2	0.2	
	5	0.001			19.23	19.29	0.3	0.1	

point. The molarity (M_s) of the sample solution is calculated from

$$M_s = \frac{VM}{nV_s}$$

where V = ml of permanganate solution taken for titration; M = molarity of the permanganate; V_s = ml of the sample solution required; n = number of moles of electrons released per mole of compound oxidized (the values of n given in Table 1 were determined empirically).

RESULTS AND DISCUSSION

Results for 0.002–0.025M solutions of some thiols, cystine and methionine are given in Table 1. The average deviation is 0.1–0.5%.

A number of oxidants such as iodine,[9] iodoso-compounds,[10] lead(IV),[11] periodate,[12] ferricyanide,[13] copper(II),[14] tetrathionate,[15] *N*-iodosuccinimide,[16] chloramine-T and -B,[17] cerium(IV),[18] interhalogens,[19] iodate,[20] bromate[21] have been employed in the oxidimetric determination of mercaptans. The oxidation product is usually the corresponding disulphide. The stoichiometry of the oxidation is greatly influenced by the nature of the mercapto compound, the nature of the oxidant, and the reaction conditions. Most iodometric methods employ iodine in acidic or neutral medium.[3] Occasionally iodine is used in alkaline medium, but in concentrated alkali the extent of reaction depends on the order of reagent addition, the temperature and time, and the concentration of the alkali.[21] Sometimes the overoxidation becomes more pronounced as the dilution of the sample increases.[1] With *o*-iodosobenzoate, the oxidation proceeds to the disulphide at pH 7 but at lower pH there is a tendency for overoxidation.[10] In the ferricyanide methods, the iodine or cerium(IV) used to titrate the ferrocyanide produced can further oxidize the disulphide.[22] The oxidative titrimetry of some mercaptans can therefore become erroneous as a result of partial oxidation of the disulphide formed.

In the procedures proposed here, this problem is eliminated because oxidation beyond the disulphide stage is complete and reproducible. A further advantage of this is the larger consumption of permanganate since its reduction is a 1-electron reaction instead of the 5-electron reaction that occurs in acid medium, and the equivalent weights of the analytes are very small (see Table 1). The major disadvantage is that the burette has to be rinsed out with each sample solution in turn. To some extent this is offset by the advantage that the volume of sample solution needed in the titration increases with dilution of the sample, thus improving the precision.

Acknowledgement—The thanks of the authors are due to the University Grants Commission, New Delhi, for financial assistance to one of them (K.K.T.).

REFERENCES

1. J. P. Danhey and M. Y. Oester, *J. Org. Chem.*, 1967, **32,** 1491.
2. J. P. Danhey, C. P. Egan and J. Switalski, *ibid.*, 1971, **36,** 2530.
3. M. R. F. Ashworth, *The Determination of Sulphur-Containing Groups*, Vol. 2, pp. 20, 38. Academic Press, London, 1976.
4. K. Kalinowski, J. Bersztel, J. Fecko and Z. Zwierzchowski, *Acta Polon. Pharm.*, 1957, **14,** 77.
5. C. Willgerodt, *Ber.*, 1885, **18,** 331.
6. I. M. Kolthoff and R. Belcher, *Volumetric Analysis*, Vol. III, pp. 33, 34. Interscience, New York, 1957.
7. H. Stamm, *Angew. Chem.*, 1934, **47,** 791.
8. A. I. Vogel, *A Text Book of Quantitative Inorganic Analysis*, 3rd Ed., pp. 282, 284. Longmans, London, 1971.
9. J. W. Kimball, R. L. Kramer and E. E. Reid, *J. Am. Chem. Soc.*, 1921, **43,** 1199.
10. L. Hellarman, F. P. Chinard and P. A. Ramsdell, *ibid.*, 1941, **63,** 2551.
11. K. K. Verma and S. Bose, *Anal. Chim. Acta*, 1973, **65,** 236.
12. J. Ahmed and S. Bose, *J. Indian Chem. Soc.*, 1973, **50,** 506.
13. A. E. Mirsky, *J. Gen. Physiol.*, 1941, **24,** 725.
14. S. B. Sant and B. R. Sant, *Anal. Chem.*, 1959, **31,** 1879.
15. J. Macleod, *J. Gen. Physiol.*, 1941, **24,** 725.
16. A. Srivastava, *Talanta*, 1979, **26,** 917.
17. D. S. Mahadevappa and N. M. H. Gowda, *ibid.*, 1975, **22,** 771.
18. A. Piotrowska, *Acta Polon. Pharm.*, 1970, **27,** 131.
19. A. Srivastava and S. Bose, *J. Indian Chem. Soc.*, 1974, **51,** 736.
20. B. C. Verma, S. M. Ralhan and N. K. Ralhan, *Z. Anal. Chem.*, 1972, **259,** 367.
21. G. Aravamudan and C. R. Rao, *Talanta*, 1963, **10,** 231.
22. B. R. Sant and S. B. Sant, *ibid.*, 1960, **3,** 261.
23. K. K. Tiwari and R. M. Verma, *ibid.*, 1981, **28,** 397.
24. *Idem, Microchem. J.*, in the press.
25. K. K. Verma, A. Srivastava, J. Ahmed and S. Bose, *Talanta*, 1978, **25,** 469.

Talanta, Vol. 30, No. 6, pp. 443–445, 1983
Printed in Great Britain

0039-9140/83/060443-03$03.00/0
Pergamon Press Ltd

SPECTROPHOTOMETRIC DETERMINATION OF FORMALDEHYDE IN AIR

PRATIMA VERMA and V. K. GUPTA*
Department of Chemistry, Ravishankar University, Raipur, 492 010, India

(*Received* 1 *October* 1982. *Accepted* 20 *December* 1982)

Summary—A spectrophotometric method for the determination of formaldehyde in air is described, based on the colour reaction of formaldehyde, *p*-aminoazobenzene and sulphur dioxide in hydrochloric acid medium. Beer's law is obeyed at 505 nm in the range 2–12 μg of formaldehyde per 25 ml of final solution (0.08–0.48 ppm). Optimum conditions for colour development, and possible interferences, have been studied.

Formaldehyde is one of the most important air pollutants, deriving from the partial oxidation of organic matter, particularly fuels, and is a normal constituent of automobile and aero-engine exhaust products.[1,2] It is also found in the waste gases from incinerators as well as in the effluents from plastic, textile and other industries.[3] Formaldehyde irritates the mucous membrane and causes eye irritation.[2] The Threshold Limit Value is 3 mg/m^3,[4] but formaldehyde causes irritation at lower levels than this.

A large number of reagents have been proposed for the spectrophotometric determination of formaldehyde in air.[5–9] West and Gaeke[10] developed a method using pararosaniline and formaldehyde for the estimation of sulphur dioxide, and this has been modified by several investigators for determination of formaldehyde.[11,12] Knisely and Throop[13] recommended *p*-aminoazobenzene for the spectrophotometric determination of sulphur dioxide, as it is chemically similar to pararosaniline but contains only one amino group, gives better sensitivity and is readily available in higher purity.

This paper describes a method based on the reaction between sulphur dioxide, *p*-aminoazobenzene and formaldehyde, modified for the determination of submicrogram amounts of formaldehyde in air. A pink dye is formed when formaldehyde reacts with *p*-aminoazobenzene and sulphur dioxide in acidic medium. The absorbance obeys Beer's law over the range 2–12 μg of formaldehyde per 25 ml of final solution. The pink dye shows an absorbance maximum at 505 nm, with a molar absorptivity of 4.5×10^4 l.mole^{-1}.cm^{-1}. The optimum reaction conditions for full colour development have been investigated.

EXPERIMENTAL

Apparatus

An ECIL model GS-685 spectrophotometer and a Carl Zeiss Spekol were used with 1-cm matched glass cells. Midget impingers of 35 ml capacity were used for air sampling, and calibrated rotameters were used for measuring the air flow-rates.

Reagents

p-*Aminoazobenzene solution (0.02%).* Prepared in aqueous ethanol (25% v/v alcohol) from reagent recrystallized from alcohol.

Standard formaldehyde solution. One ml of 30–40% formaldehyde solution diluted to 100 ml and standardized titrimetrically[14] and further diluted with 0.005*M* hydrochloric acid to give a 6-μg/ml working formaldehyde standard.

Sulphite solution (0.1%). Prepared from anhydrous sodium sulphite and double distilled water.

All chemicals used were of analytical reagent grade.

Procedure

Two impingers, each containing 10 ml of 0.005*M* hydrochloric acid were connected in series and then to a rotameter and a vacuum pump. Air was drawn through the system at *ca.* 1.5 l./min, then the solutions were quantitatively transferred to a 25-ml standard flask and 1 ml each of the *p*-aminoazobenzene and sulphite solutions were added. The solution was mixed and kept for 20–25 min. The acidity was then adjusted to between 0.4 and 1.2*M* hydrochloric acid and the solution made up to the mark with doubly distilled water. The absorbance of the pink dye was measured at 505 nm against distilled water and the amount of formaldehyde was computed from a calibration graph prepared in a similar manner after correction for the absorbance of a reagent blank measured at the same wavelength.

RESULTS AND DISCUSSION

The absorption spectra are shown in Fig. 1. The absorbance of the reagent blank was measured at the same wavelength and subtracted from all sample readings.

Effect of varying the reaction condition

The effect of acidity, both before and after addition of sulphite solution, was studied. It was found that a minimum acidity of 0.02*M* hydrochloric acid was essential before addition of sulphite solution, but up to 0.1*M* hydrochloric acid could be used without change in the absorbance. After addition of the sulphite solution the hydrochloric acid concentration

*To whom correspondence should be sent.

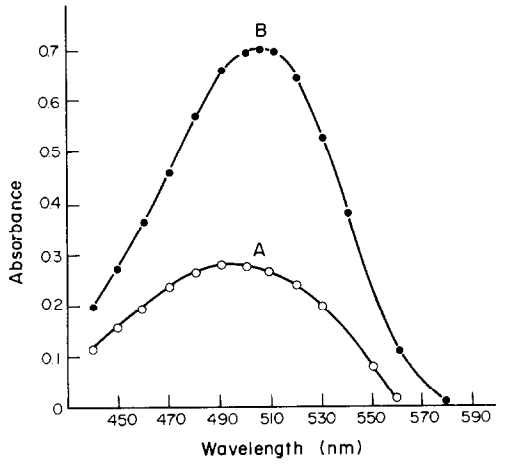

Fig. 1. Absorption spectra: A, reagent blank; B, reagent plus 7 μg of formaldehyde in 25 ml.

needed to be increased to at least 0.4*M* for full colour development, and with 0.4–1.2*M* hydrochloric acid the absorbance was constant.

The time necessary for full colour development was found to be 20 min, and the absorbance remained constant for a further 90 min. Varying the temperature between 20 and 35° had no serious effect on the results.

It was observed that as the quantity of *p*-aminoazobenzene was increased the absorbance of both the reagent blank and the sample solutions increased by the same amount. The amount of sulphur dioxide present should be at least ten times the stoichiometric amount needed for the level of formaldehyde present. A large excess of sulphur dioxide does not affect the absorbance of the solutions.

Beer's law, molar absorptivity and reproducibility

The colour system obeys Beer's law over the range 2–12 μg of formaldehyde per 25 ml of final solution. The molar absorptivity is 4.5×10^4 $l.mole^{-1}.cm^{-1}$.

The reproducibility was checked by replicate determination of 6 μg of formaldehyde over a period of 7 days. The standard deviation found was ± 0.025 μg.

Effect of foreign species

To assess the validity of the method, the effect of foreign species commonly found with formaldehyde was studied. The tolerance limits for several foreign species are shown in Table 1. Several common organic species, *viz.* other aldehydes and hydrocarbons, do not interfere. The interference from nitrogen dioxide is removed by the addition of 1 ml of 3% sulphamic acid solution, and that of sulphide can be removed by passing the air sample through a tube containing lead acetate solution.

Collection efficiency

A modified Wilsons' procedure[15] was used to investigate the collection efficiency of the absorbing solution.[16] Purified air was passed through an evaporation chamber preheated to 60–70°. Known amounts of formaldehyde were added from a microburette and evaporated from the chamber. The formaldehyde borne on the air stream was collected in the absorbing solution. At a flow-rate of 1.5 l./min, approximately 85% absorption was achieved in the first impinger and 15% in the second when two impingers were used with 10 ml of absorption solution in each.

Comparison with other methods

Since the method was specially devised for the determination of formaldehyde in air, a comparison with other commonly used methods[5–9,16] was worthwhile. Instability of the colour and interferences from co-pollutants are the main drawbacks of methods based on Schiff's reagent,[5] MBTH[9] and phenylhydrazine.[8] The comparison is summarized in Table 2.

Acknowledgement—The authors are grateful to Professor S. G. Tandon, Head of Department of Chemistry, Ravishankar University, Raipur, for providing laboratory facilities.

REFERENCES

1. W. Leithe, *The Analysis of Air Pollutants*, p. 229. Ann Arbor Science, Ann Arbor, 1973.

Table 1. Interferences and tolerable limits* of other species in the determination of 6 μg of formaldehyde

Inorganic		Organic			
Cd^{2+}	10	Ethanol	25	Acetone	0.25
Zn^{2+}	6	Benzaldehyde	2.5	Aniline	0.25
Pb^{2+}	2.5	Ethylamine	2.5	Benzene	0.25
Hg^{2+}	1	Isobutyl methyl ketone	2	Urea	0.25
Cu^{2+}	0.6	Formic acid	1	Toluene	0.2
NH_3	0.6	Nitrobenzene	0.5	Acetaldehyde	0.1
H_2S	0.6	Acetic acid	0.25	Phenol	0.08
NO_2†	0.5				
Fe^{3+}	0.1				
VO_3^-	0.1				

*Amounts (mg) which cause a 2% error.
†Masked up to this level by 1 ml of 3% sulphamic acid.

Table 2. Comparison of some spectrophotometric methods for the determination of formaldehyde in air

Reagents	Colour λ_{max}, *nm*	Medium	Beer's law range, *μg/25 ml*	Molar absorptivity, *l.mole^{-1}.cm^{-1}*	Colour stability	Absorption efficiency, %	Interferences
Schiff's reagent[5]	Violet 550	HCl	*	3.5×10^3	30 min	72	SO_2, NO_2^- alcohol, phenol
Chromotropic acid[6,7]	Purple 578	H_2SO_4	5–100	1.57×10^4	24 hr	78–97	SO_2, NO_2^-, NO_3^- hydrocarbons
Phenylhydrazine[8]	Red 520	4*M* HCl	2–36	3.42×10^4	15 min	—	—
3-Methyl-2-benzothiazolone hydrazone[9]	Blue 670	Slightly acidic	1.2–23	6.50×10^4	40 min	84	SO_2, aromatic amines
Oxaldihydrazone, Cu(II)[16]	Blue 620	pH 5.8–7.0	15–90	7.7×10^3	150 min	95–96	Sulphur compounds
p-Aminoazobenzene, SO_2 (present method)	Pink 505	0.02–0.1*M* and 0.4–1.2*M* HCl	2–12	4.5×10^4	90 min	85†	See Table 1

*Beer's law not obeyed.
†First impinger (100% with two impingers in series).

2. F. A. Patty, *Industrial Hygiene and Toxicology* Vol. II, 2nd Ed., p. 1959. Interscience, New York, 1963.
3. P. L. Magill and R. M. Benoliel, *Ind. Eng. Chem.*, 1952, **44,** 1347.
4. *Threshold Limit Values, 1980.* HMSO Publication EH 15/80.
5. A. C. Rayner and J. M. Jephcott, *Anal. Chem.*, 1961, **33,** 627.
6. A. P. Altshuller, D. L. Miller and S. L. Sleva, *ibid.*, 1961, **33,** 621.
7. P. W. West and B. Sen, *Z. Anal. Chem.*, 1956, **153,** 177.
8. M. Tanenbaum and C. E. Bricker, *Anal. Chem.*, 1951, **23,** 354.
9. E. Sawicki, R. T. Hauser, T. W. Stanley and W. Elbert, *ibid.*, 1961, **33,** 93.
10. P. W. West and G. C. Gaeke, *ibid.*, 1956, **28,** 1816.
11. R. R. Miksch, D. W. Anthon and L. Z. Fanning, *ibid.*, 1981, **13,** 2118.
12. R. Hryniewicz and H. Wielogorska, Ochr. Powietrza, 1976, **10,** 153; *Chem. Abstr.*, 1977, **86,** 194261e.
13. S. J. Kniseley and L. J. Throop, *Anal. Chem.*, 1966, **38,** 1270.
14. A. I. Vogel, *Elementary Practical Organic Chemistry*, Part 3, *Quantitative Organic Analysis*, p. 828. Longmans, London, 1971.
15. K. W. Wilson, *Anal. Chem.*, 1958, **30,** 1127.
16. J. Nair and V. K. Gupta, *Talanta*, 1979, **26,** 962.

Talanta, Vol. 30, No. 6, pp. 446–448, 1983
Printed in Great Britain

0039-9140/83/060446-03$03.00/0
Pergamon Press Ltd

THE REACTION OF PHENYLARSENAZO WITH CHROMIUM(III)

SUN FU-SHENG*
Department of Chemistry, China University of Science and Technology, Hefei, Anhui, People's Republic of China

(*Received* 31 *December* 1981. *Revised* 22 *November* 1982. *Accepted* 2 *December* 1982)

Summary—The conditions for the reaction between phenylarsenazo (PAA) (2-[(2-arsonophenyl)azo]-7-(phenylazo)-1,8-dihydroxynaphthalene-3,6-disulphonic acid) and chromium(III) have been studied. A blue 1:1 complex is formed at pH 2.2 on heating the reactants at 100° for 15 min. It has maximum absorption at 635 nm and is stable for at least 24 hr. The molar absorptivity is 3.3×10^4 l.mole^{-1}.cm^{-1}. Beer's law is obeyed in the chromium concentration range 0–1.4 μg/ml. The reaction has been successfully applied to determination of chromium in alloy steel.

Diphenylcarbazide[1,2] is an important reagent for the spectrophotometric determination of chromium, but it has some shortcomings. For example, its solution is unstable, and chromium(III) must be oxidized to chromium(VI) for the determination.

Several reagents for chromium(III) have been developed, such as TAR,[3] Sunchromine Blue R,[4] PAR[5] and Arsenazo III.[6] The first two are sensitive enough but have poor selectivity. The PAR reaction requires heating for 45 min. Arsenazo III is considered the most sensitive reagent for chromium(III).

Savvin considers that the reactions of Arsenazo III with metal ions depend only on the radicals on one side of the chromotropic acid.[7] We have therefore conceived the idea of synthesizing reagents where the Arsenazo I structure is retained but there is no arsonic acid group at the *o*-position of the azo radical on the other side of the chromotropic acid. We have synthesized a series of such reagents and found that several have higher sensitivity than Arsenazo III for chromium (III). Phenylarsenazo (PAA) is one of them.

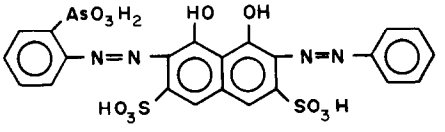

Phenylarsenazo

EXPERIMENTAL

Synthesis of PAA

To 3.4 g (0.037 mole) of aminobenzene add 8 ml of concentrated hydrochloric acid and 20 ml of water. Cool to 0° in an ice-bath. Add a solution of 2.8 g (0.041 mole) of sodium nitrite in 10 ml of water with constant stirring.

Dissolve 19.1 g (0.03 mole) of arsenazo I in 70 ml of 10% lithium hydroxide solution and cool to 0°. Add to this, with constant stirring, the solution of diazotized aminobenzene (at 0–5°). The solution turns blue-violet. Stir for 1 hr and let stand overnight.

Add 40 ml of concentrated hydrochloric acid to the mixture, and filter off after settling. Wash the residue with a little dilute hydrochloric acid and discard the filtrate. Immerse the residue in hydrochloric acid (1 + 1) for several hr, filter off the precipitate and wash it with dilute hydrochloric acid.

Dissolve the precipitate in 500 ml of 2% sodium hydroxide solution by heating on a water-bath, and filter immediately. To the filtrate add 70 ml of concentrated hydrochloric acid with constant stirring. Let stand for several hr, and filter off the precipitate. Wash it successively with a little dilute hydrochloric acid, water, ethanol and acetone. Dry the product at 40° (yield 13.7 g).

Reagents

Standard chromium(III) solution. Dissolve 0.500 g of pure chromium in 20 ml of concentrated hydrochloric acid and a little water by heating gently. Cool, transfer into a 500-ml standard flask and dilute to the mark with water. Dilute 100-fold to obtain a 10-μg/ml solution, adding 1 ml of concentrated hydrochloric acid per litre in the course of the dilution.

Phenylarsenazo solution, 0.1%.

Procedure

To a solution containing <35 μg of chromium(III), in a test-tube, add a drop of Thymol Blue solution and then 0.5*M* sodium hydroxide dropwise until the colour turns to yellow. Then add 2 ml of 0.02*M* hydrochloric acid and 3 ml of 0.1% PAA solution and dilute to about 15 ml with water. Heat in a boiling water-bath for 15 min, cool, transfer to a 25-ml standard flask, dilute to the mark with water, and mix. Measure the absorbance at 635 nm against a reagent blank treated similarly.

RESULTS AND DISCUSSION

Chromium(III) forms a blue complex with PAA in acid medium. The absorption spectra of the reagent and the chromium(III) complex at pH 2.7 are shown in Fig. 1. The reagent has maximum absorption at 550 nm, and the complex at 630 nm. The absorbance is maximal (Fig. 2) in the pH range 2.0–2.8. Hence all further studies were made at pH 2.2.

*Present address: Chemical Engineering Department, Wuxi Institute of Light Industry, Wuxi, Jiangsu, People's Republic of China.

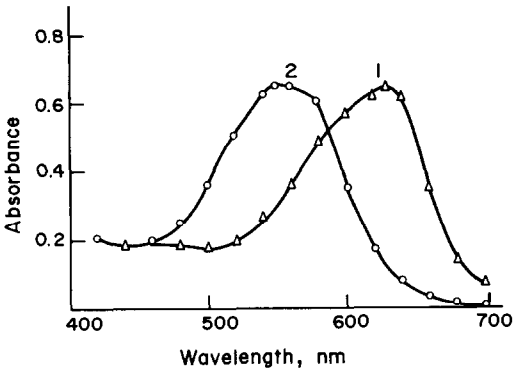

Fig. 1. Absorption spectra of Cr(III)–PAA complex and reagent blank. 1, Cr(III)–PAA, $1.92 \times 10^{-5}M$; 2, PAA, $1.92 \times 10^{-5}M$.

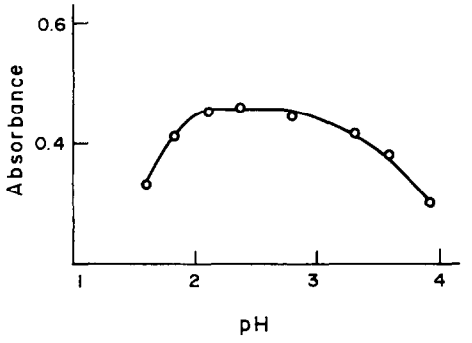

Fig. 2. Effect of acidity on absorbance of complex. Cr(III) 20 μg.

It is found that 1 ml of 0.1% PAA solution is sufficient for up to 20 μg of chromium(III), so 2 ml are recommended for the general procedure.

The reaction is inconveniently slow at room temperature, but comes to completion within 12 min if the mixture is heated in a boiling water-bath. Hence heating for 15 min is recommended. The complex is stable at room temperature for at least 24 hr.

Table 1. Effect of diverse ions [15 μg of chromium(III) in 25 ml]

Foreign ion	Tolerance level, μg
Fe(III), Cu(II), Sn(II), Al(III), Th(IV), Ga(III), La(III), Er(III), Cr(VI)	15
Ti(IV), Zr(IV), V(V)	60
Pb(II), Ca(II)	75
W(VI), Bi(III)	150
$NH_4(I)$, Ac^-, EDTA	1500
Mn(II), Zn(II), Co(II), Ni(II), Mo(VI), SiO_3^{2-}	150
SO_4^{2-}, PO_4^{3-}, NO_3^-	1500

Job's method and the slope-ratio method both show the complex to have a 1:1 mole-ratio. Beer's law is obeyed up to 1.4 μg of chromium(III) per ml at 635 nm. The molar absorptivity is 3.3×10^4 $l.mole^{-1}.cm^{-1}$, which makes it more sensitive than the Arsenazo III method.

Effect of other ions

The effect of about 30 ions on the determination of 15 μg of chromium(III) was tested (Table 1). The selectivity of PAA is not high, but after the colour development the selectivity can be improved by increasing the acidity of the solution. If the hydrochloric acid concentration is raised to at least 1M, the chromium(III) complex is still stable for 24 hr but the interference of copper(II), tin(II), vanadium(IV), lead, calcium, gallium, erbium, tungsten(VI), zirconium and ammonium becomes negligible.

Determination of chromium in alloy steels

If the steel sample is dissolved in dilute nitric acid, the iron(III) produced seriously interferes in the determination of chromium(III). To deal with this interference we reduce the iron(III) to iron(II) with hydroxylamine hydrochloride, and increase the acidity

Table 2. Determination of chromium in alloy steels

Sample	Composition of the alloy steel, %	Chromium found, %	Average, %	Error, %
BISI No. 165-3	C:0.52, Si:0.16 Mn:0.56, P:0.020 S:0.0056, Cr:0.57, Ni:1.55, Mo:0.20	0.56 0.56 0.555	0.558	−2.1
BISI No. 609	C:0.16, Si:0.33, Mn:1.01, P:0.020 S:0.007, Cr:1.08, Ni:0.14, Ti:0.049	1.09 1.08 1.09	1.09	+0.9
BAMI 20 CrMo	C:0.205, S:0.016 Si:0.295, Mn:0.54, P:0.020, Cr:0.95, Mo:0.20	0.98 0.98 0.96	0.97	+2.1
ISI, AISC No. 7136	C:0.15, Si:0.29, Mn:2.06, Ci:0.036 Ni:0.023, P:0.015 N:0.030, Mo:0.004, Co:0.008, Cr:0.51, V:0.41	0.51 0.51 0.50	0.507	−0.6

of the solution after the colour development. We have found that a minimum of 2.5 ml of 5% hydroxylamine hydrochloride solution is needed for a solution containing 2 mg of iron(III), and recommend use of 3.0 ml.

To prepare the calibration graph, standards are made by taking 0.1-g portions of chromium-free carbon steel in 125-ml conical flasks and adding 0, 200, 400, 600, 800, 1000 and 1200 μg of chromium(III) (0–1.2 ml of 1-mg/ml standard solution). The samples are dissolved in 5 ml of nitric acid (1 + 3), and the solutions boiled to decompose carbides. The solutions are cooled to room temperature, transferred into 100-ml standard flasks, diluted to the mark with water, and mixed. Then 2-ml portions of these solutions are treated as described in the procedure. Samples are dissolved and analysed similarly (without addition of standard chromium solution).

Results

Chromium in four alloy steels were determined. The samples came from Beijing Iron and Steel Institute (BISI), Beijing Accurate Mechanical Institute (BAMI), the Iron and Steel Institute, Ashan Iron and Steel Company (ISI, AISC). The results are given in Table 2.

REFERENCES

1. M. Bose, *Anal. Chim. Acta*, 1954, **10,** 209.
2. H. Sano, *ibid.*, 1962, **27,** 398.
3. B. Surahmanyam and M. C. Eshwar, *Mikrochim. Acta*, 1976 **II,** 579.
4. K. Uesugi and Y. Katsube, *Bull. Chem. Soc. Japan*, 1965, **38,** 2010.
5. S. G. Nagarkar and M. C. Eshwar, *Indian J. Technol.*, 1975, **13,** 377.
6. O. A. Tataev and V. K. Guseinov, *J. Anal. Chem. USSR*, 1975, **30,** 935.
7. S. B. Savvin, *ibid.*, 1962, **17,** 785.

Talanta, Vol. 30, No. 6, pp. 449–453, 1983
Printed in Great Britain.

0039-9140/83/060449-05$03.00/0

ANALYTICAL DATA

THE STABILITY CONSTANTS OF PdEDTA AND ITS CHLORIDE COMPLEXES

J. KRAGTEN
Natuurkundig Laboratorium der Universiteit van Amsterdam, Valckenierstraat 65, 1018 XE Amsterdam, The Netherlands

and

L. G. DECNOP-WEEVER
Laboratorium voor Analytische Chemie der Universiteit van Amsterdam, Nieuwe Achtergracht 166, 1018 WV Amsterdam, The Netherlands

(*Received* 19 *October* 1982. *Accepted* 18 *January* 1983)

Summary—From the position of the equilibrium Th + PdEDTA $\rightleftharpoons$ Pd + ThEDTA, the stability constant of PdEDTA can be related to that for ThEDTA. If $\log K_{ThEDTA} = 25.3$ is taken as the most reliable value currently available, $\log K_{PdEDTA} = 25.6 \pm 0.2$ is found ($NaClO_4$ medium, $21 \pm 1°$). Repetition of the experiments at different chloride concentrations gives an estimated $\log K = 5.3 \pm 0.1$ for the equilibrium $PdEDTA + Cl^- \rightleftharpoons PdEDTACl^-$. The stability constants of ThEDTA and PdEDTA are not very dependent on ionic strength in the range 0.1–1.0.

In a previous communication[1] it was established that the only value[2] for the stability constant of Pd(II)EDTA known up to 1977 is obviously too low, and that the value $\log K_{PdEDTA} = 26.4$, although found by combining stability constants related to different ionic strengths, provisionally seemed more realistic. Also some preliminary data were reported for the ternary chloride complexes of PdEDTA.

At the moment of publication we were unaware of results published by Anderegg and Malik shortly before.[3,4] They examined the equilibrium

$$PdBr_4^{2-} + LuEDTA^- + H^+ \rightleftharpoons HPdEDTABr^{2-} + Lu^{3+} + 3Br^- \quad (1)$$

by measuring the Pd–Br absorption. Their value, $\log K_{PdEDTA} = 26.4$, corroborates ours although it is an approximation for the same reason. Their measurements were made at pH 2.8, 20°, $I = 0.1$ in sodium perchlorate medium.[3,4] More accurate values are claimed for potassium bromide and sodium bromide media ($I = 1$, 20°) ($\log K_{PdEDTA} = 25.5$ and 24.5 respectively).

In order to establish the stability constant of PdEDTA more precisely, our investigations of the position of the equilibrium

$$PdEDTA^{2-} + Th^{4+} \rightleftharpoons ThEDTA + Pd^{2+} \quad (2)$$

have been extended and refined.

The basic idea is that equilibrium (2), once attained, hardly shifts if the free thorium remaining in the mixture is determined quickly by titration. From the titration result and the known analytical concentrations (C_{Pd}, C_{EDTA} and C_{Th}), the position of equilibrium (2) can be established. By combining reaction (2) with the protolytic side-reactions of the various species, the system is completed and the stability constant of PdEDTA can be related to that of ThEDTA.

To establish ternary complex formation between PdEDTA and chloride ions some experiments have been done in perchlorate medium containing added chloride. The stability constant of $PdH_2EDTACl^-$ has been determined from the results.

THEORY

In the following equations Y represents fully deprotonated EDTA. Conditional concentrations are indicated by primes, and charges are omitted for convenience. The mass-balance equations are:

$$C_{Th} = [Th'] + [ThY'] \quad (3)$$

$$C_Y = [ThY'] + [PdY'] + [Y'] \quad (4)$$

$$C_{Pd} = [Pd'] + [PdY']. \quad (5)$$

In practice, equimolar quantities of Pd and Th are used. EDTA is added in such an amount that always $C_{Pd} < C_Y < C_{Pd} + C_{Th}$. Under these conditions, and since the conditional constants of PdEDTA and ThEDTA are large (under our experimental condi-

tions both $\log K'$ values are >10), [Y'] can be neglected in equation (4).

The equilibrium equation related to equation (2) is

$$V = \frac{K'_{PdY}}{K'_{ThY}} = \frac{[PdY'][Th']}{[ThY'][Pd']}. \quad (6)$$

It is obvious from equations (3)–(6) that when [Th'] has been determined, all concentrations are known, and so will V.

EXPERIMENTAL

In the first preliminary experiments, V was found to vary with C_Y. This was attributed to inaccuracy, probably arising from use of equation (5), where [Pd'] is found as the difference between two large quantities, and thus has a large relative error. Improvement of the accuracy seemed so crucial that all experiments were done with calibrated glassware. Reagents were added by weight, the corresponding volumes being found from densities determined in advance. During the experiments the ionic strength I was kept constant at $0.2M$ (sodium perchlorate). Reagent solutions and the equilibrating mixtures were stored in pretreated polyethylene bottles.

The stock solutions of palladium, thorium and EDTA had to be made very carefully in order to keep them stable. Both metal ions have a strong tendency to hydrolyse and their solutions should be kept fairly acidic; their concentrations were determined with an error of about 0.3%. All water used was doubly distilled from quartz.

Thorium solution. A $10^{-2}M$ thorium(IV) solution was made by dissolving $Th(NO_3)_4.2H_2O$ (*p.a.*, Merck) in $1M$ perchloric acid. This solution was diluted to $10^{-3}M$ with $10^{-2}M$ perchloric acid. The concentration was determined by direct photometric titration with standardized EDTA and Semi-Xylenol Orange (SXO) as the indicator (wavelength 533 nm, pH 2.0). The SXO was purified by extraction. Xylenol Orange should not be used, as it leads to systematic deviations which are not negligible.[5]

Palladium solution. About 100 mg of metallic palladium, cut into pieces, was heated with nitric acid (1 + 1), washed with water and acetone, dried and weighed accurately. As chloride had to be absent in the first experiments, the metal could not be dissolved in *aqua regia* but was dissolved in 5 ml of concentrated nitric acid to which 5 ml of 30% hydrogen peroxide was added in portions. It dissolves slowly. The necessary removal of excess acid had to be performed with care. The best way was to reduce the volume to a few ml by heating under an infrared lamp. The process had to be watched and controlled carefully; local overheating was prevented by keeping the beaker walls moistened with the reflux, to prevent formation of metallic deposits. The solution was transferred quantitatively to some dilute nitric acid ($pC_H = 0.5$) and diluted to 100 ml with the same dilute acid (to prevent manipulation errors[6,7]). This solution (about $10^{-2}M$ in Pd) was diluted to $10^{-3}M$ with $0.1M$ nitric acid and standardized by back-titrating the excess of EDTA with thorium, with SXO as indicator. It was verified that, within the titration time of some minutes, the equilibrium $Pd + Y \rightleftharpoons PdY$ does not shift noticeably to the left.

EDTA solutions. Dried EDTA (3.72 g, *p.a.*, Merck) was dissolved in water and diluted accurately to 1 litre. This solution was diluted tenfold ($\sim 10^{-3}M$; pH 5). For its standardization, metallic copper of spectrographic purity was cleaned with nitric acid (1 + 1) at room temperature, washed with water and acetone, dried under nitrogen, then weighed and dissolved in concentrated nitric acid. This solution was diluted to volume with $10^{-4}M$ nitric acid and titrated with the EDTA photometrically, with TAR [4-(2-thiazolylazo)resorcinol] as indicator (515 nm, $1M$ acetate buffer, pH ~ 5).

The $10^{-3}M$ EDTA was used for the equilibrium investigations. A $10^{-4}M$ solution was prepared for titration of the free thorium ions in the equilibrated mixtures.

It is known that in some cases the addition of EDTA of pH 5 to metal solutions of lower pH initiates hydrolysis which may influence the accuracy unfavourably. Because of the high accuracy wanted, several titrations were done with EDTA acidified to pH ≤ 2, but the results were not improved. Acidification of the EDTA stock led to a slow decrease in concentration, presumably because of the low solubility of EDTA in this pH region; pH 5 was selected finally for the stock solutions.

The equilibrium mixture

The reaction between thorium and EDTA is rapid; the reaction between palladium and EDTA is slow. Several experiments were done to find out whether equilibrium was attained.

With the sequence of addition, palladium, EDTA, thorium, equilibrium was reached within 24 hr; with addition in the reverse order it took 12 days to obtain the same results. The first sequence was adopted throughout the definitive experiments.

The reaction mixtures were prepared as follows. In 50-ml standard flasks, 0.1 ml of $2M$ nitric acid, 0.5 ml of $10^{-3}M$ palladium and either 0.6 ml (series A) or 0.75 ml (series B) of $10^{-3}M$ EDTA were placed, the flask being weighed after each addition. After 15 min, 0.5 ml of $10^{-3}M$ thorium was added and weighed. After another 15 min the flask was filled up to the mark with a $0.2M$ sodium perchlorate/$0.01M$ nitric acid mixture. The solutions were then set aside for at least 2 days.

The experimental conditions correspond to $pC_H = 1.70$, $I = 0.2$ (sodium perchlorate) and $T = 21 \pm 1°$. Finally, 10-ml aliquots were transferred into a 20-ml titration cell, 1 ml of $10^{-4}M$ SXO was added and the solutions were titrated spectrophotometrically (535 nm) with $10^{-4}M$ EDTA from a microburette (Metrohm E457).

RESULTS AND DISCUSSION

The repeatability within the series A and B, each comprising 12 determinations, was fairly good (standard deviation of $\log V = 0.08$). Nevertheless the mean values differed significantly: $\log V = 2.04$ for series A and $\log V = 1.53$ for series B. Although the difference corresponds to only a 1.5% difference in the titration results, several attempts were made to explain this phenomenon.

Modification of the model to postulate that only inert Pd_2Y, or inert PdThY or a very thorium-labile PdThY is formed, is not satisfactory. The formation of only inert Th_2Y can explain the phenomenon mathematically, but such a complex is very unlikely to exist, for physicochemical reasons.[8–10]

The limited solubility of EDTA near pH 2 should not interfere as the limit is never reached. Amine-containing impurities in EDTA having a great affinity for Pd and not for Th cannot explain the difference either.

It is worthy of note that the difference between the series disappears when chloride is present at concentations $>10^{-2}M$, in which case palladium is present mainly as $PdCl_n$.

The mean value $\log V = 1.8$ (± 0.2) was taken for the calculation of $\log K_{PdY}$. Although not altogether satisfactory, this suffices for our purposes, in view of

Table 1. $\log \alpha_{Y(H)}$ *vs.* pC_H for sodium perchlorate medium at various ionic strengths

I \ pC_H =	log $\alpha_{Y(H)}$					
	0	1.0	1.5	1.70	2.0	3.0
0.01	23.22	18.13	15.85	15.02	13.86	10.87
0.1	22.71	17.62	15.36	14.54	13.42	10.57
0.2	22.55	17.46	15.20	14.39	13.28	10.48
1.0	22.74	17.65	15.38	14.56	13.44	10.66

the errors in log K'_{ThY} and in the various side-reaction coefficients involved.

For the calculation of K_{PdY}, we need the conditional constant for ThEDTA and the side-reaction coefficient $\alpha_{Y(H)}$; both should refer to our experimental conditions ($I = 0.2$, sodium perchlorate medium and room temperature). These are not directly available in the literature and were evaluated as done previously for the chloro-complexes of palladium[11] by using Guggenheim's modifications of the Debye–Hückel equation for ion-activity coefficients. In the Appendix the procedure is elucidated for the stepwise stability constants of EDTA. From these data, Table 1 was drawn up for $\alpha_{Y(H)}$ at various pC_H and I. For ThEDTA the value log $K_{ThY} = 23.2$ is advocated in many data books.[12–15] From our own experience (because of the low concentration at which Th^{4+} at low pH can be titrated), it was evident that this value is too low. To explain their titration results Pijpers *et al.*[16] adopted log $K' = 11.9$ for the conditional constant at $pC_H = 2.0$ ($I = 0.01$, perchloric acid medium and room temperature), and this value is more consistent with our findings.

From the reliable value[17] (independent of ionic strength) log $K_{ThY(H)} = 1.98$, whence log $\alpha_{ThY(H)} = 0.3$, the absence of hydroxide complex formation at low concentrations[6] (log $\alpha_{Th(OH)} = 0.0$) and log $\alpha_{Y(H)} =$ 13.86 (Table 1), the value log $K_{ThY} = 25.5$ can be deduced, which is probably a better estimate. This value also agrees with an earlier result (log $K_{ThY} = 25.3$) obtained by Bottari and Anderegg[17] from equilibrium studies with iron(III) at room temperature and in sodium perchlorate medium ($I = 0.1$). Their value will be adopted as the most reliable available for the moment.

For adaptation of this value to $I = 0.2$, the necessary values of z^2 and $B(I)$ were estimated from Baes and Mesmer's tables,[18] by using Pitzer and Mayorga's monotonic function $F(I)$[19] for the higher ionic charges (Table 2). From Table 2, log $K_{ThY} = 25.3$ and equation (A6) (Appendix), it follows that at $I = 0.2$ we have log $K_{ThY} = 25.1$. It now remains to evaluate K_{PdY}, which is found from equation (6) after taking into consideration all the side reactions. This leads to the equation

$$\log K_{PdY} = \log K_{ThY} + \log V - \log \alpha_{PdY(H)} + \log \alpha_{Pd(OH)} + \log \alpha_{ThY(H)} - \log \alpha_{Th(OH)}. \quad (7)$$

Anderegg and Malik[3] studied the protonation of PdY at $I = 1.0$ and found the species PdHY, PdH_2Y and PdH_3Y with the stepwise protonation constants log $Q_1 = 3.01$, log $Q_2 = 2.31$ and log $Q_3 = 0.9$.

If the procedure in the Appendix is used to adapt these values to $I = 0.2$, with the usual B values for uni–univalent and uni–bivalent interactions, it turns out that the values for log Q_i are not very dependent on I:

$$\log Q_1 = 3.5 - 2.0\left(\frac{I^{1/2}}{1 + I^{1/2}}\right) + 0.5\,I$$

$$\log Q_2 = 2.5 - 1.0\left(\frac{I^{1/2}}{1 + I^{1/2}}\right) + 0.3\,I$$

$$\log Q_3 = 0.9.$$

For our conditions, this leads to log $\alpha_{PdY(H)} = 1.9$ and the distribution of PdY, PdHY, PdH_2Y and PdH_3Y being 1%, 22%, 67% and 10% respectively under our experimental conditions.

For the calculation of log $\alpha_{Pd(OH)}$ we follow Baes and Mesmer[18] in their conclusion that log $*\beta_1 = -2.3 \pm 0.1$ and log $*\beta_2 = -4.8 \pm 0.2$ are good estimates for the hydrolysis constants; thus log $\alpha_{Pd(OH)} = 0.12$. Although the log $*\beta_i$ values are rather uncertain, log $\alpha_{Pd(OH)}$ is fairly reliable; its value is small because of the low pC_H and therefore it is rather insensitive to changes in log $*\beta_i$.

Application of equation (A6) (Appendix) to log $K_{ThY(H)}$ shows that because $\Delta z^2 = 0$ and $b \sim 0$, this constant hardly changes with I. Thus, for $pC_H = 1.70$, log $\alpha_{ThY(H)} = 0.46$. It has already been noted that log $\alpha_{Th(OH)} = 0.0$ at pC_H 2. This will certainly hold at lower pC_H so we eventually derive log $K_{PdY} = 25.6$ for the stability constant after substitution of the appropriate values in equation (7). When equation (A6) is applied to PdY and reasonable values are taken for z^2 and B, it turns out, that in the ionic strength range 0.1–1.0, log K_{PdY} will change by not more than 0.2 with I (log $K_{PdY} = 25.7$ and 25.4 for I 0.1 and 1.0). This behaviour has also been found for FeY and ThY.[17] These fluctuations with I are of the same

Table 2. The values of z^2 and B(I) that correspond to equation (A3) (Appendix) for calculating the ionic activity coefficient

Ion	z^2	$B(0)$	$B(\infty)$	$B(0.1)$	$B(0.2)$	log $\gamma(0.1)$	log $\gamma(0.2)$
Th^{4+}	16	10.8	0.7	6.8	5.6	−1.28	−1.41
ThY	0	—	—	~0	~0	0	0
Y^{4-}	4	—	—	0.48	0.48	−0.44	−0.54

Table 3. Experiments in chloride-containing media

$[Cl^-]$, M	0.006	0.015	0.03	0.06
pCl	2.22	1.82	1.52	1.22
$\Delta\log V^*_{exp}$	$-0.86\ (\pm 0.1)$	$-1.53\ (\pm 0.02)$	$-2.16\ (\pm 0.02)$	$-2.80\ (\pm 0.02)$
$\log \alpha_{Pd(Cl)}$	3.85	4.98	5.91	6.91
$\log \alpha_{PdH_2Y(Cl)}$	2.99	3.45	3.75	4.11
$\log \beta_1$	5.21	5.27	5.27	5.33

*The $\Delta\log V$ values are related to $\log V = 1.80$.
(Experimental conditions: $I = 0.2$, ($NaCl + NaClO_4$) medium, $pC_H = 1.70$, room temperature $21 \pm 1°$).

magnitude as the expected error in $\log K_{PdY}$, which arises mainly from the errors in $\log K_{ThY}$ and $\log V$. At the moment we think that 0.2 is a realistic estimate of this error.

The chloride complexes of PdEDTA

Anderegg and Malik[3] determined the stability constants of the chloro complexes of PdEDTA and its protonated forms at $I = 1.0$ (sodium perchlorate medium). Their values are unexpectedly low. On calculation of the conditional constant related to these values, taking into account the strong tendency of palladium to form Pd–Cl compounds, it turns out that even in $10^{-3}M$ chloride, titrations of palladium should be impossible. This does not agree with experiments; obviously our preliminary values[1] are more reliable.

In Table 3 the changes in $\log V$ found experimentally are presented, together with the relevant values of $\log \alpha_{Pd(Cl)}$.[11]

Neither thorium nor ThY has any affinity for chloride, so the change in $\log V$ with $[Cl^-]$ is caused by only the side-reactions described by the coefficients $\log \alpha_{Pd(Cl)}$ and $\log \alpha_{PdY(Cl)}$.

From the previous section we know that PdH_2Y predominates under our experimental conditions, which implies that $\alpha_{PdY(Cl,H)}$ can be approximated by

$$\alpha_{PdH_2Y(Cl)} = 1 + \beta_1[Cl^-] + \beta_2[Cl^-]^2 + \ldots \quad (8)$$

Then, since

$$\Delta \log V = \log \alpha_{PdH_2Y(Cl)} - \log \alpha_{Pd(Cl)} \quad (9)$$

we can first try to explain the experimental results by only the second term in equation (8):

$$\log \alpha_{PdH_2Y(Cl)} = \log \beta_1[Cl] \quad (10)$$

Table 3 shows that the values of $\log \beta_1$ do not differ significantly from each other, so it can be assumed that only one chloride ion is attached to the PdH_2Y species; the constant for the equilibrium $PdH_2Y + Cl \rightleftharpoons PdH_2YCl$ can be taken as $\log K = 5.3 \pm 0.1$.

Acknowledgement—We are much indebted to Mr. René Sepers for his contribution to the experimental work, which sometimes had to be performed at a painstakingly accurate level.

REFERENCES

1. J. Kragten, *Talanta*, 1978, **25**, 239.
2. W. M. MacNevin and O. H. Kriege, *J. Am. Chem. Soc.*, 1955, **77**, 6149.
3. G. Anderegg and S. C. Malik, *Helv. Chim. Acta*, 1976, **59**, 1498.
4. G. Anderegg, in *Proc. Summer School on Stability Constants*, (Bivigliano, Florence, Italy, June 1974), P. Paoletti, R. Barbucci and L. Fabbrizzi (eds.), p. 27.
5. J. Kragten, *Z. Anal. Chem.*, 1973, **264**, 356.
6. *Idem, Atlas of Metal–Ligand Equilibria in Aqueous Solution*, Horwood, Chichester, 1977.
7. *Idem, Talanta*, 1977, **24**, 483.
8. A. A. McConnell and R. H. Nuttall, *Inorg. Chim. Acta*, 1976, **19**, 253.
9. R. H. Nuttall and D. M. Stalker, *Talanta*, 1977, **24**, 355.
10. A. A. McConnell, R. H. Nuttall and D. M. Stalker, *ibid.*, 1978, **25**, 425.
11. J. Kragten, *ibid.*, 1980, **27**, 375.
12. G. Anderegg, *Critical Survey of Stability Constants of EDTA Complexes*, IUPAC Chemical Data Series No. 14. Pergamon, Oxford, 1978.
13. A. E. Martell and R. M. Smith, *Critical Stability Constants*, Vol. 1. Plenum Press, New York, 1974.
14. L. G. Sillén and A. E. Martell, *Stability Constants of Metal–Ion complexes*, Special Publication No. 17. Chemical Society, London, 1964.
15. *Idem, op. cit.* Supplement No. 1, Spec. Publ. No. 25, 1971.
16. C. J. C. Pijpers, L. G. Decnop-Weever, G. den Boef and W. E. van der Linden, *Mikrochim. Acta*, 1976 **I**, 667.
17. E. Bottari and G. Anderegg, *Helv. Chim. Acta*, 1976, **50**, 2349.
18. C. F. Baes and R. E. Mesmer, Jr., *The Hydrolysis of Cations*, p. 436. Wiley–Interscience, New York, 1976.
19. K. S. Pitzer and G. Mayorga, *J. Phys. Chem.*, 1973, **77**, 2300.
20. E. A. Guggenheim, *Thermodynamics*, p. 357. North-Holland, Amsterdam, 1959.
21. S. Glasstone, *Introduction to Electrochemistry*, 7th Ed., p. 140. Van Nostrand, Princeton, 1956.
22. J. Kragten and L. G. Decrop-Weever, *Talanta*, 1983, in the press.

APPENDIX

For adapting the stability constants to other ionic strengths we used Guggenheim's modifications of the Debye–Hückel equation[20] for ion activity coefficients γ. The general equations are

$$\log \gamma_R = -Az_R^2 \frac{I^{1/2}}{(1 + I^{1/2})} + \sum_{X'} B_{R,X'} m_{X'} \quad (A1)$$

$$\log \gamma_X = -Az_X^2 \frac{I^{1/2}}{(1 + I^{1/2})} + \sum_{R'} B_{R',X} m_{R'} \quad (A2)$$

where R denotes a particular cation species and R′ all cation species, X and X′ denote the same for anions, z is the ionic charge, m the molality and A is a temperature-dependent constant ($=0.511$ at room temperature). As the uni–univalent electrolyte sodium perchlorate is present in excess, only the interactions with sodium perchlorate contribute substantially to the sum term in equations (A1) and

(A2), which means that these equations can be replaced by

$$\log \gamma = -0.511 \frac{I^{1/2}}{(1 + I^{1/2})} + B(I)I \qquad \text{(A3)}$$

For many common electrolytes the interaction coefficients B have been estimated experimentally.[18] When localized high ionic charges are involved, as for instance in the case of Fe^{3+} and Th^{4+} ions, it is necessary to use the extended form of equation (A3) where B depends on I.[18] For uni–univalent interactions B may be taken as constant and lying in the range 0.10–0.20; for bi–univalent interactions B will usually lie in the range 0.4–0.8.

With EDTA, the electric charges of Y^{4-}, HY^{3-} and H_2Y^{2-} are spread out as unit charges over the nitrogen atoms and carboxyl groups. In the original derivation of the Debye–Hückel equation,[21] the total electric work W of all ions of the ith kind is proportional to $N_i z_i^2$, where N_i is the number of ions with ionic charge z_i. If EDTA is regarded as n_i separate ionic unit charges, then $W_{EDTA} \sim n_i N_i z_i^2 = n_i N_i$, so

$$\ln \gamma_i \sim \frac{\partial W}{\partial N_i}$$

is proportional to n_i. This means that in equation (A3) z^2 has to be replaced by n_i. The values of B for the different EDTA species will be close to the value for uni–univalent interactions.

For any chemical reaction the activity constant K and concentration constant Q are related through the activity coefficients γ

$$K = \frac{a_{12}}{a_1 a_2} = Q \frac{\gamma_{12}}{\gamma_1 \gamma_2} \qquad \text{(A4)}$$

with, for EDTA:

$$Q_n = \frac{[H_n Y^{n-4}]}{[H_{n-1} Y^{n-5}][H^+]} \qquad \text{(A5)}$$

Substitution of equation (A3) in equation (A4) leads to the general formula for the stability constant

$$\log Q = \log K + 0.511\, \Delta z^2 \left(\frac{I^{1/2}}{I^{1/2} + 1} \right) - bI \qquad \text{(A6)}$$

Table A1. Values of $z^2(n_i)$ and B, related to equation (A3) for the ionic activity coefficients of the EDTA species in sodium perchlorate medium

Ion	Value of "z^2"(n_i) eqn. (A3)	B
H^+	1	0.18
H_6Y^{2+}	2	0.34
H_5Y^+	1	0.18
H_4Y	0	0
H_3Y^-	1	0.18
H_2Y^{2-}	2	0.10
HY^{3-}	3	0.22
Y^{4-}	4	0.48

Table A2. The stability constants for stepwise protonation of EDTA in sodium perchlorate medium as a function of I (at 21 ± 1°); $\log Q_5$ and $\log Q_6$ are independent of I as both Δz^2 and b are zero

$$\log Q_1 = 10.40 - 1.02 \frac{I^{1/2}}{1 + I^{1/2}} + 0.44\, I$$

$$\log Q_2 = 6.42 - 1.02 \frac{I^{1/2}}{1 + I^{1/2}} + 0.30\, I$$

$$\log Q_3 = 2.88 - 1.02 \frac{I^{1/2}}{1 + I^{1/2}} + 0.10\, I$$

$$\log Q_4 = 2.17 - 1.02 \frac{I^{1/2}}{1 + I^{1/2}} + 0.36\, I$$

$$\log Q_5 = 1.45$$

$$\log Q_6 = -0.10$$

where Δz^2 is the algebraic sum of the values of z^2 (or $|n|$) of numerator and denominator [equation (A5)] and b analogously the sum of the B values.

From equation (A5) it is obvious that $\log \gamma_{H^+}$ appears in every equation for Q_n and that $\log \gamma_{H_iY}$ generally appears in the equations for both $\log Q_i$ and $\log Q_{i-1}$, thus interrelating the six equations (A6) for EDTA. From the data in the literature[12–15,22] about the stability constants of EDTA in sodium perchlorate medium at different ionic strengths, a consistent set of values for z^2 and B could be evaluated that satisfied the interrelationship between $\log Q_i$ and the B values already known[18] (Table A1). In Table A2 the formulae are given for the stability constants which follow from the data in Table A1, in combination with the literature data[12–15] ($\log Q_5$ and $\log Q_6$ are from solubility measurements;[22] their magnitude however, plays a minor role in our calculations of K_{PdY}).

Table A3. The values of the stepwise and overall stability constants of EDTA for sodium perchlorate medium at different ionic strengths

I =	0.01	0.1	0.2	1.0
$\log Q_1$	10.31	10.20	10.17	10.33
$\log Q_2$	6.33	6.20	6.16	6.21
$\log Q_3$	2.79	2.64	2.58	2.47
$\log Q_4$	2.08	1.96	1.93	2.02
$\log Q_5$	1.45	1.45	1.45	1.45
$\log Q_6$	−0.1	−0.1	−0.1	−0.1
$\log \beta_1$	10.31	10.20	10.17	10.33
$\log \beta_2$	16.64	16.40	16.33	16.54
$\log \beta_3$	19.43	19.04	18.91	19.01
$\log \beta_4$	21.51	21.00	20.84	21.03
$\log \beta_5$	22.96	22.45	22.29	22.48
$\log \beta_6$	22.86	22.35	22.19	22.38

Talanta, Vol. 30, No. 7, pp. 455–458, 1983
Printed in Great Britain.

0039-9140/83 $3.00+0.00

SELECTIVE COLLECTION OF SELENIUM(IV) ON ANION-EXCHANGE RESIN WITH AZOTHIOPYRINE DISULPHONIC ACID

MORIO NAKAYAMA, MASAHIKO CHIKUMA and HISASHI TANAKA
Faculty of Pharmaceutical Sciences, Kyoto University, Sakyo-ku, Kyoto 606, Japan
and
TOMOO TANAKA
Meiji College of Pharmacy, Nozawa, Setagaya, Tokyo 154, Japan

(*Received* 7 *September* 1982. *Revised* 29 *November* 1982. *Accepted* 2 *February* 1983)

Summary—Azothiopyrine disulphonic acid (ATPS) has been shown to be terfunctional, namely it can form a selenotrisulphide by reaction of its thiol group with selenium(IV), bind to an anion-exchange resin by ion-exchange through its sulphonate group, and be strongly physically adsorbed on the ion-exchange resin. ATPS adsorbed on the resin does not bleed into solution even in the presence of sodium chloride and hydrochloric acid. The collection of selenium(IV) is practically complete when ATPS is added to a selenium(IV) solution and the reaction product is collected on the anion-exchange resin. Selenium(IV) is not satisfactorily collected, however, by reaction with anion-exchange resin loaded with ATPS. The sorbed selenium can be eluted [as Se(IV)] with 13*M* nitric acid and directly determined fluorometrically in the eluate.

The biological activity of selenium has been of interest since its recognition as a nutritionally essential element, in glutathione peroxidase.[1,2] In addition, selenium compounds decrease the toxic effect of mercury compounds, and the role of selenium as a biological protector against highly toxic metals has been suggested.[3] The danger with this element, however, stems from the comparatively narrow concentration gap between the essential level and the toxic level, and methods for accurate determination of low levels are still in demand.

Co-precipitation[4] and adsorption on XAD-resin[5] or activated carbon[6] have been reported as collection methods for selenium, but all are lacking in selectivity. This paper deals with development of a method for the selective collection of selenium(IV) with a new chelating agent, azothiopyrine disulphonic acid (ATPS) (Fig. 1), which has already been used for the collection of mercury.[7,8] This reagent has three important analytical properties: ion-exchange, chelate-formation and physical adsorption on an ion-exchange resin. Qualitative tests of ATPS with selenium indicated high selectivity and reactivity in an acidic medium, suggesting its application in a trapping system for selenium(IV), especially if it is used with an anion-exchange resin.

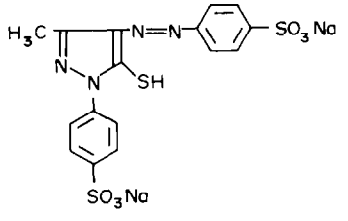

Fig. 1. ATPS.

EXPERIMENTAL

Apparatus

Absorption spectra in the ultraviolet and visible regions were measured with a Hitachi 330 spectrophotometer. A Shimadzu RF-500 spectrofluorophotometer was used for the fluorometric determination of selenium(IV) with 2,3-diaminonaphthalene (DAN).

Reagents

Disodium 4,4′-(4-diazenediyl-5-mercapto-3-methyl-1,2-diazacyclopenta-2,4-diene-1-yl)dibenzenesulphonate (ATPS) was prepared as previously reported.[9] A standard solution of selenium(IV) was prepared from selenious acid (Wako Pure Chemical Industries, Ltd.). Amberlite IRA-400 (8% cross-linking) in the chloride form, 100–200 mesh, was used as the anion-exchange resin. All reagents used were of analytical-grade quality.

Thin-layer chromatography

Equivalent amounts of ATPS and selenium(IV) were added to 0.5*M* hydrochloric acid at 4°. After 12 hr, the pH was raised to 4 by dropwise addition of sodium hydroxide solution. Standard solutions of ATPS and its disulphide were prepared similarly. These three solutions were spotted on a cellulose-coated plate. Isoamyl alcohol–acetone–water mixture (5:6:5 v/v) was used as development solvent.

Collection of selenium(IV)

Batch method. The efficiency of collection of selenium(IV) was examined by the following procedures.

System A. One gram of the anion-exchange resin was stirred with 100 ml of aqueous solution containing 0.2 mmole of ATPS, at 30°, until the supernatant became colourless. The resin thus loaded with ATPS was filtered off, washed with water and methanol, and dried *in vacuo*. To portions of 2-mg/l. selenium(IV) solution in 0.1–1.0*M* hydrochloric acid, 100 mg of the loaded resin were added. The mixture was shaken for about 5 hr at 50°, and the resin was then collected on a fritted-glass funnel. An appropriate volume of filtrate was taken and analysed fluorometrically[10] for selenium(IV) with DAN.

System B. To 48 ml of hydrochloric acid of various concentrations, 1 ml of $10^{-2}M$ ATPS solution and 1 ml of 100-mg/l. selenium(IV) solution were added. This mixture

was stirred for 15 min at 50°, and then 100 mg of the anion-exchange resin in the chloride form were added. The mixture was shaken for 1 hr at 30°, and the resin was collected and analysed for selenium(IV) for system A.

Column method. Examination of the reaction conditions led to the following optimal procedure. The selenium(IV) sample (200 ml) solution was made 2*M* in hydrochloric acid and 2 ml of $10^{-2}M$ ATPS were added. The reaction was allowed to proceed at 0° (ice-bath) for 6 hr and then the mixture was applied to a column (1.0 cm bore, 5.0 cm length) of the anion-exchange resin. [If the concentration of selenium(IV) was very low, 4 ml of $10^{-2}M$ ATPS were added to 500 ml of sample acidified in the same way.] The flow-rate through the column was adjusted to 40 ml/hr with a peristaltic pump. The column was then washed with 100 ml of distilled demineralized water. The selenium sorbed was eluted with 13*M* nitric acid (10 ml) at a flow-rate of 20 ml/hr. The eluate was neutralized with ammonia solution and analysed fluorometrically with DAN.

RESULTS AND DISCUSSION

Two approaches to the collection of selenium(IV) were tried, one (A) being sorption of the selenium on resin loaded with ATPS, and the other (B) being formation of the Se(IV)–ATPS complex in solution, followed by sorption on the non-loaded anion-exchange resin.

First, the reaction of ATPS with selenium(IV) was investigated. Some thiols have been proposed as reagents for spectrophotometric determination of selenium(IV),[11,12] and so have thiopyrine and its derivatives.[13] ATPS is exceptionally stable even in 10*M* hydrochloric acid[9] so its reaction with selenium(IV) was studied in 0.1–10*M* hydrochloric acid media. A distinct colour change from red to yellow is observed in this reaction. The maximum absorption band of ATPS occurs at 398 nm, whereas that of the reaction mixture is at 345 nm. The reaction of ATPS with selenium(IV) is found to be accelerated by increasing the concentration of hydrochloric acid and the temperature (Fig. 2). A slight red turbidity caused by release of elemental selenium is observed when the concentrations of ATPS and selenium(IV) are raised and the reaction mixture is allowed to stand at 30–50° for about 3 hr. The rate of formation of elemental selenium is dependent on the temperature. At 90°, elemental selenium is generated in a matter of minutes. However, when the reaction is done at 0° the spectral change takes place in about 5 hr, and no red turbidity is observed.

The molar ratio of ATPS to selenium(IV) in the complex formed in 0.5*M* hydrochloric acid at 50° has been found to be 4:1 by the molar-ratio and continuous-variation methods, the absorbance being monitored at 345 nm. The reaction takes about 15 min and there is no release of elemental selenium during this period. These results suggest that the reaction between selenium(IV) and ATPS in hydrochloric acid proceeds according to equation (1), based on analogy with the reactions of selenite with some thiols, coenzyme A, cysteine,[14] glutathione[15] and

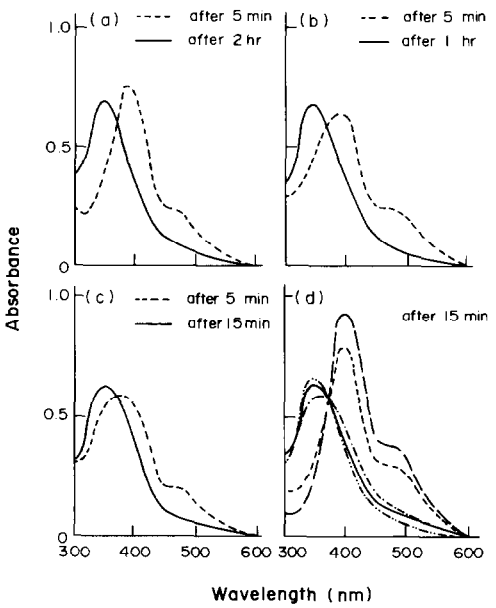

Fig. 2. Absorption spectra of the reaction products of ATPS with selenium(IV). ATPS $4 \times 10^{-5}M$, Se(IV) $8 \times 10^{-5}M$, (a) 0.2*M* HCl (at 30°); (b) 0.5*M* HCl (at 30°); (c) 1.0*M* HCl (at 30°); (d) ····· 0.5*M* HCl (at 0°), —·— 0.5*M* HCl (at 30°), —— 0.5*M* HCl (at 50°), --- ATPS only, —··— ATPS + I_2.

thiopyrine[16] to form selenotrisulphides:

$$4RSH + H_2SeO_3 \rightarrow R\text{–}S\text{–}Se\text{–}S\text{–}R + R\text{–}S\text{–}S\text{–}R + 3H_2O \quad (1)$$

Some selenotrisulphides have been found to decompose and to release elemental selenium according to equation (2):[14,16]

$$R\text{–}S\text{–}Se\text{–}S\text{–}R \rightarrow R\text{–}S\text{–}S\text{–}R + Se \quad (2)$$

The shift of the absorption band from 398 nm to 345 nm is attributed to the formation of the selenotrisulphide and the disulphide. It is difficult to distinguish them spectrophotometrically, because their absorption spectra are so similar. In fact, the absorption spectrum of the reaction mixture was similar to that of the product of oxidation of ATPS with iodine, as shown in Fig. 2. In the case of thiopyrine, the absorption spectrum of the selenotrisulphide is also very similar to that of the disulphide.

The thin-layer chromatogram of this reaction mixture showed two spots with similar colour intensity. The R_f value of the orange spot (0.75) was identical to that of the product (R–S–S–R) from iodine oxidation of ATPS. The other spot ($R_f = 0.68$) was yellowish orange in colour and considered to be that of the selenotrisulphide produced from ATPS. Although the R_f values are not very different, the colour difference is distinct enough for the two spots to be distinguishable.

These results indicate formation of the fairly stable selenotrisulphide in acid medium according to equa-

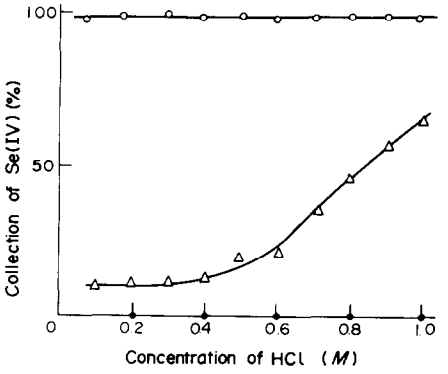

Fig. 3. Collection of selenium(IV) by systems A and B. ATPS 0.01 mmole, Se(IV) 100 μg, resin 100 mg (Amberlite CG-400), —○— Se-ATPS + resin (system B), —△— Se + ATPS-resin (system A), —●— Se + resin.

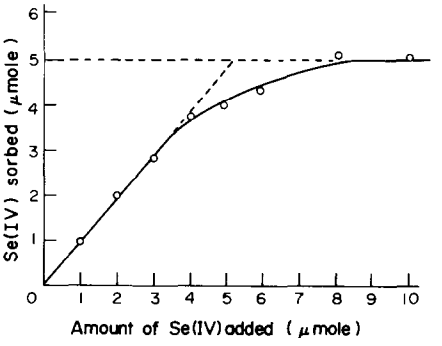

Fig. 4. Amount of selenium(IV) collected on the anion-exchange resin by system B. ATPS 0.02 mmole, anion-exchange resin 100 mg (Amberlite CG-400).

tion (1), but it is important to do the reaction at low temperature in order to avoid complete decomposition of the selenotrisulphide.

Collection of selenium(IV)

Selenium(IV) was collected by a batch method (A) and a column method (B).

Batch method. As shown in Fig. 3, with system A, uptake of selenium(IV) on the ATPS-resin increased with hydrochloric acid concentration. The ATPS-resin sorbed 10% of the selenium from the 0.1*M* acid and 65% from the 1.0*M* acid. Slight leakage of ATPS from the anion-exchange resin was found when the concentration of hydrochloric acid was higher than 1.0*M*. No uptake of free selenium(IV) on the unloaded anion-exchange resin was found when the concentration of hydrochloric acid was 0.2–1.0*M*.

On the other hand, the product of reaction of ATPS with selenium(IV) was almost completely sorbed on the anion-exchange resin in 0.1–1.0*M* hydrochloric acid when system B was used. When the reaction mixture was shaken with the anion-exchange resin there was no detectable production of elemental selenium. Hence system B was the method of choice for the collection of selenium(IV). Its capability for collecting selenium(IV) was therefore tested, 0.02 mmole of ATPS in 0.5*M* hydrochloric acid being used, as shown in Fig. 4. The effect of increasing amounts of selenium(IV) was examined. The maximum amount of selenium(IV) sorbed was about 0.005 mmole and the binding ratio of selenium(IV) to ATPS on the resin was found to be about 1:4, which is supporting evidence that the reaction is as described in equation (1). Figure 4 shows that complete uptake of the selenium(IV) requires at least a 7-fold amount of ATPS.

The effect of other ions, such as chloride, copper(II) and cadmium(II), on the collection of selenium(IV) was examined (Fig. 5). Sodium chloride does not interfere, because of the strong physical adsorption of ATPS onto the ion-exchange resin. This can be contrasted with the behaviour of some other chelating agents which bear ion-exchange groups but lack the capability for physical adsorption, and hence are readily displaced into the solution.[16] Cadmium(II) and copper(II), which are capable of chelate formation with ATPS, interfere when present in concentration five times that of the selenium(IV), in 0.2*M* hydrochloric acid medium, but not in 0.6–1.0*M* hydrochloric acid. This indicates that in the presence of copper(II) and cadmium(II), ATPS reacts selectively with selenium(IV) in strongly acid medium, where these cations cannot form their chelates with ATPS.

Column method. Because of its success in batch operation, system B was tested for the column collection of selenium(IV). The results indicated that to form the selenotrisulphide completely and avoid its decomposition it is best to react ATPS with selenium(IV) at low temperature (0°) in 2*M* hydrochloric acid, and then apply the reaction product to a column packed with the anion-exchange resin. Nitric acid will elute selenium from the anion-exchange resin, together with the disulphide of ATPS, and the eluate can be directly used for the fluorometric determination of selenium with DAN, because the selenium is eluted in the quadrivalent state. In contrast, in other collection methods[5] complicated treatments are necessary to convert the selenium into Se(IV) for the fluorometric determination. In the column procedure, the anion-exchange resin can be regenerated but the ATPS is lost because of its oxidation to the disulphide by nitric acid.

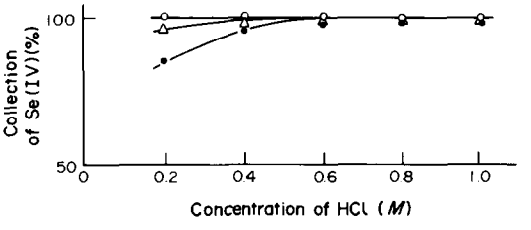

Fig. 5. Collection of selenium(IV) from solutions containing sodium chloride, copper(II) or cadmium, by system B. ATPS 0.01 mmole, Se(IV) 100 μg, resin 100 mg, —○— 0.5*M* NaCl, —△— 10 mg/l. Cd^{2+}, —●— 10-mg/l. Cu^{2+}.

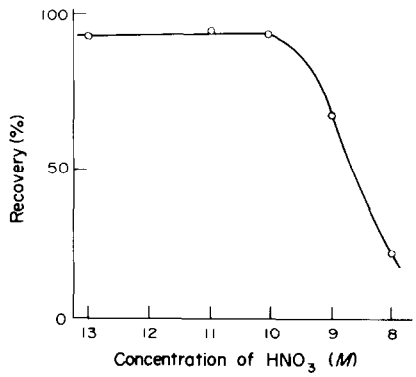

Fig. 6. Elution of selenium with nitric acid. ATPS 0.02 mmole, Se 100 μg, anion-exchange column 10 × 50 mm.

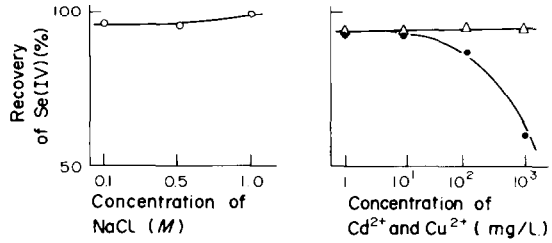

Fig. 7. Recovery of selenium(IV) from solutions containing sodium chloride, copper(II) or cadmium. ATPS 0.02 mmole, Se(IV) 100 μg, —○— NaCl, —△— Cd^{2+}, —●— Cu^{2+}.

The elution of selenium with various concentrations of nitric acid is shown in Fig. 6. More than 90% of the selenium is eluted as Se(IV) with 10–13*M* nitric acid.

Interference by a few other ions was tested for (Fig. 7). Sodium chloride (0.1–1.0*M*) did not interfere in the column method (or the batch method), owing to the strong physical sorption of ATPS on the anion-exchange resin. Cadmium (1–100 mg/l.) did not interfere. The interference of copper(II) was negligible at concentrations below 10 mg/l. In the absence of these foreign ions, the mean recovery of selenium(IV) from a solution containing 1 mg/l. was 93.8% (relative standard deviation 1.9%, 6 determinations) and in the presence of sodium chloride (0.5*M*), copper(II) and cadmium (each at the 10 mg/l. level) was 91.6% (relative standard deviation 3.5%, 6 determinations). However, when the concentration of copper(II) was increased, the recovery of selenium decreased (to 60% at Cu/Se w/w ratio of 10^3); the spectrum of the reaction mixture was then similar to that of the disulphide of ATPS, obtained by oxidation with iodine. The copper(II) interference was therefore presumably due to oxidation of the ATPS. Addition of 4 ml of 0.01*M* iodine to the reaction system decreased the recovery of selenium(IV) to 44%. Hence, it can be concluded that the interference of low concentrations of copper(II) is not significant, but the presence of large amounts of oxidizing agents may decrease the recovery of selenium(IV). Selenium(IV) was found not to cause any spectral change of ATPS under the conditions used for the collection of selenium(IV).

To assess the applicability of the method to biological and environmental samples containing only trace amounts of selenium(IV), a sample containing selenium(IV) at the 10-μg/l. level was tested. The recovery was only 78% (relative standard deviation 9%, 6 determinations), which was not very satisfactory. A search for better terfunctional reagents, having higher reactivity with selenium and forming a more stable selenotrisulphide has therefore been begun.

The method presented here has the following advantageous features for collection of selenium(IV). The reagent has a thiol group and reacts with selenium(IV) to form a selenotrisulphide even in strongly acidic medium, and the product is separable by means of an ion-exchanger, which makes the method highly selective. In addition, the eluate containing selenium(IV) can be used for the fluorometric determination with DAN without further treatment. The anion-exchange resin can be used repeatedly.

Acknowledgement—Financial support from the Ministry of Education, Science and Culture of Japan (Grant-in-Aid No. 587017) is gratefully acknowledged.

REFERENCES

1. T. C. Stadtman, *Science*, 1974, **183,** 195.
2. J. T. Rotruck, A. L. Pope, H. E. Ganther, A. B. Swanson, D. G. Hafeman and W. G. Hoekstra, *ibid.*, 1973, **179,** 588.
3. H. E. Ganther, C. Goudie, M. L. Sunde, M. J. Kopecky, P. Wagner, S. H. Oh and W. G. Hoekstra, *ibid.*, 1972, **175,** 1122.
4. Th. A. Kouimtzis, M. C. Sofoniou and I. N. Papadoyannis, *Anal. Chim. Acta*, 1981, **123,** 315.
5. Y. Sugimura and Y. Suzuki, *J. Oceanog. Soc. Jap.*, 1977, **33,** 23.
6. H. J. Robberecht and R. E. Van Grieken, *Anal. Chem.*, 1980, **52,** 449.
7. M. Chikuma, M. Nakayama, T. Tanaka and H. Tanaka, *Talanta*, 1979, **26,** 911.
8. M. Nakayama, M. Chikuma, H. Tanaka and T. Tanaka, *ibid.*, 1982, **29,** 503.
9. T. Tanaka, K. Tanaka, M. Nakayama, M, Chikuma and H. Tanaka, *Chem. Pharm. Bull.*, 1981, **29,** 165.
10. K. Hiraki, O. Yoshii, H. Hirayama, Y. Nishikawa and T. Shigematsu, *Bunseki Kagaku*, 1973, **22,** 712.
11. A. I. Busev, *Talanta*, 1964, **11,** 485.
12. H. Yoshida, M. Taga and S. Hikime, *Bunseki Kagaku*, 1965, **14,** 1109.
13. T. Tanaka, H. Katagihara and N. Iritani, *ibid.*, 1971, **20,** 291.
14. H. E. Ganther, *Biochemistry*, 1968, **7,** 2898.
15. *Idem, ibid.*, 1971, **10,** 4089.
16. M. Chikuma, M. Nakayama, T. Itoh, H. Tanaka and K. Itoh, *Talanta*, 1980, **27,** 807.

Talanta, Vol. 30, No. 7, pp. 459–464, 1983
Printed in Great Britain.

0039-9140/83 $3.00+0.00

OPTIMIZATION OF INSTRUMENTAL PARAMETERS FOR SQUARE-WAVE ANODIC STRIPPING VOLTAMMETRY

E. B. BUCHANAN, JR. and D. D. SOLETA
Department of Chemistry, University of Iowa, Iowa City, IA 52242, U.S.A.

(*Received* 10 *May* 1982. *Revised* 17 *November* 1982. *Accepted* 1 *February* 1983)

Summary—Experimental parameters associated with the use of a square-wave potential waveform during the stripping procedure have been examined for their effect on the sensitivity of ASV. Voltamperograms for 10-ng/ml solutions of lead and of cadmium were recorded under the various experimental conditions. Peak heights obtained experimentally were compared with those calculated from an equation describing the rate of decay of the measured current. Calibration graphs were constructed for lead and cadmium over the range 0.1–1.6 ng/ml, and the two metals were determined in samples of the local water supply.

Square-wave voltammetry has been demonstrated to be a highly sensitive technique for the measurement of trace metals in aqueous solutions.[1-3] The improvement in sensitivity is achieved through more efficient discrimination between the charging and the faradaic currents. When it is coupled with anodic stripping techniques, sensitivities as high as 0.1–1 ng/ml have been obtained.[4] The potential-waveform utilized in this type of stripping procedure consists of a staircase voltage upon which is superimposed a series of square-waves, as shown in Fig. 1. The use of this more complex waveform introduces a number of new experimental parameters into the stripping process. This paper reports an examination of the effects of these parameters and their interplay upon the overall sensitivity of the method.

The parameters considered are those associated with the square-wave scanning potential and include (*a*) the square-wave amplitude, (*b*) the square-wave half-period and (*c*) the scan-rate of duration of each 5-mV step. Additional parameters examined are those related to the current measurement, namely the transition-sample delay period and the sample aperture period. The conventional stripping parameters of deposition time and drop-size of the hanging mercury drop electrode (HMDE) were also studied.

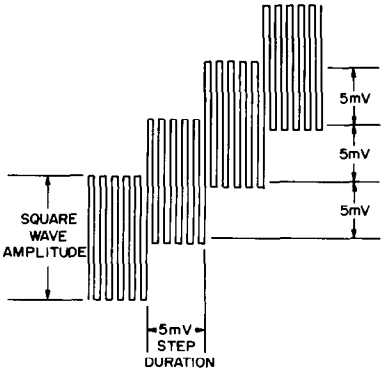

Fig. 1. Square-wave staircase-potential waveform.

The total current, i_T produced at the working electrode is the sum of the charging, i_C, and faradaic, i_F, currents:

$$i_T = i_C + i_F \tag{1}$$

The decays of the charging and faradaic currents are given by:

$$i_{C_t} = Ae^{(-t/RC)} \tag{2}$$

$$i_{F_t} = Bt^{-1/2} \tag{3}$$

where A and B are proportionality constants, t is the time (in μsec) after the square-wave transition, and R and C are the resistance and double-layer capacitance of the cell and electrode.[5] Combining these equations gives an expression for the total instantaneous current, i_{T_t} through the cell:

$$i_{T_t} = Ae^{(-t/RC)} + Bt^{-1/2} \tag{4}$$

Thus, the shape of the current–time curve is independent of the repetition frequency of the square-wave, when viewed over the life of a single half-period of the square-wave.

The enhancement in sensitivity attributable to square-wave voltammetry occurs because the two current components, charging current and faradaic current, are separable on the basis of time. Figure 2 is a graphical representation of the time-dependence of the total current flow resulting from the applied potential. The total time during which current flows is divided into three sections, the transition-sample delay period, the sample aperture period and a slack period. The ratio of charging and faradaic currents during the complete cycle changes from mostly charging, during the transition-sample delay period, to mostly faradaic, during the sample aperture period

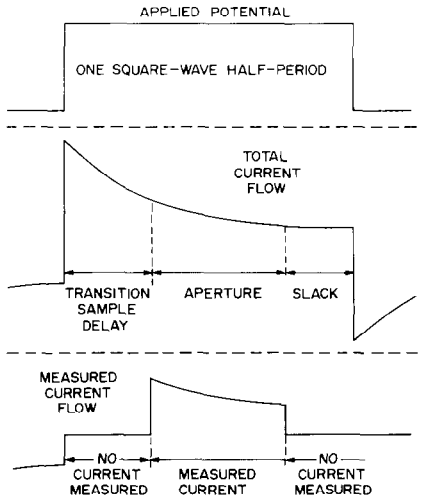

Fig. 2. Applied potential and resulting current flows.

because the charging current decays faster than the faradaic current.

The ratio of faradaic to charging current in the measured current flow is maximized by adjustment of the transition-sample delay period, during which no current is measured, and the sample aperture period, during which the current flow is measured. The slack period, although seldom employed, is available to make up the period in time between the closure of the sampling operation and the commencement of the next square-wave signal.

EXPERIMENTAL

Apparatus

The square-wave anodic stripping voltammetry (SWASV) instrument with mini flow-through cell has already been described.[4] Voltamperograms were recorded on a Heath Servo-Recorder Model EU-20B. A Tektronix Type 535A Dual-Trace Oscilloscope was used to monitor the current decay signal. A silver/silver chloride reference electrode was used with an unfired Vycor tip as the solution-to-electrode interface.

Reagents

Distilled water passed through Barnstead "Ultrapure" and "Organic Removal" cartridges was used in the preparation of all solutions. Stock solutions of cadmium and lead were prepared from reagent-grade cadmium chloride and lead carbonate. Reagent-grade hydrochloric acid, ammonium chloride, potassium nitrate and nitric acid were used in preparing the stripping solution for the matrix exchange method. Nitrogen was employed to deaerate the stripping solution, and was freed from oxygen by bubbling it through an aqueous chromium(II) scrubber solution before use.

SQUARE-WAVE VOLTAMPEROGRAPH

1. Sq.-wave amp. select (0, 5, 10, 25, 50)	mV
2. Sq.-wave half-period	μsec
3. Deposition time	sec
4. Transition-sample delay	μsec
5. Sample aperture	μsec
6. Initial potential (< = +/−2000 mV)	mV
7. Final potential (< = +/−2000 mV)	mV
8. 5-mV step duration	msec
9. Sensitivity (1, 2, 3, 4)	
A. Drop size (1, 2, 3, 4)	

Fig. 3. Menu display of operating parameters.

Procedure

A series of fourteen optimization studies was made. Figure 3 shows the operating parameters called the "Menu", as displayed on the CRT of the SWASV instrument. Tables 1 and 2 list the values assigned to the particular Menu parameters for each of the optimization studies indicated by the column heading. The parameters listed as variable in the tables are described below. The cadmium and lead ion concentrations were 10 ng/ml. The supporting electrolyte for the cadmium solutions was 0.01*M* hydrochloric acid, and for the lead solutions was 0.1*M* ammonium chloride.

Amplitude. The square-wave amplitude was varied between 50 and 10 mV peak-to-peak and its effect on peak-height and baseline as well as on the resolution of adjacent peaks was studied. For lead the sensitivity was maintained at 4 (equivalent[4] to a multiplication-factor of 440) in all cases except for the 50-mV amplitude, where it was reduced to 3 (≡ × 220) in order to keep the trace on scale.

Deposition time. Measurements were made of peak-heights as a function of the deposition time, with cadmium and lead solutions of constant concentration. The deposition time was varied between 30 and 120 sec.

Drop-size. Peak-heights were examined as the drop-size was varied between the four available with the instrument used. The drop-sizes themselves were evaluated by collecting and weighing a number of drops.

Transition-sample delay. Sample delays from 200 to 700 μsec were employed. Preliminary experiments indicated that maximum sensitivity would be achieved when the aperture and sample delay periods were equal to the half-period of the square-wave. Accordingly, in these experiments the sample delay period and the aperture period were adjusted so that their sum was the square-wave half-period.

Table 1. "Menu" parameters for cadmium experiments

Menu parameter number	Parameter examined				
	Half-period	Amplitude	Deposition time	Scan-rate	Drop-size
1, *mV*	50	Var	50	50	50
2, *μsec*	Var	2000	2000	2000	2000
3, *sec*	60	60	Var	60	60
4, *μsec*	400	400	400	400	400
5, *μsec*	Var	1600	1600	1600	1600
6, *mV*	−700	−800	−800	−700	−700
7, *mV*	−475	−400	−400	−450	−475
8, *msec*	2000	2000	2000	Var	2000
9	2	2	1 & 2	2	3
10	3	3	3	3	Var

Table 2. "Menu" parameters for lead experiments

Menu parameter number	Parameter examined						
	Half-period	Sample delay	Amplitude	Deposition time	Aperture	Scan-rate	Drop-size
1, *mV*	50	50	Var	50	50	50	50
2, *μsec*	Var	2000	2000	2000	2000	2000	2000
3, *sec*	60	60	60	Var	60	60	60
4, *μsec*	400	Var	400	400	400	400	400
5, *μsec*	Var	Var	1600	1600	Var	1600	1600
6, *mV*	−550	−550	−550	−550	−550	−550	−550
7, *mV*	−150	−150	−150	−150	−150	−150	−150
8, *msec*	2000	2000	20 00	2000	2000	Var	2000
9	4	3	4	3	4	3	3
A	3	3	3	3	3	3	Var

Aperture. Peak-heights were observed as the sample aperture was varied between 200 and 1600 μsec.

Scan-rate (5-mV step duration). The step durations were varied between 200 and 5000 msec.

Square-wave half-period. For these studies the sample aperture period was made 400 μsec shorter than the square-wave half-period.

Decay rate. To evaluate the rate of decay of the instantaneous faradaic current flow over a single half-period, a square-wave half-period of 6000 μsec was used. The transition-sample delay and sample aperture periods were adjusted so that the measured current flow was examined over nine different time intervals during the 6000-μsec half-period. The peak-height on the voltamperogram for each time interval was taken as proportional to the average value of the instantaneous faradaic current for that interval of the 6000-μsec half-period.

Calibration graphs for cadmium and lead over the concentration range from 0.1 to 1.6 ng/ml were prepared. The supporting electrolyte used was 0.05*M* potassium nitrate containing 4 drops of concentrated nitric acid per litre.

Water samples collected in polypropylene containers were acidified with 1 ml of concentrated hydrochloric acid per gallon of sample. Samples were prepared for analysis by adding 3.0 g of potassium nitrate and 4 drops of concentrated nitric acid per litre of sample.

RESULTS AND DISCUSSION

The results of the optimization of the square-wave amplitude are shown in Fig. 4. When smaller square-wave amplitudes were used, peak-heights became smaller, baselines became smoother, and resolution of adjacent peaks was improved. Figure 4 shows voltamperograms for the 10-ng/ml lead ion solution, obtained with square-wave amplitudes of 50, 25 and 10 mV. The improvement in resolution of the peak for the impurity in the lead solution, when smaller square-wave amplitudes are used, is obvious. Larger square-wave amplitudes provide greater sensitivity at the expense of poorer resolution of overlapping peaks. It should be noted that the 50-mV voltamperogram was recorded with a sensitivity-setting half of that used for the other curves.

The peak-height increases linearly with increase in deposition time, but the gain in sensitivity is achieved at the expense of longer analysis time.

Figure 5 shows the experimental results for variation of the size of the mercury drop. The instrument allows selection from four preset drop-sizes. The change in drop-size is obtained by doubling the time for which the mercury-flow control-value is held open. There should theoretically be a linear increase in current flow with increase in the surface area of the drop, but it is apparent from Fig. 5 that there is a second (and constant) factor partially controlling the surface area of the drop. This factor is an instrumental artifact and though constant for a given electrode

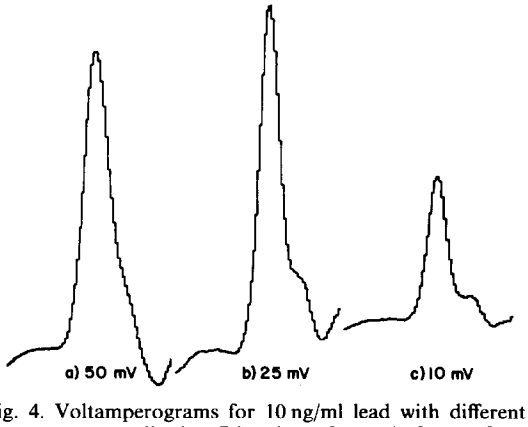

Fig. 4. Voltamperograms for 10 ng/ml lead with different square-wave amplitudes. Direction of scan is from left to right.

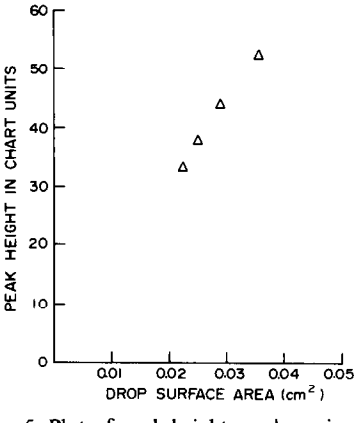

Fig. 5. Plot of peak-height *vs.* drop-size.

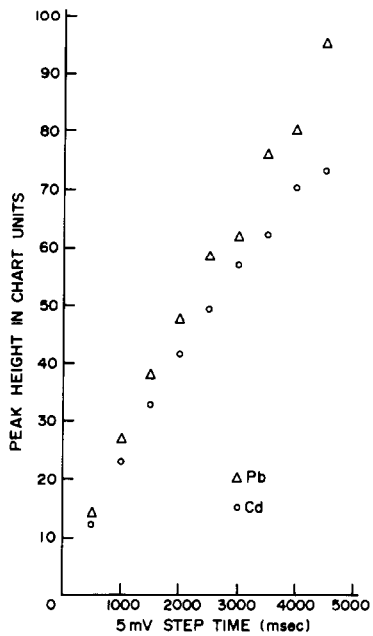

Fig. 6. Plot of peak-height *vs.* 5-mV step duration.

assembly may differ between assemblies. It is the result of the finite closure time of the mercury-flow valve, which is a significant fraction of the time that the valve is open. Stronger springs and higher voltages would materially shorten this closure time, if desired. Though the greatest sensitivity was obtained with the largest drop-size, the setting 3 (0.028 cm^2 surface area) was chosen, because the drops obtained with setting 4 did not remain attached to the HMDE for the longer analysis times.

Figure 6 shows the results from the study of the 5-mV step duration experiments. The increase in peak-height at longer step durations is caused by the increased number of square-wave transitions occurring during a single 5-mV step. A single response value is obtained for each 5-mV step. This response is derived from a gated integrator operating over the life of the 5-mV step duration. The gate on the integrator is open for integration only during the sample aperture period. An increase in the duration of the 5-mV step produces a corresponding increase in the number of sample aperture periods and accordingly increases the gate-open integration time, which hence produces an increase in response. If the current measured at each step is larger, the peak current will also be larger. This implies that the optimal conditions would use long 5-mV step durations. The disadvantage of this is that the single-analysis time would increase. A 500-mV scan would take 100 sec if the 5-mV step duration was 1000 msec. The same scan would take 500 sec with a 5-mV step duration of 5000 msec. This argument does not take into consideration the fact that there would also be some depletion of the metal from within the drop if longer times were used. A 5-mV step duration of 2000 msec was chosen as suitable for the analysis of solutions containing metals at the ng/ml level.

The results for optimization of the sample aperture period are shown in Fig. 7. The larger peak-heights at longer sample aperture periods are due to the increase in the time period over which the current flow is measured. The plot shows that for optimum measuring conditions the sample aperture period should be as long as possible. The practical optimum value of the sample aperture period is limited by the

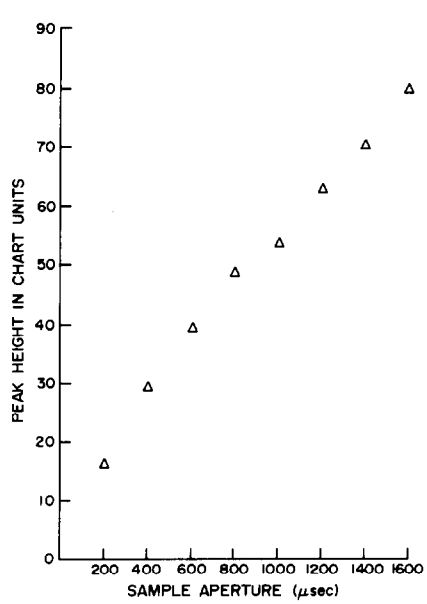

Fig. 7. Plot of peak-height *vs.* sample aperture.

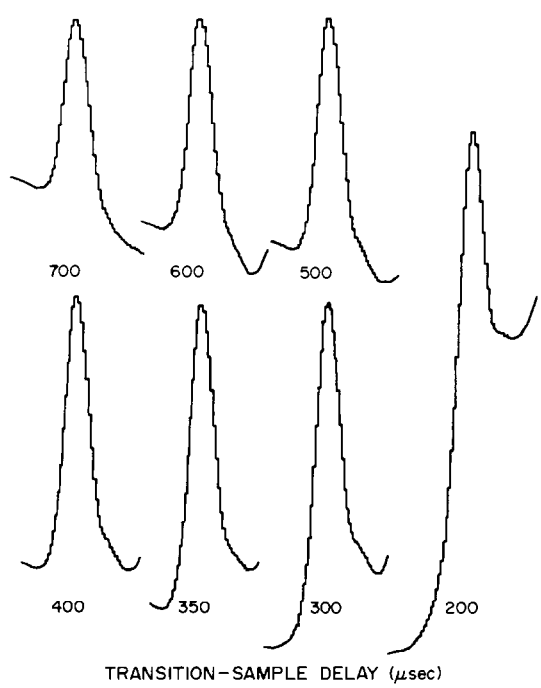

Fig. 8. Voltamperograms for lead, with various transition-sample delay periods. Direction of scan is from left to right.

transition-sample delay period and the duration of the square-wave half-period.

Figure 8 shows several voltamperograms of a 10-ng/ml lead solution, for various transition-sample delay periods. There is an increased peak-height and a more sloping baseline with decrease in the transition-sample delay period. A larger portion of the total current flow is measured at shorter transition-sample delay periods, resulting in an increase in the charging and faradaic currents composing the measured current flow. The increase in faradaic current in the measured current flow is desirable, and produces larger peak-heights when shorter transition-sample delay periods are used. However, the ratio of charging to faradaic current in the measured current flow increases at shorter transition-sample delay periods because of the faster decay of the charging current. This higher ratio of charging to faradaic current in the measured current flow produces the sloping baseline. The optimum transition-sample delay period is then one in which the slope of the baseline does not interfere with the measurement of the peak produced by the faradaic current. These criteria neglect the effects of adsorption on the current flow and select the minimum transition-sample delay period which will provide a reasonably flat baseline. A transition-sample delay period of 400 μsec was considered the most appropriate.

The results of the optimization study of the square-wave half-period are shown in Fig. 9. The data show the optimum square-wave half-period to be between 1500 and 2000 μsec. The occurrence of an optimum value indicated at least two opposing factors contributing to the shape of the curve. The data produced by the decay-rate experiment were used to identify these factors. Table 3 shows the results of several voltamperograms obtained from the same solution with a constant aperture period and square-wave half-period but with an increasing transition-sample delay. These experiments had the effect of moving the measurement window along the current decay curve for a single square-wave half-period, and thus the peak-height obtained from each experiment was proportional to a current measured during that portion of the square-wave half-period. Taken together and plotted as a function of the transition-sample delay period plus the mean of the sample aperture period, these peaks gave a curve representative of the current decay curve, of the type shown in Fig. 2. A non-linear least-squares fit of equation (4) (by the method of successive approximation with residual sum of squares[6]), to the experimental peak-heights and their median time of measurement produced numerical values for A, B, and RC in equation (4). These values are shown below in equation (5), which is the resulting expression for the measured current flow. A comparison of the experimental peak-heights for the nine time intervals, with those calculated by using equation 5, is shown in Table 3.

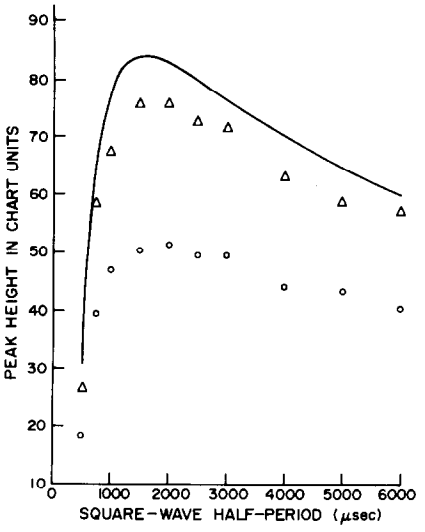

Fig. 9. Comparison of calculated and experimental peak-heights at various square-wave half-periods. △, Pb; ○, Cd; — calculated.

$$i_{T_t} = 23.9e^{-t/2110} + 1224.9t^{-1/2} \qquad (5)$$

An equation having been obtained that accurately described the current decay signal during the sampling time, it was then used to calculate the optimum square-wave half-period. When equation (5) is integrated over the sample aperture time, the value obtained will be the current produced for that time period during one square-wave half-period. Multiplying the current for one half-period by the number

Table 3. Comparison of experimental and calculated peak-heights based on decay-rate data

Time interval, μsec	Median time, μsec	Exptl. peak-ht., *chart units*	Calc. peak-ht., *chart units*
500–750	625	66.0	66.7
750–1000	875	58.0	57.2
1000–1500	1250	48.6	47.8
1500–2000	1750	39.2	39.7
2000–2500	2250	33.6	34.0
2500–3000	2750	29.6	29.8
3000–4000	3500	25.4	25.3
4000–5000	4500	21.2	21.2
5000–6000	5500	18.6	18.3

Table 4. Analysis of water supply samples

Sample	Cadmium, *ng/ml*	Lead, *ng/ml*
Well water	0.3 ± 0.05	1.5 ± 0.1
Municipal water	0	1.0 ± 0.05
Softened municipal water	0.1	0.5 ± 0.05

of half-periods occurring during a 5-mV step gives the total current for that step. This calculation was performed by a computer program that varied the value of the square-wave half-period. The 5-mV step duration period was set at 2000 msec and the transition-sample delay period at 400 μsec. Starting with a square-wave half-period of 500 μsec, equation (5) was integrated from 400 to 500 μsec. The resulting value was multiplied by 4000, which is the number of 500-μsec half-periods that occur during a 2000-msec 5-mV step to produce the peak-height value for a square-wave half-period of 500 μsec. The calculation was repeated with the square-wave half-period increased in 100-μsec steps until a value of 6000 μsec was reached, the multiplication factor being correspondingly reduced. Longer square-wave half-periods produced larger current values for one square-wave half-period, owing to the increase in the integration time of equation (5), but this was offset by the corresponding decrease in the number of half-periods occurring during a 2000-msec 5-mV step, *i.e.*, in the current multiplication factor. These are the two opposing factors that produce the optimum value of the square-wave half-period. An optimum value of 1600 μsec was calculated by the computer program. The calculated peak-heights for square-wave half-periods ranging from 500 to 6000 μsec are shown in Fig. 9, along with the experimentally determined values for lead and cadmium.

Calibration graphs were prepared for cadmium and lead over the concentration range ranging from 0.1 to 1.6 ng/ml, with a 3-min deposition period. The cadmium and lead peaks occurred at -515 mV and -330 mV respectively *vs.* a silver/silver chloride reference electrode. The data points for lead produced a line with a slope of 22.7 ± 0.5 chart units per ng/ml and a correlation coefficient of 0.9987. For cadmium the slope was 48.1 ± 0.6 chart units per ng/ml and the correlation coefficient 0.9997.

Three local water supplies were analysed; well water, municipal water, and softened municipal water. The results of the analyses are shown in Table 4. The increase in the cadmium concentration in the softened water sample is probably due to cadmium present in the sodium chloride used in the water-softening process.

The optimization experiments provided insight into the factors that produce the maximum response of the SWASV technique to trace metal ions. Adjustment of the square-wave, current measurement and drop-size parameters to their optimum settings prior to an analysis allows the analyst to obtain the maximum sensitivity from the SWASV instrument before resorting to increased deposition times to provide the required sensitivity. The result is faster sample through-put, owing to the shorter individual analysis time.

REFERENCES

1. M. S. Krause and L. Ramaley, *Anal. Chem.*, 1969, **41**, 1365.
2. J. A. Turner, J. H. Christie, M. Vukovic and R. A. Osteryoung, *ibid.*, 1977, **49**, 1904.
3. E. B. Buchanan, Jr. and W. J. Sheleski, *Talanta*, 1980, **27**, 955.
4. E. B. Buchanan, Jr. and D. D. Soleta, *ibid.*, 1982, **29**, 207.
5. A. B. Bond, *Modern Polarographic Methods in Analytical Chemistry*, p. 391. Dekker, New York, 1980.
6. J. H. Pollard, *A Handbook of Numerical and Statistical Techniques*, p. 275. Cambridge University Press, New York, 1979.

Talanta, Vol. 30, No. 7, pp. 465–470, 1983
Printed in Great Britain.

0039-9140/83 $3.00+0.00

A GROUP SEPARATION BASED ON ANION- AND CATION-EXCHANGE FROM HYDROFLUORIC ACID MEDIUM

APPLICATION TO MULTIELEMENT NEUTRON-ACTIVATION ANALYSIS OF NIOBIUM

R. CALETKA and V. KRIVAN
Sektion Analytik und Höchstreinigung, Universität Ulm, Oberer Eselsberg N-26, D-7900 Ulm, Ulm/Donau, F.R.G.

(*Received* 6 *December* 1982. *Accepted* 29 *January* 1983)

Summary—A group separation procedure for the determination of 33 elements has been developed and applied to the neutron-activation analysis of niobium. It is based on cation- and anion-exchange chromatography in HF media and separates the elements into five groups suitable for gamma spectrometry. The recoveries and their reproducibilities have been studied by the radiotracer technique. Recovery $\geqslant 95\%$ (mean deviation $\leqslant 3\%$) was obtained for all the elements tested. For a 12-hr irradiation at a thermal neutron flux of 8×10^{13} n.cm^{-2}.sec^{-1}, the limits of detection for a niobium matrix vary between 0.6 pg (for Mn) and 0.6 μg (for Fe).

In general, hydrofluoric acid is an excellent solvent for the elements of the fourth, fifth and sixth rows of the periodic table that tend to hydrolyse, polymerize or precipitate even at fairly low pH values. In hydrofluoric acid these elements form highly stable anionic complexes which are readily sorbed on strong anion-exchangers and extractable as ion-association complexes. On the other hand, hydrofluoric acid, being a moderately weak acid ($pK_a = 3.17$), facilitates the sorption of a number of other elements in cationic form on cation-exchange resins, as well as solvent extraction of their chelates.

In recent years, we have studied the behaviour of elements on anion- and cation-exchangers[1,2] and in solvent extraction with diantipyrilmethane,[3,4] dithizone and diethyldithiocarbamate.[5] These studies have permitted the development of separation procedures based on extraction and ion-exchange from hydrofluoric acid media. These separations have been used in the analysis of niobium and other refractory metals by activation with neutrons[6,7] or charged particles,[8,9] and by X-ray fluorescence spectrometry after separation of the matrix, and preconcentration.[10] They have also been used in the analysis of plant materials by X-ray fluorescence spectrometry and neutron activation.[11,12]

In the present paper, a new group separation is described, which is based on combined anion- and cation-exchange from hydrofluoric acid medium. It enables the rapid separation of at least 33 elements into 5 groups, application to neutron-activation analysis of niobium being given as an example.

EXPERIMENTAL

Samples

Samples of metallic niobium (*ca.* 100 mg) were cut with a diamond saw and etched in a mixture of hydrofluoric and nitric acids (9:1 v/v), washed with doubly distilled water, and wrapped in aluminium foil for irradiation. After irradiation, the samples were repeatedly etched, weighed and dissolved.

Standards

Standardization was done by a single comparator method using zirconium and gold for the simultaneous determination of the factors α and f,[13] and by a conventional method (involving simultaneous multielement standardization) for Co, Cu, Hf, Ir, La and U.

Irradiation

Samples and standards were irradiated simultaneously in the Karlsruhe FR-2 reactor at a thermal neutron flux of 8×10^{13} n.cm^{-2}.sec^{-1} for 12 hr. The separation was performed about 4–5 hr after the end of the irradiation.

Reagents

All reagents were of "*pro analysi*" grade. Dowex-1 × 8 and Dowex-50W × 8, both 100–200 mesh, were obtained from Fluka. The radiotracers used for investigation of the separation method were prepared by irradiating the pure metals or compounds in the Karlsruhe FR-2 reactor. The radiochemical purity of the tracers were checked by γ-ray spectrometry; simultaneous group labelling with three or four radioisotopes and counting by γ-ray spectrometry were used.

Apparatus

Plastic 2-ml syringes (without pistons) were used for making the columns, which had an active bed 45 mm in depth and 8 mm in diameter. The syringes were closed with polyethylene caps having a hole for interconnection of the columns. The columns filled with Dowex-1 resin had an active bed 100 × 8 mm and were made from plastic pipettes closed with Luer caps. The columns for the selective separation of copper had an active bed of 45 × 8 mm and were filled with Dowex-1 × 8 in the Cu(I)-form, made by reducing copper(II) chloride solution in 2*M* hydrochloric acid with sulphur dioxide and mixing it with Dowex-1 (about 0.2 meq per g of wet resin); the resin was then placed in the column, washed, and kept in distilled water.

A peristaltic pump (Ismatec ip-4, Zürich) was used in the elution, several column systems being operated simultaneously.

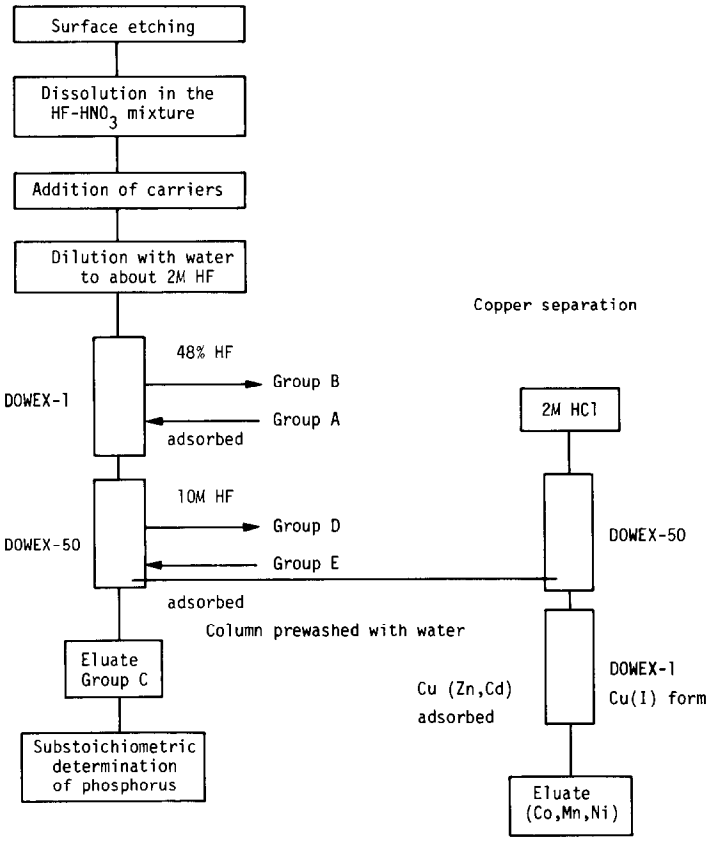

Fig. 1

The fractions obtained after group separation were counted with a high-resolution γ-ray spectrometer consisting of an Ortec Ge(Li)-detector and a Canberra "Series 80" multichannel analyser. The energy resolution of the system was 0.9 keV FWHM for the 1332 keV γ-ray of ^{60}Co. The counting time varied from about 600 to 10^4 sec, depending on the activity of the sample.

Chemical procedure

Figure 1 gives the flow-chart of the radiochemical procedure. After surface decontamination and weighing, the irradiated sample was placed in a 20-ml disposable syringe which was then closed with its piston. The sample was dissolved in 0.5 ml of 48% hydrofluoric acid and a minimum of 63% nitric acid (about 0.3 ml) as reported earlier.[4] Immediately after dissolution, for each indicator radionuclide 50–100 μg of inactive element was added as carrier, the solution was diluted with distilled water to give 8–10 ml total volume (and hydrofluoric acid concentration $\sim 2M$) and loaded into the column system. The elution was done with 15 ml of $2M$ hydrofluoric acid at a flow-rate of 0.5–0.7 ml/min. The columns were then decoupled and further eluted with 25 ml of concentrated hydrofluoric acid (for the Dowex-1 column) and $10M$ hydrofluoric acid (for the Dowex-50 column). For the separation of copper, the cation-exchange column was prewashed with water and a new Dowex-1 column in the Cu(I)-form was connected to it in the sequence shown in Fig. 1. A volume of 25 ml of $2M$ hydrochloric acid was passed through these two columns, whereby copper (together with zinc and cadmium) was left on the lower column, while cobalt, manganese and nickel were eluted.

RESULTS AND DISCUSSION

Radiochemical procedure

A survey of the sorption behaviour of the elements on Dowex-1 and Dowex-50 resins from hydrofluoric acid of various concentrations is given in Table 1. This summary was compiled from previously published data;[1,2,14–17] the behaviour of Np and Te was studied in the present work. As no element referred to in Table 1 is sorbed on both Dowex-1 and Dowex-50 from $2M$ hydrofluoric acid, a system consisting of coupled columns of the two exchangers can be used for the first separation, into three groups, as follows.

(1) Elements which remain on the Dowex-1. This group comprises weakly hydrolysable elements which form stable negatively charged fluoride complexes.

(2) Elements retained on the Dowex-50. This group includes the alkali, alkaline-earth and rare-earth metals, yttrium and bivalent transition metals.

(3) Elements passing through both columns. Many tervalent metal ions, Np(V), Se(IV) and PO_4^{3-} ions belong to this group.

The columns are then eluted for further separation. In the treatment of the Dowex-1 column with concentrated hydrofluoric acid, all elements except Nb, Ta,

Table 1. Summary of ion-exchange behaviour of elements in hydrofluoric acid*

Group	Element	Dowex-1 × 3		Dowex-50 × 8	
		2 ± 1*M* HF	48% HF	2 ± 1*M* HF	10*M* HF
A	Nb, Ta, W, Sb(V), As(V)†	●	●	○	○
B	Be, Sc, Zr, Hf, Ti, Sn(IV), Te(IV), V(V), Pa, Mo, Re(VII)	●	○	○	○
C	Al, Cr, Fe(III), Ga, In,‡ Bi(III),‡ As(III), Sb(III). V(IV), Se(IV), PO_4^{3-}, Np(V)	○	○	○	○
D	Na, K, Rb, Cs, Mg, (Eu)§	○	○	●	○
E	Ag, Cd, Co, Cu, Mn, Ni, Pb, Zn, Ca, Sr, Ba, La, Y	○	○	●	●

*Black circles indicate sorption; open circles indicate that the elements will be found in the eluate.
†Partial elution (about 25–30%) of arsenic with 48% HF was found.
‡For the elution of In and Bi 4*M* HF or larger volumes of 2*M* HF must be used.[2]
§About 88% of europium is eluted with 10*M* HF.

W and Sb(V) are rapidly eluted. The alkali metals and magnesium can be separated from bivalent transition elements by washing the Dowex-50 column with 10*M* hydrofluoric acid, the first group being eluted and the second remaining on the column. This further subdivision results in the five groups (A–E) shown in Fig. 1 and Table 1.

The yield of each element in the complete separation procedure was determined by adding the necessary radiotracers during dissolution of the inactive niobium matrix. Only those elements detectable in refractory metals by neutron-activation analysis were tested. The results obtained from at least three replicate experiments are given in Table 2.

Group A. The retention of Nb (matrix), Ta and W on Dowex-1 was quantitative; the decontamination factors measured for these elements, the radionuclides of which represent the main radioactivity of neutron-irradiated niobium, were higher than 10^6. None of these elements can be eluted with 25 ml of concentrated hydrofluoric acid. On further elution, traces of tungsten appear in the eluate. The elution of tungsten depends on the extent of saturation of the column, *i.e.*, on the amount of sample. Antimony(V), mercury and gold are also retained on Dowex-1 when concentrated hydrofluoric acid is used as eluent, but because of the high activity of the long-lived radionuclides of Ta and W, their determination in niobium by direct counting of the Dowex-1 column (or after elution) is impossible. Arsenic(V) is also retained on Dowex-1 from dilute hydrofluoric acid, but about 30% is eluted with the concentrated acid.

Group B. The uptake of all the elements of this group on the anion-exchanger is quantitative (≥99.5%). Elution with 25 ml of concentrated hydrofluoric acid results in 87–99.8% of the radioactivities being transferred to the eluate. The only elements which are not separated satisfactorily are molybdenum and rhenium. On further elution, tungsten gradually appears in the eluate, making the determination of the elements of this group difficult. To avoid this, a stepwise elution with collection of 1-ml fractions is recommended. For measurement, only those fractions free from tungsten activity are used. In this way, yields of 95 ± 3% can be obtained for Mo and Re.

Group C. The elements of this group are sorbed on neither column. The yields for all the elements in this group were better than 95%. Anomalous ion-exchange behaviour was observed for chromium, which forms three different complexes in hydrofluoric

Table 2. Yields and detection limits

Element	Yield, %	Detection limit, *ng*
Fraction A (Dowex-1)		
Nb (matrix)	≥99.9	—
Ta	≥99.9	*
W	≥99.9	*
Sb	96.2 ± 1.2	—
Hg	99.8 ± 0.1	—
Au	99.9 ± 0.1	—
Fraction B (48% HF)		
Hf	99.8 ± 0.1	0.4
Zr	99.8 ± 0.1	10
Th (^{233}Pa)	99.7 ± 0.2	0.3
Mo	90–95	25
Re	87–92	0.02
Sn	95.7 ± 2.1	10
Sc	97.3 ± 1.2	0.05
Te	98.1 ± 0.8	—
Fraction C (2*M* HF)		
Fe	99.0 ± 0.3	10
Se	99.2 ± 0.3	5
Cr	98.6 ± 0.8	3
U (^{239}Np)	96.1 ± 1.7	0.005
Ga	97.3 ± 1.3	—
Fraction D (10*M* HF)		
Na	99.6 ± 0.2	0.05
K	99.5 ± 0.3	0.5
Rb	99.0 ± 0.6	30
Cs	98.5 ± 1.2	10
Eu	~88	—
Fraction E (Dowex-50)		
Ag	99.9 ± 0.1	0.05
Cd	97.8 ± 0.6	1
Co	99.5 ± 0.3	0.2
Cu	99.8 ± 0.1	0.01
La	95.6 ± 2.2	0.02
Mn	99.5 ± 0.2	0.006
Ni	98.3 ± 1.1	10
Zn	99.2 ± 0.4	50
Y	97.8 ± 1.3	—

*Determined by instrumental neutron-activation analysis.

acid.[2] Since 98.6% of the chromium was found in the eluate, only non-sorbable species are formed under the given experimental conditions. However, prolonged standing of the solute at room temperature before the separation causes a decrease in the yield. After the γ-radioactivity of the eluate has been measured, phosphorus can be selectively separated. The application of substoichiometric extraction of molydophosphate with tetraphenylarsonium chloride for this purpose was reported earlier.[17]

Group D. The elution of alkali metals from the cation-exchanger column with 10*M* hydrofluoric acid is nearly quantitative. This elution should be done only when relatively high radioactivity due to sodium or potassium is encountered.

Group E. A nearly quantitative uptake was exhibited by all the elements of this group. If necessary, the elements can be eluted with hydrochloric or nitric acid.[18,19] The elution of copper merits special attention. The 511-keV radiation of ^{64}Cu can interfere with the annihilation radiation of the other radionuclides, and the 1345-keV radiation has an intensity of only 0.48%. Therefore, a selective separation of copper is required. The isotopic exchange between Cu(II) in the 2*M* hydrochloric acid eluate and Cu(I) fixed on an anion-exchange resin (recommended by Malvano *et al.*[20]) is used for this purpose. In addition to copper, any cadmium and zinc are also retained, while cobalt, manganese and nickel remain in solution. The total yield for copper is better than 97%. The separation of copper and cobalt on a Dowex-1 × 8 column (connected to the Dowex-50 column) by elution with 8*M* hydrochloric acid was not successful.

The alkaline-earth and rare-earth metals and yttrium were not studied in more detail, but can be quantitively sorbed on Dowex-50 from 10*M* hydrofluoric acid, as described previously.[2] Only the heavier lanthanides are eluted (partially) with 10*M* hydrofluoric acid, *e.g.*, about 88% of europium. Neirinckx *et al.*[21] found that the lanthanides (La, Ce, Sm and Eu) are sorbed on Dowex-1 from 1*M* hydrofluoric acid and are not eluted even by 22*M* hydrofluoric acid. The discrepancy between their results and ours can be explained by assuming the precipitation of insoluble fluorides of rare earths and thorium, used as carriers by Neirinckx *et al.* (1 mg for each element in 15 ml of 1*M* hydrofluoric acid).

The fact that Nb, Ta and W are strongly retained by an anion-exchanger even in concentrated hydrofluoric acid, while Hf, Mo, Re, Pa (from Th), Sc, Sn, Zr and almost all other cations are not, is the outstanding feature of this separation technique when applied to the analysis of niobium (and probably also of tantalum and tungsten). In the experiments described above, the solution to be separated was loaded onto a two-stage column with the anion-exchanger at the top. As is evident from the summary in Table 1, the columns could also be used in reverse order, but in model experiments with irradiated niobium samples, it was found that if this arrangement is used, the decontamination factors for the radionuclides responsible for the main radioactivity (Nb, Ta and W) are decreased by a factor of up to 100. For analysis of some matrices, however, the sequence of Dowex-50 followed by Dowex-1 could be advantageous. With this arrangement, gold, mercury, the platinum metals and some other elements remain sorbed on the first (cation-exchanger) column and can be determined.

In the preliminary experiments with matrices labelled *in situ* by irradiation, the sorption behaviour of some elements which occur in two or more oxidation states, *e.g.*, As, Re, Ir, Sb, was found to differ from that obtained in experiments involving the conventional labelling by addition of radiotracers. In the irradiation experiments, up to 60% of As, 15% of RE, 15% of IR and 10% of Sb were found along with group C. These apparent discrepancies are due to the formation of lower oxidation states of these elements during dissolution of the metals, in spite of the use of oxidative conditions. The stable higher oxidation states necessary for quantitative recovery can be achieved either by evaporation almost to dryness, or by oxidation (with hydrogen peroxide, chlorine or bromine).

Strongly reducing conditions exist during the dissolution of metals such as Al, Hf, Ti or Zr in pure hydrofluoric acid. Under these conditions, iron and tin are present in the bivalent form and are retained on cation-exchangers. Arsenic and a fraction of the antimony are in the tervalent form, pass through both columns, and are found along with group C. Under these conditions neptunium remains mainly on the anion-exchanger. Elements which are more electropositive than the matrix, and are present as impurities in the sample or are added as carriers, may be deposited in elemental form during the etching or dissolution. Some examples of this behaviour have already been discussed.[4] From these results it can be concluded that in some cases model experiments using the conventional tracer technique (addition of a suitable radioisotope to the system investigated) do not provide accurate estimates of yields, and therefore *in-situ* labelling of doped materials should be used.

Analysis of niobium samples

The procedures described was applied to the analysis of niobium of various grades of purity. The results obtained are summarized in Table 3. Niobium types Nb-P, Nb-ES and Nb-WCT are commercially available. Niobium-WCT was prepared by remelting under vacuum in an electron-beam furnace and was used at the Max-Planck-Institut für Metallforschung, Stuttgart, for further purification to yield Nb-R-1 and Nb-R-2.[22] The results obtained for Nb-P and Nb-P and Nb-WCT in this work are compared with those obtained by the technique developed earlier in our laboratory.[7] The last three materials are of the

Table 3. Contents of trace elements in niobium of different grades of purity (weight per g of sample)

Element	Nb-P*	Nb-P	Nb-WCT*	Nb-WCT	Nb-ES	Nb-R1	Nb-R2
Co	42 ± 1.5 μg	33.2 ± 0.5 μg	<0.2 ng	<1.8 ng	5.9 ± 0.2 ng	<2 ng	2.2 ± 0.8 ng
Cr	10.8 ± 1.5 μg	15.8 ± 0.5 μg	5.3 ± 1.5 μg	6.0 ± 0.5 ng	37.5 ± 2.5 ng	30 ± 8 ng	690 ± 10 ng
Cu	0.54 ± 0.06 μg	0.68 ± 0.12 μg	55 ± 11 ng	0.32 ± 0.01 μg	69 ± 7 ng	180 ± 25 ng	6 ± 2 ng
Fe	130 ± 12 μg	120 ± 10 μg	<60 ng	<0.7 μg	0.92 ± 0.08 μg	0.87 ± 0.12 μg	8.15 ± 0.78 μg
Hf	0.4 ± 0.1 μg	0.4 ± 0.05 μg	15.0 ± 2.2 ng	12 ± 2 ng	10.7 ± 1.0 μg	<5 ng	<5 ng
K	<10 ng	<85 ng	<4 ng	<10 ng	<10 ng	215 ± 76 ng	0.56 ± 0.18 μg
						192 ± 35 ng§	0.74 ± 0.40 μg§
Mn	—	—	31 ± 5 ng	18.5 ± 4.0 ng	0.15 ± 0.07 ng	0.28 ± 0.09 ng	4.4 ± 0.3 ng
							4.8 ± 1.6 ng§
Mo	191 ± 5 μg	164 ± 11 μg	2.4 ± 0.4 ng	0.75 ± 0.22 μg	2.9 ± 0.4 μg	170 ± 30 ng	32 ± 8 ng
Na	38 ± 4 ng	20.2 ± 0.4 ng	11.5 ± 1.1 ng	15 ± 3 ng	15.1 ± 0.8 ng	29.7 ± 2.3 ng	180 ± 25 ng
						33.3 ± 3.0 ng§	171 ± 48 ng§
Ni	66 ± 6 μg	70 ± 4 μg	<0.1 μg	<0.1 μg	<40 ng	<0.1 μg	<0.1 μg
P†	—	46.6 ± 5.8 μg	—	60.8 ± 7.5 ng	1.8 ± 0.2	23.8 ± 15.2 ng	8.2 ± 2.6 ng
Re	—	7.9 ± 1.1 μg	—	1.5 ± 0.4 ng	30 ± 5 ng	<0.3 ng	<0.3 ng
Se	0.32 ± 0.08 μg	0.40 ± 0.08 μg	86 ± 8 ng	53 ± 8 ng	0.41 ± 0.08 μg	43 ± 12 ng	34 ± 5 ng
Sn	33.3 ± 2.8 μg	34.3 ± 1.8 μg	0.23 ± 0.04 μg	0.25 ± 0.05 μg	—	85 ± 15 ng	—
Ta	0.8%	3730 ± 20 μg§	163 μg	147 ± 6 μg§	900 ± 28 ng§	5.4 ± 0.2 μg§	2.30 ± 0.15 μg§
U	—	10.5 ± 1.5 μg	—	0.17 ± 0.03 ng	20.5 ± 1.5 ng	<0.5 ng	<0.5 ng
W	980 μg	928 ± 10 μg§	7 ± 1 μg	6.8 ± 0.3 μg§	115 ± 5 μg§	122 ± 15 ng§	38 ± 9 ng§
Zr	2.08 ± 0.12 μg	2.2 ± 0.3 μg	<0.3 μg	<1 μg	21 ± 2 μg	<1 μg	<1 μg

*From reference 7.
†From reference 17.
§Determined by instrumental neutron-activation analysis.

same origin as those used in that work,[7] but from a different batch.

The results given in Table 3 were obtained by using gold as the standard. Comparison with results obtained by using multielement standards shows that the difference is only $\pm 5\%$, which is less than the inhomogeneity of the samples analysed. Limits of detection which can be obtained in analysis of 100 mg of high-purity niobium are listed in Table 2.

Acknowledgements—Financial assistance was provided by the Bundesministerium für Forschung und Technologie, Bonn. The authors would like to thank the Institut für Radiochemie, Kernforschungszentrum Karlsruhe, for making available all irradiation facilities, and Dr. K. Schulze for supplying the high-purity niobium samples. Thanks are also due to Mr. C. Vorwalter for his technical assistance.

REFERENCES

1. W. G. Faix, R. Caletka and V. Krivan, *Anal. Chem.*, 1981, **53,** 1719.
2. R. Caletka and V. Krivan, *Talanta*, 1983, **30,** 543.
3. R. Caletka, *J. Inorg. Nucl. Chem.*, 1981, **43,** 1619.
4. R. Caletka and V. Krivan, *Z. Anal. Chem.*, 1982, **313,** 125.
5. *Idem, ibid.*, 1982, **311,** 177.
6. W. G. Faix, R. Caletka and V. Krivan, *Anal. Chem.*, 1981, **53,** 1594.
7. R. Caletka, W. G. Faix and V. Krivan, *J. Radioanal. Chem*, 1982, **72,** 109.
8. C. S. Sastri and V. Krivan, *Anal. Chim. Acta*, 1982, **141,** 399.
9. C. S. Sastri, R. Caletka and V. Krivan, *J. Radioanal. Chem.*, 1982, **70,** 273.
10. H. Knote and V. Krivan, *Anal. Chem.*, 1982, **54,** 1858.
11. H. F. Haas, V. Krivan and H. M. Ortner, *Anal. Chim. Acta*, in the press.
12. H. F. Haas and V. Krivan, *Z. Anal. Chem.*, in the press.
13. A. Simonits, F. De Corte, L. Moens and J. Hoste, *J. Radioanal. Chem.*, 1982, **72,** 209.
14. J. P. Faris, *Anal. Chem.*, 1960, **32,** 520.
15. T. A. Farraro, *Talanta*, 1968, **15,** 923.
16. *Idem, ibid.*, 1969, **16,** 669.
17. R. Caletka, C. Vorwalter and V. Krivan, *Anal. Chim. Acta*, 1982, **141,** 393.
18. F. Nelson, T. Murase and K. A. Kraus, *J. Chromatog.*, 1964, **13,** 503.
19. F. W. Strelow, R. Rethemeyer and C. J. C. Bothme, *Anal. Chem.*, 1965, **37,** 106.
20. R. Malvano, P. Grosso and M. Zanardi, *Anal. Chim. Acta*, 1968, **41,** 251.
21. R. Neirinckx, F. Adams and J. Hoste, *ibid.*, 1969, **46,** 165.
22. K. K. Schulze, *J. Met.*, 1981, **33,** 33.

Talanta, Vol. 30, No. 7, pp. 471–474, 1983
Printed in Great Britain

0039-9140/83 $3.00+0.00
Pergamon Press Ltd

APPLICATION OF CELLULOSE ANION-EXCHANGERS TO SEPARATION OF PALLADIUM FROM PLATINUM OR IRIDIUM WITH GLYCINE AS COMPLEXING AGENT AND ATOMIC-ABSORPTION SPECTROMETRY FOR DETECTION

KRYSTYNA BRAJTER and KRYSTYNA SŁONAWSKA
Department of Chemistry, University of Warsaw, Warsaw, Poland

(*Received* 27 *August* 1982. *Revised* 11 *January* 1983. *Accepted* 21 *January* 1983)

Summary—The use of glycine as complexing agent for chromatographic separation of palladium from platinum, or palladium from iridium, on cellulose anion-exchangers has been investigated and found possible over a wide range of concentration ratios. The method can be used for analysis of Pd–Ir alloys. The nature of the complexes taking part in the ion-exchange has been identified.

The great similarity in the properties of certain platinum metals necessitates preliminary separation before their determination at trace levels,[1-4] even if a highly selective method such as atomic-absorption spectrometry (AAS) with electrothermal excitation is used, especially when some of the metals are present in much larger amount than the others.[5-7]

The present work establishes conditions for separating large amounts of palladium from small amounts of platinum or iridium by ion-exchange, before determination by AAS.

The cellulose ion-exchangers, Cellex D and Cellex T, were used, since their low capacity and affinity for platinum-metal chloro-complexes are particularly useful for separation of platinum metals.[8-10] Glycine is used as complexing agent to improve the selectivity.

EXPERIMENTAL

Exchangers

The cellulose ion-exchangers DEAE (diethylaminoethylcellulose) and TEAE (triethylaminocellulose), supplied by Bio-Rad Laboratories as Cellex D and Cellex T, were used. The capacities were 0.88 meq/g for Cellex D and 0.74 meq/g for Cellex T (elemental analysis indicated capacities of 0.80 and 0.69 meq/g, respectively). The ion-exchangers were used in the chloride or hydroxide form. The columns were 25 cm long, 9.8 mm in bore, and had Rotaflo TF 12/Cl/13 stopcocks.

The batch-type experiments showed that Cellex T gave slightly better differentiation between the platinum metals, so Cellex T was preferred for the column work.

Solutions

Solutions of Pt(IV) of definite concentration were obtained by diluting a solution of H_2PtCl_6 containing 14.14% of platinum, and standardized by precipitation of the ammonium salt.[12] The palladium solution was prepared by dissolving $PdCl_2$ in 10 ml of concentrated hydrochloric acid, evaporating to low bulk and diluting; it was standardized gravimetrically with dimethylglyoxime.[13] The iridium solution was obtained by diluting a standard solution of H_2IrCl_6 containing 3.42% of iridium. Rhodium(III) solution was obtained by dissolving $RhCl_3 \cdot 3H_2O$ in 10 ml of concentrated hydrochloric acid, evaporating to low bulk and diluting; it was standardized gravimetrically with thionalide.[14]

Determination of metal-ion retention (batch method)

The ion-exchanger (200 mg) was mixed with 20 ml of metal ion solution (Pt $2.1 \times 10^{-4}M$, Pd $2.3 \times 10^{-4}M$, Ir $2.1 \times 10^{-4}M$, Rh $2.5 \times 10^{-4}M$), the test solution (metal ion + complexing agent) being adjusted to the desired pH with sodium hydroxide solution after addition of the exchanger. The mixture was shaken for 24 hr, then the concentration of metal ion in the solution was measured by graphite-furnace AAS (Perkin–Elmer 300 spectrophotometer and HGA-72 furnace). The conditions of determination are collected in Table 1. To eliminate the effect of background on absorbance, blank tests were run.

Column separation

A 5-ml portion of solution containing similar amounts of the metal ions (as chloro-complexes) at pH 1–2 was added to a column of 1.2 g of Cellex T in chloride form (bed height 12.5 cm), and the metal ions retained were eluted with the following eluents (at a flow-rate of 0.7 ml/min), 10-ml fractions being collected.

For Pd–Pt separation: Pd—80 ml of $0.01M$ glycine (pH 6.4); Pt—100 ml of $0.01M$ glycine (pH 13.0).

For Pd–Ir separation: Pd—80 ml of $0.01M$ glycine (pH 6.4); Ir—150 ml of $1.5M$ hydrochloric acid/$0.01M$ hydroxylamine.

Larger amounts of resin were used when the metals were present in very dissimilar amounts.

Table 1. Conditions for determination of Pt, Pd and Ir by AAS

Element	Wavelength, *nm*	Band-width, *Å*	Sample, *μl*
Pt	266.0	7	20
	273.4	2	10, 20
Pd	244.7	2	10, 20
	340.4	2	20
Ir	264.0	7	10, 20
Rh	340.3	2	10, 20
	351.0	2	10, 20

When smaller amounts of resin were used (*e.g.*, 0.6–0.8 g of Cellex T), Pd(II) could be eluted with 80 ml of 0.01*M* glycine (pH 6.4), and Pt(IV) with 50 ml of 0.01*M* glycine (pH 13.0), at a flow-rate of 1 ml/min.

Analysis of Pd–Ir alloy

A weighed sample of the alloy (0.1159 g) was dissolved in *aqua regia* and the solution evaporated to dryness. The residue was dissolved in 5 ml of 0.1*M* hydrochloric acid, transferred to a 50-ml standard flask and made up to volume; 5 ml of this solution were introduced into a colum filled with Cellex T in chloride form. Palladium and iridium were eluted as described above.

RESULTS AND DISCUSSION

Glycine is used in this work to alter the affinity of Pt(IV), Pd(II), Ir(IV), Ir(III) and Rh(III) for Cellex D and Cellex T in their chloride and hydroxide forms. Its effect is illustrated in Figs. 1 and 2. The results obtained earlier[6] for Pd(II) and Pt(IV) are also used in Fig. 1. In the batch experiments a constant 1:100 molar ratio of metal to ligand was maintained and the amount of metal ion was 3–5% of the ion-exchanger capacity.

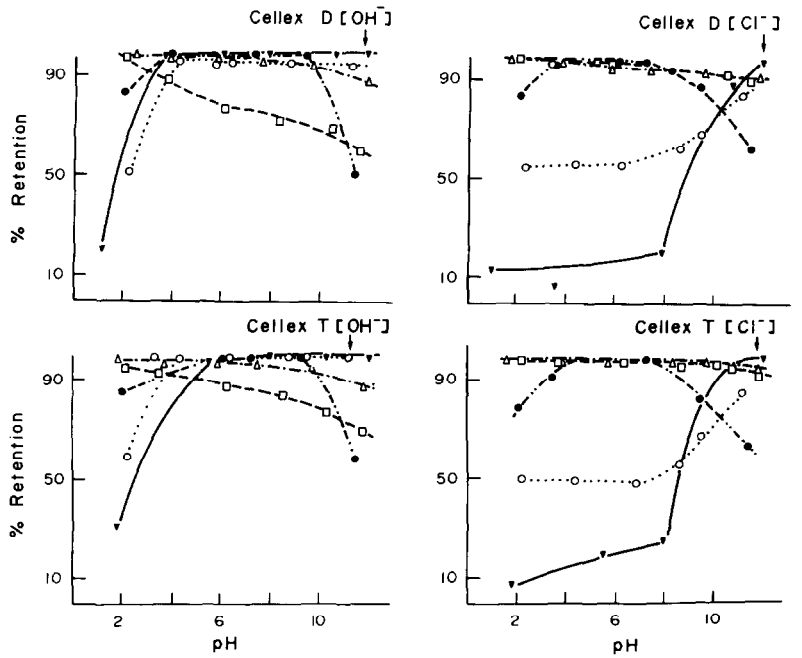

Fig. 1. Retention of platinum-metal ions in absence of organic ligand, as a function of pH, □--□, Pt(IV); △—·△, Pd(II); ●···●, Ir(IV); ○···○, Ir(III); ▼——▼, Rh(III).

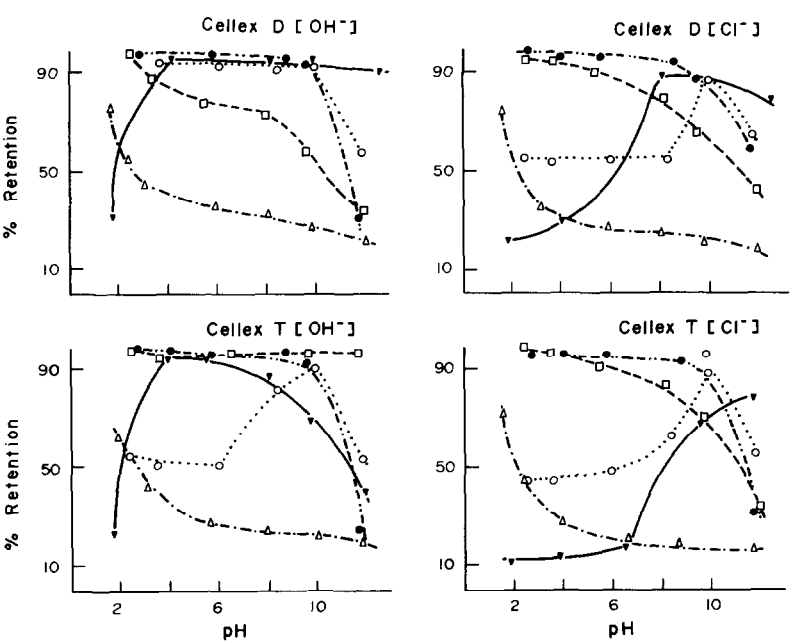

Fig. 2. Retention of platinum-metal ions in presence of glycine, as a function of pH. Symbols as in Fig. 1.

The affinity is expressed in terms of the fraction of added metal that is retained on the resin. From Fig. 1, the affinity of the chloro-complexes of Pd(II), Pt(IV), Ir(IV) and Ir(III) is too similar for them to be separated. Figure 2 shows the effect of adding glycine, which considerably decreases the affinity of Pd(II) for the exchangers, over a wide pH range.

The retention of Pt(IV) and Ir(III) is also lowered by the presence of hydroxylamine, especially at high pH, but not as much as that of Pd(II). There is not much change in the retention of Ir(IV). These conclusions from the batch studies are confirmed by the column work. The batch studies show that the difference in retention between Pd(II) and Ir(IV) or between Pd(II) and Pt(IV) is the greatest at about pH 6. A glycine solution at pH 6.4 gives quantitative column separation of Pd(II) from Ir(IV) or Pt(IV); Figs. 3–5. This pH is chosen because it is the pH of 0.01*M* glycine solution. Iridium is eluted with a solution of hydrochloric acid, glycine and hydroxylamine [to reduce Ir(IV) to Ir(III)]. Alternatively

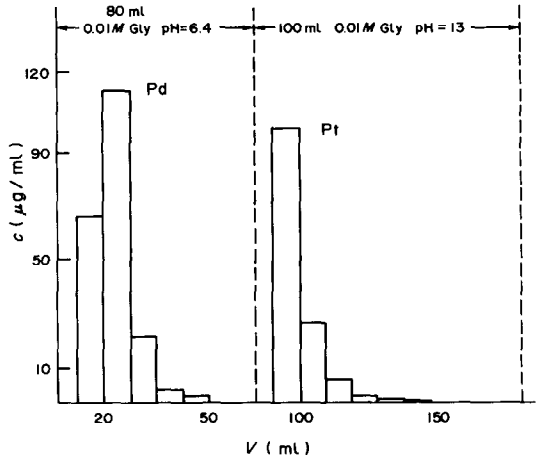

Fig. 3. Elution curves of Pd(II) and Pt(IV) on Cellex T in chloride form.

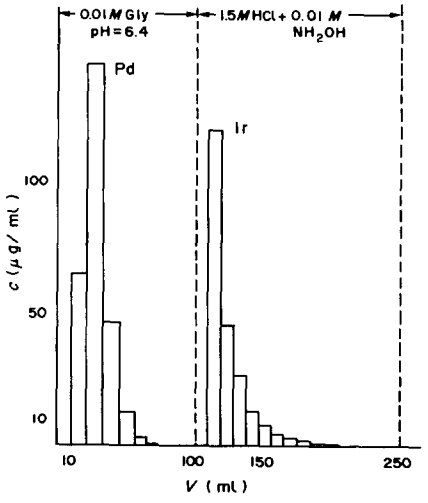

Fig. 4. Elution curves of Pd(II) and Ir(IV) on Cellex T. Ir eluted with HCl/hydroxylamine solution.

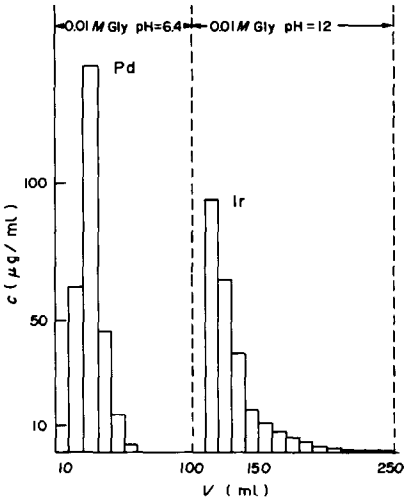

Fig. 5. Elution curves of Pd(II) and Ir(IV) on Cellex T. Ir eluted with 0.01*M* glycine at pH 12.0.

Ir(IV) can be eluted quantitatively with 0.01*M* glycine at pH 12.0. Both eluents gave the same shape of elution curve for iridium were observed (Figs 4 and 5). Platinum is eluted with 0.01*M* glycine at pH 13.0. Some results for separation of these pairs of platinum metals are shown in Tables 2 and 3.

These conditions were worked out for separation of approximately equal weights of the two metals, but were found to be equally suitable for much wider weight ratios, *e.g.*, 300:1 ratio of iridium to palladium or 7500:1 ratio of palladium to platinum. Hence it should be possible to determine as little as 0.013% of platinum in palladium. The Pd(II)–Ir(IV) separation has been applied to the analysis of a Pd–Ir alloy [Pd 98%, Ir 2%; found: Pd 97.3 ± 1.1%, Ir 1.95 ± 0.07% (95% confidence limits)].

Ion-exchange on the macro scale is rather time-consuming, so we decided to shorten the method by

Table 2. Results of separation of Pd(II) from Pt(IV) on Cellex T (Cl^-)

Taken, *mg*		Found,* *mg*	
Pd	Pt	Pd	Pt
2.39	2.00	2.36–2.38	1.96–1.99
2.39	3.74	2.33–2.39	3.67–3.73
1.20	3.74	1.17–1.21	3.65–3.73
0.10	5.61	0.097–0.100	5.57–5.60

*Range of four determinations.

Table 3. Results of separation of Pd(II) from Ir(IV) on Cellex T (Cl^-)

Taken, *mg*		Found,* *mg*	
Pd	Ir	Pd	Ir
2.39	1.85	2.36–2.38	1.82–1.84
2.39	0.93	2.36–2.38	0.88–0.91
5.99	0.93	5.89–5.94	0.89–0.92
1.20	3.70	1.16–1.21	3.65–3.69
12.0	0.16	11.79–11.86	0.16

*Range of four determinations.

Table 4. The effect of bed-height (weight of resin) on amount of Ir(IV) found in the Pd(II) fraction

Taken, *mg*		Cellex T,	Bed-height,	Ir in Pd,
Pd	Ir	*g*	*cm*	%
30.0	0.16	1.2	12.5	2.9
		1.4	15.0	1.5
		1.5	16.5	0.5
		1.6	19.0	0
60.0	0.16	1.2	12.5	4.8
		1.4	15.0	3.2
		1.5	16.5	2.4
		1.6	19.0	1.5
		1.8	21.5	0.8
		1.9	23.0	0

Table 5. Results of separation of Pd(II) from Pt(IV) on Cellex T (Cl^-)

Ion-exchanger,	Taken, *mg*		Found,* *mg*	
g	Pd	Pt	Pd	Pt
1.4	30.0	0.18	28.9–29.4	0.17–0.18
1.7	60.0	0.18	59.1–59.8	0.17–0.18
0.5	6.0	0.04	5.9–6.0	0.038–0.040
0.6	30.0	0.04	29.0–29.6	0.039–0.040
0.6	60.0	0.04	58.9–59.8	0.039–0.040
0.8	300.0	0.04	289–297	0.039–0.040

*Range for four determinations.

operating on the micro scale. The amounts of platinum metals suitable for the work were limited by the sensitivity of AAS as the detection method. If only small amounts of the strongly retained platinum metals are present, a shorter column can be used. The results obtained are shown in Tables 4 and 5. It appears that the separation of 0.16 mg of iridium from over 300 times as much palladium needs a bed height of 23 cm. Separation of 0.04 mg of platinum from 300 mg of palladium needs a bed height of only about 8 cm (0.8 g of ion-exchanger). The analysis time is then less than 2 hr.

An important limitation is set by the effect of palladium[5,6] on the AAS signals for platinum and iridium (Fig. 6).

From the results obtained, conclusions may be drawn as to the nature of the complexes taking part in the ion-exchange process.

The linear relation (zero slope) found between log K_d and log $[L]$ points to the presence of an uncharged palladium complex, most probably $Pd(glyc)_2$, already reported in the literature.[15] On the other hand, the Ir(IV) and Pt(IV) complexes (slope -1) are similarly found to have a single negative charge. This may suggest the presence of complexes such as $[Pt(glyc)_2OH]^-$ and $[Ir(glyc)_3Cl]^-$, assuming there is reduction of Pt(IV) to Pt(II) and of Ir(IV) to Ir(III).

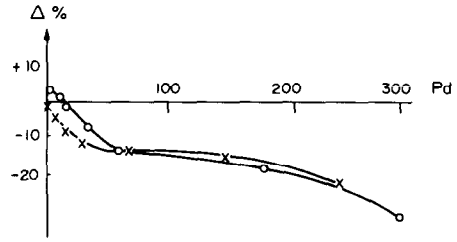

Fig. 6. Effect of Pd on the AAS signals of Ir (○) and Pt (×); expressed as relative change in signal (△%).

Such reductions have been reported[16,17] for Pt(IV). The batch studies showed that there was lower retention of iridium in presence of glycine when hydroxylamine was added as a reducing agent to keep the iridium in the Ir(III) oxidation state. This may possibly indicate formation of mixed-ligand complexes.

We have also made spectral studies of solutions containing the platinum metals and glycine at various pH values, with compositions corresponding to those in the batch studies. The positions of the absorbance maxima, as compared with the corresponding literature data, agreed with the chromatographic results concerning the charges and assumed compositions of the complexes. No kinetic problems seemed to arise, even with iridium, which is known to form inert complexes. Presumably this was because of the pH ranges used for the chromatography.

REFERENCES

1. W. M. MacNevin and W. B. Crummett, *Anal. Chem.*, 1953, **25,** 1628.
2. *Idem, Anal. Chim. Acta*, 1954, **10,** 323.
3. F. von S. Toerien and M. Levin, *J. South Afr. Chem. Inst.*, 1974, **27,** 87.
4. *Idem, ibid.*, 1974, **27,** 91.
5. G. Everett, *Analyst*, 1976, **101,** 348.
6. E. Adriaenssens and P. Knoop, *Anal. Chim. Acta*, 1973, **68,** 37.
7. K. Brajter, K. Słonawska and Z. Vorbrodt, *Chem. Anal. Warsaw*, 1982, **27,** 239.
8. K. Brajter and B. Gankowski, *Talanta*, 1977, **24,** 761.
9. K. Brajter and K. Słanawska, *Chem. Anal. Warsaw*, 1979, **24,** 273.
10. *Idem, Talanta*, 1980, **27,** 745.
11. Bio-Rad Laboratories Catalogue, 1976.
12. R. Gilchrist, *Anal. Chem.*, 1953, **25,** 1617.
13. G. H. Ayres and E. W. Berg, *ibid.*, 1953, **25,** 980.
14. N. K. Pshenitsin and I. V. Prokofeeva, *Zh. Neorgan. Khim.*, 1957, **2,** 569.
15. G. Anderegg and A. Malik, *Helv. Chim. Acta*, 1976, **59,** 1498.
16. L. M. Volshtein, *Koord. Khim.*, 1975, **1,** 595.
17. A. A. Grinberg, Kan Yuan and Y. S. Varshavskii, *Dokl. Akad. Nauk SSSR*, 1964, **154,** 375.
18. K. A. Gladyshevskaya and I. V. Prokofeeva, *Zh. Neorgan. Khim.*, 1968, **13,** 1370.

Talanta, Vol. 30, No. 7, pp. 475–480, 1983
Printed in Great Britain

0039-9140/83 $3.00 + 0.00
Pergamon Press Ltd

THE DETERMINATION OF THIOLS WITH DIPHENYLPICRYLHYDRAZYL AS A SPECTROPHOTOMETRIC REAGENT

DONALD B. HUNSAKER, JR.
*Oak Ridge National Laboratory, Post Office Box X, Oak Ridge, TN 37830, U.S.A.

and

GEORGE H. SCHENK
Department of Chemistry, Wayne State University, Detroit, MI 48202, U.S.A.

(*Received* 22 *July* 1982. *Revised* 17 *December* 1982. *Accepted* 17 *January* 1983)

Summary—Diphenylpicrylhydrazyl (DPPH), a stable, intensely purple free radical, is used as a reagent in the quantitative determination of various aromatic and aliphatic thiols by indirect spectrophotometric analysis. Plots of degree of reaction *vs.* time show that thiophenol and its derivatives react more quickly than aliphatic thiols with DPPH. Calibration plots are linear over the concentration range $0.05–3.00 \times 10^{-5} M$ thiol. The average relative error is in the range 1–2% and the absolute standard deviations range up to $0.50 \times 10^{-6} M$.

The stable free radical α,α-diphenyl-β-picrylhydrazyl (DPPH) has been used extensively in the past as a spectrophotometric analytical reagent.[1–4] Its advantages are (1) its intense purple colour, (2) its ability to react quantitatively with compounds of interest, (3) a pronounced variation in the rates of such reactions, and (4) no observed tendency to dimerize.

The DPPH radical is electron-deficient and undergoes reactions in which it functions as an oxidizing agent by gaining an electron. It abstracts a hydrogen atom from various hydrogen-atom donors (*e.g.*, =NH, –OH, –SH). Upon gaining a hydrogen atom, the intensely purple DPPH is reduced to the yellow compound α,α-diphenyl-β-picrylhydrazine (DPPH:H).

The basis for use of DPPH in spectrophotometric analysis is that the decrease in absorbance at the 520-nm absorption maximum of DPPH is a measure of the amount of hydrogen-atom donor present. Schenk and co-workers used DPPH to determine dihydric phenols,[1,2] and Papariello and Janish successfully determined phenols and amines with the DPPH method.[3,4] These earlier works plus the similarity of thiols to amines and phenols encouraged us to investigate the determination of thiols with DPPH.

A wide variety of analytical methods have been reported for the determination of thiols, including titrimetry with tetrathioate, iron(III), cystine, and hexacyanoferrate(III);[5] thin-layer chromatography with use of Dragendorff's reagent;[6] and atomic-absorption spectrometry of silver salts of thiols.[7] However, other spectrophotometric methods for thiols are of most relevance to this paper. Aliphatic thiols have been determined by using the reaction between the thiol anion and 3-3′-dithiobis(6-nitrobenzoic acid) (Ellman's reagent) at pH 8.0 to form the highly-coloured *p*-nitrothiophenol anion.[8] The reaction of Ellman's reagent with many thiols is rapid and sensitive, and lends itself to spectrophotometric analysis.[9] Novak *et al.* modified the method slightly by developing dithiodianil reagents that produce a colour change more easily detected by visual observation than that produced by Ellman's reagent.[9] A method for the simultaneous determination of the oxidized and reduced forms of thiols in solution by using the reaction between ammonium tetrachloropalladate(II) and thiols or disulphides to form complexes of uncertain structure but with unique spectra has been reported by Dupre and Aureli.[10] None of the methods above is based on indirect spectrophotometry, and none is focused on unifunctional thiols (*i.e.*, organic compounds with –SH as the only functional group).

Indirect spectrophotometry is of value when a strongly-absorbing reagent is available, as is the case with DPPH and thiols. The primary drawback to indirect spectrophotometry is that at low concentrations of analyte the absorbance is high, and the error in reading the absorbance scale is greater.[11] Consequently, the method is best suited to systems that provide a linear plot of absorbance *vs.* concentration of analyte at low to medium absorbance values. The past success of indirect spectrometry with DPPH[3,4,12] is undoubtedly due to the existence of these conditions.

The reaction between DPPH and thiols has also been studied in detail from a non-analytical standpoint. Russell reported that the abstraction of the

*Operated by Union Carbide Corporation under contract W-7405-eng-26 with the U.S Department of Energy.

hydrogen atom from the thiol by DPPH, as illustrated in Fig. 1, is the rate-determining step in the DPPH/thiol reaction mechanism.[13] Consequently, aromatic thiols are more reactive than aliphatic because once a hydrogen atom is abstracted from an aromatic compound by DPPH, a radical species is formed in which the unpaired electron can be delocalized throughout the aromatic system. Aliphatic thiols, on the other hand, have limited means of stabilizing the unpaired electron and are therefore less reactive.

With the DPPH/thiol reaction, as with any free-radical system, secondary reactions can complicate the decolorization of DPPH; however, as Papariello and Janish point out, the assumption that the DPPH/thiol reaction occurs principally as shown in Fig. 1 is indeed valid. In other words, the side-reactions are thought to exert a small effect.

Brook *et al.* have also stated that the DPPH/thiol reaction occurs as shown in Fig. 1, provided that dilute solutions are used, and that the DPPH is added to the thiol.[14] Russell has shown that the DPPH/thiol reaction is second-order overall; he proposed the rate expression[13] $R_{DPPH} = 2k[DPPH][RSH]$. Ewald also reports that the DPPH/thiol reaction is second-order.[15]

In the present work, aliquots of thiol solution are added to solutions of DPPH, and the resulting decolorization is monitored by spectrophotometric measurement near the 520-nm absorption maximum of DPPH. Calibration graphs are prepared from thiol solutions of known concentrations. The degree of reaction occurring between DPPH and a particular thiol is calculated by comparing the absorbance of the DPPH/thiol solutions with that of a DPPH "blank" solution. The purities of the thiols are determined by iodine titrimetry. This procedure allows for a precise, accurate determination of aromatic thiols. Aromatic compounds and multifunctional thiols containing other hydrogen-atom donors (*e.g.*, –OH, =NH) are possible interferences; however, aliphatic hydrogen-atom donors should not interfere with the determination of aromatic thiols.

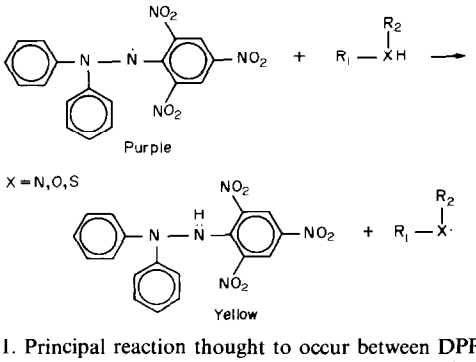

Fig. 1. Principal reaction thought to occur between DPPH and hydrogen-atom donor to form α,α-diphenyl-β-picrylhydrazine. Note that R_2 is not present when X is a sulphur or oxygen atom.

EXPERIMENTAL

Apparatus

All the experimental data were obtained with a Beckman DB spectrophotometer. Selected analyses were repeated with a Cary 14 spectrophotometer and a Bausch and Lomb Spectronic 20 spectrophotometer.

Reagents

All the chemicals used were reagent grade or equivalent. The DPPH, thio-β-naphthol, and 2-mercapto-6-nitrobenzothiazole were obtained from Eastman Kodak. Aldrich supplied the thiobenzoic acid, benzyl mercaptan, *p*-bromothiophenol, *p*-chlorothiophenol, *p*-thiocresol, and tert.-butyl mercaptan. The thiophenol was obtained from Matheson, Coleman, and Bell, and the thioacetic acid from Evans. All solvents used were of spectroscopic quality. The principal solvent, "Gold Shield" ethyl alcohol (absolute ethanol), was dried over "Drierite" for at least 24 hr before use.

Solutions of DPPH were prepared by weighing 100 mg of the compound into a 25-ml standard flask, dissolving in 5.0 ml of acetone, and diluting to volume with absolute ethanol. This solution was used to make 1.0×10^{-4} and $4.0 \times 10^{-4}M$ stock solutions by appropriate dilution with absolute ethanol. All DPPH solutions, including the stock solutions, were prepared fresh daily to minimize errors from *in situ* decomposition of DPPH; however, DPPH solutions kept in foil-covered tightly-stoppered flasks under a nitrogen atmosphere exhibit a loss of free radical activity not exceeding 2–4%/week.[12] Thus, laboratories performing routine thiol analyses by this method could prepare stock solutions only as needed.

Thiol solutions were prepared by weighing 0.3 mmole of thiol into a 25-ml standard flask, dissolving in acetone (if insoluble in alcohol), and diluting to volume with absolute ethanol. A $1 \times 10^{-4}M$ stock solution was then made by diluting 0.5 ml of the solution to volume in a 50-ml standard flask with absolute ethanol. All thiol solutions, including the stock solutions, were prepared fresh daily, and were stored in foil-covered tightly stoppered flasks until used.

The $0.05N$ iodine solution was prepared by weighing about 7 g of iodine into a 1-litre standard flask, and dissolving and diluting to the mark with 95% ethanol. The 5% aqueous potassium iodide solution was prepared in 1-litre quantities. The $0.1N$ sodium thiosulphate solution was prepared by dissolving 25 g of $Na_2S_2O_3 \cdot 5H_2O$, in 1 litre of freshly boiled and cooled distilled water, with addition of 0.1 g of sodium carbonate as stabilizer. The $0.1N$ sulphuric acid was prepared by pipetting 6.95 ml of the concentrated acid into 50 ml of distilled water in a 250-ml standard flask, and diluting to the mark with distilled water.

Procedures

Preparation of analytical plots. Because deviations from direct proportionality between absorbance and concentration are minimized in the 15–65% transmittance range,[16] the DPPH method was studied at each extreme of this range, two concentrations of DPPH being used in the preparation of two calibration plots for each thiol. The $8.00 \times 10^{-5}M$ DPPH blank gave a transmittance of about 20% and the $2.00 \times 10^{-5}M$ DPPH blank a transmittance of about 63%. Analytical plots in the $2.0–200 \times 10^{-7}M$ thiol concentration range were prepared by adding 0.005–0.05 μmole of thiol to 2.0 ml of $1.0 \times 10^{-4}M$ DPPH in a 10-ml standard flask, mixing, diluting to volume with absolute ethanol, tightly stoppering the flask, and measuring the absorbance at 540 mm with a high-precision spectrophotometer after completion of the reaction. The DPPH and thiol were allowed to react in a light-proof container to avoid the slow photochemical reduction of DPPH to DPPH:H that occurs in sunlight and at 520 mm.[2] A blank

was prepared by pipetting 2.0 ml of $1.0 \times 10^{-4}M$ DPPH solution into a 10-ml standard flask and diluting to volume with absolute ethanol, and measured similarly to the standards. Measurements were made at 540 nm, rather than at 520 nm (the absorption maximum of DPPH) to avoid interference from the absorption of DPPH:H. [If a high-precision spectrophotometer is not available, per cent transmittance (%T) can be measured and converted into absorbance.] The absorbance was plotted *vs.* concentration of thiol. Calibration plots were prepared daily to minimize errors and interferences. Plots covering the 2.00×10^{-6}–$6.00 \times 10^{-5}M$ range were similarly prepared, with 0.04–0.20 μmole of thiol added to 2.0 ml of $4.0 \times 10^{-4}M$ DPPH in a 10-ml standard flask and the blank prepared with 2.0 ml of $4.0 \times 10^{-4}M$ DPPH in a 10-ml standard flask.

Determination of reaction time. To determine the time needed for a particular series of DPPH/thiol solutions to react completely, the absorbances for the blank and the lowest thiol concentration in the series were measured as a function of time, the solutions being kept in the dark between readings. The reaction was assumed to be complete when the absorbance was constant for at least 4 min. The time elapsed from solution preparation to the mid-point of this region was taken as the reaction time for the particular series.

Accuracy studies. A series of DPPH/thiol solutions of various thiol concentrations was prepared, covering the range for a given calibration plot. The solutions were allowed to react in the dark for the appropriate time and the absorbance of each was measured at 540 nm. The analytical calibration plot was used to determine the experimental thiol concentration of each solution. The accuracy of the method was determined by comparing the experimental thiol concentration with the expected thiol concentration. These studies served as a check on the calibration plots.

Precision studies. To ascertain the precision of the method, a series of DPPH/thiol solutions, all of the same thiol concentration, was prepared. Each solution was allowed to react in the dark for the amount of time required for completion of reaction. Absorbance readings for each solution were taken, and were used to obtain the experimental concentrations from the standard plot, and the standard deviation was calculated.

Determination of thiol purity. The purity of the thiols was determined by titration with iodine, as follows. A 0.1N sodium thiosulphate solution was prepared as described in Kolthoff *et al.*[17] and used to standardize the 0.05N solution of iodine in ethanol, as described in Stone.[18] Various analytical procedures employing iodine titrations[17-21] were tried in order to determine the purity of the thiols. Because these methods were not successful, the following procedure was developed. A 1.0–2.0 mg quantity of thiol was weighed into an iodine flask and dissolved in 50 ml of 95% ethanol. For liquid thiols, an ampoule was used to introduce the thiol into the flask; the ampoule was broken by shaking with glass beads after addition of the solvent. The dissolved thiol was titrated with the 0.05N iodine, with starch added as indicator near the end-point.

RESULTS AND DISCUSSION

Reaction-time measurements

The amount of time for completion of the DPPH/thiol reaction varied significantly, depending on the thiol. As can be seen from Table 1, thiophenol and its derivatives, and thio-β-naphthol, reacted very quickly (5.0 min). On the other hand, benzyl mercaptan required 15.0 min to react, and 2-mercapto-6-nitrobenzothiazole and tert.-butyl mercaptan required 90 and 120 min respectively. Excluding benzyl mercaptan and tert.-butyl mercaptan, the average degree of reaction was 111% (absolute standard deviation +5.6%).

The stability of the radicals in the rate-determining step can be used to explain the observed differences in reaction time. Thiophenol and thio-β-naphthol react most rapidly because they form the most stable radicals after the hydrogen atom has been abstracted from the SH group, the rate-determining step. At the other extreme, tert.-butyl mercaptan and 2-mercapto-6-nitrobenzothiazole react much more slowly because their radical intermediates are less stable. Furthermore, steric factors are probably responsible for further slowing of the rate of the tert.-butyl mercaptan/DPPH reaction. Thioacetic acid reacts more rapidly than tert.-butyl mercaptan, probably because the radical intermediate gains stability from resonance involving the carbonyl group.

The reaction times reported in Table 1 are for the most dilute thiol solutions and thus represent the slowest reaction rate measurable by this method at a given DPPH concentration (assuming a second-order reaction). Therefore, for a given series of thiol solutions, the more concentrated ones will react completely in the time required for the most dilute solution to react.

Figure 2 shows a plot of absorbance (A) *vs.* time for a mixture of 2-mercapto-6-nitrobenzothiazole

Table 1. Reaction times and degree of reaction for selected thiols

Thiol	Reaction time, *min*	1-electron reaction, %
Thio-β-naphthol	5.0	105
Thiobenzoic acid	5.0	111
Benzyl mercaptan	15.0	57
Thiophenol	5.0	113
p-Chlorothiophenol	5.0	105
p-Bromothiophenol	5.0	111
p-Thiocresol	5.0	118
2-Mercapto-6-nitrobenzothiazole	90.0	120
Thioacetic acid	50.0	107
tert.-Butyl mercaptan	120.0	2

[DPPH] = $8.00 \times 10^{-5}M$.

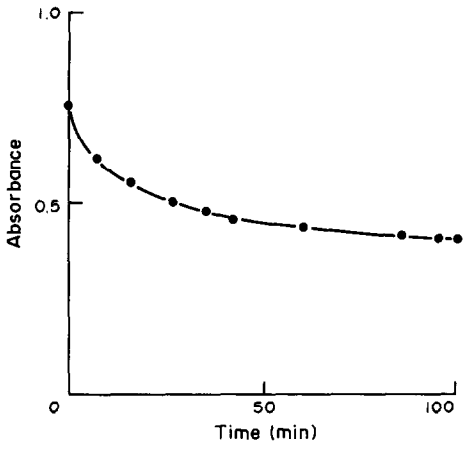

Fig. 2. Plot of absorbance *vs.* time for a mixture of 2-mercapto-6-nitrobenzothiazole ($3.00 \times 10^{-5}M$); [DPPH] $= 8.00 \times 10^{-5}M$.

($3.00 \times 10^{-5}M$) and DPPH ($8.00 \times 10^{-5}M$). As can be seen, the curve became asymptotic to $A = 0.400$, thus suggesting cessation of reaction when this absorbance was reached.

Degree of reaction

The reaction time was taken as the mid-point of the 4-min period within which the absorbance of the reaction mixture did not change measurably. Although such a criterion gives an indication of cessation of the reaction, it does not provide a numerical estimate of the amount of DPPH that has reacted with the thiol.

To ascertain the degree of reaction between the DPPH and thiol, the following equation was used:

$$\text{Degree of reaction} = \left(\frac{A_b - A_m}{A_b}\right) \times \Big([\text{DPPH}]/[\text{RSH}]\Big) \times 100\% \quad (1)$$

where A_b = DPPH blank absorbance, and A_m = DPPH/thiol mixture absorbance. The equation assumes a one-electron DPPH/thiol reaction, as postulated in Fig. 1. All the data required are available from the spectrophotometric analysis. The thiol and DPPH concentrations used in the equation are the initial (total) concentrations in the solution measured.

If the DPPH/thiol reaction always exhibits 1:1 stoichiometry, the degrees of reaction should be comparable. The values listed in Table 1 exhibit a standard deviation of 5.6% (excluding benzyl mercaptan and tert.-butyl mercaptan), which is approximately 5% of the mean value of 111%. These results suggest that the stoichiometry is indeed 1:1.

Equation (1) was used to calculate the degrees of reaction listed in Table 1. The 57% reaction for benzyl mercaptan was puzzling, because very little error was expected in this determination. A possible explanation might be that this is the only thiol which has a benzyl radical as its intermediate; if, as a consequence, it does not react with DPPH stoichiometrically, the use of equation (1) would not be valid. The value for tert.-butyl mercaptan was expected, because this compound did not furnish linear analytical plots, possibly owing to radical instability and steric hindrance caused by the methyl groups.

The degree of reaction can also be determined graphically from the linear analytical plot to serve as a check of the values obtained by calculation. The graphical method involves extrapolating the linear portion of the plot to intersect the abscissa. The resulting intercept theoretically represents the thiol concentration at which all of the DPPH has reacted. Hence, division of the initial DPPH concentration by this thiol concentration should give the degree of reaction.

The values found by the graphical method agreed with those found by calculation. For the DPPH concentration of $2.00 \times 10^{-5}M$, the average was 113%, with an absolute standard deviation of +7.1%. At a DPPH concentration of $8.00 \times 10^{-5}M$, the average was 115%, with an absolute standard deviation of +7.5%. The benzyl mercaptan and tert.-butyl mercaptan data were excluded from the graphical analysis.

The data for degree of reaction can be used to represent graphically the relative rate of the DPPH/thiol reaction, by a plot of degree of reaction *vs.* time. Figure 3 shows the relative reaction rates for tert.-butyl mercaptan ($2.64 \times 10^{-4}M$), thioacetic acid ($5.05 \times 10^{-6}M$), *p*-bromothiophenol ($9.00 \times 10^{-6}M$) and 2-mercapto-6-nitrobenzothiazole ($1.50 \times 10^{-5}M$). The curve for the reaction between DPPH and tert.-butyl mercaptan is at the bottom of Fig. 3. As can be seen, the reaction is indeed very slow, for

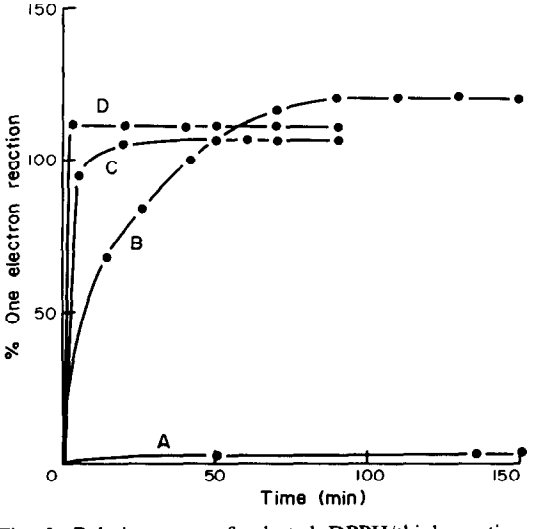

Fig. 3. Relative rates of selected DPPH/thiol reactions. [DPPH] $= 8.00 \times 10^{-5}M$. (A) tert.-Butyl mercaptan. (B) 2-Mercapto-6-nitrobenzothiazole. (C) Thioacetic acid. (D) *p*-Bromothiophenol.

the reasons given above. At the other extreme is the curve for *p*-bromothiophenol, which reacts very rapidly with DPPH. Thioacetic acid and 2-mercapto-6-nitrobenzothiazole react at intermediate rates, as would be predicted from the reaction time data (Table 1).

The degree of reaction studies serve to provide graphical representations of the DPPH/thiol reaction rates. These reaction rate curves could very well be used to "screen" classes of compounds to find those for which the method is useful. For example, all the *para*-substituted thiophenols would be expected to yield reaction rate curves very similar to the *p*-bromothiophenol plot, and hence would be very suitable for analysis by the method. The rate data also suggest that aromatic thiols could be easily determined in the presence of aliphatic thiols, with no interference.

That the degree of one-electron reaction averaged over 100% for both the calculated values (111%) and the graphical values (115%) (excluding benzyl mercaptan and tert.-butyl mercaptan) may have been caused by self-dimerization, photochemical decomposition of DPPH, the reaction of impurities with the DPPH, or the DPPH/thiol reaction not occurring with 1:1 stoichiometry. Self-dimerization of DPPH is not a likely cause, however, since it exhibits little tendency to dimerize (a trait that makes it a desirable analytical reagent). Photochemical decomposition is also not a very likely cause, because great care was taken that the solutions should react in the dark. Impurities are not likely to be the major cause either, because they would need to be capable of decolorizing DPPH, and they would also need to be of lower equivalent weight than the thiols, to cause a positive deviation. The likelihood that both of these conditions were met for most of the thiols studied appears remote. A somewhat more likely explanation is that the DPPH/thiol reaction did not always occur with 1:1 stoichiometry. In calculating the degree of one-electron reaction, it is assumed that one mole of DPPH is decolorized by one mole of thiol, and that the resulting thiol radical dimerizes to form a disulphide. This is the mechanism postulated by Brook *et al.* for the reaction between DPPH and thiol in dilute solutions.[14] If, however, the thiol radical is in the presence of many DPPH molecules, it will react with the DPPH to form DPPH:SR, which means that two moles of DPPH have been consumed for one mole of thiol.[14] The very nature of the method used in the present work, indirect spectrophotometry, requires that the reagent (DPPH) be present in at least a slight excess. Typically, a 10-fold molar excess was used, and thus it is possible that the DPPH/SR· reaction occurred to some extent. However, the solutions used were dilute enough for this mechanism not to be predominant in the DPPH/thiol reaction (or the degree of reaction would have approached 200%).

Spectrophotometric calibration plots

Linear analytical plots over various concentration ranges were obtained for all the thiols studied except tert.-butyl mercaptan. Table 2 summarizes the thiols studied and the concentration ranges over which the plots were linear for studies with a DPPH concentration of $2 \times 10^{-5} M$.

The slopes of the analytical plots are also presented in Table 2; with the exception of benzyl mercaptan, the slopes are quite similar for the different thiols, indicating that the reaction stoichiometries were all quite uniform, with the DPPH reacting only with the SH group of each thiol (as postulated in Fig. 1), and that the structure of the thiol has very little effect on the degree of reaction. Of special interest are the values for thiophenol, *p*-chlorothiophenol, *p*-bromothiophenol, and *p*-thiocresol; the slopes indicate that the *para*-substitution has very little effect on the DPPH/thiol reaction. Papariello and Janish obtained similar results for amines.[4] Because of the similarity of the plots, it is feasible to use a single calibration plot for determination of a series of *para*-substituted thiols.

As already mentioned, the analytical plots were linear only over a certain concentration range. For all the thiols studied, deviation from linearity occurred as the concentration of thiol was increased;

Table 2. Analytically useful concentration ranges and slopes of linear plots for selected thiols

Thiol	Concentration range for linear plot, μM	Slope of linear plot, $10^6 \times$ A.*l.mole*$^{-1}$
Thio-β-naphthol	0.0–1.50	−0.014
Thiobenzoic acid	0.0–1.50	−0.010
Benzyl mercaptan	0.0–7.00	−0.003
Thiophenol	0.0–3.00	−0.015
p-Chlorothiophenol	0.0–5.00	−0.013
p-Bromothiophenol	0.0–3.00	−0.012
p-Thiocresol	0.0–3.00	−0.014
Thioacetic acid	0.0–4.00	−0.006
2-Mercapto-6-nitrobenzothiazole	0.0–5.00	−0.007
tert.-Butyl mercaptan	—	—

[DPPH] = $2.00 \times 10^{-5} M$. A = absorbance.

Table 3. Determination of selected thiols with DPPH

Thiol	Present, μM	Found, μM
Thio-β-naphthol	0.505	0.505
Thiobenzoic acid	0.489	0.487
Benzyl mercaptan	3.00	3.00
Thiophenol	1.00	1.01
p-Chlorothiophenol	3.00	2.92
p-Bromothiophenol	1.00	1.01
p-Thiocresol	1.00	1.01
Thioacetic acid	1.52	1.49
2-Mercapto-6-nitrobenzothiazole	3.03	3.00

[DPPH] = $2.00 \times 10^{-5}M$.

typically this deviation consisted of a concave trend in the calibration line at "high" thiol concentrations, indicating that the decrease in absorbance of the DPPH has been less than expected for direct proportionality to the thiol concentration.

The observed non-linearity could be due to a number of factors acting singly or in unison. First, it could be a manifestation of incomplete reaction, as suggested by Reilley and Hildebrand;[11] however, the initial molar ratios of DPPH to thiol (approximately 10:1) should have ensured that sufficient DPPH was present to react completely with the thiol. A second possibility is that it is a result of the uncertainties associated with detecting low thiol concentrations at the end of the reaction. Third, it could have been caused by reaction products or by-products absorbing at 540 nm. The method is based on the assumption that the DPPH is the only species (in the mixture of DPPH and thiol) that is absorbing at 540 nm. If this assumption is invalid, because of other reaction species (*e.g.*, RSSR, DPPH:H, or DPPH:RS) absorbing at this wavelength, then the calibration plots would have curved upward with increasing thiol concentration. Further research is needed to isolate and correct the cause of the non-linearity, thus extending the analytically useful range of the method.

Analysis results

Table 3 summarizes the statistical results of determining selected thiols by the DPPH method. The relative error averaged about 1%, and the absolute standard deviations ranged from 0 to $0.11 \times 10^{-6}M$. When the analysis was repeated with a DPPH concentration of $8.0 \times 10^{-5}M$, the average relative error was approximately 2% and the standard deviations ranged from 0 to $0.45 \times 10^{-6}M$.

These results indicate that for the particular thiols and concentrations used, interfering side-reactions exert minimal influence. Repeating the analyses with different spectrophotometers produced similar results for the accuracy and precision.

Multifunctional thiols were not investigated in this study, but it can be predicted that the DPPH method is unlikely to allow selective determination of the SH group when the other hydrogen atom donors (–OH, =NH) are present in the same molecule. From the success of the DPPH method for amine and phenol determinations,[3,4] the DPPH method would probably yield a determination of the total amount of hydrogen-atom donor present. Similarly, mixtures containing aromatic thiols, amines, and phenols could probably not be selectively analysed for only one of the hydrogen-atom donors; however, aromatic species in the presence of aliphatic species could probably be determined, with minimal interference, owing to the difference in reaction rates.

Acknowledgements—The authors wish to thank Dr. H. E. Zittel and Dr. M. J. Kelly, Energy Division, Oak Ridge National Laboratory, for reviewing this manuscript.

REFERENCES

1. G. H. Schenk and N. Swieczkowski, *Talanta*, 1971, **18**, 230.
2. G. H. Schenk and D. Brown, *ibid.*, 1967, **14**, 257.
3. G. J. Papariello and M. A. Janish, *Anal. Chem.*, 1966, **38**, 211.
4. *Idem, ibid.*, 1965, **37**, 900.
5. K. K. Verma,*Talanta*, 1979, **26**, 277.
6. B. N. Prosad, G. B. Kawale, S. V. Padalikar and V. D. Joglekar, *Sci. Cult. India*, 1980, **46**, 275.
7. J. S. Marhevka and S. Siggia, *Anal. Chem.*, 1979, **51**, 1259.
8. G. L. Ellman, *Arch. Biochem. Biophys.*, 1959, **82**, 70.
9. T. J. Novak, S. G. Pleva and J. Epstein, *Anal. Chem.*, 1980, **52**, 1851.
10. S. Dupre and M. Aureli, *Anal. Biocehm.*, 1980, **105**, 97.
11. C. N. Reilley and G. P. Hildebrand, *Anal. Chem.*, 1959, **31**, 1763.
12. M. S. Blois, *Nature*, 1958, **181**, 1199.
13. K. E. Russell, *J. Phys. Chem.*, 1954, **58**, 437.
14. A. G. Brook, R. J. Anderson and J. T. Van Patot, *Can. J. Chem.*, 1958, **36**, 159.
15. A. H. Ewald, *Trans. Faraday Soc.*, 1959, **55**, 792.
16. D. A. Skoog and D. M. West, *Fundamentals of Analytical Chemistry*, 2nd Ed., pp. 666–667. Holt, Rinehart & Winston, New York, 1969.
17. I. M. Kolthoff, E. B. Sandell, E. J. Meehan and S. Bruckenstein, *Quantitative Chemical Analysis*, 4th Ed., p. 849, pp. 964–983. Macmillan, New York, 1969.
18. K. G. Stone, *Determination of Organic Compounds*, pp. 184–192. McGraw-Hill, New York, 1956.
19. S. Siggia, *Quantitative Organic Analysis via Functional Groups*, 3rd Ed., pp. 578–579. Wiley, New York, 1963.
20. A. I. Vogel, *Elementary Practical Organic Chemistry*, pp. 799–800. Longmans, London, 1958.
21. D. P. Harnish and S. Tarbell, *Anal. Chem.*, 1968, **21**, 968.

Talanta, Vol. 30, No. 7, pp. 481–485, 1983
Printed in Great Britain.

0039-9140/83 $3.00+0.00

DETERMINATION OF MERCURY IN WATER BY ELECTRO-DEPOSITION AND LOW-PRESSURE RING-DISCHARGE EMISSION SPECTROSCOPY

H. Z. WREMBEL
Department of Physics, Teaching University, Słupsk, Poland

(*Received* 21 *December* 1981. *Revised* 19 *November* 1982. *Accepted* 12 *January* 1983)

Summary—The application of low-pressure ring-discharge atomic-emission spectroscopy, combined with electro-deposition on copper and platinum, to the determination of trace mercury in water has been investigated. Distilled water, artificial Baltic Sea water, artificial sea-water, and various natural waters were examined. The results obtained show that the method is suitable for the intended purpose.

The importance of mercury-assay at ultratrace levels (0.01–1 μg/l) in environmental waters is well known, and several methods for that purpose have been developed. Their detection limits, accuracy, precision *etc.* are in general adequate for research as well as routine work but most of the methods have drawbacks such as very expensive equipment; need for highly qualified laboratory staff; radiation hazard to the operator; relatively high power consumption; time consumption in an analysis. Thus there is much interest in development of new analytical methods which will eliminate some of these disadvantages.

Many recent studies have used electrolytic preconcentration (to lower the detection limits and eliminate matrix interferences) in conjunction with spectroscopic methods of trace-metal analysis. Most of these methods are indirectly applied to assay for mercury, or seem easy to adopt for this purpose. Heavy metals can be electro-deposited on metallic wires[1–8] or on graphite.[9–14] Deposition on metallic wires is mainly combined with emission spectroscopy, and deposition on graphite seems to be mostly combined with absorption spectroscopy.

The utility of low-pressure ring-discharge atomic-emission spectroscopy for the determination of ultratraces of mercury in water has already been shown.[15–19] In the present work it is combined with electrolytic preconcentration on copper and platinum mesh cathodes.

EXPERIMENTAL

Equipment

The spectrometric instrumentation was a modified version of that used earlier.[15–19] Several components were replaced by more suitable ones and some improvements were made in the analytical procedure, giving better sensitivity and lower detection limits. The apparatus used consisted essentially of:

(*i*) the spectral lamp (laboratory made) with a discharge cell made from "Vitreosil" HPQ-quartz (Fig. 1);

(*ii*) the photometric arrangement, made up of a monochromator with a 68° silica prism (SPM-2, Carl Zeiss, Jena), a silica lens (50 mm in diameter, focal length 100 mm), and a photomultiplier tube (M 12 FVC 51, Werk für Fernsehelektronik, East Berlin);

(*iii*) the recording equipment, consisting of a chart-recorder (K-200, Carl Zeiss, Jena), an electrometer (219A, UNITRA ZRK, Warsaw) and a digital multimeter (V 543, MERATRONIK, Warsaw);

(*iv*) a vacuum stage made up of a vacuum pump (BL-82 UNITRA, Koszalin), oil separator (laboratory made) and a vacuum gauge (PSO-69, ZOPAP, Warsaw);

(*v*) the power supply unit, made up of three power supplies (ES-131, ZALMED; ZWN-25, BUTJ; IZS-1/60, INCO, Warsaw), an oscillator (GM-2, INCO, Warsaw),

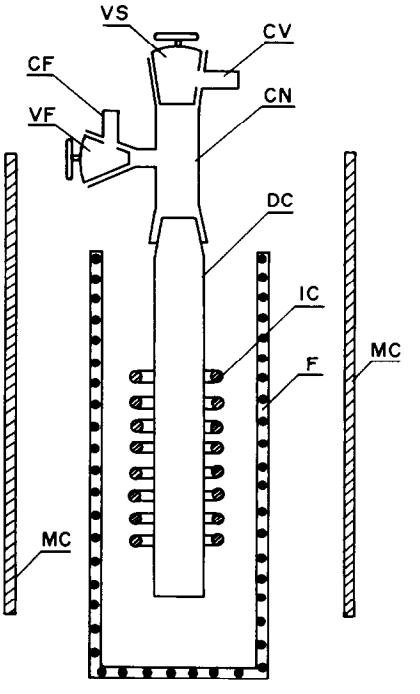

Fig. 1. The spectral lamp; CF—connection to the fill-gas reservoir, VF—fill-gas valve, MC—antimagnetic coating, DC—discharge cell, F—furnace, RC—radiofrequency coil, CN—connector, CV—connection with the vacuum compartment, VS—vacuum valve.

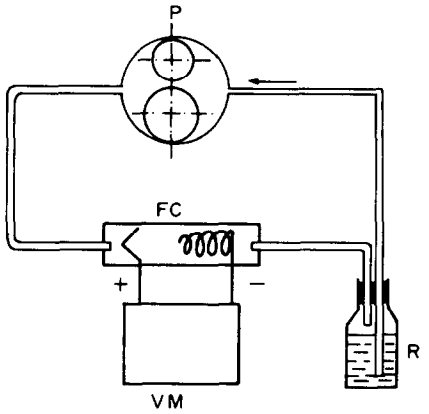

Fig. 2. The flow-through cell assembly; P—pump, FC—flow-through cell, VM—voltmeter, R—reservoir.

proportional amplifier (laboratory made), mixing stage (PPM-4A, ZOPAN, Warsaw) and frequency meter (PFL-21, ZOPAN, Warsaw).

Procedure

The mercury content of the water samples investigated was determined by measuring the intensity of the Hg I 253.65-nm resonance line relative to the He I 388.86-nm line. The peak intensity of the mercury line should be a direct measure of the mercury concentration, but in general is not a reliable measure as it is affected by a number of factors such as the instrumental operating parameters, vacuum conditions, varying conditions in the excitation of the atomic gas, *etc.* It is therefore better to use the internal standard method, with measurement of the intensity relative to that for a known amount of reference element (helium in this case).

In the low-pressure ring-discharge plasma the atomic lines of both mercury and helium are strongly excited. All the most sensitive lines (*raies ultimes*) of atomic mercury appear in the discharge even at very low concentrations (10^6 atoms/cm^3) of mercury in the plasma. The Hg I 546.07 and 578.97-nm lines and the He I 587.56-nm line in the plasma are also very intense and can be used as analytical lines, but the monochromator resolution is better for work in the ultraviolet than the visible region. The 253.65-nm mercury line is particularly intense and clearly isolated from the background.[15,16]

The mercury in a given volume of sample is deposited electrolytically in the discharge cell of the spectral lamp in a manner similar to that described earlier.[20] A flow-though cell is used for the electro-deposition, with copper or platinum mesh cathodes (total area about 9 cm^2) and a platinum-wire anode (total area 4.5 cm^2).

To a 180-ml sample of water, 20 ml of concentrated nitric acid (mercury-free quality) and 0.02 g of potassium iodide are added, in a 250-ml PTFE container, from which the mixture is continuously circulated by pump at about 30 ml/min through the flow-through cell for 35 min. The electrolysis is done at 3 V and a current of 0.01–0.5 A. The general layout is shown in Fig. 2.

After the electrolysis the cathode is carefully dried with an air-stream and then placed inside the discharge cell of the lamp. The lamp is then pumped down to a pressure of about 0.01 mmHg, flushed several times with helium, and finally filled to a pressure of 10 mmHg with this element. The vacuum system is switched off from the lamp and the discharge cell is preheated to about 525°, the working temperature of the lamp, by means of the external d.c. furnace. The low-pressure ring-discharge is then initiated.

The image of about half the length of the plasma (*i.e.*, the radiation passing through the window in the metal cylinder round the lamp) is projected by the silica lens onto the slit of the monochromator. With a slit-width of 20 μm the spectral resolution is sufficient to reduce most of the possible effects of line overlap (at 250 nm the spectral band-width is 20 pm). The intensities of the Hg I 253.65-nm line and the He I 388.86-nm line are measured with the photomultiplier tube and electrometer system and their ratio is plotted against mercury content.

The test samples (distilled water; artificial Baltic Sea water;[21,22] artificial sea-water;[23] some natural waters) are acidified to pH $\leqslant 2$ with mercury-free concentrated nitric acid and stored in PTFE containers or silica bottles after addition of 0.1 g of potassium iodide per litre. These containers, the discharge cell, and the glass parts of the spectral lamp are carefully cleaned with powerful metal-free detergent, then treated with nitric acid and rinsed with doubly distilled demineralized water. To avoid memory effects, after each series of measurements on a given sample of water the discharge cell is heated for several hours at a temperature of about 1130° and the glass parts of the lamp at a temperature of about 425°. Blank values are regularly determined.

Plasma source

The low-pressure ring-discharge plasma is formed inside the evacuated discharge cell of the spectral lamp by induction of an oscillating magnetic field. The discharge cell (12.8 mm internal diameter, 150 mm long) is manufactured of "Vitreosil" HPQ-quartz. The rest of the lamp is made of Pyrex glass. The discharge cell can be heated to about 525° with an external d.c. furnace. The lamp is shielded from the influence of accidental electromagnetic fields by a coaxial metal cylinder (internal diameter 100 mm, with a 30 × 25 mm window for passage of the discharge cell radiation). The general layout of the lamp is shown in Fig. 1.

The lamp is powered by a VHF oscillator with an applied field frequency of 60 MHz. The power input into the plasma area of the discharge cell is 1.3 W/cm^3 (total power input efficiency approximately 30%). Under these conditions a bright plasma (with strong mercury and helium atomic lines) is obtained. The torch "strikes" immediately the oscillator power is turned on.

RESULTS AND DISCUSSION

Quantitative analysis

The calibration graph for low levels has the customary spectroanalytical equation:

$$x_j = a C^b \tag{1}$$

which is easy to handle for computation purposes, since

$$\log C = \frac{1}{b}(\log x_j - \log a) \tag{2}$$

where x_j is the relative intensity of the Hg 253.65-nm line [i.e. $x_j = x(\text{Hg } 253.65)/x(\text{He } 388.86)$], C is the

Table 1. Values of the experimental constants of the calibration function for mercury-contaminated distilled water, for electro-deposition on platinum and copper lattice cathodes

Cathode	a	b
Pt	6.3×10^5	1.112
Cu	6.1×10^5	1.110

mercury concentration (in g/l.), and a and b are constants which differ slightly (Table 1) according to which type of cathode is used. This last effect is due to several factors, mainly the efficiency of the deposition (preconcentration) of mercury on the electrode, and the efficiency of evaporation of the mercury from the cathode surface.

Limits of detection

In the analytical spectroscopy of extremely small amounts of an element, the key problem is the limit of detection. Unfortunately the commonly used terminology is not uniform and various authors use different definitions.[25-31] In this work we use the definitions given by Boumans,[32] and estimate the detection limits from the blank x_B and its standard deviation s_B, by means of the equation

$$x_i = x_B + k_i s_B \qquad (3)$$

The limit of detection C_L is then the concentration corresponding to the signal x_L for $k_i = 3$, the limit of identification C_I corresponds to the signal for $k_i = 6$, and the limit of determination C_D is given by the signal for $k_i = 10$. At the C_L and C_D values given by these definitions the relative standard deviations are 50 and 10% respectively. The values obtained for mercury in distilled water are shown in Table 2.

Table 2. The limits of C_L (detection), C_I (identification), and C_D (determination) in mercury-contaminated distilled water, for electro-deposition on platinum and copper

Cathode	C_L, ng/l.	C_I, ng/l.	C_D, ng/l.
Pt	0.004	0.02	0.5
Cu	0.006	0.03	0.5

The applicability of the method to determination of mercury in various kinds of water was investigated. The method proved useful for the purpose, but as in earlier work,[17,19] in which freeze-drying was used as the preconcentration method, the limits obtained (Table 3) for the sea-waters were markedly higher than those for distilled water.

Table 3. The limits of C_L (detection), C_I (identification), and C_D (determination) in various kinds of mercury-contaminated waters: D—distilled, B_A—artificial Baltic Sea water, B_N—natural Baltic Sea water, S_A—artificial sea-water; electro-deposition on platinum

Type of water	C_L, ng/l.	C_I, ng/l.	C_D, ng/l.
D	0.004	0.02	0.5
B_A	0.03	0.09	1.0
B_N	0.04	0.1	2.0
S_A	0.06	0.2	4.0

Precision and accuracy

The precision[31] is expressed as the relative standard deviation (RSD) for 10 replicate determinations on the same sample. In Figs. 3 and 4 the RSD is plotted against mercury concentration, for use of both kinds of cathode with distilled water contaminated with mercury.

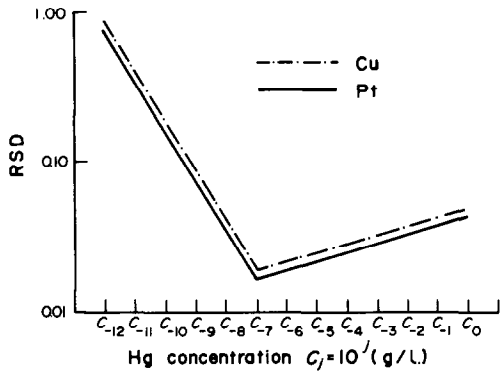

Fig. 3. The changes in the RSD (illustrating the precision of the method) as a function of the Hg concentration, for electro-deposition on: Pt—platinum, Cu—copper lattice cathode.

The better precision was obtained with the platinum electrode, and was minimal (1–4%) for mercury concentrations > 10 ng/l. The precision was slightly worse for sea-water samples.

The accuracy was estimated by means of a series of control determinations (Table 4). Slightly better accuracy was achieved with the platinum electrode. The accuracy was further investigated with the sea-waters (and the platinum electrode). The natural Baltic Sea water was freed from mercury by reduction of mercury compounds to the elemental state and flushing the mercury out with a stream of argon.[33,34] The calibration was then done in the same way as for the other kinds of water, by use of the multiple-addition

Table 4. The results of control measurements with electro-deposition on copper and platinum-mesh cathodes, from distilled water contaminated with mercury

Cathode	Hg added, ng/l.	Hg found, ng/l.	RSD, %	n
Cu	100.0	99.8 ± 0.3	1.4	21
Pt	100.0	99.7 ± 0.3	1.5	21

Note. The values of C given in Tables 4–8 were calculated from

$$C = \langle C \rangle \pm \frac{SD}{\sqrt{n}}; \quad \langle C \rangle = \frac{1}{n}\sum_i^n C_i;$$

SD = standard deviation; n = number of measurements.

Table 5. The results of control measurements for electro-deposition on platinum, for D—distilled water, B_A—artificial Baltic Sea water, B_N—natural Baltic Sea water, S_A—artificial sea-water

Kind of water	Hg added, ng/l.	Hg found, ng/l.	RSD, %	n
D	100.0	99.8 ± 0.3	1.4	21
B_A	100.0	99.4 ± 0.6	2.6	21
B_N	100.0	98.9 ± 0.6	2.9	21
S_A	100.0	99.2 ± 0.7	3.1	21

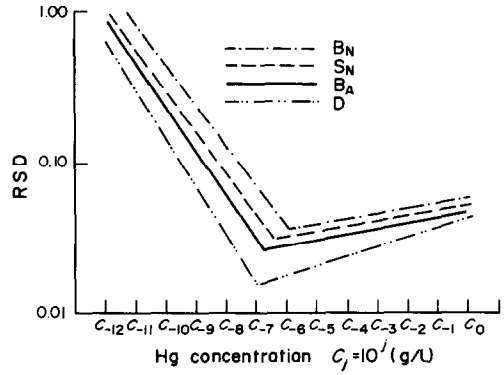

Fig. 4. The changes in the RSD (with electro-deposition on platinum) as a function of the Hg concentration in several kinds of water: D—distilled water, B_A—artificial Baltic Sea water, B_N—natural Baltic Sea water, S_A—artificial sea-water.

method.[31] The accuracy was slightly lower than that obtained for the distilled water, especially in the case of the artificial sea-water. Table 5 gives the results.

Interferences

The analytical signal x_j is affected by the matrix solutes in the water sample, as is generally the case with spectroanalytical methods. For saline waters x_j is markedly decreased (especially for mercury lines in the ultraviolet) in comparison with the value for distilled water containing the same nominal amount of mercury, but the decrease is much smaller than that obtained when freeze-drying is used for preconcentration. The main effect was on the 253.65-nm mercury line. The decrease is attributed mainly to absorption of the emitted radiation by the microlayer of sodium chloride which gathers on the inner walls of the discharge cell. Supporting evidence for this was obtained by running a series of samples with the same mercury content, but containing only certain components of the artificial sea-water (Fig. 5).

The method is also highly sensitive to the presence of water in the discharge cell of the lamp, because even small amounts of liquid water give a large volume of vapour, and this makes the discharge very unstable or even (in extreme cases) extinguishes it. Hence the electrode has to be very carefully dried. Unfortunately, it is possible for variable amounts of mercury to be lost from the cathode during the drying process, resulting in increased error.

Applications

The sensitivity and precision of the method show that it is generally applicable to assay for mercury in environmental waters, and results for various samples are given in Tables 6–8, and are in good agreement with those reported by various workers[35–49] and obtained by several different methods. The rivers investigated showed relatively high mercury concentration, especially the Odra, which is also strongly polluted with other species.[48,49]

Table 6. The average mercury concentration in natural precipitation

Kind of precipitation	*C*, *ng/l.*	RSD, %	*n*
Rain	190 ± 7	50	185
Snow	160 ± 15	57	37

Table 7. The mercury concentration in the waters of the Baltic

Origin of the sample	*C*, *ng/l.*	RSD, %	*N*
Shore area	50 ± 8	72	21
Open sea area	40 ± 5	68	30
Stolp Bank	45 ± 7	76	24

Table 8. The mercury concentration in several rivers

River	*C*, *ng/l.*	RSD, %	*n*
Odra	485 ± 65	67	25
Słupia	205 ± 20	66	46
Wisła	385 ± 45	64	30

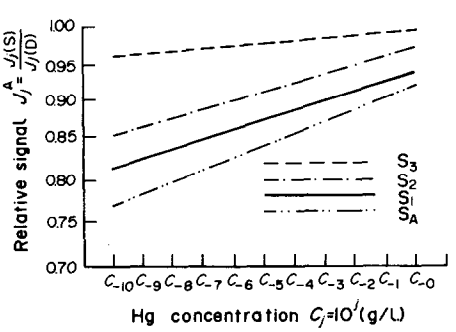

Fig. 5. The relative signal intensity (normalized to that for distilled water) obtained for: S_A—artificial sea-water, S_1—solution of the chloride and sodium salts in S_A, S_2—solution of the remaining salts in S_A, S_3—solution of the heavy-metal nitrates in S_A, as a function of the Hg concentration.

Acknowledgements—This work was supported by the Polish Academy of Sciences under grant MR-I.15. I am grateful to Professor J. Dera and to Professor K. Korzeniewski for many valuable discussions, critical remarks and assistance during preparation of this paper.

REFERENCES

1. W. Lund and B. Larsen, *Anal. Chim. Acta*, 1974, **70**, 299.
2. *Idem*, *ibid.*, 1974, **72**, 57.
3. J. Dawson, D. Ellis, T. Hartley and M. Evans, *Analyst*, 1944, **99**, 602.
4. M. P. Dawson and D. G. Davis, *Anal. Chem.*, 1975, **47**, 2003.
5. W. Lund, Y. Thomassen and P. Døvle, *Anal. Chim. Acta*, 1977, **93**, 53.
6. V. E. Krasilshchik and T. G. Manova, *Zh. Analit. Khim.*, 1975, **30**, 971.
7. H. Z. Heinrichs, *Z. Anal. Chem.*, 1975, **273**, 197.
8. E. Desimoni, *Ann. Chim. Roma*, 1979, **69**, 381.

9. Y. Thomassen, B. V. Larsen, F. J. Langmyhr and W. Lund, *Anal. Chim. Acta*, 1976, **83,** 103.
10. R. E. Sturgeon and C. L. Chakrabarti, *Anal. Chem.*, 1977, **49,** 90.
11. C. Fairless and A. J. Bard, *Anal. Lett.*, 1975, **5,** 433.
12. G. E. Batley and J. P. Matousek, *Anal. Chem.*, 1977, **49,** 2031.
13. V. Z. Krasilshchik, N. M. Kuzmin and E. Ya. Neiman, *Zh. Analit. Khim.*, 1979, **34,** 2045.
14. H. Z. Wrembel, Z. Frąckowiak and K. Kido, *Oceanologia*, 1981, **13,** 105.
15. H. Z. Wrembel, *Stud. Mater. Oceanolog.* 1977, **17,** 415.
16. *Idem, ibid.*, 1977, **19,** 128.
17. *Idem, Chem. Analit. (Warsaw)*, 1979, **24,** 793.
18. *Idem, UP PRL Patent*, No. 109 219.
19. *Idem, Oceanologia*, 1981, **13,** 93.
20. G. Kaiser, D. Götz, P. Schoch and G. Tölg, *Talanta*, 1975, **22,** 889.
21. R. A. Horne, *Marine Chemistry*. Wiley, New York, 1969.
22. A. Trzosińska, *Stud. Mater. Oceanolog.*, 1977, **17,** 165.
23. *Polska Norma; Zastępcza woda morska*, PKN, PN-66/C-06502, 1966.
24. H. Z. Wrembel, *Oceanologia*, 1981, **13,** 113.
25. H. Kaiser and H. Specker, *Z. Anal. Chem.*, 1956, **149,** 46.
26. K. Laqua, W. D. Hagenah and H. Wächter, *ibid.*, 1967, **225,** 142.
27. H. Specker, *Angew. Chem.*, 1968, **80,** 297.
28. R. Gabriel, *Anal. Chem.*, 1970, **42,** 1439.
29. J. Minczewski, J. Chwastowska and R. Dybczyński, *Analiza Śladowa*. WNT, Warsaw, 1973.
30. H. Moenke, *Atomspektroskopische Spurenanalyse*. AV, Leipzig, 1974.
31. J. D. Winefordner, *Trace Analysis*. Wiley, New York, 1976.
32. P. W. J. M. Boumans, *Spectrochim. Acta*, 1978, **33B,** 625.
33. H. Z. Wrembel, in: W. Parczewski *et al.*, *Wykorzystanie Badań Meteorologicznych i Oceanograficznych z Obszarów Oceanów, Mórz Oraz Strefy Brzegowej w Gospodarce Morskiej*. WSM, Szczecin, 1980.
34. *Idem, Acta Geophys.*, 1982, **33,** 39.
35. U. Förstner and G. Müller, *Schwermetalle in Flüssen und Seen*. Springer, Berlin, 1974.
36. A. Stock, *Naturwissenschaften*, 1934, **22,** 390.
37. J. G. Sherbin, *Mercury in Canadian Environment*. Environmental Protection Agency, Ottawa, 1979.
38. R. A. Duce, J. G. Quin, C. E. Olney, S. R. Piotrowicz, B. J. Ray and T. L. Wade, *Science*, 1972, **176,** 161.
39. A. Brzezińska and A. Trzosińska, *Stud. Mater. Oceanolog.*, 1976, **14,** 68.
40. K. Pedersen and B. Larsen, *Kemiske og Biologiske Undrsøceler Baeltprojekt*. Miljøstrelsen, Copenhagen, 1976.
41. L. Brügmann, *Acta Hydrochim. Hydrobiol.*, 1979, **7,** 409.
42. *Idem, Chem. Erde*, 1979, **38,** 292.
43. *Idem, Oceanologia*, 1981, **13,** 93.
44. K. Brzozowska, H. Podfigurne and M. Kosek, *Ann. Acad. Med. Gedan.*, 1973, **3,** 17.
45. A. Brzezińska, T. Bogacka, R. Taylor and A. Trzosińska, *Oceanologia*, 1979, **11,** 85.
46. E. Andrulewicz, *Stud. Mater. Oceanolog.*, 1976, **15,** 79.
47. K. Korzeniewski, *Badania Sozologiczne w Brzegowej Strefie baĹtyku Polskiego Wybrzeża Środkowego*. WSP, SĹupsk, 1978.

Talanta, Vol. 30, No. 7, pp. 487–492, 1983
Printed in Great Britain.

0039-9140/83 $3.00+0.00

MECHANISM OF EXTRACTION OF THE PALLADIUM(II) THIOCYANATE COMPLEX BY POLYETHER FOAM

SARGON J. AL-BAZI and ARTHUR CHOW
Department of Chemistry, University of Manitoba, Winnipeg, Manitoba, Canada

(*Received* 4 *November* 1982. *Accepted* 6 *January* 1983)

Summary—The mechanism of sorption of the palladium(II) thiocyanate complex by polyether-type polyurethane foam has been investigated. At low thiocyanate concentration, palladium is most likely extracted as $Pd(SCN)_2$. The results obtained in the presence of enough thiocyanate for formation of the $Pd(SCN)_4^{2-}$ complex are in disagreement with several possible mechanisms for sorption of the anionic metal complex by the foam, such as adsorption, solvent extraction, ligand addition or exchange, and weak or strong base anion-exchange. The extraction of $Pd(SCN)_4^{2-}$ at high pH increased in the order $Li^+ < Na^+ < Cs^+ < Rb^+ < K^+ < NH_4^+$ which is in good relation with the "cation-chelation" mechanism. This mechanism was also found predominant in the extraction of $Pd(SCN)_4^{2-}$ complex from hydrochloric acid solutions.

For several solvent-extraction systems, the mechanism through which palladium is extracted from the aqueous phase is mainly explained as due to formation of a neutral complex, with general formula PdX_2L_2,[1-7] for example, the extraction of $Pdpy_2(SCN)_2$ by methyl isobutyl ketone.[7]

The extraction of palladium as an ion-association complex of the type $2C^+ \cdot PdX_4^{2-}$ has also been reported,[8-10] where C^+ is a counter-ion. For instance, palladium is extracted as $[H_3O^+] \cdot [HPd(SCN)_4^-]$ by butanol or isoamyl alcohol and as $2[H_3O^+] \cdot [Pd(SCN)_4^{2-}]$ by cyclohexane in benzene.[10]

The possible mechanisms by which polyether-type polyurethane foam could act in such systems are described later in the paper. The purpose of the present work was to investigate the mechanism of sorption of palladium as a thiocyanate complex from aqueous solutions by polyether-type polyurethane foam.

EXPERIMENTAL

Apparatus

A model 306 Perkin-Elmer atomic-absorption spectrophotometer was used for the determination of palladium. Spectrophotometric measurements were made with a Varian model 634S spectrophotometer and the pH values were determined with a Fisher Accumet model 520 pH-meter. An automatic controlled-temperature multiple squeezer was used for squeezing the foam in the sample solutions.

Reagents

Polyether-type polyurethane foam (No. 1338M) sheets were obtained locally and cut into small cubes of approximately 1 g each. These foam cubes were washed and dried as previously described.[11]

A stock solution of $4.7 \times 10^{-3} M$ (500 μg/ml) palladium was prepared from $PdCl_2$ in 0.1 M hydrochloric acid, and a 5.0 M stock solution of potassium thiocyanate was prepared in doubly distilled and demineralized water.

Procedure

The sample solution was prepared in a 100-ml standard flask by diluting a known amount of the stock solutions of palladium, thiocyanate and any other reagents to volume with water.

The extraction and calculation were done by the procedures already described.[11]

RESULTS AND DISCUSSION

There are several possible mechanisms for the sorption of metal ions from aqueous solution by polyether-type polyurethane foam. The predominant one will depend upon the conditions of sorption and the species sorbed. In the "surface adsorption" mechanism, the metal ion is adsorbed at some sites on the polymer surface. For palladium, the high foam capacity (0.81 mole/kg) indicates that an absorption rather than an adsorption process is at work. Because of the high values of foam capacity obtained for the sorption of different metals, the surface adsorption mechanism has also been rejected by other workers.[12-14] The absorption isotherm for the sorption of palladium from acidic thiocyanate solutions by polyether-type polyurethane foam is plotted in Fig. 1. The amount of metal on the foam increases linearly with its concentration in the initial solution, up to $9.4 \times 10^{-4} M$. At higher concentrations the equilibrium amount of palladium on the foam is independent of the initial concentration in solution, which indicates saturation of the foam.

In the "solvent extraction" mechanism, it is proposed that the polyether foam acts as a polymeric analogue of diethyl ether in solvating the sorbed species. According to this mechanism, the metal ions are extracted as a neutral complex of the type $H_{(n-m)}MX_n$ [M = metal (with charge $m+$), X = halide or pseudohalide] or an ion-association complex

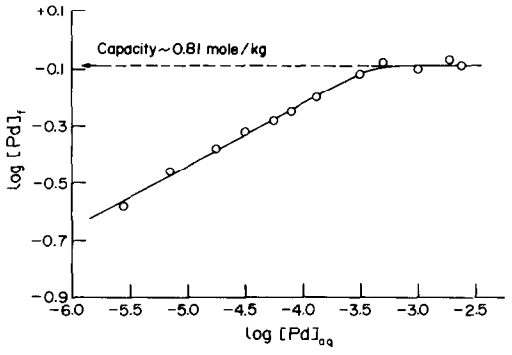

Fig. 1. Effect of initial palladium concentration on the sorption of palladium. Conditions: 50 ± 1 mg of foam; 95 ml of solution $0.5M$ in HCl, 6×10^{-3}–$5.6 \times 10^{-2}M$ in KSCN (the concentration of which is directly proportional to that of palladium, to minimize interference by thiocyanic acid).

$(n-m)[C^+]\cdot[MX_n^{(n-m)-}]$ where C^+ is a bulky cation. The equilibrium between 49 ± 1 mg of foam and 95 ml of $1 \times 10^{-4}M$ palladium solution in $6 \times 10^{-3}M$ thiocyanate medium containing various amounts of hydrochloric acid was therefore studied. Figure 2 shows that as the hydrochloric acid concentration was increased from 0.1 to $0.5M$, the degree of palladium extraction increased slowly from 95% (log $D = 4.55$) to 98% (log $D = 4.99$). At higher acidity the degree of extraction remained independent of acid concentration. The effect of lower acidities was studied under the same conditions and is also shown in Fig. 2. The pH was varied from 1.0 to 10.7 by the addition of lithium hydroxide or hydrochloric acid. The degree of extraction decreased sharply from 95% at pH 1.0 to 54% (log $D = 3.35$) at pH 4.0 and then slowly to 42% (log $D = 3.14$) at pH 10.7. The absorption spectra of the solutions, before the extraction, showed that the absorbance band at 308 nm, which is assigned to the $Pd(SCN)_4^{2-}$ complex,[8,15-18] was not changed in either intensity or shape by change in the acidity of the solution. These results suggest that hydrochloric acid only influences the distribution of the palladium thiocyanate complex between foam

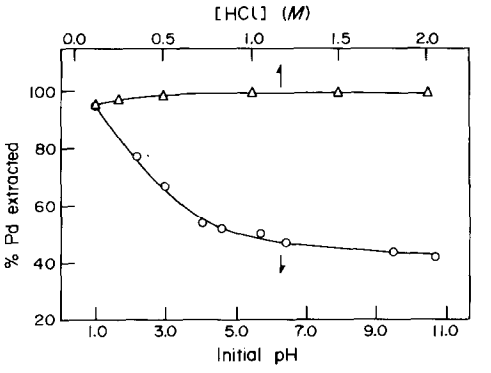

Fig. 2. Effect of acidity of solution on the sorption of palladium. Conditions: 49 ± 1 mg of foam; 95 ml of solution $1 \times 10^{-4}M$ in Pd(II), $6 \times 10^{-3}M$ in KSCN.

Table 1. Effect of lithium chloride concentration on the extraction of palladium: [Pd(II)] $1 \times 10^{-4}M$; pH 2.7; solution volume 95 ml; foam weight 50 ± 1 mg; temperature 25.0 ± 0.1°C

[LiCl], M	Extraction, %	log D
0.0	24	2.79
0.1	10	2.31
0.5	7	2.13
1.0	2	1.53

and solution, and not formation of the extractable species. The results in Fig. 2 indicate that more than 40% of the palladium is extracted from basic solutions where the formation of the neutral protonated species $H_2Pd(SCN)_4$ is not possible. It is also obvious that approximately $0.5M$ hydrochloric acid is sufficient for maximum extraction of palladium, a much lower concentration than that ($3M$) reported by Paria and Majumdar[19] for the extraction by ethyl acetate. These results, as well as the high distribution coefficients ($\sim 10^5$) obtained in comparison to the value of 0.02 reported for the extraction of palladium from acidic thiocyanate solutions by diethyl ether,[20] indicate that it is difficult to treat the polyether polyurethane foam as an analogue of diethyl ether.[21,22] Furthermore, the $Pd(SCN)_4^{2-}$ complex was completely recovered from the foam with acetone, which does not agree with the fact that the polarity of urethane polymers has been estimated to be very similar to that of acetone.[23] From these results it can be concluded that factors other than a simple ether-like "solvent extraction" mechanism operate in the distribution of $Pd(SCN)_4^{2-}$ between foam and aqueous phase.

The sorption of the metal ion through a "ligand addition or exchange" mechanism has also been suggested[12] and is attributed to the fact that polyurethane foam contains a large number of lone electron pairs on its nitrogen and oxygen atoms, these being supposed to be involved in co-ordinate bonding to the metal:

$$MX_n^{m-} + zL \rightleftharpoons [MX_{(n-z)}L_z]^{(m-z)-} + zX^-$$

$$MX_n^{m-} + zL \rightleftharpoons [MX_nL_z]^{m-}$$

where L represents the lone pair and its associated atom in the polyurethane.

Several investigations were therefore made of the sorption of palladium from both chloride and thiocyanate solutions. In one experiment, the effect of different chloride concentrations ranging from zero to $1M$ was studied. The results given in Table 1 indicate that the amount of palladium sorbed on the foam decreases with increasing chloride concentration. The ultraviolet-region spectrum of the solution containing no lithium chloride showed two characteristic maxima at 204 and 234 nm. The addition of lithium chloride resulted in a shift in these

absorption bands to 220 and 278 nm and these bands showed maximum absorbance at lithium chloride concentrations greater than 0.5*M*. The absorbance bands at 204 and 234 nm most likely correspond to $PdCl_2$, while those at 220 and 278 nm have been assigned to $PdCl_4^{2-}$ by various workers.[15,24] These results indicate that the neutral $PdCl_2$ is extractable by the foam, whereas $PdCl_4^{2-}$ is not. The low degree of extraction from 0.1*M* lithium chloride indicates that the affinity of polyether foam for palladium through the "ligand *substitution*" mechanism, *i.e.*,

$$PdCl_4^{2-} + 2L \rightleftharpoons PdCl_2L_2 + 2Cl^-$$

is very low in comparison to that of many solvent extractants[1,2,5,6,25,26] which can give ligand substitution even at hydrochloric acid concentrations > 1*M*. Since most palladium complexes are square planar,[27] the species sorbed is probably $PdCl_2L_2$ [formed by the *addition* of 2L to $PdCl_2$].

To determine the efficiency of polyurethane foam for palladium extraction from thiocyanate solutions at high pH, a series of solutions (95 ml) at pH 5.8 ± 0.4 with thiocyanate concentrations ranging from 4×10^{-4} to $1 \times 10^{-2}M$ was equilibrated for 20 hr with foam cubes each weighing 50 ± 1 mg. The results (Fig. 3) indicate that extraction increases with increasing thiocyanate concentration up to $1.2 \times 10^{-3}M$ where 72% (log $D = 3.68$) of the palladium is extracted, and then slowly decreases again, reaching 39% (log $D = 3.09$) at $1 \times 10^{-2}M$ thiocyanate. The absorbance of these solutions at 308 nm is also shown in Fig. 3 and indicates that at thiocyanate concentrations higher than $1.6 \times 10^{-3}M$ the formation of the $Pd(SCN)_4^{2-}$ complex is almost complete, and independent of thiocyanate concentration. Since the extraction decreases at thiocyanate concentrations $> 1.2 \times 10^{-3}M$, it seems likely that $Pd(SCN)_2$ is the species extracted, rather than $Pd(SCN)_4^{2-}$:

$$PdCl_2 + 2SCN^- \rightleftharpoons Pd(SCN)_2 \overset{SCN^-}{\rightleftharpoons} Pd(SCN)_4^{2-}$$

$$\downarrow\uparrow$$

$$\overline{Pd(SCN)_2} + \overline{2L} \rightleftharpoons \overline{Pd(SCN)_2L_2}$$

where the bars indicate the foam phase. The extraction of a neutral thiocyanate complex by polyether foam was reported by Abbas *et al.*[28] who indicated that $Fe(SCN)_3L_3$ was the species sorbed from solutions containing iron and thiocyanate in molar ratio 1:3.

When the effect of thiocyanate concentration was studied at pH 2.7 ± 0.1, a higher degree of extraction was obtained (Fig. 3). Since the effect of thiocyanate concentration on the absorbance of these solutions at 308 nm was similar to that at pH 5.8 ± 0.4 (Fig. 3), the higher extraction for thiocyanate concentrations $< 1.2 \times 10^{-3}M$ is mainly due to the simultaneous extraction of $Pd(SCN)_2$ and $Pd(SCN)_4^{2-}$, whereas, for solutions containing more than $1.2 \times 10^{-3}M$ thiocyanate it is most likely due to the sorption of $Pd(SCN)_4^{2-}$ complex.

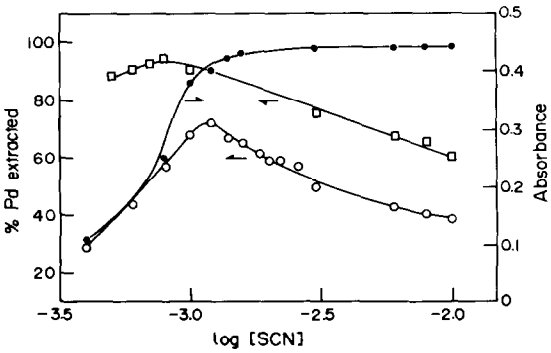

Fig. 3. Effect of thiocyanate concentration on the formation and sorption of palladium(II) thiocyanate complex. Conditions for spectrophotometry (●): [Pd(II)] = $1 \times 10^{-4}M$, pH = 5.8 ± 0.4, $\lambda = 308$ nm, path-length = 1 mm. Conditions for extraction: 50 ± 1 mg of foam; 95 ml of $1 \times 10^{-4}M$ Pd(II); (○) pH = 5.8 ± 0.4; (□) pH = 2.7 ± 0.1.

The decrease in extraction at thiocyanate concentrations $> 1.2 \times 10^{-3}M$ suggests that sorption does not take place by either the ligand addition or exchange mechanisms:

$$Pd(SCN)_4^{2-} + zL \rightleftharpoons [Pd(SCN)_4L_z]^{2-} \quad (z = 1 \text{ or } 2)$$

$$Pd(SCN)_4^{2-} + 2L \rightleftharpoons Pd(SCN)_2L_2 + 2SCN^-$$

The first possibility is ruled out because the co-ordination number of the palladium would increase to five or six, which is rare for palladium(II) complexes and has not been observed in their solvent extraction.[29,30] In the ligand substitution mechanism, the replacement of the strongly bound[31-34] sulphur atom by the nitrogen or oxygen atoms on the foam is unlikely and has not been reported even for strongly donating solvents.[29,30] Therefore in the presence of excess of thiocyanate, palladium is extracted as $Pd(SCN)_4^{2-}$, which is the complex formed in the aqueous solution before extraction. This was further evidenced by the foam changing colour to the golden yellow (due to the $Pd(SCN)_4^{2-}$ complex) of the solution before extraction. These results correlate with those reported by Hamon[12] which showed that the $Co(SCN)_4^{2-}$ complex present in the initial solution was extracted by the foam.

It was suggested by Bowen[13] that the extraction of anionic metal complexes could be due to the polyurethane foam acting as a weak or strong anion-exchanger. The feasibility of existence of anion-exchange sites arises from the tendency of both the nitrogen atoms of the urethane linkage and the ether oxygen atoms to accept protons to give

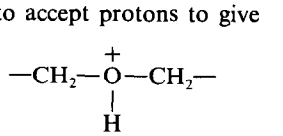

or

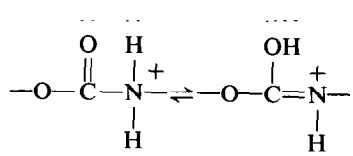

and hence the polyether-type polyurethane foam will have anion-exchange sites of various strengths. This mechanism may contribute significantly to the sorption of anionic metal complexes in the presence of high concentrations of strong acids. As mentioned in connection with the effect of pH on extraction of the $Pd(SCN)_4^{2-}$ complex (Fig. 2), more than 40% was extracted from basic solutions, where protonation of the foam is improbable. Furthermore, 95% of the palladium was extracted at pH 1.0, which is unlikely to be acidic enough for protonation of the foam. Therefore, the sorption of $Pd(SCN)_4^{2-}$ through the "anion-exchange" mechanism is considered improbable.

Recently Hamon *et al.*[35] suggested the "cation-chelation" mechanism (CCM) for the sorption of anionic metal complexes. According to this mechanism, polyether-based polyurethane foam can chelate metal ions in a similar way to their chelation by cyclic and linear polyethers, most likely owing to the polyether chains adopting a helical configuration around the cations. Thus the sorption of ion-association complexes containing cations such as Na^+, K^+, NH_4^+, H_3O^+, Rb^+, Ag^+, Tl^+, Ba^{2+}, Sr^{2+}, Pb^{2+} by polyether foam is attributed to specific chelation of the cation by the polyether segment of the foam. It is further considered that the extent of sorption depends not only on the chelation affinity of the cation (which depends on its size and charge) but also on the nature and hydrophobicity of the anionic metal complex. To test whether the CCM is involved

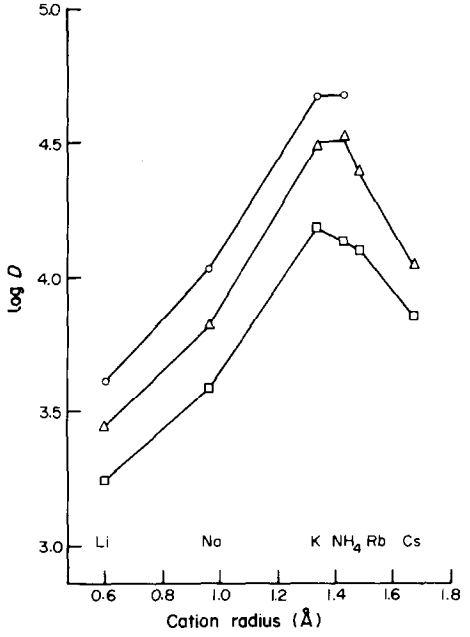

Fig. 4. Effect of the size of various univalent cations on the distribution of the palladium thiocyanate complex between foam and aqueous solution. Conditions: 50 ± 1 mg of foam; 95 ml of solution $1 \times 10^{-4}M$ in Pd(II), $6 \times 10^{-3}M$ in KSCN; (□) 0.1*M*, (△) 0.25*M*, (○) 0.5*M* salt concentration; pH = 6.0 ± 0.2 except for NH_4Cl solution (pH = 4.3 ± 0.2).

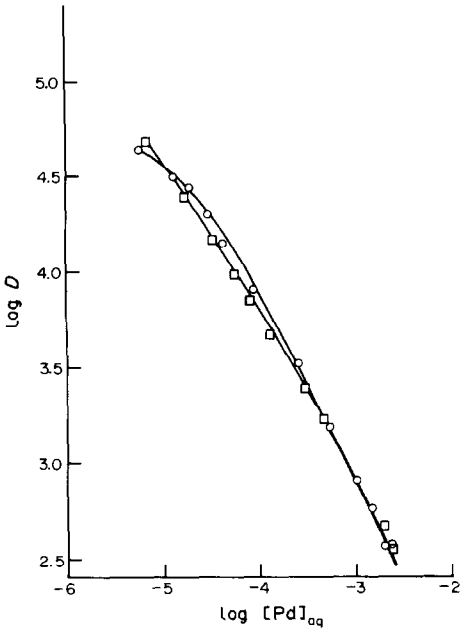

Fig. 5. Plots of log *D* *vs.* log of equilibrium palladium concentration in the presence of hydrochloric acid or potassium chloride. Conditions: 50 ± 1 mg of foam; 95 ml of solution, (○) 0.5*M* KCl, pH = 5.5 ± 0.4; (□) 0.5*M* HCl; 6×10^{-3}–$5.6 \times 10^{-2}M$ in KSCN (concentration of which is directly proportional to that of palladium to minimize interference by thiocyanic acid or potassium thiocyanate).

in sorption of the $Pd(SCN)_4^{2-}$ complex by polyether foam, the effect of the chlorides of Li^+, Na^+, K^+ and NH_4^+ was investigated, at pH 6.0 ± 0.2 except for ammonium chloride, for which pH 4.3 ± 0.2 was used in order to prevent formation of the $Pd(NH_3)_4^{2+}$ complex.[36–38] It was found that when the salt concentration rose from zero to 0.5*M*, the extraction increased from 50% (log $D = 3.28$) to 69% (log $D = 3.28$) for Li^+, 85% (log $D = 4.02$) for Na^+ and 96% (log $D = 4.68$) for K^+ and NH_4^+. The spectra of these solutions showed that the absorbance band of the $Pd(SCN)_4^{2-}$ complex at 308 nm was the same for all the solutions. Thus the differences in the degree extraction from the different media must be due to differences in the distribution of $Pd(SCN)_4^{2-}$ between foam and solution and not to differences in the degree of formation of the complex. When the results for a fixed salt concentration are plotted as a function of the cation size (Fig. 4), it is obvious that the effect of the cations on the efficiency of polyurethane foam for palladium extraction increases in the order $Li^+ < N^+ < Cs^+ < Rb^+ < K^+ \sim NH_4^+$. This order corresponds to that obtained previously[35,39] and indicates that the CCM is the major means of extraction of the $Pd(SCN)_4^{2-}$ complex by polyether-type polyurethane foam.

Complexation of the hydronium ion, H_3O^+, by crown ethers[40] and cryptates[41] has been reported, and its behaviour as a counter-ion in the sorption of anionic metal complexes by the CCM has also been suggested.[35] Therefore, the extraction of $Pd(SCN)_4^{2-}$

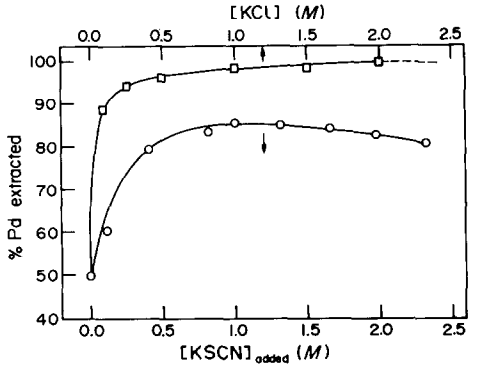

Fig. 6. Comparison of palladium thiocyanate extraction as a function of potassium chloride or thiocyanate concentration. Conditions: 50 ± 1 mg of foam; 95 ml of solution $1 \times 10^{-4}M$ in Pd(II), $6 \times 10^{-3}M$ in KSCN, pH ≈ 6.1 ± 0.1.

from acidic solutions by the "cation-chelation" mechanism is also possible, and this would fit with the fact already noted, that the acid concentration needed for the palladium extraction is lower than that reported for extraction into ethyl acetate.[19] To confirm this, the effect of the metal-ion concentration on the sorption of palladium from 0.5*M* hydrochloric acid or potassium chloride solutions at pH 5.5 ± 0.4 was studied. The similarities in the capacity of the foam (0.81 mole/kg) and the equilibrium palladium concentration as a function of the amount of palladium sorbed (Fig. 5) are strong evidence that the $Pd(SCN)_4^{2-}$ complex is extracted through the CCM even from acidic solutions.

To determine the effect of other anions on the extractability of the $Pd(SCN)_4^{2-}$ complex, the degree of sorption from $1 \times 10^{-4}M$ palladium solution at pH 6.1 ± 0.1 was studied as a function of chloride and thiocyanate concentrations. The results given in Fig. 6 indicate that in both series of solutions (*i.e.*, chloride and thiocyanate), the extraction at first increases sharply with anion concentration and then levels off (and eventually decreases slightly in the thiocyanate system) and that at a given concentration, chloride gives better extraction than thiocyanate.

These results can be explained by assuming a competition between $Pd(SCN)_4^{2-}$ and X^- ions ($X^- = SCN^-$ or Cl^-) for the chelated potassium ions, and that this is highly dependent on the hydrophobicity of the X^- ions. The hydrophobicity is determined by size, charge density and the ability to form strong hydrogen bonds with water. This is illustrated in Fig. 7, which shows the sorption of the anionic metal complex as taking place through two steps.

1. Extraction of the ion-association complex of the anionic metal complex and the cation through a simple mechanism which is highly dependent on the hydrophobicity of both ions and explains the fact that the extractability of $Pd(SCN)_4^{2-}$ greatly exceeds that of $PdCl_4^{2-}$.

2. Dissociation of the ion-association complex, whereby the cation can occupy a cavity in the foam and the anionic metal complex will act as a counter-ion to neutralize the charge of the chelated cation.

In the "cation-chelation" mechanism, the second step is the extraction-determining step and is highly dependent on how well the cation fits the cavity in the foam. This step in the mechanism explains why cation effect on the efficiency of extraction $Pd(SCN)_4^{2-}$ decreases in the order $K^+ > Rb^+ > Cs^+$ (Fig. 4) which is the opposite of their ability for ion-association complex formation and is not what might be expected on the basis of simple ion-pair extraction into an organic solvent.[42] However, it must be remembered that in the presence of Rb^+ and Cs^+, the extraction

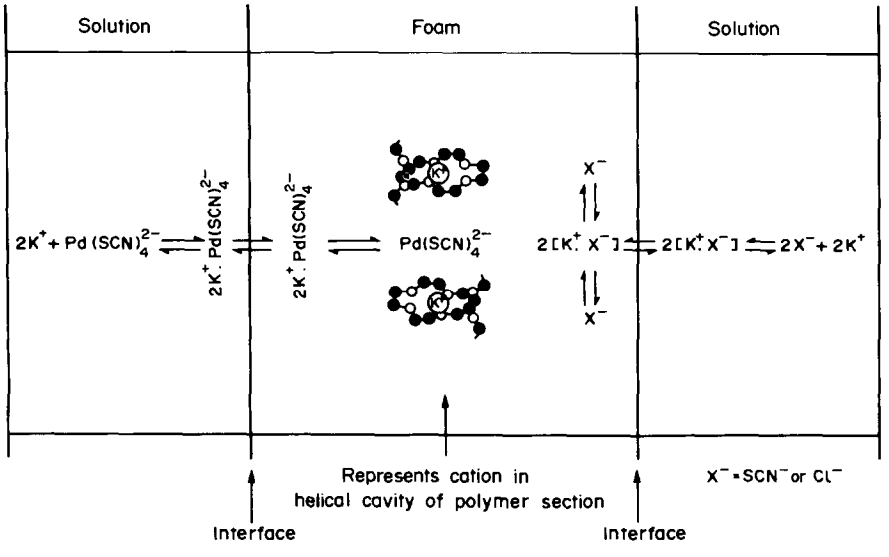

Fig. 7. Proposed two-step extraction mechanism. ○, Oxygen; ●, CH_2.

of $Pd(SCN)_4^{2-}$ through the "ion-association" mechanism may play a significant role in the sorption process. For large cations such as Et_4N^+ and Bu_4N^+ the simple "ion-association" complex extraction may even be the predominant mechanism as indicated by Hamon[12] for extraction of the $Co(SCN)_4^{2-}$ complex.

From the diagram it is also apparent that if considerable extraction of another ion-association complex containing the same cation as the anionic metal complex, $MX_n^{(n-m)-}$, occurs either during or after the extraction of $MX_n^{(n-m)-}$, then the latter may be desorbed by an "anion-exchange" mechanism. This is the reason why the sorption of $Pd(SCN)_4^{2-}$ complex decreases with potassium thiocyanate concentrations $>1M$ (Fig. 6). The anion-exchange behaviour of polyether foam differs from that of the solid and liquid anion-exchangers by the fact that the exchange mechanism operates *after* the extraction of the ion-association complex.

Finally, the sorption of $Pd(SCN)_4^{2-}$ through the CCM explains the following results, obtained in other experiments.

1. In the presence of $2M$ potassium chloride, an average of 99% (log $D = 5.12$) of the palladium was extracted at pH values ranging from 1.0 to 10.5, but in its absence, the extraction decreased with increasing basicity of the solution (Fig. 2).

2. The metal could be recovered with high efficiency when the foam was treated with acetone, probably owing to swelling of the foam and resultant release of the chelated cation.

3. The extraction of palladium from $6 \times 10^{-3}M$ thiocyanate/$0.5M$ ammonium chloride medium dropped from 96% at pH 4.0 to 75% at pH 6.3 and to zero at pH 7.4, owing to the formation of $Pd(NH_3)_4^{2+}$ in basic solution.

Conclusions

The relatively high extraction of palladium from solutions containing low thiocyanate and chloride concentrations is mainly due to the extraction of the neutral species PdX_2 ($X = Cl^-$ or SCN^-). On the other hand, in the presence of high thiocyanate concentration, the sorption of the anionic metal complex, $Pd(SCN)_4^{2-}$ from highly acidic solutions and also from solutions at high pH and containing Li^+, Na^+, K^+ or NH_4^+ ions is through the "cation-chelation" mechanism.

Acknowledgement—This work was supported by the Natural Sciences and Engineering Research Council of Canada.

REFERENCES

1. M. Mojski, *Talanta*, 1978, **25,** 163.
2. *Idem, ibid.*, 1980, **27,** 7.
3. P. Senise and F. Levi, *Anal. Chim. Acta*, 1964, **30,** 509.
4. W. J. Holland, R. A. Dimenna and R. J. Walker, *Mikrochim. Acta*, 1972, 183.
5. P. Dunn and W. J. Holland, *ibid.*, 1977 **I,** 363.
6. Yu. A. Zolotov, O. M. Petrukhin, V. N. Shevchenko, V. V. Dunina and E. G. Rukhadze, *Anal. Chim. Acta*, 1978, **100,** 613.
7. J. H. W. Forsythe, R. J. Magee and C. L. Wilson, *Talanta*, 1960, **3,** 330.
8. R. J. Magee and M. A. Khattak, *Microchem. J.*, 1964, **8,** 285.
9. D. J. Nicolas, *Natl. Inst. Metall., Repub. S. Afr., Project No.* 01374, 5 December 1974.
10. A. M. Golub and G. V. Pomerants, *Ukr. Khim. Zh.*, 1965, **31,** 104.
11. S. J. Al-Bazi and A. Chow, *Talanta*, 1982, **29,** 507.
12. R. F. Hamon, *Ph.D. Thesis*, University of Manitoba, 1981.
13. H. J. M. Bowen, *J. Chem. Soc.*, 1970, 1082.
14. G. A. Horsfall, *M.Sc. Thesis*, University of Manitoba, 1977.
15. A. A. Biryukov and V. I. Shlenskaya, *Russ. J. Inorg. Chem.*, 1967, **12,** 1362.
16. S. B. Joshi, M. D. Pundalik and B. N. Mattoo, *Indian J. Chem.*, 1973, **11,** 1297.
17. V. I. Shlenskaya, V. P. Khvostova and V. M. Peshkova, *J. Anal. Chem. USSR*, 1962, **17,** 596.
18. K. S. De Haas, *J. Inorg. Nucl. Chem.*, 1973, **35,** 3231.
19. P. K. Paria and S. K. Majumdar, *Indian J. Chem.*, 1976, **14A,** 820.
20. G. H. Morrison and H. Freiser, *Solvent Extraction in Analytical Chemistry*, pp. 129, 136. Wiley, New York. 1957.
21. H. D. Gesser, E. Bock, W. G. Baldwin, A. Chow, D. W. McBride and W. Lipinsky, *Sepn. Sci.*, 1976, **11,** 317.
22. J. J. Oren, K. M. Gough and H. D. Gesser, *Can. J. Chem.*, 1979. **57,** 2032.
23. A. Chapiro, M. Lamothe and T. LeDoan, *Eur. Poly. J.*, 1978, **14,** 647.
24. J. Vorlíček and J. Doležal, *Z. Anal. Chem.*, 1972, **260,** 369.
25. E. E. Rakovskii, N. V. Shvedova and L. D. Berliner, *J. Anal. Chem. USSR*, 1974, **29,** 1933.
26. R. J. Walker and W. J. Holland, *Mikrochim. Acta*, 1973, 591.
27. F. R. Hartley, *The Chemistry of Platinum and Palladium*. Wiley, Toronto, 1973.
28. M. N. Abbas, A. Vertes and T. Braun, in the press.
29. F. E. Beamish, *The Analytical Chemistry of The Noble Metals*. Pergamon Press, Oxford, 1966.
30. F. E. Beamish and J. C. Van Loon, *Recent Advances in the Analytical Chemistry of the Noble Metals*. Pergamon Press, Oxford, 1972.
31. J. Lewis, R. S. Nyholm and P. W. Smith, *J. Chem. Soc.*, 1961, 4590.
32. O. W. Howarth, R. E. Richards and L. M. Venanzi, *ibid.*, 1964, 3335.
33. A. Sabatini and I. Bertini, *Inorg. Chem.*, 1965, **4,** 959.
34. D. Forster and D. M. L. Goodgame, *ibid.*, 1965, **4,** 715.
35. F. R. Hamon, A. S. Khan and A. Chow, *Talanta*, 1982, **29,** 313.
36. W. M. MacNevin and W. B. Crummett, *Anal. Chem.*, 1953, **25,** 1628.
37. *Idem, Anal. Chim. Acta*, 1954, **10,** 323.
38. S. Singh, *J. Radioanal. Chem.*, 1975, **24,** 5.
39. A. S. Khan, *Ph.D. Thesis*, University of Manitoba, 1982.
40. R. M. Izatt, B. L. Haymore and J. J. Christensen, *J. Chem. Soc., Chem. Commun.*, 1972, 1308.
41. J. Cheney and J. M. Lehn, *ibid.*, 1972, 487.
42. G. Schill, in *Ion Exchange and Solvent Extraction*, Vol. 6, J. A. Marinsky and Y. Marcus (eds.), pp. 1–57. Dekker, New York, 1974.

Talanta, Vol. 30, No. 7, pp. 493–496, 1983
Printed in Great Britain.

0039-9140/83 $3.00+0.00

DETERMINATION OF BARIUM IN SULPHIDE ORES, CONCENTRATES AND OTHER GEOLOGICAL SAMPLES BY FLAME ATOMIC-ABSORPTION SPECTROMETRY

K. D. SHARMA
Central Research and Development Laboratory, Hindustan Zinc Limited, Zinc Smelter—313024, Udaipur, India

(*Received* 23 *February* 1982. *Revised* 14 *December* 1982. *Accepted* 5 *January* 1983)

Summary—A rapid, precise and selective analytical method has been developed for estimation of barium in geological samples by flame atomic-absorption spectrometry. The method consists of precipitation of barium sulphate with ammonium sulphate, followed by dissolution of the sulphates in EDTA at pH 10. The barium in this solution is measured by AAS with a nitrous oxide–acetylene flame. Appreciable amounts of lead, calcium and strontium can be tolerated in the method, which has been applied for estimation of barium in sulphide ores and concentrates of lead, zinc and copper, and is feasible for estimation of barium from 20.0 ppm to the per cent level in such geological samples.

In the Rajpura Dariba Mines near the Udaipur district of Rajasthan, barium occurs as barite ($BaSO_4$) and witherite ($BaCO_3$) along with lead–zinc ores. After removal of lead and zinc minerals by conventional froth flotation, efforts are made to separate barite concentrate, as this can be used[1,2] as a weighting agent in drilling fluids, owing to its high specific gravity. In the estimation of barium in such ore samples by conventional gravimetric and titrimetric methods, lead, calcium and strontium interfere as they also form insoluble sulphates. Heyn and Schupak[3] have described a procedure for selective precipitation of barium sulphate by complexation of Ba, Ca and Sr at pH 10 with EDTA and then release of the barium by lowering the pH to 4.5–5.0 by hydrolysis of ammonium persulphate, which simultaneously produced the sulphate required.

Přibil and Maričová[4] proposed obtaining a pure barium sulphate precipitate by addition of ammonium sulphate to a solution in which heavy-metal ions were complexed with EDTA at pH 4.5–5.0. This method was tried in this laboratory, but was not found suitable for low concentrations of barium. Therefore, there still seemed a need for a method for rapid determination of barium in such samples. Other techniques such as neutron-activation analysis,[5,6] mass spectrometry[7,8] and graphite-furnace atomic-absorption spectrometry[9] are either expensive or time-consuming. A flame atomic-absorption method using a nitrous oxide–acetylene flame has therefore been developed and is reported in this communication. This method has successfully been employed for estimation of barium in sulphide ores and concentrates of lead, zinc and copper.

EXPERIMENTAL

Reagents

All the chemicals used were of recognized analytical grade. Doubly distilled water was used throughout. A stock barium standard solution (Ba 1000 mg/l.) was prepared by dissolving 1.438 g of $BaCO_3$ in 20.0 ml of 1.0*M* hydrochloric acid and diluting the solution to 1000 ml.

Working standards (1–10 ppm) were prepared daily by diluting suitable aliquots of the stock standard solution, 2.0 ml of 4% EDTA solution and 3.0 ml of 5% sodium hydroxide solution being added for each 100 ml of working standard. These solutions were used for the atomic-absorption spectrometry calibration graph, which is linear over the concentration range 1–10 ppm barium.

Apparatus

A Pye Unicam SP1900 atomic-absorption spectrophotometer was used, with a fuel-rich nitrous oxide–acetylene flame. A Pye Unicam barium hollow-cathode lamp was used and the absorbance readings at 553.56 nm were integrated for 4 sec. The instrumental settings were those reported in the literature.[10,11]

Procedures

Barium in ores and zinc, copper and barium concentrates. To a weighed ore or concentrate sample containing 0.1–50 mg of barium, add 15.0 ml of concentrated hydrochloric acid followed by 10.0 ml of concentrated nitric acid and heat till a syrupy state is achieved. Add 5.0 ml of concentrated hydrochloric acid, cool, dilute to 100 ml and add 10.0 ml of 10% ammonium sulphate solution. Keep the solution on a hot water-bath for half an hour. Decant the supernatant liquid through a Whatman No. 42 or equivalent filter paper, then transfer and wash the precipitate with 1% ammonium sulphate solution. Transfer the filter paper and precipitate to the original beaker, add 5–10 ml of 4% EDTA solution and 3.0 ml of 5% sodium hydroxide solution (or one pellet of solid sodium hydroxide) and dilute to about 50 ml. Heat on a hot-plate to dissolve the sulphates and finally filter through a small amount of filter-paper pulp into a suitable size of standard flask. Dilute to volume after addition of one pellet of sodium hydroxide per 100 ml of final volume and measure the barium by AAS.

Barium in lead concentrate. Decompose a suitable amount of sample with *aqua regia* as above, then add 5.0 ml of concentrated nitric acid. Heat to evaporate the excess of nitric acid. Cool, dilute, precipitate the sulphates, wash the precipitate with two 10.0-ml portions of hot 10% ammonium acetate solution and continue as in the previous procedure.

Titrimetric determination. To compare the results obtained for the barium in the geological samples with those

found by an independent method, the following procedure was used.

Attack the sample as described above, add 5.0 ml of concentrated hydrochloric acid (or 5.0 ml of concentrated nitric acid, if the amount of lead in solution is expected to be more than 50 mg) and precipitate the sulphates. Wash the precipitate with two 10.0-ml portions of hot 10% ammonium acetate solution, transfer the precipitates to the original beaker and dissolve them in 4% EDTA solution as described above. Dilute the solution to about 200 ml and adjust the pH to 4.5–5.0 with ammonium acetate/acetic acid buffer. Heat to boiling and precipitate barium sulphate by adding two 10.0-ml portions of 10% cobalt sulphate solution. Digest the barium sulphate precipitate on a hot water-bath, let it settle and filter it off on a Whatman No. 42 paper. Wash the precipitate with hot 1% ammonium sulphate solution till the filtrate is free from cobalt and EDTA. Dissolve the precipitate in excess of 0.05*M* EDTA and back-titrate the surplus at pH 10 with 0.05*M* magnesium chloride, using Eriochrome Black T as indicator.

Table 1. Effect of foreign ions on estimation of barium by flame atomic-absorption

Barium taken, *mg*	Foreign ion added, *mg*			Barium found,* *mg*
	Pb	Sr	Ca	
76.2	10	—	—	76.4
76.2	20	—	—	76.7
76.2	30	—	—	76.7
76.2	50	—	—	76.7
125	—	5	—	126.8
125	—	10	—	127.3
125	—	20	—	135.0
76.2	50	—	25	75.4
76.2	50	—	50	74.8
76.2	50	—	75	76.7
76.2	50	—	100	75.4
124	50	10	100	123.3

*Mean of 3 replicates.

RESULTS AND DISCUSSION

In classical wet analysis[12–14] barium is separated as the sulphate. It may then be determined gravimetrically, or titrimetrically after dissolution in standard EDTA solution. However, in the presence of lead, strontium or calcium, the barium must be separated before the precipitation, to avoid contamination with the sulphates of these elements. This can be achieved by masking[4] with EDTA at pH 4.5–5.0 (the solubility products are $10^{-9.87}$ for $BaSO_4$, $10^{-7.79}$ for $PbSO_4$, $10^{-6.49}$ for $SrSO_4$ and $10^{-5.62}$ for $CaSO_4$). These methods are not very suitable for low concentrations of barium, however, and are fairly time-consuming for routine analyses of geological samples. A flame atomic-absorption method has, therefore, been developed for estimation of barium in such samples.

After decomposition of the sulphides with *aqua regia*, ammonium sulphate is added to precipitate all the barium along with other sulphates. The precipitated sulphates are dissolved in EDTA at pH 10 and this solution is used for AAS measurement of the barium. To obtain comparison results a titrimetric method can be used. After decomposition of the sample, the sulphates are precipitated. The precipitate is washed with ammonium acetate to remove most of the lead sulphate and then dissolved in EDTA to mask the remaining calcium, strontium and lead at pH 4.5–5.0. Barium is released, and precipitated as $BaSO_4$ at this pH by addition of cobalt sulphate.

Large amounts of lead can be masked with EDTA at pH 4.5–5.0 owing to the high stability constant of the lead–EDTA complex (the logarithms of the stability constants at 20° and 0.1*M* ionic strength are:[14] lead–EDTA 18.2, calcium–EDTA 10.59, strontium–EDTA 8.63 and barium–EDTA 7.76).

Table 1 shows the effect of cations that give insoluble sulphates, on the estimation of barium. Calcium and lead have no effect on the atomic-absorption signals due to barium. Up to 10 mg of strontium will cause less than 2% error, but larger amounts cause positive errors. Table 2 compares the barium values obtained by AAS and by the titrimetric method. Lower values for barium were obtained by the titrimetric method for samples containing less than 1% barium. Hence no comparison figures are reported for the copper concentrate sample. For the zinc tailing sample, where the barium content is only 45 ppm, the titrimetric method could not be used at all.

Lead and calcium are only partly precipitated along with the barium in the method developed. Table 3 gives the amount of lead and calcium precipitated with barium in one experiment. There is no

Table 2. Results for various samples

Sample	Ba in sample,* %	Barium added,† *mg*	Recovery, %	Ba found by titration,§ %
Barium ore 1	8.62	50	96	8.55
Barium ore 2	8.05	100	92	7.95
Barium concentrate	48.8	40	98	49.1
Zinc concentrate	0.86	50	94	0.70
Lead concentrate	1.25	50	95	1.12
Copper concentrate	0.35	25	98	—
Zinc tailings	0.0045	—	—	—

*Average of 5 or more estimations.
†Added as aliquots of standard barium solution to the solid samples before decomposition.
§Average of 3 estimations.

Table 3. Extent of precipitation of lead and calcium in the AAS method

Sample	Barium in the sample taken, *mg*	Lead			Calcium		
		Total in sample, *mg*	Precipitated, *mg*	Fraction precipitated, %	Total in sample, *mg*	Precipitated, *mg*	Fraction precipitated, %
Barium ore 1	43.1	10.0	0.70	7.0	7.5	0.03	0.4
Barium ore 2	40.25	4.0	0.15	3.8	15.0	0.06	0.4
Zinc concentrate	8.6	19.0	0.5	2.6	6.0	0.03	0.5
Copper concentrate	3.5	35.0	1.5	4.3	8.0	0.04	0.5
Lead concentrate	12.5	678.0	50.0	7.4	10.0	0.06	0.6

effect of calcium and lead on the AAS signal due to barium. However, most of the lead and calcium can be separated from barium by using the acid concentrations given in the procedure, and washing the precipitate with ammonium acetate solution.

The effect of the EDTA and sodium hydroxide concentration on the AAS readings was also studied.

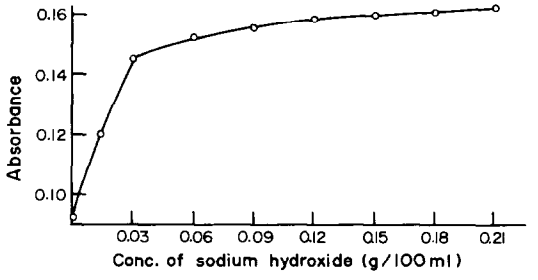

Fig. 1. Effect of sodium hydroxide concentration on absorbance reading for fixed amount of barium.

Up to 2.0 g of EDTA per 100 ml of solution has no effect; larger amounts than this can cause frequent solid deposition in the burner slot. If the sodium hydroxide concentration is less than 0.12 g per 100 ml of solution, the absorbance readings are lowered because of barium ionization in the flame (Fig. 1). Hence a sodium hydroxide concentration of 0.15 g per 100 ml is recommended.

The statistical analysis of several determinations of barium in the same sample is given in Table 4. The data show that the method is fairly precise. The reliability intervals for 95% and 99% confidence limits have been calculated by the method reported by Dean and Dixon.[15] Down to 100 μg of barium has been quantitatively precipitated and estimated by this method. Hence by use of a 5.0-g sample, a barium concentration as low as 20.0 ppm may be conveniently estimated. The detection limit for barium in the solution to be used for the AAS measurement is 0.16 ppm. The method is fairly rapid and 12 samples

Table 4. Statistical analysis of the results

Sample	No. of determinations	Mean Ba found, %	Relative std. devn., %	Reliability interval		Approximate composition of the sample
				(95% confidence limit)	(99% confidence limit)	
Barium ore	7	8.62	0.3	8.6 ± 0.31	8.62 ± 0.48	Zn—6%, Pb—2%, Cu—0.5%, Fe—4%, SiO_2—45%, Ca—1.5%
Zinc concentrate	7	0.86	3.9	0.86 ± 0.10	0.86 ± 0.16	Zn—54.0%, Pb—1.9%, Cu—1.0%, Fe—5.0%, Ca—0.6%, S—30.5%
Lead concentrate	7	1.25	3.6	1.25 ± 0.12	1.25 ± 0.16	Pb—67.8%, Fe—1.7%, Zn—3.5%, Ca—1.0%, S—13.0%
Copper concentrate	6	0.35	4.0	0.35 ± 0.04	0.35 ± 0.06	Cu—25.5%, Fe—22.5%, Zn—2.4%, Pb—3.5%, S—26.0%
Barium concentrate	5	48.8	0.5	48.8 ± 0.10	48.8 ± 0.16	Ba—48.8%, S—11.5%

can be conveniently analysed by a single analyst in a 6–8 hr working day.

Applications

Barium in sulphide ores and zinc, lead, copper and barium concentrates has been determined by this method. Amounts of barium added to the samples before the decomposition were recovered quantitatively. The barium content found by the proposed method in a variety of samples is in good agreement with that obtained by the titrimetric method. The method is simple, rapid and precise and is recommended for routine determination of barium in sulphide ores, concentrates and other such geological samples.

Acknowledgements—The author is thankful to the management of Hindustan Zinc Limited for granting permission to publish the data. The assistance of colleagues from the analytical division, *viz.* Messrs. S. C. Bhanawat, M. P. Jain, R. L. Menaria and S. K. Rawariya is also acknowledged.

REFERENCES

1. N. Cornell, *Engng. Mining J.*, 1978, **179,** 208.
2. A. R. D. Orr, *Mining Annual Review*, 1981, 117.
3. A. H. A. Heyn and E. Schupak, *Anal. Chem.*, 1954, **26,** 1243.
4. R. Přibil and D. Maričová, *Chem. Listy*, 1952, **46,** 542.
5. K. K. Turekian, *Geochim. Cosmochim. Acta*, 1968, **32,** 603.
6. K. K. Turekian and D. G. Johnson, *ibid.*, 1966, **30,** 1153.
7. T. J. Chow, *Science*, 1976, **193,** 57.
8. T. J. Chow and E. D. Goldberg, *Geochim. Cosmochim. Acta*, 1960, **20,** 192.
9. M. S. Epstein and A. T. Zander, *Anal. Chem.*, 1979, **51,** 915.
10. P. J. Whiteside, *Pye Unicam Atomic Absorption Data Book*, p. 10. Pye Unicam Ltd., Cambridge, 1975.
11. W. J. Price, *Analytical Atomic Absorption Spectrometry*, p. 187. Heydon, London, 1978.
12. A. I. Vogel, *A Text Book of Quantitative Inorganic Analysis*, 3rd Ed., p. 445. Longmans, London, 1975.
13. N. H. Furman, *Standard Methods of Chemical Analysis*, 6th Ed., Vol. 1, pp. 138–152. Van Nostrand, New York, 1962.
14. F. J. Welcher, *The Analytical Uses of Ethylenediaminetetracetic Acid*. Van Nostrand, New York, 1965.
15. R. B. Dean and W. J. Dixon, *Anal. Chem.*, 1951, **23,** 636.

Talanta, Vol. 30, No. 7, pp. 497–504, 1983
Printed in Great Britain

0039-9140/83 $3.00+0.00
Pergamon Press Ltd

SPECTROPHOTOMETRIC DETERMINATION OF TANTALUM IN ORES AND MILL PRODUCTS WITH BRILLIANT GREEN AFTER SEPARATION BY METHYL ISOBUTYL KETONE EXTRACTION OF TANTALUM FLUORIDE

ELSIE M. DONALDSON
Mineral Sciences Laboratories, Canada Centre for Mineral and Energy Technology, Energy, Mines and Resources Canada, Ottawa, Canada

(*Received* 22 *November* 1982. *Accepted* 28 *December* 1982)

Summary—A method for determining ~0.001% or more of tantalum in ores and mill products is described. After fusion of the sample with sodium carbonate, the cooled melt is dissolved in dilute sulphuric–hydrofluoric acid mixture and tantalum is separated from niobium and other matrix elements by methyl isobutyl ketone extraction of its fluoride from 1*M* hydrofluoric acid–0.5*M* sulphuric acid. The extract is washed with a hydrofluoric–sulphuric acid solution of the same composition to remove co-extracted niobium, and tantalum is stripped with dilute hydrogen peroxide. This solution is acidified with sulphuric and hydrofluoric acids and evaporated to dryness, and the residue is dissolved in oxalic–hydrofluoric acid solution. Tantalum is ultimately determined spectrophotometrically after extraction of the blue hexafluorotantalate–Brilliant Green ion-association complex into benzene from a 0.05*M* sulphuric acid–0.5*M* hydrofluoric acid–0.2*M* oxalic acid medium. The apparent molar absorptivity of the complex is 1.19×10^4 l.mole^{-1}.mm^{-1} at 640 nm, the wavelength of maximum absorption. Common ions, including iron, aluminium, manganese, zirconium, titanium, molybdenum, tungsten, vanadium, tin, arsenic and antimony, do not interfere. Results obtained by this method are compared with those obtained by an X-ray fluorescence method.

The Canadian Certified Reference Materials Project (CCRMP) is involved in the certification of a tantalum ore for its tantalum content. As part of this project, and for use in routine work in the CANMET chemical laboratory, a reasonably simple and reliable spectrophotometric method was required for the determination of ~0.001% or more of tantalum in diverse ores and mill products. The method should also be applicable to extracts and other solutions resulting from solvent extraction processes designed to recover tantalum from ores and concentrates and to separate it from niobium. Niobium is usually present in ores containing tantalum and it interferes to a certain extent in all known spectrophotometric methods for the determination of tantalum. Consequently, it was considered that a suitable method would involve the preliminary separation of tantalum from most of the niobium and from other matrix elements by extraction of tantalum fluoride from a hydrofluoric acid medium.

Probably the most widely used methods currently employed for the spectrophotometric determination of tantalum are those based on solvent extraction of the ion-association complexes formed between hexafluorotantalate and basic-dye cations of the triphenylmethane type such as Methyl Violet, Crystal Violet, Malachite Green and Brilliant Green.[1–4] Other similar but less frequently employed methods involve the use of xanthene (Rhodamine 6G, Rhodamine 6J and Butylrhodamine),[2,3] oxazine (Capri Blue, Nile Blue and Melba Blue),[5] triazine (Methylene Blue) and acridine (Acridine Orange) dyes.[6] These methods are characterized by high sensitivity, and are all considerably more selective and can tolerate much larger amounts of niobium, than those based on chelation systems involving chromogenic reagents such as pyrocatechol, pyrogallol, tribromopyrogallol, tiron, stilbazo, Alizarin Red S, quinalizarin, Pyrocatechol Violet, phenylfluorone,[7] Bromopyrogallol Red[8] and 1-(2-pyridylazo)-2-resorcinol.[9] Consequently, this type of spectrophotometric finish was considered to be the most promising for the present work, and because only triphenylmethane dyes were immediately available, the applicability of a dye of this type was investigated. Early work showed that the extraction of hexafluorotantalate–triphenylmethane complexes is greatly dependent on the concentration of sulphuric acid and that the optimum ranges of pH required for the extraction of the Methyl Violet and Crystal Violet complexes are very narrow. Those required for the Malachite Green and Brilliant Green complexes are somewhat broader.[2] Malachite Green has been recommended for the determination of tantalum in iron, steel[10,11] and niobium metal[12,13] and

in silicon,[14] boron, uranium, zirconium and uranium–zirconium alloys.[15] However, some preliminary work with this dye yielded erratic and inconsistent results, possibly because the compound used was relatively old and of unknown purity. Brilliant Green (Basic Green 1) has also been used previously[16–18] but most of the methods based on this dye appear in obscure Soviet and other journals not readily accessible to Western readers. Furthermore, the abstracts of these papers do not provide much information on the optimum conditions required for the extraction and spectrophotometric determination of tantalum. Because initial tests with Brilliant Green yielded promising results, it was chosen for further study.

The proposed method is based on the separation of tantalum from niobium and other matrix elements by methyl isobutyl ketone (MIBK) extraction of its fluoride complex from a 1*M* hydrofluoric acid–0.5*M* sulphuric acid mixture. The tantalum is stripped into dilute hydrogen peroxide and ultimately determined spectrophotometrically after extraction of the hexafluorotantalate–Brilliant Green complex into benzene from a 0.05*M* sulphuric acid–0.5*M* hydrofluoric acid–0.2*M* oxalic acid medium. Results obtained for ores and mill products by this method have been compared with those obtained by an X-ray fluorescence (XRF) method.

EXPERIMENTAL

Apparatus

Pear-shape 125- and 500-ml polypropylene separatory funnels, 50-, 100-, 200-, 500- and 1000-ml plastic standard flasks and 15-ml plastic centrifuge tubes equipped with plastic stoppers were used. Graduated "Nalgene" pipettes were used for adding all the reagents. Glass pipettes were used for preparation of the dilute tantalum solutions and for taking aliquots of the sample solutions for the MIBK and benzene extractions.

Reagents

Standard tantalum solution, 100 μg/ml. Transfer 0.1000 g of pure tantalum metal (Note 1) to a 100-ml platinum dish and add ~8 ml of concentrated hydrofluoric acid and ~3 ml of concentrated nitric acid. Cover the dish with a "Teflon" cover and warm gently until the metal has dissolved. Remove the cover, add ~5 ml of 50% v/v sulphuric acid and evaporate the solution to dryness, then wash down the sides of the dish with water and evaporate the solution to dryness again. Add ~15 ml of water and 7 ml of concentrated hydrofluoric acid, warm gently, if necessary (Note 2), to dissolve the salts, then transfer the solution to a 1-litre plastic standard flask (Note 3) and dilute to volume with water. Dissolve 6 g of oxalic acid in ~70 ml of warm water contained in a 250-ml "Teflon" beaker (Note 4), then dilute this solution and 5 ml of the tantalum stock solution to volume with water in a 100-ml plastic standard flask, to prepare a 5-μg/ml tantalum solution in 0.5*M* oxalic acid.

Brilliant Green, 0.2% solution. Transfer to a brown plastic bottle an amount of Brilliant Green sufficient for the number of extractions required. Add the required volume of water and shake to dissolve the dye. Allow the solution to stand for 1 hr, then use it within ~30 min. (The Brilliant Green used in this work had a total dye content of 94%; it was obtained from the Fisher Scientific Company, Fair Lawn, New Jersey, U.S.A., and was used without further purification.)

Sulphuric acid (0.25M)–hydrofluoric acid (2.5M) solution. From a graduated pipette, add 7 ml of concentrated sulphuric acid to ~300 ml of water contained in a 500-ml plastic standard flask, mix and allow the solution to cool to room temperature, Add 45 ml of concentrated hydrofluoric acid and dilute to volume with water.

Hydrofluoric acid (1M)–sulphuric acid (0.5M) solution. Add 55 ml of 50% v/v sulphuric acid and 36 ml of concentrated hydrofluoric acid to ~500 ml of water contained in a 1-litre plastic standard flask and dilute to volume with water.

Oxalic acid, 6% solution. Dissolve 30 g of oxalic acid in 500 ml of water contained in a 600-ml "Teflon" beaker, by heating gently. Allow the solution to cool to room temperature, then transfer it to a plastic bottle (Note 4).

Hydrofluoric acid, 2M. Store in a plastic bottle.

Sulphuric acid, 50% v/v.

Hydrogen peroxide, 5% v/v. Dilute 10 ml of 30% w/v hydrogen peroxide to 200 ml with water.

Benzene. Add ~0.5 g of quinol (Note 5) to ~600 ml of reagent-grade benzene contained in a 1-litre flask. Using a mechanical shaker, shake for ~1 hr, then, using phase-separating paper, filter the solvent into a brown 1-litre bottle.

MIKB, equilibrated. Shake ~200 ml each of reagent-grade MIBK and 1*M* hydrofluoric acid–0.5*M* sulphuric acid solution for about 1 min in a 500-ml plastic separatory funnel. After the layers have separated, drain the lower aqueous layer into a second 500-ml plastic separatory funnel (Note 6).

Procedures

Calibration curve. From a burette, add 1, 2, 3, 4, 5 and 7 ml of 5-μg/ml standard tantalum solution to six 125-ml polypropylene separatory funnels marked at 25 ml, then add 9, 8, 7, 6, 5 and 3 ml, respectively, of 6% oxalic acid solution. Add 10 ml of 6% oxalic acid solution to two further 125-ml separatory funnels for use as blanks (Note 7). Add 5 ml of 0.25*M* sulphuric acid–2.5*M* hydrofluoric acid solution to each funnel (Note 8). Add 5 ml of 0.2% Brilliant Green solution (aged for 1 hr) to two of the flasks (Note 9), dilute to the 25-ml mark with water, then without delay, add by pipette* 25 ml of benzene, stopper the funnels and shake them for 2 min. Proceed in a similar manner with the extraction of the tantalum hexafluoride–Brilliant Green complex from the remaining solutions, taken in pairs, then drain off and discard the lower (aqueous) layers. Drain the benzene layers into 15-ml plastic centrifuge tubes (Note 10), stopper the tubes and allow the extracts to stand for at least 30 min. Measure the absorbance of each extract at 640 nm against benzene as reference, using 10-mm cells (Note 11). Correct the absorbances by subtracting the mean of the absorbances obtained for the blanks (Note 12). Plot μg of tantalum *vs.* absorbance.

Ores and mill products. Depending on the expected tantalum content, transfer 0.1–0.8 g of powdered sample, containing not more than 400 mg of niobium and 8 mg of tantalum, to a 30-ml platinum crucible containing 4.0 ± 0.1 g of sodium carbonate (Notes 13 and 14). Mix thoroughly, then cover the crucible with a platinum lid and fuse the mixture over a blast burner for ~8 min. Allow the crucible and cover to cool for several minutes, then transfer them to a covered 400-ml "Teflon" beaker containing ~75 ml of water, 15 ml of 50% v/v sulphuric acid and 2 ml of concentrated hydrofluoric acid. When the melt has dissolved, remove the crucible and cover after washing them thoroughly with water, then cover the beaker (Note 15) with a "Teflon" cover and evaporate the solution to ~75 ml to remove carbon dioxide and the excess of hydrofluoric acid. Allow the solution to cool to room temperature, then add

*An automatic or safety pipette should be used.

7 ml of concentrated hydrofluoric acid (Note 16) and mix thoroughly. Transfer the solution to a 200-ml plastic standard flask, dilute to volume with water, mix and allow the solution to stand until any calcium sulphate or other insoluble material has settled.

Transfer a suitable aliquot (10, 20 or 25 ml) of the solution to a 125-ml polypropylene separatory funnel marked at 25 ml and, if necessary, dilute to the mark with 1*M* hydrofluoric acid–0.5*M* sulphuric acid solution. Using a plastic graduated cylinder, add 25 ml of equilibrated MIBK, stopper the funnel and shake it for 2 min. Allow the layers to separate, then drain the lower (aqueous) layer into a second 125-ml separatory funnel and wash the ketone phase by shaking it for ~30 sec with 10 ml of 1*M* hydrofluoric acid–0.5*M* sulphuric acid solution. Drain the aqueous layer into the second funnel and repeat the washing step. Add 25 ml of equilibrated MIBK to the second funnel containing the combined aqueous phase and wash solutions and extract the solution again by shaking for 1 min. After the layers have separated, drain off and discard the lower (aqueous) layer. Wash the ketone layer twice with 10-ml portions of 1*M* hydrofluoric acid–0.5*M* sulphuric acid solution as described above, discarding each aqueous layer. Run the second extract into the first funnel and wash the second funnel with MIBK from a plastic squeeze-type wash-bottle.

Add 20 ml of 5% hydrogen peroxide solution to the combined extracts, stopper the funnel and shake it for 1 min. Allow the layers to separate, then drain the lower (aqueous) layer into a 100-ml platinum dish and wash the stem of the funnel with water. Repeat the stripping step twice more by shaking the extract for ~30 sec each time with first 10 ml and then 5 ml of 5% hydrogen peroxide solution. Wash the stem of the funnel with water each time and collect the washings in the platinum dish (Note 17). Cover the dish with a "Teflon" cover, heat the solution to destroy the hydrogen peroxide, then remove the cover, add 1 ml of 50% v/v sulphuric acid and 3 or 4 drops of concentrated hydrofluoric acid (Note 18) and evaporate the solution to dryness.

If the aliquot taken for the MIBK extraction contains 35 μg or less of tantalum, add 10 ml of 6% oxalic acid solution to the platinum dish and evaporate the solution to ~5 ml. Add 5 ml of 0.25*M* sulphuric acid–2.5*M* hydrofluoric acid solution, warm gently for ~1 min (Note 2) to dissolve the salts, then transfer the solution to a 125-ml polypropylene separatory funnel marked at 25 ml, rinsing the dish with ~3-ml portions of water, so that the total volume of solution in the separatory funnel does not exceed 20 ml. Prepare two blank solutions as described for the calibration, then proceed with the addition of Brilliant Green solution and the subsequent extraction and determination of tantalum as described above.

If the aliquot taken for the MIBK extraction contains more than 35 μg of tantalum, then, depending on the expected tantalum content, add sufficient oxalic acid in crystalline form for 3 g to be present for each 50 ml of final solution. Add sufficient 2*M* hydrofluoric acid for 2.5 ml to be present for each 50 ml of final solution (Note 19), then heat the solution gently to dissolve the oxalic acid. To prevent crystallization of the oxalic acid, transfer the solution (Note 3), while still warm, to a plastic standard flask of appropriate size (50–200 ml), cool to room temperature and dilute to volume with water. Transfer a suitable aliquot (5 or 10 ml) of this solution (Note 20) to a 125-ml polypropylene separatory funnel. If necessary, add sufficient 6% oxalic acid solution for the total volume of the solution to be 10 ml, then add 5 ml of 0.25*M* sulphuric acid–2.5*M* hydrofluoric acid solution. Prepare two blank solutions as described for the calibration, then proceed with the extraction and determination of tantalum as described above.

Notes

1. If tantalum metal is not available, the standard solution (~0.2*M* in hydrofluoric acid) can be prepared by fusing 0.1221 g of tantalum pentoxide with 3 g of sodium carbonate in a covered platinum crucible. The cooled melt should be dissolved in ~250 ml of water containing 9.3 ml of concentrated hydrofluoric acid and the resulting solution diluted to volume with water in a 1-litre plastic standard flask.

2. The solution should not be heated too strongly, or hydrofluoric acid will be lost by volatilization.

3. The transfer can be facilitated by using a plastic funnel in the neck of the flask.

4. "Teflon" or plastic ware is recommended for the preparation and storage of solutions, to avoid boron contamination from borosilicate glass.

5. Quinol is added to destroy any organic peroxides present in the benzene and to help prevent aerial oxidation of the dye in the tantalum–Brilliant Green extract.

6. The acid layer can be used for a second equilibration of MIBK.

7. Because of the ease with which the solutions can become contaminated with boron contained in the dust in the laboratory, it is recommended that two blank solutions should be prepared and that the mean of the two results should be used to correct the absorbances of the tantalum extracts. During the author's experimental work, the absorbance of the blank for different solutions prepared from the same batch of Brilliant Green varied from ~0.06 to 0.11 (measured against benzene as reference).

8. The funnels should not be left unstoppered for too long, or hydrofluoric acid will be lost by volatilization.

9. Addition of the Brilliant Green solution to only two solutions at a time, followed by immediate extraction of the tantalum complex, is recommended because the dye is photosensitive. A low result will be obtained if the extraction is not performed within 3 or 4 min after addition of the dye. The brown bottle containing the dye solution should also be capped or covered after each use to minimize the introduction of light, and the extracts should be kept out of direct sunlight.

10. Centrifuge tubes cleaned with nitric acid or previously employed for solutions containing nitric acid should not be used, because plastic absorbs oxides of nitrogen and these cause the blue extract to intensify in colour because of the reaction of nitrogen compounds with Brilliant Green.[4,12,16] After use the tubes should be washed with methanol and then water.

11. The absorbance of the extract should be measured as quickly as possible after it has been transferred to the cell, to avoid aerial oxidation of the dye and minimize action of the fluoride on the glass cells (which could cause a high result for tantalum because of the formation of the tetrafluoroborate–Brilliant Green complex[14]). The cell may also become coated with a film of tantalum oxide, which produces erratic results. It is recommended that after each series of tests the cells used for measurement of the extracts should be quickly dipped into ~1% hydrofluoric acid and then immediately washed thoroughly with water, followed by methanol. Although this is a rather drastic method for cleaning cells, the absorbance of a cell treated in this manner increased by only about 0.03 after constant use for about 5 months. It is possible that soaking the cells in an acidic hydrogen peroxide solution might also be effective.

12. The benzene can be used again if the extracts are collected and the tantalum is stripped from about 500 ml of combined extract by shaking for ~1 min each time with four 100-ml portions of 5–10% sulphuric acid, then washing twice with ~100-ml portions of water, and finally adding ~0.5 g of quinol.

13. It is not necessary to run a reagent blank.

14. The amount of sodium carbonate used should be kept within the specified limits because the volume of 50% sulphuric acid subsequently added is that required to neu-

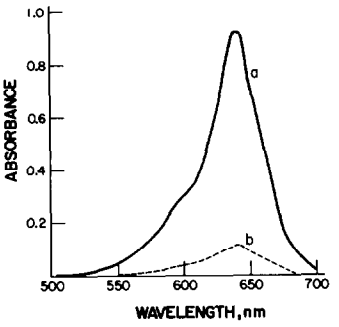

Fig. 1. Absorption spectrum (10-mm cells) of the hexofluorotantalate–Brilliant Green complex in benzene. (a) Tantalum (35 μg) extracted into 25 ml of benzene and measured against a reagent blank; (b) reagent blank measured against benzene.

tralize 4 g of sodium carbonate and give a final sulphuric acid concentration of 0.5*M*.

15. The solution should be kept almost completely covered during the evaporation, to avoid loss by spray.

16. The solution should not be allowed to stand for too long at this point, or hydrofluoric acid will be lost by volatilization.

17. The MIBK can be washed with water and then used again after equilibration with 1*M* hydrofluoric acid–0.5*M* sulphuric acid solution as described.

18. Hydrofluoric acid is added (and the solution evaporated to dryness) to ensure that any boron present is removed by volatilization as boron trifluoride before the final extraction step.

19. For final sample solution volumes of 50, 100 and 200 ml, add 3, 6 and 12 g of oxalic acid and 2.5, 5 and 10 ml of 2*M* hydrofluoric acid, respectively.

20. This step should be performed rapidly to minimize contamination of the solution with boron resulting from the reaction of hydrofluoric acid with the glass pipette. For the reason given in Note 7, it is recommended that two aliquots of the sample solution should be taken for the final extraction step and the mean result used.

RESULTS AND DISCUSSION

Extraction and spectral characteristics of the hexafluorotantalate–Brilliant Green complex

Figure 1 shows the absorption spectrum of the blue hexafluorotantalate–Brilliant Green complex in benzene and that of a corresponding reagent blank. The apparent molar absorptivity of the complex is 1.19×10^4 l.mole^{-1}.mm^{-1} at 640 nm, the wavelength of maximum absorption. This is in good agreement with the value reported by several previous investigators,[16] *viz.* 1.2×10^4 l.mole^{-1}.mm^{-1}.

Benzene, toluene and chlorobenzene are the best extractants for hexafluorotantalate–triphenylmethane dye complexes because they readily extract the complexes but not the dyes themselves.[1] Because benzene is usually used, it was also chosen for this work, but the other two solvents could be used if preferred (though it would be necessary to investigate the conditions to be used). To avoid oxidation of the complex, the benzene was previously saturated with quinol to destroy the organic peroxides present. Up to at least 35 μg of tantalum can be extracted from 25 ml of aqueous solution in one step with 25 ml of benzene when a 2-min shaking period is used. Tests showed that erratic and often high results, probably due to aerial oxidation of the leuco base of the dye (which is soluble in benzene[15]), will be obtained if the extracts are centrifuged to remove water droplets. Reproducible results can be obtained if the extracts are allowed to stand for ~30 min before the absorbance measurements are made, and if the measurements are made as quickly as possible after the extracts have been transferred to the glass cells. High results will be obtained if the extracts are allowed to remain for too long in contact with the glass. This is probably due to the presence of traces of fluoride in the extract, which react with the glass and yield the tetrafluoroborate–Brilliant Green complex. Similar effects have been reported by other investigators.[2,14,15] Beer's law is obeyed for up to at least 35 μg of tantalum and the absorbance of the complex remains constant for at least 24 hr if the extracts are kept out of direct sunlight (in the polypropylene separatory funnels used for the extraction or in tightly stoppered plastic centrifuge tubes).

Factors influencing the formation and extraction of the tantalum complex

Effect of Brilliant Green concentration and of time. In the initial work, the absorbance of extracts, derived from tantalum solutions to which freshly prepared Brilliant Green solution was added, decreased when the solutions were allowed to stand for 5–30 min before the extraction step, but the decrease in the absorbance of corresponding blanks, from ~0.16 to 0.06, was smaller. Previous investigators have found that basic triphenylmethane dyes are photosensitive[2] and that the Brilliant Green–hexafluorotantalate complex is unstable in aqueous media and should be extracted immediately after addition of the dye.[18] It has also been reported that aqueous solutions of Brilliant Green[19] and other triphenylmethane and basic dyes such as Crystal Violet, Methyl Violet, Methylene Blue and Acridine Orange are unstable because of the formation of dimers.[20] Consequently, it was considered that the behaviour described above was probably caused by a combination of these three effects. Ultimately, it was found that reproducible results and reasonably low and constant blanks could be obtained by preparing and keeping the Brilliant Green solution in an opaque brown plastic bottle, and letting it stand for ~1 hr before use. According to Fogg *et al.*,[19] this is approximately the time required for the dimers formed in ~10^{-3}*M* aqueous solution to dissociate into the monomer. Because absorbance values obtained when the Brilliant Green solution was used 2 hr after preparation were slightly low (by ~0.02–0.03 at the 0.7 absorbance level), it is recommended that the solution should be used within ~30 min after the 1-hr standing period. The extraction step should also be performed within 3 or 4 min after the addition of the dye solution. Although Fogg

et al.[19] recommend the use, when possible, of ethanolic solutions of Brilliant Green to avoid the formation of dimers, this was not feasible in this work because of the resulting co-extraction of the dye. The optimum concentration of Brilliant Green (≥94% pure) required for complex formation was found to be ~0.04% (0.004*M*). If necessary, the dye can be purified by continuous extraction with anhydrous acetone.[21,22]

Effect of oxalic, sulphuric and hydrofluoric acid concentrations

Most methods based on the extraction of hexafluorotantalate complexes with triphenylmethane and other dyes involve the presence of oxalic acid during the extraction step. However, Tarayan *et al.*[6] showed that up to ~1.5 times greater sensitivity can be obtained in the absence of this competitive complexing agent, because of the greater proportion of tantalum present in the reactive monomeric form. They recommend that oxalic acid should not be present during the extraction step. Although preliminary work confirmed that the molar absorptivity is ~1.3 times greater when tantalum is extracted from sulphuric–hydrofluoric acid media alone, the results obtained were very erratic and inconsistent. Further work showed that reproducible results can be obtained when tantalum is extracted in the presence of ~0.15 to at least 0.2*M* oxalic acid.

Table 1 shows the importance of the sulphuric acid concentration in the extraction of the tantalum complex under the proposed conditions. The extraction of the complex is constant from ~0.02–0.07*M* sulphuric acid. A concentration of 0.05*M* was chosen for further work.

The optimum range of hydrofluoric acid concentration is ~0.3–0.5*M*. A concentration of 0.5*M* was chosen. At higher concentrations, the magnitude of the blank increases because of the presence of traces of boron in the acid. The use of sodium, potassium or ammonium fluoride is not recommended, because they usually contain larger amounts of boron.

The optimum concentrations of ammonium oxalate, sulphuric and hydrofluoric acids found in an earlier investigation[16] have been reported (in the abstract) as 0.2, 0.8 and 0.5*M*, respectively. Although these oxalate and hydrofluoric acid concentrations, as well as the apparent molar absorptivity (1.2×10^4 $l.mole^{-1}.mm^{-1}$), are in good agreement with those found in the present work, the reported sulphuric acid concentration is considerably higher. Later investigators recommend extraction from 0.5*M* sulphuric acid.[18] Under the conditions used in this work, only about 85 and 50% of the tantalum present is extracted from 0.5 and 0.8*M* sulphuric acid, respectively.

Table 1. Effect of sulphuric acid concentration on the extraction of the tantalum complex (25 μg of Ta)

$[H_2SO_4]$, M	Absorbance
0	0.610
0.02	0.653
0.04	0.650
0.05	0.661
0.06	0.664
0.07	0.651
0.08	0.643
0.10	0.636
0.20	0.590

Separation of tantalum by MIBK extraction of tantalum fluoride

The extraction of tantalum fluoride into ketones, usually MIBK, from hydrofluoric acid–hydrochloric acid or hydrofluoric acid–sulphuric acid solutions, is the most widely used method for separating tantalum from the bulk of niobium and/or from other elements before its determination by spectrophotometric and other methods.[23–27] Stevenson and Hicks[23] found that the extraction of tantalum and niobium is more selective from hydrofluoric acid–sulphuric acid solutions, because the chloro-complexes of iron(III), molybdenum(VI), tin(IV), antimony(V) and arsenic(III) are co-extracted from hydrofluoric acid–hydrochloric acid media.[27] Later, Nishimura *et al.*[28] showed that from ~1*M* hydrofluoric acid–0.5*M* sulphuric acid tantalum is ~95% extracted into an equal volume of MIBK, whereas niobium is only ~2% extracted. This was confirmed in the present work. Consequently, because of its selectivity, the separation of tantalum from niobium by a double MIBK extraction from hydrofluoric–sulphuric acid medium, in conjunction with a suitable washing step to remove co-extracted niobium, was investigated.

Preliminary tests, using MIBK pre-equilibrated as described in the proposed method, were made with solutions containing 50 mg of tantalum-free niobium and up to 1 mg of tantalum. The tantalum-free niobium was prepared by extracting 50 ml of 1*M* hydrofluoric acid–0.5*M* sulphuric acid solution containing 500 mg of niobium with three 50-ml portions of MIBK; the aqueous phase was washed with chloroform to remove residual MIBK, then evaporated to dryness in the presence of sulphuric acid, and the residue was dissolved in dilute hydrofluoric acid. Aliquots of this solution, to which suitable volumes of appropriate standard hydrofluoric acid solutions of tantalum were added, were evaporated to dryness and the residues were dissolved in 1*M* hydrofluoric acid–0.5*M* sulphuric acid solution before MIBK extraction. To remove co-extracted niobium, the MIBK extracts were shaken separately for ~30 sec with 10 ml of hydrofluoric acid–sulphuric acid solution of the same composition as that used for the extraction. The tantalum lost in washing the first MIBK extract was recovered by adding the wash solution to the aqueous phase from the first extraction, and using this combined solution for the second MIBK extraction. The

Table 2. Effect of washing* on the separation of tantalum from niobium by MIBK extraction

Nb taken, *mg*	Ta taken, *μg*	Ta found, *μg*	
		One wash of each MIBK extract	Two washes of each MIBK extract
50	0	6.6	0.3
50	5	9.5	4.9
50	10	15.3	11.0
50	25	27.8	25.2
50	100	101.7	101.5
50	500	499	498
50	1000	992	1008

*With 10 ml of 1*M* hydrofluoric acid–0.5*M* sulphuric acid solution.

aqueous solution from the washing of the second MIBK extract was discarded. Because of the high distribution ratio of tantalum fluoride between MIBK and the aqueous phase under the chosen conditions of acidity, very little or none of the small amount of tantalum remaining in the aqueous phase after the first extraction step will be lost to the wash solution during the washing of the second MIBK extract. Table 2 shows that with a single wash of each MIBK extract, complete recovery of the added tantalum was obtained only for the test solutions containing $\geqslant 100$ μg of tantalum, for which an aliquot of the final solution containing only part of the co-extracted niobium was taken for the determination of tantalum. High results, owing to the presence of all the co-extracted niobium during the final determination step, were obtained for the solution containing $\leqslant 25$ μg of tantalum. Analysis of the final solutions for niobium (by an unpublished method developed by the author, with PAN as reagent) showed that a single wash of each extract (as described above) left ~ 350 μg of niobium in the combined MIBK extracts, out of 50 mg taken. Further tests showed that two washes of each extract with 10 ml of 1*M* hydrofluoric acid–0.5*M* sulphuric acid solution will effectively reduce the residual niobium to a level (~ 110–150 μg) at which it will not interfere in the determination of microgram quantities of tantalum.

Effect of diverse ions

Previous investigators[23,24] found that only selenium(VI), tellurium(VI) and small amounts of titanium and molybdenum are co-extracted into ketones from 0.4*M* hydrofluoric acid–6*M* sulphuric acid solutions. Tests showed that under the proposed conditions up to at least 50 mg of iron(III), 40 mg of phosphate, 20 mg of aluminium, zirconium, titanium(IV), tin(IV), manganese(II), tungsten(VI), molybdenum(VI), calcium, magnesium, arsenic(III), arsenic(V), antimony(III), antimony(V), chromium(III) and copper(II) and up to at least 10 mg of vanadium(V) can be present during the MIBK extraction step without causing error in the tantalum result. A small amount of chromium(VI) is co-extracted, which, during the stripping step with hydrogen peroxide is reduced to blue perchromic acid which remains largely in the MIBK phase. However, the small amount that accompanies the tantalum can cause a low result. Interference from chromium(VI) can readily be avoided by reducing it with hydrogen peroxide after dissolution of the sodium carbonate melt, followed by vigorous boiling of the solution to destroy the excess of peroxide before the MIBK extraction step. Small amounts of residual hydrogen peroxide can be destroyed by the addition of potassium permanganate solution.

Boron interferes seriously in the determination of tantalum with Brilliant Green and other triphenylmethane dyes because it forms extractable tetrafluoroborate ion-association complexes.[4,12,15] Interference from any boron present in the solution after the stripping step is avoided by treating the solution with sulphuric and hydrofluoric acids, followed by evaporation to dryness to remove boron as volatile boron trifluoride.[4,12] Boron will not interfere if it is present in the initial sample solution,

Table 3. Recovery of tantalum from a synthetic niobium ore*

Matrix and nominal composition, %	Total Ta present, %	Ta found, %
Nb ore OKA-1 (31.3 Ca, 2.8 Fe, 2.4 Si, 1.3 Mg, 1.1 Mn, 1.0 Sr, 1.1 P, 0.9 Al, 0.4 Nb)	0.0089	0.009_0
	0.0139	0.014_5
	0.0539	0.052_0
	0.1039	0.10_3
	0.204	0.20_0
	0.504	0.50_8
	1.004	1.02_4

*The mean value for tantalum in OKA-1 found by the proposed method is 0.0039% (cf. Table 5—calculated from % Ta_2O_5).

Table 4. Determination of tantalum in CCRMP ores and in diverse mill products

Sample	Nominal composition, %	Ta_2O_5 found, % XRF*	Ta_2O_5 found, % Proposed method
CCRMP-TAN-1 Tantalum ore	71.5 SiO_2, 1.5 K, 0.5 Ca, 0.2 Fe, 0.02 Nb	0.257†	0.295, 0.303
CCRMP-HV-1 Copper-molybdenum ore	33.9 Si, 6.6 Al, 1.9 Fe, 1.4 Ca, 2.8 K, 0.2 Ti, 0.5 Cu, 0.3 S	—	0.010_7‡
CCRMP-PR-1 Molybdenum ore	39.2 Si, 2.4 Al, 1.3 Fe, 1.4 Ca, 2.0 K, 0.6 Mo, 0.8 S	—	0.011_7‡
CCRMP-BH-1 Tungsten ore	0.4 W, 38.0 Si, 3.5 Al, 3.2 Fe, 0.5 Ca, 0.4 Mg, 1.7 K, 0.4 Ti, 0.8 S	—	0.011_0‡
CCRMP-TLG-1 Tungsten ore	0.1 W, 21.5 Si, 3.0 Al, 17.5 Fe, 16.6 Ca, 2.7 Mg, 0.4 K, 0.1 Ti, 1.3 Mn, 0.1 S	—	0.011_5‡
Pyrochlore feed—1	~60 Nb_2O_5	0.189	0.216, 0.217
—2	~60 Nb_2O_5	0.179	0.211
Rougher tails—1§		0.035#	0.040, 0.041
—2§		0.071#	0.069, 0.067
—3§		0.05#	0.038, 0.037
—4§		0.062#	0.045, 0.049, 0.042
Mill heads—1		0.16#	0.140, 0.146
—2		0.25#	0.235, 0.223
—3		0.19#	0.172, 0.157
Cleaner tails—1		0.34#	0.357, 0.341
—2		0.47#	0.508, 0.516
Rougher tails concentrate—1		3.72#	3.71, 3.75

*XRF determinations done at CANMET and other organizations, with either sodium tetraborate or lithium metaborate for fusion.
†Mean of 5 results.
‡0.0122% Ta_2O_5 present, *i.e.*, 80 μg of tantalum added to a 0.8-g sample.
§Sample was very coarse and gritty and contained black particles and pieces of mica.
#The approximate chemical composition of the sample is not known but it contains niobium, titanium and iron.

because it is not co-extracted into MIBK. Nitrate causes a high result for tantalum because it also forms an ion-association complex with Brilliant Green.[4,16] Although nitric acid and/or nitrates are not used in this method, they can readily be removed before the determination of tantalum by evaporating the solution to dryness in the presence of sulphuric acid. The effects of selenium(VI) and tellurium(VI) were not investigated, because they are not usually present in tantalum- and niobium-bearing ores. However, if these elements were present, they would probably be in the quadrivalent state after fusion of the sample with sodium carbonate.[29]

Applications

Table 3 shows that the results obtained by the proposed method for a series of synthetic niobium ores, in which the added tantalum was varied from 0.005 to 1%, agree favourably with the calculated amount present. In these tests, the required volumes of appropriate standard hydrofluoric acid solutions of tantalum were added to the platinum crucibles and the solutions were evaporated to dryness before the addition of the ore and sodium carbonate. Table 4 shows that the results obtained for four diverse CCRMP ores, to which a known amount of tantalum was added, agree with the amount added. The results obtained for a CCRMP ore, TAN-1, which is currently undergoing certification for tantalum, and for various pyrochlore feed samples and mill products that had previously been analysed for tantalum by XRF, are in reasonably good agreement with the XRF values. However, those obtained for rougher tails sample 4 are not in good agreement with each other, because of the inhomogeneity of this sample. It is considered that the results obtained by the proposed method are probably more accurate than the XRF values because reliable XRF results necessitate careful corrections for interelement effects.[30] The results shown in Tables 3 and 4 are, except for tantalum contents below ~0.03%, the means of the results obtained for two aliquots of the final solution. All the results shown in Table 4 are for individual subsamples.

Table 5 shows that the precision of the results for tantalum at the 0.005–0.5% level is reasonably good. Except for OKA-1, these results are the means of the results obtained for two aliquots of each final solution.

The proposed method is applicable to niobium metal if the solution or aliquot taken for the MIBK extraction step contains not more than 50 mg of

Table 5. Precision for tantalum in ores and mill products

	Ta_2O_5 found, %		
	OKA-1	TAN-1	Cleaner tails—2
	0.0045_2	0.295	0.508
	0.0051_3	0.303	0.516
	0.0042_7	0.303	0.524
	0.0047_6	0.305	0.521
	0.0050_1	0.294	0.508
Mean	0.0047_4	0.300	0.515
Standard deviation	0.00035	0.00510	0.00734
Relative standard deviation, %	7.4	1.7	1.4

niobium. After decomposition of the sample with nitric and hydrofluoric acids, the solution should be evaporated to dryness in the presence of sulphuric acid, followed by the dissolution of the residue in 1*M* hydrofluoric acid–0.5*M* sulphuric acid solution (or the required volumes of 50% v/v sulphuric acid and concentrated hydrofluoric acid) before the extraction step. Tantalum can also be determined in MIBK or tributylphosphate extracts and in strip and scrub solutions resulting from solvent-extraction recovery processes. After dilution of a suitable aliquot of the extract (depending on the niobium and expected tantalum content) with a threefold or greater volume of toluene to reduce the viscosity, tantalum can be stripped by shaking the extract 4 or 5 times, for ~1 min each time, with an equal volume of 10% v/v hydrogen peroxide–2% v/v hydrofluoric acid solution. Sufficient 50% sulphuric acid should be added to the resulting solution for the final concentration to be ~0.5*M*, then 100 mg of iron(III), as sulphate, should be added to catalyse the decomposition of hydrogen peroxide and the solution should be boiled vigorously for 20–30 min to destroy the peroxide and remove most of the hydrofluoric acid. After cooling the solution, potassium permanganate should be added to destroy any residual hydrogen peroxide, then sufficient concentrated hydrofluoric acid should be added to give a final concentration of ~1*M*. After dilution of the solution to the required volume, a suitable aliquot can be taken for the MIBK extraction step. Aliquots of strip and scrub solutions can be evaporated to dryness in the presence of sulphuric acid, followed by the addition of sufficient concentrated hydrofluoric acid and 50% sulphuric acid for the final concentrations to be 1 and 0.5*M*, respectively. This solution, or a suitable aliquot, after dilution of the solution to a definite volume with water, can be taken for the MIBK extraction step.

The proposed method is suitable for samples containing ~0.001–1% of tantalum but samples containing up to ~4% can also be analysed with reasonable accuracy. It is emphasized that reliable results can only be obtained if care is taken to adhere strictly to the conditions recommended for the preparation and preliminary treatment of the photosensitive Brilliant Green solution, for the extraction of the complex as described in Note 9, and for the final spectrophotometric measurement of the extracts as described in Note 11.

REFERENCES

1. I. P. Alimarin and S. V. Makarova, *Zh. Analit. Khim.*, 1964, **19,** 90.
2. S. V. Makarova and I. P. Alimarin, *ibid.*, 1964, **19,** 564.
3. *Idem, ibid.*, 1964, **19,** 847.
4. N. S. Poluektov, L. I. Kononenko and R. S. Lauer, *ibid.*, 1958, **13,** 396.
5. S. V. Elinson, A. N. Nevzorov, M. V. Belogortseva, N. A. Mirzoyan and S. N. Mordvinova, *ibid.*, 1974, **29,** 1234.
6. V. M. Tarayan, E. N. Ovsepyan and S. R. Barkhudaryan, *ibid.*, 1971, **27,** 19.
7. H. A. Flaschka and A. J. Barnard, Jr., *Chelates in Analytical Chemistry*, Vol. 2, p. 295. Dekker, New York, 1969.
8. Wen-Chun Sung, Sung-Yu Liu, Chi-Heng Hsu and Tse-Chung Wang, *Fen Hsi Hua Hsueh*, 1980, **8,** 536; *Chem. Abstr.*, 1981, **95,** 143477k.
9. R. Kojiyama and M. Watanabe, *Bunseki Kagaku*, 1966, **15,** 153; *Chem. Abstr.*, 1968, **68,** 9089x.
10. I. Janoušek and D. Čechová, *Chemist- Analyst*, 1966, **55,** 19.
11. K. Furuya, K. Fujimura and C. Tsurumi, *Bunseki Kagaku*, 1971, **20,** 535; *Chem. Abstr.*, 1971, **75,** 83901s.
12. Y. Kakita and H. Gotô, *Anal. Chem.*, 1962, **34,** 618.
13. O. Grossmann, *Z. Anal. Chem.*, 1969, **245,** 135.
14. K. Bhattacharya, D. V. Jayawant and T. K. S. Murthy, *Indian At. Energy Comm., Bhabha At. Res. Cent., Rept.*, B.A.R.C.-511, 1970.
15. A. R. Eberle and M. W. Lerner, *Anal. Chem.*, 1967, **39,** 662.
16. A. N. Nevzorov and L. A. Bychkov, *Sovrem. Metody Khim. Spektral. Anal. Mater.*, 1967, 180; *Chem. Abstr.*, 1968, **68,** 18414b.
17. I. Tsukahara, *Bunseki Kagaku*, 1967, **16,** 583; *Chem. Abstr.*, 1968, **68,** 18413a.
18. N. V. Bausova and E. M. Lebedeva, *Tr. Inst. Khim., Akad. Nauk SSSR, Ural. Filial*, 1970, **17,** 195; *Chem. Abstr.*, 1971, **74,** 25573e.
19. A. G. Fogg, A. Willcox and D. T. Burns, *Analyst*, 1976, **101,** 67.
20. E. M. Zadorozhnaya, B. I. Nabivanets and N. M. Maslei, *Zh. Analit. Khim.*, 1974, **29,** 993.
21. A. G. Fogg, C. Burgess and D. T. Burns, *Analyst*, 1970, **95,** 1012.
22. C. Burgess, A. G. Fogg and D. T. Burns, *Lab. Pract.*, 1973, **22,** 472.
23. P. C. Stevenson and H. G. Hicks, *Anal. Chem.*, 1953, **25,** 1517.
24. G. R. Waterbury and C. E. Bricker, *ibid.*, 1957, **29,** 1474.
25. M. L. Theodore, *ibid.*, 1958, **30,** 465.
26. C. L. Luke, *ibid.*, 1959, **31,** 904.
27. J. H. Hill, *Analyst*, 1966, **91,** 659.
28. S. Nishimura, J. Moriyama and I. Kushima, *Trans. Jap. Inst. Met.*, 1964, **5,** 39.
29. I. M. Kolthoff and P. J. Elving, *Treatise on Analytical Chemistry*, Part II, Vol. 7, p. 147. Interscience, New York, 1961.
30. R. W. Moshier, *Analytical Chemistry of Niobium and Tantalum*, p. 197. Macmillan, New York, 1964.

Talanta, Vol. 30, No. 7, pp. 505–508, 1983
Printed in Great Britain.

0039-9140/83 $3.00+0.00

LASER ATOMIC-IONIZATION DETERMINATION OF CAESIUM IN FLAMES

V. I. CHAPLYGIN, N. B. ZOROV and YU. YA. KUZYAKOV
Department of Chemistry, Moscow State University, Moscow 117234, U.S.S.R.

(*Received* 19 *November* 1982. *Accepted* 23 *December* 1982)

Summary—The laser atomic-ionization (AI) method has been developed for determination of caesium in flames. The limit of detection for caesium in pure aqueous solution is 4 pg/ml. The interference of Li, Na, K, Rb, Ca and Fe with the AI signal of caesium has been investigated and explained. The analytical potential of this method has been demonstrated by determination of caesium in water samples, in the concentration range 0.1–1 ng/ml.

It is known that the highly sensitive method of laser atomic-ionization* (AI) spectrometry is a valuable new analytical tool, possessing exciting potential for analytical chemistry.[5,6] This method relies on detection of the changes in an electrical current (due to collisional ionization of laser-excited atoms) passed through a flame into which the analyte solution is sprayed. The dye lasers used are tuned to appropriate discrete atomic transitions. Despite its many attractive features this method has not been widely used for analysis of complex real samples, mainly because of its susceptibility to severe matrix-ionization interference, especially when the sample contains a large (cathode) detecting the ions formed is outside the amount of easily ionized elements and the electrode flame.[7–9] To reduce such interferences it has been suggested, for example, to use a cathode inside the flame, and direct the laser beam into the flame very close to the surface of the cathode.[10,11]

This paper examines the conditions for laser atomic-ionization determination of caesium in a flame. The effect of easily ionized elements (Li, Na, K, Rb, Ca) and also of Fe on the AI signal was investigated for the 1, 10 and 100 ng/ml caesium levels. It should be mentioned that the traditional methods of flame atomic-emission and atomic-absorption (and also flameless atomic-absorption) give a detection limit above 1 ng/ml for caesium,[12] and it is known that the alkali and alkaline-earth metals give significant interference in AI determination of caesium. Laser-induced atomic fluorescence in combination with electrothermal atomization of the sample gives a detection limit of 0.02 ng/ml (1.2 pg in 60 μl of sample[13]) for caesium in aqueous solution, but the reproducibility is not so good (14% at the 0.1 ng/ml level). Also the electrothermal atomization method is rather slow and more complicated than determination in the flame.

*The name "atomic ionization" was suggested by Zorov *et al.*[1]. We feel that this name is more generally descriptive than others used in the literature for the same effect, such as stepwise photoionization of atoms,[2] optogalvanic spectroscopy,[3] resonance ionization spectroscopy,[4] and laser-enhanced ionization (LEI) spectrometry.[5]

EXPERIMENTAL

Reagents

Aqueous alkali-metal standards were prepared from the reagent-grade metal chlorides and high-purity water. Calcium stock solution was prepared by dissolving the reagent grade carbonate in reagent-grade hydrochloric acid, and iron stock solution was prepared by dissolving iron metal in a mixture of hydrochloric and nitric acids. The stock solution concentrations were 1 and 10 mg/ml. The water used was distilled twice in a quartz still and then demineralized with the "Milli-Q" system (to give ~20 MΩ.cm resistivity).

Apparatus

This is shown in Fig. 1. The laboratory-made 300-kW nitrogen laser (1) was operated at a frequency of 5 Hz and the laser pulse-duration was 12 nsec. This laser was used to pump a tunable dye laser (2). Instead of the Hänsch design[14] a grazing-incidence dye laser without beam expander[15] was used first for atomic-ionization analysis. The laser power (20 kW) was measured with an IMO-2 energy meter. The dye-laser pulse-duration was about 10 nsec and the linewidth was about 0.005 nm. A $5 \times 10^{-3} M$ solution of the

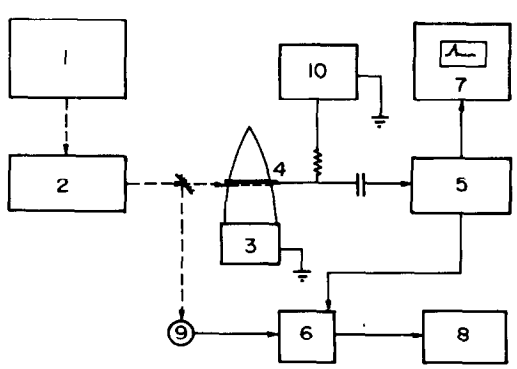

Fig. 1. Block scheme of the experimental apparatus: 1—nitrogen laser; 2—dye laser; 3—burner; 4—cathode; 5—amplifier; 6—analogue-to-digital converter; 7—oscilloscope; 8—digital display; 9—photodiode; 10—high-voltage source.

organic dye Coumarin 47 in ethanol was used as the active material. The dye laser was tuned to excite the $6^2S_{1/2}$–$7^2P^0_{3/2}$ transition of atomic caesium at 455.5 nm by monitoring the fluorescence signal from an electrically heated electrodeless discharge caesium lamp.

The laser beam (diameter about 1–1.5 mm) was directed into the flame at a region on the axis of the circular Mèker-type burner (3). In the present work we used the premix burner from a Carl Zeiss AAS-1 atomic-absorption spectrophotometer (solution uptake rate 4 ml/min). The laser beam was centred in the flame under and parallel to the 0.6-mm diameter stainless-steel rod (4), which was used as a cathode and maintained at a negative high voltage (usually −600 V) with respect to the burner head, which was used as the anode.

The atomic-ionization signal was amplified by a laboratory-made broad-band amplifier (frequency response bandwidth 10 MHz, sensitivity 20 μV, gain 500) and processed with an analogue-to-digital converter (6). The RC high-pass filter was on the input of an amplifier (R = 50 kΩ, C = 300 pF) rejecting the d.c. background current and the associated low-frequency noise caused by normal fluctuations of the flame conductivity. The atomic-ionization signal pulse was displayed on the S1-70 oscilloscope (7) for visual monitoring of the shape and amplitude of the pulses. The analogue-to-digital converter integrated the gated part of the signal pulse, with a 1 μsec gate-width. The output signal was the average response of 10 pulses and was read out on a digital display (8). The signal-registration system was triggered by a photodiode (9) which monitored the laser pulse.

Procedure

A propane–butane–air flame was used in the present work and the flow-rates were adjusted (0.6 and 6 l./min for fuel and support gas respectively) to maximize the AI signal. The optimum height of the cathode above the burner head was found to be 20–22 mm.

For determination of very low concentrations of caesium it was found necessary to remove the memory effect from the previous sample by aspirating into the flame first 0.01M hydrochloric acid for 25–30 sec and then high-purity demineralized water until the caesium signal had decreased to the noise level of the registration system.

RESULTS AND DISCUSSION

Determination of caesium in aqueous CsCl solution

Aqueous caesium standards were prepared in calibrated transparent Teflon standard flasks from 1000 μg/ml caesium stock solution by serial dilution, down to 10^{-5} μg/ml. The total dilution error did not exceed 3%.

A linear calibration graph was obtained over four orders of magnitude of concentration (from 0.01 to 400 ng/ml). The detection limit (4 pg/ml) for caesium in pure aqueous solutions was limited by the noise of the registration system, which was larger than the blank signal for caesium in the high-purity water. The detection limit was defined as the concentration of analyte which would give a signal equal to three times the standard deviation of the blank signal (calculated from 20 replicates of the blank).

The relative standard deviation of 10 determinations of caesium at the 0.1 ng/ml level was 6%.

The magnitude of the AI signal was essentially the same for any voltage between 600 and 1600 V applied to the electrode, indicating that the efficiency of ion-collection was close to 100% even at an applied voltage of 600 V.

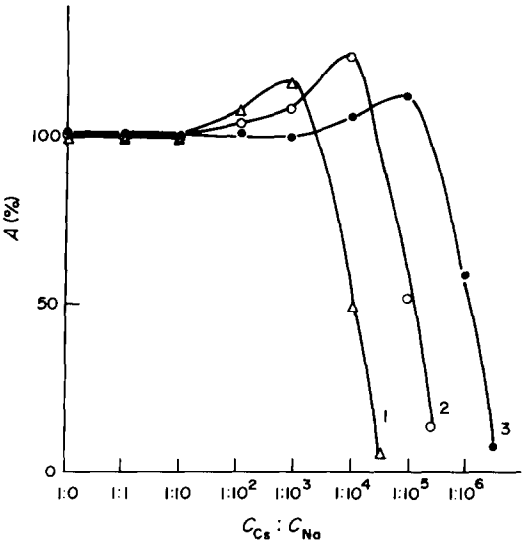

Fig. 2. Dependence of AI signal for caesium (% nominal signal A) on C_{Cs}:C_{Na} ratio for different caesium concentrations: 1—100; 2—10; 3—1 ng/ml.

Interference of easily ionized elements

The effect of various concentrations of such elements as Li, Na, K, Rb, Ca and Fe on the AI signal of caesium was investigated. These elements usually accompany caesium in natural samples, and all of them except Fe are easily ionized. The effect was investigated for three caesium concentrations (1, 10 and 100 ng/ml).

Figure 2 shows that the effect of sodium on the signal depends only on the concentration of sodium, and not on the concentration ratio C_{Cs}:C_{Na}. For

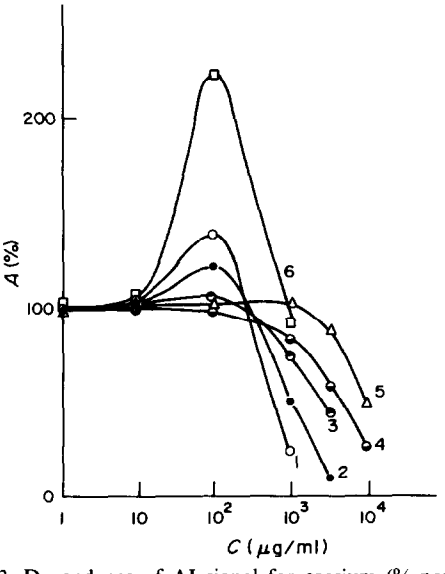

Fig. 3. Dependence of AI signal for caesium (% nominal signal A) (C_{Cs} = 10 ng/ml) on concentration of added elements: 1—K; 2—Na; 3—Li; 4—Ca; 5—Fe; 6—Rb.

Table 1. Determination of caesium in water samples (*ng/ml*)

	Tap-water I	Tap-water II	Distilled water	Demineralized water ("Milli-Q" installation)
Calibration-graph method	0.6 ± 0.1	0.40 ± 0.03	0.11 ± 0.01	<0.004
Standard-addition method	1.0	0.6	0.10	—

example, the signal is decreased by 50% at a sodium concentration of 1000 μg/ml for all three concentrations of caesium.

This signal depression by the addition of easily ionized elements can be explained by the mechanism suggested by Green *et al.*[8] With an increase in concentration of the easily ionized element the positive-ion space charge around the cathode, due to thermal ionization, increases in magnitude. This space charge shields the cathode, thus reducing the field at the measurement site, and the conditions for caesium ion collection are abruptly impaired.

In contrast to the results reported by Havrilla and Green,[9] who used a cathode outside the flame, in our experiments the AI signal magnitude did not essentially change with increasing applied voltage up to 1600 V. Further, the tolerance of the AI signal to the concentration of sodium in the flame was improved by two orders of magnitude. The analyte signal was depressed by 50% by a sodium concentration of 10 μg/ml when the "external" cathode was used, compared to the 1000 μg/ml found in the present work. It should be noted that when Rb solutions with concentrations higher than 1000 μg/ml are aspirated (applied voltage 600 V) the conditions of signal detection are disturbed because of arcing in the flame. A similar effect arises at high concentrations of K, Na, Li or Ca with increasing applied voltage up to 1400–1600 V.

Figure 3 shows the dependence of the caesium AI signal ($C_{Cs} = 10$ ng/ml) on the concentration of added elements. As the concentration of easily ionized element increases, the AI signal is at first enhanced. This may be due to the added elements acting as ionization buffers (swamping method), the presence of the easily ionized element suppressing the ionization of the analyte, and thereby increasing the proportion of free caesium atoms in the flame. This enhancement was noticeable in the case of potassium ($C_K = 100$ μg/ml) and considerable in the case of rubidium ($C_{Rb} = 100$ μg/ml). Another reason for the signal enhancement could be the presence of caesium as an impurity in the RbCl used. According to the analysis of the reagent-grade RbCl, this could amount to 1.3×10^{-3}% Cs, and with increasing concentration of Rb the total concentration of Cs would also increase. The caesium content of the other alkali-metal salts used was considerably lower and did not effect the AI signal.

It is also possible to transfer excitation energy between close atomic energy-levels of caesium and rubidium through the vibrational levels of some molecular species in the flame, followed by collisional ionization of the excited rubidium atom. The caesium atom provides the energy and can be excited again during the same laser pulse, and then may be ionized. In this manner signal enhancement should be produced. To clarify the process of caesium signal enhancement in the presence of potassium and rubidium more detailed experiments should be done.

Once the concentration of easily ionized element has become high enough for formation of a considerable space charge, the AI signal of caesium abruptly decreases. It is interesting to see from Fig. 3 that the suppression effect is the greater, the lower the ionization potential of the matrix species.

Hence to eliminate the effect of an easily ionized matrix species it is sufficient to dilute the sample solution so that the concentration of this matrix species in the flame is rather low. Naturally, this is only applicable if the detection limit of the analyte is very low.

Determination of caesium in water samples

To illustrate its possibilities, the AI method has been successfully applied to the determination of caesium in various samples of tap water, distilled water and demineralized water. The analysis was done by both the calibration-graph and standard-addition methods. The results are presented in Table 1. It was found by emission spectrometry that the total content of Na, K and Ca did not exceed 30 μg/ml in tap-waters I and II, so the level of easily ionized elements was not sufficient to affect the determination of caesium.

REFERENCES

1. N. B. Zorov, Yu. Ya. Kuzyakov and O. I. Matveev, *Zh. Analit. Khim.*, 1982, **37**, 520.
2. R. V. Ambartzumian, V. N. Kalinin and V. S. Letokhov, *Pis'ma ZhETF*, 1971, **13**, 305.
3. R. B. Green, R. A. Keller, G. G. Luther and P. K. Schenk, *Abstr. Pittsburgh Conf. Anal. Chem. Appl. Spectrosc.*, Cleveland, Ohio, 1977, p. 120.
4. G. S. Hurst, M. G. Payne, S. D. Kramer and J. P. Young, *Rev. Modern Phys.*, 1979, **51**, 767.
5. G. C. Turk, J. C. Travis, J. R. DeVoe and T. C. O'Haver, *Anal. Chem.*, 1978, **50**, 817.
6. A. S. Gonchakov, N. B. Zorov, Yu. Ya. Kuzyakov and O. I. Matveev, *Anal. Lett.*, 1979, **12**, 1037.
7. G. C. Turk, J. C. Travis, J. R. DeVoe and T. C. O'Haver, *Anal. Chem.*, 1979, **51**, 1890.

8. R. B. Green, G. J. Havrilla and T. O. Trask, *Appl. Spectrosc.*, 1980, **34,** 561.
9. G. J. Havrilla and R. B. Green, *Anal. Chem.*, 1980, **52,** 2376.
10. N. B. Zorov, Yu. Ya. Kuzyakov, O. I. Matveev and V. I. Chaplygin, *Zh. Analit. Khim.*, 1980, **35,** 1701.
11. G. C. Turk, *Anal. Chem.*, 1981, **53,** 1187.
12. P. Frigieri, R. Trucco, I. Ciaccolini and G. Pampurini, *Analyst*, 1980, **105,** 651.
13. J. P. Hohimer and P. J. Hargis, Jr., *Appl. Phys. Lett.*, 1977, **30,** 344.
14. T. W. Hänsch, *Appl. Opt.*, 1972, **11,** 895.
15. I. Shoshan, N. N. Danon and U. P. Oppenheim, *J. Appl. Phys.*, 1977, **48,** 4495.

Talanta, Vol. 30, No. 7, pp. 509–513, 1983
Printed in Great Britain.

0039-9140/83 $3.00+0.00

DETERMINATION OF CADMIUM IN URINE BY EXTRACTION AND FLAMELESS ATOMIC-ABSORPTION SPECTROPHOTOMETRY

COMPARISON OF URINE FROM SMOKERS AND NON-SMOKERS OF DIFFERENT SEX AND AGE

MOHAMMAD JAWAID, BIRGER LIND and CARL GUSTAF ELINDER
National Institute of Environmental Medicine and Department of Environmental Hygiene, Karolinska Institute, P.O. Box 60208, S-10401 Stockholm, Sweden

(*Received* 23 *March* 1982. *Revised* 20 *September* 1982. *Accepted* 25 *October* 1982)

Summary—A method is presented for determining cadmium in urine by flameless atomic-absorption spectrophotometry after extraction. The sample is dried, ashed in the presence of nitric acid, and then the residue is dissolved in hydrochloric acid. Cadmium is extracted as its tetrahexylammonium iodide complex into methyl isobutyl ketone. The organic phase is analysed for cadmium by atomic-absorption spectrophotometry with electrothermal atomization. The median urinary excretion of cadmium for smokers aged 50–64 has been found to be 0.7 and 0.75 μg/l. for males and females respectively, the values for non-smokers being 0.25 and 0.4 μg/l.

Urine is a readily accessible biological material which can be used for the assessment of environmental and occupational exposure to metals. The amount of cadmium excreted in the urine has been used to estimate the body burden of cadmium in various populations.[1] Available data indicate that urinary excretion of cadmium reflects body or kidney burden, and to a lesser extent recent exposure.[2,3] The urinary concentration of cadmium in normal, non-occupationally exposed persons is low, often less than 1 μg/l.,[4] and therefore highly sensitive analytical methods are required. Atomic-absorption spectrophotometry (AAS) with electrothermal atomization (ETA) meets this demand, but non-specific absorptions due to the complex matrix pose considerable problems,[2] despite the use of background correction.

Liquid–liquid extraction to separate the metal before its determination by AAS provides a method of reducing the interference from the matrix, and improving the sensitivity by concentrating the metal in a small volume of an organic solvent. Most solvent-extraction systems demand stringent control to achieve selective and quantitative extraction of the metal into the organic phase and to leave the bulk of the matrix in aqueous solution. Pretreatment of the sample, to convert the element of interest into extractable form may involve loss in various steps[5] and contamination from reagents (even "Suprapur" quality reagents are no exception).[6]

Quaternary ammonium salts have been reported to be useful reagents for the extraction of metal ions from aqueous solutions.[7,8] Maeck *et al.*[9] have shown that cadmium can be quantitatively extracted into methyl isobutyl ketone in the presence of tetrahexylammonium iodide from a wide range of concentrations of hydrochloric acid. Viets[10] used Aliquat 336 (tricaprylmethylammonium chloride) and reported 100% extraction of cadmium from 1–6*M* hydrochloric acid.

In the present paper a new extraction procedure for determination of cadmium in urine is described. The method does not demand stringent control of factors such as pH, and therefore is simpler and more rapid than an earlier method.[3] It is based on extraction by the method of Maeck *et al.*[9] followed by determination of cadmium in the organic phase by AAS with electrothermal atomization. The method has been used to determine cadmium in urine collected from a small random sample of the general population of Sweden.[11]

EXPERIMENTAL

Apparatus

A Perkin–Elmer atomic-absorption spectrophotometer, model 373, was used for cadmium measurements at 228.8 nm (band-pass 0.7 nm), with a cadmium electrodeless discharge lamp or hollow-cathode lamp, and deuterium-lamp background correction. The Perkin–Elmer HGA 500 electrothermal atomization unit was programmed as follows.

	Temperature, °C	Ramp time, *sec*	Hold time, *sec*
Drying	150	20	5
Charring	450	6	30
Atomization	2200	1	10
Cleaning	2500	1	2
Cooling	20	1	10

The purging gas was 99.99% pure argon, at an internal flow-rate of 100 ml/min (atomization step). Injections (20 μl) of standards or test solutions were done with a Perkin–Elmer AS-40 automatic sampler into standard graphite tubes.

The areas under the atomization-signal peaks were integrated by the instrument, printed out on a Perkin–Elmer PRS-10 printer and used for evaluating the results. A Perkin–Elmer 56 two-pen recorder was utilized to check the electrothermal programme. One pen recorded the shape and peak-height of the deuterium-compensated cadmium signals. The other recorded the non-specific absorption of the light emitted by the deuterium lamp. The interface between the instrument and the recorder was constructed at this Institute.

Reagents

The hydrochloric acid and nitric acid (Merck "Suprapur") were both delivered in glass containers. The methyl isobutyl ketone (MIBK) (Merck, *pro analysi*) was saturated with water. The tetrahexylammonium iodide (THAI), Eastman Kodak *purum*, was used as a 2.5% (0.05*M*) solution in MIBK saturated with water. Cadmium standards were prepared by appropriate dilutions of a commercial "standard" solution (BDH, 1 ml = 1.00 ± 0.005 mg of Cd). Fresh working standards were prepared each day immediately before use. Water was distilled and subsequently demineralized. All glassware was carefully washed with reagent grade nitric acid and rinsed many times with water.

Urine samples

Urine samples were obtained from 207 persons (99 males and 108 females) aged between 19 and 72, randomly selected from the general population of two major cities of Sweden, Stockholm and Västerås. The urine samples were collected during the daytime at this Institute. For females, urine was collected in disposable paper cups and poured into acid-washed polyethylene flasks. These paper cups had been checked on several occasions to ensure that they would not contaminate the urine. In the case of males, urine samples were collected directly in the polyethylene flasks. A small amount, 10 mg, of sodium azide was added to each flask to prevent bacterial growth. The samples were then stored in a freezer at −20°. A portion (10 ml) from each urine sample was set aside for creatinine determination. The amount of creatinine in the urine was determined for all the samples (except one that was accidentally omitted), as follows. A filtered urine sample was diluted 400 times with an auto diluter (Hook and Tucker). Equal volumes (2 ml each) of the diluted sample and the picric acid reagent (150 ml of saturated picric acid solution + 35 ml of 10% sodium hydroxide solution + 500 ml of distilled water) were mixed and the absorption was measured with a spectrophotometer (Vitatron). The calibration curves was prepared by running standards (0–4 g/l.) in exactly the same manner. The accuracy of the method was continuously checked by analysing reference urine samples simultaneously with the sample batch. The specific gravity of the urine was determined with a Goldberg refractometer.

Procedure

A urine sample (~3 g) was accurately weighed in a clean (acid-washed) 10-ml borosilicate extraction tube, 0.5 ml of nitric acid ("Suprapur") was added, and after mixing, the tube was placed in an oven at 105° overnight to evaporate the sample to dryness and then in a muffle furnace at 450° for 12 hr to ash the sample.[5] After cooling, the residue was dissolved in exactly 3 ml (Gilson pipette) of 6*M* hydrochloric acid ("Suprapur"), with mixing on a "Whirlimixer" (Fisons Scientific Apparatus, U.K.). The solution was then diluted with 3 ml of demineralized water (Gilson pipette) and 1 ml of 2.5% THAI solution in MIBK was added (Eppendorf pipette). The solution was shaken for about 30 sec on the "Whirlimixer" and centrifuged at 3000 rpm for about 3 min. About 0.5 ml of the clear transparent ketone phase was transferred to a sampling cup in the autosampler and 20 μl were injected into the graphite cuvette of the electrothermal analyser and analysed by AAS, according to the programme already given. Each sample solution was injected in triplicate and the mean was used to evaluate the signals. The calibration graph was prepared by running standards (and blanks) that were treated in exactly the same way as the samples, with omission of the dry-ashing step. Pooled and spiked human urines, checked by neutron-activation analysis, were run as quality-control samples to test the accuracy of the method. The routine analysis included two quality-control samples of each cadmium concentration and two blanks (empty tubes) run through the whole method.

RESULTS AND DISCUSSION

Sample treatment and extraction

The extraction procedure was first tested on urine samples that had not been dry-ashed. The samples were acidified with 3*M* hydrochloric acid and cadmium was extracted with the THAI–MIBK system. This procedure gave cadmium concentrations that were only 75–85% of those obtained after dry-ashing. This is in accord with Sperling and Bahr,[13] who extracted cadmium from urine into MIBK with ammonium pyrrolidine dithiocarbamate and concluded that it was not possible to extract all the cadmium without a complete digestion of the sample. Dry-ashing is necessary to destroy proteins and other organic ligands which can bind cadmium and inhibit complete extraction. Further, it has been observed that emulsions may form when a high-protein urine sample is shaken with MIBK, and that these emulsions cannot be separated into two clear phases even by prolonged centrifuging. To obtain complete oxidation, a small amount (0.5 ml per 3 g of urine) of nitric acid is added before drying and dry-ashing. This procedure gives a perfectly white amorphous ash which dissolves easily in hydrochloric acid.

It has been suggested[10] that iodide should be added to the aqueous phase in order to achieve complete extraction of cadmium. This was tested in the system described above, but was found to be unnecessary since it did not result in a higher recovery of cadmium. In agreement with Maeck *et al.*[9] it was found that cadmium could be quantitatively extracted into

Table 1. Effect of THAI and HCl concentration on extraction

THAI Concentration	Cadmium, *ng/g*		[Hcl], M
	Added	Found*	
0	10	<0.2	3
0.01% ($2 \times 10^{-4}M$)	10	<0.2	3
0.1% ($2 \times 10^{-3}M$)	10	7.8 ± 0.2	3
1.0% ($2 \times 10^{-2}M$)	10	10.3 ± 0.2	3
2.5% ($5 \times 10^{-2}M$)	10	10.0 ± 0.1	3
2.5%	10	9.9 ± 0.1	1
2.5%	10	10.3 ± 0.1	5

*Mean (of three determinations) ± standard deviation.

Table 2. Comparisons between the results (Cd, *ng/g*) obtained with 2.5 and 5.0% THAI

Urine	APDC extraction*	2.5% THAI†	5.0% THAI†
80:313	1.5	1.7 ± 0.1	1.5 ± 0.1
79:31	3.6	3.7 ± 0.1	3.4 ± 0.2
78:19	4.6	4.7 ± 0.3	4.5 ± 0.5
Detection limit	—	0.1	0.1

*Mean of two determinations by the method of Elinder *et al.*[3]
†Mean (of 6 replicates) ± standard deviation.

MIBK from a wide range of hydrochloric acid concentrations, and that the addition of iodide was not necessary if quaternary amines were used as extractants. The following extraction mechanism is postulated:

$$Cd^{2+}_{aq} + 4Cl^{-}_{aq} \rightleftharpoons [CdCl^{2-}_{4}]_{aq}$$

$$2R_4NI_o + [CdCl^{2-}_{4}]_{aq} \rightleftharpoons [(R_4N)_2CdCl_4]_o + 2I^{-}_{aq}$$

where the subscripts (aq and o) refer to the aqueous and organic phases, respectively, but there may also be an exchange reaction between $CdCl^{2-}_{4}$ and I^- to give CdI^{2-}_{4}, and extraction of more than one cadmium species. This does not affect the amount of cadmium found, so long as the extraction is quantitative.

Table 1 demonstrates the influence of the THAI concentration on the extraction of a 10 ng/g cadmium solution, from ~3*M* hydrochloric acid medium. Quantitative extraction can be achieved with a reagent concentration of 1% or more (0.02*M*). Since a number of other metals present in urine, notably Cu, Hg, Pb and Zn, may also be partially extracted under these conditions, an extractant concentration of about 2.5% (0.05*M*) was used throughout to maintain a sufficient excess of reagent.

Accuracy and precision

Table 2 presents a comparison between the proposed method and an APDC extraction method previously used at this Institute.[1,3] There is no significant difference in the results obtained with 2.5% and 5% THAI solution. Thus the 2.5% reagent is sufficient for urines having a cadmium concentration up to 4.6 ng/g. For higher concentrations it may be wise to dilute the urine before extraction.

Table 3 presents results for spiked urine samples, analysed by the present method. The values are the means of six replicate determinations, a hollow-cathode lamp being used for one series and an electrodeless discharge lamp (EDL) for the other. There were no major differences in the results although the EDL gave a lower detection limit (0.1 ng/g). Recovery of added cadmium averaged 96%, and the coefficient of variation was about 10%. The results also compare well with those of neutron-activation analysis (NAA). NAA cannot always be regarded as an exact method, however; the duplicate analysis of the urine samples spiked at the 2.0 ng/g cadmium level gave 2.7 and 1.9 ng/g.

Figure 1 shows a comparison between the results obtained by the proposed method and by an earlier

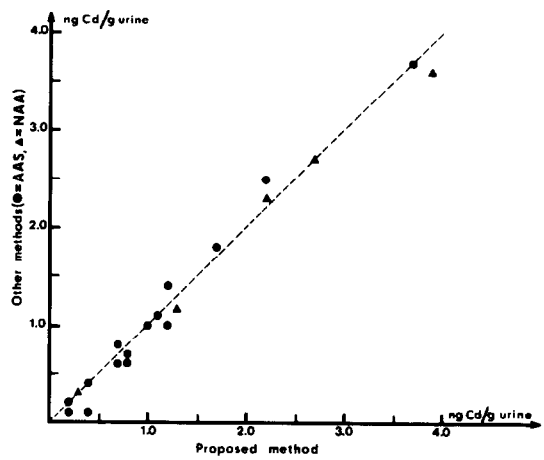

Fig. 1. Comparison between urinary cadmium concentrations found by the proposed method and by an AAS–ETA method formerly in use[3] at this institute (●) as well as by neutron-activation analysis (NAA) (▲).

Table 3. Comparison between the cadmium results (*ng/g*) obtained by the proposed method and by NAA

	Proposed method*		Amount recovered*		
Urine	HCL	EDL	HCL	EDL	NAA†
Unspiked pooled urine	0.3 ± 0.1	0.3 ± 0	—	—	0.3, 0.4
Spiked with 1.0 ng/g	1.2 ± 0.1	1.3 ± 0.1	0.9 ± 0.1	1.0 ± 0.1	1.2, 1.1
Spiked with 2.0 ng/g	2.5 ± 0.2	2.2 ± 0.1	2.2 ± 0.2	1.9 ± 0.1	2.7, 1.9
Spiked with 4.0 ng/g	4.1 ± 0.3	3.9 ± 0.4	3.8 ± 0.3	3.6 ± 0.4	3.6, 3.6
Reference urine (I)	—	2.7 ± 0.1	—	—	2.8, 2.6
Detection limit	0.2	0.1			

*Mean (of 6 replicates) ± standard deviation: HCL = hollow-cathode lamp; EDL = electrodeless discharge lamp.
†Neutron activation analysis, duplicate samples.

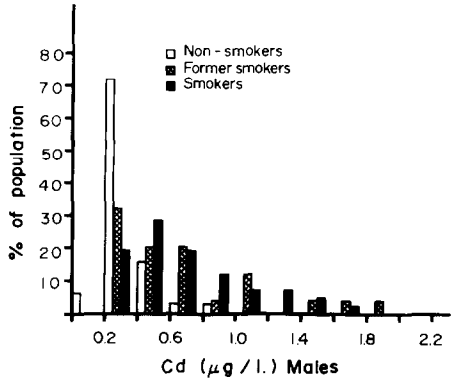

Fig. 2. Frequency distribution of urinary cadmium concentration among males in different smoking categories.

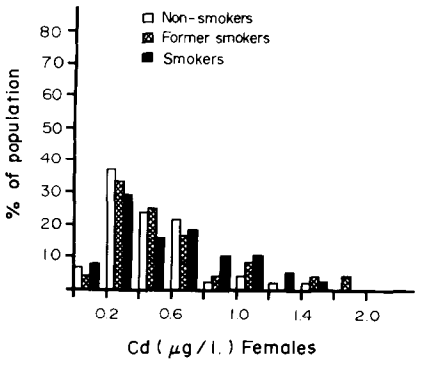

Fig. 3. Frequency distribution of urinary cadmium concentration among females in different smoking categories.

method described by Elinder *et al.*[3] Fifteen different samples of urine, with cadmium concentrations ranging from 0.2 to 4.2 ng/g, were run independently on two different instruments by the two methods. It should be pointed out that the earlier method requires about 50 g of sample for duplicate analyses, and that careful adjustment of pH is necessary for the quantitative extraction of cadmium. The results were all in good agreement, the correlation coefficient being 0.985 ($n = 15$) for the two extraction methods and 0.995 ($n = 5$) for the present method and NAA.

The whole procedure, from weighing to centrifugation, is carried out in the same extraction tube. The number of steps and reagents has been reduced to an absolute minimum, so the proposed method is much less prone to errors caused by loss of the metal in different steps[5] or by contamination from the reagents.

Urinary excretion of cadmium

Data on the urinary excretion of a substance can be presented in various ways, the most straightforward being as μg/l. The drawback is that different urine samples frequently have a variable degree of dilution and a diluted sample cannot readily be compared with a concentrated one. A common way of making urine samples more comparable is to adjust the results to refer to a certain specific gravity,[14] corresponding to a certain degree of dilution, or to use creatinine as a reference metabolite, quoting μg per g of creatinine. Adult males excrete about 1.7 g of creatinine per 24 hr and females about 1.0 g.[15]

Table 4. Urinary excretion of cadmium among *n* males (median), expressed as μg/g of creatinine and μg/l. of urine, adjusted to specific gravity of 1.016*

	Non-smokers			Former smokers			Current smokers		
Age	μg/g	μg/l.	*n*	μg/g	μg/l.	*n*	μg/g	μg/l.	*n*
19–34	0.2	0.2	18	0.3	0.3	6	0.25	0.35	12
35–49	0.2	0.2	7	0.4	0.4	7	0.4	0.4	9
50–64	0.25	0.25	6	0.75	1.05	6	0.7	0.7	13
65–72	0.3	0.4	1	0.55	0.65	6	1.0	1.05	8
All	0.2	0.2	32	0.5	0.5	25	0.55	0.6	42

*The results are usually given with one significant figure. In some cases, where the number of samples in the subgroup was even, the median value has been estimated as the average of the higher and the lower values, and given with a second decimal place.

Table 5. Urinary excretion of cadmium among *n* females (median), expressed μg/g of creatinine and μg/l of urine, adjusted to specific gravity of 1.016*

	Non-smokers			Former smokers			Current smokers		
Age	μg/g	μg/l.	*n*	μg/g	μg/l.	*n*	μg/g	μg/l.	*n*
19–34	0.25	0.2	8	0.2	0.25	6	0.3	0.3	18
35–49	0.4	0.45	8	0.45	0.4	6	0.55	0.65	6
50–64	0.4	0.4	17	0.55†	0.6	11	0.85	0.75	10
65–72	0.5	0.6	13	0.6	0.5	1	1.2	0.75	4
All	0.4	0.4	46	0.5§	0.5	24	0.5	0.5	38

*See footnote to Table 4.
†$n = 10$.
§$n = 23$.

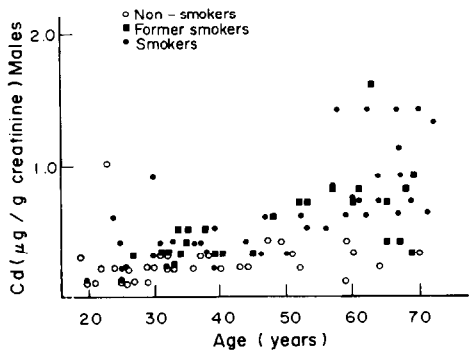

Fig. 4. Urinary excretion of cadmium in relation to age (μg/g of creatinine) for male non-smokers, former smokers and current smokers.

This difference should be borne in mind when data for the two sexes are compared. In this study the results are presented either as μg/l., adjusted to a specific gravity of 1.016, or as μg per g of creatinine.

There was considerable scatter in the excretion of cadmium by different individuals, the overall range being 0.1–1.9 μg/l. with a median of 0.4 μg/l. The frequency distributions (Figs. 2 and 3) were skewed and closer to a logarithmic than a normal distribution. Therefore median values are given in Tables 4 and 5, which present data on the urinary excretion of cadmium by males and females in different age and smoking categories. Smokers in all age groups had higher urinary excretion of cadmium than did non-smokers. On average, in Sweden the concentration of cadmium in the urine of a smoker is about twice that of a non-smoker of the same age. Former smokers usually give values intermediate between those of non-smokers and current smokers, but generally closer to those for non-smokers. Figures 4 and 5 present the variation, with age, of the urinary excretion of cadmium among non-smokers, current and former smokers, for males and females. It is evident that age also has a significant influence on the urinary excretion of cadmium. Persons aged 50–65 had a urinary excretion of cadmium about twice that of those aged below 35. These observations are not new, but confirm earlier reports.[1–4,12] It has been noticed that urinary excretion of cadmium follows the same pattern as does the kidney or body burden of cadmium, and suggested that it can be used as an indicator of the kidney or body burden of cadmium,[1,3,4] especially since it is not correlated with the daily intake of this metal.[3] The urinary excretion of cadmium appears to give a more reliable measure of the body burden than do measurements of blood cadmium. Blood cadmium levels among smokers are about 10 times those among non-smokers, whereas the body burden is about twice that of non-smokers.[11] Thus, blood cadmium among smokers reflects the degree of recent exposure to inhalation. On the other hand, the urinary excretion of cadmium by smokers is about twice that for non-smokers, which is in agreement with the ratio found for tissue cadmium.

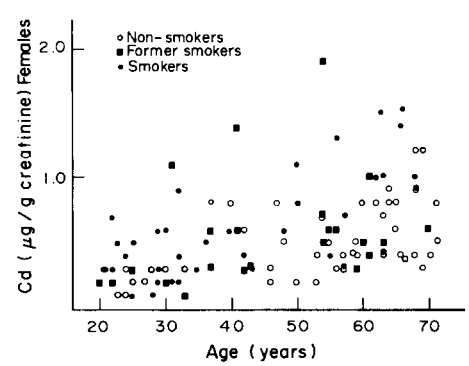

Fig. 5. Urinary excretion of cadmium in relation to age (μg/g of creatinine) for female non-smokers, former smokers and current smokers.

Acknowledgements—This work was financially supported by the National (Swedish) Environment Protection Board. The authors are grateful to Bo Nilsson and Jan Edelsjö for skilful experimental assistance. Rolf Åberg is thanked for preparing tables and graphs.

REFERENCES

1. T. Kjellström, *Environ. Health Perspect.*, 1979, **28**, 169.
2. L. Friberg, M. Piscator, G. F. Nordberg and T. Kjellström, *Cadmium in the Environment.* Chemical Rubber Co., Cleveland, Ohio, 1974.
3. C-G. Elinder, T. Kjellström, L. Linnman and G. Pershagen, *Environ. Res.*, 1978, **15**, 473.
4. L. Friberg, G. F. Nordberg and V. B. Vouk (eds.), *Handbook on the Toxicology of Metals*, p. 365. Elsevier/North Holland Biomedical Press, Amsterdam, 1979.
5. T. Kjellström, B. Lind, L. Linnman and G. F. Nordberg, *Environ. Res.*, 1974, **8**, 92.
6. V. W. Oelschläger and L. Bestenlehner, *Landwirtsch. Forsch.*, 1974, **27**, 62.
7. C. W. McDonald and F. L. Moore, *Anal. Chem.*, 1973, **45**, 983.
8. C. W. McDonald and T. Rhodes, *ibid.*, 1974, **46**, 300.
9. W. J. Maeck, G. L. Booman, M. E. Kussy and J. E. Rein, *ibid.*, 1961, **33**, 1775.
10. J. G. Viets, *ibid.*, 1978, **50**, 1097.
11. C-G. Elinder, L. Friberg, B. Lind and M. Jawaid, *Environ. Res.*, 1983, in the press.
12. N. E. Kowal, D. E. Johnson, D. F. Kraemer and H. R. Pahren, *J. Toxicol. Environ. Health*, 1979, **5**, 1014.
13. K. R. Sperling and B. Bahr, *Z. Anal. Chem.*, 1980, **301**, 31.
14. H. B. Elkins and L. D. Pagnotto, *Arch. Environ. Health*, 1969, **18**, 996.
15. S. Jackson, *Health Phys.*, 1966, **12**, 843.

Talanta, Vol. 30, No. 7, pp. 515–518, 1983
Printed in Great Britain

0039-9140/83 $3.00+0.00
Pergamon Press Ltd

SHORT COMMUNICATIONS

RAPID-SCAN PULSE VOLTAMMETRY

LEON ASHLEY and SOLOMON L. LEVINE*
IBM Instruments, Inc., P.O. Box 332, Danbury, CT 06810, U.S.A.

(*Received* 26 *March* 1982. *Revised* 24 *August* 1982. *Accepted* 26 *January* 1983)

Summary—In pulse voltammetry slow scan-rates (1–5 mV/sec) are generally used, so long scan-times are needed to cover reasonable potential ranges. Data are presented to show that fast pulse voltammetry with stationary electrodes and the dropping mercury electrode can provide useful analytical data which fit the theory of conventional pulse voltammetry. The possibility of reducing the capacitive currents and increasing the apparent faradaic current in cyclic pulse voltammetry is also shown.

Since the introduction of pulse polarography[1] and its evaluation for use in trace analysis,[2] the pulse techniques have been used in a wide variety of analyses, and use made of their many and well-discussed advantages. However, one disadvantage of pulse techniques is that the scan-rates generally range from 1 to 5 mV/sec, so relatively long times are needed to scan a reasonable potential range.

To increase the scan-rate, the entire potential range can be applied to a single mercury drop, or stationary electrodes can be used [as in differential pulse voltammetry (DPV)] or square-wave voltammetry.[3–5] DPV has also been used with a single mercury drop[6] and reports of fast DPV have been presented,[7–12] besides at least one on differential pulse stripping voltammetry[13] and one on fast alternate-drop pulse polarography.[14] Combination of rapid scanning with pulse techniques requires short drop-times or pulse repetition times. In all the works cited above, the instruments used were either home-made, or commercial models modified to provide drop or repetition times down to 100 msec.

Data are presented here to show the effects of rapid-scan differential pulse and alternate-drop voltammetry and polarography at scan-rates of up to 100 and 900 mV/sec, respectively, with use of unmodified analogue instrumentation. It is also noted that cyclic pulse voltammetry can be used. A primary benefit of rapid-scan pulse voltammetry is the substantially reduced analysis time, an important factor when the scan constitutes a major fraction of the total analysis time.

EXPERIMENTAL

All voltamperograms were recorded with an IBM Instruments EC/225 Voltammetric Analyzer and 7424MT X–Y recorder. The differential pulse and alternate-drop pulse potential voltamperograms were recorded at rates from 5 mV/sec to 1 V/sec, with drop and pulse-repetition rates of 1–10 per sec and pulse amplitudes from 5 to 115 mV.

An IBM Instruments voltammetric cell with an SCE reference and platinum-wire coil counter-electrode was used. The working electrodes used were a dropping mercury electrode (DME) with a drop-knocker (mercury flow-rate 4.55 mg/sec for 0.1 sec drop-time and 4.38 mg/sec for 1.0 sec drop-time), an IBM Instruments Model A6011 glassy-carbon electrode and a Metrohm E410 hanging mercury-drop electrode (HMDE). The glassy-carbon electrode was used as received, and occasionally repolished with 0.2-μm alumina.

Systems with well-understood electrode processes were studied to determine the effects of fast scanning, and all the solutions were prepared from reagent-grade or ultrahigh-purity chemicals. These included 0.2 m*M* solutions of ferrocene and 10-methylphenothiazine (K and K Laboratories) in a pH-4.8 methanolic acetate buffer prepared by dissolving 13.6 g of sodium acetate trihydrate in 50 ml of water, adjusting the pH with glacial acetic acid (~5.8 ml) and diluting to 1 litre with methanol. Cadmium, lead and zinc solutions were prepared from either the pure metal dissolved in the appropriate acid (hydrochloric or nitric) or from J. T. Baker "Dilut-it" standards. The supporting electrolyte was 0.1*M* potassium nitrate.

The nitrogen used for deoxygenation of solutions was piped to the laboratory from a reservoir of liquid nitrogen and used without further purification. It was passed through distilled water before the solution in the polarographic cell and was passed over the solution surface while the voltamperograms were recorded.

RESULTS AND DISCUSSION

Figures 1a and 1b show differential pulse voltamperograms of ferrocene and 10-methylphenothiazine scanned at 5 and 100 mV/sec respectively, the glassy-carbon electrode being used. In both cases, the peaks are well-defined and analytically usable, but the rapid scan was recorded in only 9 sec, whereas the slow scan took 180 sec. With a pulse-repetition rate

*Present address: IBM Corporation, 1701 North Street, Endicott, NY 13760, U.S.A.

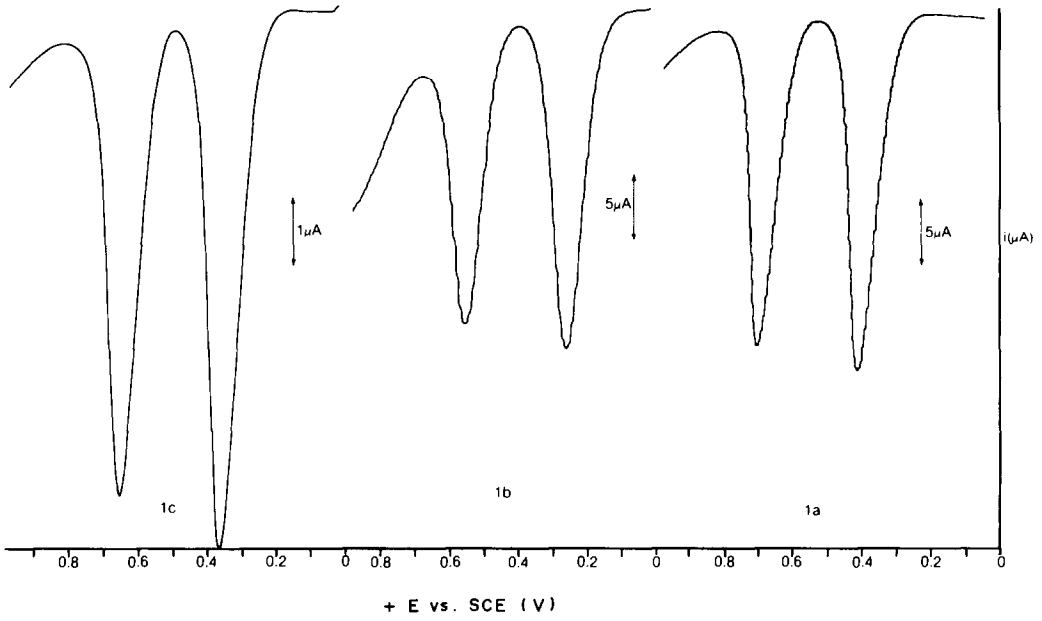

Fig. 1. Voltamperograms of 0.2 m*M* ferrocene and 10-methylphenothiazine in methanolic acetate buffer (glassy-carbon electrode). a, DPV: scan-rate = 5 mV/sec; 1.0/sec pulse-repetition. b, DPV: scan-rate = 100 mV/sec; 10/sec pulse-repetition. c, ADV: scan-rate = 500 mV/sec; 10/sec pulse-repetition.

of 10 per sec, 100 mV/sec is the fastest scan-rate that can be used without distortion of the peaks.

The theoretical relationships for conventional (slow) differential pulse polarography are also valid for this rapid scanning technique. Plots of current and peak-width at half peak-height as functions of pulse amplitude for fast scanning compare favourably with those for slow scanning, as shown in Figs. 2 and 3, and in general with the theoretical plots.[2] The similarity is further shown by comparing the fraction of maximum current obtainable (as a function of pulse amplitude) with that theoretically predicted from the $(\delta - 1)/(\delta + 1)$ term of the equation for differential pulse current.[2,15] Table 1 shows these data normalized to a pulse amplitude of 100 mV for these 1-electron transfer reactions. All the peak potentials in the rapid scans were shifted from the half-wave potential by the predicted[2] $\Delta E/2$, within 2–3 mV.

Alternate-drop pulse polarography is a relatively new technique designed to compensate completely for the capacitive backgrounds arising from extrusion of the mercury drop from the DME.[16] In this technique, alternate drops are subjected to a constant-amplitude pulse superimposed on the ramp; intervening drops are held at the pulse potential for the life of the drop. The current output is the difference between the currents for the pulsed and non-pulsed drops. With the solid electrodes used in this portion of the work, the measurement is made on alternate pulses and the pulse is applied at alternate pulse-repetition times; hence the name alternate-pulse (AP) voltammetry. A

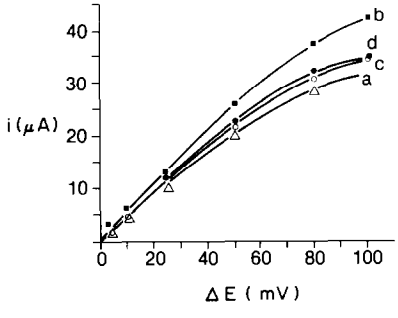

Fig. 2. Current (*i*) *vs.* pulse amplitude (ΔE). Rapid-scan DPV: scan-rate = 100 mV/sec; 10/sec pulse-repetition. Conventional DPV: scan-rate = 5 mV/sec; 10/sec pulse-repetition. a, Ferrocene (conventional); b, ferrocene (rapid-scan); c, 10-methylphenothiazine (conventional); d, 10-methylphenothiazine (rapid-scan).

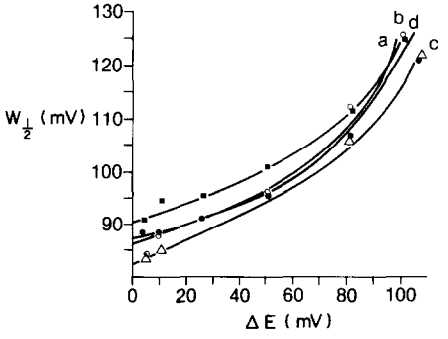

Fig. 3. Peak-width ($W_{1/2}$) at half-height, as a function of pulse amplitude (ΔE). a, Ferrocene (conventional); b, ferrocene (rapid-scan); c, 10-methylphenothiazine (conventional); d, 10-methylphenothiazine (rapid-scan).

Table 1. Fraction of maximum current obtainable, as a function of pulse amplitude (normalized to 100 mV)

Pulse amplitude, *mV*	Theoretical *i*, %	Ferrocene *i*, % (Slow DP)*	Ferrocene *i*, % (Fast DP)†	Ferrocene *i*, % (Fast AD)§	10-Methylphenothiazine *i*, % (Slow DP)	10-Methylphenothiazine *i*, % (Fast DP)
10	12.9	16.1	14.8	—	15.3	15.6
25	31.9	31.6	33.4	41.8	29.2	34.9
50	60.4	—	61.0	60.4	—	59.1
80	86.9	87.4	87.9	86.9	87.8	92.6
100	100.0	100.0	100.0	100.0	100.0	100.0
115	107.6	—	110.0	—	—	—

*Drop-time 1.0 sec; scan-rate 5 mV/sec.
†Drop-time 0.1 sec; scan-rate 100 mV/sec.
§Drop-time 0.1 sec; scan-rate 500 mV/sec.

similar compensation is obtained for the capacitive contribution to the background currents. Figure 1c shows an AP voltamperogram scanned at 500 mV/sec, showing the well-defined peaks and somewhat lower background current at the more positive potentials. This technique could be used at scan-rates up to 900 mV/sec before the peak distortion became large enough to make the curves unusuable. The distortion manifests itself as skewed, ill-defined peaks, because the current-follower and sample/hold circuitry is not fast enough to keep up at the higher scan-rates. All other effects were similar to those in fast-scan differential pulse work, as stated above.

Reduction processes were followed by both slow and fast pulse polarography, with various concentrations of the three metal ions and use of both the DME and HMDE. Polarograms obtained for $10^{-4}M$ solutions of the three metal ions at 100-mV/sec scan-rate and 0.1-sec drop-time and 10/sec pulse repetition were analytically usable, but the currents obtained were only 20–25% of those obtained from more conventional polarograms (5 mV/sec, 1.0-sec drop-time and 1/sec pulse repetition). The lower currents are due to the smaller electrode areas obtained with the short drop-times. With the HMDE, currents obtained for the slow and fast DPV scans were comparable; in the AP scans, the currents were smaller, as expected.

The decrease in current due to the small drop areas limits the analytical sensitivities of fast scan with the DME to about $10^{-6}M$ for these ions as opposed to about $10^{-8}M$ with slower scans. Figures 4a and b show typical fast DP scans with the DME; Fig. 3b was scanned with a 0.1-sec time-constant filter on the output. Although the curve is smoothed, there is also the expected shift in peak potentials.

The DP and AP techniques are both designed to reduce the background, particularly the capacitive current, in d.c. polarography. Reducing this current should result in better defined peaks with a higher

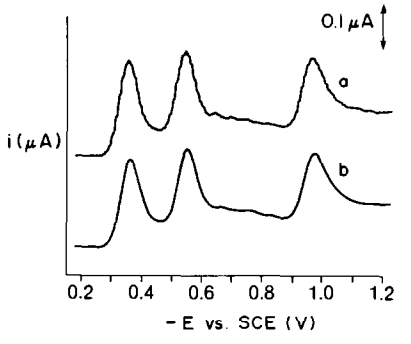

Fig. 4. Polarograms of $10^{-4}M$ Pb^{2+}, Cd^{2+} and Zn^{2+} in $0.1M$ KNO_3 (DME). Conditions: $\Delta E = 50$ mV; scan-rate = 100 mV/sec; drop-time 0.1 sec and pulse repetition 10/sec. a, No output filter; b; 0.1-sec time-constant output filter.

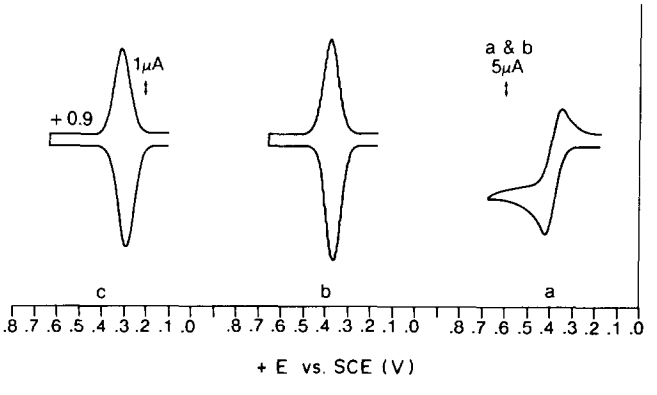

Fig. 5. Rapid-scan cyclic pulse voltamperograms of 0.2 mM ferrocene in methanolic acetate buffer (glassy-carbon electrode). a, d.c., scan-rate 100 mV/sec; b, AP, scan-rate 500 mV/sec, pulse repetition 10/sec; c, DP, scan-rate 100 mV/sec, pulse repetition 10/sec.

apparent current in cyclic voltammetry. Cyclic DP and AP voltammetry at the faster scan-rates both proved feasible, as shown in Fig. 5 for ferrocene. The backgrounds for voltammetry of these organic compounds on the glassy-carbon electrode are lower than those obtained in conventional d.c. cyclic voltammetry. This should allow the use of lower analyte concentrations in cyclic voltammetry.

The data presented indicate that rapid-scan pulse polarography and voltammetry show promise as time-saving tools; scans over reasonable potential ranges can be accomplished in seconds as opposed to a few minutes at the more conventional slower rates. However, the rapid scans require higher concentrations than the slower scan-rates do. With the DME in particular, the practical detection limit is relatively high (10^{-4}–$10^{-6}M$) because of the increase in background and the smaller currents caused by the small drop areas obtained in rapid scans.

With cyclic voltammetry, the background signal obtained with solid electrodes is lower than that of d.c. positive-potential cyclic scans with a glassy-carbon electrode. The pulsed cyclic scans give easier current measurements and lower detection limits. More work is necessary, however, to refine these techniques and utilize their advantages.

REFERENCES

1. G. C. Barker and A. W. Gardner, *AERE Harwell*, C/R 2297, 1958.
2. E. P. Parry and R. A. Osteryoung, *Anal. Chem.*, 1965, **37**, 1634.
3. L. Ramaley and M. S. Krause, Jr., *ibid.*, 1969, **41**, 1362.
4. J. H. Christie, J. A. Turner and R. A. Osteryoung, *ibid.*, 1977, **49**, 1899.
5. J. A. Turner, J. H. Christie, M. Vukovic and R. A. Osteryoung, *ibid.*, 1977, **49**, 1904.
6. H. Blutstein and A. M. Bond, *ibid.*, 1976, **48**, 248.
7. K. C. Burrows, M. P. Brindle and M. C. Hughes, *ibid.*, 1977.
8. G. D. Christian, *J. Electroanal. Chem.*, 1969, **22**, 33.
9. S. C. Rifkin and D. H. Evans, *Anal. Chem.*, 1976, **48**, 1616.
10. *Idem*, *ibid.*, 1976, **48**, 2174.
11. K. C. Burrows, *Ph.D. Thesis*, Lehigh University, 1979.
12. M. C. Hughes, E. F. Blaedel, Jr. and J. Grossman, Presented at 1981 Pittsburgh Conference on Analytical Chemistry and Applied Spectroscopy, Atlantic City, March, 1981.
13. P. Valenta, L. Mark and H. Rutzel, *J. Electroanal. Chem.*, 1977, **82**, 327.
14. J. A. Turner and R. A. Osteryoung, *Anal. Chem.*, 1978, **50**, 1496.
15. A. J. Bard and L. R. Faulkner, *Electrochemical Methods*, pp. 190–196. Wiley, New York, 1980.
16. J. H. Christie, L. L. Jackson and R. A. Osteryoung, *Anal. Chem.*, 1976, **48**, 242.

Talanta, Vol. 30, No. 7, pp. 519–522, 1983
Printed in Great Britain

0039-9140/83 $3.00+0.00
Pergamon Press Ltd

ACETOTHIOACETANILIDE AS A GRAVIMETRIC REAGENT FOR PALLADIUM, PLATINUM AND RHODIUM

TARASANKAR PAL and JYOTIRMOY DAS
Chemistry Department, University of Burdwan, Burdwan 713104, India

(*Received* 14 *January* 1981. *Revised* 20 *October* 1982. *Accepted* 25 *January* 1983)

Summary—Acetothioacetanilide, $CH_3CO \cdot CH_2 \cdot CS \cdot NH \cdot C_6H_5$, is found to be a very suitable gravimetric reagent for Pd(II), Pt(II) and Rh(III). The complexes [composition, $M(C_{10}H_{10}NOS)_2$ for M = Pd(II) and Pt(II), and $Rh(C_{10}H_{10}NOS)_3$] are stable and can be weighed after drying at 105–110°. Separation from base metals has been studied, and a structural interpretation made from DTA, TG and infrared data.

Much attention has been paid to sulphur as a ligand atom in determination and separation of platinum metals, but most of the complexes are unsuitable for gravimetric purposes, owing to their thermal instability. Few reagents are available for the separation of these metal ions, but there are several for determination of individual members of the group.[1–9] Thionalide[10] and thiosalicylamide[11] have been studied but are not effective for the separation of the noble metals. 2-Mercaptobenzothiazole[12] precipitates only platinum and rhodium, and 2-mercaptobenzoxazole[13] is suitable for only rhodium. Some semicarbazides and semicarbazones are used for palladium[14] and platinum.[15–17] Though substituted thioureas[18] are gradually replacing other reagents because of their analytical potential, suitable gravimetric procedures still need to be developed.

The conditions for the use of acetothioacetanilide as a gravimetric reagent for platinum, palladium and rhodium were studied in this investigation. The procedure described below is not only very selective but also has high precision and accuracy. Separation from almost all other platinum metals, and of palladium(II) and platinum(II) from one another, is possible. The use of the reagent for the determination of zinc, cadmium and mercury has already been reported.[19]

EXPERIMENTAL

Reagents

Acetothioacetanilide. The reagent was prepared by the method due to Barnikow *et al.*[20] Thiodiacetoacetanilide was first prepared from acetylacetone and phenylisothiocyanate, and on hydrolysis produced acetothioacetanilide. This was recrystallized from 40% aqueous ethanol. The pale yellow product (m.p. 64°) is soluble in all common organic solvents, and appreciably soluble in water at about pH 7. It is a mild reducing agent (redox potential 0.64 V). Its dissociation constant has been determined by Bjerrum titration and found to be 3.09×10^{-9}. The reagent decomposes slowly after 2–3 months unless preserved in a dark cool place, preferably in a refrigerator. Three ethanolic solutions of the reagent were used [concentrations 5% (0.26*M*), 7.5% (0.39*M*) and 11% (0.57*M*)].

Palladium(II), platinum(II) and rhodium(III) solutions. Palladium(II) chloride, platinum(II) chloride and rhodium(III) chloride (Johnson–Matthey) were dissolved separately in dilute hydrochloric acid and the solutions were standardized by conventional methods[12,21,22] and diluted as desired.

All chemicals used were of analytical reagent or guaranteed reagent grade.

Procedures

Palladium(II). A measured amount of the stock palladium(II) solution containing 4.4–17.6 mg of the metal was diluted to about 200 ml with water, 2 g of potassium chloride were added and the pH was adjusted to 3.0 with 3*M* hydrochloric acid. The solution was heated to 80–90° on a water-bath and 100% excess of 5% acetothioacetanilide solution was added dropwise with constant stirring. After digestion on the water-bath for about 30 min the granular dull red precipitate was filtered off on a sintered-glass crucible (porosity 4), washed with warm water (~60°), dried at 100° and weighed as $Pd(C_{10}H_{10}NOS)_2$, containing 21.65% of the metal.

Platinum(II). A known amount of solution containing 12–50 mg of platinum(II) was diluted to about 200 ml with water, 2 g of potassium chloride were added and the pH was adjusted to about 2.0 with 3*M* hydrochloric acid. The mixture was heated to 90–95° on a water-bath and 100% excess of 7.5% acetothioacetanilide solution was added dropwise with constant stirring. After digestion on the water-bath for 45–60 min the granular dark red precipitate was collected and washed as for the palladium compound, dried at 100–110° and weighed as $Pt(C_{10}H_{10}NOS)_2$, containing 33.69% of the metal. Platinum(IV) can be reduced with hydroxylamine hydrochloride before addition of the reagent, or with the reagent itself if a large enough excess is used.

Rhodium(III). A portion of solution containing 3.6–10.9 mg of rhodium(III) was diluted to 150 ml after addition of 1 g of ammonium chloride, and the pH was adjusted to

Table 1

Complex	Required, %			Found, %		
	M	N	S	M	N	S
PdL_2	21.60	5.57	6.51	21.7	5.7	6.5
PtL_2	33.50	4.81	11.00	33.7	4.8	11.1
RhL_3	15.10	6.13	14.13	15.1	6.2	14.1

about 6.0 with 1*M* ammonia solution. The mixture was heated to 80–90° on a water-bath and 100% excess of reagent solution was added with constant stirring. After digestion for 45–60 min on the boiling water-bath the orange-yellow precipitate was collected and washed as for the palladium compound, dried at 120° and weighed as $Rh(C_{10}H_{10}NOS)_3$, containing 14.93% of rhodium.

RESULTS AND DISCUSSION

Nature of the complexes

The complexes are fairly soluble in the common organic solvents. They were analysed for nitrogen by the Dumas method and for sulphur by its conversion into sulphate. The metal contents were determined by oxidative decomposition of the complex. The results in Table 1 indicate 1:2 complexation of palladium and 1:3 complexation of rhodium.

Thermogravimetric studies

Appropriate weights of the complexes were mixed with aluminium oxide and heated at 12°/min. The thermogravimetric curves showed that the thermal stability of the complexes was in the order Pd < Pt < Rh. All three complexes can be weighed directly after drying at about 100°. The complexes are hygroscopic but the uptake of water over a 24-hr period is too slow to be of significance and the water is readily removed on heating at below 100°, with no decomposition of the complex, as the first decomposition temperatures are 110°, 120° and 220° for palladium, platinum and rhodium respectively; decomposition is complete at 820° for palladium and 640° for platinum and rhodium under dynamic heating conditions. The losses in weight are 79.8% for palladium, 66.3% for palladium and 70.0% for rhodium, in agreement with expectation. Hence care must be taken in drying the palladium and platinum complexes. The decomposition patterns for palladium and rhodium are the same but differ from that for platinum.

Spectral information

From the NMR spectrum of the ligand it appears that enolization similar to that of acetylacetone takes place. It is evident that the compound behaves as a bidentate ligand.

The infrared spectra of the ligand and complexes indicate co-ordination through C=O→M and chelation through C–S–M. The band at 1628 cm^{-1} is quite sharp and intense, indicating that the carbonyl group is not enolized, and this is further corroborated

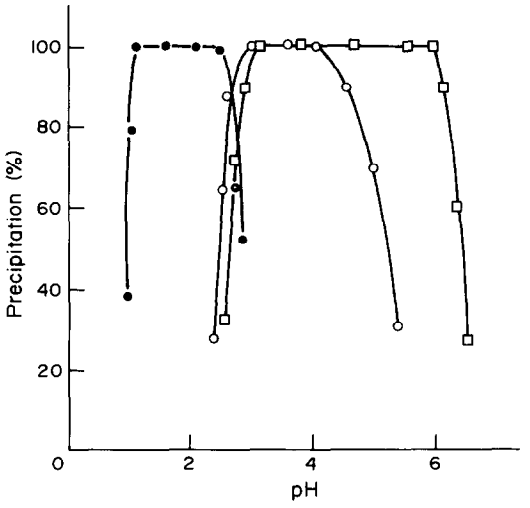

Fig. 1. Variation of degree of precipitation with pH. Palladium —○—; platinum —●—; rhodium —□—.

by the absence of any broad enol O–H stretching absorption at 2700–2500 cm^{-1}. The displacement of this band is greatest for the Rh-complex, indicating[23] strong co-ordination of the type C=O→M. The C=O stretching frequency is shifted to 1610–1555 cm^{-1} in the complexes, and the C–S stretching frequency of the ligand at 1220 cm^{-1} is shifted to 1160–1250 cm^{-1}, suggesting a 6-membered ring.

The rhodium complex is diamagnetic, indicating the octahedral low-spin arrangement of the electrons in the split *d*-orbitals. The orange-red colour of the complex suggests transition from the $^1A_{1g}$ ground-state to the $^1T_{1g}$ and $^1T_{2g}$ excited states. The magnetic-moment data for the palladium and platinum complexes indicate square-planar structures.

Table 2. Tolerance limits

Ion	Tolerated amount, *mg*, for		
	Pd (9 mg)	Pt (19 mg)	Rh (7 mg)
Ca^{2+}	100	100	100
Mg^{2+}	100	100	100
Sr^{2+}	100	100	100
Ba^{2+}	100	100	100
As(V)	100	100	100
Cr^{3+}	80	60	100
Cd^{2+}	—	—	80
Ni^{2+}	80	60	100
Zn^{2+}	100	100	100
Fe^{3+} *	100	100	100
Al^{3+}	100	80	100
Co^{2+}	—	60	100
Mo(VI)	80	60	100
Mn^{2+}	100	100	100
V(IV)	100	80	100
Os(VIII)	80	30	60
Ir(III)	80	30	60
Ru(III)	80	30	60
Pt(II)	—	—	50
Pd(II)	—	15	30
Rh(III)	—	—	—
U(VI)	100	90	100

*In presence of sodium potassium tartrate

Table 3. Individual determination of palladium, platinum and rhodium

	Taken, mg	Weight of ppte, mg		Metal found, mg	
Pd(II)	8.8	40.8	40.8	8.8	8.8
	13.3	61.2	61.3	13.2	13.3
	17.7	81.6	81.7	17.7	17.7
Pt(II)	12.5	37.3	37.0	12.6	12.5
	19.2	57.3	57.0	19.3	19.2
	38.3	113.7	113.6	38.3	38.3
Rh(III)	3.6	24.3	24.3	3.6	3.6
	7.3	48.6	48.6	7.3	7.3
	10.9	72.9	72.9	10.9	10.9

Effect of reagent concentration and pH

Approximately 100% excess of reagent was found necessary for quantitative precipitation. Palladium starts to precipitate at pH 2.5 and platinum at 1.0, the ranges for quantitative precipitation being 3.0–4.1 and 1.8–2.6 respectively. At higher pH, precipitation is incomplete. For rhodium, the pH range for complete precipitation is 3.0–6.0. At lower pH there is a tendency towards incomplete precipitation. The effect of pH is shown in Fig. 1. The precipitation of platinum has a long induction period, and takes at least 45 min to begin, at a temperature of 80–90°.

Effect of sequestering agents

Tartrate, acetate and citrate do not interfere, so they can be used as masking agents. EDTA cannot be used for masking in the determination of platinum, because of the low pH of precipitation.

Effect of diverse ions

The precipitation of platinum along with palladium cannot be avoided when the procedure given above is used, but can be prevented by adding the potassium chloride 15 min after the reagent solution; this enhances the rate of coagulation of the palladium complex, which can then be filtered off after 25–30 min (the platinum precipitates later). For the separation of rhodium from other platinum metals it is best to precipitate it at the higher limit of the pH range (6.0). At lower pH there is risk of co-precipitation of the other metal ions. Tartrate masks iron(III), and prevents its interference. Mercury(II) interferes, but small amounts can be removed by rapid precipitation with H_2S at around pH 3.0. Fluoride, chloride, bromide, nitrate, nitrite and sulphate do not interfere. Silver and gold(III) interfere by forming complexes with the reagent, and which rapidly decompose to give the sulphides.

Tolerance limits for other ions are given in Table 2.

Determination of palladium, platinum and rhodium

Results for determination of the metals in pure solutions are given in Table 3. Several synthetic mixtures were analysed under conditions corresponding to dissolution of alloys with *aqua regia* (4 parts HCl, 1 part HNO_3, 1 part H_2O) at 70° under reflux, following by fusion of the residue with sodium hydroxide and peroxide[24] and dilution of the combined solution to 100 ml. Suitable aliquots were analysed with acetothioacetanilide. In samples Nos. 1 and 4 palladium and platinum were determined. In sample No. 2 palladium was precipitated first by controlling the pH, and filtered off after 25–30 min. The palladium precipitate coagulates within 20 min, whereas the platinum precipitation does not start before the elapse of at least 45 min, otherwise these determinations would not be possible. The separation of palladium and rhodium in samples Nos. 3 and 5 by controlling the pH is not difficult. The results are all presented in Table 4.

Table 4. Determination of palladium, platinum and rhodium in complex mixtures

No.	Composition, mg/100 ml*	Found, mg/100 ml*
1	Pd 35, Pt 10, Rh 5, Os 10, Ir 15, Ru 5, Ni 20	Pd 35.0, 34.9
2	Pd 50, Pt 10, Rh 20, Ni 20	Pd 50.1, 50.2 Pt 9.9, 9.9
3	Pd 70, Rh 10, Ni 10, Fe 10	Pd 70.1, 70.0 Rh 9.9, 10.0
4	Pt 45, Rh 10, Ru 10, Os 5, Fe 20, Ni 20	Pt 45.1, 45.2
5	Pd 10, Rh 6, Os 15, Ir 15, Ru 10, Ni 24, Fe 20	Rh 6.0, 6.0 Pd 10.0, 10.0
6	Pt 15, Rh 8, Ru 15, Fe 15, Ni 32, Co 15	Rh 8.0, 8.0 Pt 15.0, 15.1

*Of stock solution (see text).

Precision and accuracy

The relative standard deviations were 0.1, 0.2 and 0.1% for palladium, platinum and rhodium respectively. Typical 95% confidence limits for the means are Pd 8.8 ± 0.07 mg, Pt 19.2 ± 0.12 mg, and Rh 7.3 ± 0.01 mg (10 determinations).

REFERENCES

1. J. J. B. Nevado, J. A. Muñoz Leyva and M. R. Ciba, *Talanta*, 1976, **23**, 257.
2. V. M. Peshkova, V. I. Shlenskaya and A. I. Rashevskaya, *Ser. Fiz. Mat. i Estetuen*, Nauk, 1954, No. 3, 83; *Chem. Abstr.*, 1954, **48**, 13529i.
3. A. Kawase, *Bunseki Kagaku*, 1963, **12**, 714.
4. A. K. Majumdar and M. M. Chakraborty, *Naturwissenschaften*, 1957, **44**, 511.
5. J. A. W. Dalziel and D. Kealey, *Analyst*, 1964, **89**, 411.
6. P. Champ, P. Fauconnier and C. Duval, *Anal. Chim. Acta*, 1958, **10**, 443.
7. N. K. Pshenitsyn and N. V. Fedeorenko, *Zh. Neorgan. Khim.*, 1957, **2**, 2375.
8. J. E. Currah, W. A. E. McBryde, A. J. Cruikshank and F. E. Beamish, *Ind. Eng. Chem., Anal. Ed.*, 1948, **18**, 120.
9. W. J. Allen and F. E. Beamish, *Anal. Chem.*, 1950, **22**, 451.

10. T. Umemura, *Nippon Kagaku Zasshi*, 1940, **61,** 26.
11. K. Sur and S. C. Shome, *Anal. Chim. Acta*, 1969, **48,** 145.
12. L. Ubaldini and L. Nebbia, *Chem. Ind. (Milan)*, 1951, **33,** 360.
13. R. L. Haines and D. E. Ryan, *Can. J. Res.*, 1949, **27B,** 72.
14. T. Komatsu, T. Kida and Z. Hiroaki, *Nippon Kagaku Zasshi*, 1956, **77,** 1437.
15. T. Naito, *Bunseki Toshiyaku*, 1949, **3,** 84.
16. T. Naito, Y. Y. Kinoshita and J. Hayoshi, *J. Pharm. Soc. (Japan)*, 1949, **69,** 361.
17. S. Komatsu and J. Ishizak, *Nippon Kagagu Zasshi*, 1960, **81,** 1623.
18. S. C. Shome, M. Mazumdar and M. K. Chakraborty, *J. Indian Chem. Soc.*, 1977, **54,** 225.
19. T. Pal and J. Das, *ibid.*, 1977, **55,** 1154.
20. G. Barnikow, H. Kunzek and D. Richter, *Annalen.*, 1966, **695,** 49; *Chem. Abstr.*, 1966, **65,** 20051.
21. G. H. Ayres and E. W. Berg, *Anal. Chem.*, 1953, **25,** 980.
22. A. J. Vogel, *A Text Book of Quantitative Inorganic Analysis*, 3rd Ed., p. 510. Longmans, London, 1962.
23. L. Bellamy and R. F. Braunch, *J. Chem. Soc.*, 1954, 4491.
24. K. Kodama, *Quantitative Inorganic Analysis*, p. 231. Interscience, New York, 1963.

Talanta, Vol. 30, No. 7, pp. 523–526, 1983
Printed in Great Britain.

0039-9140/83 $3.00+0.00

THE EFFECT OF ORGANIC MATTER AND COLLOIDAL PARTICLES ON THE DETERMINATION OF CHROMIUM(VI) IN NATURAL WATERS

SUSUMU OSAKI
Radioisotope Center, Kyushu University, Hakozaki, Higashi-ku, Fukuoka, 812 Japan

TOMOE OSAKI
Faculty of Engineering, Fukuoka Institute of Technology, Shimowaziro, Higashi-ku, 811-02 Japan

and

NOBUHIRO HIRASHIMA and YOSHIMASA TAKASHIMA
Department of Chemistry, Faculty of Science, Kyushu University, Hakozaki, Higashi-ku, Fukuoka, 812 Japan

(*Received* 19 *October* 1982. *Accepted* 21 *January* 1983)

Summary—The chromium(VI) contents of two water samples, a river water and a sea-water, were determined by means of solvent extraction with APDC (ammonium pyrrolidinedithiocarbamate) into chloroform and by co-precipitation with iron(III) hydroxide. The analytical results depended on the separation method used, possibly because of differences in the behaviour of the chemical species of chromium in natural waters. Various chromium species, including simple inorganic ions, organic complexes, Cr(III) adsorbed on inorganic colloids and Cr(III) combined with organic polymers, were prepared, and their analytical characteristics were investigated.

Most of the separation methods used for the determination of Cr(VI) in natural waters can be divided into two types: solvent extraction,[1–4] in which Cr(VI) is extracted with DDTC (diethyldithiocarbamate) or APDC (ammonium pyrrolidinedithiocarbamate) *etc.* into MIBK (4-methyl-2-pentanone) whereas Cr(III) is not, and co-precipitation,[5–8] in which Cr(III) is collected with Fe(III) hydroxide, Al(III) hydroxide, *etc.*, which show little tendency to co-precipitate Cr(VI). It has been confirmed that Cr(VI) ions and Cr(III) ions added as spikes to natural waters can be quantitatively separated by these methods. Although little is known about the chemical forms of chromium in natural waters, the existence of organic Cr(III) complexes can be inferred by analogy with other metals in natural waters.[9–11] If the sample contains organic Cr(III) complexes which are extractable into the organic solvent used, the analytical value for Cr(VI) obtained by the solvent extraction methods will be higher than the true value. On the other hand, some of the organic Cr(III) complexes, *e.g.*, the Cr(III)–EDTA complex, are not co-precipitated with Fe(III) hydroxide.

The chromium(VI) contents of two samples, a river water and a sea-water, have been determined by both the solvent extraction and the co-precipitation method. The results for a given sample differed according to the method used, possibly because of differences in the chemical behaviour of the chromium species present. To study the effect of organic matter and colloidal particles on the determination, nine chromium species, including simple inorganic species, organic complexes, Cr(III) adsorbed on inorganic colloids and Cr(III) combined with organic polymers, have been prepared and their behaviour in the separation procedures investigated.

EXPERIMENTAL

Preparation of chromium species

Chromate ions. A ^{51}Cr-labelled sodium chromate solution with an activity of 140 mCi per mg of Cr was purchased from Daiichi Radioisotope Laboratory. A chromate solution was prepared by diluting the ^{51}Cr solution with distilled water. The purity of this chemical form was checked by solvent extraction with tetrabutylammonium hydroxide into chloroform and was above 98%.

Chromium(III) ions. A labelled chromium(III) solution in 0.1*M* hydrochloric acid was prepared by reducing the ^{51}Cr solution with sodium sulphite. The excess of reducing agent was removed by boiling.

Chromium(III) adsorbed on colloidal Fe(III) hydroxide. To 500 ml of distilled water, 1 mg of ferric ions and an adequate amount of the labelled chromium(III) solution were added. The solution was adjusted to pH 6 with 1*M* ammonia solution. The colloidal solution was centrifuged at 35000 rpm for 60 min and the activity of the solid was measured. It corresponded to pratically 100% adsorption of the ^{51}Cr.

Chromium(III) adsorbed on colloidal silica. A 3.5% sodium silicate solution was desalted on a column of cation-exchange resin, Bio-Rad AG 50 W × 8.[12] The effluent was adjusted to pH 9 with 1.5% sodium hydroxide solution, and concentrated slowly to one-fifth of its original volume. The labelled chromium(III) solution was added to the colloidal silica solution at pH 6. The chromium was about 100% adsorbed.

Chromium(III) adsorbed on colloidal aluminosilicate. A 0.01*M* aluminium nitrate solution was mixed with an equal volume of $10^{-3}M$ sodium silicate.[13] The mixture was adjusted to pH 9 with 0.1*M* sodium hydroxide and aged for 24 hr. The labelled chromium(III) solution was added to the solution at pH 6. The degree of adsorption was about 95%.

Chromium–EDTA complex. The labelled chromium(III) solution was added to $10^{-3}M$ EDTA and the pH was adjusted to 5 with 1*M* ammonia solution. The solution was heated for 10 min at 90°. The complex formed was assumed to be $Cr(H_2O)EDTA^-$.[14]

Chromium glycinate complex. The labelled chromium(III) solution was added to $10^{-3}M$ glycine and the solution was heated at 50° for 24 hr, then left standing for 1 week at room temperature.[15] The product seems to be a mixture of $Cr(H_2O)_4gly^{2+}$ and $Cr(H_2O)_2(gly)_2^+$.

Chromium(III) bound and/or adsorbed by tannic acid. The labelled chromium(III) solution was added to 1.5-mg/ml tannic acid solution prepared from reagent grade tannic acid and distilled water. The solution was adjusted to pH 5 and heated for 1 hr at 90°. A 2-ml portion of the solution was passed through a column of XAD-2 (volume 5 ml) to estimate the amount of chromium(III) bound to tannic acid. The column was washed with 10 ml of acetate buffer (pH 5), followed by 10 ml of methanol. About 23% of the initial activity was found in the initial effluent and the acetate effluent. The activity of the methanol effluent was measured and indicated that about 40% of the chromium(III) was bound by the tannic acid, the remainder being hydrolysed[16] to species sorbed on XAD-2 resin but not eluted with methanol.

Chromium(III) bound to and/or adsorbed on humic acid. The labelled chromium(III) solution was added to 34-μg/ml humic acid solution prepared from reagent grade humic acid purified by the method described by Clem and Hodgson.[17] The solution was adjusted to pH 5 and heated for 1 hr at 90°. A 2-ml portion of the solution was passed through a cation-exchange (Biorad AG 50 W × 8) column (volume, 5 ml) to estimate the degree of binding to the humic acid. The column was washed with 10 ml of acetate buffer solution (pH 5) and the activity of the effluent was measured. Hydrolysed Cr(III) species were exchanged and/or sorbed by the cation-exchange resin under these conditions.

Determination of Cr(VI) and total Cr by the solvent extraction method

The sample was filtered through a 0.45-μm membrane as soon as possible after collection, and stored at 5°. Chromate labelled with ^{50}Cr purchased from Oak Ridge National Laboratory was added as a spike to two 100-ml portions of sample. Chromium(III) in one portion was oxidized with 0.02*M* ceric ammonium nitrate to determine the total chromium content. Chromium(VI) was extracted with APDC into chloroform. The organic phase was evaporated and the residue ashed by ignition. The stable-isotope ratio of chromium in the residue was measured with a mass spectrometer (JEOL 05RB). This method has been described in detail by Osaki *et al.*[4]

Determination of Cr(III) and total Cr by the co-precipitation method

The method developed by Fukai and Vas[6] was modified. Instead of the radioisotope, the stable isotope ^{50}Cr was used. Chromium(III) labelled with ^{50}Cr was added as a spike to the filtered sample and mixed well with it. The solution was divided into two 500-ml portions. Chromium(VI) was reduced with sodium sulphite in one portion to determine the total chromium content. Iron(III) hydroxide was formed in each solution, filtered off, and then dissolved in 1*M* sulphuric acid. The Cr(III) in the solution was oxidized with 0.02*M* ceric ammonium nitrate. Finally the chromium(VI) was extracted with APDC into chloroform and its stable-isotope ratio measured as above.

Separation of chromium species spiked

Solvent extraction. River water and sea-water were filtered through 0.45-μm membranes. Then 100 ml of the filtered sample and 1 ml of a solution containing both Cr(VI) and Cr(III) labelled with ^{51}Cr were mixed well in a separating funnel. The solution was adjusted to pH 2 with 1*M* hydrochloric acid and extracted with two 100 ml portions of chloroform after addition of 2 ml of 1% APDC solution. The organic phase was washed with distilled water and its activity measured with a well-type scintillation counter (Aloca SC-5).

Co-precipitation. The filtered sample was divided into two 500-ml portions which were transferred to flasks. To each flask, 1 ml of a solution containing both Cr(VI) and Cr(III) labelled with ^{51}Cr was added and mixed in well. To one flask, 2 ml of 6*M* hydrochloric acid and 100 mg of sodium sulphite were added and nitrogen was bubbled through the solution for 1 hr. Then to each flask 1 mg of iron(III) in 0.1*M* hydrochloric acid was added and the solution was adjusted to pH 8 with 1*M* ammonia solution. The solutions were heated for 1 hr and finally boiled. After cooling, the precipitates were filtered off on 1.2-μm filters, washed, and dissolved with 30 ml of warm 0.1*M* sulphuric acid. The activities of these solutions were then measured.

RESULTS AND DISCUSSION

The chromium(VI) contents of the river water and sea-water were determined by the solvent extraction method [$Cr(VI)_E$] and the co-precipitation method [$Cr(VI)_P$]. The results are given in Table 1. For the river water, $Cr(VI)_E$ is higher than $Cr(VI)_P$, but the reverse is the case for the sea-water. The results suggest that unidentified chromium species which contribute to the error of the analytical methods for Cr(VI) are present to a significant extent in these samples.

Because of the high solubility of chromate ions and their high oxidizing power, Cr(VI) is unlikely to be bound to organic matter or adsorbed on colloidal particles. In contrast, because of the very low solubility of hydrolysed Cr(III) ions,[18] Cr(III) in natural waters is predominantly bound to organic matter or adsorbed on colloidal particles. We assume that these organic and/or colloidal Cr(III) species contribute to the error in the analytical Cr(VI) value.

Table 1. Determination of Cr(VI) and Cr(III) in natural waters by the solvent extraction and co-precipitation methods

	Total Cr, μg/l.	Cr(III), μg/l.	Cr(VI), μg/l.
River water*			
Solvent extraction	0.38	(0.0)†	0.38
Coprecipitation	0.47	0.19	(0.28)§
Sea-water‡			
Solvent extraction	0.33	(0.18)†	0.15
Coprecipitation	0.32	0.02	(0.30)§

*Collected from the Muromi River, Fukuoka, Japan.
†The values are the differences between the total Cr and Cr(VI) concentrations.
‡Collected from the shore of Shingu, Fukuoka, Japan.
§The values are the differences between the total Cr and Cr(III) concentrations.

Table 2. Recovery of chromium spikes in sea-water

Species spiked	Co-precipitation, % without reduction	Co-precipitation, % with reduction	Solvent extraction, %
Chromate ions	4.8, 4.1	100, 87.7	89.4, 71.4
Chromic ions	91.1, 97.3	96.7, 95.5	1.3, 0.2
Cr–Fe hydroxide	100, 100	98.9, 100	0.4, 0.5
Cr–silica	100, 100	100, 100	0.0, 0.0
Cr–aluminosilicate	94.0, 100	100, 100	0.0, 0.0
Cr–glycine	95.2, 100	94.9, 98.0	0.0, 0.0
Cr–EDTA	0.0, 0.0	0.0, 0.0	0.8, 1.4
Cr–tannic acid	100, 85.1	100, 92.8	0.0, 0.0
Cr–humic acid	94.8, 96.7	94.8, 94.7	0.0, 0.0

To verify this assumption, various Cr(III) species were prepared and their behaviour in the separation procedures was observed. The results are shown in Tables 2 and 3. The first and second species in the tables are the simplest species of Cr(III) and Cr(VI), respectively, which are normally used for studying analytical methods for these species. When chromium(III) ions were added in neutral solution, they were immediately hydrolysed. About 4% of the chromate ions added as a spike to sea-water was co-precipitated on Fe(III) hydroxide. Partial adsorption of Cr(VI) in sea-water on Fe(III) hydroxide has been reported by Cranston and Murray.[7] It is difficult to understand the mechanism of this adsorption. Chromate ions added as a spike to river water are rarely precipitated on Fe(III) hydroxide. The degree of co-precipitation of chromium(III) apparently ranged from 87 to 100%, perhaps because of incomplete recovery from the precipitate. The extraction of chromate ions was also incomplete. The isotope-dilution method or the standard-additions method has been used in practice to compensate for incomplete recovery. If the chromium in natural waters were present only as these simple species, chromium(VI) should be determinable with error of $< 5\%$ by either the solvent extraction or the co-precipitation method.

Chromium(III) adsorbed on inorganic colloids was completely co-precipitated with Fe(III) hydroxide. Since colloidal particles tend to accumulate at a phase interface, some of them are expected to be partially transferable into an organic phase. The experimental results, however, show that Cr(III) adsorbed on inorganic colloids is scarcely transferred at all into the organic phase except that a small fraction of Cr(III) adsorbed on aluminosilicate and added to the river water was transferred into the organic phase.

The chromium glycinate complex was completely co-precipitated with Fe(III) hydroxide, whereas the Cr–EDTA complex was not. Neither complex was extracted with APDC into chloroform.

Chromium(III) bound to and/or adsorbed on the high molecular-weight organic substances humic acid and tannic acid was co-precipitated with Fe(III) hydroxide but not extracted with APDC into chloroform.

The chromium(III) species which contribute to the error of the analytical method for Cr(VI) could not be identified in this study. Unless the main Cr(III) species present in natural waters, and their characteristics, are known, it is difficult to rule out the possibility of a large error in the determination of Cr(VI). Recently, Nakayama *et al.*[19] improved the co-precipitation method for chromium speciation in natural waters, and classified the chromium in sea-water as inorganic Cr(III), organic Cr(III) and Cr(VI). This method, however, may also be subject to the possibility of the error described above.

REFERENCES

1. T. R. Gilbert and A. M. Clay, *Anal. Chim. Acta*, 1973, **67**, 289.
2. K. Hiiro, T. Owa, M. Takaoka, T. Tanaka and A. Kawahara, *Bunseki Kagaku*, 1976, **25**, 122.

Table 3. Recovery of chromium spikes in river water

Species spiked	Co-precipitation, % without reduction	Co-precipitation, % with reduction	Solvent extraction, %
Chromate ions	0.8, 1.3	94.5, 89.0	83.8, 91.7
Chromic ions	100, 100	99.3, 100	0.7, 1.5
Cr–Fe hydroxide	94.5, 100	94.3, 94.1	0.0, 0.0
Cr–silica	96.3, 100	99.3, 95.3	0.3, 0.4
Cr–aluminosilicate	100, 98.9	100, 84.9	4.2, 4.2
Cr–glycine	100, 100	100, 100	0.0, 0.0
Cr–EDTA	2.0, 0.8	1.2, 1.6	0.0, 0.0
Cr–tannic acid	91.7, 100	100, 89.5	0.0, 0.0
Cr–humic acid	89.5, 88.7	94.0, 81.7	0.0, 0.0

3. G. J. de Jong and U. A. Th. Brinkman, *Anal. Chim. Acta*, 1978, **98**, 243.
4. S. Osaki, T. Osaki, S. Shibata and Y. Takashima, *Bunseki Kagaku*, 1978, **25**, 385.
5. L. Chuecas and J. P. Riley, *Anal. Chim. Acta*, 1966, **35**, 240.
6. R. Fukai and D. Vas, *J. Oceanog. Soc. Japan*, 1967, **23**, 298.
7. R. E. Cranston and J. W. Murray, *Anal. Chim. Acta*, 1978, **99**, 275.
8. T. Yamamoto, S. Kadowaki and J. H. Carpenter, *Geochem. J.*, 1974, **8**, 123.
9. T. M. Florence and G. E. Batley, *Talanta*, 1977, **24**, 151.
10. *Idem, ibid.*, 1976, **23**, 179.
11. Y. Sugimura, Y. Suzuki and Y. Miyake, *Deep Sea Research*, 1978, **25**, 309.
12. Y. Iguchi (ed.), *New Experimental Chemistry Course*, Vol. 18, p. 330. Maruzen, Tokyo, 1977.
13. R. Brance and E. Matijevic, *Colloid Polymer Sci.*, 1977, **255**, 153.
14. G. Doppler and R. Patzak, *Z. Anal. Chem.*, 1956, **152**, 45.
15. H. Matsukawa, M. Ohta, S. Takata and R. Tsuchiya, *Bull. Chem. Soc. Japan*, 1965, **38**, 1235.
16. V. von Meyenburg, O. Siroky and G. Schwarzenbach, *Helv. Chim. Acta*, 1973, **56**, 1099.
17. R. G. Clem and A. T. Hodgson, *Anal. Chem.*, 1978, **50**, 102.
18. S. Osaki, T. Osaki, M. Setoyama and Y. Takashima, *J. Chromatog.*, in the press.
19. E. Nakayama, T. Kuwamoto, H. Tokoro and T. Fujinaga, *Anal. Chim. Acta*, 1981, **131**, 247.

Talanta, Vol. 30, No. 7, pp. 527–528, 1983
Printed in Great Britain.

0039-9140/83 $3.00+0.00

SOME OBSERVATIONS CONCERNING THE DIRECT TITRATION OF NITRITE WITH CERIUM(IV)

U. MURALIKRISHNA,* K. SUBRAHMANYAM, M. V. S. SURYANARAYANA and MANNAM KRISHNAMURTHY
Analytical Chemistry Laboratories, Department of Chemistry, Andhra University, Waltair 530003, India

(*Received* 21 *October* 1982. *Accepted* 12 *January* 1983)

Summary—Direct titration of nitrite with cerium(IV), with ferroin as indicator, is shown to give satisfactory results if the acidity is kept between 0.033 and 0.055*M* at the end-point. Loss of nitrous acid owing to volatilization and decomposition is discussed. From 10 to 60 mg of sodium nitrite can be estimated with a standard deviation of 5 μg and an average error of 0.2%.

Titrimetric methods of determining nitrite have been critically reviewed by Cool and Yoe,[1] and surveyed by Kolthoff *et al.*[2] According to Alexeyev,[3] only indirect methods are suitable, but a direct reductometric titration with ascorbic acid in phosphoric acid medium has recently been reported.[4]

From the literature it appears that the direct oxidimetric titration of nitrite is adversely affected by loss of nitrous acid by decomposition, which depends on the acidity, and by volatilization. The earlier procedures therefore relied largely on adding nitrite to an acidified solution of the oxidant, with adequate precautions in the addition step. Further, in the direct methods the titrand solutions seem not to have been diluted to more than 100 ml,[1] and further dilution to minimize the loss due to volatalization does not appear to have been tried.

There are also contradictory reports with regard to the error in the direct titration of permanganate with nitrite.[5]

These aspects led us to investigate further the direct titration of nitrite with ceric sulphate.

EXPERIMENTAL

Ceric sulphate solution (0.05*M*) was prepared and standardized.[6] Sodium nitrite solution (0.025*M*) was prepared and standardized with ceric sulphate by an indirect method.[7] Analytical grade reagents and doubly distilled water were used.

RESULTS AND DISCUSSION

The effect of dilution of the titrand solution on loss of nitrous acid by volatilization was examined, the titrand acidity being kept constant at the 0.25*M* concentration used in the indirect determination.[7] From the results (Table 1) it can be seen that with increasing dilution there was greater recovery, and dilution to 300 ml seemed both convenient and adequate. However, the question of decomposition of nitrous acid remained open, and was examined as follows. So that a significant amount of nitric oxide (a product of the decomposition of nitrous acid in presence of acid) would be obtained, 25-ml portions of 2*M* nitrite were adjusted to give different acidities after dilution to a total volume of 300 ml and any gas liberated was flushed into a solution of acidified (0.05*M*) ferrous ammonium sulphate. The qualitative observations made are given in Table 2.

It can be seen that the decomposition decreases with decrease in the acid concentration and is minimal at acidity lower than 0.05*M*.

The effect of varied acidity on the titration of nitrite (titrand solution volume 300 ml) with ceric sulphate was therefore examined, and the results are presented in Table 3.

From Tables 1 and 3 it is obvious that the direct titration of nitrite with ceric sulphate is possible provided the solution is adequately diluted to minimize the loss due to volatilization and the acidity is low enough for decomposition to be prevented.

Table 1. Effect of dilution on the titration of 25.00 mg of nitrite with cerium(IV); overall acidity 0.25*M*

Total volume, *ml*	$NaNO_2$ found, *mg*	Recovery, %
100	23.74	95.0
150	23.92	95.7
200	24.04	96.2
250	24.19	96.8
300	24.25	97.0
350	24.25	97.0

*Present address: Professor and Head, Department of Chemistry, A.U.P.G.E. Centre, Nuzvid 521201, India.

Table 2. Effect of acidity on the decomposition of nitrous acid (25 ml of 2*M* nitrite at different acidities, diluted to 300 ml; the nitrous oxide formed by the decomposition of nitrous acid was flushed into 50 ml of 0.1*M* ferrous ammonium sulphate)

Overall acidity, M	Colour with iron(II)
0.500	Dark, brown, almost black
0.300	Dark brown
0.200	Brown
0.150	Brownish yellow
0.100	Yellow
0.075	Light yellow
0.050	Colourless
0.025	Colourless

Table 3. Effect of acidity on the titration of 25.00 mg of sodium nitrite with cerium(IV) (total volume 300 ml)

Acidity at the end-point, M	$NaNO_2$ found, *mg*	Recovery, %
0.500	24.02	96.5
0.250	24.25	97.0
0.120	24.48	97.9
0.090	24.72	98.9
0.070	24.80	99.2
0.060	24.88	99.5
0.055	24.95	99.8
0.050	25.00	100.0
0.045	25.00	100.0
0.040	25.00	100.0
0.035	25.00	100.1
0.030	25.09	100.4
0.025	25.32	101.3
0.020	26.08	104.3
0.015	27.94	114.8

Final acidities between 0.055 and 0.035*M* are found to be suitable. At acidities higher than 0.055*M* errors arise from the decomposition of nitrite. With acidities lower than 0.035*M* the results are erratic, the nitrite probably not being quantitatively oxidized, which is consistent with the observations made by Beckuts.[1]

Table 4. Results for determination of sodium nitrite with cerium(IV); total volume 300 ml, overall acidity 0.04*M*

Amount taken, *mg*	Amount found,* *mg*	Standard deviation, *mg*
8.02	8.01	0.04
16.04	16.07	0.03
32.08	32.09	0.03
48.12	48.09	0.02
64.16	64.04	0.03

*Average of four determinations.

Recommended procedure

A sample of nitrite solution (equivalent to 10–60 mg sodium nitrite) is treated with enough water and 0.5*M* sulphuric acid to give an overall acidity of 0.035–0.055*M* in a total volume of 300 ml at the end-point, including the acidity associated with the titrant. The solution is titrated with 0.05*M* cerium(IV) sulphate solution in 0.5*M* sulphuric acid, with 1 or 2 drops of 0.025*M* ferroin as indicator, to the colour change from light orange to colourless. The titration can be completed within 3–4 min. Results are presented in Table 4.

Acknowledgement—KS and MVSS thank the UGC, New Delhi and MK thanks the CSIR, New Delhi, for the award of research fellowships.

REFERENCES

1. R. D. Cool and J. H. Yoe, *Ind. Eng. Chem., Anal. Ed.*, 1933, **5**, 112.
2. I. M. Kolthoff, R. Belcher, V. A. Stenger and G. Matsuyama, *Volumetric Analysis*, Vol. III, pp. 69, 140, 182, 310, 435, 526, 591 and 641. Interscience, New York, 1957.
3. V. Alexeyev, *Quantitative Analysis*, 2nd Ed., p. 350. Mir Publishers, Moscow, 1979.
4. N. Rukmini, V. S. N. P. Kavitha and K. Rama Rao, *Talanta*, 1980, **27**, 593.
5. I. M. Kolthoff, R. Belcher, V. A. Stenger and G. Matsuyama, *op. cit.*, p. 70.
6. A. I. Vogel, *Text Book of Quantitative Inorganic Analysis*, 4th Ed., p. 365. Longmans, London, 1978.
7. *Idem*, *op. cit.*, p. 369.

Talanta, Vol. 30, No. 7, pp. 529–530, 1983
Printed in Great Britain

0039-9140/83 $3.00+0.00
Pergamon Press Ltd

APPLICATION OF METHOPROMAZINE FOR THE EXTRACTIVE SPECTROPHOTOMETRIC DETERMINATION OF PLATINUM

ANATOL KOJŁO and HELENA PUZANOWSKA-TARASIEWICZ
Department of Chemistry, Warsaw University Division, Białystok, Poland

(*Received* 11 *November* 1981. *Revised* 20 *November* 1982. *Accepted* 9 *December* 1982)

Summary—Optimum conditions have been established for the formation and extraction of the complex of methopromazine with platinum(IV) in hydrochloric acid and an extractive spectrophotometric method for the determination of platinum is described.

In a previous paper it was reported that methopromazine (MPM) is a suitable reagent for the extractive spectrophotometric determination of palladium(II).[1] The present paper deals with the application of MPM for the extraction of platinum(IV). We have found that MPM complexes platinum(IV) rapidly in the presence of copper(II) as catalyst. The product can be quantitatively extracted into chloroform. This property has been exploited for the development of an extractive spectrophotometric method for the determination of platinum(IV). The method is more selective than some earlier ones.[2–4]

EXPERIMENTAL

Reagents

Platinum(IV) solution, 0.01M. Prepared from potassium chloroplatinate, in 1*M* hydrochloric acid. Standardized gravimetrically by reduction to platinum metal.[5]

Methopromazine maleate [2-methoxy-10-(3-dimethylaminopropyl)phenothiazine maleate, SPECIA, Paris] was used as a 0.01*M* solution in 0.2*M* hydrochloric acid. The solution was stored in an amber-coloured bottle in a refrigerator.

Copper(II) sulphate solution, 0.1M. All chemicals used were of analytical purity.

Extraction of platinum

The coloured platinum complex formed with methopromazine in hydrochloric acid in the presence of copper(II) as catalyst can be extracted by chloroform–methanol mixture (1:1 v/v) or chloroform–butanol (9:1). The intensity of the colour depends on the acidity of the solution, the MPM and copper(II) concentrations, and the nature of the solvent used. Suitable amounts of potassium chloroplatinate solution, 5*M* hydrochloric acid, 0.1*M* copper(II) sulphate and 0.01*M* methopromazine maleate were mixed in a 50-ml separating funnel and diluted to 10 ml with water. The mixture was allowed to stand for 10 min. Then a 1:1 v/v mixture of chloroform and methanol was added in small portions, each being shaken for 3 min with the aqueous phase. The extracts were combined in 15-ml standard flask. The absorbance was measured at once at 665 nm against a reagent blank as reference.

RESULTS AND DISCUSSION

Optimal conditions for extraction

The blue complex has maximum absorption in the organic phase at 665 nm (Fig. 1). The molar absorptivity is 2.6×10^4 l.mole^{-1}.cm^{-1}.

A study of the effect of the concentrations of the reagents (Fig. 2) showed that the optimal concentrations are 1–1.5*M* hydrochloric acid, 0.02–0.03*M* copper(II) sulphate and 0.008–0.01*M* methopromazine maleate in the aqueous phase. The colour of the complex, in presence of copper(II) as catalyst, is fully developed in 5 min after mixing the reagents. The aqueous solution can be left for about 10 min before the extraction, because the absorbance is constant for standing periods between 5 and 12 min. The absorbance of the extract is constant for at least 20 min. The absorbance of the complex formed in sulphuric, phosphoric or acetic acid medium is lower than that for reaction in hydrochloric acid.

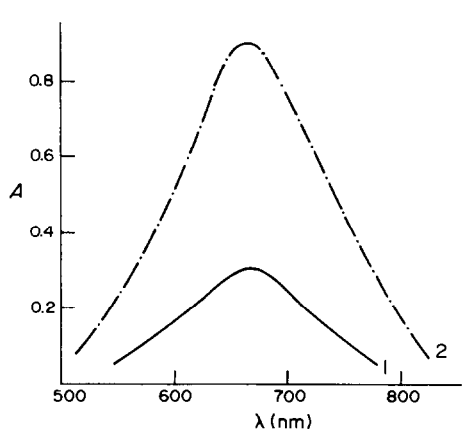

Fig. 1. Absorption spectra of the platinum(IV)–MPM complexes in chloroform, 1, Pt + MPM; 2, Pt + $CuSO_4$ + MPM; 1*M* HCl, 7.5×10^{-5}*M* Pt, 9×10^{-3}*M* MPM, 2.5×10^{-2}*M* $CuSO_4$ in the aqueous solution.

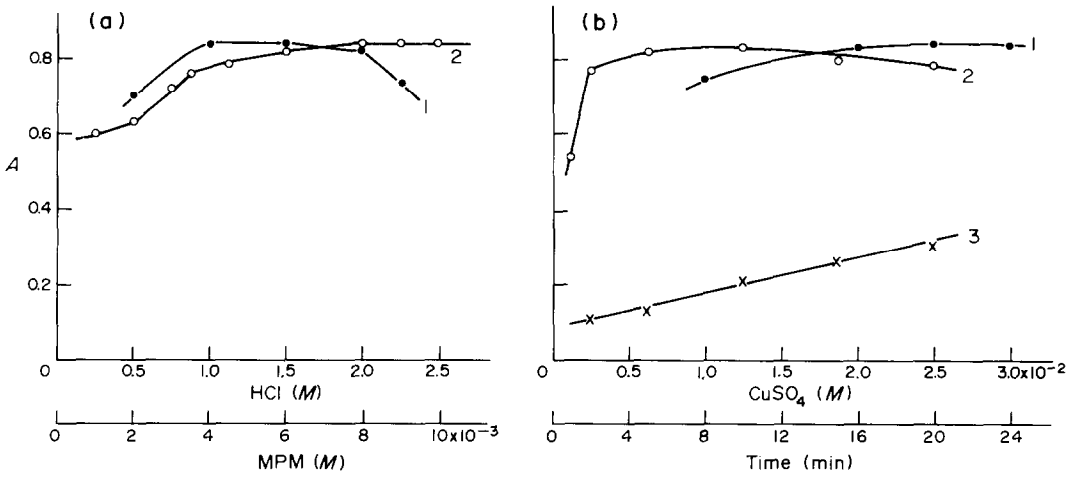

Fig. 2. Dependence of absorbance of the platinum(IV)–MPM complex on time and reagent concentrations: (*a*) 1, effect of [HCl]; 2, effect of [MPM]; $5 \times 10^{-5}M$ Pt, $2.5 \times 10^{-2}M$ $CuSO_4$, $9 \times 10^{-3}M$ MPM (curve 1); $1M$ HCl (curve 2), $\lambda = 665$ nm; (*b*) 1, effect of [$CuSO_4$]; effect of time on colour development of platinum(IV)–MPM complex with $CuSO_4$ (curve 2) and without $CuSO_4$ (curve 3) in the aqueous phase; $\lambda = 665$ nm.

Extractive determination of platinum

In a 50-ml separating funnel place a sample solution containing 10–80 μg of platinum(IV), 2 ml of $5M$ hydrochloric acid, 2.5 ml of $0.1M$ copper(II) sulphate, 4.5 ml of $0.02M$ methopromazine maleate and dilute to 10 ml with water. Then proceed according to the procedure outlined above.

Beer's law is obeyed over the platinum concentration range 1–8 μg/ml in the organic solvent. The reproducibility of the measurements, expressed as a relative standard deviation, is 0.2–1.5%, depending on the platinum concentration. Job's method and the equilibrium shift method both show the complex to be 1:2 Pt:MPM.

Effect of diverse ions

The metal ions Na^+, K^+, Mg^{2+}, Ca^{2+}, Ba^{2+}, Zn^{2+}, Ni^{2+}, Co^{2+}, Mn^{2+}, Cd^{2+}, Al^{3+}, Cr^{3+} do not interfere. The tolerance limits (μg/ml) for other ions in the determination of platinum(IV) at the 5-μg/ml level are: Fe^{3+} (130), Ru^{3+} (100), Rh^{3+} (350), Pd^{2+} (30), Os^{8+} (100), Ir^{3+} (30), Au^{3+} (4.5), Ag^+ (5), Br^- (2000), I^- (20). If a 9:1 v/v mixture of chloroform and butanol is used for the extraction, platinum(IV) (1–8 μg/ml, $\lambda_{max} = 665$ nm) and palladium(II) (5–20 μg/ml, $\lambda_{max} = 477$ nm) can be determined in the same sample solution by the procedure described above. The error of the determinations of these metals is about $\pm 2\%$.

Comparison with other methods

The method is more sensitive than the method using diethazine hydrochloride as reagent.[3] Many other methods involve either heating for a long time for maximum colour development (*e.g.*, acenaphthenequinone monoxime[6] and *o*-aminophenol-*p*-sulphonic acid[7] require about 2 hr). Reagents such as potassium iodide,[8] dibenzyldithioxamide,[9] α-benzoinoxime[10] and 2,3-quinoxaline dithiol[11] require 0.5–18 hr to give maximum colour development.

REFERENCES

1. H. Puzanowska-Tarasiewicz, A. Kojło and M. Tarasiewicz, *Chem. Analit. (Warsaw)*, 1980, **25**, 1053.
2. H. S. Gowda and K. S. Jagadeesh, *Talanta*, 1978, **25**, 416.
3. *Idem*, *Mikrochim. Acta*, 1979 **I**, 183.
4. H. S. Gowda and K. A. Padmaji, *J. Indian Chem. Soc.*, 1979, **56**, 568.
5. F. E. Beamish, *The Analytical Chemistry of the Noble Metals*. Pergamon Press, Oxford, 1966.
6. S. K. Sandhwani and P. Rajendra Singh, *Talanta*, 1973, **20**, 248.
7. A. K. Majumdar and J. G. Sen Gupta, *Z. Anal. Chem.*, 1960, **117**, 265.
8. F. G. R. Ardagh, F. S. Seaborne and N. S. Grant, *Can. Chem. Met.*, 1924, **8**, 117, 140.
9. J. T. Pyle and W. D. Jacobs, *Talanta*, 1962, **9**, 761.
10. P. K. Paria and S. K. Majumdar, *Zh. Analit. Khim.*, 1976, **279**, 207.
11. H. F. Janota and G. H. Ayres, *Anal. Chem.* 1964, **36**, 138.

Talanta, Vol. 30, No. 7, pp. 531–533, 1983
Printed in Great Britain

0039-9140/83 $3.00+0.00
Pergamon Press Ltd

THE USE OF CHLORANIL FOR SPECTROPHOTOMETRIC DETERMINATION OF SOME TRANQUILLIZERS AND ANTIDEPRESSANTS

EL-SEBAI A. IBRAHIM, A. S. ISSA, M. A. ABDEL SALAM and M. S. MAHROUS
Pharmaceutical Chemistry Department, Faculty of Pharmacy, Alexandria University, Alexandria, Egypt

(*Received* 20 *May* 1982, *Revised* 26 *December* 1982. *Accepted* 18 *January* 1983)

Summary—Chlorpromazine hydrochloride, promethazine hydrochloride, promazine hydrochloride, perphenazine, thioridazine hydrochloride, chlorprothexine, opipramol hydrochloride, amitriptyline hydrochloride, imipramine hydrochloride and hydroxyzine hydrochloride are estimated in their pure state and in pharmaceutical formulations by means of the reaction of the free bases with chloranil in dioxan–ethanol medium to give a coloured product with maximal absorbance at 550 nm. The method is precise, accurate and specific and recommended for routine analysis for the drugs mentioned.

Chloranil has been used for determination of amino-acids,[1] aliphatic and aromatic amines,[2] and tertiary amines (but not their salts).[3] We now describe its use for the estimation of tranquillizers and anti-depressants. The most widely used methods for this currently in use involve non-aqueous titration,[4] two-phase titration,[5–7] or precipitation with tetraphenylborate[8–10] or ammonium reineckate.[11] Titration with lead, copper, cadmium or zinc picrate,[12] potassium iodobismuthate[13] or the thiocyanate complex of chromium[14] or zinc[15] has been reported for the evaluation of many phenothiazine derivatives. Photometric titration with ceric sulphate has also been used for determination of phenothiazines.[16] Titan Yellow forms complexes with phenothiazines, and these can be extracted with ethyl acetate and measured at 405 nm.[17] Eriochrome Black T also forms complexes with phenothiazines, in chloroform, which can be measured at 510–520 nm.[18] Ferric chloride,[19] potassium bromate,[20] hydrogen peroxide[21] and *p*-benzoquinone[22] have been applied for estimating phenothiazines colorimetrically. Phenothiazines have been determined colorimetrically with aconitic anhydride as reagent[23] and titrimetrically with iodine monochloride.[24]

Opipramol and imipramine have been determined by precipitation with potassium hexacyanochromate (III) and back-titration of excess of reagent.[25] Imipramine and amitriptyline can be determined polarographically.[26] Amitriptyline has been estimated in sulphuric acid medium at 238 nm,[27] and colorimetrically with potassium permanganate.[28] Hydroxyzine forms a coloured complex with cobalt thiocyanate, which can be measured at 620 nm,[29] and it can also be determined with sodium tetraphenylborate.[30] Chloramine-T has been used as a reagent for the evaluation of phenothiazines and chlorprothexine.[31] Phenothiazines as well as imipramine, amitriptyline, hydroxyzine and chlorprothexine can be determined colorimetrically with Nitrazine Yellow.[32]

EXPERIMENTAL

Reagent

A 0.5% solution of chloranil in dioxan.

Procedure

For drug salts. Dissolve about 50 mg of the drug salt in 10 ml of water in a separatory funnel. Alkalize the solution with sodium hydroxide solution and extract the drug base with four portions of chloroform (10, 10, 5 and 5 ml). Dry the combined extracts over anhydrous sodium sulphate, transfer the solution to a 50-ml standard flask and make up to volume with chloroform. Transfer an aliquot containing 1–6 mg of the drug base to a 10-ml standard flask and evaporate to dryness on a boiling water-bath. Dissolve the residue in 5 ml of ethanol, add 2 ml of chloranil reagent, dilute to volume with ethanol and let stand for 15 min. Measure the absorbance at 550 nm against a reagent blank.

For drug bases. Treat a known volume of ethanolic solution containing 1–6 mg of the drug base, in a 10-ml standard flask, with 2 ml of chloranil reagent, dilute to volume and measure at 550 nm after 15 min, against a reagent blank.

For tablets. Weigh and powder 20 tablets. Transfer a weighed portion, equivalent to about 50 mg of the drug, to a 50-ml glass-stoppered flask containing 15 ml of 1*M* hydrochloric acid. Shake the mixture for 20 min and filter the solution into a 50-ml separatory funnel. Shake the residue for 5 min with an extra 5 ml of 1*M* hydrochloric acid and filter. Alkalize the combined filtrate with sodium hydroxide solution and proceed with the chloroform extraction *etc.*, as for drug salts.

Table 1. Results obtained by the chloranil and B.P. 1980 methods

Compound*	Chloranil method		B.P. 1980 method	
	Taken,† mg/100ml	Recovery, %	Taken† mg/100ml	Recovery, %
1. Chlorpromazine·HCl	20–40	100.9 ± 0.9	50.0	99.6 ± 1.3
Neurazine ampoules[M] (25 mg/ml)	20–40	103.7 ± 1.4	0.5	104.1 ± 1.5
Neurazine tablets[M] (25 mg/tab.)	20–40	97.1 ± 1.5	0.5	97.3 ± 0.5
2. Promethazine·HCl	20–40	100.0 ± 1.0	50.0	98.7 ± 0.7
Promantine ampoules[M] (25 mg/ml)	20–40	104.6 ± 1.0	0.5	104.2 ± 0.9
Laboratory-made tablets§	20–40	98.7 ± 1.1	—	— —
3. Promazine·HCl	20–40	100.9 ± 0.8	25.0	101.0 ± 0.4
Sparine vials[W] (50 mg/ml)	20–40	103.8 ± 0.9	0.5	102.9 ± 0.3
4. Perphenazine	20–50	99.5 ± 1.0	50.0	99.2 ± 1.1
Trilafone tablets[Sc] (8 mg/tab.)	20–50	98.8 ± 1.4	0.5	102.2 ± 0.9
5. Thioridazine·HCl	20–40	101.2 ± 0.9	25.0	101.0 ± 0.6
Melleril tablets[Sp] (100 mg/tab.)	20–40	104.0 ± 1.6	0.25	103.4 ± 0.8
6. Imipramine·HCl	20–40	99.5 ± 0.9	50.0	100.7 ± 0.3
Tofranil tablets[G] (25 mg/tab.)	20–40	98.2 ± 0.6	0.5	99.2 ± 0.9
7. Amitriptyline·HCl	20–40	99.9 ± 0.8	50.0	101.6 ± 0.9
Tryptizole tablets[K] (25 mg/tab.)	20–40	103.1 ± 1.2	1.0	102.4 ± 0.6
8. Chlorprothexine	20–40	99.6 ± 0.9	50.0	98.4 ± 0.3
Taractan tablets[R] (15 mg/tab.)	20–40	97.2 ± 1.0	45.0	97.1 ± 0.2
9. Hydroxyzine·2HCl	20–50	100.6 ± 1.1	50.0	101.0 ± 1.4
Atarax tablets[C] (15 mg/tab.)	20–50	99.1 ± 1.6	50.0	101.3 ± 0.5
10. Opipramol·2HCl	20–40	100.6 ± 0.6	50.0	99.4 ± 0.6
Insidone tablets[G] (50 mg/tab.)	20–40	102.6 ± 1.2	50.0	103.0 ± 0.2

*M = Misr; W = Wyeth; Sc = Schering; Sp = Swisspharma; G = Geigy; K = Kahira; R = Roche; C = CID.

†Refers to concentration of solution used for final measurement. The recovery is given ± standard deviation.

§Tablets prepared with 10 mg of drug and tablet fillers composed of lactose 90, starch 7, talc 2.7 and magnesium stearate 0.3 parts.

For ampoules and vials. Transfer a known volume of the sample, containing about 50 mg of the drug, to a 50-ml separatory funnel. Alkalize, extract with chloroform *etc.*, as already described.

RESULTS AND DISCUSSION

Attempts were made to use chloranil for determination of tertiary-amino type tranquillizers and antidepressants by the procedure reported for primary and secondary amines,[1,2] but failed.

The procedure of Sass *et al.*[3] for determination of simple tertiary amines by warming with chloranil in toluene as solvent also failed to give any colour. More polar solvents such as ethanol, methanol and water were therefore tried and found to give good colour development, but the chloranil is insoluble in these solvents, and precipitates. Chloranil solution in dioxan was tried, but the reaction mixture had to be warmed to produce a colour. However, with a dioxan–ethanol mixture (1:4 v/v) as solvent, a violet colour was formed in the cold and reached its maximum intensity in 15 min.

Various authors have tried to explain the mechanism of the interaction between chloranil and tertiary amines. Foster[33] suggested the reaction gave a charge-transfer complex, with chloranil acting as electron acceptor and the base as electron donor. Sass *et al.*[3] suggested it was a quaternization reaction, with liberation of chloride ions:

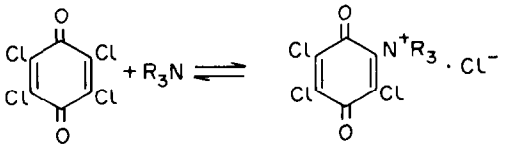

We therefore isolated the violet product by distilling the solvent at reduced pressure, and found that the compound gave a violet solution in water, and that a white precipitate was formed when this solution was treated with silver nitrate and nitric acid.

The dioxan–alcohol solution of the product also gave a white precipitate with silver nitrate, but a reagent blank test did not. We regard this as confirmation of the mechanism proposed by Sass *et al.*[3] The colour developed in the dioxan–alcohol mixture was found to be stable for about 2 hr, after which it started to fade.

The common tablet fillers such as lactose, talc, starch and magnesium stearate were found not to interfere.

Beer's law is valid over the concentration ranges listed in Table 1; the regression equations indicated a small positive intercept on the ordinate. The applicability of the chloranil method to some of the commercial preparations has been checked (Table 1).

REFERENCES

1. F. Al-Sulimany and A. Townshend, *Anal. Chim. Acta*, 1973, **66,** 195.
2. T. S. Al-Ghabsha and S. A. Rahim, *ibid.*, 1976, **95,** 189.
3. S. Sass, J. J. Kaifman, A. A. Cardenas and J. J. Martin, *Anal. Chem.*, 1958, **30,** 529.
4. J. Milne, *J. Pharm. Assoc.*, 1959, **48,** 117.
5. J. Blazek and M. Travincková, *Cesk. Farm.*, 1975, **24,** 100.
6. S. Rolski and Z. Zakrzewski, *Farm. Pol.*, 1969, **25,** 621.
7. F. M. Albert, H. Aftalion and R. Simionovicic, *Rev. Chem. (Bucharest)*, 1968, **19,** 383.
8. Gh. Morait, V. Turcylat and Gh. Ciogolea, *Farmacia (Bucharest)*, 1970, **18,** 267.
9. J. Dobrecky and B. E. Gonzales, *Rev. Asoc. Bioquim. Argent.*, 1969, **34,** 168.
10. S. Prinzanti and V. Dalpiaz, *Boll. Chim. Farm.*, 1972, **111,** 512.
11. A. Olech, *Acta Pol. Pharm.*, 1972, **29,** 57.
12. M. Gajewska, *Chem. Anal. (Warsaw)*, 1973, **18,** 651.
13. H. Basinska and M. Tarasiewicz, *Acta Pol. Pharm.*, 1969, **26,** 343.
14. A. Olech, *ibid.*, 1973, **30,** 505.
15. B. Dembinski and N. Novakowski, *Farm. Pol.*, 1974, **30,** 423.
16. S. P. Agarwal and M. I. Blake, *J. Pharm. Sci.*, 1969, **58,** 1011.
17. H. Puzanowska-Tarasiewicz and M. Tarasiewicz, *Farm. Pol.*, 1973, **29,** 1009.
18. F. Pellerin, J. A. Gautier, O. Barat and D. Damay, *Chim. Anal. (Paris)*, 1963, **45,** 395.
19. M. K. Youssef and I. A. Attia, *Indian J. Pharm.*, 1975, **37,** 121.
20. M. Tarasiewicz and H. Puzanowska-Tarasiewicz, *Farm. Pol.*, 1970, **26,** 393.
21. H. Basinska, H. Puzanowska-Tarasiewicz and M. Tarasiewicz, *Chem. Anal. (Warsaw)*, 1970, **15,** 405.
22. J. Mounier and B. Viossat, *Ann. Pharm. Franç.* 1968, **26,** 429.
23. Y. A. Beltagy, A. S. Issa and M. S. Mahrous, *Egypt. J. Pharm. Sci.*, 1978, **19,** 107.
24. *Idem, Talanta*, 1978, **25,** 349.
25. A. Olech, *Acta Pol. Pharm.*, 1975, **32,** 73.
26. O. Rojos S., H. Garcia M., R. Bravo O. and G. Neumann S., *An. R. Acad. Farm.*, **42,** 1976, 281.
27. K. Worm, *Acta Pharmacol. Toxicol.*, 1969, **27,** 439.
28. E. J. Wallace and V. E. Dahl, *J. Forensic Sci.*, 1967, **12,** 484.
29. I. M. Rouchdi, S. A. Soliman and M. H. Sadek, *U.A.R.J. Pharm. Sci.*, 1971, **12,** 353.
30. S. Bronislaw and J. Bolelaws, *Acta. Pol. Pharm.*, 1966, **23,** 573.
31. A. S. Issa, Y. A. Beltagy and M. S. Mahrous, *Talanta*, 1978, **25,** 710.
32. Y. A. Beltagy, A. S. Issa and M. S. Mahrous, *Egypt. J. Pharm. Sci.*, 1977, **18,** 211.
33. R. Foster, *Organic Charge Transfer Complexes*, Vol. 15, p. 313. Academic Press, New York, 1969.

Talanta, Vol. 30, No. 7, pp. 534–536, 1983
Printed in Great Britain

0039-9140/83 $3.00+0.00
Pergamon Press Ltd

A DECOMPOSITION PROCEDURE FOR THE DETERMINATION OF ARSENIC IN MARINE SAMPLES

W. A. MAHER*
Department of Oceanography, The University of Southampton, Southampton SO9 3TU, England

(*Received* 1 *November* 1982. *Accepted* 12 *January* 1983)

Summary—The use of wet and dry ashing procedures to decompose marine biological tissues and to degrade organoarsenic compounds to inorganic arsenic for analysis by zinc-column arsine generation and atomic-absorption spectrophotometry was investigated. Wet ashing with nitric, sulphuric and perchloric acids (10:2:3 v/v) released the largest percentage of arsenic from fish tissue and quantitatively degraded methylated and other organoarsenic compounds to inorganic arsenic. The arsenic concentrations found when standard reference materials were ashed with this acid mixture were in agreement with the certified values.

Most procedures used to determine total arsenic require it to be in inorganic form. To decompose biological tissues and to degrade organoarsenic compounds, wet- or dry-ashing is normally employed.

Dry-ashing procedures involve heating samples to 400–700° and may result in the loss of arsenic if an ashing aid is not used.[1] Quantitative recoveries from inorganic and methylated arsenic compounds have been obtained when a magnesium oxide–magnesium nitrate ashing aid was used.[2] However, loss of arsenic has been reported even when an ashing aid was used.[3]

For wet-ashing, it is usually recommended that a combination of nitric, sulphuric and perchloric acids be used, as most biological components are mineralized by this mixture and oxidizing conditions are maintained which minimize the loss of volatile arsenic compounds.[4] Digestion with nitric acid is recommended to remove halides and prevent loss of arsenic as the volatile trichloride.[5] Complete recovery of arsenic from fish tissues containing methylated arsenic compounds has been reported.[2] In contrast, other investigators[6,7] suggest that normal wet-ashing procedures will not release arsenic from compounds such as dimethylarsenic salts and that wet-ashing with nitric and sulphuric acids in combination with a catalyst, for example, vanadium pentoxide, is required.[3]

The conflicting results reported in the literature created uncertainty as to which ashing procedures would be suitable for decomposing marine biological tissues. In this study the efficiencies of several wet- and dry-ashing procedures for decomposing marine biological tissues and degrading organoarsenic compounds were investigated.

The suitability of the extracts for the determination of arsenic as inorganic arsenic by zinc-column arsine generation and atomic-absorption spectrophotometry[8] was also examined.

EXPERIMENTAL

Apparatus

The zinc-column arsine generator and atomic-absorption detection system have been described previously.[8] An aluminium heating block and 2.5-cm bore Pyrex test-tubes were used for all wet-ashings. Dry-ashing was performed in 100-ml Pyrex beakers covered with watch glasses.

Reagents

All reagents were of analytical grade. Arsenic(III) oxide and arsenic(V) oxide were dissolved in 0.1*M* sodium hydroxide to give 1000 μg/ml arsenic concentrations. Organoarsenic standards (As 1000 μg/ml) were prepared by dissolving disodium methylarsonate, sodium dimethylarsinate, *o*-arsanilic acid and phenylarsine oxide, respectively, in 2*M* hydrochloric acid. The solutions were standardized by graphite-furnace atomic-absorption spectrophotometry, by comparison with standards made by dissolving the pure element in hydrochloric acid.

Preparation of fish tissue

Muscle tissues from *Merluccius merluccius* was freeze-dried, ground to pass a 350-μm sieve and stored at −2° until required.

Recommended decomposition procedure

Weigh the sample into a Pyrex test-tube, add 5 ml of concentrated nitric acid, place a glass bulb on top and leave the mixture for at least 12 hr to allow some oxidation to take place, thus avoiding foaming on heating. Place the tube in the aluminium block and heat until the evolution of brown fumes ceases. Cool the tube, add 10 ml of a nitric–sulphuric–perchloric acid mixture (5:2:3 v/v) and raise the

*Present address: Department of Physical and Inorganic Chemistry, University of Adelaide, G.P.O. Box 498, Adelaide, S.A. 5001, Australia.

Table 1. Comparison of sample decomposition procedures

Procedure	Arsenic: Released, μg/g*	Arsenic: Recovery of spike,† %	Comments	Reference
Dry ashing Addition of $Mg(NO_3)_2$	—	—	Excessive foaming, not suitable	7
Dry ashing HNO_3 predigestion Addition of MgO	16 ± 1	85 ± 6	Foaming occurs on evaporation to dryness; hard to redissolve ash	13
Dry ashing Addition of $MgO/Mg(NO_3)_2$	18.8 ± 0.5	95 ± 4	Slight foaming when ashed	2
HNO_3/H_2SO_4 (10:5 v/v)	10.7 ± 0.4	85 ± 5	Interference in reduction to arsine	10
HNO_3/H_2SO_4 (10:5 v/v) Addition of ammonium oxalate at end	10.7 ± 0.4	88 ± 5	Interference in reduction to arsine	
$HNO_3/H_2SO_4/H_2O_2$ (10:5:10 v/v)	11.0 ± 0.4	85 ± 3	Interference in reduction to arsine	14
HNO_3/H_2SO_4 (10:5 v/v) Addition of V_2O_5	9.7 ± 0.2	83 ± 3	Interference in reduction to arsine High blanks	3
$HNO_3/H_2SO_4/HClO_4$ (10:2:3 v/v)	22.2 ± 0.9	99 ± 5	Complete dissolution; No interference (peak broadening) in reduction of arsenic to arsine by zinc column	15

*Average of four replicates.
†Average of three replicates.

temperature of the aluminium block to remove the nitric acid. After refluxing with the perchloric and sulphuric acids for 3–4 hr, remove the glass bulb and continue heating until dense fumes of sulphur trioxide appear.

Determination of arsenic

Dissolve or dilute the sample with 2*M* hydrochloric acid, then add potassium iodide and ascorbic acid and leave for 40 min for the inorganic arsenic present to be reduced to the tervalent form. Pass the solution through a zinc reductor column, and decompose the evolved arsine in a heated carbon-tube furnace, measuring the atomic absorption of the arsenic at 193.7 nm.[8]

RESULTS AND DISCUSSION

Evaluation of ashing procedures

The efficiency of the ashing procedures was evaluated by measuring the release of arsenic as inorganic arsenic from the prepared fish tissue. The procedures tested and the amounts of arsenic obtained, together with the recoveries of an arsenic(III) spike, are shown in Table 1.

Dry-ashing with magnesium nitrate was unsatisfactory as foaming and charring of samples often occurred during heating.

Most of the wet-ashing procedures tested were also unsatisfactory, because of interference in the determination step. Peak broadening during the arsine generation suggested that not all the arsenic present had been degraded to inorganic arsenic. Any monomethyl and dimethylarsenic compounds present in extracts will be reduced to the corresponding arsine in the zinc reductor column and evolved, but at slower rates,[9] and cause peak broadening.

Preliminary studies showed that the presence of nitric acid even at concentrations below 0.05*M* will suppress arsine generation. Therefore incomplete removal of nitrogen compounds from the extracts may have caused low recoveries of the inorganic arsenic(III) spikes. The addition of ammonium oxalate or vanadium pentoxide to remove nitrogen compounds[3,10] did not produce any significant improvement. The addition of perchloric acid removed all interferences, and gave quantitative recovery of the arsenic(III) spike. The use of a nitric–sulphuric–perchloric acid mixture (10:2:3 v/v) for ashing samples was further investigated.

Decomposition of inorganic and organoarsenic compounds

The efficiency of the nitric–sulphuric–perchloric acid mixture in converting organoarsenic compounds into inorganic arsenic was investigated (Table 2). The recommended sample decomposition procedure was used; each arsenic compound was added to 5 ml of concentrated nitric acid and refluxed before the addition of the other acids. In all cases recoveries were greater than 93%, showing that this acid mixture is

Table 2. Recovery of arsenic from inorganic and organoarsenic compounds after ashing with nitric, sulphuric and perchloric acids (10:2:3 v/v)

Compound*	Recovery†
As_2O_3	99.7 ± 0.2
As_2O_5	99.8 ± 0.3
$CH_3AsOONa_2$	93.5 ± 0.8
$(CH_3)_2AsOOH$	96 ± 2
$NH_2C_6H_4AsO(OH)_2$	100 ± 2
C_6H_5AsO	96.4 ± 0.5

*Amount taken equivalent to 10 μg of arsenic.
†Mean of three replicates.

Table 3. Recovery of arsenic from NBS standard reference materials after ashing with nitric, sulphuric and perchloric acids (10:2:3 v/v)

Material	Found*, $\mu g/g$	Certified, $\mu g/g$	Recovery, %
Orchard Leaves NBS 1571	9.7 ± 0.2	10 ± 2	97 ± 2
Oyster Tissue NBS 1566	13.1 ± 0.3	13.4 ± 1.9	98 ± 2

*Mean of five determinations.

suitable for converting organoarsenic compounds known to exist in marine organisms[11,12] into inorganic arsenic.

Accuracy and precision

The accuracy of the recommended ashing procedure was assessed by the analysis of standard reference materials. As shown in Table 3, the arsenic concentrations obtained were in agreement with the certified values.

The precision of the recommended ashing procedure was estimated from 9 replicate analyses of the freeze-dried fish muscle tissue. The relative standard deviation was 1.7% (As 22.9 ± 0.4 μg/g).

Conclusion

The use of a nitric–sulphuric–perchloric acid mixture (10:2:3 v/v) for the ashing of marine organisms was found to produce extracts suitable for the determination of arsenic as inorganic arsenic by zinc-column arsine generation and atomic-absorption spectrophotometry.

REFERENCES

1. T. T. Gorsuch, *Analyst*, 1959, **84**, 135.
2. K. H. Tam and H. B. S. Conacher, *J. Environ. Health*, 1977, **B12**, 213.
3. J. F. Uthe, H. C. Freeman, J. R. Johnston and P. Michalik, *J. Assoc. Off. Anal. Chem.*, 1974, **57**, 1363.
4. W. R. Penrose, *C.R.C. Crit. Rev. Env. Control*, 1974, **4**, 465.
5. J. E. Portmann and J. P. Riley, *Anal. Chim. Acta*, 1964, **31**, 509.
6. J. G. Lamberton, B. L. Arbogast, M. L. Deinzer and L. Norris, *Am. Ind. Hyg. Assoc. J.*, 1976, 418.
7. P. J. LeBlanc and A. L. Jackson, *J. Assoc. Off. Anal. Chem.*, 1973, **56**, 383.
8. W. A. Maher, *Talanta*, 1982, **29**, 532.
9. *Idem*, *Ph.D. Thesis*, University of Southampton, 1980.
10. M. Kurokawa, M. Kaneko, N. Nishiyama, S. Fukui and S. Kanno, *J. Hyg. Chem.*, 1975, **21**, 77.
11. J. S. Edmonds and K. A. Francesconi, *Nature*, 1977, **265**, 436.
12. W. A. Maher, *Anal. Chim. Acta*, 1981, **126**, 157.
13. W. L. Hoover, J. R. Melton, P. A. Howard and J. W. Bassett, *J. Assoc. Off. Anal. Chem.*, 1974, **57**, 18.
14. I. M. Orheim and H. H. Bovee, *Anal. Chem.*, 1974, **46**, 921.
15. R. P. Sharma and J. L. Shupe, *Sci. Total Environ.*, 1977, **7**, 55.

Talanta, Vol. 30, No. 7, pp. 537–542, 1983
Printed in Great Britain.

0039-9140/83 $3.00+0.00

ANALYTICAL DATA

MACROSCOPIC AND MICROSCOPIC IONIZATION CONSTANTS OF THE THIOL AND AMINE GROUPS IN 1-METHYL-4-MERCAPTOPIPERIDINE

H. BARRERA, J. C. BAYON, P. GONZALEZ-DUARTE, J. SOLA and J. VIVES
Departament de Química Inorgànica, Universitat Autònoma de Barcelona, Bellaterra, Barcelona, España

(*Received* 25 *August* 1982. *Revised* 17 *December* 1982. *Accepted* 18 *January* 1983)

Summary—The acid dissociation constants of 1-methyl-4-mercaptopiperidine ($pK_1 = 9.51$, $pK_2 = 11.33$), the 1,1-dimethyl-4-mercaptopiperidinium ion ($pK_A = 9.59$) and 1-methyl-4-(methylthio)piperidine ($pK_B = 10.18$) have been determined potentiometrically in 3*M* sodium perchlorate (10% methanol) medium. The ultraviolet absorption of the mercaptide ion has been used to determine the relative proton affinity of the sulphur and nitrogen functions in 1-methyl-4-mercaptopiperidine under the same conditions, and its four microscopic constants ($pK_a = 9.49$, $pK_b = 10.23$, $pK_c = 11.34$, $pK_d = 10.60$) have been calculated; pK_A has also been determined spectrophotometrically. From the results obtained, it can be concluded that the thiol group is more acidic than the amine group and that the Adams relation, $K_a + K_b = K_1$, holds very well when it is assumed that the spectrophotometric values for K_a and K_b can be replaced by K_A and K_B respectively.

The acid dissociation constants of several β-mercaptoamines have been reported[1,2] but there is very little such information about γ-mercaptoamines. This knowledge is fundamental for investigation of their complexation of metal ions[3–7] and determination of the stability constants of the complexes.

From our data[4–6] on solid metal complexes of 1-methyl-4-mercaptopiperidine (**I**), we conclude that this compound behaves as a unidentate neutral ligand, in the zwitterionic form $^-S\text{–}C_5H_9\overset{+}{N}\text{–}(CH_3)H$. Thus, equilibrium solution studies should provide a model for the behaviour of simple thiol ligands, the metal complexes of which have not been extensively investigated, mainly because of their very slight solubility in aqueous solution.

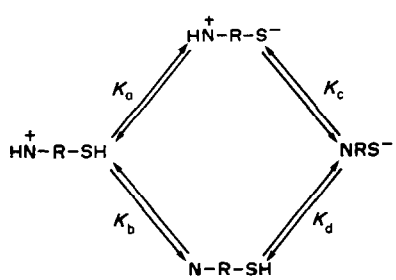

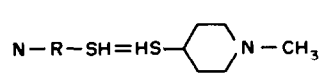

(**I**)

A study of the behaviour of 1-methyl-4-mercaptopiperidine in aqueous methanol (9:1 v/v) solution, at constant ionic strength (3*M* $NaClO_4$) and temperature (25°) is reported here. It includes determination of the macroscopic dissociation constants (K_1 and K_2) of the protonated cation and of the microscopic constants, K_a, K_b, K_c and K_d, corresponding to the equilibria shown above.

The microscopic constants were evaluated by two methods. One is based on the assumption that K_a and K_b are roughly equal to the dissociation constants of the 1,1-dimethyl-4-mercaptopiperidinium ion, K_A, and the 1-methyl-4-(methylthio)piperidinium ion, K_B, respectively. The other uses direct spectrophotometric determination. The Adams equation,[8] $K_1 = K_a + K_b$, holds well if the spectroscopically determined K_a and K_b values are replaced by K_A and K_B.

EXPERIMENTAL

Syntheses

1-Methyl-4-mercaptopiperidine hydrochloride. 1-Methyl-4-mercaptopiperidine was synthesized[9] and purified[10] until at least 99.5% pure. The product was converted into its hydrochloride with dry HCl gas and the white crystals, m.p. 174–5°, were recrystallized from cyclohexane–chloroform (1:5 v/v).

1-Methyl-4-(methylthio)piperidine hydrochloride. A methanolic solution of methyl iodide (106 mmole in 30 ml) was slowly added to a refluxing methanolic solution of 1-methyl-4-mercaptopiperidine (97 mmole in 30 ml) and refluxing was continued for 30 min. After removal of most of the methanol under reduced pressure, 15 ml of water were added. The pH was raised to about 12 and the solution was

extracted with cyclohexane. The extract was dried over potassium carbonate and the cyclohexane removed under reduced pressure. The residue was distilled at 65° under nitrogen and at reduced pressure (14 mmHg). The colourless liquid produced was kept in the freezer under an inert atmosphere. Acidimetric determination of the amine group indicated 99.7 ± 0.2% purity. The product was converted into its hydrochloride with dry HCl gas (hygroscopic white crystals, m.p. 126–7°): $C_7H_{16}NSCl$ requires C 46.27%, H 8.87%, N 7.71%, Cl 19.51%; found: C 46.1%, H 9.0%, N 7.7%, Cl 19.5%.

1,1-Dimethyl-4-mercaptopiperidinium chloride. A mixture of 6.5 ml of 30% hydrogen peroxide and 15 ml of water was slowly added to 1-methyl-4-mercaptopiperidine (76 mmole). The disulphide separated immediately and was filtered off. A solution of the disulphide and 282 mmole of methyl iodide in 50 ml of methanol was refluxed for 2 hr. After cooling, {bis[4-*N*-dimethylpiperidinium] disulphide} iodide (**II**, X = I⁻) separated out.

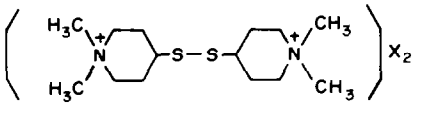

(II)

The iodide, dissolved in 20 ml of water, was converted into the chloride (**II**, X = Cl⁻) by addition of 5 ml of 30% hydrogen peroxide and 6.5 ml of concentrated hydrochloric acid. Most of the iodine produced was filtered off and the rest extracted with carbon tetrachloride. The chloride was then reduced by refluxing for 2 hr with tin in 80 ml of 2*M* hydrochloric acid. After cooling, 1,1-dimethyl-4-mercaptopiperidinium trichlorostannate(II) (**III**) precipitated, m.p. 138–9°.

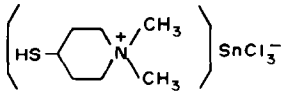

(III)

Hydrogen sulphide was passed into a solution of 26 mmole of **III** in 50 ml of 0.25*M* hydrochloric acid. Tin(II) sulphide was filtered off. The filtrate was evaporated nearly to dryness and the residue dissolved in hot ethanol under nitrogen. After cooling, a white crystalline solid separated, m.p. 235–7°. $C_7H_{16}NSCl$ requires C 46.27%, H 8.87%, N 7.71%, Cl 19.51%; found: C 46.0%, H 9.0%, N 7.6%, Cl 19.5%.

Potentiometric measurements

Reagents and apparatus. The sodium perchlorate stock solution was prepared and analysed according to Biedermann.[11] Sodium hydroxide solution was prepared from a freshly filtered 50% solution and CO_2-free water. Methanol and the perchlorate stock solution were boiled separately under nitrogen before addition of concentrated sodium hydroxide solution to a suitable mixture of the two. Stock perchloric acid was prepared from the 70% reagent. Stock solutions of the three compounds were prepared with a free hydrogen-ion concentration, *h*, of *ca.* 20 m*M* (the first two from the hydrochlorides); all of them kept for about two weeks without evidence of oxidation. Methanol (*p.a.*) was used without further purification.

The silver electrode (prepared according to Brown[12]) and a hydrogen electrode (prepared according to reference 13) were used in combination with a Crison Digilab 517 potentiometer (precision ±0.1 mV). A "Wilhelm" glass apparatus was used for the salt bridge and reference half-cell.[14] The titration vessel, salt bridge and last wash-bottle for the oxygen-free nitrogen used were submerged in an oil thermostat at 25.0 ± 0.1°. The hydrogen electrode reached constant potential within 20 min for acidic solutions and 40 min for basic ones, the readings remaining constant for at least 24 hr.

Procedure. Solutions of different concentrations (*L*) of the test compounds in 10% v/v aqueous methanol and an excess of perchloric acid were titrated. The test solution in the titration vessel was composed of $L + H + 3.0M$ ClO_4^- + 10% v/v CH_3OH, where *L* denotes the total concentration of test compound and *H* the analytical hydrogen-ion concentration in the test solution, which was varied by adding from the burette a certain volume of solution S_1 or S_2, which had the compositions:

$$S_1 = H_1 + (3.0 - H_1)M\ Na^+ + 3.0M\ ClO_4^- + 10\%\ v/v\ CH_3OH$$

$$S_2 = -OH + 3.0M\ Na^+ + (3.0 - OH)M\ ClO_4^- + 10\%\ v/v\ CH_3OH$$

The reversibility of the system was checked by back-titrations. The initial value of the free hydrogen-ion concentration, *h*, in the test solution was determined potentiometrically,[15] with the cell

Ag, AgCl	2.99*M* $NaClO_4$ 0.01*M* NaCl 10% v/v CH_3OH	3*M* $NaClO_4$ 10% v/v CH_3OH	Test solution	H_2 electrode

the hydrogen electrode being calibrated in concentration units.[16] Then *h* was calculated from

$$E = E_0 + 59.16 \log h + E_j \qquad (1)$$

where E_0 is the calibration constant determined before each titration[16] (and checked at the end), and E_j is the liquid-junction potential (always negligible under our experimental conditions). E_0 was calculated at each titration point by use of the Gran functions.[15]

Spectrophotometric measurements

Reagents and apparatus. The methanol, perchloric acid, sodium dihydrogen phosphate and boric acid were of the best grade supplied by Merck, and used without further purification. Sodium hydroxide and sodium perchlorate solutions were prepared and analysed as before. Oxygen-free nitrogen was passed through the distilled water and the methanol for 1 hr before they were used for making solutions. A Beckman Acta-III spectrophotometer equipped for measurement at constant temperature (25.0 ± 0.1°) was used with matched 1-cm quartz cells. All pH-measurements (Radiometer PHM-4 pH-meter) were made at the same temperature.

Buffer solutions. These were prepared, under nitrogen, by adding different volumes of a 2*M* NaOH/0.02*M* H_3BO_3/0.02*M* NaH_2PO_4/3*M* $NaClO_4$/10% v/v CH_3OH solution to a 0.02*M* H_3BO_3/0.02*M* NaH_2PO_4/3*M* $NaClO_4$/10% v/v CH_3OH solution. After each addition the free hydrogen-ion concentration, *h*, was determined and

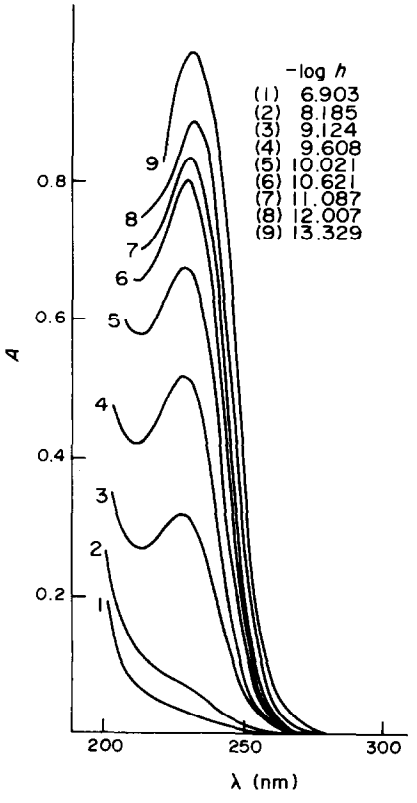

Fig. 1. Absorption spectra of $1.6 \times 10^{-4}M$ 1-methyl-4-mercaptopiperidine in $3M$ $NaClO_4$–10% v/v CH_3OH solutions at 25°.

25 ml of the buffer were withdrawn; h was calculated by equation (1) from the emf of the cell

$$H_2(g)Pt\,|\,BS\,\|\,3M\ NaClO_4,\ 10\%\ v/v\ CH_3OH\,|\,Ag/AgCl\ electrode$$

where BS denotes the buffer solution.

Procedure. This was essentially that of Benesch and Benesch.[17] The absorption spectra of solutions made by diluting 100.0 μl of 1-methyl-4-mercaptopiperidine solution (Agla microsyringe) to volume in a 10-ml standard flask with buffer solution were measured against the buffer as reference, and are shown in Fig. 1. The same procedure was used for 1,1-dimethyl-4-mercaptopiperidinium chloride.

CALCULATIONS AND RESULTS

Potentiometry

1-Methyl-4-mercaptopiperidine hydrochloride. The species in solution were of the type BH_j, where j is an integer, $0 \leqslant j \leqslant 2$, and B denotes the completely deprotonated ligand. Values for log h and $\bar{j}$ (the average number of protons bound) were calculated from the primary data and the calculated value for K_w ($pK_w = 14.16$) in the medium used, by means of

$$E = E_0 \pm 59.16 \log h$$

$$\bar{j} = (H - h + K_w/h)/L$$

Plots of $\bar{j}$ against $(-\log h)$ for the four titrations done are given in Fig. 2. By expressing $\bar{j}$ as a function of the macroscopic constants and by means of a graphical method, a first estimate for K_1 and K_2 was obtained. Numerical treatment of the data with the program MINIQUAD 75[18] in conjunction with a VAX/VMS computer gave the values shown in Table 1.

1,1-Dimethyl-4-mercaptopiperidinium chloride and 1-methyl-4-(methylthio)piperidine hydrochloride. The same method was used. The only difference from the previous case is that the maximum value for j is 1. A plot of $\bar{j}$ against $(-\log h)$ for one set of four titrations is given in Fig. 3. The other set was comparable in precision. The same numerical treatment of the data was based on estimating pK_A and pK_B as the $-\log h$ values for the corresponding $\bar{j} = 0.5$. The best values are given in Table 1.

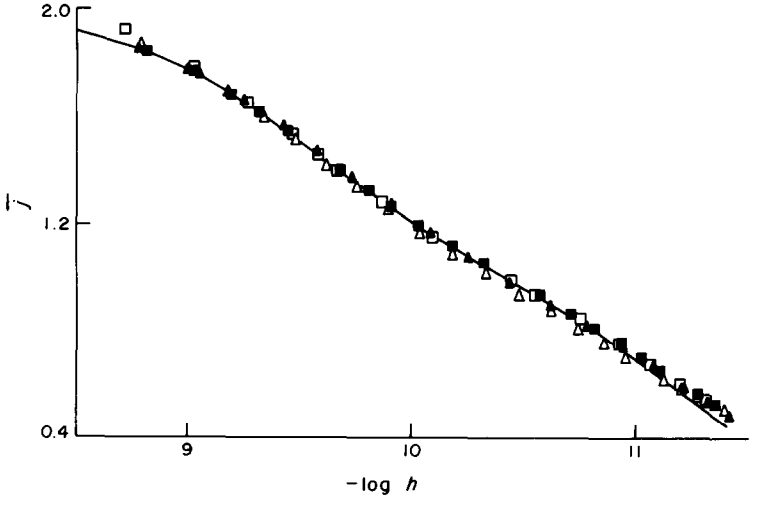

Fig. 2. Formation curve $\bar{j}$ *vs.* $(-\log h)$ for 1-methyl-4-mercaptopiperidine at various initial concentrations. △, 3.05 mM; □, 3.93 mM; ▲, 5.06 mM; ■, 7.00 mM.

Table 1. Acid dissociation constants at 25.0 ± 0.10 in 3.0*M* $NaClO_4$ and 10% v/v CH_3OH aqueous solution

Compound	Acid dissociation constants* Potentiometric method	Spectrophotometric method
1-Methyl-4-mercaptopiperidine	$pK_1 = 9.51 \pm 0.01$ $pK_2 = 11.33 \pm 0.01$ $U'(K) = 1.8 \times 10^{-6}$ (108 points) $\sigma = 1.0 \times 10^{-4}$	$pK_a = 9.49 \pm 0.05$ $pK_b = 10.23 \pm 0.05$ $pK_c = 11.34 \pm 0.05$ $pK_d = 10.60 \pm 0.05$
1,1-Dimethyl-4-mercaptopiperidinium chloride†	$pK_A = 9.59 \pm 0.01$ $U'(K) = 2.5 \times 10^{-6}$ (113 points) $\sigma = 1.0 \times 10^{-4}$	$pK_A = 9.62 \pm 0.05$
1-*Methyl*-4-(methylthio)piperidine†	$pK_B = 10.18 \pm 0.01$ $U'(K) = 1.0 \times 10^{-6}$ (108 points) $\sigma = 6.8 \times 10^{-5}$	

$U'(K)$ given as $\sum_n (\bar{j}_{cal} - \bar{j}_{exp})^2$, n being the number of points

*Mean ± standard deviation.
†J.V. Doctoral Thesis.

Spectrophotometry

The absorption spectra of the test solutions showed only one band, in the region 215–300 nm, for strongly alkaline but not strongly acid media (see Fig. 1). In both cases, the absorption maximum shifted from 227 to 230 nm with increasing pH. These facts are in agreement with data reported for several aminothiols[17] and allow the conclusion that the absorption at 227 nm is due to $H\overset{+}{N}RS^-$ and at 230 nm to NRS^-. The molar absorptivity of the latter form was calculated as $\log \varepsilon = 3.792$ at 230 nm for both compounds (1-cm cells).

Making the same assumptions as Benesch and Benesch,[17] we write

$$A = C_S \varepsilon_S + C_{SH} \varepsilon_{SH}$$

where A is the maximum absorbance at *ca.* 230 nm,

$$C_S = [H\overset{+}{N}RS^-] + [NRS^-],$$

$$C_{SH} = [H\overset{+}{N}RSH] + [NRSH]$$

(brackets indicate concentrations), and ε_S and ε_{SH} denote the corresponding molar absorptivities, obtained from measurements of solutions at very high and very low pH respectively.

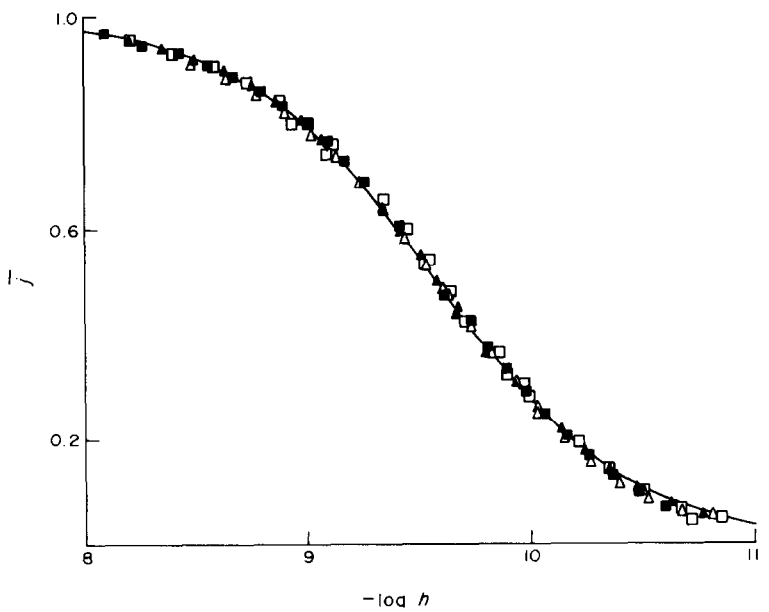

Fig. 3. Formation curve $\bar{j}$ *vs.* $(-\log h)$ for 1,1-dimethyl-4-mercaptopiperidinium ion at various initial concentrations. △, 4.78 m*M*; □, 9.55 m*M*; ▲, 14.32 m*M*; ■, 19.10 m*M*.

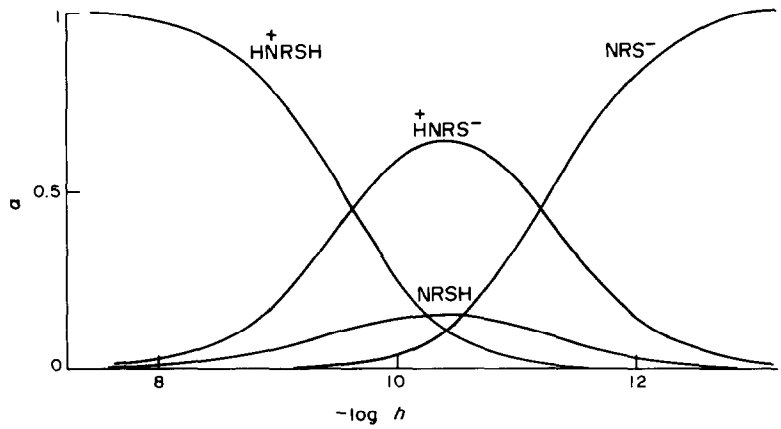

Fig. 4. Distribution curves for 1-methyl-4-mercaptopiperidine as a function of pH, calculated from the microscopic constants in Table 1.

By substituting $\lim A_{(pH\to 14)} = A_S = \varepsilon_S C$, $\lim A_{(pH\to 0)} = A_{SH} = \varepsilon_{SH} C$ and $C = C_S + C_{SH}$ the fraction of molecules with the thiol group dissociated, α_S, can be calculated from

$$\alpha_S = \frac{C_S}{C} = \frac{A - A_{SH}}{A_S - A_{SH}}$$

This variable, α_S, is related to three independent microscopic constants, *e.g.*, K_a, K_b and K_c, by

$$\alpha_S = \frac{K_a K_c + K_a h}{h^2 + K_a h + K_b h + K_a K_c} \qquad (2)$$

and will depend only on K_a and K_b if the following equality is introduced:

$$K_1 K_2 = K_a K_c$$

To find the values of K_a and K_b that were most compatible with the experimental data, a minimizing program was written in BASIC and run on an HP-9830A calculator. This program searched for the values of K_a and K_b that would minimize $U(K)$, where

$$U(K) = \sum_n (\alpha_{S,exp} - \alpha_{S,calc})^2$$

n being the number of points. Final values for the constants ($K_1 K_2 = K_a K_c = K_b K_d$) for 1-methyl-4-mercaptopiperidine are given in Table 1.

A simpler form of equation (2), $\alpha_S = K_A/(h + K_A)$, and analogous numerical treatment were used for 1,1-dimethyl-4-mercaptopiperidinium chloride. The final value for K_A is also given in Table 1.

DISCUSSION

The formation curve of the 1-methyl-4-mercaptopiperidinium ion (Fig. 2) clearly indicates that the two deprotonation steps do not occur completely separately. By plotting α_S *vs.* $-\log h$ it can be concluded that the degree of ionization of the $-SH$ group when its proton is the first removed, is 85%, and consequently that the acidity of this group is greater than that of the protonated amine group ($pK_a = 9.49$, $pK_b = 10.23$). This result is in agreement with those reported for β-mercaptoamines.[2,17]

The pK_A value found for the 1,1-dimethyl-4-mercaptopiperidinium ion is practically independent of the method used, 9.62 (spectrophotometric), 9.59 (potentiometric), supporting the view of Danehy and Parameswaran[1] that for thiols neither method has an intrinsic advantage over the other.

Comparison of pK_A and pK_B with pK_a and pK_b (Table 1) suggests that either *S*-methyl or *N*-methyl substitution on the 1-methyl-4-mercaptopiperidinium ion has very little influence on the acidity of the other group. This supports the view[19] that in certain cases this is a valid method for estimating microscopic constants.

From the constants given in Table 1, the validity of the Adams relation, $K_1 = K_a + K_b$, can be checked: $pK_1 = 9.51$, $-\log(K_a + K_b) = 9.42$; the agreement is better if pK_A and pK_b are used instead of pK_a and pK_b: $-\log(K_A + K_B) = 9.49$, which may be attributed to the higher accuracy of the potentiometric method, or possibly to systematic errors in the determinations.

From the microscopic constants, the distribution of the 1-methyl-4-mercaptopiperidine species in the medium used can be calculated as a function of pH and is given in Fig. 4. The predominance of the zwitterionic form, $H\overset{+}{N}RS^-$, over the uncharged form, NRSH, at all pH values explains the behaviour of this γ-mercaptoamine as a unidentate neutral ligand[4-6] and validates the assumptions made about the geometries of its soluble zinc(II) complexes.[10]

REFERENCES

1. J. P. Danehy and K. N. Parameswaran, *J. Chem. Eng. Data*, 1968, **13**, 386.
2. Ya L. Kostyukovskii, Yu A. Bruk, L. V. Pavlova, N. M. Slavachevskaya, A. V. Kokushkina, B. S. Mirkin and I. A. Belen'kaya, *Zh. Obshch. Khim.*, 1972, **42**, 662.
3. J. W. Wrathall and D. H. Busch, *Inorg. Chem.*, 1963, **2**, 1182.

4. M. C. Briansó, J. L. Briansó, W. Gaete, J. Ros and C. Suñer, *J. Chem. Soc. Dalton Trans.*, 1981, 852.
5. J. C. Bayón, M. C. Briansó, J. L. Briansó and P. González-Duarte, *Inorg. Chem.*, 1979, **18**, 3478.
6. J. C. Bayón, I. Casals, W. Gaete, P. González-Duarte and J. Ros, *Polyhedron*, 1982, **1**, 157.
7. H. Barrera, J. C. Bayón, P. González-Duarte, J. Sola and J. M. Viñas, *ibid.*, 1982, **1**, 647.
8. E. Q. Adams, *J. Am. Chem. Soc.*, 1916, **38**, 1503.
9. H. Barrera and R. R. Lyle, *J. Org. Chem.*, 1962, **27**, 641.
10. J. C. Bayón and P. González-Duarte, *J. Chem. Soc. Dalton Trans.*, 1982, 487.
11. G. Biedermann, *Ark. KEMI*, 1956, **9**, 277.
12. A. S. Brown, *J. Am. Chem. Soc.*, 1934, **56**, 646.
13. *Some Laboratory Methods*, Department of Inorganic Chemistry, Royal Institute of Technology, Stockholm, 1959.
14. W. Forsling, S. Hietanen and L. G. Sillén, *Acta Chem. Scand.*, 1952, **6**, 901.
15. G. Gran, *Analyst*, 1952, **77**, 661.
16. L. Pehrsson, F. Ingman and A. Johansson, *Talanta*, 1976, **23**, 769.
17. R. E. Benesch and R. Benesch, *J. Am. Chem. Soc.*, 1955, **77**, 5877.
18. P. Gans, A. Sabatini and A. Vacca, *Inorg. Chim. Acta*, 1976, **18**, 237.
19. M. A. Grafius and J. B. Neilands, *J. Am. Chem. Soc.*, 1955, **77**, 3389.

Talanta, Vol. 30, No. 7, pp. 543–545, 1983
Printed in Great Britain.

0039-9140/83 $3.00+0.00

CATION-EXCHANGE OF 43 ELEMENTS FROM HYDROFLUORIC ACID SOLUTION

R. CALETKA and V. KRIVAN
Sektion Analytik und Höchstreinigung, Universität Ulm, Oberer Eselsberg N-26, D-7900, Ulm/Donau, F.R.G.

(*Received* 25 *November* 1982. *Accepted* 26 *January* 1983)

Summary—The cation-exchange behaviour of 43 elements in 1–24*M* hydrofluoric acid has been investigated by means of the radiotracer technique. Under certain conditions the alkali, alkaline-earth, rare-earth and bivalent transition metal ions are retained on Dowex-50W × 8, whereas ions forming stable anionic fluoro-complexes are not.

Although the analytical usefulness of anion-exchange from hydrofluoric acid media is well known, and the data have been summarized in a number of monographs and reviews, less information is available on the behavour of elements in systems consisting of a cation-exchange resin and hydrofluoric acid solution. The retention of 36 elements on Dowex-50W × 8 from 0.1*M* hydrofluoric acid was studied under dynamic conditions by Fritz *et al.*[1] Strong sorption was observed for Ag, Be, Co, Cr, Cu, Fe(II), In, La, Mg, Ni, Pb, Th and Y, the other elements being eluted with either 0.1*M* or 1*M* hydrofluoric acid. The same concentrations of hydrofluoric acid in the presence of equal concentrations of nitric or sulphuric acid have been used in a batch distribution study of 27 elements between Dowex 50W × 8 and the solution, by Danielsson.[2] Headridge and Dixon[3] reported the distribution of Al, Cr, Cu, Fe, Mn, Ni and V between Zeo-Karb 225 and 1*M* hydrofluoric acid. The sorption of more than 30 elements on Dowex-50W × 8 from 6*M* hydrofluoric acid was studied by Girardi *et al.*,[4] and of Nb, Pa and Ta on the same resin from 0.01–15*M* hydrofluoric acid by Keller.[5] For a number of elements, sorption on Dowex-50 paper from 0.5*M* hydrofluoric acid was investigated by Lederer.[6]

Cation-exchange from hydrofluoric acid media has been utilized in several separation procedures. Danielsson and Ekström[7,8] and De Wispelaere *et al.*[9] used it for the separation and preconcentration of Ag, Co, Cu, In, Mg, Mn, Na, Ni, Pb, lanthanides and Zn at the ppm-level in pure iron. Hibbs and Wilkins[10] used cation- and anion-exchange columns in series for the separation of Al, Ni and Ti. A procedure for separation of rare earths and yttrium from high-purity zirconium on Dowex-50 from 3.5*M* hydrofluoric acid was reported by Hettel and Fassel.[11] Separation techniques reported by Kirk *et al.*[12] and Smet *et al.*[13] are based on the retention of Ag, Co, Cs, Cu, Ga, K, Na, Pb, Rb and Zn on Dowex-50 from 0.1*M* hydrofluoric acid.

The incompleteness and inconsistency of the published data on cation-exchange from hydrofluoric acid solution have prompted the present work in which the sorbability of 43 elements on a strong cation-exchanger from 1–24*M* hydrofluoric acid was systematically studied.

EXPERIMENTAL

The distribution data were obtained by the batch method with determinations done by the radiotracer technique, except for magnesium, for which atomic-absorption spectrometry was used.

Most of the radiotracers were prepared by irradiation of the pure metals or compounds in a nuclear reactor; ^{87}Y and ^{203}Pb were prepared by irradiation of strontium nitrate and thallium respectively in the isochronous cyclotron at Kernforschungszentrum, Karlsruhe. The radiotracer ^{7}Be was obtained from NEN Chemicals, GmbH. Stock solutions in 10*M* hydrofluoric acid were used. The radiochemical purity of the tracers was checked by high-resolution γ-ray spectrometry.

The distribution ratio D, defined as the ratio of the total amount of a species per gram of dry resin to total amount per ml of solution, was measured at $20 \pm 1°$. For this purpose, 2 ml of solution containing 10 μg of the labelled element (in the case of Ca, Eu, La, Sr, Tc and Y no carrier was added) were mixed with 50 mg of vacuum-dried Dowex-50W × 8 (50–100 mesh, prewashed H^+-form, Fluka product) for 24 hr. Because of the danger of adsorption of some species, *e.g.*, Ag, Au(I), Ca, Eu, La, Y, on the walls of the plastic vessels, the solutions were prepared shortly before use.

For experiments under dynamic conditions, columns with an active bed of 100–200 mesh resin, 45 mm in length and 8 mm in diameter, were used.

RESULTS AND DISCUSSION

For those elements with measurable D-values, the results are illustrated in Fig. 1. The quoted values are

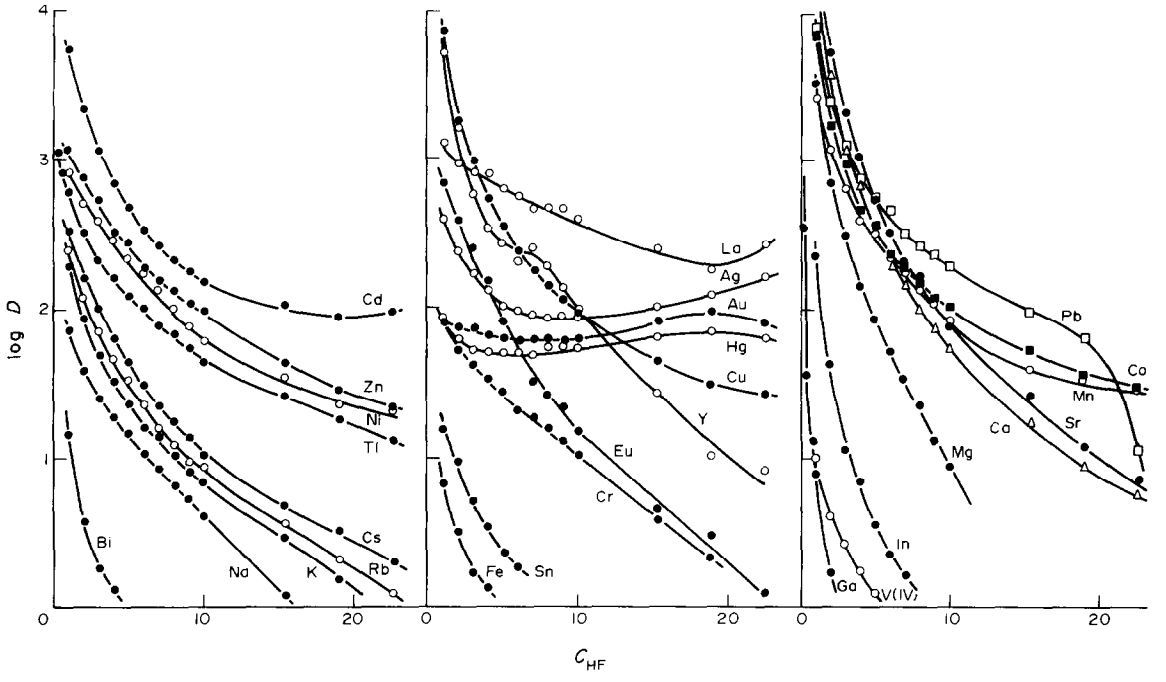

Fig. 1. Distribution coefficients for the system Dowex-50W × 8–hydrofluoric acid solution; D = distribution coefficient (ml/g); C_{HF} = concentration of hydrofluoric acid (M).

averages of at least two determinations. No significant retention ($D \leqslant 2$) from hydrofluoric acid solutions of concentration from 1 to 24M was detected for As(III,V), Be, Hf, Ir(III,IV), Mo, Nb, P(V), Re(VII), Sb(III,V), Sc, Se(IV), Ta, Tc(VII), W and Zr. Gallium was sorbed only from dilute hydrofluoric acid; in the range 0.1–2M hydrofluoric acid, the dependence of D on [HF] can be expressed as $\log D_{Ga} = 0.931 - 2.294\log[HF]$. The highest distribution ratios were obtained for the alkaline-earth metal ions from dilute hydrofluoric acid, *e.g.*, from 1M hydrofluoric acid, $\log D_{Ca} = 4.28$ and $\log D_{Sr} = 4.36$. The D-values did not differ substantially when the following pairs of oxidation states were used: Au(I, III), Fe(II,III), Sn(II,IV) and Tl(I,III). This behaviour can be attributed to the oxidation of Fe(II) and Sn(II) by atmospheric oxygen, and to the reduction of Au(III) and Tl(III) by the resin. It follows from the column experiments that Fe(II) and Sn(II) are strongly retained on the cation-exchanger from 2M hydrofluoric acid under dynamic conditions, since the oxidation to Fe(III) and Sn(IV) then takes place only slowly.

Peculiar behaviour was observed in the case of chromium(III), three species of which could be identified under dynamic conditions. Two of them were easily eluted with 2M hydrofluoric acid, but the third was retained on the column. The amount of the sorbable species decreased strongly when the solution was preheated (see Fig. 2). A similar observation was made by Danielsson[2] for hydrofluoric acid solutions and by Nelson *et al.*[14] for hydrochloric acid solutions. This behaviour is caused by the formation of hydrated isomers of fluoride (or, presumably, chloride) complexes.[15]

For most elements, our results are in accordance with those reported by other authors, the only exceptions being the data on Be, Cd, Mn and Zn obtained

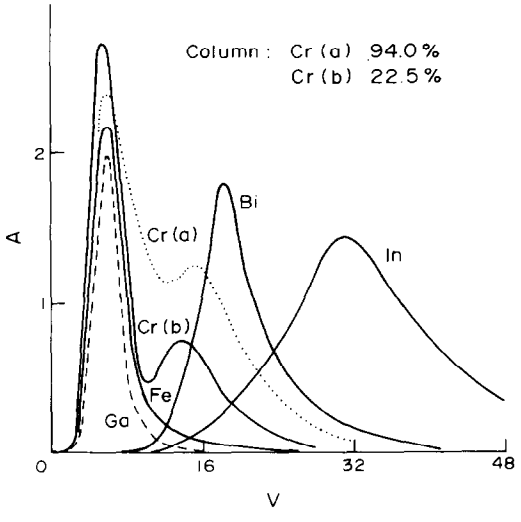

Fig. 2. Elution of Bi, Cr, Ga and In from a Dowex-50W × 8 column with 2M HF. Column 45 × 8 mm, flow-rate 0.5 ml/min, volume applied for separation 5 ml. Cr(a) at room temperature; Cr(b), heated under an infrared lamp for 30 min before separation. A, radioactivity of the eluate (arbitrary units); V, volume of the eluate (ml).

by Fritz *et al.*[1] and those on Nb and Ta obtained by Keller.[5] Fritz *et al.* reported the elution of Cd and Zn + Mn with 0.1 and 1*M* hydrofluoric acid respectively, while Be was retained on the cation-exchanger column under dynamic conditions. Our results showed that Be could easily be eluted with 2*M* hydrofluoric acid, and that Cd, Mn and Zn were retained on the Dowex-50 column even when 10*M* hydrofluoric acid was used for elution. For the sorption of Nb and Ta on Dowex-50, Keller found *D*-values between 10 and 30 for 1*M* hydrofluoric acid. In the present work, no significant retention ($D \leqslant 2$) could be found, and these results are in accordance with those obtained for dynamic conditions. Strong retention on Dowex-50 from 2–10*M* hydrofluoric acid under dynamic conditions was also observed for Ag, Co, Cu, Ni, Pb and Y. Bi and In can be eluted with 2*M* hydrofluoric acid (see Fig. 2), but the 4*M* acid is more suitable. Alkali metals and Mg are retained from 2*M* hydrofluoric acid, but can be eluted with the 10*M* acid. The individual separation of alkali metals was achieved with 8*M* hydrofluoric acid on a larger column (120 × 8 mm). In accordance with the batch work, lanthanum and yttrium are sorbed on the column from 10*M* hydrofluoric acid, but europium is 88% eluted. It can be assumed that precipitation of the insoluble fluorides of the alkaline earth metals, lanthanides and yttrium influences the behaviour of these elements when their concentrations exceed those corresponding to the conditional solubility products at the acid concentrations used.

From earlier studies on cation-exchange it can be concluded that the distribution ratios decrease with increasing concentration of a strong mineral acid also present in the solution. The sorption of cobalt from 1*M* hydrofluoric acid in the presence of 0.1–2*M* nitric acid was examined in greater detail. The behaviour can be described by the equation $\log D_{Co}$ (1*M* HF) = 1.368–1.986 $\log[HNO_3]$. Ammonium fluoride also causes a decrease in the sorption of cobalt. For ammonium fluoride concentrations up to 1*M* in 1*M* hydrofluoric acid, the following linear dependence was observed: $\log[(D^0_{Co} - D_{Co})/D_{Co}] = 2.736 + 2.541 \log[NH_4F]$, where $D^0_{Co} = 7100$. The competitive sorption of ammonium ions and formation of fluoride complexes can be suggested as reasons for this behaviour. The presence of up to 15*M* formic acid in the 1*M* hydrofluoric acid medium does not have any significant influence on the D_{Co} value. It can be assumed that the behaviour of other bivalent transition element ions will be similar.

Acknowledgements—This project was financially supported by the Bundesministerium für Forschung und Technologie, Bonn. The authors wish to thank the Kernforschungszentrum Karlsruhe, for providing, free of charge, irradiation facilities.

REFERENCES

1. J. S. Fritz, B. B. Garralda and S. K. Karraker, *Anal. Chem.*, 1961, **33,** 882.
2. L. Danielsson, *Acta Chem. Scand.*, 1965, **19,** 1859.
3. J. B. Headridge and E. J. Dixon, *Analyst*, 1962, **87,** 32.
4. F. Girardi, R. Pietra and E. Sabbioni, *J. Radioanal. Chem.*, 1970, **5,** 141.
5. C. Keller, *Radiochimica Acta*, 1963, **1,** 147.
6. M. Lederer, *J. Chromatog.*, 1959, **2,** 209.
7. L. Danielsson and T. Ekström, *Acta Chem. Scand.*, 1966, **20,** 2402.
8. *Idem, ibid.*, 1966, **20,** 2415.
9. C. De Wispelaere, J. P. Op De Beeck and J. Hoste, *Anal. Chim. Acta*, 1974, **70,** 1.
10. L. E. Hibbs and D. H. Wilkins, *Talanta*, 1959, **2,** 16.
11. H. J. Hettel and V. A. Fassel, *Anal. Chem.*, 1955, **27,** 1311.
12. M. Kirk, E. G. Perry and J. M. Arritt, *Anal. Chim. Acta*, 1975, **8,** 163.
13. T. Smat, J. Hertogen, R. Gijbels and J. Hoste, *ibid.*, 1978, **101,** 45.
14. F. Nelson, T. Murase and K. A. Kraus, *J. Chromatog.*, 1964, **13,** 503.
15. K. Nowak and A. Pasternak, *J. Radioanal. Chem.*, 1976, **31,** 167.

Talanta, Vol. 30, No. 8, pp. 547–554, 1983
Printed in Great Britain.

0039-9140/83 $3.00+0.00

A BROMIDE-SELECTIVE ELECTRODE–REDOX ELECTRODE CELL FOR THE POTENTIOMETRIC DETERMINATION OF BROMINE AND FREE RESIDUAL CHLORINE

D. MIDGLEY
Central Electricity Research Laboratories, Kelvin Avenue, Leatherhead, Surrey, England

(*Received* 29 *November* 1982. *Accepted* 9 *March* 1983)

Summary—A potentiometric cell consisting of a bromide-selective electrode and a platinum redox electrode is sensitive to free residual chlorine (FRC) when the sample solution is treated before measurement with reagents to give pH 5 and a bromide content of 0.1*M*. The calibration graph of e.m.f. *vs.* log [FRC] is linear over the [FRC] range from about 0.05 to 50 mg/l. (the highest level tested). Not all forms of bromide-selective electrode prove suitable, but one with a silver bromide single-crystal membrane has been found to give a theoretical calibration slope, whereas one with an Ag_3SBr compressed pellet membrane gave a sub-Nernstian response. The response to combined residual chlorine (CRC) is negligible but if both FRC and CRC are present, the sample treatment is likely to cause a reduction in FRC concentration. Tests have shown that a similar bias can be found with the commonly used DPD colorimetric method.

The concentration of free residual chloride (FRC) is a measure of the disinfecting power remaining in a solution that has been dosed with chlorine or sodium hypochlorite and is also an indicator of the toxicity of a chlorinated discharge. Chemically, FRC consists of chlorine, hypochlorous acid and hypochlorite ion. If bromide is present in the solution, bromine (and its complexes), hypobromous acid and hypobromite will also be formed, give positive results in tests for FRC and have powers of disinfection similar, but not identical, to those of the chlorine species.

An EEC directive[1] sets an upper limit of 5 μg/l. for chlorine in fresh waters "needing protection or improvement in order to support fish life". A method of monitoring specifically for FRC would be of use in biological research into the effect of chlorination on aquatic fauna, since FRC and other (combined) forms of residual chlorine are likely to differ in their toxicities towards any individual species.

Methods for determining FRC have been reviewed[2-4] and one of the greatest difficulties is distinguishing FRC from combined residual chlorine (CRC), which consists of the chloramines, NH_2Cl, $NHCl_2$ and NCl_3 and organic chloramines. Amperometric titration is capable of high sensitivity and has good selectivity for FRC, but is relatively inconvenient to perform and is ill-suited to field work with portable apparatus or to continuous on-line measurement. Voltammetric and galvanic sensors are mainly used for on-line monitoring, but some portable apparatus is available; the sensitivity and selectivity of this equipment vary considerably between individual instruments and are generally not well characterized. A wide variety of colorimetric reagents has been used for the determination of FRC,[4] with very mixed results with regard to selectivity. The most commonly used is DPD (*N*,*N*-diethyl-*p*-phenylenediamine), the method being suitable for field and laboratory measurements, but not particularly so for on-line monitoring. The limit of detection of the DPD method is about 20 μg/l.

The characteristics required for a method of determining FRC are, therefore, good selectivity with respect to CRC, ability to measure μg/l. levels, and suitability for use in portable and on-line apparatus. A combination of a platinum redox electrode and an iodide-selective membrane electrode has performed very well in the determination of TRC.[5-7] A similar system for FRC determination has been devised in which FRC oxidizes bromide to bromine and so controls the e.m.f. of a cell comprising a platinum electrode and a bromide-selective membrane electrode. The results of tests with this system are reported here.

THEORY

The potentiometric cell consists of a bromide-selective electrode and a platinum (redox) electrode immersed in a buffered FRC solution to which bromide has been added. The FRC components will oxidize bromide to bromine, hypobromous acid or hypobromite, the proportions of each product depending on pH.

$$Cl_2 + 2Br^- \rightleftharpoons Br_2 + 2Cl^-$$
$$HOCl + Br^- \rightleftharpoons HOBr + Cl^-$$
$$OCl^- + Br^- \rightleftharpoons OBr^- + Cl^-$$

Any molecular bromine produced can also form complexes with bromide and chloride ions in solution:

$$Br_2 + Br^- \rightleftharpoons Br_3^-$$
$$Br_2 + Cl^- \rightleftharpoons Br_2Cl^-$$

The bromide-selective electrode responds to the bromide concentration:

$$E_{Br} = E^0_{Br} - k \log [Br^-] \quad (1)$$

The platinum electrode responds to the bromine–bromide redox equilibrium

$$E_{Pt} = E^0_{Pt} - \frac{k}{2} \log \frac{[Br^-]^2}{[Br_2]} \quad (2)$$

The slope factor, k, in equations (1) and (2) is theoretically equal to $2.303\,RT/F$, where R is the gas constant, T the absolute temperature and F the Faraday constant.

The overall cell potential is given by the difference between equations (1) and (2)

$$E = E^0_{Pt} - E^0_{Br} + \frac{k}{2} \log [Br_2] \quad (3)$$

Equation (3) shows that a cell of this type responds to the free bromine concentration independently of the bromide concentration. This could not be achieved with a cell using, for example, a platinum electrode and a saturated calomel reference electrode, which would have an e.m.f. proportional to log $([Br^-]^2/[Br_2])$. An arrangement of the type proposed also has the advantage of not having a liquid junction and thus avoids the systematic and random errors associated with it. A further practical advantage, particularly for continuous monitoring, is that the electrodes require very little maintenance.

Although the response indicated by equation (3) may be useful in some applications, *e.g.*, thermodynamic studies, for analytical purposes it is generally desired to relate the e.m.f. to the FRC concentration. To achieve a calibration in terms of FRC, constraints on the pH and bromide concentration must be introduced because of the equilibria summarized in equation (4):

$$\begin{aligned}[FRC] &= [Br_2] + [HOBr] + [OBr^-] + [Br_3^-] + [Br_2Cl^-] \\ &= [Br_2]\left\{1 + \frac{1 + K_a[H^+]}{K_H[Br^-][H^+]} + \beta_1[Br^-] + \beta_2[Cl^-]\right\} \\ &= \alpha[Br_2] \end{aligned} \quad (4)$$

where K_a is the dissociation constant of hypobromous acid, β_1 and β_2 are the formation constants of the bromide and chloride complexes of bromine and K_H is the hydrolysis constant for the equilibrium

$$Br_2 + H_2O \overset{K_H}{\rightleftharpoons} HOBr + Br^- + H^+ \quad (5)$$

Substitution in equation (3) gives

$$E = E^0_{Pt} - E^0_{Br} - \frac{k}{2} \log \alpha + \frac{k}{2} \log [FRC]$$

In the analytical procedure, the solution is buffered and bromide is added in such excess that its concentration is virtually constant. Under these conditions, α is effectively constant and we can write the equation for the calibration in the familiar Nernstian form as

$$E \cong \text{constant} + \frac{k}{2} \log [FRC] \quad (6)$$

where constant $\cong E^0_{Pt} - E^0_{Br} - \frac{1}{2}k \log \alpha$. Activity coefficients have been omitted from this treatment, since the excess of bromide makes the ionic strength virtually constant.

EXPERIMENTAL

Apparatus

Most of the work was done with a Philips IS-550-Br bromide-selective electrode with an Ag_3SBr membrane and an EIL type EPT-23 platinum electrode. Other types of bromide-selective electrodes were also tried, namely the Radiometer F1022Br with a single-crystal AgBr membrane and the Růžička "Selectrode" (Radiometer F3012) impregnated with AgBr or Ag_2S/AgBr mixtures. An EIL type 1380 230 mercury–mercury(I) sulphate reference electrode with a 1*M* sodium sulphate filling solution was used in tests with the bromide-selective electrodes. Potentials were measured with a Corning 110 digital pH-meter reading to 0.1 mV.

Spectroscopic measurements were made with Pye-Unicam SP1750 and SP6-500 spectrophotometers.

Reagents

Chemicals were of analytical reagent grade unless otherwise specified.

FRC standard solutions. Sodium hypochlorite solution (BDH laboratory reagent, 10–14% available chlorine) was diluted to make a suitable stock solution ($Cl_2 \sim 1000$ mg/l.) which was standardized iodometrically with sodium thiosulphate. Further standards were prepared by dilution immediately before use.

CRC (monochloramine) standard solutions. Monochloramine solutions were prepared by reaction of 0.5*M* sodium hypochlorite and 0.5*M* ammonia followed by ether extraction and then stripping into demineralized water.[8] The solutions were standardized iodometrically with sodium thiosulphate. The ultraviolet spectra of such solutions indicated that no FRC was present.

Mixed FRC and CRC solutions. Concentrated ammonia solution was added to sodium hypochlorite solution (Cl_2 100 mg/l.) in molar ratios between 3 and 0.3. The ratio of monochloramine to hypochlorite was calculated from the absorbances at 245 nm and 294 nm.

Acetate buffer (pH 4). Prepared by dissolving 243 g of sodium acetate trihydrate and 480 g of glacial acetic acid in water and diluting to 1 litre. The pH-5 buffer was prepared by adding sodium hydroxide pellets to the pH-4 buffer until the correct pH was indicated by a glass electrode.

Citrate buffer (pH 6). Citrate acid monohydrate (4.0 g) and 23.8 g of trisodium citrate dihydrate were dissolved in water and made up to 100 ml.

Bromide solutions, 1M and 0.1M. These were prepared using 119 g and 11.9 g KBr per litre of water.

DPD reagents. Commercial DPD (*N,N*-diethyl-*p*-phenylene diamine) reagents were used, either as tablets (BDH), or solutions (Wallace and Tiernan Ltd., Tonbridge).

Water. Water from a nuclear-grade mixed-bed demineralization unit (Elga Spectrum) was used for the preparation of reagent and standard solutions. The chlorine demand of this water was found[7] to be <5 μg/l. (usually <2 μg/l.).

Procedure

Ten ml of bromide solution (0.1 or 1.0*M*) were added to 90 ml of sample solution, followed by 1 ml of buffer solution. The electrodes were immersed in the treated sample solution, which was stirred gently and the e.m.f. was noted when it became steady.

RESULTS

The response predicted by equation (6) could be obtained only if certain types of bromide-selective electrodes were used. Moreover, the choice of reaction conditions was critical if the response was to be selective.

Optimum reaction conditions

Calibration curves at pH 4, 5 and 6 for the cell incorporating the Philips electrode are shown in Fig. 1 for solutions containing 10 ml of 0.1*M* potassium bromide per 90 ml of standard solution. At pH 6 the response was slow even with hypochlorite solutions and a linear response was not obtained. Although the response to hypochlorite had a longer linear range at pH 4 than at pH 5 (extending down to about 0.5 mg/l. FRC compared with about 2 mg/l.), interference by chloramines at the lower pH would have been severe, as shown by the proximity of the two calibration curves at pH 4. At pH 5, however, the response to chloramines was negligible.

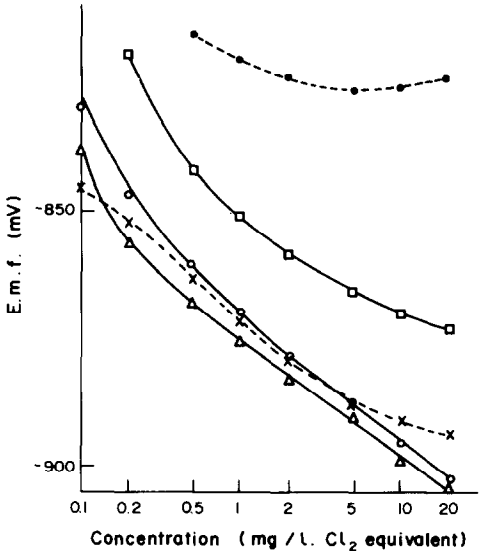

Fig. 1. Calibration with hypochlorite (——) and chloramine (– – –) in presence of 0.1*M* bromide. △, ×, pH 4; ○, ●, pH 5; □, pH 6.

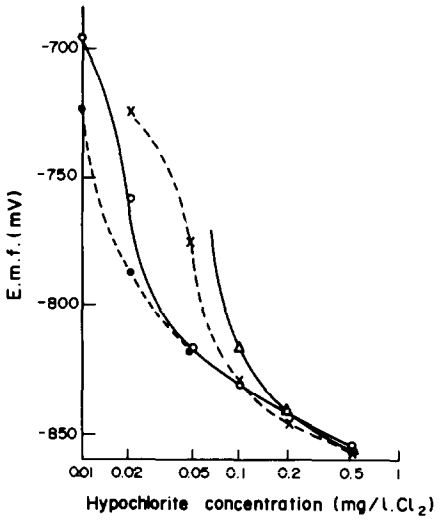

Fig. 2. Effect of bromide concentration and pH on calibration. ○ 0.1*M* KBr, pH 5; △ 0.01*M* KBr, pH 5; ● 0.1*M* KBr, pH 4; × 0.01*M* KBr, pH 4.

The linear parts of the hypochlorite calibration graphs had slopes of 22–24 mV/decade, which was considerably below the theoretically expected value of 29 mV/decade. The shift of e.m.f. between hypochlorite calibrations at pH 4 and pH 5 was in the direction expected from equation (5), *i.e.*, at higher pH the proportion of bromine fell. The deviations from linearity at low concentrations indicated a deficiency of bromine in the test solution: this may have arisen from consumption of FRC by compounds in the water used to prepare the standards, or because at low concentration and in weakly acidic solution, bromine was produced so slowly that no change in e.m.f. was perceptible in the time (5–10 min) allowed for measurements. Previous work[7] with water from the same source indicated a chlorine demand of less than 2 μg/l., which would have been insufficient to produce the curvature in Fig. 1. In order to increase the rate of reaction and therefore extend the linear calibration range, the concentration of bromide added was increased tenfold. Figure 2 shows that the linearity of calibration then extended to much lower concentrations (0.1 mg/l.). The linear sections of the calibrations were shifted to less negative e.m.f. values with the more concentrated bromide reagent, indicating a lower free bromine concentration. This shift arose from the increased tendency of the bromine to form the tribromide complex (Br_3^-) at the higher bromide concentration. The observed shifts were, however, not as large as predicted from the stability constants.

The optimum conditions for the reaction, therefore, require 0.1*M* bromide and pH 5 in the solution presented to the electrode and these were used in the subsequent work. It may be noted that the non-theoretical responses obtained in this part of the work arose from the properties of the Philips electrode (see below). When a single-crystal membrane electrode

was used, the response was almost Nernstian and the shifts due to changes in bromide concentration were almost theoretical.

Bromide-selective electrodes

The previous section revealed an unexpected non-Nernstian response, so four different types of bromide-selective electrodes were investigated. In these tests the e.m.f. of the platinum–bromide electrode pair was not measured directly. Instead each electrode potential was measured with respect to a common mercury–mercury(I) sulphate reference electrode, so that the origin of the non-Nernstian response could be traced. The response of the platinum–bromide electrode pair to FRC was obtained from the difference between the e.m.f. values for the bromide–reference and platinum–reference pairs. Measurements were made at pH 5, the optimum found in the previous section, and the bromide and FRC concentrations were varied independently. The response to bromide in the absence of FRC was satisfactory in three cases, but in the presence of FRC two of the bromide-selective electrodes were useless and one became non-Nernstian in response. The results for the two better electrodes in FRC/0.1*M* bromide solutions are shown in Table 1, together with calculated values allowing for tribromide formation and hydrolysis of bromine and hypobromous acid, but assuming no redox interference with the bromide-selective electrode.

The Radiometer F1022Br single-crystal membrane electrode gave a Nernstian response in bromide solutions and nearly near-Nernstian response when used in conjunction with a platinum electrode to measure FRC.

Its potential in bromine-containing solutions changed with FRC concentration according to theory (Table 1). This type of electrode does not respond to redox potentials and is most suitable for measurements of FRC concentration.

In the absence of free residual chlorine the Philips IS-550-Br electrode gave theoretical responses to bromide (59–60 mV per tenfold change in concentration), but the platinum–bromide electrode cell made with it had a non-Nernstian response to FRC (22–24 mV per tenfold change in concentration). Table 1 shows that the potential of the platinum electrode changed almost as expected from theory, but that of the Philips IS-550-Br changed much more than expected. It was inferred, therefore, that the electrode had a response to the Br_2–Br^- redox couple in addition to the simple response to bromide. However, since the calibration graph obtained with the Philips IS-550-Br and platinum pair did not change with time and showed good linearity in the range tested, the Philips electrode should be suitable even though the sensitivity is lower than theoretical. Similar results were obtained with another Philips IS-550-Br electrode.

A Růžička "Selectrode"[9] impregnated with a mixture of silver sulphide and silver bromide had a near-theoretical response in bromide solutions but on addition of FRC its potential increased by about 800 mV. This may be attributed to oxidative attack by FRC on the sulphide in the membrane, leading to a release of silver ions and a large positive shift in potential. No use could be made of the electrode for FRC determination.

A Růžička "Selectrode" impregnated with silver bromide showed considerable drift in bromide solutions and on addition of FRC gave a fixed e.m.f. of +36 mV when coupled with the platinum electrode, *i.e.*, it was responding only to the Br_2–Br^- redox couple and not as a bromide-selective electrode. This electrode was of no use for measuring FRC concentrations.

Selectivity

Figure 1 shows that the Philips electrode had a negligible response to chloramine at pH 5, but in further tests with solutions containing both FRC and CRC, the results were all low. Two series of tests with the Philips IS-550-Br were performed to investigate this bias. In the first series chloramine was added to FRC solutions in which the electrode had already reached equilibrium, thus allowing the interactive effects of the two forms of residual chlorine to be investigated. In the second series the electrode was

Table 1. Observed and theoretical e.m.f. values for bromide and platinum electrodes (0.1*M* Br^-/pH 5 acetate buffer)

FRC concentration, *mg/l.*		1	2	4	6	10
Bromide-electrode potential, *mV*	Series I (Philips IS-550-Br)	0	1.8	4.6	5.9	8.1
	Series II (Radiometer F1022Br)	0	0.1	0.3	0.5	0.8
	Theoretical	0	0.1	0.2	0.5	0.8
Platinum-electrode potential,* *mV*	Series I	0	10.1	19.4	24.4	30.9
	Series II	0	10.7	20.1	24.9	31.0
	Theoretical	0	9	18.1	23.5	30.5
Cell e.m.f.,* *mV*	Series I	0	−8.3	−14.8	−18.5	−22.8
	Series II	0	−10.6	−19.8	−24.4	−30.2
	Theoretical	0	−8.9	−17.9	−23.0	−29.7

*The values in each series are normalized with respect to that for 1-mg/l. FRC.

Table 2. Effect of adding chloramine and ammonia solutions to test solutions containing FRC

[FRC], *mg/l.*	Apparent loss of FRC (%) on addition of: Equivalent quantity of chloramine	Residual ammonia after extraction
0.1	6	0
1.0	83	26
10.0	94	78

immersed in solutions containing both FRC and CRC, which would correspond to practice, but at concentrations high enough for the proportions of FRC and CRC to be found from ultraviolet spectrophotometry. After dilution, the solutions in this series were also analysed by the DPD colorimetric method.

Addition of chloramine after measurement of FRC. Fixed volumes of 1 *M* bromide and pH-5 buffer were added to standard FRC solutions and the e.m.f. values recorded. To each FRC solution, once a steady e.m.f. had been reached, an equivalent quantity (with respect to chlorine content) of concentrated chloramine solution was added and the change in e.m.f. was recorded. As shown in Table 2, the changes in e.m.f. represented a significant loss of FRC, indicating that the FRC had reacted with the chloramine itself or with residual ammonia from the chloramine preparation.

To resolve the contributions made by chloramine and ammonia to the loss of FRC, the tests were repeated with the final aqueous extract from a monochloramine "preparation"[8] in which no hypochlorite was added. Since no chloramine could be formed, any loss of FRC could only be caused by reaction with ammonia carried over in the extractions. Table 2 shows that the loss of FRC was smaller than with addition of chloramine. Furthermore, the change in e.m.f. on addition of the ammonia solution was complete within about 10 sec, compared with 2–3 min on addition of chloramine solutions. It can be inferred that the bromine or hypobromous acid in the test solution reacted mainly with the chloramine. Indications of a reaction between hypobromous acid and chloramine have also been found[10] by polarography and ultraviolet spectrophotometry. The dilution of the FRC on addition of the chloramine or ammonia solution accounted for a fall in FRC concentration of only 0.01–1%, and was insignificant.

The response-time of the electrode differed in FRC and CRC solutions. Figure 3 shows the results for two series of successive additions, one of FRC and one of CRC. The response to an increase in FRC was rapid, being complete in 10–30 sec, depending on the concentration. The addition of CRC, however, first produced a positive shift in e.m.f. (indicating less residual chlorine) before the e.m.f. returned to a more negative e.m.f. over a period of 2–3 min.

Premixed solutions containing both FRC and CRC. Mixtures of hypochlorite and ammonia at pH 11.5 were analysed by ultraviolet spectrophotometry and by potentiometry with the Philips IS-550-Br electrode. In Fig. 4 the potentiometric results are plotted against the FRC concentrations determined from the absorbance at 294 nm (λ_{max} for the hypochlorite ion) for different FRC:CRC ratios. The CRC concentration was determined from the absorbance at 245 nm (λ_{max} for monochloramine). No other absorbance peaks were detected in the range 190–350 nm. It is apparent that the potentiometric results were much lower than the spectrophotometric ones unless the FRC was present in considerable excess. In the mixed solutions the electrode took about 5 min to reach a steady potential, which was much slower than in solutions containing only FRC (Fig. 3).

The FRC concentrations of the solutions used in obtaining Fig. 4 were much higher than are found in cooling water (except in the immediate vicinity of the

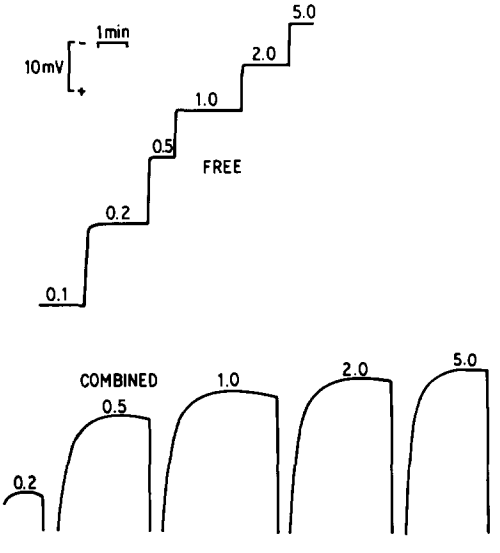

Fig. 3. Response curves for free and combined residual chlorine (concentrations shown in mg/l., Cl_2).

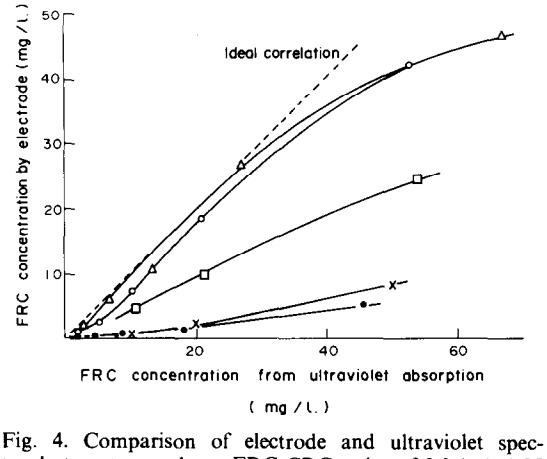

Fig. 4. Comparison of electrode and ultraviolet spectrophotometry results at FRC:CRC ratios of 2.0 (△), 1.25 (○), 1.0 (□), 0.63 (×), 0.36 (●).

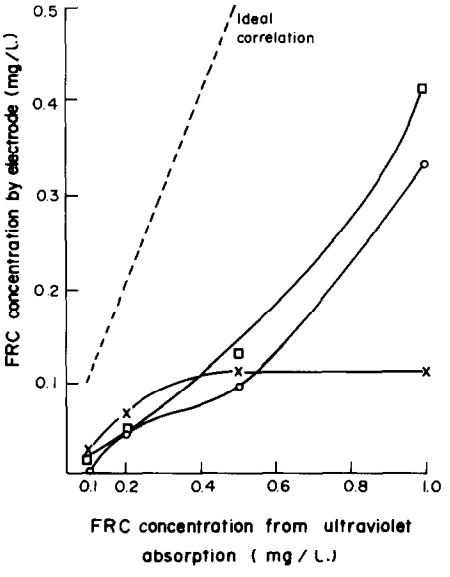

Fig. 5. Comparison of electrode and ultraviolet spectrophotometry results at FRC:CRC ratios of 1.35 (○), 0.92 (□), 0.59 (×). Electrode measurements were made after, and absorbance measurements before, 100-fold dilution.

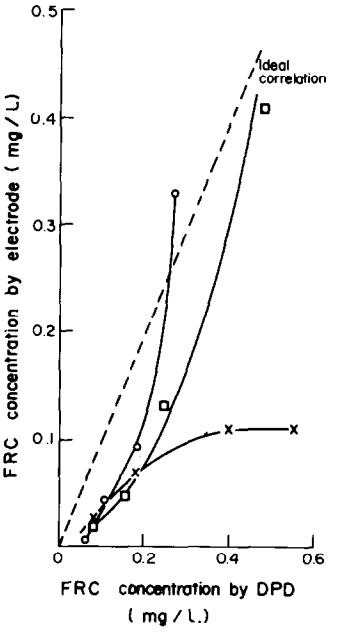

Fig. 7. Comparison of electrode and DPD results at FRC:CRC ratios of 1.35 (○), 0.92 (□), 0.59 (×).

dosing point). A further series of tests was run in which the solutions were diluted a hundredfold before measurement with the electrode but after measurement of the absorbance at 294 nm, absorbance measurements being considered impracticable with the dilute solutions. The results in Fig. 5 again showed that the electrode gave a low reading in mixtures of FRC and CRC.

Comparison with the DPD colorimetric method. Solutions were analysed by both the potentiometric method and the DPD colorimetric method[11] at various ratios of FRC to CRC (determined by ultraviolet spectrophotometry as described above). The results for the concentrated solutions, corresponding to Fig. 4, are shown in Fig. 6. The solutions were diluted a hundredfold before analysis with DPD. The results corresponding to Fig. 5 are shown in Fig. 7, the solutions being diluted a hundredfold before measurement by both the electrode and DPD methods.

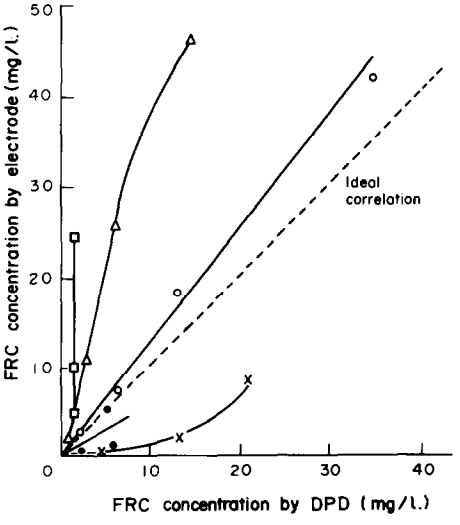

Fig. 6. Comparison of electrode and DPD results at FRC:CRC ratios of 2.0 (△), 1.25 (○), 1.0 (□), 0.63 (×), 0.36 (●). Electrode measurements were made before, and DPD results after, 100-fold dilution.

No consistent relationship between the DPD and electrode results can be seen, although both methods gave results lower than expected from ultraviolet spectrophotometry. The bias in the DPD method was smallest when the ratio of FRC to CRC was small, whereas the bias in the electrode results was smallest at high ratios of FRC to CRC. Neither method appeared to give reliable results for mixtures of FRC and CRC.

DISCUSSION

Analytical performance of the potentiometric method

The electrochemical cell gives a linear response to the logarithm of the FRC concentration and if a single-crystal membrane electrode for bromide is used, the slope of the response graph is almost theoretical (29 mV per decade). Other types of bromide-selective electrode, however, may yield a sub-Nernstian response because of redox interference, or even no useful response at all. The choice of reaction conditions is critical, in that at pH 4 combined residual chlorine will interfere and at pH 6 the oxidation of bromide is incomplete: pH 5 is a good compromise, giving a linear calibration for FRC down to 0.05 mg/l. and no significant response to combined residual chlorine. A high bromide con-

centration also favours the rapid formation of bromine and a level of 0.1*M* in the reaction mixture is recommended.

The greatest failing of the method is its response when the test solutions contain both FRC and CRC. The reaction conditions necessary result in a shift in the equilibrium between the various species present, or enable irreversible reactions to proceed more rapidly: in either case the FRC concentration is considerably reduced. This problem is not unique to the potentiometric method, since most methods involve at least a change in pH and it is possible that bias in the analysis of FRC–CRC solutions is more serious than is commonly thought.

This bias with mixtures of FRC and CRC is likely to restrict the application of the potentiometric method in general analysis. It could be used for measurements of FRC when CRC is known to be absent, but there would be little advantage, if any, over the use of the total residual chlorine electrode.[5-7] The method might also be used to detect the appearance of FRC in waters expected to contain only CRC, even though the bias prevents an accurate determination.

In circumstances where CRC is known to be absent, as in thermodynamic or kinetic laboratory studies of FRC reactions, the potentiometric method could find many uses. For instance, concern for the environment has prompted much work on the halogenation of organic compounds in aqueous solution,[12] with possible consequences for the treatment of cooling water, sewage effluent and drinking water.

The advantages of the potentiometric method over other analytical methods are uncertain, because of the lack of results in the literature for mixtures of FRC and CRC. Direct amperometric methods for FRC are prone to interference by CRC[13-15] and would, therefore, seem worse than the potentiometric method in this respect. Colorimetry with DPD was better than potentiometry at low FRC:CRC ratios but worse at high ratios; the number of tests in this study, however, was too small for the advantages of one method or the other to be definitely ascertained. One advantage of the potentiometric method is that the bias is also associated with an abnormally slow response, as in Fig. 3 and therefore should be detectable, though not quantifiable.

Performance of bromide-selective electrodes

The differences in the results obtained with four different types of bromide-selective electrode show that the chemical composition and physical constitution of the membrane are critical factors in the performance of the method. An electrode with a membrane consisting of a single crystal of silver bromide, as in the Radiometer F1022Br, has a nearly theoretical response to FRC, but all the other types showed the influence of redox reactions. A redox effect was not expected with the single-crystal electrode, because silver bromide[16] is exclusively an ionic conductor with $t_{Ag^+} = 1.0$.

A membrane consisting of many crystals of silver bromide supported on a conducting substrate, however, may show a very large redox effect, *e.g.*, the AgBr-"Selectrode" gives a constant cell e.m.f. when coupled with a platinum electrode and is therefore useless for FRC determination.

Most commercially produced bromide-selective electrodes have membranes comprising silver bromide and silver sulphide, sometimes as the compound Ag_3SBr. The Radiometer S42415 Ag_2S/AgBr mixture used for impregnating the "Selectrode" is believed to be co-precipitated:[9] with this mixture, large shifts in e.m.f. occur, as if the sulphide in the membrane were being oxidized by the FRC in solution and the electrode is consequently of no use for FRC determination.

The Philips IS-550-Br has a compressed pellet membrane believed to be Ag_3SBr, *cf.* van de Leest and Geven.[17] The conductivity[18] of Ag_3SBr is not purely ionic, with $t_{Ag^+} = 0.98$–0.99, and redox interference with the electrode is therefore possible. Although these electrodes give a non-ideal calibration graph in the potentiometric determination of FRC, their performance is acceptable. Most commercial bromide-selective electrodes are of the Ag_2S/AgBr compressed pellet type and would be expected to behave roughly the same as the Philips type.

The classical electrode of the second kind (silver–silver bromide) was not tested, since its potential was expected to be dominated by redox effects in the conditions of FRC measurement,[19] unless a pore-free surface could be obtained.

Acknowledgements—The author acknowledges the considerable help given by Mr. N. A. Dimmock with the experimental work. This work was done at the Central Electricity Research Laboratories and is published with the permission of the Central Electricity Generating Board.

REFERENCES

1. *Anon., Off. J. European Communities*, No. L222/1 (14.8.78).
2. D. Midgley, *Proc. Intern. Conf. Local Generation and Use of Chlorine and Hypochlorite*, Society of Chemical Industry, London, 1980.
3. G. R. Helz, J. W. Gretz, P. Higgens, J. C. Peterson, A. C. Siglio and R. Sugam, *EPRI EA*-929, Electric Power Research Institute, Palo Alto, 1978.
4. N. J. Nicolson, *Analyst*, 1965, **90**, 187.
5. L. P. Rigdon, G. J. Moody and J. W. Frazer, *Anal. Chem.*, 1978, **50**, 465.
6. G. Scarano and M. G. Saroglia, in *Condenser Biofouling Control*, J. F. Garey, R. M. Jorden, A. H. Aitkne, D. T. Burton and R. H. Gray (eds.), p. 373. Ann Arbor, 1980.
7. N. A. Dimmock and D. Midgley, *Talanta*, 1982, **29**, 557.
8. J. Kleinberg, M. Tecotzky and L. F. Audrieth, *Anal. Chem.*, 1954, **26**, 1388.
9. E. H. Hansen, C. G. Lamm and J. Růžička, *Anal. Chim. Acta*, 1972, **59**, 403.

10. A. Bousher, P. Brimblecombe and D. Midgley, *CERL Note* RD/L/2162N81, Central Electricity Research Laboratories, Leatherhead, 1981.
11. A. T. Palin, *J. Inst. Water Engineers*, 1974, **28,** 139.
12. D. Midgley, *Power Industry Res.*, 1981, **1,** 1.
13. N. A. Dimmock and D. Midgley, *Water Res.*, 1979, **13,** 1101.
14. *Idem*, *ibid.*, 1979, **13,** 1317.
15. J. J. Morrow and R. N. Roop, *J. Am. Water Wks. Assoc.*, 1975, **67,** 184.
16. F. Bénière, in *Physics of Electrolytes*, Vol. 1, J. Hladik (ed.), p. 299. Academic Press, London, 1972.
17. R. E. Van de Leest and A. Geven, *J. Electroanal. Chem.*, 1978, **90,** 97.
18. M. Koebel, N. Ibl and A. M. Frei, *Electrochim. Acta*, 1974, **19,** 287.
19. C. Harzdorf, *Anal. Chim. Acta*, 1982, **136,** 61.

Talanta, Vol. 30, No. 8, pp. 555–564, 1983
Printed in Great Britain

0039-9140/83 $3.00 + 0.00
Pergamon Press Ltd

DERIVATIVES OF CARBOHYDRAZIDE, THIOCARBOHYDRAZIDE AND DIAMINOGUANIDINE AS PHOTOMETRIC ANALYTICAL REAGENTS—I

1,3-bis[(2-PYRIDYL)METHYLENEAMINO]THIOUREA AND 1,3-bis[(2-PYRIDYL)METHYLENEAMINO]GUANIDINE

F. J. BARRAGAN DE LA ROSA, J. L. GÓMEZ ARIZA and F. PINO
Department of Analytical Chemistry, Faculty of Chemistry, University of Seville, Seville, Spain

(*Received* 23 *November* 1981. *Revised* 10 *January* 1983. *Accepted* 24 *February* 1983)

Summary—1,3-Bis[(2-pyridyl)methyleneamino]thiourea (PMAT) and 1,3-bis[(2-pyridyl)methyleneamino]-guanidine (PMAG) have been prepared. They have been examined and characterized by infrared and ultraviolet spectroscopy. A spectrophotometric method has been used for determination of the protonation constants of the reagents. Finally, a spectrophotometric survey has been made of the reactions of various cations with PMAT and PMAG.

Carbohydrazide and thiocarbohydrazide may be considered the final members of the structural sequence urea/thiourea, semicarbazide/thiosemicarbazide and carbohydrazide/thiocarbohydrazide, and also to have close links with carbamic/thiocarbamic and carbazic/thiocarbazic acids, as well as the aminoguanidines.

Carbohydrazide, thiocarbohydrazide and their derivatives, are interesting substances with numerous biochemical, pharmacological, industrial and other uses. Diaminoguanidine derivatives are no less varied in their applications.

In analytical chemistry, thiocarbohydrazide is useful for identification and estimation of both organic and inorganic compounds.[1–4] It precipitates aldehydes and ketones quantitatively. With certain ions, including U(VI), Mo(VI), Ni, Bi and Cu(II), carbohydrazide and thiocarbohydrazide form characteristic precipitates, which have been examined thermogravimetrically.[1,3] Numerous colour tests for anions and cations are based on the complexing power of these reagents.[5–7] More recent studies have included the reactions of carbohydrazide with Cu(II)[8] and $FeNO^{2+}$,[9,10] and of thiocarbohydrazide with Cd,[11–14] Cu(II),[15,16] Co(II) and Ni,[17,18] and Cr(III), Pb, Mn(II), Zn and V(V).[13] The metal complexes of various thiocarbohydrazide derivatives have been used to identify the binding sites and the molecular structures of the complexes.[18–25] However, these reagents are still little used in analytical chemistry, except for diphenylcarbazide and diphenylthiocarbazide, which are already classical photometric reagents, and it is interesting to consider the use of other carbohydrazide, thiocarbohydrazide and diaminoguanidine derivatives.

During the last 10 years or more the possibilities for analytical use of pyridine thiosemicarbazones, semicarbazones and 4-phenylthiosemicarbazones have been reported from this department, and numerous reagents for the photometric determination of metal ions have been proposed.[26–30] Attention is now focused on use of the 1,5-thiocarbohydrazide and 1,5-diaminoguanidine derivatives of pyridine (PMAT and PMAG respectively) for analogous purposes. The structural resemblance between thiosemicarbazones and thiocarbohydrazones allows possible syntheses to be envisaged and metal ion reactivity to be predicted.

The diaminoguanidine derivatives do not seem to have been used analytically.

EXPERIMENTAL

Reagents

Synthesis. The reagents were prepared in the usual way for Schiff's bases. Either thiocarbohydrazide or diaminoguanidine hydrochloride (0.01 mole) was dis-

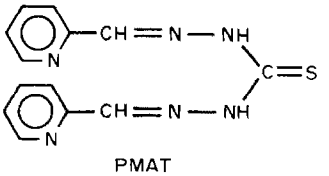

PMAT

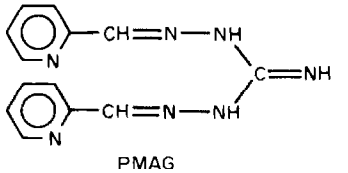

PMAG

solved in 40 ml of distilled water, a solution of 2-pyridinecarboxaldehyde in 10 ml of ethanol was slowly added, and the mixture was stirred for 1 hr at room temperature. For the diaminoguanidine derivatives, the aqueous solution of the dihydrazide was neutralized with potassium hydroxide before the condensation step. The yellow crystalline products were filtered off and recrystallized from ethanol. The yields were about 80%. The microanalytical results were as follows

PMAT (m.p. 200–201°)	C	H	N	S
Calculated for $C_{13}H_{12}N_6S$, %	54.9	4.2	29.5	11.3
Found, %	54.6	4.4	29.3	11.4
PMAG (m.p. 208–209°)				
Calculated for $C_{13}H_{13}N_7$, %	58.4	4.5	36.7	
Found, %	57.2	4.9	35.6	

The results for PMAG were not very satisfactory.

Other reagents. Salts and solvents of analytical-reagent grade purity or better were used throughout. All metal ion solutions were standardized.

Procedures

Determination of acid-dissociation constants. A 1-ml aliquot of a solution of PMAT or PMAG ($5 \times 10^{-4}M$) in ethanol was placed in a 25-ml standard flask and the pH was adjusted with buffers which also maintained the ionic strength at 0.1; solutions with extremely high pH were made by the procedure of Schwarzenbach and Sulzberger.[31] The solution was then made up to the mark with distilled water and mixed, and the absorbance measured at a suitable wavelength. Absorbance *vs.* pH curves were plotted for each reagent and the pK_a values were calculated from the inflexion points on graphs of $\Delta A/\Delta$ pH *vs.* pH. The stability of the ethanolic and aqueous reagent solutions at different pH values had previously been checked.

Spectrophotometric study of the reagent–metal ion reactions. The spectra of the chelates were recorded for samples with the reagent in excess (about 100-fold). The general procedure was to mix 15 ml of 0.03% (w/v) ethanolic reagent solution, enough metal ion solution to give a suitable absorbance and 5 ml of buffer solution (pH 4.6) and dilute with water to known volume. The colour was allowed to develop to a maximum (a few minutes). The absorbance remained constant for at least 24 hr.

To determine the effect of pH the absorbance was measured at suitable wavelengths from samples prepared as just described but without the buffer solution, and with their pH adjusted to different values with sodium hydroxide and hydrochloric acid.

RESULTS AND DISCUSSION

Infrared spectra

The infrared spectra of the reagents are complicated because the aromatic portion of the molecules causes numerous bands and their overlap makes detailed assignments difficult. However, the assignments for the spectrum of pyridine are well established,[32,34] and so are those for thiocarbohydrazide;[35] the infrared spectra of some dicarbohydrazones[36] and dithiocarbohydrazones[37] have also been described and discussed and their similarity with those of secondary amides noted.

PMAT. The principal bands and their assignments are given in Table 1. The well-defined band at 3050 cm^{-1} is characteristic of aromatic C–H stretching frequencies. Coupled with this band are the expected aromatic C=C ring vibration frequencies at about 1590, 1500 and 1450 cm^{-1}. The spectrum in the "double-bond" region (1700–1450 cm^{-1}) is further complicated by the presence of the C=N frequency of the pyridine ring and that of the azomethine group at 1610–1600 cm^{-1}, the peak at 1560–1550 cm^{-1} attributed to CNH vibration, and a weak band at 1625 cm^{-1} which may be due to an N–C–N stretching vibration. The band at 3440 cm^{-1} is due to the N–H stretching frequency.

A strong band observed in the 1300–1200 cm^{-1} region is probably due to the C=S stretching frequency. Complications in this region are the bands for the expected ring vibrations and C–H deformation of the pyridine ring at about 1200 cm^{-1}. At lower frequencies in the range 1000–600 cm^{-1}, there are many strong absorptions that can also be attributed to the C–H deformation of the pyridine ring. The presence of two strong bands at 990 and 705 cm^{-1} is indicative of the presence of the pyridine ring. Most of the other bands overlap to such an extent that assignment would be extremely speculative.

PMAG. As expected, the spectrum of PMAG is similar in nature and complexity to that of PMAT (Table 1). The identification of individual bands is again difficult because of the high degree of overlap. The most important difference is the absence of the C=S stretching frequency. The C=N, C=C, CNH and N–C–N bands occur in the 1640–1400 cm^{-1} region and the pyridine C–H deformation bands at 1200–900 cm^{-1}.

Ultraviolet spectra

The spectra of aqueous solutions of both reagents are pH-dependent (Fig. 1). The PMAT spectrum at pH 4.0–9.3 is attributed to the uncharged species (RH), with $\lambda_{max} = 327$ nm, that at pH 1.8

Table 1. Infrared spectra

Frequency, cm^{-1}		Intensity		
PMAT	PMAG	PMAT	PMAG	Assignment
3440	3440	m	m	N–H stretch
3050	3030	m	m	aromatic C–H stretch
1625–1400	1640–1400	s (multiplet)	s	C=N, C=C, CNH, NCN stretch
1300–1200		s		C=S stretch, pyridine C–H deformations
	1200–900		s (multiplet)	pyridine C–H deformations
900	990	s	s	pyridine deformation
900–600	900–600	s (multiplet)	s (multiplet)	C–H in-plane deformations

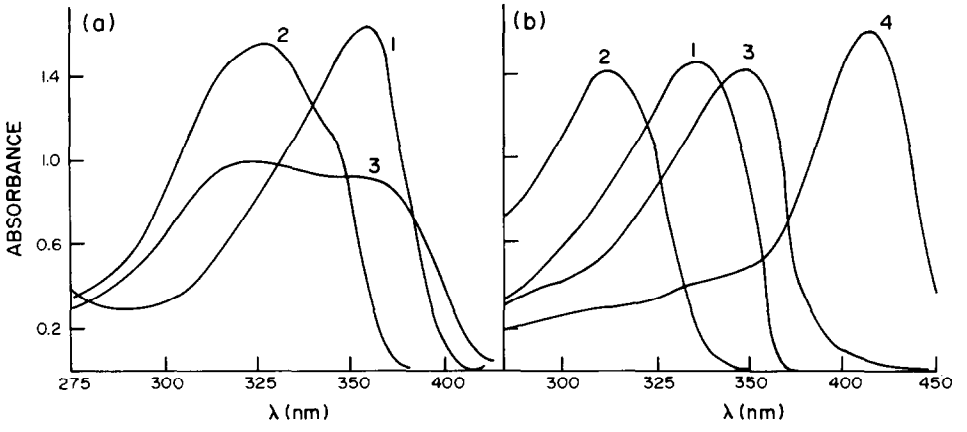

Fig. 1. Absorption spectra of the reagents at different pH values: PMAT, (1) pH 1.80, (2) pH 5.30, (3) pH 10.3. B; PMAG, (1) pH 1.0, (2) pH 4.5, (3) pH 10.6, (4) pH 15.0. $C_R = 4 \times 10^{-5} M$.

($\lambda_{max} = 360$ nm) to the fully protonated species (RH_3^{2+}), and that at pH 10.5 to the anion R^-. The spectral shifts in the pH range 2–4 are more difficult to interpret, because the constants for protonation of the two pyridine nitrogen atoms are too close.

The influence of pH on the spectra of PMAG in aqueous solution is still more marked. As can be seen from Fig. 1, the spectral curves can be ascribed to the four species that can be expected structurally (RH_3^{3+}, RH_2^{2+}, RH^+ and R, with λ_{max} at 335, 310, 348 and 414 nm respectively), therefore this reagent has three protonation constants, with no overlap. The protonation of the second pyridine nitrogen atom occurs at higher pH for PMAG than for PMAT. This behaviour can be explained on the assumption that the basicities of the pyridine nitrogen atoms of PMAG are dissimilarly affected by the weak acid group $>C{=}NH_2^+$ (the imine group of PADAG is present as $>C{=}NH_2^+$ because of its strong basic character).

Reagent equilibria in the absence of metal ions

Graphical analysis of protonation reactions. Buděšínský[38] developed a technique based on computer calculation of the molar absorptivities (ϵ_i) and protonation constants (β_i) of individual protonated species of a reagent (R) from $2(N - i + 1)$ linear equations of the type

$$\sum_i^N (A - C_R \epsilon_i)[H]^i \beta_i = 0$$

which result from the combination of the mass balance and total absorbance equations

$$C_R = [R] \sum_i^N [H]^i \beta_i;$$

$$A = [R] \sum_i^N \epsilon_i [H]^i \beta_i;$$

$$0 \leqslant i \leqslant N \quad \text{and} \quad \beta_0 = 1.$$

However, a much simpler but quite satisfactory procedure[38] was used in the present work. When only the fully protonated or deprotonated form is present in extremely acidic or alkaline medium respectively, the molar absorptivities of these forms may easily be calculated from $\epsilon_0 = A_0/C_R$ and $\epsilon_N = A_N/C_R$ where C_R is the total concentration of the ligand and A_0 or A_N is the measured absorbance. At any range of acidity between both extremes, provided only two forms co-exist in significant amounts, the absorbance will be the sum of the individual absorbances, and the protonation constant $K_n = [H_nR]/[H][H_{n-1}R]$ may be calculated from the condition that log K_n will be equal to the pH at which $[H_nR] = [H_{n-1}R]$ and hence at which $A_n/\epsilon_n = A_{n-1}/\epsilon_{n-1}$. It follows that at pH = log K_n the absorbance (which will be called $A_{1/2}$) is given by $A_{1/2} = (\epsilon_n + \epsilon_{n-1})C_R/2$. The values of ϵ_n and ϵ_{n-1} for the wavelength of measurement must be obtained by measurements at pH values at which virtually only the form of interest exists.

The use of this method requires fulfilment of two conditions:

(*i*) the appearance of an isosbestic point in a set of spectral curves for different acidities;

(*ii*) the presence of only the complexes H_nR and $H_{n-1}R$ as main species in solution in the acidity range concerned.

It is then necessary to analyse graphically the absorbance *vs.* pH graph to find whether only one proton participates in the acid–base equilibrium reaction. The method involves the graphical transformation of the absorbance–pH plot into the incremental form [$(A-A_{n-a})$ *vs.* pH] and substitution of the slope of this graph into the equation

$$\Delta A/\Delta \text{pH} = -0.575a(A_n - A_{n-a})$$

where the value of a indicates the number of protons interchanged; hence the simplified method can be used only when $a = 1$.

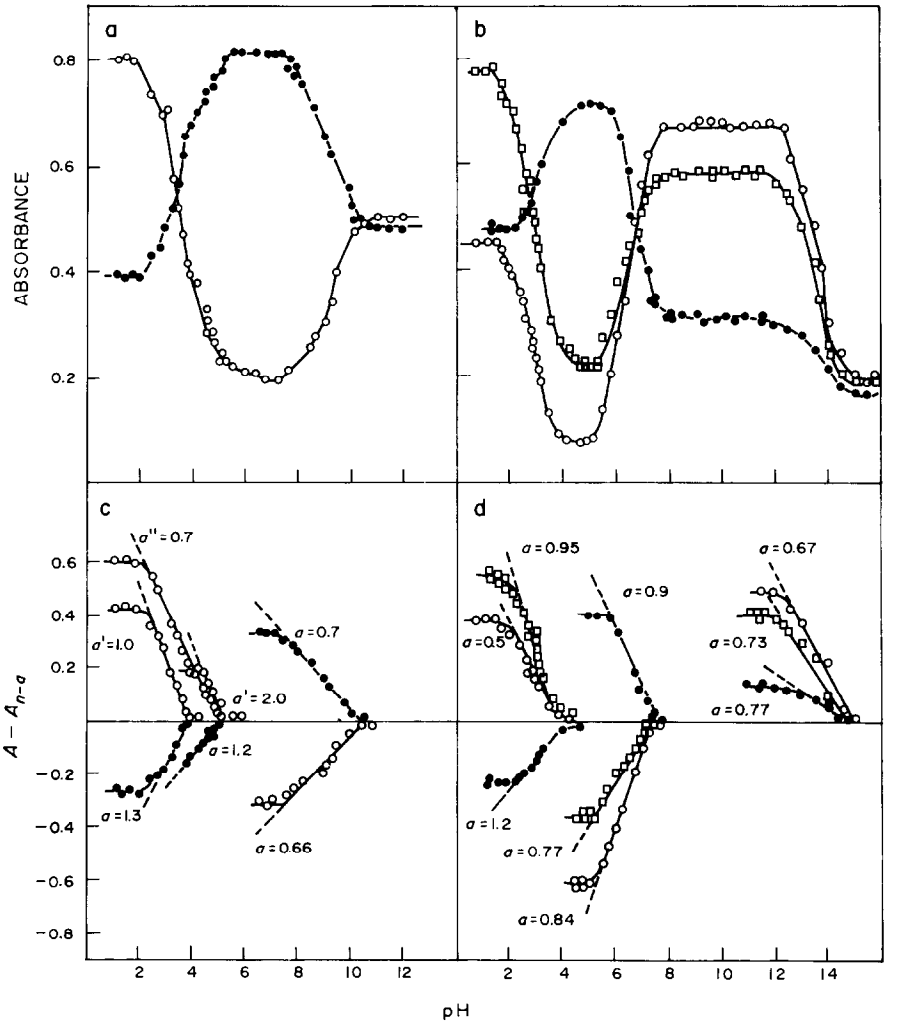

Fig. 2. Effect of pH on the absorbance of the reagents. a and b: absorbance–pH plots for PMAT and PMAG. c and d: $(A_n - A_{n-a})$ pH graphs for PMAT and PMAG. a and c: ● 325 nm, ○ 360 nm; b and d: ● 310 nm, □ 335 nm, ○ 350 nm. $C_R = 4 \times 10^{-5} M$.

The shape of several *A vs.* pH curves at different wavelengths for PMAT and PMAG can be seen from Figs. 2a and 2b, respectively, and of the incremental forms from Figs. 2c and 2d.

The *A vs.* pH graphs for PMAT are plotted for measurements at 360 and 325 nm, and in both cases exhibit a break-point in acid medium and another in alkaline medium; in the acid region there is apparently an inflexion point which divides the steep part of the graph (especially for the 325-nm plot) into two sections with different slopes (Fig. 2a). This could be explained as due to consecutive deprotonation of the two pyridinium nitrogen atoms, as can be seen in Fig. 2c, since the values for *a* calculated from the $(A - A_{n-a})$ *vs.* pH plot, for 325 nm, before and after the inflexion point, are close to 1. The change in the slope in the 360-nm plot is less marked and the results from the incremental plot disagree with what can be assumed from the structure of the reagent, since the *a* values (represented in Fig. 2c as *a'*) are 1 and 2 for the sections of curve either side of the inflexion point, which is not possible because only two protons are involved in the equilibrium, and if the inflexion point is treated as an artefact, a single *a* value ($a'' \sim 1$) is obtained. Therefore the measurements at 325 nm seem to give more reliable results. This wavelength was therefore used for determination of the protonation constants of the reagent; the log K_n values obtained are rather close, however (log $K_3 = 3.2$, log $K_2 = 4.5$), and consequently only approximate.

For PMAG, hydrogen-bonding is suggested as the reason for the greater difference between the protonation constants for the pyridine nitrogen atoms, and the absorbance–pH plots (Fig. 2b) show three well-discernible breaks (for measurements at 310, 335 and 350 nm), each corresponding to a deprotonation step, without the overlap exhibited for PMAT. This

Table 2. Stepwise stability constants of hydrogen complexes

	$\log K_n = \log [H_nR]/[H]^a [H_{n-a}R]$			
Reagent	$n=1$ $a=1$	$n=2$ $a=1$	$n=3$ $a=1$	$n=3$ $a=2$
PMAT	9.1	—	—	3.6
PMAG	13.6	6.4	2.8	—

Table 3. Isosbestic points in absorption spectra of reagents

Reagent	Species	pH	λ_{isos}, *nm*
PMAT	R^-, HR	10.0–7.0	348
	HR, H_3R^{2+}	5.0–2.0	340
PMAG	R, HR^+	15.0–12.0	370
	HR^+, H_2R^{2+}	8.0–5.0	326
	H_2R^{2+}, H_3R^{3+}	4.5–1.5	322

Table 4. Maximum molar absorptivities of individual protonated species*

	$\epsilon \times 10^{-4}$, $l.mole^{-1}.cm^{-1}$ for λ_{max} (*nm*)			
Reagent	R	HR	H_2R	H_3R
PMAT	2.25 (356)	3.85 (327)	—	3.90 (360)
PMAG	4.00 (414)	3.50 (348)	3.55 (310)	3.60 (335)

*Charges are omitted.

is in accordance with the results in Fig. 2d in which the consecutive values for a are all close to 1.

The calculated protonation constants are collected in Table 2. Table 3 shows the wavelengths of the isosbestic points, and the corresponding pairs of complexes present in the solution. Table 4 shows the maximum molar absorptivity of individual complex species.

COMPLEX FORMATION EQUILIBRIA

Study of the spectra

Comparison of the absorption spectra of (2-pyridinecarboxaldehyde)thiosemicarbazone (PAT) metal complexes[26] with those of the PMAT complexes, and again those of the (2-pyridine carboxaldehyde)aminoguanidine (PAG) complexes with those of the PMAG complexes supplies the data needed to deduce the differences in reactivity with metal-ions, caused by the additional

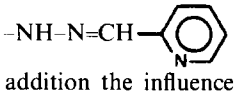

grouping. In addition the influence of sulphur and nitrogen (in the >C=S and >C=NH_2^+ groupings, respectively) as co-ordinating atoms may be established.

In Table 5 we summarize the results obtained in acetate-buffered medium. Several broad conclusions may be drawn. PMAT and PMAG are better photometric reagents than PAT and PAG since the absorption bands are shifted to longer wavelengths and the molar absorptivities are generally increased. In addition the PMAG–metal complexes are formed in more acidic medium. PMAT is more reactive than PMAG and gives greater sensitivities; on the other hand, the absorption band shift is greater for the PMAG complexes, which can increase the selectivity.

Influence of pH

The absorbance of various reagent–metal ion systems as a function of pH is shown in Figs. 3 and 4, for PMAT and PMAG respectively. Such diagrams allow the utility of a ligand to be rapidly discerned.

For PMAT, the pH–absorbance curves have been plotted at the wavelength of maximum absorption and at a somewhat longer wavelength (420 nm) to

Table 5. Photometric characteristics of the complexes in solution

	PMAT		PAT*		PMAG		PAG†	
Cation	λ_{max}, *nm*	ϵ_{max}§	λ_{max}, *nm*	ϵ_{max}§	λ_{max}, *nm*	ϵ_{max}§	λ_{max}, *nm*	ϵ_{max}§
Cu(II)	400	16.5	360	22.0	430	15.2	380	13.0 (NaOH)
Co(II)	395	58.8	410	7.4	450	37.5		
Ni(II)	410	21.1	385	19.0	435	16.4	390	9.9 (NH_3/NH_4^+)
Fe(III)	405	107.7	360	14.0	450	45.7	375	16.6 (NaOH)
Fe(II)	384	34.4						
	550–570 sh	3.3	360	16.8	420	31.3	380	11.8
	620	4.5	610	5.8	570	13.6		
Zn(II)	394	11.2	‡					
Cd(II)	400	34.6	‡		405	28.7		
Hg(II)	396	57.7	‡					
Hg(I)	390	18.4	‡					
Pd(II)	392	23.4	‡		414	7.2		
					480	5.9	440	3.4 (HAC/Ac^-)
Bi(III)	400	12.6	‡					
In(III)	410	37.2						

*See reference 26.
†See reference 39,
§10^3 $l.mol^{-1}.cm^{-1}$.
‡Colour reaction, but molar absorptivity not reported in reference 26.

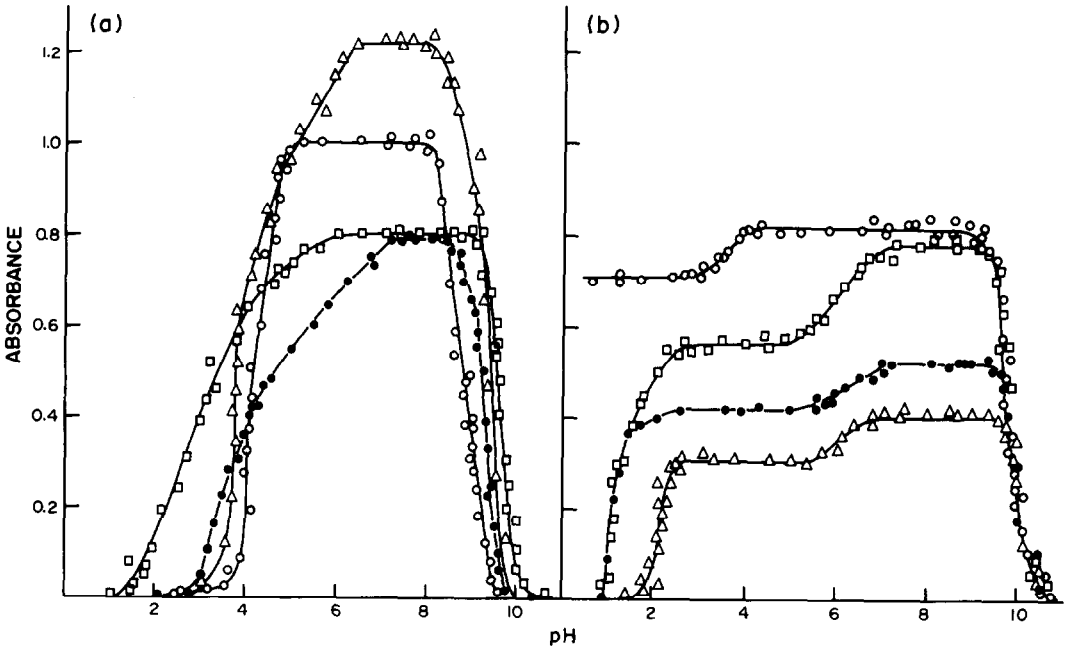

Fig. 3. Complex-absorbance *vs.* pH plots for PMAT. (a): ○, Co(II) (395 nm); ●, Cu(II) (400 nm); □, Ni(II) (410 nm); △, Zn(II) (430 nm). $C_M = 2$ ppm Cu(II), Ni(II) and Zn(II); 1 ppm Co(II).

avoid the reagent background. All four metals studied show similarities in their pH–absorbance curves: at the shorter wavelengths the reagent also absorbs. The absorbance is independent of pH only when the reagent is in the neutral form and its absorption maximum is shifted hypsochromically (see Fig. 1). The plots for 420 nm show two pH-independent zones which can be due to either uncharged (RH) or singly-protonated species participating in the complexation reaction. The cobalt reaction produces a spectrum different from the others, with the absorbance constant at pH lower than 1.0, whereas the other curves show a sharp break in this region.

The graphs for the PMAG complexes differ from those of the PMAT compounds, Fig. 4, and the measurements are made at about the wavelength of

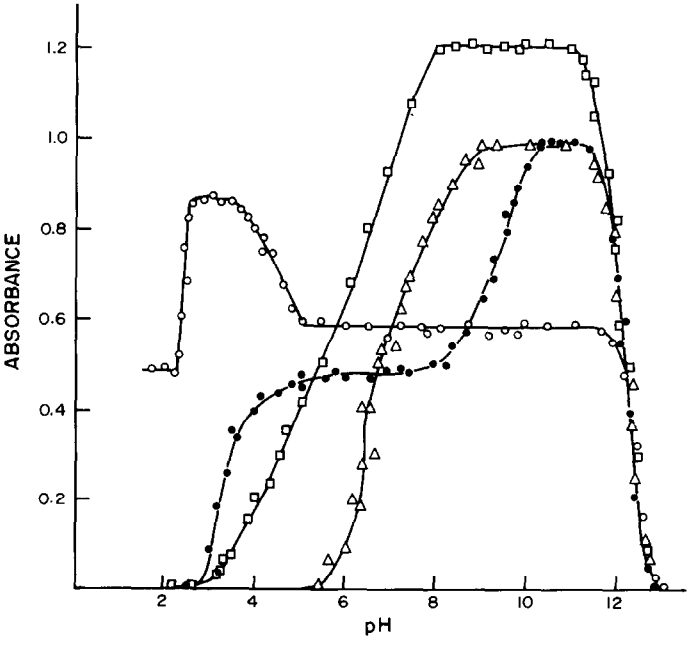

Fig. 4. Complex-absorbance *vs.* pH plots for PMAG. ○ Co(II) (450 nm, 1 ppm); ● Cu(II) (430 nm, 3 ppm); □ Ni(II) (435 nm, 2 ppm); △ Cd(II) (405 nm, 3 ppm).

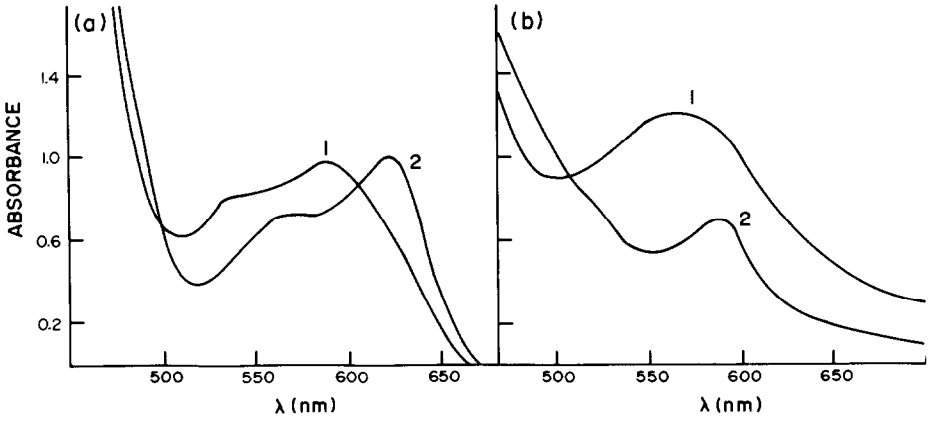

Fig. 5. Absorption spectra of the iron(II) complexes at different pH values. (a) Fe(II)–PMAT: 1, pH 2.7; 2, pH 8.4. (b) Fe(II)–PMAG: 1, pH 5.4; 2, pH 9.2. $C_{Fe} = 5$ ppm.

maximum absorption. Nickel and cadmium behave differently from copper and cobalt. The first two show constant and maximal absorbance at pH 8–11 where PMAG is in the singly-protonated form (RH^+); therefore the formation of RH^+–metal complexes can be postulated to explain the pH-dependence of the absorbance of these systems.

The plot for the Cu(II)–PMAG system has two plateaus but the molar ratio of the components remains the same (Cu:L = 1:2), so the two pH-independent zones are presumably due to participation of two differently protonated forms of the reagent. The Co(II)–PMAG plot also exhibits two plateaus, but these are associated with two different molar ratios of the complex, corresponding to CoL_2 at low pH and to CoL at high.

The pH-dependence of the iron(II) systems (Fig. 5) deserves separate consideration. First, Fe(II)–PMAT forms a green complex in acetate buffer and at higher pH values, and a red complex in more acidic medium. Both types of solution show another absorption maximum (at 385 and 410 nm respectively) due to the presence of a yellow complex of different molar ratio (see following section). The Fe(II)–PMAG system forms only one complex, at about pH 4 (Fig. 5b) with λ_{max} at 570 and 420 nm, and its spectrum shifts bathochromically and hypochromically at higher pH values, to give λ_{max} 590 and 450 nm, and is destroyed in more acid medium. To keep the iron in the bivalent state it is necessary to add ascorbic acid.

The pH–absorbance plots for Fe(II), Fig. 6, support the conclusions reached concerning the number of complexes formed. The resemblance in shape of the 590 and 560 nm curves for PMAT and the 570 and 590 nm curves for PMAG, confirms the analogous nature of the complexes formed at ~pH 4, which we call the red complex. However, the 620-nm curve for PMAT has a different shape, indicating a change in the nature of the species (the green complex). Absorbance–pH curves for PMAT and PMAG are included in Fig. 6 for reference, and suggest that the red complex is formed when one of the pyridine

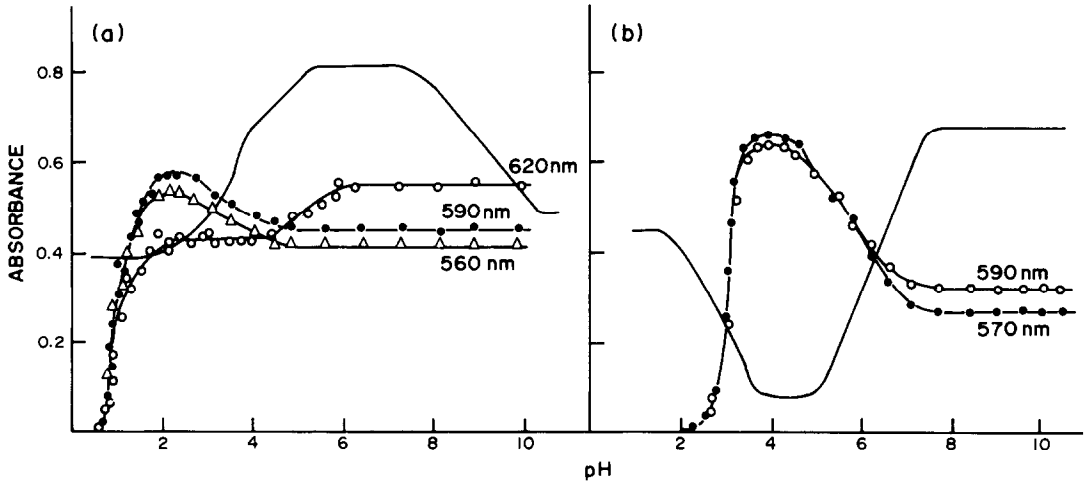

Fig. 6. Absorbance–pH plots for iron(II) complexes. (a) PMAT; (b) PMAG. Solid lines are absorbance–pH plots for the reagents alone: (a) $\lambda = 325$ nm, (b) $\lambda = 350$ nm.

nitrogen atoms is unprotonated, so the first narrow pH-independent region for Fe(II)–PMAT occurs at pH 2–3, *i.e.*, when the reagent molecule loses the first proton; the same applies to Fe(II)–PMAG at pH 3–4.5. The green complex is apparently formed by the reagent species which has both pyridine nitrogen atoms unprotonated (Fig. 6a).

Nature of the complexes

Published results[26,27,39–41] on the composition of the transition metal complexes of pyridine thiosemicarbazones show that mononuclear ML_2 complexes are generally formed. Ablov and Belichuk,[41] however, assert that 2-pyridylmethylene thiosemicarbazone acts as a terdentate ligand forming octahedral complexes with transition metal ions as shown in the structure.

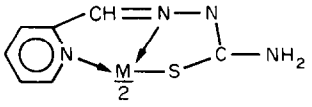

Other studies of the metal complexes of thiocarbohydrazide[11,13,16,17] and its derivatives, especially mono- and bis-(salicylmethylene)hydrazone[22–25] and nicotinoyl and benzoylhydrazide[18–20] present data which enable the ligand atoms or groupings to be identified.

Thiocarbohydrazide forms 5-membered chelate rings with a sulphur atom and a nitrogen atom as donors, forming ML_2 complexes with Cu(II), Cd(II), Co(II), Ni(II) and Zn(II):

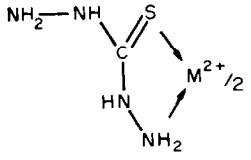

However, the behaviour of substituted thiocarbohydrazides is variable, depending on whether unsymmetric or symmetric derivatives are considered; the first can act (*i*) as unidentate *S*-donor ligands,[18,21] forming complexes of the type $[M^{n+}R_2Cl_n]$, where M = Ni(II) or Cu(I); (*ii*) bidentate ligands in which co-ordination occurs through the sulphur atom and the terminal nitrogen atom to give

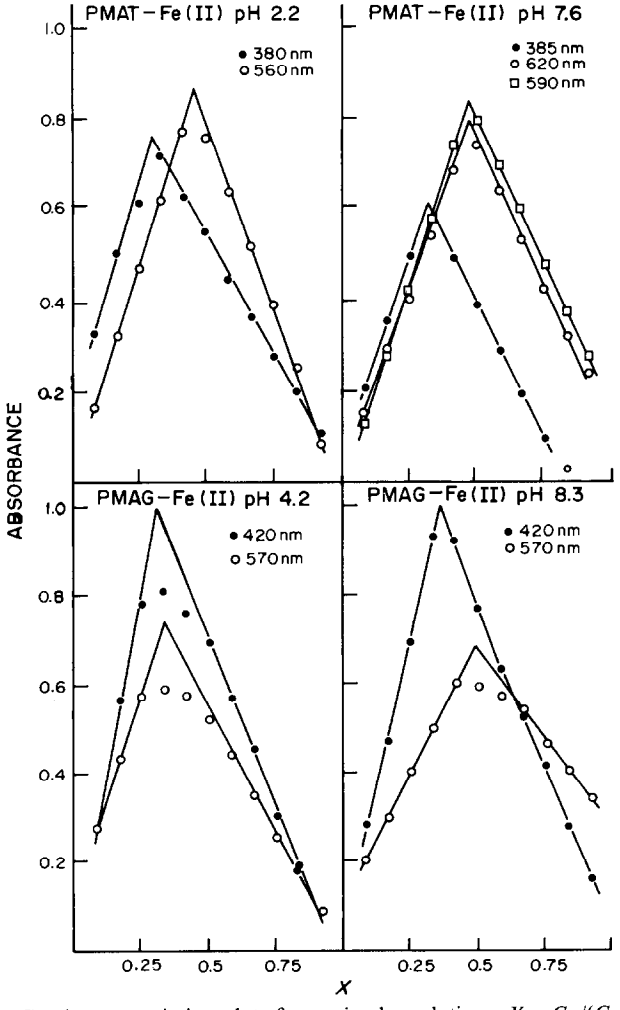

Fig. 7. Continuous-variation plots for equimolar solutions. $X = C_M/(C_M + C_R)$.

$[NiRCl_2]\cdot 4H_2O$,[18] or $[M^{n+}(HR)_2Cl_n]$ where M = Co(II),[20] Ni(II),[19] Cu(I);[21] (*iii*) as terdentate ligands when the side-chain has an additional co-ordinating site, such as the phenolic oxygen atom in 1-salicyloyl-4-phenylthiocarbohydrazide.[25] The symmetrical derivatives, such as bis-(salicylmethylene)-thiocarbohydrazone,[22,23] form 1:1 complexes with quadridentate co-ordination through the two oxygen atoms and two azomethine nitrogen atoms.

Job's method was used for determining the molar ratio of the complexes under study. For the PMAT complexes, the wavelength and pH used for the measurements were chosen on the basis of the following considerations: (*a*) the unsymmetrical shape of the absorption spectra of the complexes, especially for cobalt(II), suggests that another complex besides the main one is present in the solution and causes an additional absorption on the right-hand side of the bands; (*b*) the two absorbance plateaus on the absorbance–pH plots for certain wavelengths. For these reasons, we applied the continuous-variations method at pH 4.5 and 7.6, and at two wavelengths. The measurements at λ_{max} for the cobalt(II) and nickel complexes indicated a 1:2 molar ratio (cation:reagent); measurements at 450 nm indicated existence of a 1:1 complex. Zinc also exhibits 1:2 stoichiometry but there is also evidence of a 2:1 complex. For copper(II) a 1:1 molar ratio was found, with evidence for both a 1:2 and a 2:1 (metal:ligand) complex.

For the PMAG systems measurements were made at λ_{max} and two pH values, 2.5 and 10.3. Nickel, copper(II) and cadmium all gave 1:2 complexes but cobalt(II) formed a 1:1 complex at pH 10.3 and a 1:2 complex at pH 2.5.

The equilibria of iron(II) with PMAT and PMAG are considered separately for the reasons given above. For the Fe(II)–PMAT system Job's method was applied at pH 7.6 and 2.2 and the measurements were made at 385 nm (yellow complex), 560 and 590 nm (red complex), and 620 nm (green complex). The results collected in Fig. 7 indicate a 1:2 stoichiometry for the yellow complex and a 1:1 for the red and green complexes. Fe(II)–PMAG was studied at pH 8.3 and 4.2, and 420 and 570 nm; Fig. 7 shows that the yellow complex (at 420 nm) has the same 1:2 molar ratio at both pH values but for the red complex (570 nm) the stoichiometry changes from 1:1 at pH 8.3 to 1:2 at pH 4.2.

On the basis of the results of the various studies the following structures seem probable for the PMAT complexes.

Molar ratio 1:2
Co^{2+}, Ni^{2+}, Zn^{2+}

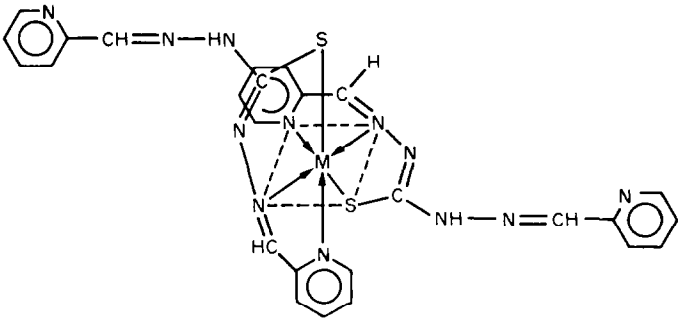

Molar ratio 1:1
(octahedral configuration) Co^{2+}, Ni^{2+}

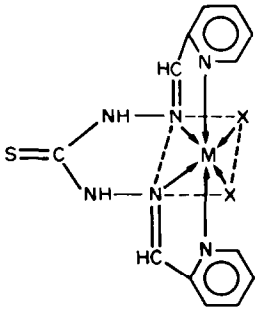

Molar ratio 1:1
(tetrahedral configuration) Cu^{2+}

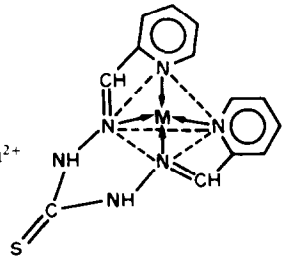

We present no data to support these structures, and they can only be considered as a hypothesis. The structures take into account only the co-ordination sites of the ligands and previously reported configurations of the complexes. The protonation status of some of the co-ordinating atoms has been considered. Structures for the PMAG complexes are not been proposed because no corresponding literature data have been found.

REFERENCES

1. N. P. Bun-Hoi, T. B. Loc and N. D. Xuong, *Bull. Soc. Chim. France*, 1955, 694.
2. C. Duval and N. D. Xuong, *Mikrochim. Acta*, 1956, 747.
3. C. Duval and T. B. Loc, *ibid.*, 1956, 458.
4. *Idem, Compt. Rend.*, 1955, **240,** 1097.
5. E. Campi, G. Ostacoli, A. Vanni and E. Casorati, *Ric. Sci., Rend. Sez. A*, 1964, **6,** 341; *Chem. Abstr.*, 1965, **62,** 15490.
6. B. Steiger, *Mikrochemie*, 1934, **16,** 193.
7. D. Williams and F. M. Nakhla, *Bull. Inst. Mining. Met.* 1951, No. 533, 257; *Chem. Abstr.*, 1951, **45,** 6956 *g*.
8. M. J. M. Campbell and R. Grzeskwiak, *Inorg. Nucl. Chem. Lett.*, 1976, **12,** 545.
9. G. Martini and E. Tiezzi, *Z. Naturforsch.*, 1973, **28B,** 300; *Chem. Abstr.*, 1974, **80,** 89284t.
10. G. Martini, N. Niccolai and E. Tiezzi, *J. Phys. Chem.*, 1975, **79,** 1721.
11. F. Bigoli, A. Braebanti, A. M. M. Lanfredi, A. Tiripicchio and M. Tiripicchio Camellini, *Inorg. Chim. Acta*, 1971, **5,** 392.
12. F. Bigoli, E. Leporati and M. A. Pellinghelli, *Cryst. Struct. Commun.* 1976, 5; *Chem. Abstr.*, 1976, **85,** 115101f.
13. Z. A. Savel'eva, S. V. Larionov, A. V. Nikolaev, L. I. Nasonova and G. N. Dolenko, *Ser. Khim. Nauk*, 1977, No. 4, 73.
14. K. Dwarakanath, D. N. Sathganarayana and K. Volka, *Bull. Soc. Chim. Belg.*, 1978, **87,** 677; *Chem. Abstr.*, 1979, **90,** 78670w.
15. Z. A. Savel'eva, S. V. Larionov, A. V. Kolaev, T. F. Kolomiets and A. A. Shklyaev, *Izv. Sib. Otd. Akad. Nauk. SSSR. Ser. Khim. Nauk*, 1973, **5,** 69; *Chem. Abstr.*, 1973, **79,** 152376w.
16. F. Bigoli, M. A. Pellinghelli, A. Tiripicchio and M. Tiripicchio Camellini, *Acta Crystallog.*, 1975, B31; *Chem. Abstr.*, 1975, **82,** 66702e.
17. B. Singh and K. P. Thakur, *J. Inorg. Nucl. Chem.*, 1974, **36,** 1735.
18. K. N. Dutt and N. C. Chakder, *ibid.*, 1970, **32,** 2303.
19. *Idem, Inorg. Chim. Acta*, 1971, **5,** 188.
20. *Idem, J. Inorg. Nucl. Chem.*, 1971, **33,** 393.
21. *Idem, Inorg. Chim. Acta*, 1971, **5,** 536.
22. R. Singh, J. P. Srivastava and L. K. Mishra, *Indian J. Chem.*, 1977, **15A,** 805; *Chem. Abstr.*, 1978, **88,** 98458v.
23. N. V. Gerbeleu and K. M. Indrichan, *Koord. Khim.*, 1977, **3,** 1527; *Chem. Abstr.* 1978, **88,** 15268j.
24. G. C. Macarovici and S. Barbu, *Rev. Roum. Chim.*, 1978, **23,** 1035; *Chem. Abstr.*, 1978, **89,** 208329j.
25. A. K. Srivastava, V. B. Rana and M. Mohan, *J. Inorg. Nucl. Chem.*, 1974, **36,** 2118.
26. J. M. Cano Pavon, *Ph.D. Thesis*, 1971.
27. M. P. M. Martínez, D. Pérez Bendito and F. Pino, *Anales Real Soc. Españ. Fis. Quim.*, 1960, **69,** 747.
28. J. L. Gómez Ariza, *Ph.D. Thesis*, 1976.
29. M. T. Martínez Aguilar, *Ph.D. Thesis*, 1977.
30. M. González Balairón, *Ph.D. Thesis*, 1978.
31. G. Schwarzenbach and R. Sulzberger, *Helv. Chim. Acta*, 1944, **27,** 348.
32. C. H. Kline and J. Turkevich, *J. Chem. Phys.*, 1944, **12,** 300.
33. L. Corssin, B. J. Fax and R. C. Lord, *ibid.*, 1953, **21,** 1170.
34. J. K. Wimshurst and H. J. Bernstein, *Can. J. Chem.*, 1957, **35,** 1185.
35. F. Kurzer and M. Wilkinson, *Chem. Rev.*, 1970, **70,** 111.
36. D. M. Wiles and T. Suprunchuck, *Can. J. Chem.*, 1968, **46,** 701.
37. S. Barba and C. G. Macarovici, *Rev. Roum. Chim.*, 1978, **23,** 1243.
38. B. Buděšínský, *Talanta*, 1969, **16,** 1277.
39. D. J. Leggett and W. A. E. McBryde, *ibid.*, 1974, **21,** 1005.
40. *Idem, ibid.*, 1975, **22,** 781.
41. A. V. Ablov and N. I. Belichuk, *Zh. Neorgan. Khim.*, 1969, **14,** 179.

Talanta, Vol. 30, No. 8, pp. 565–570, 1983
Printed in Great Britain.

0039-9140/83 $3.00+0.00

COMPLEXES OF OXOVANADIUM(IV) WITH POLYAMINOCARBOXYLIC ACIDS

JUDITH FELCMAN
Departamento de Química da Pontifícia Universidade Católica do Rio de Janeiro, Brasil

and

J. J. R. FRAÚSTO DA SILVA
Centro de Química Estrutural, Instituto Superior Técnico, Lisboa, Portugal

(*Received* 27 *October* 1982. *Accepted* 24 *February* 1983)

Summary—The stability constants for a series of oxovanadium(IV) complexes of polyaminocarboxylic acids were determined by potentiometry. The values obtained are almost equal to those of the corresponding nickel(II) complexes. The complexes formed by terdentate and quadridentate ligands contain 2 and 1 co-ordinated water molecules, respectively. These dissociate at pH ~4 in the first case, to give dimers—$(VO)_2(OH)_2L_2$—and at about pH ~7, in the second case, to give the mononuclear hydroxo species VO(OH)L. Hydrolysis of the 1:1 aquo-complexes is preferred to the formation of 2:1 ligand: metal complexes even in the presence of a 10-fold molar excess of ligand. These results are of interest for better understanding of the behaviour of oxovanadium(IV) in biological systems.

Vanadium is nowadays recognized as an essential element, at least for the development of certain laboratory animals; a deficiency of it leads to reduction of growth, impairment of reproductive capability, altered blood-cell and blood-lipid levels, impairment of hard-tissue metabolism and other anomalies.[1]

The biological basis for the occurrence of these effects is still unknown, but it was found recently that vanadium is involved in certain enzymatic reactions, notably those of the ATPase, and the interest in the study of the role of this element received a new impetus.[2]

Before this discovery, unusually high concentrations of vanadium had been found in the blood of certain tunicates, such as the ascidean *Phallusia mamillata* (about 8 mg of vanadium in a 40-g adult animal),[3] and in the toadstool *Amanita muscaria* (120 ppm dry weight).[4] In the first case, vanadium appears to be present as V(III) or V(III) + V(IV) bound to water, and it is located in a special type of blood cells called vanadocytes, in sulphuric acid medium (1.8*M*). Neither the biological function of the vanadocytes nor the role of the vanadium has been unambiguously established.[5]

In the case of the toadstool, it was reported that vanadium is distributed all over the plant in the form of an ML_2 complex of VO^{2+} with *N*-hydroxyiminodi-α-propionic acid ("amavadin") where the ligand is bidentate.[6] The biological function of this complex and the reason why the ligand is selective for vanadium are unknown.

The elucidation of these problems requires better knowledge of the complex equilibria of vanadium in aqueous solution, a field which has been rather neglected and for which very few reliable data exist. This is particularly true in the case of the complexes formed by the amino-acids and by the polyaminocarboxylic acids, although these are relevant for the understanding of the possible interaction of vanadium with likely biological ligands.

Since the oxovanadium(IV) ion VO^{2+} seems to be directly or indirectly involved in all the cases referred to above, it seemed of interest to undertake the study of the formation of some of its complexes. In the present work we report the results obtained with a series of polyaminocarboxylic acids differing in number of donor atoms and in geometry of chelation. They are represented by the general formulae **I–III**, explained by Table 1.

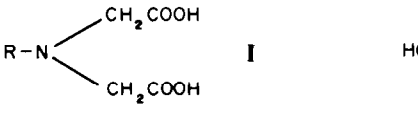

I

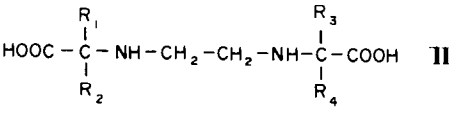

II

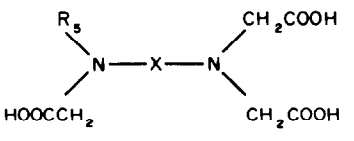

III

Table 1. Ligands used

Type	Substituents	Name	Abbreviations
I	$R = -H$	Iminodiacetic acid	IDA
	$R = -CH_3$	Methyliminodiacetic acid	MIDA
	$R = -NH_2$	Hydrazine-*N,N'*-diacetic acid	HDA
	$R = -CH_2CH_2OH$	Hydroxyethyliminodiacetic acid	HEIDA
	$R = -CH_2COOH$	Nitrilotriacetic acid	NTA
	$R = -CH(CH_3)COOH$	2-Methylaceticiminodiacetic acid	MNTA
	$R = -CH_2C_5H_5N$	Pyridine 2-methyliminodiacetic acid	PMIDA
	$R = -C_6H_4(COOH)$	*o*-Carboxyphenyliminodiacetic acid	CFIDA
	$R = -C_3H_2N_2O_3$	Uramildiacetic acid	UDA
II	$R_1,R_2,R_3,R_4 = -H$	Ethylenediamine-*N,N'*-diacetic acid	EDDA
	$R_1,R_3 = -CH_3$	Ethylenediamine-*N,N'*-di-α-propionic acid	EDDPA
	$R_1,R_2,R_3,R_4 = -CH_3$	Ethylenediamine-*N,N'*-di-isobutyric acid	EDDIBA
III	$R_5 = -CH_2COOH$ $X = -CH_2-CH_2-$	Ethylenediaminetetra-acetic acid	EDTA
	$R_5 = -CH_2COOH$ $X = -(CH_2)_2-O-(CH_2)_2-O-(CH_2)_2-$	Ethyleneglycol bis(aminoethylether) tetra-acetic acid	EGTA
	$R_5 = -(CH_2)_2-CH_2COOH$ $X = C_6H_{10}$	*Trans*-cyclohexanediaminetetra-acetic acid	DCTA
	$R_5 = -CH_2CH_2OH$ $X = -CH_2-CH_2-$	*N*-hydroxyethylethylenediaminetriacetic acid	HEDTA

Besides being of interest for the understanding of the role of vanadium in biology, the results are also of importance for analytical chemists, who are frequently confronted with the lack of data for vanadyl complexes.

Some of the ligands have been studied before,[7-11] but the conditions used were different and in certain cases the results presented raised doubts since they were obviously at variance with published literature values (*e.g.*, NTA for which pk_3 is too low and log $K_{(VO)L}$ too high) so they were repeated for the sake of consistency.

The set of values established in this work allows the development of a series of general principles concerning the behaviour of VO^{2+} polyaminocarboxylate systems.

EXPERIMENTAL

Reagents

Hydrazine-*N,N'*-diacetic acid (HDA), 2-methylaceticiminodiacetic acid (MNTA), *o*-carboxyphenyliminodiacetic acid (CFIDA), pyridine-2-methyliminodiacetic acid (PMIDA), ethylenediamine-*N,N'*-di-isopropionic acid (EDDPA) and ethylenediamine-*N,N'*-di-isobutyric acid (EDDIBA) were synthesized in our laboratories by condensing the appropriate amines with chloroacetic, α-chloropropionic and α-chloroisobutyric acids, respectively, following standard procedures.

The other ligands were commercial products available from various sources (BDH, K & K and Fluka).

In all cases the products were recrystallized from water/ethanol mixtures until their purity was 99.5% or higher, as determined by titration with standard alkali.

Oxovanadium(IV) sulphate solution. A standard 0.1*M* solution of oxovanadium(IV) sulphate was prepared by dissolving the appropriate amount of $VOSO_4 \cdot 5H_2O$ (BDH) in 1*N* sulphuric acid and determining the content of VO^{2+} by permanganate titration. Contact with the atmosphere was reduced to a minimum. The solution was stable for several months.

Dilutions from this standard were made when necessary, and the excess of acid was determined from titrations (with standard alkali) of 1:1 mixtures of VO^{2+} and EDTA (a well-defined end-point is obtained when EDTA is completely titrated, and the excess of acid is easily calculated), avoiding the more complicated procedure based on ion-exchange.

Carbonate-free potassium hydroxide, $C_B = 0.100$ or 1.00*M*. Prepared directly from Merck "Titrisol" vials, under nitrogen and in recently boiled-out demineralized water. This provided a satisfactory carbonate-free titrant, identical to that prepared by the more laborious procedure of Schwarzenbach and Biedermann.[12]

Potassium nitrate. The ionic strength of the solutions was adjusted to 0.10*M* by adding adequate amounts of a concentrated potassium nitrate solution prepared from an analytical-grade product.

Demineralized water was used throughout the work for preparation of solutions.

Instruments

The pH measurements and titrations were made with a Procyon digital pH-meter, using a combination electrode calibrated at low and high pH with appropriate acid solutions or buffers with ionic strength of approximately 0.1*M*. Values were read to 0.001 pH units and the reproducibility was 0.003 pH units or better.

Technique

The ionization constants of the ligands and the stability constants of the oxovanadium(IV) complexes of the polyaminocarboxylic acids were determined by potentiometric (pH) titrations of mixtures of the ion and the ligands over a range of concentrations (5×10^{-4}–5×10^{-3}*M*). Details of the experimental procedures have been given previously.[13]

The measurements were made in media of ionic strength 0.1*M* maintained with potassium nitrate; the temperature was controlled to $25.0 \pm 0.1°$ by circulating water through the double-walled titration cell. The ionic product of water at 25° in potassium nitrate medium was taken to be the same as in a potassium chloride medium.[14]

Tables of experimental results are not given but will be made available upon request; some experimental titration curves are presented as examples.

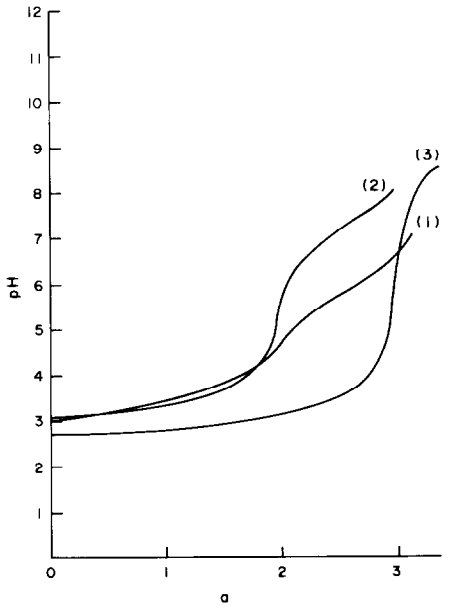

Fig. 1. Titration curves of MIDA (1), EDDA (2) and HEDTA (3) in the presence of VO^{2+}; $T = 25°C$; $I = 0.1M$ (KNO_3); "a" is the number of moles of titrant KOH added per mole of ligand.

CALCULATIONS

The expressions used to calculate the stability constants of the proton and vanadium complexes were derived in the usual manner by considering the mass-balances for the ligand and for the metal and introducing the electroneutrality condition.[13] When hydroxo-complexes are formed (ionization of co-ordinated water in $VO(H_2O)L$ species), Sillén's normalized-curves method[15,16] was employed. A more detailed account of these cases will be presented later.

RESULTS AND DISCUSSION

Typical titration curves of the ligands in the presence of equimolar amounts of VO^{2+} are shown in Fig. 1; for comparison, we have selected a terdentate, a quadridentate and a potentially sexidentate complexing agent (which actually acts as quinquedentate, see below).

The curves show that oxovanadium(IV) forms quite stable complexes with these ligands [it will be shown later that their stability constants are almost equal to those of the corresponding nickel(II) complexes], and that in the cases of the terdentate and quadridentate ligands a further hydrogen ion is titrated, which can only come from hydrolysis of a co-ordinated water molecule, to give a hydroxo-species.

In the case of the quadridentate ligands, the hydrolysis is independent of the concentration of the aquo complex—see Fig. 2—showing that only a mononuclear species is formed. This contrasts with the situation found for the terdentate ligands,[9,10] in which polynuclear hydroxo-complexes are formed by olation, the dimers being predominant in the range of pH studied (Fig. 3). It should be noted that in both cases, at the pH values where hydrolysis occurs, the pH readings are rather unstable and decrease slowly; this is probably due to the competition for OH^- ions to form oxovanadium(IV) hydroxide and its higher polymerization products.

It is not obvious which co-ordination positions are occupied by the ligands and which by the water molecules, since there is, in principle, a choice of equatorial and axial sites and there is also the possibility of formation of square pyramidal structures in which a quadridentate ligand may occupy all the available sites.

The problem has already been studied by NMR relaxation techniques and it was concluded that in the cases examined (which included the NTA and PMIDA complexes), whatever the structure of the $VO(H_2O)L$ complex, the resulting hydroxo-group occupied one of the equatorial positions in an approximately octahedral configuration.[17]

All these observations, and the fact that for the sexidentate ligands no hydrolysis is observed, are consistent with a co-ordination number of 6 for

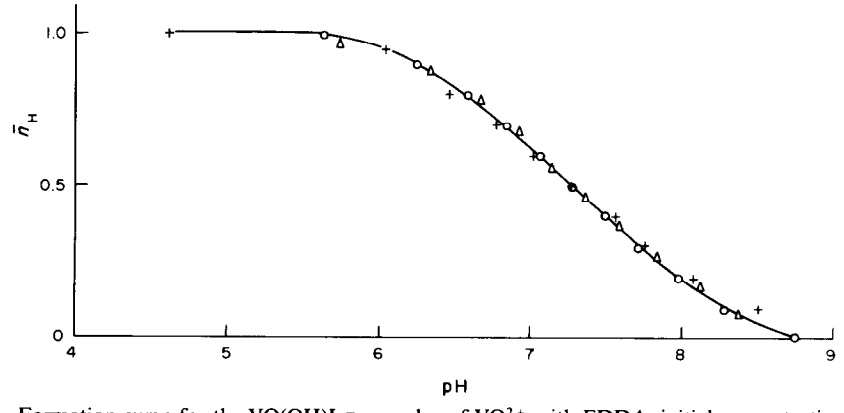

Fig. 2. Formation curve for the $VO(OH)L^-$ complex of VO^{2+} with EDDA; initial concentration of the 1:1 aquo-species $VO(H_2O)L$: △ $2.0\ 8 \times 10^{-3}M$; ○ $1.00 \times 10^{-3}M$; + $5.00 \times 10^{-2}M$.

vanadium(IV), which leaves a total of 5 co-ordination positions available for other ligands in the case of the oxovanadium(IV) cation VO^{2+}.

Hence, for the complexes of the quadridentate ligands, only one co-ordination site remains with a co-ordinated water molecule, whereas for the complexes of terdentate ligands, two water molecules remain co-ordinated. Apparently the co-ordination sphere cannot be expanded, so the complexes of quadridentate ligands hydrolyse to give a mononuclear hydroxo complex—VO(OH)L—but the complexes of terdentate ligands can dimerize to form $(VO)_2(OH)_2L_2$ species with two hydroxide bridges, as in **IV** (*a*) or (*b*)

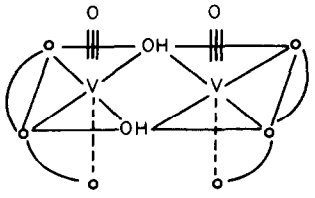

(*a*)

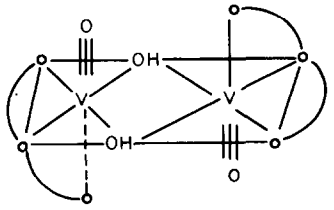

(*b*)

IV

Titrations of solutions containing a considerable excess of ligand over metal (typically 10:1 molar ratio) show that the hydrolysis of the co-ordinated water molecule in the 1:1 complex is still preferred to the formation of 2:1 complexes, which should not have any co-ordinated water molecules unless not fully co-ordinated. This is still more pronounced in the cases of the complexes of simple amino-acids, where the formation of hydroxo-species is predominant even at pH values below 4 (unpublished results obtained by us).

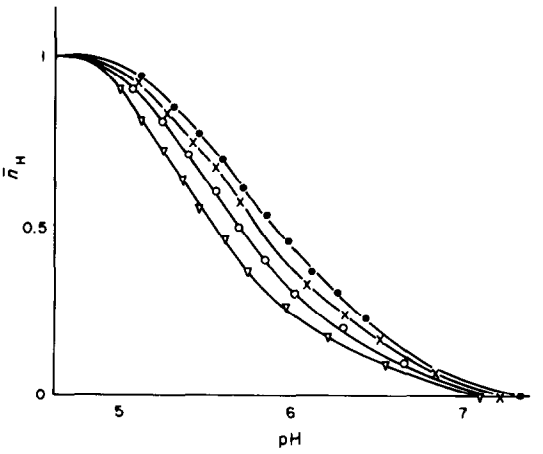

Fig. 3. Formation curve for the $VO(OH)L^-$ complex of VO^{2+} with IDA; initial concentration of the 1:1 aquo-species $VO(H_2O)L$. ● $5 \times 10^{-4}M$; × $1 \times 10^{-3}M$; ○ $2 \times 10^{-3}M$; △ $5 \times 10^{-3}M$.

These facts are relevant in biological terms since it has been proposed that "amavadin"—the VO^{2+} complex of *N*-hydroxyiminodi-α-propionic acid said to be present in the toadstool *Amanita muscaria*—is a 2:1 complex where the ligand behaves as bidentate (like an amino-acid) and the fifth co-ordination position is occupied by one water molecule.[6] This proposal is questionable in view of the observations above and the conditions prevalent in the plant. It is not unlikely that the species isolated has been modified by the process of extraction*. Table 2 summarizes the values of the stability constants of the oxovanadium(IV) complexes of polyaminocarboxylic acids obtained in this work or available in the literature. The values of the acid dissociation constants of the ligands agree well with the literature values and are included in the table for quick reference. The main exception is that of pk_3 and $\log K_{(VO)L}$ for NTA, for which other authors found, at $T = 25°$ and $I = 0.5M$, $pk_3 = 8.58$ and $\log K_{(VO)L} = 7.15$.[11]

As expected, the stability of the complexes increases with the number of co-ordinating groups of the ligand, and for ligands of analogous co-ordinating capability it increases with the basicity of the ligand when steric effects are not operative (which is the case of the EDDIBA complex compared with that of EDDA).

Curiously, when steric effects are absent, the values of the stability constants $\log K_{(VO)L}$ are mostly almost equal to the corresponding values for the nickel(II) complexes [see Table 2 where these were included for comparison together with the corresponding values for the copper(II) and lead(II) complexes] and a

*After this paper was submitted for publication we obtained fairly pure samples of synthetic *N*-hydroxyiminodi-α-propionic acid (the natural ligand of "amavadin"). Preliminary studies show that the *N*-hydroxyl group lowers the basicity of the nitrogen atom of the ligand to such an extent ($pk_2 = 5.6$) that, at biological pH, the concentration of "free ligand" may compete effectively with OH^-, and ML_2 complexes with VO^{2+} can be formed preferentially to the dimers. As will be reported in a future paper, this may be one reason why nature selected such an unusual ligand: to exclude the dimers which would otherwise form. In any case, the values obtained for the stability constants of *N*-hydroxyiminodi-α-propionic acid with the oxovanadium(IV) ion—$\log K_{ML} = 6.8$ and $\log K_{ML_2} = 13.1$—are higher than would be expected for bidentate behaviour of the ligand as suggested by Kneifel and Bayer.[6] Thus the possibility of a co-ordinated water molecule in natural "amavadin" is open to question; it may well be the result of the process of extraction, but no evidence or argument can be presented against the structure proposed.

Table 2. Stability constants for the VO^{2+}, Ni^{2+}, Cu^{2+} and Pb^{2+} complexes of several polyaminocarboxylic acids

Type	Ligand Abbreviation	Acid dissociation constants				Oxovanadium(IV) complexes			Other complexes		
		pk_1	pk_2	pk_3	pk_4	$\log K_{(VO)L}$	$-\log K^{H}_{(VO)L}$		$\log K_{NiL}$	$\log K_{CuL}$	$\log K_{PbL}$
I	IDA	2.63 ± 0.01	9.32 ± 0.01	—	—	8.98 ± 0.03	(9.30)[a]	5.8 ± 0.1	8.13	10.57	7.41
	MIDA	2.10 ± 0.02	9.55 ± 0.03	—	—	9.56 ± 0.03	(9.44)[b]	5.8 ± 0.1	8.67	11.04	7.97
	HDA	2.87 ± 0.02	7.25 ± 0.01	—	—	7.61 ± 0.02	—	5.2 ± 0.1	7.19	8.1	—
	HEIDA	2.37 ± 0.02	8.80 ± 0.02	—	—	9.60 ± 0.01	(9.26)[b]	5.3 ± 0.1	(5.11)[b]	9.33	11.72	9.45
	NTA	2.17 ± 0.02	2.30 ± 0.02	9.66 ± 0.02 (8.98)[b]	—	11.47 ± 0.02	(12.30)[b]	7.06 ± 0.03	(7.15)[b]	11.50	12.94	11.34
	MNTA	2.58 ± 0.02	9.85 ± 0.02	—	—	11.77 ± 0.01	—	7.30 ± 0.01	—	11.21 ± 0.01	—	—
	PMIDA	2.82 ± 0.02	8.23 ± 0.03	—	—	11.30 ± 0.03	—	6.61 ± 0.03	(6.45)	11.22	—	10.31[b]
	CFIDA	2.61 ± 0.02	2.97 ± 0.01	7.72 ± 0.02	—	9.49 ± 0.03	—	6.97 ± 0.02		9.48	10.93	—
	UDA	1.7 ± 0.1	2.67 ± 0.02	9.58 ± 0.01	—	>14		7.18 ± 0.01		13.12	14.10	12.73
II	EDDA	6.48 ± 0.01	9.47 ± 0.02	—	—	13.40 ± 0.02	—	7.29 ± 0.01	—	13.65	16.2[a]	—
	EDDPA	6.74 ± 0.01	9.58 ± 0.02	—	—	13.34 ± 0.02	—	7.50 ± 0.02	—	12.2	15.2[b]	10.0[b]
	EDDIBA	7.0 ± 0.01	9.85 ± 0.01	—	—	12.23 ± 0.01	—	7.88 ± 0.02	—	10.79 ± 0.05	—	—
III	EDTA (1)	2.0	2.68	6.11	10.17	18.77		—		18.52	18.70	17.88
	EGTA	2.46	2.82	8.90	9.51	10.48 ± 0.04*		5.58 ± 0.05		9.19*	12.61*	10.28*
	DCTA (1)	2.42	3.59	6.12	12.3	20.1		—		20.20	21.92	20.24
	HEDTA	2.19 ± 0.02	5.36 ± 0.01	9.82 ± 0.02	—	17.12 ± 0.07		—		17.1	17.5	15.5

All values quoted with standard deviations are from the present work; other values were obtained from references 24 and 25, except the following: (*a*) ref. 9; (*b*) ref. 11.
*Log $K_{M(HL)}$

Fig. 4. Correlation between the stability constants of oxovanadium(IV) complexes (log $K_{(VO)L}$) and those of the corresponding nickel(II) complexes 1—HDA; 2—IDA; 3—MIDA; 4—HEIDA, 5—CFIDA; 6—MNTA; 7—PMIDA; 8—NTA; 9—EDDA; 10—HEDTA; 11—EDTA; 12—DCTA.

linear correlation with slope close to unity (0.95) and a small positive intercept (0.7) exists (Fig. 4).

Similar correlations can be obtained between the stability constants (log K_{ML}) of the vanadyl and the copper(II) or lead(II) complexes, but they are not so good. The slopes are close to 1 in both cases but the intercepts are higher for lead and lower for copper complexes, as expected from the values in Table 2. Of all the common metals, nickel gives the best correlations and closest similarity.

This allows prediction of unknown values for oxovanadium(IV) complexes, particularly in cases when the superimposition of hydrolysis equilibria makes it impossible or difficult to determine them experimentally.

For example, the values previously reported[18,19] for the complexes of the amino-acids are likely to be incorrect, because standard potentiometric titration techniques were used to measure the stability constants. The buffer regions of the titration curves used for the calculations correspond to the hydrolysis of co-ordinated water molecules rather than to the displacement of the protons bound to the nitrogen atoms of the ligands, which would occur at higher pH (see comments in reference 20).

A single exception is the oxovanadium(IV)–glycine system, which was studied by spectrophotometry[20] but, even so, not completely (the formation of hydroxo-species was not considered). A recent potentiometric study does consider this possibility, and opens the way to a comprehensive study of these systems.[21]

It is interesting to note that the correlation shown in Fig. 4 also holds for ligands such as EDTA or DCTA, which are potentially sexidentate ligands. Since VO^{2+} cannot accept more than five donor groups, the same must be true for nickel in these cases, as was indeed found in the solid state.[22]

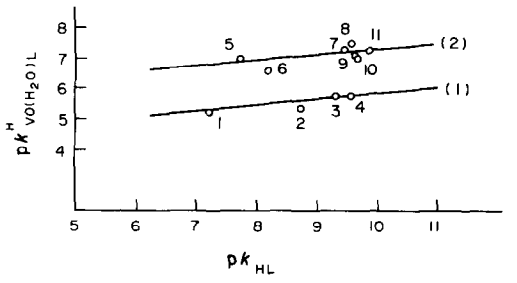

Fig. 5. Correlation of the proton dissociation constants of co-ordinated water molecules and the basicity of (1) the terdentate and (2) the quadridentate complexing agents: 1—HDA; 2—HEIDA; 3—IDA; 4—MIDA, 5—CFIDA; 6—PMIDA; 7—EDDA; 8—EDDPA; 9—UDA; 10—NTA; 11-MNTA.

The values obtained for the dissociation constants of the co-ordinated water molecules—$pk^{H}_{VO(H_2O)L}$ or log β_{11}†—show that this process becomes more difficult the higher the number of co-ordinated groups and the higher the basicity of the ligand [measured by the value of pk_n for the corresponding ligand or pk_{n-1} in the case of protonated complexes $VO(H_2O)HL$, as for the EGTA complex].

Figure 5 illustrates these observations and it can be seen that two straight lines are obtained for correlation of $pk^{H}_{(VO)(H_2O)L}$ with pk_n for each group of complexing agents—terdentate and quadridentate.

It would be expected that the ease of dissociation of a proton from the co-ordinated water would depend on the electron-withdrawing power of the vanadium atom and that this power would be decreased both by the number of negatively charged co-ordinated carboxylate groups and by the degree of donation of electrons by the co-ordinated nitrogen atoms of the ligands. Hence, in the cases of EDDA and NTA the values of $pk^{H}_{(VO)(H_2O)L}$ are almost equal, although the first ligand is co-ordinating through 2 nitrogen atoms and 2 carboxylate groups, and the second through one nitrogen atom and 3 carboxylate groups. However, the effect of basicity is small (Fig. 5) and the value of $pk^{H}_{(VO)(H_2O)L}$ seems to be determined mainly by the total number of co-ordinating groups of the ligand, or, which is really the same thing, by the number (and position) of co-ordinated water molecules in the complexes. Since the location of the co-ordinated water is also relevant, in the cases of EDDA and NTA the donor groups seem to be co-ordinated to the same sites even though their structures, linear and branched, might allow different possibilities.

The case of pyridine-2-methyliminodiacetic acid is anomalous, showing that either the geometry of chelation is not so favourable or that the pyridine nitrogen atom (apparently co-ordinated to the equatorial position[23]) is less effective than the carboxylate group of NTA in decreasing the electron-withdrawing power of vanadium.

Hydroxyliminodiacetic acid and EGTA apparently behave as terdentate towards VO^{2+}; their neutral oxygen atoms are very weak donors and although they seem to be co-ordinated (the values of the stability constants of their respective complexes are higher than for correspondent terdentate ligands), they do not alter significantly the electron-withdrawing power of the vanadyl ion.

A final remark concerns the EDDA, EDDPA and EDDIBA complexes, where the successive introduction of methyl groups in the acetic acid chains of the first ligand increases the basicity of the resulting ligand but not the stability of the corresponding complexes. This is due to steric factors, but the vanadyl ion seems to be less affected than other common transition-metal ions; the reason for this is not at present clear.

†$pk^{H}_{VO(H_2O)L} = \log \beta_{11} = [VO(HO)L][H^+]/[VO(H_2O)L]$.

REFERENCES

1. L. L. Hopkins and H. E. Mohr, *Fed. Proc.*, 1974, **33,** 6.
2. T. J. B. Simons, *Nature*, 1979, **281,** 337.
3. H. J. Bielig, E. Bayer, H. Dell, G. Rohns, H. Mollinger and W. Rüdiger, *Protides of the Biological Fluids*, 1966, **14,** 197.
4. E. Bayer and H. Kneifel, *Z. Naturforsch.*, 1972, **27b,** 207.
5. I. G. Macara, G. C. McLeod and K. Kustin, *Biochem. J.*, 1979, **181,** 457.
6. H. Kneifel and E. Bayer, *Angew. Chem., Intern. Ed.*, 1973, **12,** 508.
7. G. Schwarzenbach and J. Sanders, *Helv. Chim. Acta*, 1953, **36,** 1089.
8. G. Schwarzenbach, R. Gut and G. Anderegg, *ibid.*, 1954, **37,** 937.
9. A. Napoli and L. Pontelli, *Gazz. Chim. Ital.*, 1973, **103,** 1219.
10. A. Napoli, *ibid.*, 1975, **105,** 1073.
11. *Idem, J. Inorg. Nucl. Chem.*, 1977, **39,** 463.
12. G. Schwarzenbach and W. Biedermann, *Helv. Chim. Acta*, 1948, **31,** 331.
13. J. J. R. Fraústo da Silva, *Rev. Port. Quím.*, 1965, **7,** 230.
14. T. Moeller and R. Ferrius, *J. Inorg. Nucl. Chem.*, 1961, **20,** 261.
15. L. G. Sillén, *Acta Chem. Scand.*, 1956, **10,** 803.
16. F. J. C. Rossotti and H. Rossotti, *Determination of Stability Constants*. McGraw-Hill, New York, 1961.
17. K. Wüthrich and R. E. Connick, *Inorg. Chem.*, 1968, **7,** 7.
18. O. Farooq, A. V. Malik, N. Ahmad and S. M. F. Rahman, *J. Electroanol. Chem.*, 1970, **24,** 464.
19. M. V. Chidamharam and P. K. Bhattacharya, *Indian J. Chem.*, 1970, **8,** 941.
20. H. Tomiyasu and G. Gordon, *J. Coord. Chem.* 1973, **3,** 47.
21. I. Fabian and I. Nagypál, *Talanta*, 1982, **29,** 71, and references therein,.
22. G. S. Smith and J. L. Hoard, *J. Am. Chem. Soc.*, 1959, **81,** 556.
23. S. Ooi, M. Nischizawe, K. Matsumoto, H. Kuroya and K. Saito, *Bull. Chem. Soc. Japan*, 1979, **52,** 452.
24. L. G. Sillén and A. E. Martell, *Stability Constants of Metal-Ion Complexes*, Supplement No. 1. Chemical Society, London, 1971.
25. A. E. Martell and R. M. Smith, *Critical Stability Constants*. Plenum Press, New York, 1974.

Talanta, Vol. 30, No. 8, pp. 571–577, 1983
Printed in Great Britain.

0039-9140/83 $3.00 + 0.00

DETERMINATION OF COPPER IN URINE BY CARBON-FURNACE ATOMIC-EMISSION SPECTROMETRY

J. MARSHALL and J. M. OTTAWAY
Department of Pure and Applied Chemistry, University of Strathclyde, Cathedral Street, Glasgow, Scotland

(*Received* 20 *December* 1982. *Accepted* 23 *February* 1983)

Summary—A method is described for the direct determination of copper in urine at normal (10–30 μg/l.) levels by carbon-furnace atomic-emission spectrometry. Wavelength modulation is used to achieve automatic background correction for scatter-signals produced by the furnace and matrix. The accuracy of the method has been assessed by comparison with continuum-source atomic-fluorescence and carbon-furnace atomic-absorption methods. Relative standard deviations of about 4–5% can be achieved for either the platform or probe atomization techniques.

Relatively few applications of carbon-furnace atomic-emission spectrometry (CFAES) have been reported. This can be attributed, in part, to a lack of suitable instrumentation during the early development of the technique, particularly with regard to automatic background correction. Despite this, useful analytical procedures have been developed, using conventional atomic-absorption instruments for the determination of lithium in copper,[1] trace metals in steels[2] and barium in potable waters and sediments.[3] The introduction of wavelength modulation as a means of automatically correcting for background signals arising from the furnace has extended the range of analytical applications of CFAES, allowing the analysis of more complex samples.[4–7] The development of a new instrument, incorporating an echelle monochromator and wavelength modulation, has resulted in a significant improvement in sensitivity.[8] Detection limits for many elements are comparable to or superior to those obtained by carbon-furnace atomic-absorption spectrometry (CFAAS), suggesting that CFAES may be useful for a wide range of analytical applications.

The determination of urinary copper excretion is of established value in the diagnosis and treatment of Wilson's disease.[9] Elevated levels of copper in urine have been demonstrated for other conditions such as nephrotic syndrome,[10] copper intoxication[11] and burn injuries.[12] In general, the determination of increased levels of copper poses no great analytical problems and a number of colorimetric techniques have been successfully applied. However, when normal levels of copper (10–30 ng/ml) in urine are to be determined, *e.g.*, for metabolic balance studies, few methods offer the required sensitivity. Atomic spectrometric techniques have been employed since 1967, when Parker *et al.*[13] described the determination of urinary copper by flame atomic-absorption spectrometry. In this method, the copper was preconcentrated by chelation and extraction, and similar methods have subsequently been described.[14,15] For routine analytical application, however, it is desirable that a simple, rapid and accurate method is found which does not require elaborate sample pretreatment. A method based on flame atomic-absorption spectrometry has been proposed by Dawson *et al.*[16] for the direct determination of copper in urine. High scale expansion (×15) was employed to achieve the required sensitivity with a single-beam instrument. Spector *et al.*[17] have reported that greater experimental stability is obtained by using a double-beam instrument, but in general, methods based on flame atomic-absorption spectrometry involve measurements close to the detection limit in the determination of normal levels of copper in urine. The reliability of such results could therefore be in doubt because of insufficient sensitivity and precision close to the detection limit. Recently, Halls *et al.*[18] described a method for the direct determination of copper in urine by carbon-furnace atomic-absorption spectrometry. The only sample pretreatment required involved a 1:1 dilution of the urine with distilled water. The results showed good agreement with those obtained by extraction followed by CFAAS. The levels found were also in agreement with those established by flame methods.[17]

It would appear that a CFAES method for the determination of copper in urine might prove a suitable alternative in view of the sensitivity problems encountered with other techniques. In this paper, the development of a CFAES method for the direct determination of copper in urine is described. The accuracy of the method was assessed by comparison with methods based on continuum-source atomic-fluorescence spectrometry[19] and carbon-furnace atomic-absorption spectrometry.[18]

Table 1. Analytical instrumentation

Unit	Spectrametrics SMI III echelle monochromator focal length 0.75 m f/10 aperture reciprocal linear dispersion 0.062 nm/mm at 200 nm 0.25 nm/mm at 800 nm slit-widths, vertical 0.2 mm horizontal 0.5 mm
Detector	Hamamatsu R292 photomultiplier tube
Amplification	Ortec Brookdeal 5002 current pre-amplifier Ortec Brookdeal 9503D lock-in amplifier
Wavelength modulation	Quartz mechanical chopper. Detection frequency 40 Hz. Unit and power supply made in the laboratory[8]
Recorder	Servoscribe R541.20 potentiometric recorder
Atomizer	Perkin–Elmer HGA 72 carbon furnace Tubes and platforms coated with pyrolytic graphite *in situ*.[20] Pure pyrolytic graphite for probe manufacture supplied by Philips[22]
Focusing lens	$f = 130$ mm

EXPERIMENTAL

Instrumentation

All measurements were made with a Perkin–Elmer HGA 72 electrothermal atomizer, and an echelle spectrometer incorporating a wavelength-modulation background-correction system. The application of this instrument to the measurement of furnace atomic-emission signals has been described elsewhere.[8] The components which comprise this system are detailed in Table 1. Furnace-operating conditions employed in the determination of copper in urine are summarized in Table 2. The furnace was operated with tubes coated *in situ* with pyrolytic graphite, and platform[20] or probe[21] atomization as indicated in the text. Samples were dispensed manually from a micropipette of the appropriate volume. Atomic-emission signals for copper were measured at 324.75 nm and displayed on a chart-recorder.

Reagents

Standard copper solutions (0–100 ng/ml copper) were prepared freshly, as required, from a 1000-μg/ml stock solution and were acidified with nitric acid to a final acid concentration of $10^{-2}M$.

Procedure

Urine samples were collected in acid-washed polythene containers and acidified by addition of 5 ml of "Aristar" concentrated sulphuric acid to each 24-hr sample.[18] The sample was shaken thoroughly before measurement and was analysed by direct injection of the solution into the furnace, followed by calibration against aqueous standard solutions of copper. Apart from dilution of the sample in some cases to allow measurement within the linear calibration range of the method, no other sample pretreatment was used. Pipette tips were washed before the analysis, by pipetting distilled water, and normally the first sample was rejected to avoid any possible contamination.

RESULTS AND DISCUSSION

Background correction

Halls *et al.*[18] have reported a CFAAS method for the direct determination of copper in urine. A 1:1 dilution step was incorporated in the method to allow for high background signals resulting from complex matrices. A deuterium lamp was used for background correction. However, at the wavelength of 324.75 nm used for the copper determination, the intensity of the deuterium lamp is relatively weak, making correction for high background signals more difficult and resulting in increased noise. The magnitude of the background signal observed will also be related to some extent to the design of the atomizer. Background-correction problems in atomic-absorption spectrometry result from non-specific attenuation of the light-sources by scatter from particles, and from specific molecular absorptions. In CFAES, a continuum background signal is produced, which consists of tube-wall radiation scattered by particles and molecules into the monochromator.[23] When a sample is analysed, the scattering of tube-wall radiation will be increased and the extent of the background signal produced will be dependent on the concentration of matrix present in the sample. For this reason, it has proved difficult to use CFAES as an analytical technique for the determination of real samples without some method of correcting for large and variable background signals. It has been demonstrated that a system of wavelength modulation (such as that incorporated into the echelle spectrometer employed in the present study) can provide satisfactory correction for this type of background signal. The atomic-emission signal emanating from the furnace can be attenuated by matrix effects such as scatter and non-specific absorption. However, interferences of this type can be corrected for in atomic emission by the use of a standard-addition procedure. The effect of the matrix on the signal from a urine sample of known copper concentration was studied. It is possible to monitor the uncorrected CFAES signal from the pre-amplifier output in the echelle

Table 2. Temperature programme for HGA 72 atomizer*

Stage	Temperature, °C	Time, *sec*
Dry	300 (400)	30
Ash	900	30
Atomize	2500	8 (10) (Gas stop)

*Argon was used as the purge gas. Sample volumes of 50 μl for platform atomization, and 20 μl for probe atomization were employed. Modifications to the furnace programme required for probe atomization[21] are indicated in brackets.

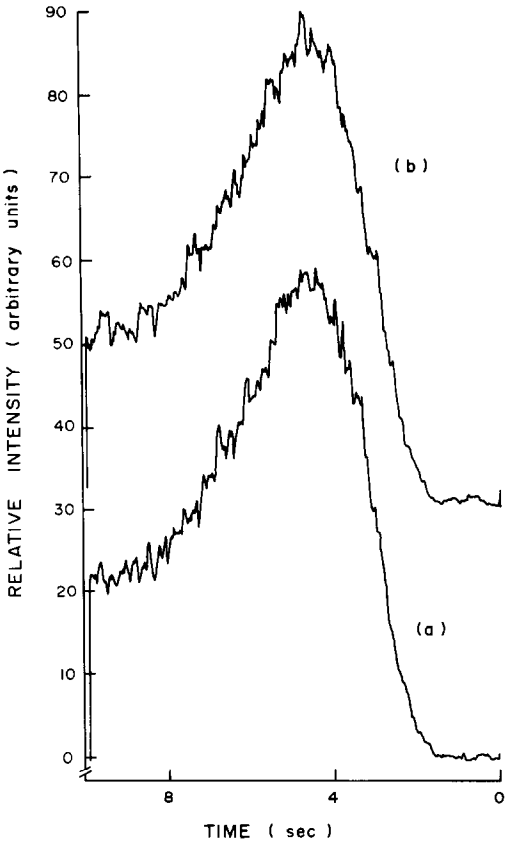

Fig. 1. CFAES signals obtained for (a) 50 μl of 40 ng/ml aqueous copper standard solution; (b) 50 μl of a urine sample containing ~40 ng/ml copper. Measurements made at 324.75 nm without background correction. The base-line for curve (b) is at 30 arbitrary units.

spectrometer system. The signal thus produced will have components from the normal tube background, matrix scatter of tube-wall radiation and the analyte atomic-emission signal. Signals for a 40-ng/ml aqueous standard solution of copper and a urine sample containing a similar copper concentration are shown in Fig. 1. There is very little difference between the signals obtained, indicating that the intensity of scattered light reaching the detector at the wavelength of the atomic-emission line for copper is small in comparison to the atomic-emission signal intensity. In addition, it is clear that the time of appearance of the signals and the time of the peak emission intensities are the same for the aqueous standard solution and the urine sample.

The scatter-signal from a urine sample was measured at a series of wavelengths and compared to the background signal obtained from a blank firing of the tube at each of the points on the wavelength scale. The results are illustrated in Fig. 2. The scatter-signal is clearly larger than the tube-background signal, but is still small with respect to the atomic-emission signal. The total signal due to scatter at the wavelength of the copper atomic-emission line corresponds to a copper concentration of 2.3 ng/ml. It is probable that the use of the high-resolution echelle spectrometer reduces the total amount of continuum radiation falling on the detector. It has been confirmed, however, that a substantial scatter-signal is present at the wavelength of interest and that a method of background correction is required.

A further wavelength scan was made at wavelengths much closer to the copper atomic-emission line to ascertain whether any spectral interference was present resulting from, for example, molecular emission from the urine sample. The modulation waveform was displayed on an oscilloscope. No spectral overlaps were observed within the wavelength modulation interval, and the emission signal produced appeared to be due to copper present in the sample.

The calibration graph obtained for copper by CFAES with platform atomization is shown in Fig. 3. Above about 80 ng/ml the plot deviates from linearity and this was the upper limit of concentration used for direct calibration. It was possible to employ a direct calibration procedure because the slope of the graph was very close to that produced by standard additions of copper to urine sample. If a systematic error were present, *e.g.*, as a result of chemical interference or scatter by matrix particles, the slope of the standard-addition plot would be expected to differ from that of the calibration graph. It would appear from the results shown in Fig. 3 that practically no such interference was present. It was found, however, that the precision obtained for the CFAES determination of copper in urine was somewhat worse than that obtained for aqueous copper standard solutions. This is to be expected, as a result of viscosity differences resulting from variations in the high dissolved solids content of urines. Additional error is also likely to result from noise (introduced by the matrix) on the analyte signal. A typical reproducibility for urine samples analysed directly by

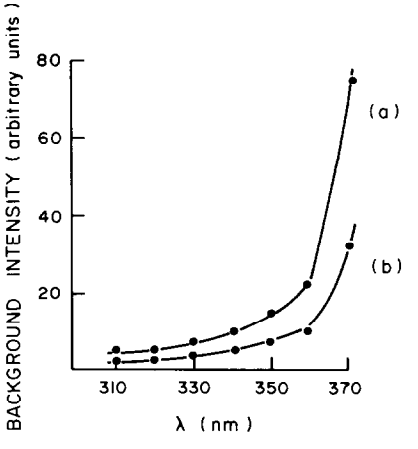

Fig. 2. Variation of background with respect to wavelength in the region of the CFAES analytical line for copper (324.75 nm). (a) Scattered background signal in the presence of a urine sample; (b) background signal obtained from a blank firing of the tube.

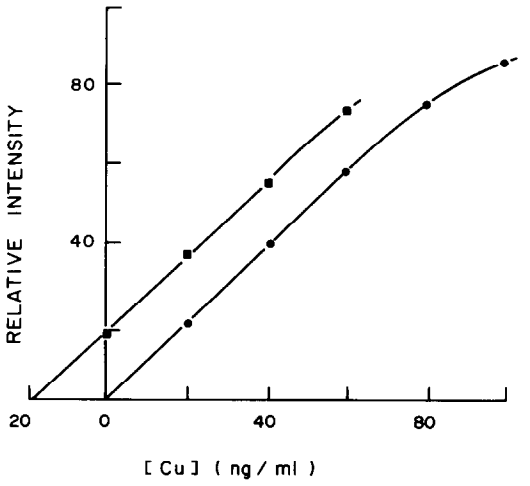

Fig. 3. Determination of copper in a pooled normal urine sample. (●) Calibration graph; (■) standard additions of copper to the urine sample. Measurements made at 324.75 nm by CFAES with platform atomization.

CFAES is given in Fig. 4. The noise in the CFAES signals is due in part to fluctuation in the background intensity transmitted, as a result of variation in the vapour-phase concentration of matrix particles during the emission measurement. There is also an increased shot-noise contribution which is proportional to the square root of the total intensity reaching the photomultiplier and resulting from scatter of continuum radiation from the tube wall into the monochromator by the matrix. The a.c. components of the background signal can be transmitted through the wavelength modulation detection system, resulting in noise which will affect the overall detection limit. The practical detection limit for copper by the method was 0.5 ng/ml.

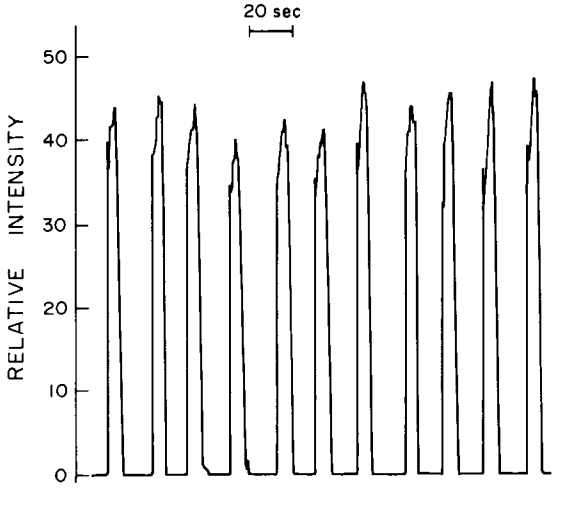

Fig. 4. Reproducibility of CFAES signals for copper in undiluted urine by platform atomization. R.S.D. 5.1% for 50-μl aliquots of a urine sample containing ~20 μg/ml copper.

Table 3. Comparison of results obtained by atomic-fluorescence spectrometry (AFS) and carbon-furnace atomic-emission spectrometry (CFAES)

Urine sample	Concentration of copper, μg/l. AFS[19]	CFAES*
1	35	31
2	45	43.5
3	37	33
4	31	32
5	33	27
6	42	44
7	37	35.5
8	55	56.5
9	54	52
10	27	27

*Direct determination on undiluted urine samples.

Comparison with AFS method

A series of trials was undertaken to compare the accuracy of the furnace emission method with that of other methods used for the determination of copper in urine. The first of these was a comparison with a continuum-source flame atomic-fluorescence method described elsewhere.[19] The CFAES results shown in the second column of Table 3 were obtained by direct analysis of the undiluted urine samples. The regression equation was of the form $Y = BX + A$ where Y is the dependent variable, in this case assumed to be the CFAES result, and X is the test result of the comparative method. The slope of the line was 1.06 ± 0.09 and the intercept -3.9 ± 3.9. The correlation coefficient was 0.969. These results provide evidence that the CFAES method is suitable for the determination of copper in urine. It should be noted that the two techniques have fundamentally different theoretical bases, and hence are unlikely to suffer the same systematic bias. Since furnace and flame atomization mechanisms are also substantially different, it seems reasonable to assume that no systematic error is involved in the CFAES method.

Comparison with CFAAS method

To establish its accuracy the CFAES method was also compared in trials with the CFAAS method developed by Halls *et al.*[18] Each sample was divided into two portions which were separately analysed, one by each method. The results obtained for a set of urine samples are given in Table 4. Fair agreement was obtained between the CFAAS and CFAES results. Regression analysis (CFAES = Y, CFAAS = X) gave a correlation coefficient of 0.992, slope 0.986 ± 0.04, intercept 2.4 ± 2.5. Initially some problems were encountered in achieving contamination-free analysis. One of the reasons for using a direct method of analysis was to minimize sample-handling and hence the risk of contamination. The CFAES method described in this paper involves only the direct sampling of the urine

Table 4. Comparison of results obtained by carbon-furnace atomic-absorption spectrometry (CFAAS) and carbon-furnace atomic-emission spectrometry (CFAES)

Urine sample	Concentration of copper, $\mu g/l$. CFAAS[18]	CFAES*
1	27	31
2	14.5	15
3	8.5	11
4	161	165
5	15	14
6	25	25
7	19	21
8	27	29
9	16	30

*Direct determination on undiluted urine samples.

Table 5. Comparison of results obtained by CFAAS and CFAES

Urine sample	Concentration of copper, $\mu g/l$. CFAAS[18]	CFAES*
1	23.5	24
2	15.5	18
3	47	47
4	18	22.5
5	11.5	15
6	18.5	21
7	19	20
8	18	24
9	25.5	28
10	21	30.5

*Direct determination on undiluted urine samples. Correlation coefficient 0.956; slope of regression equation 0.883 ± 0.095; intercept 5.78 ± 2.25.

and its introduction into the furnace by micropipette. Contamination could only arise from the original separation of the sample into separate containers, during transport, or during the introduction of the sample into the furnace. However, copper is such a common element in a laboratory environment that it is very easy to contaminate samples with it. The results shown in Table 4 were obtained only by analysis of the same half of the sample analysed by CFAAS. The half of the sample analysed originally by CFAES showed considerably higher values, indicative of contamination. Halls *et al.*[18] have indicated that co-precipitation of copper with insoluble materials can be a problem in the determination of copper in urine and that variable losses can occur which make comparative studies extremely difficult. In order to limit the co-precipitation of copper, samples were acidified to a concentration of $0.1M$ sulphuric acid. It was found during the course of the present study that precipitation still occurred in some samples. This indicates that problems in the determination may be related to specific samples rather than to a systematic bias in a general method, and be due to variations in matrix composition. It is known that the matrix composition of urine varies widely from sample to sample and that for certain samples this may present specific analytical problems. The extent of precipitation in a given sample is likely to be related to the length of storage of the sample prior to analysis. This time may be critical in the determination of copper in urine, since different degrees of precipitation may occur between sample sets and also from sample to sample prior to analysis. A further set of samples was analysed by the CFAES and CFAAS methods within 48 hr in order to avoid any problems which might arise as a result of storage. It should be noted that the samples analysed in the comparative study with the AAS method were analysed on the same day. The results obtained for the CFAAS and CFAES analyses are presented in Table 5. Although a small bias towards higher values is apparent in the CFAES results, it is clear that relatively good agreement can be achieved by a direct method if the samples are analysed at the same time.

Standard reference materials for clinical analysis for trace metals are less readily available than in other areas of analysis. It is difficult to produce a standard synthetic mixture representative of a clinical fluid, since each sample is unique to the individual patient. Furthermore, concentrations of both matrix components and analyte vary so widely from sample to sample that it is difficult to represent the analytical problem adequately by using a synthetic mixture. The problem is further complicated by a lack of suitable techniques which could accurately define the concentration present in the standard sample. For this reason, a range of values in which the analytical results should fall is often quoted. Urinary copper determinations are routinely performed as tests for Wilson's disease, where elevated levels are normally evident. Standard urine samples therefore normally contain relatively high copper levels. Two samples were analysed by CFAES and CFAAS. The first was a standard urine (pooled human urine with copper added) of known composition and the second a urine sample from a patient with Wilson's disease. The results are shown in Table 6. As the concentrations in the neat urine samples were outwith the linear calibration range of the CFAES method, dilutions of 1:5 and 1:10 respectively were made. The CFAES

Table 6. Analysis of urine samples of high copper content by CFAAS and CFAES

Sample	Concentration of copper, $\mu g/l$. CFAAS[18]	CFAES*	Accepted range
Standard urine sample†	260	245 ± 11	140–300 (mean 220)
Wilson's disease sample§	500	520 ± 23	—

*50-μl samples, platform atomization.
†Lypochek Quantitative Control Urine II, from Environmental Chemical Specialities, California. Diluted 1:5 with distilled water before CFAES analysis.
§Diluted 1:10 with distilled water before CFAES analysis.

results show reasonable agreement with the CFAAS values and fall within the accepted range of the standard certificate value, although this range is relatively wide. It is evident that with a dilution step the CFAES method can provide acceptable results. Indeed, it may be that the routine use of a dilution of 1:5 or more would eliminate any possibility of matrix interference for particular samples, whilst retaining sufficient sensitivity for the analysis to be performed.

Probe atomization

Slavin *et al.*[24] have reported that the use of a platform allows the atomization of the sample in a furnace tube close to isothermal conditions. The sample experiences a higher temperature in the vapour phase when platform atomization is used than it does in atomization from the tube wall. This leads to an improvement in the dissociation of analyte species. However, for certain elements the peak free-atom concentration occurs some time before the maximum tube temperature has been reached, even when platform atomization is used.[20] Thus in cases where complex matrices are present, the temperature of the furnace may not be sufficiently high at the time of sample vaporization to dissociate the sample completely. Incomplete atomization might therefore be a contributory factor to the difficulty of analysing particular samples. Several authors have proposed that the sample could be introduced into the furnace on a probe made of tungsten or graphite, once the maximum tube temperature has definitely been established.[21,25–28] It has been shown that matrix interferences can be greatly reduced by using this technique[21,28,29] and it was expected that the use of probe atomization could prove beneficial in the determination of copper in urine.

A set of urine samples was analysed directly without dilution, by CFAES with probe atomization.[21] The results are compared in Table 7 with those obtained by CFAAS. The results obtained by probe atomization do not appear to give significantly better agreement than those obtained in previous trials using platform atomization. However, the fact that

Table 7. Comparison of results obtained by CFAAS and CFAES using probe atomization

Sample	Concentration of copper, $\mu g/l$. CFAAS[18]	CFAES with probe*
1	27	20
2	62	55
3	36	36
4	5	24
5	20	19
6	23	29
7	104	85
8	83	80
9	20	23
10	9	20

*Direct analysis of undiluted urine samples (20 μl).

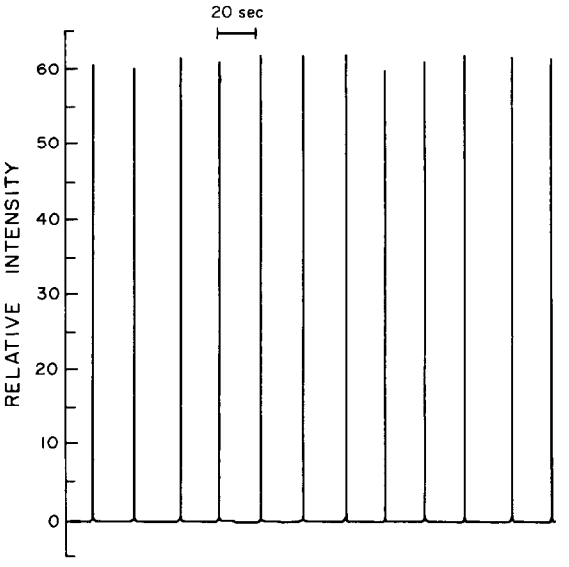

Fig. 5. Reproducibility of probe-atomization CFAES signals for copper in undiluted urine. R.S.D. 1.0% for 20-μl aliquots of a urine sample containing ~80 ng/ml copper.

satisfactory agreement is achieved for some samples but not for others may indicate that a problem exists in the determination of particular samples. The precision of the method was improved by using probe atomization. Replicate determinations of a urine sample containing 80 ng/ml copper are shown in Fig. 5. It is probable that the degree of sample contamination limits the precision, since the r.s.d. values at lower concentrations (*e.g.*, 20 ng/ml) were of the order of 4%. However, different sample volumes were employed for the platform and probe methods and therefore a comparison of the precision on this basis may not be exact.

CONCLUSIONS

CFAES appears to be a useful analytical tool for the determination of copper in urine. The major problems in the analysis appeared to result from the irreproducible nature of the sample, rather than any inherent error in the method of measurement employed. As CFAES is an emission technique it is possible to utilize a standard-addition procedure to correct for scatter and molecular absorption interferences where direct calibration against aqueous standard solutions is unsatisfactory. Alternatively, because of the high sensitivity afforded by the CFAES method, the sample could be diluted to minimize possible matrix interferences for particular samples. In the collaborative studies undertaken in this work sample stability and contamination contributed significantly to the difficulty in performing useful analytical comparisons. In view of the precision of the CFAES and comparative methods, the agreement obtained is considered acceptable. Recently, CFAES has been successfully applied to the

determination of chromium, manganese and lead in clinical fluids.[30] The technique would appear to have potential for application to a wide range of clinically important trace element determinations, particularly if utilized for simultaneous multi-element analysis.[31]

Acknowledgements—This work was made possible by the award of grants (to J.M.O.) by the Royal Society for the purchase of the HGA 72 atomizer and by the SERC for the purchase of the echelle spectrometer. The authors are also grateful for the provision of pure pyrolytic graphite by Pye Unicam Ltd. and Philips Research Laboratories. The co-operation of Dr. D. J. Halls and Dr. G. S. Fell of Glasgow Royal Infirmary in the provision of urine samples and comparative CFAAS analyses is also gratefully acknowledged.

REFERENCES

1. F. Shaw and J. M. Ottaway, *Anal. Lett.*, 1975, **8,** 911.
2. J. M. Ottaway and F. Shaw, *Anal. Chim. Acta*, 1978, **99,** 217.
3. L. Ebdon, R. C. Hutton and J. M. Ottaway, *ibid.*, 1978, **96,** 63.
4. M. S. Epstein, T. C. Rains and T. C. O'Haver, *Appl. Spectrosc.*, 1976, **30,** 324.
5. R. C. Hutton, J. M. Ottaway, T. C. Rains and M. S. Epstein, *Analyst*, 1977, **102,** 429.
6. M. S. Epstein and A. T. Zander, *Anal. Chem.*, 1979, **51,** 915.
7. M. S. Epstein, T. C. Rains, T. J. Brady, J. R. Moody and I. L. Barnes, *ibid.*, 1978, **50,** 874.
8. J. M. Ottaway, L. Bezur and J. Marshall, *Analyst*, 1980, **105,** 1130.
9. E. J. Underwood, *Trace Elements in Human and Animal Nutrition*, 3rd Ed. Academic Press, New York, 1971.
10. K. E. Mason, *J. Nutr.*, 1979, **109,** 1981.
11. N. Holtzmann, D. A. Elliot and R. Heller, *N. Engl. J. Med.*, 1966, **275,** 347.
12. G. Carr and A. W. Wilkinson, *Clin. Chim. Acta*, 1975, **61,** 199.
13. M. M. Parker, F. L. Humoller and D. J. Mahler, *Clin. Chem.*, 1967, **13,** 40.
14. F. W. Sunderman and N. D. Rosel, *Am. J. Clin. Pathol.*, 1967, **48,** 286.
15. D. C. Cowell, *Med. Lab. Technol.*, 1973, **30,** 133.
16. J. B. Dawson, D. J. Ellis and H. Newton-John, *Clin. Chim. Acta*, 1968, **21,** 33.
17. H. Spector, S. Glusman, P. Jatlow and D. Seligson, *ibid.*, 1971, **31,** 5.
18. D. J. Halls, G. S. Fell and P. M. Dunbar, *ibid.*, 1981, **114,** 21.
19. J. Sneddon, *Ph.D. Thesis*, University of Strathclyde, 1980.
20. L. Bezur, J. Marshall, J. M. Ottaway and R. Fakhrul-Aldeen, *Analyst*, in the press.
21. J. Marshall, S. K. Giri, D. Littlejohn and J. M. Ottaway, *Anal. Chim. Acta*, 1983, **147,** 173.
22. B. Lersmacher, *Ger. Offen.* 2949275 (Cl. GOINZ1/03), 25th June 1981.
23. D. Littlejohn and J. M. Ottaway, *Analyst*, 1977, **102,** 553.
24. W. Slavin and D. C. Manning, *Spectrochim. Acta*, 1980, **35B,** 701.
25. B. V. L'vov and L. A. Pelieva, *Zh. Analit. Khim.*, 1978, **33,** 1572.
26. D. C. Manning, W. Slavin and S. Myers, *Anal. Chem.*, 1979, **51,** 2375.
27. W. Slavin and D. C. Manning, *Spectrochim. Acta*, 1982, **37B,** 955.
28. S. K. Giri, D. Littlejohn and J. M. Ottaway, *Analyst*, 1982, **107,** 1095.
29. J. M. Ottaway, *At. Spectrosc.*, 1982, **3,** 91.
30. J. M. Ottaway, L. Bezur, R. Fakhrul-Aldeen, W. Frech and J. Marshall in *Trace Element Analytical Chemistry in Medicine and Biology*, p. 575. de Gruyter, Munich, 1980.
31. J. Marshall, D. Littlejohn, J. M. Ottaway, J. M. Harnly, N. J. Miller-Ihli and T. C. O'Haver, *Analyst*, 1983, **108,** 178.

Talanta, Vol. 30, No. 8, pp. 579–586, 1983
Printed in Great Britain.

0039-9140/83 $3.00+0.00

A COMPUTATIONAL APPROACH TO THE SPECTROPHOTOMETRIC DETERMINATION OF STABILITY CONSTANTS—II

APPLICATION TO METALLOPORPHYRIN–AXIAL LIGAND INTERACTIONS IN NON-AQUEOUS SOLVENTS

D. J. LEGGETT,* S. L. KELLY, L. R. SHIUE, Y. T. WU, D. CHANG and K. M. KADISH

Department of Chemistry, University of Houston, Houston, TX 77004, U.S.A.

(*Received* 29 *September* 1982. *Accepted* 14 *February* 1983)

Summary—The ability of the computer program SQUAD to deduce a plausible equilibrium model, associated stability constants and spectra of individual species is described. The original version of SQUAD has been extensively modified and these changes are detailed. In particular a "user-friendly" method of data input has been implemented that simplifies familiarization with the program. Brevity of program code has been sacrificed in favour of the new data input and error-checking features of SQUAD, with beneficial results. The application of SQUAD to five non-aqueous metalloporphyrin–axial ligand interactions exemplifies the program's ability to handle widely different types of equilibrium systems.

The Benesi–Hildebrand method[1] has been extensively used to evaluate the stability constants of metalloporphyrin–axial ligand complexes. For the general reaction

$$M + L \rightleftharpoons ML \quad (1)$$

where M is any metal ion or metalloporphyrin and L is any ligand, the following equations may be written:

$$C_M = [M] + [ML] \quad (2)$$

$$C_L = [L] + [ML] \quad (3)$$

$$\beta_{101} = [ML]/[M][L] \quad (4)$$

The subscripts for β refer to the number of metal ions, hydroxide or hydrogen ions, and ligand ions, respectively, associated with that stability constant. The studies are most often performed in a non-aqueous, non-donor solvent, in which case the middle subscript is then always zero. Making use of Beer's law:

$$A = \epsilon_M[M] + \epsilon_L[L] + \epsilon_{ML}[ML] \quad (5)$$

it can be shown[1] that

$$\log \frac{(A - A_0)}{(A_c - A)} = \log C_L + \log \beta_{101} \quad (6)$$

where A is the absorbance, at a preselected wavelength, of a solution having a known molarity of ligand, C_L and known molarity of metal, C_M, A_0 is the absorbance, measured at the same wavelength, of a solution where $C_L = 0$, and A_c is the measured absorbance of a solution for which $C_L \gg C_M$ so that the absorbance is constant with increasing C_L. Thus a plot of the left-hand side of equation (6) against log C_L should give a straight line which intersects the abscissa at $-\log C_L$, which will be equal to $\log \beta_{101}$.

The Benesi–Hildebrand (B–H) method may be generalized to handle equilibrium systems in which the stoichiometry of the complex formed is unknown. In this situation equation (4) becomes

$$\beta_{10n} = [ML_n]/[M][L]^n \quad (7)$$

and equation (6) becomes

$$\log \frac{(A - A_0)}{(A_c - A)} = n \log C_L + \log \beta_{10n} \quad (8)$$

Thus the slope of the straight line in the log–log plot provides the stoichiometric coefficient for the complex.

Inherent in this method is the assumption that only one complex is formed. This situation is not too frequently encountered and when there is more than one complex present the B–H plots of log $[(A - A_0)/(A_c - A)]$ *vs.* log C_L will show considerable curvature. It has been argued[2] that the plots may still yield information concerning the stoichiometry and stability constants of the complexes, but except under

*Author for correspondence. Present address: Dow Chemical USA, Texas Division, Freeport, TX 77541, U.S.A.

the most favourable conditions, encountered when complexes of *widely differing stability are formed*, this claim is not valid.

This method, and many similar approaches,[3] have the common drawback that they are only applicable if one and only one complex exists under the conditions of measurement. However, in general, more than one complex will exist in solution unless $C_L \gg C_M$ or $C_M \gg C_L$. Moreover, when several complexes are present, their nature may not be readily determinable from simple continuous-variation or molar-ratio experiments. Therefore, more sophisticated and rigorous data-processing techniques need to be adopted.

Several general computer programs are currently available[4,5] that permit various equilibrium models to be fitted to the experimental data, by change of one or more *data cards*. This type of program is clearly more desirable than one where the program code needs to be rewritten for each new model tested. The majority of programs developed to date require potentiometric data as input, which may either be obtained from measurements of pH *vs.* volume of base, or of ion-sensing electrode potentials.

Spectrophotometry is a widely used technique for the study and determination of equilibrium constants but only a few programs are available to process the data.[4,5] Spectrophotometric measurements are generally less precise than potentiometric ones, both inherently and because of the need to prepare several separate solutions. A further complication arises from the fact that for fitting an equilibrium model to absorbance measurements, not only are the stability constants to be determined, but the molar absorptivities for each species, at each wavelength, are also to be evaluated. The situation is not as bad as it might seem, since the evaluation of molar absorptivities and stability constants is done at two levels within most programs, patterned after an approach suggested by Sillén.[6]

The program used in the studies described here is SQUAD.[7,8] It is designed to calculate the best values for the stability constants of the proposed equilibrium model by employing a non-linear least-squares approach. The program is completely general in scope, having the capability to refine stability constants for the general complex $M_m M'_l H_j L_n L'_q$, where m, l, n, $q \geqslant 0$ and j is positive (for protons), negative (for hydroxide ions) or zero. Therefore, the same program may be used to study acid–base equilibria for ligands that are weak acids (or bases); metal-ion hydrolysis; complexes of the type ML_n or M_mL_n; mixed-ligand (or mixed-metal) complexes; protonated or hydroxo complexes. SQUAD was originally designed to process absorbance data from aqueous solutions. Recently extensive modifications have been made to the program that now permit the analysis of data from any type of solution. The algorithms employed in SQUAD and their relationships to each other are shown in Fig. 1. The overall *modus operandi* will be described briefly and then greater attention will be paid to the novel data-input method.

The input data consist of: (*a*) the absorbance values $A_{i,k}$, for each spectrum, giving a total of I for each wavelength, and a grand total of NW; (*b*) the total metal and ligand concentrations, $C_{M,i}$, $C_{L,i}$, pH_i (pH for aqueous and mixed solvents only) and path-length b_i, for each spectrum; (*c*) any known or previously determined molar absorptivities ($\epsilon_{j,k}$) for the jth species at the kth wavelength; (*d*) the stoichi-

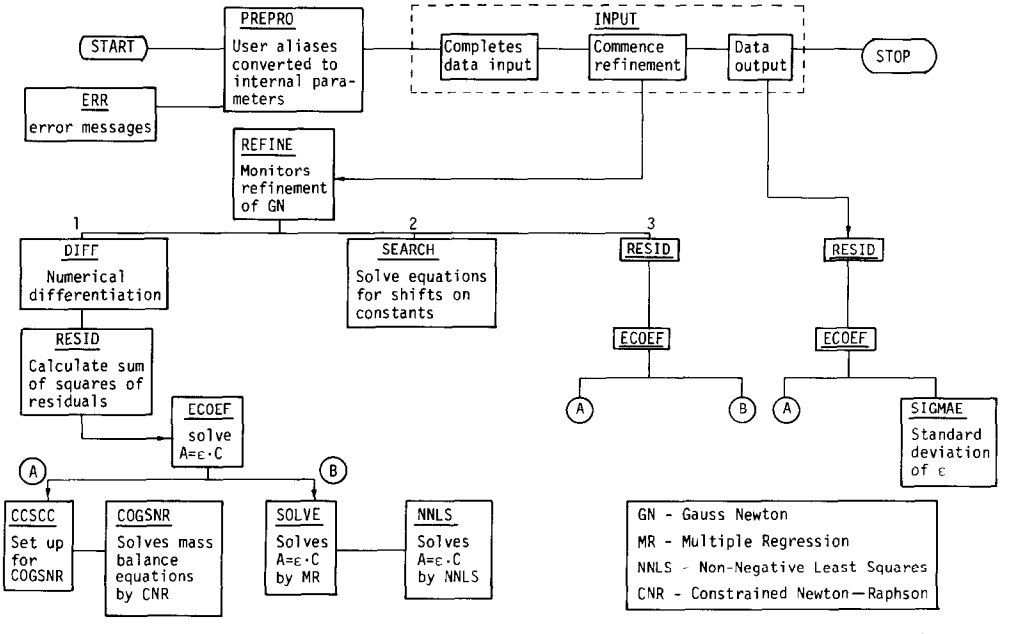

Fig. 1. Block diagram of SQUAD, showing the inter-relationships among the various algorithms.

ometry and stability constant for the jth species together with an indication of which constants are to be refined. The data are read in by subroutines PREPRO and INOUT. Once data input is complete the refinement process is commenced. The Gauss–Newton non-linear least-squares algorithm is used to minimize U, where

$$U = \sum_{1}^{I} \sum_{1}^{NW} (A_{i,k}^{\text{calc.}} - A_{i,k}^{\text{obs.}})^2 \qquad (9)$$

Subroutine REFINE controls the minimization in two major steps. First the Jacobian and Hessian matrices are built up by numerical differentiation using Sterling's central difference method. This involves, for the current set of stability constants, calculating the concentrations of all species contributing to each spectrum. In essence, the mass-balance equations are solved, given $C_{M,i}$, $C_{L,i}$ and β_j, yielding $[\text{species}]_{i,j}$. These calculations are performed by subroutines CCSCC and COGSNR. The first of these performs "book-keeping" functions for the second, which solves the mass-balance equations by using a controlled Newton–Raphson algorithm. Once the $[\text{species}]_{i,j}$ values have been found, the set of linear equations, derived from Beer's law,

$$A_{i,k} = [\text{species}]_{i,j} \epsilon_{j,k} b_i \qquad (10)$$

is solved, within the subroutines ECOEF, SOLVE and/or NNLS, for the molar absorptivities of each species, j, wavelength by wavelength. ECOEF provides the book-keeping for SOLVE. Two possible algorithms may be selected within SOLVE. Either a conventional multiple regression (MR) technique is used to solve the system of linear equations, or NNLS, a non-negative linear least-squares algorithm, is chosen. NNLS is employed when molar absorptivities are found to be negative when the MR algorithm is used. Full details of MR and NNLS have already been published.[8] Once the $\epsilon_{j,k}$ values have been calculated, the $A_{i,k}^{\text{calc.}}$ matrix is evaluated for the current set of constants. Control returns to REFINE and then proceeds to subroutine SEARCH where the shifts for the refining constants are calculated. Assuming that the refinement process is working smoothly, the new values of the constants will provide a better numerical fit to the data, *i.e.*, lower U, than the previous set of constants. This is checked in the third step by repeating the sequence of calls, starting at subroutine RESID. If the changes in the refining constants are all less than 0.001, refinement is considered to be complete. Otherwise, a new refinement cycle is started.

It is most important with computer programs of this size that the method of data-input should be as straightforward as possible. This is particularly true for first-time users and potential users with little or no programming experience. Considerable attention has been devoted to achieving this end and the method of data-input will now be described.

Table 1

A SUITABLE TITLE	
A SUITABLE SUBTITLE	
DICTIONARY:	
.	Section 1
.	
END:	
SPECIES:	
.	Section 2
.	
.	
END:	
OTHER:	
.	Section 3
.	
.	
DATA:	
.	Section 4
.	
.	
MOL. ABS.:	
.	Section 5
.	
.	
END:	
.	
.	
.	
.	
BASELINE:	
.	Section 6
.	
.	
.	
SPECTRA:	
.	Section 7
.	
.	
.	
-AMAX	

The data deck consists of seven major sections, some of which may be omitted. Each section starts with a key word and most finish with the key word END. The basic layout of the data deck is shown in Table 1. The DICTIONARY section provides SQUAD with the "aliases" (4-character identification words) that the user will employ to identify the components of the complexes. Consider, as an example, a study involving the interactions between zinc, imidazole and a porphyrin, designated TBDH. To begin communication between SQUAD and the user, "aliases" must be supplied for the program-recognizable variables MTL1 (first metal in complex), MTL2 (second metal), LIG1 (first ligand in complex), LIG2 (second ligand), PROT (the proton as ligand), HYDR (hydroxide ion as ligand).

The second section of the data deck is used to describe the model and to indicate whether stability constants are to be refined (VB) or held constant (FB) and whether molar absorptivities are to be calculated (VE) or not (FE). SQUAD will use the dictionary to construct its internal vectors and arrays that describe the stoichiometry of each complex in the model being

Table 2. The set-up of the dictionary and species data for SQUAD

```
DICTIONARY:
MTL1 = ZN; LIG1 = IMID; LIG2 = TBDH:
END:
SPECIES:
ZN(1) IMID(1); 3.30; FB; FE:
ZN(1) IMID(2); 5.87; FB; FE:
ZN(1) TBDH(1); 4.31; VB; VE:
ZN(1) TBDH(2); 7.44; VB; VE:
ZN(1) IMID(1) TBDH(1); 6.91; VB; VE:
END:
```

fitted to the data. For example, the interactions of zinc, imidazole and TBDH are believed to give rise to five complexes, Zn(Imid), $Zn(Imid)_2$, Zn(TBDH), $Zn(TBDH)_2$ and Zn(Imid) (TBDH). The zinc–imidazole system has already been studied and the relevant stability constants and molar absorptivities are known. The first two sections of the data deck are shown in Table 2. Since the molar absorptivities of the zinc–imidazole system had been previously determined they are included in the data deck at Section 5. The layout of these values is shown in Table 3.

The examples given above of three of the sections of the data deck illustrate the simplicity by which models can be specified to SQUAD and also the ease with which a model description may be changed. Although the method of data input is straightforward, key-punching errors can occur, such as mis-spelling TBDH or omitting a semicolon or parenthesis. Extensive error checks are performed throughout the data-input phase and the conversion of user-specified descriptions into internal data for SQUAD. Thus, an incorrectly constructed data deck will be detected by the program rather than by the compiler.

Section 3 (OTHER), which is optional, is used to indicate whether the molar absorptivity of any of the *components* is to be calculated, or whether the molar absorptivities of more than one species are the same. Section 4 (DATA) contains information such as the starting and finishing wavelengths and the wavelength increment; whether the β or the log β values are to be refined; whether the multiple regression or the non-negative linear least-squares method is to be used to solve the system of linear equations arising from Beer's law; and so on. Section 5 (BASELINE), which is optional, allows for baseline corrections to be performed. Section 6 (SPECTRA) will contain the recipe concentrations used for each spectrum, the pH (if applicable) of each solution, the path-length for each spectral measurement and the absorbance readings at each incremental wavelength. The final card in the data deck is labelled minus one and is used to indicate the physical end of data to be processed.

Table 3. Section 5 for inputting molar absorptivities to SQUAD

```
MOL.ABS.:
ZN(1) IMID(1); ZN(1) IMID(2):
END:
```

ϵ^1_{ZnImid}	$\epsilon^1_{ZnImid_2}$
ϵ^2_{ZnImid}	$\epsilon^2_{ZnImid_2}$
.	.
.	.
.	.
.	.
.	.
ϵ^K_{ZnImid}	$\epsilon^K_{ZnImid_2}$

ϵ^K_{ZnImid} and $\epsilon^K_{ZnImid_2}$ are the molar absorptivities of Zn(Imid) and $Zn(Imid)_2$ at the kth wavelength.

EXPERIMENTAL

The various metalloporphyrins, discussed below, were purified by previously published procedures.[9] Spectra of solutions containing various porphyrin:axial ligand ratios (C_M:C_L) were recorded with a Cary 14 spectrophotometer at $21.0 \pm 1.0°$ or a Tracor Northern Rapid Scan Spectrophotometer. In all instances non-bonding solvents were used, due precautions being taken to avoid evaporation throughout the solution preparation and data acquisition. The spectral traces were manually digitized at 1.25, 2.5 or 5.0 nm intervals, 20–45 absorbance readings per spectrum being taken. Absorbance values were read from the top of the trace, to within ± 0.003 absorbance units. Although it may be instructive to record several spectra, one on top of another, this practice is to be discouraged when obtaining data that will be processed by SQUAD. Difficulties in aligning the starting position of the pen on the paper, and possible confusion of traces, especially where cross-over points exist, far outweigh the benefits gained from being able to view trends in peak maxima shifts as a function of ligand concentration. The absorbance values, so obtained, are the major part of the data for SQUAD. Additional data required have been specified and described earlier.

RESULTS

The reactions of imidazole and pyridine with TPPMn(III)ClO_4, TPPCd, TPPMg and TPP-Ru(CO); pyridine with TPPCu; and DMSO with TPPMn(III)ClO_4 and TPPRu(CO) will be used to illustrate the applicability of SQUAD and to unravel

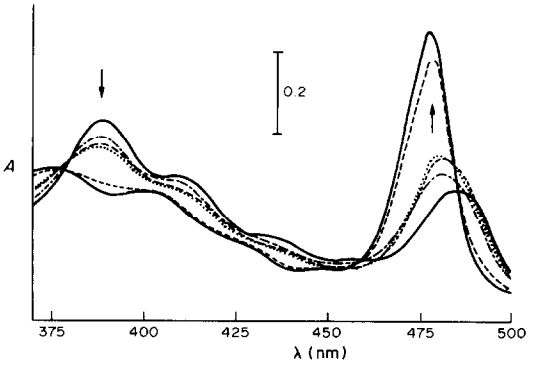

Fig. 2. Representative spectra obtained during the titration of $5.0 \times 10^{-5}M$ TPPMn(III)ClO_4 with pyridine, in $0.1M$ TBAP, $C_2H_4Cl_2$. Arrows indicate spectral trends observed when changing C_M:C_L from 1:0 to 1:4000.

Table 4. Stability constants for metalloporphyrin–axial ligand interactions

Equilibrium system	$\log \beta_{101} \pm \sigma_{\log \beta_{101}}$	$\log \beta_{102} \pm \sigma_{\log \beta_{102}}$	σ_{Data}	λ start; λ stop; number of wavelengths; number of spectra
TPPMn(III)ClO$_4$				
Imidazole	$4.35 \pm 0.43_4$	$7.45 \pm 0.04_0$	0.006	360; 500; 29; 12
Pyridine	$4.08 \pm 0.47_9$	$6.99 \pm 0.07_8$	0.008	360; 500; 29; 10
DMSO	$3.49 \pm 0.01_9$	$5.74 \pm 0.02_1$	0.003	360; 500; 29; 13
TPPCd				
Imidazole	$4.23 \pm 0.08_5$	—	0.009	555; 640; 18; 16
Pyridine	$3.37 \pm 0.06_4$	—	0.007	555; 640; 18; 16
TPPMg				
Imidazole	$4.98 \pm 0.03_4$	$5.19 \pm 0.10_2$	0.003	555; 640; 18; 16
Pyridine	$3.63 \pm 0.04_1$	$2.90 \pm 0.03_4$	0.006	555; 640; 18; 16
TPPRu(CO)				
Imidazole	$4.96 \pm 0.02_4$	—	0.004	510; 567; 5; 24; 14
Pyridine	$4.63 \pm 0.01_4$	—	0.003	510; 567; 5; 24; 14
DMSO	$4.53 \pm 0.02_7$	—	0.003	510; 567; 5; 24; 15
TPPCu				
Pyridine	$-1.28 \pm 0.00_7$	—	0.002	525; 580; 45; 7

equilibria that in several instances could not be interpreted by using conventional techniques.

TPPMn(III)ClO_4 interactions with imidazole, pyridine and DMSO give rise to relatively small spectral changes,[10] Fig. 2. Previous studies on (*p*-CH_3)TPPMnCl complexes with pyridine[11] noted the absence of clear isosbestic points, and attempts to determine the nature of the species in solution proved inconclusive. Our attempts to interpret the data in the manner suggested by Walker *et al.*[2] for iron porphyrins did not alleviate the situation. A qualitative examination of the spectral changes over the $C_M:C_L$ range from 1:0 to 1:4000 indicated the formation of more than two species in equilibrium. No wavelength (in the 360–500 nm region) could be found that would provide the appropriate slopes for the B–H plots.

In contrast, analysis of the absorbance data by SQUAD provided clear evidence of existence of the ML and ML_2 complexes. The difficulties encountered when using the B–H method are traceable to the close similarities of the spectra for M and ML, particularly for L = pyridine (Fig. 2) and the fact that overlapping equilibria exist. Table 4 lists the results of the refinement process for these three ligands.

The TPPMg equilibrium systems with pyridine and imidizole[9] illustrate a situation where reliable equilibrium constants were unobtainable without the use of SQUAD. The magnitudes of the stability constants, Table 4, and the observed spectral changes, together pose considerable problems. The addition of the first axial ligand, forming ML, is characterized by a very small red shift (~3 nm) and only a slight increase in absorbance, Fig. 3A, but β_1 is about 10^4–10^5. In direct contrast, the formation of ML_2 is accompanied by large red shifts (~25 nm), dramatic absorbance changes, Fig. 3B, but a very small K_2 ($=\beta_{102}/\beta_{101}$). The equilibria for both ligands may be considered as two distinct steps. B–H analysis of the data, considering formation of ML and ML_2 separately, did not provide any useful answers. The minimal spectral changes associated with the formation of ML would not be expected to provide any suitable wavelength for such data assessment. However, it is somewhat surprising that little conclusive evidence could be gleaned by the B–H method from the data relevant to the formation of ML_2, other than that ML_2 is a weak complex. Previous studies of TPPMg with pyridine and other axial ligands have

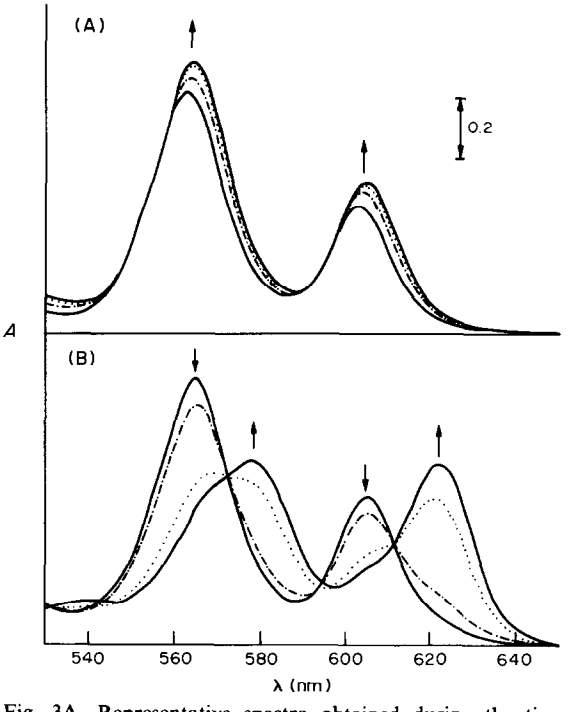

Fig. 3A. Representative spectra obtained during the titration of $5.0 \times 10^{-5}M$ TPPMg with pyridine in $0.1M$ TBAP, CH_2Cl_2. Arrows indicate spectral trends observed when changing $C_M:C_L$ from 1:0 to 1:1000.

Fig. 3B. As for Fig. 3A but illustrating spectral trends observed when changing $C_M:C_L$ from 1:4000 to 1:223000.

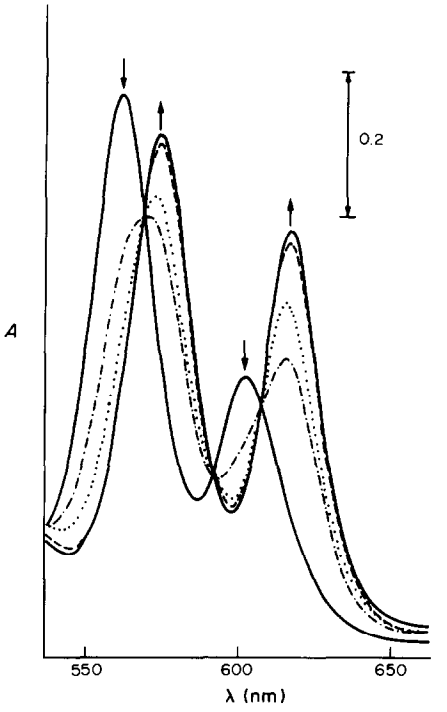

Fig. 4. Representative spectra obtained during the titration of $5 \times 10^{-5}M$ TPPCd with pyridine in $0.1M$ TBAP, $CHCl_3$. Arrows indicate spectral trends observed when changing $C_M:C_L$ from 1:0 to 1:100.

reported only approximate values or a single value for $M \rightarrow ML \rightarrow ML_2$.[12,13]

Interactions of TPPCd with pyridine and imidazole were investigated by use of B–H plots and SQUAD. These two approaches provided values of log β_{101} that were in reasonable agreement for each equilibrium system. The results shown in Table 4 are taken from the SQUAD analysis of the data. These may be compared with, for example, log $\beta_{101} = 3.28$ and 4.31 for TPPCd with pyridine and imidazole, respectively, obtained by using absorbance data at 625 nm and the B–H approach. Other selected wavelengths gave a spread of values for log β_{101} that spanned the values obtained from SQUAD. These systems are inherently amenable to the B–H methodology since only ML is formed and there are significant differences in the spectra of complexed and uncomplexed TPPCd, Fig. 4.

The addition of DMSO, pyridine and imidazole to TPPRu(CO)[14] results in spectral shifts of less than 8 nm and absorbance changes of no more than 15%, Fig. 5. Although only ML is formed, B–H analysis of the data yielded slopes ranging from 0.8 to 1.2, leading to considerable uncertainty in the value of log β_{101} as determined from B–H plots. However, analysis by SQUAD of the absorbance data from the interactions of the 20 ligands with TPPRu(CO) permitted meaningful deductions to be made concerning the nature of the bonding in TPPRu(CO) axial interactions with nitrogenous bases.

The reaction of pyridine with TPPCu exemplifies

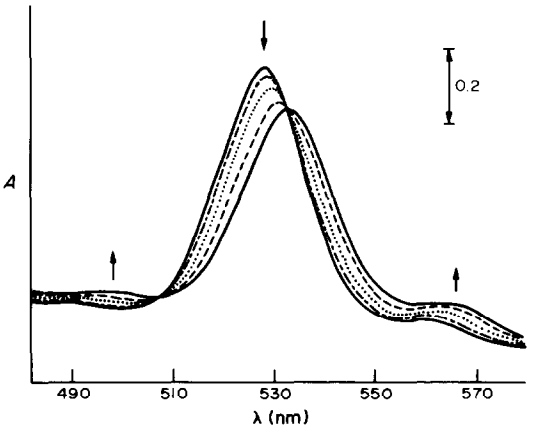

Fig. 5. Representative spectra obtained during the titration of $5.0 \times 10^{-5}M$ TPPRu(CO) with pyridine in $0.1M$ TBAP, CH_2Cl_2. Arrows indicate spectral trends observed when changing $C_M:C_L$ from 1:0 to 1:1.

the ability of SQUAD to process data arising from extremely weak interactions. For this study the reference cell contained the same molarity of ligand as was used in the sample cell, for each spectrum. This precaution was taken to minimize refractive index changes due to the high concentration of pyridine ($1–8M$) required to achieve any significant degree of complexation. Fig. 6. No evidence was found, during data processing, for any complexes other than ML. The stability constant found was in excellent agreement with previously reported results.[12]

DISCUSSION

The results presented above demonstrate that SQUAD is capable of providing reliable estimates of stability constants that best describe the available

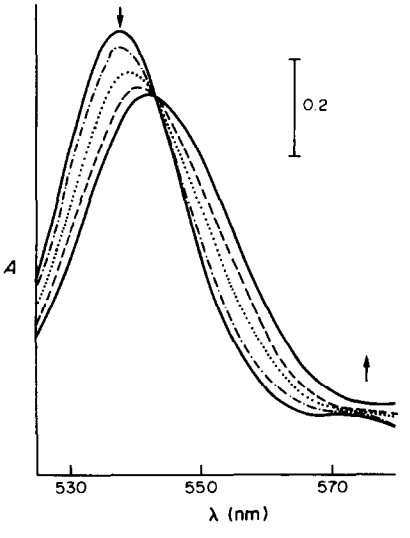

Fig. 6. Representative spectra obtained during the titration of $5 \times 10^{-5}M$ TPPCu with pyridine in $0.1M$ TBAP, CH_2Cl_2. Arrows indicate spectral trends observed when changing $C_M:C_L$ from 1:0 to 1:200,000.

data. However the question "how do we know that the answers are correct?" must be dealt with. Although the numerical reliability of SQUAD is not in doubt, the values of stability constants obtained from 15 spectra and 20 absorbance values per spectrum, for example, can only be considered to be applicable *to that set of data.* Assuming that no gross errors have been made in solution preparation *etc.*, it *may* be safe to assume that these refined values, from one set of data, are descriptive of the metal–ligand equilibrium system. It is *wiser* though, to repeat the experiment, making fresh stock solutions of metal and ligand and using different $C_M:C_L$ for the spectra. Values of constants from different data sets that are in agreement, within experimental uncertainty, lend credence to the reliability of the numbers and the proposed model.

Initial acceptance of the stability-constant values derived from any set of absorbance data, may be governed by a number of statistical parameters calculated by SQUAD. The "standard deviation in the absorbance data", σ_{DATA}, calculated from the set of stability constants at the end of each refinement cycle is, in essence, an overall measure of the fit of the model to the data. Realistically, we may expect that any single absorbance value will be accurate to ± 0.003 (for a Cary 14 spectrophotometer). Consequently, we would expect that if the fit between data and model were perfect there would be a residual, due to experimental error and uncertainty, of between about ± 0.003 and ± 0.005. Thus inspection of σ_{DATA}, based on the *refined* stability constants, will indicate how closely we have come to a "perfect" fit. Although there is no hard and fast rule, values of $\sigma_{DATA} > \sim 0.01$ indicate that a good fit has *not* been obtained. SQUAD will also provide estimates of the standard deviation of each refined constant, σ_{CONST}. Generally, values of σ_{CONST} of the order of 1% of the particular constant are indicative of a good fit. Clearly the lower σ_{CONST} is (below 1%) the better the fit.

These remarks pose the question "what if σ_{DATA} and σ_{CONST} are greater than the recommended levels?" Several answers are possible. If the equilibrium model being fitted to the data considers only ML but in reality both ML and ML_2 are formed, the fit may worsen as the concentration of ligand, relative to metal increases, *i.e.*, as ML_2 starts to predominate. This may result in high σ_{DATA} and σ_{CONST}. The trend will be visible most clearly in the values of σ_{SPECT} (the standard deviation of *each* spectrum), increasingly bad fits being observed for higher ligand concentrations. The reverse situation would be one where the model was ML *and* ML_2 but the data were representative of a system consisting of only ML. Again σ_{DATA} would be unacceptably high, but σ_{SPECT} would not necessarily indicate bad fits for low ligand concentrations, relative to the metal, compared to higher concentrations. SQUAD would attempt to "remove" ML_2 from numerical consideration by successively reducing the value of $\log \beta_{102}$ until $[ML_2]$, for all spectra taken, was effectively zero. This would be shown by a rapidly increasing σ_{CONST} for $\log \beta_{102}$ and termination of the refinement process if σ_{CONST} became greater than 200.

The second major cause for large values of σ_{DATA} and σ_{CONST} arises from gross experimental error in making stock solutions or preparing solutions for a specific spectrum. The former error is sometimes difficult to detect until a new experiment is performed. The latter problem is readily seen from inspection of each σ_{SPECT} value. An anomalously high value indicates a problem with that particular spectrum. If the data for that spectrum are removed from the data-set, σ_{DATA}, σ_{CONST} and σ_{SPECT} should be reduced when the data are reprocessed but the values of the refined constants should *not* be substantially different. Sloppy technique will cause random errors to be introduced at each stage of the experiment, with the result that all σ values will be high and the refinement will take a large number of cycles, if it can be achieved at all. Care should be taken, however, to distinguish poor manipulative technique from impurities in metal or ligand. Obviously, samples of metal and ligand should be purified as carefully as possible without resorting, in the first instance, to extreme measures. Nothing is to be gained by inordinate time spent on purifications followed by inadequate precautions taken in preparing solutions.

Assessment of the quality of the data and the model may also be obtained, indirectly, from inspection of the calculated molar absorptivities. One particularly useful feature of SQUAD is the ability to calculate molar absorptivities of species even though the stability constant is not being refined. In the studies described earlier, irrespective of whether the model was ML alone or ML *and* ML_2, the molar absorptivities for the complex(es) *and* the uncomplexed metalloporphyrin were calculated. The values obtained for free metalloporphyrin were then compared with those obtained from absorbance studies of solutions containing various concentrations of only the porphyrin. Close agreement between the results from the simple Beer's law calculations and from SQUAD provided extra assurance for the validity of the proposed model as well as the purity of the metalloporphyrin.

A second diagnostic indicator arises from the calculated molar absorptivities for each species, which when plotted provide spectra for individual species. Clearly, within the ultraviolet–visible region, the shape of each species spectrum should be a smooth continuous curve bearing some resemblance to portions of the observed spectra for various $C_M:C_L$ ratios. Severely disjointed plots are strongly indicative of a less than adequate fit of the model to the data.

It is also possible that negative values for the molar absorptivities are returned. Although this situation may often be traced to poor quality data or an

incorrect model, there is another cause. Consider two species in solution, having concentrations of 1.753×10^{-5} and $3.14 \times 10^{-6} M$. At some wavelength the absorbance is observed to be 0.141. By use of the multiple regression algorithm, values of 1.11×10^{4} and -1.73×10^{4} $l.mole^{-1}.cm^{-1}$ are found for the molar absorptivities of these two species, at the wavelength concerned. However, solving the same linear equations by the non-negative linear least-squares algorithm yields values of 8.5×10^{3} and 1.0×10^{2} $l.mole^{-1}.cm^{-1}$ for the same species. It should be noted that within SQUAD, the linear equations arising from Beer's law are solved wavelength by wavelength, from absorbance data and the appropriate species concentrations, for each spectrum. Therefore, we are dealing with an over-determined set of simultaneous equations. Since a negative molar absorptivity has no chemical significance, the cause of these negative values must be sought. It is assumed that the equilibrium model is correct and the data are as reliable as the spectrophotometer can produce, *i.e.*, ± 0.003 absorbance units. That a multiple regression treatment of the data gives rise to a negative molar absorptivity is attributable to the very small contribution (0.2%) of the second species to the observed absorbance at that wavelength. In this particular instance, the molar absorptivity is in fact close to zero. Non-negative linear least-squares analysis precludes the calculation of negative values for molar absorptivities and provides numbers that are in agreement with the qualitative observations—namely that the second species does not absorb radiation at this wavelength. A more detailed discussion of this point has already been published,[8] where the validity and use of NNLS have been amply demonstrated.

Clearly, there will be times when the multiple regression algorithm will calculate negative molar absorptivities, but the correctness of the model will still be in doubt. In these situations switching to the non-negative least squares algorithm should be done *only as a last resort* and efforts should be made to establish independently whether or not one species has negligible interaction with radiation at the particular wavelength(s).

Conclusions

The usefulness of SQUAD for determining stability constants from metalloporphyrin–axial ligand interactions has been clearly demonstrated. For most of the examples chosen the constants were not obtainable by conventional graphical or single-wavelength techniques. The program is completely general and no "simplifying" assumptions are required such as [free ligand] = [total ligand] or selection of "appropriate" wavelengths. In passing it should be noted that simplifying assumptions, used to obtain stability constant values, may well complicate theories that have been based on the values obtained from such methodologies.

SQUAD also produces individual species spectra for each complex present in solution. Careful examination of the output from SQUAD can act as a valuable guide to remedying shortcomings in experimental technique. The program is easy to use and requires no knowledge of FORTRAN. The arrangement of the data deck has been designed to be "user-friendly" and many instructive error messages are available to assist the user in rectifying any mistakes that may have occurred. Listings of SQUAD, user's manual, sample data and outputs are available (from DJL) and specific arrangements can be made for obtaining a tape copy of program and data.

Acknowledgements—We gratefully acknowledge the support of the National Science Foundation (Grant No. CHE-7921536, to KMK) and the Robert A. Welch Foundation (Grant No. E-680, to KMK, and E-755, to DJL).

REFERENCES

1. R. W. Ramette, *J. Chem. Educ.*, 1967, **44,** 647.
2. F. Walker, M.-W. Lo and M. T. Ree, *J. Am. Chem. Soc.*, 1976, **98,** 5552.
3. W. A. E. McBryde, *Talanta*, 1974, **21,** 979.
4. D. J. Leggett, *Am. Lab.*, 1982, **14,** (No. 1), 29.
5. F. Gaizer, *Coord. Chem. Rev.*, 1979, **27,** 195.
6. L. G. Sillén and G. Warnquist, *Arkiv Kemi*, 1968, **31,** 315.
7. D. J. Leggett and W. A. E. McBryde, *Anal. Chem.*, 1975, **47,** 1065.
8. D. J. Leggett, *ibid.*, 1978, **50,** 718.
9. K. M. Kadish and L. R. Shiue, *Inorg. Chem.*, 1982, **21,** 1112.
10. S. L. Kelly and K. M. Kadish, *ibid.*, 1982, **21,** 3631.
11. G. N. La Mar and F. A. Walker, *J. Am. Chem. Soc.*, 1975, **97,** 5103.
12. J. R. Miller and G. D. Dorough, *ibid.*, 1952, **74,** 3977.
13. C. B. Storm, A. H. Corwin, R. R. Arellano, M. Martz and R. Weintraub, *ibid.*, 1966, **88,** 2525.
14. K. M. Kadish, D. J. Leggett and D. Chang, *Inorg. Chem.*, 1982, **21,** 3618.

Talanta, Vol. 30, No. 8, pp. 587–591, 1983
Printed in Great Britain.

0039-9140/83 $3.00 + 0.00

SPECTROPHOTOMETRIC DETERMINATION OF LITHIUM IN BLOOD SERUM WITH THORON

JAY K. TRAUTMAN, VICTOR P. Y. GADZEKPO and GARY D. CHRISTIAN*
Department of Chemistry, BG-10, University of Washington, Seattle, WA 98195, U.S.A.

(*Received* 15 *September* 1982. *Revised* 13 *January* 1983. *Accepted* 12 *February* 1983)

Summary—Lithium is determined in blood serum by reaction with thoron [1-(*o*-arsenophenylazo)-2-naphthol-3,6-disulphonic acid, sodium salt] in an alkaline acetone medium. A bathochromic shift in the thoron spectrum results and the change in absorbance at 480 nm is measured against the reagent as reference. Proteins are removed with trichloroacetic acid, and the effect of serum electrolyte is compensated for by adding a synthetic serum electrolyte to the reagent blank. Results of analysis of serum samples from manic depressive patients by this method agree with atomic-absorption spectroscopy results with an average error of −1.1% for forty samples, with a correlation coefficient of 0.987.

Lithium salts are administered to psychiatric patients diagnosed as manic depressive. The concentration of lithium ion in the blood is maintained at between approximately 0.5 and 1.0m*M*. At slightly higher concentrations, however, lithium is toxic. Adverse side-effects appear at concentrations around 2.0–2.5-m*M*.[1] Higher levels can be fatal. It is therefore necessary that clinics administering lithium therapy should have available a method for determining lithium in blood.

This determination is usually performed by flame photometry or atomic-absorption spectrophotometry,[1] but the use of a flame and compressed gases is one which clinics, for reasons of safety or convenience, may prefer to avoid and an alternative method would be desirable.

Organic reagents having either an $-AsO(OH)_2$ or a $-PO(OH)_2$ group *ortho* to an azo group have been reported as complexing agents for lithium. The complex formation results in a bathochromic shift of the reagent spectrum.[2] It has been reported by Thomason[3] and Lazarev and Lazareva[2] that microgram amounts of lithium can be determined spectrophotometrically with thoron [1-(*o*-arsenophenylazo)-2-naphthol-3,6-disulphonic acid, sodium salt] in alkaline aqueous acetone medium. The interferences reported for sodium, calcium and magnesium are low enough to warrant investigation of this reagent for determination of lithium in blood. We report here a successful method based on this reaction.

EXPERIMENTAL

Instrumentation

A Varian Superscan 3 ultraviolet–visible double-beam spectrophotometer was used for all absorbance measurements. The band-pass was 10 nm and 1-cm quartz cells were used. A Beckman 152 "microfuge" was used for centrifugation. A 50-μl Beckman micropipette with disposable tips was used for dispensing small volumes. The lithium concentration of the blood serum samples was determined with a Perkin–Elmer 560 atomic-absorption spectrophotometer. Sodium analyses were done with a Jarrel–Ash Model 955 "Atom Comp" inductively-coupled plasma spectrometer.

Reagents

All chemicals were reagent grade unless otherwise specified. The thoron was a product of ICN Pharmaceuticals Inc.; the lithium chloride used for standards was from Fisher Scientific Co.; the potassium hydroxide pellets were from Mallinckrodt; the trichloroacetic acid (TCA) was from J. T. Baker; the acetone was technical grade produced by Cascade.

Thoron reagent. Separate stock solutions of thoron (0.27%) and potassium hydroxide (made by dissolving 4 g of pellets containing approximately 85% KOH, in 100 ml of water) were prepared in demineralized water. The thoron reagent solution was prepared by adding 10 ml of the stock thoron solution, 20 ml of the potassium hydroxide solution, 60 ml of acetone and 10 ml of demineralized water to a 100-ml flask and mixing. The final volume was somewhat less than 100 ml. For the best results, the thoron reagent solution should be prepared on the day of use. The individual stock solutions are stable for several months.

Serum preparation

The serum proteins were precipitated with trichloroacetic acid (TCA). A 100-μl aliquot of blood serum was added to 100 μl of 15% TCA solution in a 250-μl disposable plastic centrifuge tube. The mixture was centrifuged for 2–3 min and the supernatant liquid was used for analysis.

Serum electrolyte blank

A simulated solution of blood electrolytes for use as a compensatory blank was prepared by dissolving the following in demineralized water and diluting to 500 ml: NaCl 4.01 g, KH_2PO_4 0.09 g, $CaCl_2 \cdot 2H_2O$ 0.0935 g, $ZnCl_2$ 0.006 g, KCl 0.105 g, $MgCl_2 \cdot 6H_2O$ 0.124 g, $FeCl_3 \cdot 6H_2O$ 0.009 g. A 1:1 v/v mixture of this solution and the 15% TCA solution was used as a blank.

Serum analysis

To determine the lithium content of a serum sample, 3 ml of thoron reagent were pipetted into each of two spec-

*Author for correspondence.

trophotometric cells. A difference spectrum was run to establish a baseline. The absorbance reading at 480 nm was adjusted to zero. Then 100 μl of serum supernatant were pipetted into the sample cell; the cell was shaken gently and the time noted. A 100-μl aliquot of the 1:1 TCA–electrolyte blank solution was added to the reference cell. After 2 min, the absorbance at 480 nm was read. The time between the introduction of the serum sample into the cell and the recording of the response was kept constant from trial to trial, because though the reaction reaches about 90% completion essentially instantaneously, the remainder of the reaction is slow.

Calibration

Aqueous lithium chloride standards were used for the calibration. A 50-μl aliquot of 1m*M* lithium standard was added to the sample cell containing 3 ml of thoron reagent, and 50 μl of demineralized water were pipetted into the reference cell, also containing 3 ml of thoron reagent. A difference reading was taken at 480 nm after 2 min. This standard corresponds to a 0.5m*M* lithium concentration in the sample supernatant or 1m*M* in the original sample. The calibration curve was slightly non-linear over the concentration range studied (Fig. 1), but the use of a single 1m*M* standard gives satisfactory results for serum values, as evidenced below. The standard should be run at the same time as the sample analysis, because there is a slight and gradual change in the thoron reagent during the day.

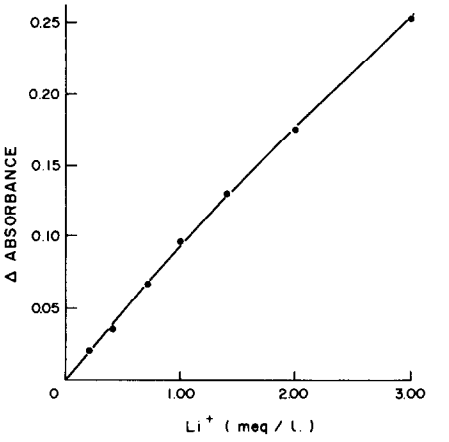

Fig. 1. Calibration curve for lithium standards approximating to the physiological concentration range for lithium-treated patients.

RESULTS AND DISCUSSION

Lithium response

The probable structure for the complex of lithium ion with thoron, deduced from studies of the reaction of bisazo derivatives of chromotropic acid with alkaline-earth cations by Savvin and Petrova,[4] is shown below

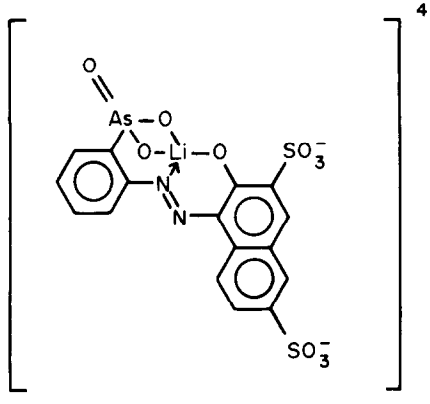

The reaction of thoron with lithium results in a bathochromic shift in the thoron absorption spectrum (Fig. 2). The maximum absorption of the thoron reagent is at around 445 nm; that of the complex is shifted to a slightly longer wavelength. The greatest difference between the two spectra is at 480 nm (Fig. 3). A 1m*M* lithium sample changes the reagent absorbance at 480 nm by about 4% (for the reagent concentration used).

Reagent properties

The thoron reagent solution proved to be unstable with time. The colour of the solution lightened noticeably and, more importantly, its effectiveness as a reagent for lithium was diminished. In a 24-hr period both the absorbance of the thoron reagent at 445 nm and the difference response for a 1m*M* lithium sample were decreased by about 10%. However, when kept separately as aqueous solutions, the components of the thoron reagent solution were found to be stable.

The optimal concentrations of the reagent constituents were determined by the simplex optimization method.[5] The recommended concentrations are not optimized in terms of magnitude of lithium response. It was found that there were advantages in reducing the acetone and the potassium hydroxide concentrations; lowering the acetone content stabilized the reagent (*i.e.*, it reduced the amount of aeration upon mixing, so readings could be made more quickly), and lowering the alkalinity decreased the intensity of the reagent colour, thus reducing the signal noise. Neither alteration was large enough, though, to have much effect on the lithium response.

Sample properties and interferences

Table 1 lists the difference responses for the reaction of some interfering substances with the thoron reagent at 480 nm. In lithium-spiked control blood samples, the interfering elements were successfully swamped out by preparing both the sample and the

Table 1. Relative responses of interfering substances (each solution treated in the same way as the lithium standard)

Interferent	[Li^+] equivalent to response, *m*M
Na^+ (3200 ppm)	0.6
Ca^{2+} (103 ppm)	0.1
Mg^{2+} (58 ppm)	0.1
Blood electrolyte solution	0.5
Albumin (7%)	0.2
Serum	1.1

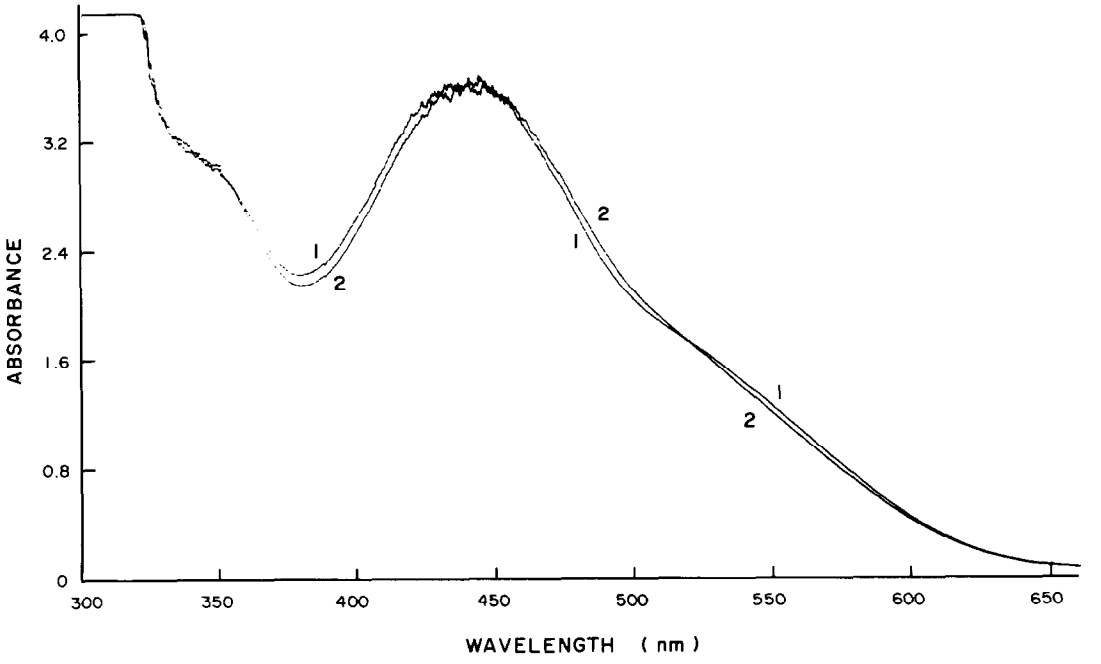

Fig. 2. Spectrum of (1) 3 ml of thoron reagent solution plus 50 μl of water, and (2) 3 ml of thoron reagent solution plus 50 μl of 1mM lithium standard.

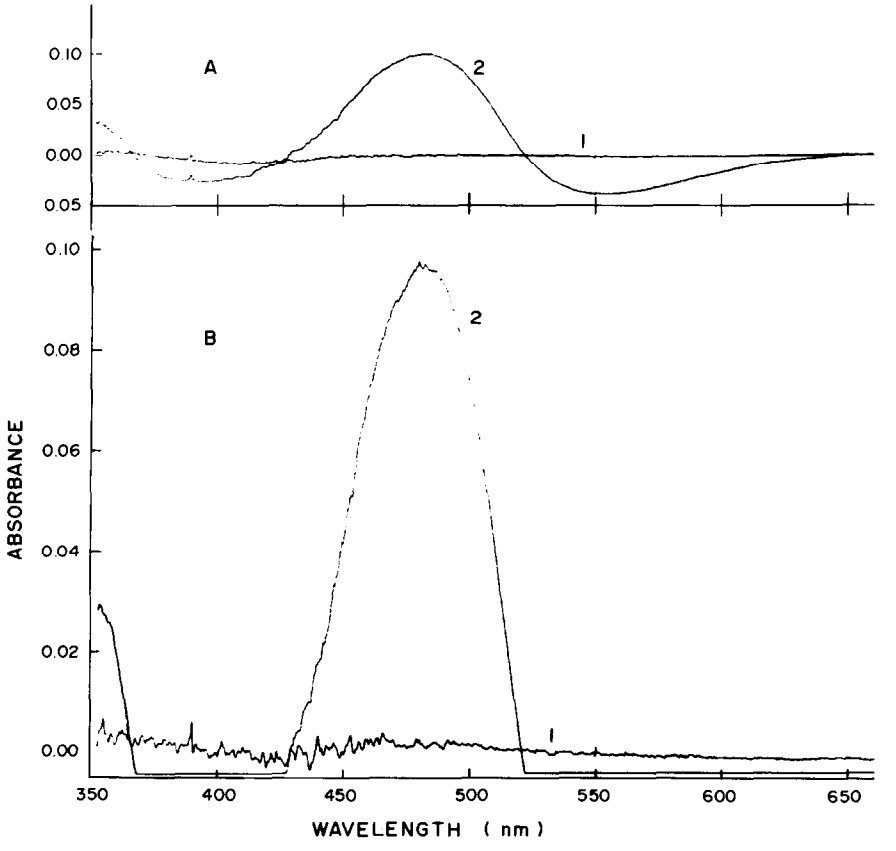

Fig. 3. Difference spectrum, obtained by the recommended procedure, for 1mM lithium standard. A, Absorbance 0.5 full scale. B, Absorbance 0.1 full scale.

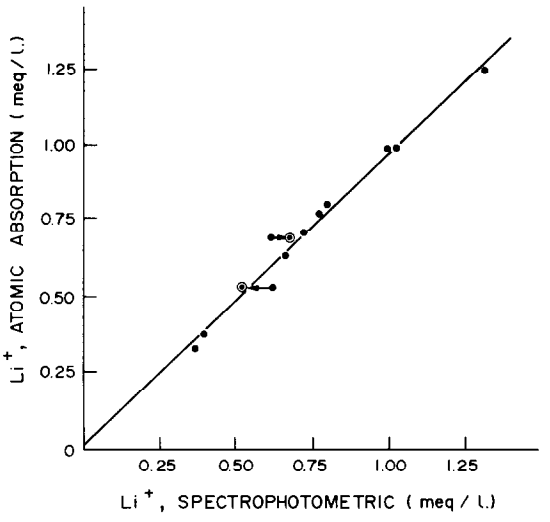

Fig. 4. Correlation plot for serum lithium values determined by the present method and by atomic-absorption spectrophotometry.

reference solutions with thoron reagent containing a sodium concentration essentially the same as that of the serum supernatant. The lithium response was reduced by 50% by this environment, and the reaction proceeded more slowly, but accurate results were obtained. When other samples were analysed, however, it became evident that different sera give significantly different absorbances with the same thoron reagent. The value given in the table for serum is an average response, and the variations from it proved to be large enough to cause as much as 100% error in some lithium determinations. Though the albumin response was relatively small, it became apparent that the individual serum fluctuations were due to protein interactions with the thoron. Perhaps globulin or other proteins exhibit significant response.

Denaturation of the serum proteins with tetramethylammonium hydroxide lessened the variations, but precipitation of the proteins was much more effective and essentially eliminated all protein response. Two precipitation methods were tested. Both the barium hydroxide/zinc sulphate and the trichloroacetic acid methods worked well[6], but the use of TCA was more convenient and faster. The acid nature of the protein-free filtrate decreased the lithium response by about 5%, so the potassium hydroxide concentration was correspondingly increased (to the 4% recommended in the procedure) to correct for this.

A solution of blood electrolytes was then made for addition to the reference cell. A 1:1 v/v mixture of this solution and the TCA solution, when used as the reference for the 1:1 TCA–serum supernatant mixture, gave zero difference reading at 480 nm, for a number of test sera.

With this procedure, samples containing known amounts of lithium (determined by atomic absorption) yielded responses comparable to those of corresponding aqueous lithium standards. For automation of the method it should be possible to use a dialysis system to separate the lithium from the serum proteins.

Serum analyses

Forty samples from manic depressive patients were analysed in groups of ten on four different days. A plot of values found by the thoron method *vs.* values found by atomic absorption for one set is shown in Fig. 4; the correlation coefficient was 0.986 and the least-squares slope (m) and intercept (b) were 0.964 and 0.012, respectively. The corresponding averages of all four sets were $r = 0.987$, $m = 0.988$, $b = 0.011$, demonstrating consistent results. A Student t-test for the 40 samples resulted in a calculated t-value of 1.00, which is less than the tabulated t-value for even an infinite number of samples at the 90% confidence level, indicating no significant difference between the two methods.[6]

Accuracy and precision

There is a random but controllable error inherent in this system, which may be attributed to the mechanics of pipetting micro volumes. Replicate measurements were made on a number of serum samples, each with a lithium concentration of about 1mM. The relative difference between the thoron-method values for two separately prepared test solutions from each of 40 different sera averaged 5%, and the difference of either value for a given pair of samples from the atomic-absorption value for that serum was approximately 3%, *i.e.*, the two thoron values straddled the atomic-absorption value. The pipetting precision could obviously be improved by using a 100-μl pipette for the sample and TCA, rather than two 50-μl volumes for each.

The only fundamental interference stems from the propensity for thoron to react with sodium. In sera sodium is present in concentrations some 140 times that of lithium. This quantity of sodium gives a response equivalent to a 0.6mM lithium concentration in the sample, and is corrected for in the procedure given. The sodium concentration does not vary much from one sample to another, but if abnormal will cause an error in the lithium determination. For instance, the two data points for the samples at the tails of the arrows in Fig. 4 were redetermined by the thoron procedure, and both were again as shown. Likewise, the atomic-absorption values were corroborated by re-evaluation. Finally, the two samples were analysed for sodium by inductively-coupled plasma spectroscopy (ICP). From the sodium–thoron absorbance data and the ICP data for the deviations from the expected 3200 ppm value for sodium, corrections for the sodium effect were made which placed the two points very nearly on the line (circled points in Fig. 4). For this set of measurements the thoron values were, on average, 2.3% higher than the AAS values; applica-

tion of the sodium corrections reduced this difference to 1.2%. For the set of 40 sera the means of the uncorrected thoron values were (on average) 1.1% lower than the AAS values. If sodium measurements are routinely made along with the lithium measurements, automatic corrections can be made to ensure highly accurate lithium measurements.

The present method offers an alternative to flame methods for serum lithium measurements. Measurement of a single sample requires only a few minutes. Automation would allow rapid and precise measurements.

Acknowledgements—The financial assistance of Beckman Instruments, Inc. is gratefully acknowledged. The authors are indebted to Dr. Robert Labbe and to Ann Melchior for providing lithium samples analysed by atomic-absorption.

REFERENCES

1. N. W. Tietz (ed.), *Fundamentals of Clinical Chemistry*, pp. 899–900, p. 878. Saunders, Philadelphia, 1970.
2. A. I. Lazarev and V. I. Lazareva, *Zh. Analit. Khim.*, 1968, **23,** 36.
3. P. F. Thomason, *Anal. Chem.*, 1956, **28,** 1527.
4. S. B. Savvin and T. V. Petrova, *Zh. Analit. Khim.*, 1969, **24,** 177.
5. D. E. Long, *Anal. Chim. Acta*, 1969, **46,** 193.
6. G. D. Christian, *Analytical Chemistry*, 3rd Ed. Wiley, New York, 1980.

Talanta, Vol. 30, No. 8, pp. 593–603, 1983
Printed in Great Britain

0039-9140/83 $3.00 + 0.00
Pergamon Press Ltd

NECESSARY AND SUFFICIENT CONDITIONS FOR THE APPEARANCE OF EXTREMA ON CONCENTRATION DISTRIBUTION CURVES IN COMPLEX EQUILIBRIUM SYSTEMS

ISTVÁN NAGYPÁL and MIHÁLY T. BECK
Department of Chemistry, L. Kossuth University, H-4010 Debrecen, Hungary

ANDREAS D. ZUBERBÜHLER
Institute of Inorganic Chemistry of the University, Spitalstrasse 51, CH-4056 Basel, Switzerland

(*Received* 9 *December* 1982. *Accepted* 3 *February* 1983)

Summary—It is shown that species distribution curves with at least one minimum may be found in most equilibrium systems with three or more components. Whether such concentration minima are actually observed then depends on the values of the equilibrium constants and on the total (analytical) concentrations of the components. A general algorithm is given for the necessary and sufficient conditions for the appearance of extrema in multicomponent systems. Three-component systems are studied in more detail and special attention is given to the limiting case of a horizontal inflection, *i.e.*, the point where the concentration minimum just disappears. Two well-studied chemical examples, the Cu^{2+}–diethylenetriamine–OH^- and Hg^{2+}–Cl^-–OH^- systems are discussed, along with a simple model system showing as many as five extrema on a single distribution curve.

Recently, a number of examples have been given of the existence of extrema on the concentration distribution curves of species formed in three- and multicomponent complex equilibrium systems.[1–9] Some of the rules governing concentration distributions, the classification of three-component equilibrium systems with special regard to concentration minima, and the definition of the thermodynamic and stoichiometric asymmetry responsible for the minima have been discussed in earlier papers.[10–12] Stoichiometric asymmetry means that at least one species is missing from the set of stepwise equilibria or that the maximum number of ligands is different in the series of complexes with different components. Evidently, stoichiometric asymmetry is a limiting case of thermodynamic asymmetry.[12]

Stoichiometric (and/or thermodynamic) asymmetry is therefore a *necessary condition* for the presence of concentration minima. If the condition is fulfilled, then the total concentrations and the formation constants determine whether concentration minima are indeed exhibited or not.

In this paper we wish to present a general method to determine the *sufficient conditions* for the appearance of concentration minima. Specific attention is given to *points of horizontal inflection* where the minima just appear or disappear. The effect of the magnitude of the formation constants and the total concentrations on the manifestation of concentration minima is illustrated for two examples taken from the literature and also for a relatively simple model system in which one of the species can exhibit as many as five extrema along the distribution curve.

MATHEMATICAL ANALYSIS

Any equilibrium system is fully characterized by the system of equations (1) expressing the mass balance based on the law of mass action:

$$\begin{aligned} T_1 &= \sum_{j=1}^{n} \alpha_{j1}[S_j] = \sum_{j=1}^{n} \alpha_{j1}\beta_j \prod_{i=1}^{k} [c_i]^{\alpha_{ji}} \\ &\vdots \\ T_k &= \sum_{j=1}^{n} \alpha_{jk}[S_j] = \sum_{j=1}^{n} \alpha_{jk}\beta_j \prod_{i=1}^{k} [c_i]^{\alpha_{ji}} \end{aligned} \qquad (1)$$

where:

k = number of components c_i in the system;
n = number of species S_j in the system, including the components;
$T_1 \ldots T_k$ = total concentrations of the components;
α_{ji} = stoichiometric numbers, giving the number of components c_i in the species S_j;
$\beta_j = [S_j]/\prod_{i=1}^{k} [c_i]^{\alpha_{ji}}$ = formation constant of species S_j (the formation constants of the components are unity by definition).

The concentration distribution in terms of equation (1) means that the total concentrations $T_2 \ldots T_k$ are kept constant while the concentration of c_1 is changed and the species concentrations are calculated and plotted against $-\log[c_1]$. Thus $-\log[c_1]$ is the independent variable, the concentrations of the species are dependent variables and the values of $T_2 \ldots T_k$, $\beta_1 \ldots \beta_n$ are the parameters of the system under consideration. The functions $[S_j] = [f([c_1])]$, however, can be expressed explicitly only in excep-

tionally simple cases, whereas equation (1) normally represents an implicit function system.

The rules for obtaining the analytical derivatives of implicit function systems can be found in every textbook of mathematical analysis. In spite of this, the various derivatives necessary for the computer calculations based on equation (1) are almost exclusively calculated numerically.[13-15] The use of analytical derivatives of equation (1) has been discussed by Bugaevsky *et al.*[16] and later by Nagypál *et al.*[17] It has been incorporated into recent computer programs for the calculation of stability constants,[18,19] and leads to the following system of equations:

$$\frac{\partial T_2}{\partial \ln[c_1]} = \sum_{j=1}^{n} \alpha_{j1}\alpha_{j2}[S_j] + \sum_{l=2}^{k}\left(\sum_{j=1}^{n} \alpha_{j2}\alpha_{jl}[S_j]\right)\frac{\partial \ln[c_l]}{\partial \ln[c_1]} = 0$$

$$\vdots$$

$$\frac{\partial T_k}{\partial \ln[c_1]} = \sum_{j=1}^{n} \alpha_{j1}\alpha_{jk}[S_j] + \sum_{l=2}^{k}\left(\sum_{j=1}^{n} \alpha_{jk}\alpha_{jl}[S_j]\right)\frac{\partial \ln[c_l]}{\partial \ln[c_1]} = 0 \qquad (2)$$

Expression (2) is a system of $k-1$ linear equations for the $\partial \ln[c_l]/\partial \ln[c_1]$ derivatives. It can be used easily to study the distribution of any species S_j as a function of $[c_1]$ or $-\log[c_1]$. This is achieved by selecting S_j to be the component c_k and by using the appropriate determinants for $\partial \ln[c_k]/\partial \ln[c_1]$. This selection of S_j as the last component c_k generally requires a suitable transformation of the stoichiometric coefficients in equation (1). Examples of such transformations will be given later.

As indicated by equation (2), the determinants needed to express the $\partial \ln[c_k]/\partial \ln[c_1]$ derivatives are of order $k-1$, and the elements of the determinants are the different sums of the species concentrations multiplied by the appropriate stoichiometric coefficients. Thus both the numerator and the denominator consist of $(k-1)$-fold products of these concentration sums. These products of the concentration sums may be rearranged to the corresponding sums of the concentration products. This rearrangement is given for the general three-component system ($k = 3$). First, equation (2) is transformed into (3):

$$-\sum_{j=1}^{n} \alpha_{j1}\alpha_{j2}[S_j] = \sum_{j=1}^{n} \alpha_{j2}^2[S_j]\frac{\delta \ln[c_2]}{\partial \ln[c_1]} + \sum_{j=1}^{n} \alpha_{j2}\alpha_{j3}[S_j]\frac{\partial \ln[c_3]}{\partial \ln[c_1]}$$

$$-\sum_{j=1}^{n} \alpha_{j1}\alpha_{j3}[S_j] = \sum_{j=1}^{n} \alpha_{j2}\alpha_{j3}[S_j]\frac{\partial \ln[c_2]}{\partial \ln[c_1]} + \sum_{j=1}^{n} \alpha_{j3}^2[S_j]\frac{\partial \ln[c_3]}{\partial \ln[c_1]} \qquad (3)$$

from which the analytical expression for the species distribution [equation (4)] is directly obtained:

$$\frac{\partial \ln[c_3]}{\partial \ln[c_1]} = -\frac{\left(\sum_{j=1}^{n} \alpha_{j2}^2[S_j]\right)\left(\sum_{j=1}^{n} \alpha_{j1}\alpha_{j3}[S_j]\right) - \left(\sum_{j=1}^{n} \alpha_{j1}\alpha_{j2}[S_j]\right)\left(\sum_{j=1}^{n} \alpha_{j2}\alpha_{j3}[S_j]\right)}{\left(\sum_{j=1}^{n} \alpha_{j2}^2[S_j]\right)\left(\sum_{j=1}^{n} \alpha_{j3}^2[S_j]\right) - \left(\sum_{j=1}^{n} \alpha_{j2}\alpha_{j3}[S_j]\right)^2} \qquad (4)$$

For the further transformation of (4) into the desired sum of concentration products, let us take two species, S_p and S_q, with stoichiometric numbers p_1, p_2, p_3 and q_1, q_2, q_3. Their role in the numerator and the denominator is given by equations (5) and (6), respectively.

$$\{(p_2)^2[S_p] + (q_2)^2[S_q]\}\{p_1p_3[S_p] + q_1q_3[S_q]\} - \{p_1p_2[S_p] + q_1q_2[S_q]\}\{p_2p_3[S_p] + q_2q_3[S_q]\} = -(p_1q_2 - q_1p_2)(p_1q_3 - q_2p_3)[S_p][S_q] \qquad (5)$$

$$\{(p_2)^2[S_p] + (q_2)^2[S_q]\}\{(p_3)^2[S_p] + (q_3)^2[S_q]\} - \{p_2p_3[S_p] + q_2q_3[S_q]\}^2 = (p_2q_3 - q_2p_3)^2[Sp][S_q] \qquad (6)$$

It is seen that the concentration products in the numerator are multiplied by the product of the determinants formed from the first two and the last two columns of the matrix composed of the stoichiometric numbers of S_p and S_q:

$$\begin{vmatrix} p_1 & p_2 & p_3 \\ q_1 & q_2 & q_3 \end{vmatrix}$$

At the same time, the concentration products in the denominator are multiplied by the square of the determinant formed from the last two columns of the same matrix. Substituting this result into (4) easily gives the final equation (7) for the analytical derivative:

$$\frac{\partial \ln[c_3]}{\partial \ln[c_1]} = \frac{\sum_{p=1}^{n}\sum_{q=p}^{n}(p_1q_2 - q_1p_2)(p_2q_3 - q_{2p3})[S_p][S_q]}{\sum_{p=1}^{n}\sum_{q=p}^{n}(p_2q_3 - q_2p_3)^2[S_p][S_q]} \qquad (7)$$

A similar, although more tedious, analysis shows that this relation is generally true, *i.e.*, all of the possible $(k-1)$-fold concentration products are found in the numerator, each multiplied by the determinants of the first $(k-1)$ and of the last $(k-1)$ columns of the matrix formed from the stoichiometric numbers of the $(k-1)$ species in question. In the denominator the same concentration products are multiplied by the square of the latter

determinant, as indicated by equation (8):

$$\frac{\partial \ln[c_k]}{\partial \ln[c_1]} = \frac{\sum_{p=1}^{n}\sum_{q=p}^{n}\cdots\sum_{y=x}^{n} \det\begin{vmatrix} p_1p_2\cdots p^{(k-1)} \\ q_1q_2\cdots q_{(k-1)} \\ \\ x_1x_2\cdots x_{(k-1)} \\ y_1y_2\cdots y_{(y-1)} \end{vmatrix} \det\begin{vmatrix} p_2p_3\cdots p_k \\ q_2q_3\cdots q_k \\ \\ x_2x_3\cdots x_k \\ y_2y_3\cdots y_k \end{vmatrix} [S_p][S_q]\cdots[S_x][S_y]}{\sum_{p=1}^{n}\sum_{q=p}^{n}\cdots\sum_{y=x}^{n} \det\begin{vmatrix} p_2p_3\cdots p_k \\ q_2q_3\cdots q_k \\ \\ x_2x_3\cdots x_k \\ y_2y_3\cdots y_k \end{vmatrix}^2 [S_p][S_q]\cdots[S_x][S_y]} \tag{8}$$

It follows from equation (8) that the denominator is always positive, so only the numerator has to be studied in order to study the possibility of extrema on the distribution curves. If all the terms in the numerator have the same sign, then no extremum can exist, but in the opposite case there may be extrema on the distribution curve. The number and the positions of extrema for a given set of $T_2 \ldots T_k$ and $\beta_1 \ldots \beta_n$ may be determined if the equations for the mass balances for $T_2 \ldots T_k$ are solved under the additional condition that the numerator of equation (8) vanishes. No general method is known, however, for finding the number of physically sensible roots, *i.e.*, the number of roots for which the concentrations of all components c_i are within the appropriate limits $0 < [c_i] < T_i$, and the problem has to be solved by numerical trial and error methods.

For our present purposes, however, it is satisfactory to see whether there *may* be a minimum on the distribution curve or not. In other words, it is enough to see whether the second derivative may or may not be positive at the zero point of the first derivative. Moreover, if both derivatives are zero, then there is a horizontal inflection on the distribution curve.

Because we are looking for the sign of the second derivative at the zero point of the first, only the numerator of equation (8) has to be differentiated with respect to $\ln[c_1]$, while the denominator remains unchanged. For the sake of simplicity, this is given here for the three-component system, but the considerations can easily be extended to the multicomponent case. The partial derivative of equation (7) is given by equation (9):

$$\left(\frac{\partial^2 \ln[c_3]}{\partial \ln[c_1]^2}\right)_{\left(\frac{\partial \ln[c_3]}{\partial \ln[c_1]}=0\right)} = \frac{\sum_{p=1}^{n}\sum_{q=p}^{n}(p_1q_2 - q_1p_2)(p_2q_3 - q_2p_3)[S_p][S_q]\left\{\frac{\partial \ln[S_p]}{\partial \ln[c_1]} + \frac{\partial \ln[S_q]}{\partial \ln[c_1]}\right\}}{\sum_{p=1}^{n}\sum_{q=p}^{n}(p_2q_3 - q_2p_3)^2[S_p][S_p]} \tag{9}$$

Since $\partial \ln[c_3]/\partial \ln[c_1] = 0$, equation (9) can be rearranged. First, from the definition of the equilibrium constants, we obtain

$$\frac{\partial \ln[S_p]}{\partial \ln[c_1]} = p_1 + p_2\frac{\partial \ln[c_2]}{\partial \ln[c_1]}$$

$$\frac{\partial \ln[S_q]}{\partial \ln[c_1]} = q_1 + q_2\frac{\partial \ln[c_2]}{\partial \ln[c_1]} \tag{10}$$

Secondly, the derivative $\partial \ln[c_2]/\partial \ln[c_1]$ [equation (11)] may be obtained directly from equation (3):

$$\left(\frac{\partial \ln[c_2]}{\partial \ln[c_1]}\right)_{\left(\frac{\partial \ln[c_3]}{\partial \ln[c_1]}=0\right)} = -\frac{\sum_{j=1}^{n}\alpha_{j1}\alpha_{j2}[S_j]}{\sum_{j=1}^{n}\alpha_{j2}^2[S_j]} \tag{11}$$

Substituting (10) and (11) into equation (9), we finally arrive at (12):

$$\left(\frac{\partial^2 \ln[c_3]}{\partial \ln[c_1]^2}\right)_{\left(\frac{\partial \ln[c_3]}{\partial \ln[c_1]}=0\right)} = \frac{\sum_{p=1}^{n}\sum_{q=p}^{n}\sum_{j=1}^{n}(p_1q_2 - q_1p_2)(p_2q_3 - q_2p_3)(p_1 + q_1)\alpha_{j2}^2 - (p_2 + q_2)\alpha_{j1}\alpha_{j2})[S_p][S_q][S_j]}{\sum_{j=1}^{n}\alpha_{j2}^2[S_j]\sum_{p=1}^{n}\sum_{q=p}^{n}(p_2q_3 - q_2p_3)^2[S_p][S_q]} \tag{12}$$

We can see from equation (12) that the second derivative at the zero point of the first derivative may be given in the form of a table (*e.g.*, Table 3). Its left-hand column contains the concentration products $[S_p][S_q]$, multiplied by $(p_1q_2 - q_1p_2)(p_2q_3 - q_2p_3)$. The column headings of the table give the species S_j, for which $\alpha_{j2} \neq 0$; the appropriate numbers $(q_1 + p_1)\alpha_{j2}^2 - (p_2 + q_2)\alpha_{j1}\alpha_{j2}$ are given in the table. The sum of the concentration products multiplied by the products of the coefficients in the left-hand column and in the table gives the numerator of equation (12). Its sign describes the nature (maximum, minimum, point of horizontal inflection) of the extremum which has been found previously by using equation (7) or (8). Some examples of the use of these equations now follow.

COPPER(II)–DIETHYLENETRIAMINE SYSTEM

This system has been studied by Kaden and Zuberbühler;[20] the data given in their work are collected in Table 1. Charges are omitted for simplicity. In the Cu^{2+}/dien system there are two species, H_2L and MLH_{-1}, which may actually exhibit concentration minima, depending on the choice of total concentrations; their distribution curves and the behaviour of the other species will now be analysed in detail. The system is relatively complicated, but the equilibrium processes can be separated into those occurring in two pH regions. Below pH 7, the formation of ML is the only important complexation reaction and the system can be described simply in terms of the species H_3L, H_2L, HL, and ML.

To illustrate the use of equation (7), Table 2 contains the description of the system and the concentration products in the numerator of the first derivatives, by using the various species as component c_3.

Table 1. Composition matrix and formation constants of the species formed in the system copper(II)–diethylenetriamine[20]

	Stoichiometric numbers			
Species	$c_1 = H$	$c_2 = L$	$c_3 = M$	$\log\beta$
H	1	0	0	0
L	0	1	0	0
M	0	0	1	0
HL	1	1	0	10.06
H_2L	2	1	0	19.35
H_3L	3	1	0	24.04
ML	0	1	1	15.94
ML_2	0	2	1	20.86
ML_2H	1	2	1	29.58
MLH_{-1}	−1	1	1	6.55

It is seen from Table 2 that the concentrations of M and H_3L increase monotonically while those of L and ML decrease monotonically with increasing $[H^+]$. Extrema are possible only in the concentrations of HL and H_2L. The second derivatives at the extrema of [HL] and $[H_2L]$ are collected in Tables 3 and 4.

The left-hand column in each table contains the concentration products of the first derivative. To obtain the numerator of the second derivative at the zero point(s) of the first, these concentration products should be multiplied by the concentration in the column heading and the coefficient in the table. Finally these concentration products should be summed [see equation (12)]. Because the second derivatives given in the tables are valid only at the zero point(s) of the first, if any integer is added to the columns, the relation remains valid. On examination of the coefficients and signs of the concentration products given in Table 3, it can be seen that the only concentration product in the second derivative that is multiplied by a positive number is [M][ML][ML]. All the others are multiplied by negative numbers or

Table 2. Composition matrices for the system copper(II)–diethylenetriamine at pH values up to 7 with the various different species taken as third components; concentration products of the numerator of the first derivatives of the distribution curves

	Stoichiometric coefficients																	
	c_1	c_2	c_3	c_1	c_2	c_3	c_1	c_2	c_3	c_1	c_2	c_3	c_1	c_2	c_3	c_1	c_2	c_3
Species	H	L	M	H	M	L	H	M	HL	H	M	H_2L	H	M	H_3L	H	M	ML
H	1	0	0	1	0	0	1	0	0	1	0	0	1	0	0	1	0	0
L	0	1	0	0	0	1	−1	0	1	−2	0	1	−3	0	1	0	−1	1
M	0	0	1	0	1	0	0	1	0	0	1	0	0	1	0	0	1	0
HL	1	1	0	1	0	1	0	0	1	−1	0	1	−2	0	1	1	−1	1
H_2L	2	1	0	2	0	1	1	0	1	0	0	1	−1	0	1	2	−1	1
H_3L	3	1	0	3	0	1	2	0	1	1	0	1	0	0	1	3	−1	1
ML	0	1	1	0	1	1	−1	1	1	−2	1	1	−3	1	1	0	0	1
numerator*	+[HL][ML] +2[H_2L][ML] +3[H_3L][ML]			−[M][HL] −2[M][H_2L] −3[M][H_3L] −[HL][ML] −2[H_2L][ML] −3[H_3L][ML]			+[M][ML] +[L][M] +[L][ML] −[M][H_2L] −[H_2L][ML] −2[M][H_3L] −2[H_3L][ML]			+[M][ML] +2[L][M] +2[L][ML] +[M][HL] +[HL][ML] −[M][H_3L] −[H_3L][ML]			+3[L][M] +3[L][ML] +2[M][HL] +[M][H_2L] +3[M][ML] +2[HL][ML] +[H_2L][ML]			−[M][HL] −2[M][H_2L] −3[M][H_3L]		

*cf. equation (7).

Table 3. The numerator of the function $\partial^2 \ln[HL]/\partial \ln[H]^2$ at the zero point(s) of the first derivative

S_j	[M]	[ML]
First derivative*	$\{(p_1+q_1)\alpha_{j2}^2-(p_2+q_2)\alpha_{j1}\alpha_{j2}\}[S_j]$†	
+[M][ML]	−1	1
+[L][M]	−1	0
+[L][ML]	−2	−1
−[M][H_2L]	1	2
−[H_2L][ML]	0	1
−[M][H_3L]	2	3
−2[H_3L][ML]	1	2

*$(p_1q_2-q_1p_2)(p_2q_3-q_2p_3)[S_p][S_q]$.
†cf. equation (12).

Table 4. The numerator of the function $\partial^2 \ln[H_2L]/\partial \ln[H]^2$ at the zero point(s) of the first derivative

S_j	[M]	[ML]
First derivative*	$\{(p_1+q_1)\alpha_{j2}^2-(p_2+q_2)\alpha_{j1}\alpha_{j2}\}[S_j]$†	
+2[M][ML]	−2	2
+2[L][M]	−2	0
+2[L][ML]	−4	−2
+[M][HL]	−1	1
+[HL][ML]	−3	−1
−[M][H_3L]	1	3
−[H_3L][ML]	−1	1

*$(p_1q_2-q_1p_2)(p_2q_3-q_2p_3)[S_p][S_q]$.
†cf. equation (12).

zero. However, if −1 is added to the right-hand column of Table 3, the coefficients of all the concentration products will be negative or zero, which means that the second derivative will always be negative. Therefore only one extremum occurs on the distribution curve of HL and this is a maximum.

If the data in Table 4 are analysed correspondingly, it can be seen that whatever number is added to any of the columns, there always remain concentration products of both signs. Therefore [H_2L] may have more than one extremum and there may be a minimum on the concentration distribution curve.

An especially interesting point of the distribution curve $[H_2L]=f(pH)$ occurs when both the first and second derivatives are zero and there is a point of horizontal inflection. This point is represented by the following system of equations:

mass-balance equations:

$$T_L=[L]+[HL]+[H_2L]+[H_3L]+[ML] \quad (13)$$

$$T_M=[M]+[ML] \quad (14)$$

from the rearrangement of the numerator of the first derivative:

$$([H_3L]-[HL]-2[L])([M]+[ML])=2[M][ML] \quad (15)$$

from the rearrangement of the numerator of the second derivative:

$$(4[L]+[HL]+[H_3L])([M]+[ML])^2 = 4[M][ML]([ML]-[M]) \quad (16)$$

Equations (13)–(16) cause [H], [L] and [M] to be overdetermined, so T_L or T_M or one of the formation constants must be left to be calculated. Obviously, in a real chemical system, the formation constants are fixed. The "natural" parameter would be the ratio of the total concentrations, T_L/T_M. For the further analysis of the system, however, we allow β_{ML} to be freely calculated along with [H], [L] and [M].

Equations (14) and (15) may be transformed simply into (17) and (18):

$$[M]=\frac{T_M}{1+\beta_{ML}[L]} \quad (17)$$

$$(\beta_{H_3L}[H]^3-\beta_{HL}[H]-2)(1+\beta_{ML}[L])=2\beta_{ML}[M] \quad (18)$$

Substituting equation (18) into (17) and multiplying by [L] gives:

$$[L](\beta_{H_3L}[H]^3-\beta_{HL}[H]-2)(1+\beta_{ML}[L]) = 2T_M\frac{\beta_{ML}[L]}{1+\beta_{ML}[L]} \quad (19)$$

and combination of equations (15) and (16), after some rearrangement, leads to

$$\beta_{ML}[L]=\frac{3\beta_{H_3L}[H]^3-\beta_{HL}[H]}{\beta_{H_3L}[H]^3-3\beta_{HL}[H]-8} \quad (20)$$

Substituting this result into (19) gives

$$[L]=2T_M\frac{(3\beta_{H_3L}[H]^3-\beta_{HL}[H])}{(\beta_{H_3L}[H]^3-3\beta_{HL}[H]-8)}\frac{(\beta_{H_3L}[H]^3-3\beta_{HL}[H]-8)}{(\beta_{H_3L}[H]^3-\beta_{HL}[H]-2)}\frac{(\beta_{H_3L}[H]^3-3\beta_{HL}[H]-8)}{(4\beta_{H_3L}[H]^3-4\beta_{HL}[H]-8)^2} \quad (21)$$

Finally, substitution into (13) leads to

$$T_L/T_M=\frac{3\beta_{H_3L}[H]^3-\beta_{HL}[H]}{4(\beta_{H_3L}[H]^3-\beta_{HL}[H]-2)} + \frac{(3\beta_{H_3L}[H]^3-\beta_{HL}[H])(\beta_{H_3L}[H]^3-3\beta_{HL}[H]-8)}{8(\beta_{H_3L}[H]^3-\beta_{HL}[H]-2)^3}\frac{(1+\beta_{HL}[H]+\beta_{H_2L}[H]^2+\beta_{H_3L}[H]^3)}{} \quad (22)$$

The surprising result is that the pH of the horizontal inflection unequivocally determines the T_L/T_M ratio. If the T_L/T_M ratios are calculated from equation (22) at different pH values, then all of the unknowns, [L], [M], β_{ML}, can be calculated by means of the explicit formulae above. The relationship between T_L/T_M and $\log\beta_{ML}$ at the point of horizontal inflection is shown in Fig. 1. A minimum in the distribution curve can occur only if the points determined by T_L/T_M and $\log\beta_{ML}$ are inside the area determined by the "borderlines" of the horizontal inflection. Some specific features of this area are as follows.

(1) If $\log\beta_{ML}$ is less than 7.806 or if the ratio T_L/T_M is higher than 26.15, then no minimum is possible in the system.

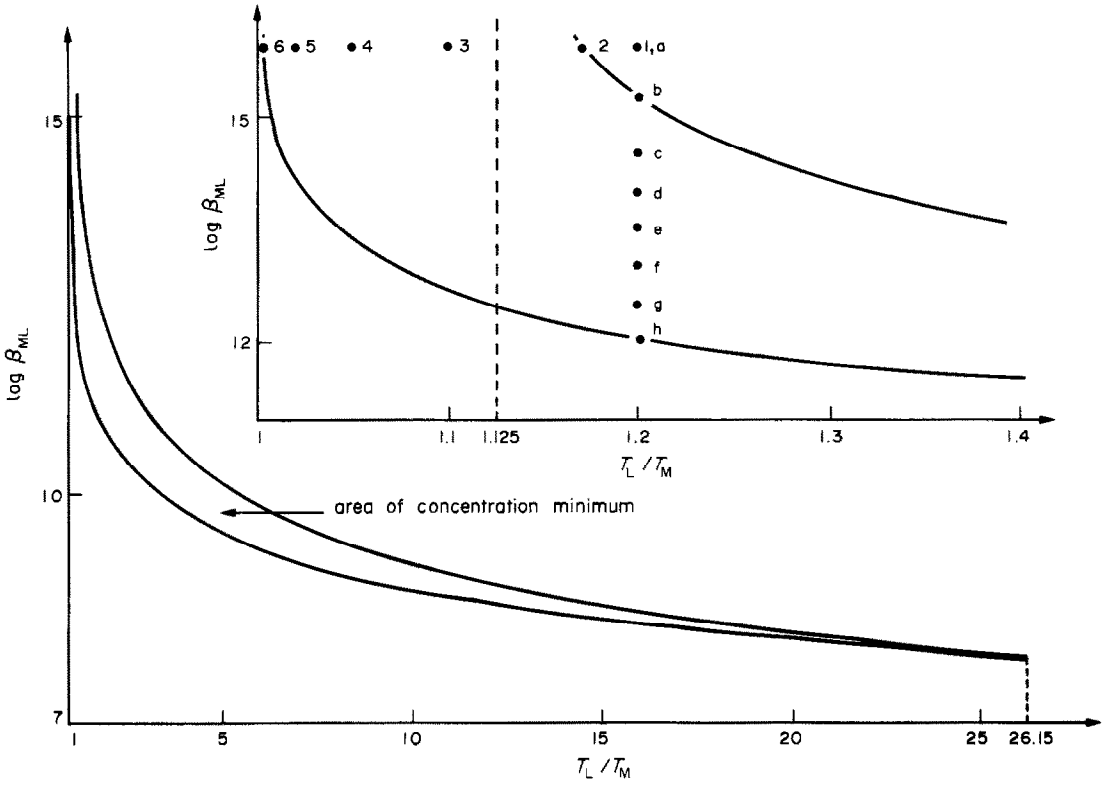

Fig. 1. Interdependence of $\log\beta_{ML}$ and the ratio of total concentrations T_L/T_M for the points of horizontal inflection on the distribution curves of H_2L in the system Cu^{2+}–dien. Inset: same function with extended T_L/T_M scale. The points on the inset correspond to the distribution curves in Figs. 2 (1–6) and 3(*a*–*h*).

(2) All $\log\beta_{ML}$ values above 7.806 will allow a minimum.

(3) At very high β_{ML} values $T_L/T_M = 1$ is approached asymptotically for the minimum condition.

(4) The experimental value $\log\beta_{ML} = 15.94$ will lead to a minimum on the distribution curve, as long as T_L/T_M is between 1.0024 and 1.164. Thus a minimum on the distribution curve of H_2L can easily be observed in the real system Cu^{2+}–dien.

The relationships illustrated in Fig. 1 are also shown on the distribution curves of H_2L in Figs. 2 and 3. The T_L/T_M ratios and the $\log\beta_{ML}$ values corresponding to the distribution curves are shown in Fig. 1 by appropriate numbers or letters. Figure 2 illustrates the appearance of the horzontal inflection, the development of a minimum and finally its disappearance through a second horizontal inflection, as can be predicted from the inset portion of Fig. 1 by using the experimental value of 15.94 for $\log\beta_{ML}$. In a similar way, Fig. 3 shows the effect of changing $\log\beta_{ML}$ for $T_L/T_M = 1.2$.

The simplified model discussed so far is valid for the copper(II)–diethylenetriamine system only up to pH 7. At higher pH values, the additional species CuL_2H, CuL_2, and CuL(OH) ($= CuLH_{-1}$) are formed. In this pH range, however, there is no significant amount of H_3L in the solution, so this species was not included in the analysis. The composition matrix was used to get the first derivatives and the results are collected in Table 5.

It is seen from the coefficients of the concentration products collected in Table 5 that only the concentration of H_2L is a strictly monotonic function of pH, and that there may be extrema on the distribution curves of all the other species.

We can now discuss the chemical meaning of the coefficients of the concentration products. It follows from equation (7) that the concentration products of a pair of species are found in the numerator only if neither of the determinants formed from the first and last two columns of the matrix

$$\begin{vmatrix} p_1 & p_2 & p_3 \\ q_1 & q_2 & q_3 \end{vmatrix}$$

is zero. This means that this matrix supplemented with the stoichiometric vector (1,0,0)(c_1) or (0,0,1) (c_3) will give a non-singular 3 × 3 matrix. In other words, a chemical equilibrium can always be written between c_1, c_3, and the two species forming the concentration product. If the species c_1 and c_3 are on the same side of the chemical equilibrium, then an

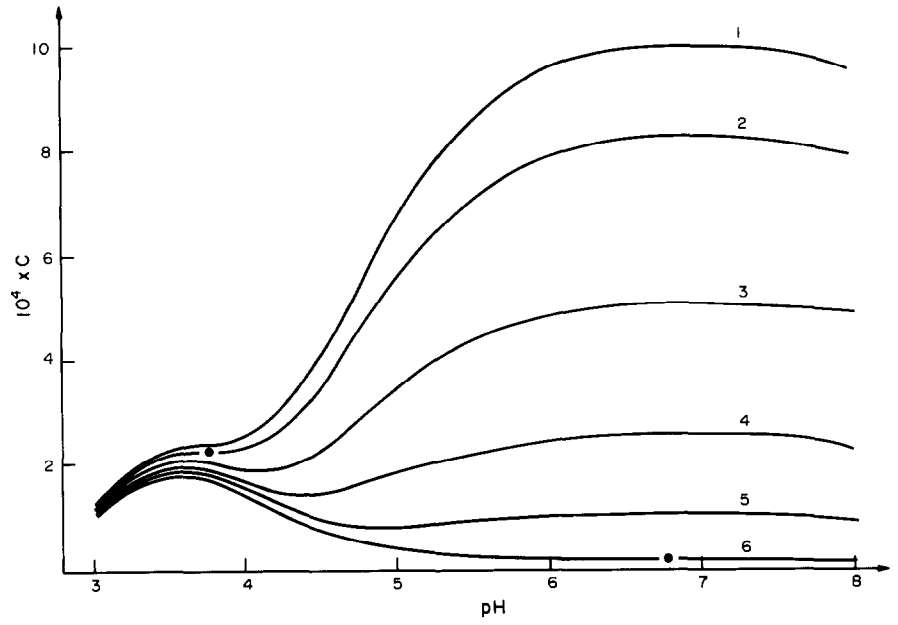

Fig. 2. Concentration distribution of H_2L in the system Cu^{2+}–dien at various total ligand concentrations. $T_M = 0.005M$. $T_L/T_M = 1.2$ (1), 1.164 (2), 1.1 (3), 1.05 (4), 1.02 (5), 1.0024 (6). The points on curves 2 and 6 denote the horizontal inflection.

increase of $[c_1]$ decreases $[c_3]$, and the sign of the concentration product is negative. If they are on opposite sides, then an increase of $[c_1]$ increases $[c_3]$, and the sign of the concentration product is positive. A detailed proof has been given earlier.[12] As an example, the various equilibria (and the appropriate concentration product signs) corresponding to the concentration product $[ML][ML_2H]$ in Table 5 are

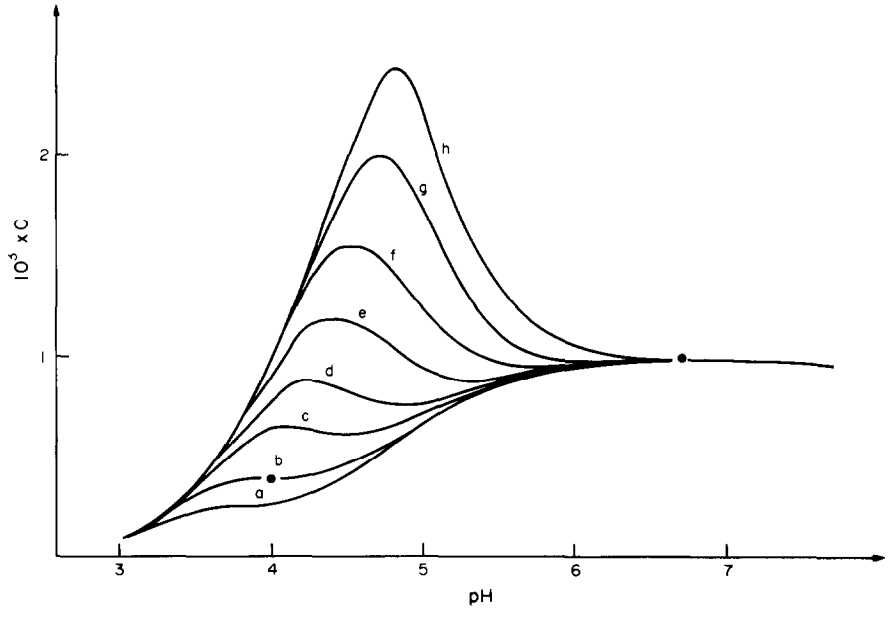

Fig. 3. Concentration distribution of H_2L in a model system corresponding to Cu^{2+}–dien with various $\log\beta_{ML}$ values. $T_M = 0.005M$, $T_L = 0.006M$. $\log\beta_{ML} = 15.94$ (*a*), 15.271 (*b*), 14.5 (*c*), 14.0 (*d*), 13.5 (*e*), 13.0 (*f*), 12.5 (*g*), 12.091 (*h*). The points on curves *b* and *h* denote the horizontal inflection.

given by

$$\begin{array}{l} \overset{+1}{\overbrace{\mathrm{H}+2\mathrm{ML} \rightleftharpoons \mathrm{ML_2H}+\mathrm{M}}} \\ \overset{-1}{\overbrace{\mathrm{ML_2H} \rightleftharpoons \mathrm{ML}+\mathrm{L}+\mathrm{H}}} \\ \overset{+1}{\overbrace{\mathrm{ML}+\mathrm{H_2L} \rightleftharpoons \mathrm{ML_2H}+\mathrm{H}}} \\ \overset{-1}{\overbrace{\mathrm{ML_2H}(+0\mathrm{ML}) \rightleftharpoons \mathrm{ML_2}+\mathrm{H}}} \\ \overset{-1}{\overbrace{\mathrm{ML}(+0\mathrm{ML_2H}) \rightleftharpoons \mathrm{MLH_{-1}}+\mathrm{H}}} \end{array} \qquad (23)$$

The analysis of the second derivatives of the distribution curves showed that the *stoichiometry* by itself would permit the manifestation of a minimum on the distribution curves of the free metal ion, of the proton complex HL and of the metal complexes ML, MLH_{-1} and ML_2H. If, however, the stability constants of the real system Cu^{2+}/dien are also considered, it turns out that a minimum can occur only on the distribution curve of the mixed hydroxo complex MLH_{-1}. The equilibria responsible for the concentration minimum of MLH_{-1} are given by equations (24) and (25):

$$\mathrm{ML} \rightleftharpoons \mathrm{MLH_{-1}} + \mathrm{H} \qquad (24)$$

$$\mathrm{MLH_{-1}} + \mathrm{H_2L} \rightleftharpoons \mathrm{ML_2} + \mathrm{H} \qquad (25)$$

In this system, ML is formed at a relatively low pH. The pK value for ML [equation (24)] is 9.49, so the formation of MLH_{-1} begins at pH ~8. The formation of ML_2 begins at the same pH, and causes the concentration of MLH_{-1} to decrease with increasing pH [equation (25)]. As the pH is raised further the extent of this process diminishes because of the decrease in $[H_2L]$. Thus $[MLH_{-1}]$ increases again.

It is seen that the only positive concentration product in the numerator of the first derivative is $[H_2L][ML_2]$, in accordance with the considerations above. The change of the concentration product $[HL][ML_2H]$ with negative coefficient is strictly parallel to the change of $[H_2L][ML_2]$. It follows from this that a minimum in the concentration distribution appears only if $\beta_{H_2L}\beta_{ML_2} > \beta_{HL}\beta_{ML_2H}$ or $pK^{H}_{HL} > pK^{H}_{ML_2}$. This relation is valid for the present system; the protonation constant for HL is higher than that for ML_2.

Because the presence of a minimum in $[MLH_{-1}]$ is a real possibility in the copper(II)–diethylenetriamine system, the parameters of the horizontal inflection were also calculated at $T_M = 0.005M$. This is a rather tedious calculation, because the mass-balance equation for the metal ion contains five terms, equation (7) for the first derivative fourteen and equation (12) for the second derivative as many as 38 terms, with the unknowns [H], [L] and [M] at different powers. The solution of the system of equations led to the following results: $[L] = 1.38 \times 10^{-4}M$, $[M] = 2.47 \times 10^{-16}M$, pH = 9.225. These data yield $T_L = 0.01167M$.

The concentration distribution of MLH_{-1} in the copper(II)–diethylenetriamine system at $T_M =$

Table 5. Coefficients of the concentration products in the numerator of the first derivatives of the distribution curves in the system copper(II)–diethylenetriamine

Concentration product	3rd component*							
	M	L	HL	H_2L	ML	ML_2	ML_2H	MLH_{-1}
[L][m]	0	0	1	2	0	0	1	−1
[L][ML]	0	0	1	2	0	0	1	−1
[L][ML_2]	0	0	1	2	0	0	1	−1
[L][ML_2H]	−1	0	1	2	−1	−1	0	−2
[L][MLH_{-1}]	1	0	1	2	1	1	2	0
[M][HL]	0	−1	0	1	−1	−2	−1	−2
[M][H_2L]	0	−2	−1	0	−2	−4	−3	−3
[M][ML]	0	0	1	2	0	0	1	−1
[M][ML_2]	0	0	4	8	0	0	4	−4
[M][ML_2H]	0	−2	2	6	−2	−4	0	−6
[M][MLH_{-1}]	0	1	2	3	1	−2	3	0
[HL][ML]	1	−1	0	1	0	−1	0	−1
[HL][ML_2]	2	−1	0	1	1	0	1	0
[HL][ML_2H]	1	−1	0	1	0	−1	0	−1
[HL][MLH_{-1}]	2	−1	0	1	1	0	1	0
[H_2L][ML]	2	−2	−1	0	0	−2	−1	−1
[H_2L][ML_2]	4	−2	−1	0	2	0	−1	1
[H_2L][ML_2H]	3	−2	−1	0	1	−1	0	0
[H_2L][MLH_{-1}]	3	−2	−1	0	1	−1	0	0
[ML][ML_2]	0	0	1	2	0	0	1	−1
[ML][ML_2H]	1	−1	0	1	0	−1	0	−1
[ML_2][MLH_{-1}]	2	−1	0	1	1	0	1	0
[ML_2H][MLH_{-1}]	3	−2	−1	0	1	−1	0	0

*The second component is L for M, and M for all other species; the first component is H throughout.

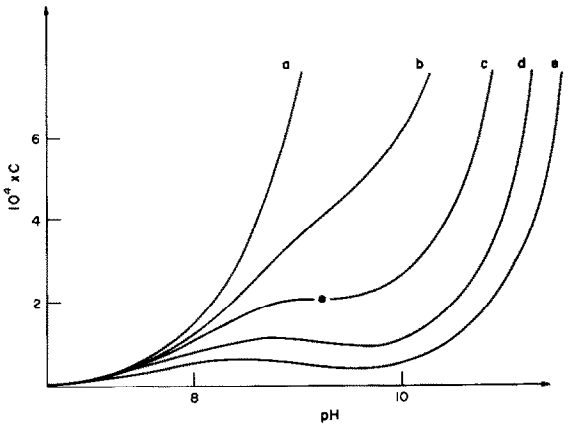

Fig. 4. Concentration distribution of MLH_{-1} in the system Cu^{2+}–dien. $T_M = 0.005M$, $T_L = 0.008M$ (*a*), $0.010M$ (*b*), $0.01167M$ (*c*, point of horizontal inflection), $0.015M$ (*d*), $0.02M$ (*e*).

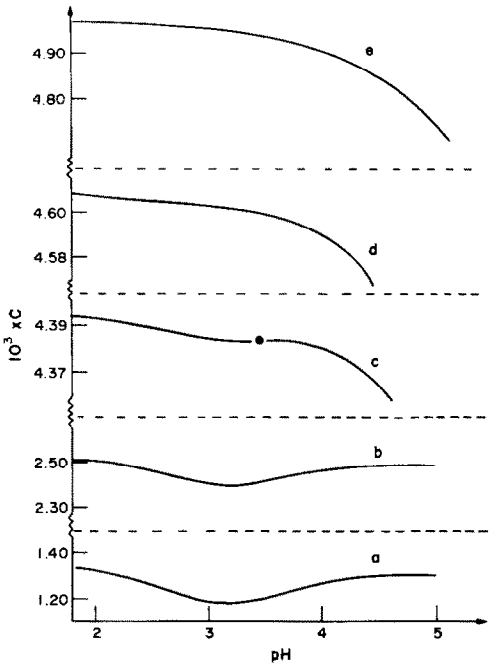

Fig. 5. Concentration distribution of $HgCl_2$ in the system Hg^{2+}–Cl–OH^-. $T_M = 0.005M$; $T_L = 0.005M$ (*a*), $0.007M$ (*b*), $0.00937M$ (*c*, point of horizontal inflection), $0.0096M$ (*d*), $0.01M$ (*e*).

$0.005M$ and different values for T_L is given in Fig. 4. At low T_L, no minimum is observed. For $T_L = 0.01167M$ we have a point of horizontal inflection (curve *c*) and at still higher T_L a concentration minimum is formed. No second point of horizontal inflection is found on the distribution curve of MLH_{-1} as T_L is increased up to $T_L = 10M$.

HYDROLYSIS IN THE Hg^{2+}–Cl^- SYSTEM

The concentration minima found in the real copper(II)–diethylenetriamine system and the minima which, in principle, may occur in similar systems are the consequence of stoichiometric asymmetry. It is not stoichiometric, but thermodynamic asymmetry that occurs in the Hg^{2+}–OH^-–Cl^- system, studied by Sjöberg.[5] A minimum occurs in the concentration of $HgCl_2$ as the pH is raised at constant T_{Cl}/T_{Hg} ratio. This is illustrated in Fig. 5. The first and second derivatives of the function $[HgCl_2] = f(\text{pH})$ are given in Table 6.

It follows from the concentration products of the first derivative that an extremum may occur only if either of the following relations is valid (charges are omitted):

$$[HgCl][HgOH] > 2[Hg(OH)Cl][Hg] \quad \text{or} \quad K_1^{Cl}K_1^{OH} > 2\beta_{11} \tag{26}$$

$$2[HgCl][Hg(OH)_2] > [Hg(OH)][Hg(OH)Cl] \quad \text{or} \quad 2K_1^{Cl}K_2^{OH} > \beta_{11} \tag{27}$$

The formation constants collected in Table 7 indicate that only the second relation is true in the present system, so the equilibrium

$$2HgCl + 2OH \rightleftharpoons HgCl_2 + Hg(OH)_2 \tag{28}$$

corresponding to the concentration product $[HgCl][Hg(OH)_2]$ is responsible for the minimum. The solution of the equations for $T_{Hg} = 0.005M$ and

Table 6. Numerator of the first derivative of the function $\log[HgCl_2] - f[\log(OH)]$ and the numerator of the second derivative at the zero point of the first

S_j	[Cl]	[Hg]	[HgOH]	$[Hg(OH)_2]$	[HgCl]	[Hg(OH)Cl]
First derivative*			$\{(p_1+q_1)\alpha_{2j}^2 - (p_2q_2)\alpha_{j1}\alpha_{j2}\}[S_j]$†			
[HgCl][HgOH]	1	4	−2	−8	1	−2
$2[HgCl][Hg(OH)_2]$	2	8	2	−4	2	−1
−2[Hg][Hg(OH)Cl]	1	4	−2	−8	1	−2
−[HgOH][Hg(OH)Cl]	2	8	2	−4	2	−1
−[Cl][HgOH]	1	4	2	0	1	0
$-2[Cl][Hg(OH)_2]$	2	8	6	4	2	1
−[Cl][Hg(OH)Cl]	1	4	4	4	1	1

*$(p_1q_2 - q_1p_2)(p_2q_3 - q_2p_3)[S_p][S_q]$, cf. equation (7).
†cf. equation (12).

Table 7. Formation constants of the species in the system Hg^{2+}–Cl^-–OH^- at low chloride concentration[5]

Species	$\log\beta^*$
HgCl	7.22
$HgCl_2$	14.00
HgOH	10.64
$Hg(OH)_2$	22.20
Hg(OH)Cl	18.35

*$pK_w = 14.22$.

the first and second derivatives gives the following data for the point of horizontal inflection: $[Cl^-] = 3.963 \times 10^{-6}M$, $[Hg^{2+}] = 2.792 \times 10^{-6}M$, $[OH^-] = 1.659 \times 10^{-11}M$ ($pK_w = 14.22$, so pH = 3.44). These data determine the total chloride concentration: $T_{Cl} = 9.37 \times 10^{-3}M$. In Fig. 5 we see the minimum of $[HgCl_2]$ for $T_{Hg} = 0.005M$ and $T_{Cl} = 0.005M$ or $0.007M$, the point of horizontal inflection for $T_{Cl} = 0.00937M$, and its disappearance at still higher chloride concentrations. Further calculations show that the minimum is present over the whole range $0 < T_L < 0.00937M$.

A MODEL SYSTEM WITH FIVE EXTREMA

Although no more than one minimum in the concentration distribution of a given species has been described up to now for any real chemical system, the possibility of two or more minima cannot be excluded. Probably the simplest model system with two minima and three maxima consists of the species HL, L, M, ML_2 and $M(OH)_4$. The result of a model calculation on this extremely asymmetric system is illustrated in Fig. 6.

The peculiar distribution of the species HL can be explained as follows: in the absence of metal ion the concentration of HL would increase with increasing pH up to $(pK_1 + pK_2)/2$ (pH = 6 in the present example). The formation of ML_2, however, decreases [HL] through the equilibrium

$$M + 2HL \rightleftharpoons ML_2 + 2H \qquad (29)$$

This process is completed at about pH 4, so [HL] increases again. As mentioned, [HL] would normally begin to decrease at pH > 6. In this pH range, however, the equilibrium

$$ML_2 + 4H_2O \rightleftharpoons M(OH)_4 + 2H + 2HL \qquad (30)$$

takes place, and this increases [HL] as the pH is raised. Finally [HL] decreases again because of its dissociation to free ligand L.

AN ALGORITHM FOR THE ANALYSIS OF CONCENTRATION DISTRIBUTIONS

From the considerations illustrated above, the following general procedure can be given for the analysis of concentration distributions of three-component systems.

1. The composition matrix is transformed to make the species of interest the third component.
2. The coefficients of all the possible concentration products are calculated according to the formula given in the numerator of equation (7).

   If all the coefficients are positive, the concentration of the given species always increases with the increase in $[c_i]$.

   If all the coefficients are negative, then the concentration of the given species always decreases with increase in $[c_i]$.
3. If there are products of both signs, then the second derivative should be collected in a table

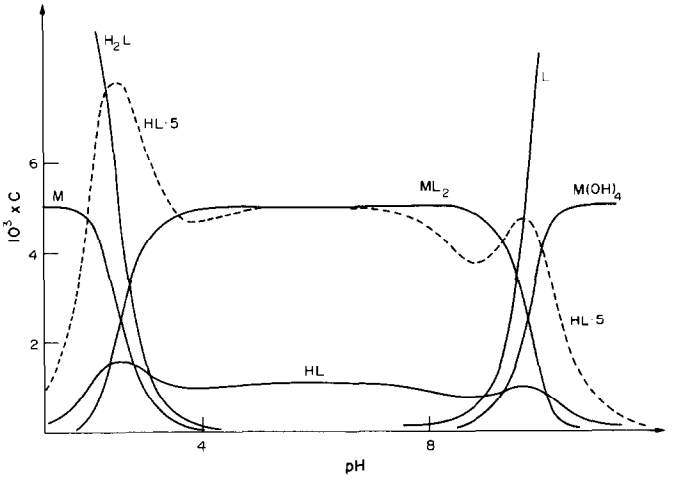

Fig. 6. Concentration distribution of the species HL in a model system. $T_L = 0.011M$, $T_M = 0.005M$, $\log\beta_{HL}$9.00, $\log\beta_{H_2L} = 12.00$, $\log\beta_{ML_2} = 8.50$, $\log\beta_{MH_{-4}} = -25.00$. Dashed line indicates 5 times the concentration of HL for better illustration.

and it should be studied in order to find out whether a uniform sign of the concentration products could be generated by adding optional positive or negative numbers to the columns of the table.

If uniform negative signs can be generated then the extremum may only be a maximum.

If uniform positive signs can be generated, then the extremum may only be a minimum (only model systems of this type have been found until now).

4. If both signs occur in the first and second derivative, then more than one extremum can be found, depending on the values of the stability constants.

The next step is to state the possible correlations between the concentration products with positive and negative signs. If they are found to be interdependent, *i.e.*, if they can be expressed with different formation constants but the same power of the component concentrations, then the relative values of the appropriate formation constants determine whether a concentration minimum may or may not occur in the given real system.

If this analysis shows the possibility of more than one extremum, then one of the mass-balance equations and the equations relating to the derivatives should be solved to get the free concentrations at the point of horizontal inflection.

The considerations discussed so far could be extended to four- and multicomponent systems. As we have seen, the possibility of a horizontal inflection is almost general for the species present in a relatively simple three-component system, so it is possible that in more complicated systems it is those species which cannot show horizontal-inflection or concentration minima at suitable total concentrations and with appropriate formation constants that are the exceptions.

REFERENCES

1. R. P. Agarwall and D. D. Perrin, in *Coordination Chemistry in Solutions*, E. Högfeldt (ed.). Berlinska Boktryekeriet, Lund, 1972.
2. M. L. Rouche and D. R. Williams, *J. Chem. Soc. Dalton*, 1976, 1355.
3. E. Schippert, *Inorg. Chim. Acta*, 1977, **21,** 35.
4. D. L. Rabenstein, R. Ozubko, S. Libich, G. A. Evans, M. Fairhust and G. Suwanprakorn, *J. Coord. Chem.*, 1974, **3,** 26.
5. S. Sjöberg, *Acta Chem. Scand.*, 1977, **A31,** 705.
6. L. Harju, *Talanta*, 1975, **22,** 1029.
7. A. Gergely and T. Kiss, *Inorg. Chim. Acta*, 1976, **16,** 51.
8. I. Nagypál and F. Debreczeni, *ibid.*, 1982, **57,** 125.
9. K. S. N. Iyer, S. Lau, S. H. Laurie and B. Sarkar, *Biochem. J.*, 1978, **169,** 61.
10. I. Nagypál and M. T. Beck, *Inorg. Chim. Acta*, 1975, **14,** 17.
11. *Idem, J. Phys. Chem.*, 1980, **84,** 722.
12. *Idem, Coord. Chem. Rev.*, 1982, **43,** 233.
13. I. G. Sayce, *Talanta*, 1968, **15,** 1397.
14. N. Ingri and L. G. Sillén, *Ark. Kemi*, 1964, **23,** 47.
15. I. Ting-Po and G. H. Nancollas, *Anal. Chem.*, 1972, **44,** 1940.
16. A. A. Bugaevsky and L. E. Nikishina, *Talanta*, 1981, **28,** 977 and references therein.
17. I. Nagypál, I. Páka and L. Zékány, *ibid.*, 1978, **25,** 549.
18. A. D. Zuberbühler and Th. A. Kaden, *ibid.*, 1982, **29,** 203.
19. L. Zékany and I. Nagypál, in *Modern Inorganic Chemistry*, D. Leggett (ed.). Plenum Press, New York, to be published; L. Zékany and I. Nagypál, *XXII I.C.C.C. Abstracts*, Budapest, 1982, p. 449.
20. Th. A. Kaden and A. D. Zuberbühler, *Helv. Chim. Acta*, 1971, **54,** 1361.

Talanta, Vol. 30, No. 8, pp. 605–608, 1983
Printed in Great Britain

0039-9140/83 $3.00 + 0.00
Pergamon Press Ltd

SHORT COMMUNICATIONS

INVESTIGATION INTO THE DETERMINATION OF PHENOLS EXTRACTED FROM AUTOMOBILE EXHAUST GASES

SABRI M. FARROHA, ALBERTINE E. HABBOUSH and ALA-MAHDI AL-SAEED
College of Science, University of Baghdad, Baghdad, Iraq

(*Received* 3 *September* 1981. *Revised* 26 *October* 1982. *Accepted* 19 *February* 1983)

Summary—A method is described in which phenols extracted from the condensate of automobile exhaust gases are determined directly by GLC. The quantities of various phenols found are calculated by using tridecane as an internal standard. The emission of phenols from cars running on fuels containing different concentrations of aromatics, and on leaded and lead-free fuels, has also been considered. The results show that the concentration of total phenols is dependent on the type of sample, and is strongly dependent on the concentration of aromatic hydrocarbons and of tetraethyl-lead in the fuel.

Phenols are known to be present in automobile exhaust gases.[1-3] They are of interest because they indicate incomplete oxidation of the gasoline and more importantly because they have been shown to be promoters of the carcenogenicity of polynuclear aromatic hydrocarbons such as benzo(α)pyrene.[4,5] However, a serious problem in the separation of such compounds is that of peak asymmetry, and derivatives of phenols have often been used in order to eliminate tailing.[6-8] The ethers formed for use in these methods are not stable in the presence of water or traces of free acid, and sterically hindered phenols react slowly and incompletely. Therefore, a more quantitative and direct method for the gas chromatographic determination of phenols extracted from automobile exhaust-gas condensate was considered necessary.

The present investigation concentrated on devising a direct GLC method for the determination of phenols extracted from automobile exhaust-gas condensate. In addition, the effect of the type of fuel on emission of phenols was examined.

EXPERIMENTAL

Apparatus

A Beckman GC-45 gas chromatograph equipped with a flame-ionization detector was used, with a 10-mV recorder. The optimal carrier-gas (nitrogen) flow-rate of 30 ml/min at NTP was used. The columns were made of stainless-steel tubing (6 ft long and $\frac{1}{4}$ in. o.d.) filled with 20% w/w liquid phase on Chromosorb W, (80–100 mesh). The column temperature was controlled to within ±1°.

Materials

The pure phenols and tridecane used were obtained from Fluka. No further purification was needed, as each of the compounds gave only one peak, with a stable base-line.

Preparation of automobile exhaust-gas samples

The sample volumes (2–3 m^3) of raw automobile exhaust gas were measured by flowmeter. The phenols were trapped in a 500-ml round-bottomed flask fitted with a double-wall condenser (Fig. 1), and containing 250 ml of 1*M* sodium hydroxide at ice-water temperature. The free phenols were released from the trapping solution by acidification with hydrochloric acid and extraction with two 50-ml portions of chloroform. The combined chloroform extract was divided into two parts, which were treated as follows.

Procedure A

Half of the combined chloroform extract was evaporated to a final volume of 5 ml by passage of an air stream across the container at room temperature, and 1 μl was injected directly onto the column of the chromatograph, by means of a 1-μl Hamilton syringe. A typical chromatogram of the free phenols present in exhaust-gas condensate is shown in Fig. 2.

The optimum experimental conditions for the analysis were selected according to the results of a previous study of phenolic compounds on a series of polysiloxane and polyester liquid phases.[9]

Procedure B

The rest of the combined chloroform extract was treated with 25 ml of 0.15% *o*-nitroaniline solution in 1*M* hydrochloric acid, freshly diazotized at 0° with 0.75 ml of 10% sodium nitrite solution. After shaking, the mixture was made alkaline by the addition of 2 ml of 20% sodium carbonate solution,[7] then acidified with hydrochloric acid; the azo-dyes were then completely extracted with successive portions of diethyl ether. The ethereal chloroform phase was dried over anhydrous magnesium sulphate and evaporated to dryness with a stream of cool air. The residue of azo-dyes was dissolved in chloroform and made up to a specific volume, then analysed by gas chromatography under the same conditions as for procedure A. A typical chromatogram is shown in Fig. 3.

The diazo-dyes of the individual phenols were also prepared [10] and chromatographed (0.1-μl samples) under the same conditions as for the analysis, in order to identify the phenols present in the exhaust-gas samples.

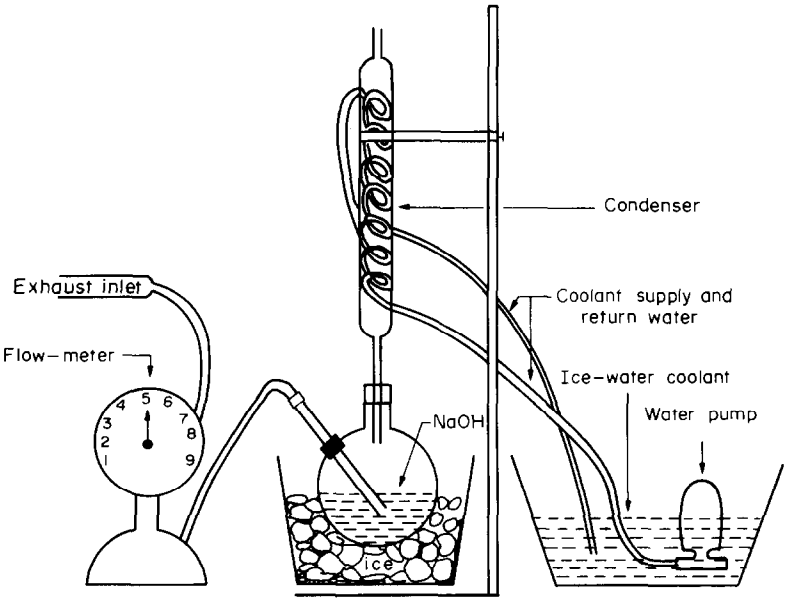

Fig. 1. Collection system for exhaust gas.

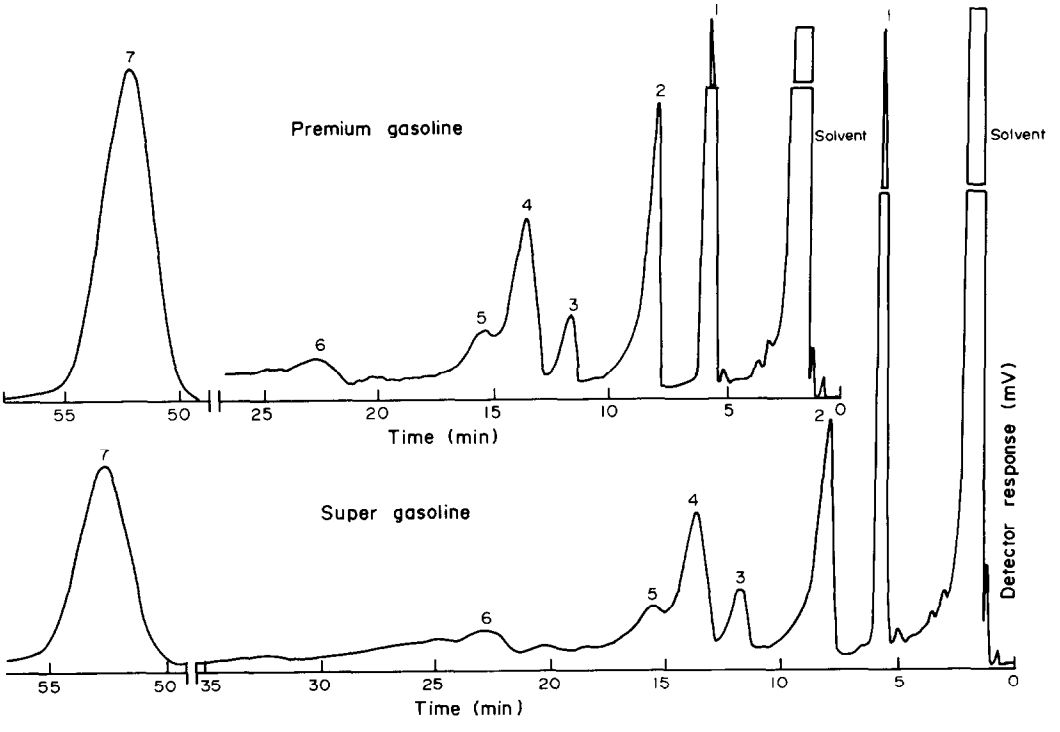

Fig. 2. Chromatograms of the phenolic fraction of the exhaust gas from combustion of premium and super gasoline. Peaks numbered as in Table 2.

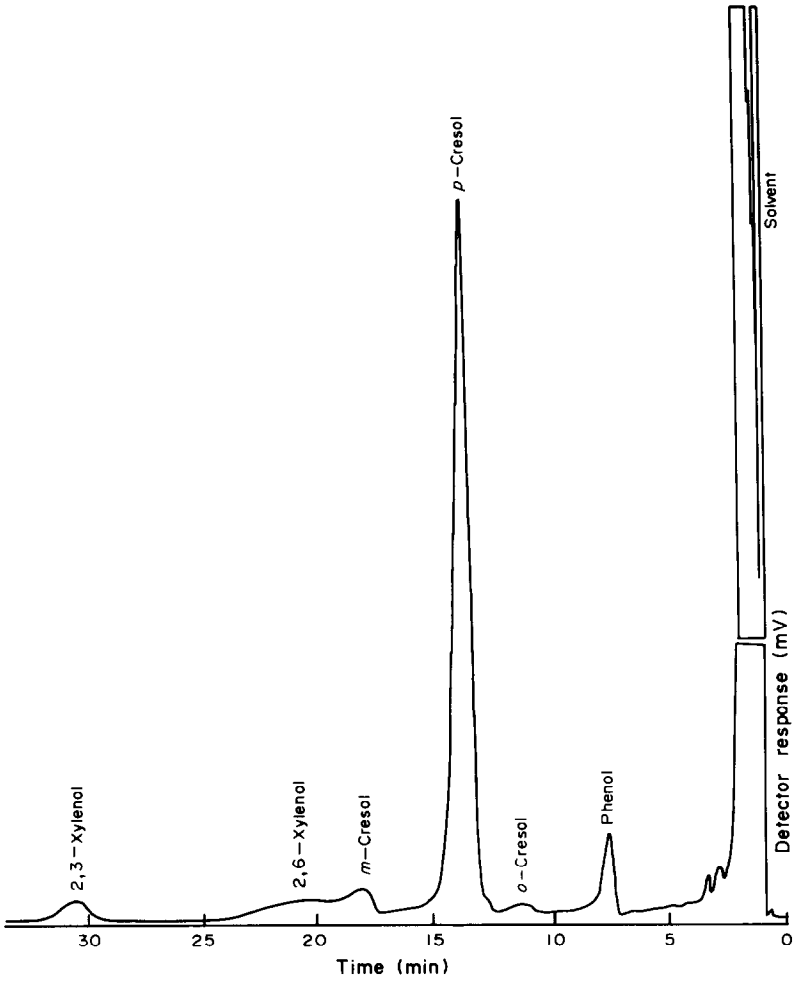

Fig. 3. Chromatogram of azo-dyes derived from phenols in exhaust gas.

Quantitative analysis

Synthetic mixtures of pure phenols (standard mixtures) were prepared by mixing 0.30 g of each of the eight phenols. Then 0.0213 g of tridecane was added as internal standard to 0.280 g of the phenol mixture, and this was diluted with 2.30 g of acetone. From this mixture 0.1-μl portions were injected into the gas chromatograph, and the relative response factors (F_x) were calculated according to the equation:

$$F_x = \frac{A_x W_i}{A_i W_x}$$

where A_i and A_x are the areas of the chromatographic peaks of the tridecane and the phenol, and W_i and W_x are the weights of tridecane and phenol, respectively. The values of the response factors in Table 2 are the means of five results.

For the analysis of exhaust-gas condensates, 0.5-g portions were spiked with 0.4 mg of tridecane as internal standard, and 1-μl portions were injected into the gas chromatograph. The quantities of the various phenols found in the exhaust gas were calculated from the appropriate peak areas on the chromatograms.

Table 1. Conditions for chromatography of free phenols

Column type	OV-101
Column temperature	120°C
Detector temperature	170°C
Carrier gas-flow	30 ml/min
Injected sample	1 μl

RESULTS AND DISCUSSION

The results for the phenols found in the automobile exhaust-gas condensate are shown in Table 3. The value for each phenol is the mean of five results and

Table 2. Analysis of the synthetic phenol mixture and the response factors relative to the internal standard (tridecane)

Peak number	Compound	Area, cm^2	Response factor, F
1	Phenol	2.08	0.566
2	*o*-Cresol	2.32	0.631
3	*m*- and *p*-Cresol	3.38	0.459
4	2,6-Xylenol	2.85	0.775
5	2,4 and 2,5-Xylenol	4.20	0.571
6	3,5-Xylenol	2.46	0.669
7	2,3-Xylenol	3.80	1.033
8	3,4-Xylenol	1.62	0.440
9	Tridecane	2.80	1.000
10	*o*-Xylene	3.45	1.233

Table 3. Levels of phenols in exhaust-gas condensate

Peak number	Compound	Premium gasoline Area cm^2	Premium gasoline Yield,* mg/l.	Super gasoline Area, cm^2	Super gasoline Yield,* mg/l.
1	*o*-Xylene	3.81	16.5	3.48	20.8
2	Phenol	2.60	24.6	1.92	25.0
3	*o*-Cresol	0.76	6.4	0.72	8.3
4	*m*- and *p*-Cresol	2.73	31.8	2.38	38.0
5	2,6-Xylenol	1.12	7.7	0.91	8.5
6	2,3-Xylenol	0.72	3.7	0.56	3.8
	Total		90.7		104.4

*Yield is expressed as mg of phenol per litre of fuel burned.

Table 4. Composition of the test fuels

Compound	Super gasoline, %	Premium gasoline, %
Benzene	3.1	1.8
Toluene	12.2	5.2
m- and *p*-Xylene	13.0	8.0
o-Xylene	7.0	5.0
Ethylbenzene	3.5	2.8
n-Propylbenzene	0.5	—
Diethylbenzene	1.5	1.4
Aromatic $C_{10}+$	11.0	7.0
Total aromatics	51.8	31.2
Paraffins	48.2	68.8
Tetraethyl lead, *ml/l.*	0.8	0.8

is expressed as mg of phenol produced by combustion of 1 litre of fuel.

The data obtained show that the concentration of total phenols differs for the various samples examined and is strongly dependent on the concentration of aromatic hydrocarbons in the fuel (Table 4).

In addition, the presence of tetraethyl-lead (TEL) in the fuels causes a significant reduction in the phenol emission, which can be explained by the hypothesis that the lead produced when the TEL decomposes to form methyl radicals reacts with the $OH^{\cdot}$ free-radicals which arise[11] in the combustion processes, to form lead oxide and $H^{\cdot}$ radicals according to the equation:

$$Pb + OH^{\cdot} \rightarrow PbO + H^{\cdot}$$

This reaction could reduce the number of $OH^{\cdot}$ radicals available for the formation of phenols.

Acknowledgement—The authors are thankful to the College of Science, University of Baghdad, for providing every facility to accomplish the work.

REFERENCES

1. E. D. Barber, E. Sawicki and S. Mepherson, *Anal. Chem.*, 1964, **36,** 2442.
2. D. Hoffman and E. L. Wynder, *J. Air Pollution Control Assoc.*, 1963, **13,** 322.
3. T. W. Stanley, E. Sawicki and H. Johnson, *Microchim. Acta*, 1965, 48.
4. R. K. Boutwell and D. K. Bosch, *Cancer Res.*, 1959, **19,** 413.
5. E. L. Wynder and D. Hoffman, *Cancer*, 1961, **14,** 1306.
6. A. C. Bhattacharyya, A. Bhattacharjee, O. K. Guha and A. N. Basu, *Anal. Chem.*, 1968, **40,** 1873.
7. G. B. Crump, *J. Chromatog.*, 1963, **10,** 21.
8. M. Mattsson and G. Peterson, *J. Chromatog. Sci.*, 1977, **15,** 546.
9. Ala-Mahdi Al-Saeed, *M.Sc. Thesis*, University of Baghdad, 1980.
10. F. Wild, *Characterisation of Organic Compounds*, 2nd Ed, p. 231. University Press, Cambridge, 1962.
11. B. B. Chakraborty and R. Long, *Combustion and Flame*, 1968, **12,** 226.

Talanta, Vol. 30, No. 8, pp. 609–610, 1983
Printed in Great Britain

0039-9140/83 $3.00+0.00
Pergamon Press Ltd

TITRIMETRIC MICRODETERMINATION OF URIC ACID AND THIOGLYCOLLIC ACID BY AMPLIFICATION REACTIONS

F. A. ABEED, M. JASIM and D. AMIN
Department of Chemistry, College of Science, Mosul University, Mosul, Iraq

(*Received* 19 *October* 1982. *Accepted* 17 *February* 1983)

Summary—A simple amplification method for determination of 0.05–2 mg of uric acid or thioglycollic acid has been worked out. It depends on iodine oxidation of the uric acid or thioglycollic acid solutions, removal of the excess of iodine, oxidation of the resulting iodide with bromine, and iodometric titration of the resulting iodate. The coefficient of variation ranges from 0.7 to 2.4% for uric acid and from 0.5 to 1.9% for thioglycollic acid, depending on the amount of the acid.

In alkaline solution, 1 molecule of uric acid is readily oxidized by 2 equivalents of iodine, thioglycollic acid is quantitatively oxidized by iodine to dithioglycollic acid:[1]

$$C_5H_4O_3N_4 + I_2 \rightarrow C_5H_2O_3N_4 + 2HI$$

$$2CH_2SHCOOH + I_2 \rightarrow (SCH_2COOH)_2 + 2HI$$

Mayr and Gebauer[2] showed that thioglycollic acid solutions are rapidly oxidized by air and therefore dissolved the acid in air-free water, for the determination.

A titrimetric determination of as little as 1 mg of uric acid has been reported by Raber and Dielacher,[3] who used oxidation with bromate/bromide mixture or ceric sulphate. Various other titrimetric methods[4–8] have been reported for determination of thioglycollic acid, but they vary in analysis time and sensitivity.

In an attempt to develop a simple, reliable and sensitive method for determination of uric acid and thioglycollic acid, we have extended our use of iodine and the Leipert amplification procedure.[9,10]

EXPERIMENTAL

Reagents

All chemicals used were of analytical-reagent grade.

Thioglycollic acid solutions. Aqueous solutions (concentrations 0.1 and 1.0 mg/ml) were prepared in air-free water.

Uric acid solutions. Aqueous solutions (concentrations 0.1 and 1.0 mg/ml) were prepared by dissolving the acid in a few drops of 1*M* sodium hydroxide and diluting with distilled water.

Sodium thiosulphate solutions, 0.01 and 0.001N. Standardized against potassium iodate solutions of similar normality.

Iodine solution. Prepared by dissolving about 0.6 g of pure iodine in 500 ml of pure dry chloroform.

Solutions of formic acid (80%), hydrochloric acid (1*M*) and bromine water (saturated) were also used.

Procedure

In a 50-ml separating funnel, mix a suitable volume (up to 10 ml) of sample solution (containing 0.05–2 mg of uric acid or thioglycollic acid) and 5 ml of iodine solution and add water (if necessary) to give a total aqueous phase volume of 10 ml. Stopper the funnel and shake the contents vigorously. Separate the organic layer (for uric acid, acidify the aqueous phase by addition of 0.5 ml of 1*M* hydrochloric acid before the separation). Remove the last traces of iodine from the aqueous layer by extraction with two 10-ml portions of chloroform. Transfer the aqueous phase quantitatively to a 50-ml conical flask. Add 3 ml of bromine and swirl or stir for 3 min. Destroy the excess of bromine by addition of 5 ml of formic acid, add about 0.5 g of potassium iodide, and titrate the liberated iodine with 0.01*N* thiosulphate (for less than 0.5 mg of uric acid or thioglycollic acid, use 0.001*N* thiosulphate), using starch as indicator. Run a blank determination.

1 ml of 0.01*N* thiosulphate ≡ 0.140 mg of uric acid

1 ml of 0.01*N* thiosulphate ≡ 0.0767 mg of thioglycollic acid

RESULTS AND DISCUSSION

Uric acid and thioglycollic acid are quantitatively oxidized when treated with iodine. The iodide formed can be dealt with by the Leipert amplification procedure,[11] after extraction of the excess of iodine with chloroform.

Preliminary studies confirmed that thioglycollic acid solutions are rapidly oxidized by air,[2] and that the sample must be dissolved in air-free water for analysis. It was found that 5 ml of 0.12% iodine solution oxidizes up to 2 mg of uric acid or thioglycollic acid quantitatively. Any iodine left in suspension in the aqueous phase would cause high results, so must be removed by washing the aqueous phase with chloroform.

In the determination of uric acid, the aqueous phase must be acidified before separation from the chloroform phase, in order to decompose any hypoiodite formed by reaction of the alkaline sample solution with the iodine reagent.

The present method gave satisfactory results (Table 1), the recoveries ranging from 94.0 to 99.5%

Table 1. Microdetermination of uric acid and thioglycollic acid by the 6-fold amplification method

Compound	Weight, *mg* Taken	Found*	Recovery, %	Coefficient of variation, %
Uric acid	0.050	0.047	94.0	2.4
	0.100	0.098	98.0	
	0.500	0.496	99.2	1.7
	1.000	0.995	99.5	
	2.000	1.982	99.1	0.7
Thioglycollic acid	0.050	0.049	98.0	1.9
	0.100	0.099	99.0	
	0.500	0.497	99.4	1.2
	1.000	1.000	100.0	
	2.000	1.988	99.4	0.5

*Mean of 5 determinations.

for 0.05–2.0 mg of uric acid, and from 98.0 to 100% for 0.05–2.0 mg of thioglycollic acid. The coefficients of variation were 2.4, 1.7 and 0.7% for 0.05, 0.5 and 2 mg of uric acid, respectively (5 replicates), and 1.9, 1.2 and 0.5% for 0.05, 0.5 and 2.0 mg of thioglycollic acid (5 replicates). The blank value was 0.05 ml of 0.01*N* thiosulphate.

REFERENCES

1. I. M. Kolthoff and R. Belcher, *Volumetric Analysis*, Vol. III, p. 388. Interscience, New York, 1957.
2. C. Mayer and A. Gebauer, *Z. Anal. Chem.*, 1938, **113**, 189.
3. H. Raber and M. Dielacher, *Sci. Pharm.*, 1969, **37**, 129; *Anal. Abstr.*, 1970, **19**, 512.
4. S. I. Obtemperanskaya and N. N. Kalinina, *Zh. Analit. Khim.*, 1971, **26**, 1407.
5. R. C. Paul, S. K. Sharma, N. Kumar and R. Parkash, *Talanta*, 1975, **22**, 311.
6. R. C. Paul, N. Kumar and R. Parkash, *J. Indian Chem. Soc.*, 1975, **52**, 1970.
7. N. Krishnamurthy and K. R. Rao, *Indian J. Chem.*, 1977, **15A**, 569.
8. S. Ashutosh, *Talanta*, 1979, **26**, 917.
9. D. Amin and M. S. Al-Ajely, *ibid.*, 1981, **28**, 955.
10. D. Amin, K. Y. Saleem and W. A. Bashir, *ibid.*, 1982, **29**, 694.
11. T. Leipert, *Mikrochemie*, 1929, 266.

Talanta, Vol. 30, No. 8, pp. 611–613, 1983
Printed in Great Britain.

0039-9140/83 $3.00+0.00

SELECTIVE COMPLEXOMETRIC DETERMINATION OF MERCURY WITH THIOCYANATE AS MASKING AGENT

K. N. RAOOT, SARALA RAOOT and V. LALITHA KUMARI
Defence Metallurgical Research Laboratory, Kanchanbagh, Hyderabad-500258, India

(*Received* 24 *August* 1982. *Revised* 25 *January* 1983. *Accepted* 20 *February* 1983)

Summary—A method is proposed for selective complexometric determination of mercury, thiocyanate being used as masking agent. An excess of EDTA is added and the surplus is back-titrated at pH 5–6 with lead nitrate, Xylenol Orange or Methylthymol Blue being used as indicator. Thiocyanate is then added to decompose the mercury-EDTA complex and the liberated EDTA is titrated with lead nitrate. The interference of various cations has been studied.

Direct EDTA titrations of mercury[1] are of poor selectivity owing to co-titration of other metal ions. The usual practice is to determine the sum of mercury and associated cations and then to decompose the mercury-EDTA complex selectively with masking agents such as thiosemicarbazide[2] or cysteine[3] and titrate the liberated EDTA. In these methods, however, copper causes serious interference. Potassium iodide[4] was suggested by Ueno as masking agent in alkaline medium for estimating mercury in the presence of copper, but then many other cations interfere. Thiosulphate[5] has also been reported as masking agent for mercury in alkaline medium, but the effect of copper was not studied. Singh[6] described determination of mercury in presence of various cations, with thiourea as masking agent, the titration being done at pH 5–6, with Xylenol Orange or Methylthymol Blue as indicator, and this method is definitely superior to those referred to earlier. The interference of copper was avoided by controlling the pH at 5.5 and cooling the solution to 15°. Experience with this method, however, reveals that good results for mercury in presence of copper are obtained only when a minimal excess of thiourea is used, and this restriction causes problems in analysis of samples of completely unknown composition.

The reagents mentioned above were also used earlier for masking of mercury[1] to prevent it from reacting with EDTA during the complexometric estimation of other cations. Barcza and Kőrös[7] used thiocyanate to mask mercury during the titration of bismuth at pH 1. The mercury–thiocyanate complex could then be decomposed with silver ions and the liberated mercury(II) titrated with EDTA at pH 5–6 in the same solution. However, thiocyanate does not seem to have been employed previously for selective decomposition of the mercury–EDTA complex. We found that mercury interfered seriously when thiocyanate was used for decomposition of the palladium-EDTA complex,[8] so decided to investigate whether thiocyanate can decompose the mercury–EDTA complex quantitatively, leading to a selective method for mercury; results are presented here. After a combined titration, the mercury–EDTA complex is selectively decomposed with thiocyanate and the EDTA released is titrated with lead nitrate solution at pH 5–6, to the Xylenol Orange or Methylthymol Blue end-point. The method tolerates a large number of cations, including copper, with no need for the manipulation of titration conditions that is necessary when thiourea is used.

EXPERIMENTAL

Reagents

Mercuric nitrate solution. Prepared by dissolving 1.0 g of pure mercury in the minimum amount of nitric acid, making up to 1 litre and standardizing.

*EDTA solution, 0.01*M.

*Lead nitrate solution, 0.01*M.

Xylenol Orange and Methylthymol Blue indicators, 0.1% aqueous solutions.

Solutions of various cations (1 mg/ml) were prepared. Analytical-reagent grade chemicals were used whenever possible.

Determination of mercury in presence of other ions

To a solution containing 5–50 mg of mercury and varying amounts of foreign metal ions, add excess of 0.01*M* EDTA and dilute to 100 ml with distilled water. Adjust the pH to 5–6 with solid hexamine. Add a few drops of Xylenol Orange or Methylthymol Blue indicator and back-titrate the excess of EDTA with 0.01*M* lead nitrate. Add 2–10 ml of 5% ammonium thiocyanate solution (2 ml for each 10 mg of mercury), shake and titrate the liberated EDTA with 0.01*M* lead nitrate to the same end-point as in the first titration.

Application to samples

Dissolve 0.1–0.2 g of sample in the minimum amount of nitric acid by slow heating. If tin is present, filter off the precipitated metastannic acid. Dilute the solution or filtrate to volume in a 100-ml standard flask. Transfer a suitable aliquot to a 250-ml conical flask, add excess of 0.01*M*

Table 1. Determination of mercury in presence of foreign metal ions

Ion, *mg*		Mercury, *mg* Taken	Found	
Ag^{+}	40.0	15.0	14.89	14.93
	20.0	25.0	24.97	25.17
Cu^{2+}	5.0	50.0	50.25	50.05
	25.0	5.0	4.93	5.02
Zn^{2+}	25.0	20.0	20.06	19.86
	12.5	30.0	29.99	30.29
Ni^{2+}	20.0	5.0	4.97	5.06
	10.0	25.0	24.97	24.77
Pb^{2+}	20.7	8.0	7.98	8.06
	10.4	40.0	40.02	39.82
Cd^{2+}	20.0	6.0	6.02	5.94
	5.0	25.0	25.18	24.98
Co^{2+}	25.5	8.0	7.98	7.94
	10.2	50.0	49.85	50.05
Mn^{2+}	5.0	15.0	15.13	15.17
	3.0	10.0	10.11	10.07
Ca^{2+}	25.0	10.0	9.95	9.91
	10.0	30.0	29.99	29.79
Mg^{2+}	35.0	15.0	14.85	14.97
	10.0	50.0	50.15	49.75
Pd^{2+}	15.0	8.0	7.98	8.06*
	6.0	15.0	14.93	14.93†
Bi^{3+}	24.0	10.0	10.03	9.95
	12.0	40.0	40.02	40.22
Al^{3+}	15.0	8.0	7.98	8.06
	7.5	30.0	29.99	30.19
Fe^{3+}	25.5	5.0	5.02	5.02
	5.1	50.0	50.35	49.95
Y^{3+}	21.0	12.0	11.92	11.96
	7.0	25.0	24.98	25.18
La^{3+}	24.0	9.0	9.07	8.90
	6.0	27.0	26.78	26.98
Gd^{3+}	18.0	6.0	5.98	6.06
	6.0	50.0	49.95	49.75
Sm^{3+}	18.9	15.0	14.93	14.89
	6.3	30.0	30.09	30.19
Rh^{3+}	12.0	12.0	14.04	12.08§
	9.0	25.0	24.77	24.97§
Ir^{3+}	12.9	15.0	15.01	15.09§
	6.4	25.0	24.98	25.18§
Ru^{3+}	3.6	12.0	11.96	11.92§
	6.2	9.0	9.03	9.03§
Pt^{4+}	8.0	20.0	20.06	19.86§
	16.0	18.0	17.94	18.15§
Ti^{4+}	10.0	25.0	25.18	25.18
	15.0	6.0	6.02	5.94
Oxalate	500	20.0	19.96	20.16
Tartrate	700	25.0	25.08	25.08
Borate	400	20.0	20.06	19.86
Citrate	600	25.0	25.08	24.87
Chloride	195	20.0	20.16	20.16
	300	20.0	19.94	19.94§

*Dimethylglyoxime used to mask palladium.
†Palladium masked with 1,2,3-benzotriazole.
§Excess of chloride removed by precipitation with silver nitrate; 2–3-fold excess of thiocyanate added.

EDTA, dilute to 100 ml with distilled water, adjust the pH to 5–6 with hexamine and complete the determination as described above.

RESULTS AND DISCUSSION

The decomposition of the mercury–EDTA complex with thiocyanate is instantaneous and quantitative at pH 5–6 at room temperature. There is no change in the pH of the solution on addition of the masking agent and hence no need to adjust the pH for the titration of the liberated EDTA, which can be performed immediately. Many cations can be tolerated (Table 1). Copper, which either interfered or was tolerated only after manipulation of certain conditions in earlier methods, has no adverse effect at all on the present method. Small quantities of mercury can conveniently be estimated in the presence of large amounts of copper. An interesting feature of the present method is that not only does copper not interfere, but it can be determined after the mercury, by heating with ascorbic acid to release EDTA from the copper complex[9] and then titrating it. Thiocyanate releases EDTA quantitatively from the palladium–EDTA complex[8] and thus palladium interferes seriously; however, this can be prevented by masking it with dimethylglyoxime[10] or benzotriazole.[11] Manganese gives some trouble in the end-point detection, particularly when more than 5 mg of it is present. Calcium and magnesium, though known to complex only weakly with EDTA at pH 5–6, make the Xylenol Orange end-point protracted. Methylthymol Blue, however, gives a sharp end-point in the presence of these metal ions.

Table 2. Determination of mercury in samples

Sample	Mercury, *mg* Taken	Found§
Dental amalgam*	32.0	31.9
		32.0‡
42% Hg–Zn alloy†	40.5	40.5
		40.4 #
15% Hg–Sn alloy†	21.5	21.6
		21.5 #

*Dental alloy powder (67.0% Ag, 25.0% Sn, 4.0% Cu, 0.5% Zn) from Dental Products of India, Bombay, was mixed thoroughly with pure mercury in 1:1 ratio and allowed to solidify.
†Alloy prepared and checked for homogeneity.
§Mean of 2 estimations.
‡Value of complexometric titration with thiourea as masking agent.
Result by thiocyanate titration.

Chloride up to 200 mg is tolerated, but larger quantities result in drawn-out end-points. In that case, the chloride can be removed by adding excess of silver nitrate solution and filtering off the precipitated silver chloride. For titration of the filtrate, it is necessary to add enough thiocyanate to yield the soluble thiocyanate complex of silver. This approach can also be used when determining mercury in the presence of platinum group metals, which are usually present as chloro-complexes and accompanied by chloride. Results given in Table 1 show that for quantities of mercury varying from 5 to 50 mg the error did not exceed 1%.

The method has been employed for the estimation of mercury in a dental amalgam sample and two

alloys (Table 2). The results by the present method are in close agreement with those obtained by the standard procedures. The method may also be found useful in the determination of mercury in pharmaceutical and chemical preparations.

Acknowledgement—Grateful thanks are due to Dr. P. Rama Rao, Director, DMRL, for permission to communicate this paper.

REFERENCES

1. T. S. West, *Complexometry with EDTA and Related Reagents*, p. 105. BDH, Poole, 1969.
2. J. Körbl and R. Přibil, *Chem. Listy*, 1957, **51**, 667.
3. W. Berndt and J. Sara, *Talanta*, 1961, **8**, 653.
4. K. Ueno, *Anal. Chem.*, 1957, **29**, 1669.
5. P. Curro and G. Calabro, *Atti Soc. Peloritana Sci. Fis. Mat. Nat.*, 1965, **11**, 49.
6. R. P. Singh, *Talanta*, 1969, **16**, 1447.
7. L. Barcza and E. Kőrös, *Chemist-Analyst*, 1959, **48**, 94.
8. K. N. Raoot, S. Raoot and V. L. Kumari, *Anal. Lett.*, in the press.
9. K. N. Raoot, S. Raoot, B. V. Rao and D. P. Lahiri, *Indian J. Technol.*, 1976, **14**, 254.
10. K. N. Raoot and S. Raoot, *Indian J. Chem.*, 1974, **12**, 1007.
11. K. N. Raoot, S. Raoot and V. G. Vaidya, *ibid.*, 1979, **18A**, 90.

Talanta, Vol. 30, No. 8, pp. 614–616, 1983
Printed in Great Britain.

0039-9140/83 $3.00 + 0.00

SEMI-XYLENOL ORANGE AND ITS PURIFICATION BY HIGH-PRESSURE LIQUID CHROMATOGRAPHY

F. SMEDES, L. G. DECNOP-WEEVER and NGUYEN TRONG UYEN*
Laboratory for Analytical Chemistry, University of Amsterdam, Nieuwe Achtergracht 166, Amsterdam, The Netherlands

J. NIEMAN and J. KRAGTEN
Physical Laboratory, University of Amsterdam, Valckenierstraat 65, 1018 XE Amsterdam, The Netherlands

(*Received* 20 *December* 1982. *Accepted* 7 *February* 1983)

Summary—By Mannich condensation of *o*-Cresol Red, iminodiacetic acid and formaldehyde, Semi-Xylenol Orange (SXO) has been prepared in a 10-hr batch-procedure with a yield of about 30%. From the crude product SXO has been isolated by reversed-phase HPLC with perchloric acid–acetone mixtures as the mobile phase and C_{18}-bonded silica as the stationary phase. The SXO fraction was freed from accompanying perchloric acid by a second separation on the same column, with water as eluent. After elution with acetone, the SXO was crystallized by evaporation.

Semi-Xylenol Orange (SXO), a homologue of Xylenol Orange (XO) allows very accurate complexometric titrations of zirconium[1] and thorium.[2,3] Both SXO and XO are triphenylmethane-type indicators, but with XO large titration errors may occur, especially with ter- and quadrivalent metals at concentrations below $10^{-3}M$. The origin of these errors is the predominant formation of the binuclear $M_2(XO)_q$ ($q = 1$ or 2) complexes.[3-6] In this respect SXO is a more favourable indicator as it forms only the mononuclear complexes $M(SXO)_q$ ($q = 1$ or 2).

In order to establish unambiguously the composition of the Th–SXO complexes, including their degree of protonation and stability, we needed SXO in a high degree of purity. SXO is not commercially available (though fairly pure XO can be obtained), so we had to synthesize and purify SXO ourselves.

Olson and Margerum[7] described a procedure for the synthesis of XO by Mannich condensation. This procedure has been adopted and optimized for SXO. After the Mannich condensation the reaction mixture mainly consists of SXO, XO, Cresol Red and iminodiacetic acid. The by-products have to be removed, as they all tend to form metal complexes. Several investigators have attempted to purify SXO. Partition chromatography on a cellulose column[8,9] and preparative thin-layer chromatography,[10] both combined with ion-exchange chromatography, have been applied to obtain the pure dye in the free acid form, but the methods are laborious and time-consuming. As reversed-phase high-pressure liquid chromatography (HPLC), previously applied to the purification of XO,[11] does not suffer from these drawbacks, this separation method was adopted by us for the purification of SXO on a semi-preparative scale. By automation of the equipment, high-quality SXO could be obtained at a relatively high production rate.

EXPERIMENTAL

Synthesis of SXO

The SXO is synthesized through Mannich condensation of *o*-Cresol Red, iminodiacetic acid and formaldehyde. The reaction scheme is as follows.

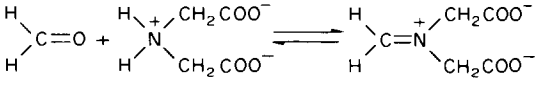

The Mannich base produced reacts with ketones in the enol form:

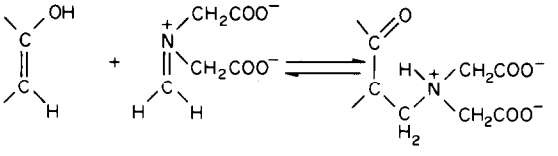

Thus with *o*-Cresol Red we get SXO:

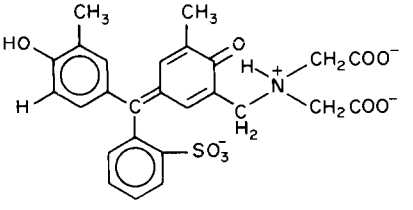

To stimulate the production of SXO, the *o*-Cresol Red should be present in excess. If the Mannich base predominates, the disubstituted product XO will predominate.

Procedure

o-Cresol Red (Merck, *p.a.*, 3.8 g, 10 mmole) was dissolved in 40 ml of acetic acid (96%, Baker); 1.8 g (10 mmole) of

*On leave from Chemistry Department, University of Hanoi.

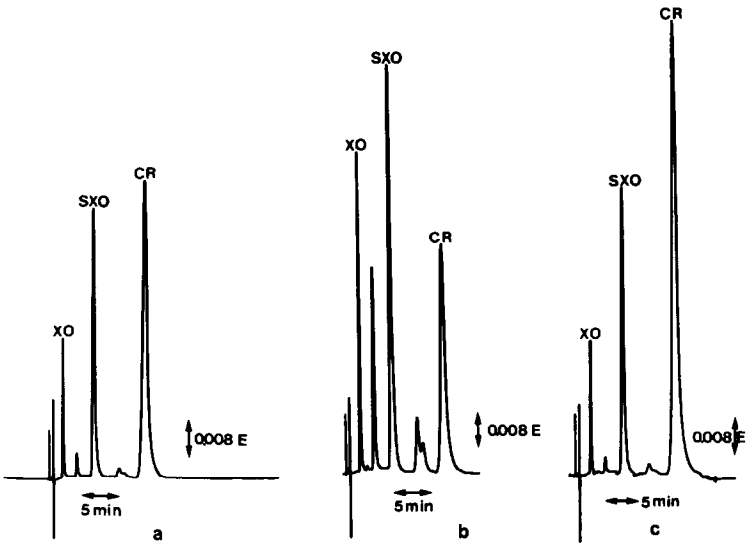

Fig. 1. Chromatograms of the reaction products: (a) after 11 hr of heating; (b) after 28 hr; (c) after 28 hr and continuous addition of formaldehyde and iminodiacetic acid. Flow-rate 2 ml/min; injection volume 20 μl.

disodium iminodiacetate (Fluka) was dissolved in 4 ml of water. Both solutions were mixed in a three-necked flask fitted with a condenser, and brought to 65°; then 1 ml of 33% formaldehyde solution (Merck) was added (≡ 10 mmole), with magnetic stirring. After 6 hr another 1 ml of the formaldehyde solution was added to compensate for losses due to polymerization. After 10 hr the acetic acid was removed by vacuum distillation at 65° in a rotary evaporator. The residue was dissolved in 150 ml of water and used as stock for purification. The optimum experimental conditions of the Mannich condensation with respect to yield, time and by-products were determined by following the progress of the reaction during 28 hr, by HPLC (Fig. 1). During the first 11 hr only XO and SXO are formed (Fig. 1a). After that time the production of other, partly unidentified, compounds increases sharply (Fig. 1b), and the production of XO is relatively favoured. The best compromise is to stop heating after about 10 hr; 28% of the initial *o*-Cresol Red has then been transformed into SXO.

In order to minimize the formation of by-products we also investigated a slightly different procedure in which a formaldehyde–iminodiacetic acid mixture was added continuously. Although less of the by-products is formed, only 20% yield is obtained even after 28 hr of heating (Fig. 1c); the first procedure is superior.

Chromatographic conditions

The liquid chromatograph was built from parts from various sources and consisted of two reciprocating pumps (Orlita, Giessen, GFR); a pneumatic high-pressure injection valve (Rheodyne, U.S.A.) fitted with a 20-μl or 1000-μl loop; a variable wavelength spectrophotometer (LC4, Pye, U.K.) set at 400 nm. The analytical and the preparative column were made of 316 stainless steel and had dimensions of 150 × 4.6 mm and 125 × 10 mm respectively.

The columns were filled with octadecyl-modified silica (Hypersil ODS, Shandon, U.K.) by means of the slurry technique recommended by the manufacturer.

The analytical separations were performed with a mixture of 0.06*M* perchloric acid and acetone (4:1 v/v) as the mobile phase. For the preparative separations a slightly different composition (0.05*M* perchloric acid and acetone; 82:18 v/v) was found to be a good compromise between rapid production of pure SXO and resolution of SXO from neighbouring peaks when the column was overloaded.

The preparative purification of SXO was automated with a programmable timer. The complete set-up is schematically shown in Fig. 2. The 1000-μl sample loop is filled with the reaction mixture by means of a peristaltic pump. Then the mixture (containing about 40 mg of reaction products) is injected into the preparative column and a fixed fraction of the SXO peak (Fig. 3) is collected (about 8 mg). In order to remove the more strongly retained reaction products rapidly, the column is flushed with 40 ml of pure acetone, delivered by a second pump (Fig. 2). Before the next injection of crude material the column is equilibrated again with the mobile phase. This method allows the production of 200 mg of SXO per day.

The acetone is evaporated from the combined SXO fractions, leaving an aqueous solution of SXO and perchloric acid. To remove the perchloric acid the solution is pumped through the preparative column, which is pre-eluted with water. Under these conditions SXO is strongly sorbed on the reversed-phase column packing, in contrast to

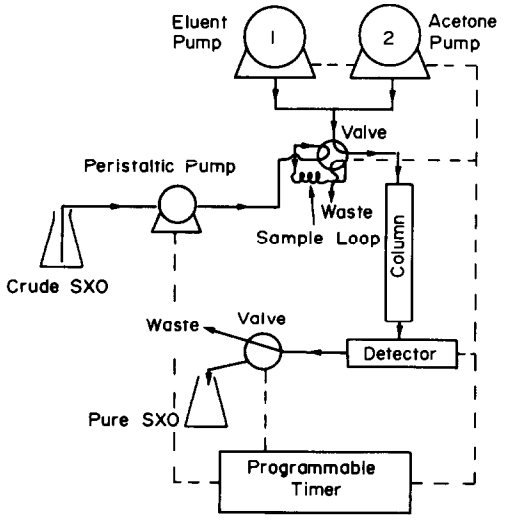

Fig. 2. Schematic representation of the automated preparative HPLC apparatus.

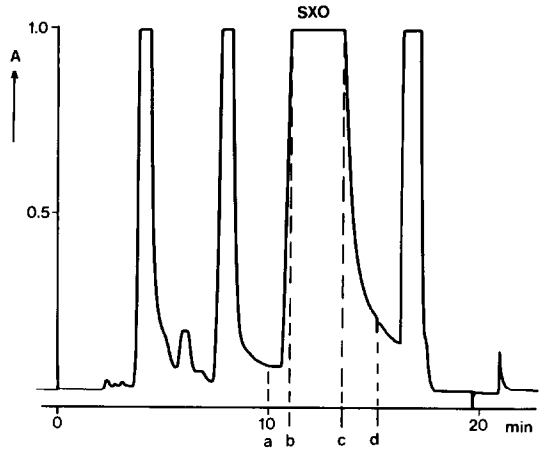

Fig. 3. Preparative separation of SXO. At *a* the timer is switched to peak-height sensitivity, after which the SXO peak is separately collected between *b* and *c*. At *d*, acetone is running in to clean the column. After 20 min, the column is stabilized with the original eluent and is ready for the next run. Flow-rate 11 ml/min; injection volume 1000 μl.

the perchloric acid, which is not retained and can be removed by flushing with water. The SXO is desorbed from the column with pure acetone, giving a concentrated solution from which very pure SXO is obtained by evaporation, and drying in a vacuum desiccator for 2 days at 60°.

DISCUSSION

For the elution of XO, Nakada *et al.*[11] used 5% aqueous acetic acid–methanol (80:20 v/v) as the mobile phase and C_{18}-bonded silica (Microbondapak C_{18}, Waters Associates, U.S.A.) as the stationary phase. With our column, this eluent gave very bad peak shapes and low efficiency. Replacing the acetic acid by perchloric acid improved the peak shapes remarkably, presumably because of better ion-association between SXO and perchloric acid. In order to avoid possible formation of methyl esters of SXO during the after-treatment at elevated temperatures, acetone was used as organic modifier instead of methanol.

An NMR spectrum of the purified product confirmed that SXO was the component isolated. However, a small amount of acetone turned out to be occluded in the crystals. From the peak integrals a 0.3 mole ratio of acetone to SXO was estimated, which corresponds to 97.1% w/w SXO.

From multiparametric non-linear curve-fitting of Job curves of Th–SXO mixtures taken at 19 different wavelengths,[12] in which the SXO content is introduced as one of the unknown parameters to be adapted, a weight content of 96.1% was found, which would correspond to a mole ratio of acetone to SXO of 0.39 and is in good agreement with the results of elemental analysis: 59.4% C, 4.8% H, 27.7% O, 2.3% N and 5.4% S (theory requires 59.4% C, 5.0% H, 27.4% O, 2.5% N and 5.7% S).

An analysis of variance of the procedure for multiparametric curve-fitting gave no evidence for the existence of other coloured ligand-forming products in the purified product.

Conclusion

Semi-Xylenol Orange can be prepared in a 10-hr batch-procedure with a minimum of by-products and a yield of about 30%. The SXO formed can be conveniently isolated from the crude reaction products by preparative reversed-phase HPLC. The purified SXO is obtained in crystalline form from the acetone used as eluent, and though minor amounts of acetone remain occluded in the crystals, they do not interfere in investigations of the composition of the Th–SXO system. No species were detected that could interfere in the investigation either by giving side-reactions with Th or by absorbing at the wavelengths used.

Acknowledgement—We are much indebted to Dr. J. C. Kraak for his support of the experimental work and critical reading of the manuscript.

REFERENCES

1. J. Kragten and A. Parczewski, *Talanta*, 1981, **28**, 149.
2. C. J. C. Pijpers, L. G. Decnop-Weever, G. den Boef and W. E. van der Linden, *Mikrochim. Acta*, 1976 **I**, 667.
3. J. Kragten, *Z. Anal. Chem.*, 1973, **264**, 356.
4. *Idem*, *Talanta*, 1971, **18**, 311.
5. *Idem*, *Mikrochim. Acta*, 1971, 821.
6. *Idem*, *Analyst*, 1971, **96**, 106.
7. D. C. Olson and D. W. Margerum, *Anal. Chem.*, 1962, **34**, 1299.
8. M. Murakami, T. Yoshino and S. Harasawa, *Talanta*, 1967, **14**, 1293.
9. H. Sato, Y. Yokoyama and K. Momoki, *Anal. Chim. Acta*, 1977, **94**, 217.
10. M. Yamada and M. Fujimoto, *Bull. Chem. Soc. Japan*, 1976, **49**, 693.
11. S. Nakada, M. Yamada, T. Ito and M. Fujimoto, *ibid.*, 1977, **50**, 1887.
12. J. Kragten, in preparation.

Talanta, Vol. 30, No. 8, pp. 617–619, 1983
Printed in Great Britain

0039-9140/83 $3.00 + 0.00
Pergamon Press Ltd

ANALYTICAL REACTIONS OF 5-AMINO-OROTIC ACID

B. ROY, AJAI K. SINGH* and R. P. SINGH
Department of Chemistry, Indian Institute of Technology, New Delhi-110016 and University of Delhi, Delhi-110007, India

(*Received* 27 *August* 1982. *Accepted* 5 *February* 1983)

Summary—The potential of 5-amino-orotic acid (AOA) for spectrophotometric determination of metal ions is explored. Only the reactions with copper(II), cobalt(II) and osmium(VIII) are sensitive and suitable for this purpose. Ternary complexes of copper(II) formed with AOA and ammonia or pyridine can also be used for photometric determination of the metal and given better sensitivity and selectivity than the binary complex. Optimum conditions for determination of all the three metal ions have been established.

Orotic acid is a promising analytical reagent[1,2] for many metals, including alkali and alkaline-earth metals. The main drawback is the comparatively low stability of its metal complexes, which is due to the poor co-ordinating tendency of ring nitrogen, the only available site for formation of a stable chelate ring with the carboxylic group.

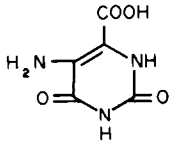

(AOA)

This results in poor selectivity and sensitivity. The inclusion of a potent donor site at the 5-position could improve both these aspects. In view of this 5-amino-orotic acid (AOA) has been studied and the results are reported in this communication. It has been already found the most suitable derivative of orotic acid for gravimetric determination of alkali metals.[2] Of the various species investigated, only Cu(II), Co(II) and Os(VIII) form coloured complexes suitable for spectrophotometric determination.

EXPERIMENTAL

Reagents

Pure AOA (Aldrich Chemicals) was converted into the ammonium salt,[3] which was used for preparing a 0.01*M* stock solution, which was stable for 2–3 weeks. Standard solutions of Cu(II), Co(II) and Os(VIII) were prepared from $CuSO_4 \cdot 5H_2O$, $CoSO_4 \cdot 7H_2O$ and OsO_4 respectively. The first two were dissolved in doubly-distilled water and the last in 0.01*M* sodium hydroxide, and the solutions were standardized[4,5] either volumetrically or gravimetrically.

Dilute hydrochloric acid and sodium hydroxide solution were used for pH adjustments. Pyridine was always distilled before use. Solutions for interference studies were prepared by dissolving the analytical-grade chemicals in doubly distilled water.

Unicam SP600 and Perkin–Elmer 554 spectrophotometers, with matched 10-mm glass cells, were used for absorbance measurements.

*To whom correspondence should be addressed.

RESULTS AND DISCUSSION

The light yellow AOA solution (λ_{max} 320 nm, ε_{max} 1.6×10^3 $l.mole^{-1}.cm^{-1}$) reacts with group VIII metal ions and copper(II), forming coloured complexes, but many of these species are unsuitable for photometric determination because they are unstable or formed only in concentrated solutions. However, the reactions with copper(II), cobalt(II) and osmium(VIII) are sensitive and suitable for the purpose. The ternary Cu(II)–AOA–NH_3 or pyridine complexes are found better than the binary complex. Optimum conditions for the determinations and effect of diverse ions are described below.

Determination of copper

Copper(II) forms a yellow complex (λ_{max} 370 nm, ε_{max} 1.48×10^4 $l.mole^{-1}.cm^{-1}$) which is not extractable into organic solvents and has composition 1:2 (metal:ligand), as determined by Job's method. The binary complex is used for the photometric determination of the metal, the procedure being as follows. Adjust a suitable aliquot containing 9–24 μg of copper to pH 9–10.8 after addition of 2 ml of $5 \times 10^{-3}M$ AOA. Dilute to 10 ml, measure the absorbance at 370 nm against a reagent blank and deduce the metal content from a calibration curve. The relative standard deviation is 2% for 1.6-μg/ml copper concentration. At least a 30-fold molar ratio of ligand to metal is required for full colour development. The complex is stable for more than 24 hr.

The tolerance limits for various ions (mg/ml) in determination of 1.6 μg/ml copper are: F^-, Cl^-, Br^-, NO_3^- (8); $S_2O_3^{2-}$, SO_4^{2-}, NO_2^-, SCN^- (0.1); $C_2O_4^{2-}$, tartrate, citrate (0.2), I^- (0.015): Ca^{2+}, Ba^{2+}, Sr^{2+}, Pb^{2+}, Al^{3+}, Zn^{2+} (0.5); Cd^{2+}, Sn^{2+}, Mn^{2+} (0.05); Hg^{2+} (0.01); Ag^+ (0.025, masked with Cl^-); Fe^{3+} (0.030, masked with F^-); Ni^{2+} (0.025); Pd^{2+} (0.5); Pt^{4+} (0.7), Ir^{3+}, Rh^{3+} or Ru^{3+} (1); Au^{3+} (0.04). Thiourea, cyanide, EDTA, cobalt(II) and osmium(VIII) interfere seriously.

On addition of ammonia or pyridine to the cop-

Table 1. Characteristics of ternary copper complexes

Characteristic	Complex	
	Cu–AOA–NH_3	Cu–AOA–pyridine
λ_{max}, *nm*	405	405
ϵ_{max}, $l.mole^{-1}.cm^{-1}$	5×10^4	4.8×10^4
pH for formation	9.5–10.5	9.5–10.5
Stability, *hr*	24	24
Accurate range for determination, $\mu g/ml$	0.2–1.4	0.2–1.2
Molar ratio of AOA to Cu needed for full colour development	$\geqslant 20$	$\geqslant 20$
Relative standard deviation for 0.63 μg/ml, %	1.6	2

per(II)–AOA system, the λ_{max} of the coloured species shifts towards longer wavelength by 35 nm and there is a more than threefold increase in the sensitivity, indicating the formation of a ternary complex with ammonia or pyridine. The ternary complex does not result if the bases are added at pH < 5.0. The metal:AOA:pyridine or NH_3 ratio in these complexes has been found to be 1:1:2 by Job's method, and a test with Amberlite IR 120 cation-exchange resin shows they are cationic. The following structures are tentatively proposed.

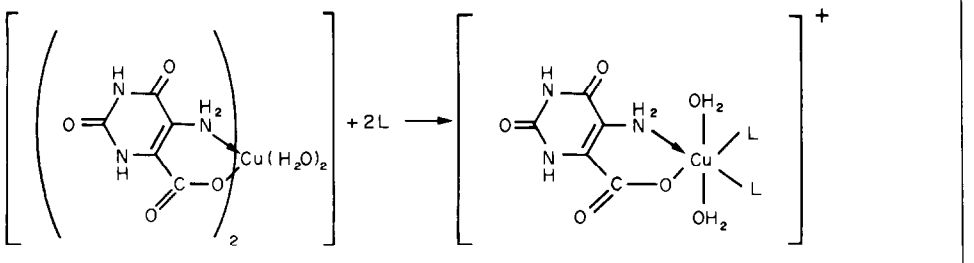

Binary complex Ternary complex

L = pyridine or NH_3

The ternary complexes can be used for the determination of copper. Optical constants for these complexes and optimum conditions for determination are summarized in Table 1.

The procedure is as follows. To a suitable aliquot add 1.5 ml of $2 \times 10^{-3}M$ AOA and 3 ml of $2 \times 10^{-3}M$ ammonia or pyridine solution. Bring the pH to 10, make up to volume in a 10-ml standard flask and measure the absorbance at 405 nm against a reagent blank. The order of addition of AOA and base is somewhat critical. The AOA must be added first, or low absorbances are obtained. For maximum colour development the ammonia or pyridine must be in at least 60-fold molar ratio to copper, but not more than 150-fold (probably further replacement of AOA with the base molecules).

Thiourea, cyanide, EDTA, cobalt(II) and osmium(VIII) always interfere. Tolerance limits (μg/ml) for other ions are given in parentheses below.

Cu(II)–AOA–NH_3 system. F^-, Cl^-, Br^-, SO_4^{2-}, NO_3^- (5000); NO_2^-, $S_2O_3^{2-}$, SCN^- (500); $C_2O_4^{2-}$ (300); tartrate, citrate (200), I^- (80); Ca^{2+}, Ba^{2+}, Sr^{2+}, Pb^{2+}, Pd^{2+} (500); Al^{3+}, Zn^{2+}(400); Cd^{2+}, Sn^{2+}, Mn^{2+} (50); Fe^{3+} (130, masked with F^-); Ag^+ (20, masked with Cl^-); Ni^{2+} (25); Hg^{2+} (10); Ru^{3+} (300); Pt^{4+} (700); Rh^{3+}, Ir^{3+} (100); Au^{3+} (50).

Cu(II)–AOA–pyridine system. F^-, Cl^-, Br^- (5000); NO_3^-, SO_4^{2-} (4000); NO_2^-, $S_2O_3^{2-}$, $C_2O_4^{2-}$ (500); SCN^-, tartrate, citrate (200); I^- (80); Ca^{2+}, Sr^{2+}, Ba^{2+} (500); Pb^{2+}, Al^{3+} (400); Zn^{2+} (300); Cd^{2+}, Sn^{2+}, Mn^{2+} (50); Fe^{3+} (140, masked with F^-); Ag^+ (25, masked with Cl^-); Ni^{2+} (25); Hg^{2+} (15); Ru^{3+}, Pt^{4+}, Rh^{3+} (200); Ir^{3+}, Pd^{2+} (100); Au^{3+} (50).

Comparison with other reagents[6,7] for copper shows that AOA is more sensitive than most ligands, especially in the ternary systems, and more selective than most of the commonly used reagents such as dithizone, PAN, oximes, nitroso-R-salt, neocuproine, bathocuproine, cuprotest, rubeanic acid, various dyes, hydrazones and 8-hydroxyquinoline. The simplicity of the procedure is another advantage.

Determination of copper in alloys

The copper contents of brass, gunmetal and BCS 181/2 alloy (4% Cu–Al alloy) have been estimated by means of the ternary systems. Results are reported in Table 2.

Determination of cobalt

Interaction of AOA with cobalt results in a yellow complex (λ_{max} 370 nm, ϵ_{max} 1.56×10^4 $l.mol^{-1}.cm^{-1}$)

Table 2. Determination of copper in alloys

Alloy	Copper present, %	Copper found,*% Ammonia method	Std. devn.	Pyridine method	Std. devn.
Brass	65.0	64.9	1.3	65.0	1.3
Gunmetal	87.1	87.0	2.0	87.0	2.2
BCS 181/2 4% Cu–Al alloy	4.0	3.98	0.01	3.96	0.01

*Average of six determinations.

having a metal:ligand ratio 1:2, as determined by Job's method. The complex is uncharged (it is not sorbed by either a cation- or an anion-exchange resin), and the structure tentatively assigned to it is the same as that for the binary copper complex. For maximum absorbance at least a 30-fold molar ratio of reagent to metal is needed, at pH 9–10. To a solution (containing 5–38 μg of cobalt(II)) add 2 ml of $5 \times 10^3 M$ AOA, adjust to pH 9.5, dilute volume in a 10-ml standard flask and measure the absorbance at 370 nm against a reagent blank. Deduce the cobalt content from a calibration graph. The absorbance is constant for a week. The standard deviation of the absorbance is 0.005 (mean absorbance 0.39 for 1.5 μg/ml Co).

In the determination of 1.5 μg/ml cobalt, the tolerance limits (μg/ml) for various ions are: F^-, Cl^-, Br^- (8000); I^- (200); $C_2O_4^{2-}$ (5000); SO_4^{2-} (2000), NO_3^-, NO_2^-, $S_2O_3^{2-}$ (1000); SCN^-, citrate, tartrate (50); EDTA (400); thiourea (300); Ca^{2+}, Sr^{2+}, Ba^{2+} (400); Cd^{2+}, Sn^{2+}, Al^{3+} (500); Mn^{2+}, Pb^{2+} (200); Sn^{2+}, Hg^{2+} (50); Fe^{3+} (25, masked with F^-); Cu^{2+} (30, masked with thiourea); Ru^{3+}, Rh^{3+} (50); Au^{3+}, Ir^{3+} (30); Pt^{4+}, Pd^{2+} (20); Ag^+ (15, masked with Cl^-), Ni^{2+} (10). Cyanide and osmium(VIII), however, interfere seriously.

AOA is among the more sensitive and selective reagents for cobalt;[6,7] it is less sensitive but more specific than the azo-dyes and the procedure is simpler.

The complex has been used for the photometric determination of cobalt in 'K' monel wire and nilo-K wire (Table 3).

Determination of osmium

Osmium reacts instantaneously at pH 4.5–6.5 with AOA, forming a 1:2 M:L brownish red complex (λ_{max} 500 nm, ϵ_{max} 2.6×10^4 l.mole^{-1}.cm^{-1}) which is not extractable and is stable for 12 hr. At least 20-fold molar ratio of AOA to osmium is required for maximum colour development. The procedure for the photometric determination is as follows. To a solution containing 28–50 μg of osmium(VIII) add 1.5 ml of $5 \times 10^3 M$ AOA, adjust to pH 5, dilute to volume in a 10-ml standard flask and read the absorbance at 500 nm against water. Determine the osmium content from a calibration graph. The standard deviation of the absorbance is 0.006 (mean absorbance 0.65 for 4.8 μg/ml Os).

Table 3. Determination of cobalt in alloys

Alloy	Cobalt, % Certified	Found	Standard deviation*
'K' Monel wire	0.51	0.50	0.04
Nilo-K wire	17.4	17.7	0.02

*For six determinations.

The amounts of foreign ions (μg/ml) tolerated in estimation of 4.8 μg of Os per ml are: F^-, Cl^-, Br^-, I^- (8000); $C_2O_4^{2-}$, tartrate (5000); $S_2O_3^{2-}$, SCN^- (1000); BO_3^{3-}, PO_4^{3-}, acetate (500); NO_3^-, EDTA (2000); NO_2^-, SO_3^{2-}, SO_4^{2-} (1500); thiourea (200); Ca^{2+}, Sr^{2+}, Ba^{2+}, Ni^{2+} (5000); Sn^{2+}, Hg^{2+}, Mn^{2+} (100); Al^{3+}, Pb^{2+} (200); Zn^{2+}, Cd^{2+} (500), Sb^{3+}, As^{3+}, Bi^{3+} (150); Cu^{2+}, Co^{2+} (50); Fe^{3+} (50, masked with F^-); Ag^+ (30, masked with Cl^-); Au^{3+} (10); Ru^{3+} (50); Pt^{4+} (40); Pd^{2+} (25). Cyanide, Rh^{3+} and Ir^{3+} interfere seriously.

From these observations it can be concluded that introduction of the amino group into the 5-position in orotic acid increases the sensitivity considerably. AOA is superior to many reagents for copper and cobalt. For osmium, the sensitivity is as good as that of most reagents,[5,8] but rhodium(III) and iridium(III), which are found associated with it in natural sources, interfere and prior separation of the osmium is then necessary.

Acknowledgement—One of us (B.R.) is grateful to the National Council of Educational Research and Training, New Delhi, for the award of a fellowship.

REFERENCES

1. A. K. Singh, B. Mukherjee, R. P. Singh and M. Katyal, *Talanta*, 1982, **29**, 95.
2. M. Katyal, W. A. E. McBryde and A. K. Singh, *Pyrimidines: Analytical Aspects*. South Asian Press, New Delhi, 1981.
3. A. K. Singh and R. P. Singh, *Indian J. Chem.*, 1979, **17A**, 469.
4. A. I. Vogel, *A. Textbook of Quantitative Inorganic Analysis*, 4th Ed. Longmans, London, 1979.
5. F. E. Beamish, *The Analytical Chemistry of the Noble Metals*. Pergamon Press, London, 1966.
6. E. B. Sandell and H. Onishi, *Photometric Determination of Traces of Metals*. Wiley, New York, 1978.
7. F. D. Snell, *Photometric and Fluorometric Methods of Analysis (Metals)*, Part I. Wiley, New York, 1978.
8. F. E. Beamish and J. C. Van Loon, *Recent Advances in the Analytical Chemistry of the Noble Metals*. Pergamon Press, London, 1972.

Talanta, Vol. 30, No. 8, pp. 620–622, 1983
Printed in Great Britain.

0039-9140/83 $3.00 + 0.00

THE EXTRACTION AND DETERMINATION OF THIOCYANATE COMPLEXES BY USE OF POLYURETHANE FOAM

A. CHOW and S. L. GINSBERG
Department of Chemistry, University of Manitoba, Winnipeg, Manitoba, Canada

(*Received* 27 *August* 1982. *Revised* 8 *January* 1983. *Accepted* 4 *February* 1983)

Summary—Metal thiocyanate solutions were extracted with polyether-type polyurethane foam and the metal contents determined by X-ray fluorescence. Iron, cobalt and zinc were extracted individually and collectively from 3.0*M* NH_4Cl and 1.0*M* NH_4SCN solutions. Similarly platinum and palladium could be simultaneously extracted from 0.12*M* NH_4SCN and 5.0*M* NH_4Cl for subsequent determination. The metal extractions were more than 95% complete and the determination of one metal was not affected by the presence of the others.

The direct determination of preconcentrated metal complexes may offer the advantages of higher metal concentrations, lower amounts of matrix and interferents, and faster analyses. Metal complexes extracted into polyurethane foam can be determined non-destructively by use of neutron activation,[1] radiochemical tracers,[2–5] visual colorimetry,[6,7] and by X-ray fluorescence.[8] The extraction of several metal thiocyanates by polyurethane has been described,[9–17] and it appears that multielement extractions and determinations might be possible for a variety of species.

The present paper describes the extraction of platinum and palladium, or of iron, cobalt and zinc, from thiocyanate solutions with polyether-type polyurethane foam, and the subsequent determination of these metals on the polymer by X-ray fluorescence.

EXPERIMENTAL

Apparatus

Atomic-absorption spectrometry was used to evaluate the efficiency of metal extraction as reported previously.[8] An energy-dispersive X-ray fluorescence system[8] was used with a polyurethane-foam sample-holder held at a fixed distance from the source and detector by 4-μm thick Mylar film. Uniform foam discs (2.0 cm diameter, 1.6 cm thick) were cut from commercial, polyether-type polyurethane foam sheet by compressing it with a large brass block and rotating a sharpened brass tube (2.0 cm diameter) in a corresponding hole drilled through the block. The discs were thoroughly cleaned[8] before use.

Cobalt and zinc solutions were made by dissolving the metals in hydrochloric acid and diluting to produce a 1000-ppm standard in 1% v/v acid. A 1000-ppm iron solution was prepared similarly in 5% v/v nitric acid. Platinum and palladium solutions were prepared from $PtCl_2$ and $PdCl_2$ in 0.12*M* hydrochloric acid. Solutions (5.0*M*) of ammonium chloride and ammonium thiocyanate were prepared from the reagent-grade salts in water. Because it contained trace amounts of iron, the 5*M* thiocyanate solution was filtered through polyurethane foam to remove this background contaminant. All water used was distilled and demineralized.

Extraction of iron, cobalt and zinc

Previous work with the thiocyanate system[8] has shown that the extraction of cobalt is most efficient from high ionic strength solutions. For the present experiments, 50 ml of a solution of an appropriate amount of the test metal in 3.0*M* ammonium chloride/1.0*M* ammonium thiocyanate medium were extracted with a single 0.127 ± 0.001 g foam disc, by manual squeezing with a flat-bottomed plunger in a glass cell. The extractions were repeated to establish the minimum extraction time for the individual complexes. For 1–5 ppm solutions of iron, cobalt or zinc, 10 min were sufficient but for 5–10 ppm solutions 20 min were required. After the extraction the solutions contained less than 0.05 ppm of the metals, even though equilibrium was not obtained. This corresponds to an extraction coefficient of 8×10^3–8×10^4 for cobalt thiocyanate, which may be compared with the $> 10^6$ reported previously.[12,13] The use of non-equilibrium conditions makes this method more practical since only a small amount of the test element is left unextracted, and the time needed is far less than the minimum of 6 hr required to establish equilibrium.

Extraction of platinum and palladium

Low thiocyanate concentrations provide the most efficient extraction of platinum and palladium.[16,17] For the present studies of the extraction of palladium alone, 0.006*M* ammonium thiocyanate/2*M* ammonium chloride medium was used, and for platinum alone or with palladium, 0.12*M* ammonium thiocyanate/5*M* ammonium chloride medium. The extraction of platinum with or without palladium required the samples to be heated at 90° for 10 min before extraction. Samples (100 ml) were extracted for 30 min with 0.128 ± 0.001 g foam discs, with an automatic squeezer.[12] The extraction efficiency for 1–10 ppm platinum or palladium solution was at least 95%.

Analysis

Before X-ray fluorescence analysis, the foams were squeezed dry and then air-dried overnight. The sample foam was placed in the hole cut in the polyurethane-foam sample-holder attached to the X-ray fluorescence exciter/detector unit. The fluorescence spectrum was accumulated for 100 sec and the peak areas for each metal were integrated individually. Each foam was counted at least three times on each side. The results indicate that repeated counting of the same side had a variation of less than $\pm 3\%$ and that the two sides agreed within $\pm 5\%$.

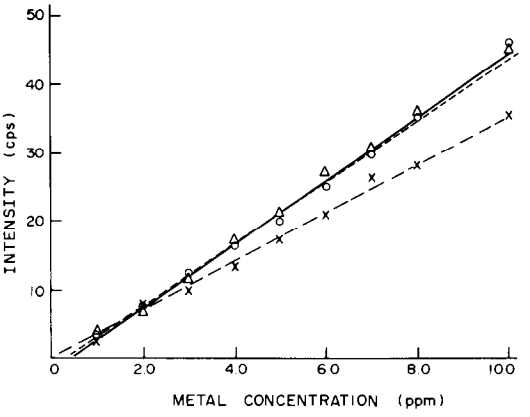

Fig. 1. X-Ray fluorescence intensity for iron, cobalt and zinc. Conditions: 50 ml of solution containing 1–10 ppm of metal in 3.0*M* NH_4Cl and 1.0*M* NH_4SCN, extracted with 0.127 g of polyurethane foam; × --- × iron; △-----△ zinc; ○——○ cobalt.

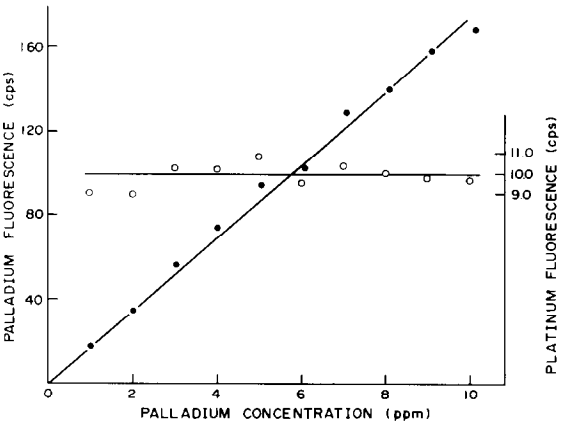

Fig. 3. The effect of varying palladium concentration on the X-ray fluorescence of platinum. Conditions as for Fig. 2 but 1 ppm of platinum and 1–10 ppm of palladium: ● palladium; ○ platinum.

Several variations in the sample-holder arrangement were evaluated such as distance of the sample above the detector, change in sample-holder design, and confinement of the sample to a smaller volume but none provided significantly better precision or sensitivity than the method outlined and all were less convenient. Regular commercial foam was adequate for use in the procedure, but Hypol® foam appeared more free from metals than the others tested. Polyester foam does not give large distribution coefficients and does not provide rapid extraction.

The average X-ray fluorescence values obtained for individual iron, cobalt and zinc samples were a reasonably linear function of the metal concentrations (Fig. 1). Mixtures of iron, cobalt and zinc in concentration combinations of 1 + 1 + 1, 1 + 1 + 0, 1 + 5 + 5, 0 + 5 + 5 and 5 + 5 + 5 ppm were also extracted, and the number of counts obtained by X-ray fluorescence were compared with those obtained for the corresponding concentrations of the individual elements. The results indicated that there is little or no mutual interference between these elements in either the extraction or the X-ray fluorescence determination. The values for zinc and cobalt were within ± 5% of those obtained in the absence of the other metals. The values for iron were not as accurate, owing to some effect of the other elements on the X-ray fluorescence background for iron. This difficulty causes inaccuracy in determination of iron at the 1-ppm level, but reasonably correct values are obtained at the 5-ppm level. A higher count rate would significantly increase the precision of the analysis and permit a more sensitive determination.

The individual X-ray fluorescence calibration curves for platinum and palladium were linear up to at least 8 ppm. The extraction and determination of 1 ppm palladium in the presence of up to 10 ppm platinum and of 1 ppm platinum in the presence of up to 10 ppm palladium are completely unaffected by the second metal. The fluorescence count rate for the metal determined remained constant within ±4.5% in the presence of 1–10 ppm of the other metal. The higher sensitivity for platinum and palladium than for iron, cobalt and zinc allows more precise determination. In addition the rapid equilibration with the polyurethane foam gives a more consistent and quantitative extraction of platinum and palladium.

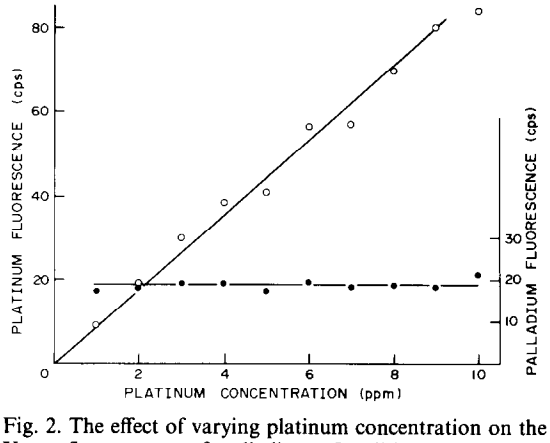

Fig. 2. The effect of varying platinum concentration on the X-ray fluorescence of palladium. Conditions: 100 ml of solution containing 1 ppm of palladium and 1–10 ppm of platinum in 5.0*M* NH_4Cl and 0.12*M* NH_4SCN, extracted with 0.128 g of polyurethane foam: ○ platinum; ● palladium.

CONCLUSION

The simultaneous determination of several elements at low concentrations is possible by combining polyurethane foam extraction with X-ray fluorescence analysis. Longer extraction times and larger sample volumes would extend the methods to lower concentrations and more sophisticated X-ray equipment could extend the lower limit of analysis by one or two orders of magnitude. The major limiting factor is the background which depends on freedom from overlap of the peaks for the extracted elements with each other or with those of the elements already present in the polyurethane foam. These procedures require the simultaneous quantitative extraction of the metal complexes and are therefore dependent on the solution chemistry of the system. The thiocyanate system is a particularly useful one, but many complexing agents can be used for the simultaneous extraction of a variety of metals.

Acknowledgements—This work was financially supported by the Natural Sciences and Engineering Research Council

of Canada and by the Research Board, University of Manitoba.

REFERENCES

1. P. Schiller and G. B. Cook, *Anal. Chim. Acta*, 1971, **54,** 364.
2. S. Palagyi and T. Braun, *J. Radioanal. Chem.*, 1979, **51,** 267.
3. S. Palagyi and E. Bila, *Radiochem. Radioanal. Lett.*, 1978, **32,** 87.
4. T. Braun and S. Palagyi, *Anal. Chem.*, 1979, **51,** 1697.
5. S. Palagyi and R. Markusova, *Radiochem. Radioanal. Lett.*, 1978, **32,** 103.
6. T. Tanaka, K. Hiiro and A. Kawahara, *Bunseki Kagaku*, 1973, **22,** 523; *Chem. Abstr.*, 1973, **79,** 87234.
7. T. Braun and A. B. Farag, *Anal. Chim. Acta*, 1974, **73,** 301.
8. A. Chow, G. T. Yamashita and R. F. Hamon, *Talanta*, 1981, **28,** 437.
9. T. Braun, A. B. Farag and M. P. Maloney, *Anal. Chim. Acta*, 1977, **93,** 191.
10. T. Braun and A. B. Farag, *ibid.*, 1978, **98,** 133.
11. T. Braun and M. N. Abbas, *ibid.*, 1980, **119,** 113.
12. R. F. Hamon, *Ph.D. Thesis*, University of Manitoba, 1981.
13. R. F. Hamon and A. Chow, *Abstracts 60th CIC Conference*, Montreal, Canada, 1977.
14. M. P. Maloney, G. J. Moody and J. D. R. Thomas, *Proc. Chem. Soc. Anal. Div.*, 1977, **14,** 244.
15. T. Braun and M. N. Abbas, *Anal. Chim. Acta*, 1982, **134,** 321.
16. S. J. Al-Bazi and A. Chow, *Anal. Chem.*, 1981, **53,** 1073.
17. *Idem*, *ibid.*, in the press.

Talanta, Vol. 30, No. 8, pp. 623–626, 1983
Printed in Great Britain.

0039-9140/83 $3.00+0.00

ANALYTICAL DATA

SOLUBILITY AND PROTONATION OF EDTA, DCTA AND DPTA IN ACIDIC PERCHLORATE MEDIUM

J. KRAGTEN
Natuurkundig Laboratorium der Universiteit van Amsterdam, Valckenierstraat 65, 1018 XE Amsterdam, The Netherlands

L. G. DECNOP-WEEVER
Laboratorium voor Analytische Chemie, Nieuwe Achtergracht 166, Amsterdam, The Netherlands

(*Received* 14 *January* 1983. *Accepted* 8 *February* 1983)

Summary—From measurements of solubility as a function of pC_H, the protonation constants of EDTA, DCTA and DTPA for the first dissociation and addition steps have been determined. The following values were found: EDTA: $\log K_6 = -0.10 \pm 0.05$, $\log K_5 = 1.45 \pm 0.02$, $\log K_4 = 1.95 \pm 0.02$ and $\log K_3 = 2.50 \pm 0.03$;DCTA: $\log K_5 = 1.78 \pm 0.02$, $\log K_4 = 2.30 \pm 0.02$ and $\log K_3 = 3.50 \pm 0.03$; DTPA: $\log K_7 = 0.75 \pm 0.03$, $\log K_6 = 1.22 \pm 0.02$ and $\log K_5 = 2.08 \pm 0.02$. The experiments were done in acidic perchlorate medium ($I = 1.0$) at room temperature (21°).

For the proton release steps of EDTA, DCTA and DTPA, fairly reliable stability constants are now available,[1–5] but the constants related to proton addition are denoted as tentative in IUPAC compilations[3,5] or are not compiled at all because of the limited number of reliable data available in the literature.

For the establishment of the stability constants of the palladium complexes[6] and the titration conditions for thorium, zirconium and bismuth, reliable data were needed. Hence we decided to determine these protonation constants from the change of the solubility at low pC_H ($= -\log [H^+]$) by making use of the straight-line adaptation technique successfully applied before to the protolysis of rare-earth metals.[7–12]

Since our experiments range down to pC_H 0, an ionic strength of 1.0 was selected. The medium chosen—$(Na,H)ClO_4$—is the one least likely to take part in side-reactions with multiply charged metal ions.

THEORY

From the reaction scheme for protonation of the ligand H_4Y in equilibrium with solid H_4Y

$$\begin{array}{c} H_6Y^{2+} \rightleftharpoons H_5Y^{+} \rightleftharpoons H_4Y \rightleftharpoons H_3Y^{-} \rightleftharpoons H_2Y^{2-} \rightleftharpoons HY^{3-} \rightleftharpoons Y^{4-} \\ \uparrow\downarrow \\ \{H_4Y\}_{solid} \end{array} \quad (1)$$

we can write for the solubility equilibrium

$$[H_4Y]^{max} = K_{s4} \quad (2)$$

and for the overall protonation constant of H_iY

$$\beta_i = \frac{[H_iY^{i-4}]}{[Y^{4-}][H^+]^i} \quad (3)$$

If the analytical concentration C_Y is the total amount of H_4Y in solution, we get for the maximum value of C_Y, occurring when the solution is saturated,

$$pC_Y^{max} = -\log\left[\sum_{i=0}^{6}\left\{10^{-(i-4)pC_H + (\log\beta_i - \log\beta_4 + \log K_{s4})}\right\}\right]. \quad (4)$$

In the pC_Y–pC_H diagram each term in the summation corresponds to a straight line with a distinct slope. The set of lines with the equations

$$pC_Y^{max} = 2pC_H + (-\log K_{s4} + \log\beta_4 - \log\beta_6),$$
$$pC_Y^{max} = pC_H + (-\log K_{s4} + \log\beta_4 - \log\beta_5), \quad etc.$$

surrounds the precipitation region. The actual borderline of the precipitation region which corresponds to equation (4) can be considered to be the smoothed line bounded by the lowest-lying straight-line segments[7–9] (Fig. 1).

To fit the actual line to the measured points an iterative calculation procedure is used. First, the straight-line segments are positioned approximately. From their points of intersection approximate values for the equilibrium constants can be found. These estimates are substituted in equation (4) and a curve is found, which usually does not fit exactly. Its position can be improved by shifting the straight-line

segments and hence the actual line. The procedure is repeated until the actual curve has as good as possible a (least-squares) fit to the experimental points.

An analogous procedure was used earlier for determination of the protolysis constants of some rare-earth metals.[7-12]

For a pentabasic acid (DTPA) a formula similar to equation (4) can be developed

$$pC_Z^{max} = -\log\left[\sum_{i=0}^{7}\{10^{-(i-5)pC_H + (\log\beta_i - \log\beta_5 + \log K_{a5})}\}\right] \quad (5)$$

The fitting procedure remains essentially the same.

EXPERIMENTAL

The solubility measurements were done for the pC_H range 0–3.8. To saturated solutions of EDTA, DCTA and DTPA in water, 1*M* perchloric acid was added to give approximately the desired pC_H. Solid sodium perchlorate was added to make the ionic strength 1.0. The solutions were shaken for 24 hr (room temperature, 21°). The equilibrated solutions were centrifuged.

The pC_H was measured in the supernatant solution, from which some 5-ml aliquots were taken in 100-ml flasks and diluted to the mark. Depending on the pC_Y^{max} known from preliminary experiments, 0.050–10.00 ml were taken for microtitration with a bismuth solution (0.005*M*, pC_H 1.0). The titrations were done at pC_H 1.5 after adjustment with ammonia or perchloric acid. The end-point was detected photometrically (Zeiss PMQ II; 530 nm), with PAR as indicator.[13] DCTA was also determined by titration with Ce(III) with hexamine buffer at pH 5.5 and Xylenol Orange as indicator (575 nm).

The pC_H measurements were made with a glass electrode. The calomel reference electrode was connected through a saturated ammonium nitrate bridge in order to prevent clogging of the junction with potassium perchlorate precipitate. The electrode system was calibrated directly in pC_H units.[14-17] For this purpose several solutions were prepared with known acidities ranging from 0.1*M* perchloric acid to 0.001*M* perchloric acid and made up to $I = 1.0$ with sodium perchlorate. The pC_H values were established through acidimetric titration. It turned out that the measured and calculated pC_H values showed a linear relationship down to pC_H 1.0. From the slope of *E vs.* pC_H, an electrode efficiency of 98.3% was found, a common value for the type of glass electrode used.[19]

At pC_H below 1.0, a discrepancy arises between the measured values and the true pC_H values (up to 0.15 at $pC_H = 0$). The deviation can be attributed to the change in the liquid-junction potential at high acidity. Within experimental error, the deviation follows the Henderson equation.[20,21] For pC_H below 1, corrections were applied to the measured values.

RESULTS AND DISCUSSION

Figures 1 and 2 show the experimental results, together with those of Anderegg[22] for EDTA and DCTA. For EDTA the best fit to the experimental points is obtained with the equation

$$pC_{EDTA} = -\log[10^{-2pC_H - 2.10} + 10^{-pC_H - 2.00} + 10^{-3.45} + 10^{pC_H - 5.40} + 10^{2pC_H - 7.90}] \quad (6)$$

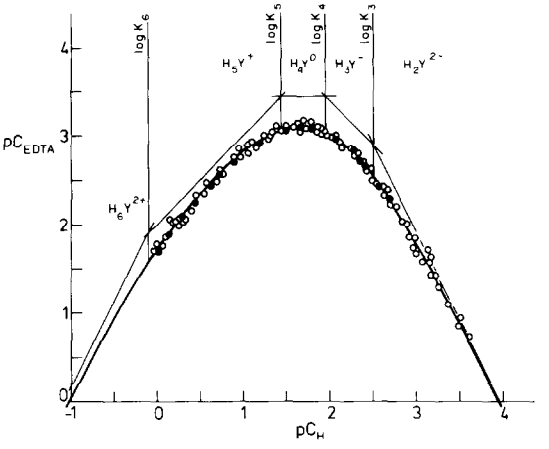

Fig. 1. The solubility of EDTA *vs.* pC_H. The circles correspond to our own measurements; the dots are results obtained by Anderegg.[22] The vertical lines separate the regions of predominance of the various ionic species. The straight-line segments are related to the exponents of equation (4) and play a role in the iterative curve-fitting procedure.

The stability constants β_i are found by comparing the exponents of equations (6) and (4) (Table 1). The stepwise stability constants ($\log K_i = \log\beta_i - \log\beta_{i-1}$) have been indicated in Fig. 1 (and Fig. 2); they follow from the intersection points of the straight-line segments for which $pC_H = \log K_i$ (Fig. 1).

For DCTA and DTPA the "best-fit" equations are respectively

$$pC_{DCTA} = -\log[10^{-pC_H - 1.52} + 10^{-3.30} + 10^{pC_H - 5.60} + 10^{2pC_H - 9.10}] \quad (7)$$

and

$$pC_{DTPA} = -\log[10^{-2pC_H + 0.28} + 10^{-pC_H - 0.47} + 10^{-1.69} + 10^{pC_H - 3.77} + 10^{2pC_H - 7.37}] \quad (8)$$

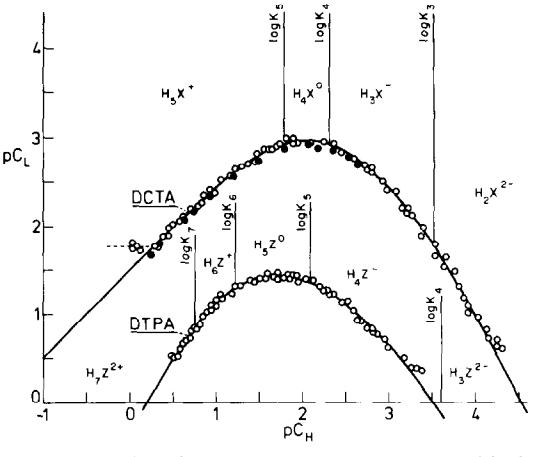

Fig. 2. Solubility of DCTA and DTPA *vs.* pC_H, with the corresponding log K_i values positioning the vertical lines separating the regions of predominance. The circles correspond to our measurements; the dots are results obtained by Anderegg.[22]

Table 1. The stability constants for the stepwise protonation of EDTA, DCTA and DTPA

Ligand	I	Medium	Temp., °C	Method	$\log K_{sn} = \log [H_nL]^{max}$	$\log K_7$	$\log K_6$	$\log K_5$	$\log K_4$	$\log K_3$	References
EDTA	1.0	(Na,H)ClO$_4$	21	solubility	−3.45 (±0.04)	—	−0.10 (±0.05)	1.45 (±0.02)	1.95 (±0.02)	2.50 (±0.03)	this work
	1.0	(Na,H)ClO$_4$	20	solubility	−3.33	—	−0.12	1.4	2.2	2.3	22
	1.0	—	25	—			0.0				1–4
	0.1	—	25	titration				1.5	2.0	2.68	1–4
	0.1	—	20	titration				1.5	2.0	2.66	1–4
DCTA	1.0	(Na,H)ClO$_4$	21	solubility	−3.30 (±0.04)	—	—	1.78 (±0.02)	2.30 (±0.02)	3.50 (±0.03)	this work
	1.0	(Na,H)ClO$_4$	20	solubility	−3.19	—	—	1.72	2.41	3.52	22
	1.0	(K,H)Cl	25	titration				(1.49)	2.41	3.21	23
	0.1	—	20	titration		—	—	—	2.42	3.53	1–4
DTPA	1.0	(Na,H)ClO$_4$	21	solubility	−1.69	0.75 (±0.03)	1.22 (±0.02)	2.08 (±0.02)	3.6 (±0.3)	—	this work
	1.0	(K,H)Cl		titration		(0.88)	(1.67)	2.29	2.50	4.13	23
	0.1	—	20–25	titration		—	—	1.82	2.66	4.30	1–4

The resulting stability constants are given in Table 1.

The pC_H regions in which the measurements could be made were 3.5 log units wide for EDTA and DCTA, but only 2.8 units for DTPA. The regions are restricted for different reasons. Dissolving DTPA in $1M$ perchloric acid until the solution is saturated leads to a solution characterized by $pC_H = 0.5$ and $pC_{DTPA} = 0.5$ (hence $C_{DTPA} = 0.3M$). The phenomenon is caused by the fact that the 0.3 mole of DTPA consumes 0.6 mole of H^+, producing H_7Z^{2+} which predominates in accordance with our findings (Fig. 2). Since $1M$ perchloric acid is the highest acidity possible for $I = 1.0$, $pC_H = 0.5$ is the lower limit of the experimental pC_H region.

For DCTA no experiments could be done at pC_H below 0.4; a compound differing from DCTA precipitated at higher acidity. Elemental analysis and NMR confirmed that a DCTA–perchlorate salt was formed (Anderegg[22] proposed the same compound for pH below 0.2).

At the high side of the pC_H region, the solubility tended to give deviating results at $pC_L < 0.5$ for all ligands. Presumably the ionic medium cannot then be regarded as solely sodium perchlorate. Anyway, it sets an upper limit to the regions.

If the position of the experimental points on the pC_H scale is considered, along with the expression $pC_H^{intersection} = \log K_i$, it will be obvious that in those regions where many experiments have been performed the precision of the relevant $\log K_i$ values will be satisfactory. Consequently $\log K_4^{DTPA}$ (= 3.6) obtained by extrapolation, can be regarded as approximate; indeed, $\log K_4^{DTPA}$ can be found more precisely from titration experiments. In this respect, Anderegg's results, determined in a narrower pC_H region and obtained from fewer measurements, can be regarded as less accurate (especially $\log K_3^{EDTA}$, $\log K_4^{EDTA}$, $\log K_4^{DCTA}$ and $\log K_5^{DCTA}$). From our least squares minimization it turned out that $(\log K_3 + \log K_4)$ can be established more accurately than $(\log K_3 - \log K_4)$. In this respect, the sum value from Anderegg's results for EDTA agrees remarkably well with ours. The errors given in Table 1 are found from our least-squares fit.

From the literature[4,23] it is known that the temperature dependence of the protonation constants determined by us is fairly low ($d\log K/dT < 0.03/5°$). This means that constants determined at different temperatures are comparable.

Another consequence is that no precautions are necessary to stabilize the temperature. Our experiments were done at ambient temperature (21 ± 1°).

In the appendix of a previous paper[6] it was shown that the stability constants of EDTA

$$K_5 = \frac{[H_5Y^+]}{[H_4Y][H^+]} \quad \text{and} \quad K_6 = \frac{[H_6Y^{2+}]}{[H_5Y^+][H^+]}$$

are independent of the ionic strength I and of the nature of the medium, because changes of the ionic activity coefficients in the numerator are balanced by

those in the denominator. The same arguments can be used for K_5 of DCTA and K_6 and K_7 of DTPA; this implies that data obtained at different ionic strengths are comparable (Table 1).

Mioduski[23] determined stability constants of DCTA and DTPA by fitting titration curves. Since his experiments were restricted to pC_H values above 3.2 and 2.3 respectively, obviously because of solubility problems, comparison of his results with ours is hardly possible.

Finally it is remarkable that the data for $\log K_{sn}$, which reflect the (low) solubility of EDTA and DCTA, are so obviously absent in most data books. They should be introduced.

CONCLUSION

Solubility measurements can usefully be applied for establishing the stability constants of EDTA, DCTA and DTPA in a region where titration experiments can give only approximate values. Since our solubility curves are based on a large number of experiments by different technicians, the constants determined can be regarded as reliable and filling a gap in the literature.

REFERENCES

1. L. G. Sillén and A. E. Martell, *Stability Constants of Metal–Ion Complexes*, Special Publ. No. 17, Chem. Soc., London, 1964.
2. *Idem, op. cit. Supplement No. 1*, Spec. Publ. No. 25, 1971.
3. G. Anderegg, *Critical Survey of Stability Constants of EDTA Complexes*. Pergamon Press, Oxford, 1978.
4. A. E. Martell and R. M. Smith, *Critical Stability Constants*, Vol. 1. Plenum Press, New York, 1974.
5. E. P. Serjeant and B. Dempsey, *Ionisation Constants of Organic Acids in Aqueous Solution*. Pergamon Press, Oxford, 1979.
6. J. Kragten, *Talanta*, 1983, **30,** 449.
7. J. Kragten and L. G. Decnop-Weever, *ibid.*, 1978, **25,** 147.
8. *Idem, ibid.*, 1979, **26,** 1105.
9. *Idem, ibid.*, 1980, **27,** 1047.
10. *Idem, ibid.*, 1982, **29,** 219.
11. *Idem, ibid.*, 1983, **30,** 131.
12. *Idem, ibid.*, 1983, **30,** 134.
13. *Idem, Z. Anal. Chem.*, 1973, **264,** 356.
14. W. A. E. McBryde, *Analyst*, 1969, **94,** 337.
15. *Idem, ibid.*, 1971, **96,** 739.
16. R. G. Bates in *Analytical Chemistry. Essays in the Memory of A. Ringbom*, E. Wänninen (ed.), p. 23. Pergamon Press, Oxford, 1977.
17. R. G. Bates, *Determination of pH*, 2nd Ed., Ch. 9. Wiley, New York, 1973.
18. R. E. Mesmer and C. F. Baes, Jr., *J. Solution Chem.*, 1974, **3,** 307.
19. D. Midgley and K. Torrance, *Analyst*, 1979, **104,** 63.
20. E. A. Guggenheim, *Thermodynamics*, 4th Ed. North-Holland, Amsterdam, 1959.
21. S. Glasstone, *An Introduction to Electrochemistry*, 7th Ed. Van Nostrand, London, 1956.
22. G. Anderegg, *Helv. Chim. Acta*, 1967, **50,** 2333.
23. T. Mioduski, *Talanta*, 1980, **27,** 299.

Talanta, Vol. 30, No. 8, pp. 627–629, 1983
Printed in Great Britain.

0039-9140/83 $3.00+0.00

ANNOTATION

ELECTRO-DEPOSITION AS A PRECONCENTRATION STEP IN ANALYSIS OF MULTICOMPONENT SOLUTIONS OF METALLIC IONS

JAMES L. ANDERSON and ROMAN E. SIODA
Department of Chemistry, University of Georgia, Athens, GA 30602, U.S.A.

(*Received* 27 *October* 1982. *Accepted* 3 *February* 1983)

Summary—An explanation is given for the observation that in the preconcentration of trace metals by electro-deposition, the yield of deposited metal is lower if an oxidant is present. The effect is related to the competition between the deposition and dissolution kinetics of the metal.

Achieving high sensitivity in analysis of solutions containing metal ions is generally no problem, when techniques such as atomic-absorption, neutron-activation or fluorescence analysis are applied. Problems can arise, however, when the test solution contains many metal ions, especially when some are present at very high concentration and hinder the determination of the less abundant components. In addition, some of the components can initially be present in quantities below the detection limits of the analytical method employed.[1] Problems of this type are frequently encountered in analysis for trace-metal components in sea, lake and other natural waters, industrial waste streams, blood and other physiological liquids.[2–4] A technique which can help to remove some of these obstacles is the application of electro-deposition as a preconcentration step and a means of separation of electroactive from non-electroactive metals. This technique has been applied successfully in the above-cited works.

However, the authors cited[2–4] ran into the unexpected problem that in all cases of electro-deposition it was impossible to deposit all the electroactive metal present in solution, despite long electrolysis times, of many hours or even days. Instead, it was observed that in each case an "equilibrium" concentration of the metal remained in solution, the limiting value of which decreased with decrease in the initial concentration of the metal ion in solution before the electro-deposition step. Another unexpected finding was that the apparent first-order rate constants of the deposition processes were not constant, but appreciably decreased with diminishing concentration of metal ions in the initial solution. These authors were not able to explain their unexpected but interesting findings. It should be strongly pointed out that interest in these phenomena is not only theoretical, but to an even larger extent practical, as they limit the efficiency and thus the applicability of electro-deposition as a preconcentration step.

The explanation of these observations readily follows, however, from much earlier work of many authors on the electro-deposition of radio-elements from solutions of very low concentration, 10^{-6}–$10^{-16}M$.[5–10] These and other authors have found that the process of deposition from these low concentrations reflects the competition between at least two opposing processes: simultaneous electro-deposition and dissolution. The differential kinetic equation which best describes the observed experimental results at low initial concentrations is

$$-\frac{dc}{dt} = k_1 c - k_2(c_0 - c) \tag{1}$$

where c is the concentration of the metal ion in solution at time t, c_0 is the initial concentration at time $t = 0$, k_1 is the rate constant of deposition and k_2 the rate constant of dissolution.[7] On integration of (1), the following equations are obtained:

$$c = c_0\left[\frac{k_1 e^{-(k_1+k_2)t} + k_2}{k_1 + k_2}\right] \tag{2}$$

or

$$t = \left(\frac{1}{k_1 + k_2}\right) \ln\left\{\frac{k_1 c_0}{k_1 c_0 - k_2(c_0 - c)}\right\} \tag{2'}$$

At long electrolysis times ($t \to \infty$), the concentration predicted by equation (2) approaches a limiting value

$$c_{eq} = \frac{k_2 c_0}{k_1 + k_2} \tag{3}$$

where c_{eq} is the long-time or steady-state equilibrium concentration of the metal ion in solution. Equation

(3) shows that the limiting ratio of final to initial concentration, c_{eq}/c_0, should be a constant, independent of the initial concentration c_0, if the competitive electro-deposition/dissolution mechanism is taking place. The limiting ratio is determined solely by the ratio of the rate constant of dissolution to the sum of the rate constants of electro-deposition and dissolution. This is an important result, indicating that the only means of reducing the final concentration ratio further is to enhance the rate of electro-deposition relative to dissolution, *e.g.*, by adding protective reagents to inhibit the dissolution.

Figure 1 illustrates the variation of $\ln(c/c_0)$ with $(k_1 + k_2)t$ for a series of values of the dissolution/electro-deposition rate constants ratio, k_2/k_1. When the dissolution step is much slower than the electro-deposition, the plot reduces to the linearity for simple first-order kinetic behaviour. As the relative importance of the dissolution kinetics increases, the curves deviate increasingly from those for simple first-order kinetics, eventually reaching constant values of $\ln(c/c_o)$ at long times, as predicted by equations (2) and (3). Differentiation of equation (2) yields an instantaneous rate

$$-\frac{dc}{dt} = k_1 c_0 e^{-(k_1 + k_2)t} \qquad (4)$$

which corresponds to simple first-order kinetics (line 0.0 in Fig. 1) governed solely by the rate of electro-deposition at short times [deviation less than 5% for $(k_1 + k_2)\ t < 0.05$]. For $(k_1 + k_2)t > 0.05$, the deviation from linear behaviour occurs earlier and its magnitude increases, as the rate of dissolution increases relative to the rate of electro-deposition (*i.e.*, as k_2/k_1 increases). Such an outcome can be expected, provided that there is less than a monolayer of deposit present at the electrode surface, since the kinetics of electro-deposition and especially of dissolution will be affected by the surface coverage for sub-monolayer deposition. Thus, for a given electrolysis started with known c_0, by determining k_1 from kinetic measurements at the early stages of electrolysis and use of equation (4), and determining c_{eq} after a sufficiently long time of electrolysis, we can calculate both k_1 and k_2 by using equation (3).

In our view, the dissolution term in equation (1) should also depend, especially in the case of metals having a positive standard reduction potential, on the presence and concentration of oxidizing agents in the deposition solution. It is a long-standing and common practice, applied even in the very early studies of the electro-deposition of radio-elements,[5-10] to have nitric acid present in the deposition solution. This practice was also applied in the cited works[2-4] on use of electro-deposition as a preconcentration and separation step in the trace analysis of multi-component solutions. It seems probable to us that the nitric acid present in the solution could increase the dissolution rate of deposited metals by increasing k_2, which to a first approximation can be considered proportional to the concentration of the oxidant ([Ox]):

$$k_2 = k_2'[\mathrm{Ox}] \qquad (5)$$

where k_2' is a new constant. Equation (5) is based on the assumption that the dependence of k_2 on oxidant concentration is first-order, although it is fully possible that it may be of higher or fractional order. From equation (5) it follows that increasing the oxidant concentration increases the rate constant of dis-

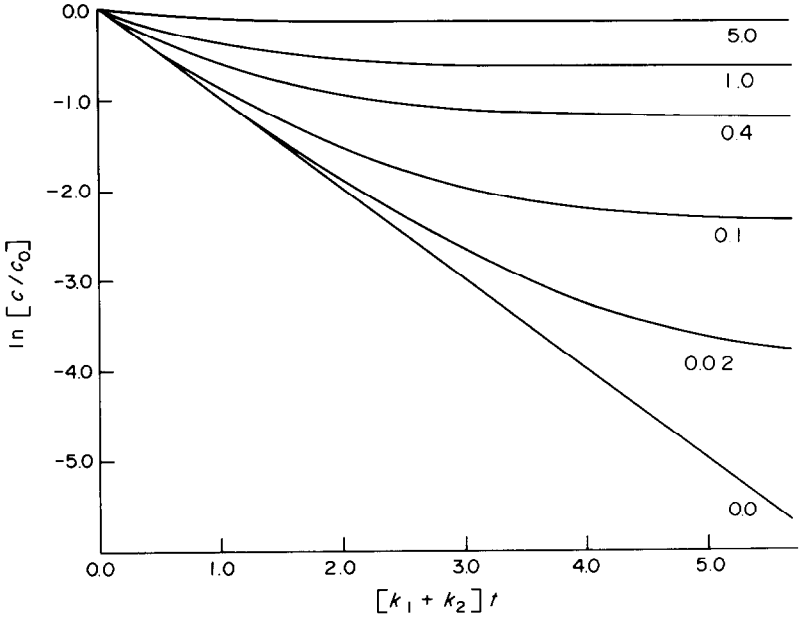

Fig. 1. The calculated dependence of $\ln(c/c_0)$ on $(k_1 + k_2)t$ values for the various k_2/k_1 ratios given in the plot.

solution k_2, and according to equation (3) also increases the equilibrium concentration c_{eq} in comparison with that for a solution that does not contain oxidant. The apparent pseudo first-order rate constant of the overall deposition process should also be smaller in the presence than in the absence of the oxidant.

The last conclusion has been borne out by our experiments in which 120 ml of $0.050M$ copper sulphate solution in $0.30M$ sulphuric acid was electrolysed on a platinum-foil electrode (total surface area approximately 22 cm^2) at a constant current of 0.5 A. The anode was a piece of platinum wire. The electrolysis was done at room temperature, and the solution was mixed by a magnetic stirrer. After 3.5 hr of electrolysis the concentration of copper ions in solution had decreased to $2.14 \times 10^{-5}M$, or 0.043% of the initial concentration, as determined by inductively-coupled plasma emission spectroscopy. In a second experiment under identical conditions, except that the solution was also made $0.185M$ in nitric acid, the final concentration of copper ions after the same electrolysis time was $7.62 \times 10^{-4}M$, or 1.52% of the initial concentration, about 36 times that obtained in the absence of nitric acid. This seems to us a convincing proof that addition of an oxidant, in this case nitric acid, to the solution from which copper is electrodeposited, decreases the apparent rate of deposition. The apparent pseudo first-order rate constants calculated from the initial and final concentrations were 6.2×10^{-4} sec^{-1} for the first experiment, and 3.3×10^{-4} sec^{-1} for the second.

Acknowledgements—The authors gratefully acknowledge financial assistance from the U.S. Environmental Protection Agency under Grant R808084010 (J.L.A.) The valuable assistance of Dr. Charles Anderson and Dr. Thomas Hoover from the U.S. Environmental Protection Agency Laboratory in Athens, Georgia, in making ICP measurements is also gratefully acknowledged. The authors also acknowledge helpful discussion with Professor L. B. Rogers, and the experimental help of Miss M. Izadi.

REFERENCES

1. D. E. Leyden and W. Wegscheider, *Anal. Chem.*, 1981, **53**, 1059A.
2. K. Jørstad and B. Salbu, *ibid.*, 1980, **52**, 672.
3. K. Jørstad, B. Salbu and A. C. Pappas, *ibid.*, 1981, **53**, 1398.
4. J. Muhlbaier, C. Stevens, D. Graczyk and T. Tisue, *ibid.*, 1982, **54**, 496.
5. G. Hevesy and F. Paneth, *Physik. Z.*, 1914, **15**, 797.
6. K. F. Herzfeld, *ibid.*, 1913, **14**, 29.
7. F. Joliot, *J. Chim. Phys.*, 1930, **27**, 119.
8. M. Haissinsky, *ibid.*, 1932, **29**, 453.
9. C. Haenny and P. Reymond, *Helv. Chim. Acta*, 1954, **37**, 2067.
10. M. Haissinsky, *Nuclear Chemistry and Its Applications*, Chapter 20. Addison-Wesley, New York, 1964.

Talanta, Vol. 30, No. 9, pp. 631–648, 1983
Printed in Great Britain

0039/9140/83 $3.00 + 0.00
Pergamon Press Ltd

COLLECTION AND ATOMIC SPECTROSCOPIC MEASUREMENT OF METAL COMPOUNDS IN THE ATMOSPHERE: A REVIEW

JOSEPH SNEDDON
Department of Chemistry, New Mexico State University, Las Cruces, NM 88003, U.S.A.

(*Received* 26 *February* 1982. *Revised* 24 *August* 1982. *Accepted* 11 *March* 1983)

Summary—A review is given of the collection of metal compounds in the atmosphere and their subsequent measurement by atomic spectroscopy. Collection is principally by filtration, impaction or electrostatic precipitation. Atomic absorption, emission and fluorescence have all been used for the analysis, atomic absorption being the most favoured.

Air pollution is of ever-increasing concern. Solid airborne particles, varying widely in chemical composition, size, shape, homogeneity and concentration, are often referred to as "dust", regardless of origin. Examples of size ranges of various particles are shown in Table 1.[1] Particles more than 100 μm in diameter tend to settle out of the air by gravitation fairly rapidly, whereas smaller particles are dispersed by winds over considerable distances before returning to the earth's surface by sedimentation. The harmfulness of dust depends not only on the chemical composition but also on the particle size.[2] It is accepted that small particles are more dangerous than larger ones because they are carried more efficiently into the lungs. Airborne dust is generated naturally by winds removing particulate matter from the

Table 1. Approximate size ranges of airborne particles*

Substance	Diameter, μm	
	Minimum	Maximum
Rain drops	500	5000
Human hair	35	200
Stoker fly-ash	10	800
Pollen	10	100
Plant spores	10	35
Red blood cells (adults)	7.5	
Cement dust	3	100
Water vapour (natural mist, 60–500 μm; natural fog and clouds, 2–60 μm)	2	500
Foundry dusts	1	1000
Pulverized-coal fly-ash	1	50
Metallurgical dust	0.5	100
Ground talc	0.5	50
Insecticide dusts	0.3	35
Sulphur trioxide mist	0.3	3
Paint pigments	0.1	5
Alkaline fume	0.5	5
Ammonium chloride fume	0.1	3
Oil smoke	0.1	1
Salt nuclei (from sea-water)	0.03	0.5
Colloidal silica	0.02	0.005
Metallurgical fume	0.01	2.2
Resin smoke	0.01	1
Tobacco smoke	0.01	1
Normal oxide fume	0.01	0.5
Magnesium oxide fume	0.01	0.4
Carbon black	0.01	0.3
Combustion nuclei	0.01	0.1
Viruses and proteins	0.003	0.005
Gas molecules	0.0001	0.0006

*Data from ASTM D 1357-57 (Reference 1).

Table 2. Compounds frequently determined in polluted air

Acrolein	Hydrogen sulphide
Aldehydes (aliphatic)	Methanol
Ammonia	Metals
Carbon disulphide	Nitrates
Chlorine	Nitric oxide
Chromium trioxide and salts of chromic	Nitrogen dioxide
	Oxidants
Fluorides (inorganic)	Phenols
Formaldehyde	Sulphates (particulate)
Hydrochloric acid and chlorides	Sulphur dioxide
Hydrogen cyanide	Sulphuric acid mist

earth's surface, but in industrial and domestic areas, dust is also generated by man or machinery under his control.

The analysis of dust has long been the concern of the environmentalist, industrial hygienist and analytical chemist. The introduction of legislation in the United Kingdom[3] conferred new and wide-ranging responsibilities on employers, involving a legal obligation to be aware of hazards, particularly in processes used within their industry. Similar legislation in the United States is controlled by the Occupational Safety and Health Act. In addition, the United States Environmental Protection Agency (EPA) maintains some control over the introduction of new and potentially harmful substances into industrial use. For chemical substances in work-room air, the American Conference of Governmental Industrial Hygienists (ACGIH) publishes a list of Threshold Limit Values (TLVs)[4] based on experiments on animals, human volunteers, reports of medical cases and industrial experience. A list of substances which are more frequently determined as particulate and gaseous pollutants in air is given in Table 2.[5] A recent publication by Moreton and Falla[6] describes the state of the art in the determination of airborne pollutants in the welding and surface-coatings industry. The Alpha Intersociety Committee of the American Public Health Association[7] has listed methods for sampling and analysing pollutants in the atmosphere.

Of increasing interest is the study of the environmental and biological effects of atmospheric pollution by metallic compounds. Several physical meth-

Table 3. Comparison of techniques used to measure metals in the atmosphere

Technique	Advantages	Disadvantages
Atomic spectroscopy	Over 70 elements can be determined at low levels. Modest cost and ready availability. Aqueous samples give good precision and accuracy. Solid sampling may be possible. Analysis is fast, automated or computer-controlled. Good selectivity. Single or multi-element analysis.	Matrix and interelement interferences. Solid sampling can result in poor precision. Destructive.
Mass spectrometry	Overall elemental coverage with low detection limits. Favourable speed of analysis. Gaseous samples give good precision and accuracy. Good selectivity.	Limited to elements or compounds which can be volatilized. High cost. Poor reproducibility for solid samples. Difficult to automate. Destructive
Neutron-activation analysis	Overall elemental coverage at low detection limits, if both fast and slow neutron sources are available. Good precision and accuracy. Non-destructive. Good selectivity.	High cost and limited availability. Difficult to automate.
X-Ray diffraction	Polymorphic forms of one chemical species may be identified. Solids (crystalline) are analysed directly. Non-destructive.	Mixtures may require preliminary chemical separation. Identification of unknowns may be slow.
Anodic-stripping voltammetry	Acceptable precision and accuracy with low detection limits for samples in solution. Possible to automate determination of three or four elements simultaneously. Modest cost and good availability.	Limited to about 30 elements. Matrix and interelement interferences. Speed of analysis limited by deposition time. Selectivity may be poor for some combinations of elements. Liquid samples essential.
X-Ray fluorescence spectrometry	Applicable normally to elements of atomic number $\geqslant 11$. Solid samples may be analysed directly. Single-element and simultaneous analyses. Automation and computer control commercially available. Non-destructive.	Particle size may affect results. Standardization difficult with solid samples. High cost. Matrix effects: chemical pretreatment usually needed.

ods for the analysis of airborne particles for metals have been described,[8] including X-ray fluorescence,[9,10] neutron-activation analysis,[11] anodic-stripping voltammetry,[12,13] mass spectrometry,[14] X-ray diffraction[15] and atomic spectroscopic techniques,[16–19] each with its own merits and disadvantages. A comparison of these techniques, shown in Table 3, shows that atomic spectroscopy offers many advantages over these other techniques in terms of speed, sensitivity, range of elements, precision, accuracy, possible automation and cost. However, for certain elements the other techniques may be better.

This paper reviews the collection of metal compounds from the atmosphere, their dissolution and their determination by atomic spectroscopy.

SAMPLING

Sampling systems for airborne pollutants generally consist of three parts: a means of collecting an air sample, a device to trap the pollutants and a means of measuring the amount of air sampled.

The techniques used include sedimentation,[20,21] centrifugal collection in cyclones which trap particulate matter,[22] condensation to separate fractions and thermal precipitation.[23] The particle size range collected will depend on the method of collection (Table 4). Though these methods have been used with varying degrees of success, the most suitable methods for collection are by filtration, impaction or electrostatic precipitation.[24]

Filtration

Filtration is the most frequently used method, particularly in industrial hygiene work, because of ease of operation, low cost and the availability of relatively pure filter materials.

A filter assembly consists of a sampling head, the filter and a pump. The sampling head should be constructed of a material which will not contaminate the sample,[25] *e.g.*, stainless steel and/or Teflon. The filter and holder should also not contain trace metals which might influence the analytical results and complicate sample preparation. Even the pump, particularly the motor, can cause contamination with copper[26] and lead. The physical size and porosity of the filter will influence the air flow: the flow-rate of air through a filter depends on the pressure differential and the temperature and will decrease as the pores in the filter get clogged up during sampling. Table 5 summarizes the different types of filters and their advantages and disadvantages. The pump should have a calibrated flow-rate indicator or total-volume gas meter. Wood[27] has described the requirements to be met by an ideal sampling pump.

Table 6, which gives a general survey of the field of analysis of air and gases for metals and their compounds, includes applications of the filters which have been used to collect particulate matter from the air. Because of their high mechanical strength, glass fibre filters have been used by a number of workers, despite their high chemical blanks. Cellulose and membrane filters have become increasingly popular

Table 4. Size ranges for collection of particles

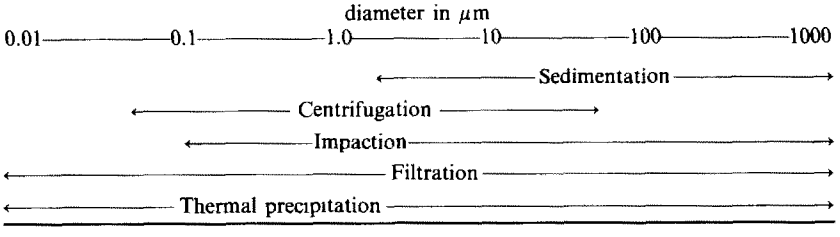

Table 5. Filter types

Depth filters—Random matrix of fibres giving tortuous channels of varying size; particles are trapped at varying depths in the filter.

Advantages. High loading capacity and cheapness.

Disadvantages. No defined pore size, low strength.

Materials. Cellulose: cheap, tough, widely available, resistant to dilute chemical solutions but easy to decompose by ashing or wet-oxidation; low metal content makes cellulose filters suitable for direct analysis of particles by XRF.

Glass fibre: high mechanical strength, resistant to moderate chemical attack; high concentrations of metal ions present may interfere in direct XRF work; good for organics.

Membrane filters—rigid continuous polymer with fine holes of uniform and defined size; particles are held on the surface.

Advantages. Good separation of particles of different sizes; high pore density, so quicker filtration.

Disadvantages. Low loading capacity, so clog quickly.

Materials. Poly(vinylidine fluoride) and Teflon: both chemically inert, hydrophobic, stable towards solvents; Teflon can be used at up to 250° in air.

Cellulose esters (acetate and nitrate): hydrophilic, readily combusted, giving negligible ash.

Poly(vinyl chloride): hydrophobic, low water uptake, so ideal for gravimetric analysis.

Silver: convenient for determination of organics and for X-ray diffraction analysis of crystalline particles.

Table 6. Collection, treatment and method of measurement of metal compounds

Element	Sample collection	Sample treatment	Technique	Reference	Comments
Ag	Sample air stream introduced into the primary air supply to the flame.		Flame AAS	28	Detection limit 3 $\mu g/m^3$.
Ag (AgI)	1-μm nylon membrane filter; flow-rate 12 l./min.	Soak filter in 10 ml of acetone and agitate mechanically.	ETAAS	29	Sensitivity 3×10^4 AgI nuclei at $-15°$.
Ag	Collection on 8×10 in. glass fibre filter.	Cut a 0.4-in.^{2} piece into small pieces and place in a borosilicate glass test-tube; add 1.5 ml of H_2SO_4/HNO_3 and heat for 1 hr at 250°. Dilute to 15 ml and centrifuge to remove particulate matter.	Flame AAS	30	Automatic method; sensitivity 1 $\mu g/l$.
As	Whatman No. 41 filter paper. Air pumped at 1.2 m^3/min for 24 hr.	Cut out and ash 25- and 5-mm discs; take up residue in ml of 4M HNO_3.	ETAAS	31	Substantial losses of arsenic during low-temperature ashing.
As	Arsine gas diluted with clean air.		Radiofrequency rod atomizer and ETAAS	32	Ambient air gave an arsenic signal.
Be	Air filtered through a porous graphite cup which is then inserted between electrodes and used as the atom cell.		ETAAS	33	Concentrations of beryllium of 2–20 $\mu g/m^3$ detected in 50 ml of air.
Be	Gelman type-E glass fibre filter. Air flow-rate of 60 l./min for 2–3 days to give a total volume of 570 m^3.	Digest in a Pt dish with 2 ml of HNO_3 and 3 ml of HF; heat to near dryness, cool, add 2 ml of H_2SO_4, heat to fumes of SO_3.	ETAAS	34	Detection limit 12 pg.
Br, Cl halogenated organic compounds	Analyte desolvated, electrothermally vaporized and swept into plasma to produce cationic emission from halogen.		MIPOES	35	Detection limit 8 ng for Br and Cl.
Organic carbon	Suspended particulate matter dispersed in Pt boat, dried at 85° for 10 min, volatilized and measured directly.		MIPOES	36	Detection limit 0.4 μg for dissolved carbon.
Cd	Whatman No. 41 cellulose filter paper; 24 hr collection equivalent to 400–1200 m^3 of air.	Dissolve Cd in 50 ml of 0.1M HNO_3, aided by ultrasonic vibration.	ETAAS	37	Half of filter allows a concentration of 0.2 ng/m^3 to be determined.
Cd	Modified graphite cup with 0.22-μm Millipore filter; titanium punch was used to cut 2.8-mm diameter piece. 200-ml air sample collected.	Place filter directly in the cup of a carbon rod atomizer and add 2 μl of 1000-ppm H_3PO_4.	ETAAS	38	Detection limit 8 ng/m^3. Cigarette smoke contained 0.1 $\mu g/m^3$ Cd.
Cd	Direct determination.		Radiofrequency rod atomizer and ETAAS.	39	Detection limit 0.1 pg.

Cd	Glass fibre or cellulose filter; flow-rate 1.13–1.60 m^3/min for up to 24 hr.	Add dropwise 1 ml of HF and heat; and add 1–2 ml of HNO_3, boil and filter through Whatman No. 41; rinse with 10 ml of warm water.	Flame AAS or ETAAS	40	Analytical method for occupational hygiene.
Cu	Electrostatic precipitation on a tungsten rod followed by direct injection of rod into the furnace for analysis; aerosol generated by carbon rod atomizer and sampled at various flow-rates from 1.5 to 14 l./min; laboratory air also sampled.		ETAAS	41	Collection efficiency depended on particle size, applied voltage, geometry of system and flow-rate.
Cu	Electrostatic precipitation and impaction on carbon tube for analysis; aerosol generated as in reference 41; laboratory air also sampled.		ETAAS	42	Collection efficiency depended on particle size, applied voltage, geometry of system and flow rate.
Cu	Delbag microsampler filter type 99/7 used for 24 hr.	Dry ash at 400–450°, dissolve in 5 ml of 30% HCl and let stand for 5 hr; add 2 ml of 65% HNO_3 and let stand 3 hr.	Flame AAS	26	Concern with copper contamination from sampling pump.
Hg	Collection on gold-plated quartz wool.		CVAAS	43	400 litres of air gave 1.5 ng/m^3. Ambient background level 1.0–4.0 ng/m^3.
Hg	Millipore monitor with filter replaced by three layers of carbon-loaded paper. Sample volume 10 m^3 at flow-rate of 200 l./hr.	Boil filter for 20 min with 20 ml of HNO_3, cool and filter; wash filter with 5 ml of 50% HNO_3 and dilute.	CVAAS	44	0.2 μg determined.
Hg	Absorption trap contained 25 ml of 4% $KMnO_4$, 25 ml of 10% H_2SO_4 and 50 ml of distilled water. Air sampled at 40 l./min for 25 min.	Transfer contents to a cylinder and wash trap with 1 ml of 20% $N_2OH \cdot HCl$ solution.	CVAAS	45	Outdoor concentrations of mercury ranged from 0 to 70 ng/m^3 and increased on misty and foggy days.
Hg	Porous graphite filter tube plated with thin layer of gold inside; used as atom cell.		ETAAS	46	Sensitivity of 0.06 μg/m^3 for 50 ml of air.
Hg	Straight glass tube packed with two 1-in. sections (180 mg) of 20/40 mesh activated impregnated charcoal.	Heat the impregnated charcoal at 600–800° for 1 hr before use.	Tantulum boat and flame AAS	47	Detection limit 0.2 μg for 10 litres of air.
Hg	Electrostatic accumulation in furnace separated by glass fibre plugs; integrated air sample of 10 litres.		ETAAS	48	Detection limit 50 ng/m^3.
Hg	Mercury in air is amalgamated on 1–2 g of clean silver wool inside a borosilicate glass tube heated by nichrome wire.	Heat tube to 400°; inert gas stream carries released mercury at 200 ml/min to analyser.	CVAAS	49	Detection limit 3 ng; calibration from 0.5 to 594 ng. Analysed ambient Hg levels from 15 ng/m^3 to 10 μg/m^3 for 24-hr sampling time.
Hg	Air sample is scrubbed with hydrochloric acid.		Flame AAS	50	Four separate analyses gave 0.068–0.12 μg/m^3.

(continued)

Table 6—*continued*

Element	Sample collection	Sample treatment	Technique	Reference	Comments
Hg	Direct continuous analysis.		Radiofrequency rod atomizer and ETAAS.	51	Sensitivity 0.1 $\mu g/m^3$.
Hg	Air drawn through carbon tube which is plated with 1.5 mg of gold on inside; air drawn through carbon cup which is then used as the atom cell.		ETAAS	52	Sensitivity 0.3 ng.
Hg	Collection of air in 5 or 10 litre bag; for direct analysis.		CVAAS	53	Less than 1 $\mu g/l$. detectable.
Hg	Collector contained gold-plated quartz wool; air sampled at 15 l./min for 1–2 hr.	Heat collector to 650° and sweep out the mercury in a stream of purified nitrogen into the optical cell.	CVAAS	54	Mercury concentrations in the range 11–568 ng/m^3 found for different locations.
Hg	Mercury vapour collected on 1 cm of gold wire exposed in air for 5 min.	Thermally desorb mercury from the wire.	Flame AFS	55	Concentration levels of mercury in the range 0–120 $\mu g/m^3$ found.
Hg	Air bubbled through Barnes's reagent (3% KI/0.25% I_2).	Mercury reduced by 0.5 ml of 5% $SnCl_2$ or 0.5 ml of 40% hydrazine hydrate solution.	ETAAS	56	Sensitivity 0.2 ng.
Hg	0.2–1 litre of air aspirated through a quartz collection tube lined with Au-Pt alloy gauze.	Quartz tube closed and inserted into cold-vapour accesory.	CVAAS	57	Detection limit 2 $\mu g/m^3$ for a 1-litre air sample.
Hg	Absorption on Hopcalite granules.	Dissolve the mercury by washing four times with HNO_3.	CVAAS	58	Concentration levels of 0.04–2.6 mg/m^3 found.
Hg	Gases from an incinerator drawn through a stainless-steel tube; mercury collected by oxidation in absorption bottle filled with 75 ml of 4% $K_2Cr_2O_7$/20% HNO_3, and amalgamation on Au.	Transferred to a 500-ml standard flask and diluted with demineralized water.	CVAAS	59	Detection limit 1 ng; 121–163 $\mu g/m^3$ found.
Hg	Air drawn through absorber at 2.5–3.5 l./min; prefilter removed particulate mercury. Activated charcoal, silver-coated sea sand and gold-plated sea sand investigated as absorbers.	Desorb mercury and sweep into analyser with stream of nitrogen.	CVAAS	60	Detection limit 0.1 ng; urban environment levels 6.7–7.3 ng/m^3 found.
Particulate mercury, methylmercury chloride, mercuric chloride, Hg, and dimethyl mercury.	Sequential selective absorption tubes containing Au, Ag and Cu.	Drive off mercury by heating.	d.c. discharge: spectral emission detector	61, 62	Detection limit 0.01 ng. Possible to determine 0.1–0.5 ng/m^3 mercury in a 100 litre air sample.

Hg	Pass air through a tube containing silver wool.	Drive off mercury by heating.	CVAAS	63	Applicable to range 0.02–10 $\mu g/m^3$ for collection flow-rate of 100–200 ml/min for 24 hr.
Hg	Draw gas through one tube containing MnO_2 and another tube containing cellulose and activated charcoal.	Dissolve the MnO_2 in HCl/HNO_3 mixture. Combust the cellulose and activated charcoal in an oxy–hydrogen flame and condense the mercury for determination.	CVAAS	64	Limit of detection 0.01–0.02 μg; suitable for estimation of mercury in air, hydrogen or gas.
Hg, particulate and volatile	Air passed through a Gelman quartz fibre filter at 2.5–3.5 l./min with a membrane pump.	Release the mercury and collect it on gold-coated sand absorber.	CVAAS	65	High levels of mercury found in a polarography laboratory.
Mn	Collection on micro-particulate filters.		Flame AAS	66	For 12 different locations, concentrations of 0.07–0.13 $\mu g/m^3$ of manganese were found.
Methyl cyclopentadienyl manganese tricarbonyl (MMT)	Approximately 15 m^3 of air collected and retained in a freezer until analysed.	Trap MMT in a small loop of a gas chromatograph sampling valve.	ETAAS	67	Air samples from an underground car park contained 0.1–0.3 ng/m^3 MMT. No MMT was found at street level.
P	Phosphorus-containing air generated by passing metered cylinder air through a Pyrex tube containing filter paper impregnated with triethyl phosphate, and drawn into the burner.		Flame emission spectroscopy with cool H_2 flame.	68	Linear range from 0.9 μg/l. to 2 mg/l.
Pb	Whatman No. 41 cellulose filter paper; 24-hr collection equivalent to	Remove lead from filter with 50 ml of 0.1*M* HNO_3 and ultrasonic vibration.	ETAAS	69	Use of 1/8 of filter gave routine sensitivity of 0.1 $\mu g/m^3$.
Pb	Modified graphite sampling cup with 0.22-μm Millipore filter. Air sample of 200 ml.	Add excess of H_3PO_4 just before the analysis.	ETAAS and comparative study by flame AAS.	70	Sensitivity of 0.1 $\mu g/m^3$ with a 200-ml sample.
Pb	Particulate matter caught on a 0.45-μm Millipore membrane filter, organic lead absorbed in ICl solution; 2.5 m^3 of air sampled at 2 l./min over 24 hr.	Extract ICl solution with ammonium pyrrolidinedithiocarbamate and methyl isobutyl ketone.	Flame AAS	71	Organic lead in the range 0.1–4 $\mu g/m^3$ found.
Pb	Glass or cellulose filter; flow-rate 1.13–1.60 m^3/min for up to 24 hr.	Add dropwise 1 ml of HF and heat; add 1–2 ml of HNO_3, boil and filter through Whatman No. 41 paper; rinse with 10 ml of warm water.	Flame or ET-AAS	72	Analytical method for occupational hygiene.
Pb	Porous graphite cup.	Insert the cup in an isothermal furnace.	ETAAS	73	Sensitivity 0.005 $\mu g/m^3$ for 100 ml of air.
Pb	Millipore organic membranes.	Dissolve membranes in acetone and extract with 50% HNO_3.	Flame AAS	74	Principally concerned with interferences.

(*continued*)

Table 6—*continued*

Element	Sample collection	Sample treatment	Technique	Reference	Comments
Pb	37-mm diameter Millipore MF cellulose ester filter (0.8 μm); flow-rate 2.7 l./min for 10 min.	Soak filter in 2.0 ml of 1 + 1 HNO_3, heat, decant into a 10-ml flask and wash filter with 2-ml portions of warm distilled water.	ETAAS	75	Sensitivity 0.1 $\mu g/m^3$. Lead measured in streets of Oslo found to be 0.1–12.2 $\mu g/m^3$.
Pb	Glass fibre filters.		ETAS	76	XRF and ETAAS compared.
Pb	Air pumped through an 8 × 10 in. glass fibre filter at 100 m^3/hr for 24 hr.	Heat a 1-in. strip at 150° for 1 hr and extract with HCl/HNO_3; centrifuge to remove suspended material.	Flame AAS and spark-excited ES	77	203 samples analysed with detection limit of 0.1 $\mu g/m^3$ (AAS) and 800 samples with detection limit of 0.15 $\mu g/m^3$ (ES).
Pb	Atmospheric particulates collected on Millipore EH or HA filters.	Remove lead from filter with 0.1*M* HNO_3 (15 min in ultrasonic bath).	Flame AAS	78	0.39–37 $\mu g/m^3$ found.
Pb	8 × 10 in. flash-fired glass fibre filter used for 24 hr.	Ignite for 1 hr at 500°, extract with 50% HNO_3, filter and evaporate to 3–4 ml.	Flame AAS	79	0.1–3.8 $\mu g/m^3$ found (38 separate analyses).
Pb	Modified cup (similar to that in reference 66) but containing two cups, one for a blank, the other for sample; 200 ml of automobile exhaust sampled.	As reference 66.	ETAAS	80	2.44 ug/m^3 found in streets of Hobart.
Pb	Air samples filtered through a graphite crucible used for carrier distillation (ASTM No. 5–3); 100–500 ml of air drawn by a plastic syringe.	Insert into heated graphite furnace.	ETAAS	81	Sensitivity 5 pg.
Pb	Modified graphite cup with 0.22-μm Millipore filter in base; 200–400 ml of air sampled.	Add 2 μl of 0.1% H_3PO_4 before analysis.	ETAAS	82	Absolute sensitivity 42 pg; 0.3–8.6 $\mu g/m^3$ lead found in air in Hobart.
Pb	Impaction on Ta foil which is then used in a specially constructed atomization cell.		ETAAS	83	Sensitivity 0.4 pg and detection limit 0.02 $\mu g/m^3$ obtained for a 6-min sampling period.
Pb	3-cm Millipore disc filters, quartered for dissolution.	Heat filter with 5 ml of 50% HNO_3 at 100° for 30 min, evaporate to dryness, redissolve in few drops of $HNO_3/HClO_4$; evaporate to dryness, heat with 1 ml of HNO_3 and dilute.	ETAAS	84	Automatic analysis
Pb	Air pumped through glass fibre filters at 1.5 m^3/min.	Heat filters for 60 min at 500°, then heat in HNO_3 at 95° for 45 min.	Flame AAS	85	A maximum of 1.6 $\mu g/m^3$ in June, minimum of 0.5 $\mu g/m^3$ in April, found in a 1-yr study in West Berlin.
Pb	Electrostatic accumulation from 100–300 ml of air collected over 30–90 sec.		ETAAS	86	Detection limit 1 pg.
Pb	Direct deposition by electrostatic precipitation of atmospheric particulates.		ETAAS	87	

Pb	Glass fibre filters; particulate matter collected by high-volume samplers over 24 hr.	HNO_3 extraction.	ETAAS and spark-excited OES	88	Evaluation of EPA reference method for lead in suspended particulate matter from ambient air.
Pb	Cellulose filters (0.8 × 1 in.); 24-hr sampling with a high volume sampler.	Transfer 0.5-cm^2 discs to a nichrome microsampling cup for direct introduction into atom cell.	Flame AAS	82	Correlation between this method and X-ray fluorescence spectrometry was good. For a 24-hr period mean lead concentrations of 0.001–5 $\mu g/m^3$ were found.
Pb	Duplicate Nuclepore membrane filters; 3 m^3 of air collected by low-volume vacuum pump at flow-rate of 24 l./min for ~2 hr.	Extract lead with hot HNO_3.	Flame AAS	90	Ratios of indoor/outdoor lead concentrations for three separate analysis were 0.82, 0.63 and 0.87.
Pb	Collect dust samples and weigh (~0.2 g) on glass fibre filter.	A. Extract by refluxing with 1 + 1 HNO_3. B. Fuse with alkali at 900° and extract with HNO_3.	Flame AAS	91	Principally concerned with sample treatment.
Pb	Membrane filter type Synpor-3; 0.5–1 m^3 samples.	Dissolve the membrane in HNO_3/H_2O_2, evaporate, dissolve residue in 2 ml of 0.5% tartaric acid solution.	Flame AAS	92	Amount of Pb from 0.6 to 13 μg on filters in Budapest.
Pb	Air sampled continuously.	Pass the air over white-hot carbon rods into a heated absorption chamber for measurement.	Radiofrequency atomizer and ETAAS	93	Sensitivity for lead in air was 0.16 $\mu g/m^3$ with absolute sensitivity of 0.3 pg.
Pb	Standard collection by high-volume samplers.	Standard method.	Flame AAS	94	Survey of ambient air levels of lead in El Paso, Texas, 1972–1979.
Pb	Collection on glass fibre filters with a high-volume sampler.		Flame AAS	95	Downward trend found in lead concentrations in Ontario from 1971 to 1979.
Tri-alkyl lead chlorides	Collection with a gas chromatograph.		MIPOES	96	
$Pb(CH_3)_3$ and $Pb(C_2H_5)_4$	Midget impinger, containing 15 ml of 0.1*M* ICl; particulate matter removed on a 0.45-μm cellulose acetate filter; flow-rate 3 l./min to collect at least 10 ng of lead.	Extract the buffered ICl with dithizone in presence of EDTA; decompose with HNO_3/H_2O_2 and analyse.	ETAAS	97	Detection limit 0.2 $\mu g/m^3$ for 10-min sample.
Alkyl Pb	70 litres of air passed through a series of 4 traps at −72° with atmospheric particulates collected first on Whatman No. 41 paper.	Use liquid chromatograph for separation.	ETAAS	98	Total concentration of atmospheric alkyl lead was 14 ng/m^3.
$Pb(CH_3)_4$ (TAL)	Particulate matter removed from air on a 47 mm Nuclepore membrane filter, then TAL trapped cryogenically.	Use liquid chromatography for separation.	ETAAS	99	Concentrations of TAL around Antwerp varied from 0.3 ng/m^3 in rural environment to 400 ng/m^3 near a gasoline station.

(continued)

Table 6—*continued*

Element	Sample collection	Sample treatment	Technique	Reference	Comments
$Pb(CH_3)_4$ and $Pb(C_2H_5)_4$	3-μl aliquots of gasoline injected into chromatograph column.	Use liquid chromatography for separation.	ETAAS	100	Absolute detection limit of 40 pg for $Pb(CH_3)_4$ and 90 pg for $Pb(C_2H_5)_4$.
Tetra-alkyl lead	$Pb(CH_3)_4$ collected in a cold trap containing SE-52 Chromosorb at $-80°$.	Separate TAL from absorbent by freeze drying, concentrate with an organic solvent, separate by gas chromography.	MIPOES	101	Limit of detection <17 ng/m^3, which implies absence of tetra-alkyl leads above a concentration of 0.3 μg/m^3.
Molecular lead	Particulate matter removed by graphite disc and air passed through a carbon bed which absorbs the non-filtered lead. 500 ml of air used at a flow-rate of 200 ml/min.	Heat carbon bed to 1500° to evolve lead.	Radiofrequency atomizer and ET-AAS	102	Weather conditions affect the concentration of lead; lead concentration depends on traffic density; some vapour-phase lead may be inorganic.
Organic Pb	0.22-μm Millipore filter to trap particulate matter, then organic lead absorbed in a tube filled with 10% Apiezon L on 60/80-mesh silanized acid-washed Universal support and sealed.	Pass nitrogen at 800 ml/min through the tube heated to 130°, then mix with air supply to flame.	Flame AAS	103	Levels of 0.003 μg/m^3 for 0.06 m^3 of air sampled over 30–40 min.
Inorganic and organic lead	Whatman No. 41 filter to collect inorganic lead and ICl solution to collect organic lead; flow-rate 3 l./min.	Ash a 7-cm^2 piece of the filter at low temperature for 1 hr; dissolve the residue in 1 ml of 0.5*M* HNO_3; add 20 ml of 46% ammonium citrate solution (pH = 11.1) + 40 μl of 0.1*M* EDTA to the ICl solution and selectively extract organic lead with dithizone.	ETAAS	104	For a 6-hr sampling period, 10 ng/m^3 inorganic lead and 8 ng/m^3 organic lead were found.
Alkyl lead	Direct injection of tetra-alkyl lead compounds.	Separate by gas chromatography.	Flame AAS, flame AFS and ETAAS	105	Concluded that ETAAS was the most sensitive and suitable technique.
Pt	Collected air sample on filters.	Leach Pt from filter with 1*M* HCl or *aqua regia*.	ETAAS	106	Platinum levels of 3–5 μg for five samples.
Sb (as SbH_3)	Air sample passed through pyridine–silver diethyldithiocarbamate solution for direct analysis.		ETAAS	107	Detection limit 0.07 mg/m^3 for 30-min sampling at 0.5 l./min.
V	Glass fibre or cellulose filter; flow-rate 1.13–1 60 m^3/min for up to 24 hr.	Add dropwise 1 ml of HF and heat; add 1–2 ml of HNO_3, boil, filter through Whatman No. 41 paper, wash with 10 ml of warm water.	Flame AAS or ETAAS	108	Method for occupational hygiene.
As, Ba, Ca, Cd, Cr, Cu, Fe, Mn, Ni, Pb, Tl, V and Zn	Glass fibre and membrane filters; 24-hr sampling at 1.5 m^3/min.	Ash 1/8 of strip of filter at 150° for 1 hr, then add to 8 ml of HCl and 32 ml of HNO_3, reflux for 3 hr, concentrate to 1–2 ml, cool and dilute as required.	Flame AAS	109	Detection limits from 0.002 μg/m^3 for zinc to 0.02 μg/m^3 for arsenic.

Cd, Cs, Cr, Cu, Fe, Mn, Ni, Pb, V and Zn	Filter paper and Gelman Type A glass filter with sampling for 24 hr.	Convert metal salts into sulphates with H_2SO_4, then ash at 500°.	Flame AAS	110	Ten different samples of Cd, Cu, Pb and Zn showed a range of values from 0.1 $\mu g/m^3$ for Cd to 59 $\mu g/m^3$ for Pb.
Cd, Hg, Pb and Zn	Environmental particulates volatilized directly into plasma for analysis.		MIPOES	111	Used for speciation of halides, sulphides and sulphates of Cd, Hg and Zn.
Be, Bi, Cd, Cr, Cu, Mn, Ni, Pb, Sn, Ti, V and Zn	Air pumped through a Gelman membrane filter at 30 l./min for 7 days.	Dissolve filter in acetone, centrifuge particulate matter, wash with acetone, dry, mix with NaF and graphite powder.	Powder–d.c. arc emission spectroscopy.	112	
Cd, Cu, Fe Pb and Zn	Whatman No. 41 filter with total loading of 100–500 $\mu g/cm^2$.	Treat 10 cm^2 of filter paper with 7.5 ml of HNO_3, boil off excess and dissolve residue in 2.5 ml of HNO_3 and 10 ml of demineralized water.	ETAAS and flame AAS (Zn)	113	
Cd, Co, Cr, Cu, Pb, Mn, Ni and Zn	8 × 10 in. glass fibre filter with four half-sheet samples cut into pieces.	Add 100 ml of HCl to pieces of filter and digest for 30 min at low heat; decant dissolved solids and rinse filters with 3 × 15 ml of water; evaporate to dryness and take up in 10 ml of HCl and 10 drops of HNO_3.	Flame AAS	114	Concentrations from a low of 0.002 $\mu g/m^3$ for cadmium to a high of 0.77 $\mu g/m^3$ for copper.
As, Be, Cd, Co, Cr, Cu, F, Hg, Mn, Mo, Ni, Pb Sn, V and Zn	Cyclone probe sampler. Different positions sampled for 3–5 min each.	Dissolve samples in $HCl/HNO_3/HClO_4$.	ETAAS	115	
Al, Be, Bi, Cu, K, Li, Mg, Mn, Na, Pb, Rb, Si, Sr, Ti and V	Polystyrene filters of Delbag Luftfilter type 99/97 were used with air sampled for 24 hr.	Dry-ash at 400–425° for 12–16 hr; dissolve residue in mixture of HF, HCl and HNO_3.	Flame AAS	118	Detection limits from a low of 0.04 $\mu g/m^3$ for chromium to a high of 0.8 $\mu g/m^3$ for silicon.
Al, Ca, Cd, Cr, Cu, Fe, Pb, Mg, Ni, Si, Sn and Zn	25-mm filter paper; sample time varied according to dirt level in area monitored.		Direct reading emission spectroscopy	119	
Al, Be, Cr, Co, Hg, Mg, Ni, Pb, Ti, V, W and Zn	Spectroscopic graphite electrodes used as filters.		Emission spectroscopy	120	Absolute detection limits from a low of 1 ng for beryllium to a high of 5 ng for tungsten.
As, Cd, Cu, Pb and Zn	Deposition collected on samplers every 2 months. Collection area 0.032 m^2.	Transfer sample to a clean polyethylene bottle, add 5 ml of HNO_3; treat sample as in reference 30.	Flame AAS	121	Measurement of atmospheric fall-out in the vicinity of a base-metal smelter plant.

(*continued*)

Table 6—*continued*

Element	Sample collection	Sample treatment	Technique	Reference	Comments
Cd, Cu, Pb and Zn	Air sampled in an 8-stage Anderson Impactor System at 20 l./min for 14–27 days.	Rinse collection stage for each plate four times with 10% HNO_3, mix with 7.5 ml of $HNO_3/HClO_4$ and heat to dissolve metals; dilute to 25 ml.	Flame AAS	122	Concentration of metals near lead smelter showed that 66% of the lead, 88% of the cadmium, 73% of the zinc and 54% of the copper was composed of particles smaller than 4.7 μm.
Cr, Pb, Sb and Zn	Air in stack sampled by cascade impactor before and after emission from coal-fired power plant and from cotton gin for 10 min to 24 hr.	Cut filters into strips; ash in Pyrex boats for 30 min at low temperature.	ETAAS	123	Relationship between metal concentration and particle size found.
Pb and Zn	Particulates in ambient air, waste gases and automobile exhaust fumes were collected.	Dissolve samples in 6*M* HCl and concentrated HNO_3 (50 + 5 ml); filter off insolubles.	Flame AAS	124	Concentration of lead in final solution 1–10 mg/l and zinc 1–5 mg/l.
Al, Ca, Cu, Fe, Mg, Si and Zn	Sample collected on a Mylar film at a flow-rate of 9 l./min and dried. Individual particles selected under microscope and vaporized with laser discharge.		Spark emission spectroscopy	125	
Cd, Cr, Cu, Fe, K, Mn, Na, Ni, Pb, V and Zn	Gelman glass fibre filter; a few collections in a Delbag Microsorbon type filter (for sodium); constant flow-rate of 27 m^3/hr for 1 week.	Digest in $HNO_3/HClO_4$ mixture.	Flame AAS	126	"High" concentrations of chromium, iron, manganese, nickel, vanadium and zinc found in Rio de Janeiro; high lead concentrations attributed to traffic.
Pb and Zn	Collection on a membrane filter.	Digest in $HNO_3/HClO_4$ acid mixture.	Flame AAS	127	Principally concerned with enhancement of signal by acid.
Be and Mn	Whatman No. 41 filter and Nuclepore polycarbonate membrane filter.	Destroy filter paper by boiling with $HNO_3/HClO_4$; decompose membrane filter by low-temperature ashing and dissolve residue in HF/HNO_3 mixture.	ETAAS	128	Detection limit 100 ng of manganese.
Cd and Zn	Sample in form of a solid or evaporated solution was deposited on a small tantulum rod, which was fed into the furnace.	Remove organic matter by ashing in a muffle furnace at 450–500° for 8–12 hr.	Radiofrequency atomization and AAS and AES	129	Detection limit of 5 pg for cadmium and zinc by AAS and 6 and 8 pg respectively for cadmium and zinc by AES.
Cd and Hg	Direct determination.		Radiofrequency atomization and ETAAS	130	Concentration ranges of 0.18–0.29 $\mu g/m^3$ for cadmium and 1.9–4.7 $\mu g/m^3$ for mercury.
Cd and Hg	Hg collected in scrubbing solution of HNO_3 and H_2SO_4; Cd collected by trapping in 1*M* HNO_3.		ETAAS	131	Concluded method unsuitable for direct determination of metals in air.
Ag, Be, Cd, Hg, Pb and Se	Air drawn through a porous graphite tube which is then used as the atomization cell; 10-litre air sample.		ETAAS	132	Sensitivities from a low of 0.1 $\mu g/m^3$ for cadmium to a high of 0.02 $\mu g/m^3$ for selenium.

Ge, Sb and methyl-germanium	25-mm diameter Gelman type A–E glass fibre filter; 8–10 m^3 of air sampled.	Digest sample with 0.1*M* NaOH; add 40 ml of distilled water and HCl/10% oxalic acid solution to adjust pH to 1. Convert into volatile hydrides with $NaBH_4$.	d.c. atomic emission detector	133	Detection limits of 0.4 ng for antimony and germanium. Low concentrations of inorganic antimony and germanium found but no organometallics.
Cd, Cu, Fe, Mg, Ni, Pb and V.	Collected on a high-volume sampler for 24 hr.		Flame AAS	134	Concentrations in New York measured
Al, Ca, Cd, Co, Cr, Fe, Mg, Mn, Ni, Pb and Zn	Porous graphite cell and Nuclepore polycarbonate membrane.	Treat filters with 10 ml of HCl in an ultrasonic bath.	ETAAS	116	Detection limits from a low of 0.0017 $\mu g/m^3$ for magnesium to a high of 0.167 $\mu g/m^3$ for tin.
Cu, Cr, Mn and Ni	Air pumped through a Millipore organic membrane filter for 8 hr.	Add 1 ml of acetone to the filter in a Pt dish, evaporate to dryness and ash at 550° for 1 hr; extract residue with 5 ml of HNO_3 and dilute as required.	Flame AAS	117	Concentrations ($\mu g/100$ m^3 of air) were 5.4–57.5 for copper, 11–509 for chromium, 3.3–8.5 for nickel and 10.1–70 for manganese.
Al, Bi, Cd, Cr, Fe, Pb, Mn, Mo, Ni, Sn, V and Zn	Silver membrane filter. Sampling flow-rate of 30 l./min for 7–10 days to give a sample weight of 10–100 mg.	Add 10 ml of 2*M* HNO_3 containing 5 ppm In and Co (as internal standards) + 200 mg of high purity graphite + 5 ml of 1*M* HCl to sample in a 100-ml Teflon beaker.	d.c. arc emission spectroscopy	135	Concentration levels from a high of 0.25–5 $\mu g/m^3$ for cadmium to a low of 1.3–25 $\mu g/m^3$ for bismuth.
Ca, Cu, Mg and Fe	Cellulose filter paper. Air sampled for 24 hr.	Ash 1/4 of filter at 500–550° for 1 hr, fuse with Na_2CO_3, dissolve in distilled water, add 2 ml of HCl and dilute as required.	Flame AAS	136	21 sampling sites in Chicago showed the following values for particulate matter: Ca 1.09–6.10 $\mu g/m^3$, Mg 0.60–2.28 $\mu g/m^3$, Fe 0.86–4.04 $\mu g/m^3$ and Cu 0.35–1.46 $\mu g/m^3$.
Mn, Pb and V	Gelman type A glass fibre filter; flow-rate 0.57 m^3/min for 1 week.	Digested in HNO_3 and $HClO_4$.	Flame AAS	137	Long-term concentration measurements of manganese, lead and vanadium in New York.
Al, As, Ba, Be, Ca, Cd Cr, Cu, Fe, K, Mg, Mn Mo, Na, Nb, Ni, P, Pb, Sn, Ti, V and Zn	A 0.3.μm Gelman type A–E glass fibre filter; flow-rate of 1.2 m^3/min for 24 hr, high-volume sampler.	An acid digestion procedure.	ICPAES	138	Increase in arsenic, cadmium, copper, lead and zinc found in the vicinity of a lead/zinc smelter plant.
As and Cd	Used high-volume samplers and a standard method.	Standard method.	Flame AAS	139	Survey of ambient air levels of arsenic and cadmium in El Paso, Texas 1972–1979.
Cu, Cr, Mn, Ni, Fe and Pb	A 20 × 25 cm glass fibre type A–E filter.	Solids digested in 20% HNO_3.	Flame AAS	140	Concentration of these metals in Naples not high.
Cd, Fe, Pb and Zn	Whatman No. 42 filter paper; 3-mm discs used for the analyses.	Furnace volatilization of filter disc.	Flame AFS	141	Results agreed well with standard atomic absorption procedure.

(*continued*)

Table 6—*continued*

Element	Sample collection	Sample treatment	Technique	Reference	Comments
Ag, Al, Cr, Cu, Fe, Ga, Mn, Mo, Ni, Pb, Sn, Ti, V and Zn	A Gelman GA-3 cellulose acetate membrane filter used; air sampled at 20 l./min continuously for one month with a low-volume sampler.	Ash the filters at low temperature and dissolve residue in HNO_3.	Arc emission spectroscopy	142	Applied to monthly determinations in Kobe City.
Ag, Be, Cd, Cu, Fe, Mn, and Pb	Direct impaction of laboratory air on a graphite furnace for analysis; maximum flow-rate of 10 l./min.		ETAAS	143	Concentrations from low of 2 ng/m^3 for beryllium to high of 47 ng/m^3 for copper.

ETAAS = Electrothermal atomization atomic-absorption spectroscopy.
Flame AAS = Flame atomic-absorption spectroscopy.
CVAAS = Cold vapour atomic-absorption spectroscopy.
Flameless AFS = Flameless atomic-fluorescence spectroscopy.
Flame AFS = Flame atomic-fluorescence spectroscopy.
OES = Optical-emission spectroscopy.
MIPOES = Microwave-induced plasma optical-emission spectroscopy.
ICPAES = Inductively-coupled plasma atomic-emission spectroscopy.

as they introduce fewer interferences into the chemical analysis. Other filters include nylon membranes, quartz fibre, polystyrene and silver membranes.

Dissolution of solids on filters

The particulate matter collected on the filter has to be dissolved for chemical analysis (though for some physical methods such as X-ray fluorescence the whole filter may be used). In some cases the sample may be dissolved, leaving the filter (glass fibre) more or less untouched, in others (paper filters) everything will be dissolved. Decomposition procedures are mentioned briefly in Table 6.

When glass-fibre filters are used, sample decomposition may be achieved with sulphuric and nitric acid,[40,72,108] heating at 150° for 1 hr followed by extraction with a mixture of hydrochloric and nitric acids,[77,109] ignition at 500° for 1 hr followed by extraction with 50% nitric acid,[79,85] leaching with nitric acid,[88,91,140] fusion with alkali at 900° followed by extraction with nitric acid,[91] dissolution in hydrochloric acid,[114] or mixture of nitric and perchloric acids,[126,138] or sodium hydroxide solution followed by addition of hydrochloric and oxalic acids to adjust the pH to 1 for conversion of some elements into their hydrides by sodium borohydride.[133]

Cellulose filters have been decomposed with nitric acid,[32,38,69,75,78,104,113] in a mixture of hydrofluoric and nitric acids,[40,72,108] or of nitric, perchloric and hydrofluoric acids,[85,128] or have been ashed at 500°,[110] or at 500° followed by fusion with sodium carbonate and dissolution of the residue with hydrochloric acid,[136] or by direct volatilization in the furnace.[141]

Membrane filters have been dissolved in acetone,[74,112,117] decomposed with hot concentrated nitric acid,[90] or nitric acid and hydrogen peroxide followed by dissolution of the residue in 0.5% tartaric acid,[92] or in a mixture of hydrochloric and nitric acids,[109] or of nitric and perchloric acids,[127] or ashed at low temperature followed by dissolution of the residue in a mixture of hydrofluoric and nitric acids.[128,142]

Nylon filters have been dissolved in acetone,[29] polystyrene filters ashed at 400–425° for 12–16 hr (followed by dissolution of the residue with a mixture of hydrofluoric, hydrochloric and nitric acids)[125] and silver membranes in nitric acid.[137]

Impactors and impingers

A pump can be used to draw an air sample through a sampling device where the air stream impinges on a solid surface or a solution in such a way that the particles are deposited.

A typical impinger bottle has a sampling tube 10 mm in diameter, with an outlet orifice 1.5 mm in diameter and a gradual bend to prevent larger particles from colliding with the tube wall. The impinger is operated at a flow-rate of about 2.4 l./min and a linear gas velocity of 1.2 m/sec by a filter pump. The dust particles are retained in the fluid into which the sampling tube dips. To ensure high collection

efficiency, three impingers can be used in series and the solutions combined.

Robinson and Araktingi[131] collected mercury in a solution of nitric and sulphuric acids containing two drops of 5% potassium permanganate solution and cadmium in 1*M* nitric acid. Gardner[45] collected mercury in a 4% solution of potassium permanganate in 10% sulphuric acid. Delaughter[50] used hydrochloric acid to collect mercury, whereas Hwang *et al.*[56] used Barnes's reagent (3% potassium iodide/0.25% iodine) for mercury collection. Organic lead[71] and tetra-alkyl lead[97,104] have been collected in iodine monochloride solution. Stibine has been collected in a pyridine–silver diethyldithiocarbamate solution.[107] However, absorption by a liquid-impinger is generally regarded as unsatisfactory because it may be far from complete and many particles, particularly the smaller ones, may not be wetted and will pass through unabsorbed.

Dry impinger methods with a cascade impactor are generally used when some information on particle size is desired.[122,123] The theory of the cascade impactor and the first instrument were described by May:[144] it consisted of a system of four jets and sampling slides in series. The jets were progressively finer, so that the speed of the air stream increased and finer particles were impacted on the slides and thus removed from the air stream. A size-grading thereby resulted, which assisted in assessing the samples. In this system the last jet gave a linear velocity of 34 m/sec and the whole system achieved good collection efficiency for particle sizes down to 1 μm and a density of 1 g/cm^3. Since then, cascade impactors of various designs have been used.[145–150] The most widely used is the Anderson sampler[147] which has the tage of being simple and inexpensive. The particle sizes collected by this system are approximately the same as those for the May impactor, the 50% cut-off point at the last stage being at about 0.5 μm. By using a higher flow-rate Hu[150] has extended the range down to 0.1–0.2 μm.

Impaction has been used by Woodriff and co-workers,[33,46,52,73,81,132] who collected particulate matter by drawing an air sample through a porous graphite cup, which was then inserted between electrodes and used as the atom cell. Roques and Mathieu[83] collected particles by impaction on a tantalum foil which was then transferred to a specially constructed atom cell. Seeley and Skogerboe[120] collected particles on spectroscopic graphite electrodes which were subsequently analysed by emission spectroscopy. Bezur *et al.*[143] collected solids from laboratory air by direct impaction on a graphite furnace. A number of workers have used impaction on absorbent material to collect particulate matter. Moffit and Kupal[47] collected mercury on impregnated charcoal. Mercury has also been collected on silver wool,[49,63] gold-plated quartz wool,[43,54] gold–platinum gauze,[57] Hopcalite granules,[68] manganese dioxide,[64] cellulose and activated charcoal[64] and in sequential selective absorption tubes containing gold, silver and copper.[61,62] The anti-knock component in petrol, methylcyclopentadienyl manganese tricarbonyl was collected in a small-loop gas-chromatographic sampling valve.[67] Brodie and Matoušek[38,70] used a modified cup sampler to collect particles from 200 ml of air sample. The method was modified by Noller and Bloom[80] to correct for a blank. This sampling cup was the forerunner of a commercially available air microsampler.[151] An iodine monochloride solution has been used to collect tetramethyl and tetraethyl lead[97] and organic lead.[104] Cold traps have been used to collect alkyl lead[98] and tetra-alkyl lead.[99,101] Lead compounds in gaseous form have been collected on a carbon bed.[102]

Electrostatic precipitation

The role of the corona discharge in the electrical separation of particles from gases has been recognized since the last century. Unlike solids or liquids, gases contain practically no free electrons or ions and are therefore almost perfect electrical insulators. However, when the potential difference between electrodes immersed in a gas is increased sufficiently, a point is reached at which the gas ionizes and the conductivity increases greatly. This transition from the insulating to the conducting state is called an electrical breakdown or gas discharge. The dominant ion-production mechanism in the corona is ionization by electron impact, in which free electrons in the gas acquire energy from an applied electric field and collide violently with gas molecules and literally knock electrons out of them. The net result is the creation of additional free electrons and positively charged gaseous ions. For this process to occur, the colliding electron must possess a minimum energy which is characteristic of the molecule or atom bombarded and is known as the ionization potential. For most atoms and molecules the ionization energy is in the range 5–25 eV, *e.g.*, 13.6 for hydrogen and 24.6 for helium. Electrons are singularly effective ionizers since they gain relatively high energies from the electric field on account of the long mean-free path between their collisions with gas molecules and they retain virtually all their kinetic energy in elastic collisions with gas molecules and yet transfer virtually all of it when they make inelastic (ionizing) collisions.

The unipolar corona, used in electrostatic precipitation, is a stable self-maintaining gas discharge between an emitting electrode, such as a fine wire and a receiving, or passive, electrode such as a cylinder or plate. The electrodes are normally a few inches apart and gas pressures of about 1 atmosphere are used.

A negative corona is far superior to a positive one for electrical precipitation because in practice it is not unusual to find that the spark-over voltage for the negative corona is as much as twice that for the positive corona and, in addition, the positive corona often tends to be unstable and sporadic. For these

reasons the unipolar negative corona is used almost exclusively for industrial precipitation. Practically all industrial furnace and process gases as well as air contain appreciable proportions of electronegative gases such as oxygen, water vapour, carbon dioxide and frequently sulphur dioxide. The corona can be visualized as consisting of two primary zones. The first is the active or glow region around the discharge wire and is composed of a cloud of positive and negative ions, free electrons and both excited and normal molecules, all interacting with one another and with the discharge wire. The second zone contains neutral molecules plus a minute fraction of negative ions and free electrons which have been created in the active zone around the discharge wire and move toward the collecting electrode under the influence of the electric field.

To date, electrostatic precipitation from air for analysis by atomic spectroscopy has been little used. Richards and Badami[152] estimated crysotile by X-ray diffraction after passing 1000 m^3 of air through a 20-kV corona discharge. They concluded that the sample flow-rate and the size distribution of the particles collected affected the collection efficiency. Torsi and co-workers[48,87,88] used electrostatic precipitation to collect particles from the laboratory atmosphere. The collecting electrode was subsequently transferred to an electrothermal atomizer for analysis. However, an adequate means of standardization was not achieved. Bezur *et al.*[41] collected aerosol particles, generated by a carbon-rod atomizer, by electrostatic precipitation on a tungsten rod and then fitted this rod into a graphite furnace for analysis. The method was extended to laboratory air samples. They concluded that the collection efficiency depended on particle size, applied voltage, geometry of the system and sampling flow-rate. Further work by Bezur *et al.*[42] combined electrostatic precipitation and impaction of particles in a graphite furnace.

COMPARISON OF ATOMIC SPECTROSCOPIC METHODS OF ANALYSIS

The most frequently used technique for determining atmospheric trace metals is atomic absorption. Instruments using flames are widely available at reasonable cost, and when samples are provided in solution the matrix effects are not serious. A disadvantage of flame spectroscopy is that direct analysis of solids is difficult, though attempts have been made to introduce a particulate-contaminated air sample directly into the air supply of a burner.[28,68]

An attractive alternative to a flame as source is an electrothermal atomizer, particularly for atomic absorption. The greater sensitivity thus achieved has led to this often being the preferred atom cell. A major advantage of the electrothermal atomizer is that the direct analysis of metal compounds collected from the atmosphere by impaction[151] or electrostatic precipitation[41,48,71,87,88] is now feasible, and automation[153,154] a real possibility. A disadvantage is that multi-element analysis is not possible, although an electrothermal atomizer used as an emission source does offer this possibility.[155]

The unique properties of mercury allow this element to be determined by the cold-vapour atomic-absorption method after release from the sample solution.

Despite its inherent sensitivity, atomic fluorescence[55,105,141] has found little use as a means of analysing for metals and their compounds in the atmosphere, possibly because of the lack of commercially available systems.

Atomic-emission spectroscopy, on account of its multi-element capability, has been used where a number of different metals have to be determined but has also been used for single-element analysis. A number of sources have been utilized, including flame,[68] spark,[77,88,125] plasma[35,36,96,101,111,138] and arc.[112,119,142] Plasma emission-spectroscopy appears to offer the most serious competition to electrothermal-atomization atomic absorption. The detection limits are also low, but the linearity is much better, often extending over five or six orders of magnitude rather than the very limited range of one order for atomic absorption. The high temperature of the plasma, *ca.* 8000–16000°, ensures complete atomization, thus minimizing chemical matrix interferences, but ionization is prevalent, and the spectra contain many more lines than do those from flames. A further advantage of the plasma is that certain non-metals, including the halogens, phosphorus, sulphur and carbon, can also be determined, whereas they cannot easily be determined by atomic absorption. The major drawback would appear to be that direct presentation of solid samples presents problems which have not yet been fully overcome.

A more recent use of atomic spectroscopy has been the determination of volatile lead[96,98–103,105] and manganese[67] organometallic compounds by trapping and separation on a gas chromotographic column, and detection by use of an electrothermal atomizer or plasma.

APPLICATIONS

Table 6 also summarizes the determination of trace metals in atmospheric particulate matter. The metals which have been examined most closely are the toxic ones, lead,[69–105] closely followed by mercury[43–65] and cadmium.[37–40] Levels of lead of 0.3–8.6 $\mu g/m^3$ have been found in Hobart,[80,82] 0.5–1.6 $\mu g/m^3$ in Berlin,[85] 0.2–12.2 $\mu g/m^3$ in Oslo[75] and 0.6–13 $\mu g/m^3$ in Budapest.[94] Surveys of lead levels have also been made in Texas[94] and Ontario.[95] Levels of tetra-alkyl lead in Antwerp have been reported to vary from 0.3 ng/m^3 in a rural environment to 400 ng/m^3 near a gasoline station.[99] Multi-element analysis for metals in the atmosphere in Rio de Janeiro,[126] New York,[134] Chicago,[136] New York City,[138] El Paso,[139] Naples[140] and Kobe City,[142] has also been done.

REFERENCES

1. American Society for Testing and Materials, *ASTM Standards on Methods of Atmospheric Sampling and Analysis*, Philadelphia, 1962.
2. D. F. S. Natusch and J. R. Wallace, *Science*, 1974, **186,** 695.
3. *Health and Safety at Work Act*, 1974, Chapter 37, H.M.S.O., London.
4. *Documentation of the Threshold Limit Values for Substances in Workroom Air*, American Conference of Government Hygienist, Cincinnati, 3rd Ed., 1975.
5. M. Katz, *Measurement of Air Pollutants*, World Health Organization, Geneva, 1969.
6. J. Moreton and N. A. R. Falla, *Analysis of Airborne Pollutants in Working Atmospheres*, The Chemical Society, London, 1980.
7. M. Katz (ed.), *Methods of Air Sampling and Analysis*, 2nd Ed., American Public Health Association, Washington, 1977.
8. H. Malissa (ed.), *Analysis of Airborne Particles by Physical Methods*, CRC Press, Florida, 1978.
9. D. C. Camp, J. A. Cooper and J. R. Rhodes, *X-Ray Spectrom.*, 1974, **3,** 47.
10. D. C. Camp, A. L. Vanlehn, J. R. Rhodes and A. H. Pradzynski, *ibid.*, 1975, **4,** 123.
11. P. R. Harrison, K. A. Rahn, R. Dams, J. A. Robbins, J. W. Winchester, S. S. Brar and D. M. Nelson, *J. Air Poll. Control. Assoc.*, 1971, **21,** 563.
12. P. R. Harrison, W. R. Matson and J. W. Winchester, *Atmos. Environ.*, 1971, **5,** 613.
13. G. Colovos, G. S. Wilson and J. Moyers, *Anal. Chim. Acta*, 1973, **64,** 457.
14. R. Brown, M. L. Jacobs and H. E. Taylor, *Intern. Lab.*, 1973, Jan/Feb, 32.
15. K. W. Olson and R. K. Skogerboe, *Environ. Sci. Technol.* 1975, **9,** 227.
16. W. J. Price, *Spectrochemical Analysis by Atomic Absorption*, Heyden, London, 1979.
17. J. C. Van Loon, *Analytical Atomic Absorption Spectroscopy*, Academic Press, New York, 1980.
18. J. A. Dean and T. C. Rains (eds.), *Flame Emission and Atomic Absorption Spectrometry*, Vols. 1–3, Dekker, New York, 1969–1975.
19. C. W. Fuller, *Electrothermal Atomization for Atomic Absorption Spectrometry*, The Chemical Society, London, 1977.
20. B. Linsky, *Report on Design of the Detroit Dust Fall Collector*, Bureau of Smoke Inspection and Abatement, Detroit, 1952.
21. M. Sachs and W. Munroe, *State Control of Air Pollution*, Symposium on Air Pollution, Wagner College, Staten Island, New York, March 1954.
22. C. V. Kanter, R. G. Lunche and A. P. Fudrich, *Air Poll. Control. Assoc. Meeting*, Buffalo, 1956.
23. M. T. Gordon and C. Orr, *Air Poll. Control Assoc. Meeting*, Chattanooga, 1954.
24. J. Y. Hwang, *Anal. Chem.*, 1972, **44,** No. 14, 20A.
25. *Methods for the Sampling and Analysis of Fume and Welding and Allied Processes*, Part I, British Standards Institution Draft for Development DD/54, 1977.
26. G. L. Hoffman and R. A. Duce, *Environ. Sci. Technol.*, 1971, **5,** 1134.
27. J. D. Wood, *Ann. Occup. Hyg.*, 1977, **20,** 3.
28. H. W. Edwards, *Anal. Chem.*, 1969, **41,** 1172.
29. J. P. Lacaux, P. V. Dinh and J. Beguin, *At. Absorp. Newsl.*, 1974, **13,** 49.
30. P. N. Vijan and G. R. Wood, *ibid.*, 1974, **13,** 33.
31. P. R. Walsh, J. L. Fasching and R. A. Duce, *Anal. Chem.*, 1976, **48,** 1012.
32. J. W. Robinson, R. Garcia, G. Hindman and P. Slevin, *Anal. Chim Acta*, 1974, **69,** 203.
33. D. Siemer, J. F. Lech and R. Woodriff, *Spectrochim. Acta*, 1973, **28B,** 469.
34. R. J. Bettger, A. C. Ficklin and T. F. Rees, *At. Absorp. Newsl.*, 1975, **14,** 124.
35. J. W. Carnahan and J. A. Caruso, *Anal. Chim. Acta*, 1982, **136,** 261.
36. D. G. Mitchell, K. M. Aldous and E. Canelli, *Anal. Chem.*, 1977, **49,** 1235.
37. M. Janssens and R. Dams, *Anal. Chim. Acta*, 1974, **70,** 25.
38. K. G. Brodie and J. P. Matoušek, *ibid.*, 1974, **69,** 200.
39. J. W. Robinson, D. K. Wolcott, P. J. Slevin and G. D. Hindman, *ibid.*, 1973, **66,** 13.
40. I.U.P.A.C., *Pure Appl. Chem.*, 1974, **40,** 37.
41. L. Bezur, J. Sneddon and J. M. Ottaway, to be published.
42. *Idem*, to be published.
43. F. Slemr, W. Seiler, C. Eberling and P. Roggendorf, *Anal. Chim. Acta*, 1979, **110,** 35.
44. J. H. Janssen, J. E. Van Den Enk, R. Bult and D. C. De Groot, *ibid.*, 1976, **84,** 319.
45. D. Gardner, *ibid.*, 1976, **82,** 321.
46. J. F. Lech, D. D. Siemer and R. Woodriff, *Spectrochim. Acta*, 1973, **28B,** 435.
47. A. E. Moffitt, Jr. and R. E. Kupal, *At. Absorp. Newsl.*, **9,** 113.
48. G. Torsi, E. Desimoni, F. Palmisano and L. Sabbatini, *Analyst*, 1982, **107,** 96.
49. S. J. Long, D. R. Scott and R. J. Thompson, *Anal. Chem.*, 1973, **45,** 2227.
50. B. Delaughter, *At. Absorp. Newsl.*, 1970, **9,** 49.
51. J. W. Robinson, P. J. Slevin, G. D. Hindman and D. K. Wolcott, *Anal. Chim. Acta*, 1972, **61,** 431.
52. D. Siemer, J. Lech and R. Woodriff, *Appl. Spectrosc.*, 1974, **28,** 68.
53. L. A. Krause, R. Henderson, L. P. Shortwell and D. A. Culp, *J. Am. Ind. Hyg. Assoc.*, 1971, **32,** 331.
54. Z. Yoshida and K. Motojima, *Anal. Chim. Acta*, 1979, **106,** 405.
55. J. E. Scott and J. M. Ottaway, *Analyst*, 1981, **106,** 1076.
56. J. Y. Hwang, P. A. Ullucci and A. L. Malenfant, *Can. Spectrosc.*, 1971, **16,** 100.
57. P. Schierling and K. H. Schaller, *At. Spectrosc.*, 1981, **2,** 91.
58. A. O. Rathje, D. H. Marcero and D. Dattilo, *J. Am. Ind. Hyg. Assoc.*, 1974, **35,** 571.
59. R. Dumarey, R. Heindryckx and R. Dams, *Environ. Sci. Technol.*, 1981, **15,** 207.
60. R. Dumarey, R. Heindryckx, R. Dams and J. Hoste, *Anal. Chim. Acta*, 1979, **107,** 159.
61. R. S. Braman and D. L. Johnson, *Environ. Sci. Technol.*, 1974, **8,** 996.
62. D. L. Johnson and R. S. Braman, *ibid.*, 1974, **8,** 1003.
63. T. J. Kneip, R. S. Ajemian, J. R. Carlberg, J. Driscoll, L. Kornreich, J. W. Loveland, J. L. Moyers and R. J. Thompson, *Health Lab. Sci.*, 1974, **11,** 342.
64. Report prepared for "Bureau International Technique du Chlore", *Anal. Chim. Acta*, 1979, **108,** 1.
65. R. Dumarey, R. Heindryckx and R. Dams, *ibid.*, 1980, **116,** 111.
66. W. R. Pierson, D. E. McKee, W. W. Brachaczek and J. W. Butler, *J. Air Poll. Control Assoc.*, 1978, **28,** 692.
67. M. Coe, R. Cruz and J. C. Van Loon, *Anal. Chim. Acta*, 1980, **120,** 171.
68. M. J. Prager and W. R. Seitz, *Anal. Chem.*, 1975, **47,** 148.
69. M. Janssens and R. Dams, *Anal. Chim. Acta*, 1973, **65,** 41.
70. J. P. Matoušek and K. G. Brodie, *Anal. Chem.*, 1973, **45,** 1606.
71. L. J. Purdue, R. E. Enrione, R. J. Thompson and B. A. Bonfield, *ibid.*, 1973, **45,** 527.
72. I.U.P.A.C., *Pure Appl. Chem.*, 1974, **40,** 35.

73. J. F. Lech, D. Siemer and R. Woodriff, *Environ. Sci. Technol.*, 1974, **8,** 840.
74. J. Y. Hwang, *Can. Spectrosc.*, 1971, **16,** 1.
75. S. H. Omang, *Anal. Chim. Acta*, 1971, **55,** 439.
76. B. Magyar and H. Vonment, *Z. Anal. Chem.*, **280,** 115.
77. D. R. Scott, D. C. Hemphill, L. E. Holboke, S. J. Long, W. A. Loseke, L. J. Pranger and R. J. Thompson, *Environ. Sci. Technol.*, 1976, **10,** 877.
78. J. L. Moyers, W. H. Zoller, R. A. Duce and G. L. Hoffman, *ibid.*, 1972, **6,** 68.
79. C. D. Burnham, C. E. Moore, E. Kanabrocki and D. M. Hattori, *ibid.*, 1969, **3,** 472.
80. B. N. Noller and H. Bloom, *Anal. Chem.*, 1977, **49,** 346.
81. R. Woodriff and J. F. Lech, *ibid.*, 1972, **44,** 1323.
82. B. N. Noller and H. Bloom, *Atmos. Environ.*, 1975, **9,** 505.
83. Y. Roques and J. Mathieu, *Analusis*, 1973, **2,** 481.
84. C. J. Pickford and G. Rossi, *Analyst*, 1978, **103,** 341.
85. H. W. Georgii and D. Jost, *Atmos. Environ.*, 1971, **5,** 725.
86. G. Torsi, E. Desimoni, F. Palmisano and L. Sabbatini, *Anal. Chem.*, 1981, **53,** 1035.
87. G. Torsi and E. Desimoni, *Anal. Lett.*, 1979, **12,** 1361.
88. S. J. Long, J. C. Suggs and J. F. Walling, *J. Air Poll. Control Assoc.*, 1979, **29,** 28.
89. D. G. Pachuta and L. J. Cline Love, *Anal. Chem.*, 1980, **52,** 444.
90. M. Halpern, *J. Air. Poll. Control Assoc.*, 1978, **28,** 689.
91. D. B. McDonnell and J. C. Hilborn, *ibid.*, 1978, **28,** 933.
92. K. Szivós, L. Pólos, I. Fehér and E. Pungor, *Period. Polytech. Chem. Eng.*, 1974, **18,** 281.
93. H. P. Loftin, C. M. Christian and J. W. Robinson, *Spectrosc. Lett.*, 1970, **3,** 161.
94. J. S. Hubert, R. M. Candelaria, B. Rosenblum and H. G. Applegate, *J. Air Poll. Control Assoc.*, 1981, **31,** 259.
95. K. C. Heidorn and I. Z. Rohac, *ibid.*, 1981, **31,** 1097.
96. S. A. Estes, P. C. Uden and R. M. Barnes, *Anal. Chem.*, 1981, **53,** 1336.
97. S. Hancock and A. Slater, *Analyst*, 1975, **100,** 422.
98. B. Radziuk, Y. Thomassen, J. C. Van Loon and Y. K. Chau, *Anal. Chim. Acta*, 1979, **105,** 255.
99. D. Chakraborti, S. G. Jiang, P. Surkijn, W. De Jonghe and F. Adams, *Proc. Anal. Div. Chem. Soc.*, 1981, **18,** 347.
100. W. De Jonghe, D. Chakraborti and F. Adams, *Anal. Chim. Acta*, 1980, **115,** 89.
101. D. C. Reamer, W. H. Zoller and T. C. O'Haver, *Anal. Chem.*, 1978, **50,** 1449.
102. J. W. Robinson, L. Rhodes and D. K. Wolcott, *Anal. Chim. Acta*, 1975, **78,** 474.
103. R. M. Harrison, R. Perry and D. H. Slater, *Atmos. Environ.*, 1974, **8,** 1187.
104. W. De Jonghe and F. Adams, *Anal. Chim. Acta*, 1979, **108,** 21.
105. B. Radziuk, Y. Thomassen, L. R. P. Butler, J. C. Van Loon and Y. K. Chau, *ibid.*, 1979, **108,** 31.
106. G. L. Everett, *Analyst*, 1976, **101,** 348.
107. J. B. Cross, *Anal. Chem.*, 1979, **51,** 2033.
108. I.U.P.A.C., *Pure Appl. Chem.*, 1974, **40,** 38.
109. R. J. Thompson, G. B. Morgan and L. J. Purdue, *At. Absorp. Newsl.*, 1970, **9,** 53.
110. T. Y. Kometani, J. L. Bove, B. Nathanson, S. Siebenberg and M. Magyar, *Environ. Sci. Technol.*, 1972, **6,** 617.
111. C. F. Bauer and D. F. S. Natusch, *Anal. Chem.*, 1981, **53,** 2020.
112. A. Sugimae, *ibid.*, 1974, **46,** 1123.
113. P. Geladi and F. Adams, *Anal. Chim. Acta*, 1978, **96,** 229.
114. M. Beyer, *At. Absorp. Newsl.*, 1969, **8,** 23.
115. J. M. Ottaway and D. C. Hough, *Proc. Anal. Div. Chem. Soc.*, 1975, **12,** 319.
116. B. C. Begnoche and T. H. Risby, *Anal. Chem.*, 1975, **47,** 1041.
117. J. Y. Hwang and J. Feldman, *Appl. Spectrosc.*, 1970, **24,** 371.
118. L. E. Ranweiler and J. L. Moyers, *Environ. Sci. Technol.*, 1974, **8,** 152.
119. D. W. Lander, R. L. Steiner, D. H. Anderson and R. L. Dehm, *Appl. Spectrosc.*, 1971, **25,** 270.
120. J. L. Seeley and R. K. Skogerboe, *Anal. Chem.*, 1974, **46,** 415.
121. W. G. Franzin, G. A. McFarlane and A. Lutz, *Environ. Sci. Technol.*, 1979, **13,** 1513.
122. C. R. Dorn, J. O. Pierce, P. E. Phillips and G. R. Chase, *Atmos. Environ.*, 1976, **10,** 443.
123. R. E. Lee, H. L. Crist, A. E. Riley and K. E. MacLeod, *Environ. Sci. Technol.*, 1975, **9,** 643.
124. P. Hermann, *Spectrochim. Acta*, 1975, **30B,** 15.
125. H. Uchida, F Adachi, O. Mori and R. Negishi, *Bunseki Kagaku*, 1975, **24,** 325.
126. H. L. Trindade, W. C. Pfeiffer, H. Londres and C. L. Costa Riberio, *Environ. Sci. Technol.*, 1981, **15,** 84.
127. W. W. Brachaczek, J. W. Butler and W. R. Pierson, *Appl. Spectrosc.*, 1974, **28,** 585.
128. P. Geladi and F. Adams, *Anal. Chim. Acta*, 1979, **105,** 219.
129. Y. Talmi, *Anal. Chem.*, 1974, **46,** 1005.
130. C. M. Christian and J. W. Robinson, *Anal. Chim. Acta*, 1971, **56,** 466.
131. J. W. Robinson and Y. E. Araktingi, *ibid.*, 1973, **63,** 29.
132. D. D. Siemer and R. Woodriff, *Spectrochim. Acta*, 1974, **29B,** 269.
133. R. S. Braman and M. A. Tompkins, *Anal. Chem.*, 1978, **50,** 1088.
134. B. P. Leaderer, *J. Air Poll. Control Assoc.*, 1978, **28,** 321.
135. A Sugimae, *Appl. Spectrosc.*, 1974, **28,** 458.
136. M. E. Hoschler, E. L. Kanabrocki, C. E. Moore and D. M. Hattori, *ibid.*, 1973, **27,** 185.
137. P. J. Lioy, R. P. Mallon and T. J. Kneip, *J. Air Poll. Control Assoc.*, 1980, **30,** 153.
138. A. J. Lynch, N. R. McQuaker and D. F. Brown, *ibid.*, 1980, **30,** 257.
139. J. S. Hubert, R. M. Candelaria, B. Rosenblum, R. Munoz and H. G. Applegate, *ibid.*, 1981, **31,** 261.
140. M. Mansi, V. Romano and F. Senatore, *ibid.*, 1981, **31,** 881.
141. J. Ip, Y. Thomassen, L. R. P. Butler, B. Radziuk and J. C. Van Loon, *Anal. Chim. Acta*, 1979, **110,** 1.
142. S. Imai, Y. Kusaka, H. Tsuji and Y. Hishiya, *ibid.*, 1979, **108,** 103.
143. L. Bezur, J. Sneddon and J. M. Ottaway, to be published.
144. K. R. May, *J. Sci. Instrum.*, 1945, **22,** 187.
145. W. E. Ranz and J. B. Wong, *Ind. Eng. Chem.*, 1952, **44,** 1371.
146. G. R. Gillespie and H. F. Johnstone, *Chem. Eng. Prog.*, 1955, **51,** 74F.
147. A. A. Anderson, *Bacteriol.*, 1958, **76,** 471.
148. J. A. Brink, *Ind. Eng. Chem.*, 1958, **50,** 645.
149. R. I. Mitchell and J. M. Pilcher, *ibid.*, 1959, **51,** 1039.
150. J. Nan-Hai Hu, *Environ. Sci. Technol.*, 1971, **5,** 251.
151. *Air microsampler for trace metal analysis*, Varian–Techtron, Victoria, Australia.
152. A. L. Richards and D. V. Badami, *Nature*, 1971, **234,** 93.
153. L. Bezur, J. Sneddon and J. M. Ottaway, in preparation.
154. D. Pritty, J. Sneddon, A. McLean, L. Bezur and J. M. Ottaway, in preparation.
155. J. M Ottaway, R. C. Hutton, D. Littlejohn and F. Shaw, *Wissensch. Zeit der Karl-Marx Universität, Leipzig*, 1979, **28,** 457.

Talanta, Vol. 30, No 9, pp. 649–654, 1983
Printed in Great Britain.

0039/9140/83 $3.00 + 0.00

PHOTOCHEMICAL ANALYSIS STUDIES—V*

PHOTOCHEMICAL ENHANCEMENT OF THE FLUORESCENCE SIGNAL OF THE ANTIMALARIAL PLASMOCID IN LIQUID SOLUTION AND ON SILICA-GEL THIN LAYERS

JEAN-JACQUES AARON,† JOELLE FIDANZA and MAME DIABOU GAYE
Laboratoire de Chimie Physique Organique et d'Analyse Instrumentale, Département de Chimie, Faculté des Sciences, Université de Dakar, Dakar-Fann, Sénégal

(*Received* 28 *January* 1983. *Accepted* 29 *March* 1983)

Summary—Ultraviolet irradiation converts the antimalarial plasmocid into a highly fluorescent photoproduct. The effect of pH, solvent composition and irradiation time on the photochemical enhancement of the fluorescence signal of plasmocid has been investigated in solution and on silica-gell thin layers. A significant increase in the fluorescence intensity in very acidic medium is explained by the formation of a triprotonated plasmocid species. The photochemical–fluorescence enhancement factors are particularly large, ranging between about 10 and 20 on silica-gel thin layers. Linear calibration plots are obtained over a concentration range of nearly three orders of magnitude. The photochemical–fluorimetric detection limit of plasmocid on thin layers is 10 ng. The results presented demonstrate the potential of thin-layer phototochemical fluorimetry as a sensitive analytical method.

Photochemical kinetic analysis is a method based on the photodecomposition of the sample into a photoproduct which can be measured spectrophotometrically, fluorimetrically or electrochemically.[1] Of particular interest is the recent use of photoreactions to increase the sensitivity of the fluorescence detection of organic compounds, in the ng/ml range.[2–10] The possibility of combining photochemical processes and detection of fluorescent photoproducts with high-pressure liquid chromatography (HPLC) or thin-layer chromatography (TLC) has also been investigated recently by several research groups.[11–21]

Post-column photochemical reactors coupled with HPLC have been used to induce photoconversion into fluorescent photoproducts of pharmaceutically important compounds such as cannabinol,[11] diethylstilbestrol,[12] clobazam, phenothiazines,[13–15,17,18] and clomiphene.[16] Detection limits were reported to be in the ng and pg range.

Recent work from our group[19–21] has been concerned with application of photochemical reactions to the improvement of fluorescence detection of antimalarial aminoquinoline derivatives in TLC.

The effect of pH, alkali-metal halides, eluent composition, and irradiation time on the fluorescence signal of chloroquine and its photoproduct on silica-gel thin layers was investigated.[19,20] The influence of irradiation time and solvent composition in the photochemical-fluorimetric determination of primaquine on silica-gel chromatoplates was also studied.[21]

In the present paper, we report on plasmocid dihydriodide, an 8-aminoquinoline derivative (see structure in Table 1), which possesses well-known antimalarial properties[22] related to its binding to deoxyribonucleic acid.[23] So far, only paper chromatography has been used for its determination and separation.[24] It was the goal of this study to investigate the effect of pH, solvent composition and irradiation time on the photochemical enhancement of the fluorescence signal of plasmocid, and to show the usefulness of photochemical fluorimetry as a sensitive analytical method for determination of the compound.

EXPERIMENTAL

Reagents

Plasmocid [8-(3-diethylaminopropylamino)-6-methoxyquinoline] dihydriodide was purchased from Aldrich (Beerse, Belgium). Solvents used were analytical-grade methanol, absolute ethanol, propan-2-ol, acetone, acetonitrile, tetrahydrofuran and concentrated phosphoric acid. Distilled water was used for solutions.

Precoated 5 × 20 cm silica-gel 60 TLC plates (Merck) were used.

Instrumentation

Ultraviolet absorption spectra were obtained with a Beckman model 3600 spectrophotometer, and a Perkin-Elmer model MPF-44B spectrophotofluorimeter was used for determining excitation and emission fluorescence spectra.

Fluorimetric measurements were performed with a Turner model 111 filter fluorometer, with a 110–850 lamp (7–54 excitation and 2-A emission filters), equipped with a Camag model 110–710 automatic TLC scanner, and a Kipp & Zonen model BD-12 recorder; 10% and 1% neutral

*Part IV, J. J. Aaron, S. A. Ndiaye and J. Fidanza, *Analusis*, 1982, **10**, 433.
†Author to whom all correspondence should be addressed.

density filters were used according to the fluorescence intensity.

For the photolysis, a 200-W Osram mercury arc lamp was used in an Oriel model 6137 housing and run by an Oriel model 8500 power supply.

Photochemical–fluorimetric procedures

Portions (20 μl) of plasmocid solution were spotted on silica-gel TLC plates with a 50-μl microsyringe. The plates were dried with a hot-air current, and put in an oven at 110° for about 5 min. The dried plates were placed on the Camag TLC scanner at about 60 cm from the mercury arc lamp, and irradiated for a fixed time with the image of the mercury arc focused on the plasmocid spots. The fluorescence intensity of the spots was then recorded as a function of time by automatic scanning of the plates with the Turner fluorometer.

For the photochemical–fluorimetric measurements in liquid solution, 3 ml of plasmocid solution were put in a cylindrical quartz tube, and irradiated for a fixed time at about 60 cm from the mercury arc lamp. The fluorescence intensity was then measured. The solution temperature was regularly checked, in order to avoid possible overheating by the mercury arc lamp, leading to losses of liquid by evaporation.

RESULTS AND DISCUSSION

Fluorescence and ultraviolet absorption characteristics

Ultraviolet irradiation of plasmocid, which has weak native fluorescence, resulted in drastic changes of its fluorescence characteristics in phosphoric acid medium as well as on silica-gel thin layers. Excitation and emission fluorescence data are given in Table 1. It can be seen that there is a 26-nm blue-shift of the fluorescence emission maximum on irradiation. This is in contrast to the red-shift observed for chloroquine[20] and primaquine.[21] There is a 7-fold increase in relative fluorescence intensity at the emission maximum on irradiation of plasmocid.

Table 1. Structure and fluorescence properties of plasmocid dihydriodide*

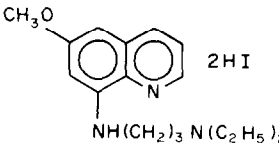

	Fluorescence properties	
	Before irradiation	After irradiation†
λ_{ex}, *nm*	321,355	355
λ_{em}, *nm*	503	477
I_{FS}§	7	50

*Experimental conditions: plasmocid concentration $10^{-4}M$ in $0.66M$ aqueous H_3PO_4 solution.
†Irradiation time 53 min.
§Relative fluorescence intensity at the maximum fluorescence emission band.

The absorption spectra of plasmocid in phosphoric acid solutions, after different irradiation times, are shown in Fig. 1. There are three main bands, with maxima at 405, 330 and 260 nm. On irradiation for 10 min, the 405-nm and 330-nm bands disappear and the 260-nm band is decreased in intensity. This last band is still further decreased in intensity on further irradiation for 25 min.

Our results suggest the formation of a highly fluorescent photoproduct, which is relatively weaker than plasmocid as an ultraviolet absorber.

Influence of pH

The effect of pH on the fluorescence intensity of plasmocid was studied in solution and on silica-gel thin layers. Phosphoric acid solutions were used for the Hammett H_0 acidity scale[25] from -1.6 to 1.0 and

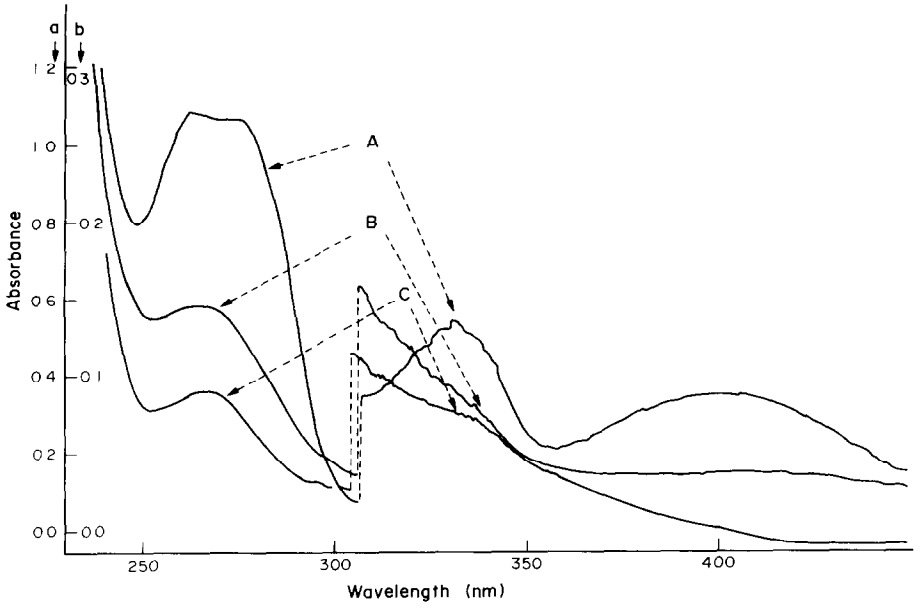

Fig. 1. Ultraviolet absorption spectra of plasmocid at different stages of the photochemical reaction. Plasmocid concentration 54 ppm. Irradiation times: A, 0; B, 9 min; C, 24 min. Absorbance scale a corresponds to wavelengths < 305 nm and absorbance scale b corresponds to wavelengths > 305 nm.

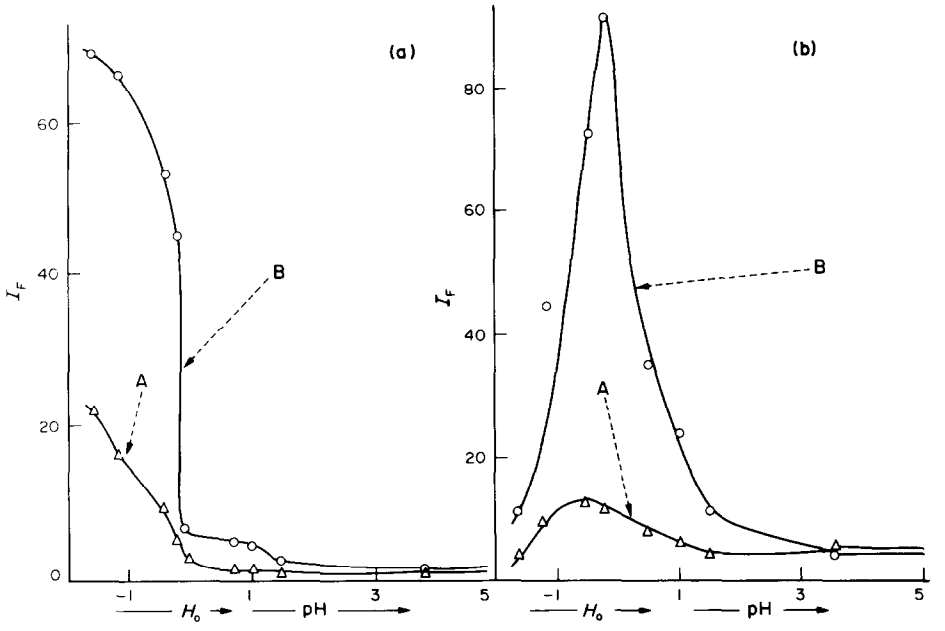

Fig. 2. Effect of pH and H_0 on the fluorescence intensity (I_F) of plasmocid. (a) In solution; plasmocid concentration 54 ppm; A, no irradiation; B, irradiation time 10 min. (b) On silica-gel thin layers; plasmocid concentration 27 ppm; A, no irradiation; B, irradiation time 6 min.

the pH range 1–4, and sodium hydroxide was added for the pH range 6–13.

The fluorescence intensity of plasmocid in solution is practically constant from pH 13 down to pH 4, decreases very slightly until pH 1.5 is reached, and increases strongly at an H_0 value of about zero (Fig. 2a, curve A). This enhancement of the fluorescence signal in very acidic medium is probably due to addition of a third proton to the already doubly protonated plasmocid, according to the equilibrium shown below. We calculated a pK value of about -0.8 for ground-state dissociation of the third proton (on the basis of the inflection point on the graph of fluorescence intensity *vs.* pH), which may be compared with the pK value of 3.0 previously reported for the ground-state dissociation of the second proton in this system.[23]

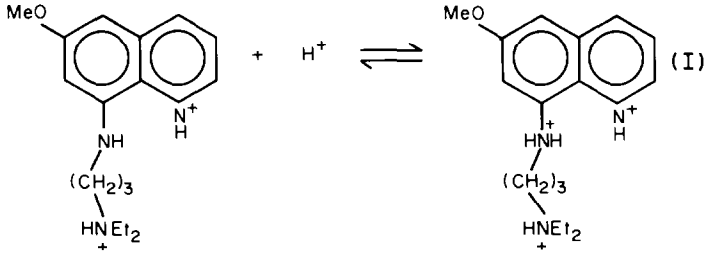

Curve B (in Fig. 2a) shows the dramatic effect of irradiation on the fluorescence of plasmocid at high acidity. This effect can be attributed to photodecomposition of the triply protonated plasmocid to give a highly fluorescent product.

A similar effect is shown when plasmocid is irradiated on silica-gel thin layers (Fig. 2b) and can be explained in the same way. The decrease in fluorescence intensity at acidities greater than $H_0 = -1$ is probably due to quenching by high concentrations of phosphate species adsorbed on the silica-gel substrate.

Effect of the solvent composition

The effect of solvent composition on the relationship between fluorescence signal and irradiation time was investigated for phosphoric acid alone and in binary mixture with acetone, methanol, ethanol, propan-2-ol, acetonitrile or tetrahydrofuran. The time needed to reach maximum fluorescence depends on the organic solvent used and is longer for irradiation of solutions than of thin layers (Figs. 3 and 4). It also increases with increasing polarity of the organic solvent.

This behaviour is the same as that of chloroquine and primaquine,[20,21,26] and confirms the usefulness of silica-gel as a substrate for the rapid

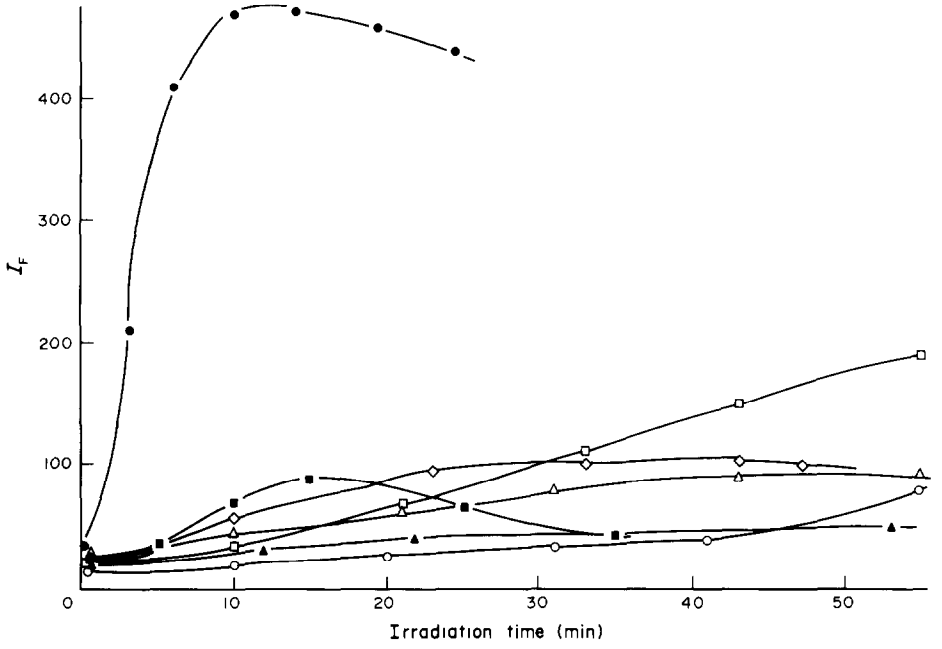

Fig. 3. Photolysis of plasmocid (54 ppm) in 1:1 v/v mixtures of organic solvent and 0.66*M* phosphoric acid, ● acetone–H_3PO_4; ■ iPrOH–H_3PO_4; ○ EtOH–H_3PO_4; ▲ MeOH–H_3PO_4; △ MeCN–H_3PO_4; □ THF–H_3PO_4; ◇ H_3PO_4, 0.66*M*

photochemical–fluorimetric determination of these antimalarial compounds.

Photochemical fluorescence enhancement

Tables 2 and 3 give the relative fluorescence signals and photochemical fluorescence enhancement factors for plasmocid in various phosphoric acid–organic solvent mixtures.

The photochemical fluorescence enhancement factors, defined as the ratio of the relative fluorescence signal for the irradiated sample and for the non-irradiated sample, were much larger than unity for all the solvent systems studied, and, except for the acetone system, were greater for measurements on thin layers than in solutions, so silica-gel thin layers are the preferred medium.

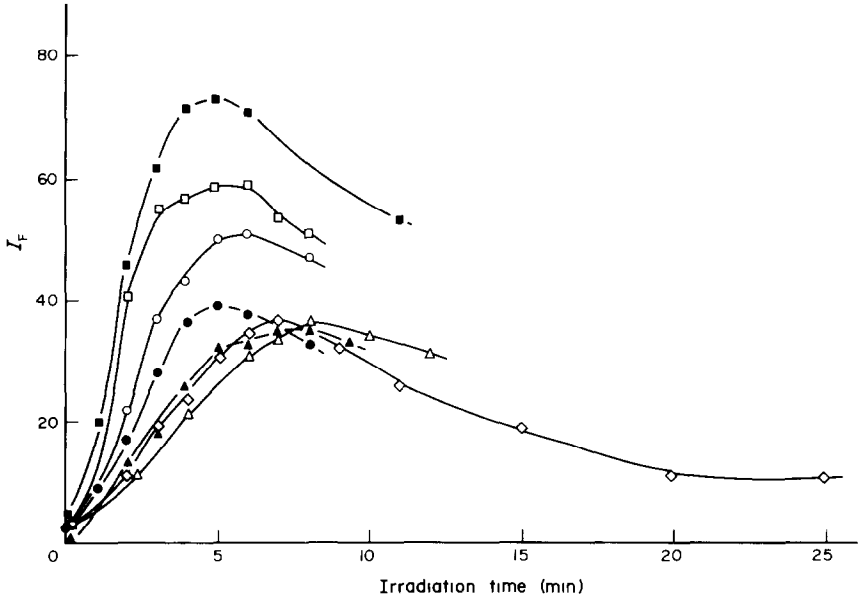

Fig. 4. Photolysis of plasmocid (54 ppm) adsorbed on silica-gel thin layers from 0.66*M* phosphoric acid–organic solvent 1:1 v/v mixtures. ● acetone–H_3PO_4; □ iPrOH–H_3PO_4; ○ EtOH–H_3PO_4; ▲ MeOH–H_3PO_4; △MeCN–H_3PO_4; □ THF–H_3PO_4; ◇ H_3PO_4, 0.66*M*.

Table 2. Comparison of fluorescence intensity of plasmocid (27 ppm) before and after ultraviolet irradiation in solution

Solvent system*	Relative fluorescence intensity		Photochemical fluorescence enhancement factor§	Irradiation time, *min*
	Non-irradiated	Irradiated†		
Acetone–H_3PO_4	32	470	14.7	11
iPrOH–H_3PO_4	21	81	3.8	15
EtOH–H_3PO_4	12	85	7.1	56
MeOH–H_3PO_4	24	50	2.1	53
MeCN–H_3PO_4	23	91	4.1	58
THF–H_3PO_4	20	190	9.5	55
H_3PO_4 0.66*M*	11	101	9.2	43

*Mixtures of organic solvent and 0.66*M* aqueous H_3PO_4, 1:1 v/v.
†Maximum relative fluorescence intensity measured at the optimal irradiation time (given in column 5).
§See text for definition.

Table 3. Comparison of fluorescence intensity of plasmocid (54 ppm) before and after ultraviolet irradiation on silica-gel thin layers

Solvent system	Relative fluorescence intensity		Photochemical fluorescence enhancement factor§	Irradiation time, *min*
	Non-irradiated	Irradiated†		
Acetone–H_3PO_4	4	39	9.7	5
iPrOH–H_3PO_4	4	73	18.2	5
EtOH–H_3PO_4	3	51	17.3	7
MeOH–H_3PO_4	2	35	17	8
MeCN–H_3PO_4	3	36	12	8
THF–H_3PO_4	3	59	19.6	5
H_3PO_4 0.66*M*	3	36	12	6

*Mixtures of organic solvent and 0.66*M* aqueous H_3PO_4, 1:1 v/v.
†§See corresponding footnotes in Table 2.

The enhancement factors for plasmocid are much larger than those for chloroquine[20] (2.2–3.4) and primaquine[21] (1.3–5.4).

Calibration graphs and detection limits

Log–log plots of the fluorescence intensity *vs.* initial concentration of plasmocid in 0.66*M* phosphoric acid medium were linear ($r = 0.990$) over a concentration range of nearly three orders of magnitude: 0.05–100 μ g/ml for measurements in solution and 0.5–100 μg/ml for the thin-layer measurements. The reproducibility was about 5%. The detection limits, defined as the concentration or amount of compound giving a signal-to-noise ratio of 3:1, are 50 ng/ml for the measurements in solution and 10 ng for the thin-layer measurements (which is much lower than the detection limit of 50 μg reported[24] for paper chromatography).

CONCLUSION

The results given here and in our previous papers[20,21] show that the photolysis of 4- and 8-aminoquinoline derivatives on silica-gel thin layers leads to the formation of more strongly fluorescent photoproducts. Under the optimal conditions, the fluorimetric detection limits for the photoproducts of chloroquine, primaquine and plasmocid are between 0.9 and 10 ng. Optimal irradiation times are between 30 sec and 5 min for these compounds.

These results clearly demonstrate the potential of the thin-layer photochemical-fluorimetric method for the sensitive, simple and rapid determination of these antimalarial compounds.

REFERENCES

1. J. M. Fitzgerald, in *Analytical Photochemistry and Photochemical Analysis*, p. 745. Dekker, New York, 1971.
2. R. J. Lukasiewicz and J. M. Fitzgerald, *Anal. Chem.*, 1973, **45**, 511.
3. *Idem*, *Appl. Spectrosc.*, 1974, **28**, 151.
4. V. R. White, C. S. Frings, J. E. Villafranca and J. M. Fitzgerald, *Anal. Chem.*, 1976, **48**, 1314.
5. J. J. Aaron, J. E. Villafranca, V. R. White and J. M. Fitzgerald, *Appl. Spectrosc.*, 1976, **30**, 159.
6. J. J. Aaron, *Methods Enzymol.*, 1980, **67**, 140.
7. P. Hadju and D. Damm, *Arzneim-Forsch.*, 1976, **26**, 2141.
8. H. M. Hill, J. Chamberlain, P. Hadju and D. Damm, *Biophys. Drug Dispos.*, 1979, **1**, 1.
9. D. W. Mendenhall, H. Kobayashi, F. M. L. Shih, L. A. Sternson, T. Higuchi and C. Fabian, *Clin. Chem.*, 1978, **24**, 1518.
10. Y. Golander and L. A. Sternson, *J. Chromatog.*, 1980, **181**, 41.
11. P. J. Twitchett, P. L. Williams and A. C. Moffat, *ibid.*, 1978, **149**, 683.
12. A. T. R. Williams, S. A. Winfield and R. C. Belloli, *ibid.*, 1982, **235**, 461.

13. A. H. M. T. Scholten, U.A. Th. Brinkman and R. W. Frei, *Anal. Chim. Acta*, 1980, **114,** 137.
14. A. H. M. T. Scholten, P. L. M. Welling, U. A. Th. Brinkman and R. W. Frei, *J. Chromatog.*, 1980, **199,** 239.
15. A. H. M. T. Scholten and R. W. Frei, *ibid.*, 1979, **176,** 349.
16. P. J. Harman, G. L. Blackman and G. Phillipou, *ibid.*, 1981, **225,** 131.
17. U. A. Th. Brinkman, P. L. M. Welling, G. De Vries, A. H. M. T. Scholten and R. W. Frei, *ibid.*, 1981, **217,** 463.
18. M. Uihlein and E. Schwab, *Chromatographia*, 1982, **15,** 140.
19. J. Fidanza and J. J. Aaron, *Analusis*, 1981, **9,** 118.
20. J. J. Aaron and J. Fidanza, *Talanta*, 1982, **29,** 383.
21. J. J. Aaron, S. A. Ndiaye and J. Fidanza, *Analusis*, 1982, **10,** 433.
22. P. E. Thompson and L. M. Werbel, in *Antimalarial Agents: Chemistry and Pharmacology*, p. 100. Academic Press, New York, 1972.
23. L. P. Whichard, C. R. Morris, J. M. Smith and D. J. Holbrook, Jr., *Mol. Pharmacol.*, 1968, **4,** 630.
24. A. E. Mshvidobadze, B. I. Chumburidee and O. V. Sardjeveladze, *Aptechn. Delo*, 1963, **12,** 30.
25. J. E. Leffler and E. Grunwald, in *Rates and Equilibria of Organic Reactions*, p. 269. Wiley, New York, 1963.
26. J. J. Aaron and J. Fidanza, unpublished results.

Talanta, Vol 30, No. 9, pp. 655–658, 1983
Printed in Great Britain.

0039/9140/83 $3.00 + 0.00

POLAROGRAPHIC DETERMINATION OF PHOSPHORUS

R. PARDO, E. BARRADO, Y. CASTRILLEJO and P. SANCHEZ BATANERO
Departamento de Química Analítica, Facultad de Ciencias, Universidad de Valladolid, Valladolid, España

(*Received* 26 *August* 1982. *Revised* 14 *January* 1983. *Accepted* 29 *March* 1983)

Summary—A method has been developed for the determination of phosphorus, as phosphate, by means of the catalytic polarographic wave for the reduction of hydrogen peroxide in the presence of Mo(VI). This reduction is combined with the previous formation and extraction of 12-molybdophosphoric acid. Depending on the extractant chosen, ethyl acetate or methyl isobutyl ketone, the determination limit is 2.3 or 3.1 μg/l. respectively. The procedure has been applied to certified steel samples with good results.

The formation of heteropolymolybdic acids has been widely used as the basis for indirect determination of the hetero-atom. Various methods have been reported for the determination of phosphorus, as phosphate, after its conversion into 12-molybdophosphoric acid (12-MPA). The sensitivity achieved varies according to the technique used to measure the molybdenum attached to the hetero-atom: 1 mg/l. by ASS,[1] 20 μg/l. by X-ray fluorescence,[2] 5 mg/l. by spectrophotometry,[3] and 0.1 mg/l. by differential pulse polarography.[4]

The sensitivity can be enhanced by measurement of the polarographic waves or peaks resulting from the catalytic reduction of some oxidants, such as perchlorate or nitrate, in the presence of Mo(VI). Hight *et al.*[5] proposed the use of nitrate and evaluation of the catalytic wave by differential pulse polarography (DPP). A determination limit of 9 μg/l. was reported.

In the present work we used a similar approach, with hydrogen peroxide as the oxidant, which also undergoes polarographic reduction catalysed by Mo(VI).[6] In this case, DPP could not be used, but d.c. polarography was found to provide good results because of the high sensitivity of the catalytic reduction. The proposed procedure combines this sensitive polarographic indicator reaction with the 12-fold multiplication provided by formation of 12-MPA, and gives a detection limit of 2.3 μg/l. Because of the nature of the reduction, it is necessary to separate the 12-MPA by extraction with an organic solvent.

The procedure has been applied to the determination of phosphorus in drinking water and in certified Cr–Ni steel samples.

EXPERIMENTAL

Apparatus

The d.c. polarograms were recorded on a Radiometer P04d polarographic analyser with a dropping mercury electrode and a saturated calomel reference electrode. A sweep-rate of 100 mV/min was used. A Radiometer 29 pH-meter was used with a Radiometer GK 2401C combined electrode. The temperature was controlled by using a double-wall polarographic cell and a Selecta recirculation thermoregulator. Deaeration was not required in the final procedure, but was done with nitrogen during the preliminary studies.

Reagents

Standard phosphate solution. Dissolve 7.099 g of dried sodium dihydrogen phosphate in 1 litre of demineralized water and store in polythene. This solution is $5.00 \times 10^{-2}M$. Prepare less concentrated standard solutions by dilution.

Standard molybdate solution. Dissolve 12.36 g of ammonium paramolybdate tetrahydrate in 1 litre of demineralized water and store in polythene. This solution is $1.00 \times 10^{-2}M$. Prepare less concentrated solutions by dilution.

Molybdate solution, 2%. Prepare and store in polythene. All reagents were of analytical grade, and demineralized water was used throughout.

Procedures

Standardization of molybdate solution. Acidify the solution with acetic acid (5 ml per 200 ml) and heat nearly to boiling. Add 4% lead acetate solution slowly until no further precipitation occurs and then about 5% excess. Let the precipitate settle for a few minutes, then filter off hot on ashless filter paper. Wash the precipitate with hot water until free from lead acetate. Dry and ignite it in a porcelain crucible at red heat for about 20 min, and weigh as $PbMoO_4$.

Amplification reaction. Transfer a known volume of sample solution into a separating funnel. Add 2 ml of 2% molybdate solution and dilute with water to 25 ml. Add 1 ml of 5*M* sulphuric acid and after 15 min 1 ml more of the acid and 15 ml of the organic solvent. Shake the mixture for 3 min and then separate the organic phase. Wash the organic phase with two 10-ml portions of 0.8*M* sulphuric acid and then strip the molybdate with 25 ml of 1*M* sodium hydroxide. Acidify this aqueous extract with 0.8*M* sulphuric acid to about pH 2.5. Add 4 ml of 5*M* sulphuric acid and 10 ml of 0.2*M* hydrogen peroxide and dilute to volume in a 100-ml standard flask. Transfer an aliquot of this solution into the polarographic cell and run a d.c. polarogram between 0.40 and 0.00 V (*vs.* SCE). Deaeration is not required, but the temperature must be constant (25.0 ± 0.1°). Measure the current at 0.20 V. Run a blank solution.

Find the phosphorus concentration of the sample from a calibration graph constructed by use of known phosphate solutions under the same conditions.

Analysis of steel samples. Place a 0.1-g sample, accurately weighed, in a 250-ml Erlenmeyer flask. Add about 70 ml of hydrochloric acid (1 + 3) and a few drops of concentrated nitric acid (to ensure that all the phosphorus is in phosphate form). Heat until dissolution is complete, then add 2 ml of 20% hydroxylamine hydrochloride solution, and heat to boiling. Cool the solution, transfer it into a 100-ml standard flask and dilute to the mark with demineralized water. Analyse an aliquot of this solution according to the recommended procedure, using ethyl acetate as extractant.

RESULTS AND DISCUSSION

The proposed procedure involves several steps: (1) formation of 12-MPA in the aqueous phase, (2) extraction with an organic solvent and (3) and determination of the Mo(VI) by means of the indicator reaction. The Mo(VI) is determined by measurement of the catalytic reduction of hydrogen peroxide in the presence of Mo(VI). The mechanism of the reaction was proposed by Kolthoff and Parry[6] and can be briefly described as:

$$MoO_4^{2-} + H_2O_2 \xrightarrow[-H_2O]{} MoO_5^{2-} + 2H^+ + 2e^- \longrightarrow MoO_4^{2-} + H_2O$$
$$\uparrow \qquad\qquad +H_2O_2 \qquad\qquad \downarrow$$

Figure 1 shows the polarograms obtained for solutions which contain, respectively, Mo(VI), H_2O_2 and Mo(VI) + H_2O_2. In acidic media Mo(VI) gives three irreversible waves (curve a) between 0.10 and −0.90 V (*vs.* SCE), which have no analytical applications. Hydrogen peroxide is also reduced in acid media but at more positive potentials (curve b). When both species are present in the solution, a catalytic current appears at 0.20 V (curve c). If the current for the hydrogen peroxide reduction is subtracted from the catalytic current, a peak is obtained, the height of which depends on the Mo(VI) concentration, provided the pH and the peroxide concentration are constant.

A series of experiments with 0.5*M* sulphuric acid, $5 \times 10^{-6}M$ molybdate and various hydrogen peroxide concentrations was performed. Figure 2 shows the currents obtained, as well as the currents corresponding to the peroxide reduction. The latter became significant for peroxide concentrations higher than 0.02*M*, and therefore this value was chosen for use in the determination. The catalytic current is measured at 0.20 V (*vs.* SCE) and therefore prior deaeration of the solutions is not necessary.

An acidic medium is necessary for the catalytic current to be obtained. Nitric[7] and perchloric[8] acid also give catalytic waves with molybdate, but they are different from those studied here, and hence sulphuric acid was used. Figure 3 shows the effects produced by changing the sulphuric acid concentration. As can be deduced from this figure, a 0.20*M* sulphuric acid medium is optimal. The apparent shift in intercept with change in acidity is probably due to a shift in the distribution of the various isopolymolybdate species formed, and hence in the reaction with hydrogen peroxide.

Because of the catalytic nature of the process, the temperature is another important factor to take into

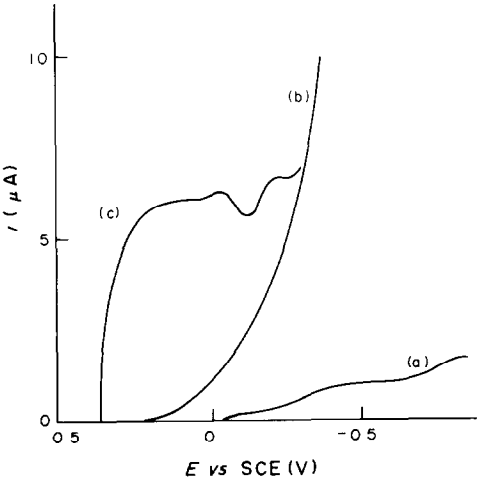

Fig. 1. Polarograms obtained for: (a) $5 \times 10^{-6}M$ Mo(VI); (b) 0.02*M* H_2O_2; (c) $5 \times 10^{-6}M$ Mo(VI) + 0.02*M* H_2O_2.

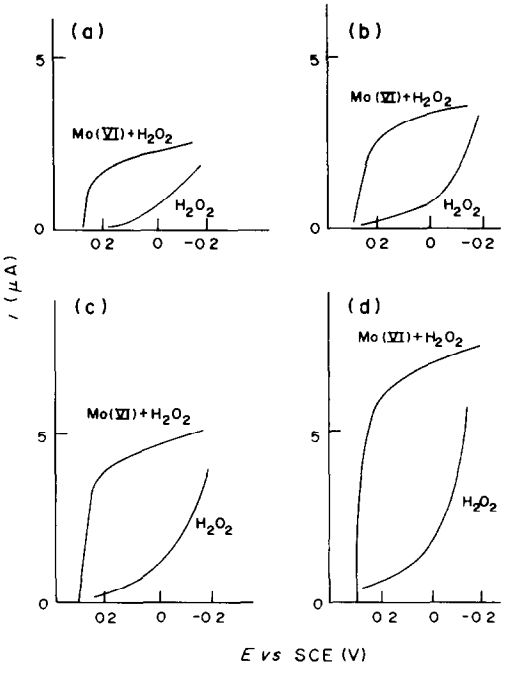

Fig. 2. Variation of wave height with H_2O_2 concentration, with [Mo(VI)] = $5 \times 10^{-6}M$, [H_2SO_4] = 0.5*M* (currents due to H_2O_2 alone are also given). [H_2O_2]: (a) 0.01*M*; (b) 0.02*M*; (c) 0.03*M*; (d) 0.04*M*.

account. A temperature coefficient of 5%/deg was obtained, high enough to require all polarograms to be run at constant temperature (25.0 ± 0.1°).

With all the significant parameters fixed, a calibration line for Mo(VI) can be constructed. It is linear from $7 \times 10^{-7}M$ to $1.3 \times 10^{-5}M$ molybdate. The presence of phosphate in the measurement medium affects neither the shape nor the height of the polarograms.

For formation of the 12-MPA an acidic medium and an excess of Mo(VI)[9] are required. This excess of molybdate is the reason for separation of the 12-MPA being necessary, so that only the molybdate present in the MPA is determined polarographically.

The optimum pH for formation of the 12-MPA is about 1.0 and is obtained with sulphuric acid. To find the optimum amount of Mo(VI) to form the heteropoly acid quantitatively, several solutions containing the same phosphate concentration ($5 \times 10^{-7}M$) and various excesses of Mo(VI) were extracted and stripped, and the aqueous extracts polarographed: use of more than 2 ml of 2% molybdate solution gave constant current. Therefore that amount was chosen, and provides a molybdate/phosphate ratio > 1000.

The efficiency of various organic solvents for extraction of 12-MPA has been discussed by several authors.[10-14] The main conclusion is that 12-MPA is best extracted with oxygen-containing solvents such as ethers and ketones. Various solvents were studied by us and the best results were obtained with ethyl acetate and methyl isobutyl ketone (MIBK), which provided extraction efficiencies of 94.6% and 78.5% respectively. The use of isobutyl acetate was rejected because of the low extraction efficiency (< 60%) and also because the results obtained varied very much with temperature. This last problem does not occur with ethyl acetate or MIBK. Only one extraction is used, and the pH is lowered after the formation of the 12-MPA but before its extraction, to provide the best efficiency.[3]

It is necessary to wash the organic phase with sulphuric acid and also to run a blank (for the whole procedure) alongside the standard phosphate solutions and the samples, because of the molybdic acid extracted with the 12-MPA.

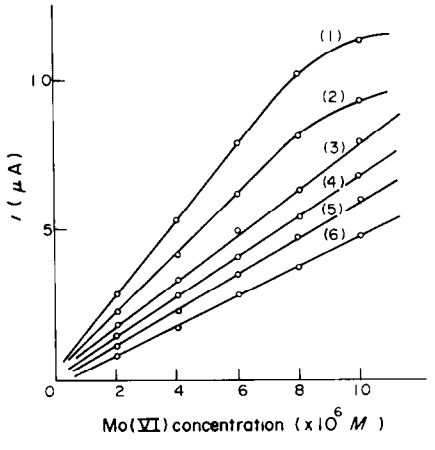

Fig. 3. Variation of the calibration graph for Mo(VI) with H_2SO_4 concentration ($[H_2O_2] = 0.02M$) $[H_2SO_4]$: (1) $0.10M$; (2) $0.15M$; (3) $0.20M$; (4) $0.25M$; (5) $0.35M$; (6) $0.55M$.

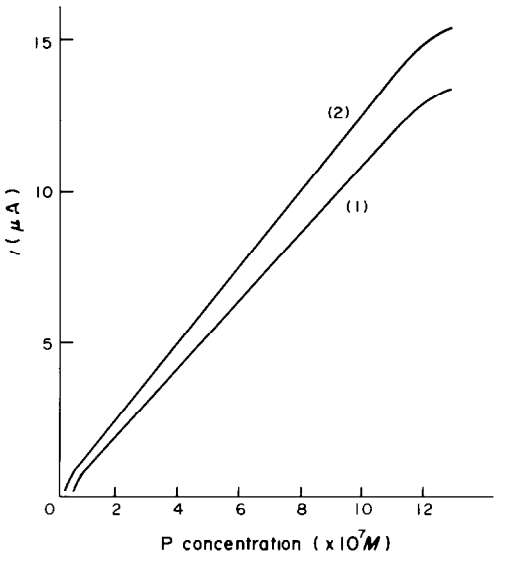

Fig. 4. Calibration graphs for phosphate. (1) MIBK as extractant; (2) ethyl acetate as extractant.

Before the polarographic analysis, the heteropoly acid is stripped into aqueous solution with sodium hydroxide solution. The pH of this extract is then adjusted to about 2.5 with sulphuric acid, which gives the correct conditions for the indicator reaction.

Figure 4 shows the calibration graphs for pure phosphate solutions with MIBK (curve 1) and ethyl acetate (curve 2) as extractants. Ethyl acetate is preferred since it gives a lower determination limit and a higher recovery of phosphate, *i.e.*, a greater slope of the calibration line. The "dip" at the lowest phosphorus concentrations is probably due to incomplete formation of the heteropoly acid. Interference may be expected from all those elements which form heteropoly acids with molybdate, that are extracted along with the 12-MPA and cause positive errors. To study this the recommended procedure was applied to solutions containing various concentrations of germanium, arsenic and silicon. More selective results were obtained by using ethyl acetate as extractant, and the concentrations of these elements at which no catalytic current was obtained (the tolerance limits), were respectively 5.5×10^{-7}, 9.6×10^{-6} and $6.0 \times 10^{-6}M$. If the concentrations of the interferents are higher than these limits, the method can still be applied by diluting the sample, provided the original molar ratio of interferent to phosphorus does not exceed 4:1 for Ge, 60:1 for As and 40:1 for Si.

PRACTICAL APPLICATIONS

Phosphate in drinking waters

Owing to the low concentrations of the interfering elements in this type of sample, the recommended

Table 1. Analysis of two standard chromium-manganese steels by applying the recommended procedure (ethyl acetate as extractant)

Sample	P certified, %	P found		
		Mean, %	Std devn., %	*n*
1	0.0215	0.0209	8×10^{-4}	7
2	0.0174	0.0173	1×10^{-4}	7

procedure can be applied directly, without modification. The result obtained (mean of 10 determinations) was $21.1 \pm 0.9\ \mu g/l.$ of phosphorus as phosphate, at a confidence level of 95%. The samples were also analysed by a routine spectrophotometric procedure,[15] with preconcentration by evaporation of 200 ml of sample to 10 ml in a polythene beaker. The result obtained was $24 \pm 3\ \mu g/l.$ (6 determinations, confidence level of 95%).

Phosphorus in steels

When the recommended procedure was applied directly to solutions of steel samples, low results were obtained. The reason may be formation of a mixed molybdate–iron(III)–phosphate complex[16] which is stable over a wide pH range. This complex can act in two ways: first by lowering the degree of formation of the 12-MPA (by competitive complex formation) and secondly by being less efficiently extracted than the 12-MPA.[3] The problem can be dealt with by reducing the iron(III) to iron(II) with hydroxylamine hydrochloride, before the extraction.

Table 1 shows the results obtained when the method was applied to two standard samples, with ethyl acetate as extractant. The interfering elements were at levels below their tolerance limits. The results agree very well with the certified values and confirm the validity of the proposed procedure, which provides greater sensitivity than previous methods.

REFERENCES

1. G. F Kirkbright, A. M. Smith and T. S. West, *Analyst*, 1967, **92**, 411.
2. D E Leyden, W. K. Nonidez and P. W. Carr, *Anal. Chem.*, 1975, **47**, 1449.
3. G. L. Pina, T. I. Thikomirova and E. N. Dorokhova, *Talanta*, 1981, **28**, 665.
4. A. G. Fogg and K. S. Yoo, *Anal. Lett.*, 1976, **9**, 1035
5. S. C. Hight, F. Bet-Pera and B. Jaselkis, *Talanta*, 1982, **29**, 721.
6. I. M. Kolthoff and E. P. Parry, *J. Am. Chem Soc.*, 1951, **73**, 5315.
7. M. G. Johnson and R. J. Robinson, *Anal. Chem.*, 1952, **24**, 366.
8. G. P. Haight, *ibid.*, 1951, **23**, 1505.
9. Z. Halász and E. Pungor, *Talanta*, 1971, **18**, 557.
10. C. Wadelin and M. G. Mellon, *Anal. Chem.*, 1953, **25**, 1668.
11. T. Kumamaru, Y. Otari and Y. Yamamoto, *Bull. Soc. Chem. Japan*, 1967, **40**, 429.
12. J Paul, *Mikrochim. Acta*, 1965, 833.
13. S. J. Simon and D. F Boltz, *Anal. Chem.*, 1975, **47**, 1758.
14. G. Linden, S. Turk and B. Tarodo de la Fuente, *Chim. Anal. Paris*, 1971, **53**, 244.
15. *Official Methods of Analysis of the Association of Official Analytical Chemists*, 12th Ed., A.O.A.C., Washington, 1975.
16. E. N. Dorokhova, Z. F. Shakova and L A. Sazanova, *Zh. Analit. Khim.*, 1966, **21**, 884.

Talanta, Vol. 30, No. 9, pp. 659–664, 1983
Printed in Great Britain

0039/9140/83 $3.00+0.00

DIFFUSION COEFFICIENTS AND COMPLEX EQUILIBRIA IN SOLUTION—III*

GRAPHICAL EVALUATION OF FORMATION CONSTANTS FROM DIFFUSION COEFFICIENTS

D. R. CROW
Department of Physical Sciences, The Polytechnic, Wolverhampton, England

(*Received* 28 *February* 1983. *Accepted* 24 *March* 1983)

Summary—The values of the individual diffusion coefficients of the complexes participating in a metal–ligand system of equilibria may be estimated when provisional values of the formation constants have been calculated from diffusion currents. In this paper a new graphical method, involving average diffusion coefficients observed for metal–ligand systems, is described. The method is applied to four such systems, chosen for the particular characteristics shown by them.

Once an approximate value for k, in the relation $\bar{n} = k\Delta i_d$, has been obtained and provisional values of formation constants established as described previously,[1] it is possible to obtain refined values by the use of mean diffusion coefficients of simultaneously diffusing complex and aquo ions. Graphs of $\log F_0'[X]$ *vs.* $\log[X]$ for the four systems reported on here are shown in Fig. 1. These give some indication of the variation in certainty of the value of k from system to system; some, such as the cadmium–thiourea and lead–thiourea systems, show quite clear linear limiting regions, while others, *e.g.*, the cadmium–benzimidazole and cadmium–allylthiourea systems, do not.

Although preliminary analysis, in terms of Δi_d data, may indicate the formation of (say) four complex species, it is by no means certain that this degree of co-ordination is developed, to the virtual exclusion of lower ones, in the region of the highest ligand concentrations used. However, a fair estimate may be made at this stage of the value of $\bar{n}$ at one or more of the higher *experimental* values of ligand concentration. This is achieved by insertion of the provisional values of the various formation constants (β_{MX_j}) into the relation

$$\bar{n} = \frac{\sum_0^N j\beta_{MX_j}[X]^j}{\sum_0^N \beta_{MX_j}[X]^j} \quad (1)$$

This allows estimation of $(\Delta i_d)_{max}$ for the condition that $\bar{n}$ approaches n_{max}, calculation of the limiting value of i_d at full co-ordination of the metal ion, and evaluation of D_{MX_N}. Since a linear relationship between $(D_{MX_j})^{1/2}$ and j has been established, all the D_{MX_j} values now follow and, as a consequence, so do the values of the functions $(\bar{D} - D_{MX_j})$ for all complexes over the entire ligand concentration range. An example will make this clear: from the preliminary formation-constant data reported earlier for the lead–thiourea system, the value of $\bar{n}$ at [thiourea] = 1.0M is 3.37. The value of Δi_d at this concentration is 2.59 μA. Thus, when $\bar{n} = n_{max} = 4$, $\Delta i_d = 3.07$ μA. Since in the absence of thiourea $i_d = 10.07$ μA, the limiting value of the diffusion current at $\bar{n} = 4$ must be 7.00 μA. Assuming that D_M may be taken as the infinite dilution value of 9.80×10^{-6} cm^2/sec at 25°, the capillary constant of the dropping electrode is estimated to be 3.217 mg$^{2/3}$. sec$^{1/6}$, and the limiting diffusion coefficient (D_{MX_4}) then becomes 4.74×10^{-6} cm^2/sec. It is now a straightforward matter to obtain, by interpolation, the diffusion coefficients of the species with co-ordination numbers from 1 to 3 (Table 1).

Once the individual values, D_{MX_j}, are known, it is possible to obtain values of $(\bar{D} - D_{MX_j})$ over the experimental range of ligand concentration and to apply directly the relationship

$$(D_M - \bar{D}) = (\bar{D} - D_{MX})\beta_{MX}[X] + \cdots + (\bar{D} - D_{MX_N})\beta_{MX_N}[X]^N \quad (2)$$

In a manner similar to that of Leden, the function G_1 may be defined as:

$$G_1 = \frac{(D_M - \bar{D})}{[X]} = (\bar{D} - D_{MX})\beta_{MX} + \cdots + (\bar{D} - D_{MX_N})\beta_{MX_N}[X]^{N-1} \quad (3)$$

Equation (3) implies that a graph of G_1 *vs.* [X] should produce an intercept on the G_1 axis of $(\bar{D} - D_{MX})\beta_{MX}$ as [X]→0. Now $(\bar{D} - D_{MX})$, in common with other such functions, varies very sharply with [X] at low values of this variable. Consequently, for many systems it is difficult to obtain a reliable value for the

*Part II—*Talanta*, 1982, **29**, 739.

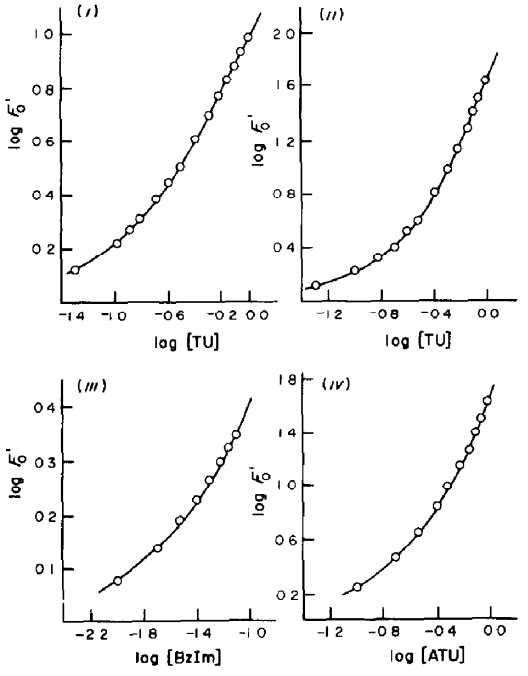

Fig. 1. Graphs of log $F_0'[X]$ *vs.* log [X]: (*i*) cadmium–thiourea, (*ii*) lead–thiourea (*iii*) cadmium–benzimidazole, (*iv*) cadmium–allylthiourea.

intercept. A graph showing less curvature is obtained by plotting values of G_1 against corresponding values of $(\bar{D} - D_{MX})$ appropriate to the ligand concentrations used. In practice, the limiting region of this graph, near to the values of $(\bar{D} - D_{MX})$ where [X] approaches zero, is almost linear and a small extrapolation to the value of $(\bar{D} - D_{MX})$ at [X] = 0 gives a good assessment of the value of $[G_1/(\bar{D} - D_{MX})]_{[X]=0}$, *i.e.*, of β_{MX}.

It is usually found that there is good agreement between the values of β_{MX} obtained by these means and by use of the pseudo-formation curve, even with a rather poor assessment of the constant, k, in the latter procedure. For example, in the case of the cadmium–thiourea system, the intercepts of the plots of $F_1'[X]^k$ *vs.* [thiourea] vary only from 15 for the lowest value of $k = 3$, to 25 for $k = 4$ (Table 2). It is in any case necessary to reconcile the values of β_{MX} obtained by the two methods. If the method under discussion does *not* give a β_{MX} value in essential agreement with that produced from the analysis of the pseudo-formation curve, it will almost certainly be necessary to revise the whole set of values of $(\bar{D} - D_{MX_i})$ functions. The case of the cadmium–allylthiourea system demonstrates this well. However, for most systems so far studied by these means,

Table 1. Values of diffusion coefficients of complexes present in the lead–thiourea system [607 $nm^{2/3}t^{1/6}C = 3.217 \times 10^{-3}\,mg^{2/3}.sec^{1/6}.mol.l^{-1}$; $i_d([X] = 0) = 10.07\ \mu A$]

Species	M	MX	MX_2	MX_3	MX_4
D, $10^{-6}\ cm^2/sec$	9.80	8.36	7.04	5.83	4.74

Table 2. Variation of the intercepts of the $F_1'[X]^k$ vs. [thiourea] plots for the cadmium–thiourea system

k	3.0	3.4	3.5	3.63	3.7	4.0
Intercept (β_{MX})	15	18	20	20	22	25

the required agreement is met, a fact giving ground for confidence both in the values of $(\bar{D} - D_{MX_i})$ used and in the means by which they are estimated.

Values of a new function, G_2, at each ligand concentration may now be calculated; G_2 is defined as

$$G_2 = \frac{G_1 - (\bar{D} - D_{MX})\beta_{MX}}{[X]} = (\bar{D} - D_{MX_2})\beta_{MX_2} + \cdots + (\bar{D} - D_{MX_N})\beta_{MX_N}[X]^{N-2} \quad (4)$$

It is perhaps worth stressing at this point that since values of the function $(\bar{D} - D_{MX})$ are now known with fair reliability over the whole range of [X] values (either by confirmation through the β_{MX} value obtained, or by reassessment by using the value of β_{MX} derived from the pseudo-formation curve) it follows that $(\bar{D} - D_{MX_2}) \ldots (\bar{D} - D_{MX_N})$ are known with equal reliability. A graph may now be plotted of G_2 *vs.* $(\bar{D} - D_{MX_2})$; the intercept at the value of $(\bar{D} - D_{MX_2})$ corresponding to [X] = 0 yields the value of β_{MX_2} directly. Also, a plot of G_2 *vs.* [X] gives, in principle, an intercept equal to $(\bar{D} - D_{MX_2})\beta_{MX_2}$ at [X] = 0 zero. Again, the first graph, being approximately linear in the important region, is preferable to the second, which may well show even steeper curvature than the G_1 plot.

It should be noted that, in defining G_2 (and subsequent similar functions), it is the value of the *varying* function $(\bar{D} - D_{MX})\beta_{MX}$, [or in subsequent functions, $(\bar{D} - D_{MX_2})\beta_{MX_2}$ etc.] *at each value of* [X] that is subtracted from G_1 before division by [X]. In this respect the technique differs from that of Leden[2] and introduces the advantage that the increased scatter of points for the higher derived functions, and the cumulative uncertainties, are of less significance than in that method.

It can easily be seen that the final function, G_N, is given by

$$G_N = \frac{G_{N-1} - (\bar{D} - D_{MX_{N-1}})\beta_{MX_{N-1}}}{[X]} = (\bar{D} - D_{MX_N})\beta_{MX_N} \quad (5)$$

It clearly follows from equation (5) that $G_N/(\bar{D} - D_{MX_N})$ should be constant and equal to β_{MX_N}.

EXPERIMENTAL

Most of the data used in the present paper derive from experimental results reported or quoted earlier.[1,3] For the cadmium–allylthiourea system (for which there appear to be no published formation-constant data) values of diffusion currents were obtained manually at 25° from individually plotted polarograms. The working solutions were $5 \times 10^{-4}M$ in Cd^{2+}, $0.1M$ in potassium nitrate and had

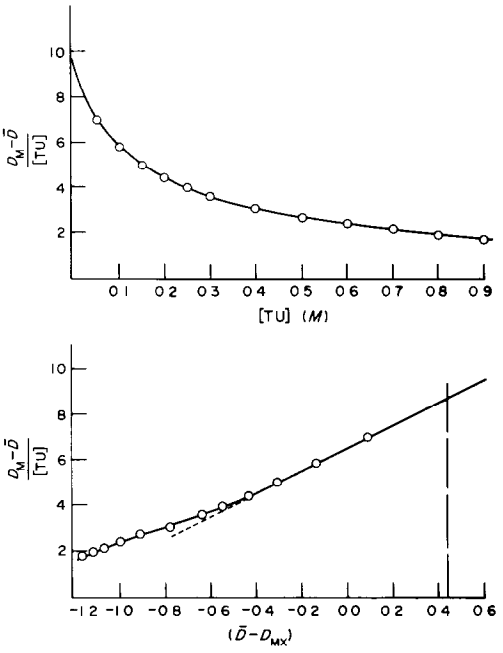

Fig. 2. G_1 plots for the cadmium–thiourea system: (*i*) G_1 *vs.* [TU]; intercept ~8.5–9.5; (*ii*) G_1 *vs.* $(\bar{D} - D_{MX})$;

$$[G_1]_{[TU]=0} \atop {(\bar{D}-D_{MX})=0.44} \Big\} = 8.80.$$

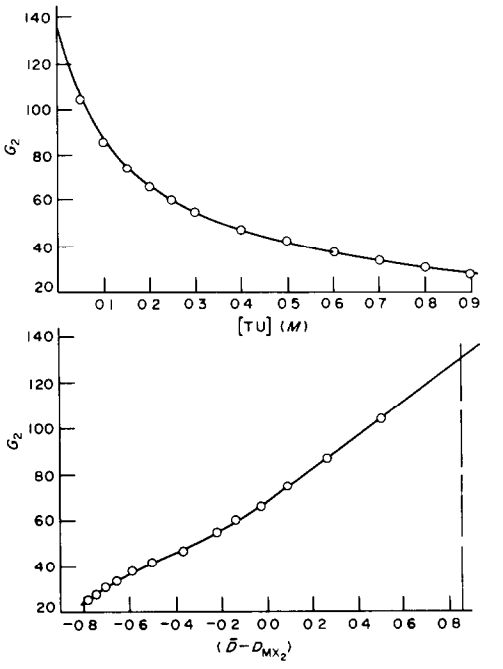

Fig. 3. G_2 plots for the cadmium–thiourea system: (*i*) G_2 *vs.* [TU]; intercept ~130–140; (*ii*) G_2 *vs.* $(\bar{D} - D_{MX_2})$;

$$[G_2]_{[TU]=0} \atop {(\bar{D}-D_{MX_2})=0.85} \Big\} = 135.$$

allylthiourea concentrations varying from zero to 1.0M; all solutes were of analytical grade. This system is the first showing irreversible electrode reactions that has been investigated by means of $\bar{D}$ data according to the method described.

RESULTS AND DISCUSSION

Cadmium–thiourea

Values of the $(\bar{D} - D_{MX_j})$ functions, together with those of the functions G_1–G_4, are collected in Table 3.* Graphs of significance in the analysis of the data are collected in Figs. 2–5.

It is seen that the values of the first three overall formation constants agree favourably with those estimated previously; the value of the highest constant is, however, considerably lower than that obtained from the pseudo-formation curve, but agrees favourably with the value reported by Migal and Tsiplyakova[4] for media of rather lower ionic strength than that used here.

Constancy of the value of $G_4/(\bar{D} - D_{MX_4})$ was not obtained at ligand concentrations above 0.4M, although the final graph appears to allow a fairly unambiguous assessment of β_{MX_4}.

*In this and subsequent analyses, the factor of 10^{-6} is omitted from G, $\bar{D}$ and $(\bar{D} - D_{MX_j})$ data; this is a matter of convenience since the factor may be eliminated from both sides of equations (3)–(5).

Table 3. Plotting functions and other data required for the calculation of the value of formation constants in the cadmium–thiourea system (G and D values have units of 10^{-6} cm^2/sec)

[TU], M	$\bar{D}$,	G_1	$(\bar{D} - D_{MX})$,	G_2	$(\bar{D} - D_{MX_2})$,	G_3	$(\bar{D} - D_{MX_3})$,	G_4	$(\bar{D} - D_{MX_4})$,	$G_4/(\bar{D} - D_{MX_4})$
0.0	7.20		0.44		0.85		1.25		1.65	
0.05	6.85	7.00	0.09	104.0	0.50	490	0.90	1520	1.30	1169
0.10	6.62	5.80	−0.14	86.0	0.27	431	0.67	1230	1.07	1149
0.15	6.45	5.00	−0.31	74.7	0.10	392	0.50	1080	0.90	1200
0.20	6.32	4.40	−0.44	66.0	−0.03	354	0.37	920	0.77	1195
0.25	6.21	3.96	−0.55	59.8	−0.14	328	0.26	832	0.66	1261
0.30	6.12	3.60	−0.64	54.7	−0.23	304	0.17	753	0.57	1321
0.40	5.98	3.05	−0.78	46.6	−0.37	264	0.03	625	0.43	1453
0.50	5.85	2.70	−0.91	41.8	−0.50	243	−0.10	578	0.30	1927
0.60	5.76	2.40	−1.00	37.3	−0.59	219	−0.19	510	0.21	—
0.70	5.69	2.16	−1.07	33.7	−0.66	198	−0.26	454	0.14	—
0.80	5.64	1.95	−1.12	30.4	−0.71	179	−0.31	403	0.09	—
0.90	5.60	1.78	−1.16	27.8	−0.75	163	−0.35	360	0.05	—
1.00	5.57	1.63	−1.19	25.4	−0.78	149	−0.38	324	0.02	—

$\beta_{MX} = 20 \pm 2$; $\beta_{MX_2} = 159 \pm 30$; $\beta_{MX_3} = 460 \pm 100$; $\beta_{MX_4} = 1164 \pm 200$.

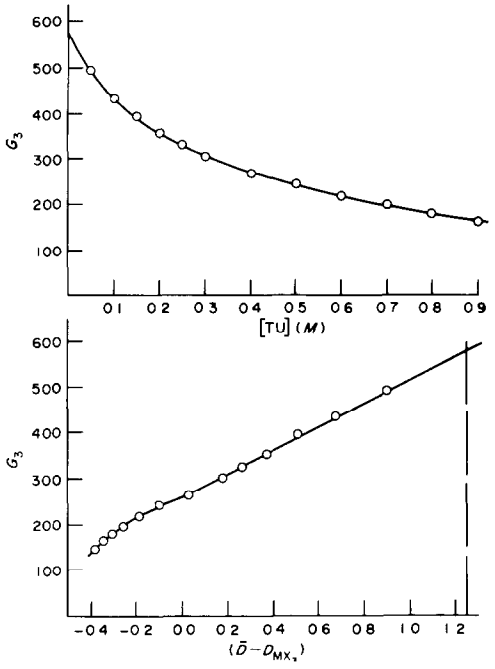

Fig. 4. G_3 plots for the cadmium–thiourea system: (*i*) G_3 *vs.* [TU]; intercept ~ 550–600; (*ii*) G_3 *vs.* $(\bar{D} - D_{MX_3})$;

$$[G_3]_{\substack{[TU]=0 \\ (\bar{D}-D_{MX_3})=1.25}} = 575.$$

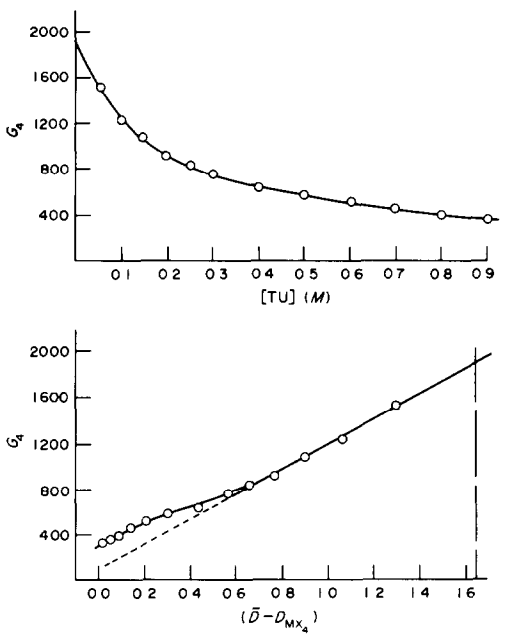

Fig. 5. G_4 plots for the cadmium–thiourea system: (*i*) G_4 *vs.* [TU]; intercept ~ 1800–2000; (*ii*) G_4 *vs* $(\bar{D} - D_{MX_4})$.

$$[G_4]_{\substack{[TU]=0 \\ (\bar{D}-D_{MX_4})=1.65}} = 1920.$$

limiting slope = 1160.

Lead–thiourea

The analysis was done in the same way as for cadmium with the same ligand. The results obtained are included with others for comparison purposes in Table 4. In this case an analysis using an alternative set of $(\bar{D} - D_{MX_3})$ data yielded values of $G_4/(\bar{D} - D_{MX_4})$ which showed better constancy, the variation being from 71 to 110 over the whole range of ligand concentration (0.1–1.0*M*).

Cadmium–benzimidazole

This is a case where to infer the value of the proportionality constant between Δi_d and $\bar{n}$ from the limiting slope of the log $F_0'[X]$ *vs.* log [X] graph would

Table 4. Overall and stepwise formation constants for the lead–thiourea system, obtained by five methods

	β_1	β_2	β_3	β_4
a	6	13	90	109
b	6	30	40	100
c	7.1	23	45	80
d	7.3 ± 1	24 ± 4	53 ± 10	90 ± 20
e	4	11	95	110
	k_1	k_2	k_3	k_4
a	6	2.7	6.9	1.2
b	6	5	1.3	2.5
c	7.1	3.2	2	1.8
d	7.3	3.3	2.2	1.7
e	4	2.8	8.6	1.2
	k_2/k_1	k_3/k_2	k_4/k_3	
a	0.45	2.6	0.17	
b	0.83	0.26	1.92	
c	0.45	0.63	0.9	
d	0.45	0.66	0.77	
e	0.70	3.07	0.14	

a From pseudo-formation curve.
b From pseudo-formation curve (alternative treatment).
c From $(\bar{D} - D_{MX_i})$ data.
d From alternative $(\bar{D} - D_{MX_i})$ data.
e From the shift in half-wave potential.

Table 5. Comparison of the values of overall formation constants of complex species present in the cadmium–benzimidazole system at 25°

Method	β_1	β_2	β_3
$\Delta E_{1/2}$ (DeFord and Hume)	85	2.8×10^3	1.55×10^4
Pseudo-formation curve	85	2.8×10^3	1.65×10^4
$(\bar{D} - D_{MX_i})$ functions	94 ± 10	$2.8 \pm 0.2 \times 10^3$	$1.59 \pm 0.04 \times 10^4$

be grossly misleading. There is *nothing* to tell us that *three* complexes are formed—except independently determined half-wave potential data—and it is the object of the present exercise *not* to depend upon these.

Graphical treatment of the $F_0'[X]^k$, [X] data for a range of values of k, according to the method described in Part II, leads to the conclusion that k is ~ 4.3. This value provided three formation-constant values agreeing well with those obtained previously from half-wave potentials. Calculation of the effective value of $\bar{n}$ for the highest benzimidazole concentration used ($0.08M$), in terms of the β values obtained from the pseudo-formation curve, gave $\bar{n}$ as ~ 1.9. This figure, combined with Δi_d data, made it possible to generate values for the diffusion coefficients of the various species. Analysis in terms of $(\bar{D} - D_{MX_i})$ functions gave values for the formation constants which agreed favourably with those obtained earlier (Table 5).

Cadmium–allylthiourea

The apparent symmetry of the pseudo-formation curve might suggest that the maximum co-ordination number for this system is 2.[5] Since for this case it seemed that a limiting value of $\bar{D}$ was clearly indicated, from the observed trend in diffusion currents, it was initially assumed that this (2.92×10^{-6} cm^2/sec) approximated to D_{MX_2}; D_{MX} was estimated accordingly, and analysis in terms of the supposed $(\bar{D} - D_{MX})$ and $(\bar{D} - D_{MX_2})$ functions was attempted without recourse to any manipulation of the pseudo-formation curve data. This approach proved to be quite incorrect on two counts; the maximum co-ordination number is, in fact, 4 and not 2, and the limiting value of $\bar{D}$ is not so obvious as it might appear. Consequently, the graph of G_2 *vs.* $(\bar{D} - D_{MX_2})$, as initially conceived, showed no linear limit and nothing approaching constancy of values for the function $G_2/(\bar{D} - D_{MX_2})$ over the ligand concentration range.

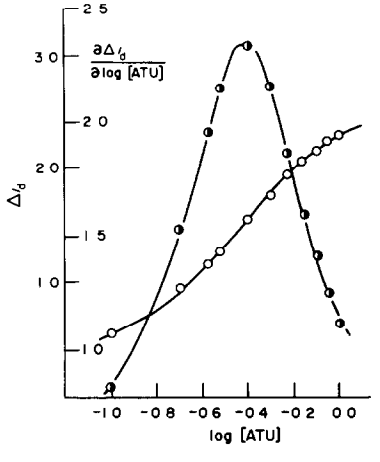

Fig. 6. Pseudo-formation curve (○) and its derivative (◑) for the system cadmium–allylthiourea. The apparent symmetry of the curves masks the fact, shown by detailed analysis, that $N = 4$.

Subsequent analysis of the data of the pseudo-formation curve, using a value of 1.69 for k, revealed the existence of *four* complex species with the following provisional values for their overall formation constants: $\beta_1 = 10$; $\beta_2 = 40$; $\beta_3 = 80$; $\beta_4 = 360$. Once again, the value of β_4, as obtained by this provisional assessment, is noticeably higher than would be expected in terms of the preceding sequence of β_1–β_3 values. Such an overestimate seems to be a fairly common feature of all analyses based on integration of formation curves.

An initial analysis with $(\bar{D} - D_{MX_i})$ functions (and the following values for the diffusion coefficients: $D_{MX} = 6.25 \times 10^{-6}$; $D_{MX_2} = 5.02 \times 10^{-6}$; $D_{MX_3} = 3.92 \times 10^{-6}$; $D_{MX_4} = 2.92 \times 10^{-6}$ cm^2/sec) proved to be unsatisfactory. Formation-constant values $\beta_1 = 15$, $\beta_2 = 81$, $\beta_3 = 225$ were generated, but the value of β_4 was quite indefinable. The apparent values of $G_4/(\bar{D} - D_{MX_4})$ varied from 426 at $0.1M$ ligand concentration to 6043 at $1.0M$! The large discrepancy between the two values of β_1 (one derived from the pseudo-formation curve and the other from the preliminary values of $D_{MX} - D_{MX_4}$) given above), was a particularly obvious feature of this system. This discrepancy suggested that the value of $(\bar{D} - D_{MX})$ at [X] = 0 which had been used to generate $\beta_1 = 15$, was significantly lower than its true value and implied that the whole range of values of $(\bar{D} - D_{MX_i})$ required reassessment. Fortunately, in this case it was fairly clear that the intercept of the plot of $(\bar{D} - D_{MX})/[X]$ *vs.* [X] was 14.1, so if the value $\beta_1 = 10$ obtained from the pseudo-formation curve is taken to be reliable (and there would now seem to be sufficient precedents for assuming this) then $(\bar{D} - D_{MX})_{[X]=0} = 1.41$. This value contrasts markedly with the initially assessed value of 0.95. The whole set of $(\bar{D} - D_{MX_i})$ functions was recalculated on this basis. A much more satisfactory analysis was now possible, which finally yielded the data $\beta_1 = 10$; $\beta_2 = 40$; $\beta_3 = 89$; $\beta_4 = 110$. The limiting region of the G_4 *vs.* $(\bar{D} - D_{MX_4})$ graph was clearly linear with a slope of 110, the limiting value of $G_4/(\bar{D} - D_{MX_4})$ at [X] = 0 was 109, and the

values of the function over the whole ligand concentration ranged varied only between 109 and 250.

CONCLUSIONS

In general there is a tendency for analysis by means of a pseudo-formation curve to give a value for the formation constant of the highest complex which is considerably higher than that obtained from mean diffusion coefficients.

Uncertainty in assessing the value of the highest formation constant would seem to be considerably reduced by means of the graphical treatment described. Ideally, the value of $G_N/(\bar{D} - D_{MX_N})$ should remain constant with variation in concentration of the ligand. The more nearly this is the case in practice, the more nearly correct the experimental and derived data may be considered to be. Thus, though for the cadmium–thiourea system there is a clear limiting slope and intercept, the values of $G_4/(\bar{D} - D_{MX_4})$ show a clear upward trend for ligand concentrations in excess of $0.4M$ (below which the values vary more randomly) and suggest that the experimental diffusion currents are too low. This could well be so since the values were estimated from a curve drawn through a comparatively small number of somewhat scattered points. For the lead–thiourea system the situation is improved, the values of $G_4/(\bar{D} - D_{MX_4})$ increasing regularly but over a small range. For the cadmium–benzimidazole system the overall trend of values of $G_3/(\bar{D} - D_{MX_3})$ is *downwards* (from 15,900 to 11,660) with increase in concentration of benzimidazole, but the variation is random in the lower half of the concentration range. The comparatively small overall decline suggests a small underestimate in the shifts of current. From the analysis described for the cadmium–allylthiourea system, it is clear that the smaller the variation in $G_4/(\bar{D} - D_{MX_4})$, the more realistic is the calculated value of β_4 likely to be. Even in the most successful analyses, however, the departures from constancy occur in the region of ligand concentration where currents approaching the limiting value are encountered; quite small errors in values of $(\bar{D} - D_{MX_j})$ functions can induce large changes in the ratios considered. Fortunately the analysis described is able to include data for low ligand concentrations in its treatment of all derived G functions, and this provides a tempering of the uncertainties.

It is found that the method outlined produces a sequence of values of both overall and stepwise constants which is generally in line with expectation and there is found to be greater consistency in the values of k_2/k_1, k_3/k_2, *etc.* There remain problems associated with the production of the initial current data, an aspect to be considered in some detail in Part IV.

REFERENCES

1. D. R. Crow, *Talanta*, 1982, **29**, 733, 739.
2. I. Leden, *Z. Phys. Chem., Leipzig*, 1941, **188**, 160.
3. D. R. Crow, *J. Electroanal. Chem. Interfac. Electrochem.*, 1968, **16**, 137.
4. P. K. Migal and V. A. Tsiplyakova, *Russ. J. Inorg. Chem.*, 1963, **8**, 319; 1964, **9**, 333.
5. L. G. Sillén, *Acta Chem. Scand.*, 1956, **10**, 186.

Talanta, Vol 30, No. 9, pp 665–676, 1983
Printed in Great Britain.

0039/9140/83 $3 00+0.00

THE DEVELOPMENT OF SAMPLING AND GAS CHROMATOGRAPHY–MASS SPECTROMETRY ANALYTICAL PROCEDURES TO IDENTIFY AND DETERMINE THE MINOR ORGANIC COMPONENTS OF LANDFILL GAS

B. I. BROOKES*
Regional Chemist's Department, Strathclyde Regional Council, 8 Elliot Place, Glasgow, Scotland

P. J. YOUNG
Waste Research Unit, Building 146.3, Harwell Laboratory, Oxfordshire, England

(*Received* 17 *February* 1983. *Accepted* 21 *March* 1983)

Summary—Modified drive-in piezometers provided quick and inexpensive probes to give access to the undiluted landfill gas below ground level. Samples collected on Tenax GC and Porapak Q adsorption tubes were thermally desorbed and injected into a gas chromatograph through a cold trap. Aqueous condensate samples were injected directly by syringe. Chromosorb 101, Tenax GC and Triton X100/KOH packed columns, and an SE30 capillary column were used, together with full-scan and selective-ion mass spectrometry. Limits of detection, all less than 1 mg/m^3, and calibration correlation coefficients were determined for the least tractable components, *i.e.*, free acids, amines and alcohols. A detection limit of 0.1 mg/m^3, based on anisole as internal standard, was estimated for all other compounds. The standard deviation for the whole procedure, with full-scan mass spectrometry, was $\pm 55\%$ of the mean. A large part of this was due to an instrumental error, standard deviation = 33% of the mean, that was inherent in the manual operation of the mass-spectrum chart-recorder. These procedural errors were insignificant in comparison with the variations caused by the type of site and the age of the fill.

All wastes disposed of by landfill release decomposition products to the atmosphere. The production of the major components of landfill gas such as methane and carbon dioxide is now well documented,[1,2] but there are very few data on the many other compounds released. Landfill odours are widespread and undesirable, and recent concern has been directed at possible long-term health risks associated with the gas. The object of this research, funded by the Department of the Environment, was an initial survey of the minor components in landfill gas, and to relate the results to the presence of odours and to the recommended limits for toxic vapours.[3] This paper describes the gas chromatography–mass spectrometry (GC/MS) methods that have been developed to identify and determine the constituents in the gas, and the validation of their use.

EXPERIMENTAL

Sampling probes

Methane production within landfills has been studied for several years but the probes conventionally in use for extracting the gas have the following disadvantages for the monitoring of vapours.

(*a*) The pipes are wide, >100 mm, and their insertion requires the excavation of pits or the preparation of boreholes, which is time-consuming and expensive.

(*b*) This process disturbs the fill adjacent to the pipe and may cause significant ingress of air below ground, and disturbance of the local microbiological fauna. Although reliable measurements of methane can be made within a few days of installation, it cannot be assumed that a representative vapour sample will be obtained, even within the lifetime of the probe.

To overcome these difficulties, "Casagrande" drive-in piezometers, from Soil Instruments Ltd., have been adapted for use as probes. Each one has a conical tip and a cadmium-plated mild steel pipe which is perforated over a length of 300 mm. Further lengths of galvanized iron pipe can be added and the whole hammered into the waste with a post-hammer. Before use the perforated tips are degreased, rinsed with acetone, dried at 100°, cleaned with compressed air and sealed in polythene until required. The pipes are also cleaned and sealed in polythene. The insertion of the probe is quick and inexpensive, and it is possible to drive in several pipes on each site and check the evolution of gas from each before deciding which to sample. Probes can be inserted to depths up to 4.3 m. No problems of air ingress need be encountered even at depths of only 1 m below ground level.

Sampling procedures

Figure 1 shows a schematic diagram of the apparatus. The full trapping procedure employs three Tenax GC adsorption tubes, two Porapak Q adsorption tubes and a condensate trap, as summarized in Table 1. The use of

*To whom correspondence should be addressed.

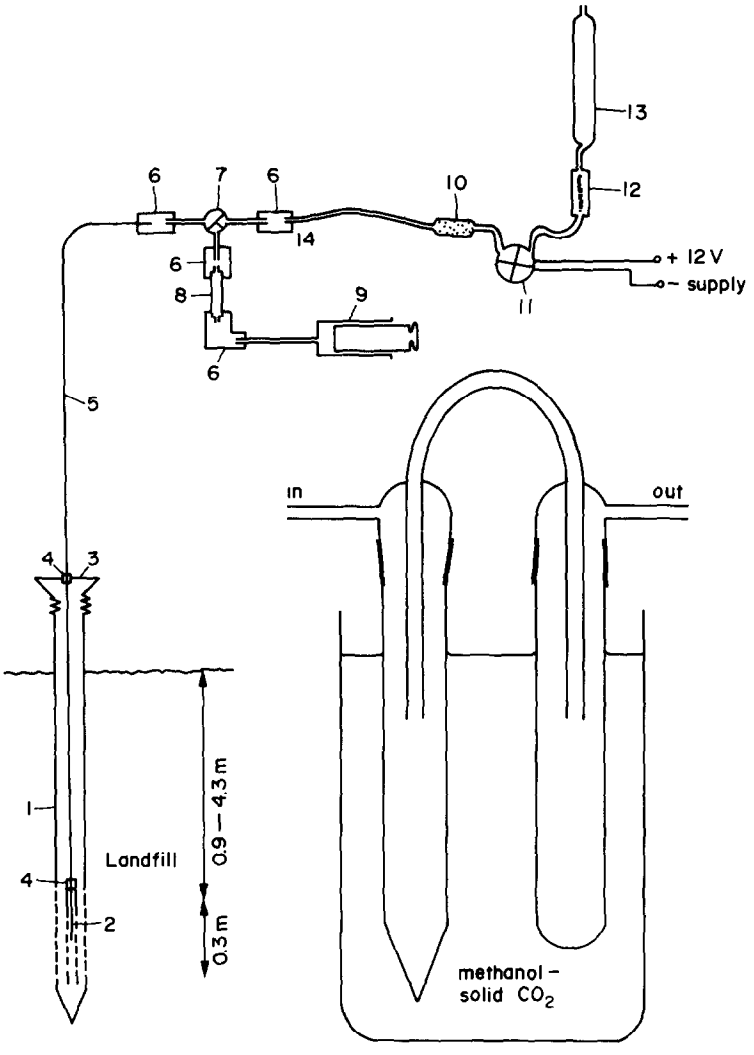

Fig. 1. Schematic diagram of sampling apparatus (not to scale); condensate trap shown in inset. 1. Piezometer probe. 2. Perforated aluminium sample line guard. 3. Threaded probe cap. 4. PVC seal coated with PTFE tape. 5. PTFE sampling tube (3 mm o.d. × 5 m). 6. Chemcon PTFE compression coupling. 7. PTFE/glass T-tap. 8. Adsorption tube, either Porapak Q in solid CO_2 or Tenax GC at ambient temperature. 9. Glass syringe. 10. Activated carbon adsorption tube. 11. Diaphragm pump. 12. Rotameter. 13. Bubble flowmeter. 14. Position for insertion of grab samplers and condensate trap (inset).

Table 1. A summary of the sampling and analytical techniques

Trap	Gas volume, *l.*	Chromatography column	Objective
Tenax GC at ambient temperature	0.025	SE30 Capillary	non-polar species and a general "fiingerprint"
Porapak Q at −80°C	0.1	Chromosorb 101	acid and neutral compounds and low molecular-weight compounds
Condensate trap at −80°C	7.5	(*i*) Chromosorb 101	water-soluble acidic and neutral compounds
		(*ii*) Tenax GC	water-soluble basic and neutral compounds
		(*iii*) Triton X100/KOH	water-soluble basic and neutral compounds

Tenax GC as a general-purpose trapping medium has been widely reported.[4-6] The tubes used here have 0.13 g of 60/80 mesh beads packed in a 6-mm o.d. glass tube. The inlet is terminated with 1-mm bore glass tubing to prevent back-diffusion during sampling. The Porapak Q tubes are made from 12 mm o.d. stainless steel, terminated with 6 mm o.d. inlets and outlets, and packed with 1 g of the 60/80 mesh beads. Adsorption tubes are purged before use with a flow of pure nitrogen at 170° for 1 hr. Tenax GC tubes are prestandardized by injection of 1 μl of methanol containing 25 ng of anisole, according to the method of Brookes;[7] most of the methanol is removed by purging with pure nitrogen at room temperature for 5 min at a flow-rate of 200 ml/min. Anisole is particularly suitable as an internal standard because it has a distinctive mass spectrum and middle of the range volatility, and is only rarely found in environmental samples. The Porapak Q tubes are not prestandardized.

The condensate trap is of all-glass construction, with two limbs connected in series by conical joints (see inset in Fig. 1). The limbs are immersed in a bath of methanol and solid carbon dioxide (at $-80°$) during sampling. The total-liquefaction procedure developed by Rasmussen[8] and Penkett[9] for sampling normal atmospheres by total condensation of a whole-air sample at liquid-nitrogen temperature was considered as an alternative to the condensate trap, but rejected because of the risk of producing an explosive mixture of liquid methane and oxygen. Such a technique could also encounter procedural difficulties with landfill gases containing hydrogen, which does not condense at liquid-nitrogen temperature.

Traps and tubes are sealed with stainless-steel Swagelok closures fitted with PTFE ferrules.

Bulk gas samples are collected in stainless-steel grab samplers for methane, carbon dioxide, hydrogen, oxygen, nitrogen and hydrogen sulphide analysis.

The following sampling procedures have been adopted.

The best probe with respect to gas generation and location is selected. The PTFE tube, with the aluminium guard in place, is lowered into position and the probe sealed with the screw cap. Throughout the sampling procedure gas is drawn through the PTFE tube by means of the diaphragm pump. Small sample volumes are drawn from the main flow at the T-tap, but large volumes, *i.e.*, more than 500 ml, are sampled by connecting the trap into the main flow line.

Gas sampling. A preliminary methane measurement is made with a "Gascoseeker" or other portable thermal-conductivity instrument, and further measurements are made at regular intervals to ensure that all sampling operations proceed at rates lower than the rate of gas production in the probe. A fall in the methane level indicates that the sample abstraction rate is too high.

For chromatographic gas analysis, a grab sampler is connected in the main gas flow and sufficient gas is drawn through to displace the air completely.

Tube sampling. A volume of 25 ml of gas is drawn through a Tenax GC tube at ambient temperature, with a syringe. When a Porapak Q tube is used for sampling, the second half of its length is covered with powdered solid carbon dioxide to cool it to $-80°$, then 100 ml of gas are sampled.

Condensate sampling. A volume of 7.5 litres of gas is drawn through the trap (which is kept at $-80°$) at flow-rates of up to 250 ml/min.

Analysis

No adverse effects have been observed from storage of samples at room temperature, but it is better to store the samples in solid carbon dioxide until needed for analysis.

Samples are recovered from the Tenax GC tubes by desorption at 160° for 13 min, and transferred with a helium flow of 10 ml/min into a 3 mm o.d. stainless-steel trap at liquid-nitrogen temperature (in this work an automated instrument supplied by GN Instrumentation Consultancy Ltd. was used). The sample is flash-vaporized at 200°, and passes through a 10:1 splitter into a 50 m × 0.3 mm i.d. SE30 capillary column programmed for heating from 0 to 120° at 4°/min. The sub-ambient temperatures are achieved initially by pouring liquid nitrogen into a tray of the GC oven. When the nitrogen has evaporated, the subsequent rise in temperature can be controlled in the usual way by the temperature programmer. The column used in this work had a high phase-loading on a deactivated glass capillary and was supplied by GC2 Chromatography Ltd., Cheshire. The eluate from the column is passed directly into a VG Micromass MM16F mass spectrometer, operated in the full-scan mode from $m/z = 34$ to $m/z = 230$, at 1 scan/sec. The mass spectra are recorded on an SE Laboratories Ltd. UV chart-recorder with manual push-button control, but this operation interrupts the chromatograph record for 5 sec and frequently cuts off the top of a GC peak. This is referred to as "peak chopping".

The Porapak Q tubes are cooled to $-80°$ before removal of the closures, to prevent the pressure inside the tube from expelling the contents. The samples are desorbed as from the Tenax GC tubes but with a helium flow of 20 ml/min, and are flash-vaporized directly into a 1 m × 2 mm i.d. 80/100 mesh Chromosorb 101 column at 50°. The temperature is programmed to rise at 10°/min to 230°, starting 2 min after the injection. The column is connected to the mass spectrometer through a jet separator, and initially the instrument scans from m/z 22 to 220 every 1.5 sec. The scan range is adjusted to $m/z = 34$–230 after 5 min, by which time the very low molecular-weight compounds have been eluted.

The condensate trap should be stored in solid carbon dioxide. Before its analysis, the sample is condensed into the bottom of the first limb. A 1-μl injection of the aqueous condensate is analysed on the Chromosorb 101 column, by the same operating procedure as for the Porapak Q adsorption tube samples.

Basic compounds are determined by direct injection of 1 μl into a 1 m × 2 mm i.d. 60/80 mesh Tenax GC column at 50°, programmed to rise in temperature to 200° at 10°/min, starting 2 min after the injection. The mass spectrometer is operated in the same way as for the analyses on the Chromosorb 101 column. After these analyses, the volume of condensate may be determined gravimetrically.

All of these analyses were terminated at elution of naphthalene.

Selective ion-monitoring. Isothermal chromatography, with sample injection at higher temperatures, gives improved sensitivity and reproducibility for polar compounds, but results in a crowded chromatogram, and selective ion-monitoring is required to distinguish the compounds of interest. Some procedures which can be used are given below.

(*a*) Carboxylic acids are analysed on the Chromosorb 101 column by monitoring (1-sec cycle) the fragment ions with m/z 45, 46 and 60. The tube sample, or 2 μl of condensate, is injected at 160°.

(*b*) Most low molecular-weight amines can be analysed on a Triton X100/KOH column by monitoring (1-sec cycle) the ions with $m/z = 31$, 30, 45 and 44. One μl of condensate is injected at 110°. The column used in this work is a modification of that described by Keay and Hardy[10] and contains two packing materials with the following compositions: (1) Silocell C22 (80–100 mesh), 40 g; Triton X100, 10 g; potassium hydroxide (analytical grade), 1.4 g; (2) Silocell C22 (80–100 mesh), 20 g; Triton X100, 5 g; potassium hydroxide (analytical grade), 4.2 g. A 1 m × 3 mm i.d. column is filled to within 9 cm of the inlet with packing (1), and the remainder is filled with packing (2).

Calibration procedures

All peak heights from the analysis of a Tenax GC tube sample are recorded relative to the peak height for the anisole internal standard. Specific response factors relative

to anisole are determined either by sampling and analysing standard atmospheres produced in the atmosphere generator described by Brookes,[11] or by direct injection of standard solutions. The second method is not suitable for compounds giving peaks which would be obscured by a solvent peak. For analysis of other samples separate standards are injected and analysed before each sample.

All of the non-polar compounds listed in Table 6 have been shown to have response factors similar to that of anisole, and approximate concentrations ($\mu g/m^3$) for such compounds are calculated by using the expression $25\ h/h_a V$, where h and h_a are the peak heights for the compound and anisole, respectively, V is the sample volume (in litres) and 25 ng of anisole are used as internal standard.

For compounds for which this expression is unlikely to be satisfactory, and for all selective ion-monitoring analyses, calibration is done with the most appropriate standards available—usually the compounds themselves.

RESULTS AND DISCUSSION

Reproducibility

The reproducibility of the technique and the regularity of the gas emission was examined during the study of the first site in the survey. Three complete sampling runs were carried out in succession with the same probe, so giving three sets of samples, taken at 1-hr intervals. A comparison of the analyses of the Tenax samples on the SE30 capillary column is given in Table 2. The compounds were selected so that a minimum of five measurements was summed in each case. (The errors affecting individual measurements are discussed separately below.) The largest standard deviation for any group was 27% of the mean and a paired comparison of the data gave an overall standard deviation of 15%. These variations were similar to those normally encountered with emissions from more tractable sources, for example solids in flue gases.[12]

The deviations observed in these results were believed to be due to the sampling techniques, since the random analytical errors would be smoothed by the process of summing the results into compound groups. The relative standard deviation for repeated measurements of a compound at the same probe was 55%, but a large part of this resulted from an instrumental error (r.s.d. 33%) due to the peak-chopping effect caused by the manual operation of the UV chart recorder. This instrumental error was avoided in the latter part of the survey by analysing one tube without acquisition of spectra and using this result for the quantitative assessment. Two other tubes from the same probe were analysed with data-acquisition to give the identifications.

In the final assessment the errors for individual compound concentrations were smaller than those reported above, because the results reported from each site were based on not one but at least two sample analyses.

The analyses of the Porapak Q and condensate samples on packed columns produced similar, though much less detailed, results. The first site studied did not yield any of the highly polar compounds for which the packed column analyses were intended, although high concentrations of C_1–C_4 alcohols were observed at some of the other sites. The use of Porapak Q adsorption tubes for the atmospheric sampling of alcohols has been studied by Halliday.[13,14] That work was carried out in association with one of the present authors (B.I.B.) and the adsorption tubes and analytical procedures were essentially similar to those used here. Procedural calibrations, in which simulated air samples were prepared by injecting standard solutions of alcohols into tubes and drawing clean air through them before analysis, yielded linear calibration graphs for ethanol and propan-2-ol, as the following data show:

	Ethanol	Propan-2-ol
Number of points	6	7
Correlation coefficient	0.998	0.998
Y intercept (relative to maximum peak height), %	1	1

The analyses of Porapak Q samples for alcohols were sometimes impaired by interference from co-eluted hydrocarbons. This could have been overcome by selective ion-monitoring, but a more elegant procedure made use of the aqueous condensate sample. By injection of only the aqueous phase, the interference of these hydrocarbons could be avoided.

A typical chromatogram for the analysis of carboxylic acids with full-scan monitoring is shown in Fig. 2a. Tests showed that the MS response to formic and acetic acids in a moist sample was subject to large variation when injections were made with the chromatography column at 50°. Although water vapour has an adverse effect on MS response, we believe the primary problem is caused by the partial condensation of the water at the head of the column, which introduces a third phase into the chromatography. The alternative procedures, whereby moist samples were injected onto a hot column, avoided this problem, but because of the crowded chromatogram obtained at high operating temperatures, selective ion-monitoring was necessary to distinguish the compounds of interest. Figure 2b shows the chromatogram for the analysis of an aqueous solution containing 16 mg/l. each of formic, acetic, propionic and n-butyric acids. A calibration plot of peak height against concentration for a series of injections covering the range 16–200 mg/l. exhibited good linearity, as indicated by the statistical data in Table 3. Most chromatographic procedures for polar compounds require preconditioning of the column with the sample to be analysed before a final determination is made. However, for the analysis illustrated in Fig. 2b and Table 3 this was not necessary, as is shown by the data in Table 4 for a series of consecutive injections of carboxylic acids in aqueous solution. There is no significant variation in the results between the 1st and 7th, and the 2nd and 6th injections despite 3 intermediate injections of a much more concentrated solution. Figure 2c shows the chromatogram for the blank injection.

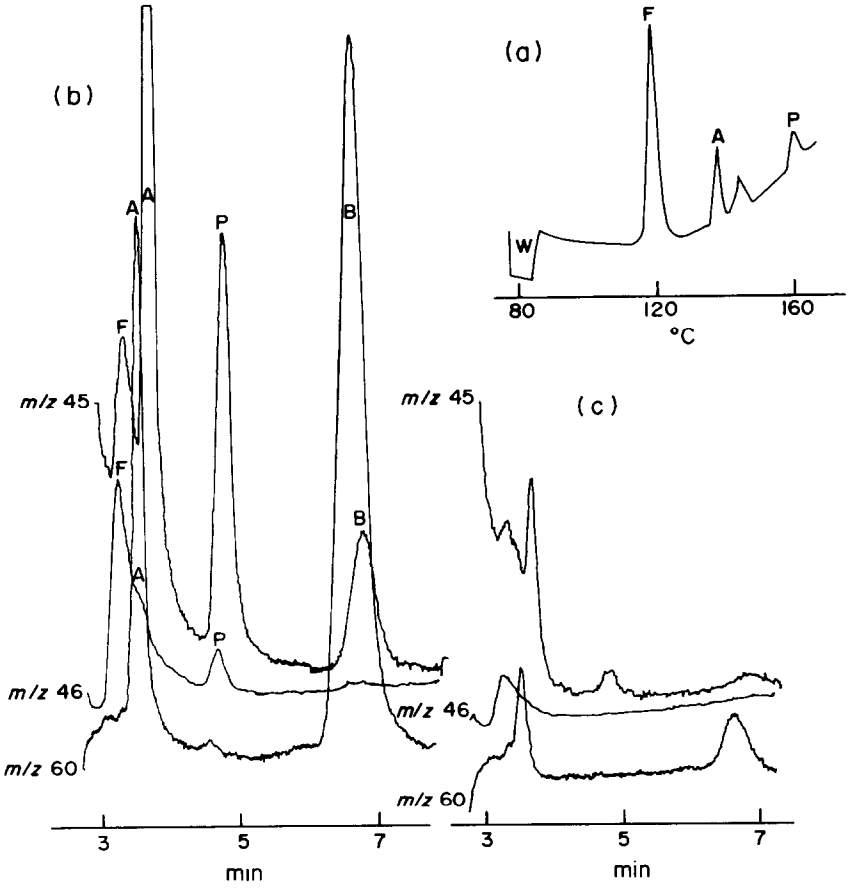

Fig. 2. Analysis of carboxylic acids. (a) A Porapak Q sample of a standard atmosphere containing 5 mg/m^3 of formic, acetic and propionic acids, analysed on Chromosorb 101, injection at 50°C, temperature programmed heating at 10°C/min, with integrated ion-monitoring. (b) An aqueous standard containing 16 mg/l. of formic, acetic, propionic and n-butyric acids (equivalent to a condensate of a standard atmosphere containing 0.4 mg/m^3 of each) analysed on Chromosorb 101, injection at 160°C, isothermal chromatography with selective ion-monitoring. (c) An aqueous blank analysed by the same procedure as (b). *Key*: W, water; F, formic acid; A, acetic acid; P, propionic acid; B, n-butyric acid.

Table 2. Variations between Tenax GC samples taken from the same site

	Probe samples				Relative standard deviation, %	Vent sample	Dilution factor, probe to vent
	A	B	C	Mean			
Total vapours	670 mg/m^3	614 mg/m^3	966 mg/m^3	750 mg/m^3	25	186 mg/m^3	4.0
Methane (20°C, 1 atm)	66.8% v/v	66.3% v/v	—	66.6% v/v	0.5	19.8% v/v	3.4
Relative concentration of each group	%	%	%	%		%	
C_4–C_6 alkane	0.44	0.63	0.4	0.49	25	0.75	2.5
C_7–C_8 alkane	1.6	2.1	2.3	2.0	18	1.8	4.6
C_9–C_{10} alkane	12	18	17	15	20	26	2.3
C_{11}–C_{12} alkane	5.6	9.1	7.8	7.5	24	5.0	5.9
C_5–C_7 alkene*	1.2	0.9	1.0	1.0	15	1.4	2.9
C_8–C_9 alkene	2.5	2.2	2.6	2.4	9	4.2	2.3
C_{10} alkene	5.8	8.2	10	8.0	27	16	2.2
C_{11}–C_{12} alkene	4.9	4.6	5.0	4.8	4	7.4	2.7
alkylbenzenes	40	28	35	34	18	22	6.3
other	27	21	19	22	18	16	5.7

*"Alkene" is used here to include all unsaturated non-aromatic hydrocarbons.

Table 3. Calibration data for carboxylic acids on Chromosorb 101 with selective ion-monitoring of aqueous standards ranging from 16 to 200 mg/l.

	Formic acid	Acetic acid	Propionic acid	n-Butyric acid
Number of data	11	12	12	11
Correlation coefficient	0.992	0.998	0.9996	0.9997
Y intercept (relative to largest peak height)	−0.05	−0.01	−0.01	−0.03

Similar sensitivity and reproducibility have been obtained for amines on the Triton X100/KOH column, as shown by the statistical data in Table 5 for methylamine, isopropylamine, tert.-butylamine and n-butylamine. Alcohols were considered as possible interferents in this analysis since they have similar volatility, polarity and fragment ions, but the chromatograms in Fig. 3 show that even large concentrations are separated from these amines on the Triton X100/KOH column. Figure 3c shows a typical blank chromatogram for the injection of pure water. The small peak corresponding to methanol is probably derived from the methanol used as solvent in the preparation of the column packing.

Figure 3a illustrates the detection of isopropylamine and tert.-butylamine at the 5 mg/m^3 level in a standard atmosphere sample analysed on the Tenax GC column with full-scan monitoring. As with carboxylic acids, this type of analysis gave poorer chromatography and reproducibility. The full-scan methods for polar compounds were included in the preliminary survey because they avoided any restriction on the compounds that could be observed. A data-acquisition system would allow re-analysis of the acquired data with a variety of SIM procedures to cover all compounds of interest. The full-scan procedures for polar compounds, as illustrated in Figs. 2a and 3a were used in the absence of such a system.

This discussion of reproducibility can be placed in perspective by considering that a comparison of all results for all six sites in the survey showed that only 3% of them exhibited site-to-site variations of less than 1 order of magnitude, 39% had variations of 1–2 orders of magnitude and 47% had variations of 2–3 orders of magnitude. In this context the variation found in the data from one site, including that introduced by instrumental errors, can be considered insignificant.

Systematic errors

In addition to the random errors there are possible sources of biased error which cannot be quantified by repetition.

Sampling errors. The site discussed above, where three samples were taken from the same probe (see Table 2) also provided an opportunity to test whether the probe and sample line had any effect on the constituents of the sample. Subsidence had opened an 80-mm diameter vent above refuse of similar age to that at the probe and, eight weeks after the earlier probe samples, Tenax GC samples of the gases issuing from the vent were taken at a position 150 mm above the surface of the fill. A comparison of the ratios of the various components in the two sets of samples gives a partial measure of the accuracy of the technique. In the right-hand column of Table 2 the relative concentrations of the compounds measured in the probe sample are compared with those measured at the vent. The methane analysis indicated that the landfill gas coming from the vent had been diluted by a factor of 3.4 by the surrounding air. This compares with a dilution factor of 4.0 calculated from the total vapour concentrations. For each group of compounds the difference between the two measurements is within a factor of 2, and a paired comparison of the two sets of data gives the overall standard deviation as 57% of the mean.

Table 4. Reproducibility of consecutive injections of carboxylic acids on Chromosorb 101, with selective ion-monitoring

		Peak height, *mm*			
Injection sequence	Concentration, *mg/l.*	Formic acid	Acetic acid	Propionic acid	n-Butyric acid
1	0.0	2.5	10	1	1
2	16	18	34	24	39
3	400	804	835	690	1120
4	400	—	865	685	1095
5	400	815	830	670	1068
6	16	13	29	24	42
7	0.0	2.8	4.5	1.2	3.4

Table 5. Calibration data for amines on the Triton X100/KOH column with selective ion-monitoring of aqueous standards ranging from 20 to 200 mg/l.

	Methylamine	Isopropylamine	tert.-Butylamine	n-Butylamine
Number of data	9	9	9	9
Correlation coefficient	0.990	0.998	0.999	0.999
Y intercept (relative to largest peak height)	−0.05	−0.05	+0.01	−0.03

The use of the PTFE sample line to conduct the gases and vapours to the surface of the landfill was preferred to a procedure in which sample tubes were lowered into the tip, since this had been shown to carry considerable risk of errors resulting from contact with the solid and liquid materials in the fill. The continuous flow of at least 50 ml/min of landfill gas through the sample line throughout the sampling period helped to overcome any problems from adsorption on the wall of the tubing.

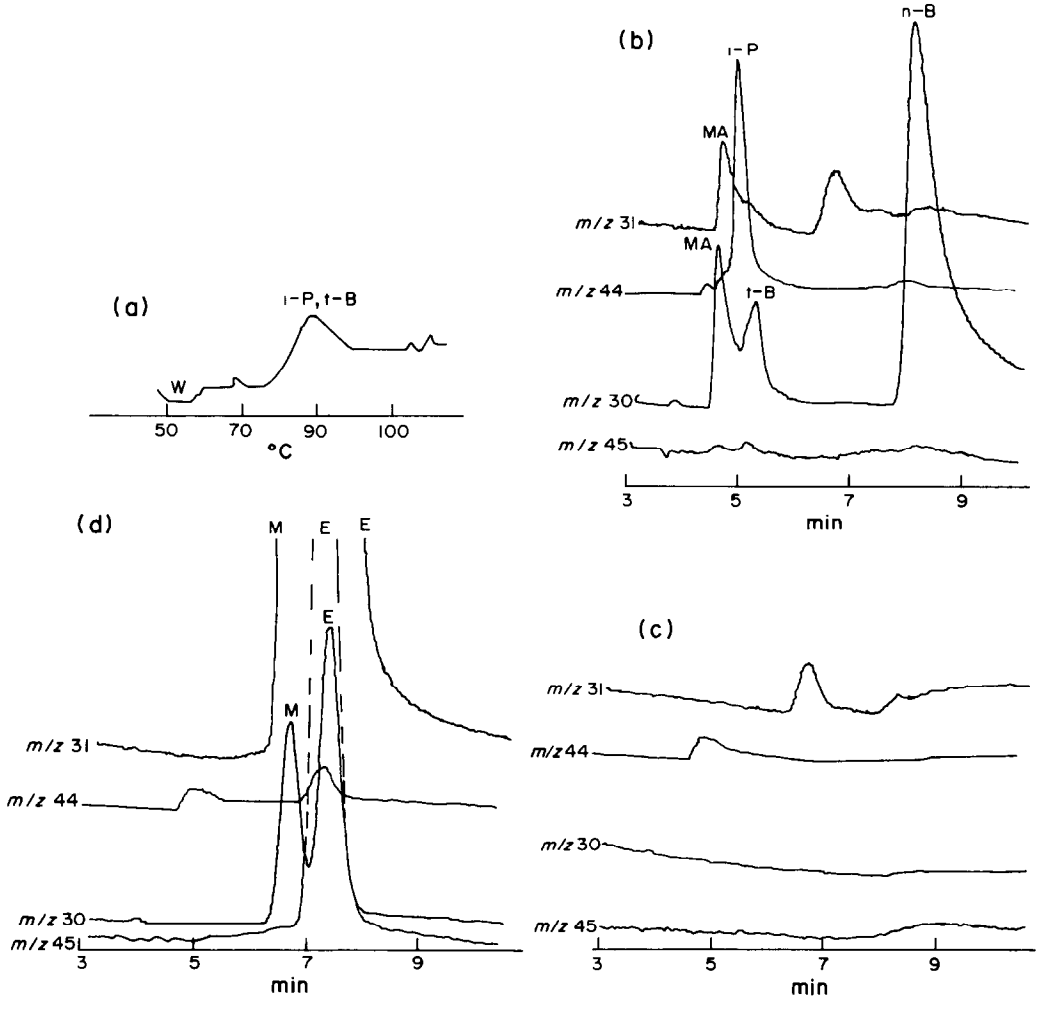

Fig. 3. Analysis for amines. (a) A condensate sample of a standard atmosphere containing 5 mg/m^3 of methylamine, isopropylamine, and tert.-butylamine analysed on Tenax GC, injection at 50°C, temperature programmed heating at 10°C/min, with integrated ion-monitoring. (b) An aqueous standard containing 20 mg/l. of methylamine, isopropylamine, tert.-butylamine and n-butylamine (equivalent to a condensate of a standard atmosphere containing 1.0 mg/m^3 of each) analysed on Triton X100/KOH, injection at 110°C, isothermal chromatography with selective ion-monitoring. (c) An aqueous blank analysed by the same procedure as (b). (d) An aqueous solution, containing 400 mg/l. of methanol and ethanol, analysed by the same procedure as (b). *Key*: W, water; MA, methylamine; i-P, isopropylamine; t-B, tert.-butylamine; n-B, n-butylamine; M, methanol; E, ethanol.

Most of the compounds were present at concentrations below that of their saturated vapours at ambient temperature and so sample loss by condensation would not be a problem. However, moisture did condense in the sample line above ground at some sites and losses of water-soluble compounds to the liquid phase may have occurred. It is arguable that such effects would be an acceptable part of the procedure since they must also occur for the natural emission of the landfill gases as they reach the surface. However, cold-trap condensate samples were collected during the survey to ensure the recovery of all the water-soluble species.

Calibration factors. In the analysis of the Tenax GC samples, anisole was used as the initial calibration standard for all the compounds, and the difference between the true calibration and that based on anisole constituted a systematic error. This would not interfere with comparative assessment of variations between sites but would affect the accuracy of individual measurements. Table 6 lists the calibration factors for a number of volatile compounds with respect to anisole. Except for the markedly polar compounds, in the second half of the table, all the factors are below 2. Since this was similar to the random errors discussed above, anisole was adopted as a general calibrant for such compounds.

The polar compounds in Table 6 all gave poor peak shape in the SE30 chromatograms, and most of them were completely miscible with water. For such compounds individual calibrations were performed with the most appropriate standards available—usually the compounds themselves.

Instrumental error. GC peak-chopping, caused by manual operation of the UV chart recorder, introduces a reduction in the peak height displayed on the recorder. A comparison of the chromatograms of the two samples referred to above, of which one was recorded without acquisition of mass spectra, showed that the peak-chopping reduced the peak height by an average of 27%. No correction factor was introduced into the calculations to allow for this effect, but the full peak height of the internal standard, anisole, was recorded.

Chromatographic performance. The injection of a sample containing μl-quantities of water, or other polar compound, into a GC column at a temperature below the boiling point of the compound can lead to loss of chromatographic performance for all or part of the subsequent analysis. This phenomenon seriously reduces the GC peak heights and also affects the limit of detection. However, it is readily recognizable because of the impairment of peak shape, and it was not a major problem in any of the survey analyses.

Artefacts from the trapping media. Significant peaks for various compounds are often observed in "blank" chromatograms run for both Porapak Q and Tenax

Table 6. Calibration factors relative to anisole

Compound	Medium*	$\frac{\text{Anisole peak height}}{\text{Compound peak height}}$†
For the SE30 capillary column:		
chloroform	L	1.0
trichloroethylene	A	1.4
tetrachloroethylene	A	0.63
n-butyl acetate	A	1.0
n-heptane	A	1.3
n-decane	A	1.2
1-octene	A	0.56
benzene	A	1.1
toluene	A	0.91
ethylbenzene	A	0.83
p-xylene	A	0.77
o-xylene	A	0.71
1,3,5-trimethylbenzene	A	0.56
1,2,4-trimethylbenzene	A	0.67
methylstyrene	A	0.63
naphthalene	A	0.71
1-methylnaphthalene	A	0.83
phenol	L	11
For the chromosorb 101 column with integrated ion-monitoring:		
ethanol	L	24
acetic acid	L	21
2-methylpropan-1-ol	L	4.3
butan-1-ol	L	5.2
ethanethiol	L	17
dimethyl sulphide	L	4.1
tetrahydrothiophene	L	2.0
n-butylamine	L	32

*L = standard solution; A = standard atmosphere.
†For equal weights of anisole and compound.

Table 7. List of compounds detected, and the results for one of the sites

Compound	Results for one site: Number of GC peaks	Results for one site: Concentration, mg/m^3
Alkanes		
Propane	0	<2
Butanes	1	14
Pentanes	2	105
Hexanes	2	100
Heptanes	3	99
Octanes	2	17
Nonanes	6	147
Decanes	6	125
Undecanes	2	12
Alkenes		
Butadiene	0	<1
Butenes	2	18
Pentadienes	0	<2
Pentenes	1	0.5
Hexenes	1	15
Heptadienes	0	<2
Heptenes	0	<2
Octenes	5	21
Nonadienes	1	5
Nonenes	2	22
Decenes	7	82
Undecenes	0	<2
Cycloalkanes		
Cyclopentane	0	<2
Cyclohexane	1	33
Methylcyclopentane	0	<2
Dimethylcyclopentanes	1	1
Ethylcyclopentane	0	<2
Methylcyclohexane	1	15
Trimethylcyclopentanes	0	<2
Dimethylcyclohexanes	0	<1
Trimethylcyclohexanes	0	<2
Propylcyclohexanes	0	<2
Butylcyclohexanes	0	<2
Terpenes		
Limonene	1	240
Other terpenes	5	160
? Menthene	1	14
Aromatic hydrocarbons		
Benzene	1	5
Toluene	1	15
Styrene	1	7
Xylenes	2	34
Ethylbenzene	1	14
Methylstyrene	0	<2
C_3-Alkylbenzenes	4	36
C_4-Alkylbenzenes	3	5.8
C_5-Alkylbenzenes	0	<2
Halogenated compounds		
Chloromethane	1	1
Chlorofluoromethane	1	1
Dichloromethane	1	140
Chlorodifluoromethane	1	4
Dichlorofluoromethane	1	5
Chloroform	0	<1
Dichlorodifluoromethane	1	10
Trichlorofluoromethane	1	20
Chloroethane	1	25
1,1-Dichloroethane	1	120
1,2-Dichloroethane	0	<2
Vinyl chloride	1	16
1,1,1-Trichloroethane	1	29
1,2-Dichloroethylenes	1	68

continued

Table 7—*continued*

Compound	Results for one site: Number of GC peaks	Results for one site: Concentration, mg/m^3
Trichloroethylene	1	10
Tetrachloroethylene	1	250
1,1-Dichlorotetrafluoroethane	1	1
1,2-Dichlorotetrafluoroethane	0	<2
1,1,1-Trichlorotrifluoroethane	0	<2
Bromoethane	0	<2
Chloropropanes	0	<2
Dichlorobutenes	0	<2
Chlorobenzene	0	<2
Dichlorobenzenes	0	<2
Organosulphur compounds		
Carbonyl sulphide	0	<1
Carbon disulphide	1	5
Methanethiol	1	60
Ethanethiol	0	<1
Dimethyl sulphide	1	14
Dimethyl disulphide	1	10
Diethyl disulphide	0	<2
Butanethiols	0	<2
Pentanethiols	0	<2
Alcohols		
Methanol	0	<2
Ethanol	1	>810
Propan-1-ol	1	110
Propan-2-ol	1	>22
Butan-1-ol	0	<2
Isobutanol	0	<0.1
Butan-2-ol	1	110
Esters		
Ethyl acetate	1	60
Methyl butyrate	1	5
Ethyl propionate	1	50
Propyl acetate	1	50
Isopropyl acetate	1	6
Methyl pentanoate	1	1
Ethyl butyrate	1	350
Propyl propionate	1	200
Butyl acetate	1	60
Ethyl pentanoate	1	20
Propyl butyrate	1	100
Ethers		
Dimethyl ether	0	<2
Methyl ethyl ether	0	<2
Diethyl ether	0	<2
Dipropyl ethers	0	<2
Other oxygenated compounds		
Acetone	0	<1
1,3-Dioxolane	1	5
Butan-2-one	1	38
Tetrahydrofuran	0	<1
Pentan-2-one	0	<2
Methylfurans	0	<2
Dimethylfurans	0	<2
? Camphor/fenchone	0	<2

GC sorption tubes. Even with the low desorption temperatures employed in this work, Porapak Q gives rise to alkylstyrene compounds, so these were ignored in the analyses of the Porapak Q samples. Although there are literature reports which maintain that Tenax GC does not give rise to artefacts,[5,15] others have suggested this may occur[16,17] and the suppliers have acknowledged that C_1 and C_2 alkylbenzenes can be observed.[18] In the course of other studies the authors have observed production of a variety of compounds, including phenol, benzaldehyde and benzyl alcohol. The production of artefacts from Tenax GC is variable—the same tube may give a clean blank on one occasion and a highly con-

taminated one on another. The quantities of C_1 and C_2 alkylbenzenes which arise as artefacts are too small to interfere in the survey and the other compounds were not observed. Higher alkylbenzenes can be produced from Tenax GC sample tubes in very significant quantities (several μg), but in the authors' experience they are always accompanied by benzaldehyde, and so their observation and measurement in the survey (in which no benzaldehyde was found) was regarded as valid. Overall, therefore, there was no problem from artefacts. A new product, Tenax TA, which is claimed to suffer fewer problems than Tenax GC, has not yet been tested by the authors. No artefacts are produced on a Tenax GC chromatographic column, however.

Limits of detection

The detection limit depended not only on the observation and resolution of a GC peak but on the ability to identify it from the mass spectrum. For non-polar compounds chromatographed on the SE30 column this limit corresponded to a concentration of typically 0.1 mg/m^3 in the original 25-ml sample. For compounds co-eluted with a much larger quantity of another substance, the detection limit was assessed as ten times the minimum, *i.e.*, typically 1.0 mg/m^3.

Specific tests were made to determine the detection limits for polar compounds, using all the sampling techniques and the integrated ion-monitoring procedures. Three sets of standard atmospheres containing (*a*) formic, acetic and propionic acids; (*b*) methylamine, isopropylamine and tert.-butylamine; (*c*) pyridine, were generated by the dynamic technique developed by Brookes.[11] In order to simulate the conditions applying to landfill gas, the humidity of the atmospheres was raised by passing the inlet air through heated water in a bubbler before its admixture with the vapours of the test compounds. The water temperature was that calculated to give the equivalent of 100% humidity at 31°. The whole apparatus was warmed with heating tapes to prevent condensation, and sampling was done with the same PTFE sample line and other apparatus used for on-site sampling. A chromatogram for atmospheric samples containing carboxylic acids is shown in Fig. 2a, and for amines in Fig. 3a. Methylamine was not detected in any of the analyses since the integrated ion analysis of the eluate from the SE30 column did not include the fragment ions of methylamine, and although methylamine can be chromatographed adequately on Tenax GC, under the conditions used its peak will be obscured by the water peak (Fig. 3a). For basic compounds in general, the limit of detection was assessed as 10 mg/m^3. The Porapak Q samples permitted the detection of the acids at 5 mg/m^3. For determination none of these integrated ion procedures would have been reliable and further analysis by a selective ion-monitoring technique would have been required. The detection limits (mg/m^3) estimated for a range of compounds analysed by the SIM procedures (Figs. 2 and 3) were as follows: formic acid 0.6, acetic acid 0.6, propionic acid 0.3, n-butyric acid 0.2, methylamine 0.6, isopropylamine 0.6, tert.-butylamine 0.6, n-butylamine 0.3.

No individual measurements were made for finding the limits of detection for alcohols, but from the work of Halliday,[13,14] which used procedures similar to those reported here, the limit of detection on Chromosorb 101 with full-scan MS was estimated to be 2 mg/m^3. A lower limit should be possible with selective ion-monitoring.

Conclusions

Table 7 shows the complete list of all the species observed in the survey, together with the analytical results obtained from one of the sites. The methods allowed the identification and determination of these compounds with sufficient accuracy and reproducibility to show up significant variations between their source concentrations at six different sites. They also permitted the estimation of potential odour intensities and toxicity levels.[3] Limits of detection have also been assessed for important compounds not yet observed in the survey.

The analyses for polar compounds by selective ion-monitoring techniques and with sample injection at high temperatures, were found to give much better reproducibility and sensitivity than the alternative full-scan/cold-injection procedures did.

Acknowledgements—The survey of landfill gas emissions is funded by the Department of the Environment, and the development of the GC–MS analytical procedures is funded by Strathclyde Regional Council.

REFERENCES

1. J. F. Rees, *Proc. Landfill Gas Symposium*, 6 May 1981, Paper 2, Harwell Laboratory, Harwell, England.
2. J. F. Rees and I. Viney, *Leachate Quality and Gas Production from a Domestic Refuse Landfill. The Implications of Water Saturated Refuse at Aveley Landfill*, Report R-10328, February 1982; HMSO, London.
3. P. J. Young and A. Parker, *The Identification and Possible Environmental Impact of Trace Gases, Vapours and Metallic Compounds found in Landfill Gas*, to be published.
4. K. J. Krost, E. D. Pellizzari, S. G. Walburn and S. A. Hubbard, *Anal. Chem.*, 1982, **54**, 810.
5. E. D. Pellizzari, *Environmental Protection Agency Rept.*, EPA-600/2-79-057, March 1979, Research Triangle Institute, P.O. Box 12194, Research Triangle Park, NC 27709, U.S.A.
6. R. H. Brown and C. J. Purnell, *J. Chromatog.*, 1979, **178**, 79.
7. B. I. Brookes, *Analyst*, 1979, **104**, 698.
8. R. A. Rasmussen, *Am. Lab.*, July 1972, 19.
9. S. A. Penkett, N. J. D. Prosser, R. A. Rasmussen and M. A. K. Khalil, *J. Geophys. Res.*, 1981, **86**, 5172.
10. J. N. Keay and R. Hardy, *J. Sci. Food Agric.*, 1972, **23**, 9.
11. B. I. Brookes, *Analyst*, 1981, **106**, 403.

12. P. G. W. Hawksley, S. Badzioch and J. H. Blackett, *Measurement of Solids in Flue Gases*. The Institute of Fuel, London, U.K., 1977.
13. M. M. Halliday and K. B. Carter, *Br. J. Anaesth.*, 1978, **50,** 1013.
14. D. Campbell, P. D. Davis, M. M. Halliday and I. MacDonald, *ibid.*, 1980, **52,** 885.
15. E. D. Pellizzari, J. E. Bunch, R. E. Berkley and J. McRae, *Anal. Lett.*, 1976, **9,** 45.
16. M. B. Neher and P. W. Jones, *Anal. Chem.*, 1977, **49,** 512.
17. M. J. Lewis and A. A. Williams, *J. Sci. Food Agric.*, 1980, **31,** 1017.
18. *Chrompack News*, 1982, **9,** No. 5.

Talanta, Vol. 30, No. 9, pp. 677–682, 1983
Printed in Great Britain.

0039/9140/83 $3.00+0.00

DETERMINATION OF CHLORIDE, NITRATE, SULPHATE AND TOTAL SULPHUR IN ENVIRONMENTAL SAMPLES BY SINGLE-COLUMN ION CHROMATOGRAPHY

J. A. HERN,[1] G. K. RUTHERFORD[2] and G. W. VANLOON[1]
Departments of [1]Chemistry and [2]Geography, Queen's University, Kingston, Ontario, Canada

(*Received* 15 *February* 1983. *Accepted* 21 *March* 1983)

Summary—The analytical performance characteristics of a single-column ion chromatography system are reported. The data were obtained by using conductivity detection as well as by an indirect ultraviolet technique. The method has been applied to the determination of Cl^-, NO_3^- and SO_4^{2-} in samples of rain, sewer water, and soil-pore water. Also described are two methods which allow ion chromatographic analysis of $CaSO_4$-extractable nitrate in soils, and total sulphur in soils, marine sediments and plant tissue.

Ion chromatography (IC) is a variant of high-pressure liquid chromatography, applicable to analysis for inorganic ions. The instrument consists of an efficient ion-exchange column through which a suitable eluent is pumped. A loop-type injection valve is used to introduce the sample into the eluent stream and onto the column. The ions are retained to varying degrees and therefore emerge from the column after characteristic retention times.

The first report of this technique was by Small *et al.*[1] The method they developed uses a carbonate/bicarbonate buffer as eluent and incorporates a second "suppressor" column in addition to the analytical column. The suppressor column—a cation-exchange column—serves to remove eluent metal cations so that the emerging solution contains protons, carbon dioxide and the analyte anions. The conductivity of the weak carbonic acid electrolyte is low, making it possible to detect the other anions with a conductivity flow cell and meter. It is necessary to regenerate the suppressor column regularly since it becomes saturated with cations from the eluent solution. Recently, a hollow-fibre suppressor system has been developed which eliminates the need for a separate regeneration step. The eluent passes through a hollow fibre constructed of cation-exchange membrane material, while a counterflowing stream of very dilute acid outside the fibre continuously reconverts the resin into the hydrogen-ion form.[2,3]

A second type of ion chromatography—non-suppressed, or single-column IC—is also possible. No suppressor column is used and the eluents are of relatively low conductivity. Two types of detectors are compatible with a single-column system. Most commonly used is a conductivity meter which electronically compensates for background conductivity.

An ultraviolet detector may also be used if the eluent buffer includes an organic acid which absorbs in an appropriate region of the ultraviolet. Inorganic anions which do not absorb in that region appear as troughs in the baseline, allowing indirect detection.

Since conventional HPLC instrumentation is employed in single-column IC, the equipment cost can be considerably lower than with the two-column instrument. Regeneration of a suppressor column is not required, and the analytical characteristics of the two techniques are comparable. This paper describes the performance of a single-column ion chromatograph using both conductivity and ultraviolet detectors.

Environmental samples

Natural waters—rain, lake and soil-pore water—have traditionally been analysed for anions by spectrophotometric methods, but these methods are subject to interference from other species present, especially in soil solutions. For example, chloride and nitrite interfere with the widely-used nitrophenoldisulphonic acid method for nitrate.[4] Routine spectrophotometric anion analysis is time-consuming, and though it is possible to handle large numbers of samples efficiently by the use of an auto-analyser, a heavy investment in equipment and reagents is necessary for each species being determined, and there must be sufficient sample to allow determination of all the anions of interest.

Ion chromatography is gaining wide acceptance as a useful method for the determination of anions in environmental samples. Determinations of species such as F^-, Cl^-, Br^-, NO_2^-, NO_3^-, SO_4^{2-}, AsO_4^{3-} and PO_4^{3-} have all been reported, although most current literature is concerned with systems using eluent suppression.[5,6]

Ion chromatography permits the simultaneous analysis of an aqueous solution for Cl^-, NO_3^- and SO_4^{2-}. The method is well suited to analysis of lake,

stream, rain and soil-pore water. These water samples are, however, relatively clean and contain only low concentrations of additional organic and inorganic constituents.

Analysis of environmental samples requiring dissolution or extraction may present greater difficulties. The ion-exchange resin used in the IC system has low capacity (of the order of μeq/g), and the detector measures a property of the bulk eluent solution, not just of the analyte (as would be the case with direct ultraviolet detection of organic compounds). As a result, any ionic species present in the sample at high concentration relative to the analyte may cause column overloading, with loss of resolution, and severe baseline fluctuations at the detector. This has precluded the use of IC for many samples with high levels of total ionic species, or requiring pretreatment with concentrated reagents.

Such samples include the inorganic salt solutions used to extract "available" nutrient anions from soil. Also included are solutions prepared for total elemental analysis from solid samples such as soils and plant tissue. Pretreatment by wet ashing with strong acids or fusion at high temperature introduces large amounts of ionic material and so prevents direct ion chromatographic analysis.

In addition to water analysis for Cl^-, NO_3^-, and SO_4^{2-}, this paper describes the use of ion chromatography for two more difficult analyses, (a) for soil nitrate extractable into aqueous calcium sulphate solution, and (b) for total sulphur in soils, sediments and plant tissue.

EXPERIMENTAL

Apparatus

A Spectra-Physics Model 3500 HPLC instrument was used in conjunction with a Vydac 302 IC anion-exchange column, a Valco UHPa-N60 injection port and a Rheodyne Model 7302 2-μm column inlet filter. Detection was by a Vydac Model 6000 CD conductivity cell and meter, or a Spectra-Physics Model 230 ultraviolet detector. The retention times, heights and areas of peaks were recorded and measured with a Hewlett Packard 3390A integrating recorder. A block diagram of the system is given in Fig. 1.

Reagents

The eluent was $4.0 \times 10^{-3}M$ aqueous phthalic acid buffer adjusted to pH 5.0 with sodium borate, when conductivity detection was used. A $1.0 \times 10^{-3}M$ phthalate buffer adjusted to pH 4.0 was used with the ultraviolet detector. Mixed standards containing Cl^-, NO_3^- and SO_4^{2-} were prepared from the analytical-reagent grade potassium salts.

Procedure

Samples high in suspended particulate matter were filtered through a 1.2-μm filter before analysis. Most samples, however, were injected directly.

An eluent flow-rate of 2.0 ml/min was used with a pump pressure of 900 psig. For all samples a 250-μl sample loop was used.

The conductivity meter includes controls to offset the baseline conductivity and was adjusted to send a net zero baseline signal to the recorder. To achieve a zero baseline output from the ultraviolet detector, the reference cell was filled with eluent and the balance control adjusted to compensate for any minor differences in sample and reference cells. Reversal of the recorder leads resulted in positive peaks for analyte species, which could be integrated by the recorder. A wavelength of 280 nm and a detector sensitivity of 0.08 AUFS (absorbance units full scale) were used, although higher absorbance range settings were necessary for ion concentrations greater than 25 μg/ml.

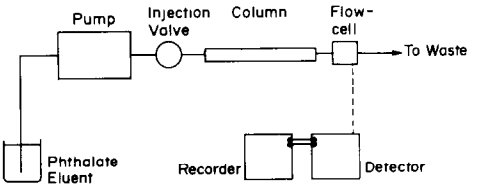

Fig. 1. Block diagram of single-column ion chromatograph.

RESULTS AND DISCUSSION

Conductivity detection

A typical chromatogram obtained with conductivity detection is shown in Fig. 2. The first peak in the chromatogram (retention time $t_R = 95$ sec) was the pseudo-peak[7] due to cations in the sample plus anions displaced from the column by analyte anions. The pseudo-peak was usually large and could be either positive or negative, depending on the total concentration of ions moving with the solvent front.

Following the pseudo-peak, Cl^-, NO_3^- and SO_4^{2-} were eluted at $t_R = 200$, 280 and 430 sec respectively.

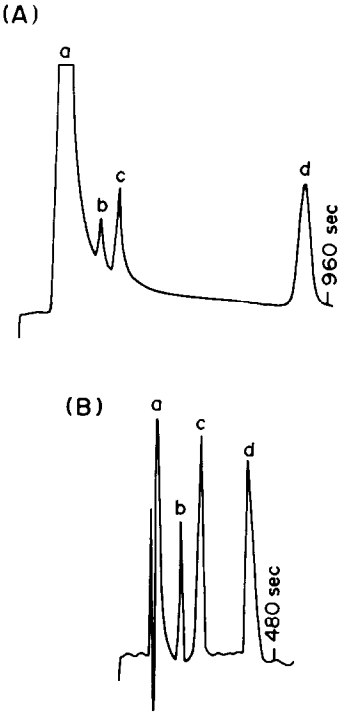

Fig. 2. Typical ion chromatogram of water samples: A, ultraviolet detector (1 μg/ml, 0.02 AUFS); B, conductivity detector (25 μg/ml); a, pseudo-peak; b, Cl^-; c, NO_3^-; d, SO_4^{2-}.

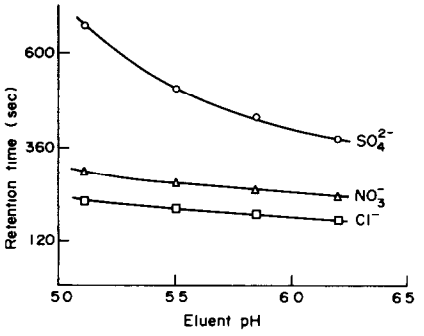

Fig. 3. Retention times of Cl^-, NO_3^- and SO_4^{2-} as a function of pH for $2.0 \times 10^{-3}M$ phthalate eluent.

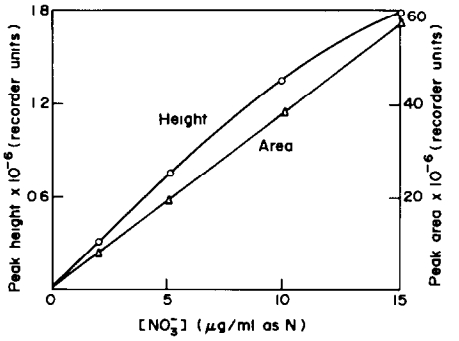

Fig. 4. Nitrate calibration by peak-height and peak-area measurements, with conductivity detection.

The retention times and resolution were dependent on the ionic strength of the eluent and its pH. Retention times, particularly for SO_4^{2-} and other strongly retained anions, were markedly pH-dependent, with longer retention times at lower pH (Fig. 3). The eluent pH must therefore be adjusted carefully for good reproducibility to be obtained. Sample pH between 2 and 7 did not affect the position or size of the peaks.

The ionic strength of the eluent was adjusted by varying the phthalic acid concentration. Although separation of the three anions of interest could be achieved at any phthalic acid concentration in the range $1.0–4.0 \times 10^{-3}M$, the shortest retention time possible for SO_4^{2-} was desired, in order to speed up the analysis. The optimum combination of short retention time and resolution was obtained at $4.0 \times 10^{-3}M$. For the resolution, defined as $R = (t_{R_A} - t_{R_B})/(Y_A + Y_B)$, where Y = peak width, a value of 1.0 or greater is considered sufficient for quantitative analysis. For the NO_3^- and Cl^- peaks, values of $R = 8.3$ and 3.3 were obtained with $2.0 \times 10^{-3}M$ and $4.0 \times 10^{-3}M$ eluent solutions, respectively.

Calibration lines for all three anions were curved when peak-height measurements were used, but were linear for peak-area measurements. Typical calibration lines for NO_3^- are shown in Fig. 4. Linear ranges and sensitivities for all species are given in Table 1. The peaks broadened at higher concentrations, and overlap of the Cl^- and NO_3^- signals, when both ions were present at concentrations above about 120 μg/ml, began to cause small deviations from linearity. Calculated in terms of molar concentrations, the sensitivity was about twice as great for SO_4^{2-} as for Cl^- and NO_3^-. Over a 6-month period the sensitivities varied by less than $\pm 7\%$, but there was some loss of column efficiency, and this necessitated a decrease in the eluent pH to maintain the resolution and retention times reported.

Detection limits are listed in Table 2 and are defined as twice the standard deviation of the baseline noise.

Other anions can be detected by ion chromatography. With the $4.0 \times 10^{-3}M$ pH-5.0 phthalate buffer, NO_2^- gave a peak at $t_R = 240$ sec, Br^- at $t_R = 245$ sec and $S_2O_3^{2-}$ at $t_R = 545$ sec. None of these species was found in any of the water samples

Table 1. Linear concentration ranges and sensitivities of ion chromatographic analysis, based on area measurements

	Linear range, $\mu g/ml$		Sensitivity (*area. counts.ml* μg^{-1})	
Anion	Conductivity	UV	Conductivity	UV
Cl^-	0–120	0–25	1.50×10^4	4.45×10^4
NO_3^- (as N)	0–120	0–30	3.86×10^4	1.17×10^5
SO_4^{2-} (as S)	0–140	0–50	3.77×10^4	2.54×10^5

Table 2. Detection limits for anions in aqueous solution (250-μl sample loop)

	Detection limit based on peak area, $\mu g/ml$	
Anion	Conductivity	UV
Cl^-	0.6	0.2
NO_3^- (as N)	0.2	0.07
SO_4^{2-} (as S)	0.2	0.03

examined. When all three were added to standard samples containing Cl^-, NO_3^- and SO_4^{2-}, however, all species except Br^- and NO_2^- could be resolved. These last two species could be resolved with a $2.0 \times 10^{-3}M$ pH-5.0 buffer, although at the expense of increased retention time for SO_4^{2-}. A peak for SO_3^{2-} was also obtained, but it had the same retention time as the SO_4^{2-} peak. Gjerde *et al.*[7] using a variety of conditions, were also unable to resolve these two peaks.

Ultraviolet detection

The use of an ultraviolet detector to monitor eluent absorbance as a means of detecting non-absorbing anions in ion chromatography is called indirect photometric chromatography (IPC) and was reported by Small and Miller.[8] This detection system offers the advantages of single column IC as well as greater sensitivity and lower detection limits than are possible with conductivity detection. Maximum versatility is obtained with a variable-wavelength detector, but since fixed-wavelength detectors are more common as standard HPLC equipment, the latter was used for the water analyses reported in this paper.

The factors influencing optimum chromatographic resolution are identical for the two types of detector, but the fixed-wavelength detector places an additional constraint on the eluent concentration. The absorbance of the eluent at the wavelength of the detector should be between 0.2 and 0.8 in the detector cell[7] and the absorbance of a $4 \times 10^{-3}M$ phthalic acid solution is too high. For that reason a $1 \times 10^{-3}M$ solution was chosen as eluent. As a result, the peaks were broader, and retention times longer than with the higher concentration buffer.

Linear concentration ranges, and sensitivity for the eluent and wavelength used are given in Table 1, and detection limits in Table 2. The smaller linear concentration range obtained with ultraviolet detection is mainly due to the use of a lower eluent concentration. As the analyte concentration becomes significant relative to eluent concentration, peak resolution is lost. Overlap of the broader Cl^- and NO_3^- peaks at concentrations above $25\ \mu g/ml$ causes deviations from linearity.

The choice of detector depends on the intended use. For routine analysis of samples containing high concentrations of anions, conductivity detection is satisfactory in terms of speed and simplicity. The ultraviolet detector offers greater sensitivity and lower detection limits and thus is well suited to analysis of low concentration samples.

Soil water samples that are coloured by organic matter should be analysed by conductivity measurement to avoid potential problems associated with the ultraviolet absorption of the organic species.

Analysis of water samples

Subsequent analyses were obtained with conductivity detection except where otherwise noted.

Calibration line and standard-additions procedures were used on a single soil-pore water sample as a means of determining whether or not matrix interferences occurred in the analysis. The calibration curve was constructed by use of five aqueous standards with concentrations from 0 to $15\ \mu g/ml$. In the standard-additions method, the sample was spiked with four successive additions, up to a maximum added concentration of $12.8\ \mu g/ml$. The results and the calculated confidence intervals are given in Table 3. The close agreement of the results indicates that for this sample there are no substantial matrix interferences. All other analyses in this paper were obtained by use of the calibration curve procedure.

Comparative analyses of various soil-pore water, sewer water and rain samples are reported in Table 4. Results for SO_4^{2-} were obtained by IC as well as by a turbidimetric procedure[9] and for NO_3^- by IC and by the spectrophotometric procedure of Norman and Stucki.[10] Cl^- was determined by IC and by potentiometric titration. The results are comparable in accuracy and precision.

The soil-pore water samples analysed were obtained from field and laboratory studies on Canadian Shield podzols and brunisols. Many of the low-value samples were from B and C horizon material, and the high values usually occurred in samples taken from the L and H layers. Some of these latter samples were highly coloured with soluble humic materials but there is no evidence that this affected the results obtained by conductivity detection.

Analysis of soils for extractable NO_3^-

Ion chromatography has been used in the determination of NO_3^- extractable from soil, but the extracting solutions are dilute ($10^{-2}M$ potassium chloride, for example).[11] Other more concentrated extracting solutions have also been recommended, such as saturated aqueous calcium sulphate solution.[12] In this solution the equilibrium concentration of sulphate is sufficient to mask any peak due to extracted NO_3^- if analysis by IC is attempted. A means of removing the sulphate after extraction, while quantitatively retaining the nitrate, was therefore sought.

Lead sulphate has a K_{sp} of approx. 1×10^{-8}, or an equilibrium sulphate concentration of less than

Table 3. Analysis of soil-pore water [mean (95% confidence interval)]

	NO_3^-, $\mu g/ml$ as N	SO_4^{2-}, $\mu g/ml$ as S
Calibration line method	1.2 (0.1)	3.1 (0.5)
Standard-additions method	1.2 (0.1)	3.1 (0.5)

Table 4. Mean values (95% confidence intervals) for the analysis of water samples by ion chromatography and other methods, analyses performed in triplicate

Sample		SO_4^{2-}, μg/ml as S		NO_3^-, μg/ml as N		Cl^-, μg/ml	
		IC	Turbidimetric†	IC	UV	IC	Potentiometric
Soil-pore water	G1	22.30 (0.48)	23.02 (0.85)	2.89 (0.17)	2.91 (0.09)	ND	—
	G2	9.35 (0.26)	9.16 (0.42)	1.59 (0.18)	1.57 (0.09)	ND	—
		9.28 (0.25)*		1.52 (0.30)*		ND*	
	G3	12.59 (0.34)	11.91 (0.60)	2.58 (0.17)	2.74 (0.30)	ND	—
Sewer water	S1	7.63 (0.26)	7.42 (0.58)	3.57 (0.16)	4.04 (0.08)	10.64 (0.30)	11.48
	S2	3.91 (0.30)	3.91 (0.27)	3.21 (0.18)	3.49 (0.08)	3.80 (0.25)	3.97
		4.01 (0.40)*		3.28 (0.23)*		4.83 (1.3)*	
Rain water	R1	0.20 (0.50)	0.44 (0.20)	ND	ND	ND	—
		0.23 (0.30)*		ND*		ND*	
	R2	1.60 (0.30)	1.75 (0.36)	0.86 (0.20)	0.91 (0.09)	ND	—
		1.74 (0.36)*		0.87 (0.30)*		ND*	
Lake water	L1	9.13 (0.48)	—	ND	—	28.22	—

ND = None detected.
*Ion chromatography with ultraviolet detection.
†Standard deviation based on 3 measurements—turbidimetry only.
— = No analysis done.

10 μg/ml, which is low enough to permit the IC analysis. Adding a soluble lead salt to the extractant, however, merely replaces the sulphate with an equivalent amount of a second anion, which will give the same interfering effect. This problem can be overcome by charging a cation-exchange resin with lead, the resin acting as an insoluble counter-ion. When the sulphate-containing soil extract is passed through a column of such a lead-charged resin, $PbSO_4$ precipitates and is trapped in the column. The NO_3^- passes through and may be collected in the effluent.

A 0.5-ml bed of Dowex 50W-X8 (200–400 mesh) hydrogen-form resin was prepared in a Bio-Rad disposable polypropylene column. The resin was flushed with 5 ml of 10% lead acetate solution, and rinsed with 10 ml of demineralized water. One ml of soil extract solution was introduced into the column, and after it had passed into the resin bed, was followed by a few ml of water. The lead sulphate precipitate was visible as it formed in the column. The first 0.25 ml of effluent immediately following sample introduction was discarded and the next 2.0 ml were collected in a graduated tube. An aliquot of this sample was then injected directly onto the ion chromatograph for NO_3^- determination.

Table 5. Nitrate recovery during SO_4^{2-} removal by a lead-charged cation-exchange column

Trial	NO_3^- added, μg of N	NO_3^- found, μg of N	Recovery, %
1	46.9	46.9	100.0
2	46.9	46.2	98.5
3	46.9	46.7	99.6
4	46.9	46.7	99.5
5	46.9	47.6	101.5

A recovery study was performed to test for any loss of NO_3^- during the clean-up of solutions containing added NO_3^- in the presence of $CaSO_4$. Results are listed in Table 5.

The use of the lead-charged cation-exchange column provides a means of removing the bulk of the sulphate, with essentially quantitative recovery of NO_3^-, although a twofold dilution of the soil extract results.

Other extracting solutions are also commonly employed in the determination of available soil nutrients, for example[13] $CaCl_2$ or KCl solutions for extraction of NO_2^- and NO_3^-. A similar principle has been applied to the separation of Cl^- and Br^- from complex matrices by collection of the halides on a silver-charged resin, followed by elution and determination.[14] Resins charged with silver could also provide a means of removing excess of Cl^-, allowing analysis of $CaCl_2$ or KCl soil extracts by ion chromatography.

Total sulphur determination

Determination of total sulphur in plant and soil material by spectrophotometric methods requires conversion of all the sulphur into SO_4^{2-} or S^{2-}. Neither approach yields a sample suitable for ion chromatographic analysis if methods involving Na_2CO_3 or Na_2O_2 fusions are used. Other pretreatments have been reported,[15] but they also involve the use of concentrated reagents, so they too do not yield samples suitable for IC.

The combustion of samples in an oxygen atmosphere has been used for the clean oxidation of many types of samples. No excess of ionic material is introduced into the sample during oxidation, leaving it "clean" enough for analysis by ion chromatography.

Table 6. Total sulphur analysis by ion chromatography

Sample	Found, %	Certificate value, %	
NBS-1571, Orchard Leaves	0.20 (0.03)*	0.19	
NRC-MESS-1, Marine Sediment		0.72 (0.03)	0.72 (0.05)
NRC-BCSS-1, Marine Sediment		0.40 (0.03)	0.36 (0.05)
Canmet SO-2, Soil	0.037 (0.02)	0.034 (0.01)	
Canmet SO-4, Soil	0.059 (0.02)	0.044 (0.04)†	

*Figures in parentheses are 95% confidence interval, based on six measurements.
†Individual certificate values obtained by combustion, XRF and SSMS range from 0.03 to 0.09% for soil SO-4.

A study was undertaken to determine whether or not this technique would be effective for soils, marine sediments and plant tissue.

The combustion was performed in a 250-ml Schöniger flask with 40–60 mg of sample in the usual way.[16] The absorption solution in the flask was 5 ml of demineralized water plus 3 drops of 50% H_2O_2. After the combustion the flask was shaken vigorously, then left for 10 min. The contents were transferred quantitatively to a 25-ml standard flask and made up to volume with demineralized water. This sample was then analysed by ion chromatography as already described.

To ensure a low blank, a sulphur-free flame was used to light the paper wick, not a match. In the case of soils and sediments, an insoluble inorganic residue remained after combustion. Filtration of the samples before injection was not necessary if the solids were allowed to settle out before the sample was withdrawn.

Five standard reference materials were analysed by this method to test for completeness of oxidation of all sulphur to SO_4^{2-}. Results are given in Table 6.

For samples low in total sulphur, a large weight of sample may be used, but a larger flask should also be used to accommodate safely the greater volume of combustion gases.

Cl^- and NO_3^- peaks were also found in the chromatograms of these samples. Simultaneous quantitative analysis was not possible, however. Recoveries of total N as NO_3^- were typically less than 50% and variable.

The Schöniger flask combustion of plant and soil samples followed by ion chromatographic analysis is a rapid, simple and accurate method of analysing for total sulphur content. Fusion at high temperature or treatment with concentrated reagents is not necessary, and recovery is quantitative. The high inorganic content of the soils and sediments presents no problems in the combustion step.

Conclusion

Single-column ion chromatography is well suited to rapid, simultaneous analysis for anions in aqueous environmental samples. The relative simplicity and ease of operation are conducive to routine analysis, particularly with the availability of modern data-handling systems which can be directly interfaced with the detector. No interruption of operation is necessary to regenerate a suppressor column, and indirect ultraviolet detection provides lower detection limits than previously possible with conductivity measurements.

Analyses by IC are not restricted to "clean" water samples only. Pretreatment with a lead-charged cation-exchange resin permits the analysis of samples high in SO_4^{2-}, as in the determination of "available" soil NO_3^-.

Oxygen combustion of a solid environmental sample yields the total sulphur content as a sulphate-containing solution which can be analysed directly. The result is a simple and accurate method for total sulphur determination by ion chromatography.

Acknowledgements—This work was supported by DSS contract number ISU80-00350. We are also grateful for support to J.A.H. through a Queen's Graduate Award and would like to thank R. Helleur for assistance in setting up the chromatographic system.

REFERENCES

1. H. Small, T. S. Stevens and W. C. Bauman, *Anal. Chem.*, 1975, **47**, 1801.
2. T. S. Stevens, J. C. Davis and H. Small, *ibid.*, 1981, **53**, 1488.
3. T. S. Stevens, G. L. Jewett and R. A. Bredeweg, *ibid.*, 1982, **54**, 1206.
4. C. A. Black (ed.), *Methods of Soil Analysis*, Part I, p. 1213. American Society of Agronomy, 1965.
5. L. D. Hansen, B. E. Richter, D. K. Rollins, J. D. Lamb and D. J. Eatough, *Anal. Chem.*, 1979, **51**, 633.
6. H. Small, *ibid.*, 1983, **55**, 235A.
7. D. T. Gjerde, J. S. Fritz and G. Schmuckler, *J. Chromatog.*, 1979, **186**, 509.
8. H. Small and T. E. Miller, Jr., *Anal. Chem.*, 1982, **54**, 462.
9. B. C. Verma, K. Swaminathan and K. C. Sud, *Talanta*, 1977, **24**, 49.
10. R. J. Norman and J. W Stucki, *Soil Sci. Soc. Am. J.*, 1981, **45**, 347.
11. W. A. Dick and M. A. Tabatabai, *ibid.*, 1979, **43**, 899.
12. C. A. Black, *op. cit.*, p. 1216.
13. *Idem, op. cit.*, p. 1187.
14. D. D. Siemer, *Anal. Chem.*, 1980, **52**, 1874.
15. A. Steinbergs, O. Iismaa, J. R. Freney and N. J. Barrow, *Anal. Chim. Acta*, 1962, **27**, 158.
16. W. Schöniger, *Mikrochim. Acta*, 1955, 123; 1956, 869.

Talanta, Vol 30, No. 9, pp. 683–686, 1983
Printed in Great Britain.

0039/9140/83 $3.00+0.00

DETERMINATION OF CHROMIUM(VI) IN NATURAL WATERS BY THE SORPTION OF CHROMIUM–DIPHENYLCARBAZONE WITH XAD-2 RESIN

SUSUMU OSAKI
Radioisotope Centre, Kyushu University 16, Hakozaki, Higashi-ku, Fukuoka, 812 Japan

TOMOE OSAKI
Faculty of Engineering, Fukuoka Institute of Technology, Shimowaziro, Higashi-ku, Fukuoka, 811–02 Japan

YOSHIMASA TAKASHIMA
Department of Chemistry, Faculty of Science, Kyushu University 33, Hakozaki, Higashi-ku, Fukuoka, 812 Japan

(*Received* 19 *October* 1982. *Revised* 17 *February* 1983. *Accepted* 11 *March* 1983)

Summary—The sorption of the chromium(III)–diphenylcarbazone complex (Cr–DPC) with XAD-2 has been investigated, for use in the separation of Cr(VI) from Cr(III) species in natural waters. Cr–DPC is formed from the reaction of Cr(VI) with diphenylcarbazide, but Cr(III) species give no reaction in aqueous solution. The addition of sodium chloride or sodium β-naphthalenesulphonate markedly enhances the sorption. The Cr–DPC sorbed on XAD-2 can be almost completely eluted with organic solvents, especially methanol, but about 5% of it is irreversibly sorbed and cannot be eluted. The excess of diphenylcarbazide and some of the organic matter in natural waters are also sorbed on XAD-2 but most of this can also be eluted with methanol. Organic matter which interferes with measurement of the absorbance of Cr–DPC can almost all be removed by extraction with chloroform. By use of these techniques, Cr(VI) in sea-water has been determined by the standard-addition method. Although about 50 litres of sea-water are necessary for the analysis, organic and colloidal Cr(III) species do not interfere.

Solvent extraction and co-precipitation are generally used for the determination of Cr(III) and Cr(VI) in natural waters. Part of the organically bound Cr(III), however, might be extracted with the solvent used for extraction of the Cr(VI) and part of any inert Cr(III) complexes might not be co-precipitated with the iron(III) hydroxide or other species used for the co-precipitation of Cr(III). Such errors are discussed in a companion paper.[1] The well-known diphenylcarbazide method[2] is one of the most suitable methods for the determination of ionic Cr(VI) in water. The magenta complex, Cr(III)–diphenylcarbazone (Cr–DPC), is formed from the reaction of Cr(VI) with diphenylcarbazide, but Cr(III) species do not react directly with diphenylcarbazide and diphenylcarbazone in aqueous solution.[3] The sensitivity, however, is too low for determination of Cr(VI) in natural waters. Yoshimura *et al.*[4] improved the sensitivity by using an ion-exchange resin and applied the method to the determination of total chromium in natural waters. XAD-2 resin is used for concentration and separation of many organic compounds,[5,6] including organometallic complexes.[7] In order to develop a new analytical method for Cr(VI) in natural waters, the sorption of Cr–DPC with XAD-2 resin has been investigated.

EXPERIMENTAL

Reagents and apparatus

Analytical-grade reagents were used whenever possible. XAD-2 resin (purchased from the Rohm and Haas Corp.) was crushed in a ceramic mortar and sieved. The 100–200 mesh fraction was washed successively with 4*M* hydrochloric acid, distilled water, 4*M* sodium hydroxide, distilled water and methanol and then dried at room temperature. Cr(VI) stock solution was prepared by dissolving potassium dichromate in water, and further diluted as required. Diphenylcarbazide solution was prepared by dissolving 250 mg of reagent in 100 ml of acetone. Sodium β-naphthalenesulphonate solution was prepared by dissolving 23 g of the reagent-grade material in 1 litre of water and filtered through a fine sintered-glass filter. Redistilled water was used throughout.

Absorbances were measured with a Hitachi 200–10 double-beam spectrophotometer, with 10-cm or 1-cm cells.

Stability of Cr–DPC

*In 0.05*M *sulphuric acid.* In a 1-litre standard flask, *ca.* 600 ml of water, 20 ml of 2.5*M* sulphuric acid, 4 ml of 101-μg/ml Cr(VI) solution, 15 ml of diphenylcarbazide solution and 10 ml of sodium β-naphthalenesulphonate solution were mixed and the solution was diluted to volume with water and transferred into a polyethylene bottle. At given time intervals, small portions (10 ml) were removed and their absorbance measured at 542 nm against water.

In methanol. An aliquot (100 ml) of the freshly prepared solution just described was passed through an XAD-2

column (column volume 10 ml). The coloured complex was eluted from the XAD-2 with *ca.* 40 ml of methanol, the effluent being collected in a 50-ml standard flask and diluted to volume with methanol. The absorbance of the methanol solution was measured at 542 nm at various times, against methanol.

On XAD-2. In a 100-ml standard flask, *ca.* 60 ml of water, 5 ml of 1*M* sulphuric acid, 3 ml of 10.1-μg/ml Cr(VI) solution, 2 ml of diphenylcarbazide solution and 1 ml of sodium β-naphthalenesulphonate solution were mixed and the solution was diluted to 100 ml and passed through an XAD-2 column (column volume 10 ml). After a given time, the coloured complex was eluted with *ca.* 40 ml of methanol and the effluent diluted to 50 ml with methanol. The absorbance was measured at 542 nm against methanol

Sorption of Cr–DPC on XAD-2

Batch method. In a 250-ml standard flask, *ca.* 100 ml of water, 5 ml of 2.5*M* sulphuric acid, 5 ml of 5-μg/ml Cr(VI) solution, 4 ml of diphenylcarbazide solution and appropriate amounts of sodium β-naphthalenesulphonate solution or 3*M* sodium chloride were mixed and the solution was diluted to volume. In an Erlenmeyer flask, 500 mg of XAD-2 were placed and wetted with 5 ml of methanol. The solution was poured into the flask and stirred for 30 min by a magnetic stirrer. The XAD-2 was filtered off on a sintered-glass filter. The absorbance of the filtrate was measured at 542 nm against water.

Column method. Into polyethylene containers, 0.050, 1, 2, 5 or 10-litre portions of distilled water were placed and 5 ml of 10-μg/ml Cr(VI) solution were added to each. Appropriate amounts of concentrated sulphuric acid, diphenylcarbazide solution and sodium β-naphthalenesulphonate solution were added to give overall concentrations of 0.05*M* sulphuric acid, 0.15m*M* diphenylcarbazide and 2m*M* sodium β-naphthalenesulphonate. XAD-2 resin was wetted with 20 ml of methanol and then mixed with 500 ml of water. This slurry was poured into the column (diameter 20 mm, bed volume 15 ml). A supply tube leading from the sample bottle was attached to the top of the column, and the test solution was drawn through the column by suction. The flow-rate was about 200 ml/min at the start and became steadily slower owing to the packing of the resin in the column. When 10 litres of sample solution had passed through the column, the flow-rate was only about 100 ml/min. After passage of the sample, the resin was washed with 50 ml of water and eluted first with 30 ml of acetone and then with 20 ml of methanol. The eluate was placed in a 100-ml separating funnel with 25 ml of 0.05*M* sulphuric acid and extracted with three 25-ml portions of chloroform, being shaken for 1 min with each. The aqueous phase was filtered through paper to remove droplets of organic phase, and then diluted to volume in a 50-ml standard flask with water. The absorbance of the solution was measured at 440 and 542 nm against water

Determination of Cr(VI) in sea-water

To 10-litre portions of sample, Cr(VI) (0, 1, 2, 3 or 4 μg) was added, together with 26 ml of concentrated sulphuric acid, 375 mg of diphenylcarbazide (dissolved in *ca.* 50 ml of acetone) and 4.5 g of sodium β-naphthalenesulphonate (dissolved in *ca.* 200 ml of water). The mixture, in a polyethylene container, was well stirred by a magnetic stirrer. The procedures for the sorption on an XAD-2 column, the elution with acetone and methanol, the purification with chloroform and the measurement of the absorbance were the same as just described in the section on the column method. The concentration of Cr(VI) in the sample was determined graphically by the standard-addition method

All experiments were done at room temperature.

RESULTS AND DISCUSSION

Stability of Cr–DPC

The spectrophotometric determination of Cr(VI) with diphenylcarbazide has been widely studied,[2,3] and it has been shown that the absorbance of the coloured complex in aqueous solution decreases with standing time, at a rate which depends on the acidity, temperature and so on. The stabilities of Cr–DPC in aqueous solution, in methanol and on XAD-2 were investigated before the study on sorption of Cr–DPC by XAD-2. The results are shown in Table 1. Under the conditions used, the absorbance of Cr–DPC was little affected by standing times of a few hours.

Sorption of Cr–DPC by XAD-2 resin

The sorption of Cr–DPC by XAD-2 resin was investigated by the batch method (Fig. 1). Cr–DPC in aqueous solution is extracted into a suitable solvent if sodium chloride[8] or sodium β-naphthalenesulphonate[9] is added. As this suggests, the sorption of Cr–DPC on XAD-2 is also enhanced by the addition of sodium chloride or sodium β-naphthalenesulphonate, the latter being the more effective. When the concentration of sodium β-naphthalenesulphonate is 1.5m*M* or above, Cr–DPC is nearly quantitatively sorbed by XAD-2. Since the Cr(VI) concentrations of most natural waters are very low (0.01–0.5 μg/l.), more than 10 litres of sample water will be necessary to give enough Cr(VI) for the Cr–DPC absorbance to be measurable, but sample volumes larger than about 2 litres make the batch method difficult to operate.

As the results of the batch experiments suggested, Cr–DPC in 2m*M* sodium β-naphthalenesulphonate solution is sorbed nearly at the top of the XAD-2 column. When an XAD-2 column 20 mm in diameter and 15 ml in bed volume was used, at flow-rates up to 200 ml/min, no Cr–DPC was detected in the effluent.

Table 1. Effect of the standing time on the stability of Cr–DPC in various media

Standing time, *hr*	Decrease in absorbance		
	0.05*M* H_2SO_4	methanol	XAD-2
$\frac{1}{6}$	(100)†	(100)†	—
$\frac{1}{3}$	100	99.7	—
$\frac{2}{3}$	99.2	99.7	—
1	98.9	99.5	(100)*
2	98.9	99.5	100
4	98.5	—	100
24	95.1	—	97.6
48	85.6	—	94.2

*Cr–DPC on XAD-2 was eluted with methanol after a given standing time, and the absorbance of the eluate was measured at 542 nm against methanol.

†The absorbances obtained in these experiments were taken as reference (100)%.

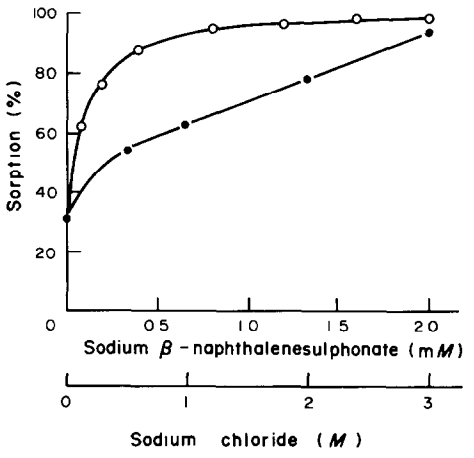

Fig. 1. Effect of the concentration of sodium chloride (●) and sodium β-naphthalenesulphonate (○) on the sorption of Cr–DPC on XAD-2 resin.

No aqueous solution could be found that would elute Cr–DPC from XAD-2. Preliminary experiments with organic solvents showed that methanol was most effective as an eluent. About 5% of the Cr–DPC, however, still remained on the XAD-2, even when a large amount (more than 10 column volumes) of methanol was used. The irreversible adsorption is possibly due to the change of Cr–DPC on XAD-2 into an unidentified brown substance. The brown substance can be eluted with methanol after passage of 4*M* sodium hydroxide through the column.

Measurement of the absorbance of CR–DPC

As XAD-2 resin is an excellent sorbent for many organic compounds, most of the organic compounds in natural waters and the excess of diphenylcarbazide will also be sorbed on the XAD-2. Because 10 litres of natural water samples are needed, the excess of diphenylcarbazide and significant quantities of the organic compounds in the sample water are concentrated in the eluate from the XAD-2 column. Some of these compounds give an intense brown colour which interferes in the measurement of the Cr–DPC absorbance. Therefore, most of these compounds should be separated. For this purpose, liquid–liquid extraction with chloroform from dilute sulphuric acid medium was used. The brown compounds are mainly transferred to the organic phase, and the Cr–DPC is left in the aqueous phase. The methanol remains mostly in the aqueous phase, which decreases the sensitivity of the analysis. Acetone can be used for the elution instead of methanol, and is mostly transferred to the organic phase in the extraction, but unfortunately acetone is less effective than methanol in the elution. Therefore, successive elution with acetone and methanol was used. A large fraction of the Cr–DPC in the XAD-2 column was eluted with 30 ml of acetone and the remainder with 20 ml of methanol.

It is impossible to separate the other organic compounds from the eluate completely by chloroform extraction. When a 10-litre sample of sea-water was used, the absorption spectrum of the eluate purified by chloroform extraction was a composite of the spectra of Cr–DPC and other organic matter (Fig. 2). Because Cr–DPC in aqueous solution is rather unstable, the absorption of the Cr–DPC disappears on standing for about 10 days. Unfortunately, the absorbance of the other organic matter increases slightly with standing time, so the exact background spectrum cannot be obtained in this way. We can only assume that the *shape* of the background spectrum, (c) in Fig. 2, will not change during the 10 days. The absorbance of the Cr–DPC at 542 nm [$(Cr–DPC)_{542}$] is then estimated from the absorbances of the purified eluate at 440 nm [$(eluate)_{440}$] and 542 nm [$(eluate)_{542}$] by means of the equation:

$$(Cr–DPC)_{542} = 1.038(eluate)_{542} - 0.215(eluate)_{440}$$

This equation is based on the following data:

$$(Cr–DPC)_{440}/(Cr–DPC)_{542} = 0.177$$
$$(org)_{440}/(org)_{542} = 4.83$$
$$(eluate)_{440} = (Cr–DPC)_{440} + (org)_{440}$$
$$(eluate)_{542} = (Cr–DPC)_{542} + (org)_{542}$$

where $(Cr–DPC)_{440}$, $(org)_{440}$ and $(org)_{542}$ are the absorbances of Cr–DPC at 440 nm and those of the other organic matter in the purified eluate at 440 and 542 nm, respectively. The $(org)_{440}/(org)_{542}$ ratio was obtained from a blank experiment with 10 litres of distilled water and was very similar to that for curve (c) in Fig. 2. Diphenylcarbazide, its degradation products, and β-naphthalenesulphonate may be present in the purified eluate, and contribute strongly to the absorbance of the solution. Naturally the suggested ratio is probably somewhat variable, depending on which organic compounds are present.

Determination of Cr(VI) in sea-water

Chromium(VI) in various volumes (50 ml–10 litres) of distilled water was separated by means of the XAD-2 column, and the $(Cr–DPC)_{542}$ values were

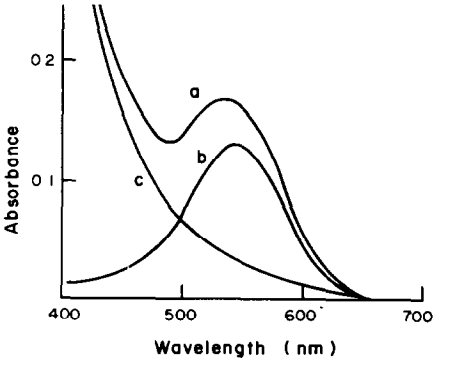

Fig. 2. Absorption spectrum of the solution finally separated from 10 litres of sea-water by the XAD-2 column (a) and the estimated spectra of Cr–DPC (b) and other organic matter (c) in the solution.

Table 2. Effect of sample volume on the yield of Cr–DPC in the column separation

Sample volume, *litres*	Yield, %
0.05	94.6, 95.7
1	93.1
2	94.4
5	87.5, 86.4
10	84.1, 82.4

measured as described above. The results are listed in Table 2. The yields decreased with increasing sample volume, possibly on account of an increase in the irreversible sorption of Cr–DPC on XAD-2. The reproducibility of duplicate runs was good, which suggests that these techniques can be applied to the determination of trace amounts of Cr(VI) by the standard-addition method.

Chromium(VI) in sea-water from the shore of Shingu, Fukuoka, Japan was determined after filtration of the sample through a 0.45-μm membrane. The result is shown in Fig. 3. To estimate the reagent blank, the procedure was applied to sample volumes of 5 and 10 litres. From Fig. 3, the amounts of Cr(VI) found were 0.83 and 1.50 μg in the 5- and 10-litre samples respectively. The Cr(VI) concentration in the sample and the amount in the reagent blank are calculated to be 0.13 μg/l. and 0.16 μg, respectively.

The average yields found were 72% for the 10-litre sample and 75% for the 5-litre from the estimated slopes of the plots in Fig. 3 to the slope of a calibration graph for Cr–DPC. These values are about 10% lower than the corresponding values shown in Table 2. The lower concentration of Cr(VI) in the sample may have affected the rate of decomposition of Cr–DPC or the irreversible sorption of Cr–DPC on XAD-2.

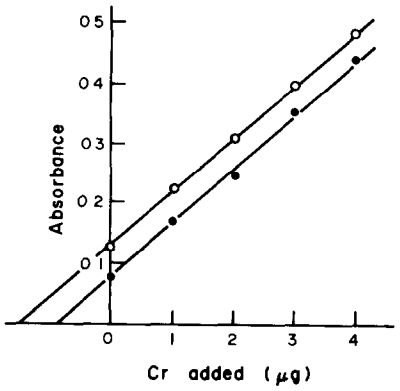

Fig. 3. Determination of Cr(VI) in 10 litres (○) and 5 litres (●) of sea-water by the standard-addition method.

It is difficult to determine Cr(VI) in natural waters accurately, without adequate knowledge about organic and colloidal Cr(III). The method developed in this study may be one of the more suitable methods for determining ionic (reactive) Cr(VI) in natural waters, although a large sample volume is necessary.

REFERENCES

1. S. Osaki, T. Osaki, N. Hirashima and Y. Takashima, *Talanta*, 1983, **30**, 523.
2. E. B. Sandell, *Colorimetric Determination of Traces of Metals*, 3rd Ed., p. 392. Interscience, New York, 1959.
3. G. J. Willems, N. M. Blaton, O. M. Peaters and C. J. De Ranter, *Anal. Chim. Acta*, 1977, **88**, 345.
4. K. Yoshimura and S. Ohashi, *Talanta*, 1978, **25**, 103.
5. A. K. Burnham, C. V. Calder, J. S. Fritz, G. A. Junk, H. J. Suec and R. Willis, *Anal. Chem.*, 1972, **44**, 139.
6. P. V. Rossum and R. G. Webb, *J. Chromatog.*, 1978, **150**, 381.
7. K. L. Cheng and H. V. Guh, *Microchim. Acta*, 1978 **I**, 55.
8. J. E. Delaney, *Sanitalk*, 1953, **1**, 9.
9. E. V. Kovalenko and V. I. Petrashen, *Tr. Komis. po Analit. Khim., Akad. Nauk SSSR, Inst. Geochim. i Analit. Khim.*, 1965, **15**, 101.

Talanta, Vol 30, No. 9, pp. 687–691, 1983
Printed in Great Britain.

0039/9140/83 $3.00+0.00

A SIMPLE AUTOMATIC SYSTEM USING THE HP-85 MICROCOMPUTER FOR PROGRAMMED POTENTIOMETRIC TITRATION

GEORGI VELINOV
Faculty of Pharmacy, Medical Academy, 15 Ekz. Josif Street, Sofia, Bulgaria

NEDKO TODOROV and SIMEON KARAMPHILOV
ITKR, Bulgarian Academy of Sciences, Sofia, Bulgaria

(*Received* 23 *November* 1982. *Accepted* 23 *February* 1983)

Summary—A simple way of constructing an automatic titration system is proposed, based on combination of a digital pH-meter and an automatic burette with an HP-85 microcomputer. An inexpensive interface unit based on a MOTOROLA 6800 has been developed, which permits communication of the computer with the pH-meter and the burette. The system constructed is very flexible and can find wide application in potentiometric titration and direct potentiometry with different kinds of ion-selective electrodes.

The reviews published by Betteridge and Goad[1] and by the initiative of *Talanta*[2] show unambiguously that the use of microprocessors enters widely into analytical chemistry and the modern analyst has to change his outlook in order to take advantage of this new technique. Microprocessors are of special interest to analytical chemistry, because of their possibilities for control and automation of analysis, especially through utilization of digital instruments for measurements. In this connection potentiometric titration is a method which can comparatively easily be automated.

Two approaches are possible for the construction of microprocessor-controlled systems for potentiometric titration: (1) utilizing specialized microprocessor-controllers, and (2) adapting commercially available microcomputers. The first approach has been used by several authors[3–6] for the construction of automatic titrators; its main advantage is the low cost of the microprocessor chips. The essential disadvantage is the necessity to create the whole organization of the system control, which is usually hardware. This approach to creation of automatic titrators is preferable when serial analyses are performed or the instruments[7] are multi-purpose and constructed for the determination of the inflection (equivalence) points on the titration curves.

The second approach, using microcomputers such as the COMMODORE PET, APPLE II, HP-85, *etc.*, has the great advantage of using high-level organization of the microcomputer system and implementation of algorithmic languages (mainly BASIC). The great possibilities of this approach were shown by Frazer *et al.*[8] A main disadvantage of this tactic is the need for interface modules to link the computer with the instruments, especially if the laboratory is equipped with instruments of different types that are not suitable for direct communication with the computers.

In the present work a simple means is proposed for the creation of an automatic system for potentiometric titration, with use of the HP-85 microcomputer. An inexpensive interface unit has been developed which allows connection between the computer and different types of automatic burette and digital pH-meter. The system uses an adaptive algorithm to make the measurements as well as digital and graphical representation of the results.

EXPERIMENTAL

Apparatus

Automatic titration system. The system was based on a digital OP-208 pH-meter with accuracy of ±0.1 mV and BCD output, a Radiometer type ABU-12 automatic burette accurate to ±0.001 ml, and an HP-85 microcomputer, with HP–IB interface and I/O ROM memory extension. The system ensures direct transfer of data and control commands between the measuring instruments (the pH-meter and the burette) and the computer. Also, a special coupling has been developed which permits simultaneous measurements of the output of another instrument such as a spectrophotometer or an HPLC detector, along with that from the pH-meter. The functions of the system are shown in Fig. 1. The first stage of the system converts the data from the pH-meter into suitable form for acceptance by the computer. In the second stage the data are treated according to a definite algorithm, and then control commands are sent to the burette.

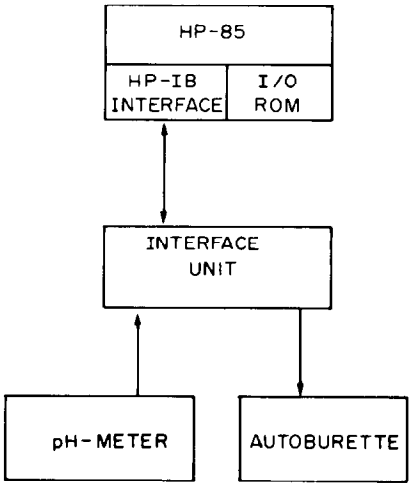

Fig. 1. Titration system with microcomputer HP-85.

The construction of the computer permits communication with external devices working according to the IEEE 488 (HP-IB) standard for data transfer. The pH-meter and the burette used have no controllers for data transfer according to this standard, so an interface unit for this purpose has been developed.

The HP-IB interface module. The HP-85 works according to the HP-IB standard if it is connected with the interface module and the I/O ROM memory extension. A full description of these modules is given in the computer manual.

The HP-IB interface module has 8 lines for data transfer, 3 protocol lines and 5 control lines. This imposes strict requirements with respect to the transfer and the use of "intelligent" controllers. In these conditions the system is flexible and has possibilities for extension. The functions of the separate lines are shown in Table 1.

Description of the interface unit. The interface card of this unit is shown in Fig. 2. A MOTOROLA 6820 peripheral interface adapter (PIA) is used. The data transfer in this configuration is made according to another standard, requiring a combination of both software and hardware. The PIA has 6 internal registers, shown in the user's manual. The initiation is performed by means of controlling bytes according to the HP-IB. The digital information entering from the pH-meter by the peripheral registers PRA and PRB is accepted. This information is transformed under program control and is then suitable for use according to the HP-IB transfer. The two control registers of the PIA (CRA and CRB) are used to transform the commands from HP-IB to the relays operating the burette and the switch for the entrance signals. Signal ATN directly commands the duplicate switch relay; signal SRQ accepts the highest digit from pH-meter.

Software. The software consists of four subroutines and one main program to give the data array for further treatment by the user. The subroutines perform: (1) initiation of the PIA, (2) data reading (mV) and translation from inverted BCD code into decimal code, (3) running the burette for a definite time to give a defined increment of titrant (*e.g.*, when a 2.5-ml burette is used, the INCREMENTS button is in the "ON" position and the speed of the piston is set at "20", the program-set time of 10.5 sec gives a 0.100-ml portion of titrant), and (4) graphical representation of the results as they are being obtained (an auto-scaling procedure chooses the scale for the graph).

The programs are written in BASIC with some additional input–ouptut instructions for communication with the external instruments.

Experimental test of the system

The system was tested by an acid–base titration with glass and calomel electrode. A very weak base—amidopyrine ($pK_b = 9.0$)—was titrated in water with standard hydrochloric acid. This case was chosen in order to illustrate the possibilities of the system for giving good results under unfavourable conditions. The titration aims at quantitative determination and identification of the substance by means of precise determination of the equivalence point and the protolysis constant.

The execution of the program involves the following stages:

—data acquisition (ml, mV) after addition of equal portions of the titrant;

—division of the data into two groups: before and after neutralization;

—treatment of the data after neutralization according to the Gran equation[9] for strong protolytes and calibration of the galvanic cell as described elsewhere;[10]

—treatment of the data before neutralization according to the extended Gran equation[11] adapted for bases; calculation of the equivalence point and the pK-value of the amidopyrine;

Table 1. The function of the lines of the HP-IB interface module

Function	Coupling	Remark
DATA LINES	1, 2, 3, 4, 13, 14, 15, 16	DI01–DI08
CONTROL LINES		
ATN	11	ATTENTION
IFC	9	INTERFACE CLEAR
SRQ	10	SERVICE REQUEST
EOI	5	END OR IDENTIFY
REN	17	REMOTE ENABLE
TRANSFER LINES		
NRFD	7	NOT READY FOR DATA
NDAC	8	NO DATA ACCEPTED
DAV	6	DATA VALID

The HP-IB uses negative logic.

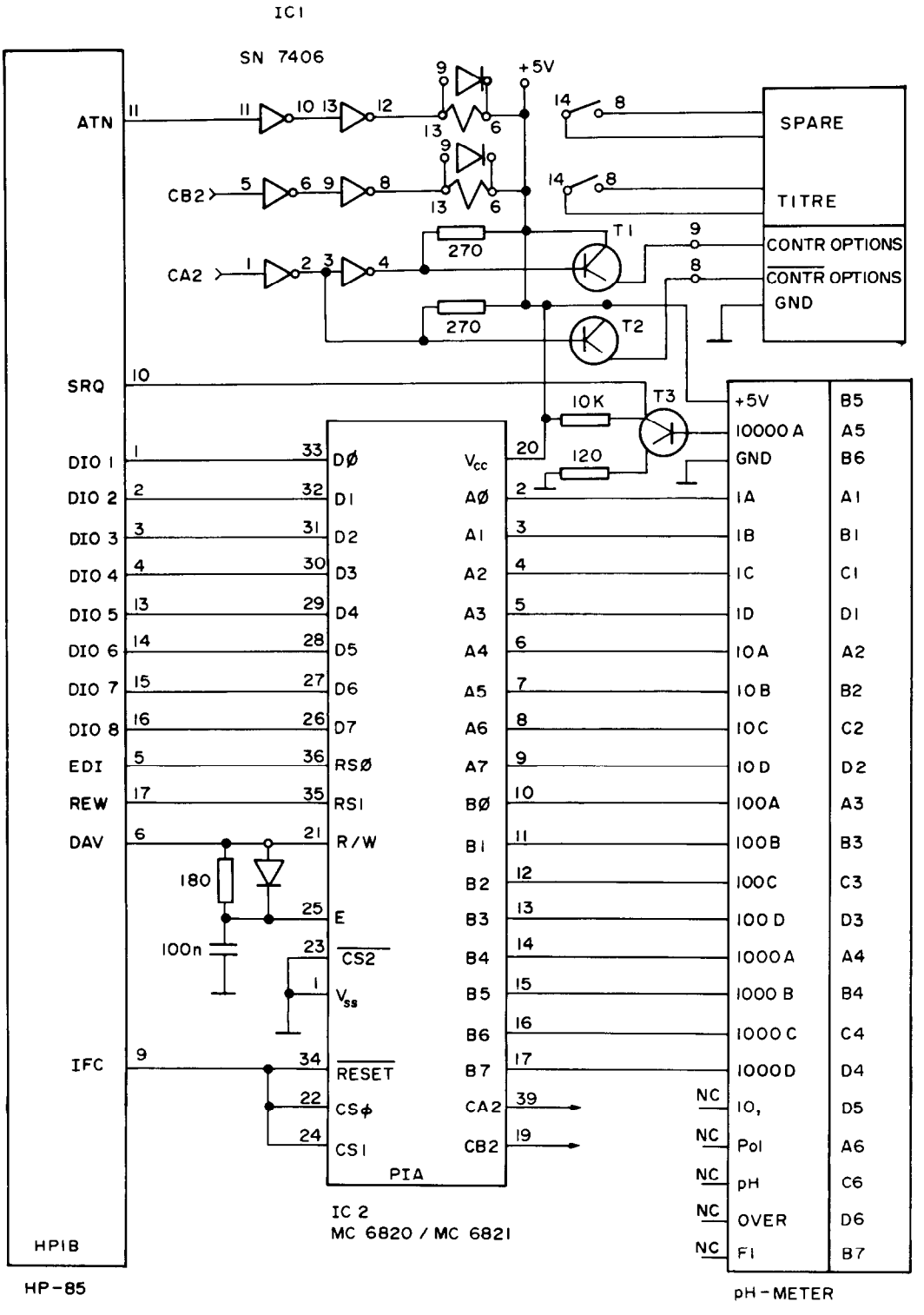

Fig. 2. Block diagram of the interface unit for communication of HP-85 with the pH-meter and the burette.

—graphical presentation of the pH-curve and its linear plot on the CRT display of the computer;

—copying of the curves and the final results on the thermal printer (see Fig. 3).

The BASIC listing for data acquisition is given in the Appendix.

The experimental test shows that communication between the computer and the instruments proceeds

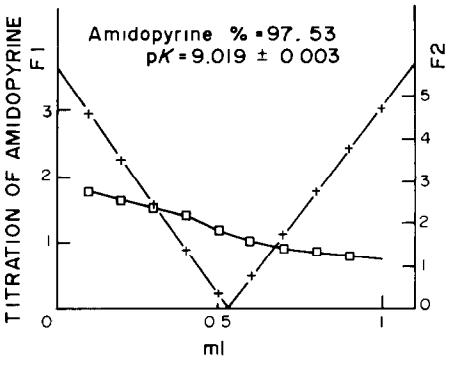

Fig. 3. The final results for the titration of amidopyrine, presented on the CRT display of the HP-85 and copied on the thermal printer. F1 and F2 denote the non-exponential parts of the linear plot functions.

according to the logic of the programme. The analysis takes 4–5 min. The results have high reproducibility: the standard deviations are not greater than 0.001 ml for the equivalence volume, and 0.005 for the pK-value. The mean error in a series of determinations is not greater than $\pm 0.2\%$.

In conclusion it must be stressed that the automatic system constructed is very flexible and "intelligent", with great possibilities. It can be used successfully in research work, and in chemical and industrial laboratories for potentiometric titrations and direct potentiometric measurements with different types of ion-selective electrodes.

Acknowledgements—The authors are indebted to the Ministry of Chemical Industry of P. R. Bulgaria for financial support of this work. One of them (G.V.) is indebted to the Professor Omortag Budevsky for introducing him to the field of equilibrium analysis.

REFERENCES

1. D. Betteridge and T. B. Goad, *Analyst*, 1981, **106**, 257.
2. *Talanta*, 1981, **28**, No. 7B.
3. O. Ginstrup, *Chem. Instrum.*, 1973, **4**, 141; S. Gobom and J. Kovács, *Chem. Scr.*, 1972, **2**, 103; J. T. Stock and K. D. Wolter, *Analyst*, 1976, **101**, 786; F. Dellavalle and G. Mori, *Ann. Chim. Roma*, 1976, **66**, 753; P. V. Früh, L. Meier, H. Rutishauser and O. Širokỳ, *Anal. Chim. Acta*, 1977, **95**, 97; L. Pehrsson and F. Ingman, *Talanta*, 1977, **24**, 79.
4. D. J. Leggett, *Anal. Chem.*, 1978, **50**, 718.
5. A. H. Wu and H. W. Malmstadt, *ibid.*, 1978, **50**, 2090.
6. H. Gampp, M. Maeder, A. D. Zuberbühler and T. A. Kaden, *Talanta*, 1980, **27**, 513.
7. Radiometer Titrator No. DTS 633, Mettler Titrator No. SR 10; Metrohm Titroprocessor E636; Pye Unicam Ion-selective Analyser No. PW 9416.
8. J. Frazer, A. M. Kray, W. Selig and R. Lim, *Anal. Chem.*, 1975, **47**, 869.
9. F. J. C. Rossotti and H. Rossotti, *J. Chem. Educ.*, 1965, **42**, 377.
10. J. Tencheva, G. Velinov and O. Budevsky, *J. Electroanal. Chem.*, 1976, **68**, 65.
11. L. Pehrsson, F. Ingman and A. Johansson, *Talanta*, 1976, **23**, 769.

APPENDIX

Program for Data-Acquisition

```
10 REM **DATA ACQUISITION PROCEDURE
20 GOSUB 560
30 DISP "NUMBER OF MEASUREMENTS"
40 BEEP 500,200
50 INPUT N0
60 DISP "PERIOD IN SECONDS"
70 BEEP 500,200
80 INPUT N1
90 DISP "ACCURACY IN MILLIVOLTS"
100 BEEP 500,200
110 INPUT N2
120 DISP "TIME FOR TITRATION IN SECONDS"
130 BEEP 500,200
140 INPUT N3
150 DISP "INITIAL VOLUME"
160 BEEP 500,200
170 INPUT N4
180 OPTION BASE 1
190 DIM M(50,3)
200 REM COM OR SOMETHING ELSE
210 FOR J=1 TO N0
220 GOSUB 620
230 Z0=Y3
240 WAIT 1000*N1
250 GOSUB 620
260 Z1=Y3
270 IF ABS(Z0-Z1)>N2 THEN GOTO 220
280 WAIT 1000*N1
290 GOSUB 620
300 Z2=Y3
310 IF ABS(Z2-Z0)>N2 THEN GOTO 220
320 IF ABS(Z2-Z1)>N2 THEN GOTO 220
330 Z=Z2
340 IF J=2 THEN GOSUB 910
350 IF J>2 THEN GOSUB 1200
360 LET M(J,1)=J
370 LET M(J,2)=Z
380 LET M(J,3)=J*N3
390 X5=203
400 BEEP 200,150
410 BEEP 100,150
420 BEEP 200,150
430 GOSUB 720
440 WAIT N3*1000
450 X5=195
460 GOSUB 720
470 BEEP
480 NEXT J
490 CLEAR
500 DISP "N0";TAB(7);"MILLIVOLTS";TAB(19);
    "T";"    ";"V0=";N4
510 FOR K=1 TO N0
520 DISP M(K,1);TAB(7);M(K,2);TAB(18);
    M(K,3)
530 NEXT K
540 BEEP 200,3000
550 END
560 RESET 7
570 CONTROL 7,2 ; 80,195
580 CONTROL 7,2 ; 84,195
590 CONTROL 7,2 ; 16,195
600 CONTROL 7,2 ; 20,195
610 RETURN
620 CONTROL 7,2 ; 88,0
630 STATUS 7,3 ; X0
640 CONTROL 7,2 ; 24,0
650 STATUS 7,2 ; X2,X1
660 X3=BIT(X2,5)
670 GOSUB 830
680 RETURN
690 CONTROL 7,2 ; 80,X4
700 CONTROL 7,2 ; 84,X4
710 RETURN
720 CONTROL 7,2 ; 16,X5
730 CONTROL 7,2 ; 20,X5
740 RETURN
750 REM INVBCD TO DEC CONV
760 Y8=0
770 Y9=0
780 FOR I=0 TO 3
790 IF BIT(X,I)=0 THEN Y8=Y8+2^I
800 IF BIT(X,I+4)=0 THEN Y9=Y9+2^I
810 NEXT I
820 RETURN
830 X=X0
840 GOSUB 760
850 Y0=Y8
860 Y1=Y9
870 X=X1
880 GOSUB 760
890 Y3=1000*X3+100*Y9+10*Y8+1*Y1+.1*Y0
900 RETURN
910 GCLEAR
920 Y4=M(1,2)
930 Y5=400
940 Y6=Y4-300
950 IF Z-Y4>0 THEN Y6=Y4-10
960 FOR I1=0 TO 2000 STEP 10
970 IF Y6-I1<10 THEN GOTO 990
980 NEXT I1
990 SCALE 1,N0,I1,Y6+Y5
1000 XAXIS I1,1
1010 YAXIS 1,10
1020 FOR I0=2 TO N0-1 STEP 2
1030 MOVE I0,I1
1040 LABEL ""&VAL$(I0)
1050 NEXT I0
1060 MOVE 1,I1
1070 Y7=100
1080 IF Y5<101 THEN Y7=50
1090 IF Y5<51 THEN Y7=10
1100 FOR I2=I1 TO Y6+Y5
1110 IF FP(I2/Y7)=0 THEN GOSUB 1170
1120 NEXT I2
1130 MOVE 1,Y4
1140 DRAW 1,Y4
1150 DRAW 2,Z
1160 RETURN
1170 MOVE 1,I2
1180 LABEL "_"&VAL$(I2)
1190 RETURN
1200 DRAW J,Z
1210 RETURN
1220 ! ####end of data acquisition#####
     ##################################
1230 ! ####beginning of calculations###
     ##################################
```

Talanta, Vol. 30, No. 9, pp. 693–694, 1983
Printed in Great Britain

0039/9140/83 $3.00+0.00
Pergamon Press Ltd

SHORT COMMUNICATIONS

DETERMINATION OF THIOCARBONATE IN THE PRESENCE OF SULPHITE, THIOSULPHATE AND THIOCYANATE BY TITRATION WITH *o*-HYDROXYMERCURIBENZOATE

K. SINGH and B. A. FODEKE
Department of Chemistry, Ahmadu Bello University, Zaria, Nigeria

(*Received* 7 *October* 1982. *Accepted* 29 *March* 1983)

Summary—A direct titrimetric method has been developed for the determination of thiocarbonate in the presence of sulphite, thiosulphate and thiocyanate, by titration with *o*-hydroxymercuribenzoate, with sodium nitroprusside as indicator.

Potassium and sodium thiocarbonates have proved useful analytical reagents as an alternative to gaseous hydrogen sulphide in qualitative[1] and quantitative[2,3] analysis. Thiocarbonate has been estimated gravimetrically[4] as Tl_2CS_3. Indirect titrimetric methods[5–7] of determination of thiocarbonate with iodine, potassium iodate, chloramine-T, potassium ferricyanide, potassium permanganate and sodium vanadate have been reported, but suffer interference from sulphite, thiosulphate and thiocyanate, which are also oxidized. No direct titrimetric method (with visual indication of the end-point) for determination of thiocarbonate when present together with sulphite, thiosulphate and/or thiocyanate has been described, though indirect methods are known,[8–10] in which *o*-hydroxymercuribenzoate (HMB) is used as reagent.

This communication describes a direct method, based on titration with HMB, with sodium nitroprusside as indicator. Thiocarbonate instantaneously develops a purple complex with sodium nitroprusside (stable over the pH range 8.0–11.5), whereas sulphite, thiosulphate and thiocyanate do not produce any colour; this colour is discharged by addition of excess of HMB, thus making visual end-point detection possible in the titration of thiocarbonate, selectively and directly, in the presence of sulphite, thiosulphate and thiocyanate. Any sulphide present is co-titrated, however, giving a 1:1 reaction with HMB when nitroprusside is used as indicator.[11]

EXPERIMENTAL

Reagents

Standard HMB solution, 0.05*M*. Prepared by dissolving 16.04 g of the anhydride, (Merck, analytical-reagent grade), in 100 ml of 0.1*M* sodium hydroxide and diluting with water to volume in a 1-litre standard flask.

Sodium nitroprusside indicator. Freshly prepared 1% aqueous solution.

Potassium thiocarbonate solution, 1*M*. Prepared and standardized as reported earlier,[4] and diluted as required.

"*Combined sulphur*" *solution*. Solutions of sodium sulphite, sodium thiosulphate and potassium thiocyanate (all analytical-reagent grade), about 0.2*M* with respect to sulphur, were mixed in equal proportions (by volume).

Procedure

To a sample of thiocarbonate solution containing 15–75 mg of thiocarbonate sulphur and a varied amount of "combined sulphur" solution, 5 ml of 1*M* sodium hydroxide were added and the solution was diluted to 100 ml. After addition of 1 ml of indicator the purple solution was immediately titrated with 0.05*M* HMB till colourless or faint yellow.

RESULTS AND DISCUSSION

The determination of 14–101 mg of thiocarbonate sulphur in the presence of 32–96 mg of total sulphite, thiosulphate and thiocyanate sulphur with HMB solutions ranging in concentration from 0.03 to 0.10*M* gave excellent results with a standard deviation of only 0.02 mg. It is evident that thiocarbonate and HMB react in 1:1 mole ratio. Two mechanisms are possible; either the thiocarbonate group replaces the OH-group of the HMB, or the thiocarbonate undergoes hydrolysis to give carbon disulphide and a sulphide ion which displaces the OH-group of HMB.

The formation of carbon disulphide was confirmed by a positive response to a colorimetric test.[12] In this test a drop of the reaction solution produced a stable pink colour when mixed with elemental sulphur dissolved in acetone.

The results obtained with samples containing more than 75 mg of thiocarbonate sulphur were high. This was attributed to the slow reaction between the carbon disulphide generated and the alkali present, resulting in the formation of thiocarbonate and carbonate:

$$3CS_2 + 6OH^- \rightarrow 2CS_3^{2-} + CO_3^{2-} + 3H_2O$$

This reaction is favoured at about 40° (a temperature attainable as room temperature in Zaria) but can easily be avoided by cooling the sample solution in ice for a while before titration.

Acknowledgement—The authors thank the Head of the Chemistry Department for providing facilities and taking a keen interest in the work.

REFERENCES

1. K. N. Johri, *Chemical Analysis Without H_2S, Using Potassium Trithiocarbonate*, Asia Publishing House, Bombay, 1968.
2. K. N. Johri and K. Singh, *Bull. Chem. Soc. Japan*, 1967, **40,** 990.
3. K. N. Johri and N. K. Kaushik, *Chromatographia*, 1976, **9,** 326.
4. K. N. Johri and K. Singh, *Indian J. Chem.*, 1965, **3,** 158.
5. *Idem, Analyst*, 1965, **90,** 745.
6. K. N. Johri and N. K. Kaushik, *ibid.*, 1968, **93,** 791.
7. K. Singh, P. G. Bhatia and R. D. Gupta, *Talanta*, 1982, **29,** 47.
8. M. Wroński, *Anal. Chem.* 1960, **32,** 133.
9. *Idem, Z. Anal. Chem.*, 1961, **183,** 361.
10. *Idem, Talanta*, 1981, **21,** 173.
11. *Idem, Chem. Anal. (Warsaw)*, 1957, **2,** 385.
12. T. Urbanski, *Talanta*, 1962, **9,** 799.

Talanta, Vol. 30, No. 9, pp. 695–698, 1983
Printed in Great Britain

0039/9140/83 $3.00+0.00
Pergamon Press Ltd

CONSTANT-CURRENT POTENTIOMETRIC TITRATION OF ORTHOPHOSPHATE WITH CETYLPYRIDINIUM CHLORIDE: A FEASIBILITY STUDY

WALTER SELIG
Lawrence Livermore National Laboratory, University of California, Livermore, California 94550, U.S.A.

(*Received* 18 *November* 1982. *Accepted* 8 *March* 1983)

Summary—The feasibility of constant-current potentiometric titration of orthophosphate with cetylpyridinium chloride has been studied. The phosphate solution is acidified with hydrochloric acid to pH 1.1–1.3 and an excess of molybdate solution added. For 1 mg of phosphorus (as phosphate) the optimum Mo:P ratio is about 40. Cetylpyridinium chloride reacts stoichiometrically with 12-molybdophosphate, in 3:1 ratio. The optimum cathodic polarizing current is 1.1 μA. The blanks for molybdate are relatively small, constant and non-stoichiometric.

A vast amount of literature exists on the determination of orthophosphate. A recent summary appeared in 1979.[1] Most of the wet analytical methods are based on formation of the 12-molybdophosphate anion. In fact, according to Babko,[2] for the determination of small quantities of phosphorus or silicon, heteropoly acid formation is the only suitable chemical method.

Macháček and Malát[3] recently described some new spectrophotometric procedures for phosphate, based on extraction of the ion-association complexes of 12-molybdophosphoric acid, its "molybdenum blue" reduction product, or 11-molybdovanadophosphoric acid, with a cationic detergent. We have already used quaternary ammonium halides (cationic detergents) for the determination of a variety of inorganic and organic anions,[4–13] and now present a feasibility study on the use of cetylpyridinium chloride (CPC) for the direct titration of orthophosphate as the 12-molybdophosphate.

EXPERIMENTAL

Reagents

The titrant was approximately 0.05*M* cetylpyridinium chloride (CPC), prepared by dissolving 17.9 g of the monohydrate in about 200 ml of hot water, cooling to room temperature, and diluting to 1 litre with cold distilled water. It was standardized by titration of a known amount of sodium dihydrogen phosphate. The molybdate solution was prepared by dissolving 100 g of sodium molybdate dihydrate in 1 litre of distilled water and filtered through Whatman No. 541 paper. The phosphate solution contained approximately 200 μg of phosphorus per ml and was prepared from ACS reagent-grade sodium dihydrogen phosphate monohydrate.

Apparatus

The titration system was controlled by a Tektronix 4051 graphics system, as previously described.[14] This system can impress a constant polarizing current of 0–10 μA (in either direction) on the electrodes. Potential differences were monitored with a single-junction Ag/AgCl reference electrode (0.1*M* sodium nitrate salt bridge) and a Beckman No. 39271 platinum thimble, as well as other electrodes.

Stirring was provided by a magnetic stirrer. The stirring motor was separated from the titration vessel by a water-cooled plate and an earthed (grounded) aluminium plate.

Procedure

The solutions contained 1 mg of phosphorus (as sodium dihydrogen phosphate), 5 ml of 2.5*M* hydrochloric acid, and 5 ml of molybdate solution, and were diluted to 25 ml with distilled water in a 50-ml beaker containing a Teflon-covered stirring bar. The platinum electrode was cathodically polarized at a constant current of 1.1 μA. The current source was turned on approximately 30 sec before the start of a titration. The titrant was added at 0.33 ml/min. Titrations were performed at room temperature (23 $\pm$ 1°).

Titration end-points were calculated according to Savitsky and Golay,[15] with 25 points used for obtaining the convolute for a third-order second derivative. The zero crossing was found by linear interpolation near the change in sign of the convolute.

RESULTS AND DISCUSSION

The method for the determination of orthophosphate by precipitation as quinoline molybdophosphate, and subsequent acid–base titration,[16] has been regarded as the most promising method for the determination of this anion.[17] It has been compared with several other methods and indeed found superior.[18] On the basis of the previous work[4–13] on use of quaternary ammonium halides for potentiometric titration of various anions, we decided to explore the feasibility of direct titration of phosphate as 12-molybdophosphate, with CPC.

Initial experiments were based on a standard colorimetric method[19] which specifies that not more than 1 mg of phosphorus (as orthophosphate) in 5 ml of

2.5*M* nitric or perchloric acid is reacted with 5 ml of 10% sodium molybdate dihydrate solution. Because perchlorate is precipitated by CPC,[4,7] nitric acid was chosen for the exploratory work. A poly(vinyl chloride)/dioctylphthalate-coated spectroscopic graphite rod, which had previously been used as indicating electrode in titrations with CPC,[20] yielded poor titration curves and poor reproducibility. Somewhat better curves were obtained when a small amount of molybdophosphoric acid was incorporated in the plastic coating, as shown in Fig. 1(a), but were still not considered good enough to be analytically useful. Poor curves were also obtained with an Orion No. 93–05 fluoroborate ion-selective electrode.

Consistent results were obtained with a platinum indicator electrode, as shown in Fig. 1(b), but the curves were quite shallow and the magnitude of the break was small. Vinnikov and Kostareva[21] had reported the determination of non-ionic surfactants in the presence of barium ions by potentiometric titration with molybdophosphoric acid, a cathodically polarized platinum electrode being used, and this polarized electrode system was found to give greatly improved end-point breaks in the titration of molybdophosphate with CPC, as shown in Fig. 1(c).

The next step was to optimize the type and amount of acid, the polarizing current, and the amount of molybdate used.

The acids investigated were nitric, sulphuric, and hydrochloric, at a concentration of 2.5*M*. Nitric acid yielded a small titration blank, which could be attributed to formation of its slightly soluble cetylpyridinium salt which, however, is soluble in hot water. Hydrochloric acid yielded the largest breaks and was thenceforth used. The optimum pH was between 1.05 and 1.30, although reasonable titration curves were obtained at any pH between 0.85 and 1.75. A suitable pH can be ensured by using 3 ml of 2.5*M* hydrochloric acid in a volume of 25 ml.

The cathodic polarization current was varied over a wide range, and affected the shape and magnitude of the titration curves profoundly. The optimum current was 1.1 μA; good results were obtained with 0.9–1.2 μA.

The blank due to the excess of molybdate is probably the only detrimental factor in the method. It arises from the moderate solubility of cetylpyridinium molybdate. However, at the high acidity used for the titration with CPC, this blank is small and quite reproducible. It can be estimated by the relationship

$$\text{blank} = 0.155 \times (\text{ml of } 10\% \text{ sodium molybdate solution}) - 0.098 \text{ ml of } 0.05M \text{ CPC}$$

The blank corrections found for 1–10 ml of molybdate are listed in Table 1, which also gives the calculated values based on this equation. The correlation coefficient is 0.995. For 1 mg of phosphorus the best titration curves were obtained with 2–3 ml of molybdate, as shown in Fig. 1(d).

Table 2 presents statistics for the standardization of 0.05*M* CPC with 0.8002 mg of phosphorus (as sodium dihydrogen phosphate). The steepest and most reproducible titration curves were obtained with 3 ml of molybdate at an Mo:P ratio of 48. Smaller

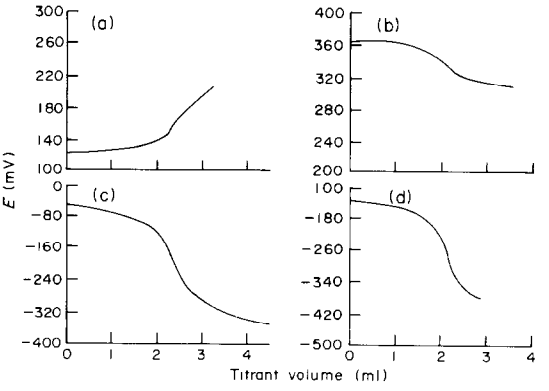

Fig. 1. Titration curves of approximately 1 mg of P (as phosphate) will 0.05*M* CPC. (a) PVC/DOP-coated graphite sensor containing 12-molybdophosphoric acid; (b) platinum sensor, unpolarized; (c) platinum sensor, $-1.0\,\mu$A; (d) platinum sensor, $-1.1\,\mu$A, 3 ml of 2.5*M* HCl, 2 ml of molybdate.

Table 1. Blank corrections for molybdate

Molybdate added, *ml*	0.05*M* CPC required, *ml* Found*	Calculated
1	0.05 (10)	0.06
2	0.21 (9)	0.21
3	0.38 (3)	0.37
4	0.55 (3)	0.52
5	0.68 (6)	0.68
10	1.44 (3)	1.45

*Number of replicates is given in parentheses.

Table 2. Standardization of approx. 0.05*M* CPC: effect of amount of molybdate

Molybdate added, *ml*	Mo:P	Molarity found Mean	Standard deviation	Number of replicates	Remarks
5	80	0.0553	0.0011	4	
3	48	0.0549	0.0008	4	Best curves
2	32	0.0474	0.0008	5	
1	16	0.0611	0.0012	5	Shallow curves

amounts of molybdate, according to the data, are insufficient for complete reaction, and larger amounts cause larger blank values.

Attempts to use addition of excess of CPC and back-titration with sodium dodecyl sulphate,[8] were unsuccessful.

We have isolated some of the precipitate obtained in the titration of the molybdate blanks. It was a very fine material which was difficult to filter. Its elemental analysis (C 42.5%, H 6.4%, N 2.2%) corresponds to anhydrous cetylpyridinium tetramolybdate ($C_{42}H_{76}N_2O_{13}Mo_4$, molecular weight 1200.8, requires C 42.01%, H 6.36%, N 2.33%). The sequence of reactions leading to the formation of this precipitate is probably

$$4MoO_4^{2-} + 6H^+ \rightarrow Mo_4O_{13}^{2-} + 3H_2O \quad (1)$$

$$Mo_4O_{13}^{2-} + 2C_{21}H_{38}N^+ \rightarrow (C_{21}H_{38}N)_2Mo_4O_{13} \quad (2)$$

where $C_{21}H_{38}N^+$ is the cetylpyridinium cation.

We have also isolated some of the precipitate from the phosphomolybdate titrations. The small amount of cetylpyridinium tetramolybdate present, which is approximately 3% of the total, can be removed by washing the precipitate with hot water. The precipitate was filtered off, air-dried and analysed. The analysis gave C 28.2%, H 4.3%, N 1.7%; $C_{63}H_{114}N_3PO_{40}Mo_{12}$ (m.w. 2735.9) requires C 27.66%, H 4.20%, N 1.70%. These results confirm that the reaction is

$$3C_{21}H_{38}NCl + H_3(PO_4 \cdot 12MoO_3) \rightarrow (C_2H_{38}N)_3PO_4 \cdot 12MoO_3 + 3HCl \quad (3)$$

The material was analysed thermogravimetrically on a Perkin-Elmer TGS-2 instrument with computer-controlled data-acquisition and plotting capability. The thermogram shown in Fig. 2 is similar to that reported for quinolinium phosphymolybdate[22] in almost all features, but cetylpyridinium phosphomolybdate does not contain any water of hydration.

Preliminary experiments have shown that silicate, arsenate and germanate also form cetylpyridinium heteropolymolybdates and may react stoichiometrically. Addition of citric acid to the phosphate solution before the addition of molybdate results in the phosphomolybdic acid not being formed.[23] This feature may be used in the determination of silicate in the presence of phosphate, but a strict time schedule is necessary, since silicomolybdate is also destroyed by citric acid, though much more slowly than phosphomolybdate.[24]

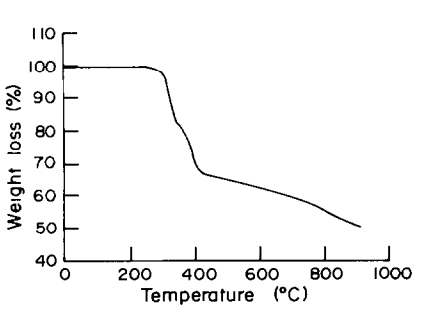

Fig. 2. Thermal decomposition of tricetylpyridinium dodecamolybdophosphate

According to Kauffman and Vartanian,[25] as many as 36 different elements have been reported to function as central atoms in distinct heteropoly anions. It may thus be possible to determine about one third of all the elements in the periodic table, as heteropoly anions.

Work is in progress exploring the lower limits of our method and examining the recovery of phosphate over a wide range. An expected difficulty is that for each quantity of phosphate there will probably be an optimum amount of molybdate. Other possible titrants such as quinoline, 2-methylpyridine,[26] 2,4-dimethylquinoline,[27] *etc.*, will be investigated.

Acknowledgements—The writer thanks Raul Canez for carrying out many of the titrations, Glendon L. Crossman for the thermogravimetric analysis and Lewis J. Gregory for the elemental analyses. The work was performed under the auspices of the U.S. Department of Energy by the Lawrence Livermore National Laboratory under Contract No. W-7405-ENG-48.

REFERENCES

1. W. J. Williams, *Handbook of Anion Determination*, pp. 445–485. Butterworths, London, 1979.
2. A. Babko, *Talanta*, 1968, **15**, 721.
3. V. Macháček and M. Malát, *Microchem. J.*, 1981, **26**, 307.
4. W. Selig, *Talanta*, 1979, **26**, 1061.
5. *Idem*, *Mikrochim. Acta*, 1979 **II**, 373.
6. *Idem*, *ibid.*, 1979 **II**, 437.
7. *Idem*, *Talanta*, 1980, **27**, 357.
8. *Idem*, *Z. Anal. Chem.* 1980, **300**, 183.
9. *Idem*, *Microchem. J.*, 1980, **25**, 200.
10. *Idem*, *Lawrence Livermore Natl. Lab. Rept.* UCID-18785, 1980; *Chem. Abstr.*, 1981, **95**, 27275s.
11. *Idem*, *Mikrochim. Acta*, 1981 **II**, 251.
12. *Idem*, *Propellants Expl.*, 1981, **6**, 96.
13. *Idem*, *Z. Anal. Chem.*, 1982, **312**, 419.
14. *Idem*, *Mikrochim. Acta*, 1978 **II**, 75.
15. A. Savitsky and M. J. E. Golay, *Anal. Chem.*, 1964, **36**, 1627.
16. H. N. Wilson, *Analyst*, 1951, **76**, 65.
17. R. Belcher and C. L. Wilson, *New Methods of Analytical*

Chemistry, 2nd Ed., pp. 322–330. Reinhold, New York, 1964.
18. R. Craven and E. V. Schwehr, *Fertiliser Society and S.A.C. Joint Symposium on Fertiliser Analysis*, 1960, *Proceedings*, Nos. 63, 139.
19. D. F. Boltz and M. G. Mellon, *Anal. Chem.*, 1948, **29,** 749.
20. W. Selig, *Anal. Lett.*, 1982, **15,** 309.
21. Y. Y. Vinnikov and L. A. Kostareva, *Zh. Analit. Chim.*, 1980, **35,** 547.
22. W. W. Wendlandt and W. M. Hoffman, *Anal. Chem.*, 1960, **32,** 1011.
23. H. N. Wilson, *Analyst*, 1954, **79,** 535.
24. R. A. Chalmers and A. G. Sinclair, *Anal. Chim. Acta*, 1966, **34,** 412.
25. G. B. Kauffman and P. F. Vartanian, *J. Chem. Educ.*, 1970, **47,** 212.
26. A. M. G. MacDonald and A.-M. Rivero, *Anal. Chim. Acta*, 1967, **37,** 525.
27. C. C. Miller and R. A. Chalmers, *Analyst*, 1958, **78,** 24.

Talanta, Vol. 30, No. 9, pp 699–701, 1983
Printed in Great Britain

0039/9140/83 $3.00+0.00
Pergamon Press Ltd

A NEW METHOD OF CAESIUM DETERMINATION BY THERMAL DECOMPOSITION OF CAESIUM TETRATHIOCYANATOBISMUTHATE(III)

ANDRZEJ CYGAŃSKI and TOMASZ MAJEWSKI
Institute of General Chemistry, Technical University of Łódź, 90–924 Łódź, Poland

(*Received* 11 *May* 1982. *Revised* 4 *January* 1983. *Accepted* 21 *March* 1983)

Summary—A thermal method of caesium determination is reported. The method is based on precipitation of $Cs[Bi(SCN)_4]$, thermal decomposition of this compound at 500°, absorption of the evolved SO_2 in Na_2HgCl_4 solution, and finally titration of the acid formed. The method can be used to determine caesium in the presence of potassium, ammonium and rubidium. When rubidium is present, caesium and rubidium can be determined simultaneously on the basis of the weight of the precipitate and the amount of sulphur dioxide evolved.

Determination of caesium in presence of the potassium group is very difficult.[1] The methods used for this purpose can be divided according to whether a separation is used.[2] The separation methods require another caesium determination after separation has been completed. There are only a few methods (of either type) for caesium determination in the presence of rubidium and potassium. The most noteworthy of the separation methods are Strecker and Diaz's[3] precipitation of $Cs_3SbCl_6 \cdot FeCl_3$ (modified by Moser and Ritschel[4] and applied by Fresenius,[5] O'Leary and Papish's[6] caesium precipitation with tungstosilicic acid, and the Wells and Stevens[7] method based on the difference between the solubilities of the chlorides and sulphates of these metal ions in alcohol. The direct determination methods are precipitation of $Cs_3Bi_2I_9$,[8–10] $Cs_2Na[La(NO_2)_6]$,[11] $Cs[B(C_6H_4F)_4]$,[12] $Cs_{12}Mg_8[Fe(CN)_6]_7$,[13] and $Cs[Cr(NH_3)_2(SCN)_4$.[14] and have low tolerance levels for rubidium.

The subject of the present paper is the thermal method of caesium determination, by precipitation of caesium tetrathiocyanatobismuthate(III), followed by its thermal decomposition. Caesium tetrathiocyanatobismuthate, reported only recently,[15] has been used for gravimetric and titrimetric determination of caesium,[16] but these methods cannot be used in the presence of rubidium. The thermal method, on the other hand, can be used to determine caesium not only in the presence of potassium and ammonium ions, but also when rubidium is present. Moreover, caesium and rubidium can be determined simultaneously.

EXPERIMENTAL

Principle

The method of caesium determination is based on precipitation of caesium tetrathiocyanatobismuthate.[15] When heated to 500° the precipitate is thermally decomposed according to the reaction[17]

$$6Cs[Bi(SCN)_4] + 45O_2 = 3Cs_2SO_4 + 2Bi_2S_3 + 2Bi + 15SO_2 + 24CO_2 + 12N_2 \quad (1)$$

The sulphur dioxide evolved is absorbed in sodium tetrachloromercurate(II) solution:[18]

$$HgCl_4^{2-} + 2SO_2 + 2H_2O = Hg(SO_3)_2^{2-} + 4H^+ + 4Cl^- \quad (2)$$

The hydrochloric acid liberated is titrated with 0.1 *M* sodium hydroxide and the amount of caesium calculated according to equation (2).

Determination of the sulphur dioxide evolved is the basic principle of the method, so the amount evolved was determined in relation to the temperature of the thermal decomposition (Fig. 1) of $Cs[Bi(SCN)_4]$.

Apparatus

The equipment needed includes a furnace fitted with temperature control, a rotameter, and bubblers to absorb the gases liberated.

Reagents

Precipitant. A 0.5*M* $H[Bi(SCN)_4$ solution, saturated with $Cs[Bi(SCN)_4]$, prepared as follows. Distil ammonium thiocyanate and sulphuric acid[19] to obtain an 18–20% thiocyanic acid solution. Dilute this to 14%, and then react it with basic bismuth carbonate for 2–3 hr [add 100 ml of 14% HNCS solution to 20 g of $(BiO)_2CO_3$]. Filter off the undissolved

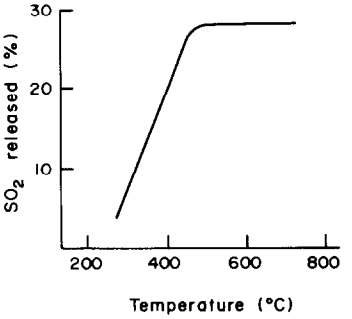

Fig. 1. Relationship between amount of sulphur dioxide evolved and temperature of the thermal decomposition of caesium tetrathiocyanatobismuthate(III).

carbonate. If the HNCS solution is left to react with the $(BiO)_2CO_3$ for too long, crystals of $Bi(SCN)_3$ are formed on the surface of the carbonate, which slows the reaction and decreases the concentration of tetrathiocyanatobismuthic acid in the solution. Finally add 0.6 g of caesium carbonate (for 100 ml of the solution) to the filtrate. Yellow crystals of $Cs[Bi(SCN)_4]$ very soon precipitate. Stir the solution, cover the beaker with a watch-glass and leave it for 24 hr. Filter the solution just before use. The bismuth concentration should be about 0.5*M*, and the $SCN^-:Bi^{3+}$ ratio 4.0–4.5. The reagent is usable for about 2 weeks. After that, light yellow plates of $Bi(SCN)_3$ separate out.

Saturated $Cs[Bi(SCN)_4]$ solution in 0.25M *nitric acid.* This solution must be prepared with special care since caesium tetrathiocyanatobismuthate is fairly soluble in 0.25*M* nitric acid. Obtain $Cs[Bi(SCN)_4]$ by adding, gradually, 2 g of caesium carbonate to 50 ml of 0.5*M* $H[Bi(SCN)_4]$. Filter off the precipitate after 2–3 hr, wash it two or three times with 0.3*M* nitric acid, and again with a 3:1 v/v mixture of benzene and absolute ethanol. Dry the crystals on filter paper, at room temperature. Shake 3 g of the crystals with 40 ml of 0.25*M* nitric acid for 6 hr, filter, and leave the solution for crystallization to take place. When crystals of $Cs[Bi(SCN)_4]$ have formed on the bottom of the beaker, the solution is ready for filtering (just before use for washing the precipitate).

Absorbent for sulphur dioxide. Dissolve 27.2 g of mercury(II) chloride and 11.7 g of sodium chloride in water and dilute to 1 litre.

Standard solutions

Caesium carbonate standard solution. Dissolve about 50 g of $Cs_2CO_3 \cdot 2H_2O$ in water and dilute to 1 litre. Standardize by precipitation of caesium as $CsClO_4$,[5] or $Cs_3Bi_2I_9$.[9]

Rubidium carbonate standard solution. Dissolve about 40 g of Rb_2CO_3 in water and dilute to 1 litre. Standardize by determination of rubidium as $RbClO_4$.[5]

*Sodium hydroxide solution, 0.1*M.

Procedure

Evaporate the caesium solution (carbonate, nitrate or sulphate) almost to dryness, then add the precipitation reagent according to Table 1. Stir the solution, cover the beaker with a watch-glass, and leave it for 8 hr. Yellow crystals are formed a few minutes after the reagent is added. Collect the coarsely crystalline precipitate on a porosity-3 sintered-glass crucible. Use some of the filtrate to transfer the precipitate quantitatively, then remove the suction and add 3–4 ml of saturated $Cs[Bi(SCN)_4]$ solution in 0.25*M* nitric acid to the precipitate. After the wash solution has percolated through the crucible, wash the precipitate several times (under suction) with small amounts (2–3 ml) of 3:1 v/v mixture of benzene and absolute ethanol. Place the crucible and its contents in a fused-silica tube through which a current of air (10 l./hr) can be passed, and put the tube in the crucible furnace. Pass the air from the tube through three bubblers, each containing 25 ml of 0.1*M* sodium tetrachloromercurate(II) solution. Raise the temperature of the furnace to 500° while maintaining the flow of air. Transfer the solutions from the bubblers into a 250-ml conical flask and titrate with 0.1*M* sodium hydroxide, using Methyl Red as indicator. Table 2 gives some results for determination of caesium.

Table 1. Amount of precipitant solution to be added for various amounts of caesium

Caesium, *mg*	Volume of precipitant, *ml*
20	6
40	6
80	8
120	10
160	12
200	14
240	16

Table 2. Determination of caesium by thermal procedure

Taken, *mg*	Found, *mg*	Error, %
19.2	19.6	+2.1
33.5	33.3	−0.6
67.0	66.0	−1.5
100.5	101.6	+1.1
134.0	134.0	0
167.5	166.0	−0.9
268.0	264.2	−1.4

Determination of caesium and rubidium

Rubidium also forms a precipitate with tetrathiocyanatobismuthate(III), but it is more soluble than the caesium salt.[15] These compounds are isostructural and their thermal decompositions proceed in a similar way.[17] $Rb[Bi(SCN)_4]$ is co-precipitated with $Cs[Bi(SCN)_4]$, which makes the caesium determination by weighing or titration impossible. If the weight of precipitate and the amount of sulphur dioxide liberated from it by thermal decomposition are determined, both the caesium content and the amount of co-precipitated rubidium can be found. It is just as easy to determine the whole of the rubidium present, and this is done by using a larger excess of precipitant (which must be saturated with both the salts to be precipitated) and a wash solution saturated with both caesium and rubidium tetrathiocyanatobismuthates.

Precipitation and wash solutions. Make the precipitation solution by adding 0.6 g of caesium carbonate to 100 ml of 0.5*M* $H[Bi(SCN)_4]$ solution, as already described. Stir the solution and leave it for 24 hr. Filter off the $Cs[Bi(SCN)_4]$ precipitate and add 4 g of rubidium carbonate to 80 ml of the solution. Stir the solution and leave it for 24 hr.

Filter off the large $Rb[Bi(SCN)_4]$ crystals and use the solution for precipitation. The volumes needed are given in Table 4.

The wash solution is a saturated solution of $Cs[Bi(SCN)_4]$ and $Rb[Bi(SCN)_4]$ in 0.25*M* nitric acid. Shake 3 g of $Cs[Bi(SCN)_4]$ with 40 ml of 0.25*M* nitric acid for 6 hr, filter, and leave the filtrate for crystallization of $Cs[Bi(SCN)_4]$. Filter and shake 25 ml of the filtrate for 6 hr with 5 g of $Rb[Bi(SCN)_4]$. Filter and leave the solution for crystallization of $Rb[Bi(SCN)_4]$. Filter again before use.

Procedure. This is the same as for caesium, except for the precipitation and wash solutions.

The caesium content is calculated from the following equations.

$$m = m_1 + m_2 \tag{3}$$

$$\frac{5}{2}\left(\frac{m_1}{M_1} + \frac{m_2}{M_2}\right) = \frac{m_{SO_2}}{M_{SO_2}} \tag{4}$$

where m is the weight of the precipitate, m_1 the weight of $Cs[Bi(SCN)_4]$ and m_2 that of $Rb[Bi(SCN)_4]$, M_1 and M_2 are the corresponding formula weights, m_{SO_2} is the weight of sulphur dioxide liberated and M_{SO_2} is the formula weight of SO_2.

Solving equations (3) and (4) gives equation (5), for m_1.

$$m_1 = \frac{0.00949\ m - 0.0312\ m_{SO_2}}{0.000784} \tag{5}$$

The weight of caesium present is then 0.2314 m, and that of the rubidium is 0.2003 $(m - m_1)$.

Analysis of pollucite

Treat a 0.2-g sample of powdered mineral with 15 ml of concentrated hydrochloric acid and evaporate, with frequent stirring, to dryness. Repeat the evaporation after addition of another 15 ml of concentrated hydrochloric acid. Heat the residue with 30 ml of distilled water at the boiling point for 20 min, then filter through a porosity-3 crucible, and wash the precipitate several times with small portions of hot water. Evaporate the filtrate to dryness and add 7 ml of the caesium and rubidium precipitant to the residue. Stir the solution, cover the beaker with a watch-glass and set it aside for 8 hr. Filter off the precipitate, wash it with the solution saturated with $Cs[Bi(SCN)_4]$ and $Rb[Bi(SCN)_4]$ and finally with benzene–alcohol mixture, as already described. Complete the determination as described for caesium and rubidium determination.

Determination of caesium and rubidium in a pollucite sample (from Auburn, Maine, U.S.A., by courtesy of the Mineralogy Museum, Institute of Geological Sciences, University of Wrocław) gave 25.6% Cs_2O and 1.7% Rb_2O, in agreement with the results obtained by other methods (25.4% Cs_2O by the iodobismuthate method, 1.6% Rb_2O by flame photometry).

RESULTS AND DISCUSSION

The results obtained show that the method is sufficiently accurate. The thermal method is more rapid than gravimetric determination. The essential advantage is that caesium can be determined in the presence of rubidium, or both can be determined simultaneously.

The method can be used to determine caesium in the presence of rubidium (with precipitant saturated with $Cs[Bi(SCN)_4]$) only if the ratio between Rb and Cs does not exceed 2:1 (Table 3). When rubidium is present in higher ratios than this, the caesium tetrathiocyanatobismuthate is not completely precipitated. This limitation on the applicability of the method is characteristic of methods for caesium determination in the presence of rubidium. For example, Tananajew and Harmasz[8] claim that the $Cs_3Bi_2I_9$ method can be used when the rubidium:caesium ratio is 10:1, but Feldman[20] found that the results are too high even at 4:1 ratio of Rb to Cs. Plyushchev and Korshunov[9] suggested that the ratio should not be higher than 3:1, and Tadashi[10] considers it should be 2:1.

When caesium is determined by the thermal method, however, this limitation does not apply if the precipitant and wash solution are both saturated with $Cs[Bi(SCN)_4$ and $Rb[Bi(SCN)_4]$, and in that case caesium and rubidium can both be determined even if the Rb:Cs ratio is 10:1 (Table 4).

The method is the first thermal method for simultaneous determination of caesium and rubidium.

Table 3. Determination of caesium in presence of rubidium

Caesium, *mg*		Rubidium taken, *mg*	Ratio Cs:Rb	Error for caesium, %
Taken	Found			
33.5	34.1	72.3	0.47	−1.8
67.0	66.9	84.8	0.79	−0.2
100.5	98.8	57.8	1.7	−1.7
167.5	168.7	28.9	5.8	+0.7
100.5	98.8	14.4	7	−1.7
167.5	166.9	14.4	11.6	−0.4

REFERENCES

1. R. Fresenius and G. Jander, *Handbuch der analytischen Chemie*, Vol. III, *Quantitative Bestimmungs und Trennungsmethoden; Elemente der Ersten Hauptgruppe*, p. 402. Springer, Berlin, 1940.
2. K. Bogusławska and A. Cygański, *Chem. Anal. (Warsaw)*, 1980, **25**, 687.
3. W. Strecker and F. O. Diaz, *Z. Anal. Chem.*, 1925/26, **67**, 321.
4. L. Moser and E. Ritschel, *ibid.*, 1927, **70**, 184.
5. L. Fresenius, *ibid.*, 1931, **86**, 182.
6. W. I. O'Leary and I. Papish, *Ind. Eng. Chem., Anal. Ed.*, 1934, **6**, 108.
7. R. C. Wells and R. E. Stevens, *ibid.*, 1934, **6**, 439.
8. N. A. Tananajew and E. P. Harmasz, *Z. Anal. Chem.*, 1932, **89**, 259.
9. V. E. Plyushchev and B. G. Korshunov, *Zh. Analit. Khim.*, 1955, **10**, 115.
10. H. Tadashi, *Bull. Inst. Chem. Res. Kyoto Univ.*, 1959, **37**, 132; *Anal. Abstr.*, 1960, **7**, 1665.
11. N. K. Dutt, *J. Indian Chem. Soc.*, 1945, **22**, 65.
12. C. E. Moore, F. P. Cassaretto, H. Posvic and I. I. McLafferty, *Anal. Chim. Acta*, 1965, **35**, 1.
13. K. Bogusławska and A. Cygański, *Z. Anal. Chem.*, 1971, **273**, 288.
14. I. L. Bagbanly, M. V. Shirai, N. Ch. Rustamov and L. M. Mamedova *Uch. Zap. Azerb. Gos. Univ., Ser. Khim. Nauk*, 1977, No. 2, 3; *Ref. Zh. Khim.*, 1978, 14G 101.
15. A. Cygański, *Roczniki Chem.*, 1965, **39**, 193.
16. *Idem, Chem. Anal. (Warsaw)*, 1967, **12**, 765.
17. *Idem, Talanta*, 1977, **24**, 361.
18. P. W. West and G. C. Gaeke, *Anal. Chem.*, 1956, **28**, 1816.
19. W. Glund, K. Keller and W. Klempt, *Ber.*, 1926, **59**, 1384.
20. R. W. Feldman, *Z. Anal. Chem.*, 1935, **102**, 102.

Table 4. Determination of caesium and rubidium

Taken, *mg*		Precipitant, *ml*	Ratio Rb:Cs	Found, *mg*		Error, %	
Cs	Rb			Cs	Rb	Cs	Rb
19.1	28.7	10	1.5	19.5	28.1	+2.1	−2.2
19.1	57.9	10	2.9	18.6	58.8	−2.6	+1.5
19.1	202.6	20	10.6	18.5	205.2	−3.1	+1.3
38.3	202.6	20	5.3	38.9	199.2	+1.6	−1.7
38.3	115.8	15	3.0	37 9	117.0	−1.0	+1.0
100.5	115.8	20	1.2	99.2	118.3	−1.3	+2.2
191.4	57.9	20	0.3	189.2	58.9	−1.7	+1.7

Talanta, Vol 30, No. 9, pp. 702–704, 1983
Printed in Great Britain

0039/9140/83 $3.00 + 0.00
Pergamon Press Ltd

AN IMPROVED, AUTOMATED XYLENOL ORANGE METHOD FOR THE COLORIMETRIC DETERMINATION OF ALUMINIUM

ANTHONY C. EDWARDS and MALCOLM S. CRESSER
Department of Soil Science, Aberdeen University, Meston Walk, Aberdeen AB9 2UE, Scotland

(*Received* 14 *January* 1983. *Accepted* 12 *March* 1983)

Summary—An automated colorimetric procedure is described for the determination of aluminium, based on its complex with Xylenol Orange. Ethanol is used to accelerate the reaction and EDTA to mask iron. The procedure has been applied successfully to natural waters, soil extracts and plant digests.

The determination of aluminium in natural waters, plant digests and soil extracts is currently attracting increasing attention through widespread interest in the effects of "acidic" rain. These sample solutions frequently contain 2 μg or less of the element per ml. At such levels the precision of flame atomic-absorption spectrometry is poor, and the very high dissolved-solids content of many of the soil extractants can cause severe clogging of the burner slot. Colorimetric methods are therefore potentially attractive. Of the numerous colorimetric procedures which have been proposed, that of Pritchard,[1] based on Xylenol Orange, is sensitive and reproducible. Selectivity is improved by masking iron with EDTA.[1] Unfortunately the procedure is slow, requiring 90 min heating at 40° for colour development and a further 60 min at room temperature for complete reaction of the iron–Xylenol Orange complex with EDTA.

Dodson and Jennings[2] showed that the rate of reaction between aluminium and Xylenol Orange could be greatly increased by use of an ethanolic solution of the indicator. However, the advantage gained by reducing the colour development time and by use of semi-automation was offset by the necessity for prior removal of iron(III) by solvent extraction.[2] The procedure described below obviates the need for separation of iron(III) by reverting to the use of EDTA masking, but employs an ethanolic solution of the reagent and moderate heating (at 55°) to accelerate colour formation and bleaching of the iron complex. The procedure has been fully automated to allow aluminium determinations over the range 0–1 or 0–15 μg/ml at a rate of 40 per hr.

EXPERIMENTAL

Reagents

Aluminium stock solution (1000 μg/ml). Dissolve 17.58 g of analytical-reagent grade potassium aluminium sulphate [$AlK(SO_4)_2 \cdot 12H_2O$] in 100 ml of 2*M* sulphuric acid and dilute to 1 litre.

Acetate buffer. Dissolve 136 g of analytical-reagent grade hydrated sodium acetate in approximately 900 ml of demineralized water, adjust to pH 3.8 with hydrochloric acid and dilute to 1 litre. Add 2 ml of 30% Tween 80 solution and mix thoroughly.

*Disodium EDTA solution (0.0125*M). Dissolve 1.164 g of analytical-grade reagent in demineralized water, dilute to 250 ml and add 1 ml of 30% Tween 80 solution.

Xylenol Orange solution. Dissolve 0.0375 g of reagent in a small quantity of demineralized water, add 75 ml of ethanol and two drops of 1*M* hydrochloric acid to give a clear orange solution. Dilute to 100 ml and add 1 ml of concentrated Tween 80. Leave to stand for one day before use to avoid problems from small bubbles.

Note. The surfactant is added *after* dilution to standard volume, to avoid the inconvenience of the foaming caused if it is added first.

Apparatus

For automated colorimetric determinations, a Technicon AAII AutoAnalyzer was used, with the manifold shown in Fig. 1 and 520 nm filters. Polyvinyl "solvent resistant" tubing (Sterilin Instruments, Alton, Hampshire) was used in all lines coming into contact with the ethanol. Manual spectrophotometric measurements were made with a Cecil Instruments CE 505 double-beam spectrophotometer, with 10-mm matched cells.

Atomic-absorption determinations were done with a Baird A3400 Atomic Absorption Spectrometer, with a nitrous oxide–acetylene flame. Potassium was added (to give a 5000 μg/ml concentration) when necessary as an ionization buffer.

Procedure

Prepare calibration standards covering the range 0–1 or 0–15 μg/ml aluminium, as required. For analysis of potassium chloride extracts from soil, prepare standards with the extractant solution used. For acid digests of ashed plant material, prepare standards in acid of the appropriate concentration, and just before the determination adjust samples and standards to pH 3–4 with sodium hydroxide and dilute to fixed volume. "Free" aluminium in natural waters may be determined directly, with use of aqueous standards.

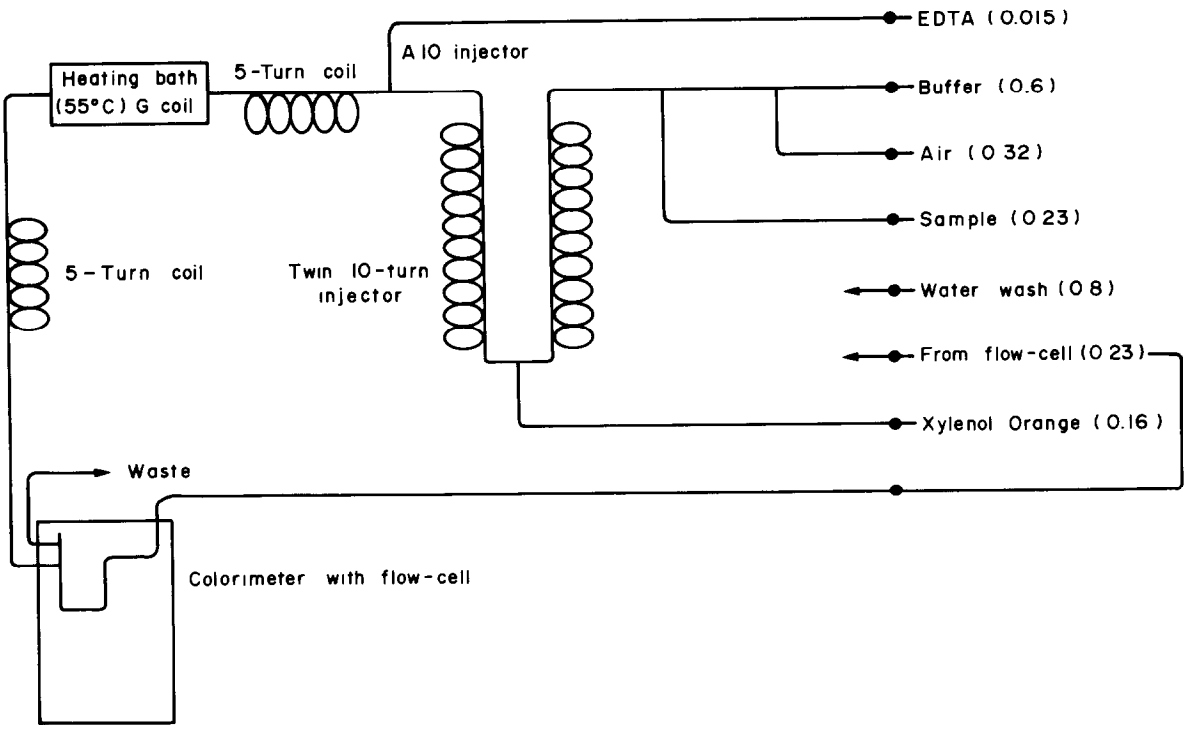

Fig. 1. Manifold for automated determination of aluminium. Figures in parentheses are flow-rates in ml/min.

RESULTS AND DISCUSSION

Reagent solution

Dodson and Jennings[2] found it necessary to free their sample of Xylenol Orange from Semi-Xylenol Orange by cation-exchange, but this was found unnecessary for any of the three separate batches of commercial reagent (one from Hopkin & Williams, Chadwell Heath, Essex, two from BDH Chemicals Ltd., Poole, Dorset) used in this study.

Use of ethanol to accelerate complex formation

It has been stated that the colour-forming reaction is complete within 5 min if a 50% v/v ethanol medium is used.[2] A lower concentration of ethanol is found to be quite adequate for the automated procedure described here. The reason for the increased reaction rate is not known, but may be suppression of dissociation of the reagent.

Masking of iron (III)

An interfering iron(III) complex also forms rapidly in dilute ethanolic solution. However, as in purely aqueous systems,[1] the iron complex reacts with EDTA much more rapidly than the aluminium complex does. The time required for complete destruction of the iron complex was investigated by preparing a series of 10-μg/ml iron(III) standards, and completing the analysis manually with a standard development time of 10 min and "bleaching" times of 0, 2, 4, 6, 8, 10 and 20 min, the reaction flasks being shaken in a water-bath at 55° to speed up the process. A time of 8 min was adequate for quantitative decolorization. To avoid too high an ethanol vapour pressure, higher temperatures were not used. Some degree of heating is necessary, however, as the reaction is so slow at room temperature that a long delay coil would be necessary in the automated method. To confirm that the manifold shown in Fig. 1 gave adequate time for complete removal of iron interference, a series of iron standards up to 100 μg/ml was analysed; the absorbance observed was in each case less than 0.002.

Interference from phosphate and fluoride

Phosphate, in 25-fold w/w ratio to aluminium, caused no interference in the determination of aluminium at the 0.4-μg/ml level, but at 125-fold ratio depressed the absorbance by 5.0%. This is a tolerable error for most environmental samples. Interference from fluoride was more severe: Table 1 shows the suppression caused by 0.5–40 μg/ml fluoride levels in the measurement of 1–5 μg/ml aluminium solutions. In practice, fluoride will rarely be encountered at such high levels in environmental samples.

Importance of pH control

For acidic digests of plant material or acidic concentrates of water samples,[3] it was found necessary to adjust the sample pH to 3–4. Use of higher pH values

Table 1. Effect of increasing amounts of fluoride on the determination of aluminium at the 1, 3 and 5 μg/ml level

	Aluminium found, μg/ml				
	Fluoride (μg/ml)				
Aluminium, μg/ml	0.5	1.0	5	10	40
1	0.95	0.98	0.52	0.25	0.03
3	2.85	2.80	1.38	0.75	0.13
5	4.90	4.78	2.43	1.38	0.25

could in some instances cause low recoveries of aluminium if the neutralized samples were left to stand for more than a few minutes before analysis.

Analysis of potassium chloride extracts of soils

To check the accuracy of the method, seven 1*M* potassium chloride extracts from a range of peats were also analysed by atomic-absorption spectrometry. Table 2 shows that the results from both procedures agreed within the limits of experimental error. No error was caused by the absorbance of dissolved organic matter from these samples. This was confirmed by running the manifold with aqueous ethanol (75 ml of ethanol + 25 ml of water + 1 ml of Tween 80) in the reagent line; samples then gave no measurable absorbance (*i.e.*, absorbance < 0.002).

Table 2. Results of duplicate determinations of aluminium in 1*M* potassium chloride extracts of peats by atomic-absorption spectrometry and the proposed procedure

	Aluminium concentration, μg/ml			
	Proposed procedure		AAS	
Sample No.				
96	0.94	0.94	0.96	0.90
120	0.75	0.77	0.70	0.70
158	0.70	0.70	0.68	0.74
211	0.49	0.46	0.50	0.46
229	0.30	0.27	0.24	0.35
235	0.47	0.49	0.40	0.44
236	0.61	0.60	0.64	0.56

Table 3. Stability of acid digests (of ashed Sitka spruce needles) analysed by the proposed procedure

	Al concentration found, μg/g	
Sample No.	Immediately	After 1 month
282	220	230
290	220	225
385	150	165
389	187	170
400	120	125

Reproducibility

Table 2 demonstrates the reproducibility of the procedure for extracts from peat. Table 3 shows results for hydrochloric acid digests of five ashed samples of Sitka spruce needles, analysed both immediately after preparation and after storage for one month. The results show that the acid digests are stable and need not be analysed immediately.

Analysis of waters

The method has been successfully applied both to "free" aluminium in drainage water removed from organic soils by suction and to river water samples after preconcentration.[3] As expected, for some drainage water samples the colorimetric procedure gave slightly but significantly lower results than flame atomic-absorption spectrometry, since the latter technique, unlike colorimetry, will determine any aluminium present in polymerized ionic form as well as that present as monomeric aquo-ions.

Acknowledgements—The authors are indebted to the Agricultural Research Council for the award of a grant to purchase the AutoAnalyzer, and to the Natural Environment Research Council for the award of a Research Studentship.

REFERENCES

1. D. T. Pritchard, *Analyst*, 1967, **92**, 103.
2. A. Dodson and V. J. Jennings, *Talanta*, 1972, **19**, 801
3. J. M. Reid, D. A. MacLeod and M. S. Cresser, *Earth Surface Processes and Landforms*, 1981, **6**, 447.

Talanta, Vol 30, No. 9, pp 705–707, 1983
Printed in Great Britain

0039/9140/83 $3.00+0.00

MICRODETERMINATION OF THE DEGREE OF HYDRATION OF POLYSACCHARIDES AND GLYCOPROTEINS

F. B. SHERMAN
N.D. Zelinski Institute of Organical Chemistry, Academy of Sciences of the USSR, Leninski Prospect 47, Moscow B-334, USSR

(*Received* 3 *February* 1983. *Accepted* 10 *February* 1983)

Summary—In the hydration of polysaccharides and glycoproteins a "glass transition effect" has been discovered, *i.e.*, a phase transition, at certain critical values of the relative water-vapour pressure $(p/p_s)_{gt}$, of lyophilized preparations to a new state which is accompanied by a "glass transition" of the samples. The dependence of $(p/p_s)_{gt}$ on the content of polysaccharide and glycoprotein has been shown. Conditions have been found which make it possible to measure the absolute value of the degree of hydration of such biopolymers at any values of p/p_s, by means of Karl Fischer titration.

The moisture content of carbohydrates and carbohydrate-containing products can be reliably determined by many methods; gravimetric methods, azeotropic distillation and the Karl Fischer method are frequently used.[1,2] When drying methods are used, syrups, molasses, honey and other viscous products are first dispersed on pumice, quartz, or Filter-Cel.[1]

In using the Karl Fischer method for measuring the degree of hydration of polysaccharides and glycoproteins containing more than 10% carbohydrate, over a wide range of relative water-vapour pressure (p/p_s), we ran into certain difficulties connected with a phase transition of the hydrated samples—the "glass transition effect"—at high values of p/p_s [which we will designate by $(p/p_s)_{gt}$]: at $p/p_s > 0.8$, only part of the hydration water is determined by the Karl Fischer method.[3,4]

This paper presents the conditions which make it possible to measure the absolute values of hydration (H) of polysaccharides and glycoproteins at any p/p_s ratio by means of a direct titration with the Karl Fischer reagent, defines the p/p_s values at which the samples undergo phase transition $[(p/p_s)_{gt}]$, and shows the dependence of $(p/p_s)_{gt}$ on the composition of such biopolymers.

EXPERIMENTAL

Samples investigated

Dextran T-20 (Fluka), rheopolyglucin, polyglucin, blood group substance (BGS) with activity factor (H + A),[5] immunoglobulin M and egg albumin (Table 1).

Method of measuring the hydration level

Samples of biopolymers with different degrees of hydration were obtained under dynamic conditions[6] at predetermined p/p_s values; the absolute value of hydration was determined by direct titration of a biopolymer sample (1–3 mg) with the standard Karl Fischer reagent, by two methods: (1) titration by the usual procedure[7] at 20° in methanol medium; quantitative results were obtained only for preparations hydrated at $p/p_s < 0.8$; (2) titration in a water-jacketed cell kept at 50–70°, with a 1:1 v/v mixture of dimethylformamide and methanol as titration medium; in this case swelling of the "vitrified" samples was observed, and the water of hydration reacted with the Fischer reagent quantitatively, irrespective of the value of p/p_s.

RESULTS AND DISCUSSION

In the course of obtaining isothermal curves with lyophilically dried preparations of dextrans and glycoproteins at $p/p_s \geqslant 0.8$, it was observed that there was a sharp transition of the loose powder to a new state, accompanied by "vitrification" of the preparations (Table 1). At $p/p_s \geqslant (p/p_s)_{gt}$ the apparent level of hydration, as is determined by Karl Fischer titration in methanol, stops rising and even decreases with increase in p/p_s. At the same time, measurement of H by the weighing method shows that at $p/p_s > (p/p_s)_{gt}$ the hydration of the preparations steadily continues to grow, and is accompanied by vitrification of the sample.

The "glass transition effect" can apparently be explained by a co-operative recombination in the system of stable hydrogen bonds between water molecules and hydroxyl groups of carbohydrate chains in the biopolymer, when the water vapour reaches a critical pressure, given by $(p/p_s)_{gt}$. After such a transition, *i.e.*, at $p/p_s \geqslant (p/p_s)_{gt}$, only a part of the water of hydration of the preparations of polysaccharides and glycoproteins is titrated by the Karl Fischer reagent in methanol.

Table 1. The dependence of the "glass transition effect" and maximum hydration on the nature of a carbohydrate-containing biopolymer

Biopolymer	Molecular weight	Carbohydrate content %	Glass trans. effect $(p/p_s)_{gt}$	Glass trans. effect H_s,† *mmole H_2O/g*	Maximum H_s,† *mmole H_2O/g*
Dextran T-20	20×10^3	100	0.80	12.03	16.40
Rheopolyglucin	35×10^3	100	0.80	—	14.44
Polyglucin	70×10^3	100	0.80	—	12.22
BGS_1*	30×10^4	80	0.83	11.50	14.20
BGS_2*	27.5×10^4	73	0.83	12.06	15.52
BGS_3*	19×10^4	45	0.86	13.30	19.30
Immunoglobulin M	93×10^4	12 3	0.92	28.15	40.00
Egg albumin	44.5×10^3	1.8	—	—	17.01

*BGS—initial mucopolysaccharide sample of blood group substance with activity (H + A); BGS_2 and BGS_3—preparations of BGS after partial splitting of carbohydrates from it, by acid[9] and enzymic[10] hydrolysis.
†Average of 4–6 determinations; relative standard deviation, $S_r = 0.12\%$.

As can be seen from Table 1, the value of $(p/p_s)_{gt}$ for dextran is independent of the polysaccharide molecular weight. Glycoproteins with varying carbohydrate content also undergo the transition at certain values of p/p_s, and with decrease in the content of carbohydrates in the peparation $(p/p_s)_{gt}$ shifts towards higher p/p_s values, *i.e.*, the "glass transition effect" is observed at higher hydration values (Table 1). The same relationship is also observed for maximum hydration values at $p/p_s \simeq 0.96$–1.00 under stationary conditions (H_s):H_s rises with decrease in the carbohydrate content in the glycoprotein preparations. In the case of dextrans, H_s decreases with increase in the molecular weight (Table 1).

When the carbohydrate content is low, for instance in the case of egg albumin, the "glass transition effect" cannot be observed visually, but the processes causing it apparently still take place, since the quantitative dehydration of egg albumin in a flow of dry nitrogen requires a temperature of 135–145°, *i.e.*, 50° higher than that for dehydration of globular proteins containing no carbohydrates.[8]

From Fig. 1 it appears that $(p/p_s)_{gt}$ for egg albumin should be given by $p/p_s \simeq 0.95$. However, staging the experiment at such a high water-vapour pressure may result in condensation of water vapour in the adsorption tube of the dynamic unit[5] and this will certainly lead to higher H values.

Therefore, the "glass transition effect" for immunoglobulin M and the temperature effect for egg albumin, which are observed for glycoproteins with a low carbohydrate content, are also due to the positions of the polar groups in the carbohydrate residues on the macromolecule surface.

Figure 2 presents isotherms of water vapour adsorption by dextran T-20 under dynamic conditions. As can be seen from Table 1, the "glass transition effect" for this preparation is observed when the water-vapour pressure reaches the value given by $p/p_s = 0.80 \pm 0.02$.

The absolute degree of hydration of a dextran T-20 preparation can only be quantitatively determined by Karl Fischer titration in methanol medium (method 1) in the course of obtaining isothermal curves of

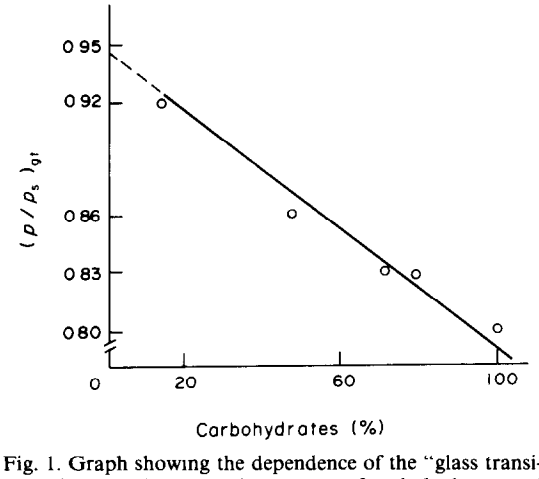

Fig. 1. Graph showing the dependence of the "glass transition effect", $(p/p_s)_{gt}$, on the content of carbohydrates and carbohydrate-containing biopolymers.

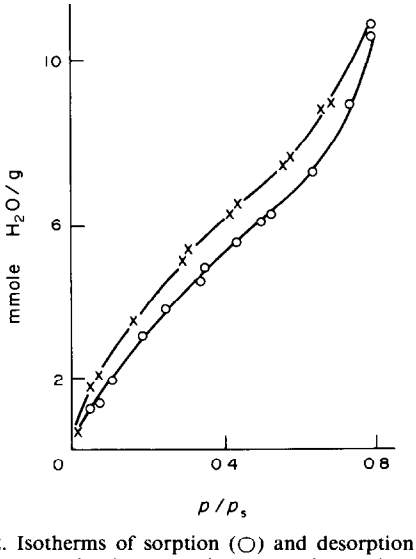

Fig. 2. Isotherms of sorption (○) and desorption (×) of water vapour by dextran T-20 preparation under dynamic conditions in nitrogen flow at 25°.

water vapour sorption at $p/p_s < (p/p_s)_{gt}$. H values obtained from the hydration isotherm at $p/p_s \geq (p/p_s)_{gt}$ and practically all H values obtained from the dehydration isotherm, when measured by method 1, give low and non-reproducible results; about 10–25% of the water of hydration is so firmly bound by dextran T-20 that it cannot be titrated with the Karl Fischer reagent. In order to obtain the absolute H values, the water of hydration in vitrified samples should be titrated by the Karl Fischer method in a mixture of methanol with DMF (method 2).

The micromethod that we propose here for determining the absolute moisture content of carbohydrate-containing biopolymers with changing water-vapour activity can be employed for moisture control in sugar-containing products in the confectionery, perfumery and pharmaceutical industries, as well as for obtaining isothermal curves for the hydration of polysaccharides and glycoproteins under dynamic conditions.

Acknowledgements—The author expresses his gratitude to L. M. Likhosherstov for donating the blood-group substance preparations and to Yu. I. Khurgin for useful discussion of the work.

REFERENCES

1. J. Mitchell and D. M. Smith, *Aquametry*, 2nd Ed., Vols. 1–3. Wiley, New York, 1977–1980.
2. A. Pande, *Handbook of Moisture Determination and Control*, Vols. 1–4. Dekker, New York, 1974–1975.
3. F. B. Sherman and Yu. I. Khurgin, in *Khimiya i biokhimiya uglevodov*, N. K. Kochetkov (ed.), p. 101. Pushyno, USSR, 1982.
4. *Idem*, in *Konformatsionnye izmeneniya biopolimerov v rastvorakh*, G. M. Mrevlishvily (ed.), p. 146. Metsniereba, Tbilisi, USSR, 1980.
5. V. A. Derevitskaya, *Pure Appl. Chem.*, 1981, **53**, 89.
6. V. A. Klimova, U. Tusupkaliev, F. B. Sherman, Yu. I. Khurgin and A. B. Klyachko-Gurvich, *Izv. Akad. Nauk SSSR, Ser. Khim.*, 1973, 2111.
7. V. A. Klimova, in *Basic Methods of Microanalysis of Organic Compounds*, 2nd Ed., p. 180. Khimiya, Moscow, 1975.
8. F. B. Sherman, U. Tusupkaliev, V. A. Klimova and Yu. I. Khurgin, *Izv. Akad. Nauk SSSR, Ser. Khim.*, 1973, 1401.
9. L. M. Likhosherstov, M. D. Martynova and V. A. Derevitskaya, *Biokhimiya*, 1968, **33**, 1135.
10. N. K. Kochetkov, S. G. Kara-Murza and V. A. Derevitskaya, *Izv. Akad. Nauk. SSSR, Ser. Khim.*, 1965, 2212.

Talanta, Vol. 30, No. 9, pp. 709–712, 1983
Printed in Great Britain.

0039/9140/83 $3.00+0.00

ANALYTICAL DATA

EQUILIBRIUM AND CALORIMETRIC STUDY OF THE HYDRATION OF ANION-EXCHANGE RESINS

A. MARTON, É. KOCSIS* and J. INCZÉDY
Department of Analytical Chemistry, University of Veszprém, P.O. Box 158, H-8201 Veszprém, Hungary

(*Received* 25 *January* 1983, *Accepted* 21 *March* 1983)

Summary—The adsorption of water vapour on anion-exchangers of various degrees of cross-linking (×2, ×4, ×8, ×10) and in different ionic forms (Cl^-, Br^-, I^-) was studied by the isopiestic technique. The calculated integral free-energy changes were independent of the degree of cross-linking of the resins. With increase in the number of adsorbed water molecules the free-energy functions approached limiting values which were characteristic for the counter-ions. The free-energy change was combined with the enthalpy of water sorption (obtained from direct calorimetric measurements) to obtain the entropy change due to the water uptake. Both the enthalpy and the entropy functions indicated the existence of several processes during the adsorption of water, among which the most relevant are hydration, swelling of the matrix, and dilution of the internal electrolyte of the ion-exchanger.

The most important property of ion-exchangers is the selectivity which, as a rule, is the result of manifold ionic and molecular interactions. The ion-exchange proper is always accompanied by a transfer of electrolyte and water. The adsorption of water molecules has been mostly studied for cation-exchangers.[1,2] In the present work the thermodynamic parameters ΔG, ΔH and ΔS for the sorption of water by strongly basic anion-exchange resins are reported. The results of such investigations are not only important for a better understanding of the selectivity of ion-exchangers but are also generally useful for interpretation of systems where water molecules are immobilized on polar surfaces such as protein membranes and other biological systems. In this respect ion-exchangers can be considered as reproducible model materials.[3]

EXPERIMENTAL

Dowex 1 (100–200 mesh) anion-exchange resins with various degrees of cross-linking (×2, ×4, ×8 and ×10) were converted into their chloride, bromide and iodide forms. The capacities were determined by the usual methods[4] and the values obtained are given in Table 1.

The water-sorption equilibria of the resins were studied by the isopiestic technique described by Dickel and Hartmann.[5] The resin samples were first dried in a vacuum oven at 50° for 48 hr then transferred to small flat dishes and stored in the vapour atmosphere of desiccators containing various saturated salt solutions which gave the following water activities ($a_w = p/p°$) at 25°: 0.07, 0.333, 0.428, 0.577, 0.807, 0.925 and 0.980.[1] After 4 or 5 weeks of equilibration the water content of the resins was determined by drying for 24 hr at 95° in a vacuum drying pistol containing phosphorus pentoxide as desiccant.

Dry resins for the calorimetric measurements (see below) were handled in a special dry-box filled with nitrogen that had been dried over phosphorus pentoxide.

The integral heat of hydration of the dry and partially hydrated resins was determined by a direct calorimetric technique using an LKB-8700 solution calorimeter. The reaction vessel of the calorimeter was filled with 100 ml of distilled water and the dry or partially hydrated resin stored in the desiccators was weighed in thin glass ampoules of 0.5 cm^3 nominal volume. The overall performance of the calorimeter as well as the calibrations were made in the same way as described earlier [6].

For determination of the water content of the fully swollen resins the excess of water was removed by centrifuging the resin samples at 3000 rpm for 10 min. The water content was then determined by drying as described above.

Table 1. Ion-exchange capacity (c_d) of the resins

Ionic form	DVB,*%	c_d, *meq/g*†
Cl^-	2	4.60
	4	4.06
	8	3.67
	10	3.56
Br^-	2	3.80
	4	3.39
	8	3.15
	10	3.12
I^-	2	3.24
	4	2.94
	8	2.80
	10	2.74

*Divinylbenzene.
†Of dry resin.

*Present address: Department of Atomic Physics, Institute of Physics, Technical University of Budapest, Budafoki út 8, H-1111 Budapest, Hungary.

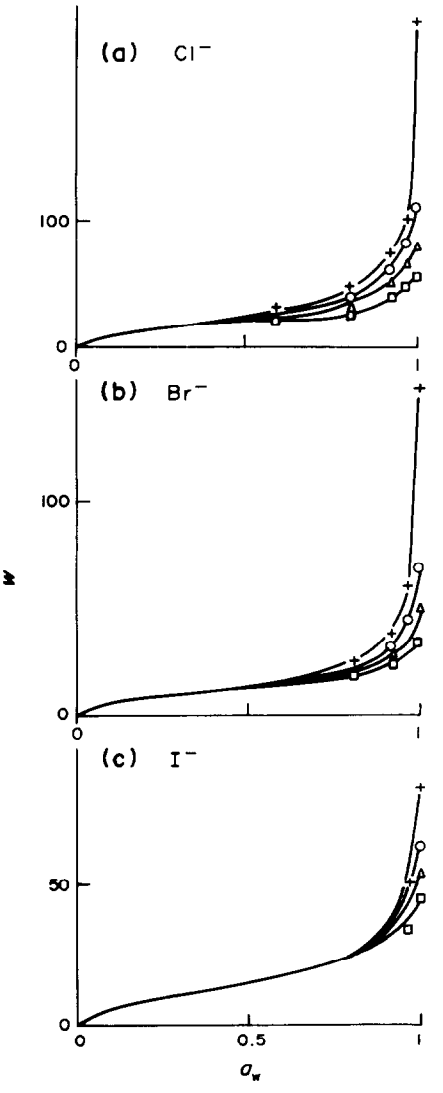

Fig. 1. Water-sorption isotherms of the chloride (a), bromide (b) and iodide (c) form resins with various degrees of cross-linking, at 298 K. + ×2; ○ ×4; △ ×8; □ ×10.

RESULTS AND DISCUSSION

Calculation of the free-enthalpy changes

The water-vapour adsorption isotherms of the resins studied are shown in Fig. 1. In the low water-activity region the quantity of water adsorbed (w) is practically independent of the degree of cross-linking of the resin, but becomes very strongly dependent on the DVB content as a_w is increased.

The free-energy change of the adsorption process can be calculated from the data of the isotherms by the following equation:[7]

$$\Delta G = zRT \ln a_w - RT \int_0^{a_w} z \, d \ln a_w \qquad (1)$$

where R and T have their usual meanings; z is the number of moles of water per equivalent of active group and is calculated from

$$z = \frac{w}{100} \times \frac{1}{18} + \frac{1000}{c_d} \qquad (2)$$

The second term in equation (1) can be obtained by graphical integration of the isotherms plotted as z *vs.* a_w. In Fig. 2 the calculated ΔG values are shown as a function of the z values. The points on the curves give the free-energy change when one equivalent of dry resin takes up z mole of water. As z increases, ΔG approaches a limit that depends only on the nature of the counter-ion, but not on the degree of cross-linking of the resin: $\Delta G(\mathrm{RCl}) = -23.2$ kJ/eq, $\Delta G(\mathrm{RBr}) = -17.7$ kJ/eq, $\Delta G(\mathrm{RI}) = -11.3$ kJ/eq. If these values are plotted against the reciprocal of the crystallographic radius of the counter-ions then a straight line is obtained (Fig. 3).

This linear relationship can be interpreted in terms of the Born charging equation for the free-energy charge of hydration of the ions:

$$\Delta G_{\mathrm{hydr}} = -\frac{Z^2 e^2}{8\pi\varepsilon_0 r}\left(1 - \frac{1}{\varepsilon_r}\right) \qquad (3)$$

where e is the charge of an electron, ε_0 is the permittivity of free space, ε_r is the relative permittivity of the medium (water), Z and r are the charge and radius of the ion.

The adsorption of water molecules on ion-exchangers is simultaneously accompanied by hydration, dilution, swelling, *etc.* The linear relationship given above, however, seems to indicate the decisive role of the hydration.

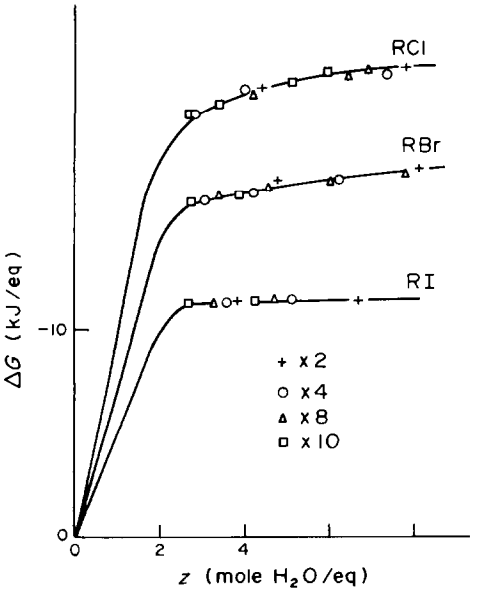

Fig. 2. Free-energy changes accompanying water adsorption by the ion-exchangers studied.

The enthalpy functions and their interpretation

The reaction taking place in the calorimeter is either

$$RX + (z+n)H_2O \rightleftharpoons RX.(H_2O)_{(z+n)} \Delta H_d \quad (4)$$

(when dry resin is used for the measurements) or

$$RX.(H_2O)_z + nH_2O \rightleftharpoons RX.(H_2O)_{(z+n)} \Delta H_w \quad (5)$$

(when partially hydrated resins are investigated). From these measurable heat effects the enthalpy change sought:

$$RX + zH_2O \rightleftharpoons RX.(H_2O)_z \Delta H \quad (6)$$

can be obtained by the application of Hess's law:

$$\Delta H = \Delta H_d - \Delta H_w \quad (7)$$

The measured ΔH_d values were independent of the degree of cross-linking of the resin and were characteristic for the counter-ion: $\Delta H_d(RCl) = -31.3$ kJ/eq, $\Delta H_d(RBr) = -23.5$ kJ/eq, $\Delta H_d(RT) = -11.2$ kJ/eq.

When reaction (5) is studied at various values of z, an interesting change in the shape of the calorimetric curves can be observed (Fig. 4).

As Fig. 4 clearly indicates, the overall process involves both exothermic and endothermic processes, as has been proposed by other authors.[1,2] Experimental verification of this postulation, however, has not been presented. The exothermic process is certainly hydration, whereas the endothermic contribution is due to the swelling of the resin matrix as well as to the dilution of the internal electrolyte. The changes of the calculated ΔH values as a function of z are given in Fig. 5.

Similarly to the case in Fig. 2, the points of the ΔH function represent the enthalpy change of the process when one equivalent of dry resin absorbs z mole of water. No experimental data are available for small values of z but it can be supposed, to a good approximation, that in this region the course of the curves is independent of the degree of cross-linking.

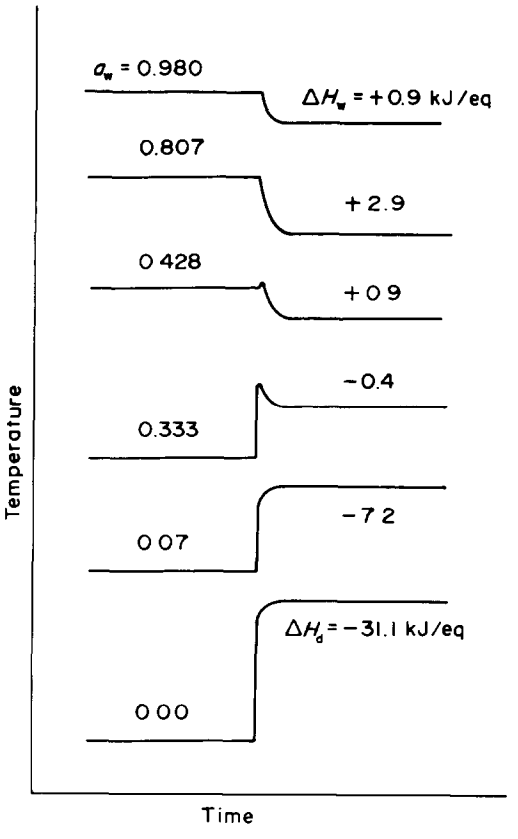

Fig. 4. Typical change in the calorimetric curves for the reaction (2% DVB)RCl.$(H_2O)_z + nH_2O \rightleftharpoons$(2% DVB)RCl. $27H_2O$, for various values of z.

At higher values of z, however, the curves diverge and after reaching a maximum they tend to the limiting ΔH_d values. The position of the maximum of the curves depends on the counter-ion: chloride ($z = 5$), bromide ($z = 3.5$) and iodide ($z = 2.5$). Curves simi-

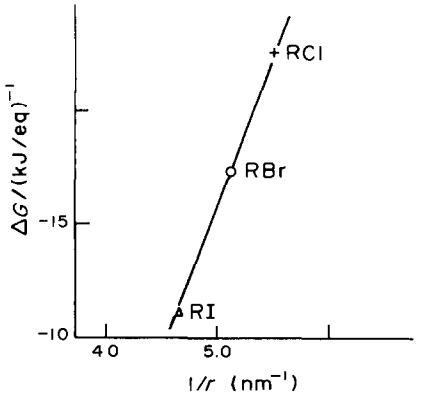

Fig. 3. Change of the ΔG values for water adsorption by the chloride, bromide and iodide form resins as a function of the reciprocal of the radius of the counter-ions.

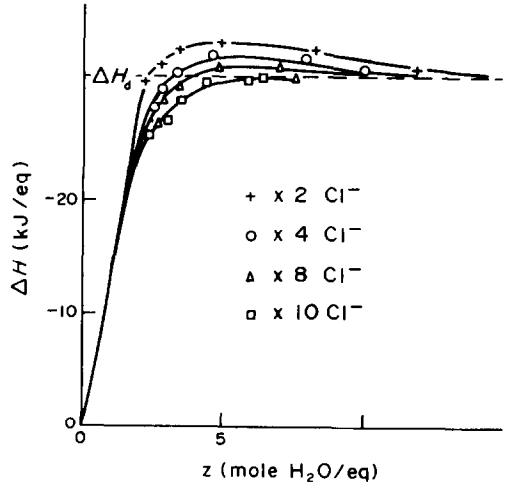

Fig. 5. Integral enthalpy changes accompanying the water uptake of the chloride-form resins with various degrees of cross-linking.

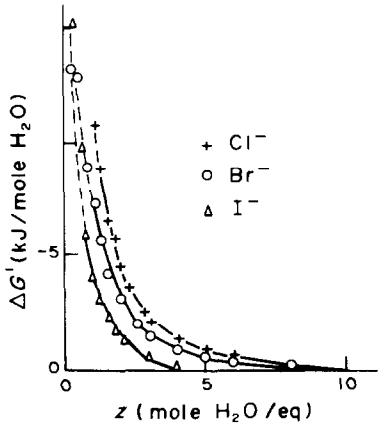

Fig. 6. Differential free-energy changes for water uptake by the resins studied.

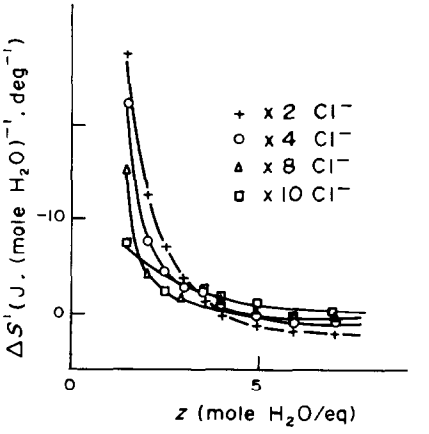

Fig. 8. Differential entropy changes for water uptake by the chloride-form resins with various degrees of cross-linking.

lar to those presented for the chloride-form resins were obtained for the bromide and iodide forms, but are omitted for brevity.

Calculation of the entropy functions

Graphical differentiation of the ΔG *vs.* z and ΔH *vs.* z curves gives the values of these thermodynamic parameters for the uptake of one mole of water ($\Delta G'$ and $\Delta H'$).

The differential free-energy curves for the resins studied and the enthalpy curves for the chloride-form resins are shown in Figs. 6 and 7.

Apart from the initial (and uncertain) parts of the curves (drawn as dotted lines) the $\Delta G'$ and $\Delta H'$ functions both demonstrate that the energy contribution caused by the uptake of one mole of water decreases with increasing value of z.

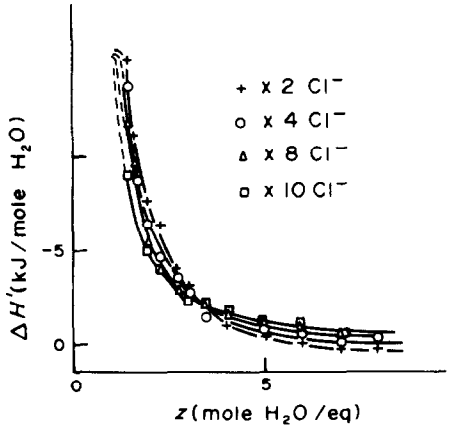

Fig. 7. Differential enthalpy changes for water uptake by the chloride-form resins with various degrees of cross-linking.

From the familiar $\Delta S' = (\Delta H' - \Delta G')/T$ equation the differential entropy change of the water uptake can also be calculated (Fig. 8).

The shape of the differential entropy curves can be interpreted in terms of the processes mentioned in the discussion of the ΔG and ΔH functions. The negative entropy changes are in accordance with orientation of the water molecules during hydration of the counter-ions [the standard hydration entropies of the ions are[8] (J.mole^{-1}.deg^{-1}) $\Delta S°(Cl^-) = -86.9$, $\Delta S°(Br^-) = -74.8$, $\Delta S°(I^-) = -57.3$]. A negative entropy contribution is also caused by the stretching of the polymer network of the resin. As Fig. 8 shows, above a certain value of z the entropy change becomes positive, which is a clear indication of the existence of further process(es). The positive entropy contribution is caused by the mixing effect due to dilution of the internal electrolyte of the ion-exchanger.

REFERENCES

1. G. Dickel, H. Degenhart, K. Haas and J. W. Hartmann, *Z. Phys. Chem. (Frankfurt)*, 1959, **20,** 121.
2. K. Gärtner and J. Giesmann, *Z. Phys. Chem. (Leipzig)*, 1965, **228,** 129.
3. G. N. Ling, C. Miller and M. M. Ochsenfeld, *Ann. N.Y. Acad. Sci.*, 1973, **204,** 6.
4. J. Inczédy, *Analytical Applications of Ion Exchangers*, p. 120. Pergamon Press, New York, 1966.
5. G. Dickel and J. W. Hartmann, *Z. Phys. Chem. (Frankfurt)*, 1960, **23,** 1.
6. R. J. Irving, M. H. Abraham, J. E. Salmon, A. Marton and J. Inczédy, *J. Inorg. Nucl. Chem.*, 1977, **39,** 1433.
7. F. Helfferich, *Ion Exchange*, p. 100. McGraw-Hill, New York, 1962.
8. B. E. Conway, *Ionic Hydration in Chemistry and Biophysics*, p. 351. Elsevier, Amsterdam, 1981.

Talanta, Vol. 30, No 9, pp. 713–716, 1983
Printed in Great Britain.

0039/9140/83 $3.00 + 0.00

ANNOTATIONS

LASER-EXCITED FLUORESCENCE LINE-NARROWING: AN ANALYTICAL STUDY

D. BOLTON* and J. D. WINEFORDNER†
Department of Chemistry, University of Florida, Gainesville, FL 32611, U.S.A.

(*Received* 10 *February* 1983. *Accepted* 16 *March* 1983)

Summary—The limits of detection obtained by fluorescence line-narrowing spectroscopy for 6 polynuclear aromatic hydrocarbons are compared with those obtained by low-temperature and room-temperature fluorescence, and the merits of the technique are discussed.

The need to develop sensitive and selective techniques suitable for the detection of polynuclear aromatic hydrocarbons (PAHs) has led to considerable advances in the past few years. Several techniques based on the optical luminescence of these compounds have been proposed. The optical luminescence spectra of these compounds are seen to consist of bonds with a full width at half maximum (FWHM) of 100–300 cm^{-1} at room temperature. Room-temperature luminescence is therefore relatively unsuitable for the analysis of complex mixtures, owing to the effects of inhomogeneous broadening.

There are basically three approaches for reducing the effects of inhomogeneous broadening in molecular luminescence spectroscopy. These are matrix isolation spectroscopy (MIS), Shpol'skii solvent spectroscopy (SSS) and fluorescence line-narrowing spectroscopy (FLNS).

First reported in the 1950s, MIS attempts to reduce the energy of interaction of an analyte molecule with its surrounding environment by employing an inert host material such as argon.[1,2] Recent work concerning the analytical application of MIS has been surveyed by Wehry and Mamantov.[3]

The Shpol'skii effect takes advantage of a phenomenon first reported by Shpol'skii *et al.* in 1952.[4] When certain organic species, such as PAHs, are placed in frozen polycrystalline snows consisting of n-alkane hosts, highly resolved absorption and emission spectra are observed. This is attributed to the incorporation of analyte molecules into sites within the crystalline lattice, minimizing the heterogeneity of the environment of the analyte molecules.[5] This approach for obtaining high-resolution absorption and emission spectral data has been the subject of extensive work, with regard to both the physical nature of the phenomenon and its application to chemical analysis.

Wehry and Mamantov has reviewed the current status of SSS with particular emphasis on its potential for the selective determination of PAHs.[3] Only those aspects relevant to the ultimate analytical use of this technique are mentioned here.

Some shortcomings of SSS have been discussed by Lukasiewicz and Winefordner.[6] The effect is highly dependent upon selection of an appropriate host (solvent), precluding the use of a single solvent.[7] The spectral resolution attainable improves as the sample temperature is lowered.[8] In addition, other factors such as freezing rate,[9–13] analyte concentration,[10,13,14] and matrix effects,[9,15] can also affect the spectral resolution.

There are some additional problems that have a direct bearing on the quantitative usefulness of the Shpol'skii effect. The linear dynamic range is generally less than three orders of magnitude.[16–21] Furthermore, since most compounds are less soluble at lower temperatures, solute aggregation can occur unless the freezing is rapid and the analyte concentration low.[13,22–24]

Another approach for reducing the effects of inhomogeneous broadening, and one that serves as the basis for FLNS, was first suggested by Feld and Javan[25] and later demonstrated by Szabo.[26,27] In this early work, FLNS was used to produce narrow line ($\Delta\bar{\nu} \sim 0.002\ cm^{-1}$) emission of the 6934 Å Cr^{3+} transition in ruby. The technique was extended to organic species by Personov *et al.* in 1972.[18,19] More recent studies have established the physical nature of the phenomenon.[28–31]

The fluorescence line-narrowing requires the selective excitation of a subset of species occupying similar lattice sites in the solid state. The phenomenon can be observed in virtually any solvent medium. Assuming

*Present address: Department of Chemistry, University of Denver, Denver, CO 80208, U.S.A.
†Author to whom correspondence should be addressed.

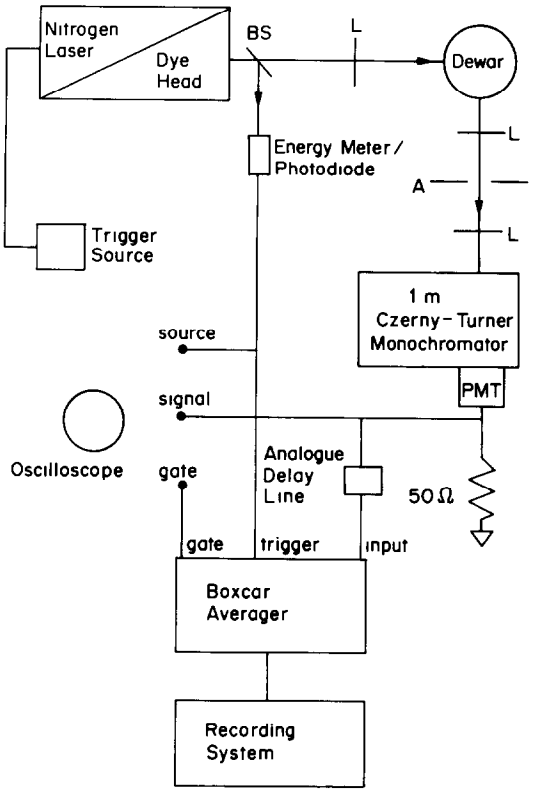

Fig. 1. Block diagram of the experimental apparatus for FLNS measurements.

that emission occurs from the same excited electronic state, the resulting emission spectrum is seen to consist of many well-resolved bands.

Each band in the emission spectrum is seen to consist of two parts, a narrow zero-phonon line and a broader phonon wing.[32] This type of band structure is evidence that the effects of inhomogeneous band-broadening have been minimized.

In order to observe line-narrowed fluorescence emission, the solute in question must be excited with a source having a band-width which is small compared with that of the absorbing species.[33] This implies that the limiting fraction of the species thus excited is small:

$$\frac{n_{ex}}{n_T} = \frac{\Delta\lambda_{ex}}{\Delta\lambda_{abs}}$$

where $\Delta\lambda_{ex}$ represents the line-width of the source, $\Delta\lambda_{abs}$ the absorption line-width, and n_{ex} and n_T are the number of excited analyte species and total number of analyte species, respectively.

To render the effects of thermal broadening negligible, the use of sample-cooling equipment (*e.g.*, an immersion helium-filled Dewar flask) is required. Although more convenient sample-cooling devices are commercially available, such as closed-cycle refrigeration systems, such systems have not yet been successfully utilized for FLNS.

The analyte must be excited in the vicinity of its 0–0 vibronic absorption band.[28] Since 0–0 transition wavelengths are not readily available for many organic species, selection of an appropriate excitation wavelength is not as straightforward as in conventional fluorimetry.

Assuming the criteria above are met, emission spectra can be measured in which the vibronic line-widths are limited by the line-width of the source of excitation. In practice, however, the observed spectral resolution is often limited by instrumental factors (such as monochromator band-pass).

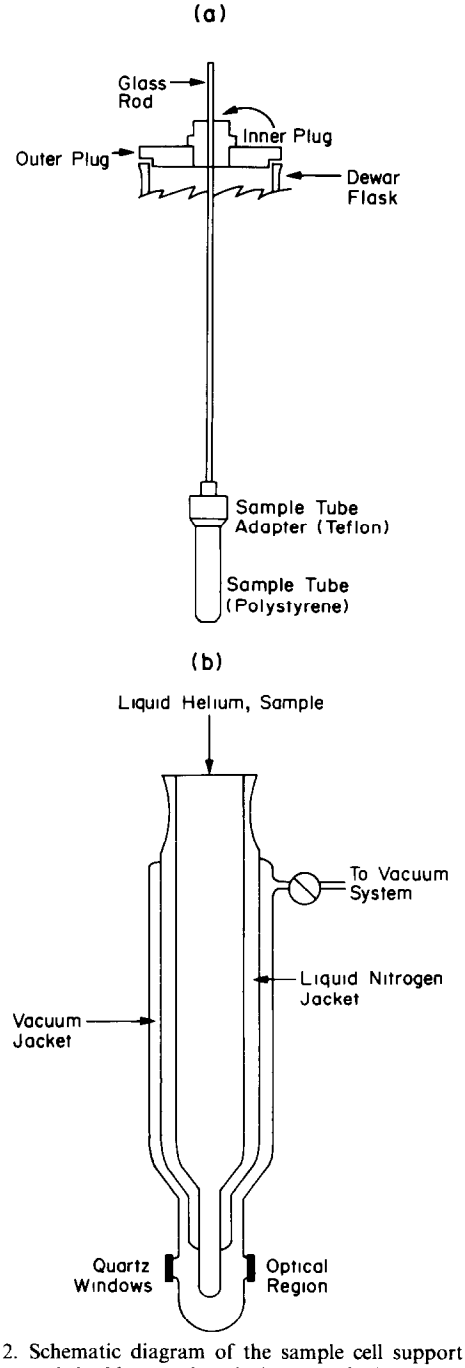

Fig. 2. Schematic diagram of the sample cell support (a) and double-nested optical Dewar flask (b).

Table 1. Experimental apparatus and operating conditions

Nitrogen-laser	Model UV24, Molecton Corp. (Sunnyvale, CA); operated at repetition rate of 30 Hz.
Dye-laser	Model DLII, Molecton Corp. (Sunnyvale, CA); operated with PBD and BBQ dyes.
Dewar flask	Model 30368, Pope Scientific, Inc. (Menomonee Falls, WI).
Collection optics	Two 102-mm focal length, 51-mm diameter, fused silica planoconvex lenses, each placed 51 mm from sample centre and monochromator entrance slits, respectively. Aperture between two lenses used to match f-number to that of monochromator.
Monochromator	Model H1000, Instruments SA, Inc. (Metuchen, NJ); 1-m Czerny-Turner monochromator; operated with a spectral band-pass of 1 Å.
Photomultiplier	Model 6256B, EMI Electron Tubes (Middlesex, GB); operated at voltage of 1.3 kV.
Energy meter	Model J3-05DW, Molectron Corp. (Sunnyvale, CA).
Photodiode/trigger circuit	Laboratory-constructed.
Analogue delay line	Model V2552050, Allen Avionics.
Boxcar averager	Model 162 gated integrator used with Model 164, Princeton Applied Research (Princeton, NJ); operated with 20 nsec aperture time, 1 msec sampling time constant, and 1 sec mainframe (low-pass filter) time-constant.
Strip-chart recorder	Model 5000, Fisher Scientific (Pittsburgh, PA).

Probably the most unusual aspect of FLNS is that large changes in spectra may be produced by small changes in excitation wavelength. A change in excitation wavelength produces two effects. First, the entire emission spectrum is seen to shift with excitation wavelength in the vicinity of the 0–0 vibronic absorption band.[33] If the energy corresponding to the wavelength of excitation exceeds the 0–0 absorptive transition by more than about 1500 cm^{-1}, significant band-broadening can occur.[34,35] This is attributed to the rapid release, to the matrix, of the excess of energy accompanying vibrational relaxation, leading to rapid local site-melting.

In this paper, we deal with some quantitative aspects of FLNS and report limits of detection (LODs) and emission band-widths for six PAHs.

EXPERIMENTAL

Instrumentation

A block diagram of the experimental apparatus appears in Fig. 1. A nitrogen-pumped tunable dye-laser was used as the source of excitation. The dyes PBD [2-phenyl-5-(4-biphenyl)-1,3,4-oxadiazole] and BBQ [4,4‴-bis(butyloctyl)-quaterphenyl] were used to cover the wavelength ranges 360–380 and 380–400 nm, respectively. Part of the dye-laser output was directed toward a pyroelectric detector by means of a small quartz plate. This facilitated optimization of the laser system before preparation of the helium-filled Dewar flask. The laser beam was focused onto the sample cell, which consisted of a 13-mm o.d. polystyrene culture tube suspended within the inner section of a 2-litre double-nested Dewar helium flask. The tube was supported by a Teflon sleeve attached at one end to the culture tube cap and at the other to a 2-ft piece of 8-mm diameter glass rod supported at the top of the Dewar flask by a Teflon plug, as depicted in Fig. 2. This arrangement permitted introduction and removal of samples from the liquid-helium bath without requiring recharging of the Dewar flask with coolant. The luminescence excited was then collected by a quartz lens and focused onto the entrance slits of a 1-m monochromator. In order to reduce stray light, an aperture was placed between the collimating and focusing lenses to match the f-number of the collection optics to that of the monochromator. The output of the photomultiplier tube was connected to the boxcar-averager signal input through an analogue delay line fitted with switch-selection of delays in the range 0–255 nsec. The output of the boxcar was attenuated by a laboratory-constructed instrumentation amplifier/attenuator before being input to the strip-chart recorder. The experimental apparatus and operating conditions used are summarized in Table 1.

Reagents

All PAHs used in this study were supplied by Aldrich Chemical Co. and were used without further purification. The composition of the solvent from which all the glasses used were made was 2:1:1 v/v glycerol:ethanol:water. The glycerol and ethanol were laboratory-reagent grade and used without further purification.

Procedures

Stock solutions of all compounds used in this study were prepared in ethanol and stored at 5°. These stock solutions were removed from the refrigerator and brought to room temperature before serial dilutions were made from them. A small volume (*ca.* 5 ml) was decanted into the corresponding culture tube, which was then introduced into the Dewar flask in analogous fashion to a procedure reported by Brown *et al.*,[36] after introduction of liquid nitrogen and liquid helium into the insulating and sample jackets of the Dewar flask, respectively.

RESULTS AND DISCUSSION

The emission spectrum of each PAH examined in this study was recorded in order to determine the optimum emission wavelength for quantitative measurement. The limits of detection (LODs) and relative standard deviations for each of these compounds are given in Table 2. The emission band-widths for all of the PAH studies were indistinguishable from the monochromator band-pass. The linear dynamic ranges for all compounds studied were less than 3 orders of magnitude, similar to ranges reported in previous studies with Shpol'skii matrices.[16–21]

These data suggest that FLNS is as much as five orders of magnitude less sensitive than conventional room-temperature fluorimetry.[37] It should be noted, however, that a similar comparison with

Table 2. Comparison of limits of detection for six PAHs by FLNS, low-temperature fluorescence (LTF), and room-temperature fluorescence (RTF)

	FLNS				LTF	RTF
Compound	λ_{ex}^{a}, Å	λ_{em}^{a}, Å	LOD[b], ng/ml	RSD[c], %	LOD[d], ng/ml	LOD[d], ng/ml
Anthracene	3640	3803	200	6.8	90	0.002
2-Methylanthracene	3845	3863	100	7.0	3	0.003
9-Methylanthracene	3825	3906	100	5.9	2	0.003
9,10-Dimethylanthracene	3940	4017	1000	5.2	20	0.006
Perylene	4340	4412	100	6.3	90	0.001
Pyrene	3640	3722	300	8.4	70	0.04

[a]Wavelengths are uncorrected for instrumental response and were determined with a 1-Å spectral band-pass.

[b]Fluorescence measurements were made with a 1-Å spectral band-pass. The limit of detection is that concentration which gives a signal 3 times the standard deviation of 8 blanks.

[c]Relative standard deviations based on 8 determinations of a 1000-ng/ml solution.

[d]Fluorescence analytical figure of merit measurements were made with an 80-Å spectral band-pass. The limit of detection is that concentration which gives a signal 3 times the standard deviation of 16 blanks.

conventional low-temperature fluorimetry is more favourable.

The relatively high LODs obtained for the six PAHs studied can be attributed to the high background signals observed. Two additional factors that contributed to the high LODs were irreproducible placement of the sample with respect to the incident beam, and the formation of small bubbles around the sample cell. The effect of the first of these was minimized by placing a small Teflon block at the bottom of the Dewar flask, with a cavity in which the sample tube could rest. This resulted in more reproducible placement of the lowered sample tube, although the problem was not completely eliminated. The second problem became worse after the lower section (tail) of the Dewar flask was damaged and had to be repaired. One way to circumvent such problems would be to utilize a closed-cycle refrigeration system for sample-cooling, in place of an immersion Dewar flask; the evaluation of such a configuration is currently under way.

Acknowledgement—This work was supported by Contracts NIH-GM11373-19 and DOE-DE AS05 780R06022 MOD.A003.

REFERENCES

1. E. Whittle, D. A. Dows and G. C. Pimentel, *J. Chem. Phys.*, 1954, **22**, 1943.
2. I. Norman and G. Porter, *Nature*, 1954, **174**, 508.
3. E. L. Wehry and G. Mamantov, *Anal. Chem.*, 1979, **51**, 643A.
4. E. V. Shpol'skii, A. A. Ilina and L. A. Klimova, *Dokl. Akad. Nauk SSSR*, 1952, **87**, 935.
5. C. Pfister, *Chem. Phys.*, 1973, **2**, 171.
6. R. J. Lukasiewicz and J. D. Winefordner, *Talanta*, 1972, **19**, 381.
7. E. V. Shpol'skii, *Sov. Phys. Usp.*, 1963, **6**, 411.
8. A. Colmsjo and U. Stenberg, *Chem. Scripta (Sweden)*, 1977, **11**, 220.
9. L. A. Mishina and L. A. Nakhimovskaya, *Opt. Spectrosc.*, 1974, **36**, 298.
10. N. S. Dokunikhin, V. A. Kizel, M. N. Sapozhnikov and S. L. Solodar, *ibid.*, 1968, **25**, 42.
11. D. M. Grebenshchikov, N. A. Kovizhynkh and S. A. Kozlov, *ibid.*, 1974, **37**, 155.
12. G. L. Bebel and J. D. Laposa, *J. Mol. Spectrosc.*, 1972, **41**, 249.
13. J. J. Dekkers, G. P. Hoornweg, C. MacLean and N. H. Velthorst, *ibid.*, 1977, **68**, 56.
14. T. N. Bolotnikova, *Opt. Spectrosc.*, 1959, **7**, 138.
15. E. V. Shpol'skii and T. N. Bolotnikova, *Pure Appl. Chem.*, 1974, **37**, 183.
16. G. F. Kirkbright and C. G. deLima, *Analyst*, 1974, **99**, 338.
17. B. S. Causey, G. F. Kirkbright and C. G. deLima, *Analyst*, 1976, **101**, 367.
18. R. I. Personov, E. I. Al'shits and L. A. Bykovskaya, *JETP Lett.*, 1972, **15**, 431.
19. *Idem*, *Opt. Commun.*, 1972, **6**, 169.
20. G. E. Fedoseeva and A. Y. Khesina, *J. Appl. Spectrosc. USSR*, 1968, **9**, 838.
21. G. E. Kamil'tseva and A. Y. Khesina, *ibid.*, 1966, **5**, 196.
22. R. J. McDonald and B. K. Selinger, *Aust. J. Chem.*, 1971, **24**, 249.
23. R. J. McDonald, L. M. Logan, J. G. Ross and B. K. Selinger, *J. Mol. Spectrosc.*, 1971, **40**, 137.
24. R. A. Keller and D. E. Breen, *J. Chem. Phys.*, 1965, **53**, 2562.
25. M. J. Feld and A. Javan, *Phys. Rev.*, 1969, **177**, 549.
26. A. Szabo, *Phys. Rev. Lett.*, 1970, **25**, 924.
27. *Idem*, *ibid.*, 1971, **27**, 323.
28. E. I. Al'shits, R. I. Personov, A. M. Pyndyk and V. I. Stogov, *Opt. Spectrosc.*, 1975, **39**, 156.
29. L. A. Bykovskaya, R. I. Personov and B. M. Kharlamov, *Chem. Phys. Lett.*, 1974, **27**, 80.
30. R. I. Personov, E. I. Al'shits, L. A. Bykovskaya and B. M. Kharlamov, *Sov. Phys. JETP*, 1974, **38**, 912
31. R. I. Personov and E. I. Al'shits, *Chem. Phys. Lett.*, 1975, **33**, 85.
32. L. A. Bykovskaya, R. I. Personov and Y. V. Romanovskii, *Anal Chim Acta*, 1981, **125**, 1.
33. W. C. McColgin, A. P. Marchetti and J. H. Eberly, *J. Am. Chem. Soc.*, 1978, **100**, 5622.
34. K. Cunningham, J. M. Morris, J. Funfschilling and D. F. Williams, *Chem. Phys. Lett.*, 1975, **32**, 581.
35. R. I. Personov and B. M. Kharlamov, *Opt. Commun.*, 1973, **7**, 417.
36. J. C. Brown, J. A. Duncanson and G. F. Small, *Anal. Chem.*, 1980, **52**, 1711.
37. A. Jurgensen, *Ph.D. Thesis*, University of Florida, 1981

Talanta, Vol. 30, No. 9, pp. 717–720, 1983
Printed in Great Britain

0039/9140/83 $3.00+0.00
Pergamon Press Ltd

TITRIMETRIC DETERMINATION OF ALUMINIUM IN ZINC–ALUMINIUM ALLOYS, WITH EDTA AND A Cu(II)-SELECTIVE ELECTRODE

HENRY F. STEGER
Mineral Sciences Division, Canada Centre for Mineral and Energy Technology, 555 Booth Street, Ottawa, Canada

(*Received* 25 *August* 1982. *Revised* 15 *December* 1982. *Accepted* 24 *February* 1983)

Summary—The end-point for the titration of EDTA with Cu(II), as measured by a Cu(II)-selective electrode, varies with pH and temperature. Moreover, the effect of pH and temperature on the behaviour of this electrode differs according to whether fluoride is present. As a consequence, the determination of aluminium in zinc–aluminium alloys by the Freegarde and Allen method with use of a Cu(II)-selective electrode must be performed with close control of pH and temperature to maximize accuracy and repeatability.

In 1979, the Canadian Certified Reference Materials Project (CCRMP) initiated a programme to confirm that the homogeneity of a suite of seven zinc–aluminium alloys (Al 7–30%) was sufficient for their use as reference standards for emission and X-ray fluorescence spectrometry. The determination of aluminium was first attempted by use of a modified Freegarde and Allen method.[1,2] In this, an excess of ethylenediaminetetra-acetic acid (EDTA) is added to the sample and the mixture is boiled to form the Al–EDTA complex; the uncomplexed EDTA is titrated with a zinc solution in the presence of a small amount of copper(II), with Xylenol Orange as indicator. The EDTA complexed with the aluminium is released by adding fluoride and boiling, and is titrated with zinc in the same way. The second titration corresponds to the aluminium in the sample. The relative standard deviation of 46 results was 1.7% (for 28.9% Al), which was too high to warrant any conclusions concerning homogeneity of the alloy. Some of this poor repeatability was attributed to errors arising from visual detection of the two end-points.

The Cu(II)-selective electrode has been found effective in Cu(II)–EDTA titrations[3,4] and also in the back-titration of uncomplexed 1,2-diaminocyclohexanetetra-acetic acid (DCTA) with copper(II) in the indirect determination of aluminium.[5] The application of this electrode to the determination of aluminium by the unmodified Freegarde and Allen method with copper(II) as titrant ultimately gave a relative standard deviation of 0.4% for 47 determinations. This paper reports the differences observed in the behaviour of the Cu(II)-selective electrode in fluoride-free and fluoride-bearing titration media, as a result of which close control of pH and temperature is required if this repeatability is to be achieved.

EXPERIMENTAL

Reagents

All solutions were prepared from analytical grade chemicals and demineralized water.

Apparatus and titration procedure

A Mettler Automatic Titrater was used with an Orion 94-29 Cu(II)-selective electrode and saturated calomel electrode.

Samples were adjusted to and kept at the desired titration temperature in a thermostatically controlled water-bath. Between titrations, the electrodes were stored in $10^{-3}M$ copper(II) kept at the temperature of the water-bath. Overnight, the electrodes were stored in demineralized water.

The samples were titrated as follows. The $\sim 0.1M$ copper titrant was added at maximum rate to within 0.5 ml of the estimated end-point and the electrode was allowed to reach constant potential. Titrant was then added at the minimum rate possible, 0.003 ml/sec (with the titrater operated manually), to 0.1–0.15 ml beyond the end-point. This excess was, of course, considered in calculating the titrant volume equivalent to the EDTA released from its aluminium complex. A derivative plot ($\Delta E/\Delta V$) was used to find the end-point.

General procedure

The samples for titration consisted of solutions of various quantities of zinc–aluminium alloy or other metals, a maximum of 20 ml of $0.05M$ EDTA and sufficient water to give a volume of 70 ml. The pH was adjusted to 4.3–4.8 with sodium hydroxide (pH-meter), and then by addition of 10 ml of acetate buffer of the required pH (for concentration, see discussion). The solution was boiled for 5 min, cooled and titrated. After addition of 30 ml of sodium fluoride solution (~ 42 g/l.), the solution was again boiled for 5 min, cooled and titrated. Samples which did not contain aluminium were not boiled, but otherwise were handled as described.

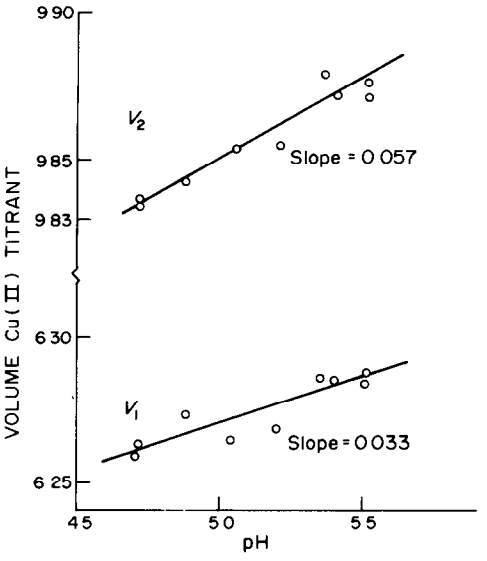

Fig. 1. The relationship between pH and V_1, the volume of Cu(II) titrant equivalent to surplus EDTA after complexation of 10.00 mg of aluminium in fluoride-free medium, and V_2, the volume of Cu(II) titrant equivalent to the EDTA liberated when 10.00 mg of aluminium are complexed with fluoride in fluoride-bearing medium.

RESULTS AND DISCUSSION

The initial attempts to determine aluminium with use of a Cu(II)-selective electrode were made by the Freegarde and Allen method with the recommended buffer of 1.5% sodium acetate–0.5% acetic acid and the samples were cooled to approximately room temperature after boiling. The agreement obtained between equal aliquots of a given sample that were prepared and titrated in the same run was in general acceptable. However, the agreement between results from different runs was variable. For example, the mean value of four determinations in each of four consecutive runs was 29.16, 28.88, 28.37 and 29.16% Al for alloy No. 1. This poor repeatability was found to be due to a difference between the effect of small differences in the pH of replicate aliquots both in one run and in different runs, and between the temperatures of replicate aliquots in different runs, on the response of the Cu(II)-selective electrode in fluoride-free and fluoride-bearing media. The small differences in pH arose from a variable loss of acetic acid from the samples during boiling, as a result of which the pH could not be maintained at better than 4.9 ± 0.1 for the first back-titration and at 5.7 ± 0.2 for the second. Use of a buffer containing 7.5% sodium acetate and 8% acetic acid gave better pH control, at 5.11 ± 0.03 and 5.45 ± 0.06 respectively for the two titrations. Small differences in temperature were easily eliminated by cooling in a constant-temperature bath. The repeatability of results was found to be independent of the time spent by the samples in the bath after they had reached bath-temperature.

The volume of copper(II) titrant needed to reach the end-point indicated by the Cu(II)-electrode increased slightly with pH in the range 4.2–5.6, regardless of the composition of the titration medium. The pH was varied with buffers consisting of 7.5% sodium acetate solution containing 1–20% v/v acetic acid; and was measured before the titration. Figure 1 illustrates the results for the titration of 10 ml of 1-mg/ml aluminium solution plus 20 ml of 0.05*M* EDTA. Table 1 reports the values of the slope and its 95% confidence intervals for V_1, (the volume of titrant used in the back-titration after Al–EDTA complex formation), V_2, (the total volume of titrant used for both back-titrations), and V_3, the volume of titrant corresponding to the quantity of aluminium, which is given by $V_2 - V_1$, when these are plotted as a function of pH. Although the overlap of the 95% confidence limits indicates that there is no statistical significance in the difference between the three slopes, the relative magnitudes of these slopes together with the difference between the slopes found for V_1 for EDTA alone in fluoride-free and fluoride-bearing media, imply a physical significance. The variation of 0.4 in the pH after the decomposition of the Al–EDTA complex, observed for replicate samples when the 1.5% sodium acetate–0.5% acetic acid buffer is used, could therefore result in apparent differences of up to ~ 0.008 ml in V_3.

This variation in the titrant volume used, with pH, can be explained as follows. After the equivalence-point in the titration of EDTA with Cu(II), the potential of the Cu(II)-selective electrode depends on the concentration of the excess of copper, and this potential is independent of pH in the range 3–6.[6–8] Before the equivalence-point, the potential of the electrode depends solely on the concentration of the excess of EDTA.[7,9] A decrease in pH causes a shift in the potential of the electrode to more positive values,[7,10,11] in the same manner as does a decrease in the

Table 1. Effect of pH on Cu(II)-electrode response

Titration medium	Slope ± 95% confidence interval, *ml/pH*		
	V_1	V_2	V_3
EDTA only, no F^-	0.0356 ± 0.0061	—	—
EDTA only, F^-	0.0614 ± 0.0097	—	—
EDTA, Al^{3+}	0.033 ± 0.012	0.057 ± 0.017	0.024 ± 0.017
EDTA, Al^{3+}, Zn^{2+}	0.014 ± 0.008	0.039 ± 0.010	0.021 ± 0.013
EDTA, Zn–Al alloy	0.025 ± 0.015	0.046 ± 0.020	0.020 ± 0.013

Table 2. Effect of temperature on Cu(II)-electrode response

Titration medium	Slope ± 95% confidence interval, *ml/pH*		
	V_1	V_2	V_3
EDTA only, no F^-	-0.00072 ± 0.00054	—	—
EDTA only, F^-	-0.00028 ± 0.00028	—	—
EDTA, Al^{3+}, Zn^{2+}	-0.00093 ± 0.00046	0.00041 ± 0.00034	0.00078 ± 0.00039
EDTA, Zn–Al alloy	-0.00068 ± 0.00056	0.00038 ± 0.00035	0.00102 ± 0.00048

concentration of EDTA.[7,11] Consequently, differences between the pH values of the solutions titrated cause the electrode to indicate differences between the concentrations of free EDTA at the same point in the titration, and hence differences in the apparent equivalence-point volumes. It has been suggested that the dependence of the electrode response on pH is a result of the protonation equilibria of the complexing ligand.[11] If this is indeed so, it would appear that the Cu(II)-selective electrode is responsive to the $HEDTA^{3-}$ and possibly $EDTA^{4-}$ forms of the ligand.

The effect of temperature on the end-point was roughly linear in the range 15–35 as shown in Table 2, but the effect is different for fluoride-free and fluoride-bearing media. Hence the apparent aluminium content of a given sample will increase with an increase in the temperature of titration. For example, a difference of 5° in the titration temperature of two aliquots from a given sample would give a difference of ~0.005 ml between the apparent volumes of 0.1*M* copper solution used. This difference is the same as the standard deviation calculated for the volume of titrant used for 24 replicate aliquots from a sample of alloy No. 1 (7.5% sodium acetate–8% acetic acid buffer and constant temperature).

The variation in the end-point with temperature is due to two effects. Changes in sample volume with temperature need not be considered in potentiometric titrations. The standard potential and the slope of the Nernst equation

$$E = E_0 + \frac{RT}{zF} \log a_{\text{}}$$

for behaviour of an electrode are both temperature-dependent.[12] Although this dependence can strongly affect the accuracy of potentiometric determination of concentrations by a single-measurement procedure, it is generally only of minor consequence in a potentiometric titration. The titration of EDTA with Cu(II) is an exception because the electrode responds to Cu(II) with a slope of $RT/2F$ after the equivalence-point but is thought to respond to Cu(I) (at the solution–electrode interface) with a slope of RT/F before the equivalence point.[9] A change in temperature can also change the pH of a sample by altering the equilibrium of the acetate buffer.[13] The effect of pH changes has been discussed above.

The effect of temperature on the end-point and so on the repeatability of titration would be more evident from comparison of the titrant volumes for replicates in different batches than from those within a batch. The between-batch repeatability observed in this study was poorer than the within-batch repeatability, and this can probably be attributed to differences in temperature between the various sets of experiments performed in the initial attempts to determine aluminium.

Fluoride-free samples could be titrated consecutively without any affect on the "sharpness" of the derivative plots. For fluoride-bearing media, however, the "sharpness" of the successive plots degenerated rapidly unless the electrode was treated in a special fashion. Figure 2 shows the $\Delta E/\Delta V$ *vs.* V curve obtained for fluoride-bearing media for (a) 16–20, (b) 20–24 and (c) >24 consecutive titrations. This degeneration was unchanged if an equal number of titrations in fluoride-free media were interspersed among those in fluoride-bearing media, as would be the procedure for the determination of aluminium. Interference by fluoride with the potential of a Cu(II)-selective electrode has been noted previously.[14]

The shape of plots (b) and (c) in Fig. 2 suggests that the degeneration is due to the occurrence of more than one end-point for the titration. This suggests the formation of a sparingly-soluble film of a fluoride compound on the surface of the electrode*. Similar behaviour has been observed for chloride, which interferes with the Cu(II)-selective electrode[14–17] and forms on the electrode surface a dark, dull tarnish which is readily removed by light polishing.[15] Although no such film could be visually detected at any time in this study, it was found that a light polishing of the electrode surface restored the "sharpness" of the derivative end-point. The degeneration of response of the electrode on continuous use in fluoride-bearing medium could also be avoided by storage of the electrode overnight in demineralized water and in $10^{-3}M$ copper(II) solution between batches of titrations. The cumulative formation of the suggested film is therefore prevented by its physical removal or by dissolution in fluoride-free medium. This last procedure was used in this study, so the difference between the end-points obtained in fluoride-free and fluoride-bearing media is relevant to all the titrations, *i.e.*, it is an ever-present effect which does not appear only after some critical film thickness on the electrode surface has been attained.

Figure 3 depicts the effect of fluoride concentration

*The electrode then becomes responsive to fluoride; this is supportive evidence for formation of a "fluoride" film.

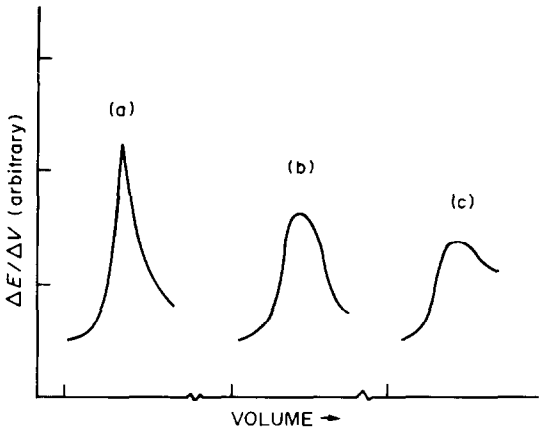

Fig. 2. The degeneration of the sharpness of the $\Delta E/\Delta V$ *vs.* V curve with the number of titrations performed.

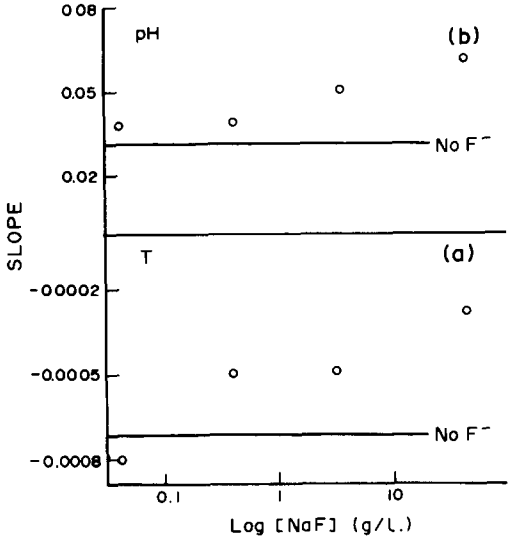

Fig. 3. The relationship between the slope of the plot of the end-point against (a) T and (b) pH and the concentration of NaF. The solid line represents the slope of the end-point for the fluoride-free solution

on the slopes of the plots of the equivalence-point volume of Cu(II) titrant as a function of temperature or pH: [NaF] refers to the stock solution, of which 30 ml were added to the sample; [F^-] in the sample is therefore approximately 3[NaF]/11. Figure 3 shows that the extent of the change in the end-point increases with increasing [NaF] in the manner expected. The nature of this interference by fluoride is undergoing further investigation.

This study has demonstrated that the end-point obtained with the Cu(II)-selective electrode responds to changes in pH and temperature differently in fluoride-free and fluoride-bearing media. It is consequently important to control the pH and temperature closely in the determination of aluminium in zinc–aluminium alloys by the Freegarde and Allen method, to maximize the accuracy and repeatability.

REFERENCES

1 M. Freegarde and B. Allen, *Analyst*, 1960, **85**, 731.
2. E. Mark and E. M. Donaldson, *Internal Tech. Rept*, CANMET, Energy, Mines and Resources Canada, 1979.
3. E. W. Baumann and R. M. Wallace, *Anal. Chem.*, 1969, **41**, 2072
4. A. Varma, *Talanta*, 1981, **28**, 785.
5. L. Šůcha and M. Suchánek, *Anal. Lett.*, 1970, **3**, 613.
6. G. Nakagawa, H. Wada and T Hayakawa, *Bull. Jap Chem. Soc.*, 1975, **48**, 424.
7. G. J. M. Heijne and W. E. van der Linden, *Anal. Chim Acta*, 1978, **96**, 13.
8. J. W. Ross, Jr. and M. S. Frant, *Anal Chem.*, 1969, **41**, 1900.
9. A. Hulanicki and A. Lewenstam, *Talanta*, 1976, **23**, 661.
10. V. K. Olson, J. D. Carr, R. D. Hargens and R. K. Force, *Anal. Chem.*, 1976, **48**, 1228.
11. I. Sekerka and J. F. Lechner, *Anal. Lett.*, 1978, **11**, 415.
12. R. J. Simpson, in *Ion-Selective Electrode Methodology*, A. K. Covington, (ed.), Vol. I, p. 55. CRC Press, Boca Raton, U.S.A., 1979.
13. L. G. Sillén and A. E. Martell (eds.), *Stability Constants*, Special Publication No. 17, The Chemical Society, London, 1969.
14. D. Midgley, *Anal. Chim. Acta*, 1976, **87**, 19.
15. D. J Crombie, G J Moody and J. D. R. Thomas, *Talanta*, 1974, **21**, 1094.
16. G. B. Oglesby, W. C. Duer and F. J. Millero, *Anal. Chem.*, 1977, **49**, 877.
17. J. C. Westall, F. M. M. Morel and D N Hume, *ibid*, 1979, **51**, 1792.

Talanta, Vol 30, No. 9, pp. 721–723, 1983
Printed in Great Britain

0039-9140/83$3.00 + 0.00
Pergamon Press Ltd

SPECTROPHOTOMETRIC DETERMINATION OF GALLIUM(III) AFTER SOLVENT EXTRACTION OF ITS CHLORO-COMPLEX WITH RHODAMINE B

YUKO HASEGAWA, TETSUYA INAGAKE, YUJI KARASAWA and ATSUSHI FUJITA
Department of Chemistry, Science University of Tokyo Kagurazaka, Shinjuku-ku, Tokyo, 162, Japan

(*Received* 15 *July* 1982. *Revised* 30 *January* 1983. *Accepted* 24 *February* 1983)

Summary—In the spectrophotometric determination of Ga(III) after extraction of its chloro-complex with Rhodamine B, addition of sodium chloride has been found to be very effective for improving the sensitivity and broadening the operating conditions, *e.g.*, a wider range of acid and dye concentration can be employed. The improvement is due to increased extraction of the gallium in the presence of sodium chloride.

The determination of traces of gallium(III) by measuring the absorbance of a benzene solution of the tetrachlorogallate–Rhodamine B ion-pair[1,2] has been regarded as one of the best methods for this element. However, the absorbance obtained is very dependent on the experimental conditions, such as concentrations of hydrochloric acid and the dye, and the volume ratio of the organic and aqueous phases.[2] As pointed out by Culkin and Riley,[3] this is due to incomplete extraction of Ga(III) under the conditions employed in the Onishi and Sandell method,[1] and if suitable conditions for better extraction could be found, the sensitivity would be enhanced and the experimental conditions less critical. Culkin and Riley[3] used a mixture of chlorobenzene and carbon tetrachloride as solvent, which was claimed to make the extraction quantitative, but still used a high hydrochloric acid concentration (6.5*M*), and the method suffered from various interferences. The present paper proposes an improvement by using extraction from 2.5*M* hydrochloric acid saturated with sodium chloride, instead of the 6*M* hydrochloric acid medium hitherto used.

EXPERIMENTAL

Gallium(III) stock solution was made by dissolving gallium metal (99.99% pure) in nitric acid, evaporating the excess of acid and diluting to the desired volume. The solution was standardized by EDTA titration, with morin as indicator.[4]

A simple procedure was developed to permit calculation of the distribution ratio, D, when only the absorbance (A) of the extracted species can be measured. The complex is first equilibrated between equal volumes of the organic and aqueous phases. Then,

$$D = \frac{[\mathrm{Ga(III)}]_{o(\mathrm{total})}}{[\mathrm{Ga(III)}]_{a(\mathrm{total})}}$$

where $[\mathrm{Ga(III)}]_o = [\mathrm{Rh^+ GaCl_4^-}]_o = A/\epsilon$, where ϵ is the molar absorptivity of the complex. An aliquot of the equilbrated aqueous phase is shaken with an equal volume of pure organic solvent. Since the conditions of extraction are identical, the value of D is assumed to remain the same as in the first extraction, and

$$D = \frac{[\mathrm{Ga(III)}]_{o,\mathrm{I}}}{[\mathrm{Ga(III)}]_{o,\mathrm{II}} + [\mathrm{Ga(III)}]_{a,\mathrm{II}}} = \frac{[\mathrm{Ga(III)}]_{o,\mathrm{II}}}{[\mathrm{Ga(III)}]_{a,\mathrm{II}}}$$

where $[\mathrm{Ga(III)}]_{o,\mathrm{I}} = A_\mathrm{I}/\epsilon$ and $[\mathrm{Ga(III)}]_{o,\mathrm{II}} = A_\mathrm{II}/\epsilon$, the subscripts I and II indicating the first and second extractions, respectively. By suitable manipulation the equation

$$D = (A_\mathrm{I} - A_\mathrm{II})/A_\mathrm{II}$$

can be derived.

Recommended procedure

In a stoppered glass tube take 5.0 ml of a gallium solution (concentration in the range 10^{-6}–$10^{-5}M$) in 2.5*M* hydrochloric acid containing 0.10% Rhodamine B and 0.6% titanium(III) chloride, saturate the solution with sodium chloride (about 1 g is needed) and add an equal volume of benzene. Shake the tube for 10 min, and then centrifuge it. Measure the absorbance of the benzene phase at 565 nm within 1 hr. Up to $7 \times 10^{-3}M$ iron(III), $1.2 \times 10^{-4}M$ antimony(III), and $10^{-4}M$ thallium(I) will not interfere. The apparent molar absorptivity of the tetrachlorogallate–Rhodamine B complex is 9.8×10^4 l.mole^{-1}.cm^{-1}.

RESULTS AND DISCUSSION

In the Onishi and Sandell method, the maximum absorbance is obtained by use of 6*M* hydrochloric acid concentration which must be maintained throughout because a small change in it causes a large decrease in the absorbance (*cf.* Fig. 49 in reference 2). This critical dependence of the absorbance on the hydrochloric acid concentration was confirmed in the present study. For example, when Ga(III) was extracted from 5.3, 6.0 and 6.5*M* hydrochloric acid with the Rhodamine B concentration recommended by Onishi and Sandell, the absorbances found were 0.45, 0.65, and 0.45, respectively. It was also observed that when sodium chloride was present in the aqueous phase, the absorbance was higher than when the

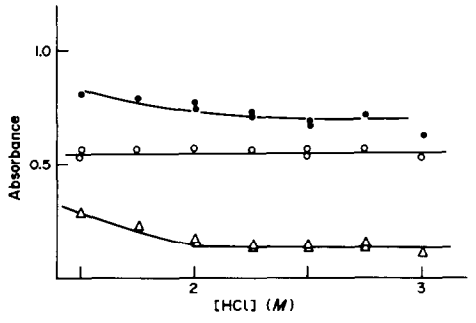

Fig. 1. Absorbance of the benzene extract as a function of the acidity; (●) measured against pure benzene; (○) measured against the reagent blank; initial aqueous solutions $6 \times 10^{-6}M$ Ga(III) and 0.1% Rhodamine B. (△) Reagent blank measured against pure benzene; initial aqueous solution 0.1% Rhodamine B.

acidity was the same but the sodium chloride was absent. For example, when the $5.3M$ acid solution was saturated with sodium chloride, the absorbance of the extract increased to 1.1. The relative increase obtained by saturating the solution with sodium chloride is still larger when the acid concentration is lower. The absorbance is nearly independent of acid concentration in the range 1.5–$3M$ when the solution is saturated with the salt (Fig. 1).

Figure 2 shows the dependence of the absorbance on the dye concentration under the conditions of the Onishi and Sandell method and the present method. The absorbance of the conventional method is always dependent on the dye concentration, but is independent of it (at least in the range 0.07–0.18%) when the solution is saturated with sodium chloride.

To find the molar ratio of metal to dye in the extract, the dependence of the distribution ratio on the dye concentration was examined, when the aqueous phase was $2.5M$ hydrochloric acid saturated with sodium chloride. The logarithm of the distribution ratio was proportional to the logarithm of the dye concentration in the range from 1×10^{-5} to $1 \times 10^{-3}M$ (D ranged from 0.1 to 7), indicating that a 1:1 Ga(III)–Rhodamine B species is extracted. It

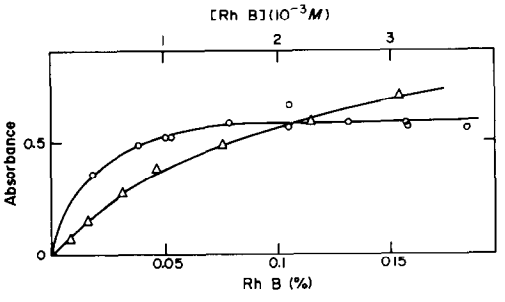

Fig. 2. Absorbance of the benzene extract as a function of the dye concentration. Initial aqueous solution: (○) $6 \times 10^{-6}M$ Ga(III) in $2.5M$ HCl saturated with NaCl; (△) $1.2 \times 10^{-5}M$ Ga(III) in $6M$ HCl.

has been established by Culkin and Riley[4] that the gallium is present as the tetrachlorogallate anion in the species extracted, so the extraction can be written as:

$$GaCl_4^- + Rh^+ \rightleftharpoons Rh^+ GaCl_{4(o)}^-$$

$$K_{ex} = [Rh^+ GaCl_4^-]_o / [GaCl_4^-][Rh^+] \quad (1)$$

The difference in effect of the dye concentration on the absorbance for the present method and the Onishi and Sandell method, as shown in Fig. 2, may be explained as follows. The method is based on measurement of the tetrachlorogallate–Rhodamine B ion-pair in the benzene phase and this absorbance depends on the degree of extraction, given by

$$E = \frac{[Rh^+GaCl_4^-]_o \times 100}{[Ga(III)]_{total}}\% = \frac{D \times 100}{(V_a/V_o) + D} \quad (2)$$

where D is the distribution ratio and V_a/V_o the phase-volume ratio: D itself is dependent on the Rhodamine B concentration, but E is practically independent of it if $D \gg V_a/V_o$. For example, when the dye concentration is $2 \times 10^{-3}M$, the aqueous phase is saturated with sodium chloride and $V_a/V_o = 1$, the distribution ratio is 13; doubling the dye concentration doubles the distribution ratio. However, the value of E changes only from 93 to 96%. On the other hand, under the conditions of the Onishi and Sandell method, D is 0.4 (at the phase-volume ratio of 0.65), and E is only 38% when a dye concentration of $7.5 \times 10^{-4}M$ is employed. Doubling the dye concentration would increase the value of E to 55%, which is still far from quantitative extraction.

There are two main factors that decide the value of D. One is stoichiometric in character, depending on the effective concentration of Rhodamine B, and the other is non-stoichiometric, depending on the solvent system selected and the salting-out effect by co-existing electrolytes. It is well known that Rhodamine B is readily protonated, and that the fraction in the singly-charged form involved in the ion-pair formation is reduced when the acidity is increased. Our use of lower acidity and saturation with sodium chloride therefore serves several purposes. It increases the effective concentration of the dyestuff and also maintains the chloride concentration at the level used in the earlier methods. Further addition of sodium chloride gives a salting-out effect on the ion-pair between the Rhodamine B cation and tetrachlorogallate. Of the series of alkali metal halides, sodium chloride improves the extraction of the ion-pair most effectively. Culkin and Riley found their mixed solvent to be more efficient than benzene as solvent for the ion-pair when a high hydrochloric acid concentration was used. Our work shows that the efficiency of benzene as the solvent is impaired by use of a high acidity.

Though our method is more sensitive than the Onishi and Sandell method and less affected by

variation in the experimental conditions, it suffers somewhat more interference from ions such as iron(III) and antimony(III), and the reagent blank is a little higher. Addition of titanium(III), as recommended by Culkin and Riley,[5] lowers the blank and decreases the effect of iron(III) by reducing it to an oxidation state which does not form an extractable ion-association complex with chloride and Rhodamine B. The presence of 0.6% titanium(III) chloride is found to be suitable. The tolerance limits are then 390 ppm of Fe(III), 10 ppm of Tl(I) and 15 ppm of Sb(III), in the determination of ~0.054 ppm of Ga(III) in the sample solution. These values compare favourably with those indicated by Riley and Culkin.[5]

Acknowledgement—The authors are grateful to Dr R. A. Chalmers, University of Aberdeen, and Professor Tatsuya Sekine, Science University of Tokyo, for valuable discussions and encouragement in this study, and also express their appreciation to Mr Takeshi Ito for his assistance.

REFERENCES

1. H. Onishi, *Anal. Chem.*, 1955, **27**, 832; H. Onishi and E. B. Sandell, *Anal. Chim. Acta*, 1955, **13**, 159.
2. E. B. Sandell, *Colorimetric Determination of Traces of Metals*, 3rd Ed., p. 473. Interscience, New York, 1965.
3. F. Culkin and J. P. Riley, *Anal. Chim. Acta*, 1961, **24**, 413.
4. K. Ueno, *Chelatometry*, 3rd Ed., p. 170. Nankodo, Tokyo, 1957.
5. F. Culkin and J. P. Riley, *Analyst*, 1958, **83**, 208.

Talanta, Vol. 30, No. 10, pp. 725–739, 1983
Printed in Great Britain

0039-9140/83 $3.00 + 0.00

DETECTION METHODS FOR HIGHLY TOXIC ORGANOPHOSPHONATES

A LITERATURE SURVEY

S. J. SMITH*
Department of Chemistry, Imperial College of Science and Technology, London S.W.7., England

(*Received* 28 *September* 1982. *Accepted* 19 *March* 1983)

Summary—A review is given of the literature on the methods available for the detection of the organophosphonate compounds known as the "nerve gases".

THE HISTORY OF NERVE WEAPONS

After the universal revulsion at the effects of gases used in the Great War, a conference met in 1925 at Geneva and debated prohibiting the use of dangerous gases in warfare. A treaty—the Geneva Protocol—was signed by 38 countries, including all the major powers (except the U.S.S.R., which signed later), to the effect that each would not use toxic gases or bacteriological weapons in warfare.[1–4] To be binding, the Protocol had to be ratified by individual governments: after the rest of Europe, Germany ratified in 1929, Britain in 1930 and the United States in 1975. Britain and other countries appended limiting clauses, including the right to reply with chemical weapons if attacked with them. Research was not limited. The chief lethal war gases at the time of the Protocol included chlorine, phosgene, mustard gas, lewisite and hydrogen cyanide.

Work in the 1930s in Germany on the properties of organophosphorus compounds as pesticides revealed a compound that was highly lethal to man.[3–6] Details were kept secret, but research was intensified and by the end of the Second World War it was discovered that German workers had discovered three highly toxic compounds, all of which were derivatives of phosphonic acid. These compounds were named and later given code letters, as below:

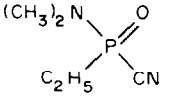

Tabun, GA

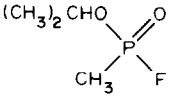

Sarin, GB

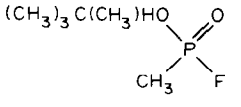

Soman, GD

They are all volatile liquids, with faint, sweet smells and in the right concentrations, all have rapid and fatal effect on mammalian life. Toxicity increases from Tabun to Soman.

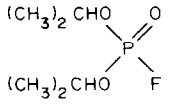

DFP

Research in Britain had been devoted to improvement of the First World War gases,[4] but one discovery was the far less potent liquid nerve agent di-isopropyl fluorophosphate (DFP),[7,8] though its development had not left the experimental stage. In Germany, however, by the end of the war a plant capable of producing 3000 tons of Tabun per month was available;[4] 12,000 tons had been prepared,[3–6] and it was used to fill shells and bombs. The German leadership thought that the Allies had also developed nerve agents (in fact the then secret insecticide DDT was the cause of their concern). Although Germany had the research and production facilities to enable the use (with possibly devastating consequences) of nerve weapons, they were never deployed, partly through fear of retaliation, but mainly because their use was not expedient. British scientists were unaware of the massive enemy nerve-gas operation.

At the end of the War, both the U.S.A. and the U.S.S.R. captured information on the German nerve gases, and research into chemical warfare has continued in both countries. Several new agents have been discovered: some are variants on the German originals, such as cyclohexyl Sarin GF, or ethyl Sarin, with greater toxicity but otherwise similar properties. Others, such as agent VX (the formula of which was

*Present address: Department of Instrumentation and Analytical Science, UMIST, P.O. Box 88, Manchester, England.

secret until quite recently[1]) are involatile liquids which are used as aerosols and are far more toxic. Other and deadlier agents have possibly been synthesized, but still remain secret.

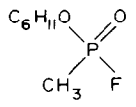

Cyclohexyl Sarin, GF

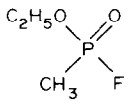

Ethyl Sarin

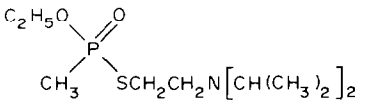

VX

Nerve weapons have been stock-piled in both the U.S.A. and U.S.S.R.—each side supposing them necessary as a deterrent.[2-5] In Great Britain, only experimental quantities are produced.

Increasing opposition to chemical weapons and an accidental release of agent VX in Utah in March 1968, which killed over 6000 sheep, resulted in the announcement in November 1969 that the U.S. government was to order the cessation of production of nerve agents and the destruction of some stockpiles.[2-4] This "demilitarization" programme was one reason for the development of sensitive detection methods.

Recent reports[2-5] suggest that this policy will shortly be reversed, with massive budgets being assigned to the development and production of nerve gases in the U.S.A. New concepts include the creation of "binary weapons", in which two chemicals that react to form the nerve agent are mixed in the gas projectile only after it has been fired, thus increasing safety of storage and transportation.

Nerve gases are only one element of the extensive armoury of chemical and biological warfare. Other types of gas weapon are significant,[3-5,9-12] but are not discussed here. Biological weaponry is also a matter of current concern.

CHEMICAL AND BIOLOGICAL ACTIVITY

The simple agents DFP, GA, GB, GD, GF and ethyl Sarin can be easily synthesized by reaction of an alkyl or alkylamido phosphonodichloridate with appropriate reagents.[7,8,13,14] These and agent VX (no syntheses available), are moderately good phosphorylating agents and are powerful inhibitors of the enzymes involved in nerve function.

A simplified description of nerve action is as follows.[12-14] Impulses are transmitted along nerve fibres by changing electrical potentials. At the end of the fibres, release of the compound acetylcholine (in humans) is stimulated. This diffuses across the synapse (a gap of about 10^{-8} m between nerve ending and muscle), after which it causes a change in electrical potential on the muscle and initiates muscular contraction. At this point, the acetylcholine is hydrolysed by the enzyme acetylcholinesterase: the hydrolysis products no longer activate the muscle, so it can relax. The impulses, each requiring the release and hydrolysis of acetylcholine, causing muscular contraction and relaxation, occur many thousands of times per second. A similar mechanism controls glandular functions.

The hydrolysis of acetylcholine depends on the formation of an initial complex with the enzyme, with subsequent release of choline, and thence hydrolysis of the esterified enzyme:

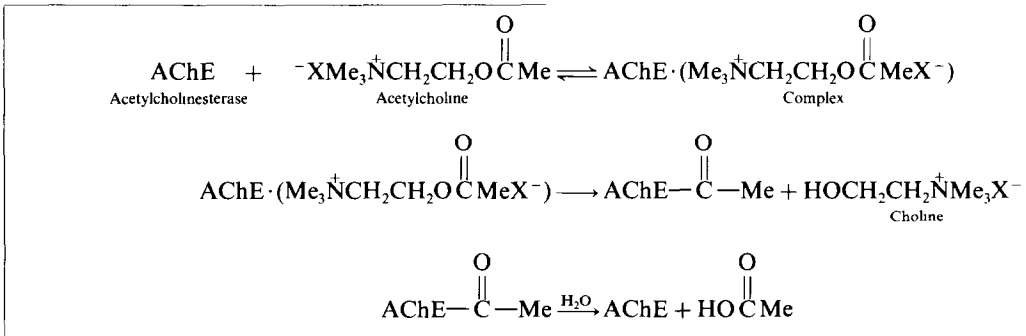

All organophosphorus pesticide and chemical warfare agents of general form $R^1R^2P(O/S)X$, where R^1, R^2 are alkyl or alkoxy groups and X a good leaving group, are fairly good phosphorylating agents, because of the group X. Such compounds can form stable complexes with a cholinesterase enzyme and then prevent enzyme function by phosphorylation. The phosphorylation is difficult to unblock, because the required hydrolysis is very slow.

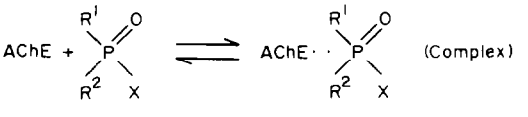

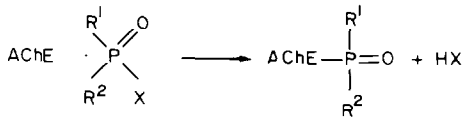

(S may replace O for some pesticides.) As a result of this action, organophosphorus agents are often called "anticholinesterases".

The effectiveness of a nerve agent depends on the stability of the intermediate enzyme/agent complex and on the ease of hydrolysis of the agent. An easily hydrolysed (good phosphorylating) agent will be consumed before reaching the enzyme and the hydrolysis products—phosphoric or phosphonic acids—are not toxic.

Antidotes to these agents have been developed,[2,12,13] but their application in a case of nerve-gas poisoning is limited because of the very quick effectiveness of the toxins. Some antidotes are active by competition—they offer a site that is more readily phosphorylated than the enzyme—such as atropine. Others, of pyridinium oxime type, attack the phosphorylated enzyme and release the free cholinesterase.

Only very low concentrations of nerve agents are necessary to produce, rapidly, extremely unpleasant symptoms. Concentrations are usually expressed in mg/m^3 for air contamination. For toxicity tests, exposure is expressed as the product of concentration and time ($mg.min.m^{-3}$).

For Sarin, for example,[12] a level of 15 $mg.min.m^{-3}$ causes "mild" symptoms in man, whereas 70 mg. $min.m^{-3}$ is rapidly fatal. Symptoms range from dramatic contraction of the eye pupil (miosis), through (with increasing concentrations) breathing difficulties, glandular over-function, such as sweating and salivation, twitching, nausea, involuntary urination and defaecation, to severe convulsions, coma and death by respiratory failure, or heart failure in some animals. Fuller descriptions are given in the literature[13,15,16] and some workers have described the effects subjectively.[7,8]

The concentrations of nerve agents that will prove lethal depend on both atmospheric conditions and the physical condition of those affected. Only approximate values can be found: it appears that for Sarin 50–100 $mg.min.m^{-3}$ is about the lethal breathing dose;[12] the values are doubled for percutaneous absorption. For VX, 0·4 mg entering the body is sufficient to kill.[2] As nerve agents are lethal both by inhalation of the vapour and by absorption of the liquid through the skin, there are serious consequences if the agents are ever released—overall body protection is required for safety, even at low concentrations. As such low levels of nerve agents are found to be detrimental, highly sensitive detection methods are necessary.

Under natural conditions, the compounds GA, GB, GD and GF (the G-agents) are all degraded fairly rapidly, being unstable in the presence of some metal cations[17] and at pH ranges differing considerably from neutrality. VX is not quickly degraded naturally and can contaminate water and land for prolonged periods.

Nerve agents are soluble and stable in most common solvents. In water, the stability to hydrolysis depends strongly on pH. For laboratory work, organophosphorus compounds are usually handled in solution in ethanol or propan-2-ol, but water is sometimes used as the solvent.

NATURE OF THE DETECTION METHODS

Detection systems are available for use in the laboratory and, more importantly, in the field. They can be grouped as follows.

General laboratory methods. These use standard analytical equipment, such as gas chromatography, mass spectrometry *etc.* Reports on their use usually include nerve agents as part of a wider study of organophosphorus compounds.

Specific laboratory methods. These include specific detectors, but more commonly a chemical reaction between a nerve agent (usually in solution) and a substrate is followed by instrumental detection of the products.

Field portable instrumental monitors. These are usually small devices designed to give an alarm if the concentration of nerve agents in the atmosphere exceeds a certain level. They are often continuous monitors, designed for prolonged air sampling, with apparatus and reagents prepared for such use. Reports of these instruments are scarce, because they are items of military equipment.

Field-test systems. These are simple spot-tests to establish quickly whether the air or a water supply is contaminated with nerve agents, and involve simple, quick and definite colorimetric tests. Again, reports are rare.

The aim of this review is to describe developments since 1970 in these detection methods. Many older methods are often still in use, however, and as some of the newer ideas are basically improvements on older designs it is necessary in several cases to refer to the earlier methods. The detection methods will be dealt with according to the analytical technique used, and each section may encompass any of the system groups outlined above, though the more specific methods are considered before the general ones.

The security considerations outlined previously may contribute to the report not being completely up to date.

COLORIMETRIC DETECTION METHODS

Procedures involving colorimetry are probably the largest group of detection methods for nerve agents. They are subdivided below by the type of chemical reaction required to give the coloured species.

Cholinesterase methods

The off-shore dumping of weapons containing nerve agents may lead to the contamination of sea-water. As the agents are potent even at low concentrations, highly sensitive detection methods are required. A system based on the reaction of agents with excess of cholinesterase, the surplus of which is determined colorimetrically, has been devised by the U.S. Army chemical warfare establishment, Edgewood Arsenal, and is useful at the μg/l. level.[18]

Acetylcholinesterase (from electric eels) is treated with the nerve agent sample solution, which partially phosphorylates the enzyme present. The amount of enzyme remaining will depend on the period of treatment and the concentrations of the reactants. Under specified conditions it can be related to the nerve agent concentration. The enzyme activity before and after the reaction can be determined spectrophotometrically with a mixture of acetylthiocholine and 5,5′-dithiobis(2-nitrobenzoic acid) as reagent.

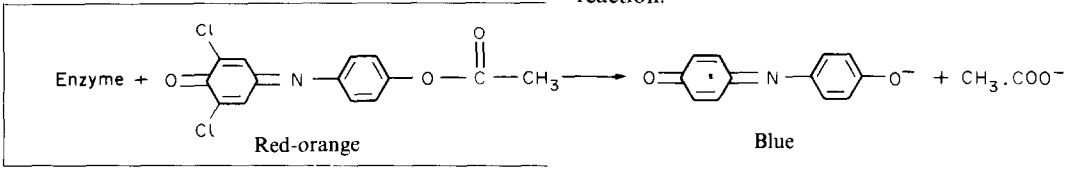

Since the cholinesterase cannot distinguish between the components of a mixture of inhibitors, a procedure relying on the different stabilities of agents at various pH levels is used. For example, a sea-water sample contaminated with GB and VX is treated with a solution of eel acetylcholinesterase in pH-7.2 buffer at 25° for 30 hr, then a portion is reacted with the spectrophotometric reagent for exactly 1 hr and the absorbance is measured at 412 nm against a blank prepared from uncontaminated sea-water, buffer and colour reagent. The whole procedure is applied to a set of standards for calibration and the total concentration of GB and VX is found.

To determine the VX, the GB must be selectively hydrolysed by adjustment to pH 10 with sodium hydroxide solution. The solution is extracted with methylene chloride, which is then acidified with dilute hydrochloric acid and evaporated to dryness. The residue is dissolved in water and treated as for the combined GB/VX determination. Subtraction of the two results gives the GB concentration.

The specificity for the highly toxic agents was demonstrated by testing with less toxic compounds of similar structure. The sensitivity towards such interferents was so low that the concentrations needed to give a comparable response would be far higher than those likely to occur. Further resolution could be obtained by use of a different cholinesterase, such as butyrylcholinesterase. The characteristic rates of reaction of different organophosphorus compounds with cholinesterases were proposed as an identification method.

The sensitivities and reaction rates for GB in the presence of various ions were determined and optimum conditions for reagent and sample storage were given. The use of other photometric reagents was studied. Many kinetic investigations were made, but no detection limits were quoted.

A simple, quick field-test for contamination of drinking water by nerve agents has been reported.[19] It consists of a small plastic "ticket" enclosing two glass-fibre discs impregnated with butyrylcholinesterase. One end of the ticket (one disc) is wetted with pH-8 buffer solution, and then with a solution of 2,6-dichloroindophenyl acetate in ligroin. The disc quickly turns blue. The other disc is dipped in the suspect water and then the colour reagent is applied. If the water contains a harmful level of nerve agent, this disc remains colourless. A blue colour like that of the "control" end indicates that the water is safe as regards anticholinesterase compounds. The control disc is used to ensure that the "ticket" is functioning. The blue colour is a consequence of the reaction:

If a sufficient amount of anticholinesterase agent is present, the enzyme is inhibited, resulting in non-production of the blue colour. The system has been in use in the U.S. Army for many years.

Gamson *et al.*[19] reported various tests of the method, in particular the reaction times for different agents (at 10, 50 and 100 ng/ml concentrations) under various conditions of pH (6, 7 and 8) and temperature (0 or 20°). The contaminating agents tested were Sarin, VX and parathion, a potent insecticide.

For both Sarin and VX it was found that exposure of the disc to a 100-ng/ml solution for 5 min always gave complete inhibition, but for 10-ng/ml solutions complete inhibition required exposure for times from 15 to over 25 min. For VX, the rate of inhibition was greater at pH 6 than at pH 8, except for the 10-ng/ml level at 20°, whereas for Sarin the rate was the same at all three pH values at low concentrations, but decreased with increasing pH at higher concentrations. The rate of inhibition was generally greater at the higher temperature. The longer reaction times for detection of low concentrations were an incentive for modification of the system.

More recently, a study[20] has been made of indoxyl acetate as colour reagent, this having been found acceptable in tests in the earlier work.[18] The effect of storage at elevated temperatures of papers impregnated with indoxyl acetate was examined. The compound was found to decompose appreciably under extreme conditions, but since these would not normally be encountered, indoxyl acetate was considered a possible alternative reagent.

An automated analyser for colorimetric detection of inhibited acetylcholinesterase has been described.[21] The unit was required to detect GB at the 1 $\mu g/m^3$ level and VX at the 0.1 $\mu g/m^3$ level in air. Samples could be fed in as solutions from a scrubber–concentrator (for field work) or as solutions in dilute acid for laboratory testing. The samples were incubated with enzyme and then reacted with acetylthiocholine iodide (ATCI) to give thiocholine, which gives a coloured product with 5,5′-dithiobis(2-nitrobenzoic acid) (DTNB). The principal reactions are:

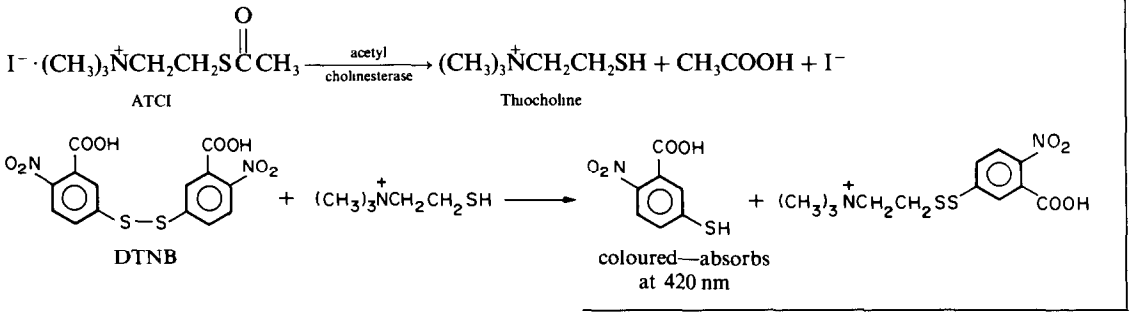

In the laboratory procedure, automatic sampling was employed. Blank samples, consisting of dilute hydrochloric acid only, were included periodically for washing the apparatus. Pumps were used to deliver appropriate quantities of reactants. The sample solution, an enzyme solution and air were mixed and incubated in a coil at 32°. The mixture passed on to another coil, where ATCI and buffered DTNB were added. Colour developed, and was measured in a single-channel cell, and recorded. The sampling rate was 20/hr. The absorbance decreased linearly with increasing concentration of agent present. The results were found to be reproducible and sensitive. There were no apparent interferents, and the signals were insensitive to sample pH. The method is thus convenient and reliable.

A method that is similar in principle,[22] but not automated, is based on reaction for 30 min at 25° with a standard solution of horse serum butyrylcholinesterase in aqueous buffer, followed by addition of an aqueous solution of freshly synthesized 2-azobenzene-1-naphthyl. After 10 min, a mixture of dilute hydrochloric acid and acetone is added, which gives an intense red colour due to the formation of 2-azobenzene-2-naphthol. This colour is measured at about 500 nm. The results are reproducible but the reagent synthesis is complex, and similar modern methods are more sensitive (the detection limit is 0.1–0.5 μg/ml for Sarin in water).

A cholinesterase method has been developed for use as a field air-test.[23] Air is drawn through a paper filter impregnated with a cholinesterase solution in phosphate buffer and gelatine. The paper is then treated with a developing solution, comprising, for example, indoxyl acetate and potassium ferricyanide and ferrocyanide in a phosphate buffer. The enzyme hydrolyses the indoxyl acetate to indoxyl, which is then aerially oxidized to indigo. Various indoxylphenols can be used in place of indoxyl acetate. If the enzyme on the paper has been inhibited by a nerve agent, no colour is produced.

This straightforward field detection method gave reliable results, with a lower detection limit of 2 μg of GB.

Peroxophosphonate colorimetric methods

One of the earliest works on detection methods for Tabun and Sarin was the Schoenemann Report,[24] based on a lecture given in Berlin in 1944 by R. B. R. Schoenemann, while work on nerve agents was still secret. The fundamental report gave an account of both colorimetric and luminescence methods based on the same reaction.

It was found that paper impregnated with copper sulphate, hydrogen cyanide and luminol gave a luminescence with such agents as Tabun, hydrogen cyanide and arsenicals. The papers served as good spot-test indicators. Sarin gave no reaction and also suppressed the blank value due to the cyanide.

Further work showed that the copper sulphate and hydrogen cyanide could be replaced by hydrogen peroxide, and luminol by another easily oxidizable substrate, such as benzidine or *o*-tolidine. A paper spotted successively with H_2O_2, nerve agent, *o*-tolidine in acetic acid solution and 10% sodium hydroxide or ammonia solution gave a red-orange colour if the agent was active. The report proposed mechanisms for this reaction, with peroxophosphonates acting as key intermediates.

Over a hundred compounds of similar structure to Tabun and Sarin were tested. The results indicated that, in general, only compounds containing a labile metalloid–halogen (or pseudohalogen) bond gave a positive reaction.

A modified spot-test was also described, which used a filter paper impregnated with hydrogen peroxide, to which a solution of *o*-tolidine in benzene was added. A drop of warfare agent in solution was placed centrally on it, and the colour developed over ammonia. A six-stage colour chart was made for semiquantitative estimation of agent concentrations.

Field tests were carried out, by releasing clouds of Tabun over watch-glasses containing benzene or toluene and the resulting solutions were tested. It was

also found that Tabun and Sarin could be readily adsorbed by silica gel and relevant tests were made. Nerve agents were introduced as solutions, or pumped in air through silica-gel columns, and solutions of H_2O_2, *o*-tolidine and ammonia were added. After colour development, semiquantitative estimations could be made, or an electrical colorimeter used, with determination by comparison with standards. The detection limit was found to be 2 ng/m^3 for Sarin and 4 ng/m^3 for Tabun. Chlorine and cyanogen interfered strongly with the detection, but since they also discoloured the gel, such measurements could be detected and disregarded. Use of large-size gel tubes facilitated greater sensitivity.

The chemiluminescence reaction could be employed in a similar way, by using silica gel impregnated with H_2O_2 and luminol. Agents were pumped through the column, followed by an ammonia solution. Detection limits and sensitivity were found to be the same as for the colorimetric method.

In a colorimetric variation on the Schoenemann procedure[25] the phosphonate to be detected is reacted with hydrogen peroxide or perborate to form a peroxophosphonate. This has much greater oxidative ability than H_2O_2 or BO_3^-, and can be used to convert an amine group into a diazo species, which can be estimated colorimetrically. The reactions for Sarin (for example) are:

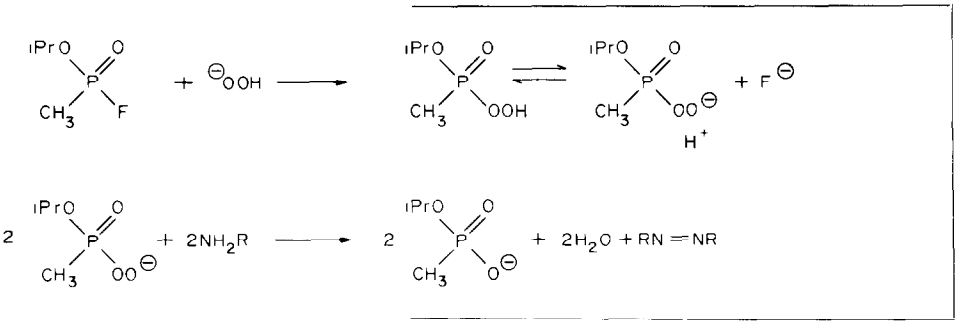

Various amines were tested, and an analytical procedure was developed. The method was simple—calibration graphs were obtained by adding benzidine in acetone solution to known solutions of nerve agent, followed by aqueous sodium perborate solution (made daily). Absorbances were recorded after 20 min. Sodium perborate provides the correct pH (around 10) as well as the peroxo species for the reaction. The procedure was then applied to unknown agent solutions and concentrations determined from the calibration plots.

The time for colour development decreases with increasing alkalinity, but at pH > 11 the organophosphorus compound is hydrolysed in preference to reaction with perborate, so colour intensity is lost. In the correct pH range, the reaction with perborate is 100 times as fast as the hydrolysis. The detection limit was 1 μg of Tabun or Sarin.

The method worked for many organophosphate and organophosphonate compounds. The products of the hydrolysis reaction did not interfere, nor did ions commonly found in water, up to 1-mg levels. Other possible interferents were removed during the reagent preparation.

A successful field monitor based on this reaction was reported in 1958.[26] It was based on detection of the red colour formed when a nerve agent reacts with a combined solution of *o*-dianisidine and sodium pyrophosphate peroxide (which acts in the same way as perborate).

The mechanical system used pumped a drop of a mixture of sodium pyrophosphate, hydrogen peroxide and *o*-dianisidine solutions onto a paper tape. A timing motor operated so that a fresh portion of tape was wetted every 5 min. The tape passed across a port, through which the air sample was pumped by a piston (through a paper prefilter). Light from a flashlight-bulb was reflected by the tape to two phototubes, one of which monitored the wetted paper before the air sample was blown through it, and the other monitored it after sampling. If a red colour developed on the tape, owing to the presence of G-agents in the air, the imbalance in the amount of light reaching the two phototubes was detected electronically. A 30% imbalance triggered both light and sound alarms. A reflectance method was preferred because of the large range of absorbance of the product. The machine was designed to operate for up to 12 hr continuously.

Some likely interferents were tested, such as screening smoke, vapours from explosives and certain gases. Of these, the only interferents were an HCl/H_2SO_4 mixture, which inhibited the agent, and chlorine and nitrogen dioxide, which gave false positives (but the amounts needed to do this greatly exceeded any possible natural concentrations, and since these gases are themselves toxic, an alarm was desirable anyway).

Some results for alarm times and reliability for Sarin were given: the alarm responded in an average of 5 sec for Sarin concentrations over 2 ppm and in 1 min for 0.1 ppm, all with 100% successful tests. At lower concentrations, the sampling time needed was longer and success rate lower: for 0.02 ppm, the average alarm time was 2 min (98% successes) and for 0.01 ppm the average time was 5 min (58% successes). However, these levels are well below the lethal con-

centrations (at which the unit responded rapidly and reliably).

The unit was tested under extreme climatic conditions, and "rough handling" tests were made. With some exceptions, the device was suitable for all service applications. It could be powered from a vehicle battery and required servicing every 12 hr with fresh solutions and tape.

Two remarkably simple and quick spot-tests for nerve gases were described by Egyptian workers.[27] They are based on the properties of the peroxophosphonate species.

For the first test, one drop of 3% thallous sulphate solution is placed on a spot-plate and a drop of 3% potassium sodium carbonate solution is added, followed by one drop of 5% urea peroxide solution. Addition of a drop of alkyl phosphonate solution gives an immediate brown precipitate, or colour, in comparison with a blank. The lower limit of detection is 5–15 μg of agent.

To be suitable as a field test, this method would require some type of bubbler and concentrator to dissolve any aerial nerve agent, so the benefit of the speed of the test is lost. The test is based on peroxophosphonate catalysing the oxidation of Tl(I) by peroxide in alkaline medium, with precipitation of TlO(OH).

In the second test, one drop of a solution of *o*-dianisidine hydrochloride in acidified methanol and water, with hydrogen peroxide present, is mixed with a drop of 3% potassium sodium carbonate solution. Addition of one drop of a nerve agent solution causes a red colour to develop, compared with a blank. The lower limit of response is 0.1–5 μg.

The reaction mechanism is identical to that for phosphonofluoridates and amines detailed above. These workers also repeated the colorimetry with *o*-dianisidine tested by Gehauf *et al.*,[25] but with hydrogen peroxide and potassium sodium carbonate instead of perborate. The colour was found to form within 2 min, compared with the 20 min for the perborate method; 0.1–5 μg of GB, DFP or dimethyl diaminophosphofluoridate could be detected.

Oxime/cyanide colorimetric methods

There are a number of detection methods based on the reaction of organophosphonates with certain oximes to yield cyanide, which itself reacts with the oxime, eventually leading to more cyanide production than consumption. The use of specific reagents allows colorimetric detection.

The chemistry behind one of the current systems has been reported.[28] The oxime used is 1-phenyl-1,2,3-butanetrione-2-oxime [isonitrosobenzoylacetone (IBA)]. This reacts with an organophosphonate to liberate cyanide, by a Beckmann fragmentation. The cyanide then itself reacts with the oxime.

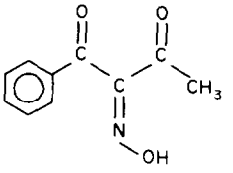

Isonitrosobenzoyl acetone, IBA

For an oxime of the R·CO·NOH·CO·R′ type the reaction is

$$CN^- + R\cdot CO\cdot NOH\cdot CO\cdot R' \rightarrow R\cdot COCN + R'\cdot COCN + OH^-$$

The two organic products both react with OH^- to give cyanide:

$$R\cdot COCN + 2OH^- \rightarrow R\cdot COO^- + CN^- + H_2O$$

$$R'\cdot COCN + 2OH^- \rightarrow R'\cdot COO^- + CN^- + H_2O$$

Thus the initial level of CN^- is doubled. The OH^- ions are provided by addition of alkali. The cyanide produced is reacted with *p*-nitrobenzaldehyde and *o*-dinitrobenzene to give a coloured product:

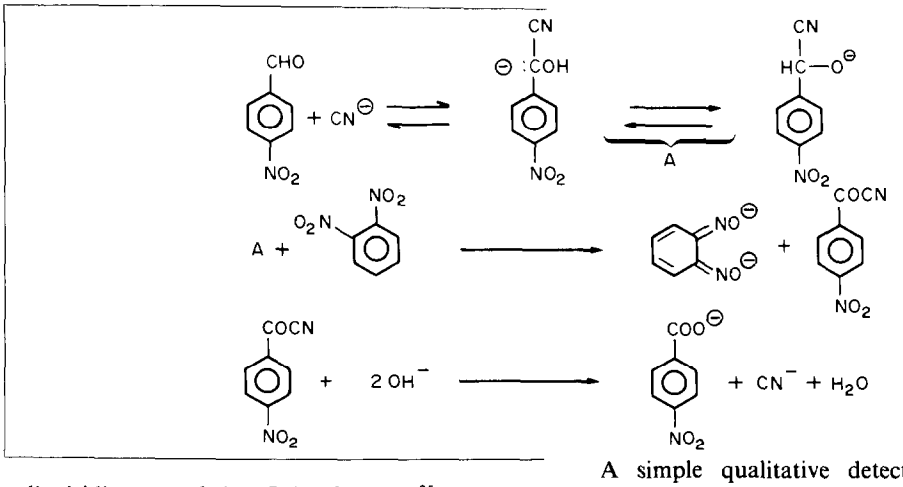

A simple qualitative detection procedure was described.[28] One drop each of methylene chloride solutions of IBA, *p*-nitrobenzaldehyde and *o*-dinitrobenzene were applied to a small tube packed with silica gel and the solvent was removed by an airstream. The air was then sucked through the tube and the addition of a drop of dilute sodium hydroxide

solution to the tube gave a blue colour if the air contained nerve agent; 0.12 and 0.3 μg of GB could be detected in 5 and 3 min respectively. In the absence of nerve agent, the tube packing changed colour in 8–10 min, owing to base-initiated fragmentation of the oxime. Less than 0.1 μg of GB was undetectable.

A modification to the sampling procedure has been published more recently.[29] The same detection system is used, and an adaptation of an existing sampling device used for field detection.[30]

Air is drawn through a replaceable detection tube by compression and release of a rubber bulb. The detection tube, containing the reagents (as before) on silica gel, is then removed and to it is added one drop of 0.5*M* sodium hydroxide. The colour change is observed in about 5 min.

Results for detection were reported for GA, GB and GD: for GB they were those already given.[28] Additional tests with GA and GD indicated that as little as 0.1 μg could be detected within 5 min.

Other, earlier, reports on the oxime/cyanide procedure have been found,[31–34] showing the evolution of reagents and methods to the present system.

The U.S. Army's "M8" nerve agent alarm depends on the estimation of cyanide produced by the reaction of phosphonates with IBA. Attempts have been made to find a better substrate than IBA.[35] Thirty-three similar compounds were investigated, to find those superior in reactivity and stability. The approach adopted was (*a*) to maximize the rate of CN^- production, by micellar catalysis or adjustment of rates and equilibria and (*b*) to minimize the rate of decomposition of keto-oxime by variations in structure to hinder nucleophilic attack.

The report concentrated on the rate equations and their consequences, and on reaction profiles and mechanism for each stage. Several conclusions were reached. Brønsted catalysis holds for most of the oximes examined and the use of micelles to limit the reactivity of hydrophilic oximes with DFP is limited. The concentration of liberated cyanide, is, alone, no indication of the amount of oxime consumed; OH^- and oximate are also important nucleophiles. Since all routes of decomposition of the oxime involve the protonated form, its stability is enhanced by alkaline conditions. In all the work done, no single oxime was found to better IBA.

An abstract[36] describes the use of cards impregnated with 1,3,5-trinitrobenzene solution for detection of VX. A deep stain is produced on the card. Photographing the cards with microfilm provides input for an automatic spot sizer and counter. The details of this report are contained in a U.S. Patent, which as been physically removed from, or covered up in, patent records. It was probably released by mistake for abstracting.

LUMINESCENCE AND FLUOROMETRIC METHODS

Nearly all these methods involve the peroxophosphonate species, which react with a suitable compound to give a product that gives chemiluminescence or fluorescence.

Luminescence methods

The principle of this technique is the measurement of light emitted by the decay of excited species formed in a chemical reaction. The work by Schoenemann, detailed earlier,[24] was the first report of application of the method to nerve agent detection.

An early, but fundamental, chemiluminescence technique was described by Goldenson.[37] It was based on the action of a nerve agent on luminol in the presence of peroxide. The reagent was a solution of luminol and sodium perborate (with trisodium phosphate to increase the solubility of the luminol), aged for 3 days, as more reproducible results were thus obtained.

A microphotometer was assembled in a light-tight box, with the photomultiplier tube fully exposed and a specially constructed cell positioned adjacent to it. For low levels of nerve agents, the luminescence from the reaction is very small, so the full sensitivity of the apparatus is required. Portions of nerve agent in propan-2-ol added to the luminol/perborate solution in the cell gave a blue-green luminescence which reached peak intensity in about 15 sec. The intensity varied linearly with agent concentration, giving a simple quantitative test. The detection limits were 0.5 μg of Tabun or Sarin. Strong apparent interference by chloride was suppressed by adding thiosulphate.

This method is particularly suitable for continuous automatic monitoring of the atmosphere. Unlike fluorometric and colorimetric methods, no light supply is required, so a "clockwork" detector—using a spring-driven pump and a barrier photocell—was proposed. Continuous use of this apparatus would be difficult, however, because of the rates of reaction.

A similar technique was recently reported by Fritsche,[38] who used luminol and chloride, which was found to promote the luminescence strongly. To suppress metal-ion interferences EDTA was also added. The apparatus consisted of a light-tight box with a photomultiplier inside connected to a recorder, and a closable aperture for the insertion of the reaction cell. The contents of the cell could be stirred mechanically.

A sodium perborate solution and a luminol solution (luminol, trisodium phosphate, EDTA and sodium chloride) were mixed in the cell and gave a background signal, due to oxidation of luminol by perborate, which decayed to a steady level in about 4 min. A dilute methanolic solution of organophosphonate was added and the resultant increase in luminescence was recorded as a peak above the background.

The peak-area was said to be linearly related to the amount of agent added, over three orders of magnitude. It was claimed that compounds could be

identified from the characteristic time interval needed to reach maximum intensity. Detection limits were 0.5 ng for DFP, Sarin and Soman, 1 ng for Tabun and 10 ng for VX.

Fluorometric methods

Although reported over 25 years ago,[39] the indole–perborate method is still in use. In the presence of peroxide (sodium perborate), an alkylphosphonate forms a peroxophosphonate as already described above. This can oxidize indole to fluorescent intermediates and thence to non-fluorescent indigo.

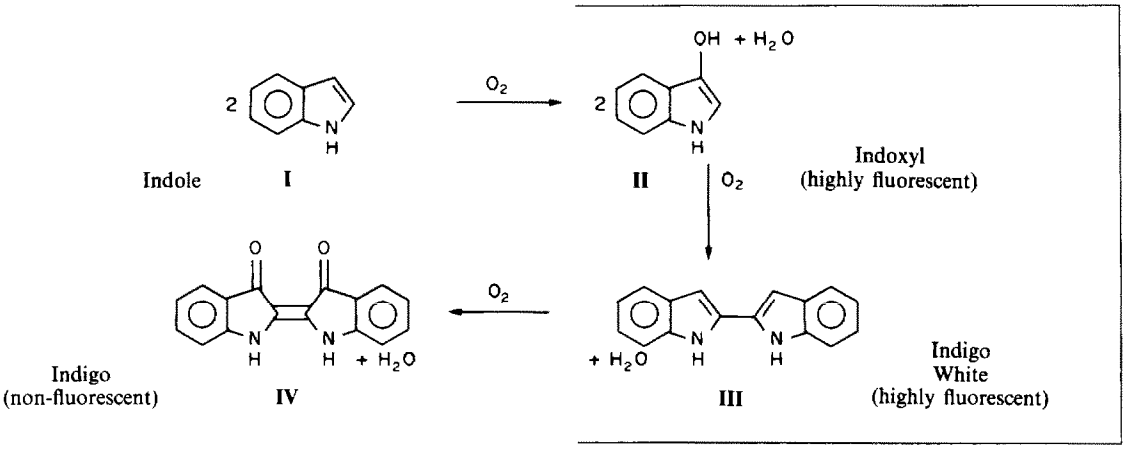

Compounds **II** and **III** are slightly coloured, and fluoresce intensely blue-green when excited at 300–400 nm. The transition from **I** to **II** requires the most oxidizing capacity.

The procedure is to mix an acetone solution of indole with aqueous sodium perborate solution and add this to an anhydrous propan-2-ol solution of Sarin. The maximum fluorescence at 460–490 nm is measured after 30–60 sec with an acidic quinine solution as reference standard and corrected for the blank (fluorescence from reagents and solvents). The calibration graph is linear. Levels as low as 5 mg/m^3 are detectable.

The method is far more sensitive than the colorimetric methods and it is suggested that it might detect as little as 1 ng of Sarin. The drawback of the technique is the short lifetime of the compound **II**, which necessitates almost immediate measurement. Some automatic systems for nerve gas analysis based on the indole–perborate reaction have been surveyed.[40]

A fluorometric detection system based on release of fluoride ions by hydrolysis has been reported.[41] After alkaline hydrolysis of an organophosphorofluoridate (*e.g.*, GB, GD), the product is dissolved in water and neutralized with dilute acid. An aliquot of this solution is then added to an ethanolic solution of the aluminium oxinate complex. The fluorescence of the solution is compared with that of a reagent blank solution. The decrease in fluorescence of the aluminium oxinate complex (caused by competitive formation of aluminium fluoride complexes) is proportional to the amount of organophosphorus agent. Detection limits are 13 μg/m^3 for GB and 10 μg/m^3 for GD, well below the toxic levels.

ELECTROCHEMICAL METHODS

Electrochemical methods are some of the more sensitive techniques found. Two types have been reported.

Cholinesterase methods

Direct potentiometric measurement of cholinesterase solutions reacting with nerve agents is highly sensitive. The first report based on this was a U.S. Patent in 1962.[42] Since details of more modern methods will be provided below, only the essentials of this report are given.

Platinum electrodes are immersed in a buffered aqueous solution containing the nerve agent and a substrate (*e.g.*, acetyl- or butyrylthiocholine iodide) with a reference electrode. The potential between the reference electrode and the positive electrodes is monitored as a function of time. At a noted time, a solution of the appropriate cholinesterase is added, and the change in potential with time is observed. The change is caused by depolarization of the positive electrode by the action of the enzyme on the substrate, and is linearly related to the concentration of enzyme. Presence of an anticholinesterase reduces the enzyme activity and hence the potential change. Calibration plots give the concentration of anticholinesterase.

The method is moderately sensitive ($\sim$g/m^3 level, which is relatively poor for nerve agent studies) and fairly accurate.

The chemistry behind the development and operation of a bench detector for nerve agents was described in a report[43] on part of the work in the "demilitarization" programme for U.S. chemical agents. The objective was detection of 0.1-μg/m^3

levels of GB in air, or 0.01 $\mu g/m^3$ VX in air, in 15 min or less.

During the first 2 min of a 3-min detection cycle, the nerve agent dispersed in the air sample was collected in a concentrator. The aqueous agent solution was pumped through an enzyme pad, which consisted of a cholinesterase distributed on a polymer support and inhibited an equivalent amount of the enzyme. During the last minute of the cycle, the change in activity of the enzyme pad was determined automatically by simultaneously passing a substrate stream, air and an electric current through the cell. The best substrate was acetylthiocholine iodide in tris buffer. The cell voltage was measured with a high-impedance voltmeter and was a function of the enzyme activity; inhibition of the enzyme by nerve agent increased the cell voltage. Thus increases in the voltage were indicative of the presence of cholinesterase inhibitors in the air sampled, and were used to trigger alarms. The system has clear applications as a field detector.

With this system, it was possible to detect as little as 0.1 $\mu g/m^3$ GB in air, in 6–9 min, and no interference was found. For the objective of 0.01 $\mu g/m^3$ for VX a higher air-sampling rate was required.

The acetyl-type cholinesterases and thiocholines were found to give the best response. Different concentrations of enzyme in the pads were tried, and various pad materials, such as urethane foam, investigated. The electrochemical cell consisted of platinum electrodes in a plastic housing. Cup-shaped electrodes were found best; platinum black and grey were tried, and the conditioning of the electrodes was described. The apparatus was slightly modified for bench detection of the agents and a "Solution Sampling Enzyme Alarm" (SSEA) described.

A companion report[44] describes an "Immobilized Enzyme Alarm" (IEA) which uses the same detection procedure as the SSEA, but the peripheral systems, in particular the air-sampling, were studied in detail and improved. Various concentrator designs were studied: the object of the concentrator was to dissolve the nerve agent, contained in a large volume of air, in a small volume of solvent, rapidly. Wire spiral and wet-wall concentrators were evaluated, but the design chosen was a "spin concentrator", where water passes down a cylinder against a tangential air-flow. This was very efficient: 3–5 ml of water could absorb the agents from air flowing at 70–90 l./min, there was no need to separate air from water after the absorption and the first test cycle could give an alarm. Several other modifications to the SSEA procedure were made, such as doubling the cycle time and recirculating sample solutions, which enabled the easy detection at the desired level of 0.01 $\mu g/m^3$ VX in air.

Electrochemical measurement of an enzyme hydrolysis product, thiocholine, is the basis of the British "NAIAD" nerve gas alarm.[45] In this system, air is drawn through a cholinesterase-impregnated pad, through which is pumped butyrylthiocholine. Nerve agent contamination in the air inhibits the enzyme activity, and the consequent reduction in the concentration of normal reaction product, thiocholine, is detected by a graphite electrode, initiating an alarm signal. This rugged, compact system operates automatically for up to 12 hr at a time and is suitable for use in harsh climatic and battle conditions.

Ion-specific electrode method

This procedure[46] involves alkaline hydrolysis of an organophosphorofluoridate, such as Sarin, and potentiometric measurement of the resulting fluoride concentration. With alkali, Sarin undergoes S_N2 hydrolysis:

The resulting acid is quite harmless.

In a plastic vessel at controlled temperature, a small amount of concentrated sodium hydroxide solution is added to the sample Sarin solution (about 400 ppm) in propan-2-ol. A little glacial acetic acid is added, followed by some TISAB containing fluoride (90 ng/ml). A fluoride electrode and a standard calomel electrode are immersed in the solution, and the potential is recorded after 10 min. A blank is run with water and a calibration graph made. The procedure can be automated.

A differential method can be adopted to increase the sensitivity. The use of a buffer containing fluoride permits work at well above the detection limit of the electrode (which is about 10 ng/ml). The greatest sensitivity thus achievable was 20–30 ng/ml for Sarin. The results agreed with those found by an independent colorimetric method.

Detection of fluoride from enzymic hydrolysis was attempted, but was unsuccessful, as fluoride is not liberated when an organophosphorofluoridate reacts with a cholinesterase. It was proposed that the method would be applicable to the detection of Soman, DFP and, with an appropriate electrode, Tabun.

GAS CHROMATOGRAPHY

Gas chromatography (GC) has proved to be one of the more versatile methods for determination of organophosphorus compounds.

Various column support materials have been investigated[47] under identical conditions, by use of flame-ionization detection (FID), with three organophosphorus test compounds: parathion, dimethoate (both insecticides) and VX. The supports were Chromosorb W HP; Chromosorb G AW-DMCS: Gas Chrom Q; Haloport F (Teflon) and Corning GLC 110 (textured glass beads). The stationary phases used were OV-1 and OV-101.

With Gas Chrom Q and Chromosorb G, small quantities of dimethoate and VX gave prolonged retention with tailing of the peaks (which could not be prevented). Parathion gave a constant retention time for the microgram range used, but also exhibited tailing.

Teflon was found useful for parathion and dimethoate, but adsorption of VX was very strong, and it could not be detected even when injected in only microgram quantities. A column containing glass beads gave good peaks for all compounds tested, down to the lowest levels detectable by FID.

Further tests indicated that OV-101 was better overall than OV-1 as the stationary phase. The best combination found for the detection of VX-type compounds was OV-101 on glass beads, which gave good sensitivity, with sharp peaks and little or no tailing.

Gas chromatography was important in the "demilitarization" programme.[48] The process for demilitarization of Sarin involves its decomposition with strongly alkaline brines. It is thus necessary to detect any residual Sarin in the resulting solid salts and brine slurries. Methods were given for the recovery of the agent from these media. The processes developed were also suitable for detection of agents in air bubblers, soils and as exudates from munitions.

Limits for detection of Sarin were set as $3\,\mu g/m^3$ in demilitarization stack effluent, $0.3\,ng/m^3$ as the maximum permissible ground-level concentration and <1 ppm w/w in solids. Sarin in munitions contains a large proportion of tributylamine (TBA) as a stabilizing agent. Since this and decomposition products might interfere in the GC work, realistic tests were made with mixtures of Sarin, TBA, di-isopropylmethyl phosphonate (DIMP) and Sarin pyroester ($[(iPrO)MeP(O)]_2O$), the last two being possibly interfering decomposition products.

Studies were made on columns of Gas Chrom Q support with a variety of moderately to highly polar stationary phases. The sensitivity (detection limit), resolution and interferences were the important factors. Flame-photometric detection was used throughout. All the stationary phases tested gave a sensitivity of 0.5 ng of Sarin or better, except DC-LSX-3-0295 (5 ng). Resolution was generally good, though that with QF-1 was poor for samples with high DIMP levels. Most stationary phases were free from interference, except Carbowax 20M and QF-1, which were subject to interference from TBA. Tenax gave good sensitivity even with high TBA levels, but was no good for testing brines or salts. The results of the tests indicated that EGSS-X and FFAP gave the most suitable columns, though only the latter was usable with electron-impact mass spectrometry (EIMS) combined with gas chromatography. In EIMS, Sarin gives a peak at $m/z = 99$; the EGSS-X column, while otherwise ideal, itself gives this signal.

Each type of column was suitable in some way, but the best stationary phase for general use was EGSS-X, or FFAP for EIMS work. The minimum detectable level for Sarin was 0.3 ng. Accuracy at the 15-ng level was ± 2.2 ng and the standard deviation at the 100-ng level was 1.3 ng.

Further studies were made on the decomposition of Sarin, particularly the reaction mechanisms. The possibility of recombination of decomposition products in the column was postulated, since certain results indicated this. Of particular note was the result that Sarin could be detected at low levels in the presence of similar compounds at a thousand times greater concentration.

In a report on structure–response relationships in gas chromatography[49] there was a thorough survey of the GC responses of 53 organophosphorus compounds. The results were examined to determine any relation between GC signal and the molecular structure, particularly as regards substituents on the phosphorus atom.

All the compounds were chromatographed on a Gas Chrom Q column, with a flame-photometric detector (FPD), which measures the HPO group concentration. Certain compounds were also run with a nitrogen–phosphorus detector (NPD) in the phosphorus mode, which measures the species PO or $PO_2^{\cdot}$ as intermediate radicals. For some others, a flame-ionization detector (FID) was used, which detects carbon and hydrogen species. Purities for some substances were checked independently, notably by a hydrolytic method for G-agents,[50] or a thioate procedure for VX. Sample concentrations were in the range 1–200 ng/μl (g/m^3).

For FPD, the signal recorded was proportional to the concentration of the HPO species reaching the detector (similarly to $PO^{\cdot}$ and $PO_2^{\cdot}$ for NPD), so the comparison of different compounds required the calculation of a molar response, as below:

$$P = \frac{30.98 \times 100}{\text{molecular weight of compound}}\ \%w/w$$

$$\text{Relative response} = \frac{\text{integrated area}}{\text{concentration injected}}$$

$$\text{Molar response} = \frac{\text{Relative response}}{P(\%w/w)}$$

DIMP was used as a standard to allow for day to day instrument variations. For some organophosphate and phosphonate compounds, there was a narrow range of molar response, generally between 19.6 and 20.6, for FPD. For compounds of the Tabun type, possessing the $(CH_3)_2NP$ group, there was a wide disparity in the molar responses: 17.1–39.4 (FPD), with Tabun lowest of the group. It was found that phosphonofluoridates, such as Sarin, had higher molar responses than compounds containing alkyl–amino–alkyl groups, such as VX. For the former type, G-agents, the responses were almost directly proportional to the molecular weights of the compounds. Though it was not tested with many

nerve agents, NPD gave higher responses, which were again in rough proportion to the molecular weight. NPD is generally more sensitive than FPD to phosphorus.

As the sensitivity of FPD or NPD detection depends on how much sample reaches the detector, the throughput characteristics of the column, and the stability of substances in it are important. Tests were made with stationary phases of different polarities, increasing in the order SE-30 < OV-17 < QF-1. Of the nerve agents, only Sarin and VX were tested: VX (like DIMP) gave greatest molar response on OV-17; the responses for Sarin varied only slightly—highest with SE-30 but only about 2.5% less than with the generally used QF-1.

The throughput of the column is related to the retention time. Under similar conditions for each compound, the retention index was compared with the molar response. This index is related to the time spent in the heated column, in comparison with a standard series of hydrocarbons. The FPD response apparently had no direct correlation with molar response.

Within a given homologous series, the FPD sensitivity was linear with respect to molar concentrations of phosphorus; this relationship did not hold for comparison of analogues. Alkyl–amino–alkyl compounds had a molar response pattern different from that of other compounds. It was found that structure had a bearing on FPD sensitivity and there was a linear relationship (of molar response to size of substituent) for most compounds. For FPD, NPD (and FID) the response obtained varied according to the species of ions reaching the detector—in particular, the molar response pattern of VX type compounds was attributed to intramolecular fission and intermolecular reaction at the detector.

A report on phosphorus-sensitive molecular-emission cavity analysis (MECA) concerned the adaptation of MECA to cope with a flowing sample stream, such as that from an HPLC column.[51] A wheel with 40 cavities punched in its circumference is rotated so that each cavity in turn (containing one drop of eluate) is heated to remove the solvent and then further heated to produce the molecular-emission signal. The detection limit for non-toxic organophosphorus compounds was 100 ng. Single-cavity MECA has also recently been described,[52] in connection with measurement of HPO species by FPD for the detection of nanogram amounts of phosphorus.

An important study has been made of possible detection methods for use in continuous atmospheric monitoring in establishments for destruction of chemical weapons.[53] Nearly 22,000 kits containing a variety of chemical weapons had been distributed throughout the U.S. for military training purposes and all were to be destroyed.

Automated gas chromatography was found to be the best system. With the appropriate detector, GC was sensitive to nearly all possible agents, but required a preconcentrator. With a cyclic system using two preconcentrators alternately, an approach to "real time" monitoring could be achieved.

PLASMA CHROMATOGRAPHY AND MASS SPECTROMETRY

Reports of nerve agent detection by these methods are found as parts of wider surveys of organophosphorus compounds. A number of organophosphorus compounds have been studied with a commercial BETA IV plasma chromatograph.[54] The principle of plasma chromatography is as follows.[55]

A carrier gas (moist air or nitrogen) is subjected to a 60-keV electron discharge emitted from ^{63}Ni foil. This generates ions such as $(H_2O)H^+$, $(H_2O)NO^+$ and (from air) $(H_2O)O_2^-$. A trace of the sample compound is added to the excited gas, and undergoes reactions forming dissociated species and quasi-molecular ions. The ions flow as a plasma down a tube with a potential gradient between its ends (Fig. 1). An ion pulse is sent through the injection grid to the electrometer detector. As these ions move through the nitrogen drift gas, their velocities are determined by interactions with the nitrogen molecules, giving a "mobility spectrum" which can be detected and recorded. An elaborate electronic system is used to control the instrument and interpret the data, which are presented as mobility coefficients, K, defined as $K = d/\tau E$ where d = drift length, τ = drift time, E = electric field, and are converted into reduced mobility coefficients, K_0, for standard conditions, by means of

$$K_0 = \frac{273\ KP}{760\ T}$$

where P is the working pressure (mmHg) and T the working temperature (absolute).

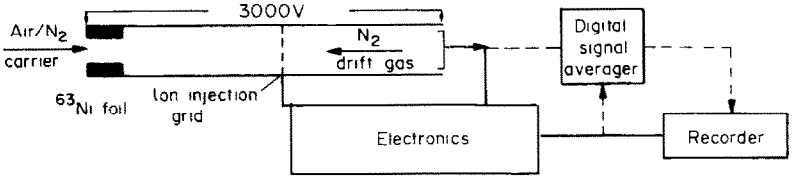

Fig. 1.

Reduced mobility coefficients are calculated for each peak of interest in the spectrum. Usually, the spectra are complicated, and correlation of plasma-chromatography and mass-spectrometry data is required for interpretation. General rules have been found, however: for a molecule M, the species MH^+ is always likely; the chemistry of a compound as regards equilibrium in air is a useful guide to the species found and there is a roughly linear relationship between the mobility and the logarithm of the mass of the ion. There are several problems, however: for resolution, a mass difference of 10–20% between a pair of ions is necessary; thermal decomposition at the inlet may occur, and the hydration or dehydration of molecule-ions leads to close peaks, which may obscure the data, but this is a minor problem with nerve agents.

Results quoted for some nerve agents confirmed the general patterns given: the protonated molecule was a common species and usually gave the highest K_0 values and largest peaks. Singly or multiply hydrated protonated molecules were usually responsible for other peaks and the K_0 values decreased with increasing hydration. For GD, however, peaks with K_0 values higher than for the simply protonated form were caused by molecule-ions which had lost parts of the pinacolyl carbon chain: the K_0 values increased with the size of the fragment lost. VX was found to give a lower K_0 value than those usual for G-agents. Anomalies were discussed, but no information relevant to nerve agents was given. K_0 values may prove useful for characterization of the agents.

Mass spectrometry has been studied for the characterization and identification of a variety of organophosphorus compounds.[56] The electron impact and chemical ionization techniques were used. Amongst other compounds, the nerve agents GA, GB, GD, VX and the "lethal" SV (*O*-ethyl-*O*-di-isopropylaminoethylmethylphosphonothioate) were studied. Samples were introduced from a gas chromatograph into an evacuated chamber, where electron impact or chemical ionization took place. Electron-impact mass spectrometry was found to be satisfactory for all nerve agents, but certain expected peaks did not appear. For chemical ionization, methane, ethane and isobutane were used as the reactant. Methane and isobutane gave good results (strong well-defined peaks), with the latter giving simple spectra. The technique was not very suitable for nerve gas detection because of the lengthy interpretation of results.

In contrast to this laboratory method, a portable quadrupole mass-spectrometer for the monitoring of organic vapours in the field has been found suitable for analysis of a wide range of organic vapours.[57] It fitted into two suitcases, had a special sampler and filter, used modern electronics, displayed the results on a television screen and was a compact and efficient system. The device had a great many commercial and military applications.

OTHER METHODS

Titrimetric methods

Two techniques have been found: both are quite old, but one[50] was reported as being a standard method for many organophosphorus compounds.[49] Both methods are for accurate determination of relatively high concentrations of alkylphosphorus halides (g/l. levels).

One technique[58] requires the reaction of excess of sodium pyrophosphate peroxide with an alcoholic solution of the sample, which generates the peroxophosphonate from a phosphonate. Acidification of the solution destroys this species, but leaves the unreacted sodium pyrophosphate peroxide intact and this can then be determined iodometrically. Good results are obtained.

A more important method is a hydrolytic estimation,[50] suitable for phosphate, phosphonate and pyrophosphate anhydride compounds. An aqueous sample solution, to which a mixed indicator (thymolphthalein and Methyl Red) has been added, is titrated with sodium hydroxide first to a yellow end-point (of Methyl Red) and then to a blue end-point (of thymolphthalein). The first titration step liberates the phosphoric/phosphonic acid from the sample, and the second neutralizes it.

Separation on a silica-gel column allows detection of the compounds in the presence of the pyroester. To the aqueous washings of the column eluate, indicator is added, followed by excess of hydroxide, and back-titration with dilute acid.

Piezoelectric crystal studies

The use of coated piezoelectric crystals as detectors is a relatively new development in analytical chemistry. Results have been published for organophosphorus pesticides, but not for nerve agents, so the utility of the method for this purpose is not yet publicly known.

The theory and principles of piezoelectric detection have been given in a review.[59] Most work is concerned with finding suitable coatings for the piezoelectric crystal. Initial tests for pesticides were made with inorganic metal salts (such as $FeCl_3$) as coatings.[60] The chemisorption of DIMP under high vacuum conditions, to give a metal salt complex, was noted. Results were good for some pesticides, such as paraoxon. Oxime coatings, such as the cobalt complex of isonitrilobenzoylacetone, were later found to be satisfactory.[61] These gave good results for a number of potent pesticides, but air pollutants tended to interfere.

The latest coatings tried are those of carboxylic acid salts of transition metals, their complexes with ethylenediamine, and similar polymer-bonded complexes.[62] The polymer complex XAD-4–Cu^{2+} has been found to give the best reversibility and lifetime, but there is slight interference from vehicle exhaust gases.

The piezoelectric methods clearly have applications for future development in the field of nerve gas detection.

Olfactory detection

Unlike many other chemical warfare agents, nerve gases are almost totally undetectable by the senses until casualties occur. Although instrumental field-detection methods are well developed, a simple system to enable sensory detection would be desirable for "surprise situations".

The use of isocyanides as the means of olfactory detection has been proposed.[63] They can be formed simply by reaction of an electrophile with a formamide and are detectable by smell at very low concentrations. For example, methyl isocyanide has an olfactory detection threshold of 7 $\mu g/m^3$ and a recognition threshold ten times higher. Although they have a horrible smell, most isocyanides have low toxicity for mammals.

Tests with Sarin indicated that it did not react directly with any formamides, but Tabun reacted with *N*-(tert.-butyl)formamide to give an isocyanide characterizable by gas chromatography.

The dehydration of a formamide required in this reaction depends on the nucleophilic strength of the formyl oxygen atom and on the electrophilic strength of the phosphorus compound. The nucleophilicity of oxygen can be increased by using the salt form of the amide. The lithium salt of *N*-(tert.-butyl)formamide was found to react satisfactorily with nerve agents, but was too rapidly hydrolysed in air for general application.

Metal-ion complexation also offers the possibility of increasing the nucleophilicity of oxygen. The mixed-ligand octahedral *N*-methylformamide (NMF) complexes of magnesium, manganese, cobalt, nickel and zinc, the square-planar copper complexes and the tetrahedral zinc and cadmium complexes have been made and tested, in the solid state, with nerve agents. Only the tetrahedral zinc complexes were found to react, as the oxygen atoms in the octahedral complexes were too sterically hindered to be able to attack the phosphorus compounds. The complex $Zn(NMF)_2Cl_2$ was found to be best. Its other halide analogues were less effective, but some aqueous substitution complexes of the same form were almost as successful. Mechanistic studies indicated that the initial step involved attack by nerve agent on the metal.

Field tests were carried out on the compounds, and some interferents (such as ammonia) found, which decreased the sensitivity. Ranges for the sensory detection of isocyanides were between 0.6 and 6 $\mu g/m^3$. However, the applications of the complexes were limited, because a solvent was required for the formamide, and the reaction rate with Sarin was slow. The method could be used for other chemical hazards though, and *p*-toluenesulphonyl chloride was extensively tested.

A detector based on the colorimetric detection of the isocyanide was devised, which utilized the oxidation of an aromatic amine by copper(II) in the presence of organophosphorus agents (like Schoenemann's first tests[24]). The absolute limit of detection was 10^{-7} g of agent. Other methods for the detection of isocyanides have been reported.[30]

CONCLUSION

The scope of this literature report was recently published detection methods for nerve gases. There has been a remarkable amount of effort and work put in by researchers all over the world in this highly specialized area.

Unfortunately, no general summary or recommendation of detection methods can be given, because each technique, device or system has its individual merits or failures. In general, the fact that a description of a method has been published indicates some use or possibilities for it.

Of note is the large volume of material published by the U.S. Army's research laboratories at Edgewood Arsenal, Maryland. The British equivalent, the Chemical Defence Establishment at Porton Down, appears to have published little about detection methods.

The ethics of the creation, proliferation and use of nerve weapons are certainly of vital and current concern. Little is known about the possible effects of widespread use of these gases, but the results would probably be terrible and devastating.

By the nature of the subject, this report cannot be complete. The security controls on developments associated with nerve weapons usually mean that accounts of detection methods are not published immediately on completion, or in full.

Acknowledgement—The original form of this report was presented for assessment as part of the third year of the undergraduate chemistry course at Imperial College, London. The helpful advice and criticism given by Dr. L. Pratt, Senior Tutor in Chemistry at Imperial College, during its preparation were greatly appreciated.

REFERENCES

1. M. S. Meselson, *Sci. Am.*, 1970, **222,** No. 5, 15.
2. L. R. Ember, *Chem. Eng. News*, 15 December 1980, 22.
3. R. Harris and J. Paxman, *How Close is Chemical Warfare?*, Sunday Telegraph Supplement, No. 286, 21 March 1982.
4. *Idem, A Higher Form of Killing: The Secret Story of Gas and Germ Warfare*, Chatto & Windus, London, 1982.
5. *Overcast with Outbreaks of Yellow Rain*, BBC radio programme, 21 January 1983.
6. M. F. Sartori, *Chem. Rev.*, 1951, **48,** 225.
7. B. C. Saunders and H. McCombie, *Nature*, 1946, **157,** 286
8. B. C. Saunders and G. J. Stacey, *J. Chem. Soc.*, 1948, 695.
9. H. McCombie and B. C. Saunders, *Nature*, 1946, **158,** 382.

10. F. N. Woodward, A. H. Williams, R. Brown, E. J. Gasson, H. McCombie, A. Hamilton and R. C. G. Moggridge, *J. Chem. Soc.*, 1948, 35, 38, 42, 44, 47.
11. B. C. Saunders and G. J. Stacey, *ibid.*, 1949, 919.
12. J. Emsley and D. Hall, *The Chemistry of Phosphorus*, pp. 502–508. Harper & Row, New York, 1976.
13. D. F. Heath, *Organophosphorus Poisons*, Pergamon Press, London, 1961.
14. D. Corbridge, *Phosphorus: An Outline of its Chemistry, Biochemistry and Technology*, p. 319. Elsevier, Amsterdam, 1976.
15. C. A. De Candole, W. W. Douglas, C. Lovatt-Evans, R Holmes, K. E. V. Spencer, R. W. Torrance and K. M. Wilson, *Brit. J. Pharmacol.*, 1953, **8,** 466.
16. *Phosphorus and its Compounds*, Vol. II, J. R. Van Wazer (ed.), p. 1926. Interscience, London, 1961.
17. J. Epstein and D. H. Rosenblatt, *J. Am. Chem. Soc.*, 1958, **80,** 3596.
18. H. O. Michel, E. C. Gorder and J. Epstein, *Environ. Sci. Technol.*, 1973, **7,** 1045.
19. R. M. Gamson, D. W. Robinson and A. Goodman, *ibid.*, 1973, **7,** 1137.
20. T. J. Novak, L. W. Daasch and J. Epstein, *Anal. Chem.*, 1979, **51,** 1271.
21. D. H. Tomlinson and H. L. Feller, *U.S. Govt. Rept.*, AD A025796, 1976.
22. J. Epstein, M. Demek and V. C. Wolff, *Anal. Chem.*, 1957, **29,** 1050.
23. C. Gelman and D. M. Kramer, *U.S. Patent* 3049411, 1962.
24. R. B. R. Schoenemann, *New Reaction for Detection of Metalloid–Non Metal Halogen Linkage*, P.B.119877, Office of Publication Board, U.S. Dept. of Commerce, August 1944.
25. B. Gehauf, J. Epstein, G. B. Wilson, B. Witten, S. Sass, V. E. Bauer and W. H. C. Rueggerberg, *Anal. Chem.*, 1957, **29,** 278.
26. J. C. Young, J. R. Parsons and H. E. Reeber, *ibid.*, 1958, **30,** 1236.
27. S. S. M. Hassan and S. A. I. Thoria, *Microchem. J.*, 1973, **18,** 622.
28. E. J. Poziomek, E. V. Crabtree and P. N. Kramer, *ibid.*, 1969, **14,** 150.
29. *Idem*, *U.S. Patent*, 3910763, 1975.
30. E. V. Crabtree, E. J. Poziomek and D. J. Hoy, *Talanta*, 1967, **14,** 857.
31. D. N. Kramer and R. D. Morin, *U.S. Patent*, 2926072, 1960.
32. A. L. Green and B. Saville, *J. Chem. Soc.*, 1956, 3887.
33. B. Saville, *Analyst*, 1957, **82,** 269.
34. S. Sass, W. D. Ludemann, B. Witten, V. Fisher, A. J. Sisti and J. I. Miller, *Anal. Chem.*, 1957, **29,** 1346.
35. R. A. Kenley, R. Swidler and G. E. Manser, *U.S. Govt. Rept.*, AD A081553, 1978.
36. H. E. Thompson and F. M. Noonan, *U.S. Patent* 3877874, 1974; *Chem. Abstr.*, 1975, **83,** 136516.
37. J. Goldenson, *Anal. Chem.*, 1957, **29,** 877.
38. U. Fritsche, *Anal. Chim. Acta*, 1980, **118,** 179.
39. B. Gehauf and J. Goldenson, *Anal. Chem.*, 1957, **29,** 276.
40. R. H. Cherry, G. M. Edey, C. O. Badgett, R. D. Eanes and H. R. Smith, *ibid.*, 1958, **30,** 2139
41. M. I. Yanbastier, *Dokl. Bulg. Akad. Nauk*, 1973, **26,** 1447.
42. P. L. Cannon, Jr. and D. N. Kramer, *U.S. Patent*, 3275534, 1966.
43. L. H. Goodson and W. B. Jacobs, *U.S. Govt. Rept.*, AD A009763, 1975.
44. *Idem*, *ibid.*, AD A036372, 1976.
45. Thorn E.M.I., *Automation Publication* 577/2/E, England, 1981.
46. H. DeClerq, J. Mertens and D. L. Massart, *Arch. Toxicol.*, 1973, **31,** 185.
47. I. Lindgren and B. Jansson, *J. Chromatog.*, 1975, **106,** 385.
48. T. L. Fisher, R. J. Steiger and G. A. Parker, *U.S. Govt. Rept.*, AD B015464, 1976.
49. S. Sass and G. A. Parker, *J. Chromatog.*, 1980, **189,** 331.
50. L. K. Beach and S. Sass, *Anal. Chem.*, 1961, **49,** 1890.
51. M. J. Cope, *Anal. Proc.*, 1980, **17,** 273.
52. R. Belcher, S. Bogdanski, O. Osibanjo and A. Townshend, *Anal. Chim. Acta*, 1976, **84,** 1.
53. E F. Colburn, Jr., *Conf. Sens. Environ. Pollut.*, (*Conf. Proc.*) *4th, 1977*, 1978, 489.
54. J. M. Preston, F. W. Karasek and S. H. Kim, *Anal. Chem.*, 1977, **49,** 1747.
55. F. W. Karasek, *ibid.*, 1974, **46,** 710A.
56. S. Sass and T. L. Fisher, *Org. Mass Spectrom.*, 1979, **14,** 257.
57. R. W. Meier, *Am. Ind. Hyg. Soc. J.*, 1978, **39,** 233.
58. S. Sass, I. Master, P. M. Davis and N. Beitsch, *Anal. Chem.*, 1960, **32,** 285.
59. J. Hlavay and G. G. Guilbault, *ibid.*, 1977, **49,** 1890.
60. E. P. Scheide and G. G. Guilbault, *ibid.*, 1972, **44,** 1764.
61. W. M. Shackleford and G. G. Guilbault, *Anal. Chim. Acta*, 1974, **73,** 383.
62 G. G. Guilbault, J Affolter, Y. Tomita and E. S. Kolesar, Jr., *Anal. Chem.*, 1981, **53,** 2057.
63. E. J. Poziomek, G. L. Boshart, E. V. Crabtree, R. Dehn, J. M. Green, D. J. Hoy, R. A. Mackay, G. T. Prior, H. Stone and M. Tanabe, *Microchem. J.*, 1971, **16,** 136.

Talanta, Vol 30, No. 10, pp. 741–744, 1983
Printed in Great Britain

0039-9140/83 $3.00 + 0.00

CONSTRUCTION OF A PERMANGANATE ION-SELECTIVE ELECTRODE AND ITS APPLICATION TO POTENTIOMETRIC TITRATIONS

MASAMITSU KATAOKA, NAOKI UNJYO and TOMIHITO KAMBARA
Department of Chemistry, Faculty of Science, Hokkaido University, Kita 10, Nishi 8, Kita-ku, Sapporo 060, Japan

(*Received* 22 *March* 1982. *Revised* 22 *March* 1983. *Accepted* 5 *May* 1983)

Summary—The construction of a liquid-membrane type permanganate ion-selective electrode and its application to potentiometric titrations are described. The benzylcetyldimethylammonium–permanganate ion-pair in the aqueous phase is easily extracted into nitrobenzene and the extract is employed as the liquid ion-exchange membrane of the ion-selective electrode. The electrode gives Nernstian response to permanganate in the concentration range from 10^{-6} to $10^{-1}M$, and the potential is almost independent of pH over the range from 3.0 to 10.5. The electrode can be used as indicator electrode in potentiometric titrations with permanganate.

Potassium permanganate is widely used in redox titrations, including the measurement of chemical oxygen demand (COD).[1] It also serves as the end-point indicator in such titrations, but for the highest accuracy a correction must be made to allow for the slight excess necessary.

Potentiometric redox titrations with potassium permanganate can be done with a platinum or glassy-carbon indicator electrode, but these electrodes are not specific for permanganate, and the potential is not particularly stable. Baczuk and Dubois[2] have suggested that the commercially available liquid-membrane type perchlorate ion-selective electrode is also sensitive to periodate, perrhenate and permanganate, but have not pursued the idea. We have now prepared and used a permanganate-sensitive electrode of the liquid-membrane type.

EXPERIMENTAL

Reagents

A 0.1M stock solution of potassium permanganate was prepared by dissolving 15.8 g of the reagent in 1 litre of demineralized water, boiling the solution, letting it stand for 1 day, and filtering. The solution was standardized against sodium oxalate, then stored in a dark bottle, in the dark in a refrigerator.

Benzylcetyldimethylammonium chloride ($BCDMA^+Cl^-$) was obtained from Wako Pure Chemicals Co. and a 0.01M stock solution prepared by dissolving 3.96 g of reagent in 1 litre of water.

All chemicals used were of analytical reagent grade.

Apparatus

All emf measurements were made with an Orion microprocessor "Ionalyzer", model 901, connected to a Hitachi model 056 recorder. A Toa HS-305D double-junction calomel electrode was employed as the reference electrode, with its outer cell filled with 0.01M potassium nitrate.

Preparation of liquid ion-exchange membrane

To 5 ml of 2mM potassium permanganate in a 100-ml separatory funnel were added 1 ml of 0.01M $BCDMA^+Cl^-$ solution and 10 ml of nitrobenzene (NB). The mixture was shaken for 10 min and allowed to stand for 10 min, then the organic phase was separated, and dried with anhydrous sodium sulphate. The liquid-membrane electrode barrel used was the same as that described previously.[3,4]

The potential of the electrode in the presence of foreign anions is given by the Nikolskii–Eisenman equation:[5]

$$E = E^0 - \frac{2.303\ RT}{F} \log \left(a_{MnO_4^-} + \sum_{j=1}^{n} K_j a_j^{1/z_j}\right) \qquad (1)$$

where $a_{MnO_4^-}$ and a_j are the activities of the permanganate ion and the jth foreign ion, K_j is the selectivity coefficient and z_j is the absolute value of the charge on the jth ion.

The cell system including the ion-selective electrode is shown by:

Platinized Pt electrode	Internal reference solution, 0.01M $KMnO_4$	Liquid ion-exchanger, 1mM $BCDMA^+$–MnO_4^- in NB	Sample solution containing MnO_4^-	0.01M KNO_3 solution	SCE or Ag/AgCl
		Ion-selective electrode			

RESULTS AND DISCUSSION

Selection of ion-exchange counter-ion

Four quaternary ammonium cations, *viz.* Capriquat (methyltrioctylammonium chloride, Cq^+Cl^-), Zephiramine (benzyldimethyltetradecylammonium chloride, $Zeph^+Cl^-$), Victoria Blue ($C_{33}H_{32}N_3Cl^-$, VB^+Cl^-), and $BCDMA^+Cl^-$ were tested as counter-

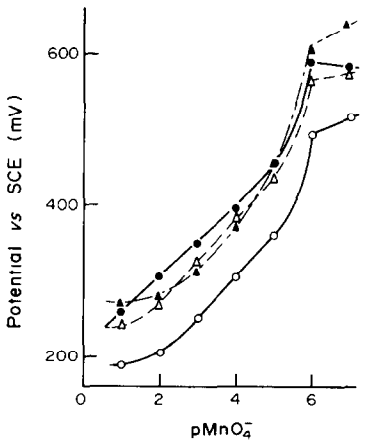

Fig. 1. Selection of ion-exchange counter-ion; —○— Capriquat, ---△--- Zephiramine, —●— $BCDMA^+$, ---▲--- Victoria Blue. Concentration of ion-pair in nitrobenzene: 0.2m*M*. Temperature 19.0°C.

ions. The ion-pair concentration in the nitrobenzene ion-exchange membrane solution was kept to 0.2m*M*. As shown in Fig. 1, only the BCDMA electrode showed Nernstian response in the permanganate concentration range from 10^{-6} to $10^{-1}M$.

Selection of the ion-pair concentration

The effect of the ion-pair concentration in the ion-exchange membrane is shown in Fig. 2. When the concentration is higher than 0.2m*M*, the electrode exhibits good Nernstian response and high stability of potential. Since the permanganate in the nitrobenzene extract gradually decomposes to give manganese dioxide, the membrane must be prepared every two weeks. In view of this, we chose 1.0m*M* for the ion-pair concentration in the membrane. A platinized platinum electrode is used as the internal

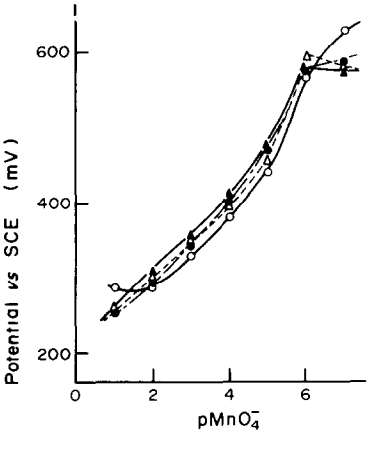

Fig. 2. Selection of $BCDMA^+$–MnO_4^- ion-pair concentration in the ion-exchange membrane. Ion-pair concentration, m*M*; —○— 0.05, ---●--- 0.5, ---△--- 1.0, —▲— 2.0. Internal reference solution: 0.01*M* $KMnO_4$. Temperature 20.0°C.

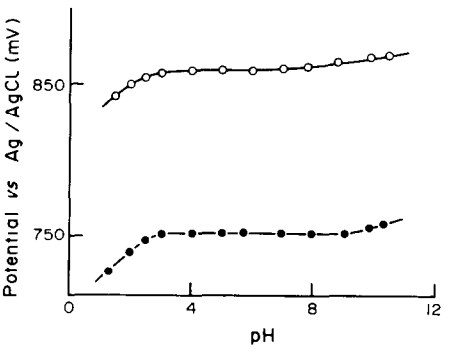

Fig. 3. Electrode response as a function of pH. Permanganate ion concentration: —○— $10^{-5}M$, —●— $10^{-3}M$. Ionic strength 0.15 (sodium sulphate).

reference electrode, because the silver–silver chloride electrode is not suitable, owing to oxidation of the chloride by permanganate. A 0.01*M* permanganate solution is used as the internal reference solution.

Electrode response as a function of pH

The effect of pH on the electrode-potential is shown in Fig. 3. The pH was adjusted with 0.1*M* sulphuric acid and 0.1*M* sodium hydroxide containing an appropriate amount of permanganate. The total ionic strength of the test solution was kept at 0.15*M* with potassium sulphate. The response of the electrode to 10^{-5} and $10^{-3}M$ permanganate was almost independent of pH in the range from 3.0 to 10.5.

Response time

The electrode gives 95% of full response in about 3 sec when the concentration is changed by a factor of 10, and the electrode potential is stable for 40 min.

Selectivity

The selectivity coefficients for various anions were evaluated by the mixed-solution method of Srinivasan and Rechnitz.[6] The permanganate concentration was varied from 10^{-4} to $10^{-5}M$, while the concentration of the competing anion was kept constant. The electrode shows good selectivity with respect to the most common anions. It is well known that

Table 1. Selectivity coefficients $K_{MnO_4^-,J}$

Anion	$-\log K_{MnO_4^-,J}$
ClO_4^-	−1 38
IO_4^-	−0.08
IO_3^-	2.40
BrO_3^-	2.62
ClO_3^-	2.87
HCO_3^-	2.92
$CH_3CO_2^-$	3 03
BO_2^-	3 11
NO_3^-	3.11
Br^-	3.23
H_2PO_4	3.38
Cl^-	3.41

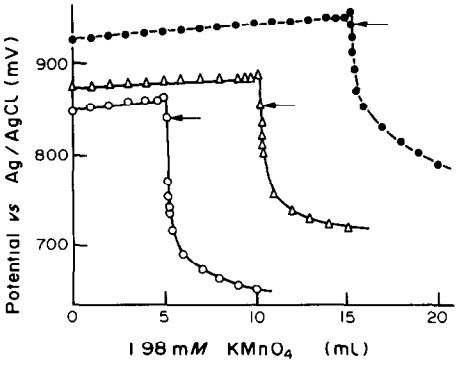

Fig. 4. Potentiometric titration of *ca.* 0.01*M* $FeSO_4$ with 1.98m*M* $KMnO_4$. $FeSO_4$ taken, ml; —○— 5, —△— 10, —●— 15. Arrows show the colour change at the visual end-point.

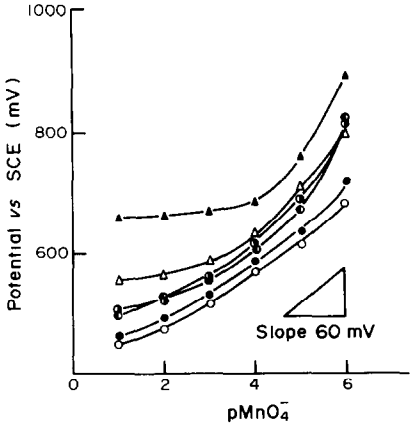

Fig. 5. Effect of temperature on calibration curve. ○, 24.5°; ●, 29.5°; ◐, 34.8°; ◑, 40.0°; △, 45.0°; ▲, 49.0°.

chloride and bromide are gradually oxidized by permanganate in neutral aqueous media, but the reaction is very slow. Since some anions, such as iodide and nitrite, are rapidly oxidized, their selectivity coefficients cannot be evaluated. The electrode shows poor selectivity for perchlorate, periodate and some anionic detergents.

Potentiometric titrations

The electrode can be successfully used in potentiometric permanganate titrations. Typical titration curves for 0.01*M* ferrous sulphate with 1.98m*M* permanganate at pH 2 are shown in Fig. 4. A slight excess of permanganate gives a sharp potential jump. The visual end-points, corrected for the blank, are also shown.

Results for the determination of four reductants by the electrode method and the visual method are compared in Table 2. The *F*- and *t*-tests reveal that no significant difference between the means and variances of the two sets of results.

Determination of COD

In the Japanese Industrial Standards method,[1] the solution temperature should be kept in the range 55–60°. Figure 5 shows the temperature-dependence of the electrode response. The response is almost Nernstian at temperatures below about 40° but markedly non-Nernstian at higher temperatures.

The procedure recommended for COD determination is to dilute a suitable volume of sample to 100 ml with water, add 10 ml of 6*M* sulphuric acid, *ca.* 1 g of silver sulphate and 10 ml of 0.005*M* permanganate, heat in a boiling water-bath for 30 min, then add 10 ml of 0.0125*M* sodium oxalate, cool to 40°, and titrate potentiometrically with 0.005*M* permanganate. A blank is run and the appropriate correction made.

The method has been applied to several pure organic compounds, and the results are tabulated in Table 3.

Table 2. Comparison of potentiometric and visual titrations

Sample	Volume of permanganate solution, *ml**		F_0†	t_0†
	Potentiometric method	Visual method		
Oxalate	$10.21_2 \pm 0.027$	$10.21_4 \pm 0.030$	1.234	0.138
Iron(II)	$9.77_0 \pm 0.026$	$9.79_4 \pm 0.036$	1.930	1.486
Ferrocyanide	$9.93_6 \pm 0.007$	$9.93_8 \pm 0.010$	2.333	0.447
Nitrite	$9.94_0 \pm 0.034$	$9.94_5 \pm 0.033$	1.077	0.333

*Mean and standard of five titrations of 10-ml portions of *ca.* 10m*M* sample with 1.98m*M* $KMnO_4$.

†$F_{(4,4,0.025)} = 9.60$; $t_{(8,0.05)} = 2.306$.

Table 3 COD of pure materials

Sample	0.002*M* $KMnO_4$ required, *ml*		F_0†	t_0†
	Potentiometric method	Visual method		
Potassium sodium tartrate	4.59 ± 0.10	4.56 ± 0.08	1.621	0.706
Formic acid	8.62 ± 0.01	8.57 ± 0.03	7.154	2.750
Soluble starch	3.53 ± 0.25	3.58 ± 0.23	1.154	0.163
Ethyl acetate	7.06 ± 0.26	7.12 ± 0.27	0.964	2.240
Mixed sample§	7.70 ± 0.05	7.68 ± 0.08	2.412	2.217

*Mean and standard deviation of 5 titrations.

†See Table 1.

§Composition: potassium sodium tartrate, formic acid, soluble starch, ethyl acetate and glycerine.

Table 4. Comparison of COD measurements

Source of supply	0.005*M* $KMnO_4$ required, *ml**		F_0†	t_0†
	JIS method	Potentiometric method		
Shinkawa	3.79 ± 0.35	3 77 ± 0 37	1.09	0 055
Toyohira	4 70 ± 0 21	4.69 ± 0 18	1 14	0 125
Fushiko	3.14 ± 0.21	2.94 ± 0 24	1.67	1 480
Sōsei	2.00 ± 0.24	1 98 ± 0 13	3.60	0 187

*Mean and standard deviation of 5 determinations (sample volume 50 ml)
†See Table 1.

It has also been applied to some waste-water samples from Sapporo city (Table 4).

REFERENCES

1. JIS K 0102-1979, *Testing Method for Industrial Waste Water*.
2. R. J. Baczuk and R. J. Dubois, *Anal. Chem.*, 1968, **40**, 685.
3. M. Kataoka and T. Kambara, *J. Electroanal. Chem.*, 1976, **73**, 279.
4. *Idem*, *Denki Kagaku*, 1976, **43**, 654.
5. G. Eisenman, *Glass Electrodes for Hydrogen and Other Cations*, Dekker, New York, 1969.
6. K. Srinivasan and G. A. Rechnitz, *Anal. Chem.*, 1969, **41**, 1203.

Talanta, Vol 30, No. 10, pp. 745–749, 1983
Printed in Great Britain

0039-9140/83 $3.00 + 0.00
Pergamon Press Ltd

AN ION-SELECTIVE ELECTRODE METHOD FOR DETERMINATION OF CHLORINE IN GEOLOGICAL MATERIALS

P. J. ARUSCAVAGE and E. Y. CAMPBELL
U.S. Geological Survey, Reston, VA 22092, U.S.A.

(*Received* 26 *August* 1982. *Revised* 25 *February* 1983. *Accepted* 26 *April* 1983)

Summary—A method is presented for the determination of chlorine in geological materials, in which a chloride-selective ion electrode is used after decomposition of the sample with hydrofluoric acid and separation of chlorine in a gas-diffusion cell. Data are presented for 30 geological standard materials. The relative standard deviation of the method is estimated to be better than 8% for amounts of chloride of 10 μg and greater.

The accurate determination of chlorine in geological materials is important to much current research at the U.S. Geological Survey in connection with evaluation of proposed mechanisms for the transport and deposition of metals in these materials, and its application for mineral exploration.

The determination is generally done by spectrophotometry,[1–6] X-ray fluorescence analysis[7–9] and neutron-activation analysis.[10–14] The chloride-selective electrode has also been used,[15,16] but in order to obtain accurate determinations by this method, chlorine must be separated completely from the sample matrix. This requirement normally adds considerably to the analysis time and results in poorer limits of detection because of increased volumes of sample and larger blanks. In this new procedure, distillation of the chlorine from the sample during its decomposition in a gas-diffusion cell solves these problems and permits advantage to be taken of the low cost and simplicity of operation of the ion-selective electrode.

To assess the accuracy of the method, 30 geological standard materials from several sources have been analysed. In addition, a one-factor analysis of variance was done on 11 U.S. Geological Survey standard rocks to test for bottle-to-bottle differences as a possible source for the variation of chlorine contents published in the literature.

EXPERIMENTAL

Reagents

Oxidizing solution: 1 part of 5% $KMnO_4$ in 15% w/v H_2SO_4 + 4 parts of concentrated (48%) HF. Reducing solution: 16% KOH and 0.8% anhydrous sodium sulphite.

Apparatus

Orion combination chloride-selective electrode model 96-17.* Orion ion analyser, model 901. Oscillating plate. Gas-diffusion cells: illustrated in Fig. 1.

Procedure

For samples containing 25–3000 ppm of chloride, weigh 200 mg of sample (100 mesh or finer) into the outer chamber of the diffusion cell. Measure 2.5 ml of the reducing solution into the centre chamber of the cell. Measure 3.0 ml of the oxidizing solution into the outer chamber and cap the cell immediately. Prepare a blank and several standards containing from 2 to 600 mg of chloride by measuring standard sodium chloride solutions into the outer chambers of separate cells and treat them as described for the samples. Place the cells on a gently oscillating surface, at room temperature. After 16–20 hr (overnight) remove the cells from the oscillating surface. Open the blank, stir the centre chamber contents with a small Teflon rod and then insert the chloride electrode into the centre chamber. After conditioning the electrode in the blank solution for 30 min, remove the electrode. Open the cells (one at a time), stir, and then read the potential differences for the standards and samples for a period of 10 min each or until the readings are stable. Plot the calibration graph (μg of chloride *vs.* mV, semi-log paper) and determine the chloride content of the samples.

RESULTS AND DISCUSSION

The colorimetric determination of chlorine after separation in a gas-diffusion cell has been described,[17,18] but this technique for the separation of chlorine has not been applied more universally, apparently because the design of the cell for decomposing samples with hydrofluoric acid is inadequate. However, if the cells are fabricated from TPFE (Teflon), which is very easily worked by machine, the use of hydrofluoric acid presents no problem. The details of the cells, which are totally machined from a solid cylinder of Teflon, 2.5 in. in diameter, are shown in Fig. 1. Thus, in one operation we are able to decompose the sample, distil the chlorine from the

*The use of trade names in this publication is for descriptive use only and does not constitute endorsement by the U.S. Geological Survey.

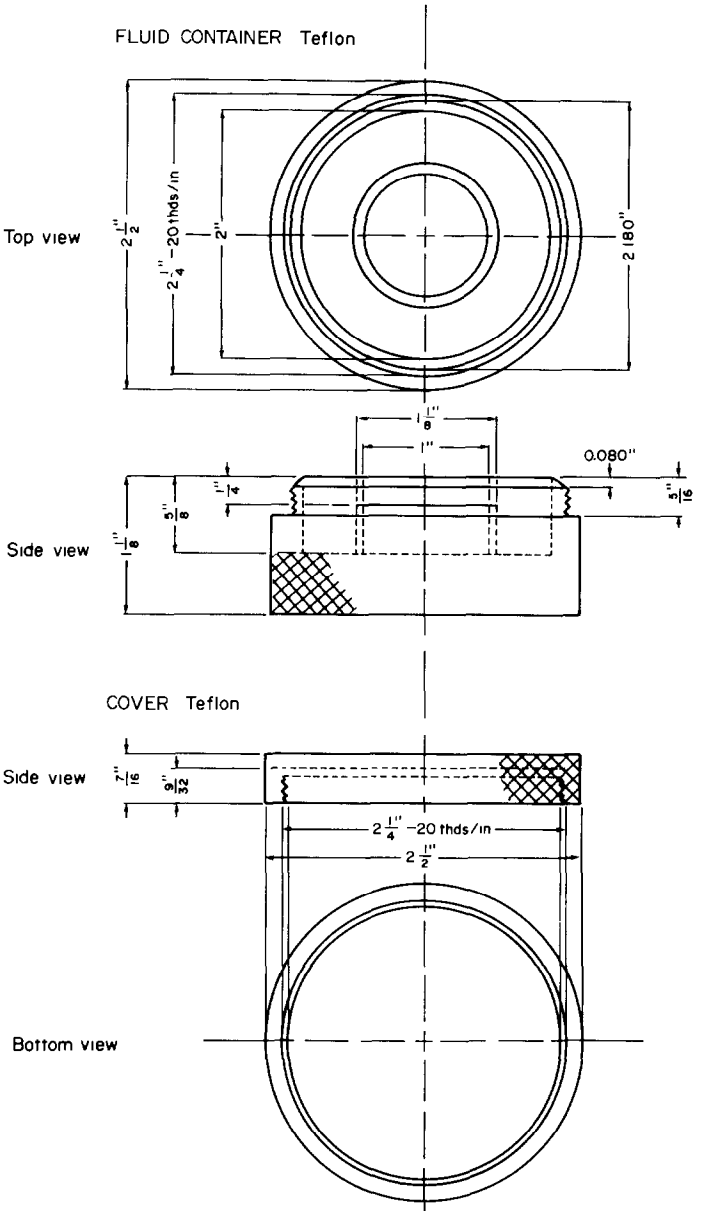

Fig. 1. Gas-diffusion cell.

rock matrix and collect the gas in a basic sulphite solution suitable for determination by the chloride-selective electrode.

The amount of hydrofluoric acid added is the minimum necessary for complete decomposition of a 200-mg sample of silicate rock, thus ensuring the lowest blank possible. The amount of potassium permanganate is in excess of that needed to oxidize most geological samples, but certain types of samples such as highly reducing sulphides may require additional permanganate. However, these samples have not been investigated. The amount of potassium hydroxide is calculated from the amount of hydrofluoric acid added, so that the final solution has a pH of 4–5; this allows the electrode reading to be determined directly after the cells have been opened.

Although in the past the distillation was done from a stationary cell,[17,18] we have obtained more consistent results by gently oscillating the sample to produce more thorough decomposition and distillation of the sample.

The calibration graph was linear from 20 to 500 μg of chloride and had a slope of 59 mV/pCl, consistent with the theoretical Nernstian slope. Below 20 μg of chloride the slope deviates from Nernstian because of kinetic effects at the electrode interface. The distillation–extraction efficiency for both samples and standards was determined by using radioactive ^{36}Cl

tracer. Approximately 90% of the chlorine was recovered in the inner chamber and less than 1% remained in the outer chamber after an overnight (16-hr) digestion. This implies that 10% of the chlorine remained in the vapour phase when the cells were opened. Because the percentage recovery is very consistent (±2%), the losses do not prejudice the results significantly.

We tested 500 and 1000 μg quantities of bromide and iodide under the same experimental conditions, to study their possible interference in the determination. We found that the signal from 1 μg of bromine was equivalent to 0.66 μg of chlorine and that from 1 μg of iodine was equivalent to 0.011 μg of chlorine. Because the concentration of iodine and bromine in rocks is typically smaller than that of chlorine by a factor of 50–100, the error produced in the determination of chlorine would be only about 1%.

The results of a one-factor (bottle-to-bottle) analysis of variance on 11 U.S. Geological Survey standard rocks are shown in Table 1. From tables of F-values at 5% uncertainty, the value for significance is 5.4 for 2 degrees of freedom (bottles) and 6 degrees of freedom (determinations). Therefore, no significant differences was found in the chlorine content from bottle to bottle for each of the standard rocks examined. The variations in the values published in the literature are thus probably due to errors in analytical technique or to contaminated samples. The precision of the method, expressed as relative standard deviation (RSD), is better than 8% for all samples except DTS-1.

Table 2 shows the results for chlorine determined in this work for 30 geological standard materials and also some values reported in the literature for the same samples. Also shown in Table 2 are estimated values from several compilations of data.[19–21] A mean and standard deviation of all the literature values, including the mean from this procedure, were also calculated for those samples for which values have been obtained by at least four different procedures. To eliminate any outliers, those values more than two standard deviations from the mean were eliminated,

Table 1. Chlorine (ppm) in 11 U.S. Geological Survey standard rocks

Rock	Bottle No.	Individual results	F (0.95)	Mean ± SD	RSD, %
G-2	1	51, 53, 49	4.16, NS	50 ± 3	6.0
	2	45, 48, 47			
	3	53, 53, 48			
GSP-1	1	340, 330, 325	3.26, NS	339 ± 8	2.4
	2	340, 340, 350			
	3	350, 340, 340			
RGM-1	1	520, 550, 540	0.425, NS	530 ± 17	3.2
	2	520, 535, 515			
	3	515, 515, 560			
QLO-1	1	253, 270, 260	0.605, NS	255 ± 13	5.1
	2	250, 260, 235			
	3	233, 260, 270			
AGV-1	1	128, 113, 120	0.229, NS	119 ± 5	4.2
	2	115, 115, 122			
	3	118, 115, 123			
BCR-1	1	70, 60, 68	0.037, NS	66 ± 4	6.1
	2	65, 63, 69			
	3	65, 60, 70			
BHVO-1	1	105, 95, 106	0.034, NS	102 ± 5	4.9
	2	102, 103, 98			
	3	103, 108, 95			
DTS-1	1	32, 28, 33	0.073, NS	31 ± 5	16
	2	39, 21, 32			
	3	35, 30, 32			
PCC-1	1	75, 80, 83	0.064, NS	80 ± 4	5.0
	2	83, 81, 78			
	3	82, 73, 85			
SDC-1	1	42, 45, 43	0.566, NS	42 ± 3	6.4
	2	42, 46, 41			
	3	41, 45, 37			
SCO-1	1	65, 68, 68	1.59, NS	64 ± 5	7.6
	2	65, 63, 53			
	3	61, 69, 62			

NS = not significant.
SD = standard deviation.
RSD = relative standard deviation.

Table 2. Chlorine (ppm) in 30 international geological standard materials

Rock type	Producer	Sample	This work (N)	Literature values	Mean ± SD (N) of methods	Values from compilations
Granite	USGS	G-2	50 (6)	55[5], 54[8], 145[9]*, 53[10], 59[11], 60[13], 75[16], 91[22]	64 ± 14 (7)	100[20], 50[21]
	CRPG	GA	214 (2)	180[9]		300[20]
	CRPG	GH	59 (2)	100[1]		100[20]
	NIM	G	273 (2)	210[9]		200[20]
Granodiorite	USGS	GSP-1	340 (6)	338[2], 340[4], 304[5], 305[8], 340[9], 311[10], 300[11], 315[13], 351[16], 354[22]	326 ± 21 (10)	340[20], 300[21]
	GSJ	JG-1	56 (2)	190[9], 57[11], 53[15]		59[20], 200[21]
Syenite	USGS	STM-1	518 (2)	415[1], 408[3], 420[7], 431[10], 452[12], 458[13]	443 ± 38 (7)	440[19], 500[20]
	CCRMP	SY-2	143 (2)			130[20]
	CCRMP	SY-3	180 (2)			140[20]
Rhyolite	USGS	RGM-1	530 (6)	590[1], 492[3], 580[5], 440[7], 440[12], 540[13], 525[14]	517 ± 57 (8)	490[19], 500[20]
Latite	USGS	QLO-1	255 (6)	231[1], 226[3], 194[5], 192[7], 225[12], 224[13], 220[14]	220 ± 20 (8)	214[19], 250[20]
Andesite	USGS	AGV-1	119 (6)	110[2], 119[3], 320[4]*, 108[8], 225[9]*, 115[10], 100[11], 106[13]	111 ± 7 (7)	185[20], 110[21]
Tonalite	USGS	TLM-1	275 (2)			
Basalt	USGS	BCR-1	66 (6)	62[2], 62[4], 59[5], 62[6], 64[8], 55[9], 58[10], 59[11], 54[13]	60 ± 4 (10)	58[20], 50[21]
	USGS	BHVO-1	102 (6)	110[1], 95[5], 92[7], 96[12], 93[13], 87[14]	96 ± 8 (7)	92[19]
	USGS	BIR-1	23 (2)			
	GSJ	JB-1	204 (2)	190[9], 200[15]		175[20], 190[21]
Diabase	USGS	W-2	245 (2)			
	USGS	DNC-1	43 (2)			
Gabbro	USGS	GSM-1	278 (2)			
	CCRMP	MRG-1	187 (2)			150[20]
Norite	NIM	N	47 (2)	45[9]		100[20], 100[21]
Dunite	USGS	DTS-1	31 (6)	33[4], 10[6], 45[9], 9.4[10], 10[11], 12[13]	21 ± 15 (7)	11[20], 11[21]
	USGS	DTS-2	37 (2)			
	NIM	D	235 (2)	340[9]		400[20], 400[21]
Peridotite	USGS	PCC-1	80 (6)	74[4], 85[6], 115[9], 66[10], 72[11], 76[13]	72 ± 33 (7)	80[20], 60[21]
Pyroxenite	NIM	P	70 (2)	145[9]		200[20], 100[21]
Schist	USGS	SDC-1	42 (2)	29[1], 40[3], 38[7], 32[13], 17[14]	33 ± 9 (6)	30[19]
Shale	USGS	SGR-1	33 (6)	20[1], 7800[3]*, 44[7], 21[14]	30 ± 11 (4)	29[19]
	USGS	SCO-1	64 (6)	53[1], 363[3]*, 67[7], 51[13], 34[14]	54 ± 13 (5)	48[19]

SD = standard deviation.
* = not used in calculation of mean.
(N) = number of results used in calculation.
USGS = U.S. Geological Survey.
CPRG = Centre de Recherches Pétrographiques et Géochimiques, France.
NIM = National Institute of Metallurgy, South Africa.
GSJ = Geological Survey of Japan.
CCRMP = Canadian certified research mineral project.
Ref. 22 = Average of 4 values by differing procedures.
Note: the results of Moore[5] are means of 9 determinations by use of a carbonate–thiocyanate procedure.

and a new mean and standard deviation were calculated. These data show that the samples GSP-1, AGV-1 and BCR-1 are the best characterized standards; their relative standard deviations are less than 7% for the pooled results by all the methods. These are followed by BHVO-1, STM-1, QLO-1, RGM-1 and G-2, all of which have an RSD of less than 14%. The poorest agreement among the methods is for the ultramafic rocks, probably because of their generally lower chlorine content, and for the shales, possibly because of interference by the large amounts of organic matter.

The generally satisfactory agreement of our results with the literature values indicates that the proposed method is accurate for a wide variety of geological materials. Clearly there is a need for additional data obtained by independent methods for several samples where unacceptable discrepancies remain, such as G-2, NIM D, NIM P and GH, and also for continued updating of compilation values, which are often used as the "true concentration" by many laboratories.

REFERENCES

1. R. Fuge, *Geostand. Newsl.*, 1981, **5**, 183.
2. *Idem*, *Chem. Geol.*, 1976, **17**, 37.
3. G. Troll and A. Farzanah, *Geostand. Newsl.*, 1980, **4**, 37.
4. W. H. Huang and W. D. Johns, *Geochim. Cosmochim. Acta*, 1967, **31**, 597.
5. R. Moore, U.S. Geological Survey, Reston, Va., 1980, Private communication.
6. P. J. Cattermole and R. Fuge, *Geochim. Cosmochim. Acta*, 1969, **33**, 295.
7. B. P. Fabbi and L. F. Espos, *U.S. Geol. Survey Prof. Paper*, No. 840, 1976, 89.
8. *Idem*, *Appl. Spectrosc.*, 1972, **26**, 293.
9. W. B. Stern, *Geostand. Newsl.*, 1977, **1**, 181.
10. O. Johansen and E. Steinnes, *Geochim. Cosmochim. Acta*, 1967, **31**, 1107.
11. C. K. Unni and J. C. Schilling, *Anal. Chim. Acta*, 1978, **96**, 107.
12. O. Johansen and E. Steinnes, *Geostand. Newsl.*, 1979, **3**, 47.
13. J. Rosenberg, *Radiochem. Radioanal. Lett.*, 1979, **40**, 115.
14. G. E. Gordon, W. B. Walters, W. H. Zoller, D. C. Anderson and M. P. Farley, *Techn. Rept.* ORO-5173-008, Department of Chemistry, University of Maryland, College Park, Md., 1979.
15. H. Akaiwa, H. Kawamuto and K. Hasagewa, *Talanta*, 1979, **26**, 1027.
16. S. J. Haynes and A. H. Clark, *Economic Geol.*, 1972, **67**, 378.
17. E. J. Conway, *Biochem. J.*, 1935, **29**, 2221.
18. C. J. Rodden, *Analytical Chemistry of the Manhattan Project*, p. 297. McGraw-Hill, New York, 1950.
19. E. S. Gladney and W. E. Goode, *Geostand. Newsl.*, 1981, **5**, 31.
20. S. Abbey, *Geol. Survey Canada Paper*, No. 80-14, 1980.
21. F. J. Flanagan, *Geochim. Cosmochim. Acta*, 1973, **37**, 1189.
22. S. J. Haynes, *Talanta*, 1978, **25**, 85.

Talanta, Vol. 30, No 10, pp 751–754, 1983
Printed in Great Britain

0039-9140/83 $3.00 + 0.00

PROCEDURES FOR ISOLATION AND DETERMINATION OF THORIUM

ALAN D. WESTLAND and CHIRAN J. KANTIPULY
Department of Chemistry, University of Ottawa, Ottawa, Ontario, Canada

(*Received* 1 *March* 1983. *Accepted* 24 *April* 1983)

Summary—The cation-exchange behaviour of micro and trace quantities of thorium on Dowex 50-X8 in the presence of carbonate and phosphate has been studied. Carbonate causes loss of thorium to the column effluent at pH ≥ 10. In the presence of phosphate, thorium is incompletely sorbed in the pH range 2–4.5, the loss being maximum at pH 3.8. Outside this range, thorium is quantitatively sorbed and recovered. A method that does not employ ion-exchange has been developed for the microdetermination of thorium in phosphate solution. The phosphate is precipitated as bismuth phosphate and thorium is leached from the precipitate with ammonium carbonate solution and determined with Arsenazo III. Uranium, molybdenum and vanadium are removed with Alamine 336. The results obtained for a standard ore are in excellent agreement with the certified value.

There is considerable interest in the behaviour of trace levels of the actinides in the environment. It is expected that thorium will be used as a nuclear fuel and this makes it important to determine it in the two phases of uranium process streams if it is to be stockpiled. Existing methods for thorium determination require separation from the rare-earth and other interfering elements such as U, Zr, Hf, V and Mo.

Separation of thorium from solutions containing significant amounts of phosphate can be incomplete.[1] Carbonate also complexes thorium strongly. As carbonate and phosphate are important constituents of ground-water and other natural water systems, these two anions may play an important role in the complexation, absorption and other reactions of thorium in natural samples. Phosphate is also present in uranium process streams.

Cation-exchange is frequently used to isolate thorium from interfering elements, but the published data do not lead to unambiguous predictions of the cation-exchange behaviour of thorium when carbonate and phosphate are present.[2,3] We have therefore investigated the sorption and recovery of thorium in microgram and trace quantities as a function of pH. As the ion-exchange procedure is time-consuming, owing to the need to evaporate a considerable volume of sulphuric acid (the eluate), an alternative method of separating phosphate was developed. This was incorporated into a complete method for thorium determination, which was tested in the presence of uranium, molybdenum and vanadium.

EXPERIMENTAL

Apparatus

Photometric readings were made with a Unicam SP 1800 spectrophotometer and ^{234}Th beta-counting was done with a Beckman 3133P scintillation counter.

Reagents

Standard thorium solution $Th(NO_3)_4 \cdot 4H_2O$ (Baker analytical grade) was used as supplied. A stock solution containing 100 ppm Th was prepared by dissolving the salt in doubly distilled water and adding nitric acid to give a final acid concentration of 1 *M*, and standardized gravimetrically by evaporating aliquots to dryness in a crucible and igniting Working solutions (5 ppm Th) were freshly prepared by diluting the stock solution with 1 *M* nitric acid.

Arsenazo III solution, 0.05%.

Alamine 336 solution. Thirty-five ml of reagent (General Mills, Ltd.) were diluted to 500 ml with a 3:1 v/v mixture of petroleum ether (b.p. 40–50°) and *o*-xylene.

Carrier-free ^{234}Th tracer.[4] Two g of $UO_2(NO_3)_2 \cdot 6H_2O$ (Baker, A. R.) in 10 ml of water were converted into the carbonate complex by addition of saturated ammonium carbonate solution until the initial precipitate of carbonate dissolved; then 2 ml of freshly prepared 6% aqueous cupferron solution were added. ^{234}Th was extracted at pH 8–8.5 into 10 ml of chloroform. The extraction was repeated and the extracts were combined. The ^{234}Th was stripped with 10 ml of 3 *M* nitric acid containing 2–3 ml of saturated bromine water. The aqueous phase was washed twice with chloroform and boiled for 2 min to eliminate traces of chloroform. The volume was finally adjusted to 25 ml.

Preparation of cation-exchange columns. Dowex 50-X8 (20–50 mesh) in the H^+-form was prewashed with dilute sulphuric acid, followed by water. The height of the resin bed was 10 cm and the diameter 1.5 cm. A similar column was converted into the NH_4^+-form by conditioning with 2 *M* ammonium chloride.

Procedures

Photometric determination. The sample solution was evaporated to dryness, 5 ml of 70% perchloric acid were added and the solution was again taken to dryness, after which 1 ml of concentrated hydrochloric acid was added and the solution was again evaporated to dryness. One ml of concentrated hydrochloric acid and 5 ml of water were added and the solution was transferred to a 25-ml standard flask. A 5-ml portion of 8% oxalic acid solution was added, followed by 1 ml of Arsenazo III solution. The solution was diluted to volume with water The absorbance was measured at 660 nm in a 1-cm cell. A calibration curve was prepared as described by Abbey,[5] for the concentration range 0–1.2 μg/ml Ammonium salts, when present, were destroyed with concentrated nitric and hydrochloric acids.[6]

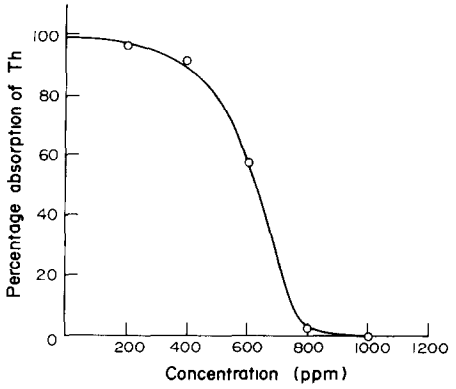

Fig. 1. Relation between sorption of thorium on Dowex 50-X8 and carbonate concentration.

Scintillation counting. ^{234}Th was used as carrier-free tracer. The sample solution was evaporated to dryness, 1 ml of concentrated hydrochloric acid was added and the solution transferred to a 20-ml scintillation vial (Fisher). The volume was 12 ± 1 ml at this point. A 3-ml portion of "Sentiverse" (Fisher) was added and the solution mixed and counted in an open channel of the counter, with the gain set at 280. The efficiency of the counter for ^{14}C ($E_{max} = 0.156$ MeV) was 95%. Since E_{max} for ^{234}Th is 0.263 MeV, we assume the efficiency for this isotope was greater than 95%.

Cation-exchange behaviour of thorium

Microgram quantities and trace levels of thorium in 1*M* nitric acid were sorbed on Dowex 50-X8 and recovered by elution with 500 ml of 1.8*M* sulphuric acid. The amounts recovered were determined by the two procedures above.

Effect of carbonate Solutions containing 770 ppm of carbonate caused cation-exchange beds in the H^+-form to break up owing to evolution of CO_2. In the NH_4^+-form the cation-exchanger behaved normally. The sorption of thorium from solutions of 1 ppm concentration was completely inhibited by the presence of carbonate at a concentration of 1 mg/ml and pH = 10. The relation between percentage sorption and carbonate concentration is shown in Fig. 1. This behaviour is similar to that of uranium and is attributed to the formation of anionic carbonate-complexes, *e.g.*, $Th(CO_3)_5^{6-}$.[2]

Effect of phosphate. A study was made of the sorption of thorium on Dowex 50-X8 (H^+-form) as a function of pH and at a phosphate concentration of 520 ppm. Thorium was lost to the effluent in the pH range 2–4.5; the maximum loss (~30%) occurred at pH 3.8, as shown in Fig. 2. Outside this pH range, sorption of thorium was quantitative and the

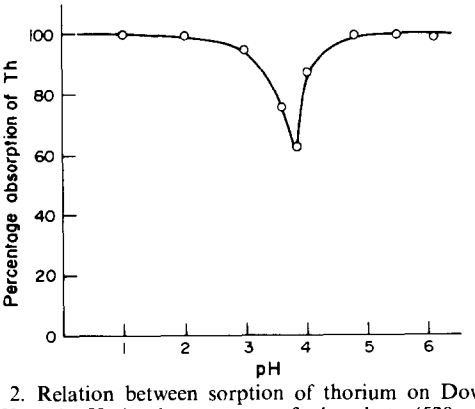

Fig. 2. Relation between sorption of thorium on Dowex 50-X8 and pH, in the presence of phosphate (520 ppm PO_4^{3-})

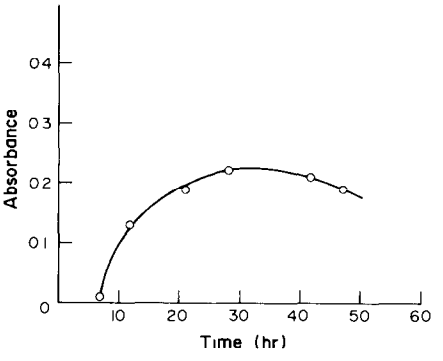

Fig. 3. Effect of phosphate on the absorbance of thorium–Arsenazo III

element was quantitatively recovered by elution with 500 ml of 1.8*M* sulphuric acid.

The work of Langmuir *et al.* leads us to suggest that the following equilibria are responsible for the behaviour observed.[7]

$$Th^{4+} + 2H_3PO_4 \rightleftharpoons Th(HPO_4)_2 + 4H^+$$

$$Th(HPO_4)_2 \overset{OH^-}{\rightleftharpoons} Th[Th(OH)_3]_m^{(4+m)+} + 2PO_4^{3-}$$

The species $Th(H_2PO_4)^{3+}$ and $Th(HPO_4)^{2+}$ are doubtless also formed at pH values $\leqslant 2$. At low pH values, cations are favoured in the equilibria, so there is sorption by the resin The neutral species $Th(HPO_4)_2$ is important at intermediate pH values and this causes losses to occur At higher pH values, hydroxo polycations form and these too are sorbed and tightly bound.[12] Condensation polymerization is also observed for plutonium. Toth *et al.* report that polymerization occurs very rapidly with this element in aqueous nitric acid.[8]

Phosphate also interferes with the formation of the coloured Th–Arsenazo III complex.[9] We found that phosphate at a concentration of 0.76 mg/ml delayed the appearance of the complex for a period of 7 hr. After this, the absorbance increased to a maximum after about 30 hr and then again decreased (Fig. 3), but never reached the value observed when phosphate was absent.

Separation of phosphate

An alternative method for the isolation of thorium from samples containing phosphate and uranium has been developed. The phosphate is precipitated by the addition of bismuth nitrate. The solubility product of $BiPO_4$ is reported to be 1.3×10^{-23} at 20 .[10] The precipitate carries down much of the thorium, but this may be leached from the precipitate with warm saturated ammonium carbonate solution. The carbonate added also causes precipitation of the excess of bismuth.

If the quantity of phosphate is insufficient to ensure good nucleation of $BiPO_4$, additional phosphate is added to bring its concentration to at least 0.5 mg/ml. A 0.1*M* solution of bismuth nitrate is added slowly until the precipitation of $BiPO_4$ is complete. An equal volume of saturated ammonium carbonate solution is added and the mixture kept on a steam-bath for 40 min. The precipitate is removed on a medium porosity sintered-glass filter and washed with saturated ammonium carbonate solution. The ammonium carbonate is then eliminated by addition of concentrated hydrochloric and nitric acids and boiling.[6]

The efficiency of the separation was examined by treating solutions that contained 0.5 mg of phosphate and 1.0 μg of thorium per ml. A trace of ^{234}Th was also present. The β activity of both precipitate and solution was determined The results given in Fig. 4 show that the incorporation of thorium into the precipitate increased with time of standing

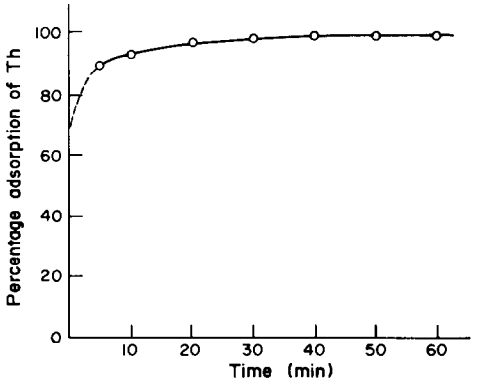

Fig. 4. Incorporation of thorium into a precipitate of $BiPO_4$.

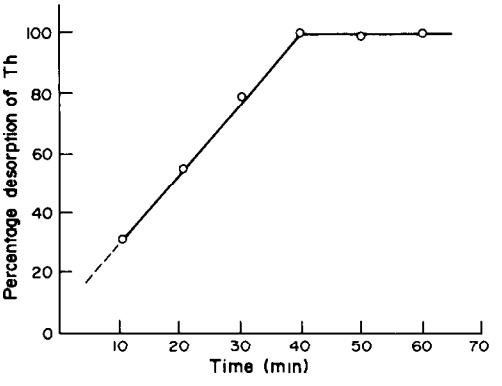

Fig. 5. Leaching of thorium from a precipitate of $BiPO_4$ by heating with $(NH_4)_2CO_3$ solution.

and was complete within 50 min from the time of precipitation. The effect of leaching is shown in Fig. 5 and it is seen that 98 ± 2% of the thorium was recovered by digestion for 40 min.

A further step, a solvent extraction with a tertiary amine (Alamine 336), is necessary in the analysis of ores, concentrates and mill liquors. Uranium mill raffinate normally contains phosphate, molybdate, vanadate and residual uranium. The following procedure is recommended.

The sample solution should have a volume of *ca.* 25 ml. Its pH is adjusted to 1.0–2.5 (but not higher) with dilute nitric acid. The sample is placed in a separatory funnel and shaken with an equal volume of Alamine 336 solution. The extraction is repeated after readjustment of the pH of the aqueous phase by addition of a further 2 ml of 6*M* nitric acid. The aqueous phase is subsequently boiled to expel traces of organic solvent, then cooled. The procedures for the elimination of phosphate and for the photometric determination are then applied.

Effect of UO_2^{2+}. In the absence of phosphate, neither U nor Th was extracted into a petroleum ether solution of Alamine 336. When various amounts of $UO_2(NO_3)_2$ and phosphate were added to aliquots of standard thorium solution, uranium entered the organic phase. It is recommended that the concentration of uranium be no greater than 0.1 mg/ml.

Effect of molybdate. Molybdenum behaved in much the same manner as uranium. When both were added to solutions containing Th and 3 mg of phosphate per ml at a pH of 1.0–2.5, both U and Mo were quantitatively removed by solvent extraction and Th was quantitatively recovered in the aqueous phase. It is well known that molybdate condenses with phosphate in an acid medium and that the heteropoly species is extractable.

Effect of vanadate. Both U and Th were quantitatively extracted in the presence of vanadate at an initial pH < 2. At pH > 2, only partial extraction of each element was observed. We believe that Th and U form extractable heteropoly species with vanadium at low pH. It has been reported[11] that at pH 2–8 the major species in vanadate solutions are $V_3O_9^{3-}$, $V_4O_{12}^{4-}$, $HV_6O_{17}^{3-}$, $HV_{10}O_{28}^{5-}$ and $H_2V_{10}O_{28}^{4-}$. Some of these anions might combine with Th^{4+} and UO_2^{2+} to form neutral heteropoly groups. However, when phosphate was also present, V and U, but not Th, were extracted into the organic phase at pH 1–2.5. In this situation, uranium may form a complex similar to phosphomolybdovanadate,[12] which is extracted in the protonated form. The thorium in the aqueous phase may be isolated and determined by applying the procedures for the elimination of phosphate and for photometric determination.

Results of the extraction experiments are shown in Table 1. Thorium recoveries were quantitative except when large quantities of interfering elements resulted in the formation of precipitates.

Analysis of a certified reference material

The validity of the procedure was verified by analysing a certified ore, arkose sandstone, supplied by the Department of Energy, Mines and Resources, Ottawa (CANMET), catalogue number DL-la. The certified mean value for thorium was 0.0076% and the 95% confidence limits were 0.0072–0.0079%. The material was reported to contain uraninite, brannerite and possibly monazite and ura-

Table 1. Recovery of thorium in the presence of phosphate,* uranium, molybdenum and vanadium

Th taken, μg	Other elements present, mg			Th recovered, μg
	U	Mo	V	
25.0(3)†	0.25	—	—	25.0 ± 0.2
250.0(3)	2.5	—	—	248.9 ± 0.7
25.0(3)	3.0	—	—	24.3 ± 1.1
25.0(1)	—	—	—	§
600.0(1)	2.5	—	—	§
25.0(4)	0.25	37.0	—	24.8 ± 0.4
250.0(3)	0.25	42.0	—	247.9 ± 2.3
250.0(1)	0.25	76.0	—	§
25.0(3)	0.25	—	20.0	25.0 ± 0.5
250.0(3)	0.25	—	30.0	249.1 ± 1.6
250.0(1)	0.25	—	40.0	§

*In all cases $[PO_4^{3-}] = 3$ mg/ml. Initial volume 25 ml.
†The number of replicate samples appears in brackets.
§Precipitation occurred; solvent extraction was not possible.

Table 2. Recovery of thorium after removal of potassium as perchlorate

K^+ precipitated, *mg*	Th added, *μg*	Th recovered, *μg*
0	25.0	25.0
50.7	25 0	24.9
72 5	25.0	25.0
145.1	15.0	15.2
217.7	15.0	15.0
290.2	25.0	24.9

nothorite. As sodium interferes in the determination of thorium with Arsenazo III, the sample was fused in a mixture of potassium superoxide and potassium hydroxide. A 0.5-g portion of the finely powdered ore was mixed with 1 g of potassium superoxide (Alpha, Ventron) and 0.5 g of potassium hydroxide in a zirconium crucible.[13] The mixture was fused and heated to redness over an open flame for 3–5 min. The cooled crucible was placed in a 250-ml beaker and the melt dissolved with 50 ml of 2*M* nitric acid. The solution was evaporated to dryness on a steam-bath. The residue was heated to dehydrate silicic acid, and after addition of 1*M* nitric acid, the silica was collected on a Whatman No. 41 paper. The filtrate was again evaporated to dryness in order to render insoluble a further small amount of silicic acid. The residue was treated with acid as before and the silica collected on a fresh filter. The two washed precipitates were combined and ignited at 700° in a platinum dish. The silica was removed by heating with a mixture of sulphuric and hydrofluoric acids. The platinum dish was washed with 1*M* nitric acid and the washings added to the combined filtrates. The solution was made up accurately to 100 ml and a 50-ml aliquot taken. This was evaporated to 30 ml and then cooled in ice. Potassium was precipitated by addition of cold 20% perchloric acid. The precipitate was separated on a medium porosity sintered-glass filter and washed with more cold perchloric acid. The solution was evaporated to dryness and the salts were taken up in 30 ml of 1*M* nitric acid. The procedures for solvent extraction, removal of phosphate and photometric determination were then applied.

The thorium values obtained with four samples of the ore were 0.0074, 0.0072, 0.0075 and 0.0075%, all within the 95% confidence limits.

The removal of potassium by precipitation as perchlorate presented no difficulties. We tested the recovery of thorium for a range of potassium concentrations and found all the thorium in the filtrate in all cases The results of these experiments are given in Table 2.

The procedure developed in the present work for samples in solution is more rapid than that involving the ion-exchange procedure and the effects of dissolution of the ion-exchanger are avoided. The procedures are useful when a chemical method of determination is to be used and this also applies when it is necessary to obtain a chemical yield in a radiochemical assay.

Acknowledgement—The authors are grateful to the Government of India for a scholarship granted to C.J.K.

REFERENCES

1. R. J. Callow, *The Industrial Chemistry of Lanthanons, Yttrium, Thorium and Uranium*, 1st Ed., p. 133. Pergamon Press, Oxford, 1967
2. J. Korkisch, *Atomic Energy Review*, Vol. 8, **3**, IAEA, Vienna, 1970.
3. O. Menis, D. L. Manning and G. Goldstein, *Anal. Chem.*, 1957, **29**, 1426.
4. G. A. Cowan, *Preparation of Carrier-free ^{234}Th Tracer*, LA-1721, 2nd Ed., Los Alamos Scientific Laboratory of Univ. of California, New Mexico, 1954.
5. S. Abbey, *Anal. Chim. Acta*, 1964, **30**, 176.
6. W. F. Hillebrand, G. E. F. Lundell, H. A. Bright and J. I. Hoffman, *Applied Inorganic Analysis*, 2nd Ed., p. 133. Wiley, New York, 1953.
7. D. Langmuir and J. S. Herman, *Geochim. Cosmochim. Aca*, 1980, **44**, 1753.
8. L. M. Toth, H. A. Friedman and M. M. Osborne, *J. Inorg. Nucl. Chem.*, 1981, **43**, 2929.
9. H. Onishi and K. Sekine, *Talanta*, 1972, **19**, 473.
10. W. F. Linke, *Solubilities of Inorganic and Metal Organic Compounds*, 4th Ed., Vol. 1, p. 437. Am Chem. Soc., Washington D.C., 1958.
11. M. T. Pope and B. W. Dale, *Quart. Rev.*, 1968, **22**, 527.
12. G. A. Tsigdinos, *Heteropoly Compounds of Molybdenum and Tungsten*, in *Topics in Current Chemistry*, Vol. 76, p. 1. Springer-Verlag, Berlin, 1978
13. A. D. Westland and C. Kantipuly, unpublished results.

Talanta, Vol 30, No. 10, pp 755–760, 1983
Printed in Great Britain

0039-9140/83 $3.00 + 0.00

CATION-EXCHANGE BEHAVIOUR OF THE PLATINUM GROUP AND SOME OTHER RARE ELEMENTS IN HYDROBROMIC ACID–THIOUREA–ACETONE MEDIA*

C. H.-SIEGFRIED W. WEINERT and FRANZ W. E. STRELOW
National Chemical Research Laboratory, P.O. Box 395, Pretoria 0001, Republic of South Africa

(*Received* 28 *February* 1983. *Accepted* 22 *April* 1983)

Summary—Ion-exchange distribution coefficients and elution curves are presented for copper(I), silver, gold(I), palladium, platinum(II), rhodium(III), iridium(III), ruthenium(III), osmium(III), mercury(II), thallium(I), tellurium(II), lead and bismuth in mixtures of thiourea, hydrobromic acid, acetone and water, with the cation-exchange resin AGW50W-X4. The system affords excellent separations of rhodium, mercury, silver (or copper), tellurium, gold, and palladium (or platinum) from each other.

In a previous paper[1] it was shown that the presence of thiourea (Tu) in hydrochloric acid media selectively enhances the sorption of some elements, including the platinum and copper-group metals, mercury and tellurium, on strongly acid sulphonated polystyrene (AG50W) resins. The possibility of separating these metals from each other was not investigated except for a suggestion that rhodium and iridium can be separated by exploiting the fact that their anionic chloro-(aquo-)complexes undergo ligand-exchange with thiourea only very slowly, to form cationic thiourea complexes. The distribution coefficients of most of the other elements mentioned above were too high to facilitate their stepwise elution with practicable volumes of aqueous thiourea and hydrohalic acid solutions even though some separation factors, for example those between silver and gold, were reasonably large.

Preliminary work indicated that (*a*) the distribution coefficients decrease sharply and selectively with increasing concentration of the organic solvent present, and (*b*) hydrobromic acid is more effective than hydrochloric acid for the elution of thiourea complexes. An organic solvent–thiourea–hydrobromic acid system was therefore selected for further study. Acetone was chosen as the organic solvent because of its low dielectric constant, ready availability and complete miscibility with water. Some earlier work by Toerien and Levin[2,3] had already given an indication of the usefulness of this system for the separation of small amounts (2 mg each) of rhodium (or iridium), silver, gold and platinum (or palladium).

*This paper represents part of a D.Sc. Thesis by C.H.-S.W. Weinert to be submitted to the University of Pretoria, Republic of South Africa.

EXPERIMENTAL

Reagents

AG50W-X4 cation-exchange resin (100–200 and 200–400 mesh particle size) in the hydrogen form was obtained from Bio-Rad laboratories, Richmond, Ca.

Water was distilled, and for further purification, passed through an Elgastat demineralizer.

Only reagents of analytical-reagent quality were used. In the preparation of mixed solvents, volume changes on mixing were disregarded. For example, 0.50*M* HBr–0.10*M* Tu in 80% acetone was prepared by mixing 100 ml of aqueous 2.50*M* HBr–0.50*M* Tu solution with 400 ml of acetone. Stock solutions each containing 0.050 mole of a given element per litre, were prepared from the pure (>99.9%) metals or salts. Thallium(I), silver, mercury(II) and lead were used as analytical quality salts. The metals were dissolved by heating with a suitable combination of hydrochloric acid and nitric acid (for Pd, Pt, Au, Cu, Te, Bi), or by heating with these acids in a Teflon(PTFE)-lined pressure bomb at temperatures up to 290° (for Rh, Ir, Os, Ru). The stock solutions contained hydrochloric acid (1.0*M* concentration), and in most cases small amounts of nitric acid ($\leq 0.15M$), except for the thallium, silver and lead solutions, which contained only nitric acid (0.01*M*).

Apparatus

Borosilicate glass tubes of 20 mm internal diameter, and about 400 mm length, were used as columns. They were each fitted with a fused-in No. 2 porosity sintered-glass plate and a burette tap at the bottom, and a B19 ground-glass joint at the top to receive a separating funnel of 500 ml capacity which acted as a reservoir for eluting agents. The columns were filled with a slurry of AG50W-X4 resin (200–400 mesh, H^+-form) until the settled resin bed reached a mark indicating a volume of 43 ml (10 g of dry resin).

Most analytical determinations were done by atomic-absorption spectrometry with a Varian Techtron AA-5 instrument. Standards were made up with solution matrices closely matching those for the samples. Copper nitrate was used as a releasing agent (plus bromine to destroy thiourea) for the determination of some elements (Rh, Ir, Os, Ru). A nitrous oxide–acetylene flame was used whenever possible, to minimize interferences from unsuspected contaminants.

Some elements (Hg, Te) were determined by well-known spectrophotometric techniques,[4] with measurements made with a Zeiss PMQ II spectrophotometer.

Table 1. Distribution coefficients in 0.50*M* HBr–0.10*M* thiourea at various acetone concentrations

Element	Acetone, % v/v 0	40	60	80	90
Bi(III)	27.1	3.3	2.0	—	—
Pt(II)	—	—	—	107	39.5
Pd(II)	—	—	—	79.0	26.1
Te(II)	899	94.3	36.9	8.7	3.8
Hg(II)	1040	18.0	<1	—	—
Pb(II)	18.0	4.3	2.8	—	—
Au(I)	925	79.3	32.4	17.9	9.3
Cu(I)	354	13.7	4.7	—	—
Ag(I)	151	8.9	4.9	—	—
Tl(I)*	21.2	ppt	—	—	—
Ru(III)	211	352	614	457	253
Rh(III)	18.8	31.2	25.4	16.0	14.0
Ir(III)	2.6	2.9	3.5	3.4	4.3
Os(III)	4	5	6	4	5

*0.05 mmole.

Distribution coefficients

The resin (AG50W-X4, 100–200 mesh, H^+-form) was dried at 80° in a ventilated drying oven, and stored in a desiccator over anhydrous silica gel. Residual moisture was determined by drying at 110°. The weight of the resin was corrected accordingly.

Distribution coefficients, *D*, were determined by mixing 2.500 g of dry resin with 250 ml of solution containing 0.50 mmole of the element of interest, and equilibrating for 24 hr (mechanical shaker) in a room thermostatically controlled at 20 + 2°. Before transfer to the equilibration mixture, each aliquot of stock solution (except in the case of Tl^+, Ag^+ and Pb^{2+}) was evaporated to a moist residue on a steam-bath, and again after addition of about 10 ml of concentrated hydrobromic acid; this was done to ensure that at the start the elements were present mainly as bromide complexes. The salts resulting from this procedure were dissolved in the correct amount of hydrobromic acid for transfer.

After equilibration, the resin and solution were separated by filtration, and the element examined was determined in both fractions. Distribution coefficients were calculated with the usual equation:[5]

$$D = \frac{\text{(amount of element sorbed, g)} \times \text{(amount of solution, ml)}}{\text{(amount of element not sorbed, g)} \times \text{(amount of dry resin, g)}} \quad (1)$$

Some distribution coefficients were determined by the column (elution) method, and the equation:[5]

$$D = \frac{V_{max} - V_0}{m_r} \quad (2)$$

where V_{max} is the volume (ml) of eluent at peak maximum, m_r the weight (g) of dry resin in the column, and V_0 the dead space in the column (assumed to be 15 ml for a 10-g column).

A basic set of results is presented in Table 1. Some additional data are shown in Fig. 1, or mentioned in the discussion.

Elution curves

A mixture of 0.05 mmole of each element in 50 ml of aqueous 0.50*M* HCl–0.50*M* Tu was sorbed on the column, with rinsing four times with a total volume of 50 ml of 0.50*M* HCl–0.10*M* Tu, followed by elution with the agents described below.

Elution of Ag(I), Cu(I) and Hg(II) (Fig. 2). (*a*) 950 ml of 0.10*M* HBr–0.10*M* Tu in 60% acetone to elute Ag(I) and Cu(I); (*b*) 250 ml of 0.20*M* HBr–0.01*M* Tu in 60% acetone to elute Hg(II).

Elution of Te(II) and Au(I) (Fig. 3). 950 ml of 0.10*M* HBr–0.01*M* Tu in 90% acetone.

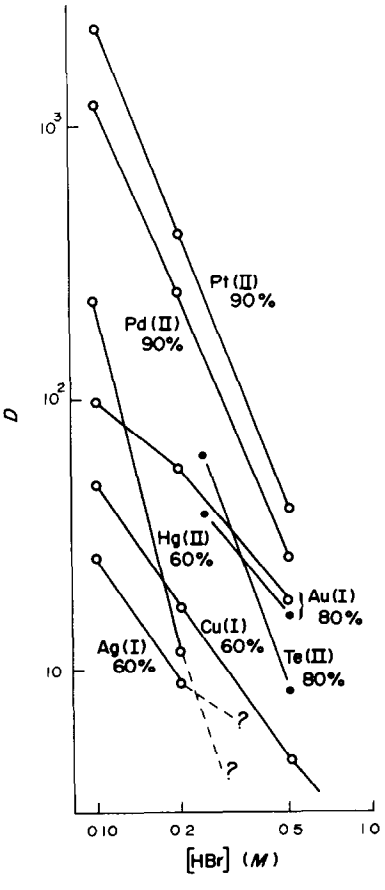

Fig. 1. Logarithmic plots of the distribution coefficients of some elements as a function of HBr concentration at 0.10*M* thiourea and various acetone concentrations. Open circles refer to the batch equilibration method, closed circles to the column (elution) method. Percentages refer to acetone concentration.

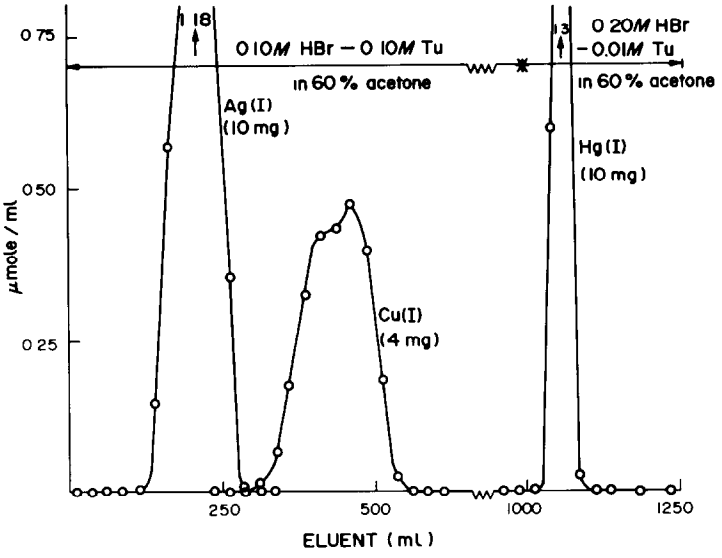

Fig. 2. Elution curve for Ag(I), Cu(I) and Hg(II). Column: 10 g (43 ml) of AG50W-X4, 200–400 mesh, H^+-form; internal diameter = 2.0 cm. Flow-rate 3.0 ± 0.3 ml/min.

Elution of Au(I) and Pd(II) (*Fig. 4*). 950 ml of 0.25*M* HBr–0.01*M* Tu in 90% acetone (Pd[II] only partially eluted).

Elution of Pd(II) and Pt(II) (*Fig. 5*). 500 ml of 0.50*M* HBr in 90% acetone. The resin was subsequently ashed, the ash dissolved after fusion with a mixture of potassium pyrosulphate ($K_2S_2O_7$) and sodium chloride, and tested for µg-amounts of palladium and platinum (with negative results).

Stepwise elution of Rh(III), Ag(I), Au(I) and Pt(II) (*Fig. 6*). A solution of 0.05 mmole of each element in 50 ml of 0.50*M* hydrochloric acid was cooled to about 5° in an ice-bath. Solid thiourea (1.9 g) was added with thorough stirring, and the solution immediately transferred onto the column together with any undissolved thiourea. The solution was allowed to pass through the column without delay. Fractions were collected from the beginning of this step ("sorption"). Rinsing was done with cold (5°) 0.5*M* HCl–0.10*M* Tu (50 ml). This was followed by (*a*) 250 ml of cold (5°) 0.5*M* HCl–0.10*M* Tu, which was allowed to approach room temperature as elution proceeded, and (*b*) 200 ml of 0.5*M* HCl–0.01*M* Tu. The sequence up to this point served to elute Rh(III) as quantitatively as possible. Ag(I) was then eluted with 500 ml of 0.10*M* HBr–0.01*M* Tu in 60% acetone, Au(I) with 500 ml of 0.25*M* HBr–0.01*M* Tu in 90% acetone, and Pt(II) with 400 ml of 0.87*M* HBr–0.01*M* Tu in 90% acetone. Subsequent elution with 250 ml of 2.0*M* HCl–2% Br_2 recovered a small residue, consisting only of gold (*ca.* 20 µg). The resin was finally ashed, and tested (after fusion with $K_2S_2O_7$–NaCl) for µg-amounts of Rh, Ag, Au and Pt (with negative results).

Eluting agents used solely for the determination of *D*-values are specified in Fig. 1 or in the discussion. The flow-rate was kept at 3.0 ± 0.3 ml/min. Evaporation of acetone was minimized by inverting a small beaker over the mouth of the separating funnel. The column was allowed to drain completely after each addition of solution. Care was

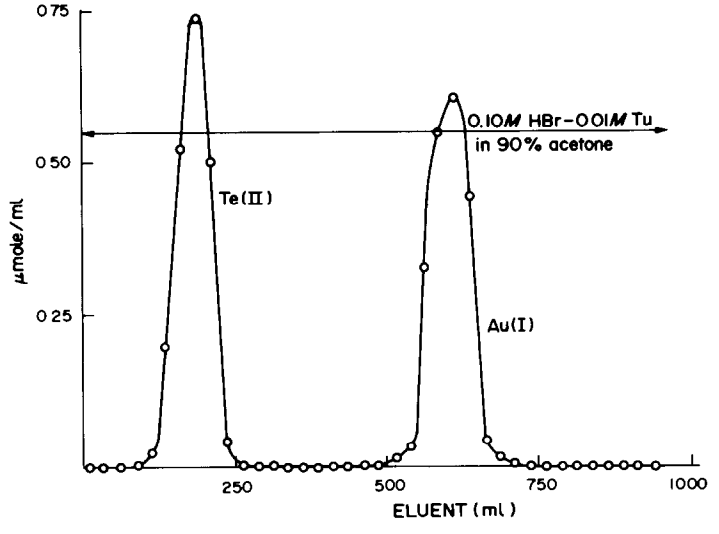

Fig. 3. Elution curve for Te(II) and Au(I). Column and flow-rate as for Fig. 2.

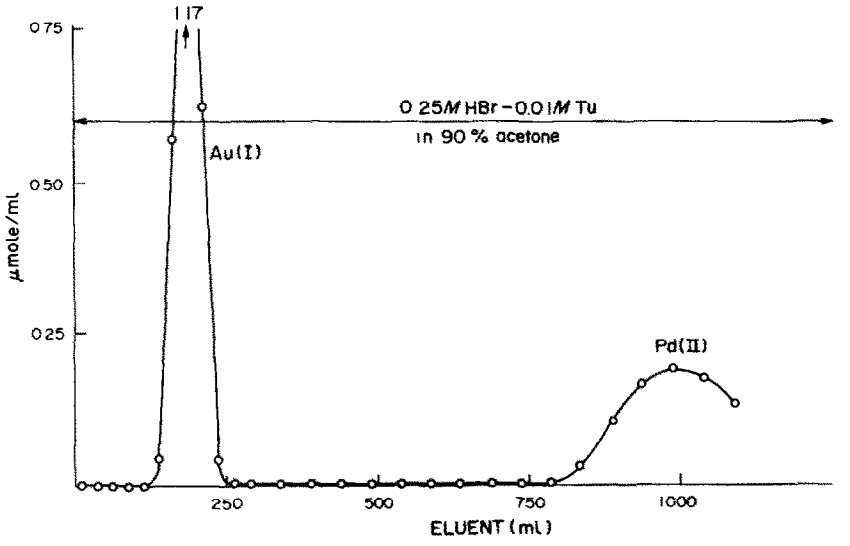

Fig. 4. Elution curve for Au(I) and Pd(II). Column and flow-rate as for Fig. 2.

taken to minimize disturbance of the resin bed surface. Fractions (25 ml) were collected automatically, and each was analysed for each element present. The experimental elution curves are shown in Figs. 2–6.

DISCUSSION

In the stock solutions, the elements were present in their most common oxidation states, as evidenced by their colour or history. When thiourea was added, some of the elements were reduced, *viz.* Cu(II)→Cu(I), Au(III)→Au(I), Pt(IV)→Pt(II), Ir(IV)→Ir(III), Os(IV, VI)→Os(III), and Te(IV)→Te(II), and these oxidation states stabilized by complexation.

The distribution coefficients obtained for Rh(III), Ir(III), Os(III) and Ru(III) were not equilibrium values. This could be verified, at least for Rh(III), Os(III) and Ru(III), because they form characteristic deeply coloured complexes with thiourea. After the resin had been separated, a slow build-up of the deeply coloured complexes in the separated solutions could be observed. The coloured complexes were rapidly sorbed when a little extra resin was added. The process of separating the resin, allowing the colour to develop, and adding more resin could be repeated many times before all the metal ions were sorbed. The kinetic ligand-exchange behaviour of Ir(III) could be assumed to be similar.[1] By elution experiments with 0.5–0.9*M* HBr–0.10*M* Tu in 90% acetone it was established that the thiourea complexes of Pd(II), Pt(II), Ir(III), Rh(III), Ru(III) and Os(III) were retained very strongly, and eluted in that order.

Effect of acetone concentration

The results in Table 1 show that the distribution coefficients decreased sharply as the acetone concentration was increased, except for the four elements discussed above.

Effect of HBr concentration

Hg(II), Cu(I), Ag(I), Au(I), Te(II), Pd(II) and Pt(II) showed substantially enhanced sorption in acetone-free solutions, and were studied in detail. Figure 1 shows logarithmic plots of the distribution coefficients as a function of hydrobromic acid concentration at fixed acetone and Tu (0.10*M*) concentrations. It demonstrates that the distribution coefficients for the bivalent metals decrease much more sharply with an increase in hydrobromic acid

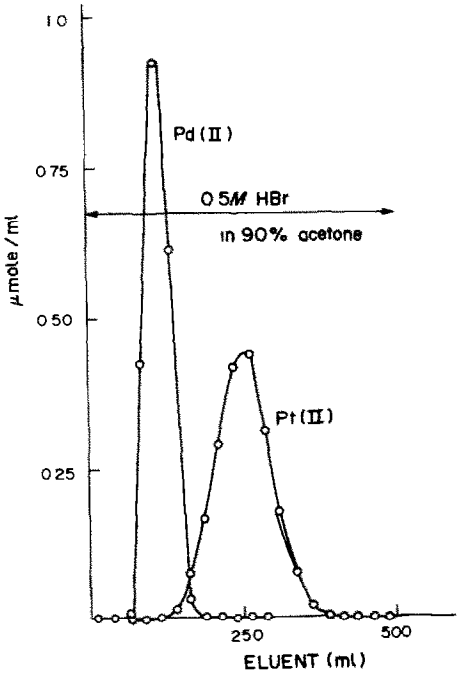

Fig. 5. Elution curve for Pd(II) and Pt(II). Column and flow-rate as for Fig. 2.

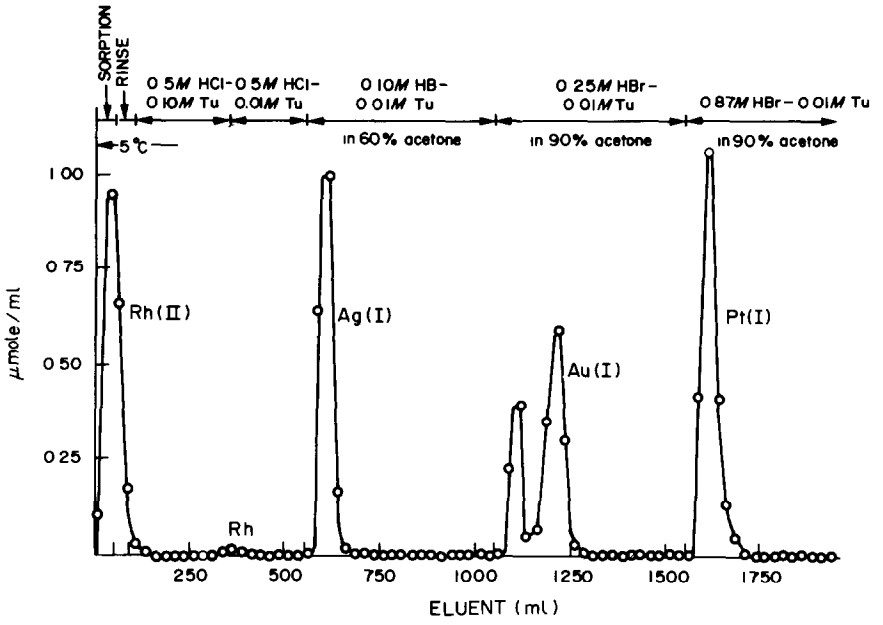

Fig. 6. Elution of Rh(III), Ag(I), Au(I) and Pt(II). Column and flow-rate as for Fig. 2.

concentration than those for the univalent ones. A slope of about −2.5 seems to be typical for the former and one between about −1.0 and −1.5 for the latter. At any fixed hydrobromic acid, Tu and acetone concentration the D-values for the univalent and bivalent metals increase in the order $Ag(I) < Cu(I) \ll Au(I)$, and $Hg(II) \ll Te(II) \ll Pd(II) < Pt(II)$ respectively. Since the distance between two curves in Fig. 1 may be taken as a direct measure of the separability of the respective elements, the figure shows that good separations should be possible between Cu(I) (or Ag[I]) and Au(I), Hg(II) and Te(II), and Te(II) and Pd(II) (or Pt[II]), over a wide range of eluent compositions. The only condition is that the D-value of the element to be eluted first must be approximately 10 to ensure (*a*) its elution with a reasonably small volume of eluent, and (*b*) adequate retention of the element to be eluted next.[5] In principle, it seems to be possible to find a hydrobromic acid concentration at any given acetone concentration (or *vice versa*) which will satisfy this condition for any of the pairs of elements mentioned above. The choice is limited only by the fact that concentrated mixtures of hydrobromic acid, Tu and acetone tend to decompose.

Figure 1 also illustrates that—in general terms—separation factors between univalent, M(I), and bivalent metals, M(II), decrease with increasing hydrobromic acid concentration [$D_{M(II)} > D_{M(I)}$], and then increase again with a reversal in selectivity [$D_{M(II)} < D_{M(I)}$]. A good separation of Cu(I) (or Ag[I]) from the most critical bivalent metal, Hg(II), was obtained with 0.10*M* HBr-0.10*M*Tu in 60% acetone [$D_{M(II)} < D_{M(I)}$; Fig. 2]. It should be possible to separate Au(I) from Hg(II) with rapid elution of the latter [$D_{M(II)} < D_{M(I)}$] with *e.g.*, 0.20*M* HBr–0.10*M* Tu in 60% acetone as eluent.

Effect of thiourea concentration

Further work showed that the D-values for Te(II) (and Hg[II]) decreased much more sharply as the Tu concentration was decreased than did those for Au(I) (or Ag[I] or Cu[I]). This fact was utilized to elute Te(II) well ahead of Au(I) with 0.10*M* HBr–0.01*M* Tu in 90% acetone (Fig. 3).

The D-values for Au(I) decreased slightly more sharply with a decrease in Tu concentration than did those for Pd(II). This made possible the separation of Au(I) from Pd(II) with a reasonably rapid elution of Au(I) (Fig. 4).

The Ag(I)–Cu(I) and Pd(II)–Pt(II) pairs showed only small differences in behaviour. Good separations of these pairs would require the use of impracticably large columns and elution volumes. The best separations that could be obtained with 10-g columns are illustrated in Figs. 2 and 5. The elution curve in Fig. 5 was obtained with a thiourea-free eluting agent, and illustrates the extraordinary stability of the Pt(II) and Pd(II) Tu complexes with respect to substitution by bromide ions. Their distribution coefficients were found to decrease only slightly when the Tu concentration was varied between 0.10 and 0.01*M* Tu at HBr concentrations between 0.10 and 0.50*M* and from 80 to 90% acetone.

The data presented here and in our previous paper indicate a variety of possible separations by stepwise elution which should be particularly useful in the analysis of certain sulphide-bearing ores. For example, it should be possible to elute Bi, Cu(I), Hg(II),

Te(II), Au(I) and Pt(II) in that order, with appropriate amounts of 1.0*M* HCl–0.10*M* Tu (Bi), 0.10*M* HBr-0.10*M* Tu in 60% acetone (Cu[I]), 0.20*M* HBr–0.01*M* Tu in 60% acetone (Hg[II]), 0.10*M* HBr–0.10*M* Tu in 90% acetone (Te[II]), 0.25*M* HBr–0.01*M* Tu in 90% acetone (Au[I]), and 0.80*M* HBr in 90% acetone (Pt[II]). Another possibility is illustrated in Fig. 6. Development with thiourea and initial elution were done at low temperature in order to suppress the formation of cationic Rh(III)–Tu complexes.[1] Some incipient reaction of Tu with one of a variety of possible Rh(III)–chloride–aquo complexes which may be present in the stock solution is probably responsible for the sorption of a small amount of Rh(III) which is eluted, after the main fraction, with 0.50*M* HCl–0.01*M* Tu. For accurate work, a correction may have to be applied for a small amount of Au(I) which is not eluted with the main Au(I)-fraction. Since similar amounts of gold tend to remain on the column during elution with thiourea-free solutions,[6] it is suspected that this small amount is sorbed as a relatively kinetically inert (aquo-?) complex.

Small amounts of iridium can be eluted together with Rh(III). Larger amounts ($\geqslant$2 mg) rapidly give an insoluble precipitate with Pt(II) or Pd(II). This leads to incomplete recoveries not only of Ir(III), but also of Pt(II) and Pd(II), which are lost in amounts related to the amount of iridium present. In the absence of Pt(II) and Pd(II), Ir(III) (10 mg) was found to accompany Rh(III) quantitatively.

The double peak for gold in the main Au(I)-fraction was found to be associated with elements co-sorbed as thiourea complexes, *e.g.* Ag(I), Pd(II) and Pt(II). The amount of gold appearing in the second peak seemed to be roughly proportional to the amount of the other element(s) present. When no sorbable thiourea complexes other than those of gold were present in the sample solution, all the gold appeared at the position of the first peak. Further evidence suggested that the gold appearing in the second peak must have remained closer to the top of the column during the elution of Ag(I) than that appearing in the first peak. The presence of the additional complexes may have caused a localized decrease in the free bromide concentration at the top of the column. As a consequence, stronger retention of part of the gold could have occurred.

Ruthenium(III) and osmium(III) are best separated before the sorption step. They tend to be eluted as two major fractions, accompanying Rh(III) and Pt(II) respectively. Traces appear in the intermediate fractions. Some Ru(III) tends to be sorbed almost irreversibly, possibly as a cationic aquo-complex, unless treated with concentrated hydrobromic acid (or hydrochloric acid) shortly before the addition of thiourea.

Because of limited solubility some elements can be tolerated in amounts not much in excess of 0.05 mmole each. We have, however, been able to demonstrate that a mixture containing 0.05 mmole of each of Rh(III), Ag(I) and Au(I), together with 0.50 mmole each of Pt(II) and Pd(II) can be separated by the elution sequence shown in Fig. 6. Pd(II) accompanies Pt(II) apparently quantitatively. Rapid transfer of the (cold) sample solution (100 ml) to the column ensures that Pt(II), which tends to precipitate as $[PtTu_4]Cl_2$,[1] does so only on the column. Here it dissolves during the elution sequence, and seems to cause no further complications. Large amounts (100 mg) of Cu(I) or Ag(I) are found to be soluble in the sorption medium, but form a precipitate within the column during elution with 0.10*M* HBr–0.01*M* Tu in 60% acetone. This results in poor recoveries of Cu(I) or Ag(I), and appreciable amounts of these elements appear in the subsequent elution steps.

REFERENCES

1. C. H.-S. W Weinert, F. W. E. Strelow and R G. Böhmer, *Talanta*, 1983, **30**, 413.
2. F. von S. Toerien and M. Levin, *J. S. Afr. Chem. Inst.*, 1974, **27**, 91.
3. F. von S. Toerien and M. Levin, Unpublished work.
4. O. G. Koch and G. A. Koch-Dedic, *Handbuch der Spurenanalyse*, 2nd Ed., Springer-Verlag, Berlin, 1974.
5. F. W. E. Strelow, *Anal. Chem.*, 1960, **32**, 1185
6. *Idem*, Private communication.

Talanta, Vol. 30, No. 10, pp. 761–765, 1983
Printed in Great Britain.

0039-9140/83 $3.00 + 0.00

DETERMINATION OF MICRO AMOUNTS OF OXYGEN IN SILICON BY INERT-GAS FUSION

HE HUANNAN, LI YUEZHEN, ZHAO GUANDI, YAN RONGHUA, LU QINGREN and QI MINGWEI
Shanghai Institute of Metallurgy, Academy of Sciences of China, Shanghai, China

(*Received* 14 *January* 1983. *Accepted* 15 *April* 1983)

Summary—A chromatographic inert-gas fusion method using an Ni–Sn fusion bath and helium as carrier gas has been developed for determining micro amounts of oxygen in silicon. With the Ni–Sn bath, the oxygen determination can be done at lower temperatures (1650–1700°) in a heated graphite crucible than in an empty crucible (with no molten metal bath) in which the sample is directly in contact with the carbon. Four samples can be analysed in succession in a single crucible with a relatively short time for oxygen extraction (5 min). Careful control of experimental conditions, and the use of a water-cooled quartz tube and a small unshielded graphite crucible have resulted in a lower blank (0.1 μg of oxygen), and better reproducibility, enabling oxygen in silicon to be determined down to 1 ppm. A calibration curve for determining oxygen in single crystals of silicon by measuring the infrared absorption at 9 μm has been constructed and gives results agreeing with those obtained by α-particle activation analysis.

The development of large-scale integrated circuits has created an increasing demand for single-crystal silicon of ever higher purity. The physical parameters which have in the past been used as a measure of purity are now not sufficient to guarantee the quality of single-crystal silicon. Oxygen is one of the most important impurities which can affect the electrical performance and reliability of silicon devices.

For the inert-gas fusion determination of oxygen in silicon, baths of molten platinum,[1] iron,[2] copper,[3] and tin[3] have been used, or the molten-metal bath can be omitted,[4] but a nickel–tin bath does not appear to have been used before for this determination. It offers some advantages, however: according to the phase diagram, the melting points of all Si–Ni alloys are lower than that of pure nickel, the solubility of carbon in nickel is moderate, and tin lowers the viscosity of the bath and prevents the absorption of gases. We have investigated the Ni–Sn bath technique for the determination of oxygen in silicon and compared it with the other metal-bath techniques: the results demonstrate that it is reliable.

A calibration curve for determining interstitial oxygen in single-crystal silicon by measuring the infared absorption at 9 μm at room temperature has been constructed by use of the helium carrier inert-gas fusion/gas chromatographic method. Careful control of experimental conditions and improvements in the preparation of specimens have resulted in a lower blank for inert-gas fusion analysis and in better reproducibility. The calibration curve obtained (the calibration constant is 6.2×10^{-4} atom%/cm^{-1}) is better than those in the published literature.[5–8]

EXPERIMENTAL

Specimen preparation

Specimens were prepared as $0.7 \times 0.7 \times 0.5$ cm dice cut from single-crystal silicon ⟨111⟩ of N type and P type (CZ, FZ) and weighing approximately 0.57 g. The six faces were polished with Syton (colloidal silica) and then the pieces were cleaned by sequential immersion in basic and acidic hydrogen peroxide before the inert-gas fusion analysis. According to Henderson,[5] an oxide film 13–15 Å thick is left after such cleaning. In construction of the calibration curve of absorption at 9 μm *vs.* oxygen content determined by inert-gas fusion, the oxygen content in the surface film was deducted. As the surface area of each of our specimens was 2.38 cm^2, the average volume of the oxide film should have been 3.3×10^{-7} cm^3 and the total oxygen 3.9×10^{-7} g (assuming an SiO_2 density of 2.2 g/cm^3), so the oxygen content in the oxide film (average thickness 14 Å) corresponded to 1.2×10^{-4} atom% oxygen for each die (0.57 g).

Specimens used for activation analysis were slices 1.8 cm in diameter and 0.2 cm thick, with both sides polished with Syton. For each slice, four infrared absorption readings at different spots were taken and the results averaged.

Inert-gas fusion apparatus

A schematic diagram of the inert-gas fusion and gas chromatographic system is shown in Fig. 1. It consists of the gas-extraction, collection, and measurement units. The furnace is a 30-kW induction unit, operating at a frequency of 300–500 kHz. The furnace assembly is shown in Fig. 2. The unshielded graphite crucible (50 mm long, bore 11 mm, wall thickness 3.5 mm) is placed in the transparent water-cooled quartz tube (volume about 250 ml, including the sampling arm).

The helium is purified by passage through columns of molecular sieves 13X and 5A at −196°.

The gases liberated from the specimen are transferred from the extraction system by a stream of purified helium (at 250 ml/min) and trapped at −196° in a concentration column consisting of a silica tube 20 cm long and 4 mm in diameter packed with molecular sieve 5A (10–20 mesh). The concentration of carbon monoxide in the gases is measured

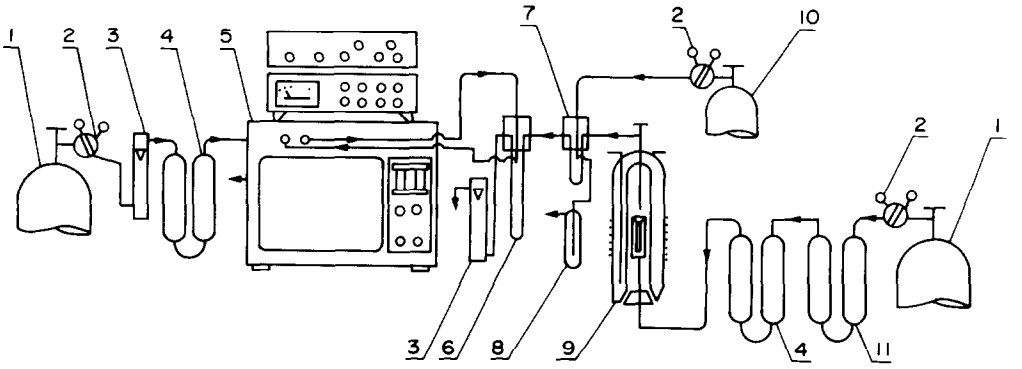

Fig. 1. Helium carrier-gas fusion gas chromatographic apparatus. 1, He tank; 2, gas regulator; 3, gas flowmeter; 4, 5A molecular sieve (−196°C); 5, gas chromatograph; 6, concentration column; 7, standard gas sampling valve; 8, bubbler; 9, high-frequency reaction furnace; 10, CO standard gas tank; 11, 13X molecular sieve.

by gas chromatography with a 2 m × 4 mm chromatographic column packed with molecular sieve 13X (20–30 mesh) and maintained at 75°. The helium flow-rate is 50 ml/min. The recorder sensitivity is 1.0 mV for full scale deflection. The bridge current of the gas-chromatograph katharometer is 195 mA. The sensitivity of the gas chromatographic method is 1.5×10^{-2} μg of oxygen per mm of peak-height.

A standard CO gas mixture (1% CO in helium) and standard samples of low carbon steel are used for calibration of the apparatus.

Procedure

The graphite crucible is thoroughly outgassed in a stream of purified helium at approximately 2100°. The blank at the operating temperature can in this way be reduced to less than 0.1 μg of oxygen. Before the first sample is analysed, 4 g of nickel and 0.6 g of tin are added to the crucible to prepare a molten metal bath. The bath is outgassed at 1750° for 10 min, then the temperature is lowered to approximately 1700° (operating temperature controlled at 1690 ± 30°) while samples are being analysed. The gas liberated is analysed after a collection time of 5 min. Before each new sample is analysed, a further 2 g of nickel and 0.3 g of tin are added to the crucible. Four samples are analysed in succession in a single crucible, the blank being checked before and after each sample. All the oxygen of the silicon sample is converted into carbon monoxide by reaction with carbon dissolved in the bath. At the same time as the sample is dropped into the crucible, the helium line from the furnace is connected to the concentration column at −196° for 5 min, at the end of which the valve is turned to connect the chromatograph to the column. At the same instant the Dewar vessel containing liquid nitrogen is lowered and boiling water applied to the trap so that the flow of helium from the carrier supply carries the carbon monoxide into the molecular sieve 13X column in the chromatograph. The amount of carbon monoxide is estimated from the chromatogram and the oxygen content of the specimen is then calculated.

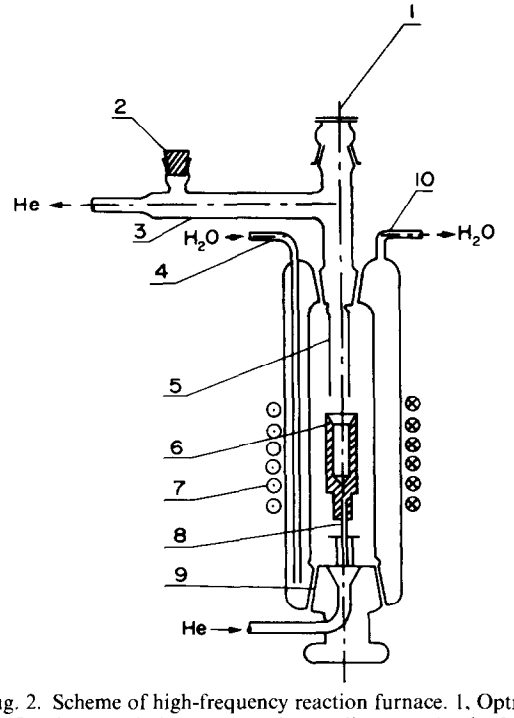

Fig. 2. Scheme of high-frequency reaction furnace. 1, Optical flat; 2, ground-glass stopper; 3, sampling arm; 4, inlet for cooling water; 5, sampling tube; 6, graphite crucible; 7, high-frequency induction coil, 8, tungsten rod; 9, ground-silica stopper; 10, outlet for cooling water.

Infrared spectrophotometry and α-particle activation-analysis

Each specimen is examined by infrared spectrophotometry on a Perkin–Elmer 577 instrument and the absorption coefficient at 9 μm determined by the differential absorption method in order to eliminate lattice-band interference. The area exposed is a circle 5 mm in diameter, and the full width at the half maximum of the oxygen-in-silicon band (ΔH) is 32–35 cm^{-1}. Five readings are taken and averaged for each die. The absorption coefficients are also corrected for multiple surface reflection.

To minimize effects arising from inhomogeneity in the oxygen distribution, the specimens are prepared as 0.7 × 0.7 × 0.5 cm dice so that they just fill the exposure area (diameter 0.5 cm) of the spectrophotometer. Each sample is analysed first by the infrared method and then by the inert-gas fusion method, so that the infrared absorption coefficient can be correlated exactly with the oxygen content.

A beam of 31.2-MeV α-particles is used for irradiation in the activation analysis. Both surfaces of the irradiated slice are deeply etched in order to eliminate surface contamination. Determination of the oxygen content is based on the nuclear reaction $^{16}O(\alpha,pn)^{18}F$.[12] After the nuclear reaction, two 3 × 3-in. NaI(Tl) crystals and a γ–γ coincidence-counting unit are used for measuring the ^{18}F activity. The detection limit of this method is 0.07×10^{-4} atom% oxygen content.

RESULTS AND DISCUSSION

Blank of the inert-gas fusion method

The detection limit of the reduction fusion method depends on the blank for the gas analysis system. In this method, as a water-cooled quartz tube and a small graphite crucible were used, the amount of graphite was minimized and it was not necessary to use graphite powder for insulation. Under these conditions, after the graphite crucible had been outgassed sufficiently at approximately 2100°, the blank for the gas analysis system remained at a value lower than 0.1 μg of oxygen, one order of magnitude smaller than those reported in the literature.[8,9] The quality of the graphite crucible is very important and it is preferable to use crucibles made from graphite of high purity, compactness and density. The purity of the helium is also of utmost importance. To minimize the blank from the furnace system it is necessary to connect the helium purification unit to the water-cooled furnace with stainless-steel or copper tubing. Plastic or rubber tubing is not suitable at all because of its high permeability to gases.

If the outgassing temperature of the graphite crucible is lower than 2000° or if the outgassing time is not sufficient, the residual oxides in the crucible wall will be reduced to carbon monoxide, thus increasing the blank and giving high results. However, the outgassing temperature should not be too high either—if heated above 2200°, the graphite will be extensively vaporized and the vapour will condense on the cooler part of the silica tube to form an active sublimate which will absorb a certain amount of the carbon monoxide from the specimen. In this case, the result of the analysis will be low.

Comparison of the Ni–Sn bath with other baths

Results obtained from different baths are listed in Table 1. The dimensions of all the specimens were 0.7 × 0.7 × 0.5 cm.

It can be seen from Table 1 that the Ni–Sn bath gives more reproducible results and more nearly complete recovery of oxygen in silicon. As a fresh bath was prepared for each successive sample, the fluidity of the bath was maintained, and the reaction was both rapid and quantitative. The preliminary experiments demonstrated that the results obtained with the Ni–Sn bath were in agreement with those for the Pt–Sn bath (1800°). Because of the high cost of platinum the Ni–Sn bath is preferred.

Table 2. Parallel analysis by inert-gas fusion and infrared spectrophotometry

Date	Absorption coefficient, cm^{-1}	Oxygen content, 10^{-4} atom%
7.3.80	2.44	15.3
7.3.80	2.47	14.8
3.5.80	2.49	15.8
23.5.80	2.50	15.0
15.4.81	2.46	14.8
18.4.81	2.41	14.6
18.4.81	2.45	14.6

Results of inert-gas fusion and infrared spectrophotometry

On different days, 7 samples were measured by the infrared absorption method and by the inert-gas fusion method. The results are shown in Table 2.

The reproducibility is good, as shown in Table 2. In the Ni–Sn bath technique, the temperature of analysis is low, but the viscosity of the bath is also low, so the gases are released easily. In the empty crucible method (with no molten-metal bath), during the consecutive additions of single-crystal silicon samples, silicon carbide forms continuously, the viscosity of the bath increases and complete extraction of the carbon monoxide formed in the reduction process becomes more difficult. In order to obtain a stable operating temperature, it is necessary to keep the position of the graphite crucible constant relative to the induction coil. When the temperature is controlled in the range 1690 ± 30°, this can be done more reproducibly than at higher temperatures.

Infrared spectrophotometry for oxygen determination in single-crystal silicon, as calibrated by inert-gas fusion analysis

The infrared absorption, α-particle activation and reduction fusion methods are the three main possibilities for measuring the oxygen content of single-crystal silicon, and of these the 9-μm infrared absorption method is the quickest, most convenient and cheapest, and is also non-destructive. However, the absorption coefficient is only a relative value and the reduction fusion method or the activation method must be used for calibration. Owing to the inherent

Table 1. Comparison of results obtained with an Ni–Sn bath and other baths

Analysis No.	Oxygen content of single-crystal Si A, 10^{-4} atom%				
	With no molten metal bath		Cu bath	Pt bath	Ni–Sn bath
	1900°	1700°	1500°	1800°	1700°
1	15.7	15.8	21.5	17.8	22.4
2	16.4	20.2	12.3	17.4	20.2
3	6.2	12.8	13.0	13.4	22.0
4	7.6	—	—	12.1	22.2

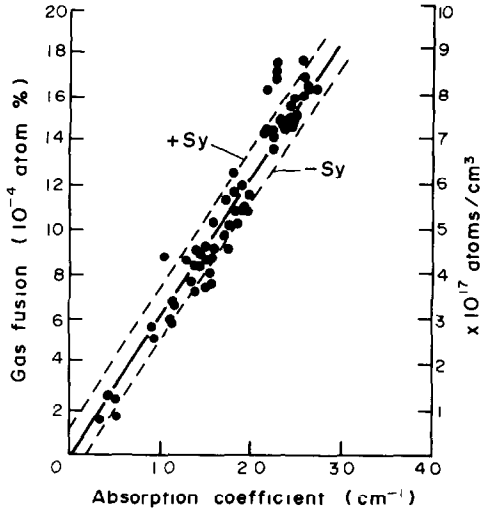

Fig. 3. The calibration curve for gas fusion results *vs.* infrared absorption coefficient (300 K).

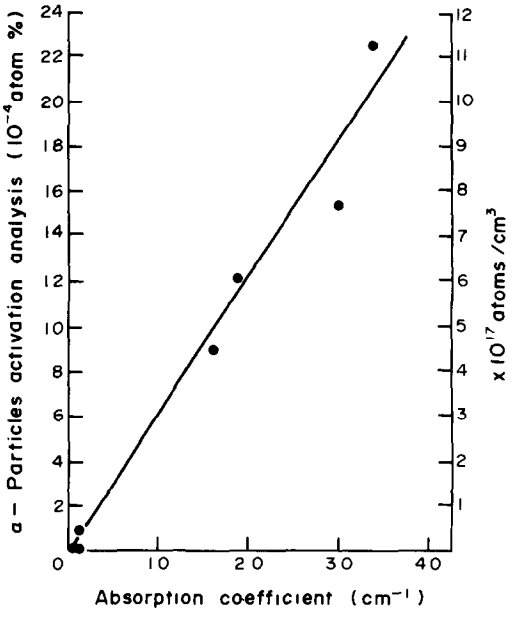

Fig. 4. The relationship between activation analysis and infrared absorption coefficient (300 K).

difficulties of these reference methods for calibration, there are several different calibration curves in the literature. The range of calibration coefficient values is 4.9–9.63 × 10^{-4} atom%/cm^{-1}.[6-9] Since 1971, in the ASTM Standard Test Method, Baker's data[8] have been adopted. In 1977, a standard method (DIN) has been proposed in West Germany on the basis of Graff's data.[9] Because of these differences, we have attempted to establish a more accurate calibration curve.

Sixty-seven pairs of data points from gas fusion analysis and infrared spectrophotometry were fitted to the regression line $y = a + bx$, where $a = -1.15$, $b = 6.7 \times 10^{-4}$ atom%/cm^{-1}, with correlation coefficient $r = 0.965$. If the intercept is made zero, we have $y = b'x$. The calculated value of $b' = 6.2 \times 10^{-4}$ atom%/cm^{-1} (calibration constant). The calibration curve is shown in Fig. 3. The standard deviation of the residuals is $s_y = 1.2 \times 10^{-4}$ atom%.

Seven pairs of data points from activation analysis and infrared spectrophotometry were treated in the same way and yielded $a = -0.16$, $b = 6.2_3 \times 10^{-4}$ atom%/cm^{-1}, $r = 0.988$, $b' = 6.1_7 \times 10^{-4}$ atom %/cm^{-1}, $s_y = 1.5 \times 10^{-4}$ atom%. The calibration curve is shown in Fig. 4.

As the blank for inert-gas fusion analysis can be lowered to less than 0.1 μg of oxygen, the lower limit of oxygen content which can be determined is somewhere below 2 × 10^{-4} atom%. Earlier values were not so low.[6-9]

Owing to the improvements in specimen preparation and the fact that the infrared absorption coefficients of the dice were measured individually, there was no influence of inhomogeneous distribution of oxygen content. In addition, because of the higher precision of the inert-gas fusion analysis, the correlation coefficient for our calibration curve (0.972) was better than that of Baker's.[8]

The standard deviation of the residuals can be used as the criterion for the accuracy of the y value: it is 1.2 × 10^{-4} atom% in our experiment and about 9.5 × 10^{-4} atom% in Baker's (calculated from his data).

The calibration constants obtained by Baker,[8] Graff[9] and in our work are shown in Table 3. The calibration graphs shown in Figs. 3 and 4 are more accurate than those of Baker and Graff and the agreement between the two calibration curves obtained in this work is better than for others in the literature.[8,9]

Table 3. Comparison of the calibration constants (10^{-4} atom%/cm^{-1}) for the two methods

Reference	Calibration constant: Gas fusion analysis	Calibration constant: Infrared absorption coefficient	Calibration constant: Activation analysis	Calibration constant: Infrared absorption coefficient
Baker[8]	9.63 ± 2.29		8.1	
Graff[9]	4.9 ± 0.2		5.9	
This paper	6.2 ± 0.1		6.2 ± 0.4	

According to our calibration graph (300 K), the calibration equation is

$$N_0 = 3.1 \times 10^{17}\,\alpha \text{ atoms/cm}^3$$

or

$$N_0 = 6.2 \times 10^{-4}\,\alpha \text{ atoms\%}$$

where α is the infrared absorption coefficient.

Acknowledgements—The authors thank Professor Wu Tzu-liang and Professor Wang Houchi (Shanghai Institute of Metallurgy, Academy of Sciences of China) for their guidance and Zhang Jiading and Hua Zhifen (Shanghai Nuclear Institute, Academy of Sciences of China) for their assistance in performing the activation analysis.

REFERENCES

1. A. Colombo, *Anal. Chim. Acta*, 1976, **81**, 397.
2. P. D. Donovan, J. L. Evans and G. H. Bush, *Analyst*, 1963, **88**, 771.
3. J. J. Engelsman, A. Meyer and J. Visser, *Talanta*, 1966, **13**, 409.
4. G. G. Devyatykh, V. V. Balabanov, N. V. Larin and Yu. V. Revin, *Zh. Analit. Khim.*, 1973, **28**, 2254.
5. R. C. Henderson, *J. Electrochem. Soc.*, 1972, **119**, 775.
6. W. Kaiser, P. H. Keck and C. F. Lange, *Phys. Rev.*, 1956, **101**, 1264.
7. W. Kaiser and P. H. Keck, *J. Appl. Phys.*, 1957, **28**, 882.
8. J. A. Baker, *Solid-State Electronics*, 1970, **13**, 1431.
9. K. Graff, E. Grallath, S. Ades, G. Goldbach and G. Tölg, *ibid.*, 1973, **16**, 887.
10. *Annual Book of ASTM Standards*, Part 43, F 121-71, 1971.
11. W. R. Thurbor, *NBS Technical Note*, 529, 1970.
12. *The Determination of Trace Amount of Oxygen in Silicon by Proton and α-Particles Activation Analysis*, Shanghai Nuclear Institute, Academy of Sciences of China, April, 1978.

Talanta, Vol. 30, No 10, pp 767–770, 1983
Printed in Great Britain.

0039-9140/83 $3 00 + 0 00

GAS-CHROMATOGRAPHIC DETERMINATION OF THE PRODUCT DISTRIBUTION IN THE SYNTHESIS OF SODIUM BOROHYDRIDE

TAPIO SALMI
Laboratory of Industrial Chemistry, Department of Chemical Engineering, Åbo Akademi, 20500 Turku 50, Finland

(*Received* 1 *March* 1983. *Accepted* 15 *April* 1983)

Summary—A gas-chromatographic method has been developed for determination of the sodium borohydride and methanol content of alkaline aqueous solutions of $NaBH_4$. From the ratio between $NaBH_4$ and CH_3OH the product distribution in $NaBH_4$ synthesis from NaH and $B(OCH_3)_3$ in mineral oil can be calculated and the amount of the by-product $NaBH(OCH_3)_3$ formed can be estimated. A separation and extraction procedure for the mineral oil dispersion must precede the gas-chromatographic analysis. Sodium borohydride is determined by measurement of the 2-propanol formed after treatment of the solution with acetone, whereas methanol can be determined directly by gas chromatography, with 1-propanol as internal standard. The analysis of the synthesis products is thus the separation and detection of simple alcohols.

Sodium borohydride is extensively used in the pulp and textile industries as a storable raw material for production of the bleaching chemical, dithionite, which is easily obtained from alkaline $NaBH_4$ solutions and sulphur dioxide. The commercial synthesis method most used for the production of sodium borohydride is the reaction between sodium hydride and trimethyl borate:[1,2]

$$4NaH_{(s)} + B(OCH_3)_{3(l)} \rightarrow NaBH_{4(s)} + 3NaOCH_{3(s)} \quad (1)$$

Reaction (1) is performed at temperatures >250° in a high-boiling inert mineral oil, in which the NaH is dispersed and $B(OCH_3)_3$ is added as a liquid. The reactions can be done industrially in continuous reactors.[2] Sodium borohydride is often used as an alkaline solution, which is stable for several years.[3] An alkaline solution is easily obtained from the mineral oil dispersions by treatment with water:

$$NaBH_4 + 3NaOCH_3 + H_2O \rightarrow NaBH_{4(aq)} + 3CH_3OH + 3NaOH_{(aq)} \quad (2)$$

When reaction (1) is performed at temperatures lower than 250°, $NaBH_4$ is not the only reaction product; methoxy-containing borohydrides begin to appear as by-products.[4] The best known of these compounds is sodium trimethoxyborohydride, $NaBH(OCH_3)_3$, which also can be synthesized selectively from NaH and $B(OCH_3)_3$ at lower temperatures (>60°):[4]

$$NaH_{(s)} + B(OCH_3)_{3(l)} \rightarrow NaBH(OCH_3)_{3(s)} \quad (3)$$

The methoxy-containing by-products will be destroyed during the water treatment of mineral oil dispersions:

$$NaBH(OCH_3)_3 + 2H_2O \rightarrow NaBO_{2(aq)} + 3CH_3OH + H_2 \quad (4)$$

In studying the synthesis of $NaBH_4$ over a broad temperature range, it is of great interest to determine both the degree of conversion of sodium hydride and the product distribution between $NaBH_4$ and $NaBH(OCH_3)_3$. Although several analytical methods for the determination of $NaBH_4$ are reported in the literature[1,4–7] little attention has been paid to the distribution of the synthesis products. As far as we know, the only method reported for the determination of the reaction products is a gas volumetric procedure, where the hydride content is measured as the volume of hydrogen liberated when borohydrides are treated with an acidic water solution and the boron content is measured by titration with sodium hydroxide in the presence of mannitol.[1,4,8] It is quite clear that this method is tedious and impractical, particularly when water solutions of borohydride are the final goal of the synthesis. The solid compounds must first be separated from the dispersion by washing with a suitable hydrocarbon solvent, *e.g.*, hexane, and then the borohydrides must be extracted with a selective solvent, *e.g.*, isopropylamine. In the work with aqueous solutions of $NaBH_4$ there is thus a need for a more straightforward analytical procedure.

THEORY

From reactions (2) and (4) it can be seen that the ratio between methanol and $NaBH_4$ gives information about the amount of by-product formed, so analysis for both the $NaBH_4$ and the methanol content of the aqueous solutions is desirable.

The reducing properties of $NaBH_4$ are used in an indirect spectrophotometric method proposed by Lichtenstein and Mras.[7] Acetone reacts with $NaBH_4$

to give 2-propanol according to the reaction

$$4(CH_3)_2CO + BH_4^- + 3H_2O \rightarrow 4(CH_3)_2CHOH + H_2BO_3^- \quad (5)$$

Lichtenstein and Mras base their method on a spectrophotometric measurement of acetone. The absorbance of the solution is compared with that of a standard solution with the same initial concentration of acetone. The difference ΔA between the absorbance values yields the borohydride concentration:

$$c_{NaBH_4} = \frac{\Delta A}{4\varepsilon l} \quad (6)$$

where ε is the molar absorptivity of acetone and l is the path-length of the cell. The sodium borohydride content of the solution can, however, also be related to the 2-propanol formed according to reaction (5). After addition of acetone the $NaBH_4$ and CH_3OH contents of the solution can be determined by gas chromatography. The $NaBH_4$ concentration is simply given by

$$c_{NaBH_4} = \frac{c_{(CH_3)_2CHOH}}{4} \quad (7)$$

If it is further assumed that the only by-product is trimethoxyborohydride, the methanol comes from two sources and the stoichiometric equations (2) and (4) give the expression

$$n_{CH_3OH} = 3n_{NaBH_4} + 3n_{NaBH(OCH_3)_3} \quad (8)$$

which also can be written as

$$n_{NaBH(OCH_3)_3} = \left(\frac{n_{CH_3OH}}{3n_{NaBH_4}} - 1\right) n_{NaBH_4} \quad (8')$$

where n is the number of moles of compound indicated by subscript.

From (8′) it can easily be seen that a ratio $n_{CH_3OH}/n_{NaBH_4} > 3$ indicates that some by-product is formed. The yields of $NaBH_4$ and $NaBH(OCH_3)_3$ can then be calculated:

$$\phi_{NaBH_4} = \frac{n_{NaBH_4}}{n_{0,B(OCH_3)_3}} = \frac{4n_{NaBH_4}}{n_{0,NaH}} \quad (9)$$

$$\phi_{NaBH(OCH_3)_3} = \phi_{NaBH_4}\left(\frac{n_{CH_3OH}}{3n_{NaBH_4}} - 1\right) \quad (10)$$

where n_0 is the initial number of moles of compound used. It should be mentioned that equation (9) assumes that stoichiometric quantities of sodium hydride and trimethyl borate were used in the synthesis.

EXPERIMENTAL

Apparatus

A Varian 1400 gas chromatograph with FI-detector and a capillary column was used. The stationary phase was SE-30 (0.3 μm film thickness). The column temperature was 30° and the detector temperature 150°.

Chemicals

The acetone, 1-propanol, 2-propanol and methanol used were of analytical grade. They were used without further purification, with the exception of the acetone, which was dried over anhydrous sodium sulphate and then fractionally distilled. $NaBH_4$ was synthesized from NaH and $B(OCH_3)_3$ of synthesis quality (>98% purity). The methods used for synthesizing NaH and $NaBH_4$ are described elsewhere.[9,10]

Procedures

A 4–5 g sample of oil dispersion, corresponding to a theoretical amount of approximately 0.004 mole of $NaBH_4$, is placed in a separatory-funnel, 10–15 ml of hexane are added and the dispersion is stirred for 5 min. The sample is then centrifuged for 20 min at 700 rpm, whereby complete sedimentation of the solid particles is achieved. The liquid phase containing mineral oil, hexane and possibly small amounts of unreacted trimethyl borate is sucked away. This washing procedure with hexane is repeated 2 or 3 times After the last centrifugation and removal of hexane phase, 10 ml of an aqueous sodium hydroxide solution (pH = 12.3) are added. The solid phase dissolves in the aqueous phase according to equations (2) and (4). Some liberation of hydrogen is observed, from the hydrolysis of NaH and methoxyborohydrides. The samples are so small that no appreciable temperature increase is observed. When the degree of conversion of NaH is very low, however, the reaction can become hazardous because of hydrogen evolution.

Because the mineral oil is washed away, the hexane and water phases are easily separated and no centrifugation is necessary. The aqueous phase is transferred from the separatory-funnel to a 50-ml standard flask. The separatory-funnel is further shaken with three 10-ml portions of sodium hydroxide solution (pH = 12.3) and the aqueous phases are added to the 50-ml flask. After this procedure it may be assumed that all the $NaBH_4$ and CH_3OH from the original product dispersion is quantitatively collected in the flask. Then 2–3 ml of acetone are added, which corresponds to 100% excess. After 30 min the reaction between borohydride and acetone is complete[7] and the solution can be diluted with distilled water to 50 ml. Then 2.00 ml of the resulting solution and 5.00 ml of a standard 1-propanol solution containing 8.40 g/l, are added to a 50-ml standard flask and diluted to volume with distilled water. The solution is now ready for a gas-chromatographic analysis, with injection of a 2–3 μl sample. The separation and analysis procedure is illustrated in Fig. 1. A typical chromatogram is presented in Fig. 2.

The 2-propanol and methanol contents of the solution are calculated by integrating the peak areas in the chromatogram and taking into account the calibration factors according to the formula

$$m_i/m_{st} = f_i(A_i/A_{st}) \quad (11)$$

where m_i and m_{st} are the weights of determinand in the sample and standard respectively, f_i is the calibration factor, and A_i and A_{st} are the corresponding peak areas.

The calibration factors of 2-propanol and methanol with respect to 1-propanol were determined by injection of standard solutions. Several solutions of known composition were prepared and the calibration factors were calculated according to equation (11) by linear regression. The calibration factor determined for methanol was 1.73 and for 2-propanol 1.15.

RESULTS AND DISCUSSION

The reaction between acetone and $NaBH_4$ was tested by Lichtenstein and Mras[7] and the comparison with several other analytical methods showed that results from the spectrophotometric determination agreed well with the results obtained by other tech-

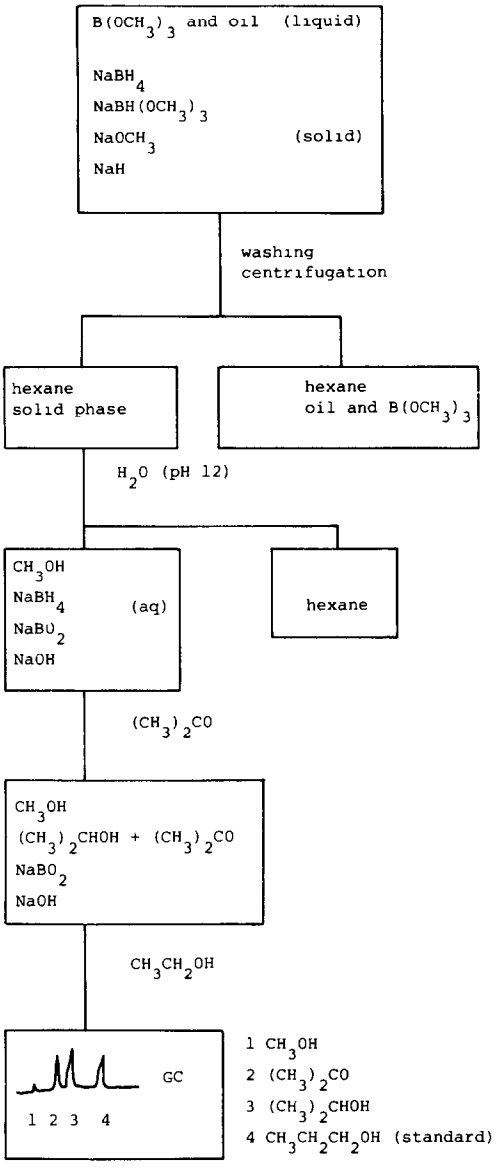

Fig. 1. Separation scheme for determination of $NaBH_4$ and by-products in a mineral oil dispersion.

niques. Therefore it was not necessary here to test the suitability of reaction (5) but only to compare the results from a spectrophotometric analysis with the results obtained from a gas-chromatographic one.

For this purpose a sample containing about 0.2 g of $NaBH_4$ of *purum* quality was dissolved in 20 ml of an aqueous sodium hydroxide solution (pH = 12.3) and 3.00 ml of purified acetone were added. After half an hour the solution was diluted accurately with distilled water to 50 ml. Then 2.00 ml of this solution were mixed with 5 ml of the standard solution ($c_{CH_3(CH_2)_2OH}$ = 8.40 g/l.) in a 50-ml standard flask and diluted to volume. A reference solution for the spectrophotometric analysis was prepared in the same way but without acetone. These solutions were then analysed both spectrophotometrically and gas-

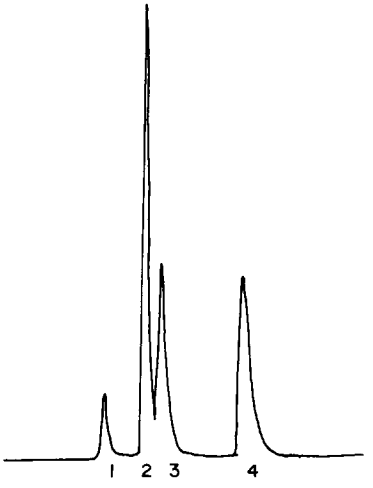

Fig. 2. Chromatogram for analysis of an $NaBH_4$ synthesis. 1 = CH_3OH; 2 = $(CH_3)_2CO$; 3 = $(CH_3)_2CHOH$; 4 = $CH_3(CH_2)_2OH$.

chromatographically. The photometric measurement was made at 265 nm, where the molar absorptivity of acetone is 17.63 l.mole^{-1}.cm^{-1}.[7] The results from the gas chromatographic determination can be found in Table 1. Six GC determinations of $NaBH_4$ gave 0.2164 g $NaBH_4$ as the mean, whereas the photometric determinations gave 0.2147 g. This indicates that the two methods give comparable results. The possibility of determining the acetone content of the solution has not been studied, because it is more natural to calculate the borohydride content of the solution directly from the 2-propanol formed. Chromatograms obtained from the sample solution and the reference solution used in the spectrophotometric analysis can be seen in Fig. 3. In analysis of the synthesis products a fourth peak appears in the chromatogram, namely a methanol peak (Fig. 2).

The proposed separation and analysis procedure is simpler and less time-consuming than the procedures used previously,[1,4,8] especially when it is essential to study the synthesis products. In particular, the gas-chromatographic method is preferred to the spectrophotometric one if the synthesis of $NaBH_4$ has been done in a mineral oil, because some colloidal impurities will contaminate the aqueous phase during the water extraction of the product dispersion.

Table 1. Determination of $NaBH_4$ by GC

Sample	A/A_{st}	m_{NaBH_4}, g
1	1.1477	0.2195
2	1.1522	0.2204
3	1.1439	0.2188
4	1.1058	0.2115
5	1.1422	0.2184
6	1.0972	0.2098
		$\bar{m}$ = 0.2164

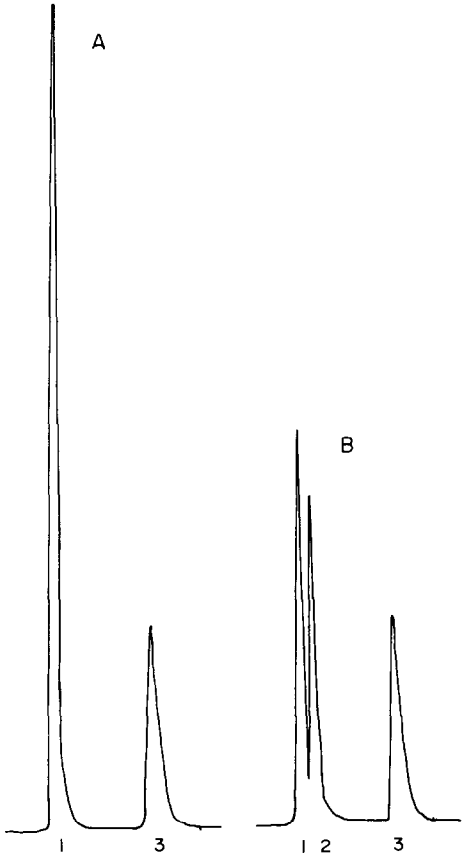

Fig. 3 Chromatograms from reference (A) and sample (B) solutions, 1 = $(CH_3)_2CO$; 2 = $(CH_3)_2CHOH$; 3 = $CH_3(CH_2)_2OH$.

The proposed method could further be tested, for example, by analysing only for $NaBH(OCH_3)_3$. No 2-propanol should be formed, because methoxy-containing borohydrides are unstable in aqueous solution. A more suitable stationary phase for separation of alcohols (*e.g.* Carbowax) could be used; ethanol could then be used as the internal standard, instead of 1-propanol, but it is not suitable with the SE 30 used in the present work, because of low resolution.

Acknowledgements—The author is indebted to Professor L. Hummelstedt and Assistant Professor L.-E. Lindfors for many valuable discussions during this investigation.

REFERENCES

1. H. J. Schlesinger, H. C. Brown and A. E. Finholt, *J. Am. Chem. Soc.*, 1953, **75**, 205.
2. W. S. Fedor, M. D. Banus and D. P. Ingalls, *Ind. Eng. Chem.*, 1957, **49**, 1664.
3. M. M. Kreevoy and R. W. Jacobson, *Ventron Alembic*, 1979, **15**, 2.
4. H. C. Brown, H. J. Schlesinger, I. Scheft and D. M. Ritter, *J. Am. Chem. Soc.*, 1953, **75**, 192.
5. C. Harzdorf, *Z. Anal. Chem.*, 1966, **210**, 12.
6 A. R. Shah, D. K. Padma and A. R. V. Murthy, *Analyst*, 1972, **97**, 17.
7. I. E. Lichtenstein and J. A. Mras, *J. Franklin Inst.*, 1966, **281**, 481.
8. V. I. Mikheeva, I. N. Dymova, A. A. Vysheslavtsev and N. G. Eliseeva, *Russ. J. Inorg. Chem.*, 1967, **12**, 1062.
9. B. Sjoberg, *M.Sc. Thesis*, Åbo Akademi, 1980
10. T. Salmi, *M.Sc. Thesis*, Åbo Akademi, 1980.

Talanta, Vol 30, No 10, pp 771–775, 1983
Printed in Great Britain

0039-9140/83 $3.00 + 0.00
Pergamon Press Ltd

CATALYTIC THERMOMETRIC TITRATIONS

TIBOR F. A. KISS
Institute of Pharmaceutical Chemistry, University of Münster, D-4400 Münster, G.F.R.

(*Received* 7 *August* 1980. *Revised* 14 *January* 1983. *Accepted* 15 *April* 1983)

Summary—A review is given of the principles, instrumentation and applications of catalytic thermometric titrations.

Homogeneous catalysed reactions were first applied as identification reactions in qualitative analysis[1–3] and for acceleration of titration reactions in quantitative analysis.[4–8] Later, these reactions were used for the determination of numerous substances[9–13] by means of the rate of reaction, which is directly proportional to the catalyst concentration to be measured.

In the last decade they have been employed for indication of the end-point in titrimetric analysis.[12,14,15] In a direct titration the determinand must be an inhibitor of the catalysed reaction (the indicator reaction) to be used for end-point detection and a high concentration of the indicator reagents is added to the inhibitor, which is then titrated with a standard solution of the catalyst. Before the end-point, the inhibitor reduces the catalyst concentration (and hence its activity) practically to zero by precipitation, complex formation or neutralization. At the end-point the first excess of the catalyst immediately accelerates the catalytic reaction. In a very short time a large amount of the indicator-reagent mixture reacts and the resultant concentration changes can be detected by visual,[16–19] photometric,[14,20–28] potentiometric,[23,28,29] biamperometric[14,19] or thermometric means,[19,30–32] thus indicating the end-point. Here we review thermometric detection with exothermic indicator reactions, and the related catalytic thermometric titrations.

METHODS

The methods can be classified according to the type of titration or type of reaction, etc.

Type of titration

Direct titration is done as described above. *Reverse titration* is done similarly but in this case it is the catalyst that is to be determined, and a known volume of standard inhibitor solution (plus indicator reagents) is titrated with the sample solution containing the catalyst. In *back-titration* the catalyst is determined by addition of a standard solution of inhibitor in excess to the sample, followed by addition of the indicator reagents and back-titration of the surplus inhibitor with a standard solution of the catalyst. In a *displacement titration*[18] the determinand is titrated with a suitable standard solution (or *vice versa*) in the presence of the indicator reagents. The catalyst is added to the sample solution before the titration and must be "blocked" by formation of a sufficiently stable compound with a inhibitor. It must also be capable of release from this compound by displacement caused by a small excess of titrant, so that it starts the indicator reaction.

Instead of titration of the inhibitor with the catalyst, as in all the methods above, the catalyst can be titrated with the inhibitor.[23] In this case one component of the indicator-reaction system is added to the inhibitor solution and the other to the catalyst solution. The end-point is indicated by cessation of the indicator reaction (which takes place only until the catalyst has been removed by reaction with the inhibitor).

Enzyme-catalysed reactions[24] are also used as indicator reactions for determination of metal ions that can activate or inhibit the enzyme. In this method a very low concentration ($10^{-4}M$) of an activator or an inhibitor or a mixture of both is titrated with EDTA. The titration is very tedious, however, as the reaction rate of the indicator system has to be determined spectrophotometrically after each addition of titrant.

Type of reaction

Catalytic thermometric titrations can be classified as acid–base, complexometric, and precipitation, the principles of which are well known. The inhibition of the catalyst could also be achieved by oxidation or reduction, but such methods have not yet been developed, because the indicator reactions are mostly redox reactions themselves, which could cause interference in the determination reaction. The titrations can be done in aqueous or non-aqueous media, according to the system used.

End-point location

The *reaction rate* can be measured accurately.[20–22] A series of solutions is prepared, each having the same concentration of inhibitor to be determined, and the same concentration of indicator–reagent

mixture. To each solution a known volume of standard catalyst solution is added, increasing from zero to ~100% excess. The indicator-reaction rate is determined photometrically for each solution. The slopes of the graphs of log absorbance *vs.* time are plotted against the concentration of catalyst. Before the end-point the slopes (tan α) are constant and practically zero, but increase linearly with catalyst concentration after it. The end-point is given by the intersection of the extrapolated straight lines. So far only photometric measurement of the rate has been used, but thermometric measurement could also be used.

The *temperature can be monitored during the titration.*[12,14] This is a simplified form of the method just mentioned. The titrand is added at constant rate from a motor-driven syringe burette to the vigorously stirred sample solution and the temperature-volume curve is registered with a chart-recorder. The end-point is again the intersection of two extrapolated straight lines.

In *comparative titration*[33] two identical indicator reagent mixtures of high concentration are prepared and brought to the same temperature. The sample solution containing the catalyst to be determined is added to one, and the other is titrated with a standard solution of the catalyst until the reaction rates of both solutions (as shown by the rates of temperature change) are the same.

In the *simultaneous indication method*[34,35] a series of sample solutions is prepared, each containing the same (but unknown) concentration of the inhibitor and the same concentration of one component of the indicator-reaction mixture. To each solution is added a known volume of standard catalyst solution, increasing from zero to 100% excess. Then to each is added the same quantity of the second component of the indicator reaction. The time t needed for the indicator reaction to proceed to the same preselected extent for each sample solution is measured. Then $1/t$ is proportional to the concentration of the catalyst, and the end-point is given by the intersection of the two straight lines in a plot of $1/t$ *vs.* volume. Colour indicator-reactions have been used so far, with visual observation, but thermometry could be used for exothermic indicator-reaction.

For the *indicator reaction* numerous homogeneous catalysed redox reactions and one enzyme-catalysed reaction[24] have been used, of pseudo-zero, first, second or higher order. Exchange reactions of unidentate and multidentate ligand complexes, heterogeneous, micro-heterogeneous and most enzyme-catalysed reactions have not yet been applied, although they are very sensitive and specific.

The determinations can be done on all scales from macro down to ultramicro. A very small excess of catalyst causes consumption of a large amount of the indicator reagent mixture in a very short time, so the end-point is remarkably sensitive and very easily seen even in ultramicro determinations.

THEORY

Although the theory of thermometric titrations is well established,[36-38] that of the catalytic thermometric methods also involves the kinetics and mechanisms of the reactions and these have so far been incompletely investigated. For example, Mottola[12,14] and Goizman[39] have described mathematically the temperature *vs.* volume curve for direct continuous catalytic thermometric titration with first or second order indicator reactions but the dependence of the kinetic constants on various factors and side-reactions has not been considered.

To sum up, the sensitivity and accuracy are proportional to the change in catalyst concentration at the end-point, the inhibition effect, the rate of the titration reaction, the difference between the constants of the catalysed and non-catalysed indicator reaction and the thermometric effect of the indicator reaction, and inversely proportional to the induction period of the catalysed reaction, the temperature effect of the titration reaction, and the rate of the non-catalysed indicator reaction. These effects depend on many different factors, including the solvents used and the influence of foreign substances. Catalytic action is usually rather specific, so few foreign ions interfere with the indicator reaction by catalysis. Naturally, foreign ions reacting with substances present in the titrand must be absent, or must be masked.[40,41]

Before the end-point, the heats of mixing of titrant and titrand, of stirring and of volatilization produce a linear increase in temperature. This effect can be diminished by decreasing the sensitivity of the recorder, but the temperature jump at the end-point will usually be sufficiently large and sharp for precise end-point indication.[41] Alternatively, the heat of mixing of the titrant can be compensated for by addition of a non-reacting species to give an equal and opposite heat of dilution.[42]

APPLICATIONS

Neutralization titrations in non-aqueous solution

Determination of acids.[30-32,43-45,52] The hydroxide-catalysed dimerization of acetone has been used as indicator reaction for the direct and continuous titration of acids, hydroxy-acids, phenols, phenolic acids, keto-enols, imides and aromatic nitro compounds with potassium hydroxide, in acetone medium. Various acids have similarly been determined by coulometric generation of the base at a platinum cathode in acetone or a mixture of acetone and diacetone alcohol as solvent.[47]

Determination of bases.[30-32,45-50] The proton-catalysed indicator reaction between acetic or propionic anhydride and water, various alcohols or hydroquinone, in acetic acid, acetic anhydride, propionic anhydride or nitromethane as solvent, has been used for titration of many bases (antipyrine,

brucine, cinchonine, flagyle, inversal, caffeine) and salts, with perchloric acid or coulometrically generated hydrogen ions.

The dehydration of formic acid and the acetic anhydride–hydroquinone indicator reaction—both catalysed by hydrogen ions—serve for titration of tertiary amines with internally generated hydrogen ions in formic acid or acetic anhydride medium.

The proton-catalysed polymerization of monomers such as methylstyrene and isobutyl vinyl ether has been used as indicator reaction, and the monomers as solvents, for the titration of amines, amides and some basic sulphur and phosphorus compounds, either with perchloric acid in acetic acid or with boron trifluoride etherate in dioxan. The polymerization of ethyl vinyl ether has been used for end-point detection in the iodine titration of hydrazines, organic bases and water.[52]

Precipitation titrations in aqueous solution[31,32,40,41,53–55]

The iodide-catalysed Ce(IV)–As(III) and Ce(IV)–Sb(III) indicator reactions have used for direct and reverse titration of Ag^+, Hg^{2+} and Pd^{2+} with I^- and for determination of several anions [Cl^-, Br^-, I^-, SCN^-, CN^-, $Fe(CN)_6^{4-}$, S^{2-}] by addition of excess of Ag^+, Hg^{2+} or Pd^{2+} and back-titration with I^-, and for the displacement titration of Ag^+, Hg^{2+}, Pd^{2+} and SCN^- with SCN^- in presence of AgI, HgI_2 or PdI_2 as the blocked form of the catalyst.

The same indicator reactions have also been used in titration with externally coulometrically generated I^-, both for direct titration of Ag^+ and Hg^{2+} and back-titration of excess of Ag^+ (in the determination of I^-, Br^- and SCN^-).

Complexometric titrations[19,24,40,55–57]

The decomposition of H_2O_2 (catalysed by Mn^{2+}, Cu^{2+} and Pb^{2+}), the reactions between H_2O_2 and resorcinol (catalysed by Mn^{2+}, Cu^{2+} and Fe^{3+}), hydroquinone (catalysed by Fe^{3+}, Cu^{2+}), dimethyl-*p*-phenylenediamine (catalysed by Cu^{2+} and Fe^{3+}), catechol (catalysed by Cu^{2+}) or hydrazine (catalysed by Cu^{2+}) have been used as indicator reactions for the direct titration of EDTA, DCTA and NTA, for reverse titrations of the catalysts with the chelating agents, for the determination of cations by back-titration of excess of chelating agent with catalyst cations, and for the displacement titration of EDTA and various cations in presence of Mn–EDTA as the blocked form of the catalyst.

The Co^{2+}-catalysed H_2O_2-tartaric acid indicator reaction has been used for the determination of Co^{2+} by the comparative titration procedure.

Complexometric titrations in non-aqueous solutions have some advantages over the corresponding titrations in aqueous medium, the end-point temperature break being bigger and sharper, mainly because of the increased chelate stability and catalytic activity. Typical examples are the use of the Mn^{2+}-catalysed decomposition of H_2O_2 in ethanolamine, dimethylsulphoxide (DMSO) or DMSO–formamide mixture, and the Mn^{2+}-catalysed reaction between H_2O_2 and resorcinol in DMSO as indicator reactions for the direct titration of EDTA, DCTA and NTA, the reverse titration of Mn^{2+} with these chelating agents, and the determination of several metals by back-titration of excess of DCTA or EDTA with Mn^{2+}.

The reactions available for masking interfering ions in non-aqueous (DMSO) solvents are the same as those for aqueous media, *e.g.*, Al^{3+} can be masked with triethanolamine in determination of alkaline-earth metals or with fluoride in titrations of Cu^{2+}, Ni^{2+} and Zn^{2+}. Cd^{2+}, Cu^{2+}, Ni^{2+}, Co^{2+}, Zn^{2+}, Cd^{2+} can be masked with cyanide in the determination of alkaline-earth metals.

INTRUMENTATION

The apparatus is similar to that used in thermometric titrations, and consists of the titration vessel, stirrer, means of adding the titrant, and means of locating the end-point.

The titration vessel

In titrations with a catalytic end-point, a high degree of adiabaticity of the titration system is unnecessary, so the titration vessels used can be simpler than those for non-catalytic thermometric titrations. If the heat of the indicator reaction is high, the titration can be performed in a simple beaker, or in a beaker fitted into a block of polystyrene or even filter paper. For precise work a Dewar vessel can be used. The titration vessel has a lid with apertures to admit the thermistor, the inlet tube for titrant, *etc.*

The stirrer

A local excess of titrant must be avoided, because it would initiate the irreversible indicator reaction and cause a premature end-point, so efficient stirring of the titration solution is required. Rotary-paddle, magnetic and vibratory stirrers are all used.

Addition of the titrant

For *incremental addition* of the titrant, any convenient burette (micro or semimicro, classical, piston or micrometer-syringe) can be used, with or without thermostatic control. As the rate of the indicator reaction and the change in temperature of the titrant are functions of time, the temperature is measured at a fixed interval, usually 1 min, after addition of an increment of titrant.

Continuous addition of the titrant eliminates the main disadvantage of incremental addition, its slowness. Macro, micro or ultramicro motor-driven micrometer-syringe burettes can be used.

Constant current *coulometric generation* of titrant can also be used. For example, in acetic or propionic anhydride medium hydrogen ions can be internally generated at a mercury (sodium perchlorate support-

ing electrolyte) and/or platinum (hydroquinone supporting electrolyte) anode.[31,47] Hydroxide ions can be generated at a platinum cathode,[47] with sodium perchlorate (in acetone or a mixture of acetone and diacetone alcohol) as supporting electrolyte. Iodide can be externally generated by cathodic polarization of a silver–silver iodide electrode and used as titrant for determination of Ag^+. Strychnine has been titrated with hydrogen ions externally generated with sodium perchlorate and hydroquinone as supporting electrolyte in acetic anhydride–acetic acid mixture.

End-point location

With *continuous addition* of titrant and use of a thermistor for temperature measurement, various Wheatstone bridge circuits have been used[43,46,53,57] for plotting the temperature–volume curve, either directly or as a first or second derivative curve.[31] The differential technique can be used to improve the sensitivity of detection of the end-point. In this the temperature is measured with two thermistors which have the same resistance but different response times, connected in opposition and immersed in the titrand. When the temperature changes, the response of one of the thermistors is slower than that of the other, and the difference in response is greatest when the temperature change is at its fastest, *i.e.*, at the end-point. The titration end-point can thus be determined very easily, especially with small quantities of substances.[31]

Automatic apparatus

The automation of thermometric or catalytic thermometric titration apparatus began with the continuous addition of titrant from a flow-burette and later with the use of the syringe-burette, and continued with the introduction of electrical temperature detection and recording of the titration curve. Full automation was achieved[58] by use of a digital timer and constant rate of titrant addition, together with use of a transistor circuit to convert the temperature change into a linearly decreasing voltage which was differentiated to give a square-wave voltage with amplitude proportional to the rate of temperature change, and period equal to the duration of the change. This signal was amplified and fed to the end-point detector. Stern *et al.*[59] amplified the out-of-balance potential from the Wheatstone bridge. The potential was then filtered, differentiated and applied to the control unit of a Sargent–Malmstadt automatic titrator, which amplified the signal and differentiated it twice; the abrupt signal-change at the end-point then triggered a relay system to stop the titration.

DISCUSSION

The advantages and disadvantages can conveniently be discussed with reference to other catalytic techniques and means of end-point detection.

Comparison with other catalytic end-point indicators

Thermometric monitoring of the indicator reaction has certain advantages over potentiometric, visual, photometric and biamperometric detection. Not all indicator reactions can be followed potentiometrically, since a suitable electrode with fast enough response time may not be available. Only colour-change, gas-producing and precipitate-forming indicator reactions can be monitored visually, and there may be interference from the presence of suspensions or coloured foreign substances. The biamperometric, conductometric and similar electrometric methods are also limited by numerous factors. In contrast, the thermometric method is generally applicable because all the indicator reactions have a large thermal effect which can be precisely measured with a thermistor and simple equipment. This detection method is usable for coloured suspensions and can be fully automated. Further, it is applicable on the macro, micro and ultramicro scale, and can be used in aqueous and non-aqueous media. The end-point break is often so sharp that no extrapolation is needed. Finally, it is possible to locate back-titration end-points that cannot be determined with other catalytic or non-catalytic methods. For example, when the back-titration product is more stable or insoluble (*e.g.*, AgI) than the compounds to be determined (*e.g.*, AgBr), the normal indicator methods will not work, because of the exchange reaction of excess of titrant with the product (in this case, of I^- with AgBr). The catalytic thermometric back-titrations can be realized, however, because at the end-point the first excess of the catalyst starts the indicator reaction—which is registered immediately by the thermistor—before the catalyst can react in the slow exchange (displacement) reaction. The rate of addition of the catalyst has to be optimized, of course: if it is too slow the displacement reaction can predominate; if it is too fast a premature end-point will be observed.

Comparison with non-catalytic end-point indication

When the concentration of the determinand decreases, the end-point jump also decreases when non-catalytic methods are used. In contrast, with catalytic end-point detection the first small excess of catalyst at the end-point causes reaction of a large amount of indicator-reagent mixture in a very short time. This high concentration change is easily detected because of the large accompanying physical effect. Hence catalytic titrations are generally more sensitive and accurate than those using non-catalytic end-point indication. The catalysed indicator reaction, and therefore the corresponding end-point indication, is generally more specific than the non-catalytic methods.

Comparison with direct catalytic determination

Continuous catalytic titration has the advantage

that it is not necessary to keep the experimental conditions constant, and the titration gives more precise results than the direct catalytic determination. It is also much faster, since no calibration graph is needed.

The main disadvantage is that the indicator reagent mixture has to be added in high concentration, so the products of the indication reaction will be produced in high concentration, and components of the indicator system may react with substances present in the titrand, *e.g.*, sulphide or ferrocyanide cannot be determined by back-titration of an excesss of Ag^+, or Pd^{2+} with iodide in presence of Ce(IV) + As(III) indicator-reagent mixture, because the Ce(IV) oxidizes these anions.

It is also necessary to add the titrant at constant and optimal rate, which is sometimes rather slow. This disadvantage can be overcome by adding most of the required volume of titrant to the sample *before* addition of the indicator reagent mixture, and then titrating the remainder of the determinand.

A further disadvantage is that the titration reaction must give a titrand concentration jump at the endpoint. Therefore, the concentrations that can be determined are not as low as is possible with the direct catalytic determinations.

REFERENCES

1. F. Feigl, *Tüpfelanalyse*, Vols. I and II, Akademischer Verlag, Frankfurt/Main, 1960.
2. H. Weisz, *Microanalysis by the Ring Oven Technique*. Pergamon Press, Oxford, 1961.
3. H. Weisz and T. F. A. Kiss, *Bull. Chem. Soc. Belgrade*, 1969, **34,** 419.
4. J. P. Phillips, *Automatic Titrations*. Academic Press, New York, 1959.
5. R. E. Cover and L. Meites, *J. Phys. Chem.*, 1963, **67,** 1528.
6. J. J. Lingane, *Electroanalytical Chemistry*. Interscience, New York, 1958.
7. P. W. Carr and L. Meites, *J. Electroanal. Chem.*, 1965, **12,** 373.
8. P. W. Carr and J. Jordan, *Anal. Chem.*, 1973, **45,** 634.
9. W. J. Blaedel and G. P. Hicks, in *Advances in Analytical Chemistry and Instrumentation*, Vol. 3, C. N. Reilley (ed.), p. 126. Interscience, New York, 1964.
10. K. B. Yatsimirskii, *Kinetic Methods of Analysis*. Pergamon Press, Oxford, 1966.
11. Z. Arkosi, *Thesis*. Juris-Verlag, Zürich, 1956.
12. H. A. Mottola, *MPI Appl. Notes*, 1971, **6,** No. 3,17.
13. H. B. Mark, Jr. and G. A. Rechnitz, *Kinetics in Analytical Chemistry*. Interscience, New York, 1968.
14. H. A. Mottola, *Talanta*, 1969, **16,** 1267.
15. E. Greenhow, *Chem. Rev.*, 1977, **77,** 835.
16. H. Weisz and V. Muschelknautz, *Z. Anal. Chem.*, 1966, **215,** 17.
17. H. Weisz and T. Janjić, *ibid.*, 1967, **227,** 1.
18. D. Klockow and L. García Beltrán, *ibid.*, 1970, **249,** 304.
19. H. Weisz and S. Pantel, *Anal. Chim. Acta*, 1972, **62,** 361.
20. K. B. Yatsimirskii and T. I. Fedorova, *Dokl. Akad. Nauk SSSR*, 1962, **143,** 143.
21. *Idem, Zh. Analit. Khim.*, 1963, **18,** 1300.
22. T. I. Fedorova and K. B. Yatsimirskii, *ibid.*, 1967, **22,** 283.
23. H. Weisz, S. Pantel and H. Ludwig, *Z. Anal. Chem.*, 1972, **262,** 269.
24. B. Kratochvil, S. L. Boyer and G. L. Hicks, *Anal. Chem.*, 1967, **39,** 45.
25. H. A. Mottola, M. S. Haro and H. Freiser, *ibid.*, 1968, **40,** 1263.
26. H. A. Mottola and H. Freiser, *ibid.*, 1968, **40,** 1266.
27. H. A. Mottola, *ibid.*, 1970, **42,** 630.
28. T. P. Hadjiioannou, E. A. Piperaki and D. S. Lapastathopoulos, *Anal. Chim. Acta*, 1974, **68,** 447.
29. H. Weisz and D. Klockow, *Z. Anal. Chem.*, 1967, **232,** 321.
30. V. Vajgand, F. Gaál, Lj. Zrnić, S. Brusin and D. Velimirović, *Proc. 3rd Anal. Chem. Conf. Budapest*, 1970, I. Buzás (ed.), Vol. II, p. 443. Akadémiai Kiadó, Budapest, 1970.
31. V. Vajgand and F. F. Gaál, *Proc. 2nd. Conf. Appl. Phys. Chem., Veszprém*, 1971, Vol. I, p. 683. Akadémiai Kiadó, Budapest, 1971.
32. V. J. Vajgand, F. F. Gaál, Lj. P. Zrnić-Zeremski and V. I. Sörös, *Proc. 3rd ICTA, Davos 1971*, H. G. Wiedemann (ed.), Vol. 2, p. 437. Birkhäuser, Basel, 1972.
33. I. Sajó, *Talanta*, 1968, **15,** 578.
34. J. Bognár, *Mikrochim. Acta*, 1963, 397, 801.
35. J. Bognár and Sz. Sárosi, *ibid.*, 1963, 1072; 1966, 534; 1969, 463.
36. H. J. V. Tyrrell and A. E. Beezer, *Thermometric Titrimetry*. Chapman & Hall, London, 1968.
37. L. S. Bark and S. M. Bark, *Thermometric Titrimetry*. Pergamon Press, Oxford, 1969.
38. G. A. Vaughan, *Thermometric and Enthalpimetric Titrimetry*. Van Nostrand Reinhold, London, 1973.
39. M. S. Goizman, *Zavodsk. Lab.*, 1971, **37,** 11, 64; *Dokl. Akad. Nauk SSSR*, 1969, **184,** 599.
40. T. Kiss, *Z. Anal. Chem.*, 1970, **252,** 12.
41. *Idem, Rev. Res. Fak. Sci. Novi Sad*, 1971, **1,** 139.
42. I. Sajó and B. Sipos, *Talanta*, 1967, **14,** 203.
43. G. A. Vaughan and J. J. Swithenbank, *Analyst*, 1965, **90,** 594; 1970, **95,** 890.
44. E. J. Greenhow and L. A. Dajer de Torrijos, *ibid.*, 1979, **104,** 801.
45. V. J. Vajgand and F. F. Gaál, *Bull. Chem. Soc. Belgrade*, 1966, **31,** 103.
46. *Idem, Talanta*, 1967, **14,** 345; 1968, **15,** 699.
47. V. J. Vajgand, F. F. Gaál and S. S. Brusin, *ibid.*,1970, **17,** 415.
48. V. J. Vajgand, F. F. Gaál and S. S. Brusin, *ibid.*, 1970, **17,** 415.
49. E. J. Greenhow and L. E. Spencer, *Analyst*, 1973, **98,** 81, 98.
50. E. J. Greenhow, *ibid.*, 1977, **102,** 584.
51. *Idem, Chem. Ind. (London)*, 1972, 466.
52. E. J. Greenhow and L. E. Spencer, *Analyst*, 1974, **99,** 82; 1973, **98,** 485.
53. H. Weisz, T. Kiss and D. Klockow, *Z. Anal. Chem.*, 1969, **247,** 248.
54. T. Kiss, *Proc. Euroanalysis I, Heidelberg 1972*, p. 55.
55. K. C. Burton and H. M. N. H. Irving, *Anal. Chim. Acta*, 1970, **52,** 441.
56. H. Weisz and T. Kiss, *Z. Anal. Chem.*, 1970, **249,** 302.
57. T. Kiss, *Mikrochim. Acta*, 1972, 420; 1973, 847.
58. P. T. Priestley, *Analyst*, 1963, **88,** 194.
59. M. J. Stern, R. Withnell and R. J. Raffa, *Anal. Chem.*, 1966, **38,** 1275.

Talanta, Vol. 30, No 10, pp 777–781, 1983
Printed in Great Britain.

0039-9140/83 $3.00 + 0.00

GRAPHICAL REPRESENTATION OF POLYNUCLEAR ACID–BASE AND COMPLEX EQUILIBRIA

G. RAMIS RAMOS, M. C. GARCIA ALVAREZ-COQUE and C. MONGAY FERNANDEZ
Departamento de Química Analítica, Facultad de Ciencias Químicas, Universidad de Valencia, Valencia, Spain

(*Received* 28 *October* 1982. *Revised* 21 *December* 1982. *Accepted* 22 *February* 1983)

Summary—A calculation procedure for diagrams of $\log C_M = f(pL)$ at various values of the ratio of analytical concentrations, C_L/C_M, in polynuclear binary systems is described. The diagrams are useful in the resolution of analytical problems of practical interest involving acid–base equilibria (such as the preparation of buffer solutions) and complex equilibria. The presence of a solid phase is also considered.

In a previous work,[1] a calculation procedure was developed for determination of the concentration of the species in equilibrium in binary systems involving the formation of polynuclear complexes. In that work, a numerical and a graphical method, based on the resolution of the system of simultaneous equations of the mass balances for the central ion and for the ligand (in analytical concentrations C_M and C_L), were proposed. The numerical method requires the resolution of the system by iterating simultaneously with respect to the two variables, *viz.* the free concentrations of central ion and ligand. On the other hand, in the graphical method, the two balances are drawn independently; each of the two equations is iterated with respect to a single variable.

In this work, a method for rapid representation of the diagram for $\log C_M = f(pL)$ at different concentration ratios $q = C_L/C_M$ is proposed. The mass balances are transformed so that only one of the equations requires iterative calculation with respect to a single variable. It is noteworthy that there is always a single diagram for each system, in contrast to the distribution and logarithmic concentration diagrams, which are different at different values of C_M in the presence of polynuclear species.

When only mononuclear species are present, it is not necessary to make use of iterative procedures to construct the diagrams, as some authors indicate for complex formation equilibria.[2,3]

It may be considered that the treatment of acid–base systems is more general than the treatment of complex-ion systems, since the former involves the additional equilibrium of dissociation of water. Also, polynuclear species are frequently found in acid–base equilibria (including the hydrolysis of metal ions). For these reasons, the present paper deals with acid–base systems. It is necessary only to omit the dissociation of water to make the treatment applicable to any complex equilibrium.

For simplicity, in this paper the diagrams are drawn by taking equilibrium constants at zero ionic strength, with the exception of the diagram for boric acid, which has been constructed for 0.5*M* ionic strength, in order to make experimental verification possible.

CALCULATION AND DIAGRAMS

In an aqueous solution, where a central ion, M, and a ligand, L, react to form mononuclear and polynuclear complexes, the concentration of the species M_jL_i is given by $\beta_{ij}m^j l^i$, where $m = [M]$ and $l = [L]$ and β_{ij} is the formation constant of M_jL_i at the working ionic strength.

In order to define the system completely, it is necessary to solve the mass-balance equations for M and for L. In acid–base equilibria, the balance for L includes the term K_w/l, which takes account of the hydrogen ions or hydroxide ions from the dissociation of water. When $l = [H^+]$, the total concentration of hydrogen ion will be $C_H + K_w/[H^+]$, where C_H is the concentration of strong acid dissolved; for a strong base with concentration C_{OH}, the proton concentration will be $[OH^-] - C_{OH} = K_w/[H^+] - C_{OH}$ (equivalent to $C_H + K_w/[H^+]$, if $C_H = -C_{OH}$). Similar expressions are obtained when $l = [OH^-]$. For other ligands the term K_w/l is omitted.

Thus, the general mass-balance equations are:

$$C_M = m + \sum j\beta_{ij}m^j l^i \tag{1}$$

$$C_L + \frac{K_w}{l} = l + \sum i\beta_{ij}m^j l^i \tag{2}$$

Mononuclear systems

When only mononuclear species are present, the curves for $\log C_M = f(pL)$ at various q values are given by:

$$C_M = \frac{\left(l - \frac{K_w}{l}\right)\left(1 + \sum \beta_i l^i\right)}{q + \sum (q - i)\beta_i l^i} \tag{3}$$

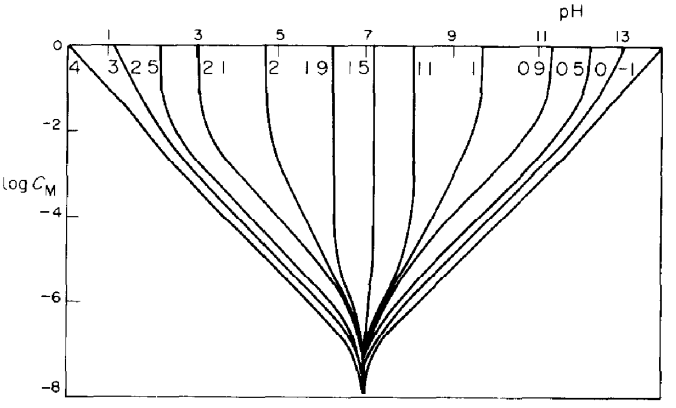

Fig. 1. Log $C_M = f(\text{pH})$ for phosphoric acid. The numbers on the lines are the q values. The cumulative protonation constants at 25°C and zero ionic strength are, $\log \beta_1 = 12.38$, $\log \beta_2 = 19.59$, $\log \beta_3 = 21.71$ and $pK_w = 14.00$.[4]

Figure 1 shows $\log C_M = f(\text{pH})$ for phosphoric acid. The values $q = 0$, 1, 2 and 3 represent solutions of PO_4^{3-}, HPO_4^{2-}, $H_2PO_4^-$ and H_3PO_4, respectively, and the values in the range $0 < q < 3$ correspond to various buffer solutions. The values $q > 3$ correspond to mixtures of H_3PO_4 with a strong acid, and negative values of q correspond to solutions of phosphate in excess of strong base.

On dilution ($C_M \to 0$), all the lines on the diagram converge to $\text{pH} = \frac{1}{2} pK_w$. When L is other than the proton or hydroxide, pL always increases with dilution, giving rise to diagrams of different appearance.[3]

Analytical problems of practical interest can be solved readily with such diagrams. Thus, the pH of a mixture of 10 ml of $0.45M$ KH_2PO_4 and 5 ml of $0.1M$ H_3PO_4, diluted to 250 ml ($C_M = 0.2$, $q = 2.1$) may be directly obtained from Fig. 1; *viz.* pH = 3.25. If the usual logarithmic diagram is used, it is not easy to establish the proton condition, as there is not a suitable reference level.

Vertical lines are observed at high values of C_M, corresponding to buffer solutions for which the pH does not change on dilution. To find the corresponding pH, it may be assumed that the vertical segments coincide with the vertical asymptotes of the curves, which can be obtained by setting the denominator of equation (3) equal to zero:

$$q + (q-1)\beta_1 l + (q-2)\beta_2 l^2 + \ldots + (q-n)\beta_n l^n = 0 \quad (4)$$

This equation only has positive real roots when $0 < q < n$. Outside of this range, there are no vertical asymptotes. For a single-proton system, the asymptotes appear at

$$\text{pH} = \log K + \log \frac{1-q}{q} \quad (5)$$

This expression is equivalent to the Henderson equation.

Polynuclear systems

When polynuclear species are present, it is not possible to express C_M explicitly in terms of l. In this case, from (1) and (2):

$$\left(mq - l + \frac{K_w}{l}\right) + \sum (qj - i)\beta_{ij} m^j l^i = 0 \quad (6)$$

This equation allows the calculation of m as a function of l for any q value by means of an iterative procedure. If m and l are known, C_M can immediately be calculated from (1).

The diagram for boric acid is shown in Fig. 2. The curves are similar to those for mononuclear systems, except when the concentration of the polynuclear species is significant (at high C_M values). In this particular diagram, deviations occur when $C_M > 0.03M$ ($\log C_M > -1.5$). Thus, for a solution containing $0.125M$ $Na_2B_4O_7$ and $0.2M$ NaOH ($C_M = 0.5$, $q = 0.1$), a value of 10.45 can be read for $-\log h$. If polynuclear species were not considered, $-\log h$ would be 9.85.

The solution of equation (6) leads in some cases (*e.g.*, $q = 0.9$) to two real roots, both with a chemical meaning, indicating that in the presence of polynuclear species, the pH of the solution may increase and then decrease on dilution. In addition, it may be observed that at high values of C_M, a tenfold dilution changes the pH by more than one unit; this is higher than the change produced by tenfold dilution of a strong acid, and it occurs mainly as a result of depolymerization with production of free central ions ($H_2[B(OH)_4]_3^- \rightleftharpoons 2H[B(OH)_4] + B(OH)_4^-$). These $B(OH)_4^-$ ions have a much greater affinity for protons (boric acid is a very weak acid) than have the $H_2[B(OH)_4]_3^-$ ions, so protons are removed from solution, causing the pH to increase.

A direct application of the diagram is the calculation of the composition of buffer solutions of known ionic strength. A horizontal line represents a series of solutions with constant concentration of the

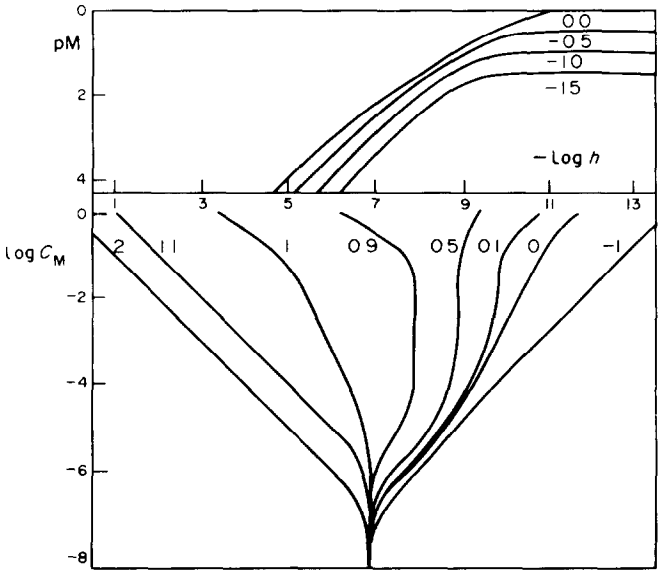

Fig. 2. Boric acid. Upper part: $pM = f(-\log h)$ diagram at various $\log C_M$ values. Lower part: $\log C_M = f(-\log h)$ diagram at different q values. The cumulative protonation constants ($I = 0.5$, 25°C) are: $\log \beta_1 = 8.89$, $\log \beta_{1,2} = 8.74$, $\log \beta_{2,3} = 19.95$, $\log \beta_{2,4} = 20.46$. ($jB(OH)_4^- + iH^+ \rightleftharpoons H_i[B(OH)_4]_j^{(i-j)-}$, $\log \beta_{i,j}$) and $pK_w = 13.74$.[1]

buffer system. The diagram indicates in which ratios the reagents must be mixed in order to get the desired values of $-\log h$. For the preparation of these solutions, the contribution of the system to the ionic strength must be known, *i.e.*, pM must be known. Therefore plots of $pM = f(-\log h)$ at various C_M values may be used [equation (1)]. Such a diagram is plotted in the upper part of Fig. 2 for various values of C_M.

The diagram for various q values could also easily be plotted, since the corresponding points have been obtained by solving equation (6). Nevertheless, the lines of this diagram have zones of high slopes, where the reading of pM becomes imprecise. Therefore, the representation shown in Fig. 2 is preferable.

For the preparation of the buffers, the pM value should be read from the upper part of Fig. 2 so that the concentration of the various species in solution can be calculated. Thus, for a solution containing 5.367 g of boric acid in 100 ml of 0.434*M* KOH ($C_M = 0.868$, $q = 0.50$), it may be found from the diagrams that $-\log h = 9.33$ and $pM = 0.75$, whence the ionic strength is 0.50*M*. We have prepared this solution, measured its pH with a Crison Digilab 517 pH-meter, and found it to be 9.38. This value, accepting the Davies equation and 9 Å for the ionic parameter of the proton, corresponds to:

$$-\log h = pH + \log f_{H^+} = 9.31$$

which agrees satisfactorily with the value obtained from the diagram.

Two other solutions were prepared from the one mentioned, by dilution of 50 and 25 ml to 100 ml and addition of 1.954 and 2.878 g of KCl, respectively, in order to keep the ionic strength at 0.50*M*. The measured pH values were 9.23 and 9.12, corresponding to the $-\log h$ values 9.16 and 9.05. The values of $-\log h$ read from the diagram are 9.19 and 9.07. If the concentrations of polynuclear species had not been significant, the pH of the buffer solution would scarcely have changed on dilution.

This behaviour was also checked for $q = 0.9$, where the variation of $-\log h$ on the diagram is more important. Four solutions of 0.5*M* ionic strength were prepared with decreasing C_M (0.487*M*, 0.347*M*, 0.241*M* and 0.153*M*). The values of $-\log h$ corresponding to the experimental pH values were 6.90, 7.16, 7.38 and 7.59, verifying the high variation of pH on dilution.

Presence of solid phase

When a sparingly soluble substance, M_aL_b, precipitates, a direct relationship exists between m and l through the solubility product, K_s. The solubility, S, in terms of the central ion in solution, is given by:

$$C_M = aS = K_s^{1/a} l^{-b/a} + \sum j\beta_{ij} K_s^{j/a} l^{[i-(b/a)j]} \qquad (7)$$

In Fig. 3, the solubility curve corresponding to the hydrolysis of chromium(III) is plotted together with the $\log C_M = f(pH)$ curves. The value of q at each point of the solubility curve can be obtained from (1) and (2) by substituting for m in terms of l:

$$q = \frac{\left(l - \frac{K_w}{l}\right) + \sum i\beta_{ij} K_s^{j/a} l^{[i-(b/a)j]}}{K_s^{1/a} l^{-b/a} + \sum j\beta_{ij} K_s^{j/a} l^{[i-(b/a)j]}} \qquad (8)$$

In the case of chromium(III) hydroxide, it may be observed that the limiting value of q for no precip-

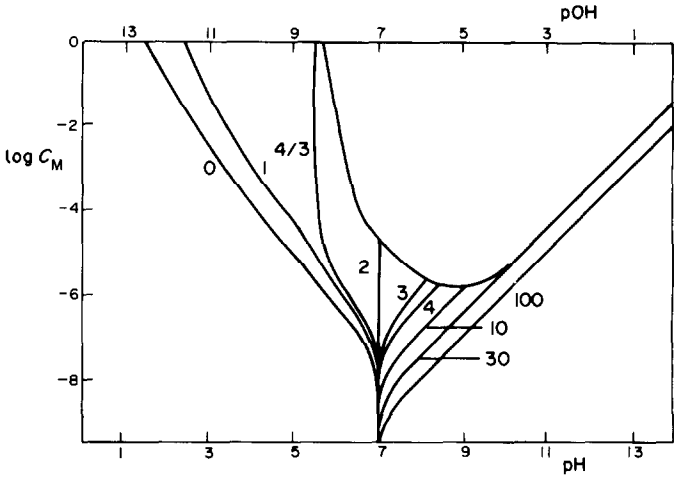

Fig. 3. Log $C_M = f$(pOH) diagram and solubility curve for the hydrolysis of chromium(III). Formation constants of the hydroxo-complexes are: $\log \beta_1 = 10.0$, $\log \beta_2 = 18.3$, $\log \beta_3 = 24.0$, $\log \beta_4 = 28.6$, $\log \beta_{2,2} = 22.94$, $\log \beta_{4,3} = 47.85$; $pK_s = 30$ and $pK_w = 14.00$ ($I = 0$, 25°C).[5]

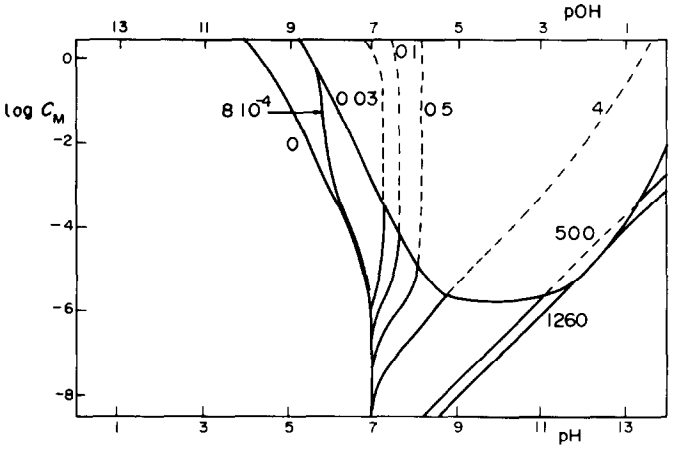

Fig. 4. Log $C_M = f$(pOH) diagram and solubility curve for the hydrolysis of zinc(II). Formation constants of the hydroxo-complexes are: $\log \beta_1 = 5.04$, $\log \beta_2 = 11.1$, $\log \beta_3 = 13.6$, $\log \beta_4 = 14.8$, $\log \beta_{1,2} = 5$, $\log \beta_{6,2} = 26.2$; $pK_s = 16.86$ and $pK_w = 14.00$ ($I = 0$, 25°C).[5]

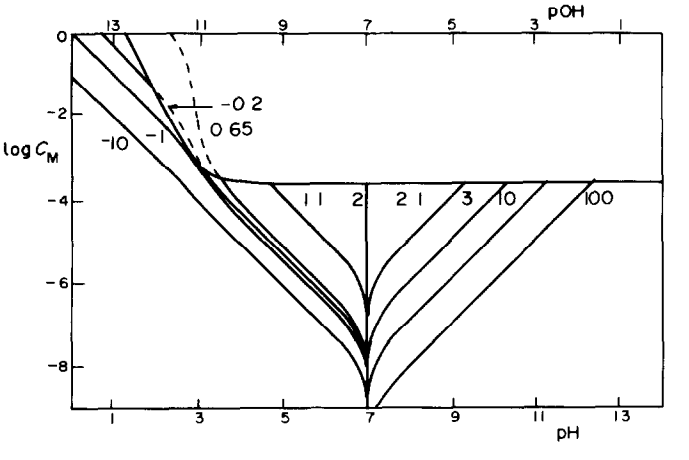

Fig. 5. Log $C_M = f$(pOH) diagram and solubility curve for the hydrolysis of mercury(II). Formation constants of the hydroxo-complexes are: $\log \beta_1 = 10.6$, $\log \beta_2 = 21.83$, $\log \beta_{1,2} = 10.67$, $\log \beta_{3,3} = 35.58$; $pK_s = 25.44$ and $pK_w = 14.00$ ($I = 0$, 25°C).[5]

itation in basic medium corresponds to the asymptote to the solubility curve.

In the calculation of the limit of equation (8), as $l \rightarrow \infty$, three different cases may be distinguished, depending on the maximum value of $i - bj/a$, which may be equal to, bigger than or smaller than unity.

Chromium(III) hydroxide, where the maximum value of $(i - 3j)$ (corresponding to the 1:4 complex) is unity, is representative of the first case. The limit of q is:

$$q = \frac{1 + 4\beta_4 K_s}{\beta_4 K_s} = 30$$

This value represents the minimum ratio of the analytical concentrations of strong base and chromium(III) for the hydroxide not to precipitate in basic medium.

A representative example of the second case is given by the precipitation of zinc hydroxide (Fig. 4), where the maximum value of $(i - 2j)$ is 2 because of the presence of the 1:4 and 2:6 complexes. The asymptote exists for:

$$q = \frac{4\beta_4 K_s + 6\beta_{6,2} K_s^2}{\beta_4 K_s + 2\beta_{6,2} K_s^2} = 4$$

In this case the asymptote extends into the region representing the solid phase, indicating that the curves for q values bigger than 4 will intercept the solubility curve at two points, until a maximum q value corresponding to the tangent of the curve is reached. This value, along the solubility curve, can be obtained by equating to zero the derivative of expression (8) with respect to pL. For zinc this value is $q = 1260$. At higher values of q no solid phase appears. Thus, in a strong base solution with $q = 500$, the hydroxide first precipitates and then redissolves on further dilution.

When the maximum value of $i - bj/a$ is smaller than unity, the limit of q is ∞ and all the curves extend into the "solid phase region" for basic medium, and no redissolution of the precipitate is possible. This is the case with mercury(II) (Fig. 5), where the maximum value of $(i - 2j)$ is zero (1:2 complex).

In a similar way, it is possible to study the behaviour of the systems in acid medium, and to determine the limit of expression (8) when $l \rightarrow 0$. The various cases that may be distinguished depend on the minimum value of $(i - bj/a)$, which may be equal to, bigger than or smaller than $-b/a$ or -1.

In the examples above, the minimum values of $(i - bj/a)$ are -5 (3:4 complex of chromium) and -3 (2:1 complex of zinc, and 2:1 and 3:3 complexes of mercury). In these three cases $(i - bj/a) < -b/a < -1$ and the asymptotes appear at $q = 4/3$ for chromium, $q = 1/2$ for zinc and

$$q = \frac{\beta_{2,1} K_s^2 + 3\beta_{3,3} K_s^3}{2\beta_{2,1} K_s^2 + 3\beta_{3,3} K_s^3} = 0.65$$

for mercury. The tangent to the solubility curve, calculated by equating to zero the derivative of equation (8), exists at $q = 8 \times 10^{-4}$ (pH = 5.55) for zinc and at $q = -0.62$ (pH = 2.75) for mercury.

In Fig. 5 the curves for q values between $+0.65$ and -0.62 correspond to solutions which precipitate and redissolve by dilution. For other cases (*e.g.*, zinc hydroxide), the upper intercepts of the solubility curve appear at C_M values that are too high to possess any analytical meaning.

Acknowledgements—The authors wish to thank Prof. I. Nagypál, L. Kossuth University, Debrecen, Hungary, for his suggestions.

REFERENCES

1. G. Ramis Ramos, M. C. García Alvarez-Coque and C. Mongay Fernández, *An. Quím.*, 1983, **79B**, 244.
2. J. N. Butler, *Ionic Equilibrium: A Mathematical Approach*, Addison-Wesley, California, 1964.
3. I. Nagypál and M. T. Beck, *Talanta*, 1982, **29**, 473.
4. Y. Lurie, *Handbook of Analytical Chemistry*, Mir, Moscow, 1975.
5. C. F. Baes, Jr. and R. E. Mesmer, *The Hydrolysis of Cations*, Wiley, New York, 1976.

Talanta, Vol. 30, No. 10, pp. 783–786, 1983
Printed in Great Britain.

0039-9140/83 $3.00 + 0.00

SHORT COMMUNICATIONS

TRACE METAL ASSAY OF U_3O_8 POWDER BY ELECTROTHERMAL AAS

A. G. PAGE, S. V. GODBOLE, MADHURI J. KULKARNI, N. K. PORWAL, S. S. SHELAR* and B. D. JOSHI
Radiochemistry Division, Bhabha Atomic Research Centre, Trombay, Bombay 400085, India

(*Received* 25 *January* 1983. *Accepted* 15 *April* 1983)

Summary—Methods have been developed for the direct determination of Ag, Ca, K, Li, Mg, Na, Pb, Sn and Zn in U_3O_8 powder samples by electrothermal AAS. Nanogram and lower amounts of these elements have been determined with a relative standard deviation of 6–16% in mg amounts of sample (either alone or mixed with an equal weight of graphite). The results for NBL reference samples were in reasonable agreement with the certified values. X-Ray diffraction studies on the residues left from the graphite mixtures after the atomization cycle, confirmed the formation of uranium carbide (UC_2).

Atomic-absorption spectrometry (AAS) with electrothermal atomization has recently been applied to the determination of trace metals in nuclear fuel materials and uranium solutions.[1–5] Electrothermal atomization offers scope for AAS analysis of solid samples.[6–8] The refractory nature of U_3O_8 makes it particularly suitable for trace metal assay by atomization of powder samples, as shown by our earlier studies on the estimation of Cd and Li[9] and of Co, Cr, Cu, Mn and Ni.[10] We also found that addition of graphite to the U_3O_8 sample had a beneficial effect on the atomization of some of these trace metals. Further work has therefore been done on the direct determination of nanogram amounts of Ag, Ca, Li, Mg, Pb and Sn in U_3O_8 samples with use of samples and standards mixed in 1:1 proportion with pure graphite. Owing to the significant amounts of K, Na and Zn in the graphite used, it was omitted in the determination of these elements. The methods developed have been used for analysis of a set of seven U_3O_8 standards obtained from the New Brunswick Laboratory, and the nature of the effect of the addition of graphite has been studied.

EXPERIMENTAL

Apparatus

A Varian Techtron AA-6 atomic-absorption spectrometer with CRA-63 carbon cup atomizer with BC-6 hydrogen-continuum background corrector was used. The graphite cups used for atomization of the powder samples had a pyrolytic coating to reduce sample losses. The carbon cup atomizer can be enclosed in a glove box for analysis of radioactive samples.

A specially designed Perspex funnel was used for quantitative transfer of the weighed sample into the graphite cup. Small quartz crucibles were used for weighing 1–5 mg amounts of samples. High-purity argon at a flow-rate of 4.5 l./min was used to provide the inert-gas sheath round the atomizer to prevent oxidation of the cup. Single element hollow-cathode lamps were used and operated at the prescribed optimum currents.

Preparation of standards and samples

A homogeneous mixture containing a large number of the metallic elements determined in quality-control analysis of uranium was made by grinding together their high-purity oxides, nitrates or carbonates, as appropriate, for 1 hr. No halides were used, as these had earlier been found[11] to cause inefficient atomization and produce non-specific absorption. A fraction of the mixture was mixed with high-purity analysed U_3O_8 powder to make a master standard. Two sets of seven graded trace-metal standards (5 g of each standard) were then prepared by diluting the master standard with (*i*) U_3O_8 powder and (*ii*) a 1:1 w/w mixture of U_3O_8 and high-purity graphite powder. The trace-metal concentration ratio between successive standards in both series was 2–2.5. Bulk amounts of finely ground U_3O_8 and U_3O_8 + C standards were also prepared for specific X-ray studies on the uranium compounds formed at different atomization temperatures.

Portions of seven NBL standards (98-1 to 98-7) for trace-metal impurities in U_3O_8 were mixed with an equal weight of graphite. These mixtures and the undiluted standards were then used as samples, along with the synthetically prepared samples, to check the standardization procedure for each element. Some of the NBL standards, particularly 98-1 to 98-5, were further diluted with analysed pure U_3O_8 when necessary to bring the amount of element to be determined into the calibration range.

Procedure

The sample weight for U_3O_8-based standards and samples was 5 mg and that for the graphite-mixed standards was 1 mg. Because graphite is less dense than U_3O_8 powder, the 1 mg of U_3O_8 + C standard occupied nearly the same volume as the 5 mg of U_3O_8 standard. The losses during

*Present address: Toshniwal Bros. Pvt, Ltd., Bombay, India.

Table 1 Experimental conditions for analysis of U_3O_8 powder

Element	Analytical line, *nm*	Bandwidth for monochromator, *nm*	Atomization: Voltage setting (Temp, °C)	Atomization: Time, *sec*
Ag	328.07	0 5	8 (2400)	3
Ca	422.67	0.5	7 (2100)	4
K	766.5	0.5	6 (1720)	4
Li	670.78	0 5	7 (2100)	4
Mg	285.2	0.2	6 (1720)	4
Na	330 2 330 3	0.5	7.5 (2250)	4
Pb	217 00	1.0	6.5 (1920)	3
Sn	235.48	0.5	8.5 (2540)	4
Zn	213.86	0.5	6.1 (1760)	3

transfer of sample into the graphite cup were less than 5% in both cases.

Because solid samples were used, the temperature used for the drying step was kept at about 120° to remove any moisture in the samples. The ashing step used a temperature of about 160° for 5–10 sec. The atomization temperatures and times were optimized for each element. Since the maximum permissible amounts of these elements in uranium were not too low, no special efforts were made to improve the detection limits. The optimized working conditions are given in Table 1. The graphite cup was emptied and replaced between successive firings, a fresh cup being used for each element. The precision was determined by repeated analysis of a synthetic sample containing the trace elements at concentrations in the middle of the ranges. The NBL reference samples were then analysed and the determinations for the analyte elements were made from the working curves. The U_3O_8 and $U_3O_8 + C$ standards (5-mg and 1-mg portions separately) were atomized at different temperatures in the range 1000–2540°, the procedure being repeated several times at each temperature so that enough residue could be collected for X-ray diffraction examination. A fresh graphite cup was used for each atomization temperature and type of sample.

RESULTS AND DISCUSSION

The earlier studies on the addition of graphite to the U_3O_8 powder had indicated two advantages: an increase in analytical signal because of increased rate of reduction of oxide to metal, and a longer life of the graphite cup because of the free carbon in the sample itself. There was also improved precision. Hence it seemed sensible to extend the use of this method. The optimum proportion of graphite to U_3O_8 was found to be generally 1:1. For the determination of K, Na and Zn the high absorbance signals for these elements from the graphite used, and the poor reproducibility, made the use of graphite inadvisable, and for these elements the U_3O_8 powder was analysed directly.

Absorbance measurements made with the uranium 358.49-nm line showed that the signals for an empty cup and for cups carrying U_3O_8 or $U_3O_8 + C$ charges were the same at any of the atomization temperatures used for the trace analysis, indicating that there was no detectable vaporization of uranium from either type of sample.

The calibration data are summarized in Table 2. The absolute detection signal is improved considerably by the graphite addition and just 0.5 mg of U_3O_8 sample is sufficient to give the high sensitivity required in trace analysis. The precision (r.s.d.) ranges between 6 and 16%, so a sufficient number of replicates should be run. The optimized atomization

Table 2. Analytical results for U_3O_8 powder

Element	Matrix	Estimation range*, *ppm*	Detection limit†, *ng*	Sensitivity§, (*absorbance*/*ng*)	Rel. std devn., %
Ag	$U_3O_8 + C$	0.1–10	0.026	0.348	11.3
Ca	$U_3O_8 + C$	5–100	3.7	0.038	12.7
K	U_3O_8	2.5–50	1	0.0074	10.0
Li	$U_3O_8 + C$	0 5–10	0.043	0.368	15.5
Mg	$U_3O_8 + C$	1–50	1.94	0.006	12.3
Na	U_3O_8	2–100	8 0	0 0018	7 4
Pb	$U_3O_8 + C$	0 5–10	0.15	0.209	6 1
Sn	$U_3O_8 + C$	0 5–50	0.14	0 055	16.4
Zn	U_3O_8	0.5–10	4.0	0.046	11.1

*Values expressed in ppm on U_3O_8 basis for 5-mg amount of U_3O_8 matrix or 1 mg amount of 1:1 $U_3O_8 + C$ matrix

†Concentration corresponding to absorbance (X_L) obtained by using the relation $X_L = \bar{X}_{Bl} + 3S_{Bl}$ where $\bar{X}_{Bl}$ = mean absorbance for the standard blank, S_{Bl} = standard deviation for these measurements

§Slope of the analytical curve.

temperature for Mg was 1700° in these studies, much lower than the 2700° found optimal[5] for analysis of uranium solutions. The considerably lower atomization temperature for the determination of Mg in powder samples mixed with graphite indicates that the solid state reduction of oxide to metal has a lower threshold than the corresponding reaction in uranyl nitrate solutions. The lower atomization temperature reduces the rate of deterioration of the cup and increases its life.

Analysis of NBL standards

The NBL standards used here contain 30 elements in graded proportions and have been analysed for the trace metals by one or more of the following methods: (1) atomic-absorption spectrometry, (2) emission spectroscopy, (3) polarography, (4) spark-source mass-spectrometry, (5) spectrophotometry. The results obtained for the 9 elements examined in the present work, together with the certified values, are given in Table 3. For some elements it was necessary to dilute the sample with analysed pure U_3O_8 to bring the concentration into the linear range of the calibration graph. The results are in reasonable agreement with the certified values except for NBL 98-1 in the case of Ca, K, Li, Mg, Na, Sn and Zn. This is probably due to dilution errors involved in making suitable dilutions with pure U_3O_8 for the respective standards. Interelement interferences appear to be negligible.

Role of the added graphite

The X-ray diffraction studies on the residues left in the graphite cup after the atomization cycle indicate that in the absence of added graphite most of the U_3O_8 remain unchanged at temperatures up to 1400° but it is then increasingly reduced to UO_2 at higher temperatures, with total conversion into UO_2 as 2200°. When graphite is added to the sample, however, UO_2 formation is complete even at 1700° and formation of UC_2 begins at 1900°. The proportion of uranium carbide increases with atomization temperature, and at 2400° most of the charge is reduced to UC_2. A very small proportion of UC was also found. Such carbide species have also been found in high-temperature mass-spectrometry studies.[12]

The absence of uranium in the vapour phase can thus be ascribed to the stability of UO_2 and UC_2 in an argon atmosphere. Further, as the sample temperatures are often lower than the set atomization temperatures, the higher thermal conductivity of graphite is likely to decrease this temperature difference, thereby increasing the efficiency of volatilization and dissociation of the analyte.

These studies show that AAS with electrothermal atomization is suitable for the direct determination of a number of trace metals in U_3O_8 with only a few mg of sample.

Table 3. Analysis of U_3O_8 reference standards from NBL

Element	98-7		98-6		98-5		98-4		98-3		98-2		98-1		
	Present work	Certified value	Present work	Certified value	Present work	Certified value	Present work	Certified value	Present work	Certified value	Present work	Certified value	Present work	Certified value	Reference method*
Ag	<0.1	<0.1	0.2	0.2 ± 0.1	0.35	0.2 ± 0.0$_5$	0.6	0.4 ± 0.0$_6$	2.0	1.2 ± 0.1	3.4	2.3 ± 0.2	7.2	6.4 ± 1.4	(1), (3)
Ca	<5	0.8 ± 0.2	<5	1.6 ± 0.2	<5	3.6 ± 0.3	7.0	8.0 ± 0.3	21	18.8 ± 0.7	38	37.1 ± 1.0	140	95.1 ± 2.7	(1)
K	<2.5	<0.5	8.3	10.9 ± 0.4	18	25.3 ± 0.9	50	61.0 ± 1.2	110	124.9 ± 2.6	280	264.6 ± 4.0	350	669.5 ± 2.8	(1)
Li	<0.5	<0.1	<0.5	0.4 ± 0.0$_5$	1.5	0.9 ± 0.0$_4$	3.1	2.5 ± 0.0$_5$	4.9	5.0 ± 0.0$_7$	9.4	9.9 ± 0.1	30.2	24.5 ± 0.1	(1)
Mg	<1	1.0 ± 0.0$_8$	4	2.8 ± 0.0$_5$	5.7	4.5 ± 0.0$_4$	13	9.2 ± 0.1	26	16.6 ± 0.2	33.6	32.2 ± 0.2	61	80.5 ± 0.3	(1)
Na	<2	<0.5	4.2	3.6 ± 0.3	9.2	9.7 ± 2.6	30	33.1 ± 2.7	90	86.6 ± 1.3	178	176.4 ± 1.2	248	387.7 ± 3.0	(1)
Pb	<0.5	0.8 ± 0.2	2	1.9 ± 0.6	4	3.0 ± 0.5	9.3	5.2 ± 0.9	11.7	10.7 ± 0.9	18	19.0 ± 1.2	45	48.8 ± 1.8	(2), (3)
Sn	0.9	0.6 ± 0.0$_6$	1.3	1.2 ± 0.4	1.6	1.9 ± 0.7	3.5	4.7 ± 0.4	6.3	9.6 ± 1.5	14.2	17.6 ± 0.7	33	48.5 ± 2.7	(4)
Zn	0.8	1.6 ± 0.4	7.6	10.6 ± 1.2	15	18.9 ± 3.1	37.5	49.2 ± 2.1	85	97.4 ± 4.5	208	193.9 ± 2.9	235	491.5 ± 11.8	(1), (2)

*The methods used by NBL to characterize the reference material are: (1) atomic-absorption spectrometry; (2) polarography; (3) spark-source mass-spectrometry; (4) spectrophotometry.

Acknowledgements—The authors are thankful to Shri D. M. Chackraburtty and Dr K. D. Singh Mudher for their help in the X-ray diffraction studies.

REFERENCES

1. G Bagliano, F. Benischek and I. Huber, *At. Absorp. Newsl.*, 1975, **14**, 45.
2. M. Buffereau and J. Robichet, *Method. Phys. Anal. (GAMS)*, 1971, **7**, 138.
3. B. M. Patel, P. M Bhatt, N. Gupta, M. M. Pawar and B. D. Joshi, *Anal. Chim. Acta*, 1979, **104**, 113.
4. B. M. Patel, N. Gupta, P. J. Purohit and B. D. Joshi, *ibid.*, 1980, **118**, 163.
5. B. M. Patel, A. G. Page, T. R. Bangia, M. D. Sastry and B. D. Joshi, *Intern. Symp. Trace Analysis and Technological Applications*, Bombay, February 1981.
6. F. J. Langmyhr, *Talanta*, 1977, **24**, 277
7. *Idem*, *Analyst*, 1979, **104**, 993.
8. B. V. L'vov, *Talanta*, 1976, **23**, 109.
9. A. G. Page, S. V. Godbole, S. B. Deshkar and B. D. Joshi, *Anal. Lett.*, 1978, **11**, 619.
10. A. G. Page, S. V. Godbole, M. J. Kulkarni, S. S. Shelar and B. D. Joshi, *Z. Anal. Chem.*, 1979, **296**, 40.
11. A. G. Page, S. V. Godbole, M. J. Kulkarni, N. K. Porwal and B. D. Joshi, Annual Convention of Chemists, Madras, December 1981.
12. S. K. Gupta and K. A. Gingreich, *J. Chem. Phys.*, 1979, **71**, 3072.

Talanta, Vol 30, No 10, pp 787–788, 1983
Printed in Great Britain.

0039-9140/83 $3 00 + 0.00

A NEW COLORIMETRIC METHOD FOR THE DETERMINATION OF CARBON DISULPHIDE AND ITS APPLICATION TO THE ANALYSIS OF SOME DITHIOCARBAMATE FUNGICIDES

BALBIR CHAND VERMA,* R. K. SOOD and H. S. SIDHU
Department of Chemistry, Himachal Pradesh University, Simla 171005, India

Summary—A new and convenient colorimetric method for determination of carbon disulphide, based on its transformation into bright yellow potassium benzyl trithiocarbonate through reaction with benzyl mercaptan and potassium hydroxide in tert.-butyl alcohol, has been successfully applied to determination of some dithiocarbamate fungicides in their formulations. The method possesses a distinct advantage in that it is free from all sources of errors/problems which are associated with the xanthate method for the analysis of these materials. The proposed method is precise and accurate and hence recommended for routine analysis of technical formulations containing dithiocarbamate fungicides.

The use of dithiocarbamates as agricultural fungicides has necessitated methods for their determination. A variety of techniques have been used for the determination of these materials but the method based on evolution of carbon disulphide from these fungicides by digestion with dilute sulphuric acid is generally applicable. The gas is absorbed in alcoholic potassium hydroxide solution and the xanthate formed titrated with iodine in neutral solution. The method is subject to two significant sources of error.[1] The first is due to hydrogen sulphide, which may be formed from sulphide impurities and/or degradation products in the acid hydrolysis of dithiocarbamates. To eliminate or at least minimize this error, the carbon disulphide evolved is washed with lead acetate solution before it is absorbed in the alcoholic potassium hydroxide solution. The second error arises from the susceptibility of xanthate solutions to hydrolysis:

$$CH_3OCS_2K + H_2O \rightarrow CH_3OH + COS + KSH$$
$$KSH + KOH \rightarrow K_2S + H_2O$$
$$COS + KOH \rightarrow CO_2 + KSH$$

The production of sulphide causes the results to be high, because the sulphide produced consumes twice as much iodine as would the xanthate hydrolysed.

In addition to these sources of error, difficulties are experienced in detection of the starch end-point. Matuszak,[2] on the basis of exhaustive work on the establishment of suitable conditions for the iodimetric titrations of xanthate formed from carbon disulphide, pointed out that the alcoholic potassium hydroxide solution used as absorber must always be fresh and the xanthate solution should be cooled to 0° and neutralized to the phenolphthalein end-point with acetic acid before the titration with aqueous iodine, in order to increase the permanency of the starch end-point. Making the starch end-point sharper by cooling of the xanthate solution before titration has also been recommended by other workers.[3,4]

These sources of error and other problems associated with the xanthate method arise from the oxidimetric nature of the method. A new colorimetric method free from these errors and problems has now been developed for the determination of carbon disulphide, and adapted to the analysis of dithiocarbamate fungicides such as ziram, ferbam and thiram, in their technical formulations.

The method consists in absorbing the evolved carbon disulphide in a solution of benzyl mercaptan and potassium hydroxide in 80% tert.-butyl alcohol, to form the bright yellow potassium benzyl trithiocarbonate (**I**):

$$C_6H_5CH_2SH + CS_2 + KOH \rightarrow C_6H_5CH_2S{-}\overset{\overset{S}{\|}}{C}{-}SK + H_2O$$

(I)

The absorbance of **I** is measured at 430 nm against a reagent blank. Tertiary butyl alcohol, besides serving as the medium for the quantitative transformation of carbon disulphide into potassium benzyl trithiocarbonate, also stabilizes the yellow colour. Beer's law is followed in the concentration range 14–150 μg/ml in the solution measured. The proposed method is simple, accurate and precise and is recommended for routine analysis of carbon disulphide samples and dithiocarbamate fungicides in their formulations. The method possesses distinct advantages over the xanthate method in that there is no interference from hydrogen sulphide, an impurity that is generally associated with carbon disulphide

*Author for correspondence.

Table 1. Assay of some commercial dithiocarbamate fungicides

Active ingredient		Active ingredient found,* % Present method	Xanthate method
Ziram	I	26.9 (0.3)	26.8 (0.2)
	II	29.7 (0.3)	29.4 (0.3)
Ferbam	I	75.2 (0.3)	74.9 (0.3)
Thiram	I	74.5 (0.3)	74.5 (0.2)
	II	74.7 (0.2)	74.3 (0.3)

*Values are means of five determinations, with standard deviations in brackets.

samples and evolved as a gas during acidic decomposition in the analysis of dithiocarbamates. The apparatus employed for the analysis is essentially the same as that described by Lowen and Pease,[5] with the difference that the hydrogen sulphide absorber is eliminated and the carbon disulphide absorber is the solution of benzyl mercaptan and potassium hydroxide in tert.-butyl alcohol.

EXPERIMENTAL

Reagents

Carbon disulphide ("Baker analyzed" 100%, estimated chromatographically) was used as received. Benzyl mercaptan was distilled before use. Tertiary butyl alcohol ("Baker analyzed") was used as such for preparing its 80% v/v solution in water. Ziram and ferbam required for preparing calibration curves were prepared and purified in the laboratory by reported methods.[6] Thiram (Fluka) was recrystallized before use.

Carbon disulphide absorber solution: Benzyl mercaptan (0.2M) and potassium hydroxide (0.1M) in 80% tert.-butyl alcohol.

Procedures

Calibration graph for carbon disulphide. To 8 ml of absorber solution various volumes (0.1–1.0 ml) of carbon disulphide solutions in ethanol, acetonitrile, isopropyl alcohol or tert.-butyl alcohol were added slowly and with shaking. The volume of the solution was then made up to 10 ml with absorber solution. The absorbance of the bright yellow solution thus obtained was measured at 430 nm against a reagent blank.

Calibration graphs for ziram, ferbam and thiram. Aliquots (1–5 ml) in chloroform of ziram, ferbam and thiram were introduced into the reaction flask of the apparatus. The experimental details of digestion and absorption are the same as those described by Lowen and Pease.[5] The analysis was concluded by measuring the absorbance of the absorber solution (10 ml) at 430 nm against a reagent blank. The results of analysis of some technical formulations containing ziram, ferbam and thiram are given in Table 1.

RESULTS AND DISCUSSION

The absorption spectrum of the yellow potassium benzyl trithiocarbonate solution is shown in Fig. 1. The molar absorptivity at 430 nm is 2.10×10^2 l. mole^{-1}.cm^{-1}. Hydrogen sulphide, even when present in up to tenfold ratio to carbon disulphide, does not cause any interference.

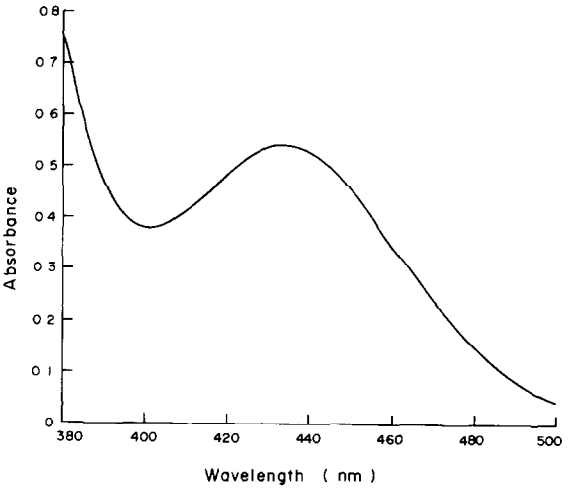

Fig. 1.

That carbon disulphide is quantitatively transformed into potassium benzyl trithiocarbonate has been established[8] by performing the absorption in the absence of potassium hydroxide and titrating the potassium benzyl trithiocarbonic acid with potassium hydroxide, with phenolphthalein as indicator (trithiocarbonic acids are strong acids,[7] K for ethyl trithiocarbonic acid being 2.8×10^{-2}). During the titration, the solution becomes yellow, and the colour changes sharply to yellow pink at the end-point. The excess of mercaptan does not interfere under the conditions used (a pink colour appears immediately on addition of the first drop of potassium hydroxide in the blank titration). The volume of potassium hydroxide used corresponds to the amount of potassium benzyl trithiocarbonic acid and consequently of carbon disulphide.

The method for determination of carbon disulphide has been successfully adapted to analysis of some dithiocarbamate fungicide formulations. The standard deviation is in the range 0.2–0.3% (Table 1).

Acknowlegement—The authors thank the Indian Council of Agricultural Research for financial support.

REFERENCES

1. J. H. Karchmer (ed.) *The Analytical Chemistry of Sulfur and its Compounds*, Part II, p. 623. Wiley–Interscience, New York, 1972.
2. M. P. Matuszak, *Ind. Eng. Chem., Anal. Ed.*, 1932, **4**, 98.
3. J. D. Patterson, *J. Assoc. Off. Agr. Chemists*, 1950, **33**, 788.
4. A. Stevenson, *J. Sci. Food Agr.*, 1964, **15**, 509.
5. W. K. Lowen and H. L. Pease, in *Analytical Methods for Pesticides, Plant Growth Regulators and Food Additives*, G. Zweig (ed.), Vol. III, p.69. Academic Press, New York, 1964.
6. G. D. Thorn and R. A. Ludwig, *The Dithiocarbamates and Related Compounds*, p. 7. Elsevier, Amsterdam, 1962.
7. E. E. Reid, *Organic Chemistry of Bivalent Sulphur*, Vol. IV, p. 178. Chemical Publishing Co., New York, 1962.
8. B. C. Verma and S. Kumar, *Talanta*, 1978, **25**, 291.

Talanta, Vol 30, No. 10, pp 789–791, 1983
Printed in Great Britain

0039-9140/83 $3 00 + 0.00
Pergamon Press Ltd

COULOMETRIC GENERATION OF HYDROGEN IONS BY OXIDATION OF MERCURY IN ANHYDROUS ACETONE

RANDJEL P. MIHAJLOVIĆ
Faculty of Science, Radoja Domanovića 12, Kragujevac, Yugoslavia

and

VILIM J. VAJGAND
Institute of Chemistry, University of Belgrade, Studentski trg 16, Yugoslavia

(*Received* 26 *May* 1982. *Revised* 17 *March* 1983. *Accepted* 26 *April* 1983)

Summary—The application of a mercury anode for the quantitative generation of H^+ ions in anhydrous acetone has been investigated. From the changes of anode potential with current density in 0.25*M* sodium perchlorate in anhydrous acetone it has been established that in this solvent mercury is oxidized at a potential which is much more negative than the oxidation potentials of the bases to be titrated, the indicator used and the solvent. Protons generated in this way have been used for titration of some organic bases, with either visual or potentiometric end-point detection. The oxidation of mercury in anhydrous acetone and the reaction of mercury ions with acetone have been found to proceed with 100% current efficiency.

Anhydrous acetone is a very suitable solvent for the determination of weak organic acids and bases, either individually or in mixtures. Fritz and Yamamura[1] have used it as the medium for potentiometric titration of weak organic acids; Cundiff and Markunas[2] have titrated mixtures of mineral and carboxylic acids in it, and Malmstadt and Vassallo[3] have used it for titration of acid mixtures with tri-n-butylammonium hydroxide, with either potentiometric or visual end-point detection. For titration of organic acid mixtures Malyshev[4] has used potassium hydroxide in methanol as titrant.

Fritz and Burgett[5] have titrated organic bases in acetone, individually or in mixtures, with perchloric acid in dioxan, with visual or potentiometric end-point detection.

Streuli *et al.*[6] titrated organic acids by generating hydroxide ions in acetone containing 1% of water, tetraethylammonium bromide and sodium perchlorate; Fritz and Grainner used a lower concentration of water (0.2%).[7] Christian has titrated weak organic bases in acetone containing 10% of water and a high concentration of lithium perchlorate (3*M*).[8]

Coulometric titration of organic bases in acetone by generation of protons from the oxidation of water is unsuitable since in this solvent the bases are oxidized at the platinum electrode at potentials which are significantly more negative than the oxidation potential of water; it is known that the presence of water in an organic solvent interferes with the determination of organic bases.

Hence, coulometric generation of protons in acetone requires the presence of an anode depolarizer, the oxidation potential of which is more negative than that of the base to be titrated or of other species in the solution.

In this paper, we describe the quantitative production of protons in anhydrous acetone by electrolytic oxidation of mercury.

EXPERIMENTAL

Reagents

All chemicals used were of p.a. purity (Merck). Before use the acetone was purified according to Kreshkov *et al.*[9]

Liquid bases (butylamine, pyridine, piperidine and isobutylamine) were first dried over fused potassium hydroxide and then fractionally distilled under reduced pressure. Suitable amounts of the bases were weighed into standard flasks, dissolved in anhydrous acetone and diluted to the mark. The base concentration was checked by coulometric titration in acetonitrile.[10] Portions (0.8–1.5 ml) of the base solutions were delivered from a microburette fitted with a Teflon stop-cock.

As supporting electrolyte 0.25*M* sodium perchlorate in acetone was used and a 0.1% solution of Methyl Red in acetone for photometric end-point detection.

Apparatus

The apparatus for photometric end-point detection (Fig. 1) consisted of a current source and an electrolytic vessel. The current source was a current stabilizer ("Vinča", Belgrade), and the generating current was measured with a precise milliammeter ("Iskra", Kranj).

The anolyte was separated from the catholyte by a porosity-4 sintered-glass disc. The anolyte volume was 2–3 ml; a platinum spiral of 28 mm^2 area was used as the cathode, and a mercury pool with a surface area of 2 cm^2 as the anode.

The apparatus for potentiometric titration is shown in Fig. 2. The catholyte and anolyte were again separated by a sintered-glass disc. The volume of catholyte was about 5 ml, and of the anolyte about 15 ml. The cathode was a platinum spiral and the anode a mercury pool with surface

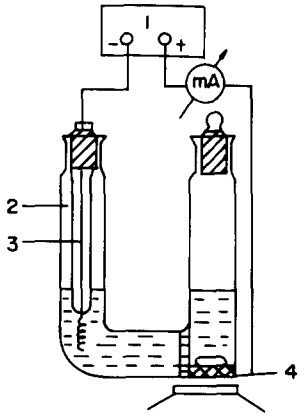

Fig. 1. Schematic diagram of the apparatus for coulometric titration of bases with visual end-point detection. 1, Current-stabilizer; 2, electrolytic vessel; 3, Pt-cathode; 4, Hg-anode.

area of 7 cm^2. The indicator electrode was an H_2/Pd-wire spiral electrode (14.3 mm^2 area),[11] and the reference electrode a modified calomel electrode containing methanolic potassium chloride solution. Potential changes were measured with a Radiometer pHM-26 pH-meter.

Procedures

Photometric end-point detection. Put enough mercury into the anode compartment just to cover the bottom, and then 0.25*M* sodium perchlorate solution in anhydrous acetone to the same level into the anode and cathode compartments; add a drop of indicator and a known volume of the base to be determined, to the anolyte. Insert the platinum spiral into the catholyte, turn on the stirrer, then simultaneously switch on the chronometer and the current source and electrolyse till the colour of the solution changes from yellow to violet. To the same solution add the next sample and analyse it in the same way. In this manner 3 or 4 samples can be analysed in the same supporting electrolyte. The current efficiency can be determined from the coulometric titration of a known amount of base.

Potentiometric end-point determination. Put electrolyte in the cathode and anode compartments, insert the platinum spiral into the catholyte and in the anode compartment put mercury, the H_2/Pd electrode, the modified calomel electrode and a known volume of solution of the base being determined. Switch on the current source for a known time to generate a known amount of protons, and then measure the potential, and repeat the procedure for each titration point. Make the generation periods shorter in the equivalence-point region. Find the titration end-point by the classical method from a derivative plot.

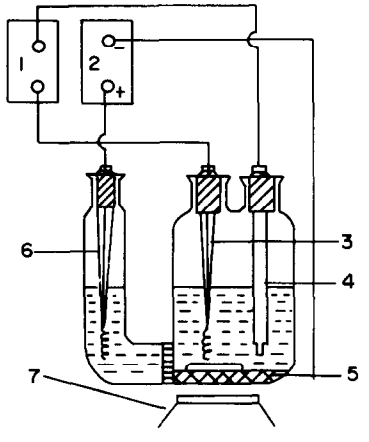

Fig. 2. Schematic diagram of the apparatus for coulometric titration of bases with potentiometric end-point detection. 1, pH-meter; 2, current stabilizer; 3, indicator electrode; 4, calomel electrode; 5, Hg-anode; 6, Pt-cathode; 7, magnetic stirrer.

RESULTS AND DISCUSSION

It is known[12] that mercury(II) ions react with acetone to give protons:

$$Hg^{2+} + 2CH_3COCH_3 \rightarrow Hg(CH_2COCH_3)_2 + 2H^+ \quad (1)$$

Mercury(I) reacts similarly:

$$Hg_2^{2+} + 2CH_3COCH_3 \rightarrow Hg_2(CH_2COCH_3)_2 + 2H^+ \quad (2)$$

All our preliminary investigations, as well as the results obtained in quantitative determination of bases, are consistent with these equations. The mercury salts formed are soluble in acetone, but some other ketones with an α-methylene group which we have investigated form precipitates, producing protons as well.

The validity of the reactions above was confirmed coulometrically by generating protons in the absence of bases and then titrating the liberated acid with acetone solutions of bases.

In order to avoid the preparation of standard solutions of mercury salts for the generation of protons according to equations (1) and (2), we have investigated the possibility of coulometric generation of mercury ions by oxidation of mercury in 0.25*M* sodium perchlorate solution in acetone. Therefore the changes of anode potential at different current densities were measured, for various electrolyte compositions. Plots of current *vs.* voltage were obtained under experimental conditions similar to those used for the coulometric titrations. From the curves given in Fig. 3 we conclude that in anhydrous acetone

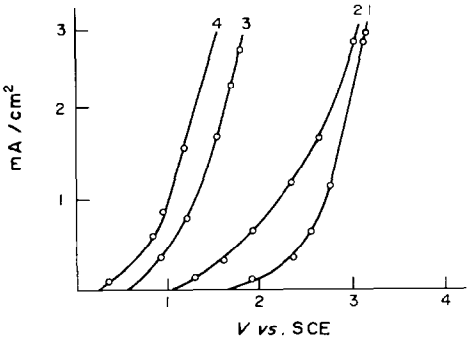

Fig. 3. Change of anode potential (*vs* SCE) with current density in 0.25*M* sodium perchlorate solution in anhydrous acetone: 1, solvent; 2, Methyl Red; 3, triethylamine; 4, mercury.

Table 1. Coulometric titration of bases

Base	Photometric end-point			Potentiometric end-point		
	No. of detns.	Taken, *mg*	Recovery,* %	No. of detns.	Taken, *mg*	Recovery* %
α,α′-Bipyridyl	7	3.687	100.0 ± 0.4			
Triethanolamine	6	5.709	100.0 ± 0.3	5	17.127	100.1 ± 0.1†
Butylamine	7	2.527	99.9 ± 0.4	6	7.578	100.0 ± 0.2†
Isobutylamine				5	7.813	100.1 ± 0.4†§
Pyridine	10	3.149	100.0 ± 0.2	4	9.447	99.9 ± 0.2†
Piperidine	8	5.475	100.0 ± 0.1			

*±Standard deviation.
†H_2/Pd indicator electrode.
§Glass indicator electrode.

mercury is oxidized at a potential which is more negative than that of the titrated base, the indicator or the supporting electrolyte. Small amounts of water (0.05%) affect neither the curves nor the results obtained. The water content of the solvent was determined by a Karl Fischer titration.

In order to establish whether the oxidation of mercury and the reaction of its ions with acetone are quantitative, we have titrated some organic bases with protons generated according to equations (1) and (2). The titration end-points were detected either photometrically, with a Methyl Red as indicator, or potentiometrically with a calomel reference electrode and a glass or H_2/Pd indicator electrode.

Since the reaction of mercury ions with acetone gives rise to the formation of slightly ionized compounds which are very soluble in acetone [$Hg_2(CH_3COCH_2)_2$ and $Hg(CH_3COCH_2)_2$], the change of indicator colour at the titration end-point is very sharp and the results obtained are very reproducible. Eight titrations of 5.475-mg amounts of piperidine gave a mean recovery of 100.0%, standard deviation 0.07%.

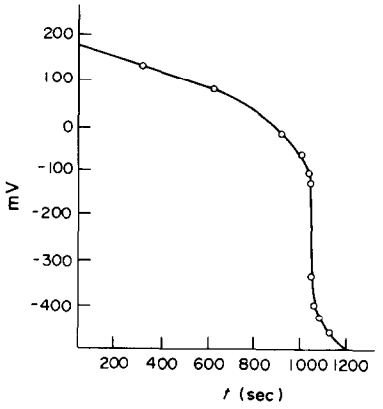

Fig. 4. Coulometric titration of piperidine with protons generated by mercury oxidation in anhydrous acetone.

The results obtained in the determination of some organic bases with either photometric or potentiometric end-point detection are given in Table 1. In the potentiometric titrations with the H_2/Pd indicator electrode, the potential is instantaneously established throughout. Figure 4 shows a typical titration plot for piperidine, and shows that the potential jump at the equivalence end-point is higher than 300 mV. For bases of medium strength the potential jump ranges from 200 to 250 mV, and even for very weak bases it is not less than 60 mV. Both the photometric and potentiometric titrations give good reproducibility.

From the results obtained in Table 1 it is seen that the current efficiency is 100%, from which it may be concluded that mercury in anhydrous acetone can be successfully applied for the quantitative coulometric generation of protons.

REFERENCES

1. J. S. Fritz and S. S. Yamamura, *Anal. Chem.*, 1957, **29**, 1079.
2. R. H. Cundiff and P. C. Markunas, *ibid.*, 1958, **30**, 1447, 1450.
3. H. V. Malmstadt and D. A. Vassallo, *ibid.*, 1959, **31**, 206.
4. A. I. Malyshev, *Zavodsk. Lab.*, 1962, **28**, 927.
5. J. S. Fritz and C. A. Burgett, *Anal. Chem.*, 1972, **44**, 1673.
6. C. A. Streuli, J. J. Cincotta, D. L. Mariele and K. K. Mead, *ibid.*, 1964, **36**, 1371
7. J. Fritz and F. E. Grainner, *Talanta*, 1968, **15**, 939.
8. D. G. Christian, *Anal. Chim. Acta*, 1969, **46**, 77.
9. A. P. Kreshkov, L. N. Bykova and N. A. Kazaryan, *Kislotno-osnovnoe titrovanie v nevodnykh rastvorakh*, Khimiya, Moscow, 1967.
10. V. J. Vajgand and R. P. Mihajlović, *Talanta*, 1969, **16**, 1311.
11. *Idem*, *Bull. Soc. Chem., Belgrade*, 1975, **40**, 96.
12. R. Montequi, A. Doadrio and M. F. Santiso, *Inform. Quim. Anal.*, 1957, **11**, 1; *Chem. Abstr.*, 1957, **51**, 10298e.

Talanta, Vol 30, No. 10, pp 792–794, 1983
Printed in Great Britain

0039-9140/83 $3 00 + 0 00

SPECTROPHOTOMETRIC DETERMINATION OF TETRACYCLINES AND CEPHALOSPORINS WITH AMMONIUM VANADATE

M. M. ABDEL-KHALEK and M. S. MAHROUS
Department of Pharmaceutical Chemistry, Faculty of Pharmacy, University of Alexandria, Alexandria, Egypt

(*Received* 15 *December* 1982. *Revised* 3 *April* 1983. *Accepted* 22 *April* 1983)

Summary—A spectrophotometric method for the determination of some tetracyclines as well as some cephalosporins is described. The drug is boiled with ammonium vanadate solution in sulphuric acid medium for 10 min and the absorbance of the colour developed is measured at 750 nm. The proposed method can be successfully applied to the determination of tetracycline hydrochloride, oxytetracycline hydrochloride, doxycycline hyclate, demeclocycline hydrochloride, chlortetracycline hydrochloride, cephalothin sodium, cephaloridine and cephapirin sodium. These drugs can be determined either in pure form or in pharmaceutical preparations.

Several methods have been reported for the quantitative determination of tetracyclines. These include fluorimetric,[1-3] chromatographic[4,5] and titrimetric[6] methods. Cephalosporins have been determined iodometrically after hydrolysis with alkali[7,8] and titrimetrically with *N*-bromosuccinimide[9] or potassium iodate.[10] Spectrophotometric methods based on the use of hydroxamic acid,[11] hydroxylamine hydrochloride,[12] and acetone–sodium hydroxide[13] have also been reported. Other methods use fluorimetry,[14-16] high-pressure liquid chromatography[17,18] and polarography.[19,20]

This paper describes the spectrophotometric determination of some tetracyclines and cephalosporins with ammonium vanadate in sulphuric acid medium. The method is applied to the analysis of various pharmaceutical preparations for these drugs.

EXPERIMENTAL

Apparatus

A Perkin-Elmer Model 550 S spectrophotometer with matched 1.00-cm quartz cells was used for absorbance measurements.

Reagents

Ammonium vanadate solution, 10%. Prepared by dissolving 10 g of ammonium vanadate in boiling 50% v/v sulphuric acid and diluting to 100 ml with 50% v/v sulphuric acid. This solution is stable for 3 days.

Test solutions. Freshly prepared 1-mg/ml solutions of tetracyclins and cephalosporins in water. Laboratory reference standards were used for calibration.

General procedure

Transfer 5 ml of an aqueous solution containing from 1.0 to 5.0 mg of the drug into a 50-ml conical flask. Add 10 ml of ammonium vanadate solution and 10 ml of concentrated sulphuric acid, mix well and boil gently for 10 min on a sand-bath. Cool, transfer to a 50-ml standard flask and dilute to volume with water. Cool thoroughly for 5 min, and then measure the absorbance at 750 nm against a blank treated similarly.

For injections. Transfer an accurately known weight of the sample, equivalent to 30 mg of the drug, into a 50-ml standard flask, and dissolve it in water, then make up to volume with water. Transfer 5 ml of this solution into a 50-ml conical flask and complete the assay as described above.

For capsules and tablets. Weigh accurately a quantity of the mixed contents of 20 capsules or of 20 powdered tablets, equivalent to 30 mg of the drug, and transfer it into a 50-ml standard flask. Add 30 ml of methanol, shake for 10 min and make up to volume with methanol. Filter, then transfer 5 ml of the filtrate into a 50-ml conical flask and evaporate to dryness. To the residue, add 5 ml of water and complete the assay as described under the general procedure.

RESULTS AND DISCUSSION

The proposed method has been used for the quantitative estimation of various tetracyclines and cephalosporins by oxidation with ammonium vanadate in sulphuric acid medium. The effect of varying the heating period was studied and it was found that gentle boiling for 10 min is sufficient. The blue colour developed is measured 5 min after dilution and mixing. It is stable for 3 hr.

The blue colour is attributed to the vanadium (IV) produced by reduction of vanadium(V) by tet-

Table 1. Regression equations for the calibration graphs (range 0.02—0.10 mg/ml)

Compound	Regression equation*
Tetracycline. HCl	$A = 0.000 + 6.11C$
Oxytetracycline. HCl	$A = 0.000 + 5.40C$
Doxycycline hyclate	$A = 0.006 + 9\ 90C$
Demeclocycline. HCl	$A = 0.002 + 6.32C$
Chlortetracycline. HCl	$A = 0.002 + 5.58C$
Cephalothin sodium	$A = 0\ 002 + 7.15C$
Cephaloridine	$A = 0.000 + 5.93C$
Cephapirin sodium	$A = 0.002 + 4.70C$

*A = absorbance at 750 nm (1-cm cells); C = concentration (mg/ml).

Table 2. Determination of tetracyclines and cephalosphorins by the ammonium vanadate procedure, compared with the official method

Compound	Found* ± S.D. % Proposed method	Official method (ref.)	t_{calc} †	F_{calc} ‡
Tetracycline. HCl powder	100.0 ± 0.4	100.1 ± 0.7 (21)	0.40	3.79
Tetracycline capsules (Adwic)	102.3 ± 0.8	101.7 ± 0.6 (21)	2.00	1.36
Micycline capsules (Misr)	97.2 ± 0.9	97.5 ± 0.5 (21)	0.95	1.57
Oxytetracycline. HCl powder	100.1 ± 0.7	99.9 ± 0.4 (21)	0.54	1.95
Oxytetrin capsules (Memphis)	101.6 ± 1.2	101.3 ± 0.5 (21)	0.82	4.54
Doxycycline hyclate powder	99.6 ± 0.6	—	—	—
Vibramycin capsules (Pfizer)	102.5 ± 0.8	—	—	—
Demeclocycline. HCl powder	99.9 ± 0.6	99.9 ± 1.0 (21)	0.05	3.53
Demeclocycline. HCl tablets§	98.6 ± 0.7	99.0 ± 0.3 (21)	1.99	4.80
Chlortetracycline. HCl powder	100.7 ± 0.5	—	—	—
Chlortetracycline. HCl tablets§	98.9 ± 0.7	—	—	—
Cephalothin sodium powder	99.7 ± 0.5	99.7 ± 0.4 (7)	0.31	1.20
Keflin injections (Lilly)	101.3 ± 0.8	101.2 ± 0.2 (7)	1.09	1.47
Cephaloridine powder	100.7 ± 0.4	100.7 ± 0.3 (7)	0.40	1.47
Keflodin injections (Lilly)	101.4 ± 1.0	101.2 ± 0.2 (7)	1.77	5.00
Cephapirin sodium powder	99.7 ± 0.2	—	—	—
Cephatrexyl injections (Bristol)	100.7 ± 0.6	—	—	—

*Average of 6 determinations.
†Theoretical value 2.23 ($p = 0.05$).
‡Theoretical value 5.34 ($p = 0.05$).
§Laboratory-prepared tablets containing the drug, lactose, talc, starch and magnesium stearate.

racyclines or cephalosporins. Beer's law is valid for tetracyclines and cephalosporins in the range of 20–100 μg/ml in the final solution. The regression equations in Table 1 were calculated from the calibration graphs.

Extraction of tetracyclines from powdered tablets or the contents of capsules with methanol, eliminates any interference by the excipients usually added, such as lactose, glucose and starch.

Table 2 gives the results obtained by application of the suggested method and an official method[7,21] to the determination of tetracyclines and cephalosporins in pure form and in pharmaceutical preparations. Both sets of results are compared statistically by the Student t-test and the variance ratio.[22] The calculated values of t did not exceed the theoretical value, which indicates that there is no significant difference between the two mean recoveries. The variance ratio, F, also shows there is no significant difference between the precision of the two methods.

REFERENCES

1. H. Poiger and C. Schlatter, *Analyst*, 1967, **101,** 808.
2. E. Ragazzi and G. Veronese, *J. Chromatog.*, 1977, **132,** 105.
3. A. Regosz, *Pharmazie*, 1977, **32,** 681.
4. E. Ragazzi and G. Veronese, *J. Chromatog.*, 1977, **134,** 223.
5. K. Tsuji and J. Robertson, *J. Pharm. Sci.*, 1976, **65,** 400.
6. I. Haroun and F. Khattab, *Indian J. Pharm.*, 1978, **40,** 12.
7. *British Pharmacopoeia 1980,* H.M. Stationery Office, London, 1980.
8. S. Okada, K. Hattori and T. Takano, *Bull. Chem. Soc. Japan*, 1965, **38,** 2186.
9. J. F. Alicino, *J. Pharm. Sci.*, 1976, **65,** 300.
10. J. R. Grime and B. Tan, *Anal. Chim. Acta*, 1979, **105,** 369.
11. W. W. Holl, M. O'Brien, J. Filan, T. R. Mazeika, A. Post, D. Pitkin and P. Actor, *J. Pharm. Sci.*, 1975, **64,** 1232.
12. D. L. Mays, F. K. Bangert, W. C. Cantrell and W. G. Evans, *Anal. Chem.*, 1975, **47,** 2229.
13. L. P. Marrelli, *J. Pharm. Sci.*, 1972, **61,** 1647

14. R. Aikawa, M. Nakano and T. Arita, *Chem. Pharm. Bull.*, 1976, **24,** 2350.
15. R. H. Barbhaiya and P. Turner, *J. Pharm. Pharmacol.*, 1976, **28,** 791.
16. A. F. Heald, C. E. Ita and E. C. Schreiber, *J. Pharm. Sci.*, 1976, **65,** 768.
17 V. Hartmann and M. Roediger, *Chromatographia*, 1976, **9,** 266.
18. J. S. Wold and S. A. Turnipseed, *J. Chromatog.*, 1977, **136,** 170.
19. J. A. Squella, L. Nunez-Vergara and E. M. Gonzalez, *J. Pharm. Sci.*, 1978, **67,** 1466.
20. *Idem, J. Assoc. Off. Anal. Chem.*, 1979, **62,** 556.
21. *U.S. Pharmacopoeia 1980*, 20th Revision, Mack Publishing Company, Easton, Pa., 1980.
22. L Saunders and R. Fleming, *Mathematics and Statistics*, 2nd Ed., pp. 192–197. Pharmaceutical Press, London, 1971

Talanta, Vol. 30, No 10, pp. 795–797, 1983
Printed in Great Britain

0039-9140/83 $3.00 + 0.00
Pergamon Press Ltd

INDIRECT SPECTROPHOTOMETRIC DETERMINATION OF CYANIDE BY MEANS OF THE COLOUR REACTION OF SILVER WITH CADION 2B IN PRESENCE OF TRITON X-100

ZHU YU-RUI, WEI FU-SHENG* and YIN FANG
Department of Chemistry, China University of Science and Technology, Hefei, China

(*Received* 21 *January* 1983. *Accepted* 15 *April* 1983)

Summary—Silver gives a colour reaction with cadion 2B in the presence of the non-ionic surfactant Triton X-100, and the suppression of the colour by competitive complexation of the silver can be used for the spectrophotometric determination of cyanide. Cyanide in waste water can be separated by distillation from other ions that also interfere, and then determined.

Cadion 2B reacts with silver at pH 9.2 in the presence of the non-ionic surfactant Triton X-100 to form a red-violet complex with a molar absorptivity of 1.0×10^5 l.mole^{-1}.cm^{-1} at 565 nm.[1] This sensitive colour reaction is suppressed by cyanide. This paper reports how the suppression can be utilized in analysis of industrial waste water for cyanide.

The method developed is more sensitive than the other indirect spectrophotometric determinations of cyanide, such as those based on the Ag^+–phen–BPR,[2–4] Ni^{2+}–5–Br-PADAP,[5] and Cu^{2+}–CAS–CPC systems.[6] Compared with the pyridine–pyrazolone,[7] isonicotinic acid–pyrazolone[8] and pyridine–barbituric acid systems,[9] the colour system and reagents used here are rather stable, non-toxic and odourless.

EXPERIMENTAL

Reagents

Standard silver solution (1.00 mg/ml). Dissolve 0.1580 g of analytical-reagent grade silver nitrate in distilled water and make up to volume in a 100-ml standard flask. Dilute to a final concentration of 20 μg/ml as a working standard.

Standard cyanide solution. Dissolve 1.000 g of analytical grade potassium cyanide in distilled water and make up accurately to 1000 ml. Standardize with 0.01 *M* silver nitrate. Dilute to give a final cyanide concentration of 2.00 μg/ml, as a working standard.

Cadion 2B solution. Dissolve 0.04 g of the reagent in 100 ml of ethanol.

Triton X-100, 5% aqueous solution.

Sodium tetraborate, 5% aqueous solution.

Procedure

To a 25-ml standard flask, add 20 μg of silver, 2 ml of 5% sodium tetraborate solution, 1 ml of 5% Triton X-100 solution, not more than 10 μg of cyanide and mix well. Then add 1.5 ml of cadion 2B solution, dilute to the mark with distilled water and mix well. Measure the absorbance at 565 nm in a 1-cm cell against a reference blank solution containing no cyanide or silver.

Separation of cyanide by distillation

Place the cyanide-containing sample in a 500-ml all-glass distillation apparatus (if necessary, dilute to 250 ml with distilled water). Add 2 g of tartaric acid and 2 ml of 10% zinc acetate solution, connect up the distillation apparatus, and distil rapidly. Collect the distillate in an absorption flask containing 5 ml of 0.1 *M* sodium hydroxide. Stop distilling when the distillate volume reaches 45 ml, and dilute it to volume in a 50-ml standard flask with distilled water. Determine the cyanide in an aliquot according to the procedure above.

RESULTS AND DISCUSSION

Mechanism of the determination

In sodium tetraborate solution, in the presence of Triton X-100, cyanide complexes silver and thus suppresses the colour reaction of the silver with cadion 2B. The effect is shown in Fig. 1. A molar ratio plot indicates that the complex anion $Ag(CN)_2^-$ is formed.

Effect of pH

The absorbance obtained in the presence of 4.0 μg of cyanide was determined by the general procedure, at various pH values. Constant absorbance (Fig. 2) was obtained at pH 8.8–9.8, so a pH of 9.2 was selected for determination of cyanide.

Effect of cadion 2B concentration

Figure 3 shows that the difference, ΔA, between the absorbances for the silver complex with and without cyanide present is dependent on the amount of cadion 2B added. If less than 0.6 ml of 0.04% cadion 2B solution is added, ΔA is zero because there is not sufficient cadion 2B to combine with all 20 μg of silver ion. If 1.2–3.0 ml of 0.04% cadion 2B solution is added, ΔA is maximal and constant. Hence 1.5 ml of the reagent is recommended in the procedure.

*Present address: China National Environmental Monitoring Center, Beiyuan, Beijing, China.

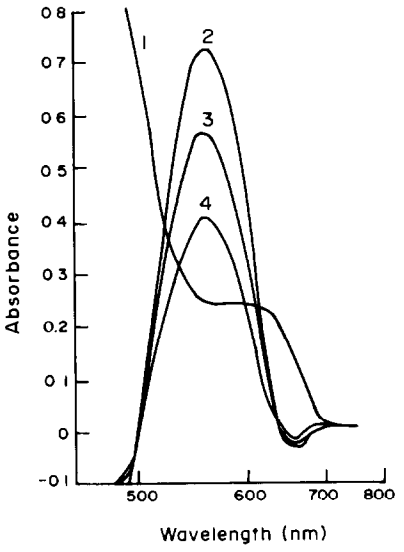

Fig. 1. Absorption curves: 1, 0.0024% cadion 2B solution against water; 2, 20 μg of Ag^+ + 0.0024% cadion 2B solution against reagent blank; 3, 20 μg of Ag^+ + 2.0 μg of CN^- + 0.0024% cadion 2B solution against reagent blank; 4, 20 μg of Ag^+ + 4.0 μg of CN^- + 0.0024% cadion 2B solution against reagent blank.

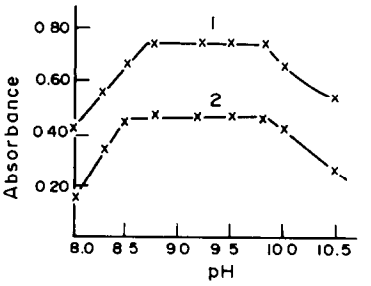

Fig. 2. Effect of pH: 1, 20 μg of Ag^+ + 0.0024% cadion 2B solution against reagent blank, 2, 20 μg of Ag^+ + 4.0 μg of CN^- + 0.0024% cadion 2B solution against reagent blank.

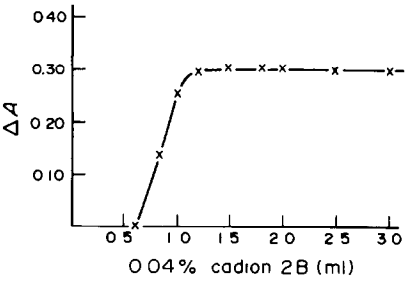

Fig. 3. Effect of cadion 2B concentration in determination of 4μg of CN^-.

Effect of temperature

Cyanide reacts with the silver instantaneously. A temperature of 10–40° for colour development does not affect the stability of the silver complex or the absorbance difference. The development of colour is complete within 3 min and ΔA remains constant for at least 24 hr.

Table 1. Recovery of cyanide by distillation

CN^- taken, μg	Form taken	Found, μg
10.0	KCN	10.1
20.0	KCN	20.0
40.0	KCN	41.6
100.0	KCN	98.4
200.0	KCN	192.2
100.0	$Zn(CN)_4^{2-}$	99.5
100.0	$Cd(CN)_4^{2-}$	93.3
100.0	$Fe(CN)_6^{4-}$	3.9
100.0	$Fe(CN)_6^{3-}$	3.9
100.0	$Co(CN)_6^{3-}$	0.0

Effect of order of addition of reagents

It does not matter whether the cyanide is added before or after formation of the silver–cadion 2B complex.

Adherence to Beer's law

A series of standard cyanide solutions was prepared and the absorbance of each was measured. ΔA was a linear function of amount of cyanide from 0.5 to 10 μg.

Precision

Ten replicate determinations of 4.0 μg of cyanide gave a mean absorbance of 0.306 with a relative standard deviation of 2.9%. The recoveries of cyanide by distillation of HCN and collection in alkali are listed in Table 1. Of the complex cyanides, only those that are labile give reasonable recovery.

Table 2. Analysis of waste water

Sample*	No. of detns.	Average [CN^-], *ppm*	RSD, %	Isonicotinic acid–pyrazolone method, *ppm*
1	13	24.4	2.1	24.0
2	8	51.9	2.5	50.0
3	10	20.0	3.0	21.8
4	9	82.2	2.3	80.0
5	5	0.017	5.9	0.018

*1,2: From an electroplating works.
3,4: From coking coal.
5: From domestic sewage.

Determination of cyanide in waste water

Sulphide, chloride, bromide and iodide interfere unless separated. Sulphide can be removed at pH 11 by adding small portions of powdered lead carbonate.[7] The distillation procedure eliminates the effect of Cl^-, Br^- and I^-.

The results for five samples are given in Table 2.

REFERENCES

1. F. S. Wei and F. Yin, *Talanta*, 1983, **30**, 190.
2. R. M. Dagnall and T. S. West, *ibid.*, 1964, **11**, 1627.
3. R. M. Dagnall, M. T. El-Ghamry and T. S. West, *ibid.*, 1968, **15**, 107.
4. J. H. Huang and Z. Q. Liu, *J. Univ. Chungshan*, 1978, **3**, 88.
5. F. S. Wei, Y. Q. Liu, F. Yin and N. K. Shen, *Talanta*, 1981, **28**, 694.
6. Y. Y. Zhu and W. B. Qi, *Fenxi Huaxue*, 1981, **9**, 692.
7. *Standard Methods for the Examination of Water and Waste Water*, 13th Ed., pp. 397, 404. American Public Health Association, American Water Works Association and Water Pollution Control Federation, 1971.
8. G. V. L. N. Murty and T. S. Viswanhan, *Anal. Chim. Acta*, 1961, **25**, 293.
9. K. Ishii, T. Iwamato and K. Yamanishi, *Bunseki Kagaku*, 1973, **22**, 448.

Talanta, Vol 30, No 10, pp 798–800, 1983
Printed in Great Britain

0039-9140/83 $3 00 + 0 00
Pergamon Press Ltd

OXIDIMETRIC ESTIMATION OF CHLORAMPHENICOL WITH AROMATIC SULPHONYL MONOHALOAMINES

B. JAYARAM and S. M. MAYANNA
Department of Chemistry, Central College, Bangalore University, Bangalore 560001, India

(*Received* 4 *October* 1982. *Revised* 6 *April* 1983. *Accepted* 15 *April* 1983)

Summary—The reaction between chloramphenicol and chloramine-T, chloramine-B, bromamine-B or bromamine-T has been found to proceed quantitatively over a wide range of experimental conditions. Simple titrimetric procedures for the estimation of chloramphenicol with *N*-haloamines have been developed. Oxidation of the antibiotic involves a four-electron change and the products of oxidation have been identified. The methods are useful for the estimation of this antibiotic in medicinal formulations.

Chloramphenicol, the first of the broad-spectrum antibiotics, has been assayed by spectrophotometric,[1,2] polarographic,[3] GLC[4] and HPLC[5] techniques, but some of the methods described are rather tedious. Titrimetric procedures include oxidation with periodate, the excess of which is determined by arsenite–iodine titration,[6] an argentometric titration,[7] acid hydrolysis followed by dichromate titration of the base produced,[8] and an iodometric procedure.[9] Titrimetric estimations of CP have been reported by Yalcindag[10] and Eremina *et al.*,[11] but we have been unable to obtain details.

Aromatic sulphonyl monohaloamines have been used as versatile oxidizing agents[12–14] for assay of organic and inorganic compounds. Here we describe their use for estimation of chloramphenicol by back-titration methods which are elegant, simple, fairly rapid and suitable for the assay of medicinal formulations.

EXPERIMENTAL

Chloramphenicol was purified by extraction from water with ethyl acetate. Colorimetric assay[1] of the sample showed the purity to be 99.9%. A standard solution (1 mg/ml) was prepared in doubly distilled water or buffer solution.[15] Chloramine-T (CAT) was purified by the method of Morris *et al.*[16] Chloramine-B[17] (CAB), bromamine-T[18] (BAT) and bromamine-B[19] (BAB) were prepared and purified by standard procedures. Approximately 0.05*N* solutions of the oxidants were prepared in distilled water and standardized iodometrically. All other reagents used were of analytical grade.

Preliminary studies

Direct titration at room temperature (26 ± 2°) was found impracticable, because the oxidation is not instantaneous, so a back-titration procedure was developed.

In preliminary experiments 5 ml of $10^{-3}M$ chloramphenicol solution were added to a known and excessive (40–60%) volume of oxidant (0.005*N*) containing various amounts of acid, base or buffer (and copper sulphate in the case of CAT and CAB) in an iodine flask. The reaction mixture was set aside and occasionally shaken. Then 20 ml of 3*M* sulphuric acid and 10 ml of 10% potassium iodide were added and the liberated iodine was titrated to a starch end-point, with 0.01*M* sodium thiosulphate. A blank titration was performed under identical conditions.

The extent of oxidation of chloramphenicol in various media in 30 min is given in Table 1. Oxidation with CAT and CAB is not feasible at pH 1–10, but is complete in 0.05–0.10*M* sodium hydroxide containing copper sulphate (at the 5–20 × $10^{-5}M$ level). With BAT and BAB, oxidation is slow at pH < 6, and incomplete in 30 min at pH 6–10. The reaction is complete with both oxidants, in 0.05–0.01*M* sodium hydroxide medium even in the absence of copper(II). At least 40 min reaction time must be allowed, to ensure completion of the oxidation at room temperature (26 ± 2°), but only 20 min will be needed at 40°. From statistical evaluation of the results (coefficients of variance) it appears that the precisions given by the four oxidants are in the order CAT > CAB > BAT > BAB.

Table 1. Extent of oxidation of chloramphenicol with *N*-haloamines in various media

Medium	$\left(\frac{\text{mole of oxidant consumed}}{\text{mole of antibiotic taken}}\right)$			
	CAT	CAB	BAT	BAB
0.05*M* NaOH	0.0	0.0	2.00	1.98
0.10*M* NaOH	0.0	0.0	2.00	2.00
0.05*M* NaOH + 5 × $10^{-5}M$ Cu^{2+}	2.00	2.01	—	—
0.05*M* NaOH + 2 × $10^{-4}M$ Cu^{2+}	2.00	2.00	—	—
0.1*M* NaOH + 5 × $10^{-5}M$ Cu^{2+}	1.99	1.99	—	—
0.5*M* NaOH + 5 × $10^{-5}M$ Cu^{2+}	1.35	1.78	—	—

Time 30 min; temperature 26 ± 2°C; [oxidant] = 5 × $10^{-3}N$; [antibiotic] = 1 × $10^{-3}M$.

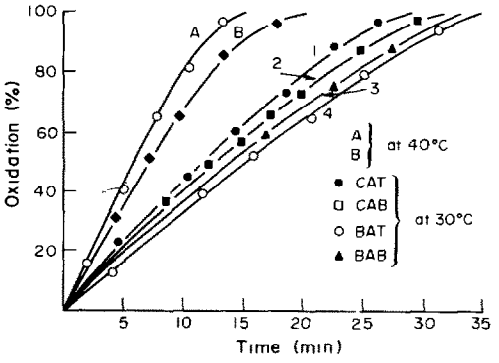

Fig. 1. Variation of % oxidation of chloramphenicol by *N*-haloamines with time. 1, 2—0.1*M* NaOH + $5 \times 10^{-5}M$ $CuSO_4$; 3, 4—0.1*M* NaOH; [CP] = $1 \times 10^{-3}M$; [oxidant] = $1 \times 10^{-2}M$.

Recommended procedure

Pipette a suitable volume (*e.g.*, 5 ml) of a solution containing between 0.5 and 15 mg of chloramphenicol into an iodine flask. Add 50 ml of 0.005*N* oxidant. Add enough sodium hydroxide and copper sulphate solutions to give the required concentrations (0.01–0.05*M* NaOH and $5–20 \times 10^{-5}M$ $CuSO_4$ for CAT and CAB; 0.05–0.1*M* NaOH for BAT and BAB). After about 40 min (30 min with CAT), add 20 ml of 3*M* sulphuric acid and 10 ml of 10% potassium iodide solution and titrate the liberated iodine with thiosulphate solution to a starch end-point (V_1 ml). Run a blank under identical conditions (V_2 ml). The amount of chloramphenicol (x mg) in the sample is given by the equation

$$x = 80.75Y(V_2 - V_1) \quad (1)$$

where Y is the molarity of the thiosulphate solution.

Table 2. Estimation of chloramphenicol in authentic samples with *N*-haloamines

Antibiotic taken, *mg*	Antibiotic found, *mg*			
	CAT	CAB	BAT	BAB
0.5	0.5	0.51	0.5	0.5
1.0	1.01 (0.99)*	0.99	1.00	1.01
1.5	1.48	1.49	1.51	1.51
2.0	2.0 (1.95)*	2.01	2.02	2.01
3.0	3.02	3.01	2.98	3.02
4.0	3.97	3.98	4.02	3.98
5.0	5.03 (5.01)*	4.97	5.03	5.04
7.5	7.48	7.53	7.47	7.46
10.0	9.97 (10.01)*	10.02	10.03	9.96

*Colorimetric values[1] are given in parentheses.

Analysis of medicinal preparations

In medicinal formulations, CP is generally associated with excipients such as benzocaine, propylene glycol, phenyl mercuric nitrate, phenol and ointment base, all of which have been found to interfere in the method just given. The excipients must therefore be removed[1,20,21] before the assay for chloramphenicol. The methods are given below.

Capsules. Grind the contents of 10 capsules to a fine powder. Weigh about 50 mg of this and transfer it to a beaker containing 10 ml of distilled water. Adjust the pH to 8.3 and transfer the mixture into a separatory funnel. Extract with three 25-ml portions of ethyl acetate, transferring the aqueous layer to a clean dry separatory funnel each time. Collect the ethyl acetate layers in a dry beaker, and evaporate to dryness. Dissolve the residue in 50 ml of distilled water and take 5 ml of the solution for titration.

Tablets. Grind about 10 tablets to a fine powder. Weigh out 500 mg and transfer to a beaker containing 100 ml of benzene, stir for 5 min, then filter off the residue and wash it with benzene. Dry the residue, weigh 100 mg of it into a beaker, and add 100 ml of distilled water. Adjust the pH of the solution to 8.3 and transfer it into a separatory funnel. Extract with ethyl acetate (3 × 25 ml) and complete the determination as for capsules.

Eye drops. Add 1 ml of sample to a beaker containing about 50 ml of distilled water, adjust the pH to 8.3 and transfer to a separatory funnel. Extract with ethyl acetate (3 × 25 ml) as for capsules. Evaporate the combined extracts to dryness, dissolve the residue in 10 ml of water and titrate.

Ear drops and injection. Take 1 ml of sample and about 10 ml of distilled water in a separatory funnel. Extract with diethyl ether (3 × 25 ml). Extract the aqueous layer with ethyl acetate (3 × 25 ml) as for capsules. Evaporate the combined extracts to dryness. Dissolve the residue in 100 ml of distilled water and take 5 ml for the estimation.

Eye ointment. Weigh about 1 g of ointment and dissolve it in about 10 ml of cyclohexane. Precipitate the ointment base by addition of ethyl alcohol (~ 50 ml). Filter off on a dry filter paper and wash with ethyl alcohol. Evaporate the filtrate and washings to dryness under reduced pressure. Dissolve the residue in 50 ml of water and take 5 ml for titration.

Table 3. Estimation of chloramphenicol in various medicinal formulations with *N*-haloamines

Medicinal formulation	Excipients present	Antibiotic present, *mg*	Antibiotic found, *mg*			
			CAT	CAB	BAT	BAB
Tablet	Approved colour	3.37*	3.35 (3.36)	3.35	3.38	3.34
Capsule	—	6.57*	6.53 (6.55)	6.53	6.53	6.52
Eye drops	Phenyl mercuric nitrate	5.0†	4.96 (4.98)	4.90	4.90	5.16
Ear drops	Benzocaine + propylene glycol	5.0§	4.97 (4.96)	4.99	4.96	4.98
Eye ointment	Ointment base	10.0‡	9.94 (9.97)	9.95	9.98	9.97
Injection	Phenol + propylene glycol	12.5§	12.32 (12.38)	12.34	12.42	12.54

*mg/10 mg. †mg/ml. ‡mg/g. §mg/0.1 ml. Colorimetric values[1] in parentheses.

RESULTS AND DISCUSSIONS

The recovery was determined with samples containing known amounts of chloramphenicol (Table 2) and medicinal formulations (Table 3), and compared with the results obtained colorimetrically.[1] The methods of sample preparation are designed to remove interfering compounds; benzene extraction removes colouring matter, ether extraction removes phenol, propylene glycol and benzocaine, and the alcohol treatment precipitates ointment base. The error is generally 1% or less. The reactions can be represented by:

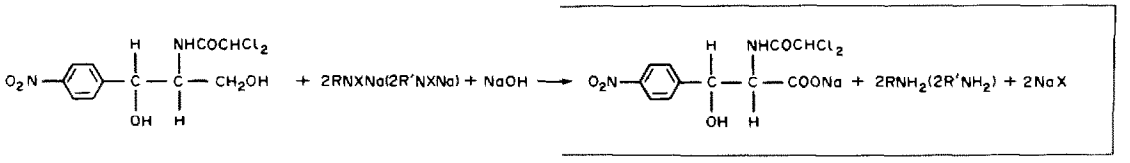

where $R = p\text{-}CH_3C_6H_4SO_2-$, $R' = C_6H_5SO_2-$ and $X = Cl$ or Br. The oxidants undergo four-electron reduction to the sulphonamides.

The presence of foreign ions such as Na^+, K^+, Ba^{2+}, Cl^-, SO_4^{2-}, ClO_4^-, PO_4^{3-} (up to an ionic strength of 0.2*M*) had no influence on the rate of oxidation, but with CAT and CAB, higher concentrations of copper has a considerable catalytic effect. The oxidation stoichiometry is unaffected by reversal of the order of addition of the reagents.

Acknowledgements—The authors are grateful to Prof. G. K. N. Reddy, Head, Department of Chemistry, Bangalore University, Bangalore, for laboratory facilities. They also wish to thank Prof. D. S. Mahadevappa, Department of Chemistry, Mysore University, Mysore and Prof. P. P. Thampi, Govt. Pharmacy College, Bangalore for helpful discussions. One of them (B.J) acknowledges a research fellowship from the UGC, New Delhi, India, under the F.I.P.

REFERENCES

1. (*a*) K. Jan and L. Agnieszka, *Chem. Anal. Warsaw*, 1977, **22**, 755. (*b*) F. D. Snell and C. T. Snell, *Colorimetric Methods of Analysis*, Vol. IV AAA, p. 178. Van Nostrand Reinhold, New York, 1971. (*c*) *British Pharmacopeia-73*, Vol. II, p. 525. DHSS, University Printing House, Cambridge, 1980.
2. Kirk-Othmer, *Encyclopaedia of Chemical Technology*, 3rd Ed., Vol. 2, p. 926. Interscience, New York, 1978.
3. (*a*) K. Fossdal and E. Jackson, *Anal. Chim. Acta*, 1971, **56**, 105. (*b*) G. B. Hess, *Anal. Chem.*, 1950, **22**, 649.
4. *Encyclopaedia of Industrial Chemical Analysis*, F. D. Snell and C. L. Hilton (eds.), Vol. 5, p. 496. Interscience, New York, 1967.
5. H. A. Ruessel, *Chromatographia*, 1978, **11**, 341.
6. A. Valseth and A. Wickstrøm, *Medd. Norsk Farm. Selskap*, 1955, **17**, 345; *Chem. Abstr.*, 1956, **50**, 5979a.
7. *Analytical Profiles of Drug Substances*, K. Florey (ed.), Vol. 4, p. 77. Academic Press, New York, 1975.
8. U. M. Chandra and P. Pandey, *LABDEV* (*Kanpur*), 1967, **5**, 338.
9. I. P. Koka, *Mater. S'ezda Farm. B. SSR, 3rd.*, 1977, 132; *Chem. Abstr.*, 1980, **92**, 47268h.
10. O. N. Yalcindag, *Folia Pharm.* (*Istanbul*), 1962, **4**, 536; *Chem. Abstr.*, 1962, **57**, 4762i.
11. Z. I. Eremina, N. S. Astakhina, K. V. Emel'yanenko and R. A. Protsenko, *Farmatsiya Resp. Mezhved. Sb.*, 1975, **2**, 59; *Ref. Zh. Khim.*, 1976, 20349.
12. M. M. Campbell and G. Johnson, *Chem. Rev.*, 1978, **78**, 65.
13. S. M. Mayanna and B. Jayaram, *Analyst*, 1981, **106**, 729.
14. S. M. Mayanna and K. V. Uma, *Talanta*, 1981, **28**, 259.
15. A. Findlay, *Practical Physical Chemistry*, p. 268. Longmans, London, 1954.
16. J. C. Morris, J. A. Salazar and M. A. Wineman, *J. Am. Chem. Soc.*, 1948, **70**, 2036.
17. A. Chrzaszczewska, *Bull. Soc. Sci., Lett. Lódź Classe III*, *3*, 1952, **16**, 5; *Chem. Abstr.*, 1955, **49**, 212.
18. C. G. R. Nair, R. L. Kumari and P. I. Senan, *Talanta*, 1978, **25**, 525.
19. D. S. Mahadevappa and M. S. Ahmed, *ibid.*, 1980, **27**, 669.
20. D. Halit, *Ann. Pharm. Franc.*, 1961, **19**, 477.
21. F. Vláčil and J. Synek, *Collection Czech. Chem. Commun.*, 1964, **29**, 1618.

Talanta, Vol. 30, No 10, pp. 801–804, 1983
Printed in Great Britain.

0039-9140/83 $3.00 + 0.00

ANNOTATIONS

UNEXPECTED DEPENDENCE OF THE PROTONATION CONSTANT OF 2,2′-BIPYRIDYL ON IONIC STRENGTH

KLÁRA SZABÓ
Institute of Chemistry, Janus Pannonius University, H-7644 Pécs, Hungary

ISTVÁN NAGYPÁL and ISTVÁN FÁBIÁN
Institute of Inorganic and Analytical Chemistry, Lajos Kossuth University, H-4010 Debrecen, Hungary

(*Received* 23 *March* 1983. *Accepted* 26 *April* 1983)

Summary—The protonation constants of 2,2′-bipyridyl and ammonia have been determined by pH titration at 25°, at ionic strengths of 0.1, 0.2, 0.5, 1.0, 1.5 and 2.0*M* obtained by using $LiNO_3$, $NaNO_3$, KNO_3, $LiClO_4$ and $NaClO_4$ as background electrolytes. The protonation constants generally change by about 0.3–0.4 log units for both ligands in nitrate media. A similar change in the protonation constant of ammonia was observed in perchlorate media. There is, however, a change of about 0.8–0.9 log units in the protonation constant of bipyridyl in the perchlorate media. This phenomenon is interpreted by postulating ion-pair formation between perchlorate and the protonated form of bipyridyl, $HBp^+ + ClO_4^- \rightleftharpoons HBp^+ . ClO_4^-$ with formation constants of 0.54 in 2*M* lithium nitrate and 0.45 in 2*M* sodium nitrate.

The transition-metal complexes of 2,2′-bipyridyl have been studied by many authors. A critical review of the equilibrium data has recently appeared under the auspices of the IUPAC Commission on Equilibrium Data.[1] This review includes values for the protonation constants, with the critical comment "to be rejected" for a value of $pK = 4.62$, found by Davies and Dunning[2] for 1*M* KNO_3 medium at 30.3°. The reason for this comment was that the protonation constant was expected to have no significant dependence on ionic strength, and all the values determined at ionic strength 0.1 and 25° were in agreement, with a mean of 4.42 ± 0.05.

In a recent work on the kinetics of equilibria in the copper(II)–bipyridyl–glycine system, the protonation constant was determined in 1*M* potassium chloride at 25° and found to be 4.63.[3] This value should also be evaluated as "to be rejected" if the criterion above is correct. Repeated experiments and efforts to find any systematic error were unsuccesful. We therefore decided to make a systematic study of the effect of ionic strength on the protonation constant of bipyridyl at 25°, using ionic strengths of 0.1, 0.2, 0.5, 1.0, 1.5 and 2.0*M*, obtained with $LiNO_3$, $NaNO_3$, KNO_3, $LiClO_4$ and $NaClO_4$ as background electrolytes. For comparison, the protonation constant of ammonia was also determined in the same solutions. Some measurements were done in the mixed electrolytes $LiNO_3$–$LiClO_4$ and $NaNO_3$–$NaClO_4$.

EXPERIMENTAL

The salts used to maintain the ionic strength were purified by recrystallization, until regular V-shaped Gran-functions[4] were found for the strong acid–strong base titration curves. "Reanal" bipyridyl and ammonia were used; no acid–base impurity could be detected; the concentrations of their solutions agreed to within 0.1–0.2% with the expected values. Carbonate-free solutions of base were used for the potentiometric titrations.

A Radiometer PHM-52 pH-meter, with GK-2301B electrode (filled with saturated sodium chloride solution), was used for the pH measurements. The ligand concentration in all solutions to be titrated was 0.01*M*. The ligand stock solutions contained about a 60% excess of the appropriate acids, so the first part of each titration curve was a strong acid–strong base titration, followed by the titration of the protonated ligand.

EVALUATION OF THE TITRATION CURVES

The first part of the titration curve may be used to calibrate the electrode system for $-\log[H^+]$ on the basis of the method proposed by Irving *et al.*[5] This part of the titration curve may also serve for the determination of the concentration of the excess of

Table 1. The logarithm of the protonation constants of 2,2′-bipyridyl and ammonia as a function of ionic strength in various background electrolytes

Test substance	Ionic strength, M	$LiNO_3$	$NaNO_3$	KNO_3	$LiClO_4$	$NaClO_4$
2,2′-Bipyridyl	0.1	4.41_5	4.40_6	4.39_7	4.44_1	4.42_7
	0.2	4.46_0	4.43_6	4.43_4	4.50_4	4.49_5
	0.5	4.53_7	4.54_4	4.53_2	4.61_0	4.65_8
	1.0	4.64_7	4.68_3	4.64_4	4.78_2	4.89_2
	1.5	4.73_8	4.81_9	4.74_5	4.93_3	5.10_0
	2.0	4.83_6	4.92_6	4.81_8	5.08_0	5.33_1
Ammonia	0.1	9.30_6	9.22_4	9.20_5	9.28_8	9.22_7
	0.2	9.30_5	9.27_2	9.22_2	9.29_9	9.26_7
	0.5	9.35_1	9.31_7	9.30_2	9.36_8	9.32_5
	1.0	9.42_8	9.41_0	9.40_4	9.43_9	9.39_7
	1.5	9.48_0	9.50_5	9.48_0	9.49_3	9.49_6
	2.0	9.53_5	9.55_8	9.57_3	9.58_5	9.59_1

acid. From that part of the curve where the deprotonation takes place, the protonation constant and the total ligand concentration can be determined. Finally, from the section at pH above ~11, where the deprotonation is practically completed, the pK_w^c value defined by the concentrations can be calculated.

Taking into account the mass-balances, the dilution of the solution during the titration, and the equations

$$-\log[H^+] = p(H) - I$$

$$pK_w^c = p(H) - I - \log[OH^-]$$

which represent the curves at pH below ~3 and above ~11 respectively, the volume of titrant can be explicitly expressed as a function of $(H) = 10^{-p(H)}$ with the parameters I, pK_w^c, T_H^0, T_L^0 and $\log K_{HL}$:

$$V = V_0 \frac{T_H^0 - (H)B + K_w^c/[(H)B] - T_L^0 K_{HL}(H)B/[1 + (H)BK_{HL}]}{C_b + (H)B - K_w^c/[(H)B]}$$

where p(H) is the pH-reading, I is a calibration term to convert p(H) into $-\log[H^+]$,[5] $B = 10^I$, T_H^0 is the total proton concentration in the initial solution, T_L^0 is the total ligand concentration in the initial solution, K_{HL} is the protonation constant of the ligand, [HL]/[H] [L], V_0 is the volume of the initial solution, and C_b is the concentration of the basic titrant.

A program was written to calculate T_H^0, T_L^0, pK_w^c, I and $\log K_{HL}$, or *any combination* of them if some of them have fixed predetermined values, by minimizing the sum of the squares of the differences between the measured and back-calculated volumes. For this work, the I and $\log K_{HL}$ values were calculated and T_H^0, T_L^0 and pK_w^c were predetermined and fixed. The titration curves were used for evaluation up to pH ~7 with bipyridyl, and up to pH ~9.7 with ammonia. Up to these pH values, pK_w^c has no influence on the parameters calculated, so $pK_w^c = 13.8$ was used throughout the calculations.

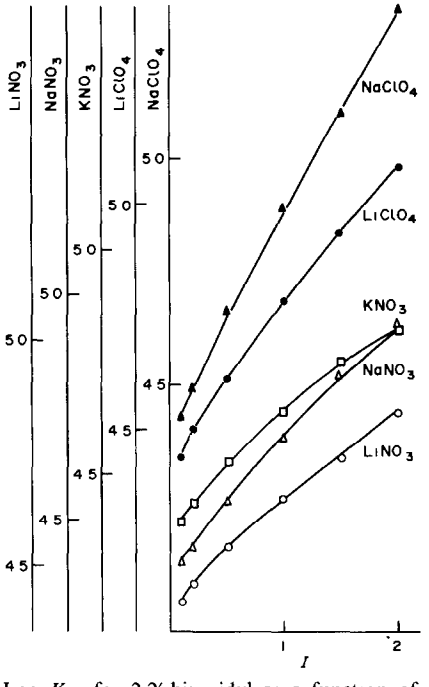

Fig. 1. Log K_{HL} for 2,2′-bipyridyl as a function of ionic strength in various background electrolytes.

RESULTS AND DISCUSSION

The log K_{HL} values calculated in the various salt solutions are given in Table 1. The dependence of log K_{HL} on ionic strength in the presence of various background electrolytes is shown in Figs. 1 and 2.

Figure 2 shows that the dependence of log K_{HL} for ammonia on ionic strength is roughly the same in all electrolytes. For bipyridyl, however, the dependence of log K_{HL} on ionic strength is quite different in solutions of different electrolytes. In lithium nitrate or in potassium nitrate, the increase in log K_{HL} with increasing ionic strength is roughly the same as for ammonia. The change in log K_{HL} between ionic strength 0.1 and 2.0M is about 0.1 higher when the background electrolyte is sodium nitrate. A sur-

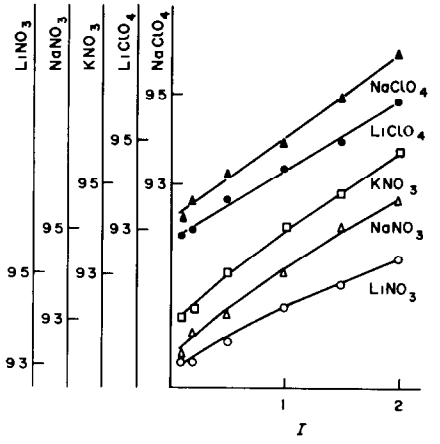

Fig. 2. Log K_{HL} for ammonia as a function of ionic strength in various background electrolytes.

Table 2. The logarithm of the protonation constant for 2,2′-bipyridyl and ammonia in mixed $NaNO_3$–$NaClO_4$ and $LiNO_3$–$LiClO_4$ electrolytes

C_{salt}, M			
$LiNO_3$	$LiClO_4$	2,2′-Bipyridyl	Ammonia
2.0	0.0	4.83_6	9.53_5
1.9	0.1	4.84_5	9.53_9
1.8	0.2	4.87_5	9.54_4
1.7	0.3	4.89_8	9.54_8
1.6	0.4	4.91_0	9.53_9
1.5	0.5	4.93_7	9.53_4
$NaNO_3$	$NaClO_4$		
2.0	0.0	4.92_6	9.55_8
1.9	0.1	4.94_2	9.55_1
1.8	0.2	4.96_1	9.54_3
1.7	0.3	4.98_0	9.54_0
1.6	0.4	4.99_9	9.54_6
1.5	0.5	5.00_9	9.56_5

prisingly large change in the protonation constant is observed in perchlorate media.

A possible explanation of the peculiar ionic-strength dependence of log K_{HL} for bipyridyl in perchlorate media is the formation of ion-pairs by the protonated bipyridyl and the perchlorate ions.

To get evidence for ion-pair formation in these systems, the dependence of log K_{HL} for bipyridyl and ammonia was studied in $2M$ ($NaNO_3 + NaClO_4$) and in $2M$ ($LiNO_3 + LiClO_4$) in the concentration range 2.0–1.5M nitrate and 0–0.5M perchlorate. The results are given in Table 2. For interpretation of the results, it is assumed that the measured protonation constants are apparent constants defined by:

$$K^{m}_{HL} = \frac{[HBp^+] + [HBp^+ClO_4^-]}{[H^+]\,[Bp]}$$

$$= K^{0}_{HL}(1 + K_{ip}[ClO_4^-])$$

where K^{m}_{HL} is the measured protonation constant in presence of perchlorate, K^{0}_{HL} is the protonation constant in $2M$ nitrate and $K_{ip} = [HBp^+ClO_4^-]/([HBp^+]\,[ClO_4^-])$.

Since the total perchlorate concentration was at least ten times that of protonated bipyridyl, the relationship $T_{ClO_4^-} \cong [ClO_4^-]$ is valid, *i.e.*,

$$K^{m}_{HL} = K^{0}_{HL} + K^{0}_{HL} K_{ip} T_{ClO_4^-}$$

The straight lines defined by these equations are shown in Fig. 3. It is seen that the slope is practically zero for ammonia (*i.e.*, there is no significant ion-pair formation), but there is a definite positive slope in the case of bipyridyl. The formation constant of the ion-pair is 0.54 in $2M$ lithium nitrate and 0.45 in $2M$ sodium nitrate. It is seen, moreover, that log K_{HL} values for ammonia in $2M$ lithium nitrate and in $2M$ sodium nitrate are the same, whereas there is a considerable difference between the log K_{HL} values for bipyridyl in the presence of these two electrolytes.

It should be stressed that the ion-pair formation constants given are valid in $2M$ nitrate media, where the ion-pairs $HBp^+NO_3^-$ may also be formed. The data given represent the *difference* between the abilities for ion-pair formation in perchlorate and nitrate media. Moreover, this interpretation of the unexpected dependence of the protonation constant of bipyridyl on ionic strength is only a possible and plausible assumption. Further work is in progress to attempt to prove it.

On the subject of critical evaluation of equilibrium data, the results of the work described here serve to

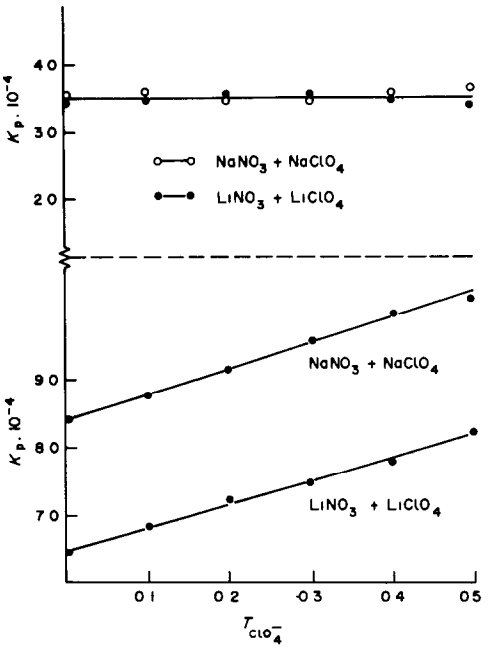

Fig. 3. Upper part: the logarithm of the protonation constant of ammonia as a function of perchlorate concentration in $2M$ ($LiNO_3 + LiClO_4$) and in $2M$ ($NaNO_3 + NaClO_4$). Lower part: the same function for 2,2′-bipyridyl.

act as a warning that qualification notes should be used with extreme care. An unexpected result is not necessarily wrong, and extrapolation by using well-known general formulae may be completely misleading.

Acknowledgements—We are indebted to Dr. L. D. Pettit, Prof. G. Anderegg and Prof. E. Högfeldt for reading the manuscript and for their critical comments. We are also indebted to Mrs. Katalin Biró for her skilful technical assistance.

REFERENCES

1. W. A. E. McBryde, *A Critical Review of Equilibrium Data for Proton and Metal Complexes of 1,10-Phenanthroline, 2,2′-Bipyridyl and Related Compounds*, IUPAC, Chemical Data Series, No. 17. Pergamon Press, Oxford, 1978.
2. R. L. Davies and K. W. Dunning, *J. Chem. Soc.*, 1965, 4168.
3. F. Debreczeni and I. Nagypál, *Inorg. Chim. Acta*, 1981, **57**, 135.
4. G. Gran, *Acta Chem. Scand.*, 1950, **4**, 559.
5. H. M. Irving, M. G. Miles and L. D. Pettit, *Anal. Chim. Acta*, 1967, **38**, 475.

Talanta, Vol. 30, No. 10, pp 805–809, 1983
Printed in Great Britain

0039-9140/83$3.00/0 + 0.00

LABORATORY DATA-ACQUISITION CAPABILITIES OF MICROCOMPUTER HIGH-LEVEL LANGUAGES

R. L. A. SING, S. W. MCGEORGE and E. D. SALIN*
Department of Chemistry, McGill University, Montreal, Quebec, Canada

(*Received* 16 *March* 1983. *Accepted* 25 *March* 1983)

Summary—A comparison is made of the efficiency and precision of various high-level languages in data-acquisition programs for microcomputers.

Microprocessors have become increasingly important in the laboratory. Automated experiments can provide rapid sample throughput, minimize operator errors, provide immediate calculation of results and allow the convenient storage of data for later retrieval and report-writing. In a scientific laboratory it is most efficient if programming is done in a high-level language such as BASIC, FORTRAN or PASCAL rather than directly in assembler, the language of the processor. The scientific laboratory is computation-intensive and a few lines of a high-level language can do what might require hundreds of lines of assembly-level coding. Therefore, most laboratory requirements can be met more rapidly by using high-level languages. Development, debugging and maintenance of high-level language programs are also much easier, since the statements are more "English" and "algebraic" in appearance and meaning. Scientists and technicians have often received training in a high-level language, traditionally FORTRAN. The input/output features of high-level languages allow programmers to develop visually appealing, "user friendly" programs with greater ease than is possible with assembly-level programming. Finally, high-level language programs are machine-independent, thereby providing a high degree of portability.

A major application of laboratory computers is data-acquisition, so the capabilities of high-level languages for this are of considerable interest.

In the recording of wave-forms, it is often essential that the acquisition interval be extremely precise, particularly with such techniques as the Fourier transform. Programmers often rely on the software to provide the time interval for the acquisition, and, if assembler programming is used, it is possible to ensure that all possible paths through the software or hardware result in the same time interval. The price paid for the convenience of high-level language programming is a certain loss of control over the internal operations of the program. These internal operations are designed for rapid execution, which may entail by-passing sections of code in one case and not in another. The structure of the languages is a proprietary secret, so the packages must be evaluated experimentally to determine their limitations for real-time use.

The two main ways of translating high-level languages into machine code involve the use of interpreters and compilers. For interpreter languages, of which BASIC is the most common example, high-level statements are converted into some executable form one line at a time and then immediately executed before the next statement in the program is dealt with. The end result is usually slower execution; however, program development is enhanced by the ability to execute programs immediately. Interpreters are often quite compact and can easily be run from read only memory (ROM). Compiler languages such as FORTRAN and PASCAL are completely converted into machine code before execution. They are therefore faster, but require disk-based systems, since large amounts of storage are required for the source code, the object code, the compiler, the linker and the associated libraries. While compiler programs execute rapidly, their development is more tedious and time consuming.

Previous work by Salin *et al.*[1] has indicated that acquisition rates can vary significantly between CPUs and languages. In this study, four high-level languages, Interpreter BASIC, Compiler BASIC, PASCAL and FORTRAN, have been run on a 4-MHz Z-80 CPU S-100 bus-based system and compared with a program written in optimized assembler code. In addition, several other manufacturers' versions of Interpreter BASIC have been compared by running on a variety of popular microprocessor-based computers (APPLE II, IBM PC, AIM-65). Table 1 lists the versions of the languages which were compared, along with their manufacturers.

BASIC (Beginners All Purpose Symbolic Instruction Code) is traditionally an interpreter language, popular for microprocessor systems because the interpreter can be conveniently put into ROM and used without expensive mass-storage devices. BASIC is also relatively easy to learn. This has led to much development and to the appearance of compiler

*Author for correspondence.

Table 1. High-level language versions

CPU/Language	Manufacturer	Size, *kbytes*
Z-80 (4 MHz)		
—Interpreter BASIC-80 (MBASIC)	Microsoft, 10800 N.E. Eighth, Suite 819, Bellevue, WA 98004	24
—Compiler BASIC-80	Microsoft	*
—FORTRAN-80	Microsoft	*
—PASCAL MT+	Digital Research, P.O. Box 579, Pacific Grove, CA 93950	*
6502 (1 MHz)		
—AIM-65 BASIC	Microsoft	8
—APPLESOFT	Apple Computer Inc., 10260 Bandley Drive, Cupertino, CA 95014	10
8088 (6 MHz)		
—IBM Personal Computer Advanced BASIC	IBM Corp., Personal Computer, P.O. Box 1328, Boca Raton, FL 33432	16

*Variable, depending on program library subroutine requirements.

versions of BASIC for microcomputers. Programs can be developed quickly with the interpreter and can then be compiled to give a faster-running program.

PASCAL is a highly structured language favoured by professional programmers. It is a compiler language, the power of which lies in its ability to manipulate varied and complex data types and structures. For evaluation, the PASCAL MT+ version was selected since it has a number of features which make it particularly useful for real-time data-acquisition. The foremost of these is its ability to utilize "in-line" assembly-level instructions.

FORTRAN (FORmula TRANslator) is an older, widely taught, compiler language, the strength of which lies in its ability to perform extensive calculations. A number of versions of FORTRAN exist for microcomputers though these are not so successful as the PASCAL versions.

EXPERIMENTAL

For this evaluation, the problem of the acquisition and storage of 9–16 bit (2 byte) data from an analogue-to-digital converter has been selected as an appropriate benchmark. Data points of 9–16 bits were selected since they represent resolutions ranging from 0.2 to 0.001%, which would prove adequate for most instrumental acquisitions. The following assumptions were made in order to ensure that the evaluation was free from hardware constraints. The analogue-to-digital converter was assumed to have a conversion time short enough for the conversion to be complete before the software was ready to read the next data value, thereby eliminating the need to check for the "End of Conversion" signal. Further, it was assumed that the converter would be triggered by a "Start Conversion" signal provided by the computer and that this signal would be automatically generated by a parallel input/output port. These assumptions are valid for most modern equipment. To provide accurate information about the acquisition processes, the "Start of Conversion" signal was monitored with an oscilloscope. This allowed the observation of any irregularities in the acquisition interval.

For all the evaluations, the routine shown in Fig. 1 was followed. Figure 2 shows the BASIC version of this routine, on which all the other routines were modelled. In all cases, standard, straightforward programming appropriate to the languages in general and not just to the specific versions studied was used, and optimization through the use of programming "tricks" was avoided. Such optimization can always be applied to any of the programming languages, but will seriously detract from the ease of programming and maintenance, and the portability that are so desirable in high-level languages.

RESULTS AND DISCUSSION

The experimental results are summarized in Table 2, which characterizes three different aspects of data-acquisition routines written in high-level languages: rate, timing, and size. These aspects will be treated separately.

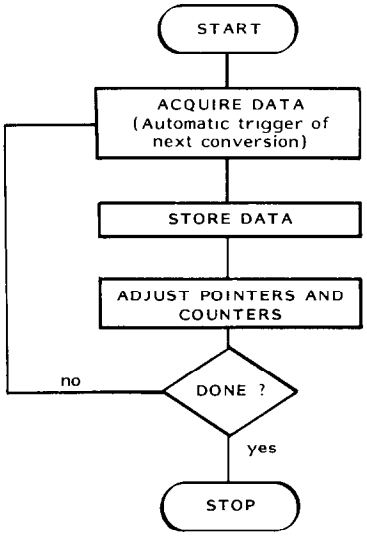

Fig. 1 Data acquisition flow diagram.

BASIC Acquisition Routine

```
 5 REM ALL VARIABLES INTEGER
10 DEFINT A-Z
15 REM INPUT START AND END MEMORY LOCATIONS
20 INPUT ST,EN
30 FOR I = ST TO EN STEP 2
35 REM READ AND STORE LOW BYTE THEN HIGH BYTE
40 POKE I,INP(24)
50 POKE I+1,INP(36)
60 NEXT I
70 STOP
```

Note: All REM (Remark) statements are removed for experiments.

Fig. 2. BASIC acquisition routine.

Acquisition rate

Table 2 confirms that the order of acquisition rate is assembler > compiler > interpreter, as expected. The surprising revelation is that compiler BASIC, using integer indexes, can yield rates which are as high as 30% of the highest obtained (with the optimized assembler version). Therefore, with compiler BASIC, all but very high rate (> 15 kHz) acquisition problems can be accommodated. Examination of the machine code generated by the compiler indicates that it does indeed optimize as claimed by the manufacturer. The FORTRAN and PASCAL programs are slower than the BASIC compiler program using integers, though by only an order of magnitude. This is because the FORTRAN program implements the POKE (direct memory modification) command as a subroutine and PASCAL has no direct equivalent of the POKE command. For both these languages, the acquisition rate can be increased by using version-specific programming elements; for example, PASCAL can acquire data at 10 kHz if pointers are used. Furthermore, PASCAL MT$^+$ allows in-line assembly-code insertion and can thereby acquire data at the same rate as the assembler routine.

The interpreter versions of the programs are comparatively quite slow, but would still be sufficiently fast for many applications such as gas chromatography, liquid chromatography, electrothermal atomic-absorption, differential scanning calorimetry, polarography and anodic-stripping voltammetry. Transients as short as 0.1–0.02 sec could be accurately recorded, given the 50–200 Hz acquisition rates. This represents a considerable improvement over the strip-chart recorders which are often used to record transient signals.

Common to the interpreter and compiler languages is the substantial increase in acquisition speed provided by the use of integer indexes rather than real indexes in the loops, as dramatically demonstrated by the real and integer versions of the compiler BASIC program. Since calculations using real numbers require floating point algorithms and multi-word storage, their execution is much slower than integer calculations. With the Z-80 in particular, integer

Table 2. Maximum acquisition frequencies and program sizes for various high-level programming languages

Language	Acquisition frequency, *Hz*	Size, *bytes*	Acquisition interval description
Z-80 assembler	51.0×10^3	20	Regular
PASCAL MT$^+$	3.50×10^3	4862	Regular
FORTRAN-80	4.73×10^3	6595	Regular
MBASIC integer	220	177	Regular
MBASIC real	152	175	Regular
COMPILER BASIC integer	15.4×10^3	6144	Regular
COMPILER BASIC real	368	6656	Irregular
6502 assembler	27.8×10^3	63	Regular
AIM-65 BASIC normal	56.7	204	Irregular
AIM-65 BASIC optimized	122	199	Irregular
APPLESOFT	53.4	248	Irregular
IBM BASIC integer	178	165	*
IBM BASIC real	130	163	*

*Not recorded.

arithmetic is quite rapid, since it is implemented by using the 16-bit register pairs. When the interpreter is used, much of the execution time is spent in the interpretation process and the arithmetic processes represent a substantially smaller fraction of the total execution time. Therefore, the difference in execution speeds between the real and integer versions of the interpreter programs (45%) is less dramatic than for the compiler programs (4000%).

The 6502 assembler data-acquisition routine is about half as fast as the Z-80 routine. This is mainly because the Z-80 has 16-bit register pairs which can be used for counting and memory indexing, whereas the 6502 has only 8-bit index registers and hence requires page-turning procedures. The 6502-based BASICs (AIM BASIC and APPLESOFT) had about half the speed of interpreter BASIC-80 and the two did not differ substantially. AIM BASIC performs all calculations with real numbers, so the possibility of increasing speed by use of integers is not available. The APPLE offers two paths for the use of integers, APPLESOFT and APPLE INTEGER BASIC, but neither accepted a simple FOR loop with integer variables.

AIM BASIC demonstrated the increase of acquisition speed available by applying certain speed hints suggested by the manufacturers. The speed could be doubled by (1) using variables instead of constants, (2) declaring frequently used variables early in the program, (3) using names of only 1 or 2 characters for variables, (4) re-using variables and using multi-statement lines. These speed hints apply generally to all interpreter languages, but must be used carefully. For example, interpreting short constants (1–3 digits) may be faster than locating the variable in the variable list if it is lower down on the list than 3rd or 4th.

Program timing

As mentioned above, maintaining a constant time interval between acquisitions is always possible when programming in assembler. For the Z-80 assembler acquisition routine, uniform acquisition intervals were easy to obtain since the use of the 16-bit register pairs for counting and memory indexing resulted in single-path execution. For the 6502 assembler routine, the page-turning needed every 128 points necessitated careful adjustment of the different program branch lengths if a constant time interval was to be maintained. Nonetheless, it was possible to obtain uniform acquisition intervals.

The three compiler languages maintained constant time intervals when integer indexes were used for loops. This was determined in all cases by using an oscilloscope and a digital frequency/period meter. For compiler BASIC, it was possible to verify the precision by analyzing the assembler code generated by the compiler. For PASCAL and FORTRAN this verification was not possible because the code contained calls to library subroutines. The interpreter BASIC (MBASIC) routine maintained a constant time interval with integer indexes because integer arithmetic can be implemented as single-precision arithmetic through the use of the Z-80's 16-bit register pairs.

For all the BASICs, interpreter and compiler, use of real numbers rather than integer numbers resulted in irregular acquisition intervals. The irregularity manifested itself as a sudden shift in the acquisition interval. The shift occurred at varying stages in the acquisition routine, depending on the number of points acquired. Shifts as large as 3% were observed for compiler BASIC, in which arithmetic occupies a larger portion of the total execution time. Irregularities in the acquisition interval are expected since the floating-point arithmetic routines were designed by the manufacturers to execute as fast as possible. This often involves by-passing certain portions of the multiple-precision arithmetic not necessary for a given calculation. As a result, the acquisition interval may "jitter", though it may not be possible to observe this with the oscilloscope.

The irregularity in the acquisition interval is of great concern for any work based on precise frequency and requiring accurate recording of waveforms. In addition, any use of the cumulative time interval of the acquisition routine may suffer from the effects of the irregular time interval. This may not be a serious problem in laboratories which always make measurements relative to standards; at least self-consistent results could be expected, but absolute measurements made with software in which the acquisition interval is irregular may be subject to rather serious errors. All BASICs using real indexes for looping, and all the ROM-based 6502 BASICs (APPLE, COMMODORE, AIM-65), are subject to irregular acquisition intervals and the problems associated with them.

To ensure regular timing intervals while working with high-level languages which cannot benefit from the regular time intervals provided by integer arithmetic, hardware timing procedures should be used, so timing hardware is needed. Many computer systems have available a clock or timer-integrated circuit which is accessible to the high-level program. The software must wait for the end of the timing interval before proceeding with the actual acquisition. In this case, the maximum acquisition rate would be somewhat less than that obtained in the evaluation.

Program size

The size of the acquisition software is of great importance since it limits the available memory and consequently the number of data points which can be acquired at high data-rates. The assembler routines studied are quite compact, but they would be substantially larger if they were to include the additional software required for interaction with the user and to perform any real-time calculations. Furthermore, such programs would require major programming

effort. The interpreter BASIC programs themselves are quite compact, requiring about 150–200 bytes, but size of the interpreters must also be taken into account in calculation of the actual amount of memory used by interpreter programs. For ROM-based BASICs (APPLE and AIM-65), no additional RAM space is consumed by the interpreter itself, so the programs are indeed space-efficient. However, disk-based BASIC interpreters occupy a substantial amount of RAM memory, and also, many of these require that the operating system remain resident for proper operation, thereby further reducing the memory available for data storage. In a 64-kbyte system as much as 32 kbytes may be taken up by the BASIC and the operating system, leaving only the other 32 kbytes for the program and data storage. The apparently excessively large size of the compiler programs, for the brief sections of code written, results from the need for linkage of a core of library routines for initial operation, mathematical operations and user interaction. Large portions of the software are not executed, but the library structure requires that they still be linked. As a result, larger source programs would probably not lead to proportionately larger object code. Generally, compiler programs are less memory-consuming than their interpreter counterparts, because of the size of the interpreter itself.

In cases where real-time calculations are not required, memory constraints can be alleviated by having two separate routines, one for data acquisition and the other for calculations. Once the acquisition is complete, the calculation routine can replace the acquisition routine and continue processing. All of the disk-based high-level languages allow the chaining or overlaying of routines. Storage of data on secondary storage devices with post-acquisition processing is an alternative for low-speed acquisition problems.

CONCLUSIONS

It is important that the laboratory computer-user be acutely aware of the limitations of and errors introduced by the data-acquisition system. The data given here clearly indicate that irregularities in acquisition rate can occur when certain types of computer language are used. The error will generally not be important at low frequencies, but will increase in significance as the maximum acquisition-frequency is approached. It should also be noted that slight changes in the use of certain languages can produce regular acquisition intervals. It is especially important to note that very high data-acquisition rates are possible with some high-level languages, so the laboratory scientist can probably avoid having to program in assembler to gain a significant speed advantage. We find it very interesting that the newer 16-bit 6-MHz 8088 did not perform significantly differently from the 4-MHz Z-80 for comparable programs.

REFERENCE

1. E. D. Salin, M. W. Blades and G. Horlick, *Talanta*, 1981, **28**, 519.

Talanta, Vol. 30, No. 11, pp. 811–818, 1983
Printed in Great Britain.

0039-9140/83 $3.00 + 0.00

GC/MS DETERMINATION OF INCIDENTAL PCBs IN COMPLEX CHLORINATED-HYDROCARBON PROCESS AND WASTE STREAMS

RANDLE S. COLLARD*
Dow Chemical USA, Louisiana Division, Plaquemine, LA 70764, U.S.A.

MORRIS M. IRWIN, JR.
Dow Chemical USA, Michigan Division, Midland, MI 48640, U.S.A.

(*Received* 28 *March* 1983. *Accepted* 8 *June* 1983)

Summary—An electron-impact gas chromatography/mass spectrometry method using selected ion monitoring for the determination of incidental polychlorinated biphenyls in complex chlorinated-hydrocarbon samples is described. Ions in the molecular-ion cluster for each degree of chlorination (from monochloro- to decachlorobiphenyl) are monitored. Individual PCB isomers are used as standards. Validation data collected for several complex chlorinated-hydrocarbon matrices in three different laboratories had a relative precision (2σ) of 20% with a limit of detection ($3 \times$ standard deviation of base-line noise) of 5 ppm for a single isomer at any degree of chlorination. The method has been used for the determination of incidental PCBs in more than 1000 samples from more than 30 different chlorinated-hydrocarbon sample matrices.

The manufacture, processing, distribution and use of any substance containing polychlorinated biphenyls (PCBs) at a concentration of 50 ppm or greater were prohibited by Environmental Protection Agency (EPA) ruling 40 CRF 761.[1] As a result of a court ruling, the EPA has recently published new concentration limits for the ban.[2] The new limits are 10 μg/m^3 in air, 100 μg/l. in water, and 2 μg/g in products or wastes. PCBs are defined in the ruling as "any chemical substance or combination of substances that is limited to the biphenyl molecule that has been chlorinated to varying degrees." Under this definition, there are 209 isomeric PCBs (including the three monochlorobiphenyls).

Most of the PCBs that have been manufactured and distributed were specific groups of isomers, *e.g.*, the heat-transfer fluids, and these classical fluids have long been considered synonymous with the name PCBs. The ruling, however, controls all 209 isomers regardless of their source or the distribution of the isomers. As a result, numerous chlorinated-hydrocarbon process and plant wastes which contain non-classical PCBs have come under the ruling. These streams do not contain the classical PCB fluids produced as a result of the direct chlorination of biphenyl. Instead, a host of processes, reactants and conditions lead to the formation of various PCBs as undesired by-products. For example, Hutzinger *et al.*[3] list more than 40 different chemical reactions which produce PCBs. To differentiate them from the classical PCB fluids, these by-product PCBs are referred to as incidental PCBs.

The determination of incidental PCBs (some of which contain more than 70% Cl) in complex chlorinated-hydrocarbon streams presents an entirely different set of analytical problems from those encountered with classical PCBs. The classical PCB fluids have been well characterized[4,5] and can be completely analysed by determining only those 60 or so PCB isomers the fluids contain. The PCB content and isomer distribution of most chlorinated-hydrocarbon process and waste streams have not been characterized, however. Further, the isomer distribution is subject to change with variation in process. Therefore, analysis of these streams requires a method which can determine each of the 209 isomeric PCBs.[2]

The methods for determining classical PCBs,[3,5–7] *e.g.*, electron-capture gas chromatography (ECD), require the analyst to recognize on the chromatogram the isomer pattern of a particular classical PCB fluid or mixture of fluids and then to compare one or more peaks with a standard taken through the procedure. Pattern recognition is necessary because the usual chromatographic technique of peak for peak comparison cannot be used, since not all isomers are available as standards. Pattern-recognition techniques are satisfactory for determining the PCB content of classical PCB fluids because these fluids were produced by the controlled chlorination of biphenyl to give a consistent distribution or pattern of isomers, and standards of these fluids are readily available. Pattern-recognition techniques cannot be used for the determination of incidental PCBs which may form in chlorinated-hydrocarbon process and waste streams, because the isomer distribution in

*Author for correspondence.

such systems is unknown and is subject to change with variations in process. Unfortunately, standardization of the ECD methods for the determination of incidental PCBs in complex chlorinated-hydrocarbon matrices is not possible with the approximately 80 commercially available PCB isomers. It is not possible to use just a few isomers as ECD standards for all 209 isomers, since there is such a wide variation in response factor both between isomers with different degrees of chlorination and between isomers with the same degree of chlorination.[3,8] The lack of availability of all 209 isomers would also require the analyst to treat all peaks within the entire PCB retention-time range as belonging to authentic PCBs. Even with a good sample clean-up, ECD determinations would give erroneously high results for complex chlorinated-hydrocarbon process and waste streams.

Perchlorination has also been suggested as a technique for determination of PCBs,[3] but is completely non-specific with respect to degree of chlorination. In chlorinated-hydrocarbon process and waste stream samples, for which the isomer distribution is unknown, use of the perchlorination technique would require the yield of decachlorobiphenyl from each isomer to be the same. However, the yield has been found to depend on both degree of chlorination and structure.[3,9] Also, biphenyl and some non-PCB species are converted into decachlorobiphenyl by the perchlorination procedure and would interfere.[9] It is necessary, therefore, to find a method which can be used to determine all 209 isomeric PCBs. In order to prove that a stream contained less than 50 ppm, the original EPA-ban limit, a method would be necessary which could determine each of the 209 PCB isomers individually with a sensitivity such that the limit of detection for the sum of all 209 isomers would be 50 ppm. There is currently no method which has been validated for all complex chlorinated-hydrocarbon samples at the originally mandatory 50-ppm total PCBs limit or at the new limit of 2 ppm for the PCBs forming any particular peak.

Gas chromatography/mass spectrometry (GC/MS) has been used successfully to determine polychlorinated biphenyls in non-classical samples.[10] GC/MS is the only method found which can specifically determine incidental PCBs in complex chlorinated-hydrocarbon process and waste streams. The electron-impact (EI) GC/MS method described here uses selected ion monitoring (SIM) to monitor several ions for each degree of chlorination. Mixtures of individual PCB isomers of each degree of chlorination are used to standardize the method. The validated method described below was supplied to the EPA and its contractor by Dow as the suggested screening method for the analysis of incidental PCBs in complex chlorinated-hydrocarbon matrices.[11]

Table 1. Masses of ions monitored for determining incidental PCBs

Degree of chlorination	Ion masses
Cl_1	188 (M), 190 (M + 2)
Cl_2	222 (M), 224 (M + 2)
Cl_3	256 (M), 258 (M + 2)
Cl_4	290 (M), 292 (M + 2)
Cl_5	324 (M), 326 (M + 2)
Cl_6	358 (M), 360 (M + 2)
Cl_7	392 (M), 394 (M + 2)
Cl_8	428 (M + 2), 430 (M + 4)
Cl_9	462 (M + 2), 464 (M + 4)
Cl_{10}	498 (M + 4), 500 (M + 6)

EXPERIMENTAL

This method was used on several hundred samples in three Dow facilities to determine incidental PCBs in several different chlorinated-hydrocarbon process and waste streams. In addition to the Finnigan 1020-OWA GC/MS described here, a Hewlett-Packard 5985A and a Finnigan 4000 were used to perform analyses in the other laboratories. The analyses were essentially identical, with minor variations due to individual limitations and capabilities of the GC/MS systems.

Apparatus

A Finnigan 1020-OWA quadrupole GC/MS was used in the SIM–EI mode for analyses. The signals for the selected ions (see Table 1) were integrated at 66 msec/amu (1.5 sec repetition rate). A 6-ft long 2-mm bore glass column packed with 3% OV-210 on Chromosorb WHP (100–120 mesh) and designed for on-column injection was used. The column was temperature programmed for heating from 90° to 230° at 8°/min. The injector temperature was 230° and the separator temperature 240°. Helium was used as the carrier gas, at a flow-rate of 25 ml/min.

Reagents

Standards of individual PCB isomers were obtained from Analabs (North Haven, Connecticut) and Ultra Scientific (Hope, Rhode Island). Dilute solutions of standards and samples were prepared in *o*-xylene ("Distilled-in-Glass" grade, Burdick & Jackson Labs., Muskegon, Michigan) and refrigerated.

Procedure

The samples were weighed (0.50–2.00 g) and diluted to 10 ml with *o*-xylene. Aliquots (4 μl) were injected, and the volatilized solvent was diverted for 2 min, after which the components eluted were admitted into the mass spectrometer. Incidental PCBs were detected by monitoring selected ions specific for each degree of chlorination, as components were eluted from the chromatographic column. Integrated peak-height measurements were recorded. A calibration for each set of analyses was made daily, with at least three concentrations of mixtures of pure PCB isomers for each degree of chlorination.

RESULTS AND DISCUSSION

The data presented here were obtained with a Finnigan 1020-OWA GC/MS system. The other GC/MS systems used gave similar results.

The PCBs were first identified by determining whether or not coincident peaks at all of the masses monitored for a particular degree of chlorination had the correct ion-intensity ratios, within experimental error. Figure 1 shows a set of ion chromatograms obtained from a mixture of PCB isomer standards. When authentic PCBs were found in a sample, the peak height for the ion giving the highest signal was

used for quantification in order to maximize the sensitivity. For chlorinated-hydrocarbon samples for which the peak-height ratios were incorrect or when one or more of the masses monitored did not correspond to a peak, the maximum amount of PCBs which could be hidden under the peak showing the least interference was calculated (Fig. 2). In Fig. 2, the peak heights for peaks A, A′, C and C′ were used to authenticate and measure incidental PCBs. Since peak B was too high for the expected isotope ratio, the peak height of B′ was used to calculate the maximum amount of PCB that could be hidden

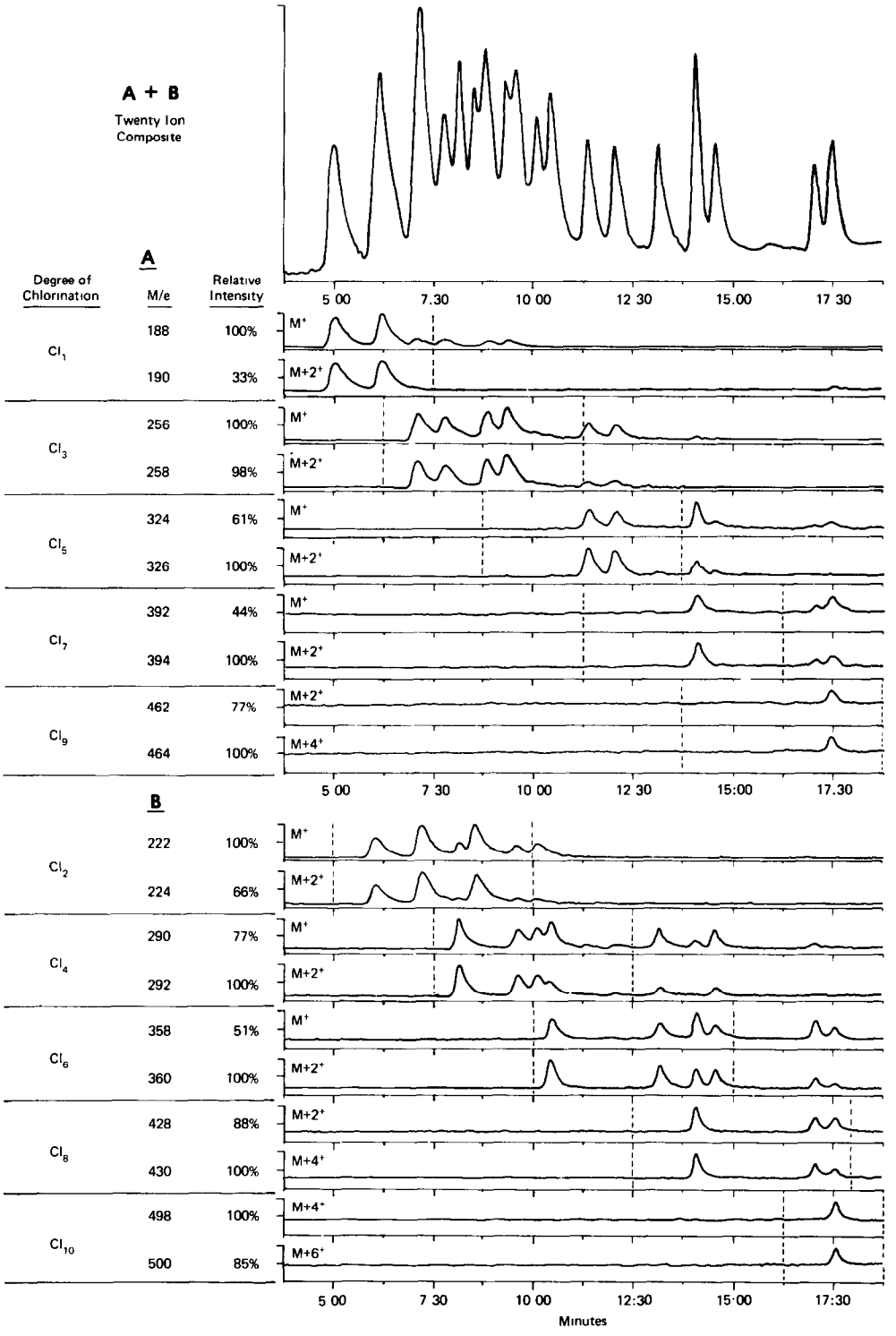

Fig. 1. Composite and individual selected-ion chromatograms of several PCB isomers.

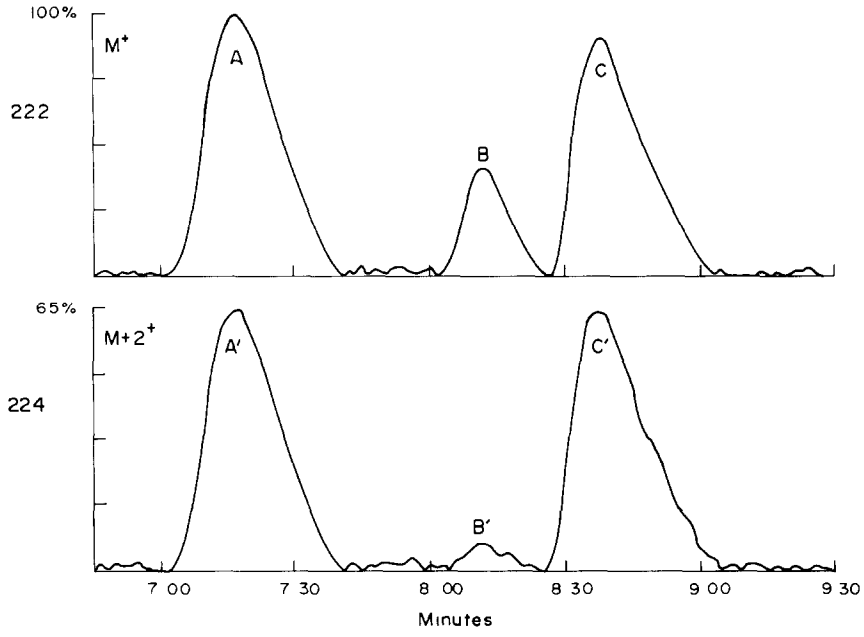

Fig. 2. Selected-ion chromatograms of a chlorinated-hydrocarbon sample. Peaks A,A′ and C,C′ in each chromatogram are of authentic PCBs and peaks B,B′ are due to interference(s).

under the peak for the mass with the least interference. Peak heights were used, rather than the integrated areas calculated by the data system.

Automatic area integrations such as those made by the Finnigan 1020-OWA or the HP 5992 were found to be less than satisfactory for these complex samples, as illustrated in Fig. 3. Although only peaks B and C contained authentic PCBs as indicated from isotope-ratio measurement, the data system automatically integrated the area for peaks A + B + C at one mass and peaks B′ + C′ + D′ at the other mass. The peak heights reported by the data system for the peaks C and C′ must, therefore, be used for quantification. When using such systems, which prevent the analyst from manually defining the area to be integrated for complex samples, it is necessary to sum the peak-height measurements manually to quantify the incidental PCBs. In this manner, the ratio of the peak heights for B and B′ to those reported by the data system for C and C′ would be evaluated manually. The sums for B + C and B′ + C′ would then be used to calculate the total amount of PCBs. Considerable effort is needed and care must be taken when using this technique for chlorinated-hydrocarbon process and waste streams. The manual area-calculations possible with the more sophisticated GC/MS data systems are preferable.

Since not all of the PCB standards were available, exact retention-time windows could not be set for each degree of chlorination. Broad windows were set, equal in width to the retention window for the first and last isomer eluted for each degree of chlorination, plus or minus 10% of the total analysis time. When the number of standard isomers available was extremely limited, the window set in this way was too small, so the window was set wide enough to include the signals for the adjacent degrees of chlorination. In no case have PCBs been detected outside these retention windows.

The lack of all 209 isomers also prevented the determination of a response factor for each. It was thus necessary to use a mixture of a few isomers to determine an average response factor to be used for

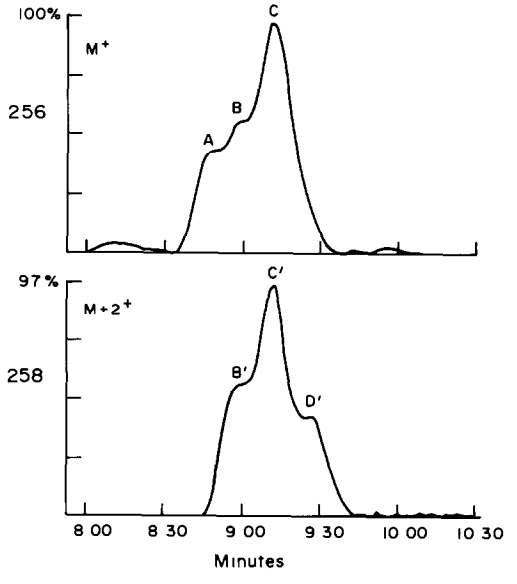

Fig. 3. Selected-ion chromatograms illustrating the limitations of automated area calculations.

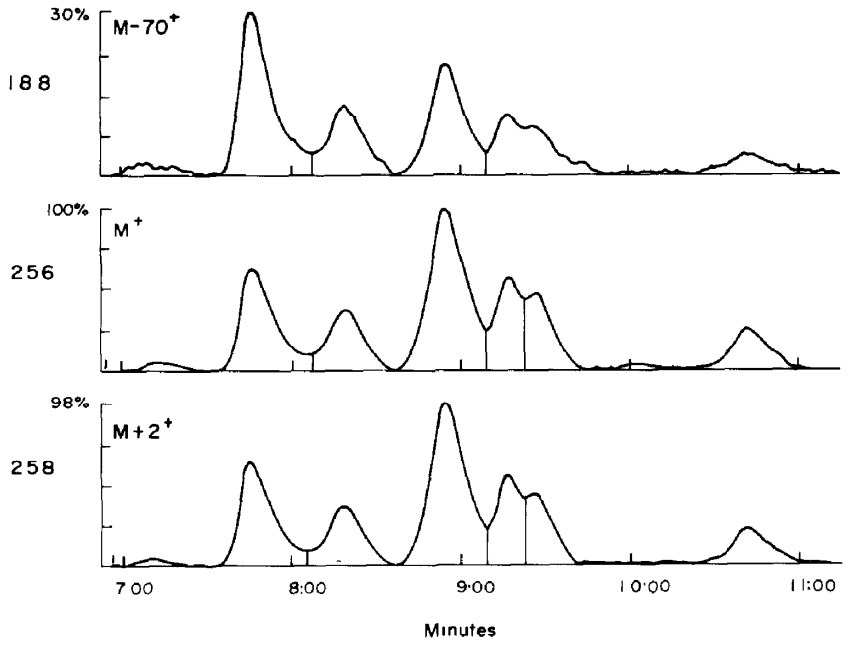

Fig. 4. Molecular and $(M-70)^+$ selected-ion chromatograms for a sample containing trichlorobiphenyls.

a particular degree of chlorination. A limited investigation of the variation in response factors among some of the commercially available PCB isomers was made for the principal ions from isomers of several degrees of chlorination. The values reported in Table 2 for the M^+ (molecular), $(M-70)^+$ (loss of 2 Cl) and $(M-35)^+$ (loss of Cl) ions of several tetrachlorobiphenyl isomers are representative of the isomers studied. The response factors for the tetrachlorobiphenyl isomers studied varied by at most a factor of 2 for both the M^+ and the $(M-70)^+$ ions. Recent work by Martelli *et al.* confirms this range for 45 PCB isomers.[12] They found that the response factors for groups of chlorobiphenyls, from mono- to octa-, varied by a factor of about two or less for a given degree of chlorination. The $(M-35)^+$ ion signals were very weak and their relative responses ranged from 1 to 78. The molecular ions and the $(M-70)^+$ ions gave the most intense response and had only relatively small response differences, so were chosen for monitoring the incidental PCBs (Fig. 4). The particular ions listed in Table 1 were chosen to minimize interferences for the samples being determined and to obtain the maximum sensitivity. Other or additional ions, or even full scans when the incidental PCB levels are sufficiently high, could be used for other types of samples. Quantification, however, should be done with ions in the molecular ion cluster whenever possible. As can be seen from Table 2, the use of an individual isomer for calibration purposes could lead to significant error. For this reason the method was standardized with mixtures of individual isomers and an average response factor for each degree of chlorination was used for determination of the incidental PCBs in samples.

Table 3 illustrates the significant variation in the response factors for various degrees of chlorination. The response for each degree of chlorination was a

Table 2. Relative GC/MS response factors for several tetrachlorobiphenyls

Isomer	M^+	$(M-35)^+$	$(M-70)^+$
2, 2′, 4, 4′	1.4	29	1.6
2, 2′, 3, 3′	1.0	78	1.7
2,3,5,6	2.0	10	1 8
2,2′,4,5′	1.3	36	1.6
2,3,4,5	1.6	3.5	1.3
2,2′,3,5′	1.0*	48	1.4
2,2′,6,6′	1.6	20	1.6
2,3′,4′,5	1.5	1.5	1.2
3,3′,4,4′	1 5	1.0*	1.0*
Average	1.4	25	1.4
Relative standard deviation, %	22	102	18

*Value used as reference.

Table 3. Relative PCB GC/MS response factors for various degrees of chlorination

Degree of chlorination	*M/e* used for quantification	Relative response factor	Relative precision (95% confidence), %
Cl_1	188	9.42	4 4
Cl_2	222	6 79	5.3
Cl_3	256	5.17	4.9
Cl_4	292	4.25	7.7
Cl_5	326	2.92	7 4
Cl_6	360	3.12	6.2
Cl_7	394	2.38	6.4
Cl_8	430	2.21	7.1
Cl_9	464	1.00*	5 8
Cl_{10}	498	1 79	5.8

*Value used as reference.

Table 4. Relative precision of incidental PCB measurements (Sample 1)

Degree of chlorination	Found, *ng*											Relative precision (95%), %
	1	2	3	4	5	6	7	8	9	10	Mean	
Cl_1	1.1	1.2	1.3	1.1	1.2	1.6	1 5	1 6	1 6	1 6	1.4	31
Cl_2	5 7	5.7	5.9	5.5	5.5	5.3	4.6	5.9	5.1	5.6	5.5	15
Cl_3	6.9	7.2	6.8	7.0	7.0	6.5	6.1	7.2	6.9	7.2	6.9	10
Cl_4	3 3	3.4	3.6	3 4	3.4	2.9	2.7	3.2	2.9	3.2	3.2	17
Cl_5	1 8	1 7	1 7	1.7	1.7	1 5	1.4	1 4	1.5	1.5	1 6	18
Cl_6	1.2	1.2	1 2	1 1	1 2	0.9	0 9	1 0	1 0	1 0	1 1	23
Cl_7	ND*	ND	ND	ND	ND	ND	ND	ND	ND	ND	—	—
Cl_8	ND	ND	ND	ND	ND	ND	ND	ND	ND	ND	—	—
Cl_9	ND	ND	ND	ND	ND	ND	ND	ND	ND	ND	—	—
Cl_{10}	1.1	1.0	1 0	1.0	1.0	1.1	1.1	1.0	1.1	1.0	1.0	10

*ND = none detected; LOD 1 ng.

linear function of concentration. Generally, the molar response decreases with increasing degree of chlorination, but this loss in sensitivity is offset by the smaller number of interferences at higher degrees of chlorination. Thus the actual limits of detection for real samples spiked with standards were very nearly the same for each degree of chlorination. The average relative precision at the 95% confidence level ($RP = 2\sigma$) for replicate standards was 6% (Table 3). The precision of the method was established by analysing two samples five times each on two different days. The data shown in Tables 4 and 5 give an average RP of 18%. Thus compounds which gave peak-height ratios within 20% of the correct values for ions monitored for that degree of chlorination were taken to be authentic PCBs.

The types of matrices analysed by the method in our laboratories contained mixtures of a wide range of aliphatic, aromatic and polymeric (tar) chlorinated hydrocarbons. The chlorine content of the samples varied from about 10% to more than 70%. Solutions of a "PCB-free" chlorinated-hydrocarbon sample were spiked with individual PCB isomers at concentrations equivalent to 1–10 ng of PCB in the volume injected, to determine recoveries. Recoveries in this sample matrix ranged from 95 to 103% for the ten degrees of chlorination (Table 6). Recoveries for the method are actually a measure of the matrix effect, which usually decreases the response. Although the recovery for this sample averaged 100%, values from other samples were as low as 65%. Consequently the recovery must be determined for each type of matrix.

Table 5. Relative precision of incidental PCB measurements (Sample 2)

Degree of chlorination	Found, *ng*											Relative precision (95%), %
	1	2	3	4	5	6	7	8	9	10	Mean	
Cl_1	6.8	6.6	7.2	6 9	7.0	7.5	7.6	8.3	7.3	7.7	7 3	14
Cl_2	37.3	36 3	38.0	37.4	35.9	31 4	32.2	34.1	31 0	32.3	34.6	16
Cl_3	45.5	47.7	46.1	46.2	45.8	39 5	39.0	42.8	39 4	41.8	43.4	15
Cl_4	24.8	25.4	25 6	25.9	25.7	21.2	21.1	23.3	21 3	23 2	23.8	17
Cl_5	12.8	12.4	12.6	13.4	13.0	10.8	10.8	11 7	10.7	11.1	11.9	18
Cl_6	9.4	9.4	9.6	9 6	9 8	7.8	7.9	8.1	7 8	8.3	8.8	19
Cl_7	6.0	6.0	5 9	5 9	6.4	4.5	4.9	4 9	4.8	4 8	5 4	25
Cl_8	4 6	5.3	5.2	5.5	5.4	4 3	4.3	4.6	4 6	4.6	4 8	19
Cl_9	5.3	5.7	5.8	5 9	5.8	4 3	4.4	4.8	4 7	4.9	5.2	24
Cl_{10}	5.7	5 9	5.8	6 0	6.0	4.9	5 1	5.7	5.1	5.5	5.6	14

Table 6. Recoveries of incidental PCB from a spiked chlorinated-hydrocarbon matrix

Degree of chlorination	Run 1			Run 2			Run 3			Mean recovery, %
	Added, *ng*	Found, *ng**	Std. devn., *ng*	Added, *ng*	Found, *ng*†	Std. devn., *ng*	Added, *ng*	Found, *ng*§	Std. devn., *ng*	
Cl_1	2.0	1.9	0.05	10.0	9.7	0 2	20 0	19 0	1 1	96
Cl_2	3.0	3.0	0.08	15.0	14.8	0.4	30 0	28 1	1 3	98
Cl_3	4.0	4 1	0 09	20.0	19 7	0 7	40 0	38.1	1 6	99
Cl_4	3 0	2.8	0 21	15.0	15.3	0.9	30.0	27.9	0.8	96
Cl_5	2.0	1.8	0.12	10.0	10.0	0.3	20.0	18.6	0 8	95
Cl_6	3.0	2.8	0.15	15.0	15.2	0 6	30 0	28 9	1 0	97
Cl_7	1.0	1 0	0 15	5.0	5 2	0 2	10.0	9 8	0.3	103
Cl_8	2 0	2 0	0.08	10.0	10.3	0.2	20.0	20 0	0 2	100
Cl_9	1.0	1.0	0.06	5 0	5 1	0.3	10 0	10.1	0.2	99
Cl_{10}	1.0	0 9	0 10	5.0	5.0	0.3	10 0	9 7	0 1	96

*Mean value of 5 determinations
†Mean value of 3 determinations
§Mean value of 2 determinations.

The limit of detection (LOD = 3 × standard deviation of base-line noise) for this method was 1.0 ng of a single PCB isomer injected, when twenty ions were monitored simultaneously. This represents an LOD of 5 ppm for each chromatographic peak for a 4.0-μl injection of a 0.5-g sample dissolved in 10 ml of *o*-xylene. Owing to sample matrix effects, this is slightly higher than the specification limits for the instrument performance and slightly higher than LODs found for standard mixtures in pure *o*-xylene. Limiting effects were the presence of components having ion fragments with the same masses as those monitored for the PCBs, limited sample solubility, and components of sufficiently high concentration to cause ion-molecule reactions or space-charge effects in the ion source.

Several classical PCB clean-up techniques[3] were tested as a means of decreasing levels of interferents but none significantly improved the LOD. The LOD was not the same for all sample matrices, however. In some matrices, owing to lower interferent levels or higher solubility, the LOD was as low as 1 ppm for a single chromatographic peak. The 5-ppm LOD represents the LOD which could be achieved for all of the sample matrices analysed. In guidelines recently proposed for environmental monitoring, the lower limit of quantification (LOQ) was defined as 10 × standard deviation of base-line noise (or 3.3 × LOD).[13] For the chlorinated-hydrocarbon matrices analysed, the LOQ was thus 3.3 ng (17 ppm) for a particular chromatographic peak. Values were found for PCB levels between the LOD and LOQ, however. As can be seen from the precisions reported in Tables 5 and 6, such values are much less precise than those that are greater than the LOQ.

This LOQ of 17 ppm is significantly higher than the 2-ppm limit for products and wastes mandatory in the revised EPA ruling. The EPA limit is predicated on the sensitivity of a capillary GC/electron-impact mass-spectrometer (CGC/EIMS) and on the use of an unspecified extraction and concentration of the incidental PCBs from a 50-g sample into 1 ml of solution, an aliquot of which is injected into the CGC/EIMS for analysis. Numerous extraction and concentration techniques were suggested in the EPA support documents,[11] and the setting of the 2-ppm limit in the light of matrix effects encountered in actual samples was discussed[2] in the ruling: "However, in the analysis of other (more complex) samples, interferences and matrix effects were significant, and resulted in a LOQ that was two orders of magnitude higher than the lower quantitation limit of the analytical instrument." Despite these findings, the ruling then states: "EPA's estimate of a reasonable allowance for interferences and matrix effects is one order of magnitude higher than the average lower quantitation limit of CGC/EIMS as estimated by EPA." Thus the limit set was based on a 2-ppm LOQ even though a 20-ppm LOQ was the best that could be achieved for some complex samples.

As stated earlier, extractions and concentrations of the type suggested by the EPA[2,3] were attempted on several complex matrices previously analysed by the SIM GC/MS method. However, none of these techniques significantly improved the LOD of the method for very complex chlorinated-hydrocarbon waste samples. These samples contain up to 90% chlorine and the incidental PCBs are extremely difficult to separate from the wide variety of other highly chlorinated compounds present. Thus the SIM GC/MS method reported was developed without any extraction and concentration step and the selected-ion monitoring technique was employed to obtain maximum sensitivity. For complex chlorinated waste samples, no validated method has yet been reported which can provide the 2-ppm LOQ made mandatory by the EPA ruling.

This method has also been successfully used to determine the level of classical PCB fluids in transformer-oil samples which gave very high ECD interference. Mixtures of individual PCB isomers were used as standards and no attempts were made to identify the fluids. Generally, however, an extensive clean-up such as one of those reviewed by Hutzinger,[3] followed by ECD determination, is more satisfactory for such samples.

CONCLUSION

Classical electron-capture gas chromatography methods used for the determination of classical PCB fluids are not satisfactory for the determination of incidental PCBs in complex chlorinated-hydrocarbon matrices. EC methods rely upon pattern recognition since not all isomers are available as standards and there is such a wide variation in response factors among the PCBs. Even if all 209 standards were available, however, EC detection could not be used for the incidental PCBs in the matrices without a clean-up able to remove the wide variety of other chlorinated hydrocarbons from the sample. Furthermore, any technique which cannot quantify incidental PCBs in the presence of other chlorinated hydrocarbons and which cannot use just a few isomers as standards for all 209 isomers is unacceptable for the determination of incidental PCBs in complex chlorinated-hydrocarbon matrices. Although less sensitive than EC detection, SIM GC/EIMS is the only technique developed to date which has the necessary selectivity to be used for accurately determining chlorinated biphenyls in complex chlorinated-hydrocarbon process and waste streams. The method reported has been used for the determination of incidental PCBs in more than 1000 samples from more than 30 different chlorinated-hydrocarbon sample matrices.

Acknowledgements—The authors wish to express their thanks to M. J. Phinney and K. L. Hodges for their suggestions during the preparation of this manuscript and

to The Dow Chemical Company USA for encouraging the publication of this work.

REFERENCES

1. *Federal Register*, **44,** 31514–31568, 31 May 1979.
2. *Ibid.*, **47,** 46980–46996, 21 October 1982.
3. O. Hutzinger, S. Safe and V. Zitko, *The Chemistry of PCB's*, Chapter 12. CRC Press, Boca Raton, Florida, 1974.
4. D. Sissons and D. Welti, *J. Chromatog.*, 1971, **60,** 15.
5. L. D. Sawyer, *J. Assoc. Off. Anal. Chemists*, 1978, **61,** 272.
6. R. G. Webb and A. C. McCall, *J. Chromatog. Sci.*, 1973, **11,** 366.
7. L. D. Sawyer, *J. Assoc. Off. Anal. Chemists*, 1978, **61,** 282.
8. L. Fishbein, *J. Chromatog.*, 1972, **68,** 345.
9. P. L. Levins, C. E. Rechsteiner and J. L. Stauffer, *Report* 1979, EPA/600/7-74/047; Order No. PB-293360, 90 pp., Avail. NTIS, from *Govt. Rept. Announce Index (US)*, 1979, **79,** No. 14, 81.
10. G. W. Tindall and P. E. Wininger, *J. Chromatog.*, 1980, **196,** 109.
11. USEPA, OPTS, EED, *Methods of Analysis For Incidentally Generated PCBs, Literature Review and Preliminary Recommendations. Draft Interim Report, Review* 2, 1 April 1982.
12. G. P. Martelli, M. G. Castelli and R. Fauelli, *Biomed. Mass Spec.*, 1981, **8,** 347.
13. W. Crummett *et al.*, *Anal. Chem.*, 1980, **52,** 2242.

Talanta, Vol. 30, No. 11, pp. 819–823, 1983
Printed in Great Britain.

0039-9140/83 $3.00 + 0.00

USE OF AN ELECTROSTATIC PRECONCENTRATION SYSTEM TO IDENTIFY INTERFERENCES IN ATOMIC-ABSORPTION SPECTROMETRY

PAULA A. MICHALIK and ROGER STEPHENS*
Trace Analysis Research Centre, Department of Chemistry, Dalhousie University, Halifax, N.S., Canada

(*Received* 25 *March* 1983. *Accepted* 6 *June* 1983)

Summary—Interference effects can be identified by deviations from ideality of the slopes of the concentration curves generated with an electrostatic trapping system. The technique is employed to detect spectral interferences in atomic-absorption measurements, due to the presence of sodium chloride, and caused by imperfect background correction. The electrostatic trap is found to be a particularly convenient means of obtaining the required concentration curves because the device gives a ready control of the concentration factor, reliable performance for a range of different solutions, and ease of use in dealing with the necessary number of samples.

Electrostatic concentration methods have been used to collect airborne particles[1–3] and to achieve preconcentration of aqueous solutions for chemical analysis.[4–6] The procedure employed in the latter application comprises initial conversion of the sample solution into an aerosol, followed by desolvation and collection of the dry particles in a fixed volume of water. This technique is effective for the concentration of samples with a low matrix content, but fails when large amounts of matrix salts are present, because of precipitation of matrix salts in the collecting solution. Under these circumstances the apparatus must be modified to permit the isolation of matrix salts which precipitate when the collector reaches saturation.[6]

Although the performance of an electrostatic concentrator is consistent over a wide range of conditions, matrix effects which influence it can still arise. This is particularly the case when there is precipitation and isolation of matrix salts (because it is possible that some analyte will be retained within the precipitate). Furthermore, the risk of encountering matrix effects which influence the subsequent analysis is usually greater than that for the original solution, since the concentrated solution is saturated with the salts which precipitate during the concentration step. It has been found that, in addition to concentrating the sample, the electrostatic trap can be used to identify the occurrence of either type of matrix effects, *i.e.*, those affecting the concentration process and those influencing the subsequent analysis. The procedure is to compare the concentration curve for the species of interest with an ideal curve. Differences between the two can then be used to determine the existence of matrix effects and, in favourable cases, to deduce their possible causes.

*Author for correspondence.

Matrix effects can be divided into classes which influence the concentration curve in different ways. One specific class is considered here, that of spectral interference in atomic-absorption spectrometry.

If a solution is concentrated in an electrostatic trap and a small portion of the collecting solution is analysed at increasing time intervals, a concentration curve can be constructed by plotting the observed concentration in the collector against the concentration factor, defined as the trapping efficiency multiplied by the volume of analyte solution and divided by the volume of the collector solution. The trapping efficiency is measured by the methods described previously[4–6] and is assumed to be constant in the absence of matrix effects. Comparison of such a concentration curve with a standard curve, prepared either by concentration of the pure analyte solution or directly by constructing a calibration graph by use of standards of the appropriate concentration, allows various types of matrix effects to be identified. Thus, for instance, any matrix effect which influences the method of analysis will cause the observed concentration curve to deviate from its ideal value over the concentration range which is affected, and also cause the observed curve to show a discontinuity at the point where matrix precipitation occurs (*i.e.*, where the matrix concentration in the collector ceases to change with time). Some qualitative forms which are expected for various types of concentration curve are shown in Fig. 1; case C represents the type of interference discovered in the present work.

To achieve the type of comparison illustrated in Fig. 1, the observed and ideal curves must be displayed on the same scale. This is straightforward if the initial concentration of the test solution is known (since the concentration factor for a particular system can be measured). Deductions concerning the presence or absence of matrix effects for that test solution then follow directly. That is the approach taken here.

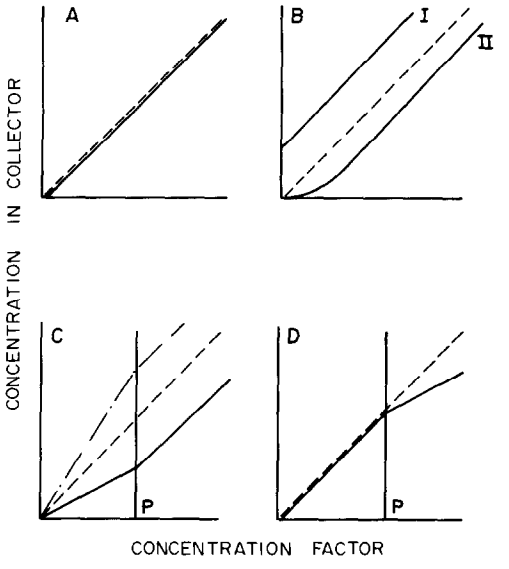

Fig. 1. Concentration curves illustrating possible matrix effects. The line P indicates the point of matrix precipitation. (---) Ideal curve determined with appropriate calibration standards. A—Ideal and standard curves coincide throughout their range, no matrix effects. B—(I) Contamination adds a fixed concentration to the collector; (II) adsorption loss at low collector concentrations. C—Prior to matrix precipitation, concentration curve deviates owing by an additive matrix effect. D—After precipitation of matrix, the curve deviates owing to a matrix effect which influences the preconcentration.

However, if the procedure is applied to a solution of unknown concentration, the relation between the concentration axes for the ideal and test-solution curves is also unknown, and the two cannot be compared directly (since any measurement of concentration yields a value which has already been affected by any matrix effect present). Under these circumstances it is necessary to modify the procedure. One possible modification is to construct two concentration curves, one for the unknown solution and the other for the unknown solution spiked with a known amount of analyte, both concentration steps being continued past the point of matrix precipitation. This variant of the method has not yet been examined in detail and will not be considered further at present.

EXPERIMENTAL

The apparatus was tested with cadmium, copper and lead, with sodium chloride as matrix salt. Solutions of each element were made up in demineralized distilled water as reference solutions, and in solutions containing 35, 3.5, 0.35 and 0.035 g of sodium chloride per litre. All solutions were acidified to pH ~ 2 with Baker "Ultrex" hydrochloric acid. Concentration was done with an electrostatic trap, with a liquid collector and a cooled filter for matrix precipitation, as previously described.[6] Each point on each concentration curve was determined by means of a separate concentration step, in order to provide a sufficient volume of solution for replicate measurement by various methods. The concentration curves were extended beyond the point at which the collector solution became saturated with sodium chloride and precipitation of the matrix occurred. The concentrated collector solution was analysed by the method of standard additions, the techniques used being anodic-stripping voltammetry, flame atomic-absorption, and graphite-furnace atomic-absorption. The conditions used for the different methods of analysis are summarized below.

Anodic-stripping voltammetry (ASV)

The samples were analysed by differential pulse polarography with an EG & G (Princeton Applied Research) Model 174A polarographic analyser equipped with a glassy-carbon electrode. The mercury film was formed by plating from a $1 \times 10^{-4} M$ mercuric chloride solution for 6 min at -0.8 V. The deposition step for samples involved plating for 3 min at -1.0 V and the stripping involved scanning at 2 mV/sec over a range of 1 V. The initial concentration of cadmium and copper was 2 μg/l., and that of lead was

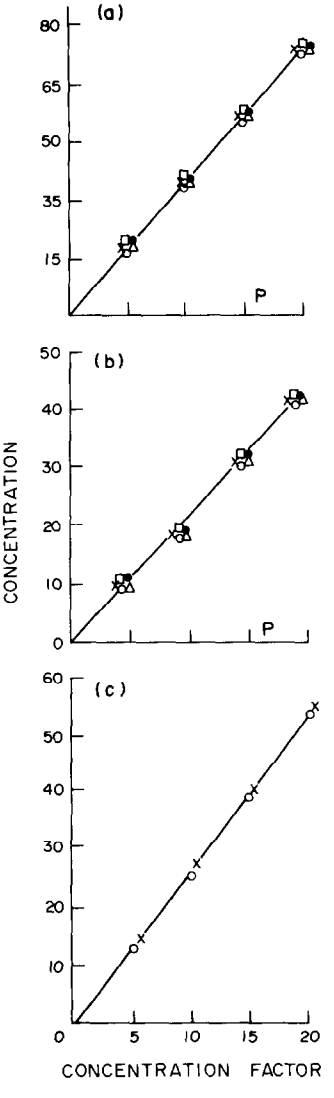

Fig. 2. Concentration curves determined by ASV. (a) Cd, (b) Cu, (c) Pb; ○, ●, □, ▽, ×, represent the ideal curve, and matrix dilution factors of 0, 1, 10, 100 and 1000. P marks matrix precipitation for the undiluted solutions. For lead the initial NaCl concentration was restricted to 0.035 g/l., to ensure linearity of the calibration curve.

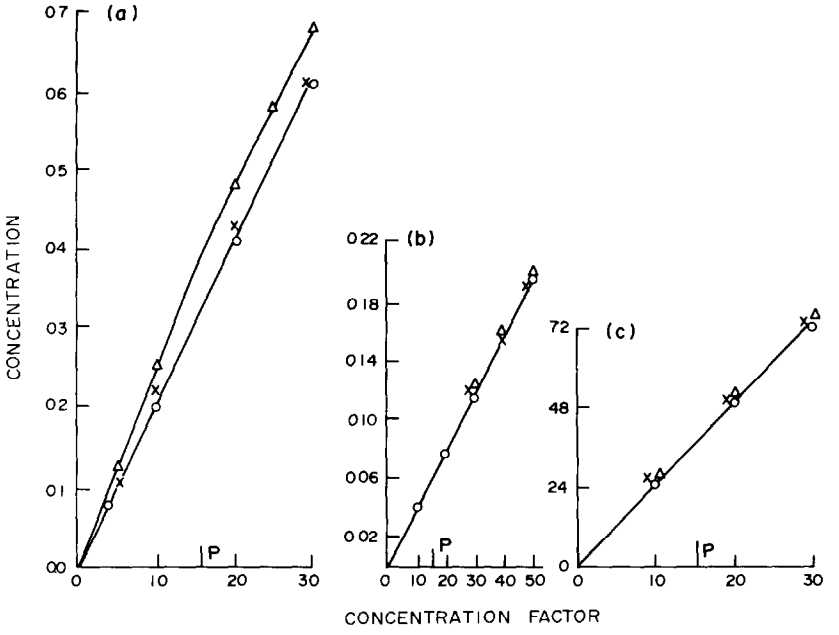

Fig. 3. Concentration curves for (a) Cd, (b) Cu, (c) Pb, determined by FAAS. ○, ×, ▽ show the ideal curve, and results with Zeeman and 2-line background-correction respectively, for an initial NaCl concentration of 35 g/l.

governed by its level in the sodium chloride, which gave a concentration of ~2.5 μg/ml for a sodium chloride concentration of 35 g/l.

Graphite-furnace atomic-absorption spectrometry (GFAAS)

A Varian AA475 spectrometer equipped with a Perkin–Elmer HGA 2200 furnace assembly and a deuterium background-corrector was used. Because of the elevated salt concentrations in most samples, matrix modifiers were used with samples containing >0.35% sodium chloride. Cadmium was determined by the method described by Guevremont *et al.*,[7] with EDTA as matrix modifier. Ammonium nitrate was used as matrix modifier in the determination of copper, according to the method of Ediger *et al.*[8] Initial concentrations were the same as those used with ASV.

Flame atomic-absorption spectrometry (FAAS)

The initial concentration of cadmium was increased to 20 μg/l. for all FAAS measurements. All results were obtained on a single-beam Varian AA5 spectrometer, with the standard 8-cm air–acetylene burner. Background correction was effected by the two-line method, a second reading being taken at the appropriate correction line for each sample. The Sn 224.6, Ag 328.1 and Mg 285.2 nm lines respectively were used for background correction of the Cd 228.8, Cu 324.1 and Pb 283.3 nm analytical lines. All measurements were repeated with a laboratory-built spectrometer with Zeeman background-correction at the source.[9]

RESULTS AND DISCUSSION

The concentration curves obtained by the various methods of analysis are shown in Figs. 2–5. In each figure the ideal curve is that obtained with the standard solution of the corresponding element, and any deviations of the other curves are interpreted as a measure of an interference associated with the presence of sodium chloride. The results obtained when ASV was used as the method of analysis (Fig. 2) show close agreement between the various curves. This demonstrates that neither the trapping procedure itself nor the subsequent analysis by ASV is greatly influenced by the presence of sodium chloride.

Greater deviations are seen in the case of FAAS measurements (Figs. 3 and 4). In view of the ASV results, and because the slopes of the various curves

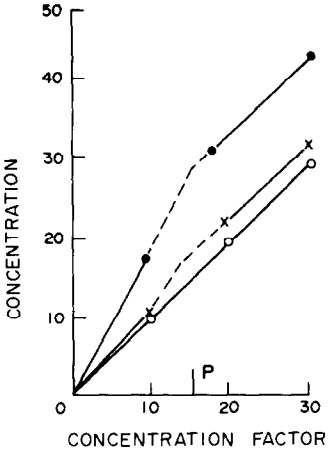

Fig. 4. Concentration curves for Pb determined by FAAS without background correction. ○, ×, ● represent the ideal curve, and observed results for the 283.3 and 217.0 nm Pb lines, respectively. NaCl concentration 35 g/l.

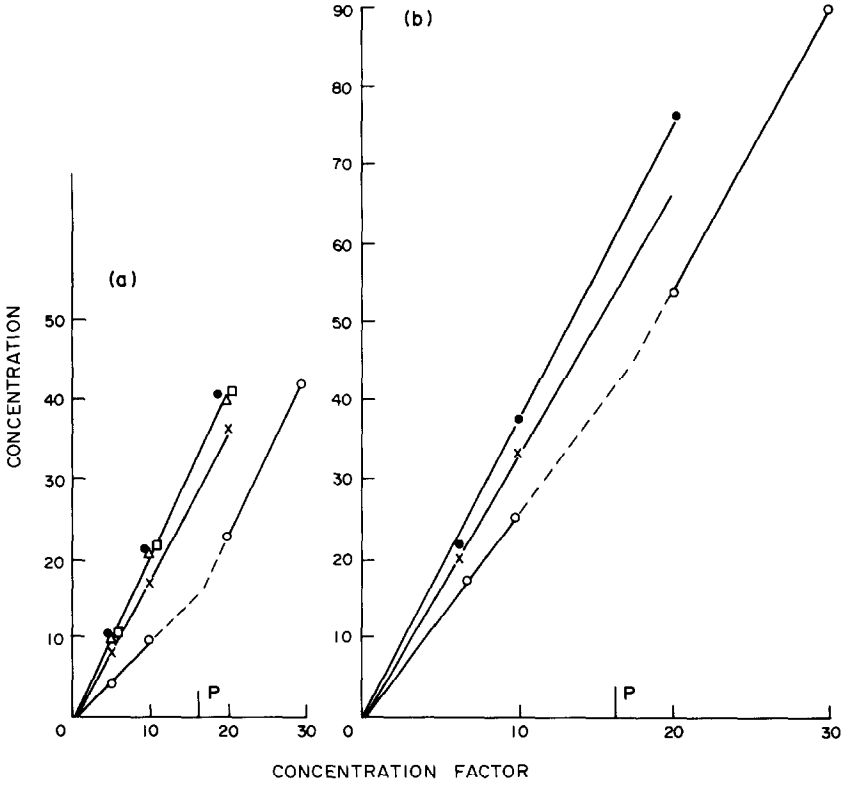

Fig. 5. Concentration curves determined by GFAAS. (a) Cd, (b) Cu; ●, ○, ×, □, ▽ show the ideal curve, and the curves for initial NaCl concentrations of 35, 3.5, 0.35, 0.035 g/l., respectively.

in Figs. 3 and 4 become parallel after precipitation of the sodium chloride matrix commences, it is assumed that the deviations are associated with interference in the analysis, primarily spectral interference. The reasons for this conclusion are given below. Thus when the more efficient Zeeman background-correction is employed, the interference is markedly reduced. When no background correction at all is employed (the curves for lead, in Fig. 4) the interference becomes appreciably greater for the shorter wavelength, suggesting that scatter by particles is contributing at least partly to the effect.

The interference effects observed for GFAAS are shown by the deviations of the concentration curves in Fig. 5 to be greater than those for FAAS. However, the fact that each curve essentially follows the ideal slope after precipitation of the matrix has occurred shows that the interference is again spectral, rather than caused by any uncompensated change in the atomization behaviour, caused by the presence of sodium chloride. This conclusion is unaffected by the fact that the deviations in Fig. 5 are in the opposite sense to those in Figs. 3 and 4, as discussed below.

Influence of spectral interferences

Let c be the initial solution concentration, f the concentration factor, and p the efficiency with which trapped material is released and converted into a form suitable for measurement. The absorbance of an atomic-line source, A_A, is given by

$$A_A = ({}_AK_a p_a c_a + {}_AK_b p_b c_b) f$$

where ${}_AK$ is the absorption coefficient and the subscripts a, b refer to absorption by atomic and background absorbing species respectively. The corresponding expression for the background correction source is

$$A_B = ({}_BK_a p_a c_a + {}_BK_b p_b c_b) f$$

and the observed signal, s, is given by

$$s = A_A - A_B = (\Delta K_a p_a c_a + \Delta K_b p_b c_b) f \qquad (1)$$

where $\Delta K = {}_AK - {}_BK$. The determination of the concentration in the collector by a standard-addition procedure is assumed to provide a satisfactory measure of s. For the ideal solution

$$c_b = 0 \quad \text{and} \quad s = \Delta K_a p_a^0 c_a f \qquad (2)$$

where p_a^0 is the ideal value of p_a. Thus if the slopes of the s *vs.* f curves of equations (1) and (2) are equal beyond the point of matrix precipitation, then differentiating equations (1) and (2) shows that p_a and p_a^0 are also equal. This does not automatically guar-

antee that matrix effects are absent, but only that, if present, they cancel. The absence of mutually cancelling matrix effects contained in p (or f) in the present experiments is shown by the combination of the AAS results with the ASV data of Fig. 2.

Given that p_a and p_a^0 are equal at the point of matrix precipitation, the difference between the observed and ideal curves in Figs. 3–5 must arise primarily from the $\Delta K_b p_b c_b$ term in equation (1), *i.e.*, it is a spectral interference caused by incomplete background correction ($\Delta K_b \neq 0$). The direction of the deviation between the observed and ideal curves is given by the sign of ΔK_b. Thus when ${}_A K_b > {}_B K_b$, ΔK_b is positive (undercorrection), and the observed curve is higher than the ideal curve (Figs. 3, 4) and *vice versa* when ${}_A K_b < {}_B K_b$ (Fig. 5).

CONCLUSIONS

These experiments demonstrate the ability of an electrostatic trap to identify an interference which affects the method of analysis and to determine the cause of that interference. The results also show that for the high salt concentrations dealt with here, the background correction capabilities of both the two-line and deuterium methods are suspect, whereas the Zeeman correction technique is satisfactory, in agreement with the findings of other workers.[10–15] The results obtained with GFAAS show that the matrix-modifier techniques of Guevremont *et al.*[7] and of Ediger *et al.*[8] were successful in giving reproducible atomization during these experiments, irrespective of the presence of sodium chloride, thereby providing evidence for the validity of these techniques under extreme conditions.

This use of concentration curves to identify interference effects can, in principle, be applied with any method of preconcentration. However, the electrostatic trap is especially convenient for the purpose since the concentration proceeds uniformly and predictably with time, and provides a break at the point of matrix precipitation, which aids distinction between different types of matrix effect. The automatic nature of the trap proves to be an additional advantage here, since the necessarily large number of samples used can be concentrated with a minimum of effort.

Acknowledgements—The authors are indebted to the Natural Sciences and Engineering Research Council of Canada for support of this work. P.A.M. thanks the Walter C. Sumner Foundation for the award of a scholarship.

REFERENCES

1. G. Torsi and E. Desimoni, *Anal. Lett.*, 1979, **12,** 1361.
2. G. Torsi, E. Desimoni, F. Palmisano and L. Sabbatini, *Anal. Chem.*, 1981, **53,** 1035.
3. *Idem, Anal. Chim. Acta*, 1981, **124,** 143.
4. P. A. Michalik and R. Stephens, *Talanta*, 1981, **28,** 37.
5. *Idem, ibid.*, 1981, **28,** 43.
6. *Idem, ibid.*, 1982, **29,** 443.
7. R. Guevremont, R. E. Sturgeon and S. S. Berman, *Anal. Chim. Acta*, 1980, **115,** 163.
8. R. D. Ediger, G. E. Peterson and J. D. Kerber, *At. Absorpt. Newsl.*, 1974, **13,** 61.
9. R. Stephens, *Talanta*, 1978, **25,** 435.
10. F. J. Fernandez, S. A. Myers and W. Slavin, *Anal. Chem.*, 1980, **52,** 741.
11. G. R. Carnrick, W. Slavin and D. C. Manning, *ibid.*, 1981, **53,** 1866.
12. K. G. Brodie and P. R. Liddell, *ibid.*, 1980, **52,** 1059.
13. *Idem, ibid.*, 1980, **52,** 1256.
14. P. Frigieri and R. Trucco, *Spectrochim. Acta*, 1980, **35B,** 113.
15. B. Magyar and H. Vonmont, *ibid.*, 1980, **35B,** 117.

Talanta, Vol. 30, No. 11, pp. 825–830, 1983
Printed in Great Britain

0039-9140/83 $3.00 + 0.00
Pergamon Press Ltd

INFRARED SPECTROMETRY FIELD-METHOD FOR IDENTIFICATION OF NATURAL SEEP-OILS*

DOUGLAS F. GRANT
Division of Natural Sciences and Mathematics, Stockton State College, Pomona, NJ 08240, U.S.A.

DELYLE EASTWOOD
Department of Nuclear Energy, Brookhaven National Laboratory, Upton, NY 11973, U.S.A.

(*Received* 17 *February* 1983. *Accepted* 2 *June* 1983)

Summary—An infrared field-method has been developed which is capable of distinguishing between oils originating from natural seepage in the Santa Barbara (California) Channel region and closely similar oils from offshore drilling platforms. The technique involves a minimum of sample preparation and the use of simple infrared instrumentation which can be operated by non-technical personnel. Natural seep-oil samples were collected from the surface of the water, underwater, and from beaches in the area. The non-seep oils were obtained from production wells which were located in the same geographical areas as the seepage and were from several different well depths corresponding to different geological zones. Natural seep-oils are more aromatic than the production oils, and this difference is evidenced by observed differences in the spectra for both weathered and unweathered oils. These spectral differences between seep and non-seep oils have been found to persist after exposure to weathering for a week.

Natural seepage of petroleum into the oceans is estimated to be in the range from 0.2 to 1 million metric tons per year. This constitutes a significant contribution world-wide even though it appears to be less than that from tankers and ship bilge discharges.[1] In the Western hemisphere, significant natural seepages are found in Newfoundland, Alaska, the Gulf of Mexico, and California, especially off the coast near Santa Barbara.[2] The Santa Barbara area has an estimated natural seepage of at least 50–70 barrels daily.[3] The most important seepage occurs just offshore of Coal Oil Point, which lies a few miles west of Santa Barbara proper (Fig. 1). This section of California, with a history of chronic oil seepage, thus provides a unique problem from the standpoint of distinguishing natural seep-oil from man-made spills.

Earlier researchers[4-6] found infrared spectroscopy to be a useful method for categorizing natural seeps and asphalts. An infrared field-method has now been developed which is capable of distinguishing oils due to natural seepage in the Santa Barbara (California) Channel region, from closely similar oils from offshore drilling platforms. This method is also capable of distinguishing between closely similar production oils and can provide information on the geological origin of the oil. An earlier version[7] of this method was developed for classification of spilled oils according to type.

Natural seep-oil samples were collected from the surface of the water, underwater, and from the beaches. The non-seep oils were obtained from production wells in the same geographical areas as the seepage and from several different well depths corresponding to different geological zones. Samples examined in the present study included 41 production oils, 15 seep-oils and 13 beach-tar samples. Of the seep-oils, 13 were from surface oil-slicks and 2 were underwater samples taken directly from the seeps, one from Coal Oil Point and the other from nearby Isla Vista. Figure 2 is an underwater photograph of the natural oil seepage at a depth of 60 ft in the Isla Vista area. The sand and turbidity of the ocean floor at this depth reduced visibility considerably, but a section of an oil "pot" can be seen with one of its oil

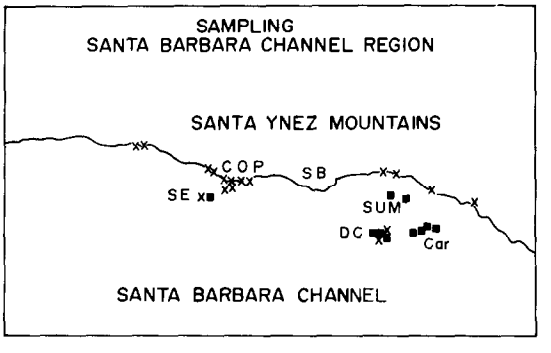

Fig. 1. Map of Santa Barbara Channel region. Rectangles represent offshore drilling platforms. Crosses represent places where natural seep or beach tar samples were collected. Abbreviations: S.E. South Elwood; C.O.P. Coal Oil Point; S.B. Santa Barbara; D.C. Dos Cuadras; SUM. Summerland; Car. Carpenteria. The distance from S.E. to SUM. is 18 miles.

*Research done at the U.S. Coast Guard Research and Development Center, Groton, CT 06340, U.S.A. The opinions or assertions contained herein are the private ones of the writers and are not to be construed as official or reflecting the views of the Commandant or the Coast Guard at large.

Fig. 2. Underwater photograph of the natural oil seepage in the Isla Vista seepage area.

droplets about to break away and float to the surface. The "pot" (approximately 4 ft in diameter) contained hundreds of droplets that gave the appearance of a boiling pot of oil.

The major offshore oil fields are South Elwood, Carpenteria, Summerland and Dos Cuadras. The geology and geochemistry of the Santa Barbara area are discussed in reference 8. The Dos Cuadras oil field is the most productive. The range of oils (as measured by aromaticity) from the Dos Cuadras field appears representative of the range of oils found in the other fields, (as estimated from the aromaticity as shown in the infrared spectra); consequently, detailed discussion will focus on oils from the Dos Cuadras field.

One of the shallower zones in the Dos Cuadras field, the brown zone (average well depth 1000 ft), is the most productive within the Dos Cuadras field. Infrared spectra of the brown-zone oil most nearly resemble those of the natural seeps. Oil from this zone is highly aromatic; its API gravity ranges from 18° to 22°.[8] The oil from the deepest, "green", zone (average well depth 3000 ft), is much less aromatic and has a higher API gravity (32°). These variations in aromaticity and API gravity with depth agree with what would be expected petrochemically.[9]

EXPERIMENTAL

Sample preparation

Samples were collected in pretreated glass jars fitted with Teflon-lined lids. Surface slicks were sampled with perforated Teflon strips. The oils were refrigerated at 45°F, but not frozen, to avoid dewaxing or fractionation prior to analysis.

Samples were dried by heating to 60°C in a water-bath, adding anhydrous magnesium sulphate, and centrifuging at 2500 rpm for up to several hours. For the heaviest seep samples, complete removal of water was very difficult. Fortunately, this did not lead to interference in the spectral regions of interest.[10]

Instrumentation

Infrared specta were recorded in both the laboratory and the field. In the laboratory, a sealed demountable cell with silver bromide windows and a 0.1–mm Teflon spacer was used with either a double-beam Perkin-Elmer 467 infrared spectrophotometer or a single-beam Wilks Miran I variable-filter infrared spectrophotometer. In the field, only the Wilks instrument was used, with a Wilks mini-cell (0.1 mm path-length and silver bromide windows). Since emphasis was placed on development of a field method, most of the spectra were run on the Wilks Miran spectrophotometer in both the absorbance and transmittance modes. Several double-beam spectra were recorded for comparison. The transmittance mode was used because a large data-base of transmission spectra was available, and the absorbance mode because it had a scale-expansion facility.

The Wilks Miran spectrophotometer has high photometric accuracy ($\pm 0.5\%$) for a single-beam field instrument. Although the resolution is relatively low (0.25 μm at 11 μm), this instrument proved completely satisfactory for our purposes.

Instrument settings for the Miran are listed in Table 1. In the "oil-fingerprint" region of the spectra (8–14 μm), the absorbance scale from 0 to 1 was used between 8 and 11 μm,

Table 1. Instrument settings for Miran spectra oil identification

Time constant	0.25 sec
Slit-width	0.50 mm
Scale expansion	10× = 1–2 absorbance (at $\lambda > 11\,\mu m$)
	1× = %T or 0–1 absorbance
Variable gain	90% at 3.34 μm (0.05 mm polystyrene)
Cell (step A)	Sealed demountable AgBr, 0.1 mm
(step B)	RIIC disposable, AgBr, 0.1 mm
	or Wilks mini-cell AgBr, 0.1 mm

and the scale from 1 to 2 was used for the 11–14 μm region. The gain was adjusted at a wavelength of 3.34 μm with reference to a standard 0.05-mm polystyrene film. To achieve satisfactory spectral overlays with the single-beam instrument, it was found necessary to use the same Teflon spacer, because there was $\sim \pm 15\%$ variation in thickness of the spacers. Five replicate measurements were made for each sample.

RESULTS AND DISCUSSION

Figure 3 shows a comparison between the double-beam spectra of unweathered green and brown (deepest and shallowest) zone oils from the Dos Cuadras oil field. The spectra differ considerably in the region between 700 and 800 cm^{-1}, especially in the relative intensities of the 725 and 747 cm^{-1} peaks. These spectral differences reflect variations in the relative concentrations of aliphatics and aromatics, and show a higher percentage of aromatics in the brown-zone production oil.

Figure 4 shows a similar comparison of double-beam spectra between the brown-zone oil and unweathered natural seeps (collected underwater directly from their sources). The unweathered natural seeps have strong carbonyl peaks at 1710 cm^{-1} whereas the unweathered brown-zone oil does not. Mattson[6] previously pointed out this distinction, which unfortunately disappears after two days of weathering. After this period, examination of the 747/725 cm^{-1} (13.5/13.8 μm) ratio, which is an indication of the relative aromatic-aliphatic content of the oil, is also required in order to distinguish the more aromatic seep-oils from non-seep-oils.

A comparison of Miran single-beam transmission spectra of three Dos Cuadras production oils from

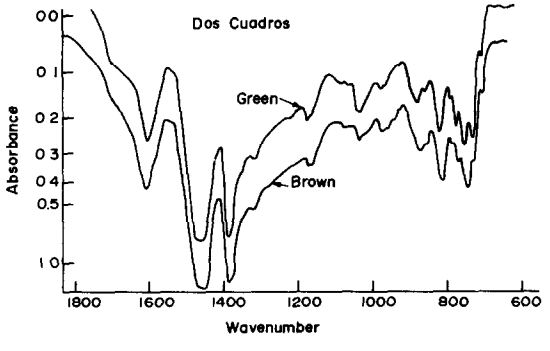

Fig. 3. Double-beam spectra of unweathered green and brown-zone oils from Dos Cuadras oil field.

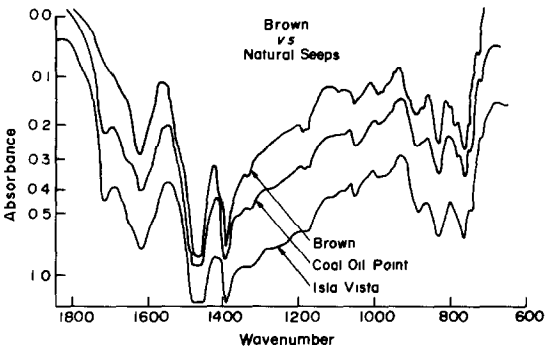

Fig. 4. Double-beam spectra of brown-zone oil (Dos Cuadras) and two unweathered natural seeps.

different depths (brown, purple and green zones, *i.e.*, in order of increasing depth) with the spectrum of the Coal Oil Point natural seep, collected at source, is shown in Fig. 5. The carbonyl peak at 5.85 μm can be observed in the spectrum for the natural seep. At 7.5 μm the differences in infrared absorption which correspond to differences in the API gravity or density of the oil[7] are particularly distinct.

Figure 6 shows absorption spectra obtained with the Miran instrument for the same oils. The oils can easily be distinguished by comparing the 13.5 and 13.8 μm peaks. The more aromatic the oil, the larger is the 13.5/13.8 μm peak ratio. This ratio technique shows that the natural seep is more aromatic than the most aromatic production oil (brown Dos Cuadras).

A similar estimation of aromaticity can be made by comparing production oils from different fields, as shown in Fig. 7. The brown-zone (Dos Cuadras field) oil is the most aromatic, the Vacqueros oil (Sum-

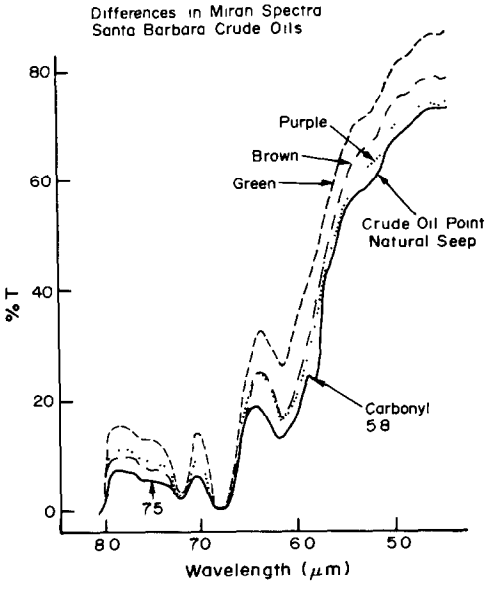

Fig. 5. Miran single-beam transmission spectra of Dos Cuadras production oils (brown, purple and green zones in order of increasing depth) and Coal Oil Point natural seep.

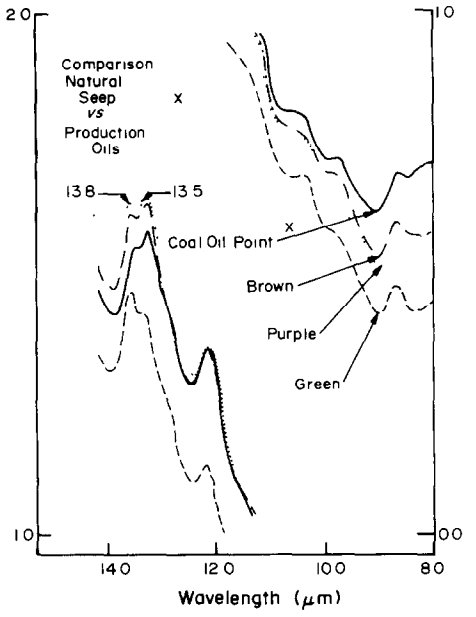

Fig. 6. Miran single-beam absorption spectra of Dos Cuadras production oils (brown, purple and green zones in order of increasing depth) and Coal Oil Point natural seep. Absorbance scale 0–1 for 8–11 μm, 1–2 for 11–14 μm.

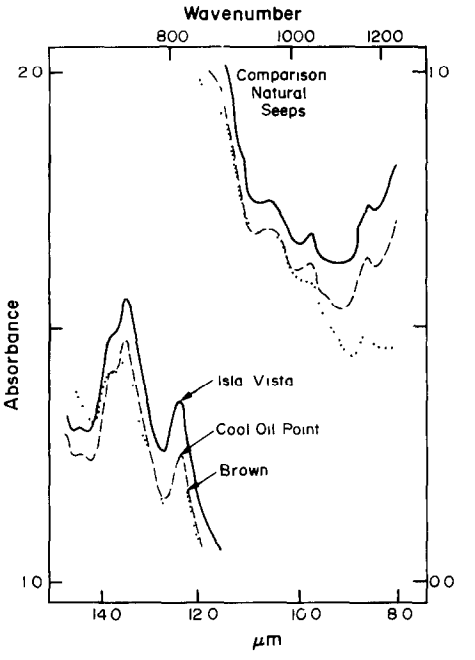

Fig. 8. Miran single-beam absorption spectra of two underwater natural seeps and brown-zone oil (Dos Cuadras). Scales as for Fig. 7.

merland field) is intermediate, and the onshore Rincon field oil is the most aliphatic.

Figure 8 compares the Miran absorption spectra of two underwater seep samples and the brown-zone (Dos Cuadras) oil. These seeps can readily be distinguished from the brown-zone oil by comparison of the 13.5 and 13.8 μm peaks (*i.e.*, by the difference in aromaticity). All the natural seep samples from surface slicks and the beach-tar samples had similar infrared spectra. However, since their weathering histories and exact sources were unknown, their spectra are not included, though they were consistent with the results shown. The tars and slick samples showed a high aromaticity and quite low concentration of aliphatics.

Weathering is an important variable in the problem of distinguishing between seep-oils and non-seep-oils. By the time the oils wash ashore, they have often been extensively weathered. Figure 9 compares the double-beam spectra of natural seep and brown-zone (Dos Cuadras) samples, each weathered for three days in outside troughs with sea-water circulating at a constant water temperature of 20°. After the three days,

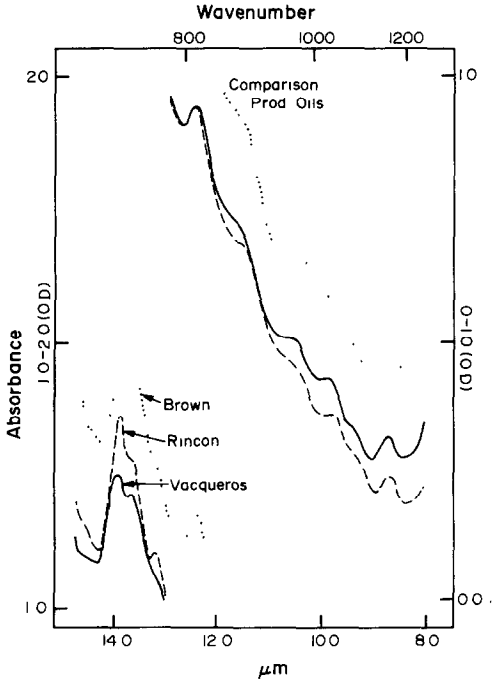

Fig. 7. Miran single-beam absorption spectra of production oils from different fields. Scales as for Fig. 7.

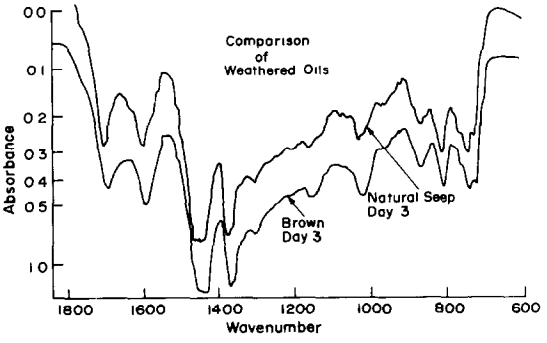

Fig. 9. Double-beam spectra of natural seep and brown zone (Dos Cuadras) samples, each weathered for three days.

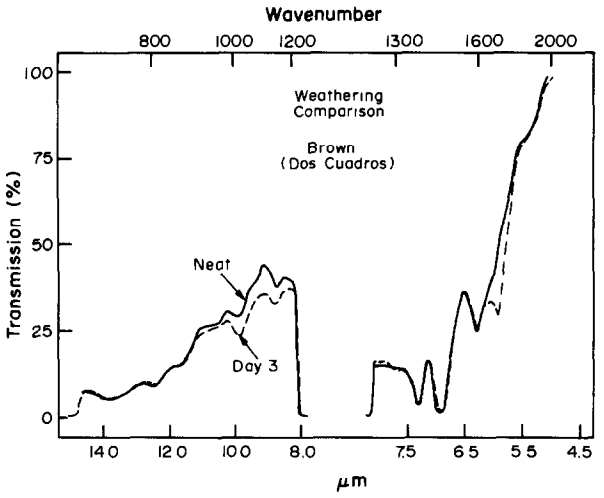

Fig. 10. Miran single-beam transmission spectra of brown-zone oil for neat sample and 3-day weathered sample.

the spectrum of the brown-zone oil had developed a large carbonyl peak at $\sim 1710\,cm^{-1}$, but it was still smaller than that for the natural seep; the differences in the 800–700 cm^{-1} region still persisted. Additional infrared studies on weathering seep and production oils indicated that these spectral differences between brown-zone oil and natural seep-oil persist on weathering for up to one week.[11]

A comparison of Miran transmission spectra for neat and 3-day weathered brown-zone oil is shown in Fig. 10. The carbonyl peak has appeared in the weathered sample. Figure 11 shows the corresponding absorption spectra. The 13.5/13.8 μm peak ratio changes markedly on weathering, so the weathered brown-zone oil appears more aliphatic and therefore spectrally less similar to a seep-oil than before weathering. Figure 12 shows the Miran absorption spectra of weathered and unweathered natural seep samples. Although the spectrum of a weathered natural seep-oil compares closely with that of an unweathered brown-zone oil in the 13.5–13.8 μm region, an unweathered brown-zone oil has no carbo-

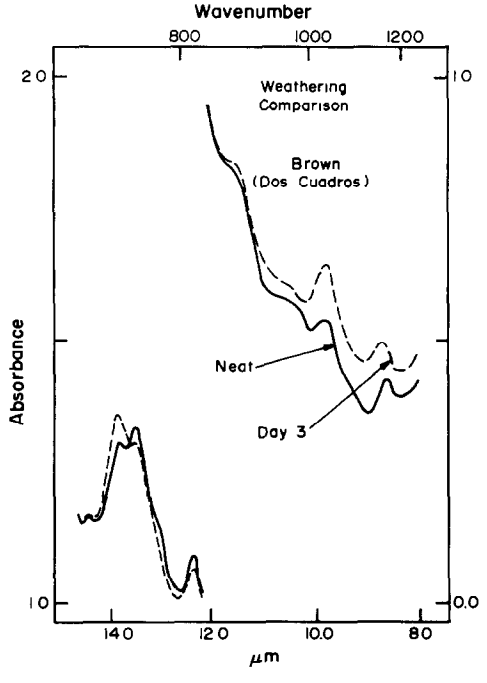

Fig. 11. Miran single-beam absorption spectra of brown-zone oil for neat sample and 3-day weathered sample. Scales as for Fig. 7.

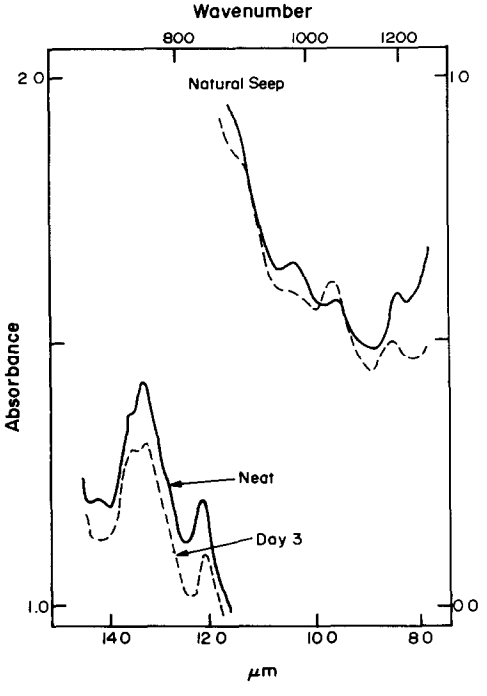

Fig. 12. Miran single-beam absorption spectra of natural seep sample for neat sample and 3-day weathered sample. Scales as for Fig. 7.

nyl peak at 1710 cm^{-1}. Consequently, discrimination between seep- and non-seep-oils is still possible.

In this study, comparisons were made by using spectral overlays. Provided the precautions mentioned were taken, good spectral overlays were always obtained. Seep and production oils can also be differentiated quantitatively by means of the ratio of the 13.5 and 13.8 μm peaks but the sloping base-line of the single-beam instrument must be taken into account. A new computerized model of the Miran instrument makes an automatic correction to give a flat base-line similar to that for a double-beam instrument.

In summary, a rapid on-site method to distinguish seep- from non-seep-oils by use of low-cost, portable, infrared instrumentation has been developed. This method has been used at the Santa Barbara Coast Guard Group, and also for oil-spill identification work. This method, with modifications,[12] should be applicable in other areas of active natural seepage, but tests of this were beyond the scope of the present project. Geochemists may find the potential for comparing oils from different geological zones in the same field useful for rapid on-site analysis of production oil.

Acknowledgements—The authors thank Clara D. Craver of Chemir Laboratories for valuable technical consultation, Terry O'Connell and other Coast Guard personnel for help in sample collection, Chris Brown and Mark Ahmadjian of the University of Rhode Island for help with weathering studies, Scott Fortier for experimental assistance and William A. Saner and Martha S. Hendrick for helpful discussions.

REFERENCES

1. J. N. Butler, *Sci. Am.*, 1975, **232,** No. 6, 90.
2. T. C. Johnson, *Natural Oil Seeps In or Near the Marine Environment: A Literature Survey*, U.S. Coast Guard Project No. 714141/002 NTIS AD723310, March 1971, p.5.
3. A. A. Allen, R. S. Schlueter and P. G. Mikolaj, *Science*, 1970, **170,** 974.
4. A. A. Rosen, L. R. Musgrave and J. J. Lichtenberg, *Characterization of Coastal Oil Pollution by Submarine Seeps*, State Water Pollution Control Board, Publication No. 21, Part 2, Sacramento, California, 1959.
5. C. D. Smith (Craver), C. C. Schuetz and R. S. Hodgson, *Ind. Eng. Chem., Prod. Res. Dev.*, 1966, **5,** 153.
6. J. S. Mattson, H. B. Mark, Jr., R. L. Kolpack and C. E. Schutt, *Anal. Chem.*, 1970, **42,** 234.
7. D. Eastwood, K. Cichon, D. F. Grant and A. P. Bentz, *Field Classification of Oils With the Wilks Miran I Infrared Analyzer*. Pittsburgh Conference on Analytical Chemistry and Applied Spectroscopy, Cleveland, Ohio, March, 1975.
8. *Geology and Petroleum Development and Seismicity of the Santa Barbara Channel Region, California, U.S. Geol. Surv. Paper*, 679, 1969.
9. P. F. Andreev, A. I. Bogomolov, A. F. Dobryanskii and A. A. Karstev, *Transformation of Petroleum in Nature*, Pergamon Press, New York, 1968.
10. Chemistry Branch, *Oil Spill Identification System*. U.S. Coast Guard Final Report No. DOT-CG-D-52-77, National Technical Information (NTIS) Accession No. ADAO44750, June 1977.
11. C. W. Brown, University of Rhode Island, Kingston, RI, private communication.
12. C. D. Craver, Chemir Laboratories, Glendale, MO, Private communication.

Talanta, Vol. 30, No. 11, pp. 831–835, 1983
Printed in Great Britain.

0039-9140/83 $3.00 + 0.00

MEASUREMENT OF Ag, Te AND Pd IN GEOCHEMICAL REFERENCE MATERIALS BY MASS SPECTROMETRIC ISOTOPE-DILUTION ANALYSIS

R. D. Loss, K. J. R. Rosman and J. R. de Laeter
School of Physics and Geosciences, Western Australian Institute of Technology, Kent Street, Bentley, 6102 Western Australia, Australia

(*Received* 22 *November* 1982. *Revised* 30 *March* 1983. *Accepted* 27 *May* 1983)

Summary—Procedures are described which permit mass spectrometric isotope-dilution analysis to be used to determine Ag, Te and Pd in rock samples at the ng/g level. The concentrations (ng/g) of Ag, Te and Pd were found to be 25.7 ± 0.7, 1.2 ± 0.6 and 0.08 ± 0.05 respectively in BCR-1 and 3.5 ± 0.2, 4.2 ± 0.7 and 2.9 ± 1.7 respectively in PCC-1.

Geochemical reference materials are available from a variety of sources.[1] They are intended principally for instrument calibration and for developing and testing methods of rock analysis. Since the first detailed compilation of analytical data of the now famous G-1 and W-1 "standard rocks" in 1951 by Fairbairn *et al.*,[2] there has been a large increase in the number and variety of reference materials available to analysts. The history of their development is interesting and has recently been reviewed briefly by Abbey[3] and Date.[4]

Although tremendous effort has been devoted to the preparation of these samples, their usefulness is significantly limited by the lack of accurate data on some chemical constituents, particularly those present in trace amounts. Roelandts[5] has discussed this problem and has indicated that it is soluble with the aid of "new" analytical techniques having higher sensitivity, precision and accuracy than those normally used for geoanalysis. Mass spectrometric isotope-dilution (MSID) is one such technique identified by Roelandts[5] as having the required attributes. Unfortunately it is seldom used by analytical chemists, because it is relatively slow and costly. It is not new, however, and is routinely used in geochronology laboratories and in the standards laboratories of most nations. In view of the problems currently existing in geoanalysis and environmental analysis it is surprising that it is not more widely used.

In this paper we outline the principles of MSID and describe the procedures we have developed for determining silver, tellurium and palladium in geochemical reference materials (GRMs) at the ng/g level. Analyses of the U.S. Geological Survey samples BCR-1 and PCC-1 have been used to illustrate the results which can be achieved. The technique offers good accuracy and sensitivity and can measure picogram quantities of these elements.

EXPERIMENTAL

Mass spectrometric isotope-dilution

Details of the MSID technique have been given by Webster.[6] Briefly, an accurately known amount of a highly enriched stable isotope (the tracer) of the element to be determined is allowed to equilibrate with the sample solution. A compound of the element is then isolated in pure form by standard chemical techniques and its isotopic composition is measured by mass spectrometry. From the known isotopic composition of the natural element and the tracer, the amount of natural element present in the sample can be calculated. One of the principle advantages of the method is that quantitative separation of the element is not essential.

Since the procedures used for tellurium and palladium differ substantially from those used in previous work[7,8] they will be described in some detail. Silver is separated by an ion-exchange procedure similar to that developed by Kelly *et al.*[9]

Samples

The samples are suppled as powders sealed in polyethylene bags or glass bottles. The spread of results from different laboratories is large enough for the packaging not to be a significant source of error, but if the precision is improved, packaging may pose a serious problem. In this study no attempt was made to detect differences between different batches of the same rock.

Reagents

The preliminary stages of reagent purification were performed in laboratories supplied with coarsely filtered air, and the final distillation stage was done in laminar-flow clean-air streams.

High-purity water. Tap water was demineralized by ion-exchange and distilled in Pyrex. It was further purified by sub-boiling distillation in a quartz still, then stored in acid-leached high-density polyethylene (LPE) containers.

Hydrochloric and nitric acids. The analytical grade reagents were distilled first in a quartz sub-boiling still, then in a two-bottle Teflon still.

Ion-exchange resins. Bio-Rad AG50 X8 cation-exchanger and AG1 X8 anion-exchanger (100–200 mesh) were stored in 4*M* and 2*M* hydrochloric acid respectively, and cleaned and conditioned immediately before use.

Apparatus

Beakers machined from Teflon (PTFE) rod were employed for sample digestion and evaporation. They were cleaned prior to each analysis by immersion in hot *aqua regia* for 48 hr, then hot analytical grade hydrochloric acid for a further 48 hr. Immediately before use they were covered with Teflon lids and refluxed with high-purity dilute nitric acid for several hours. The ion-exchange resin was supported on acid-leached quartz wool in quartz or Vycor tubes.

Procedures

Preparation of the tracer. In this study a tracer solution containing the enriched stable isotopes ^{107}Ag, ^{124}Te and ^{102}Pd was prepared from materials supplied by Oak Ridge National Laboratory, and standardized by the MSID method against fresh solutions of the metals (Johnson-Matthey "Spec-pure"), accurately prepared. Particular care was taken with the standardization, as it determined the ultimate accuracy of the analyses. Tellurium and palladium were dissolved in dilute nitric acid and *aqua regia* respectively. Although some difficulty was experienced in keeping silver in solution, this was eventually achieved by dissolution in 2.5*M* nitric acid and dilution with 0.5*M* nitric acid, to give a final acid concentration of 1*M*. This solution was carefully shielded from light, and within a few hours the more dilute solution used for the standardization was prepared by dropwise addition of the concentrated solution to 6*M* hydrochloric acid. The concentrations of silver, tellurium and palladium in the tracer solution were found to be 108.7 ± 0.9, 51.7 ± 0.5 and 19.77 ± 0.07 ng/g, respectively.

Decomposition. Samples (0.2–0.5 g) were digested in Teflon beakers together with an accurately weighed amount of tracer. Next 15 g of *aqua regia* were added, and the mixture was left to stand for 2–4 hr, then refluxed for 2–3 hr. The acid was evaporated and 10 g of concentrated hydrofluoric acid were added. After standing overnight the acid was gently evaporated, another 10 g of acid were added and the evaporation was repeated. After addition of 10 g of 9*M* hydrochloric acid and evaporation to dryness the final residue was taken up in 15 g of 9*M* hydrochloric acid.

Ion-exchange separation. The digested sample was loaded onto a 2-ml anion-exchange column in 9*M* hydrochloric acid and washed with 5 column-volumes (CV) of 9*M* hydrochloric acid. Under these conditions the silver is present in the effluent and the tellurium and palladium are strongly retained by the resin. The resin was then washed with 5 CV of 4*M* hydrochloric acid followed by 5 CV of 3*M* hydrochloric acid, and tellurium was eluted with 8 CV of 0.5*M* hydrochloric acid. After washing of the resin with 5 CV of 1*M* nitric acid and 20 CV of 0.1*M* hydrochloric acid, palladium was eluted with 8 CV of 0.03*M* ammonium chloride/0.03*M* ammonia solution. This eluate was then treated with *aqua regia* and evaporated to dryness, to remove ammonium salts.

The silver fraction (in 9*M* hydrochloric acid) was evaporated to dryness, taken up by heating with 3 g of 3*M* hydrochloric acid and diluted with water to three times its volume. This solution was transferred to a 1-ml anion-exchange column. Cationic species were removed from the resin by washing with 4 CV of 1*M* hydrochloric acid followed by 20 CV of 0.01*M* hydrochloric acid. Silver was then eluted with 6 CV of 1*M* nitric acid. The residue obtained from the evaporation of this solution was sufficiently pure for isotopic analysis.

Tellurium required a further two stages of cation-exchange processing. The 0.5*M* hydrochloric acid solution from the first column was transferred directly to a column containing 1.5 ml of cation-exchange resin. Under these conditions most constituents of the solution other than tellurium are retained by the resin. Any tellurium remaining on the resin was eluted with 6 CV of 0.5*M* hydrochloric acid. The eluate containing the tellurium was evaporated to dryness with a few drops of nitric acid to avoid possible loss of tellurium and the residue was redissolved in a few ml of 0.5*M* hydrochloric acid. The procedure was repeated on a column containing 1 ml of resin. The final residue was sufficiently pure for isotopic analysis.

Although quantitative separation of the silver, tellurium and palladium is not essential, a relatively high yield ensures that maximum quantities of each element are available for isotopic analysis. The yields for complete extraction were 98, 90, and 54% for Ag, Te and Pd, respectively. Two blanks were carried through with each batch of 10 samples analysed.

Mass spectrometry

Isotopic-abundance measurements were made on an AEI MS12 mass spectrometer with a 31-cm radius 90° magnetic sector, fitted with an electron-multiplier and modified for thermal ionization of solid samples. The ion currents corresponding to each isotope were amplified, then digitized with the aid of a digital voltmeter. Data acquisition was performed under computer control, by a "peak-hopping" method. A Hall probe was employed to sense the magnetic field. The measurement system was calibrated to provide linearity of better than 2 parts in 10^5 down to 10% of full-scale reading or less. The ease with which ions are produced by thermal ionization is dependent on the ionization potential of the element and the work function and temperature of the ionizing surface.[10] Because of the high ionization potentials of Te (9.01 eV) and Pd (8.3 eV) these two elements normally produce ion beams too weak to be measured. However, by transfer of the sample to the filament surface together with an ion-enhancing agent such as phosphoric acid–silica gel mixture,[11] measurable beams can be produced from nanogram samples. Samples were loaded onto rhenium filaments (0.76×0.03 mm) which were degassed at 1600° in a vacuum for 30 min before addition of the sample.

Silver. The procedures developed by Kelly *et al.*[9] were followed with only minor changes. The silver sample, in 9*M* hydrochloric acid, was transferred to a rhenium filament and evaporated to dryness by passage of a current of 1 A. The activator was added to the filament and the mixture bonded on by evaporation of the solution and increase in the current to give red heat for 3–5 sec. A white fine-pored deposit was formed. The sample was heated under vacuum in the mass spectrometer to 850–900° for 10 min and then to a final temperature of 1000 ± 5° over a 15-min interval. Ion currents of about 10^{-13} A were produced for 60 min from 10 ng of natural Ag. Although Ag has no isobaric interferences, peaks due to residual hydrocarbon vapours, were occasionally detected on the high-mass side of $^{107}Ag^+$ and $^{109}Ag^+$. The hydrocarbon interference was essentially eliminated by including a cold finger (cooled with liquid nitrogen) in the ion-source region and operating the mass spectrometer with a resolution of about 800.

During any isotopic analysis the lighter isotopes are preferentially lost from the filament. For silver this leads to a time-dependent change in the 109/107 isotope abundance ratio which, if not carefully controlled, will result in small inaccuracies in the final result. By use of the procedures of Kelly *et al.*[9] satisfactory control of the mass fractionation was achieved for a wide range of sample sizes. The precision within and between analyses is indicated in Fig. 1(a) where measured isotope abundance ratios for natural (Johnson–Matthey "Spec-pure") samples of between 10 and 700 ng are shown. Each point represents the mean of 6 sets of 12 ratios. The data show that no bias due to mass-fractionation effects is introduced as the size of the sample analysed decreases.

Kelly *et al.*[9] have shown that AsS^+ ions can interfere with silver isotope abundance measurements. Since these ions cannot be resolved from the silver ions at the resolution

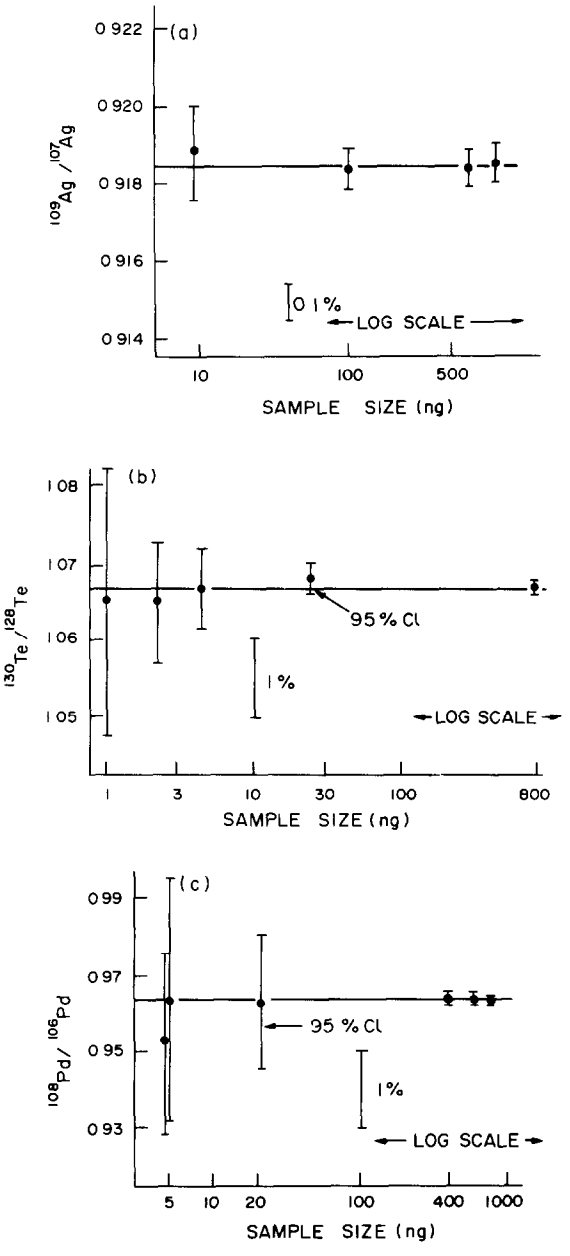

Fig. 1. Variation of isotope abundance ratio with sample size, showing the precision of the measurements and the absence of bias due to mass fractionation. The uncertainties shown are 95% confidence limits. (a) Silver, (b) tellurium and (c) palladium.

employed, this can lead to measurement errors. To obviate this possibility a number of precautions were taken. A second anion-extraction stage, incorporating nitric acid elution of the silver, minimized contamination by sulphur.[9] The choice of a silver-107 spike meant that the 107-isotope abundance was always greater than the 109-abundance, and thus the fractional error due to interference at $m/z = 107$ was reduced. Also the ion currents were generally large and the ratios were monitored for at least 2 hr to ensure that they conformed to a standard time-dependent isotope fractionation pattern. In addition, numerous measurements made in a parallel study on natural silver from terrestrial rocks did not reveal any significant contamination due to AsS^+.

Tellurium and palladium. For most elements the efficiency of ionization depends on the purity of the sample. In the case of tellurium and palladium extracted from natural materials, where levels are frequently in the low ng/g range, high sample purity is essential. To achieve this, microelectro-deposition was used as a final purification step and as an aid in binding the sample to the filament. The sample was transferred in a drop of 9*M* hydrochloric acid to a rhenium filament and evaporated to dryness. A small drop of 2.5*M* ammonium chloride–2.5*M* ammonia mixture was added and the sample cathodically deposited onto the filament. A short strip of acid-leached (nitric acid) high-purity platinum ribbon was used as the second electrode. Electro-deposition efficiencies greater than 90% were achieved in 5 min at plating voltages of ~3.5 V for tellurium and ~5 V for palladium. The deposits were insoluble in water, which permitted rinsing to remove impurities. The activator was then added and bonded to the filament by gentle evaporation of the liquid and increase in the filament current to give red heat for 3–5 sec.

The mass spectrometric procedure used for tellurium is essentially that used by Smith *et al.*[7] Samples were heated to 1000° for 10 min then to between 1250 and 1300° over a period of 15 min. The 128/124 and 126/124 isotope abundance ratios were measured. The spectrum was scanned at regular intervals to check for contamination peaks which could lead to inaccuracies in the measured ratios. Since tin could interfere at $m/z = 124$, its presence was tested for at $m/z = 118$, but none was ever detected. Hydrocarbon peaks were generally present early in an analysis but were minimized by using the precautions described previously for silver. The achievable precision for a range of sample sizes is shown in Fig. 1(b); 2-ng samples yielded ion currents of 10^{-15}–10^{-14} A which lasted for about 60 min and gave precisions of about 1%.

The mass spectrometric procedure for palladium is similar to that described by Mermelengas *et al.*[12] Samples were heated to 1000° for 10 min then to 1150–1200° during the next 15 min. The 104/102 and 106/102 isotope abundance ratios were measured. The mass spectrum was routinely scanned before analysis to check for interferences from cadmium and hydrocarbons. The presence of cadmium was tested for at $m/z = 111$, but was never observed. Contamination peaks were often initially present at $m/z = 104$ and 106 but soon decayed to a negligible level. The achievable precision for a range of sample sizes is shown in Fig. 1(c); 2-ng samples yielded ion currents of 10^{-15} A for about 30 min and gave precisions of about 2% in the isotopic ratios.

The inclusion of the electro-deposition step yielded a significant improvement in the precision of the isotope-abundance measurements that could be achieved on ng amounts of palladium and tellurium extracted from rocks. No detectable improvement occurred when samples of laboratory-reagent tellurium or palladium were treated in this way.

RESULTS AND DISCUSSION

Replicate analyses of GRMs BCR-1 and PCC-1 are given in Table 1. To provide the most likely concentrations for each GRM the data for each element have been averaged and the between-analyses variation is shown alongside the mean. The error given is at the 95% confidence limit. The errors indicate that fairly high accuracy is obtained even at the 1 ng/g level. The errors shown for individual analyses are 95% confidence limits. Uncertainties associated with calibration standards, weighing errors, isotopic abundance ratios and the analytical

Table 1. Ag, Te and Pd contents of geochemical reference materials BCR-1 and PCC-1

	Concentration,* *ng/g*		
	Ag	Te	Pd
BCR-1	27.7 ± 0.4	0.6 ± 0.5	0.1 ± 0.8
	24.4 ± 1.9	2.5 ± 1.8	0.1 ± 0.4
	26.3 ± 1.1	0.7 ± 0.4	0.0 ± 0.6
	25.4 ± 0.9	1.5 ± 0.3	0.09 ± 0.05
	25.5 ± 0.3	0.9 ± 0.5	0.1 ± 0.2
	25.2 ± 1.0	0.8 ± 0.5	
	25.7 ± 1.2	1.2 ± 0.3	
	25.8 ± 0.6		
	25.3 ± 0.5		
Mean	25.7 ± 0.7	1.2 ± 0.6	0.08 ± 0.05
PCC-1	3.6 ± 0.6	3.8 ± 0.3	3.3 ± 0.3
	3.6 ± 1.2	4.8 ± 0.7	1.3 ± 0.5
	3.4 ± 0.9	3.9 ± 0.4	3.2 ± 0.4
	3.4 ± 0.2†	4.4 ± 0.4†	3.7 ± 1.0†
Mean	3.5 ± 0.2	4.2 ± 0.7	2.9 ± 1.7

*The errors shown are 95% confidence limits. Errors given for individual analyses are indications of accuracy. The error of the mean is based on the between-analyses variation only.
†1.9-g sample. See Results and Discussion.

blank have been taken into account. At low concentrations the uncertainty in the blank is the main source of error, while at higher concentrations the uncertainties in the isotopic abundance ratios tend to dominate. Most replicate analyses show good agreement, although there is one exception for Ag in BCR-1, one for Te in BCR-1 and one for Pd in PCC-1. Since all known errors have been accounted for, these wide differences may be the result of heterogeneities in these rocks.

In the initial stages of this work difficulties were experienced in achieving reproducible chemical extraction efficiencies for tellurium. This was overcome by treating the sample with hot 9*M* hydrochloric acid instead of 2*M* hydrochloric acid before transferring it to the ion-exchange column. This ensured that the tellurium was present in the quadrivalent state, which is strongly retained on anion-exchange resins. To remove a substantial amount of iron from the resin it must be washed with dilute hydrochloric acid ($<3M$). To avoid loss of tellurium at this stage, only small volumes of reagent were used. The cation-exchange stages provide an effective means of isolating tellurium from the remaining elements. The bulk of these are retained on the resin during washing with 0.5*M* hydrochloric acid, and tellurium is quantitatively eluted. Although these elements are more strongly retained at hydrochloric acid concentrations lower than 0.5*M*, significantly larger volumes are required to elute all the tellurium and there is risk of breakthrough by elements such as sodium and potassium.

The chemical procedures for palladium described by Mermelengas *et al.*[12] have also been modified to improve the extraction efficiency of the ion-exchange separation. This has been achieved by eluting palladium from the anion-exchange resin with a mixture of ammonium chloride and ammonia rather than ammonia alone. The cation-exchange stage has also been replaced by an electro-deposition stage.

The analytical blank was determined by adding a known weight of tracer solution to a Teflon beaker and following the same chemical procedure as that used for the sample. Considerable care was taken to obtain an accurate estimate of the analytical blank. So that problems related to inadequate cleaning procedures could be detected, the blanks were run with the regular digestion beakers and columns, not with special ones reserved for blanks. Following some relatively large fluctuations in the earlier batches of samples, the blanks settled to 0.2 ± 0.3 ng for Ag, 0.15 ± 0.10 ng for Te and 0.29 ± 0.10 or 0.12 ± 0.10 ng for Pd (the values are the most likely ± the calculated uncertainty). Fluctuations in the early Te blanks were accommodated by using the corresponding batch blank rather than the value given above. Two values are shown for Pd, since a substantial improvement was achieved when improved chemical cleaning procedures for the laboratory ware were adopted. In the digestion of PCC-1 a small residue remained undissolved after the normal digestion procedure. To assess the error introduced by neglecting this residue, a 1.9-g sample was treated by the normal procedure and the residue was dissolved in a Teflon pressure bomb. The two solutions were spiked separately and the results combined to give the total concentration (last value, Table 1). Only minor amounts of Ag, Pd and Te were present in the residue, indicating that the error incurred by neglecting its contribution was negligible.

The published data for silver in BCR-1 and PCC-1 are numerous, a representative set being given by Govindaraju *et al.*[13] The BCR-1 values, which were obtained by a variety of analytical techniques, range from 11 to 54 ng/g with a mean of about 30 ng/g. A recent compilation by Abbey [1] gives values of 35(?) ng/g for BCR-1 and 10(?) ng/g for PCC-1. Our values are significantly lower than these. Relatively few measurements have been made for tellurium in GRMs. BCR-1 is the most commonly analysed and is frequently used as a reference sample for lunar and meteorite studies. The published values for tellurium in BCR-1 vary considerably (49 ng/g, Hughes;[14] <90 ng/g, Mignonsin and Roelandts;[15] 5.61 ng/g, Hertogen *et al.*;[16] 5.5 ng/g, Keays *et al.*;[17] <5 ng/g, Greenland and Campbell;[18] <4 ng/g, Ebihara *et al.*).[19] The two lowest values are consistent with our value of 1.2 ± 0.6 ng/g. An earlier measurement from our laboratory[7] indicated that the value for BCR-1 was between 2 and 5 ng/g. We believe that the present value is more accurate than the earlier value. Only a few determinations of tellurium in PCC-1 have been published. Beaty and Manuel[20] reported <8 ng/g, while an earlier measurement in our laboratory[6] yielded a value between 0 and 3 ng/g. We believe that the present value of 4.2 ± 0.7 ng/g is more accurate than the earlier value.

The isotopic analysis of palladium in GRMs is particularly difficult, owing to the small concentrations involved. In the past 5 years we have refined

both the chemical and mass spectrometric procedures for handling palladium. The blank, which was 1.2 ng in 1978[8] has now been reduced by almost an order of magnitude. Owing to the relatively low extraction efficiency at that time, the blank seems to have been underestimated in some cases, which led to artificially high concentrations. This is particularly true of BCR-1 and PCC-1 which gave values of 10 and 9 ng/g respectively, compared with the present values of 0.08 ± 0.05 and 2.9 ± 1.7 ng/g. Flanagan[21] gave preferred values of 12 and 13 ng/g for BCR-1 and PCC-1 respectively. The significantly lower value we now find for BCR-1 is supported by the recent values of <0.03 ng/g by Wolf *et al.*[22] and <2.2 ng/g by Ebihara *et al.*[19] Comparisons of recent data are not possible for PCC-1 as no values have been reported since 1978.[8] In general it appears that reliable data on palladium in GRMs are rare and confined to the MSID and neutron-activation analysis techniques.

CONCLUSION

The accurate determination of minor constituents in GRMs is essential if these materials are to achieve their full potential as reference samples for instrument calibration and procedural development. However, there are relatively few techniques available with the sensitivity and accuracy needed to make these measurements. Even though the MSID method is relatively slow and requires highly experienced personnel and costly equipment, it offers the advantages of high accuracy and sensitivity for many elements. This paper shows how the MSID technique can be applied to the measurement of silver, tellurium and palladium in rock samples where concentrations are in the low ng/g region.

Acknowledgements—The authors wish to thank the agencies who provided GRMs for this project, Mr. A. Planken and Mr. A. Cruise for technical assistance and Mrs. D. Rosman, Mrs. C. Green and Mrs. J. Miller for assisting with the preparation of the manuscript. This project was supported by The Australian Research Grants Scheme.

REFERENCES

1. S. Abbey, *Geostandards Newsl.* 1980, **4,** 163.
2. H. W. Fairbairn, W. G. Schlecht, R. E. Stevens, W. T. Dennen, L. H. Ahrens and F. Chayes, *U.S. Geol. Surv. Bull.* 1951, **980,** 1.
3. S. Abbey, *Anal. Chem.*, 1981, **53,** 529A.
4. A. R. Date, *Anal. Proc.*, 1982, **19,** 7.
5. I. Roelandts, *Chem. Geol.*, 1981, **32,** 155.
6. R. K. Webster, in *Methods in Geochemistry*, A. A. Smales and L. R. Wager (eds.), p. 202. Interscience, New York, 1960.
7. C. L. Smith, J. R. de Laeter and K. J. R. Rosman, *Goechim. Cosmochim. Acta*, 1977, **41,** 676.
8. J. R. de Laeter and N. Mermelengas, *Geostandards Newsl.*, 1978, **2,** 9.
9. W. R. Kelly, F. Tera and G. J. Wasserburg, *Anal. Chem.*, 1978, **50,** 1279.
10. I. Langmuir and K. H. Kingdom, *Proc. Roy. Soc.*, 1925, **A 107,** 61.
11. A. E. Cameron, D. H. Smith and R. L. Walker, *Anal. Chem.*, 1969, **41,** 525.
12. N. Mermelengas, K. J. R. Rosman and J. R. de Laeter, *Intern. J. Mass Spectrom. Ion Phys.*, 1981, **37,** 1.
13. K. Govindaraju, J. Morel and N. L'Homel, *Geostandards Newsl.*, 1977, **1,** 137.
14. T. C. Hughes, *J. Radioanal. Chem.*, 1980, **59,** 7.
15. E. P. Mignonsin and I. Roelandts, *Chem. Geol.*, 1975, **16,** 137.
16. J. Hertogen, M. J. Janssens and M. Palme, *Geochim. Cosmochim. Acta*, 1980, **44,** 2125.
17. R. R. Keays, R. Ganapathy, J. C. Laul, U. Krahenbuhl and J. W. Morgan, *Anal. Chim. Acta*, 1974, **72,** 1.
18. L. P. Greenland and E. Y. Campbell, *ibid.*, 1976, **87,** 323.
19. M. Ebihara, R. Wolf and E. Anders, *Geochim. Cosmochim. Acta*, 1982, **46,** 1849.
20. R. D. Beaty and O. K. Manuel, *Chem. Geol.*, 1973, **12,** 155.
21. F. J. Flanagan, *U.S. Geol. Surv. Prof. Paper*, 1976, **840,** 131.
22. R. Wolf, G. R. Richter, A. B. Woodrow and E. Anders, *Geochim. Cosmochim. Acta*, 1980, **44,** 711.

Talanta, Vol. 30, No 11, pp. 837–840, 1983
Printed in Great Britain.

0039-9140/83 $3.00 + 0.00

SUBTRACTIVE DIFFERENTIAL PULSE VOLTAMMETRY FOLLOWING ADSORPTIVE ACCUMULATION OF ORGANIC COMPOUNDS

JOSEPH WANG* and BASSAM A. FREIHA
Department of Chemistry, New Mexico State University, Las Cruces, NM 88003, U.S.A.

(*Received* 15 *March* 1983. *Accepted* 25 *May* 1983)

Summary—Subtractive differential pulse voltammetry following adsorptive preconcentration of organic compounds at solid electrodes is described. Different preconcentration periods are used, and the difference between the oxidation (stripping) currents is recorded. Background currents which are independent of the preconcentration period cancel out. Combining the enhanced peak current, due to the preconcentration step, with the background current correction of the subtractive mode, gives improved sensitivity and/or allows the use of shorter preconcentration periods. Chlorpromazine and dopamine have been used as test systems. A detection limit of around $1 \times 10^{-9} M$ has been obtained for chlorpromazine with a 10-min preconcentration period. Applicability to clinical samples is illustrated by the determination of chlorpromazine in whole blood and urine.

Electrochemistry of electroactive reactants confined to electrode surfaces is under active study in a number of laboratories. The adsorption process has been utilized as a selective preconcentration step, which enhances the differential pulse voltammetric response subsequently recorded.[1-6] The resulting differential pulse peak currents depend on the length of the preconcentration step and the rate of solution mass-transport to the surface of the electrode. While the adsorptive accumulation step enhances the analytical peak current, the background current (due to surface redox reactions and solvent decomposition) controls the detectability in very dilute solutions.

The adsorptive accumulation approach is analogous to anodic stripping voltammetry (ASV) in which extremely low detection limits are achieved by electroplating metal ions onto mercury electrodes prior to the actual measurement step. On the basis of the similarity to ASV, we suggest incorporating a subtractive (differential) approach, commonly employed in trace metal determination, for correcting the background current in pulse voltammetry of adsorbable organic compounds. Subtractive techniques have a long history in electroanalytical measurements. In subtractive ASV, different deposition times on the working electrode (or on two matched electrodes) are used and the difference between the resulting stripping currents is used.[7-9] Better detectability than that of conventional ASV is obtained because the difference between the responses is free from most background current components (*i.e.*, background currents which are independent of the deposition period cancel).

The present work is aimed at adapting the subtractive stripping approach to measurement of organic analytes which can be accumulated by adsorption or extraction on carbon electrodes. Equation (1) describes the difference in currents obtained at different preconcentration periods, T_1 and T_2.

$$\Delta i = (i_{p(T_1)} + i_b) - (i_{p(T_2)} + i_b) = i_{p(T_1)} - i_{p(T_2)} \quad (1)$$

where $i_{p(T)}$ is the faradaic current due to the redox reaction of the surface-bound species and i_b the background current. As will be shown below, the differential pulse background current is usually independent of the preconcentration period and is thus compensated when one total current is subtracted from the other. In most cases (and as in ASV), T_2 is made zero to maintain maximum speed of analysis. However, when a medium-exchange procedure is employed,[4] a very short T_2 (usually 15 sec) is used. The characteristics and advantages of this methodology have been elucidated by application to the measurement of chloropromazine and dopamine at the nM concentration level: it is known that these compounds can be accumulated on carbon paste and platinum electrodes, respectively.[1,6]

EXPERIMENTAL

Apparatus

A 0.75-cm diameter home-made carbon paste electrode and a 0.2-cm diameter platinum electrode (Model PTE, Bioanalytical Systems) served as the working disk electrodes in the chlorpromazine and dopamine experiments, respectively. The carbon electrode was mounted on a rotating disk assembly (Model PIR, Pine Instruments Co.), but a magnetic stirrer was employed in conjunction with the platinum electrode. The carbon paste was prepared by thoroughly mixing 2.5 g of graphite powder (Acheson Graphite, Grade 38, Fisher) and 1.5 g of Nujol oil. The paste surface was smoothed on a deck of smooth-surfaced paper with a circular motion. A fresh carbon surface was

*Author for correspondence.

prepared every day. Pyrex glass cells (100 and 10 ml) were used in the chlorpromazine and dopamine studies, respectively. The working electrode, an Ag/AgCl reference electrode, and a spectroscopic graphite electrode were inserted into the cells through holes in their covers. The blood experiments were performed at a microelectrode prepared by packing carbon paste in Teflon tubing (0.3 mm bore); a 2-ml glass cell was used in these experiments. All experiments were done with a Princeton Applied Research Model 364 polarographic analyser (in conjunction with a Houston Omniscribe strip-chart recorder), or with a Sargent-Welch Model 4001 polarograph.

Reagents

Chlorpromazine and dopamine sample solutions were prepared in demineralized water and ethanol, respectively. Stock solutions of chlorpromazine and dopamine (Sigma Chemical Co.), each $5 \times 10^{-4}M$, were prepared fresh every day. Portions of these solutions were diluted as required for standard-addition experiments. Supporting electrolytes were $0.1M$ phosphate buffer (pH 7.4) prepared from analytical grade KH_2PO_4 and K_2HPO_4 in 1:4 molar ratio and $0.1M$ hydrochloric acid. Rhesus monkey whole blood samples (from the NMSU Primate Center), were stored at 4°. Human urine samples from a healthy volunteer were used shortly after collection.

Procedures

Chlorpromazine measurements. A 100-ml aliquot of supporting electrolyte solution was introduced into the cell. The working electrode was pretreated by continuously changing the potential between −0.5 and +1.0 V at 50 mV/sec for 10 min. The "background" voltamperogram, to be subtracted from the "analytical" (with preconcentration) voltamperogram, was recorded first. It was obtained by applying the preconcentration potential (0 V) to the stationary electrode, waiting 45 sec for the current to decay, and then scanning the current *vs.* potential curve from 0 to +1.0 V at the scan-rate chosen for the subsequent "analytical" scan. The preconcentration potential was then applied to the electrode for a time selected according to the analyte concentration, while the electrode was rotated. The rotation was then stopped, and after 45 sec the "analytical" voltamperogram was recorded over the potential range from 0 to +1.0 V. The electrode was then kept at +0.8 V for a few minutes (3 and 5 at the $10^{-8}M$ and $10^{-7}M$ levels respectively) to clean it by removal of the remaining adsorbed chlorpromazine; completeness of removal was indicated by the next "background" voltamperogram.

Dopamine measurements. Dopamine was preconcentrated from ethanol onto an electrode disconnected from the potentiostat. The electrode was then transferred to a $0.1M$ hydrochloric acid solution where the measurement was performed. The "background" and "analytical" voltamperograms were obtained after 15 and 120 sec preconcentration periods, respectively. After this the electrode was kept at +0.7 V for 1 min, then placed in ethanol in an ultrasonic bath for 2 min, to remove the remaining dopamine.

The subtractive voltamperograms were obtained by using the Tektronix 4010 terminal of PROPHET (a time-sharing computer system operated by the National Institute of Health). The "background" and "analytical" curves were converted into digitized forms; subtraction of the "background" scan from the "analytical" one yielded the digitized subtractive curve. The three curves were transformed into analogue form and displayed graphically by means of the Tektronix 4631 copy unit.

RESULTS AND DISCUSSION

Figure 1A compares differential pulse voltamperograms for $2 \times 10^{-8}M$ chlorpromazine, these being obtained in the conventional mode with (b) and without (a) preconcentration, and in the subtractive mode (c). The curve without preconcentration was recorded before the "analytical" (with 5 min preconcentration) curve, and was subtracted from it to obtain the desired subtractive curve. Conventional differential pulse voltammetry following the preconcentration period does not provide sufficient sensitivity for measurements in the vicinity of the limits of the useful potential range; the desorption/stripping peak (at +0.7 V) coalesces with the high differential pulse background due to solvent decomposition and surface redox reactions [curve (b)]. Therefore, a 5-min preconcentration is not sufficient for convenient determinations at the $10^{-8}M$ level. The subtractive mode discriminates against the background components (as indicated by its flat baseline), and permits the desired measurement; in view of the better detectability, the preconcentration period may be shortened, as described later in this paper. Similar advantages are observed in Fig. 1B, in which $5 \times 10^{-7}M$ dopamine was determined by preconcentrating it from ethanol. In this case, the "background" and "analytical" curves were recorded for preconcentration times of 15 and 120 sec, respectively; measurements were performed after transfer of the electrode to a $0.1M$ hydrochloric acid solution. The subtractive curve (c) shows a well-defined dopamine peak, free from interference by decomposition of the solvent.

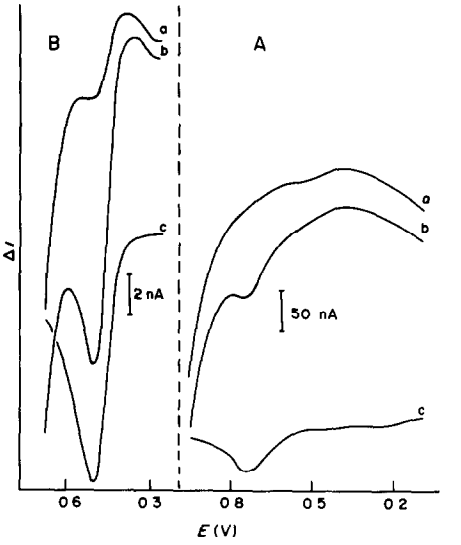

Fig. 1. Differential pulse voltamperograms for $2 \times 10^{-8}M$ chlorpromazine (A) and $5 \times 10^{-7}M$ dopamine (B). (a) "Background" curve [$T_2 = 0$(A) and 15 sec (B)]. (b) "Analytical" curve [$T_1 = 5$ (A) and 2 min (B)]. (c) The subtractive response (b) − (a). Scan-rate, (A) 5 and (B) 10 mV/sec. Amplitude, (A) 50 and (B) 25 mV. Convection during preconcentration; 1600-rpm rotation (A) and 500-rpm stirring (B).

Experiments were done to establish the optimum conditions for the preconcentration. Figure 2 shows the effects of the preconcentration parameters (time

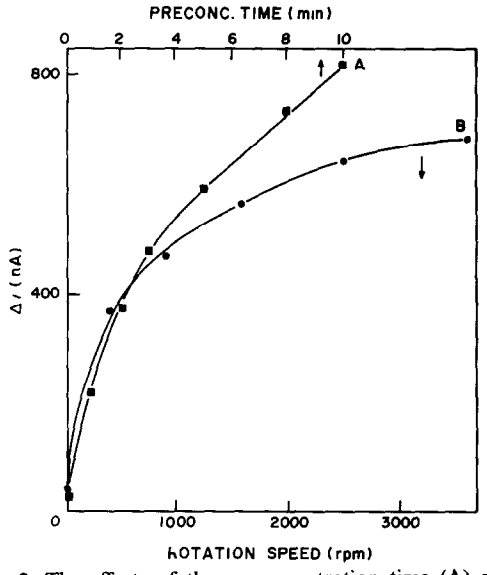

Fig. 2. The effects of the preconcentration time (A) and rotation speed (B) on the subtractive differential pulse peak current. $2.5 \times 10^{-7}M$ (A) and $5 \times 10^{-7}M$ (B) chlorpromazine in $0.1M$ phosphate buffer. Scan-rate and amplitude as for Fig. 1. Rotation speed (A) 1600 rpm. Deposition period (B) 2 min.

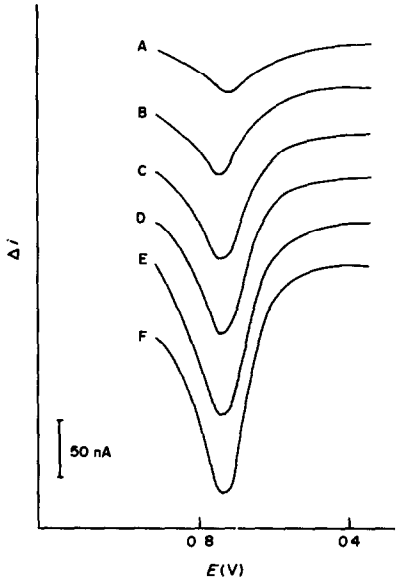

Fig. 3. Subtractive differential pulse voltamperograms obtained after successive concentration increments of $2 \times 10^{-8}M$ chlorpromazine (A–F). Preconcentration for 3 min with 1600-rpm electrode rotation. Supporting electrolyte, scan-rate and amplitude, as for Fig. 1.

and rotation speed) on the chlorpromazine peak current. A curvature is observed in the current *vs.* preconcentration-time plot, in contrast to the linear dependence usually obtained in stripping analysis for trace metals; this is due to the different nature of the accumulation processes (adsorption/extraction instead of electrolytic plating). Similar curvatures have been reported by other workers.[1,2] As in stripping analysis of trace metals, the preconcentration period is chosen to achieve a balance between sensitivity and speed. For convenient determination of concentrations ranging from 2 to 200 nM, the corresponding deposition times (at 1600 rpm) range from 10 to 1 min. At concentrations higher than 200 and 1000nM, conventional differential pulse measurements with 1 min preconcentration and without it, respectively, are sufficient. The dependence of current on rotation speed (during preconcentration) is also different from that observed in trace-metal stripping analysis. As the rotation speed increases, the peak current rises rapidly at first and then more slowly. The current obtained at 0 rpm is only 6% and 3% of the currents at 400 and 3600 rpm, respectively; this indicates that forced convection plays a major role in the accumulation process. When replotted on a log–log graph the data of Fig. 2B yield a straight line (not shown) with a slope of 0.27. The rate of accumulation depends on the rates of mass-transport to the surface and adsorption at the surface. In trace-metal stripping analysis, a slope of 0.5 for such a log–log plot characterizes the mass-transport effect on electrolytic deposition at a rotating disk electrode.

Quantitative evaluation is based on the linear correlation between the peak current and the solution bulk concentration. Figure 3 shows subtractive voltamperograms obtained after successive standard additions of chlorpromazine, each addition effecting a $2 \times 10^{-8}M$ increase in concentration; 3-min preconcentration periods were employed. The peak current was proportional to the chlorpromazine concentration; the successive $2 \times 10^{-8}M$ increments yielded subtractive peak current increments of 39, 38, 35, 30, 31 and 30 nA. Least-squares fitting yielded the equation $\Delta i_p = (16.3 \pm 0.4)C + (10.5 \pm 0.3)$ (correlation coefficient, 0.998) where Δi_p is in nA and the chlorpromazine concentration is $C \times 10^{-8}M$. This indicates that the amounts of chlorpromazine adsorbed (during the preconcentration step) are proportional to its bulk concentration. While $2 \times 10^{-8}M$ chlorpromazine can easily be determined in the subtractive mode with a 3-min preconcentration (Fig. 3A), 5-min periods are not sufficient in the conventional mode [Fig. 1A(b)].

To evaluate the detectability in the subtractive mode, differential pulse voltamperograms were recorded for $7.5 \times 10^{-9}M$ chlorpromazine following a 10-min preconcentration (Fig. 4). The conventional differential pulse voltamperogram (recorded after the preconcentration period, curve B) does not show a detectable response. In contrast, the subtractive response (curve C) yields a definite peak. The bump in the background current (at around +0.55 V), which merges with the chlorpromazine peak, as well as the solvent decomposition current, is compensated. A detection limit of around $1 \times 10^{-9}M$ may be estimated from the signal-to-noise characteristics of the response.

For effective background subtraction the adsorbed

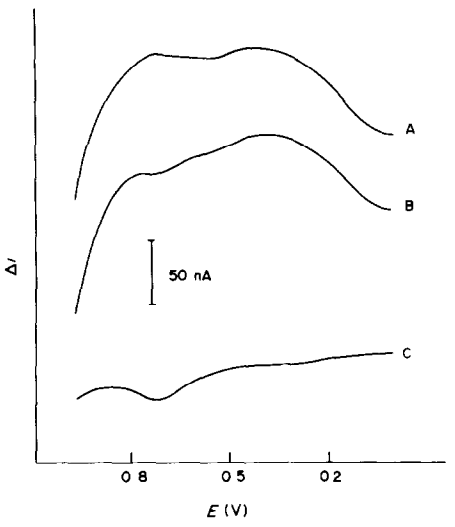

Fig. 4. Differential pulse voltamperograms for $7.5 \times 10^{-9}M$ chlorpromazine in $0.1M$ phosphate buffer. (A) "Background" curve (no preconcentration). (B) "Analytical" curve (10 min preconcentration with 2500-rpm electrode rotation). (C) The subtractive response. Scan-rate and amplitude as for Fig. 1.

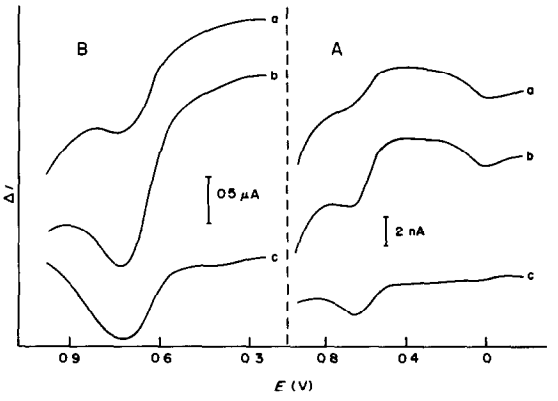

Fig. 5. Differential pulse voltamperograms for chlorpromazine in blood (A) and urine (B). (a) "Background" curve [$T_2 = 0$ (A) and 15 sec (B)]. (b) "Analytical" curve [T_1 3 (A) and 1 min (B)]. (c) The subtractive response. Samples: (A) rhesus monkey whole blood spiked with $5 \times 10^{-5}M$ chlorpromazine; (B) human urine diluted by a factor of 4 and spiked with $5 \times 10^{-6}M$ chlorpromazine. Scan-rate 0.5, (A) and 0.6 V/min (B). Amplitude 50 (A) and 25 mV (B). Convection during preconcentration: 500-rpm stirring (A) and 1600-rpm rotation (B).

compound must not change the background current, *i.e.*, identical background currents must be obtained in the "background" and "analytical" scans. In subtractive stripping analysis for trace metals with mercury-film electrodes, incomplete background correction may be the result of changes in the film activity in the cycles with and without deposition.[9,10] Although the adsorption process on bare carbon changes the electrode surface more than does electrolytic plating into mercury electrodes, a relatively high degree of background correction is obtained. This is indicated by the flat baseline of all the subtractive voltamperograms shown in this paper. Some experiments performed over more than 3 hr of continuous operation yielded flat subtractive baselines throughout.

The precision was estimated by 6 successive measurements of $1.2 \times 10^{-7}M$ chlorpromazine, with the same electrode surface (conditions as for Fig. 3). The mean subtractive peak current found was 170 nA, with a range of 159–194 nA and a relative standard deviation of 7.5%. These data indicate that cleaning the electrode (by holding it at +0.8 V) is effective and that relatively reproducible results are obtainable. The precision obtained in this study compares favourably with that (15–30% relative standard deviation) reported for other adsorbable compounds at submicromolar concentration levels.[2]

To demonstrate the applicability of the subtractive differential pulse method to real samples, blood and urine samples were spiked with chlorpromazine (Fig. 5). A 0.3-mm diameter carbon-paste microelectrode, a 2-ml sample, and a miniature cell with tiny stirring bar were used in the blood experiment. The medium-exchange procedure[4] was employed in the urine study to minimize background currents due to electroactive urine constituents. In both cases, the advantage of using the subtractive mode (curves c) is obvious, as background currents are compensated.

Applicability of the method to analyses of other reactants confined to the electrode surfaces is obvious. Work is in progress to exploit the enhanced sensitivity and selectivity of this method for *in vivo* monitoring of drugs following their administration. The shorter preconcentration period of the subtractive method would be advantageous for obtaining rapid responses, as desired in such monitoring. It would also be advantageous in the development of rapid (clinical or quality control) flow-analysers.

Acknowledgements—The authors wish to thank L. Hutchins for her assistance in the experimental work, and S. Selim for the samples of monkey blood.

REFERENCES

1. T. R. Jarbawi and W. R. Heineman, *Anal. Chim. Acta*, 1982, **135**, 359.
2. H. Y. Cheng, L. Falat and R. L. Li, *Anal. Chem.*, 1982, **54**, 1384.
3. R. P. Baldwin, D. Packett and T. M. Woodcock, *ibid.*, 1981, **53**, 540.
4. J. Wang and A. B. Freiha, *Anal. Chim. Acta*, 1983, **148**, 79.
5. R. Kalvoda, *ibid.*, 1982, **138**, 11.
6. J. W. Siria and R. P. Baldwin, *Anal. Lett.*, 1980, **13**, 577.
7. R. Kemula, *Pure Appl. Chem.*, 1967, **15**, 283.
8. J. Wang and M. Ariel, *J. Electroanal. Chem.*, 1977, **85**, 289.
9. S. D. Brown and B. R. Kowalski, *Anal. Chim. Acta*, 1979, **107**, 13.
10. J. Wang and B. Greene, *ibid.*, 1982, **144**, 137.

Talanta, Vol. 30, No. 11, pp. 841–844, 1983
Printed in Great Britain

0039-9140/83 $3.00 + 0.00

METAL SPECIATION BY FLOW-INJECTION ANALYSIS

B. P. BUBNIS, M. R. STRAKA and G. E. PACEY
Department of Chemistry, Miami University, Oxford, OH 45056, U.S.A.

(*Received* 18 *November* 1982. *Revised* 16 *March* 1983. *Accepted* 9 *May* 1983)

Summary—A two-channel switching valve is incorporated in the flow-injection manifold for on-line control of the metal speciation of Fe(II)/Fe(III) and Cr(III)/Cr(VI). 1,10-Phenanthroline is used for the iron determinations and diphenylcarbazide for chromium. The absorbances are measured at 512 and 540 nm, respectively. When a 30-μl injection loop is used, the response is linear for 0.5–30.0 ppm Fe and 0.5–40.0 ppm Cr. The relative standard deviation in each case is approximately 1%. The method allows at least 180 injections per hour.

Flow-injection analysis (FIA) is a rapidly developing technique for the analysis of many clinical and environmental samples. The method offers distinct advantages in flexibility, reproducibility, and sample throughput over conventional methods. It can readily be adapted for the determination of metals.

It has been widely shown that the relative toxicity of a metal is dependent on the oxidation state. For instance, Fe(II) is required for proper transport and storage of oxygen in higher animals by means of haemoglobin and myoglobin. The oxidized forms, methaemoglobin and metmyoglobin, which contain Fe(III), will not bind oxygen.[1] Another example is Cr(III)/Cr(VI). Cr(III) has been hypothesized as acting as a co-factor with insulin at the cellular level, and Cr(VI) has been shown to induce dermatitis, ulcers, bronchitis and pulmonary carcinomas.[2]

Flow-injection techniques for metal speciation in samples have yet to appear in the literature. Our objective in this project was to show that FIA can, indeed, be used to perform this task rapidly and sequentially. It is important, of course, to ensure that no change in the oxidation states of the metals in the sample can take place during the sample preparation, and FIA is again advantageous since in many instances this can be done directly in the flow stream.

To allow determination of two oxidation states of a particular element, a two-channel flow-through switching valve was incorporated in the manifold of the FIA system. The properly timed addition of an appropriate oxidant or reductant through the valve allows complete conversion into a single oxidation state, so that a pair of measurements (one before and one after the reagent addition) will give the concentration of both species.

Thus for Fe(II)/Fe(III), use of 1,10-phenanthroline as the spectrophotometric reagent, with measurement at 512 nm, will give the concentration of Fe(II) in the sample, and then addition of a reducing agent such as ascorbic acid to the flow-stream to reduce the Fe(III) will give the total iron concentration. The concentration of Fe(III) is obtained by difference.

EXPERIMENTAL

Reagents

Solutions were prepared as described in the literature.[3] All chemicals were used without further purification. All water was prepared with a Barnstead "Nanopure" system.

1,10-Phenanthroline solution, 0.25%. 1,10-Phenanthroline (0.500 g) was added to 100 ml of water heated to 60° to aid in dissolving the reagent. The solution was allowed to cool before dilution to 200 ml with water.

Acetate buffer solution pH 3.7. Ammonium acetate solution (2*M*, 16 ml) mixed with 184 ml of 2*M* acetic acid.

Ascorbic acid solution, 1.0%

Standard iron solutions. A stock solution containing 500 ppm Fe(II) was prepared by dissolving 3.51 g of ammonium iron(II) sulphate hexahydrate in a mixture of 20 ml of concentrated sulphuric acid and 50 ml of water, then diluting to 1 litre with water. A stock solution of 500 ppm Fe(III) was prepared by making a 500 ppm Fe(II) stock solution, and adding 0.02*M* potassium permanganate until a persistent pink colour was obtained, before the dilution to 1 litre. Working solutions containing Fe(II) and Fe(III) were prepared in the range 0.50–30.0 ppm by proper dilution of the standard stock solutions.

1,5-Diphenylcarbazide solution, 0.14%, in acetone

Ceric ammonium nitrate solution, 0.4%. Ceric ammonium nitrate (4.0 g) was dissolved in 0.50*M* nitric acid and the solution was diluted to 1 litre.

Standard chromium solutions. A stock solution of Cr(III) was prepared by dissolving 7.70 g of chromium nitrate in 200 ml of water and diluting to 1 litre. A stock solution of Cr(VI) was prepared by dissolving 3.74 g of potassium chromate in 200 ml of water and diluting to 1 litre. Working solutions containing Cr(III) or Cr(VI) were prepared by proper dilution of the standard stock solutions.

Procedure

The flow system for the Fe(II)/Fe(III) and Cr(III)/Cr(VI) determinations are described in Figs. 1 and 2, respectively. The manifold, 30-μl dual injector and a dual peristaltic pump were housed in a Tecator 5020 Flow Injection Analyzer. An additional peristaltic pump (Gilson Minipuls 2) was used for both systems. Absorbances were measured at

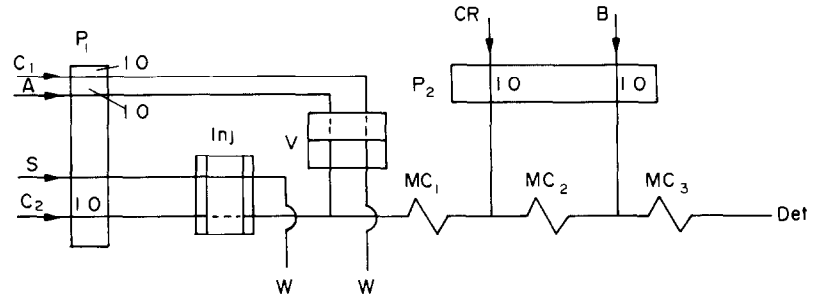

Fig. 1. Flow diagram for Fe(II)/Fe(III) determinations. P_1 and P_2 represent the peristaltic pumps used, with the flow-rates of the reagents indicated (ml/min). C_1 indicates the carrier stream which passes through the flow-through valve; C_2 indicates the carrier stream which passes through the injector. Both C_1 and C_2 are 0.014*M* HNO_3. A is the reducing agent, ascorbic acid. S is the sample solution which fills the sample loop. Inj is the 2-channel injection valve. At the time of injection, the sample loop replaces the carrier stream (segmented line) for the appropriate length of time before returning to its original postion. V represents the 2-channel flow-through valve, positioned to allow ascorbic acid to enter the flow stream. The complexing reagent, 1,10-phenanthroline, is indicated by CR. The pH-3.7 buffer is B. MC_1, MC_2 and MC_3 corresponds to mixing coils of 30, 30 and 50 cm length, respectively. W indicates waste collection.

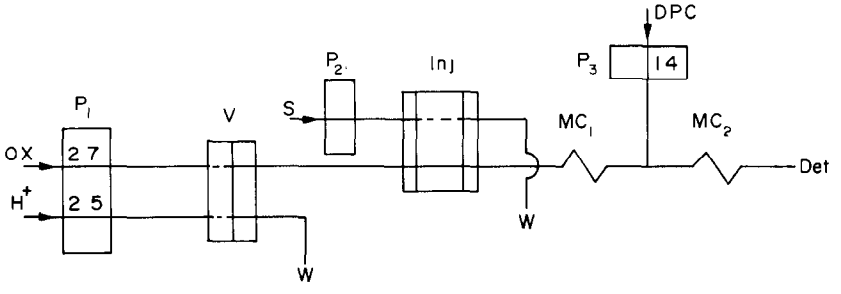

Fig. 2. Flow diagram for Cr(III)/Cr(VI) determinations. P_1 and P_2 represent the peristaltic pumps housed in the Tecator 5020 analyser, with the flow-rates of the reagents indicated (ml/min). P_3 represents the additional peristaltic pump used to introduce DPC (1,5-diphenylcarbazide solution) the complexing reagent. OX represents the ceric ammonium nitrate solution, and H^+ the 1.0*M* H_2SO_4. V is the 2-channel flow-through valve, S the sample solution which fills the 30-μl injection loop, and Inj the dual injector. MC_1 and MC_2 correspond to mixing coils of 60 and 90 cm length, respectively. W indicates waste collection.

512 and 540 nm with a Perkin-Elmer 124 double-beam spectrophotometer equipped with a Helma 10-mm flow-through cuvette. Recordings were made with a Fisher series 5000 recorder. The two-channel switching valve (Fig. 3) was made of "Plexiglas" in our own laboratory.

RESULTS AND DISCUSSION

When a determination is done by FIA, it is essential to know (*a*) how much the original sample solution is diluted on its way to the detector, and (*b*) the time lapse between sample injection and read-out.[4] The dispersion (*D*) is defined as the ratio of the analyte concentrations before and after the dispersion process has taken place in the element of fluid that yields the analytical read-out. For the manifolds described in Figs. 1 and 2, *D* was found to be 5.0 and 7.0 respectively. The residence times (*t*), defined as the time elapsed between sample injection and appearance of the peak maximum, were 7.5 and 8.0 sec. The axial dispersions (defined as half the peak-width at 62.5% of maximum peak height) were 2.0 and 7.1 sec.

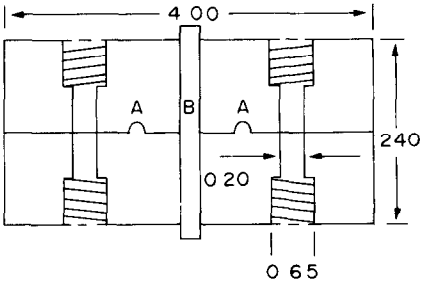

Fig. 3. Dimensions (cm) and design of switching valve, A denotes a tongue and groove system to hold the valve in correct position for channel switching, B is the locking screw holding the valve together.

Iron

The method used the well-known phenanthroline method for determination of iron(II), with absorbance measurement at 512 nm. A 30-μl sample was injected into the carrier stream and analysed for iron(II) with and without reduction of any iron(III) present, by introduction of ascorbic acid solution through the switching valve, as appropriate. As shown in Fig. 4, the corresponding peak heights for equal concentrations of Fe(II) and Fe(III) were equal within experimental error. This allows use of a single

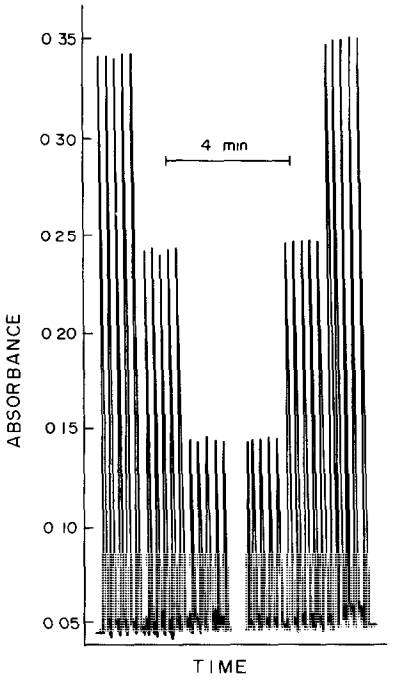

Fig. 4. Absorbance of equal concentrations of Fe(II)/Fe(III) injected into the system. From left to right: 30, 20 and 10 ppm Fe(II). Fe(III) injections of 10, 20 and 30 ppm are then presented. Each standard was injected five times.

calibration curve for both species, Fe(II) directly, and Fe(III) from the difference between the Fe(II) and the total iron concentrations. Figure 5 shows a typical calibration curve. The linear range was 0.5–30.0 ppm Fe and the relative standard deviation was less than 1.5% (calculated by the range method). Increasing the injection loop volume to 100 μl should lower the detection limit to ~0.05 ppm Fe and the relative standard deviation to less than 1.0%. This value approaches the detection limit of 0.005 ppm obtainable by conventional atomic-absorption spectrophotometry.[5] Table 1 shows the accuracy and precision of the method. All mean total Fe values were within 0.5 ppm of the true value (standard error of the mean <2%). The concentrations at high potentially interfering elements affect the determination of iron at the 10.0-ppm level are 15 ppm for nickel, 50 ppm for zinc and 70 ppm for copper. Nickel has the greatest potential as an interferent, but in environmental samples will rarely occur in high enough ratio to iron to cause difficulty.

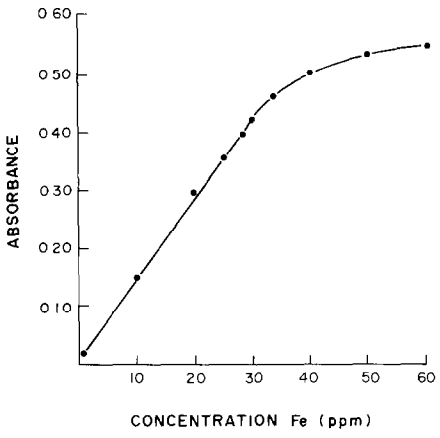

Fig. 5. Linear dynamic range of Fe determinations; means of five 30-μl injections of each sample (s.d. < 1%).

Figure 6 depicts the reproducibility of the method. By using the flow-through switching valve we were able to determine both Fe(II) and Fe(III), and accomplish at least one speciation determination per minute.

Chromium

Chromium(VI) was determined with 1,5-diphenylcarbazide, the coloured species formed being a chelate of Cr(III) [formed by reduction of Cr(VI) by the diphenylcarbazide] and the resulting diphenylcarbazone.[6–9] The absorbance of the complex was measured at 540 nm. Figure 2 depicts the manifold

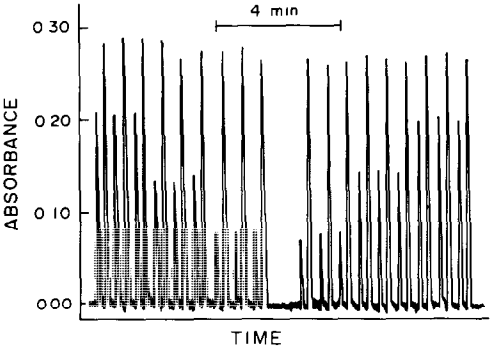

Fig. 6. Reproducibility of 2-channel flow-through valve control of the metal speciation of Fe(II)/Fe(III). Total Fe in all cases was 20 ppm. From left to right the Fe(II) concentrations were 15, 10 and 5 ppm respectively (injection volume 30 μl).

Table 1. Accuracy of the method for Fe(II)/Fe(III) determinations; mean of triplicate analyses (values in parentheses are the true values)

	Fe(II), *ppm*	Fe(III), *ppm*	Total Fe, *ppm*	Error, %
1	10.8 ± 0.2 (10.0)	7.0 (7.5)	17.8 ± 0.2 (17.5)	1.7
2	4.9 ± 0.3 (4.9)	16.5 (17.0)	21.4 ± 0.2 (21.9)	1.2
3	11.5 ± 0.2 (11.0)	7.3 (7.5)	18.7 ± 0.2 (18.5)	1.2

Table 2. Accuracy of the method for Cr(III)/Cr(VI) determinations; means of triplicate analyses. The (values in parentheses are the true values)

	Cr(III), *ppm*	Cr(VI), *ppm*	Total Cr, *ppm*	Error, %
1	5.4	19.8 ± 0.1	25.2 ± 0.3	0.6
	(5.0)	(20.0)	(25.0)	
2	9.2	15.3 ± 0.1	24.5 ± 0.2	2.0
	(10.0)	(15.0)	(25.0)	
3	9.8	5.2 ± 0.1	15.0 ± 0.2	0.0
	(10.0)	(5.0)	(15.0)	

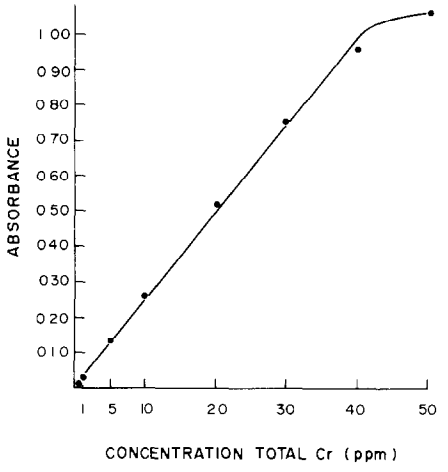

Fig. 7. Linear dynamic range for total Cr (means of five 30-μl injections, s.d. < 1%).

used. The carrier stream was 1*M* sulphuric acid, and ceric ammonium nitrate was used to oxidize Cr(III) to Cr(VI) for total Cr determination since the direct reaction of Cr(III) with diphenylcarbazone in aqueous solution was too slow for use. The calibration graph was linear from 0.5 to 20.0 ppm Cr(VI). Figure 7 shows the linearity of the calibration graph for total chromium. The use of peak-height measurements makes it necessary to use a constant concentration of oxidizing agent, since the oxidation of the Cr(III) is incomplete (in the reaction time used) if the Ce(IV) concentration is too low ($< 3.5 \times 10^{-3} M$), and the surplus oxidant also gives an absorbance signal at 540 nm. This oxidant absorbance results in a variable baseline signal for the Cr(VI) determination, and in the apparent net signal for Cr(VI) decreasing (linearity) with increasing Ce(IV) concentration, since the Cr(VI) and total chromium determinations are run alternately (in that order). The Cr(III) is taken as the difference. A further consequence is that full advantage cannot be taken of the rapid on-line switching capability of the two-channel flow-through valve, which has to be operated manually under these circumstances. Use of a detector connected on-line to a computer would permit automatic switching, however, and increase the sampling rate. The error for total chromium does not exceed 2.0%, but is higher for Cr(III) and Cr(VI) individually (Table 2).

Conclusions

Automated flow systems have greatly decreased the analysis time for clinical samples. Unfortunately, a given sample may need to be prepared in different ways for the necessary information to be acquired, and then more than one manifold will be required. The major advantage of the multiple valve described here is that it allows use of the same manifold for two different reactions. This allows true automation of the system. By use of the computer capacity available in many laboratories, it should be possible to arrange on-line switching so that a wide range of analyses can be run without changing the primary unit.

Acknowledgements—We would like to thank Tecator Corporation for the use of the 5020 analyser and Sigma Xi for funding this project.

REFERENCES

1. J. E. Huheey, *Inorganic Chemistry*, 2nd Ed., Harper & Row, New York, 1978.
2. E. Berman, in *Toxic Metals and their Analysis*, L. C. Thomas (ed.), Heyden, Philadelphia, 1980.
3. J. Mortatti, F. J. Krug, L. C. R. Pessenda and E. A. G. Zagatto, *Analyst*, 1982, **107**, 659.
4. J. Růžička and E. Hansen, *Flow Injection Analysis*, Wiley, New York, 1981.
5. R. D. Beaty, *Concepts, Instrumentation and Techniques in AAS*, Perkin-Elmer Corp., 1978.
6. H. Sano, *Anal. Chim. Acta*, 1962, **27**, 398.
7. E. V. Kovalenko and V. I. Petrashen, *J. Anal. Chem. USSR*, 1963, **18**, 645.
8. E. Najdeker, *Proc. Soc. Anal. Chem.* 1971, **8**, 194.
9. H. Marchart, *Anal. Chim. Acta*, 1964, **30**, 11.

Talanta, Vol. 30, No. 11, pp. 845–850, 1983
Printed in Great Britain.

0039-9140/83 $3.00 + 0.00

DETERMINATION OF ARSENIC BY GALVANOSTATIC STRIPPING ANALYSIS AND ITS APPLICATION TO STEELS

JIŘÍ LEXA
Chemical Laboratories, Central Research Institute, Škoda Works, Pilsen, Czechoslovakia

KAREL ŠTULÍK*
Department of Analytical Chemistry, Charles University, Albertov 2030, 12840 Prague 2, Czechoslovakia

(*Received* 11 *February* 1983. *Accepted* 5 *May* 1983)

Summary—Arsenic can be determined by galvanostatic stripping analysis with a modified gold-film electrode, prepared by simultaneous electro-deposition of gold and arsenic on a glassy-carbon support. This initially deposited arsenic is stripped from the film before the electrode is used for the analysis, but its presence during the formation of the film apparently leads to uniformly distributed crystallization sites for the subsequent determination of arsenic, so that the precision of the determination is better than that obtained with an unmodified gold-film electrode. The pre-electrolysis is performed potentiostatically in a stirred solution of 7*M* hydrochloric acid, at a potential from −0.10 to −0.35 V (*vs.* Ag/AgCl). If the galvanostatic stripping step is performed in quiescent solution after a 6-sec rest-period, at a current of 2–12 μA, then for a 100-sec pre-electrolysis time the calibration curve is linear up to an arsenic concentration of about 2 μg/ml and the limit of determination is 8 ng/ml. In the analysis of steel, the arsenic must first be separated by selective extraction of arsenic(III) bromide into toluene and back-extraction into the supporting electrolyte. A single extraction is virtually 100% quantitative. The relative error of the determination in steels is a few per cent and the results are in good agreement with the certified values for reference materials and with the results obtained by X-ray fluorescence analysis.

Arsenic can be determined with high sensitivity by electrochemical stripping analysis (*e.g.*, a determination limit of 0.02 ng/ml has been reported for differential pulse voltammetry with a gold electrode,[1] which is similar to that obtained with the AAS hydride method[2]). Gold metal or gold-film electrodes are most often used for the stripping determination of arsenic, because, as shown, *e.g.*, by Kaplin *et al.*,[3] interaction between arsenic and the gold of the electrode surface is weak and thus the reproducibility of the determination is good and the electrode surface need not be regenerated after each determination. However, these authors also observed two arsenic peaks during potentiostatic stripping from a gold electrode and ascribed the more negative one to the stripping of arsenic from a species produced by Au–As interaction and the more positive one to stripping of the pure arsenic phase.[4] The favourable effect of Au^{3+} ions present in the supporting electrolyte on the sensitivity of the determination of arsenic has been explained[5] as due to simultaneous deposition of gold and arsenic on the support; this prevents complete coverage of the support by elemental arsenic, which would decrease the efficiency of the pre-electrolysis on account of the low electrical conductance of arsenic.

Most stripping determinations of arsenic with gold electrodes have involved a potentiostatic anodic stripping step.[1,3–10] Only Jagner *et al.*[11] proposed a potentiometric stripping determination, employing chemical oxidation of elemental arsenic on the electrode surface by Au^{3+} ions present in the supporting electrolyte. This paper describes the galvanostatic stripping determination of arsenic with a gold-film electrode, which, to our knowledge, has not yet been used for this purpose but offers certain general advantages. Galvanostatic stripping is readily automated, the experimental data are often more easily handled than those from potentiostatic stripping, and the method is more universal than potentiometric stripping and places less stringent requirements on the choice of supporting electrolyte composition. (For details of galvanostatic stripping see, for example, references 13 and 14).

The main problem in the analysis of metallic materials is selectivity. For steels, we have obtained very good results[12] by extracting arsenic(III) bromide into toluene and back-extracting the arsenic into an aqueous supporting electrolyte, so we have employed this principle in the present work. An additional advantage of the extraction is the simultaneous reduction of As(V), obtained during the sample decomposition, to electroactive As(III).

EXPERIMENTAL

Apparatus

The measurements were performed on a semiautomatic instrument of our own construction,[15] permitting prepro-

*Author for correspondence.

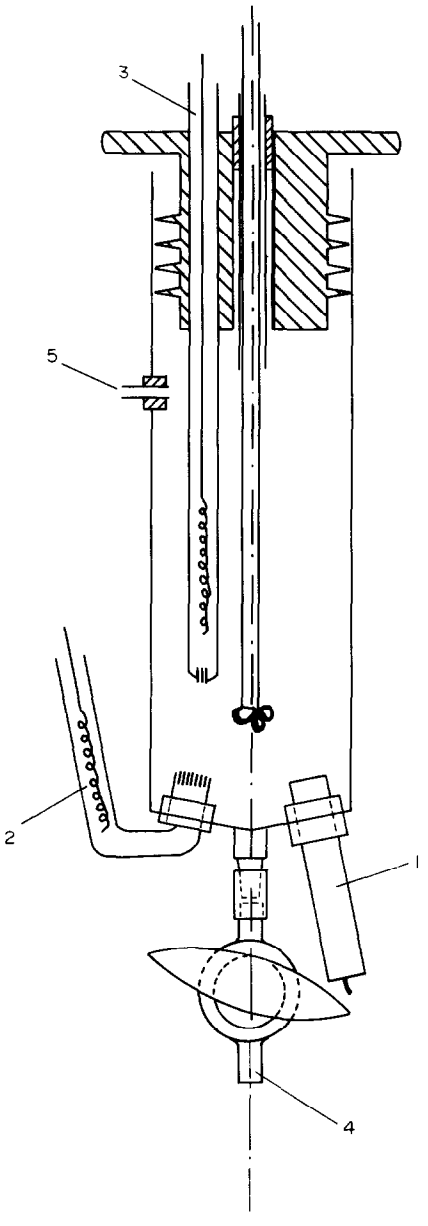

Fig. 1. The electrolytic cell. 1—working electrode, 2—counter electrode, 3—reference electrode, 4—tube for aspiration and outlet of the sample, 5—tube connected to a peristaltic pump by means of which the pressure in the vessel can be decreased or increased, thus introducing or discarding the test solution.

gramming of all the measuring stages and automatic display of the time needed to reach a given potential. The stripping curves were recorded on an RE 511.20 chart-recorder (Smiths, England). A three-electrode circuit was used, consisting of a stationary glassy-carbon disk electrode (GC20; Tokay Electrode Mfg., Nagoya, Japan), 5.27 mm in diameter, cemented into a glass tube with epoxy resin, a silver chloride reference electrode (1*M* hydrochloric acid; potential −0.020 V *vs.* SCE) and a platinum counter-electrode separated from the working electrode chamber by a porous glass plug. The working electrode was polished first with metallographic papers (4/0 and 6/0, SIA, Switzerland) and then with a 1-μm alumina suspension (Struers Scientific Instruments, Denmark), rinsed thoroughly with water, then degreased with acetone and prepolarized in 0.5*M* sulphuric acid for 50 sec at +1.00 V and for 100 sec at −1.00 V. The electrode was disconnected from the potentiostat at the latter potential, rinsed with water and immediately electrolytically coated with gold. The procedure was repeated before each renewal of the gold film, with omission of only the polishing with the metallographic papers.

The electrolysis vessel (Fig. 1)[16] permits introduction and removal of the test solution through a single tube, by pressure variation. This cell has the advantage that it is possible to aspirate the (lower) aqueous phase after the extraction, without the need to separate the phases mechanically. Small solution volumes were measured with Eppendorf micropipettes (FRG). The extractions and back-extractions were performed in 25- and 10-ml standard flasks, respectively, closed with polyethylene stoppers.

Reagents

All chemicals used were of *p.a.* purity (Lachema, Czechoslovakia and Merck, FRG) and were not further purified. A standard solution of As^{3+} (0.1 mg/ml) was prepared by dissolving 0.1320 of arsenious oxide in 20 ml of 2*M* sodium hydroxide, diluting with water to about 100 ml, adding 10 ml of dilute sulphuric acid (1 + 5) and diluting with water to 1000 ml. A standard solution of Au^{3+} (1 mg/ml) was prepared by dissolving 0.1000 g of pure gold in a small amount of *aqua regia*, evaporating to dryness, dissolving the residue in 5 ml of concentrated hydrochloric acid and diluting with water to 100 ml.

All measurements were made at room temperature and the potentials referred to the silver–silver chloride electrode (1*M* hydrochloric acid).

The stripping curves for low arsenic concentrations (at a current of 2μA) were evaluated by the usual chronopotentiometric technique (see, for example, reference 13). At higher arsenic concentrations (at a current of 12 μA), the stripping time was obtained by measuring the time (t_{strip}) from the beginning of the stripping step to the attainment of a potential of +0.30 V, and subtracting the corresponding value for the blank.

Procedure

Weigh out 0.200 g of steel and dissolve it in 10 ml of hydrochloric/nitric acid mixture (3:1 v/v) in a covered 100 ml beaker. Then add 20 ml of sulphuric acid (1 + 1) and evaporate the solution to about half its initial volume. Rinse the walls of the beaker with a small amount of water, add 2 ml of concentrated formic acid and again evaporate to about half the initial volume. Transfer the solution to a 25-ml standard flask, rinse the beaker with 1 ml of 1*M* iron(II) sulphate into the flask, add 5.0 ml of 4*M* potassium bromide, cool the flask to room temperature, add 1.00 ml of toluene and make up to the mark with water. Shake the stoppered flask for 2 min then, after phase separation, pipette 0.500 ml of the organic phase into a 10-ml standard flask containing 10 ml of the supporting electrolyte (7*M* hydrochloric acid). Back-extract the arsenic by inverting the stoppered flask several times. After phase separation, aspirate part of the lower (aqueous) phase into the electrolysis vessel. Apply the pre-electrolysis/stripping cycle twice and find the arsenic content from the second stripping curve. Measure the time from the beginning of the stripping step to the instant when the electrode attains a potential of +0.300 V (I_{strip} = 12 μA) or +0.150 V (I_{strip} = 2 μA). After each determination, rinse the electrolysis vessel with ethanol and then with water.

RESULTS AND DISCUSSION

Electrode preparation

It has been found that the concentration of hydrochloric acid in the solution for the preparation of the

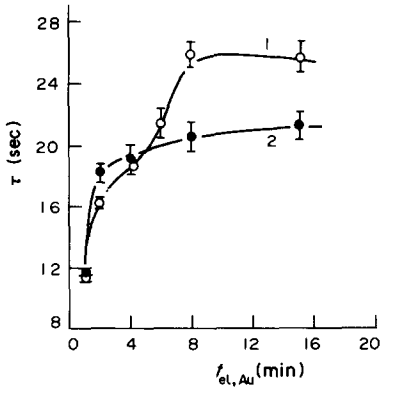

Fig. 2. The effect of $E_{el,Au}$ and $t_{el,Au}$ on the sensitivity and precision of the determination of arsenic. Electrode preparation: 7*M* HCl + 2.5 × 10^{-4}*M* Au^{3+}, $E_{el,Au} = -0.150$ V (1), $E_{el,Au} = -0.300$ V (2). Determination of arsenic: 7*M* HCl + 1.00 μg/ml As; $E_{el,As} = -0.350$ V, $t_{el,As} = 100$ sec, $I_{strip} = 12$ μA.

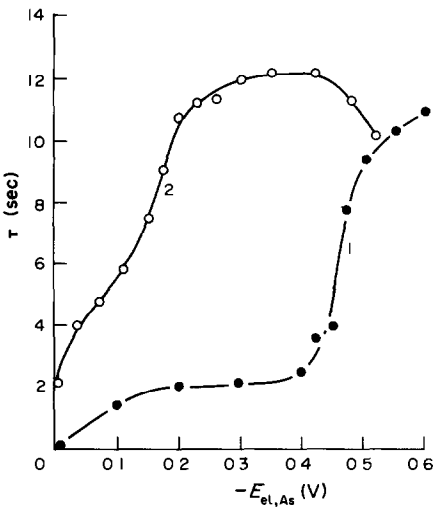

Fig. 3. The effect of the pre-electrolysis potential on the transition time of arsenic for unmodified (1) and modified (2) gold film electrodes. Electrode preparation: 7*M* HCl + 2.5 × 10^{-4}*M* Au^{3+} + c_{As}; $c_{As} = 0$ μg/ml (1), $c_{As} = 2$ μg/ml (2); $E_{el,Au} = -0.350$ V; $t_{el,Au} = 100$ sec. Determination of arsenic: 7*M* HCl + 0.5 μg/ml As; $t_{el,As} = 100$ sec; $I_{strip} = 12$ μA.

gold-film electrode has little effect on the analytical properties of the electrode. Therefore, the same acid concentration was used as that of the electrolyte for the determination, *i.e.*, 7*M*, selected on the basis of the literature data.[5,11] The concentration of gold(III) in the solution was 2.5 × 10^{-4}*M*.

The effect of the two important parameters, the pre-electrolysis potential $E_{el,Au}$ and the electrolysis time $t_{el,Au}$, on the analytical properties of the gold film was studied by repeated determinations of arsenic at two $E_{el,Au}$ values and various electrolysis times (Fig. 2). Each stripping determination was repeated ten times in the same solution and Fig. 2 contains the average transition times, together with the confidence intervals for a significance level of $\alpha = 0.05$. The highest sensitivity is obtained for $E_{el,Au} = -0.150$ V and $t_{el,Au} \geqslant 8$ min (Fig. 2, curve 1). However, the curves exhibit two transition times, corresponding to potentials $E_{\tau/2} = +0.05$ and $+0.15$ V, indicating inhomogeneity of the layers of elemental arsenic on the gold-film surface. Also the sensitivity of this determination varies with time. Gold films prepared at $E_{el,Au} \leqslant -0.300$ V and $t_{el,Au} \geqslant 6$ min (Fig. 2, curve 2) have somewhat better properties and the first transition time (here with $E_{\tau/2} = +0.12$ V) amounts to only about 5% of the sum of the two transition times.

It has been observed that the presence of arsenic(III) in the plating solution has a marked effect on the quality of the gold film and that film electrodes modified by simultaneous deposition of arsenic with the gold have much better analytical properties than do unmodified electrodes. This is demonstrated by the dependence of the arsenic transition time on the arsenic pre-electrolysis potential, $E_{el,As}$, for modified and unmodified electrodes (Fig. 3) and by the shapes of the stripping curves (Fig. 4). Apparently the co-deposition of arsenic leads to formation of uniformly distributed crystallization centres for arsenic in the surface layers of the gold film, even if the arsenic is electrochemically stripped from the electrode before it is used for the determinations. The sensitivity of the determination of arsenic depends on the surface area of the electrode, but is practically independent of the thickness of the gold film. If the pre-electrolysis potential is shifted to values more negative than the optimal value, the sensitivity of the determination decreases irreversibly. The gold-film electrode can be used for one working day without significant change in the sensitivity, but storage over-

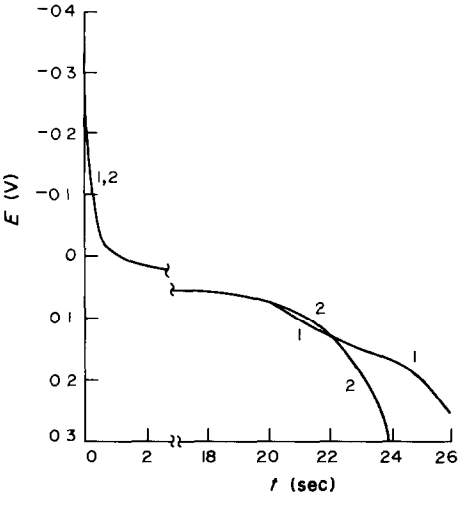

Fig. 4. Galvanostatic stripping curves for arsenic with unmodified (1) and modified (2) gold film electrodes. Electrode preparation: 7*M* HCl + 2.5 × 10^{-4}*M* Au^{3+} + $c_{As} = 0$ μg/ml (1), $c_{As} = 0.2$ μg/ml (2); $E_{el,Au} = -0.050$ V; $t_{el,Au} = 10$ min. Determination of arsenic: 7*M* HCl + 1 μg/ml As; $E_{el,As} = -0.350$ V; $t_{el,As} = 100$ sec; $I_{strip} = 12$ μA.

night causes about 50% decrease in the sensitivity, and the film must be renewed.

When the deposition–stripping cycle is repeated in the same solution, the precision of the arsenic determination improves. The first stripping curve is poorly reproducible and thus the second curve was always used to determine the transition time. From the point of view of film-surface stability toward organic solvents (which is important because the practical application to steels requires solvent extraction) it is better to use longer gold plating times ($t_{el,Au} > 5$ min) and lower concentrations of arsenic(III) in the plating solution ($c_{As} \approx 0.2$ μg/ml). If the supporting electrolyte is saturated with toluene, the sensitivity of the arsenic determination decreases by about 10% for both unmodified and modified electrodes, but the precision of the determination with the modified electrode is better [for the determination of arsenic at a concentration of 1 μg/ml, the relative standard deviation (ten measurements) is 2.8% for the unmodified electrode and 1.4% for the modified electrode].

Therefore, the following procedure is used for the electrode preparation: the gold film is plated on the pretreated glassy carbon at a potential of $E_{el,Au} = -0.050$ V for 10 min from a solution that is $7M$ in hydrochloric acid, $2.5 \times 10^{-4}M$ in Au^{3+} and $2.7 \times 10^{-6}M$ (0.2 μg/ml) in As^{3+}. Then the arsenic is galvanostatically stripped into the plating solution at a current of 12 μA until the electrode potential becomes +0.300 V. The electrode is rinsed with water and transferred to the sample solution.

Determination of arsenic

It follows from the literature[5,11–13] that hydrochloric acid is the most suitable supporting electrolyte for the electrochemical stripping determination of arsenic. It can be seen from Fig. 5 that the optimal hydrochloric acid concentration is about $7M$, in agreement with earlier results.[5,11]

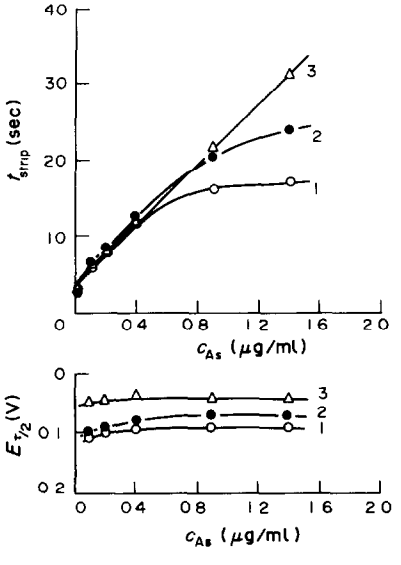

Fig. 5. The effect of the hydrochloric acid concentration on the linearity of the calibration and on the stripping potential of arsenic. 1.4M (1), 3.5M (2), 7M (3); $E_{el,As} = -0.350$ V; $t_{el,As} = 100$ sec, $I_{strip} = 12$ μA; modified gold film electrode.

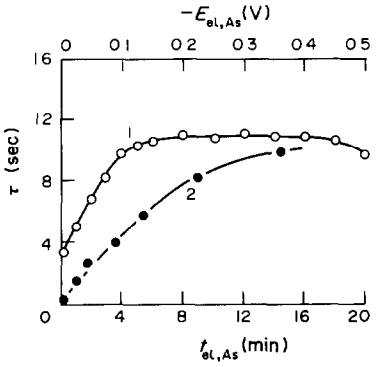

Fig. 6. The effect of the potential (1) and time (2) of pre-electrolysis on the arsenic transition time. 7M HCl; $c_{As} = 0.5$ μg/ml (1), $c_{As} = 0.1$ μg/ml (2); $E_{el,As} = -0.350$ V (2); $t_{el,As} = 100$ sec (1); $I_{strip} = 12$ μA; modified gold film electrode.

The dependence of the arsenic transition time on the pre-electrolysis potential and time in this solution are given in Fig. 6, and the effect of the arsenic pre-electrolysis potential on the linearity of the calibration curve is demonstrated in Fig. 7. It can be seen that $E_{el,As}$ should be about −0.35 V for a linear calibration curve over a sufficiently wide arsenic concentration range to be obtained, and that the sensitivity of the determination increases with increasing pre-electrolysis times up to about 15 min. As it was found that rest periods greater than 4 sec after the pre-electrolysis in stirred solutions have no effect on the shape of the stripping curves, a 6-sec rest period was used in the determinations.

Typical stripping curves recorded under these conditions are shown in Fig. 8 and the analytical parameters for the determination are summarized in Table 1. It can be seen from the table that a decrease in the

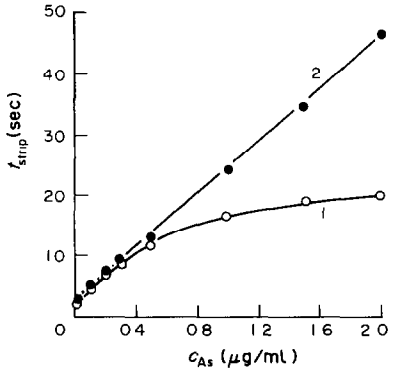

Fig. 7. The effect of the pre-electrolysis potential on the linearity of the calibration. 7M HCl, $E_{el,As} = -0.100$ V (1); $E_{el,As} = -0.350$ V (2); $t_{el,As} = 100$ sec; $I_{strip} = 12$ μA; modified gold film electrode.

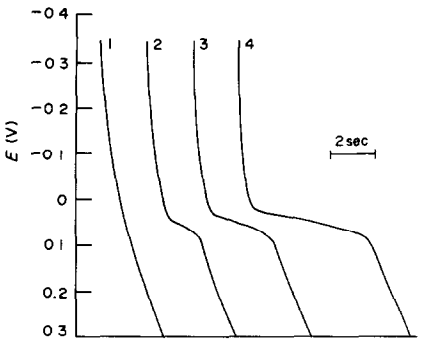

Fig. 8. Typical galvanostatic stripping curves of arsenic. 7*M* HCl; $E_{el,As} = -0.350$ V; $t_{el,As} = 100$ sec., $I_{strip} = 12$ μA; modified gold film electrode; $c_{As} = 0$ (1), 0.05 (2), 0.10 (3) and 0.20 (4) μg/ml.

stripping current from 12 to 2 μA does not lead to a sixfold increase in the sensitivity of determination as might be expected from the theory, but that the increase is only about 3.5-fold. This is probably due to oxidation of the elemental arsenic during longer stripping times by atmospheric oxygen dissolved in the supporting electrolyte; this effect would also somewhat limit the possibilities for improving the measuring sensitivity by increasing the pre-electrolysis time. Some trial measurements in de-aerated solutions showed that the removal of oxygen does cause an increase in the measuring sensitivity.

Extraction of arsenic

To attain sufficient selectivity for the determination of arsenic in steels, the extraction method described previously[12] was employed. We have found that the extraction of arsenic(III) bromide from sulphuric acid medium into toluene permits the selective determination of arsenic in pure antimony and tin by the present method, when $c_{H_2SO_4} \leqslant 7M$ and $c_{Br^-} > 0.5M$. It is possible to determine 0.01% arsenic in common steels in the presence of 0.1% antimony with a relative error of *ca.* +10%, with $c_{H_2SO_4} \cong 8M$ and $c_{Br^-} \cong 0.8M$. When the steel is oxidatively decomposed with a 3:1 v/v mixture of hydrochloric and nitric acids, then 1% of selenium and 2% of germanium do not interfere.

To decompose the small amount of bromine formed in the aqueous phase by the oxidation of hydrogen bromide by atmospheric oxygen, a small amount of ascorbic acid or ferrous sulphate is added. Ferrous sulphate is preferable because its acidic solutions are more stable.

When 24 ml of aqueous phase are extracted with 1 ml of toluene, equilibrium with virtually 100% extraction is attained within 1 min; to provide a safety margin, we subsequently used a 2-min extraction time. The back-extraction into 7*M* hydrochloric acid is virtually instantaneous and quantitative recovery is attained simply by inverting the stoppered flask several times. However, to prevent loss of arsenic by back-extraction into water, the extract must be protected against atmospheric moisture and the pipette must be thoroughly dried. To prevent deposition of toluene on the electrode, only part of the aqueous phase after back-extraction is aspirated into the electrolytic vessel and the vessel is rinsed with ethanol and then water after the measurement.

Application to steels

A 3:1 v/v mixture of hydrochloric and nitric acids, which will dissolve all types of steel, with oxidation of arsenic to As(V) without formation of the volatile chloride, was used to decompose the samples. Most of the acid mixture was removed by evaporation with sulphuric acid and the residual nitric acid by addition of formic acid, to prevent precipitation of ferric sulphate on prolonged evaporation. To prevent possible oxidation of As^{3+} by bromine formed during the extraction, ferrous sulphate was added to the aqueous phase before the extraction.

The calibration curve was then linear from 1 to 200 ppm As in the sample and the determination limit 0.7 ppm. The parameters of the calibration curve are given in Table 2. They were obtained by analysing pure iron with an arsenic content of less than 0.7 ppm, to which various amounts of arsenic were

Table 1. Characteristics of the calibration regression lines for the direct determination of arsenic in the 7*M* HCl base electrolyte

I_{strip}, μA	Number of measurements	$b \pm s_b$ ($sec.\mu g^{-1}.ml$)	$a \pm s_a$, *sec*	Correlation coefficient	Limit of detection, $\mu g/ml$
2	6	71 ± 3	0.1 ± 0 2	0.997	0.008
12	8	21.4 ± 0.4	−0.1 ± 0.4	0.999	0.06

c_{As} = 0.005–0 150 and 0.05–2.00 μg/ml; $E_{el,As} = -0$ 350 V; $t_{el,As} = 100$ sec; modified gold film electrode; 3*s* criterion used for the limit of detection. Equation: $\tau = bc_{As} + a$

Table 2. Characteristics of the calibration regression straight lines for the determination of arsenic in steel

I_{strip}, μA	Number of measurements	$b \pm s_b$ ($sec.\mu g^{-1}.ml$)	$a \pm s_a$, *sec*	Correlation coefficient	Limit of detection, *ppm*
2	6	0.72 ± 0.02	0.1 ± 0.2	0.998	0.7
12	8	0.183 ± 0.003	0.4 ± 0.3	0.999	5.0

Sample weight, 0.2 g; c_{As} = 0.5–15 and 5–200 ppm; $E_{el,As} = -0.100$ V and −0 350 V; $t_{el,As} = 100$ sec; modified gold film electrode; 3*s* criterion used for the limit of detection. Equation: $\tau = bc_{As} + a$

Table 3. Precision and accuracy of the determination of arsenic in steel ($\alpha = 0.05$)

Reference material	Certified content of As, %	C, %	Si, %	Ni, %	Cr, %	Cu, %	Mo, %	V, %	Co, %	Ti, %	W, %	Arsenic found (%) RFA	GSA, $L_{1,2}$	n
ČKD 170	0.030	0.2	0.8	0.2	2.0	0.1	1.3	0.0	0.0		0.3	0.030	0.030 ± 0.002	3
ČKD 171	0.015	0.1	0.0	1.9	2.8	0.0	0.0	0.3	0.0		0.0	0.015	0.015 ± 0.001	3
V 4108	0.008			10.0	18.0					0.5		0.007	0.007 ± 0.001	3
V 4109	0.023			10.0	18.0					0.5		0.021	0.021 ± 0.001	3
ČKD 226	0.03	2.5	3.6	0.1	1.8	0.3	0.2	0.2	0.1		0.1	0.030	0.032 ± 0.002	5
ČKD 229	0.015	2.7	0.7	2.3	0.2	0.1	0.1	0.0	0.1		0.0	0.015	0.015 ± 0.001	3
ČKD 230	0.005	2.6	1.0	1.1	0.1	1.0	0.0	0.0	0.0		0.0	0.005	0.006 ± 0.001	5
V 4103	0.010			3.7	12.5		0.3					0.010	0.010 ± 0.001	3

RFA—X-ray fluorescence analysis; GSA—galvanostatic stripping analysis; $L_{1,2} = \bar{x} \pm st_\alpha/\sqrt{n}$; n = number of parallel determinations.

added. The method was verified by analysing eight reference materials (see Table 3). It can be seen that the agreement with the certified contents of arsenic and with the results of X-ray fluorescence analysis is satisfactory.

As the method is highly selective, it is readily applicable to analysis of a great variety of materials.

REFERENCES

1. G. Forsberg, J. W. O'Laughlin, R. G. Megargle and S. R. Koirtyohann, *Anal. Chem.*, 1975, **47**, 1586.
2. *Guide to Techniques and Application of Atomic Spectroscopy*, Perkin–Elmer, Norwalk, 1980.
3. A. A. Kaplin, N. A. Veits, N. M. Mordvinova and G. G. Glukhov, *Zh. Analit. Khim.* 1977, **32**, 687.
4. *Idem, Zavodsk. Lab.*, 1977, **43**, 1051.
5. P. H. Davis, G. R. Dulude, R. M. Griffin, W. R. Matson and E. W. Zinc, *Anal. Chem.* 1978, **50**, 137.
6. A. A. Kaplin, N. A. Veits, N. M. Mordvinova and V. E. Morozova, *Zh. Analit., Khim.*, 1978, **33**, 1972.
7. A. A. Kaplin and N. T. Rud, *ibid.*, 1980, **35**, 1093.
8. T. W. Hamilton and J. Ellis, *Anal. Chim. Acta*, 1980, **119**, 225.
9. S. W. Lee and J. C. Méranger, *Anal. Chem.*, 1981, **53**, 130.
10. F. G. Bodewig, P. Valenta and H. W. Nürnberg, *Z. Anal. Chem.*, 1982, **311**, 187.
11. D. Jagner, M. Josefson and S. Westerlund, *Anal. Chem.*, 1981, **53**, 2144.
12. J. Lexa and K. Štulík, *Talanta*, 1982, **29**, 1089.
13. F. Vydra, K. Štulík and E. Juláková, *Electrochemical Stripping Analysis*, Horwood, Chichester, 1976.
14. F. Opekar, *Chem. Listy*, 1981, **75**, 132.
15. J. Lexa, *Technical Report*, Škoda Works, 1983.
16. *Idem, Chem. Listy*, 1983, **77**, 436.

Talanta, Vol. 30, No. 11, pp. 851–855, 1983
Printed in Great Britain.

0039-9140/83 $3.00 + 0.00

RAPID AND SELECTIVE CHELATOMETRIC TITRATION OF ZINC IN NON-FERROUS ALLOYS

ZHOU NAN*
Shanghai Research Institute of Materials, The Ministry of Machine Building Industry, Shanghai, People's Republic of China

LU ZHI-REN and GU YUAN-XIANG
The Third Factory of Shanghai Reagent Chemicals, Shanghai, People's Republic of China

(*Received* 20 *December* 1982. *Revised* 18 *March* 1983. *Accepted* 27 *April* 1983)

Summary—A rapid titrimetric method for the determination of Zn (≥ 5%) in zinc, aluminium and copper alloys is proposed. It is based on the chelation of Zn(II) with HEDTA as titrant in an ethanolic aqueous medium. The end-point is detected with hydrazidazol, a new indicator developed in China. Up to at least 6% Mn in the alloy does not interfere. Direct determination of Zn(II) is rendered possible by using a combination of masking agents. A separation is needed only if nickel is also present. A decided advantage of this method is its high selectivity. The standard deviation was found to be 0.07 mg and the coefficient of variation to vary from 0.2 to 0.5%. The method has been successfully used to determine Zn in different kinds of non-ferrous alloys, especially those containing Mn.

The chelatometric titration of Zn(II) is one of the widely used analytical methods. Unfortunately many metal ions interfere. Four titrations are required for the determination of Zn(II) in the presence of Cu(II), Pb(II) and Ni(II) by the Přibil and Veselý method.[1] The cumulative error of the four titrations may be appreciable. The methods recommended by ASTM[2,3] are accurate but time-consuming. Moreover, masking with cyanide followed by demasking is not now generally accepted as good practice. Hence in the case of copper alloys containing ≥5% of Zn, the Zn is usually determined by difference.[4]

The interference caused by Mn(II) is extremely difficult to eliminate. The literature on the masking of Mn is rather confusing[5] and conflicting. All the masking agents used so far, including carboxymethylmercaptosuccinic acid[6] are found to be rather unsatisfactory.

A selective titrimetric method for the determination of Zn(II) in the presence of other commonly encountered metal ions, especially Mn, which is highly desirable in practice, is still lacking and deserves further study. In order to solve this difficult problem in analytical chemistry a selective titrant and a metallochromic indicator specific or nearly specific for Zn(II) must be used. In this paper HEDTA, *N*-(2-hydroxyethyl)ethylenediamine-*N*,*N*′,*N*′-triacetic acid, is suggested as the titrant instead of EDTA, and hydrazidazol as the indicator. Hydrazidazol is the trivial name proposed for 1-(2-butyrohydrazidonaphthylazo)-2-hydroxy-4-nitrobenzene, which is an entirely new reagent recently developed by us. Detailed information about this new reagent will be reported in the near future. This new approach makes possible a rapid and selective method for the determination of Zn(II). It has been successfully applied to the determination of Zn (≥5%) in different kinds of non-ferrous alloys, especially those containing Mn.

*To whom correspondence and requests for reprints should be sent. Present address: 999 Dong Chang Zhi Lu, Shanghai, People's Republic of China

EXPERIMENTAL

Reagents

Analytical-reagent grade chemicals were used unless otherwise specified.

Hydrogen peroxide, 30%.

Sodium hydroxide solution, 20%.

Ethanol, 95% *v*/*v*.

Saturated sodium bicarbonate solution.

Sodium fluoride solution, 4%.

Ascorbic acid solution, 5%. Freshly prepared before use.

Thiourea solution. Dissolve 5 g of thiourea and 1 g of ascorbic acid in water and dilute to 100 ml. Freshly prepared before use.

Barium chloride dihydrate solution, 1%.

Potassium sulphate solution. Dissolve 15 g of potassium sulphate in water and dilute to 450 ml.

1,10-Phenanthroline solution in ethanol, 0.1%.

Dimethylglyoxime solution in ethanol, 1%.

Hexamine solutions, 15% *and* 30%. Freshly prepared before use.

Naphthyl Red solution in ethanol, 0.05%.

Hydrazidazol solution in acetone, 0.05%.

*Zinc standard solution, 0.02*M. Dissolve 3.255 g of zinc oxide of SRM grade in 50 ml of 2*M* hydrochloric acid by warming. Cool and dilute to 500 ml. Add 2 drops of Naphthyl Red solution and 30% hexamine solution dropwise till the appearance of a yellow colour. Transfer to a 2-litre standard volumetric flask, dilute to volume and mix.

HEDTA standard solution. Dissolve 11.13 g of anhydrous *N*-(2-hydroxyethyl)ethylenediamine-*N*,*N*′,*N*′-triacetic acid in 700 ml of water by warming, cool to room temperature and add 2 drops of Naphthyl Red solution and saturated sodium bicarbonate solution dropwise till the appearance of

a yellow colour. Transfer to a 2-litre standard flask, dilute to volume and mix. Standardize as follows. Pipette 25.00 ml of 0.02*M* standard zinc solution into a 400-ml Teflon beaker. Add 20 ml of water, 5 ml of ascorbic acid solution and 2 drops of 1,10-phenanthroline solution. Acidify to pH 2 with hydrochloric acid (1 + 1). From a burette add 20 ml of HEDTA solution and stir thoroughly with a Teflon rod. Add 40 ml of ethanol, 2 or 3 drops of hydrazidazol solution and sodium bicarbonate solution dropwise till a purple colour appears. Then add 4 ml of 30% hexamine solution and titrate with the HEDTA solution to an abrupt colour change from blue to bright red. Add another 2 ml of 30% hexamine solution and titrate again with HEDTA, repeating this until the red colour of the indicator remains unchanged on further addition of hexamine. Calculate the titre T of the HEDTA as mg of Zn per ml, from:

$$T = \frac{0.02 \times 65.38 \times V_2}{V_1} = \frac{1.3076 V_2}{V_1}$$

where V_1 = volume of standard zinc solution used (ml) and V_2 = volume of HEDTA solution used (ml).

Procedures

Determination of Zn in zinc–aluminium alloys. Transfer 0.25 g of the sample, weighed to the nearest 0.1 mg, into a 250-ml beaker. Add 10 ml of hydrochloric acid (1 + 1) followed by a few drops of hydrogen peroxide. Warm till dissolution is complete, then boil to destroy excess of hydrogen peroxide. Cool to room temperature, transfer to a 250-ml standard flask, dilute to volume and mix. Pipette 50 ml of the sample solution into a 400-ml Teflon beaker. Add the following reagents in succession, stirring thoroughly with a Teflon rod after each addition: 10 ml each of the sodium fluoride and thiourea solutions, 2 drops of 1,10-phenanthroline solution, 25 ml of HEDTA from a burette, 40 ml of ethanol, 2 or 3 drops of hydrazidazol solution, and saturated sodium bicarbonate solution dropwise till a purple colour appears. Then add 4 ml of 15% hexamine solution and titrate with HEDTA to an abrupt colour change from blue to bright red. Complete the titration as in the HEDTA standardization by repeated addition of hexamine and titration. Calculate the percentage of Zn from % Zn = 100 TV/G where G is the sample weight in the aliquot taken for titration, T = the titre (Zn, mg/ml) the standard HEDTA solution, V = the volume used (ml).

Determination of Zn in aluminium alloys. Transfer 0.20 g of the sample, weighed to 0.1 mg, to a 250-ml beaker. Add 10 ml of sodium hydroxide solution. When the reaction subsides, warm till decomposition of the sample is complete, adding a few drops of hydrogen peroxide if necessary. Add 80 ml of water and 20 ml of hydrochloric acid (1 + 1), stir vigorously to make the solution clear and boil gently to destroy excess of hydrogen peroxide. Cool to room temperature, transfer to a 200-ml standard flask, dilute to volume and mix. Pipette 50 ml of the sample solution into a 400-ml Teflon beaker. Add the same reagents and titrate as for zinc–aluminium alloys, but use 15 ml of the sodium fluoride solution.

Determination of Zn in copper alloys containing no Ni. Transfer 0.20 g of the sample, weighed to 0.1 mg, to a 250-ml beaker. Add 5 ml of hydrochloric acid followed by a few drops of hydrogen peroxide. Warm till dissolution is complete, adding 1 or 2 drops of hydrofluoric acid if necessary. Boil gently to destroy excess of hydrogen peroxide. Cool to room temperature, transfer to a 100-ml standard flask, dilute to volume and mix. Pipette 25 ml into a 400-ml Teflon beaker. Add the following reagents in succession and stir thoroughly with a Teflon rod after each addition: 10 ml of sodium fluoride solution, 40 ml of thiourea solution, 2 drops of phenanthroline solution, 3 ml each of the barium chloride and potassium sulphate solutions, 40 ml of ethanol, 5 ml of standard HEDTA solution from a burette, 2 or 3 drops of hydrazidazol solution and saturated sodium bicarbonate solution dropwise till a purple colour appears. Then complete the titration as described above.

Determination of Zn in copper alloys containing Ni. Weigh out, dissolve and dilute the sample as for other copper alloys, adding a few drops of nitric acid to complete the dissolution if necessary. Pipette 25 ml of the sample solution into a 400-ml beaker. Add the following reagents and mix thoroughly after each addition: 10 ml of sodium fluoride solution, 40 ml of thiourea solution, 2 drops of 1,10-phenanthroline solution, 3 ml each of the 30% hexamine, barium chloride and potassium sulphate solutions, 1 drop of Naphthyl Red solution and saturated sodium bicarbonate solution dropwise until the colour changes from red to yellow. Then add 5 ml of dimethylglyoxime solution dropwise, stir vigorously for 1–2 min and filter off the precipitate on a medium porosity filter paper. Wash the beaker and filter paper with water 3 or 4 times. Collect the combined filtrate and washings in a 400-ml Teflon beaker containing 5 drops of hydrochloric acid (1 + 1). Add 35 ml of ethanol and saturated sodium bicarbonate solution dropwise till the disappearance of the red colour. Then add hexamine and complete the titration as described above.

RESULTS AND DISCUSSION

Choice of titrant

Titrants other than EDTA, such as triethylenetetramine[7] and tetraethylenepentamine[8] have been suggested, but the chelation of Zn(II) with such polyamines requires a higher pH, at which unfavourable side-reactions of zinc may arise.

The interference caused by Mn(II) may be ascribed to the formation constant of its EDTA-chelate not being sufficiently low. Theoretically speaking, the selective titrant to be searched for should fulfil the following requirements: (1) the lower the conditional formation constant of its Mn-chelate the better; (2) the conditional formation constant of its Zn-chelate must be sufficiently large (log $K' \geqslant 8$); (3) the larger the difference between the conditional formation constants of its Zn- and Mn-chelates the better. Of these, (3) is the main criterion.

The relevant data for six chelating agents are summarized in Table 1 for comparison. Though these values refer to aqueous medium, the effect of a given ethanol content should be essentially the same for all the chelates, so the differences between the constants for the zinc and manganese complexes should not be substantially changed. HEDTA is the logical choice. The conditional formation constant of its zinc chelate at pH 5–7 would be sufficiently high to permit a direct titration. It should be emphasized that for HEDTA ($\log K_{ZnL} - \log K_{MnL}$) is 3.8, so any interference caused by Mn(II) may be assumed to be due to post-titration but not co-titration.

Choice of indicator

The indicators commonly used, such as Xylenol Orange, are unsuitable since they also react with Mn(II) to form coloured chelates in the pH range 5–7. Absolutely necessary is a selective metallochromic indicator which should meet the following

Table 1. Formation constants of some chelates of Zn(II) and Mn(II)[9]

Chelate		log K_{ML}	log K_{ZnL} − log K_{MnL}	log K'_{ML} pH 5	6	7
EDTA	Zn	16.5	2.5	10.0	11.8	13.2
	Mn	14.5		7.5	9.3	10.7
HEDTA	Zn	14.5	3.8	9.2	10.6	11.7
	Mn	10.7		5.4	6.8	7.9
NTA	Zn	10.5	3.1	5.7	6.7	7.7
	Mn	7.4		2.6	3.6	4.5
DCTA	Zn	18.7	1.9	10.7	12.5	13.8
	Mn	16.8		8.8	10.6	11.9
DTPA	Zn	18.0	2.5	8.7	10.7	12.7
	Mn	15.5		6.2	8.2	10.2
EGTA	Zn	12.8	1.3	4.3	6.3	8.3
	Mn	11.5		3.0	5.0	7.0

requirements under the conditions for titrating Zn(II): (1) it should not react with Mn(II) to form coloured chelates; (2) its colour change should take place before the post-titration of Mn(II). Preliminary experiments showed that hydrazidazol, an entirely new indicator recently developed by us, serves the purpose. The indicator is prepared as an acetone solution, which is very stable. It should be pointed out that it does not react with Zn(II) in aqueous solution, but does in an ethanolic aqueous medium. In such a medium the greenish blue colour of the zinc–indicator complex begins to appear at an apparent pH of 5.9–6.2, depending on the amount of Zn(II) present. This colour reaction is very sensitive. In the absence of Zn(II) the indicator remains bright red at pH $\leqslant$ 8. Therefore a very sharp end-point can be obtained, indicated by the colour change from blue to bright red. This colour change is best observed if the titration is done in a translucent Teflon beaker.

Hydrazidazol exhibits its absorption maximum at 510 nm; that of the zinc chelate is at 640 nm. Within the pH range 5–7 its bright red colour remains unchanged in the presence of 43 cationic species, but it forms coloured chelates with Ti(IV) (orange), Fe(III) (yellow), Fe(II) (brown), Cu(II) (purple), Ni(II) and Co(II) (green). The interferences caused by such coloured chelates can be readily eliminated by adding a combination of masking agents, as described below under "Effects of diverse ions and ligands". Hence it is a very selective metallochromic indicator.

Effect of ethanol

The final volume of the titration system may vary from 50 to 200 ml. The optimum concentration of ethanol was found to be 20–40% v/v, but too much ethanol causes high results (Table 2).

Table 2. Effect of ethanol on the titration of Zn(II) at pH 6.5

Ethanol, % *v/v*	0.02*M* Zn(II) taken, *ml*	0.02*M* HEDTA used, *ml*
20	26.00	26.00
25	24.00	24.05
35	17.00	16.95
40	23.00	23.00
62	27.00	27.90

Effect of pH

All the pH values of the ethanolic aqueous solutions reported in this paper are apparent values, because aqueous standard buffers were used for calibration. The optimum pH for determination of Zn(II) was found to be 6–7, at which hydrazidazol functions very well. This range applies only in the absence of Mn(II). In its presence the upper limit of pH was found to be 6.6. Therefore precise pH control is of prime importance. As metal–metallochromic indicator complexes function as narrow-range acid–base indicators,[10] the Zn(II)–hydrazidazol complex can function as the indicator for the rough pH adjustment of an acidified sample solution with sodium bicarbonate. In order to obtain the desired pH a definite amount of hexamine is then added. Zinc can be titrated selectively in the presence of manganese(II) only if the complexation of the manganese does not begin before that of the zinc is practically complete.

Unfortunately ordinary buffers were found to be unsuitable in such an ethanolic aqueous solution, and the addition of hexamine is repeated to remove the protons liberated during the titration. Generally 2–4 additions suffice. In this way zinc can be selectively titrated in the presence of up to at least 6 mg of manganese without interference (Table 3). Therefore it should be possible to determine zinc directly in the

Table 3. Effect of Mn(II) on the titration of Zn(II)

Mn(II) added, *mg*	Zn, *mg* Taken	Found	Error, *mg*
—	3.40	3.36	−0.04
	4.05	4.01	−0.04
	10.08	10.14	+0.06
	13.87	13.80	−0.07
3	4.92	4.97	+0.05
	13.25	13.34	+0.09
	14.51	14.58	+0.07
	15.18	15.10	−0.08
	15.17	15.17	0.00
	15.28	15.23	−0.05
	16.40	16.35	−0.05
	25.85	25.76	−0.09
	34.59	34.65	+0.06
	44.13	44.07	−0.06
	44.77	44.85	+0.06
6	9.15	9.15	0.00
	52.30	52.23	−0.07

Table 4. Effects of some reagents on the titration of 19.61 mg of Zn(II)

Reagent added, mg		Zn found, mg	Error, mg
Ascorbic acid	500	19.61	0.00
1,10-Phenanthroline	0.5	19.59	−0.02
Thiourea	6000	18.82	−0.79
	3500	18.82	−0.79
	2500	19.67	+0.06
Sodium fluoride	1000	19.60	−0.01
	500	19.61	0.00
Ammonium fluoride	1000	19.67	+0.06
Dimethylglyoxime	50	19.60	−0.01
Sodium chloride	3500	19.69	+0.08
Sodium acetate	1000	19.67	+0.06
Sodium tartrate	500	19.59	−0.02
Barium chloride	30	19.59	−0.02
Potassium sulphate	100	19.63	+0.02

above-mentioned alloys, the manganese content of which rarely, if ever, exceeds 6%. Obviously this is a decided advantage.

To minimize the number of additions of hexamine it is recommended to estimate in advance the consumption of titrant and add the bulk of it all at once to the solution to be titrated. If the same total amount of hexamine is added all at once, manganese does interfere. In the absence of manganese a 30% hexamine solution may be used instead of the 15% solution.

Effects of diverse ions and ligands

Effects of some reagents in common use were studied and the results obtained are shown in Table 4.

It is obvious that many metal ions interfere, and must be masked. Be(II), Al(III), Fe(III), Ti(IV), Ge(IV), Si(IV), Zr(IV), Nb(V), Sb(V), Mo(VI), W(VI) and the lanthanides can be masked with sodium or ammonium fluoride. Potassium fluoride, as suggested by Přibil,[11] gives less satisfactory results in ethanolic aqueous medium.

Pb(II) is most conveniently co-precipitated with barium sulphate. The precipitate thus formed need not be filtered off, and its solubility is depressed by the addition of ethanol. Consequently it is possible to reduce the amounts of the co-precipitants used. Ten-ml aliquots of 0.01*M* Pb(II) and 0.02*M* Zn(II) standard solutions were mixed in Teflon beakers, diluted to 70 ml and treated with different amounts of barium chloride and potassium sulphate at pH 2–3, then the zinc was titrated. The results are shown in Table 5, and show that up to 20 mg of Pb(II) can be masked by co-precipitation with 30 mg of barium chloride and 100 mg of potassium sulphate.

Cu(II) is usually masked by thiourea, but the complex formed tends to make the solution turbid at the pH for the titration. In order to obtain a colourless and perfectly clear solution at this pH the mixture of ascorbic acid, thiourea and 1,10-phenanthroline, originally suggested as a chelate-decomposing agent,[12] was used instead and proved to be very satisfactory.

As is well known, both Ni(II) and Co(II) interfere in the titration of Zn(II). It was found that up to 1 mg of Co(II) can be effectively masked by 5 ml of 1% ethanolic solution of dimethylglyoxime at pH 6. The colour of the soluble chelate thus formed is not so deep as to obscure the colour change of the hydrazidazol indicator system at the end-point. The interference caused by up to 4 mg of Ni(II) can be eliminated by adding dropwise the same amount of dimethylglyoxime at the same pH, followed by vigorous stirring for 1–2 min and filtration. Although precipitation is incomplete, the residual nickel in the nearly colourless filtrate remains masked and does no harm. If the dimethylglyoxime solution is added dropwise with vigorous stirring till no more precipitate appears, and then 5 ml in excess, even 50 mg of nickel can be rendered harmless (Table 6).

If the zinc is previously complexed with a suitable amount of hexamine, no loss is found after this precipitation and filtration. It should be borne in mind that the volume of dimethylglyoxime reagent added also contributes to the concentration of ethanol in the titration solution.

In practice the masking agents should be added before the ethanol, and they may be used in combination for different purposes. As a general rule it is recommended to add successively (at pH 2–3): (1) fluoride, (2) thiourea mixed with ascorbic acid, (3) 1,10-phenanthroline, (4) barium chloride, (5) potassium sulphate. The interferences caused by 40 mg of Cu(II), 20 mg of Pb(II), 3 mg of Fe(III) and 3 mg of Mn(II) can thus be eliminated. Přibil reported that fluoride fails to mask Fe(III) in the presence of Mn(II),[11] no such failure was observed in the mixed solvent medium used in our experiments. The only abnormality experienced due to the presence of Fe(III) masked with sodium fluoride was that sometimes, but not always, the blue colour of the Zn–hydrazidazol chelate became paler and was gradually bleached. This can be readily remedied, however, by adding a further 2 drops of the indicator. Dimethylglyoxime should be added last since its reaction with Co(II) and Ni(II) needs a higher pH, which can be conveniently indicated by the colour change of Naphthyl Red.

The effect of Cd(II) was not studied since it can be readily eliminated with iodide, as suggested by Ringbom.[13]

Table 5. Effect of co-precipitation of Pb(II) on the titration of Zn(II); taken, Zn(II) 13.08 mg, Pb(II) 20.72 mg

Co-precipitants added, mg		Zn found, mg	Error, mg
$BaCl_2 \cdot 2H_2O$	K_2SO_4		
—	165	13.73	+0 65
10	35	13.80	+0.72
20	100	12 95	−0.13
20	140	12.88	−0.20
30	100	13.08	0.00
30	165	13.14	+0.06
100	165	12.94	−0.14
30	100	13.07*	−0.01

*Pb(II) absent.

Table 6. Titration of 19.61 mg of Zn(II) in the presence of diverse metal ions

Metal ions added, *mg*	Masking agents*	Zn found, *mg*	Error, *mg*
Ca(II) 10	—	19.61	0.00
Cr(III) 0 2	—	19.64	+0.03
Mo(VI) 10	—	19.55	−0.06
Mg(II) 10	—	19.66	+0.05
Be(II) 10	a	19.67	+0.06
Ce(III) 5	a	19.55	−0.06
La(III) 12	a	19.56	−0.05
Sn(IV) 50	a	19.52	−0.09
Ti(IV) 10	a	19.68	+0.07
Al(III) 50	a	19.50	−0.11
Fe(III) 5	a	19.55	−0.06
Zr(IV) 10	a	19.53	−0.08
Pr(III) 5	a	19.57	−0.04
Co(II) 1	f	19.72	+0.11
Ni(II) 4	f	19.53	−0.08
50	f	19.51	−0.10
Cu(II) 40	b+c	19.68	+0.07
Cu(II) 35, Fe(III) 5	a+b+c	19.54	−0.07
Cu(II) 41, Ni(II) 4	b+c+f	19.64	+0.03
Cu(II) 35, Pb(II) 10	b+c+d+e	19.57	−0.04
Fe(III) 3, Mn(II) 3	a	19.66	+0.05
Cu(II) 40, Fe(III) 3, Mn(II) 3	a+b+c	19.67	+0.06
Cu(II) 40, Pb(II) 20, Fe(III) 3, Mn(II) 3	a+b+c+d+e	19.52	−0.09
Sn(IV) 10, Sb(III) 1, P(V) 0.1, Si(IV) 2	a	19.48	−0.13

*(a) Sodium fluoride; (b) thiourea mixed with ascorbic acid; (c) 1,10-phenanthroline; (d) barium chloride; (e) potassium sulphate; (f) dimethylglyoxime.

Table 7. Determination of Zn in some non-ferrous alloys

Sample	Composition, %	Zn found, %	
		Proposed method	Other methods*
Copper alloy, HNi 65–5	Cu 66, Ni 6.5	27.12	27.05[a]
ZHMn 55-3-1	Cu 55, Mn 3, Fe 1	37.53	37.44[a]
	Cu 60, Ni 16.5, Mn 3	20.15	20.04[a]
	Cu 62, Mn 3.5, Al 5, Fe 3	26.12	26.03[a]
673-3	Cu 58, Al 1, Fe 1, Mn 0.5, Sn 0.5	38.38	38.30[b]
601	Cu 82, Pb 5, Sn 3.5 Ni 1	8.28	8.32[b]
Aluminium alloy, ZL401	Al 81, Si 8	9.39	9.33[c]
Zinc alloy, ZZnAl 10-5	Al 10, Cu 5	83.11	82.97[d]
	Sn 14, Cu 6	79.34	79.25[d]
	Sn 75	24.78†	24.89[d]

*(a) ASTM E478-76; (b) certified value; (c) ASTM E34-78; (d) with EDTA as titrant and Xylenol Orange as indicator.
†HEDTA not added in bulk in advance.

The effects of diverse metal ions are summarized in Table 6.

The proposed method is highly selective and versatile in practical applications. Its standard deviation was found to be 0.07 mg ($n = 18$) and its coefficient of variation varies from 0.2 to 0.5%.

Applications

The proposed method has been used to determine zinc in different kinds of non-ferrous alloys. Some analytical results are shown in Table 7.

By this rapid titrimetric method accurate and reproducible results can be obtained. The error is $\leq 0.2\%$. It is expected that this new method will find many other applications in analytical chemistry.

Acknowledgements—Grateful thanks are due to all members of the Directorate of SRIM for encouragement in this work and for permission to publish this paper.

REFERENCES

1. R. Přibil and V. Veselý, *Chemist-Analyst*, 1964, **53**, 38.
2. ASTM, *1978 Annual Book of ASTM Standards*, p. 137. ASTM, Philadelphia, 1978.
3. *Ibid*, p. 788.
4. *Ibid*, p. 142.
5. B. C. Sinha and S. Dasgupta, *Talanta*, 1978, **25**, 693.
6. H. Yamaguchi, K. Iwasaka, K. Yamaguchi and K. Ueno, *Bunseki Kagaku*, 1967, **16**, 703.
7. C. N. Reilley and M. V. Sheldon, *Chemist-Analyst*, 1957, **46**, 59.
8. N. C. Johnson, *Clin. Chem.*, 1962, **8**, 497.
9. A. Ringbom, *Complexation in Analytical Chemistry*. pp. 322–351. Interscience, New York, 1963.
10. R. A. Chalmers and F. I. Miller, *Analyst*, 1971, **96**, 97.
11. R. Přibil and V. Veselý, *Talanta*, 1965, **12**, 385.
12. R. P. Singh, *ibid.*, 1972, **19**, 1421.
13. A. Ringbom, *op. cit.*, p. 150.

Talanta, Vol. 30, No. 11, pp. 857–860, 1983
Printed in Great Britain

0039-9140/83 $3.00 + 0.00
Pergamon Press Ltd

SHORT COMMUNICATIONS

DETERMINATION OF THALLIUM IN CADMIUM AND LEAD BY GRAPHITE-FURNACE ATOMIC-ABSORPTION SPECTROMETRY WITH SAMPLE VAPORIZATION FROM A PLATFORM

JÁNOS FAZAKAS
Centre for Analytical Spectrochemistry, Bd. Marasti 61, R-71331 Bucharest, Romania

DAN M. MARINESCU
Air Pollution Laboratory, Institute of Meteorology and Hydrology, Sos Afumati 1581, P.O.B. 11-2, R-72400 Bucharest, Romania

(*Received* 15 *March* 1983. *Accepted* 5 *May* 1983)

Summary—When the sample is vaporized from the wall of a graphite furnace it is not possible to determine thallium in cadmium and lead by AAS without matrix matching of the standards. In the case of a lead matrix and vaporization from the wall, the thallium signal is barely distinguishable from the base-line. When the sample is vaporized from a platform, and the peak area is used for measurement, pure aqueous standards may be used for instrument calibration. The peak heights and areas of the thallium signals are considerably enhanced by vaporization from a platform (peak height 1.7-fold and peak area 2.6-fold in pure aqueous solutions as compared to vaporization from the wall). The enhancement factors are larger in presence of the cadmium or lead matrix since here the reduced interference also makes a contribution.

Thallium is one of the less studied elements in both flame and graphite-furnace atomic-absorption spectrometry (AAS). Recent interest in this element stems partly from its use in the semiconductor industry and partly from the high toxicity of some of its chemical forms.

Thallium has been determined in cobalt and nickel alloys,[1] nickel-base alloys,[2,3] high-purity nickel,[4] cadmium[5] and semiconductor silicon.[6] The determination of thallium in several geological standards has also been reported.[7,8]

L'vov suggested[9,10] that sample vaporization from a platform may overcome many interferences. This was later proved, at least for lead.[11] Subsequent papers discussed the use of the platform technique for the direct analysis of bovine liver,[12] oyster tissue,[13] plastics[14] and biological materials.[15] Slavin and Manning[16] noted that the interference of sodium chloride and magnesium chloride in determination of thallium is lower when platform vaporization is used instead of wall vaporization.

The purpose of the present work was to study the determination of thallium in cadmium and lead. Since no standard materials were available for instrument calibration it was decided to study the possibility of using pure aqueous standards. To the best of our knowledge the methods published in the literature all made use of some form of matrix-matching of samples and standards.

EXPERIMENTAL

A Perkin–Elmer HGA-500 was used to atomize samples. With ramp setting 0 and at temperatures over *ca.* 800° this atomizer works in the temperature feed-back mode (heating rate *ca.* 2000°/sec). An AS-1 autosampler was used for dispensing 20-μl samples into the graphite tube. Pyrolytically coated graphite tubes and platforms made of pyrolytic graphite were used. Argon was used as purge gas, with "gas-stop" during atomization. Samples were dried at 120° for 30 sec with a ramp of 5 sec when vaporizing from the wall and at 200° for 30 sec with a ramp of 1 sec when vaporizing from a platform. Ashing was done at 400° in all cases. Ramp setting 0 was used in the atomization phase. Other details of the experimental system have been described elsewhere.[17] Temperatures quoted in this paper refer to the furnace wall. The platform temperature is usually lower.

The thallium standards were obtained by diluting a commercially available stock solution. According to the manufacturer (Pierce Inorganics B.V.) the standard was prepared from thallous sulphate. The matrices were simulated by use of 1000-mg/l. Cd and Pb solutions. According to the manufacturer (Merck) these were prepared from cadmium chloride and lead nitrate respectively. To prevent interference by chloride, the cadmium solution was made 0.1*N* in sulphuric acid.

Absorbances were measured with a Perkin–Elmer 5000 spectrometer. A deuterium-lamp background corrector was

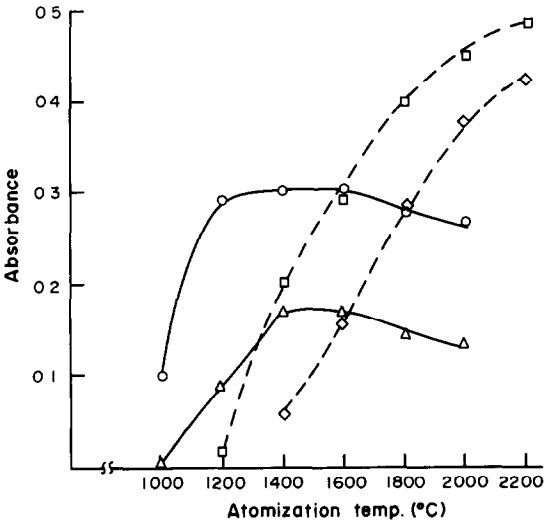

Fig. 1. Peak heights for 0.1-mg/l. thallium as a function of atomization temperature, for pure aqueous solutions and in presence of 1000-mg/l. Cd. For working conditions see Experimental. ○, 0.1 ppm Tl (wall); △, 0.1 ppm Tl + 1000 ppm Cd (wall); □, 0.1 ppm Tl (platform); ◇, 0.1 ppm Tl + 1000 ppm Cd (platform).

used in all measurements. A thallium hollow-cathode lamp was used as the light-source and operated at 8 mA. The 276.97-nm resonance line was used, with a band-pass of 0.7 nm. The peak-monitoring time was fixed at 5 sec.

RESULTS AND DISCUSSION

Optimization of response

Thallium in cadmium matrix (Tl_{Cd}). Vaporization from the wall gave considerably lower signals for Tl_{Cd} than for Tl. It is shown in Fig. 1 that the peak height for Tl_{Cd} is only half that for the same amount of Tl. It is also to be noted that whereas the Tl signal reaches a plateau at around 1200°, for Tl_{Cd} the plateau is reached only at 1400°. At >1600° the peak heights decrease in both cases, but the relative sensitivity of the Tl_{Cd} signal does not improve.

Vaporization from a platform remarkably improves the peak height for Tl. As noted in an earlier paper,[17] the heating rate of the platform used is lower than that of the furnace walls. However, because of the delay of vaporization, the convective losses are lower than those for wall vaporization. As a result the peak height for Tl is enhanced *ca.* 1.7-fold relative to vaporization from the wall. The enhancement factor for Tl_{Cd} is even larger, 2.5-fold, which certainly means that at least part of the interferences encountered in vaporization from the wall can be explained as due to a vapour-phase occlusion or dissociation mechanism. The higher vapour temperature obtained with vaporization from the platform obviously improves the chances of efficient atomization. It is possible that the use of higher atomization temperatures would improve the peak heights even further. However, because of traces of oxygen present in the argon used,

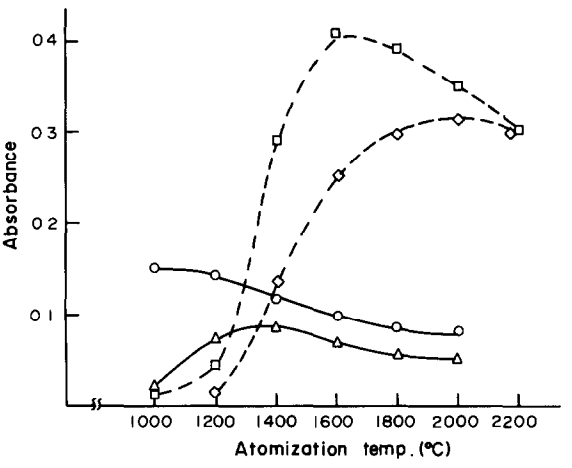

Fig. 2. Peak areas of 0.1-mg/l. thallium as a function of atomization temperature, for pure aqueous solutions and in presence of 1000-mg/l. Cd. For working conditions see Experimental. Symbols as in Fig. 1.

atomization temperatures >2200° considerably shortened the useful life of the graphite tubes.

Figure 2 shows that use of peak area with vaporization from the wall gives much better results for Tl_{Cd} than peak height. Whereas for Tl the peak-area signal decreases steadily with increasing atomization temperature, for Tl_{Cd} the signal increases with temperature up to 1400°. As in the case of peak-height measurements this again points to a vapour phase interference mechanism. Figure 2 also shows that even at an atomization temperature of 2000° there is still a considerable difference between the Tl and Tl_{Cd} signals. Moreover, at temperatures higher than 1400° the relative sensitivity of the Tl_{Cd} signal does not increase further.

Figure 2 also shows the peak-area results obtained with vaporization from a platform. It can be seen that for Tl the best sensitivity is achieved at 1600°. The sensitivity for Tl with vaporization from a platform at 1600° is 2.6 times better than that with vaporization from the wall at 1000°. Atomization tem-

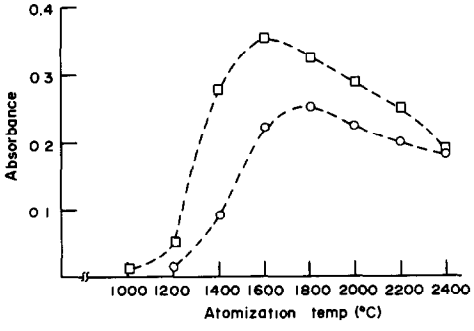

Fig. 3. Peak areas of 0.1-mg/l. thallium as a function of atomization temperature for pure aqueous solutions and in the presence of 1000-mg/l. Pb. Vaporization from a platform. For working conditions see Experimental. □, 0.1 ppm Tl (platform); ○, 0.1 ppm Tl + 1000 ppm Pb (platform).

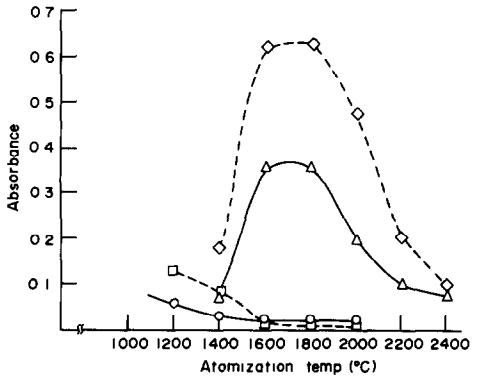

Fig. 4. Background absorption of a cadmium matrix (1000-mg/l.) as a function of atomization temperature. For working conditions see Experimental. ○, peak height, wall vaporization; □, peak area, wall vaporization; △, peak height, platform vaporization; ◇, peak area, platform vaporization.

peratures > 1600° will reduce the peak area, probably because the increased diffusion rate of the atoms results in a shorter mean residence time. In the case of Tl_{Cd} the peak area with platform vaporization is 3.5 times that with vaporization from the wall. It can be seen from Fig. 2 that the Tl_{Cd} signal continues to increase with atomization temperature up to 2000° (that is, 400° higher than for Tl). It is remarkable that at 2200° the Tl and Tl_{Cd} curves cross. It may therefore be concluded that with vaporization from a platform, atomization at 2200° and measurement of peak areas, *pure aqueous standards may be used for instrument calibration when determining* Tl_{Cd}.

Thallium in a lead matrix (Tl_{Pb}). Wall vaporization of thallium in a lead matrix (Tl_{Pb}) gives low signals at the 0.1-mg/l. Tl level, for both peak height and area. In fact the Tl_{Pb} signal is barely distinguishable from the base-line. Therefore Fig. 3 shows only results obtained with vaporization from a platform. Only peak area is shown in Fig. 3 since even with the highest atomization temperature used, the peak-height readings for Tl_{Pb} were rather low. It is to be noted that the peak area of Tl_{Pb} is highest at 1800°, which is 200° higher than the temperature for the maximum Tl signal and 200° lower than that for the highest Tl_{Cd} signal (Fig. 2). The peak-area curves for Tl and Tl_{Pb} cross at 2400°. It may therefore be concluded that with vaporization from a platform, atomization at 2400° and use of peak areas, *pure aqueous standards may be used for instrument calibration when determining* Tl_{Pb}.

Background absorption

Figure 4 shows the background absorption as a function of atomization temperature. With vaporization from the wall, the background absorption decreases steadily with increasing atomization temperature. With vaporization from a platform the background absorption increases with temperature up to *ca.* 1800°, but decreases considerably at higher atomization temperatures. It is to be noted that in all cases the background absorption of the lead matrix (not shown in Fig. 4) is higher than that of the cadmium matrix. However, in all circumstances investigated by us, the background absorption is small enough to be efficiently compensated by the deuterium background-corrector of the instrument. The background absorption was contrary to our expectation that it would be lower for platform vaporization. We cannot advance any explanation for this apparently anomalous phenomenon. A similar behaviour was noted by Slavin and Manning[11] when determining lead in a chloride matrix.

Table 1. Thallium content of some metals and compounds

Sample	Thallium content, *ppm*	
	Standard addition	Direct
Cd metal A	18.2	18.3
Cd metal B	30.8	29.9
$Pb(NO_3)_2$	21 1	20.5
$CdSO_4$	18.7	19.0

Peak-area results were used in all cases, with vaporization from a platform. Atomization at 2200° for the cadmium matrix and 2400° for the lead matrix. Metal samples were dissolved in dilute nitric acid; salts were dissolved in demineralized water and slightly acidified (up to 0.05% in HNO_3). For other details see Experimental.

Analysis of real samples

Since no reference materials were available to us, we have compared our results obtained by use of aqueous standards, with results obtained by the method of standard additions. The results show good agreement and are given in Table 1.

CONCLUSION

With vaporization from a platform, thallium may be determined in a cadmium or lead matrix, with pure aqueous standards for instrument calibration. The background absorption is small enough to be handled efficiently by the background-corrector of the instrument. The direct analysis of real samples compares favourably with results obtained by standard additions. Interference by the cadmium and lead matrix seems to be due to a vapour phase occlusion mechanism, *i.e.*, molecular aggregates of the matrix, containing some analyte, are ejected from the furnace before vaporization of the analyte can occur.

It should be noted that since carbide coatings will prevent some matrix occlusion interferences,[18] recoveries could be even better with vaporization from the wall, but this approach has not been attempted for the time being.

Based on our previous experience it would seem likely that thallium can also be determined directly in a zinc matrix. However, we were unable to determine thallium in a copper or nickel matrix, as recoveries barely exceeded 5–6% even with platform vaporization.

REFERENCES

1. O. Kujirai, T. Koboyashi and E. Sudo, *Z. Anal. Chem.*, 1979, **297**, 398.

2. A. A. Baker, J. B. Headridge and R. A. Nicholson, *Anal. Chim. Acta*, 1980, **113,** 47.
3. J. Y. Marks, G. C. Welcher and R. J. Spelman, *Appl. Spectrosc.*, 1977, **31,** 9.
4. J. E. Forrester, V. Lenecka, J. R. Hohnston and W. L. Ott, *At. Abs. Newsl.*, 1979, **18,** 73.
5. E. Norval and W. N. Gries, *Anal. Chim. Acta*, 1976, **83,** 393.
6. I. G. Yudelevich and N. F. Beizel, *Izv. Sib. Otd. Akad. Nauk SSSR Ser. Khim. Nauk*, 1978, **6,** 94.
7. H. Heinrichs, *Z. Anal. Chem.*, 1979, **294,** 345.
8. F. O. Simon, E. Y. Campbell and P. J. Aruscavage, *J. Res. U.S. Geol. Surv.*, 1977, **5,** 579.
9. B. V. L'vov, L. A. Peliaeva and A. I. Sharnopolsky, *Zh. Prikl. Spektr.*, 1977, **27,** 395.
10. B. V. L'vov, *Spectrochim. Acta*, 1978, **33B,** 153.
11. W. Slavin and D. C. Manning, *Anal. Chem.*, 1979, **51,** 261.
12. C. L. Chakrabarti, C. C. Van and W. C. Li, *Spectrochim. Acta*, 1980, **35B,** 93.
13. *Idem, ibid.*, 1980, **35B,** 547.
14. W. J. Price, T. C. Dymott and P. J. Whiteside, *ibid.*, 1980, **35B,** 3.
15. E. J. Hinderberger, M. L. Kaiser and S. R. Koirtyohann, *At. Spectrosc.*, 1981, **2,** 1.
16. W. Slavin and D. C. Manning, *Spectrochim. Acta*, 1980, **35B,** 701.
17. J. Fazakas, *Anal. Lett.*, 1982, **15,** 245.
18. *Idem*, to be published.

Talanta, Vol. 30, No. 11, pp 861–863, 1983
Printed in Great Britain

0039-9140/83 $3.00 + 0.00
Pergamon Press Ltd

SOLID-STATE HALIDE ION-SELECTIVE ELECTRODES: STUDIES OF QUATERNARY AMMONIUM HALIDE SOLUTIONS AND DETERMINATION OF SURFACTANTS

H. GOMATHI, G. SUBRAMANIAN, NAVIN CHANDRA and G. PRABHAKARA RAO
Central Electrochemical Research Institute, Karaikudi-623 006, Tamil Nadu, India

(*Received* 22 *February* 1982. *Revised* 17 *March* 1983. *Accepted* 13 *May* 1983)

Summary—The feasibility of using homogeneous membrane-type halide ion-selective electrodes in solutions containing cationic surfactant compounds was examined. The results established the applicability of these electrodes for monitoring halide ions in solution without interference by the surfactants. The data also provided a basis for estimation of the surfactant in solution through the halide content. Two typical plating-bath compositions containing CTAB have been successfully analysed for their surfactant content by this procedure.

Tetra-alkyl ammonium compounds having surface-active properties have a wide variety of industrial applications, *e.g.*, as antistatic agents, textile softeners, foam depressants, flotation chemicals, asphalt and petroleum additives, corrosion inhibitors and pigment dispersion agents. The cationic surface-active agents with antibacterial properties are used as sanitizing and antiseptic agents, germicides, fungicides and components in cosmetic formulations.[1] In plating and metal-finishing baths these compounds have been used as addition agents to improve the quality of deposits. Another application is as maximum suppressors in polarographic analysis. Conventionally, these compounds are determined by absorptiometric, titrimetric or gravimetric methods.[2] Cationic surfactants can be titrated potentiometrically with anionic surfactants, and *vice versa*.[3] Quaternary ammonium halides can also be titrated argentometrically, with adsorption indicators or potentiometrically. The potentiometric method with silver metal electrodes may not be useful when oxidizing species are present. The silver sulphide–silver halide solid-state ion-selective electrodes (ISEs), on the other hand, are generally immune to oxidizing and reducing components present in the solution,[4] and because they can be used in comparatively dilute, turbid and coloured solutions without difficulty, are useful for industrial analyses. However, very little is known about the effect of adsorption, which the quaternary ammonium ions exhibit, on the performance of the ion-selective electrodes. Studies on the performance of liquid-membrane calcium ISEs in the presence of surfactants[5,6] indicate interference by these compounds, but another study[7] shows that surfactants have no influence on the LaF_3 single-crystal fluoride ISE. No such studies have been made on silver sulphide–silver halide homogeneous solid-state ion-selective electrodes. Some ISEs sensitive to quaternary ammonium ions have been reported, but have short life, large response times and a change in slope with usage.[6,8]

In the present communication, we report the response of silver sulphide–silver halide homogeneous solid-membrane ion-selective electrodes in quaternary ammonium halide solutions.

EXPERIMENTAL

Reagents

Doubly distilled water was used for preparing test solutions. Twice recrystallized analytical grade sodium nitrate was used as background electrolyte. BDH cetyltrimethylammonium bromide (CTAB), tetramethylammonium chloride (TMAC) and tetramethylammonium iodide (TMAI), and HICO (India) cetyltrimethylammonium chloride (CTAC), tetramethylammonium bromide (TMAB), tetradecyltrimethylammonium bromide (TTAB) and octadecyltrimethylammonium bromide (OTAB) were used without further purification. Stock solutions of quaternary ammonium halides were prepared and the test solutions made by successive dilution.

Apparatus

Ag_2S–AgBr, Ag_2S–AgCl and Ag_2S–AgI solid-membrane Br^-, Cl^- and I^- ISEs developed in our laboratory were used. The potentials of the electrodes were measured against a double-junction calomel reference electrode (1*M* potassium chloride) with a high-impedance digital pH/mV-meter (Chemtrix Model 60A) having a sensitivity of ± 1 mV, the solutions being stirred with a magnetic stirrer. When not in use, the electrodes were stored in doubly distilled water.

Procedure

In experiments on the response behaviour of the electrodes, their potentials in solutions with successively increasing concentrations of quaternary ammonium halides were measured. After each measurement the electrode was washed thoroughly with doubly distilled water and blotted dry before immersion in the next solution.

For potentiometric titrations, 10 ml of quaternary ammonium halide test solution were diluted to 100 ml with sodium nitrate solution to make the final solution 0.1*M* in sodium

nitrate, and the solution was titrated with 0.1*M* silver nitrate, the potential being read 2 min after each addition. The readings were taken at 0.4-ml intervals.

To investigate the suitability of the Br^- ISE for determination of quaternary ammonium ions in solutions of industrial interest, two typical examples[10] of metal-plating baths were examined. These were an acid copper-plating bath and an alkaline zinc-plating bath having the following compositions.

Copper bath

$CuSO_4 \cdot 5H_2O$	100 g/l.
H_2SO_4	30 g/l.
CTAB	5×10^{-5}–$10^{-2}M$

Zinc bath

$ZnSO_4 \cdot 7H_2O$	71 g/l.
EDTA	100 g/l.
NaOH	20 g/l.
CTAB	5×10^{-5}–$10^{-2}M$.

RESULTS AND DISCUSSION

The bromide ISE gave a linear response down to $5 \times 10^{-5}M$ bromide concentration in solutions of 0.10*M* ionic strength (adjusted with sodium nitrate) with a slope of 56 mV/decade at 25° for sodium bromide, TMAB, TTAB and OTAB, and 53 mV/decade for CTAB (*cf.* Fig. 1). For CTAB the slope depended slightly on the pH of the solution. The slope was 56 mV/decade for acid solutions (*e.g.*, the copper-plating bath) and 53 mV/decade for neutral and alkaline solutions (*e.g.*, the zinc-plating bath).

The chloride ISE gave a linear response (slope 58 mV/decade at 25°) to chloride down to $10^{-4}M$ concentration, for sodium chloride or CTAC or TMAC

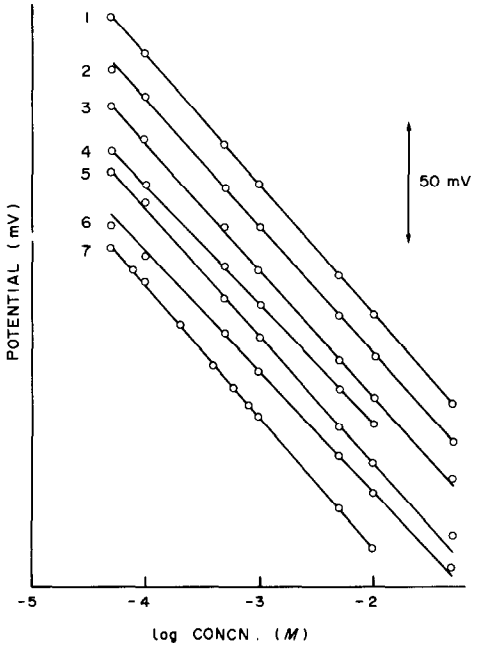

Fig. 1. Response of Br^- ISE. 1—NaBr, 2—TMAB, 3—TTAB, 4—CTAB, 5—OTAB in $NaNO_3$ background electrolyte; 6 and 7—CTAB in zinc-plating bath and copper-plating bath respectively.

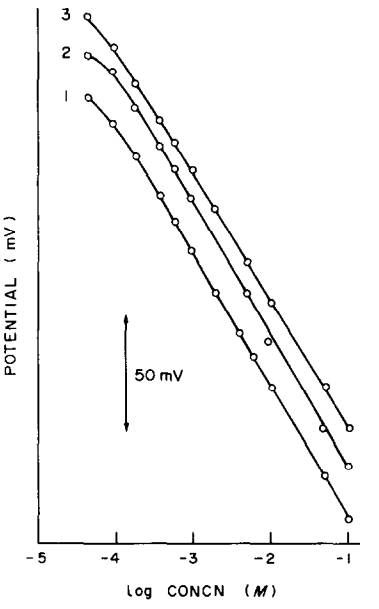

Fig. 2. Response of Cl^- ISE. 1—NaCl, 2—CTAC, 3—TMAC in $NaNO_3$ background electrolyte.

in 0.10*M* ionic strength solutions (sodium nitrate) (*cf.* Fig. 2).

The iodide ISE gave linear response down to $10^{-6}M$ iodide concentration for TMAI or sodium iodide, with a slope of 60 mV/decade at 25°.

It is therefore concluded that these electrodes can be used successfully to monitor halide ions in the presence of quaternary ammonium ions, irrespective of the length of the alkyl chains. If the only source of halide ion in the test solution is a quaternary ammonium compound, the halide ISEs can be used for indirect determination of the concentration of these compounds. These results also show the utility of the bromide ISE for monitoring the concentration of CTAB in typical plating baths where it is present at low levels, falling within the range of concentrations reported here. In addition, the electrodes can be used as indicator electrodes in potentiometric titrations (which are known to give better analytical results than calibration curves, standard addition or analyte-addition methods). A representative set of results of analysis by visual (Mohr method) and potentiometric (ISE) titration with 0.1*M* silver nitrate for the seven quaternary ammonium compounds studied is given in Table 1. The plot of $\Delta E/\Delta V$ *vs* the volume of 0.1*M* $AgNO_3$ added for corresponding potentiometric titrations is shown in Fig. 3. From the results given in Table 1 it is seen that the results obtained by the two methods agree within about 1%, except in the case of TMAI where the deviation is higher (about 3%). The self-consistency of both the potentiometric and visual titration methods was found to be better than 0.5%. The results obtained by titrimetric methods are also in close agreement with the weights of compounds taken (incorporated in Table 1) except in the case of OTAB and CTAC

Table 1. Comparative results of estimation of quaternary ammonium halides by potentiometric and visual titration methods

Compound	Taken, g/l.	Found, g/l. Potentiometric titration	Found, g/l. Visual titration
CTAB	35.56	35.5	35.1
TMAB	16.10	16.3	16.3
OTAB	*	45.4	45.9
TTAB	23.33	23.2	23.3
TMAC	10.96	10.9	10.9
CTAC	*	17.1	17.3
TMAI	15.42	15.8	15.3

*Compounds are impure. Refer to text for comments on the impurities and their relevance to the observed analytical results.

where large deviations have been noted (15.3% and 41.4% respectively). Lack of purity in the case of the last two compounds was suspected to be responsible for the observed deviations and was confirmed by elemental analysis of these compounds (figures in brackets are the expected theoretical values):

OTAB: C = 59.2% (64.24%); H = 11.4% (11.82%); N = 4.6% (3.56%); Br = 21.7% (20.37%)

CTAC: C = 59.7% (71.3%); H = 12.7% (13.24%); N = 4.6% (4.38%); Cl = 11.5% (11.09%).

No residue was obtained on ignition of the compounds, and only the one halogen was found in each. Direct determination of the halogen by dissolving the sample in water and titrating potentiometrically with silver nitrate gave the same halogen figures as those reported above.

If the impurity is taken as water then correction for this would indicate that the "CTAC" had a number average formula of approximately $C_{15}H_{34}NCl$. A similar calculation was impossible for the OTAB since the atomic ratio of nitrogen to halogen was about 1.2 instead of unity.

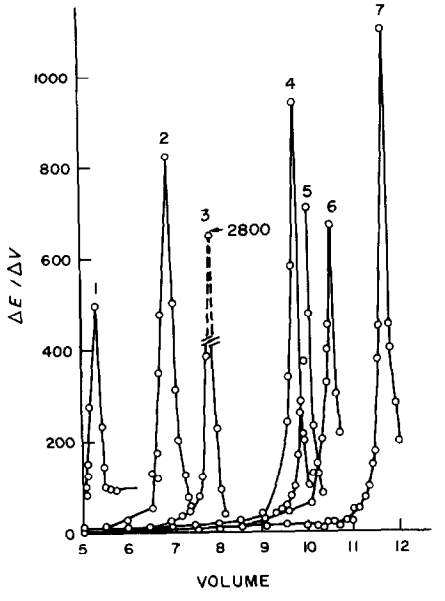

Fig. 3. Plot of $\Delta E/\Delta V$ *vs.* volume of 0.10*M* $AgNO_3$ added. 1—CTAC, 2—TTAB, 3—TMAI, 4—CTAB, 5—TMAC, 6—TMAB, 7—OTAB.

Acknowledgements—The authors are thankful to Dr. V. K. Venkatesan for his keen interest in the work, Dr. K. S. Rajagopalan, Director, for his permission to publish this paper, and Dr. R. A. Chalmers, Editor, for kindly providing the elemental analysis data reported in the paper.

REFERENCES

1. E. Jungermann, in *Cationic Surfactants*, E. Jungermann (ed.), p. 1. Dekker, New York, 1970.
2. J. T. Cross, in *Cationic Surfactants*, E. Jungermann (ed.), Chapter 13. Dekker, New York, 1970.
3. B. J. Birch and R. N. Cockcroft, *Ion-Selective Electrode Revs.* 1981, **3**, 1.
4. G. Subramanian, N. Chandra and G. Prabakara Rao, unpublished work.
5. A. Craggs, G. J. Moody, J. D. R. Thomas and B. J. Birch, *Analyst*, 1980, **105**, 426.
6. R. A. Llenado, *Anal. Chem.*, 1975, **47**, 2243.
7. R. Pakalns and J. Y. Farrar, *Water Res.*, 1976, **10**, 1087.
8. G. E. Baiulescu and V. V. Coşofreţ, *Applications of Ion-Selective Membrane Electrodes in Organic Analysis*, Chapters 10 and 11. Horwood, Chichester, 1977.
9. S. G. Cutler, P. Meares and D. G. Hall, *J. Electroanal. Chem.*, 1977, **85**, 145.
10. K. S. Indira and H. V. K. Udupa, *Met. Finish.*, 1973, **71**, No. 5, 92.

Talanta, Vol. 30, No. 11, pp. 864–866, 1983
Printed in Great Britain.

0039-9140/83 $3.00 + 0.00

CONCENTRATION OF YTTRIUM SUBGROUP IMPURITIES IN HIGH-PURITY YTTRIUM OXIDE BY TBP–NH_4SCN EXTRACTION CHROMATOGRAPHY

ZHANG TAO
Hunan Research Institute for Rare Earth Metallurgy, Changsha, Hunan, People's Republic of China

(*Received* 5 *November* 1982. *Revised* 10 *February* 1983. *Accepted* 12 *May* 1983)

Summary—Separation factors for all the yttrium subgroup elements and yttrium, extracted with TBP from 0.45*M* NH_4SCN solution at 24–42° have been determined and found to be ≥ 1.9. Eight yttrium subgroup impurities in high-purity yttrium oxide have been concentrated by means of TBP–NH_4SCN extraction chromatography at 32° before spectroscopic determination. Analysis of one real sample and two synthetic samples gave average recoveries of 80–100%.

The rare-earth impurities in yttrium oxide are determined by emission spectrometry, X-ray fluorescence, mass spectrometry and X-ray excited optical-fluorescence spectrometry.[1–3] For the analysis of high-purity yttrium oxide, however, it is necessary to concentrate the rare-earth impurities before determination.

The separation of yttrium from other rare-earth elements has been reviewed,[1–4] but few of the methods are concerned with the analysis of high-purity yttrium oxide. Cation-exchange chromatography with α-hydroxyisobutyric acid[5] or citric acid[6] as eluent and extraction chromatography with 2-ethylhexyl hydrogen 2-ethylhexylphosphonate, HEH(EHP), as stationary phase[7] have been used for the separation of cerium subgroup impurities from high-purity yttrium oxide. Cation-exchange chromatography with ammonium acetate as eluent can also be used for the separation of yttrium subgroup impurities in high-purity yttrium oxide.[8] With HEH(EHP)[9] or naphthenic acid[10] as the stationary phase, two methods of extraction chromatography, which can be used for concentration of both cerium subgroup and yttrium subgroup impurities in high-purity yttrium oxide, have been reported. Extraction chromatography with a column containing di(2-ethylhexyl) phosphoric acid (HDEHP) is frequently used for this purpose.[11–13]

Several reports on the separation of rare-earth elements by solvent extraction of the thiocyanate complexes into tributyl phosphate (TBP) have been published,[14–25] but application to the determination of yttrium subgroup impurities in pure yttrium oxide does not seem to have been described. In a previous work on the thermodynamic functions associated with solvent extraction of rare earths in the TBP–NH_4SCN system it was observed that the distribution ratio for yttrium is smaller than that for other rare-earths.[26] This paper reports an extraction chromatographic method for concentrating yttrium subgroup impurities in high-purity yttrium oxide before their determination by emission spectrometry.

EXPERIMENTAL

Reagents

Tributyl phosphate. The chemical reagent grade material was washed successively with three volumes of 0.2*M* sodium hydroxide, three volumes of 0.2*M* hydrochloric acid and five volumes of water.

Yttrium oxide, 99.999% purity.

Individual rare earths. About 99.95% purity.

Ammonium thiocyanate. Analytical reagent grade.

Diethylenetriaminepenta-acetic acid, DTPA. Analytical reagent grade.

Preparation and operation of chromatographic column

Silanized porous silica spheres, 120–180 mesh (100 g) were slurried with 50 ml of TBP dissolved in 150 ml of diethyl ether. The solvent was evaporated by gentle stirring under an infrared lamp. Enough of the coated silica spheres were packed into a glass tube (20 mm bore, 700 mm long) with a sintered-glass plate at the bottom, to give a bed height of 650 mm. The column was evacuated and filled with water. Before use, it was washed with 2*M* hydrochloric acid and equilibrated with 0.45*M* ammonium thiocyanate. The column was placed in a box kept at $32 \pm 1°$.

A suitable amount of the rare earths to be separated was dissolved in 4*M* hydrochloric acid and the solution evaporated. The residue was dissolved in 10–15 ml of 1*M* ammonium thiocyanate and the solution was fed into the column. The rare earths were eluted with 0.45*M* ammonium thiocyanate at a linear flow-rate of 0.75 cm/min.

Determination of separation factors

Static method. Ten ml of a solution containing an individual rare-earth element chloride (0.001*M* $RECl_3$ in 0.45*M* ammonium thiocyanate, pH 5.2 ± 0.2) and 10 ml of TBP (pre-equilibrated with 0.45*M* ammonium thiocyanate) were placed in a 25-ml stoppered Nessler tube and shaken for 5 min. After centrifuging, 5 ml of the aqueous phase were transferred to a 50-ml crucible and titrated with 0.0002*M* or 0.00005*M* DTPA with Xylenol Orange as indicator. The concentration of rare earth in the organic phase at equilibrium was deduced from the difference between the initial analytical concentration of rare earth in the aqueous phase and that at equilibrium.

Dynamic method. One ml of rare-earth solution, corresponding to 10 mg of Y_2O_3 and 10 mg of a second rare-earth

oxide (RE_xO_y) in 0.45*M* ammonium thiocyanate was fed into the chromatographic column and the components were eluted with 0.45*M* ammonium thiocyanate. Each 5-ml fraction of effluent was titrated with 0.001*M* or 0.0005*M* DTPA (indicator Xylenol Orange). Elution curves were plotted and the separation factors calculated as described previously.[27]

The rare-earth determination was as described earlier[28] but DTPA was used instead of EDTA.

Spectrography

A 4-m grating spectrograph (Model DFS-13-2, made in the Soviet Union, reciprocal linear dispersion 2 Å/mm) was used under the following conditions.

Lower electrode, 3 mm deep and 3 mm i.d. undercut cup.
Upper electrode, tapered.
Sample-to-buffer (graphite) ratio, 1:1.
Excitation chamber, dynamic atmosphere chamber.
Gas composition, O_2:Ar = 1:4 v/v.
Gas flow-rate, 5 l./min.
Arc current (d.c.), 10 A.
Exposure time, 90 sec.
Analytical line (Å)/internal standard line (Å)/concentration range (ppm):

Gd (3422.46)/Y (3420.9)/5–300
Tb (3324.4)/Y (3317)/10–300
Dy (3645.4)/Y (3700.7)/5–300
Ho (3398.98)/Y (3420.9)/5–300
Er (3906.32)/Y (3909)/5–300
Tm (3425.1)/Y (3420.9)/5–300
Yb (3289.37)/Y (3317)/1–50
Lu (3359.56)/Y (3420.9)/5–300

RESULTS AND DISCUSSION

Separation factors

All the separation factors listed in Table 1 are at least 1.9. With increase in temperature, the separation factor $S_{Gd/Y}$ decreases, $S_{Yb/Y}$ and $S_{Lu/Y}$ increase and the others show only slight changes.

Chromatographic separation

Earlier results[26] have shown that the ammonium thiocyanate concentration has no appreciable effect on the separation factors. From Table 1 it can be seen that a temperature of 40° is satisfactory for the chromatographic separation of yttrium subgroup elements from yttrium. However, for practical reasons the lower temperature of 32 ± 1° and an ammonium thiocyanate concentration of 0.45*M* were adopted.

Table 1. Effect of temperature on separation factors

Lanthanide	Separation factor,* $S_{RE/Y}$					
	Static method					Dynamic method†
	23.8°	28.0°	32.0°	36.8°	42.0°	32 ± 1°
Gd	2.7	2.4	2.3	2.1	2.0	2.2
Tb	2.4	2.3	2.4	2.2	2.2	2.3
Dy	2.3	2.3	2.2	2.1	2.1	2.1
Ho	1.9	2.0	2.0§	2.0	2.0	1.9‡
Er	2.0	2.1	2.2	2.1	2.1	2.0
Tm	2.2	2.4	2.4	2.4	2.5	2.2
Yb	2.7	3.0	3.1	3.2	3.3	3.0
Lu	2.9	3.3	3.4§	3.5	3.7	3.3‡

*A solution containing 10 mg of yttrium oxide and 10 mg of an individual yttrium subgroup rare-earth oxide was fed into the column. Figures given are the mean of 2 determinations unless otherwise indicated.

†Aqueous phase or eluent was 0.45*M* NH_4SCN.

‡Mean of 4 determinations, standard deviation 0.11 for $S_{Ho/Y}$ and 0.15 for $S_{Lu/Y}$.

§Mean of 5 determinations, standard deviation 0.12 for $S_{Ho/Y}$ and 0.15 and 0.25 for $S_{Lu/Y}$.

The elution curves of yttrium and holmium are shown in Fig. 1. It can be seen that the chromatographic peak corresponding to 600 mg of Y_2O_3 is distorted, but the retention volume for holmium is almost independent of the amount of Y_2O_3. It was found that 600 ml of eluent removed all but 1–2 mg of the 600 mg of Y_2O_3 added.

Procedure for analysis of samples

Dissolve 600 mg of a sample of Y_2O_3 in 10 ml of 4*M* hydrochloric acid, warm gently to evaporate excess of acid

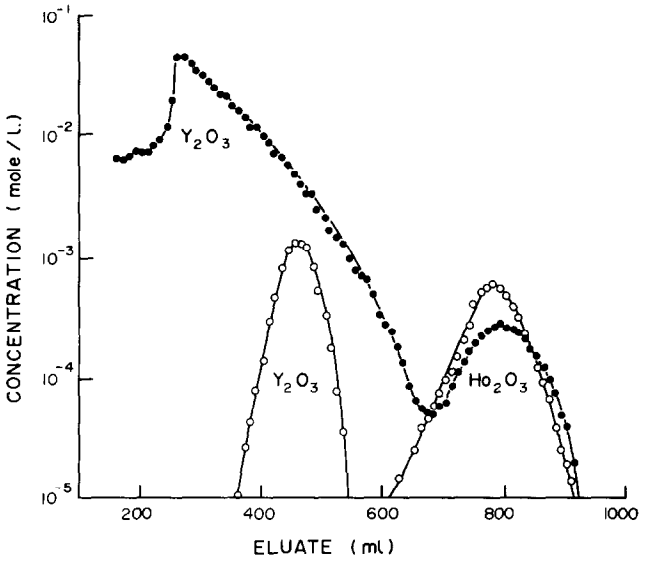

Fig. 1. Elution curves for yttrium and holmium. Column, 20 × 620 mm (TBP/silica spheres = 1/2). Column free volume, 103 ml. Eluent, 0.45*M* NH_4SCN solution. Temperature, 32 ± 1°. Flow-rate, 0.75 $ml.cm^{-2}.min^{-1}$. Volume of RE solution fed to column, 10 ml. 0—10 mg of Y_2O_3 + 11 mg of Ho_2O_3; ●—600 mg of Y_2O_3 + 7 mg of Ho_2O_3.

Table 2. Spectroscopic analysis of yttrium subgroup impurities in high-purity yttrium oxide

Sample	RE_xO_y	Added, *ppm*	Total found, *ppm*	Rel. std. devn., %	Recovery, %
1	Gd_2O_3		0.44*	13	
	Tb_4O_7		Nil		
	Dy_2O_3		0.99*	13	
	Ho_2O_3		0.60*	12	
	Er_2O_3		0.68*	13	
	Tm_2O_3		Nil		
	Yb_2O_3		0.10*	9	
	Lu_2O_3		Nil		
2†	Gd_2O_3	1.00	1.37	14	93
	Tb_4O_7	2.00	2.00*	5	100
	Dy_2O_3	1.00	1.88	13	89
	Ho_2O_3	1.00	1.50	8	90
	Er_2O_3	1.00	1.48	8	80
	Tm_2O_3	1.50	1.31	13	87
	Yb_2O_3	0.12	0.200	12	83
	Lu_2O_3	1.50	1.46*	14	99
3†	Gd_2O_3	1.40	1.61	7	83
	Tb_4O_7	8.00	7.24*	13	91
	Dy_2O_3	2.00	2.78*	16	90
	Ho_2O_3	1.40	1.72	9	80
	Er_2O_3	1.40	1.93	18	89
	Tm_2O_3	2.00	1.65	14	83
	Yb_2O_3	0.50	0.57	8	94
	Lu_2O_3	2.00	1.88*	17	94

*Mean of 5 results; values without an asterisk are the mean of 6 results.
†Prepared by adding known amounts of impurities to Sample 1.

and dissolve the residue in 10 ml of 0.45*M* ammonium thiocyanate. The pH of the sample solution thus prepared is about 5. Transfer the solution to the chromatographic column, and elute the yttrium with 0.45*M* ammonium thiocyanate saturated with TBP, at a flow-rate of 0.75 $ml.cm^{-2}.min^{-1}$. Discard the first 100 ml of eluate (column free volume), and collect the next 500 ml (fraction 1) in a 500-ml standard flask for recovery of the yttrium. Elute the residual yttrium and yttrium subgroup impurities with 0.1*M* hydrochloric acid, collecting 300 ml of eluate (fraction 2). Add 35 ml of fraction 1 (containing 42 mg of Y_2O_3) to fraction 2. Recover the rare-earths from this mixture by precipitation as hydroxides and oxalates (successively) and ignite the oxalates to the oxides. Mix the oxides with an equal amount of graphite powder, pack the mixture in two undercut electrodes and excite in a d.c. arc.

One real sample and two synthetic samples (prepared by adding eight yttrium subgroup impurities to the real sample) were analysed repeatedly and the recoveries were found to be 80–100%. The results of these analyses are summarized in Table 2.

Acknowledgements—The author is indebted to his colleague Huang Lin-guang for the spectroscopic determination and to Xu Min-liang, at Central-South Institute of Mining and Metallurgy, China, for reading the manuscript.

REFERENCES

1. Chemistry Department, Wuhan University, *Analytical Chemistry of Rare Earths*, Science, Beijing, 1981.
2. D. I. Ryabchikov and V. A. Ryabukhin, *Analytical Chemistry of Yttrium and the Lanthanide Elements*, Ann Arbor–Humphrey, Ann Arbor, 1970.
3. O. B. Michelsen, *Analysis and Application of Rare Earth Materials*, Universitesforlaget, Oslo, 1973.
4. J. Korkisch, *Modern Methods for the Separation of Rarer Metal Ions*, Pergamon Press, Oxford, 1969.
5. Laboratory of Analytical Chemistry, Wuhan University, *Wuhan Daxue Xuebao (Ziran Kexue)*, 1974, No. 2, 5.
6. V. A. Ryabukhin, N. G. Gatinskaya and A. N. Ermakov, *Zh. Analit. Khim.* 1977, **32**, 909.
7. Lu An-chiu, Cheng Ying-ke and Li Duan-lin, *Fenxi Huaxue*, 1979, **7**, 97.
8. Changchun Institute of Applied Chemistry, Academia Sinica, *ibid.*, (*Trial Publication*), 1972, 21.
9. Han Cheng-kui, Jing Wei-min, Lu An-chiu, Li Duan-lin, Shang-guan Xin-xian, He Shi-wei, Ou Jing and Peng Chun-lin, in *Selected Papers of the Second National Conference on Analysis of Rare Earths*, p. 273. Baotou Research Institute for Metallurgy, 1979.
10. Peng Chun-lin, Pei Ai-li, Wu Shao-le, Ji Yong-yi, Yan Bai-zhen, Sui Xi-yun and Liu Chun-lan, *Huaxue Xuebao*, 1979, **37**, 267.
11. E. Herrman, H. Grosse-Ruyken and V. A. Chalkin, *J. Chromatog.*, 1973, **87**, 351.
12. E. Herrman, in *Analysis and Application of Rare Earth Materials*, O. B. Michelsen (ed.), p. 39. Universitiesforlaget, Oslo, 1973.
13. G. I. Shmanenkova, M. G. Zemskova, Sh. G. Melamed, G. P. Pleshakova and G. V. Sukhov, *Zavodsk. Lab.*, 1969, **35**, 897.
14. H. Yoshida, *J. Inorg. Nucl. Chem.*, 1962, **24**, 1257.
15. D. F. Peppard and G. W. Mason, *U.S. Patent*, 1963, 3 110 556.
16. W. Fischer, K. J. Bramekamp, M. Klinge and H. P. Pohlmann, *Z. Anorg. Allg. Chem.*, 1964, **329**, 44.
17. A. M. Golub and M. I. Olevinskii, *Ukr. Khim. Zh.*, 1965, **31**, 12.
18. T. Sekine, *Bull. Chem. Soc. Japan*, 1965, **38**, 1972.
19. A. M. Golub and A. N. Borshch, *Zh. Neorgan. Khim.*, 1967, **12**, 522.
20. K. Naramura, *J. Inorg. Nucl. Chem.*, 1969, **31**, 455.
21. *Idem*, *ibid.*, 1970, **32**, 2265.
22. P. K. Khopkar and P. Narayanankutty, *ibid.*, 1972, **34**, 2617.
23. W. Fischer and F. Schmitt, *Japan Patent*, 75-34000, 11 November 1975.
24. A. R. Eberle and M. W. Lerner, *U.S. At. Energy Comm. Rept.*, AECD-4286, 1957.
25. B. Ceccaroli and J. Alstad, *J. Inorg. Nucl. Chem.*, 1981, **43**, 1181.
26. Zhang Tao, Unpublished work.
27. T. Braun and G. Ghersini, *Extraction Chromatography*, Elsevier, Amsterdam, 1975.
28. Hong Shui-jie and Ren Hong-de, *Huaxue Xuebao*, 1965, **31**, 91.

Talanta, Vol. 30, No. 11, pp. 867–869, 1983
Printed in Great Britain.

0039-9140/83 $3.00 + 0.00

USE OF SODIUM DODECYL SULPHATE TO CLARIFY THE END-POINT OF ANODIC-STRIPPING COMPLEXOMETRIC TITRATIONS

SHUN-ITU TANAKA, YUKIHIRO MORIMOTO, MITSUHIKO TAGA and HITOSHI YOSHIDA
Department of Chemistry, Faculty of Science, Hokkaido University, Nishi-8, Kita-10, Kita-ku, Sapporo-shi, Hokkaido, Japan

(*Received* 11 *April* 1983. *Accepted* 6 *May* 1983)

Summary—It has been found that addition of sodium dodecyl sulphate will completely suppress the dissociation of the copper–EDTA complex at the electrode surface in the anodic-stripping complexometric titration of copper and make the end-point of the titration very clear. The addition of SDS also makes it possible to titrate traces of nitrilotriacetic acid, which forms a copper complex that is less stable than the EDTA complex. The effect of SDS is presumed to be due to electrostatic repulsion between the negative charges of adsorbed SDS and the metal complex at the electrode surface.

The characterization of trace metals and estimation of organic ligands in natural waters are mainly investigated by electrochemical methods. Anodic-stripping voltammetry (ASV) is regarded as the most effective method and has been applied in many water analyses.[1–4] This is because of the high sensitivity of the method and its ability to distinguish between free metal, labile metal complex and inert metal complex.

However, problems in the use of ASV for the estimation of organic ligands have been pointed out.[5,6] Shuman and Woodward reported that when ethylenediaminetetra-acetic acid (EDTA) is titrated with cadmium, dissociation of the metal complex takes place at the electrode surface during the deposition and it becomes difficult to locate the end-point on the titration curve.[6] The validity of calculating conditional stability constants of metal complexes from the titration curves obtained by the ASV method has been disputed on the grounds of dissociation and electrolysis of the complexes during the deposition step.[7,8]

To prevent this dissociation Hanck and Dillard tried making the measurements at low temperature[9] but it was impossible to inhibit the dissociation completely.

It is well known that surfactants present in the supporting electrolyte solution are adsorbed on a mercury electrode surface and have various effects on the electrode reaction. Generally, a charged surfactant is known to inhibit the electrode reaction of a depolarizer having the same sign of charge as the surfactant and to accelerate the electrode reaction of a depolarizer with opposite charge.[10,11] It might be possible to utilize this surfactant property to control the electrode reaction, *i.e.*, to suppress electrolysis of the metal complex and reduce only the free metal ion.

In this paper, we report the effect of a surfactant such as sodium dodecyl sulphate (SDS) on the anodic-stripping complexometric titration of EDTA and nitrilotriacetic acid (NTA) with copper.

EXPERIMENTAL

Apparatus

A PAR-174A polarographic analyser and a PAR-315A automated control unit were used to record the stripping voltammograms. The working electrode was a Metrohm Model E410 hanging mercury drop electrode (HMDE) and the counter-electrode was a platinum wire. A saturated calomel electrode was used as reference electrode.

Reagents

The standard copper solution was prepared by dissolving electrolytic copper (99.999% pure) in concentrated nitric acid and diluting to 0.01*M*. The EDTA solution was prepared from $Na_2H_2Y \cdot 2H_2O$ and standardized complexometrically with 1-(2-pyridylazo)-2-naphthol as indicator. The solution of NTA was standardized with Chrome Azurol S as indicator. The SDS was biochemical grade. Other reagents were of analytical reagent grade.

Procedure

Acetate buffer solution (0.1*M*, 20 ml) containing EDTA or NTA was placed in the electrolysis cell and nitrogen was passed through the solution for 15 min. Deposition was performed at −0.5 V *vs.* SCE, with stirring, for 2 min, followed by a 15-sec rest period and an anodic potential scan at 5 mV/sec (in the differential pulse mode). The pulses were applied every 0.5 sec; the pulse height was 50 mV. The copper titrant was added in 20-μl portions with an Eppendorf micropipette until 100% excess was present. The titration curve was obtained by plotting peak-height of the copper stripping wave against volume of titrant added.

RESULTS AND DISCUSSION

Titration curve for EDTA

The ASV deposition potential can be selected from knowledge of the stripping polarography of the copper–EDTA complex. If the metal complex does not dissociate, only the free copper ion should be electrolytically reduced, and the metal complex

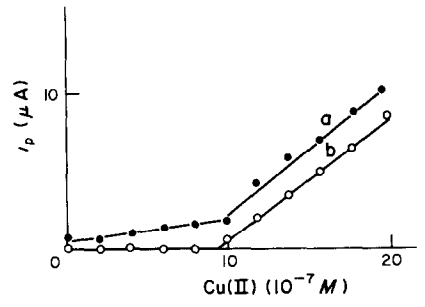

Fig. 1.

should not be electrolysed at potentials more positive than −0.7 V *vs.* SCE. However, even when the deposition potential is −0.5 V *vs.* SCE and the amount of free copper ion is made negligible by the presence of excess of EDTA, a slight copper stripping peak is observed. As reported by Shuman and Woodward,[6] this seems not to be associated with dissociation of the metal complex in the bulk solution, but with its dissociation at the electrode surface. Therefore the titration curve for EDTA has a small copper peak current before the equivalence point, as shown in Fig. 1a.

The conditional formation constant can be calculated from the slope of the line obtained from a plot of peak current against $C_m/(C_l - C_m)$, where C_m is the concentration of added metal and C_l is the concentration of ligand, and the slope of the titration curve after the equivalence point, as described by Shuman and Woodward.[12] The value obtained from the titration curve in Fig. 1a was log $K' = 7.46$ at pH 4 and lower by about one order of magnitude than the literature value[13] (log $K' = 8.7$). Figure 1b shows the titration curve obtained in the presence of 10^{-3}% SDS; the peak current before the equivalence point is almost zero and the slope of the line after the equivalence point is equal to that in the absence of SDS. Moreover the end-point of this titration curve is very clear. It can be therefore presumed that SDS prevents dissociation of the metal complex but has little influence on reduction of free copper ion.

The effect of other surfactants was also investigated. The presence of 10^{-3}% Triton X-100 suppressed not only the dissociation of metal complex but also decreased the reduction of free copper ion by a factor of 2. The presence of 10^{-3}% gelatine or poly(vinyl alcohol) did not completely prevent the dissociation. Laurylamine, a cationic surfactant, had little effect on the peak current before the equivalence point.

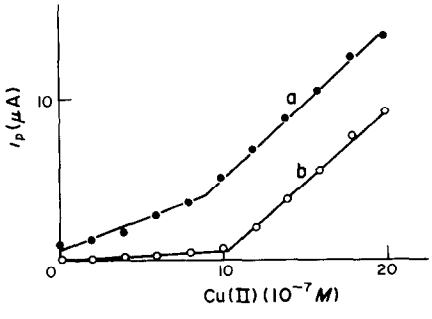

Fig. 2.

It was confirmed from the electrocapillary curve in the supporting electrolyte solution containing 10^{-3}% SDS that SDS is adsorbed on the mercury electrode surface over the range from −0.4 to −1.0 V *vs.* SCE.

Consequently, the effect of SDS on dissociation of the metal complex at the electrode seems to be due to the adsorbed SDS on the electrode electrostatically or sterically preventing the metal complex from approaching the electrode surface. In particular, it is presumed that electrostatic repulsion between the negative charges of the adsorbed SDS and the copper–EDTA complex is the main reason, because the anionic surfactants, such as SDS, are more effective in preventing electrolysis of the metal complex.

Titration curve for NTA

Since the formation constant of the copper–NTA complex is lower than that of copper–EDTA, it has hitherto seemed impossible to determine NTA by the anodic-stripping complexometric titration method. The titration curve obtained in our laboratory is shown in Fig. 2a. The end point is rather vague and cannot be improved by increasing the pH for the titration. Addition of SDS makes the end-point of the titration clear, as shown in Fig. 2b. However, it is impossible to eliminate the dissociation effect completely, even by increasing the SDS concentration to 3×10^{-3}%.

The conditional formation constant of the copper–NTA complex, determined from the titration curve, is log $K' = 5.66$ in the absence of SDS, which is one order of magnitude lower than the literature value[13] (log $K' = 6.5$), but in the presence of 3×10^{-3}% SDS, the value is log $K' = 6.48$, in agreement with the literature value.

Determination of EDTA and NTA

Analytical results for EDTA and NTA are given in Table 1. The determination of EDTA at pH 4.0 gave a small negative error, which increased with decreasing EDTA concentration. The relative standard

Table 1. Determination of EDTA and NTA (0.1 *M* acetate buffer, 1×10^{-3}% SDS, deposition for 2 min at −0.5 V *vs.* SCE)

Sample	pH	Taken, μM	Found, μM	Relative error, %	R.S.D., %
EDTA	4.0	0.53	0.51	−3.8	1.3
	4.0	0.21	0.19	−9.5	2.1
	4.0	0.11	0.09	−18.1	1.0
NTA	5.0	1.02	1.03	+1.0	—
	4.0*	0.51	0.49	−3.9	4.1
	4.0*	0.20	0.21	+5.0	4.9

*5×10^{-3}% SDS.

deviation (5 runs) was $<2\%$. The determination of 0.2–1.0μM NTA had a relative error of $<5\%$.

REFERENCES

1. T. M. Florence and G. E. Batley, *Talanta*, 1977, **24,** 151.
2. R. G. Clem and A. T. Hodgson, *Anal. Chem.*, 1978, **50,** 102.
3. T. M. Florence and G. E. Batley, *J. Electroanal. Chem.*, 1977, **75,** 791.
4. G. A. Bhat, R. A. Saar, R. B. Smart and J. H. Weber, *Anal. Chem.*, 1981, **53,** 2275.
5. J. R. Tuschall and P. L. Brezonik, *ibid.*, 1981, **53,** 1986.
6. M. S. Shuman and G. P. Woodward, *ibid.*, 1973, **45,** 2032.
7. G. A. Bhat, J. H. Weber, J. R. Tuschall and P. L. Brezonik, *ibid.*, 1982, **54,** 2116.
8. M. S. Shuman, P. L. Brezonik and J. R. Tuschall, *ibid.*, 1982, **54,** 998.
9. K. W. Hanck and J. W. Dillard, *Anal. Chim. Acta*, 1977, **89,** 329.
10. N. Gundersen and E. Jacobsen, *J. Electroanal. Chem.*, 1969, **20,** 13.
11. T. Aisaka, K. Nagasawa and T. Yoshioka, *Denki-kagaku*, 1976, **44,** 674.
12. M. S. Shuman and G. P. Woodward, *Environm. Sci. Technol.*, 1977, **11,** 809.
13. A. Ringbom, *Complexation in Analytical Chemistry*, Wiley, New York, 1963.

Talanta, Vol. 30, No. 11, pp. 870–872, 1983
Printed in Great Britain.

0039-9140/83 $3.00 + 0.00

COMPLEXOMETRIC TITRATIONS CONTROLLED BY ANODIC-STRIPPING METHODS—I

VOLTAMMETRIC STRIPPING

P. GRÜNDLER
Karl Marx University Leipzig, Chemical Department, Analytical Centre, Leipzig 7010, D.D.R.

(*Received* 24 *February* 1983. *Accepted* 4 *May* 1983)

Summary—Anodic-stripping voltammetry is used to perform automatic complexometric titrations of metal ions, with high precision. The stripping peaks are converted into corresponding titrant volume increments which are added consecutively during stripping. In analysis of samples containing about 1 mmole, each of lead, indium and gallium, relative standard deviations of 0.008–0.03% were attained.

One of the most important factors governing the precision of a titration is the sensitivity of end-point detection. In most cases, end-point indication can be considered as the application of a trace-determination method to monitoring very small concentration changes in the vicinity of the equivalence point. In the case of complexometry, trace concentrations of free metal ion are to be monitored. For this purpose, stripping methods offer great advantages because of their superior sensitivity and very high signal-to-noise ratio.

Anodic stripping has already been applied for bulk analysis by Besagni *et al.*, who used the technique for determination of metal excess in non-stoichiometric solids. Their idea was to mask the stoichiometric metal content completely with a precisely weighed amount of EDTA. The small remaining excess metal concentration due to the non-stoichiometry was then determined by a single anodic-stripping analysis. Unfortunately, this simple procedure may give erroneous results if the complex formed does not fulfil the requirement of "complete masking", *i.e.*, if its conditional stability constant is not extremely high. Hence it has been found better to follow the titration curve point by point in a multicycle experiment. This has been applied to determination of gallium in non-stoichiometric gallium nitride.[2,3] In the meantime, the "potentiometric stripping" method has been applied in complexometric titration by Jagner.[4] Anodic-stripping voltammetry has also been used in titrations to find the "complexing capacity" of natural waters.[5]

End-point determination by stripping is rather tedious, since each complete determination cycle will give only one point of the titration curve. An attempt has therefore been made to develop techniques which allow not only automatic performance of each determination step, but also automation of the complete titration.

In the method presented here, after deposition of the metal, stripping is performed by a voltage sweep. The resulting current peak is converted by an analogue-to-digital (A–D) converter into pulses with a pulse-rate proportional to the instantaneous stripping current. The pulses are fed to the stepping motor of a piston burette. Each pulse causes the burette to deliver a definite volume of titrant solution. Thus, in the next cycle, as a consequence of the smaller stripping peak area, the volume delivered will be smaller, and so on. As a result, more and more closely spaced points on the titration curve are produced as the end-point is approached. Moreover, every volume increment delivered by the burette represents a measure of the peak signal. The titration curve can therefore be constructed very easily by plotting the consecutive volume increments against the cumulative volumes. The printed output from the burette system contains the complete titration information.

EXPERIMENTAL

Apparatus

A Beckman "Electroscan" was used in the scanning mode. The instrument was equipped with a "Disk" integrator which delivers pulses with a frequency proportional to the recorder deflection. The pulses were formed and amplified in a comparator circuit to give them a rectangular profile. They were fed to the input of an OP-930 automatic burette (Radelkis, Budapest). A single pulse causes the burette to deliver a volume of 2 μl.

Cell and electrodes

A 150-ml beaker equipped with a reference electrode (SCE), auxiliary electrode (platinum wire) and working electrodes was used in conjunction with a magnetic stirrer. The working electrode was a glassy carbon disc of 6 mm diameter for lead determination, and a commercial hanging mercury drop electrode (HMDE) with a drop volume of 1.5 μl for indium and gallium determination. The test solution was deaerated with pure argon before each measurement.

Chemicals

Lead nitrate stock solution was prepared from lead

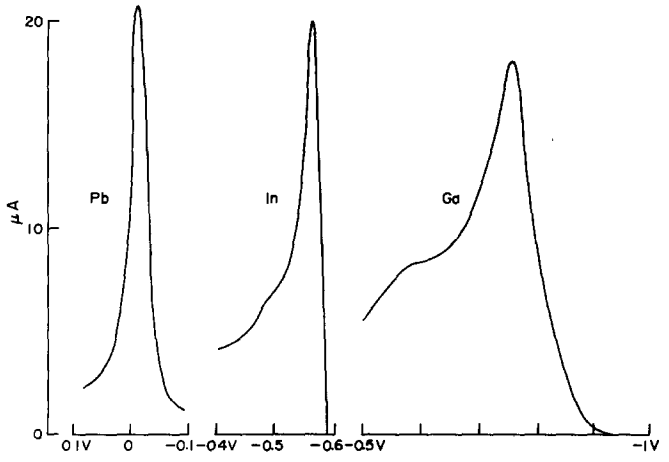

Fig. 1. ASV peak signals for $8 \times 10^{-5}M$ free metal ion in presence of $10^{-2}M$ metal–EDTA complex (0.8% uncomplexed metal). Conditions described in text.

nitrate (analytical-reagent grade) and standardized by a complexometric weight titration with amperometric end-point. Gallium and indium solutions were prepared from the very pure (99.9999%) metals, weighed on a microbalance, dissolved in *aqua regia* (gallium) or hydrochloric acid (indium), approximately neutralized, and diluted with water to a definite weight. The concentration of the stock solutions was about 0.1 mole/kg.

EDTA solutions were standardized coulometrically with zinc ions generated from zinc amalgam electrodes. The end-point was determined amperometrically with a lead dioxide electrode.[6]

Salicylic acid (pharmaceutical grade) was recrystallized twice from water. All other chemicals were reagent grade.

Working conditions

Lead determination. Electrolyte solution: $0.1M$ potassium bromide, $0.05M$ hexamine, adjusted to pH 5.1 with hydrochloric acid. Deposition for 2 min at -1.0 V onto a glassy carbon electrode. Stripping scan from -0.6 to $+0.2$ V at 10 mV/sec. Recorder sensitivity 140 μA full scale.

Indium determination. Electrolyte solution: $0.1M$ potassium bromide, $0.1M$ chloroacetate buffer, pH 3.0. Deposition for 2 min at -1.25 V on the HMDE. Stripping scan from -0.6 to 0 V at 10 mV/sec. Recorder sensitivity 70 μA full scale.

Gallium determination. Electrolyte solution: $0.005M$ salicylate, $0.1M$ acetate buffer, pH 5.0. Deposition for 5 min at -1.4 V on the HMDE. Stripping scan from -1.0 to 0 V at 10 mV/sec. Recorder sensitivity 28 μA full scale.

Titration procedure

Portions of stock metal solutions were measured out by weight from a plastic syringe weighed in a metallic case. About 99% of the metal content to be titrated was complexed by addition of an exactly weighed amount of $0.1M$ EDTA. The remaining 1% was determined precisely by the following automatic titration. After addition of the buffer and other constituents in appropriate amounts the pH was adjusted (pH-meter) and the solution deaerated. The titration was then started with the deposition step, and was done with $0.001M$ EDTA. In all cases the titration vessel contained about 1 mmole of determinable metal ion.

RESULTS AND DISCUSSION

The deposition potentials were chosen from current–potential curves for small concentrations of free metal ion in the presence of a huge excess of their EDTA complexes. Thus it was ensured that there was no decomposition of the complex during deposition of the free metal ion.

The conditions for titrant delivery were chosen so that each stripping run caused the burette to add an amount of EDTA sufficient to complex about 25–33% of the free metal ion, so, in the vicinity of the end-point, the density of the points became very high. The pulse rate of the A–D converter, *i.e.*, the number of pulses output per unit voltage input, could not be adjusted arbitrarily, so the proper conditions were realized by selecting the correct amplification of the peak signal. Typical stripping peaks are shown in Fig. 1.

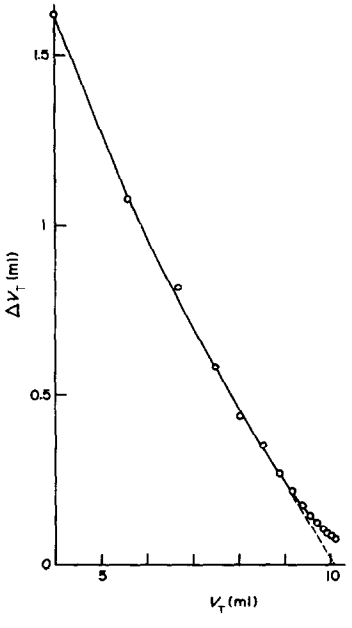

Fig. 2. Lead titration, ASV with glassy carbon electrode. ΔV_T = titrant volume increments proportional to peak area; V_T = titrant volume ($10^{-3}M$ EDTA).

Table 1. Results of lead, indium and gallium determinations

Metal titrated	Content of stock solution, g/kg		Relative standard deviation, %	Number of measurements
	Calculated*	Found		
Lead	24.886	24.884	0.03	11
Indium	11.457	11.463	0.008	11
Gallium	6.8833	6.886	0.01	24

*From results of standardization titration (lead) or weight of metal sample in stock solutions (indium, gallium).

Part of the error was attributable to improper functioning of the mechanical disc integrator which was used as an A–D converter. In some cases, at very low metal concentration, the peaks became very flat, and the integrator was not able to follow them exactly. It would be better to use an electronic A–D converter.

Figure 2 shows a typical titration curve, from which it can be seen that the contribution of the end-point determination to the overall titration error should be rather small. Even in the worst case the end-point can be found with an uncertainty of not more than ± 0.2 ml of $10^{-3}M$ EDTA. This corresponds to an overall error of 0.02% if 1 mmole of metal is to be titrated. Table 1 gives the results of some titrations of this type. The standard deviation data do not allow a clear distinction between the contributions of various weighing errors and the end-point uncertainty. It would be even more difficult to draw conclusions about systematic error, since two high-precision titrations are compared, one of them acting as a standardization. In the case of lead the titrant solution was used for standardization of the stock metal solution as well. The difference between the "calculated" and "found" values is then in effect a comparison of the two different end-point indication procedures (amperometric and ASV). In the case of indium and gallium the weight of pure metal taken is used as the reference standard, which is compared with the result of the coulometric titration used for titrant standardization.

It can be said that the method is applicable for high-precision titration. Another possible application would be the titration of very dilute metal ion solutions in the concentration range of 10^{-5}–$10^{-4}M$. With such solutions an error of only a few per cent is attainable, if the conditional stability constants are high enough. Under the conditions recommended in this paper, the conditional constants are $10^{9.6}$ for lead, $10^{14.3}$ for indium and $10^{10.3}$ for gallium.

REFERENCES

1. T. Besagni, F. Licci and L. Zanotti, *Microchem. J.*, 1978, **23**, 305.
2. E. Marx, *Diplomarbeit*, Karl-Marx-Universität Leipzig, 1980.
3. P. Gründler and E. Marx, *Acta Chim. Acad. Sci. Hung.*, in press.
4. D. Jagner and K. Årén, *Anal. Chim. Acta*, 1982, **134**, 201.
5. B. T. Hart, *Environm. Technol. Lett.*, 1981, **2**, 95.
6. T. Böttger, P. Gründler and G. Werner, *Chem. Anal. (Warsaw)*, in press.

Talanta, Vol. 30, No 11, pp. 873–875, 1983
Printed in Great Britain

0039-9140/83 $3.00 + 0.00

DETERMINATION OF THALLIUM IN LEAD SALTS BY DIFFERENTIAL PULSE ANODIC-STRIPPING VOLTAMMETRY

A. CISZEWSKI and Z. ŁUKASZEWSKI*
Institute of General Chemistry, Technical University of Poznań, 60-965 Poznań, Poland

(*Received* 2 *February* 1983. *Accepted* 4 *May* 1983)

Summary—The determination of trace levels of thallium in lead and lead salts by differential pulse anodic-stripping voltammetry has been made possible by using a surfactant as an electrochemical masking agent in addition to a complexing agent. In 0.2*M* EDTA at pH 4.5 as supporting electrolyte without surfactant, lead at concentrations below 0.5m*M* does not give a peak. When the electrolyte also contains tetrabutylammonium chloride (TBAC) at 0.01*M* concentration, lead can be tolerated at concentrations up to 0.05*M*, while the height of the thallium peak is unaffected. It is thus possible to determine 5n*M* Tl(I) in the presence of 0.05*M* Pb(II), *i.e.*, Tl at the 1×10^{-5}% level in lead. The precision of the determination (1–4%) and the recovery are satisfactory. Neither an 800-fold excess ratio of Cu(II) to Tl(I) nor a 10^7-fold ratio of Bi(III) interferes in the determination. Thallium has been determined in a range of lead salts of various degrees of purity.

Suppression of electrochemical activity by addition of a surfactant—known as electrochemical masking—can sometimes be used to permit the determination of a trace element in an otherwise difficult matrix by use of anodic-stripping voltammetry.[1] One system which can present significant difficulties in electroanalysis is that of mixtures of Tl(I) and Pb(II). These difficulties may be minimized by suitable choice of supporting electrolyte, the complexing action of which shifts the reduction potential of lead, but not that of thallium, to more negative values.[2–8] In most methods published, EDTA has been used.[3,5–7] In this way, the interference from a relatively small amount of Pb(II), up to some orders of magnitude greater than that of the thallium, may be eliminated. However, when the sample matrix is lead, a chemical separation step is normally necessary, for instance oxidation of Tl(I) to Tl(III) and extraction into diethyl ether.[9]

The objective of this study was to examine the possibility of determining thallium, as Tl(I), in the presence of very much higher concentrations of Pb(II), by differential pulse anodic-stripping voltammetry, by adding both a complexing agent and a surfactant. A successful solution to this problem would permit the determination of traces of thallium in lead without the need for a preliminary separation. The degree of suppression of the electrochemical activity of a metal ion by an inhibitor is associated with the ionic potential of the ion being determined.[10,11] The relatively small difference in the ionic potentials of Tl(I) (0.74) and Pb(II) (1.59) makes this approach difficult.

*Author for correspondence.

EXPERIMENTAL

Apparatus

A Telpod (Poland) pulse polarograph model PP-04, designed by Kowalski *et al.*, was used. Voltamperograms were displayed on an Endim (GDR) 620.02 XY-recorder. The differential pulse amplitude was 10 or 50 mV and the scan-rate 11.1 mV/sec. The Radiometer controlled-temperature Kemula electrode equipment was used. The surface area of the hanging mercury drop was 2.1 mm^2.

Reagents

Tetrabutylammonium chloride (Merck), sodium dodecylsulphate (POCh), poly(ethylene glycol) of M.W. 2×10^4 (Fluka), reagent-grade lead acetate and nitrate, analytical-grade EDTA, lead acetate and nitrate, semiconductor-grade acetic acid and nitric acid, and spectral-grade lead nitrate, lead and thallium were used. Concentrated solutions of potassium hydroxide were purified by electrolysis at a mercury cathode.[12]

Water was doubly distilled in a Heraeus quartz still. The standard solutions of Tl(I) and Pb(II) were prepared by dissolving the metals in nitric acid or acetic acid. Solutions with concentrations below 1m*M* were prepared just before use.

The medium used was 0.2*M* EDTA, pH 4.5 ± 0.1. The pH was adjusted with purified potassium hydroxide solution. The solutions examined were deaerated by passage of purified nitrogen and were brought to $20 \pm 0.2°$ before measurement.

Procedure

Determination of thallium in metallic lead. Weigh out about 0.3 g of lead, dissolve it in a few ml of hot acetic acid of semiconductor-grade, then evaporate the excess of acid. Add 0.25 ml of 1*M* tetrabutylammonium chloride and 20 ml of 0.25*M* EDTA. Adjust the pH to 4.5 ± 0.1, by dropwise addition of 10% potassium hydroxide solution, transfer the solution to a 25-ml standard flask and make up to the mark with water. Transfer the solution into the electrochemical cell and pass purified nitrogen or argon through it for 15 min. Perform the electrolytic deposition in stirred solution at −0.70 V *vs.* SCE for 5–15 min, depending on the expected thallium content. After the deposition, switch off the stirrer

wait 20 sec, then record the voltamperogram from −0.70 to 0 V *vs.* SCE. Repeat the measurement cycle twice more on the same solution, with a new mercury drop each time. Estimate the thallium according to the standard-addition method by three successive additions of a known volume of thallium(I) standard solution to the same solution, repeating the measurement cycle each time, beginning from the deposition stage. From the linear plot of peak height *vs.* amount of thallium standard added read the amount of thallium in the sample. If the volume of added thallium standard solution is less than 0.25 ml, correction for dilution may be omitted.

Determination of thallium in lead salts. Weigh out an amount of salt equivalent to about 0.3 g of lead, dissolve it in 20 ml of 0.25*M* EDTA, add 0.25 ml of 1*M* tetrabutylammonium chloride, and adjust to pH 4.5 ± 0.1 by dropwise addition of 10% electrochemically purified potassium hydroxide solution. Transfer the solution into the electrochemical cell and determine thallium as above.

RESULTS AND DISCUSSION

The use of 0.2*M* EDTA at pH 4.5 as supporting electrolyte causes a shift of the Pb(II) reduction potential from the value of about −0.5 V *vs.* SCE found for non-complexing electrolytes, to much more negative values. The lead deposited on an HMDE under these conditions gives a stripping peak at −0.49 V *vs.* SCE, *i.e.*, very close to the thallium peak (−0.48 V).

On the basis of the measurements plotted as curve *a* in Fig. 1, a deposition potential of −0.70 V *vs.* SCE was selected for the determination of thallium. Under these conditions there is no lead stripping peak for concentrations below 0.5m*M*, but at higher concentrations lead gives a stripping peak coinciding with the thallium peak, the peak-height increasing non-linearly with increasing concentration of Pb(II), (curve *a*, Fig. 2). The peak for 0.0241*M* lead is shown as curve *a* in Fig. 3. The dependence presented in curve *a*, Fig. 2, suggests that it would be difficult to determine thallium in the presence of high concentrations of lead, and impossible to determine traces of thallium in samples where the matrix is lead.

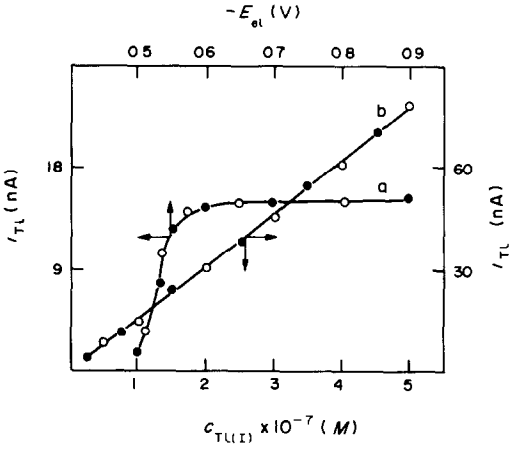

Fig. 1. (*a*) Peak current for 0.1μ*M* thallium *vs.* deposition potential, and (*b*) peak current *vs.* thallium concentration, in the absence (○) and presence (●) of TBAC. Deposition potential for (*b*) −0.70 V *vs.* SCE. Deposition time 5 min. Differential-pulse amplitude 10 mV.

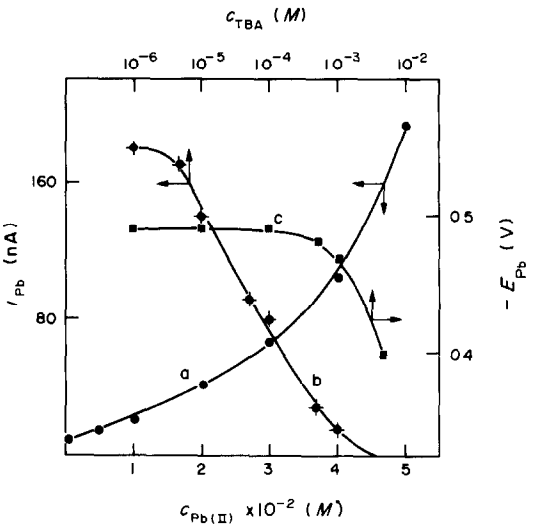

Fig. 2. Variation in size of the lead peak in the absence (*a*) and in the presence (*b*, *c*) of TBAC. (*a*) Peak current *vs.* [Pb(II)]; (*b*) peak current *vs.* [TBAC]; (*c*) peak potential *vs.* [TBAC]. Concentration of Pb(II), (*b*) and (*c*) 0.05*M*. Deposition potential −0.70 V *vs.* SCE. Deposition time 5 min. Differential-pulse amplitude 10 mV.

An attempt was made to suppress the lead peak by the addition of surfactants. Preliminary experiments showed that poly(ethylene glycol) of M.W. 2 × 10^4 or sodium dodecylsulphate did not have much effect on the height of the lead peak for 0.05*M* lead. Tetrabutylammonium chloride (TBAC) appeared to be more useful and was investigated more fully.

The influence of TBAC concentration on suppression of the peak for 0.05*M* lead is illustrated by curve *b* in Fig. 2. Changes in the peak potential for lead were also recorded (curve *c*, Fig. 2). It is apparent that a concentration of 0.01*M* TBAC is sufficient to suppress the lead peak completely. This suppression is further shown in Fig. 3. If the lead concentration is substantially higher than 0.05*M*, however, the lead peak is not completely suppressed. The lead peak potential, which can be determined before the complete suppression of the peak, becomes less negative in the presence of TBAC at concentrations higher than 0.1m*M*. As was shown earlier,[13] in the two-stage anodic-stripping cycle the main effect of surfactant is at the deposition stage.

The influence of 0.01*M* TBAC on the thallium peak was checked. Neither the height of the peak (curve *a*, Fig. 1) nor the potential (curve *b*, Fig. 1) was affected by the addition of TBAC.

The complete suppression of the lead peak at a lead concentration of 0.05*M* without affecting the thallium peak makes possible the determination of traces of thallium in a lead matrix. An example of such a determination is presented in Fig. 3, curves *c* and *d*. The thallium added corresponded to a level of 1.02 × 10^{-5}% in the lead.

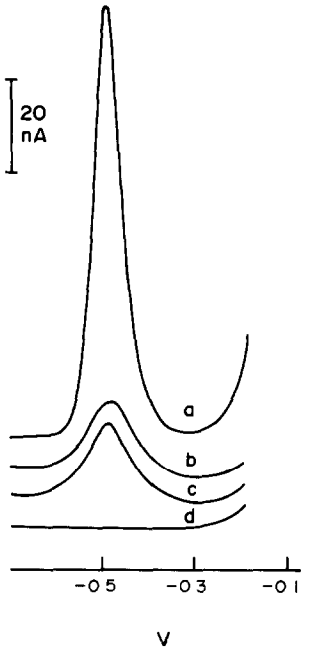

Fig. 3. Differential pulse anodic-stripping voltamperograms for (*a*) 0.0241*M* Pb(II); (*b*) 5n*M* Tl(I); (*c*) 5n*M* Tl(I) + 0.0482*M* Pb(II) + 0.01*M* TBAC; (*d*) 0.0241*M* Pb(II) + 0.01*M* TBAC. Deposition potential −0.70 V *vs.* SCE. Deposition time 15 min. Differential-pulse amplitude 50 mV.

Results showing the precision and recovery are collected in Table 1. They indicate satisfactory precision and the absence of a systematic error. The method was tested by determining the thallium content of lead salts of various degrees of purity. The results are summarized in Table 2. Assuming that 5n*M* Tl(I) can be determined with a 15-min deposition time and that the lead concentration should not exceed 0.05*M*, the lower limit of the determination is about $1 \times 10^{-5}\%$ of thallium in metallic lead and $6\text{–}7 \times 10^{-6}\%$ in lead salts.

Besides Pb(II), other ions reducible at potentials less negative than Tl(I) also interfere in the determination of Tl(I) if they are present in substantial amounts. It would be expected that Cu(II) and Bi(III), for which the reduction potentials are −0.27 and −0.55 V *vs.* SCE, respectively, would be reduced together with the thallium under the conditions of the thallium deposition (−0.70 V *vs.* SCE). Though the stripping peaks are quite far from the thallium peak (Cu −0.26 and Bi −0.14 V), if they are large, their tails will substantially increase the background current, thus causing an interference. In the presence of TBAC under the conditions described, an 800-fold ratio of Cu(II) to Tl(I) and an amount of Bi(III) similar to that of Pb(II) do not interfere in the thallium determination.

Table 1. Determination of thallium in the presence of lead and TBAC

Series	Number of tests	Added Pb, *mg*	Added Tl, *ng*	Found Tl, *ng*	Std. devn., *ng*
I	7	100	102	100	4.2
II	7	100	406	410	5.7

Table 2. Thallium content of lead salts

Lead salt	Grade	Sample weight, *g*	Thallium content, *ppm*
$Pb(CH_3COO)_2 \cdot 3H_2O$	Reagent	0.300	72(73)*
$Pb(CH_3COO)_2 \cdot 3H_2O$	A.R.	0.350	2.8
$Pb(NO_3)_2$	Reagent	0.250	20(18.5)*
$Pb(NO_3)_2$	A.R.	0.400	0.25
$Pb(NO_3)_2$	Spectral	0.400	0.06

*Spectrophotometric determination.[14]

The investigations described in this paper were performed as part of the research programme MR-I-32.

REFERENCES

1. Z. Łukaszewski, M. K. Pawlak and A. Ciszewski, *Talanta*, 1980, **27,** 181.
2. R. Neeb, *Z. Anal. Chem.*, 1962, **190,** 98.
3. M. S. Zakharov and A. G. Stromberg, *Zh. Analit. Khim.*, 1964, **19,** 913.
4. P. Bersier, K. Finger and F. von Sturm, *Z. Anal. Chem.*, 1966, **216,** 189.
5. C. Peker, M. Harlem and J. Badoz-Lambling, *ibid.*, 1967 **224,** 302.
6. R. Neeb and I. Kiehnast, *ibid.*, 1968 **241,** 142.
7. E. Temmerman and F. Verbeek, *J. Electroanal. Chem.*, 1968, **19,** 423.
8. Z. Łukaszewski, *Talanta*, 1977, **24,** 603.
9. R. G. Pats, *Zavodsk. Lab.*, 1962, **28,** 18.
10. A. Ciszewski and Z. Łukaszewski, *Anal. Chim. Acta*, 1983, **146,** 51.
11. J. Opydo, *Thesis*, Technical University of Poznań, 1982.
12. M. K. Pawlak and Z. Łukaszewski, *Chem. Anal. (Warsaw)*, 1975, **20,** 69.
13. Z. Łukaszewski, M. K. Pawlak and A. Ciszewski, *J. Electroanal. Chem.*, 1979, **103,** 217.
14. Z. Marczenko, H. Kałowska and M. Mojski, *Talanta*, 1974, **21,** 93.

Talanta, Vol. 30, No. 11, pp. 876–878, 1983
Printed in Great Britain

0039-9140/83 $3.00 + 0.00
Pergamon Press Ltd

A RAPID GEOCHEMICAL SPECTROPHOTOMETRIC DETERMINATION OF TUNGSTEN WITH DITHIOL

E. P. WELSCH
U.S. Geological Survey, Box 25046, Denver, CO 80225, U.S.A.

(*Received* 23 *December* 1982. *Revised* 12 *April* 1983. *Accepted* 22 *April* 1983)

Summary—1-g sample is decomposed with nitric and hydrofluoric acids, and after evaporation of the solution to dryness the residue is dissolved in concentrated hydrochloric acid. A clear aliquot is treated with stannous chloride to inhibit interferences. The blue tungsten dithiol complex is developed at a temperature of 85° over a half-hour period. The complex is extracted into 2 ml of heptane and the tungsten is determined spectrophotometrically with a sensitivity of 0.5 ppm. Fifty samples per man-day can be analysed in this manner.

Geochemical methods of analysis should be rapid, sensitive, and free from interferences. Atomic-absorption methods for the determination of tungsten lack the desired sensitivity, owing to the refractory nature of the oxides of the element. A method employing chemical preconcentration followed by emission spectroscopy[1] provides sensitivity but not speed. Of the many dithiol colorimetric procedures examined, several came close to fulfilling the above-mentioned criteria, but all were found wanting to some degree.

The use of dithiol in the determination of tungsten was investigated as early as 1947.[2] Since then a number of different methods have been published. Various sample decomposition procedures have been tried, ranging from fusions[3,4] to various combinations of acids.[5–7] Interference by molybdenum has been dealt with by control of acidity in the complexation step[2] or by extraction of the molybdenum dithiol complex in the presence of citric acid to mask the tungsten.[5] Molybdenum and tungsten can be complexed with dithiol and determined simultaneously,[6] but the simplest remedy is to suppress the molybdenum–dithiol reaction by reduction of the molybdenum (VI) with stannous chloride.[4,8]

The procedure proposed here uses a mixture of nitric and hydrofluoric acids for sample decomposition, which allows flexibility in choice of sample size and avoids the use of perchloric acid. Molybdenum interference is suppressed with stannous chloride. It has been found that the dithiol solution can be prepared by simply acidifying the zinc complex and adding ethanol; this eliminates the need to use thioglycollic acid, which has an offensive odour. Heptane is used instead of isoamyl acetate to extract the complex because it separates better from the aqueous phase, is less volatile, and does not turn yellow on reaction with interfering sample constituents.

This combination and modification of techniques, drawn from several accepted dithiol procedures for tungsten determination, provides a simple yet effective method for the purpose of geochemical exploration.

EXPERIMENTAL

Apparatus

A Bausch and Lomb Spectronic 100 spectrophotometer* equipped with a micro flow-through system was used. The uptake volume was set at 0.5 ml. A Laboratory Supplies Inc. heating block for 16 × 150-mm test-tubes was used to maintain a constant temperature of 85°.

Reagents

The 1.5% dithiol solution was made by acidifying 1.5 g of zinc dithiol complex with 2 ml of concentrated hydrochloric acid and adding 100 ml of ethanol (use of ultrasonic mixing facilitates the dissolution). The stannous chloride solution was made by dissolving 30 g of $SnCl_2 \cdot 6H_2O$ in 100 ml of concentrated hydrochloric acid. A 10% potassium ferricyanide solution was used for high-copper samples.

Tungsten stock solution (1000 μg/ml) was made by dissolving 0.90 g of $Na_2WO_4 \cdot 2H_2O$ in 500 ml of water. Working standards were prepared (each in triplicate) by pipetting suitably diluted stock solution (*e.g.*, 1 ml) equivalent to 0, 0.5, 1, 5, 10, and 25 μg of W into 16 × 150 mm test-tubes, followed by 1 ml of water, 4 ml of concentrated hydrochloric acid, 5 ml of stannous chloride solution and a boiling chip. The standards were placed in the heating block and treated in the same manner as the samples.

Procedure

Weigh 1.0-g sample of <80-mesh material into a 50-ml Teflon beaker. Add 5 ml of concentrated nitric acid and 20 ml of concentrated hydrofluoric acid. Evaporate to dryness and heat overnight at 125°. Moisten the residue with 2 ml of warm water and transfer it to a 16 × 150-mm test-tube with 8 ml of concentrated hydrochloric acid, mix and centrifuge. Transfer 5 ml to a second test-tube along with 5 ml of stannous chloride solution and a boiling chip. Heat the test-tube in the heating block at 85° for 10 min, add 1 ml of dithiol solution, and continue to heat at 85° for 30 min. Cool, add 2 ml of heptane, cap the tube and shake it for 1 min. Read the absorbance of the extract at 630 nm and compare with the absorbances of the standards. If the

*Any use of trade names is for descriptive purposes only and does not imply endorsement by the U.S. Geological Survey.

Table 1. A comparison of digestion methods

Sample	Tungsten found, $\mu g/g$			
	$K_2S_2O_7$ fusion	$HClO_4$–HF	*aqua regia*–HF	HNO_3–HF
GXR 1	200	200	200	177
GXR 2	2.0	1.2	1.2	2.1
GXR 3	12.0×10^3	12.0×10^3	12.0×10^3	11.9×10^3
GXR 4	20	28	16	27
GXR 5	0.4	2.8	0.4	1.2

Table 2. Replicate analyses of geochemical samples

Sample	Material	This work			Other values, $\mu g/g$	
		Range, $\mu g/g$	Mean, $\mu g/g$	R.S.D., %	Dithiol[10]	NAA[11]
GXR 1	Jasperoid	174–179	176	1.2	191	
GXR 2	Soil	2.1–2.2	2.1	2.6	2.5	1.8 ± 2
GXR 3	Spring deposit	$11.3–12.4 \times 10^3$	11.9×10^3	3.9	12.7×10^3	$10.8 \pm 0.6 \times 10^3$
GXR 4	Coppermill head	25.7–28.2	27.0	3.9	35.7	28 ± 5
GXR 5	Soil	1.2–1.3	1.3	4.3	1.6	
GXR 6	Soil	2.4–2.6	2.5	3.3	1.4	0.88 ± 18

sample reading is greater than 25 μg of tungsten, repeat the colour development and measurement with a smaller volume of the acid test solution.

RESULTS AND DISCUSSION

Sample decomposition

Five U.S. Geological Survey geochemical exploration reference samples[9] were digested by four different methods. The results are listed in Table 1.

Table 1 seems to indicate that all four methods work about equally well, though the perchloric/hydrofluoric acid and nitric/hydrofluoric acid methods do a better job on GXR 4 and 5. The nitric/hydrofluoric acid method was chosen because the evaporation is faster and does not require a special fume-hood.

Sensitivity

A 0.5-μg standard can be expected to give 0.038 absorbance, allowing detection of 0.5 μg in a 1-g sample, which is at or below the average crustal abundance of tungsten in rocks.

Precision and accuracy

Replicate analyses of the six U.S. Geological Survey geochemical exploration reference samples (Table 2) show fairly consistent and acceptably low relative standard deviations for the various sample types and tungsten levels, and give results in reasonably good agreement with values obtained by a similar colorimetric method[10] and by neutron-activation analysis (NAA).[11]

GXR 2 was roasted at 600° for 1 hr to drive off excess of organic material. GXR 4 was treated with potassium ferricyanide to precipitate copper (the sample contains about 0.7% copper).

Interference

Molybdenum interference was studied by spiking a set of tungsten-free samples with 10 μg of tungsten and increasing amounts of molybdenum from 0 to 5000 μg. The samples were then digested and the normal procedure was applied. The results indicated no interference by up to 200 μg of molybdenum and then gradual increase in signal until, with 1000 μg of molybdenum added, the normally sky-blue extract began to take on a greenish tinge indicative of the presence of the molybdenum dithiol complex, and the signal was high by 10%. The error increased smoothly with increasing molybdenum concentration, reaching 100% when 5000 μg of molybdenum had been added. The effects of several other often-mentioned interfering elements[2,6,8,12,13] were tested by adding 10, 100, and 1000-μg quantities of each to solutions containing 1 and 10 μg of tungsten. The elements tested were Bi, Co, Cu, Cr, Pb, Mn, Ni and V. Of these, only bismuth and copper showed any appreciable effect at

Table 3. Recovery of tungsten from spiked samples (average of triplicate analyses)

Sample	Present, μg	Added, μg	Found, μg	Recovery, %
GXR 1	170	200	350	90
GXR 2	1.8	1	2.8	100
GXR 3	12.5×10^3	5.0×10^3	17.4×10^3	98
GXR 4	28.4	15	43.8	102

the 1000-μg level, both causing a decrease in signal. Interference from copper can be avoided by precipitating the copper with 1 ml of 10% potassium ferricyanide solution before centrifuging the sample solution. Otherwise its tolerance level is about 200 ppm. Nearly 100% removal of copper is achieved with only about 7% loss of tungsten. Though not as often encountered in such high concentrations in geochemical samples, bismuth remains a problem. When it does cause a serious interference, complexing it with dithizone[13] may be necessary before the tungsten colour-development step.

REFERENCES

1. R. W. Leinz and D. J. Grimes, *J. Res. U.S. Geol. Survey*, 1978, **6**, 259.
2. B. Bagshaw and R. J. Truman, *Analyst*, 1947, **72**, 189.
3. P. G. Jeffery, *ibid.*, 1956, **81**, 104.
4. R. E. Stanton, *Australas. Inst. Min. Metall. Proc.*, 1970, **236**, 59.
5. K. M. Chan and J. P. Riley, *Anal. Chim. Acta*, 1967, **39**, 103.
6. K. Kawabuchi and R. Kuroda, *Talanta*, 1970, **17**, 67.
7. P. Aruscavage and E. Y. Campbell, *J. Res. U.S. Geol. Survey*, 1978, **6**, 697.
8. F. Quin and R. R. Brooks, *Anal. Chim. Acta*, 1972, **58**, 301.
9. G. H. Allcott and H. Q. Lakin, *U.S. Geol. Survey Open Rept.*, 1978, No. 78-163, p. 122.
10. S. Terashima, *Geostd. Newsl.*, 1980, **4**, 9.
11. E. S. Gladney, W. E. Gode, D. R. Porrin and C. E. Burne, *Los Alamos National Laboratories Rept.*, LA-8966-MS, 1980.
12. C. F. Bickford, W. S. Jones and J. S. Keene, *J. Am. Pharm. Assoc.*, 1948, **37**, 255.
13. S. H. Allen and M. B. Hamilton, *Anal. Chim. Acta*, 1952, **7**, 483.

Talanta, Vol. 30, No. 11, pp. 879–883, 1983
Printed in Great Britain.

0039-9140/83 $3.00 + 0.00

ANALYTICAL DATA

STRUCTURE–IONIZATION RELATIONSHIP OF TYROSINE-CONTAINING PEPTIDES

T. ISHIMITSU
Kyoto College of Pharmacy, Kyoto 607, Japan

H. SAKURAI
Faculty of Pharmaceutical Sciences, University of Tokushima, Tokushima 770, Japan

(*Received* 6 *May* 1983. *Accepted* 2 *June* 1983)

Summary—The acid–base chemistry of tyrosine-containing peptides such as enkephalin, tyrosylglycylglycine, tyrosylglycine and analogous peptides is described. For each peptide and tyrosine derivative, microscopic and macroscopic acid dissociation constants and the thermodynamic parameters for proton dissociations were determined from pH-titrations and ultraviolet absorption spectra. The relative concentrations of various ionic forms for the peptides were calculated from the microscopic constants. The concentration ratio, represented by the tautomeric equilibrium constant (K_t), showed a definite relationship to structure.

The role of structure as a determinant of the opiate activity of tyrosine-containing peptides has been recognized and reported in several investigations.[1–5] Study of the aqueous acid–base equilibria of the peptides seems likely to be of help in the elucidation of their mode of interaction with the opiate receptor.

It has been suggested[6] that determination of the microscopic proton-dissociation phenomena of compounds such as tyrosylglycylglycine and tyrosylglycine is very important for the understanding of which active molecular species may be involved in the biological functions of tyrosylglycylglycylphenylalanylmethionine (enkephalin). Enkephalin is the most important opiate peptide in the brain; it contains three functional groups (carboxy-, amino- and tyrosyl-) but its deprotonation has not been studied fully. For this reason, we have made a brief report on the structure–ionization relationships of enkephalin and related fragments in aqueous solution.[6]

In earlier papers[6–8] we suggested that determination of the microscopic proton dissociation constants (micro-constants) of a compound is extremely important for the understanding of the structure–ionization relationships of the compound. Recently, Jaureguiberry *et al.*[9] have reported a study of the conformational states of an enkephalin-related compound in different ionic conditions, by use of ^{15}N NMR spectroscopy. The micro-constants reported in that paper provided a better model for the biological action of tyrosyl residues in proteins.

In the present work, we studied the acid–base chemistry of various types of tyrosine-containing peptides in order to determine not only the structure–ionization properties of enkephalin in aqueous solution but also a possible proton-dissociation model for tyrosine-containing proteins. Both microscopic and macroscopic proton dissociation constants have been measured by means of potentiometric titrations and ultraviolet absorption spectra, and the species distribution has been calculated from the micro-constants.

EXPERIMENTAL

Materials

Enkephalin, tyrosylglycylglycine, tyrosylglycine, tyrosyltyrosine and *N*-acetyltyrosine were obtained from Sigma Chemical Co., glycyltyrosylglycine from Biochemical Co., glycylglycyltyrosine from ICN Pharmaceutical Co., tyrosine methyl ester, tyrosine ethyl ester and tyrosine amide from Nakarai Chemical Co., and glycyltyrosine from Wako Chemical Industries Ltd. The compounds were of analytical grade and used without further purification.

Absorption spectra and pH-titrations

The apparatus was as described previously.[7] The spectrum of each compound was measured at 25° (for $2 \times 10^{-4} M$ concentration). The titrations were done with a Radiometer TTT 60 Titrator and an ABU 12 Autoburette fitted with a 0.25-ml burette. The solution (10 ml containing 0.5 mmole of compound) was transferred to the temperature-controlled titration vessel. A slow stream of nitrogen was bubbled through the solution, which was stirred with a mechanically driven plastic stirrer. The pH-meter (Radiometer pHM64, G2040C glass electrode and K4040 reference electrode) was calibrated before each titration with buffers of pH 4.01 and 9.18 at 25°. An interval of 10 min was allowed for thermal equilibration before starting the titration. The compounds were titrated with carbonate-free 0.1*M* potassium hydroxide at temperatures of 1°, 15°, 25°, 35° and 45° (all ±0.1°). The ionic strength was adjusted to 0.1*M* with sodium perchlorate.

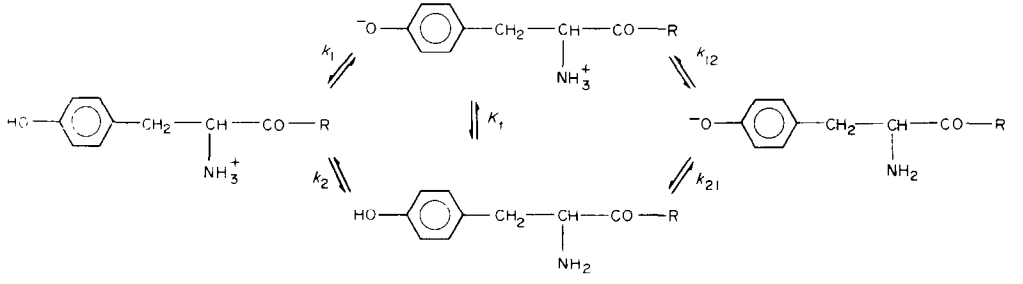

$$K_1 = k_1 + k_2 \quad (1)$$

$$K_2^{-1} = k_{12}^{-1} + k_{21}^{-1} \quad (2)$$

$$K_1 K_2 = k_1 k_{12} = k_2 k_{21} \quad (3)$$

$$K_t = \frac{k_2}{k_1} = \frac{k_{12}}{k_{21}} \quad (4)$$

Chart 1. Ionization equilibria of tyrosine-containing peptides.

Table 1. Proton dissociation constants of tyrosine-containing peptides*

	Titration				CTS method†		From micro-constants	
Compound	pK_{COOH}	pK_1	pK_2	pK_3	pK_2	pK_3	pK_1	pK_2
Enkephalin	3 68 ± 0.05	7 77 ± 0.03	9 89 ± 0.03		9 96 ± 0.08		7 61 ± 0.04	9.99 ± 0 06
Tyrosylglycylglycine	3 21 ± 0.03	7.75 ± 0.02	9.78 ± 0.06		9 92 ± 0.09		7 58 ± 0.05	10.07 ± 0 06
Glycyltyrosylglycine	3.10 ± 0 04	8.06 + 0.03	9.78 + 0 05		9.97 + 0 08		8 48 + 0.04	10.01 + 0.04
Glycylglycyltyrosine	3.18 ± 0.03	8.17 ± 0.07	9 75 ± 0 09		9.94 ± 0 07		8.33 ± 0.04	10 01 ± 0.05
Tyrosylglycine	3.51 ± 0.02	7.77 ± 0 04	10 04 ± 0.02		9 97 ± 0.07		7 89 ± 0.02	10.05 ± 0 04
Glycyltyrosine	3.24 ± 0.06	8.23 ± 0.04	10.55 ± 0.06		10 39 ± 0.04		8.36 ± 0 03	10.48 ± 0 03
Tyrosyltyrosine	2.62 ± 0.02	7 53 ± 0.03	9.89 ± 0 04	10 77 ± 0 05	9.85 ± 0 02	10 84 ± 0 05		
Tyrosine amide		7 60 ± 0 03	10.18 ± 0.02		10.13 ± 0.05		7.45 ± 0.04	10 12 ± 0.03
Tyrosine methyl ester		7.31 ± 0.03	9.92 ± 0.02		9.99 ± 0.04		7.23 ± 0 03	9 96 ± 0 04
Tyrosine ethyl ester		7.34 ± 0 02	9.91 ± 0.01		10.02 ± 0.03		7 32 ± 0 06	10.01 ± 0.01
N-Acetyltyrosine	2.83 ± 0.03		10.39 ± 0.04		10.43 ± 0 06			
N-Acetyltyrosine ethyl ester			9.99 ± 0.06		10.09 ± 0.05			
Tyrosine§	2 46 ± 0.02	9.01 ± 0.02	10.17 ± 0.02		10 05 ± 0.03		9 01 ± 0.03	10.19 ± 0.03

*$\mu = 0.1$ ($NaClO_4$). 25°.

†The pK_2 and pK_3 values, which correspond to proton dissociation from the phenolic groups, were determined by the CTS method.

§From Ishimitsu *et al*[7]

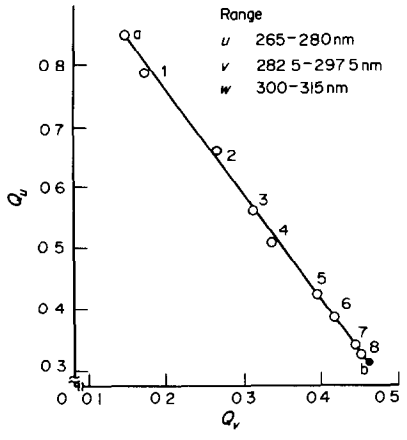

Fig. 1. Q_u–Q_v plot for enkephalin. pH values: a, 3.03; 1, 7.34; 2, 8.64; 3, 9.58; 4, 9.74; 5, 9.95; 6, 10.43; 7, 10.78; 8, 12.07; b, 12.48.

Determination of the proton-dissociation constants

The proton-dissociation constants of each compound were determined by three methods: (*a*) by complementary tristimulus colorimetry (CTS method);[10] (*b*) from the micro-constants described in the next paragraph;[7] (*c*) by the potentiometric method of Schwarzenbach.[11]

Determination of the micro-constants

The acid dissociation of the tyrosine-containing peptides is shown in Chart 1. The micro-constants were obtained as follows. From the Q_u–Q_v plot (Fig. 1), the mole fraction (q_{OH}) of singly dissociated phenolate anions was calculated for the region between *a* and *b* by use of the CTS method. The M_{OH} value defined by Edsall[12] is given by equation (5):

$$M_{OH} = \frac{[H^+]q_{OH}}{(1-q_{OH})} = \frac{k_1[H^+] + k_2k_{21}}{[H^+] + k_2} \quad (5)$$

which can be expressed as

$$k_1[H^+] - M_{OH}k_2 + k_2k_{21} - M_{OH}[H^+] = 0 \quad (6)$$

From these three values (k_1, k_2 and k_{21}), the remaining k_{12} and the proton dissociation constants, pK_1 and pK_2, were calculated from equations (1)–(3) (Chart 1).

Thermodynamic parameters

The values of the thermodynamic parameters were obtained in a manner similar to that reported earlier.[8] Plots of pK_i^T ($i = 1, 2$) against reciprocal of the absolute temperature were linear or slightly curved. From the empirical equations, the values of the free-energy (ΔG, kcal/mole), enthalpy (ΔH, kcal/mole) and entropy (ΔS, cal.mole^{-1}.deg^{-1}) changes for the proton dissociation were calculated.

RESULTS AND DISCUSSION

Proton-dissociation constants

The values obtained for the proton-dissociation constants of enkephalin and related compounds are listed in Table 1. The proton-dissociation constant for the carboxyl group is denoted by pK_{COOH}. Since the Q_u–Q_v plot, obtained from the change in absorbance caused by proton dissociation of the phenol group, was linear (Fig. 1), the proton-dissocation constants of the phenol group of tyrosine-containing peptides were calculated both by the CTS method and from the micro-constants. The values obtained by the three methods agree well. From the data given in Table 1, it can be deduced that (1) the value of pK_1 depends on the sequence of tyrosine residues in the di- and tripeptide, (2) the pK_2 values for the tripeptides are not as high as for the dipeptide, indicating the absence of intramolecular hydrogen-bonding between phenol and *C*-terminal carboxylate groups, and (3) the pK_3 value for tyrosyltyrosine is not much higher than the value expected for deprotonation of the second phenol group of catechol,[8] probably because there is no intramolecular hydrogen bonding after deprotonation of the first phenol group.

Thermodynamic parameters

Thermodynamic parameters obtained for the deprotonation of the phenol and ammonium groups of the compounds are given in Table 2. Figure 2 shows the plots of ΔH *vs.* $T\Delta S$ for the ammonium group (ΔH_1 *vs.* $T\Delta S_1$) and for the first and second phenol groups (ΔH_2 *vs.* $T\Delta S_2$, ΔH_3 *vs.* $T\Delta S_3$). The parameters for the phenol group of the peptides correlate well with the thermodynamic parameters of monophenol derivatives, indicating that deprotonation of the first phenol group of tyrosine-containing peptides proceeds like that of the first phenol group of 3,4-dihydroxyphenylpropionic acid and 3,4-dihy-

Table 2. Thermodynamic parameters for ionization of tyrosine-containing peptides at 25°C

Compound	ΔG_1	ΔG_2	ΔG_3	ΔH_1	ΔH_2	ΔH_3	ΔS_1	ΔS_2	ΔS_3
	kcal/mole			*kcal/mole*			*cal.mole^{-1}.deg^{-1}*		
Enkephalin	10.6	13 5		7.5	5 0		−10.4	−28.5	
Tyrosylglycylglycine	10.5	13.3		7.5	5.4		−10.3	−26.5	
Glycyltyrosylglycine	11.0	13.3		8.3	6.7		−9.0	−22.3	
Glycylglycyltyrosine	11.1	13.3		7.9	4.6		−10.9	−29.1	
Tyrosylglycine	10.6	13 7		7.9	5.0		−9.0	−29.3	
Glycyltyrosine	11.2	14.4		8 7	5.3		−8.4	−30.4	
Tyrosyltyrosine	10 3	13.5	14.7	7.9	5.0	6.0	−7.9	−28.9	−27.6
Tyrosine amide	10.4	13.9		8.1	3.2		−7.7	−36.5	
Tyrosine methyl ester	10.0	13.5		7 9	4.7		−6.9	−29.7	
Tyrosine ethyl ester	10.0	13 5		8 3	3.6		−5.7	−33.8	
N-Acetyltyrosine		14.2			3 7			−34.9	
N-Acetyltyrosine ethyl ester		13.6			4.2			−31.8	
Tyrosine*	12,3	13.9		10.0	5.4		−7.8	−28.5	

*From Ishimitsu *et al.*[8]

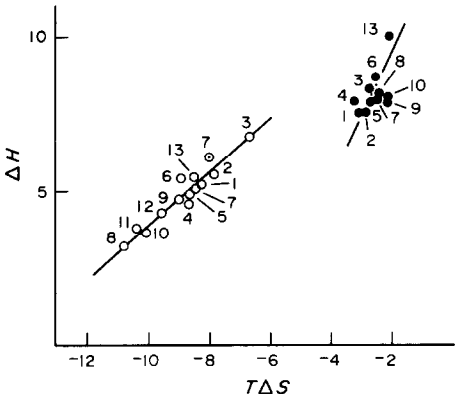

Fig. 2. Relationship between ΔH and $T\Delta S$ for tyrosine-containing peptides. 1, Enkephalin; 2, tyrosylglycylglycine; 3, glycyltyrosylglycine; 4, glycylglycyltyrosine; 5, tyrosylglycine; 6, glycyltyrosine; 7, tyrosyltyrosine; 8, tyrosine amide; 9, tyrosine methyl ester; 10, tyrosine ethyl ester; 11, *N*-acetyltyrosine, 12, *N*-acetyltyrosine ethyl ester; 13, tyrosine.

● First ionization (corresponds to pK_1)
○ First phenol ionization (corresponds to pK_2)
⊙ Second phenol ionization (corresponds to pK_3)

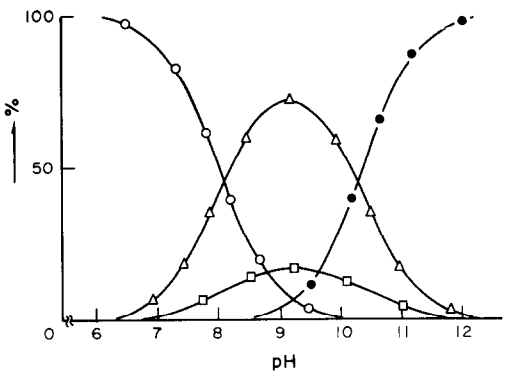

Fig. 3. Relative concentrations of various ionic forms of methionine enkephalin.

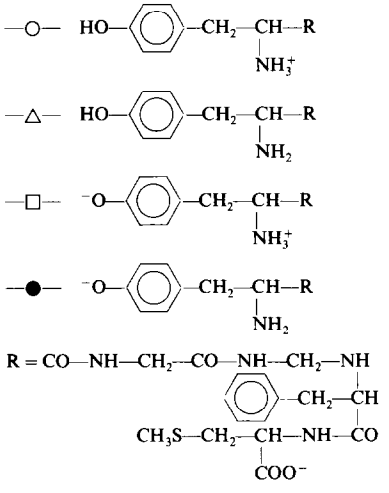

droxyphenylalanine (DOPA).[8] The parameters for the second phenol group of tyrosyltyrosine gave a similar correlation (Fig. 1), probably because of the absence of intramolecular hydrogen bonding after deprotonation of the first phenol group.

Micro-constants

Two pathways are possible for proton dissociation from enkephalin and tyrosine peptides, as shown in Chart 1. The micro-constants of the peptides (at 25°) are given in Table 3. The data also include the ratio of the number of molecules present in the phenolate–ammonium form to the number in the phenol–amino form. This ratio gives the tautomeric constant (K_t). By use of the micro-constants, the relative concentrations of the various ionic forms of the compounds were calculated as a function of pH, and the results for enkephalin and glycyltyrosylglycine are shown in Figs. 3 and 4, respectively. In *N*-terminal tyrosine-containing peptides such as enkephalin, tyrosylglycylglycine and tyrosylglycine, about 10–20% of the first ionization occurs by way of the phenolate–ammonium form between pH 8 and 10, similarly to that of tyrosine and its derivatives,[7] while for the other three peptides (glycyltyrosylglycine, glycylglycyltyrosine and glycyltyrosine) the phenolate–ammonium form contributes as little as 2–5% in the same pH range. The K_t-values and Figs. 3 and 4 show that the concentration of phenolate–ammonium form is greater in the *N*-

Table 3. Microscopic acid dissociation constants and tautomeric constants of tyrosine-containing peptides

Compound	pk_1	pk_2	pk_{12}	pk_{21}	K_t*
Enkephaline	8.61 ± 0.02	7 99 ± 0.03	9.63 ± 0.04	10.30 ± 0.04	4 2
Tyrosylglycylglycine	8.18 ± 0.03	7.71 ± 0.02	9.47 ± 0.03	10.00 ± 0.03	3 0
Glycyltyrosylglycine	9.80 ± 0.03	8.49 ± 0.03	8.85 ± 0.04	9.98 ± 0.04	20.4
Glycylglycyltyrosine	9.55 ± 0.02	8.36 ± 0.04	8 79 ± 0.04	10.01 ± 0.03	15.5
Tyrosylglycine	8.42 ± 0.03	8.04 ± 0.01	9 51 ± 0.03	9.90 ± 0.02	2.4
Glycyltyrosine	9.32 ± 0.02	8.41 ± 0.02	9 52 ± 0 04	10.43 ± 0.04	8 1
Tyrosine amide	8.58 ± 0.04	7 50 ± 0.02	8.85 ± 0.04	10.20 ± 0.02	12.0
Tyrosine methyl ester	9.15 ± 0.02	7.44 ± 0 03	8 52 ± 0 02	10 13 ± 0 03	51 3
Tyrosine ethyl ester	9.18 ± 0.01	7 37 ± 0 02	8.20 ± 0 03	10.08 ± 0.01	64 6
Tyrosine†	9.56 ± 0.03	9.16 ± 0.04	9.66 ± 0.04	10.04 ± 0 02	2.5

*K_t value calculated from k_2/k_1.
†From Ishimitsu *et al*[7]

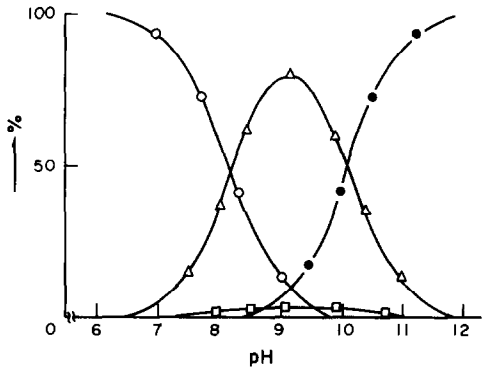

Fig. 4. Relative concentrations of various ionic forms of glycyltyrosylglycine.

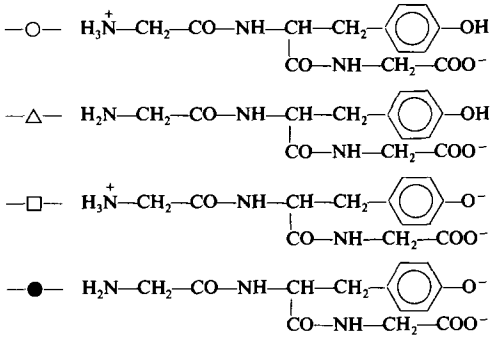

terminal tyrosine-containing peptides than in other types of peptides. Thus, alteration of a partial drug structure, especially the sequence of the tyrosine residues, may change the balance between the phenolate–ammonium and phenol–amino forms. The results presented here may be important not only for the understanding of the biological activity of enkephalin but also for characterizing the sequence of tyrosine residues in other peptides and proteins.

REFERENCES

1. H. H. Büscher, R. C. Hill, D. Romer, F. Cardinaux, A. Closse, D. Hauser and J. Pless, *Nature*, 1976, **261**, 423.
2. J. K. Change, B. T. W. Fong, A. Pert and B. Pert, *Life Sci.*, 1976, **18**, 1473.
3. B. M. Cox, A. Goldstein and C. H. Li, *Proc. Natl. Acad. Sci. USA*, 1976, **73**, 1821.
4. A. R. Day, M. Lujan, W. L. Dewey, L. S. Harris, J. A. Radding and R. J. Freer, *Res. Commun. Chem. Pathol. Pharmacol.*, 1976, **14**, 579.
5. B. A. Mogan, C. F. C. Smith, A. A. Waterfield, J. Hughes and H. W. Kosterlitz, *J. Pharm. Pharmac.*, 1976, **28**, 660.
6. T. Ishimitsu and H. Sakurai, *Intern. J. Pharm.*, 1982, **12**, 271.
7. T. Ishimitsu, S. Hirose and H. Sakurai, *Chem. Pharm. Bull.*, 1976, **24**, 3195.
8. *Idem*, *Talanta*, 1977, **24**, 555.
9. C. G. Jaureguiberry, J. Baudet, D. Florentin and B. P. Roques, *FEBS Lett.*, 1980, **115**, 315.
10. H. Flaschka, *Talanta*, 1960, **7**, 90.
11. G. Schwarzenbach, *Helv. Chim. Acta*, 1950, **33**, 947.
12. J. T. Edsall, R. B. Martin and B. R. Hollingworth, *Proc. Natl. Acad. Sci. USA*, 1958, **44**, 505.

Talanta, Vol. 30, No 11, pp 885–886, 1983
Printed in Great Britain.

0039-9140/83 $3.00 + 0.00

ANNOTATIONS

A COMMENT ON THE SIMULTANEOUS DETERMINATION OF GLASS ELECTRODE PARAMETERS AND PROTONATION CONSTANTS

H. K. J. POWELL and M. C. TAYLOR
Department of Chemistry, University of Canterbury, Christchurch, New Zealand

(*Received* 8 *November* 1982. *Accepted* 13 *May* 1983)

Summary—Recently published methods for calibration of the glass electrode as an $[H^+]$-probe are examined. Problems arising from the pH-dependence of the reference electrode liquid-junction potential are noted.

The determination of equilibrium quotients for protonation reactions and for metal–ligand equilibria involving anions of weak acids as ligands, requires values of the equilibrium hydrogen-ion concentration in solution, $[H^+]$. May *et al.*[1] recently described two direct methods for determining $[H^+]$ in solution, which did not require reference to conventional standard buffer solutions (*e.g.*, NBS buffers). The first method involved direct calibration of the glass electrode–reference electrode pair against a family of solutions of known $[H^+]$ generated from titration of a strong acid with a strong base. Least-squares values of E_{const} and S in equation (1) were derived from data in the pH ranges 2.3–2.9 and 10.8–11.3.

$$E_{cell} = E_{const} + S\log[H^+]. \quad (1)$$

This calibration was considered valid in the pH range 2.3–11.3.

A second method involved simultaneous determination of E_{const}, S, and the n protonation quotients β_1----β_n from a single direct titration of a weak acid with a strong base, followed by non-linear least-squares analysis of equation (1) and the mass-balance equations for total acid and total base (ligand), using all data points.

These two methods were considered superior to these previously published which utilize titration-generated buffers such as acetic acid–sodium acetate (pH 3.8–5.0) and ethylenediamine–ethylenediamine dihydrochloride (pH 6.5–10.3) for which concentration quotients are known accurately from measurements in cells without liquid junction or with matched liquid junctions.[2] However, the method described by May *et al.*[1] appears to overlook one fundamental problem associated with pH measurements in cells involving a liquid junction (*e.g.*, with a calomel reference electrode). It is well documented[3] that the liquid-junction potential is measurably dependent on pH at pH <4.0 and pH >9.2. This is readily established for the acid region by measurement of the pH of NBS standard buffers [for which pH(S) has been determined in cells without liquid junction]. Results from our measurements on NBS buffer solutions (pH 1.68–10.01) in cells with and without liquid junction illustrate this point (Table 1). A similar trend of negative deviations (relative to electrode response to buffers of intermediate pH) occurs at pH >9.2, but the limited number of standard buffers for this region permits a less well defined analysis.

Thus in any calibration based on measurement of pH for solutions of known $[H^+]$, the measured emf will incorporate a liquid-junction term which is (approximately) constant for pH 4.0–9.2 but becomes increasingly negative outside this range. A calibration interpolated from data at pH 2.3–2.9 and pH 10.8–11.3 will introduce an error (of *ca.* 0.03 pH) into all data subsequently collected between pH 4 and 9.2 (see Table 1). This situation will also arise in the second method of calibration when titration data outside the pH 4.0–9.2 range are used. (May *et al.*[1] reported an electrode calibration and β_i values based on titration data for glycine, pH 1.8–11.1 but gave no information to indicate that the liquid-junction potential for their electrode system was constant in that range.)

The magnitude of such errors is illustrated by calibration data for solutions of known $[H^+]$, with or without correction of the measured pH (pH_m) for variation in liquid-junction potential. With the electrode system described in Table 1 we obtained the following calibration relationships, $pH_m = Mp[H^+] + C$, for $I = 0.10M$ (potassium chloride).

Table 1. Measured pH values for standard buffers

NBS buffer*	pH (S)	pH (measured) values: Cell with liquid junction†	pH (measured) values: Cell without liquid junction§
0.05*m* Tetroxalate	1.679	1.639 ± 0.006 (15)‡	1.687 ± 0.006 (2)
0.01*m* Tetroxalate	2.157	2.123 ± 0.003 (2)	—
Hydrogen tartrate	3.557	3.550 ± 0.003 (15)	3.559 ± 0.006 (2)
Hydrogen phthalate	4.005	4.005 ± 0.004 (15)	4.005 ± 0.006 (2)
1:1 Phosphate	6.863	6.868 ± 0.006 (20)	6.868 ± 0.006 (2)
1:3.5 Phosphate	7.415	7.417 ± 0.005 (3)	—
Borax	9.183	9.188 ± 0.008 (19)	—
Carbonate/bicarbonate	10.014	9.989 ± 0.008 (10)	10.019 ± 0.006 (2)
Calcium hydroxide	12.454	12.438 ± 0.010 (7)	—

*Prepared as in reference 3.
†Beckman E-2 glass electrode (type 39004) and frit-junction calomel electrode (39071).
‡Mean ± standard deviation for number of measurements shown in parentheses.
§Ag/AgCl reference electrode in buffer solution spiked with 0.001*M* potassium chloride.

(*i*) Solutions of HCl (pH 1.7–3.0) and KOH (pH 10.9–11.9): $pH_m = 1.002p[H^+] + 0.052$.

(*ii*) The same solutions as for (*i*) with correction for liquid-junction potential variation (using data from Table 1): $pH_m = 1.001p[H^+] + 0.079$.

The relationship in (*ii*) was consistent with that derived from phthalate buffers at pH 3.0–5.5 (corrected at low pH);[4] similar results were obtained at $I = 0.04$, 0.15 and 0.20*M* (potassium chloride).

Conclusion

In cells with a liquid junction, it is *not* possible to make an accurate determination of $p[H^+]$ values in the range pH <4.0 and pH >9.2 from pH (measured) vs $p[H^+]$ calibrations in the intermediate pH range (or *vice versa*) unless allowance is made for the pH-dependence of the liquid-junction potential at low and high pH.

If the pH (measured) *vs.* $p[H^+]$ calibration is for a wide pH range but is based on data at low and high pH only, then for reliable work all pH (measured) values (for standard and unknown solutions) *must* be corrected according to the pattern of liquid-junction potentials established from measurements on standard buffers (as in Table 1).

This approach gives a linear calibration [although even without this correction a linear calibration may be achieved from a simple least-squares fit as used by May *et al.* with equation (1)]. Interpolation from the intermediate pH range is not justified, however, unless co-linearity with $[H^+]$ standards in this pH range is also established, *e.g.*, by use of titration-generated buffers formed from a weak acid and its conjugate base,[1,2] as described in *(ii)* above.

We recommend the more comprehensive calibration involving a *co-linearity* check, especially because of the limited number of standard buffers available for liquid-junction potential corrections at high pH.

REFERENCES

1. P. M. May, D. R. Williams, P. W. Linder and R. G. Torrington, *Talanta*, 1982, **29**, 249.
2. G. R. Hedwig and H. K. J. Powell, *Anal. Chem.*, 1971, **43**, 1206.
3. R. G. Bates, *Determination of pH; Theory and Practice*, 2nd Ed., Wiley–Interscience, New York, 1973.
4. J. A. Kennedy, H. K. J. Powell and M. C. Taylor, *Anal. Chim. Acta*, 1983, **147**, 351.

Talanta, Vol 30, No. 11, pp. 887–893, 1983
Printed in Great Britain

0039-9140/83 $3.00 + 0.00
Pergamon Press Ltd

REFINEMENT OF STRUCTURES PREVIOUSLY PROPOSED FOR GUM ARABIC AND OTHER *ACACIA* GUM EXUDATES

C. A. STREET
Products Research Department, Rowntree-Mackintosh, York, England

D. M. W. ANDERSON
Chemistry Department, The University of Edinburgh, Edinburgh, Scotland

(*Received* 21 *March* 1983. *Accepted* 6 *June* 1983)

Summary—In the light of advances in structural gum-chemistry, the analytical data available from earlier analytical and structural studies of gum arabic (*Acacia senegal* Willd.), and of the gum exudates from *Acacia laeta*, *A. campylacantha* and *A. seyal*, have been re-interpreted. The structures originally suggested were based on random arbitrary assignments of substituent sugars without an attempt to establish regular structures. Modelling considerations and recalculations show that the data can also be interpreted in terms of more ordered structures. These are consistent with almost all of the available experimental data and give a much clearer insight into the nature and extent of the structural differences shown by the two *Acacia* gums of commercial importance, *Acacia senegal* (gum arabic, gum hashab) and *Acacia seyal* (gum talha).

Gum arabic, defined[1] as the "dried exudation from *Acacia senegal* (L.) Willd. or the related species of *Acacia*", has been assessed toxicologically as a safe foodstuffs additive, to which the "without limit" category of Acceptable Daily Intake (ADI) was assigned[2] in 1982. Apart from its widespread uses as a foodstuffs additive, gum arabic is an important ingredient in confectionery, providing the possibility of creating different textures and other specialized effects. Trends towards automated processing require allowances for variations in the properties of natural ingredients to be preprogrammed; to allow this, a sound understanding of the structure of gum arabic and other *Acacia* gums, and of the reasons why they function uniquely in different applications, is required. The best possible structural information will also be useful in helping to define the article approved for use in foodstuffs. The complex sequence of enzymatic processes clearly involved in the biosynthesis of gum arabic suggests that its structure may contain a certain degree of order, a feature disregarded in previous structural interpretations.[3]

The analytical data published[3–6] for some *Acacia* gums have therefore been re-interpreted structurally with the aid of models, taking into account the following advances published in the past 7 years. Churms and co-workers have presented evidence[7–9] that *Acacia* gums belonging to Bentham's[10] series *Phyllodineae* and *Botryocephalae* have structures based on regular repeating subunits; there is similar evidence for galactans[11,12] and gums from *Prosopis* spp.[13] For gum arabic, it has been shown[14] that all the rhamnose residues are attached to glucuronic acid and that some galactose units, to which glucuronic acid groups are attached, can also carry small numbers of arabinofuranose units.

At this early stage of reappraisal of all the experimental data available on gum structures, attention has been restricted to those *Acacia* gums, within Bentham's[10] series *Vulgares* and *Gummiferae*, that are of greatest commercial importance. The series *Vulgares* includes gum arabic (*Acacia senegal*[3] syn. *verek*) and its close relatives *A. laeta*[4] and *A. polyacantha*[6] (syn. *campylacantha*). The series *Gummiferae* includes *Acacia seyal*[5] (gum talha). The large difference in the specific rotation of aqueous solutions of *A. seyal* gum, $[\alpha]_D$ *ca.* $+60°$, and *A. senegal* gum, $[\alpha]_D$ *ca.* $-30°$, indicates that their structures probably differ more significantly than is indicated by the structures proposed earlier.[3,5]

The modelling approach

In a previous study[3] of gum arabic it was realized that the structural fragment proposed was only one of many possible interpretations. The fragment was built up in a retrospective modelling approach[15] in which a randomly branched structure was arbitrarily assigned[3] to the essential core (*i.e.*, the branched galactan "polysaccharide E") of the complex highly-branched globular gum arabic molecules. It was recognized[3] that polysaccharide E was not a simple linear β-1,3-galactan, and that there was no evidence for the "main chain" or "backbone" model in terms of which the structure had hitherto been discussed.

In this reappraisal of the data, the main change is to assign to polysaccharide E a structure which maximizes the regularity of structure that can subsequently be assigned to its precursor, polysaccharide

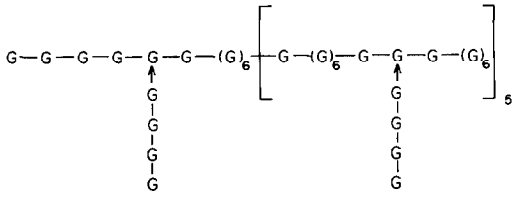

Fig. 1. *Acacia senegal* gum: polysaccharide E comprising 116 galactose residues. [ ] defines segment considered in Fig. 2–6. For key see end of paper.

D, in terms of all the other analytical data available[3] for D and E, *e.g.*, yields, molecular weights, sequential Smith-degradation data, sugar ratios *etc.* As before, this stepwise reconstruction of structures for precursors is repeated until eventually a possible structure for the whole gum, more regular than that suggested previously,[3] is attained. Other data available from autohydrolysis and other hydrolytic degradations help to allow comparisons to be made between the experimental values and those calculated from postulated structures at each stage of the model-building process.

The same process can be applied to the gums from *A. laeta*,[4] *A. seyal*[5] and *A. campylacantha*[6] (syn. *polyacantha*); for these gums some analytical data additional to those available for *A. senegal* gum aid the reconstructional modelling.

DISCUSSION

Recalculation of the gel filtration data[3] for polysaccharide E of *A. senegal* gum indicates a statistical-average molecular weight of about 1.9×10^4, about 10% higher than the single-peak value (1.7×10^4) originally reported. The amount of formic acid released on periodate oxidation of polysaccharide E to give polysaccharide F, and of F to give the final product, polysaccharide G, indicates that F and G have 6 or 7 non-reducing end-groups. G also gave some 6-*O*-β-D-galactopyranosyl galactose on partial hydrolysis, indicating some branching. These observations suggest that polysaccharide E comprises 116 galactose units, predominantly linked β-1,3- but with 6 branches connected to the chain by β-1,6-links. Symmetry suggests the structure in Fig. 1, as the evidence indicates the branches to be at least 3 units long.

Polysaccharide E was methylated and methanolysed, and the methyl sugars were determined.[3] Calculated values for the proposed structure (Fig. 1) are compared with the experimental observations[3] in Table 1. The agreement is well within experimental limits (*i.e.*, $\pm 10\%$ error).

Table 2 shows the degrees of polymerization for the precursors of polysaccharide E, deduced from the different pieces of experimental evidence.[3] In each case there is good agreement between two of the estimates, and good reasons (see Table 2) for rejecting the third, enabling a value to be chosen from which the structural changes can be deduced. Corresponding possible structures are shown in Figs. 2–6.

There is the possibility[16,17] that over-oxidation during degradation of polysaccharide A may result from incomplete removal of acidic fragments during hydrolysis in the first Smith-degradation of the whole gum. The presence of a high proportion of ruptured

Table 1. Comparison of observed and predicted methanolysis products for *A. senegal* polysaccharide E

Methyl sugar	Predicted from Fig. 1	Observed[3]
2,3,4,6-tetramethylgalactose	1 01	1
2,4,6-trimethylgalactose	15	12
2,3,4-trimethylgalactose	—	trace
2,6-dimethylgalactose	—	3*
2,4-dimethylgalactose	0.87	1

*This is probably 2,4,6-trimethylgalactose under-methylated at position 4.

Table 2. Degree of polymerization (D.P.) and sugar composition of *A. senegal* gum and its Smith-degradation products (values calculated on the basis of the value selected for the preceding polysaccharide)

	Polysaccharide					
	E	D	C	B	A	Whole gum
D.P. from formic acid released	—	128	185	275	2000*	945
D.P. from yield of polysaccharide	—	182†	220†	294†	517	751‡
D.P. from gel filtration	116	141	187	280	527	975
Selected value of D.P.	116	135	185	279	518	942
Relative numbers of sugar residues						
Galactose	116	135	179	249	340	397
Arabinose	—	—	6	30	160	292§
Glucuronic acid	—	—	—	—	18	123
4-*O*-Methylglucuronic acid	—	—	—	—	—	12
Rhamnose	—	—	—	—	—	118

*Value high, as result of over-oxidation.
†Values high, as discussed in text.
‡Value requires less galactose than present in polysaccharide A.
§Some arabinose residues (probably about 50) present as pyranose end-groups; remainder in furanose form.

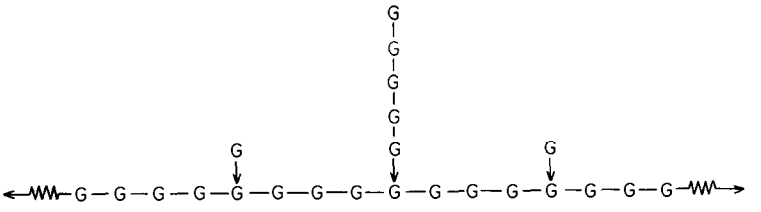

Fig. 2. *Acacia senegal* gum: polysaccharide D.

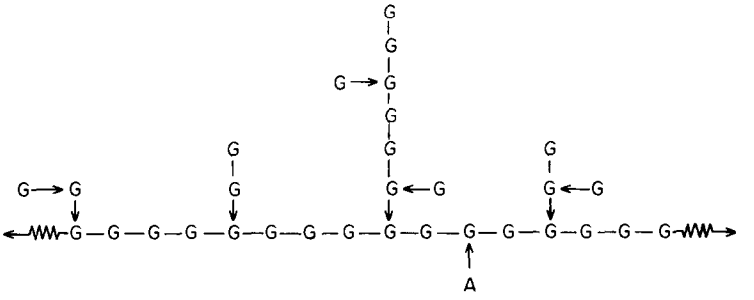

Fig. 3. *Acacia senegal* gum: polysaccharide C.

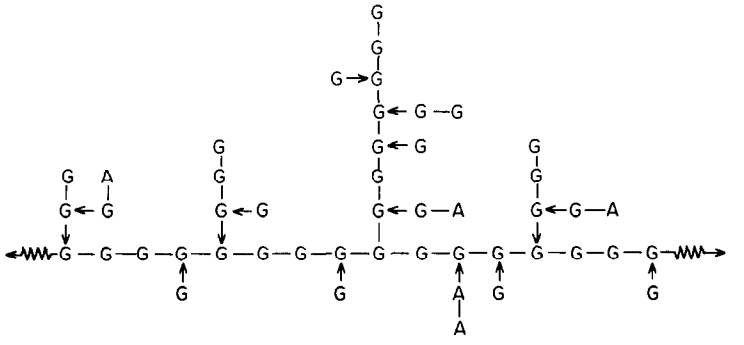

Fig. 4. *Acacia senegal* gum: polysaccharide B.

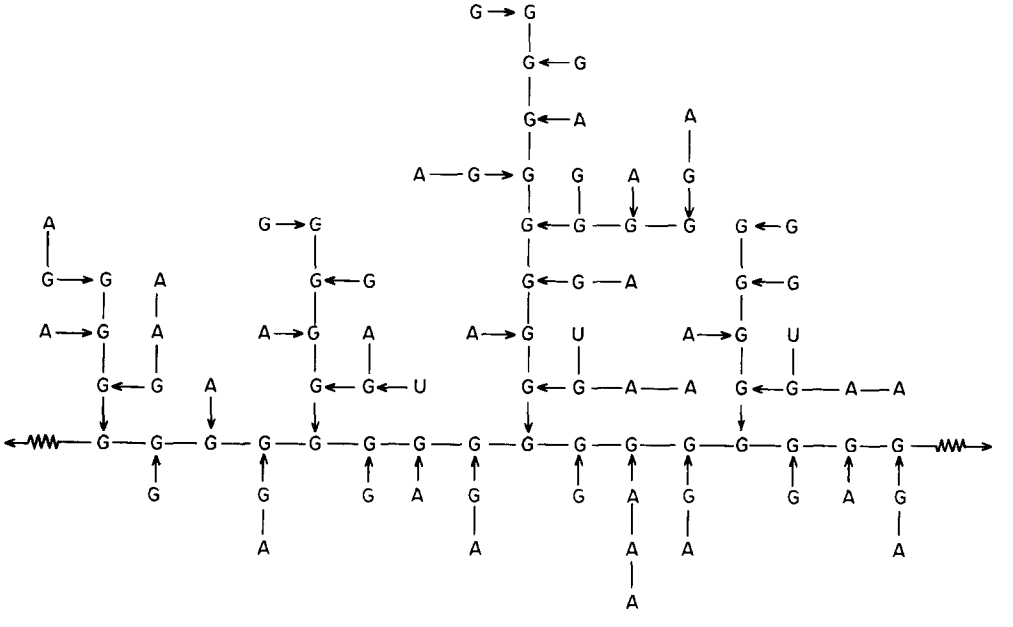

Fig. 5. *Acacia senegal* gum: polysaccharide A.

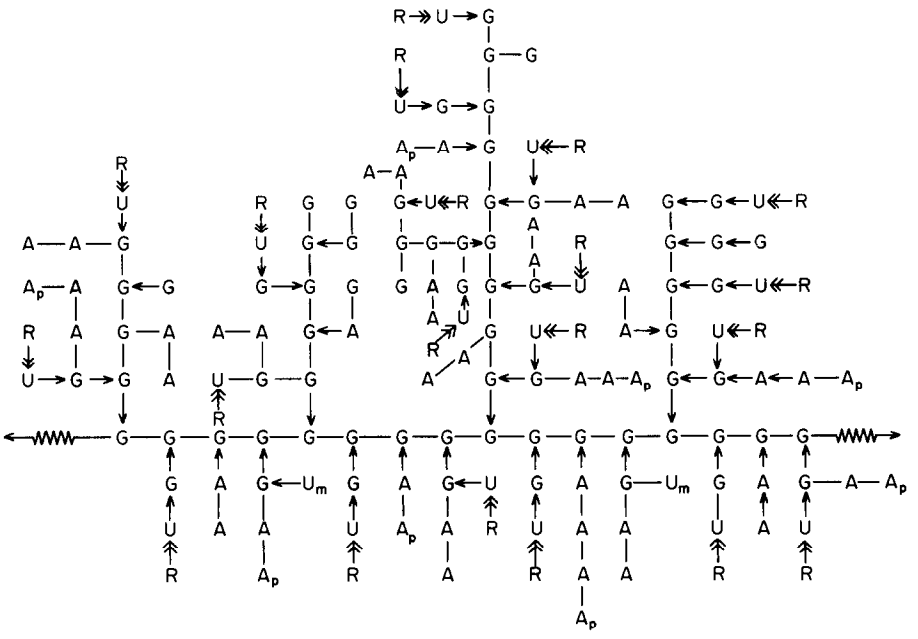

Fig. 6. *Acacia senegal* gum.

uronic acid residues in polysaccharide A would account for the otherwise theoretically anomalous yield in addition to the over-production of titratable acidity in the next degradation. Also the data[6] for *A. campylacantha* gum show that the high value for formic acid is not accompanied by a correspondingly high value for the amount of periodate reduced. Over-oxidation could also explain this anomaly. A similar but less pronounced effect is observed for *A. laeta* gum.[4]

Figure 7 shows a plot of polysaccharide yield, expressed as a percentage of the theoretical value calculated from the proposed structures, against the average molecular weights found by gel filtration[3] after dialysis. This plot is interpreted as indicating that the dialysis membrane is permeable by the fragments of smaller size. This factor invalidates any deductions based on gel-filtration data when gums from the *Gummiferae* series are considered; in these, polysaccharide A is reduced to one tenth or less of its original size in one degradation step, through cleavage of the main chain; this results in very low yields for all subsequent degradation products.

Methylation of *Acacia senegal* gum followed by methanolysis produces a range of methyl sugars which have been examined[3] by GLC. 2,4-Dimethylgalactose predominates, as required by the proposed structure. The original chromatogram revealed a high proportion of galactose end-groups and a deficiency of uronic acid relative to the initial analysis requirements; this may have resulted from incomplete separation of 2,3,4,6-tetramethylgalactose and 2,3,4-trimethylglucuronic acid, which appear as adjacent peaks in other chromatograms. The chromatogram also indicated the presence of some

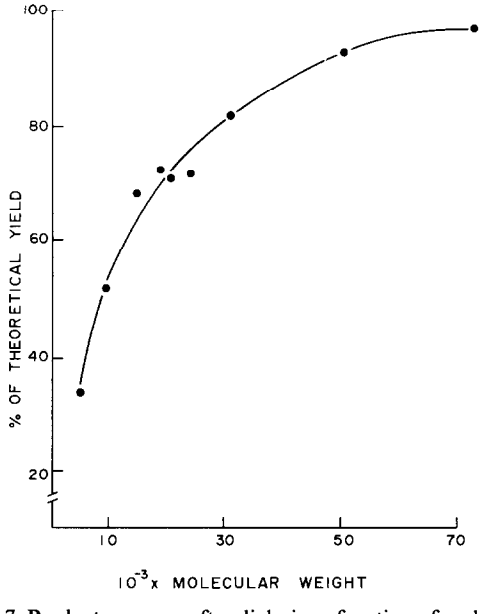

Fig. 7. Product recovery after dialysis as function of molecular weight.

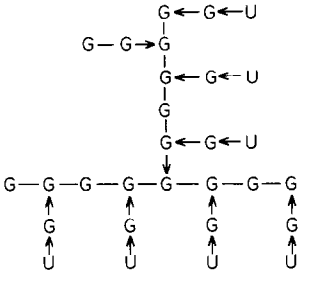

Fig. 8. *Acacia senegal* degraded gum A.

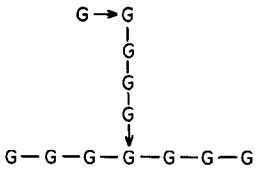

Fig. 9. *Acacia senegal* degraded gum B.

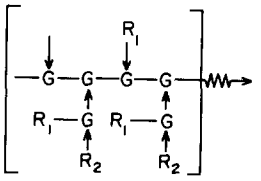

Fig. 10. Type 1 repeat unit: R_1 is an arabinose chain of varying length; R_2 may be H, U, U_m or U«—R; at the end of a branch, the unit may be incomplete.

2,3,4-trimethylarabinose but its quantity could not be determined because of incomplete resolution from 2,3,4-trimethylrhamnose.

Dividing the proposed gum structure (Fig. 6) into 3 fragments (each of which is about an eighteenth of the whole molecule) and stripping off rhamnose and arabinose gives structures typified by Fig. 8, with a molecular weight of about 5.4×10^3 (which may be compared with the 4.8×10^3 observed[3]). Some smaller fragments lost during dialysis may account for the apparent loss of galactose and glucuronic acid. Smith-degradation of the structure in Fig. 8 would give that shown in Fig. 9. The predicted and observed[3] data for these polysaccharides, degraded Gums A and B, are compared in Table 3. The agreement is within reasonable experimental error.

Applying the same approach to *A. campylacantha* gum in terms of the data available[6] gives Table 4. The structure proposed for polysaccharide 5 has only one branch on the terminal reducing group and is less branched than is suggested by the methanolysis products[6] of the methylated gum. However, as the structure is built up, good agreement between prediction and observation[6] is obtained for polysaccharides 4, 3 and 2, as shown in Table 5. Good agreement for the methylated sugars is also obtained for polysaccharide 1, although the size of the molecule is in doubt. As explained above, the degree of polymerization (D.P.) predicted from formic acid release is expected to be high as a result of incomplete removal of acidic fragments in the previous stage. The D.P. is also incompatible with the amount of periodate reduced and could only be explained structurally by very long chains of 1,6-linked galactose with some arabinose branches. Such a structure is not compatible with the methylation data. The practical yields of the 2nd–5th degradation products are expected to be only 60–70% of theoretical because of losses during dialysis and hence are much closer to the values deduced from the amount of periodate reduced. As this is not consistent with the molecular weight obtained by gel filtration it appears that some cleavage of the molecule occurs, probably at a 1,6-linkage. This may involve either division into two approximately equal parts, or removal of several side-chains of molecular weight about 5×10^3. The

Table 3. Comparison of observed and predicted methanolysis products for *A. senegal* degraded gums A and B

	Degraded gum A		Degraded gum B	
Methyl sugar	Predicted (Fig. 8)	Observed[3]	Predicted (Fig. 9)	Observed[3]
2,3,4,6-tetramethylgalactose	2	++	2	++
2,4,6-trimethylgalactose	4	++	8	++++
2,3,4-trimethylgalactose	8	+++	1	trace
2,4-dimethylgalactose	8	++++	1	<+
2,3,4-trimethylglucuronic acid	7	+++	—	—

Table 4. Degree of polymerization (D.P.) and sugar composition of *A campylacantha* gum and its Smith-degradation products

	Polysaccharide					
	5	4	3	2	1	Whole gum
D.P. from yield of polysaccharide	—	81*	90*	180*	455*	505
D.P. from gel filtration	52	60	73	110	429†	818†
D.P. from formic acid released	—	110	85	122	497‡	<483
D.P. from periodate used	—	70	78	136	250	553
Selected value of D.P.	55	63	81	134	214	432
Relative numbers of sugar residues						
Galactose	55	63	81	130	161	220
Arabinose	—	—	—	4	47	144§
Glucuronic acid	—	—	—	—	6	30
4-*O*-Methylglucuronic acid	—	—	—	—	—	8
Rhamnose	—	—	—	—	—	30

*Yield expected to be less than 100% of theoretical, hence these values are higher.
†These values suggest cleavage of the molecule during Smith-degradation.
‡This value inconsistent with the estimate based on periodate reduced and hence probably high.
§As some of these residues are in the pyranose form, the estimated degree of polymerization from formic acid assay is high.

Table 5. Comparison of predicted and observed methanolysis products from *A. campylacantha* gum and its Smith-degradation products

Polysaccharide	5		4		3		2		1*		Whole gum†
Methyl sugar	A	B	A	B	A	B	A	B	A	B	A
2,3,4,6-tetramethylgalactose	2	2	8	9	15	15	41	36	17	16	23
2,4,6-trimethylgalactose	52	20	47	38	49	45	38	40	66	65	4
2,3,4-trimethylgalactose	—	tr	—	tr	3	3	8	8	8	8	33
2,4-dimethylgalactose	1	tr	7	6	14	12	43	38	64	43	150
2,3,5-trimethylarabinose	—	—	—	—	—	tr	4	4	43	33	100‡
2,5-dimethylarabinose	—	—	—	—	—	—	—	tr	4	4	47
2,3,4-trimethylglucuronic acid	—	—	—	—	—	—	—	—	6	5	30
2,3-dimethylglucuronic acid	—	—	—	—	—	—	—	—	—	—	8
2,3,4-trimethylrhamnose	—	—	—	—	—	—	—	—	—	—	30

A, Predicted from postulated model (Fig. 10).
B, Reported.[6]
*The molecule is probably twice the size indicated.
†The molecule is probably four times the size indicated.
‡17 of these will be 2,3,4-trimethylarabinose

Table 6. Degree of polymerization (D.P.) and sugar composition of *A. laeta* gum and its Smith-degradation products

	Polysaccharide								
	8	7	6	5	4	3	2	1*	Whole gum†
D.P. from periodate used	—	65	74	82	94	126	198	450	709
D.P from formic acid released	—	64	73	81	94	116	189	378	568
D.P. from yield of polysaccharide	—	77‡	82‡	94‡	111‡	142‡	200‡	358‡	561
D.P. from gel filtration	58	76	79	—	—	—	—	—	—
Selected value of D P.	60	65	73	81	92	120	190	336	573
Relative numbers of sugar residues									
Galactose	60	65	73	81	89	114	170	218	246
Arabinose	—	—	—	—	3	6	20	107	194§
Glucuronic acid	—	—	—	—	—	—	—	11	59
4-*O*-Methylglucuronic acid	—	—	—	—	—	—	—	—	15
Rhamnose	—	—	—	—	—	—	—	—	59

*Gel filtration suggests twice the size indicated.
†Probably 3 or more times the size indicated.
‡Values all expected to be high as yield less than 100%.
§About 30 of these are in form of pyranose end-groups.

second possibility would result in low yield after dialysis, as required by the experimental observations. A further cleavage of the molecule appears to occur during the first degradation of the whole gum.

The data[4] for *A. laeta* gum lead to Table 6; the molecular weights observed for polysaccharides 1 and 6 require the assumption of cleavage at some stage, as for *A. campylacantha* gum. Some of the molecular weight data derived by gel filtration may be inaccurate.

From these deductions it can be suggested that repeat units of the form indicated in Figure 10 are involved in the structure of *Acacia* gums of the *Vulgares* series. While *A. senegal* gum appears to consist entirely of these Type 1 units with few, if any, R_2 groups consisting of hydrogen, the data for *A. laeta* gum and *A. campylacantha* gum can best be explained in terms of the insertion of an occasional Type 2 unit of the form shown in Fig. 11. One or two such Type 2 units per molecule would be adequate, with at least some R_1 chains not more than one arabinose residue in length. *A. campylacantha* gum would have a slightly higher proportion of Type 2 blocks although *n* is probably small in both cases. *A. campylacantha* gum also has a significant number of hydrogen atoms acting as R_2 groups in the Type 1 units.

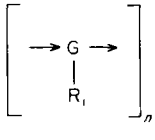

Fig. 11. Type 2 repeat unit; R_1 is an arabinose chain as in Fig. 10.

There is no substantive evidence for the Type 2 units, but this may result from the ease with which arabinose is removed during hydrolysis, the difficulty of detecting very small amounts of 1,6-linked galactotriose, and the possibility that 1,6-linked galactobiose may arise from hydrolysis of the Type 1 units. There are, however, significant amounts of 1,6-linked galactotriose in the partial hydrolysis products of gums from the *Gummiferae* series and their degradation products.[5,18,19]

Deducing the structures of the gums from the *Gummiferae* series (*e.g., Acacia seyal*) from available data[5] is extremely difficult as the gum molecules are degraded into ten or more fragments when polysaccharide 2 is prepared from polysaccharide 1 and,

in some cases, when polysaccharide 3 is prepared from polysaccharide 2. The molecular weights and product yields available do not give reliable estimates of the degradations because of large losses during dialysis. In addition, more galactose and/or arabinose than is accounted for by the Smith-degradation data appears to be eliminated from the structure at some stage. It is suggested that the structure of *A. seyal* gum consists of small blocks of two or three modified Type 1 repeat units (Fig. 10) separated by significant blocks of Type 2 repeat units.

The revised structure proposed for the gum[3] from *A. senegal* (Fig. 6) is considerably more regular than any previously proposed and similar regular structures can be proposed for the gums from *A. polyacantha*,[6] *A. laeta*[4] and *A. seyal*.[5] They are consistent with almost all of the experimental data available, yet do not differ drastically from the basic structures suggested in the earlier studies.

CONCLUSIONS

More regular structures can be assigned to these gums if the regularity assigned to the ultimate branched galactan core of the molecules is maximized. Such structures reveal more clearly the extent of the basic differences between *A. senegal* and *A. seyal* and give much clearer explanations than available hitherto for the considerable differences in performance shown by these two gums in commercial applications.

Should more precise structural detail be required it would be necessary to obtain improved analytical data, possibly by HPLC, and to reduce the inaccuracies arising from dialysis and other losses in clean-up stages, derivative formation *etc.* In particular, more detailed evidence concerning galactose–arabinose linkages would be required to augment the information available[18,19] concerning galactose linked to position 3 in arabinose; in gums of the *Vulgares* series, only one such residue per molecule is possible unless arabinose occurs in the main galactan framework. This possibility has not been detected in gums of the *Gummiferae* series, where excess of arabinose is present. Even if better analytical data could be obtained, however, it would still be necessary to carry out modelling calculations and computer simulations before significantly more detailed structures could be assigned with confidence; the basic uncertainties arising from over-oxidation, under-methylation, and sugar degradation at various stages of the structural analysis would probably continue to be limiting factors in the elucidation of such complex structures.

KEY TO FIGURES

G = D-galactopyranose; A = L-arabinofuranose; A_p = L-arabinopyranose; U = D-glucuronic acid; U_m = D-4-*O*-methylglucuronic acid; R = L-rhamnose; glycosidic bonds: —— = β-1,3-; → = β-1,6-; ↠ = α-1,4-.

REFERENCES

1. Joint Expert Committee on Food Additives, *Specifications for Identity and Purity*, Food and Nutrition Paper No. 25, FAO, Rome, 1982.
2. Joint FAO/WHO Expert Committee on Food Additives, 26 Session, Rome, April 1982.
3. D. M. W. Anderson, E. L. Hirst and J. F. Stoddart, *J. Chem. Soc. C*, 1966, 1959.
4. D. M. W. Anderson, I. C. M. Dea and R. N. Smith, *Carbohyd. Res.*, 1968, **7**, 320.
5. D. M. W. Anderson, I. C. M. Dea and E. L. Hirst, *ibid.*, 1968, **8**, 460.
6. D. M. W. Anderson and A. C. Munro, *ibid.*, 1970, **12**, 9.
7. S. C. Churms and A. M. Stephen, *ibid.*, 1975, **45**, 291.
8. S. C. Churms, E. H. Merrifield and A. M. Stephen, *ibid.*, 1977, **55**, 3.
9. *Idem*, *ibid.*, 1978, **63**, 337.
10. G. Bentham, *Trans. Linn. Soc. London*, 1875, **30**, 335.
11. S. C. Churms, E. H. Merrifield and A. M. Stephen, *Carbohyd. Res.*, 1978, **64**, C1.
12. S. C. Churms, A. M. Stephen and I. R. Siddiqui, *ibid.*, 1981, **94**, 119.
13. S. C. Churms, E. H. Merrifield and A. M. Stephen, *ibid.*, 1981, **90**, 261.
14. G. O. Aspinall and K-G. Rosell, *ibid.*, 1977, **57**, C23; *Can. J. Chem.*, 1978, **56**, 685.
15. D. M. W. Anderson, *D.Sc. Thesis*, Edinburgh University, 1968.
16. H. O. Bouveng, *Acta Chem. Scand.*, 1965, **19**, 953.
17. G. O. Aspinall, V. B. Bhavanandan and T. B. Christensen, *J. Chem. Soc.*, 1965, 2667.
18. D. M. W. Anderson and I. C. M. Dea, *Carbohyd. Res.*, 1968, **7**, 109.
19. D. M. W. Anderson and G. M. Cree, *ibid.*, 1968, **6**, 385.

Talanta, Vol. 30, No 11, pp. 894–898, 1983
Printed in Great Britain

0039-9140/83 $3.00 + 0.00

THE DENSITY OF 4-AMINOPYRIDINE, VOIDS IN CRYSTALS, AND PRECISION WEIGHING

HARVEY DIEHL and DONALD L. BIGGS
Departments of Chemistry and Earth Sciences, Iowa State University, Ames, IA 50011, U.S.A.

(*Received* 28 *February* 1983. *Accepted* 15 *April* 1983)

Summary—Erratic results in the determination of the density of 4-aminopyridine have been traced to numerous tubular cavities, some traversing the entire length of the long, thin crystals formed by sublimation. The effect of the variability in density, as it affects the correction for the buoyancy of air in a high-precision weighing, is discussed with particular reference to the value of the Faraday.

In the use of 4-aminopyridine as the primary standard chemical for a high-precision determination[1-3] of the value of the Faraday, a value for the density of the 4-aminopyridine was necessary for the calculation of the buoyancy correction for the weight of 4-aminopyridine used. Considerable uncertainty was experienced in the determination of the density of 4-aminopyridine during the work. This has now been traced to numerous tubular cavities in the crystals obtained by sublimation. The 4-aminopyridine had been sublimed in a stream of nitrogen to avoid inclusions of solvents, the bane of handling chemicals in high-precision work.

The correction for buoyancy (C) is made by using the formula

$$M_{o,vac} = M_{o,air}\left[\frac{\{1-(d_a/d_w)\}}{\{1-(d_a/d_o)\}}\right] \quad (1)$$

in which $M_{o,vac}$ and $M_{o,air}$ are the mass in vacuum and the mass observed when weighing in air, respectively, d_a is the density of air, d_o the density of the object being weighed and d_w the density of the weights. The correction (C) is obtained by rearrangement of equation (1):

$$C = M_{o,vac} - M_{o,air} = M_{o,air}\left[\frac{\{(d_w-d_a)/d_w\}}{\{(d_o-d_a)/d_o\}} - 1\right] \quad (2)$$

Differentiation of equation (2) with respect to the density of the object yields:

$$\frac{\partial(C)}{\partial(d_o)} = M_{o,air}\left[\frac{d_w-d_a}{d_w}\right] \times \left[\frac{1}{(d_o-d_a)} - \frac{d_o}{(d_o-d_a)^2}\right] \quad (3)$$

Evaluation of this differential coefficient for 1.000000 g of 4-aminopyridine weighed in air of density $d_a = 0.00115$ g/ml, with stainless-steel weights of density $d_w = 7.89$ g/ml, gives

$$\frac{\partial(C)}{\partial(d_o)} = -0.000716 \text{ ml} \quad (4)$$

The permissible uncertainty in C is the same as that in the measurement of the mass, and for an uncertainty of 1 ppm, the goal of present work on the Faraday, on a 1.000000-g sample of 4-aminopyridine, $\Delta C = 1\ \mu$g for which equation (4) yields a permissible uncertainty in the density of 4-aminopyridine of

$$\Delta d_o = 0.00140 \text{ g/ml} \quad (5)$$

The determination of density to 1 part per thousand (ppt) would appear to be straightforward and simple but in actuality proved rather difficult. We list our successive misadventures with this problem so that others may know what to look for, given a similar problem.

1. *Pycnometric method using mineral oil.* Density found, 1.2695 g/ml. Later measurements with mineral oil gave very unsatisfactory results; not only is the temperature coefficient high, but the liquid creeps, covers the outside walls of the pycnometer, and creates problems in cleaning and temperature adjustment.

2. *Pycnometric method using xylene saturated with 4-aminopyridine.* Density found, 1.2633 g/ml (preliminary; see 8, below). The results were badly scattered and proved much lower than the X-ray value and it was suspected that air remained trapped in the interstices of the bundles of the long needle- or lath-like crystals of the 4-aminopyridine in spite of shaking, and stirring with a platinum wire.

3. *X-Ray value.* Density found, 1.2710 g/ml. This value was obtained by Professor Jon C. Clardy, then at Iowa State University, from a determination of the crystal structure, by a second refinement analysis. The uncertainty was estimated to be less than 0.001 g/ml.

4. *Flotation.* Experiments were made to determine the density by a flotation method using concentrated solutions of sodium perchlorate. Not only was temperature control difficult and the procedure tiresome to carry out with the accuracy needed, but the results were ambiguous. As the densities of the solutions approached 1.26 g/ml, the crystals of 4-aminopyridine both rose and fell in the sodium perchlorate solutions.

5. *Pycnometric method using xylene saturated with 4-aminopyridine, and application of a vacuum.* Density found, 1.2682 g/ml. The 4-aminopyridine, after weighing, was covered with xylene and then subjected to vacuum, and then the pycnometer was filled and weighed. Streams of fine bubbles were observed to rise from the mass of crystals, even on second and third evacuations. See Experimental for details, and Table 1, section 5. Although this value was used in our second, "Additional Results" paper,[2] a nagging uncertainty remained as to its validity. This led to a more thorough examination of the sublimed crystals.

6. *Examination under the microscope.* Unlike crystals of primary standard potassium dichromate, which have occasional cavities containing mother liquor,[4] and unlike trishydroxymethylaminomethane, which has many cavities containing mother liquor,[5] the very long, thin crystals of sublimed 4-aminopyridine are pierced by numerous tubular cavities, frequently running the entire length of the crystal and usually open at the ends, Fig. 1. Moreover, it was observed that the immersion oil entered the tubular cavities, forming menisci, Fig. 1.

It is apparent that the streams of bubbles observed during the evacuations in the xylene–vacuum method were of air or nitrogen pulled from the tubular cavities. Presumably, on the release of the vacuum, xylene entered the cavities. The variation in the number and distribution of these air-filled cavities

Fig. 1. Photomicrograph of crystals of 4-aminopyridine obtained by sublimation. 100x. Polarized analysed light. Note tubular cavities, 25 × 1000 μm in size. A meniscus is present in some of the cavities, the immersion oil (commercial refractive-index oil, ND, 1.5150) used for the microscopic examination, having entered them.

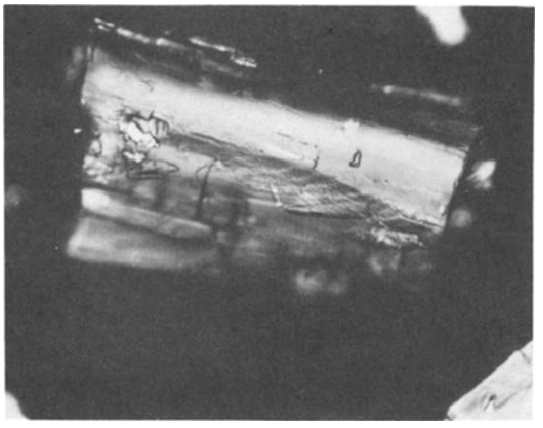

Fig. 2. Photomicrograph of 4-aminopyridine obtained by melting the sublimed crystals and allowing the melt to cool and solidify. 100x. Polarized analysed light. Crystal is 462 × 50 μm in size. The focal plane is 44 μm below the surface. The white spots are surface effects; dark areas are voids.

accounts for the behaviour when the crystals were immersed in sodium perchlorate solutions (some crystals sinking, some rising). It accounts also for the great variation in the density as measured by the pycnometer–xylene method (2, above),

A possible way around this problem is to melt the crystals of 4-aminopyridine, crush the solidified melt, determine the density, and use the melted, solidified and crushed material as the primary standard; the melting would do away with the cavities and the density should then approach the X-ray value. What was actually found (7, below) was a value much lower than the X-ray value. Examination under the microscope of the material so obtained showed the presence of numerous voids, Fig. 2.

7. *Density of 4-aminopyridine obtained by melting and cooling; pycnometric method using xylene saturated with 4-aminopyridine.* See Experimental, and Table 1, section 4. Found, 1.2597 g/ml.

8. *Repetition of pycnometer-xylene procedure to establish standard deviation.* Of the various procedures tried, the pycnometric procedure using xylene saturated with 4-aminopyridine and without a vacuum being applied appeared to approach most nearly the conditions prevailing when the sublimed crystals were weighed in air for an analysis. This procedure was repeated, with care, to learn just how great the variation might be (12 determinations; see Experimental, and Table 1, section 3). Found 1.2607 g/ml.

EXPERIMENTAL

Sublimation of 4-aminopyridine

The purification of 4-aminopyridine and the sublimation under nitrogen are described in our first paper[1] on the Faraday.

Fusion of 4-aminopyridine

Thirty-five g of sublimed crystals of 4-aminopyridine were melted under nitrogen in a glass tube immersed in a bath of mineral oil held at 165–170°. After the individual crystals

had fallen into the hot, liquid 4-aminopyridine, microbubbles continued to rise from the crystals until the whole was completely melted. After the melt had cooled and solidified, the glass tube was broken away and the fused mass of 4-aminopyridine lightly crushed.

Density measurements

Xylene was saturated with 4-aminopyridine by stirring mechanically overnight at 25° and then filtered through a fine fritted-glass filter. This liquid, and also demineralized and doubly-distilled water, was stored in glass in a constant-temperature bath of water held at 25.3 ± 0.1°.

The pycnometers used were 25-ml glass bottles with a single ground-in capillary plug. The capillary was left open at the top. [Pycnometers with built-in thermometers (ground-glass joints) and capillary plugs gave less reproducible results.] The pycnometers were cleaned with acetone, dried with a slight stream of air flowing to flush out acetone vapour, and reweighed after each operation; the weights generally returned to within 0.2 mg of the initial weight. After filling, with water or xylene, or 4-aminopyridine plus xylene, the pycnometers were lowered to the bottom of tall-form metal cans immersed in the water-bath. Thus the pycnometers did not make contact directly with the water in the constant-temperature bath. After 15–30 min, the pycnometers were withdrawn and the capillaries filled by inserting xylene saturated with 4-aminopyridine through a microsyringe with a fine needle pushed into the capillary, and then weighed immediately. The pycnometers were handled with tongs or with fingers and absorbent, lint-free tissue. Three pycnometers were used as a batch, each step being applied to all three together. Several precautions were necessary in the handling. After weighing of the pycnometers plus 4-aminopyridine, the pycnometers were placed in the constant-temperature bath for 30 min before being filled with xylene; the pycnometers plus contents, and the xylene, were thus at the same temperature and the subsequent temperature equilibration was arrived at quickly, and the amount of xylene needed in the final filling with the microsyringe was minimal. Evaporation of xylene from the open ends of the capillary plugs was sufficiently rapid to require that the temperature equilibration and weighing be made within about 30 min after filling.

The density was measured for crystals of 4-aminopyridine formed by sublimation and for 4-aminopyridine melted and solidified. The results are given in Table 1, sections 3 and 4.

In the modified, "xylene–vacuum" procedure, the weighed pcynometers containing the crystals of 4-aminopyridine were partially filled with xylene saturated with 4-aminopyridine and the pycnometers were placed in a vacuum desiccator. The pressure was reduced to 0.5 mmHg. Very small bubbles rose from the crystals. The vacuum was continued until the xylene just began to boil. The pycnometers were then filled with xylene solution and weighed. The capillary plugs of the pycnometers were then removed and each pycnometer and its contents again subjected to vacuum and the pycnometers again weighed and filled and weighed. This was repeated twice more. Even in the final evacuation, streams of microbubbles emerged from the mass of crystals. The results are given in Table 1, section 5.

The solubility of 4-aminopyridine in xylene was determined by extracting a weighed sample (56.3085 g) of the saturated solution with a large excess of standard hydrochloric acid with mechanical intermixing, separating the layers, and back-titrating the excess of acid. Found, 0.118% w/w of 4-aminopyridine.

DISCUSSION

For making the buoyancy correction, the X-ray value for the density of 4-aminopyridine is certainly not apposite because it applies only to a microscopic area of perfect crystal structure. The pycnometric methods are applied to masses of the size used in weighings for analysis and the heart of the matter lies in what is present in the voids, both during a weighing in air and during a pycnometric measurement involving a transfer liquid.

The relative standard deviations in the preliminary phases of the pycnometric measurements (0.36 ppt

Table 1. Density of 4-aminopyridine by the pycnometric method ($\bar{x}$ = average; n = number of observations; σ = standard deviation; δ = relative standard deviation; r = range; temperature 25.3 ± 0.1° throughout)

Preliminary measurements	
1. Volume of pycnometers*,	No. 38 $\bar{x}$ = 25.1627 ml; n = 4; σ = 0.0127 ml; δ = 0.51 ppt
	No. 75 $\bar{x}$ = 25.1461 ml; n = 4; σ = 0.0032 ml; δ = 0.13 ppt
	No. 82 $\bar{x}$ = 25.1140 ml; n = 4; σ = 0.0109 ml; δ = 0.43 ppt
	Average relative standard deviation: 0.36 ppt
2. Density of xylene saturated with 4-aminopyridine	
$\bar{x}$ = 0.86048 g/ml; n = 12†; σ = 0.00019 g/ml; δ = 0.22 ppt	
Density of 4-aminopyridine	
3. Crystals formed by sublimation	
x_1–x_{12}, g/ml:	1.2594, 1.2725, 1.2630, 1.2614,
	1.2644, 1.2562, 1.2396, 1.2604,
	1.2591, 1.2636, 1.2579, 1.2715
$\bar{x}$ = 1.2607 g/ml; n = 12; σ = 0.00831 g/ml; δ = 6.6 ppt; r = 0.0328 g/ml	
4. Material obtained by melting and solidifying	
x_1–x_{10}, g/ml:	1.2624, 1.2604, 1.2590, 1.2496,
	1.2595, 1.2600, 1.2792, 1.2466,
	1.2632, 1.2570
$\bar{x}$ = 1.2597 g/ml; n = 10; σ = 0.00869 g/ml; δ = 6.9 ppt; r = 0.0296 g/ml	
5. Crystals obtained by sublimation, xylene–vacuum procedure§	
x_1–x_8, g/ml:	1.2708, 1.2644, 1.2668, 1.2684
	1.2653, 1.2700, 1.2729, 1.2669
$\bar{x}$ = 1.2682 g/ml; n = 8; σ = 0.00290 g/ml; δ = 2.3 ppt; r = 0.0085 g/ml	

*By weighing filled with water.
†Four determinations in each of three pycnometers.
§Data from W. F. Koch; temperature 24 ± 0.5°.

for the determination of volume; 0.22 ppt for the density of xylene saturated with 4-aminopyridine) indicates the inherent precision of the procedure. Thus the large standard deviation of the values obtained for the density of 4-aminopyridine is real, and a true indication that the material is far from uniform. This non-uniformity is confirmed by examination with the microscope, Fig. 1. The voids are scattered randomly throughout the crystals. Presumably, because the crystals were formed in an atmosphere of nitrogen at atmospheric pressure and only slightly above room temperature, the closed voids contain nitrogen at essentially atmospheric pressure. The open-ended voids would permit later exchange with air, and presumably the gas content would also be at atmospheric pressure. During the pycnometric measurements, the xylene was probably slowly displacing the air in the voids, inasmuch as bubbles were observed to rise occasionally during the work. In the vacuum procedure, of course, the entrance of the xylene was more or less complete and the density found was higher than that determined with no application of vacuum.

What is really surprising is that voids are present in the material obtained by allowing the melted material to solidify, Fig. 2. This material consists of many quite large crystals and the voids are within individual crystals. Presumably, at the time of formation, these voids were filled with liquid 4-aminopyridine or with 4-aminopyridine vapour at the vapour pressure of molten 4-aminopyridine and later at the vapour pressure at room temperature; *i.e.*, at room temperature, these voids (being sealed) are essentially vacua, although solid 4-aminopyridine must have some vapour pressure inasmuch as it has a faint odour [to humans, and probably to birds (see *Chem. Abstr.*, 1967, **66**, 114905s for use as a bird repellent)]. Many of the voids would be exposed, of course, during the light crushing needed before transfer to the pycnometers.

Quite surprisingly, however, essentially the same density was obtained for the melted and solidified material as for the sublimed crystals, and moreover, the standard deviations and the ranges (about 4 standard deviations) were about the same for the two sets of results, Table 1, sections 3 and 4.

Of the three pycnometric values, that obtained with xylene saturated with sublimed 4-aminopyridine crystals (no vacuum) appeared most pertinent to the weighing problem and the measurement was repeated a sufficient number of times to establish fairly well the standard deviation and the range, Table 1, section 3. Two consequences follow from these findings, one general, the other related to the existing value for the Faraday.

Limitation on the validity of 4-aminopyridine as a primary chemical

With the standard deviation in the pycnometer–xylene method, Table 1, section 3, taken as a measure of the uncertainty in the density of the sublimed crystals of 4-aminopyridine, $\Delta d_o = 0.00831$ g/ml (6.59 ppt), equation (4) yields

$$\Delta C = (-0.000716)(0.00831) = -0.0000060\,g \quad (6)$$

Alternatively, taking the range, Table 1, section 3, as the worst possible case, $\Delta d_o = 0.0329$ g/ml, and equation (4) yields

$$\Delta d_o = -0.0000236\,\text{g} \quad (7)$$

These ΔC values represent, respectively, uncertainties of 6 ppm [at the 70% confidence level (± 1 standard deviation)] and 24 ppm [95% confidence level (± 2 standard deviations)] in the measurement of mass and also in the value for the Faraday.

Thus, for determining the Faraday to 1 ppm, 4-aminopyridine falls short of requirements and the disconcerting conclusion is that 4-aminopyridine, with the present techniques of weighing, simply cannot be used as the primary chemical for a determination of the value of the Faraday to better than 6, or perhaps 10, ppm error. Improving the precision of physical measurements in general, begins to be really difficult at the 1 in 10^5 level. For 4-aminopyridine, this density limitation appears at this very level, and comes from a surprising direction indeed.

The most highly precise measurement of density ever made was that of elemental silicon, by Deslattes *et al.*,[6] made on zone-refined silicon, presumably on a single crystal. Could 4-aminopyridine be grown in a single crystal? That is doubtful; our attempts to zone-refine 4-aminopyridine have always failed because the glass tubes invariably shattered from internal strains after the liquified 4-aminopyridine had emerged from the heated zone and solidified; probably polymorphs are present in the solid phase in the neighbourhood of the melting point and phase changes occur with cooling and time, with accompanying changes in volume.

Correction to the existing value for the Faraday

In the evaluation of the Faraday with 4-aminopyridine,[1,2] the final result reported[2] was $F = 96486.57$ 1972 NBS coulombs per gram-equivalent weight, the correction for buoyancy having been made by use of a density of 1.2682 g/ml. In view of the knowledge advanced above, the pycnometer–xylene (no vacuum) value for the crystals, 1.2607 g/ml, appears more appropriate, inasmuch as during the pycnometric measurements with xylene the cavities were not filled with xylene, or were filling only slowly, and thus the situation resembled more closely the conditions prevailing during weighing of the sublimed crystals for analysis. Recalculation with a change in the density from 1.2682 to 1.2607 g/ml changes the value for the Faraday to

$$F = 96486.05 \text{ 1972 NBS coulombs per gram-equivalent weight.} \quad (8)$$

The uncertainty assigned to the measurement of mass in our second, "Additional Results" paper[2] was 4 ppm (measurements at I.S.U.) and 1 ppm (measurements at N.B.S.). In view of the findings reported above, a more realistic figure [Equation (6)] is 7 ppm (70% confidence level). Combining this with the assessments of the other systematic and random uncertainties by the root sum of squares method yields a new uncertainty of 7.5 ppm for the value in equation (8).

REFERENCES

1. W. F. Koch, W. C. Hoyle and H. Diehl, *Talanta*, 1975, **22,** 717.
2. W. F. Koch and H. Diehl, *ibid.*, 1976, **23,** 509.
3. H. Diehl, *Anal. Chem.*, 1979, **51,** 318A.
4. J. Knoeck and H. Diehl, *Talanta*, 1969, **16,** 191.
5. W. F. Koch, D. L. Biggs and H. Diehl, *ibid.*, 1975, **22,** 637.
6. R. D. Deslattes, A. Henins, H. A. Bowman, R. M. Schoonover, C. L. Carroll, I. L. Barnes, L. A. Machlan, L. J. Moore and W. R. Shields, *Phys. Rev. Letters*, 1974, **33,** 463.

Talanta, Vol. 30, No. 11, pp.899-900, 1983
Pergamon Press Ltd. Printed in Great Britain

LETTER TO THE EDITOR

SIMULTANEOUS DETERMINATION OF GLASS ELECTRODE PARAMETERS AND PROTONATION CONSTANTS

SIR,

The comments of Powell and Taylor[1] on our procedure for calibrating the glass electrode as a hydrogen-ion concentration probe[2] suggest they have misread our paper in several places. For example, far from considering that calibrations obtained from titrations of strong acid with strong base are "valid in the pH range 2.3-11.3", we emphasised the undesirability of extrapolating from either of the $-\log[H^+]$ ranges 2.3-2.9 or 10.8-11.3 into the intermediate pH region. Nor did we claim our approach to be superior to one in which free hydrogen-ion concentrations are calculated from accurately known concentration quotients; indeed, we noted that "Very precise calibrations can be made in this way" provided that the necessary constants are available.

More fundamentally, Powell and Taylor do not seem to appreciate the profound difficulties which are encountered whenever standard buffers are used to calibrate the glass electrode for the determination of formation constants. They have consequently misjudged the relative importance of the various errors involved. The main point of their remarks, that the liquid-junction potential depends on hydrogen-ion concentration, is, as they say, well documented in the literature: the data shown in their Table 2 are in accord with those of many other investigators. However, it is incorrect of them to suggest we have overlooked this problem, since our paper makes several references to it. What they surely mean to do is to query our stated assumption that, for formation constant determinations (at the present state of the art), it can be neglected.

To justify such criticism, they must demonstrate not only that the effect on the formation constants really is significant, but also that it introduces greater error than their alternative procedure. They fail to do either.

Whilst it is difficult to quantify the error arising from a neglect of liquid-junction potentials, its magnitude in terms of e.m.f. can be estimated in a variety of ways. Calculations based on Henderson's equation[3] for the changes in liquid-junction potential that occur over either of the $-\log[H^+]$ ranges 2.3-2.9 and 10.8-11.3 (with respect to a saturated potassium chloride salt bridge) suggest that the error is less than 0.1 mV. A similar conclusion can be drawn from the plots over this pH region obtained from titrations of strong acid with a strong base. They are remarkably linear, as evidenced by a random distribution of residuals, and they have Nernstian slopes (within the limits of experimental error in the acid and base concentrations, 0.1%).

In contrast, the maximum error introduced by calibration with buffers probably lies in the range 2-8 mV, although it too cannot be determined exactly. Judging from the standard deviations shown by Powell and Taylor in their Table 1, this maximum error has a random component of about 1 mV arising out of the practical difficulty in reproducing the junction potential at all. There is, of course, also the systematic change in liquid-junction potential due to differences in composition between buffer and test solution which, under ideal circumstances, may amount to several millivolts.[3] In practice, even greater errors are probably generated by the transfer of reference electrodes between solutions of different electrolytes, as vividly exposed by Brezinski's recent investigation.[4]

Finally, it is relevant to note that most of the formation constants that have been determined potentiometrically over the past decade have been refined by means of computer programs which take no account of changes in liquid-junction potential (e.g., MINIQUAD[5]). A new computer program is currently being developed at UWIST which, amongst other things, will deal with this effect.[6] We are finding that, except for titrations which begin with unusually acidic solutions, errors arising from other sources (such as typical changes in ionic strength) are more important. It may therefore be concluded that, by itself, neglecting liquid-junction potential changes in our procedure for determining formation constants has had no significant effect.

Department of Applied Chemistry, PETER M. MAY
UWIST, King Edward VII Avenue,
Cardiff, Wales

7 June 1983

REFERENCES

1. H.K.J. Powell and M.C. Taylor, Talanta, 1983, 30, 885.
2. P.M. May, D.R. Williams, P.W. Linder and R.G. Torrington, ibid., 1982, 29, 249.
3. R.G. Bates, CRC Crit. Rev. Anal. Chem., 1981, 10, 247.
4. D.P. Brezinski, Analyst, 1983, 108, 425.
5. A. Sabatini, A. Vacca and P. Gans, Talanta, 1974, 21, 53.
6. P.M. May and K. Murray, unpublished work.

Talanta, Vol. 30, No. 12, pp. 901–905, 1983
Printed in Great Britain.

0039-9140/83 $3.00 + 0.00

DETERMINATION OF MANGANESE AT ng/ml LEVELS IN NATURAL WATERS BY DIFFERENTIAL PULSE POLAROGRAPHY

M. P. COLOMBINI
Istituto di Chimica Analitica dell'Università, Pisa, Italy
R. FUOCO
Istituto di Chimica Analitica Strumentale del C.N.R., Via Risorgimento 35, 56100 Pisa, Italy

(*Received* 11 *March* 1983. *Accepted* 24 *June* 1983)

Summary—A procedure based on differential pulse polarography is described for the determination of manganese at ng/ml levels in fresh, estuarine and sea-water buffered at pH 9.5 with a citrate–borate solution that also serves as supporting electrolyte. The procedure is unaffected by the potentially interfering compounds most likely to occur in natural waters. Furthermore, iron (in ascorbate–borate buffer, pH 9.5) or chromium (in ascorbate–ammonia–ammonium–chloride buffer, pH 9.8) can be determined together with manganese. Some results for the concentration of manganese, iron and chromium in the River Arno are reported.

Manganese is an essential micronutrient[1] both for plants and animal species. The level of this element in natural waters ranges from 0.001 to 1.0 μg/ml. In contaminated waters concentrations as high as 50 μg/ml are possible. The maximum allowable concentration (MAC) varies according to the use to be made, *e.g.*, the MAC is 0.05 μg/ml for domestic water supplies and 2.0 μg/ml for irrigation water.[1]

Manganese in natural waters may be determined by electrochemical techniques that provide information about the concentrations at ng/ml levels. Such techniques, being quite simple to apply and not time-consuming, are to be preferred in trace analysis for metals. However, insufficient literature information is available regarding the determination of manganese in natural waters by these techniques, and all but one[2] of the papers[2–7] dealing with it do not take into account the possible interference by other ionic species which may be present in natural waters. In the one exception,[2] which refers to an analytical method based on anodic-stripping voltammetry, some interfering elements are mentioned, but no general procedure for dealing with them is reported.

In this paper, an electrochemical procedure based on differential pulse polarography (DPP) is described for the determination of manganese at ng/ml levels. Chromium and iron can be also determined if the buffer system is changed.

EXPERIMENTAL

Apparatus

A PAR model 174 Polarographic Analyzer was employed in the differential pulse mode, with a Hewlett–Packard model 7044 X–Y recorder. Except where otherwise specified, the instrumental parameters used were: pulse-amplitude 25 mV; scan-rate 2 mV/sec; drop-time 1 sec. The electrochemical cell was equipped with a platinum wire counter-electrode, a saturated calomel electrode (SCE) as reference electrode and a dropping mercury electrode as working electrode. The nitrogen used for deaeration was first passed through a buffer solution of the same concentration as that in the cell.

Containers

Plastic containers were used for heavy-metal solutions and samples. To avoid analyte losses and sample contamination, it was found advisable to wash all containers by the procedure previously devised for glass bottles.[8]

Reagents

All the reagents were of analytical-reagent grade (Carlo Erba, Milan). Standard 0.01*M* solutions of Mn(II), Fe(II), Fe(III), Cr(III) and Cr(VI) were prepared from $MnSO_4.H_2O$, $(NH_4)_2Fe(SO_4)_2.6H_2O$, $NH_4Fe(SO_4)_2.12H_2O$, $CrK(SO_4)_2.12H_2O$ and $K_2Cr_2O_7$ respectively. The Fe(II) solution was freshly prepared daily because of instability with respect to oxidation. The Mn(II), Fe(II) and Fe(III) concentrations were checked by EDTA titration. The Cr(III) concentration was checked by redox titration after oxidation to Cr(VI). Doubly distilled water was used throughout.

Citrate solution. A 1*M* citric acid solution, adjusted to pH 9 with concentrated sodium hydroxide solution.

Ascorbate solution. A 1*M* ascorbic acid solution adjusted to pH 9 with concentrated sodium hydroxide solution.

Ammonia buffer solution. A 6*M* ammonia/3*M* ammonium chloride buffer solution (pH 9.8).

Borate buffer solution. A 0.5*M* borax/0.34 *M* sodium hydroxide buffer solution (pH 9.5).

Synthetic lake water. $NaHCO_3$ (0.16 g), $MgSO_4.7H_2O$ (0.03 g) and $CaCl_2.6H_2O$ (0.16 g) were dissolved in 1 litre of pure water. The concentration of nitrate ions was 1 ppm, except where otherwise specified.

Synthetic sea-water. NaCl (30 g), $MgSO_4.7H_2O$ (3.5 g) and $CaCl_2.6H_2O$ (2.2 g) were dissolved in 1 litre of pure water. The concentration of nitrate ions was 1 ppm, except where otherwise specified.

Nitrate solution, 0.01*M*.

Sample storage and pretreatment

To avoid undesirable changes in chemical composition, the water sample, immediately after collection, was filtered

(Sartorius membrane filter, pore size 0.45 μm), acidified with concentrated hydrochloric acid to ~pH 2 and stored at 4°. Before addition of the buffer selected for the analysis, solid sodium chloride to give a final concentration of 0.5*M*, and ascorbate or citrate solution (in 2:100 v/v ratio to the sample), were added to the acidified sample. The chloride was added in order to obtain the same slope of calibration plot for all types of natural water (N.B., for sea-water analysis this addition is not required).

Reagent blank

If pure reagents are used, the reagent blank for manganese and iron is significant only when ammonium persulphate is used for the oxidation of organic matter, and can then be determined by running a reagent blank through the procedure for the sample.

RESULTS AND DISCUSSION

The method for manganese was tested preliminarily with two different types of synthetic water samples (lake and sea-water[9]), without addition of buffer solution, in accordance with the procedures previously proposed.[3-6] As shown in Table 1, there was overlap of the manganese, iron and chromium reduction signals, the effect being greatest with the lake water. Nitrate could also be a cause of interference as it strongly influences the electrochemical reduction of chromium(III). Figure 1 shows the non-linear dependence of the differential-pulse peak current of the chromium signal ($E_p = -1.50$ V) on the chromium concentration in synthetic lake-water containing nitrate at the 1-μg/ml level which can be present in natural waters. This effect of nitrate (which is catalytic in nature) on the reduction step of chromium(III) has been noticed before[10,11] and used for the determination of nitrate. As we were unable to obtain the Saito and Himeno paper,[10] investigations were performed on synthetic lake water by d.c. polarography. It was found that the diffusion current of the reduction wave of chromium(III) ($E_{\frac{1}{2}} = -1.45$ V) was linearly dependent on concentration in the range 0.5–10 μg/ml both in the absence and presence of nitrate, but when nitrate was present a very asymmetric maximum was observed on the

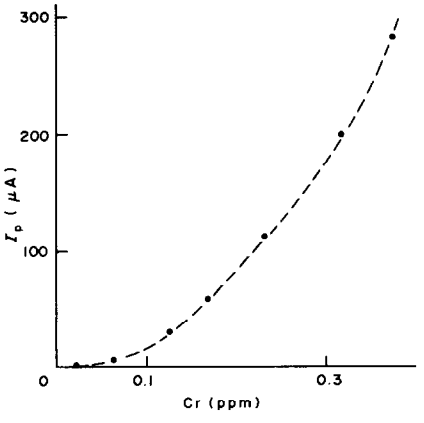

Fig. 1. Dependence of differential-pulse peak current of the signal at −1.50 V on chromium concentration in synthetic lake-water containing 1 ppm of nitrate.

Table 1. Peak potentials (E_p) of the signals, and slopes (Δ) of the calibration plots, for Mn, Fe and Cr in buffered and unbuffered synthetic waters

	Manganese			Iron			Chromium		
	E_p, V	Δ, nA.ml.ng^{-1}	S.D., nA.ml.ng^{-1}	E_p, V	Δ, nA.ml.ng^{-1}	S.D., nA.ml.ng^{-1}	E_p, V	Δ, nA.ml.ng^{-1}	S.D., nA.ml.ng^{-1}
Lake water	−1.47	0.062	0.001	−1.35	0.008	0.0005	−1.47[b]	0.040[b]	0.004
Sea-water	−1.49	0.058	0.002	−1.45	0.007	0.0006	−1.63[b]	0.035[b]	0.005
Sample + ascorbate–borate buffer	−1.52	0.038	0.001	−1.38	0.007	0.0004	−0.95[c]	—	
Sample + citrate–borate buffer	−1.56	0.047[a]	0.002	N.R.	—		−1.0[c]	—	
Sample + ascorbate–ammonia buffer	−1.52	0.036	0.001	N.R.	—		−1.62	0.048	0.003

N.R. = Not reducible; S.D. = standard deviation (12 values, each repeated three times); [a]instrumental parameters: pulse amplitude 50 mV, scan-rate 2 mV/sec, drop-time 2 sec; [b]data were obtained in absence of nitrate ions; [c]the signals are very broad and are not useful for analytical determinations.

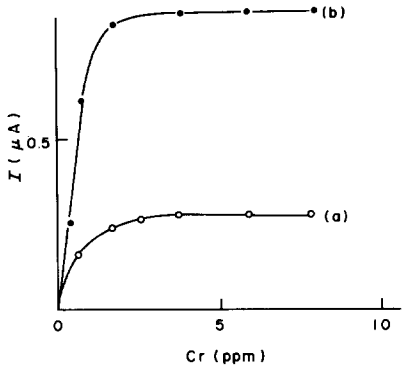

Fig. 2. Effect of increasing chromium concentration on the magnitude of the d.c. polarographic maximum in synthetic lake water containing (a) 1 ppm and (b) 3 ppm of nitrate. The current of the maximum was measured at about −1.5 V. Scan-rate 2 mV/sec, drop-time 2 sec.

reduction wave, its magnitude depending on both the chromium and the nitrate concentrations: this is shown in Fig. 2 for two different concentrations of nitrate and increasing chromium concentration.

It may be concluded that if the earlier procedures for manganese determination are used, errors may arise not only from the overlap effect but also from the nitrate effect on the chromium signal. Such errors were found to be as great as +400% for determination of manganese (0.1 μg/ml) with chromium and nitrate concentrations of 0.1 and 1 μg/ml respectively (such a chromium concentration can be found in catchment waters used for water supply[9] as well as in polluted water).

Different types of buffer solutions were then tested, with the aim of separating the signals of the various electroactive species and suppressing the nitrate effect. By the scheme shown in Fig. 3, it is possible

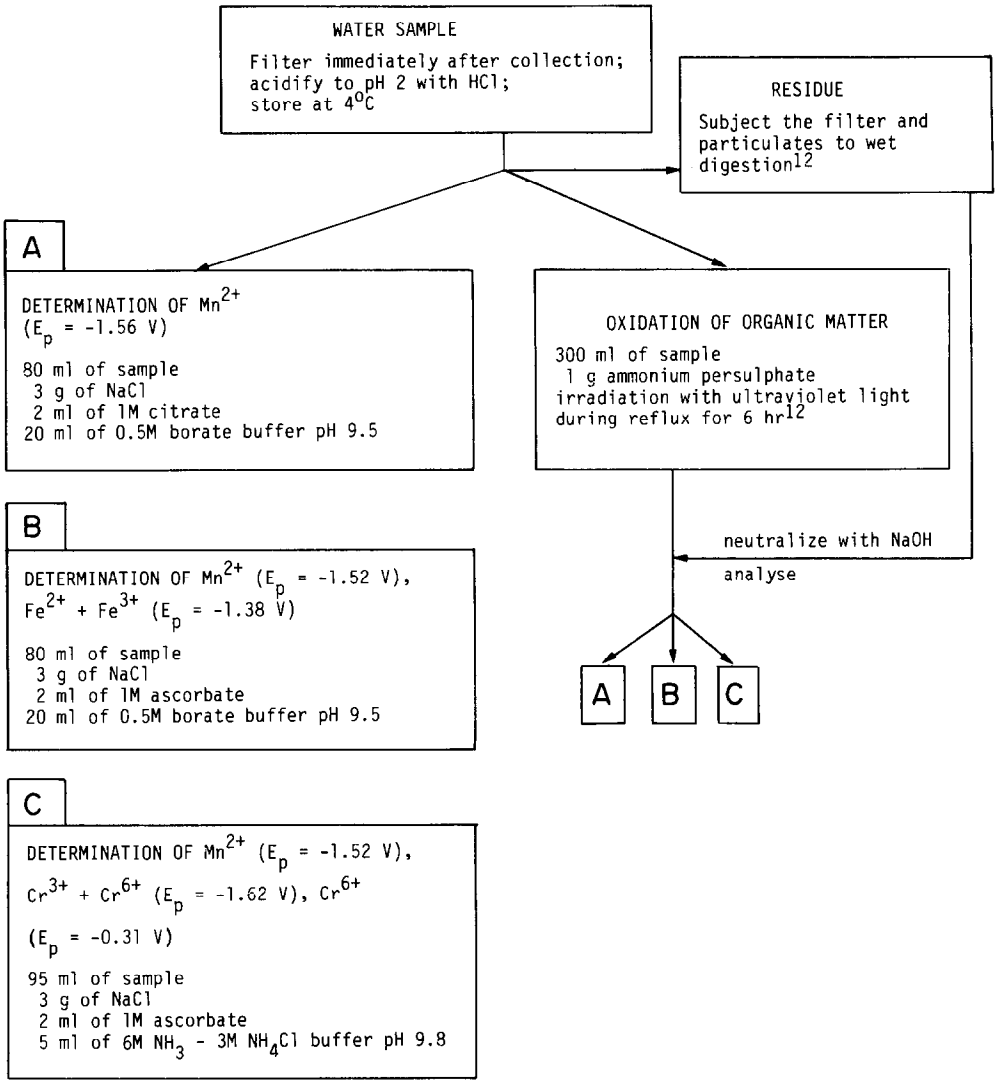

Fig. 3. Analytical procedure suggested for the determination of (A) manganese, (B) manganese and iron, (C) manganese and chromium in fresh water, estuarine water and sea-water.

to determine manganese without any interference. In particular, addition of the citrate–borate buffer to the acidified sample both shifts the peak potential for chromium ($E_p = -1.0$ V, very broad peak) and suppresses the peak for iron, since the iron is then not reducible in the working potential range. Zn^{2+}, Cd^{2+}, Pb^{2+}, Ni^{2+}, Cu^{2+}, Sn^{4+} and Co^{2+} at a concentration as high as 1 μg/ml do not interfere.

By use of the ascorbate–borate buffer, manganese and iron (as the sum of Fe^{2+} and Fe^{3+}) may be determined simultaneously in concentration ratios ranging from 0.01 to 100. Figure 4 shows the differential-pulse polarogram of a buffered synthetic sea-water sample containing 450 ng of iron and 8 ng of manganese per ml.

With the ascorbate–ammonia–ammonium chloride buffer, manganese and total chromium in concentration ratio ranging from 0.1 to 10 may be determined, the total chromium from the peak current (for Cr^{2+}/Cr) at -1.62 V and the manganese from the peak current at -1.52 V. The peak current is measured from a notional base-line drawn between the troughs on either side of the peak. Because the positioning of the base-line will depend on the signals from other species present, it is necessary to use the standard-additions method. Figure 5 shows the differential pulse polarogram of a buffered synthetic sea-water sample containing 65 ng of chromium and 70 ng of manganese per ml. The peaks at -1.40, -1.52 and -1.62 V are due to the reductions $Cr^{3+} \rightarrow Cr^{2+}$, $Mn^{2+} \rightarrow Mn$ and $Cr^{2+} \rightarrow Cr$ respectively. If both chromium(III) and chromium(VI) are present, the latter can be determined at -0.31 V, and the former calculated.[12]

Table 1 gives the peak potentials used in the analytical determinations and the slopes of the calibration plots. All these plots are linear up to a concentration of 25 μg/ml. For the determination of iron with use of the ascorbate–borate buffer, however, the linearity holds only up to 1 μg/ml, as precipitation begins at higher concentration.

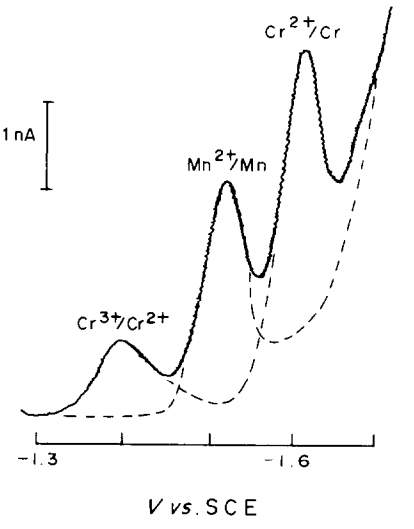

Fig. 5. Differential-pulse polarogram of synthetic sea-water sample containing ascorbate–ammonia buffer, 65 ng/ml Cr^{6+} and 70 ng/ml Mn^{2+}. The dashed lines refer to the polarograms obtained when only one of the species is present in the sample.

The detection limit is 5 ng/ml for manganese and chromium and 30 ng/ml for iron, calculated[13] as the concentration corresponding to three times the peak-to-peak noise measured on the base-line close to the expected signal.

The influence of the ascorbate–ammonia–ammonium chloride buffer on the effect of nitrate on the Cr^{3+}/Cr^{2+} reduction peak ($E_p = -1.50$ V) is interesting. It has been found that the critical factor is the concentration of ammonia and ammonium chloride, as shown in Fig. 6.

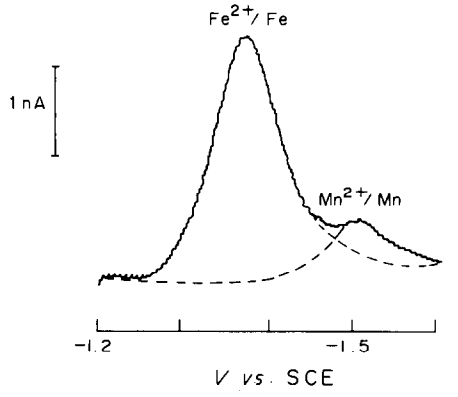

Fig. 4. Differential-pulse polarogram of synthetic sea-water samples containing ascorbate–borate buffer, 450 ng/ml Fe^{2+} and 8 ng/ml Mn^{2+}. The dashed lines refer to the polarograms obtained when only one of these species is present in the sample.

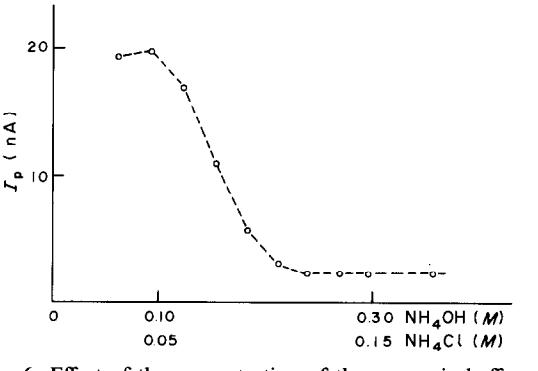

Fig. 6. Effect of the concentration of the ammonia buffer components on the differential-pulse peak current at -1.50 V for 0.24 ppm of Cr^{3+} in synthetic lake water containing 1.8 ppm of nitrate. The limiting value obtained for buffer concentrations higher than 0.25M NH_3 and 0.125M NH_4Cl is equal to that obtained in the absence of nitrate.

Table 2. Determination of manganese, iron and chromium (*ng/ml*) in water from the River Arno by the proposed procedure

Element		River Arno sample		Spiked with 60 ng/ml of each element		Spiked with 120 ng/ml of each element	
		Found	S.D.	Found	S.D.	Found	S.D.
Mn	(a)	10	0.8				
	(b)	21	1.2	83	2.3	140	1.2
Fe	(a)	N.D.	—				
	(b)	50	5.2	115	2.9	165	2.3
Cr	(a)	N.D.	—				
	(b)	N.D.	—	58	1.5	122	1.2

(a) Untreated samples; (b) samples treated with ammonium persulphate and ultraviolet light; N.D. = none detectable; S.D. = standard deviation (5 measurements).

Concentrations higher than 0.25*M* ammonia and 0.125*M* ammonium chloride suppress the effect completely. It must be stressed that the buffer composition (0.1*M* ammonia, 0.1*M* ammonium chloride) proposed in the literature[7] for manganese determination in aqueous solution cannot be used in the analysis of natural waters containing chromium and nitrate. Further experiments are in progress to elucidate this behaviour.

The proposed procedure was tested with natural and polluted water samples taken from the River Arno and from the sea around its estuary. To determine the total content of manganese, chromium and iron, an aliquot of acidified sample was refluxed for 6 hr with ammonium persulphate (0.3 g per 100 ml of sample) and at the same time, irradiated with ultraviolet light from two 150-W mercury lamps.[14] Table 2 gives the results for the River Arno sample. The slopes of the calibration plots for treated and untreated samples were obtained by the standard-additions method and were the same as those obtained for synthetic samples. This supports the conclusion that the organic and inorganic substances present in the samples do not interfere.

Conclusions

It has been shown that the polarographic determination of manganese in unbuffered natural waters is subject to strong interference because the chromium and iron signals overlap the manganese signal. In addition, the presence of nitrate enhances the chromium interference. In the proposed procedure based on DPP, citrate–borate, ascorbate–borate and ascorbate–ammonia–ammonium chloride buffers allow the determination of ng/ml levels of manganese, manganese and iron, and manganese and chromium respectively, in natural waters, without interferences.

Acknowledgements—The authors are extremely grateful to Professor Paolo Papoff (University of Pisa) for his constant interest and for helpful discussions. One of the authors (M.P.C.) acknowledges assistance from the M.P.I.

REFERENCES

1. M. Sitting, *Toxic Metals*, p. 184. Noyes Data Corp., New Jersey, 1976.
2. R. J. O'Halleran, *Anal. Chim. Acta*, 1982, **140**, 51.
3. W. Davison, *J. Electroanal. Chem.*, 1976, **72**, 229.
4. G. C. Whitnack, *Anal. Chem.*, 1975, **47**, 618.
5. S. Knox and D. R. Turner, *Estuarine Coastal Mar. Sci.*, 1980, **10**, 317.
6. G. S. Deshmukh and U. S. Waik, *Z. Anal. Chem.*, 1971, **254**, 353.
7. P. E. Sturrock and R. J. Carter, *Rept.* ERCR 0874, Georgia Institute of Technology, Atlanta, 1974.
8. M. P. Colombini, G. Corbini, R. Fuoco and P. Papoff, *Ann. Chim. (Rome)*, 1981, **71**, 609.
9. R. G. Bond and C. P. Straub, *Handbook of Environmental Control*, Vol. III, CRC Press, Ohio.
10. A. Saito and S. Himeno, *Rev. Polarog. (Japan)*, 1976, **22**, 72.
11. B. D. Seiler and J. P. Avery, *Anal. Chim. Acta*, 1980, **119**, 277.
12. R. Fuoco and P. Papoff, *Ann. Chim. (Rome)*, 1975, **65**, 155.
13. *Anal. Chem.*, 1980, **52**, 2242.
14. H. W. Nürnberg, *Pure Appl. Chem.*, 1982, **54**, 853.

Talanta, Vol. 30, No. 12, pp. 907–913, 1983
Printed in Great Britain.

0039-9140/83 $3.00 + 0.00

A SIMULTANEOUS MULTIELEMENT NON-DISPERSIVE ATOMIC-FLUORESCENCE SPECTROMETER USING MODULATED SOURCES AND FREQUENCY DISCRIMINATION OF FLUORESCENCE SIGNALS

A. D'ULIVO and P. PAPOFF

Istituto di Chimica Analitica Strumentale del C.N.R.—Istituto di Chimica Analitica dell'Università di Pisa, Via Risorgimento 35, 56100 Pisa, Italy

C. FESTA

Istituto di Chimica-Fisica dell'Università di Pisa, Via Risorgimento 35, 56100 Pisa, Italy

(*Received* 3 *February* 1983. *Accepted* 23 *June* 1983)

Summary—Commercial radiofrequency-excited electrodeless discharge lamps can be run from a square-wave modulated power supply so as to give a low level of continuous emission when modulated in the frequency range 3–10 kHz. Use of a different modulation frequency and lock-in amplifier for each lamp allows multielement non-dispersive atomic-fluorescence spectrometry to be performed. Very low detection limits have been obtained for arsenic, selenium, tin and mercury. The use of low-cost electronic components in the system largely offsets the high cost of the individual excitation power supplies and tuned a.c. detectors.

Whenever several analytes have to be measured in a number of samples, as in the characterization of an eco-system in terms of the concentrations of various chemical components, an instrumental method which allows multicomponent analysis, performed automatically either in simultaneous or sequential mode, is particularly useful.

For determination of elements, atomic spectroscopy can be used successfully provided that: (1) well defined chemical and physical conditions can be obtained so that, for each element, the rate and yield of the formation and excitation of the atoms is not much lower in the multielement mode than in the single-element mode; (2) the detector system is able to distinguish and measure each individual signal without distortion.

Non-dispersive atomic-fluorescence spectroscopy (NDAFS) suits simultaneous multielement analysis[1–6] very well, and is often superior to atomic-absorption spectroscopy (AAS), flame atomic-emission spectroscopy (FAES) and inductively-coupled plasma atomic-emission spectroscopy (ICPAES), as far as linear dynamic ranges and detection limits are concerned.[7–10]

The applicability of NDAFS depends on the availability of a line-source giving intense, low-noise spectral power, modulation of the source in the most favourable frequency range, high quantum efficiency for fluorescence of the atomic vapour, minimization of misleading optical and chemical effects, as well as of noise, in the optimized system which includes reactor, atomizer, light-traps, and electrical filters, and deconvolution and automatic allotment of each specific signal to the corresponding element.

Different arrangements for multielement analysis by NDAFS may be found described elsewhere, but all but one, that proposed by Van Loon and co-workers,[3] concern sequential, rather than simultaneous, sampling of the different atomic-fluorescence signals, with little or no possibility of measuring discrete transient signals.

Mitchell and Johansson,[1] using a time-multiplexer approach, produced a system for multielement analysis of up to six elements by use of hollow-cathode lamps (HCLs), each being excited in turn at 1 kHz for 0.1 sec. Owing to the relatively low speed of synchronization of these lamps and the optical filters employed, the frequency of sampling of the signal for each element was 1 Hz.

Palermo *et al.*,[2] and later Ip *et al.*,[5] also used a time-multiplexer approach, sequentially pulsing HCLs or electrodeless discharge lamps (EDLs) respectively. Under the experimental conditions used by Palermo, depending on the HCL used, the width of the pulse of emitted radiation was between 2 and 10 msec with a delay time of between 6 and 30 msec. In this way, assuming four lamps were used, the frequency of sampling reached 25 Hz at most.

A different time-multiplexer approach was used by Chester and Winefordner.[4] In their investigation,

concerning the potential of multielement analysis by NDAFS, they used two EDLs mechanically chopped at 465 and 260 Hz, and sampled the fluorescence signals by a single lock-in amplifier sequentially tuned to the frequency of modulation of the two lamps.

Van Loon *et al.*,[3] by using individual lock-in amplifiers, were able to monitor continuously the atomic-fluorescence of Ni, Cu and Zn, and hence use the system as a detector in liquid chromatography. HCLs were used, at modulation frequencies of 325, 285 and 80 Hz respectively.

Here we describe a system for multielement NDAFS, based on exposure of the atomic vapour simultaneously to the radiation from four radio-frequency-excited EDLs (RF-EDLs) each being modulated at a distinct frequency in the kHz range, and one photomultiplier (PM) having its output monitored continuously by four lock-in amplifiers, each tuned to the frequency of the relevant EDL. The output from each lock-in amplifier is fed to either an individual or a time-shared pen-recorder. All electronic parts (RF power supplies, modulators and lock-in amplifiers) were assembled in our laboratory from high-quality low-cost components. RF-EDLs were chosen because they can accept 100% modulation over a wide range of frequencies (3–15 kHz, with a best performance at about 8 kHz) as found earlier.[11] In contrast, microwave-excited EDLs accept only a low percentage of modulation superimposed at a high d.c. level[12,13] with the best signal-to-noise ratio (SNR) at around 20 kHz.[12] HCLs, owing to their slow response both on switching on and switching off, give a high continuous power level which rises at increased modulation frequencies, becoming particularly significant at frequencies above a few hundred Hz.[14–17]Further, RF-EDLs exhibit higher spectral radiance than do the corresponding HCLs[14,17–20] whenever volatile elements or thermally decomposable iodides are present inside the lamp bulb, as in the present case.

Low-power commercial RF-EDLs were preferred for this application since high-power pulsed RF-EDLs vary considerably in behaviour, depending on the element considered, as may be inferred from the papers of Novak and Browner.[21,22]

The system's characteristics were carefully matched in view of its application to the separation of mixed, transient signals with life-times of a few seconds or less.

FACTORS INFLUENCING SIGNAL-TO-NOISE RATIO IN MULTIELEMENT NDAFS

Assuming that the spectral distribution of the source over a wide range of frequencies is not modified by the modulation or pulsing of the light-source, and than an ideal lock-in amplifier is used, with a time-constant of zero and tuned to the frequency f, then the instantaneous output voltage for a constant concentration C of analyte and peak radiance B_s of the source is

$$V_{out} = S + N_d + N_a + N(B_s) \quad (1)$$

where the right-hand terms, expressed in volts, are S, the fluorescence signal, N_d, the noise from the photomultiplier–amplifier chain, N_a, the noise from flickering, background emission, turbulence effects *etc.*, related to the atomizer configuration, and $N(B_s)$, the noise from the source, including source fluctuation as well as the radiation reflected or scattered onto the photodetector (all noise referred to the frequency band-pass of the lock-in amplifier). When the noise depends on the concentration of analyte, C, then $N(B_s,C)$ must be considered. Assuming that S depends linearly both on C and the peak radiance of the source (B_s), then

$$V_{out} = aCbB_s + N_d + N_a + N(B_s,C) \quad (2)$$

where a is the slope of a plot of V_{out} *vs.* B_s at constant C, and b is the slope of V_{out} *vs.* C at constant B_s.

From (2) it can be inferred that the quality of the output signal and the cause of the predominant noise depend strongly on all the chemical and instrumental steps involved in the measurement and on the working modulation frequency f.

The parameter a is chemical in nature and is related to the overall efficiency of atom production from the analyte in the sample. It depends on the element, its oxidation state, the composition of the matrix and the conditions used. It is well known, for example, that to achieve reasonably high sensitivity, Se(VI) must be reduced to Se(IV) and Pb(II) oxidized to Pb(IV) before conversion into the hydrides[23,24] and that of the reagents available, sodium borohydride is particularly efficient.[25–31]

The parameter b is instrumental in nature and is related to the efficiency of obtaining, collecting and detecting the fluorescence radiation emitted by the analyte atoms. By the use of non-dispersive techniques, a consistent enhancement of b is obtained, since the fluorescence radiation measured is integrated over the working wavelength range of the photomultiplier.

It may sometimes be necessary to increase B_s, particularly at low values of a, but it must be pointed out that if any real benefit is to be gained by increasing B_s then $N_d + N_a$ must remain higher than, or of the same magnitude as, $N(B_s,C)$, since $N(B_s,C)$ increases almost linearly with B_s and the SNR does not improve.

In turn, at constant C, $N(B_s,C)$ depends on the efficiency of the light traps and on the geometry of the atomizer, as well as on the level of modulation of the light-source.

This last point has not yet been sufficiently elucidated; indeed, high-intensity lamps with a low level of modulation have been tried but gave no effect other than a significant worsening of the SNR when compared with other lamps emitting a much lower light intensity but with 100% amplitude modulation.

If the maximum radiant power emitted by a modulated source is B_s, and the level of modulation is α, $(0 < \alpha < 1)$, then the modulated radiant power is αB_s. The fluorescence emitted by the atoms of the analyte will give a total signal S of which αS is the modulated component. The a.c. amplifier will reject the d.c. component $(1 - \alpha)S$ and will consider only αS as the signal. The noise levels N_d and $N(B_s,C)$ are related during each cycle to the magnitude of S and $(1 - \alpha)S$ respectively, and will be added to the signal αS at the lock-in amplifier output. It is clear that the SNR will reach its optimum value at $\alpha = 1$, that is for 100% modulation.

When several lamps are operating at their individual modulation frequencies f_1, f_2, . . . f_i and the corresponding elements are present in the sample, the d.c. component of the signal will be the sum of the $(1 - \alpha)S_i$ contributions, and the noise at each frequency f_i will increase with lowering of the value of α. It must be noted that, at constant B_s, the absolute value of the d.c. component of the fluorescence signal depends on the concentration of the analyte. Provided that $\alpha = 1$ for all the lamps, the $N(B_s,C)$ noise is ideally the same as in single-lamp operation, and N_d, as far as shot-noise is concerned, is proportional to the square root of the sum of the signals.

In practice, shot-noise does not significantly affect the SNR when lock-in amplifiers are used. It is to be presumed, than, that the best approach in multielement simultaneous NDAFS is to find the range of modulation frequencies where α can be set very close to unity, and the fraction of total noise which is combined with the signal is kept as low as possible.

To make any improvement it would then be necessary to identify the main source of noise and to reduce it until another source of noise became predominant. The most important parameter in judging the characteristics of a measuring system is the SNR or, correspondingly, the detection limit. Since the SNR also depends on the analyte, the performances of different instruments can be compared only when the same chemical procedure is followed.

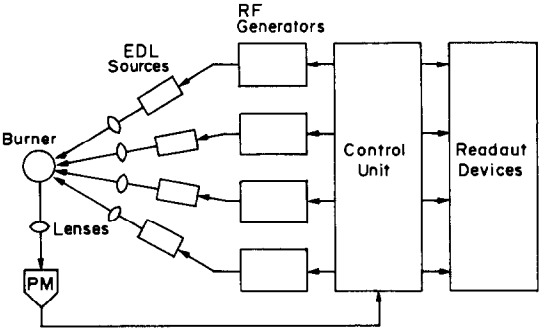

Fig. 1. Schematic diagram of the multielement non-dispersive atomic-fluorescence system.

EXPERIMENTAL

Figure 1 shows the general lay-out of the four-channel NDAFS excitation–detection system, the experimental components of which are listed in Table 1.

EDL sources and RF generators

EDLs produced by Perkin-Elmer were used. Each EDL was excited at 27 MHz and the mean power recommended by the manufacturer. Each RF generator supplied variable power up to a maximum of 45 W (expressed as the mean value) at the selected modulation frequency. The duty-cycle was always 0.5 (see Table 2). A resistive T-network was inserted between the generator and the EDL coil to achieve reasonable load-matching, on account of the considerable impedance variation in the firing transient, and the negative temperature coefficient of resistance of the lamp. This network was designed so as to dissipate about the same power as the EDL.

Control unit

Figure 2 shows a block-diagram of the control unit. A Colpitts oscillator supplied the 450-MHz driving-frequency to the frequency-dividers for the four channels, each divider being built round a 4029 CMOS integrated circuit coupled with a 4027 CMOS flip-flop. In this way square-waves were generated for each channel with frequencies of 7031, 7500, 8036 and 8554 Hz. The square-wave output controlled both the modulation of the RF power and the switching of the phase-sensitive detector in the corresponding amplifier. The composite signal at the PM output was amplified by a

Table 1. Experimental components

Item	Description and manufacturer
Sources	As, Se, Sn, Pb and Hg electrodeless discharge lamps, Perkin-Elmer
RF generators	27-MHz, 45-W, standard type, home-made
Control unit	Prototype, home-made
Photomultiplier	R-759, solar-blind type, Hamamatsu TV
Focusing lens	$f = 50$ mm, $d = 25$ mm, Suprasil quartz, Melles-Griot
Power supply	Max. 1000 V, standard type, home-made
Focusing lenses for EDLs	(a) $f = 75$ mm, $d = 25$ mm, Suprasil quartz, Melles-Griot (b) quartz lens doublets, $f = 90$ mm, $d = 25$ mm, Galileo S.p.A.
Burners	(*a*) according to Slevin *et al.*[32] (fitted on a premix chamber, IL 25958), i.d. = 10 mm, home-made (*b*) Pyrex, i.d. = 4 mm, home-made
Flame	Argon–hydrogen (entrained air)
Optical bench and accessories	Ealing Beck Ltd.

Table 2. Experimental conditions for the simultaneous determination of arsenic, selenium, tin and mercury

Radio-frequency power for EDLs	As, 8 W, Se 6 W, Sn 8 W, Hg 5 W, (expressed as mean power)
Power modulation for EDLs	Square-wave, 0–100% amplitude modulation
Modulation frequencies	As 8654 Hz, Se 8036 Hz, Hg 7500 Hz, Sn 7031 Hz
Photomultiplier voltage	750 V
Focusing height	15 mm above the burner top
Gas flow-rates	Circular burner: hydrogen 2 l./min, argon (auxiliary gas) 2 l./min, argon (carrier gas) 2 l./min: Pyrex burner: hydrogen 0.35 l./min, argon 1.0 l./min
Sample size	1 ml
Acidity	0.6*M* HCl
Reductant	1 ml of 2% $NaBH_4$ solution
RC time-constant	2 sec for circular burner; 10 sec for Pyrex burner

pre-amplifier (an FET source-follower) and fed to a band-pass filter tuned to the frequency for each channel. The band-width of these filters was sufficiently large to minimize any phase-shift fortuitously caused by any slight frequency-drift of the driving oscillator and/or the band-pass filter. The amplifiers were A 739 integrated circuits (Fairchild) with a voltage gain of 10^3. Phase-sensitive detection was achieved by using two bilateral switches of a 4066 CMOS integrated circuit. The reference signal of each channel controlled these switches, which fed the d.c. signal to the *RC* low-pass filter. The time-constant of the low-pass filter could be switched to 0.5, 2 or 10 sec. The d.c. signals were further amplified by a factor of 10 by the TL 081 operational amplifier (Texas Instruments).

This chain, of a.c. tuned-amplifier/phase-sensitive detector/d.c. amplifier, was equivalent to a dedicated lock-in amplifier. Its cost was about one tenth that of the general-purpose lock-in amplifier described by Caplan and Stern.[33]

Burners

Two different burners were tested; a circular one constructed according to Slevin *et al.*[32] and another constructed in Pyrex glass (i.d. 4 mm). An argon–hydrogen (entrained air) flame was used for both burners in conjunction with hydride evolution. The glass burner provided a mini-flame[25,26] and the circular burner was fitted on an IL 25958 premix chamber (for gas flow-rates see Table 2).

Chemicals

Stock solutions (500 ppm) of arsenic(III), selenium(IV), tin(IV) and mercury(II) were prepared from pure Sn, Hg, As_2O_3 and SeO_2, adjusted to the desired pH with concentrated hydrochloric acid (Erba), and diluted to give working standards just before use.

A 2% sodium borohydride solution was prepared, stabilized[34] by the addition of sodium hydroxide (0.1%) and then filtered. Erba RLE sodium borohydride was preferred, for its high purity and low cost.

Procedure

The NDAFS system was tested for the simultaneous determination of arsenic, selenium, tin and mercury with sodium borohydride reduction. One ml of 2% sodium borohydride solution was placed in the reaction vessel[35] and a disposable micropipette (Pabisch) containing the sample (0.2–1 ml) was placed in the injector port. Argon was then allowed to flow through the reaction vessel until stable base-lines were obtained. The sample was then injected, and the signals were recorded and peak heights measured.

RESULTS AND DISCUSSION

EDL source behaviour

Oscilloscope traces of the light-intensity emitted by arsenic, selenium, tin, mercury and lead EDLs, modulated at 7031 Hz, are shown in Figs 3, 4 and 5. Lead was included in these experiments on account of its importance in future studies on organolead pollution. A monochromator was inserted in the light-path between the EDL and the PM so as to select the following spectral resonance lines: arsenic 193.7 nm, selenium 196.0 nm, tin 286.3 nm, mercury 253.6 nm and lead 283.3 nm. The control unit was disconnected and the oscilloscope connected directly to the PM output.

The light intensities of the EDLs should follow exactly the waveform of the modulation signal applied to the RF power supplies, but a certain distortion of the modulation waveform and depth was found, differing from one lamp to another.

In our case, modulation depth was calculated as a percentage, by the equation:

$$\text{modulation depth} = \left(1 - \frac{I_{min}}{I_{max}}\right) \times 100\%$$

where I_{max} and I_{min} are the highest and lowest in-

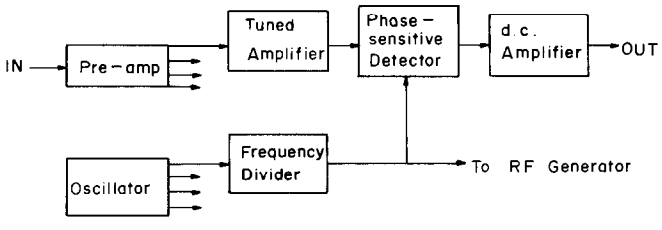

Fig. 2. Block diagram of the multichannel control unit.

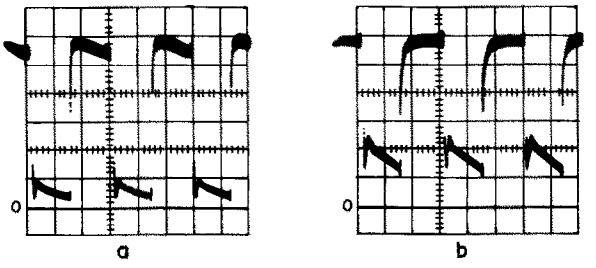

Fig. 3. Oscilloscope traces of EDL light intensities. Modulation frequency 7031 Hz. Oscilloscope scan-rate 50 μsec/div. (*a*) Arsenic EDL, 8 W, 193.7 nm; (*b*) selenium EDL, 6 W, 196.0 nm,

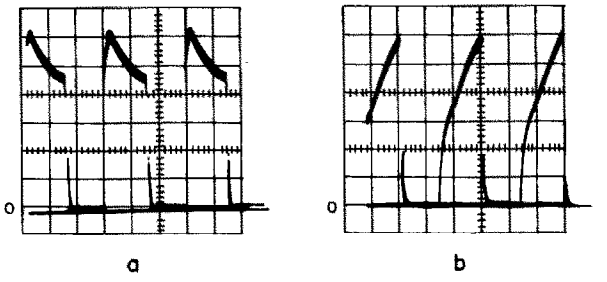

Fig. 4. Oscilloscope traces of EDL light intensities. Modulation frequency 7031 Hz. Oscilloscope scan-rate 50 μsec/div. (*a*) Lead EDL, 10 W, 283.3 nm; (*b*) tin EDL, 8 W, 286.3 nm.

tensities of the light emitted, both being measured against the zero level (see Figs 3–5). The best behaviour was shown by the mercury EDL (Fig. 5) which exhibited 100% modulation depth and only a slight distortion of the waveform. The lead and tin EDLs also exhibited 100% modulation depth but with quite severe distortion of the waveform during the cycle on-time.

The arsenic and selenium EDLs gave satisfactory on-time behaviour but quite strange behaviour during the cycle off-time (Fig. 3), their light intensity falling sharply then suddenly increasing, only to fade slowly and reach I_{min} at the end of the off-time. The modulation depth was 90% for the arsenic EDL and 75% for the selenium EDL. Similar results were obtained at a modulation frequency of 8654 Hz, and also when the monochromator was excluded, to give a non-dispersive apparatus.

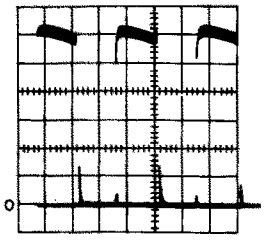

Fig. 5. Oscilloscope traces of light intensity of mercury EDL run at 5 W. Modulation frequency 7031 Hz, 253.6 nm line. Oscilloscope scan-rate 50 μsec/div.

Probably a better modulation waveform would be obtained for the lead and tin EDLs by using duty-cycle values respectively lower and higher than 0.5. However, the advantage of an improvement in SNR by adopting any duty-cycle value other than 0.5 would probably not offset the difficulties arising from the more complex control-unit circuitry required.

Analytical results

Experimental conditions for the multielement mode were a reasonable compromise of the best individual conditions for each element in terms of sample acidity and EDL focusing height above the burner top. All experimental conditions are reported in Table 2.

The half-intensity width of the recorded peaks was found to range between 7 and 9 sec when a Pyrex burner was used. This made it possible to work with the highest *RC* time-constant (10 sec) available at the output low-pass filter, with a consistent improvement in SNR. Figure 6 shows the effect of the *RC* time-constant on the recorded peak for arsenic. The relative standard deviation (10 replicates) was about 5% at the nanogram level for all elements tested. Reagent blanks were equivalent to 0.2, 0.1, 0.3 and 0.6 ng for arsenic, selenium, mercury and tin respectively. The upper limits of the linear calibration graphs were 0.3, 0.45, 0.3 and 0.4 μg for arsenic, selenium, mercury and tin respectively. Detection limits were calculated for a signal equal to twice the base-line noise, for the sake of comparison with those

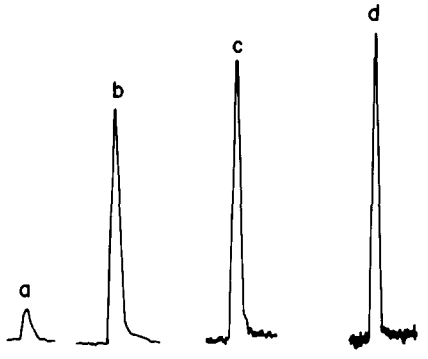

Fig. 6. Recorded peaks for arsenic. (*a*) Reagent blank, *RC* time-constant 10 sec; (*b*), (*c*) and (*d*) 1 ng of arsenic for *RC* time-constant of 10, 2 and 0.5 sec respectively.

reported in the bibliography, and are presented in Table 3.

A remarkable improvement in the detection limit was obtained for each element tested, in spite of the fact that the experimental conditions in the multi-element mode were not the best for each element. For arsenic and tin a direct comparison was possible since all but one of the same experimental conditions were used in both cases, the exception being that, for the single-element mode, Tsujii and Kuga[25,26] excited the EDLs in the continuous mode and modulated them by chopper at 27 Hz. We found improvement by a factor of 6 for both detection limits (see Table 3).

However, it must be considered that reagent blanks, rather than base-line noise levels, were the limiting factors for detection limits. It was more correct to calculate the detection limit as three times the standard deviation of a signal near blank level; the detection limits calculated in this way were 30, 60, 90 and 180 pg for arsenic, selenium, mercury and tin respectively.

The circular burner, working at higher gas flow-rates than the Pyrex burner, gave detection limits about one order of magnitude higher for all four elements, ranging from 0.2 ng for arsenic to 1 ng for tin (2 × base-line noise).

Table 3. Absolute detection limits (*pg*) (2 × base-line noise)

Element	Present work (multielement mode)	Previous work (single-element mode)
Arsenic	8[a], 200[b]	50[c], 2000[d], 100[e]
Selenium	20[a]	60[c]
Tin	100[a]	600[f]
Mercury	15[a]	50[g]

[a]Pyrex burner used.
[b]Circular burner used.
[c]Reference 25; experimental conditions as in [a] but RF-EDL chopped at 27 Hz, 0.5-ml sample size.
[d]Reference 27; 20-ml sample, 0.1*M* HCl.
[e]Reference 36; experimental conditions as in [a] but dispersive system, microwave EDLs run at 40 W (incident power), electronic modulation at 325 Hz.
[f]Reference 26; experimental conditions as in [a] but RF-EDL chopped at 27 Hz, 0.5-ml sample size.
[g]Reference 37; flameless technique, stannous chloride reduction, microwave EDL run at 25 W (incident power).

Table 4. Cross-interference effect*

Interferent, *ng/ml*		Peak-height variation, %		
		As	Se	Sn	Hg
As	50		0	0	0
	500		0	−20	0
Se	50	0		0	0
	500	0		0	0
Sn	50	0	0		0
	500	+10	0		0
Hg	50	0	0	0	
	500	0	0	0	

*All measurements performed in multielement mode. Concentration of analyte 5 ng/ml. Variation calculated as fraction of peak height for 5-ng/ml solution of analyte.

Interferences

Separately from chemical and optical effects, cross-talk was measured by the following procedure. Each lamp in turn was excited and part of its radiation reflected onto the photomultiplier in order to obtain a 500-mV signal at the relevant lock-in amplifier output. The output signals of the remaining lock-in amplifiers were measured under the same conditions (see Table 2). As a maximum peak to peak value of 0.4 mV was found, *i.e.*, twice the value obtained when all the lamps were unlit, the cross-talk was calculated to be, at most, 1:2500 (68 dB).

Detailed information about the chemical and optical cross-interferences will be given in a paper in preparation, together with the optimization procedure. However, it is worth mentioning that no evidence was found of serious cross-interferences, their extent in the multielement mode being practically the same as in the single-element procedure proposed in this paper, and very low compared to those in procedures described elsewhere.[27,31,38]

Table 4 summarizes the overall cross-interference effects of each element in turn, at concentration levels of 50 and 500 ng/ml, with the remaining three elements present in concentrations of 5 ng/ml. The only serious effects were the +10% change for arsenic in the presence of tin at 500 ng/ml, and the −20% change for tin in the presence of arsenic at 500 ng/ml.

CONCLUSIONS

From the findings above it is possible to conclude that:

(*a*) low-power, radiofrequency-excited EDLs, commercially available, give lower d.c. light levels than HCLs or microwave-excited EDLs do when modulated in the range 3–10 kHz;

(*b*) regardless of the differences in the shape of the light pulses, all the lamps tested, arsenic, selenium, tin and mercury, with a fixed duty-cycle of 0.5, proved to give a good SNR at around 8 kHz;

(*c*) with a 0.5 duty-cycle, it was possible to use a peak-radiance twice that suggested by the manufacturer for the continuous mode, without causing a noticeable decrease in the life of the lamp.

These features, together with the use of individual tuned a.c. detectors, have proved to be decisive in obtaining high noise-rejection and correspondingly low detection limits. For arsenic and tin, where comparison with the literature was possible because similar experimental conditions had been used (except for a modulation frequency of 27 Hz instead of 8kHz), an improvement by a factor of 6 was found for both.

The possible disadvantage of the high cost of individual a.c. detectors and modulated power supplies was overcome by using low-cost high-quality components in home-made apparatus.

Acknowledgements—This work was supported by C.N.R. (Rome). One of the authors (P.P.) gratefully acknowledges the financial support of Min. P.I. (40%).

REFERENCES

1. D. G. Mitchell and A. Johansson, *Spectrochim. Acta*, 1971, **26B,** 677.
2. E. F. Palermo, A. Montaser and S. R. Crouch, *Anal. Chem.*, 1974, **46,** 2154.
3. J. C. Van Loon, J. Licwa and B. Radziuk, *J. Chromatog.*, 1977, **136,** 301.
4. T. L. Chester and J. D. Winefordner, *Spectrochim. Acta*, 1976, **31B,** 21.
5. J. Ip, Y. Thomassen, L. R. P. Butler, B. Radziuk and J. C. Van Loon, *Anal. Chim. Acta*, 1979, **110,** 1.
6. U. H. Ullman, *Prog. Anal. Atom. Spectrosc.*, 1980, **3,** 87.
7. N. Omenetto and J. D. Winefordner, *ibid.*, 1979, **2,** 1.
8. T. S. West, *Analyst*, 1974, **99,** 886.
9. R. F. Browner, *ibid.*, 1974, **99,** 617.
10. G. F. Kirkbright, *ibid.*, 1971, **96,** 609.
11. M. P. Colombini, C. Festa and P. Papoff, *Atti 2° Conv. Naz. Chim. Anal., Padua, 1979*, p. 8.
12. R. M. Dagnall, M. D. Silvester and T. S. West, *Talanta*, 1971, **18,** 103.
13. D. P. Hubbard and R. G. Michel, *Anal. Chim. Acta*, 1973, **67,** 55.
14. H. Prugger, *Spectrochim. Acta*, 1969, **24B,** 197.
15. H. Prugger, R. Grosskopf and R. Torge, *ibid.*, 1971, **26B,** 191.
16. N. Omenetto, *Anal. Chem.*, 1976, **48,** 75A.
17. H. Falk, *Prog. Anal. Atom. Spectrosc.*, 1982, **5,** 205.
18. S. Murayama, M. Yasuda, M. Ito and M. Yamamoto, *Spectrochim. Acta*, 1979, **34B,** 159.
19. H. G. Human, P. J. Th. Zeegers and J. A. van Elst, *ibid.*, 1977, **29B,** 111.
20. J. M. Mansfield, M. P. Bratzel, H. O. Norgordon, D. O. Knapp, K. E. Zacha and J. D. Winefordner, *ibid.*, 1968, **23B,** 389.
21. J. W. Novak, Jr. and R. F. Browner, *Anal. Chem.*, 1978, **50,** 407.
22. *Idem, ibid.*, 1978, **50,** 1453.
23. H. W. Sinemus, M. Melcher and B. Welz, *At. Spectrosc.*, 1981, **2,** 81.
24. H. D. Fleming and R. G. Ide, *Anal. Chim. Acta*, 1976, **83,** 67.
25. K. Tsujii and K. Kuga, *ibid.*, 1978, **97,** 51.
26. *Idem, ibid.*, 1978, **101,** 199.
27. T. Nakahara, S. Kobayashi and S. Musha, *ibid.*, 1979, **104,** 173.
28. *Idem, ibid.*, 1978, **101,** 375.
29. S. Kobayashi, T. Nakahara and S. Musha, *Talanta*, 1979, **26,** 951.
30. T. Nakahara, T. Wakisaka and S. Musha, *Spectrochim. Acta*, 1981, **36B,** 661.
31. T. Nakahara, S. Kobayashi, T. Wakisaka and S. Musha, *Appl. Spectrosc.*, 1980, **34,** 194.
32. P. J. Slevin, V. I. Muscat and T. J. Vickers, *ibid.*, 1972, **26,** 296.
33. L. C. Caplan and R. Stern, *Rev. Sci. Instrum.*, 1971, **42,** 689.
34. J. R. Knechtel and J. L. Fraser, *Analyst*, 1978, **103,** 104.
35. K. C. Thompson and D. R. Thomerson, *ibid.*, 1974, **99,** 595.
36. K. C. Thompson, *ibid.*, 1975, **100,** 307.
37. J. E. Caupeil, P. W. Hendrikse and J. S. Bongers, *Anal. Chim. Acta*, 1976, **81,** 53.
38. B. Welz and M. Melcher, *ibid.*, 1981, **131,** 17.

Talanta, Vol. 30, No. 12, pp. 915–918, 1983
Printed in Great Britain.

0039-9140/83 $3.00 + 0.00

SPECTROPHOTOMETRIC DETERMINATION OF CADMIUM WITH 1-(2-PYRIDYLAZO)-2-NAPHTHOL AND NON-IONIC SURFACTANTS

APPLICATION TO ACETIC ACID EXTRACTS OF CERAMIC ENAMELS

J. MEDINA ESCRICHE, M. LLOBAT ESTELLES and F. BOSCH REIG
Department of Analytical Chemistry, Faculty of Chemistry, Valencia University, Burjasot (Valencia), Spain

(*Received* 7 *February* 1983. *Revised* 6 *June* 1983. *Accepted* 23 *June* 1983)

Summary—The Cd–PAN system in the presence of non-ionic surfactants (polyoxyethylene nonylphenols), which dissolve the reagent and complex by formation of micelles, has been studied spectrophotometrically. The optimum conditions for Cd determination are pH 9 ($Na_2B_4O_7$–$HClO_4$), 2% of surfactant and measurement at 555 nm. The complex is $Cd(PAN)_2$ and its conditional formation constant is 3.5×10^{11}. The system obeys the Lambert–Beer law, with an error of 0.9% over the Cd concentration range 0.44–1.74 ppm; the molar absorptivity is 4.94×10^4 l.mole^{-1}.cm^{-1} at 555 nm. The relative standard deviation is 0.7% and the limit of detection 0.009 μg/ml. The selectivity with respect to species important in the ceramic industry is adequate for application of the method to determination of Cd in acetic acid extracts of ceramic enamels.

One of the recent lines of spectrophotometric investigation has been concerned with use of surfactants[1,2] for improving sensitivity and selectivity by the formation of mixed species and/or micelles. The purpose of the present work was study of the Cd–PAN system in the presence of non-ionic surfactants (polyoxyethylene nonylphenols), which act as solubilizing agents by formation of micelles.

The spectrophotometric determination of metals with PAN usually involves extraction with organic solvents because of the insolubility of the reagent and complexes in aqueous solution;[3–6] this can be avoided if appropriate surfactants are added.[7–11]

EXPERIMENTAL

Reagents

Stock solution (1000 μg/ml) of Cd $(NO_3)_2 \cdot 4H_2O$, standardized gravimetrically with oxine.

Stock $10^{-3}M$ solution of *o*-PAN in methanol.

Stock 25% w/v solutions of non-ionic surfactants (polyoxyethylene nonylphenols) NEMOL K-36, K-1030 and K-2030 (Masso-Carol) with hydrophile–lipophile balances[12] of 12.6, 15.1 and 17.4 respectively.

Determination of Cd in acetic acid extracts of ceramic enamels

To eliminate interferences, extraction with sodium diethyldithiocarbamate and carbon tetrachloride is used. If a mixture of cadmium, zinc and lead is treated with 0.5% sodium diethyldithiocarbamate solution in $1M$ NH_4^+/NH_3 buffer and then extracted with carbon tetrachloride, it can be shown by atomic-absorption spectrophotometry (AAS) that about 80% of the zinc stays in the aqueous phase, and the other 20% can be eliminated from the organic phase by washing with $1M$ NH_4^+/NH_3 buffer solution. The cadmium and lead can be quantitatively stripped from the organic phase with $1M$ hydrochloric acid. The cadmium can be determined with PAN and surfactant in $0.025M$ citrate medium and up to 50 μg of Pb per ml will cause an error of not more than 3%.

The relative standard deviation (7 independent samples) is 0.9% and the limit of detection (defined as the cadmium concentration giving a signal that is twice the standard deviation of the blank) is 0.013 μg/ml. The corresponding AAS figures are 1.2% and 0.012 μg/ml.

Procedure

Add 2 g of sample to 50 ml of 4% acetic acid and let the mixture stand for 24 hr at room temperature, then filter into a 100-ml standard flask and dilute to volume with 4% acetic acid.[13]

To 10 ml of this solution add 15 ml of demineralized water, 5 ml of 20% sodium citrate solution, 20 ml of $2.5M$ $NH_4^+/2.5M$ NH_3 buffer, 5 ml of 0.5% sodium diethyldithiocarbamate solution and 10 ml of carbon tetrachloride, shake the mixture for 5 min, then separate the phases and shake the organic phase with 10 ml of $1M$ $NH_4^+/1M$ NH_3 solution for 5 min and discard the aqueous phase. Then strip cadmium by shaking the organic phase with 10 ml of $1M$ hydrochloric acid for 5 min, and separate the phases. Dilute the aqueous phase to volume in a 25-ml standard flask with demineralized water. To 5 ml of this solution add 1 ml of $1M$ sodium hydroxide, 2.5 ml of $0.25M$ sodium citrate, 2 ml of 25% NEMOL K-1030 solution, 2.5 ml of $10^{-3}M$ PAN and 10 ml of $Na_2B_4O_7$–$HClO_4$ buffer, and dilute to the mark in a 25-ml standard flask with demineralized water. Measure the absorbance at 555 nm against a reagent blank prepared in the same way.

RESULTS AND DISCUSSION

Influence of pH on the PAN–surfactant system

The presence of NEMOL K-1030 surfactant results in dissolution of the neutral form of PAN (pH 4–11);

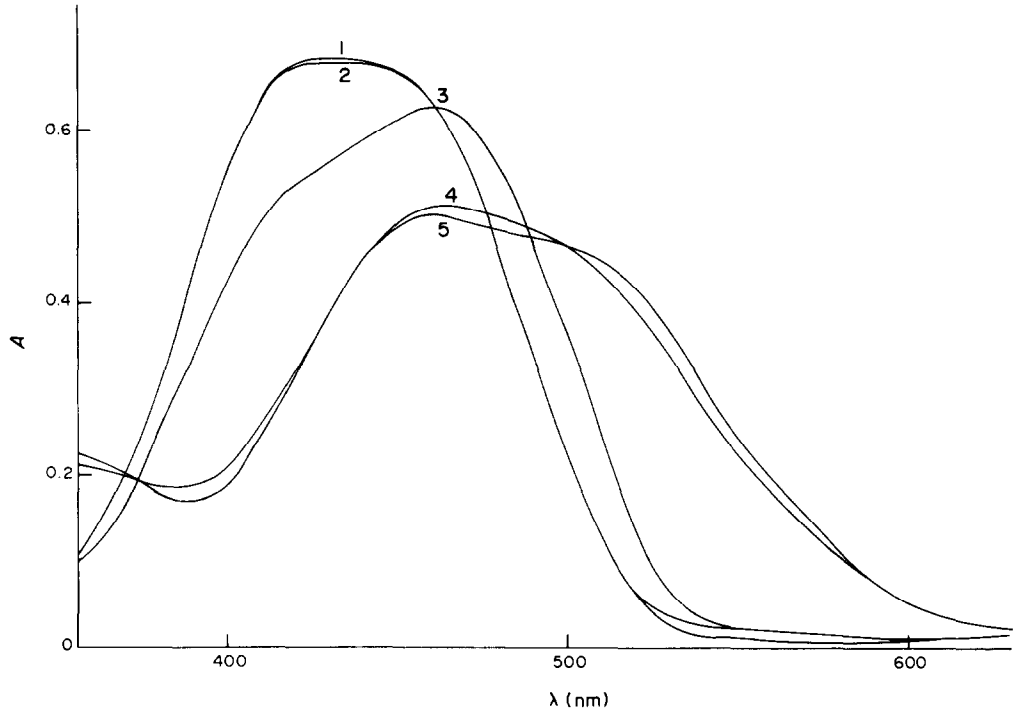

Fig. 1. Absorption spectra of PAN. Influence of pH. 1, pH 1.23; 2, pH 1.83; 3, pH 2.96; 4, pH 12.48; 5, pH 13.16; PAN $4 \times 10^{-5} M$.

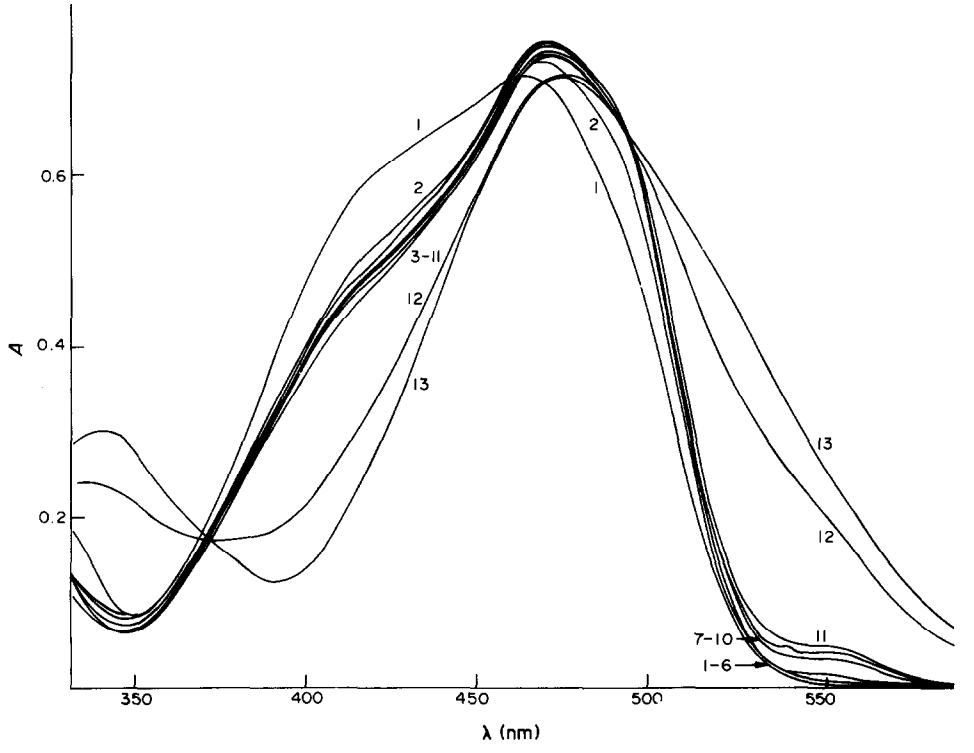

Fig. 2. Absorption spectra of PAN–NEMOL K-1030. Influence of pH.1, pH 1.26; 2, pH 1.93; 3, pH 3.21; 4, pH 4.10; 5, pH 5.08; 6, pH 6.06; 7, pH 7.10; 8, pH 8.02; 9, pH 8.83; 10, pH 10.07; 11, pH 10.88; 12, pH 12.32; 13, pH 12.85; PAN $4 \times 10^{-5} M$; NEMOL K-1030 2% w/v.

the solutions in this pH range have practically identical spectra, with a well defined maximum at 470 nm. The spectra of the protonated and deprotonated forms of PAN are modified by the surfactant; at pH <3 there is a large bathochromic shift and at pH >11 the maximum at about 465 nm disappears and a maximum appears at 475 nm (Figs. 1 and 2). By the Kwiatowsky method[14] two isosbestic points are found at 370 and 458 nm, showing the existence of three absorbent species.

By means of the Stenstrom and Goldsmith method[15] the PAN acid dissociation constants $K_1 = 9.55 \times 10^{-2}$ and $K_2 = 1.15 \times 10^{-12}$ at $1M$ ionic strength (HCl–KCl, KCl–KOH) were obtained. These values are analogous to those obtained in other solvents.[16–20]

Spectrophotometric study of surfactant–Cd–PAN system

Influence of pH. The spectra of Cd–PAN solutions in presence of NEMOL K-1030 at different acidities, ionic strength $0.1M$, and 25°, measured against PAN–surfactant blanks, show a well defined maximum at 555 nm at pH >8 (Fig. 3). A graph of absorbance at this wavelength as a function of pH indicates that the optimum working range is pH 9–10 (Fig. 4).

Influence of surfactant. Examination of the influence of three nonylphenols (NEMOL K-36, K-1030 and K-2030) on the Cd–PAN system at pH 9 ($Na_2B_4O_7$–$HClO_4$), ionic strength $0.1M$ and 25° shows that λ_{max} is 555 nm in all three cases, but the absorptivity is greatest with NEMOL K-1030.

As Cd–PAN is only slightly soluble at pH 4–11, the concentration of K-1030 needed to dissolve the compound has been studied. Concentrations $<8 \times 10^{-4}M$ do not cause dissolution and concentrations $>2.4 \times 10^{-2}M$ enhance the PAN blank absorbance and decrease the sensitivity.

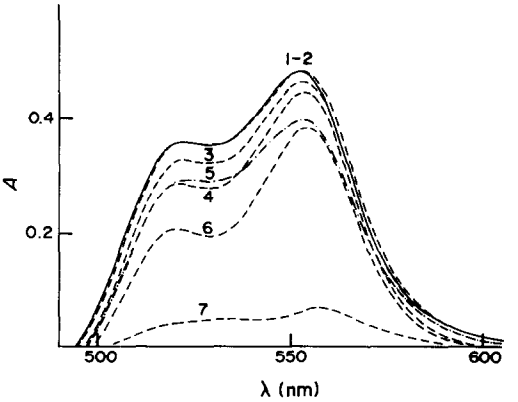

Fig. 3. Absorption spectra of Cd–PAN–NEMOL K-1030. Influence of pH. 1, pH 9.06; 2, pH 9.76; 3, pH 11.66; 4, pH 12.44; 5, pH 8.24; 6, pH 12.92; 7, pH 7.31; Cd(II) $0.96 \times 10^{-5}M$; PAN $10^{-4}M$; NEMOL K-1030 2% w/v. Reference reagent blank.

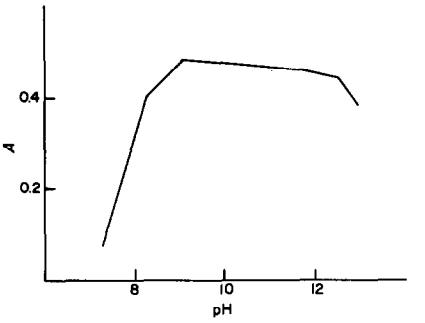

Fig. 4. Absorbance *vs.* pH for Cd–PAN–NEMOL K-1030 at 555 nm. Reference reagent blank.

Cd–PAN and PAN solutions in presence of NEMOL K-1030 at pH 8–11 are stable for at least 24 hr. The order of addition of the reagents does not matter.

Stoichiometry and stability constant. The molar-ratio, continuous-variations and slope-ratio methods all show the Cd/PAN ratio to be 1:2. The conditional stability constant is 3.47×10^{11} at pH 9.

Analytical characteristics. Beer's law is obeyed over the cadmium concentration range 0.44–1.74 μg/ml in the solution measured. The molar absorptivity is 4.94×10^4 l.mole^{-1}.cm^{-1} at 555 nm. The mean deviation of points from the line is 0.9%. The relative standard deviation S_r for 11 independent tests is 0.7% and the limit of detection C_L is 0.009 μg/ml. The selectivity with respect to important species in ceramics is shown in Table 1.

Results

Each test sample was analysed in triplicate. The results obtained by the proposed method and by AAS analysis of the initial acetic acid extracts are shown in Table 2. A single wash of the organic phase with NH_4^+/NH_3 buffer is enough to remove all the zinc in

Table 1. Influence of foreign ions on the determination of cadmium. Cd(II) 1 ppm. Maximum tolerance 3% ($4S_r$) of the original absorbance 0.434. Reference reagent blank.

Interferent	Compound taken	Concentration, *ppm*	A_{555}
PO_4^{3-}	Na_2HPO_4	500	0.437
F−	NaF	500	0.446
SiO_3^{2-}	$Na_2SiO_3 \cdot 5H_2O$	200	0.425
Ba(II)	$Ba(NO_3)_2$	500	0.444
Ca(II)	$CaCO_3$	200	0.438
Li(I)	$LiCO_3$	100	0.423
Se(IV/VI)	Se(HCl–HNO_3)*	40	0.453
Mg(II)	$Mg(NO_3)_2 \cdot 6H_2O$	20	0.445
Al(III)	$Al(NO_3)_3 \cdot 9H_2O$	10	0.425
Hg(II)	$Hg(NO_3)_2 \cdot H_2O$	2	0.433
Zr(IV)	$ZrOCl_2 \cdot 8H_2O$	1	0.449
Mn(II)	Mn(HCl)*	0.2	0.435
Pb(II)	$Pb(NO_3)_2$	0.2	0.443
Ti(IV)	TiO_2($KHSO_4 - H_2SO_4$)*	0.2	0.444
Co(IV)	$Co(NO_3)_2 \cdot 6H_2O$	0.05	0.445
Cu(II)	Cu(HNO_3)*	0.01	0.439
Zn(II)	Zn(HCl)*	0.01	0.443
Ni(II)	Ni(HNO_3)*	0.01	0.445

*Element dissolved with the species shown in parentheses.

Table 2. Comparison of results

Sample	Contents (AAS), *ppm*			Cd found, *ppm*
	Cd	Pb	Zn	
1	19.9	12.3	31.2	19.9
2	10.4	26.7	9.5	10.1
3	19.8	13.8	44.0	21.2
4	42.2	50.0	92.5	40.5
5	7.4_6	8.3	24.6	7.5_3

the analysis of enamels with a Zn/Cd ratio not higher than 2; for higher ratios more than one washing is necessary (two for samples 4 and 5). Copper, nickel and cobalt remain in the organic phase; aluminium is not extracted from the original aqueous phase.

The tolerances for cadmium in enamelled surfaces range from 0.1 to 2 μg/ml, depending on the country making the regulations.[21] The method proposed in this work can be applied to determination of cadmium in the acetic acid extracts of these surfaces,[22] by virtue of its low limit of detection and other analytical characteristics.

REFERENCES

1. K. Ueno, in *MTP Intern. Rev. Sci., Phys. Chem. Ser. One, Anal. Chem.*, 1973, **13,** 43.
2. W. L. Hinzer, in *Solution Chemistry of Surfactants*, K. L. Mittal (ed.), Vol. 1, pp. 79–127, Plenum Press, New York, 1979.
3. N. Desai and H. Gandhi, *Chim. Anal. (Paris)*, 1968, **50,** 297.
4. S. Shibata, *Anal. Chim. Acta*, 1960, **23,** 367.
5. Y. K. Tselinskii and E. V. Lapitskaya, *Metody. Analit. Khim. Reaktivov Prep.*, 1968, **15,** 92.
6. H. Akaiwa and H. Kawamoto, *Bunseki Kagaku*, 1978, **27,** 449.
7. H. Watanabe, *ibid.* 1974, **23,** 396.
8. *Idem, ibid.*, 1979, **28,** 366.
9. *Idem, Talanta*, 1974, **21,** 295.
10. K. Goto, S. Taguchi, Y. Fukue and H. Watanabe, *ibid.*, 1977, **24,** 752.
11. Q. Wen Bing, *Kao Teng Hsueh Hsiao Hua Hsueh Pao*, 1981, **2,** 385; *Chem. Abstr.*, 1981, **95,** 176231.
12. W. C. Griffin, *J. Soc. Cosmet. Chem.*, 1949, **1,** 311.
13. A. W. Norris, *Trans. Brit. Cer. Soc.*, 1950–1, **50,** 255.
14. T. Nowicka-Jankowska, *J. Inorg. Nucl. Chem.*, 1971, **33,** 2043.
15. W. Stenstrom and N. Goldsmith, *J. Phys. Chem.*, 1926, **30,** 1683.
16. E. Bishop, *Indicators*, Pergamon Press, Oxford, 1972.
17. V. M. Ivanov, A. I. Busev and N. S. Ershova, *Zh. Analit. Khim.*, 1973, **28,** 214.
18. I. G. Per'kov and I. T. Polkovnichenko, *ibid.*, 1974, **29,** 9.
19. A. Lewandowski, *Chem. Anal. (Warsaw)*, 1977, **22,** 349.
20. E. Šimuničová and D. Rúriková, *Chem. Zvesti*, 1979, **33,** 57.
21. L. Lopez Mateo, A. Ravagioli and J. E. Enrique Navarro, *Bol. Soc. Espan. Ceram. Vidrio*, 1977, **16,** 73.
22. ASTM C 738–76. *Lead and cadmium extracted from glazed ceramic surfaces.*

Talanta, Vol. 30, No. 12, pp. 919–924, 1983
Printed in Great Britain.

0039-9140/83 $3.00 + 0.00

THE BILAYER LIPID MEMBRANE AS A BASIS FOR A SELECTIVE SENSOR FOR AMMONIA

MICHAEL THOMPSON, ULRICH J. KRULL and LEAH I. BENDELL-YOUNG
Department of Chemistry, University of Toronto, 80 St. George St., Toronto, Ontario, Canada

(*Received* 28 *March* 1983. *Accepted* 22 *June* 1983)

Summary—The development of an electrochemical method for the selective sensing of ammonia gas, based on a modified bilayer lipid membrane, is described. Membrane selectivity for ammonium ion is achieved through incorporation of the antibiotic nonactin as ion-carrier. The detection limits compare favourably with those for conventional ammonia gas-sensing electrodes, but the selectivity is much superior. Theoretical evaluation of the potential sensitivity of the new gas-sensor with respect to design parameters is described.

A number of gas-sensing electrodes based on conventional electrochemistry are commercially available and are suitable for measurement of small inorganic gas molecules such as CO_2, SO_2, H_2S, NO_x and NH_3. Applications have been found in areas such as water, sewage, blood-gas and protein-concentration analysis. These systems are based on the hydrogen-ion selective electrode, the sensing tip of which is covered with a thin film of aqueous electrolyte solution. As gas diffuses into this solution to establish a partial-pressure equilibrium, associative reactions with the solvent occur, producing changes in pH. The pH of the aqueous film is directly proportional to the partial pressure of gas in the external aqueous solution or gas phase. There are three types of such gas sensors,[1] classified according to whether they are constructed with microporous hydrophobic membranes, homogeneous dense-polymer membranes which are semipermeable to gases, or with an air gap a few mm wide. Selectivity for a particular gas is obtained by use of different semipermeable membranes and pH conditions. The detection limits for some common gases are 10^{-8} *M* for H_2S, 10^{-7} *M* for NH_3 and NO_x, and 10^{-6}–10^{-5} *M* for CO_2 and SO_2.[1] These systems are often limited by contamination of the solvent or electrolyte, or by difficulties with the membranes used.

The bilayer lipid membrane (BLM) has been investigated as an electrochemical detection system for organic compounds, and offers substantial improvements over conventional electrochemical systems.[2] Chemically, this structure has a central non-polar hydrocarbon region, bounded on both sides by polar sheets of lipid head-groups which are hydrated in a supporting aqueous electrolyte.[3] Application of a small direct electrical potential difference across this structure will result in passage of a finite ion-current through the membrane. It has been suggested that an interaction between a membrane-bound receptor and a stimulant, resulting in a transmembrane ionic flux, is a suitable model for the development of a sensitive and selective electrochemical sensor. The important physical/chemical factors governing control and alteration of the transmembrane ion flux, as well as a number of successful receptor-based sensing systems, have already been studied,[2,4] and indicate the feasibility of this concept. The BLM sensor is not subject to the competitive effects which limit the use of ion-selective electrodes, since the development of an equilibrium interfacial potential is not the primary source of the analytical signal. This work describes the construction and operation of a prototype BLM gas-sensor designed to be selective for ammonia.

EXPERIMENTAL

Apparatus

Solution cell. The cell used for electrochemical investigation of the selectivity of the BLM consisted of two identical machined Perspex blocks separated by a Teflon sheet (0.1 mm thick) with a 1-mm diameter hole in it to support the BLM. An external d.c. voltage was applied across the membrane between two Ag/AgCl single-junction reference electrodes with agar salt bridges (Orion Research Inc., Cambridge, Mass). The external circuitry consisted of a d.c. power supply and a microprocessor-controlled multichannel digital electrometer (Keithley System 1, Keithley Instruments, Cleveland, OH) for data acquisition. An optical system consisting of a cold-light halogen–quartz fibre-optics illuminator and a wide-angle 20× microscope was used to investigate and monitor formation of the BLM. The solution cell and all sensitive electronic equipment were isolated in a well grounded Faraday cage.

Gas-sensor cell. The basic design of the gas-sensor electrochemical cell retained the concept of two solution compartments separated by a BLM. The BLM was formed in a standard Teflon sheet, and supported at one face by a Perspex half-cell as described above. A Teflon semipermeable membrane designed for use with an ammonia electrode (Ammonia Porous Membranes, Orion Research Inc.) was used to trap a thin layer of electrolyte at the other membrane face and act as the interface to the gas phase. The trapped aqueous layer was connected by means of a thin channel to an Ag/AgCl reference electrode, as shown in Fig. 1. A specially constructed external clamp was used to

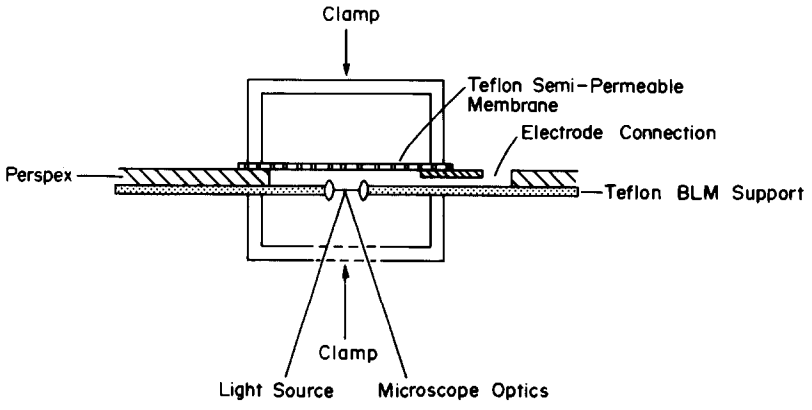

Fig. 1. Schematic of BLM support system used in the gas detection cell.

sandwich the Teflon sheet and semipermeable membrane to a central Perspex support; this made it easy to clean the apparatus and replace the Teflon. The external electrochemical equipment was as described above.

Reagents

The antibiotics valinomycin, gramicidin and nonactin were obtained from the Sigma Chemical Company, St. Louis, MO. The lipid used for BLM formation was egg phosphatidyl choline, obtained as lyophilized powder from Avanti Polar Lipids, Inc., Birmingham, AL. Cholesterol (obtained from Sigma) was recrystallized from ethanol. Electrolyte solutions were prepared from the reagent-grade chlorides of potassium, lithium, magnesium and ammonium, and doubly distilled water scrubbed free from organic compounds with an "organic removal cartridge" incorporated in the still. All other chemicals were also of reagent grade.

Procedures

The BLMs were formed from a 2% lipid, 2% cholesterol solution in n-decane that had been purified on an alumina column and dried with a molecular sieve. The lipid-containing solution was introduced into the aperture in the Teflon by means of a fine sable-hair brush, to form a lipid plug between the two 5-ml capacity compartments for the aqueous solution. The lipid plug spontaneously thinned to form a BLM, as observed optically and electrochemically. The membranes were formed under an applied d.c. potential difference of +25 mV, and were allowed to stabilize for a minimum of 10 min before any investigations were performed. Electrochemical observations involved the monitoring of transmembrane current as various reagents were added from a Gilson "Pipetman" adjustable-capacity pipette to the stirred aqueous supporting electrolyte.

The ion-selectivity of the BLM could be modified by incorporation of different antibiotics. Initial experiments were performed with the solution cell to determine which of the antibiotics giving substantial response to univalent cations were selective for ammonium ions. The change in transmembrane ion current with concentration of antibiotic added (as a solution in methanol) to the various 0.1*M* salt solutions was employed as an indicator of ion-selectivity. The concentration–response curves of BLMs modified with the chosen antibiotics were then determined, for various electrolytes. This step gave the optimum operating conditions for the gas cell, which was then tested for response to gaseous ammonia by replacement of one solution compartment by the gas-phase interface.

RESULTS AND DISCUSSION

BLM response characteristics

The design of the electrochemical cell and membrane support is similar to that for a conventional glass-electrode type gas-sensor.[5,6] The operation of the system depends on using a membrane semipermeable to ammonia gas as an interface between the fragile free BLM and the gas sample. Though part of the selectivity is provided by the semipermeable membrane, most of it comes from the polypeptides incorporated in the BLM. These compounds preferentially complex and transport ammonium ions across the membrane, so there is an increase in ion current in the presence of ammonia gas. The principle of operation is analogous to that of the diffusion-controlled Clark oxygen electrode,[7] indicating sensitivity to thickness of the Teflon membrane and to the rate of sample-stirring since ammonium ion is continuously consumed during the measurement. It is important to note that the effect of pH on the ion conductance of these BLMs is minimal in the range 3–11. Direct contact of the BLM with sample solutions at pH >11 (as commonly employed with ammonia electrodes)[8] may cause destabilization of the membrane unless the mechanical strength is increased.

Polypeptide antibiotics demonstrate a remarkable ability to distinguish between chemically similar ions, and complex such ions selectively for transport across BLMs.[3] Four major groups of antibiotics have been applied to BLMs for electrochemical investigation. These are the valinomycin, polyether, nigericin and polyene groups, of which only the valinomycins and the polyethers are very selective to Group I cations and the ammonium ion. The selectivity is a function of the stability constant of the complex and directly related to the membrane permeability constants. A summary of such constants is presented in Table 1 and contrasts the extreme selectivity differences between gramicidin, valinomycin, nonactin (all from the valinomycin group) and a polyether.

Table 1. Relative antibiotic selectivities for univalent cations

Antibiotic	Log (permeability X^+/permeability K^+)			
	Li^+	Na^+	K^+	NH_4^+
Gramicidin[9]	−0.9	−0.2	0	+0.1
Valinomycin[10]	−6	−5	0	−2
Nonactin[10]	−3	−2	0	+0.75
*Crown ether[11]	−2	−1.5	0	−0.5

*Bis(tert.-butyl)dicyclohexyl-18-crown-6.

To reduce the background ion-current of the gas sensor and maximize the sensitivity and selectivity for the ammonium ion, the BLM is made with the antibiotic of greatest selectivity for ammonium ion, and the supporting electrolyte should have low concentration and contain a cation for which the polypeptide has minimum selectivity. Figure 2 shows the change in ion-current on addition of antibiotic to membranes bathed in various electrolytes. The results indicate that of the antibiotics tested, nonactin has the greatest selectivity for ammonium ion relative to potassium and lithium. It also has equally poor selectivity for lithium and magnesium, so use of salts of either of these as supporting electrolyte will maximize analytical response to ammonium ion. The concentration–response curves for ammonium ion showed a marked increase in sensitivity as the lithium chloride concentration was reduced to a value slightly above the minimum required for stable BLM formation. Reduction of the electrolyte concentration reduces the competitive effect of lithium but may also lead to increased osmotic effects which can result in drift of background signal as the internal solution volume and electrolyte concentration vary. The membrane concentration of antibiotic also affects the overall analytical signal. The membranes used were loaded with nonactin (in equilibrium with a final aqueous solution concentration of $10^{-5}M$), but not to the point of saturation (a limit is set by membrane destabilization). The detection limit in this work was found to be approximately $10^{-6}M$, although

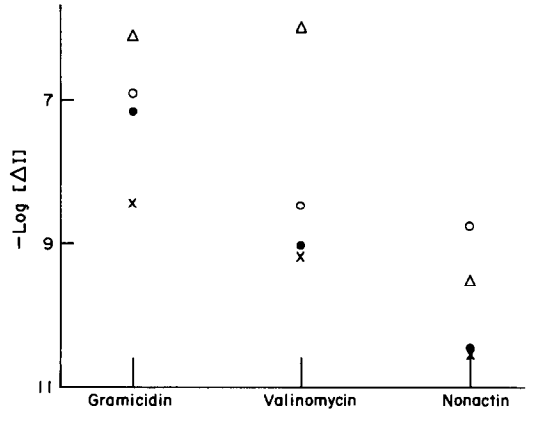

Fig. 2. Comparison of analytical signals induced by addition of different antibiotics at $10^{-6}M$ aqueous concentration, for a BLM immersed in $0.1M$ electrolyte solutions at pH 5: △ = KCl, ● = LiCl, ○ = NH_4Cl, × = $MgCl_2$. The residual current before addition of antibiotic was about 10^{-11} A.

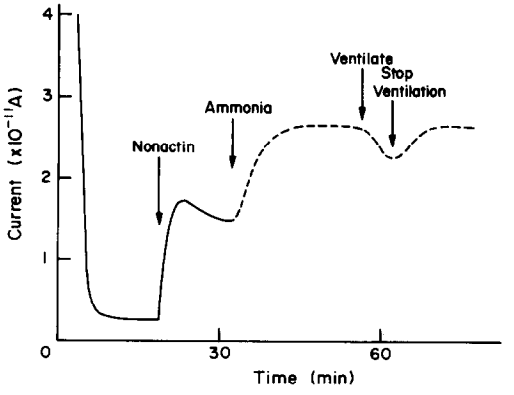

Fig. 3. Results for sensing of concentrated ammonia gas with the nonactin/LiCl system and cell design as illustrated in Fig. 1.

10^{-7}–$10^{-8}M$ may be achievable with optimization of appropriate conditions. Deviations from linearity are expected at high ammonium ion concentrations because of ionic strength effects on the response.

An attempt was made to use a sensor based on the nonactin/LiCl system to detect a high concentration of ammonia gas in an enclosed space. The results are shown in Fig. 3, and exhibit the expected time-dependence for diffusion-controlled gas permeation resulting in production of an ammonium ion population on one face of the BLM. The signal was small, owing to the 1-mm aqueous layer thickness used.

Model of BLM gas-sensor operation

To evaluate the influence of various design parameters on the BLM gas-sensor described, a mathematical model for diffusion of ammonia gas and ammonium ions in the experimental system has been developed. By use of the basic diffusion equation shown below, and the parameters summarized in Table 2, a measure of the ion current through a BLM can be obtained.

$$M = DAt(C_2 - C_1)/H \qquad (1)$$

where M = number of molecules, D = diffusion coefficient, A = area, t = time, H = thickness,

Table 2. Parameters used in calculations

Diffusion zone	Parameter	Value
Teflon membrane	Diffusion coefficient	0.2 cm^2/sec
	Area of membrane	0.005 cm^2
	Membrane thickness	0.05–0.01 cm
	Concentration of NH_4^+	1.6×10^{13}–1.5×10^9 molecules/cm^2
	Time	1 sec
Thin aqueous film	Diffusion coefficient	1×10^{-5} cm^2/sec
	Area of film	0.005 cm^2
	Zone thickness	0.1–0.01 cm
	Time	1 sec

(Calculated on basis of area of BLM and ratio $NH_4^+/NH_3 = 300$ in aqueous phase.)

Table 3. Experimental BLM ion-flux data

Aqueous ion concentration, M	Change in current, *A*	Ion flux, *ions/sec*	BLM interfacial ion density*
1×10^{-6}	3.0×10^{-12}	1.88×10^{7}	3.6×10^{7}
1×10^{-5}	1.8×10^{-11}	1.13×10^{8}	1.7×10^{8}
1×10^{-4}	1.4×10^{-10}	8.75×10^{8}	7.7×10^{8}
1×10^{-3}	1.0×10^{-9}	6.25×10^{9}	3.6×10^{9}

*Number of ions in the BLM.

C_2 = number density of molecules outside the diffusion zone and C_1 = number density of molecules inside the diffusion zone.

The diffusion problem has been simplified into a two-step time-dependent reiteration process which initially involves gas permeation through the Teflon membrane into the internal aqueous phase, to establish a localized high concentration of ammonium ion. This concentration is then used to calculate the diffusion to the BLM surface, and this combined with the active-ion transport rate [obtained from the experimental data (Table 3)] finally produces an estimate of the increase in transmembrane ion flux above the background level. The model is summarized in Fig. 4a, which shows the various diffusion zones. For simplicity, the area chosen for the calculations was the area of the BLM used in this work. This implies that the calculated current represents a minimum analytical signal since lateral diffusion is

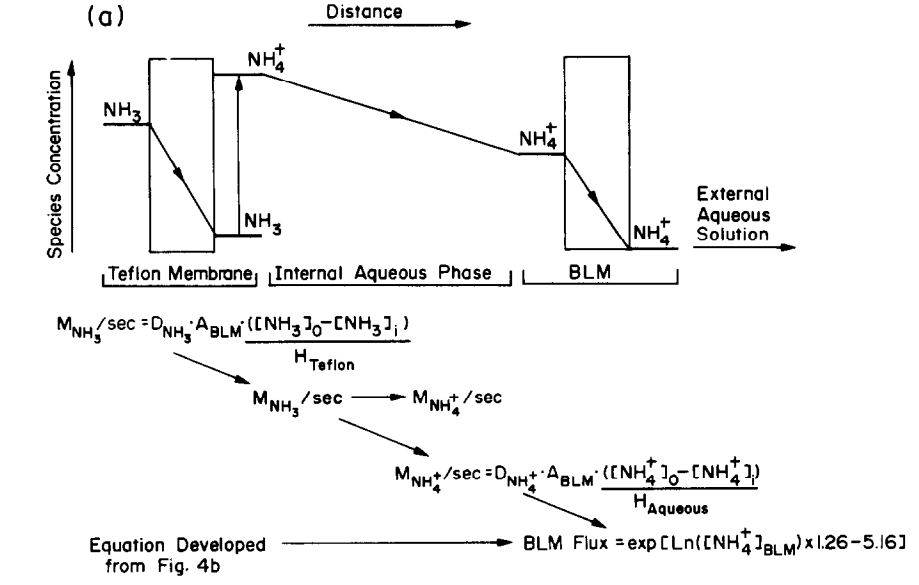

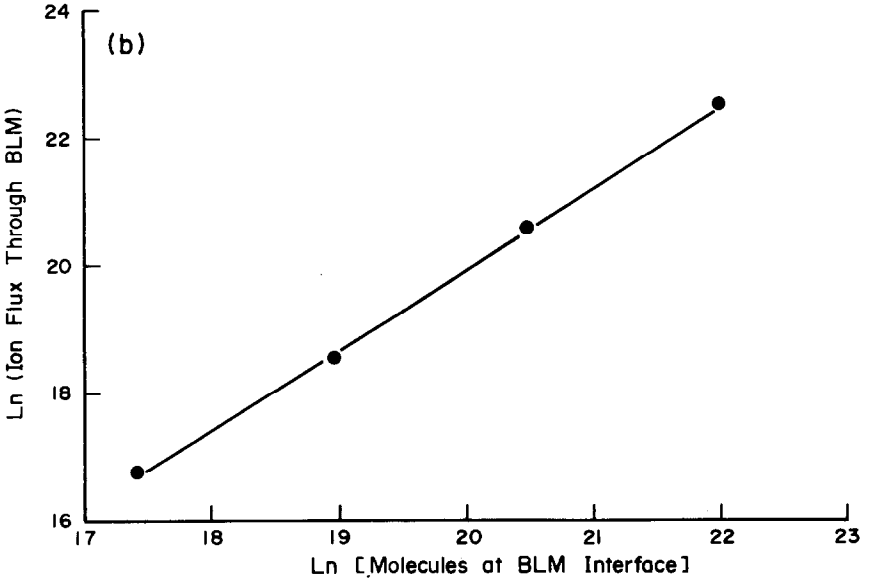

Fig. 4. (a) Schematic representation of the diffusion model employed for calculations. (b) Relationship of transmembrane ammonium ion flux to the ion number density at the BLM interface.

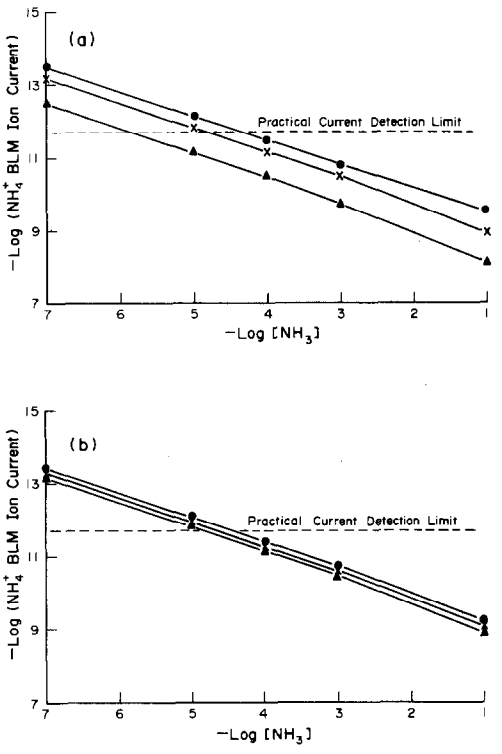

Fig. 5. (a) Calculated BLM ion current as influenced by the thickness of the thin aqueous film. ● = 0.1 cm, × = 0.05 cm, + = 0.01 cm. (b) Calculated alteration in BLM ion current, caused by variation of the thickness of the Teflon semi-permeable membrane. ● = 0.05 cm, × = 0.03 cm, + = 0.01 cm.

not considered. Table 3 gives a summary of the experimental data collected from the calibration curve. The data are further developed in Fig. 4b to illustrate the trend of observed ion current as a function of the interfacial concentration of ammonium ion. The ion-transport process apparently becomes more efficient as the available interfacial ammonium ion concentration increases. This may be due to a concerted effect caused by reduction of the fluidity of the membrane by structure perturbation by the carrier complex, and a concurrent increase in ion-transport rate. An analysis of the influence of the thickness of the Teflon membrane and underlying aqueous thin film is provided in Fig. 5. Removal of the Teflon membrane and replacement of the aqueous phase with a hydrated gel-like layer was found to give little difference from the results presented in Fig. 5b. The aqueous phase is the diffusion rate-determining zone and controls the final BLM ion current.

Analytical potential

The sensitivity of the modified BLM towards ammonium ion compares favourably with that of commercial ammonia gas-sensors. Exposure of nonactin-loaded membranes to methylamine hydrochloride concentrations up to 0.005*M* did not produce any significant analytical signal, nor did it affect subsequent determination of ammonium ion concentration, indicating a substantial selectivity advantage for the BLM-based sensor. This is necessarily the case, owing to the origin of the selectivity of these membranes. Since nonactin traps the cation in the centre of a large pseudospherical structure, and the cavity at the interior of this structure determines the binding capability,[3] complexation of the methylammonium ion is physically less easy than that of the smaller Group I and ammonium ions. Table 4 identifies common volatile amines which interfere with the conventional ammonia gas-sensor.[1] Since methylamine is the most potent interferent, and is also physically the smallest molecule listed, it seems that the BLM sensor is effectively immune to interference from such volatile amines. The selectivity of the modified BLM ammonia gas-sensor is therefore substantially greater than that of conventional sensors.

The solution experiments indicated that the 99% response time for an order of magnitude change in ammonium ion concentration is 1–2 min, which is fast enough for adequate routine laboratory use.[8] Calculations indicate that the same holds true for gas-phase sensing with the BLM electrode.

The investigation of this prototype gas-sensing system revealed the following deficiencies in design and function.

(1) The large volume of trapped aqueous electrolyte must be reduced to minimize response time and maximize analyte ion concentration.

(2) The electrochemical response should be measured by integrating the transmembrane ion-current since equilibration of the gas-phase and bulk solution concentrations cannot be attained, because of the dynamic ion-transport system involved.

(3) The BLM must be supported or altered in some manner to give it greater mechanical stability without impairing its electrochemical sensitivity. This would minimize difficulties from transmembrane pressure and osmotic pressure, and might allow elimination of the Teflon semipermeable membrane, which at present is required only for membrane support.

These deficiencies do not preclude the further development of useful BLM-based selective gas-sensors, especially in the light of recent advances in thin-layer technology involving Langmuir–Blodgett production of stable polymerized lipid films.[12] A

Table 4. Common interferents in use of the ammonia gas probe[1]

Interferent	Estimate of apparent increase (*mg/l.*) in ammonia concentration for [Interferent] = [NH_3] = 1 mg/l.
Methylamine	0.3
Ethylamine	0.2
Hydrazine	0.02
Cyclohexylamine	0.03
Octadecylamine	0.3

further area of interest involves the coupling of macroelectrode technology with the field-effect transistor (FET). The production of an ammonium ion-selective FET based on a polymer membrane loaded with nonactin has already been reported,[13] and a hybrid BLM/FET device will undoubtedly appear in the near future.

Acknowledgements—Support from the Air Resources Branch of the Ministry of the Environment, Province of Ontario, is gratefully acknowledged. We are indebted to the Natural Sciences and Engineering Research Council of Canada for provision of a Fellowship to U.J.K. Also, we thank A. Azzopardi for his assistance in design and construction of part of the gas cell.

REFERENCES

1. P. L. Bailey, *Analysis With Ion-Selective Electrodes*. Heyden, London, 1976.
2. M. Thompson and U. J. Krull, *Anal. Chim. Acta*, 1983, **147**, 1.
3. H. Ti Tien, *Bilayer Lipid Membranes*. Dekker, New York, 1974.
4. M. Thompson and U. J. Krull, *Anal. Chim. Acta*, 1982, **141**, 33.
5. W. Severinghaus, *Ann. N.Y. Acad. Sci.*, 1965, **148**, 115.
6. Orion Research Inc., *Instruction Manual 95-10*, 1971.
7. L. C. Clark, *Trans. Am. Soc. Artificial Internal Organs*, 1956, **2**, 41.
8. J. W. Ross, J. H. Riseman and J. A. Krueger, *Pure Appl. Chem.*, 1973, **36**, 473.
9. S. B. Hladky and D. A. Haydon, *Biochim. Biophys. Acta*, 1972, **274**, 294.
10. J. M. Diamond, *J. Exp. Zool.*, 1975, **194**, 227.
11. G. Szabo, G. Eisenman, R. Laprade, S. M. Ciani and S. Krasne, in *Membranes*, G. Eisenman (ed.), Vol. 2. Dekker, New York, 1973.
12. O. Albrecht, D. S. Johnston, C. Villaverde and D. Chapman, *Biochim. Biophys. Acta*, 1982, **687**, 165.
13. U. Oesch, S. Kara and J. Janata, *Anal. Chem.*, 1981, **53**, 1983.

Talanta, Vol. 30, No. 12, pp. 925–931, 1983
Printed in Great Britain.

0039-9140/83 $3.00 + 0.00

ELECTROLYTIC REDUCTION OF MOLYBDOPHOSPHATE IN AQUEOUS ACETONITRILE AND ITS APPLICATION TO FLOW-COULOMETRIC DETERMINATION OF ORTHOPHOSPHATE

T. HORI*
Department of Chemistry, College of Liberal Arts and Sciences, Kyoto University, Kyoto 606, Japan

T. FUJINAGA
Department of Chemistry, Kobe Gakuin University, Kobe 673, Japan

(*Received* 21 *February* 1983. *Accepted* 20 *June* 1983)

Summary—The formation and electrolytic reduction of molybdophosphate in aqueous solutions of various water-miscible organic solvents have been extensively investigated. Acetonitrile was found to be the most useful of these solvents. Two species of molybdophosphate are formed in aqueous acetonitrile, one of which changes spontaneously into the other, which is quite stable and undergoes a 2-electron electrolytic reduction. On the basis of these facts, a flow-coulometric method for orthophosphate has been developed, applicable to the range 5×10^{-6}–$1 \times 10^{-3}M$. It has been used for determination of orthophosphate in several phosphorus compounds, some of which are acid-labile.

On the basis of the chemistry of molybdophosphate formed in aqueous and aqueous ethanol solutions, we have already developed a flow-coulometric determination of phsophate by direct injection of 100 μl of sample into a steady flow of a mixed 0.05*M* molybdate–1.2*N* sulphuric acid reagent prepared in 20% v/v ethanol medium.[1] Molybdophosphate is formed rapidly and quantitatively and can then be electrolytically reduced. The ethanol is essential for complete formation of molybdophosphate at the high acidity needed to facilitate the electrolysis. The method has many advantages over others for phosphate: (*i*) only a 100-μl sample is needed; (*ii*) the determination takes only 2 min, so there is practically no interference from hydrolysis of other phosphorus compounds to orthophosphate; (*iii*) unstable reductants are replaced by electrolytic reduction; (*iv*) coulometric measurements have high reproducibility. The only problem is that the charging current at the working electrode in the flow-electrolysis cell is slightly perturbed by the injection of aqueous sample, which causes noise in the base-line, overlapping the true coulometric signal. This noise causes a negative error of about $5 \times 10^{-6}M$ in the phosphate concentration, but can be corrected for, since it is fairly reproducible when a fixed volume of sample is injected. Fogg and Bsebsu[2] have examined this and concluded that it can be avoided by injecting samples already mixed with acidic molybdate reagent. This lowers the determination limit to $10^{-6}M$ phosphate. However, it entails giving up the most important advantage, that of use of an extremely small volume of phosphate sample. As a compromise, Fogg and Bsebsu proposed the use of molybdate reagent acidified with sulphuric acid to give the optimal composition,[3] to which the direct injection was made.

We have now investigated the use of mixtures of water and various water-miscible organic solvents as the reaction medium and found that acetonitrile is the best for flow-coulometry. In the improved method the sample is injected into a steady flow of water which is then mixed in 1:1 ratio with a steady flow of a composite molybdate/hydrochloric acid/acetonitrile reagent. This allows quantitative conversion of phosphate into molybdophosphate (which is then electrolytically reduced) and minimizes the effect on the base-line for the charging current. Because of the conditions required for the coulometry a double-strength composite molybdate reagent is needed to compensate for the dilution by the sample-carrier stream, but fortunately the acetonitrile solution is stable enough for long-term storage, in contrast to an ethanol solution at the same concentration.

*To whom all correspondence should be addressed and who wishes to dedicate his contribution to the work to his co-author in celebration of the award of the Talanta Gold Medal to Professor Fujinaga.

EXPERIMENTAL

Reagents

Standard 0.1000M phosphate. Prepared from potassium

dihydrogen phosphate and kept in a polyethylene bottle. Working standards are made by dilution as required.

*Sodium molybdate solution 0.5*M. Kept in a polyethylene bottle.

Mixed molybdate reagent. Prepared by mixing 400 ml of 0.5*M* molybdate solution, 400 ml of concentrated hydrochloric acid and 800 ml of acetonitrile, and diluting to 2 litres with water. The reagent [0.1*M* Mo(VI)–2.4*M* HCl–40% v/v acetonitrile] can be stored in a polyethylene bottle without appreciable deterioration for at least one month. The acetonitrile (Wako Pure Chemicals GR grade) could be used without further purification, since it was found that it gave practically the same results as those obtained with acetonitrile purified[4] according to standard procedures.

Test solutions. Molybdophosphate solutions for the preliminary coulometric study were prepared by mixing known amounts of 0.1*M* phosphate solutions, 0.5*M* molybdate solution, concentrated hydrochloric acid and acetonitrile, and diluting to known volume (usually 200 ml) with water. The molybdophosphate started to form immediately after the dilution and the formation was reproducible and independent of the order of mixing, but the acetonitrile concentration had a remarkable effect on the course of formation. In solutions containing less than 20% v/v acetonitrile, formation of molybdophosphate reached equilibrium within a few minutes, whereas at higher acetonitrile concentrations a bright yellow species of molybdophosphate formed instantaneously and was then gradually converted into the ordinary species of molybdophosphate at a specific rate depending on the acetonitrile concentration. The final product was the same in both cases. The complexes can be easily distinguished by their difference in optical properties at about 420 nm, and will be referred to here as the "ordinary" and "extraordinary" forms (except that "ordinary" will be omitted when no confusion can arise).

In addition to these mixtures, several phosphorus compounds were prepared as sample materials. Of these, $Na_5P_3O_{10}$, Na_2HPO_3, adenosine-5′-triphosphate disodium salt, and D-glucose-6-phosphate disodium salt were commercially available and used as received; monomethyl phosphate and dimethyl phosphate were separated[5] from a commercially available mixture; monomethyl phosphonate was synthesized[6] from triphenyl phosphite and methyl iodide.

Apparatus

A Shimadzu UV-200 automatic recording spectrophotometer equipped with a constant-temperature housing for the cuvettes was used. Measurements were made at $25 \pm 0.2°$ (unless otherwise indicated) in quartz cuvettes (path-lengths 1, 0.2 and 0.1 cm).

In accordance with the principles of flow-electrolysis,[7] a flow-through cell[1] was constructed, combining a column electrode packed with 0.5 g of glassy-carbon fibre, a platinum counter-electrode, and a reference electrode of silver–silver chloride in saturated potassium chloride solution. The applied e.m.f. was controlled by a Hokuto Denko HA-501 potentiostat and in some cases was varied by a programme from a Hokuto Denko HB-104 function generator attached to the potentiostat. The currents were recorded on a Rika Denki R-20 recorder.

The reaction system is shown in Fig. 1. Three Pharmacia P-1 peristaltic pumps were used, one for pumping the sample-carrier of pure water and the mixed molybdate reagent, one for the solution of preformed molybdophosphate, and one for the saturated potassium chloride solution circulating at 1 ml/min round the counter-electrode of the cell. The flow-lines were 2-mm bore silicone rubber tubes. The dampers, reaction coil and delay coils were also silicone rubber tubes (1.3 cm bore × 30 cm, 3 mm bore × 30 cm, and 3 mm bore × 15 cm, respectively). The pressure column was a glass tube, 2 mm in bore and 3 cm long,

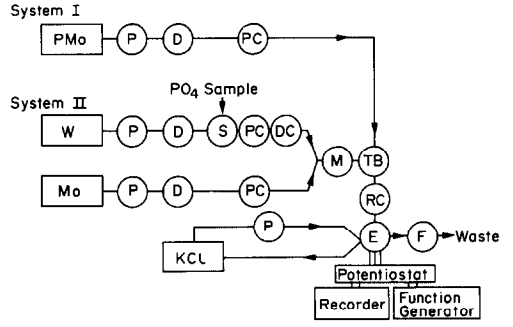

Fig. 1. Schematic representation of flow-electrolysis systems; I, for the measurement of coulopotentiograms of preformed molybdophosphate; II, for the flow-coulometry of phosphate. PMo, W, Mo, and KCl denote molybdophosphate solution, water, mixed molybdate reagent, and saturated potassium chloride solution, respectively; P denotes a peristaltic pump, D a damper, S an injection port for phosphate sample, M a mixer, DC a delay coil, PC a pressure column, TB a three-way tap, RC a reaction coil, E a flow-electrolytic cell, F a flowmeter.

packed with 50–60 mesh glass beads; the sample injection port was T-shaped as already described.[1]

System I in Fig. 1 was used for measuring coulopotentiograms of preformed molybdophosphate, and System II for the flow-coulometry of phosphate. Up to the three-way tap (TB), the systems were independent, with the reaction coil, flow-through cell and detector common to both. To reduce flow pulsation, a damper (D) was included in each line, with its inlet upwards so that there was sufficient room left for air. Smooth and steady flows were thus attained by means of the compressibility of the air, combined with the liquid resistance given by the pressure column (PC).

Measurements of coulopotentiograms

System I was used to investigate the electrochemical behaviour of molybdophosphate under various conditions. The solution of preformed molybdophosphate was pumped at 5.0 ml/min from the reservoir (PMo) to the flow-cell, the e.m.f. applied to the cell was decreased from +0.7 V at a rate of 50 mV/min and the current–voltage curve for the flow-electrolysis was recorded, resulting in a "coulopotentiogram"[7,8] for molybdophosphate. If the electrolytic process is sufficiently rapid and practically 100% efficient, the limiting current, I, on the plateau of the coulopotentiogram, is given by $I = nfCF$, where n is the number of electrons involved in the electrolytic reaction, C the concentration of the depolarizer, f the flow-rate of the sample- carrier, F the Faraday constant. On the basis of this equation, n was calculated from the known values of f and C and the values of I from the coulopotentiograms. The electrolytic characteristics of molybdophosphate were deduced by relating n to the applied potential.

Flow-coulometry for phosphate determination

System II was used for the flow-coulometry of phosphate. The phosphate sample (usually 100 μl) was injected through the injection port (S) by a calibrated microsyringe into the sample- carrier of pure water flowing at 2.5 ml/min from the reservoir (W). The sample stream, after passage through the delay coil (DC), merged with the molybdate reagent stream pumped at 2.5 ml/min from the reservoir (Mo), and was immediately mixed with it in a small mixer (M) by magnetic stirring. The delay coil was incorporated so that any baseline noise caused by the sample injection would be separated in position from the "delayed" coulometric signal. The

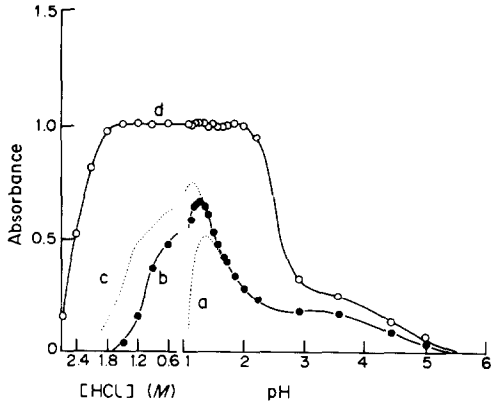

Fig. 2. Formation curves for molybdophosphate as a function of acidity in solutions composed of $1 \times 10^{-3}M$ phosphate, $0.05M$ Mo(VI), and various concentrations of (*a*) H_2SO_4, (*b*) HCl, and (*c*) $HClO_4$. Curve (*d*) illustrates the facilitation of formation by the presence of 17% v/v acetonitrile.

length of the reaction coil (RC) was chosen to give a reaction time of 25 sec so that formation of molybdophosphate was complete just before entry to the flow-cell. The molybdophosphate was preferentially reduced electrolytically in the cell at a fixed potential of +0.350 V, in a 2-electron reaction. The recorder response during the electrolysis gave a peak having an area proportional to the amount of phosphate present in the injected sample, in accordance with Faraday's law of electrolysis.

RESULTS AND DISCUSSION

Formation of molybdophosphate

The conditions for formation of molybdophosphate were preliminarily investigated by spectrophotometry. The effect of acidity is shown in Fig. 2. The curves show that the formation in purely aqueous solution is maximal at a pH of about 1, depending on which acid is d. This creates problems in the use of coulometry in the reduction, since this requires highly acidic conditions, as discussed below.

Halász and Pungor[9] account for this dependence on acidity in terms of the competitive protonation equilibria involving isopolymolybdate species such as $H_4Mo_8O_{26}$ and the eventual production[10] of cationic $HMo_2O_6^+$ and MoO_2^{2+} at high acidity. It has been pointed out[11] that the rapidity of formation of some heteropolymolybdates implies that a substantial portion of the structure must be already present in the particular isopolymolybdate present, which also helps to explain the pH effect, since the degree of condensation of the isopolymolybdate is a function of the acidity. A further complication is the stabilization of molybdate species in highly acidic solutions by association with the anions of the acid used.[12,13] These competitive equilibria always participate in the formation of molybdophosphate in strongly acidified solutions and result in a lower degree of formation at above a certain acidity. On the other hand, increasing the molybdate concentration will offset this effect to an appreciable extent, as reported by Halász and Pungor,[9] and with a molybdate concentration of about $0.1M$ the formation of molybdophosphate is maximal in 0.8–$2.4M$ perchloric acid. However, under these conditions a different species of molybdophosphate (the β-modification) is formed,[14] in agreement with the supposition[11] that the isopolymolybdate species present is a decisive factor. As pointed out by Strickland,[15] the co-existence of more than one form of heteropolymolybdate accounts for the apparent discrepancies in the spectrochemical properties of these systems.

In contrast, when an auxiliary solvent such as acetonitrile is added, the formation of molybdophosphate is markedly improved and the acidity range broadened. Addition of about 17% (v/v) of acetonitrile intensifies the yellow colour and gives a constant absorbance over an acidity range from pH 2.3 to $2.1N$ acid, irrespective of which acid is used (curve *d* in Fig. 2). This increased tolerance range for the acid concentration is particularly favourable for the coulometric work.

The amount of acetonitrile needed for maximal molybdophosphate formation was determined by spectrophotometry (Fig. 3). The absorbance of the molybdophosphate is constant for 10–20% v/v acetonitrile, and increases at higher concentrations, but the time factor is involved, and the colour at the higher acetonitrile concentrations gradually fades, eventually giving the same absorbance as that for solutions containing 10–20% of the solvent. The rapidly formed "extraordinary" complex is only slowly converted into the "ordinary" form, conversion being complete in approximately 2, 5, 14 and 40 hr at 25° for acetonitrile concentrations of 30, 40,

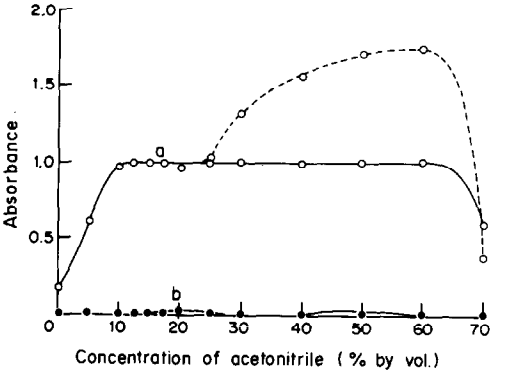

Fig. 3. Formation curves for molybdophosphate as a function of acetonitrile concentration in solutions composed of $1 \times 10^{-3}M$ phosphate, $0.05M$ Mo(VI), $1.2M$ HCl, and various amounts of acetonitrile. Absorbances measured after 10 min (dotted line, for the "extraordinary" complex) and 40 hr (solid line, for the "ordinary" complex) are plotted in curve (*a*), with those of the corresponding blank solutions in curve (*b*).

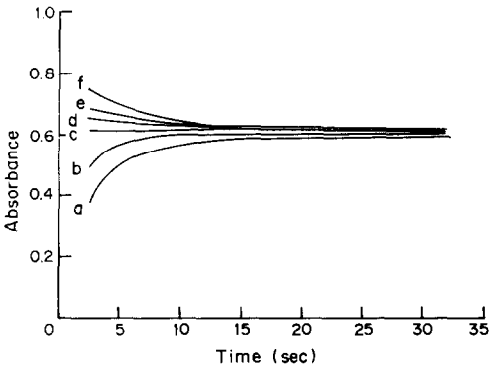

Fig. 4. Rate of formation of molybdophosphate in 20% v/v acetonitrile. A 2-ml aliquot of $6 \times 10^{-4}M$ phosphate was reacted with the same volume of $0.1M$ Mo(VI)–$2.4M$ HCl–40% v/v acetonitrile reagent at temperatures of (*a*) 10°, (*b*) 15°, (*c*) 20°, (*d*) 25°, (*e*) 30°, and (*f*) 35°.

50 and 60% v/v, respectively. The "extraordinary" molybdophosphate can be reduced electrolytically and determined coulometrically, but its electrochemical behaviour is quite different from that of the "ordinary" molybdophosphate, so a mixture of the two cannot be analysed in this way. It was thought safer to use the ordinary form, so the presence of the other complex was avoided either by keeping the acetonitrile concentration below 20%, or by leaving the solutions long enough for only the ordinary form to be present.

Rate of formation of "ordinary" molybdophosphate

In properly acidified aqueous solutions, molybdophosphate forms practically instantaneously. Javier *et al.*[16] measured the formation rate by the stopped-flow technique and confirmed that equilibrium was reached within a few seconds. We have already reported that the rate of formation is not much retarded by the presence of alcohol.[1]

The rate of formation is important for deciding the length of reaction coil needed to allow molybdophosphate to be formed quantitatively. The rate in 20% acetonitrile medium was therefore determined.

A 2-ml portion of $0.1M$ Mo(VI)/$2.4M$ HCl/40% acetonitrile mixture was placed in a 1-cm quartz cuvette and brought to the desired temperature, then 2 ml of $6 \times 10^{-4}M$ phosphate (at the same temperature) were added and quickly mixed in, care being taken to avoid production of air-bubbles. At the same time a stop-watch was started, and the absorbance at 420 nm was recorded as a function of time, and corrected for the reagent blank.

Figure 4 shows that at temperatures below ~20°, only the "ordinary" species is formed, but at higher temperatures a little "extraordinary" species is initially formed but rapidly decays. The slight differences between the final absorbances are probably due to the very short time span, and experimental error. Increasing the acetonitrile concentration decreases the rate of conversion of the "extraordinary" complex, and also results in its initial formation even at the lower temperatures.

Coulometric study

Suitable potentials for rapid and quantitative electrolytic reduction of molybdophosphate were found from the coulopotentiograms obtained by using flow system I. Typical coulopotentiograms for $2 \times 10^{-4}M$ phosphate/$0.05M$ Mo(VI)/$1.2M$ HCl are shown in Fig. 5. Curve (*a*), for purely aqueous medium, shows an ill-defined cathodic wave at around +0.35 V, in contrast to curve (*b*), for 20% acetonitrile medium, which gives a well-defined cathodic wave with a distinct plateau between +0.41 and +0.29 V. The limiting current of 3.22 mA at the plateau shows that $n = 2$, *i.e.*, a 2-electron cathodic reaction is taking place.

Curve (*c*) is for freshly prepared molybdo-

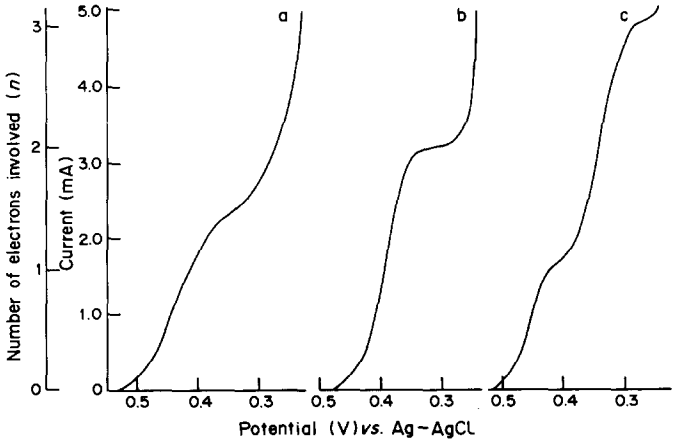

Fig. 5. Coulopotentiograms for molybdophosphate formed in solutions composed of $2 \times 10^{-4}M$ phosphate, $0.05M$ Mo(VI), $1.2M$ HCl, and the following amounts of acetonitrile: (*a*) nil, (*b*) 20% v/v, and (*c*) 40% v/v.

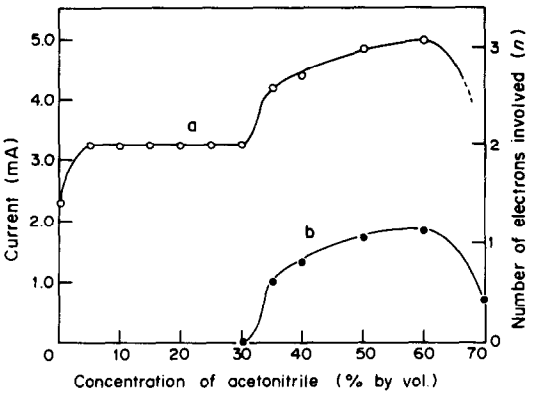

Fig. 6. Dependence of limiting current(s) of molybdophosphate on acetonitrile concentration. Molybdophosphate was formed in mixtures of $2 \times 10^{-4}M$ phosphate, $0.05M$ Mo(VI), $1.2M$ HCl, and various amounts of acetonitrile, and its coulopotentiogram was recorded 10–25 min later. The limiting currents for the main wave (*a*) and the pre-wave (when it appeared) (*b*), are plotted against the acetonitrile concentration.

phosphate in 40% acetonitrile medium, measured within 30 min of preparation. There are two distinct cathodic waves, one at potentials around +0.4 V, with $n = 1$, and the other at around +0.3 V, with $n = 3$. That is why it is essential to avoid formation of mixtures of the two molybdophosphates when the coulometric method is to be used. Coulopotentiograms of type (*c*) are obtained whenever the acetonitrile content exceeds 30% v/v.

This effect of the acetonitrile concentration is summarized in Fig. 6, which clearly confirms the interference by the "extraordinary" complex through the deviation from $n = 2$.

The effect of acidity (hydrochloric acid) on the electrolysis was examined with a constant composition of $2 \times 10^{-4}M$ phosphate and $0.05M$ Mo(VI) in the presence and absence of 20% acetonitrile. The results are shown in Fig. 7. If 20% acetronitrile

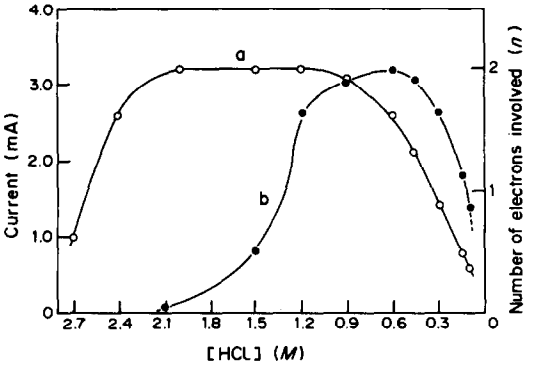

Fig. 7. Dependence of the limiting current of molybdophosphate on HCl concentration in the presence (*a*) and in absence of acetonitrile (*b*). The complex was formed in mixtures of $2 \times 10^{-4}M$ phosphate and $0.05M$ Mo(VI) [with 20% v/v acetonitrile for curve (*a*)].

medium is used, the limiting current is constant over the acidity range 1.2–2.1M hydrochloric acid.

The electrolysis of molybdophosphate should be facilitated by high acidity because it proceeds with the consumption of hydrogen ions. However, acidities high enough to facilitate the electrolysis cause partial decomposition of the complex and correspondingly diminish the limiting current. Thus, the optimal acidity in the absence of acetonitrile is limited to a narrow range around $0.6M$ as shown by curve (*b*) in Fig. 7. These opposing effects of acidity can be mitigated by such use of acetonitrile as auxiliary solvent.

Choice of auxiliary solvent

The interaction between molybdophosphate and certain water-miscible organic solvents was first pointed out by Bernhart and Wreath,[17] who observed that acetone intensifies the yellow colour of aqueous molybdophosphate solutions, and proposed its use in the spectrophotometric determination of phosphate. Chalmers and Sinclair[18] explained the effect as due to stabilization of the β-form by solvation with acetone, since they thought that co-ordinated water molecules could play a significant role in conversion into the Keggin α-form from the β-form postulated by Chalmers.[11] It is interesting that the β-structure proposed by Chalmers has been confirmed for tungstosilicic acid.[19] Utilizing the effect successfully, Chalmers and Sinclair reported sensitive methods for the determination of silicate, phosphate, arsenate and germanate,[18] and later for mixtures of phosphate and silicate.[20] Halász and Pungor[21] also used acetone in the spectrophotometric determination of phosphorus in mixtures with germanium or silicon. We reported[22] that tetrahydrofuran had a similar effect. Unlike acetone, tetrahydrofuran is transparent in the ultraviolet region, and this makes it possible to use the absorption band of molybdophosphate at about 310 nm, which has a molar absorptivity about ten times that at 410 nm.

Although these solvent effects are extremely favourable for phosphate determination, their application has been quite restricted, mainly because of spectral interference by isopolymolybdate species, and the determination limit for phosphate by the spectrophotometric method has remained at a level above $10^{-4}M$ phosphate even with full use of the solvent effect.

Fruchart and Souchay[23] found in a voltammetric study that molybdophosphate in 50% aqueous dioxan medium gives well-defined cathodic waves. We have also observed[1] a similar electrolytic reduction in 20% ethanol medium, resulting in rapid production of the corresponding "molybdenum blue". These facts suggested two methods (coulometric, reported here, and spectrophotometric, to be reported elsewhere) of highly sensitive determination of phosphate by electrolytic reduction of molybdophosphate in aqueous organic media. Many organic solvents, such

as methanol, ethanol, tetrahydrofuran, dimethylformamide, dimethylsulphoxide, methoxyethanol (methyl cellosolve), dioxan, acetone and acetonitrile, are known to intensify the yellow colour of molybdophosphate solutions, so all of them could be proposed as auxiliary solvents for use in the coulometric method, but several of them are unsatisfactory, for various reasons. The first two give partial reduction of acidic molybdate solutions during storage; the third and fourth give yellow precipitates when mixed with molybdophosphate at acidity $> 1N$; the fifth is unstable in acid solutions; the sixth, seventh, and eighth give slightly irreversible coulopotentiograms for molybdophosphate. Acetonitrile is therefore the best choice.

It is interesting that 1,2-ethanediol gives neither colour enhancement nor improvement of the coulopotentiograms. This inertness is in striking contrast to the effect of methanol and ethanol, but no reason for it has yet been found.

Species of molybdophosphate formed in aqueous and aqueous acetonitrile solutions

Although compositional and structural analyses of the "ordinary" and "extraordinary" molybdophosphate have not yet been performed because of the difficulty in isolating them from aqueous acetonitrile solutions, there can be no doubt that two different species are formed. From the spectral characteristics it seems highly probable that the "ordinary" species is the so-called α-modification, which has the Keggin structure.[24] It is also probable, from the spontaneous and non-reversible conversion of the "extraordinary" into the "ordinary" form, that the former is the β-molybdophosphate postulated[18] in analogy with β-molybdosilicate.[15] The two-step reduction for this form, and the single-step reduction of the ordinary form, might also be taken as confirmation of the existence of two structures. Whether the "extraordinary" form has the β-structure postulated by Chalmers[11] or is a dimeric species or an 11-molybdophosphate is a matter for conjecture, however. Nevertheless the kinetic stabilization of the "extraordinary" form by acetonitrile resembles the stabilizing effect of acetone on β-molybdosilicate reported by Chalmers and Sinclair,[18] and may be evidence for existence of a β-form of molybdophosphate.

Determination of orthophosphate in various phosphorus compounds

When the system II is used, each injection of phosphate sample gives a current peak with a shape essentially the same as that described earlier,[1] but with improved accuracy for low phosphate concentrations. The present method is applicable to phosphate concentrations ranging from 5×10^{-6} to $1 \times 10^{-3}M$. The coefficients of variation (ten determinations) for 5×10^{-6} and $1 \times 10^{-4}M$ phosphate standards are 3.0 and 0.7%, respectively.

The method has been applied to the determination of orthophosphate present as impurity in several phosphorus compounds, and the results are listed in Table 1. The results show fair accuracy, with no interference from hydrolytic decomposition of the matrix phosphorus compounds in the short period needed for the analysis. The method is therefore particularly suitable for determination of phosphate in labile phosphorus compounds.

The presence of high concentrations of electrolyte in the phosphate sample interferes with the coulometry, however. The interference is relatively serious with alkali-metal and neutral salts, but not with acids. In practice, the presence of acids in the sample is tolerable up to around $3M$ concentration, whereas the concentration of salts should be less than $0.1M$. The mechanism of the interference is not fully understood, but it seems that the cations of the salts form insoluble compounds with the "molybdenum blue" which temporarily cover the electrode surface and inhibit further electrolysis. This interference, however, will not often arise with ordinary phosphate

Table 1. Recovery of othophosphate present in solutions of various phosphorus compounds

Compound	Concentration, mM	Electrical charge used,* mC	Orthophosphate, $10^{-5}M$ Added	Total found	Recovery, %
Sodium phosphite	10	< 0.02	0	< 0.1	—
	10	0.96	5.0	5.0	100
Sodium triphosphate	10	6.64	0	34.4	—
	10	7.68	5.0	39.8	108
	10	8.70	10.0	45.1	107
Adenosine-5′-triphosphate	1	2.34	0	12.1	—
	1	3.51	5.0	18.2	122
D-Glucose-6-phosphate	1	1.37	0	7.1	—
	1	2.36	5.0	12.0	98
Sodium monomethylphosphate	6	0.39	0	2.0	—
	6	1.34	5.0	6.9	98
	6	2.26	10.0	11.7	97
Sodium dimethylphosphate	4	< 0.02	0	< 0.1	—
	4	0.96	5.0	4.9	98
Sodium monomethylphosphonate	4	< 0.02	0	< 0.1	—
	4	0.99	5.0	5.1	102

*Mean of three replicates.

samples, and can be easily dealt with by removal of the cations by suitable pretreatments.

Acknowledgement—The authors' thanks are due to the Ministry of Education, Science and Culture of Japan for financial support as part of the national project for environmental sciences.

REFERENCES

1. T. Fujinaga, S. Okazaki and T. Hori, *Bunseki Kagaku*, 1980, **29**, 367.
2. A. G. Fogg and N. K. Bsebsu, *Analyst*, 1981, **106**, 1288.
3. *Idem*, *ibid.*, 1982, **107**, 566.
4. E. O. Sherman and D. C. Olson, *Anal. Chem.*, 1968, **40**, 1174.
5. T. Hori, *J. Inorg. Nucl. Chem.*, 1977, **39**, 2173.
6. A. Michaelis and R. Kaehne, *Ber.*, 1898, **31**, 1048.
7. T. Fujinaga and S. Kihara, *CRC Rev. Anal. Chem.*, 1977, **6**, 223.
8. T. Fujinaga, S. Okazaki and T. Yamada, *Chem. Lett.*, 1972, 863.
9. A. Halász and E. Pungor, *Talanta*, 1971, **18**, 557.
10. Y. Sasaki and L. G. Sillén, *Acta Chem. Scand.*, 1964, **18**, 1014.
11. R. A. Chalmers, Paper presented at *IIIrd Conf. Anal. Chem.*, Prague, 1959.
12. H. M. Neumann and N. C. Cook, *J. Am. Chem. Soc.*, 1957, **79**, 3026.
13. S. Himeno, Y. Ueda and M. Hasegawa, *Inorg. Chim. Acta*, 1983, **70**, 53.
14. A. Halász and E. Pungor, *Talanta*, 1971, **18**, 569.
15. J. D. H. Strickland, *J. Am. Chem. Soc.*, 1952, **74**, 862, 868, 872.
16. A. C. Javier, S. R. Crouch, and H. V. Malmstadt, *Anal. Chem.*, 1968, **40**, 1922.
17. D. H. Bernhart and A. R. Wreath, *Anal. Chem.*, 1955, **27**, 440.
18. R. A. Chalmers and A. G. Sinclair, *Anal. Chim. Acta*, 1965, **33**, 384.
19. K. Y. Matsumoto, A. Kobayashi and Y. Sasaki, *Bull. Chem. Soc. Japan*, 1975, 48, 3146.
20. R. A. Chalmers and A. G. Sinclair, *Anal. Chim. Acta*, 1966, **34**, 412.
21. A. Halász, E. Pungor and K. Polyák, *Talanta*, 1971, **18**, 577.
22. T. Fujinaga, M. Koyama and T. Hori, *ibid.*, 1971, **18**, 960.
23. J. M. Fruchart and P. Souchay, *Compt. Rend.*, 1968, **C266**, 1571.
24. J. F. Keggin, *Proc. Roy. Soc.*, 1934, **A144**, 75.

Talanta, Vol. 30, No. 12, pp. 933–939, 1983
Printed in Great Britain

0039-9140/83 $3.00 + 0.00
Pergamon Press Ltd

INVESTIGATION OF TWO MULTICHANNEL IMAGE DETECTORS FOR USE IN SPECTROELECTROCHEMISTRY

MARY LOU FULTZ and RICHARD A. DURST
Organic Analytical Research Division, National Bureau of Standards, Washington, DC 20234, U.S.A.

(*Received* 18 *April* 1983. *Accepted* 5 *June* 1983)

Summary—Two multichannel image detectors, a vidicon and a silicon photodiode array, were investigated for their performance as detectors in ultraviolet–visible absorption spectroelectrochemical experiments. Their spectral band-pass, dispersion, dynamic range, and precision of absorbance measurements were compared. *o*-Tolidine was used as a model compound to study their performance in a spectropotentiostatic experiment using an optically transparent thin-layer electrode. Both detectors performed well, but the silicon photodiode array had twice the spectral resolution and dynamic absorbance range of the vidicon detector.

The combination of two different analytical techniques, electrochemistry and spectroscopy, has proved to be an effective approach for studying the oxidation–reduction chemistry of many different types of molecules. This technique, "spectroelectrochemistry," was developed to obtain more information about the nature of processes occurring at the electrode surface. Since Kuwana *et al.*[1] first demonstrated the feasibility of obtaining spectra at an optically transparent electrode, spectroelectrochemistry has been used to study the redox chemistry of both inorganic and organic compounds, including biological molecules. The types of information that can be obtained include (1) the spectra of electrogenerated species, (2) the formal potentials of electroactive species, (3) the number of electrons involved in the redox reaction, and (4) optical monitoring of preceding or subsequent chemical reactions.

A variety of optical methods have been coupled with electrochemical techniques. The most commonly used is absorption spectroscopy.[1,2] The optical systems used in ultraviolet–visible absorption spectrophotometry range from fixed-wavelength systems to rapid-scanning systems designed to record an absorption spectrum over a broad wavelength region. The first rapid-scanning spectrometer employed in spectroelectrochemical experiments used a mechanically driven oscillating mirror to scan the spectrum past the exit slit to the photomultiplier tube.[3] Another approach to monitoring a broad wavelength region is the use of multichannel detection systems. Multichannel detectors which simultaneously monitor all the dispersed radiation offer either of two advantages over single-channel detection systems. They can provide rapid data collection, or an improved signal-to-noise ratio proportional to the square root of the number of spectra taken.[4–6] Multichannel detectors use multiple detectors to monitor spatially separated discrete channels. The photographic emulsion is one example. Another is an array of photomultiplier tubes (PMT). This provides good sensitivity and rapid response, but the number of channels is physically limited by the size of the PMT.

Two other types of multichannel detectors commercially available are the vidicon detector and the self-scanned linear silicon-photodiode array detector. The use of a vidicon detector in the spectroelectrochemical study of molten salts has been reported.[7] Kadish and co-workers have reported the use of a silicon-photodiode array detector in the spectroelectrochemical study of metalloporphyrins.[8,9]

The vidicon detector is a two-dimensional array of photodiodes spaced 8–15 μm apart on a single silicon wafer. A continuously scanning electron beam presets all the diodes to an equal reversed-bias potential. Absorption of photons creates electron–hole pairs in the diodes, and these pairs combine to deplete the surface charge. When the electron beam scans over a partially depleted area, a recharging current flows which is proportional to the number of electron–hole pairs and thus the number of photons incident on the diode. This "electrical" spectrum image is stored in a digital memory and can be quantitatively transmitted to a display monitor or processed further. The useful wavelength region of the vidicon detectors is about 300–1100 nm. For work in the ultraviolet, a scintillator coating is added to the vidicon face. This coating is transparent to visible light, but converts ultraviolet radiation into visible wavelengths which can be detected.[10]

The silicon-photodiode array detector differs from the vidicon detector in two respects. First, it is a one-dimensional array of discrete reversed-bias photodiodes. Secondly, after being discharged by photon-generated electron–hole pairs the photodiodes are recharged electronically rather than by a

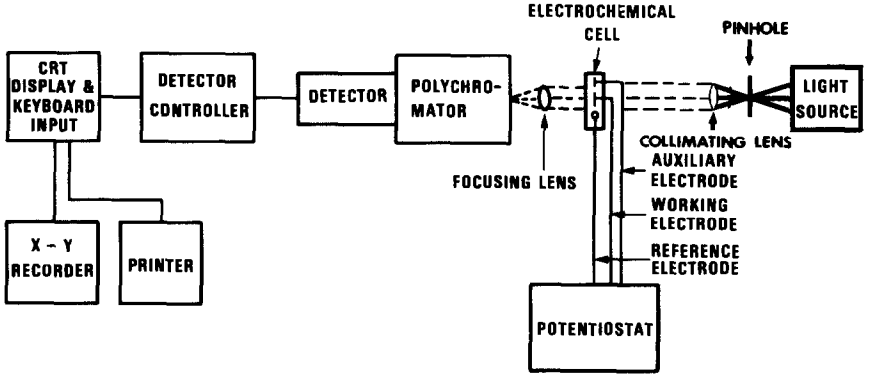

Fig. 1. Diagram of spectroelectrochemistry instrumentation.

scanning electron beam. The change in voltage on the video line is amplified, digitized, and transmitted as data for display or storage.[11]

Two multichannel image detectors, a vidicon and a silicon-photodiode array detector were studied for their suitability as detectors for ultraviolet–visible absorption spectroelectrochemistry. The resolution, dispersion, precision, accuracy and dynamic range of each system were determined. *o*-Tolidine was used as a model compound to test each system's performance and optimize the parameters for spectroelectrochemical experiments.

EXPERIMENTAL

Instrumentation

A block diagram of the instrumentation is shown in Fig. 1. The potential of the electrochemical cell was controlled with a commercially available potentiostat. The two detectors used were a silicon intensified-target vidicon, Model 1254, and a silicon-photodiode array, Model 1412, both manufactured by EG&G, Princeton Applied Research Corporation.* The data collection and storage were controlled with an OMA-2 PARC system processor. The components were secured on an optical bench to facilitate and maintain alignment. A xenon arc lamp was used for work in the ultraviolet and near ultraviolet, and a tungsten lamp for the visible region.

The 0.25-m polychromator is designed to be used with multichannel detectors. Instead of an exit slit, the instrument has an exit port on which the detector is mounted. The range of dispersed radiation focused on the detector is varied by changing the grating. Four different gratings were used in the polychromator: 150, 300, 600, and 1200 grooves/mm.

After passing through a pinhole, the light-beam is collimated with a 16-mm focal length 8-mm diameter quartz lens. This beam impinges on the sample and the transmitted beam is then focused onto the entrance slit of the polychromator, with a 60-mm focal length 25-mm diameter quartz lens.

*In order to describe experimental procedures adequately, it is occasionally necessary to identify commercial products by manufacturer's name or label. In no instance does such identification imply endorsement by the National Bureau of Standards nor does it imply that the particular products or equipment are necessarily the best available for that purpose.

RESULTS AND DISCUSSION

Detector characteristics

Absorption measurements. The spectrophotometric system is a single-beam instrument. The data collected from the detector give the transmission spectrum of the sample. Three measurements are made for calculation of the absorbance (A) by the equation

$$A = \log \frac{(I_o - I_d)}{(I - I_d)} \qquad (1)$$

where I_o is the intensity of the incident radiation, I is that of the transmitted radiation, and I_d that of the dark current. I_o and I are measured by recording the transmission spectra of the reference and sample solutions, respectively. The dark current is measured by blocking the source beam to the polychromator and recording a spectrum. These three spectra are taken in succession and recorded in floppy disk memory. The absorption spectrum calculated from the stored transmittance spectra is also stored in disk memory and can be displayed on the instrument's CRT or plotted on an X–Y recorder.

It is possible to vary the data-acquisition time of multichannel image detectors. Little improvement in the signal-to-noise ratio (SNR) of the absorption measurement can be achieved by signal-averaging many scans of the spectra. This is because the major source of noise is not white noise but rather drift in the source intensity and also some drift in the detector dark current. Therefore, the data-acquisition time was kept short to minimize errors due to drift.[12,13] For the silicon-photodiode array detector, the acquisition time was 16.5 msec for a single spectrum (1024 diodes). Ten scans were accumulated (0.165 sec). The vidicon detector was set at 40 msec per 512 channels. One hundred scans were used, giving an acquisition time of 4.05 sec.

Wavelength calibration. A 4% holmium oxide solution in 1.4M perchloric acid was used to calibrate the wavelength scale. Matched quartz 1.0-cm cells were used. The OMA-2 software has a function for calibrating the wavelength scale if at least four

Table 1. Spectral band-pass and dispersion for vidicon and silicon-photodiode array detectors

	Grating, *gr/mm*	Spectral band-pass, *nm*	Dispersion, *nm/channel*	Spectral window, *nm*
Vidicon	150	2.4	0.6	300
	300	1.5	0.3	145
	600	0.7	0.14	70
	1200	0.5	0.07	33
Silicon-photodiode array	300	1.2	0.3	300
	600	0.7	0.14	145
	1200	0.3	0.07	70

known wavelengths are entered in it. The wavelength values for the absorption peaks of holmium oxide solution are published by the American Society for Testing and Materials.[14]

Spectral band-pass and dispersion. The spectral window, that is, the range of wavelengths simultaneously viewed by the arrays, can be varied by using gratings of various dispersions. A low-pressure mercury lamp was used as a line source to measure the spectral band-pass and dispersion of the system with different gratings. The spectral band-pass values in Table 1 were obtained by measuring the peak width at half-height for several mercury lines.[17] The dispersion values were determined by measuring the number of channels between the mercury lines. A 25-μm entrance slit was used in all experiments.

The vidicon detector face is 12.5 × 12.5 mm, with the data collected into a 512 × 512 array. The silicon-photodiode array detector (SPD) is 25 mm wide and 2.5 mm high, with 1024 discrete photodiodes collecting the data. Since the SPD contains twice as many data-acquisition units for a given spectral window, it has twice the resolving power of the vidicon. This is graphically illustrated in Figs. 2 and 3, where the small side peak on the 416.3-nm absorption band of holmium oxide is better resolved by the SPD detector than by the vidicon detector, with the same grating.

The theoretical resolution of an optical system is given by the equation[15]

$$\Delta\lambda_R = R_d(W_s + W_e) \tag{2}$$

where $\Delta\lambda_R$ is the complete resolution for two slit functions, R_d is the reciprocal linear dispersion, and W_s and W_e are the entrance and exit slit-widths, respectively. For the array detectors, the exit slit-width has been taken to be that of one detector element, 25 μm for both detectors. From the experimentally determined linear dispersion, the theoretical resolution for both detectors, with the 1200 grooves/mm grating, is 0.15 nm. The observed spectral band-pass of 0.3 nm for the SPD is the limiting resolution of the polychromator.

Dynamic range. Cobalt(II) nitrate solutions in 0.1*M* perchloric acid were used to determine the absorbance range over which Beer's law is obeyed. Absorbance measurements were made at the 512 nm absorption band maximum. Absorbance *vs.* concentration plots were linear from 0 to 1.0 absorbance for the vidicon detector and from 0 to 2.0 absorbance for the SPD. Talmi[13] has reported linearity up to 4.0 absorbance for the SPD detector. The range of 0–2.0

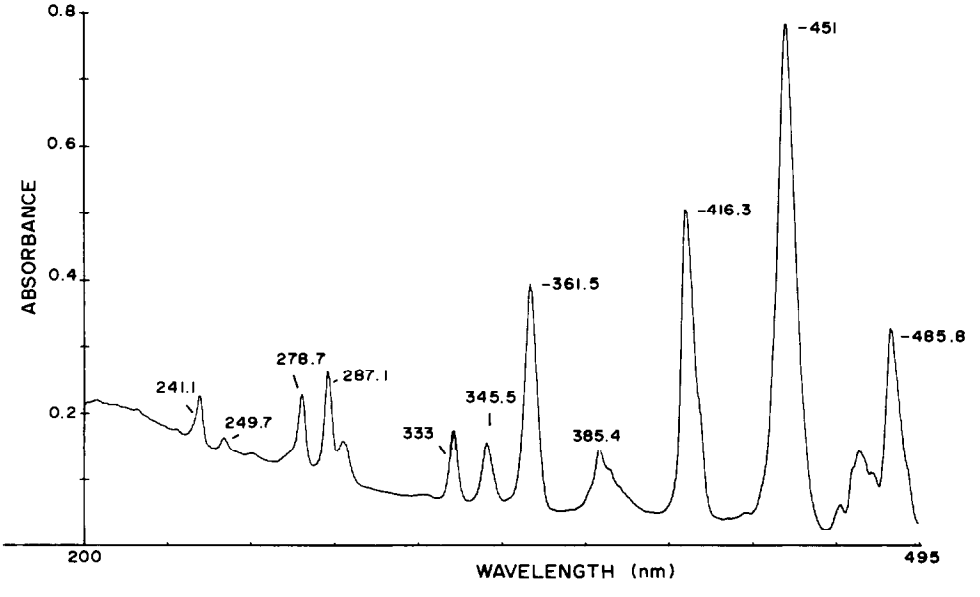

Fig. 2. Absorption spectrum of 4% holmium oxide solution in perchloric acid (vidicon detector).

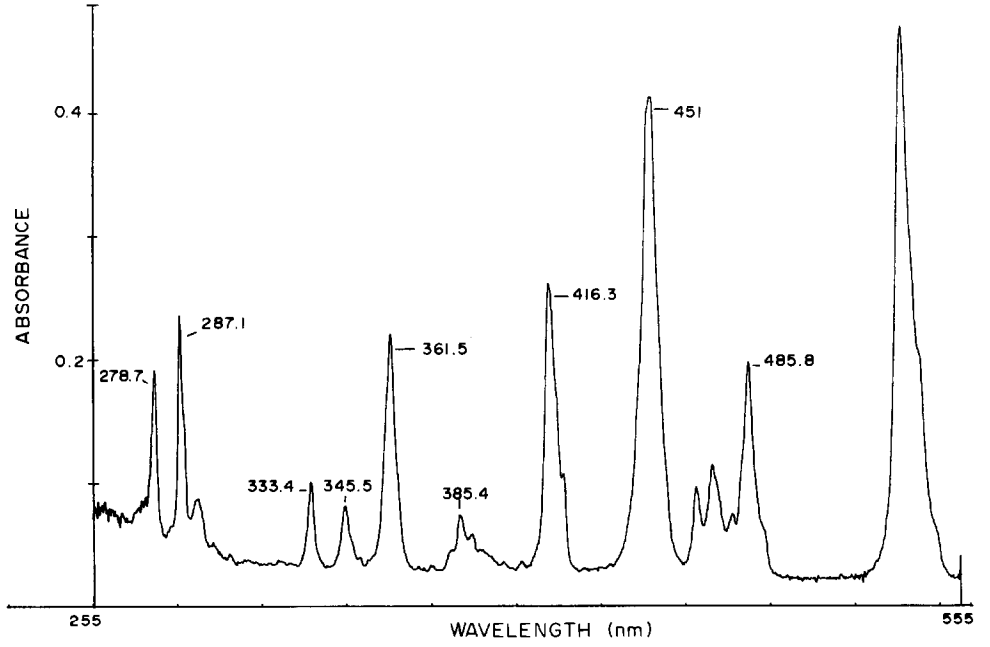

Fig. 3. Absorption spectrum of 4% holmium oxide solution in perchloric acid (silicon-photodiode array detector).

determined is that for the combination of detector and polychromator; therefore, the dynamic range of this system is presumably limited by the polychromator.

Stray radiation

A simple check for excessive amounts of stray radiation was made, with several different band-pass filters. Figure 4 shows the transmission spectrum of a 410-nm band-pass filter for the visible region. On subtraction of the dark-current signal from the transmission spectrum, no significant transmission is seen outside the band-pass region. These experiments were repeated with the xenon lamp source. Again, no measurable stray radiation in the visible region was observed.

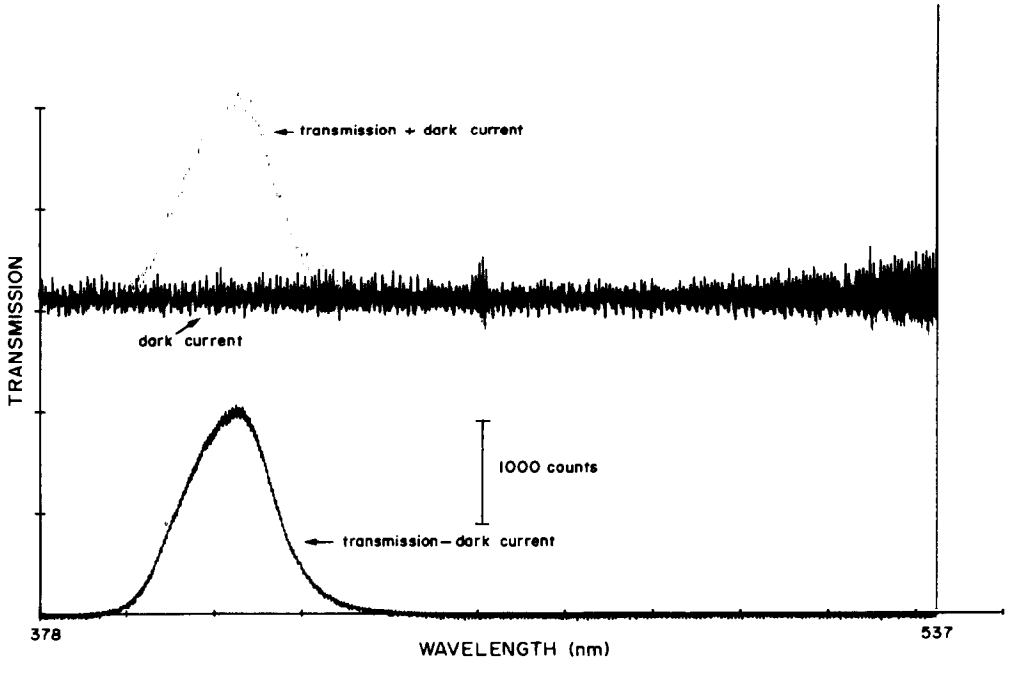

Fig. 4. Transmission spectrum for 410-nm band-pass filter.

Spectroelectrochemistry of o-*tolidine*

o-Tolidine was used as a model compound to evaluate the system's performance for spectroelectrochemical experiments. The electrochemical behaviour of *o*-tolidine is well defined[16] and its spectroelectrochemical behaviour in a thin-layer cell has also been reported.[17] *o*-Tolidine exhibits electrochemically reversible behaviour at pH < 2, with a single oxidation product having an absorption maximum at 437 nm. The reduced form does not absorb in the visible region. The formal potential and number of electrons transferred for a redox reaction can be calculated from information obtained in a "spectropotentiostatic" experiment. In this type of experiment, a potential is applied to the optically transparent thin-layer electrode (OTTLE). When equilibrium has been reached, the absorption spectrum is recorded. In an electrochemical cell, the ratio of oxidized to reduced form of a reversible electroactive species is controlled by the potential applied to the working electrode, as defined by the Nernst equation:

$$E_{\text{applied}} = E^{o\prime} + \frac{0.059}{n} \log \frac{[\text{O}]}{[\text{R}]}. \qquad (3)$$

In the OTTLE, the potential applied to the working electrode controls the concentration ratio of the redox couple in the light-path, owing to the thin-layer configuration of the cell.[18]

Figure 5 shows the absorption spectra of *o*-tolidine in a gold minigrid OTTLE at various applied potentials, recorded by use of the vidicon detector. At +0.8 V *vs.* an Ag/AgCl reference electrode (a), the solution in the OTTLE is completely oxidized ([O]/[R] > 1000). At +0.4 V (b), complete reduction is obtained ([O]/[R] < 0.001). The intermediate spectra correspond to applied potentials between +0.8 and +0.4 V *vs.* Ag/AgCl.

The absorbance at 437 nm reflects the concentration of the oxidized species in the OTTLE. By use of Beer's law, the ratio of oxidized to reduced species at each applied potential can be calculated according to the equation[17]

$$\frac{A_{\text{m}} - A_{\text{r}}}{A_{\text{o}} - A_{\text{m}}} = \frac{[\text{O}]}{[\text{R}]} \qquad (4)$$

where A_{o} is the absorbance when the species is completely oxidized, A_{r} is the absorbance when the species is completely reduced, and A_{m} is the absorbance for a mixture of the oxidized and reduced forms (see Appendix).

A plot of log [O]/[R] *vs.* E_{applied} for *o*-tolidine, as calculated from the absorbance spectra shown in Fig. 5, is linear as predicted by the Nernst equation. The slope of the plot is 29.5 mV, which corresponds to $n = 2.0$, and the intercept is 0.621 V *vs.* Ag/AgCl, the calculated formal potential of the redox system. These values agree well with previously reported data.[17]

The electrochemical cell used is the same as that reported by Murray *et al.*[2] Spectra were recorded after complete electrolysis at each potential and, in a typical experiment, about eight different potentials were applied to the electrode. Stepwise conversion from oxidized into reduced form in this manner takes about 45 min, and in this time there is a shift in the base-line of the absorption spectra. This can clearly

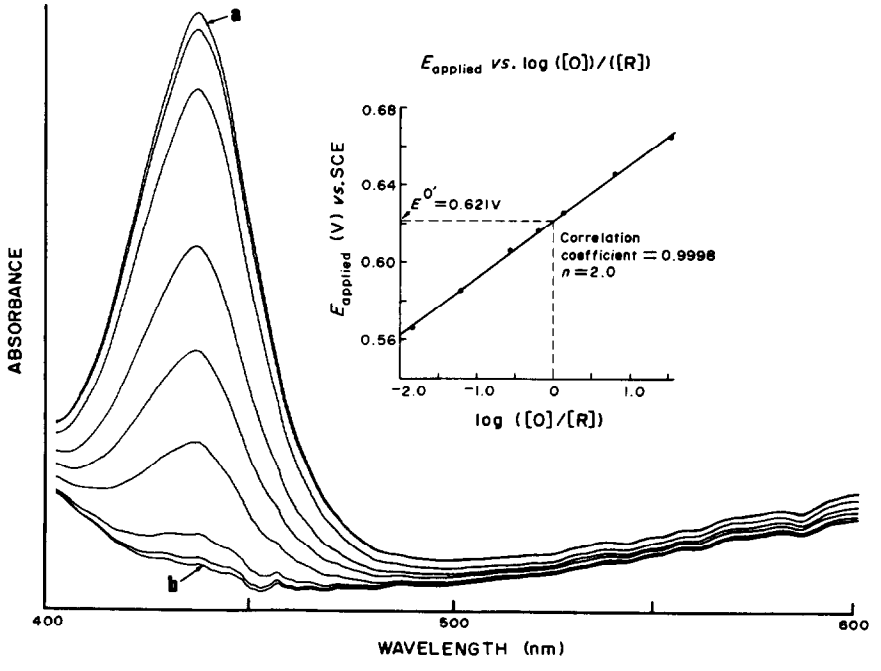

Fig. 5. Absorption spectra of 0.2 m*M* *o*-tolidine, pH < 2, in an OTTLE at various applied potentials. Insert: Nernst plot of spectra shown.

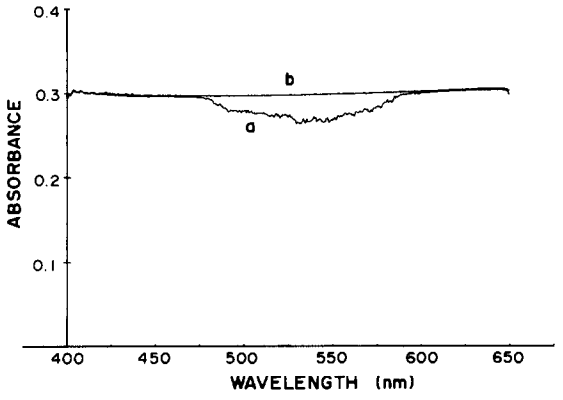

Fig. 6. Absorption spectrum of a 0.3 absorbance neutral density filter (vidicon detector and tungsten light-source). Tungsten light-source maximum set at (a) 13,000 counts and (b) 9400 counts.

be seen in Fig. 5 and is a result of drift in source intensity. Since I_0 is recorded once, at the beginning of the experiment, no compensation is made for changes in source output during the experiment. To alleviate this problem, a cell holder was constructed which would hold two OTTLEs, one for a reference and the other for the sample solutions. By recording the transmission spectra of the sample and reference OTTLEs within 20 sec of each other, it was possible to reduce the base-line drift (calculated as absorbance) from 0.02 to 0.005.

Spectropotentiostatic experiments were made for *o*-tolidine concentrations ranging from 0.01 to 2.0 m*M*. Both the xenon and tungsten lamps were used as sources, and the vidicon and silicon-photodiode array as detectors. Table 2 is a summary of the results, which are in good agreement with previously published data.[17]

One problem encountered with the vidicon detector is non-linearity of response of the photodiodes between very low and very high light-levels. The detector digitizes the light intensity detected in each channel, in units of "counts," with light levels above 16383 counts/channel saturating the detector. To obtain the largest dynamic range for the absorbance measurements, the source was set to give the maximum number of counts without saturating the detector. The absorption spectra for concentrated *o*-tolidine solutions show that when the xenon emission

Table 2. Values of $E^{\circ\prime}$ and n for *o*-tolidine

	$E^{\circ\prime}$, V *vs.* SCE	$n \pm$ s.d.
Xenon light-source Vidicon detector	0.618 ± 0.009	1.9 ± 0.1
Tungsten light-source Vidicon detector	0.614 ± 0.008	1.9 ± 0.1
Tungsten light-source Linear photodiode array	0.611 ± 0.008	1.9 ± 0.1
Previously reported values[17]		
Spectroelectrochemistry	0.614	1.9
Cyclic voltammetry	0.608 ± 0.006	
Coulometry		2.0 ± 0.11

Table 3. Precision of absorbance measurements (*o*-tolidine, OTTLE cell)

Detector	Concentration, m*M*	Mean absorbance	Standard deviation
Silicon-photodiode array	1.0	0.244	0.002
Silicon-photodiode array	0.1	0.023	0.002
Vidicon	0.1	0.0297	0.001
Vidicon	1.0	0.3000	0.0004

lines do not produce equal detector response in the spectra used for obtaining I_0 and I, the non-linear response results in appearance of feature lines in the calculated absorption spectrum. These are most pronounced at the highest absorbances. At low absorbances, where the absolute difference between I_0 and I is small and the detector response is more uniform, this effect disappears.

To minimize this problem, a tungsten light-source was used for work in the visible region. The tungsten source has a smoother emission pattern than the xenon source, but has its own limitations. Figure 6 shows absorption spectra obtained for a 0.3 absorbance neutral density (ND) filter. Curve b is the absorption spectrum when the maximum of the tungsten source was set to 9400 counts. Curve a is the spectrum when the tungsten source maximum was set to 13000 counts. The profile of the dip in curve a corresponds to the inverse of the emission profile of the tungsten source. The effect is analogous to that of stray light. It was found that this behaviour was obtained for detector counts over 10000. At less than 10,000 counts, an absorbance of 0.300 ± 0.002 was obtained for the ND filter over the wavelength range 404–668 nm. This phenomenon was not observed for the SPD detector which gave a value of 0.302 ± 0.002 over the same wavelength region for any number of counts up to 14000.

Precision of absorbance measurements

o-Tolidine has a high molar absorptivity, making its study in a very short path-length cell (0.05–0.2 mm), such as the OTTLE, a relatively easy task. However, many compounds of interest have much more weakly absorbing oxidized or reduced species. It was, therefore, desirable to determine with what precision the absorption measurements could be made.

There are several possible sources of uncertainty in the spectroelectrochemical absorption measurement. The final absorbance value is calculated from measurements of (1) the reference transmission spectrum, (2) the sample transmission spectrum, and (3) the dark current. Each of these measurements involves some inherent uncertainty. Drift in the source intensity and dark current are additional sources of uncertainty. Another major source of uncertainty is the reproducibility of placement of the sample and reference cells in the light-beam. Uncertainties resulting from source and dark-current drift were min-

imized by recording the two spectra and the dark current in as rapid succession as possible. The sample holder was secured to an optical stage and a guide bar and stops were used to ensure reproducible placement of the sample and reference cells.

The precision of the measurements with the vidicon and silicon-photodiode array detectors was determined. A 0.1 m*M* solution of *o*-tolidine in 1*M* perchloric acid/0.5*M* acetic acid was placed in the OTTLE, and a potential of +0.8 V *vs.* SCE was applied to the cell. After complete electrolysis, repetitive absorption measurements were made. The results are shown in Table 3. The precision of measurements with the vidicon is somewhat better than that with the silicon-photodiode array, especially for larger signals.

CONCLUSIONS

The vidicon and silicon-photodiode array detectors provide a rapid means of obtaining absorption spectra in the ultraviolet–visible region. The measurement precision of these detectors makes them suitable for use in spectroelectrochemical analysis. Errors due to source drift can be minimized by obtaining sample and reference spectra in rapid succession. One improvement that could be made is to make the system double-beam. This could be accomplished by splitting the source-beam to pass through both the sample and the reference cell and triggering the detector to record these spectra alternately. Both detectors perform well in spectropotentiostatic experiments, with minimal differences. The vidicon detector has greater precision by a factor of two, but the silicon-photodiode array has twice the resolution for equal spectral windows. With the polychromator used in this system, the dynamic range of the silicon-photodiode array detector for absorbance measurements is twice that of the vidicon detector. The two-dimensional array of the vidicon detector will make it more useful for kinetic studies, where time-resolved spectra can be recorded in rapid succession on specific areas of the detector.

APPENDIX

Derivation of equation (4)

Let

$$A_r = \varepsilon_r b[R_t]$$
$$A_m = \varepsilon_r b[R_m] + \varepsilon_0 b[O_m]$$
$$A_0 = \varepsilon_0 b[O_t]$$

where b is the path-length and ε the molar absorptivity for the species indicated by subscript (t = total; m = measured); also let

$$[R_m] + [O_m] = [R_t] = [O_t]$$

i.e., the sum of the concentrations of R and O at intermediate potentials must equal the total concentration of R or O.

Then

$$\frac{A_m - A_r}{A_0 - A_m} = \frac{\varepsilon_r b[R_m] + \varepsilon_0 b[O_m] - \varepsilon_r b[R_t]}{\varepsilon_0 b[O_t] - \varepsilon_r b[R_m] - \varepsilon_0 b[O_m]}$$

and cancelling b and rearranging gives

$$\frac{A_m - A_r}{A_0 - A_m} = \frac{\varepsilon_r([R_m] - [R_t]) + \varepsilon_0[O_m]}{\varepsilon_0([O_t] - [O_m]) - \varepsilon_r[R_m]}$$

Since

$$[R_m] - [R_t] = -[O_m] \quad \text{and} \quad [O_t] - [O_m] = [R_m]$$

$$\frac{A_m - A_r}{A_0 - A_m} = \frac{-\varepsilon_r[O_m] + \varepsilon_0[O_m]}{\varepsilon_0[R_m] - \varepsilon_r[R_m]} = \frac{[O_m]}{[R_m]}.$$

REFERENCES

1. T. Kuwana, R. Darlington and D. Leedy, *Anal. Chem.*, 1964, **36**, 2023.
2. R. Murray, W. R. Heineman and G. O'Dom, *ibid.*, 1967, **39**, 1666.
3. J. Strojek, G. Gruver and T. Kuwana, *ibid.*, 1969, **41**, 481.
4. R. E. Santini, M. J. Milano and H. L. Pardue, *ibid.*, 1973, **45**, 915A.
5. Y. Talmi, D. Baker, J. Jadamec and W. A. Saner, *ibid.*, 1978, **50**, 936A.
6. Y. Talmi, *Am. Lab.*, 1978, No. 3, 79.
7. G. Mamantov, V. E. Norvell and L. Klatt, *Energy Res. Abstr.*, 1979, **4**, 3207.
8. K. Kadish, L. Shive, R. Rhodes and L. Bottomley, *Inorg. Chem.*, 1981, **20**, 1274.
9. K. Kadish and R. Rhodes, *ibid.*, 1981, **20**, 2961.
10. Y. Talmi, *Optoelectronic Image Detectors in Chemistry, An Overview*, in *Multichannel Image Detectors*, Y. Talmi (ed.), American Chemical Society, Washington, DC, 1979.
11. EG&G Princeton Applied Research, *Operating Manual for Model 1412 Silicon Photodiode Array Detector.*
12. T. C. O'Haver, in *Trace Analysis: Spectroscopic Methods for Elements*, J. D. Winefordner (ed.), p. 20. Wiley, New York, 1976.
13. Y. Talmi, *Appl. Spectrosc.*, 1982, **36**, 1.
14. ASTM Designation E275-67, *Recommended Practice for Describing and Measuring Performance of Spectrophotometers*, 1982 Annual Book of ASTM Standards, Part 42, 217.
15. J. D. Winefordner, S. G. Schulman and T. C. O'Haver, *Luminescence Spectrometry in Analytical Chemistry*, p. 155. Wiley–Interscience, New York, 1972.
16. T. Kuwana and J. W. Strojek, *Disc. Faraday Soc.*, 1968, **45**, 134.
17. T. P. DeAngelis and W. R. Heineman, *J. Chem. Educ.*, 1976, **53**, 594.
18. W. R. Heineman, B. J. Norris and J. F. Goelz, *Anal. Chem.*, 1975, **47**, 79.

Talanta, Vol. 30, No. 12, pp. 941–944, 1983
Printed in Great Britain.

0039-9140/83 $3.00 + 0.00

CATALYTIC DETERMINATION OF MOLYBDENUM(VI) BY MEANS OF AN IODIDE ION-SELECTIVE ELECTRODE AND A LANDOLT-TYPE HYDROGEN PEROXIDE–IODIDE REACTION

M. KATAOKA, K. NISHIMURA and T. KAMBARA*
Department of Chemistry, Faculty of Science, Hokkaido University, Sapporo, Japan

(*Received* 4 *May* 1983. *Accepted* 1 *June* 1983)

Summary—A trace amount of molybdenum(VI) can be determined by using its catalytic effect on the oxidation of iodide to iodine by hydrogen peroxide in acidic medium. Addition of ascorbic acid added to the reaction mixture produces the Landolt effect, *i.e.*, the iodine produced by the indicator reaction is reduced immediately by the ascorbic acid. Hence the concentration of iodide begins to decrease once all the ascorbic acid has been consumed. The induction period is measured by monitoring the concentration of iodide ion with an iodide ion-selective electrode. The reciprocal of the induction period varies linearly with the concentration of molybdenum(VI). The most suitable pH and concentrations of hydrogen peroxide and potassium iodide are found to be 1.5, 5 and 10m*M*, respectively. An appropriate amount of ascorbic acid is added to the reaction mixture according to the concentration of molybdenum(VI) in the sample solution. A calibration graph with good proportionality is obtained for the molybdenum(VI) concentration range from 0.1 to 160μM. Iron(III), vanadium(IV), zirconium(IV), tungsten(VI), copper(II) and chromium(VI) interfere, but iron(III) and copper(II) can be masked with EDTA.

Many metal ions have been determined by catalytic methods, usually by colorimetric methods.[1–10] Recently, polarography,[11,12] potentiometry,[13–16] amperometry[17–19] and ion-selective electrodes[20–26] have been used in measurement of the reaction rate. We have reported the use of ion-selective electrodes in the trace determination of molybdenum(VI),[21] tungsten(VI),[21] iron(III)[22] and zirconium(IV),[22] which all catalyse the oxidation of iodide to iodine by hydrogen peroxide.

Many methods based on the Landolt reaction[27] have been developed, with use of colorimetry,[28–34] fluorimetry,[30,35] photometry[36] and potentiometry[36] for determination of the induction period.

The present paper describes the application of the Landolt reaction to the microdetermination of molybdenum(VI) by means of its catalytic effect on the hydrogen peroxide–iodide reaction, monitored with an iodide ion-selective electrode.

THEORETICAL CONSIDERATIONS

The indicator reaction used proceeds according to the stoichiometry

$$H_2O_2 + 3I^- + 2H^+ \rightarrow I_3^- + 2H_2O \qquad (1)$$

but by two paths, only one of which involves hydrogen ions. In the presence of molybdenum the rate of consumption of hydrogen peroxide can be described by[37]

$$-\frac{d[H_2O_2]}{dt} = (k_1 + k_2 c_{Mo})[H_2O_2][I^-] + (k_3 + k_4 c_{Mo})[H_2O_2][I^-][H^+] \qquad (2)$$

where c_{Mo} is the analytical concentration of molybdenum, k_1 and k_3 the rate coefficients of the uncatalysed reactions, and k_2 and k_4 those of the catalysed reactions.

To achieve the Landolt effect, ascorbic acid is added to the reaction mixture. The tri-iodide ions produced in reaction (1) are immediately reduced by the ascorbic acid, with release of the same number of hydrogen ions as those consumed in reaction (1):

$$C_6H_8O_6 + I_3^- \rightarrow C_6H_6O_6 + 3I^- + 2H^+ \qquad (3)$$

Thus, both the iodide and hydrogen-ion concentrations remain constant so long as ascorbic acid is present. With the notation

$$k_{un} = k_1[I^-] + k_3[I^-][H^+] \qquad (4)$$

and

$$k_{cat} = k_2[I^-] + k_4[I^-][H^+] \qquad (5)$$

the rate equation can be written as

$$-\frac{d[H_2O_2]}{dt} = (k_{un} + k_{cat} c_{Mo})[H_2O_2] \qquad (6)$$

This rate equation can be integrated by considering

*Present address: Hakodate Technical College, Tokuracho, 226, Hakodate, Japan.

that when the reagents are mixed ($t = 0$), $[H_2O_2] = [H_2O_2]_0$, and at the end of the induction period ($t = t_i$), $[H_2O_2] = [H_2O_2]_0 - [C_6H_8O_6]_0$ (the subscript zero indicates an initial concentration), and this leads to the expression:

$$\frac{1}{t} = \frac{k_{un} + k_{cat}c_{Mo}}{\ln \dfrac{[H_2O_2]_0}{[H_2O_2]_0 - [C_6H_8O_6]_0}} = a + bc_{Mo} \qquad (7)$$

Hence plotting the reciprocal of the reaction time against molybdenum concentration gives a straight-line calibration graph.

The concentration of iodide begins to decrease when all the ascorbic acid has been consumed. The time required for the complete consumption of ascorbic acid (the induction period) is determined by recording the potential of the iodide-ion selective electrode as a function of time.

EXPERIMENTAL

Apparatus

Potential measurements were made with a Toa HM-7A pH-meter, an I-125 iodide ion-selective electrode, and an HC-205C saturated calomel electrode, and a Hitachi 056 recorder.

Reagents

*Hydrogen peroxide solution, 0.1*M. Dilute 11.0 g of 30% H_2O_2 solution to 1 litre with water, standardize iodometrically and store in a dark bottle in a refrigerator.

*Potassium iodide stock solution, 1*M. Dissolve 166.0 g of analytical-reagent grade potassium iodide in 1 litre of water, standardize by potentiometric titration with silver nitrate and store in a dark bottle.

*Ammonium molybdate stock solution, 10.0*mM. Dissolve 1.766 g of analytical-reagent grade $(NH_4)_6Mo_7O_{24}\cdot 4H_2O$ in 1 litre of water, and standardize by adding excess of 0.01*M* EDTA and back-titrating with 0.01*M* lead nitrate, at pH 5 (Xylenol Orange as indicator).

*Ascorbic acid solution, 0.01*M. Dissolve 0.3523 g of analytical-reagent grade ascorbic acid in 200 ml of water, just before use. A 0.1*M* solution is prepared analogously, if required.

The water used in this study was demineralized and then distilled twice.

Procedure

To a 50-ml standard flask containing 5 ml of 0.1*M* hydrogen peroxide add 4 ml of 1*M* hydrochloric acid and 5 ml of 1*M* potassium chloride and dilute to the mark (solution A). To another 50-ml flask containing 0.5–770 μg of molybdenum(VI) (in the sample solution) add 10 ml of 0.1*M* potassium iodide and 10 ml of 10m*M* or 3 ml of 100m*M* ascorbic acid solution and dilute to volume (solution B). Bring both solutions to 25° in a thermostat, then transfer solution A into a 200-ml tall beaker in the thermostat, and insert the iodide ion-selective electrode and the SCE. When the e.m.f. of the electrode combination is stable, rapidly pour solution B into the beaker and at the same time switch on the recorder. The e.m.f. recorded will remain constant until all the ascorbic acid has been consumed, and then become more positive as the iodide concentration decreases.

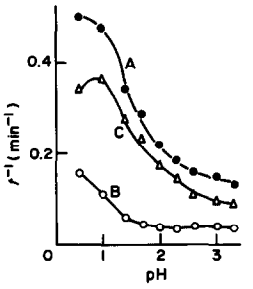

Fig. 1. Effect of pH on $1/t$. $[H_2O_2] = 5.0$m*M*, $[KI] = 10.0$m*M*, $[Asc] = 1.0$m*M*, temperature = (25 ± 0.5)°C. A: $[Mo(VI)] = 5.0\mu M$, B: blank, C: difference of the reciprocal of induction period, (A − B).

RESULTS AND DISCUSSION

Effect of pH

With fixed concentrations of potassium iodide, hydrogen peroxide, ascorbic acid and molybdenum(VI), the pH of the reaction mixture was varied by addition of various volumes of 1*M* hydrochloric acid and 1*M* potassium chloride. As shown in Fig. 1, the reciprocal of the induction period increases with decreasing pH (curve A). As the indicator reaction also proceeds slowly without catalyst (curve B), the net value is obtained by difference (curve C). The most suitable pH is 1.5, because the blank value increases at pH lower than 1.4.

Effect of hydrogen peroxide concentration

The net value of the reciprocal of the induction period is constant over the peroxide concentration range 2–10m*M* (Fig. 2) so a concentration of 5m*M* is selected as convenient and giving wide tolerance.

Effect of iodide concentration

As shown in Fig. 3, the net value of the reciprocal of the induction period increases with increasing iodide concentration, but the blank value increases rapidly when the concentration is higher than 10m*M*, and this is chosen as the most suitable concentration.

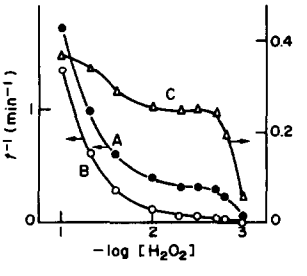

Fig. 2. Effect of the concentration of hydrogen peroxide on $1/t$. $[KI] = 10.0$m*M*, pH = 1.5, $[Asc] = 1.0$m*M*, temperature = (25 ± 0.5)°C. A: $[Mo(VI)] = 5.0\mu M$, B: blank, C: difference of the reciprocal of induction period, (A − B).

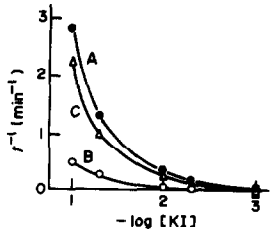

Fig. 3. Effect of the concentration of potassium iodide on $1/t$. $[H_2O_2] = 5.0mM$, pH = 1.5, [Asc] = 1.0mM, temperature = (25 ± 0.5)°C. A: [Mo(VI)] = 5.0μM, B: blank, C: difference of the reciprocal of induction period, (A − B).

Effect of ascorbic acid concentration

The induction period is proportional to the ascorbic acid concentration in the range from 0 to 3mM. The most suitable ascorbic acid concentration varies from 1 to 3mM, depending on the molybdenum(VI) concentration, because if too much is added, relative to the molybdenum(VI), the induction period is too long, but if too little is added the error is increased.

Calibration graph

The electrode potential *vs.* time curves for various catalyst concentrations in the range from 5 to 100μM are shown in Fig. 4. The arrows indicate the ends of the induction periods. The calibration plots of reciprocal of the induction period against concentration of molybdenum(VI) are linear over the concentration ranges (*a*) from 1 to 160μM, and (*b*) from 0.1 to 2.0μM (with a lower ascorbic acid concentration in the reaction mixture). The regression equations (and the 95% confidence limits) are:

$$(a)\quad \frac{1}{t} = (6.64 \pm 0.07) \times 10^4[\text{Mo(VI)}] + (5.61 \pm 0.07) \times 10^{-2}$$

Table 1. Effect of diverse ions

Ion	Concentration, μM	Error in [Mo(VI)] found, %
W(VI)	0.05	+3.2
V(IV)	3	+5.1
Cr(VI)	0.5	−4.4
Cr(III)	1000	+6.9
Zr(IV)	10	+5.3
Ca(II)	10000	−2.4
Mg(II)	20000	0.0
Fe(III)	1	+9.2
Fe(III)*	1	+0.5
Fe(III)†	10	+1.6
Zn(II)	10000	+0.5
Cu(II)	10	+5.2
Cu(II)§	10	+2.0
Mn(II)	5000	−3.2

[Mo(VI)] = 1.0μM, [KI] = 10.0mM, $[H_2O_2] = 5.0mM$, [Asc] = 1.0mM, temperature = (25 ± 0.5)°C.
*EDTA 3.0μM.
†EDTA 100μM.
§EDTA 1.0mM.

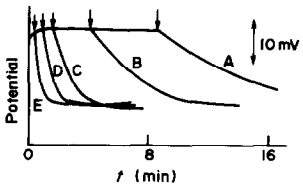

Fig. 4. Potential change of iodide ion-selective electrode with time. $[H_2O_2] = 5.0mM$, pH = 1.5, [Asc] = 3mM, temperature = (25 ± 0.5)°C. [Mo(VI)]: A, 5; B, 10; C, 30; D, 50; E, 100μM. Arrows show the appearance of the starch–iodine colour.

$$(b)\quad \frac{1}{t} = (2.01 \pm 0.01) \times 10^4[\text{Mo(VI)}] + (9.7 \pm 6.3) \times 10^{-3}$$

where (*a*) is for 3.0mM ascorbic acid (*b*) for 1.0mM ascorbic acid; t is in sec, and [Mo(VI)] in mole/l.

Alternatively, the tangent method[21–26] can be used, the rate of potential change after the induction period being plotted against the concentration of catalyst, but the rate of change for molybdenum(VI) concentrations < 2μM is too low to be useful. The induction period method is more than 20 times as sensitive as the tangent method.

Interferences

Since some other metal ions also catalyse the indicator reaction, their interference in the determination of 1μM molybdenum(VI) was tested and is summarized in Table 1. Triplicate measurements were made in the presence and absence of interferent. Iron(III), vanadium(IV), zirconium(IV), tungsten(VI), copper(II) and chromium(VI) interfere, but the effect of iron(III) and copper(II) can be reduced by masking with EDTA.

REFERENCES

1. K. B. Yatsimirskii, *Kinetic Methods of Analysis*, Pergamon Press, Oxford, 1966.
2. H. A. Laitinen and W. E. Harris, *Chemical Analysis*, 2nd Ed., Chap. 21. McGraw-Hill, New York, 1975.
3. H. B. Mark, Jr. and G. A. Rechnitz, *Kinetics in Analytical Chemistry*, Interscience, New York, 1968.
4. S. Utsumi, *Bunseki Kagaku*, 1967, **16**, 644.
5. T. Kawashima and N. Yonehara, *ibid.*, 1972, **21**, 825.
6. H. B. Mark, Jr., *Talanta*, 1972, **19**, 717.
7. A. M. Gary and J. P. Schwing, *Bull. Soc. Chim. France*, 1972, 3657.
8. T. Fukazawa and H. Yamane, *Bunseki*, 1977, 491.
9. H. A. Mottola and H. B. Mark, Jr., *Anal. Chem.*, 1980, **52**, 31R.
10. *Idem, ibid.*, 1982, **54**, 62R.
11. G. P. Haight, Jr., *ibid.*, 1951, **32**, 1505.
12. T. Kambara, N. Tanaka and K. Fukuda, *Bunseki Kagaku*, 1968, **17**, 1144.
13. H. Weisz, D. Klockow and H. Ludwig, *Talanta*, 1969, **16**, 921.
14. H. Weisz, K. Rothmaier and H. Ludwig, *Anal. Chim. Acta*, 1974, **73**, 224.
15. D. Klockow, H. Ludwig and M. A. Giraudo, *Anal. Chem.*, 1970, **42**, 1682.

16. H. L. Pardue and S. Shepherd, *ibid.*, 1963, **35,** 21.
17. C. M. Wolff and J. P. Schwing, *Bull. Soc. Chim. France*, 1976, 675.
18. *Idem*, *ibid.*, 1976, 679.
19. F. M. Barton and B. H. Loo, *J. Chem. Soc., A*, 1971, 3032.
20. A. Altinata and B. Pekin, *Anal. Lett.*, 1973, **6,** 667.
21. M. Kataoka and T. Kambara, *Bunseki Kiki*, 1972, **10,** 773.
22. M. Kataoka, Y. Yoshizawa and T. Kambara, *Bunseki Kagaku*, 1982, **31,** E171.
23. M. Kataoka and T. Kambara, *ibid.*, 1974, **23,** 1157.
24. *Idem*, *Denki Kagaku*, 1977, **45,** 674.
25. M. Kataoka, M. Takahashi and T. Kambara, *Bunseki Kagaku*, 1979, **28,** 169.
26. M. Kataoka, S. Miyagata and T. Kambara, *Nippon Kagaku Kaishi*, 1980, **10,** 1520.
27. H. Landolt, *Ber.*, 1886, **19,** 1317.
28. G. Svehla, *Analyst*, 1969, **94,** 513.
29. G. Svehla and L. Erdey, *Microchem. J.*, 1963, **7,** 206.
30. J. Bognár and O. Jellinek, *Mikrochim. Acta*, 1966, 453.
31. A. Páll, G. Svehla and L. Erdey, *Talanta*, 1970, **17,** 211.
32. G. Svehla and L. Erdey, *Microchem. J.*, 1963, **7,** 211.
33. H. Thompson and G. Svehla, *Z. Anal. Chem.*, 1969, **247,** 244.
34. H. Weitz and S. Pantel, *Anal. Chim. Acta*, 1975, **76,** 487.
35. J. Bognár and O. Jellinek, *Mikrochim. Acta*, 1968, 1013.
36. H. Weisz and K. Rothmaier, *Anal. Chim. Acta*, 1974, **68,** 93.
37. C. H. Bamford and C. F. H. Tipper (eds.), *Comprehensive Chemical Kinetics*, Vol. 6, p. 406 ff. Elsevier, Amsterdam, 1972.

Talanta, Vol. 30, No. 12, pp. 945–949, 1983
Printed in Great Britain

0039-9140/83 $3.00 + 0.00
Pergamon Press Ltd

LIQUID-STATE MEMBRANE ELECTRODE SENSITIVE TO BISMUTH(III)

WALENTY SZCZEPANIAK and MARIA REN
Faculty of Chemistry, A. Mickiewicz University, 60-780 Poznań, ul. Grunwaldzka 6, Poland

(*Received* 10 *December* 1982. *Revised* 17 *March* 1983. *Accepted* 27 *May* 1983)

Summary—A liquid ion-exchange electrode containing a tetrachloraethane solution of the complex of bismuth(III) with 5-mercapto-3-(naphthyl-1)-1,3,4-thiadiazol-2-thione is described. The electrode is sensitive to Bi^{3+}. The slope of the calibration graph (electrode potential *vs.* concentration) is 18.7 mV/pBi in the pBi range 6.5–9.5 in ammonium acetate buffer (pH = 4.0). Bivalent cations and Al(III), Fe(III) and Th(IV) do not interfere ($K_{Bi^{3+},M^{z+}} < 10^{-5}$). The dissociation constant of bismuth acetate has been determined with the aid of the electrode.

Ion-selective electrodes, with both solid and liquid membranes, have been shown to be satisfactory for univalent and bivalent cations as well as for some anions. Experience with electrodes sensitive to higher valency cations shows that the major difficulty lies in finding a suitable membrane material. Only a few attempts have been made to use liquid membrane systems in the preparation of electrodes sensitive to Fe(III),[1] Cr(III), La(III) and Th(IV).[2] Several electrodes sensitive to anionic halide-complexes of the type MX_4^-, *e.g.*, $FeCl_4^-$,[3–5] $AuCl_4^-$,[6–9] BiI_4^-,[10] have been described.

In this paper, we describe an ion-selective electrode with liquid membrane, sensitive to bismuth cations. A solution of the complex of bismuth(III) with Bismuthiol III is used as liquid ion-exchanger in this electrode. Bismuthiol III [5-mercapto-3-(naphthyl-2)-1,3,4-thiadiazolthione-2], (HL),

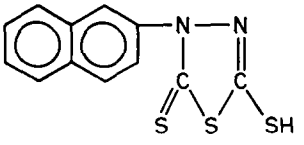

forms a bismuth complex of the type BiL_3. This complex is insoluble in water but very soluble in organic solvents such as chloroform and 1,1′,2,2′-tetrachloroethane. It is orange-yellow in colour and has been used for the determination of bismuth by extraction spectrophotometry.[11] This complex has been chosen as the active electrode substance because it has a very high extraction coefficient but dissociates to a sufficient extent to enable an ion-exchange reaction to take place between the aqueous and membrane phases. Bismuthiol III is selective and does not form complexes with cations such as Co(II) and Ni(II); its complexes with Sn(II), Sb(III), Pb(II), Zn(II), Cd(II) and Cu(II) are not extracted. Other complexes, *e.g.*, with La(III), Al(III), Th(IV), are extractable, but only very slightly.

EXPERIMENTAL

Liquid ion-exchanger

Bismuthiol III was prepared as described earlier.[12] An aqueous solution of its potassium salt ($10^{-2}M$) was mixed in 3:1 volume ratio with $10^{-2}M$ bismuth nitrate in ammonium acetate buffer at pH 4. The orange precipitate of BiL_3 was centrifuged and washed first with ammonium acetate buffer and then with water, then dried *in vacuo* over anhydrous calcium chloride, and dissolved in 1,1′,2,2′-tetrachloroethane to give a $5 \times 10^{-3}M$ solution.

Measuring cell

A Teflon ion-selective electrode,[13] in which the liquid membrane was stabilized in a porous, siliconed circular plate, was used. Alternatively a Sartorius membrane filter type SM-11306 (cellulose nitrate) was used to carry the complex. The composition of the inner solution of the electrode was $10^{-3}M$ bismuth nitrate and $10^{-2}M$ potassium chloride in ammonium acetate buffer (pH 4). A silver/silver chloride electrode with salt bridge was used as the reference electrode.

The measuring cell was

Ag	AgCl	Inner solution	Liquid membrane	Test solution	1*M* KNO_3	1*M* KCl	Ag	AgCl

The e.m.f. was measured with an N-512 pH-meter (ELPO, Poland) connected to a V-530 digital voltmeter (Meratronik, Poland) and a G_1B_1 recorder (Carl Zeiss, Jena, G.D.R.) to within 0.1 mV.

Reagents

All reagents were of analytical grade. Doubly-distilled water from a quartz still was used. The acetate buffer was 0.2*M* ammonium acetate/0.7*M* acetic acid, adjusted to pH 4.

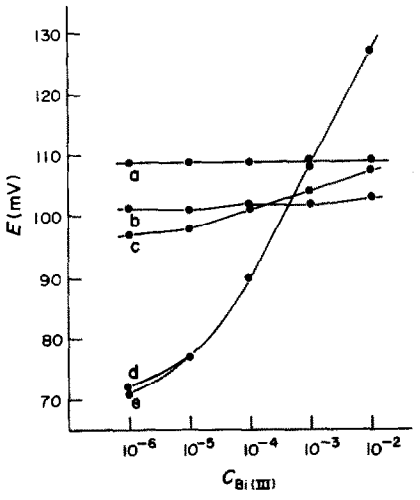

Fig. 1. Calibration curves for electrode: pure $C_2H_2Cl_4$ membrane, Bi(bismuthiol)$_3$ in tributylphosphate membrane, in nitrobenzene, in $CHCl_3$, in $C_2H_2Cl_4$.

RESULTS AND DISCUSSION

Figure 1 presents calibration curves for electrodes in which $5 \times 10^{-3}M$ solutions of BiL_3 in four different solvents (chloroform, 1,1′,2,2′-tetrachloroethane, tributyl phosphate and nitrobenzene) were used as the membrane. A curve for an electrode made with pure tetrachloroethane without the active complex is also included. The solution investigated was bismuth nitrate in ammonium acetate buffer. The most promising curves were those for the membranes made with chloroform and tetrachloroethane as solvents. Within the linear range, the slopes for these electrodes correspond to 18.7 mV/decade change in concentration, which is close to the theoretical value for an electrode sensitive to tervalent cations (19.3 mV/decade). Tetrachloroethane was preferred because of its lower volatility and lower solubility in water. Further, the electrode with the membrane made of tetrachloroethane alone showed no dependence of potential on Bi(III) concentration.

Composition of solutions investigated

The bismuth cation causes serious difficulties in ion-selective potentiometry because it hydrolyses in aqueous solution (hydrolysis constant $pk_1 = 12.4$). The slope of curve *e* in Fig. 1 suggests that the electrode is not sensitive to the hydrolysed ions such as $Bi(OH)^{2+}$ and $Bi(OH)_2^+$ but responds only to the Bi^{3+} activity. Therefore, all test solutions must be at constant pH and ionic strength so that the ratio $a_{Bi^{3+}}/C_{Bi}$ will be constant.

The extraction of the Bismuthiol III complex of bismuth is pH-dependent and the best acidity range is pH 3–4. The supporting electrolyte should therefore keep the pH constant in this range and thus prevent precipitation of basic salts. The acetate anion in the buffer forms weak complexes with Bi^{3+} at the pH used.

Activity of Bi^{3+} in the ammonium acetate buffer

There are no literature data on the stability of Bi^{3+}–acetate complexes and this makes it impossible to calculate the true activity of Bi^{3+} ions in ammonium acetate buffer. This parameter is required for determination of the selectivity coefficients and for evaluation of the sensitivity range of the electrode. For this reason we have attempted to use our electrode to determine the conditional dissociation constant

$$K = \frac{[Bi^{3+}]\,[CH_3COO^-]^3}{[Bi(CH_3COO_3]} \qquad (1)$$

for the reaction

$$Bi(CH_3COO)_3 \rightleftharpoons Bi^{3+} + 3CH_3COO^-$$

For this purpose four series (A,B,C,D) of Bi^{3+} solutions, each with bismuth concentrations of 10^{-6}, 10^{-5}, 10^{-4}, 10^{-3}, $10^{-2}M$, were prepared in ammonium acetate buffer of different concentrations. In this way a series of solutions with differing pH and acetate ion concentrations was obtained (Table 1). Calibration curves were determined for each series of solutions (Fig. 2). It was assumed that the electrode is sensitive to Bi^{3+} ions and that it has the same potential for the same Bi^{3+} activity in each series of solutions, *i.e.*, if $E_A = E_B$ then $(a_{Bi^{3+}})_A = (a_{Bi^{3+}})_B$. Hence

$$f_A[Bi^{3+}]_A = f_B[Bi^{3+}]_B \qquad (2)$$

In Bi(III) solutions in ammonium acetate buffer (pH 4) Bi^{3+} ions are lost by side-reactions such as hydrolysis and the formation of bismuth acetate complexes. The bismuth may be present in the following forms: Bi^{3+}, $BiOH^{2+}$, $Bi(OH)_2^+$, $Bi(CH_3COO)^{2+}$, $Bi(CH_3COO)_2^+$, $Bi(CH_3COO)_3$. Because at pH 4 the concentration ratio $[BiOH^{2+}]:[Bi(OH)_2^+]$ is $1:10^{-6.6}$,

Table 1. Characteristics of solutions used for the determination of the dissociation constant of $Bi(CH_3COO)_3$

Series	Buffer composition: $C_{CH_3COONH_4}$, M	C_{CH_3COOH}, M	pH	$C_{CH_3COO^-}$, M	$\frac{a_{Bi^{3+}}}{C_{Bi(III)}}$
A	0.4	1.4	4.1	0.45	1.11×10^{-6}
B	0.3	1.05	4.05	0.31	2.9×10^{-6}
C	0.2	0.7	4.0	0.187	1.21×10^{-5}
D	0.1	0.35	3.8	0.064	2.7×10^{-4}

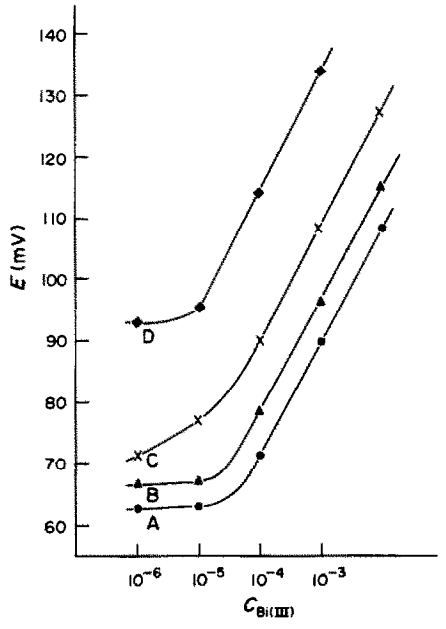

Fig. 2. Calibration curves of the electrode in the solution of Bi(III) in ammonium acetate buffer. *A*, 0.4*M* CH_3COONH_4, 1.4*M* CH_3COOH; *B*, 0.3*M* CH_3COONH_4, 1.05*M* CH_3COOH; *C*, 0.2*M* CH_3COONH_4, 0.7*M* CH_3COOH; *D*, 0.1*M* CH_3COOHN_4, 0.35*M* CH_3COOH.

only $BiOH^{2+}$ need be taken into account. Likewise, because of the large excess of acetate relative to Bi(III), $Bi(CH_3COO)_3$ is mainly formed: evidence for this comes from the shift in the electrode calibration graphs when the ammonium acetate concentration is changed. The total Bi(III) concentration can therefore be expressed as

$$C_{Bi(III)} = [Bi^{3+}] + [BiOH^{2+}] + [Bi(CH_3COO)_3] \quad (3)$$

Substitution for $[BiOH^{2+}]$ and $[Bi(CH_3COO)_3]$ in terms of the equilibrium constants *etc.*, and rearrangement, leads to

$$[Bi^{3+}] = \frac{C_{Bi(III)}}{1 + \dfrac{[OH^-]}{k_{BiOH2+}} + \dfrac{K(C_s + C_k)^3}{\alpha^3_{CH_3COO(H)}}} \quad (4)$$

where $[Bi^{3+}]$ is the concentration of Bi^{3+}, $C_{Bi(III)}$ the total concentration of Bi(III) in solution, k_{BiOH2+} the hydrolysis constant of $BiOH^{3+}$, $\alpha_{CH_3COO(H)}$ the Ringbom side-reaction coefficient for acetate and protons, K the conditional dissociation constant of $Bi(CH_3COO)_3$, C_s the concentration of CH_3COONH_4 and C_k the concentration of CH_3COOH.

By substituting values of $[Bi^{3+}]$ calculated from equation (4) into equation (2), we can derive equation (5), from which the conditional dissociation constant K of the complex $Bi(CH_3COO)_3$ can be calculated.

$$K = \frac{f_B[C_{Bi(III)}]_B \left[\dfrac{C_s + C_k}{\alpha_{CH_3COO(H)}}\right]^3_A - f_A[C_{Bi(III)}]_A \left[\dfrac{C_s + C_k}{\alpha_{CH_3COO(H)}}\right]^3_B}{f_A[C_{Bi(III)}]_A \left[1 + \dfrac{[OH^-]}{k_{BiOH}}\right]_B - f_B[C_{Bi(III)}]_B \left[1 + \dfrac{[OH^-]}{k_{BiOH}}\right]_A} \quad (5)$$

where subscripts A and B refer to the two series of measurements, and $[C_{Bi(III)}]_A$, $[C_{Bi(III)}]_B$ are the total concentrations of Bi(III) in series A and B, giving the same E value in the measurement cell (Fig. 2). The dissociation constant K for the complex $Bi(CH_3COO)_3$ was calculated from equation (5) for each pair of series, *i.e.*, AB, AC, AD, BC, BD and CD (Table 2). The average value so calculated is 6.1×10^{-7}. With this value, it was possible to calculate $[Bi^{3+}]$ and $a_{Bi^{3+}}$ in solution by using equation (4). The values of $a_{Bi^{3+}}/C_{Bi(III)}$ for each series are presented in Table 1. The activity coefficients can be calculated by the equation

$$\log f = -Z^2\left[\frac{0.51\sqrt{I}}{1 + 1.5\sqrt{I}} - 0.2I\right] \quad (6)$$

where Z is the charge on the ion and I is the ionic strength. The calculated values of $a_{Bi^{3+}}$ were plotted against E, and as a result, a single calibration curve was obtained (Fig. 3). This is a confirmation of the validity of our assumptions and shows that the value for the conditional dissociation constant of the complex is substantially correct.

Influence of pH on the electrode potential

The electrode gives correct response in the pH range 3–4, changes in electrode potential being due only to changes in $a_{Bi^{3+}}$. On the other hand, in a very acidic medium (0.1*M* nitric acid), the calibration is linear in the range 10^{-5}–$10^{-3}M$ and the slope decreases to 11 mV/p$C_{Bi(III)}$. This is a result of the decomposition of the complex and its incomplete extraction, as well as the influence of hydrogen-ion concentration on the electrode behaviour.

Table 2. Values of the dissociation constant $K_{Bi(CH_3COO)_3}$

	$C_{Bi(III)}$, M from calibration curves				$10^7 \times K$ (calculated from pairs of the series)					
E,mV	A	B	C	D	AB	AC	AD	BC	BD	CD
90	10^{-3}	4.18×10^{-4}			5.9					
95	1.96×10^{-3}		1.99×10^{-4}			4.5				
100	3.5×10^{-3}	1.49×10^{-3}	3.54×10^{-4}	1.77×10^{-5}			7.8	4.0	7.8	
120			4.17×10^{-3}	1.99×10^{-4}						6.6

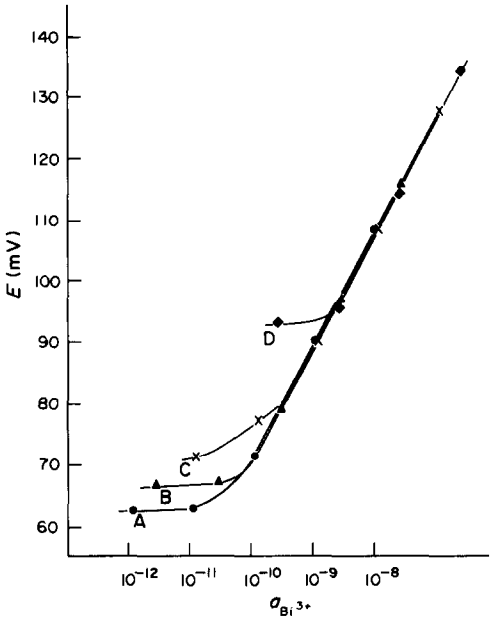

Fig. 3. Dependence of electrode potential on Bi^{3+} activity in Bi(III) solutions in ammonium acetate buffer with the following compositions: *A*, 0.4*M* CH_3COONH_4, 1.4*M* CH_3COOH; *B*, 0.3*M* CH_3COONH_4, 1.05*M* CH_3COOH; *C*, 0.2*M* CH_3COONH_4, 0.7*M* CH_3COOCH; *D*, 0.1*M* CH_3COONH_4, 0.35*M* CH_3COOH.

Effect of interfering ions

Sulphate, chloride and nitrate at a concentration of $10^{-2}M$ in pH-4 ammonium acetate buffer do not affect the calibration curve. To characterize the effect of cations on the potential of the electrode the selectivity coefficients were determined. For this purpose, electrode potentials for solutions containing Bi^{3+} ions alone and in the presence of interfering ions were measured.[14,15] The activities of Bi^{3+} in both solutions were the same. Selectivity coefficient values $K_{Bi^{3+}/M^{z+}}$ are shown in Table 3. The activities of the Bi^{3+} ions and the interfering cations were used in calculations of the selectivity coefficients. These activities differ considerably from the total concentrations of the cations (*e.g.*, $a_{Bi^{3+}}/C_{Bi(III)} = 1.2 \times 10^{-5}$), because of complex formation between the cations and the acetate anions from the buffer. The "activity" selectivity coefficients are inconvenient in analytical practice because their use requires a knowledge of the stability constants of the cation–acetate complexes and calculation of the concentration ranges of the interfering cations M^{z+}, for determination of $C_{Bi(III)}$. To avoid this problem we introduce "concentration" selectivity coefficients $K_{Bi(III)/M^{z+}}$, measured as activity values but calculated from the total concentrations of the metals. They are valid only under the conditions of pH and buffer concentration used in their determination. Some "concentration" selectivity coefficients, $K_{Bi(III)/M^{z+}}$ are also shown in Table 3.

Table 3. Values of the selectivity coefficients ($10^{-4}M$ Bi(III), $10^{-2}M$ M^{z+})

Cation	Selectivity coefficient	
	$K_{Bi^{3+}/M^{z+}}$	$K_{Bi(III)/M^{z+}}$
Th(IV)	$<5.3 \times 10^{-7}$	$<4.2 \times 10^{-4}$
Al(III)	$<6.1 \times 10^{-7}$	$<1.3 \times 10^{-3}$
Mn(II)	$<2.8 \times 10^{-6}$	$<1.3 \times 10^{-2}$
Co(II)	$<2.9 \times 10^{-6}$	$<1.3 \times 10^{-2}$
Ca(II)	$<6.9 \times 10^{-6}$	$<1.3 \times 10^{-2}$
Mg(II)	$<7.5 \times 10^{-6}$	$<1.3 \times 10^{-2}$
Ni(II)	$<1.3 \times 10^{-5}$	$<1.3 \times 10^{-2}$
Cd(II)	$<2 \times 10^{-5}$	$<1.3 \times 10^{-2}$
Zn(II)	$<4.2 \times 10^{-5}$	$<1.3 \times 10^{-2}$
Pb(II)*	9.3×10^{-5}	0.42
Fe(III)	$<1.3 \times 10^{-4}$	$<1.3 \times 10^{-3}$
Cu(II)†	0.2	>1
Hg(II)	≫1	≫1
Ag(I)	≫1	≫1

*($10^{-4}M$ Bi(III), $10^{-3}M$ Pb(II)).
†($10^{-2}M$ Bi(III), $10^{-2}M$ Cu(II)).

Considerable differences between "activity" and "concentration" selectivity coefficients are caused by the apparently higher stability of the acetate–Bi(III) complex than that of the acetate complexes of the interfering cations. It can be seen from the values of the selectivity coefficients that the electrode shows good selectivity for several bivalent cations and also for Al^{3+}, Fe^{3+} and Th^{4+}. Hg^{2+}, Ag^{+} and Cu^{2+} interfere.

Time stability of the electrode

The electrode is ready for use immediately after mounting and does not require conditioning in Bi^{3+} solution. The behaviour of the electrode was investigated by determining the calibration curve every day for 20 days (Fig. 4). Small changes in potential were observed at low concentrations of Bi(III), *i.e.*, 10^{-6} and $10^{-5}M$. For 10^{-4}–$10^{-2}M$ Bi(III) the electrode potential was stable. The stability of the membrane solution was also investigated and the calibration curves for freshly prepared solutions and those left for 3 months were found to be identical.

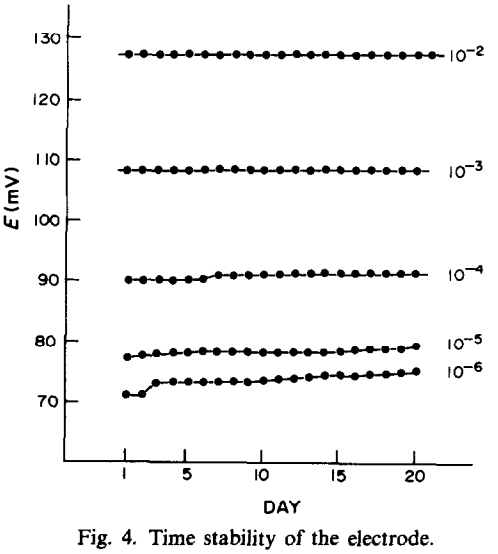

Fig. 4. Time stability of the electrode.

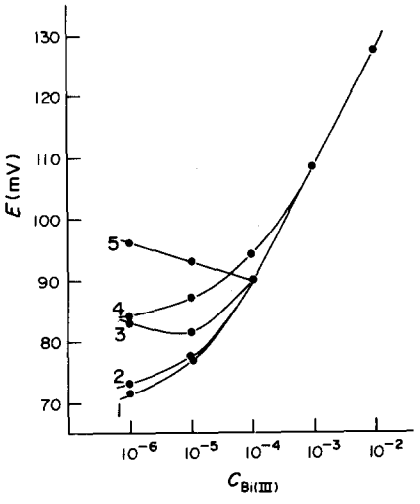

Fig. 5. Dependence of electrode potential on Bi(III) concentration in solutions containing interfering ions with concentration of $10^{-2}M$. 1, Bi(III) and Bi(III) + Zn(II) or Ni(II), Fe(III); 2, Bi(III) + Ca(II) or Mg(II), Co(II), Mn(II), Th(IV); 3, Bi(III) + Cd(II); 4, Bi(III) + $10^{-4}M$ Cu(II); 5, Bi(III) + $10^{-3}M$ Pb(II).

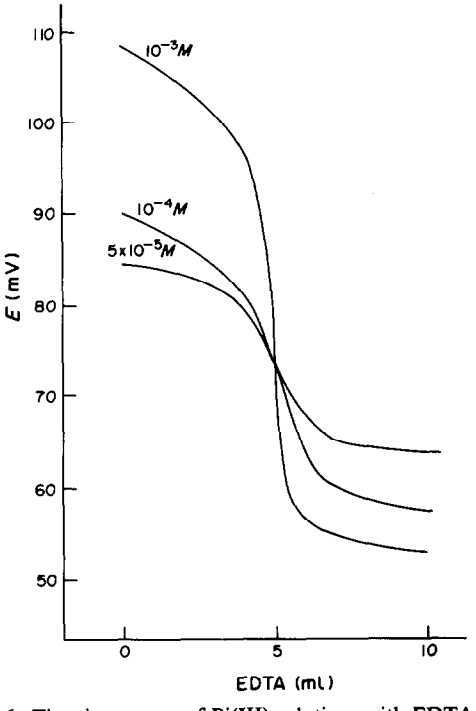

Fig. 6. Titration curves of Bi(III) solutions with EDTA in ammonium acetate buffer (pH 4).

Response time

One advantage of the electrode is its very rapid response. It reaches 95% of the final potential for 10^{-6}–$10^{-2}M$ Bi(III) in only a few seconds and gives 100% response in 3 min for $10^{-6}M$, 1 min for $10^{-5}M$ and about 10 sec for 10^{-4}–$10^{-2}M$ solutions.

Analytical applications of the electrode

Bi(III) in solution can be determined by direct potentiometry in the concentration range 10^{-5}–$10^{-2}M$. Figure 5 presents calibration curves for the electrode in the presence of various interfering ions at constant concentration. The shape of the calibration curve is not affected by $10^{-2}M$ Mg(II), Ca(III), Ni(II), Co(II), Zn(II), Mn(II), Cd(II), and Fe(III). It is also possible to determine 10^{-4}–$10^{-2}M$ Bi(III) in the presence of $10^{-3}M$ Pb(II).

Potentiometric titration

The application of the electrode for end-point detection in the titration of Bi(III) has been studied. A suitable titrant is EDTA because of the very high stability constant of the Bi–EDTA complex (log $\beta = 28.2$). Some examples of the potentiometric titration of Bi(III) solutions (10^{-3}, 10^{-4} and $5 \times 10^{-5}M$) in ammonium acetate buffer (pH 4) with EDTA (10^{-2}, 10^{-3} and $5 \times 10^{-4}M$ respectively) dissolved in the same buffer solution are illustrated in Fig. 6.

REFERENCES

1. P. Gabor-Klatmanyi, K. Tóth and E. Pungor, *Ion Selective Electrodes.* Symposium Mätrafüred–Hungary, 23–25 October 1972.
2. J. B. Harrell, A. D. Jones and G. R. Choppin, *Anal. Chem.*, 1969, **41**, 1459.
3. R. W. Cattrall and Pui Chin-Poh, *ibid.*, 1975, **47**, 93.
4. *Idem, Anal. Chim. Acta*, 1975, **78**, 463.
5. E. Hopîrtean, M. Preda and C. Liteanu, *Z. Anal. Chem.*, 1977, **286**, 65.
6. N. K. Evseeva and I. N. Kreminskaya, *Zh. Analit. Khim.*, 1976, **31**, 822.
7. V. N. Golubev and N. K. Evseeva, *Elektrokhimiya*, 1976, **12**, 263.
8. A. G. Fogg and A. A. Al-Sibaai, *Anal. Lett.*, 1976, **9**, 33.
9. A. S. Bychkov and O. M. Petukhin, *Zh. Analit. Khim.*, 1975, **30**, 2213.
10. K. Ohzeki and T. Kambara, *J. Electroanal. Chem.*, 1978, **88**, 85.
11. A. I. Busev, *Zh. Analit. Khim.*, 1968, **23**, 59.
12. *Idem, Synthesis of New Organic Reagents for Inorganic Analysis* (in Russian), Moscow University Press, 1972.
13. K. Ren and W. Szczepaniak, *Chem. Anal. (Warsaw)*, 1976, **21**, 1365.
14. G. J. Moody and J. D. R. Thomas, *Selective Ion Sensitive Electrodes*, Merrow, Watford, 1971.
15. G. J. Moody, N. S. Nassory and J. D. R. Thomas, *Talanta*, 1979, **26**, 873.

Talanta, Vol. 30, No. 12, pp. 951–954, 1983
Printed in Great Britain.

0039-9140/83 $3.00 + 0.00

STUDIES OF THE OXIDATION OF IMINODIACETIC ACID (IDA) AND NITRILOTRIACETIC ACID (NTA) WITH LEAD DIOXIDE SUSPENSION IN NITRIC ACID

TOSHIO MATSUDA and TOYOSHI NAGAI
Department of Chemistry, Ritsumeikan University, Kyoto, Japan

(*Received* 25 *January* 1983. *Revised* 18 *March* 1983. *Accepted* 24 *May* 1983)

Summary—The stoichiometry of the oxidation of IDA or NTA with lead dioxide suspension was studied by polarographic measurement and by derivative polarographic titration. One mole and two moles of Pb(IV) are reduced per mole of IDA and NTA respectively, with moderate speed at room temperature in nitric acid solutions. One mole each of carbon dioxide, formaldehyde and glycine are produced from the oxidation of 1 mole of IDA, and two moles of carbon dioxide, two moles of formaldehyde and one mole of glycine from 1 mole of NTA. The overall reaction in each case may be written as follows:

$$Pb(IV) + IDA + H_2O \rightarrow Pb(II) + CO_2 + HCHO + H_2NCH_2COOH + 2H^+$$

$$2Pb(IV) + NTA + 2H_2O \rightarrow 2Pb(II) + 2CO_2 + 2HCHO + H_2NCH_2COOH + 4H^+$$

We have recently introduced lead dioxide suspension, prepared by hydrolysis of lead tetra-acetate, as an oxidizing agent. Studies of its redox reactions with sodium oxalate,[1] chromium(III)[2] and EDTA[3] have already been reported. The reactions proceed at room temperature with definite reacting ratios. The oxidation of chromium(III) has been applied to the standardization of chromium(III) solution by potentiometric titration after prior oxidation to chromium(VI) with lead dioxide suspension.[4]

The redox reactions of chelating agents such as EDTA with various oxidizing agents have been studied in analytical and environmental chemistry, for various purposes.[5–9]

In a previous paper,[3] the stoichiometry and mechanism of the reaction between lead dioxide suspension and EDTA were studied by derivative polarographic titration (the DPT method) and determination of the products. Four moles of Pb(IV) are reduced per mole of EDTA, with moderate speed at room temperature in sulphuric acid solutions, and the products are four moles of carbon dioxide, three moles of formaldehyde and one mole of *N*-hydroxymethylethylenediamine. In the present paper, the reaction of lead dioxide suspension in nitric acid with iminodiacetic acid (IDA) and nitrilotriacetic acid (NTA), which have a simpler structure than EDTA, is investigated.

EXPERIMENTAL

Reagents and apparatus

A 0.05*M* solution of lead tetra-acetate in glacial acetic acid was prepared and standardized as reported previously.[3] The iminodiacetic acid and the nitrilotriacetic acid were recrystallized twice from hot water and dried at 90°; 0.05*M* solutions of IDA and NTA were standardized by potentiometric titration with potassium hydroxide. A 0.005*M* solution of glycine was prepared from the analytical-reagent grade chemical. Solutions of *o*-phthalaldehyde and 2-mercaptoethanol, used for the fluorometric determination, were prepared according to Roth.[10] Other solutions were prepared as reported elsewhere.[1,3] The water used was demineralized water distilled in the presence of small amounts of potassium permanganate and sodium hydroxide, in a glass apparatus.

The polarograph and potentiometer were those used previously.[2,3] A Hitachi 650-10M fluorescence spectrophotometer was used. Unless otherwise stated, all measurements and titrations were performed at 25 ± 0.2°.

Determination of the reaction stoichiometry

The reacting ratio between Pb(IV) and IDA was determined polarographically in a batchwise operation by use of a mole-ratio method as shown in Fig. 1. To each of a series of 200-ml Erlenmeyer flasks, containing 10 ml of 1*M* nitric acid and 10 ml of 1*M* potassium nitrate, diluted with 78–63 ml of distilled water, 2.00 ml of 0.05*M* lead tetra-acetate were added dropwise and hydrolysed. Then 0–15 ml of 0.01*M* IDA solution (to give constant total volume) were added. Each mixture was diluted to 100 ml and stirred for 10 min, then the remaining lead dioxide was filtered off on a 0.45 μm membrane filter (Toyo, type TM-2). The lead(II) in the filtrate was then determined polarographically. When IDA was present in excess, the lead(II) in the mixture was directly determined polarographically.

The reacting ratio between Pb(IV) and NTA was determined by the DPT method, as shown in Fig. 2. To each of a series of 100-ml electrolytic cells, containing 5 ml of 1*M* nitric acid and 5 ml of 1*M* potassium nitrate, diluted with 38 ml of distilled water, 2.00 ml of 0.05*M* lead tetra-acetate solution were added dropwise and hydrolysed. The solution was then deaerated with nitrogen, and titrated with 0.01*M* NTA. The procedures for the titration and the treatment of the platinum electrode were the same as described previously.[3]

Analysis of the products

Solutions (0.05*M*) of lead tetra-acetate and IDA or NTA were mixed in 1.5:1 molar ratio for IDA and 3:1 molar ratio for NTA, and diluted to 100 ml with 0.1*M* nitric acid, and

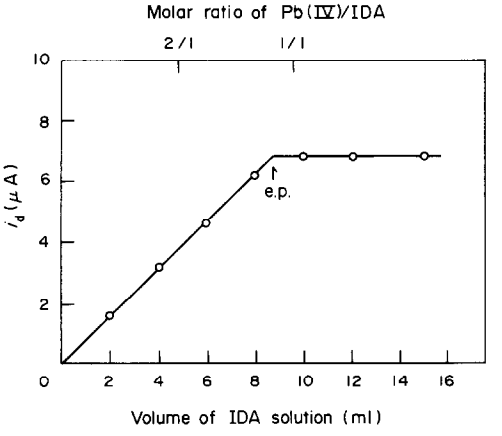

Fig. 1. Relation between the diffusion current of Pb(II) produced and the volume of IDA solution added: 2.00 ml of $4.90 \times 10^{-2}M$ lead tetra-acetate hydrolysed in $0.1M$ nitric acid and $0.1M$ potassium nitrate, and then reacted with 0–15 ml of $1.017 \times 10^{-2}M$ IDA (total volume 100 ml).

allowed to stand for 10–15 min at 25°. After the remaining lead dioxide had been collected on the membrane filter, the amounts of Pb(II), formaldehyde and glycine were determined by the following procedures, a separate sample being analysed when necessary.

Pb(II) was determined directly by polarography, and formaldehyde was determined gravimetrically with dimedone.[3]

Glycine was determined fluorimetrically[10] by the standard-addition method with *o*-phthalaldehyde and 2-merceptoethanol, as follows. Ten ml of $5M$ sulphuric acid were added to the filtrate to remove most of the lead(II), and the lead sulphate produced was filtered off. The filtrate was adjusted to pH 9 and diluted to 250 ml. Then 1–4 ml

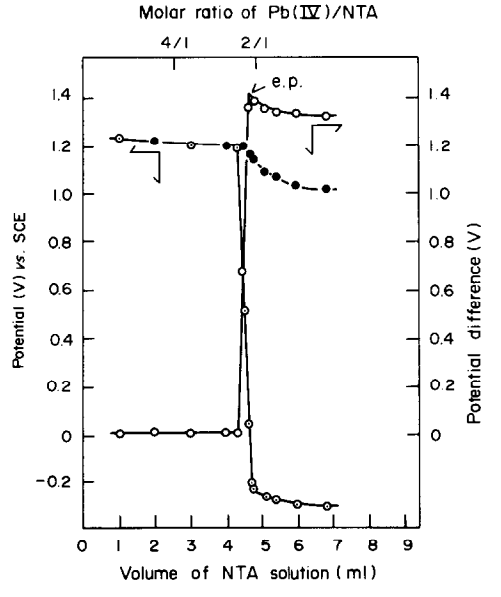

Fig. 2. Titration curve and potential changes of anode and cathode: 2.00 ml of $4.99 \times 10^{-2}M$ lead tetra-acetate hydrolysed in $0.1M$ nitric acid and $0.1M$ potassium nitrate (total volume 50 ml), and then titrated with $1.036 \times 10^{-2}M$ NTA (● anode potential; ◉ cathode potential; ○ ΔE).

volumes of $5mM$ standard glycine solution were added to 25-ml aliquots of the solution, and the mixtures were diluted to 50 ml. Then 1 ml of this solution was mixed with a mixture of 0.5 ml of *o*-phthalaldehyde solution (10 mg/ml in ethanol), 0.5 ml of 2-mercaptoethanol solution (5 μl/ml in ethanol) and 29 ml of $0.05M$ borate buffer (pH 9.0), and let stand for 25 min at room temperature. The fluorescence was measured at 450 nm with an excitation wavelength of 340 nm. The amount of glycine was calculated from the results (standard-addition method).

Carbon dioxide was determined as follows. A cylindrical cell (40 mm in diameter and 150 mm in height) was used as the reaction vessel. It was closed by a rubber stopper fitted with a tube through which nitrogen could be introduced into the reaction solution, a 10 ml burette for addition of IDA or NTA solution, and a vertically mounted condenser connected to three absorption traps. During an experiment, the jacket of the condenser was maintained at about 15° by circulation of cold water, to minimize contamination with acetic acid. Solutions of lead tetra-acetate and IDA or NTA were mixed in the vessel in 0.7:1 molar ratio for IDA and 1.5:1 molar ratio for NTA, and allowed to stand for 15 min at 25°. The vessel temperature was then raised to 90°. The carbon dioxide evolved was absorbed in the three traps, each containing 75 ml of $0.005M$ barium hydroxide, a stream of nitrogen being passed through the system for 4 hr at a flow-rate of 30–40 ml/min, as carrier gas. The excess of barium hydroxide in the traps was titrated with hydrochloric acid. A blank was run to allow correction for the unavoidable carry-over-of acetic acid.

RESULTS AND DISCUSSION

Determination of reacting ratio between Pb(IV) and IDA

Figure 1 shows an example of the relation between the diffusion current of lead(II) produced and the volume of standard IDA solution added. For each combination, equilibrium was reached within 5 min. The reacting ratio of Pb(IV) to IDA found for the reaction of 100 ml of $0.980 \times 10^{-3}M$ lead dioxide suspension in $0.1M$ nitric acid with $1.017 \times 10^{-2}M$ IDA was 1.11 ± 0.04 (7 replicates). The reacting ratio was also determined at two Pb(IV) concentrations (1.00 and 4.00 ml of lead tetra-acetate solution), two levels of acidity (0.05 and $1M$ nitric acid) and two temperatures (25 and 50°). A reaction ratio of about 1:1 was found in all cases.

Determination of the reacting ratio between Pb(IV) and NTA

Figure 2 shows a typical titration curve, giving the changes of potential difference (ΔE) between the anode and the cathode. After the end-point, the oxidation of NTA[11] is the electrode reaction at the anode. The optimum current density was obtained from the current–potential curve and the titration curve. Although a wide range of current density at the anode was suitable, the titration curve was liable to rise after the end-point when a current density below 19 nA/mm^2 was used. A sharp peak on the titration curve was obtained with a current density of 19–25 nA/mm^2. The reacting ratio of Pb(IV) to NTA obtained from the titration of 50 ml of 1.996×10^{-3} M lead dioxide suspension in $0.1M$ nitric acid with

Table 1. Determination of carbon dioxide

Conditions*		CO_2, *mmole*		
Pb(IV), *mmole*	IDA or NTA *mmole*	Calc.	Found	Molar ratio, CO_2/IDA or NTA
(A) IDA				
0.181	0.252	0.181	0.179	0.99
			0.171	0.95
			0.172	0.95
			0.173	0.96
			0.172	0.95
(B) NTA				
0.229	0.153	0.229	0.240	2.11
			0.223	1.96
			0.236	2.06
			0.233	2.04

*Total volume 50 ml.

Table 2. Determination of formaldehyde

Conditions*		HCHO, *mmole*		
Pb(IV), *mmole*	IDA or NTA, *mmole*	Calc.	Found†	Molar ratio, HCHO/IDA or NTA
(A) IDA				
0.170	0.126	0.126	0.126 ± 0.001	1.00
			0.122 ± 0.001	0.97
			0.121 ± 0.001	0.96
			0.122 ± 0.001	0.97
(B) NTA				
0.689	0.254	0.508	0.500 ± 0.008	1.97
			0.512 ± 0.003	2.02
			0.501 ± 0.005	1.97
			0.501 ± 0.003	1.97

*Total volume 100 ml.
†Average and deviation are based on three replicates on the same solution.

$1.036 \times 10^{-2}M$ NTA was 2.06 ± 0.01 (6 replicates). The reacting ratio determined at two Pb(IV) concentrations (1.00 and 5.00 ml of lead tetra-acetate solution), two acidity levels (0.05 and 1*M* nitric acid) and two temperatures (35 and 50°) was 2:1 in all cases.

Products

The determination of Pb(II) in the reaction solution confirmed the 1:1 reacting ratio for IDA and 2:1 ratio for NTA.

The results for determination of carbon dioxide are shown in Table 1. The calculated value is based on the assumption that one carboxyl group of IDA and two of NTA will be decarboxylated by the Pb(IV). The effect of the other substances present (nitric acid, acetic acid, lead nitrate, formaldehyde, glycine and surplus IDA or NTA) was studied first with a standard sodium carbonate solution under the chosen conditions. The recovery of carbon dioxide was found to be $92 \pm 2\%$ (4 replicates), and the experimental values listed in Table 1 have been corrected on this basis. The results in Table 1 indicate that one and two mole(s) of carbon dioxide are produced per mole of IDA and NTA respectively.

The results for determination of formaldehyde are shown in Table 2. The effect of the other substances present (nitric acid, acetic acid, lead nitrate, glycine and lead dioxide) was studied beforehand with a

Table 3. Determination of glycine

Conditions*		Glycine, *mmole*		
Pb(IV), *mmole*	IDA or NTA, *mmole*	Calc.	Found†	Molar ratio, Glycine/IDA or NTA
(A) IDA				
0.381	0.257	0.257	0.249 ± 0.007	0.97
			0.261 ± 0.005	1.02
			0.259 ± 0.002	1.01
(B) NTA				
0.432	0.150	0.150	0.143 ± 0.002	0.95
			0.148 ± 0.001	0.99
			0.157 ± 0.010	1.05
			0.153 ± 0.007	1.02

*Total volume 100 ml.
†Average and deviation are based on two replicates on the same solution.

standard formaldehyde solution, and the recovery was found to be 98 ± 2%. Table 2 shows that one and two mole(s) of formaldehyde are produced per mole of IDA and NTA respectively.

proceeds by the following process. IDA first loses one electron per molecule, with decarboxylation, and then a second electron before the formation of formaldehyde and glycine by hydrolysis:

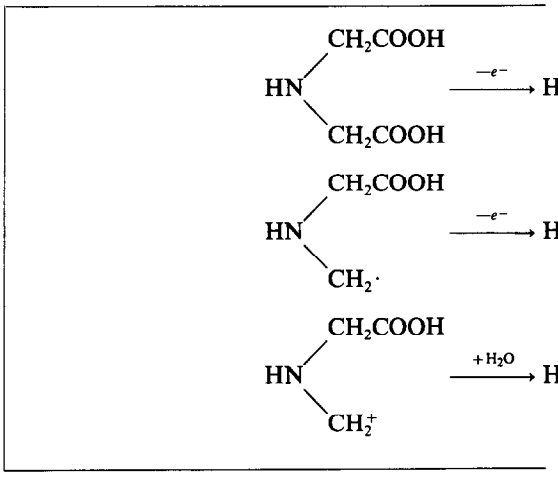

$$\mathrm{HN(CH_2COOH)_2} \xrightarrow{-e^-} \mathrm{HN(CH_2COOH)(CH_2\cdot)} + \mathrm{CO_2} + \mathrm{H^+} \quad (1)$$

$$\mathrm{HN(CH_2COOH)(CH_2\cdot)} \xrightarrow{-e^-} \mathrm{HN(CH_2COOH)(CH_2^+)} \quad (2)$$

$$\mathrm{HN(CH_2COOH)(CH_2^+)} \xrightarrow{+\mathrm{H_2O}} \mathrm{H_2NCH_2COOH} + \mathrm{HCHO} + \mathrm{H^+} \quad (3)$$

In the determination of glycine, maximum fluorescence intensity was obtained with excitation at 340 nm and measurement at 450 nm, both for the test samples and a synthetic solution with known concentrations of nitric acid, acetic acid, lead nitrate, formaldehyde, glycine and lead tetra-acetate.

The products were also examined by thin-layer chromatography with a silica gel 60 plate (Merck, No. 5626) and a developing solution consisting of equal volumes of acetone and 0.1*M* hydrochloric acid or sodium hydroxide. The chromatograms of the oxidation products of IDA and NTA showed only one spot, with R_f value identical to that for glycine.

The results for determination of glycine are shown in Table 3. The calculated value is based on the assumption that one mole of glycine will be produced per mole of IDA or NTA. The effect of other substances present was studied beforehand. The recovery was found to be 94 ± 4% for application of the whole procedure to standard glycine solutions. The results indicate that one mole of glycine is produced per mole of IDA or NTA.

CONCLUSIONS

From the results above, it can be assumed that the oxidation of IDA or NTA by lead dioxide suspension

On the other hand, NTA loses two electrons per molecule in the first step, with formation of IDA. In the second step, glycine is produced from the IDA. Therefore, the overall reaction in each case may be written as follows:

$$\mathrm{Pb(IV) + IDA + H_2O \rightarrow Pb(II) + CO_2 + HCHO + H_2NCH_2COOH + 2H^+}$$

$$\mathrm{2Pb(IV) + NTA + 2H_2O \rightarrow 2Pb(II) + 2CO_2 + 2HCHO + H_2NCH_2COOH + 4H^+} \quad (2)$$

REFERENCES

1. S. Ito, T. Matsuda and T. Nagai, *Bunseki Kagaku*, 1977, **26**, 687.
2. T. Nagai, T. Matsuda and Y. Kouji, *ibid.*, 1978, **27**, 749.
3. S. Ito, T. Matsuda and T. Nagai, *Talanta*, 1980, **27**, 25.
4. T. Nagai, T. Matsuda and Y. Kouji, *Bunseki Kagaku*, 1980, **29**, 115.
5. G. E. Batley and Y. J. Farrar, *Anal. Chim. Acta*, 1978, **99**, 283.
6. T. M. Florence, *Talanta*, 1982, **29**, 345.
7. H. Holzapfel and K. Dittrich, *ibid.*, 1966, **13**, 309.
8. S. B. Hanna, S. Al-Hashimi, W. H. Webb and W. R. Carroll, *Z. Anal. Chem.*, 1969, **246**, 231.
9. N. Tanaka, K. Gomi and T. Shirakashi, *Nippon Kagaku Kaishi*, **1975**, 444.
10. M. Roth, *Anal. Chem.*, 1971, **43**, 880.
11. K. Štulík and F. Vydra, *J. Electroanal. Chem.*, 1968, **16**, 385.

Talanta, Vol. 30, No. 12, pp. 955–958, 1983
Printed in Great Britain

0039-9140/83 $3.00 + 0.00
Pergamon Press Ltd

ANALYTICAL APPLICATIONS OF Zr(IV) AND Ti(IV) ARSENOPHOSPHATES AS ION-EXCHANGERS

K. G. VARSHNEY, S. AGRAWAL, K. VARSHNEY and A. PREMEDAS*
Chemistry Section, Z.H. College of Engineering and Technology, Aligarh Muslim University, Aligarth-202001, India

M. S. RATHI and P. P. KHANNA
Wadia Institute of Himalayan Geology, Dehradun, India

(*Received* 26 *March* 1980. *Revised* 22 *March* 1983. *Accepted* 13 *May* 1983)

Summary—The distribution of 27 metal ions between zirconium and titanium arsenophosphate and demineralized water, perchloric acid and nitric acid has been studied. On the basis of the results, several binary and ternary separations can be designed. The data have been used in application of these materials to the analysis of certain alloys and rocks.

Inorganic ion-exchangers have an advantage over their organic counterparts because of their higher stability. They are also more selective. For example, tin(IV) vanadophosphate,[1] vanadoarsenate[2] and tungstoarsenate[3] are selective for alkaline-earth metal ions. Tin(IV) arsenophosphate[4] shows good affinity for some quadrivalent metal ions such as Th^{4+} and Zr^{4+}. However, practically all the work published on these materials has been on their preparation and properties, and none on applications other than to simple binary or ternary mixtures. The present work is aimed at remedying this situation, and illustrating the wider utility of these materials.

Zirconium and titanium arsenophosphate, prepared by us earlier,[5] were selected for the study.

EXPERIMENTAL

Reagents

Zirconyl chloride (J. T. Baker), titanium(IV) chloride (s.g. 1.73, BDH), trisodium orthophosphate (BDH), and disodium hydrogen arsenate (Merck) were used. Other reagents and chemicals were of analytical grade.

Synthesis of the ion-exchange materials

Zirconium and titanium arsenophosphate (ZrAsP and TiAsP) were prepared as described earlier.[5] It was observed that when the material was converted into the H^+-form by the usual batch (equilibrium) process and washed in a column with demineralized water (DMW) or dilute nitric acid, the effluents were found (by atomic-absorption spectroscopy) to contain Al, Mg, Ca, Si, Fe and Mn. These may have arisen from impurities present in the chemicals used for the synthesis. Before use, the exchangers were therefore thoroughly washed with 1.0*M* nitric acid in a column until the effluent was free from the impurities mentioned. The material thus obtained had improved reproducibility and enhanced ion-exchange behaviour.

Distribution studies

All the metal ion solutions used were prepared in DMW except those of the tervalent and quadrivalent ions, to which a few drops of the appropriate acid were added to prevent hydrolysis. The distribution coefficients were determined[6] by equilibrating 250 mg of exchanger with 25 ml of solution containing an amount of metal ion equivalent to not more than 3% of the total ion-exchange capacity of the material and adjusted to the appropriate acidity *etc.* Titanium, uranium and cerium were determined colorimetrically[7–9] and the other metal ions by EDTA titration,[10] before and after the equilibration. The results obtained are summarized in Table 1.

Separations

Synthetic mixtures. A few synthetic binary and tertiary mixtures were prepared by mixing the metal ion solutions in the required volume ratios. For column operation, the exchanger (60–100 mesh, 2 g, H^+-form) was used in a glass tube of ~0.6 cm bore. A known volume (~0.5 ml) of sample solution was loaded on the column at a very slow flow-rate (~3–4 drops/min) and recycled through the column at least three times, with a 2–3 ml water wash between cycles, followed by elution with suitable solvents at a flow-rate of ~0.5 ml/min. The effluent was monitored qualitatively by standard spot-tests[11] to determine the elution behaviour, and then separate samples were analysed quantitatively by the methods used for the distribution studies. For brevity, the results, which were satisfactory, are omitted. Typical separations include V(IV)–Fe(III)–Ti(IV); Zn–Pb–Fe(III); Mn(II)–Fe(III); Al–Fe(III); Y–Ti(IV); Ni–Fe(III); Hg(II)–Pb; Cd–Pb; Y–Ce(IV); U(VI)–Ce(IV); La–Ce(IV); Ni–Pb; V(IV)–Pb.

Alloy and rock samples. Stock solutions of the alloys and rocks tested were prepared as follows. The alloy (~30 mg, accurately weighed) was dissolved in ~5 ml of *aqua regia*. The solution was evaporated to ~1 ml and then diluted to volume in a 100-ml standard flask with DMW. For the rock analysis, 100 mg of sample were fused with sodium hydroxide in a nickel crucible at dull red heat, followed by the leaching of the cooled melt with DMW and dilution to 1 litre (standard flask) with dilute hydrochloric acid.

For the alloy analysis 1 ml of the stock solution was loaded on the column (2 g of exchanger) at a very slow rate as described above. All the metal ions except iron(III) were eluted with 0.01*M* nitric acid. The iron(III) was then eluted with 0.1*M* nitric acid. Table 2 gives the results.

For the rock analysis 0.5 or 1 ml of the stock solution was evaporated to dryness to remove the excess of acid. The residue was taken up in DMW (~2 ml) and the solution was loaded on the exchanger (2 g) in the column, the rest of the

*Present address: Chemical Laboratory, Atomic Minerals Div., Department of Atomic Energy, Bangalore, India.

Table 1. Distribution coefficients of some metal ions on ZrAsP and TiAsP

Metal ions	Distribution coefficients									
	DMW		0.01*M* $HClO_4$		0.1*M* $HClO_4$		0.01*M* HNO_3		0.1*M* HNO_3	
	ZrAsP	TiAsP	ZrAsP	TiAsP	ZrAsP	TiAsP	ZrAsP	TiAsP	ZrAsP	TiAsP
Mg(II)	134	48	0	0	0	0	0	0	0	0
Ca(II)	188	95	0	12	0	8	0	12	0	8
Cu(II)	804	131	25	4	0	0	61	30	1	0
Co(II)	360	122	242	82	9	25	40	40	1	0
Ni(II)	217	48	12	18	8	0	10	0	9	0
Zn(II)	255	227	0	0	0	0	11	35	0	0
Cd(II)	860	291	155	44	5	20	6	15	0	0
Hg(II)	800	18	100	5	5	0	4	8	0	0
Pb(II)	TA	9.5×10^3	566	567	18	233	644	1.1×10^3	16	1.1×10^3
Mn(II)	525	4	20	0	0	0	36	0	0	0
V(IV)	480	700	4	0	4	0	220	38	0	5
Fe(III)	TA	TA	1.7×10^3	20	260	0	TA	2.9×10^3	330	500
Al(III)	TA	TA	900	0	0	0	860	TA	0	0
Cr(III)	100	—	—	—	—	—	65	—	0	—
U(VI)	713	95	298	0	27	7	290	0	20	0
Y(III)	TA	TA	180	1	27	0	2.5×10^3	160	8	4
La(III)	TA	260	61	100	27	7	260	120	40	0
Tb(III)	TA	900	25	30	0	0	30	50	0	0
Ho(III)	TA	400	400	27	0	0	40	30	0	0
Gd(III)	TA	287	520	11	0	0	52	20	0	0
Nd(III)	TA	600	460	61	0	0	50	58	0	0
Pr(III)	260	576	80	59	35	0	88	71	0	0
Dy(III)	TA	230	1.0×10^3	10	3	0	110	20	3	0
Sm(III)	140	900	435	275	0	15	50	37	0	0
Th(IV)	TA	TA	1.2×10^3	37	232	63	460	240	89	0
Ce(IV)	TA	550	443	525	525	56	525	525	440	400
Ti(IV)	TA	—	TA	—	525	—	TA	—	550	—

TA = total adsorption; (–) = not studied.

Table 2. Quantitative separation of iron (with ZrAsP, from 1 ml of stock solution of iron-base alloys)

Sample	Composition of stock solution, μg/ml					Found, μg	
	Fe	Cr	Ni	Mn	Si	Eluent 0.01*M* HNO_3 (100 ml)	Eluent 1*M* HNO_3 (100 ml)
AISI-303	222.8	56.5	26.7	4.7	1.6	Cr 55.1 Ni 26.7 Mn 4.8 Si 1.7	Fe 225
AISI-347	219.4	56.5	31.4	4.7	1.6	Cr 55.5 Ni 31.4 Mn 4.8 Si 1.7	Fe 221

procedure being the same as for the alloys. All the metal ions except Al^{3+} and Fe^{3+} were eluted with DMW as usual. Al^{3+} was removed from the column with 0.1*M* perchloric acid, and Fe^{3+} with 0.5*M* hydrochloric acid/1*M* ammonium chloride mixture. Table 3 summarizes the results.

Reproducibility of ion-exchange behaviour

Ten batches of ZrAsP were prepared and the ion-exchange capacity and K_d values determined as usual. The values were essentially the same in all cases.

DISCUSSION

The main purpose of this work was to study the distribution and separation of various metal ions on ZrAsP and TiAsP inorganic ion-exchangers. As the results show, the materials offer selectivity for a number of metal ions in various media. Though both exchangers generally show the same behaviour, in some cases they differ remarkably. For example, Ti(IV) and Y(III) are found to be strongly sorbed by ZrAsP in 0.01*M* nitric acid, but not by TiAsP, whereas Pb(II) is strongly sorbed by TiAsP in 0.1*M* nitric acid, but not by ZrAsP.

The distribution studies indicate several possible separations, some of them useful for the analysis of alloys such as ferronickel and ferromanganese. Tantalum antimonate, reported earlier,[12] also gives some

Table 3. Quantitative separation of various constituents in rocks, on ZrAsP

Rock sample	Volume of stock solution loaded, ml	Elements present, μg						Elements eluted by eluent shown, μg		
		Al	Fe	Si	Ca	Mg	Mn	DMW	0.1*M* $HClO_4$ (50 ml)	0.5*M* HCl + 1*M* NH_4Cl (50 ml)
G-2	0.5	7.70	1.34	34.6	0.98	0.37	0.01	Si 32.6 Ca 1.12 Mg 0.34	Al 8.4	Fe 1.4
G-2	1.0	15.4	2.69	69.2	1.96	0.75	0.03	Si 73.3 Ca 1.96 Mg 0.68	Al 15.8	Fe 2.7
AGV-1	0.5	8.59	3.89	29.8	2.47	0.76	0.05	Si 30.1 Ca 2.5 Mg 0.76 Mn 0.04	Al 8.6	Fe 3.8
AGV-1	1.0	17.2	6.78	59.6	4.94	1.52	0.10	Si 51.7 Ca 4.9 Mg 1.53 Mn 0.06	Al 17.2	Fe 6.7
BHVO-1	0.5	6.85	6.00	2.45	7.70	3.60	0.08	Si 2.45 Ca 7.5 Mg 3.6 Mn 0.06	Al 6.9	Fe 6.9
BHVO-1	1.0	13.7	12.0	4.90	11.4	7.20	0.17	Si 5.1 Ca 11.3 Mg 7.2 Mn 0.14	Al 14.0	Fe 11.6
BCR-1	0.5	6.86	6.70	27.26	3.48	1.74	0.09	Si 27.0 Ca 3.4 Mg 1.8 Mn 0.08	Al 7.1	Fe 6.8
BCR-1	1.0	13.7	13.4	54.5	6.97	3.48	0.18	Si 53.9 Ca 6.7 Mg 3.3 Mn 0.13	Al 14.1	Fe 13.6
PCC-1	0.5	0.36	4.14	21.1	0.27	21.7	0.06	Si 22.3 Ca 0.29 Mg 21.8 Mn 0.05	Al 0.36	Fe 4.1
PCC-1	1.0	0.73	8.28	42.1	0.55	43.5	0.12	Si 43.3 Ca 0.57 Mg 42.0 Mn 0.09	Al 0.72	Fe 8.2

of these separations, but our methods cover a wider range of composition. Titanium arsenate[13] and titanium phosphate[14] do not give these separations. TiAsP is more selective than the simple titanium arsenate for lead.

Because of its high affinity for iron and aluminium in certain media, ZrAsP has been tried for the analysis of alloys and rocks. Table 2 gives the results for the quantitative separation of iron from two standard steel samples. The error range was $\sim 1\%$ Analysis of rocks also gave satisfactory results (Table 3).

Acknowledgements—The authors are thankful to Professor M. Qureshi for research facilities and to the CSIR (India) for financial assistance.

REFERENCES

1. M. Qureshi and R. C. Kaushik, *Anal. Chem.*, 1977, **49**, 165.
2. P. S. Thind, S. S. Sandhu and J. P. Rawat, *Chim. Anal. (Warsaw)*, 1979, **24**, 65.
3. M. Qureshi, R. Kumar, V. Sharma and T. Khan, *J. Chromatog.*, 1976, **118**, 175.
4. K. G. Varshney and A. A. Khan, *J. Inorg. Nucl. Chem.*, 1979, **41**, 241.
5. K. G. Varshney and A. Premadas, *Sepn. Sci. Technol.*, 1981, **16**, 793
6. K. G. Varshney and A. A. Khan, *Talanta*, 1978, **25**, 528.
7. F. D. Snell and C. T. Snell, *Colorimetric Methods of Analysis*, 3rd Ed., Vol. II, p. 438. Van Nostrand, Princeton, 1959.
8. *Idem, op. cit.*, p. 492.
9. *Idem, op. cit.*, p. 515.
10. C. N. Reilley, R. W. Schmid and F. S. Sadek, *J. Chem. Educ.*, 1959, **36**, 555.
11. F. Feigl and V. Anger, *Spot Tests in Inorganic Analysis*, 6th Ed., Elsevier, Amsterdam, 1972.
12. M. Qureshi, J. P. Gupta and V. Sharma, *Anal. Chem.*, 1973, **45**, 1901.
13. M. Qureshi and S. A. Nabi, *J. Inorg. Nucl. Chem.*, 1970, **32**, 2059.
14. Y. V. Egorov, N. V. Dranitsina and N. N. Kagaker, *Tr. Ural. Politekh. Inst.*, 1970, **184**, 86.

Talanta, Vol. 30, No. 12, pp. 959–962, 1983
Printed in Great Britain.

0039-9140/83 $3.00 + 0.00

A PYROLYTIC CARBON FILM ELECTRODE FOR VOLTAMMETRY—III

APPLICATION TO ANODIC-STRIPPING VOLTAMMETRY

INGEMAR GUSTAVSSON and KENT LUNDSTRÖM*
Department of Analytical Chemistry, University of Uppsala, P.O. Box 531, S-751 21 Uppsala, Sweden

(*Received* 22 *April* 1983. *Accepted* 9 *May* 1983)

Summary—The potential applicability of a pyrolytic carbon film electrode in the differential-pulse anodic-stripping voltammetric determination of cadmium and lead in sea-water is demonstrated. The performance at the $10^{-10}M$ level is compared with that of a satisfactory glassy-carbon electrode. The two types of electrode display comparable behaviour in anodic-stripping voltammetry, but the pyrolytic carbon film electrode needs less pretreatment.

Anodic-stripping voltammetry (ASV) is a widely used technique in environmental studies of several important metallic trace elements. The mercury film electrode (MFE) is commonly employed for measurements at lower levels,[1] normally with a glassy-carbon electrode (GCE) serving as a satisfactory substrate for the mercury film. However, the maintenance of the substrate surface in proper condition for adequate ASV performance of the MFE becomes a serious drawback when routine assays at sub-ng/ml levels are to be undertaken. Frequent repolishing is required for glassy-carbon material, which from the outset must be of proper quality. Several alternative materials have been proposed and evaluated in order to improve the situation (*e.g.*, references 2–4). Various approaches for subtraction of the background current have also been considered.[5]

We report in this paper on the potential use of a recently introduced pyrolytic carbon film electrode (PCFE) in ASV. The fundamental properties of this type of carbon material have been described elsewhere.[6] Noteworthy are the favourable residual current characteristics,[7] permitting measurements of sub-micromolar levels of oxidizable organic compounds by differential-pulse voltammetry.[8,9] The utility of this electrode in the negative potential range is studied in the present work. It is demonstrated, in experimental comparison with a GCE, that this type of substrate for the mercury film shows great promise, in that no repolishing is needed, and ASV performance is as good as that of the GCE.

EXPERIMENTAL

Apparatus

Voltammetric measurements were made with a Princeton Applied Research 174A Polarographic Analyzer and charted with a Hewlett–Packard 7044A X–Y recorder. The time interval for current sampling in the pulse modes of the polarograph was modified to 20 msec in order to minimize interference from the mains frequency (50 Hz). The cell assembly is comprised of a quartz beaker of 100-ml capacity placed in a 'Plexiglas' housing with a screw-in lid, a nitrogen-purging device of conventional design, an Ag/AgCl reference electrode positioned in a quartz tube salt-bridge fitted at one end with a magnesia frit (Merck, catalogue No. 5809), a platinum-wire auxiliary electrode and the working electrode.

A Metrohm model 628-10 rotating electrode assembly was used with both a Metrohm glassy-carbon working electrode tip (model EA 289-1; electrode area 18.1 mm^2) and the pyrolytic carbon film electrode (PCFE) of our own manufacture. The preparation of this carbon material has been described elsewhere,[8] but for this study well-polished glassy-carbon discs (quality EB-5-GC-A from Tokai Carbon Ltd.; 3-mm thick discs cut from a 5-mm diameter rod) served as the substrate for the pyrolytic carbon film and the deposition time was reduced to 30 min. The coated discs were mounted by means of heat-shrinkable Teflon tubing to a steel piece designed to fit the screw connection of the electrode rotor. The precaution[8] of using an inert atmosphere during the heat-shrinking process was found unnecessary and hence dropped. Four PCFEs, each with an electrode area of 19.6 mm^2, were mounted for this study, different batches of prepared discs being used.

Ultraviolet irradiation was done in an air-cooled device, locally built essentially according to the design by Sipos *et al.*,[10] in which quartz tubes of 50 ml capacity were placed around a 700-W ultraviolet lamp. The quartz tubes were rigidly closed with ground-in quartz stoppers fixed with Teflon-coated stainless-steel spring-clips.

Reagents

Hydrochloric acid, sodium chloride and hydrogen peroxide were of suprapure grade (Merck). Commercially available standard stock solutions (BDH) of $Cd(NO_3)_2$, $Pb(NO_3)_2$ and $Hg(NO_3)_2$ were used throughout. Adequate purity of the water used was arrived at by double distillation (quartz still) of water from a Milli-Q water purification system, to be followed by ultraviolet irradiation as described below.

Procedure

The sea-water samples were collected and stored according to recommended procedures,[11] *i.e.*, made $0.01M$ in hydrochloric acid immediately after sampling. Approxi-

*Author for correspondence.

mately 50 ml of sample, contained in the type of quartz tube described above, was subjected to ultraviolet irradiation for at least 2 hr, after addition of 50 μl of 30% hydrogen peroxide.

Before use, the PCFE was subjected only to a thorough wash in 0.1M hydrochloric acid and subsequent rinses in water (repeated twice). A mercury film, if present, was wiped off with a wet Kleenex tissue before the washing.

The GCE received the following initial treatment. The electrode was polished for 10 min with an aqueous slurry of 1-μm alumina (BDH) on a filter paper, and then thoroughly rinsed with water. This was repeated twice. The same was then done with 0.3-μm and 0.05-μm alumina. A soft polishing disc (Winter Pellon, W. Germany) was used for the 0.05-μm polish. Finally, the electrode received the same washing treatment as the PCFE. Between samples, repolishing was done with only the 0.05-μm alumina. The electrodes were kept in the laboratory atmosphere under cover, even for long-term storage.

The voltammetric analyses were done essentially as described by Mart.[12] An approximately 40-ml sample was accurately weighed out in the cell beaker and, to achieve simultaneous plating of the mercury film, 160 μl of the $Hg(NO_3)_2$ standard solution were added to give a concentration of $2 \times 10^{-5}M$. The solution was deaerated by passage (for 10 min) of nitrogen that had been passed over a reduced copper catalyst[13] and through a wash-bottle. The deposition step was performed at -1.00 V with rotation of the working electrode at 1500 rpm, and nitrogen purging. Deposition times never exceeded 10 min. An equilibration time of 30 sec was allowed before the positive sweep was initiated, starting from -0.8 V. Settings for the differential-pulse anodic-stripping voltamperograms were sweep rate 10 mV/sec, pulse amplitude 50 mV and clock period 0.5 sec. The currents reported are the true differential-pulse currents, *i.e.*, those obtained when the internal tenfold amplification factor of the polarograph in the dpv-mode is taken into account.[14] The first measurement on a new solution was considered a conditioning run and hence always rejected. Sample concentrations were evaluated by the standard-addition method. At least two measurements were made for each concentration level (besides the conditioning run).

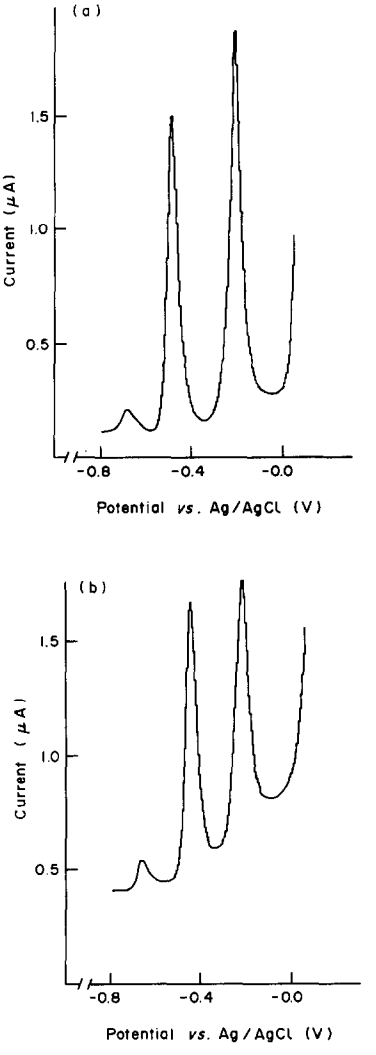

Fig. 1. Voltamperograms illustrating the typical behaviour of the two test electrodes with a Baltic Sea water sample. (a) PCFE, (b) GCE. Deposition time: 10 min in both cases.

RESULTS AND DISCUSSION

Representative voltamperograms obtained with the PCFE and the GCE are depicted in Fig. 1. The sample is near-shore Baltic Sea water and the expected presence of cadmium, lead and copper is confirmed in both voltamperograms. As discussed in more detail below, the concentrations of cadmium and lead in this sample were determined by means of standard additions and found to be 0.073 μg/l. ($6.5 \times 10^{-10}M$) and 0.98 μg/l. ($4.8 \times 10^{-9}M$) respectively (see Table 1). In general, as can be seen from Fig. 1, the two electrodes display similar ASV behaviour, and well-developed stripping peaks appear at essentially identical potentials. The peak-current responses are similar, but the residual-current characteristics of the PCFE are somewhat more favourable, with a lower magnitude and better positive cut-off. Such behaviour of the two electrodes was observed throughout this brief study, including twenty samples not explicitly accounted for in Table 1.

As estimated from eight successive measurements of cadmium and lead at the 0.5 μg/l. level, the coefficients of variation were 4.9% for cadmium and 2.5% for lead. Essentially the same figures were found for the GCE, namely 6.6% and 1.4% for cadmium and lead, respectively (five measurements only). The repeatability of the peak currents obtained with the PCFE is hence satisfactory, considering the metal concentrations under study.

The negative potential limit for the PCFE in acid media, taken as a linear sweep voltammetry residual current of 1 μA (10mM hydrochloric acid, sweep rate 10 mV/sec, starting potential -0.5 V *vs.* SCE and electrode area 19.6 mm^2), is typically -1.1 V. Similar values were found for the GCE used. A detailed characterization of the residual current behaviour of the PCFE is presented elsewhere.[7]

Table 1 summarizes the quantitative work included in this brief study. In the first sample, 0.5M sodium chloride, the levels of cadmium and lead determined represent impurities, presumably originating from the salt used. The second sample, analysed only with the

Table 1. The quantitative determination* of cadmium and lead levels in three selected water samples with the two electrodes; see text for details

	Cadmium found, $\mu g/l.$		Lead found, $\mu g/l.$	
Sample	PCFE	GCE	PCFE	GCE
0.5*M* NaCl	0.0108 ± 0.0007	0.0156 ± 0.0003	0.117 ± 0.003	0.146 ± 0.011
Standard in 10m*M* HCl	0.51 ± 0.02		0.97 ± 0.04	
Baltic Sea water	0.073 ± 0.002	0.057 ± 0.001	0.98 ± 0.02	0.99 ± 0.02

*Values reported with a confidence interval ($P = 0.90$) for the intercept of the regression line on the abscissa, *i.e.*, the concentration axis. For method of calculation, see reference 19.

PCFE, is a standard solution of cadmium and lead in 10m*M* hydrochloric acid. These two samples illustrate that two prerequisites for successful sea-water analysis are fulfilled with the PCFE, namely compatibility with high salt levels, and an adequate hydrogen overvoltage for a slightly acid medium. For the GCE, these are established characteristics. The final tests were done on an authentic Baltic Sea water sample, the third sample in Table 1. Since it was a near-shore sample (collected off the Forsmark nuclear power plant), the levels found are quite reasonable considering recent investigations in the Baltic,[15–17] as well as a previous extensive study of this specific area.[18]

Each sample was analysed once, with three standard additions (with duplicate measurements at each concentration level). The quantification of cadmium and lead in the Baltic Sea water sample, by use of the PCFE, is illustrated in Fig. 2. The confidence intervals ($P = 0.90$) for the intercept of the abscissa[19] are given in Table 1 and indicate quite satisfactory statistics of the regression lines fitted to the experimental data. Also, considering the low concentrations studied, the results with the two electrodes are in reasonable agreement.

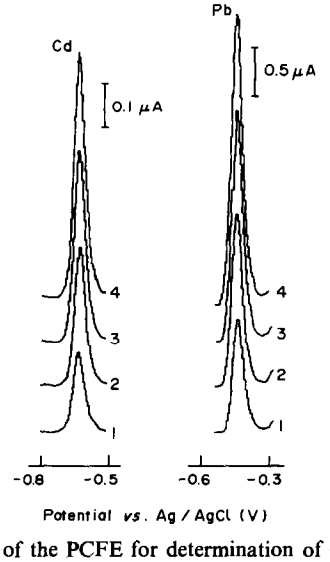

Fig. 2. Use of the PCFE for determination of Cd and Pb in a Baltic Sea water sample. (1) Sample. (2, 3, 4) Three stepwise standard additions to give an increase in concentration of 0.05 μg/l. for Cd and 0.5 μg/l. for Pb after each addition. Only one measurement at each concentration level is shown.

During the course of this study the type of electrode encasement relied on, *i.e.*, heat-shrinkable Teflon tubing, proved to be inadequate for extended periods of time. As indicated by increasing residual currents, encountered typically one week after electrode mounting, solution slowly started to penetrate the Teflon-carbon seal. An electrode that had failed in this way could be completely restored if a new Teflon cover was mounted, the same pyrolytic carbon-coated disc being used.

Hence the pyrolytic film material introduced appears to be a useful alternative to the different types of electrode materials currently used in ASV. As judged from the voltammetric behaviour, this type of carbon material seems to have remarkable long-term surface stability. The stability on storage is very promising, with no decline in performance over a six-month period. The major advantage of the PCFE for ASV is clearly the minimal treatment required before analysis. As described in the experimental section, a thorough wash suffices for the PCFE, which may be compared with the more tedious polishing procedure necessary with the GCE. The number of specimens used for this study (four, all from different batches) is, however, too small to allow final conclusions to be drawn. The comparatively simple technique for manufacturing the PCFE in the laboratory should also be stressed.

Conclusion

It has been demonstrated that the PCFE described is well comparable to the GCE for ASV determinations of trace metals at subnanomolar levels in sea-water samples. Most noteworthy are the simplified pretreatment and the long-term stability of the electrode material.

REFERENCES

1. H. W. Nürnberg, *Sci. Tot. Environm.*, 1979, **12,** 35.
2. K. Sykut, I. Cukrowski and E. Cukrowska, *J. Electroanal. Chem.*, 1980, **115,** 137.
3. M. R. Cushman, B. G. Bennett and C. W. Anderson, *Anal. Chim. Acta*, 1981, **130,** 323.
4. J. Wang, *Anal. Chem.*, 1982, **54,** 221.
5. J. Wang and B. Greene, *Anal. Chim. Acta*, 1982, **144,** 137.
6. K. Lundström, *Doctoral Thesis, Acta Universitatis Upsaliensis, Abstracts of Uppsala Dissertations from the Faculty of Science*, 1981, 617.
7. C. Urbaniczky and K. Lundström, *J. Electroanal. Chem.*, in press.

8. K. Lundström, *Anal. Chim. Acta*, 1983, **146,** 97.
9. *Idem, ibid.*, 1983, **146,** 109.
10. L. Sipos, J. Golimowski, P. Valenta and H. W. Nürnberg, *Z. Anal. Chem.*, 1979, **298,** 1.
11. L. Mart, *ibid.*, 1979, **296,** 350.
12. *Idem, ibid.*, 1980, **300,** 350.
13. M. Schütze, *Angew. Chem.*, 1958, **70,** 697.
14. Princeton Applied Research, *Operation and Service Manual, Model 174A Polarographic Analyzer*, p. V-9. Princeton Applied Research Corporation, Princeton, 1974.
15. B. Magnusson and S. Westerlund, *Mar. Chem.*, 1980, **8,** 231.
16. L. Brügmann, *Mar. Pollut. Bull.*, 1981, **12,** 214.
17. I. Gustavsson, *Acta Hydrochim. Hydrobiol.*, 1983, **3,** in press.
18. *Idem, The National Swedish Environment Protection Board*, Uppsala, Sweden, SNV-PM 1565, 1982.
19. C. Liteanu and I. Rîcă, *Statistical Theory and Methodology of Trace Analysis*, pp. 141–179. Horwood, Chichester, 1980.

Talanta, Vol. 30, No. 12, pp. 963–966, 1983
Printed in Great Britain

0039-9140/83 $3.00 + 0.00
Pergamon Press Ltd

FORMATION D'UN CHELATE CUIVRE-VANCOMYCINE: APPLICATION AU DOSAGE DE L'ANTIBIOTIQUE EN FLUX CONTINU ET DETECTION AMPEROMETRIQUE

CH. CHABENAT, D. ANDRE et P. BOUCLY
Laboratoire de Chimie Analytique Pharmaceutique, U.E.R. de Médecine et Pharmacie de Rouen, Avenue de L'Université, 76800 St Etienne-du-Rouvray, France

(*Reçu le* 22 *mars* 1983. *Accepté le* 4 *mai* 1983)

Résumé—La formation d'un chélate entre les ions cuivriques et la vancomycine, molécule à propriétés antibiotiques sur les bactéries Gram positif, est montrée par des methodes spectrales, polarographiques et potentiométriques. En particulier, les valeurs des potentiels de demi-vague de réduction et l'évolution des courbes intensité–potentiel permettent de mettre en évidence la stoechiométrie du compose d'addition formé et d'apprécier la stabilité du complexe obtenu. Cette propriété complexante est utilisée pour proposer une methode de dosage en flux continu, en utilisant une phase mobile contenant des ions cuivriques et une détection ampérometrique à l'aide d'une cellule électrochimique de type couche mince.

La vancomycine présente des propriétés antibiotiques très actives contre une grande variété de micro-organismes Gram positif. Cette molécule est difficilement dosable sélectivement par voie bactériologique, et quelques méthodes physico-chimiques ont été décrites.[1–3]

Nous proposons, ici, une méthode originale utilisant des ions métalliques comme traçeurs, et une cellule électrochimique de type couche mince en flux continu comme détecteur. L'aptitude de cette molécule à former des complexes organométalliques est d'ailleurs utilisée comme moyen de purification, au cours de sa préparation.[4]

L'ensemble de cette étude est réalisé dans un solvant mixte eau–acétonitrile (86:14 v/v); la présence de solvant organique limite les phénomènes d'adsorption aux électrodes.

L'utilisation d'un traçeur est nécessaire pour effectuer une détection électrochimique. En effet, dans le solvant seul, la détection électrochimique directe de la vancomycine donne naissance à une courbe intensité–potentiel présentant une vague mal définie à proximité de la feduction du solvant lui-même, et à un potentiel de demi-vague voisin de $-1{,}80$ V *vs.* ECS.

Le signal obtenu est inutilisable à des fins analytiques quantitatives; en particulier, les courants limites ne suivent pas les lois de la diffusion en régime stationnaire, empêchant, dans les conditions opératoires, un dosage polarographique.

La formation et les conditions de stabilité d'un complexe cuivre–vancomycine de type chélate, suffisamment stable pour utiliser le métal comme traçeur, sont étudiées par différentes méthodes physico-chimiques. L'utilisation de ces propriétés au dosage de la vancomycine en flux continu est discutée.

PARTIE EXPERIMENTALE

Appareillage

Les courbes intensité/potentiel sont tracées à l'aide d'un ensemble polarographique type Tacussel PRG 5; l'électrode

Les courbes intensité/potentiel sont tracées à l'aide d'un ensemble polarographique type Tacussel PRG 5; l'électrode de travail est, soit une électrode à goutte de mercure, soit une électrode tournante au carbone vitreux type Tacussel EDI. La cellule électrochimique est thermostatée à $25 \pm 0{,}2°$.

Les mesures potentiométriques à courant nul sont effectuées sur un pH-mètre type Tacussel Isis 20.000. L'électrode spécifique des ions cuivriques est de type Tacussel PCU 2 M.

Le circuit en flux continu utilise un chromatographe moyenne pression type Jobin Yvon LC 50 comme générateur de pression constante. La colonne est remplie d'un support inerte constitué de microbilles de verre (Alltech 40 μm). Le détecteur est une cellule électrochimique type couche mince (Fig. 1) fonctionnant en mode ampérométrique. Le potentiel est imposé à l'aide d'un potentiostat type Tacussel PRGE.

Réactifs

Solvant. Acétonitrile pour HPLC (Carlo Erba) et solution d'acétate de sodium 0,05*M* (14:86 v/v).

Phase mobile. Solution contenant Cu^{2+} à la concentration $2 \times 10^{-6}M$, dans le solvant précédent, préparée à partir de $CuCl_2 \cdot 2H_2O$ (Prolabo).

Solution de vancomycine. Vancocin HCl (Lilly) à la concentration $2 \times 10^{-2}M$ dans l'eau distillée ($=29$ mg/ml). Les injections sont de l'ordre de 1 à 5 μl, c'est-à-dire 29 à 150 μg de vancomycine.

Dosage de la vancomycine

Le principe de la technique analytique que nous proposons ici, consiste à utiliser une phase mobile liquide circulant avec une vitesse linéaire constante, en utilisant une pompe à pression de gaz inerte, dans un circuit possédant un injecteur constitué d'une membrane de type téflon, d'une colonne remplie de billes de verre sans aucun pouvoir séparateur mais permettant de réduire le volume mort au niveau du circuit, d'une cellule électrochimique type couche mince relié à un potentiostat permettant d'imposer entre deux électrodes contenues dans la cellule un potentiel con-

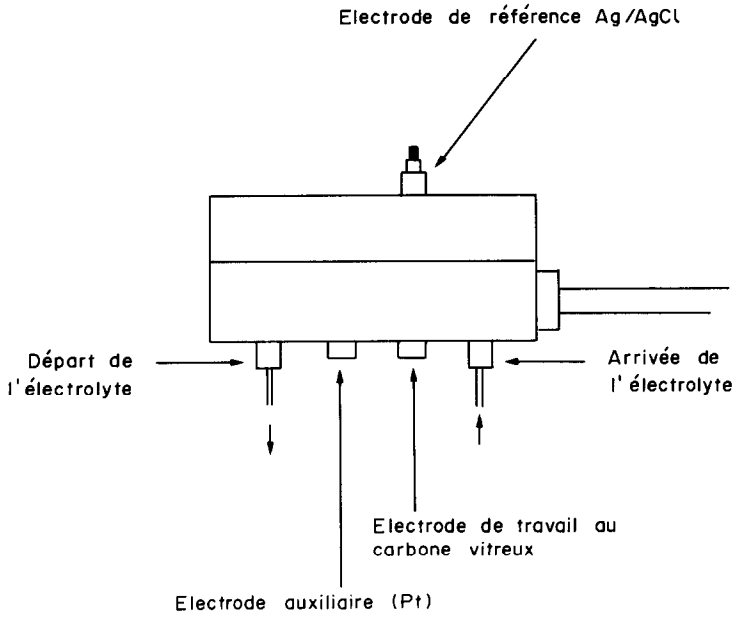

Fig. 1. Disposition de la cellule pour la détection en couche mince.

venable, et d'un enregistreur ampérométrique ou potentiométrique. La phase mobile est constituée du mélange eau–acétonitrile préalablement décrit contenant de l'acétate de sodium environ 0,05M afin d'amener la solution à un pH voisin de 7, et du chlorure cuivrique $2 \times 10^{-6}M$. Cette solution circule à travers la cellule électrochimique couche mince (Fig. 1) où il est imposé entre l'électrode de travail au carbone vitreux et la micro électrode de référence un potentiel intermédiaire entre la réduction électrochimique des ions Cu^{2+} en ions Cu^{+} et la réduction des ions Cu^{+} en Cu, soit d'après l'étude préliminaire un potentiel compris entre +0,16 et −0,20 V.

Au passage des ions cuivriques, il apparait entre les électrodes de travail et auxiliaire un courant qui est proportionnel à la concentration des ions Cu^{2+} et à la vitesse linéaire de la phase mobile.

En sortie de colonne, la vancomycine a complexé les ions cuivriques selon la réaction chimique indiquée çi-dessus, provoquant une diminution du courant proportionnelle à la concentration de vancomycine.

Les quantités de vancomycine injectées sont de l'ordre de 30 μg. La méthode proposée présente un temps d'analyse de l'ordre de quelques dizaines de secondes, fonction de la vitesse linéaire de la phase mobile. Les dosages peuvent être répétés sans limitation avec une fréquence d'environ deux par minute. La précision des dosages est de l'ordre de 5%, ce qui est suffisant pour les dosages de routine sur les médicaments terminés.

RESULTATS ET DISCUSSION

Formation d'un complexe cuivre–vancomycine

Le cuivre est choisi, préférentiellement à d'autres métaux, en raison de ses propriétés complexantes avec les molécules de structure polypeptidique. Afin d'étudier la formation et les conditions de stabilité du chélate formé, trois méthodes sont utilisées: la spectrophotométrie, la polarographie et voltampérométrie, enfin la potentiométrie à courant nul utilisant une électrode spécifique.

Etude spectrale. En fixant le pH de la solution au voisinage de la neutralité, l'addition d'ions cuivriques à une solution de vancomycine provoque l'apparition d'un maximum d'absorption vers 555 nm, attribué à la formation d'un composé d'addition. En maintenant les concentrations de cuivre et de vancomycine constantes et identiques, la densité optique atteint un maximum, à cette longueur d'onde, pour un pH compris entre 7 et 7,5, fixant ainsi la zone de pH où le complexe formé est stable. La formation du complexe peut être suivie en mesurant la variation de densité optique lors d'addition croissante d'ions cuivriques à une solution de vancomycine maintenue à pH 7 par addition d'acétate de sodium. La densité optique à 555 nm suit la loi de Beer-Lambert, proportionnellement à la concentration en ions cuivriques, puis reste constante lorsque les quantités d'ions cuivriques et de vancomycine sont identiques. Ce dernier résultat suggère la formation d'un complexe de type 1:1. Le coefficient d'extinction molécu-

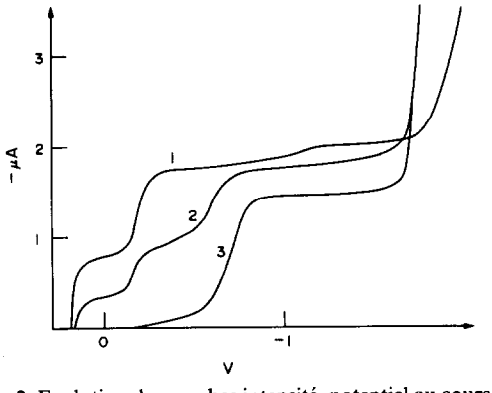

Fig. 2. Evolution des courbes intensité–potentiel au cours de la formation du complexe cuivre–vancomycine. 1—Solution de chlorure cuivrique, $10^{-3}M$; 2—après addition de vancomycine à la concentration finale de $0,5 \times 10^{-3}M$; 3—après addition de vancomycine à la concentration finale de $10^{-3}M$.

laire est voisin de 218 $l.mole^{-1}.cm^{-1}$. Cette faible valeur empêche l'utilisation de ces propriétés spectrales à des fins analytiques quantitatives suffisamment sensibles.

Etude polarographique et voltampérométrique. La formation du complexe peut être suivie par les tracés des courbes intensité–potentiel, à une électrode de mercure ou de carbone vitreux. Ces deux électrodes de travail donnent des résultats voisins. Nous présentons ici les voltampérogrammes obtenus en utilisant l'électrode de mercure. Une solution d'ions cuivriques, pure, présente deux vagues successives, en réduction, correspondant à la réduction des ions Cu^{2+} en deux étapes (Fig. 2, courbe 1), suivant les réactions électrochimiques:

$$Cu^{2+} + e^- \rightarrow Cu^+ \quad E_{1/2} = +0{,}16\,V.$$

$$Cu^+ + e^- + Hg \rightarrow Cu(Hg) \quad E_{1/2} = -0{,}20\,V.$$

En présence de quantités croissantes de vancomycine, amenée à partir d'une solution titrée, la courbe intensité–potentiel se modifie. Les courants limites correspondant aux deux vagues de réduction des ions cuivriques diminuent proportionnellement à l'ajout de vancomycine et il apparait parallèlement une nouvelle vague, située à un potentiel plus réducteur ($-0{,}75$ V). Cette vague est attribuée à la formation, en solution, d'un composé d'addition entre les ions cuivriques et la vancomycine (Fig. 2, courbes 2 et 3).

Le courant observé à $-0{,}75$ V correspond à la réduction électrochimique du chélate cuivre–vancomycine (Cu–VAN). Une étude électrochimique plus fondamentale[5] sur le mécanisme réactionnel de réduction électrochimique de ce chélate montre que la réaction électrochimique correspond à un transfert bi-électronique selon la réaction:

$$Cu\text{–}VAN + 2e^- + Hg \rightarrow Cu(Hg) + VAN.$$

Les valeurs très différentes des courants limites, observées entre les vagues de réduction correspondant au cuivre libre et celles correspondant au cuivre complexé s'expliquent facilement par la différence importante des coefficients de diffusion. Ces résultats électrochimiques peuvent être utilisés pour confirmer

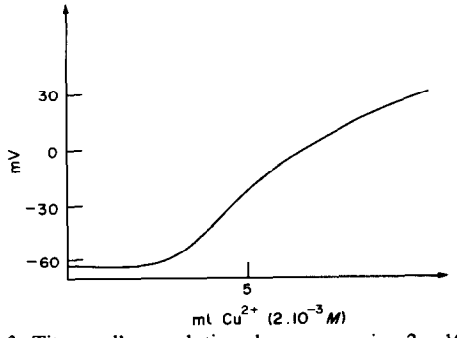

Fig. 3. Titrage d'une solution de vancomycine $2 \times 10^{-4}M$ par une solution titrée de chlorure cuivrique $2 \times 10^{-3}M$. La réaction est suivie par la mesure du potentiel d'équilibre à courant nul d'une électrode spécifique des ions cuivriques.

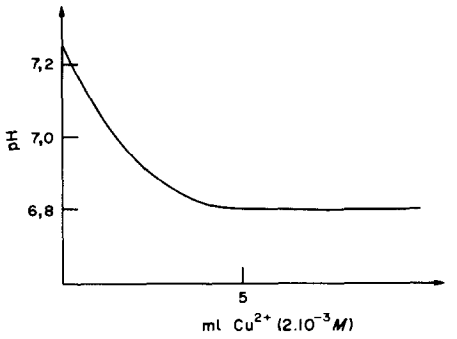

Fig. 4. Variation du pH de la solution au cours du titrage d'une solution de vancomycine par une solution titrée d'ions cuivriques, dans un solvant acétonitrile/d'acétate de Na 0,05*M*.

la stoechiométrie du complexe formé en solution. Il est en effet possible de réaliser un titrage ampérométrique à un potentiel imposé de -0.80 V, c'est-à-dire un potentiel légèrement inférieur au potentiel de réduction du complexe Cu–VAN. Dans ces conditions expérimentales, le courant circulant dans le circuit électrode de mercure–électrode auxiliaire de platine, est directement proportionnel à la concentration du complexe en solution. La courbe ampérométrique correspondant au titrage d'une solution de cuivre par une solution titrée de vancomycine, fait apparaitre un point équivalent correspondant à la formation d'un complexe 1:1, confirmant ainsi les résultats spectrophotométriques. L'utilisation d'une électrode tournante de carbone vitreux à la place de l'électrode de mercure permet de suivre la disparition du cuivre libre lors de la formation du complexe, mais le domaine d'électroactivité plus réduit ne permet pas d'observer le courant correspondant à la réduction électrochimique du composé d'addition formé.

Etude potentiométrique. La formation de ce complexe peut également être suivie par potentiométrie à courant nul, en utilisant une électrode spécifique des ions Cu^{2+} comme électrode indicatrice (*cf.* partie expérimentale). La courbe potentiométrique correspondant au titrage d'une solution de vancomycine par une solution titrée d'ions cuivriques, fait apparaître (Fig. 3) un saut de potentiel correspondant à un équivalent de cuivre ajouté, par rapport à la quantité de vancomycine initiale. Dans les conditions expérimentales, la variation de pH en fonction de l'ajout d'ions cuivriques est enregistrée (Fig. 4). Il apparait une diminution du pH au cours de la formation du complexe, qui cesse lorsqu'un équivalent de cuivre est ajouté, par rapport à la quantité de vancomycine présente au départ. Ces résultats confirment que le composé d'addition formé est un chélate. La réaction de formation du composé s'écrit:

$$Cu^{2+} + H_2VAN \rightleftharpoons Cu\text{–}VAN + 2H^+.$$

Une exploitation informatique de ces différentes courbes potentiométriques est actuellement en cours, à partir de modèles mathématiques et doit permettre la détermination précise de la constante de

complexation apparente. Notons que l'allure des courbes potentiométriques et électrochimiques permet de prévoir un complexe de stabilité importante, la réaction d'addition étant quantitative.

LITTERATURE

1. J. R. Fooks, I. J. McGilveray and R. D. Strickland, *J. Pharm. Sci.*, 1968, **57**, 314.
2. J. Rotschafer, *11th Intern. Congress Chemother. and 19th Intersci. Conf. Antimicrob. Ag. & Chemother.*, Boston, 1979.
3. J. B. L. McClain, R. Bongiovanni and S. Brown, *J. Chromatog.*, 1982, **231**, 463.
4. *Symposium on vancomycin*, Lilly Laboratory for Clinical Research, San Francisco, 16–17 November 1978.
5. Travaux personnels à publier.

Summary—The formation of a metal-complex of copper (II) with vancomycin, an antibiotic active towards Gram-positive bacteria, has been proved by spectrophotometric, polarographic and potentiometric methods. In particular, the half-wave reduction potentials and voltamperograms indicate the stoichiometry of the addition compound and the equilibrium constant. This complex has been used for determination of vancomycin by a continuous flow method with copper (II) and amperometric detection in a polarographic cell of thin-layer type.

Talanta, Vol. 30, No. 12, pp. 967–968, 1983
Printed in Great Britain

0039-9140/83 $3.00 + 0.00
Pergamon Press Ltd

SHORT COMMUNICATIONS

DETERMINATION OF ARSENIC IN GEOLOGICAL MATERIALS BY X-RAY FLUORESCENCE SPECTROMETRY AFTER SOLVENT EXTRACTION AND DEPOSITION ON A FILTER

A. E. HUBERT
U.S. Geological Survey, Box 25046, Denver, CO 80225, U.S.A.

(*Received* 21 *February* 1983. *Accepted* 1 *June* 1983)

Summary—Rock, soil, or sediment samples are decomposed with a mixture of nitric and sulphuric acids. After reduction from arsenic(V) with ammonium thiosulphate, arsenic(III) is extracted as the chloro-complex into benzene from a sulphuric-hydrochloric acid medium. The benzene solution is transferred onto a filter-paper disc impregnated with a solution of sodium bicarbonate and potassium sodium tartrate, and the benzene allowed to evaporate. The arsenic present is determined by X-ray fluorescence. In a 0.5-g sample, 1–1000 ppm of arsenic can be determined. The close proximity of the lead $L\alpha$ peak (2θ 48.73°), to the arsenic $K\alpha$ peak (2θ 48.83°) does not cause any interference, because lead is not extracted under the experimental conditions. Arsenic values obtained are in agreement with those reported for various reference samples.

Arsenic is considered to be a pathfinder or indicator element in geochemical surveys.[1] Because of the relative ease of dispersion by both physical and chemical processes, arsenic forms primary as well as secondary halos around ore deposits. The determination of arsenic at or below the crustal abundance level (1.8 ppm) provides a useful geochemical prospecting guideline for detailed surveys.

One of the early methods of arsenic determination was a colorimetric procedure involving the Gutzeit apparatus.[2] Attempts to replace the colorimetric procedure by direct determination by atomic-absorption spectrometry after sample dissolution have not been successful because of interferences caused by the light-scattering effects of other elements present, regardless of the method of atomization.

Hydride generation has been used to isolate arsenic from possible ionic interferences and for preconcentration, but the generation of arsine and the final determination by flame or flameless methods may still be affected by various ions present in the sample solutions.[3–6]

Direct determination of arsenic by X-ray fluorescence analysis of powder or pelleted samples does not provide satisfactory sensitivity at the level of crustal abundance. The usual matrix problems that arise in the determination of trace amounts of various elements are compounded by the proximity of the lead $L\alpha$ (2θ, 48.73°) and arsenic $K\alpha$ (2θ, 48.83°) peaks. Secondary arsenic peaks are less sensitive, so provide a lower count-rate and decrease the sensitivity of any direct determination technique.

The method proposed here makes use of a nitric–sulphuric acid digestion, after which ammonium thiosulphate, benzene, and hydrochloric acid are added, and arsenic(III) is extracted as the chloride into the benzene layer according to the procedure of Jewett *et al.*[7] The benzene layer is evaporated in contact with a filter-paper disc impregnated with a solution of sodium bicarbonate and potassium sodium tartrate, and the arsenic present on the disc is determined by X-ray fluorescence analysis.

EXPERIMENTAL

Apparatus

A computer-controlled Siemens SRS* wavelength-dispersive X-ray spectrometer equipped with a tungsten source (set at 50 kV and 40 mA) and a lithium fluoride 110 crystal was used. Each sample was counted for 100 sec at the arsenic $K\alpha$ peak (2θ, 48.83°) and the background was counted (2θ, 50°) for the same time. Each microgram of arsenic provided a 20-cps count-rate above background. Plastic sample cups (EC16, Chemiplex Industries) were used to hold the benzene extract and the Whatman No. 540 filter-paper discs.

Reagents

All chemicals used were of analytical-reagent grade.

Arsenic standard solution, 1000 μg/ml. Dissolve 0.132 g of As_2O_3 in 2 ml of 1*M* sodium hydroxide, acidify with 1 ml of 10% (v/v) nitric acid and dilute to 100 ml with water.

*Any use of trade names is for descriptive purposes only and does not imply endorsement by the U.S. Geological Survey.

Solution of sodium bicarbonate and potassium sodium tartrate. Dissolve 5 g of $NaHCO_3$ and 5 g of $KO_2C(CHOH)_2CONa \cdot 4H_2O$ in 100 ml of water.

Ammonium thiosulphate solution, 1%. Dissolve 1 g of $(NH_4)_2S_2O_3$ in 100 ml of water.

Calibration graph

Pipette aliquots of the arsenic standard solution containing 0, 1, 2, 5, 10, 20, 50, 100, 200 and 500 μg of arsenic into 50-ml Teflon beakers, each containing 0.5 g of rock or soil known to contain less than 0.1 μg of arsenic. Apply the digestion and extraction procedures as for the test samples. The calibration is linear over this range. The standards prepared in this manner correspond to arsenic concentrations up to 1000 ppm in the samples.

Procedure

Weigh a 0.5-g sample of pulverized rock, soil, or sediment into a 50-ml Teflon beaker. Add 2 ml of water and 10 ml or more of concentrated nitric acid, depending on the organic content of the sample. Add 5 ml of sulphuric acid and heat on a hot-plate until copious white fumes of sulphur trioxide are evolved. Allow to cool and transfer the solution to a 16 × 150 mm Pyrex test-tube fitted with a Teflon screw-cap. Add 1 ml of 1% ammonium thiosulphate solution and 5 ml of benzene and allow to cool. Teflon beakers are used because the product from the digestion can be transferred practically completely without rinsing. From a pipette add 0.1 ml of concentrated hydrochloric acid on top of the benzene layer and immediately cap the tube. Shake it for 10 min and allow the two phases to separate. Add another 0.1 ml of concentrated hydrochloric acid and shake again for 10 min, to obtain consistent results. Centrifuge the test-tube to separate the two phases. Remove the benzene layer with a pipette and place it in an EC16 sample cup. Immediately cover the benzene with a Whatman No. 540 filter-paper disc impregnated with 0.2 ml of the sodium bicarbonate–potassium sodium tartrate solution. Allow the benzene to evaporate and the filter-paper disc to dry in air, then cover the cap plug with a layer of Mylar film. Secure the Mylar film to the sample cup with a retaining ring, turn the sample cup over and shake the filter loose so that it comes to rest on the Mylar film, which is used as the support for the determination of arsenic by X-ray fluorescence.

RESULTS AND DISCUSSION

Sample digestion and solvent extraction

The procedure for sample digestion and solvent extraction is adapted from that of Jewett *et al.*,[7] which involves the extraction of arsenic as the chloro-complex from sulphuric–hydrochloric acid. These authors reported a recovery of 80–90% for arsenic in biological materials after digestion and extraction. Discs prepared by spiking a sample and following the procedure were compared with discs prepared by placing an equivalent amount of arsenic on a filter. The results confirmed that 80–90% recovery is obtained.

If a benzene extract containing arsenic is allowed to evaporate on a filter-paper disc without the sodium bicarbonate–potassium sodium tartrate solution present, the arsenic evaporates along with the benzene. Potassium sodium tartrate prevents this loss, and the sodium bicarbonate neutralizes any sulphuric acid left in the benzene layer and makes it easier to free the filter-paper disc from the bottom of the plastic cup. Any excess of sulphuric acid transferred to the plastic cup would destroy the filter paper and require the analysis to be repeated.

It is necessary to carry arsenic-spiked samples through the procedure as standards to compensate for losses in the digestion and extraction steps.

Table 1. Replicate analyses ($n = 6$) of arsenic in seven reference samples

Sample	Range *ppm*	Mean *ppm*	RSD, %*	Reported values, *ppm*
1. GXR 1 Jasperoid	420–472	448	4.0	460 ± 30†
2. GXR 2 Soil	32–36	34	3.3	31 ± 5†
3. GXR 3‡ Fe–Mn Deposit	3830–4360	4005	6.1	4000 ± 450†
4. GXR 4 Copper mill head	96–112	106	5.5	98 ± 10†
5. GXR 5 Soil	12–14	13	5.5	12 ± 3†
6. GXR 6 Soil	292–320	309	3.8	340 ± 30†
7. Mag-1 Marine mud	6–8	7	10.5	6§

*Relative standard deviation.
†Reference 8.
‡0.10-g sample.
§Reference 9.

Interferences

Samples were spiked with 1000 μg of antimony, bismuth, cobalt, copper, nickel, and lead, and analysed by the proposed procedure. Lead was not detected at the 48.73° $L\alpha$ lead peak on the filter disc prepared from samples containing 1000 μg of lead. It therefore appears that lead is not extracted under the experimental conditions and does not interfere with the arsenic detection. Under similar conditions, cobalt, copper, and nickel are also not extracted and cannot be detected. Antimony and bismuth are partially extracted, but do not interfere with the arsenic determination.

Analysis of samples

Replicate analyses of seven geological reference samples with varying matrices gave the arsenic values presented in Table 1. The mean values found by the proposed method are in general agreement with values reported in the literature.

REFERENCES

1. R. W. Boyle and I. R. Jonasson, *J. Geochem. Explor.*, 1973, **2**, 251.
2. H. Almond, *Anal. Chem.*, 1953, **25**, 1766.
3. G. F. Kirkbright and M. Taddia, *Anal. Chim. Acta*, 1978, **100**, 145.
4. G. E. M. Aslin, *J. Geochem. Explor.*, 1976, **6**, 321.
5. S. Terashima, *Anal. Chim. Acta*, 1976, **86**, 43.
6. F. D. Pierce and H. R. Brown, *Anal. Chem.*, 1977, **49**, 1417.
7. G. K. Jewett, R. P. Himes and O. U. Andens, *J. Radioanal. Chem.*, 1977, **37**, 813.
8. E. S. Gladney, D. R. Perrin, J. W. Owens and D. Knab, *Anal. Chem.*, 1979, **51**, 1557.
9. E. S. Gladney and W. E. Goode, *Geostds. Newsl.*, 1981, **5**, 1.

Talanta, Vol. 30, No. 12, pp. 969–970, 1983
Printed in Great Britain.

0039-9140/83 $3.00 + 0.00

USE OF A MANGANESE DIOXIDE COLUMN IN THE FLOW ENTHALPIMETRIC DETERMINATION OF HYDROGEN PEROXIDE

NOBUTOSHI KIBA, KAZUHITO SHIMIZU* and MOTOHISA FURUSAWA
Department of Chemistry, Faculty of Engineering, Yamanashi University, Kofu-shi, 400, Japan

(*Received* 15 *March* 1983. *Accepted* 24 *May* 1983)

Summary—A method for flow enthalpimetric determination of H_2O_2 is described. The method uses manganese dioxide to catalyse the decomposition of H_2O_2. The catalyst is stable enough to be used for at least 500 analyses. H_2O_2 in the concentration range 0.01–10m*M* is determined with coefficients of variation <2%. The method has been used for determination of glucose in a non-alcoholic beverage and wines, with glucose oxidase as the peroxide-producing enzyme.

Since a continuous-flow enthalpimetric analyser was designed and constructed by Pristley *et al.*[1] many such instruments have been described and a wide variety of reactions have been adapted for use with the instruments. Immobilized-enzyme flow enthalpimeters (enzyme thermistors) have been developed by Mosbach and Danielsson.[2,3] Immobilized catalase has been used for the determination of H_2O_2.[4–6] The catalase was immobilized on controlled-pore glass beads by glutaraldehyde cross-linking[4] and on Sepharose by antigen–antibody interaction.[5,6] A practical drawback of the method is the lack of stability, because the catalase is irreversibly inactivated by the substrate (H_2O_2). In the reversible immobilization on Sepharose by antigen–antibody interaction, however, any catalase lost can easily be replaced on the support, but because of the low mechanical stability of Sepahrose a lower flow-rate must be used in the flow system.

The decomposition of H_2O_2 is also catalysed by heavy metal ions, metal oxides, hydroxides and sulphides. Among the inorganic catalysts the metal oxides are the most active[7–9] and are readily available in rigid granule form. The purpose of the present work was to demonstrate the use of manganese oxide as catalyst in a flow system for the determination of H_2O_2.

EXPERIMENTAL

Reagents

Hydrogen peroxide (30%, Mitsubishi Gas Chemical Co.) was diluted with distilled water to give a 0.5*M* solution, which was standardized by iodometric titration. Manganese dioxide (granular, for elemental analysis, Merck) was washed with 1*M* nitric acid for 20 min, followed by rinsing with distilled water. Tris–HCl buffers (0.1 and 0.2*M*, pH 8.5) were used.

Preparation of catalyst. Sulphides and hydroxides [FeS, CuS, $Cd(OH)_2$ and $Zn(OH)_2$], which show fair catalytic activity, do not have high enough mechanical stability under pressure. Granular oxides (MnO_2, CuO, Hopcalite I (50% MnO_2, 30% CuO, 15% Co_2O_3, 5% Ag_2O) and Hopcalite II (60% MnO_2, 40% CuO) show high activity, but are progressively inactivated during the catalytic reaction.

A stable catalyst was obtained by heating MnO_2 at 500–550° for 1 hr with air blowing through the furnace at a flow-rate of 100 ml/min. The treated oxide was sieved and the 60–80 mesh fraction used.

Apparatus

The enthalpimeter and components of the flow system were similar to those previously described.[10] The two thermistors (sealed in glass tubes) were placed one in the detection column (bed 0.8 cm in diameter, 2.0 cm in length) packed with the catalyst, and the other in the reference column (0.8 × 2.0 cm) packed with inert material (glass beads, 20 mesh). The temperature of the thermistor unit was maintained at 35°. The sample volume was 2.0 ml.

Procedure

Samples (10.0 ml) were diluted with 10.0 ml of the 0.2*M* buffer solution. The 0.1*M* buffer was passed through the system at a flow-rate of 2.5 ml/min. An aliquot of diluted sample solution (2.0 ml) was introduced into the flow stream through the injector. The temperature peak was displayed on a chart-recorder and the peak-height was measured as the maximum deflection from the pre-peak base-line.

RESULTS AND DISCUSSION

The dependence of peak-height on pH of the buffer solution was studied over the pH range 7.2–10.0. Tris–HCl (pH 7.2–9.0) and Na_2CO_3–$NaHCO_3$ buffers (pH 9.0–10.0) were used. The results are shown in Fig. 1. The peak-height was constant for pH above 8.3, and almost independent of the buffer concentration in the range 0.02–0.2*M*.

The peak-height was dependent on the flow-rate and the column length. Figure 2 shows the combined effect of the two factors. A flow-rate of 2.5 ml/min and a 2.0-cm column were chosen as optimal.

*Present address: Department of Technology, Fujisangyo Co., Nirasaki-shi, 407, Japan.

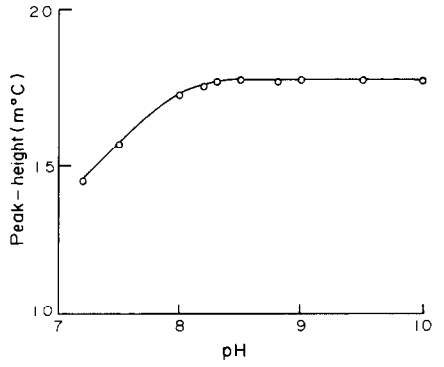

Fig. 1. Effect of pH on peak-height (1.0m*M* H_2O_2, flow-rate 2.5 ml/min).

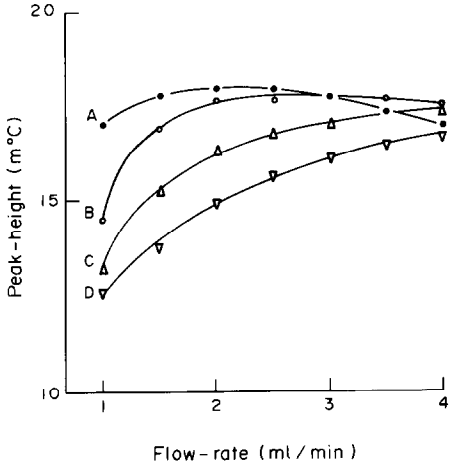

Fig. 2. Effect of flow-rate and column length on peak-height. (1.0m*M* H_2O_2, pH 8.5). Column length, cm: A 1.0, B 2.0, C 3.0), D 4.0.

Phosphate inhibited the catalyst. The presence of 0.01*M* phosphate in the buffer approximately halved the peak-height, and the peak-height gradually decreased during the catalytic reaction. The inhibition was irreversible. The presence of 0.05*M* ammonium ion caused 30% decrease in the peak-height, but this inhibition effect was reversible. The presence of 0.01*M* EDTA or pyrophosphate caused fluctuations of the base-line. Acetate, nitrate, sulphate and chlorate had no significant influence.

Table 1. Determination of H_2O_2

Sample conc., *m*M	ΔT, 10^{-3} *deg*	C.v., %
0.0102	0.172	1.8
0.0510	0.855	1.2
0.102	1.71	0.7
0.510	5.51	0.4
1.02	17.0	0.3
5.10	85.0	0.3
10.2	170	0.3

*C.v. = coefficient of variation ($n = 6$).

Table 2. Analysis of non-alcoholic beverage and wines

Sample	Glucose, %			Certificate value %
	n	$\bar{x}$	C.v., %	
Beverage	6	2.50	0.3	2.5
White wine	6	0.27	0.3	0.3
Red wine	5	0.14	0.6	0.1

The catalyst has been used continuously for 500 trials over a period of 10 days, with no decrease in peak-height for 5.0m*M* hydrogen peroxide. The analysis rate was 40/hr. Linear calibration graphs were obtained for three ranges (0.01–0.1, 0.1–1.0 and 1.0–10.0m*M*). Table 1 shows the reproducibility for solutions of known concentration.

The procedure has been applied to the determination of glucose in a non-alcoholic beverage and two wines. The degassed beverage (2.0 ml) was added to Tris–HCl buffer (0.01*M*, pH 7.5, 50 ml) containing about 2 mg of glucose oxidase (from *P. amagasakiense*, 100 U/mg). After incubation at 30° for 20 min with oxygen supplied at a flow-rate of 50 ml/min, the solution was diluted with Tris–HCl buffer (0.2*M*, pH 8.5) to 100 ml. A 2.0-ml portion was then analysed by the procedure give. The white wine (10.0 ml) was boiled for 5 min and analysed in the same way as the beverage. The red wine was filtered through polyamide gel (Bio-gel P-300, 50–100 mesh) before test. The results (Table 2) agreed with the certified values.

REFERENCES

1. P. T. Priestley, W. S. Sebborn and R. F. Selman, *Analyst*, 1965, **90**, 589.
2. K. Mosbach and B. Danielsson, *Biochim. Biophys. Acta*, 1974, **364**, 140.
3. *Idem*, *Anal. Chem.*, 1981, **54**, 83A.
4. B. Mattiasson, B. Danielsson and K. Mosbach, *Anal. Lett.*, 1976, **9**, 217.
5. B. Mattiasson, *FEBS Lett.*, 1977, **77**, 107.
6. B. Danielsson, B. Mattiasson and K. Mosbach, *Pure Appl. Chem.*, 1979, **51**, 1443.
7. S. J. Updike and M. C. Shults, *Anal. Chem.*, 1975, **47**, 1457.
8. K. G. Schick, V. G. Magearu, N. L. Field and C. O. Huber, *ibid.*, 1976, **48**, 2187.
9. A. Iwase, S. Kudo and N. Tanaka, *Anal. Chim. Acta*, 1979, **110**, 157.
10. N. Kiba, Y. Ishida, M. Tsuchiya and M. Furusawa, *Talanta*, 1983, **30**, 187.

Talanta, Vol. 30, No. 12, pp. 971–973, 1983
Printed in Great Britain

0039-9140/83 $3.00 + 0.00
Pergamon Press Ltd

THE OXIDATIVE DECARBOXYLATION OF POLYAMINOCARBOXYLIC ACIDS WITH LEAD DIOXIDE SUSPENSION IN NEUTRAL MEDIUM

A. B. EL-SAYED and M. F. EL-SHAHAT
Department of Chemistry, Faculty of Science, Ain Shams University, Cairo, Egypt

(*Received* 26 *October* 1982. *Revised* 8 *March* 1983. *Accepted* 23 *June* 1983)

Summary—The reaction between a suspension of lead dioxide and polyaminocarboxylic acids in neutral medium at 80° has been examined titrimetrically and found to involve decarboxylation in which 3 moles of PbO_2 oxidize 1 mole of the acid, the products being 3 moles of CO_2, 3 moles of HCHO, 1 mole of ethylenediaminemonoacetic acid and 3 moles of Pb(II) followed by chelation of the 3 moles of Pb(II) by an additional 3 moles of EDTA.

The oxidation of the polyaminocarboxylic acids used as sequestering agents has found applications in analytical and environmental chemistry.[1,2] MacNevin *et al.*[3] have studied the homogeneous precipitation of ferric hydroxide through release of iron(III) from its EDTA-complex by destructive oxidation of the EDTA with hydrogen peroxide. Rao *et al.*[4] used the same idea in precipitating lead smoothly as lead sulphate, and Cartwright[5] precipitated bismuth phosphate in a similar manner.

Various reports have appeared on the oxidation of EDTA with potassium permanganate,[6,7] ceric sulphate,[8–10] manganese(III)[11] and lead dioxide in sulphuric acid medium.[12]

The extent of oxidation varies with the conditions used. Thus Carroll *et al.*[9] reported that at room temperature a 4-electron oxidation of EDTA took place but with increasing temperature and reaction time a 14-electron oxidation could be achieved. The last of these studies concluded that 4 moles of CO_2, 3 moles of formaldehyde and 1 mole of *N*-hydroxymethylethylenediamine are the products of the oxidation of 1 mole of EDTA with 4 moles of PbO_2, but these conclusions depended on certain assumptions. We have made an independent investigation of the oxidative decarboxylation of some commonly used polyaminocarboxylic acids with a suspension of lead dioxide in neutral medium. We consider the study interesting, as representing use of a heterogeneous reaction in analytical chemistry, and also in connection with determination of polyaminocarboxylic acids in waste-water treatment.

EXPERIMENTAL

Reagents

Solid lead dioxide of general reagent grade was dried and used without further purification. Its purity was determined by a standard iodate method.[13] Ethylenediaminetetra-acetic acid (H_4EDTA), *trans*-1,2-diaminocyclohexane-*N*,*N*,*N*′,*N*′-tetra-acetic acid (H_4DCTA) and ethyleneglycol bis(aminoethyl ether) tetra-acetic acid (H_4EGTA) were all reagent grade, and were checked by complexometric titration[14] with 0.02*M* manganese sulphate. A carbonate-free stock solution of barium hydroxide was prepared by dissolving 40 g of the pure solid in 1 litre of boiled-out doubly distilled water, and filtering off all carbonate deposits. The solution was standardized with 0.1*M* hydrochloric acid.

Procedure

Different known weights of the dried solid lead dioxide were thoroughly mixed with a constant weight of solid polyaminocarboxylic acid (the acid being in excess), the weights being chosen to provide a wide range of molar ratios. The mixture was introduced into a reaction cell (25 cm long and 4 cm in diameter) connected in the middle of a series of ten CO_2-traps, each containing 25 ml of standard barium hydroxide solution. The first five traps removed all CO_2 from the air drawn into the system, and the second five trapped all the CO_2 released in the oxidative decarboxylation. The last trap was connected to a water pump, which was allowed to run for few minutes to remove all CO_2 from the system, then 50 ml of boiled-out doubly distilled water were introduced into the reaction cell, after which the temperature was slowly raised to 80°. The completion of the reaction was indicated by the complete disappearance of the dark brown lead dioxide.

Determination of the unreacted H_4A

At the end of the reaction the unreacted polyaminocarboxylic acid was determined by complexometric titration with 0.05*M* manganese sulphate, at pH 10 in the presence of ascorbic acid and with Eriochrome Black T as indicator. A blank was run under the same conditions to check that there was no other decomposition of the acid. The amount of the acid reacting with the lead dioxide was determined from the difference between the two titrations.

Determination of CO_2

The unreacted barium hydroxide solution in the last five traps was filtered to remove the barium carbonate, and titrated with 0.1*M* hydrochloric acid, with Methyl Orange as indicator. A blank was run with the same initial volume of barium hydroxide solution, and the difference was used for calculation of the amount of CO_2 released.

This amount was substantiated by gravimetric deter-

Table 1. Reacting ratio of PbO_2 and H_4A

H_4A	Reaction mixture: PbO_2, *mmole*	Reaction mixture: H_4A, *mmole*	Molar ratio PbO_2/H_4A: Taken	Molar ratio PbO_2/H_4A: Reacting ratio
H_4EDTA	0.029	0.342	0.085	0.729
	0.059		0.172	0.754
	0.085		0.251	0.748
	0.114		0.333	0.769
	0.163		0.476	0.751
	0.182		0.532	0.752
	0.969	3.023	0.320	0.765
	1.288	3.395	0.379	0.762
			Mean	0.754
H_4DCTA	1.051	3.057	0.343	0.736
	0.423	1.021	0.414	0.744
	0.525	1.216	0.432	0.762
			Mean	0.747
H_4EGTA	0.288	1.055	0.273	0.749
	0.354	1.121	0.316	0.741
	0.452	1.230	0.367	0.759
			Mean	0.750

mination of the precipitated barium carbonate, by conversion into barium sulphate.

Determination of formaldehyde

The apparatus used for determination of CO_2 was also used for estimating the amount of formaldehyde released in the oxidative decarboxylation, the first five traps being filled with 10% sodium sulphite solution, to prevent oxygen from entering the system, and the last five traps with 0.1*N* sodium sulphite to absorb the formaldehyde produced.

The excess of sulphite was determined iodimetrically and compared with the value for a blank run, to give the amount of formaldehyde released.

RESULTS AND DISCUSSION

Stoichiometry

Solid lead dioxide in suspension reacts mildly with polyaminocarboxylic acids in neutral aqueous medium at 80°. The reaction can be monitored by titrating the unreacted H_4A with manganese(II). The lead(II) present as $PbEDTA^{2-}$ in the solution does not affect the titration.

The results (Table 1) indicate that 3 moles of PbO_2 react with 4 moles of polyaminotetracarboxylic acid, when the acid is present in large excess, 1 mole of the acid being oxidized, and the other three complexing the lead(II) produced.

However, when the reactants were mixed in molar ratio (PbO_2/H_4A) greater than 0.6 and both the unreacted PbO_2 and H_4A were determined, the reaction was not complete even in 0.5*M* sulphuric acid medium, but approached a limiting molar ratio of 3 (Table 2), in agreement with the redox reaction proposed below; in this case there is insufficient H_4A to complex all the lead(II).

Table 2. Reacting ratio of PbO_2 and H_4EDTA in 0.5*M* H_2SO_4

Reaction mixture: PbO_2, *mmole*	Reaction mixture: H_4A, *mmole*	Molar ratio PbO_2/H_4A: Taken	Molar ratio PbO_2/H_4A: Reacting ratio
0.418	0.595	0.70	1.43
0.944		1.59	2.29
2.090		3.51	2.70
10.40	1.504	6.94	2.90

The results for the determination of lead(II) by flame atomic-absorption spectrometry and for CO_2 and HCHO are collected in Table 3. They show that 3 moles of CO_2 and 3 moles of HCHO are liberated when 3 moles of PbO_2 react with 4 moles of H_4A. This suggests that one mole of H_4A is destructively oxidized by reaction with 3 moles of PbO_2 to give a less reactive species, presumably a non-chelating agent, such as ethylenediaminemonoacetic acid in the case of H_4EDTA, and 3 moles of CO_2 and 3 moles of HCHO. The three moles of lead(II) produced are complexed by the other 3 moles of H_4A. Hence the *oxidative* reacting ratio is 1:1 PbO_2:H_4A.

Mechanism of the reaction

The reaction mechanism suggested by Nagai *et al.*[12] for the oxidation is adopted here, but under our conditions the decarboxylation process proceeds only up to its third step. The first decarboxylation step can be treated as a three-stage reaction, as shown in (1)–(3) below, and the same mechanism applies for further decarboxylation.

The overall equation for complete decarboxylation of H_4EDTA, in short, can be represented as follows:

$$3Pb^{4+} + C_{10}H_{16}N_2O_8 \xrightarrow{+3H_2O} 3Pb^{2+} + 3CO_2 + 3HCHO + C_4H_{10}N_2O_2 + 6H^+$$

The difference between our results and those of Nagai *et al.*[12] can be attributed to the difference in experimental conditions and is supported by the fact

Table 3. Molar ratios of Pb(II) to H_4A, CO_2 to H_4A and HCHO to H_4A

H_4A	Reaction mixture: PbO_2, *mmole*	Reaction mixture: H_4A, *mmole*	Molar ratios: Pb^{2+}/H_4A	Molar ratios: CO_2/H_4A	Molar ratios: $HCHO/H_4A$
H_4EDTA	0.163	0.342	0.751	0.748	0.755
	0.182		0.752	0.752	0.749
	0.969	3.023	0.765	0.739	0.738
	1.288	3.395	0.762	0.761	0.764
H_4DCTA	1.051	3.057	0.736	0.752	0.759
	0.423	1.021	0.744	0.758	0.760
	0.525	1.216	0.762	0.741	0.739
H_4EGTA	1.122	3.455	0.734	0.762	0.751
	0.474	1.234	0.755	0.743	0.749
	0.511	1.474	0.745	0.753	0.750

that the reacting ratio of cerium(IV) to EDTA varies considerably with the experimental conditions.[9] Nagai *et al.* stressed that the fourth decarboxylation step was difficult and not completely achieved. We attempted to reproduce the conditions used by Nagai *et al.*, with an initial molar ratio of 4:1 (PbO_2/H_4A), but found that some PbO_2 was left unreacted and that the maximum reacting ratio was about 3.5:1, instead of the 4:1 reported by Nagai *et al.*[12] This indicates that the fourth decarboxylation step can take place, but not necessarily completely.

Comparison of these results with those reported for oxidation with permanganate and cerium(IV) shows clearly that the reactions depend very strongly on the conditions used.

Acknowledgements—The authors wish to express their gratitude to Dr. M. F. El-Newahy, Professor of Organic Chemistry, Ain Shams University, for helpful discussion of the reaction mechanism.

REFERENCES

1. R. G. Clem and A. T. Hodgson, *Anal. Chem.*, 1978, **50,** 102.
2. P. D. Goulden and D. H. J. Anthony, *ibid.*, 1978, **50,** 953.
3. W. H. MacNevin and M. L. Dunton, *ibid.*, 1954, **26,** 1246.
4. J. Rao, A. Suryanaryana and B. R. Sant, *Talanta*, 1974, **21,** 1300.
5. P. F. S. Cartwright, *Analyst*, 1961, **86,** 688.
6. P. N. Palei and N. I. Udaltsova, *Z. Analit. Khim.*, 1960, **15,** 668.
7. M. T. Beck, *Chemist-Analyst*, 1961, **50,** 14.
8. H. Holzapfel and K. Dittrich, *Talanta*, 1966, **13,** 136.
9. *Idem, ibid.*, 1966, **13,** 309.
10. S. B. Hanna, S. Al-Hashimi, W. H. Webb and W. R. Carroll, *Z. Anal. Chem.*, 1969, **246,** 231.
11. N. Tanaka, K. Gomi and T. Shirakashi, *Nippon Kagaku Kaishi*, 1975, 444.
12. S. Ito, T. Matsuda and T. Nagai, *Talanta*, 1979, **27,** 25.
13. A. I. Vogel, *A Text-Book of Quantitative Inorganic Analysis*, 3rd Ed. p. 379. Longmans, London, 1961.
14. *Idem, op. cit.*, p. 415.

Talanta, Vol. 30, No. 12, pp. 974–976, 1983
Printed in Great Britain.

0039-9140/83 $3.00 + 0.00

DETERMINATION OF PHOSPHORUS IN SAMPLES OF VEGETABLE ORIGIN

MINERALIZATION WITH MOLTEN ALKALI AND SPECTROPHOTOMETRIC DETERMINATION

J. V. GIMENO ADELANTADO, F. BOSCH REIG, A. PASTOR GARCIA and V. PERIS MARTINEZ
Department of Analytical Chemistry, Faculty of Chemistry, University of Valencia, Burjasot (Valencia), Spain

(*Received* 14 *January* 1983. *Revised* 20 *May* 1983. *Accepted* 9 *June* 1983)

Summary—For determination of phosphorus in samples of vegetable origin (leaves and wheat flour) decomposition by means of molten alkali is proposed. Two procedures have been studied, one with dry reagents including an auxiliary oxidant, and the other with initially moist alkali with no extra oxidant. The fusion product is easily soluble and produces a solution suitable for elemental analysis. The phosphorus is determined by the molybdenum blue method. The suggested mineralization is rapid, accurate and precise.

Phosphorus is an essential element, and is found in vegetable and animal specimens both in inorganic forms such as ortho- and pyrophosphate and also in organic forms, mainly in nucleoproteins, phospholipids, sugar-phosphates and enzymes. In most cases organic phosphorus is present as a phosphate group.

Various procedures have been proposed for destroying the organic matrix and mineralizing the phosphorus. Wet-ashing uses mineral acids and their mixtures, together with other oxidants.[1–4] Dry-ashing is done with and without ashing aids.[5,6] Other techniques include oxidation with potassium permanganate in a closed tube,[7] sodium peroxide fusion,[8] and reduction by metal fusion.[9] Oxygen-flask combustion is also frequently used.[10,11]

Decomposition of organic samples by fusion with sodium hydroxide has been little used except in determination of elements such as fluorine in vegetables,[12,13] or germanium in organic compounds.[14] Recently, however,[15] a thorough study has been made of this method, resulting in a set of simple working conditions for mineralizing several elements for subsequent determination.

The present work describes fusion with molten sodium or potassium hydroxide (or a eutectic mixture of the two) to destroy the organic matrix of natural samples of vegetable origin such as leaves and wheat flour, for determination of phosphorus.

The fusion is done in an open system in a silver crucible over a Bunsen burner. Two methods are suggested: one using dry reagents and an auxiliary oxidizing agent (method D_{ox}), and the other with initially moist alkali and no auxiliary oxidant (method *W*). The phosphorus is determined by the molybdenum blue method with hydrazine as reductant.[16]

The results obtained by the suggested method are statistically compared with the certified content of the standards studied, analysed according to Pinta *et al.*[17]

For the wheat flour samples a comparative study was made of the suggested method and the AOAC method,[6] involving ashing of the samples with magnesium nitrate, and phosphorus determination by alkalimetric titration. The determination has also been done gravimetrically with ammonium phosphomolybdate and phosphomolybdic oxide[18] as the weighing forms.

EXPERIMENTAL

Alkaline fusion

In a 50-ml silver crucible melt about 3 g of sodium or potassium hydroxide pellets or a eutectic mixture of the two, and during cooling keep the crucible swirling until the alkali has solidified, then leave it to reach room temperature. Weigh 0.15 g of dried sample (wheat flour dried for 6 hr at 100°, leaves for 16 hr at 70–80°) and add it to the crucible.

Method D_{ox}. Warm the crucible with a burner and swirl it constantly until a homogeneous and half-liquid mixture of molten alkali and organic matter is obtained. Add a very small portion of solid sodium or potassium nitrate and heat the mixture strongly until the organic matter is destroyed. If a charred residue is left (usually the case), continue strong heating and addition of oxidant (not exceeding 0.1 g) with energetic mixing after each addition, repeated until oxidation is complete and a transparent melt formed.*

Method W. Add 0.5–1 ml of water to the crucible, wetting the sample and the alkali. Warm cautiously with the burner flame and swirl vigorously to obtain at relatively low temperature a homogeneous mixture of alkali and organic matter. Continue warming and stirring until the moisture

*Jacobson and Hall[19] decomposed organophosphate insecticides with a fusion mixture of sodium hydroxide and potassium nitrate (4:1) in a platinum crucible.

has evaporated. Gradually increase the heating with constant swirling until the mixture fuses, and then heat strongly until the organic matter is destroyed. If a persistent residue is left, increase the heat until a transparent melt is obtained.

Phosphorus determination

When cold, the fusion product readily dissolves on addition of small volumes of hot water (not more than 5 ml at a time). Transfer the solution to a plastic beaker and rinse out the crucible thoroughly. Neutralize the solution by adding sulphuric acid (1 + 1) dropwise with stirring, until the effervescence stops. Add slowly and with stirring 8–10 ml more acid. Boil the solution for 30 min, cool and transfer it to a 50-ml standard flask, and dilute to the mark. Transfer a 5-ml (maize or orange samples) or 10-ml (wheat flour, olive tree or eucalyptus) aliquot to a 50-ml beaker, and neutralize with dilute sodium hydroxide solution. Prepare fresh hydrazine–molybdate reagent[16] by mixing 25 ml of ammonium molybdate solution [8.5 g of ammonium heptamolybdate tetrahydrate in 500 ml of sulphuric acid (1 + 4)] and 10 ml of 0.15% hydrazine sulphate solution, and diluting to 100 ml. Add 20 ml of this molybdate–hydrazine solution to the test solution, dilute with water to 40 ml, mix and place in a boiling water-bath for 7–8 min. Cool and transfer the blue solution to a 50-ml standard flask, and dilute to the mark. Measure the absorbance in a 1-cm cell at 830 and 650 nm. Prepare a calibration graph covering the range 0.25–12.5 × $10^{-3}M$ phosphate.

RESULTS AND DISCUSSION

Both decomposition procedures mineralize the organic phosphorus easily and rapidly (10–15 min), giving a clear melt. The fusion product gives a suitable solution for determination of the phosphorus. The efficiency of method *W* is possibly due to the thorough mixing of the sample and alkali at low temperature assisting the degradation of the organic matter. The amount of hydroxide necessary is 15–20 times the weight of sample used.

Up to 0.2 g of sodium nitrate, added as auxiliary oxidant, does not interfere in the spectrophotometric determination. The amount usually used is less than 0.1 g.

The results obtained were analysed statistically (95% significance level).

Wheat flour

The results in Table 1 show that the phosphorus content found varies slightly according to the method used, diminishing in the order alkalimetric titration, gravimetry as ammonium phosphomolybdate, gravimetry as phosphomolybdic oxide, spectrophotometry, but the last gives the best agreement with the certified value. The standard deviation also diminishes in the same order.

The high results obtained by alkalimetry are probably due to adsorption of acid on the yellow precipitate, and those by weighing ammonium phosphomolybdate are due to its hygroscopic nature; phosphomolybdic oxide is not very hygroscopic, however,[18] and the results obtained by this method are practically the same as those obtained by spectrophotometry.

The precision of the spectrophotometric determination is comparable for both decomposition methods. The alkaline mineralization also gives results comparable to those obtained with the reference decomposition (*F*-test); nevertheless, the precision of the alkaline fusion method is better than that of dry ashing, lower values and variances being obtained in all cases.

Table 1. Analysis of wheat flour (series I and II, present method; series IV, AOAC method; series III, V and VI, other reference methods)

Series	Destruction of organic matter	Phosphorus determination	P found, % $\bar{x}$	s,§%	Relative std. devn., %
I	Alkaline fusion (method D_{ox})	Spectrophotometric (molybdenum blue)	0.0849* 0.0839†	0.00074 0.00074	0.6 0.6
II	Alkaline fusion (method *W*)		0.0848* 0.0843†	0.00079 0.00067	0.7 0.6
III	Ashing with magnesium nitrate		0.0848* 0.0844†	0.00132 0.00097	1.1 0.8
IV		Alkalimetric titration	0.0894	0.00386	3.1
V		Gravimetric ammonium phosphomolybdate	0.0878	0.00103	0.8
VI		Gravimetric phosphomolybdic oxide	0.0860	0.00082	0.7

*λ = 830 nm.
†λ = 650 nm.
§n = 10.

Table 2. Analysis of leaf samples[17]

Sample (certified P content, %)	Fusion method	P found, % $\bar{x}$	s,§ %	Relative std. devn., %
Maize (0.219)	D_{ox}	0.215*	0.00365	2.1
		0.214†	0.00342	2.0
	W	0.216*	0.00270	1.6
		0.216†	0.00249	1.4
Orange tree (0.15)	D_{ox}	0.150*	0.00152	1.3
		0.149†	0.00084	0.7
	W	0.150*	0.00195	1.3
		0.149†	0.00158	1.3
Olive tree (0.083)	D_{ox}	0.080*	0.00084	1.3
		0.080†	0.00084	1.3
	W	0.080*	0.00084	1.3
		0.080†	0.00084	1.3
Eucalyptus (0.085)	D_{ox}	0.082*	0.00100	1.3
		0.082†	0.00089	1.3
	W	0.082*	0.00110	1.3
		0.082†	0.00055	1.3

*λ = 830 nm.
†λ = 650 nm.
§n = 10.

Leaf samples (maize, orange tree, olive tree and eucalyptus)

Table 2 compares the certified values for the standards with the results obtained by the spectrophometric method and both mineralization techniques.

Method W gives a lower standard deviation than method D_{ox}, and measurement at 650 nm is more precise than measurement at 830 nm.

The accuracy of the proposed method is excellent for samples with high phosphorus content, and reasonable for those with lower phosphorus content. All the "Student"-t values are smaller than the tabulated values, indicating that the average results obtained are correct.

Acknowledgements—The authors thank Dr. M. Pinta, Research Director and Chief of the Spectrography Department O.R.S.T.O.M. (France), for the use of the leaf standards used in this work.

REFERENCES

1. R. Levy, *Compt. Rend.*, 1953, **236,** 1781.
2. R. A. Chalmers and D. A. Thomson, *Anal. Chim. Acta*, 1958, **18,** 575.
3. S. S. Asthana and E. B. Singh, *Sci. Cult. India*, 1977, **43,** 527.
4. M. S. Cresser and J. W. Parsons, *Anal. Chim. Acta*, 1979, **109,** 431.
5. M. Pinta, *Spectrométrie d'absorption atomique, Tome II*, Masson, Paris, 1971.
6. Association of Official Analytical Chemists, *Official Methods of Analysis*, 13th Ed., Sections 14.015–14.016, p. 213. AOAC, Washington, D.C., 1980.
7. A. A. Abramyan, R. S. Sarkisyan and M. A. Balyan, *Izv. Akad. Nauk Arm. SSR Khim. Nauk*, 1961, **14,** 561.
8. A. Kondo, *Bunseki Kagaku*, 1960, **9,** 416.
9. M. Jureček and J. Jeník, *Chem. Listy*, 1957, **51,** 1312.
10. J. F. Colaruotolo, *Ion Chromatog. Anal. Environ. Pollut.*, 1978, **149,** 67.
11. W. I. Awad, S. S. M. Hassan and S. A. Thoria, *Mikrochim. Acta*, 1976 **II,** 111.
12. R. L. Baker, *Anal. Chem.*, 1972, **44,** 1326.
13. M. Vandepute, L. Dryon, E. L. Raelboom, J. R. Istas and D. L. Massart, *Z. Anal. Chem.*, 1976, **282,** 215.
14. V. A. Klimova and M. D. Vitalina, *Zh. Analit. Khim.*, 1964, **19,** 1254.
15. J. V. Gimeno Adelantado, *Doctoral Thesis*, Valencia, 1981.
16. G. Charlot, *Dosages Colorimétriques des Eléments Minéraux*, p. 293, Masson, Paris, 1961.
17. M. Pinta and Inter-Institutes Committee, *Analusis*, 1975, **3,** 345.
18. L. Erdey, *Gravimetric Analysis*, Vol. III, p. 131. Pergamon Press, London, 1965.
19. M. Jacobson and S. A. Hall, *Anal. Chem.*, 1948, **20,** 736.

Talanta, Vol. 30, No. 12, pp. 977–979, 1983
Printed in Great Britain.

0039-9140/83 $3.00 + 0.00

POLAROGRAPHIC DETERMINATION OF PROGUANIL AND CHLORHEXIDINE

F. TOMAS VERT, F. VICENTE PEDROS, J. MARTINEZ CALATAYUD* and V. PERIS MARTINEZ
Facultad de Ciencias Químicas, Universidad de Valencia, Burjasot (Valencia), España

(*Received* 23 *March* 1982. *Revised* 29 *March* 1983. *Accepted* 7 *June* 1983)

Summary—The method is based on the cathodic wave obtained for chlorhexidine and proguanil in buffered aqueous dimethylformamide media. Concentrations up to 8×10^{-5} and $6 \times 10^{-4}M$, respectively, can be determined. The difference in behaviour at various pH values or in the presence of surface-active agents, is useful for characterization of both biguanides.

Biguanides are found in several pharmaceutical formulations and their analytical reactivity with metallic ions has been studied.[1-3] The polarographic behaviour of biguanide solutions has not previously been described, however, only the metal-ion complexes having been studied.[4-7]

Aqueous and aqueous dimethylformamide solutions of chlorhexidine (I) and proguanil (II) exhibit characteristic cathodic waves at pH values at which the two compounds are monoprotonated.[8] The wave is due to heterogeneous saturative reduction of the azomethine bonds to amino groups.[9] In the absence of the chlorophenyl group, the biguanides tested do not show this wave, and give only hydrogen evolution.[10]

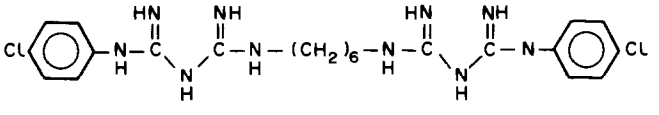

(I)

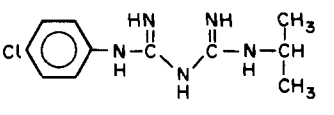

(II)

The present work deals with the polarographic differentiation of chlorhexidine and proguanil and their determination. There are few quantitative methods for biguanides. The standard method[11] is by titration with perchloric acid in acetic acid medium. A recent paper[12] deals with the HPLC separation of proguanil in serum samples.

EXPERIMENTAL

Chemicals

Chlorhexidine dihydrochloride and proguanil hydrochloride were donated by ICI Farma. Both were crystalline white powders, m.p. 249° and 237°, respectively. Thin-layer chromatograms showed only one spot (under ultraviolet radiation) for each substance. Perchloric acid titration (in acetic acid medium) gave 99.8% and 99.9% purity, respectively. All chemicals used were of analytical grade.

*To whom all correspondence should be addressed.

Apparatus

A Radiometer Polariter PO4g, with a 1250-Ω resistance SCE and a dropping mercury electrode (2.61 sec drop-time, drop-rate 3.58 mg/sec) was used, at 20°, for the analytical procedures and examination of surfactants.

A Metrohm Polarecord E-506, with an Ag/AgCl, KCl (satd.) reference and auxiliary electrodes was used for the d.c. and a.c. controlled drop-time techniques (drop-life 0.6 sec, drop-rate 2.31 mg/sec) at 20°.

Procedures

An appropriate amount of biguanide was dissolved in 2 ml of dimethylformamide and accurately diluted with pH 7.05 Britton–Robinson buffer ($0.5M$) to 25 ml. The solution was deoxygenated by passage of nitrogen for 5 min and then the polarogram was recorded.

Chlorhexidine in "Hibitane" tablets. About 0.5 g (accurately weighed) of powdered sample was dissolved in 50 ml of a 1:1 v/v mixture of pH 7.05 Britton–Robinson buffer and dimethylformamide. Four-ml portions were diluted accurately to 25 ml with the same buffer. Various volumes (0–3 ml at 0.5-ml intervals) of a standard $3.68 \times 10^{-4}M$ chlorhexidine solution in Britton–Robinson buffer (8% dimethylformamide solution) were added and the deoxygenation and polarographic steps were applied.

RESULTS AND DISCUSSION

The polarographic waves of chlorhexidine and proguanil are shown in Fig. 1. Addition of dimethylformamide increases the solubility of the biguanides and shifts the half-wave potential to less negative values, improving the resolution with respect to the wave from the medium.

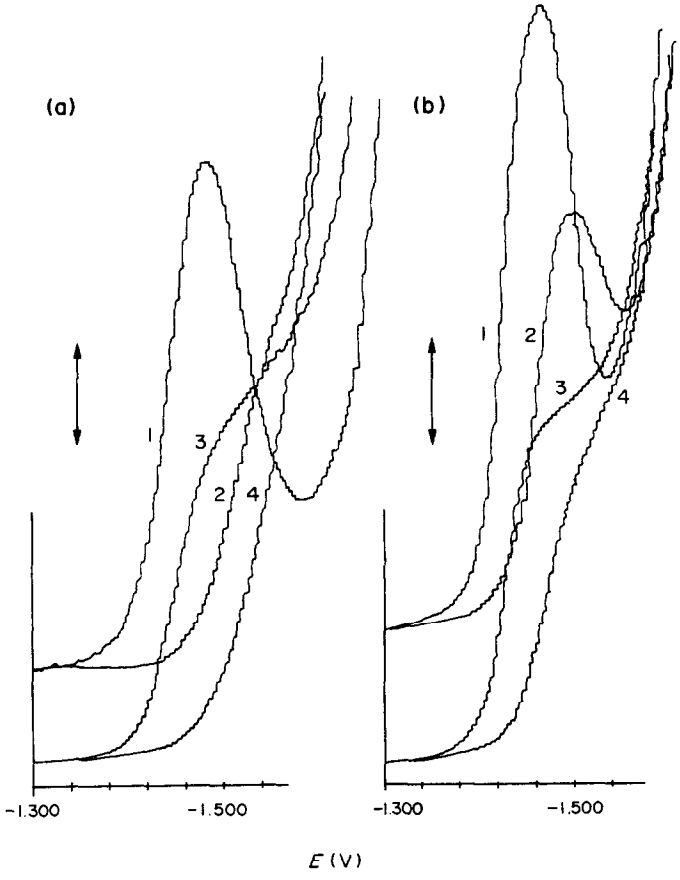

Fig. 1. Typical a.c. and d.c. waves (drop-life 0.6 sec; ΔE 30 mV; temperature 20°; 0.05M Britton–Robinson buffer, pH 6.52. (↕) 0.015 μA (a.c.) and 0.10 μA (d.c.). (a) Proguanil $4 \times 10^{-4}M$; (b) chlorhexidine $4 \times 10^{-4}M$; 1 and 2, a.c.; 3 and 4 d.c.; 2 and 4, gelatine $4 \times 10^{-2}M$.

The pH-dependence of the half-wave potential was found to be linear in both cases ($\Delta E_{\frac{1}{2}}/\Delta$ pH $\simeq -60$ mV and $Q_{act} > 3$ kcal/mole). Proguanil shows polarographic activity only at pH > 3, but chlorhexidine gives a useful wave at pH > 1.7. These two biguanides can be differentiated at pH values below 3; the wave obtained for $2 \times 10^{-4}M$ chlorhexidine solution at pH 2.25 is not disturbed by successive additions of proguanil up to a concentration of $2 \times 10^{-4}M$.

Adsorption phenomena affect the characteristics of the waves, the half-wave potentials being shifted to slightly more negative values when gelatine or Triton X-100 is added to the biguanide solution. At pH 7.05 and a proguanil concentration up to $5.7 \times 10^{-4}M$, the wave disappears at a gelatine concentration of 5.6×10^{-3}%. The effect is less marked with chlorhexidine, for which the wave at the same pH and a concentration of $8 \times 10^{-5}M$ is not affected by a 6×10^{-2}% concentration of gelatine. However, 1.5×10^{-2}% gelatine causes interference with the waves from $3.3 \times 10^{-5}M$ chlorhexidine and $3.3 \times 10^{-4}M$ proguanil.

Triton X-100 has a bigger effect than does gelatine. The limits of detection are $3.3 \times 10^{-5}M$ for chlorhexidine and $3.3 \times 10^{-4}M$ for proguanil, with 1.2×10^{-2} and 8.6×10^{-3}% Triton X-100, respectively.

The effect of the surfactants on the polarographic waves is shown in Table 1 and Fig. 1.

Table 1. Effect of surfactants on the half-wave potentials and diffusion currents (E_{start} −1.20 V, pH 7.05 Britton–Robinson buffer)

[Biguanide], M	Gelatine, %	Triton X-100, %	$E_{\frac{1}{2}}$, V	I, μA
			−1.47	1.32
Chlorhexidine	1.5×10^{-2}		−1.54	1.08
0.8×10^{-4}		1.2×10^{-2}	−1.52	0.96
			−1.57	5.10
Proguanil	2.3×10^{-3}		−1.51	3.04
5.7×10^{-4}		2.7×10^{-4}	−1.62	4.64

The analytical method is based on these results and uses d.c. polarography at the dropping mercury electrode. The polarogram is recorded over the range of applied potential from -1.2 to -1.6 V. The calibration graph is linear up $8 \times 10^{-5}M$ chlorhexidine or $6 \times 10^{-4}M$ proguanil. The half-wave potentials do not vary significantly: -1.57 V for proguanil and -1.47 V for chlorhexidine.

The Lingane constants and $n\alpha$ values calculated are 3.2 and 0.80 for proguanil, and 6.0 and 1.64 for chlorhexidine.

The relative standard deviations found were 2% for proguanil solutions and 0.4% for chlorhexidine (15 replicates).

Chlorhexidine in "Hibitane" tablets (from ICI Farma) was also determined by the standard-addition method (see procedure). The correlation coefficient was 0.999. Found 4.9 mg (declared 5 mg).

REFERENCES

1. F. Bosch, J. Martínez Calatayud and M. C. Garcia Alvarez-Coque, *Afinidad*, 1980, **37**, 137.
2. J. Hernández Méndez, F. Bosch Reig, J. Martínez Calatayud and M. C. Pascual Martí, *ibid.*, 1978, **35**, 345.
3. J. Martínez Calatayud, F. Bosch Reig and M. C. Garcia Alvarez-Coque, *Talanta*, 1982, **29**, 139.
4. B. Chakravarty, *J. Inorg. Nucl. Chem.*, 1979, **41**, 757; 1979, **41**, 1211.
5. B. Dutta, *Electrochim. Acta*, 1980, **28**, 533.
6. *Idem, J. Indian Chem. Soc.*, 1980, **57**, 429; *Indian J. Chem.*, 1980, **19A**, 669.
7. D. Sen, S. Debabratta and C. Ranjan, *J. Chem. Soc., Dalton Trans.*, 1976, 776.
8. F. Vicente, F. Tomás and M. A. Nuñez, *IV Reunión de Química (Sanitaria)*, ANQUE, Madrid, 1981.
9. F. Vicente, *Doctoral Thesis*, Valencia, 1981.
10. J. Trijueque, F. Vicente and F. Tomás, *IV Reunión de Química (Sanitaria)*, ANQUE, Madrid, 1981.
11. *British Pharmacopoeia*, HMSO, London, 1973.
12. R. R. Moody, A. B. Selkirk and R. B. Taylor, *J. Chromatog.*, 1980, **182**, 359.

Talanta, Vol. 30, No. 12, pp. 980–982, 1983
Printed in Great Britain

0039-9140/83 $3.00 + 0.00
Pergamon Press Ltd

POTENTIOMETRIC TITRATION OF SULPHATE, SULPHITE AND DITHIONATE MIXTURES, WITH USE OF A LEAD ION-SELECTIVE ELECTRODE

P. A. SISKOS,* E. P. DIAMANDIS and E. GILLIERON
Laboratory of Analytical Chemistry, University of Athens, 104 Solonos St., Athens 144, Greece

JENNIFER C. COLBERT
Chemical Thermodynamics Division, Center for Chemical Physics, National Bureau of Standards, Washington, DC 20234, U.S.A.

(*Received* 22 *December* 1982. *Revised* 20 *April* 1983. *Accepted* 2 *June* 1983)

Summary—Simple methods are described for the analysis of sulphate, sulphite and dithionate mixtures by potentiometric titration with lead perchlorate (and use of a lead ion-selective electrode). The error and precision are both about 2–5% for the sulphate concentration range 3×10^{-3}–$6 \times 10^{-4}M$. The sulphur content in fuels derived from refuse was determined by potentiometric titration after bomb-combustion and the results compared favourably with those from the standard $BaSO_4$ gravimetric method.

The environmental significance of sulphur is being increasingly recognized[1] and the analytical chemistry of sulphur compounds has therefore received much attention.[2,3] Sulphur dioxide is one of the most ubiquitous pollutants in ambient air. Its oxidation in clean, dry air is slow, but certain transition metals such as iron, copper and manganese, which are quite common constituents of urban atmospheres, may enhance it.[4] The oxidation of sulphur dioxide may lead to dithionate ($S_2O_6^{2-}$) or sulphate.[5,6] Dasgupta *et al.* first proposed the existence of dithionate in atmospheric aerosols.[6]

There are few satisfactory analytical techniques for determination of dithionates or mixtures of dithionates with other sulphur-containing anions.[2,3] Dasgupta *et al.* have proposed a method for the analysis of sulphate, sulphite and dithionate mixtures.[6] In this, sulphite is titrated with tri-iodide in one aliquot of sample. In another aliquot, sulphite is oxidized to sulphate with hydrogen peroxide and the total sulphate is titrated with barium perchlorate with Sulphonazo III or Thorin as indicator. In a third aliquot, sulphite is oxidized to sulphate, and the total sulphate is precipitated as barium sulphate and filtered off. The filtrate, containing dithionate, is oxidized with concentrated nitric acid and the resulting sulphate is determined gravimetrically. The error of this procedure for dithionate was about ±3%, and the method is time-consuming and complicated.

The present paper describes the analysis of mixtures of sulphate, sulphite and dithionate, by potentiometric titration with lead perchlorate. An aliquot of sample is titrated with lead perchlorate to obtain the sum of sulphate and sulphite. Another aliquot is acidified with perchloric acid, and the sulphur dioxide produced is removed from the solution by passage of nitrogen. The sulphate is then titrated with lead perchlorate. A third aliquot is oxidized with hydrogen peroxide to convert sulphite into sulphate and then with concentrated nitric acid to oxidize dithionate to sulphate, and the total sulphate is titrated. All the titrations are done at pH 4 in 50% aqueous methanol. The error and precision of each titration are both 2–5% for the sulphate concentration range 3×10^{-3}–$6 \times 10^{-4}M$.

The method is simple, fairly accurate and precise. It needs only one standard solution and may find application in the analysis of atmospheric and industrial particulates and aerosols for sulphite, sulphate and dithionate. It has been applied to the determination of sulphur in some fuels derived from refuse.

EXPERIMENTAL

Apparatus

An Orion model 94-82 lead electrode and model 90-02 double-junction reference electrode were used with a Corning model 12 pH/mV-meter. The salt-bridge compartment of the reference electrode was filled with 1*M* sodium nitrate to prevent precipitation of potassium perchlorate.

Reagents

All solutions were prepared with demineralized distilled water and reagent-grade materials.

*Lead perchlorate solution, 0.1*M. Dissolve 46.0 g of $Pb(ClO_4)_2 \cdot 3H_2O$ in water, dilute to 1 litre, and standardize by EDTA titration. Dilute further as needed.

*Author for correspondence.

Table 1. Results for the analysis of sulphate–sulphite mixtures

Taken, *m*M	Found, *m*M		Error, %	
$[SO_4^{2-}]+[SO_3^{2-}]$	$[SO_4^{2-}]$	$[SO_3^{2-}]$	$[SO_4^{2-}]$	$[SO_3^{2-}]$
2.000 + 0.500	2.030	0.440	+1.5	−12.0
0.500 + 2.000	0.458	1.960	−8.4	− 2.0
1.000 + 2.000	1.000	1.980	0	− 1.0
2.000 + 1.000	1.970	0.980	−1.5	− 2.0
1.000 + 1.000	1.010	0.960	+1.0	− 4.0

*Sodium sulphate solution, 0.1*M. Dissolve 14.20 g of anhydrous Na_2SO_4 in water and dilute to 1 litre. Dilute further as required.

*Sodium sulphite solution, 0.1*M. Dissolve 1.260 g of anhydrous Na_2SO_3 in freshly boiled water and dilute to 100 ml. Prepare daily and standardize by iodometric titration. Dilute further with freshly boiled water, as needed.

*Sodium dithionate solution, 0.1*M. Dissolve 24.20 g of dried $Na_2S_2O_6 \cdot 2H_2O$ (97.0%) in water and dilute to 1 litre. Standardize by oxidation with concentrated nitric acid, followed by titration with lead perchlorate as in procedure (*a*) below. Dilute further as required.

Procedures

(*a*) *Determination of sulphate and sulphite.* Pipette a 20-ml sample into a 100-ml beaker. Adjust the pH to 4 with sodium hydroxide solution or perchloric acid. Add 25 ml of methanol, immerse the electrodes in the solution, start stirring at the maximum speed at which air bubbles are not formed, and titrate with 0.01*M* lead perchlorate.

(*b*) *Determination of sulphate.* Pipette a 20-ml sample into a 100-ml beaker. Add 1.0 ml of 3*M* perchloric acid and bubble nitrogen vigorously through the solution for 15–20 min. Adjust the pH to 4 with 5*M* sodium hydroxide, add 25 ml of methanol and continue as in (*a*).

(*c*) *Determination of sulphate, sulphite and dithionate.* Pipette a 20-ml sample into an Erlenmeyer flask. Add 2 or 3 drops of 0.025*M* sodium hydroxide and 0.5 ml of 30% hydrogen peroxide. Allow 5 min for oxidation of sulphite to sulphate. Add 30 ml of concentrated nitric acid and put the loosely stoppered flask in a heated water-bath for 4 hr. The dithionate is quantitatively oxidized to sulphate. Evaporate the solution almost to dryness to remove the nitric acid, add 20 ml of water and adjust the pH to 4. Add 25 ml of methanol and continue as in (*a*).

Calculations

Plot the e.m.f. against volume of titrant and take the point of inflection as the end-point. Calculate the sulphite content from the difference between titrations (*a*) and (*b*). Calculate the dithionate content from titrations (*a*) and (*c*), remembering that 1 mole of dithionate is converted into 2 moles of sulphate.

RESULTS AND DISCUSSION

Potentiometric titration of sulphate

Ross and Frant first described the potentiometric titration of sulphate with lead, with use of a lead ion-selective electrode.[7] They used 50% aqueous dioxan medium to suppress the solubility of lead sulphate. The detection limit is $5 \times 10^{-5}M$ sulphate. Major interference is caused by cations which give an electrode response (Cu^{2+}, Hg^{2+}, Ag^+), anions which form insoluble lead salts (PO_4^{3-}) and high concentrations of chloride and nitrate. Lokka used a water–acetone mixture to suppress the solubility of lead sulphate,[8,9] but we use 50% aqueous methanol in accordance with the electrode manufacturer's instructions,[10] but no formaldehyde. The pH used (4) is the middle of the optimal range (4 ± 1).[7–10]

When sodium sulphate solutions in the range $4–20 \times 10^{-3}M$ were titrated with 0.1*M* lead perchlorate as in procedure (*a*), the error and precision were about 1%. The potential break at the equivalence point was about 85 mV. For $4–20 \times 10^{-4}M$ sodium sulphate titrated with 0.01*M* lead perchlorate the error and precision were about 1–2%, and the potential break about 45 mV.

Determination of sulphite

It was found that sulphite can also be titrated directly by the procedure for sulphate. Titration of $2–10 \times 10^{-3}M$ sulphite with 0.01*M* lead perchlorate at pH 4 [procedure (*a*)] gave an error and precision of about 1–2%, and a potential break of about 35 mV. The detection limit was $5 \times 10^{-4}M$. An alternative is to oxidize the sulphite to sulphate with hydrogen peroxide, heat to dryness to remove peroxide, which interferes with the titration,[11] dissolve the sodium sulphate in water and titrate by procedure (*a*).

Analysis of sulphate–sulphite mixtures

The sum of the sulphate and sulphite is determined [procedure (*a*)] and then the sulphate alone [procedure (*b*)] after decomposition of the sulphite. The accuracy for analysis of mixtures is shown in Table 1. There is a small systematic negative error in the determination of the sum of sulphate and sulphite,

Table 2. Results for the analysis of sulphate–sulphite–dithionate mixtures

Taken, *m*M	Found, *m*M			Error, %		
$[SO_4^{2-}]+[SO_3^{2-}]+[S_2O_6^{2-}]$	$[SO_4^{2-}]$	$[SO_3^{2-}]$	$[S_2O_6^{2-}]$	$[SO_4^{2-}]$	$[SO_3^{2-}]$	$[S_2O_6^{2-}]$
1.000 + 1.000 + 1.000	1.020	0.900	1.030	+2.0	−10.0	+3.0
1.000 + 3.000 + 1.000	1.007	2.960	1.034	−0.7	− 1.3	+3.4
3.000 + 1.000 + 1.000	2.985	0.930	0.960	−0.5	− 7.0	−4.0
1.000 + 1.000 + 3.000	0.996	0.958	2.925	−0.4	− 4.2	−2.5
2.000 + 2.000 + 2.000	2.060	1.894	1.954	+3.0	− 5.3	−2.3

Table 3. Results for the determination of sulphur in fuels derived from refuse

Sample	Sulphur, %*†	
	Gravimetry (X)	Titrimetry (Y)
1	0.250	0.220
2	0.462	0.446
3	0.238	0.234
4	0.238	0.231
5	0.095	0.100
6	0.188	0.199
7	0.463	0.478
8§	0.224	0.226

*Referred to dry weight.
†Correlation equation $Y = 0.990X$ ($r = 0.9934$, $N = 8$).
§Standard deviations ($N = 5$): gravimetry 0.012, titrimetry 0.008.

which is possibly due to the greater solubility of the lead sulphite.

Analysis of sulphate–sulphite–dithionate mixtures

Dithionate is remarkably stable towards oxidizing agents, being attacked by only by a few strong oxidants, the most suitable of which is concentrated nitric acid, but prolonged heating is needed for complete oxidation.[6] The sulphite present is oxidized first with peroxide, as otherwise there would be loss of sulphur dioxide during addition of the nitric acid. After the oxidation of dithionate the surplus nitric acid is expelled by heating almost to dryness, as nitrate interferes in the titration.[10] Table 2 shows the accuracy of the method.

The proposed methods may find application in analysis of atmospheric and industrial particulates.[12]

Determination of sulphur in fuel derived from refuse

The bomb-combustion and classical gravimetric procedure for this analysis[13] is time-consuming and tedious. We have compared the gravimetric finish with procedure (*a*), after decomposition of the sample by bomb-combustion. Table 3 shows the results.

The precision of the two methods was checked by burning five samples of the same material and analysing the resulting solutions by both methods. The means and standard deviations were 0.224 ± 0.012 and $0.226 \pm 0.008\%$, for the gravimetric and titrimetric methods, respectively. The agreement is good but the titrimetric method is more precise and takes only 30 min, whereas the gravimetric method needs 3 hr.

REFERENCES

1. B. Meyer, *Sulfur, Energy and Environment*, Elsevier, Amsterdam, 1977.
2. J. H. Karchmer (ed.), *The Analytical Chemistry of Sulfur and its Compounds*, Wiley-Interscience, New York, 1970.
3. L. Szekeres, *Talanta*, 1974, **21**, 1.
4. R. B. Schlesinger, J. L. Gurman and Lung-Chi Chen, *Atmos. Environ.*, 1980, **14**, 1279.
5. D. W. Carlyle and O. F. Zeck, Jr., *Inorg. Chem.*, 1973, **12**, 2978.
6. P. K. Dasgupta, P. A. Mitchell and P. W. West, *Atmos. Environ.*, 1979, **13**, 775.
7. J. W. Ross, Jr. and M. S. Frant, *Anal. Chem.*, 1969, **41**, 967.
8. E. J. Lokka, *Paper Puu*, 1978, **60**, 441.
9. *Idem, Acta Polytech. Scand.*, 1977, No. 137.
10. *Instruction Manual for Lead Electrode, Model 94-82*, Orion Research, 1977.
11. S. N. K. Chaudhari, F. C. Chang and K. L. Cheng, *Anal. Chem.*, 1981, **53**, 2048.
12. L. D. Hansen, L. Whiting, D. J. Eatough, T. E. Jensen and R. M. Izatt, *ibid.*, 1976, **48**, 634.
13. ASTM Standard E 711-81, *Standard Test Method for Gross Calorific Value of Refuse-Derived Fuel by the Bomb Calorimeter.*

Talanta, Vol. 30, No. 12, pp. 983–985, 1983
Printed in Great Britain

0039-9140/83 $3.00 + 0.00
Pergamon Press Ltd

STUDIES ON THE DETERMINATION OF DISSOLVED OXYGEN IN WATER

M. MALAIYANDI*
National Health and Welfare Canada, Environmental Health Centre, Health Protection Branch, Ottawa, Canada

V. S. SASTRI
Physical Metallurgy Research Laboratories, CANMET, Department of Energy, Mines and Resources, Ottawa, Canada

(*Received* 16 *November* 1982. *Revised* 4 *May* 1983. *Accepted* 27 *May* 1983)

Summary—Studies on the decomposition rates of the Mn(III) complex of cyclohexanediaminetetra-acetate (DCTA) in light and in darkness have shown that this complex is more stable than the one derived from ethylenediaminetetra-acetate. The optimum pH range for the determination of dissolved oxygen by means of the Mn(III)–DCTA complex is found to be between 3 and 4. The absorbance of this complex is independent of the amount of DCTA used (in the range 0.2–1.0 g) with water samples containing a maximum of 3.2 ppm of dissolved oxygen. Significant interferences are caused by the presence of CO_3^{2-}, HCO_3^-, $S_2O_3^{2-}$, PO_4^{3-}, I^-, NO_2^-, SO_3^{2-}, Ca^{2+}, Fe^{2+} and Fe^{3+} at 500 times the oxygen concentration.

Various methods have been proposed for the determination of dissolved oxygen in solutions since the classical work of Winkler.[1] Some are simply modifications of Winkler's method. These have been reviewed by Caritt and Carpenter,[2] who concluded that the modified Winkler's methods, though laborious, are quite reliable. Photometric methods appear to be most popular for determination of dissolved oxygen. Direct photometric methods involve the oxidation of polyphenols and aminophenols[3–6] or leuco dyes,[7] and the indirect methods involve oxidation of manganese(II) by the dissolved oxygen and reaction of the resulting manganese(III) with iodide,[8] *o*-toluidine[9] or redox indicators.[10,11] In another set of methods, the manganese(III) is complexed with EDTA[12,13] or DCTA[14] and the resultant colour intensity measured.

During the course of studies on the determination of corrosion rates of mild steel in coal–water slurries, a reliable and accurate method for the determination of micro quantities of dissolved oxygen in the medium became essential. Preliminary work showed that the Mn(III)–EDTA and Mn(III)–DCTA complexes are photosensitive even to laboratory lighting, and this factor seems to have been ignored in earlier studies.[12–14] Hence, a brief study has been made of the relative stability of the Mn(III) complexes of DCTA and EDTA. The results, as well as the influence of variables such as pH, DCTA concentration and interferences due to some cations and anions frequently found in coal–slurry waters, are reported in this paper.

EXPERIMENTAL

Reagents

All reagent solutions were made from analytical-grade chemicals. "Baker-Grade" DCTA and EDTA were obtained from a local supplier. A 1.5*M* manganese(II) chloride tetrahydrate solution was prepared.

Procedure

Samples with varying concentrations of dissolved oxygen were prepared by bubbling either oxygen or nitrogen (the latter to reduce the oxygen levels already present) through distilled water contained in 2-litre flasks. The dissolved oxygen in these stock solutions was determined by the modified Winkler's method,[7] and by using a Delta Scientific model 2010 oxygen-probe electrode. Before addition of the reagents, the dissolved oxygen content of aliquots of the stock solution was determined by the modified Winkler's method and by the oxygen-probe method, and these values were taken as standard.

For determination of the decomposition rates of Mn(III) complexes, aliquots of the stock water samples containing a known amount of oxygen were taken in two sets of 250-ml standard flasks. To each solution 4 ml of 1.5*M* manganese(II) solution were added, followed by 0.4 g of DCTA or EDTA and 4 ml of 4*M* sodium hydroxide. The flasks were wrapped in aluminium foil to minimize photochemical decomposition. After vigorous shaking of the mixtures the precipitates were allowed to settle, and 1.4 ml of 5*M* sulphuric acid were added to each flask. The mixtures were shaken and diluted to volume with water.

One set of flasks was unwrapped, and exposed to the fluorescent lighting in the laboratory; the other set remained in the dark. The decomposition rates of the Mn(III)–DCTA and Mn(III)–EDTA complexes in solution were determined by measuring the absorbances at regular intervals (approximately 2-hr intervals for the exposed solutions and approximately 24-hr intervals for those kept in the dark) at 500 and 495 nm respectively.

*To whom correspondence should be addressed.

RESULTS AND DISCUSSION

Stability of Mn(III) complexes

The visible absorption spectra of the complexes are shown in Fig. 1. Mn(III)–DCTA has an intense absorption maximum at 500 nm, while Mn(II)–DCTA gives very little absorption in the 400–600 nm region. Mn(III)–EDTA gives a spectrum similar to that of Mn(III)–DCTA, with a maximum at 495 nm. Typical first-order plots for the decomposition of Mn(III)–DCTA at pH 2.4 are shown in Fig. 2. It is apparent that the decomposition of the complex is accelerated on exposure to light. Similar observations were made with the Mn(III)–EDTA complex.

Data on the decomposition rates of Mn(III)–DCTA and Mn(III)–EDTA at pH 2.4 and 4.5 are given in Table 1. It is clear that Mn(III)–DCTA is more stable than Mn(III)–EDTA, which itself is more stable at pH 4.5 in sulphuric acid medium in the dark than in acetic acid medium under the same conditions. However, if 1 ml of 0.5% CTAB solution was added before formation of the Mn(III)–EDTA complex, the half-life of the coloured complex was found to be about $2\frac{1}{2}$ times greater than that observed without the addition of CTAB as stabilizer. This finding is in agreement with the observations made by Rahim and Mohamed.[13] In the case of Mn(III)–DCTA, however, addition of CTAB had no marked effect on the stability of the complex. This observation further substantiates the finding that Mn(III)–DCTA is more stable than Mn(III)–EDTA.

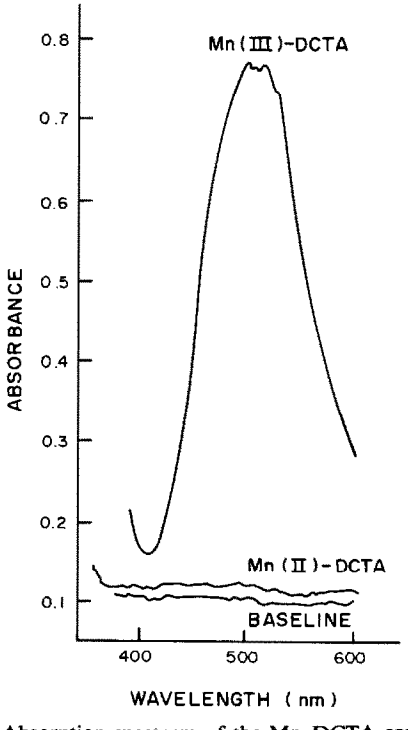

Fig. 1. Absorption spectrum of the Mn–DCTA complex.

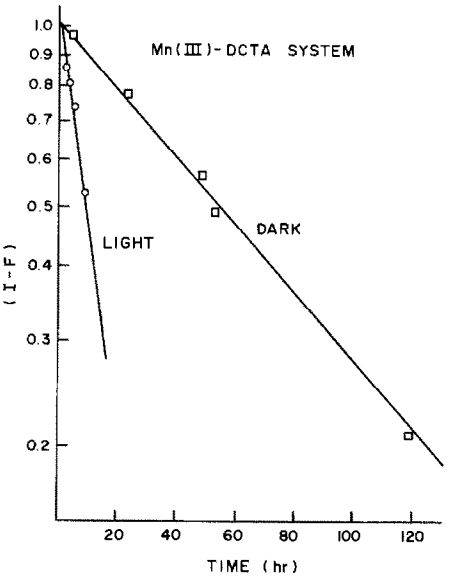

Fig. 2. Rate of photodecomposition of the Mn(III)–DCTA complex.

The effect of pH on the absorbance of the Mn(III)–DCTA complex at 500 nm is shown in Fig. 3. The absorbance increases quite sharply between pH 2.2 and 3.0, then remains constant at pH up to at least 4.1. Hence, further work was done at pH 3.0–4.0.

The effect of variation of DCTA concentration at two levels (2.4 and 3.2 ppm) of dissolved oxygen was studied and the absorbance was found to be independent of amount of DCTA added, from 0.2 to 1.0 g.

The absorbance of the Mn(III)–DCTA complex (kept in the dark) was measured for four levels of dissolved oxygen content (each in triplicate) and used to construct a calibration curve. Least-squares analysis gave a slope of 0.1312 (absorbance unit per ppm oxygen) and an intercept of 0.0328 absorbance unit. Assuming the stoichiometric formation of four moles of Mn(III)-complex per mole of dissolved oxygen, the molar absorptivity of the Mn(III)–DCTA complex was calculated to be 5321.mole^{-1}.cm^{-1}, which is higher than the 3391.mole^{-1}.cm^{-1} reported in the literature.[14]

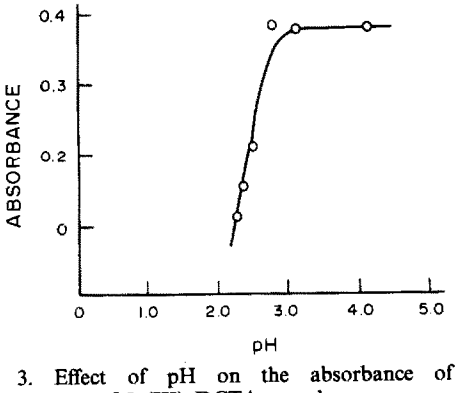

Fig. 3. Effect of pH on the absorbance of the Mn(III)–DCTA complex.

Table 1. Decomposition rates of Mn(III) complexes

System	Medium	pH	Half-life, *min*
Mn(III)–DCTA			
Dark	H_2SO_4	4.4	3240
Light	H_2SO_4	4.4	570
Mn(III)–DCTA + CTAB			
Dark	H_2SO_4	4.14	3390
Light	H_2SO_4	4.14	732
Mn(III)–EDTA			
Dark	CH_3COOH	4.5	145
Light	CH_3COOH	4.5	118
Dark	H_2SO_4	4.5	207
Light	H_2SO_4	4.5	114
Dark	H_2SO_4	2.4	285
Light	H_2SO_4	2.4	223
Mn(III)–EDTA + CTAB			
Dark	CH_3COOH	4.07	355
Light	CH_3COOH	4.07	290

A brief investigation was made of the influence of some inorganic ions usually encountered in mining waters, on the determination of dissolved oxygen with Mn(III)–DCTA. Serious interferences were observed with anions such as CO_3^{2-}, HCO_3^-, $S_2O_3^{2-}$, SO_3^{2-}, PO_4^{3-}, I^-, NO_2^-, NO_3^- and cations such as Ca^{2+}, Fe^{2+}, Fe^{3+}, when present in 500:1 ratio to oxygen. These findings are similar to the observations made by Rahim and Mohamed for the Mn(III)–EDTA method.[13] However, the method reported here is applicable to waters containing low levels of these ionic species and to coal-slurrying water containing sodium chloride at 3.5 g/l. concentration.

REFERENCES

1. L. W. Winkler, *Ber. Deut. Chem. Ges.*, 1888, **21**, 2843.
2. D. E. Caritt and J. H. Carpenter, *J. Marine Res.*, 1966, 286.
3. W. M. Mackay and R. E. Middleton, *J. Soc. Chem. Ind.*, 1898, **17**, 1127.
4. R. Tuve, *U.S. Patent*, 2440315, 27 April 1948.
5. F. W. Gilcreas, *J. Am. Water Works Assoc.*, 1935, **27**, 1166.
6. L. W. Winkler, *Z. Angew. Chem.*, 1916, **26**, 135.
7. A. H. Meyling and G. H. Frank, *Analyst*, 1962, **87**, 60.
8. W. J. Hansen and H. H. Pieters, *Anal. Chim. Acta*, 1948, **7**, 712.
9. F. R. McCrumb and W. R. Kenny, *J. Am. Water Works Assoc.*, 1929, **21**, 400.
10. J. Banks, *Analyst*, 1959, **84**, 700.
11. W. F. Stones, *Chem. Ind. London*, 1957, 37.
12. A. H. de Carvalho, J. G. Calado and M. L. Mowra, *Rev. Port. Quim.*, 1963, **5**, 15.
13. S. A. Rahim and S. H. Mohamed, *Talanta*, 1978, **25**, 519.
14. G. S. Sastry, R. E. Hamm and K. H. Pool, *Anal. Chem.*, 1969, **41**, 857.

Talanta, Vol. 30, No. 12, pp. 986–988, 1983
Printed in Great Britain

0039-9140/83 $3.00 + 0.00
Pergamon Press Ltd

DETERMINATION OF THE TOTAL IRON CONTENT OF USED LUBRICATING OILS BY ATOMIC-ABSORPTION WITH USE OF EMULSIONS

A. SALVADOR,* M. DE LA GUARDIA and V. BERENGUER
Department of Analytical Chemistry, Faculty of Chemistry, University of Valencia, Valencia, Spain

(*Received* 5 *August* 1982. *Revised* 13 *March* 1983. *Accepted* 9 *May* 1983)

Summary—A new method is proposed for the determination of the total iron content of used lubricating oils. It is based on treatment of the samples with a mixture of hydrofluoric and nitric acids (without destruction of the organic matter) and emulsification, followed by atomic-absorption measurement. This allows the use of aqueous standards and provides a simple, rapid, inexpensive and accurate method, that is not affected by the particle size of the solids in the oil.

The determination of wear metals in used lubricating oils is of great technological and analytical interest. These metals are present as suspensions with a large range of particle sizes, depending on the degree of engine wear. Because of this, the samples are remarkably heterogeneous, and serious difficulties are created in atomizing them for atomic-absorption spectroscopy (AAS).

Iron is probably the element most commonly found among the wear metals in lubricating oils, so determination of this metal could act as a guide for testing some general methods for checking engine wear.

Direct dilution methods[1–5] do not allow determination of the total iron content because the larger particles can pass through the flame without being converted into free atoms. The results obtained by these methods are strongly dependent on the particle size and much lower than those obtained by methods based on the destruction of the matrix.

Methods based on the ashing of the sample and analysis of the ash allow determination of the total iron content, but require many manipulations with consequent long analysis time and risk of contamination or loss.

To obtain a rapid and accurate method for determining total iron in used oils, with aqueous standards, we have examined the use of spraying emulsions[6–9] obtained after chemical treatment of the samples with mineral acids, without destruction of the organic matter.

EXPERIMENTAL

Apparatus

A Pye-Unicam SP 1900 atomic-absorption spectrophotometer was used, with an iron hollow-cathode lamp, under the conditions for highest sensitivity. An air–acetylene flame was used.

A Selecta Vibromatic 384 vibrator was used to mix the samples.

Reagents

Stock solution of iron (1000 ppm), prepared by dissolving 1.000 g of pure iron in 8.5 ml of concentrated hydrochloric acid and 5 ml of concentrated nitric acid (both pure grades) and diluting to 1 litre with distilled demineralized water.

Nemol K 39 (nonyl phenol polyethylene glycol ether, with 9 ethylene oxide units) (Masso y Carol), Atlox 4853 B (mixture of anionic and non-ionic surfactants) (ICI), Emulsogen LBH (mixture of surfactants with solvents), and Renex 690 (alkyl aryl polyethylene glycol ether, with 9 ethylene oxide units) (ICI), were used as emulsifiers.

Sampling

To reduce as far as possible all error due to sampling, oil samples were stored in transparent glass bottles so that the appearance of any sludge could be detected and, before sampling, samples were heated at 60° on a hot-plate, with shaking, for about 30 min. To avoid any possible difference due to sampling, the samples for both the reference and the proposed method were drawn simultaneously.

Reference method

The modified ASTM spectrophotometric method[10] was used after ashing and dissolution of the samples.

Procedure. Weigh 2–6 g of oil into a porcelain crucible, then heat it with a Bunsen burner until dry and no more smoke appears. Transfer the crucible to a muffle furnace at 550–600° and heat for 1 hr. Cool, add 1 g of potassium hydrogen sulphate per 2 g of sample and fuse. Cool, add 5 ml of hydrochloric acid (1 + 1), cover the crucible and heat gently for 30 min to dissolve the residue. Filter (Whatman No. 42 paper). Dilute the filtrate to volume in a 50-ml standard flask with distilled water. Pipette 10 ml of this solution, add 4 drops of 2,4-dinitrophenol, 5 ml of 20% sodium acetate solution, 1 ml of 10% hydroxylamine hydrochloride solution and 1 ml of 0.5% phenanthroline hydrochloride solution and dilute to 25 ml.

Prepare aqueous iron standards containing the same concentrations of reagents and measure the absorbance of samples and standards in 1-cm cells at 510 nm.

Analysis by AAS, using emulsions

Use of emulsions stabilized with various commercial

*Author for correspondence.

surfactants has been tested, the emulsions being formed either directly or after treatment of the samples with acids or acid mixtures. The results have been compared with those obtained by the reference method.

Among the procedures tested, the one based on the use of oil in water (o/w) emulsions stabilized with non-ionic surfactants after treatment of the samples with a mixture of nitric and hydrofluoric acids gave the best results.

Procedure. Weigh approximately 1 g of oil into a polyethylene bottle, add 2.5 ml of a 1:1 v/v mixture of concentrated hydrofluoric and nitric acids by means of a polyethylene syringe, close the bottle and shake it for 5 min by means of a mechanical vibrator. Then add 3 ml of methyl isobutyl ketone (MIBK), 10 ml of 20% aqueous solution of Nemol K 39 and 25 ml of water, and shake manually to form an o/w emulsion.

Prepare standards in the same way, but using new iron-free oil, and introducing known volumes of 100-ppm iron solution into the aqueous phase.

Introduce the samples and standards into an air–acetylene flame and measure their absorbance at 248.3 nm.

It is important that all volumes are accurately measured, as the solutions are not diluted to a fixed volume in standard flasks.

RESULTS AND DISCUSSION

Stability of the emulsions towards mineral acids

The determination of the total iron content of used lubricating oils by direct emulsification of the samples after acid treatment requires that the emulsions be stable, and because of this it is necessary to use very different kinds of emulsions, depending on the amount and nature of the acids employed in the treatment of the samples.

Stable water in oil emulsions containing 1 g of lubricating oil in a total volume of 50 or 25 ml can be obtained by use of the anionic surfactant Atlox 4853 B or Emulsogen LBH (0.1 g per ml of total volume) respectively, 10% v/v of aqueous phase and MIBK as diluent, but their stability towards mineral acids is limited, so they cannot be used after an acid treatment of the sample.

Water in oil emulsions containing 10 g of Nemol K 39, 1 g of lubricating oil, 3 ml of water and 25 ml of MIBK are stable for several hours in the presence of 2.5 ml of mineral acid mixtures such as hydrochloric/hydrofluoric or nitric/hydrofluoric. Moreover, water in oil emulsions containing less surfactant (10 ml of 20% Nemol K 39 solution in MIBK) but the same quantities of oil, water and MIBK, are stable in the presence of the mineral acids.

It is also possible, however, to obtain oil in water emulsions containing 1 g of lubricating oil in 50 ml, stabilized with 10 ml of 5% aqueous Renex 690 solution and containing 4 ml of benzene. In the presence of 5 ml of hydrochloric acid (1 + 1) these emulsions are stable for only some minutes, but can be regenerated by simple manual shaking. In contrast, oil in water emulsions containing 1 g of lubricating oil, 3 ml of MIBK, 10 ml of 20% aqueous Nemol K 39 solution and 25 ml of water are stable for several hours at temperatures below 25°, in the presence of 2.5 ml of various hydrofluoric/nitric acid mixtures.

Direct determination of iron in lubricating oils by use of emulsions

The concentration of iron in a sample of used lubricating oil was determined by the reference method and by atomic-absorption spectrometry applied after emulsification of the samples with Atlox 4853B or Emulsogen LBH as stabilizer.

The results given in Table 1 show that AAS analyses of these emulsions are low by about 75% compared with those obtained by the reference method. This indicates that only a small fraction of the total iron present is atomized, corresponding to the iron either in solution in the oil or present in sufficiently small particles. The results obtained are independent of the surfactant employed. For determination of the total iron content a previous treatment of the samples to dissolve all the particles is therefore necessary.

Determination by formation of emulsions after acid treatment of the samples

The simple way to avoid ashing is to attack the sample with mineral acids to dissolve all the metallic particles present in the oil, then to emulsify the oil and acid solution for spraying into the AAS flame.

Table 1. Determination of iron in used lubricating oils; comparison between the procedures employed

	Emulsion methods					
	Direct determination		Determination with previous acid treatments			Reference method
	a	b	HCl	HF/HCl	HF/HNO_3	
$\bar{x}$, μg	27	25	90.5	99	107	103
n	11	7	17	7	5	5
s, μg	2.6	1.8	1.8	1.8	1.6	2.6
s_r, %	10	7	2	2	1.5	2.5
d, %	−74	−76	−12	−4	4	—

a, Emulsions stabilized with Atlox 4853 B.
b, Emulsions stabilized with Emulsogen LBH.
$\bar{x}$, Average in 1 g of lubricating oil.
n, Number of replicates.
s, Standard deviation.
s_r, Relative standard deviation.
d, Relative difference from reference method.

Hydrochloric acid dissolves and complexes iron and to dissolve the iron particles in the oil it should be sufficient to contact the sample with a small volume of the acid. However, the results obtained in this way are found to be low by about 12% (Table 1). Other acid systems have therefore been tested (Table 1) and both the HF/HCl and HF/HNO_3 mixtures, stabilized with Nemol K39, seem suitable, but the HF/HNO_3 mixture is preferred because it dissolves all the metallic particles dispersed in the oil, including molybdenum species.[11]

Choice of procedure

Water in oil emulsions containing 10 g of Nemol give only 90% of the sensitivity given by the o/w emulsions prepared by the procedure described in the experimental section, probably because of their higher viscosity, which is responsible for the low aspiration rate and some nebulization and clogging problems. However, when stabilized by 10 ml of 20% MIBK solution of Nemol, these emulsions provide twice the sensitivity of the o/w emulsions and a detection limit of 0.9 μg of iron in the emulsion. This is very useful for the analysis of samples with low iron content, but for routine analysis the o/w emulsions are preferable because of the greater stability of the absorbance readings.

The total iron content of some used lubricating oil samples, of different origins, was determined by the procedure described in the experimental section. The results are summarized in Table 2 along with those obtained by the reference method.

The figures of merit of the method are as follows. The sensitivity, defined as the slope of the calibration curve, is an absorbance of 5.7×10^{-4} per μg of iron in the emulsion. The standard deviation of the absorbance for the blank is 4.8×10^{-4}, so if three times this absorbance is taken as the detection limit, the minimum amount of iron detectable is about 2 μg (2 ppm in a 1-g sample).

The precision, taken as the relative standard deviation for repetitive analysis, is about 1.4% at the 100-μg level and is in general better than that obtained by the reference method (Table 1).

Table 2. Determination of the total iron content in used lubricating oils by AAS, using emulsions and prior treatment of the samples with HF/HNO_3 (for symbols see Table 1)

	Emulsion method				Reference method			
Sample	$\bar{x}$	n	s	s_r	$\bar{x}$	n	s	s_r
Aircraft	107	5	1.6	1.5	103	5	2.6	2.5
Car 1	28	7	1.1	4	29	7	1.9	7
Car 2	84	7	1.0	1	82	7	4.3	5
Train	39	6	1.0	2.5	40	6	2.2	6
Car 3	198	7	3.2	1.5	200	7	2.0	10

The accuracy of the emulsion method was established by regression analysis of the values obtained by both the proposed and the reference methods.[12,13] Statistical tests of the slope and intercept show that the method is free from systematic error and requires no correction for the blank [t(intercept) = 0.3; t(slope) = 0.1; t(tabular) = 2.04 (P = 0.95)]. The mean values obtained by both methods are in agreement according to the Fisher test.[14]

CONCLUSIONS

The total iron content of used lubricating oils cannot be determined directly by AAS analysis of emulsions made from the oils, because any metallic iron present will not be atomized in the flame. Prior treatment of the sample with a mixture of hydrofluoric acid and hydrochloric or nitric acid dissolves the metallic iron without the need to ash the organic matter. Emulsification then disperses the iron species uniformly in the system. If the acid treatment and emulsification are done in the container into which the sample is weighed, risk of contamination or loss is minimized.

The procedure allows rapid and accurate determination of the total iron content and is unaffected by the particle size of the solids present. It has the advantage over the Saba and Eisentraut method,[15] that conventional aqueous standards can be used.

Acknowledgement—This work was done with the aid of a grant from Excma. Diputación Provincial of Valencia to A. Salvador.

REFERENCES

1. T. T. Bartels and M. P. Slater, *At. Absorp. Newsl.*, 1970, **9**, 75.
2. R. H. Kriss and T. T. Bartels, *ibid.*, 1970, **9**, 78.
3. J. H. Taylor, T. T. Bartels and N. L. Crump, *Anal. Chem.*, 1971, **43**, 1780.
4. R. H. Kriss and T. T. Bartels, *At. Absorp. Newsl.*, 1972, **11**, 110.
5. P. K. Hon, O. W. Lau and C. S. Mok, *Analyst*, 1980, **105**, 919.
6. V. Berenguer and J. Hernandez, *Quim. Anal.*, 1977, **31**, 2, 81.
7. M. de la Guardia, A. Salvador and V. Berenguer, *Analusis*, 1980, **8**, 448.
8. *Idem*, *Anal. Quim.*, in press.
9. *Idem*, *Analusis*, 1981, **9**, 74.
10. ASTM D-810 and D-811.
11. C. S. Saba and K. J. Eisentraut, *Anal. Chem.*, 1977, **49**, 454.
12. M. de la Guardia, A. Salvador and V. Berenguer, *Anal. Quim.*, 1981, **77B**, 1.
13. *Idem*, *ibid.*, submitted for publication.
14. Y. Lacroix, *Analyse chimique: interprétation des résultats par le calcul statistique*, Masson, Paris, 1973.
15. C. S. Saba and K. J. Eisentraut, *Anal. Chem.*, 1979, **51**, 1927.

Talanta, Vol. 30, No. 12, pp. 989–992, 1983
Printed in Great Britain.

0039-9140/83 $3.00 + 0.00

ANNOTATIONS

NANOGRAM DETECTION OF *m*-DINITROAROMATICS AND THEIR DERIVATIVES

A RE-EVALUATION OF THE SPOT-TEST BASED ON THE JANOVSKY REACTION

SYED ASHFAQ NABI, SEEMA HAQUE and PUSHKIN M. QURESHI
Department of Chemistry, Aligarh Muslim University, Aligarh 202001, India

(*Received* 17 *May* 1982. *Revised* 23 *May* 1983. *Accepted* 2 *June* 1983)

Summary—The spot-test for *m*-dinitroaromatics and their derivatives, based on the Janovsky reaction, is re-investigated. The sensitivity of the spot-test has been much enhanced by changing the solvent and using the novel "pellet" spot-test. With the "pellet" spot-test and dimethylsulphoxide, 4–50 ng of *m*-dinitroaromatic compounds and their derivatives can be detected. The change from acetone (used in the original spot-test) to dimethylsulphoxide changes the reaction product in most cases.

The past few years have seen a considerable increase in study of the reactions of polynitroaromatics, but though most of these compounds are coloured, little use has been made of the reactions in organic analytical chemistry, apart from the specific colorimetric detection of aliphatic amines.[1,2] These tests were based on anionic complexes, which have a much higher molar absorptivity than charge-transfer complexes. Four excellent reviews cover the field to 1970.[3–6]

The detection of *m*-dinitroaromatics and their derivatives is very important, as most of them show carcinogenic activity. 2,4-Dinitrotoluene, for example, has recently been shown to be an important hepatocarcinogen.[7] Further, the reactions can be used for the determination of dinitrophenyl (DNP) derivatives of amino-acids, *e.g.*, by means of their reaction with cyanide.[8]

Perhaps the oldest colorimetric reaction in this field is the interaction of *m*-dinitroaromatics and their derivatives with acetone in the presence of alkali, the so-called Janovsky reaction.[9] This method was first successfully applied to the determination of *m*-dinitroaromatics by English,[10] who claimed 0.05% of these compounds could be detected in the mononitro compounds. A spot-test published 6 years later[11] showed the practical limit ranged from 0.5 μg for *m*-dinitrobenzene to 9 μg for 3,5-dinitrobenzoic acid. However, as shown in this paper, there is great scope for increasing the sensitivity of this reaction.

A new technique, the "alkali pellet" spot-test, has been developed, which gives maximum sensitivity. It appears this will be a useful technique in those equilibrium reactions where the hydroxide ion is a reactant:

$$A + OH^- \overset{K}{\rightleftharpoons} AOH^-$$

and the equilibrium constant is favourable.

EXPERIMENTAL

Materials

Most nitroaromatics used were guaranteed-reagent grade (Merck), and were not further purified. Some were laboratory reagent grade (B.D.H. or Koch-Light) and were recrystallized until the melting points were in agreement with the literature values. The dimethylsulphoxide (DMSO) was a Baker "Analyzed Reagent", the dimethylformamide (DMF) was B.D.H. "Analar".

The micropipette used was precise to ±3%. Amberlite IRA-400 (Cl^- form) was used for the "resin spot-test".

Procedures

(*a*) Place one drop (1 μl) of a solution of the test substance in distilled ethanol in the depression of a white spot-plate, followed by one drop (~50 μl) of 30% sodium (or potassium) hydroxide solution (prepared with conductivity water). Add one drop of acetone (~50 μl) and note the colour. If the test is negative add 4 or 5 drops more acetone and again note any colour. Repeat this procedure, but replace the acetone first with DMF and then with DMSO.

(*b*) Place a few resin beads (Amberlite IRA-400, Cl^- form) in the depression of a white spot-plate. Add to the beads one drop (1 μl) of the test solution in distilled ethanol, followed by the other reagents as described in (*a*).

(*c*) Repeat procedure (*b*) with a clean pellet of sodium (or potassium) hydroxide instead of the resin beads.

RESULTS

The analytical results are tabulated in Table 1, together with a comparison with other methods. A

number of organic compounds were tested by procedures (*a*), (*b*) and (*c*) and found not to interfere with the test. They include carbohydrates [L(+)-arabinose, lactose, D(+)-malezitose, glucose, rhamnose, sucrose]; acids (acetic, formic, tartaric, phthalic, pyrogallic, oxalic); alcohols (propan-2-ol, ethyl, methyl, 2-methylpropan-2-ol, amyl, isoamyl); heterocyclic bases (pyridine, piperidine); aldehydes (formaldehyde, acetaldehyde, benzaldehyde, paraldehyde, *p*-chlorobenzaldehyde); ketones (acetophenone, cyclopentanone, cyclohexanone, propiophenone, benzophenone); hydrocarbons and their derivatives (benzene, xylene, *o*-dichlorobenzene, bromobenzene, toluene); ethers (diethyl, anisole, 1,4-dioxan); amino-acids (DL-tryptophan, L-lysine, DL-phenylalanine, L-histidine); anilides (acetanilide, benzanilide); nitriles (aceto, benzo); amides (acetamide, benzamide); amines (trimethyl, triethyl, methyl, diethyl, aniline, diphenyl); phenols (phenol, *m*-cresol, resorcinol); miscellaneous (chloroform, carbon tetrachloride, urea, thiourea).

DISCUSSION

This spot-test is based on the general reaction involving a compound that contains an aromatic ring with two or three electron-attracting groups in the *meta*-positions, and an anion suitably activated to give highly coloured complexes.[12]

A glance at Table 1 shows that the sensitivity can generally be improved by replacing the conventional spot-test by the resin spot-test and further improved by the novel "alkali pellet" spot-test.

We have also changed the solvent, and in addition to acetone (used in the original spot-test), have used two polar aprotic solvents, DMF and DMSO, which increase the sensitivity, the order being DMSO > DMF > acetone, which is also the order of the dielectric constants. DMSO has a special ability to stabilize anionic species.[13]

Test substances (nitroaromatics) which gave yellow or orange colours were not considered. 1-Fluoro-2,4-dinitrobenzene gives a violet colour with acetone, an orange-red colour with DMF and a blue-violet colour in the presence of DMSO. Therefore there is a potential for using these interactions to develop solvent polarity scales similar to those of Taft *et al.*[14,15] There is also scope for using these reactions as acidity indicators.[16,17]

The colours produced in the alkaline solutions of polynitroaromatics can be due to a variety of interactions, which will be discussed individually below.

m-*Dinitrobenzene*

The coloured species proposed (Y = OH or OD) is

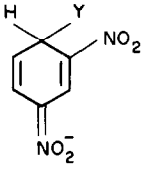

$\lambda_{max} = 526$ nm

(I)

which is stable, has $\lambda_{max} = 526$ nm, and is formed in >70 mole% DMF medium.

Table 1. Limit of detection ($\mu g/\mu l$)

Name of compound	Solvent: Acetone[a]	Solvent: DMF[b]	Solvent: DMSO[c]	Colour*	Structure proposed for coloured species in DMSO	Sensitivity relative to other tests
	3.0 (C)	4.0 (C)	0.4 (C)	OR[a]	(2a)	25 (S)
1-Chloro-2,4-dinitrobenzene	4.0 (R)	0.4 (R)	0.4 (R)	OR[b]		2000 (T)
	0.4 (P)	0.04 (P)	0.04 (P)	OR[c]		100 (V)
	0.4 (C)	0.4 (C)	0.4 (C)	V[a]		—
1-Fluoro-2,4-dinitrobenzene	0.4 (R)	4.0 (R)	4.0 (R)	OR[b]	(2b)	—
	0.4 (P)	0.04 (P)	0.04 (P)	BV[c]		—
	6.0 (C)	4.0 (C)	0.8 (C)			—
2,4-Dinitroaniline	0.4 (R)	4.0 (R)	0.04 (R)	P	(3a)	—
	0.4 (P)	0.4 (P)	0.004 (P)			—
	0.120 (C)	0.080 (C)	0.060 (C)			650 (C)
3,5-Dinitrobenzoic acid	0.04 (R)	0.032 (R)	0.028 (R)	RV	(5)	350 (T)
	0.032 (P)	0.028 (P)	0.014 (P)			75 (V)
	4.0 (C)	0.280 (C)	0.240 (C)			40 (S)
2,4-Dinitrotoluene	0.320 (R)	0.080 (R)	0.040 (R)	G	(4)	—(T)
	0.024 (P)	0.024 (P)	0.020 (P)			100 (V)
	1.0 (C)	2.0 (C)	0.100 (C)			250 (S)
2,4-Dinitrophenylhydrazine	0.4 (R)	1.0 (R)	0.100 (R)	BV	(3b)	—(T)
	0.4 (P)	0.100 (P)	0.050 (P)			—(V)
	0.160 (C)	0.080 (C)	0.040 (C)			125 (S)
m-Dinitrobenzene	0.036 (R)	0.032 (R)	0.032 (R)	RV	(1)	2500 (T)
	0.024 (P)	0.008 (P)	0.004 (P)			250 (V)
	0.140 (C)	0.120 (C)	0.095 (C)			25 (S)
1,3,5-Trinitrotoluene	0.100 (R)	0.090 (R)	0.070 (R)	R	(6)	25 (T)
	0.080 (P)	0.060 (P)	0.040 (P)			25 (V)

(C) Conventional spot-test. (P) "Pellet" spot-test. (R) Resin spot-test. (S) Seiichi.[11] (T) Tiwari *et al.*[21] (V) Verma and Dubey.[22]
*BV Blue violet, G Green, OR Orange red, P Pink, R Red, RV Red violet, V Violet.

1-Chloro-2,4-dinitrobenzene and 1-fluoro-2,4-dinitrobenzene

These are thought[5,6] to give the structures

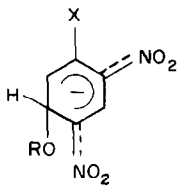

X = Cl,F

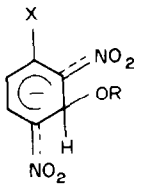

$\lambda_{max} = 500$ nm (2a)

$\lambda_{max} = 600$ nm (2b)

2,4-Dinitroaniline[19] *and 2,4-dinitrophenylhydrazine*[2]

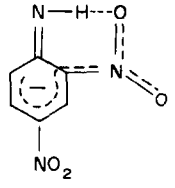

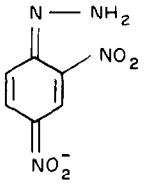

$\lambda_{max} = 380, 400, 515$ nm (3a)

$\lambda_{max} = 640$ nm (3b)

2,4-Dinitrotoluene

This reaction is fairly complicated as it can give rise to deprotonation and base addition as well as radical formation. The reaction of *p*-nitrotoluene with bases has been studied in detail[20] and has similar spectral characteristics to that of 2,4-dinitrotoluene, so an analogous reaction sequence would predict the colour-forming species to be:

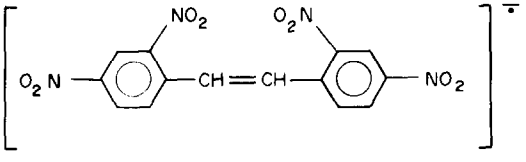

$\lambda_{max} = 630, 650$ nm

(4)

3,5-Dinitrobenzoic acid

The colour in this reaction is most probably due to base attack on the conjugate base of the acid:

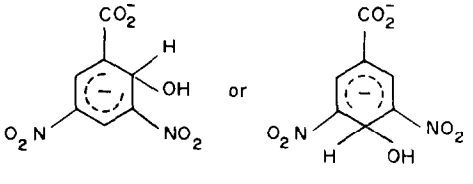

(5)

1,3,5-Trinitrobenzene[3-6]

The colour is due to base addition:

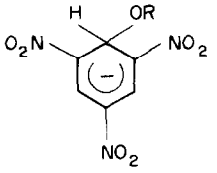

(6)

Reactions involved

The reactions on which this spot-test is based are rather different from those on which the original spot-test was based. This is because the presence or absence of acetone has a profound effect on the nature of the colour-forming reaction, and hence the colour produced. In the presence of acetone "Janovsky" adducts are formed, *e.g.*, from 1,3-dinitrobenzene:

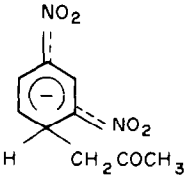

In the absence of acetone the adducts will result from base attack:[3-6]

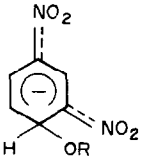

2,4-Dinitrophenol and picric acid do not give a colour under the reaction conditions. The test can be used for virtually all dinitro and trinitro compounds having two nitro groups in the *meta*-position, and is expected to be extremely sensitive.

A novel feature is the "pellet" spot-test, which gives maximum sensitivity, because of interfacial effects and the very high surface concentration of hydroxide ions.

Acknowledgements—The authors thank Professor Wasiur Rahman, Chairman, Department of Chemistry, for facilities and C.S.I.R. (India) for financial assistance.

REFERENCES

1. S. A. Nabi, A. Mohammad and P. M. Qureshi, *Talanta*, 1979, **26**, 1179.
2. M. Qureshi, S. A. Nabi, I. A. Khan and P. M. Qureshi, *ibid.*, 1982, **29**, 757.
3. R. Foster and C. A. Fyfe, *Rev. Pure Appl. Chem.*, 1966, **16**, 61.

4. E. Buncel, A. R. Norris and K. E. Russell, *Quart. Rev., Chem. Soc.*, 1968, **22,** 123.
5. M. R. Crampton, *Advan. Phys. Org. Chem.*, 1969, **7,** 211.
6. M. J. Strauss, *Chem. Rev.*, 1970, **70,** 667.
7. J. A. Bond and D. E. Rickert, *Drug. Metab. Disp.*, 1981, **9,** 10.
8. J. A. Vinson and L. D. Pepper, *Anal. Biochem.*, 1977, **83,** 357.
9. T. Canback, *Svensk. Farm. Tid.*, 1950, **54,** 1.
10. F. L. English, *Anal. Chem.*, 1948, **20,** 745.
11. O. Seiichi, *J. Pharm. Soc. Japan*, 1955, **75,** 1430.
12. E. Sawicki, *Photometric Organic Analysis*, Part 1, p. 577. Wiley-Interscience, London, 1970.
13. J. W. Larsen, K. Amin and J. H. Fendler, *J. Am. Chem. Soc.*, 1971, **93,** 2910.
14. R. W. Taft, J. L. M. Abboud and M. J. Kamlet, *ibid.*, 1981, **103,** 1080.
15. M. J. Kamlet, J. L. M. Abboud and R. W. Taft., *ibid.*, 1977, **99,** 6027.
16. K. Bowden and R. S. Cook, *J. Chem. Soc.* 1971, 1765.
17. *Idem, ibid.*, 1971, 1771.
18. E. Buncel and A. W. Zabel, *Can. J. Chem.*, 1981, **59,** 3168.
19. M. R. Crampton and P. M. Wilson, *J. C. S. Perkin Trans. II*, 1980, 1854.
20. E. Buncel and B. C. Menon, *J. Am. Chem. Soc.*, 1980, **102,** 3499.
21. R. D. Tiwari, G. Srivastava and J. P. Misra, *Analyst*, 1978, **103,** 651.
22. K. K. Verma and S. K. Dubey, *Talanta*, 1981, **28,** 485.

Talanta, Vol. 30, No. 12, pp. 993–996, 1983
Printed in Great Britain.

0039-9140/83 $3.00 + 0.00

CRITICAL EXAMINATION OF SOME COMMON REAGENTS FOR REDUCING SELENIUM SPECIES IN CHEMICAL ANALYSIS

RAGNAR BYE
Department of Chemistry, University of Oslo, Oslo 3, Norway

(*Received* 29 *March* 1983. *Accepted* 24 *May* 1983)

Summary—In an attempt to resolve apparently conflicting statements in the literature, a study has been made of the action of various reductants on selenium(VI) and selenium(IV). Chloride in hot non-oxidizing acid medium will reduce Se(VI) to Se(IV) but not further. Sulphur dioxide will reduce Se(IV) to Se, but has no effect on Se(VI). Hydrazinium salts reduce both Se(VI) and Se(VI) to Se, but hydroxylammonium salts reduce only Se(IV) to Se. Hydrogen peroxide partially reduces Se(VI) to Se(IV) but not further. If chloride is also present [to reduce Se(VI) to Se(IV)], sulphur dioxide or hydroxylammonium salts can then reduce the Se(IV) to Se, and this combined effect has led to some confusion in interpretation of experimental observations.

There is an increasing interest in determination of selenium in both organic and inorganic materials. The instrumental techniques usually employed have recently been reviewed.[1] The techniques are often very different, with respect both to the analytical reactions and the physical principles of the measuring process, but usually have in common the demand that the selenium should be in one particular oxidation state.

The oxidation numbers for selenium are −II, O, +IV and +VI. Most techniques (but not all) require that the sample is brought into solution for analysis. This is usually achieved with oxidants, resulting in selenium(IV) or selenium(VI), or a mixture of the two. For a few techniques elemental selenium is preferable or necessary, for instance for gravimetric and some X-ray and neutron-activation methods, but for most instrumental techniques selenium(IV) is required. Hence, after decomposition of the sample under conditions resulting in the presence of selenium(VI), a reduction will be necessary.

The choice of reductant is important and depends on the initial and final oxidation states obtaining in the system. The most frequently used reductants for production of selenium(IV) or elemental selenium are chloride, hydrazinium and hydroxylammonium compounds, sulphur dioxide and hydrogen peroxide. Sodium borohydride is used exclusively for producing selenium(−II) and is not considered here. In the literature there seems to exist some confusion as to the effect of the various reductants, in terms of the initial and final oxidation states of the selenium. Moreover, the composition of the reaction medium is not always considered when the reducing property of a reductant is deduced. Thus the presence of other reducing species in the solution can easily lead to erroneous conclusions concerning the effect of the reductant under test. For instance, in a recent paper it is claimed that sulphur dioxide generated from *in situ* decomposition of dimethyl sulphite reduces selenium(VI) to the element, and that this would not be possible if sulphur dioxide gas were used.[2] However, the experiments were done with fairly concentrated hydrochloric acid media, and in such solutions elemental selenium will always be obtained by use of sulphur dioxide, no matter how it is generated, because the hydrochloric acid will reduce the Se(VI) to Se(IV), which is then reduced by the sulphur dioxide. This is confirmed in the present work. In another work, chloride ions are claimed to reduce selenium(VI) to the element on prolonged boiling in hydrochloric acid.[3] This statement will be discussed later in this paper.

Quotations of results from other works can sometimes cause confusion, usually because they are incomplete. For example, it was implied in a review[1] that sulphur dioxide has been found capable of reducing selenium(VI) to selenium(IV) but this apparent contradiction of the known facts arose simply because the reviewers failed to mention that the work cited was done with solutions containing hydrazinium ions and hydrochloric acid,[4] both capable of reducing selenium(VI) to selenium(IV), which *is* reducible to selenium by sulphur dioxide.

The oxidation–reduction properties of hydrogen peroxide when reacting with selenium species may also seem somewhat contradictory, as this reagent has often been used for reducing selenium(VI) to selenium(IV), but the opposite process has also been claimed to occur.[5,6] It seems remarkable that both processes should be possible, and reasons for this will be discussed below.

The present work is hence a discussion of the oxidation–reduction properties of some common re-

Table 1

Experiment	Reaction mixture	Recovery, %
1	$Se(VI) + H_2SO_4 + N_2H_4.H_2O$	100.1
2	$Se(VI) + H_2SO_4 + N_2H_4.2HCl$	100.6
3	$Se(VI) + HCl + N_2H_4.H_2O$	99.3
4	$Se(VI) + HCl + N_2H_4.2HCl$	99.8
5	$Se(VI) + H_2SO_4 + (NH_2OH)_2.H_2SO_4$	3.0
6	$Se(VI) + H_2SO_4 + NH_2OH.HCl$	23.5
7	$Se(VI) + HCl + (NH_2OH)_2.H_2SO_4$	91.9
8	$Se(VI) + HCl + NH_2OH.HCl$	99.1
9	$Se(VI) + H_2SO_4 + SO_2$	0.7
10	$Se(VI) + HCl + SO_2$	99.1
11	$Se(VI) + H_2SO_4 + MgCl_2 + SO_2$	101.2
12	$Se(IV) + Se(VI)\ (50/50) + H_2SO_4 + SO_2$	48.4
13	$Se(VI) + H_2SO_4 + H_2O_2\ (+ SO_2)$	61.4
14	$Se(IV) + H_2SO_4 + H_2O_2\ (+SO_2)$	98.4
15	$Se(VI) + H_2SO_4\ (+SO_2)$	2.1
16	$Se(IV) + H_2SO_4\ (+SO_2)$	98.2
17	$Se(IV) + H_2SO_4 + H_2O_2$ (cold solution)	0.0

ductants for selenium species: chloride, hydrazinium compounds, hydroxylammonium compounds, sulphur dioxide and hydrogen peroxide. The reducing effects of these compounds on selenium(VI) and (IV) in various acidic media have been examined, and the results are discussed in view of the thermodynamic constants for the reacting compounds.

EXPERIMENTAL

Reagents

Se(VI) solution, 2 *g/l*. Sodium selenate (4.786 g) was dissolved in water and the solution diluted to 1000 ml.

Se(IV) solution, 2 *g/l*. Selenious acid (3.267 g) was dissolved in water and the solution diluted to 1000 ml.

Hydrazinium chloride solution, 1*M*. $N_2H_4 \cdot 2HCl$ (10.5 g) was dissolved in water and the solution diluted to 100 ml.

Hydrazinium hydrate solution, 1*M*. $N_2H_4 \cdot H_2O$ (100%, density 1.03 g/ml, 4.85 ml) was diluted to 100 ml with water.

Hydroxylammonium chloride solution, 2*M*. $NH_2OH \cdot HCl$ (13.9 g) was dissolved in water and the solution diluted to 100 ml.

Hydroxylammonium sulphate solution, 1*M*. $(NH_2OH)_2 \cdot H_2SO_4$ (16.4 g) was dissolved in water and the solution diluted to 100 ml.

Hydrogen peroxide, 30%, "pro analysi".

Sulphur dioxide. Anhydrous gas.

Procedures

Experiments 1–8. To 50.0 ml of Se(VI) solution ($\equiv$ 100 mg of Se) 50 ml of 12*M* hydrochloric acid or 33 ml of 18*M* sulphuric acid and 20 ml of hydrazinium or hydroxylammonium solution were added. The solution was diluted to 150 ml with water and the beaker heated on a boiling water-bath for 2 hr. Thereafter the precipitated elemental selenium was filtered off on a porosity-4 sintered-glass crucible and washed with water and ethanol. After drying at 110° for 2 hr the crucible was cooled and weighed.

Experiments 9 *and* 10. As for experiments 2 and 3 respectively, but the reduction solution was replaced by 20 ml of water and sulphur dioxide was passed through the solution for 2 hr, at room temperature. The mixture was then heated for 15 min on a boiling-water bath, and the selenium collected, *etc.*, as before.

Experiment 11. As for experiment 9, but 60 g of $MgCl_2 \cdot 6H_2O$ was added after the sulphuric acid.

Experiment 12. As for experiment 9, but with 100 mg of Se(VI) (as Na_2SeO_4) as well as the 100 mg of Se(IV) (as H_2SeO_3).

Experiments 13 *and* 14. To a solution of 100 mg of Se(IV) (13) or Se(VI) (14) in 10 ml of water, 65 ml of 18*M* sulphuric acid were added and the beaker was covered with a watch-glass and heated to 180° on a hot-plate. Then 20 ml of 30% hydrogen peroxide were added dropwise, with stirring of the solution. After cooling, the solution was diluted to 150 ml with water, and sulphur dioxide was passed through the solution for 2 hr. The selenium was collected and weighed as before.

Experiments 15 *and* 16. As for 13 and 14, but hydrogen peroxide was not added.

Experiment 17. Se(IV) (100 mg) was dissolved in 33 ml of 18*M* sulphuric acid, and 10 ml of 30% hydrogenperoxide were added carefully, with cooling of the solution. The mixture was left for 3 hr at room temperature, and any product collected as before.

RESULTS

The results of experiments 1–17 (means of three replicates) are shown in Table 1.

DISCUSSION

For the discussion the standard electrode potentials shown in Table 2 will be considered.

Hydrazinium compounds

Solutions of hydrazinium salts reduce Se(VI) and Se(IV) quantitatively to Se in agreement with the $E°$ values for (1), (5) and (6) and with the experimental evidence from many earlier works. The presence or absence of chloride is of no importance.

Hydroxylammonium compounds

It seems reasonable to conclude that the hydroxylammonium ion does not itself reduce Se(VI) to

Table 2

Reaction	$E°$, *V*	No.
$N_2 + 5H^+ + 4e^- \rightleftharpoons N_2H_5^+$	−0.23	(1)
$N_2O + H_2O + 4H^+ + 4e^- \rightleftharpoons 2NH_2OH$	−0.05	(2)
$Cl_2 + 2e^- \rightleftharpoons 2Cl^-$	1.35	(3)
$SO_4^{2-} + 4H^+ + 2e^- \rightleftharpoons H_2SO_3 + H_2O$	0.17	(4)
$SeO_4^{2-} + 4H^+ + 2e^- \rightleftharpoons H_2SeO_3 + H_2O$	1.15	(5)
$H_2SeO_3 + 4H^+ + 4e^- \rightleftharpoons Se + 3H_2O$	0.74	(6)
$O_2 + 2H^+ + 2e^- \rightleftharpoons H_2O_2$	0.68	(7)
$H_2O_2 + 2H^+ + 2e^- \rightleftharpoons 2H_2O$	1.77	(8)
$\frac{1}{2}O_2 + 2H^+ + 2e^- \rightleftharpoons H_2O$	1.23	(9)

Se(IV) or Se to any great extent. The results show that the degree of reduction of Se(VI) increases with increasing concentration of chloride. It must therefore be concluded that the chloride reduces Se(VI) to Se(IV), which is then reduced to Se by the hydroxylammonium ion. In view of the E° value for reaction (2) the failure of hydroxylamine to reduce Se(VI) is difficult to understand. Hydroxylamine reactions are often slow, however, and Latimer[7] has pointed out that halides seem to given faster reduction of selenate than other reductants do. It is also known that a mismatch of the electron requirements of the oxidant and reductant half-reactions can create mechanistic problems that affect the reaction kinetics.

Sulphur dioxide and chloride

Theoretically SO_2 should reduce both Se(VI) and Se(IV) to Se. However, it is generally accepted that Se(VI) is *not* reduced by SO_2,[8,9] though the contrary has been stated.[6] Likewise, it is well known that chloride is able to reduce Se(VI) to Se(IV). This is, however, not evident from the E° values. Combination of reactions (3) and (5) gives:

$$H_2SeO_3 + H_2O + Cl_2 \rightleftharpoons SeO_4^{2-} + 4H^+ + 2Cl^- \quad (10)$$

$$K_{10} = 10^{6.8}$$

Because of the very high concentration of H^+ and Cl^- (usually above $6M$) and the very low concentration of Cl_2, the reaction will be forced to the left.

As Se(IV) is easily reduced to Se by SO_2, it should theoretically be possible to obtain 100% reduction of a *mixture* of Se(VI) and Se(IV) to Se with SO_2, because the Se first formed from the reduction of Se(IV) should be capable of reducing Se(VI) to Se(IV), according to a combination of reactions (5) and (6):

$$Se + 2SeO_4^{2-} + H_2O + 4H^+ \rightleftharpoons 3H_2SeO_3 \quad (11)$$

$$K_{11} = 10^{28}$$

However, experiment 12 revealed that this reaction is not feasible, as only about 50% recovery was obtained, indicating that only Se(IV) was reduced.

It has also been claimed that chloride can reduce Se(IV) to Se on prolonged boiling with hydrochloric acid.[3] If this were possible, the following reaction, which is a combination of reactions (3) and (6), should be displaced to the left:

$$Se + 3H_2O + 2Cl_2 \rightleftharpoons 4Cl^- + H_2SeO_3 + 4H^+ \quad (12)$$

$$K_{12} = 10^{42}$$

From a thermodynamic point of view it is very difficult to understand how this could be possible. Loss of selenium from a solution of boiling concentrated hydrochloric acid could perhaps be due to volatilization of Se(IV) as $SeCl_4$ (subl. 170–196°) or $SeOCl_2$ (b.p. 176°).

All this seems to confirm the old fact that SO_2 reduces Se(IV) to Se and that Se(VI) is not reduced. However, if chloride ions are present in the acidic solution, these will reduce Se(VI) to Se(IV). Thus the sum of Se(VI) and Se(IV) can be determined. It should be noted that the chloride ions need not originate from hydrochloric acid, as might sometimes be the impression obtained from older textbooks. This is evident from experiment 11.

Hydrogen peroxide

Experiments 13 and 14 show that Se(VI) is partly reduced by H_2O_2. Reactions (7) and (8) illustrate the dual redox properties of H_2O_2, *i.e.*, that it can act both as a reductant and an oxidant. Combination of reactions (5) and (7) gives

$$H_2O_2 + SeO_4^{2-} + 2H^+ \rightleftharpoons H_2SeO_3 + H_2O + O_2 \quad (13)$$

$$K_{13} = 10^{16}$$

and of (5) and (8):

$$H_2SeO_3 + H_2O_2 \rightleftharpoons SeO_4^{2-} + H_2O + 2H^+ \quad (14)$$

$$K_{14} = 10^{21}$$

Thus both (13) and (14) seem to be spontaneous reactions. Experiments 13 and 14 show that reaction (13) is favoured although $K_{13} < K_{14}$. The reason is probably that the high concentration of H^+ will favour reaction (13) but force reaction (14) to the left.

Combination of (7) and (8) gives:

$$2H_2O_2 \rightleftharpoons 2H_2O + O_2 \quad (15)$$

$$K_{15} = 10^{37}$$

This reaction can be catalysed by many substances, and probably also by Se(IV), because in experiments 14 and 17 evolution of oxygen was observed. There could be two reasons for this. One is reaction (15), and the other is a combination of (7) + (6) giving:

$$2H_2O_2 + H_2SeO_3 \rightleftharpoons Se + 3H_2O + 2O_2 \quad (16)$$

$$K = 10^4$$

As this reaction is theoretically feasible, an experiment was done to see whether it really takes place. In experiment 17 the solution was not heated, so that any possible oxidizing effect from the hot, concentrated sulphuric acid would be avoided. After 3 hr at room temperature no precipitated selenium could be detected. With a lower concentration of acid and a higher one of peroxide, the result was still always negative. A possible explanation for the evolution of oxygen observed in experiments 14 and 17 could therefore be:

$$2H_2O_2 \xrightarrow[\text{cat.}]{\text{Se(IV)}} 2H_2O + O_2 \quad (17)$$

Experiments 15 and 16 were "blanks" for 13 and 14, *i.e.*, with no peroxide present, so that any possible effect of the sulphuric acid could be detected. No significant effects were observed.

Procedures for oxidation of selenium(IV) to selenium(VI) by means of hydrogen peroxide have been published,[5,6] but these procedures utilized passage of oxygen through the solution, and therefore reactions (5) and (9) must be considered, giving:

$$H_2SeO_3 + \tfrac{1}{2}O_2 \rightleftharpoons SeO_4^{2-} + 2H^+ \qquad (18)$$

$$K_{18} = 10^{2.7}$$

As shown, this reaction is feasible if the solution is not too acidic. In the works cited the solutions were neutral, and the results claimed are reasonable. However, in another paper, H_2O_2 alone was supposed to oxidize Se(IV) to Se(VI), but this was not examined experimentally,[10] and there is doubt whether it could really be so.

Finally it should be pointed out that the E°-values must not be used uncritically for the H_2O_2 equilibria, because these are in fact never true equilibria (on which the proper use of the thermodynamic constants is based), though the E°-values are useful in deducing which reactions can *not* take place.

The oxidation–reduction properties of hydrogen peroxide for reaction with selenium may be summarized as follows.

1. H_2O_2 is capable of reducing Se(VI) to Se(IV) (at least partly) in hot, concentrated sulphuric acid.
2. H_2O_2 does not oxidize Se(IV) to Se(VI) under such conditions.
3. H_2O_2 is theoretically capable of reducing Se(IV) to Se, but this reaction does not take place, at least not in sulphuric acid media.
4. Hot, concentrated sulphuric acid does not have any significant oxidation–reduction effect on the Se(IV)–Se(VI) system.

CONCLUSIONS

When the total amount of selenium in the solution is to be reduced to the elemental form, hydrazinium compounds are preferred, as they reduce both Se(IV) and Se(VI) irrespective of the acid used (other than nitric acid). If only Se(IV) is to be reduced, sulphur dioxide should be used, but chloride ions must be absent.

If selenium(VI) is to be reduced to selenium(VI), it seems that chloride is the most reliable reductant. Moreover, reduction by chloride can be done in both sulphuric and perchloric acid media. Chloride should also be more convenient than hydrogen peroxide, because the latter will result in evolution of gas, which can result in loss of material by spray.

As to the reducing effect of hydrogen peroxide on Se(VI), the results seem somewhat ambiguous. In view of the dual oxidation–reduction properties of peroxide this is not very surprising. Complete reduction of Se(VI) to Se(IV) by H_2O_2 could possibly be obtained by using other experimental conditions but, as mentioned above, for analytical purposes this reduction can most easily be achieved with chloride.

REFERENCES

1. H. Robberecht and R. Van Grieken, *Talanta*, 1982, **29**, 823.
2. B. V. Narayana and N. A. Raju, *Analyst*, 1982, **107**, 392.
3. G. A. Cutter, *Anal. Chim. Acta*, 1978, **98**, 59.
4. Y. K. Chau and J. P. Riley, *ibid.*, 1965, **33**, 36.
5. L. I. Gilbertson and G. B. King, *J. Am. Chem. Soc.*, 1936, **58**, 180.
6. E. R. Caley and C. L. Henderson, *Anal. Chem.*, 1960, **32**, 975.
7. W. M. Latimer, *Oxidation Potentials*, 2nd Ed., p. 84. Prentice-Hall, Englewood Cliffs, 1952.
8. A. I. Vogel, *Quantitative Inorganic Analysis*, 2nd Ed. Longmans, London, 1945.
9. I. M. Kolthoff and P. J. Elving (eds.), *Treatise on Analytical Chemistry*, Part II, Vol. 7. Interscience, New York, 1961.
10. J. M. Rankin, *Environm. Sci. Technol.*, 1973, **7**, 823.

Talanta, Vol. 30, No. 12, pp. 997–999, 1983
Printed in Great Britain.

0039-9140/83 $3.00 + 0.00

ON THE INVENTION OF CONDUCTIMETRIC TITRATION

F. SZABADVÁRY
Department of General and Analytical Chemistry, Technical University Budapest and Museum for Science and Technology, Budapest H-1521, Hungary

and

ROBERT A. CHALMERS
Department of Chemistry, University of Aberdeen, Old Aberdeen, Scotland

(*Received* 3 *November* 1982. *Accepted* 30 *July* 1983)

Summary—In contrast to the earlier statement of one of the authors according to which conductimetric titration was invented by Küster and Grüters in 1903, it is shown that Ostwald made use of this analytical method as early as the nineties of the past century. Prior to Ostwald's work, however, papers appeared in which conductimetric curves were shown, with statements about their different characteristics in the case of reaction between weak and strong acids and bases. The first of these seems to be due to Kohlrausch [together with one of his co-workers, Kreichgauer (1885)]. It does not seem to have occurred to them, however, to use this phenomenon for the purposes of analytical chemistry, namely for titrimetry.

On the basis of his research up to that time, it was stated by one of us earlier[1,2] that Küster and Grüters[3] were the first to suggest the application of conductivity measurement for analytical purposes, and that they should be considered the inventors of conductimetric titrimetry. Their experimental work on the conductivity of the sodium salts of organic acids led them to the conclusion that the end-point of the titration of acids with bases and *vice versa* is indicated by a minimum in the conductivity. Their paper does not present the results graphically as is usual nowadays, but lists them in a table. The equipment used is not described in the paper; there is only a sentence noting that the determination can be performed with the simple equipment for conductivity measurement that is available in all laboratories. Presumably the authors meant the Kohlrausch equipment usual at the time, with a bridge circuit and a telephone for detecting the null-point for bridge balance.[4] Kohlrausch, from whose work conductivity measurements originate, is not mentioned in the paper, which does not mention any previous workers in the field or give any literature references. However, there is one sentence preceding the conclusions: "zum Schluß mögen die vorstehend erhaltenen, zum Teil nicht neuen, aber oft nicht beachteten Resultate nochmals zusammengefaßt werden..." ("finally let us summarize the results, which are partially novel, but frequently not considered...").

Some time ago a copy of Ostwald and Luther's book "*Hand- und Hülfsbuch zur Ausführung physiko-chemischer Messungen*" (1902) came into the hands of one of us (F.Sz.). It is in effect a laboratory text-book with an appendix listing the laboratory exercises performed by the students in Ostwald's institute in Leipzig. It contains the following text: "Titration von Säuren und Basen durch Leitfähigkeitsbestimmung (Kohlrausch). Setzt man zu einer gelösten Base portionsweise eine Säure hinzu, so wird die spezifische Leitfähigkeit zunächst abnehmen, weil die rasch wandernden Hydroxylionen durch das langsam wandernde Anion der zugesetzten Säure ersetzt wird. Wenn die Base neutralisiert ist, so bewirkt ein weiterer Zusatz von Säure wieder ein Ansteigen der Leitfähigkeit. Im neutralen Punkt ist die Leitfähigkeit am geringsten. Das Minimum wird noch ausgesprochener, wenn man die Leitfähigkeit des zugesetzten Säurenanions in Abzug bringt. Dies ist bei der Titration schwacher Basen (resp. schwacher Säuren) sowie hydrolytisch gespaltener Salze unerläßlich, ebenso die Berücksichtigung der Volumzunahme durch das Zusetzen der Säure." ["Titration of acid and bases by measurement of conductivity (Kohlrausch). If an acid is added in portions to a dissolved base, the conductivity will first decrease, since the rapidly migrating hydroxyl ions will be replaced by the slowly migrating anions of the acid added. When the base has been neutralized, further addition of acid will result in an increase in the conductivity. At the neutral point there is a minimum in the conductivity. The minimum will be more pronounced if the conductivity of the added anions is subtracted. This is indispensable if weak bases, weak acids or hydrolysed salts are being titrated, and a correction must be applied for the volume change caused by the addition of the acid".]

This passage is a perfect description of conductimetric titration (the equipment used at the time for

conductivity measurement is presented in detail, with figures, in another chapter of the book). Some literature references follow it, but with one exception there seems no reason for their being cited: they have nothing to do with titration, and mainly deal with the application of conductivity measurement for structure determinations. The exception is a paper published in 1896 by Whitney,[5] with the title "Untersuchungen über Chromsulphat-Verbindungen". The author had obviously been working in Ostwald's institute in Leipzig, since he closed the paper with acknowledgements to his professor, Wilhelm Ostwald. The paper is essentially concerned with inorganic chemistry, but it includes some conductivity measurements, and in particular gives the following information. "Eine Methode, welche von Prof. Ostwald zur Bestimmung der Menge der freien Säure in der grünen Lösung angegeben war, beruht auf den Veränderungen in der elektrolytischen Leitfähigkeit von Lösungen, die durch successives Hinzufügen gewisser Quantitäten eines bestimmten Elektrolyts hervorgebracht werden ... Die einfachste Form dieser Erscheinung wird im Falle der Neutralisation einer Säure und eines Alkalis beobachtet. Von den möglichen Kombinationen der vorhandenen Ionen bei der Neutralisation verlangt diejenige der Wasserbildung das Verschwinden des größten Teils der OH- und H-Ionen aus der Lösung ... Wenn wir also einer Lösung von Schwefelsäure Natriumhydrat zufügen, so zeigt sich eine Verminderung der Leitfähigkeit. Diese Verminderung dauert fort, wenn nach und nach mehr von dem Alkali hinzugefügt wird und zwar so lange, bis der Punkt erreicht ist, wo Säure und Alkali in gleichwertigen Mengen vorhanden sei, über diesen hinaus resultiert aus dem weiteren Hinzufügen von Alkali ein Steigen der Leitfähigkeit. Dieses ist aus der nebenstehenden Kurve ersichtlich, wo die Abscissen die spezifische Leitfähigkeiten der Mischungen darstellen und die Ordinaten die ccm der gebrauchten 0,1 norm. NaOH Lösung, die mit 10 ccm 0,1 norm. H_2SO_4 auf ein Volumen von 100 ccm gebracht wurden". ("A method given by Prof. Ostwald to determine the amount of free acid in the green solution relies on the changes of conductivity of solutions, resulting from successive addition of certain quantities of a certain electrolyte ... The simplest form of this phenomenon is observed in the case of the neutralization of an acid and an alkali. Among the possible combinations of the ions present at the neutralization, that of water formation requires the disappearance of the major part of the OH- and H-ions from the solution ... Hence, if sodium hydroxide is added to a solution of sulphuric acid, the conductivity will decrease. The decrease continues as more and more alkali is added, until the point is reached when the acid and alkali are present in equivalent quantities: after this, further addition of alkali will result in an increase of conductivity. This is evidenced by the curves in the figure, where the abscissae represent conductivity and the ordinates the ccm of 0.1 normal NaOH solution mixed with 10 ccm 0.1 normal H_2SO_4 and made up to 100 ccm".)

Here, the paper—which otherwise is very conscientious in citing references—does not give a reference. It might be assumed that Ostwald gave this advice only verbally, and considered it so self-evident that he did not think it worth writing down. This is demonstrated by the reference in the laboratory text-book[4] to Kohlrausch, hinting that what follows is a natural consequence of Kohlrausch's work. To be sure, it is its consequence of Kohlrausch's work. To be sure, it is its consequence, since in science everything follows from something, but Kohlrausch, a physicist, never thought of any applications in analytical chemistry. It might therefore be concluded that Wilhelm Ostwald was the inventor of conductimetric titration.

This is not necessarily so, however. During discussion of this work we found a reference by Kolthoff[6] to Dutoit,[7] whose review paper led to a reference to a paper by Bertholet in 1891,[8] which gave a clear description of the abrupt change in conductivity at the equivalence point when a strong acid and weak base (or weak acid and strong base) are mixed in various proportions. Bertholet showed graphs which are in effect conductimetric titration plots, but does not seem to have realized his results could be used for analytical purposes.

Even this is not the end of the story, however. Reference to Davies[9] and Britton[10] resulted in a number of references which appear to indicate that Kohlrausch did in fact invent the technique, and that Ostwald was making rather cryptic acknowledgement of this. Miolati[11,12] refers twice to Kohlrausch as having used the method for the first time (and also to Whitney). The relevant passage by Kohlrausch[13] reads: "Starke Basen und Säuren (KOH, NaOH, HCl, H_2SO_4) zeigen ein Leitungsvermögen, welches bei der Neutralisation zuerst bis zu einem scharf markirten Punkte abnimmt, dann zunimmt. Dieser Punkt wird derjenige des neutralen Salzes sein. NaOH und H_3PO_4 schien eine mehrfach geknickte Curve zu liefern. KOH oder NaOH gab dagegen mit Essigsäure keine scharf geknickten Curven für *K*, sondern allmähliche Übergänge. Es scheint hier also ein scharf bestimmter Punkt der Neutralisation nicht zu bestehen." ["Strong bases and acids (KOH, NaOH, H_2SO_4) show a conductivity which on neutralization first decreases to a sharply marked point, then increases. This point is the same as that for the neutral salts. NaOH and H_3PO_4 appeared to yield a curve with several breaks. However, KOH or NaOH reacting with acetic acid did not give a sharply broken curve for *K*, but only gradual transitions. Here there does not seem to exist a strictly determined point of neutralization"].

This passage occurs right at the very end of a long paper, almost as an afterthought. It is immediately followed by the statement that H. Kreichgauer did

part of the work described. Whether he was responsible for the first use of conductimetric titration is not made clear, but his name should obviously be linked with that of Kohlrausch in this connection.

REFERENCES

1. F. Szabadváry, *History of Analytical Chemistry*, pp. 383–384. Pergamon Press, Oxford, 1966.
2. *Idem*, *The Development of the Methods of Analytical Chemistry* (in Hungarian), p. 384. Akadémiai Kiado, Budapest, 1960.
3. F. W. Küster and M. Grüters, *Z. Anorg. Chem.*, 1903, **35,** 454.
4. W. Ostwald and R. Luther, *Hand- und Hülfsbuch zur Ausführung physiko-chemischer Messungen*, pp. 426–427. Engelmann, Leipzig, 1902.
5. W. R. Whitney, *Z. Phys. Chem.*, 1896, **20,** 40.
6. I. M. Kolthoff, *Konduktometrische Titrationen*, p. 14. Steinkopff, Dresden, 1923.
7. P. Dutoit, *J. Chim. Phys.*, 1910, **8,** 12.
8. D. Bertholet, *Ann. Chim. Phys.*, 1891, **24,** 5.
9. C. W. Davies, *The Conductivity of Solutions*, Chapman & Hall, London, 1930.
10. H. T. S. Britton, *Conductometric Analysis*, Van Nostrand, New York, 1934.
11. A. Miolati, *Z. Anorg. Chem.*, 1900, **22,** 445.
12. A. Miolati and E. Mascetti, *Gazz. Chim. Ital.*, 1901, **31,** 93.
13. F. Kohlrausch, *Wied. Ann.*, 1885, **26,** 225.

Talanta

The International Journal of Pure and Applied Analytical Chemistry

The illustration of a Greek balance from one of the Hope Vases is reproduced here by kind permission of Cambridge University Press

Annual Subscription Rates (1983) US$300.00 (2-yr rate US$570.00)—For libraries, government laboratories, research establishments, manufacturing houses and other multiple-reader institutions. Price includes postage and insurance. £10—For *bona fide* students, who place their orders with the publisher together with a note from their professor or tutor certifying their status. Published monthly, 1 volume per annum.

Specially Reduced Rates to Individuals

In the interests of maximizing the dissemination of the research results published in this important international journal we have established a three-tier price structure. Any individual, whose institution takes out a library subscription, may purchase a second or additional subscription for personal use at a much reduced rate of US$55.00 per annum.

Microform Subscriptions and Back Issues

Back issues of all previously published volumes are available in the regular editions and on microfilm and microfiche. Current subscriptions are available on microfiche simultaneously with the paper edition and on microfilm on completion of the annual index at the end of the subscription year.

Publishing Office. Pergamon Press Ltd, Hennock Road, Marsh Barton, Exeter, Devon EX2 8RP, England (*Tel.* Exeter (0392) 51558; *Telex* 42749).

Subscription enquiries and Advertising Offices. *North America:* Pergamon Press Inc., Maxwell House, Fairview Park, Elmsford, NY 10523, U.S.A. *Rest of the World:* Pergamon Press Ltd, Headington Hill Hall, Oxford OX3 0BW, England (*Tel.* Oxford 64881).

Talanta, Vol. 30, No. 12, p. i, 1983
Pergamon Press Ltd. Printed in Great Britain

PAPERS RECEIVED

Spectrophotometric determination of halogenated 8-hydroxyquinoline derivatives: F. BELAL. (6 September 1983)
2,4-Dimethyl-6-hydroxyacetophenone oxime as an extractive photometric reagent for the determination of copper and nickel: M. J. EAPEN and V. DAMODARAN. (6 September 1983)
A rapid method for the determination of some antihypertensive and antipyretic drugs using thermometric titrimetry: U. M. ABBASI, FATEH CHAND, M. I. BHANGER and S. A. MEMON. (6 September 1983)
Flow injection analysis with gas carrier: ABDULRAHMAN S. ATTIYAT and GARY D. CHRISTIAN. (7 September 1983)
Further application of the diazotization-coupling spectrophotometric technique to the determination of aromatic amines with 8-amino-1-hydroxynaphthalene-3,6-disulphonic acid and/or *N*-(1-naphthyl)ethylenediamine as the coupling agents: GEORGE NORWITZ and PETER N. KELIHER. (22 August 1983)
The determination of trace water in organic solvents by a spectrofluorimetric method: CI YUNXIANG and JIA XIN. (7 September 1983)
Matrix modification for determination of selenium in geological samples by graphite-furnace atomic-absorption spectrometry after preseparation with sulphydryl cotton fibre: SHAN XIAO-QUAN and HU KAI-JING. (8 September 1983)
Pulse polarography of nitrosated GPC fractions of humic acids: MARIA TERESA LIPPOLIS, VITTORIO CONCIALINI and GIUSEPPE CHIAVARI. (8 September 1983)
Effect of thiocyanate on the pyridine–barbituric acid method for the spectrophotometric determination of cyanide: SHIGERU NAGASHIMA. (9 September 1983)
Spectrophotometric determination of cobalt after extraction of its 4′-(*p*-methoxyphenyl-2,2′,6′,2″-terpyridine complex with tetraphenylborate into molten naphthalene: TOHRU NAGAHIRO, JENN-LIN LIN and MASATADA SATAKE. (9 September 1983)
Simultaneous determination of acetaminophene and dextropropoxyphene napsylate in pharmaceutical preparations by reverse-phase HPLC: S. SA'SA, I. JALAL and A. RASHID. (14 September 1983)
Extractive spectrophotometric determination of molybdenum with 4-unsubstituted-5-pyrazolones: A. AHMAD, F. IK. NWABUE and G. E. EZEIFE. (19 September 1983)
Solvent extraction of the ion-pairs of chromium(VI) and molybdenum(VI) with trioctylmethylammonium chloride and benzyldimethylcetylammonium chloride: KOUSABURO OHASHI, KEIKO SHIKINA, HIROYUKI NAGATSU, IZUMI ITO and KATSUMI YAMAMOTO. (19 September 1983)
Spectrophotometric determination of trace amounts of beryllium in silicate materials: ALFRED SAUERER and GEORG TROLL. (27 July 1983)
Spectrophotometric methods for the determination of thiols with aminophenols and Fe(III): M. K. TUMMUR, T. E. DIVAKAR and C. S. P. SASTRY. (21 September 1983)
Gas chromatographic studies of copper(II) and nickel(II) chelates of bis(isovalerylacetone)ethylenedi-imine: M. Y. KHUHAWAR, A. G. M. VASANDANI and I. ARAIN. (21 September 1983)
Spectrophotometric determination of rhodium(III) with perazine dimalonate: B. KESHAVAN and P. NAGARAJA. (23 September 1983)
Multiparametric curve fitting—VI: MRFIT and MRLET, two computer programs estimating the stability constant of the prevailing M_pL_q complex and the ligand purity by photometric-titration curve analysis: MILAN MELOUN and MILAN JAVŮREK. (23 September 1983)
***p*-Phenylenediamine as a chromogenic reagent for traces of chloramine-T and *N*-chlorosuccinimide in aqueous solution:** A. K. HAREEZ and W. A. BASHIR. (23 September 1983)
Solvent extraction of noble metals with formazans—I: Comparative study on the extractability of Pt(IV), Pd(II) and Ag(I) by formazans combined with a liquid anion-exchanger: M. GROTE, U. HÜPPE and A. KETTRUP. (23 September 1983)
Critical study of the determination of tin by electrothermal atomic-absorption spectrometry using resonance and non-resonance lines: JÁNOS FAZAKAS. (23 September 1983)
Polarographic study of mixed-ligand complex stability constants and thermodynamic parameters of the reduction of Zn(II)–pyridine–thiocyanate system: JYOTI SHARMA and ARVIND KUMAR. (28 September 1983)
Characterization and elimination of the interfering effects of foreign species in atomic-absorption spectrophotometry—III: Determination of iron: A. M. ABDALLAH, M. M. EL-DEFRAWY, M. A. MOSTAFA and A. B. SAKLA. (28 September 1983)
Bestimmung von Osmiumspuren mit Dithizon mittels substöchiometrischer Isotopenverdünnungsanalyse: G. RÖBISCH, B. PFENDT and H. SCHELHORN. (18 August 1983)
Active nitrogen: A review of chemiluminescence spectrometry in analytical chemistry: HEATHER JURGENSEN and J. D. WINEFORDNER. (28 September 1983)
Solvent extraction: Atomic-absorption analysis using electrothermal atomizers—A review: A. B. VOLYNSKY, B. YA. SPIVAKOV and YU. A. ZOLOTOV. (29 September 1983)
Studies on the application of Fe–Zr mixed hydrous oxide membranes in ion-selective potentiometry: S. K. SRIVASTAVA and C. K. JAIN. (30 September 1983)
Improved tribenzylamine–silver bromide extraction/atomic-absorption spectrophotometric method for the determination of silver in ores, concentrates and zinc process solutions: ELSIE M. DONALDSON. (3 October 1983)
Potentiometric investigation of the stability of the Ag(I)-complexes of some *N*-methyl-substituted 4-H-diethylenetriamines in aqueous solution: J. YPERMAN, J. MULLENS, J.-P. FRANCOIS and L. C. VAN POUCKE. (3 October 1983)
A sensitive spectrophotometric method for the determination of hydroxylamine with *p*-nitroaniline and *N*-(1-naphthyl)-ethylenediamine: PRATIMA VERMA and V. K. GUPTA. (3 October 1983)
Determination of ascorbic acid using double-intermediate coulometry: CHAO-PING ZHANG, LING HAN and QIAN-WEN WU. (4 October 1983)
Graphical evaluation of complexometric titration curves: JOSE L. GUINON. (4 October 1983)
A study of the reaction of *N*-chlorosuccinimide with indoles and its analytical application: IMADUL ISLAM, D. D. MISRA, R. N. P. SINGH and J. P. SHARMA. (10 October 1983)

Talanta, Vol 30, No 11, p. i, 1983
Pergamon Press Ltd. Printed in Great Britain

PAPERS RECEIVED

Thermodesorptive analysis of GaAs and ZnSe surfaces: I. A. KIROVSKAYA, G. M. ZELYEVA and A. V. YURYEVA. (2 August 1983)
Titrimetric determination of phenol, resorcinol and phloroglucinol: D. AMIN and W. A. BASHIR. (2 August 1983)
Rapid photometric determination of phosphorus in iron ores and related materials as phosphomolybdenum blue: OM P. BHARGAVA and MICHAEL GMITRO. (3 August 1983)
Determination of arsenic by polyurethane foam extraction and X-ray fluorescence: A. S. KHAN and A. CHOW. (3 August 1983)
Organization and evaluation of interlaboratory comparison studies among Southern African water analysis laboratories: R. SMITH. (3 August 1983)
Molecular absorption spectrometry by electrothermal evaporation in the graphite furnace—X: Determination of chloride traces by A1C1-MA in graphite cuvettes after liquid–liquid extraction of chloride with triphenyltin hydroxide: K. DITTRICH, B. YA. SPIVAKOV, V. M. SHKINEV and G. A. VOROB'EVA. (8 August 1983)
Determination of free acidity in antimony chloride solutions: S. C. SOUNDAR RAJAN. (8 August 1983)
Open wet ashing of biological materials for the determination of mercury and other toxic elements: H. F. HAAS and V. KRIVAN. (8 August 1983)
Palladium complexes with triethylenetetraaminehexa-acetic acid: ALDO NAPOLI. (8 August 1983)
Detection and determination of phenylhydrazine: N. KRISHNA MURTY, V. JAGANNADHA RAO and N. V. SRINIVASA RAO. (8 August 1983)
Analytical applications of liquid–liquid phase equilibria: Analysis of binary mixtures of chemically similar components: S. K. SURI and MOHINDER PAL. (9 August 1983)
Oxidation–reduction reactions and the analysis of thioureas, hydrazines and ascorbic acid in fused monobromoacetic acid as a non-aqueous solvent—Part IV: J. K. PURI, JASWINDER KAUR, VIJAY SHARMA and JACK M. MILLER. (10 August 1983)
Differential pulse polarographic determination of nitrate in environmental materials: HIROTOSHI HEMMI, KIYOSHI HASEBE, KUNIO OHZEKI and TOMIHITO KAMBARA. (12 August 1983)
2-(4-Arsenophenyl)azo-7-(4-antipyril)azo-1,8-dihydroxy-3,6-naphthalene disulphonic acid, as a spectrophotometric reagent and metallochromic indicator for Bi(III): J. AZNAREZ ALDUAN and A. LOPEZ MOLINERO. (12 August 1983)
A continuous dilution calibration technique for flame atomic-absorption spectrophotometry: J. F. TYSON and J. M. H. APPLETON. (15 August 1983)
The determination of formaldehyde—A review of the methods available for trace analysis: A. D. PICKARD and E. R. CLARK. (15 August 1983)
Gravimetric determination of the mutual abundance of zirconium and hafnium, based on the *in situ* thermal decomposition of $K_4[Zr, Hf)(C_2O_4)_4]\cdot 5H_2O$: TOMITARO ISHIMORI, MASATOMI SAKAMOTO and TADAO WATANABE. (19 August 1983)
Analysis of equilibrium in heme model systems, by a successive linear regression method: LUIZ A. MORINO and HENRIQUE E. TOMA. (19 August 1983)

Talanta, Vol 30, No. 10, p. i, 1983
Pergamon Press Ltd Printed in Great Britain

PAPERS RECEIVED

Determination of hexacelsian by infrared spectroscopy: MA. CARMEN GUILLEM VILLAR and CLAUDIO GUILLEM MONZONÍS. (30 June 1983)

A new procedure for the separation of enamel and dentin in human teeth: BRUCE R. SMITH, CAROLE YOUNGBERG, DENNIS FINTON, DAVID WILLEY, THEODORE R. WILLIAMS and JANET B. VAN DOREN. (20 June 1983)

Background current subtraction in voltammetric detection for flow-injection analysis: JOSEPH WANG and HOWARD D. DEWALD. (30 June 1983)

A note on the INT-reducing property of the organophosphate pesticide malathion: N. S. SRIKANTH, M. V. BHARANIKUMAR, P. SATYAM and V. CHANDRASEKHARAM. (4 July 1983)

Coulometric titrations by a controlled-potential pulsed-charge technique with potentiometric end-point detection of acid–base precipitation and homogeneous redox systems: THEOLOGOS ANDRONIDIS, ANNA MARIA GHE and SERGIO VALCHER. (4 July 1983)

Simplified analyses of polycyclic aromatic hydrocarbons: MICHAEL J. AVERY, JOHN J. RICHARD and GREGOR A. JUNK (20 April 1983)

Spectrophotometric determination of hydrogen peroxide and peroxidase activity of food stuffs: CH. SURYAPRAKASA SASTRY, K. V. S. S. MURTY and M. VEERABHADRA RAO. (7 July 1983)

A new spectrophotometric method for assay of chloramphenicol: R. C. HIREMATH and S. M. MAYANNA. (7 July 1983)

Extraction of metals with carboxylic acids—A review: DEVENDRA SINGH, BINA GUPTA and S. N. TANDON. (13 July 1983)

Binary data acquisition from instrumentation with BDC-coded output: A hardware converter and an example of the relative software control: L. LAMPUGNANI, D. GUIDARINI and N. FANELLI. (13 July 1983)

Uranyl complexes of diaminoalkanetetra-acetic acids: M. L. SIMÕES GONÇALVES, A. M. ALMEIDA MOTA and J. J. R. FRAUSTO DA SILVA. (13 July 1983)

Influence and role of metal ions on the enzymatic catalysis of E.C. 1.2.3.2. xanthine oxidase: Application to metal trace analysis: ANNA MARIA GHE, CLAUDIO STEFANELLI and DANIELA CARATI. (13 July 1983)

Thin-layer potentiometric detection of anticardiolipin antibodies in syphilis serology by means of an ion-selective electrode: YOSHIO UMEZAWA, SUSUMU SOFUE and YOSHIAKI TAKAMOTO. (13 July 1983)

New quantitative estimations of phosphorus, arsenic and zinc with 1,3-dimorpholinopropane: TAJ ALI and IMDADULLAH. (15 July 1983)

Etude par spectroscopie Raman du chlorhydrate de cocaine: A. P. GAMOT, G. VERGOTEN and G. FLEURY. (18 July 1983)

Etude par spectrométrie Raman de corticosteroides dérivés de la fluocortolone: Triméthylacétate et caproate: A. P. GAMOT, G. VERGOTEN, M. SAUDEMON and G. FLEURY. (18 July 1983)

La microscopie Raman: un nouvel outil analytique. Son utilisation dans l'identification du triméthylacétate et du caproate de fluocortolone isolés d'une forme galénique: A. P. GAMOT, G. VERGOTEN, M. SAUDEMON and G. FLEURY. (18 July 1983)

New spectrophotometric determination of exchangeable calcium with khimduchlorophosphonazo I: QIU XING-CHU, ZHU YING-QUAN and ZHANG YU-SHENG. (18 July 1983)

Spectrophotometric determination of phenothiazines, tetracyclines and chloramphenicol with sodium cobaltinitrite: M. S. MAHROUS and M. M. ABDEL-KHALEK. (18 July 1983)

Multiparametric curve fitting—V: General ABLET program, the system for regression analysis in solution equilibria studies: MILAN MELOUN and JOSEF ČERMÁK. (22 July 1983)

Determination of micro amounts of uranium by the molybdenum blue method: V. K. BHARGAVA, M. S. OAK, A. R. JOSHI and V. B. SAGAR. (22 July 1983)

Investigation of contributions to physical dispersion in flow injection systems: E. H. RUDOLF VON BARSEWISCH, ROBERT A. HASTY and RAY M. A. VON WANDRUSZKA. (1 August 1983)

Dosage de dérivés de l'acide phenylpropionique a activité pharmacologique par titrage coulométrique: G. KANOUTE, E. NIVAUD, B. PAULET and P. BOUCLY. (8 July 1983)

Determination polarographique de facteurs vitaminiques P: Rutine et ses dérivés: F. FAHRAT, M. KALLEL, D. CANTIN, A. CAIOLA and J. ALARY. (8 July 1983)

Sampling and analysing mixtures of sulphate, sulphite, thiosulphate and polythionate: CARL O. MOSES, D. KIRK NORDSTROM and AARON L. MILLS. (15 July 1983)

Talanta, Vol. 30, No 9, p. i, 1983
Pergamon Press Ltd. Printed in Great Britain

PAPERS RECEIVED

Extractive-fluorimetric determination of ultratraces of lead with 18-crown-6 and eosin: A. SANZ-MEDEL, D. BLANCO GOMIS, E. FUENTE and S. ARRIBAS JIMENO. (7 June 1983)
Simultaneous determination of glass electrode parameters and protonation constants: PETER M. MAY. (7 June 1983)
The pH-dependence of the UV spectrum of the linear bonding P–P hexamer oxoanion: TOSHIO NAKASHIMA and HIROHIKO WAKI. (9 June 1983)
Some applications of ligand–exchange—III: Preparation and properties of phenol–formaldehyde resin in the iron(III) form: B. M. PETRONIO and A. LAGANÀ. (14 June 1983)
A study of the conditions for the quantitative reaction between 2,4-dinitro-1-chlorobenzene and amines: ABDEL FATTAH A. MOUSA and M. M. AYAD. (14 June 1983)
Adsorption behaviour of bismuth on hydrous lead dioxide, from bismuth–EDTA solution: SHINICHI ITO, TOSHIO MATSUDA and TOYOSHI NAGAI. (14 June 1983)
Flow enthalpimetric determination of glucose, based on oxidation by 1,4-benzoquinone with use of an immobilized glucose oxidase column: NOBUTOSHI KIBA, TOSIMITSU and MOTOHISA FURUSAWA. (14 June 1983)
A new functional resin for the selective collection of selenium(IV), prepared by the conversion of anion-exchange resin with bismuthiol-II: MORIO NAKAYAMA, KAZUO ITOH, MASAHIKO CHIKUMA, HIROMU SAKURAI and HISASHI TANAKA. (15 June 1983)
Determination of uranium in wet phosphoric acid: HELENA GÓRECKA and HENRYK GÓRECKI. (3 May 1983)
Selenium in human urine: Determination, speciation and concentration levels: H. J. ROBBERECHT and H. A. DEELSTRA. (17 June 1983)
Rapid assays based on immobilized bioluminescent enzymes and photographic detection of light emission: K. GREEN, L. J. KRICKA, G. H. G. THORPE and T. P. WHITEHEAD. (20 June 1983)
An enzyme-catalysed method for the determination of mercury traces in carbonated soft drinks, by the Hg^{2+} inhibition of β-fructofuranosidase: J. MASŁOWSKA and J. LESZCZYŃSKA. (20 June 1983)
Thallimetric oxidations—III: Estimation of malonic acid. S. R. SAGI, K. APPA RAO and M. S. PRASADA RAO. (22 June 1983)
Determination of total tin in geological materials by electrothermal atomic-absorption spectrophotometry with a tungsten-impregnated graphite furnace: LIYI ZHOU, T. T. CHAO and A. L. MEIER. (23 June 1983)
Solvent extraction–spectrophotometric determination of phosphate with molybdate and Malachite Green in river and sea waters: SHOJI MOTOMIZU, TOSHIAKI WAKIMOTO and KYOJI TÔEI. (23 June 1983)
Investigation on the use of thermometric titrimetry for the determination of acidic substances in wine: O. E. S. GODINHO, J. A. COELHO, A. P. CHAGAS and L. M. ALEIXO. (24 June 1983)
Twin-spray flame atomic-absorption spectrometric determination of antimony, bismuth and mercury in geochemical samples: XIAN-AN YU, GAO-XIANG DONG and CHUN-XUE LI. (24 June 1983)
Potentiometric determination of plutonium by sodium bismuthate oxidation: M. M. CHARYULU, V. K. RAO and P. R. NATARAJAN. (24 June 1983)

Talanta, Vol. 30, No. 8, p. i, 1983
Pergamon Press Ltd. Printed in Great Britain

PAPERS RECEIVED

Selective and sensitive spectrophotometric method of determination of copper(II) in basic medium with TQA (Indcop): ANIL KUMAR CHAKRABARTI. (10 May 1983)
Pyrocatecholsulphonphthalein complexan as an analytical reagent: RU-QIN YU, ZHENG-QI ZHANG and ZHI-HUA ZHANG. (10 May 1983)
Determination by HPLC of trifluoroacetic levels in plasma and urine of patients anesthetized with halothane: M. IMBENOTTE, A. BRICE, F. ERB and J. M. HAGUENOER. (11 May 1983)
A sensitive chiral determination of heroin by means of induced cholesteric mesophases: GIOVANNA BERTOCCHI, GIOVANNI GOTTARELLI and ROMANO PRATI. (12 May 1983)
Electrochemical studies on micellar solutions: WAHID U. MALIK and M. J. JOSEPH. (12 May 1983)
Determination of bismuth(III) by direct potentiometry and potentiometric titration by means of a bismuth ion-selective electrode: WALENTY SZCZEPANIAK and MARIA REN. (13 May 1983)
Acidity constants, neutralization enthalpies and some reactions of 3-styryl, 2-mercaptopropenoic and 3-(1-naphthyl)-2-mercaptopropenoic acids: A. IZQUIERDO, E. BOSCH and J. L. BELTRAN. (17 May 1983)
A programmable positioning stepper-motor controller with a multibus/IEEE 796 compatible interface: P. PAPOFF and D. RICCI. (17 May 1983)
The surfactant-sensitized analytical reaction of niobium with 8-hydroxyquinoline-5-suiphonic acid: J. I. GARCIA ALONSO, M. E. DIAZ GARCIA and A. SANZ MEDEL. (17 May 1983)
Method of sample digestion: An important factor in the determination of metallic elements by atomic-absorption spectrophotometry: JULIUS YINKA OLAYEMI and KEHINDE OLOLADE OSIPITAN. (18 May 1983)
Well defined conditions for the analysis of trioctylamine by gas–liquid chromatography: AMER M. AL-ANI. (18 May 1983)
The use of simplex optimization in the calculation of proton dissociation constants: JOHN D. STONG. (6 May 1983)
Determination of indium and thallium by hydride generation and atomic-absorption spectrometry: DU YAN, ZHANG YAN, GUANG-SHEN CHENG and AN-MO LI. (23 May 1983)
An investigation of the conditions for the titrimetric determination of cadmium with use of a cadmium ion-selective electrode: GÜLER SOMER. (24 May 1983)
Determination of low levels of bromide in fresh water after chromatographic enrichment: ULLA LUNDSTRÖM, ÅKE OLIN and FOLKE NYDAHL. (24 May 1983)
Preconcentration techniques for trace element analysis of water: N. KALLITHRAKAS-KONTOS and A. A. KATSANOS. (24 May 1983)
Extraction of ruthenium thiocyanate and its separation from rhodium by polyurethane foam: SARGON J. AL-BAZI and ARTHUR CHOW. (24 May 1983)
Interaction of zinc(II) and copper(II) with soil-derived humic acid, as investigated by flotation: S. SAITO, M. SUGAWARA and T. KAMBARA. (25 May 1983)
Verification of certified sulphur values in steel reference materials by isotope-dilution mass-spectrometry, and characterization of sulphur present on solid samples: KAZUO WATANABE. (27 May 1983)
Comparison of silver results for Canadian reference ores and concentrates and zinc processing products by acid-decomposition/, tribenzylamine–chloroform extraction/ and fire-assay/atomic-absorption spectrophotometric methods: ELSIE M. DONALDSON, E. MARK and MAUREEN E. LEAVER. (1 June 1983)
Rapid spectrophotometric determination of osmium with 1,3-cyclohexanedione bis(thiosemicarbazone) monohydrochloride: Simultaneous determination of osmium and platinum: K. HUSSAIN REDDY and D. VENKATA REDDY. (1 June 1983)
Synergic extraction and spectrophotometric determination of copper(II) with pyrimidinethiol: M. A. ANUSE and M. B. CHAVAN. (3 June 1983)
Formation and reduction of molybdothorophosphoric acid: M. BALON and M. A. MUNOZ. (6 June 1983)
High-pressure liquid chromatographic determination of some 1,4-benzodiazepines and their metabolites in biological fluids: A review: ANIL C. MEHTA. (6 June 1983)

Talanta, Vol. 30, No. 7, p. i, 1983
Pergamon Press Ltd. Printed in Great Britain

PAPERS RECEIVED

A sensitive spectrophotometric method for the determination of methyl alcohol in air and water: PRATIMA VERMA and V. K. GUPTA. (30 March 1983)
Improvement of end-point detection in the non-aqueous titration of sulphacetamide sodium: SOBHI A. SOLIMAN, SAIED BELAL and MONA BEDAIR. (30 March 1983)
Molecular absorption spectrometry by electrothermal evaporation in a graphite furnace—IX. Determination of bromide traces by AlBr molecular absorption in graphite cuvettes after liquid–liquid extraction of bromide with triphenyltin hydroxide: K. DITTRICH, B. YA. SPIVAKOV, V. M. SHKINEV and G. A. VOROB'EVA. (8 April 1983)
Application of matrix modification technique for the determination of thallium in waste water by graphite furnace atomic-absorption spectrometry: SHAN XIAO-QUAN, NI ZHE-MING and ZHANG LI. (8 April 1983)
Addition of sodium dodecyl sulphate to clarify the end-point of anodic-stripping complexometric titration curves: S. TANAKA, Y. MORIMOTO, M. TAGA and H. YOSHIDA. (11 April 1983)
Heavy-metal analysis of sediments in the Tejo Estuary, Portugal, by a rapid flameless atomic-absorption procedure: M. J. T. CARRONDO, F. REBOREDO, R. M. B. GANHO and J. F. S. OLIVEIRA. (11 April 1983)
A contribution to the use of Thorin as an analytical reagent: spectrophotometric study of the complexation with barium and application to sulphate detection in atmospheric particulates: P. BRUNO, M. CASELLI, A. TRAINI and A. ZUFFIANÒ. (11 April 1983)
2-(8-Quinolylazo)-7-phenylazochromotropic acid as an analytical reagent: RU-QIN YU, ZHI-HUA ZHANG and YA-WEN LI. (11 April 1983)
Influence of volatile hydride-forming elements on antimony determination with atomic-absorption spectrometry by the hydride generation technique: LAURI H. J. LAJUNEN, TIMO MERKKINIEMI and HANNU HÄYRYNEN. (14 April 1983)
Arc emission spectrographic determination of common and refractory elements in U_3O_8 with a mixed carrier: $AgCl + SrF_2$: M. K. BHIDE, VIJAYALAXMI R. BHANDIWAD and MITHLESH KUMAR. (20 April 1983)
Comparison of sub- and super-equivalence and substoichiometric isotope-dilution analysis for the determination of a trace amount of antimony: H. YOSHIOKA and T. KAMBARA. (21 April 1983)
GC/MS determination of incidental PCBs in complex chlorinated hydrocarbon process and waste streams: RANDLE S. COLLARD and MORRIS M. IRWIN, JR. (28 March 1983)
Titrimetric determination of some phenothiazine derivatives with ferricyanide: A. S. ISSA and M. S. MAHROUS. (21 April 1983).
Spectrophotometric determination of tranexamic acid with chloranil: ABDEL-AZIZ M. WAHBI, ESSAM A. LOTFI and HASSAN Y. ABOUL-ENEIN. (22 April 1983)
A pyrolytic carbon film electrode for voltammetry—III: Application to anodic-stripping voltammetry: INGEMAR GUSTAVSSON and KENT LUNDSTRÖM. (22 April 1983)
Selective cation-exchange separation of bismuth on a zirconium hexacyanoferrate(III) column: AJAY K. JAIN, RAJ P. SINGH and CHAND BALA. (25 April 1983)
Gel speciation studies—I: The intrinsic dissociation constant of weakly acidic cation-exchange gels: YVES MERLE and JACOB A. MARINSKY. (25 April 1983)
A comparative study of flame atomic-absorption methods for zinc determination in serum and blood plasma: M. J. SORIANO and M. DE LA GUARDIA. (26 April 1983)
Analytical properties of pyridylhydrazones derived from cyclohexanone, 1,2-cyclohexanedione and 1,3-cyclohexanedione: D. ROSALES, J. A. MUNOZ LEYVA and J. L. GOMEZ ARIZA. (26 April 1983)
Investigation of two multichannel image detectors for use in spectroelectrochemistry: MARY LOU FULTZ and RICHARD A. DURST. (26 April 1983)
Electrodeposition of Cu and Ag from solutions of μg/ml concentration, monitored by inductively-coupled plasma spectrometry: ROMAN E. SIODA. (27 April 1983)
Charge-transfer complexes of a new trinitroanisole-derivative with organic electron-donors: G. HAESEN, B. LE GOFF and P. GLAUDE. (27 April 1983)
Spectrophotometric determination of iron(II) after separation by adsorption of its ternary complex with 3-(4-phenyl-2-pyridyl)-5,6-diphenyl-1,2,4-triazine and tetraphenylborate on microcrystalline naphthalene: TORU NAGAHIRO, KATSUYA UESUGI, M. C. MEHRA and MASATADA SATAKE. (28 April 1983)
Separation and concentration of molybdenum and tungsten with chelating ion-exchange resins containing sulphur ligands: CHUEN-YING IU and PENG-JOUNG SUN. (29 April 1983)
Volumetric microdetermination of antihypertensive drugs with potassium hexacyanoferrate(III) and *N*-chlorosuccinimide: M. K. SRIVASTAVA, S. AHMAD, D. SINGH and I. C. SHUKLA. (4 May 1983)
Determination of isocyano groups on polymer supports by bromination: REZA ARSHADY and IVAR UGI. (4 May 1983)
Hydrogen peroxide–iodide reaction of Landolt type applied to the catalytic determination of molybdenum(VI) by means of an iodide ion-selective electrode: M. KATAOKA, K. NISHIMURA and T. KAMBARA. (4 May 1983)
Spectrophotometric determination of iron with 1-hydroxy-4-sulpho-2-naphthoic acid in the presence of Mn(II), Cr(III) and Pb(II): LAURI H. J. LAJUNEN, EERO AITTA and VEIJO MÄKÄRÄINEN. (5 May 1983)
Sorption–desorption studies of malathion on activated charcoal in different waters: S. R. SHARMA, H. S. RATHORE, I. ALI and S. R. AHMED. (6 May 1983)
Determination of cadmium(II) at a gold electrode in the presence of selenium(IV) by enhancement with iodide and anodic-stripping voltammetry: CUI CHUNGUO. (6 May 1983)
Detection limits and sample/surface interactions in quantitative NCI mass spectrometry: Ultratrace analysis of derivatized metals and metal-derivatized analytes: I. K. GREGOR and M. GUILHAUS. (6 May 1983)
Structure-ionization relationship of tyrosine-containing peptides: T. ISHIMITSU and H. SAKURAI. (6 May 1983)

Talanta, Vol. 30, No. 6, p. I, 1983
Pergamon Press Ltd. Printed in Great Britain

THE LOUIS GORDON MEMORIAL AWARD

The Editorial Board and Publisher of *Talanta* take great pleasure in announcing that the Louis Gordon Memorial Award for 1982 (for the paper judged to be the best written of those appearing in *Talanta* during the year) will be made to Mr. N. A. Dimmock and Dr. D. Midgley, of the Central Electricity Research Laboratories, Leatherhead, England, for their paper "Performance of the Orion 97-70 total residual chlorine electrode at low concentrations and its application to the analysis of cooling waters" (*Talanta*, 1982, **29**, 557).

THE PHARMACIA PRIZE

Pharmacia AB (Uppsala, Sweden) and the Editorial Board and Publisher of *Talanta* take great pleasure in announcing that the Pharmacia Prize for 1981–1982 (for the paper published in *Talanta* that was judged to be the best contributed from an industrial laboratory) has been awarded to Dr. Thomas R. Dulski, Carpenter Technology Corp., Reading, PA, U.S.A., for his paper "A rapid procedure for the simultaneous determination of zirconium and hafnium in high-temperature alloys by means of a spectrophotometric masking approach" (*Talanta*, 1982, **29**, 467).

Talanta, Vol. 30, No. 6, p. i, 1983
Pergamon Press Ltd. Printed in Great Britain

PAPERS RECEIVED

Spectrophotometric studies on ion-pair extraction equilibria of iron(II)– and **iron(III)–4-(2-pyridylazo)resorcinol chelates:** HITOSHI HOSHINO and TAKAO YOTSUYANAGI. (8 March 1983)
Subtractive differential pulse voltammetry following adsorptive accumulation of organic compounds: JOSEPH WANG and BASSAM A. FREIHA. (9 March 1983)
A new method of determination of the equivalence point, in application to potentiometric titration of trace amounts of halide and SCN^- ions: TADEUSZ MICHAŁOWSKI. (9 March 1983)
Comprehensive determination of precious metals in geological materials by flameless A. A. spectroscopy: G. P. SIGHINOLFI, C. GORGONI and A. H. MOHAMED. (9 March 1983)
Determination of ultratrace concentrations of nitrite in polluted waters and soil: ABHA CHAUBE, ANIL K. BAVEJA and V. K. GUPTA. (11 March 1983)
Liquid-liquid extraction of zinc(II) with potassium ethyl xanthate: A. K. CHAKRAVARTI, S. MUKHERJEE, H. K. SAHA and T. CHAKRABARTY. (11 March 1983)
Determination of manganese in natural waters by differential pulse polarography: M. P. COLOMBINI and R. FUOCO. (11 March 1983)
Fluorescence properties of some Schiff bases derived from 3-hydroxypyridine-2-aldehyde and their metal chelates. Fluorimetric determination of manganese based on its catalytic effects on the oxidation of these compounds with hydrogen peroxide: J. VAZQUEZ RUIZ, A. GARCIA DE TORRES and J. M. CANO-PAVON. (15 March 1983)
Use of a manganese oxide column in the flow enthalpimetric determination of hydrogen peroxide: NOBUTOSHI KIBA, KAZUHITO SHIMIZU and MOTOHISA FURUSAWA. (15 March 1983)
Modified normal pulse polarography of alkali-metal ions in acid solution: MINORU HARA and NOBORU NOMURA. (15 March 1983)
Determination of thallium in cadmium and lead by graphite furnace–atomic absorption spectrometry with sample vaporization from a platform: JÁNOS FAZAKAS and DAN MARINESCU. (15 March 1983)
Laboratory data-acquisition capabilities of microcomputer high-level languages: R. L. A. SING, S. W. MCGEORGE and E. D. SALIN. (16 March 1983)
Study of 1,4-dihydroxyanthraquinone as an acid–base indicator in propan-2-ol medium: Evaluation of colour-change limits through complementary chromaticity parameters: J. BARBOSA, J. SANCHEZ and E. BOSCH. (16 March 1983)
Highly selective determination of trace metal ions with 2,2′-dihydroxyazobenzene by ion-pair reversed-phase partition HPLC–spectrophotometric detection system: HITOSHI HOSHINO and TAKAO YOTSUYANAGI. (18 March 1983)
Differenzspektroskopische und pulspolarographische Untersuchungen zur Zusammensetzung der Kupfer–Alizarin S-Komplexe: TH. PRANGE, H. D. SOMMER and F. UMLAND. (21 March 1983)
Refinement of structures proposed previously for gum arabic and other acacia gum exudates: C. A. STREET and D. M. W. ANDERSON. (21 March 1983)
Evaluation of activity of magnetically treated water: VĚNCESLAV PATROVSKÝ. (21 March 1983)
A new spectrophotometric method for the determination of citric acid in water: H. S. RATHORE, S. K. SHARMA and KUSUM KUMARI. (21 March 1983)
Formation d'un chélate cuivre-vancomycine: Application au dosage de l'antibiotique en flux continu et détection ampèrométrique: CH. CHABENAT, D. ANDRE and P. BOUCLY. (22 March 1983)
The determination of stability constants of ternary complexes with the isosbestic point—spectrophotometric method—I: the copper–bipyridyl–Eriochrome Cyanine R system: SHI-FU ZOU and WEI-AN LIANG. (23 March 1983)
Unexpected dependence of the protonation constant of 2,2′-bipyridyl on ionic strength: KLÁRA SZABÓ, ISTVÁN NAGYPÁL and ISTVÁN FÁBIÁN. (23 March 1983)
Coulometric separation and titration of metal ions by means of controlled potential charge-pulse potentiometric technique: THEOLOGOS ANDRONIDIS, ANNA MARIA GHE, CESARE PAGURA and SERGIO VALCHER. (23 March 1983)
Sieve effect on filtration through membrane filters: MANABU IGAWA, TOMOKO HIYORI and MASAO TANAKA. (24 March 1983)
Anion-exchange detection of phenols and specific spectrophotometric determination of catechol: MOHSIN QURESHI, K. M. SHAMSUDDIN, PUSHKIN M. QURESHI and SYED ALI. (25 March 1983)
Application of ICAP–AES for the determination of Dy, Eu, Gd, Sm and Th in uranium after chemical separation: T. K. SESHAGIRI, Y. BABU, M. L. JAYANTH KUMAR, A. G. I. DALVI, M. D. SASTRY and B. D. JOSHI. (25 March 1983)
The use of an electrostatic preconcentration system to identify interferences: PAULA A. MICHALIK and ROGER STEPHENS. (25 March 1983)
The bilayer lipid membrane as a basis for a selective sensor for ammonia: MICHAEL THOMPSON, ULRICH J. KRULL and LEAH I. BENDELL-YOUNG. (28 March 1983)
Kinetic-spectrophotometric determination of Cu(II) and pyridine by using aerial oxidation of dimedone bisguanylhydrazone: F. SALINAS LOPEZ, J. J. BERZAS NEVADO and A. ESPINOSA MANSILLA. (29 March 1983)
Critical examination of the reducing properties of some common reductants for selenium species used in chemical analysis: RAGNAR BYE. (29 March 1983)

Talanta, Vol 30, No 5, p i, 1983
Pergamon Press Ltd Printed in Great Britain

PAPERS RECEIVED

A simultaneous multielement non-dispersive atomic-fluorescence spectrometer using modulated sources and frequency-discrimination of fluorescence signals: A D'ULIVO, C FESTA and P PAPOFF (3 February 1983)
Microdetermination of polysaccharide and glycoprotein hydration levels: F B SHERMAN (3 February 1983)
A precise spectrophotometric determination of trace level zirconium: N S B SINGH, T PREM KUMAR and G R BALASUBRAMANIAN (7 February 1983)
Development of a matrix rank method for determining the number of optically absorbing species in solution: A A BUGAEVSKY, N A MARSHALOVA and E YU ZAKHAROVA (7 February 1983)
Spectrophotometric determination of cadmium with 1-(2-pyridylazo)-2-naphthol and non-ionic surfactants: Application to acetic acid extracts of ceramic enamels: J MEDINA ESCRICHE, M LLOBAT ESTELLES and F BOSCH REIG (7 February 1983)
Polarographic behaviour of some arylazopyrimidines and their metal complexes: RAJEEV JAIN (8 February 1983)
Laser-excited fluorescence line-narrowing: Analytical figures of merit: D BOLTON and J D WINEFORDNER (10 February 1983)
Elektrochemische Untersuchung von bis(Diphenyldithiophosphin) Disulphid: ANGEL SCHISCHKOV, SHIVKO DENTSCHEV and CHRISTINA MALAKOVA (11 February 1983)
Determination of arsenic by galvanostatic stripping analysis and its application to steels: JIŘÍ LEXA and KAREL ŠTULÍK (11 February 1983)
The determination of chloride, nitrate, sulphate and total sulphur in environmental samples by single-column ion-chromatography: J A HERN, G K RUTHERFORD and G W VANLOON (15 February 1983)
Séparation et identification des produits d'hydrolyse de la tetryzoline: A NICOLAS, J M ZIEGLER and M MIRJOLET (15 February 1983)
Material consumption in spark-source mass-spectrometry: J VAN PUYMBROECK, J VERLINDEN and R GIJBELS (16 February 1983)
Complex formation of iron(III) with triphosphate in an aqueous solution: A T ORKUN and AYCA (16 Feburary 1983)
Photometric and fluorimetric kinetic determination of manganese, based on the oxidation of an anthraquinone-type compound: A NAVAS DIAZ and F SANCHEZ ROJAS (16 February 1983)
Application of personal microcomputers in the analytical laboratory—II. Long-term monitoring and control: HUGO GUTERMAN and SAM BEN-YAAKOV (16 February 1983)
Extraction of Catechol Violet, Chrome Azurol S and Eriochrome Cyanine R with chloroform solutions of liquid anion-exchangers: S PRZESZLAKOWSKI and H WYDRA (17 February 1983)
Infrared field method for natural seep-oil identification: DOUGLAS F GRANT and DELYLE EASTWOOD (17 February 1983)
Copper(II) metformin hydrochloride complexes and their utility for spectrophotometric determination of copper(II): FARAG AHMED ALY, MOHAMED A EL RYES and F EL-GHNDOUR (17 February 1982)
The development of sampling and gas chromatography–mass spectrometry analytical procedures to identify and determine the minor components of landfill gas: B I BROOKES and P J YOUNG (17 February 1983)
Determination of arsenic in geological materials by X-ray fluorescence spectrometry following solvent extraction and filter deposition: A E HUBERT (21 February 1983)
Electrolytic reduction of molybdophosphate in aqueous acetonitrile and its application to a flow-coulometric determination of orthophosphate: T HORI and T FUJINAGA (21 February 1983)
Indirect determination of cyanide in water by atomic-absorption spectrophotometry: XU BO-ZING, XU TONG-MING and FANG YU-ZHI (21 February 1982)
Spectrophotometric determination of Mn(II) with 1-(2-quinolylazo)-2,4,5-trihydroxybenzene: Microdetermination of Mn in foodstuffs: ISHWAR SINGH and Mrs POONAM (23 February 1983)
Spectroscopic analysis of simultaneous protolysis equilibria: JURGEN POLSTER (23 February 1983)
Complexometric titrations controlled by anodic stripping methods—I: Voltammetric stripping: P GRUNDLER (24 February 1983)
Determination of stability constants of complexes of H_2XY type: TADEUSZ MICHAŁOWSKI (25 February 1983)
Method of determination of stability constants of mixed complexes of $Na_iK_jH_kL$ and $Me(OH)_iB_jD_k$ type: TADEUSZ MICHAŁOWSKI (25 February 1983)
Diffusion coefficients and complex equilibria in solution—III: Graphical evaluation of formation constants from diffusion coefficients: D R CROW (28 February 1983)
The density of 4-aminopyridine, voids in crystals, and precision weighing: HARVEY DIEHL and DONALD L BIGGS (28 February 1983)
Cation-exchange behaviour of the platinum group and some other rare elements in hydrobromic acid–thiourea–acetone media: C H -SIEGFRIED W WEINERT and FRANZ W E STRELOW (28 February 1983)
Ion-chromatographic determination of metal ions in plating solutions and waste water: TAKASHI TANAKA, KAZUO HIIRO, AKINORI KAWAHARA and SHINICHI WAKIDA (1 March 1983)
Procedures for isolation and determination of thorium: ALAN D WESTLAND and CHIRAN J KANTIPULY (1 March 1983)
Gas chromatographic determination of the product distribution in the synthesis of sodium borohydride: TAPIO SALMI (1 March 1983)
Logarithmic diagrams for redox titrations: CARLO MACCÀ and G GIORGIO BOMBI (2 March 1983)
2-Thio-orotic acid as a new spectrophotometric reagent for the estimation of nickel(II): MADHULIKA SHRIVASTAVA and G S PANDEY (4 March 1983)
Some remarks on the information power and selectivity of analytical processes: J INCZÉDY (7 March 1983)
The use of emulsions in the preparation of samples and standards for analysis by atomic-absorption spectroscopy: Determination of Cu and Fe in extracts of their complexes with APDC in MIBK: M DE LA GUARDIA and M T VIDAL (7 March 1983)

Talanta, Vol 30, No. 4, p. i, 1983
Pergamon Press Ltd. Printed in Great Britain

PAPERS RECEIVED

Electrolytic separation of microquantities of lead: R. BULAJIĆ, V. VAJGAND and M. TODOROVIĆ. (11 January 1983)
A simple titrimetric method for the determination of antimony in white metal: K. SRIRAMAM, A. R. K. VARA PRASAD and P. RAVINDRANATH. (11 January 1983)
Electrochemical behaviour of cobalt and nickel at the dropping mercury electrode with ϵ-caprolactam: B. K. PURI and AHSOK KUMAR. (11 January 1983)
Determination of water in ethanol and acetone by direct injection enthalpimetry using the heat of dilution: WALLACE A. DE OLIVEIRA and CELIO PASQUINI. (12 January 1983)
Extractive spectrophotometric determination of osmium with 1-phenyl-4,4,6-trimethyl(1H, 4H)-2-pyrimedinethiol into molten naphthalene: A. WASEY, R. K. BANSAL, A. L. J. RAO and B. K. PURI. (13 January 1983)
Solubility and protonation of EDTA, DCTA and DPTA in acidic perchlorate medium: J. KRAGTEN and L. G. DECNOP-WEEVER. (14 January 1983)
Analysis of samples of vegetable origin for phosphorus by mineralization with molten alkali and spectrophotometric determination: J. V. GIMENO ADELANTADO, F. BOSCH REIG, A. PASTOR GARCIA and V. PERIS MARTINEZ. (14 January 1983)
Determination of micro amounts of oxygen in silicon: HE HUANNAN, LI YUEZHEN, ZHAO GUANDI, YAN RONGHUA, LU QINGREN and QI MINGWEI. (14 January 1983)
An improved, automated Xylenol Orange method for the colorimetric determination of aluminium: ANTHONY C. EDWARDS and MALCOLM C. CRESSER. (14 January 1983)
Use of *N*-phenyl-laurohydroxamic acid for selective absorptiometric determination of titanium(IV): H. D. GUNAWARDHANA and K. C. UDUMAN. (17 January 1983)
Reinvestigation of a procedure for determining low levels of nitrate in natural waters: H. D. GUNAWARDHANA, A. M. KUMUDINI and R. ADIKARI. (17 January 1983)
Polarographic study on simple and mixed-ligand complex formation: P. H. TEDESCO and J. MARTINEZ. (20 December 1982)
A measuring stick for hydroxide: THOMAS GAROFF. (18 January 1983)
Ein neues graphisches Auswerteverfahren zur Ermittlung stöchiometrischer Faktoren gelöster Komplexe: TH. PRANGE, U. LECHNER-KNOBLAUCH and F. UMLAND. (18 January 1983)
Kinetic determination of cobalt(II) by its catalytic effect on the atmospheric oxidation of 1,3-cyclopentanedione *bis*(4-methylthiosemicarbazone) monohydrochloride: M. ROMAN CEBA, J. C. JIMENEZ SANCHEZ and T. GALEANO DIAZ. (19 January 1983)
Paper chromatographic behaviour of some tertiary amine pollutants and an attempt at structure–activity-correlation: PUSHKIN M. QURESHI and AFSAR N. SULAIMAN. (20 January 1983)
Indirect spectrophotometric determination of cyanide by colour reaction of silver with Cadion 2B in presence of Triton X-100: ZHU YU-RUI, WEI FU-SHENG and YIN FANG. (21 January 1983)
Stability constants and thermodynamic functions of cobalt(II) and nickel(II) chelates formed with 8-quinolinyl monoethyl orthophosphate: M. F. EL-SHAHAT, E. EL-SAWI, M. Z. MOSTAFA and M. MONSHI. (21 January 1983)
Seasonal variations in groundwater quality: GEORGE W. HEUNISCH and DAVID L. WARDER. (22 December 1982)
Equilibrium and calorimetric study of the hydration of anion-exchange resins: A. MARTON, É. KOCSIS and J. INCZÉDY. (25 January 1983)
Separation of mercury(II), copper(II) and silver(I) as nitrite complexes by anion-exchange chromatography: S. O. AJAYI and N. U. EZEKWE. (25 January 1983)
Trace metal assay of U_3O_8 powder electrothermal AAS: S. S. SHELAR and B. D. JOSHI. (25 January 1983)
Studies of the oxidation of iminodiacetic acid (IDA) and nitrilotriacetic acid (NTA) with lead dioxide suspension in nitric acid: TOSHIO MATSUDA and TOYOSHI NAGAI. (25 January 1983)
A polarographic study of some quinone derivatives: S. D. POPESCU. (26 January 1983)
Synthesis, ion-exchange behaviour and analytical applications of Zr–EDTA–PO_4 anion-exchanger: S. Z. QURESHI, VINOD BANSAL and REETA BANSAL. (26 January 1983)
Photochemical analysis studies—V: Photochemical enhancement of the fluorescence signal of antimalarial plasmocid in liquid solution and on silica-gel thin-layers: JEAN-JACQUES AARON, JOELLE FIDANZA and MAME DIABOU GAYE. (28 January 1983)
Fluorimetric kinetic studies and sub-μM determination of aluminium with 2-hydroxy-1-naphthaldehyde *p*-methoxybenzoylhydrazone: P. C. IOANNOU and P. A. SISKOS. (31 January 1983)
Separation and determination of phenylhydrazine-*N*-dithiocarbamates of Ru(III), Rh(III) and Pd(II) from other group VIII metals by thin-layer chromatography and spectrophotometry: NEPAL SINGH, MEENA MEHROTRA, KALPNA RASTOGI and RAVINDRA KUMAR. (2 February 1983)
Determination of thallium in lead salts by differential pulse anodic-stripping voltammetry: Z. ŁUKASZEWSKI. (2 February 1983)

Talanta, Vol. 30, No. 3, p. i, 1983
Pergamon Press Ltd. Printed in Great Britain

PAPERS RECEIVED

Fluorimetric determination of pyrimethamine in tablet preparations of daraprim and fansidar: PYARE PARIMOO. (6 December 1982)

A group separation procedure based on anion- and cation-exchange from HF medium: Application to multielement neutron-activation determination of niobium: R. CALETKA and V. KRIVAN. (6 December 1982)

Pulse polarographic study of zinc bis(*O,O'*-dibutyldithiophosphate) in dimethylformamide: J. L. DESPORTES, J. M. MARTIN and O. VITTORI. (7 December 1982)

A new method for the selective spectrophotometric determination of 2,6-lutidine and its possible use for specific determination of a physiologically important pollutant: PUSHKIN M. QURESHI, MOHSIN QURESHI and AFSAR M. SULAIMAN. (8 December 1982)

Necessary and sufficient conditions for the manifestation of several extrema on concentration distribution curves in complex equilibrium systems: ISTVÁN NAGYPÁL, MIHÁLY T. BECK and ANDREAS D. ZUBERBÜHLER. (9 December 1982)

Synthesis and analytical properties of monobutyl esters of α-(*N*-benzylamino)salicylphosphonic acid and α-(*N*-*p*-chlorobenzylamino)salicylphosphonic acid: JERZY SIEPAK. (10 December 1982)

A liquid-state membrane electrode sensitive to bismuth ions: WALENTY SZCZEPANIAK and MARIA REN. (10 December 1982)

Spectrophotometric determination of zinc with 2-(3,5-dibromo-2-pyridylazo)-5-diethylaminophenol in the presence of anionic surfactant: TAN ZHE and SHUI-SHENG WU. (20 December 1982)

Determination of copper in urine by carbon-furnace atomic-emission spectrometry: J. MARSHALL and J. M. OTTAWAY. (20 December 1982)

Rapid and selective chelatometric titration of zinc in non-ferrous alloys: ZHOU NAN, LU ZHI-REN and GU YUAN-XIANG. (20 December 1982)

Potentiometric titration for the estimation of isomeric xylidines and triethylamine: SNEH BHATLA, M. M. RAI and S. S. SINGH. (20 December 1982)

Semi-Xylenol Orange and its purification by high-pressure liquid chromatography: F. SMEDES, L. G. DECNOP-WEEVER, NGUYEN TRONG UYEN, J. NIEMAN and J. KRAGTEN. (20 December 1982)

Determination of tungstate by laser nephelometry: G. BOISSIER, J. DREUX and O. VITTORI. (20 December 1982)

Spectrophotometric determination of iron(II) after separation by extraction of its ternary complex with 1,10-phenanthroline and tetraphenylborate into molten naphthalene: LIH-FEN CHANG, MASATADA SATAKE, TOORU KUWAMOTO and B. K. PURI. (21 December 1982)

Laser atomic-ionization determination of caesium in flames: V. I. CHAPLYGIN, N. B. ZOROV and YU. YA. KUZYAKOV. (22 December 1982)

Potentiometric titration of sulphate, sulphite and dithionate mixtures, with use of a lead ion-selective electrode: P. A. SISKOS, E. P. DIAMANDIS, E. GILLIERON and JENNIFER C. COLBERT. (22 December 1982)

Method of determination of free acid in presence of hydrolysing salts of MeA_q type—I: Essence of the method: TADEUSZ MICHAŁOWSKI. (23 December 1982)

Spectrophotometric determination of tungsten in geological materials by complexing with dithiol: E. P. WELSCH. (23 December 1982)

Determination of non-sulphide lead and zinc in lead–zinc ores: S. C. SOUNDAR RAJAN. (31 December 1982)

Some observations about the atomic-absorption spectroscopy of antimony(III) and (V) by solution nebulization and hydride generation: J. R. CASTILLO, C. MARTINEZ, J. PEREZ and M. A. BELARRA. (31 December 1982)

Talanta, Vol. 30, No. 2, p. I, 1983
Pergamon Press Ltd. Printed in Great Britain

TALANTA MEDAL

PROFESSOR TAITIRO FUJINAGA

The Publisher and Editorial Board of *Talanta* take pleasure in announcing that, with the approval of the Advisory Board, the Tenth Award of the Talanta Medal has been made to Professor Taitiro Fujinaga, of the Department of Analytical Chemistry, University of Kyoto.

Professor Taitiro Fujinaga has made outstanding contributions to analytical chemistry through his scientific research and his participation at national and international level in analytical organizations. He is the author or co-author of some 200 papers and has originated or developed many analytical techniques. The fields to which he has made major contributions include:

Differential polarography with square-wave pulses.
Current-scanning polarography and galvanostatic voltammetry.
Short-circuited amperometry with high or low potential reference-electrodes.
Electrolytic chromatography and coulopotentiometry.
Solvent extraction, especially with molten solids as solvents.
Gas chromatographic separation of metal chelates with carrier gas containing ligand vapour.
Oceanographic analysis, especially the use of co-precipitation for separation and preconcentration.

He has served IUPAC for over 20 years, has organized three major international meetings on analytical chemistry, and has been a plenary lecturer at many national and international meetings. He has given unstintingly of his time and energy in the cause of analytical chemistry and analytical research, and is widely known and respected for his achievements.

TAL 30/2—A

Talanta, Vol. 30, No. 2, p. i, 1983
Pergamon Press Ltd Printed in Great Britain

PAPERS RECEIVED

A comment on the simultaneous determination of glass electrode parameters and protonation constants: H. K. J. POWELL and M. C. TAYLOR (8 November 1982)
Studies on the determination of dissolved oxygen in water: M. MALAIYANDI and V. S. SASTRI (16 November 1982)
Thiocyanate for solvent extraction and spectrophotometry of metal ions: K. S. PATEL and H. L. KHATRI. (16 November 1982)
Extraction separation with tri-n-octylamine/benzene: Complex-adsorption oscillopolarography in determining trace zirconium in ores: YE HUA-LI and HE YOU-HUA. (16 November 1982)
Cellulose: A biopolymeric sorbent for heavy-metal traces in waters: P. BURBA and P. G. WILLMER. (17 November 1982)
A systematic study of the chromatographic behaviour of 52 cations on Sn(IV)-based ion-exchange papers in complex-forming acid systems: S. D. SHARMA and T. R. SHARMA. (17 November 1982)
Potential–pH equilibrium diagrams for the (Ag–Py–H_2O) ternary system: R. M. EL-BAHNASAWY and M. M. ABOU SEKKINA. (17 November 1982)
Thymolphthalin as an analytical reagent—I: Spectrophotometric determination of ferricyanide and ferrocyanide: M. F. SHAHAT, A. B. EL-SAYED, M M. ABDEL-BADEI and A. I. AMER. (18 November 1982)
Metal speciation by flow-injection analysis: B. P. BUBNIS, M. R. STRAKA and G. E. PACEY. (18 November 1982)
Constant-current potentiometry of orthophosphate with cetylpyridinium chloride: A feasibility study: WALTER SELIG. (18 November 1982)
Spectrophotometric investigation on the reaction of nickel with some sulphonated azo-dyes: MARIA PESAVENTO and TERESA SOLDI. (18 November 1982)
Benzohydroxamic acid as an indicator in the titrimetric determination of alkaline-earth metals: R. D. ROSHANIA and Y. K. AGRAWAL. (18 November 1982)
Spectrophotometric determination of tantalum in ores and mill products with Brilliant Green after separation by methyl isobutyl ketone extraction of tantalum fluoride: ELSIE M. DONALSON. (22 November 1982)
The measurement of Ag, Te and Pd in geochemical reference materials by mass-spectrometric isotope-dilution analysis: R. D. LOSS, K. J. R. ROSMAN and J. R. DE LAETER. (22 November 1982)
Simple creation of an automatic system for programmed potentiometric titration with an HP-85 microcomputer: GEORGI VELINOV, NEDKO TODOROV and SIMEON KARAMPHILOV. (23 November 1982)
Polarographic study of thiodiglycolate and thiodipropionate complexes of cadmium: K. C. GUPTA and TEJINDER KAUR. (23 November 1982)
Cation-exchange of 43 elements from hydrofluoric acid solutions: R. CALETKA and V. KRIVAN. (25 November 1982)
Oxydation vanadique de la khelline: Applications analytiques: J. E. HILA, M. CHASTAGNIER, M. TSITINI TSAMIS and M. HAMON. (29 November 1982)
Bromide-selective electrode–redox electrode cell for the potentiometric determination of bromine and free residual chlorine: D. MIDGLEY. (29 November 1982)
Application of the Deford and Hume modified method for quasi and irreversible processes to the chelates of Bi(III) with azomethine derivatives of 2-benzoylpyridine: M. A. GOMEZ NIETO, J. L. CRUZ SOTO, M. D. LUQUE DE CASTRO and M. VALCARCEL. (29 November 1982)
Complex formation between In(III) and 2-mercaptopropanoic acid in 3.0*M* $NaClO_4$ at 25°: SALVADOR ALEGRET, ANTONIO FLORIDO, MANUEL VALIENTE and MANUEL AGUILAR. (29 November 1982)
Spectrophotometric determination of gold(III) with 2-acetylpyridine thiosemicarbazone: C. K. BHASKARE and SUREKHA DEVI. (30 November 1982)
A computational study of the complex formation function: PAN ZHONG-XIAO and **Chang Mou-Sen.** (30 November 1982)
Spectrophotometric determination of some bivalent non-transition toxic metal ions—A review: H. B. SINGH, B. S. KAPOOR and R. L. SHARMA. (2 December 1982)
Spectrophotometric determination of tetracyclines and cephalosporins with ammonium vanadate: M. M. ABDEL-KHALEK and M. S. MAHROUS. (3 December 1982)

Talanta, Vol. 30, No. 1, p. i, 1983
Pergamon Press Ltd Printed in Great Britain

PAPERS RECEIVED

Separation of iron(II) from cobalt(II) and their determination with 2-acetyl pyridine thiosemicarbazone. Analysis of ferrites: C. K. BHASKARE and SUREKHA DEVI. (12 October 1982)
Titrimetric microdetermination of uric acid and thioglycollic acid by amplification reactions: F. A. ABEED, M. JASIM and D. AMIN. (19 October 1982)
The stability constants of Pd–EDTA and its chloride complexes: J. KRAGTEN and L. G. DECNOP-WEEVER. (19 October 1982)
Determination of chromium(VI) in natural waters by the adsorption of chromium(VI)–diphenylcarbazide with XAD-2 resin: SUSUMU OSAKI, TOMOE OSAKI and YOSHIMASA TAKASHIMA. (19 October 1982)
The effect of organic matter and colloidal particles on the determination of chromium(VI) in natural waters: SUSUMU OSAKI, TOMOE OSAKI, NOBUHIRO HIRASHIMA and YOSHIMASA TAKASHIMA. (19 October 1982)
Purification of Xylenol Orange by preparative paper chromatography: Chelate formation with zirconium: V. MICHAYLOVA, L. SŮCHA✠ and M. SUCHÁNEK. (20 October 1982)
A new colorimetric method for the determination of carbon disulphide and its applications to the analysis of some dithiocarbamate fungicides: BALBIR CHAND VERMA, J. BUTAIL, R. K. SOOD and H. S. SIDHU. (20 October 1982)
Ion-pair extractions using 12-crown-4 and its analogues: G. E. PACEY and Y. P. WU. (20 October 1982)
Estimation of 2-thio-orotic acid (6-hydroxy-2-mercaptopyrimidine-4-carboxylic acid) by mercurimetric titration: MADHULIKA SHRIVASTAVA and G. S. PANDEY. (21 October 1982)
Some observations concerning the direct titration of nitrite with cerium(IV): U. MURALIKRISHNA, K. SUBRAHMANYAM, M. V. S. SURYANARAYANA and MANNAM KRISHNAMURTHY. (21 October 1982)
The oxidative decarboxylation of polyaminocarboxylic acids with lead dioxide suspension in neutral medium: A. B. EL-SAYED and M. F. EL-SHAHAT. (25 October 1982)
Graphic representation of polynuclear acid–base and complex equilibria: G. RAMIS RAMOS, M. C. GARCIA ALVAREZ-COQUE and C. MONGAY FERNANDEZ. (26 October 1982)
Complexes of oxovanadium(IV) with polyaminocarboxylic acids: JUDITH FELCMAN and J. J. R. FRAUSTO DA SILVA. (27 October 1982)
Electrodeposition as a preconcentration step in analysis of multicomponent solutions of metallic ions: JAMES L. ANDERSON and ROMAN E. SIODA. (27 October 1982)
Titrimetric resolution of mixtures of phenol and *p*-hydroxybenzoic acid with *N*-bromocaprolactam: ASHUTOSH SRIVASTAVA and RENUKA KOCHAR. (29 October 1982)
Determination of total arsenic in marine organisms by use of a zinc column arsine generator: Evaluation of sample-ashing procedures: W. A. MAHER. (1 November 1982)
Cation-exchange in thiourea–hydrochloric acid solutions: C. H.-SIEGFRIED W. WEINERT, FRANZ W. E. STRELOW and REINHARD G. BÖHMER. (1 November 1982)
Comparison of the efficiency of extraction of chloroquine with different solvents during fluorimetric analysis: S. A. ADELUSI. (3 November 1982)
On the invention of conductimetric titration: F. SZABADVÁRY. (3 November 1982)
Mechanism of the extraction of the palladium(II)–thiocyanate complex by polyether foam: SARGON J. AL-BAZI and ARTHUR CHOW. (4 November 1982)
Concentration of yttrium subgroup impurities in high-purity yttrium oxide by TBP–NH_4SCN extraction chromatography: ZHANG TAO. (5 November 1982)
DECFAM—a new computer-oriented algorithm for the determination of equilibrium constants from potentiometric and/or spectrophotometric measurements—I: Basic principles of the method and the calculations of equilibrium concentrations in reversible systems: J. KOSTROWICKI and A. LIWO. (5 November 1982)
DECFAM—a new computer-oriented algorithm for the determination of equilibrium constants from potentiometric and/or spectrophotometric measurements—II: Methods for the determination of equilibrium constants from potentiometric and/or spectrometric data with the use of analytical expressions: J. KOSTROWICKI and A. LIWO. (5 November 1982)

Talanta, Vol. 30, No. 1, p. I, 1983
Pergamon Press Ltd. Printed in Great Britain

TALANTA ADVISORY AND EDITORIAL BOARDS

These guiding bodies have suffered a severe loss from the death of Professor Belcher, who had served continuously as Chairman of both since the inception of the journal (and more recently as Co-Chairman of the Advisory Board, with Professor Winefordner), and as a mark of respect, no attempt will be made to replace him. Professor Winefordner will become sole Chairman of the Advisory Board. A further loss to the Editorial Board was the decision of Professor Betteridge to resign from his post as Assistant Editor because of increased research commitments. He had been Assistant Editor for nearly twenty years, and his help will be greatly missed. He is not severing his connection with the journal completely, however, and will become a member of the Advisory Board. The Editorial Board and the Publisher of the journal express their sincerest gratitude to him for services rendered in the past, and expect that he will prove equally valuable in the future.

TENTH TALANTA GOLD MEDAL

Professor Taitiro Fujinaga responds — after receiving the Medal (see *Talanta,* 1983, **30**(2), facing page 75) from Dr M. Williams (on right) on behalf of the Editorial Board and Pergamon Press. Professor J. Růžička (Ninth Medal Winner) looks on.

Group photograph at presentation ceremony during the 32nd IUPAC General Assembly in Lyngby, Denmark, 18–26 August 1983. Present in the group are: Mrs. Fujinaga, Professor S. Nagakura (President of IUPAC — on her left), Professor F. Pellerin (President of IUPAC's Analytical Chemistry Division — on right of Professor Fujinaga).

Professor K. Fukui (on right), President of the Chemical Society of Japan, congratulates Professor Fujinaga at the Talanta Prize Party, held in Miyako Hotel on 3 April 1983, during the Annual Meeting of the Society.

SUBJECT INDEX

LIST OF CONTENTS

JANUARY

FEBRUARY

MARCH

APRIL

AUGUST

SEPTEMBER

OCTOBER

DECEMBER

Talanta, Vol. 30, No. 8, p. ii, 1983
Pergamon Press Ltd. Printed in Great Britain

PUBLICATIONS RECEIVED

Wilson and Wilson's Comprehensive Analytical Chemistry, Vol. XIV: G. SVEHLA (ed.). **Ion Exchangers in Analytical Chemistry, Their Properties and Use in Inorganic Chemistry:** M. MARHOL, Elsevier, Amsterdam, 1982. Pages 585. US$127.75, Dfl. 275.00

Synthetic organic ion-exchange resins were first described by Adams and Holmes nearly 50 years ago. Their work heralded the development and subsequent applications of improved "universal" and selective exchangers mainly, but not exclusively, organic in framework structure. The volume under review is devoted to such exchangers applied to the analytical chemistry of inorganic systems. The text is divided into three parts. Part 1 has a chapter on basic concepts and properties and another on selectivity, plate theory and other quantitative treatments associated with the elution process; the last-mentioned includes a treatment of gradient (concentration, pH and temperature) elution chromatography. Part 2 begins with a chapter on physical, physico-chemical and chemical properties of exchangers and their determination. Instrumentation is next considered and is succeeded by a long chapter (pp. 160–399) on applications. There is a liberal sprinkling of procedures given for separation of individual ions or groups of ions from complex mixtures, and a number of these make use of mixed solvents. Part 3 deals with characteristic properties of commercially available exchangers and provides distribution coefficients (some tabulated but many graphically presented) for various ions in representative aqueous systems. An appendix lists 96 monographs published worldwide on ion-exchange.

The important recent development, usually referred to as Ion Chromatography, introduced by Small, Stevens and Bauman in 1975, using a conductivity cell as detector, is merely included in a list with other detection techniques of relatively limited application (p. 155). This lack of coverage of a development which has contributed much to the improvement of common anion and some cation analysis is unfortunate because the previous volume (IIB) of the Treatise dealing with ion-exchange chromatography was published in 1968. However, a separate treatment of Ion Chromatography may be planned and could easily be justified. Apart from this omission, the present volume gives a well-balanced, informative and reasonably up-to-date account within the limits already noted and it can be highly recommended as a reference work on the subject in keeping with editorial intentions regarding the aim of the Treatise.

S. J. LYLE

Chromatography and Mass Spectrometry in Biomedical Sciences, 2: A. FRIGERIO (ed.), Elsevier, Amsterdam, 1983. Pages xii + 506. US $106.50; Dfl. 250.00.

This is the proceedings of the *International Conference on Chromatography and Mass Spectrometry in Biomedical Sciences* which was held at Bordighera, Italy in 1982. The various papers are grouped under five main headings—Drug Studies, Developments in Methodology, Endogenous Compounds, Clinical Studies and Environmental Studies. Generally the standard of the camera-ready papers is high, but in one or two the English is rather poor—a fault which should have been rectified by the editor or publisher.

In a review of this length it is not possible to comment on all of the papers contained in this book. Instead I have restricted my comments mainly to some of the papers with a clinical bias. Most of the papers are concerned with mass spectrometry (as the title suggests!), coupled with gas chromatography and high-pressure liquid chromatography. Two papers and a plenary lecture cover the analytical applications of ion-exchange thin-layer chromatography, in particular the detection of phenylketonuria and Maple-syrup urine disease. The technique is relatively simple and applicable as a screening technique, *e.g.*, in plant breeding programmes (p. 141) and for inherited metabolic disease (p. 159). Some coverage is also given to different forms of electrophoresis. Nagy and colleagues (p. 421) employed a combination of affinity chromatography and different types of electrophoresis in the isolation and characterization of the anorexogenic glycoprotein, satietin. As part of a study of the diagnostic and anti-tumour properties of group IIIa metals, Shukla *et al.* (p. 179), describe the binding properties of aluminium, gallium, indium and thallium with ferritin and transferrin, as determined by paper and cellulose acetate electrophoresis. A criticism of this work is the simplistic interpretation of the electropherograms of ferritin from different suppliers and the lack of consideration given to isoferritins.

Amongst the different liquid phases used in the various gas chromatographic separations described in this book, the use of nematic liquid crystals in the separation of polycyclic aromatic hydrocarbons is particularly noteworthy (p. 221), although the transition temperature of the particular liquid crystal and the relatively short operative life of liquid crystal columns does limit their routine application.

Biological fluids are complex mixtures of many different substances (carbohydrates, peptides, proteins, steroids, metal ions, nitrogeneous compounds, *etc*). Analysis of such fluids by chromatographic methods often requires some form of sample extraction or clean-up and in some cases formation of derivatives to improve chromatographic properties or facilitate detection. Several papers in this book describe improvements to established chromatographic analyses. For example, Manrique and co-workers (p. 97) report a method for nitroglycerine in plasma, which involves a single extraction step followed by isothermal gas–liquid chromatography (electron-capture detector).

Metabolic profiling is an approach to clinicochemical analysis which exploits the resolving power of chromatographic techniques. The study of propionic acidaemia in a neonate by Kuhara *et al.* (p. 449) by use of gas chromatography–mass spectrometry exemplifies the use of this technique. Unfortunately, no experimental results are shown and the significance of the analytical findings at the various stages of this rare illness are not discussed at any length.

Graeve and Delaval (p. 461) have contributed an excellent article on tandem mass spectrometry which explains the principle of the technique, illustrates its application and discusses its advantages, disadvantages and future prospects. Anyone unfamiliar with this technique would find this a very useful introduction to what appears to be an exciting analytical prospect.

This book will be of interest to many scientists engaged in biomedical research, but at the price most will borrow a library copy rather than buy it.

L. J. KRICKA

Talanta, Vol. 30, No. 7, p. ii, 1983
Pergamon Press Ltd. Printed in Great Britain

NOTICE

IV BRAZILIAN SYMPOSIUM OF ELECTROCHEMISTRY AND ELECTROANALYTICAL CHEMISTRY

São Carlos, Brazil, 15–18 April 1984

This symposium will be held in São Carlos, State of São Paolo, Brazil. The deadline for submission of titles of papers offered is 5 November 1983; the deadline for submission of abstracts is 5 February 1984. Information can be obtained from

Comissão Organizadora
IV Simpósio Brasileiro de Electroquímica e Eletroanalítica
Caixa Postal-297
13560-São Carlos, SP-Brasil

Talanta, Vol. 30, No. 3, p. ii, 1983
Pergamon Press Ltd. Printed in Great Britain

PUBLICATIONS RECEIVED

Guide-Lines to Planning of Atomic Spectrometric Analysis: B. MAGYAR, Elsevier, Amsterdam, 1982. Pages x + 273. $76.75.

The author of this book says that the title was chosen to describe its contents "as well as possible in few words". However, anyone buying the volume expecting a practical guide may well be surprised to find approximately half of the contents devoted to fundamental theory, generally with rather tenuous connections to routine analytical atomic spectroscopy. There is much useful information in the book, but the approach is very much an academic one.

The introductory chapter contains an interesting but brief general discussion of quantitative assessment of the relative merits of instrumental methods, and a short historical survey with a strong hint of nostalgia. This is followed by chapters on electromagnetic radiation, line profiles and atomic spectra and electronic structure. Chapters 5 and 6, on characteristics of atom reservoirs and their influence on sensitivity in AAS and AES and on the measurement of atomic absorption and emission respectively are more obviously useful, as are the appendices on sensitivities and on alternative wavelengths.

The price is rather high for a book produced directly from poor quality typescript, inundated with grammatical, spelling and typographic errors. The work would have benefited greatly from the services of a diligent and competent translation editor.

M. S. CRESSER

Advances in Chromatography, Vol. 19: J. C. GIDDINGS, E. GRUSHKA, J. CAZES and P. R. BROWN (editors), Dekker, New York, 1981. Pages XV + 312. S.Fr. 98.

This volume follows the style set by its predecessors. There is no unifying theme and the six chapters are quite disparate in subject matter. Few will be of direct interest to the analyst and then only to the specialist wishing to determine, for example, 2,4-D herbicide products or aldosterone and its metabolites. Nevertheless, those with the preceding 18 volumes will surely wish this to be added to the collection.

D. BETTERIDGE

Standards in Fluorescence Spectrometry: J. N. MILLER (editor), Chapman & Hall, 1981. Pages viii + 115. £8.50.

This short book consists of about 80 pages of text, arranged into eight chapters, plus an appendix of sixteen excitation/emission spectra of common organic fluorophors. The book can be read in a few hours and gives a brief account of the method of operation and theoretical background of low-resolution solution-phase fluorescence spectroscopy. The book should be a useful introduction for research workers and clinical or industrial technicians using this kind of equipment for the first time. Those planning to specialize in this field will, of course, require a much greater depth of knowledge than this short book offers.

For the most part the book stresses methods of conventional fluorimetry. There is no discussion of fluorescence decay or other time-resolved measurements, nor is there any mention of polarization phenomena (except as a potential source of error). There is no mention of sample forms other than room-temperature liquid solutions—no gases, solids or glassy solutions. No mention is made of the possible use of lasers as excitation sources. The use of double monochromators is considered, though, as are microprocessor-controlled instruments.

I personally will find this book useful for introducing new graduate students in my laboratory to the principles and techniques of routine fluorescence measurements.

R. F. BORKMAN

Talanta, Vol. 30, No. 1, p. ii, 1983
Pergamon Press Ltd. Printed in Great Britain

PUBLICATIONS RECEIVED

Marine Electrochemistry, A Practical Introduction: M. WHITFIELD and D. JAGNER (eds.), Wiley, Chichester, 1981. Pages xiii + 529. £27.50.

Marine Electroanalysis would have been a better title for this book, since it is concerned with oceanographic analysis and not at all with topics such as corrosion, desalination or any applied aspect of sea-water chemistry. A quarter of the book is taken up with "Fundamentals": a long chapter on sea-water as an electrochemical medium draws much useful information together; short ones on the classification of techniques, instrumentation, and computing are less satisfactory in that the first is a luxury in a book of this type and the others too short to do justice to the material. The "Applications" section contains full and interesting chapters on conductometry, the determination of oxygen and a review of voltammetric analysis of sea-water. The chapter "Direct Potentiometry" deals fairly well with pH, but very cursorily with ion-selective electrodes. This and the chapter on potentiometric titrations overlap more than they should, *e.g.*, both deal with the known-addition method, and both suffer as a result. Some looseness of structure may be expected from a book with ten contributors, but considered as a whole it adds up to a substantial and useful volume.

DEREK MIDGLEY

Nonisotopic Alternatives to Radioimmunoassay: Principles and Applications: LAWRENCE A. KAPLAN and AMADEO J. PESCE (eds.), Dekker, New York, 1981. Pages 352. Sw. Fr. 135.

This is Volume 10 of the excellent *Clinical and Biochemical Analysis Series*. It reviews current analytical methods capable of replacing the disadvantageous radioimmunoassay procedures with non-isotopic alternatives.

Several leading experts outline alternative methodology which can replace RIA and its associated costs, hazards and waste-disposal problems. Basic principles for achieving sufficient sensitivity with techniques such as fluorescence-based immunoassays, enzyme-coupled procedures, and nephelometry for monitoring a variety of molecules in clinical applications are presented clearly. Concise histograms, diagrams and tables add to the overall readability of the chapters, making this volume acceptable as an advanced graduate textbook. The division of the book into chapters dealing with specific techniques in detail makes it equally acceptable for professional clinical scientists and all research investigators currently using immunologically-based assays.

The chapter on diagnostic enzyme-labelled immunoassays (ELISA) exemplifies the book's theme of contrasting new methods with radioisotopic assays, and presenting problems in a clear manner. References are up-to-date and many chapters contain bibliographies which will be valuable to those wishing to become conversant with such a recently developed field.

D. M. W. ANDERSON

Thin-Layer Chromatography: Techniques and Applications (Chromatographic Science Series, Vol. 17): BERNARD FRIED and JOSEPH SHERMA, Dekker, New York, 1982. Pages 320. Sw. Fr. 148.

This volume is recommended to all those with more than a transient interest in TLC. Aimed at those involved in teaching this important analytical technique, this book will be a useful reference text rather than a direct textbook for students.

The book is divided into two parts—"General Practices of TLC" and "Applications of TLC to Different Compound Types". There are clear, concise chapters on the history, mechanism and equipment of TLC, complementary sections on development techniques qualitative evaluation and quantification, and an excellent chapter on the reproducibility of results. All chapters end with good reference sections. From the viewpoint of the typical student, the book suffers from the extensive detail of some chapters, lists of equipment and materials for specific experiments, and the lengthy compilation of manufacturers' addresses of interest largely to American readers. There is a useful Glossary and Index. This volume offers a good introduction to methods and applications of TLC and can be recommended for library acquisition.

D. M. W. ANDERSON

Talanta, Vol. 30, No. 12, p. III, 1983
Pergamon Press Ltd. Printed in Great Britain

LOUIS GORDON MEMORIAL AWARD

Presentation of the Louis Gordon Memorial Award for 1982 to Dr. Lars Kryger, Aarhus University. Left to right: Professor J. Růžička, Dr. L. Kryger, Professor N. Hofman-Bang.

Talanta, Vol. 30, No. 8, p. III, 1983
Pergamon Press Ltd. Printed in Great Britain

EDITORIAL

The first issue of *Talanta* appeared 25 years ago this month—in August 1958. Three editors, thirty volumes, several thousand papers and some millions of words later, the journal is flourishing, offers its contributors a first class publishing service, and its readers much better value for money than most of its commercial competitors. Authors and readers alike will be aware that acceptance of a paper for *Talanta* is a guarantee of quality, and that no pains are spared to ensure continuation of the journal's reputation, which has stood high from the very first issue. In many ways *Talanta* is run like a club, with a good deal of camaraderie between staff, contributors and readers. Besides its full range of publishing services (papers, reviews, annotations, analytical data, letters) it has three awards—the Talanta Medal, the Louis Gordon Memorial Award, and the Pharmacia Prize—and these alone would distinguish it from other journals in the field. *Talanta* was established to meet the demand for publication created by the rapid expansion of research in analytical chemistry in the late 1950s. At the same time, the policy was established of accepting only work that was soundly done, likely to prove useful, and of general analytical interest. The same policy is followed today, and will continue. We look forward to the next 25 years and the developments they will bring in analytical chemistry, and wish our authors and readers many happy and rewarding years of research (and reading *Talanta*).

R. A. CHALMERS

Talanta, Vol. 30, No 1, p. iii, 1983
Pergamon Press Ltd. Printed in Great Britain

CORRIGENDA

At the request of various parties concerned, the following corrections should be made to the paper by H. Ishii and K. Satoh, *Talanta*, 1982, **29**, 243.

Page 243, column 1, lines 19–22 should be replaced by:

approach for ICPES, combining the high-resolution spectrometer recently marketed by Yanoco Co. Ltd. (model UOE-1) with a commercially available ICP

Page 244, Table 1, the last two lines should be replaced by:

Optical measurement unit	Model UM-1, Yanaco Ltd. (Japan) and Model RC-125 chart recorder, Japan Spectroscopic Co., Ltd.

Page 244, Figure 1, the caption should read:

Block diagram of the optical measurement unit.

Page 247, *Acknowledgements*, line 3 should read:

advice in connection with use of the high-resolution

Talanta, Vol. 30, No. 12, pp. iii–iv, 1983
Pergamon Press Ltd. Printed in Great Britain

PUBLICATIONS RECEIVED

The Interpretation of Analytical Chemical Data by the Use of Cluster Analysis: D. LUC MASSART and LEONARD KAUFMAN. Wiley, New York, 1983. 237 pages. $45.00.

Within many areas of science, the methods of cluster analysis have proved valuable for the interpretation of multivariate information. During the past decade, analytical chemists have become increasingly aware of the potentialities of these techniques, but, so far, the majority of workers have focused on hierarchical clustering procedures and, occasionally, discovered some shortcomings.

In their book, *The Interpretation of Analytical Chemical Data by the Use of Cluster Analysis*, D. Luc Massart and Leonard Kaufman point out that some of the difficulties encountered by workers within the field may be overcome by the use of non-hierarchical clustering techniques in combination with display methods. The authors foresee that analytical chemists, who have become acquainted with these more versatile techniques, are likely to adopt a systematic use of cluster analysis. To promote this development, the authors devote a fair proportion of their book to a thorough introduction to non-hierarchical clustering methods and to a number of demonstrations of the applications. But apart from this, the book presents the entire field of cluster analysis of chemical data in a well-organized and logical manner.

The book is divided into eight chapters: Chapters 1 and 2 introduce the main concepts of cluster analysis and discuss the relations of clustering methods to mapping techniques, supervised pattern recognition and principal components analysis. Chapters 3–5 are devoted to hierarchical and non-hierarchical clustering methods, a comparison of the techniques and a discussion of possible ways of solving special problems, such as those due to incomplete data sets. Chapter 6 reviews a number of applications and, in Chapter 7, some of the available computer program packages are introduced. Finally, in Chapter 8, an illustrative problem concerning the classification, according to biosynthetic pathways, of fatty acids in goat milk is worked through in detail, and the results of the application of several clustering methods are compared and discussed.

Some of the results which are presented in the book are quite impressive, but even so, the authors discuss the subject with an appealing critical sense. In particular, they emphasize that often the classifications which can be obtained with cluster analysis do not differ much from those developed by an expert in the scientific field from which the data originate. Furthermore, they warn the reader not to trust blindly in any single clustering procedure, and they point out that as a rule, the scientist must be prepared to investigate the performance of a number of clustering strategies in order to gain insight into the data. Thus, with no intelligent user-interaction, clustering methods cannot be expected to lead to an interpretation of multivariate data. However, to the experienced scientist, the techniques may be extremely useful and help him to take simultaneously into account considerably more multivariate data and correlations than he would normally be able to perceive.

Since the book contains a thorough review of the field with many useful references, it can be recommended to chemists who are already acquainted with multivariate data analysis, but without doubt it will be of even more interest to those who want a good introduction which explains the practical details and points out the pitfalls. The text, which is accompanied by clear and explanatory illustrations, mainly uses a simplified description of the mathematics. This is adequate for readers who are chiefly interested in the correct applications. However, certain chapters are extended with mathematical sections to satisfy readers who want a deeper understanding of the mathematics. No computer programs or subroutines are listed in the book, but the text appears to contain sufficiently detailed and organized information for readers with some programming experience to use it as a basis for writing their own clustering programs.

LARS KRYGER

Progress in Analytical Atomic Spectroscopy, Vol. 4: C. L. CHAKRABARTI (editor). Pergamon Press, Oxford, 1982. v + 456 pages. £53.00; US$106.00.

The fourth volume in this useful series contains eight review articles. The first, by Delves, covers the analysis of biological and clinical materials, from sample preparation through to spectroscopic determination. It contains a wealth of practical detail from 259 references and much useful constructive criticism. Mills and Belcher present an account of the analysis of coal, coke, ash and mineral matter by atomic spectroscopy, including XRF, based upon 140 publications between 1973 and 1980, again with a useful overview of techniques and possible pitfalls in sample preparation. The comprehensive contribution (479 references) from Noller, Bloom and Arnold discusses every aspect of the analysis of atmospheric particulates for metals by graphite-furnace AAS. The first chapter in particular is a very useful introduction to this field of analysis. La Breque reviews the progress made in radioisotope-induced XRF, emphasising the relative merits and problems associated with radioisotopes, compared with the conventional X-ray tube technique, while Cresser discusses the theoretical and practical advantages and disadvantages of nebulization of small, discrete samples into flames and plasmas, and looks at applications of this approach to analysis of small samples. Matousek has made a commendable effort to give a systematic account of interferences in electrothermal atomic absorption spectrometry, including in his treatment the approaches used for their elimination and control. Sullivan offers a timely review of developments in the design and construction of lamps and sources for analytical atomic spectroscopy. Finally the volume concludes with another useful and comprehensive applications review, this one by Sychra, Lang and Sebor on petroleum and related products.

The quality of the production, like that of the articles the book contains, is generally good, the use of camera-ready copy in no way detracting from the value of the work. The series can be strongly recommended for providing authoritative accounts of value, both as updates of progress in selected fields, and also as comprehensive introductions for newcomers to specific areas of analytical atomic spectroscopy.

M. S. CRESSER

Ion Chromatography: J. S. FRITZ, D. T. GJERDE and C. POHLANDT, Hüthig, Heidelberg, 1982. x + 203 pages. DM66; $33.00.

The title of this short monograph may well suggest to the prospective reader that it will be concerned with that particular brand of ion-exchange chromatography marketed by the Dionex Corporation. The book does indeed describe and discuss the ion-exchange processes that occur in that two-column system, and gives references to a number of applications to analysis for anions and cations in the environmental, industrial and clinical fields.

However, the book also describes and discusses in some detail the newer single-column type of ion chromatography developed by the authors themselves. Since their work is fairly recent, most of the applications are proposed by them, and appear to be relatively untested. The authors obviously believe their single-column technique to be superior in many ways to the Dionex product, and they do produce considerable evidence to support this.

The result is, however, that their book is rather peculiar. It would not be of much use to the average Dionex user, who is probably already familiar with the literature, although possibly a prospective user would benefit from its study before reaching a decision.

It would be of rather more use to someone wanting to try single-column ion chromatography. Thus, methods for preparing the special ion-exchangers are given (but what is methylal, p. 102?), but the analyst wanting to set up his own system will still find a lot of information lacking. There is a discussion about detectors, but little guidance on how to set about making or buying one. *Most* disappointingly, there is no description at all of the sorts of pipes, fittings, pumps, *etc.* that are currently being used for the highly corrosive inorganic eluents used in ion chromatography.

Overall, although this book does give a useful picture of the present state of ion chromatography, I feel it is premature and not altogether satisfactory. I am sure the authors could write a much better one in 5 years' time.

MARY MASSON

Talanta, Vol. 30, No. 10, pp. iii–iv, 1983
Pergamon Press Ltd. Printed in Great Britain

NOTICES

THIRD INTERNATIONAL WORKSHOP ON TRACE ELEMENT ANALYTICAL CHEMISTRY IN MEDICINE AND BIOLOGY

GSF RESEARCH CENTRE, NEUHERBERG, F.R.G.

The dates for this meeting have been changed. The Workshop will now be held 16–18 April 1984, not 4–6 April as previously advertised.

SCIENTIFIC METHODOLOGIES APPLIED TO WORKS OF ART

FLORENCE, ITALY, 2–5 MAY 1984

This symposium, under the auspices of the Opificio delle Pietre Dure e Laboratori di Restauro di Firenze, the Progetto Finalizzato Fine e Secondaria, and the Istituto Guido Donegani di Novara, will be held for the exchange of information on application of science in research on the study, restoration and conservation of works of art. The topics are: (1) techniques and materials used for the manufacture of works of art; (2) degradation processes and materials in works of art; (3) processes and materials employed in conservation; (4) dating methods, provenance studies, and authentication. Abstracts (in English, not more than 200 words) of papers offered (presentation time 20 minutes, English or Italian) should be sent before 31 October 1983. The registration fee is 200,000 Italian lire. Further details are obtainable from

Istituto Guido Donegani S.p.A.,
Segreteria Tecnica,
Via G. Fauser 4,
28100 Novara NO,
Italy

SYMPOSIUM ON THE ROLE OF ANALYTICAL CHEMISTRY IN NATIONAL DEVELOPMENT

CAIRO UNIVERSITY, 3–7 JANUARY 1984

This symposium is organised by the Egyptian Chemical Society with the participation of some European societies of analytical chemistry. The topics are:

1—Status and prospects of chemical education and research
2—Implementation of national strategies in chemical industries
3—Trends and perspectives in analytical chemistry
  (a) Product quality control
  (b) Analytical data quality
  (c) Trace analysis
  (d) Surface analysis
  (e) Information systems
  (f) Computers
4—Analytical chemistry for national development
  (a) Life sciences
  (b) Materials science
  (c) Food production
  (d) Environmental studies

Contributions relevant to these topics are invited. Titles and abstracts should arrive before 31 October 1983. The symposium fee for overseas participants is $100. Special air-fares are available (details from Dr. M. Khater, Cairo University, Giza, Egypt). Further information may be obtained from

Professor M. Grasserbauer,
Institute of Analytical Chemistry,
TU Wien,
Getreidemarkt 9,
A-1060 Wien,
Austria
(Telex 133000 tvfawa; telephone 222-5601-4857/4837)

THE PITTSBURGH CONFERENCE ON ANALYTICAL CHEMISTRY AND APPLIED SPECTROSCOPY

ATLANTIC CITY, U.S.A., 5–10 MARCH 1984

The 35th Pittsburgh Conference and Exposition on Analytical Chemistry and Applied Spectroscopy will convene 5–10 March 1984 in Atlantic City, New Jersey, U.S.A. The following symposia have been organized for the 1984 Technical Programme:

1. Spotlight on chromatography
2. Analytical techniques using supercritical fluids
3. Advanced light sources
4. Microprobe techniques as applied to organic materials
5. New techniques in electroanalytical chemistry
6. New opportunities in mass spectrometry
7. Sample introduction for plasma and flames. how can we do it better?
8. Integrating software into laboratory systems
9. Polymer characterization
10. Industrial hygiene monitoring
11. New horizons in nuclear magnetic resonance
12. The really sensitive techniques
13. ASTM E-42—Industrial applications of surface analysis
14. Pittsburgh Analytical Chemistry Award
15. Pittsburgh Spectroscopy Award
16. Dal Nogare Award Symposium
17. The Williams-Wright Industrial Spectroscopist Award

The symposium "Spotlight on chromatography" will feature three invited symposia and an evening discussion group sponsored by the Pittsburgh Conference and organized by the International Meeting on Capillary Chromatography:

(a) Sample Preparation and Introduction
(b) Column Technology and Applications
(c) Detectors and Multidimensional Chromatography
(d) High Resolution Chromatography Discussion Session

Registration forms and further information may be obtained from

Pittsburgh Conference
437 Donald Road, Department CFP
Pittsburgh, PA 15235, U.S.A.

Talanta, Vol. 30, No. 9, pp III–IV, 1983
Pergamon Press Ltd Printed in Great Britain

PROFESSOR I. P. ALIMARIN

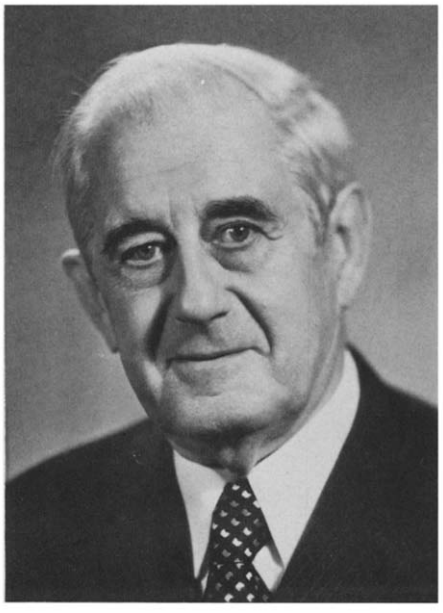

On 11 September 1983 an outstanding analytical chemist, Ivan Pavlovich Alimarin, will be 80 years old and complete 60 years of scientific and pedagogical activity.

In the 1920s he was a student at the Moscow Mining Academy and from 1923 till 1953 he worked at the Institute of Mineral Raw materials. In 1950 he received the degree of Doctor of Chemistry and was appointed to a Professorship, and in 1966 he was elected a full member of the USSR Academy of Sciences. For many years he has been in charge of important scientific bodies. He has been the head of the Department of Analytical Chemistry at the Moscow Institute of Fine Chemical Technology, since 1947 the head of the laboratory at the Vernadskii Institute of Geochemistry and Analytical Chemistry of the USSR Academy of Sciences, and since 1953 the head of the Department of Analytical Chemistry at the M.V. Lomonosov Moscow University.

His investigations have been most diverse, ranging from the theoretical basis of analytical chemistry to the development of various methods of chemical analysis for use in raw materials processing, production of rare metals, metallurgy and the nuclear and semiconductor industries.

Professor Alimarin's interests were for long concentrated on the analytical chemistry of gallium, indium, thallium, germanium and other rare elements. Some of his methods for their concentration and determination are still used in analysis of geological and other samples. He has paid particular attention to micro and ultramicro methods of chemical analysis, and has contributed considerably to the application of organic reagents, the development of concentration methods based on co-precipitation, extraction, ion-exchange and partition chromatography, the improvement of instrumental methods of analysis, such as spectrophotometry, luminescence, electrochemical methods, spectroscopy and radiochemistry. He has also made contributions to the theoretical investigation of complex-formation mechanisms and of kinetics in aqueous and non-aqueous media.

Professor Alimarin is the president of the Scientific Council on Analytical Chemistry of the USSR Academy of Sciences, the Editor-in-Chief of *Zhurnal Analiticheskoi Khimii*, a member of some other editorial boards, and a Regional Editor for *Talanta*, *Journal of Radioanalytical Chemistry* and *Radiochemical and Radioanalytical Letters*. He was a titular member of the IUPAC Analytical Chemistry Division. Professor Alimarin has also been elected an honarary member of the Society for Industrial Chemistry of France, the Society for Analytical Chemistry (now a division of the Royal Society of Chemistry), the Japan Society for Analytical

Chemistry, and the Chemical Society of the German Democratic Republic. He is a foreign member of the Academy of Sciences of Finland, and a Doctor *honoris causa* of Budapest Technical University and the Universities of Göteborg and Birmingham. In 1965 he was awarded the Talanta Gold Medal for his outstanding contributions to analytical chemistry. He has also been awarded the Purkyňe gold medal (Czechoslovakia), the Emich medal (Austria), the Hevesy medal (Hungary) and the medal of Helsinki University (Finland).

Professor Alimarin's friends and colleagues know and appreciate him not only as an outstanding scientist who has devoted many years of his life to the development of analytical chemistry but as a remarkable person and an excellent teacher for his younger co-workers. He is fond of photography and taking colour slides, collecting records, fishing and other practical and interesting hobbies.

We heartily congratulate Professor Alimarin on this glorious anniversary and wish him good health and further success in the development of analytical chemistry.

S. B. SAVVIN

Talanta, Vol. 30, No. 9, pp iii–iv, 1983
Pergamon Press Ltd. Printed in Great Britain

PUBLICATIONS RECEIVED

Analysis of Complex Hydrocarbon Mixtures: Part A—Separation Methods; Part B—Group Analysis and Detailed Analysis, Volume XIII of Wilson and Wilson's **Comprehensive Analytical Chemistry:** S. HÁLA, M. KURAŠ and M. POPL. Editor, G. SVEHLA. Elsevier, Amsterdam, 1981. Part A, pp. XIV + 382; $95.75. Part B, pp. 459; $95.75.

Though not the first work to be published on the analysis of hydrocarbon mixtures, this is certainly the most comprehensive one that I have come across. It is well planned and deals with each topic systematically and evenly, resulting, no doubt, from close team-work from the authors. Each section gives an introduction to the principles and methodology, followed by a discussion of applications to hydrocarbon analysis, well illustrated by examples and with references. It is often difficult to make a true distinction between separation and analysis in this context, but if quantification is the key to analysis, then the technique will be covered in Part B.

Part A deals with distillation and gel chromatography (together about half the book), as well as with liquid chromatography, adduct crystallization, molecular sieves, thermal methods and sundry chemical methods. I found the longer chapters both well written and very informative—students would find these accounts very helpful.

Part B covers a multitude of quantitative analytical techniques, some perhaps included from a sense of completeness, but others because they are powerful and widely used tools common to many laboratories. Of these chapers, the substantial one on mass spectrometry is least successful, with a great deal of detailed information and yet sometimes still not enough to make the matter clear. The quality of the translation editing in this chapter does not match the high standard achieved in most other chapters, but I was impressed by the chapter on GLC, finding aspects very well explained. The survey of recommended procedures will be helpful and is well referenced: it is nicely complemented by the final chapter on trace analysis of hydrocarbons in water, air and food.

These two books constitute a worthy addition to the well known series and will certainly prove valuable to a much wider readership than those engaged only in petroleum analysis. Strongly recommended, but expensive.

IAIN L. MARR

Analytical Techniques in Environmental Chemistry—2: Proceedings of the 2nd International Congress in Barcelona, 1981: edited by J. ALBAIGES. Pergamon Press, Oxford, 1982. pp x + 473. £37.50.

The first congress was held three years earlier, in 1978. The contents of this volume provide an interesting reflection of shifts of interest and emphasis in environmental analysis over this period. There have been more environmental incidents for analysts to test their methods and skills on: Seveso was discussed in the first volume, while in this volume the major spillage of several chemicals, including 12 tone of crude pentachlorophenol at New Orleans in 1980, is reported. Indeed, "Monitoring Strategies" is the heading given to a group of seven contributions, and others could well have been included in this section, covering organics in air, inorganic dusts in air, organics in water, and heavy metals in ash and sediments.

Another indication of a shift in emphasis is the increased number of papers dealing with the application of HPLC, perhaps a measure more of the increase in the use of this tool than in the development of the technique. There are, too, reports on the use of plasma sources for emission spectroscopy, describing some comparisons with older more widely established techniques.

There is much illustrative material here which will not find its way into the usual analytical journals, and for this reason the publication of this volume is to be welcomed. It makes the material available to a much wider audience than was present at the congress, and one which will certainly find this book worth reading.

IAIN L. MARR

Membrane Electrodes in Drug-Substances Analysis: VASILE V. COSOFRET, Pergamon Press, 1982. Pages xvi + 362. £29.50.

Although the title suggests a rather restricted readership, most users of ion-selective electrodes could find much of interest in this text. The book begins with a short theoretical chapter, followed by chapters on membrane-electrode characteristics, commercial membrane electrodes and analytical techniques. The next section covers general methods of analysis with electrodes, and covers determination of halogens, sulphur, phosphorus and inorganic cations. For all the species included, there is a comprehensive and fully referenced discussion of the available electrodes and procedures for their use. The main section, on determination of drug-substances, covers a very wide range of compounds. For each, the name, formula and action are given, along with, wherever possible, a detailed analytical procedure. The accompanying discussion and comments contribute significantly to the usefulness of the book. There are numerous cross-references. The text is remarkably clear and free from typographical errors for a book produced from a camera-ready typescript. References up to 1980 are included.

Inorganic Chemistry and the Earth: J. E. FERGUSSON. Pergamon Press, Oxford, 1982. pp. ix + 400. £20.00 (hard cover); £9.95 (flexicover)

It is my experience that if chemistry is taught in such a way as to balance the theory with the facts, the applications and the extensions to the outside world, it is more likely to awake interest in younger students than when it is presented purely as a rigorous academic discipline. This opinion comes from teaching environmental analysis, but those who would like to rethink their teaching of inorganic chemistry should start by reading this book.

There is no shortage of factual material or of basic concepts in the book. Mineral Resources, for example, leads via extraction of metals through thermochemistry and Ellingham diagrams to completion of the cycle with corrosion processes. Inorganic Chemicals in Everyday Use goes through the common elements (including carbon) and makes frequent reference to thermochemical data to show why the processes used are indeed feasible. Environmental cycles are presented for carbon, nitrogen, oxygen, phosphorus and sulphur, and then the pollution of air and of water is considered, with mention of quantities, concentrations, speciation, incidents, and meteorological and physiological effects. Time and again discourses on the phenomena of environmental chemistry bring us back to chemical equilibria, reaction kinetics and energetics, all put together to make a most readable account. The threat from lead gets its fair share of very balanced argument, as does that of mercury, cadmium and other toxic elements.

The publishers apologize for the direct reproduction of the (very neat)typescript: if it keeps the price within the range of students, fine, but this book would deserve proper typesetting. The question of units is a vexed one. I suppose we have to tend towards SI units these days, but I do prefer small particles to be measured in μm, not m, large amounts in tonnes, not Tg, and industrial pressures in atmospheres, not kPa. I think the vertical scale in Fig. 9.7 should be "deaths per day" and not just "deaths". In the chapter on analytical chemistry, the detection limits in Table 14.1 are very optimistic (I think I recognize the source, but it is not quoted) but the better summary in Table 14.4 puts that right. There is an extensive bibliography at the end of the book (mainly listing monographs, not journals) but I feel it would have been helpful, at least to teachers if not to students, to have indicated more often in the text where material had been taken from. But these are minor criticisms: the book should prove popular with students and staff alike, and should to a long way to make chemistry appear more interesting to general science students.

IAIN L. MARR

Talanta, Vol. 30, No. 6, pp. iii–iv, 1983
Pergamon Press Ltd. Printed in Great Britain

NOTICES

EUROANALYSIS

The 5th European Conference on Analytical Chemistry will be held in Cracow (Poland) on 26 August–1 September 1984. On behalf of the Working Party on Analytical Chemistry of the Federation of European Chemical Societies this Conference will be organized by the Polish Chemical Society and the Committee for Analytical Chemistry of the Polish Academy of Sciences. The Conference will aim, as did the earlier conferences, at the broadest possible coverage of analytical chemistry. The programme is being planned to appeal both to those practising analytical chemistry in industrial and control laboratories and to those teaching and doing research on analytical chemistry at universities and research institutes. The topics of the Conference will encompass papers dealing with all classical and instrumental analytical techniques of determination and separation. A special session will be devoted to Computer Based Analytical Chemistry (COBAC III) and to "Speciation in Trace and Environmental Analysis". The official language of the Conference will be English.

More details may be obtained from the Secretary General of the Conference:

Professor Zygmunt Kowalski
Academy of Mining and Metallurgy
Mickiewicza 30, 30-059 Kraków
Poland

THIRD INTERNATIONAL WORKSHOP ON TRACE ELEMENT ANALYTICAL CHEMISTRY IN MEDICINE AND BIOLOGY

The Third International Workshop on Trace Element Analytical Chemistry in Medicine and Biology will be held at the GSF research centre at Neuherberg, near Munich, 4–6 April 1984.

We would like the 3rd Workshop to return to the character of a workshop in the way practised in the first held in 1980. Therefore joint discussion on definite problems in trace element research will be well to the fore. Only in this way can free and effective exchange of views between analytical specialists on the one hand and biomedical specialists (the users of the analytical data) on the other be guaranteed. It is hoped that the workshop will lead to a productive scientific dialogue between these two groups in regard to the biomedical applications of trace element analytical research. The international and multi-disciplinary character of the workshop should provide a good working forum for all those interested in this subject. The workshop will be repeated at two-year intervals. The aim of the meeting is to bring together experts in the analytical and biomedical fields.

The third workshop will have "Se, Zn, Mn, metalloproteins and other modern essential trace elements" as the scientific topic. The most important aspect will be to cover all the different problems of one element (for instance, nutrition, medicine, biochemistry, analytical chemistry), within a special session, so that all new points of view can be dealt with and discussed among experts in the different fields. The content of the invited papers will have modern developments in these special fields in the foreground.

The workshop will consist of a series of invited papers on specific problem areas each followed by an extended discussion period in which all participants will be invited to take part. Short contributed papers (oral or poster presentation) are also solicited for the workshop.

Participation is open to all interested in trace element studies in the biomedical field. The registration fee (DM 200) covers attendance at the workshop, the conference abstracts and the proceedings at reduced cost as well as activities of the workshop.

All correspondence concerning the workshop should be addressed to:

Dr. P. Schramel
Gesellschaft für Strahlen- und Umweltforschung
Institut für Angewandte Physik
Physikalisch-Technische Abteilung
Ingolstädter Landstraße 1
D-8042 Neuherberg
F.R.G.

Société Belge des Sciences Pharmaceutiques
Belgisch Genootschap voor Pharmaceutische Wetenschappen

FIRST INTERNATIONAL SYMPOSIUM ON DRUG ANALYSIS

7–10 JUNE, 1983

Université Libre de Bruxelles, Belgium

The Scientific Programme will cover the principal aspects of drug analysis, including bioanalytical techniques and therapeutic drug monitoring, analytical toxicology, drug formulation analysis, pharmaceutical quality control, process control optimisation techniques, computer-aided methods of drug analysis, and recent advances in analytical technology.

Plenary lectures will be presented by: E. Stahl, P. Buri, M. Pesez, J. Alary, M. Lesne, R.A. de Zeeuw and A.C. Moffat. Keynote Lecturers will be: S.L. Ali, P.M. Bersier, R. Bouché, L.G. Chatten, J. Crommen, A. David, A.F. Fell, S. Görög, A. Hulshoff, J.N. Miller, G.J. Patriarche, L.A. Sternson and J. Volke.

Oral and poster presentations will be integrated with Discussion Sessions in workshop style on: novel spectroscopic methods, electroanalytical techniques, progress in immunoassay methods and new perspectives for detection in HPLC.

For full details of Social Programme, Commercial Exhibition and Registration contact:

Dr. C. Van Kerchove, rue Archimedestraat 11, B-1040 BRUSSELS, Belgium Tel: (02)733.98.20 (ext. 33)

The Proceedings will be published as part of the first (1983) volume of the JOURNAL OF PHARMACEUTICAL AND BIOMEDICAL ANALYSIS. Full details available on request from your nearest Pergamon office.

Talanta, Vol 30, No 5, pp iii–iv, 1983
Pergamon Press Ltd Printed in Great Britain

PUBLICATIONS RECEIVED

Solving Problems in Analytical Chemistry: STEPHEN BREWER, Wiley, New York, 1980 Pages xvi + 538 £7 75

This book aims to provide students with a detailed guide to the calculations required in beginning an analytical chemistry course It contains a large number of solved problems which show the author's extensive experience in the field This is not the first book of its type but it includes a few topics not covered in its predecessors

Simple approximation methods have been used throughout for solving problems which would otherwise have very complicated and lengthy solutions It contains six chapters The first, which deals with useful statistics and stoichiometry, covers the basic statistics and mathematics clearly, but has two very prominent typographical mistakes In the second chapter, on acid–base chemistry, an easy approach towards solving the problems of multiple buffer systems is presented This chapter could have been made more comprehensive by including more graphical representations of acid–base equilibria Chapter 3 deals with solubility and is very short In my view it would have been better to have put section 5 12 (on activities and activity coefficients) here Chapter 4, which contains a printers' error in the very first table, includes, after some basic analytical material, calculations of physical constants Though the next chapter on potentiometry gives wide coverage of the subject, some important electrochemical techniques such as conductimetry and polarography are omitted The introduction of a section on ion-selective electrodes is very welcome, however The last chapter on separations not involving precipitation is the best written in the book It conveys clearly and precisely the fundamental principles of the techniques given Realistic examples are used throughout this chapter, with detailed solutions, supported by appropriate graphs

Unlike other books on analytical chemistry, however, this volume ignores complexometry almost completely, which seems a curious oversight in view of its importance The book could have been reduced in length by decreasing the number of detailed solutions to the problems It is surely not necessary to give solutions for all the problems of the same type, some could be left (with slight hints) for the students

However, this is a useful book for those who want quick guidance to solving analytical problems without unduly complicated calculations

M I FAROOQI

Electroanalytical Chemistry: Basic Principles and Applications: J A PLAMBECK, Wiley, New York, 1982 Pages xix + 404 £27 30

As regards the Basic Principles, it is difficult to fault this book, except that it spans an uncomfortably wide range of levels, from the balancing of redox equations to advanced voltammetric and chrono-methods It would be most at home in a library, where students at every stage could enjoy a chapter or so of its lucid prose and clear layout There is a full treatment of fundamentals, comprising 143 pages on units, electronics, computers, measurements, cells, ions, mobility, electrode surfaces and kinetics There follow about 70 pages on potentiometric analysis and about 150 pages on non-equilibrium electroanalysis The "Applications" in the title are slanted towards contemporary instrumentation, presented with a palatable amount of mathematics and electronics There are useful classified references, appendices of data, definitions and abbreviations, and interesting study problems (though, alas, without answers) The reviewer would have liked a rather more generous treatment of the chemical aspects of Applications, perhaps in place of the photographs of equipment, which probably add more to the price of the book than to its value But this is a personal, and minor, grumble about a work which will surely be used with much profit, and with pleasure

H S ROSSOTTI

General Handbook of On-Line Process Analysers: D J HUSKINS, Ellis Horwood, Chichester, 1982 Pages 239 £30 00

This book is the first of a series of five being written by the author, D J Huskins Books two to five are specifically devoted to descriptions of the various methods available for process control and their applications Some applications are given in this first volume, which also outlines the various abbreviations and symbols used throughout the series It does not, however, contain any detailed descriptions of the analysers Its intention is to give the reader a better understanding of the proper and correct use of analysers In this aim it succeeds to a considerable degree

As one has come to expect from the Horwood Publishing House, this book is extremely well produced and presented in a very attractive cover That its cost of £30 is relatively high is more a reflection on the economics of scientific publications on this scale than on the true value of this book 239 pages for £30 is not a very attractive proposition to the scientist wishing to purchase his own copy of this text, but it is at this level rather than as a library reference book that this volume has its real value

The volume provides an ideal introduction to the scientist embarking on a career in process instrumentation It has a large section devoted to estimation of errors in calibration and standardisation Also stressed in some detail is the need for a precise specification of the process requirement The similarity here between process instrumentation and automatic analysers for laboratory or clinical use is noticeable since both need a reliable specification in detail of the analysis required and the objective of providing the data Perhaps the only improvement that I would like to see in this volume

is a more detailed and explained section devoted to cost justifications In the small section devoted to costing—there are only four pages—some of the costings seem extremely low It becomes more important in today's economic climate to provide a true justification of large capital expenditure

On the whole the book is a valuable addition to the scientific literature and scientists are encouraged to purchase it

PETER B STOCKWELL

Talanta, Vol. 30, No. 4, pp. iii–iv, 1983
Pergamon Press Ltd. Printed in Great Britain

PUBLICATIONS RECEIVED

Education and Teaching in Analytical Chemistry: G. E. BAIULESCU, C. PATROESCU and R. A. CHALMERS. Ellis Horwood, 1982. Pages 190. £15.00.

Despite indications to the contrary in the publisher's blurb, this book is not concerned with the mechanics of teaching (except to a very minor extent) but with the authors' philosophies concerning chemistry in a university environment, the main concern being to promote "the basic idea that analytical chemistry is an independent science". There are no detailed recommendations for syllabus content, no suggested laboratory experiments, no hints on lecture demonstrations *etc.* In some ways this is a disappointment, considering the considerable teaching expertise the authors have between them. The first short chapter concerns "teaching and education in chemistry" which spends as much time discussing the role of research as the role of the textbook. This chapter together with the 5-page introduction is the nearest the authors get to the "chalk-face". The second chapter concerning "Teaching analytical chemistry" deals with the growth of the relevant literature, a potted history of analytical reaction chemistry, some general remarks about instruments, data processing and the applications of computers. The whole philosophy of the book is encapsulated in two paragraphs in this chapter.

"The study of chemical reactions is necessary for the future chemist to learn what chemistry is, in the same manner as learning about laboratory instruments shows him how to apply them. The use of properly chosen reactions in conjunction with an appropriate instrument gives perhaps an ideal connection of theory with practice.

For these reasons, modern teaching of analytical chemistry should contain a judicious mixture of reaction chemistry and instrumentation."

One could argue with the grammar but not with the sentiment.

The third chapter is entitled "Education in analytical chemistry" and devotes considerable space to two usually neglected (but vital) topics; those of sampling and sample dissolution. The elegant way of teaching inorganic reaction chemistry through qualitative analytical chemistry and the need to understand the physical chemistry basis of reactions are stressed. The principles of some important instrumental methods are discussed. This forms the longest section in the book (some 56 pages altogether) and is subdivided into two broad categories, "composition" and "structural analysis". The chapter concludes with a discussion of the three C's of the quality of the analyst—capability, correctness and creativity. The book concludes with a short "Afterword" in which the authors peer into the future and amongst other conclusions, state "In order to develop analytical chemistry, all countries, at least in their large educational establishments, will have to develop independent departments of analytical chemistry. Whereever absent, research institutes of analytical chemistry will have to be created".

What else can one say? The book is well written, and highly readable; almost anecdotal in places (though always fully referenced) it provides a wealth of background information and stimulating ideas. It should be compulsory reading for all those involved in the teaching of chemistry in institutions of higher and further education.

J. F. TYSON

Trace Organic Sample Handling: ERIC REID (ed.), Ellis Horwood, Chichester, 1981. Pages 383. £30.00.

The publication of conference proceedings complete in book form is not always to be welcomed—the good material is diluted by the not so good and much is also published elsewhere. Having thus introduced this book—based on the material presented at a symposium (in 1979)—and adding that the complex index numbers to papers are more of an irritation than an aid to the reader, I must go on to say that much valuable material is gathered here and arranged systematically to aid the reader. I have found the more general papers to be of greater interst, with some most readable contributions from workers at the Laboratory of the Government Chemist, among others. King's rather light-hearted *Evaluation of Occupational Exposure* reminds us of many pertinent questions which we may find more convenient to forget when sampling air for trace organics. Foods and medical samples are also dealt with in later papers. I am sure that all workers in trace analysis can learn something useful from this book, and for many it could be the beginning of a new look their techniques and procedures. The book deserves to find a wide readership.

IAIN L. MARR

Applied Complexometry: RUDOLF PŘIBIL, Pergamon Press, Oxford, 1982. Pages xv + 410, £37.50.

How often has the reader opted for an atomic-absorption determination of one or more metals in a mixture when the problem might have been solved quickly and cheaply by a complexometric titration? The advantages of the second choice—no lamp to buy, only one standard solution needed—are familiar to us all, but the selection of working conditions—of pH, indicator and masking reagents—has so often seemed fraught with obstacles and lack of information that the first choice has often been the instrumental one. Now, many such problems are solved at one go by Dr. Přibil, a respected grand master of the art of complexometry. Aided by a close team of two translators and an editor who have also contributed much to the book, he presents a thorough survey of the literature, liberally sprinkled with comments and opinions based on his long practical experience, and finally recommends his preferred approach to the analysis of each combination of metals.

The determinations are discussed element by element in one third of the book, while the last third deals with applications to the analysis of alloys (*e.g.*, of aluminium, of lead and of copper), of rocks and minerals, of slags, glasses and ceramics, and of plating solutions. The introductory sections give a very clear account of the background theory of complexometric

titrations, always bearing in mind the practical applications. Even in the last section the author's sense of humour holds out "evaporation with acid is not pleasant because of the HCN liberated . . .."

It is to be hoped that this book has not arrived too late to win a few converts back to complexometry. The reviewer welcomes it wholeheartedly and recommends it to every practising analytical chemist.

IAIN L. MARR

Some Instrumental Methods for the Determination of Minor and Trace Elements in Iron, Steel and Nonferrous Metals and Alloys (Monograph 884): ELSIE M. DONALDSON, CANMET, Energy, Mines and Resources Canada, Ottawa, 1982. Pages v + 107. $15.00 (Canada), $18.00 (Other).

Seldom in recent memory has so dense and practical a guide to the analysis of metal alloys appeared. The subject here is minor and trace constituents (ranging from a few per cent down to parts-per-million) and the techniques employed are a deft series of themes and variations based on solvent extraction and co-precipitation. In most instances, alternative final measurements—spectrophotometry and flame AAS—are described for the separated and concentrated analyte, and an abundance of appended tables documents the accuracy obtainable in each case.

This monograph is clearly the distillate of a career at the bench and brims with practical lore, while showing excellent command of classical separation techniques. There are few in the field of metals analysis who would not find here some nugget of new information. Most of the book derives from Mrs. Donaldson's contributions to this journal over the past two decades, but the material has been refined into a practical guide—in most respects, a laboratory manual.

If there is a point of objection, it arises from the very thoroughness of the approach, which removes many of the procedures from consideration where the exigencies of an industrial setting make time a factor. For example, matrix-matching techniques in atomic-absorption work obviate the need for many of the separations that the book describes and are certainly faster. The spectrophotometric arsenic method described in the book employs co-precipitation with iron and solvent extraction with potassium ethyl xanthate to isolate the analyte prior to measurement of the arsenomolybdate colour. While this represents an interesting alternative approach, there appears to be no time advantage over the more common halide distillation separation.

Mrs. Donaldson appears to favour certain separation schemes over a more eclectic approach and some of the methods are lengthy indeed, but the book is both impressive and valuable. Anyone engaged in metals analysis should include a copy on their shelf of basic texts.

THOMAS R. DULSKI

Talanta, Vol. 30, No. 2, pp iii–iv, 1983
Pergamon Press Ltd. Printed in Great Britain

PUBLICATIONS RECEIVED

Manuel Pratique de Chromatographie en Phase Liquide: 2nd Ed., R. ROSSET, M. CAUDE and A. JARDY, Masson, Paris, 1982. Pages XXIV + 374. FF 280.

This book deals with all major forms of column chromatography in which a liquid acts as mobile phase. Thus, solutes participating in adsorption (on a solid), partition between immiscible liquids, ion-exchange ("ion-chromatography"), ion-pair formation, ligand-exchange and exclusion processes are covered. After some generalities, fundamental aspects of column operation such as selectivity, resolution, performance indices and optimization are considered. As expected of a handbook on chromatography, apparatus and materials for column packing are given a good deal of attention and commercial suppliers are listed in a final chapter. Good clear diagrams are provided and the bibliographies at the end of each chapter, while not usually extensive, appear to be representative of the literature and to contain work published up to and including 1980.

Much practical information suitable for beginners is provided in this manual, which could also serve as a useful introduction to more specialized monographs on column chromatography with liquid mobile phases.

S. J. LYLE

Manuel Pratique de Chromatographie en Phase Gazeuse: 3rd Ed., Edited by J. TRANCHANT and written by J. F. GARDAIS, PH. GORIN, A. PRÉVÔT, J. SERPINET, J. TRANCHANT and G. UNTZ, Masson, Paris, 1982. Pages XXII + 504. FF 350.

Since its introduction in 1952 by James and Martin, chromatography in which the mobile phase is a gas or vapour has become a major technique for the separation and determination of volatile components of simple and complex mixtures of substances. The technique has continued to develop in many directions up to the present time and a text which sets out to provide a balanced account of theory and practice is to be welcomed. This manual is the product of a collaborative exercise involving specialists in different aspects of gas chromatography. After a general introduction, there are chapters on "getting started", detectors, columns, qualitative and quantitative analysis, theoretical aspects of separations and methodology. The work ends with chapters on applications of a physico-chemical nature and in chemical analysis.

The chapter dealing with detectors serves as a useful introduction to the range of devices available today. These are illustrated by the use of clear diagrams; performance characteristics, symptoms and causes of malfunction are discussed. Other useful chapters are those dealing with conventional filled columns and capillary columns. The latter should provide a useful guide to anyone intending to set up for the first time a chromatograph using this type of column. These key chapters are adequately supported by the others in the manual, with the exception of that dealing with applications in chemical analysis. It is clearly impossible to deal adequately with such applications in 25 pages of tables. On the whole this is a useful manual providing information on practical and background theoretical matters relating to the current "state of the art" in gas chromatography.

S. J. LYLE

Ion Exchange and Solvent Extraction, Vol. 8: JACOB A. MARINSKY and YIZHAK MARCUS (eds.), Dekker, New York, 1981. Pages XI + 438. SFr 154.

This latest volume in a continuing series contains some very useful articles, all in English. These reviews (with comments) are as follows: Chap. 1: Metal extraction with hydroxyoximes (Whewell and Hanson, U.K., 94 pp.) deals extensively with the solvent extraction of copper; Chap. 2: Electrical phenomena in solvent extraction (Scibona, Danesi and Fabiani, Italy, 133 pp.) covers the theory well throughout with a lengthy section on liquid membrane potentials; Chap. 3: Extraction with solvent-impregnated resins (Warshawsky, Israel, 82 pp.) includes applications of these resins in analytical, hydrometallurgical and water-treatment processes; Chap. 4: Solvent extraction of elements of the platinum group (Gindin, USSR, 58 pp.) includes information on much work reported in less accessible Russian journals; Chap. 5: Solvent extraction from aqueous-organic media (Hála, Czechoslovakia, 42 pp.) gives a short but useful review of a relatively new branch of solvent extraction.

Each chapter has an extensive reference list and the book contains author and subject indexes. The editors have selected their authors with care and all reviews are of an adequate standard. The first three articles are particularly recommended.

J. B. HEADRIDGE

L'Atomisation Electrothermique en Spectrométrie d'Absorption Atomique et son Application dans les Etudes de l'Environnement: M. HOENIG, S. DUPIRE et R. WOLLAST, Cebedoc, Liège, 1981. Pages V + 218. FF 180; BF 1260.

This is a useful little book written in French. It contains eight chapters with the following headings: Introduction and books of a general nature (a very short chapter), The atomization process, Perturbations to the atomization process,

Practical aspects of electrothermal atomization, Apparatus, Ashing and dissolution of samples, Concentration and separation of the analyte (a very short chapter) and Determination of individual elements. This last chapter occupies half the book and includes information on Sb, Ag, As, Be, Cd, Cr, Co, Cu, Mn, Ni, Pb, Se, V and Zn. At the end of most chapters and at the end of each section in the last chapter, there is a list of references to authors mentioned in the text. Bibliographies of well-selected papers are to be found at the end of Chapters 3 and 6, and throughout Chapter 8. These are particularly useful in this final chapter and includes some papers published in 1981. The book is recommended to those interested in determining trace elements in foods, blood, urine, bone, hair, biological tissues, plant materials, atmospheric particulates, dust, soils, coal, rocks and sediments, waters and sewage sludge.

J. B. HEADRIDGE

Talanta, Vol. 30, No. 1, p. iv, 1983
Pergamon Press Ltd. Printed in Great Britain

NOTICES

INTERNATIONAL SYMPOSIUM ON ELECTROANALYSIS IN BIOMEDICAL, ENVIRONMENTAL AND INDUSTRIAL SCIENCES

5–8 April 1983, UWIST, Cardiff, Wales

The Second Circular and Registration Forms for this Symposium, organized by the Electroanalytical Group and Western Region of the Analytical Division of the Royal Society of Chemistry, are now available from the Short Courses Section, UWIST, Cardiff CF1 3NU, Wales, United Kingdom.

The scientific programme will consist of plenary and keynote lectures, the presentation of contributed papers and an exhibition of scientific equipment. Invited lectures include:

B. J. Birch (UK) on "Interfaces for Electroanalysis in Industry"
T. M. Florence (Australia) on "Electrochemical Approaches to Metal Speciation"
I. Karube (Japan) on "Amperometric and Related Determinations with Immobilized Enzymes and Micro-organisms"
J. Ladenson (USA) on "Ion-selective Electrodes in Clinical Chemistry and Medicine"
A. L. Levin (USSR) on "Electroanalytical Approach to Acid–Base Balance and Gases in Blood"
C. A. Marsden (UK) on "Electrochemical Detection of Amines and Other Compounds of Pharmacological and Neurochemical Interest"
E. Pungor/K. Tóth (Hungary) on "Environmental and Industrial Flow Analysis with Electrochemical Detection"
J. D. R. Thomas (UK) on "The Changing Scene in Electrochemical Analysis"
M. Thompson (Canada) on "Biosensors and their Uses in Flow-Injection Systems"

FIRST INTERNATIONAL SYMPOSIUM KINETICS IN ANALYTICAL CHEMISTRY

CORDOBA, SPAIN, 27–30 SEPTEMBER 1983

The scope and aims of the conference are intended to reflect the rapid development and increasing importance of kinetic methods of analysis during recent years.

The scientific programme will include catalytic methods (including enzyme-catalysed applications), differential reaction rate methods, and any aspect of kinetic nature with an impact on analytical methodology.

The symposium will consist of plenary lectures, contributed papers, and posters.

ORGANIZING COMMITTEE:
Prof. H. A. Mottola (Stillwater, Oklahoma, USA)
Prof. J. P. Schwing (Strasbourg, France)
Prof. M. Valcárcel (Córdoba, Spain)
Secretary: Prof. D. Pérez-Bendito (Córdoba, Spain)

An interesting social programme, including the get-together party, the conference dinner and several picturesque visits (Arabian Mezquita, Medina Azahara palace, Spanish wine bodega ...) will be arranged.

A special sightseeing excursion to Sevilla and/or Granada is being planned for Saturday, 1 October, for those interested.

Further information can be obtained from:

Prof. D. Pérez-Bendito
Departamento de Química Analítica
Facultad de Ciencias
Universidad de Córdoba
CORDOBA, ESPAÑA.

Talanta, Vol 30, No 5, p v, 1983
Pergamon Press Ltd Printed in Great Britain

ERRATUM

In the paper by V S. Tripathi (*Talanta*, 1983, **30**, 65), a line was accidentally transposed in the last paragraph on p. 67 The 9th line should have been the 14th, and the paragraph should read as follows.

> The proposed algorithm requires two one-dimensional arrays of size $\hat{n}$ NC, one one-dimensional array of size NC and two one-dimensional arrays of size MAXCOM (MAXCOM is rarely greater than 7 or 8) The total array requirement for the scheme is $(2\hat{n} + 1)$NC + 2MAXCOM The conventional method of using a two-dimensional array would have required an array of size NC NX It is evident that in the proposed scheme, the storage needed for stoichiometric coefficients depends only on the number of complexes plus solids and on $\hat{n}$ In other words, for fixed $\hat{n}$ and NC, the required storage is independent of the number of components in the problem. For the conventional method, the size of the NX NC array depends on both the number of complexes and the number of components The total storage requirements of some programs (for solution phase computations alone), including CHEMEQUIL ($\hat{n} = 4$), are shown in Table 3

Talanta, Vol. 30, No. 2, pp. v–vi, 1983
Pergamon Press Ltd. Printed in Great Britain

NOTICES

INTERNATIONAL SOLVENT EXTRACTION CONFERENCE DENVER, COLORADO, U.S.A.

26 AUGUST–2 SEPTEMBER 1983

SPONSORED BY: American Institute of Chemical Engineers
CO-SPONSORS: American Chemical Society, Industrial Chemistry Division The Metallurgical Society of the American Institute of Mining, Metallurgical and Petroleum Engineers

International Solvent Extraction Conferences (under the aegis of the International Committee for Solvent Extraction Chemistry and Technology) are now being held at three-year intervals at central locations throughout the world. ISEC '77 in Toronto, Canada and ISEC '80 in Liège, Belgium each attracted some 500 delegates and 150 papers. The conferences offer a broad technical programme covering all phases of solvent extraction and related technologies and feature social activities geared to both conference delegates and their guests and spouses.

The initial announcement of ISEC '83 generated 600 responses requesting future mailings and 350 offers of papers. This extremely positive reception insures an excellent conference with a diverse selection of papers. Additional details regarding ISEC '83 are now available. This update will help you plan for your attendance at ISEC '83 and provide information to members of the American Chemical Society (ACS) and The Metallurgical Society (TMS) of the American Institute of Mining, Metallurgical and Petroleum Engineers (AIME) who might not be familiar with ISEC meetings.

The format for the technical programme will generally follow the pattern at past ISEC meetings. Plenary lectures by a leading authority will open each day of technical sessions (except Friday). These will be followed by oral paper presentations Saturday afternoon and Monday, Tuesday, Thursday and Friday mornings. Monday, Tuesday and Thursday afternoons will be devoted to poster sessions. We are attempting to schedule nineteen oral sessions of five papers each on the following topics: Novel Extractants, Physical Chemistry, Analytical Chemistry, Interfacial Kinetics (including Interphase Mass Transfer), Fluid Mechanics (including Phase Separation and Interfacial Phenomena), Modelling of Extractors (including Effects of Axial Mixing), Inorganic Processes, Metallurgical Processes, Nuclear Processes, Fuel and Chemical Processes, Pharmaceutical/Biological Processes, Liquid Membranes (Emulsion), Solid Supported Liquid Membranes, Equipment, Field Performance, and Supercritical Extraction.

Note: Two sessions each are at present scheduled for Physical Chemistry, Metallurgical Processes and Nuclear Processes.

FINAL CALL FOR PAPERS

All respondents to the first circular who indicated an interest in contributing a paper have been sent a proposal form. Sessions have already been identified on the basis of returned proposals. Anyone else interested in contributing a paper should promptly contact:

Dean C. Judson King
College of Chemistry
University of California
420 Latimer Hall
Berkeley, CA 94720 USA

ACCOMMODATION AND REGISTRATION

Seven hundred rooms have been reserved at the Denver Hilton Hotel where the meeting is being held. There is frequent bus service from the Denver Airport.

The registration fee will be $300. This fee will include the proceedings of the conference (in the form of two-page summaries or extending abstracts) but *excluding* tours and meals, etc. There will be a late registration charge. Send applications to:

ISEC '83
c/o Don Nowak, Registration Manager
American Institute of Chemical Engineers 345 E. 47th St.
New York, NY 10017 USA

FACSS
FEDERATION OF ANALYTICAL CHEMISTRY AND SPECTROSCOPY SOCIETIES

The Tenth annual meeting of the Federation of Analytical Chemistry and Spectroscopy Societies (FACSS) convenes 25–30 September 1983, at the Franklin Plaza Hotel, Philadelphia, PA. The sponsoring organizations for the meeting are: the Society for Applied Spectroscopy; the Division of Analytical Chemistry of the American Chemical Society; the Association of Analytical Chemists, Inc. (Anachem); the Analysis Instrumentation Division of the Instrument Society of America; and the Chromatography Forum of the Delaware Valley. Information can be obtained from:

John O. Lephart
1983 Program Chairman
Philip Morris R & D
P.O. Box 26583
Richmond, VA 23261

Talanta, Vol 30, No 5, p vi, 1983
Pergamon Press Ltd Printed in Great Britain

NOTICES

35th G.A.M.S. CONGRESS
35th ANALYTICAL CHEMISTRY CONGRESS

PARIS, 5–9 DECEMBER 1983

This joint congress will be held in the Ecole Supérieure des Techniques Avancées (ENSTA), porte de Versailles à Paris It is organized by G A M S with the active collaboration of the French Federation of Chemistry, the Analytical Chemistry Division of the Chemical Society of France, the Analytical Chemistry Group of the Society of Industrial Chemistry, the Society of Biological Chemistry, the Society of Therapeutic Chemistry, the Society of Physical Chemistry, and the Interprofessional Committee of Laboratory Suppliers It is a national meeting, with foreign participation, conducted in French, but oral or poster communications in English may be accepted

The topics include Fundamental problems of trace analysis, Particle analysis, Data acquisition and treatment, Point analysis (extended X-ray fine absorption structure, Rutherford back-scattering spectroscopy, energy-loss spectroscopy, resonance ionization spectroscopy, optogalvanic spectrometry, optoacoustic spectrometry), Recent progress in metallurgical analysis, On-line analysis, Environmental and toxicological analysis, Pharmaceutic analysis, Recent methods in non-destructive analysis and telemetric analysis, Technical and economic problems in instrumentation, Analysis of heavy fractions of petroleum, Food and foodstuffs analysis

Abstracts of papers offered should reach G A M S , 88 Boulevard Malesherbes, 75008 Paris, by 15 May Information may be obtained from the same address

1984 WINTER CONFERENCE ON PLASMA SPECTROCHEMISTRY

SAN DIEGO, CALIFORNIA
2–6 JANUARY 1984

The 1984 Winter Conference on Plasma Spectrochemistry, sponsored by the *ICP Information Newsletter*, will feature developments in atomic plasma spectrochemical analysis by inductively coupled plasma (ICP), DC plasma (DCP), and microwave plasma (MIP) excitation sources The meeting will be from Monday, January 2 to Friday, January 6, at the Vacation Village Hotel and Convention Center in San Diego, California

Papers describing applications, fundamentals, and instrumental developments with atomic plasmas (ICP, DCP, MIP) will be presented in lecture and poster sessions General and special symposia organized and chaired by internationally recognized experts will include the following topics (1) automation in plasma spectroscopy, (2) applications to air, biologicals, chemicals, coal, food, metals, ores, plants, petroleum, soils, rocks, wastes, and waters, (3) combined plasma methods (chromatography, chemical/electrical aerosol generation, mass spectrometry), (4) excitation mechanisms, (5) modern data treatment, (6) new instrumentation, (7) sample introduction and transport phenomena, and (8) quality assurance and control programmes Five plenary and five invited review lectures will feature leading international experts Afternoon sessions will be devoted to poster presentations, and three evening discussions will focus upon new direction and techniques in plasma instrumentations, problem solving with plasma spectroscopy, and guidelines for selecting as plasma instrument

Invited and submitted papers will be published, following the meeting and after peer review, in a leading spectroscopy journal and in book form as the official conference proceedings

The preregistration fee is $175 until 21 October 1983, after that it will be $250 No registration fee is required for spouses

For information and registration forms contact the conference chairman

Dr Ramon M Barnes,
Department of Chemistry,
GRC Towers,
University of Massachusetts,
Amherst, MA 01003, U S A

THIRD INTERNATIONAL SYMPOSIUM ON ANALYTICAL APPLICATIONS OF BIOLUMINESCENCE AND CHEMILUMINESCENCE

BIRMINGHAM, 17–19 APRIL 1984

The Third International Symposium on Analytical Applications of Bioluminescence and Chemiluminescence will be held from 17 to 19 April 1984 in Birmingham, England Topics to be covered include luminescence in immunoassay, immobilized luminescent reagents, enhanced luminescence, new luminescence reagents, cellular luminescence, phagocytosis, rapid microbiology and instrumentation

If you wish to be placed on the conference mailing list, please write to

Dr L J Kricka,
Department of Clinical Chemistry,
Wolfson Research Laboratories,
Queen Elizabeth Medical Centre,
Edgbaston, Birmingham B15 2TH, England

AUTHOR INDEX